Applied Ecology and Environmental Research

International Scientific Journal

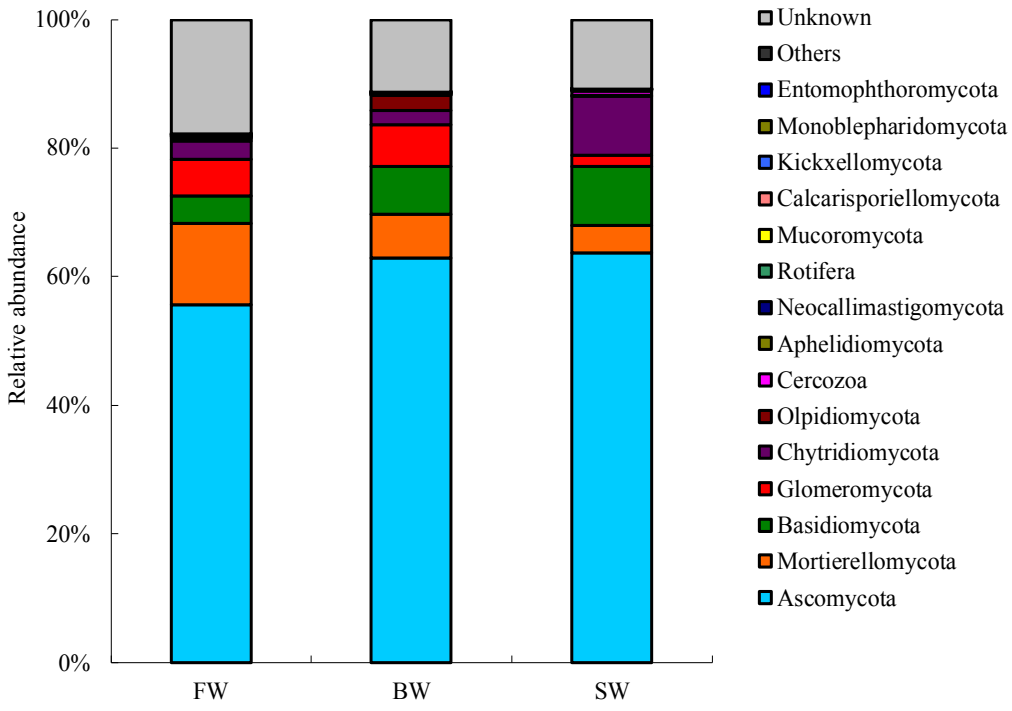

VOLUME 18 * NUMBER 4 * 2020

http://www.aloki.hu
ISSN 1589 1623 / ISSN 1785 0037
DOI: http://dx.doi.org/10.15666/aeer

PHYSIOLOGICAL AND PROTEOMIC RESPONSES OF *DENDROCALAMUS MINOR* VAR. *AMOENUS* (GHOST BAMBOO) UNDER DROUGHT STRESS

HE, T. Y.[1] – FAN, L. L.[2] – TARIN, M. W. K.[1] – SHEN, S. Y.[1] – XIE, D. J.[2] – CHEN, L. Y.[1] – RONG, J. D.[2] – CHEN, L. G.[2] – ZHENG, Y. S.[1, 2*]

[1]*College of Arts & College of Landscape Architecture, Fujian Agriculture and Forestry University, Fuzhou 350002, Fujian Province, PR China*

[2]*College of Forestry, Fujian Agriculture and Forestry University, Fuzhou 350002, Fujian Province, PR China*

**Corresponding author*
e-mail: zys1960@163.com; phone: +86-0591-8375-8750

(Received 9th Dec 2019; accepted 6th May 2020)

Abstract. *Dendrocalamus minor* var. *amoenus* was analyzed for physiological and proteomic responses under drought stress. The adverse effects of drought on *D. minor* var. *amoenus* were primarily affected by gas exchange attributes such as photosynthesis (Pn), stomatal conductance (Gs), and transpiration rate (Tr) decreased as drought intensity increased. Among chlorophyll fluorescence parameters, actual photochemical efficiency of PSII (ΦPSII), electron transport rate (ETR), and non-photochemical quenching (qN) also decreased under increasing drought stress throughout the natural dehydration process (15-30 days). Moreover, superoxide dismutase (SOD) and catalase (CAT) levels increased significantly when subjected to short drought event and then decreased rapidly under severe drought stress. Using two-dimensional gel electrophoresis (2-DE), we detected more than 500 protein spots; 41 significant differentially expressed protein spots were uncovered under drought stress. Following matrix-assisted laser desorption/ionization time-of-flight mass spectrometry (MALDI-TOF-MS) identification and BLAST of these 41 proteins spots to an NCBI or Uniprot database, 33 differential protein spots were identified. In addition to determining a suitable protocol for protein extraction from *D. minor* var. *amoenus* (or other bamboo species), this study provides important information on signal transduction pathway changes under drought stress for exploring drought resistance candidate genes in bamboo species.
Keywords: *gas exchange, chlorophyll fluorescence, gel electrophoresis, proteins spots*

Introduction

In recent years, the greenhouse effect has led to increasingly more severe environmental conditions related to global warming (Khaliq et al., 2019). In many locations, extreme drought disasters have occurred, seriously threatening the agricultural and silvicultural production as well as ecological and environmental protection efforts (Thalmann and Santelia, 2017). Drought is a significant abiotic stress factor that affects the growth and development of plants (Tayyab et al., 2018). Plant growth changes and response mechanisms under water deficit conditions have always been important scientific research subjects. Plants reduce damage caused by drought stress through changes in morphological structure, physiological responses, and biochemical processes, such as growth rate, stomatal conductance, tissue permeability, and antioxidant defense (Caruso et al., 2008; Tarin et al., 2020). When subjected to drought deficit conditions, plant responses vary greatly at three different levels; whole-plant, cellular, and molecular (Chalker-Scott, 1999).

http://www.aloki.hu ● ISSN 1589 1623 (Print) ● ISSN 1785 0037 (Online)
DOI: http://dx.doi.org/10.15666/aeer/1804_48174838

At the whole-plant level, drought deficit condition often leads to internal water imbalances, decreases cell water potential, and turgor pressure, resulting in shoot and leaf wilting and drooping. If such conditions persist, plants often lead to serious water loss from cell protoplasts and eventually plant death (Tarin et al., 2018). The adverse effects of drought stress have frequently manifested a decrease in phenotypic growth and photosynthesis, which are factors associated with changes in substance metabolism (Lawlor and Cornic, 2002; Rouhi et al., 2007; Koh et al., 2015). Photosynthetic activity and plant leaf structure are significantly impaired due to declines in stomatal closure and photosynthesis-related enzymes under drought stress (Chaves et al., 2009; Aranjuelo et al., 2010). The decrease in photosynthetic activity is caused by both stomatal and non-stomatal limitations. Under mild stress conditions, a stomatal limitation is a primary factor affecting photosynthesis; however, when severe stress damages photosynthetic organs and their structure, photosynthesis becomes increasingly influenced by non-stomatal limitation in chloroplast CO_2 fixation ability, rather than CO_2 diffusion resistance (Bota et al., 2004; Grassi and Magnani, 2005; Lawlor and Tezara, 2009).

At the cellular level, drought deficit conditions often lead to the accumulation of numerous substances that regulate osmotic pressure, including proline (PRO), soluble sugar, betaine, etc. (Kaushal and Wani, 2016). These substances increase cytoplasmic concentration levels, lower osmotic potential, and help maintain cell turgor pressure, allowing cells to continue to absorb water from the environment, sustaining plant morphological and physiological characteristics (Costa et al., 1998). Additionally, drought deficit conditions often lead to the accumulation of antioxidant enzymes (e.g., SOD and CAT), which enhance the capabilities of scavenging reactive oxygen species (ROS) such as H_2O_2 and O^{2-}, reducing their adverse effect on normal photosynthetic functions (Luna et al., 2004; Wang et al., 2009; Caverzan et al., 2016).

At the molecular level, drought deficit conditions often alter gene expression and protein synthesis (upregulation and downregulation), leading to changes in biological functions. Several molecular mechanisms of drought stress in many plants, including Arabidopsis (Zou et al., 2010), rice (Yang et al., 2012) and maize (Liu et al., 2013), were studied and elucidated by describing the quantitative trait locus (QTL), gene cloning, mutant screening, expression profiling, and functional verification of candidate genes. Specifically, the *Arabidopsis thaliana* glutathione peroxidase 3 (ATGPX3) enzyme can regulate abscisic acid (ABA) and initiate oxidative signal transduction in response to drought, leading to dynamic H_2O_2 balance in the cell (Miao et al., 2006). Unlike DNA or RNA, proteins can be directly involved in plant stress responses, and proteomics research can more intuitively reveal relationships between protein abundance and plant stress responses (Kosová et al., 2011).

Expression changes in plant proteins under drought stress can be divided into three categories: (1) signaling cascades and transcription-related proteins (e.g., protein kinase, protein phosphatase, and transcription factors); (2) functional proteins that protect the cell membrane and related proteins (e.g., embryonic period proteins, antioxidants, and osmotic-adjustment proteins); and (3) proteins associated with water and ion absorption (e.g., aquaporin and sugar transporters) (Fang and Xiong, 2015). Previous research using isobaric tags for relative and absolute quantitation (iTRAQ) and two-dimensional difference in gel electrophoresis (2D-DIGE) technology in desert poplar (*Populus euphratica*) (Bogeat-Triboulot et al., 2007), soybean (*Glycine max*) (Alam et al., 2010) and rapeseed (*Brassica napus*) (Koh et al., 2015) used proteomic analysis to reveal the

http://www.aloki.hu ● ISSN 1589 1623 (Print) ● ISSN 1785 0037 (Online)
DOI: http://dx.doi.org/10.15666/aeer/1804_48174838

effects of drought stress and related response mechanisms. Consequently, proteomic analysis can be used to identify several proteins involved in oxidative stress detoxification, signaling pathways, and protein folding.

D. minor var. *amoenus* is an important ornamental bamboo species of economic importance. Known for its exotic coloration, this plant exhibits several dark green vertical stripes interspersed with light yellow at the internodes. This bamboo species was introduced in coastal sandy areas in Fujian province as a novel windbreak and dune-fixing plant species for use in a mixed planting with wetland pine. In recent years, *D. minor* var. *amoenus* has been widely used in landscape and forest protection efforts. However, bamboo introduction to coastal sandy shelterbelt areas and its use in forest protection programs have been adversely affected because soil moisture and nutrient content are relatively low in coastal sandy soils, and environmental conditions for planting in these locations are poor. Continuous drought has also seriously affected both the ornamental characteristics of the bamboo and the survival rate of new bamboo shoots, especially during out-shoot periods. Recently, there are few studies on the drought-resistance mechanism of bamboo species with a focus on the physiology, biochemical attributes, photosynthetic pigments, water potential, photosynthetic activity (Wu et al., 2019; Tong et al., 2020). However, studies on the physiological and proteomic responses of *D. minor* var. *amoenus* under drought stress have received nearly no prior research. Therefore, efforts to investigate drought response mechanisms and enhance stress tolerance in *D. minor* var. *amoenus* will be vital to enhance landscape benefits and bamboo shoot production.

In this study, we conducted an integrated physiological and proteomic analysis of *D. minor* var. *amoenus* under drought stress. First, we optimized the protocol for protein extraction in bamboo species *D. minor* var. *amoenus*. We then assessed several physiological responses, biochemical processes, and different proteome expressions of the plant under drought stress. These results will contribute to the knowledge and understanding of the response mechanisms of bamboo species under drought stress. Additionally, they provide important information on changes in the signal transduction pathway in bamboo species under drought stress and provide an experimental basis for exploring drought resistance candidate genes of bamboo species through proteomic methods. This study is also of significant importance for future exploration of molecular genetics and transgenic breeding of bamboo species.

Materials and methods

Plant materials

Two-year-old *D. minor var. amoenus* plants were obtained from bamboo coastal sandy protection areas (Dongshan Island, Fujian, China) with similar growth conditions and directly transplanted to the Bamboo Research Institute of the Fujian Agriculture and Forestry University (*Fig. A1* in the *Appendix*). Seedlings were cultivated in plastic basins (height = 180 mm and diameter = 240 mm), containing a mixed nutrient medium of peat and matrix (1:2) in a greenhouse. The environmental conditions were 32/20 °C (day/night) with a photoperiod of 14 h under natural daylight, the relative humidity of 75-85%, and photosynthetically active radiation of 900 μmol $m^{-2}.s^{-1}$. Plants were irrigated with tap water every day to reach maximum water holding capacity. Drought stress was initiated after 6 months of normal growth. Half the bamboo plants continued to be irrigated regularly maintained in optimal water availability conditions, whereas the

http://www.aloki.hu ● ISSN 1589 1623 (Print) ● ISSN 1785 0037 (Online)
DOI: http://dx.doi.org/10.15666/aeer/1804_48174838

other half (randomly selected) was not irrigated to exposed to natural drought conditions (with water withholding). Over a month, drought plants were grown without any watering, whereas control plants were watered until basins capacity. Plant leaves used for physiological analysis were harvested at days 0, 5, 10, 15, 20, 23, 26, and 30, whereas leaves used for proteome analysis were harvested at days 0 and 26. In total 20 pots were handled (10 for drought conditions and 10 for control). At each sampling time, three biological replicates (3 or more than 3 independent pots, randomly selected with leaves at the same internode position) for each exploration were examined. Leaf samples were selected and kept on ice. Residual dirt was removed from the leaves with double-distilled water. Materials were immediately frozen in liquid nitrogen and stored at -80 °C before protein extraction and enzyme measurement.

Determination of soil water content and leaf water potential

Soil water content (SWC) and leaf water potential (LWP) of the bamboo plants were measured at days 0, 5, 10, 15, 20, 23, 26, and 30, after cessation of irrigation. LWP of the bamboo leaves was measured at different time intervals using a WP4-T potential meter (Decagon, USA) as described in a previous study (Ebrahimi-Birang and Fredlund, 2016). SWC was measured at the same time intervals as LWP, using a TZS soil moisture meter (TUOPU, China). At each sampling time, three replicates were measured for SWC and LWP.

Determination of photosynthetic and chlorophyll fluorescence parameters

Bamboo leaves were enclosed in an LI-6400XT portable photosynthesis system (LI-COR, USA) for 2.5 h from 9:00 to 11:30 am during each time node for measurement of photosynthetic parameters, including net photosynthetic rate (Pn), intercellular CO_2 concentration (Ci), stomatal conductance (Gs), and transpiration rate (Tr). Photosynthetic photon intensity and CO_2 levels inside the leaf chamber were maintained at 1000 μmol $m^{-2}.s^{-1}$ and 400 $mmol^{-1}.s^{-1}$, respectively. Water use efficiency (PWUE) and stomatal limitation values (Ls) were calculated by the following equations (Deeba et al., 2012):

$$Water\ use\ efficiency = Pn/Tr \quad \text{(Eq.1)}$$

$$Stomatal\ limitation\ = Ci/Co \quad \text{(Eq.2)}$$

where Pn is the net photosynthetic rate, Tr is transpiration rate, Ci is intercellular CO_2 concentration, and Co is the concentration of CO_2 outside the leaf, respectively.

The maximum photochemical efficiency of PSII (Fv/Fm) was measured after plant leaves had been pre-dark-adapted for 20 min within an OS5P fluorescence chamber (Opti-Sciences, USA). The actual photochemical efficiency of PSII (ΦPSII), the relative rate of photosynthetic electron transport (ETR), and non-photochemical quenching coefficient (qN) were determined simultaneously using the same device. Calculations for these parameters were done according to the instrument manufacturer's instructions (Sobrado, 2011).

Content or activity of antioxidant enzyme and osmosis substance

To determine the content or activity of physiological enzymes precisely weighed leaves were mechanically ground to powder in liquid N_2 and then homogenized in 4-

http://www.aloki.hu ● ISSN 1589 1623 (Print) ● ISSN 1785 0037 (Online)
DOI: http://dx.doi.org/10.15666/aeer/1804_48174838

fold 0.9% saline solution (V/W) to generate a 20% tissue homogenate. Homogenates were centrifuged at 4500 × *g* for 10 min and the supernatants were used for enzyme analysis. Superoxide dismutase (SOD), catalase (CAT), malondialdehyde (MDA), and proline (PRO) levels were examined using the corresponding assay kits according to the manufacturer's instructions (Nanjing Jiancheng Bioengineering Institute, Nanjing, China). Values were normalized following protein concentration determination via Coomassie Brilliant Blue method (Bradford, 1976).

Total proteins sample extraction

A process workflow for total protein extraction of *D. minor var. amoenus* leaves is shown in *Figure 1*. Detailed experimental methods follow: frozen leaves with midribs removed (0.2 g) were ground into powder in liquid N_2 in a pre-cooled mortar. The powder was incubated in 1 mL pre-chilled NP-40 protein extract buffer (0.5 M Tris-HCl, pH 8 2% [v/v]; β-mercaptoethanol, 2% [v/v] NP-40; 20 mM $MgCl_2$; 1 mM EDTA; 1 mM PMSF; and 1% PVPP). Following ultrasonication, five volumes TCA/acetone extract solution (10% [w/v] TCA and 0.07% [v/v] β-mercaptoethanol) were added and the sample was kept at -20 °C overnight to ensure complete protein precipitation. Sedimentation was centrifuged at 4 °C, at 16000 × *g* for 15 min, and the supernatant was discarded and the pellets were rinsed four times with five volumes pre-chilled TCA/acetone extract solution. The solution was left standing at -20 °C for 30 min after the addition of the extract solution for each rinse. The resultant precipitate comprised the total proteins in the leaves of *D. minor var. amoenus*. After vacuum drying, pellets were lysed with rehydration solution (4% CHAPS, 40 mM DTT, 7 M urea, 2 M thiourea, and small amounts of protease inhibitors), considered the total protein sample in this work, and stored at -80 °C (Wang et al., 2006).

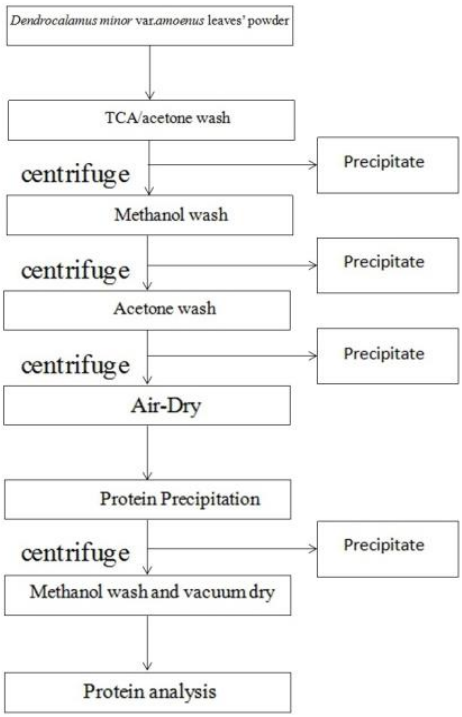

Figure 1. *Schematic workflow of total protein precipitation for D. minor var. amoenus proteome*

http://www.aloki.hu ● ISSN 1589 1623 (Print) ● ISSN 1785 0037 (Online)
DOI: http://dx.doi.org/10.15666/aeer/1804_48174838

Two-dimensional gel electrophoresis (2-DE)

Two-dimensional gel electrophoresis (2-DE) experiment was conducted following the BIO-RAD 2-DE Instruction Manual. Samples were loaded on 17 cm pH 5–8 immobilized pH gradient (IPG) strips (BIO-RAD, USA) by passive rehydration via absorption for 24 h with a loading weight and loading volume of 20 μg and 125 μL, respectively. A PROTEAN® i12™ IEF system was used to perform isoelectric focusing (IEF) at 20 ℃ and the current was limited to 50 μA per strip. IEF parameters were set as follows: 250 V (30 min), 500 V (30 min), 4000 V (boost for 3 h), 4000 V (focusing with 20000 V-h), and 500 V (hold).

Two experimental groups were frozen at -20 ℃ immediately, whereas a two-step balancing process was performed on another repeating group following first dimension electrophoresis. Equilibrate buffer (2% [w/v] SDS, 6 M urea, 20% [v/v] glycerol, 0.05 M Tris-HCl, pH 8.8, and 2% DTT) was used in the first balancing process for 15 min. In the second balancing process, equilibrate buffer (same as the first process, except that IAA was substituted for DTT) was also used for 15 min. SDS-PAGE was performed immediately after all equilibration steps were completed, using 12% separation gel and 120 V gel electrophoresis parameters, until the bromophenol blue indicator reached the gel base. After the second dimension electrophoresis, the gels were stained using a modified silver-staining method (Yan et al., 2000).

Gel with protein spots was visualized after silver staining. The spots were scanned using a UMAX Power Look 2100XL scanner (UMAX Systems, Willich, Germany) at 1000 dpi resolution in TIF format. PDQuest version 8.0.1 software (BIO-RAD, USA) was used to calculate and analyze protein spot images according to the manufacturer's instructions. Additional modifications were performed manually, after automated software detection, matching, and normalization, to reduce the potential for discrepancies during spot selection (Liu et al., 2015).

In-gel digestion and MALDI-TOF-MS identification

Differentially expressed protein spots were manually cut from the gels and were subjected to decolorization, in-gel trypsin digestion, and peptide extraction. Peptide mass fingerprint (PMF) spectrum analysis was then conducted using a 5800 MALDI-TOF-MS analyzer (Applied Biosystems, USA). Retrieval result reliability was evaluated using a ratio of peptide segment matching rate, protein score, and a sequence coverage of matched peptides in the corresponding protein, and then analyzed using biological mass spectrometry methods. A BLAST of MS spectra against the Uniprot and NCBI databases, using MASCOT2.2 software (Matrix Science, UK), was performed to search for PMF. Minimum ion scores for each identified MS data point were capped at or above 95% C. I. (Alam et al., 2010; Liu et al., 2015) to ensure result credibility.

Statistical and bioinformatics analysis

All parameters at different stress periods were statistically analyzed using SPSS 19.0 software (SPSS Science, USA). Data are reported as means with (±) standard deviation (SD). Multiple ANOVA comparisons were made using three replications; significance level was set at $P < 0.05$. Specifically, we calculated Pearson's correlation coefficient between photosynthetic parameters, SWC, and LWP.

http://www.aloki.hu ● ISSN 1589 1623 (Print) ● ISSN 1785 0037 (Online)
DOI: http://dx.doi.org/10.15666/aeer/1804_48174838

Bioinformatics analysis of the biological functions of differential proteins was performed using the Kyoto Encyclopedia of Genes and Genomes (KEGG) and Gene Ontology (GO) online analysis software. KEGG is a collection of pathway maps representing molecular interaction network information (Li et al., 2016), whereas GO is a classification system for gene function clusters that provide descriptions for genes and gene product attributes in organisms. GO uses three ontologies that describe the molecular function, cellular components, and biological processes (Li et al., 2016).

Results

Soil water content and leaf water potential

Soil water content (SWC) and leaf water potential (LWP) showed steadily decreasing trends throughout the treatment period, although no significant SWC trend differences were observed on days 15 and 20 (*Table A1* in the *Appendix*). SWC and LWP levels in the control group were maintained at 30–40% and -1.0 – -1.3 MPa, respectively, throughout the treatment period. SWC and LWP levels in the treatment group were lowered dramatically by 98% and 79% to 0.43% and -5.65 MPa, respectively. LWP decreased sharply when the treatment period was extended, whereas SWC declined slowly during days 20–30; however, this decrease was lower than that of LWP during the same timeframe.

Photosynthetic parameters

Photosynthetic parameters, including net photosynthesis (Pn), stomatal conductance (Gs), and transpiration rate (Tr), decreased significantly as the drought period was prolonged, although fluctuations in this trend were observed on days 10 and 23 (*Fig. 2*). However, declines in Pn, Gs, and Tr were slower than those in SWC. Pn, Gs, and Tr decreased by 4.38 μmol CO_2 $m^{-2} \cdot s^{-1}$, 0.11 mol H_2O $m^{-2} \cdot s^{-1}$, and 2.59 mmol H_2O $m^{-2} \cdot s^{-1}$, respectively during drought period days 0–23. Similar decreases in Pn, Gs, and Tr were noted (3.12 μmol CO_2 $m^{-2} \cdot s^{-1}$, 0.03 mol H_2O $m^{-2} \cdot s^{-1}$, and 1.32 H_2O $m^{-2} \cdot s^{-1}$, respectively) during days 23–30. *Figure 2* illustrates that Pn is more sensitive in terms of drought response than either Gs or Tr, decreasing by 7.50 μmol CO_2 $m^{-2} \cdot s^{-1}$ overall. No significant changes were observed in Ci during drought period days 0–15 compared to the control group; however, Ci also showed a downward trend during days 15–26, reaching a minimum of 395.68 μmol CO_2 mol^{-1} on day 26. PWUE increased initially, and then decreased slowly during days 5–20, before sharply decreasing after day 26. Similarly, Ls showed an upward trend during days 10–26, and then sharply decreased after days 26.

Besides, Pn, Gs, and Tr were significantly correlated with LWP ($P < 0.01$), and Pn was significantly correlated with both Gs and Tr ($P < 0.01$). Pn, Gs, and Tr were also found to be significantly correlated with SWC ($P < 0.01$) after correlation analysis was conducted between photosynthetic parameters, SWC, and LWP (*Table A2*).

Chlorophyll fluorescence parameters

Intrinsic photosynthetic efficiency of PSII (Fv/Fm) showed a decreasing trend throughout the drought stress period, and actual photochemical efficiency (ϕPSII) underwent a similar trend, both declining to minimum levels at day 30 by 28% and 82%, respectively (*Fig. 3*). Additionally, slight increases in the non-photochemical

http://www.aloki.hu ● ISSN 1589 1623 (Print) ● ISSN 1785 0037 (Online)
DOI: http://dx.doi.org/10.15666/aeer/1804_48174838

quenching coefficient (qN) were observed during days 5–15, but this parameter subsequently declined after day 15. Similarly, the apparent electron transfer rate (ETR) in the drought stress group increased slowly during days 0–10 but gradually decreased after day 10 (*Fig. 3*).

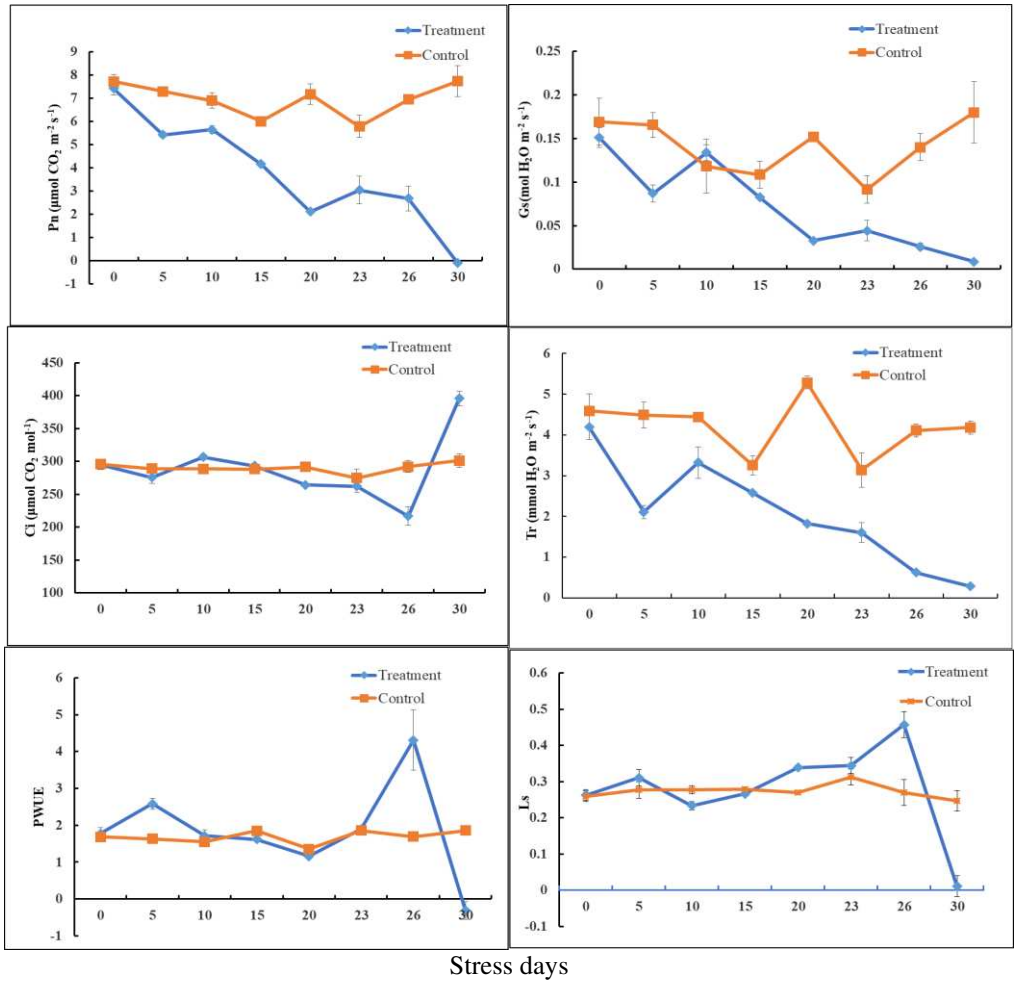

Figure 2. *Changes in photosynthetic parameters in leaves of D. minor var. amoenus under drought stress. Parameters include net photosynthetic rate (Pn), stomatal conductance (Gs), transpiration rate (Tr), intercellular CO_2 concentration (Ci), water use efficiency (PWUE), and stomatal limitation value (Ls). Vertical bars represent the standard deviations*

Antioxidant enzymes and osmotic substances

As drought conditions persisted, both PRO and MDA levels increased over time. Compared to the control group, during days 10–30, PRO levels increased 15-fold to 365 $\mu g.g^{-1}$, whereas MDA levels increased 3-fold to 14.6 $nmol.mg^{-1}$ prot. In response to drought stress, many plants increase antioxidant enzyme levels to remove ROS. Levels of two antioxidant enzymes, CAT and SOD, were measured to gauge damage response. Similar outcomes were produced in these two enzymes by drought stress, and a significant increase in SOD and CAT levels on day 10 was observed. However, a significant decrease in these two enzymes was also observed after day 10 (*Fig. 4*).

http://www.aloki.hu ● ISSN 1589 1623 (Print) ● ISSN 1785 0037 (Online)
DOI: http://dx.doi.org/10.15666/aeer/1804_48174838

Two-dimensional gel electrophoresis (2-DE) analysis

The 2-DE process was repeated thrice for each treatment group; representative gels are shown in *Figure 5*. More than 500 total protein spots were detected in silver-stained gels in each treatment. Several protein spots observed to have significant changes in abundance were also identified. These spots were identified using MALDI-TOF-MS for PMF identification. Among these, 41 protein spots were common to all gels and these were subjected to MS identification. Following MS identification, 33 protein spots were successfully identified (*Table A3*). Additionally, 23 protein spots were upregulated, 13 spots were downregulated, and 5 newly expressed spots were identified. Enlarged profiles of the 41 differentially expressed protein spots under drought stress are shown in *Figure 6.*

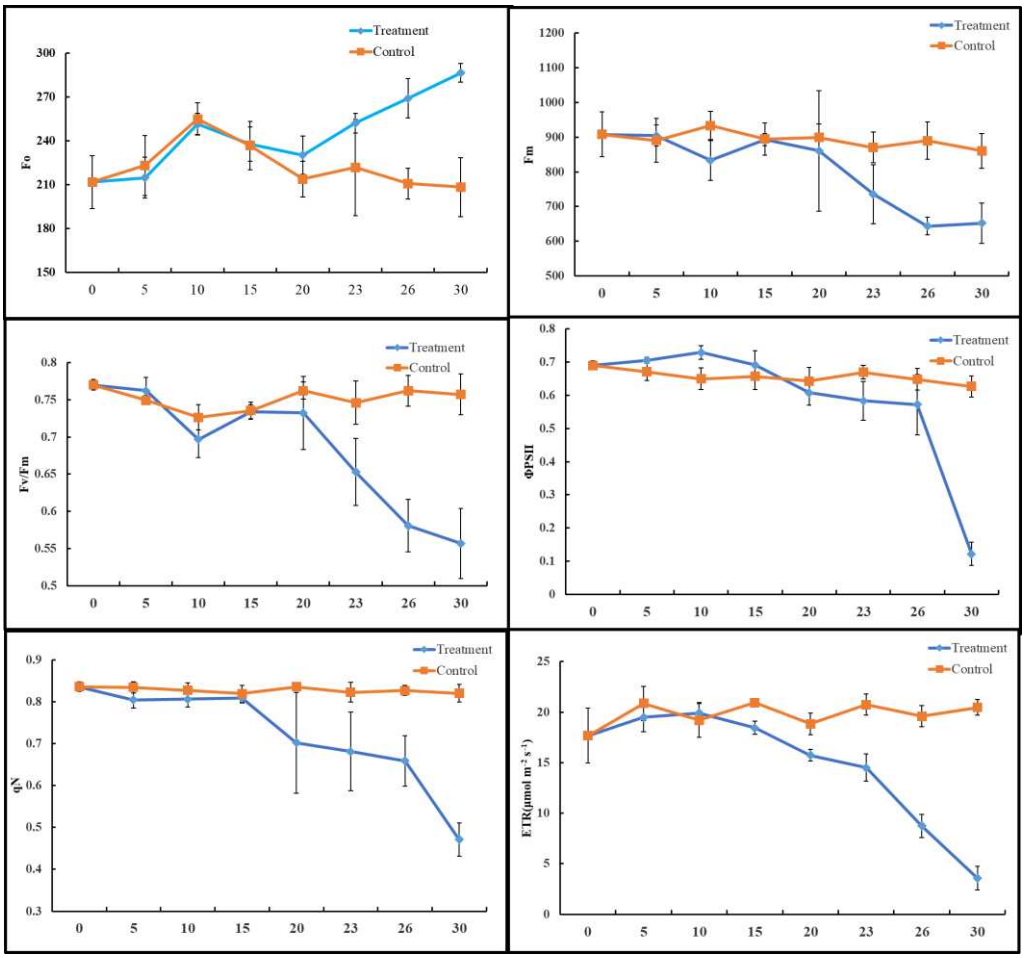

Figure 3. *Changes in chlorophyll fluorescence parameters in leaves of D. minor var. amoenus under drought stress. Parameters include initial minimum fluorescence (Fo), maximum fluorescence (Fm), quenching parameter (qN), maximum quantum yield of PSII (Fv/Fm), effective quantum yield (ϕPSII), electron transport rates (ETR). Vertical bars represent the standard deviations of the mean*

Upregulated protein spots

Upregulated protein spots were identified as oxygen-evolving enhancer protein 1 (spot 4), extra-large guanine nucleotide-binding protein 3-like isoform X2 (spot 21), 2-Cys peroxiredoxin BAS1 (spot 22), oxygen-evolving enhancer protein 2 (spot 23),

http://www.aloki.hu ● ISSN 1589 1623 (Print) ● ISSN 1785 0037 (Online)
DOI: http://dx.doi.org/10.15666/aeer/1804_48174838

calcium-dependent protein kinase (spot 29), PsbP chain A (spot 30), malate dehydrogenase (spot 31), flavin-containing monooxygenase (spot 35), glutathione S-transferase DHAR3 (spot 38), cytochrome b6-f complex iron-sulfur subunit (spot 39), and germin-like protein 8-14 (spot 40). Many upregulated proteins were associated with signaling transduction (e.g., spots 29 and 39), whereas some proteins (e.g., spots 4 and 23) were associated with photosynthesis.

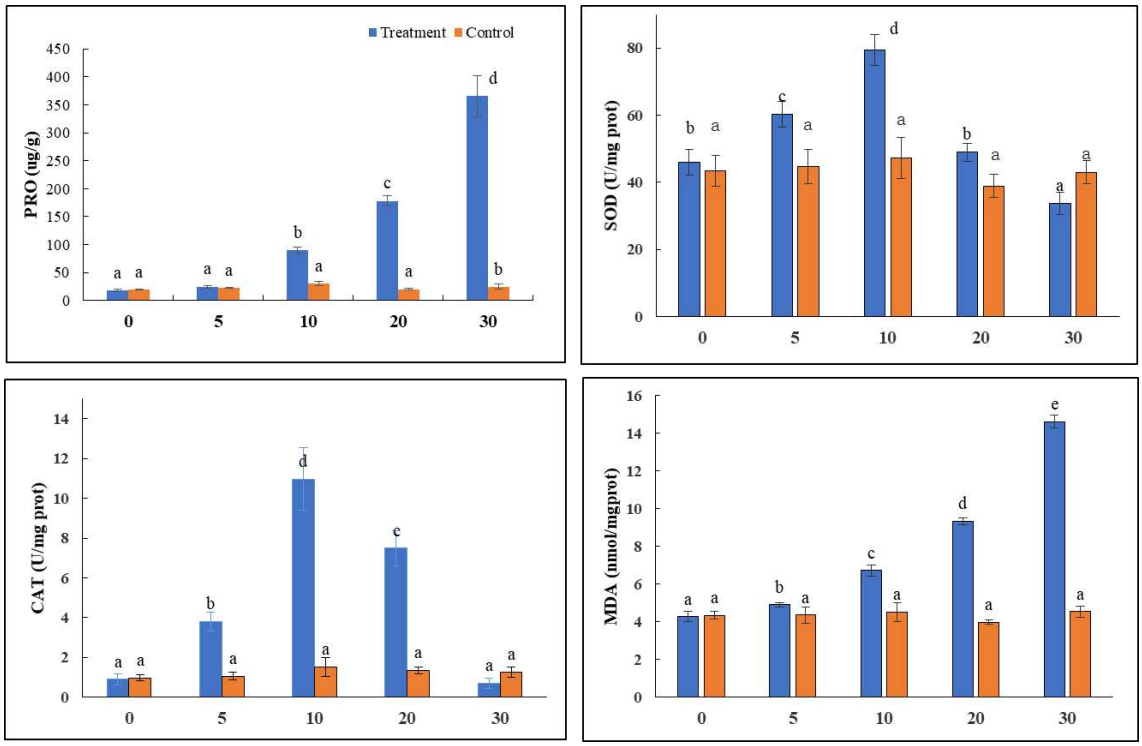

Figure 4. *Changes in proline (PRO), superoxide dismutase (SOD), catalase (CAT), and malondialdehyde (MDA) in leaves of D. minor var. amoenus under drought stress. Different letters indicate significant differences ($P < 0.05$) among various treatments with vertical bars as standard deviations*

Downregulated protein spots

Downregulated protein spots were identified as ribulose-1,5-bisphosphate carboxylase/oxygenase large subunit (spot 1), ribulose bisphosphate carboxylase small chain (spot 4), RuBisCO small subunit C (spot 5), ribosome-recycling factor (spot 16), ribulose bisphosphate carboxylase/oxygenase activase (spot 18), eukaryotic translation initiation factor 3 subunit A (spot 26), fructose-bisphosphate aldolase (spot 33), and ATP synthase CF1 beta subunit (spot 41). Many downregulated proteins were associated with photosynthesis (e.g., spots 1, 4, and 5), energy metabolism (e.g., spot 41), and translation (e.g., spot 26).

Newly expressed protein spots

Newly expressed protein spots included ferritin-1 (spot 10), transcription factor-related family protein (spot 14), and rca1 (spot 34).

http://www.aloki.hu ● ISSN 1589 1623 (Print) ● ISSN 1785 0037 (Online)
DOI: http://dx.doi.org/10.15666/aeer/1804_48174838

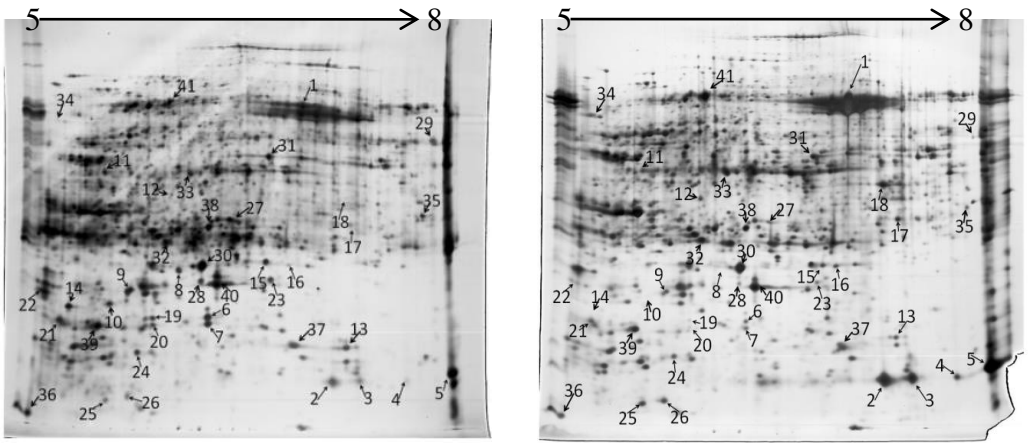

Figure 5. *Silver-stained two-dimensional proteome profiles gel of proteins extracted from leaves of D. minor var. amoenus grown under drought (left, day 0) and drought (right, day 26) conditions. In the first dimension, total protein was loaded on a 17 cm IEF strip with a linear gradient of pH 5-8. The second dimension was conducted in 12% polyacrylamide (w/v) gels (20 cm) (for details, see Materials and methods). The gel image analyses conducted with PDQuest software. The subsequent mass spectrometry analyses identified up to 41 proteins (marked by arrows) that were involved in the plant response to drought*

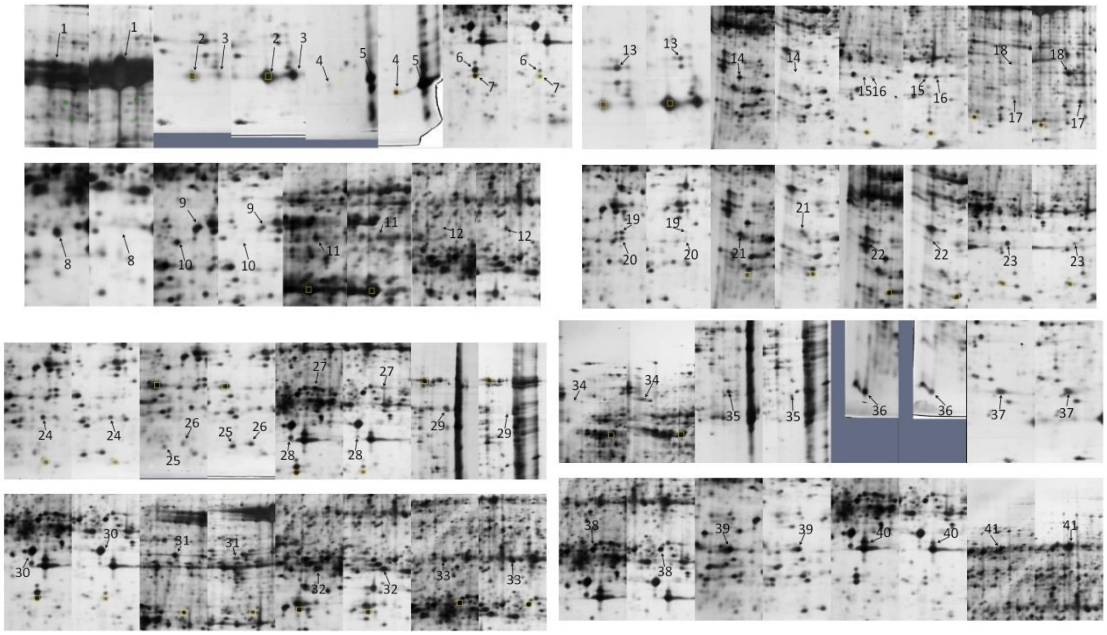

Figure 6. *Enlarged profiles of silver-stained gel of 41 differentially expressed protein spots in Figure 5 that under drought (left, day 26) and control (right, day 0) conditions. Among the same letter, left for the control group and right for the drought experimental group. The subsequent mass spectrometry analyses identified up to 41 proteins (marked by arrows) that were involved in the plant response to drought*

Bioinformatics analysis

Thirty-three differential abundance proteins were examined by GO and KEGG and classified into 19 GO terms. Of these, biological processes accounted for 10 terms,

http://www.aloki.hu ● ISSN 1589 1623 (Print) ● ISSN 1785 0037 (Online)
DOI: http://dx.doi.org/10.15666/aeer/1804_48174838

molecular functions accounted for 5 terms, and cellular components accounted for 4 terms. The most representative terms for each group included cellular processes GO: 0009987 and metabolic processes GO: 0008512; catalytic activity GO: 0003824 and binding GO: 0005488; and cell, membrane, and organelle, respectively (*Fig. 7*). KEGG pathway enrichment analysis revealed that most of these differential abundance proteins were largely involved in photosynthesis (map00195), carbon fixation in photosynthetic organisms (map00710), carbon metabolism (map01200), and glyoxylate and dicarboxylate metabolism (map00630; *Fig. 7*).

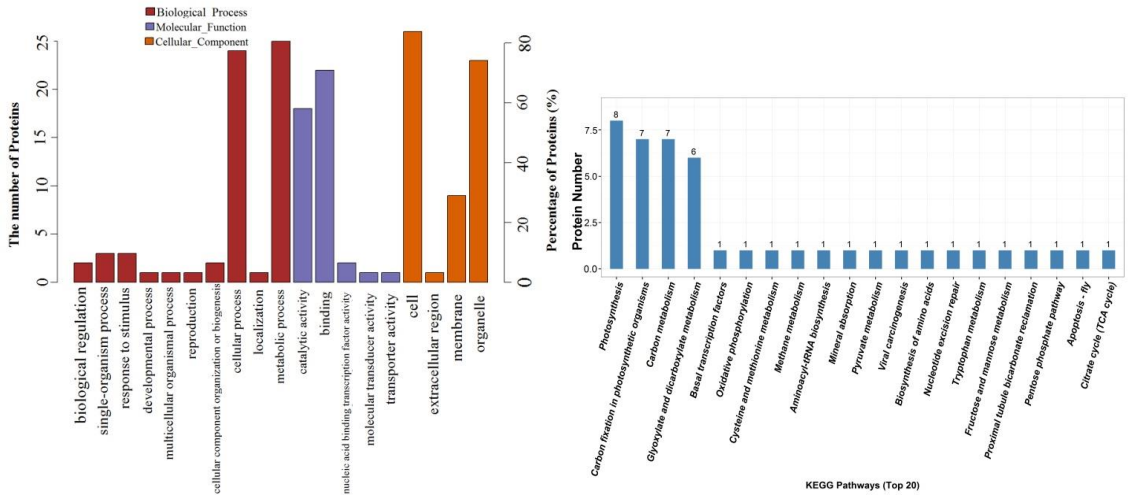

Figure 7. *GO function and KEGG enrichment analysis of differential expression proteins. GO function classification (left); KEGG pathway enrichment (right)*

Discussion

Physiological analysis under drought stress

Drought conditions intensify the various adverse effects such deficits have on plant characteristics, especially aspects related to effective soil water holding capacity, leading to irreparable leaf transpiration water loss and physical damage due to cell dehydration. These effects on plant morphological structure, physiological responses, and biochemical processes, including growth rate, stomatal conductance, tissue osmotic potential, and antioxidant defense, directly influence the normal growth and physiological processes of plants (Caruso et al., 2008; Xu et al., 2008). In this study, SWC and Pn were negatively influenced, showing a significant downward trend under prolonged drought stress. However, some fluctuations in Pn were observed on days 10 and 23, which can be attributed to fluctuations among several key environmental factors such as temperature and humidity during the treatment period. Under drought stress, the plant can decrease transpiration water loss rates by reducing stomatal conductance or through stomatal closure, although such measures also inhibit CO_2 transport efficiency in leaf cells. Stomatal and non-stomatal limitation factors hinder plant photosynthesis; intercellular CO_2 concentration (Ci) levels and stomatal limitation (Ls) rates can also help predict whether changes leading to Pn increases or decreases are primarily due to stomatal or non-stomatal limitations (Chaves et al., 2009; Lawlor and Tezara, 2009). Correlation analysis showed that Pn, Gs, and Tr were significantly associated with bamboo LWP during drought stress (*Table A2*). This is because plant transpiration

http://www.aloki.hu ● ISSN 1589 1623 (Print) ● ISSN 1785 0037 (Online)
DOI: http://dx.doi.org/10.15666/aeer/1804_48174838

intensity can be influenced by both SWC and inner-outer leaf LWP. Additionally, the physiological state of the plant itself can also regulate transpiration. In this study, we found that leaf intercellular CO_2 concentrations increased significantly ($P < 0.05$) during days 26–30, whereas Ls decreased significantly, indicating that the leaf cell structure had experienced certain levels of physical damage and illustrating the resultant photosynthetic shifts from stomatal to non-stomatal limitations.

Chlorophyll fluorescence kinetic parameters can be used to detect photosynthetic changes in plants under stress conditions quickly, accurately, and without damage to the plant leaf. Photosystem II (PSII) can be severely inhibited during drought stress. PSII also regulates electron transfer rates (ETR) and the efficiency of photochemical reactions in response to declines in carbon assimilation capacity and reduces the damage to plants caused by heat dissipation, called photoinhibition (Massacci et al., 2008). In this study, a slight increase in ETR and ΦPSII, along with a decrease in Fm and qN were observed during drought stress days 0–10, but these values did not change significantly, indicating that variation among chlorophyll fluorescence parameters is relatively small during periods of mild drought stress. *D. minor* var. *amoenus* may also maintain certain ETR and qN levels by regulating the function of photosynthetic organs structure in the leaves, as well as by reducing heat dissipation; a similar photosynthetic observation was noted in *Gossypium hirsutum* with the onset of drought stress (Massacci et al., 2008). After 10 days, fluorescence parameters ETR, ΦPSII, and qN showed a significant decrease ($P < 0.05$), indicating that PSII had been damaged to varying degrees, photosynthetic organs and enzymes had been destroyed, and the effects of excess light energy could not be protected through heat dissipation. However, Kitao and Lei elucidated that cotton plants can reduce the risk of excessive energy in PSII by maintaining higher ETR associated with higher leaf nitrogen, even if Pn was reduced by stomatal closure (Kitao and Lei, 2007). Under drought conditions, when light use in photosynthesis or heat dissipation is not enough to deal with excessive energy levels, then large amounts of reactive molecules are produced, potentially leading to oxidative damage to photosynthetic organs (Dietz and Pfannschmidt, 2011).

Proline (PRO) is an ideal osmotic adjustment material that can both increase the osmotic potential of plant cells and promote plant cell absorption rates under drought conditions, reflecting plant stress resistance capacity (Seki et al., 2007). In this study, PRO content showed a significant increasing trend, a very sensitive response to stress, and a very large change range (*Fig. 4*), indicating that the plant could improve its drought resistance capacity by increasing PRO content to adjust leaf cell osmosis rates. PRO accumulation could firstly adjust cytoplasmic inner-outer osmosis differences to prevent the inactivation of intracellular proteins and enzymes under osmotic stress. Conversely, it could also eliminate excessive ROS produced by plant stress-response mechanisms. Additionally, PRO interacts with hydrophobic protein residues to regulate drought resistance (Nanjo et al., 1999; Seki et al., 2007). As elucidated above, decreased PSII activity causes excess light photo-inhibition and promotes the formation of excessive ROS, leading to peroxidation of membrane lipids and destruction of cell structures, which results in abnormal physiological metabolism in plant cells. A set of active oxygen species scavenging systems has been formed in plants in which SOD and CAT serve as important antioxidant enzymes, scavenging ROS such as O^{2-}, OH^{-}, and H_2O_2. Similarly, membrane lipid peroxidation rates increased due to ROS accumulation in plants under drought stress, resulting in increases in MDA content (one of the final products of lipid peroxidation), and reduction in the photosynthetic capacity of plant

http://www.aloki.hu ● ISSN 1589 1623 (Print) ● ISSN 1785 0037 (Online)
DOI: http://dx.doi.org/10.15666/aeer/1804_48174838

leaves (Hughes et al., 2001). In this study, significant increases in SOD and CAT activity were detected under mild stress conditions, which could eliminate ROS in cells and reduce membrane lipid peroxidation. However, SOD and CAT contents were inhibited and subsequently decreased under severe drought conditions (*Fig. 4*). Similarly, MDA levels continued to increase significantly, which seriously damaged PSII structure and function. Thus, it was proven that the primary factors for non-stomatal Pn limitation under drought stress were enzymatic systems and photosynthetic structures (Chaves et al., 2009). It was also noted that increased CAT content levels were higher than those related to SOD, which indicates that CAT is more sensitive to water deficit conditions.

Protein involved in photosynthesis

RuBisCO (ribulose-1, 5-bisphosphate carboxylase oxygenase) is an important enzyme involved in the carbon fixation process during photosynthesis, which converts CO_2 to glucose in plants (Shi et al., 2014). RuBisCO also catalyzes RuBP, which is a primary reaction by which inorganic carbon enters the plant biosphere (Feller et al., 2007). In this study, four RuBisCO-associated proteins (spot 1: RuBisCO large subunit, spot 4: Ribulose bisphosphate carboxylase small chain, spot 5: RuBisCO small subunit C, and spot 18: RuBisCO activase) were found to be downregulated in drought-affected bamboo leaves. Similar downregulation of RuBisCO-associated proteins was also found in rice leaf sheaths under drought stress (Yamane et al., 2003; Ali and Komatsu, 2006). Similarly, two different oxygen evolution enhancing protein configurations (spot 6 OEE1 and spot 23 OEE2) were highly upregulated, suggesting a putative role in OEE water stress response, whereas RuBisCo and OEE are more closely related to photosynthesis. Photoinhibition is the primary injury that plants experience under drought stress, along with photosynthetic decreases caused by stomatal or metabolic limitations (Xu and Huang, 2010). RuBisCo subunit and RuBisCo activase are very important protein complexes highly prevalent in green plants. They are also the key enzymes related to photosynthesis and photorespiration in C3 plants; they are involved in both CO_2 fixation (during photosynthesis) and CO_2 release (during photorespiration). Both RuBisCo subunit and RuBisCo activase activity decreased as drought stress intensity increased. RuBisCo regeneration ability also decreased sharply, leading to decreases in photosynthetic rates. Jorge et al. (2006) investigated proteomic changes in *Quercus ilex* under drought stress at different growth stages in different provenances and found that both large and small RuBisCo subunits in leaves had decreased. The inhibition of, or decreases in, photosynthesis and chlorophyll fluorescence under water deficit conditions could be partially explained by such decreases in Rubisco subunits and Rubisco activase content. Additionally, OEE, which is a nuclear gene-encoded chloroplast protein, has three subunits (OEE1, OEE2, and OEE3). It is a peripheral protein in the PSII thylakoid membrane and plays an important role in water photolysis, possibly sustaining PSII oxygen release capacity (Xu et al., 2008). Furthermore, upregulated OEE was observed not only under drought stress but also in association with other abiotic stresses, such as salinity fluctuations (Gazanchian et al., 2007; Xu et al., 2010). OEE is very easy to separate from the PSII complex, resulting in increases in OEE1 and OEE2, as noted in the current study, and indicating repeat damage to the plants' photosynthetic systems. Similarly, PsbP (spot 30), a PSII oxygen-evolving complex peripheral protein in green plants, plays an important role in maintaining the oxygen releasing capacity and functional integrity of the photosynthetic system.

http://www.aloki.hu ● ISSN 1589 1623 (Print) ● ISSN 1785 0037 (Online)
DOI: http://dx.doi.org/10.15666/aeer/1804_48174838

Expression of PsbP increased in the oxygen releasing complexes of bamboo leaves under drought stress, indicating potential roles in maintaining the photosynthetic system and rate stability (Mohan et al., 1995).

Cytochrome b6-f complex metallothionein (spot 39) is a component of the cytochrome b/f complex. This complex is a membrane protein that can be isolated from thylakoid membranes and consists of four polypeptides (cytochrome f, cytochrome b6, iron-sulfur protein, and polypeptide), among which the first three are electronic carriers. Cytochrome f, also known as c type cytochrome, is closely related to mitochondrial cytochrome c1, which is involved in the transfer of photosynthetic electron. In this study, levels of cytochrome b6-f complex metallothionein increased, indicating that the protein was separated from the thylakoid membrane complex and the photosynthetic electron conduction chain was blocked. Similar upregulation of cytochrome b6-f complex metallothionein was also associated with drought stress in *Agrostis stolonifera* (Xu and Huang, 2010).

Proteins involved in energy metabolism

The substantial decline in CO_2 assimilation under water deficit conditions through the reduction in ATP levels indicated that ATP synthesis would respond to abiotic stress (Tezara et al., 1999; Deeba et al., 2012). ATP synthase, which is a key enzyme in plant energy metabolism, is widely distributed within plant chloroplasts, mitochondria, and nucleus, and provides energy requirements for metabolic activities, such as cell material transport, signal transduction, and material synthesis and decomposition. ATP synthase consists of two primary components, F0 and F1. F0 is located outside of the membrane and has three binding sites, comprised of five subunits. F1 is a transmembrane protein consisting of three subunits. ATP synthase CF1 beta subunit (spot 41) is an important component of ATP synthase, which participates in intracellular light and phosphorylation processes. The molecular functions of ATP synthase beta subunit CF1 involve the formation of non-covalent bonds between ATP and adenosine-5-monophosphate. It is an important coenzyme and enzyme activity regulator; proton transfer ATP synthase activity coupled with rotation mechanisms, operating via transmembrane rotation and reverse electrochemical gradients to transport protons, form ATP. In this study, we found that the expression of ATP synthase subunit of CF1 synthase was downregulated under drought stress. However, contradictory results have been observed in mildly drought-stressed cotton (Deeba et al., 2012) and mildly salt-stressed rice (Kim et al., 2005), in which CF1 beta subunit levels increased to enhance ATP synthesis capacity and alleviate damage to the chloroplasts and mitochondria. The authors attributed this to severe damage to the photosynthetic apparatus and metabolism enzyme inhibition during drought stress day 26. Detailed, time-interval delineated information related to this protein's response to drought conditions remains unclear in *D. minor* var. *amoenus.*

Proteins involved in stress responses

Germin-like protein (spot 40) is a kind of soluble glycoprotein that widely exists in plants. Germin-like protein is similar to Germin, which is primarily found in *Triticum aestivum,* both of which belong to the Cupin superfamily. Germin-like proteins are involved in many plant physiological and biochemical processes associated with enzymes, receptors, and structural proteins (Patnaik and Khurana, 2001). Germin-like

http://www.aloki.hu ● ISSN 1589 1623 (Print) ● ISSN 1785 0037 (Online)
DOI: http://dx.doi.org/10.15666/aeer/1804_48174838

protein may combine via ionic bonds in the extracellular matrix. Under stress conditions, the expression of germin-like proteins would be upregulated, and would then, in turn, regulate the signal transduction of H_2O_2 to protect the plant from oxidative damage. Additionally, this protein exhibits SOD-like activity, which can convert ROS into H_2O_2 in response to stress (Banerjee et al., 2010). Zhu et al. (2007) reported that expression levels of germin-like proteins were significantly increased in maize root cell walls under drought stress, indicating involvement in important roles in cell wall defense functions. Similar results were identified in *Lupinus albus* under drought stress. In this study, we found that the expression of the germin-like protein was upregulated under drought stress, which enhanced tolerance. Germin-like proteins were observed primarily through SOD and oxalate oxidase (OXO) functions under stress conditions. SOD could convert ROS into H_2O_2, and then be converted by peroxidase into H_2O, eliminating oxidase damage. OXO can catalyze oxalic acid to form H_2O_2 and CO_2, and then eliminate it via a similar process. Additionally, induced H_2O_2 could mediate plant defense responses through signaling cascades and interactions with cellulose in the cell wall, enhancing cell wall stability during stress conditions (Zhu et al., 2007).

In this study, we also found enhanced expression levels of 2-Cys peroxiredoxin BAS1 (spot 22), which participates in the removal of ROS, antioxidant defenses, and redox signaling under stress conditions. 2-Cys peroxiredoxin BAS1 is a kind of typical cysteine peroxidase-reducing protein found in plant chloroplasts and was primarily cloned from *Arabidopsis thaliana*. Additionally, 2-Cys peroxiredoxin BAS1 content in mesophyll cells was found to be higher than that of vascular sheath cells. This is because mesophyll cells use linear photosynthetic electron transfer methods, leading to the generation of higher ROS content than sheath cells, and therefore accumulating higher redoxin protein levels in mesophyll cells (Baier and Dietz, 1997). In addition to H_2O_2 reduction, 2-Cys peroxiredoxin BAS1 can also reduce peroxide and peroxide nitroso. In this study, we found that the expression of 2-Cys peroxiredoxin BAS1 was upregulated, indicating a stress-related role in *D. minor* var. *amoenus.*

We also found a new expression of ferritin-1 (spot 10). Iron (Fe) atoms easily gain and lose electrons, which can lead to intense reactions when combined with oxygen atoms or other toxic substances. In plants, ferritins are located in the protoplast and are capable of forming a holographic surface that includes more than 4,500 Fe atoms. This structure indicates that ferritins play an important role in maintaining the balance of Fe atoms and protecting Fe-mediated oxidative reactions (Bournier et al., 2013). Four multi-gene families encoding ferritins were found in *Arabidopsis*, among which ferritin-1 was the strongest response protein under iron stress. Under such conditions, ferritin-1 increased significantly from the transcriptional level to the final protein level in *Arabidopsis*, indicating that the ferritin-1 protein might also respond to abiotic stresses (Petit et al., 2001). In this study, ferritin-1 was newly expressed under drought conditions, suggesting a putative role in water deficit responses. Detailed information related to the different responses of this protein to drought-stress and iron-stress conditions requires further investigation.

Conclusion

This study provides an initial analysis of physiological and proteomic responses in leaves of the bamboo species, *D. minor* var. *amoenus*, under drought stress. Notably, the effects of mild drought stress on photosynthesis and chlorophyll fluorescence were

http://www.aloki.hu ● ISSN 1589 1623 (Print) ● ISSN 1785 0037 (Online)
DOI: http://dx.doi.org/10.15666/aeer/1804_48174838

lower than that of severe drought stress in this bamboo species, owing to compensation by other biological pathways. Severe drought stress causes leaf stomatal closure and accumulation of ROS, leading to physical damage to cell structure, while non-stomatal limitation factors assume leading roles in leaf photosynthesis and seriously affect the normal growth of plants. Analysis of stress response proteins revealed annotations of 23 upregulated, 13 downregulated, and 4 newly expressed proteins. Bioinformatics analysis showed that these differentially expressed proteins were related to photosynthesis, energy metabolism, and stress response, indicating the involvement of these proteins in response to drought stress in *D. minor* var. *amoenus*. The result of GO and KEGG classification analysis showed those differentially expressed proteins were related to photosynthesis, energy metabolism, and stress response, indicating the involvement of these proteins in response to drought stress in *D. minor* var. *amoenus*. Notably, the new expression of Ferritin-1, which reduces oxidative reactions, was studied Thus, there is a need to study the mechanism of Ferritin-1 in bamboo species under drought stress further. Taken together, these studies increase the understanding of response mechanisms of bamboo species under drought stress. Additionally, this study provides foundational information and an experimental basis for exploring drought resistance candidate genes among bamboo species.

Acknowledgements. This work was supported by the Central Fiscal Forestry Science and Technology Extension Project [2013, NO.7], the Science and Technology Major Projects of Fujian Province [2013NZ0001], the Regional Development Project of Fujian Province [2015N3015], and Program for Scientific and Technological Innovation Team for Universities of Fujian Province [2018, No.49].

REFERENCES

[1] Alam, I., Sharmin, S. A., Kim, K.-H., Yang, J. K., Choi, M. S., Lee, B.-H. (2010): Proteome analysis of soybean roots subjected to short-term drought stress. – Plant Soil 333: 491-505.

[2] Ali, G. M., Komatsu, S. (2006): Proteomic analysis of rice leaf sheath during drought stress. – J Proteome Res 5: 396-403.

[3] Aranjuelo, I., Molero, G., Erice, G., Avice, J. C., Nogués, S. (2010): Plant physiology and proteomics reveals the leaf response to drought in alfalfa (Medicago sativa L.). – J Exp Bot 62: 111-123.

[4] Baier, M., Dietz, K. (1997): The plant 2-Cys peroxiredoxin BAS1 is a nuclear-encoded chloroplast protein: its expressional regulation, phylogenetic origin, and implications for its specific physiological function in plants. – Plant J 12: 179-190.

[5] Banerjee, J., Das, N., Dey, P., Maiti, M. K. (2010): Transgenically expressed rice germin-like protein1 in tobacco causes hyper-accumulation of H2O2 and reinforcement of the cell wall components. – Biochem Biophys Res Commun 402: 637-643.

[6] Bogeat-Triboulot, M.-B., Brosché, M., Renaut, J., Jouve, L., Le Thiec, D., Fayyaz, P., Vinocur, B., Witters, E., Laukens, K., Teichmann, T. (2007): Gradual soil water depletion results in reversible changes of gene expression, protein profiles, ecophysiology, and growth performance in Populus euphratica, a poplar growing in arid regions. – Plant Physiol 143: 876-892.

[7] Bota, J., Medrano, H., Flexas, J. (2004): Is photosynthesis limited by decreased Rubisco activity and RuBP content under progressive water stress? – New Phytol 162: 671-681.

[8] Bournier, M., Tissot, N., Mari, S., Boucherez, J., Lacombe, E., Briat, J.-F., Gaymard, F. (2013): Arabidopsis ferritin 1 (AtFer1) gene regulation by the phosphate starvation

http://www.aloki.hu ● ISSN 1589 1623 (Print) ● ISSN 1785 0037 (Online)
DOI: http://dx.doi.org/10.15666/aeer/1804_48174838

response 1 (AtPHR1) transcription factor reveals a direct molecular link between iron and phosphate homeostasis. – J Biol Chem 288: 22670-22680.

[9] Bradford, M. M. (1976): A rapid and sensitive method for the quantitation of microgram quantities of protein utilizing the principle of protein-dye binding. – Anal Biochem 72: 248-254.

[10] Caruso, A., Chefdor, F., Carpin, S., Depierreux, C., Delmotte, F. M., Kahlem, G., Morabito, D. (2008): Physiological characterization and identification of genes differentially expressed in response to drought induced by PEG 6000 in Populus canadensis leaves. – J Plant Physiol 165: 932-941.

[11] Caverzan, A., Casassola, A., Brammer, S. P. (2016): Antioxidant responses of wheat plants under stress. – Genet Mol Biol 39: 1-6.

[12] Chalker-Scott, L. (1999): Environmental significance of anthocyanins in plant stress responses. – Photochem Photobiol 70: 1-9.

[13] Chaves, M. M., Flexas, J., Pinheiro, C. (2009): Photosynthesis under drought and salt stress: regulation mechanisms from whole plant to cell. – Ann Bot 103: 551-560.

[14] Costa, P., Bahrman, N., Frigerio, J.-M., Kremer, A., Plomion, C. (1998): Water-deficit-responsive proteins in maritime pine. – Plant Mol Biol 38: 587-596.

[15] Deeba, F., Pandey, A. K., Ranjan, S., Mishra, A., Singh, R., Sharma, Y. K., Shirke, P. A., Pandey, V. (2012): Physiological and proteomic responses of cotton (Gossypium herbaceum L.) to drought stress. – Plant Physiol Biochem 53: 6-18.

[16] Dietz, K.-J., Pfannschmidt, T. (2011): Novel regulators in photosynthetic redox control of plant metabolism and gene expression. – Plant Physiol 155: 1477-1485.

[17] Ebrahimi-Birang, N., Fredlund, D. G. (2016): Assessment of the WP4-T device for measuring total suction. – Geotech Test J 39: 500-506.

[18] Fang, Y., Xiong, L. (2015): General mechanisms of drought response and their application in drought resistance improvement in plants. – Cell Mol life Sci 72: 673-689.

[19] Feller, U., Anders, I., Mae, T. (2007): Rubiscolytics: fate of Rubisco after its enzymatic function in a cell is terminated. – J Exp Bot 59: 1615-1624.

[20] Gazanchian, A., Hajheidari, M., Sima, N. K., Salekdeh, G. H. (2007): Proteome response of Elymus elongatum to severe water stress and recovery. – J Exp Bot. 58: 291-300.

[21] Grassi, G., Magnani, F. (2005): Stomatal, mesophyll conductance and biochemical limitations to photosynthesis as affected by drought and leaf ontogeny in ash and oak trees. – Plant Cell Environ 28: 834-849.

[22] Hughes, S. M., Moroni-Rawson, P., Jolly, R. D., Jordan, T. W. (2001): Submitochondrial distribution and delayed proteolysis of subunit c of the H+-transporting ATP-synthase in ovine ceroid-lipofuscinosis. – Electrophoresis 22: 1785-1794.

[23] Jorge, I., Navarro, R. M., Lenz, C., Ariza, D., Jorrín, J. (2006): Variation in the holm oak leaf proteome at different plant developmental stages, between provenances and in response to drought stress. – Proteomics 6: S207–S214.

[24] Khaliq, M. A., Khan Tarin, M. W., Jingxia, G., Yanhui, C., Guo, W. (2019): Soil liming effects on CH4, N2O emission and Cd, Pb accumulation in upland and paddy rice. – Environ Pollut 248: 408-420.

[25] Kim, D., Rakwal, R., Agrawal, G. K., Jung, Y., Shibato, J., Jwa, N., Iwahashi, Y., Iwahashi, H., Kim, D. H., Shim, I. (2005): A hydroponic rice seedling culture model system for investigating proteome of salt stress in rice leaf. – Electrophoresis 26: 4521-4539.

[26] Kitao, M., Lei, T. T., (2007): Circumvention of over-excitation of PSII by maintaining electron transport rate in leaves of four cotton genotypes developed under long-term drought. – Plant Biol 9: 69-76.

http://www.aloki.hu ● ISSN 1589 1623 (Print) ● ISSN 1785 0037 (Online)
DOI: http://dx.doi.org/10.15666/aeer/1804_48174838

[27] Koh, J., Chen, G., Yoo, M.-J., Zhu, N., Dufresne, D., Erickson, J. E., Shao, H., Chen, S. (2015): Comparative proteomic analysis of Brassica napus in response to drought stress. – J Proteome Res 14: 3068-3081.
[28] Kosová, K., Vítámvás, P., Prášil, I. T., Renaut, J. (2011): Plant proteome changes under abiotic stress—contribution of proteomics studies to understanding plant stress response. – J Proteomics 74: 1301-1322.
[29] Lawlor, D. W., Cornic, G. (2002): Photosynthetic carbon assimilation and associated metabolism in relation to water deficits in higher plants. – Plant Cell Environ 25: 275-294.
[30] Lawlor, D. W., Tezara, W. (2009): Causes of decreased photosynthetic rate and metabolic capacity in water-deficient leaf cells: a critical evaluation of mechanisms and integration of processes. – Ann Bot 103: 561-579.
[31] Li, J., Ding, X., Han, S., He, T., Zhang, H., Yang, L., Yang, S., Gai, J. (2016): Differential proteomics analysis to identify proteins and pathways associated with male sterility of soybean using iTRAQ-based strategy. – J Proteomics 138: 72-82.
[32] Liu, H., Sultan MARF., Li Liu, X., Zhang, J., Yu, F., Xian Zhao, H. (2015): Physiological and comparative proteomic analysis reveals different drought responses in roots and leaves of drought-tolerant wild wheat (Triticum boeoticum). – PLoS One 10: e0121852.
[33] Liu, S., Wang, X., Wang, H., Xin, H., Yang, X., Yan, J., Li, J., Tran, L.-S. P., Shinozaki, K., Yamaguchi-Shinozaki, K. (2013): Genome-wide analysis of ZmDREB genes and their association with natural variation in drought tolerance at seedling stage of Zea mays L. – PLoS Genet 9: e1003790.
[34] Luna, C. M., Pastori, G. M., Driscoll, S., Groten, K., Bernard, S., Foyer, C. H. (2004): Drought controls on H2O2 accumulation, catalase (CAT) activity and CAT gene expression in wheat. – J Exp Bot 56: 417-423.
[35] Massacci, A., Nabiev, S. M., Pietrosanti, L., Nematov, S. K., Chernikova, T. N., Thor, K., Leipner, J. (2008): Response of the photosynthetic apparatus of cotton (Gossypium hirsutum) to the onset of drought stress under field conditions studied by gas-exchange analysis and chlorophyll fluorescence imaging. – Plant Physiol Biochem 46: 189-195.
[36] Miao, Y., Lv, D., Wang, P., Wang, X.-C., Chen, J., Miao, C., Song, C.-P. (2006): An Arabidopsis glutathione peroxidase functions as both a redox transducer and a scavenger in abscisic acid and drought stress responses. – Plant Cell 18: 2749-2766.
[37] Mohan, P., Singh, P., Dongre, A. B., Narayanan, S. S. (1995): Gossypol-gland density and free gossypol content in seed and cotyledonary leaf of upland cotton (Gossypium hirsutum). – Indian J Agric Sci 65: 66-68
[38] Nanjo, T., Kobayashi, M., Yoshiba, Y., Sanada, Y., Wada, K., Tsukaya, H., Kakubari, Y., Yamaguchi-Shinozaki, K., Shinozaki, K. (1999): Biological functions of proline in morphogenesis and osmotolerance revealed in antisense transgenic Arabidopsis thaliana. – Plant J 18: 185-193.
[39] Patnaik, D., Khurana, P. (2001): Germins and germin like proteins: an overview. – Indian J Exp Biol 39(3): 191-200.
[40] Petit, J.-M., van Wuytswinkel, O., Briat, J.-F., Lobréaux, S. (2001): Characterization of an Iron-dependent regulatory sequence involved in the transcriptional control of AtFer1and ZmFer1 plant ferritin genes by iron. – J Biol Chem 276: 5584-5590.
[41] Rouhi, V., Samson, R., Lemeur, R., Van Damme, P. (2007): Photosynthetic gas exchange characteristics in three different almond species during drought stress and subsequent recovery. – Environ Exp Bot 59: 117-129.
[42] Seki, M., Umezawa, T., Urano, K., Shinozaki, K. (2007): Regulatory metabolic networks in drought stress responses. – Curr Opin Plant Biol 10: 296-302.
[43] Shi, H., Ye, T., Chan, Z. (2014): Comparative proteomic responses of two bermudagrass (Cynodon dactylon (L). Pers.) varieties contrasting in drought stress resistance. – Plant Physiol Biochem 82: 218-228.

http://www.aloki.hu ● ISSN 1589 1623 (Print) ● ISSN 1785 0037 (Online)
DOI: http://dx.doi.org/10.15666/aeer/1804_48174838

[44] Sobrado, M. A. (2011): Leaf gas exchange and fluorescence of two teosinte species: Zea mays ssp. parviglumis and Z. diploperennis. – J Trop Agric 49: 91-94.
[45] Tarin, M. W. K., Fan, L., Tayyab, M., Sarfraz, R., Chen, L., He, T., Rong, J., Chen, L., Zheng, Y. (2019): Effects of bamboo biochar amendment on the growth and physiological characteristics of Fokienia hodginsii. – Appl Ecol Environ Res 16: 8055-8074.
[46] Tarin, M. W. K., Lili, F., Lu, S., Jinli, L., Jingwen, L., Zhiwen, D., Lingyan, C., Tianyou, H., Rong, J., Zheng, Y. (2020): Rice straw biochar impact on physiological and biochemical attributes of Fokienia hodginsii in acidic soil. – Scand J For Res 0(0): 1-10. https://doi.org/10.1080/02827581.2020.1731591.
[47] Tayyab, M., Islam, W., Khalil, F., Ziqin, P., Caifang, Z., Arafat, Y., Hui, L., Rizwan, M., Ahmad, K., Waheed, S., et al. (2018): Biochar: an efficient way to manage low water availability in plants. – Appl Ecol Environ Res 16(3): 2565-2583.
[48] Tong, R., Zhou, B., Cao, Y., Ge, X., Jiang, L. (2020): Metabolic profiles of moso bamboo in response to drought stress in a field investigation. – Science of the Total Environment 720.
[49] Tezara, W., Mitchell, V. J., Driscoll, S. D., Lawlor, D. W. (1999): Water stress inhibits plant photosynthesis by decreasing coupling factor and ATP. – Nature 401: 914.
[50] Thalmann, M., Santelia, D. (2017): Starch as a determinant of plant fitness under abiotic stress. – New Phytologist 214(3): 03-10.
[51] Wang, W., Vignani, R., Scali, M., Cresti, M. (2006): A universal and rapid protocol for protein extraction from recalcitrant plant tissues for proteomic analysis. – Electrophoresis 27: 2782-2786.
[52] Wang, W.-B., Kim, Y.-H., Lee, H.-S., Kim, K.-Y., Deng, X.-P., Kwak, S.-S. (2009): Analysis of antioxidant enzyme activity during germination of alfalfa under salt and drought stresses. – Plant Physiol Biochem 47: 570-577.
[53] Wu, X.-P., Liu, S., Luan, J., Wang, Y., Cai, C. (2019): Responses of water use in Moso bamboo (Phyllostachys heterocycla) culms of different developmental stages to manipulative drought. – For Ecosyst 6(1): 1-14.
[54] Xu, C., Huang, B. (2010): Differential proteomic responses to water stress induced by PEG in two creeping bentgrass cultivars differing in stress tolerance. – J Plant Physiol 167: 1477-1485.
[55] Xu, C., Sibicky, T., Huang, B. (2010): Protein profile analysis of salt-responsive proteins in leaves and roots in two cultivars of creeping bentgrass differing in salinity tolerance. – Plant Cell Rep 29: 595-615.
[56] Yamane, K., Hayakawa, K., Kawasaki, M., Taniguchi, M., Miyake, H. (2003): Bundle sheath chloroplasts of rice are more sensitive to drought stress than mesophyll chloroplasts. – J Plant Physiol 160: 1319.
[57] Yan, J. X., Wait, R., Berkelman, T., Harry, R. A., Westbrook, J. A., Wheeler, C. H., Dunn, M. J. (2000): A modified silver staining protocol for visualization of proteins compatible with matrix-assisted laser desorption/ionization and electrospray ionization-mass spectrometry. – Electrophor An Int J 21: 3666-3672.
[58] Yang, A., Dai, X., Zhang, W.-H. (2012): A R2R3-type MYB gene, OsMYB2, is involved in salt, cold, and dehydration tolerance in rice. – J Exp Bot 63: 2541-2556.
[59] Zhu, J., Alvarez, S., Marsh, E. L., LeNoble, M. E., Cho, I.-J., Sivaguru, M., Chen, S., Nguyen, H. T., Wu, Y., Schachtman, D. P. (2007): Cell wall proteome in the maize primary root elongation zone. II. Region-specific changes in water soluble and lightly ionically bound proteins under water deficit. – Plant Physiol 145: 1533-1548.
[60] Zou, J.-J., Wei, F.-J., Wang, C., Wu, J.-J., Ratnasekera, D., Liu, W.-X., Wu, W.-H. (2010): Arabidopsis calcium-dependent protein kinase CPK10 functions in abscisic acid-and Ca2+-mediated stomatal regulation in response to drought stress. – Plant Physiol 154: 1232-1243.

http://www.aloki.hu ● ISSN 1589 1623 (Print) ● ISSN 1785 0037 (Online)
DOI: http://dx.doi.org/10.15666/aeer/1804_48174838

APPENDIX

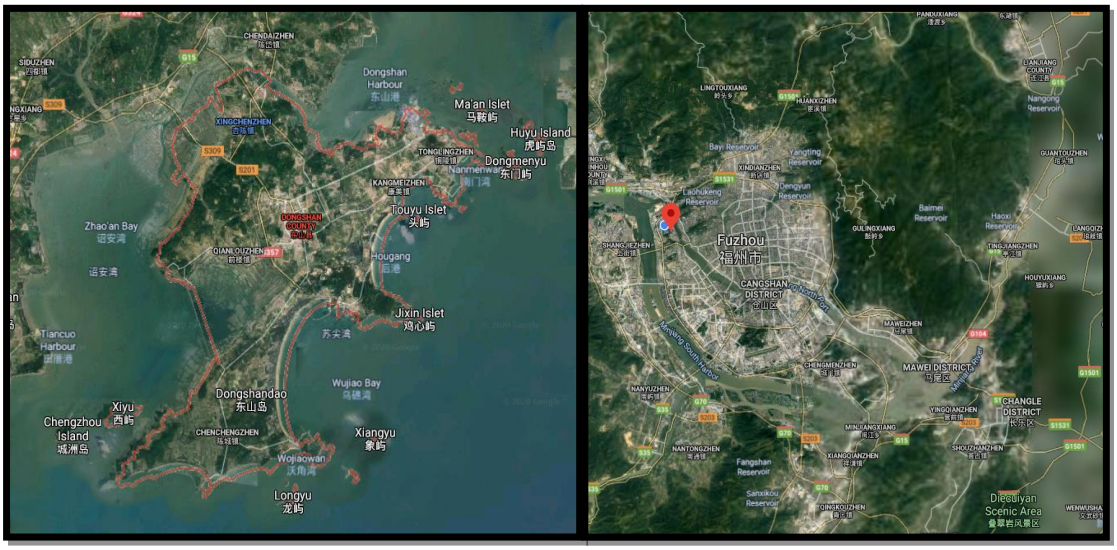

Figure A1. *Map showing the bamboo coastal sandy protection areas of Dongshan Island (left) and Bamboo Research Institute of the Fujian Agriculture and Forestry University, Fuzhou, China (right)*

Table A1. *Changes in soil water content (SWC) and leaf water potential (LWP) under drought stress*

Stress (days)	SWC (%)		LWP (MPa)	
	Treatment	Control	Treatment	Control
0	30.867 ± 1.858 f	30.867 ± 1.858 a	-1.143 ± 0.101 h	-1.237 ± 0.075 a
5	22.267 ± 1.498 e	30.567 ± 2.793 a	-2.037 ± 0.097 g	-1.05 ± 0.105 a
10	14.2 ± 0.9 d	32.433 ± 3.889 a	-2.853 ± 0.078 f	-1.237 ± 0.095 a
15	6.267 ± 0.896 c	37.733 ± 0.252 b	-3.35 ± 0.325 e	-1.043 ± 0.196 a
20	4.6 ± 0.436 c	31.867 ± 2.346 a	-3.983 ± 0.123 d	-1.207 ± 0.195 a
23	2.633 ± 0.85 b	30.967 ± 1.38 a	-4.427 ± 0.165 c	-1.087 ± 0.12 a
26	0.833 ± 0.058 a	31.5 ± 0.954 a	-4.93 ± 0.229 b	-1.213 ± 0.112 a
30	0.433 ± 0.058 a	32.9 ± 1.572 a	-5.65 ± 0.161 a	-1.187 ± 0.11 a

Measurements were conducted at each sampling time over the treatment. Each value represent means ± standard error of three replicate experiments. Data denoted by the same letter did not differ at significant levels ($P < 0.05$) according to Duncan's multiple range test

Table A2. *Correlation coefficients between photosynthetic parameters, SWC and LWP*

	LWP	SWC	Pn	Gs	Ci	Tr	PWUE
SWC	0.985**						
Pn	0.899**	0.904**					
Gs	0.921**	0.910**	0.953**				
Ci	0.170	0.167	0.196	0.274			
Tr	0.910**	0.908**	0.914**	0.962**	0.302		
PWUE	0.195	0.220	0.375	0.180	-0.613**	0.076	
LS	-0.170	-0.167	-0.196	-0.274	-1.000**	-0.302	0.613**

Parameters include net photosynthetic rate (Pn), stomatal conductance (Gs), transpiration rate (Tr), intercellular CO_2 concentration (Ci), water use efficiency (PWUE), soil water content (SWC) and leaf water potential (LWP). ** Correlation is significant at the 0.01 significance level

http://www.aloki.hu ● ISSN 1589 1623 (Print) ● ISSN 1785 0037 (Online)
DOI: http://dx.doi.org/10.15666/aeer/1804_48174838

Table A3. *Differential protein spots identified by MALDI-TOF-MS under drought stress*

Sample spot	Corresponding target	Protein name	Accession NO.	*Sources*	Theor MW	p*I*	Peptide matches	C.I.*%*
1	M19	Ribulose-1,5-bisphosphate carboxylase/oxygenase large subunit (plastid)	gi|817525241	*Neohouzeaua sp. Clark & Attigala* 1712	52851.5	6.3299	16	100
2	M20	Hypothetical protein OsJ_35814	gi|125579068	*Oryza sativa Japonica* Group	19485.9	8.87	9	100
3	M21	Hypothetical protein OsI_38046	gi|125536346	*Oryza sativa Japonica* Group	19708	9.04	9	100
4	M22	Ribulose bisphosphate carboxylase small chain, chloroplastic	gi|122234140	*Oryza sativa Japonica* Group	19633.9	9.04	9	100
5	M23	RuBisCO small subunit C	gi|158513174	*Oryza sativa Indica* Group	19633.9	9.04	7	100
6	M24	Oxygen-evolving enhancer protein 1, chloroplastic	gi|474352688	*Triticum urartu*	34407.4	5.75	10	100
7	N1	Hypothetical protein	gi|226506316	*Zea mays*	24474.4	4.99	6	100
9	N3	Hypothetical protein OsJ_01921	gi|125570526	*Oryza sativa Japonica* Group	34839.7	6.1	10	100
10	N4	Ferritin-1, chloroplastic-like	gi|514807458	*Setaria italica*	27984.2	5.67	4	100
12	N6	Uncharacterized protein	V4W9U6_9ROSI	*Citrus clementina*	42274.6	9	15	95.617
13	N7	Hypothetical protein OsJ_01921	gi|125570526	*Oryza sativa Japonica*	34839.7	6.1	7	100
14	N8	Transcription factor-related family protein	B9H470_POPTR	*Populus trichocarpa*	66182.6	6.25	21	97.77
16	N10	Ribosome-recycling factor, chloroplastic	gi|474043078	*Triticum urartu*	24755.2	8.92	5	100
17	N11	Uncharacterized protein	W5BGE9_WHEAT	*Triticum aestivum*	40596.1	9.03	7	96.716
18	N12	Ribulose bisphosphate carboxylase/oxygenase activase	gi|109940135	*Oryza sativa Japonica* Group	51421.4	5.4299	14	100
19	N13	Hypothetical protein OsJ_01921	gi|125570526	*Oryza sativa Japonica* Group	34839.7	6.1	4	100
20	N14	Hypothetical protein OsI_25003	gi|218199135	*Oryza sativa Indica* Group	108971.8	6.04	25	96.175
21	N15	Extra-large guanine nucleotide-binding protein 3-like isoform X2	gi|514817425	*Setaria italica*	70472.4	5.43	17	95.716
22	N16	2-Cys peroxiredoxin BAS1, chloroplastic	gi|514713083	*Setaria italica*	28032.5	5.97	5	99.785
23	N17	Oxygen-evolving enhancer protein 2, chloroplastic	gi|474077556	*Triticum urartu*	25485.8	8.94	7	100
26	N20	Eukaryotic translation initiation factor 3 subunit A	gi|514774931	*Setaria italica*	114747.4	9.27	15	90.854
29	N23	Calcium-dependent protein kinase, isoform AK1	gi|728449015	*Arundo donax*	2282	12	5	94.457
30	N24	Chain A, The Crystal Structure of Psbp	gi|767259516	*Zea Mays*	20117.2	5.96	5	100
31	O1	Malate dehydrogenase, cytoplasmic	gi|514816242	*Setaria italica*	35461.1	5.76	9	100
32	O2	Predicted protein	A9T5M7_PHYPA	*Physcomitrella patens* subsp.	141967.7	6.28	31	98.102
33	O3	Fructose-bisphosphate aldolase	gi|514804765	*Setaria italica*	41808.5	6.08	13	100
34	O4	rca1	gi|728675519	*Arundo donax*	44304.1	5.5	7	100
35	O5	Flavin-containing monooxygenase	A0A059AY33_EUCGR	*Eucalyptus grandis*	42130.6	8.77	18	98.908
37	O7	Hypothetical protein OsI_28915	gi|218201012	*Oryza sativa Indica* Group	26987.8	8.76	6	96.668
38	O8	Glutathione S-transferase DHAR3, chloroplastic	gi|514762575	*Setaria italica*	28944.1	7.68	7	98.992
39	O9	Cytochrome b6-f complex iron-sulfur subunit, chloroplastic	gi|475511555	*Aegilops tauschii*	23711	8.47	5	100
40	O10	Germin-like protein 8-14	gi|475618322	*Aegilops tauschii*	25959.6	8.43	3	99.887
41	O11	ATP synthase CF1 beta subunit (plastid)	gi|817524800	*Bambusa arnhemica*	53879.2	5.4699	26	100

The differentially expressed proteins were calculated according to statistically significant changes between samples using SPSS software by ANOVA-test (abundance variation at least 2-fold, $p < 0.05$). The sample spot represents the number of proteins assigned in *Figures 5* and *6*. Theor MW and pI values shown are the theoretical and experimental values. C.I.%, which is the Mascot score of the in-solution digestion protocol. Accession number and Protein name are assigned according to the NCBInr-protein sequence database

http://www.aloki.hu ● ISSN 1589 1623 (Print) ● ISSN 1785 0037 (Online)
DOI: http://dx.doi.org/10.15666/aeer/1804_48174838

SPATIOTEMPORAL VARIATION AND CLIMATE CHANGE IMPACT ON RADIAL GROWTH OF CHIR PINE (*PINUS ROXBURGHII)* IN A SUBTROPICAL PINE FOREST IN PAKISTAN

IQBAL, S.[1,2] – ZHA, T. S.[1,2*] – HAYAT, M.[1,2] – KHAN, A.[1,2] – ASHRAF, M. I.[3] – AHMAD, B.[4] – SABA, N. U.[5] – JAN, S. A.[6]

[1]*Yanchi Research Station, School of Soil and Water Conservation, Beijing Forestry University, Beijing 100083, China*

[2]*Beijing Engineering Research Center of Soil and Water Conservation, Beijing Forestry University, Beijing 100083, China*

[3]*Department of Forestry, Arid Agriculture University, Murree Road, Rawalpindi 46300, Pakistan*

[4]*Institute of Agriculture Sciences and Forestry, University of Swat, Swat 19130, Pakistan*

[5]*Faculty of Management Sciences, Riphah International University, Islamabad 44000, Pakistan*

[6]*Forest Department, Government of Khyber, Pakhtunkhwa 18300, Pakistan*

[*]*Corresponding author*
e-mail: tianshanzha@bjfu.edu.cn

(Received 18th Dec 2019; accepted 6th May 2020)

Abstract. Climate and topography both have a paramount role in defining tree species distribution. Global warming had increased the risk of climatic influences on the sustainability of subtropical pine forests. The radial growth (R_g) allows to understand the long term variation in climate change-at different temporal and spatial scales. Here, we analyzed 144 R_g chronologies from 48 different sites in a subtropical pine forest in the Murree Hills of Pakistan. The results showed a strong non-linear relationship of annual precipitation (PPT) and annual mean air temperature (T_a) with R_g. The results further indicated that previous and present summer precipitation imposed a positive impact on the R_g ($p < 0.05$). The previous summer T_a showed a significant negative effect on R_g while positively correlated during current July. The growth response analysis indicated that R_g was often limited by variation in soil moisture associated with lower PPT and higher T_a. Moreover, the dependency of R_g on PPT and T_a varied along growing degree days (GDD >5°C), at different elevations. Our findings provide a remarkable evidence that the annual R_g of *P. roxburghii* species appeared to be progressively limited by the effect of climate warming and varied spatially.
Keywords: *air temperature, chronologies, growing degree days, Murree hills, precipitation*

Introduction

An amplification in global earth surface temperature from 1880 to 2012, was observed at 0.85°C and the period from 1983 to 2012 was supposed to be the warmest thirty years since last fourteen centuries in the Northern latitudes (IPCC, 2014). How these climatic variations will dramatically affect terrestrial ecosystems is far from understood (Ma et al., 2012). Among these terrestrial ecosystems the major subtropical pine forest is predominantly distributed across indo-pacific south-western Himalayan region (Sheikh, 1993). The structure and function of forests are subject to be change by climate warming which also enhances the risk of severity in biotic and abiotic feedbacks i.e., wild fires droughts and insect outbreaks (Allen et al., 2010; Kasischke and Stocks, 2012; Price et

http://www.aloki.hu ● ISSN 1589 1623 (Print) ● ISSN1785 0037 (Online)
DOI: http://dx.doi.org/10.15666/aeer/1804_48394855

al., 2013). Consequently, it is important to know the response of pine species to increasing climate change for accurate prediction of potential variations in subtropical pine forests.

Previous studies revealed that tree ring analysis provides a high resolution proxy to reform past climatic variation change (Esper et al., 2002; Cook et al., 2004; D'Arrigo et al., 2008), which helps in comprehend the association between tree growth and climatic variables (Hughes et al., 2010; Speer, 2010). Climatic parameters and tree growth depicts a linear relationship calibrated by traditional statistical functions and it remains consistent through time period (Jones et al., 2009; Tolwinski-Ward et al., 2011). In contrast, various studies have shown the presence of nonlinear and unstable relationships among tree growth and meteorological variables due to climate warming (Visser et al., 2010; Zhang and Wilmking, 2010). In particular, it has been revealed that pine species has shown a nonlinear relationship with climate variability (Lloyd et al., 2013; Saeed et al., 2016). The white spruce growth pattern showed lessened sensitivity to temperature in high altitudes (Porter and Pisaric, 2011; Lloyd et al., 2013), pointing out the divergence concern (D'Arrigo et al., 2008). The influence of climatic variables on tree ring growth might tend to vary along altitudinal gradients in climate and growth relationship for temporal changes. Therefore, long term temporal scale radial growth analysis is required to evidently state how tree-rings responds to environmental variables.

Many hydrometeorological factors influence the tree growth among which the available soil water contents and air temperature are the key variables (Schweingruber, 1996). Therefore, ring series of long-lived trees have ability to record long-term multi-year variation in climatic circumstances (Olano et al., 2012). Tree species may respond to climatic fluctuations in more complex ways due to the nature of complex physiology (Drew et al., 2013; Zang et al., 2014). Furthermore, temporal instability between tree growth and climate mediates their response patterns due to changes in constraining factors (Briffa et al., 2002; Leburgeois et al., 2012).

Climate enforces dual adversity on subsistence and evolution of many trees and shrubs i.e., erratic, unpredictable rain and associated extreme summer droughts (Valladares et al., 2014). The effect of drought varied along altitudinal gradient (Altman et al., 2017). Dramatic shifting behavior in forest ecosystems may not be happened only by direct response to climatic variations but usually associated to disturbances caused by climate change (Ghazoul et al., 2015). As climatic conditions varied continuously, the occurrence, impact and severity of disturbances on forest ecosystems are tend to increase globally (Flannigan et al., 2009; Turner, 2010; Seidl et al., 2014) and significantly modify the forest growth, structure, function, and successional trajectories (McCullough et al., 1998). Climatic change resulting variation in precipitation and temperature patterns, however such variations does not exhibit uniform pattern over entire year. Consequently, these limiting factors have relative importance in modulating the response of tree ring formation to climate change, caused predictions more difficult.

Many researches have documented the species-specific response of growth parameters to climatic variations, although they are subjected to same environmental conditions (Fekedulegn et al., 2003; Maxime and Hendrik, 2011). During the growing season, the growth of Oak was influenced by precipitation rates and not by temperature (Bednarz and Ptak, 1990) and suffered during water deficit conditions, but could not under plentiful water availability (Pilcher and Gray, 1982). In contrast, during the 20th and 21st centuries the positive radial growth of Beech species was observed with increasing temperature (Maxime and Hendrik, 2011) that was observed to be closely associated to scarce soil water condition (Bouriaud et al., 2004). Another studies have reported the strong

http://www.aloki.hu ● ISSN 1589 1623 (Print) ● ISSN1785 0037 (Online)
DOI: http://dx.doi.org/10.15666/aeer/1804_48394855

possibility of Sycamore to largely decline in England, being more sensitive to water shortage during dry periods (Lemoine et al., 2001; Tissier et al., 2004). The responses of pine species to climate variation has been investigated in several Mediterranean and subtropical forest ecosystems. However, climate growth relationship of *P. roxburghii* in subtropical forests of Pakistan is still poorly understood.

In current study, to deeply insight on the species future persistence, we inspected the long-term continuing variation in the relationship stability between climate and growth of a subtropical Chir pine species (*P. roxburghii*). This model plant, considered as a representative species of subtropical pine zone and being significant to its functioning (Sheikh, 1993). It is uncertain that how long-term variation in climatic drivers would affect the tree growth of mature *P. roxburghii* over the previous century.

This study provides a fundamental prospective to forecast the species performance and sustainability, under the consequences of global warming. In particular, we sought to understand what kind of relationship between climate and growth is revealed by *P. roxburghii* at long-term scale and meanwhile the correlation is stable or not. We examined a complex network of tree radial ring-increment chronologies from 48 pine locations in the subtropical pine forest along different elevations in Murree Hills, Pakistan. We hypothesized that the impact of climatic factors on radial growth (R_g) of *P. roxburghii* might be varied along different elevations. The main objectives are: (1) to address the response of R_g to climatic variations by computing the domino effect of traditional linear and nonlinear functions; and (2) to explore the potential temporal variation in R_g along growing degree days (GDD), and different elevations.

Methods

Study area

The present study was conducted in Murree Hills of Pakistan (33° 47′ 15″ to 33° 54′ 47″ N and from 73° 16′ 54″ to 73° 29′ 18″ E) in September 2015 (*Fig. 1*). The study area is dominant representative part of Subtropical Chir pine forest zone (Conifer specialist group, 1996) about 33 km North-East of Islamabad, the country's capital place. The elevation range from 939 to 1873 m a. s. l. Mean monthly air temperature of the region varies gently, 35°C to 50°C in summer and 0 to 2°C in winter. Mean monthly relative humidity is 70 percent or above (Sheikh, 1993). While mean annual rainfall is around 1140 mm per year (Nizami et al., 2012). The main soil type is loamy with a variable composition of clay, sand, and silt. The sedimentary rocks are in comprises of sandstones, limestone, shales, and marls (Sheikh, 1993). The area is naturally dominated by stand of *Pinus roxburghii* (chir), managed under Punjab shelterwood silviculture system. The other related tree species are *Pinus wallichiana* (kail*), Pyrus pashia* (batangi), and *Quercus incana* (rhin). The understory vegetation contains grasses and shrubs i.e., *Dodonaea viscosa* (sanatha), *Carissa spinarum* (granda), *Myrsine africana* (khukhal), *Capparis decidua* (karir), *Adhatoda vasica* (Bahekar), *cannabis sativa* (Bang) and *Berberis lycium* species (sumblu).

Climate variables

Meteorological data was continuously collected from the meteorological station situated near the study site from 1995-2015. The climate variables used in this study includes, monthly and annual total precipitation, monthly and annual mean temperature,

http://www.aloki.hu ● ISSN 1589 1623 (Print) ● ISSN1785 0037 (Online)
DOI: http://dx.doi.org/10.15666/aeer/1804_48394855

and growing degree days (GDD > 5°C). Continuous measurements of daily precipitation were monitored by tipping bucket rain gauges (TE525MM) and air temperature with HMP45C probes (HMP155A, Vaisala). The annual total precipitation was summed from the preceding September to the current August of each year. The climate of the region is subtropical, and is defined by hot, dry and long summer seasons while gentle mild, wet winters (CWB, 2006). In the study period, mean annual temperature varied considerably.

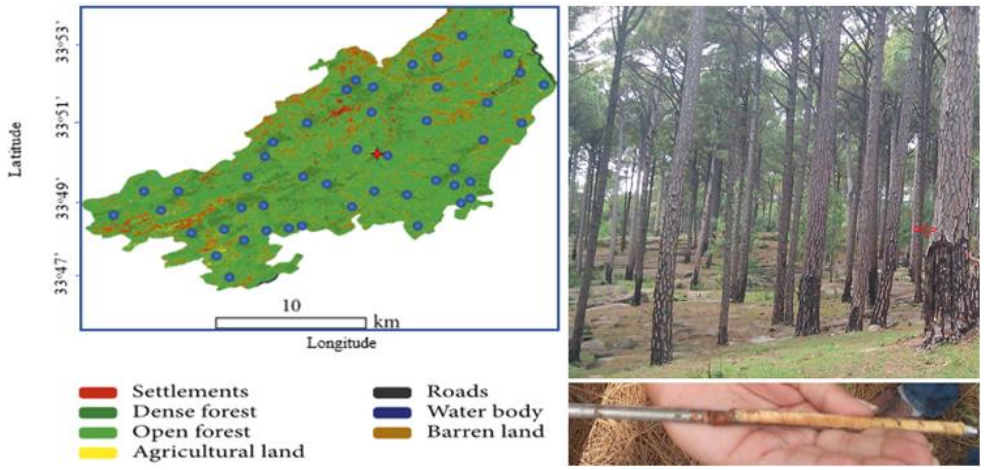

Figure 1. *Location of study sites (48 P. roxburghii stand), sampled tree and fresh tree ring core of pinus roxburghii in Murree Hills Pakistan. Sampled tree is indicated by red arrow*

Radial growth data

Trees were randomly sampled in the month of September during 2015 by following simple random sampling method. An average of three *Pinus roxburghii* trees were sampled from each site and 48 sites were sampled. The trees were cored with Pressler's increment borer (diameter 5 mm) at 1.3 m above the tree base. Each of increment cores was carefully wrapped and stored in polythene bags. In the laboratory, the cores were pasted to wooden boards, and polished after drying with successively finer grits of sandpaper (up to 600 grid) to create clearly visible tree ring sequences. All tree ring chronologies were visually cross-dated at 1st, then tree-rings of each core were counted under a dissecting microscope with 20x magnification and also by using a Velmex tree ring computing system having 0.001 mm resolution. COFECHA was used in the verification process of visual cross dating (Holmes, 1983). In addition, in order to date the trees centuries, half centuries, and decades were marked with lead pencil. Ring-widths were measured by hand using the computer program Measure J2X, a measuring table, and a microscope with 40x magnification. Rings were measured for their seasonal (dark and light bands separately) and annual growth. The standardized ring chronologies more often contains variation like natural or biological persistence. Residual chronologies were developed and less frequency persistence were removed using an autoregressive (AR) model. It considered as a bi weight dynamic approach to reduce the effect of outliers. In total, 48 Chir pine simple, residual and mean ring-width chronologies were prepared using R software (Bunn, 2008). The prepared chronologies were finalized by rechecking the ring series showing potential errors and corrected if dating miscalculation was happened (Holmes, 1986).

http://www.aloki.hu ● ISSN 1589 1623 (Print) ● ISSN1785 0037 (Online)
DOI: http://dx.doi.org/10.15666/aeer/1804_48394855

Climate-growth analysis

The relationship between climate and growth was evaluated by comparing tree ring chronologies to the climatic factors by using traditional nonlinear models and correlation analysis. Precipitation and air temperature of preceding to present growing season (May of previous year to August of current year) were tested. The significance of Pearson's correlation values was determined and the reliability of data was enhanced by bootstrapping method. The linear and nonlinear regression functions were fitted to represent the magnitude of variation in the correlation coefficients along growing degree days (GDD > 5°C) and different elevations. To analyze the growth response of *P. roxburghii* to climatic factors a multi linear mixed model was practiced, given below:

$$W_{ij} = \beta_0 + \beta_1 x_{ij} + \mu_{i1} + \mu_{i2} x_{ij} + \varepsilon_{ij} \quad \text{(Eq.1)}$$

where W_{ij} and x_{ij} denotes the tree ring chronologies and climatic factors for year i and site j; μ_{i1} and μ_{i2} are the intercept and slope values; β0 and β1 are the stable effects; ε_{ij} are site errors, μ_{i1}, μ_{i2} and εij are assumed to be independent. The parameters of linear mixed model were estimated (Bates et al., 2014) using the Matlab software (ver. R2017a, MathWorks Inc., USA).

Results

Variation in climatic factors

Seasonal variation in major climatic variables air temperature and precipitation were shown in *Fig. 2*. The long term (1995-2015) minimum, maximum, and mean air temperature from 1995-2015 were close to zero in winters and reached to seasonal maximum values during mid-summer period and peaked in June or July (*Fig. 2a*). The precipitation presented a clear seasonal trend generally varied with timing and amount (*Fig. 2b*). Winter and early springs were usually with little precipitation and the time period between July and August received most of the annual rainfall.

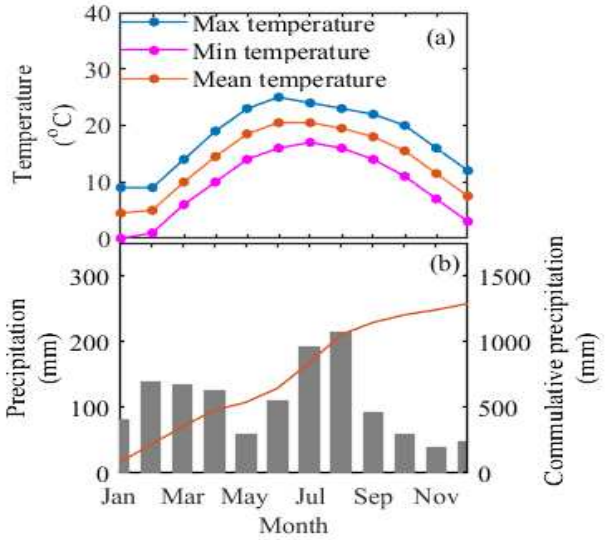

Figure 2. *Seasonal variation in (a) monthly mean minimum and maximum temperature (b) total monthly precipitation and cumulative precipitation during 1995-2015*

http://www.aloki.hu ● ISSN 1589 1623 (Print) ● ISSN1785 0037 (Online)
DOI: http://dx.doi.org/10.15666/aeer/1804_48394855

Long term variation in temperature and precipitation during the 20-year period were shown in *Fig. 3*. The annual maximum and minimum temperature ranged between 25.2-27.8°C and 12.8-14.7°C during 1995-2015. The variation in mean temperature was evident to be almost similar to the minimum temperature. The annual mean temperature was highest as 21.0°C, and lowest as 19.2°C, during 1999 and 1995, respectively (*Fig. 3b*). In addition, the slope pattern representing minimum and mean air temperature was steeper in comparison to the maximum temperature. The inter-annual mean values during 1995-2015 were 26.5 ± 0.57, 13.4 ± 0.39 and 20.90 ± 0.37°C for maximum, minimum and mean temperature respectively (*Fig. 3a,b, Table 1*). The variation was observed greater in minimum than maximum and mean temperatures with coefficient of variation 2.8, 2.01 and 1.85%, respectively. The inter-annual variation in annual total precipitation depicts an overall increasing trend whereas it varied markedly between 20 years (*Fig. 3b*). A great variation range between 590.8-1650 mm yr^{-1} was evident in the study area. The highest precipitation received in 2006 and lowest in 2000. Generally, the time period during 1999-2000 received lowest annual precipitation (*Fig. 3b*). The twenty-year inter-annual mean value of precipitation was 1190.7 ± 257.48 mm with 21% coefficient of variation (*Table 1*).

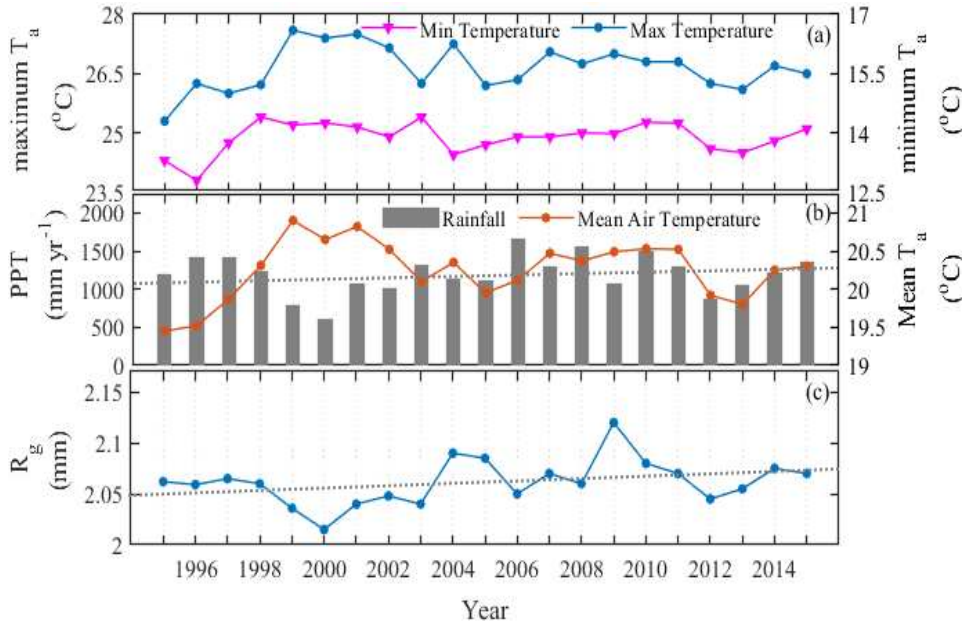

Figure 3. *Temporal variation in (a) maximum and minimum air temperature (b) precipitation and mean air temperature (c) tree radial growth (R_g) of P. roxburghii from 1995-2015. The dotted lines in b and c represents degree of slope*

Table 1. *Inter-annual variability in maximum, minimum, mean air temperature and total Precipitation over 1995-2015*

Variables	Temperature			Precipitation
	Max	Min	Mean	Mean
20 years average	26.5	13.4	20.90	1190.7
Standard deviation	0.57	0.39	0.37	257.48
Coefficient of variation (%)	2.8	2.01	1.85	21

http://www.aloki.hu ● ISSN 1589 1623 (Print) ● ISSN1785 0037 (Online)
DOI: http://dx.doi.org/10.15666/aeer/1804_48394855

Statistical parameters of R_g

The constructed chronologies based on 48 *P. roxburghii* radial growth ring-series (each point was average of three replicates at one site) followed a time span length ranged between 33-91 years (*Table 2*). The two oldest trees had 104 rings. The maximum tree radial growth (R_g) was observed in 2004, 2009, and 2014 (2.065, 2.12, and 2.07 mm, respectively) while the smallest or depressed radial growth was 2.01 mm in 2000 and 2.04 mm in 2012 (*Fig. 3c*). The inter-annual mean R_g was 2.06 mm (±0.022) with 1.06% coefficient of variation during 1995–2015, which constitute both early and late wood formation (*Fig. 3c*). The annual sensitivity (slope) of the R_g was 0.19. Moreover, the years showing no ring formation (missing ring) or fused rings were few since last 20 years and there were no absent rings in last 10 years. Contrary an insignificant rise of 0.05 mm in ring widths was observed.

Table 2. *Relative information of the site variables and standard chronologies of P. roxburghii. Elev. and std. stands for elevation and standard deviation, respectively*

Site	Elev.	Radial growth	Std.	Age	Site	Elev.	Radial growth	Std.	Age
No.	(m)	(mm)	(mm)	(Yr.)	No.	(m)	(mm)	(mm)	(Yr.)
T1	1840	2.5	0.406	80	T 25	1380	2.8	0.32	73
T 2	1800	2	0.65	60	T 26	1360	2.6	0.286	78
T 3	1750	2.25	0.536	75	T 27	1340	3	0.392	66
T 4	1790	2.5	0.71	36	T 28	1320	2.7	0.554	64
T 5	1780	2.25	0.174	47	T 29	1300	2.7	0.144	56
T 6	1700	2.5	0.39	60	T 30	1280	2.25	0.315	53
T 7	1720	2.25	0.51	44	T 31	1260	2	0.25	61
T 8	1720	2.5	0.393	72	T 32	1240	2.75	0.55	65
T 9	1600	2.75	0.401	69	T 33	1220	2.75	0.174	58
T 10	1620	2	0.54	58	T 34	1200	2.25	0.35	47
T 11	1550	2.75	0.311	91	T 35	1180	2	0.25	48
T 12	1640	2.75	0.363	77	T 36	1160	2.3	0.047	59
T 13	1610	2.5	0.585	66	T 37	1140	2.9	0.233	59
T 14	1500	2.75	0.439	66	T 38	1130	2.6	0.266	55
T 15	1400	2.75	0.257	72	T 39	1120	2.75	0.161	74
T 16	1560	2	0.392	54	T 40	1100	2.3	0.4	75
T 17	1480	2.3	0.554	64	T 41	1090	2.4	0.021	55
T 18	1520	2.7	0.693	50	T 42	1080	2.7	0.286	62
T 19	1500	2.5	0.8	61	T 43	1070	2.5	0.392	67
T 20	1480	2.9	0.576	78	T 44	1050	2.3	0.554	71
T 21	1460	2.4	0.45	41	T 45	1030	2.5	0.144	74
T 22	1440	3.1	0.619	55	T 46	1020	1.9	0.315	82
T 23	1420	3.3	0.35	63	T 47	1000	2.55	0.25	69
T 24	1400	2.4	0.508	65	T 48	980	2.2	0.052	56

http://www.aloki.hu ● ISSN 1589 1623 (Print) ● ISSN1785 0037 (Online)
DOI: http://dx.doi.org/10.15666/aeer/1804_48394855

Long-term climate–growth relationship

Fig. 3c revealed that inter annual variation in R_g clearly followed the variation pattern in precipitation and temperature, as clear rise in R_g was observed in 2004, 2005 and 2009 followed by moderate precipitation amount. Whereas significant depressions in R_g during 2000, 2001 and 2012 were clearly related with low precipitation and high temperature. In contrast, the three largest precipitation years did not exhibit any significant rise in ring widths (*Fig. 3b,c*). In fact, the ring widths formation was lower than average, with year of extreme precipitation (such as 2006 and 2010). Subsequently our findings highlighted a baseline effect, below which the R_g tend to be increased until attaining the baseline point. The R_g showed no discernable trend above from baseline effect with further precipitation. Though, it appears that low R_g (~2.01 mm) coincided with precipitation range between 690-900 mm. The larger R_g (2.1 mm and over) was supported by moderate precipitation levels of 950-1100 mm while large precipitation 1200 mm or above have adverse effects on annual growth (*Fig. 3b,c*). The results therefore point out that moderate precipitation causing larger R_g, compared to smaller and larger precipitation events resulting in reduced growth. The results are further supported by regression analysis in *Figure 4a*.

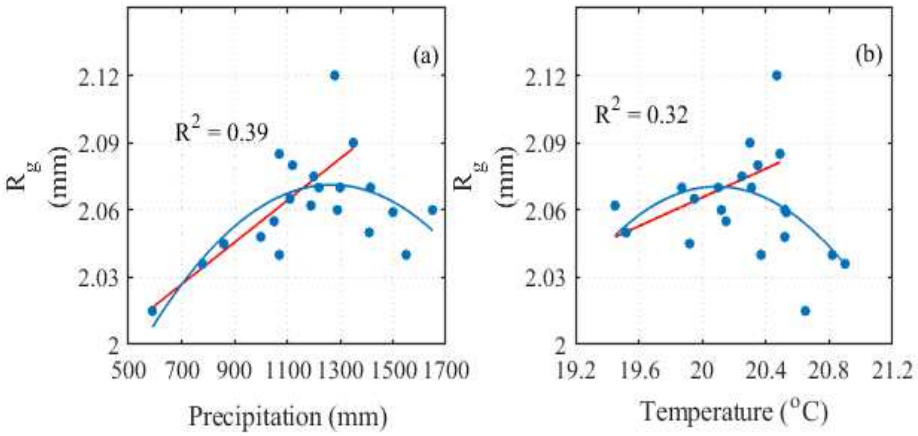

Figure 4. *Relationships between radial growth and major climatic drivers (a) precipitation and (b) temperature. Solid red lines are linear and blue lines are quadratic fitting between radial growth increement and the relevant variables. Each data point represents is annual mean from 1995-2015*

The tree R_g less influenced by mean annual temperature than precipitation (*Fig. 4a,b, Table 3*; based on Eq.1). R_g increased with increasing precipitation and temperature, then leveled off and gradually decreased showing 0.32 and 0.39 coefficient of determination respectively. Mean monthly precipitation and temperature also controls the R_g (*Fig. 5a-d*). Correlation coefficient values revealed that previous year precipitation from June-August was especially important for tree R_g ($p < 0.01$, *Fig. 5a*) and the association progressively weakened ($p = 0.05$) and turned into negative from October-December. The R_g often negatively correlated ($p < 0.05$) with preceding summer temperature of May and August (R^2 = -0.36 and -0.68, respectively) and positively correlated with October and January (R^2 = 0.45 *Fig. 5b*). In contrast, precipitation and temperature of current July showed strong positive control on R_g ($P < 0.05$; *Fig. 5c and d, Table 3*).

http://www.aloki.hu ● ISSN 1589 1623 (Print) ● ISSN1785 0037 (Online)
DOI: http://dx.doi.org/10.15666/aeer/1804_48394855

Table 3. *Estimations of the response of radial ring-width of P. roxburghii to the total monthly precipitation, and mean monthly air temperature from May-Dec of preceding year and from Jan-Aug of current year by linear mixed models (Eq.1). One and two asterisk indicate $p < 0.05$, and $p < 0.01$, respectively. SE is the standard error*

Variables	Precipitation				Temperature			
	Month	**Estimation**	**SE value**	***t* stats**	**Month**	**Estimation**	**SE value**	***t* stats**
Previous year	May	0.06*	0.026	3.19	May	-0.17*	0.024	-2.15
	June	0.13	0.025	1.362	June	-0.85	0.021	-1.05
	July	0.22**	0.026	4.53	July	-0.31*	0.021	-2.42
	August	0.37*	0.024	8.0	August	-0.22*	0.023	-5.78
	September	0.056*	0.024	3.64	September	-0.29*	0.023	-2.81
	October	-0.038*	0.025	-2.24	October	0.48*	0.023	3.55
	November	0.018	0.024	0.743	November	0.26	0.023	1.73
	December	-0.001	0.026	-0.049	December	0.51*	0.023	2.65
Current year	January	0.043	0.027	0.62	January	0.10*	0.020	2.3
	February	0.089	0.024	0.93	February	-0.07	0.020	-0.31
	March	-0.057	0.022	-0.61	March	-0.19*	0.021	-1.5
	April	-0.087	0.022	-0.85	April	0.28**	0.021	2.74
	May	0.16	0.025*	4.80	May	0.32	0.021	0.87
	June	0.247	0.022*	6.72	June	-0.097*	0.022	-1.54
	July	0.43	0.024**	1.79	July	0.27*	0.023	2.95
	August	0.068	0.023	2.77	August	0.085	0.021	2.63

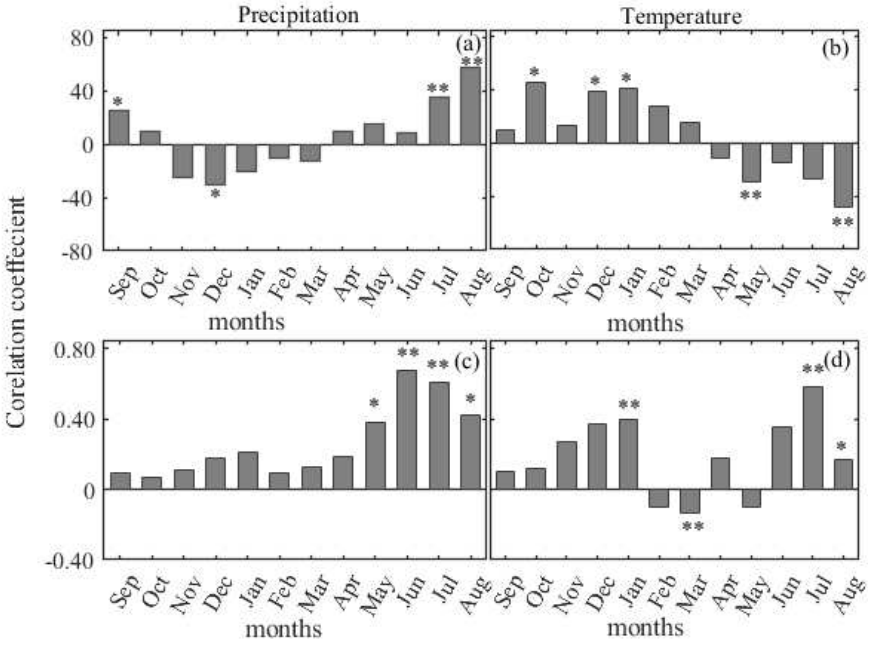

Figure 5. *Bootstrap correlations coefficients calculated among radial growth of P. roxburghii and major climatic factors i.e., monthly total precipitation of (a) preceding year from May-Jan; (c) current year from Jan-Sep, and monthly mean temperature of (b) preceding year from May-Jan; (d) current year from Jan-Sep in 1995–2015. One and two asterisks (*, **) denotes significance level at 95 and 99 % confidence ($p < 0.05$, $p < 0.01$) respectively*

http://www.aloki.hu ● ISSN 1589 1623 (Print) ● ISSN1785 0037 (Online)
DOI: http://dx.doi.org/10.15666/aeer/1804_48394855

Variation in climate-growth relationship along growing degree days (GDD > 5ºC) and different elevations

The coefficient of determination between R_g at 48 sites and total monthly precipitation of current summer decreased with increasing elevation (*Fig. 6a, p* < 0.05). In relation to elevation, *P. roxburghii* showed a robust dependency of R_g to mean summer temperature. The significant positive relationships between R_g and summer temperature was observed for higher elevations (> 1300 m), while below ~1300 m the relationships became negative (*Fig. 6b*). The correlations of previous and current summer precipitation with radial growth showed similar increasing trend but slightly differed in magnitude at high GDDs (*Fig. 6c*, *p* = 0.018, 0.025, respectively). In comparison, with increasing GDD, the influence of current and preceding summer temperatures on trees radial growth progressively declined and became negative above ~900 GDD (*Fig. 6d*, *p* = 0.041, 0.039, respectively).

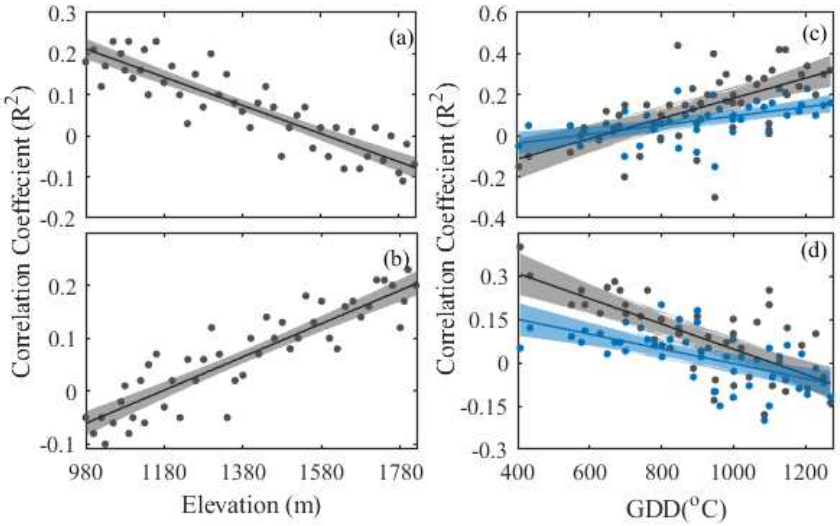

Figure 6. *Variability in correlation coefficients of radial growth with (a) total monthly precipitation and (b) mean monthly temperature of current summer along increasing elevation; (c) total monthly precipitation and (d) mean monthly temperature of preceding (blue) and current summer (grey); with growing degree days (GDD > 5◦C). The colored range shows 95% confidence level*

The response curves in *Fig. 7* showed radial growth responses to variation in temperature and soil moisture. Results indicated that radial growth affected by temperature were progressively increased and peaked its maximum in summer (July) and followed by zero effect in cold winter. Based on temperature and available soil water effected response curves, the R_g in 28 sites were mainly controlled by available soil water contents associated with precipitation (e.g., SN. 3-6 in *Fig. 7*), 9 sites were limited by temperature (e.g., SN. 7, in *Fig. 7*), and 11 sites were not affected by both variables (e.g., SN. 1, 2, 8, in *Fig. 7*). Therefore, 48 R_g trends could be grouped into 3 categories i.e., trend I (was related to soil water controlled), trend II (temperature controlled), and trend III (not controlled by both). The radial growth and three patterns were all significant (*P* < 0.05). The response curves showed the growth of *P. roxburghii* was observed to be frequently controlled by soil moisture that is directly related to precipitation and fewer by temperature, though varied among different sites.

http://www.aloki.hu ● ISSN 1589 1623 (Print) ● ISSN1785 0037 (Online)
DOI: http://dx.doi.org/10.15666/aeer/1804_48394855

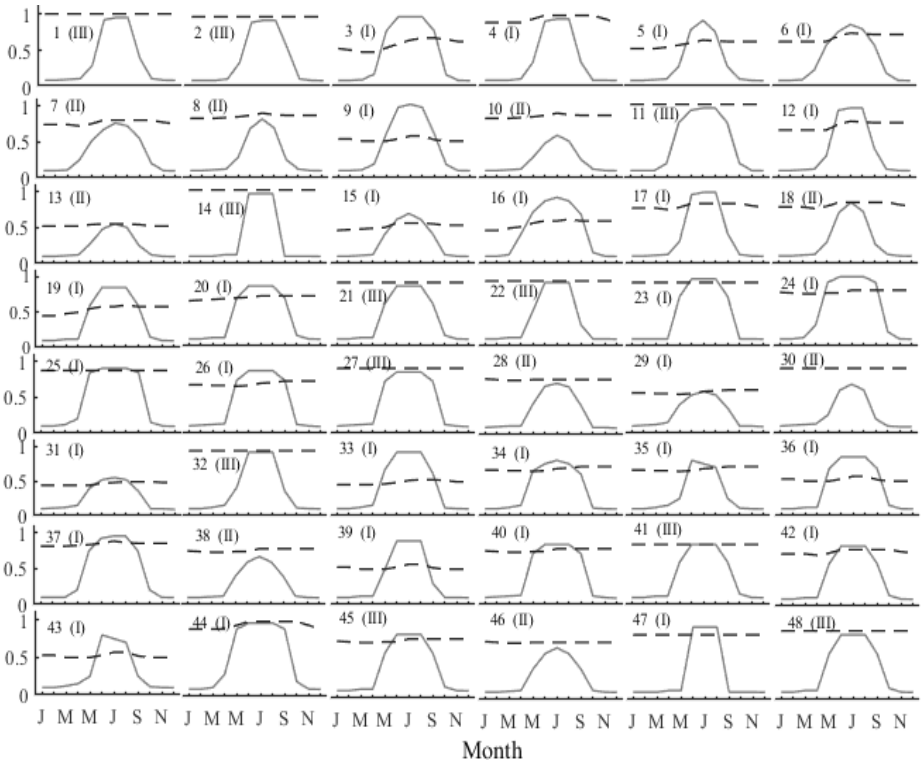

Figure 7. *Seasonal variation showing by growth response curves of temperature (the solid) and moisture level (dashed lines). The label I represents moisture controlled, II temperature controlled and III does not controlled by any of two variables. Each response graph shows the growth pattern at each site (n=48)*

Discussions

Temporal variation in R_g and its controlling mechanisms

In comparison to global average temperature, the rise was observed by 0.74°C at local levels during 1906-2005 (IPCC, 2007). This study indicated that the mean maximum and minimum temperature increases with 0.60 and 1.27°C, respectively, over long temporal scale (1995-2015). The results showed high variation in precipitation ranging between 590.8-1650 mmy^{-1} with significant rise of 21% in study area (*Fig. 3b*). The findings are in lined with previous results concluded by Grunewald et al. (2009) and Liu et al. (2010).

Previous research documented that several factors affect the tree radial growth characteristics, most of them are tree age and site specific related to management operations, however air temperature, precipitation and solar radiations were marked as broader climatic drivers (Yeh and Wensel, 2000). Our results showed that moderate precipitation range could produce larger ring growth and lower precipitation resulting smaller R_g (*Fig. 3c*). These findings are in line with previous researches which suggests that the years producing narrow rings were mainly due to low precipitation levels (Bouriaud et al., 2004; Morecroft et al., 2008). Previous researches have demonstrated the similar effects of precipitation and temperature on radial growth and ring width characteristics. It has been found that the annual radial growth (diameter increment) was more often influenced by the effect of growing season precipitation and temperature and also months preceding that season in *Pinus sylvestris, Abies alba*, *Picea abies*, *Picea sitchensis, Pseudotsuga menziesii* (Feliksik and Wilczynski, 2009). According to Khan et

http://www.aloki.hu ● ISSN 1589 1623 (Print) ● ISSN1785 0037 (Online)
DOI: http://dx.doi.org/10.15666/aeer/1804_48394855

al. (2013) radial growth of *Cedrus deodara* was found being a function of precipitation and temperature in Chitral-Hindukush, Pakistan.

Precipitation limits the growth rate of trees in many ecosystems more than temperature (Cherubini et al., 2003). However, the winter cold was key limiting factor mainly for tree species habitat in mountainous environment (Leburgeois et al., 2012; Martin-Benito et al., 2013) and for evergreen species (Granda et al., 2013). The regression results specified that the summer temperature of preceding year exerted high negative effect on R_g of *P. roxburghii,* whereas the temperature of preceding autumn and winter (Oct-Jan) had positive influence on the R_g ($p < 0.05$, *Fig. 5b*). In summer season, when temperature increases to its maximum, the rate of evapotranspiration becomes high, which results in soil water shortages (Huang et al., 2010), thus become less responsive to temperature. The previous year temperature control was in lined to carryover effect explained by Fritts (2001) and Rammig et al. (2015) that, the deficient nutrient stored during preceding year marked a substantial influence on following year growth. Equally, high temperature in preceding year had inhibit the photosynthesis that impose a decline in growth formation of tree in the subsequent year owing to the inadequate carbohydrates storage. On the other hand, high autumn and winter temperatures favors the growth rate of following year (*Fig. 5d*) by increasing the size and subsistence of buds and thus, the acclimation ability of plant (Weber et al., 2007). Another reason might include, after dormant winter period, a warm end could gently accelerate the cambial reactivation and helps in earlier leaf out, which eventually prolong the period of wood formation (Sanz-Pérez et al., 2009; Viera et al., 2014).

The previous year precipitation showed positive and significant impacts on the R_g (*Fig. 5a*). Preceding year precipitation is also important to boost radial growth formation in many species (Di Filippo et al., 2010). Soil water recharge during autumn and winter precipitation, when growth of *P. roxburghii* remain dormant, appears to be a vital element effecting tree growth rate in the subsequent growth season. This phenomenon found to be an indispensable reserve for commencement of cambial activity and early wood production (Granda et al., 2013; Martin-Benito et al., 2013). During current growing period, tree R_g was more usual positive relationship with May and June precipitation (*Fig. 5c*) and revealed a negative correlation with temperature (*Fig. 5d*). Sufficient precipitation could positively effect on radial growth through making an improvement in xylem cell production and lessen the water stress in an area (Deslauriers et al., 2016). Consequently, this phenomenon favors the positive response of radial growth to precipitation in both preceding and present growing season.

Inclusively, these findings suggest that precipitation and temperature of previous and current growing seasons are the primary controlling factors for growth rate of Chir pine. Prior to the commencement of cold in winter, the species might complete photosynthesis process to stock energy thus execute a positive influence on the tree R_g similar to various evergreen conifers (Miyazawa and Kikuzawa, 2005). Consequently, the temperature of previous year October-December was positively correlated with R_g (*Table 3, Fig. 5b*). Previous studies showed the strong effect of previous summer climate variables on radial growth (Teets et al., 2018).

Spatial variation in the climate growth relationship with GDDs

Results specified that the R_g in *P. roxburghii* was more probably to down regulated by warmer summer temperature which suggests a higher dependency of tree R_g to summer temperature in context of elevation gradient (*Fig. 6b*). Over the past decades, the

http://www.aloki.hu ● ISSN 1589 1623 (Print) ● ISSN1785 0037 (Online)
DOI: http://dx.doi.org/10.15666/aeer/1804_48394855

significant increasing trend in global temperature (IPCC, 2007) and 0.56-0.78°C in various forests of Pakistan was reported by Bukhari and Bajwa (2011). We also found that, warmer summers boosted the radial growth above ~1300 m but reduced it below this elevation (*Fig. 6b*). A winter with warmer end might prevent the soft tissues of tree i.e., roots and buds damage by freezing stress, in higher altitudes (Miller-Rushing and Primack, 2008). Correlation analyses specified the variation in climate–growth relationships with increasing elevation (Huo et al., 2017). The relationship between R_g and precipitation weakened with increasing elevation (*Fig. 6a*), due to the snow effect at higher elevation. A rise in precipitation can quickly reduce the environmental stress and stimulate the radial growth during water-deficit conditions at lower elevation and turn the relationship positive (Deslauriers et al., 2016). As a consequence, trees in the southern sites often grew in a dry and hot atmospheric conditions, so radial growth positively respond and being more sensitive to the increase of precipitation. Subsequently, the R_g was limited by temperature owing to increasing GDD and decreasing precipitation (*Fig. 6c,d*). Similar findings have been observed for silver fir species decreasing at the southern edge, likely as a consequence of the cumulative influence of severe drought (Linares and Camarero, 2010). Moreover, white spruce in Western Canada has also been reported by similar variation (Chen et al., 2017).

The results specified the monthly variation in the response of radial growth to climatic variables i.e., temperature and soil moisture at fortyeight sites (*Fig. 7*). The response curves can detect the signals of temperature influencing or moisture limiting effect on radial growth of *P. roxburghii* in the subtropical pine forest. For instance, the radial growth was limited by soil moisture in 28 sites and few sites were limited by temperature. The eleven sites were similarly effected by temperature and moisture (*Fig. 7*). The non-significant effect in eleven sits suggested that the R_g was neither restricted by precipitation nor by temperature, meanwhile could be influenced by some other site-specific factors (Gewehr et al., 2014). In addition, other site-specific factors such as micro environmental circumstances and species competition (Huang et al., 2013) may be crucial for tree growth determining at these pine sites.

Conclusion

Annual temperature and precipitation were the dominant limiting factor for the R_g of *P. roxburghii.* Summer precipitation (June-August) of previous and current year was most important for tree R_g. The previous summer temperature imposed negative impact on R_g while positive in current July. The R_g was more often limited by soil moisture associated with lower precipitation and high temperature. The control of precipitation was seen to be more significant at lower elevation (<1300 m). However, R_g showed clear dependency on summer temperature when elevation ranged above 1300 m. The approaches employed in this study for unstable temporal responses and nonlinear dependency of *P. roxburghii* to climate drivers, are related to manage and predict the effects of a substantially varied landscape. It also has the potential to forecast future resource outcomes from these forested ecosystems and vulnerability of other forests by using a combination of process-based and global circulation models. In addition, tree sensitivity to site specific climatic variables might useful to expect climate change to decrease stand growth. Due to continuous increase in global climate change, it is suggested that continuous large scale measurements are required to address the temperature and moisture induced variation in climate-growth analysis for sustainable forest management.

http://www.aloki.hu ● ISSN 1589 1623 (Print) ● ISSN1785 0037 (Online)
DOI: http://dx.doi.org/10.15666/aeer/1804_48394855

Acknowledgments. The study was supported by National Natural Science Foundation of China (NSFC) (31361130340, 31270755), and Fundamental Research Funds for the Central Universities (2015ZCQ-SB-02), a project of USCCC University of Eastern Finland, and Academy of Finland (proj. No. 14921). This research is also allied to the continuing Finnish-Chinese research collaboration project EXTREME, among University of Eastern Finland (UEF) and Beijing Forestry University (BJFU). We are thankful to Yuan Li and Mingyan Zhang for their support with the measurements and well maintenance of laboratory instruments.

Conflicts of Interest. The authors declare no conflict of interest.

REFERENCES

[1] Allen, C. D., Macalady, A. K., Chenchouni, H., Bachelet, D., McDowell, N. (2010): A global overview of drought and heat-induced tree mortality reveals emerging climate change risks for forests. – Forest Ecology and Management 259: 660-684.

[2] Altman, J., Fibich, P., Santruckova, H., Dolezal, J., Stepanek, P., Kopacek, J., Hunova, I., Oulehle, F., Tumajer, J., Cienciala, E. (2017): Environmental factors exert strong control over the climate-growth relationships of Picea abies in Central Europe. – Science of the Total Environment 609: 506-516.

[3] Bates, D., Maechler, M., Bolker, B., Walker, S. (2014): LME4: Linear mixed-effects models using Eigen and S4. – R package version 1(7): 1-23.

[4] Bednarz, Z., Ptak, J. (1990): The influence of temperature and precipitation on ring widths of oak (*Quercus robur* L) in the Niepolomice forest near cracow, southern Poland. – Tree-Ring Bulletin 50(1): 1-9.

[5] Bouriaud, O., Bréda, N., Moguéder, G., Nepveu, G. (2004): Modelling variability of wood density in beech as affected by ring age, radial growth and climate. – Trees: Structure & Function 18(3): 264-276.

[6] Briffa, K. R., Osborn, T. J., Schweingruber, F. H., Jones, P. D., Shiyatov, S. G., Vaganov, E. A. (2002): Tree-ring width and density data around the Northern Hemisphere: part 2, spatio-temporal variability and associated climate patterns. – Holocene 12: 759-78.

[7] Bukhari, S. S. B., Bajwa, G. A. (2011): Climate change trends over coniferous forests of Pakistan. – Pakistan Journal of Forestry 61: 1-14.

[8] Bunn, A. G. (2008): A dendrochronology program library in R (dplR). – Dendrochronologia 26(2): 115-124.

[9] Chen, L., Huanga, J.-G., Stadt, K. J., Comeaud, P. G., Zhai, L., Dawsone, A., Alam, S. A. (2017): Drought explains variation in the radial growth of white spruce in western Canada. – Agricultural and Forest Meteorology 233: 133-142.

[10] Cherubini, P., Gartner, B. L., Tognetti, R., Braker, O. U., Schoch, W., Innes, J. L. (2003): Identifcation, measurement and interpretation of tree rings in woody species from mediterranean climates. – Biological Reviews 78: 119-148.

[11] Cook, E. R., Esper, J., D'Arrigo, R. D. (2004): Extra-tropical Northern Hemisphere land temperature variability over the past 1000 years. – Quatenary Science Reviews 23(20): 2063-2074.

[12] D'Arrigo, R., Wilson, R., Liepert, B., Cherubini, P. (2008): On the 'divergence problem' in northern forests: a review of the tree-ring evidence and possible causes. – Global and Planetary Change 60(3): 289-305.

[13] Deslauriers, A., Huang, J. G., Balducci, L., Beaulieu, M., Rossi, S. (2016): The contribution of carbon and water in modulating wood formation in black spruce saplings. – Plant Physiology 170(4): 2072-2084.

[14] Di Filippo, A., Alessandrini, A., Biondi, F., Blasi, S., Portoghesi, L., Piovesan, G. (2010): Climate change and oak growth decline: dendroecology and stand productivity of a Turkey oak (*Quercus cerris* L.) old stored coppice in Central Italy. – Annals of Forest Science 67: 706.

http://www.aloki.hu ● ISSN 1589 1623 (Print) ● ISSN1785 0037 (Online)
DOI: http://dx.doi.org/10.15666/aeer/1804_48394855

[15] Drew, D. M., Allen, K., Downes, G. M., Evans, R., Battaglia, M., Baker, P. (2013): Wood properties in a long-lived conifer reveal strong climate signals where ring-width series do not. – Tree Physiology 33: 37-47.
[16] Esper, J., Cook, E. R., Schweingruber, F. H. (2002): Low-frequency signals in long tree-ring chronologies for reconstructing past temperature variability. – Science 295: 2250-2253.
[17] Fekedulegn, D., Hicks Jr, R. R., Colbert, J. J. (2003): Influence of topographic aspect, precipitation and drought on radial growth of four major tree species in an Appalachian watershed. – Forest Ecology and Management 6094: 1-17.
[18] Feliksik, E., Wilczynski, S. (2009): The effect of climate on tree-ring chronologies of native and nonnative tree species growing under homogenous site conditions. – Geochronometria 33: 49-57.
[19] Flannigan, M. D., Krawchuk, M. A., de Groot, W. J., Wotton, B. M., Gowman, L. M. (2009): Implications of changing climate for global wildland fire. – International Journal of Wildland Fire 18: 483-507.
[20] Fritts, H. (2001): Tree Rings and Climate. – The Blackburn Press, Caldwell.
[21] Gewehr, S., Drobyshev, I., Berninger, F., Bergeron, Y. (2014): Soil characteristics mediate the distribution and response of boreal trees to climatic variability. – Canadian Journal of Forest Research 44(5): 487-498.
[22] Ghazoul, J., Burivalova, Z., Garcia-Ulloa, J., King, L. A. (2015): Conceptualizing forest degradation. – Trends in Ecology and Evolution 30: 622-32.
[23] Granda, E., Camarero, J. J., Gimeno, T. E., Martínez-Fernández, J., Valladares, F. (2013): Intensity and timing of warming and drought differentially affect growth patterns of co-occurring Mediterranean tree species. – European Journal of Forest Research 132: 469-480.
[24] Grunewald, K., Scheithauer, J., Monget, J. M., Brown, D. (2009): Characterisation of contemporary local climate change in the mountains of southwest Bulgaria. – Climate Change 95: 535-549.
[25] Holmes, R. L. (1983): Computer-assisted quality control in tree-ring dating and measurement. – Tree-Ring Bull. 43: 69-78.
[26] Holmes, R. L., Adams, R. K., Fritts, H. C. (1986): Tree-ring chronologies of western North America: California, eastern Oregon and northern Great Basin. – Laboratory of Tree-Ring Research, University of Arizona, Tucson.
[27] Huang, J., Tardif, J. C., Bergeron, Y., Denneler, B., Berninger, F., Girardin, M. P. (2010): Radial growth response of four dominant boreal tree species to climate along a latitudinal gradient in the eastern Canadian boreal forest. – Global Change Biology 16: 711-731.
[28] Huang, J. G., Stadt, K. J., Dawson, A., Comeau, P. G. (2013): Modelling growth-competition relationships in trembling aspen and white spruce mixed boreal forests of Western Canada. – PLoS One 8(10): e77607.
[29] Hughes, M. K., Swetnam, T. W., Diaz, H. F. (2010): Dendroclimatology: Progress and Prospects. – Springer Science & Business Media.
[30] Huo, Y., Gou, X., Liu, W., Li, J., Zhang, F., Fang, K. (2017): Climate–growth relationships of Schrenk spruce (*Picea schrenkiana*) along an altitudinal gradient in the western Tianshan mountains, northwest China. – Trees 31(2): 429-439.
[31] IPCC. (2007): Synthesis report: Contribution of working groups I, II and III to the fourth assessment report of the intergovernmental panel on climate change. – IPCC, Geneva, Switzerland, pp: 1-104.
[32] IPCC. (2014): Synthesis Report: Contribution of Working Groups I, II and III to the Fifth Assessment Report of the Intergovernmental Panel on Climate Change. – In: Pachauri, R. K., Meyer, L. A. (eds.) Core Writing Team. IPCC, Geneva, Switzerland, 151p.
[33] Jones, P. D., Briffa, K. R., Osborn, T. J., Lough, J. M., Van Ommen, T. D., Vinther, B. M., Xoplaki, E. (2009): High-resolution palaeoclimatology of the last millennium: a review of current status and future prospects. – Holocene 19(1): 3-49.

http://www.aloki.hu ● ISSN 1589 1623 (Print) ● ISSN1785 0037 (Online)
DOI: http://dx.doi.org/10.15666/aeer/1804_48394855

[34] Kasischke, E. S., Stocks, B. J. (eds.) (2012): Fire, Climate Change, and Carbon Cycling in the Boreal Forest. – Springer Science & Business Media 138.
[35] Khan, N., Ahmed, M., Shaukat, S. S. (2013): Climatic signal in tree-ring chronologies of Cedrus deodara from Chitral Hindukush range of Pakistan. – Pakistan Journal of Botany 40: 195-207.
[36] Kottek, M., Grieser, J., Beck, C., Rudolf, B., Rubel, F. (2006): World Map of the Köppen-Geiger climate classification updated. – Meteorologische Zeitschrift 15: 259-263.
[37] Leburgeois, F., Mérian, P., Courdier, F., Ladier, J., Dreyfus, P. (2012): Instability of climate signal in tree-ring width in Mediterranean mountains: a multi-species analysis. – Trees 26: 715-729.
[38] Lemoine, D., Peltier, J. P., Marigo, G. (2001): Comparative studies of the water relations and the hydraulic characteristics in Fraxinus excelsior, Acer pseudoplatanus and A. opalus trees under soil water contrasted conditions. – Annals of Forest Science 58(7): 723-731.
[39] Linares, J. C., Camarero, J. J., Carreira, J. A. (2010): Competition modulates the adaptation capacity of forests to climatic stress: insights from recent growth decline and death in relict stands of the Mediterranean fir Abies pinsapo. – Journal of Ecology 98: 592-603.
[40] Liu, B., Henderson, H., Zhang, Y., Xu, M. (2010): Spatiotemporal change in China's climatic growing season: 1955-2000. – Climate Change 99: 93-118.
[41] Lloyd, A. H., Duffy, P. A., Mann, D. H. (2013): Nonlinear responses of white spruce growth to climate variability in interior Alaska. – Canadian Journal of Forest Research 43(999): 331-343.
[42] Ma, Z., Peng, C., Zhu, Q., Chen, H., Yu, G., Li, W., Zhou, X., Wang, W., Zhang, W. (2012): Regional drought-induced reduction in the biomass carbon sink of Canada's boreal forests. – Proceedings of the National Academy of Sciences U. S. A. 109(7): 2423-2427.
[43] Martin-Benito, D., Beeckman, H., Canellas, I. (2013): Influence of drought on tree ring sand tracheid features of Pinus nigra and Pinus sylvestris in a mesic Mediterranean forest. – Europian Journal of Forest Research 132: 33-45.
[44] Maxime, C., Hendrik, D. (2011): Effects of climate on diameter growth of co-occurring Fagus sylvatica and Abies alba along an altitudinal gradient. – Trees 25(2): 265-276.
[45] McCullough, D. G., Werner, R. A., Neumann, D. (1998): Fire and insects in northern and boreal forest ecosystems of North America. – Annual Review of Entomology 43: 107-127.
[46] Miller-Rushing, A. J., Primack, R. B. (2008): Effects of winter temperatures on two birch (Betula) species. – Tree Physiology 28(4): 659-664.
[47] Miyazawa, Y., Kikuzawa, K. (2005): Winter photosynthesis by saplings of evergreen broad–leaved trees in a deciduous temperate forest. – New Phytology 165(3): 857-866.
[48] Morecroft, M. D., Stokes, V. J., Taylor, M. E., Morison, J. I. L. (2008): Effects of climate and management history on the distribution and growth of sycamore (*Acer pseudoplatanus* L.) in a southern British woodland in comparison to native competitors. – Forestry 81(1): 59-74.
[49] Nizami, S. M. (2012): The inventory of the carbon stocks in sub-tropical forests of Pakistan for reporting under Kyoto Protocol. – Journal of Forestry Research 23(3): 377-384.
[50] Olano, J. M., Eugenio, M., García-Cervigón, A. I., Folch, M., Rozas, V. (2012): Quantitative tracheid anatomy reveals a complex environmental control of wood structure in continental Mediterranean climate. – International Journal of Plant Sciences 173: 137-149.
[51] Pilcher, J. R., Gray, B. (1982): The relationships between oak tree growth and climate in Britain. – Journal of Ecology 70(1): 297-304.
[52] Porter, T. J., Pisaric, M. F. (2011): Temperature–growth divergence in white spruce forests of Old Crow Flats, Yukon territory, and adjacent regions of northwestern North America. – Global Change Biology 17(11): 3418-3430.
[53] Price, D. T., Alfaro, R. I., Brown, K. J., Flannigan, M. D., Fleming, R. A., Hogg, E. H., Girardin, M. P., Lakusta, T., Johnston, M., McKenney, D. W., Pedlar, J. H. (2013):

http://www.aloki.hu ● ISSN 1589 1623 (Print) ● ISSN1785 0037 (Online)
DOI: http://dx.doi.org/10.15666/aeer/1804_48394855

Anticipating the consequences of climate change for Canada's boreal forest ecosystems. – Environmental Reviews 21(4): 322-365.

[54] Rammig, A., Wiedermann, M., Donges, J. F., Babst, F., von Bloh, W., Frank, D., Thonicke, K., Mahecha, M. D. (2015): Coincidences of climate extremes and anomalous vegetation responses: comparing tree ring patterns to simulated productivity. – Biogeosciences 12(2): 373-385.

[55] Saeed, S., Ashraf, M. I., Ahmad, A. (2016): The Bela forest ecosystem of district Jhelum, a potential carbon sink. – Pakistan Journal of Botany 48(1): 121-129.

[56] Sanz-Perez, V., Castro-Dıez, P., Valladares, F. (2009): Differential and interactive effects of temperature and photoperiod on budburst and carbon reserves in two co-occurring Mediterranean oaks. – Plant Biology 11: 142-151.

[57] Schweingruber, F. G. (1996): Tree rings and environment. – Dendroecology. Haupt, Bern, Switzerland.

[58] Seidl, R., Schelhaas, M. J., Rammer, W., Verkerk, P. J. (2014): Increasing forest disturbances in Europe and their impact on carbon storage. – Nature Climate Change 4: 806-10.

[59] Sheikh, M. I. (1993): Trees of Pakistan. – Pictoral Printers, Islamabad, Pakistan.

[60] Speer, J. H. (2010): Fundamentals of Tree-ring Research. – University of Arizona Press.

[61] Teets, A., Fraver, S., Weiskittel, A. R., Hollinger, D. Y. (2018): Quantifying climate–growth relationships at the stand level in a mature mixed-species conifer forest. – Global change biology 24(8): 3587-3602.

[62] Tissier, J., Lambs, L., Peltier, J. P., Marigo, G. (2004): Relationships between hydraulic traits and habitat preference for six Acer species occurring in the French Alps. – Annals of Forest Science 61(1): 81-86.

[63] Tolwinski-Ward, S. E., Evans, M. N., Hughes, M. K., Anchukaitis, K. J. (2011): An efficient forward model of the climate controls on interannual variation in tree-ring width. – Climate Dynamics 36(11-12): 2419-2439.

[64] Turner, M. G. (2010): Disturbance and landscape dynamics in a changing world. – Ecology 91: 2833-2849.

[65] Valladares, F., Benavides, R., Rabasa, S. G., Diaz, M., Pausas, J. G., Paula, S., Simonson, W. D. (2014): Global change and Mediterranean forests: current impacts and potential responses. – Forests and Global Change, pp: 47-75.

[66] Viera, J., Rossi, S., Campelo, F., Freitas, H., Nabais, C. (2014): Xylogenesis of Pinus pinaster under a Mediterranean climate. – Annals of Forest Science 71: 71-80.

[67] Visser, H., Büntgen, U., D'Arrigo, R., Petersen, A. (2010): Detecting instabilities in tree-ring proxy calibration. – Climate of the Past 6(3): 367-377.

[68] Weber, P., Bugmann, H., Rigling, A. (2007): Radial growth responses to drought of Pinus sylvestris and Quercus pubescens in an inner Alpine dry valley. – Journal of Vegetation Science 18: 777-792.

[69] Yeh, H. Y., Wensel, L. C. (2000): The relationship between tree diameter growth and climate for coniferous species in northern California. – Canadian Journal of Forest Research 30: 1463-1471.

[70] Zang, C., Hartl-Meier, C., Dittmar, C., Rothe, A., Menzel, A. (2014): Patterns of drought tolerance in major European temperate forest trees: climatic drivers and levels of variability. – Global Change Biology 20: 3767-3779.

[71] Zhang, Y., Wilmking, M. (2010): Divergent growth responses and increasing temperature limitation of Qinghai spruce growth along an elevation gradient at the northeast Tibet Plateau. – Forest Ecology and Management 260(6): 1076-1082.

http://www.aloki.hu ● ISSN 1589 1623 (Print) ● ISSN1785 0037 (Online)
DOI: http://dx.doi.org/10.15666/aeer/1804_48394855

INTERACTIVE EFFECTS OF ELEVATED CO_2 CONCENTRATION AND NITROGEN FERTILIZER APPLICATION ON NITROGEN DISTRIBUTION IN A COTTON–SOIL SYSTEM

LYU, N.[1,2] – SHI, L.[1] – SUN, L.[2] – LIU, F.[3] – CHEN, Y.[1*a] – YIN, F.[1*b]

[1]*Institute of Field Water Conservancy, Soil and Fertilizer Research, Xinjiang Academy of Agricultural and Reclamation Science, Shihezi 832000, Xinjiang, China (phone: +86-993-668-3300; fax: +86-993-255-3118)*

[2]*College of Economics and Management, Shihezi University, Shihezi 832003, Xinjiang, China*

[3]*College of Management and Engineering, Anhui Polytechnic University, Wuhu 241000, Anhui, China*

**Corresponding authors*
[a] *e-mail: nkycy8216@163.com; phone: +86-993-668-3731, +86-130-3132-5270; fax: +86-993-255-3118*

[b] *e-mail: nkyyfh@sohu.com; phone: +86-993-668-3699, +86-135-6773-8221; fax: +86-993-255-3118*

(Received 9th Jan 2020; accepted 6th May 2020)

Abstract. This study aimed to investigate the beneficial effects of elevated CO_2 levels and nitrogen fertilization on the nitrogen distribution in a cotton-soil system in China, using CO_2 obtained as an industrial byproduct. A semi-open-top artificial climate chamber was used to investigate the effects of ambient CO_2 concentration (360 μmol·mol^{-1}, Xinjiang) and elevated CO_2 concentrations (540 and 720 μmol·mol^{-1}) and application of nitrogen (N) fertilizer (0, 150, 300, and 450 kg·hm^{-2}) on cotton growth and available N distribution in the cotton–soil system. The results showed that the cotton biomass was positively influenced by the increase in CO_2 concentration and N application. The total N content in the cotton significantly increased with N application, and this increase was more significant with $CO_{2\ 540}$ treatment compared with $CO_{2\ 720}$ treatment. The N accumulation in buds and bolls was the highest, followed by leaves and then stems; it was the lowest in the roots. When the CO_2 concentration was elevated to 540 μmol·mol^{-1}, the soil NO_3^-–N content decreased significantly. The soil NH_4^+–N content slightly increased with 0 and 150 kg·hm^{-2} N application. When the CO_2 concentration was elevated to 720 μmol·mol^{-1}, the soil NO_3^-–N content still decreased and the soil NH_4^+–N content increased. Overall, when the CO_2 concentration was elevated, the application of 300 kg·hm^{-2} N fertilizer significantly increased the cotton biomass and the total N content. It also promoted the absorption of soil N, especially that of NO_3^-–N. The findings provided practical guides for N application in the context of elevated CO_2 concentration in cotton fields.

Keywords: *elevated CO_2 concentration, nitrogen fertilizer application, cotton growth, biomass, plant total N content, soil NO_3^-–N, soil NH_4^+–N*

Introduction

The massive emission of industrial CO_2 has become promoting global warming (Guo et al., 2013). It is expected that the atmospheric CO_2 concentration will approach 1100 μmol·mol^{-1} (ppm) by the end of the 21st century (IPCC, 2014). Doubling of the concentration of CO_2 in the atmosphere affects not only climate, but also the agroecological environment (Ainsworth et al., 2005; Kimbal et al., 2016). Current climate projections indicate that the atmosphere on the earth's surface fluctuating more

http://www.aloki.hu ● ISSN 1589 1623 (Print) ● ISSN 1785 0037 (Online)
DOI: http://dx.doi.org/10.15666/aeer/1804_48574872

frequently, and extreme weather such as hyperthermia, drought and extreme cold will appear more frequently (NOAA-ESRL, 2018). The industrial emission CO_2 storage technology is becoming more and more mature, but the rational reuse method and the related utilization quantity are still in the bottle-neck period. The reuse of industrial emission CO_2 has been the focus of climate and environment research groups (Liu et al., 2018).

CO_2 is an important raw material for plant photosynthesis. It has been proven that a certain amount of CO_2 supplied could increase the biomass and economic yield of C_3 and C_4 plants (Morgan et al., 2001; Leakey et al., 2009). N is an important component of plant proteins and chlorophyll. Thus, the N addition has both direct and indirect effects on photosynthesis, respiration, and other metabolism pathways, affecting the distribution of N nutrients in plant-soil system. Studies have found that the photosynthetic capacity and plant biomass significantly increase under elevated CO_2 and N additions (Fang et al., 2000; Xu et al., 2003; Leakey et al., 2011; José et al., 2016); this in turn promotes the absorption and metabolism of N in plants (Bloom et al., 2002; Mitchell et al., 2018). Research by Pitelka (1994) showed that an elevated CO_2 concentration was conducive to the accumulation of carbohydrates in plant tissues, thus reducing the N content of plants. Recently Other studies (Talbot et al., 2000; Kimball et al., 2001; Dong et al., 2002; Lyu et al., 2015; Cai et al., 2016; Broughton et al., 2017a) have showed that C/N values in cotton, wheat, corn, and rice increased to different degrees under doubled CO_2 concentration, with a decrease in N content in the roots of leguminous plants, but an increase in the N content of the aboveground parts (Yang, 2002; Fitzgerald et al., 2005). It might be that legumes utilized rhizobia to fix N from the air to supplement their N needs to support their rapid growth under high CO_2 concentration. Xu et al. (2004) reported that CO_2 doubling reduced the N content of *Caragana korshinskii* and *Hedysarum laeve* leaves by 10.4% and 5.06%, respectively. However, in different ecosystems, the distribution and absorption of N in different parts of the plant under high CO_2 concentration is related to the photosynthetic pathways of the plant itself, the supply of exogenous N nutrients, the nutrient status of the soil itself, and the amount of N absorbed (Oberbauer et al., 1986; Grunzweig et al., 2001; Charles et al., 2019). Therefore, following increases in CO_2 concentration, exogenous N nutrition could compensate for increased plant growth and metabolism (Stitt et al., 1999; Johnson, 2000; Yang, 2002; Zhang, 2002). It is known that a shortage of N limits the production of CO_2 (Larigauderie et al., 1998; Joel et al., 2001). Under low N conditions, the photosynthetic rates under high CO_2 concentration is lower than under normal CO_2 concentration. Further research revealed that increasing the availability and simultaneous supply of N source can prevent this photosynthetic adaptation (Guo et al., 2006; Mitchell, 2018).

There has been a significant focus of research on the response and adaptation of plants in different ecosystems under elevated CO_2 concentration and different N application and the research objects mainly focuse on horticultural plants, rice, wheat and forest. Cotton is a typical C_3 plant, and empirical and modeling studies (Morgan et al., 2007; Zhang et al., 2017; Broughton et al., 2017b; Li et al., 2020) have shown that possible increase in sensitivity of the physiology and plant productivity to enhancing atmospheric CO_2 concentration. These researches focused on the effect of CO_2 enrichment on cotton growth while the interaction mechanism of CO_2 and N coupling on cotton ecosystem is not clear. Xinjiang is a major agricultural province and is the biggest commercial cotton production base in China. Cotton plays an irreplaceable role

http://www.aloki.hu ● ISSN 1589 1623 (Print) ● ISSN 1785 0037 (Online)
DOI: http://dx.doi.org/10.15666/aeer/1804_48574872

in agricultural production and economy in China and Xinjiang. The latest statistical data (data source: National Climatic Data Center in China) and the current studies (Gao et al., 2015; Cui et al., 2019) have shown that the ambient CO_2 concentration in background air was generally about ~330-372 ppm, which is far from meeting the photosynthetic demand of cotton, and elevated CO_2 concentration can improve the light saturation point of cotton.

The objective of this study focused on the impact of elevated CO_2 and N fertilizer application in the Xinjiang cotton field ecosystem. The project used a semi-open top artificial climate chamber to investigate the response of cotton plants to increases in CO_2 at different levels of N fertilizer application. The total N content of cotton plant and the distribution of NO_3^--N and NH_4^+-N in rhizosphere soil were determined to reveal the response mechanisms of cotton and the soil to the CO_2 and N interaction. Given that the response mechanism of cotton is used to determine the optimal N application level under elevated CO_2 concentrations in cotton canopy, our results would be beneficial to guide the optimal application of N fertilizers in cotton fields under the high CO_2 concentration. Meanwhile, the findings of this study provided a technical scheme for the rational utilization of industrial CO_2 emission. It also provided a scientific basis for accurately predicting the terrestrial ecosystem response and crops yield potential model in the context of elevated CO_2 concentration, and simultaneously it will be of great significance to the healthy and sustainable development of China's cotton industry.

Materials and experimental methods

Research area

The experiment was carried out in 2016-2018 in a semi-open-top artificial climate chamber at the Xinjiang Academy of Agricultural Sciences in China (N44°18'.288, E85°59.961'). Our previous studies (Yin et al., 2011; Gao et al., 2015; Yin et al., 2016) have found that the CO_2 concentration at surface boundary layer in cotton field was generally about ~330-360 ppm from 10 a.m. to 6 p.m. Xinjiang is a typical continental arid climate, the annual precipitation in this area is ~125.0-207.7 mm, the annual evaporation is 1946 mm, the annual average temperature is ~7.5-8.2 °C, the annual sunshine hours are 2526-2874 h, with the sunshine hours in the growing season being ~1900-2000 h, and the total radiation of light per year is next to that of Qinghai-Tibet Plateau. The frost-free period is about ~160 days, and the accumulated temperature of ≥ 10 °C is ~3570-3729 °C. The basic physical and chemical properties of the soil used in the study are shown in *Table 1*. Cotton was planted on April 15 and harvested on September 30.

Table 1. *Physical and chemical properties of the soil used in the study*

Soil type	Soil texture	Soil layer (cm)	Organic matter ($g \cdot kg^{-1}$)	Alkaline hydrolysis nitrogen ($mg \cdot kg^{-1}$)	Available P ($g \cdot kg^{-1}$)	Available K ($g \cdot kg^{-1}$)	pH
Gray desert soil	Medium loam	0-20	6.94	41	21	99	8.3
		20-40	5.73	33	14	103	8.1

http://www.aloki.hu ● ISSN 1589 1623 (Print) ● ISSN 1785 0037 (Online)
DOI: http://dx.doi.org/10.15666/aeer/1804_48574872

Test materials

The test crop was cotton and the variety was Xinluzao 33, the density was 22.5 millon plant per ha; the fertilizer used was urea ($CO(NH_2)_2$), with a measured N content of 46%; CO_2 was sourced from a gas cylinder supplied by the Shihezi Tiangang acetylene plant.

Test device

The experimental set up a semi-closed open top artificial climate chamber, surrounded by a light-transmissive plastic film (blue film in a greenhouse), with a film height of 1.5 m (*Fig. 1A*). The outside of the gas chamber was connected to a CO_2 gas cylinder and CO_2 was administered via drip irrigation belt that ran inside the chamber (*Fig. 1B*). When the cotton entered the flowering period, which was the most vigorous stage of cotton growing, CO_2 was released from 12:00 to 15:00 (the illumination is strongest in Xinjiang) daily via the drip irrigation belt. The gas input was controlled by a CO_2 decompression flow valve, and the internal concentration was measured in real time through a portable infrared CO_2 concentration detector (AT-B-CO_2, Beijing Antai Jihua Technology Co., Ltd.) with S-type distribution.

A B

Figure 1. *(A) Semi-closed open top artificial climate chamber. (B) CO_2 gas cylinder and pressure reducing valve*

Experimental design

The test was carried out in a split zone design. Three CO_2 concentration levels were used: 360 μmol·mol^{-1} (CK, Xinjiang background level), 540 μmol·mol^{-1} (1.5 times higher than the background level) and 720 μmol·mol^{-1} (two times higher than the background level) (referred to as $CO_{2\,360}$, $CO_{2\,540}$ and $CO_{2\,720}$, respectively). Four levels of application N (0, 150, 300, and 450 kg·hm^{-2}; referred to as N_0, N_{150}, N_{300}, and N_{450}, respectively) were used for each CO_2 concentration based on the results of previous studies and local fertilization levels. The moderate water and fertilizer conditions in the northern cotton area of Xinjiang required 300 kg of pure nitrogen to determine the N concentration gradient for this study (Yin et al., 2010,

http://www.aloki.hu ● ISSN 1589 1623 (Print) ● ISSN 1785 0037 (Online)
DOI: http://dx.doi.org/10.15666/aeer/1804_48574872

2011). The CO_2 concentration was the main treatment, and the N fertilizer was the secondary treatment. There were 12 treatments, each repeated three times, over a total of 36 plots. Each the plot area was 42 m^2 (2.8 m × 15 m). The main treatment plots were separated by median intervals and whereas the secondary treatment plots were next to each other.

N fertilizer was applied in the form of analytical grade urea, and the phosphorus and potassium fertilizers were applied as KH_2PO_4 ($K_2O \geqslant 33.9\%$, $P_2O_5 \geqslant 51.5\%$). The fertilization measures were based on the local field requirements: thus, 30% N fertilizer was applied initially, followed by 40% at the first time of watering and 30% at the second time of watering.

The phosphate fertilizer (P_2O_5) dosage was 125 $kg \cdot hm^{-2}$, potassium fertilizer (K_2O) dosage was 54 $kg \cdot hm^{-2}$, and both were used as base fertilizers. The N fertilizer was applied according to the proportion of base application 30%, application 40% for the first irrigation and application 30% at the second water drip, respectively. The times of irrigation was nine in the whole growth period. Treatments with increased CO_2 concentrations began at the start of the cotton flowering period (July 18), under the conditions of optimal light intensity (from ~12:00 h to 15:00 h). The drip irrigation capillary system was used to inject CO_2 gas into the chamber until the desired CO_2 concentration was reached. N fertilizer was applied simultaneously with the water droplets to achieve the simultaneous application of carbon and N. The other field management measures (e.g., *verticillium* wilt control, topping and so on) were the same as used generally in cotton fields.

Test indicators and analysis methods

On 18 August (after 30 days of CO_2 gas addition), three points were selected from each treatment plot according to Z pattern and the size of each point was 2.8 m × 2 m. Ten healthy cotton plants were selected from each point and divided into their aboveground and belowground tissues, which were then heated in an over at 105 °C for 30 min and then dried at 80 °C for 24 h. The dry weight was then determined. After smashing and sieving, 10 mg of the plant sample was measured by using the standard Kjeldahl method. In each cotton plant sampling point, it was used that tubular auger (the length of auger is 1 m, bit depth is 20 cm and diameter is 3 cm) to collect fresh soil at the depth of ~0–20 cm and ~20–40 cm soil layer; 1 $mol \cdot L^{-1}$ KCl 50 mL was added to 10 g of the fresh soil sample and then shaken for 30 min. The suspension was then filtered through filter paper, and the nitrate nitrogen (NO_3^-–N) and ammonium nitrogen (NH_4^+–N) in the soil were using a Continuous Flow Analytical System (CFA). Soil moisture was determined by the drying method.

SPSS 19.0 was used to analyze the data using ANOVA and P value test significance tests. The functional relationship between CO_2 concentration and N application level was constructed by using Sigmaplot 12.5 and Excel 2007 to analyze the gradient changes in total N and soil NH_4^+–N and NO_3^-–N content. The datas in chart were the anverage of 2016–2018 year.

Results and analysis

Effects of elevated CO_2 concentration and N fertilizer application on cotton biomass

In this study, dry matter weight was adopted to analyse the changes in cotton biomass. ANOVA showed that the biomass of cotton organs and the whole plant was significantly affected by CO_2 concentration, N application and the interaction of CO_2 and N (*Table 2*). In general, the biomass of buds and bolls, stems, and the whole plant was increased significantly

http://www.aloki.hu ● ISSN 1589 1623 (Print) ● ISSN 1785 0037 (Online)
DOI: http://dx.doi.org/10.15666/aeer/1804_48574872

with CO_2 concentration elevation, whereas the biomass of leaves and roots in $CO_{2\ 540}$ concentration was higher than that in $CO_{2\ 720}$ concentration.

Gao and Guo (2003) reported that elevated CO_2 concentrations could also promote the biomass increase in desert plant, and the roots, stems, and leaves responded differently to elevated CO_2 concentrations. Some studies indicated that the initially promotion effect high concentration CO_2 on plant would gradually disappear as time going by (Chen, 2005). At the same CO_2 concentration, the biomass of different cotton organs increased with N fertilizer application increasing, with more significant increases occurring at the higher N application levels, which was consistent with the results of some researchers (Zhang et al., 1999; Stitt et al., 1999). Overall, at the flowering and boll-forming stages, the biomass of buds and bolls was the highest, followed by leaves, and lowest in stems and roots, indicating the transport of nutrients from the roots to reproductive organs.

The results also showed that the effect of elevated CO_2 concentrations on cotton biomass was closely related to the supply of mineral nutrients. When atmospheric CO_2 concentrations elevated from 350 μmol·mol^{-1} to 700 μmol·mol^{-1}, the crop yield and biomass could increase by 24–25% (Kimball, 2016), but this response would be lower in the case of water and nutrients deficiency (Oechel, 1994). Therefore, when considering the growth–promoting effects of elevated CO_2 concentrations on plant growth, it is necessary to ensure the appropriate timing of fertilizer application (Roser et al., 1999; Yang et al., 2007; Coskun et al., 2016; Zhang et al., 2017).

Table 2. *Changes in the biomass of cotton in response to elevated atmospheric CO_2 and N application (g)*

CO_2 concentration (μmol·mol^{-1})	**N fertilizer application (mg·kg^{-1})**	**Cotton organ**				
		Leaf	**Stem**	**Bud and boll**	**Root**	**Total plant**
$CO_{2\ 360}$	N_0	11.64±0.09 d	7.23±0.09 d	16.77±0.07 cd	4.07±0.16 c	39.68±0.23 d
	N_{150}	13.66±0.46 c	8.22±0.10 c	17.77±0.11 c	4.83±0.06 b	44.48±0.39 c
	N_{300}	14.29±0.15 b	9.10±0.09 b	18.85±0.05 b	5.09±0.07 ab	47.33±0.24 ab
	N_{450}	16.36±0.08 a	10.23±0.07 a	20.11±0.12 a	5.70±0.05 a	51.34±0.25 a
	Average	13.99±1.87	8.69±0.16	18.38±1.47	4.92±0.65	45.96±4.98
$CO_{2\ 540}$	N_0	12.27±0.15 d	8.41±0.15 d	16.86±0.07 d	4.94±0.07 d	42.48±0.05 d
	N_{150}	13.78±0.09 c	9.96±0.03 c	18.24±0.31 c	5.38±0.05 c	47.36±0.38 c
	N_{300}	15.91±0.14 b	10.22±0.08 b	20.42±0.57 b	6.19±0.05 ab	52.74±0.51 b
	N_{450}	17.38±0.12 a	11.17±0.08 a	22.11±0.22 a	6.56±0.09 a	57.22±0.43 a
	Average	14.83±2.10	9.94±1.04	19.41±2.49	5.77±0.70	49.95±6.07
$CO_{2\ 720}$	N_0	12.02±0.05 d	9.13±0.04 c	17.15±0.10 d	4.95±0.09 b	43.30±0.06 d
	N_{150}	13.75±0.06 c	10.96±0.06 b	19.98±0.04 c	5.18±0.10 b	49.87±0.14 c
	N_{300}	14.42±0.16 b	11.35±0.09 a	22.22±0.59 b	5.58±0.15 ab	53.57±0.64 b
	N_{450}	16.69±0.17 a	11.75±0.48 a	23.71±0.21 a	5.99±0.05 a	58.14±0.80 a
	Average	14.23±2.17	10.79±1.07	20.77±2.38	5.43±0.42	51.22±6.14
Sources of variation						
CO_2		**	**	**	*	**
N		**	**	**	*	**
CO_2 * N		*	*	**	NS	**

Different letters in the same column indicated significant difference among treatments at 0.05 level. ** indicated $P < 0.01$, * indicated $P < 0.05$, *NS* indicated no significant difference at 0.05 level

http://www.aloki.hu ● ISSN 1589 1623 (Print) ● ISSN 1785 0037 (Online)
DOI: http://dx.doi.org/10.15666/aeer/1804_48574872

Effects of elevated CO2 concentration and N fertilizer application on the total N content in different organs of cotton

The changes in total N content of leaves are shown in *Figure 2A*. Leaves are important photosynthetic organs for photosynthesis and the major source for carbohydrates. Elevated CO_2 concentrations are hypothesized to be beneficial to photosynthesis and respiration in leaves (Oberbauer et al., 1986; Wang et al., 2011; Zhang et al., 2016), which is also likely to affect nutrient absorption by the leaves. Analysis of variance showed that elevated CO_2 concentration, N fertilizer application and the interaction of CO_2 concentration and N fertilizer could significantly increase the total N content in leaves ($P = 0.005$, 0.000 and 0.002, respectively). In the same CO_2 concentration treatment, the total N content in leaves increased significantly with increasing N fertilizer application ($P = 0.012$). At the same N level, the total N content in leaves in the $CO_{2\ 720}$ treatment group was higher than that in the $CO_{2\ 540}$ treatment group, but there was no significant difference. Under high CO_2 concentrations, C_3 plants were able to adapt their photosynthesis under low N conditions (Zhou et al., 2006; Xia et al., 2019). These results indicated that when the CO_2 concentration was elevated to between 540 and 720 $\mu mol \cdot mol^{-1}$, it promoted the N absorption and utilization by leaves. The effect of elevating CO_2 concentration on the N demand resulting from increased growth was compensated by increasing N fertilizer application. Previous researches also showed that N nutrition delays the senescence of mature leaves and improves the adaptability of plant to adverse conditions (Zhang et al., 2002).

Changes in total N content in buds and bolls are shown in *Figure 2B*. This result showed that elevated CO_2 concentration and N fertilizer application had significant effects on the total N content in buds and bolls ($F = 19.13$ and 29.10, respectively), and this was also significant in terms of the interaction between CO_2 concentration and N fertilizer ($F = 2.89$). Under ambient CO_2 conditions, the total N content in buds and bolls showed a significant positive correlation with N fertilizer application dosages. When the CO_2 concentration was elevated by 0.5 and 1.0 times, the total N content in buds and bolls significantly increased, and this was more significant in the $CO_{2\ 540}$ treatment group. Compared with $CO_{2\ 360}$ treatment, when the CO_2 concentration was elevated to 540 $\mu mol \cdot mol^{-1}$, the total N content in buds and bolls at N_0, N_{150}, N_{300}, and N_{450} level increased by 12.57%, 13.41%, 28.42% and 17.50% respectively; when the CO_2 concentration was elevated to 720 $\mu mol \cdot mol^{-1}$, the total N content in buds and bolls showed had no significant changes at N_0 and N_{150} level, but increased by 14.75% and 12.50% at N_{300} and N_{450} level, respectively. In general, of the different CO_2-N combination treatments, the total N content in buds and bolls was the highest in $CO_{2\ 540}$-N_{300} treatment group.

Changes in total N content in stems are shown in *Figure 2C*. The total N content in stems increased with the increasing of N fertilizer application in each CO_2 concentration treatment. Compared with ambient CO_2 concentration treatment group, the total N content in stems increased significantly when CO_2 concentration was elevated to 540 $\mu mol \cdot mol^{-1}$ ($P = 0.703$), although there was no significant change when CO_2 concentration was elevated to 720 $\mu mol \cdot mol^{-1}$ ($P = 0.53$). This suggested that when the atmospheric CO_2 concentration was elevated to 540 $\mu mol \cdot mol^{-1}$, N fertilizer application was more beneficial to promote the N nutrition increasing in stems.

Changes in total N content in roots are shown in *Figure 2D*. There were no significant differences in total N content in roots among the different CO_2 concentration

http://www.aloki.hu ● ISSN 1589 1623 (Print) ● ISSN 1785 0037 (Online)
DOI: http://dx.doi.org/10.15666/aeer/1804_48574872

treatments ($P = 0.051$). In ambient CO_2 concentration treatment, the total N content in roots increased with increasing N fertilizer application dosages ($P = 0.016$). When the CO_2 concentration was elevated to 540 μmol·mol^{-1} and 720 μmol·mol^{-1}, the interaction of CO_2 concentration and N fertilizer application had significant effect on N content in roots and the total N content at N_{300} was lower than that at N_{150} level.

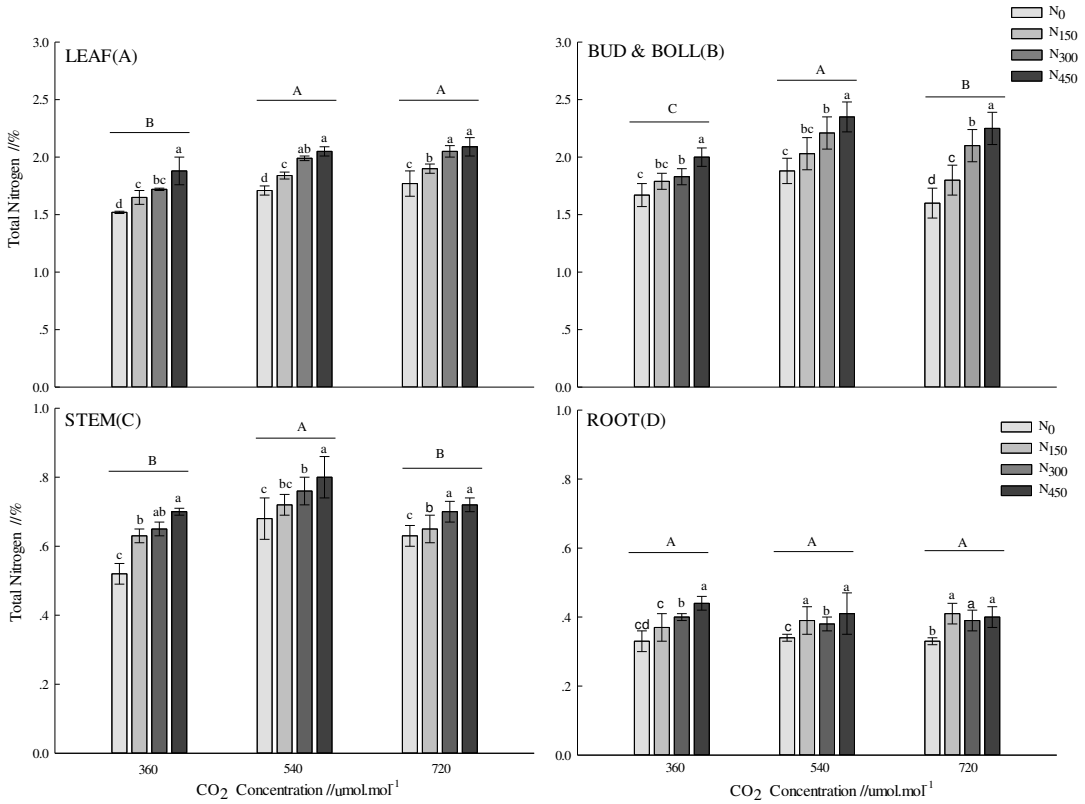

Figure 2. *Effects of elevated CO_2 and N fertilizer application on the total N distribution in cotton leaf (A), bud and boll (B), stem (C), and root (D). Different lowercase letters in the column indicated significant difference among different N treatments at $P < 0.05$. Different capital letters in the column indicate significant difference among different CO_2 treatments at $p < 0.05$*

In general, different combinations of CO_2 concentration and N fertilizer had significant effects on N absorption and utilization of different cotton organs. The total N content in buds and bolls was the highest, followed by leaves, then was in stems, being lowest was in roots. This was probably because the combination of elevated CO_2 concentrations and N fertilizer applications promoted the photosynthesis and growth metabolism of the aboveground tissues of cotton, which then needed to absorb nutrition from belowground tissues to support increase. Thus, N nutrients were transported to the buds, bolls and other vegetative organs of cotton via the roots and stems to meet the nutritional needs of reproductive growth (Hu et al., 2006; Wang et al., 2010; Yin et al., 2011).

The effects of elevated CO_2 concentration and N fertilizer application on total N in the whole cotton plant are shown in *Table 3*. When the CO_2 concentration was elevated by 0.5 times and 1.0 times, the total N content in whole cotton plant increased

http://www.aloki.hu ● ISSN 1589 1623 (Print) ● ISSN 1785 0037 (Online)
DOI: http://dx.doi.org/10.15666/aeer/1804_48574872

significantly compared with the ambient CO_2 concentration, this increasing effect was more significant in $CO_{2\ 540}$ treatment. That indicated the CO_2 concentration was elevated to 720 μmol·mol^{-1} and above would restrict N nutrient utilization by the cotton. Under the same CO_2 concentration treatment, the total N content in the whole plant increased with the N fertilizer application dosages, which was consistent with the general fertilization effect. Meantime, the interaction of elevated CO_2 concentration and N fertilizer application did have a significant effect on the total N content in the whole cotton plant ($P = 0.008$).

This suggests that when the atmospheric CO_2 concentration is elevated to ~540-720 μmol·mol^{-1}, which promotes the N nutrient absorption and accumulation in cotton plant, it would be necessary to increase the application of external N fertilizer to compensate for the nutrient absorption by the plants caused by the increasing CO_2 concentration.

Table 3. *The total N content in the whole cotton plant under different CO_2 and N treatments (%)*

Treatments	N_0	N_{150}	N_{300}	N_{450}
$CO_{2\ 360}$	4.11 ± 0.20 dC	4.63 ± 0.12 cC	4.82 ± 0.04 bB	5.08 ± 0.21 aC
$CO_{2\ 540}$	4.83 ± 0.17 dA	5.08 ± 0.12 cA	5.35 ± 0.40 bA	5.65 ± 0.17 aA
$CO_{2\ 720}$	4.56 ± 0.11 dB	4.97 ± 0.25 cAB	5.28 ± 0.06 abA	5.45 ± 0.23 aAB

The different lowercase letters in the same row indicated significant differences among different N treatments at $P < 0.05$. The same capital letters in the same column indicate no significant differences among different CO_2 treatments at $P < 0.05$

Effects of elevated CO_2 concentration and N fertilizer application on root soil NO_3^-–N content in cotton fields

The response of NO_3^-–N content to different CO_2 and N fertilizer treatments varied in the ~0–20 cm and ~20–40 cm soil layers, as shown in *Figure* 3*A* and *B*, respectively. Soil NO_3^-–N content decreased significantly with increasing CO_2 concentrations and this decrease was more significant at the $CO_{2\ 540}$ level than that at the $CO_{2\ 720}$ level. The interaction of elevated CO_2 concentration and N fertilizer application had a significant effect on the NO_3^-–N content in the ~0–20 cm soil layer and ~20–40 cm soil layer ($P = 0.032$ and 0.000, respectively).

In ambient CO_2 concentration, the NO_3^-–N content in ~0–20 cm soil layer significantly increased with increasing N fertilizer application ($P = 0.001$). When the CO_2 concentration was elevated to 540 μmol·mol^{-1}, the soil NO_3^-–N content showed no significant difference between different N application dosages ($P = 0.420$), although it was lowest at the N_{300} level. When the CO_2 concentration was elevated to 720 μmol·mol^{-1}, the soil NO_3^-–N content increased with the increase in N fertilizer application ($P = 0.040$).

At the same N fertilizer application level, the soil NO_3^-–N content in root layer decreased significantly in proportion to the elevated CO_2 concentrations. Compared with the ambient CO_2 concentration, in the $CO_{2\ 540}$ concentration treatment group, the soil NO_3^-–N content decreased by 25.90%, 25.05%, 47.77% and 37.38% at N_0, N_{150}, N_{300}, and N_{450} level, respectively; in the $CO_{2\ 720}$ concentration treatment group, the soil NO_3^-–N content decreased by 6.94%, 4.52%, 18.31% and 19.30% at N_0, N_{150}, N_{300} and N_{450} level, respectively. The NO_3^-–N content at the N_{300} and N_{450} levels was

http://www.aloki.hu ● ISSN 1589 1623 (Print) ● ISSN 1785 0037 (Online)
DOI: http://dx.doi.org/10.15666/aeer/1804_48574872

significantly lower than at N_0 and N_{150} level under elevated CO_2 concentrations. In a general, in the interaction treatment groups of CO_2 concentration and N fertilizer, the soil NO_3^-–N content was lowest in $CO_{2\ 540}$–N_{300} treatment group. Other studies reported that, at high N application levels, the soil NO_3^-–N content decreased significantly under elevated CO_2 concentrations and N fertilizer application, mainly due to N application significantly promoted the growth and metabolism of the plants (Mauney et al., 1994; Ma et al., 2004; Liu et al., 2018), increasing NO_3^-–N absorption by plants from soil, thus affecting the soil N nutrients conditions. In addition, an anaerobic environment was formed by the drip irrigation system, inhibiting soil-nitrifying microbial activity and reducing the soil NO_3^-–N content. The reduction in the soil NO_3^-–N content in the $CO_{2\ 540}$ concentration treatment was greater than that in the $CO_{2\ 720}$ concentration treatment; this suggests that the level of CO_2 enrichment was too high. If this negatively impacted the ability of cotton to adapt to higher levels of CO_2 then this would inhibit the absorption of soil nutrients by the plants.

The soil NO_3^-–N content decreased with the soil depth increasing. In the ~20–40 cm soil layer, the changes in NO_3^-–N content were the same as in the ~0–20 cm soil layer among different CO_2 concentrations and N fertilizer treatments; however, the increasing trends in NO_3^-–N content were more significant in the ~0–20 cm soil layer, given the interaction effects between the increasing CO_2 concentration and N fertilizer application.

Effects of elevated CO_2 concentration and N fertilizer application on root soil NH_4^+–N content in cotton fields

The soil NH_4^+–N content varied significantly under different CO_2 concentration and N fertilizer treatments as shown in *Figure* 3*C* and *D*. ANOVA analysis showed that elevated CO_2 concentration, N fertilizer application and the interaction of CO_2 and N all had significant effects on NH_4^+–N content in the ~0–20 cm soil layer (F = 176.7, 98.06, and 9.925, respectively) and in the ~20–40 cm soil layer (F = 191.784, 65.150, and 6.270, respectively).

In the ~0–20 cm soil layer, in the ambient CO_2 concentration, the NH_4^+–N content significantly increased with increasing N fertilizer addition (P = 0.000), and this was more significant at the N_{300} and N_{450} levels. Compared with the ambient CO_2 concentration, the NH_4^+–N content showed a slightly increase at the N_0 and N_{150} levels when the CO_2 concentration was elevated to 540 μmol·mol^{-1}, but a decrease at the N_{300} and N_{450} levels (reduced by 16.40% and 17.94%, respectively). This suggests that the interaction of CO_2 concentration and the high N fertilizer application could significant promote the NH_4^+–N nutrition absorption by cotton plants. This was consistent with the trends also recorded in the total N content in cotton plants (*Table 3*). When the CO_2 concentration was elevated to 720 μmol·mol^{-1}, the soil NH_4^+–N content was significantly increased with increasing N fertilizer application. This was consistent with previous studies on other plants, such as wheat, *Phoebe bournei* and rice (Bloom et al., 2002; Han et al., 2003; Liu et al., 2018). In rice–wheat rotation farmland ecosystems, following an increase in CO_2 concentration, soil ammonia-oxidizing bacteria decreased, as did the nitrification activity of the dominant strain, whereas the soil NH_4^+–N mass fraction increased (Lin et al., 2005). This trend was similar to the soil NO_3^-–N content; overall, the soil NH4$^+$–N content in the $CO_{2\ 540}$–N_{150} and $CO_{2\ 540}$–N_{300} treatment groups was lower than that in other CO_2–N treatment groups.

http://www.aloki.hu ● ISSN 1589 1623 (Print) ● ISSN 1785 0037 (Online)
DOI: http://dx.doi.org/10.15666/aeer/1804_48574872

Compared with the ~0–20 cm soil layer, the NH_4^+–N content in the ~20–40 cm soil increased, but not significantly. The soil NH_4^+–N content increased with increasing CO_2 concentration in the ~20–40 cm soil layer ($P = 0.000$). When the CO_2 concentration was elevated, the soil NH_4^+–N content was increased in proportion to the N application dosage.

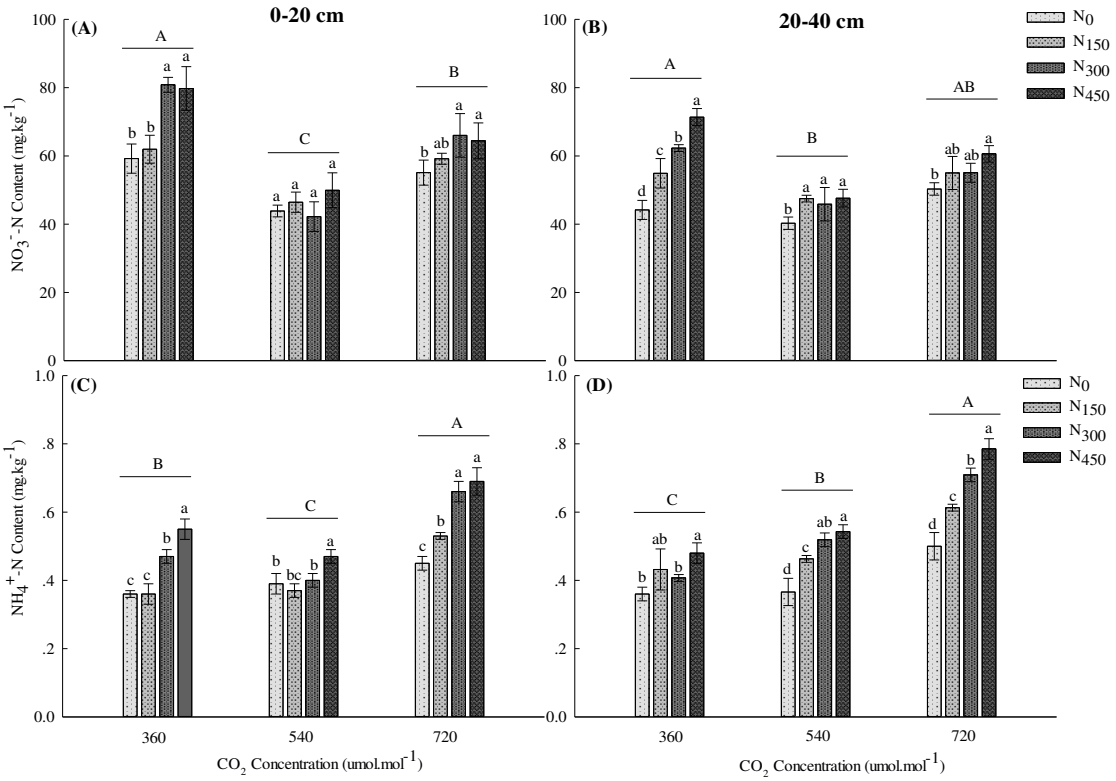

Figure 3. *Effects of elevated CO_2 concentration and nitrogen fertilizer application on NO_3^-–N content (A, B) and NH_4^+–N content (C, D) in cotton field soil. Different lowercase letters in the column indicated significant differences among different N treatments at $P < 0.05$. Different capital letters in the column indicate significant differences among different CO_2 treatments at $P < 0.05$*

Discussion

Studies have shown that elevated CO_2 concentration could promote the growth and N absorption of plants (Dijkstra et al., 2010; Xiao et al., 2017). Under the condition of enhancing CO_2 concentration, photosynthetic adaptation of C_3 plants mainly occurs under the condition of low N conditions (Stitt et al.,1999; Wang et al., 2015). Further research demonstrated that improvement in the availability of N sources and synchronous supply capacity can prevent the occurrence of adaptation (Mitchell et al., 2018).

The effect of elevated atmospheric CO_2 concentration on N uptake by plants is related to atmospheric CO_2 concentration, plant species and the form of absorbed N as well as other factors. Studies have demonstrated that cotton, wheat, corn, rice and other crops have various degrees of C/N elevation in the body under the high concentration of CO_2 and the N content of plants decreased (Lee et al., 2013), while, there was no change

http://www.aloki.hu ● ISSN 1589 1623 (Print) ● ISSN 1785 0037 (Online)
DOI: http://dx.doi.org/10.15666/aeer/1804_48574872

in legumes (Dong et al., 2002; Wang et al., 2010). This may be attributed to the fact that legume plants have *rhizobia*, which can fix N element from the air and supplement the requirement of N nutrition for rapid growth of plants under high CO_2 concentration rather than the absence of such functions in non-leguminous plants.

Previous research reported that when the CO_2 concentration was elevated to ~500–700 μmol·mol^{-1}, higher N fertilizer application promoted the N nutrition absorption and transformation by plants (Xu, 2012). In this study, there was also significant effect on cotton growth and N absorption when CO_2 concentration enrichment and N fertilizer application. As the atmospheric CO_2 concentration enriched, the biomass and N nutrition accumulation in the cotton increased, whereas the available N content in soil was decreased; this trend was most significant with the high N fertilizer application under a $CO_{2\ 540}$ concentration. Deiglmayr et al. (2004) had found that soil N availability was reduced by elevated CO_2, the increase in plant growth may only be possible when plants increase their available nitrogen uptake. Analyzing the correlation between the changes in N content in cotton and soil under different CO_2–N combination treatments showed that high N fertilizer application was beneficial to the absorption and utilization of soil N in cotton field, especially NO_3^-–N. Changes in the N content of soil are related to the forms of soil inorganic N in different regions. For example, the soil N in northern China mainly occurs in the form of NO_3^-–N; thus, cotton grown in northern regions shows the selective absorption of NO_3^-–N (Hu et al., 2006; Liu, 2010). In addition, an anaerobic environment is formed by coated cultivation, and hyperthermia and drought environments are caused by CO_2 concentrations enrichment, which will affect the activity of nitrifying microorganisms in farmland soil, which could also reduce soil the NO_3^-–N content (Chen et al., 2002; Wang et al., 2010).

Conclusions

The results showed that the increase in cotton growth was positively influenced by the increase in N application with increasing CO_2 concentration, which was most significant at $CO_{2\ 540}$ concentration treatment. During the flowering and boll-forming stages, the biomass was highest in the buds, followed by leaves, stems, and roots. When the CO_2 concentration was elevated, the total N content in the cotton plant was significant increased with the N fertilizer application increasing, and this increase effect was more significant in the $CO_{2\ 540}$ treatment than that in $CO_{2\ 720}$ treatment. The total N accumulation content in buds and bolls was the highest, followed by leaves and then stems, being lowest in the roots. The changes in soil NO_3^-–N and NH_4^+–N content were also significant with the interaction of CO_2 concentration enrichment and N fertilizer application. When the CO_2 concentration was elevated to 540 μmol·mol^{-1}, the soil NO_3^-–N content decreased significantly, the soil NH_4^+–N content slightly increased with 0 and 150 kg·hm^{-2} N application. When the CO2 concentration was elevated to 720 μmol·mol^{-1}, the soil NO_3^-–N content still decreased and the soil NH_4^+–N content increased.

Overall, when CO_2 concentration was elevated to ~540–720 μmol·mol^{-1}, the application of 300 kg·hm^{-2} N fertilizer significantly increased the cotton biomass and the total N content. It also promoted the absorption of soil N, especially of NO_3^-–N. This suggests that when N fertilizer supplied effectively, the atmospheric CO_2 concentration enrichment could promote the photosynthesis and growth metabolism of cotton, which also increase the absorption and utilization of soil N nutrients by the

http://www.aloki.hu ● ISSN 1589 1623 (Print) ● ISSN 1785 0037 (Online)
DOI: http://dx.doi.org/10.15666/aeer/1804_48574872

plants. Thus, as literature suggests that the N fertilizer application to Xinjiang cotton fields in the future should be increased when atmospheric CO_2 concentration enrichment. However, the impact of CO_2 concentration and N nutrients on cotton growth and available N utilization are governed by complicated physiological and ecological processes. Thus, the interaction of CO_2 concentration and N fertilizer requires further verification, as do the mechanisms involved in the impacts of elevated CO_2 concentration on different forms of N transformation and utilization in cotton–cropping systems.

Acknowledgements. This research was supported by National Natural Science Fund (Grant No. 40973061, the Major Scientific and Technological Projects of XPCC (Grant No. GKB00NKYGJ12NY), and the Special Fund for Agro-scientific Research in the Public Interest of China (Grant No. 20120312). We would like to acknowledge ISE Translation (http://www.internationalscienceediting.cn/) for editing this manuscript and improving its quality.

Author contribution. The authors of Ning Lyu, Lei Shi, Lingyan Sun and Fang Liu are co-first authors and contributed equally to this paper. Ning Lyu (Conceptualization, methodology, data investigation, validation and writing-original draft), Lei Shi and Ling-yan Sun (data investigation and analysis, Writing-review and editing), Fang Liu (Charts making and revision, writing-review and editing), Yun Chen and Fei-hu Yin ate co-corresponding authors (Supervision, project administration and funding acquisition,).

REFERENCES

[1] Ainsworth, E. A., Long, S. (2005): What have we learned from 15 years of free-air CO_2 enrichment (FACE)? A meta-analytic review of the responses of photosynthesis, canopy properties and plant production to rising CO_2. – New Phytologist 165: 351-372.

[2] Bloom, A. J., Smart, D. R., Nguyen, D. T., et al. (2002): Nitrogen assimilation and growth of wheat under elevated carbon dioxide. – Proceedings of the National Academy of Sciences of the United States of America 99: 1730-1735.

[3] Bloom, A. J., Burger, M., Rubio-Asensio, J. S., et al. (2010): Carbon dioxide enrichment inhibits nitrate assimilation in wheat and Arabidopsis. – Science 328: 899-903.

[4] Broughton, K. J., Smith, R. A., Duursma, R. A., et al. (2017a): Warming alters the positive impact of elevated CO_2 concentration on cotton growth and physiology during soil water deficit. – Functional Plant Biology 44(2): 267-278.

[5] Broughton, K. J., Bange, M. P., Duursma, R. A., et al. (2017b): The effect of elevated atmospheric CO_2 and increased temperatures on an older and modern cotton cultivar. – Functional Plant Biology 44(12): 1207-1218.

[6] Cai, C., Yin, X., He, S., et al. (2016): Responses of wheat and rice to factorial combinations of ambient and elevated CO_2 and temperature in FACE experiments. – Global Change Biology 22: 856-874.

[7] Charles, W. W., James, T. F. (2019): Coupled effects of atmospheric CO_2 concentration and nutrients on plant-induced soil suction. – Plant and Soil 439: 393-404.

[8] Chen, G. Y., Yong, Z. H., Liao, Y., et a1. (2005): Photosynthetic acclimation in rice leaves to free air CO_2 enrichment related to both ribulose-1,5-bisphosphate carboxylation limitation and ribulose-1,5-bisphosphate regeneration limitation. – Plant and Cell Physiology 46(7): 1036-1044.

[9] Chen, L. J., Wu, Z. J., Huang, G. H., et al. (2002): Elevated CO_2 effects the activities of soil urease and phosphatase. – Chinese Journal of Applied Ecology 13(10): 1356-1357.

[10] Coskun, D., Britto, D. T., Kronzucker, H. J. (2016): Nutrient constraints on terrestrial carbon fixation: the role of nitrogen. – Journal of Plant Physiology 203: 95-109.

[11] Cui, C., Shan, Y. L., Liu, J. H., et al. (2019): CO_2 emissions and their spatial patterns of Xinjiang cities in China. – Applied Energy 252: 1-12.

http://www.aloki.hu ● ISSN 1589 1623 (Print) ● ISSN 1785 0037 (Online)
DOI: http://dx.doi.org/10.15666/aeer/1804_48574872

[12] Deiglmayr, K., Philippot, L., Hartwig, U. A., et al. (2004): Structure and activity of the nitrate-reducing community in the rhizosphere of Lolium prenne and Trifolium repens under long-term elevated atmosphere CO_2. – FEMS Microbiology Ecology 49(3): 445-454.
[13] Dijkstra, F. A., Blumenthal, D., Morgan, J. A., et al. (2010): Contrasting effects of elevated CO_2 and warming on nitrogen cycling in a semiarid grassland. – New Phytologist 187: 426-437.
[14] Dlugokencky, E., Tans, P. (2018): NOAA/ESRL. – https://www.esrl.noaa.gov/gmd/ccgg/trends/ (accessed 10 May 2018).
[15] Dong, G. C., Wang, Y. L., Yong, H. J., et al. (2002): Effect of free-air CO_2 enrichment (FACE) on nitrogen accumulation and utilization efficiency in rice. – Chinese Journal of Applied Ecology 10: 1219-1222.
[16] Fang, J. Y., Tang, Y. H., Lin, J. D., et al. (2000): Global Ecology: Climate Change and Ecological Response. – Higher Education Press, Beijing.
[17] Fitzgerald, L. B., Stephe, A. P., Torbert, H. A., et al. (2005): Decomposition of soybean grown under elevated concentrations of CO_2 and O_3. – Global Change Biology 11: 685-698.
[18] Gao, S. H., Guo, J. P. (2003): Responses of *Aneurolepidium Chinensis* and *Stipa Baicalensis* to high CO_2 concentration and soil drought. – Journal of Soil and Water Conservation 23(6): 12-14.
[19] Gao, Z. J., Yin, F. H., Liu, Y., et al. (2014): Effect of CO_2 elevation and nitrogen application on photosynthesis, dry matter and yield of cotton. – Xinjiang Agricultural Sciences 51(8): 1430-1436.
[20] Grunzweig, J. M., Korner, C. (2001): Growth water and nitrogen relation in grass model ecosystems of the semi-arid Negev of Israel exposed to CO_2. – Oecologia 128: 251-262.
[21] Guo, H., Liu, X. M., Guo, X. L., et al. (2013): A preliminary analysis on the relationship between CO_2 concentrations and global climate change. – Journal of Subtropical Resources and Environment 8(2): 13-19.
[22] Guo, S. W., Ran, W., Zhou, Y., et al. (2006): Discussion on the change of carbon and nitrogen metabolism in rice under the condition of elevated atmospheric CO_2 concentration. – Chinese Journal of Rice Science 20(5): 560-566.
[23] Han, W. J., Liao, F. Y., He, P. (2003): The photosynthetic response of *phoebe bournei* to doubled CO_2 concentration in air. – Journal of Central South Forestry University 23(2): 62-65.
[24] Hu, M. F., Tian, C. Y., Lyu, Z. Z., et al. (2006): Effects of N rate on cotton yield and nitrate-N concentration in plant tissue and soil. – Journal of Northwest Sci-tech University of agriculture and forestry 34(4): 63-67.
[25] IPCC. Climate Change. (2014): Mitigation of Climate Change. Contribution of Working Group I to the Fifth Assessment Report of the Intergovernmental Panel on Climate Change. – Cambridge University Press, Cambridge, UK.
[26] Joel, G., Chanpin, S., Chinariello, N. R., et al. (2001): Species-specific responses of plant communities to altered carbon and nutrient availability. – Global Change Biology 7: 435-450.
[27] Johnson, D. W., Cheng, W., Ball, J. T. (2000): Effects of CO_2 and N fertilization on decomposition and immobilization in ponderosa pine litter. – Plant and Soil 224: 115-122.
[28] José, S. R. A., Arnold, J. B. (2016): Inorganic nitrogen form: a major player in wheat and Arabidopsis responses to elevated CO_2. – Journal of Experimental Botany Advance Access 23: 1-15.
[29] Kimball, B. A. (1983): Carbon dioxide and agricultural yields: an assemblage and analysis of 430 prior observations. – Agronomy Journal 75: 779-789.
[30] Kimball, B. A. (2016): Crop responses to elevated CO_2 and interactions with H_2O, N and temperature. – Current Opinion in Plant Biology 31: 36-43.

http://www.aloki.hu ● ISSN 1589 1623 (Print) ● ISSN 1785 0037 (Online)
DOI: http://dx.doi.org/10.15666/aeer/1804_48574872

[31] Kimball, B. A., Morris, C. F., Pinter, P. J. (2001): Elevated CO_2 concentrations, drought and soil nitrogen effects on wheat grain quality. – New Phytologist 2: 295-303.
[32] Larigauderie, A., Hilbert, D. W., Oechel, W. C. (1988): Effect of CO_2 enrichment and nitrogen availability on resource acquisition and resource allocation in a grass, Bromus mollis. – Oecologia 77: 554-560.
[33] Leakey, A. D. B., Ainsworth, E. A., Bernacchi, C. J., et al. (2009): Elevated CO_2 effects on plant carbon, nitrogen, and water relations: six important lessons from FACE. – Journal of Experimental Botany 60: 2859-2876.
[34] Leakey, A. D. B., Ainsworth, E. A., Bernacchi, C. J., et al. (2011): Photosynthesis in a CO_2-rich atmosphere. – Advances in Photosynthesis and Respiration 34: 733-768.
[35] Lee, K. S., Kim, H. Y., Lee, S. M., et al. (2013): Fertilizer N uptake of paddy rice in two soils with different fertility under experimental warming with elevated CO_2. – Plant and Soil 369: 563-575.
[36] Li, X. M., He, X., Smith, R., et al. (2020): Temperature alters the response of hydraulic architecture to CO2 in cotton plants (*Gossypium hirsutum*). – Environmental and Experimental Botany 2: 1-35.
[37] Lin, X. G., Hu, J. L., Chu, H. Y., et al. (2005): Response of soil ammonia-oxidizing bacteria to enriched atmospheric CO_2. – Rural Ecology environment 21(1): 44-46.
[38] Liu, J., Gloria, A. S., Theresa, O. A., et al. (2018): Effects of elevated atmospheric CO_2 and nitrogen fertilization on nitrogen cycling in experimental riparian wetlands. – Water Science and Engineering 11(1): 39-45.
[39] Liu, Y., Yin, F. H., Gao, Z. J., et al. (2016): Effect of atmospheric CO2 elevation on cotton growth under mulch drip irrigation in oasis of Xinjiang. – Jiangsu Agricultural Sciences 44(11): 108-110.
[40] Lyu, N., Yin, F. H., Chen, Y., et al. (2015): Effects of elevated atmospheric CO2 and nitrogen application on nitrogen utilization and soil urease activity. – Chinese Journal of Applied Ecology 26(11): 3337-3344.
[41] Ma, H. L., Wu, Y. H., Zhu, J. G., et al. (2009): Effect of elevated atmospheric CO_2 concentration on soil nitrogen around roots of crops. – Journal of Agro-environment Science 28(4): 849-854.
[42] Mauney, J. R., Kimball, B. A., Pinter, P. J., et al. (1994): Growth and yield of cotton in response to a free-air carbon dioxide enrichment. – Agricultural and Forest Meteorology 70: 49-67.
[43] Morgan, J. A., Milchunas, D. G., Lecain, D. R., et al. (2007): Carbon dioxide enrichment alters plant community structure and accelerates shrub growth in the shortgrass steppe. – Proceedings of the National Academy of Sciences of the United States of America 104(37): 14724-14729.
[44] Najeeh et al. (2018): Mitchell, A., Leo, M. C., Peter, D. K., et al. (2018): Effects of Elevated Atmospheric CO_2 on Nitrogen (N) Assimilation and Growth of C_3 Vascular Plants will be Similar Regardless of N-Form Assimilated. – Oxford University Press, Oxford.
[45] NOAA-ESRL. Earth's CO_2 Home Page, CO_2 now [EB/OL]. – https://www.CO_2.earth/ (accessed on 2018-12-23).
[46] Oberbauer, S. F., Sionit, N., Hastings, S. J., et al. (1986): Effects of CO_2 enrichment and nutrition on growth, photosynthesis, and nutrient concentration of Alaskan tundra plant species. – Canadian Journal of Botany 64: 2993-2998.
[47] Oechel, W. C., Cowles, S., Grulke, N., et al. (1994): Transient nature of CO_2 fertilization in arctic tundra. – Nature 371: 500-503.
[48] Pitelka, L. F. (1994): Ecosystem response to elevated CO_2. – Trends Ecology Evolution 9: 204-207.
[49] Roser, M., Bert, G. D. (1999): The influence of atmospheric CO_2 enrichment on plant-soil nitrogen interactions in a wetland plant community on the Chesapeake Bay. – Plant and Soil 210: 93-101.

http://www.aloki.hu ● ISSN 1589 1623 (Print) ● ISSN 1785 0037 (Online)
DOI: http://dx.doi.org/10.15666/aeer/1804_48574872

[50] Stitt, M., Krapp, A. (1999): The interaction between elevated carbon dioxide and nitrogen nutrition: the physiological and molecular background. – Plant Cell and Environment 6: 553-621.
[51] Talbot, J. B., Gerard, W. W., Paul, J. P., et al. (2000): Acclimation response of spring wheat in a free-air CO2 enrichment (FACE) atmosphere with variable soil nitrogen regimes. 3. Canopy architecture and gas exchange. – Photosynthesis Research 66: 97-108.
[52] Wang, J., Wang, C., Chen, N., et al. (2015): Response of rice production to elevated CO_2 and its interaction with rising temperature or nitrogen supply: a meta-analysis. – Climatic Change 130: 529-543.
[53] Wang, X. Z., Zhang, H. J., Sun, W., et al. (2010): Effects of elevated atmospheric CO_2 on paddy soil nitrogen content during rice season. – Chinese Journal of Applied Ecology 21(8): 2161-2165.
[54] Xia, Y., Hu, Z. H., Liu, C., et al. (2019): Interactive effects of different levels of elevated CO_2 concentration and nitrogen fertilization on photosynthesis and growth of winter wheat. – Research of Agricultural Modernization 40(2): 333-341.
[55] Xiao, L., Liu, G. B., Li, P., et al. (2017): Effects of nitrogen addition and elevated CO_2 concentration on soil dissolved organic carbon and nitrogen in rhizosphere and non-rhizosphere of Bothriochloa ischaemum. – Chinese Journal of Applied Ecology 28(1): 64-70.
[56] Xu, Z. Z., Zhou, G. S. (2003): Advances in the adaptability of terrestrial plants to global changes. – Progress in Natural Science 13(2): 113-119.
[57] Xu, Z. Z., Zhou, G. S., Xiao, C. W., et al. (2004): Responses of two dominated desert shrubs to soil drought under doubled CO_2 condition. – Acta Ecologica Sinica 24(10): 2186-2191.
[58] Yang, J. L. (2002): Relationship between atmospheric CO_2 and plant nitrogen nutrition. – Soil and Environment 11(2): 163-166.
[59] Yang, L. X., Wang, Y. L., Dong, G. C., et al. (2007): The impact of free-air CO_2 enrichment and nitrogen supply on grain quality of rice. – Field Crops Research 102: 128-140.
[60] Yin, F. H., Liu, H. L., Xie, Z. M., et al. (2010): Movement of N, P and K of cotton drip irrigation special fertilizer in soil and the efficiency of fertilizer utilization. – Geographical Research 29(2): 235-243.
[61] Yin, F. H., Gao, Z. J., Xie, Z. M., et al. (2011): Effects of different carbon and nitrogen fertilizer combination treatments on cotton canopy CO_2 concentration, photosynthesis and yield formation under drip irrigation in Xinjiang cotton field. – Arid Zone Research 28(4): 724-728.
[62] Yin, F. H., Chen, Y, Zeng, S. H., et al. (2016): A kind of special carbon water soluble fertilizer for drip irrigation cotton. – Invention patent ZL2014103045498.2.
[63] Zhang, F. C., Kang, S. Z., Ma, Q. L., et al. (1999): The Effects of the atmospheric CO_2 concentration increase on physiological characters and growth of cotton. – Journal of Basic Science and Engineering 7(3): 268-272.
[64] Zhang, S. Z., Yan, W., et al. (2017): Effects of elevated CO_2 concentration and temperature on some physiological characteristics of cotton (*Gossypium hirsutum* L.) leaves. – Environmental and Experimental Botany 133: 108-117.
[65] Zhang, W. F., Wang, Z. L., Yu, S. L., et al. (2002): Effect of nitrogen on canopy photosynthesis and yield formation in high-yielding cotton of Xinjiang. – Acta Agronomica Sinica 28(6): 789-796.

http://www.aloki.hu ● ISSN 1589 1623 (Print) ● ISSN 1785 0037 (Online)
DOI: http://dx.doi.org/10.15666/aeer/1804_48574872

CHANGE OF COD AND VFAS CONCENTRATION DURING THE SEQUENTIAL BATCH HIGH-TEMPERATURE ANAEROBIC DIGESTION OF CHICKEN MANURE AND STRAW

FENG, L.[1] – DU, T.[1] – ZHEN, X. F.[2*] – LI, Y. K.[3]

[1]*Liaoning Province Clean Energy Key Laboratory, Shenyang Aerospace University, Shenyang Daoyi Street 37, Shenyang 110136, China*

[2]*School of New Energy and Power Engineering, Lanzhou Jiaotong University, Lanzhou 730070, China*

[3]*College of Science, Shenyang Agricultural University, Shenyang 110086, PR China*

**Corresponding author*
e-mail: zxf283386515@163.com

(Received 9th Jan 2020; accepted 6th May 2020)

Abstract. A series of high-temperature combined anaerobic digestion tests with different mass ratios were carried out using chicken manure and straw with a high C/N ratio as the raw materials. The changing trends of CODs, CODr, CODs/CODr and VFAs and the concentration of each component were analyzed during the high-temperature anaerobic digestion of chicken manure and straw using a sequencing batch reactor. The results showed that the COD_T of the fermentation broth decreased significantly in the first 15 days, and the values of COD_T decreased from 3584.45, 3132.28, 3355.45 and 2987.39 mg/L in the initial stage to 1756.28, 1532.45, 1607.28 and 1528.33 mg/L, respectively. The degradation rates of COD_{T15} were 51.06, 55.09, 52.11 and 48.84%, respectively. At the end of the reaction (50 d), the values of the four groups of COD_T were 1223.10, 903.21, 1095.39 and 1333.46 mg/L, respectively. As the reaction proceeded to the seventh day, the maximum concentration, the VFAs of the digestive fluids from R1, R2, R3, and R7 were 3032.39, 3346.75, 3245.12 and 2794.03 mg/L, respectively. As the reaction completed, (50 d), the VFAs of the digestive fluids were 1558.34, 1547.37 and 1335.58 mg/L, respectively, in which the contents of formic acid, acetic acid, propionic acid, lactic acid, and butyric acid were 9.19-9.97%, 20.58-22.13%, 15.74-18.44%, 22.86-25.50% and 25.56-30.02%, respectively.
Keywords: *chicken manure, co-anaerobic digestion, biodegradability, gas properties*

Introduction

In recent years, the development of animal husbandry in China has led to a total annual production of livestock manure exceeding 2 billion tons (Chu et al., 2010). The inappropriate treatment of these manures will negatively affect the living environment (Li et al., 2016). Crop straw and livestock manure are the two most important types of biomass resources in China. For the anaerobic digestion of chicken manure and straw, existing studies mainly focuses on the treatment of raw materials (Linke, 2006; Naranjo et al., 2011; den Boer et al., 2012), improvement of reactor and medium-temperature anaerobic fermentation (Duan et al., 2016), and regulation of nutrients (Tauseef et al., 2013; Nasir et al., 2012; Jiménez et al., 2003). Nutrient regulation can be controlled by adding chemical reagents such as urea and ammonium bicarbonate, as well as mixing various raw materials. Based on the physical and biochemical characteristics of different raw materials, such as water content, carbon to nitrogen ratio and refractory or perishability, it can properly optimize the fluidization characteristics and nutrient structure of the fermentation material, and avoid acid suppression of perishable

http://www.aloki.hu ● ISSN 1589 1623 (Print) ● ISSN 1785 0037 (Online)
DOI: http://dx.doi.org/10.15666/aeer/1804_48734882

materials by using the appropriate proportion. The previous studies focused on the gas production characteristics of rice straw and chicken manure with different mass ratios under medium-temperature conditions. However, the parameter changes in a combined anaerobic digestion process under high-temperature conditions were not analyzed.

In this study, a self-designed bio-reactor for the anaerobic methanogenic reaction was used. The high-temperature combined anaerobic digestion tests with different mass ratios were carried out using livestock manure, i.e., chicken manure and straw with high C/N as the raw materials. The changing trend of soluble chemical oxygen demand (CODs), total chemical oxygen demand (COD_T), CODs/COD_T and volatile fatty acids (VFAs) and the concentration of each component were analyzed during high-temperature anaerobic digestion of chicken manure and straw using a sequencing batch reactor. This work will provide the basis for the mixing of raw materials for combined high-temperature dry fermentation process and further engineering application.

Materials and method

Experimental materials and inoculum

Chicken manure in the experiment came from a chicken farm in Beipiao County, Chaoyang City, Liaoning Province, China. After careful screening to remove impurities, such as stones, chicken manure collected for 3 days in a row was sent to the laboratory directly and kept at 4 °C in refrigerator. After intensive mixing in the laboratory, the collected chicken manure was used as the experimental material for high temperature anaerobic digestion. The extra 500 kg of the material was packaged as 1 kg bags and frozen in refrigerator for a further experiment of continuous high temperature dry fermentation of chicken manure (Chen et al., 2016). Stalks used in the experiments, which were from a farm in Shenbei new district, Shenyang City, Liaoning Province, were shipped to the laboratory and cut and ground to 80 mesh.

The inoculated microorganisms in the experiments were from anaerobic digested mud in a northern waste water treatment factory in Shenyang City, Liaoning Province, China. The inoculated active mud was transferred to an airtight plastic container and its temperature decreased to room temperature of about 20 °C or so during the transportation process, whereas the inoculated mud still maintained active. In the laboratory, the inoculated mud was cultivated and acclimatized at 55 °C. The acquired 5 L of active mud was transferred to a 25 L air-tight plastic bag for acclimatization. After 3 d cultivation at constant 55 °C, 2.5 kg of fresh chicken manure, which was taken in advance and kept at room temperature, was added into active mud after acclimatization for 10 d cultivation. In addition, 5 kg of fresh chicken manure kept at room temperature was acclimatized and cultivated for 10 d for a further use. Dry material masses of chicken manure, stalks, and inoculated mud were determined after heating in air dry oven for 24 h at constant temperature of 105 °C (Duan et al., 2018). The organic content was determined after 4 h heating in the muffle furnace at constant 550 °C. Main parameters of the wet basic state of chicken manure, stalks, and active mud are shown in *Table 1*.

Experimental equipment

A small scale biological and chemical reactor for anaerobic fermentation, which was designed by us, was used in the high temperature anaerobic experiments with cattle

http://www.aloki.hu ● ISSN 1589 1623 (Print) ● ISSN 1785 0037 (Online)
DOI: http://dx.doi.org/10.15666/aeer/1804_48734882

manure and stalks and is shown in *Figure 1*. The whole system was composed of two 1-L round wide-mouth bottles and one 1-L volumetric bottle, which were used for the apparatus for the digestion reaction of kitchen waste, the apparatus for the biogas collection, and the apparatus for water drainage, respectively. All apparatuses were connected with rubber tubes with anti-aging treatment to form a set of air-tight apparatuses. Air-tightness should be guaranteed in the connections. pH of the digested liquor was determined with the digital acidometer with accuracy of ± 0.01. The composition of biogas was determined by gas chromatography (Shimadzu in Japan, GC-4B).

Table 1. *Main parameters of the wet basic state of chicken manure, stalks, and active mud*

Parameters	TS/%	VS/%	pH	TC/%	TN/%
Chicken manure	27.29	23.33	6.33	46.07	4.73
Stalks	91.44	86.50	6.89	50.02	0.88
Active mud	18.12	8.36	7.41	--	--

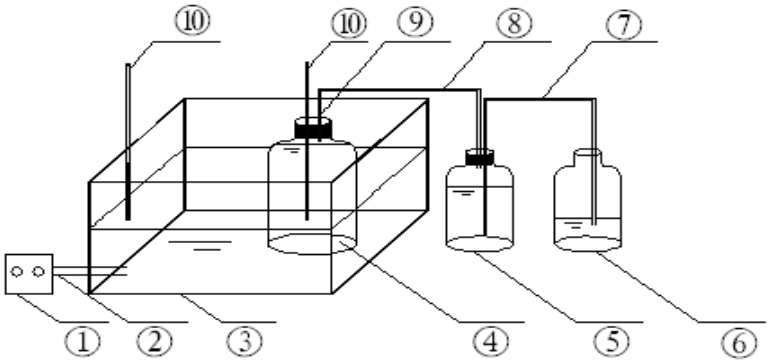

1−controller, 2-heating rod, 3-water bath, 4-sample reactor, 5-gas bottle, 6-gas bottle, 7-discharging bottle, 8-gas tube, 9-determination tube, 10-thermometer

Figure 1. *The experimental apparatus for high temperature anaerobic digestion*

Experimental scheme

The methane production experiment with chicken manure and stalks used 24 1-L air-tight wide-mouth bottles as anaerobic digestion reactors and was conducted as eight groups with three replicates for each group. The average of the three experiments was reported. Except the experiment with R0 group, which received only 300 ml of inoculated mud, which was acclimatized without any other sample, the experiments with other seven groups received 60 g samples besides the inoculum of the same concentration and volume. The material ratios for high temperature anaerobic digestion of chicken manure and stalks (m/m, %) are shown in *Table 2*.

The addition of a 50 g sample in the experiment mainly considered the volume loading of the digester. Organic acids produced by decomposition of too much material would decrease pH of the digested liquor. The resultant acid inhibition would influence the production of biogas. The volume of 1 L was set with distilled water in experiments with 8 groups. Reactors were sealed up with glass cement and put into electric-heated

http://www.aloki.hu ● ISSN 1589 1623 (Print) ● ISSN 1785 0037 (Online)
DOI: http://dx.doi.org/10.15666/aeer/1804_48734882

thermostatic water bath for constant cultivation for 50 d at 55 °C. The digested liquor was extracted with injector and put back into the reactor after pH determination with the digital acidometer with the determination frequency of one time per day. When pH values were below 6.8-7.2, $NaHCO_3$ was chosen as the regulation agent to maintain pH of the digested liquor above 6.8.

Table 2. *The material ratios for high temperature anaerobic digestion of chicken manure and stalks (m/m, %)*

	R1	**R2**	**R3**	**R4**	**R5**	**R6**	**R7**
Chicken manure	100	97	95	90	80	70	0
Stalk	0	3	5	10	20	30	100

Analytic method

Measurement of COD concentration

In a 250 mL conical beaker, 10 mL of potassium dichromate was pipetted and 100 ml of distilled water was added. Subsequently, 30 ml of concentrated sulfuric acid was incorporated using the measuring cylinder. After cooling, 3 drops of the ferrous iron indicator was added and titrated with ammonium ferrous sulfate standard solution until the yellow solution changed into bluish-green and finally to reddish-brown. All test materials were set up in three parallel test groups (Zhang et al., 2017).

Volatile fatty acids (VFAs)

Volatile fatty acid content was determined by detecting volatile organic acid (Cl-C5) using gas chromatography. The column size was HP-5, 30 m × 0.25 mm × 0.25 um, and a flame ionization detector was used. Nitrogen was used as the carrier gas, and the flow rate was kept at 50 mL/min. The injector temperature was set at 300 °C, and the detector temperature was 230 °C. The sample was filtered through a 0.45 um filter. From the filtered sample, I mL was taken and the pH was adjusted using formic acid (6 mol/L) to ensure pH < 6 for chromatographic determination (Hu et al., 2018).

Data processing

All the physical and chemical indicators in the tests were measured by setting three parallel tests. Data were tested for significance ($p = 0.05$) and correlation was analyzed using one-way ANOVA and multiple comparisons using SPSS v.18.0 (IBM Corp., Armonk, NY, USA). All data plots were drawn using Origin-8.0. The differences between treatments and physical and chemical indicators during the test were analyzed using least significance difference ($p < 0.05$) (Naranjo et al., 2011).

Results and discussion

COD concentration change during high-temperature anaerobic digestion using a sequencing batch reactor

Figure 2 shows the trends of COD_S, COD_T and COD_S/COD_T during the sequential batch high-temperature anaerobic digestion of representative chicken manure and straw

http://www.aloki.hu ● ISSN 1589 1623 (Print) ● ISSN 1785 0037 (Online)
DOI: http://dx.doi.org/10.15666/aeer/1804_48734882

in R1, R2, R3, and R7 groups. In the initial stage (1 d), the values of COD_T in R1, R2, and R3 were 3584.45-3356.45 mg/L, while the value of COD_T in R7 pure straw batch high-temperature anaerobic digestion was lower, i.e., 2987.39 mg/L. The reason is that the base of R7 is pure straw. Compared to R1 that contained pure chicken manure, R2 and R3 contained 97 and 95% chicken manure base, respectively. Straw is rich in the cellulose-hemicellulose-lignin component. Owing to the dense crystalline structure of cellulose, hemicellulose and lignin, these materials were difficult to break down. Therefore, the COD_T value of R7 was lower than the other three groups of base. During the 50-day high-temperature digestion process, the COD_T of the fermentation broth of the four groups showed a decreasing trend as a whole. This can be attributed to the high-temperature conditions during the process, in which the bacteria of hydrolysis acidification degraded the fermentation substrate to provide nutrient intermediates for the subsequent physiological metabolism of methanogenic microorganisms.

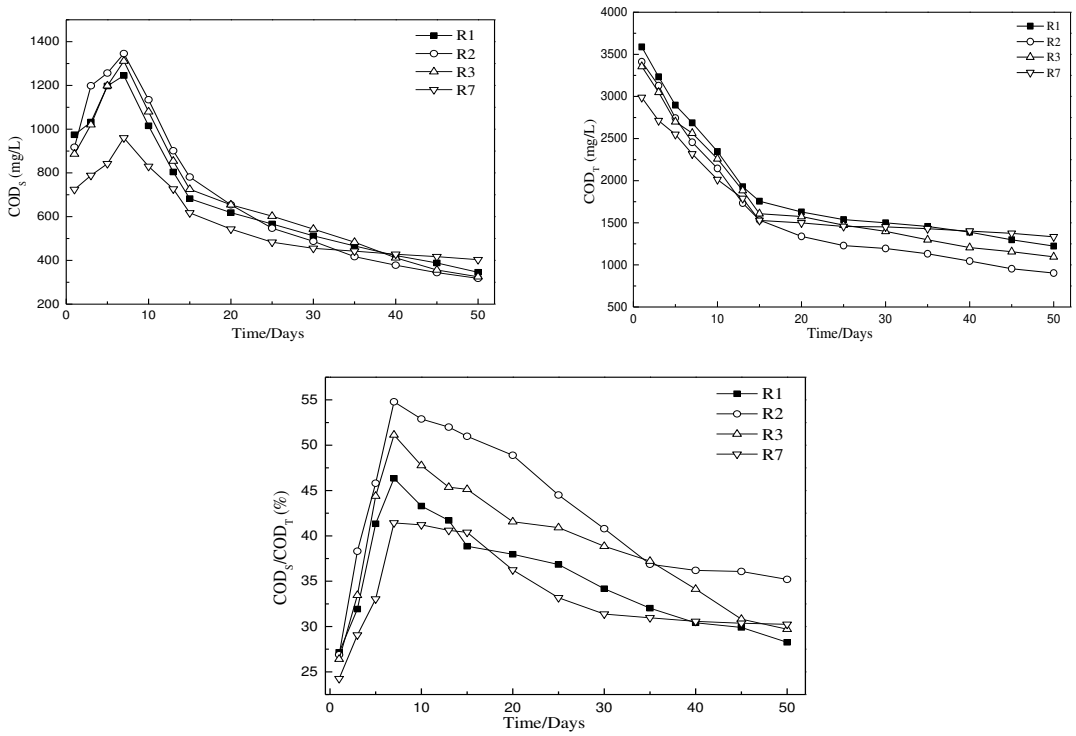

Figure 2. *Trends of COD_S, COD_T and COD_S/COD_T during sequential batch high-temperature anaerobic digestion of chicken manure and straw*

The methanogenic microorganisms used the organic acid produced in the acidification stage to produce biogas, which led to a general decline in the COD_T of the fermentation broth of the four groups of tests. The degradation rates of COD_T15 at 1-15 d were 51.06, 55.09, 52.11 and 48.84%. These rates were much higher than those in later days (16-50 d), which were 14.86, 18.44, 15.25 and 6.52%. This was mainly because the first 15 days of the initial reaction was the fastest stage of the high-temperature anaerobic digestion process. At this stage, the organic matter in the four experimental groups was mostly starch and protein, which are easy to break down. The high-temperature condition also facilitated hydrolysis and acidification, producing degradable organic matter such as monose, fatty acids and amino acids, causing pH to

http://www.aloki.hu ● ISSN 1589 1623 (Print) ● ISSN 1785 0037 (Online)
DOI: http://dx.doi.org/10.15666/aeer/1804_48734882

decrease. The decrease in pH further promoted hydrolysis and acidification of refractory organic matter in the base. On the seventh day, the pH of the digestive juice was adjusted by adding 4 g sodium bicarbonate ($NaHCO_3$) as the regulator to keep the pH above 6.8. After adding sodium bicarbonate ($NaHCO_3$), the increased pH of the four groups of biogas slurry promoted methanogens to convert organic acids into methane and carbon dioxide. As the reaction finished (50 d), the COD_T values of the four groups were 1223.10, 903.21, 1095.39 and 1333.46 mg/L, respectively. The degradation rates of COD_T50 were 65.92, 73.53, 67.36 and 55.36%.

Two main reasons account for the lower degradation rate of COD_T in the later stage. The first was the change of the base component of the high-temperature digestive juice. The degradable organic matter was rapidly broken down by methanogens under high-temperature conditions. The residual organic matter was mainly refractory organic matter, and the main component was cellulose-hemicellulose-lignin with a dense physical structure. It is difficult for the enzyme molecule and the water molecule to enter the interior and cause a hydrolysis reaction. Such substance is biodegradable, but the process takes a long time. The second was that the biochemical reaction of the fermentation broth was slowed down at the later stage due to the accumulation of metabolites. It was found that in the high-temperature anaerobic fermentation process of chicken manure and straw, the hydrolysis and acidification rate of organic matter remarkably increased at 55 °C. This led to the formation of more metabolites during the physiological metabolism process. The accumulation of metabolites had a certain inhibitory effect on the reproduction and metabolism of acid-producing methanogens in the later stage. Therefore, the degradation rate of COD_T in the later stage showed a downward trend, which was much lower than the degradation rate of COD_T in the first 15 days.

The value of COD_S at the initial stage of high-temperature anaerobic digestion solution for R7 was 724.39 mg/L, which was lower than the COD_S values of R1, R2 and R3 (974.25-886.33 mg/L). The reason is that in the R7 base, the content of straw was high and the content of starch and protein in straw was low. Since the cellulose-hemicellulose-lignin component is naturally difficult to hydrolyze, the content of insoluble organic matter was high, resulting in the lower CODs of R7 high-temperature anaerobic digestion liquid at the initial stage (1 d). As the high-temperature digestion proceeded, the COD_S values of the four groups of high-temperature anaerobic digestion liquids for R1, R2, R3 and R7 all increased and reached the peak when the reaction proceeded to the seventh day. The values of the four groups of CODs were 1245.33, 1345.69, 1311.28 and 959.89 mg/L, respectively. This is because the organic matter in the base of the four groups of fermentation broth was decomposed by the hydrolysis and acidification bacteria, and the insoluble macromolecular organic matter was hydrolyzed and acidified into small organic acids. The decrease in pH further facilitated the hydrolysis and acidification of the refractory organic matter, and dissolved in water, leading to an increase in the CODs of the four groups of fermentation broth (den Boer et al., 2012). As the reaction progressed, the CODs showed a declining trend for two reasons. The first is that the dissolved COD was utilized by methanogens to convert to carbon dioxide and methane. The second is that the relative content of dissolved COD was reduced as the concentration of total organic matter decreased. Therefore, the CODs showed a downward trend in the later stage. At the end of the reaction (50 d), the values of the four groups of CODs were 345.66, 317.89, 325.33 and 403.28 mg/L, respectively.

http://www.aloki.hu ● ISSN 1589 1623 (Print) ● ISSN 1785 0037 (Online)
DOI: http://dx.doi.org/10.15666/aeer/1804_48734882

With the high-temperature digestion reaction, the ratio of COD_S/COD_T in the high-temperature anaerobic digestion liquid of R1, R2, R3 and R7 all increased. During this period, the organic matter in the fermentation liquid was hydrolyzed and acidified, and the macromolecule was insoluble in water, which led to an increase in the CODs concentration. However, the COD_T concentration decreased as the reaction progressed, and thus the ratio of COD_S/COD_T increased. The reaction reached the peak on the seventh day, and the Should this be COD_S/COD_T ratios of the four groups of fermentation broth were 46.34, 54.78, 51.14 and 41.43%, respectively. The COD_S/COD_T ratio decreased with the reaction because the methanogens decomposed CODs, which hastened the decreasing rate of dissolved COD and thus led to a decrease in the COD_S/COD_T ratio. At the end of the reaction (50 d), the COD_S/COD_T ratios of the four groups were 28.26, 35.20, 29.70, and 30.24%, respectively.

Correlation study between VFAs and each component in sequential batch high-temperature anaerobic digestion

Figure 3 shows the variation trend of VFAs and concentration of each component in sequential batch high-temperature anaerobic digestion of chicken manure and straw. In this section, four representative experimental data of R1, R2, R3 and R7 were selected for analysis. The values of VFAs in the initial stage (1 d) were 2063.84, 1950.4, 1875.32 and 1661.66 mg/L, respectively. In total VFAs, the fraction of formic acid, acetic acid, propionic acid, lactic acid and butyric acid were R1: 8.64, 30.75, 15.37, 22.94 and 22.30%, respectively; R2: 8.03, 31.41, 15.60, 23.36 and 21.60%, respectively; R3: 7.69, 30.84, 16.01, 23.52 and 21.94%, respectively; and R7: 7.42, 32.69, 16.44, 21.36 and 22.08%, respectively. As the high-temperature anaerobic digestion proceeded, formic acid, acetic acid, propionic acid, lactic acid, butyric acid, and total VFAs all increased. The values reached the maximum peak on the seventh day of the reaction. The VFAs values of R1, R2, R3 and R7 were 3032.39, 3346.75, 3455.12 and 2794.03 mg/L, respectively. Among these digestive juices, the contents of formic acid, acetic acid, propionic acid, lactic acid and butyric acid were 9.81-10.27%, 26.28-27.28%, 16.05-17.87%, 21.59-23.13%, and 22.70-25.26%, respectively. The stage when pH decreased corresponded to the stage when VFAs concentration increased, while the stage when pH increased corresponded to the stage when VFAs concentration decreased. The pH in the pH reaction system had a corresponding relationship with the change of volatile acid content, i.e., the pH value decreased while the VFA concentration increased, and the VFA concentration reached the maximum value as the pH value reached the minimum; the pH value increased while the VFA concentration decreased. In the test and actual production, the change in the pH value can reflect the value of VFA concentration, controlling the acidizing process macroscopically (Duan et al., 2016). Subsequently, the VFAs of the digestive juices of the four experimental groups decreased. When the reaction was completed (50 d), the VFAs of the experimental digestive fluids of R1, R2, R3 and R7 were 1564.6, 1558.34, 1547.37 and 1335.58 mg/L, respectively. The contents of formic acid, acetic acid, propionic acid, lactic acid, and butyric acid were 9.19-9.97%, 20.58-22.13%, 15.74-18.44%, 22.86-25.50% and 25.56-30.02%, respectively.

The concentration of VFAs during the sequential batch high-temperature anaerobic digestion of chicken manure and straw was determined by the rate of production and consumption of formic acid, acetic acid, propionic acid, butyric acid and lactic acid. As the high-temperature anaerobic digestion proceeded, formic acid, acetic acid, propionic

http://www.aloki.hu ● ISSN 1589 1623 (Print) ● ISSN 1785 0037 (Online)
DOI: http://dx.doi.org/10.15666/aeer/1804_48734882

acid, lactic acid, butyric acid and total VFAs all increased. On the seventh day of the reaction, the presence of peak value was due to the use of base. For R1, R2 and R3, the content of chicken manure was high, of which the degradable organic matter was converted to small organic acid. However, at this stage, the methanogens were still in the period of adaptation, and the biological metabolic activity was not strong. The enzymatic reaction rate was slow, and the production rate of VFAs was greater than the metabolic rate, resulting in a decrease in the pH of the system (Yang et al., 2017). The pH drop further inhibited the activity of the methanogens, leading to the maximum of VFAs concentration on the seventh day, i.e., 3032.39, 3346.75 and 3245.12 mg/L, which showed the highest content of acetic acid, lactic acid and butyric acid. In the R4 experiment, pure straw was used as the base material, and the dense structure of the straw made hydrolysis reaction difficult (Zhou et al., 2016, 2018, 2019). Therefore, the produced content of small organic acid was relatively low, and the VFAs concentration reached 1335.58 mg/L on the seventh day.

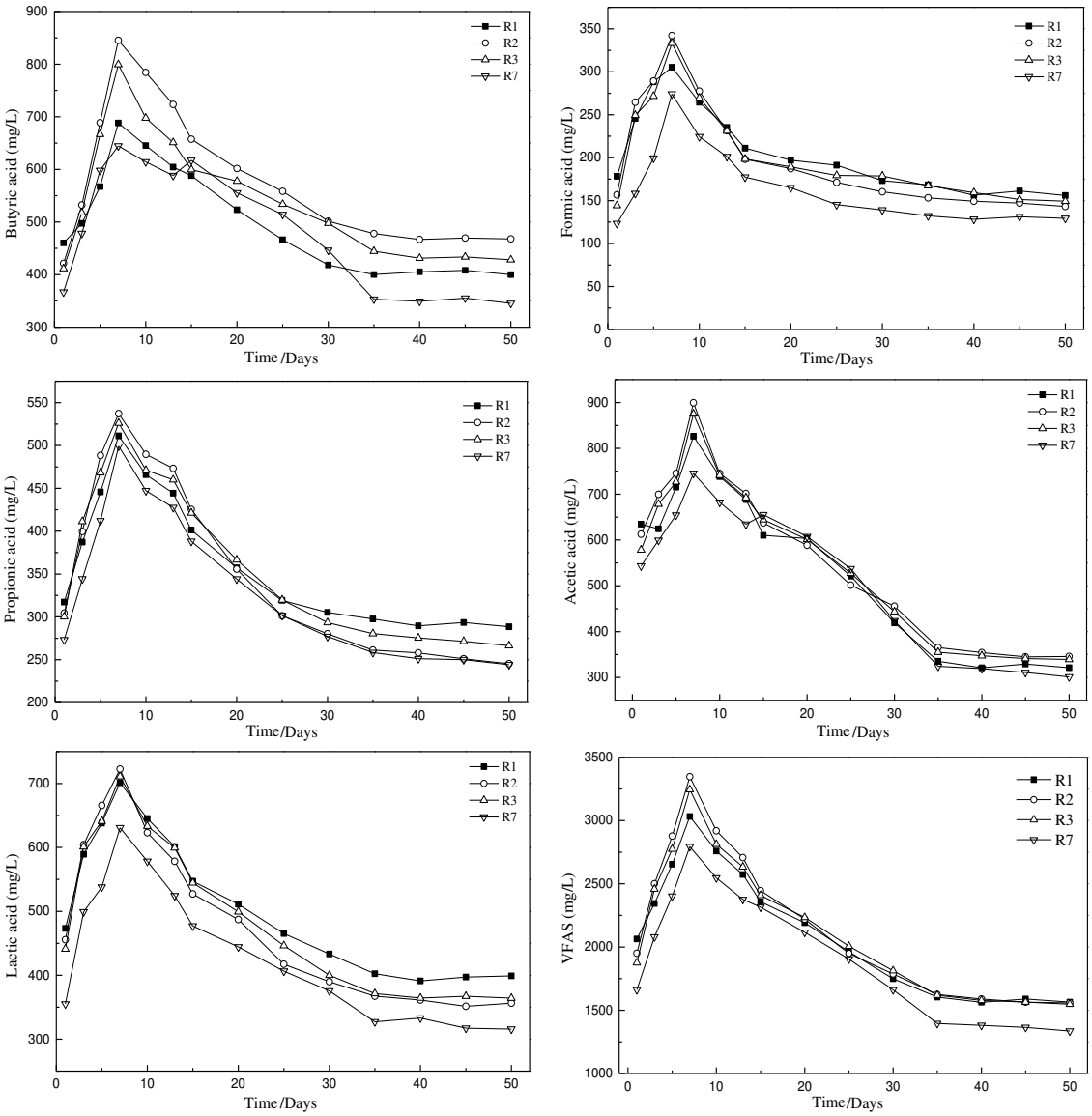

Figure 3. *Trends of VFAs and concentration of various components during sequential batch high temperature anaerobic digestion of chicken manure and straw*

http://www.aloki.hu ● ISSN 1589 1623 (Print) ● ISSN 1785 0037 (Online)
DOI: http://dx.doi.org/10.15666/aeer/1804_48734882

The main reason for the decline of VFAs in the digestive juices of the later four groups was that the pH of the digestive juice was adjusted by adding sodium bicarbonate ($NaHCO_3$) on the seventh day (Zhang et al., 2011). The methanogens in anaerobic digestion then began to adapt, and the suitable pH value also increased the anaerobic biochemical enzymatic reaction rate. This promoted the degradation of acetic acid, lactic acid and butyric acid-based VFAs, and led to the further increase in pH. When the reaction was completed (50 d), the values of VFAs in the digestive juice of R1, R2 R3 and R7 were 1564.6, 1558.34, 1547.37 and 1335.58 mg/L, respectively. Among these digestive juices, the contents of formic acid, acetic acid, propionic acid, lactic acid and butyric acid were 9.19-9.97%, 20.58-22.13% and 15.74-18.44%, 22.86-25.50% and 25.56-30.02%, respectively.

Conclusions

(1) The COD_T of the fermentation broth of R1, R2, R3 and R7 showed a downward trend. The COD_T of the fermentation broth showed a significant downward trend in the first 15 days, and COD_T values decreased from 3584.45, 3132.28, 3355.45 and 2987.39 mg/L at the initial stage to 1756.28, 1532.45, 1607.28 and 1528.33 mg/L. The degradation rates of COD_T 15 were 51.06, 55.09, 52.11 and 48.84%. At the end of the reaction (50 d), the values of the four groups of COD_T were 1223.10, 903.21, 1095.39 and 1333.46 mg/L, and the degradation rates of COD_T50 were 65.92, 73.53, 67.36 and 55.36%.

(2) The VFAs values in the initial stage of reaction (1d) of R1, R2, R3 and R4 were 2063.84, 1950.4, 1875.32 and 1166.66 mg/L, respectively. As the high temperature anaerobic digestion proceeded, formic acid, acetic acid, propionic acid, lactic acid, butyric acid and total VFAs all increased. As the reaction proceeded to the seventh day, the maximum concentration, the VFAs of the digestive fluids from R1, R2, R3 and R7, were 3032.39, 3346.75, 3245.12 and 2794.03 mg/L, respectively. At the end of the reaction (50 d), the VFAs of the four groups of experimental digestive juices were 1564.6, 1558.34, 1547.37, and 1335.58 mg/L, respectively. Among these digestive juices, the contents of formic acid, acetic acid, propionic acid, lactic acid, and butyric acid were 9.19-9.97%, 20.58-22.13%, 15.74-18.44%, 22.86-25.50% and 25.56-30.02%, respectively.

REFERENCES

[1] Chen, Z., Luo, J., Chen, X., Hang, X., Shen, F., Wan, Y. (2016): Fully recycling dairy wastewater by an integrated isoelectric precipitation–nanofiltration–anaerobic fermentation process. – Chemical Engineering Journal 283. DOI: 10.1016/j.cej.2015.07.086.

[2] Chu, C.-F., Ebie, Y., Xu, K.-Q., Li, Y.-Y., Yuhei, I. (2010): Characterization of microbial community in the two-stage process for hydrogen and methane production from food waste. – International Journal of Hydrogen Energy 35(15): 8253-8261.

[3] den Boer, E., den Boer, J., Jaroszynska, J., Szpadt, R. (2012): Monitoring of municipal waste generated in the city of Warsaw. – Waste Management and Research 30(8): 772-780.

[4] Duan, X., Wang, X., Xie, J., Feng, L., Yan, Y., Zhou, Q. (2016): Effect of nonylphenol on volatile fatty acids accumulation during anaerobic fermentation of waste activated sludge. – Water Research 105: 209-217.

http://www.aloki.hu ● ISSN 1589 1623 (Print) ● ISSN 1785 0037 (Online)
DOI: http://dx.doi.org/10.15666/aeer/1804_48734882

[5] Duan, X., Wang, X., Xie, J., Feng, L., Yan, Y., Wang, F., Zhou, Q. (2018): Acidogenic bacteria assisted biodegradation of nonylphenol in waste activated sludge during anaerobic fermentation for short-chain fatty acids production. – Bioresource Technology 268: 692-699.
[6] Hu, J., Xu, Q., Li, X., Wang, D., Zhong, Y., Zhao, J., Zhang, D., Yang, Q., Zeng, G. (2018): Sulfamethazine (SMZ) affects fermentative short-chain fatty acids production from waste activated sludge. – Science of the Total Environment 639: 1471-1479.
[7] Jiménez, A. M., Borja, R., Martín, A. (2003): Aerobic–anaerobic biodegradation of beet molasses alcoholic fermentation wastewater. – Process Biochemistry 38(9).
[8] Li, Y., Jin, Y., Li, J., Chen, Y., Gong, Y., Li, Y., Zhang, J. (2016): Current situation and development of kitchen waste treatment in China. – Procedia Environmental Sciences 31: 40-49.
[9] Linke, B. (2006): Kinetic study of thermophilic anaerobic digestion of solid wastes from potato processing. – Biomass and Bioenergy 30(10): 892-896.
[10] Naranjo, A., et al. (2011): Effects of different concentrations of NaOH pretreatment on anaerobic digestion of rice straw for biogas production. – Transactions of the Chinese Society of Agricultural Engineering 27(10): 59-63.
[11] Nasir, I. M., Ghazi, T. I. M., Omar, R. (2012): Production of biogas from solid organic wastes through anaerobic digestion: a review. – Applied Microbiology and Biotechnology 95(2): 321-329.
[12] Tauseef, S. M., Abbasi, T., Abbasi, S. A. (2013): Energy recovery from wastewaters with high-rate anaerobic digesters. – Renewable and Sustainable Energy Reviews 19: 704-741.
[13] Wang, D., Zhang, D., Xu, Q., Liu, Y., Wang, Q., Ni, B.-J., Yang, Q., Li, X., Yang, F. (2018): Calcium peroxide promotes hydrogen production from dark fermentation of waste activated sludge. – Chemical Engineering Journal 35(5): 22-32.
[14] Yang, S. F., Phan, H. V., Bustamante, H., Guo, W. S., Ngo, H. H., Nghiem, L. D. (2017): Effects of shearing on biogas production and microbial community structure during anaerobic digestion with recuperative thickening. – Bioresour. Technol. 234: 439-447.
[15] Zhang, C., Wang, W., Jia, J., Wang, A., Li, L. (2017): Study on recovery of biogas from distillers grains wastewater by USR reactor. – Procedia Engineering 205: 3743-3748.
[16] Zhang, D. D., Li, J., Guo, P., Li, P. P., Suo, Y. L., Wang, X. F., Cui, Z. J. (2011): Dynamic transition of microbial communities in response to acidification in fixed-bed anaerobic baffled reactors (FABR) of two different flow directions. – Bioresour. Technol. 102(7): 4703-4711.
[17] Zhou, M., Yang, H. N., Zheng, D., Pu, X. D., Liu, Y., Wang, L., Zhang, Y. H., Deng, L. W., (2019): Methanogenic activity and microbial communities characteristics in dry and wet anaerobic digestion sludges from swine manure. – Biochem. Eng. J. 152(15): 107-116.
[18] Zhou, M. M., Yan, B. H., Wong, J. W. C., Zhang, Y. (2018): Enhanced volatile fatty acids production from anaerobic fermentation of food waste: a mini-review focusing on acidogenic metabolic pathways. – Bioresour. Technol. 248(A): 68-78.
[19] Zhou, S., Nikolausz, M., Zhang, J. N., Riya, S., Terada, A., Hosomi, M. (2016): Variation of the microbial community in thermophilic anaerobic digestion of pig manure mixed with different ratios of rice straw. – J. Biosci. Bioeng. 122(3): 334-340.

http://www.aloki.hu ● ISSN 1589 1623 (Print) ● ISSN 1785 0037 (Online)
DOI: http://dx.doi.org/10.15666/aeer/1804_48734882

CHARACTERISTICS OF BIOGAS PRODUCTION VIA HIGH-TEMPERATURE DRY FERMENTATION OF CHICKEN MANURE AND STRAW

LI, Y. K.[1,2] – HU, X. M.[1] – FENG, L.[3]

[1]*School of Resources & Civil Engineering, Northeastern University, Shenyang 110819, PR China*

[2]*College of Science, Shenyang Agricultural University, Shenyang 110086, PR China*

[3]*Liaoning Province Clean Energy Key Laboratory, Shenyang Aerospace University, Shenyang 110136, PR China*

**Corresponding author*
e-mail: hxmin_jj@163.com

(Received 9th Jan 2020; accepted 6th May 2020)

Abstract. Dry fermentation has many advantages, such as lower water consumption, high biogas production rates, and low costs. In this paper, chicken manure and straw were combined for dry fermentation at the high temperature of 55 ± 0.2 ℃, and the changes of the production rate, pH, VFAs concentration, and other parameters of the dry fermentation process were analyzed. The results showed that during the stable period, continuous digestion was realized, and the TS content exceeded 20% in agreement with the characteristics of dry fermentation. In this stage, the TS content, biogas production rate, methane concentration, and pH were relatively stable. The VFAs content increased with the increase of the loading frequency. At the end of the stable period, the TS contents in high-temperature dry fermentation systems R1, R2, R3, and R4 increased to 21.38 ± 0.85, 22.33 ± 1.98, 23.096 ± 1.23, and 27.69 ± 2.99%, respectively. The biogas production rates maintained at 2.17–2.33, 2.40–2.63, 2.20–2.44, and 0.75–0.90 $m^3/(m^3 \bullet d)$, respectively. The methane contents in biogas stabilized at 53.33–57.22, 64.34–68.88, 61.18–66.37, and 51.32–55.45%, respectively. The systems were stable in operation, should rather be "as were the pH values and daily gas output. The HRT was determined to be 20 days.
Keywords: *chicken manure, co-fermentation, high temperature, anaerobic fermentation mechanism*

Introduction

Compared to anaerobic digestion or wet fermentation, dry fermentation has the characteristics of less water consumption, highbiogas production rates, low costs, etc. Nevertheless, dry fermentation is difficult to start, and the parameters of the process are difficult to adjust (Chu et al., 2010; Li et al., 2016; Linke, 2006). Moreover, concentrated ammonia and toxic metabolites inhibit the fermentation process. Thesedrawbacks limit popularization of the dry fermentation technology. In the past two years, encouraged by valorization of biomass resources to avoid the energy crisis, the dry fermentation technique for organic waste attracted more attention due to its advantages. In Western European countries, such as Germany, the dry fermentation technology for biogas production from domestic waste has been developed, especially for market-oriented applications (Zhang and Jahng, 2012; Chen et al., 2008; Duan et al., 2016). In 2000, the dry fermentation capacity of European domestic waste accounted for 54% of the total fermentation capacity (Tauseef et al., 2013). From 2006 to 2011, the proportion of dry fermentation in newly built anaerobic fermentation units for domestic waste further increased to 63% (Nasir et al., 2012). To date, dry fermentation is prevalently conducted at medium temperatures, and the feedstock is mainly kitchen waste. Few reports have

http://www.aloki.hu ● ISSN 1589 1623 (Print) ● ISSN 1785 0037 (Online)
DOI: http://dx.doi.org/10.15666/aeer/1804_48834895

been made on the high-temperature dry fermentation technology using livestock and poultry manure, chicken manure, and straw. The commercial applications of dry anaerobic fermentation mainly consume domestic waste instead of livestock and poultry manure. This is because the nitrogen content in livestock and poultry manure is very high and suppresses fermentation, and ammonia very easily accumulates in the dry fermentation process. Therefore, in this paper, straw was added to regulate the C/N ratio in the high-temperature dry fermentation of livestock and poultry manure to shorten HRT and improve the total solid content (TS) in the fermentation liquid above 20%. This technique targets direct feeding and discharging and stable biogas production. The high-temperature fermentation of chicken manure and straw represents a viable technical scheme for valorization of livestock and poultry manure and straw.

Experimental materials and scheme

Materials and sludge for inoculation

Chicken manure in the experiment came from a chicken farm in Beipiao County, Chaoyang City, Liaoning Province, China. 100 kg chicken manure was collected and after careful screening to remove impurities, such as stone, chicken manure collected for continuous 3 d was sent to the laboratory directly and kept at 4 °C in refrigerator (Jiménez et al., 2003; Yeoung, 2005). After intensive mixing in the laboratory, the collected chicken manure was used as the experimental material for high temperature anaerobic digestion. The extra 500 kg of the material was packaged as 1 kg bags and frozen in refrigerator for a further experiment of continuous high temperature dry fermentation of chicken manure. Stalks used in the experiments, which were from a farm in Shenbei new district, Shenyang City, Liaoning Province, were shipped to the laboratory and cut and ground to 80 mesh.

The inoculated microorganisms in the experiments were from anaerobic digested mud in a northern waste water treatment factory in Shenyang City, Liaoning Province, China. The inoculated active mud was transferred to an airtight plastic container and its temperature decreased to room temperature of about 20 °C or so during the transportation process (Rundberget et al., 2004; Wang et al., 2018; Zhang et al., 2017), whereas the inoculated mud still maintained active. In the laboratory, the inoculated mud was cultivated and acclimatized at 55 °C. The acquired 5 L of active mud was transferred to a 25 L air-tight plastic bag for acclimatization. After 3 d cultivation at constant 55 °C, 2.5 kg of fresh chicken manure, which was taken in advance and kept at room temperature, was added into active mud after acclimatization for 10 d cultivation (Hu et al., 2018; Naranjo et al., 2011). In addition, 5 kg of fresh chicken manure kept at room temperature was acclimatized and cultivated for 10 d for a further use. Dry material masses of chicken manure, stalks, and inoculated mud were determined after heating in air dry oven for 24 h at constant temperature of 105 °C (den Boer et al., 2012). The organic content was determined after 4 h heating in the muffle furnace at constant 550 °C (Duan et al., 2016). Main parameters of the wet basic state of chicken manure, stalks, and active mud are shown in *Table 1*.

Apparatus and methods

The high-temperature dry fermentation using chicken manure and straw was carried out on the basis of the previous experiment. A 4×30-liter anaerobic bioreactor (Baoxing,

http://www.aloki.hu ● ISSN 1589 1623 (Print) ● ISSN 1785 0037 (Online)
DOI: http://dx.doi.org/10.15666/aeer/1804_48834895

Shanghai) was used. The reactor content was stirred regularly through a central controller. Based on the results of the previous experiment, the feedstock with straw mass ratios of 0, 3, 5, and 100% was prepared. During the start-up stage of high-temperature dry fermentation, 3 L of anaerobic sludge for inoculation, cultivated in Shenyang North Sewage Treatment Plant, was mixed with 3 kg of the feedstock, and then the mixture was placed into the feeding tank of the bioreactor, which was equipped with an air inlet and outlet. N2 was introduced for 5 min. After oxygen was discharged from the outlet, the feeding valve was opened for the addition of feedstock into the bioreactor. In the experiment, fresh feedstock was added from the top of the bioreactor after spent materials were discharged from the bottom of the bioreactor. For fermentation, the volume of materials was set to 20 L with water, and the temperature was adjusted to 55 ± 0.2 °C (García-Ochoa et al., 1999). During the experiment, NaHCO3 was added to maintain pH of the digestion liquid above 6.8. When the system reached a stable state, hydraulic retention time (HRT) was shortened from 200 to 20 days to increase the total solid content (TS) to higher than 20%. Direct feeding and discharging and stable biogas production continued until the high-temperature dry fermentation was completed. In the last stage of the experiment, HRT was further shortened to 10 days for a destructive experiment to study the inhibition effect of the high TS content on the dry fermentation process. In the experiment, the biogas production rate, pH, volatile organic acids (VFAs) concentrations, and other parameters of the system were monitored, and the changes and relations of these parameters were analyzed. All the experiments were conducted twice, and the average values were adopted as valid data.

Table 1. *Main parameters of the wet basic state of chicken manure, stalks, and active mud*

Parameters	TS:/%	VS/%	pH	TC/%	TN/%
Chicken manure	27.29	23.33	6.33	46.07	4.73
Stalks	91.44	86.50	6.89	50.02	0.88
Active mud	18.12	8.36	7.41	--	--

TS: Total substance; VS: volatile substance; TC: total carton; TN: total nitrogen

Results and discussion

Characteristics of biogas production by the high-temperature dry fermentation

Figures 1-4 show the changes of biogas production rates, methane production rates, and methane contents in reactors R1–4. According to the changes of the loading frequency, biogas production rate, TS concentration, pH, and VFAs concentration, the whole process of high-temperature dry fermentation was divided into four periods: adaptation period (20 days, from day 1 to 20), fast-start period (30 days, from day 20 to 50), stable period (70 days, from day 51 to 120), and overload period (20 days, from day 121 to 140). The changes in biogas production rates and relevant parameters in each stage were closely related to the loading frequency. In the adaptation stage, the microorganisms did not completely adapt to the dry fermentation system, and the feedstock amount was small, leading to a low biogas production rate. After the short start-up stage, the system became stable. The temperature and biogas production rate reached high levels. When the fermentation reached the overload stage, in the excess of

http://www.aloki.hu ● ISSN 1589 1623 (Print) ● ISSN 1785 0037 (Online)
DOI: http://dx.doi.org/10.15666/aeer/1804_48834895

feedstock, the shredded straw expanded due to the high temperature and water uptake, inhibiting the reactions.

In the adaptation period (20 days, from day 1 to 20), 1 kg of feedstock was loaded at the interval of 10 days without discharging. At the same time, 10 g of sodium bicarbonate ($NaHCO_3$) was added to prohibit acidification and reaction inhibition. On the first day of the adaptation period, the TS contents in bioreactors R1–4 were 5.8 ± 0.25, 6.12 ± 0.65, 6.51 ± 0.55, and 6.99 ± 0.87%, and the biogas production rates were as low as 0.15 ± 0.06, 0.09 ± 0.02, 0.08 ± 0.04, and 0.01 ± 0.02 $m^3/(m^3 \bullet d)$, respectively. In the first 10 days (day 1 to 10) of the adaptation period, the main reason for the decrease of TS concentrations in R1–4 was that the feedstock was loaded only once, and the biochemical reactions took place in the same way as in the previous experiments. In the high-temperature dry fermentation, hydrolysis-acidification microorganisms degraded organic matter in R1–4 reactors to produce organic acids, a small portion of which was digested by anaerobic methanogenic bacteria to yield biogas. Thereby, the TS contents in this stage decreased gradually. On day 10, the TS content decreased to 4.77 ± 0.16, 5.42 ± 0.56, 5.79 ± 0.77, and 6.51 ± 0.24%, respectively. During the adaptation period, the biogas production rate increased gradually. The anaerobic active sludge for inoculation required a period to adapt to the high-temperature anaerobic digestion system. The initial stage of the reaction was similar to a stagnant stage. During the adaptation period, the anaerobic microorganisms could not grow and reproduce themselves immediately because the growth and reproduction could not occur until enzymes for metabolism of nutrients were formed after a while in the fermentation system. The number of anaerobic microorganisms increased along with the process of digestion, and the biogas production rate increased. On day 10, the biogas production rates in reactors R1–4 were 0.33 ± 0.04, 0.61 ± 0.14, 0.51 ± 0.07, and 0.14 ± 0.03 $m^3/(m^3 \bullet d)$, respectively. In this stage, feedstock was loaded at the interval of 10 days without discharging, so the HRT (day 1–20) was 200 days. The methane contents in reactors R1–4 increased from 38.45, 39.33, 40.21, and 29.31% on the first day to 47.21, 60.33, 54.35, and 45.33% on the 20th day because the number of anaerobic microorganisms increased with the improvement of adaptation to the high-temperature fermentation system. 10 g of sodium bicarbonate added elevated pH, thus improving the activity of metabolism of methanogenic bacteria and biogas production and increasing the biogas production rate. During this period, because the feedstock in R4 was only straw, the hydrolysis reaction was inhibited, and acidification took place slowly, so the biogas production rate and methane concentration were significantly lower than those of the other systems with different types of feedstock. To sum up, the process in this stage was similar to that in the previous experiment.

During the fast start-up period (30 days, from day 21 to 50), generally speaking, the TS contents in R1–4 reactors increased because the feedstock was only added without discharging during this period. The HRT (day 21–40) and HRT (day 41–50) was 60 and 40 days, respectively. During this period, the adaptation of anaerobic microorganisms to the high-temperature digestion was enhanced, and the growth rate of microorganisms increased to the maximum. The numbers of hydrolysis-acidification and methanogenic bacteria increased in geometric progression, but the feedstock was only added without discharging, so the feeding rate was higher than the metabolic decomposition rate by microorganisms, resulting in the increase of TS concentration. At the end of this fast start-up period (day 50), the TS content increased to 16.77 ± 0.65, 18.24 ± 0.29, 19.35 ± 1.08, and 21.44 ± 1.45%, respectively. During the fast start-up period, the

http://www.aloki.hu ● ISSN 1589 1623 (Print) ● ISSN 1785 0037 (Online)
DOI: http://dx.doi.org/10.15666/aeer/1804_48834895

biogas production rates in reactors R1–4 were related to the loading frequency. The production rates increased first and then decreased on each loading day. The reason is that in these days, the easily degradable organic matter in the added materials could be rapidly utilized by the anaerobic microbial community that had adapted to the high-temperature fermentation system, and hydrolysis-acidification and methanation processes occurred in these days, so the biogas production rates were high. Afterwards, the organic residue in straw degraded very slowly, leading to the decrease of biogas production rates. The biogas production rates in reactors R1–4 increased from 0.78 ± 0.09, 0.97 ± 0.11, 0.91 ± 0.12, and 0.34 ± 0.20 $m^3/(m^3 \bullet d)$ on day 21 to 1.71 ± 0.12, 2.14 ± 0.18, 2.01 ± 0.08, and 0.73 ± 0.07 $m^3/(m^3 \bullet d)$ in R 1, 2, 3 and 4 on day 50. The methane concentrations in biogas produced by high-temperature fermentation in R1–4 slightly increased. The reason is that the TS contents in the fast start-up stage increased, and the number of hydrolysis-acidification microorganisms also increased exponentially with the improvement of adaptation, promoting the hydrolysis-acidification process. The adaptation of methanogens to high-temperature anaerobic digestion was slow, and the activity of methanogens increased after the adaptation period that continued for 20 days. The addition of 10 g of sodium bicarbonate ($NaHCO_3$) maintained the pH of the systems at the level of 6.8 to improve the metabolism activity of methanogens and to enhance the utilization of organic acids in the fermentation liquid to increase the methane concentrations in biogas. On day 50, the methane contents in biogas in reactors R1–4 were 52.31, 66.25, 61.25, and 53.33%, respectively.

During the stable period (70 days, from day 51 to 120), the TS contents continuously increased. The reason is that in this period, the feedstock was added and waste was discharged every day. Because the feedstock added contained straw, the shredded straw expanded in the high-temperature fermentation systems and floated in the upper layers of CSTR reactors. Although the systems were stirred before discharging, some straw still floated, and the proportion of straw in the materials discharged was relatively small, leading to the gradual increase of TS concentrations in these systems. On day 120, the TS contents increased to 21.38 ± 0.85, 22.33 ± 1.98, 23.096 ± 1.23, and $27.69 \pm 2.99\%$, respectively. During this period, the biogas production rates in reactors R1-4 maintained at 2.17–2.33, 2.40–2.63, 2.20–2.44, and 0.75–0.90 $m^3/(m^3 \bullet d)$ in R 1, 2, 3 and 4. The biogas production rate in reactor R2 was the highest because the C/N ratio in chicken manure and straw was 9.34 and 57.04, respectively. Compared to the reactor R1 containing pure chicken manure, the content of straw in R2 was increased by 3%, so the carbon content and the C/N ratio in the feedstock of R2 were increased, promoting the physiological metabolic activity of the microbial community in the high-temperature dry fermentation process. In the fermentation process, a large amount of organic carbon was transformed into CH_4 and CO_2 by anaerobic microorganisms. On the other hand, nitrogen was only consumed in the physiological metabolism of microorganisms. When a certain proportion of carbon sources was transformed into methane and carbon dioxide, a certain amount of nitrogen was required to ensure formation of the anaerobic microbial community. The proportion of carbon and nitrogen sources should be appropriate. Therefore, R2 showed the highest biogas production rate of 2.40–2.63 $m^3/(m^3 \bullet d)$. The methane concentrations in biogas produced in the high-temperature fermentation reactors R1–4 were relatively stable and maintained at levels of 53.33–57.22, 64.34–68.88, 61.18–66.37, and 51.32–55.45% in R 1, 2, 3 and 4, respectively. The reason is that

http://www.aloki.hu ● ISSN 1589 1623 (Print) ● ISSN 1785 0037 (Online)
DOI: http://dx.doi.org/10.15666/aeer/1804_48834895

along with the high-temperature fermentation process, the organic substrate in these CSTR reactors was continuously supplied, and the hydrolysis-acidification microorganisms in these systems were balanced with methanogenic microorganisms. The former hydrolyzed and acidified the organic substrate supplied to produce organic acids, which were converted into methane by the methanogens that had adapted to the high-temperature fermentation systems. Therefore, these systems could stably produce biogas without the adjustment of pH, and the organic acids could be directly converted into methane and carbon dioxide. Therefore, the methane concentrations in biogas during this stage were the highest. Feeding and discharging could be realized each day, and 1 kg of feedstock was added each time. The HRT (day 51–120) was 20 days, and the system was stably operated.

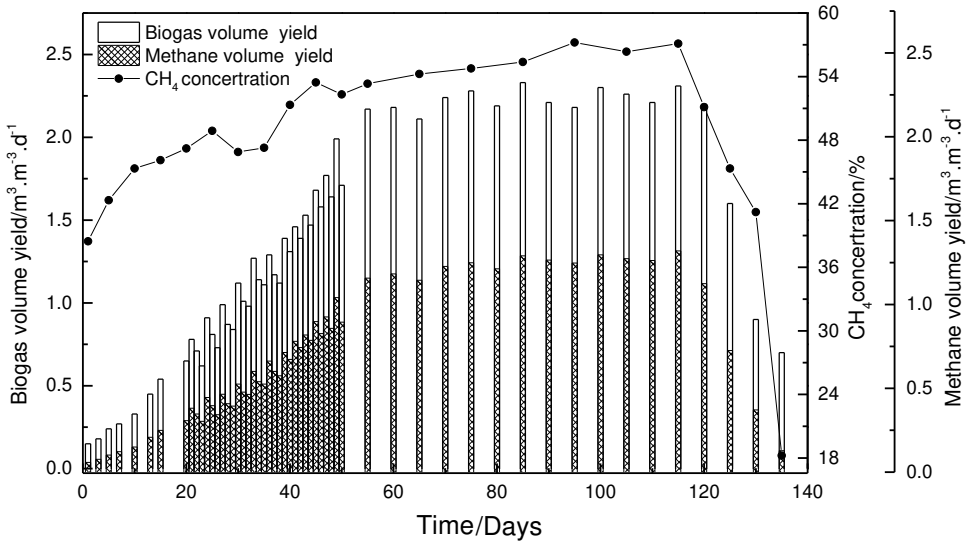

Figure 1. *Changes in the biogas production rate, methane production rate, and methane concentration in the high-temperature dry fermentation reactor R1*

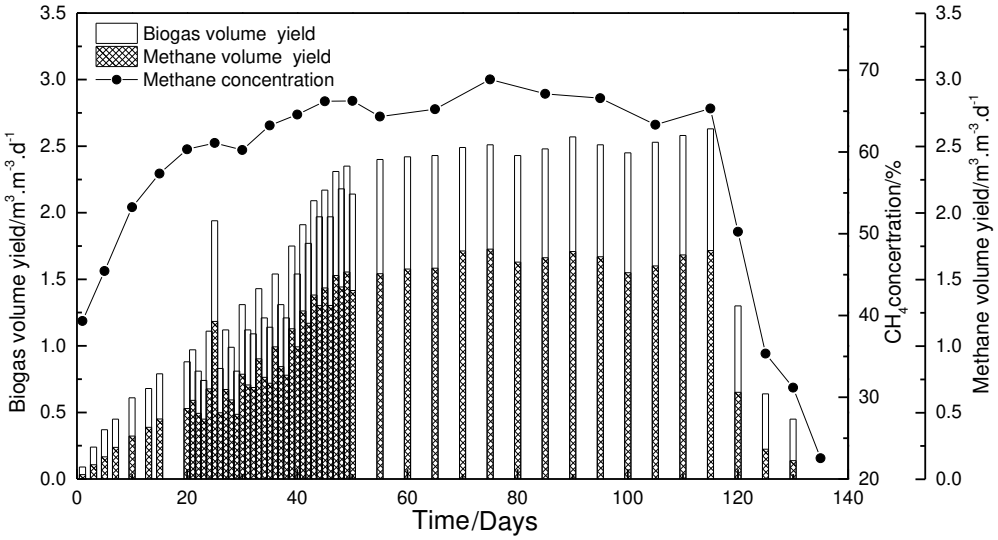

Figure 2. *Changes in the biogas production rate, methane production rate, and methane concentration in the high-temperature dry fermentation reactor R2*

http://www.aloki.hu ● ISSN 1589 1623 (Print) ● ISSN 1785 0037 (Online)
DOI: http://dx.doi.org/10.15666/aeer/1804_48834895

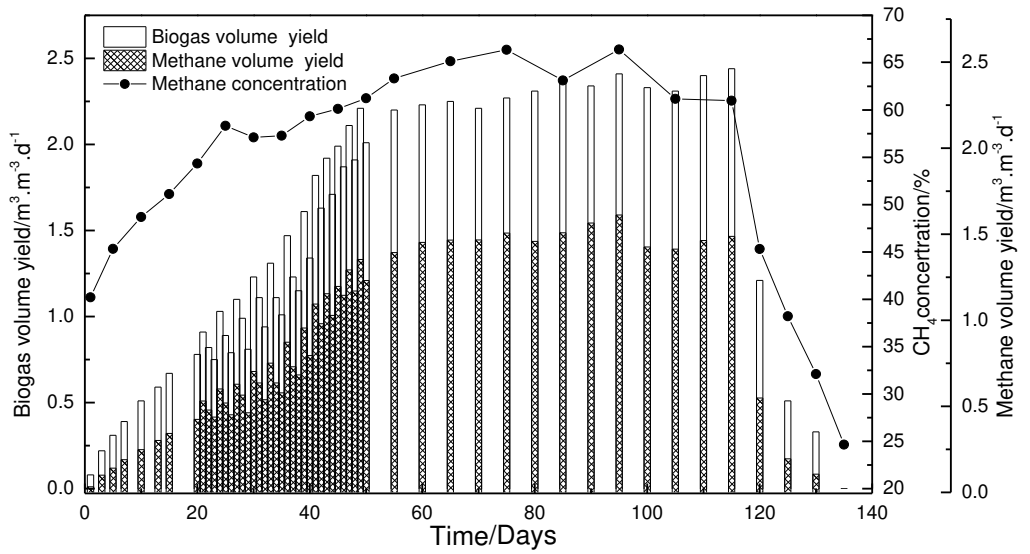

Figure 3. *Changes in the biogas production rate, methane production rate, and methane concentration in the high-temperature dry fermentation reactor R3*

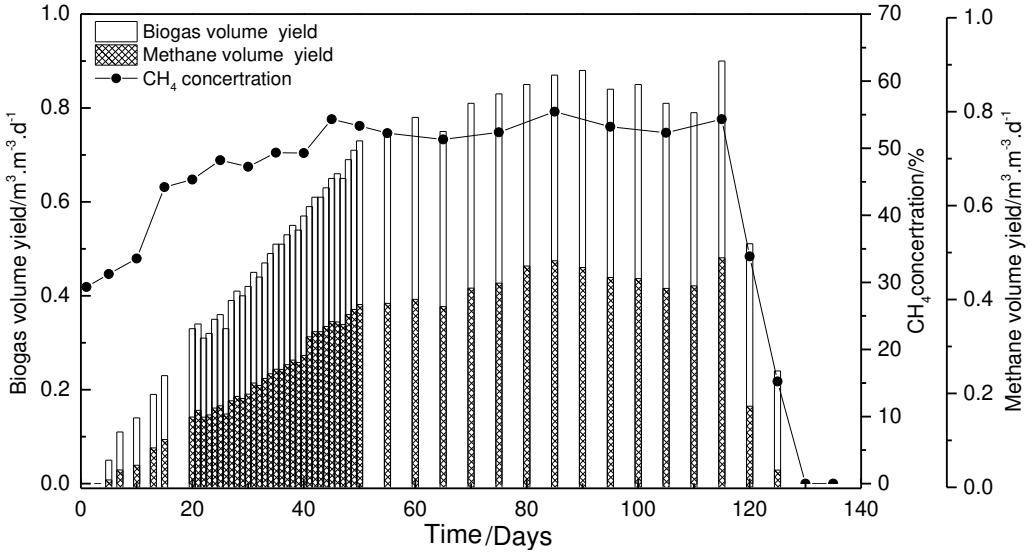

Figure 4. *Changes in the biogas production rate, methane production rate, and methane concentration in the high-temperature dry fermentation reactor R4*

During the overload period (20 days, from day 121–140), the TS concentrations in these systems significantly increased. The main reason is that when the amount of feedstock was increased, especially in reactors R2, R3, and R4 with straw as the feedstock, the large amounts of shredded straw absorbed water and expanded rapidly at high temperatures. This straw aggregated in the upper layer of CSTR reactors. Although the mixtures were vigorously stirred before discharging, the straw aggregated was difficult to discharge. As a result, the composition of these systems changed, and the proportions of straw increased due to the retention. In the last stage, the straw expanded was hard to stir and discharge, resulting in the decrease of the biogas production rate. And the chicken manure and straw were directly discharged without biochemical

http://www.aloki.hu ● ISSN 1589 1623 (Print) ● ISSN 1785 0037 (Online)
DOI: http://dx.doi.org/10.15666/aeer/1804_48834895

decomposition. Except R1, reactors R2, R3, and R4 did not yield biogas anymore, and the high-temperature dry fermentation was terminated.

Correlations between pH, TS and VFAs concentrations in the high-temperature dry fermentation

As shown in *Figures 5-8,* the changes in pH, TS and VFAs concentrations in the high-temperature dry fermentation reactors R1–4 show that the TS concentrations were positively correlated with the VFAs concentrations in all reactors. The pH was regulated with $NaHCO_3$ and maintained above 6.8 after 20 days of the adaptation period, which was favorable to the metabolic activity of methanogens. In the overload stage, with the further increase of the TS concentration, the acidification was inhibited, and the pH decreased. The reactions in reactors R1–4 were terminated.

In reactors R1–4, the pH decreased from day 1 to 10 of the adaptation period. The main reason is that the feedstock was loaded only once in the first 10 days, and the principles of biochemical reactions were similar to those in the previous experiments. During the high-temperature dry fermentation, hydrolysis-acidification microorganisms decomposed organic matter in reactors R1–4 to produce organic acids, resulting in the decline of pH in these high-temperature dry fermentation systems. However, the activity of methanogens converting organic acids into methane was relatively low, and the adaptation period of methanogens to the high-temperature dry fermentation systems was longer than that of the hydrolysis-acidification microorganisms. The decrease of pH further inhibited the metabolism of methanogens and weakened the utilization of organic acids. The pH declined gradually during the adaptation period (day 1–10), and the pH on day 10 was 6.11 ± 0.35, 5.39 ± 0.41, 5.45 ± 0.21, and 6.75 ± 0.21 in R 1, 2, 3 and 4, respectively. Among these four reactors, the pH in R2 declined to the lowest value, and the pH in R4 was the highest. The main reason is that the compositions of feedstock were different. In detail, the feedstock in R1, R2, R3, and R4 was pure chicken manure, chicken manure containing 3% straw, chicken manure containing 5% straw, and pure straw, respectively. Straw consists of cellulose, hemicellulose, and lignin, which have dense textures, greatly hampering the access of hydrolases into their internal structures and inhibiting hydrolysis reactions in R4. In contrast, the content of straw in R2 was as low as 3%, so the access of hydrolases was not impeded. Furthermore, the content of carbon in the feedstock of R2 was elevated and thus, the C/N ratio was adjusted to promote the physiological metabolism activity of the microbial community in the high-temperature dry fermentation process (Pontes and Pinto, 2006; Linke, 2006; Feng et al., 2013; Lu et al., 2012).

From day 21, the feedstock was added without discharging. In detail, from day 21 to 40, 1 kg of the feedstock was added at the interval of three days; from day 41 to 50, 1 kg of the feedstock was added at the interval of two days. At this stage, sodium bicarbonate ($NaHCO_3$) was not added, and hence the pH during the high-temperature dry fermentation in R1–4 declined from 6.65 ± 0.11, 6.53 ± 0.32, 6.58 ± 0.19, and 6.54 ± 0.32 on day 21 to 6.45 ± 0.14, 6.29 ± 0.25, 6.31 ± 0.41, and 6.39 ± 0.23 on day 50. In this stage, the VFAs concentrations increased with the increase of TS concentrations and reached 39.87 ± 2.21, 48.22 ± 2.89, 41.77 ± 2.68, and 11.23 ± 0.78 g/L, respectively in R 1, 2, 3 and 4, on day 50. The pH in the fast start-up period of high-temperature dry fermentation still decreased. The main reason is that after the adaptation stage, the metabolic activity of hydrolysis-acidification microorganisms in the high-temperature dry fermentation significantly improved, and

http://www.aloki.hu ● ISSN 1589 1623 (Print) ● ISSN 1785 0037 (Online)
DOI: http://dx.doi.org/10.15666/aeer/1804_48834895

the methanogenic microorganisms had long generation time, and the adaptation of methanogenic microorganisms was slower than that of hydrolysis-acidification microorganisms (Zheng et al., 2018; Luo and Li, 2018; Fan et al., 2008). Therefore, the microbial community grew unevenly, and the activity of hydrolysis-acidification microorganisms was higher than that of methanogenic bacteria, resulting in the decrease of pH and increase of VFAs concentration (Hua and Yong, 2009; Zheng et al., 2018). On the 50th day, the pH decreased to 6.45 ± 0.14, 6.29 ± 0.25, 6.31 ± 0.41, and 6.39 ± 0.23, and the VFAs content increased to 39.87 ± 2.21, 48.22 ± 2.89, 41.77 ± 2.68, and 11.23 ± 0.78 g/L in R 1, 2, 3 and 4.

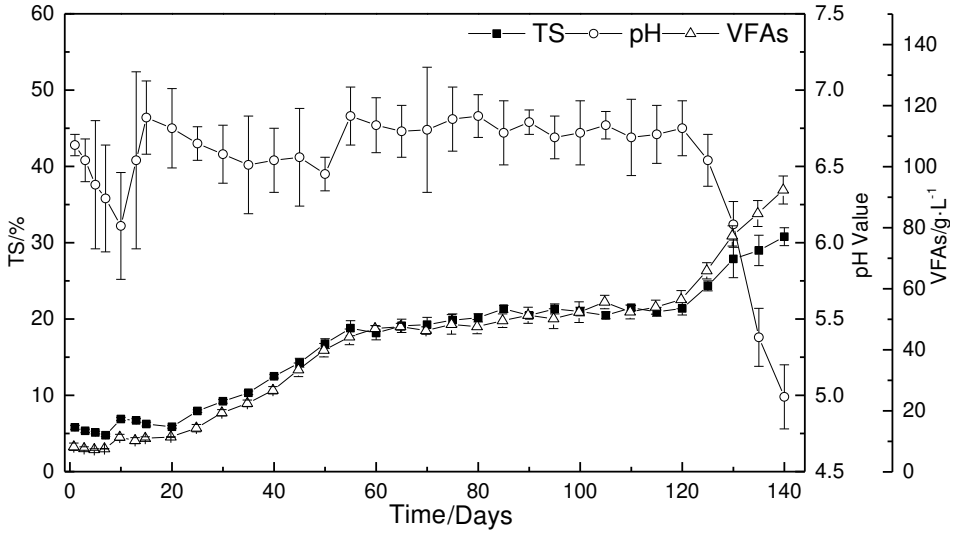

Figure 5. *Changes in pH, TS and VFAs concentrations in reactor R1*

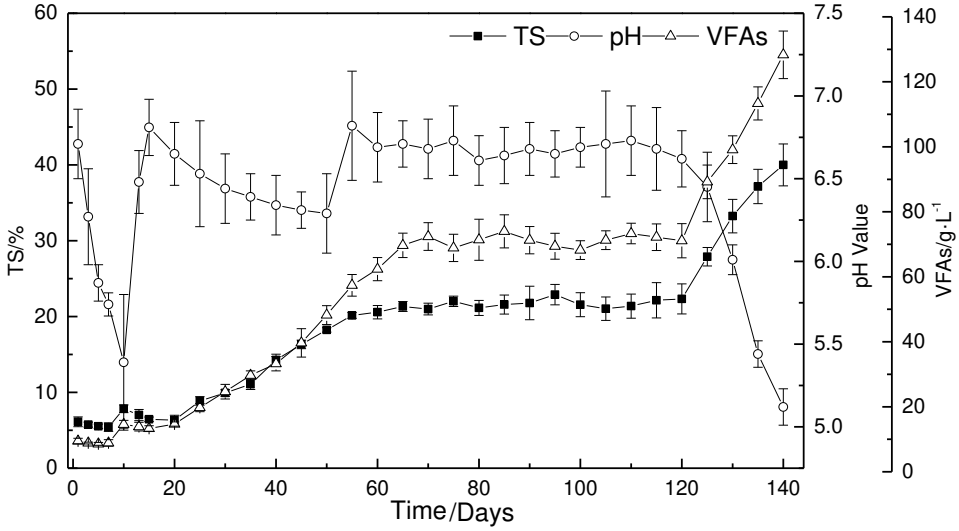

Figure 6. *Changes in pH, TS and VFAs concentrations in reactor R2*

From day 51, the feedstock was added and discharged every day. In detail, 1 L of the fermentation liquid was discharged first, and then 1 kg of the feedstock was added to the CSTR reactors. The volume of each system was increased to 1 L with water. The TS

http://www.aloki.hu ● ISSN 1589 1623 (Print) ● ISSN 1785 0037 (Online)
DOI: http://dx.doi.org/10.15666/aeer/1804_48834895

concentrations in these systems continued to increase from 18.80 ± 0.98, 20.15 ± 0.38, 20.99 ± 0.98, and 23.33 ± 1.54% on the 51st day to 21.38 ± 0.85, 22.33 ± 1.98, 23.096 ± 1.23, and 27.69 ± 2.99% on the 120th day in R 1, 2, 3 and 4, respectively. Only on the 51st day, 20 g of sodium bicarbonate ($NaHCO_3$) was added to adjust the pH of the fermentation liquid to above 6.8. Afterwards, the pH of the high-temperature dry fermentation systems self-stabilized between 6.6–6.93, and the systems ran stably. During the stable period, the concentrations of VFAs were positively correlated with the concentrations of TS and increased to 56.45 ± 2.98, 71.11 ± 5.25, 69.33 ± 3.99, and 22.08 ± 2.21 g/L, respectively, on day 120.

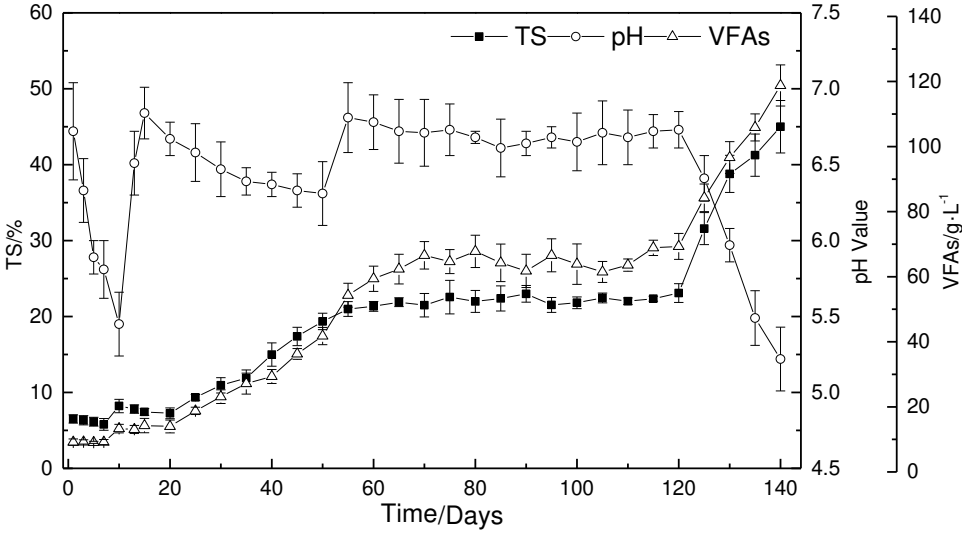

Figure 7. *Changes in pH, TS and VFAs concentrations in reactor R3*

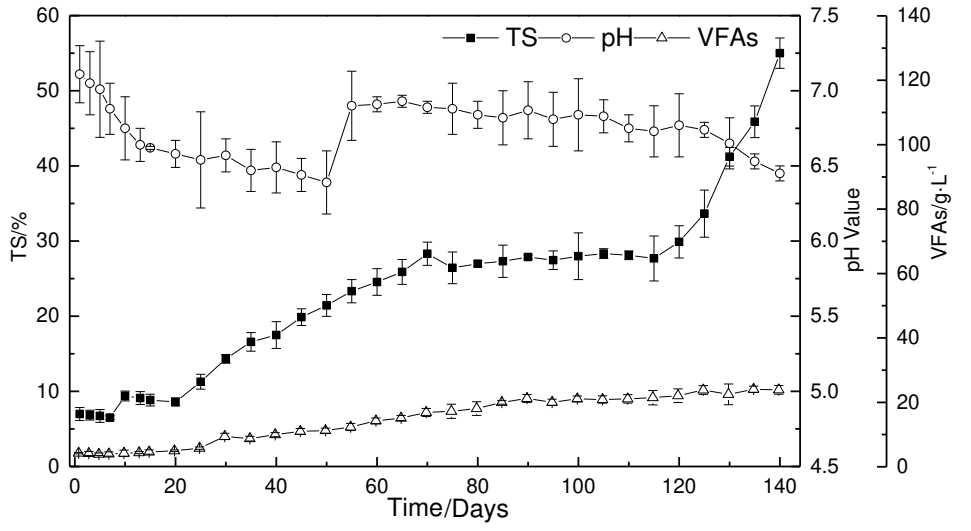

Figure 8. *Changes in pH, TS and VFAs concentrations in reactor R4*

In the stable period, feedstock was added and discharged from R1–4 every day. Only on the 51st day, the pH of the fermentation liquid was adjusted to above 6.8. Afterwards, the systems ran stably without pH adjustment. The main reason is that the

http://www.aloki.hu ● ISSN 1589 1623 (Print) ● ISSN 1785 0037 (Online)
DOI: http://dx.doi.org/10.15666/aeer/1804_48834895

metabolic activity of methanogenic bacteria was enhanced, and the high-temperature fermentation microorganisms grew evenly after the adaptation and fast start-up period. After the pH adjustment on day 51, the metabolic activity of methanogens was enhanced, and the organic acids generated from hydrolysis and acidification were directly consumed by methanogens to give methane. Therefore, the concentrations of organic acids increased in this stage, and the pH of these systems did not decline and kept constant between 6.6 and 6.93 because of the balance between the microorganisms (Luo and Li, 2018; Fan et al., 2008).

During the overload period, with higher amount of feedstock loaded, the TS concentrations in R1–4 increased significantly, resulting in a difficult discharge and decrease of pH. VFAs could not be metabolized because the reactions were inhibited, resulting in the increase of VFAs contents to 92.37 ± 4.59, 128.32 ± 7.32, 118.79 ± 6.33, and 23.88 ± 1.36 g/L in R 1, 2, 3 and 4 at the end of the reactions. Except that the biogas production rate in R1 was 0.7 ± 0.02 $m^3/(m^3 \cdot d)$, biogas was not produced in reactors R2, R3, and R4. The main reason for the stagnation of high-temperature dry fermentation is that when the amount of feedstock loaded was increased, especially in reactors R2, R3, and R4 with straw as the feedstock, the large amounts of shredded straw absorbed water and expanded rapidly at high temperatures. This straw aggregated in the upper layer of CSTR reactors. Although the mixtures were violently stirred before discharging, the straw aggregated was difficult to discharge, resulting in the changes of the composition in these systems. The proportions of straw increased due to the retention of straw. In the last stage, the straw expanded was hard to stir and discharge. The systems were obviously rancid, which was sensed during the discharge process (Zhou et al., 2019). The accumulation of organic acids led to the decrease of pH in the systems, so the chicken manure and straw were directly discharged without biochemical degradation. Except R1, biogas was not produced in reactors R2, R3, and R4, and the high-temperature dry fermentation was terminated (Yang et al., 2017).

Conclusion

(1) In the adaptation period (20 days, from day 1 to 20), along with the loading with feedstock, the TS and VFAs concentrations, biogas production rates, and pH of the systems decreased, and the ammonia concentrations increased. At the end of the adaptation period, the biogas production rate in R1, R2, R3, and R4 was as low as 0.78 ± 0.096, 0.97 ± 0.11, 0.91 ± 0.12, and 0.34 ± 0.20 $m^3/(m^3 \cdot d)$, respectively. The concentrations of methane in biogas increased to 47.21, 60.33, 54.35, and 45.33% on the 20th day, and HRT (day 1–20) was 200 days.

(2) During the fast start-up period (30 days, from day 21 to 50), semi-continuous anaerobic digestion took place. The TS concentration, biogas production rate, methane concentration, and VFAs concentration in reactor R2 increased with the increase of the loading frequency. At the end of the fast start-up period, the biogas production rate in reactors R1–3 and R4 was 1.71 ± 0.12, 2.14 ± 0.18, 2.01 ± 0.08, and 0.73 ± 0.07 $m^3/(m^3 \cdot d)$ in R 1, 2, 3 and 4, respectively. The methane concentrations in biogas increased to 52.31, 66.25, 61.25, and 53.33% on the 50th day. During the fast start-up period, the reactors were instable in operation, and the discharging and feeding could not be realized every day. The HRT (day 21–40) and HRT (day 41–50) values were 60 and 40 days, respectively.

http://www.aloki.hu ● ISSN 1589 1623 (Print) ● ISSN 1785 0037 (Online)
DOI: http://dx.doi.org/10.15666/aeer/1804_48834895

(3) During the stable period (70 days, from day 51 to 120), continuous digestion was realized, and the TS concentrations exceeded 20%, in accordance with dry fermentation. In the stable period, the TS concentrations, biogas production rates, methane concentrations, pH, and other parameters in the reactors were relatively stable. At the end of the stable period, the concentration of TS in reactors R1–3 and R4 increased to 21.38 ± 0.85, 22.33 ± 1.98, 23.096 ± 1.23, and 27.69 ± 2.99%, respectively. The biogas production rates maintained at 2.17–2.33, 2.40–2.63, 2.20–2.44, and 0.75–0.90 $m^3/(m^3 \bullet d)$, and the concentrations of methane in biogas maintained at levels of 53.33–57.22, 64.34–68.88, 61.18–66.37, and 51.32–55.45% in R 1, 2, 3 and 4, respectively. The systems were stable in operation, and pH and daily biogas output were also stable and the HRT (day 51–120) value was determined to be 20 days.

REFERENCES

[1] Chen, Y., Cheng, J. J., Creamer, K. S. (2008): Inhibition of anaerobic digestion process: a review. – Bioresource Technology 99(10): 4044-4064.
[2] Chu, C.-F., Ebie, Y., Xu, K.-Q., Li, Y.-Y., Yuhei, I. (2010): Characterization of microbial community in the two-stage process for hydrogen and methane production from food waste. – International Journal of Hydrogen Energy 35(15): 8253-8261.
[3] Chunyang Zhang, Weidong Wang, Junqi Jia, Aihua Wang, Lingling Li (2017): Study on Recovery of Biogas from Distillers Grains Wastewater by USR Reactor. – Procedia Engineering 205.
[4] den Boer, E., den Boer, J., Jaroszynska, J., Szpadt, R. (2012): Monitoring of municipal waste generated in the city of Warsaw. – Waste Management and Research 30(8): 772-780.
[5] Duan, X., Wang, X., Xie, J., Feng, L., Yan, Y., Zhou, Q. (2016): Effect of nonylphenol on volatile fatty acids accumulation during anaerobic fermentation of waste activated sludge. – Water Research 105: 209-217.
[6] Duan, X., Wang, X., Xie, J., Feng, L., Yan, Y., Zhou, Q. (2016): Effect of nonylphenol on volatile fatty acids accumulation during anaerobic fermentation of waste activated sludge. – Water Research 105: 209-217.
[7] Fan, L., Pan, J. H., Li, M. S., et al. (2008): Lactate inhibits hydrolysis of polysaccharide rich particulate organic waste. – Bioresource Technology 99(55): 2476-2482.
[8] Feng, L., Li, R. D. (2013): Process parameters of dry co-anaerobic digestion of kitchen waste and cow manure on laboratory scale. – Journal of Pure and Applied Microbiology 21(9): 777-782.
[9] García-Ochoa, F., Santos, V. E., Naval, L., Guardiola, E., López, B. (1999): Kinetic model for anaerobic digestion of livestock manure. – Enzyme and Microbial Technology 25(1).
[10] Hu, J., Xu, Q., Li, X., Wang, D., Zhong, Y., Zhao, J., Zhang, D., Yang, Q., Zeng, G. (2018): Sulfamethazine (SMZ) affects fermentative short-chain fatty acids production from waste activated sludge. – Science of the Total Environment 639: 1471-1479.
[11] Hua, W., Yong, P. (2009): Water quantity operation to achieve multi-environmental goals for a waterfront body. – Water Resources Management 23(10): 1951-1968.
[12] Jiménez, A. M., Borja, R., Martín, A. (2003): Aerobic–anaerobic biodegradation of beet molasses alcoholic fermentation wastewater. – Process Biochemistry 38(9).
[13] Li, Y., Jin, Y., Li, J., Chen, Y., Gong, Y., Li, Y., Zhang, J. (2016): Current situation and development of kitchen waste treatment in China. – Procedia Environmental Sciences 31: 40-49.
[14] Linke, B. (2006): Kinetic study of thermophilic anaerobic digestion of solid wastes from potato processing. – Biomass and Bioenergy 30(10): 892-896.

http://www.aloki.hu ● ISSN 1589 1623 (Print) ● ISSN 1785 0037 (Online)
DOI: http://dx.doi.org/10.15666/aeer/1804_48834895

[15] Lu, J., Jiang, L. N., Chen, D. J., Toyota, K., Strong, J., Wang H. L., Hirasawa T. (2012): Decontamination of anaerobically digested slurry in a paddy field ecosystem in Jiaxing region of China. – Agriculture, Ecosystems & Environment 146(1): 13-22.
[16] Luo, H., Li, F. S. (2018): Tomato yield, quality, and water use efficiency under different drip fertigation strategies. – Scientia Horticulturae 235: 181-188.
[17] Naranjo, A., et al. (2011): Effects of different concentrations of NaOH pretreatment on anaerobic digestion of rice straw for biogas production. – Transactions of the Chinese Society of Agricultural Engineering 27(10): 59-63.
[18] Nasir, I. M., Ghazi, T. I. M., Omar, R. (2012): Production of biogas from solid organic wastes through anaerobic digestion: a review. – Applied Microbiology and Biotechnology 95(2): 321-329.
[19] Pontes, R. F. F., Pinto, J. M. (2006): Analysis of integrated kinetic and flow models for anaerobic digesters. – Chemical Engineering Journal 122(1): 65-80.
[20] Rundberget, T., Skaar, I., Flaoyen, A. (2004): The presence of Penieillum and Penicillum mycotoxins in food waste. – International Journal of Food Microbiology 53(90): 181-188.
[21] Tauseef, S. M., Abbasi, T., Abbasi, S. A. (2013): Energy recovery from wastewaters with high-rate anaerobic digesters. – Renewable and Sustainable Energy Reviews 19: 704-741.
[22] Wang, D., Zhang, D., Xu, Q., Liu, Y., Wang, Q., Ni, B.-J., Yang, Q., Li, X., Yang, F. (2018): Calcium peroxide promotes hydrogen production from dark fermentation of waste activated sludge. – Chemical Engineering Journal 355: 22-32.
[23] Yang, S. F., Phan, H. V., Bustamante, H., Guo, W. S., Ngo, H. H., Nghiem, L. D. (2017): Effects of shearing on biogas production and microbial community structure during anaerobic digestion with recuperative thickening. – Bioresour. Technol. 234: 439-447.
[24] Yeoung, S. Y. (2005): High rate slurry phase decomposition of food wastes: indirect Performance estimation from dissolved oxygen. – Process Biochemistry 40(3): 1301-1306.
[25] Zhang L., Jahng, D. (2012): Long-term anaerobic digestion of food waste stabilized by trace elements. – Waste Management 32(8): 1509-1515.
[26] Zheng, J., Zhang, E. J., Wang, Y., et al. 2018. Analysis on the transport characteristics of water-biogas slurry integrated infiltration. – Journal of Lanzhou University of Technology 44(1): 58-64.
[27] Zhou, M., Yang, H. N., Zheng, D., Pu, X. D., Liu, Y., Wang, L., Zhang, Y. H., Deng, L. W. (2019): Methanogenic activity and microbial communities characteristics in dry and wet anaerobic digestion sludges from swine manure. – Biochem. Eng. J. 152(15): 107-116.

http://www.aloki.hu ● ISSN 1589 1623 (Print) ● ISSN 1785 0037 (Online)
DOI: http://dx.doi.org/10.15666/aeer/1804_48834895

QUANTITATIVE *ULVA PROLIFERA* BLOOM MONITORING BASED ON MULTI-SOURCE SATELLITE OCEAN COLOR REMOTE SENSING DATA

ZHENG, H. Y.[1] – LIU, Z.[1*] – CHEN, B.[2] – XU, H.[3]

[1]*College of Ocean Science and Engineering, Shandong University of Science and Technology, Qingdao 266590, China*

[2]*Guangxi Key Laboratory of Marine Environment Science, Guangxi Academy of Science, Nanning 530007, China*

[3]*College of Geomatics, Shandong University of Science and Technology, Qingdao 266590, China*

**Corresponding author*
e-mail: zhliu01@126.com

(Received 9th Jan 2020; accepted 6th May 2020)

Abstract. Since 2007, a large-scare green macroalgae bloom of *Ulva prolifera* has occurred every year in the Yellow Sea, and satellite ocean color remote sensing monitoring of such event is an effective technical method with important application value. For the Moderate Resolution Imaging Spectroradiometer (MODIS), Geostationary Ocean Color Imager (GOCI), Sentinel-3 Ocean and Land Colour Instrument (OLCI), Landsat8 Operational Land Imager (OLI) and Gaofen satellite (GF1) multispectral satellite data of the study area, the bloom was monitored based on spectral band difference algorithms and band-ratio algorithms. In view of the threshold selection of the detection, the scaled algae index (SAI) is less sensitive to the environment and shows accurate stability. For the five satellite ocean color sensors, this study compared their ability to monitor algal bloom on spatial and temporal scales. On the spatial scale, quantitative results of each data are specifically compared. Low spatial resolution data was found to overestimate the blooming area. On the time scale, GOCI can best monitor the dynamic changes of bloom, and the composites of algae and sea surface wind shows the dynamic evolution of blooming event in the range from May to July 2017.
Keywords: *green tide, green macroalgae bloom, NDVI, Scaled Algae Index (SAI), Floating Algae Index (FAI)*

Introduction

Ulva prolifera blooms (previously known as *Enteromorpha prolifera*) is defined as an ecological anomaly of massive green macroalgae exploding and accumulating under specific environmental conditions (Liang et al., 2008). In China, a large amount of waste on the vast coastal beaches of Jiangsu Province is thrown into the sea every spring, and the culture of the growing seaweed is polluted, which has spawned thousands of tons of *U. prolifera* (Hu et al., 2010b; Keesing et al., 2011; Naihao and Zhimeng, 2010). According to the Chinese marine bulletin, large-scale green algal blooms occur every year, often floating on the surface of scum, covered with biological or exudate beaches, with a range of up to 10,000 km^2. The *U. prolifera* disaster will cause huge losses to China's economy and will also cause damage to marine resources such as benthic animals, aquatic plants, and underwater resources (Liu et al., 2009; Shimada et al., 2008).

Ocean color remote sensing is a passive measurement technique that utilizes visible and near-infrared bands. Compared with the surrounding seawater, the increase of algal

http://www.aloki.hu ● ISSN 1589 1623 (Print) ● ISSN 1785 0037 (Online)
DOI: http://dx.doi.org/10.15666/aeer/1804_48974913

biomass leads to significant changes in satellite radiation. The law of light propagation is similar to that of common vegetation. There is a clear reflection peak near the green band at 555 nm and a distinct absorption peak near the red light at 680 nm. In the infrared band, the reflectance rises sharply to form a "red edge". At 960 nm and 1100 nm, there is an absorption peak due to water absorption (Xiao et al., 2017). With the increase of algal biomass, the reflectance of *U. prolifera* is shifted upward as a whole. Through the ocean color satellite data, we can obtain a series of bio-optical parameters such as chlorophyll concentration, sea surface temperature, fluorescence height, and seawater optical diffuse attenuation coefficient. In addition to the scientific data needed in these biogeochemical studies, ocean color remote sensing can provide near real-time monitoring of global organisms for more than 20 years. This long-term sequence data can be used to invert the evolution of floating algae and analyze time-space transformation.

Since the late 1970s, the increased demand for effective environmental monitoring for the coast has led to significant advances in the study of ocean color algorithms. Based on the difference between the spectrum of algae and surrounding seawater, various algorithms have been developed to help and monitor the blooms of *U. prolifera.* Depending on the specific spectral characteristics of *U. prolifera*, the algal patches and other features can be effectively classified by supervised or unsupervised classification; the spectral band difference algorithms and the band-ratio algorithms obtained by empirical model using in situ data sets such as chlorophyll and reflectivity is widely used in the detection of this events; the bio-optical model based on solid theoretical basis and strict equations is robust in algal classification applications. In 2008, Hu and He et al. analyzed the *U. prolifera* bloom along the coast of Qingdao during the Olympic Games using the Normalized Vegetation Index (NDVI) (Hu and He, 2008). In 2009, Hu et al. proposed a Floating Algae Index (FAI) and explored the origin of floating algae using MODIS's 2007-2013 data (Hu et al., 2010a; Hu, 2009). In 2016, Zhang Hailong et al. also proposed the Multispectral Green Tide Index (MGTI) based on GF/WFV (wide field-of-view) and HJ CCD (Huanjing satellite charge coupled device) data, and found that MGTI's overall satellite detection results for China are good (Zhang et al., 2016). The qualitative detection of blooms by ocean color remote sensing has been developed more fully (Blondeau-Patissier et al., 2014).

A wide variety of satellite sensors provide solid data support for blooms monitoring, and the use of multi-source data to monitor algae is becoming a research hotspot. Cui et al compared the ability of MODIS/Terra (EOS AM), HJ-1/CCD, Environmental Satellite (ENVISAT) Advanced Synthetic Aperture Radar (ASAR) data to detect massive green macroalgae bloom, and obtained the conclusion that spatial resolution is the main influence factor for the area of detection bloom (Cui et al., 2012). The remote sensing data of the ocean color satellites such as MODIS/Aqua (EOS PM), COMS (Communications, Ocean and Meteorological Satellite)/GOCI, Sentinel-3/OLCI, Landsat8/OLI and GF1/WFV used in this study have different spatial resolution, spectral resolution and time resolution, and also have difference with spatial coverage. What is the capability of these satellite sensors to monitor *U. prolifera* blooms? Which sensor has better performance for algal blooms detection? Is there a way to improve the performance of blooms detection? Is the effect monitored by different optical algorithms consistent? Based on the above five kinds of remote sensing data, this study analyzed the characteristics of the algorithm for qualitative monitoring, discussed the threshold selection of quantitative detection of *U. prolifera* blooms. We used the mixed

http://www.aloki.hu ● ISSN 1589 1623 (Print) ● ISSN 1785 0037 (Online)
DOI: http://dx.doi.org/10.15666/aeer/1804_48974913

pixel decomposition for area statistics, and compared a variety of data to detect the performance of algae on the spatial and temporal scales.

Materials

Study area

The Yellow Sea is located between the Chinese mainland and the Korean peninsula, with a latitude and longitude range of 32°N-37°N and 119°E-123°E. Habitually, the Yellow Sea is divided into two parts, the North Yellow Sea and the South Yellow Sea, with a line connecting the Chengshanjiao of Jiaodong Peninsula to the Changshanchuan of North Korea. The study area selected in this paper is located in the South Yellow Sea (e.g. *Fig. 1*). The sea area is rich in water mass, with coastal currents moving southward along the mainland, black tide branches entering through the Tsushima Strait, and Yangtze River freshwater flowing from the Yangtze River estuary to Jeju Island. According to the China's marine bulletin, from May to July 2017, the *U. prolifera* disaster affected the sea area near the South Yellow Sea, and the coverage area and distribution area reached the maximum on June 19, which were 281 km^2 and 29522 km^2 respectively.

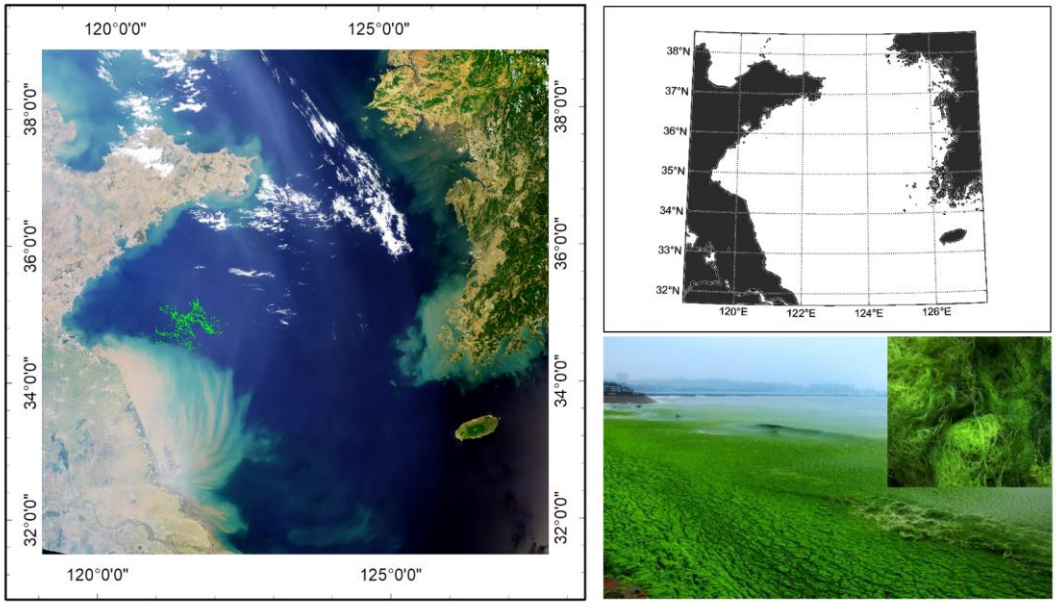

Figure 1. *Overview of the study area, the lower right is an example of green U. prolifera bloom*

Data

The important advances in the design techniques of the second and third generation ocean color satellite sensors have greatly improved the ocean color algorithm, and then the visualization of satellite images can accurately monitor blooms events such as *U. prolifera* bloom in coastal waters. In order to study the effect of the resolution on quantitative estimation of blooming area, this paper selects Aqua/MODIS with 1000 m resolution, COM/GOCI with 500 m resolution, sentinel-3/OLCI with 300 m resolution, Landsat8/OLI with 30 m resolution, GF1/WFV with a resolution of 16 m, five different

http://www.aloki.hu ● ISSN 1589 1623 (Print) ● ISSN 1785 0037 (Online)
DOI: http://dx.doi.org/10.15666/aeer/1804_48974913

spatial resolution data, they also have different spectral resolutions (e.g. *Table 1*) (the five images are imaged on May 27, 2017). The surface wind speed at 0.25° horizontal resolution are obtained from the Advanced Microwave Scanning Radiometer for Earth Observing System (AMSR). The surface wind vectors at 0.25° horizontal resolution are obtained from the Cross Calibrated Multi-Platform (CCMP) which provides consistent, gap-free long-term timeseries of the surface wind vector analysis field from July 1987 to May 2016.

Table 1. *Sensor property analysis*

Instrument	Agency/spacecraft	Spatial resolution (m)	Width (km)	Mission life	Revisit time
WFV	GF1	16	800 (Four-Taiwan Union)	2013-present	4 days
OLI	Landsat8	30	185	2013-present	16 days
OLCI	ESA-Copernicus/Sentinel-3	300	1270	2016-present	Less than 2 days
GOCI	KIOST/COMS	500	2500	2010-present	1 h
MODIS	NASA/Terra; Aqua	1000&500&200	2330	1999-present; 2002-present	1 day

Moderate Resolution Imaging Spectroradiometer (MODIS) is currently mounted on the Earth Observation System (EOS) Terra (AM) and Aqua (PM) satellites to transmit real-time data to the world via the X-band. Its main goal is to achieve a comprehensive view of solar radiation, the atmosphere, the ocean and the land from a single series of polar orbital space platforms. MODIS contains 36 bands, including 20 bands of visible light to short-wave infrared, 16 bands of thermal infrared, spatial resolution of 1-2 band of 250 m, 3-7 band of 500 m, and the remaining bands of 1000 m. The Geostationary Ocean Color Imager (GOCI) is the world's first geostationary orbit satellite imaging sensor. The GOCI is loaded on the Communications, Ocean and Meteorological Satellite (COMS) of South Korea launched in June 2010 and operated by the Korea Ocean Satellite Center (KOSC) to observe or monitor the color of the water surrounding the Korean peninsula. The OLCI is mounted on the sentinel-3 satellite. The Sentinel-3 is a polar-orbit, multi-sensor satellite system that includes sensors and optical instruments and developed by the European Space Agency as part of the Copernicus Programme to better manage the environment and understand climate change. The OLI is mounted on the American Earth observation satellite Landsat8, which runs from a near-polar circular orbit synchronized with the sun to ensure imaging of moderate solar elevations in the mid-latitudes of the Northern Hemisphere. OLI uses push-broom sensors and uses NASA's (National Aeronautics and Space Administration) technology in Advanced Land Imager sensors, which helps reduce moving parts and improve ground information. Four 16-m resolution multi-spectral cameras WFV are mounted on China's GF1. Combined with multi-spectral, high spatial resolution and high temporal resolution optical remote sensing technology, it has promoted China's satellite engineering.

http://www.aloki.hu ● ISSN 1589 1623 (Print) ● ISSN 1785 0037 (Online)
DOI: http://dx.doi.org/10.15666/aeer/1804_48974913

Remote sensing images are usually recorded with dimensionless digitized Digital Number (DN) values, and the true reflectivity is required for the algal quantization calculation, so radiometric calibration and atmospheric correction are required. The purpose of radiometric calibration is to convert the DN value into radiance. The atmospheric correction is mainly to eliminate the influence of atmospheric molecules and aerosol scattering on the reflection of the ground object. Before performing these two steps, in order to eliminate terrestrial interference, land mask processing is first performed. Multi-data quantification of algal statistic requires regional matching and therefore requires precise geometric correction to obtain geographic information. Finally, when we analyzed the performance of each resolution data, we can choose good weather condition and the range of the same area covered by the blooming patches is: 34°31'41" N -35°22'17" N, 120 °33'23"E- 122°14'14"E.

Methods

Qualitative analysis

This section specifically discusses two optical methods of detection: the band-ratio algorithms and spectral band difference algorithms.

The commonly used band ratio forms of blooming events have a ratio vegetation index RVI, a normalized vegetation index (NDVI; Rouse Jr et al., 1974), and a redeveloped enhanced vegetation index (EVI; Baret and Guyot, 1991), all of which utilize the "red edge" that appears in the near-infrared band of algae. The specific form is as follows:

$$RVI = R_{NIR} / R_R \quad \text{(Eq.1)}$$

$$NDVI = (R_{NIR} - R_R) / (R_{NIR} + R_R) \quad \text{(Eq.2)}$$

$$EVI = G \times (R_{NIR} - R_R) / (R_{NIR} + c_1 \times R_R - c_2 \times R_B + c_3) \quad \text{(Eq.3)}$$

In *Equations 1-3,* R_B, R_R and R_{NIR} are surface radiation in the blue, red and near infrared bands, respectively, c_3 is the canopy background adjustment that handles the nonlinear, differential near-infrared, and red radiation transmission through the canopy. c_1 and c_2 are coefficients of the aerosol resistance term. It uses blue bands to correct the aerosol effects in the red band. The coefficients adopted in the MODIS-EVI algorithm are; $c_3 = 1$, $c_1 = 6$, $c_2 = 7.5$, and G (gain factor) = 2.5. The range of NDVI is between -1 and 1, and the pixels covered by the U. prolifera patches are usually positive, thus distinguishing them from the ocean pixels.

The reflectance spectrum of a mixed pixel with algae changes significantly compared to the surrounding pure seawater. Compared to scattering, absorption varies more rapidly with wavelength, and two adjacent reflection spectral bands may have similar backscattering properties, but are significantly different in absorption, which can be quantified by spectral band differences. Different algorithms can be designed using spectral band differences. It is concluded that several algorithms for detecting algae have similar mathematical expressions.

Hu et al. proposed the Floating Algae Index (FAI) for macroalgae (greater than 4000 km^2) based on MODIS data. FAI uses the estimation of the difference between

http://www.aloki.hu ● ISSN 1589 1623 (Print) ● ISSN 1785 0037 (Online)
DOI: http://dx.doi.org/10.15666/aeer/1804_48974913

reflectance of near-infrared band and the linear baseline of red to short-wave infrared. Zhang Hailong et al. also proposed the Multispectral Green Tide Index (MGTI) based on GF/WFV and HJ/CCD data, defined as the difference between the reflectance of the green band and the linear baseline of the red to blue band. Fluorescence Line Height (FLH) and Maximum Chlorophyll Index (MCI; Gower et al., 2005) for red tide also have the same mathematical form (e.g. *Eqs. 4-7*).

$$FAI = R_{NIR} - R'_{NIR} \quad \text{(Eq.4)}$$

$$R'_{NIR} = R_R + (R_{SWIR} - R_R) \times \frac{\lambda_{NIR} - \lambda_R}{\lambda_{SWIR} - \lambda_R} \quad \text{(Eq.5)}$$

$$MGTI = R_G - R'_G \quad \text{(Eq.6)}$$

$$R'_G = R_G - R_B + (R_R - R_B) \times \frac{\lambda_G - \lambda_B}{\lambda_R - \lambda_B} \quad \text{(Eq.7)}$$

R_B, R_G, R_R, R_{NIR}, and R_{SWIR} are the reflectance of blue, green, red, near-infrared, and short-wave infrared, respectively. For MODIS data, Hu et al. proposed λ_R = 645 nm, λ_{NIR} = 859 nm, λ_{SWIR} = 1240 nm. Since 1240 nm results in a lower baseline and a higher FAI value, 1240 nm instead of 1640 nm or 2130 nm is selected for MODIS data. According to GF-WFV data, Zhang Hailong et al. proposed λ_B = 475 nm, λ_G = 560 nm, λ_R = 660 nm. When the spectral band difference algorithms are applied to GOCI, Sentinel3 and Landsat8, the optimal replacement band is given through comparative analysis.

Threshold selection

Threshold selection is critical to the impact of green macroalgae bloom monitoring results. For any type of optical sensor, optical algorithms such as NDVI are more or less affected by atmospheric aerosols and turbid waters, and changes in environmental factors on satellite images can lead to irregularities in algorithmic results.

When using traditional single thresholds for classification, because the sea water mass of the Yellow Sea is complex, the degree of turbidity is high, the NDVI values of many seawater pixels are positive, and they are classified as macroalgae pixels, so the region calculation with smaller thresholds contains incorrect seawater pixels, but if the threshold is too large, some algal patches with less biomass will not be detected. We framed two mixed areas (Region A, Region B, e.g. *Fig. 2*), and performed statistical histogram processing on the NDVI of the two areas, it obtained the bimodal image features (e.g. *Fig. 3*), which will be unfavorable to quantitative analysis, because it is difficult to choose a single threshold to determine the type of feature. We try to use an image processing algorithm to make the columnar statistics of the algorithm into a single peak shape to achieve semi-automatic threshold selection, which lays a good foundation for our area statistics.

The Scaled Algae Index (SAI) is a semi-automatic image processing algorithm that removes the high variability of images (Garcia et al., 2013). The SAI algorithm is derived from normalized difference algae index (NDAI; Shi and Wang, 2009), based on

http://www.aloki.hu ● ISSN 1589 1623 (Print) ● ISSN 1785 0037 (Online)
DOI: http://dx.doi.org/10.15666/aeer/1804_48974913

the algorithm results of the spectral band difference algorithms and the band-ratio algorithms obtained in Sections 3.1 and 3.2. By subtracting the local ocean pixel from the desired point, the ocean pixel is reduced to 0, algae pixels are positive. SAI takes the pixel on the optical algorithm result graph as the center, first selects the template size which match the odd-squared pixel region, performs the median convolution calculations in the spatial domain, and then subtracts the median image from the original algorithm image. (Note: terrestrial and cloud pixels are excluded from convolution calculations).

After the SAI image processing, it was found that the histogram of the region A region B is centered at 0 and the peaks overlap (e.g. *Fig. 3*), eliminating the high variability of the image. Three pure ocean regions, a, b, and c were selected, and the mixed seawater region d were selected, and their histogram distributions were compared (e.g. *Fig. 4*). After the SAI, the pixel values of the seawater in the regions a, b, and c are balanced, so we can use the tail end of the ocean pixel statistical value as the threshold to extract the algae. For any type of optical image, using the SAI algorithm will reduce the variability of the environment, making the selection of a single threshold always more reliable, and the area results are always more stable and accurate.

Mixed pixel decomposition

When using the MODIS data of 1000 m resolution to detect the blooming event, the study area of the algal patches is small, and there is a large number of mixed pixels, which makes large errors based on low resolution data, leading to misjudgment of some features. This study attempts to use the mixed pixel decomposition (Li et al., 2007; Tan et al., 2013) to calculate the blooming area on the basis of qualitatively classifying the algal pixels. The basic features are extracted from the pixels, and the proportion of the calculated features is called hyperspectral unmixing. The basic features are called endmembers, and the endmembers can be understood as pure pixels. The abundance is the proportion of each endmembers. In this paper, we choose two kinds of endmembers of *U. prolifera* and seawater. The maximum image size after SAI treatment is selected as the pure endmember of algae. The specific area calculation is divided into two steps. First, the pixels larger than the threshold in the image are designated as algae pixels, which are less than or equal to the threshold are specified as seawater pixels. The algae pixels are then scaled, and the abundance or scaling ration is limited by the largest pixels in the image.

$$S_{coverage} = \frac{SAI_{algae} - SAI_{threshold}}{MAX\ SAI_{algae} - SAI_{threshold}} * S_{piexl} \quad \text{(Eq.8)}$$

In *Equation 8,* S_{piexl} is the spatial resolution of the sensor (for example, Landsat8 is 30*30 m^2), $SAI_{threshold}$ refers to the threshold obtained in Section 3.3, and MAX SAI_{algae} refers to the pixel value of the largest image after SAI processing.

Results

Influence of spatial resolution

From the South Yellow Sea study area, randomly select 12 areas without clouds or less clouds (e.g. *Table 2*). The MODIS/Aqua, COMS/GOCI, Sentinel-3/OLCI, Landsat8/OLI and GF1/WFV images corresponding to the 12 sub-areas were subjected to atmospheric

http://www.aloki.hu ● ISSN 1589 1623 (Print) ● ISSN 1785 0037 (Online)
DOI: http://dx.doi.org/10.15666/aeer/1804_48974913

correction, geometric correction, terrestrial mask, and cloud mask pretreatment, then NDVI and SAI threshold methods were used to extract bloom information.

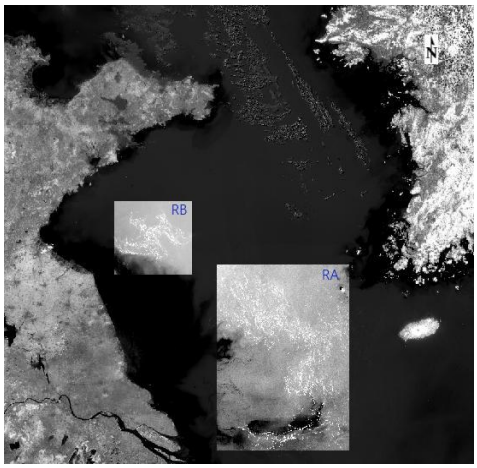

Figure 2. *The distribution of region A (31°25'41" N- 4°28'57"N, 122°40'30" - 125°10'45" E) and B (35°19'3"N - 34°29'2"N,120°39'20"E - 122°11'36"E)*

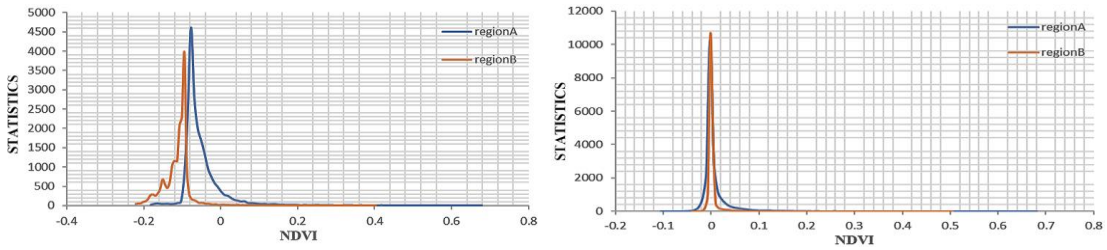

Figure 3. *NDVI statistical image of region A and B (take GOCI as an example). Left: statistics without SAI. Right: statistics through SAI*

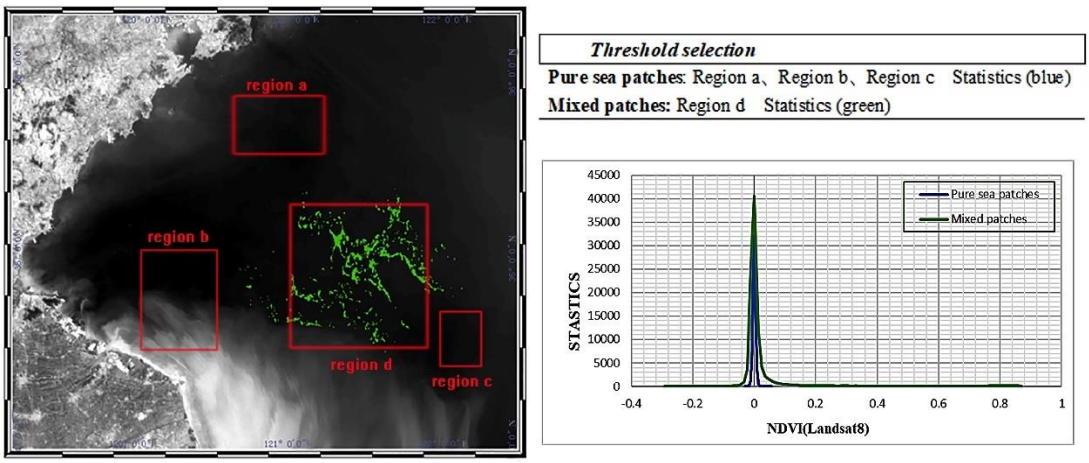

Figure 4. *Distribution of region a (35°43'5" N - 35°59'13"N, 120°24'31"E - 120°56'4"E), region b (34°33'4"N - 35°3'1"N, 119°52'59"E - 120°21'58"E), region c (34°13'59"N - 34°37'36"N, 122°16'25"W - 122°34'56"W), region d (35°19'3"N - 34°29'2"N, 122°11'36"E - 120°39'20"E) and threshold selection (take landsat8 as an example, to do histogram distribution of mixed patches and pure seawater patches)*

http://www.aloki.hu ● ISSN 1589 1623 (Print) ● ISSN 1785 0037 (Online)
DOI: http://dx.doi.org/10.15666/aeer/1804_48974913

Table 2. *Distribution of 12 sub-areas*

	Longitude	Latitude
Region 1	120°53′50″-121°16′17	35°7′34″-35°20′31″
Region 2	120°53′37″-121°18′56″	34°44′5″-34°50′99″
Region 3	121°28′17″-121°50′42″	35°4′15″-35°10′30″
Region 4	121°49′29″-122°13′72″	34°43′20″-35°6′41″
Region 5	121°9′57″-121°34′22″	34°50′17″-34°59′12″
Region 6	121°25′3″-121°37′1″	34°44′29″-34°53′55″
Region 7	121°27′28″-121°46′20″	35°6′29″-35°22′20″
Region 8	121°10′6″-121°36′40″	34°40′54″-34°51′25″
Region 9	121°20′27″-121°30′29″	34°46′59″-35°7′28″
Region 10	121°43′57″-122°0′59″	34°46′10″-34°55′26″
Region 11	120°48′22″-121°4′46″	34°45′20″-34°55′7″
Region 12	121°31′48″-121°45′42″	34°55′17″-35°1′27″

Table 3 compares the area of the algae in each of the 12 sub-areas detected by each optical sensor. We use the following form (e.g. *Eq. 9*) to compare the accuracy of different sensor algal detection areas:

$$\in = \frac{S - S_m}{S_m} \quad \text{(Eq.9)}$$

where S is the area statistics of each sensor detecting algae, S_m is the area "true value", and the algorithm will take the result of GF1/WFV as the "true value". The regression analysis of the area results of each sensor detection is shown in *Figure 5*. Based on the GF1 data of 16 m resolution, the average accuracy of algal area in different sub-areas extracted from landsat8 with a resolution of 30 m is 5.62%, and the statistical area was about 1.05 times that of GF1 result. The average precision of algal area in different sub-areas extracted from Sentinel3 with 300 m resolution was 92.9%, and the statistical area was about 1.7 times that of GF1 result. The average precision of algal area in different sub-areas extracted from GOCI with a resolution of 500 m was 172.28%, and the statistical area was about 2.3 times that of GF1 result. The average precision of algal area in different sub-areas extracted from MODIS with 1000 m resolution is 253.28%, and the statistical area is about 3 times that of GF1 result.

From the statistical results of the algal area in the 12 sub-regions of the *Table 3,* it can be seen that the spatial resolution of the satellite sensor is the main reason that affects the detection area of the green macroalgae bloom. The lower the spatial resolution, the higher the detection area. The 16 m resolution GF1 data is similar to the 30 m resolution Landsat8 data inversion of the algae, and is also the closest to the real value. The 1000 m resolution MODIS data inversion has the largest area and the lowest precision, and the overestimated error is generated relative to the 16 m resolution GF1 data. This overestimation problem can be mitigated by using mixed pixel decomposition, but it cannot be completely solved. In addition to spatial resolution, there are other factors that affect the detection area of bloom. There may be performance impact of the sensor itself, or due to the small difference in transit time between the various sensors. Due to the influence of environmental factors such as

http://www.aloki.hu ● ISSN 1589 1623 (Print) ● ISSN 1785 0037 (Online)
DOI: http://dx.doi.org/10.15666/aeer/1804_48974913

wind, flow and temperature on the sea surface, the dynamic change of this event is large, and it is difficult to accurately register between different sensors. Smaller time differences may result in changes in the biomass of the algae or algal patches rise and fall, causing deviations in pixel recognition.

Table 3. *Algal statistical results of 12 sub-areas (km^2)*

	Landsat8/OLI	*sentinel-3/OLCI*	*COMS/GOCI*	*Aqua/MODIS*	*GF1/WFV*
Region 1	4.677	7.584	11.441	16.863	4.217
Region 2	6.676	11.223	15.584	19.2183	6.226
Region 3	3.287	6.553	9.618	12.229	3.045
Region 4	3.582	6.537	10.708	14.437	3.395
Region 5	7.951	13.387	15.101	23.484	7.353
Region 6	2.783	6.568	9.301	10.290	2.730
Region 7	4.415	7.442	11.478	17.290	4.273
Region 8	8.088	13.328	15.588	21.729	8.085
Region 9	8.179	12.061	15.650	20.568	7.542
Region 10	2.887	6.874	8.016	9.586	2.731
Region 11	4.612	7.093	11.475	14.233	4.286
Region 12	2.717	5.620	9.129	10.219	2.698

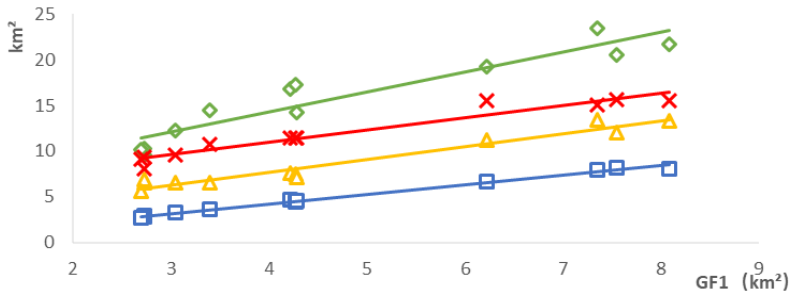

Figure 5. *Regression analysis of each sensor and GF1 sub-areas. Landsat8 (blue), MODIS (green), GOCI (red), sentinel3 (yellow)*

We selected a small area and used MODIS/Aqua, COMS/GOCI, Sentinel-3/OLCI, Landsat8/OLI and GF1/WFV data to perform NDVI calculations. The results of qualitative bloom detection are shown in *Figure 6*. Compared with the results of five different spatial resolutions of algae, the MODIS data with 1000 m resolution can only roughly reflect the drift direction of this bloom. The 500 m resolution GOCI and 300 m resolution Sentinel-3 data mostly show the jagged shape due to pixel mosaic. The Landsat8 data at 30 m resolution and the GF1 data at 16 m resolution can show a strip-like bloom drift path, showing more algae details. The higher the spatial resolution, the more detail the observable algal patches are, and the shape of the algal patches is more defined.

Comparison of U. prolifera bloom detection algorithm

The selection time was May 27, 2017, and the data of MODIS/Aqua, COMS/GOCI, Sentinel-3/OLCI, Landsat8/OLI, and GF1/WFV were used to invert the *U. prolifera* patches in the study area. Qualitative detection of blooming event used the spectral band

http://www.aloki.hu ● ISSN 1589 1623 (Print) ● ISSN 1785 0037 (Online)
DOI: http://dx.doi.org/10.15666/aeer/1804_48974913

difference algorithms and the band-ratio algorithms. The band-ratio algorithm is represented by NDVI, and the spectral band difference algorithm is represented by FAI and MGTI. Only a few ocean color sensors have the spectral requirements to meet the algorithm. Sentinel-3/OLCI, GF1/WFV, COMS/GOCI and other sensor bands are limited, while MODIS/Auqa and Landsat8/OLI can provide more spectral segments, so Sentinel-3/OLCI, GF1/WFV, COMS/GOCI take the MGTI as an example when the spectral band difference algorithm is used. For the spectral band difference algorithm of MODIS/Auqa and Landsat8/OLI, FAI is taken as an example.

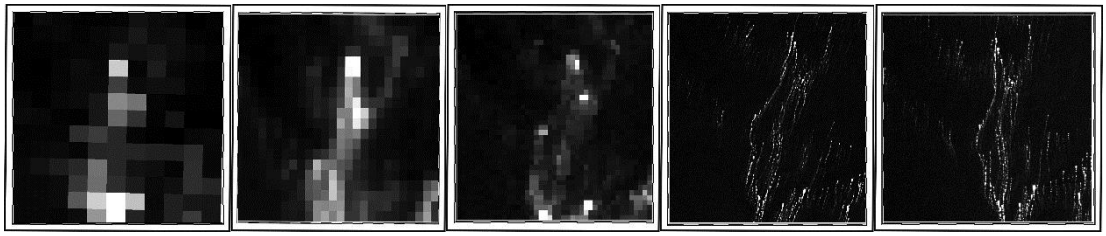

Figure 6. *From left to right, MODIS, GOCI, Sentinel3, Landsat8, GF1 NDVI detection results. Bloom (white), sea water (black) (35°10'47"N- 35°17'15"N, 120°55'41"E- 121°3'39"E)*

The results of the algal area of the study area calculated by each sensor are shown in *Table 4*. The spectral band difference algorithm of the single sensor is consistent with the area statistical result of the band-ratio algorithm, and the reliability of the extraction result is also confirmed to some extent. As shown in *Figure 7,* each sensor qualitatively detects the blooming distribution in the study area. Under the same sensor condition, the results of qualitative detection of algae by different optical algorithms are highly consistent. Compared with the band-ratio algorithm, the spectral band difference algorithm is less sensitive to observation conditions and environment, and can be seen through the "thin cloud".

U. prolifera bloom dynamic monitoring

Different time intervals for repeated observations of fixed areas on the ground by different ocean color sensors, plus cloud cover and other factors will affect the continuous and effective detection of bloom. The time resolutions of the five satellite sensors are different. The revisit time of GF1 is 4 days, the revisit time of Landsat8 is 16 days, the revisit time of Sentinel3 is less than two days, the revisit time of GOCI is 1 h, and the revisit time of MODIS is 1 day. Finding the data of each sensor from May to July 2017, and drawing the dynamic bloom drift path, the results indicate that the GOCI data can better detect the dynamic drift of the bloom(e.g. *Fig.8 (a)*), which most important reason is that it has the most valid data. The widths of MODIS, Sentinel3, and GOCI are large, and they can cover most areas where the algae, but MODIS and Sentinel3 have less available data compared with GOCI (e.g. *Fig. 8 (b, c)*). Landsat8, GF1, and Sentinel3 have small time resolution and less available data (GF1, Landsat is not shown in the figure because the data volume is too small), and because GOCI is a geostationary orbit sensor, compared to the other four sensors, it eliminates the effect of orbital movement and can efficiently target areas of interest probe. Although the time resolution of MODIS data is large, it is not recommended to use it for dynamic monitoring of algae due to the impact of cloud coverage and low spatial resolution.

http://www.aloki.hu ● ISSN 1589 1623 (Print) ● ISSN 1785 0037 (Online)
DOI: http://dx.doi.org/10.15666/aeer/1804_48974913

The cloudless GOCI image or GOCI images with few clouds in time range were selected from the Korean Ocean Satellite website. After preprocessing the images, the NDVI method was selected to extract the algal information. This study selected 6 days of yellow sea green algae bloom detection results on May 17, 2017, May 26, 2017, May 28, 2017, June 14, 2017, June 27, 2017 and July 12, 2017 for display.

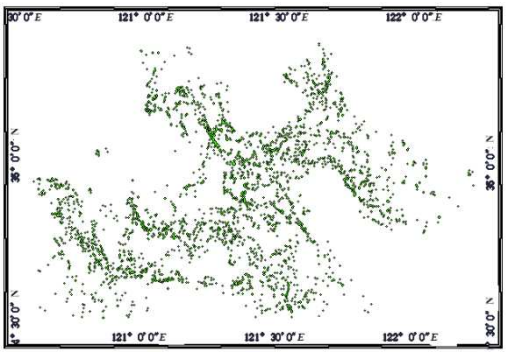

(a1) GF1/WFV NDVI results

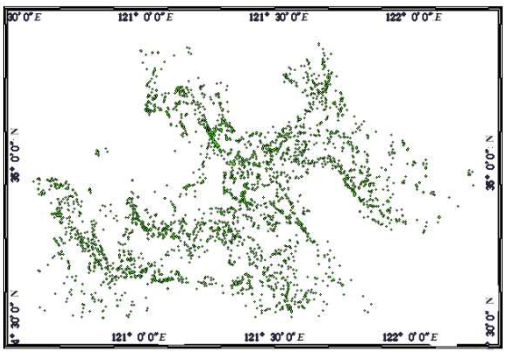

(a2) GF1/WFV MGTI results

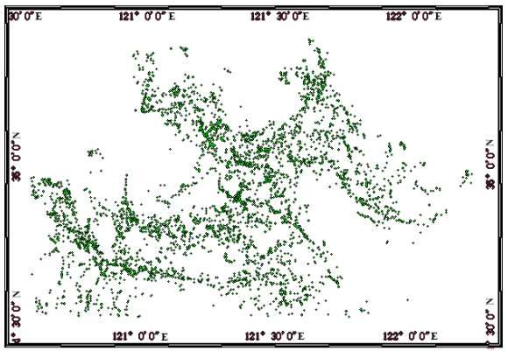

(b1) Landsat8/OLI NDVI results

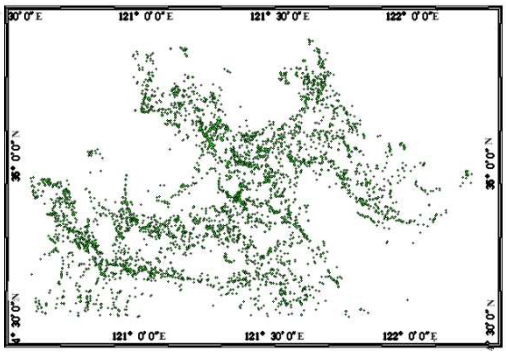

(b2) Landsat8/OLI FAI results

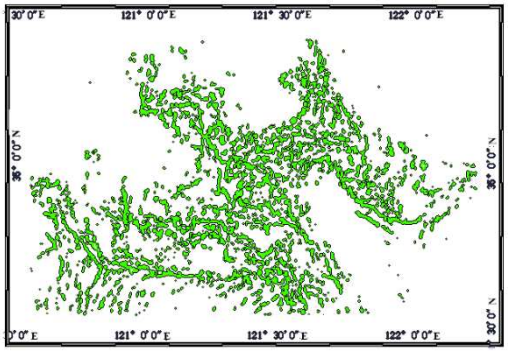

(c1) sentinel3/OLCI NDVI results

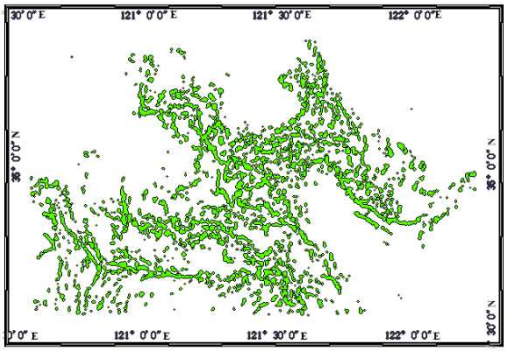

(c2) sentinel3/OLCI MGTI results

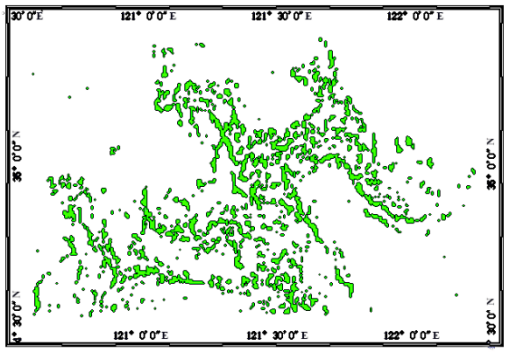

(d1) COM/GOCI NDVI results

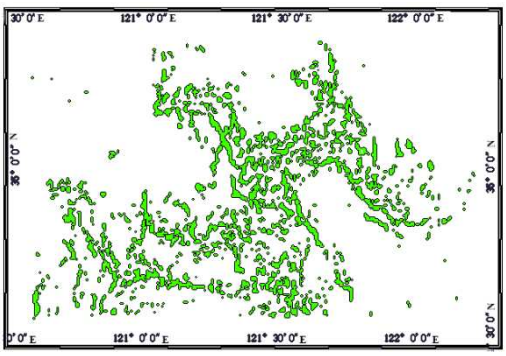

(d2) COM/GOCI MGTI results

http://www.aloki.hu ● ISSN 1589 1623 (Print) ● ISSN 1785 0037 (Online)
DOI: http://dx.doi.org/10.15666/aeer/1804_48974913

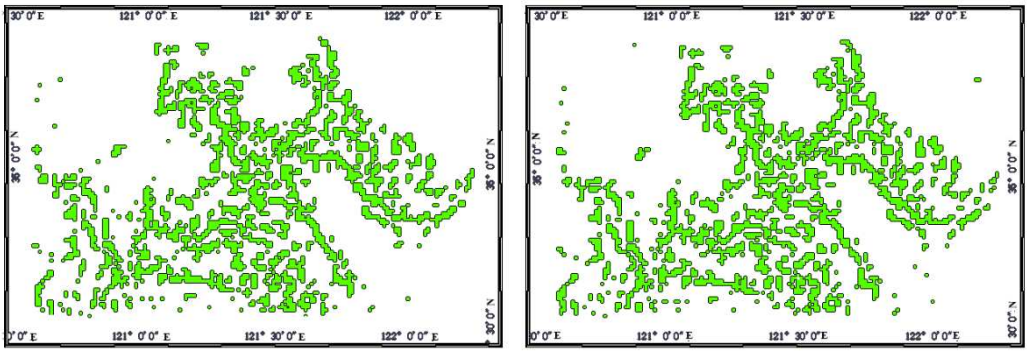

(e1) Aqua/MODIS NDVI results (e2) Aqua/MODIS FAI results

Figure 7. *Qualitative monitoring results of each sensor*

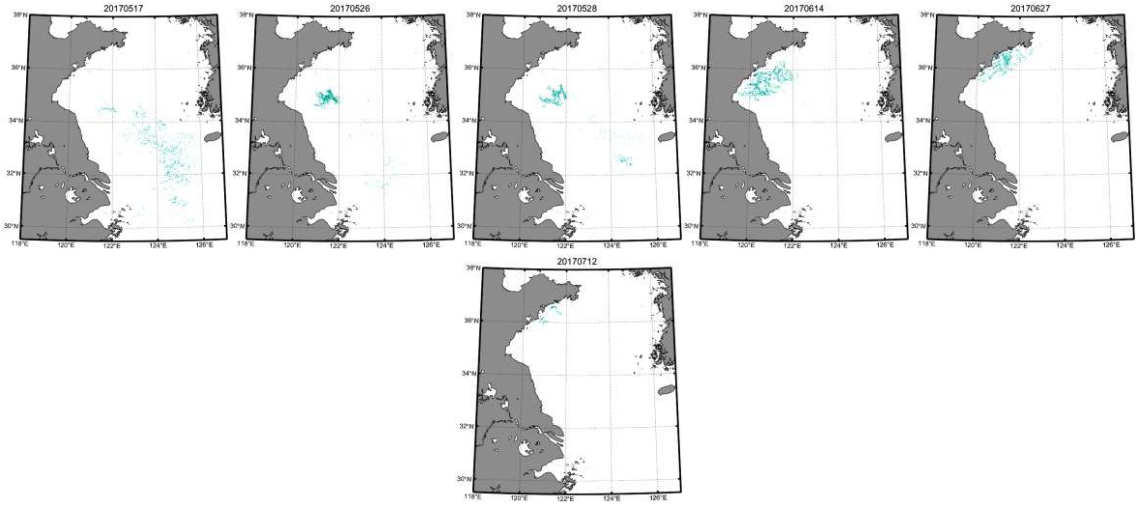

(a) Dynamic drift distribution of bloom obtained from GOCI data

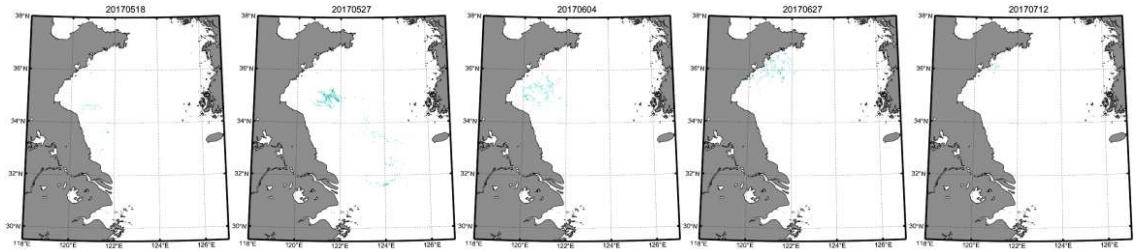

(b) Dynamic drift distribution of bloom obtained from Sentinel3 data

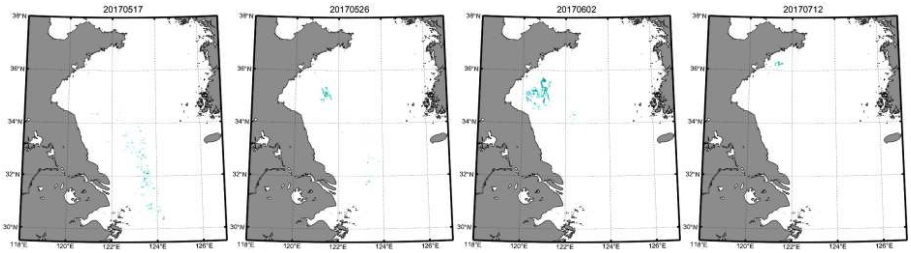

(c) Dynamic drift distribution of bloom obtained from Sentinel3 data

Figure 8. *U. prolifera distribution map from May to July 2017 obtained from GOCI, Sentinel3 and MODIS respectively*

http://www.aloki.hu ● ISSN 1589 1623 (Print) ● ISSN 1785 0037 (Online)
DOI: http://dx.doi.org/10.15666/aeer/1804_48974913

Table 4. *Statistical results of U. prolifera patches area in the study area*

Instrument	Method	Spatial resolution (m)	Area statistics results (km^2)
GF1/WFV	NDVI	16	40.939
Landsat8/OLI	NDVI	30	43.378
Sentinel-3/OLCI	NDVI	300	81.322
COMS/GOCI	NDVI	500	87.266
Aqua/MODIS	NDVI	1000	128.708
GF1/WFV	MGTI	16	41.549
Landsat8/OLI	FAI	30	43.399
Sentinel-3/OLCI	MGTI	300	80.547
COMS/GOCI	MGTI	500	83.903
Aqua/MODIS	FAI	1000	130.55

The composites of algae and sea surface wind are shown in *Figure 9,* it indicates the numerical simulation of the sea surface wind has a high correlation with the movement of the macroalgae bloom. A green macroalgae bloom appeared in May and died in July, its drift path is roughly northward along the land.

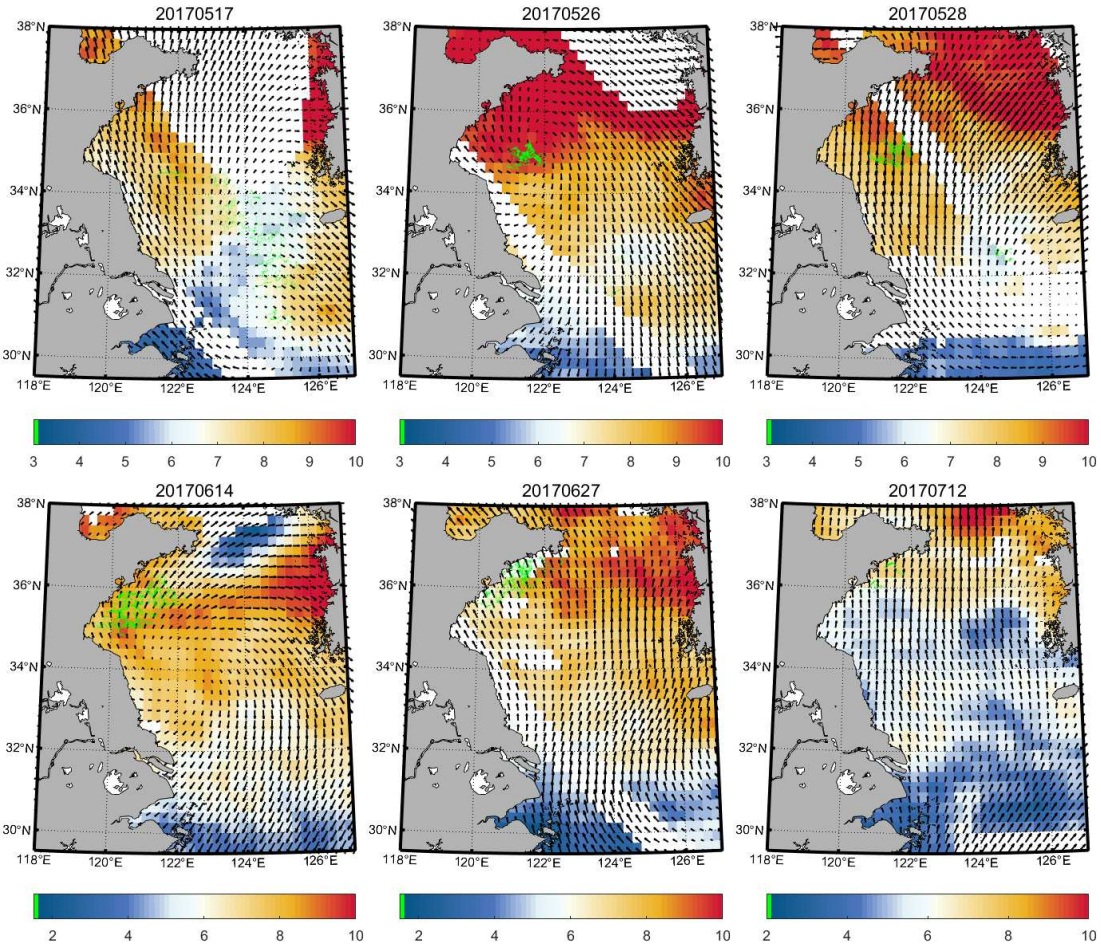

Figure 9. *The map of the surface geostrophic current speed (color), velocities (vectors) and algae obtained from GOCI data (green)*

http://www.aloki.hu ● ISSN 1589 1623 (Print) ● ISSN 1785 0037 (Online)
DOI: http://dx.doi.org/10.15666/aeer/1804_48974913

It can be seen from *Figure 9* that in May the bloom erupted and moved northward under the transport of prevailing wind (southerly and southeastern wind), that also proves that the prevailing wind is the main driving force for the movement of this event (Xing et al., 2009). Green macroalgae grows rapidly in mid-May, moves northward under the control of environmental factors, and gradually gathers in the waters near Lianyungang, from May 26th to May 28th, the drift speed of the algae was very small and there was almost no drift, which also accorded with the wind direction. The biomass of algae has reached its maximum in mid-June, and it continues to move northward and spreads. In late June and early July, the wind was blowing towards the land, it gradually disappeared due to human fishing and other reasons. A comprehensive analysis of the distribution and the biomass can be found that they are all approximately normal distribution. The distribution of *U. prolifera* is first dispersed, then aggregated and redispersed, and the biomass of algae is first increased and then decreased. This is consistent with the process of emergence, development, outbreak, and extinction of *U. prolifera*.

Discussion

In the process of using optical algorithm to detect algae, cloud pixels will cause misjudgment. Cloud pixels are displayed as high values in both FAI and NDVI. If the pixel mosaic shape is just a thin strip, it may be misunderstood as a algae pixel. The current cloud concealing algorithm is very rich, but it does not distinguish the cloud pixel completely. The algorithm of the monitor algae, we can use the RGB image for cross-checking.

More types of sensors and data assimilation methods should be used to establish relevant detection systems to deal with algal outbreaks and reduce the possibility of damage to the marine environment. In addition to optical remote sensing satellites, there are many other platforms that provide data for detecting *U. prolifera* blooms. In recent years, unmanned aerial vehicle (UAV) have become one of the important tools for obtaining high-resolution remote sensing data due to their small size, low operating cost and high flexibility. Some scholars have used UAV to conduct monitoring research on *U. prolifera* disasters. UAV observations can effectively compensate for the lack of spatial resolution and temporal resolution of traditional satellite remote sensing methods in blooming events monitoring. Optical data can detect algae suspended in the sea below a certain depth. Microwave cannot penetrate the sea surface, so it can only detect algal patches floating on the surface. However, microwave remote sensing is not affected by weather conditions and can penetrate the cloud. Microwave data such as SAR images are a good complement to all-weather monitoring of blooming events. Because the imaging mechanism of microwave image and optical image is different, we need a large number of simultaneous optical and microwave data analysis to obtain more accurate results of blooming events detection.

Conclusion

Since algal blooms is characterized by rapid growth, it is important to monitor potential algae bloom events early through satellite data. For qualitative monitoring of *U. prolifera* bloom, the use of optical algorithms for detection is reliable, and the results of the band-ratio algorithm and the spectral band difference algorithm are similar. It is important to accurately target the bands of green vegetation, the higher the spectral

http://www.aloki.hu ● ISSN 1589 1623 (Print) ● ISSN 1785 0037 (Online)
DOI: http://dx.doi.org/10.15666/aeer/1804_48974913

resolution data, the better the qualitative algae patches. For quantitative monitoring of *U. prolifera* bloom, the results of low spatial resolution data detection of area are too large, which attempted to use the mixed pixel decomposition to calculate the area to weaken the overestimation phenomenon, but this overestimation cannot be eliminated. For effective monitoring and forecasting to save time, it is recommended to use high spatial resolution sensors, of course sensor revisit time (related to the detection time interval) and the width of the image (related to the detection range) are important. Sea surface wind determines the dynamic movement direction of algae. Using satellite data numerical simulation to monitor the state of sea surface wind can effectively monitor the drift of green macroalgae.

Acknowledgements. This work was supported by the National Key R&D Program of China [Grant numbers 2017YFC1404100, 2017YFC1404104]; the Key R&D Program of Shandong [Grant numbers 2019GHY112049]; Scientific Research Foundation of Shandong University of Science and Technology for Recruited Talents [Grant numbers 2015RCJJ016]; National Natural Science Foundation of China (Grant numbers 41576024); Guangxi Key R&D Program (Project Contract numbers: Gui ke AB16380282).

REFERENCES

[1] Baret, F., Guyot, G. (1991): Potentials and limits of vegetation indices for LAI and APAR assessment. – Remote Sensing of Environment 35: 161-173.

[2] Blondeau-Patissier, D., Gower, J. F., Dekker, A. G., Phinn, S. R., Brando, V. E. (2014): A review of ocean color remote sensing methods and statistical techniques for the detection, mapping and analysis of phytoplankton blooms in coastal and open oceans. – Progress in Oceanography 123: 123-144.

[3] Cui, T. W., Zhang, J., Sun, L. E., Jia, Y. J., Zhao, W., Wang, Z. L., Meng, J. M. (2012): Satellite monitoring of massive green macroalgae bloom (GMB): imaging ability comparison of multi-source data and drifting velocity estimation International. – Journal of Remote Sensing 33: 5513-5527.

[4] Garcia, R. A., Fearns, P., Keesing, J. K., Liu, D. (2013): Quantification of floating macroalgae blooms using the scaled algae index. – Journal of Geophysical Research: Oceans 118: 26-42.

[5] Gower, J., King, S., Borstad, G., Brown, L. (2005): Detection of intense plankton blooms using the 709 nm band of the MERIS imaging spectrometer. – International Journal of Remote Sensing 26: 2005-2012.

[6] Hu, C. (2009): A novel ocean color index to detect floating algae in the global oceans. – Remote Sensing of Environment 113: 2118-2129.

[7] Hu, C., He, M. X. (2008): Origin and offshore extent of floating algae in Olympic sailing area. – Eos, Transactions American Geophysical Union 89: 302-303.

[8] Hu, C., Cannizzaro, J., Carder, K. L., Muller-Karger, F. E., Hardy, R. (2010a): Remote detection of Trichodesmium blooms in optically complex coastal waters: examples with MODIS full-spectral data. – Remote Sensing of Environment 114: 2048-2058.

[9] Hu, C., Li, D., Chen, C., Ge, J., Muller-Karger, F. E., Liu, J., He, M. X. (2010b): On the recurrent *Ulva prolifera* blooms in the Yellow Sea and East China Sea – Journal of Geophysical Research: Oceans 115: C5.

[10] Keesing, J. K., Liu, D., Fearns, P., Garcia, R. (2011): Inter- and intra-annual patterns of *Ulva prolifera* green tides in the Yellow Sea during 2007-2009, their origin and relationship to the expansion of coastal seaweed aquaculture in China. – Marine pollution bulletin 62: 1169-1182.

http://www.aloki.hu ● ISSN 1589 1623 (Print) ● ISSN 1785 0037 (Online)
DOI: http://dx.doi.org/10.15666/aeer/1804_48974913

[11] Li, S., Li, W. Z., Zhou, J. J., Zhuang, D. F. (2007): A review on endmember selection methods in the course of mixed pixel decomposition of remote sensing images. – Geography and Geo-Information Science 23(5): 35-38.
[12] Liang, Z., Lin, X., Ma, M., Zhang, J., Yan, X., Liu, T. (2008): A preliminary study of the *Enteromorpha prolifera* drift gathering causing the green tide phenomenon. – Periodical of Ocean University of China 38: 601-604.
[13] Liu, D., Keesing, J. K., Xing, Q., Shi, P. (2009): World's largest macroalgal bloom caused by expansion of seaweed aquaculture in China. – Marine Pollution Bulletin 58: 888-895.
[14] Naihao, T. Q. Z. X. Y., Zhimeng, Z. (2010): Review on the research progress on marine green tide. – Bulletin of National Natural Science Foundation of China 1: 5-9.
[15] Rouse, J. W., Haas, R. H., Schell, J. A., Deering, D. W. (1974): Monitoring vegetation systems in the Great Plains with ERTS. – NASA special publication 1974: 351-309.
[16] Shi, W., Wang, M. (2009): Green macroalgae blooms in the Yellow Sea during the spring and summer of 2008. – Journal of Geophysical Research 114: C12.
[17] Shimada, S., Yokoyama, N., Arai, S., Hiraoka, M. (2008): Phylogeography of the Genus Ulva (Ulvophyceae, Chlorophyta), with Special Reference to the Japanese Freshwater and Brackish Taxa. – In: Borowitzka, M. A. et al. (eds.) Nineteenth International Seaweed Symposium, 2008. Springer, Dordrecht, pp. 529-539.
[18] Tan, X., Yu, X. C., Zhang, P. (2013): A classification algorithm for hyperspectral images based on fuzzy mixed pixel decomposition. – Journal of Geomatics Science and Technology 30: 279-283.
[19] Xiao, Y. F., Zhang, J., Cui, T. W., Gong, J. L., Xia, S. Z., Liu, R. J., Mu, B (2017): Spectral characteristics and estimation models of floating green tide biomass on sea surface. – Acta Optica Sinica 37(4): 338-346.
[20] Xing, Q., Loisel, H., Schmitt, F., Shi, P., Liu, D., Keesing, J. (2009): Detection of the green tide at the Yellow Sea and tracking its wind-forced drifting by remote sensing. – EGU General Assembly Conference Abstracts 11: 577.
[21] Zhang, H., Sun, D., Li, J., Qiu, Z., Wang, S., He, Y. (2016): Remote sensing algorithm for detecting green tide in China coastal waters based on GF1-WFV and HJ-CCD data. – Acta Optica Sinica 36: 28-36.

http://www.aloki.hu ● ISSN 1589 1623 (Print) ● ISSN 1785 0037 (Online)
DOI: http://dx.doi.org/10.15666/aeer/1804_48974913

EFFECT OF HEAVY METALS ON SOIL MICROBIAL BIOMASS, AND NEMATODE TROPHIC GROUPS OF A PADDY SOIL AFFECTED BY LONG-RUNNING POLYMETALLIC MINING ACTIVITIES IN GUANGDONG, SOUTHERN CHINA

ZENG, Q. P.[1] – ZHU, L. A.[1*] – WANG, J. Z.[2] – CHENG, J.[1*] – LIU, Y.[1] – ZHANG, H. H.[1] – LIN, L. W.[1]

[1]*National-Regional Joint Engineering Research Center for Soil Pollution Control and Remediation in South China; Guangdong Key Laboratory of Integrated Agro-Environmental Pollution Control and Management, Guangdong Institute of Eco-Environmental Science & Technology, Guangdong Academy of Sciences, Guangzhou 510650, China*

[2]*Zhongkai University of Agriculture and Engineering, Guangzhou 510650, China*

**Corresponding authors*
e-mail: Lazhu@soil.gd.cn; 85951452@qq.com

(Received 9th Jan 2020; accepted 6th May 2020)

Abstract. While the effects of heavy metals on soil organisms are relatively well-documented, the effects of heavy metals caused by long-term sewage irrigation are poorly understood. Therefore, we collected two kinds of soil samples from a paddy field which was irrigated with sewage for more than 20 years (SIA) and the adjacent non-sewage irrigated land as control (NSIA) in Shaoguan, southern China, to assess the long-term effects of multiple metal mining activities on soil microbial biomass, nematode assemblages. The available Cu and Zn, and the total Cu, Zn, Pb and As contents in SIA were higher than those in NSIA area by 13.60, 7.69, 8.56, 2.35, 2.96 and 3.11 times on average. Heavy metals stimulated microbial biomass and nematode biomass consumption, which caused a shift in nematode groups, and the mean content of soil microbial biomass carbon (C) and nitrogen (N) in SIA drops by 25.76%, 11.10% compared to the NSIA. Organics showed a positive effect on soil microbial biomass C and N, with the same response for all types of nematodes, Available Cu and Zn, and the total Cu, Zn, Pb and As content in soils exhibited a negative effect on soil microbial biomass C and N, and each group of nematodes, which reveal that the microbial/nematode activities had been disrupted by the heavy metals.
Keywords: *long-running polymetallic mining activities, a paddy soil, mine sewage irrigation, heavy metals, soil microbial biomass, nematodes assemblages, effects, southern China*

Introduction

Ore mining making a great contribution to the economy in China, 173 kinds of minerals have been discovered and a variety of metallic minerals (e.g. copper, zinc, lead, etc.) ranked first in the world till 2017 (China Mineral Resources, CMR, 2018). In Shaoguan, a municipality in Guangdong, southern China, polymetallic mining activities have provided livelihoods for local residents since the 1958's in record (Chen, 2012).

Exploitations of ore resource accelerate industrialization process of China and improved Chinese's living standard, but it remains a momentous issue owing to incidences of health problems and environmental degradation (Cortes-Maramba et al., 2006). Ore mining is related to the increasing of soil heavy metals in environment, in general, they are deposited in ore and harmless, yet destabilized heavy metals produced by extraction pose a tremendous threat due to their potential to bioaccumulate, resistant to degradation, last for long period, high in concealment and interfere with biological processes (Heikens et al., 2001). As a result of obsolete equipment, underdeveloped

http://www.aloki.hu ● ISSN 1589 1623 (Print) ● ISSN 1785 0037 (Online)
DOI: http://dx.doi.org/10.15666/aeer/1804_49154927

technologies, unsubstantial environmental awareness etc., much tailing produced and end up in the soil, atmosphere or river (Getaneh et al., 2006; Martinez et al., 2018). According to statistics, in China, approximately 20,000,000 ha of arable land are polluted by heavy metal, accounting for 1/5 of total arable lands, including 3,300,000 ha of sewage irrigation farmland, especially in red-soil regions, where the soil is worst-polluted (Wen et al., 2008).

Mt. Dabao mine, an old large-scale region for copper exploit before Tang and Song dynasties, abandoned in 1465's, reconstructed in May 1958 and completed in 1975 (Chen, 2012). Ore mining of Mt. Dabao mine was mainly dominated by surface mining and supplemented by underground mining, where the ore is made up of pyrrhotite, pyrite, chalcopyrite, as well as minor components of galena, limonite, chalcocite, calaverite, sphalerite, and native bismuth in mineral deposits (Zhou et al., 2007). Since mining began in 1976, a large amount of acid mine drainages and mine wastes have generated without any proper treatment and dispersed downslope into the Hengshi River, which is mainly employed to irrigate agricultural land for vegetables and crops (Zhuang et al., 2009). Past investigations have demonstrated that about 83 villages, 585×10^4 m^2 paddy fields, and 21×10^4 m^2 ponds were polluted owing to mining activities around the mine (Zhou et al., 2004). Until 2006, water diversion irrigation realized in Mt. Dabao mine, yet cumulative effects of heavy metals pollution and environmental ecological impact will last for a considerable time (Chen, 2012). In recent years, the researchers mostly concentrated on research polluted characteristics of soil (Zhou et al., 2007), water (Chen et al., 2007), plant (Zhuang et al., 2009, 2013), distribution (Liao et al., 2016; Li et al., 2009) and migration (Chen et al., 2015, 2018; Wang et al., 2019) of heavy metals, assessment of soil heavy metals contamination (Zhao et al., 2012; Shu et al., 2018) etc., few information is available either on nematodes structure or soil microbial mass of the mine sites.

Soil microbial biomass is the source and library of nutrients available for plant growth (Thakura et al., 2019), drives substance conversion and nutrient circulation in soil, and represents active parts of soil nutrients, including soil biomass carbon and nitrogen (Singh et al., 2018). Nematodes, the most abundant and ubiquitous multicellular organisms in soil, which distributed widely, identified easily with sample structure, and play a critical role in soil functioning. Nematodes can regulates bacterial and fungal populations, impact the decomposition of organic matter and influence nitrogen-carbon cycle in soil (Chen et al., 1999; Ingham et al., 1985; Savin et al., 2001). Soil microbial biomass and nematode communities, the center among soil-based biological communities, a sensor to disturbance of soil ecosystem, are sensitive to environmental changes, and using its change trend to evaluate soil quality and pollution has been a hot spot in international researches in the field of different soil ecosystem, e.g. farmland, forest, grassland, wetland, etc. (Yang et al., 2018; Wu et al., 2019; Čerevková et al., 2020). Nevertheless, the change of soil microbial biomass and nematode communities are poorly understood in agricultural field ecosystem which was irrigated with sewage for more than 20 years in polymetallic mining areas.

Our objectives were to (a) determine the extent of pollution, comprehensively that of Cu, Zn, Pb, and As (Wang et al., 2016) caused by sewage irrigation owing to polymetallic mining; (b) assess the long-term influences of metals pollution on the soil microbial and nematode communities; (c) infer the relationship among soil microbial biomass, nematode parameters and soil physicochemical factors following sewage irrigating.

http://www.aloki.hu ● ISSN 1589 1623 (Print) ● ISSN 1785 0037 (Online)
DOI: http://dx.doi.org/10.15666/aeer/1804_49154927

Materials and methods

Study sites and soil sampling

The area of Mt. Dabao mine (113°40′~113°43′E, 24°30′~24°36′N) is situated in the northern part of Guangdong, southern China. The region has a subtropical monsoon climate with an average annual temperature of 20.3 ℃ and precipitation of 1782.7 mm. Our sampling area is on both side of Hengshui River and predominantly covered with paddy (*Fig. 1*). Parts of the selected area have been subjected to sewage irrigation owing to polymetallic mining and processing upstream, while other areas irrigated with unpolluted water were uninfluenced and regarded as non-polluted control. The soils at study area are waterloggogenic paddy in gray brown, distributed fairly evenly throughout all sewage area and basically within sandy sticky clay loam to clay loam (*Fig. 2*).

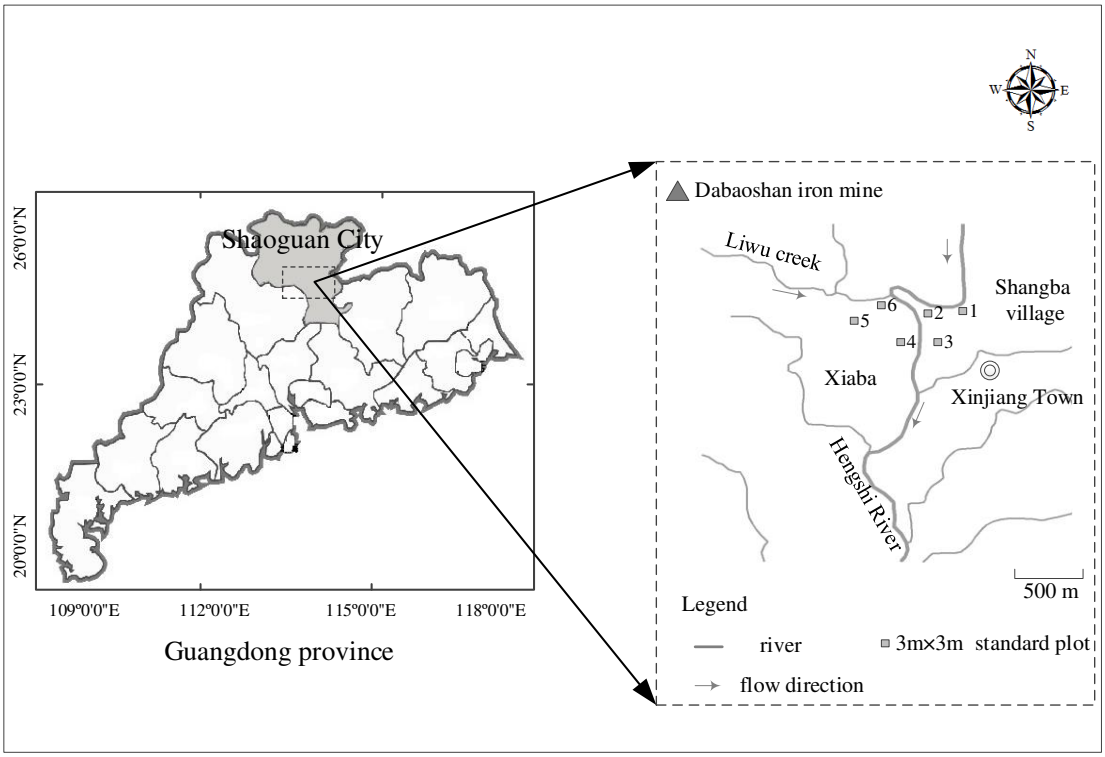

Figure 1. *Map of research plots at Dabaoshan polymetallic mine area*

Soil samplings were taken in March, 2006. The study area was divided into 6 sampling areas-S1, S2, S3, S4, S5 and S6 (*Table 1*). 6 soil samplings, each consist of 3 composite sampling, were randomly collected in excess of 10 m interdistance from each area. S4, S5 and S6 were situated in right of Hengshui River near Xiaba Village, which were irrigated with wastewater discharge from Mt. Dabao mining activities upstream, thus we a priori referred to them as 'sewage irrigation' area (SIA) as opposed to the 'non-sewage irrigation' area (NSIA), S1, S2 and S3. 6 composite samples each consist of 1000 g (a composite of 3 samples combined), were obtained from the upper 10 cm using a wooden shovel. Soil samples were put into ziplocked plastic bags and sealed tightly in a preservation box until laboratory processing. From each soil samples, 500 g

http://www.aloki.hu ● ISSN 1589 1623 (Print) ● ISSN 1785 0037 (Online)
DOI: http://dx.doi.org/10.15666/aeer/1804_49154927

were stored in 4 °C and used to the measurement of soil microbial biomass and nematode communities, another were used for nutrients, soil characteristics and heavy metal analyses.

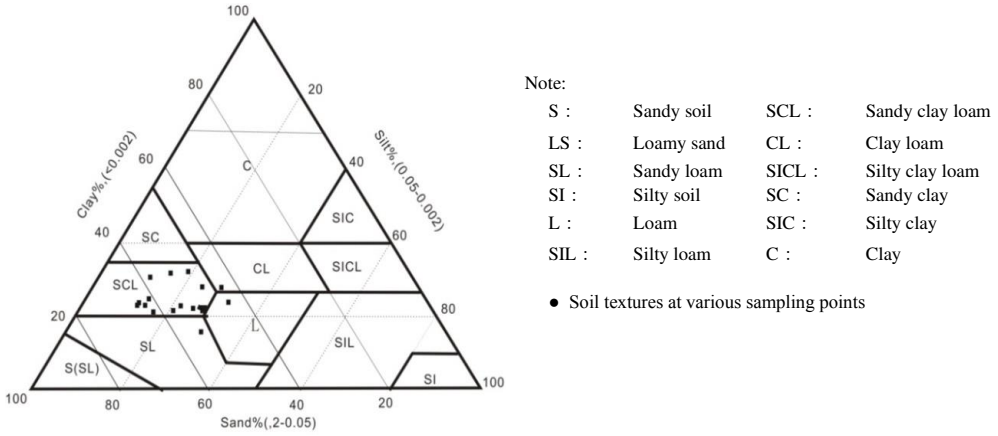

Figure 2. *Triangle diagram of soil texture distribution at sampling points of Dabaoshan polymetallic mine area*

Soil properties

Soil pH of the subsamples was measured in the soil suspension of a 1:2.5 soil: water mixture by PHS-25 (ISRIC, 1995). Soil water content (S.W.C) of the subsamples was detected gravimetrically as percentage of dry mass by drying the samples to a constant weight at 105 ℃. Soil organic matter (S.O.M) of the subsamples was measured by the Walkley–Black's procedure (Nelson et al., 1982). Soil content of total N was obtained by the Kjeldahl method (Bremner et al., 1982) Soil content of available Cu and Zn were analyzed using an atomic adsorption spectrophotometer (AAS, jena vario). Soil content of Cu, Zn were determined using a flame atomic adsorption spectrophotometer (AAS, jena vario 6). Soil content of Pb was measured using graphite furnace atomic absorption spectrophotometer (GFAAs, Jena ZEENIT 60). Soil content of As was detected using a spectrophotometer (AFS-8230).

Soil microbial

Soil microbial biomass was analyzed using a chloroform fumigation- K_2SO_4 extraction method. 50-g fresh soil subsamples were adjusted to 40% water-holding capacity and fumigated in a $CHCl_3$-saturated atmosphere in a desiccator for 24 h at 25 ℃ in the dark, CO_2 released from cells lyse of soil microbial death was absorbed by sodium hydroxide solution. Then, the fumigated and corresponding nonfumigated (control) subsamples were transferred to 0.2-L glass jars and add 0.1 L K_2SO_4 (0.5 mol·L^{-1}), keep the soil suspension of a 1:4 soil:water mixture, vibrating (300 r·min^{-1}) at 25 ℃ for 30 min, filtrated and measured immediately or stored at -18 ℃.

Soil microbial biomass (C_{mic}) was measured by Carbon- automatic analysis (Phoenix 8000) and C_{mic} was calculated as

$$C_{mic} = [(CO_2\text{-C from fumigated soil}) - (CO_2\text{-C from control sample})] / kc \quad \text{(Eq.1)}$$

http://www.aloki.hu ● ISSN 1589 1623 (Print) ● ISSN 1785 0037 (Online)
DOI: http://dx.doi.org/10.15666/aeer/1804_49154927

Extract sample nitrified with 0.2 ml $CuSO_4$ (0.19 $mol \cdot L^{-1}$) and 5 ml H_2SO_4, then using Flow injection nitrogen analyzer (FIAStar 500) to determined soil microbial biomass (N_{mic}), and N_{mic} was calculated as

$$N_{mic} = [(NH_4^+\text{-N from fumigated soil}) - (NH_4^+\text{-N from control sample})] / kc \quad \text{(Eq.2)}$$

by using kc of 0.45 (Zang et al.; 2015).

Soil microbial C/N ratio can be used as indicator to evaluate the capability and effectiveness of nitrogen supply in soil (Xiao et al., 2003), and calculated as

$$C / N = C_{mic} / N_{mic} \quad \text{(Eq.3)}$$

The change of microbial quotient reflects the conversion efficiency of organic substances input into the soil to microbial biomass carbon, the greater it is, the faster the soil organic carbon circulates (Gao et al., 2015), and Q_{mic} calculated as

$$Q_{mic} = C_{mic} / T_{S.O.C} \quad \text{(Eq.4)}$$

The conversion coefficient SOM and $T_{S.O.C}$ was 1.724 (Qiu et al., 2015).

Nematodes

In ecological studies, soil nematodes are usually divided into 5 trophic groups, usually Bacterivores (BF), Fungivores (FF), Plant-parasites (PP), Omnivores and Predators are considered as the mayor trophic habits (Chen et al., 2003; Hodda et al., 1994; Porazinska et al., 1999; Nagy et al., 2004; Weiss et al., 1991). The nematode community was analyzed by absolute abundance of individuals 100 g^{-1} dry soil.

Statistical analysis

The data presented in this work are reported as oven-dried weight. All data in this work were subjected to statistical analysis of variance using the SPSS procedure (version 18.0, IBM). The sampling data measured for normality using a Kruskal Wallis test (version 12, Statistica). Significant differences among soil samples were identified by one way analysis of variance (ANOVA) to detect the differences in soil concentration of heavy metals, soil conmicrobial biomass and soil nematodes assemblages among SIA and NSIA followed by Least Significant Difference (LSD) tests ($P < 0.05$), the relations between soil microbial biomass C & N and soil nematode community structure versus soil environmental factors were inferred by Spearman correlation.

Results

Effects of 20 years' sewage irrigation on soil physical and chemical properties and heavy metal concentration in paddy fields

There is a significant difference in soil pH between NSIA and SIA, and the soil of both areas is basically acidic, while the pH value of SIA is lower than that of NSIA (*Table 1*). In the case of permanent framing, sewage irrigation has no significant effect on soil organic matter, total nitrogen and soil water content. There are significant differences in available Cu and Zn, and the total Cu, Zn, Pb and As contents in the

http://www.aloki.hu ● ISSN 1589 1623 (Print) ● ISSN 1785 0037 (Online)
DOI: http://dx.doi.org/10.15666/aeer/1804_49154927

0~10 cm deep soil of paddy fields between SIA and NSIA. The concentration of heavy metals ranged between 2.93-67.17 mg/kg for available Cu, 1.66-22.00 mg/kg for available Zn, 21.27-280.67 mg/kg for Cu, 68.47-315.00 mg/kg for Zn, 41.20-212.67 mg/kg for Pb, 14.67-74.10 mg/kg for As. The available Cu and Zn, and the total Cu, Zn, Pb and As contents in paddy fields of SIA are higher than those in paddy fields of NSIA by 13.60, 7.69, 8.56, 2.35, 2.96 and 3.11 times on average. Soil in the SIA is stronger in acidity and suffers higher pollution overall.

Table 1. *Statistical summary of the general descriptive parameters and heavy metal contents. Mean values for SIA and NSIA*

Soil properties	NSIA			SIA		
	S1	S2	S3	S4	S5	S6
Basic soil properties						
pH	5.73 ± 0.12 a	5.42 ± 0.39 b	5.65 ± 0.20 a	5.71 ± 0.24 a	4.63 ± 0.30 c	4.75 ± 0.36 c
S.W.C (%)	0.17 ± 0.00 a	0.20 ± 0.01 a	0.29 ± 0.02 a	0.34 ± 0.12 a	0.28 ± 0.08 a	0.30 ± 0.04 a
S.O.M (g/kg)	22.3 ± 1.14 c	19.7 ± 2.43 d	28.6 ± 0.39 a	25.8 ± 0.38 b	27.0 ± 1.81 ab	21.5 ± 3.11 c
N (g/kg)	1.22 ± 0.01 a	1.23 ± 0.10 a	1.61 ± 0.10 a	1.50 ± 0.42 a	1.44 ± 0.50 a	1.23 ± 0.13 a
Available Cu (mg/kg)	3.06 ± 0.19 e	2.93 ± 0.31 e	5.59 ± 0.40 d	41.23 ± 21.34 c	49.17 ± 12.43 b	67.17 ± 14.67 a
Available Zn (mg/kg)	2.66 ± 0.32 e	1.66 ± 0.14 f	2.97 ± 0.18 d	12.80 ± 8.50 c	21.26 ± 21.17 b	22.00 ± 7.79 a
Heavy metals(mg/kg)						
Cu	21.27 ± 2.14 f	23.07 ± 1.86 e	34.33 ± 2.87 d	173.33 ± 56.37 c	219.00 ± 33.06 b	280.67 ± 23.35 a
Zn	139.23 ± 68.21 d	68.47 ± 10.11 f	119.00 ± 1.00 e	206.67 ± 61.58 c	247.00 ± 85.16 b	315.00 ± 19.16 a
Pb	61.67 ± 8.36 d	41.20 ± 16.18 f	47.87 ± 6.51 e	107.27 ± 25.54 c	126.67 ± 21.03 b	212.67 ± 22.48 a
As	14.67 ± 0.64 f	16.77 ± 3.10 d	15.47 ± 2.30 e	20.53 ± 5.15 c	51.23 ± 16.55 b	74.10 ± 17.96 a

Total soil sampling 18. Mean ± standard deviation, S.W.C soil water content, S.O.M soil organic matter, (a, b and c). Significant difference ($p < 0.01$) between 6 sampling sites

Effect of 20 years' sewage irrigation on soil biomass C and N in paddy fields

In the NSIA and SIA, from *Equation 1,* the soil microbial biomass C content ranges in 740.3~1,600.3 mg/kg and 705.8~1093.3 mg/kg with a mean of 1,154.3 mg/kg and 856.9 mg/kg respectively; from *Equation 2,* the soil microbial biomass N content ranges in 92.04~217.63 mg/kg and 141.83~167.14 mg/kg with a mean of 174.28 mg/kg and 154.93 mg/kg respectively, and both the means and mathematical statistics suggest that there is a significant difference between heavy metals effects on soil microbial biomass C and N of paddy fields. From *Equation 3,* in the NSIA and SIA, the soil microbial biomass C/N ratio ranges in 0.34~1.74 and 0.42~0.77 with a mean of 0.87 and 0.56, respectively. From *Equation 4,* the soil microbial quotient ranges in 5.72~9.82 and 5.16~6.98 with a mean of 8.40 and 5.93, respectively (*Fig. 3*).

Effect of 20 years' sewage irrigation on different groups of soil nematode in paddy fields

There are significant differences in quantity of various soil nematodes between the SIA and NSIA (*Fig. 4*), the NSIA is 2.73 times of the SIA in quantity of soil nematodes, and the density of soil nematodes in both areas follows the rule below: bacterivores > plant parasites > predators > omnivores. The density of bacterivores, plant-parasites and fungivores in the NSIA are clearly higher than that in the SIA by 2.44, 0.80 and 4.48 times respectively, but the quantity of omnivores and predators was not so different and that of fungivores changes greatly.

http://www.aloki.hu ● ISSN 1589 1623 (Print) ● ISSN 1785 0037 (Online)
DOI: http://dx.doi.org/10.15666/aeer/1804_49154927

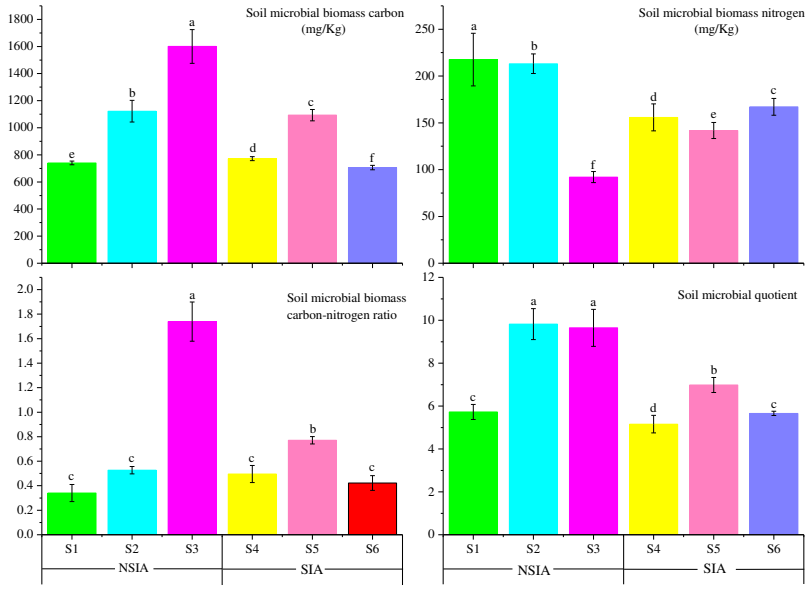

Figure 3. *Characteristics of soil microbial biomass C and N, soil microbial C/N ratio, microbial quotient in SIA and NSIA. (Different lower-case letters refer to the level of significance 5% that the difference between standard samples reaches)*

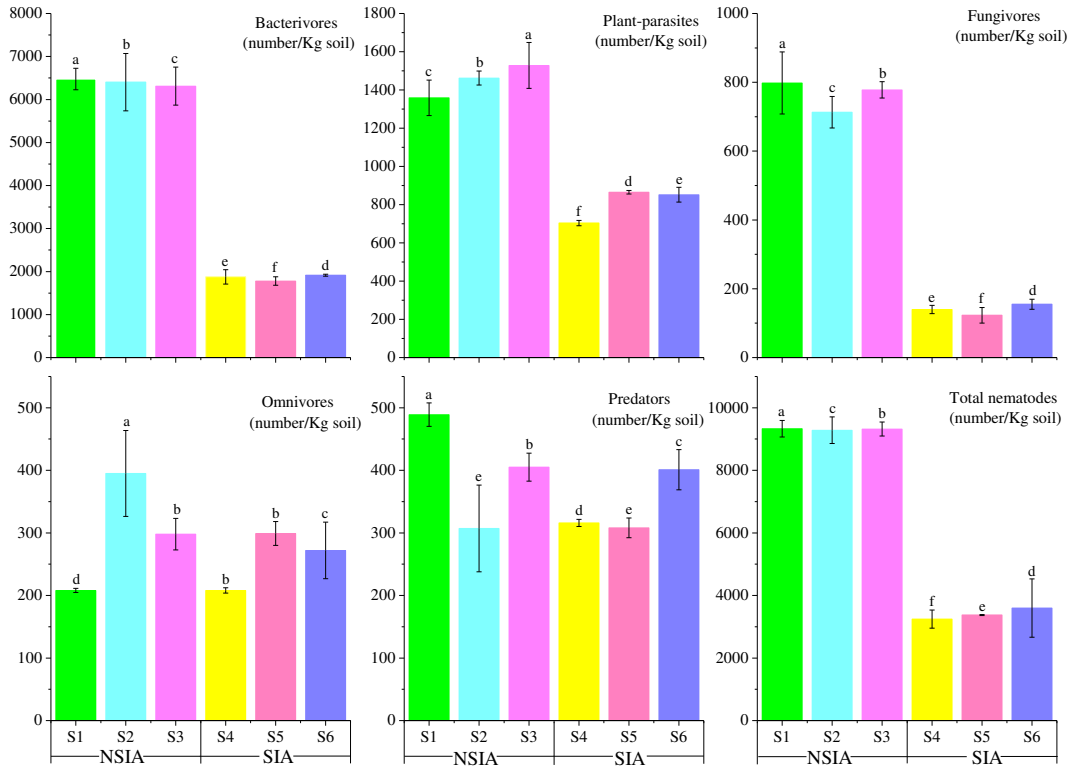

Figure 4. *Characteristics of each type of nematodes in SIA and NSIA. (Note: Different lower-case letters refer to the level of significance 5% that the difference between standard samples reaches)*

http://www.aloki.hu ● ISSN 1589 1623 (Print) ● ISSN 1785 0037 (Online)
DOI: http://dx.doi.org/10.15666/aeer/1804_49154927

Correlation analysis of soil microbial biomass C & N and nematode group structure versus soil environmental factors

Soil microbial biomass C has significant positive correlation with organics and significant negative correlation with available Cu, and the total Zn, Pb contents; soil microbial biomass N has significant positive correlation with organics; bacterivores, fungivores and the total quantity of nematodes have extremely significant positive correlation with pH and extremely significant negative correlation with available Cu and Zn, and the total Cu, Zn, Pb and As contents; plant parasites has significant positive correlation with pH and extremely significant negative correlation with available Cu and Zn, and the total Cu, Zn, Pb and As contents (*Table 2*).

Table 2. *Correlation of soil microbial biomass C & N and soil nematode community structure versus soil environmental factors*

	pH	Organics	Total nitrogen	Water content	Available Cu	Available Zn	Cu	Zn	Pb	As
Soil microbial biomass C	0.137	0.530*	0.121	0.033	-0.471*	-0.397	-0.450	-0.509*	-0.545*	-0.358
Soil microbial biomass N	0.114	0.647*	0.126	0.177	-0.215	-0.240	-0.226	-0.214	-0.098	-0.118
Bacterivores	0.622**	-0.208	-0.024	-0.435	-0.951**	-0.940**	-0.952**	-0.885**	-0.824**	-0.725**
Plant parasites	0.475*	-0.131	-0.012	-0.397	-0.894**	-0.863**	-0.889**	-0.839**	-0.773**	-0.615**
Fungivores	0.634**	-0.164	-0.018	-0.425	-0.943**	-0.932**	-0.944**	-0.858**	-0.809**	-0.719**
Omnivores	-0.276	-0.272	-0.032	-0.144	-0.241	-0.194	-0.222	-0.401	-0.258	0.006
Predators	0.312	-0.099	-0.045	-0.251	-0.290	-0.308	-0.304	-0.041	-0.052	-0.104
Total quantity of nematodes	0.599**	-0.200	-0.023	-0.433	-0.942**	-0.928**	-0.942**	-0.874**	-0.812**	-0.704**

* and ** means the significance at the level of 5% and 1% respectively, n = 18

Discussion

(1) Heavy metals that are resistant to degradation and difficult to migrate accumulate continually in soil and become permanent pollutants, not only change soil's physical and chemical properties, affecting crops growth, but also enter human bodies via the food chain and endanger human health and life (Huang et al., 2018). The result of the research indicates that, after 20 years' irrigation with mine sewage, the mean content of soil microbial biomass C in paddy fields of the SIA drops by 25.76% compared with the NSIA, and the mean content of soil microbial biomass N drops by 11.10%. These manifest that composite heavy metals of high contents have significantly affected soil microbial biomass C and N, because soil microbes in paddy fields of the mine area has long suffered intimidation of heavy metals, and composite heavy metals of high contents have led to changed size of soil microbial groups by destroying protein structure and functions as well as the integrity of cytomembranes, etc., thus affecting the form, growth, and development, and metabolism of microbes in soil (Leita et al., 1995). The results from researches of Jiang et al. (2010) and Wang et al. (2003) on microbe communities in soil polluted by composite heavy metals also proved this. The reduction of microbial quotient due to the concentration of heavy metals indicates that the content of heavy metals in high concentration limits the circulation rate of organic carbon in soil, which may be correlated with the intimidation on microbial biomass imposed by heavy metals. Results from many researches demonstrate that as the concentration of heavy metals rise, the quantity of fungus with higher resistance in soil

http://www.aloki.hu ● ISSN 1589 1623 (Print) ● ISSN 1785 0037 (Online)
DOI: http://dx.doi.org/10.15666/aeer/1804_49154927

increases, thus rendering the increase (Khan et al., 1998) of microbial biomass C/N ratio. Results from some researches prove, however, the decrease (Wang et al., 2003) of microbial biomass C/N ratio with increasing content of heavy metals. The result from this experiment is consistent with the research result of the latter, i.e. the effect of heavy metals in high concentration decreases soil microbial biomass C/N ratio (44%), which may be attributable to farming habits or multiple actions of composite heavy metals changed some functional groups of soil microbial communities and community structure.

(2) Soil nematodes are small secondary biological groups leeching on to soil environments and its communities are more vulnerable to effect of soil's physical and chemical properties. The sewage in the mine area contain available Cu and Zn, and the total Cu, Zn, Pb and As with high concentration, all of which enter soil directly in various areas in running water, affecting structure of nematode communities in soil. The result from this research indicates that bacterivores, plant parasites, fungivores, omnivores and predators in soil of the SIA are 244.29%, 79.64%, 447.61%, 15.66% and 17.17% lower than those in the NSIA respectively; and in both the SIA and NSIA, bacterivores are the most in quantity and fungivores vary the most in quantity possibly because a vast majority of organisms in soil is bacteria and therefore bacterivores are dominant in various trophic types regardless of SIA or NSIA; omnivores and predators are most sensitive to the environment (Popovici, 1992), the result of this experiment indicate that these two nematodes were least affected, when soil is polluted by heavy metals, under the action of external pressure, the species diversity in the ecosystem diminishes while the dominance of few species rises, according to the "Pressure Hypothesis" advanced by Odum, a renowned ecologist in USA (Pennanen et al., 1996). Therefore, within a certain range of concentration, heavy metals in soil would stimulate the growth of soil nematodes to some degree; in the area surveyed in the experiment, it mainly contributes to growth of some kinds of omnivores and predators in soil.

(3) Results from correlation analysis demonstrate that soil microbial biomass C and N have significant positive correlation with organics, consistent with previous conclusions (Bruggen et al., 2000; Yu et al., 2003), indicating microbial biomass C and N can represent soil's fertility; the significant negative correlation of soil microbial biomass C with available Cu, Zn and Pb proves that the available Cu, Zn and Pb in heavy metals with high concentration interfere with soil organism activity, the result from the research of Kao et al. (2006) indicates the addition of heavy metals into soil will reduce considerably soil biomass C and N, and Guo et al. (2018) gets the same conclusion from the research on effect of addition of exogenous Cd on soil microbes in red-soil paddy fields. Soil nematodes are closely tied to soil's physical and chemical properties which can lead to change in quantity and diversity of nematodes, and of which pH, Zn, Cr, Cu and Pb have considerable effect on soil nematodes (Liu et al., 2012). The results from research indicate, pH has a significant/extremely significant positive correlation with plant parasites, bacterivores, fungivores, total quantity of nematodes, revealing soil pH affects significantly the quantities of nematodes of all nutrient types, and the quantity of soil nematodes is affected by both the total content and the effective form of heavy metals in soil (Yang et al., 2019). Bacterivores, plant parasites, fungivores and total quantity of nematodes have extremely significant negative correlation with available Cu and Zn, and the total Cu, Zn, Pb and As content, which is consistent with the conclusion from researches of Weiss et al. (1991), but totally different with those from researches of Park et al. (2011), Wang et al. (2012) and

http://www.aloki.hu ● ISSN 1589 1623 (Print) ● ISSN 1785 0037 (Online)
DOI: http://dx.doi.org/10.15666/aeer/1804_49154927

Li et al. (2006), possibly because the difference in spatial distribution and soil parent materials of soil for sampling.

Conclusion

Overall, with backward technology, the content of available Cu and Zn, and the total Cu, Zn, Pb and As content in Hengshi River increased sharply owing to long-running polymetallic mining activities. Mine sewage irrigation reduced soil microbial biomass C and N, bacterivores, plant parasites, fungivores, and with no obvious effect on omnivores and predators. The significantly positive correlations between soil microbial biomass C and N with organics indicate that Organic matter is an important source of nutrients for microorganisms. Soil microbial biomass C and N, bacterivores, plant-parasites, fungivores and the total quantity of nematodes has a significant negative correlation with the content of available Cu and Zn, and the total Cu, Zn, Pb and As content, which suggesting that Heavy metal stimulated microbial biomass and nematode biomass consumption.

Our study indicates that mine sewage irrigation led to a decline in soil quality in the diggings. Hence, protection of biodiversity from safe irrigation is urgently needed in farmland ecosystems, as any heavy metals affecting the survival of microorganisms and nematodes will affect the recovery of farmland ecosystems, and more related research should be done in the future.

Acknowledgements. This work was supported by the Natural Science Foundation of Guangdong Province (06025926). Special thanks to teachers FU and ZHOU from South China Botanical Garden, Chinese Academy of Sciences for their guidance and analysis of the nematode experiment.

REFERENCES

[1] Bremner, J. M., Mulvaney, C. S. (1982): Nitrogen: Total Content. – In: Page, A. L., Miller, R. H., Keeney, D. R. (eds.) Methods of Soil Analysis, Part 2. 2nd Ed. Agron. Monogr. 9. Agronomy Society of America and Soil Science Society of America, Madison, WI, pp. 595-624.

[2] Bruggen, A. H. C. V., Semenov, A. M. (2000): In search of biological indicators for soil health and disease suppression. – Applied Soil Ecology 15(1): 0-24.

[3] Čerevková, A., Ivashchenko, K., Miklisová, D., et al. (2020): Influence of invasion by Sosnowsky's hogweed on nematode communities and microbial activity in forest and grassland ecosystems. – Global Ecology and Conservation 21: e00851.

[4] Chen, A., Lin, C., Lu, W., et al. (2007): Well water contaminated by acidic mine water from the Dabaoshan mine, South China: chemistry and toxicity. – Chemosphere 70(2): 248-255.

[5] Chen, J., Ferris, H. (1999): The effect of nematode grazing on nitrogen mineralization during fungal decomposition of organic matter. – Soil Biology and Biochemistry 31: 1265-1279.

[6] Chen, L., Li, Q., Liang, W. (2003): Effect of agrochemicals on nematode community structure in a soybean field. – Bull. Environ. Contam. Toxicol. 71: 755-760.

[7] Chen, M. Q., Lu, G. N., Guo, C. L., et al. (2015): Sulfate migration in a river affected by acid mine drainage from the Dabaoshan mining area, South China. – Chemosphere 119: 734-743.

http://www.aloki.hu ● ISSN 1589 1623 (Print) ● ISSN 1785 0037 (Online)
DOI: http://dx.doi.org/10.15666/aeer/1804_49154927

[8] Chen, M. Q., Lu, G. N., Wu, J. X., et al. (2018): Migration and fate of metallic elements in a waste mud impoundment and affected river downstream: a case study in Dabaoshan mine, South China. – Ecotoxicology and Environmental Safety 164: 474-483.
[9] Chen, S. X. (2012): Soil and Water Loss Characteristics and Heavy Metal Tolerant Plants Selection of Dabaoshan Mine of Guangdong. – Nanjing Forestry University, Nanjing (in Chinese).
[10] Cortes-Maramba, N., Reyes, J. P., Francisco-Rivera, A. T., et al. (2006): Health and environmental assessment of mercury exposure in a gold mining community in Western Mindanao, Philippines. – Journal of Environmental Management 81: 126-134.
[11] Gao, S. J., Cao, W. D., Bai, J. S., et al. (2015): Long-term application of winter green manures changed the soil microbial biomass properties in red paddy soil. – Acta Pedologica Sinica 52(04): 902-910 (in Chinese).
[12] Getaneh, W., Alemayehu, T. (2006): Metal contamination of the environment by placer and primary gold mining in the Adola region of Southern Ethiopia. – Environmental Geology 50: 339-352.
[13] Guo, B. L., Chen, X. M., Jing, F., et al. (2018): Effects of exogenous cadmium on microbial biomass and enzyme activity in red paddy soil. – Journal of Agro-Environment Science 37(09): 1850-1855 (in Chinese).
[14] Heikens, A., Peijnenburg, W. J. G. M., Hendriks, A. J. (2001): Bioaccumulation of heavy metals in terrestrial invertebrates. – Environmental Pollution 113: 385-393.
[15] Hodda, M., Wanless, F. R. (1994): Nematodes from an English chalk grassland, population ecology. – Pedobiologia 38: 530-545.
[16] Huang, Y., Chen, Q. Q., Deng, M. H., et al. (2018): Heavy metal pollution and health risk assessment of agricultural soils in a typical peri-urban area in Southeast China. – Journal of Environmental Management 207: 159-168.
[17] Ingham, R. E., Trofymov, J. A., Ingham, E. R., et al. (1985): Interaction of bacteria, fungi, and their nematode grazers, effects on nutrient cycling and plant growth. – Ecological Monographs 55: 119-140.
[18] ISRIC (1995): Procedures of Soil Analysis. Technical Paper 9. – International Soil Reference and Information Certre, FAO-UN: 9.1-9.13.
[19] Jiang, J., Wu, L., Li, N., et al. (2010): Effects of multiple heavy metal contamination and repeated phytoextraction by Sedum plumbizincicola on soil microbial properties. – European Journal of Soil Biology 46(1): 0-26.
[20] Kao, P. H., Huang, C. C., Hseu, Z. Y. (2006): Response of microbial activities to heavy metals in a neutral loamy soil treated with biosolid. – Chemosphere 64(1): 63-71.
[21] Khan, K. S., Xie, Z. M., Huang, C. Y. (1998): Effects of cadmium, lead, and zinc on size of microbial biomass in red soil. – Pedosphere 8(1): 27-32.
[22] Leita, L., Nobili, M., Muhlbachova, G., et al. (1995): Bioavailability and effects of heavy metals on soil microbial biomass survival during laboratory incubation. – Biology and Fertility of Soils 19(2-3): 103-108.
[23] Li, Y. T., Becquer, T., Dai, J., et al. (2009): Ion activity and distribution of heavy metals in acid mine drainage polluted subtropical soils. – Environmental Pollution 157: 1249-1257.
[24] Li, Q., Jiang, Y., Liang, W. J. (2006): Effect of heavy metals on soil nematode communities in the vicinity of a metallurgical factory. – Journal of Environmental Sciences 18(2): 323-328.
[25] Liao, J. B., Wen, Z. W., Ru, X., et al. (2016): Distribution and migration of heavy metals in soil and crops affected by acid mine drainage: public health implications in Guangdong Province, China. – Ecotoxicology and Environmental Safety 124: 460-469.
[26] Liu, B. B. (2012): Studies on the Characteristics of Soil Nematodes Community by Several Different land Use Types in Jiangsu Province. – NanJing Agricultural University, Nanjing (in Chinese).

http://www.aloki.hu ● ISSN 1589 1623 (Print) ● ISSN 1785 0037 (Online)
DOI: http://dx.doi.org/10.15666/aeer/1804_49154927

[27] Martinez, J. G., Torres, M. T., dos Santos, G., et al. (2018): Influence of heavy metals on nematode community structure in deteriorated soil by gold mining activities in Sibutad, southern Philippines. – Ecological Indicators 91: 712-721.
[28] Ministry of Natural Resources (2018): China Mineral Resources. – Geological Publishing, Beijing (in Chinese). http://www.yueyang.gov.cn/lxzfw/24733/24760/24821/24864/26888/content_1462180.html.
[29] Nagy, M., Bakonyi, G., Bongers, T., et al. (2004): Effects of microelements on soil nematode assemblages seven years after contaminating an agricultural field. – Sci. Tot. Environ. 320: 131-143.
[30] Nelson, D. W., Sommers, L. E. (1982): Total Carbon, Organic Carbon, and Organic Matter. – In: Page, A. L. (ed.) Methods of Soil Analysis, Part 2. 2nd Ed. American Society of Agronomy, Madison, WI, pp. 539-79.
[31] Popovici, I. (1992): Nematodes as indications of ecosystem disturbances due to pollution. – Stud Univ Babes-Royal Biol 37(2): 15-27.
[32] Porazinska, D. L., Duncan, L. W., McSorley, R., et al. (1999): Nematode communities as indicators of status and processes of a soil ecosystems influenced by agricultural management practices. – Applied Soil Ecology 13: 69-86.
[33] Park, B. Y., Lee, J. K., Ro, H. M., et al. (2011): Effects of heavy metal contamination from an abandoned mine on nematode community structure as an indicator of soil ecosystem health. – Applied Soil Ecology 51: 17-24.
[34] Pennanen, T., Frostegard, A., Fritze, H., et al. (1996): Phospholipid fatty acid composition and heavy metal tolerance of soil microbial communities along two heavy metal-polluted gradients in coniferous forests. – Applied and Environmental Microbiology 62(2): 420-428.
[35] Qiu, L. J., Huang, G. L., Shuai, Q., et al. (2015): Reconstruction of the Conversion Relationship between Organic Matter and Total Organic Carbon in Calcination Method and its Application in Shale Analysis. – Rock and Mineral Analysis 34(2): 218-223 (in Chinese).
[36] Savin, M. C., Gorres, J. H., Neher, D. A. et al. (2001): Uncoupling of carbon and nitrogen mineralization: role of microvorous nematodes. – Soil Biology and Biochemistry 33: 1463-1472.
[37] Shu, X. H., Zhang, Q., Lu, G. N., et al. (2018): Pollution characteristics and assessment of sulfide tailings from the Dabaoshan mine, China. – International Biodeterioration & Biodegradation 128: 122-128.
[38] Singh, J. S., Gupta, V. K. (2018): Soil microbial biomass: a key soil driver in management of ecosystem functioning. – Science of the Total Environment 634: 497-500.
[39] Thakura, M. P., Del Real, I. M., Cesarz, S. (2019): Soil microbial, nematode, and enzymatic responses to elevated CO_2, N fertilization, warming, and reduced precipitation. – Soil Biology and Biochemistry 135: 184-193.
[40] Wang, C. L., Dong, Z. C., Xia, X. Q. (2012): Soil contamination by heavy metals in jinan city and its biological characteristics. – Geology in China 39(03): 818-826.
[41] Wang, G. B., Lu, L., Wei, G. L., et al. (2016): Analysis and evaluation of heavy metal pollution for water and soils in Dabaoshan sewage irrigation area. – Environmental Science & Technology 39(S2): 444-448 (in Chinese).
[42] Wang, X. L., Xu, J. M., Yao, H. Y., et al. (2003): Effects of Cu, Zn, Cd and Pb compound contamination on soil microbial community. – Acta Scientiae Circumstantiae 23(1): 22-27 (in Chinese).
[43] Weiss, B., Larink, O. (1991): Influence of sewage sludge and heavy metals on nematodes in arable soil. – Biology and Fertility of Soils 12: 5-9.

http://www.aloki.hu ● ISSN 1589 1623 (Print) ● ISSN 1785 0037 (Online)
DOI: http://dx.doi.org/10.15666/aeer/1804_49154927

[44] Wen, Y. F., Zhao, J. Q. (2008): Effect of grazing on soil fertility and phosphorus availability in the red soil region, Northeast Yunnan. – Acta Pedologica Sinica 45(3): 569-572 (in Chinese).
[45] Wu, S., Cheng, J. L., Xu, X. Y., et al. (2019): Polyploidy in invasive Solidago canadensis increased plant nitrogen uptake, and abundance and activity of microbes and nematodes in soil. – Soil Biology & Biochemistry 138.
[46] Xiao, Y., Xie, G. D., An, K. (2003): The function and economic value of soil conservation of ecosystems in Qinghai, Tibet Plateau. – Acta Ecologica Sinica 23(11): 2367-2376 (in Chinese).
[47] Yang, M. L., Ma, Y. H., Huang, W. X. (2019): Study on the correlation between available state, total amount and pH of Soil Cd and Pb. – Guangdong Agricultural Sciences 46(4): 74-80.
[48] Yang, X., Xue, C., Su, L. X., et al. (2018): Exploring patterns of < Italic > Camellia < /Italic > seed cake application in relation to plant growth, soil nematodes and microbial biomass. – Soil Science & Plant Nutrition 64(2): 253-264.
[49] Yu, S., He, Z. L., Zhang, R. G., et al. (2003): Soil basal respiration and enzyme activities in the root-layer soil of tea bushes in a red soil. – Chinese Journal of Applied ecology 14(2): 179-183 (in Chinese).
[50] Zang, Y. F., Hao, M. D., Zhang, H. Q., et al. (2015): Effects of wheat cultivation and fertilization on soil microbial biomass carbon, soil microbial biomass. – Acta Ecologica Sinica 35(05): 1445-1451.
[51] Zhao, H. R., Xia, B. C., Fan, C., et al. (2012): Human health risk from soil heavy metal contamination under different land uses near Dabaoshan mine, Southern China. – Science of the Total Environment 417-418: 45-54.
[52] Zhou, J. M., Dang, Z., Situ, Y. et al. (2004): Distribution and characteristics of heavy metals contaminations in soils from Dabaoshan mine area. – Journal of Agro-Environment Science 23(6): 1172-1176 (in Chinese).
[53] Zhou, J. M., Dang, Z., Cai, M. F., et al. (2007): Soil heavy metal pollution around the Dabaoshan mine, Guangdong Province, China. – Pedosphere 17(5): 588-594.
[54] Zhuang, P., McBride, M. B., Xia, H. P., et al. (2009): Health risk from heavy metals via consumption of food crops in the vicinity of Dabaoshan mine, South China. – Science of the Total Environment 407: 1551-1561.
[55] Zhuang, P., Li, Z. A., Zou, B., et al. (2013): Heavy metal contamination in soil and soybean near the Dabaoshan mine, South China. – Pedosphere 23(3): 298-304.

http://www.aloki.hu ● ISSN 1589 1623 (Print) ● ISSN 1785 0037 (Online)
DOI: http://dx.doi.org/10.15666/aeer/1804_49154927

EFFECT OF CH_4 EMISSION REDUCTION OF WATER, FERTILIZER AND BIOCHAR REGULATION METHOD ON A RICE FIELD IN THE NORTHEASTERN COLD AREA OF CHINA

LIN, Y. Y. [1,2] – YI, S. J.[2,3*] – ZHANG, Z. X.[4] – WANG, M. X.[4] – NIE, T. Z.[5]

[1]*College of Civil Engineering and Water Conservancy, Heilongjiang Bayi Agricultural University, Heilongjiang Daqing 163319, China*

[2]*Quality Supervision and Testing Center for Agricultural Processed Products of the Ministry of Agriculture (Daqing), Heilongjiang Daqing 163319, China*

[3]*College of Engineering, Heilongjiang Bayi Agricultural University, Heilongjiang Daqing 163319, China*

[4]*Key Laboratory of Efficient Use of Agricultural Water Resources, Ministry of Agriculture, Harbin, Heilongjiang 150030, China*

[5]*School of Water Conservancy and Electric Power Heilongjiang University, Harbin, Heilongjiang 150080, China*

**Corresponding author*
e-mail: yishujuan_2005@yeah.net

(Received 24th Nov 2019; accepted 6th May 2020)

Abstract. The objective of this study was to analyse the black soil rice fields of the northeastern cold region of China**,** D311 optimal design scheme with three factors secondary saturation was adopted and static opaque chamber - gas chromatographic method was utilized to analyze the effect of irrigation amount, nitrogen fertilizer and straw biochar on the emission of the greenhouse gas CH_4 from rice fields, the study determined the optimal application scheme of water and fertilizer for emission control. The results show that the order of influence for these factors from the highest to the lowest is: biochar > nitrogen fertilizer > water; effect of irrigation amount on CH_4 emission is increased at first, followed by a decrease. Increase of nitrogen fertilizer and biochar can significantly reduce CH_4 emission loads; interaction between two factors has an inhibitory effect on CH_4 emissions and it is shown as below: nitrogen fertilizer + biochar > water + biochar > water + nitrogen fertilizer; in combination with the yield, when emission reduction target of rice field CH_4 is controlled at 20~40% of normal emission, the optimized application scheme in combination of water, fertilizer and biochar is the following: irrigation amount 4,930-5,310 m^3/hm^2, nitrogen application amount 96.93-107.74 kg/hm^2 and biochar application amount 19.71-24.12 t/hm^2.
Keywords: *cold black soil, rice, irrigation and fertilization, biochar dosage, CH_4 emission*

Introduction

The reason for global warming lies in the increase of greenhouse gas concentration in the atmosphere. CH_4 as an important greenhouse gas in the atmosphere has already contributed to as much as 15% for greenhouse effect. Hence, CH_4 has become a key factor affecting global climate following CO_2 (Wang, 2001; Jiang, 2001; Wang et al., 2008). Hence, rice fields are main anthropogenic source for CH_4 emission. About $3.1*10^{10}$~$1.12*10^{11}$ kg released annually from rice fields accounts for 5~19% proportion in CH_4 emission load to the atmosphere (Zou et al., 2009; IPCC, 2007).

http://www.aloki.hu ● ISSN 1589 1623 (Print) ● ISSN 1785 0037 (Online)
DOI: http://dx.doi.org/10.15666/aeer/1804_49294939

Therefore, the reduction of greenhouse gas CH_4 emission from rice fields has a great significance in mitigating climate change in China.

There are many factors affecting CH_4 emission from rice fields. It is shown from the study that irrigation mode of rice fields plays an important role in CH_4 emission. Compared with submerged irrigation, CH_4 emission from rice fields under inadequate irrigation will be significantly reduced (Peng et al., 2010; Li et al., 2005). Similarly, fertilization measures have an important impact on CH_4 emission from rice fields. It is shown from the study that the application of fertilizer can increase NH_4^+-N concentration, but growth of CH_4 oxidizing bacteria is also promoted. The promoted CH_4 oxidizing bacteria oxidize more CH_4, which results in the reduction of CH_4 emission from rice fields (Zou et al., 2005; Cai et al., 1997; Ma et al., 2007). Biochar can play an important role in the global carbon geochemical cycle, climate change and environmental system because of its strong ability of nitrogen and carbon fixation. It has become a hot topic in atmospheric science and environmental science fields (Liu, 2011.). The study shows that applying biochar to soil can significantly improve soil quality and permeability. While fixing atmospheric CO_2, soil CH_4 emission (Karhua et al., 2011; Qin et al., 2012) was also affected. Indoor pot experiments performed by Rondon showed that CH_4 emission decreased by 20.4% (Rondon et al., 2007) when 2 kg/m^2 biochar was added to the soil for cultivation of forage and soybean.

At present, although many scholars have conducted in-depth studies on the effects of water, fertilizer and biochar management on CH_4 emissions from rice fields (Shi et al., 2011; Yuan et al., 2008; Liang et al., 2004; Knoblauch et al., 2008; Xu et al., 2015), they are basically individual single-factor studies, but the effects of integrated management on CH_4 emissions from rice fields (factor coupling effect) are rarely reported. The objective of this study was mainly to analyze the coupling effects of three factors water, nitrogen fertilizer and biochar on CH_4 emissions from rice fields. In combination with CH_4 emission reduction targets during rice growing reason, optimal water, fertilizer and biochar application schemes are sought so as to provide the field management technology reference for CH_4 emission reduction in black soil rice fields in the cold area of Northeastern China.

Materials and methods

Overview of experimental sites

The experiment was carried out at the Rice Irrigation Test Center Station (125°44'E, 45°63'N) in Heping Town, Qingan County, Suihua City, Heilongjiang Province from May to October, 2018, which is a typical cold black soil area. With 2.5 ℃ annual mean temperature, 550 mm annual mean precipitation, 750 mm annual mean evaporation from water surface, 156~171 d hydrothermal growth period of crops and 128 d frost free period all year round, the area based on the climatic characteristics is classified as continental monsoon climate in cold temperature zone. As rice soil is an albic soil type, the soil here has 1.01 g/cm^3 unit weight and 61.8% porosity. The basic physicochemical properties of the soil are the followings: organic matter mass ratio 41.4 g/kg, pH value 6.40, total nitrogen mass ratio 15.06 g/kg, total phosphorus mass ratio 15.23 g/kg, total potassium mass ratio 20.11 g/kg, alkali hydrolysis nitrogen mass ratio 154.36 mg/kg, available phosphorus mass ratio 25.33 mg/kg and available potassium mass ratio 157.25 mg/kg.

http://www.aloki.hu ● ISSN 1589 1623 (Print) ● ISSN 1785 0037 (Online)
DOI: http://dx.doi.org/10.15666/aeer/1804_49294939

Experimental design

Saturated D311 optimal design (Xu, 1997) is used in the experiment to study the effects of irrigation amount, nitrogen fertilizer and biochar on CH_4 emission in rice growing season under controlled irrigation conditions. Water and fertilizer are applied based on the application standard of local farmers, namely 2,500~7,500 kg/hm^2 irrigation amount, 50-150 kg/hm^2 nitrogen fertilizer (pure nitrogen) and 0~40 t/hm^2 biochar. The detailed design plan is shown in *Tables 1* and *2*.

Table 1. *Encoding table for factor level*

Encoding value			Practical value		
X_1	X_2	X_3	W (m^3/hm^2)	N (kg/hm^2)	BC (t/hm^2)
2	2	2	7500	150	40
1.414	1.414	1	6800	135	30
0	0	0	5000	100	20
-1.414	-1.414	-1	3200	65	10
-2	-2	-2	2500	50	0

W (X1) - water, N (X2) - nitrogen fertilizer, BC (X3) - biochar

Table 2. *Optimal design treatment table of saturated D-311*

Treatment no.	Encoding value			Practical value			CH_4 emission load (kg/hm^2)
	X_1	X_2	X_3	W (m^3/hm^2)	N (kg/hm^2)	BC (t/hm^2)	
1	0	0	2	5000	100	40	121.29
2	0	0	-2	5000	100	0	209.71
3	-1.414	-1.414	1	3200	65	30	179.42
4	1.414	-1.414	1	6800	65	30	179.95
5	-1.414	1.414	1	3200	135	30	158.29
6	1.414	1.414	1	6800	135	30	150.45
7	2	0	-1	7500	150	10	164.63
8	-2	0	-1	2500	50	10	147.99
9	0	2	-1	5000	100	10	165.49
10	0	-2	-1	5000	100	10	178.17
11	0	0	0	5000	100	10	144.42

W (X1) - water, N (X2) - nitrogen fertilizer, BC (X3) - biochar

Eleven treatments with three repetitions are arranged in randomized block. Each block covers a 10 m*10 m = 100 m^2 area. Around the block, rice was also planted so as to add the protection line. With the same rice seedling raising, transplanting, plant protection, medication and other technical measures as well as field management conditions, the blocks were separated with impervious treatment measures to decrease the effect of lateral infiltration on the test, namely plastic sheets and cement ridges were used as seepage isolation materials around the blocks. They were buried 40 cm deep into the surface of the field. Pipeline water supply was adopted. Each pipeline was equipped with water meters so as to control the irrigation amount. Nitrogen fertilizer was applied according in 5:3:2 ratio of base fertilizer, tillering fertilizer and spike

http://www.aloki.hu ● ISSN 1589 1623 (Print) ● ISSN 1785 0037 (Online)
DOI: http://dx.doi.org/10.15666/aeer/1804_49294939

fertilizer. P fertilizer used as base fertilizer was applied at a time with 45 kg/hm^2 application amount. K fertilizer was applied twice as base fertilizer and 8.5 leaf age (panicle primordium differentiation stage) with 1:1 ratio. With 80 kg/hm^2 application amount, biochar was applied to the surface of the soil and then evenly mixed with plowing soil by rotary tiller. The tested fertilizers are urea (containing N 46%), diammonium phosphate (containing N18%, containing P_2O_5 46%) and potassium fertilizer (containing 40% K_2O). The tested biochar is the s rice traw biochar product supplied by Liaoning Golden Future Agriculture Technology Co., Ltd. The physical and chemical data are shown in *Table 3*.

Table 3. *Physicochemical data of rice straw biochar*

	PH (H2O)	**C (%)**	**N (%)**	**P (%)**	**K (%)**	**CEC (cmol.kg^{-1})**	**Surface area (m^2·g^{-1})**	**Void area (cm^3.g^{-1})**
Rice traw biochar	10.2	42.7	0.76	0.16	1.07	44.7	81.8	0.08

The rice varieties tested were Longqing Rice No. 3 with the planting density of 4 plants per hole, 25 holes per square metre. Base fertilizer was applied on 6 May and transplantation was performed on 17 May. Tillering fertilizer was applied on 31 May, earing fertilizer was applied on 19 July and the rice was harvested on 20 September. 127 d growth period of rice was divided into period of seedling establishment (May 17-May 30), tillering period (May 31-July 7), jointing and booting period (July 8-July 25), heading to flowering period (July 26-August 4), milk ripe period (August 5-August 24) and yellow ripening period (August 25-September 20).

Gas collection and determination

Gas sampling and selection were carried out on sunny days by static opaque chamber-gas chromatography method. The box is a cuboid with a cross section of 18 cm side length. It is made of plexiglass. Insulation material (sponge and aluminum foil) is pasted on the outside of the box to reduce the gas temperature change in the box caused by solar radiation during sampling. In the early growth stage, the box was 90 cm high and the box increased to 130 cm high after heading stage. A three-way valve gas recovery hole is on the box side 30 cm from the top connecting the three-way valve and gas collector. One fan is built at top of the sampling box so as to mix gas uniformly in the box during sampling. Before transplanting, a wooden base is placed in the sampling basin and aligned with the mud surface. During gas sampling, the sampling box is gently placed on the base of the concentric-circle-liked frame. The water in the base flume guarantees the gas isolation between the inside and outside of the sampling box during sampling. One week after rice transplantation, detection was started. The detection was performed from 10:00 to 12:00 (Li et al., 1998; Epstein and Burke, 1998). At each treatment, gas was collected for three times in parallel weekly until one week before harvest. About 100 mL gas in the box was extracted with a syringe during sampling. Samples were collected at 0, 5, 10 and 15 min, respectively. Afterwards, the gas in the syringe was transferred to the aluminium foil sampling bag immediately, and the sampling bag was brought back to the laboratory in time for determination.

Gas CH_4 concentration was detected with Shimadzu GC-14B meteorological chromatograph along with hydrogen flame ionization detector (FID) and thermal

http://www.aloki.hu ● ISSN 1589 1623 (Print) ● ISSN 1785 0037 (Online)
DOI: http://dx.doi.org/10.15666/aeer/1804_49294939

conductivity detector (TCD) at 200 ℃ and 100 ℃ temperature. The separation materials were GDX-502 and Porapak Q, respectively and the column temperature was 100 ℃ and 55 ℃. The standard gas was provided by the National Standard Materials Center. The gas collection device is shown in *Figure 1*.

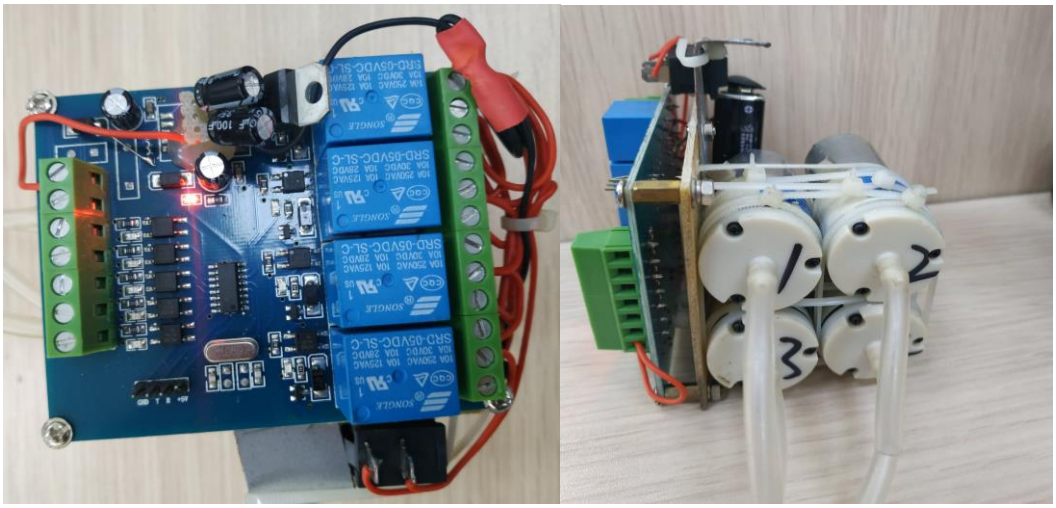

Figure 1. *A device for automatically collecting static chamber greenhouse gases*

Calculation method and data analysis

The following formula was used to calculate CH_4 emission flux from rice field (Zheng et al., 1998): $F = \rho \cdot h \cdot dc / dt \cdot 273/(273 + T)$, where F is gas emission flux ($mg.m^{-2}.h^{-1}$), ρ is gas density under standard state ($kg.m^{-3}$), h is box height (m), dc/dt is the gas concentration change rate in the sampling box ($mL \cdot m^{-3} \cdot h^{-1}$), 273 is the gas equation constant and T is the average temperature in the sampling box during the sampling process (℃). According to the relationship curve between gas concentration and time, the gas emission flux was calculated. The emission load during the growing season was the accumulated products of average flux value of each growing period and total duration in the growing period (Singh et al., 1996).

The data were analyzed with Excel 2003, SPSS 17.0 and MATLAB 7.0, using regression analysis and variance analysis to process the experimental data.

Results and analysis

Emission load effect function of CH_4 in growing season

The coding values X_1(W), X_2(N) and X_3(C) in *Table 1* were taken as independent variables and the average emission value of CH_4 in the growing season in *Table 2* were taken as the dependent variables for quadratic polynomial regression analysis so as to obtain the regression equation among CH_4 emissions load, irrigation amount, nitrogen fertilizer and biochar.

$$Y = 161.92 + 1.43X_1 - 6.05X_2 - 10.31X_3 - 1.05X_1X_2 - 2.73X_1X_3 - 2.89X_2X_3 - 5.05X_1^2 - 1.21X_2^2 - 0.57X_3^2 \quad \text{(Eq.1)}$$

http://www.aloki.hu ● ISSN 1589 1623 (Print) ● ISSN 1785 0037 (Online)
DOI: http://dx.doi.org/10.15666/aeer/1804_49294939

F test was performed for the regression equation: $F = 5.16 > (F_{0.01}(10, 20)) = 3.37$). The regression equation has a very significant relationship, that is the equation can reflect the relationship among CH_4 emission load in growing season and irrigation amount, nitrogen fertilizer and biochar. The absolute value of the first term coefficient of the regression equation is the basis for judging the influence degree of each factor on CH_4 emission. Therefore, the influence degree of the equation on CH_4 emission load from high to low was biochar, nitrogen fertilizer and water.

Single factor effect analysis

"Dimension reduction method" was adopted for the above main effect model. Any two factors were fixed at zero code value so as to determine the influencing effect of a single factor on the emission load of CH_4 during the growing season, and then respectively obtain single-factor effect equation and draw single-factor effect curve (*Eq. 2*).

$$Y_1 = 161.92 + 1.43X_1 - 5.05X_1^2 \quad \text{(Eq.2)}$$

$$Y2 = 161.92 - 6.05X_2 - 1.21X_2^2 \quad \text{(Eq.3)}$$

$$Y3 = 161.92 - 10.31X_3 + 0.57X_3^2 \quad \text{(Eq.4)}$$

It can be observed from *Figure 2* that within the coding value range, the effect from irrigation amount on CH_4 emission amount is promoting at first and then restraining. Increase of nitrogenous fertilizer and charcoal can significantly restrain CH_4 emission load.

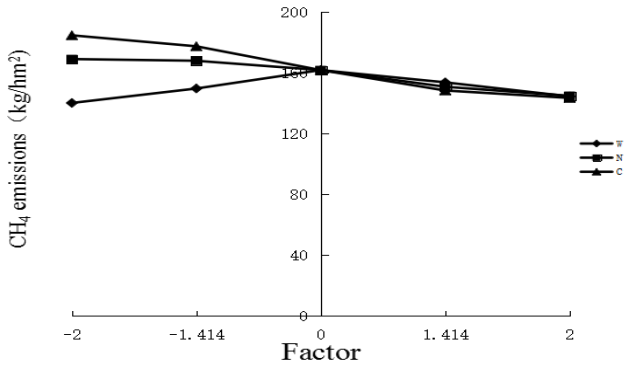

Figure 2. *Single-factor effect curve diagram. (X1 - water, X2 - nitrogen fertilizer, X3 - biochar)*

Interactive effect analysis of factor

Any factor is fixed at zero code value to obtain the interactive effect equation of two other factors and the equation is shown below:

$$Y_{12} = 161.92 + 1.43X_1 - 6.05X_2 - 1.05X_1X_2 - 5.05X_1^2 - 1.21X_2^2 \quad \text{(Eq.5)}$$

$$Y_{13} = 161.92 + 1.43X_1 - 10.31X_3 - 2.73X_1X_3 - 5.05X_1^2 - 0.57X_3^2 \quad \text{(Eq.6)}$$

$$Y_{23} = 161.92 - 6.05X_2 - 10.31X_3 - 2.89X_2X_3 - 1.21X_2^2 - 0.57X_3^2 \quad \text{(Eq.7)}$$

http://www.aloki.hu ● ISSN 1589 1623 (Print) ● ISSN 1785 0037 (Online)
DOI: http://dx.doi.org/10.15666/aeer/1804_49294939

A diagram is drawn for the interactive effect equation of these two factors (*Fig. 3*). It can be seen from *Figure 3,* the interaction between two factors has an inhibitory effect on CH_4 emission and the effect degree on CH_4 emission load from high to low is as follows: nitrogen fertilizer + biochar, water + biochar and water + nitrogen fertilizer. As can be seen from *Figure 3a* and *b,* when irrigation amount is fixed at a certain level, CH_4 emission load decreases with the increase of the application of nitrogen fertilizer and biochar. However, when nitrogen fertilizer or biochar is fixed at a certain level, the effect of irrigation amount on CH_4 emission increases or decreases and no obvious emission reduction can be obtained; it can be observed from *Figure 3c* that with increase in application quantity of nitrogen fertilizer and biochar, CH_4 emission decreased significantly. Thus, increase of biochar application quantity has a significant effect on CH_4 emission reduction effect.

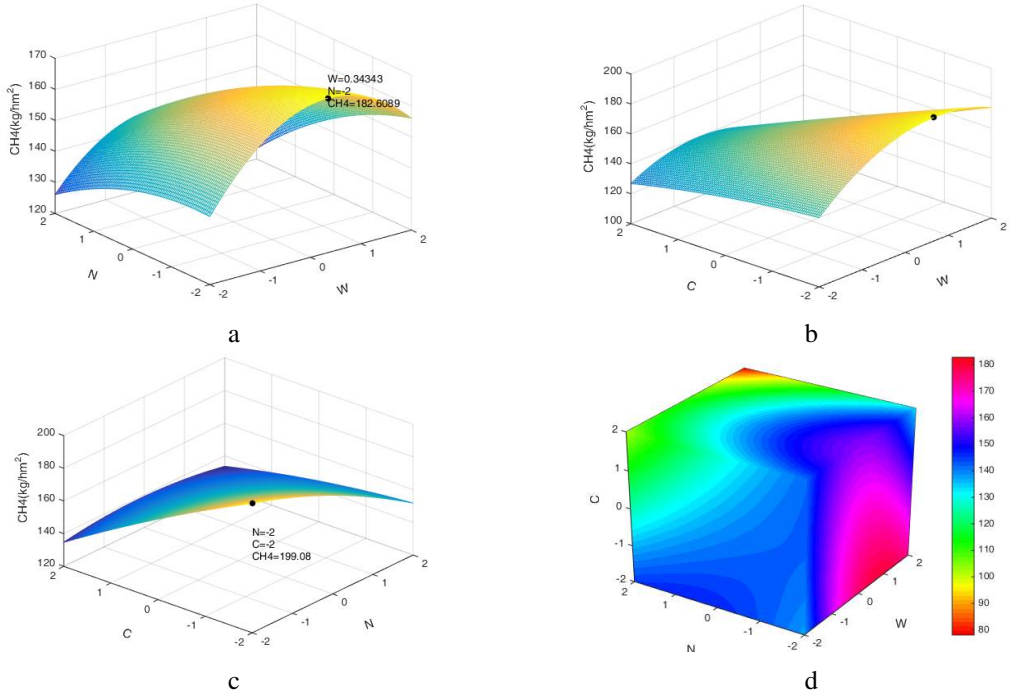

Figure 3. *Interactive effect analysis between two factors related to emission load of methane in growing season. Interactive effect curve diagram between (a) irrigation amount and nitrogenous fertilizer, (b) irrigation amount and biochar and (c) nitrogenous fertilizer and biochar. (d) Interactive effect four-dimension diagram among irrigation amount, nitrogenous fertilizer and biochar. (W - water, N - nitrogen fertilizer, C - biochar)*

Analysis for management and optimization plan of water, fertilizer and biochar

Frequency analysis method was used to optimize the main effect model. The coding values were divided into five levels (-2, -1.414, 0, 1.414, 2) within the experimental design range to constitute $T = 5^3 = 125$ treatment combinations. Combining with the yield, the emission reduction target of CH_4 in rice fields during the growing season was controlled within 20-40%, because all the factors of treatment No. 11 are at zero level in this experiment, so they are regarded as normal treatment, that is, 60~80% (86.65~115.54 kg/hm^2) normal emission load of CH_4 in growing season was selected for frequency analysis to obtain 50 optimization results for the management simulation

http://www.aloki.hu ● ISSN 1589 1623 (Print) ● ISSN 1785 0037 (Online)
DOI: http://dx.doi.org/10.15666/aeer/1804_49294939

equation between water fertilizer and biochar in CH_4 emission load during the growing season. Frequency analysis of gas emission flux is shown in *Table 4*.

Table 4. *Water and fertilizer and biochar application plan with CH_4 emission of 86.65~115.54 kg/hm^2 in the rice growing season*

Coding value	Irrigation amount		Nitrogenous fertilizer		Biochar	
	Times	Frequency/%	Times	Frequency/%	Times	Frequency/%
-2	9	18	9	18	4	8
-1.414	9	18	10	20	12	24
0	9	18	9	18	21	42
1.414	10	20	10	20	8	16
2	13	27	12	24	5	10
Average value	0.19 0.11		0.08 0.11		0.09 0.08	
Standard error confidence interval (95%)	-0.0564~0.2480		-0.1230~0.3094		-0.0287~0.4124	
Optimal plan (kg/hm^2)	4930~5310		96.93~107.74		19.71~24.12	

Discussion

Irrigation amount has an important influence on CH_4 emission load from rice fields. It is shown from the study that relatively small irrigation amount can promote gas exchange between soil and atmosphere, destroy the anaerobic conditions of soil and inhibit the activity for production of CH_4 bacteria. However, increase of soil aeration promotes CH_4 emission directly into the atmosphere to a certain extent. Whereas, in case of sufficient water quantities, the rice field will keep a deep water layer for long time. The air and soil is blocked by water layer, which may close some stomata and reduce CH_4 emissions via plants (Ding, 1997; National Information Bulletin on Climate Change of the People's Republic of China, 2004). This is consistent with the study results.

Nitrogen fertilizer application amount CH_4 has an important influence on CH_4 emission from rice field. The experimental results showed that the nitrogen fertilizer applied has obviously a negative effect on CH_4 emission load from black soil rice field in the growing season, which is basically consistent with the results of Shangguan et al. (1996) and others think that urea could reduce CH_4 emission of rice fields. However, Liang et al. (2002) and others believe that urea has different effects on CH_4 release (promoting or inhibiting), possibly because it can increase the soil pH value. In most cases,When urea was applied to acid soil, the increase of pH value of soil became favorable to the formation of CH_4, Whereas, most black soils are neutral and alkaline. After urea is applied to neutral and alkaline soils, increased pH value restrains formation of CH_4. Therefore, the effect of nitrogen fertilizer application on CH_4 emission of rice fields requires to be further studied.

The results show that biochar application can effectively reduce CH_4 emission load of rice fields. The reason may be that input of biochar effectively improves soil aeration, reduces soil water-soluble organic carbon content, thus improving soil fertility. In addition, biochar input as a carbon source can provide sufficient matrix for CH_4 oxidizing bacteria and reduce CH_4 emissions via oxidation (Liang et al., 2002).

http://www.aloki.hu ● ISSN 1589 1623 (Print) ● ISSN 1785 0037 (Online)
DOI: http://dx.doi.org/10.15666/aeer/1804_49294939

Conclusion

(1) Water, nitrogen and biochar have different degree of effects on CH_4 emission load of rice fields during growing season. The analysis results show that the effects of three factors on CH_4 emission load are as follows: biochar > nitrogen fertilizer > water; effects of irrigation amount on CH_4 emissions are increase at first and then decrease. Increase of nitrogen fertilizer and biochar can significantly reduce CH_4 emission load.

(2) The interaction of two factors can inhibit CH_4 emission during growing season. The results show that the effects on CH_4 emissions are as follows: nitrogen fertilizer + biochar > water + biochar > water + nitrogen fertilizer; when irrigation amount is fixed at a certain level, CH_4 emission amount decreases with the increase of application amount of nitrogen fertilizer and biochar. However, when nitrogen fertilizer or biochar is fixed at certain level, the increase of irrigation amount may cause CH_4 emission load increase or decrease. There is no obvious emission reduction effect. With increase of application amount of nitrogen fertilizer and biochar, CH_4 emission amount decreased significantly. Thus, increase in application amount of biochar has an obvious effect on CH_4 emission reduction.

(3) In combination with the yield, it is to reduce CH_4 emission load of rice fields in the growing season is controlled from 20 to 40%. The frequency analysis method is used to optimize the main effect model. The optimized combined application plan of water, fertilizer and biochar was determined as follows: irrigation amount 4,930~5,310 m^3/hm^2, nitrogen application amount 96.93~107.74 kg/hm^2 and biochar quantity 19.71~24.12 $t/hm^{2.}$

In this study, we tried to add biochar into the soil to realize joint coupling with water and fertilizer, and established a mathematical model of CH_4 emission load during the growing season of rice fields in the Northeast of China about water, nitrogen and biochar. The model can reflect the relationship between CH_4 emission from rice field and water, fertilizer and biochar through significance test, so as to make quantitative research on water, fertilizer and biochar more convenient. Therefore, the research has a good application prospect. However, the coupling effects of water, fertilizer and biochar on seasonal CH_4 emissions of rice fields have only been preliminarily discussed in this paper, but no qualitative research has been carried out. In the process of further in-depth study, data of different growth stages for many years should be accumulated to make the model more perfect with practical guiding significance.

Acknowledgments. Thank you for the support from Common Subsidy Scheme for Postdoctor of Heilongjiang Province (LBH-Z18255), Heilongjiang Bayi Agricultural University Support Program for San Heng San Zong (TDJH201803), Talent Introduction Plan of Heilongjiang Bayi Agricultural University (XYB201801), Postdoctor Work Station for Agricultural Processed Product Quality Supervision and Inspection Test Center (Daqing) of Ministry of Agriculture.

REFERENCES

[1] Cai, Z. C., Xing, G. X., Yan, X. Y., Xu, H., Tsuruta, H., Yagi, K., Minami, K. (1997): Methane and nitrous oxide emissions from rice paddy fields as affected by nitrogen fertilizers and water management. – Plant and Soil 196(1): 7-14.

[2] Ding, Y. H. (1997): IPCC main scientific achievements and problems for scientific assessment report about the second climate change. – Advances in Earth Science 12(2): 158-163.

http://www.aloki.hu ● ISSN 1589 1623 (Print) ● ISSN 1785 0037 (Online)
DOI: http://dx.doi.org/10.15666/aeer/1804_49294939

[3] Epstein, H. E., Burke, L. C. (1998): Plant functional type effects on trace gas fluxes in the short grass steppe. – Biogeochemistry 42(1-2): 145-168.
[4] IPCC (2007): Climate Change 2007: Mitigation of Climate Change. – Contribution of Working Group III to the Fourth Assessment Report of The Intergovernmental Panel on Climate Change. Cambridge University Press, Cambridge, pp. 63-67.
[5] Jiang, Y. (2001): Grainfield is pure emission ground of greenhouse gases. – Environmental Science of China 21(2): 136.
[6] Karhua, K., Mattila, T., Bergström, I., Kristiina, R. (2011): Biochar addition to agricultural soil increased CH_4 uptake and water holding capacity - results from a short-term pilot field study. – Agriculture, Ecosystems and Environment 140(31): 309-313.
[7] Knoblauch, C., Marifaat, A. A., Haefele, M. S. (2008): Biochar in rice-based system: impact on carbon mineralization and trace gas emissions. – Bioresource Technology 95(32): 255-257.
[8] Liang, B. C., Wang, X. L., Ma, B. L. (2002): Maize root-induced change in soil organic carbon pools. – Soil Science Society of America Journal 66(13): 845-847.
[9] Liang, W., Zhang, Y., Yue, J., Wu, J., Shi, Y., Huang, G. H. (2004): Effect of long-term nitrogen application on emission of CH_4 and N_2O from black soil water and dry land. – Journal of Ecology 23(3): 44-48.
[10] Li, D. X., Peng, S. Z., Xu, J. Z., Ding, J. L., He, Y., Yu, J. Y. (2005): Ecological and environmental effect of rice field under water-saving irrigation condition. – Journal of Hohai University (Natural Science Edition) 33(6): 629-633.
[11] Li, J., Wang, M. X., Cheng, D. Z. (1998): Selection of sampling time for non-continuous measurement of methane emission from rice fields. – Journal of Graduate School of Chinese Academy of Sciences 15(1): 24-29.
[12] Liu, Y. X. (2011): Effect of Biomass Carbon Input on Soil Nitrogen Erosion and Greenhouse Gas Emission Characteristics. – Zhejiang University, Hangzhou.
[13] Ma, J., Li, X. L., Xu, H., Han, Y., Cai, Z. C., Yagi, K. (2007): Effects of nitrogen fertilizer and wheat straw application on CH4 and N2O emissions from a paddy rice field. – Australian Journal of Soil Research 45(5): 359-367.
[14] National Information Bulletin on Climate Change of the People's Republic of China. (2004): National Information Bulletin on Climate Change. – China Planning Press, Beijing.
[15] Peng, S. Z., Yang, S. H., Xu, J. Z. (2010): Influence from control irrigation on comprehensive emissions of CH_4 and N_2O from rice field along with greenhouse effect. – Advances in Water Science 21(2): 235-240.
[16] Qin, X. B., Li, Y. E., Wan, Y. F., Shi, S. W., Liao, Y. L., Liu, Y. T., Li, Y. (2012): Effect from rice straw returning way on greenhouse gas emission strength under no-tillage condition. – Journal of Agricultural Engineering 28(6): 210-216.
[17] Rondon, M. A., Lehmann, J., Ramirez, J., Pilar, M. (2007): Biological nitrogen fixation by common beans (Phaseolus vulgaris L) increases with bio-char additions. – Biology and Fertility of Soils 43(13): 699-708.
[18] Shangguan, X. J., Wang, M. X. (1996): Transmission of Rice Field CH_4. – China Environmental Science Press, Beijing.
[19] Shi, S. W., Li, Y. E., Wan, Y. F., Qin, X. B., Gao, Q. Z. (2011): Emission of CH_4 and N_2O from double cropping rice field under different nitrogen and phosphate fertilizer dosage. – Environmental Science 32(7): 1899-1907.
[20] Singh, J. S., Sing, S., Raghubanshi, A. S., Singh. S., Kashyap, A. K. (1996): Methane flux from rice /wheat agroecosystem as affected by crop phenology, fertilization and water lever. – Plant and Soil 183(2): 323-327.
[21] Wang, F., Li, Y. H., Zhao, T. C., Chen, C. (2008): Ningxia CO_2, CH_4, N_2O greenhouse gas emission estimation and emission reduction measures. – Resources and Environment of Arid Region 22(11): 73-77.

http://www.aloki.hu ● ISSN 1589 1623 (Print) ● ISSN 1785 0037 (Online)
DOI: http://dx.doi.org/10.15666/aeer/1804_49294939

[22] Wang, M. X. (2001): Methane Emission from Rice Field of China. – Science Press, Beijing, pp. 85-87.
[23] Xu, D., Zhang, Z. X., Lin, Y. Y. (2015): Pot experiment for water and fertilizer optimization for control and emission of CH_4 from black soil rice field. – Resources and Environment of Arid Area 29(4): 172-177.
[24] Xu, Z. R. (1997): Regression Analysis and Test Design. – China Agriculture Press, Beijing, pp. 102-143.
[25] Yuan, W. L., Cao, C. G., Cheng, J. P., Xie, N. N. (2008): Evaluation for CH_4 and N_2O emission and greenhouse effect under intermittent irrigation model. – Chinese Agricultural Science 41(12): 4294-4300.
[26] Zheng, X. H., Wang, M. X., Wang, Y. S., Shen, R. X., Li, J. (1998): Comparison of manual and automatic methods for measurement of methane emission from rice paddy fields. – Advances Atmospheres Science 15(4): 569-579.
[27] Zou, J. W., Huang, Y., Jiang, J. Y., Zheng, X. H., Sass, R. L. (2005): A 3-year field measurement of methane and nitrous oxide emissions from rice paddies in China: effects of water regime, crop residue, and fertilizer application. – Global Biogeochemical Cycles 19(2): 20-21.
[28] Zou, J. W., Huang, Y., Qin, Y. M., Liu, S. W., Shen, Q. R., Pan, G. Y., Lu, Y. Y., Liu, Q. H. (2009): Changes in fertilizer-induced direct N2O emissions from rice fields during rice-growing season in China between 1950s and 1960s. – Global Change Biology 15(21): 229-242.

http://www.aloki.hu ● ISSN 1589 1623 (Print) ● ISSN 1785 0037 (Online)
DOI: http://dx.doi.org/10.15666/aeer/1804_49294939

EVALUATION OF ECOREGION-BASED VOLUME EQUATIONS FOR SCOTS PINE (*PINUS SYLVESTRIX*) IN THE EASTERN DAXING'AN MOUNTAINS, NORTHEAST CHINA

MBANGILWA, M. M.[1] – HE, P.[1] – JIANG, L. C.[1*]

[1]*Key Laboratory of Sustainable Forest Ecosystem Management-Ministry of Education, School of Forestry, Northeast Forestry University, Harbin 150040, China*

[*]*Corresponding author*
e-mail: jlichun@nefu.edu.cn

(Received 13th Dec 2019; accepted 6th May 2020)

Abstract. In this research total volume equations were developed for Scots pine (*Pinus sylvestris* var. mongolica) in Northeast China. Eighteen total volume equations were fitted to volumes from Forest Inventory Analysis data of the Eastern Daxing'an Mountains in Northest China. Eight ecoregions including: Xinlin (XL), Tahe (TH), Huzhong (HZ), Shibazhan (SBZ), Hanjiayuan (HJY), Xilinji (XLJ), Tuqiang (TQ), Amuer (AME) belonging to two regions including: The northwest of the northern slope of Yilehuli Mountains (NWYLHLM) and The southeast of the northern slope of Yilehuli Mountains (SAYLHLM) were identified and the best volume equations were tested to determine if the differences between ecoregions were statistically significant. Results varied by ecoregion. Average bias prediction error ranged from -1.2% to 7.5% in XL, from -0.8% to 11.7% in TH, from -13.9% to 0.08% in HZ, from -3.5% to 10.3% in SBZ, from -8.9% to 0.9% in HJY, from -2.5% to 10.4% in XLJ, from -11.6% to 9.4% in TQ and from -11.7% to 1.5% in AME. However, the ecoregion-based volume equation developed in this study could provide more accurate information on tree growth and development of forest ecosystems to managers and planners.
Keywords: *conifer species, prediction error, ecoregion, total volume, forest management*

Introduction

Northeastern China is divided into four vegetation regions which include cold-temperate deciduous coniferous forest region, the temperate mixed evergreen coniferous-deciduous broad-leaved forest region, the warm temperate deciduous broad-leaved forest region, and the temperate steppe region (Qian, 2003). Temperate coniferous forests are geographically and taxonomically diverse, found on five continents (North America, Europe, Asia, South America and Africa) (Frelich, 2016). The latter constitute a type of terrestrial habitat defined by the World Wildlife Fund (WWF, 2012, 2019). Temperate coniferous forests are found predominantly in areas with warm summers and cool winters, and vary in their kinds of plant life. These forests are common in the coastal areas of regions that have mild winters and heavy rainfall, or inland in drier climates or mountainous areas. Many species of trees inhabit these forests including pine (Mongolian Scots pine), cedar, fir, and redwood (WWF, 2012, 2019) including the giant sequoia and the coastal sequoia (large known trees) in California and Fitzroya which live more than three thousand years in Chile (Frelich, 2016).

Mongolian Scots pine (*Pinus sylvestris* var. mongolica) is one of the major tree species in the network of Three-North Shelterbelt for windbreak and sand stabilisation in China (Wang et al., 2012). It is a geographic variety of Scots pine (*P. sylvestris*) and is widely distributed in northern China (Wang et al., 2017). It is considered as a crucial

http://www.aloki.hu ● ISSN 1589 1623 (Print) ● ISSN1785 0037 (Online)
DOI: http://dx.doi.org/10.15666/aeer/1804_49414958

ecological species in northern China, especially in sandy areas, due to its great adaptability to infertile soils and cold and arid habitats (Han et al., 1998; Wang et al., 2017). Its natural distribution is mainly located in the sandy soils of northeast China. Since it has high tolerance to cold, drought, soil infertility and grows naturally in the sandy land, this species had been introduced to the edge of sandy lands in northern China to protect nearby lands from moving sand dunes since the 1950s (Wang et al., 2012). Since its wind-sheltering functions are strongly correlated with the architecture and ecophysiological processes of each tree, the model-assisted analysis of the cover architecture and the functional dynamics of the Mongolian Scots pine would be useful to better understand its structure role and behavior in windbreak ecosystems of arid and semi-arid regions in China (Wang et al., 2012). For this investigation, we present a study of the model of Volume Equations based on Scots pine ecoregions in northeastern China.

Volume is referred to quantity and it is the common widely used measure of wood quantity in forest mensuration. Total stem volume equations are the commonly used tools in quantifying timber stocks (García-Espinoza et al., 2018). According to Li (2019), surveying is the determination of the diameters, heights or volumes of a standing tree or cut products such as sawn logs, as well as the determination or prediction of the growth rate. The volume equation is defined as various mathematical statements applied to the determination of quantities (Shuaibu, 2014). It is imperative to increase the supply of lumber, poles and picketing materials for socio-economic development through adequate forest stand measurements to determine and improve the quantity and quality of these stands. Adegoke et al. (2010) stated that the socio-economic development of any country depends largely on the efficient use of its natural resources. The importance of direct measurements of standing trees can not be overstated to obtain basic data on the relationship between different tree dimensions and volume used to estimate the volumes of other standing trees. Clutter et al. (1983) and Husch et al. (2003) explained that the stem volume of a tree is considered a function of the independent variables (diameter, height) and shape expressed as follows: V = f (D, H, F) where V = volume, D = diameter in cm, H = total height, market value or height up to a specific limit and F = shape measurement such as Girrard shape class or absolute shape quotient.

Diameter and height measurements are essential variables in determining volume. According to Shuaibu and Alao (2013), the diameter of a tree is a random variable that depends on age and height. Therefore, the size distribution of tree diameter in stands describes forest structure and can be used to estimate stand volume and biomass, forest biodiversity and density management. Although volume equations have been studied for many years, they continue to attract forest research. Indeed, there is no single theory of volume that can be used satisfactorily for all species; no single volume model is best for all purposes and volume equations must be more accurate, flexible, valid and normal in their predictions. Forestry measures also need to be improved as market requirements for timber, poles and firewood have become more specific in recent years and current stock volumes and future growth potential are important information for sustainable forest management (Shuaibu and Alao, 2016).

The objective of this study is to evaluate tree volume equations for Scots pine tree species (*Pinus sylvestrix* var mongolica) in the boreal forests of northeastern China and set up a comparison of the inequalities between the volume-diameter relationships between the eight ecoregions; see if these volume equations are statistically justified to

http://www.aloki.hu ● ISSN 1589 1623 (Print) ● ISSN1785 0037 (Online)
DOI: http://dx.doi.org/10.15666/aeer/1804_49414958

verify ecoregion differences for selected Scots pine species and to assess the associated bias when a regional model is compared to individual ecoregion models.

Materials and Methods

Study area and data

The study was conducted in the cold temperate forest regions of the Eastern Daxing'an Mountains who are the largest area of boreal forests in China (Hu et al., 2017) and is taking particularly the Northern slope of Yilehuli Mountains in Heilongjiang Province, northeast China (from 121° 12′E to 127° 00′E and from 50° 10′N to 53° 33′N) (*Figure 1*). The elevation of the area ranges from 300 to 1520 m above the sea level. The mean annual rainfall ranges from 500 to 750 mm and mean annual temperature is from -1 to -2.8°C (Enzinga and Jiang, 2019).

Figure 1. *The geographical location of study area in the Northeast China*

The two major regions (Zhang et al., 1992) employed are depicted in *Figure 1* and include:

- Region 1: The northwest of the northern slope of Yilehuli Mountains (NWYLHLM) which includes four subregions: Xilinji (XLJ), Tuqiang (TQ), Amuer (AME), Huzhong (HZ).
- Region 2: The southeast of the northern slope of Yilehuli Mountains (SAYLHLM) which includes four subregions: Xinlin (XL), Tahe (TH), Shibazhan (SBZ), Hanjiayuan (HJY).

A total of 1294 destructively sampled *Pinus sylvestrix* var. mongolica trees species were used in this investigation. These trees were felled throughout the forest inventory areas of northeast China and all sampled trees were selected to ensure a representative distribution across a range of height and diameter classes within stands varying in

http://www.aloki.hu ● ISSN 1589 1623 (Print) ● ISSN1785 0037 (Online)
DOI: http://dx.doi.org/10.15666/aeer/1804_49414958

density, height, site condition, age and stand structure. Diameters at breast height (DBH, defined as 1.3 m above the ground) outside bark were measured for all sampled trees. Trees were felled to measure total height and their diameter outside bark near ground and at 2, 4, 6, 8, 10, 15, 20, 30, 40, 50, 60, 70, 80 and 90% of total height. Measurements for two perpendicular diameters (over bark) were taken in each part and arithmetically averaged. Smalian's formula (*Eq.1*) was used to calculate the log volumes in cubic meters. Total stem volume (over bark) above stump was computed by adding the logs volumes (over bark) and volume of the top section. Trees possessing broken tops, obvious cankers or crooked boles were excluded from the analysis. Summary statistics for tree diameter and total volume are provided for each subregion, the NWYLHLM, and SAYLHLM regions and all data combined (Overall) in *Table 1*.

Table 1. *Summary statistics of tree diameter (DBH) at breast height, total height (H), total volume (V) for regional and ecoregional data sets for Scots pine*

	DBH (cm)					H (m)				V (m^3)			
Ecoregion	**N**	**Mean**	**STD**	**Min**	**Max**	**Mean**	**STD**	**Min**	**Max**	**Mean**	**STD**	**Min**	**Max**
XL	**65**	35.79	9.70	8.60	64.00	18.52	2.35	10.80	23.30	0.94	0.55	0.03	3.78
TH	**120**	19.63	11.20	5.00	49.00	13.91	5.23	5.90	26.50	0.32	0.40	0.01	2.03
HZ	**135**	30.09	12.68	5.40	57.60	17.50	3.33	5.00	23.90	0.76	0.56	0.01	2.28
SBZ	**68**	19.90	10.69	5.40	41.30	14.31	4.05	7.10	24.20	0.31	0.35	0.01	1.66
HJY	**335**	25.05	10.86	5.20	54.00	18.41	4.46	6.10	25.60	0.56	0.48	0.01	2.61
XLJ	**189**	18.81	10.94	5.00	52.30	15.46	4.31	7.10	23.90	0.31	0.36	0.01	1.74
TQ	**184**	28.22	12.11	6.30	50.70	18.45	4.31	5.80	25.70	0.72	0.60	0.01	2.38
AME	**198**	36.16	11.88	5.30	55.90	19.68	3.77	7.04	25.40	1.09	0.63	0.01	2.55
NWYLHLM	**706**	**28.29**	**13.49**	**5.00**	**57.60**	**17.81**	**4.29**	**5.00**	**25.70**	**0.72**	**0.62**	**0.01**	**2.55**
SAYLHLM	**588**	**24.53**	**11.72**	**5.00**	**64.00**	**17.03**	**4.85**	**5.90**	**26.50**	**0.52**	**0.49**	**0.01**	**3.78**
Overall	**1294**	**26.58**	**12.85**	**5.00**	**64.00**	**17.46**	**4.57**	**5.00**	**26.50**	**0.63**	**0.58**	**0.01**	**3.78**

Note: N-sample size (number of trees), STD-standard deviation, Min.-minimum, Max.-maximum

Data and Methods

Smalian's Formula

$$V = \frac{S_1 + S_2}{2} \times l \qquad \text{(Eq.1)}$$

where:
V= is the Volume of logs in m^3,
S_1= is the area at the small end of the log in m^2,
S_2= is the area at the large end of the log in m^2,
l= is the length of the log in m.

Base volume model selection

A total of eighteen volume equations (*Table 2*) were selected from the literature (Alegria and Tome, 2011; Özçelik, 2019). In these studies, several models of volume equations are used in different forms to develop tree volume equations (Saraçoğlu, 1988; Bi and Hamilton, 1998; Bailey, 1994; Yavuz, 1999; Mısır and Mısır, 2004; Teshome, 2005; Akindele and LeMay, 2006; Perez, 2008; Alegria and Tome, 2011; Hjelm and Johansson, 2012; Stolarikova et al., 2014; Malata et al., 2017; Lee et al., 2017; Özçelik

http://www.aloki.hu ● ISSN 1589 1623 (Print) ● ISSN1785 0037 (Online)
DOI: http://dx.doi.org/10.15666/aeer/1804_49414958

and Çevlik, 2017; Kitikidou et al., 2017; Sakıcı et al., 2018). These equations were examined and evaluated to select the best model for further analysis.

Table 2. *Volume functions selected for evaluation*

Function form	References	Number
$V = a + (b D^2 h)$	Borset (1954)	(1)
$V = aD^bH^c$	Bailey (1994)	(2)
$V = (a + b D)^2$	Perez and Kanninen (2003)	(3)
$V = aD^2H$	Spurr (1952)	(4)
$V = \frac{D^2}{a + {}^b/_H}$	Honer (1967)	(5)
$V = a + b D^2H + cH$	Rachid-Casnati et al. (2014)	(6)
$V = \frac{D^2H}{a + bD}$	Takata (1958)	(7)
$V = a + bD^cH^d$	Burkhart (1977)	(8)
$V = a + b (H/D)^c D^2H$	Teshome (2005)	(9)
$V = D^2(a + bH)$	Ogaya (1968)	(10)
$V = aD^2 + b D^2H - cD^2H^2 - dH + e DH^2$	Eriksson (1973)	(11)
$V = a + b D^2H + cD^3H + d D^2H^2 + e H$	Bi and Hamilton (1998)	(12)
$V = a(D^2H)^b$	Malata et al. (2017)	(13)
$V = a(D^2)^b H^c$	Malata et al. (2017)	(14)
$V = a + b D^2 + cD^2H^2$	Alegria and Tome (2011)	(15)
$V = a + b D + c D^2 + dD^2H^2$	Alegria and Tome (2011)	(16)
$V = a + b DH + cDH^2 + d D^2H^2$	Alegria and Tome (2011)	(17)
$V = a + b D + c DH^2 + d D^2H^2$	Alegria and Tome (2011)	(18)

Note: V = total Volume (m^3); D = diameter at breast height outside bark (cm); H = total height (m); a, b, c, d, e = parameters to be estimated

Through comparisons, the Schumacher and Hall (Bailey, 1994) function (model 2) was found to provide consistent and accurate results, and was therefore considered one of the best non-linear functions to describe the total volume of the Scots pine and selected as the base model:

$$V = aD^bH^c \quad \text{(Eq.2)}$$

where V is volume in cubic meter (m^3), D is the tree diameter at breast height (DBH) (cm), H is the total height (m), (a, b, and c) are the parameters.

Equation 2 was fit to: (1) the overall data, (2) the NWYLHLM region data (region 1), (3) the SAYLHLM region data (region 2) and (4) each of the eight ecoregions separately. The PROC NLIN procedure in the Statistical Analysis System (SAS Institute, Inc. 2002) was utilized to estimate the model parameters and model statistics.

To assess whether the total volume equations are different among regions and ecoregions, the non-linear extra sum of squares method was used (Bates and Watts, 1988; Neter et al., 1996). This method demands the fitting of full and reduced models and has commonly been applied to evaluate if separate models are necessary for different species or different ecoregions and geographic regions (Huang et al., 2000; Peng et al., 2001; Zhang et al., 2002; Castedo-Dorado et al., 2005; Corral-Rivas et al.,

http://www.aloki.hu ● ISSN 1589 1623 (Print) ● ISSN1785 0037 (Online)
DOI: http://dx.doi.org/10.15666/aeer/1804_49414958

2007). The full model corresponds to different sets of parameters for each subregions and is gotten by enlarging each parameter by including an associated parameter and a dummy variable to distinguish among ecoregions. The reduced model corresponds to the same set of global parameters for all ecoregions. Using Indicator (dummy) variable approach for the *Equation 2*, the full model of the volume function can be written as:

$$V = \left(a + \sum_{i=1}^{k} a_i r_i \right) D^{\left(b+\sum_{i=1}^{k} b_i r_i\right)} H^{\left(c+\sum_{i=1}^{k} c_i r_i\right)} \quad \text{(Eq.3)}$$

where:
V = volume parameter tested,
r_i = indicator variable for regions and ecoregions,
D = tree dbh (in cm),
a,b, c = parameters to be estimated from the data,
k = the number of indicator variables.

Evaluate the overall volume differences among ecoregions

This procedure involves the use of seven indicator variables (k=7) which are needed in *Equation 3* for eight ecoregions in the full model form in this case. They are defined as follows:

If subregion = XL, $z_1 = 1$, all other zi = 0.
If subregion = TH, $z_2 = 1$, all other zi = 0.
If subregion = HZ, $z_3 = 1$, all other zi = 0.
If subregion = SBZ, $z_4 = 1$, all other zi = 0.
If subregion = HJY, $z_5 = 1$, all other zi = 0.
If subregion = XLJ, $z_6 = 1$, all other zi = 0.
If subregion = TQ, $z_7 = 1$, all other zi = 0.
If subregion = AME, all other zi = 0.

While the reduced model form is represented by a three parameters model (*Equation 2*) representing the volume relationship across all ecoregions.

Evaluate the volume differences between the two regions

To test the difference between region NWYLHLM and SAYLHLM, one indicator variable (k=1) can be defined: if region = NWYLHLM, z_1 =1; and if region = SAYLHLM, $z_1 = 0$. Similarly, the full model (*Equation 3*) has 6 estimable parameters.

Evaluate the volume differences between the eight ecoregions

A total of 28 ecoregion pairs can be formulated to test the pairwise differences between the eight ecoregions. The 28 testing pairs require 28 full models that take the form of *Equation 3*, and 28 reduced models that take the form of *Equation 2*. For example, to test the difference between ecoregion TH vs. HZ, one indicator variable (k=1) can be defined: if ecoregion = TH, z_1 =1; and if ecoregion = HZ, $z_1 = 0$. Similarly, the full model (*Equation 3*) has 6 estimable parameters. All the reduced models for these tests take the form of *Equation 2* with 3 parameters.

http://www.aloki.hu ● ISSN 1589 1623 (Print) ● ISSN1785 0037 (Online)
DOI: http://dx.doi.org/10.15666/aeer/1804_49414958

Evaluate statistic

The significance of the full and reduced model comparisons were based on an F-test of the form:

$$F = \frac{\frac{SSE_R - SSE_F}{df_R - df_F}}{\frac{SSE_F}{df_F}} \quad \text{(Eq.4)}$$

where SSE_R is the error sum of squares of a reduced model with the degrees of freedom df_R, and SSE_F is the error sum of squares of a full model with the degrees of freedom df_F. This test statistic is F-distributed for a non-linear model if the data used represent a large sample generally; the F-test is significant if the P-value for the test is less than 0.05.

In order to understand the consequences of inappropriate application of a volume model in different ecoregions, each of the eleven models (global model, regional model 1 (NWYLHLM 1), regional model 2 (SAYLHLM 2), and 8 ecoregional models was used to predict total volume of trees for each ecoregion.

To quantify the magnitude of the prediction error when a specific region model is used, the average volume prediction error ($\bar{\varepsilon}$), the standard error of the prediction error (S_e), and the prediction bias as a percentage of average "real" volume (% bias) were calculated and defined as:

$$\bar{\varepsilon} = \frac{\sum_{i=1}^{m}(\hat{V}_i - V_i)}{m} \quad \text{(Eq.5)}$$

$$S_e = \sqrt{\frac{\sum_{i=1}^{m}(\varepsilon - \bar{\varepsilon})^2}{m-1}} \quad \text{(Eq.6)}$$

$$Bias(\%) = {}^{\bar{\varepsilon}}/_{\bar{V}} \times 100 \quad \text{(Eq.7)}$$

where:
m= Number of trees,
V_i= Data reported volume for tree i,
$\hat{V}_i$ = Predicted volume for tree i,
$\bar{V}$= Mean data reported volume.

Results and Discussion

Model fitting to regional and ecoregional data

Based on the different data sets, *Equation 2* was separately fitted using non-linear least squares. Parameter estimates and MSE for each ecoregion and region are displayed in *Table 3*. In all situations, parameter estimates and model forms were statistically significant (P<0.01). Among the eight ecoregional models, the lowest MSE value was found in the TH ecoregion, and the highest MSE value was found in the AME ecoregion. The parameter estimates varied among the eight ecoregions, indicating that each ecoregion may have a different volume with DBH and H relationship from others. The three regional models also have different parameter estimates.

http://www.aloki.hu ● ISSN 1589 1623 (Print) ● ISSN1785 0037 (Online)
DOI: http://dx.doi.org/10.15666/aeer/1804_49414958

Table 3. *Parameter estimates and MSE of volume function for the regional and ecoregional models*

Ecoregions	N	a	b	c	MSE
XL	65	0.000020	2.0737	1.0984	0.0121
TH	120	0.000029	1.8453	1.2382	0.00078
HZ	135	0.000200	1.9262	0.5259	0.00522
SBZ	68	0.000015	1.8184	1.5004	0.00233
HJY	335	0.000081	2.1093	0.6063	0.00657
XLJ	189	0.000132	1.8660	0.7028	0.0012
TQ	184	0.000044	1.5513	1.4665	0.0146
AME	198	0.000117	1.9022	0.7312	0.0159
NWYLHLM	**706**	**0.000111**	**1.9041**	**0.7453**	**0.0109**
SAYLHLM	**588**	**0.000034**	**2.0686**	**0.9313**	**0.0063**
Overall	**1294**	**0.000075**	**1.9719**	**0.7906**	**0.00915**

Note: N-sample size (number of tree), a, b, c-three parameters of volume model, MSE-model mean squared error

Comparison of the total volume equations between regions and ecoregions

Table 4 shows the testing results for the differences of the overall volume models for the eight ecoregions. The F-test indicates that there are differences among the total volume models from eight ecoregions ($P < 0.0001$). This implies that the overall model is not sufficient to describe the volume with DBH and H relationships for the eight ecoregions selected. The difference between the different regions (NWYLHLM-SAYLHLM) was also tested and the P-values were less than 0.0001 for the two regional paired comparisons. This means that the difference in volume between the two geographic regions is also statistically significant. The same approach was used to test for differences among the eight ecoregions (*Table 4*). Among the 28 pairs of ecoregion comparisons, only three ecoregion pairs (e.g., XL versus SBZ, HZ versus AME, and SBZ versus TQ) showed the non-significant difference ($P>0.05$).

Prediction errors of applying overall and regional volume equations to each ecoregion

According to the tests above, there were significant differences for many paired comparisons of the volume model among the eight ecoregions and between regions. Inappropriately applying a total volume model in these ecoregions may result in prediction biases. To understand the consequences, all eleven models (overall model, NWYLHLM model, SAYLHLM model and eight sub-regional models) were used to predict total tree volume for each ecoregion individually.

If the overall model was used to predict the volume of trees in each ecoregion, excessive or underestimated predictions were made for different ecoregions. On average, the overall model under-estimated (i.e., positive Bias %) tree volume from 0.1% to 3.2% for ecoregions AME, HJY, TQ, and HZ, and over-estimated (i.e., negative Bias %) tree volume about -2.1% to -8.1% in ecoregions XL, XLJ, SBZ and TH (*Table 5*).

Applying the NWYLHLM regional model to each ecoregion would result in similar patterns and magnitudes of the prediction errors as the overall model. This model under-estimated tree volumes in the HZ (1.9%), AME (0.07%), and over-estimated tree volumes in the XL (-3.01%), TH (-11.1%), SBZ (-9.8%), HJY (-1.4%), XLJ (-9.3%) and TQ (-0.0735%) (*Table 6*).

http://www.aloki.hu ● ISSN 1589 1623 (Print) ● ISSN1785 0037 (Online)
DOI: http://dx.doi.org/10.15666/aeer/1804_49414958

Table 4. *F-test for testing the difference between regions and among eight ecoregions*

Subregions	n	Full Model			Reduced Model			Extra sum of squares		
		SSE_F	PF	df_F	SSE_R	PR	df_R	$df_R - df_F$	F-value	P-value
Overall	**1294**	**9.8339**	**30**	**1267**	**11.8065**	**3**	**1291**	**24**	**10.5898**	**0.0000**
NWYLHLM-SAYLHLM	1294	11.3292	**6**	1288	11.8065	33	1291	3	18.0893	0.0000
XL - TH	185	0.8429	6	179	0.9774	3	182	3	9.5188	0.0000
XL - HZ	200	1.4410	6	194	1.7510	3	197	3	13.9109	0.0000
XL - SBZ	133	0.9032	6	127	0.9322	3	130	3	1.3577	0.2587
XL - HJY	400	2.9341	6	394	3.1322	3	397	3	8.8686	0.0000
XL - XLJ	254	0.9753	6	248	1.2592	3	251	3	24.0628	0.0000
XL - TQ	249	3.4031	6	243	3.9713	3	246	3	13.5243	0.0000
XL - AME	263	3.8440	6	257	4.0791	3	260	3	5.2411	0.0015
TH - HZ	255	0.7807	6	249	1.2053	3	252	3	45.1421	0.0000
TH - SBZ	188	0.2428	6	182	0.2786	3	185	3	8.9416	0.0000
TH - HJY	455	2.2737	6	449	2.6379	3	452	3	23.9775	0.0000
TH - XLJ	309	0.3150	6	303	0.3822	3	306	3	21.5336	0.0000
TH - TQ	304	2.7428	6	298	2.8935	3	301	3	5.4611	0.0011
TH - AME	318	3.1836	6	312	3.4648	3	315	3	9.1839	0.0000
HZ - SBZ	203	0.8409	6	197	1.1099	3	200	3	21.0047	0.0000
HZ - HJY	470	2.8718	6	464	3.0242	3	467	3	8.2085	0.0000
HZ - XLJ	324	0.9131	6	318	1.1756	3	321	3	30.4673	0.0000
HZ - TQ	319	3.3409	6	313	3.8997	3	316	3	17.4522	0.0000
HZ - AME	333	3.7817	6	327	3.8206	3	330	3	1.1204	0.3408
SBZ - HJY	403	2.3340	6	397	2.5168	3	400	3	10.3639	0.0000
SBZ - XLJ	257	0.3753	6	251	0.4846	3	254	3	24.3789	0.0000
SBZ - TQ	252	2.8030	6	246	2.8453	3	249	3	1.2369	0.2968
SBZ - AME	266	3.2439	6	260	3.4207	3	263	3	4.7232	0.0031
HJY - XLJ	524	2.4062	6	518	2.8629	3	521	3	32.7782	0.0000
HJY - TQ	519	4.8339	6	513	5.6557	3	516	3	29.0706	0.0000
HJY - AME	533	5.2748	6	527	5.5064	3	530	3	7.7127	0.0000
XLJ - TQ	373	2.8752	6	367	3.2028	3	370	3	13.9407	0.0000
XLJ - AME	387	3.3161	6	381	3.6265	3	384	3	11.8870	0.0000
TQ - AME	382	5.7438	6	376	6.1290	3	379	3	8.4049	0.0000

Note: N – sample size, SSE_F – error sum of squares of the full model, df_F – degrees of freedom of SSE_F, SSE_R – error sum of squares of reduced model, df_R – degrees of freedom of SSE_R, P is the number of parameters

Table 5. *Prediction error of applying the overall model for each ecoregion*

Subregions	N	$\bar{V}$(m)	$\hat{V}$(m)	$\bar{\varepsilon}$	S_e	t	Bias (%)
XL	65	0.9352	0.9547	-0.0195	0.1183	-1.3284	-2.0835
TH	120	0.3198	0.3456	-0.0258	0.0479	-5.9040	-8.0736
HZ	135	0.7603	0.7360	0.0243	0.0768	3.6748	3.1946
SBZ	68	0.3136	0.3329	-0.0194	0.0629	-2.5392	-6.1728
HJY	335	0.5550	0.5516	0.0034	0.0852	0.7356	0.6167
XLJ	189	0.3128	0.3319	-0.0191	0.0507	-5.1842	-6.1184
TQ	184	0.7181	0.7117	0.0064	0.1329	0.6504	0.8876
AME	198	1.0919	1.0904	0.0015	0.1269	0.1655	0.1367

Note: N – sample size, $\bar{V}$ – average of observed tree volume, $\hat{V}$ – average of predicted tree volume from the model, S_e – standard deviation of prediction error

http://www.aloki.hu ● ISSN 1589 1623 (Print) ● ISSN1785 0037 (Online)
DOI: http://dx.doi.org/10.15666/aeer/1804_49414958

Table 6. *Prediction errors of applying regional models to each ecoregion*

Reg-Eco	N	$\bar{V}$(m)	$\hat{V}$(m)	$\bar{\varepsilon}$	S_e	t	Bias (%)
NWYLHLM - XL	65	0.9352	0.9633	-0.0281	0.1255	-1.8056	-3.0053
NWYLHLM - TH	120	0.3198	0.3554	-0.0356	0.0502	-7.7685	-11.1237
NWYLHLM - HZ	135	0.7603	0.7455	0.0148	0.0756	2.2782	1.9507
NWYLHLM - SBZ	68	0.3136	0.3443	-0.0307	0.0659	-3.8394	-9.7935
NWYLHLM - HJY	335	0.5550	0.5626	-0.0076	0.0879	-1.5896	-1.3757
NWYLHLM - XLJ	189	0.3128	0.3419	-0.0291	0.0493	-8.1208	-9.3051
NWYLHLM - TQ	184	0.7181	0.7186	-0.0005	0.1312	-0.0546	-0.0735
NWYLHLM - AME	198	1.0919	1.0911	0.0008	0.1253	0.0886	0.0722
SAYLHLM - XL	65	0.9352	0.9362	-0.0009	0.1099	-0.0702	-0.1024
SAYLHLM - TH	120	0.3198	0.3301	-0.0103	0.0448	-2.5288	-3.2368
SAYLHLM - HZ	135	0.7603	0.7177	0.0426	0.0837	5.9206	5.6079
SAYLHLM - SBZ	68	0.3136	0.3139	-0.0003	0.0566	-0.0498	-0.1091
SAYLHLM - HJY	335	0.5550	0.5359	0.0190	0.0837	4.1592	3.4277
SAYLHLM - XLJ	189	0.3128	0.3168	-0.0040	0.0548	-1.0091	-1.2857
SAYLHLM - TQ	184	0.7181	0.7037	0.0144	0.1389	1.4091	2.009
SAYLHLM - AME	198	1.0919	1.0908	0.0011	0.1367	0.1135	0.1009

Note: N – sample size, $\bar{V}$ – average of observed tree volume, $\hat{V}$ – average of predicted tree volume from the model, S_e – standard deviation of prediction error

The same approach was used for SAYLHLM regional model to each ecoregion (*Table 6*). SAYLHLM regional model under-estimated tree volumes in the HZ (5.6%), HJY (3.4%), TQ (2.01%), AME (0.1%) and over-estimated tree volumes in the XL (-0.1%), TH (-3.2%), SBZ (-0.1%) and XLJ (-1.3%).

Prediction errors of applying ecoregional equation to each ecoregion

When the eight ecoregional models were applied to each ecoregion, they generally performed well in the ecoregions in which the models were developed. Otherwise, the models produced the prediction errors. The prediction biases ranged from -1.2% to 7.5% in XL, from -0.8% to 11.7% in TH, from -13.9% to 0.08% in HZ, from -3.5% to 10.3% in SBZ, from -8.9% to 0.9% in HJY, from -2.5% to 10.4% in XLJ, from -11.6% to 9.4% in TQ and from -11.7% to 1.5% in AME (*Table 7*). *Figure 2* shows the mean prediction errors across 5-cm diameter classes when ecoregional models are applied to predict tree volume in each of the eight ecoregions separately. This further confirmed that ecoregional model developed in that ecoregion performed well for most diameter classes.

The expected results show that the different ecoregions have large differences in climatic, soil and ecological conditions. Corral-Rivas et al. (2007) and Brooks and Wiant (2008) reported in their study of the use of stump diameter to estimate DBH and tree volumes (V) at El Salto, Durango, Mexico and Ecoregion-based local volume equations for Appalachian hardwoods, USA. Part of the differences between the dbh and volume models between tree species may be caused by differences in genetics, growing conditions, and site quality. Previous studies of different species have also revealed differences between ecoregion-based height-diameter models (Huang, 1999; Huang et al., 1999; Zhang et al., 2002; Peng et al., 2004; Brooks and Wiant, 2005; Özçelik et al., 2014, 2016; Chourou, 2014; Enzinga and Jiang, 2019). In our case, the updated ecoregion classification in the cold temperate coniferous forest regions of Eastern Daxing'an Mountains (*Figure 1*) provides comprehensive information on changes in the relationships between ecoregions and tree species of *Pinus silvestrix* along ecological and macroclimatic gradients from different regions. These ecoregions are characterized by large climatic regimes that include temperature and precipitation, soil moisture and nutrient regimes, and succession and vegetation types (Hills, 1959, 1960; CEC, 1997; ELC Working Group, 2000).

http://www.aloki.hu ● ISSN 1589 1623 (Print) ● ISSN1785 0037 (Online)
DOI: http://dx.doi.org/10.15666/aeer/1804_49414958

Table 7. *Prediction errors of applying a specific ecoregion model to each ecoregion*

Subregions	N	$\bar{V}$(m)	$\hat{V}$(m)	$\bar{\varepsilon}$	S_e	t	Bias (%)
XL model							
XL - XL	65	0.9352	0.9193	0.0159	0.1079	1.1904	1.7047
XL - TH	120	0.3198	0.3235	-0.0037	0.0435	-0.9268	-1.1510
XL - HZ	135	0.7603	0.7036	0.0567	0.0908	7.2498	7.4529
XL - SBZ	68	0.3136	0.3044	0.0092	0.0518	1.4662	2.9399
XL - HJY	335	0.5550	0.5326	0.0224	0.0865	4.7333	4.0319
XL - XLJ	189	0.3128	0.3114	0.0014	0.0568	0.3298	0.4359
XL - TQ	184	0.7181	0.7038	0.0142	0.1429	1.3528	1.9851
XL - AME	198	1.0919	1.0904	0.0015	0.1454	0.1451	0.1373
TH model							
TH - XL	65	0.9352	0.8686	0.0666	0.1334	4.0237	7.1185
TH - TH	120	0.3198	0.3224	-0.0026	0.0288	-0.9789	-0.8052
TH - HZ	135	0.7603	0.6713	0.0889	0.1109	9.3206	11.7032
TH - SBZ	68	0.3136	0.3044	0.0092	0.0510	1.4795	2.9203
TH - HJY	335	0.5550	0.5331	0.0219	0.1026	3.9010	3.9401
TH - XLJ	189	0.3128	0.3149	-0.0021	0.0432	-0.6728	-0.6765
TH - TQ	184	0.7181	0.6861	0.0319	0.1248	3.4741	4.4509
TH - AME	198	1.0919	1.0322	0.0597	0.1345	6.2439	5.4667
HZ model							
HZ - XL	65	0.9352	0.9858	-0.0506	0.1323	-3.0819	-5.4076
HZ - TH	120	0.3198	0.3641	-0.0443	0.0619	-7.8473	-13.8603
HZ - HZ	135	0.7603	0.7635	-0.0032	0.0716	-0.5242	-0.4252
HZ - SBZ	68	0.3136	0.3564	-0.0428	0.0754	-4.6792	-13.6435
HZ - HJY	335	0.5550	0.5639	-0.0089	0.0878	-1.8544	-1.6029
HZ - XLJ	189	0.3128	0.3472	-0.0345	0.0486	-9.7367	-11.0184
HZ - TQ	184	0.7181	0.7175	0.0005	0.1366	0.0545	0.0765
HZ - AME	198	1.0918	1.0928	-0.0009	0.1273	-0.1049	-0.0869
SBZ model							
SBZ - XL	65	0.9352	0.8832	0.05199	0.1277	3.2817	5.5595
SBZ - TH	120	0.3198	0.3296	-0.0098	0.0459	-2.3302	-3.0569
SBZ - HZ	135	0.7603	0.6820	0.0783	0.1181	7.6986	10.2934
SBZ - SBZ	68	0.3136	0.3064	0.0071	0.0471	1.2503	2.2755
SBZ - HJY	335	0.5550	0.5563	-0.0013	0.1063	-0.2239	-0.2343
SBZ - XLJ	189	0.3128	0.3236	-0.0108	0.0566	-2.6365	-3.4702
SBZ - TQ	184	0.7181	0.7194	-0.0013	0.1355	-0.1343	-0.1868
SBZ - AME	198	1.0919	1.0770	0.0148	0.1489	1.4032	1.3601
HJY model							
HJY - XL	65	0.9352	0.9928	-0.0576	0.1201	-3.8677	-6.1634
HJY - TH	120	0.3198	0.3484	-0.0286	0.0627	-5.0008	-8.9488
HJY - HZ	135	0.7603	0.7617	-0.0014	0.0833	-0.1998	-0.1886
HJY - SBZ	68	0.3136	0.3368	-0.0232	0.0711	-2.6901	-7.3933
HJY - HJY	335	0.5550	0.5499	0.0051	0.0807	1.1471	0.9116
HJY - XLJ	189	0.3128	0.3307	-0.0179	0.0609	-4.0378	-5.7259
HJY - TQ	184	0.7181	0.7179	0.0002	0.1433	0.0218	0.0321
HJY - AME	198	1.0919	1.1206	-0.0287	0.1360	-2.9686	-2.6277
XLJ model							
XLJ - XL	65	0.9352	0.8785	0.0567	0.1523	2.9991	6.0591
XLJ - TH	120	0.3198	0.3278	-0.0081	0.0514	-1.7201	-2.5235
XLJ - HZ	135	0.7603	0.6815	0.0788	0.1006	9.0999	10.3661
XLJ - SBZ	68	0.3136	0.3189	-0.0053	0.0689	-0.6373	-1.6998
XLJ - HJY	335	0.5550	0.5157	0.0393	0.1088	6.6097	7.0821
XLJ - XLJ	189	0.3128	0.3155	-0.0027	0.0344	-1.1024	-0.8816
XLJ - TQ	184	0.7181	0.6546	0.0635	0.1431	6.0196	8.8414
XLJ - AME	198	1.0919	0.9887	0.1032	0.1432	10.1385	9.4492
TQ model							
TQ - XL	65	0.9352	0.8789	0.0563	0.1721	2.6386	6.0235
TQ - TH	120	0.3198	0.3498	-0.0300	0.0449	-7.3275	-9.3986
TQ - HZ	135	0.7603	0.6890	0.0713	0.1423	5.8229	9.3779
TQ - SBZ	68	0.3136	0.3308	-0.0172	0.0529	-2.6879	-5.4961
TQ - HJY	335	0.5550	0.5847	-0.0297	0.1261	-4.3129	-5.3526
TQ - XLJ	189	0.3128	0.3491	-0.0363	0.0542	-9.2083	-11.6156
TQ - TQ	184	0.7181	0.7269	-0.0088	0.1204	-0.9941	-1.2288
TQ - AME	198	1.0919	1.0513	0.0405	0.1503	3.7956	3.7123

http://www.aloki.hu ● ISSN 1589 1623 (Print) ● ISSN1785 0037 (Online)
DOI: http://dx.doi.org/10.15666/aeer/1804_49414958

Subregions	N	$\bar{V}$(m)	$\hat{V}$(m)	$\bar{\varepsilon}$	S_e	t	Bias (%)
AME model							
AME - XL	65	0.9352	0.9672	-0.0320	0.1258	-2.0523	-3.4251
AME - TH	120	0.3198	0.3571	-0.0373	0.0513	-7.9756	-11.6782
AME - HZ	135	0.7603	0.7487	0.0116	0.0750	1.8000	1.5289
AME - SBZ	68	0.3136	0.3463	-0.0327	0.0668	-4.0393	-10.4336
AME - HJY	335	0.5550	0.5646	-0.0096	0.0877	-1.9954	-1.7236
AME - XLJ	189	0.3128	0.3434	-0.0307	0.0498	-8.4672	-9.8101
AME - TQ	184	0.7181	0.7206	-0.0025	0.1314	-0.2590	-0.3494
AME - AME	198	1.0919	1.0938	-0.0019	0.1253	-0.2191	-0.1787

Note: N – sample size, $\overline{V}$ – average of observed tree volume, $\hat{V}$ – average of predicted tree volume from the model, S_e – standard deviation of prediction error

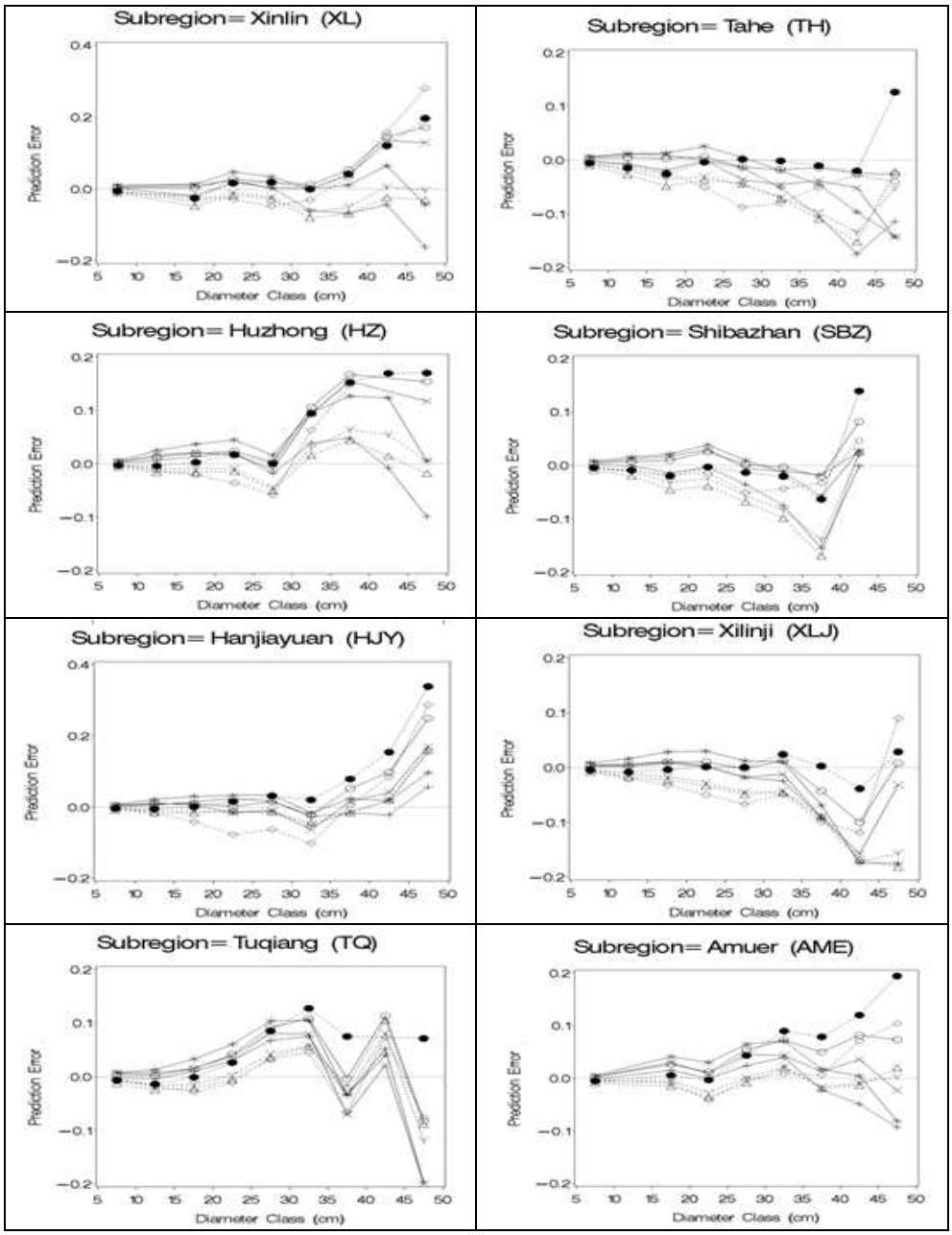

Figure 2. *Average prediction errors (m) across 5-cm diameter classes when each ecoregional model is applied to predict total volume in each of the eight ecoregions with symbols: XL (star), TH (circle), HZ (triangle), SBZ (X), HJY (plus), XLJ (dot), TQ (diamond) and AME (Y)*

http://www.aloki.hu ● ISSN 1589 1623 (Print) ● ISSN1785 0037 (Online)
DOI: http://dx.doi.org/10.15666/aeer/1804_49414958

Enzinga and Jiang (2019) provide comprehensive analysis of the climatic characteristics of the eastern Daxing'an Mountains which include the two regions (NWYLHLM and SAYLHLM) selected for the study. In addition, local ecological conditions such as vegetation types also affect growth and productivity as well as species dominance in these ecoregions For example, in the 8 subregions selected for the study, it was demonstrated that the Scots pine (*Pinus Sylvestrix* var. mongolica) population was not present in the NDXAM region containing the subregions: Songling (SL), Jiagedaqi (JGDQ) within which the Scots pine stand was not observed by observing the previous 10 subregions of the Daxing'an mountains. Therefore, the combination of all climatic, environmental and vegetation factors plays an important role in determining the different volume relationships among the 8 ecoregions linked to our study.

These results are consistent with the last and recent results reported by Brooks and Wiant (2008), Li and Zeng (2016), and Liu and Jiang (2016). Based on six ecoregions from Central Appalachian, Unites States, Brooks and Wiant (2008) evaluated the ecoregion-based volume equations for six hardwood species and found that the average bias between a regional model with a single species and specific forms of ecoregion ranged from -9.1 to 8.5% for the gross volume of board feet, from -3.5 to 9.2% for the gross volume of marketable cubic feet, and -9.5 to 16.7% for the weight of the marketable dry bole. Li and Zeng (2016) used the datasets of Larix spp. from four regions (northeastern, northern, northwestern, and southwestern) of China and same total volume equation used in our study to test the difference among regions. Their results indicated that the difference of volume estimates was noticed between northeastern and northern regions, northern and northwestern regions. Based on the classification in eastern Daxing'an Mountains, Northeast China by Zhang et al. (1992), three regions were identified. Liu and Jiang (2016) evaluated the regional difference of volume estimates using dahurian larch (*larix gmelinii*) datasets from eastern Daxing'an Mountains. Results indicated that volume models were significant difference among different regions, therefore, region-based volume equation is required to avoid increasing prediction error. Enzinga and Jiang (2019) evaluated the region and subregion-based height-diameter models for dahurian larch (*larix gmelinii*) in Eastern Daxing'an Mountains which led to conclusions demonstrating that there were distinct variations in height-diameter relationships for Dahurian larch between the different sub-regions in three forest regions and that usually, height-diameter models based on ecoregions report forecasts more reliably on a regional basis and avoid likely errors that may arise when applying the models in other areas. The same is true in the case of our study on ecoregional assessments based on volume equation models in Northeast China.

Conclusion

In the study, the total tree volume equations were developed for *Pinus sylvestrix* var mongolica in northeastern China. Using dummy variables and the non-linear extra sum of squares procedure, the volume with diameter and total height relationship was not the same for all ecoregions when tested by regions and ecoregions of Scots pine. For comparisons by ecoregion, statistical differences in total volume were found in many ecoregions, which can be explained in part by the longitudinal, latitudinal and elevation properties that exist in the soil, the length of the season, growth rates and annual precipitation rates in these regions. This brings us to prove the importance of the

http://www.aloki.hu ● ISSN 1589 1623 (Print) ● ISSN1785 0037 (Online)
DOI: http://dx.doi.org/10.15666/aeer/1804_49414958

relationship between the volume, the diameter and the total height of the trees of the *Pinus sylvestrix* var mongolica species studied.

Differences in height and diameter reported for the same northeast China ecoregions are probably the main factor behind the different volume models. The average bias varies at different percentage levels for the market value of wood in the two regions, the equations for total volume of trees specific to Scots pine and ecoregions are presented and can be easily used in situations of wood intrusion into the eight ecoregions, although there are significant volume relationships between the *Pinus sylvestrix* species in the two regions studied for this case. The inappropriate application of overall or regional volume models to these different ecoregions for Scots pine in Eastern Daxing'an Mountains can in this case lead to significant errors in the estimation of total volumes.

Apart from all these inverstigations we recommend the following:

- Develop different models for different ecoregions wherever the data are favorable;
- Furthermore, the difference in the growth of *Pinus sylvestrix* between the two regions as well as the eight ecoregions being explained in a summary manner, climatic research must be done in order to determine the factors responsible of the difference in tree growth between the two regions and the eight ecoregions on the one hand and on the other, to better understand the variations in the volume-diameter and height relationship on large scales;
- In the light of the results obtained during this study, the predicted volumes of *Pinus sylvestrix* Var Mongolica trees, obtained through the development of models of volume equations in the two regions, can be used as explanatory variables for the calculation of the allowable cut by forestry managers. However, it is preferable to use the volume that has been predicted from ecoregional models since it enjoys, to our knowledge, unprecedented precision.
- Regarding the GIS aspect, the main objective of this article being to reflect the differences between regions and ecological regions from total volume models, in the future, we will recommend cartographic studies related to remote sensing at the level of different regions and ecoregions using GIS-based methods and finally to develop a quantitative and multivariate regionalization model capable of delineating ecoregions on several levels from remote sensed information and other spatial data on environmental and natural resources so have a general vision of the evolution of the forest cover and the landscape for each defined region and ecoregions. The development of the model will thus provide a new useful approach to the mapping of ecoregions for resource managers and researchers.

Acknowledgments. This research was financially supported by the National Key R &D Program of China (grant No. 2017YFB0502700), National Natural Science Foundation of China (31570624), Applied Technology Research and Development Plan Project of Heilongjiang Province (GA19C006), and Fundamental Research Funds for Central Universities (2572019CP15).

REFERENCES

[1] Adegoke, F. F., Akinyemi, G. O., Ige, P. O., Ogunwande, O. A., Ogunade, J. O. (2010): Forestry Development; A recipe for the Nation's Economic Recession. – In: Popoola, L. (ed.) The Global Economic Crisis and Sustainable Renewable Natural Resources Management. Proceedings of the 33rd Annual FAN Conference, Benin City, Edo State, Nigeria.

http://www.aloki.hu ● ISSN 1589 1623 (Print) ● ISSN1785 0037 (Online)
DOI: http://dx.doi.org/10.15666/aeer/1804_49414958

[2] Akindele, S. O., LeMay, V. M. (2006): Development of tree volume equations for common timber species in tropical rain forest area of Nigeria. – Forest Ecology and Management 226: 41-48.
[3] Alegria, C., Tome, M. (2011): A set of models of individual tree merchantable volume prediction for *Pinus pinaster* Aiton in central inland of Portugal. – European Journal of Forest Research 130: 871-879.
[4] Bailey, R. L. (1994): A Compatible Volume-Taper Model Based On the Schumacher and Hall Generalized Constant Form Factor Volume Equation. – Forest Science 40(2): 303-313.
[5] Bates, D. M., Watts, D. G. (1988): Nonlinear regression analysis and its applications. – Wiley, New York.
[6] Bi, H., Hamilton, F. (1998): Stem volume equations for native tree species in southern New South Wales and Victoria. – Australian Forestry 61(4): 275-286.
[7] Børset, O. (1954): Volume computation of standing aspen. – Commun Norweigan For Assoc 43: 397-447.
[8] Brooks, J. R., Wiant, H. V. Jr. (2005): Evaluating ecoregion based height-diameter relationship of five economically important Appalachian hardwood species in West Virginia. – Proceedings of the seventh annual forest inventory and analysis symposium; October 3-6, 2005; Portland, ME. Gen. Tech. Rep. WO-77. Washington, DC: U.S. Department of Agriculture, Forest Service: 237-242.
[9] Brooks, J. R., Wiant, H. V. Jr. (2008): Ecoregion-based local volume equations for Appalachian hardwoods. – Northern Journal of Applied Forestry 25: 87-92.
[10] Burkhart, H. E. (1977): Cubic-foot volume of loblolly pine to any merchantable top limit. – Southern Journal of Applied Forestry 1(2): 7-9.
[11] Castedo, F., Barrio, M., Parresol, B. R., Alvarez, J. G. (2005): A stochastic height–diameter model for maritime pine ecoregions in Galicia (northwestern Spain). – Annals of Forest Science 62: 455-465.
[12] CEC (Commission for Environmental Cooperation) (1997): Ecological Regions of North America: Toward a common perspective. – CEC, Montreal. 71 p and maps.
[13] Chourou, W. (2014): Development and evaluation of height-diameter models of gray pins and black spruce at the provincial and ecoregional scale of Alberta and Quebec. – Univ. of Quebec in Montreal. Master's thesis, 81p.
[14] Clutter, J. L., Fortson, J. C., Pienaar, L. V., Brister, G. H., Bailey, R. L. (1983): Timber Management: A Quantitative Approach. – Wiley, New York.
[15] Corral-Rivas, J. J., Barrio-Anta, M., Aguirre-Calderon, O. A., Dieguez-Aranda, U. (2007): Use of stump diameter to estimate diameter at breast height and tree volume for major pine species in El Salto, Durango (Mexico). – Forestry 80: 29-40.
[16] ELC Working Group (2000): The Ecoregions and Ecodistricts of Ontario. – Ecological Land Classification Program, Ont. Min. Nat. Resour., Sault Ste Marie, ON.
[17] Enzinga, G. Y., Jiang, L. C. (2019): Evaluation of region and subregion-based height-diameter models for dahurian larch (larix gmelinii) in daxing'an mountains in china. – Applied Ecology and Environmental Research 17(6): 13567-13591. http://www.aloki.hu, ISSN 1589 1623 (Print), ISSN 1785 0037 (Online).
[18] Eriksson, H. (1973): Volymfunktioner för stående träd av ask, asp, klibbal och contorta-tall. [Tree volume functions for ash, aspen, alder and lodgepole pine in Sweden (*Fraxinus excelsior* L., *Populus tremula* L., *Alnus glutinosa* (L.) Gartn., *Pinus contorta* Dougl. var. *latifolia* Engelm.)]. – Skogshögskolan, Institutionen för skogsproduktion, Stockholm. Rapporter og Uppsatser nr. 26-1973. 26p.
[19] Frelich, L. E. (2016): Temperate Coniferous Forests. – In: Gibson, D. (ed.) Oxford Bibliographies in Ecology. New York: Oxford University Press, October 2016. http://www.oxfordbibliographies.com/view/document/obo 9780199830060/ obo-9780199830060-0162.xml?rskey=bkX55P&result=67.

http://www.aloki.hu ● ISSN 1589 1623 (Print) ● ISSN1785 0037 (Online)
DOI: http://dx.doi.org/10.15666/aeer/1804_49414958

[20] García-Espinoza, G. G., Aguirre-Calderón, O. A., Quiñonez-Barraza, G., Alanís-Rodríguez, E., De Los Santos-Posadas, H. M., García-Magaña, J. J. (2018): Taper and Volume Systems Based on Ratio Equations for Pinus pseudostrobus Lindley in Mexico. – Forests 9(6): 344.
[21] Han, G., Zhang, G., Yang, W. (1998): Quantitative analysis on principle eco-climatic factors of limiting natural reforestation of *Pinus sylvestris* var. *mongolica* on sandy land. – Sci. Silvae Sin. 35: 22-27. (Google Scholar).
[22] Hills, G. A. (1959): A Ready Reference to the Description of the Land of Ontario and its Productivity. – Preliminary Report. Ontario Department of Lands and Forests, Division of Research, Maple. 142p.
[23] Hills, G. A. (1960): Comparison of forest ecosystems (vegetation and soil) in different climatic zones. – Silva Fennica 105: 33-39.
[24] Hjelm, B., Johansson, T. (2012): Volume equations for poplars growing on farmland in Sweden. – Scandinavian Journal of Forest Research 27: 561-566.
[25] Honer, T. G. (1967): Standard volume tables and merchantable conversion factors for the commercial tree species of central and eastern Canada. – Can. Dept. Forestry Rural Devel., For. Mgmt. Res. And Serv. Inst. Info. Rep. FMR-X-5.
[26] Hu, T., Sun, L., Hu, H., Weise, D., Guo, F. (2017): Soil Respiration of the Dahurian Larch (*Larix gmelinii*) Forest and the Response to Fire Disturbance in Daxing'an Mountains, China. – Scientific Reports 7: 2967. DOI: 10.1038/s41598-017-03325-4.
[27] Huang, S. (1999): Ecoregion-based individual tree height-diameter models for lodgepole pine in Alberta. – Western Journal of Applied Forestry 14: 186-193.
[28] Huang, S., Titus, S. J., Wiens, D. P. (1999): Comparison of nonlinear height-diameter functions for major Alberta tree species. – Canadian Journal of Forest Research 22: 1297-1304.
[29] Huang, S., Price, D., Morgan, D., Peck, K. (2000): Kozak's variable-exponent taper equation regionalized for white spruce in Alberta. – West J Appl For 15(2): 75-85. (Cross Ref Google Scholar).
[30] Husch, B., Beers, T. W., Kershaw Jr., J. A. (2003): Forest Mensuration. – 4th ed., John Wiley and Sons, Inc., New Jersey, USA. 443p.
[31] Jiang, L., Brooks, J. R., Wang, J. (2005): Compatible taper and volume equations for yellow-poplar in West Virginia. – Forest Ecology and Management 213: 399-409. (Cross Ref Google Scholar).
[32] Kitikidou, K., Milios, E., Radoglou, K. (2017): Single-entry volume table for Pius brutia in panted peri-urban forest. – Annals of Silvicultural Research 41(2): 74-79.
[33] Lee, D., Seo, Y., Choi, J. (2017): Estimation and validation of stem volume equations for *Pinus densiflora, Pinus koraiensis*, and *Larix kaempferi* in South Korea. – Forest Science and Technology 13: 77-82.
[34] Li, H., Zeng, W. (2016): Validation and comparison of two-variable tree volume tables for Larix spp. in different regions of China. – Scientia Silvae Sinicae 52(6): 157-162. (in Chinese).
[35] Li, F. (2019): Forest Mensuration, Beijing. – China Forestry Publishing House.
[36] Liu, J., Jiang, L. (2016): Compatible tree volume equations and heteroscedasticity for dahurian larch in different regions of Daxing'anling. – Forest Research 29(3): 317-323. (in Chinese).
[37] Malata, H., Ngulube, E. S., Missanjo, E. (2017): Site Specific Stem Volume Models for Pinus patula and Pinus oocarpa. – Hindawi International Journal of Forestry Research. Article ID 3981647.
[38] Misir, N., Misir, M. (2004): Developing double-entry tree volume table for Ash in Turkey. – Kafkas University, Artvin Faculty of Forestry 3(4): 135-144.
[39] Neter, J., Kutner, M. H., Nachtsheim, C. J., Wasserman, W. (1996): Applied linear statistical models. – McGraw-Hill, New York. 1048p.

http://www.aloki.hu ● ISSN 1589 1623 (Print) ● ISSN1785 0037 (Online)
DOI: http://dx.doi.org/10.15666/aeer/1804_49414958

[40] Ogaya, N. (1968): Kubierungsformeln und Bestandesmassenformeln. – Inaugural. Doctoral dissertation, Dissertation-. Univ., Nat.-Math. Fak, Freiburg.
[41] Özçelik, R., Yavuz, H., Karatepe, Y., Gürlevik, N., Kiriş, R. (2014): Development of ecoregion-based height–diameter models for 3 economically important tree species of southern Turkey. – Turk J Agric For 38(3): 399-412. Tübitak doi: 10.3906/tar-1304-115.
[42] Özcelik, R., Karatepe, Y., Gürlevik, N., Canellas, I., Crecente-Campo, F. (2016): Development of ecoregion-based merchantable volume systems for *Pinus brutia* Ten and *Pinus nigra* Arnold in southern Turkey. – Journal of Forestry Research 27(1): 101-117.
[43] Özçelik, R., Çevlik, M. (2017): Batı Akdeniz Yöresi doğal sedir meşcereleri için hacim denklemleri. – Turkish Journal of Forestry 18: 68-86.
[44] Özçelik, R., Altınkaya, H. (2019): Comparison of tree volume equations for brutian pine stands in Eğirdir district. – Turkish Journal of Forestry 20(3): 149-156.
[45] Peng, C., Zhang, L., Liu, J. (2001): Developing and validation nonlinear height-diameter models for major tree species of Ontario's boreal forest. – Northern Journal of Applied Forestry 18: 87-94.
[46] Peng, C., Zhang, L., Zhou, X., Dang, Q., Huang, S. (2004): Developing and evaluating tree height-diameter models at three geographic scales for black spruce in Ontario. – Northern Journal of Applied Forestry 21: 83-92.
[47] Pérez, D., Kanninen, M. (2003): Aboveground biomass of Tectona grandis plantations in Costa Rica. – Journal of Tropical Forest Science 15(1): 199-213.
[48] Perez, D. (2008): Growth and volume equations developed from stem analysis for *Tectora grandis* in Costa Rica. – Journal of Tropical Forest Science 20: 66-75.
[49] Qian, H., Yuan, X. Y., Chou, Y. L. (2003): Forest Vegetation of Northeast China. – In: Kolbek, J., Šrůtek, M., Box, E. O. (eds.) Forest Vegetation of Northeast Asia. Geobotany, vol 28. Springer, Dordrecht.
[50] Rachid Casnati, C., Mason, E. G., Woollons, R., Resquin, F. (2014): Volume and taper equations for *P. teada* (L.) and *E. grandis* (Hill ex. Maiden). – Agrociencia Uruguay 18(2): 47-60.
[51] Sakıcı, O. E., Sağlam, F., Seki, M. (2018): Single-and Double-entry volume equations for Crimean pine stands in Kastamonu Regional Directorate of Forestry. – Turkish Jounral of Forestry 19(19): 20-29.
[52] Saraçoğlu, N. (1988): Stem volume table for Alder (*Alnus glutinosa* Gaertn subsp. *Barbata* (C.A. Mey.) Yalt.). – Tr. J. Of Agriculture and Forestry 22: 215-225.
[53] SAS Institute Inc. (2002): SAS/STAT Online User's Guide, Version 9.0. – SAS Institute Inc., Cary, NC.
[54] Shuaibu, R. B., Alao, J. S. (2013): Centrality of Forestry Education in Environmental Sustainability. – In: Labode, P., Ogunsanwo, O. Y., Adekunle, V. A. J., Azeez, I. O., Adewole, N. O. (eds.) The Green Economy: Balancing Environmental Sustainability & Livelihoods in an Emerging Economy. Proceedings of the 36th Annual Conference of Forestry Association of Nigeria (FAN) held in Uyo, Akwa Ibom State, Nigeria, pp 262-267.
[55] Shuaibu, R. B. (2014): Stem Taper and Tree Volume Equations for *Tectona grandis* (Teak) in Agudu Forest Reserve, Nasarawa State, Nigeria. – Unpublished Thesis in the Department of Forestry and Wood Technology Submitted to School of Post Graduate Studies, Federal University of Technology Akure, in Partial Fulfilment of the Requirements for the Award of Master of Agricultural Technology, (M. Agric. Tech.) Degree in Forest Inventory and Biometrics, 112p.
[56] Shuaibu, R. B., Alao, J. S. (2016): Multiple Linear Regression Tree Stem Volume Equations for the Estimation of Merchantable Volume of *Azadirachta Indica* (Neem Tree) in North-West Region of Nigeria. – International Journal of Forestry and Horticulture (IJFH) 2(1): 1-10. ISSN 2454-9487. www.arcjournals.org.
[57] Spurr, S. H. (1952): Forest Inventory. – Ronald Press, New York, 476p.

http://www.aloki.hu ● ISSN 1589 1623 (Print) ● ISSN1785 0037 (Online)
DOI: http://dx.doi.org/10.15666/aeer/1804_49414958

[58] Stolarikova, R., Salek, L., Zeahradnik, D., Dragoun, L., Jerabkova, L., Marusak, R., Merganic, J. (2014): Comparison of tree volume equations for small-leaved lime (*Tilia cordota* Mill.) in the Czech Republic. – Scandinavian Journal of Forest Research 29: 757-763.
[59] Takata, K. (1958): Construction of universal diameter-height-curves. – Journal of Japanese Forest Society 40: 1.
[60] Teshome, T. (2005): Analysis of individual tree volume equations for *Cupressus Lusitanica* in Munessa Forest, Ethiopia. – Southern African Forestry Journal 203: 27-32.
[61] Wang, F., Letort, V., Lu, Q., Bai, X., Guo, Y., Reffye, P., Li, B. (2012): A Functional and Structural Mongolian Scots Pine (Pinus sylvestris var. mongolica) Model Integrating Architecture, Biomass and Effects of Precipitation. – PLoS ONE 7(8): e43531. doi:10.1371/journal.pone.0043531.
[62] Wang, H., Wan, P., Wang, Q., Liu, L., Zhang, G., Hui, G. (2017): Prevalence of Inter-Tree Competition and Its Role in Shaping the Community Structure of a Natural Mongolian Scots Pine (*Pinus sylvestris* var. mongolica) Forest. – Forests 8(3): 84.
[63] WWF. (2012): Temperate Coniferous Forest Ecorgegions. – http://wwf.panda.org/about_our_earth/ecoregions/about/habitat_types/selecting_terrestrial_ecoregions/habitat05.cfm.
[64] WWF. (2019): Temperate Coniferous Forest Ecorgegion.
[65] Yavuz, H. (1999): Volume equations and volume tables for Black pine in Taşköprü. – Turkish Journal of Agriculture and Forestry 23: 1181-1188.
[66] Zhang, W., Sheng, W., Jiang, Y., Zhou, Z., Wang, X. (1992): Classification of forest site system in China. – Forest Research 5(3): 251-262. (in Chinese).
[67] Zhang, L., Peng, C., Huang, S., Zhou, X. (2002): Development and evaluation of ecoregion-based jack pine height-diameter models for Ontario. – Forestry Chronicle 78(4): 530-538.

http://www.aloki.hu ● ISSN 1589 1623 (Print) ● ISSN1785 0037 (Online)
DOI: http://dx.doi.org/10.15666/aeer/1804_49414958

IMPACT OF NATURAL *AZOLLA FILICULOIDES* POWDERS ON SOME PHYSIOLOGICAL, NUTRITIONAL AND BIOLOGICAL PARAMETERS OF COMMON CARP (*CYPRINUS CARPIO* L.)

SHAIMA, S. M.[1*] – BAKHAN, R. H.[1] – KARZAN, F. N.[2] – RABAR, M. R.[1] – AVAN, A. S.[1] – NASREEN, M. A.[3]

[1]*College of Agricultural Engineering Science, University of Sulaimani, Awal Road, Sulaimani, Iraq*

[2]*Bakrajo Technical Institute, Sulaimani Polytechnic University, Bakrajo, Sulaimani, Iraq*

[3]*College of Veterinary Medicine, University of Sulaimani, Sulaimani, Iraq*

**Corresponding author*
e-mail: shaima.mahmood@univsul.edu.iq; phone: +964-770-139-3650

(Received 11th Jan 2020; accepted 6th May 2020)

Abstract. This study was carried out to evaluate antioxidant roles of natural *Azolla filiculoides* on the physiological and biological aspects of young common carp. The fish were fed 0 (control), 2.50, 5.00 and 7.5% of azolla powder for 8 weeks. There were significant differences among treatments for weight gain, specific growth rate and relative growth rate. Also, significant differences were observed ($p < 0.05$) for RBC, Hgb, MCV, PLT and WBC. On the other hand, there were no significant differences for MCH, MCHC, Granules, Lymphocyte and Monocyte. AST, total protein, globulin and albumin in fish plasma were significantly higher ($p < 0.05$) for those fed with 2.50, 5.00 and 7.5% azolla than those in treatment 1(control). The highest blood glucose value was in T1 (control) which significantly differs from that in 3 and 4. There was a significant difference in plasma cholesterol of fish fed with azolla compared to control, as well as in values of triglyceride between treatment 4 and all others. Finally, there were significant differences for Hepatosomatic index, Spleenosomatic index and condition factor. The results of this study confirmed that natural azolla (5.00 and 7.5% g kg-1 feed) had significant effects on physiological, nutritional and biological parameters of common carp.
Keywords: *fern, hematological, biochemical, antioxidant, carp*

Introduction

In intensive aquaculture farm systems, feed should be high quality and rich in protein because it is important in guaranteeing higher rates of production (Narejo et al., 2010; Hardy, 1996). The feed is required to be well balanced with all the essential nutritional contents. The aquaculture feed is reasonably expensive, irregular, and in short supply for many third world countries. Major parts of fish production cost in intensive and semi-intensive aquaculture operations are in feed contents. Feed constitutes must be selected carefully since fish feed in aquaculture will play a significant role in the feeding and economic success of cultured fish. One of the high-quality sources of protein in aquaculture is fish meal and an ever more expensive contents of commercial fish culturing.

The worldwide production of fish meal was stabilized at 6 to 7 million tons in 1985, the prices of that feed component has increased (Fao, 2006). As a result, conducting research on the utilization of traditional sources of protein as components to substitute fish meal in fish diets has received rising attention by nutritionists of fish in the entire world. A number of vegetable sources have revealed to be precious to substitute fish

http://www.aloki.hu ● ISSN 1589 1623 (Print) ● ISSN 1785 0037 (Online)
DOI: http://dx.doi.org/10.15666/aeer/1804_49594968

meal in fish feed, either partly or fully. The utilazation of *sesbania* seeds (*sesbania aculeata* l.), *moringa* leaf (*moringa oleifera* lamarck), *mucuna* seeds (*mucuna pruriens* l.), duckweed (*spirodela polyrrhiza* l. Schleiden), *azolla* lamarck, etc. in feeds for *O. Niloticus* had produced hopeful outcomes (Fasakin et al., 2001; Hossain et al., 2002; Siddhuraju and Becker, 2003; Afuang et al., 2003; Fiogbé et al., 2004). Recently using of aquatic fern azolla in feeding of fish is of great interest.

Floating freshwater, azolla is one of the important aquatic plants with high biomass and production of protein that could be used directly in fish feeding or feed components of a substitute source of protein (Radhakrishnan et al., 2014). Azolla has reached its significance in aquaculture because of higher content of crude protein (13% to 30%) and composition of essential amino acid (eaa) (richin lysine) than the majority of green forage crops and other aquatic macrophytes (Panigrahi et al., 2014). Despite its attractive nutritive qualities and comparative simplicity to produce in ponds, papers on utilization of azolla in aquaculture are particularly restricted. On the other hand, azolla is well recognized in a number of shellfish such as black tiger shrimp *penaeus monodan* (Sudaryano, 2006) and finfish such as carps (Youssouf, 2012) and nile tilapia (Maity and Patra, 2008).

These species of fish have been reported to exchange raw protein from azolla into the most excellent edible protein, therefore, decrease the production cost of diets (Datta, 2011). In addition, it is noted to contain vital constitutes which improve fish performance. Cohen et al. (2002) stated the incidence of the 3-deoxyanthocyanins which are the only known flavonoids of azolla. Furthermore, Mithraja et al. (2011) reported a variety of antioxidants like phyto-constituents such as tannins, phenolic contents and flavonoids from azolla crude extract. According to the above the objectives of the recent experiment evaluate the physiological, nutritional and biological effects of azolla in common carp.

Materials and methods

Experimental fish

The experiment was done in 8 weeks on 60 common carp *C. carpio* L. brought from local fish ponds in Daquq/Kirkuk/Iraq. Fish weights ranged between 60.4 – 62.8 g. Fish were distributed in experimental plastic tanks with a mean initial weight of 61.7 g. Laboratory pre-acclimation (not added azolla) and feeding with commercial pellets (their percentage of ingredients and chemical composition are seen in *Tables 1* and 2) were carried out for 21 days prior to the real feeding trials.

Experimental system

Twelve plastic tanks (70 l water) were used in this trial for four treatments each with three replicates. Proper continuous aeration was added to each tank by using Chinese air compressors, hailea aco-318. Each replicate was stocked with five fish. The replicates were randomly placed to reduced differences among treatments. A daily cleaning by siphoning method was applied to remove remained feeds and feces from the system. The experimental trial represented four treatments with three replicates; each with five fish per replicate as below:

t1: diet without any addition, t2: adding 2.5% azolla/kg diet, t3: adding 5% azolla/kg diet, t4: adding 7.5% azolla/kg diet.

http://www.aloki.hu ● ISSN 1589 1623 (Print) ● ISSN 1785 0037 (Online)
DOI: http://dx.doi.org/10.15666/aeer/1804_49594968

Table 1. *Chemical composition of the different types of diet by NRC (1993)*

Ingredients	Crude protein (%)	Crude fat (%)	Dry matter (%)	Crude fiber (%)	Energy (kcal/kg)
Animal protein concentrate	40	5	92.9	2.2	2107
Yellow corn	8.9	3.6	89	2.2	3400
Soybean meal	48	1.1	89	7	2230
Barely	11	1.9	89	5.5	2640
Wheat bran	15.7	4	89	11	1300
Azolla	21.5	3.3	91.9	16.1	3917

Table 2. *Composition of experimental diet*

Ingredients (%)	Control 1st treatment	2nd treatment	3rd treatment	4th treatment
Yellow corn	15%	15%	15%	15%
Wheat bran	15%	15%	15%	15%
Animal concentrate protein	20%	20%	20%	20%
Barley	15%	15%	15%	15%
Soya bean meal 48%	35%	32.5	30	27.5
Azolla	0	2.5	5	7.5
Total	100			
Calculated chemical composition				
Crud protein	28.06			
Gross energy (kcal/kg feed)	2242.7			

Diet formulation

Experimental diets contained standard ingredients found in Sulaimani City markets, enriched with azolla. The items were mixed to obtain dough. Then, electrical mincer was used for pelleting by kenwood multi-processors. The samples were dried at room temperature for four days and crushed to obtained fine particles. Daily feeding was carried out twice at 9:00 a. m. and at 2:00 p.m. with 3% of body weight. Fish in every tank was weighed together bimonthly. The feeding levels were then recalculated according to new weights. The only modification on the fish feed was that the soybean had been replaced by azolla. The feeding trial continued for 8 weeks.

At the end of the experimental period, three fish were randomly taken from each experimental group. All fish samples were weighed and their length was measured individually. The blood samples from each fish of the different groups were collected from the caudal vein. Whole blood samples were collected in small plastic vials containing heparin and stored under cold condition (Al-koye, 2013).

The following parameters were measured: erythrocyte count (rbcs: 10^{12}cells/l), mean corpuscular hemoglobin (mch; pg), mean corpuscular hemoglobin concentration (mchc; g/dl), mean corpuscular volume (mcv; fl), hemoglobin (hb; g/dl) and platelet (plt; 10^9cells/l), differential leukocyte count (10^9cells/l), granulocytes%, lymphocytes%, monocytes%.

http://www.aloki.hu ● ISSN 1589 1623 (Print) ● ISSN 1785 0037 (Online)
DOI: http://dx.doi.org/10.15666/aeer/1804_49594968

Biochemical parameters

Alanine aminotransferase activity (alt), aspartate aminotransferase activity (ast), total proteins, globulin (g/dl), albumin (g/dl) albumin were examined.

To determine growth and feed utilization parameters fish were weighed (g) together for all replicate in every two weeks. Feed consumption of each replicate was read just by the obtained biomass in every two weeks.

Weight gain (g/fish) = mean of weight (g) at the end of the experimental period – weight (g) at the beginning of the experimental period.

$$\text{Weight gain (g/fish)} = w2 - w1 \quad \text{(Eq.1)}$$

where: W_2: fish weight (g) at the end of experimental period, W_1: fish weight (g) at the beginning of the experimental period.

Daily weight gain (dwg) (g/day) = weight gain / experimental period

$$= w2 - w_1 / t \quad \text{(Eq.2)}$$

T: time between w2 and w1 (84 days).

Relative growth rate (rgr%) = weight gain / initial weight x 100

$$= w2 - w_1 / w_1 \times 100 \text{ (Brown, 1957)} \quad \text{(Eq.3)}$$

Specific growth rate (sgr) = (ln final body weight–ln initial body weight]

$$\text{/experimental period) x100} = (\text{in } w2 - \text{in } w1) / t) \times 100 \text{ (Lagler, 1956)} \quad \text{(Eq.4)}$$

$$\text{Feed conversion ratio (fcr)} = \text{total feed fed (g) / total wet weight gain (g) (Uten, 1978)} \quad \text{(Eq.5)}$$

$$\text{Feed efficiency ratio (fer)} = \text{total weight gain (g) / total feed fed (g) (Uten, 1978)} \quad \text{(Eq.6)}$$

Health (biological) parameters

All fish specimens were dissected and the abdominal cavity was opened to weigh each organ alone, and they were calculated as follows.

$$\text{Intestine weight index\%} = \text{intestine weight (gm) / fish weight (gm)} \times 100 \quad \text{(Eq.7)}$$

$$\text{Intestine length index\%} = \text{intestine length (cm) / fish length (cm)} \times 100 \quad \text{(Eq.8)}$$

$$\text{Condition factor} = \text{fish weight (gm) / fish length (cm)}^3 \quad \text{(Eq.9)}$$

$$\text{Gill index\%} = \text{gill weight (gm) / fish weight (gm)} \times 100 \quad \text{(Eq.10)}$$

$$\text{Fish weight index\%} = \text{fish weight without viscera (gm) / fish weight (gm)} \times 100 \quad \text{(Eq.11)}$$

$$\text{Meat weight index\%} = \text{fish weight without viscera \& head (gm) / fish weight (gm)} \times 100 \quad \text{(Eq.12)}$$

http://www.aloki.hu ● ISSN 1589 1623 (Print) ● ISSN 1785 0037 (Online)
DOI: http://dx.doi.org/10.15666/aeer/1804_49594968

Water quality

Some essential water quality parameters were measured during the experimental period. These included water dissolved oxygen (mg/l) using O2-meter (OAKTON Singapore), water temperature °C using thermometer ranging between zero to 100 °C, water pH using a pH meter (HANNA Romania).

Statistical analysis

The trial was conducted by one way (ANOVA) with completely randomized design (crd) and general linear models (glm) procedure of xlstat 2016 version.02.28451. Duncan's test was used to compare treatment means.

Results

Physical and chemical properties of water quality during the experiment were the followings: the water temperature ranged between (24-25 °C) and the level of dissolved oxygen concentration in the plastic tanks was between 7-8.5 mg/l and water pH value was between 7 and 8.3.

There were significant differences ($p < 0.05$) in weight gain among treatment 4 with other treatments, the highest values of weight gain were observed in treatment 4. The relative growth rate, specific growth rate, food conversion ratio and food efficiency ratio of the *C. carpio* were significantly affected by feeding fish with azolla. Except food conversion ratio other parameters got the highest values with those in control (*Table 3*).

Table 3. *Effect of replacing soyameal with azolla on growth and feed utilization parameters of young common carp (C. carpio)*

Parameters	t1 Control	t2 2.5% *azolla*	t3 5% *azolla*	t4 7.5% *azolla*
Weight gain	9.347 ± 0.42 B	9.44 ± 1.41 B	8.867 ± 0.26 B	18.767 ± 0.64 A
Relative growth rate	15.271 ± 0.56 B	15.354 ± 2.30 B	14.223 ± 0.38 B	30.595 ± 1.37 A
Specific growth rate	4.02 ± 0.03	4.152 ± 0.02 B	4.111 ± 0.037 B	4.388 ± 0.10 A
Food conversion ratio	1.513 ± 0.05 A	1.579 ± 0.25 A	1.579 ± 0.05 A	0.778 ± 0.03 B
Food efficiency ratio	0.657 ± 0.02 B	0.667 ± 0.09 B	0.635 ± 0.02 B	1.290 ± 0.04 A

Different letter in same rows mean significant differences ($p < 0.05$)

Mean values for rbc, hgb, mcv, mch, mchc, mcv, plt, wbc, granules, lymphocyte and monocyte are presented in *Table 4* as mean ± se. According to the results, there were significant differences ($p < 0.05$), for rbc, hgb, mcv, plt and wbc. However, there were no significant differences for mch, mchc, granules, lymphocyte and monocyte.

Values of ast, total protein, globulin and albumin in fish plasma were significantly higher ($p < 0.05$) in treatment 2, 3 and 4 than those in treatment 1 (control). While the highest activity of alt was in t1 (control) while in treatment 2, 3 and 4, it was 32.17 ± 3.63. The highest blood glucose value was in t1 (control) and significantly differ with treatment 3 and 4 ($p < 0.05$, *Table 5*).

There was a significant difference ($p < 0.05$) in plasma cholesterol levels among control with other treatments, the highest value was in control which was (4.345 ± 0.24)

http://www.aloki.hu ● ISSN 1589 1623 (Print) ● ISSN 1785 0037 (Online)
DOI: http://dx.doi.org/10.15666/aeer/1804_49594968

while there were insignificant differences among treatment 2, 3 and 4. The results indicated a significant difference in values of triglyceride between treatment 4 with other treatments, triglyceride value in treatment 4 (4.20 ± 0.42, *Table 6*) was higher than in other treatments. Although significant differences were observed in ldl, hdl and vldl levels, the highest values of ldl and vldl were noted in treatment 1 (control) while the highest value of hdl was found in treatment 3 (*Table 6*).

Table 4. *Effect of replacing soymeal with azolla on some haematological indices of young common carp (C. carpio)*

Parameters	t1 Control	t2 2.5% *azolla*	t3 5% *azolla*	t4 7.5% *azolla*
Rbcs (10^{12}cells/l)	1.923 ± 0.13 B	1.705 ± 0.27 B	2.033 ± 0.13 B	2.748 ± 0.10 A
Hb (g/dl)	96.25 ± 2.01 C	122.00 ± 2.41 B	124.25 ± 1.88 B	137.25 ± 3.11 A
Mch (pg)	61.50 ± 4.64 A	79.17 ± 16.18 A	63.475 ± 2.96 A	77.625 ± 10.04 A
Mchc (g/dl)	251 ± 19.39 A	378 ± 59.14 A	263.75 ± 13.60 A	331 ± 45.33 A
Mcv (fl)	221.325 ± 8.15 B	232.05 ± 7.78 AB	248.075 ± 2.87 A	434.35 ± 6.28 AB
Plt (10^9cells/l)	42 ± 7.12 B	44.25 ± 9.44 B	90 ± 6.05 A	57.25 ± 21.33 AB
Wbc (10^9cells/ l)	228.80 ± 2.30 B	262.475 ± 7.55 A	236.40 ± 5.74 B	245.825 ± 8.54 AB
Granulocytes (%)	56.25 ± 2.13 A	57.45 ± 2.17 A	55.82 ± 1.04 A	59.60 ± 1.13 A
Lymphocytes (%)	9.925 ± 0.83 A	9.325 ± 1.64 A	10.60 ± 0.47 A	7.225 ± 1.00 A
Monocytes (%)	33.825 ± 1.49 A	33.225 ± 0.94 A	33.575 ± 1.28 A	33.175 ± 0.29 A

Different letter in same rows mean significant differences ($p < 0.05$)

Table 5. *Effect of replacing soymeal with azolla on some blood biochemical parameters of young common carp (C. carpio)*

Parameters	t1 Control	t2 2.5% *azolla*	t3 5% *azolla*	t4 7.5% *azolla*
Alanine aminotransferase activity (alt) (u/L)	32.17±3.63 A	26.17±2.91 AB	19.03±1.64 B	21.26±1.66 B
Aspartate aminotransferase activity (ast) (u/L)	53.275±2.26 B	61.725±1.21 A	65.075±0.97 A	65.903±2.03 A
Total proteins (g/L)	37.293±2.51 C	39.983±3.34 BC	47.96±1.21 A	45.743±1.53 AB
lood glucose (mmol/L)	6.3±0.42 A	4.785±0.23 AB	3.673±0.73 B	4.083±0.79 B
Globulin (g/L)	18.15±0.24 A	21.48±0.11 A	25.87±0.14 A	22.54±0.6 A
Albumin (g/L)	19.24±0.14 A	18.45±0.71 A	22.18±0.4 A	23.12±0.05 A

Different letter in same rows mean significant differences ($p < 0.05$).

Table 6. *Effect of replacing soymeal with azolla on growth blood lipid profile of young common carp (C. carpio)*

Parameters	t1 Control	t2 2.5% *azolla*	t3 5% *azolla*	t4 7.5% *azolla*
Cholesterol (mmol/L)	4.345 ± 0.24 A	3.085 ± 0.16 B	3.378 ± 0.23 B	3.015 ± 0.01 B
Triglyceride (mmol/L)	1.85 ± 0.19 B	1.875 ± 0.17 B	1.875 ± 0.27 B	4.20 ± 0.42 A
LDL (mmol/L)	2.98 ± 0.68 A	2.39 ± 0.61 A	0.773 ± 0.25 B	0.673 ± 0.22 B
HDL (mmol/L)	2.025 ± 0.14 B	1.925 ± 0.11 B	2.725 ± 0.08 A	1.950 ± 0.32 B
VLDL (mmol/L)	0.375 ± 0.03 AB	0.375 ± 0.03 AB	0.375 ± 0.05 AB	0.338 ± 0.02 B

Different letter in same rows mean significant differences ($p < 0.05$).

http://www.aloki.hu ● ISSN 1589 1623 (Print) ● ISSN 1785 0037 (Online)
DOI: http://dx.doi.org/10.15666/aeer/1804_49594968

Significant differences ($p < 0.05$) were noted in treatments in all parameters that are listed in *Table 7*. For hepatosomatic index, spleenosomatic index and condition factor treatment 4 had the highest values compared to other treatments. However, the highest values of gillsomatic index and meat weight index were observed in treatment 3.

Table 7. *Effect of replacing soymeal with azolla on some physio-biological parameters of young common carp (C. carpio)*

Parameters	t1 Control	t2 2.5% *azolla*	t3 5% *azolla*	t4 7.5% *azolla*
Hepatosomatic index	1.482 ± 0.08 B	1.563 ± 0. 10 AB	1.920 ± 0.16 A	1.55 ± 0.18 AB
Spleenosomatic index	0.192 ± 0.08 B	0.399 ± 0.03 A	0.221 ± 0.04 AB	0.234 ± 0.05 AB
Kidneysomatic index	0.517 ± 0.08 AB	0.353 ± 0.08 B	0.680 ± 0.11 A	0.460 ± 0.02 AB
Gillsomatic index	3.448 ± 0.04 B	3.461 ± 0.11 B	3.694 ± 0.11 AB	1.950 ± 0.32 B
Intestine weight index	2.523 ± 0.21 AB	2.528 ± 0.20 AB	2.912 ± 0.14 A	2.105 ± 0.13 B
Fish weight index	85.799 ± 0.97 AB	90.588 ± 2.37 A	86.678 ± 0.50 AB	84.25 ± 2.26 B
Meat weight index	54.365 ± 1.07 B	55.015 ± 0.27 B	58.742 ± 0.34 A	55.036 ± 0.52 B
Condition factor	1.399 ± 0.02 C	1.526 ± 0.07 BC	1.627 ± 0.3 AB	1.756 ± 0.06 A

Different letter in same rows mean significant differences ($p < 0.05$)

Discussion

Azolla seems to be an excellent replacer of protein from high cost sources such as fish meal. Fish species belong to family *cyprinidae* stated to have diverse ranges of azolla inclusion levels in the feed. The majority of studies observed enhanced feed utilization and better growth in rohu at 10-50% azolla inclusion level in the feed (Panigrahi et al., 2014; Datta, 2011). While orange fin labeo (Gangadhar et al., 2017), catla (Umalatha et al., 2018), silver carp and mrigal (Tuladhar, 2003), grass carp (Majhi et al., 2006), and thai silver barb (Das et al., 2018), stated to have a range between 10-25% azolla inclusion levels in the diet (Kumari et al., 2017). Same results have been observed by many researchers with some aquatic plants supplemented diet such as duck weed (Hassan and Edwards, 1992; Saini and Mathur, 2003). The reasons for the diverse addition levels may be due to the existence of ω-6 fatty acids (Mohanty and Dash, 1995), nutritional value of the plants such as the gross energy content of the diet and the dietary protein (Shireman et al., 1983; Du et al., 2005) which is assimilated in a different way, depends on habits of feeding of the species (example, calta vs ruhu). Also, different enzymes in the fish gut plays a significant role in the feed digestion and utilization (Dabrowski and Glogowski, 1977).

The present study observed that the level of azolla in diets affects the growth and feed utilization efficiency of common carp. High level of azolla in diets resulted in higher growth. These trends of noted differences in growth v and fcr followed the results noted by Fasakin et al. (2001) and Fiogbé et al. (2004). Weight gains were 9.44 ± 1.41 (2.5% azolla), 8.867 ± 0.26 (5% azolla) and 18.767 ± 0.64 (7.5% azolla), (Nekoubin and Sudagar, 2013) reported that there was an increased weight for grass carp that fed with azolla was 5.04 ± 0.53. In addition, specific growth rates were 4.152 ± 0.022.5% azolla), 4.111 ± 0.037 (5% azolla) and 4.388 ± 0.10 (7.5% azolla) (Nekoubin and Sudagar, 2013) noted that the specific growth rate was 0.31 ± 0.02 in their experiment.

http://www.aloki.hu ● ISSN 1589 1623 (Print) ● ISSN 1785 0037 (Online)
DOI: http://dx.doi.org/10.15666/aeer/1804_49594968

Study on last research showed that biochemical parameters affect species (Catton, 1951), age (Hutton, 1967), water temperature (Hesser, 1960) and diet (Smith, 1968). In the present study different levels of azolla had significant effects on most of the hematological and biochemical parameters. Some studies seem to indicate that the type and rate of fish consumption, and its growth, are related to the chemical content or nutritive value of the plants, such as the gross energy content of the diet and the dietary protein (Shireman et al., 1983; Du et al., 2005). Nekoubin and Sudagar (2013) stated that feeding grass carp with azolla had not have any significant effect on rbc, wbc and mchc, while had significant effects on hgb, mcv, mch and mcv. Values of rbcs (10^{12}cells/l) were 1.705 ± 0.27 (2.5% azolla), 2.033 ± 0.13 (5% azolla) and 2.748 ± 0.10 (7.5% azolla). Nekoubin and Sudagar (2013) noted that rbc values for grass carp that fed with azolla was 1.83 ± 0.12. Furthermore, wbc (10^{9}cells/l) values were 262.475 ± 7.55 (2.5% azolla), 236.40 ± 5.74 (5% azolla) and 245.825 ± 8.54 (7.5% azolla). Nekoubin and Sudagar (2013) reported that wbc value for grass carp that fed with azolla was 7.4 ± 1.9.

According to the results of the present study azolla significantly affected the lipid profile (cholesterol, triglericide, ldl, hdl and vldl) of common carp, these results were confirmed by Nekoubin and Sudagar (2013) who stated that feeding grass carp with azolla significantly affected the lipid profile of the mentioned fish.

Conclusion

According to our results it was shown that natural azolla powders had significant effect on physiological parameters such as RBC, WBC and Hb and lipid profile. Also, it affected biological and nutritional parameters such as weight gain, relative growth rate and specific growth rate of common carp. This suggests that azolla could be used to feed common carp in aquaculture. While this study recommends future studies on azolla as feed to common carp in real conditions such as a pond culture system.

Acknowledgements. Authors would like to express their thanks to the Animal Science Department of the College of Agricultural Science Engineering, University of Sulaimani for their help.

REFERENCES

[1] Afuang, W., Siddhuraju, P., Becker, K. (2003): Comparative nutritional evaluation of raw, methanol extracted residues and methanol extracts of moringa (*Moringa oleifera* Lam.) leaves on growth performance and feed utilization in Nile tilapia (*Oreochromis niloticus* L.). – Aquaculture Research 34: 1147-1159. https://doi.org/10.1046/j.1365-2109.2003.00920.x.

[2] Al-Koye, H. (2013): Effect of using Spirulina spp. instead of fishmeal on growth, blood picture and microbial load of common carp Cyprinus carpio. – MSc Thesis, College of Agriculture, University of Salahaddin, Erbil, Iraq.

[3] Brown, M. E. (1957): Experimental Studies of Growth. – In: Brown, M. E. (ed.) Physiology of Fishes. Vol. I. Academic Press, New York, pp: 361-400.

[4] Catton, W. T. (1951): Blood cell formation in certain teleost fishes. – Blood 6: 39-60.

[5] Cohen, M. F., Sakihama, Y., Takagi, Y. C., Ichiba, T., Yamasaki, H. (2002): Synergistic effect of deoxyanthocyanins from the symbiotic fern *Azolla* on hrm A gene induction in

http://www.aloki.hu ● ISSN 1589 1623 (Print) ● ISSN 1785 0037 (Online)
DOI: http://dx.doi.org/10.15666/aeer/1804_49594968

the Cyanobacterium *Nostoc punctiforme*. – Mol Plant Microbe Interact 15: 875-882. https://doi.org/10.1094/MPMI.2002.15.9.875.

[6] Dabrowski, K., Glogowski, J. (1977): Studies on the role of exogenous proteolytic enzymes in digestion processes in fish. – Hydrobiologia 54: 129-134. https://doi.org/10.1007/BF00034986.

[7] Das, M., Rahim, F. I., Hossain, M. A. (2018): Evaluation of fresh Azolla pinnata as a low-cost supplemental feed for Thai Silver Barb Barbonymus gonionotus. – Fishes 3: 1-11. https://doi.org/10.3390/fishes3010015.

[8] Datta, S. N. (2011): Culture of *Azolla* and its efficacy in diet of *Labeo rohita.* – Aquaculture 310: 376-379. https://doi.org/10.1016/j.aquaculture.2010.11.008.

[9] Du, Z. Y., Liu, Y. J., Tian, J. T., Wang, Y., Liang, G. Y. (2005): Effect of dietary lipid level on growth, feed utilization and body composition by juvenile grass carp (*Ctenopharyngodon idella*). – Aquaculture Nutrition 11: 139-146. https://doi.org/10.1111/j.1365-2095.2004.00333.x.

[10] FAO (2006): The State of the World Fisheries and Aquaculture. – FAO, Rome.

[11] Fasakin, E. A., Balogun, A. M., Fagbenro, O. A. (2001): Evaluation of sun-dried water fern, *Azolla africana*, and duckweed, *Spirodela polyrrhiza*, in practical diets for Nile tilapia, *Oreochromis niloticus*, fingerlings. – Journal of Applied Aquaculture 11(4): 83-92. https://doi.org/10.1300/J028v11n04_09.

[12] Fiogbé, E. D., Micha, J. C., Van Hove C. (2004): Use of a natural aquatic fern, *Azolla microphylla*, as a main component in food for omnivorous-phytoplanktonophagous tilapia, *Oreochromis niloticus* L. – Journal of Applied Ichthyology 20: 517-520. https://doi.org/10.1111/j.1439-0426.2004.00562.x.

[13] Gangadhar, B., Umalatha, H., Hegde, G., Sridhar, N. (2017): Digestibility of dry matter and nutrients from *Azolla* pinnata by *Labeo calbasu* (Hamilton, 1822) with a note on digestive enzyme activity. – Fish Technology 54: 94-99. https://doi.org/10.21077/ijf.2017.64.3.69091-11.

[14] Hassan, M. S., Edwards, P. (1992): Evaluation of Duckweed (Lemna perpusilla and Spirodela polyrrhiza) as feed for Nile tilapia (Oreochromis niloticus). – Aquaculture 104: 315-326. https://doi.org/10.1016/0044-8486(92)90213-5.

[15] Hardy, R. W. (1996): Alternate protein sources for salmon and trout diets. – Animal Feed Science Technology 59: 71-80. https://doi.org/10.1016/0377-8401(95)00888-8.

[16] Hesser, E. F. (1960): Method for routine fish hematology. – The Progressive Fish Culturist 22: 164-170. https://doi.org/10.1577/1548-8659(1960)22[164:MFRFH]2.0.CO;2.

[17] Hossain, M. A., Focken, U., Becker, K. (2002): Nutritional evaluation of Dhaincha (*Sesbania aculeata*) seeds as dietary protein source for tilapia *Oreochromis niloticus*. – Aquaculture Research 33: 653-662. https://doi.org/10.1046/j.1365-2109.2002.00690.x.

[18] Hutton, K. E. (1967): Characteristics of the blood of adult pinke salmon at three stages of maturity. – Fishery Bulletin of the Fish and Wild Life Service 66: 195-202.

[19] Kumari, R., Ojha, M. L., Saini, V. P., Sharma, S. K. (2017): Effect of *Azolla* supplementation on growth of rohu (*Labeo rohita*) fingerlings. – Journal of Entomology and Zoology Studies 5: 1116-1119.

[20] Lagler, F. (1956): Fresh Water Fishery Biology. – Brown Company, Dubuque, IA, pp: 131-135, 159-166.

[21] Maity, J., Patra, B. C. (2008): Effect of replacement of fishmeal by *Azolla* leaf mael on growth, food utilization, pancreatic protease activity and RNA/DNA ratio in the fingerlings of *Labeo rohita* (Ham.). – Canadian Journal of Pure and Applied Science 2: 323-333.

[22] Majhi, S. K., Das. A., Mandal, B. K. (2006): Growth performance and production of organically cultured grass carp *Ctenopharyngodon idella* (Val.) under mid-hill conditions of Meghalaya; North Eastern India. – Turkish Journal of Fisheries and Aquatic Sciences 6: 105-108.

http://www.aloki.hu ● ISSN 1589 1623 (Print) ● ISSN 1785 0037 (Online)
DOI: http://dx.doi.org/10.15666/aeer/1804_49594968

[23] Mithraja, M. J., Antonisamy, J. M., Mahesh, M., Paul, Z. M., Jeeva, S. (2011): Phytochemical studies on *Azolla pinnata* R. Br., *Marsilea minuta* L. and *Salvinia molesta* Mitch. – Asian Pacific Journal Tropical Biomedicine. https://doi.org/10.1016/S2221-1691(11)60116-0.

[24] Mohanty, S. N., Dash, S. P. (1995): Evaluation of *Azolla caroliniana* for inclusion in carp diet. – Journal of Aquatic and Tropical Ecology 10: 343-353.

[25] Narejo, N. T., Dars, B. A., Achakzai, G. D. (2010): Preparation of low-cost fish feed for the culture of Labeo rohita (Hamilton) in glass aquaria. – Sindh University Research Journal (Sci. Ser.) 42: 7-10.

[26] Nekoubin, H., Sudagar, M. (2013): Effect of different types of plants (*Lemna* Sp., *Azolla filiculoides* and *Alfalfa*) and artificial diet (with two protein levels) on growth performance, survival rate, biochemical parameters and body composition of grass carp (Ctenopharyngodon idella). – Journal of Aquaculture Research Development 4: 167. https://doi.org/10.4172/2155-9546.1000167.

[27] Panigrahi, S., Choudhary, D., Sahoo, J. K., Das, S. S., Rath, R. K. (2014): Effect of dietary supplementation of *Azolla* on growth and survibility of *Labeo rohita* fingerlings. – Asian Journal of Animal Science 9: 33-37.

[28] Radhakrishnan, S., Saravana, B. P., Seenivasan, C., Shanthi, R., Muralisankar, T. (2014): Replacement of fishmeal with Spirulina platensis, Chlorella vulgaris and *Azolla pinnata* on non-enzymatic and enzymatic antioxidant activities of *Macrobrachium rosenbergii*. – The Journal of Basic & Applied Zoology 67: 25-33. http://dx.doi.org/10.1016/j.jobaz.2013.12.003.

[29] Saini, V. P., Mathur, S. (2003): Supplementation of duckweed (*Lemna minor*) in the experimental diet of *Labeo rohita* (Ham.). – Geobios 30: 213-216.

[30] Siddhuraju, P., Becker, K. (2003): Comparative nutritional evaluation of differentially processed mucuna seeds [*Mucuna pruriens* (L.) DC. Var. *utilis* (wall exWight) Baker ex Burck)] on growth performance, feed utilization and body composition in Nile tilapia (*Oreochromis niloticus* L.). – Aquaculture Research 34: 487-500. https://doi.org/10.1046/j.1365-2109.2003.00836.x.

[31] Smith, C. E. (1968): Hematological Changes in coho salmon fed folic acid deficient diet. – Journal of the Fisheries Research Board of Canada 25: 151-156. https://doi.org/10.1139/f68-009.

[32] Shireman, J. V., Rottman, R. W., Aldridge, F. J. (1983): Consumption and growth of hybrid grass carp fed four vegetation diets and trout chow in circular tanks. – Journal of Fish Biology 22: 685-693. https://doi.org/10.1111/j.1095-8649.1983.tb04228.x.

[33] Sudaryano, A. (2006): Use of *Azolla* (*c* meal as a substitute for defatted soybean meal in diets of juvenile black tiger shrimp (*Penaeus monodon).* – Journal of Coastal Development 9: 145-154.

[34] Tuladhar, B. (2003): Comparative study of fish yields with plant protein sources and fish meal. – Our Nature 1: 26-29. https://doi.org/10.3126/on.v1i1.300.

[35] Umalatha, H., Gangadhar, B., Hegde, G., Sridhar, N. (2018): Digestibility of three feed ingredients by *Catla catla* (Hamilton 1822). – Oceanography and Fish Open Access Journal 5: 555-672. https://doi.org/10.19080/OFOAJ.2018.05.555672.

[36] Uten, F. (1978): Standard methods and terminology in finfish nutrition. – Pro. World Smp. Finfish Nutrition and Technology 11: 20-23.

[37] Youssouf, A. (2012): Water quality and sediment features in ponds with Nile tilapia (*Oreochromis niloticus* L.) fed *Azolla*. – Journal of Fisheries and Aquaculture 3: 47-51.

http://www.aloki.hu ● ISSN 1589 1623 (Print) ● ISSN 1785 0037 (Online)
DOI: http://dx.doi.org/10.15666/aeer/1804_49594968

RESPONSE OF SOIL FUNGAL COMMUNITY STRUCTURE AND DIVERSITY TO SALINE WATER IRRIGATION IN ALLUVIAL GREY DESERT SOILS

GUO, H. N. – HUANG, Z. J. – LI, M. Q. – MIN, W.*

Department of Resources and Environmental Science, Shihezi University, Shihezi, Xinjiang 832003, PR China
(e-mails: ghnshzu@163.com; hzjshzu@163.com; lmqshzu@163.com)

**Corresponding author*
e-mail: minwei555@126.com; phone: +86-139-9953-6214

(Received 1st Feb 2020; accepted 25th May 2020)

Abstract. Saline water irrigation can change the soil environment, thereby influencing soil microbial processes. In this study, a nine years saline water irrigation experiment had been conducted in Shihezi, Xinjiang Province, China, to investigate the composition and diversity of the soil fungal community. Our results showed that irrigation with either brackish or saline water significantly increased soil salinity and Available Phosphorus, but reduced soil pH, SOC, TN, and Available Kalium. Saline water irrigation significantly decreased operational taxonomic units (OTUs), ACE, Chao1, and Shannon indices but increased Simpson indices. The dominant fungal phyla were *Ascomycota, Mortierellomycota, Basidiomycota, Glomeromycota*, and *Chytridiomycota*. Irrigation with either brackish or saline water significantly reduced the abundance of *Mortierellomycota* but increased the abundance of *Ascomycota* and *Basidiomycota*. In addition, saline water irrigation significantly decreased the relative abundance of *Glomeromycota* compared with fresh water irrigation, but significantly increased the relative abundance of *Chytridiomycota*. Redundancy analysis (RDA) results showed that salinity (ECe) was the primary factors driving the changes in soil fungal community composition. LEfSe analysis demonstrated fungal potential biomarkers decreased by saline water irrigation. These results increase our understanding of soil ecological processes in soils that are increasingly salinized.
Keywords: *water salinity, environmental variables, community composition, LEfSe analysis, high-throughput sequencing*

Introduction

Fresh water scarcity is a world-wide problem, particularly in arid regions where irrigation is necessary for crop production. Xinjiang Province in northwest is classified as a temperate arid climate area which is characterized by low annual precipitation, high evaporation, water shortage and soil salinization (Wang et al., 2011; Zhang et al., 2019). These factors substantially threaten the sustainability of agriculture in this region, the main agricultural water sources in Xinjiang generally contain soluble salts (Zhou et al., 2009). Saline water may be used for irrigation in areas if appropriate crop and water management practices are used (Malash et al., 2012; Mojid and Hossain, 2013). Therefore, it is important to identify best management practices for avoiding salt accumulation in the root zone when saline water is used for irrigation. Drip irrigation is widely regarded as the most promising method for saline water irrigation (Karlberg et al., 2007). Salts introduced during the early stages of saline water irrigation can be effectively leached by subsequent applications. However, even with careful management, irrigation with saline water combined with high evapotranspiration continually intensifies salinization in arid soils. Soil salinity is a critical problem in many arid and semiarid areas, leading not

http://www.aloki.hu ● ISSN 1589 1623 (Print) ● ISSN 1785 0037 (Online)
DOI: http://dx.doi.org/10.15666/aeer/1804_49694985

only to the deterioration of soil biophysical properties but also to declines in soil microbial biomass and metabolic efficiency. Soil salinization also affects the composition and diversity of soil microbial communities (Yu et al., 2011; Li et al., 2015a). Soil microorganisms are increasingly recognized as the most sensitive bioindicators in the soil ecosystem, and there is growing interest in managing soil microorganisms to improve the soil environment (Ludwig-Müller, 2015).

Soil microbial communities are particularly complex and dynamic, which directly participate in some important ecological processes in soil. The composition of microbial communities varies largely across environments, displaying distinct responses to changing soil environment changes (Zhang et al., 2015; Amini et al., 2016). Microbial communities directly participate in many important ecological processes in soil, including organic matter decomposition, aggregate formation, and nutrient cycling. Soil microbial diversity and community structure, soil microbial biomass, respiration and enzymatic activities have been increasingly used as relevant indicators of soil quality (Canfora et al., 2015; Srivastava et al., 2016). Decreasing soil osmotic potential with increasing soil salinity has been found to reduce not only water availability to microbes but also microbial activity and biomass (Rietz and Haynes, 2003; Yuan et al., 2007; Chowdhury et al., 2011a, b). High salinity can suppress soil microbial growth and activity (Yuan et al., 2007; Elmajdoub et al., 2014). Soil salinity over a critical level has a strong negative impact on microbial respiration (Setia et al., 2011). Jackson and Vallaire (2009) and Neubauer (2013) observed that enzyme activity is negatively correlated with soil salinity. Salinity has been implicated as a major factor regulating bacterial composition and diversity across many different habitats (Lozupone and Knight, 2007). Morrissey and Franklin (2015) found that changes in soil microbial communities may occur gradually with exposure to elevated salinity. Soil fungi are important determinants of soil fertility and ecosystem services as they participate in all biogeochemical cycles. Therefore, a salinity gradient is likely to influence fungal diversity. While its impact on bacterial communities has been thoroughly studied, the influence of soil salinity on fungal communities has been largely overlooked.

Fungal are one of the main groups of soil microorganisms, which play an important role in nutrient cycling, pollutant degradation, and ecological restoration (Yang et al., 2015). However, scientists know less about soil fungal communities than other organisms. Thus, soil fungal have been compared to “Earth’s dark matter” (Jansson and Prosser, 2013). Most studies on saline soil have focused on bacterial composition and diversity. Little is known about how long-term saline water irrigation affects fungal community structure, composition, and diversity. The objective of this field experiment was to investigate the effects of irrigation water salinity on soil fungal communities diversity and composition using high throughput sequencing of the fungal internal transcribed spacer (ITS) region. We hypothesized that nine years saline water irrigation decreases soil nutrients and fungal communities diversity, changing fungal communities structure in a gray desert soil in China. Using this methodology to identify fungal taxa can elucidate the status and function of soil fungal communities in saline water-irrigated soil and quantify the effects of environmental changes on soil fungal communities. We believe this research can increase understanding about how saline water irrigation changes soil structure and function by influencing soil microbial processes. This information is useful for managing soil and saline water resources in arid and semiarid regions.

http://www.aloki.hu ● ISSN 1589 1623 (Print) ● ISSN 1785 0037 (Online)
DOI: http://dx.doi.org/10.15666/aeer/1804_49694985

Materials and methods

Site description

A nine years saline water irrigation field experiment was conducted at the Shihezi University Agricultural Experimental Station, Xinjiang Province, China (44°18′ N, 86°02′ E, 450 m above sea level). The experiment site has a temperate continental climate. The mean annual temperature in this region is 7.0 °C with about 170 frost-free days per year. The mean annual precipitation is 210 mm, and the mean annual potential evaporation is 1660 mm. The groundwater table is more than 6 m deep. The soil at the site is an alluvial, gray desert soil, classified as a Calcaric Fluvisol in the FAO/UNESCO System. Some of the soil properties (0–20 cm depth) at the start of the experiment in 2009 were as follows: bulk density, 1.33 g cm^{-3}; pH, 7.48; electrical conductivity (EC_e), 2.51 dS m^{-1}; organic matter, 16.84 g kg^{-1}; total nitrogen, 1.08 g kg^{-1}; available phosphorus (AP), 25.86 mg kg^{-1}; and available potassium (AK), 253 mg kg^{-1}.

This experiment had been conducted in the site for a period of nine years using a completely randomized block design with three replicates of three irrigation water salinity treatments. The three treatments were (1) fresh water: noted as FW, electrical conductivities (ECw) of the irrigation water was 0.35 dS m^{-1}; (2) brackish water: noted as BW, electrical conductivities (ECw) of the irrigation water was 4.61 dS m^{-1}; (3) saline water: noted as SW, electrical conductivities (ECw) of the irrigation water was 8.04 dS m^{-1}. The diagram of the experimental plot layout was presented in *Figure 1*. The fresh water was obtained from a well in study area. The brackish or saline water were obtained by adding equal weight of $CaCl_2$ and NaCl to the well water. A tank was used to store brackish or saline water and the ECw (Irrigation water Electrical conductivity) of the desired irrigation water salinity was calibrated using a conductivity meter.

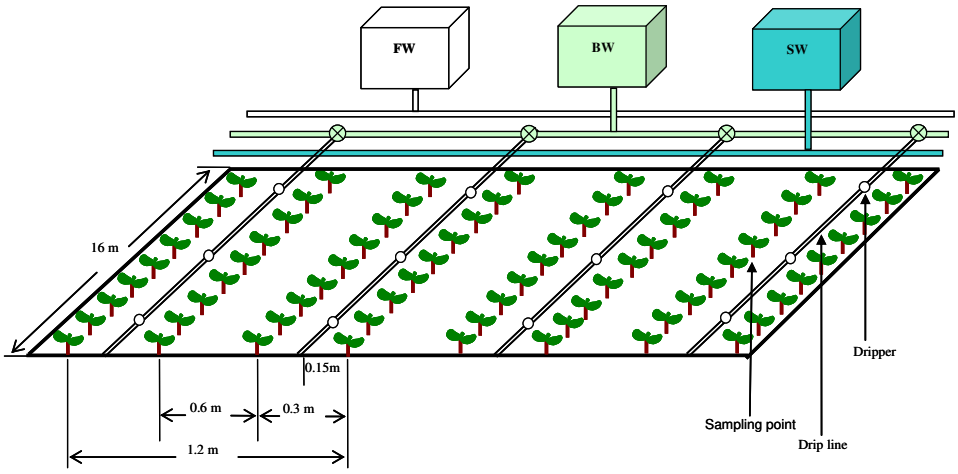

Figure 1. *Diagram of the experimental plot layout*

Cotton can tolerate soil salinity up to a given threshold (7.7 dS m^{-1}), as a moderately salt-tolerant crop, cotton is considered as a model crop to understand salinity tolerance. The crop is cotton (*Gossypium hirsutum L. cv Xinluzao No. 52*) and usually planted in late-April and harvested in late-September on the experiment plots each year. Each plot (1.2 m wide × 16 m long) had four rows. The plots were mulched with one sheet of plastic film. Two drip irrigation lines were installed under the plastic film. Phosphorous

http://www.aloki.hu ● ISSN 1589 1623 (Print) ● ISSN 1785 0037 (Online)
DOI: http://dx.doi.org/10.15666/aeer/1804_49694985

(P_2O_5) 105 kg ha^{-1} and potassium (K_2O) 60 kg ha^{-1} were applied at planting. Nitrogen fertilizer (urea) was applied through the drip irrigation system in five equal amounts during each growing season. An irrigation experiment using different irrigation water salinity (EC of water = 0.35, 4.61, or 8.04 dS m^{-1}) had been conducted at the study site for eight years (2009-2016) before the start of this experiment. The same irrigation amount (450 mm) was applied to each plot during the cotton-growing season, and the same cultivation techniques were used during the 2017 of the study.

Soil sampling

Three soil samples were collected from the 0–20 cm depth of each plot on July 28, 2017 (e.g. the ninth year of the study). The N fertilizer had been applied on June 27, July 4, July 12, July 19, and July 26 of that year. The soil samples were mixed and then passed through a 2 mm to remove stones and roots. Soil samples for DNA extraction were frozen at -80 °C. Soil samples for chemical analyses were stored at 4 °C.

Soil chemical analyses

Air-dried and sieved soil subsamples were analyzed for the following physical and chemical properties: Soil salinity (ECe) was measured with a DDS-308A conductivity meter (Shanghai Precision & Scientific Instrument Inc., Shanghai, China). Soil pH was measured in a soil-water (1:2.5, w/v) slurry using a compound electrode (PE-10; Sartorious, Germany). Soil organic carbon (SOC) was measured using the $K_2Cr_2O_7$-H_2SO_4 oxidation–reduction titration method. Soil total N was measured using the semimicro-Kjedahl digestion method. Available kalium (AK) and Available Phosphorus (AP) were determined using the flame photometry and molybdenum antimony resistance colorimetric method, respectively.

Soil microbial analysis

DNA extraction

Soil total bacterial DNA was extracted from 0.25 g of a fresh soil sample using MoBio Powersoil™ DNA Isolation kits (MoBio Laboratories, Carlsbad, CA, USA) according to the manufacturer's protocol. The concentration and purification of DNA were measured using a NanoDrop 2000 UV-vis spectrophotometer (Thermo Fisher Scientific, Waltham, MA, USA), and DNA quality was measured by 0.8% agarose gel electrophoresis. The DNA was stored at -20 °C before analysis.

PCR amplification

To analyze the taxonomic composition of the soil fungal community, the entire region of the 18S rRNA gene was selected for amplification and subsequent high-throughput sequencing of the PCR products. The PCR amplification of the fungal internal transcribed spacer (ITS) region was performed using the forward primer ITS5-1737F (5′-GGAAGTAAAAGTCGTAACAAGG-3′) and the reverse primer ITS2-2043R (5′-GCTGCGTTCTTCATCGATGC-3′). The PCR reaction system for preparing the templates contained 5 μL of Q5 reaction buffer (5×), 5 μL of Q5 High-Fidelity GC buffer (5×), 0.25 μL of Q5 High-Fidelity DNA Polymerase (5 U/μL), 2 μL (2.5 mM) of dNTPs, 1 μL (10 uM) of each forward and reverse primer, 2 μL of DNA Template, and 8.75 μL of ddH_2O. Thermal cycling was carried out with an initial denaturation at 95 °C

http://www.aloki.hu ● ISSN 1589 1623 (Print) ● ISSN 1785 0037 (Online)
DOI: http://dx.doi.org/10.15666/aeer/1804_49694985

for 3 min followed by 33 cycles of 95 °C for 30 s, annealing at 55 °C for 30 s, extension at 72 °C for 45 s, and a final extension step at 72 °C for 10 min.

Illumina MiSeq platforms sequencing

PCR amplicons were purified with Agencourt AMPure Beads (Beckman Coulter, Indianapolis, IN) and quantified using the PicoGreen dsDNA Assay Kit (Invitrogen, Carlsbad, CA, USA). After the individual quantification step, amplicons were pooled in equal amounts, and pair-end 2×300 bp sequencing was performed using the Illlumina MiSeq platform with a MiSeq Reagent Kit v3 at Beijing Biomarker Technology Co., Ltd (Beijing, China). Each replicate was analyzed three times by high-throughput sequencing. The median of three measurements was used as the value for each replicate.

Data analyses

The one-way analysis of variance (ANOVA) and Pearson correlation analysis were conducted using SPSS statistical program (version SPSS 19.0). The difference between the groups used Tukey's test method ($P < 0.05$). The sequence data were analyzed using QIIME and R packages (v3.2.0). The diversity and richness index were analyzed using Mothur software (version 1.30.1). The visualization analysis of classification and abundance used MEGAN. Linear discriminant analysis effect size (LEfSe) was performed to detect differentially abundant taxa across groups using the default parameters.

Results

Soil properties

Soil ECe, pH, SOC, TN, AK, and AP were significantly affected by irrigation water salinity (*Table 1*). Soil ECe and AP increased as water salinity increased, whereas soil pH, SOC, TN, and AK decreased.

Table 1. *Selected soil properties as influenced by irrigation water salinity*

Water salinity	ECe	pH	SOC (g/kg)	TN (g/kg)	AK (mg/kg)	AP (mg/kg)
FW	3.04 c	7.96 a	10.34 a	0.74 a	252 a	7.24 c
BW	7.94 b	7.76 b	9.98 b	0.70 b	213 b	8.92 b
SW	11.36 a	7.75 b	9.46 b	0.64 c	184 c	11.24 a

FW, BW, and SW stand for irrigation water salinities (electrical conductivity, EC) of 0.35, 4.61, and 8.04 dS m^{-1}, respectively. ECe, SOC, TN, AK, and AP stand for saturation conductivity, soil organic carbon, total N, available kalium, and available phosphorus, respectively. Different letters within a column indicate significant differences at $P < 0.05$

Sequencing analysis and alpha diversity

The soil fungal coverage among the soil samples was greater than 99%, indicating that the depth reasonably represented actual situation of the samples (*Table 2*). Irrigation water salinity significantly influenced the number of OTUs. The number of OTUs was significantly less in SW than in FW and BW. The SW treatment significantly reduced the ACE and Chao1 index. However, BW and SW treatments significantly increased Simpson index.

http://www.aloki.hu ● ISSN 1589 1623 (Print) ● ISSN 1785 0037 (Online)
DOI: http://dx.doi.org/10.15666/aeer/1804_49694985

Table 2. *Soil fungal community richness and diversity indexes as influenced by irrigation water salinity*

Water salinity	Sequence number	OTU	Coverage (%)	ACE	Chao1	Simpson	Shannon
FW	63980 a	426 a	0.9995	439 a	445 a	0.0526 c	3.86 a
BW	63047 a	435 a	0.9995	447 a	448 a	0.0627 b	3.83 a
SW	63619 a	408 b	0.9995	419 b	421 b	0.0691 a	3.68 a

FW, BW, and SW stand for irrigation water salinities (electrical conductivity, EC) of 0.35, 4.61, and 8.04 dS m^{-1}, respectively. OTUs, operational taxonomic units. Different letters within a column indicate significant differences at $P < 0.05$

Soil properties (ECe, pH, SOC, TN, AK, and AP) affected fungal community diversity indexes (*Table 3*). Pearson correlation coefficients showed that ACE, Chao1, and Shannon indexes were negatively correlated with ECe but positively correlated with soil SOC, TN, and AK. However, the Simpson indexes had the opposite effect.

Table 3. *Correlations among selected soil properties and diversity indexes*

	ECe	PH	SOC	TN	AK	AP
ACE	-0.503*	0.243	0.523*	0.597*	0.459	-0.383
Chao1	-0.610*	0.400	0.608*	0.689**	0.558*	-0.441
Simpson	0.624*	-0.581*	-0.419*	-0.518*	-0.545*	0.520*
Shannon	-0.599*	0.439	0.509*	0.535*	0.550*	-0.625*

ECe, saturation conductivity; SOC, soil organic carbon; TN, soil total nitrogen; AK, available kalium; AP, available phosphorus. **Correlation is significant at the 0.01 level. *Correlation is significant at the 0.05 level

Soil fungal community structures

Irrigation water salinity significantly influenced the relative abundance of the dominant fungal phyla in each sample (*Fig. 2*). *Ascomycota* (55.54–63.72%), *Mortierellomycota* (4.26–12.65%), *Basidiomycota* (4.41–9.23%), *Glomeromycota* (1.60–6.45%), and *Chytridiomycota* (2.25–9.30%) were the five most dominant phyla. Those five phyla accounted for 81.06%, 85.81%, and 88.10% of the total relative abundance in FW, BW, and SW, respectively. Irrigation water salinity significantly influenced the composition of the fungal communities. The BW and SW treatments significantly reduced the relative abundance of *Mortierellomycota*, *Rotifera*, and *Entomophthoromycota* ($P < 0.05$), but significantly increased the relative abundance of *Ascomycota, Basidiomycota,* and *Mucoromycota* ($P < 0.05$). The BW treatment significantly decreased the relative abundance of *Cercozoa* compared with FW, but significantly increased the relative abundance of *Olpidiomycota* ($P < 0.05$). The SW treatment significantly decreased the relative abundance of *Glomeromycota* compared with FW, but significantly increased the relative abundance of *Chytridiomycota* and *Cercozoa* ($P < 0.05$). In addition, irrigation water salinity had no significant effect on the relative abundance of *Aphelidiomycota*, *Neocallimastigomycota*, *Mucoromycota*, *Calcarisporiellomycota*, and *Kickxellomycota* ($P > 0.05$).

http://www.aloki.hu ● ISSN 1589 1623 (Print) ● ISSN 1785 0037 (Online)
DOI: http://dx.doi.org/10.15666/aeer/1804_49694985

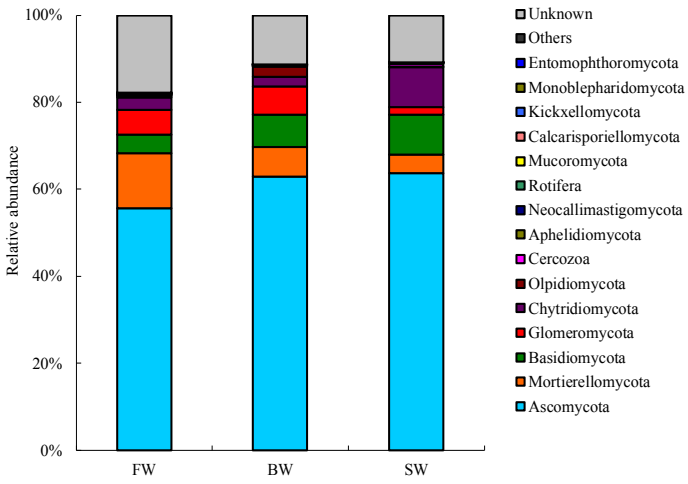

Figure 2. *Relative abundance of the fifteen most common fungal phyla were influenced by irrigation water salinity. (FW, fresh water (0.35 dS m^{-1}); BW, saline water (4.61 dS m^{-1}); SW, saline water (8.04 dS m^{-1}), respectively)*

Soil fungal phyla level of the different irrigation water salinity were divided into three groups (*Fig. 3*), indicating that fungal community in FW, BW or SW share the high similarity. A more detailed description was as follows: fresh water irrigation (FW) had the higher relative abundance of *Aphelidiomycota, Monoblepharidomycota, Mortierellomycota, Entomophthoromycota*, and *Rotifera* phyla. Howerer, irrigation with brackish water irrigation (BW) remarkably increased the relative abundance of *Glomeromycota, Mucoromycota, Olpidiomycota, Calcarisporiellomycota, Kickxellomycota, Basidiomycota, Ascomycota,* and *Neocallimastigomycota* phyla. Irrigation with saline water (SW) remarkably increased the relative abundance of *Cercozoa, Anthophyta, Chytridiomycota, Basidiomycota, Ascomycota*, and *Neocallimastigomycota* phyla.

Irrigation water salinity significantly affected the distribution of soil fungal at the genus level (*Fig. 4*). *Chaetomium* was the most abundant genus (7.54–14.79%) followed by *Mortierella* (4.26–12.63%), *Curvularia* (0.85–5.38%), *Fusarium* (1.01–1.71%), and *Verticillium* (0.35–6.19%). Combined, these five genus accounted for 23.96%, 26.81%, and 24.06% of the total relative abundance in FW, BW, and SW, respectively. Compared with FW treatment, both BW and SW treatments significantly decreased the relative abundance of *Mortierella, Entoloma*, and *Tetracladium* ($P < 0.05$), but significantly increased the relative abundance of *Curvularia* and *Mycosphaerella* ($P < 0.05$). Compared with FW, BW significantly increased the relative abundance of *Cyathus* and *Olpidium*, SW significantly increased the relative abundance of *Chaetomium, Fusarium, Vishniacozyma,* and *Chrysosporium* ($P < 0.05$). In contrast, SW significantly reduced the relative abundance of *Dominikia* ($P < 0.05$). In addition, irrigation water salinity had no significant effect on the relative abundance of *Verticillium, Aspergillus,* and *Spizellomyces* ($P > 0.05$).

A heatmap showed that the relative distribution of the fungal groups varied among the treatments (*Fig. 5*). Each column of the heatmap shows the relative abundance of a different fungal genus in the soil sample. The columns of the heatmap are ordered according to the salinity of the soil sample. The cluster structure shows three main groups of fungal genus which share a peculiar composition and abundance among the

http://www.aloki.hu ● ISSN 1589 1623 (Print) ● ISSN 1785 0037 (Online)
DOI: http://dx.doi.org/10.15666/aeer/1804_49694985

sites, indicating that bacterial community in FW, BW or SW share the high similarity. A more detailed description is as follows: fresh water irrigation (FW) had the higher relative abundance of *Entoloma, Cryptococcus, Talaromyces, Acremonium, Aspergillus, Pyrenochaetopsis, Dominikia, Tetracladium, Glomus, Thielaviopsis, Conidiobolus, Spizellomyces, Mortierella, Plectosphaerella,* and *Acrocalymma* genus. Howerer, irrigation with brackish water irrigation (BW) remarkably increased the relative abundance of *Stagonosporopsis, Curvularia, Alternaria, Metarhizium, Psathyrella, Verticillium, Neonectria, Olpidium,* and *Gibberella* genus. Irrigation with saline water (SW) remarkably increased the relative abundance of *Leptosphaeria, Lectera, Fusarium, Preussia, Chrysosporium, Chaetomium, Stachybotrys, Mycosphaerella, Ochroconis,* and *Vishniacozyma* genus.

RDA and correlation analysis

The correlations between soil properties and the relative abundance of fungal phylum are given in *Table 4*. Four phylum (*Mortierellomycota, Glomeromycota, Rotifera,* and *Entomophthoromycota*) were negatively correlated with soil ECe and AP, however, these phylum were positively correlated with pH, SOC, TN, and AK. Two phylum (*Basidiomycota, Cercozoa*) were positively correlated with soil ECe and AP, however, *Basidiomycota* and *Cercozoa* were negatively correlated with soil pH, SOC, TN, and AK. Redundancy analysis was performed to determine the influence of various environmental parameters on fungal community structure. As shown in *Figure 6,* Axes 1 and 2 explained 67.93% of the variation in soil fungal community based on phylum level. The RDA plots of fungal community structure clearly show that ECe (Explain% = 18.59%, $p = 0.046$) is the one longer arrow. These results indicated that ECe has strong influence on soil fungal communities.

Table 4. *Correlation between soil properties parameters (ECe, pH, SOC, TN, AK, and AP) and the relative abundance of fungal phylum*

	ECe	**pH**	**SOC**	**TN**	**AK**	**AP**
Ascomycota	0.521	-0.527	-0.646	-0.478	-0.604	0.753*
Mortierellomycota	-0.963**	0.929**	0.800**	0.871**	0.939**	-0.819**
Basidiomycota	0.733*	-0.690*	-0.799**	-0.724*	-0.744*	0.625
Glomeromycota	-0.694*	0.395	0.746*	0.771*	0.709*	-0.763*
Chytridiomycota	0.34	-0.232	-0.110	-0.319	-0.245	0.074
Olpidiomycota	-0.023	-0.338	0.213	0.138	0.095	-0.251
Cercozoa	0.668*	-0.354	-0.764*	-0.773*	-0.695*	0.699*
Aphelidiomycota	-0.304	0.476	0.199	0.198	0.323	-0.331
Neocallimastigomycota	0.302	-0.335	-0.258	-0.28	-0.367	0.09
Rotifera	-0.754*	0.826**	0.656	0.703*	0.723*	-0.638
Mucoromycota	0.385	-0.654	-0.268	-0.329	-0.308	0.106
Calcarisporiellomycota	-0.122	-0.129	0.325	0.267	0.113	-0.31
Kickxellomycota	-0.097	-0.231	0.194	0.116	0.164	-0.222
Monoblepharidomycota	-0.436	0.556	0.116	0.195	0.369	-0.147
Entomophthoromycota	-0.903**	0.957**	0.719*	0.806**	0.878**	-0.718*

ECe, saturation conductivity; SOC, soil organic carbon; TN, soil total nitrogen; AK, available kalium; AP, available phosphorus. **Correlation is significant at the 0.01 level. *Correlation is significant at the 0.05 level

http://www.aloki.hu ● ISSN 1589 1623 (Print) ● ISSN 1785 0037 (Online)
DOI: http://dx.doi.org/10.15666/aeer/1804_49694985

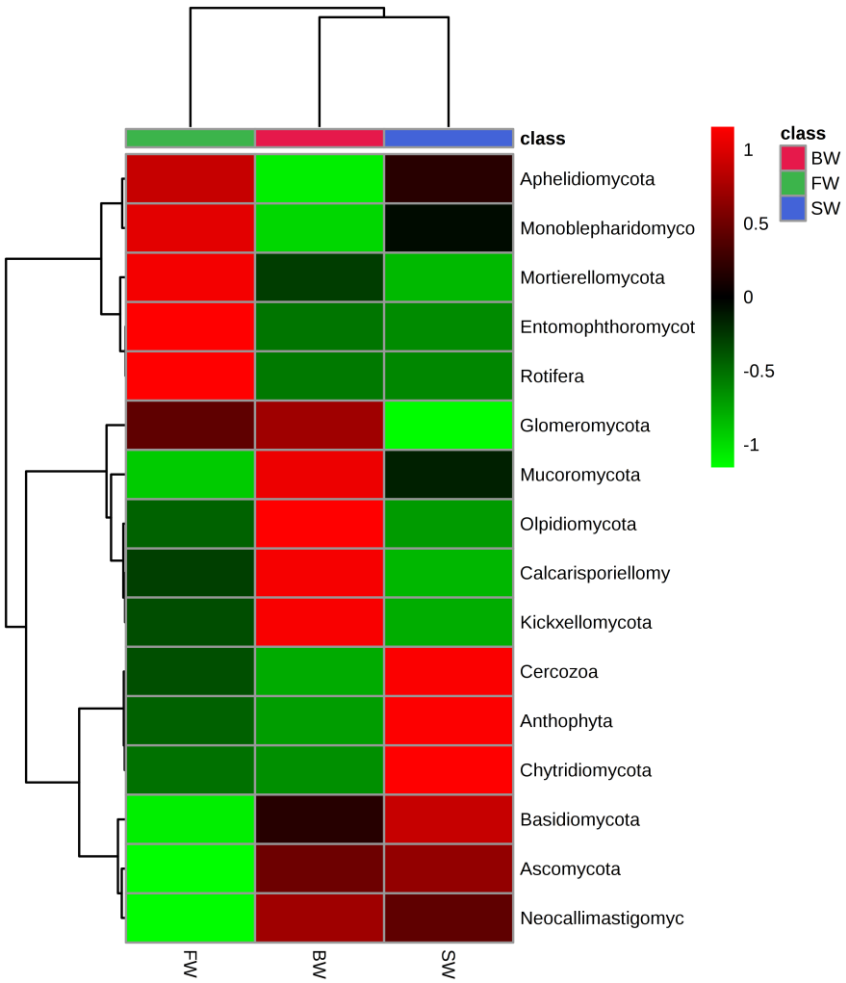

Figure 3. *Heatmap showing the most relative abundance of dominant fungal phyla. The relative values are indicated by color intensity with the legend indicated at the bottom corner. (FW, fresh water (0.35 dS m^{-1}); BW, saline water (4.61 dS m^{-1}); SW, saline water (8.04 dS m^{-1}), respectively)*

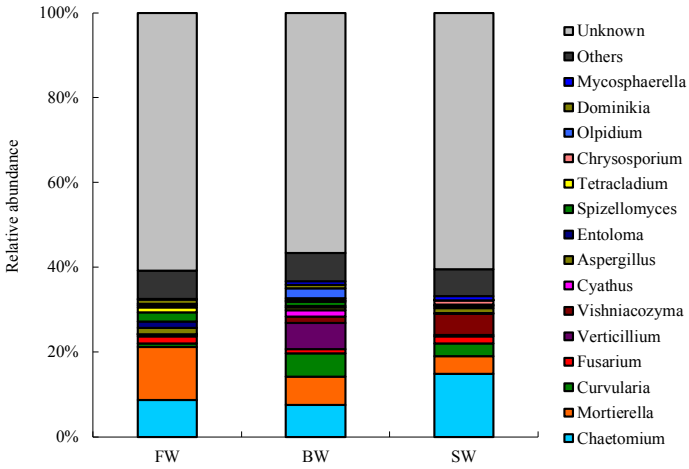

Figure 4. *Relative abundance of the fifteen most common fungal genus were influenced by irrigation water salinity. (FW, fresh water (0.35 dS m^{-1}); BW, saline water (4.61 dS m^{-1}); SW, saline water (8.04 dS m^{-1}), respectively)*

http://www.aloki.hu ● ISSN 1589 1623 (Print) ● ISSN 1785 0037 (Online)
DOI: http://dx.doi.org/10.15666/aeer/1804_49694985

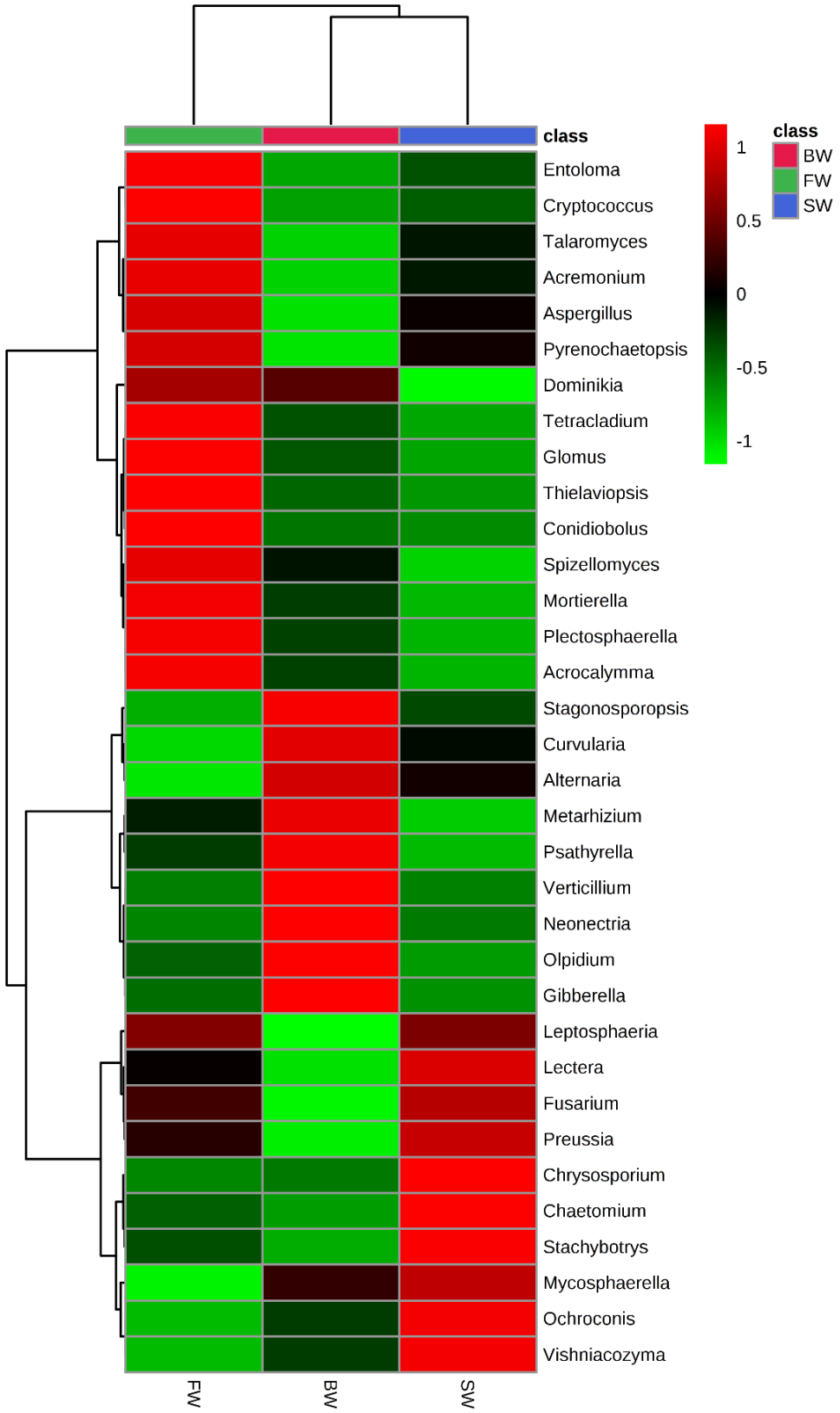

Figure 5. *Heatmap showing the most relative abundance of dominant fungal genus. The relative values are indicated by color intensity with the legend indicated at the bottom corner. (FW, fresh water (0.35 dS m^{-1}); BW, saline water (4.61 dS m^{-1}); SW, saline water (8.04 dS m^{-1}), respectively)*

http://www.aloki.hu ● ISSN 1589 1623 (Print) ● ISSN 1785 0037 (Online)
DOI: http://dx.doi.org/10.15666/aeer/1804_49694985

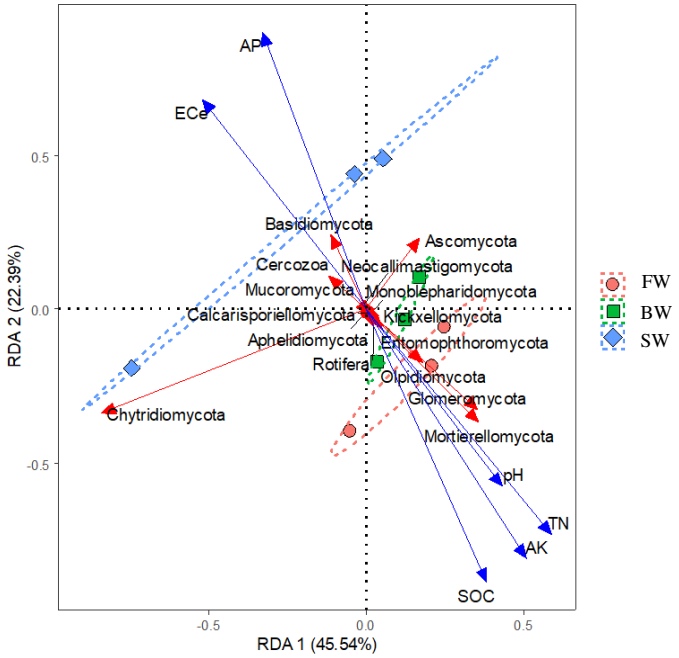

Figure 6. *Redundancy analysis (RDA) results of samples based on the phylum levels. (FW, fresh water (0.35 dS m^{-1}); BW, saline water (4.61 dS m^{-1}); SW, saline water (8.04 dS m^{-1}), respectively; ECe, saturation conductivity; SOC, soil organic carbon; TN, soil total nitrogen; AK, available kalium; AP, available phosphorus)*

The correlations between soil properties and the relative abundance of fungal genus are given in *Table 5*. Four genus (*Mortierella, Entoloma, Tetracladium,* and *Dominikia*) were negatively correlated with soil ECe and AP, however, these phylum were positively correlated with pH, SOC, TN, and AK. Two genus (*Vishniacozyma, Chrysosporium,* and *Mycosphaerella*) were positively correlated with soil ECe and AP, however, *these* genus were negatively correlated with soil pH, SOC, TN, and AK. In addition, *Chaetomium* was negatively correlated with soil TN. The correlation of soil bacterial community structures with environmental factors were analyzed by RDA (*Fig. 7*). Axis 1 and axis 2 together explained 68.56% of the total variation in the compositions of soil fungal community. The RDA plots of fungal community structure clearly show that the one longer arrows were ECe (Explain% = 25.49%, $p = 0.013$). These results indicated that ECe has strong influence on soil fungal communities.

Differential microbial composition

A cladogram generated by LEfSe showed significant differences in taxa among the treatment groups (*Fig. 8*). In total, 26 bacterial clades presented significantly different among the different clades, 8 for the FW treatment, 11 for BW treatment, and 5 for the SW treatment, indicating that the potential biomarkers increased by the brackish water irrigation, however, the potential biomarkers decreased by saline water irrigation. In addition, *Dothideomycetes*, *Pleosporales, Pleosporaceae, Curvularia, Curvularia_hawaiiensis, Auriculariales, Olpidium, Olpidiaceae, Olpidiales, Olpidiomycetes, Olpidiomycota,* and *Olpidium_brassicae* as an indicator bacteria for BW by LEfSe analysis, *Vishniacozyma_tephrensis, Tremellomycetes*, *Tremellales, Vishniacozyma*, *and Bulleribasidiaceae* were indicator bacteria for SW treatment.

http://www.aloki.hu ● ISSN 1589 1623 (Print) ● ISSN 1785 0037 (Online)
DOI: http://dx.doi.org/10.15666/aeer/1804_49694985

Table 5. *Correlation between soil properties parameters (ECe, pH, SOC, TN, AK, and AP) and the relative abundance of fungal genus*

	ECe	pH	SOC	TN	AK	AP
Chaetomium	0.551	-0.368	-0.639	-0.689*	-0.562	0.59
Mortierella	-0.963**	0.929**	0.800**	0.871**	0.939**	-0.820**
Curvularia	0.532	-0.791*	-0.289	-0.389	-0.484	0.219
Fusarium	0.128	0.148	-0.383	-0.353	-0.212	0.35
Verticillium	0.059	-0.155	-0.004	0.189	-0.07	0.295
Vishniacozyma	0.734*	-0.584	-0.798**	-0.770*	-0.746*	0.595
Cyathus	0.11	-0.418	0.077	0.117	-0.074	0.033
Aspergillus	-0.349	0.494	0. 134	0.229	0.293	-0.181
Entoloma	-0.721*	0.840**	0.534	0.605	0.681*	-0.554
Spizellomyces	-0.389	0.344	0.303	0.299	0.363	-0.424
Tetracladium	-0.962**	0.972**	0.869**	0.881**	0.951**	-0.775*
Chrysosporium	0.681*	-0.504	-0.802**	-0.806**	-0.703*	0.705*
Olpidium	-0.025	-0.334	0.211	0.138	0.099	-0.25
Dominikia	-0.869**	0.645	0.908**	0.880**	0.874**	-0.881**
Mycosphaerella	0.928**	-0.882**	-0.847**	-0.860**	-0.924**	0.710*

ECe, saturation conductivity; SOC, soil organic carbon; TN, soil total nitrogen; AK, available kalium; AP, available phosphorus. **Correlation is significant at the 0.01 level. *Correlation is significant at the 0.05 level

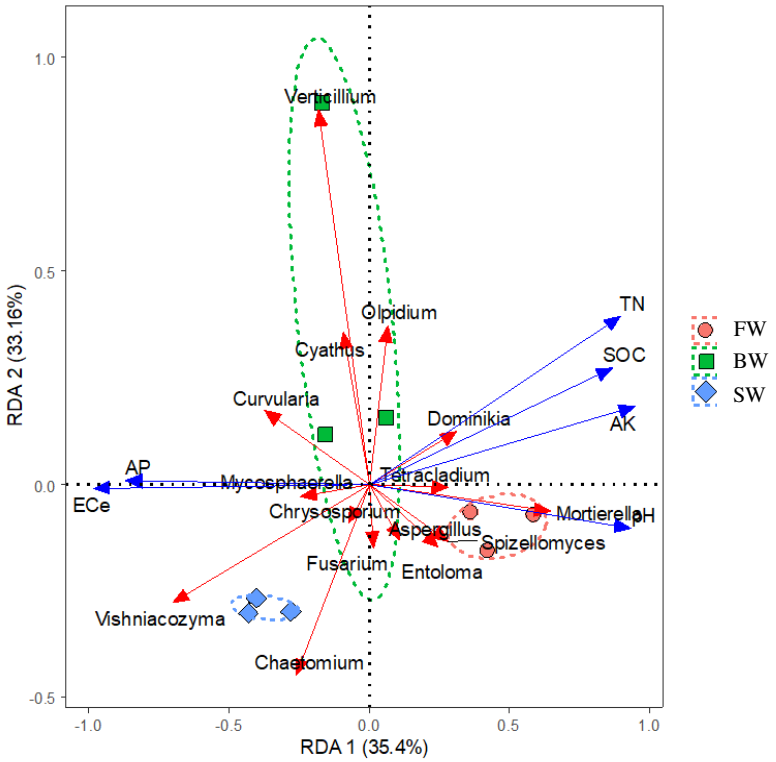

Figure 7. *Redundancy analysis (RDA) results of samples based on the genus levels. (FW, fresh water (0.35 dS m^{-1}); BW, saline water (4.61 dS m^{-1}); SW, saline water (8.04 dS m^{-1}), respectively; ECe, saturation conductivity; SOC, soil organic carbon; TN, soil total nitrogen; AK, available kalium; AP, available phosphorus)*

http://www.aloki.hu ● ISSN 1589 1623 (Print) ● ISSN 1785 0037 (Online)
DOI: http://dx.doi.org/10.15666/aeer/1804_49694985

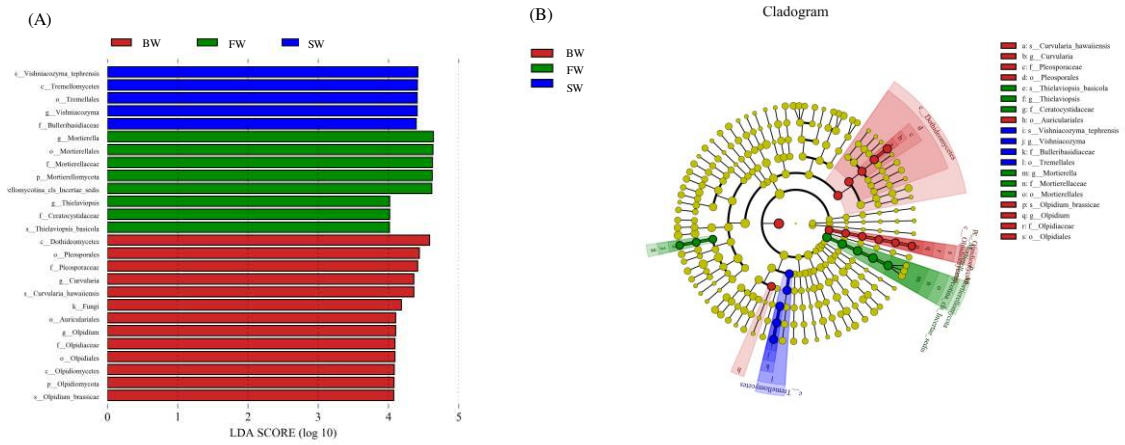

Figure 8. *A linear discriminant analysis effect size (LEfSe) method identified significant differences in the abundance of fungal taxa in all of the treatments. (A) linear discriminant analysis (LDA) score; (B) Cladogram. Taxa with significantly different abundances among treatments are represented by colored dots, and from the center outward, they represent the kingdom, phylum, class, order, family, and genus levels, respectively. The colored shadows represent trends of the significantly different taxa. Each colored dot has an effect size LDA score. Only taxa meeting an LDA significance threshold of > 4 are shown. (FW, fresh water (0.35 dS m^{-1}); BW, saline water (4.61 dS m^{-1}); SW, saline water (8.04 dS m^{-1}), respectively)*

Discussion

Saline water irrigation has received increasing attention, the future of irrigated agriculture will need to include the use of saline water especially in developing countries where there is extreme shortage of freshwater, particularly in arid regions (Letey and Feng, 2007). However, saline water irrigation in arid regions will load salt in the root zone, change soil physicochemical properties. The results of this study indicated that BW and SW both significantly increased soil salinity and Available Phosphorus, but reduced soil pH, SOC, total N, Available Kalium. These changes in soil physicochemical properties may affect soil biological effectiveness.

Fungal play an important role in the soil ecosystem, which strongly influence ecosystem structure and function and are vital components of soil microbial communities with a series of important roles, such as parasitism, decomposition, pathogenesis and symbiosis (Altieri, 1999; Neher, 1999; Van der Putten et al., 2007; Aguilar-Trigueros et al., 2014). Fungal diversity and community structure were important index for evaluating the health and stability of the soil ecosystem. It is therefore necessary to increase understanding about the influence of saline water irrigation on the diversity and ecological function of soil microorganisms. Our results indicate that saline water irrigation significantly reduced the ACE and Chao1 index. This finding agrees with the findings of Cortés-Lorenzo et al. (2016) who showed that high salinity reduced fungal diversity. The effects of salinity grade on the richness (ACE, Chao1) and Shannon diversity are congruent to the negatively correlation between soil salinity and Shannon index, supporting that the diversity of fungal community decreases with increasing soil salinity, a pattern was also demonstrated by Guo and Gong (2014).

It is well known that environmental changes may affect soil fungal community composition and structure (Li et al., 2015b). Many studies have found that soil

http://www.aloki.hu ● ISSN 1589 1623 (Print) ● ISSN 1785 0037 (Online)
DOI: http://dx.doi.org/10.15666/aeer/1804_49694985

microbial community composition may be affected by salinity (Lozupone and Knight, 2007; Llamas et al., 2008; Chowdhury et al., 2011b) because microbial genotypes differ in their tolerance of low osmotic potential (Mandeel, 2006; Llamas et al., 2008). In our study, the dominant phyla in all treatment were *Ascomycota, Mortierellomycota, Basidiomycota, Glomeromycota*, and *Chytridiomycota*. Combined, these phyla accounted for 81.06–88.10% of the relative abundance in the FW, BW, and SW treatments. In comparison, Mohamed and Martiny (2011) detected more *Ascomycota* (78%), fewer *Basidiomycota* (6%) and a greater number of basal fungal lineages (16%), including *Glomeromycota, Chytridiomycota* and *BFL1-3* in different soil (salt, brackish and freshwater marsh). Our findings are partly consistent with previous studies which found that the fungal community was mainly composed of *Ascomycota*, *Basidiomycota*, *Chytridiomycota, Glomeromycota, Zygomycota,* and *Blastocladiomycota* (Maza-Márquez et al., 2016; Xu et al., 2017). Sequence abundance in this study showed that *Ascomycota* were the most abundant phylum. Some researchers have noted the prevalence of *Ascomycota* (Wang et al., 2015; Xu et al., 2017). Most *Ascomycota* are saprophytic fungal, which can degrade soil labile organic matter. In this study, *Ascomycota* phylum abundance was negatively correlated with soil SOC. In our study, BW and SW both strongly reduced the abundance of *Mortierellomycota*, but increased the abundance of *Basidiomycota*. *Basidiomycota* are important decomposers, which can cause wood decay and decompose wood cellulose. Wang and Guo (2016) also reported that the majority of fungal belonged to *Basidiomycota* in mild-salt-tolerant communities. In addition, we observed that saline water irrigation significantly decreased the relative abundance of *Glomeromycota* compared with fresh water irrigation, but significantly increased the relative abundance of *Chytridiomycota*. However, brackish water irrigation had no significant effect on the relative abundance of *Glomeromycota* and *Chytridiomycota*. The fact that fungal composition varied at all levels of taxonomic resolution along the gradient of irrigation water salinity suggests that fungal adaption to salinity (or covarying environmental parameters) occurs at many genetic scales (Martiny et al., 2009). Therefore, soil fungal communities adapted to salinity stress by adjusting their species composition.

Conclusions

In this study, we quantified the effects of nine years of saline water irrigation on soil properties and fungal community structure under drip-irrigated cotton. Saline water irrigation can change soil physicochemical properties, which thereby influence soil microbial processes. Fungal communities in the different irrigation water salinity were markedly different. Our results show that salinity (ECe) was a major environmental factor structuring the soil fungal community. saline water irrigation significantly reduced OTUs, ACE and Chao1 index. In addition, diversity of fungal community decreases with increasing soil salinity. The dominant fungal phyla were *Ascomycota, Mortierellomycota, Basidiomycota, Glomeromycota*, and *Chytridiomycota*. Saline water irrigation reduced the abundance of *Mortierellomycota* and *Glomeromycota,* but increased that of *Basidiomycota*, *Ascomycota and Chytridiomycota* were not significantly affected by saline water irrigation. In addition, the dominant fungal genus were *Chaetomium*, *Mortierella*, *Curvularia*, *Fusarium*, and *Verticillium*. Statistical analysis (LEfSe) demonstrated that fungal potential biomarkers decreased by saline water irrigation. The results of this study increase understanding about (i) the effects of

http://www.aloki.hu ● ISSN 1589 1623 (Print) ● ISSN 1785 0037 (Online)
DOI: http://dx.doi.org/10.15666/aeer/1804_49694985

irrigation water salinity on fungal community structure under irrigated cotton and (ii) the role of environmental variability as a predictor of fungal community composition. In addition, saline irrigation will increase soil salinity, thereby affecting soil N transformations. In the future, we should focus on the effect of saline water irrigation on soil nitrogen transformation and its key microbiological process, providing a theoretical basis for the rational use of saline water resources in arid regions and the effective management of N and the regulation of the N cycle.

Acknowledgments. This work was jointly funded by The National Natural Science Foundation of China [41661055], the Youth Innovation Talent Cultivation Program of Shihezi University [CXRC201706].

REFERENCES

[1] Aguilar-Trigueros, C. A., Powell, J. R., Anderson, I. C., Antonovics, J., Rillig, M. C. (2014): Ecological understanding of root-infecting fungal using trait-based approaches. – Trends in Plant Science 19(7): 432-438.
[2] Altieri, M. A. (1999): The Ecological Role of Biodiversity in Agroecosystems. – In: Paoletti, M. G. (ed.) Invertebrate Biodiversity as Bioindicators of Sustainable Landscapes. Elsevier, Amsterdam, pp. 19-31.
[3] Amini, S., Ghadiri, H., Chen, C., Marschner, P. (2016): Salt-affected soils, reclamation, carbon dynamics, and biochar: a review. – Journal of Soils and Sediments 16(3): 939-953.
[4] Canfora, L., Malusà, E., Salvati, L., Renzi, G., Petrarulo, M. C., Benedetti, A. (2015): Exploring short-term Impact of two liquid organic fertilizers on Solanum lycopersicum L. rhizosphere Eubacteria and Archaea diversity. – Applied Soil Ecology 88: 50-59.
[5] Chowdhury, N., Marschner, P., Burns, R. (2011a): Response of microbial activity and community structure to decreasing soil osmotic and matric potential. – Plant and Soil 344(1-2): 241-254.
[6] Chowdhury, N., Marschner, P., Burns, R. G. (2011b): Soil microbial activity and community composition: impact of changes in matric and osmotic potential. – Soil Biology and Biochemistry 43(6): 1229-1236.
[7] Cortés-Lorenzo, C., González-Martínez, A., Smidt, H., González-López, J., Rodelas, B. (2016): Influence of salinity on fungal communities in a submerged fixed bed bioreactor for wastewater treatment. – Chemical Engineering Journal 285: 562-572.
[8] Elmajdoub, B., Barnett, S., Marschner, P. (2014): Response of microbial activity and biomass in rhizosphere and bulk soils to increasing salinity. – Plant and Soil 381(1-2): 297-306.
[9] Guo, X., Gong, J. (2014): Differential effects of abiotic factors and host plant traits on diversity and community composition of root-colonizing arbuscular mycorrhizal fungi in a salt-stressed ecosystem. – Mycorrhiza 24(2): 79-94.
[10] Jackson, C. R., Vallaire, S. C. (2009): Effects of salinity and nutrients on microbial assemblages in Louisiana wetland sediments. – Wetlands 29(1): 277-287.
[11] Jansson, J. K., Prosser, J. I. (2013): Microbiology: the life beneath our feet. – Nature 494(7435): 40.
[12] Karlberg, L., Rockström, J., Annandale, J. G., Steyn, J. M. (2007): Low-cost drip irrigation-A suitable technology for southern Africa? An example with tomatoes using saline irrigation water. – Agricultural Water Management 89(1): 59-70.
[13] Letey, J., Feng, G. L. (2007): Dynamic versus steady-state approaches to evaluate irrigation management of saline waters. – Agricultural Water Management 91: 1-10.

http://www.aloki.hu ● ISSN 1589 1623 (Print) ● ISSN 1785 0037 (Online)
DOI: http://dx.doi.org/10.15666/aeer/1804_49694985

[14] Li, C. J., Lei, J. Q., Zhao, Y., Xu, X. W., Li, S. Y. (2015a): Effect of saline water irrigation on soil development and plant growth in the Taklimakan Desert Highway shelterbelt. – Soil and Tillage Research 146: 99-107.
[15] Li, Y. J., Wang, H., Zhao, J. N., Huangfu, C. H., Yang, D. L. (2015b): Effects of tillage methods on soil physicochemical properties and biological characteristics in farmland: a review. – The Journal of Applied Ecology 26(3): 939-948.
[16] Llamas, D. P., de, Cara, Gonzalez, M., Gonzalez, C. I., Lopez, G. R., Marquina, J. T. (2008): Effects of water potential on spore germination and viability of Fusarium species. – Journal of Industrial Microbiology & Biotechnology 35(11): 1411-1418.
[17] Lozupone, C. A., Knight, R. (2007): Global patterns in bacterial diversity. – Proceedings of the National Academy of Sciences 104(27): 11436-11440.
[18] Ludwig-Müller, J. (2015): Bacteria and fungi controlling plant growth by manipulating auxin: balance between development and defense. – Journal of Plant Physiology 172: 4-12.
[19] Malash, N. M., Ali, F. A., Fatahalla, M. A., Hatem, M. K., Tawfic, S. (2012): Response of tomato to irrigation with saline water applied by different irrigation methods and water management strategies. – International Journal of Plant Production 2: 101-116.
[20] Mandeel, Q. A. (2006): Biodiversity of the genus Fusarium in saline soil habitats. – Journal of Basic Microbiology 46(6): 480-494.
[21] Martiny, A. C., Tai, A. P., Veneziano, D., Primeau, F., Chisholm, S. W. (2009): Taxonomic resolution, ecotypes and the biogeography of Prochlorococcus. – Environmental Microbiology 11(4): 823-832.
[22] Maza-Márquez, P., Vilchez-Vargas, R., Kerckhof, F. M., Aranda, E., González-López, J., Rodelas, B. (2016): Community structure, population dynamics and diversity of fungal in a full-scale membrane bioreactor (MBR) for urban wastewater treatment. – Water Research 105: 507-519.
[23] Mohamed, D. J., Martiny, J. B. (2011): Patterns of fungal diversity and composition along a salinity gradient. – The ISME Journal 5(3): 379.
[24] Mojid, M. A., Hossain, A. Z. (2013): Conjunctive Use of Saline and Fresh Water for Irrigating Wheat (Triticum aestivum L.) at Different Growth Stages. – The Agriculturists 11: 15-23.
[25] Morrissey, E. M., Franklin, R. B. (2015): Evolutionary history influences the salinity preference of bacterial taxa in wetland soils. – Frontiers in Microbiology 6: 1-12.
[26] Neher, D. A. (1999): Soil community composition and ecosystem processes: comparing agricultural ecosystems with natural ecosystems. – Agroforestry Systems 45(1-3): 159-185.
[27] Neubauer, S. C. (2013): Ecosystem responses of a tidal freshwater marsh experiencing saltwater intrusion and altered hydrology. – Estuaries and Coasts 36(3): 491-507.
[28] Rietz, D. N., Haynes, R. J. (2003): Effects of irrigation-induced salinity and sodicity on soil microbial activity. – Soil Biology and Biochemistry 35: 845-854.
[29] Setia, R., Marschner, P., Baldock, J., Chittleborough, D., Verma, V. (2011): Relationships between carbon dioxide emission and soil properties in salt-affected landscapes. – Soil Biology and Biochemistry 43(3): 667-674.
[30] Srivastava, P. K., Gupta, M., Singh, N., Tewari, S. K. (2016): Amelioration of sodic soil for wheat cultivation using bioaugmented organic soil amendment. – Land Degradation & Development 27(4): 1245-1254.
[31] Van der Putten, W. H., Klironomos, J. N., Wardle, D. A. (2007): Microbial ecology of biological invasions. – The ISME Journal 1(1): 28.
[32] Wang, J., Bao, J., Su, J., Li, X., Chen, G., Ma, X. (2015): Impact of inorganic nitrogen additions on microbes in biological soil crusts. – Soil Biology and Biochemistry 88: 303-313.

http://www.aloki.hu ● ISSN 1589 1623 (Print) ● ISSN 1785 0037 (Online)
DOI: http://dx.doi.org/10.15666/aeer/1804_49694985

[33] Wang, R., Kang, Y., Wan, S., Hu, W., Liu, S., Liu, S. (2011): Salt distribution and the growth of cotton under different drip irrigation regimes in a saline area. – Agricultural Water Management 100(1): 58-69.
[34] Wang, Y. Y., Guo, D. F. (2016): Response of Soil Fungal Community Structure to Salt Vegetation Succession in the Yellow River Delta. – Current Microbiology 73(4): 595-601.
[35] Xu, F., Cai, T., Yang, X., Sui, W. (2017): Soil fungal community variation by large-scale reclamation in Sanjiang plain, China. – Annals of Microbiology 67(10): 679-689.
[36] Yang, H. X., Guo, S. X., Liu, J. R. (2015): Characteristics of arbuscular mycorrhizal fungal diversity and functions in saline-alkali land. – The Journal of Applied Ecology 26(1): 311-320.
[37] Yu, Z., Wang, G., Jin, J., Liu, J., Liu, X. (2011): Soil microbial communities are affected more by land use than seasonal variation in restored grassland and cultivated Mollisols in Northeast China. – European Journal of Soil Biology 47(6): 357-363.
[38] Yuan, B. C., Li, Z. Z., Liu, H., Gao, M., Zhang, Y. Y. (2007): Microbial biomass and activity in salt affected soils under arid conditions. – Applied Soil Ecology 35(2): 319-328.
[39] Zhang, P. P., Xu, S. Z., Zhang, G. J., Pu, X. Z., Wang, J., Zhang, W. F. (2019): Carbon cycle in response to residue management and fertilizer application in a cotton field in arid northwest china. – Journal of Integrative Agriculture 18(5): 1103-1119.
[40] Zhang, T., Wang, N. F., Zhang, Y. Q., Liu, H. Y., Yu, L. Y. (2015): Diversity and distribution of fungal communities in the marine sediments of Kongsfjorden, Svalbard (High Arctic). – Scientific Reports 5: 14524.
[41] Zhou, J. L., Wu, B., Wang, Y. P., Guo, X. J. (2009): Distribution and quality assessment of medium salinity groundwater in plain areas in Tarim Basin, Xinjiang. – China Rural Water Hydropower 9: 32-36.

http://www.aloki.hu ● ISSN 1589 1623 (Print) ● ISSN 1785 0037 (Online)
DOI: http://dx.doi.org/10.15666/aeer/1804_49694985

THE HYDROLOGICAL INFLUENCE OF FOREST HARVESTING INTENSITY ON STREAMS: A GLOBAL SYNTHESIS WITH IMPLICATIONS FOR POLICY

FAROOQI, T. J. A.[1*] – ABBAS, H.[2] – HUSSAIN, S.[3]

[1]*School of Ecology and Nature Conservation, Beijing Forestry University, Beijing 100083, China*

[2]*College of Forest Science, Beijing Forestry University, Beijing 100083, China*

[3]*Research Center of Forest Management and Engineering of National Forest and Grassland Administration, Beijing Forestry University, Beijing 100083, China*

**Corresponding author*
e-mail: tanzeelfarooqi_21@yahoo.com

(Received 4th Feb 2020; accepted 22nd May 2020)

Abstract. The hydrological properties of the clearcutting of forested catchments were widely investigated by analyzing runoff in the pre- and post-harvesting periods. Deforestation worldwide is primarily to meet the wood and fiber products demand for household and industry. It is a widely known phenomenon that deforestation enhances the streamflow and water yield. However, due to the complexity of forest structure and functions, little is known about the exact estimation of a percent increase in water yield after various harvesting intensities of conifers and broadleaved forest globally. To assess these effects, this study analyzed 145 catchments dataset collected from 21 publications. The study evaluates the influence of 25, 50, 75, and 100% deforestation on streamflow. Moreover, changes in the context of various variables like treatment years, elevation, area and mean annual precipitation were also analyzed. Overall comparison showed that after harvesting of broadleaved water yield increases up to 8-23% and in needle-leaved up to 9-28%. The study provides scientific insight into the essential role that annual precipitation, area, elevation, and year of treatment play in influencing hydrology. This research suggests that a target specific approach should be adopted in future forest management under the umbrella of integrated research to mitigate the challenges of climate change.
Keywords: *climate change, streamflow, annual precipitation, water yield, broadleaved, needle-leaved*

Introduction

The ever-increasing trend in the human population has caused an upsurge the overexploitation of natural resources, especially the degradation of forests in terrestrial ecosystems. Forests are essential to life on Earth, providing numerous ecosystem services (Costanza et al., 1997) such as fruits, honey, oil, pickle, biocontrol, pollination, Carbon sink, water, and nutrient recycling as well as biodiversity conservation (Nasi et al., 2002; Badshah et al., 2017; Wang et al., 2017; Masiero et al., 2019; Ullah et al., 2019b; Muhammad et al., 2020). Among all the forest ecosystem services, carbon sinks and water provision to down- stream are the two primary services which act as essential cogs in the carbon and water cycle by playing their active role in forest processes and functions. However, there are some trade-offs between gain in forest productivity and ecosystem water balance (Farooqi et al., 2019b). Due to brimming of the population in the world has led to an increase in anthropogenic disturbance which are the primary cause of changes in forest composition over a period characterized by drastic changes in both land use and cover resulting increase in fossil fuel emissions and influencing environmental condition (Law et al., 2002; Houghton, 2012; Siddique et al., 2020). This situation is getting worst in

http://www.aloki.hu ● ISSN 1589 1623 (Print) ● ISSN 1785 0037 (Online)
DOI: http://dx.doi.org/10.15666/aeer/1804_49875009

developing countries because of massive deforestation and fire incidences (Khan et al., 2019; Ullah et al., 2019a; Ali et al., 2020).

Despite all the conflicting debates on retaining and removing forests (Popkin, 2019), for sequestrating carbon which enhances productivity, it is overwhelmingly considered the top priority (Krankina et al., 1997; Ruddell et al., 2007). As far as their interaction with water is concerned in this modern era, forests are also recognized in two important terminologies "upstream" as a source of water in streams and rivers (Zhang et al., 2017), and "upwind" as a source of precipitation (van der Ent et al., 2010; Ellison et al., 2012, 2017) however, these trends are bound to the localities and regions.

Deforestation is mainly considered as a positive aspect of increasing the streamflow and runoff, which is ultimately utilized by the industry and household (Bosch and Hewlett,1982; Jones and Post, 2004). Meanwhile, the expansion of forests reduces this water flow leading to 52% of half dryness and 13% of complete dryness of streams in the world (Andréassian, 2004; Jackson et al., 2005). The result is decline in water availability to downstream users (van Dijk and Keenan, 2007), especially dry areas are more vulnerable to this situation. However, the phenomenon of annual runoff is generally dependent on annual precipitation and evapotranspiration. The greater the precipitation, the less evapotranspiration will ultimately enhance runoff and vice versa (Komatsu et al., 2011). The proportionate contribution of precipitation to streamflow varies by how interception and evapotranspiration are influenced by vegetation development stage, rooting depth and health. However, this may differ widely according to vegetation type (Calder, 1999; Zhang et al., 2001). Because the main components of evapotranspiration are canopy transpiration and interception loss (Van Wijk et al., 2001; Vertessy et al., 2001; Wilson et al., 2001). Interception losses from coniferous and broadleaved forests were presented by (Huber and Iroume, 2001; Komatsu et al., 2011), depending on rainfall and forest characteristics (Iroume and Huber, 2002).

In the past, many research investigations have evaluated the effect of logging operation on the global variation in water yield depending on different forest types and structure (Hornbeck et al., 1993; Troendle et al., 2001; Andreassian, 2004; Adams and Flower, 2006; Komatsu et al., 2011), especially the impacts of forest harvesting of broadleaves and conifers forests on runoff and water yield (Komatsu et al., 2011). Yet questions and misconceptions linger regarding the influence of forest harvesting operations on streamflow under the variety of climatic, physiographic factors, and forest management constraints. It has been shown that considerable change in streamflow after forest cutting can be observed when more than 20% of the forest cover declined (Stednick, 1996). However, many previous studies of broadleaf and conifers forests reported that the annual runoff improved by 10-70%, depending on the size of the harvesting intensity (Keppeler and Ziemer, 1990; Fahey, 1994; Swank et al., 2001; Farooqi et al., 2020a). Similarly, some reported the effects of timber removal only in the first years after final harvest (David et al., 1994; Bari et al., 1996), whereas, others investigated up to 6-23 years after the event (Ruprecht and Stoneman, 1993; David, 1994; Fahey, 1994). This variation in results widely depending on forest type, harvesting technique, climate as well as the topography of the area.

Although forest harvesting has positive impacts on streamflow and water yield, it also has many adverse implications on the whole ecosystem. Therefore, predefined knowledge about forest types can be helpful for understanding and implementing afforestation/deforestation programs in the context of minting the balance between forest carbon sequestration and water conservation. This will provide future assistance to regional forestry planning and forest management. In this case, the negative influences of forest on

http://www.aloki.hu ● ISSN 1589 1623 (Print) ● ISSN 1785 0037 (Online)
DOI: http://dx.doi.org/10.15666/aeer/1804_49875009

streamflow might be to control the proportion of forest cover at the catchment scale, which has the potential to modify the streamflow regime (Zhang et al., 2012). This fact is essential to get a better understanding of the affiliation between runoff concerning forest cover proportion (Brown et al., 2013).

To satisfy the rapidly increasing burdens on water supply and other ecosystem services, a practical approach for managing forests (afforestation/deforestation) is needed to achieve the multifunctional benefits. That mainly addresses the tradeoff between carbon sink and water yielding, which is urgently required (*Fig. 1*). The present article aimed to investigate the effects of various degrees of deforestation on the hydrological properties of different streams with forested catchments, as well as the influence of precipitation afterward.

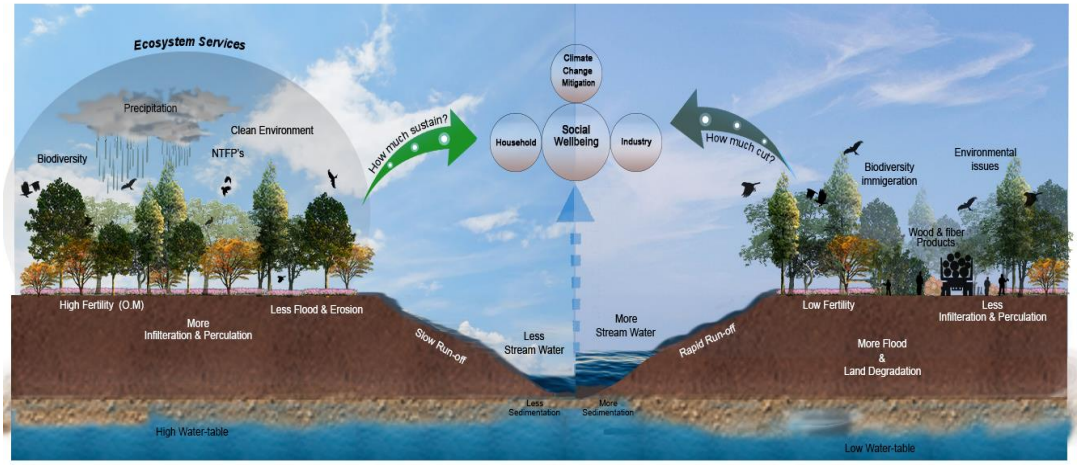

Figure 1. *The diagram showing the importance of retaining and removing forest, and their overall impacts on socio-economic development under the umbrella of efficient forest management strategies for climate change mitigation*

Materials and methods

Data collection and processing

We have compiled this large dataset of deforestation studies and their impacts on water yield from research articles published peer review journals. The sample consists of total of 64 watershed sites of conifers forest stand and 81 sites belonging to broadleaf forest stand, totaling 300 observations from all over the world. This study compiled the dataset from 21 peer-reviewed journals as well as reports of governmental and nongovernmental research institutes, representing many parts of the world (*Appendix 5*). The forest types were classified into conifers and broadleaf depending upon the dominant species of the forest stand as well as information available in the publication. Information gathering included deforestation intensities on water yield and streamflow before and after treatment. Elevation, age, area, yearly record after treatment and mean annual precipitation were determining from the publication for each site. All those sites which showed no significant increase in water yield after harvesting were discarded to get reliable and expressible estimate of computed harvesting intensities of 25, 50, 75 and 100%. The harvesting intensities were set according to the previous researches guidelines i.e. considerable change in water yield after harvesting was mainly observed when 20% or more area was cut (Bosch and Hewlett, 1982; Stednick, 1996). The percent change in water yield after harvesting was computed with the help of formula as shown in *Equation 1*.

http://www.aloki.hu ● ISSN 1589 1623 (Print) ● ISSN 1785 0037 (Online)
DOI: http://dx.doi.org/10.15666/aeer/1804_49875009

$$\text{Change in water yield (\%)} = \frac{\text{Increase in water yield after treatment}}{\text{Total available water in stream before and after treatment}} * 100 \quad \text{(Eq.1)}$$

*where stream water before and after treatment in equation.1 is in mm

Testing of significance

First the Normality test i.e. Shaprio-wilk test was performed, this test showed that the conditions of normality and homogeneity of variance were not met and that has been visual represented in QQ plot. Later nonparametric Kruskal–Wallis tests were applied before by Farley et al. (2005) in a kind of synthesis analysis. In each case, the dependent variable was either the proportional change in water yield following change in factors of evaluation i.e. deforestation percentage. The significance test suggests that the water yield rate is not the same in each of the two or more harvesting intensities ($P < 0.05$). Even if we rejected the null hypothesis of no difference, the test does not tell us either the two similar intensities of broadleaved and needle-leaved differ significantly from each other. To compare two groups at a time used the Wilcoxon Rank test.

Results

The results of Shaprio-wilk test rejected normality at $P < 0.0001$ (*Appendix 1*); the results of the QQ plot showed the visual representation, i.e., the distribution of variables for conifers and broadleaves forest groups of all four harvesting intensities. Many points in both ends fall out of the line and are away from the confidence envelope (Appendix 2). Similarly, the Kruskal-Wallis test showed a highly significant increase in streamflow (%) after deforestation in broadleaved and conifers forests of the global dataset at $P < 0.0001$ as mentioned in *Appendix 3*. These results reveal that the percent increase in water yield after treatment of 25, 50, 75, and 100% harvesting intensities in the broadleaved forest was 8, 15, 20, and 23%, respectively. However, this increase was significantly higher in conifers than broadleaved with increase of 9, 17, 23 and 28% in water yield respectively (*Figure 2)*. Therefore, the overall results of needle-leaved are significantly higher than broadleaved forest stand after treatment as illustrated in *Appendix 3*. Similar results have shown from Wilcoxon rank test while comparing similar harvesting intensities of both the forest vegetation types at ($P < 0.05$) in (*Appendix 4*).

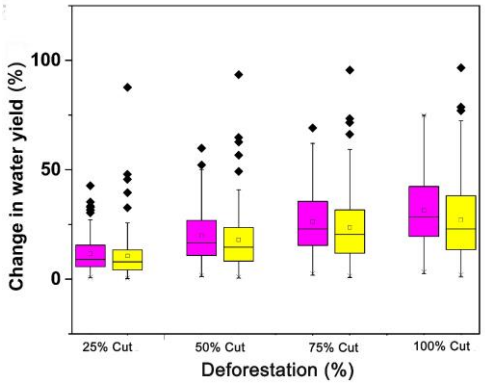

Figure 2. *Results showing the percent increase in water yield after different harvesting intensities in broadleaved and needle leaved forests of the world at P<0.05. (Yellow color indicating broadleaved and pink representing needle-leaved forest)*

http://www.aloki.hu ● ISSN 1589 1623 (Print) ● ISSN 1785 0037 (Online)
DOI: http://dx.doi.org/10.15666/aeer/1804_49875009

The relationship between annual precipitation and change in water yield (mm) as well as an increase in water yield (%) after harvesting is shown in *Figure 3*. The results showed that in higher annual precipitation regions (>1000 mm), streamflow in mm also increased more than in lower annual precipitation regions (<1000 mm). However, the post-harvest increase in percent change of water yield was higher in the low rainfall area than in high precipitation regions.

The regression analysis in *Figure 4a* and *b* also demonstrated this relationship. The figure illustrated that as long as the annual precipitation (mm) is increasing, the water yield or streamflow (mm) after the treatment also increasing with positive linear trend of $R^2 = 0.35$ at $P < 0.0001$ (*Fig. 4a*). Similarly, the relationship between annual precipitation (mm) and percent increase in water yield or increase in streamflow (%) after treatment showed declining trend with $R^2 = 0.10$, $P < 0.0001$ (*Fig. 4b*), indicating that the percent increase in water yield after treatment was observed from low precipitation to high precipitation regions.

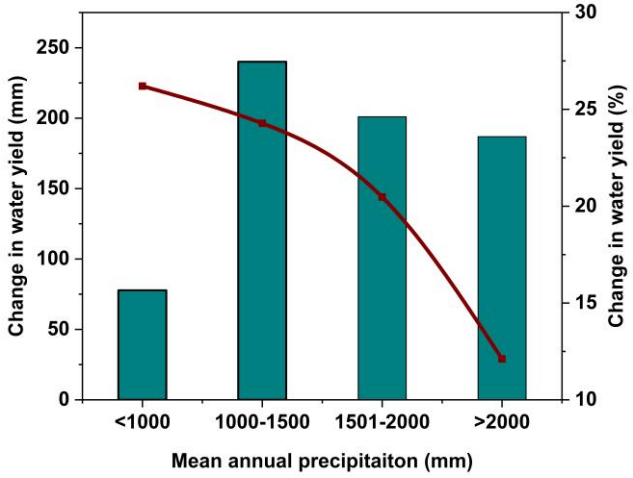

Figure 3. *Representing the influences of annual precipitation on change in water yield (mm) and percent change in water yield (%) after harvesting of the study sites (Green bars are representing Change in water yield (mm), brown line showing Change in water yield (%)*

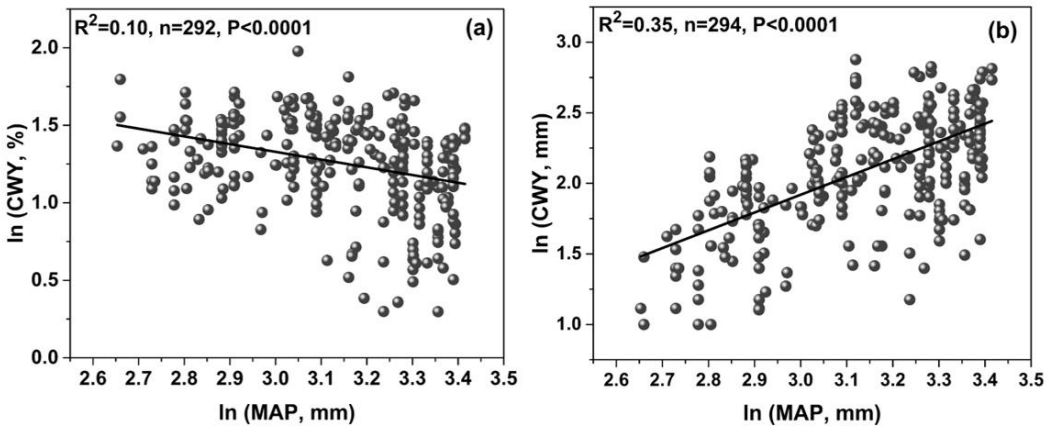

Figure 4. *Illustrating the log transformed linear relationship between mean annual precipitation (mm) and change in water yield CWY (mm) and percent change in water yield CWY (%) after treatment of global catchment sites. (MAP-mean annual precipitation)*

http://www.aloki.hu ● ISSN 1589 1623 (Print) ● ISSN 1785 0037 (Online)
DOI: http://dx.doi.org/10.15666/aeer/1804_49875009

To further explain, the role of forest types and their interaction with annual precipitation and change in water yield after treatment was assessed in *Figure 5*. The figure indicated that the majority of the broadleaved forests of this study belong to high precipitation areas than needle-leaved forests.

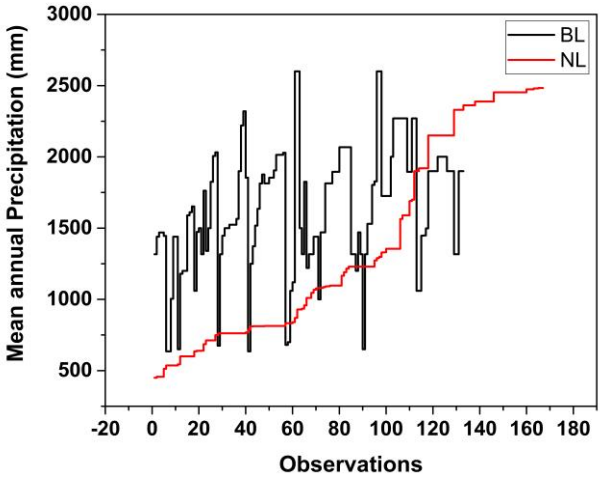

Figure 5. *Representing the presence of needle-leaved (NL) and broadleaved (BL) forests observations taken from different precipitation regions of the world in dataset of our study*

Similarly, in the dataset majority of the bigger catchment (<150 ha) with higher elevation (<2500 m) were found in lower precipitation regions (>1000 mm) as shown in *Figure 6.*

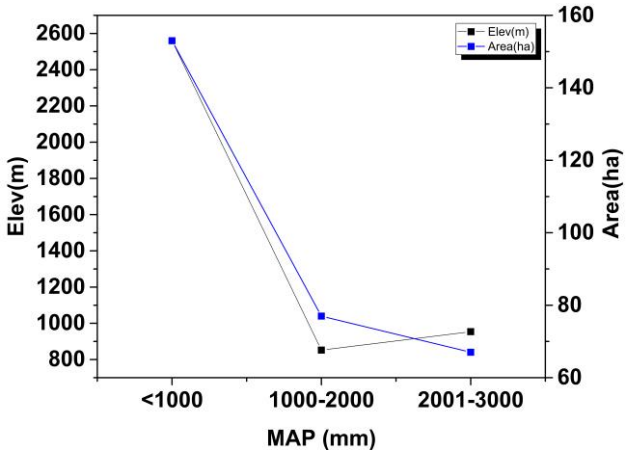

Figure 6*. Showing the distribution of mean annual precipitation (mm) at different elevation and forest cover areas of study sites. (MAP-mean annual precipitation)*

As far as post-treatment regrowth and recovery of vegetation are concerned, the broadleaf showed significant declining trend at $P < 0.0001$, however these results are non-significant in case of needle-leaved the forests as represented in *Figure 7a* and *b*.

http://www.aloki.hu ● ISSN 1589 1623 (Print) ● ISSN 1785 0037 (Online)
DOI: http://dx.doi.org/10.15666/aeer/1804_49875009

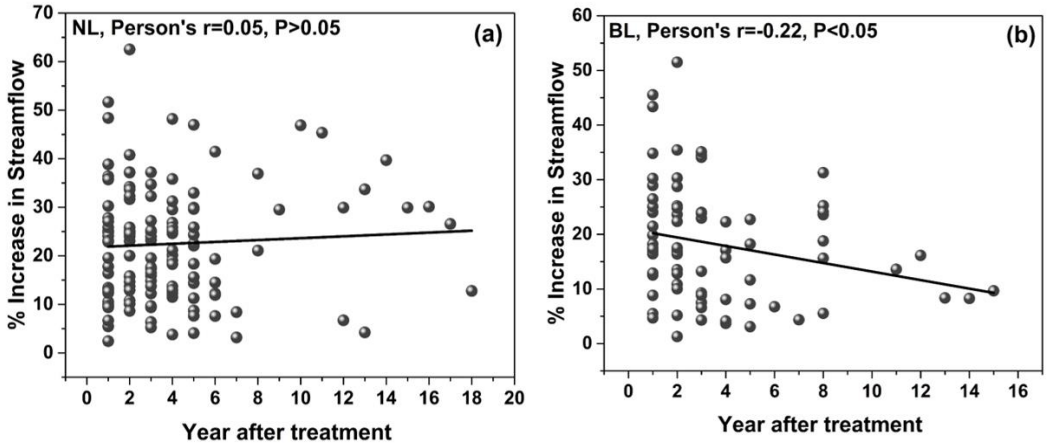

Figure 7. *Illustrating the relationship between year after treatment and increase in streamflow (%) of global catchment sites. (NL-needle-leaved, BL-broadleaved forest)*

The change in water yield/streamflow after harvesting in mm decrease from lower to higher elevation level (<1000 to 3000 m). However, the percent increase in streamflow after harvesting showed an increasing trend from a lower elevation to higher (<1000 to 3000 m), as shown in *Figure 8.*

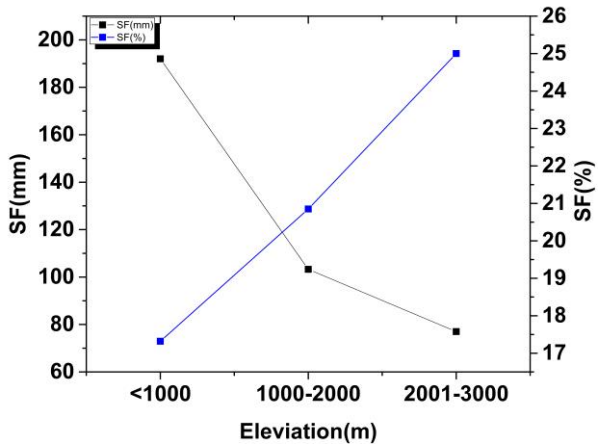

Figure 8. *Showing the trend of increase in streamflow (mm) and percent increase in streamflow (%) after harvesting at different level of elevation. (SF-streamflow)*

Similarly, in the forest area less than or equal to 100 ha showing 20% increase in streamflow after harvesting, but this trend was at its peak in forest cover of 101-300 ha with maximum percent increase in SF of around 26%, afterword > 300 ha indicating abrupt decline in percent increase of SF up to (18.2%). This is also worth noted that change in water yield in mm is greater (220 mm) in the forests consisting of < 100 ha area followed by decline up to 65-100 mm in forest cover of 101-300 ha land as shown in *Figure 9.*

http://www.aloki.hu ● ISSN 1589 1623 (Print) ● ISSN 1785 0037 (Online)
DOI: http://dx.doi.org/10.15666/aeer/1804_49875009

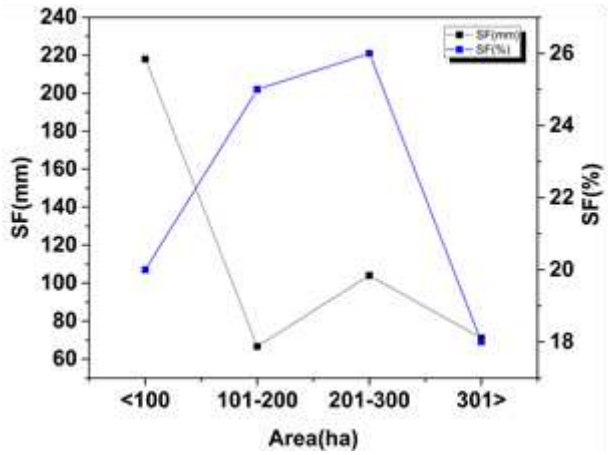

Figure 9. *Showing the trend of increase in streamflow (mm) and percent increase in streamflow (%) after harvesting at different forest cover area (ha). (SF-streamflow)*

Discussion

Forest types and hydrology

On a global level, there is a significant research gap about exact identification of the increase in water yield (%) and streamflow (mm) of different forest harvesting intensities. However, mixed results of varying harvesting intensities have found in previous research investigations (Bosch and Hewlett, 1982; Hornbeck et al., 1993; Stednick, 1996; Troendle et al., 2001; Pike and Rob, 2003; Andreassian, 2003; Adams and Flower, 2006; Komatsu et al., 2011). The plausible reason behind this variability might be due to different site/location, climate type, vegetation type, forest structure, origin, stand age, treatment years, harvesting technique, season of treatment, soil as well as other methodological and technical constraints. The results of this analysis indicated that needle-leaved forest has resulted a greater change in water yield (%) after harvesting than broadleaved when compared to different forest harvesting intensities of 25-100%. This increase in water yield of broadleaved was (8-23%) and needle-leaved (9-27%) after treatment is shown in *Figure 2*. In the previous research investigations, it was indicated that the considerable change in streamflow after timber harvesting occurred when more than 20% of the forest cover was reduced (Bosch and Hewlett, 1982; Stednick, 1996). However, phenomenon has contradicted and reveals that in some of the catchment studies, lesser harvesting intensity has had measurable increases in water yield than the area with 100% harvest depending on the catchment site and topographic factors. For example, with 15% of the basal catchment area could be cut for a considerable upsurge in annual water yield at the catchment scale in the Rocky Mountain region, whereas 50% in the Central Plains, although system responses are variable (Stednick, 1996). Similarly, the results from previous studies are also in accordance with the findings of this study indicating that the influence of different harvesting intensities on percent change in water yield is higher in needle-leaved than broadleaved forest. A recent global synthesis indicated that 68% removal of broadleaved forest leads to increase of just 16% of stream flow (Farooqi et al., 2020a). Another regional study in New Zealand showed that native deciduous forest clear-felling caused average increase of 70% on five years of treatment (Fahey, 1994) on the

http://www.aloki.hu ● ISSN 1589 1623 (Print) ● ISSN 1785 0037 (Online)
DOI: http://dx.doi.org/10.15666/aeer/1804_49875009

other side in a southern Appalachian Mountains (USA) 59 ha of mixed hardwood stand clearcutting enhanced streamflow just 28% after the first year of treatment (Swank et al., 2001). In two catchment studies in Australia one was patch-cut to remove 22% of basal area of Wicksend catchment, and the Willbob catchment was thinned to remove 12% of basal area of eucalyptus forests. This caused an annual increase in streamflow by 10% in the first three years after logging at Wicksend, and by 31% for the first four years at Willbob (Lane and Mackay, 2001).

Consequently, mixed results have recorded in case of needle-leaved deforestation. For example, the removal of 14 million board feet of lodgepole pine (*Pinus contorta*) from about 25 percent of the Brownie Creek basin formed an average of 147 mm extra water yield per annum, which is equal to 52% of the increase in annual water yield (Burton, 1997). The study of continental/maritime hydroclimatic regions of the United States in naturally regenerated conifers stands after 50% clear cut and 50% partial cut treatments reported increased water yields of 270 mm (36%) and 140 mm (23%) respectively (Hubbart et al., 2007). Similarly, a global study revealed that with 71% deforestation of needle leaved forests caused an increase of 27% in water yield in down streams (Farooqi et al., 2020a). These results agreed that in needle-leaved forest of large coverage >2000ha might produce significant or drastic increase in water yield and increase the risk of severe flooding (Burton, 1997).

Forest types and precipitation

Annual precipitation impacts the scale of water yield intensifications that follow timber harvest operations in forested watersheds (Keppeler and Ziemer,1990; Brown et al., 2005; Adams and Fowler, 2006; Komatsu et al., 2011). The results in this study indicated the significant increase in annual streamflow (mm) in higher precipitation areas compared to lower regions of the world as shown in *Figure 2* and the linear trend in the relation between annual precipitation and increase in streamflow (mm) is recorded in *Figure 3b*. This shows that the plantation schemes can be successful established in high precipitation region in order to achieve carbon objectives because abundance of water in these regions will not only helpful in enhancing the growth and productivity but also atmospheric circulation. Similarly, the percent increase in water yield after harvesting is lower than in low precipitation regions of the world (*Figs. 2* and *3a*), because the water available in the region is already in sufficient quantity, therefore after harvesting big change even show little difference. Moreover, the more evaporative losses can act positive in enhancing precipitation having sufficient energy to lift the additional atmospheric moisture high enough to condense and form clouds (Jackson et al., 2005). However, the precise estimation of hydrological implications of large watersheds (> 1000 km2) are largely lacking due to more complex for structure and other confounding factors.

It is also worth noting that in this dataset majority of vegetation at comparatively lower precipitation regions is needle-leaved compare to broadleaved found in higher precipitation regions (*Fig. 5*). A recent past, Farooqi et al. (2020a) highlighted the influences of precipitation on percent increase in water yield after-harvesting in broadleaved and conifers forests, however, he did not elaborate on these impacts and their causing factors. The reason behind all of these results might be vegetation affects the proportion of precipitation that is evaporated and transpired and, consequently, the amount available for soil moisture storage, groundwater recharge, and dry weather streamflow of broadleaved and needle-leaved forests (Komatsu et al., 2011). The

http://www.aloki.hu ● ISSN 1589 1623 (Print) ● ISSN 1785 0037 (Online)
DOI: http://dx.doi.org/10.15666/aeer/1804_49875009

variation in transpiration in the forests is because of the leaf area index as well as stomatal conductance (Kelliher et al., 1995; Raupach, 1995), whereas the interception losses also vary according to leaf area index (Komatsu et al., 2008; Muzylo et al., 2009). These interception losses were thoroughly discussed in the previous research investigations of coniferous and broadleaved forests (Huber and Iroume, 2001; Komatsu et al., 2011), while Iroume and Huber (2002) demonstrated that there are many factors associated with these losses influenced by rainfall and forest characteristics like species, density, age, etc. It is generally believed that the streamflow response depends on the mean annual precipitation of the area (Bosch and Hewlett, 1982; Ruprecht and Stoneman, 1993; Iroumé et al., 2000). Increases in streamflow (mm) are generally most significant in areas of high rainfall, but they are short-lived due to rapid regrowth of vegetation (Bosch and Hewlett, 1982; Ruprecht and Stoneman, 1993; David, 1994; Fahey, 1994; Swank et al., 2001). The decreasing trend toward pre-disturbance levels is of interest because regeneration has been reported in diverse environments, silvicultural and forest species dominance (Fahey, 1994; Bosch and Hewlett, 1982; Cornish, 1993; Hornbeck et al., 1993). For example, reductions in streamflow below pre-disturbance levels have been observed as isolated cases in needle-leaved evergreen planted a forest of the temperate region in southern Chile. Indicated that the 120% increase in runoff might be partly due to the higher rainfall during the post-harvesting period (Iroumé et al., 2006). Another study on the jarrah forest in south-western Australia reveals that the subsequent recovery of vegetation cover has led to water yields returning to pre-disturbance levels after an estimated 12-15 years (Ruprecht and Stoneman, 1993). The deciduous conversion to pine, forest harvesting in moderate-to-high rainfall areas causes a 60-80% increase in water yield for three-five years after clear-felling. It was also noted that the yields should return to pre-harvesting levels within six-eight years, depending on the silvicultural regime adopted (Fahey, 1994).

In the present study results, the significant decline trend in water yield ($P < 0.0001$) after the first year of broadleaved forests removal till it reaches to the pretreatment stage as shown in *Figure 6* might be connected to their coppiced nature which might be the reason for rapid regeneration after deforestation. For example, in a study conducted in Central Portugal, when a coppicing a fast-growing species of eucalyptus due to the fast regrowth of the forest stands recorded that the hydrological effects of clearcutting were short-lived (David,1994), in Coweeta, a mature hardwood coppice stand the first cutting required 23 years' recovery time to reach pretreatment level in striking contrast the second cutting achieved this level just within 16 years (Swank et al., 1970). Therefore, water use strategies were developed according to the variation in developmental stages as well as the available water resources (Su et al., 2014). The result of these studies demonstrate that annual water yield increases obtained from complete forest cutting in coppice catchment can be more short-lived in second rotation. Because of the difference in basal area, LAI, species density as well as letter fall production of first stand enhances fertility and water retention in the soil, which boost the regrowth of second cutting. Moreover, the only way forward of gaining large increase in annual water yield is to manage regrowth and control dense sprouting and rapid crown development.

Forest types and water use

The main distinction between the percent increase in water yield after harvesting in conifers versus broadleaved as shown in *Figure 2* might be due to the efficient water use of broad-leaved than in conifers. Evergreen conifers tend to have a higher water use

http://www.aloki.hu ● ISSN 1589 1623 (Print) ● ISSN 1785 0037 (Online)
DOI: http://dx.doi.org/10.15666/aeer/1804_49875009

due to high interception losses which are maintained throughout the whole year, and particularly during the winter period when conditions are usually wettest and windiest. During the vegetative period, interception rates are also often higher in conifer stands because of more leaf area indices. The differences are most pronounced during the dormant season when interception rates are low in hardwood stands. For example, two studies in the European forests have found that average yearly interception rates are around 25% for broadleaves species and about 45% for coniferous species (Augusto et al., 2002; Calder et al., 2003).

Canopy transpiration is often thought to increase asymptotically with leaf area index (L) for a species (Meinzer and Grantz, 1991; Raupach, 1995; Arneth et al., 1996; Oren et al., 1996). It was assumed that annual transpiration does not differ considerably between broadleaf and coniferous forests (Roberts, 1983; Harding et al., 1992; Cannell, 1999). Large-scale afforestation resulted a rise in evapotranspiration, hence dropping in-stream flows (Farley et al., 2005; Sun et al., 2006, 2008), therefore impacting the effectiveness of water conservation strategy of plants at leaf or individual level. Quantifying the productivity-water loss tradeoffs at the ecosystem level is the primary parameter to analyze the carbon-water relationship in different forest types (Li et al., 2019). Many studies at ecosystem level have demonstrated that broadleaved forest have higher productivity and less water loss than needle-leave forests (Tan et al., 2015; Gower et al., 2001). This might be because deciduous leaves have higher rates of photosynthesis per unit leaf mass during favorable conditions than evergreens, given their higher leaf nitrogen content and specific leaf area, higher intrinsic photosynthetic capacity, and the reduced internal competition for light and carbon dioxide (Catovsky et al., 2002). For example, deciduous oaks compensate for having a shorter growing season by attaining a higher capacity to assimilate carbon for a given amount of intercepted solar radiation during the well-watered spring period. At saturating light levels, deciduous oaks gained carbon at six times the rate of evergreen oaks (Baldocchi et al., 2010).

This water utilization behavior of the broadleaf and conifers may directly and significantly impact the hydrology and water yield of the forest. For example, the first study (Swank and Douglass, 1974) to examine differences in annual runoff and evapotranspiration (ET) between broadleaf and coniferous forests was performed in the United States using the paired-catchment method. Annual flow decreased with the conversion from broadleaf to coniferous forest. Changes in yearly runoff due to vegetation changes indicate changes in annual ET. Thus, the results indicate lower annual ET for broadleaf forests than for coniferous forests, suggesting that the presence of broadleaf forests is more beneficial from the viewpoint of water availability in down-stream. In another study, long-term records of streamflow following the conversion of hardwood stands to conifers show reduced water yield (Hornbeck et al., 1997; Komatsu et al., 2009). For example, this trend has been instigated in Japan (Komatsu et al., 2009). More extensive evidence of the lower annual evapotranspiration for broadleaf forests compared to coniferous forests was provided by surveying the results of numerous paired-catchment studies (Bosch and Hewlett, 1982). A very latest survey of a global dataset also demonstrated that ET of broadleaf forests is lower than coniferous, resulting in a higher annual runoff for broadleaf. The study also suggested that this condition is only valid for broadleaf deciduous forests (Komatsu et al., 2011). The differences between conifers and deciduous trees are often incorporated into large-scale models because of differences in xylem anatomy (vessels versus tracheids), leaf

http://www.aloki.hu ● ISSN 1589 1623 (Print) ● ISSN 1785 0037 (Online)
DOI: http://dx.doi.org/10.15666/aeer/1804_49875009

longevity, leaf area index, and growing season (Roberts and Rosier, 2005). Therefore, from all these survey results it is concluding that the increase in annual runoff due to deforestation tended to be lower of broadleaf forests than coniferous forests, which suggests the generality of the yearly ET for gaining growth and productivity of broadleaf forests is lower than coniferous forests.

Conclusion

In the past, many afforestation projects were established without knowing their carbon and water interaction. The difference of change in water yield (%), as well as an increase in streamflow (mm) after harvesting of broadleaved and needle-leaved forest in low and high precipitation regions, along with other adjoining factors are giving us a clue as to how the future afforestation policy needs to be revised. When, where, and why to plant/cut the tree is important questions to address. The results showed that needle-leaved forests in lower precipitation regions are expected to consume more water than broadleaved in higher rainfall regions. This study can speculate from these results that afforestation and conversion of broadleaved to conifers or mixed in higher precipitation regions might be more useful to get maximum productivity. Conversely, in lower precipitation regions scattered plantation of broadleaved primarily deciduous species along with shrubs and grasses might be an option to maintain the carbon and water tradeoff of global forests. However, sustainable forest management and targeted planning for establishment of future plantations need to take into account a broader prospective of multifunctional objectives is prerequisite to mitigate the future challenges of climate change.

Acknowledgements. TJA Farooqi acknowledges the financial support of the China Scholarship Council and Ministry of Science and Technology of China (Grant No. 2016YFC0502104). Author would also like to thank Miss. Fionnuala McCully, from School of Environmental Sciences, University of Liverpool, UK for her valuable suggestions and improvement for the manuscript. Author would also to thanks Mr. Muhammad Amir Siddique from School of Landscape Architecture, Beijing Forestry University, 100083, Beijing, China for his help in drawing *Figure 1* on photoshop software and fruitful suggestions.

Conflict of Interests. Authors declare that there is no conflict of interests.

REFERENCES

[1] Adams, K. N., Fowler, A. M. (2006): Improving empirical relationships for predicting the effect of vegetation change on annual water yield. – Journal of Hydrology 321: 90-115. https://doi.org/10.1016/j.jhydrol.2005.07.049.

[2] Ali, T., Gulzar S., Arroj, S.S., Muhammad, B., Ullah, F., Ahmad, N., Ullah, S (2020): Integrating spectral indices, topographic factors, and field data into detecting post-fire burn severity. Bulletin of the *Transilvania* University of Braşov Series II. 13(62):1 (*In press)*

[3] Anderson, H. W., Hoover, M. D., Reinhart, K. G. (1976): Forests and water: effects of forest management on floods, sedimentation, and water supply. – General Technical Report PSW-018. Berkeley, CA. US Department of Agriculture, Forest Service, Pacific Southwest Forest and Range Experiment Station 115: 18.

[4] Andréassian, V. (2004): Waters and forests: from historical controversy to scientific debate. – Journal of hydrology 291: 1-27. https://doi: 10.1016/j.jhydrol.2003.12.015.

http://www.aloki.hu ● ISSN 1589 1623 (Print) ● ISSN 1785 0037 (Online)
DOI: http://dx.doi.org/10.15666/aeer/1804_49875009

[5] Arneth, A., Kelliher, F. M., Bauer, G., Hollinger, D. Y., Byers, J. N., Hunt, J. E., McSeveny, T. M., Ziegler, W., Vygodskaya, N. N., Milukova, I., Sogachov, A. (1996): Environmental regulation of xylem sap flow and total conductance of Larix gmelinii trees in eastern Siberia. – Tree Physiology 16: 247-255.
[6] Badshah, M., Ahmad, A., Muneer, M., Rehman, A., Wang, J., Khan, M. (2017): Evaluation of the forest structure, diversity and biomass carbon potential in the southwest region of Guangxi, China. – Applied Ecology and Environmental Research 18(1): 447-467.
[7] Baldocchi, D. D., Ma, S., Rambal, S., Misson, L., Ourcival, J. M., Limousin, J. M., Pereira, J., Papale, D. (2010): On the differential advantages of evergreenness and deciduousness in Mediterranean oak woodlands: a flux perspective. – Ecological Applications 20: 1583-1597.
[8] Bari, M. A., Smith, N., Ruprecht, J. K., Boyd, B. W. (1996): Changes in streamflow components following logging and regeneration in the southern forest of Western Australia. – Hydrological Processes 10: 447-461.
[9] Bent, G. C. (2001): Effects of forest-management activities on runoff components and ground-water recharge to Quabbin reservoir, central Massachusetts. – Forest Ecology and Management 143: 115-129.
[10] Bosch, J. M., Hewlett, J. D. (1982): A review of catchment experiments to determine the effect of vegetation changes on water yield and evapotranspiration. – Journal of Hydrology 55: 3-23.
[11] Brechtel, H. M., Fuhrer, H. W. (1991): Water yield control in beech forest. A paired watershed study in the Krofdorf forest research area. – 20th General Assembly of the International Union of Geodesy and Geophysics, Vienna, Austria 8: 477-84.
[12] Brown, A. E., Zhang, L., McMahon, T. A., Western, A. W., Vertessy, R. A. (2005): A review of paired catchment studies for determining changes in water yield resulting from alterations in vegetation. – Journal of hydrology 310(1-4): 28-61.
[13] Brown, A. E., Western, A. W., McMahon, T. A., Zhang, L. (2013): Impact of forest cover changes on annual streamflow and flow duration curves. – Journal of Hydrology 483: 39-50. https://doi.org/10.1016/j.jhydrol.2012.12.031.
[14] Burton, T. A. (1997): Effects of basin-scale timber harvest on water yield and peak streamflow 1. – JAWRA Journal of the American Water Resources Association 33: 1187-1196. https://doi.org/10.1111/j.1752-1688.1997.tb03545.x.
[15] Calder, I. R. (1999): The Blue Revolution: Land Use and Integrated Water Resources Management. – Earthscan, London.
[16] Calder, I. R., Reid, I., Nisbet, T. R., Green, J. C. (2003): Impact of lowland forests in England on water resources: application of the hydrological land use change (HYLUC) model. – Journal of Water Resources Research 39(11).
[17] Cannell, M. G. R. (1999): Environmental impacts of forest monocultures: water use, acidification, wildlife conservation, and carbon storage. – New Forests 17: 239-262.
[18] Catovsky, S., Holbrook, N. M., Bazzaz, F. A. (2002): Coupling whole-tree transpiration and canopy photosynthesis in coniferous and broad-leaved tree species. – Canadian Journal of Forest Research 32: 295-309.
[19] Cheng, J. D. (1989): Streamflow changes after clear-cut logging of a pine beetle-infested watershed in southern British Columbia, Canada. – Water Resources Research 25: 449-56.
[20] Cornish, P. M. (1993): The effects of logging and forest regeneration on water yields in a moist eucalypt forest in New South Wales, Australia. – Journal of Hydrology 150: 301-322. https://doi.org/10.1016/0022-1694(93)90114-O.
[21] Cosandey, C., Andréassian, V., Martin, C., Didon-Lescot, J. F., Didon-Lescot, J. F., Lavabre, J., Folton, N., Mathys, N., Richard, D. (2005): The hydrological impact of the Mediterranean forest: a review of French research. – Journal of Hydrology 301: 235-49.

http://www.aloki.hu ● ISSN 1589 1623 (Print) ● ISSN 1785 0037 (Online)
DOI: http://dx.doi.org/10.15666/aeer/1804_49875009

[22] Costanza, R., d'Arge, R., de Groot, R., et al. (1997): The value of the world's ecosystem services and natural capital. – Nature 387: 253-260.
[23] David, J. S., Henriques, M. O., David, T. S., Tomé, J., Ledger, D. C. (1994): Clearcutting effects on streamflow in coppiced Eucalyptus globulus stands in Portugal. – Journal of Hydrology 162: 143-154. https://doi.org/10.1016/0022-1694(94)90008-6.
[24] Ellison, D., Futter, M. N., Bishop, K. (2012): On the forest cover-water yield debate: from demand to supply side thinking. – Global Change Biology 18: 806-820.
[25] Ellison, D., Morris, C. E., Locatelli, B., Sheil, D., Cohen, J., Murdiyarso, D., Gutierrez, V., Van Noordwijk, M., Creed, I. F., Pokorny, J., Gaveau, D. (2017): Trees, forests and water: cool insights for a hot world. – Global Environmental Change 43: 51-61.
[26] Fahey, B. (1994): The effect of plantation forestry on water yield in New Zealand. – New Zealand Forestry 39: 18-23.
[27] Fahey, B., Jackson, R. (1997): Hydrological impacts of converting native forests and grasslands to pine plantations, South Island, New Zealand. – Agricultural and Forest Meteorology 84: 69-82.
[28] Farley, K. A., Jobbagy, E. G., Jackson, R. B. (2005): Effects of afforestation on water yield: a global synthesis with implications for policy. – Global Change Biology 11: 1565-1576. DOI: 10.1111/j.1365-2486.2005. 01011.x.
[29] Farooqi, T. J. A., Hayat, U., Roman, M., Abbas H., Hussain S. (2020a): Comparative study determining the impacts of broadleaved and needle leaved forest harvesting on hydrology and water yield: state of knowledge and research outlook. – International Journal of Biosciences 16(2): 231-240. http://dx.doi.org/10.12692/ijb/16.2.231-240.
[30] Farooqi, T.J.A., Li, X., Yu, Z., Liu, S. and Sun, O.J. (2020b): Reconciliation of research on forest carbon sequestration and water conservation. –Journal of Forestry Research, pp.1-8. https://doi.org/10.1007/s11676-020-01138-2.
[31] Fritsch, J. M. (1990): Les effets du de´frichement de la foreˆt amazonienne et de la mise en culture sur l'hydrologie des petits bassins versants. – PhD Thesis. Universite´ des Sciences et Techniques du Languedoc, Montpellier.
[32] Gower, S., Krankina, O., Olson, R., Apps, M., Linder, S., Wang, C. (2001): Net primary production and carbon allocation patterns of boreal forest ecosystems. – Ecological Applications 11: 1395-1411.
[33] Harding, R. J., Hall, R. L., Neal, C. (1992): Hydrological Impacts of Broadleaf Woodlands: Implications for Water Use and Water Quality. – National Rivers Authority Report 115/03/ST. HSMO, London.
[34] Hornbeck, J. W., Adams, M. B., Corbett, E. S., Verry, E. S., Lynch, J. A. (1993): Long-term impacts of forest treatments on water yield: a summary for Northeastern USA. – Journal of Hydrology 150: 323-344. DOI: 10.1016/ 0022-1694(93)90115-P.
[35] Hornbeck, J. W., Martin, C. W., Eagar, C. (1997): Summary of water yield experiments at Hubbard Brook experimental forest, New Hampshire. – Canadian Journal of Forest Research 27(12): 2043-2052.
[36] Houghton, R. A., House, J. I., Pongratz, J., Van Der Werf, G. R., DeFries, R. S., Hansen, M. C., Le Quéré, C., Ramankutty, N. (2012): Carbon emissions from land use and land-cover change. – Biogeosciences 9: 5125-5142.
[37] Hubbart, J. A., Link, T. E., Gravelle, J. A., Elliot, W. J. (2007): Timber harvest impacts on water yield in the continental/maritime hydroclimatic region of the United States. – Forest Science 53: 169-180.
[38] Huber, A., Iroumé, A. (2001): Variability of annual rainfall partitioning for different sites and forest covers in Chile. – Journal of Hydrology. 248: 78-92.
[39] Iroume, A., Huber, A. (2002): Comparison of interception losses in a broadleaved native forest and a ´ Pseudotsuga menziesii plantation in the Andes Mountains of southern Chile. – Hydrological Processes 16: 2347-2361.
[40] Jackson, R. B., Jobbágy, E. G., Avissar, R., Roy, S. B., Barrett, D. J., Cook, C. W., Farley, K. A., Le Maitre, D. C., McCarl, B. A., Murray, B. C. (2005): Trading water for

http://www.aloki.hu ● ISSN 1589 1623 (Print) ● ISSN 1785 0037 (Online)
DOI: http://dx.doi.org/10.15666/aeer/1804_49875009

carbon with biological carbon sequestration. – Science 310: 1944-1947. DOI: 10.1126/science.1119282.

[41] Jones, H. S., Beets, P. N., Kimberley, M. O., Garrett, L. G. (2011): Harvest residue management and fertilisation effects on soil carbon and nitrogen in a 15-year old *Pinus radiate* plantation forest. – Forest Ecology Management 262: 339-347. https://doi.org/10.1016/j.foreco.2011.03.040.

[42] Jones, J. A., Post, D. A. (2004): Seasonal and successional streamflow response to forest cutting and regrowth in the northwest and eastern United States. – Water Resources Research 40(5).

[43] Kabeya, N., Chappell, N. A., Tych, W., Shimizu, A., Asano, S., Hagino, H. (2016): Quantification of the effect of forest harvesting versus climate on streamflow cycles and trends in an evergreen broadleaf catchment. – Hydrological Sciences Journal 61: 16-27.

[44] Kelliher, F. M., Leuning, R., Raupach, M. R., Schulze, E. D. (1995): Maximum conductances for evaporation from global vegetation types. – Agricultural and Forest Meteorology 73: 1-16.

[45] Keppeler, E. T., Ziemer, R. R. (1990): Logging effects on streamflow: water yield and summer low flows at Caspar Creek in north-western California. – Water Resources Research 26: 1669-1679.

[46] Khan, O.J., Muhammad, B., Ali T, Ullah S., Ali M. (2019): Underlying factors of deforestation and its effects in Sanger Valley District Swat. – Journal of Biodiversity and Environmental Sciences 15(5):14-28.

[47] Komatsu, H., Shinohara, Y., Kume, T., Otsuki, K. (2008): Relationship between annual rainfall and interception ratio for forests across Japan. – Forest Ecology and Management 256: 1189-1197. DOI: 10.1016/j. foreco.2008.06.036.

[48] Komatsu, H., Kume, T., Otsuki, K. (2009): Changes in low flow with the conversion of a coniferous plantation to a broad-leaved forest in a summer precipitation region, Japan. – Ecohydrology 2(2): 164-172.

[49] Komatsu, H., Kume, T., Otsuki, K. (2011): Increasing annual runoff—broadleaf or coniferous forests? – Hydrol Process 25: 302-318. https://doi.org/10.1002/hyp.7898.

[50] Krankina, O. N., Dixon, R. K., Kirilenko, A. P., Kobak, K. I. (1997): Global climate change adaptation: examples from Russian boreal forests. – Climatic Change 36: 197-216.

[51] Lane, P. N. J., Mackay, S. M. (2001): Streamflow response of mixed species eucalypt forests to patch cutting and thinning treatments. – Forest Ecology and Management 143: 131-142. https://doi.org/10.1016/S0378-1127(00)00512-0.

[52] Law, B. E., Falge, E., Gu, L. V., Baldocchi, D. D., Bakwin, P., Berbigier, P., Davis, K., Dolman, A. J., Falk, M., Fuentes, J. D., Goldstein, A.(2002): Environmental controls over carbon dioxide and water vapor exchange of terrestrial vegetation. – Agricultural and Forest Meteorology 113: 97-120.

[53] Li, X., Farooqi, T. J. A., Jiang, C., Liu, S., Sun, O. J. (2019): Spatiotemporal variations in productivity and water use efficiency across a temperate forest landscape of Northeast China. – Forest Ecosystems 6: 22. https://doi.org/10.1186/s40663-019-0179-x.

[54] Masiero, M., Pettenella, D., Boscolo, M., Kanti Barua, S., Animon, I., Matta, R. (2019): Valuing Forest Ecosystem Services: A Training Manual for Planners and Project Developers. – Food and Agriculture Organization of the United Nations, Rome.

[55] Meinzer, F. C., Grantz, D. A. (1991): Coordination of stomatal, hydraulic, and canopy boundary properties: do stomata balance conductance by measuring transpiration? – Physiologia Plantarum 83: 324-329.

[56] Muhammad, B., Ilahi, T., Ullah, S., Wu, X., Siddique, M. A., Khan, M. A., Badshah, M. T., Jia, Z (2020) Litter decomposition and soil nutrients prince rupprecht's (larix principis-rupprechtii) plantations area in Saihanba, Northern China. – Applied Ecology and Environmental Research (*In press*)

http://www.aloki.hu ● ISSN 1589 1623 (Print) ● ISSN 1785 0037 (Online)
DOI: http://dx.doi.org/10.15666/aeer/1804_49875009

[57] Muzylo, A., Llorens, P., Valente, F., Keizer, J. J., Domingo, F., Gash, J. H. C. (2009): A review of rainfall interception modelling. – Journal of Hydrology 370: 191-206. DOI: 10.1016/j.jhydrol.2009.02.058.
[58] Nasi, R., Wunder, S., Campos, J. J. (2002): Forest ecosystem services: can they pay our way out of deforestation? – A Discussion Paper Prepared for the GEF Forestry Roundtable to be Held in Conjunction with the UNFF II, Costa Rica on March 11, 2002.
[59] Oren, R., Zimmerman, R., Terborgh, J. (1996): Transpiration in upper Amazonian floodplain and upland forests in response to drought breaking rains. – Ecology 77: 968-973.
[60] Pearce, A. J., Rowe, L. K., O'Loughlin, C. L. (1980): Effects of clearfelling and slash-burning on water yield and storm hydrographs in evergreen mixed forests, western New Zealand. – Proceedings on the Influence of Man on the Hydrological Regime with Special Reference to Representative and Experimental Basins, Helsinki, June 1980. IAHS-AISH Publication No 130, pp. 119-127.
[61] Pike, R., Scherer, R. (2003): Overview of the potential effects of forest management on low flows in snowmelt-dominated hydrologic regimes. – Journal of Ecosystems and Management 3: 3.
[62] Popkin, G. (2019): How much can forests fight climate change? – Nature. DOI: 10.1038/d41586-019-00122-z.
[63] Raupach, M. R. (1995): Vegetation–atmosphere interaction and surface conductance at leaf, canopy and regional scales. – Agricultural and Forest Meteorology 73: 151-179.
[64] Roberts, J. (1983): Forest transpiration: a conservative hydrological process? – Journal of Hydrology 66: 133 – 141.
[65] Roberts, J., Rosier, P. (2005): The impact of broadleaved woodland on water resources in lowland UK: III. The results from Black Wood and Bridgets Farm compared with those from other woodland and grassland sites. – Hydrology and Earth System Sciences 9: 614-620.
[66] Rowe, L. K., Jackson, R., Fahey, B. (2002): Land use and water resources: hydrological effects of different vegetation covers. – SMF2167, Report. 5.
[67] Ruddell, S., Sampson, R., Smith, M., Giffen, R., Cathcart, J., Hagan, J., Sosland, D., Godbee, J., Heissenbuttel, J., Lovett, S., Helms, J. (2007): The role for sustainably managed forests in climate change mitigation. – Journal of Forestry 105: 314-319.
[68] Ruprecht, J. K., Stoneman, G. L. (1993): Water yield issues in the jarrah forest of south-western Australia. – Journal of Hydrology150: 369-391.
[69] Sahin, V., Hall, M. J. (1996): The effects of afforestation and deforestation on water yields. – Journal of Hydrology 178: 293-309.
[70] Siddique, M.A., Dongyun, L., Li, P., Rasool, U., Khan, T.U., Farooqi, T.J.A., Wang, L., Fan, B. and Rasool, M.A. (2020): Assessment and simulation of land use and land cover change impacts on the land surface temperature of Chaoyang District in Beijing, China. – PeerJ *8*:p.e9115.
[71] Scott, D. F., Scott, D. F. (2000): A Re-analysis of the South African Catchment Afforestation Experimental Data. – Water Research Commission, Pretoria.
[72] Smith, P. J. T. (1987): Variation of water yield from catchments under grass and exotic forest, east Otago. – Journal of Hydrology 26: 175-184.
[73] Stednick, J. D. (1996): Monitoring the effects of timber water yield harvest on annual. – Journal of Hydrology 176: 79-95.
[74] Su, H., Li, Y., Liu, W., Xu, H., Su, H., Li, Y., Liu, W., Xu, H., Sun, O. J. (2014): Changes in water use with growth in Ulmus pumila in semiarid sandy land of northern China. – Trees *28*: 41-52.
[75] Sun, G., Zhou, G. Y., Zhang, Z. Q., Wei, X., McNulty, S. G., Vose, J. M. (2006): Potential water yield reduction due to forestation across China. – Journal of Hydrology 328: 548-558.

http://www.aloki.hu ● ISSN 1589 1623 (Print) ● ISSN 1785 0037 (Online)
DOI: http://dx.doi.org/10.15666/aeer/1804_49875009

[76] Sun, G., Zuo, C. Q., Liu, S. Y., Liu, M., McNulty, S. G., Vose, J. M. (2008): Watershed evapotranspiration increased due to changes in vegetation composition and structure under a subtropical climate. – J Am Water Resource Association 44: 1164-1175.
[77] Swank, W. T., Helvey, J. D. (1970): Reduction of streamflow increases following regrowth of clearcut hardwood forests. – Symposium on the Results of Research on Representative and Experimental Basins, December 1970, UNESCO-IASH, Leuven, pp. 346-360.
[78] Swank, W. T., Douglass, J. E. (1974): Streamflow greatly reduced by converting deciduous hardwood stands to pine. – Science 185: 857-859.
[79] Swank, W. T., Vose, J. M., Elliot, K. J. (2001): Long-term hydrologic and water quality responses following commercial clearcutting of mixed hardwoods on a southern Appalachian catchment. – Forest Ecology and Management 143: 163-178.
[80] Swift Jr, L. W., Swank, W. T. (1981): Long term responses of streamflow following clearcutting and regrowth/Réactions à long terme du débit des cours d'eau après coupe et repeuplement. – Hydrological Sciences Journal 26: 245-56.
[81] Tan, Z. H., Zhang, Y. P., Deng, X. B., Song, Q. H., Liu, W. J., Deng, Y., Tang, J. W., Liao, Z. Y., Zhao, J. F., Song, L., Yang, L. Y. (2015): Interannual and seasonal variability of water use efficiency in a tropical rainforest: results from a 9-year eddy flux time series. – Journal of Geophysical Research: Atmospheres 120: 464-479.
[82] Troendle, C. A., Wilcox, M. S., Bevenger, G. S., Porth, L. S. (2001): The Coon Creek water yield augmentation project: implementation of timber harvesting technology to increase streamflow. – Forest Ecology and Management 143: 179-187.
[83] Ullah, F., Ullah, S., Ashraf, M, I., Ali T., Abbas H., Muhammad, B., Badshah, M, T. (2019a): REDD+impacts on the livelihood of the community and their involvement in the policymaking process. – Journal of Biodiversity and Environmental Sciences 15(1): 102-110.
[84] Ullah S., Muhammad B., Amin R., Abbas H., Muneer, M. (2019b): Sensitivity of arbuscular mycorrhizal fungi in old-growth forests: direct effect on growth and soil carbon storage. – Applied Ecology and Environmental Research 17: 13749-13758.
[85] Van der Ent, R. J., Savenije, H. H., Schaefli, B., Steele-Dunne, S. C. (2010): Origin and fate of atmospheric moisture over continents. – Water Resources Research 46(9).
[86] van Dijk, A. I. J. M., Keenan, R. J. (2007): Planted forests and water in perspective. – Forest Ecology and Management 251: 1-9. https://doi.org/10.1016/j.foreco.2007.06.010.
[87] Van Wijk, M. T., Dekker, S. C., Bouten, W., Kohsiek, W., Mohren, G. M. J. (2001): Simulation of carbon and water budgets of a Douglas-fir forest. – Forest Ecology and Management 145: 229-241.
[88] Vertessy, R. A., Watson, F. G. R., O'Sullivan, S. K. (2001): Factors determining relations between stand age and catchment water balance in mountain ash forests. – Forest Ecology and Management 143: 13-26.
[89] Wang, J., Zhang, D., Farooqi. T. J. A., Ma, L., Deng, Y., Jia, Z. (2017): The olive (Olea europaea L.) industry in China: its status, opportunities and challenges. – Agroforestry Systems 9: 395-417. DOI: 10.1007/s10457-017-0129-y.
[90] Webb, A. A. (2009): Streamflow response to Pinus plantation harvesting: Canobolas State forest, southeastern Australia. – Hydrological Processes 23: 1679-89.
[91] Wilson, K. B., Hanson, P. J., Mulholland, P. J., Wilson, K. B., Hanson, P. J., Mulholland, P. J., Baldocchi, D. D., Wullschleger, S. D. (2001): A comparison of methods for determining forest evapotranspiration and its components: sap-flow, soil water budget, eddy covariance and catchment water balance. – Agricultural and Forest Meteorology 106: 153-168.

http://www.aloki.hu ● ISSN 1589 1623 (Print) ● ISSN 1785 0037 (Online)
DOI: http://dx.doi.org/10.15666/aeer/1804_49875009

[92] Zhang, L., Dawes, W. R., Walker, G. R. (2001): Response of mean annual evapotranspiration to vegetation changes at catchment scale. – Water Resources Research 37: 701-708.
[93] Zhang, L., Zhao, F. F., Brown, A. E. (2012): Predicting effects of plantation expansion on streamflow regime for catchments in Australia. – Hydrology and Earth System Sciences 16: 2109-2121.
[94] Zhang, M., Liu, N., Harper, R., Li, Q., Liu, K., Wei, X., Ning, D., Hou, Y., Liu, S. (2017): A global review on hydrological responses to forest change across multiple spatial scales: importance of scale, climate, forest type and hydrological regime. – Journal of Hydrology 546: 44-59. DOI: 10.1016/j.jhydrol.2016.12.040.

APPENDIX

Appendix 1. *Normality test results of Shaprio-wilk reject normality at P < 0.05*

H.I.	DF	Statistics	P-value	Decision at level (5%)
25%NL	167	0.87663	1.6514E-10	Reject normality
25%BL	133	0.6918	2.38698E-15	Reject normality
50%NL	167	0.92063	6.51603E-8	Reject normality
50%BL	133	0.83991	1.02842E-10	Reject normality
75%NL	167	0.9465	5.95852E-6	Reject normality
75%BL	133	0.90299	8.54516E-8	Reject normality
100%NL	167	0.96282	1.93127E-4	Reject normality
100%BL	133	0.92935	3.17434E-6	Reject normality

H.I.: harvesting intensity (%)

Appendix 2. *QQ plot representing the distribution of change in water yield (%) after 25, 50, 75 and 100% of harvesting intensities of the dataset. The scores are negatively skewed (fewer scores at the low end)*

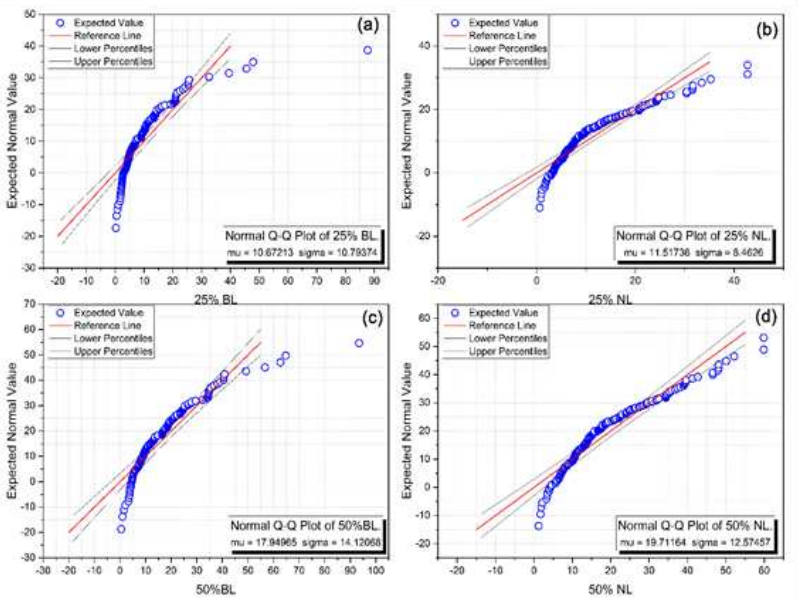

http://www.aloki.hu ● ISSN 1589 1623 (Print) ● ISSN 1785 0037 (Online)
DOI: http://dx.doi.org/10.15666/aeer/1804_49875009

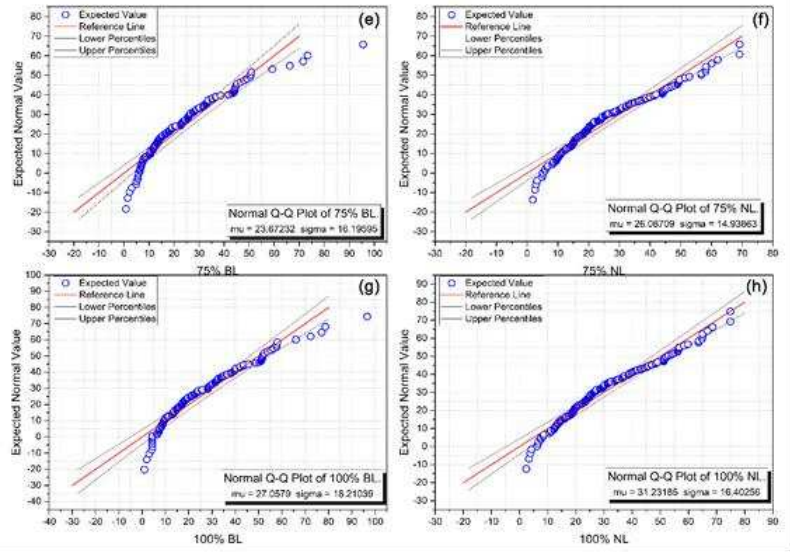

Appendix 3. *Kruskal-Wallis ANOVA, representing the descriptive statistic results of different harvesting intensities of broadleaved (BL) and needle leaved (NL) forests on change in water yield (%)*

H.I.	N	Min	Q1	Median	Q3	Max
"25%NL"	167	0.61635	5.71968	9.04704	15.52163	42.71476
"25%BL"	133	0.25043	4.24867	7.88758	13.50434	87.69458
"50%NL"	167	1.22515	10.82046	16.59292	26.87225	59.86033
"50%BL"	133	0.4996	8.15101	14.62185	23.79504	93.44391
"75%NL"	167	1.82653	15.39764	22.98264	35.53398	69.10673
"75%BL"	133	0.74753	11.74769	20.43853	31.89731	95.53162
"100%NL"	167	2.42063	19.5279	28.463	42.36111	42.36111
"100%BL"	133	0.99423	13.54604	22.96223	38.15074	96.61086

H.I: harvesting intensity (%), P < 0.0001, Chi-square = 295.027

Appendix 4. *Wilcoxon signed ranks test*

Paired sample	W	Z	P-value
"25%BL"-"25%NL"	5869	3.17332	0.00151
"50%BL"-"50%NL"	5903	3.24968	0.00116
"75%BL"-"75%NL"	5927	3.30358	9.54597E-4
"100%BL"-"100%NL"	6206	3.93016	8.48907E-5

*P < 0.05

Appendix 5. *Data set used in the synthesis*

Broadleaved forest								
Source	**Catchment**	**Country**	**Elv. (m)**	**Soil type**	**Area (ha)**	**MAP (mm)**	**MAS (mm)**	**DF (%)**
Bosch and Hewlett (1982)	Coweeta 13	USA	810	Sandy clay loam	16	1900	889	100

http://www.aloki.hu ● ISSN 1589 1623 (Print) ● ISSN 1785 0037 (Online)
DOI: http://dx.doi.org/10.15666/aeer/1804_49875009

Bosch and Hewlett (1982)	Coweeta 19	USA	960	Sandy clay loam	28	2001	1222	22
Bosch and Hewlett (1982)	Coweeta 1	USA	840	Sandy clay loam	16	1725	739	100
Bosch and Hewlett (1982)	Coweeta 28	USA	1200	Sandy clay loam	144	2270	1532	65
Bosch and Hewlett (1982)	Coweeta 17	USA	885	Sandy clay loam	14	1895	775	100
Bosch and Hewlett (1982)	Coweeta 22	USA	1035	Sandy clay loam	34	2068	1275	50
Bosch and Hewlett (1982)	Coweeta 3	USA	825	Sandy clay loam	9	1814	607	100
Bosch and Hewlett (1982)	Coweeta 10	USA	975	Sandy clay loam	86	1854	1072	30
Bosch and Hewlett (1982)	Coweeta 41	USA	1065	Sandy clay loam	29	2029	1285	53
Bosch and Hewlett (1982)	Coweeta 6	USA	793	Sandy clay loam	9	1854	838	80
Bosch and Hewlett (1982)	Kericho Sambret	Kenya	2200	Deep friable clay	688	1905	416	34
Bosch and Hewlett (1982)	Kimakia A	Kenya	2440	Deep friable clay	35	2014	568	100
Bosch and Hewlett (1982)	Fernow 1	USA	755	Stony silt loam	30	1524	584	85
Bosch and Hewlett (1982)	Fernow 2	USA	780	Stony silt loam	15	1500	660	36
Bosch and Hewlett (1982)	Fernow 5	USA	780	Stony silt loam	36	1473	732	20
Bosch and Hewlett (1982)	Fernow 3	USA	805	Stony silt loam	34	1500	607	13
Bosch and Hewlett (1982)	Fernow 7	USA	800	Stony silt loam	24	1469	788	50
Bosch and Hewlett (1982)	Fernow 6	USA		Stony silt loam	22	1440	493	50
Bosch and Hewlett (1982)	Leading Ridge WS2	USA	385	Silt loam	43	1004	321	20
Bosch and Hewlett (1982)	Placer County Ws C	USA	168	Clay loam	5	635	145	99
Bosch and Hewlett (1982)	Maimai M7	New Zealand	300	Stoney silt loam	4	2600	1500	100
Bosch and Hewlett (1982)	Maimai M9	New Zealand	310	Stoney silt loam	8	2600	1500	75
Andréassian (2004)	Leading Ridge 2	USA			43	1060	440	86
Andréassian (2004)	Dantzoud	Armenia			14100	680	413	11
Andréassian (2004)	Girants	Armenia			12200	700	224	7
Bent (2001)	Dickey brook	USA	308		308	1250	430	32
Brechtel and Fuhrer(1991)	Krofdorf A1	Germany	336	Rocky	9.3	650	300	100
Fahey and Jackson (1997)	Big bush DC1	New Zealand			8.6	1530	610	83
Fahey and Jackson (1997)	Big bush DC4	New Zealand			20.2	1530	670	94
Fritsch (1992)	Hakhoum	Armenia			####	675	268	7
Sahin and Hall (1996)	WS2L.R.	USA	360	Silt loam	43	1060	440	43
Sahin and Hall (1996)	WS4H.B	USA	606	Sandy loam	36	1340	860	33
Stednick (1996)	Coweeta 7	USA	900	Loam	59	1825	1140	100
Stednick (1996)	Fernow 3	USA	805	Silt loam	34	1500	610	91
Stednick (1996)	Ouachita, OKWS10	USA		Loam	5.7	1317	1652	50
Stednick (1996)	Ouachita, OKWS12	USA		Loam	5.9	1317	1652	100
Stednick (1996)	Ouachita, OKWS14	USA		Loam	4.3	1317	1652	50

http://www.aloki.hu ● ISSN 1589 1623 (Print) ● ISSN 1785 0037 (Online)
DOI: http://dx.doi.org/10.15666/aeer/1804_49875009

Stednick (1996)	Ouachita, OKWS15	USA		Loam	5.1	1317	1652	100
Stednick (1996)	Ouachita, OKWS17	USA		Loam	4.2	1317	1652	50
Stednick (1996)	Ouachita, OKWS18	USA			4.1	1317	1652	100
Anderson et al. (1976)	WN-Carolina 1	USA			15	1828	787	100
Anderson et al. (1976)	WN-Carolina 3	USA			9	1803	610	100
Anderson et al. (1976)	WN-Carolina 5	USA			28	2006	1219	22
Anderson et al. (1976)	WN-Carolina 6	USA			83	1854	1067	30
Anderson et al. (1976)	WN-Carolina 7	USA			28	2032	1295	35
Anderson et al. (1976)	NW-Virginia 1	USA			22	1448	762	100
Anderson et al. (1976)	NW-Virginia 3	USA			23	1447	762	50
Anderson et al. (1976)	NW-Virginia 5	USA			33.4	1498	635	14
Hornbeck et al. (1993), Kabeya et al. (2015)	Pennsylvani LR-WS3	USA	340		104	1060	440	43
Hornbeck et al. (1993), Kabeya et al. (2015)	Pennsylvani LR-WS2	USA	360		43	1060	440	24
Swift and Swank (1981)	Coweeta 13	USA	810	Clay loam	16	1900	889	100
Swift and Swank (1981)	Coweeta 37	USA	1300	Sandy clay loam	44	2220	1604	100
Swift and Swank (1981)	Coweeta 28	USA	1200		144	2320	1534	65
Andréassian (2004)	Karuah/Kokata	Australia			97.4	1565	531	29
Andréassian (2004)	Karuah/Coachwood	Australia			37.5	1447	362	61
Andréassian (2004)	Karuah/Corkwood	Australia			41.1	1636	505	40
Andréassian (2004)	Karuah/Jackwood	Australia			12.5	1373	311	79
Andréassian (2004)	Karuah/Bollygum	Australia			15.1	1518	505	32
Andréassian (2004)	Monda 1	Australia		Rocky Krasnozems	6.3	1876	702	75
Andréassian (2004)	Monda 2	Australia		Rocky Krasnozems	4	1813	550	75
Andréassian (2004)	Monda 3	Australia		Rocky Krasnozems	7.3	1763	632	75
Andréassian (2004)	Myrtle 2	Australia		Rocky Krasnozems	30.5	1590	852	74
Andréassian (2004)	Picaninny	Australia			53	1180	332	78
Andréassian (2004)	Black Spur 1	Australia		Rocky Krasnozems	17	1652	504	60
Andréassian (2004)	Black Spur 3	Australia		Rocky Krasnozems	7.7	1612	530	60
Andréassian (2004)	Wicksend	Australia			68	1200	440	22
Andréassian (2004)	Wilbob	Australia			86	1200	392	12
Andréassian (2004)	Clem creek	Australia		Rocky clay loam	46.4	1445	190	95
Andréassian (2004)	Yarragil 4L	Australia			126	1120	4.3	66
Sahin and Hall (1996)	Hansen	Australia		Gravel	80	1200	232	75
Komatsu et al. (2011), Pearce et al. (1980)	Maimai M7	New Zealand				2600	1550	100
Pearce et al. (1980)	Maimai M9	New Zealand				2600	1550	75
Stednick (1996)	Fernow 3	USA	805	Silt loam	34	1500	610	13
Stednick (1996)	Fernow 5	USA	760	Silt loam	36	1470	760	20
Stednick (1996)	Fernow 6	USA		Silt loam	22	1440	490	50
Stednick (1996)	Fernow 7	USA	800	Silt loam	24	1470	790	50
Stednick (1996)	Leading Ridge PA2	USA	358	Silt loam	43	1000	320	20
Stednick (1996)	Coweeta, NC7	USA	900	Loam	59	1825	1140	100
Stednick (1996)	Grant forest GA18	USA	165	Sandy loam	33	1220	470	100
Stednick (1996)	Ouachita, OKWS10	USA		Loam	6	1317	1652	50
Stednick (1996)	Ouachita, OKWS12	USA		Loam	6	1317	1652	100
Stednick (1996)	Ouachita, OKWS14	USA		Loam	4	1317	1652	50
Stednick (1996)	Ouachita, OKWS15	USA		Loam	4	1317	1652	100
Stednick (1996)	Ouachita, OKWS17	USA		Loam	4	1317	1652	50

http://www.aloki.hu ● ISSN 1589 1623 (Print) ● ISSN 1785 0037 (Online)
DOI: http://dx.doi.org/10.15666/aeer/1804_49875009

Needle-leaved forest								
Source	**Catchment**	**Country**	**Elev. (m)**	**Soil type**	**Area (ha)**	**MAP (mm)**	**MAS (mm)**	**DF (%)**
Bosch and Hewlett (1982)	Needle Branch	USA	312	Sand stone	71	2483	1885	82
Bosch and Hewlett (1982)	Deer Creek	USA	312	Sand stone	303	2474	1906	25
Bosch and Hewlett (1982)	H.J. Andrews 1	USA	700	Clay loams	96	2388	1376	100
Bosch and Hewlett (1982)	H.J. Andrews 3	USA	760	Clay loams	101	2388	1346	30
Bosch and Hewlett (1982)	H.J. Andrews 6	USA	900	Volcaniclastics	13	2150	1290	100
Bosch and Hewlett (1982)	H.J. Andrews 7	USA	900	Volcaniclastics	21	2150	1290	60
Bosch and Hewlett (1982)	H.J. Andrews 10	USA	500	Volcaniclastics	9	2330	1650	100
Bosch and Hewlett (1982)	Coyote Creek 1	USA	901	Gravelly loam	59	1230	627	50
Bosch and Hewlett (1982)	Coyote Creek 2	USA	901	Gravelly loam	68	1230	630	30
Bosch and Hewlett (1982)	Coyote Creek 3	USA		Gravelly loam	50	1230	630	100
Bosch and Hewlett (1982)	Workman Creek, NF	USA	2225	Clay loam	100	813	86	73
Bosch and Hewlett (1982)	Workman Creek, SF	USA	2165	Clay loam	129	813	87	83
Bosch and Hewlett (1982)	Fool Creek	USA	3200	Permeable soil	289	762	283	40
Bosch and Hewlett (1982)	Castle Creek	USA	8207	Soil of igneous origin	364	639	71	17
Bosch and Hewlett (1982)	Beaver Creek 1	USA	1700	Stony clay	124	457	24	100
Bosch and Hewlett (1982)	Beaver Creek 3	USA	1600	Stony clay	146	457	18	83
Bosch and Hewlett (1982)	Wagon Wheel Gap	USA	3110	Rocky clay loam	81	536	157	100
Burton (1997)	Brownie Creek	USA	3082	Sand stone	2134	787	300	25
Troendle et al. (2001), Pike andScherer (2003)	Coon creek	USA			1673	870	440	24
Cosandey (1990)	Latte	France			20	1900	1278	100
Stednick (1996)	Workman Ce.AZ	USA	2225	Clay loam	100	833	86	32
Stednick (1996)	N.Fork	USA	2225	Clay loam	100	810	86	32
Stednick (1996)	Wagonwheel Gap.CO	USA	3110	Rocky clay loam	81	544	157	100
Stednick (1996)	Chicken Creek M.OR1	USA	1523	Ash		1355	472	50
Stednick (1996)	Chicken Creek M.OR2	USA	1523	Ash		1355	460	50
Stednick (1996)	Chicken Creek M.OR3	USA	1523	Ash		1355	372	50
Stednick (1996)	Fool Creek, CO	USA	3200	Granite	289	760	280	40
Stednick (1996)	Fraser Forest, CO	USA	3200	Granite	289	712	283	66
Stednick (1996)	Deadhorse Cr. CO	USA	3120	Granite	270	762	500	36
Stednick (1996)	White Spar C	USA	1420	Quartz	5	450	43	100
Stednick (1996)	Castle Creek, AZ	USA		Igneous	364	640	71	17
Stednick (1996)	Deer Creek, OR	USA	312	Marine sand stone	303	2480	1910	25
Stednick (1996)	Needle Branch, OR	USA	312	Perm sand stone	71	2480	1885	82
Stednick (1996)	Blue Mts1	USA	1523	Ash		1355	472	50
Stednick (1996)	Blue Mts2	USA	1523	Ash		1355	460	50
Stednick (1996)	Blue Mts3	USA	1523	Ash		1355	372	50
Stednick (1996)	St Louis creek	USA	3200	Granite	289	712	283	100

http://www.aloki.hu ● ISSN 1589 1623 (Print) ● ISSN 1785 0037 (Online)
DOI: http://dx.doi.org/10.15666/aeer/1804_49875009

Stednick (1996)	Thomas creek, AZ	USA	2600	Loamy	227	768	500	34
Stednick (1996)	Willow creek, AZ	USA		Loam		749	512	62
Anderson (1976)	Western Oregon 1	USA			93	2362	1447	100
Anderson (1976)	Colorado 2	USA			281	762	279	40
Anderson (1976)	Arizona 2	USA			100	812	86	32
Cheng (1989)	Camp Creek, BC	USA	1920	Granite	3390	600	140	30
Cheng (1989)	Hinton, Alberta	Canada			1497	513	147	50
Cheng (1989)	Cabin Creek, Alberta	Canada			212	840	310	21
Scott et al. (2000)	Biesieviei	South Africa	580		27.2	1298	593.6	100
Scott et al. (2000)	Bosboukloof	South Africa	671		200.9	1564	245.9	100
Scott et al. (2000)	Witklip-6	South Africa	1080		165.3	929	259.7	100
Scott et al. (2000)	WitkliP-5	South Africa	1340		108	929	261.7	51
Webb (2009)	Canobolas A	Australia	1200		55.3	1080	289	100
Webb (2009)	Canobolas B	Australia	1180		55.4	1080	247	100
Cosandey (1990)	Latte	France			20	1900	1278	100
Adams and Flower (2006)	Maimai M5	New Zealand		Gritty silt loam	2.31	2453	1578	100
Adams and Flower (2006)	Maimai M8	New Zealand		Gritty silt loam	3.84	2453	1213	95
Adams and Flower (2006), Rowe et al. (2002)	Glenbervie, Logbridge	New Zealand			12.6	1920	830	100
Adams and Flower (2006), Rowe et al. (2002)	Glenbervie, Pines	New Zealand			15.5	1920	760	100
Adams and Flower (2006), Rowe et al. (2002)	Moumoukai, Central	New Zealand		Clay loam	11.42	1690	660	100
Komatsu et al. (2011), Adams and Flower (2006)	Moumoukai, South	New Zealand		Clay loam	14.98	1700	646	100
Adams and Flower (2006), Rowe et al. (2002)	Purukohukohu, Puruki	New Zealand		Sandy loam to loamy sand	34.4	1590	540	100
Adams and Flower (2006), Rowe et al. (2002)	Pakuratahi	New Zealand		Silt loam	345	1097	380	87
Adams and Flower (2006)	Moutere, C13	New Zealand			7.65	1010	64	100

MAP: mean annual precipitation, MAS: mean annual streamflow, DF: deforestation, Elv.: elevation

http://www.aloki.hu ● ISSN 1589 1623 (Print) ● ISSN 1785 0037 (Online)
DOI: http://dx.doi.org/10.15666/aeer/1804_49875009

GENETIC DIVERSITY AND PHYLOGENETIC RELATIONSHIPS IN THE *BAMBUSA* GENUS AS REVEALED BY RAPD MARKERS

RONG, J. D.[1] – ZHANG, Y. H.[2] – FAN, L. L.[1] – YU, Z. J.[1] – CHEN, L. G.[1] – TARIN, M. W. K.[3] – ZHANG, Z. X.[1] – CHEN, L. Y.[3] – ZHENG, Y. S.[1*]

[1]*College of Forestry, Fujian Agriculture and Forestry University, Fuzhou, Fujian 350002, PR China*

[2]*Fujian Vocational College of Agriculture, Fuzhou, Fujian 350007, PR China*

[3]*College of Arts & College of Landscape Architecture, Fujian Agriculture and Forestry University, Fuzhou, Fujian 350002, PR China*

**Corresponding author*
e-mail: zys1960@163.com; phone: +86-0591-8375-8750

(Received 5th Feb 2020; accepted 22nd May 2020)

Abstract. Understanding the genetic diversity and divergence within *Bambusa* has important implications for conservation and sustainable use. In this study, genetic diversity and phylogenetic relationships between 28 species/varieties of *Bambusa* were evaluated based on 16 randomly amplified polymorphic DNA (RAPD) primers screened from 96 primers. A total of 218 bands were amplified using these 16 primers, yielding DNA fragments of 290–3000 bp. The number of bands and percentage of polymorphism were 211 and 96.79%, respectively, indicating high inter and intraspecific genetic diversity within *Bambusa*. In clustering analysis, genetic distances ranged from 0.2139 to 0.7647. The 28 bamboo species/varieties were classified into six groups at a genetic distance of 0.6138, consistent with traditional classification results. Our results indicated a high degree of polymorphism at RAPD loci, suggesting that the RAPD markers are effective for the analysis of genetic diversity and phylogenetic relationships in the genus. The results of this study provide a theoretical basis for germplasm conservation, classification, and evolutionary studies of *Bambusa* species/varieties.
Keywords: *molecular diversity, genetic relationships, RAPD, bamboos*

Introduction

The genus *Bambusa*, which belongs to the Bambusoideae subfamily, is highly abundant in China and has a wide range of applications. More than a hundred *Bambusa* species have been described and classified into three subgenera, i.e., *Subgen Bambusa*, *Subgen Lingnania,* and *Subgen Leleba*, with *Bambusa chungii*, *Bambusa multiplex* cv. *Fernleaf,* and *Bambusa arundinacea* as the respective type species. China, in particular, boasts approximately 60 *Bambusa* species, which are mainly distributed in the eastern, southern, and southwestern regions (Editorial Committee of Flora of China, Chinese Academy of Sciences, 1996; Zhu et al., 2017). *Bambusa* is characterized by sympodial rhizomes and has relatively high economic, aesthetic, and ecological value. Therefore, in-depth research on the genus is beneficial for the conservation of biodiversity within bamboo resources in China (Ma et al., 2007).

Although *Bambusa* species propagate by asexual reproduction, adaptations to different habitats and long-term evolution have resulted in genetic variation. The high genetic diversity in *Bambusa* poses certain challenges for the accurate differentiation and identification of *Bambusa* species (Lou et al., 2011). In addition, as bamboo species have low flowering and fruiting rates, the determination of interspecific relationships

http://www.aloki.hu ● ISSN 1589 1623 (Print) ● ISSN 1785 0037 (Online)
DOI: http://dx.doi.org/10.15666/aeer/1804_50115021

within *Bambusa* based on morphological markers, such as the morphological characteristics of flowers and fruits, or other markers, such as isozymes, is extremely difficult (Lin et al., 2008). Therefore, the quest for effective markers has become a key topic in phylogenetic studies of *Bambusa*.

Advances in molecular biology have substantially improved DNA marker techniques, enabling the direct comparison of genetic material without the influence of external environmental factors (Liu et al., 2015). Such techniques are increasingly used for analyses of genetic diversity and phylogenetic relationships within *Bambusa*. Randomly amplified polymorphic DNA (RAPD) marker detection, using electrophoresis and PCR (Mutharaian et al., 2018), has several advantages, such as its high sensitivity, low cost, and ease, enabling the acquisition of large quantities of information (Xia et al., 2001); accordingly, this approach is widely used for studies of genetic diversity (He et al., 2019; Tanzeem et al., 2019; Leandro et al.2019; Subramanyam et al., 2010), phylogenetic relationships (Amom et al., 2020; Liu et al., 2016), variety identification (Odunayo et al., 2019; Archana et al., 2013), and DNA fingerprinting (Mei et al., 2014; Afshari et al., 2016). However, few studies have utilized RAPD to evaluate *Bambusa*. In this study, 28 *Bambusa* species/varieties were used as test materials for a RAPD-based analysis of genetic diversity and phylogenetic relationships to provide a theoretical basis for germplasm conservation, classification, and evolutionary studies of *Bambusa* species/varieties.

Materials and methods

Test materials

The test materials were obtained from 28 *Bambusa* species/varieties from the Bamboo Cultivation Base of the Fujian Agriculture and Forestry University, Fuzhou, China in August 2018. *Table 1* provides basic information for the test materials. Fresh uninfested leaves (3–6 g) were harvested from each plant and stored in a -80 °C ultra-low temperature freezer until genomic DNA extraction.

Methods

DNA extraction and detection

Genomic DNA was extracted using the CTAB method (Zhang et al., 2014), and the concentration was measured using a NANODROP 2000 spectrophotometer. Electrophoresis was performed using a 1.0% agarose gel; briefly, 9 μL of template DNA was mixed with 1.5 μL of 6× loading buffer and subjected to 120 V (5 $V \cdot cm^{-2}$) for 30 min, using 1× TBE as the electrophoresis buffer. The electrophoresis results were analyzed using a gel imaging system. The size of the DNA ladder marker (No. B500347, Sangon Biotech) is 100-3000 bp. Total DNA that satisfied the study requirements was diluted to a 20 $ng \cdot \mu L^{-1}$ and stored in a -20 °C freezer before further use.

Primer screening

A total of 96 random oligonucleotide primers of 10 bp were purchased from Sangon Biotech Co., Ltd. (Shanghai, China) and used for the preamplification of the total DNA of certain *Bambusa* species/varieties. Then, 16 primers that produced bands with high

http://www.aloki.hu ● ISSN 1589 1623 (Print) ● ISSN 1785 0037 (Online)
DOI: http://dx.doi.org/10.15666/aeer/1804_50115021

clarity, stability, degree of polymorphism, and reproducibility were selected for the RAPD analysis with the total DNA of all 28 bamboo species/varieties. *Table 2* shows a list of selected primers and sequences.

Table 1. *Summary of test materials*

No.	Species/variety name
1	*Bambusa sinospinosa*
2	*B. rutila*
3	*B. subaequalis*
4	*B. gibba*
5	*B. ventricosa*
6	*B. remotiflora*
7	*B. cerosisssima*
8	*B. textilis* cv. *Maculata*
9	*B. textilis* var. *gracilis*
10	*B. tulda*
11	*B. eutuldoides McClure* var. *viridi-vittata*
12	*B. pervariabilis*
13	*B. longispiculata*
14	*B. tuloides*
15	*B. subtruncata*
16	*B. boniopsis*
17	*B. vulgaris*
18	*B. vulgaris* cv. *Vittata*
19	*B. vulgaris* cv. *Wamin*
20	*B. gibboides*
21	*B. albo-lineata*
22	*B. lenta*
23	*B. contracta*
24	*B. multiplex*
25	*B. multiplex* cv. *Alphonse-Karr*
26	*B. multiplex* cv. *Silverstripe*
27	*B. multiplex* cv. *Fernleaf*
28	*B. multiplex* var. *riviereorum*

Table 2. *List of primers and sequences*

Primer	Sequence 5′–3′	Primer	Sequence 5′–3′
S4	GGACTGGAGT	S69	CTCACCGTCC
S5	TGCGCCCTTC	S431	TCGCCGCAAA
S13	TTCCCCCGCT	S1219	CTGATCGCGG
S26	GGTCCCTGAC	S2093	TCGGTGAGTC
S32	TCGGCGATAG	S1408	GTTACGGACC
S36	AGCCAGCGAA	S1412	CCTGTACCGA
S45	TGAGCGGACA	S1420	CTTCTCGGAC
S67	GTCCCGACGA	S1421	TCCCAGCAGA

http://www.aloki.hu ● ISSN 1589 1623 (Print) ● ISSN 1785 0037 (Online)
DOI: http://dx.doi.org/10.15666/aeer/1804_50115021

RAPD-PCR and the detection of amplification products

PCR was performed using a LabCycler PCR System (SensoQuest International Ltd). The reaction system for RAPD-PCR consisted of the following: 2.0 μL of 10× buffer, 3.5 mmol·L^{-1} Mg^{2+}, 0.4 mmol·L^{-1} dNTPs, 0.6 μmol·L^{-1} primer, 3.0 U of *Taq* polymerase, 40 ng of template DNA, and sterile ddH_2O for a total volume of 20 μL.

The RAPD-PCR protocol was as follows: initial denaturation at 94 °C for 2 min, denaturation at 94°C for 30 s, annealing at 34 °C for 30 s, and extension at 70 °C for 90 s for 38 cycles; final extension at 72 °C for 7 min. The PCR products were stored in a 4 °C refrigerator, and detection was subsequently performed by electrophoresis on a 1.0% agarose gel.

Statistical analysis

POPGENE version 3.2 was used to determine the total number of bands and the number of polymorphic bands amplified by each primer (Yeh et al., 1999). The bands produced at the same site by different primers were counted for each sample, assigning a value of 1 if a band was present and 0 if a band was absent. DPS 18.10 was used to analyze genetic diversity, perform a clustering analysis, and construct a phylogenetic tree of the tested *Bambusa* species/varieties (Tang et al., 2013).

Results and analysis

Analysis of RAPD marker polymorphism

Among 96 random RAPD primers used for preamplification, 16 primers produced bands with high clarity, degree of polymorphism, and stability and were selected for marker amplification from all 28 *Bambusa* species/varieties. *Figures 1* and *2* show the representative gel electrophoresis results obtained with primers S32 and S431. In total, 218 clear bands were obtained with the 16 primers, and 211 of these bands were polymorphic. On average, 13.63 bands and 13.19 polymorphic bands were obtained for each primer. The percentages of polymorphism for the primers ranged from 77.78% to 100% and the average percentage was 96.79% (*Table 3*). Each primer produced 6–21 bands and 5–21 polymorphic bands, with fragment lengths of 190–3000 bp. These results indicate that genetic diversity is high within *Bambusa*. This high diversity suggests that the genus possesses a strong ability to adapt to various environments. Furthermore, interspecific genetic differences within *Bambusa* can be effectively elucidated by RAPD markers.

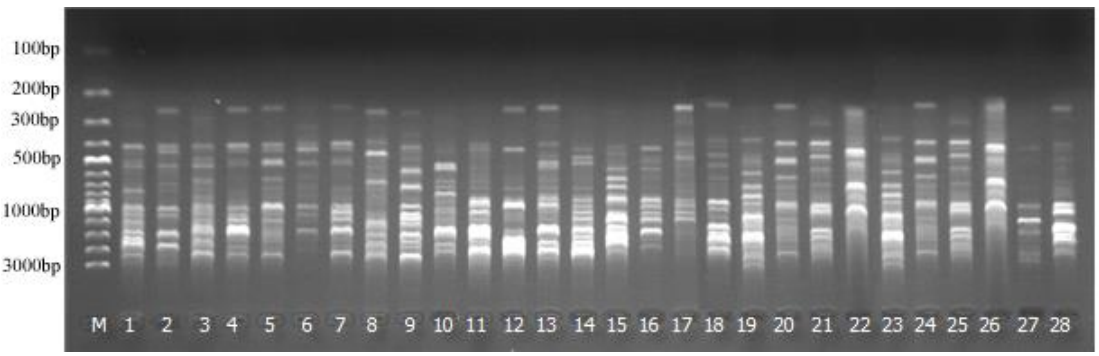

Figure 1. *Electrophoresis results for 28 Bambusa samples amplified using RAPD S32*

http://www.aloki.hu ● ISSN 1589 1623 (Print) ● ISSN 1785 0037 (Online)
DOI: http://dx.doi.org/10.15666/aeer/1804_50115021

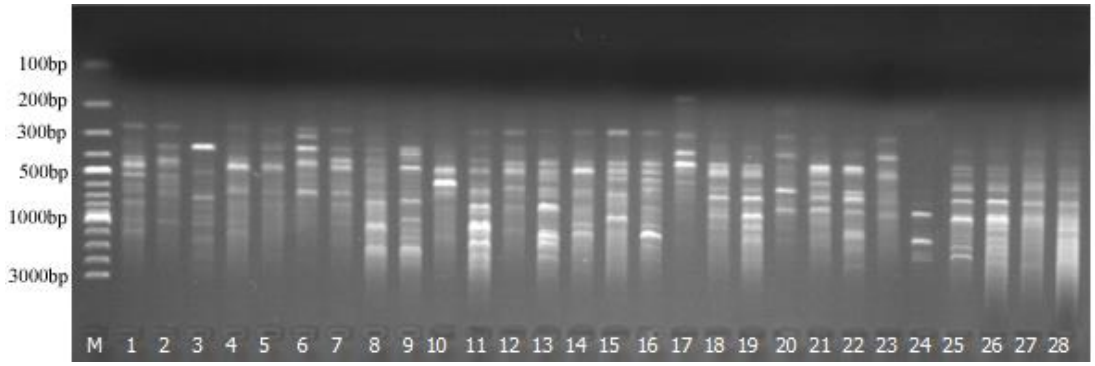

***Figure 2**. Electrophoresis results for 28 Bambusa samples amplified using RAPD S431*

***Table 3.** RAPD primers and percentages of polymorphism*

Primer	Total no. of bands	No. of polymorphic bands	Percentage of polymorphism (%)
S4	14	14	100
S5	12	12	100
S13	17	17	100
S26	10	9	90.00
S32	21	21	100
S36	9	7	77.78
S45	6	5	83.33
S67	13	12	92.31
S69	13	13	100
S431	15	15	100
S1219	12	11	91.67
S2093	13	13	100
S1408	14	13	92.86
S1412	15	15	100
S1420	17	17	100
S1421	17	17	100
Total	218	211	96.79
Average	13.63	13.19	96.79

Analysis of genetic distances and genetic diversity among the Bambusa species/varieties

For the 16 primers, a data matrix was generated from the genomic fingerprint, and pairwise genetic distances among the various *Bambusa* species/varieties were calculated using DPS 18.10 based on Jaccard's formula (Yhang et al., 2010) (*Table 4*). The average genetic distance was 0.5597 and the range was 0.2139–0.7647, indicating a relatively high average and a high degree of variation. As shown in *Table 4*, the genetic distances within the genus *Bambusa* were mostly around 0.5, indicating good genetic stability. The genetic distances between variants or cultivars of the same species were lower than those for comparisons between different species. For instance, the genetic distances among *B. multiplex* cv. *Alphonse-Karr*, *B. multiplex* cv. *Silverstripe*, *B. multiplex* cv. *Fernleaf,* and *B. multiplex* var. *riviereorum*, belonging to *Bambusa*

http://www.aloki.hu ● ISSN 1589 1623 (Print) ● ISSN 1785 0037 (Online)
DOI: http://dx.doi.org/10.15666/aeer/1804_50115021

subgen. *Leleba*, were relatively low, while the genetic distance between *B. subaequalis* (belonging to *Bambusa* subgen. *Bambusa*) and *B. subtruncata* (belonging to *Bambusa* subgen. *Leleba*) was high. These results demonstrate that the phylogenetic relationships among *Bambusa* species/varieties are consistent with the morphological classification and that RAPD markers are effective indicators of genetic diversity in *Bambusa* species/varieties.

Table 4. *The genetic distance matrix for 28 Bambusa species/varieties*

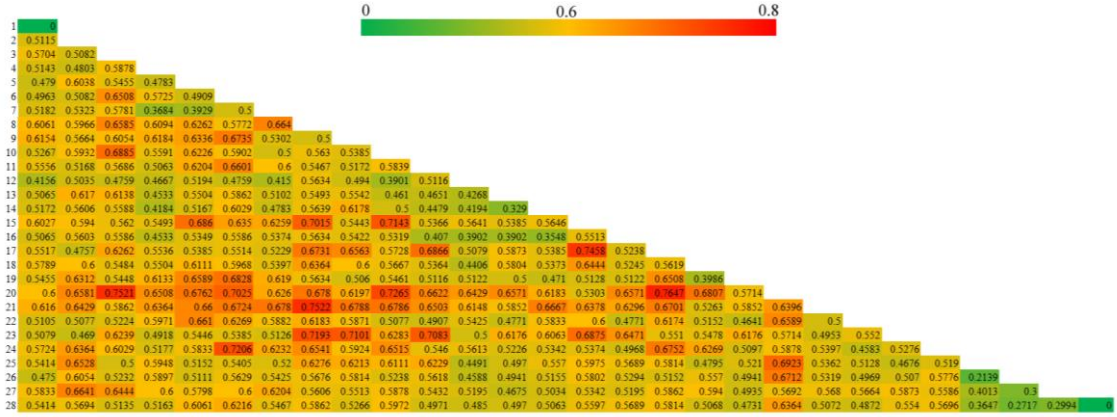

1	0																										
2	0.5115	0																									
3	0.5704	0.5082	0																								
4	0.5143	0.4803	0.5878	0																							
5	0.479	0.6038	0.5455	0.4783	0																						
6	0.4963	0.5082	0.6508	0.5725	0.4909	0																					
7	0.5182	0.5323	0.5781	0.3684	0.3929	0.5	0																				
8	0.6061	0.5966	0.6585	0.6094	0.6262	0.5772	0.664	0																			
9	0.6154	0.5664	0.6054	0.6184	0.6336	0.6735	0.5302	0.5	0																		
10	0.5267	0.5932	0.6885	0.5591	0.6226	0.5902	0.5	0.563	0.5385	0																	
11	0.5556	0.5168	0.5686	0.5063	0.6204	0.6601	0.6	0.5467	0.5172	0.5839	0																
12	0.4156	0.5035	0.4759	0.4667	0.5194	0.4759	0.415	0.5634	0.494	0.3901	0.5116	0															
13	0.5065	0.617	0.6138	0.4533	0.5504	0.5862	0.5102	0.5493	0.5542	0.461	0.4651	0.4268	0														
14	0.5172	0.5606	0.5588	0.4184	0.5167	0.6029	0.4783	0.5639	0.6178	0.5	0.4479	0.4194	0.329	0													
15	0.6027	0.594	0.562	0.5493	0.686	0.635	0.6259	0.7015	0.5443	0.7143	0.5366	0.5641	0.5385	0.5646	0												
16	0.5065	0.5603	0.5586	0.4533	0.5349	0.5586	0.5374	0.5634	0.5422	0.5319	0.407	0.3902	0.3902	0.3548	0.5513	0											
17	0.5517	0.4757	0.6262	0.5536	0.5385	0.5514	0.5229	0.6731	0.6563	0.5728	0.6866	0.5079	0.5873	0.5385	0.7458	0.5238	0										
18	0.5789	0.6	0.5484	0.5504	0.6111	0.5968	0.5397	0.6364	0.6	0.5667	0.5364	0.4406	0.5804	0.5373	0.6444	0.5245	0.5619	0									
19	0.5455	0.6312	0.5448	0.6133	0.6589	0.6828	0.619	0.5634	0.506	0.5461	0.5116	0.5122	0.5	0.471	0.5128	0.5122	0.6508	0.3986	0								
20	0.6	0.6581	0.7521	0.6508	0.6762	0.7025	0.626	0.678	0.6197	0.7265	0.6622	0.6429	0.6571	0.6183	0.5303	0.6571	0.7647	0.6807	0.5714	0							
21	0.616	0.6429	0.5862	0.6364	0.66	0.6724	0.678	0.7322	0.6788	0.6786	0.6503	0.6148	0.5852	0.6667	0.6378	0.6296	0.6701	0.5263	0.5852	0.6396	0						
22	0.5105	0.5077	0.5224	0.5971	0.661	0.6269	0.5882	0.6183	0.5871	0.5077	0.4907	0.5425	0.4771	0.5833	0.6	0.4771	0.6174	0.5152	0.4641	0.6589	0.5	0					
23	0.5079	0.469	0.6239	0.4918	0.5446	0.5385	0.5126	0.7193	0.7101	0.6283	0.7083	0.5	0.6176	0.6063	0.6875	0.6471	0.551	0.5478	0.6176	0.5714	0.4953	0.552	0				
24	0.5724	0.6364	0.6029	0.5177	0.5833	0.7206	0.6232	0.6541	0.5924	0.6515	0.546	0.5613	0.5226	0.5342	0.5374	0.4968	0.6752	0.6269	0.5097	0.5878	0.5397	0.4583	0.5276	0			
25	0.5414	0.6528	0.5	0.5948	0.5152	0.5405	0.52	0.6276	0.6213	0.6111	0.6229	0.4491	0.497	0.557	0.5975	0.5689	0.5814	0.4795	0.521	0.6923	0.5362	0.5128	0.4676	0.519	0		
26	0.475	0.6054	0.5232	0.5897	0.5111	0.5629	0.5425	0.5676	0.5814	0.5238	0.5618	0.4588	0.4941	0.5155	0.5802	0.5294	0.5152	0.557	0.4941	0.6712	0.5319	0.4969	0.507	0.5776	0.2139	0	
27	0.5833	0.6641	0.6444	0.6	0.5798	0.6	0.6204	0.5606	0.5513	0.5878	0.5432	0.5195	0.4675	0.5034	0.5342	0.5195	0.5862	0.594	0.4935	0.5692	0.568	0.5664	0.5873	0.5586	0.4013	0.3	0
28	0.5414	0.5694	0.5135	0.5163	0.6061	0.6216	0.5467	0.5862	0.5266	0.5972	0.4971	0.485	0.497	0.5063	0.5597	0.5689	0.5814	0.5068	0.4731	0.6364	0.5072	0.4872	0.554	0.5696	0.3647	0.2717	0.2994	0

Cluster analysis of Bambusa species/varieties

Based on the RAPD-PCR amplification results, phylogenetic relationships within *Bambusa* were analyzed with the raw genotypic data matrix using DPS 18.10 (Tang et al., 2013). A cluster analysis was performed based on genetic distances using the Nei–Li maximum distance method (Zaya et al., 2017), and a dendrogram was constructed (*Fig. 3*; *Table* 5). The clustering results indicate that the 28 *Bambusa* species/varieties could be classified into six groups at a genetic distance of 0.57 (L1). (1) Group 1 (genetic distance = 0.6038) included 8 species/varieties (*B. sinospinosa*, *B. remotiflora*, *B. rutila*, *B. contracta*, *B. vulgaris*, *B. gibba*, *B. cerosisssima*, and *B. ventricosa*); Group 2 (genetic distance = 0.5634) included 4 species/varieties (*B. textilis* cv. *Maculata*, *B. textilis* var. *gracilis*, *B. tulda*, and *B. pervariabilis*); (3) Group 3 (genetic distance = 0.5484) included 3 species/varieties (*B. subaequalis*, *B. vulgaris* cv. *Vittata*, and *B. vulgaris* cv. *Wamin*); (4) Group 4 (genetic distance = 0.4651) included 4 species/varieties (*B. eutuldoides McClure* var. *viridi-vittata*, *B. longispiculata*, *B. tuloides*, and *B. boniopsis*); (5) Group 5 (genetic distance = 0.5776) included 7 species/varieties (*B. albo-lineata*, *B. lenta*, *B. multiplex*, *B. multiplex* cv. *Alphonse-Karr*, *B. multiplex* cv. *Silverstripe*, *B. multiplex* cv. *Fernleaf*, *B. multiplex* var. *riviereorum*); (6) Group 6 (genetic distance = 0.5303) included 2 species/varieties (*B. subtruncata* and *B. gibboides*).

Groups 1 and 2 exhibited a genetic distance of 0.7193, with *B. sinospinosa*, *B. rutila*, *B. gibba,* and *B. ventricosa* (all belonging to *Bambusa* subgen. *Bambusa*) forming a distinct cluster, and *B. remotiflora*, *B. cerosisssima*, *B. textilis* cv. *Maculata,* and *B. textilis* var. *gracilis* (all belonging to *Bambusa* subgen. *Lingnania*) clustering together. However, *B. subaequalis*, which belongs to *Bambusa* subgen. *Bambusa*, did not cluster with species in the same subgenus; instead, it formed a group with the majority of members of *Bambusa* subgen. *Leleba,* as evidenced by the shorter genetic distances. In

http://www.aloki.hu ● ISSN 1589 1623 (Print) ● ISSN 1785 0037 (Online)
DOI: http://dx.doi.org/10.15666/aeer/1804_50115021

Group 3, *B. vulgaris* cv. *Vittata* and *B. vulgaris* cv. *Wamin*, which are both members of *Bambusa* subgen. *Leleba* and variants of *B. vulgaris*, did not cluster together with *B. vulgaris*; instead, they formed a cluster with *B. subaequalis* of *Bambusa* subgen. *Bambusa* (genetic distance, 0.5484). In Group 5, *B. multiplex* was distinctly clustered with its cultivated variants *B. multiplex* cv. *Alphonse-Karr*, *B. multiplex* cv. *Silverstripe*, *B. multiplex* cv. *Fernleaf,* and *B. multiplex* var. *riviereorum*, consistent with traditional classification results. However, *B. multiplex* cv. *Alphonse-Karr*, *B. multiplex* cv. *Silverstripe*, *B. multiplex* cv. *Fernleaf,* and *B. multiplex* var. *riviereorum* did not clustered together with *B. multiplex*; instead, they clustered together with *B. multiplex*, *B. lenta,* and *B. albo-lineata* (genetic distance, 0.5776). This indicates that divergence in *B. multiplex* resulted in greater genetic similarity with *B. lenta* and *B. albo-lineata*.

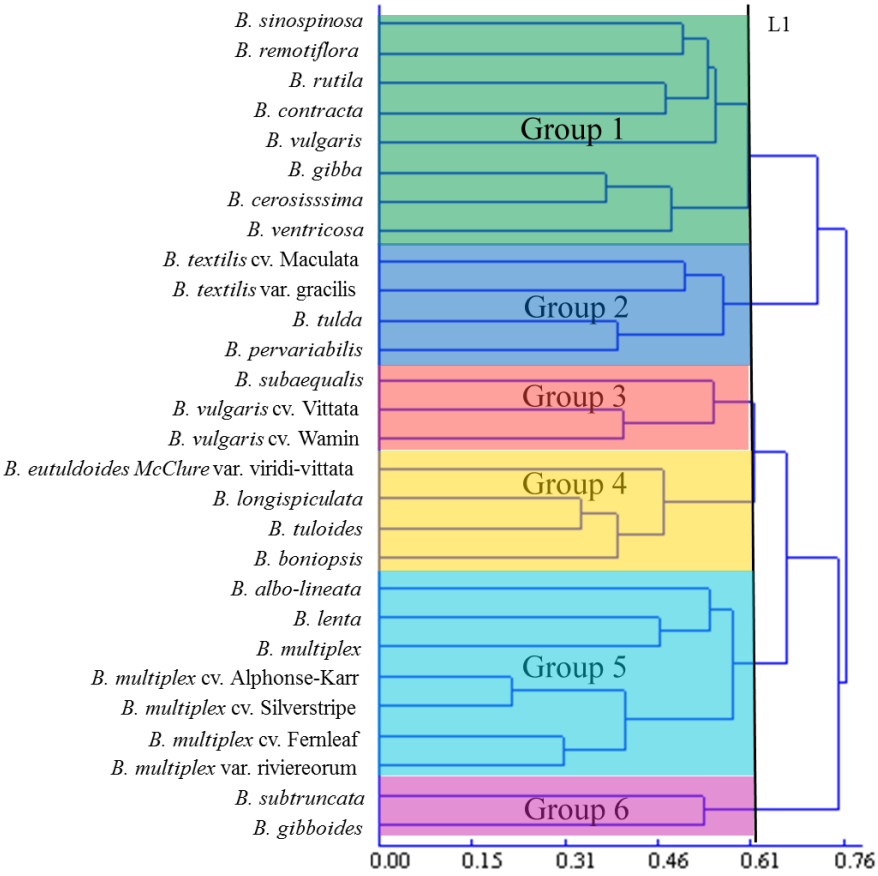

Figure 3. *Dendrogram of the 28 Bambusa species/varieties based on RAPD markers*

Discussion

Previous research has demonstrated that the main determinants of the stability and reproducibility of RAPD analyses are temperature conditions, reagent concentrations, and the duration of various PCR steps (Bi et al., 2011). The application of the RAPD method for the investigation of interspecific relationships (including subspecific classes) within *Bambusa* is rare, with a literature search yielding a single study by Nayak et al (2003) involving only a few *Bambusa* species. In this study, we adopted the RAPD technique for the analysis of genetic differences and phylogenetic relationships among 28 *Bambusa* species/varieties. The amplification patterns of certain primers consisted of

http://www.aloki.hu ● ISSN 1589 1623 (Print) ● ISSN 1785 0037 (Online)
DOI: http://dx.doi.org/10.15666/aeer/1804_50115021

a variety of bands with significant differences. Amplification using 16 primers produced 218 clear bands, with 96.79% (211 bands) polymorphism. Therefore, a high level of polymorphism within *Bambusa* was detected with RAPD molecular markers, demonstrating that the approach is practical and effective for genetic analyses of the genus.

Table 5. *Clustering and genetic distances of the 28 Bambusa species/varieties*

T Number	I Linked level	J Indexing of clustering order	Distance
1	26	25	0.2139
2	28	27	0.2994
3	14	13	0.3290
4	7	4	0.3684
5	12	10	0.3901
6	16	13	0.3902
7	19	18	0.3986
8	27	25	0.4013
9	24	22	0.4583
10	13	11	0.4651
11	23	2	0.4690
12	5	4	0.4783
13	6	1	0.4963
14	9	8	0.5000
15	20	15	0.5303
16	2	1	0.5385
17	22	21	0.5397
18	18	3	0.5484
19	17	1	0.5517
20	10	8	0.5634
21	25	21	0.5776
22	4	1	0.6038
23	11	3	0.6138
24	21	3	0.6667
25	8	1	0.7193
26	15	3	0.7521
27	3	1	0.7647

The average genetic distance range of values were high. These results show that *Bambusa* possesses high genetic diversity and relatively complex interspecific genetic relationships (Zhan et al., 2015). The genus is highly influenced by various factors, such as geographical location, climate fluctuations, and various evolutionary processes (Lou et al., 2011), leading to the establishment of a diverse gene pool.

A clustering analysis based on RAPD markers showed that the 28 *Bambusa* species/varieties could be clearly distinguished. The species/varieties were classified into 6 groups, consistent with results based on morphological properties. Compared with Nayak et al. (2003), a larger number of primers and samples were used in this study. However, the results of the two studies were largely consistent and in agreement

http://www.aloki.hu ● ISSN 1589 1623 (Print) ● ISSN 1785 0037 (Online)
DOI: http://dx.doi.org/10.15666/aeer/1804_50115021

with Loh et al. (2000), who adopted amplified fragment length polymorphism (AFLP) markers for the analysis of genetic diversity and relationships. In Group 3, *B. vulgaris* cv. *Vittata* and *B. vulgaris* cv. *Wamin*, both members of *Bambusa* subgen. *Leleba* and variants of *B. vulgaris*, were not initially clustered with *B. vulgaris*; instead, they were clustered with *B. subaequalis* of *Bambusa* subgen. *Bambusa* and only formed a cluster with *B. vulgaris* at a genetic distance of 0.7647. This can be explained by variation in *B. vulgaris* cv. *Vittata* and *B. vulgaris* cv. *Wamin* or anthropomorphic disturbance; further research is required to determine the exact cause. In Group 5, except for *B. albo-lineata*, the genetic distances among other species/varieties were less than 0.5, indicating that genetic traits within the group were relatively stable. All species/varieties within this group belong to *Bambusa* subgen. *Leleba* according to the traditional classification described in the Flora of China. In particular, *B. multiplex* cv. *Alphonse-Karr* and *B. multiplex* cv. *Silverstripe*, which are both cultivated varieties of *B. multiplex*, exhibited high genetic similarity. Sun et al. (Sun et al., 2005) utilized ribosomal DNA ITS sequences in a study of *B. subaequalis* and *B. multiplex* cv. *Fernleaf*, and suggested that the two species are sister species. Based on the results of the present study, *B. subaequalis* and *B. multiplex* cv. *Fernleaf* are closely related, further supporting the sister-group relationship.

Conclusions

Genetic diversity and phylogenetic relationships within *Bambusa* can be reliable and reproducibly evaluated based on RAPD markers. The 28 tested *Bambusa* species/varieties possess high genetic diversity and complex phylogenetic relationships. When combined with morphological features, the results of this study can provide a theoretical basis for germplasm conservation, classification, and evolutionary analyses of *Bambusa* species/varieties. It is obligatory to fortify the collection, identification, and excavation of the germplasm resources of *Bambusa* to augment the genetic diversity of breeding materials. Continuous development of biotechnology, in bamboo research will be required to address more problems. Bamboo genome research, gene mechanism, transgenic technology, and cloning technology can be a new direction in bamboo research.

Acknowledgments. This work was supported by Science and Technology Major Projects of Fujian Province [2013NZ0001], Fujian Agriculture and Forestry University Science and Technology Development Fund Project [KF2015085]. The author thanks anonymous reviewers who provided helpful suggestions and critical comments on this manuscript.

REFERENCES

[1] Afshari, A., Jamshidi, A., Razmyar, J. (2016): Genomic diversity of *Clostridium perfringens* strains isolated from food and human sources. – Iranian Journal of Veterinary Research 17: 160-164.

[2] Amom, T., Tikendra, L., Apana, N., Goutam, M., Sonia, P., Koijam Arunkumar, S., Potshangbam, A., Rahaman, H., Nongdam, P. (2020): Efficiency of RAPD, ISSR, iPBS, SCoT and phytochemical markers in the genetic relationship study of five native and economical important bamboos of North-East India. – Phytochemistry. https://doi.org/10.1016/j.phytochem.2020.112330.

http://www.aloki.hu ● ISSN 1589 1623 (Print) ● ISSN 1785 0037 (Online)
DOI: http://dx.doi.org/10.15666/aeer/1804_50115021

[3] Archana, C. P., Deepu, V., Geetha, S. P., Indira, B. (2013): RAPD assessment for identification of clonal fidelity of microrhizome induced plants of Turmeric (*Curcuma longa* L.) cultivars. – International Food Research Journal 20: 3325-3328.
[4] Bi, Y., Du, X., Zhong, Z. (2011): Advances in the application of biological techniques in *Bambusa*. – Journal of Bamboo Research 30: 57-62.
[5] Editorial Committee of flora of China, Chinese Academy of Sciences (1996): Flora of China: Vol. 9, Vol. 1. – Science Press, Beijing, pp. 48-49.
[6] He, T. Y., Qu, Y. Q., Chen, L. Y., Xu, W., Rong, J. D., Chen, L. G., Fan, L. L., Tarin, M. W. K., Zheng, Y. S., (2019): Genetic diversity analysis of Dendrocalamopsis beecheyana var. Pubescens based on ISSR markers. – Appl. Ecol. Environ. Res. 17: 12507-12518.
[7] Leandro, P., Santiago, V., Ana, F., Jaime, P., Adrián, R. (2019): Genetic diversity, population structure, and relationships in a collection of pepper (Capsicum spp.) landraces from the Spanish Centre of Diversity revealed by genotyping-by-sequencing (GBS). – Horticulture Research. DOI: 10.1038/s41438-019-0132-8.
[8] Lin, S., Ding, Y., Zhang, H. (2008): Pollen germination percentage and the floral character of five bamboo species. – Scientia Silvae Sinicae 44: 159-163.
[9] Liu, D., Yang, L., Fang, Z., Liu, Y., Zhuang, M., Zhang, Y., Li, Z., Lyu, H. (2015): Progress of Brassica crops molecular breeding. – Journal of Agricultural Science and Technology 17: 15-22.
[10] Liu, S., Wang, X., Jiang, C., Yuan, W., Zhang, J. (2016): RAPD-PCR analysis on different germplasm resources of *Curcumae Rhizoma*. – Chinese Traditional and Herbal Drugs 47: 3098-3102.
[11] Loh, J. P., Kiew, R., Set, O., Gan, L. H., Gan, Y. Y. (2000): A study of genetic variation and relationships within the bamboo subtribe Bambusinae using amplified fragment length polymorphism. – Annals of Botany (London) 85: 607-612.
[12] Lou, Y., Yang, H., Zhang, Y., Li, X., Lin, X., Fang, W. (2011): Analysis of genetic variation of some bamboo species by AFLP, ISSR and SRAP. – Journal of Fujian College of Forestry 31: 38-43.
[13] Ma, N., Chen, G., Yuan, J. (2007): Bamboo biodiversity and conservation strategies in China. – Scientia Silvae Sinicae 43: 105-109.
[14] Mei, Z., Md, A., Zeng, W., unjiang Fu, J. (2014): DNA fingerprints of living fossil Ginkgo biloba by using ISSR and improved RAPD analysis. – Biochemical Systematics and Ecology 36: 98-103.
[15] Mutharaian, V. N., Kamalakannan, R., Mayavel, A., Makesh, S., Kwon, H., Kang, K. (2018): DNA polymorphisms and genetic relationship among populations of Acacia leucophloea using RAPD markers. – Journal of Forestry Research 29: 1-8.
[16] Nayak, S., Rout, G. R., Das, P. (2003): Evaluation of genetic variability in bamboo using rapd markers. – Plant Soil and Environment 49: 24-28.
[17] Odunayo, J., Abeeb, A. (2019): Molecular evaluation of Garcinia kola Heckel accessions using RAPD markers. – American Journal of Molecular Biology 9: 41-51.
[18] Subramanyam, Rao, D., Devanna, N., Aravinda, A. (2010): Evaluation of genetic diversity among Jatropha curcas (L) by RAPD analysis. – Indian Journal of Biotechnology 9: 283-288.
[19] Sun, Y., Xia, N., Lin, R. (2005): Phylogenetic analysis of Bambusa (Poaceae: Bambusoideae) based on internal transcribed spacer sequences of nuclear ribosomal DNA. – Biochemical Genetics 43: 603-612.
[20] Tang, Q., Zhang, C. (2013): Data Processing System (DPS) software with experimental design, statistical analysis and data mining developed for use in entomological research. – Insect Science 20: 254-260.
[21] Tanzeem, F., Ashutosh, S., Vageeshbabu, S., Somashekar, P., Srinivasa Rao, M. (2019): Genetic diversity estimates of Santalum album L. through microsatellite markers: implications on conservation. – American Journal of Plant Science 10: 462-485.

http://www.aloki.hu ● ISSN 1589 1623 (Print) ● ISSN 1785 0037 (Online)
DOI: http://dx.doi.org/10.15666/aeer/1804_50115021

[22] Xia, M., Zhou, X., Zhao, S. (2001): RAPD analysis on genetic diversity of natural populations of *Pinus koraiensis*. – Acta Ecologica Sinica 21: 730-737.
[23] Yang, R., Sun, Z., Xiang, Y. (2010): SSR analysis of genetic diversity among 14 bamboo species in Phyllostachys. – Journal of Bamboo Research 29: 11-14, 20.
[24] Yeh, F. C., Yang, R. (1999): Microsoft Window-Based Freeware for Population Genetic Analysis (POPGENE Ver. 1.31). – University of Alberta, Alberta.
[25] Zaya, D. N., Molano-Flores, B., Feist, M. A., Koontz, J. A., Coons, J. (2017): Assessing genetic diversity for the USA endemic carnivorous plant *Pinguicula ionantha* R. K. Godfrey (Lentibulariaceae). – Conservation Genetics 18: 171-180.
[26] Zhan, M., Yang, Y., Cheng, Z., Su, G., Hu, W., Chen, H., Huang, Q. (2015): Genetic diversity of olive varieties based on SRAP markers. – Scientia Silvae Sinicae 51: 157-164.
[27] Zhang, Y., Shi, M., De, J., Suo, N., La, D. (2014): Extraction of genomic DNA from *Chenopodium foetidum* and detection of its RAPD. – Journal of Tibet University 29: 13-16.
[28] Zhu, Z., Cai, H., Bi, S., Zhong, Z., Du, X. (2017): A study on the examination guideline of distinctness, uniformity and stability of *Bambusa*. – Journal of Bamboo Research 36: 44-48, 65.

http://www.aloki.hu ● ISSN 1589 1623 (Print) ● ISSN 1785 0037 (Online)
DOI: http://dx.doi.org/10.15666/aeer/1804_50115021

Supplementary File S1.

No.	Name	Sequence	No.	Name	Sequence
RAPD primers					
1	A02	TGCCGAGCTG	11	B07	GGTGACGCAG
2	A03	AGTCAGCCAC	12	B09	TGGGGGACTC
3	A08	GTGACGTAGG	13	B10	CTGCTGGGAC
4	A09	GGGTAACGCC	14	C02	GTGAGGCGTC
5	A15	TTCCGAACCC	15	C06	GAACGGACTC
6	A16	AGCCAGCGAA	16	C07	GTCCCGACGA
7	A17	GACCGCTTGT	17	C08	TGGACCGGTG
8	A18	AGGTGACCGT	18	C10	TGTCTGGGTG
9	B03	CATCCCCCTG	19	C14	TGCGTGCTTG
10	B04	GGACTGGAGT	20	C16	CACACTCCAG
ISSR primers					
1	814	$(CT)_8TG$	8	HB8	$(GA)_6GG$
2	844A	$(CT)_8AC$	9	HB9	$(GT)_6GG$
3	844B	$(CT)_8GC$	10	HB10	$(GA)_6CC$
4	17898A	$(CA)_6AC$	11	HB11	$(GT)_6CC$
5	17898B	$(CA)_6GT$	12	HB12	$(CAC)_3GC$
6	17899A	$(CA)_6AG$	13	HB13	$(GAG)_3GC$
7	17899B	$(CA)_6GG$	14	HB14	$(CTC)_3GC$
NUCmer primers					
Rx1	F10337514	TGAGAAGGGTTTAGTTTGCAC CTGTGAATAGGCAGAAAGGTC	Rx18	M12975375	TGATGGACTGGACTGTGAC CCATTTTCTCTGATGCCTGC
Rx2	F11806232	TGCTTGTTAAGGGAGCCACG ACCCACCCAAAAAACAGAGAAG	Rx19	M13446011	GCCACAAGAACAAGATATTGC GAGGAACCCCATTGATAAAGC
Rx3	F12098636	TGAACTCAAATATCTGGAGCTG CCAAGTAACCCAATGGAGATAC	Rx20	M15402427	ATGTAAATCGGGTAGTGAATCG CAACATAACAACCACGAAGTTC
Rx4	F12109005	GCCTCGAAATGACTGCAAG CATGCAGCACTGAATCTCG	Rx21	M1704617	GAAAAAAGCTCTTCTTTCCGC AGGCATAAAGTGCCACAAC
Rx5	F20713033	TGAAATTGGTGCTCTTCCAAC CCTCGTCAAGATTTGTTTCCG	Rx22	M17432556	AGAACAGGCAAGAATGTCTATC CTTCTCGAACAGCAGTAGC
Rx6	F2310454	CGAGGAAATCAAATGGAGCATC CCATAGACTGCGAAAACCC	Rx23	M19428070	GGAGTTTAACCTACGGTAGGG ACCGTGCATACTCAATCAAAG
Rx7	F25581559	GGTTACAGATGTGCAGGATG ACAAGATGCGTGAGAGCAG	Rx24	M21206660	CAAACCAAAGGATGAAACTCAC TGATTAATGTTTCCTTGGCCC
Rx8	F26050110	GCTTAAGATTTGATGCTCTTGC GAATCTTTTCCCCTTGCCTG	Rx25	M22110263	AGTGGGTTTGGGGGATTTG TTCAGTACAACTACCAAGCAC
Rx9	F36548753	CGAGACAAGCTAAGTCTGAAC GACAAGATTCAACCCTAGCTTC	Rx26	M22146179	AGCTGCAAACAACATGGAC AGAGGCGAAACTTTTCCTAAC
Rx10	F3663458	TTGAAACAAGCTGGATATAGCC CAAAAATACGACTTTCCATGCC	Rx27	M24152935	AGCAATCCTACGTGACAGC TCTAGATTGAAAGAGGGGGTG
Rx11	F37007195	TGATTTCCTCATCAAGCAACAC TTAAGTTCTTTGGGTTCCGAC	Rx28	M25938614	TTGAGGCATACCTCTCACC TGTGGGATGATTTGAAGACAC
Rx12	F44091788	TCTACTTCCAATTGCAACGATG GGGCTTGTTTGTTGACTTTG	Rx29	M2696007	TCAAGAGTGCTTGGCACAG CTTGAATTTACGCAGCATCAG
Rx13	F5567539	CGCATTTTTATGGTGCTGC GCTCCATCCAATCTTCCAGG	Rx30	M27531625	AGGGAGAAGTGAATGGTGGC ATCTACGAAACCACCTGTAACC
Rx14	F5883398	TGCAGTTTCCAAAGTCGTTAG CAATCCTGCTCATTAAGCTCG	Rx31	M31773413	GCTCCTATGTTCTGGCACAC CCGTTATGATAGATCGGATTGC
Rx15	F5936656	GTCACAATGGAGCAATTTTACC ACAGCTTGATTCAATCTGGTC	Rx32	M32128495	AGATGGCCTAGTGATATACGC GTTTAGTACGACTACCTTCCAC
Rx16	F6118470	ACATCTGGGAATCAACTTCAC CCCAAACGAGAAAAGAAGCTG	Rx33	M35343149	TGTGACCTAAGAGTGTCCTC TGACATGCTCACATGAAATAGC
Rx17	F6386942	CATCTTTTGTTCTTGGGATTCG CCATGAAACAGGTCCATGAG	Rx34	M44553680	TGTTTCTAAAGCCTAGTTGCC TTTGCTCTCGGTTTGCAC
			Rx35	M6969018	ACTTGCCAGACTCTAAGAAAAG TCCACTATTCCCATAAACATGC

(a)

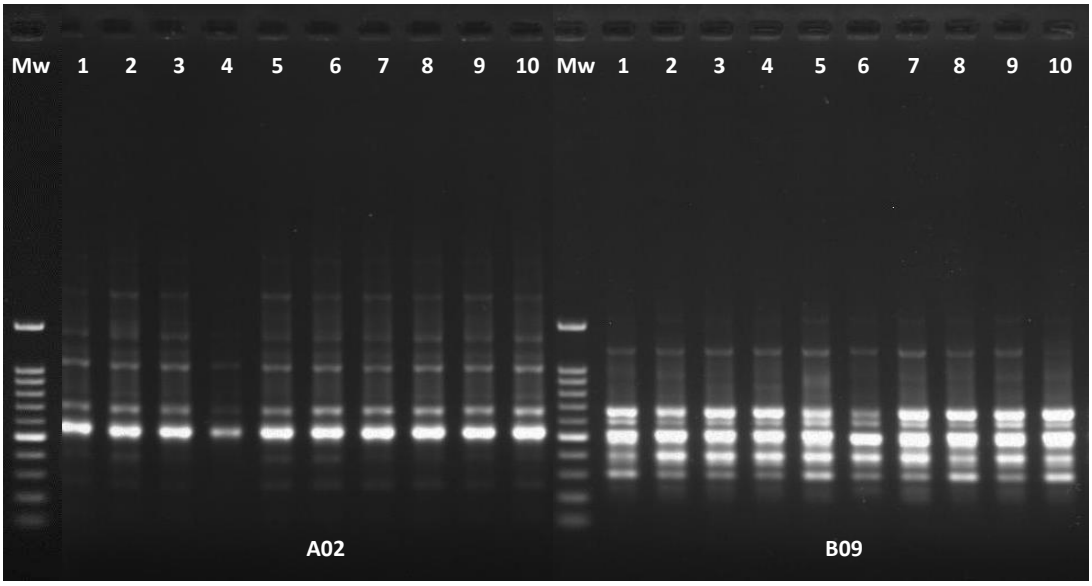

(b)

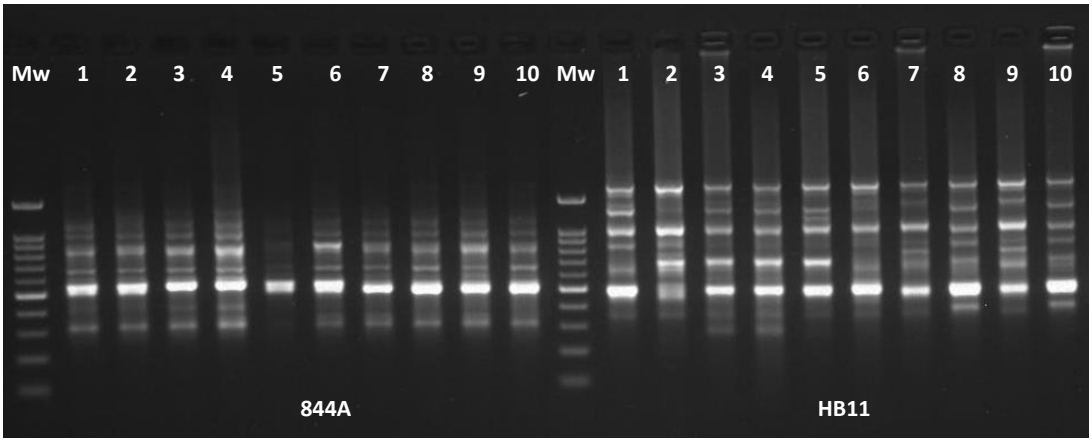

Supplementary File S2.

(c)

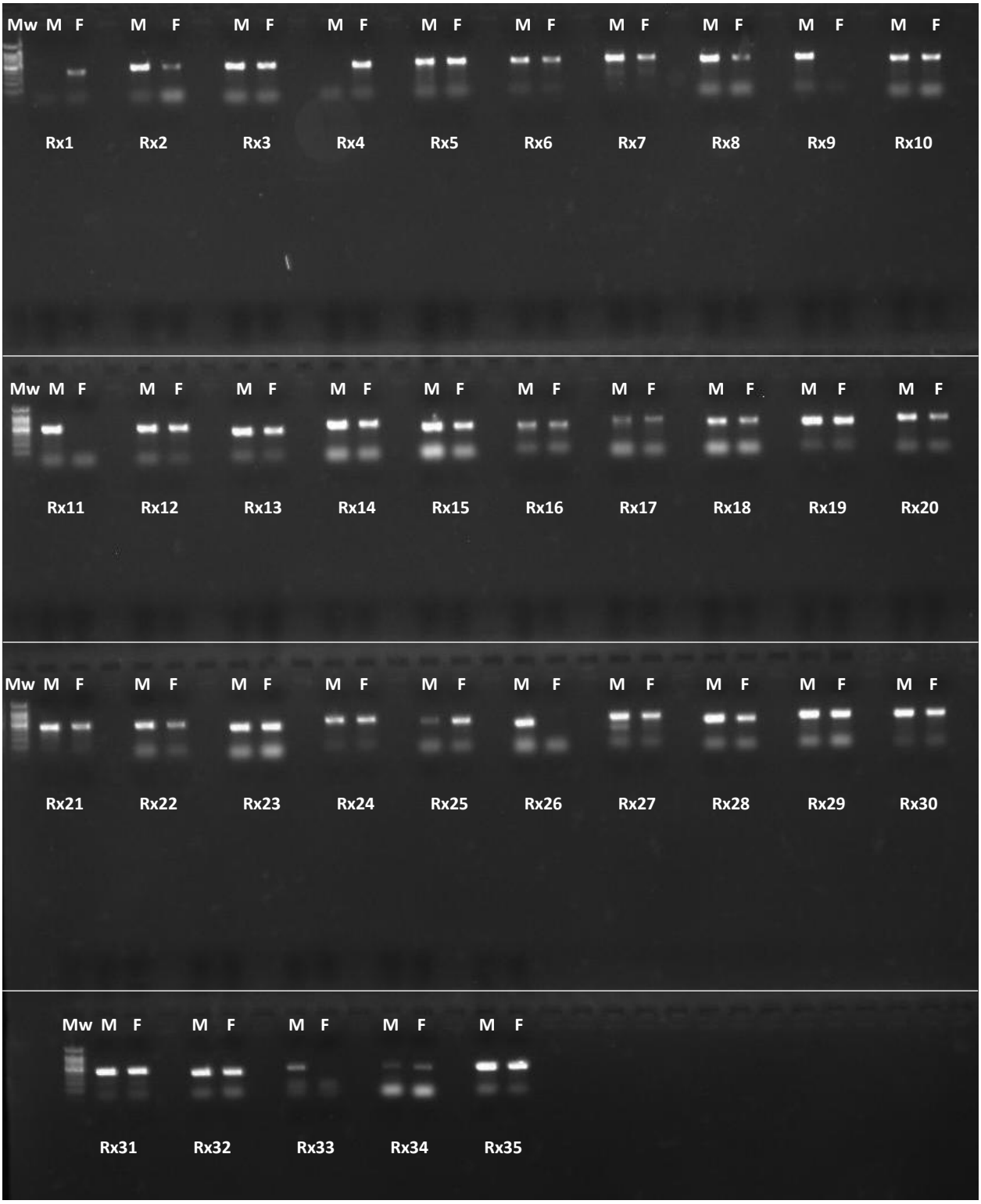

Supplementary File S2. Continued

(d)

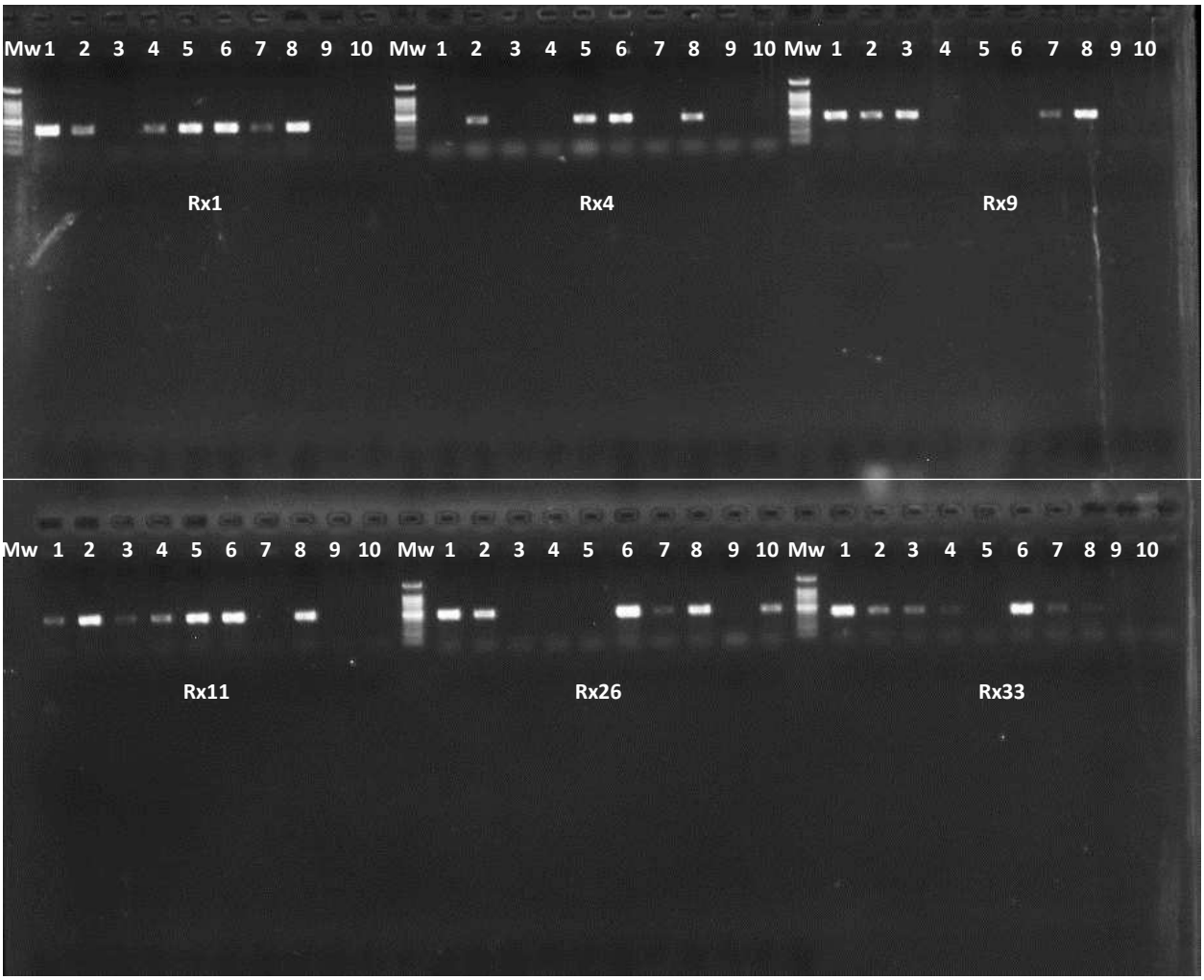

Supplementary File S2. Continued

Consensus

1. J1-F
2. J2-F
3. J3-F
4. J4-F
5. J5-F
6. J6-F
7. J7-F
8. J8-F
9. J9-F
0. J10-F

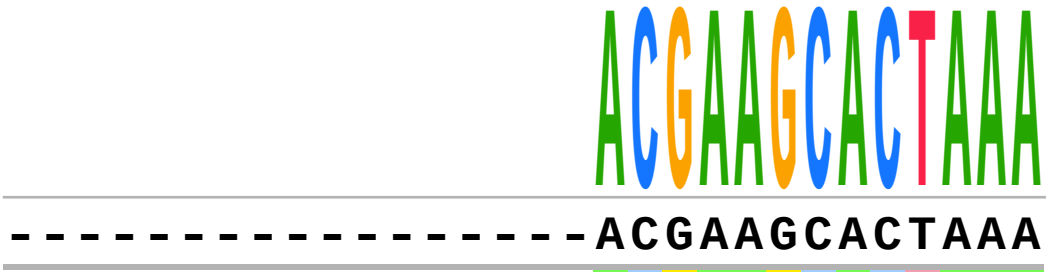

	----------ACGAAGCACTAAA	
1	----------ACGAAGCACTAAA	13
2	----------ACGAAGCACTAAA	13
3	----------ACGAAGCACTAAA	13
4	----------ACGAAGCACTAAA	13
5	----------ACGAAGCACTAAA	13
6	----------ACGAAGCACTAAA	13
7	----------ACGAAGCACTAAA	13
8	----------ACGAAGCACTAAA	13
9	----------ACGAAGCACTAAA	13
10	----------ACGAAGCACTAAA	13

ACTAGGGGATAAATGAGCCGAATCGAGCCA

1	ACTAGGGGATAAATGAGCCGAATCGAGCCA	43
2	ACTAGGGGATAAATGAGCCGAATCGAGCCA	43
3	ACTAGGGGATAAATGAGCCGAATCGAGCCA	43
4	ACTAGGGGATAAATGAGCCGAATCGAGCCA	43
5	ACTAGGGGATAAATGAGCCGAATCGAGCCA	43
6	ACTAGGGGATAAATGAGCCGAATCGAGCCA	43
7	ACTAGGGGATAAATGAGCCGAATCGAGCCA	43
8	ACTAGGGGATAAATGAGCCGAATCGAGCCA	43
9	ACTAGGGGATAAATGAGCCGAATCGAGCCA	43
10	ACTAGGGGATAAATGAGCCGAATCGAGCCA	43

AGCACCTCCTTTTTTGAACTCGATCTCGAT

1	AGCACCTCCTTTTTTGAACTCGATCTCGAT	73
2	AGCACCTCCTTTTTTGAACTCGATCTCGAT	73
3	AGCACCTCCTTTTTTGAACTCGATCTCGAT	73
4	AGCACCTCCTTTTTTGAACTCGATCTCGAT	73
5	AGCACCTCCTTTTTTGAACTCGATCTCGAT	73
6	AGCACCTCCTTTTTTGAACTCGATCTCGAT	73
7	TGCACCTCCTTTTTTGAACTCGATCTCGAT	73
8	TGCACCTCCTTTTTTGAACTCGATCTCGAT	73
9	TGCACCTCCTTTTTTGAACTCGATCTCGAT	73
10	TGCACCTCCTTTTTTGAACTCGATCTCGAT	73

GAGACTTATCAAGCTCGAGTTTAAGCCGAG

1	GAGACTTATCAAGCTCGAGTTTAAGCCGAG	103
2	GAGACTTATCAAGCTCGAGTTTAAGCCGAG	103
3	GAGACTTATCAAGCTCGAGTTTAAGCCGAG	103
4	GAGACTTATCAAGCTCGAGTTTAAGCCGAG	103
5	GAGACTTATCAAGCTCGAGTTTAAGCCGAG	103
6	GAGACTTATCAAGCTCGAGTTTAAGCCGAG	103
7	GAGACTTATCAAGCTCGAGTTTAAGCCGAG	103
8	GAGACTTATCAAGCTCGAGTTTAAGCCGAG	103
9	GAGACTTATCAAGCTCGAGTTTAAGCCGAG	103
10	GAGACTTATCAAGCTCGAGTTTAAGCCGAG	103

CTCTTATTGAACTTTCAAACCTTTGCTTGA

1	CTCTTATTGAACTTTCAAACCTTTGCTTGA	133
2	CTCTTATTGAACTTTCAAACCTTTGCTTGA	133
3	CTCTTATTGAACTTTCAAACCTTTGCTTGA	133
4	CTCTTATTGAACTTTCAAACCTTTGCTTGA	133
5	CTCTTATTGAACTTTCAAACCTTTGCTTGA	133
6	CTCTTATTGAACTTTCAAACCTTTGCTTGA	133
7	CTCTTATTGAACTTTCAAACCTTTGCTTGA	133
8	CTCTTATTGAACTTTCAAACCTTTGCTTGA	133
9	CTCTTATTGAACTTTCAAACCTTTGCTTGA	133
10	CTCTTATTGAACTTTCAAACCTTTGCTTGA	133

GCTCNAATTGATAAGGTATTAGTCTATTTG

1	GCTCGAATTGATAAGGTATTAGTCTATTTG	163
2	GCTCGAATTGATAAGGTATTAGTCTATTTG	163
3	GCTCGAATTGATAAGGTATTAGTCTATTTG	163
4	GCTCGAATTGATAAGGTATTAGTCTATTTG	163
5	GCTCGAATTGATAAGGTATTAGTCTATTTG	163
6	GCTCAAATTGATAAGGTATTAGTCTATTTG	163
7	GCTCAAATTGATAAGGTATTAGTCTATTTG	163
8	GCTCAAATTGATAAGGTATTAGTCTATTTG	163
9	GCTCAAATTGATAAGGTATTAGTCTATTTG	163
10	GCTCAAATTGATAAGGTATTAGTCTATTTG	163

ATATTCAACTCAACTTGGCTCATTAGCCTG

1	ATATTCAACTCAACTTGGCTCATTAGCCTG	193
2	ATATTCAACTCAACTTGGCTCATTAGCCTG	193
3	ATATTCAACTCAACTTGGCTCATTAGCCTG	193
4	ATATTCAACTCAACTTGGCTCATTAGCCTG	193
5	ATATTCAACTCAACTTGGCTCATTAGCCTG	193
6	ATATTCAACTCAACTTGGCTCATTAGCCTG	193
7	ATATTCAACTCAACTTGGCTCATTAGCCTG	193
8	ATATTCAACTCAACTTGGCTCATTAGCCTG	193
9	ATATTCAACTCAACTTGGCTCATTAGCCTG	193
10	ATATTCAACTCAACTTGGCTCATTAGCCTG	193

ATTGAACCGATTCAAGCCTGTTATCTACAC

1	ATTGAACCGATTCAAGCCTGTTATCTACAC	223
2	ATTGAACCGATTCAAGCCTGTTATCTACAC	223
3	ATTGAACCGATTCAAGCCTGTTATCTACAC	223
4	ATTGAACCGATTCAAGCCTGTTATCTACAC	223
5	ATTGAACCGATTCAAGCCTGTTATCTACAC	223
6	ATTGAACCGATTCAAGCCTGTTATCTACAC	223
7	ATTGAACCGATTCAAGCCTGTTATCTACAC	223
8	ATTGAACCGATTCAAGCCTGTTATCTACAC	223
9	ATTGAACCGATTCAAGCCTGTTATCTACAC	223
10	ATTGAACCGATTCAAGCCTGTTATCTACAC	223

GAGCTGAGCTAATTATGGAGCTAAATCAAG

1	GAGCTGAGCTAATTATGGAGCTAAATCAAG	253
2	GAGCTGAGCTAATTATGGAGCTAAATCAAG	253
3	GAGCTGAGCTAATTATGGAGCTAAATCAAG	253
4	GAGCTGAGCTAATTATGGAGCTAAATCAAG	253
5	GAGCTGAGCTAATTATGGAGCTAAATCAAG	253
6	GAGCTGAGCTAATTATGGAGCTAAATCAAG	253
7	GAGCTGAGCTAATTATGGAGCTAAATCAAG	253
8	GAGCTGAGCTAATTATGGAGCTAAATCAAG	253
9	GAGCTGAGCTAATTATGGAGCTAAATCAAG	253
10	GAGCTGAGCTAATTATGGAGCTAAATCAAG	253

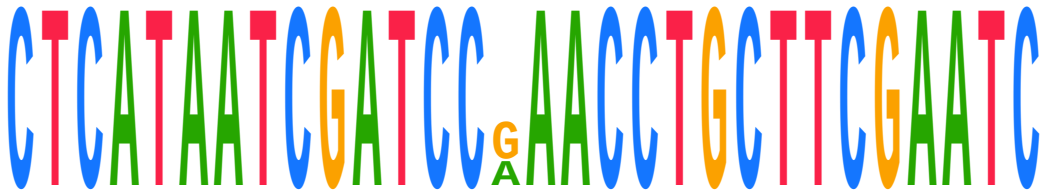

CTCATAATCGATCCGAACCTGCTTCGAATC

1	CTCATAATCGATCCGAACCTGCTTCGAATC	283
2	CTCATAATCGATCCGAACCTGCTTCGAATC	283
3	CTCATAATCGATCCGAACCTGCTTCGAATC	283
4	CTCATAATCGATCCGAACCTGCTTCGAATC	283
5	CTCATAATCGATCCGAACCTGCTTCGAATC	283
6	CTCATAATCGATCCGAACCTGCTTCGAATC	283
7	CTCATAATCGATCCAAACCTGCTTCGAATC	283
8	CTCATAATCGATCCAAACCTGCTTCGAATC	283
9	CTCATAATCGATCCAAACCTGCTTCGAATC	283
10	CTCATAATCGATCCAAACCTGCTTCGAATC	283

GAGCTCACTATCAAGCTAAGCTATTTAAGT

1	GAGCTCACTATCAAGCTAAGCTATTTAAGT	313
2	GAGCTCACTATCAAGCTAAGCTATTTAAGT	313
3	GAGCTCACTATCAAGCTAAGCTATTTAAGT	313
4	GAGCTCACTATCAAGCTAAGCTATTTAAGT	313
5	GAGCTCACTATCAAGCTAAGCTATTTAAGT	313
6	GAGCTCACTATCAAGCTAAGCTATTTAAGT	313
7	GAGCTCACTATCAAGCTAAGCTATTTAAGT	313
8	GAGCTCACTATCAAGCTAAGCTATTTAAGT	313
9	GAGCTCACTATCAAGCTAAGCTATTTAAGT	313
10	GAGCTCACTATCAAGCTAAGCTATTTAAGT	313

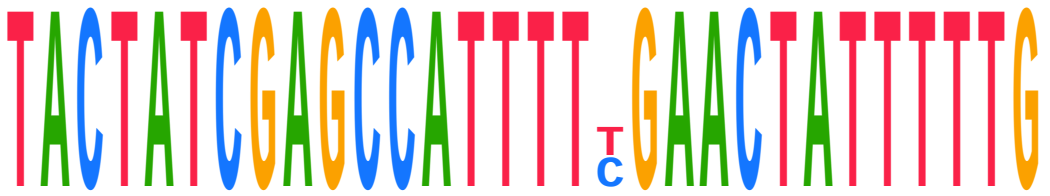

TACTATCGAGCCATTTTNGAACTATTTTTG

1	TACTATCGAGCCATTTTCGAACTATTTTTG	343
2	TACTATCGAGCCATTTTCGAACTATTTTTG	343
3	TACTATCGAGCCATTTTCGAACTATTTTTG	343
4	TACTATCGAGCCATTTTCGAACTATTTTTG	343
5	TACTATCGAGCCATTTTCGAACTATTTTTG	343
6	TACTATCGAGCCATTTTTGAACTATTTTTG	343
7	TACTATCGAGCCATTTTTGAACTATTTTTG	343
8	TACTATCGAGCCATTTTTGAACTATTTTTG	343
9	TACTATCGAGCCATTTTTGAACTATTTTTG	343
10	TACTATCGAGCCATTTTTGAACTATTTTTG	343

AGCTAATACCTATTGTTAACGAACCATTAA

1	AGCTAATACCTATTGTTAACGAACCATTAA	373
2	AGCTAATACCTATTGTTAACGAACCATTAA	373
3	AGCTAATACCTATTGTTAACGAACCATTAA	373
4	AGCTAATACCTATTGTTAACGAACCATTAA	373
5	AGCTAATACCTATTGTTAACGAACCATTAA	373
6	AGCTAATACCTATTGTTAACGAACCATTAA	373
7	AGCTAATACCTATTGTTAACGAACCATTAA	373
8	AGCTAATACCTATTGTTAACGAACCATTAA	373
9	AGCTAATACCTATTGTTAACGAACCATTAA	373
10	AGCTAATACCTATTGTTAACGAACCATTAA	373

TATTAACGACTCAAAACATCTCCCGTTCGA

1	TATTAACGACTCAAAACATCTCCCGTTCGA	403
2	TATTAACGACTCAAAACATCTCCCGTTCGA	403
3	TATTAACGACTCAAAACATCTCCCGTTCGA	403
4	TATTAACGACTCAAAACATCTCCCGTTCGA	403
5	TATTAACGACTCAAAACATCTCCCGTTCGA	403
6	TATTAACGACTCAAAACATCTCCCGTTCGA	403
7	TATTAACGACTCAAAACATCTCCCGTTCGA	403
8	TATTAACGACTCAAAACATCTCCCGTTCGA	403
9	TATTAACGACTCAAAACATCTCCCGTTCGA	403
10	TATTAACGACTCAAAACATCTCCCGTTCGA	403

ACTCGGCTCGTTAATGTTATGGAGTTTGCT

1	ACTCGGCTCGTTAATGTTATGGAGTTTGCT	433
2	ACTCGGCTCGTTAATGTTATGGAGTTTGCT	433
3	ACTCGGCTCGTTAATGTTATGGAGTTTGCT	433
4	ACTCGGCTCGTTAATGTTATGGAGTTTGCT	433
5	ACTCGGCTCGTTAATGTTATGGAGTTTGCT	433
6	ACTCGGCTCGTTAATGTTATGGAGTTTGCT	433
7	ACTCGGCTCGTTAATGTTATGGAGTTTGCT	433
8	ACTCGGCTCGTTAATGTTATGGAGTTTGCT	433
9	ACTCGGCTCGTTAATGTTATGGAGTTTGCT	433
10	ACTCGGCTCGTTAATGTTATGGAGTTTGCT	433

CAAACTCGGCTCGATAAGCTTTCAAGCTCC

1	CAAACTCGGCTCGATAAGCTTTCAAGCTCC	463
2	CAAACTCGGCTCGATAAGCTTTCAAGCTCC	463
3	CAAACTCGGCTCGATAAGCTTTCAAGCTCC	463
4	CAAACTCGGCTCGATAAGCTTTCAAGCTCC	463
5	CAAACTCGGCTCGATAAGCTTTCAAGCTCC	463
6	CAAACTCGGCTCGATAAGCTTTCAAGCTCC	463
7	CAAACTCGGCTCGATAAGCTTTCAAGCTCC	463
8	CAAACTCGGCTCGATAAGCTTTCAAGCTCC	463
9	CAAACTCGGCTCGATAAGCTTTCAAGCTCC	463
10	CAAACTCGGCTCGATAAGCTTTCAAGCTCC	463

CAAAATGAACATGAACAAGTTGCAATCGAT

1	CAAAATGAACATGAACAAGTTGCAATCGAT	493
2	CAAAATGAACATGAACAAGTTGCAATCGAT	493
3	CAAAATGAACATGAACAAGTTGCAATCGAT	493
4	CAAAATGAACATGAACAAGTTGCAATCGAT	493
5	CAAAATGAACATGAACAAGTTGCAATCGAT	493
6	CAAAATGAACATGAACAAGTTGCAATCGAT	493
7	CAAAATGAACATGAACAAGTTGCAATCGAT	493
8	CAAAATGAACATGAACAAGTTGCAATCGAT	493
9	CAAAATGAACATGAACAAGTTGCAATCGAT	493
10	CAAAATGAACATGAACAAGTTGCAATCGAT	493

TTCAAAAACGAGTAGTTTAGAATATTTGGT

1	TTCAAAAACGAGTAGTTTAGAATATTTGGT	523
2	TTCAAAAACGAGTAGTTTAGAATATTTGGT	523
3	TTCAAAAACGAGTAGTTTAGAATATTTGGT	523
4	TTCAAAAACGAGTAGTTTAGAATATTTGGT	523
5	TTCAAAAACGAGTAGTTTAGAATATTTGGT	523
6	TTCAAAAACGAGTAGTTTAGAATATTTGGT	523
7	TTCAAAAACGAGTAGTTTAGAATATTTGGT	523
8	TTCAAAAACGAGTAGTTTAGAATATTTGGT	523
9	TTCAAAAACGAGTAGTTTAGAATATTTGGT	523
10	TTCAAAAACGAGTAGTTTAGAATATTTGGT	523

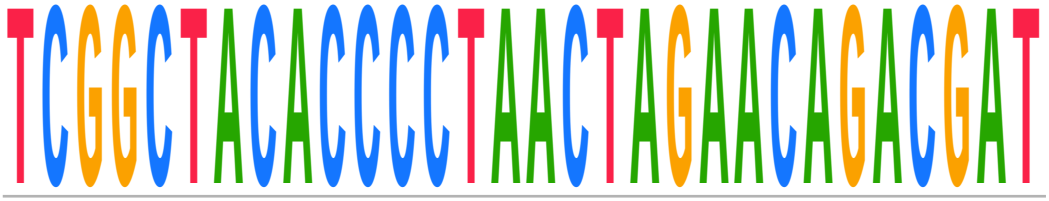

TCGGCTACACCCCTAACTAGAACAGACGAT

1	TCGGCTACACCCCTAACTAGAACAGACGAT	553
2	TCGGCTACACCCCTAACTAGAACAGACGAT	553
3	TCGGCTACACCCCTAACTAGAACAGACGAT	553
4	TCGGCTACACCCCTAACTAGAACAGACGAT	553
5	TCGGCTACACCCCTAACTAGAACAGACGAT	553
6	TCGGCTACACCCCTAACTAGAACAGACGAT	553
7	TCGGCTACACCCCTAACTAGAACAGACGAT	553
8	TCGGCTACACCCCTAACTAGAACAGACGAT	553
9	TCGGCTACACCCCTAACTAGAACAGACGAT	553
10	TCGGCTACACCCCTAACTAGAACAGACGAT	553

ATTGAGCAAGGCAATTACGTAATAAGCTAT

1	ATTGAGCAAGGCAATTACGTAATAAGCTAT	583
2	ATTGAGCAAGGCAATTACGTAATAAGCTAT	583
3	ATTGAGCAAGGCAATTACGTAATAAGCTAT	583
4	ATTGAGCAAGGCAATTACGTAATAAGCTAT	583
5	ATTGAGCAAGGCAATTACGTAATAAGCTAT	583
6	ATTGAGCAAGGCAATTACGTAATAAGCTAT	583
7	ATTGAGCAAGGCAATTACGTAATAAGCTAT	583
8	ATTGAGCAAGGCAATTACGTAATAAGCTAT	583
9	ATTGAGCAAGGCAATTACGTAATAAGCTAT	583
10	ATTGAGCAAGGCAATTACGTAATAAGCTAT	583

TCAATGGATGAAAAGGTGAAATAAAAACTT

1	TCAATGGATGAAAAGGTGAAATAAAAACTT	613
2	TCAATGGATGAAAAGGTGAAATAAAAACTT	613
3	TCAATGGATGAAAAGGTGAAATAAAAACTT	613
4	TCAATGGATGAAAAGGTGAAATAAAAACTT	613
5	TCAATGGATGAAAAGGTGAAATAAAAACTT	613
6	TCAATGGATGAAAAGGTGAAATAAAAACTT	613
7	TCAATGGATGAAAAGGTGAAATAAAAACTT	613
8	TCAATGGATGAAAAGGTGAAATAAAAACTT	613
9	TCAATGGATGAAAAGGTGAAATAAAAACTT	613
10	TCAATGGATGAAAAGGTGAAATAAAAACTT	613

CGTTCATACATTGAAGAAAGATACTAGCAG

1	CGTTCATACATTGAAGAAAGATACTAGCAG	643
2	CGTTCATACATTGAAGAAAGATACTAGCAG	643
3	CGTTCATACATTGAAGAAAGATACTAGCAG	643
4	CGTTCATACATTGAAGAAAGATACTAGCAG	643
5	CGTTCATACATTGAAGAAAGATACTAGCAG	643
6	CGTTCATACATTGAAGAAAGATACTAGCAG	643
7	CGTTCATACATTGAAGAAAGATACTAGCAG	643
8	CGTTCATACATTGAAGAAAGATACTAGCAG	643
9	CGTTCATACATTGAAGAAAGATACTAGCAG	643
10	CGTTCATACATTGAAGAAAGATACTAGCAG	643

AGATTAGGTAATAAGCTATTCAATAAATTT

1	AGATTAGGTAATAAGCTATTCAATAAATTT	673
2	AGATTAGGTAATAAGCTATTCAATAAATTT	673
3	AGATTAGGTAATAAGCTATTCAATAAATTT	673
4	AGATTAGGTAATAAGCTATTCAATAAATTT	673
5	AGATTAGGTAATAAGCTATTCAATAAATTT	673
6	AGATTAGGTAATAAGCTATTCAATAAATTT	673
7	AGATTAGGTAATAAGCTATTCAATAAATTT	673
8	AGATTAGGTAATAAGCTATTCAATAAATTT	673
9	AGATTAGGTAATAAGCTATTCAATAAATTT	673
10	AGATTAGGTAATAAGCTATTCAATAAATTT	673

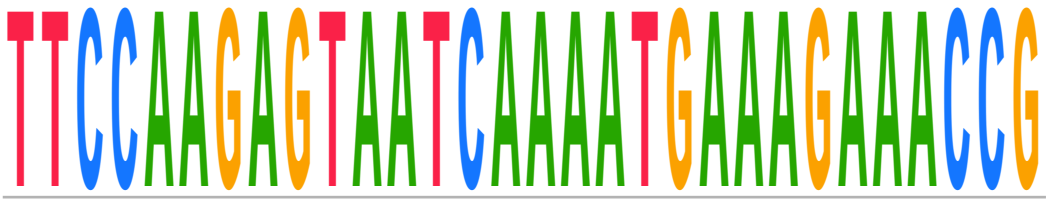

TTCCAAGAGTAATCAAAATGAAAGAAACCG

1	TTCCAAGAGTAATCAAAATGAAAGAAACCG	703
2	TTCCAAGAGTAATCAAAATGAAAGAAACCG	703
3	TTCCAAGAGTAATCAAAATGAAAGAAACCG	703
4	TTCCAAGAGTAATCAAAATGAAAGAAACCG	703
5	TTCCAAGAGTAATCAAAATGAAAGAAACCG	703
6	TTCCAAGAGTAATCAAAATGAAAGAAACCG	703
7	TTCCAAGAGTAATCAAAATGAAAGAAACCG	703
8	TTCCAAGAGTAATCAAAATGAAAGAAACCG	703
9	TTCCAAGAGTAATCAAAATGAAAGAAACCG	703
10	TTCCAAGAGTAATCAAAATGAAAGAAACCG	703

GACAGTACTCCTAAAGGACTTGCCTTATAA

1	GACAGTACTCCTAAAGGACTTGCCTTATAA	733
2	GACAGTACTCCTAAAGGACTTGCCTTATAA	733
3	GACAGTACTCCTAAAGGACTTGCCTTATAA	733
4	GACAGTACTCCTAAAGGACTTGCCTTATAA	733
5	GACAGTACTCCTAAAGGACTTGCCTTATAA	733
6	GACAGTACTCCTAAAGGACTTGCCTTATAA	733
7	GACAGTACTCCTAAAGGACTTGCCTTATAA	733
8	GACAGTACTCCTAAAGGACTTGCCTTATAA	733
9	GACAGTACTCCTAAAGGACTTGCCTTATAA	733
10	GACAGTACTCCTAAAGGACTTGCCTTATAA	733

GTAGCAACATCTTGCCAACTGAGCTTTCTG

1	GTAGCAACATCTTGCCAACTGAGCTTTCTG	763
2	GTAGCAACATCTTGCCAACTGAGCTTTCTG	763
3	GTAGCAACATCTTGCCAACTGAGCTTTCTG	763
4	GTAGCAACATCTTGCCAACTGAGCTTTCTG	763
5	GTAGCAACATCTTGCCAACTGAGCTTTCTG	763
6	GTAGCAACATCTTGCCAACTGAGCTTTCTG	763
7	GTAGCAACATCTTGCCAACTGAGCTTTCTG	763
8	GTAGCAACATCTTGCCAACTGAGCTTTCTG	763
9	GTAGCAACATCTTGCCAACTGAGCTTTCTG	763
10	GTAGCAACATCTTGCCAACTGAGCTTTCTG	763

CCTTCGAATTCCACGGAAACATAATCAACG

1	CCTTCGAATTCCACGGAAACATAATCAACG	793
2	CCTTCGAATTCCACGGAAACATAATCAACG	793
3	CCTTCGAATTCCACGGAAACATAATCAACG	793
4	CCTTCGAATTCCACGGAAACATAATCAACG	793
5	CCTTCGAATTCCACGGAAACATAATCAACG	793
6	CCTTCGAATTCCACGGAAACATAATCAACG	793
7	CCTTCGAATTCCACGGAAACATAATCAACG	793
8	CCTTCGAATTCCACGGAAACATAATCAACG	793
9	CCTTCGAATTCCACGGAAACATAATCAACG	793
10	CCTTCGAATTCCACGGAAACATAATCAACG	793

TCATCAAGTTGTCTTCGCTTTTTGGGTTGG

1	TCATCAAGTTGTCTTCGCTTTTTGGGTTGG	823
2	TCATCAAGTTGTCTTCGCTTTTTGGGTTGG	823
3	TCATCAAGTTGTCTTCGCTTTTTGGGTTGG	823
4	TCATCAAGTTGTCTTCGCTTTTTGGGTTGG	823
5	TCATCAAGTTGTCTTCGCTTTTTGGGTTGG	823
6	TCATCAAGTTGTCTTCGCTTTTTGGGTTGG	823
7	TCATCAAGTTGTCTTCGCTTTTTGGGTTGG	823
8	TCATCAAGTTGTCTTCGCTTTTTGGGTTGG	823
9	TCATCAAGTTGTCTTCGCTTTTTGGGTTGG	823
10	TCATCAAGTTGTCTTCGCTTTTTGGGTTGG	823

CATTC----------------

1	CATTC----------------	828
2	CATTC----------------	828
3	CATTC----------------	828
4	CATTC----------------	828
5	CATTC----------------	828
6	CATTC----------------	828
7	CATTC----------------	828
8	CATTC----------------	828
9	CATTC----------------	828
10	CATTC----------------	828

Sequence Logo: 50% GC base composition

Consensus Threshold: >50%

Compare to: the consensus

Bases that match the reference are marked with 4-color highlighting.

Created: 29 Dec 2019

Last Modified: 29 Dec 2019

Consensus

1. J9-R
2. J8-R
3. J7-R
4. J5-R
5. J1-R
6. J2-R
7. J3-R
8. J4-R
9. J6-R
0. J10-R

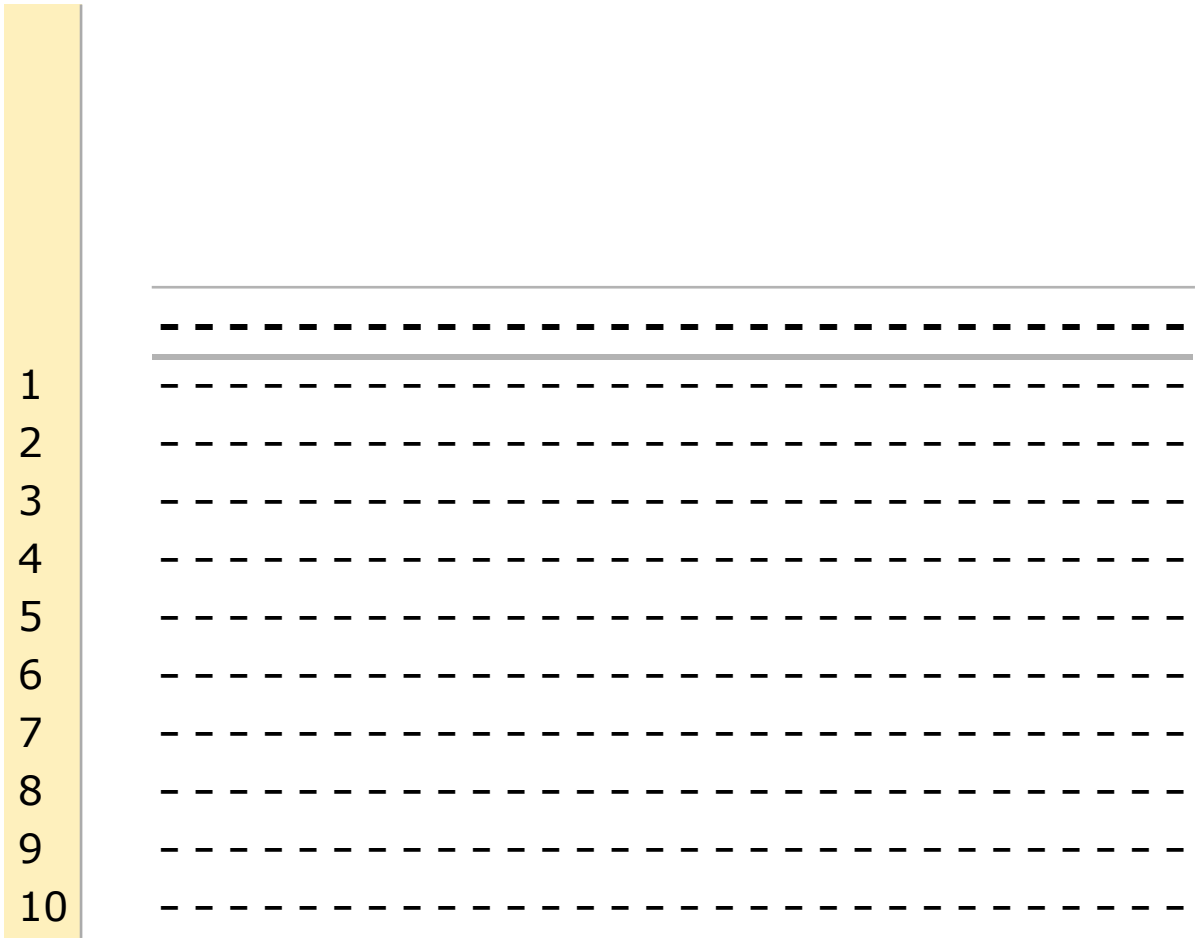

```
   ------------------------------
1  ------------------------------
2  ------------------------------
3  ------------------------------
4  ------------------------------
5  ------------------------------
6  ------------------------------
7  ------------------------------
8  ------------------------------
9  ------------------------------
10 ------------------------------
```

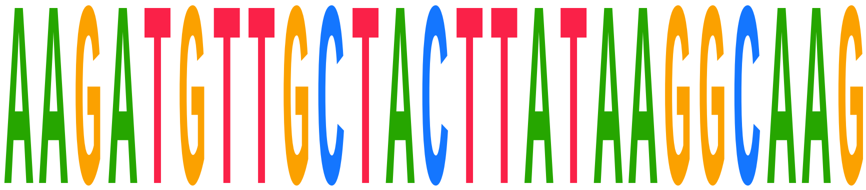

```
   -----AAGATGTTGCTACTTATAAGGCAAG
1  -----AAGATGTTGCTACTTATAAGGCAAG 25
2  -----AAGATGTTGCTACTTATAAGGCAAG 25
3  -----AAGATGTTGCTACTTATAAGGCAAG 25
4  -----AAGATGTTGCTACTTATAAGGCAAG 25
5  -----AAGATGTTGCTACTTATAAGGCAAG 25
6  -----AAGATGTTGCTACTTATAAGGCAAG 25
7  -----AAGATGTTGCTACTTATAAGGCAAG 25
8  -----AAGATGTTGCTACTTATAAGGCAAG 25
9  -----AAGATGTTGCTACTTATAAGGCAAG 25
10 -----AAGATGTTGCTACTTATAAGGCAAG 25
```

TCCTTTAGGAGTACTGTCCGGTTTCTTTCA

1	TCCTTTAGGAGTACTGTCCGGTTTCTTTCA	55
2	TCCTTTAGGAGTACTGTCCGGTTTCTTTCA	55
3	TCCTTTAGGAGTACTGTCCGGTTTCTTTCA	55
4	TCCTTTAGGAGTACTGTCCGGTTTCTTTCA	55
5	TCCTTTAGGAGTACTGTCCGGTTTCTTTCA	55
6	TCCTTTAGGAGTACTGTCCGGTTTCTTTCA	55
7	TCCTTTAGGAGTACTGTCCGGTTTCTTTCA	55
8	TCCTTTAGGAGTACTGTCCGGTTTCTTTCA	55
9	TCCTTTAGGAGTACTGTCCGGTTTCTTTCA	55
10	TCCTTTAGGAGTACTGTCCGGTTTCTTTCA	55

TTTTGATTACTCTTGGAAAAATTTATTGAA

1	TTTTGATTACTCTTGGAAAAATTTATTGAA	85
2	TTTTGATTACTCTTGGAAAAATTTATTGAA	85
3	TTTTGATTACTCTTGGAAAAATTTATTGAA	85
4	TTTTGATTACTCTTGGAAAAATTTATTGAA	85
5	TTTTGATTACTCTTGGAAAAATTTATTGAA	85
6	TTTTGATTACTCTTGGAAAAATTTATTGAA	85
7	TTTTGATTACTCTTGGAAAAATTTATTGAA	85
8	TTTTGATTACTCTTGGAAAAATTTATTGAA	85
9	TTTTGATTACTCTTGGAAAAATTTATTGAA	85
10	TTTTGATTACTCTTGGAAAAATTTATTGAA	85

TAGCTTATTACCTAATCTCTGCTAGTATCT

1	TAGCTTATTACCTAATCTCTGCTAGTATCT	115
2	TAGCTTATTACCTAATCTCTGCTAGTATCT	115
3	TAGCTTATTACCTAATCTCTGCTAGTATCT	115
4	TAGCTTATTACCTAATCTCTGCTAGTATCT	115
5	TAGCTTATTACCTAATCTCTGCTAGTATCT	115
6	TAGCTTATTACCTAATCTCTGCTAGTATCT	115
7	TAGCTTATTACCTAATCTCTGCTAGTATCT	115
8	TAGCTTATTACCTAATCTCTGCTAGTATCT	115
9	TAGCTTATTACCTAATCTCTGCTAGTATCT	115
10	TAGCTTATTACCTAATCTCTGCTAGTATCT	115

TTCTTCAATGTATGAACGAAGTTTTTATTT

1	TTCTTCAATGTATGAACGAAGTTTTTATTT	145
2	TTCTTCAATGTATGAACGAAGTTTTTATTT	145
3	TTCTTCAATGTATGAACGAAGTTTTTATTT	145
4	TTCTTCAATGTATGAACGAAGTTTTTATTT	145
5	TTCTTCAATGTATGAACGAAGTTTTTATTT	145
6	TTCTTCAATGTATGAACGAAGTTTTTATTT	145
7	TTCTTCAATGTATGAACGAAGTTTTTATTT	145
8	TTCTTCAATGTATGAACGAAGTTTTTATTT	145
9	TTCTTCAATGTATGAACGAAGTTTTTATTT	145
10	TTCTTCAATGTATGAACGAAGTTTTTATTT	145

CACCTTTTCATCCATTGAATAGCTTATTAC

1	CACCTTTTCATCCATTGAATAGCTTATTAC	175
2	CACCTTTTCATCCATTGAATAGCTTATTAC	175
3	CACCTTTTCATCCATTGAATAGCTTATTAC	175
4	CACCTTTTCATCCATTGAATAGCTTATTAC	175
5	CACCTTTTCATCCATTGAATAGCTTATTAC	175
6	CACCTTTTCATCCATTGAATAGCTTATTAC	175
7	CACCTTTTCATCCATTGAATAGCTTATTAC	175
8	CACCTTTTCATCCATTGAATAGCTTATTAC	175
9	CACCTTTTCATCCATTGAATAGCTTATTAC	175
10	CACCTTTTCATCCATTGAATAGCTTATTAC	175

GTAATTGCCTTGCTCAATATCGTCTGTTCT

1	GTAATTGCCTTGCTCAATATCGTCTGTTCT	205
2	GTAATTGCCTTGCTCAATATCGTCTGTTCT	205
3	GTAATTGCCTTGCTCAATATCGTCTGTTCT	205
4	GTAATTGCCTTGCTCAATATCGTCTGTTCT	205
5	GTAATTGCCTTGCTCAATATCGTCTGTTCT	205
6	GTAATTGCCTTGCTCAATATCGTCTGTTCT	205
7	GTAATTGCCTTGCTCAATATCGTCTGTTCT	205
8	GTAATTGCCTTGCTCAATATCGTCTGTTCT	205
9	GTAATTGCCTTGCTCAATATCGTCTGTTCT	205
10	GTAATTGCCTTGCTCAATATCGTCTGTTCT	205

AGTTAGGGGTGTAGCCGAACCAAATATTCT

1	AGTTAGGGGTGTAGCCGAACCAAATATTCT	235
2	AGTTAGGGGTGTAGCCGAACCAAATATTCT	235
3	AGTTAGGGGTGTAGCCGAACCAAATATTCT	235
4	AGTTAGGGGTGTAGCCGAACCAAATATTCT	235
5	AGTTAGGGGTGTAGCCGAACCAAATATTCT	235
6	AGTTAGGGGTGTAGCCGAACCAAATATTCT	235
7	AGTTAGGGGTGTAGCCGAACCAAATATTCT	235
8	AGTTAGGGGTGTAGCCGAACCAAATATTCT	235
9	AGTTAGGGGTGTAGCCGAACCAAATATTCT	235
10	AGTTAGGGGTGTAGCCGAACCAAATATTCT	235

AAACTACTCGTTTTTGAAATCGATTGCAAC

1	AAACTACTCGTTTTTGAAATCGATTGCAAC	265
2	AAACTACTCGTTTTTGAAATCGATTGCAAC	265
3	AAACTACTCGTTTTTGAAATCGATTGCAAC	265
4	AAACTACTCGTTTTTGAAATCGATTGCAAC	265
5	AAACTACTCGTTTTTGAAATCGATTGCAAC	265
6	AAACTACTCGTTTTTGAAATCGATTGCAAC	265
7	AAACTACTCGTTTTTGAAATCGATTGCAAC	265
8	AAACTACTCGTTTTTGAAATCGATTGCAAC	265
9	AAACTACTCGTTTTTGAAATCGATTGCAAC	265
10	AAACTACTCGTTTTTGAAATCGATTGCAAC	265

TTGTTCATGTTCATTTTGGGAGCTTGAAAG

1	TTGTTCATGTTCATTTTGGGAGCTTGAAAG	295
2	TTGTTCATGTTCATTTTGGGAGCTTGAAAG	295
3	TTGTTCATGTTCATTTTGGGAGCTTGAAAG	295
4	TTGTTCATGTTCATTTTGGGAGCTTGAAAG	295
5	TTGTTCATGTTCATTTTGGGAGCTTGAAAG	295
6	TTGTTCATGTTCATTTTGGGAGCTTGAAAG	295
7	TTGTTCATGTTCATTTTGGGAGCTTGAAAG	295
8	TTGTTCATGTTCATTTTGGGAGCTTGAAAG	295
9	TTGTTCATGTTCATTTTGGGAGCTTGAAAG	295
10	TTGTTCATGTTCATTTTGGGAGCTTGAAAG	295

CTTATCGAGCCGAGTTTGAGCAAACTCCAT

1	CTTATCGAGCCGAGTTTGAGCAAACTCCAT	325
2	CTTATCGAGCCGAGTTTGAGCAAACTCCAT	325
3	CTTATCGAGCCGAGTTTGAGCAAACTCCAT	325
4	CTTATCGAGCCGAGTTTGAGCAAACTCCAT	325
5	CTTATCGAGCCGAGTTTGAGCAAACTCCAT	325
6	CTTATCGAGCCGAGTTTGAGCAAACTCCAT	325
7	CTTATCGAGCCGAGTTTGAGCAAACTCCAT	325
8	CTTATCGAGCCGAGTTTGAGCAAACTCCAT	325
9	CTTATCGAGCCGAGTTTGAGCAAACTCCAT	325
10	CTTATCGAGCCGAGTTTGAGCAAACTCCAT	325

AACATTAACGAGCCGAGTTCGAACGGGAGA

1	AACATTAACGAGCCGAGTTCGAACGGGAGA	355
2	AACATTAACGAGCCGAGTTCGAACGGGAGA	355
3	AACATTAACGAGCCGAGTTCGAACGGGAGA	355
4	AACATTAACGAGCCGAGTTCGAACGGGAGA	355
5	AACATTAACGAGCCGAGTTCGAACGGGAGA	355
6	AACATTAACGAGCCGAGTTCGAACGGGAGA	355
7	AACATTAACGAGCCGAGTTCGAACGGGAGA	355
8	AACATTAACGAGCCGAGTTCGAACGGGAGA	355
9	AACATTAACGAGCCGAGTTCGAACGGGAGA	355
10	AACATTAACGAGCCGAGTTCGAACGGGAGA	355

TGTTTTGAGTCGTTAATATTAATGGTTCGT

1	TGTTTTGAGTCGTTAATATTAATGGTTCGT	385
2	TGTTTTGAGTCGTTAATATTAATGGTTCGT	385
3	TGTTTTGAGTCGTTAATATTAATGGTTCGT	385
4	TGTTTTGAGTCGTTAATATTAATGGTTCGT	385
5	TGTTTTGAGTCGTTAATATTAATGGTTCGT	385
6	TGTTTTGAGTCGTTAATATTAATGGTTCGT	385
7	TGTTTTGAGTCGTTAATATTAATGGTTCGT	385
8	TGTTTTGAGTCGTTAATATTAATGGTTCGT	385
9	TGTTTTGAGTCGTTAATATTAATGGTTCGT	385
10	TGTTTTGAGTCGTTAATATTAATGGTTCGT	385

TAACAATAGGTATTAGCTCAAAAATAGTTC

1	TAACAATAGGTATTAGCTCAAAAATAGTTC	415
2	TAACAATAGGTATTAGCTCAAAAATAGTTC	415
3	TAACAATAGGTATTAGCTCAAAAATAGTTC	415
4	TAACAATAGGTATTAGCTCAAAAATAGTTC	415
5	TAACAATAGGTATTAGCTCAAAAATAGTTC	415
6	TAACAATAGGTATTAGCTCAAAAATAGTTC	415
7	TAACAATAGGTATTAGCTCAAAAATAGTTC	415
8	TAACAATAGGTATTAGCTCAAAAATAGTTC	415
9	TAACAATAGGTATTAGCTCAAAAATAGTTC	415
10	TAACAATAGGTATTAGCTCAAAAATAGTTC	415

NAAAATGGCTCGATAGTAACTTAAATAGCT

1	AAAAATGGCTCGATAGTAACTTAAATAGCT	445
2	AAAAATGGCTCGATAGTAACTTAAATAGCT	445
3	AAAAATGGCTCGATAGTAACTTAAATAGCT	445
4	GAAAATGGCTCGATAGTAACTTAAATAGCT	445
5	GAAAATGGCTCGATAGTAACTTAAATAGCT	445
6	GAAAATGGCTCGATAGTAACTTAAATAGCT	445
7	GAAAATGGCTCGATAGTAACTTAAATAGCT	445
8	GAAAATGGCTCGATAGTAACTTAAATAGCT	445
9	AAAAATGGCTCGATAGTAACTTAAATAGCT	445
10	AAAAATGGCTCGATAGTAACTTAAATAGCT	445

TAGCTTGATAGTGAGCTCGATTCGAAGCAG

1	TAGCTTGATAGTGAGCTCGATTCGAAGCAG	475
2	TAGCTTGATAGTGAGCTCGATTCGAAGCAG	475
3	TAGCTTGATAGTGAGCTCGATTCGAAGCAG	475
4	TAGCTTGATAGTGAGCTCGATTCGAAGCAG	475
5	TAGCTTGATAGTGAGCTCGATTCGAAGCAG	475
6	TAGCTTGATAGTGAGCTCGATTCGAAGCAG	475
7	TAGCTTGATAGTGAGCTCGATTCGAAGCAG	475
8	TAGCTTGATAGTGAGCTCGATTCGAAGCAG	475
9	TAGCTTGATAGTGAGCTCGATTCGAAGCAG	475
10	TAGCTTGATAGTGAGCTCGATTCGAAGCAG	475

GTTCGGATCGATTATGAGCTTGATTTAGCT

1	GTTCGGATCGATTATGAGCTTGATTTAGCT	505
2	GTTCGGATCGATTATGAGCTTGATTTAGCT	505
3	GTTCGGATCGATTATGAGCTTGATTTAGCT	505
4	GTTCGGATCGATTATGAGCTTGATTTAGCT	505
5	GTTCGGATCGATTATGAGCTTGATTTAGCT	505
6	GTTCGGATCGATTATGAGCTTGATTTAGCT	505
7	GTTCGGATCGATTATGAGCTTGATTTAGCT	505
8	GTTCGGATCGATTATGAGCTTGATTTAGCT	505
9	GTTCGGATCGATTATGAGCTTGATTTAGCT	505
10	GTTTGGATCGATTATGAGCTTGATTTAGCT	505

CCATAATTAGCTCAGCTCGTGTAGATAACA

1	CCATAATTAGCTCAGCTCGTGTAGATAACA	535
2	CCATAATTAGCTCAGCTCGTGTAGATAACA	535
3	CCATAATTAGCTCAGCTCGTGTAGATAACA	535
4	CCATAATTAGCTCAGCTCGTGTAGATAACA	535
5	CCATAATTAGCTCAGCTCGTGTAGATAACA	535
6	CCATAATTAGCTCAGCTCGTGTAGATAACA	535
7	CCATAATTAGCTCAGCTCGTGTAGATAACA	535
8	CCATAATTAGCTCAGCTCGTGTAGATAACA	535
9	CCATAATTAGCTCAGCTCGTGTAGATAACA	535
10	CCATAATTAGCTCAGCTCGTGTAGATAACA	535

GGCTTGAATCGGTTCAATCAGGCTAATGAG

1	GGCTTGAATCGGTTCAATCAGGCTAATGAG	565
2	GGCTTGAATCGGTTCAATCAGGCTAATGAG	565
3	GGCTTGAATCGGTTCAATCAGGCTAATGAG	565
4	GGCTTGAATCGGTTCAATCAGGCTAATGAG	565
5	GGCTTGAATCGGTTCAATCAGGCTAATGAG	565
6	GGCTTGAATCGGTTCAATCAGGCTAATGAG	565
7	GGCTTGAATCGGTTCAATCAGGCTAATGAG	565
8	GGCTTGAATCGGTTCAATCAGGCTAATGAG	565
9	GGCTTGAATCGGTTCAATCAGGCTAATGAG	565
10	GGCTTGAATCGGTTCAATCAGGCTAATGAG	565

CCAAGTTGAGTTGAATATCAAATAGACTAA

1	CCAAGTTGAGTTGAATATCAAATAGACTAA	595
2	CCAAGTTGAGTTGAATATCAAATAGACTAA	595
3	CCAAGTTGAGTTGAATATCAAATAGACTAA	595
4	CCAAGTTGAGTTGAATATCAAATAGACTAA	595
5	CCAAGTTGAGTTGAATATCAAATAGACTAA	595
6	CCAAGTTGAGTTGAATATCAAATAGACTAA	595
7	CCAAGTTGAGTTGAATATCAAATAGACTAA	595
8	CCAAGTTGAGTTGAATATCAAATAGACTAA	595
9	CCAAGTTGAGTTGAATATCAAATAGACTAA	595
10	CCAAGTTGAGTTGAATATCAAATAGACTAA	595

TACCTTATCAATTNGAGCTCAAGCAAAGGT

1	TACCTTATCAATTTGAGCTCAAGCAAAGGT	625
2	TACCTTATCAATTTGAGCTCAAGCAAAGGT	625
3	TACCTTATCAATTTGAGCTCAAGCAAAGGT	625
4	TACCTTATCAATTCGAGCTCAAGCAAAGGT	625
5	TACCTTATCAATTCGAGCTCAAGCAAAGGT	625
6	TACCTTATCAATTCGAGCTCAAGCAAAGGT	625
7	TACCTTATCAATTCGAGCTCAAGCAAAGGT	625
8	TACCTTATCAATTCGAGCTCAAGCAAAGGT	625
9	TACCTTATCAATTTGAGCTCAAGCAAAGGT	625
10	TACCTTATCAATTTGAGCTCAAGCAAAGGT	625

TTGAAAGTTCAATAAGAGCTCGGCTTAAAC

1	TTGAAAGTTCAATAAGAGCTCGGCTTAAAC	655
2	TTGAAAGTTCAATAAGAGCTCGGCTTAAAC	655
3	TTGAAAGTTCAATAAGAGCTCGGCTTAAAC	655
4	TTGAAAGTTCAATAAGAGCTCGGCTTAAAC	655
5	TTGAAAGTTCAATAAGAGCTCGGCTTAAAC	655
6	TTGAAAGTTCAATAAGAGCTCGGCTTAAAC	655
7	TTGAAAGTTCAATAAGAGCTCGGCTTAAAC	655
8	TTGAAAGTTCAATAAGAGCTCGGCTTAAAC	655
9	TTGAAAGTTCAATAAGAGCTCGGCTTAAAC	655
10	TTGAAAGTTCAATAAGAGCTCGGCTTAAAC	655

TCGAGCTTGATAAGTCTCATCGAGATCGAG

1	TCGAGCTTGATAAGTCTCATCGAGATCGAG	685
2	TCGAGCTTGATAAGTCTCATCGAGATCGAG	685
3	TCGAGCTTGATAAGTCTCATCGAGATCGAG	685
4	TCGAGCTTGATAAGTCTCATCGAGATCGAG	685
5	TCGAGCTTGATAAGTCTCATCGAGATCGAG	685
6	TCGAGCTTGATAAGTCTCATCGAGATCGAG	685
7	TCGAGCTTGATAAGTCTCATCGAGATCGAG	685
8	TCGAGCTTGATAAGTCTCATCGAGATCGAG	685
9	TCGAGCTTGATAAGTCTCATCGAGATCGAG	685
10	TCGAGCTTGATAAGTCTCATCGAGATCGAG	685

TTCAAAAAAGGAGGTGCTTGGCTCGATTCG

1	TTCAAAAAAGGAGGTGCTTGGCTCGATTCG	715
2	TTCAAAAAAGGAGGTGCTTGGCTCGATTCG	715
3	TTCAAAAAAGGAGGTGCTTGGCTCGATTCG	715
4	TTCAAAAAAGGAGGTGCTTGGCTCGATTCG	715
5	TTCAAAAAAGGATGTGCTTGGCTCGATTCA	715
6	TTCAAAAAAGGAGGTGCTTGGCTCGATTCG	715
7	TTCAAAAAAGGAGGTGCTTGGCTCGATTCG	715
8	TTCAAAAAAGGAGGTGCTTGGCTCGATTCG	715
9	TTCAAAAAAGGAGGTGCTTGGCTCGATTCG	715
10	TTCAAAAAAGGAGGTGCTTGGCTCGATTCG	715

GCTCATTTATCCCCTAGTTTTAGTGCTTCG

1	GCTCATTTATCCCCTAGTTTTAGTGCTTCG	745
2	GCTCATTTATCCCCTAGTTTTAGTGCTTCG	745
3	GCTCATTTATCCCCTAGTTTTAGTGCTTCG	745
4	GCTCATTTATCCCCTAGTTTTAGTGCTTCG	745
5	GCTCATTTATCCCCTAGTTTTAGTGCTTCG	745
6	GCTCATTTATCCCCTAGTTTTAGTGCTTCG	745
7	GCTCATTTATCCCCTAGTTTTAGTGCTTCG	745
8	GCTCATTTATCCCCTAGTTTTAGTGCTTCG	745
9	GCTCATTTATCCCCTAGTTTTAGTGCTTCG	745
10	GCTCATTTATCCCCTAGTTTTAGTGCTTCG	745

TTGAGTAGTTGGACCTGAACTGGTCTTTGA

1	TTGAGTAGTTGGACCTGAACTGGTCTTTGA	775
2	TTGAGTAGTTGGACCTGAACTGGTCTTTGA	775
3	TTGAGTAGTTGGACCTGAACTGGTCTTTGA	775
4	TTGAGTAGTTGGACCTGAACTGGTCTTTGA	775
5	TTGAGTAGTTGGACCTGAACTGGTCTTTGA	775
6	TTGAGTAGTTGGACCTGAACTGGTCTTTGA	775
7	TTGAGTAGTTGGACCTGAACTGGTCTTTGA	775
8	TTGAGTAGTTGGACCTGAACTGGTCTTTGA	775
9	TTGAGTAGTTGGACCTGAACTGGTCTTTGA	775
10	TTGAGTAGTTGGACCTGAACTGGTCTTTGA	775

TTT

1	TTT	778
2	TTT	778
3	TTT	778
4	TTT	778
5	TTT	778
6	TTT	778
7	TTT	778
8	TTT	778
9	TTT	778
10	TTT	778

Sequence Logo: 50% GC base composition

Consensus Threshold: >50%

Compare to: the consensus

Bases that match the reference are marked with 4-color highlighting.

Created: 29 Dec 2019

Last Modified: 29 Dec 2019

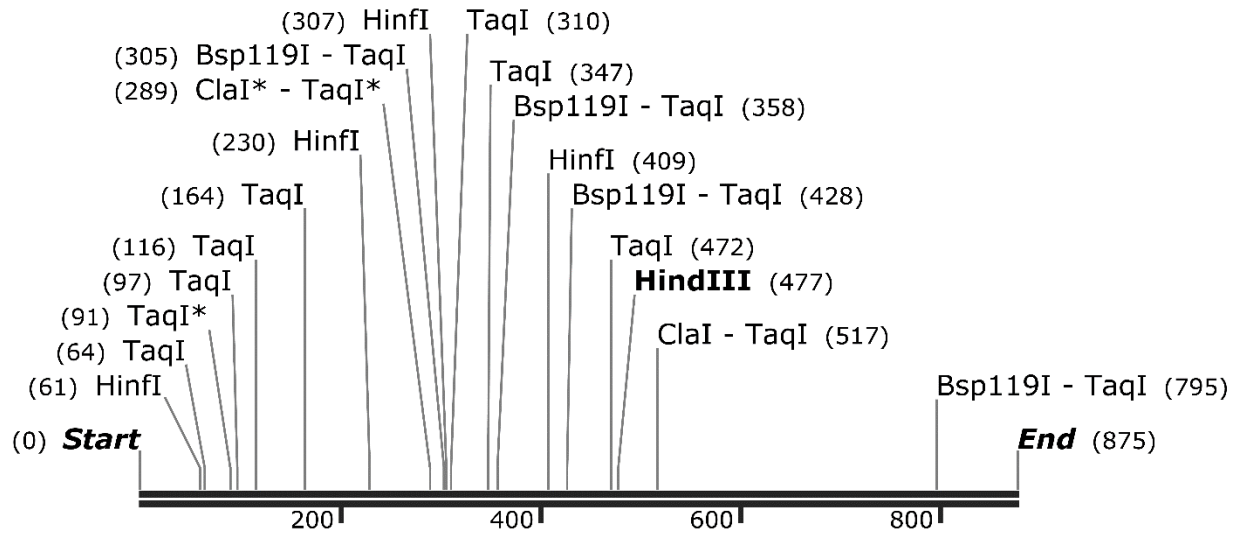

Supplementary File S5.

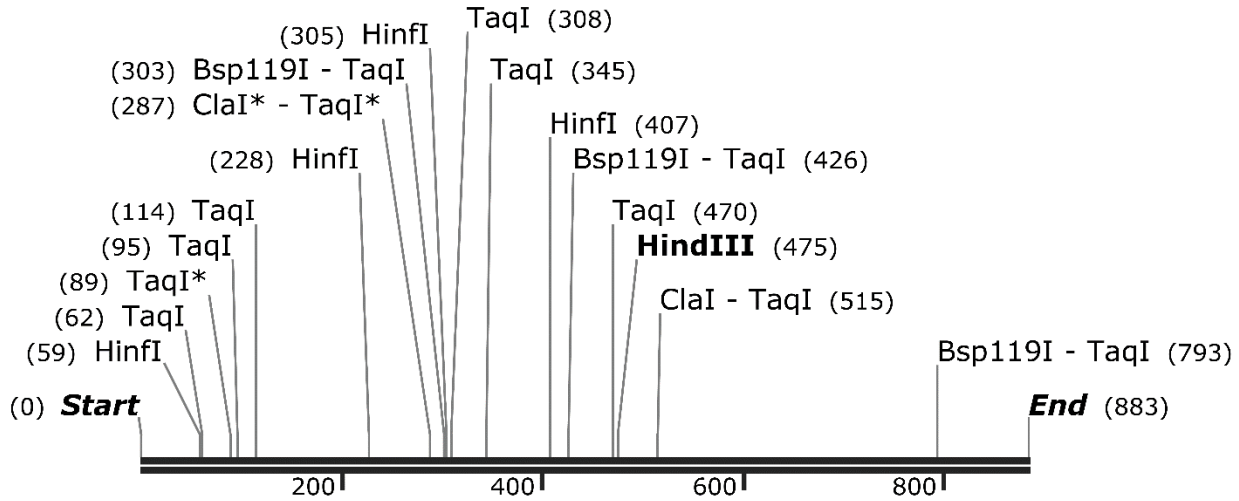

Supplementary File S6.

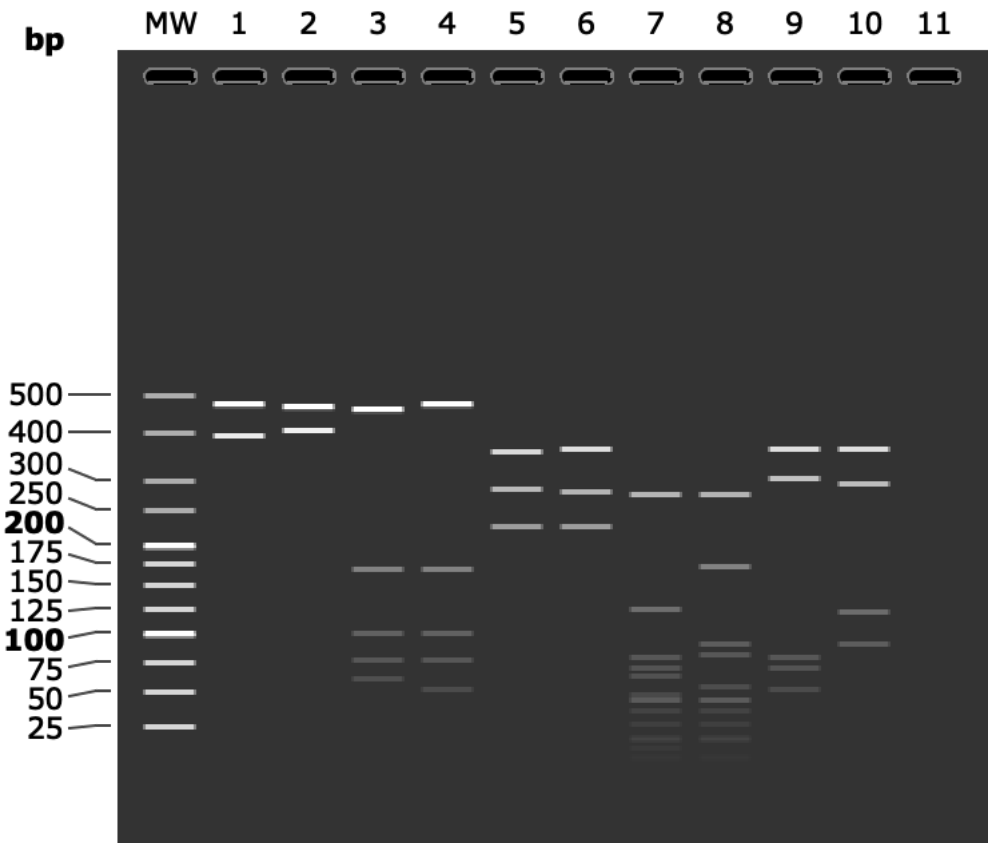

2.0% agarose

MW: HyperLadder™ 25 bp

1: J1
HindIII
1. 477 bp = Start (0) – HindIII (477)
2. 398 bp = HindIII (477) – End (875)

2: J6-F
HindIII
1. 468 bp = Start (0) – HindIII (468)
2. 408 bp = HindIII (468) – End (876)

3: J1
HinfI
1. 466 bp = HinfI (409) – End (875)
2. 169 bp = HinfI (61) – HinfI (230)
3. 102 bp = HinfI (307) – HinfI (409)
4. 77 bp = HinfI (230) – HinfI (307)
5. 61 bp = Start (0) – HinfI (61)

4: J6-F
HinfI
1. 476 bp = HinfI (400) – End (876)
2. 169 bp = HinfI (52) – HinfI (221)
3. 102 bp = HinfI (298) – HinfI (400)
4. 77 bp = HinfI (221) – HinfI (298)
5. 52 bp = Start (0) – HinfI (52)

5: J1
ClaI

1. 358 bp = ClaI (517) – End (875)
2. 289 bp = Start (0) – ClaI (289)
3. 228 bp = ClaI (289) – ClaI (517)

6: J6-F
ClaI

1. 368 bp = ClaI (508) – End (876)
2. 280 bp = Start (0) – ClaI (280)
3. 228 bp = ClaI (280) – ClaI (508)

7: J1
TaqI

1. 278 bp = TaqI (517) – TaqI (795)
2. 125 bp = TaqI (164) – TaqI (289)
3. 80 bp = TaqI (795) – End (875)
4. 70 bp = TaqI (358) – TaqI (428)
5. 64 bp = Start (0) – TaqI (64)
6. 48 bp = TaqI (116) – TaqI (164)
7. 45 bp = TaqI (472) – TaqI (517)
8. 44 bp = TaqI (428) – TaqI (472)
9. 37 bp = TaqI (310) – TaqI (347)
10. 27 bp = TaqI (64) – TaqI (91)
11. 19 bp = TaqI (97) – TaqI (116)
12. 16 bp = TaqI (289) – TaqI (305)
13. 11 bp = TaqI (347) – TaqI (358)
14. 6 bp = TaqI (91) – TaqI (97)
15. 5 bp = TaqI (305) – TaqI (310)

8: J6-F
TaqI

1. 278 bp = TaqI (508) – TaqI (786)
2. 173 bp = TaqI (107) – TaqI (280)
3. 90 bp = TaqI (786) – End (876)
4. 81 bp = TaqI (338) – TaqI (419)
5. 55 bp = Start (0) – TaqI (55)
6. 45 bp = TaqI (463) – TaqI (508)
7. 44 bp = TaqI (419) – TaqI (463)
8. 37 bp = TaqI (301) – TaqI (338)
9. 27 bp = TaqI (55) – TaqI (82)
10. 19 bp = TaqI (88) – TaqI (107)
11. 16 bp = TaqI (280) – TaqI (296)
12. 6 bp = TaqI (82) – TaqI (88)
13. 5 bp = TaqI (296) – TaqI (301)

9: J1
Bsp119I

1. 367 bp = Bsp119I (428) – Bsp119I (795)
2. 305 bp = Start (0) – Bsp119I (305)
3. 80 bp = Bsp119I (795) – End (875)

4. 70 bp = Bsp119I (358) – Bsp119I (428)
5. 53 bp = Bsp119I (305) – Bsp119I (358)

10: J6-F
Bsp119I

1. 367 bp = Bsp119I (419) – Bsp119I (786)
2. 296 bp = Start (0) – Bsp119I (296)
3. 123 bp = Bsp119I (296) – Bsp119I (419)
4. 90 bp = Bsp119I (786) – End (876)

VALIDATION AND DETECTION OF SEX-SPECIFIC MARKERS IN JOJOBA (*SIMMONDSIA CHINENSIS*) PLANTS IN SAUDI ARABIA

BAFEEL, S.* – BAHIELDIN, A.

Department of Biological Sciences, Faculty of Science, King Abdulaziz University, Jeddah, Kingdom of Saudi Arabia

**Corresponding author*
e-mail: sbafil@kau.edu.sa

(Received 10th Feb 2020; accepted 6th May 2020)

Abstract. The main target of the present study is the validation of sex-specific markers previously described and the detection of new markers for further use in breeding programs of jojoba in Saudi Arabia. The used molecular approaches included random amplified polymorphic DNA (RAPD), inter-simple sequence repeat (ISSR), Cleavage-amplified polymorphic sequence (CAPS) and amplified fragment length polymorphism (AFLP). RAPD and ISSR analyses were not useful in determining the sex of jojoba. CAPS with the J888 marker indicated the presence of two new sex-specific SNPs and consequent presence of several sex-specific markers. AFLP analysis successfully resulted in the recovery of several male- and female-specific markers. Whole genome sequencing was also done to detect new and validate already-known sex-specific markers. Use of NUCmer module resulted in no new sex-specific markers. BLAST analysis to validate sequence-related amplified polymorphism (SRAP) marker indicated its existence. Analysis of the possible functioning of *OGI/MeGI* sex determination system in jojoba was not proven. In conclusion, a number of sex-specific markers were detected in jojoba plants growing in Saudi Arabia might help promoting the biofuel production industry in Saudi Arabia and the Arab region as a new approach to be adopted in the near future.
Keywords: *RAPD, CAPS, AFLP, WGS, BLAST, NUCmer, SRAP, OGI/MeGI*

Introduction

Biofuels can be either bioalcohol or biodiesel. The latter is made of renewable resources that are generated from plants like jojoba and jatropha (Pinzi et al., 2009). Comparing biofuels to fossil fuels indicates that the first reduces pollution and greenhouse effects. Jojoba (*Simmondsia chinensis* (Link) C. K.) is a perennial and plant native to Arizona, southern California and northern Mexico (Benzioni, 1995). The plant is dioecious, e.g., bearing male and female flowers on different plants with the axillary inflorescences of male plants harbor a number of 3-20 flowers, while axillary inflorescences of female plants harbor single flower (Ince and Karaca, 2011). The use of jojoba in biofuel production is advantageous because the plant is non-edible, unlike corn or sugarcane, and can be irrigated with low quality water and cultivated in areas with high levels of drought, salinity and heat. Jojoba possesses unique favorable properties, such as low acidity and viscosity, good oxidation stability and its oil possesses < 3% triglyceride and is highly resistant to oxidation (El-Mallah and El-Shami, 2009). Jojoba oil has several applications that make it economically feasible (Passerini and Lombardo, 2000). It is used in lubricants, pharmaceuticals and cosmetics, besides its potential use in industry, e.g., plastics, printer ink, surfactants and leather lubricants (Inca and Karaca, 2010).

The most common method for jojoba breeding is the non-sexual propagation along with the selection of plants with desirable characteristics (Vaknin et al., 2003; Tobares et al., 2004; Benzioni et al., 2005). However, there is a shortage of yield with the use of

http://www.aloki.hu ● ISSN 1589 1623 (Print) ● ISSN 1785 0037 (Online)
DOI: http://dx.doi.org/10.15666/aeer/1804_50235035

clones or cuttings in commercial plantations, therefore, the application of supplemental pollination results in an increased seed yield (Coates et al., 2006). Further analysis indicated that selection of appropriate male and female genotypes for plantation and breeding studies is mandatory. However, further recovery of low yield results mainly from the high female to male plant ratio (Benzioni and Ventura, 1998; Coates et al., 2006). The plantation with seeds usually results in 84% male and 16% female plants whereas only 10% male plants are desirable for optimal yield (Agarwal et al., 2008). This ratio can be easily manipulated by planting male plants distantly far from the existing females. For economical plantation of jojoba, there is a need to identify the sex of the plant at the seedling stage. Early identification of sex will also lead to increased efficiency of a plantation program by allowing proper layout of field arrangement of male and female seedlings and early elimination of unwanted plants.

Unfortunately, sex can be determined morphologically, as indicated earlier, at mature stages when plants are 3-year-old or older, while sex is difficult to be determined at earlier stages. However, sex in young seedlings was determined at the molecular level so far but with less success. Therefore, it is important to find effective molecular or DNA markers that can reliably be used in the easy determination of sex at early stages of plant development. DNA markers have several advantages as they exhibit high allelic variation, being neutral to the environmental conditions (Tan et al., 2003; Karaca et al., 2004), besides being used in sex identification in several plant crop species including basket willow (*Salix viminalis* L.) (Alstrom-Rapaport et al., 1998), *Atriplex garrettii* (Ruas et al., 1998), *Viola pubescens* Aiton (Culley and Wolfe, 2000), nutmeg (*Myristica fragrans* Houtt.) (Shibu et al., 2000), *Pistacia* sp. (Kafkas et al., 2001), *Mercurialis annua* (Khadka et al., 2002), hemp (Torjek et al., 2002), *Eucommia ulmoides* Oliv (Xu et al., 2004), hop (*Humulus lupulus* L.) (Danilova and Karlov, 2006), *Encephalartos natalensis* (Prakash and van Staden, 2006), *Carica papaya* (Chaves-Bedoya and Nunenz, 2007), *Carica papaya* (Gangopadhyay et al., 2007), bermudagrasses (*Cynodon* spp.) (Karaca and Ince, 2008), subtropical carrot (Jhang et al., 2010), *Calamus simplicifolius* (Li et al., 2010) and jojoba (Mohasseb et al., 2009; Ince et al., 2010; Agarwal et al., 2011; Ince and Karaca, 2011; Heikrujam et al., 2014; Kumar et al., 2019).

The present study aims at validating a number of sex-specific markers previously used in jojoba towards further usage in breeding programs of jojoba growing in Saudi Arabia. Results of this study might help determining sex in jojoba more efficiently, thus, promoting the biofuel production industry in Saudi Arabia and the Arab region, a new approach possibly adopted in the near future.

Materials and methods

DNA extraction

The analysis involved a number of five male and five female plants growing at King Abdulaziz Farm station at Hada El-Sham near Jeddah, Kingdom of Saudi Arabia. Flash-frozen leaf materials from individual plants were crushed into a fine powder in a microcentrifuge tube using a sterilized metal rod and DNAs were isolated from leaves following the modified procedure of Gawel and Jarret (1991). Isolated DNAs were, then, treated with RNase A (10 mg/ml) and incubated at 37 °C for 30 min to remove RNA contaminants. DNA concentrations were estimated by measuring optical density at 260 nm according to the equation: DNA concentration (ug/ml) = OD260 X 50x dilution factor.

http://www.aloki.hu ● ISSN 1589 1623 (Print) ● ISSN 1785 0037 (Online)
DOI: http://dx.doi.org/10.15666/aeer/1804_50235035

Random amplified polymorphic DNA (RAPD) and inter-simple sequence repeat (ISSR) analyses

For RAPD analysis, a number of 20 random 10*mer* primers (Operon Technology, USA) from groups A, B and C was used in determining sex in male and female jojoba plants (*Appendix 1*). PCR was carried out in 25 µl reaction volume containing 1x PCR buffer, 4 mM $MgCl_2$, 0.2 mM dNTPs, 20 pmole primer, 2 units Taq DNA polymerase and 25 ng template DNA. PCR amplification was performed in a Perkin Elmer 2400 thermocycler (Germany), programmed to fulfill 40 cycles after an initial denaturation cycle for 4 min at 94 °C. Each cycle consisted of a denaturation step at 94 °C for 1 min, an annealing step at 37 °C for 2 min, and an extension step at 72 °C for 2 min, followed by a final extension cycle for 7 min at 72 °C.

For ISSR, 14 primers were used in detecting polymorphic bands between male and female plants (*Appendix 1*). PCR analysis was performed in 25 µl reaction and amplification was programmed to fulfill 40 cycles after an initial denaturation cycle for 4 min at 94 °C. Each cycle consisted of a denaturation step at 94 °C for 1 min, an annealing step at 40 °C for 80 s, and an extension step at 72 °C for 2 min, followed by a final extension cycle for 7 min at 72 °C. Amplicons were run on agarose gel (Wide Mini-Sub Cell GT Systems, Bio-Rad) at 120 V/50 mA (PowerPac Universal Power Supply, Bio-Rad) for 45 min, then gel stained with ethidium bromide (0.3 ug/ml) and visually examined with an UV transilluminator and photographed using a CCD camera (UVP, UK).

Cleavage-amplified polymorphic sequence (CAPS)

CAPS was generated for the J888 marker using the primer pair 5`-AGACCCAGAGCACACACAGC-3` (forward) and 5`-AGACCCAGAGGATGAGGAATG-3` (reverse) to recover 888 bp as previously described (Ince and Karaca, 2011). The amplicons were shipped to BGI, China for Sanger sequencing and sequences were analyzed via using SnapGene® in order to detect Single Nucleotide Polymorphism (SNP) markers and make predicted restriction analysis towards the detection of possible polymorphic sex-specific bands.

Amplified fragment length polymorphism (AFLP)

AFLP analysis was performed using the two combinations EcoRI-GC/MseI-GCG and EcoRI-TAC/MseI-GCG of the AFLP Analysis System I (Invitrogen, cat. no. 10544-013) following manufacturer's protocol. Genomic DNAs of the five male and five female samples were digested with EcoRI and MseI restriction enzymes in which EcoRI and MseI adapters were ligated to the digested DNA fragments. Pre-amplification was carried out using EcoRI primer plus one extension base at the 3' position (G or T) and MseI primer plus one extension base at the 3' position (G) to amplify fragments that contain complementary sequences.

Whole genome sequencing

Whole genome sequencing was done for one male and one female randomly-selected jojoba samples at BGI, China. About 60 million 100-bp paired-end reads were generated from sequencing libraries with 500-bp insert. Data were filtered to remove the low-quality reads and trim adaptor using Fastp package

http://www.aloki.hu ● ISSN 1589 1623 (Print) ● ISSN 1785 0037 (Online)
DOI: http://dx.doi.org/10.15666/aeer/1804_50235035

(https://www.ncbi.nlm.nih.gov/pmc/articles/PMC6129281/). The remaining sequencing reads from the two samples were *de novo* assembled via velvet (v1.2.10) without length cutoff as described (https://www.ebi.ac.uk/~zerbino/velvet/). Contigs recovered from the two sexes were further used in detecting either new or previously-known sex-specific markers in jojoba. The raw data was deposited in the Short Read Archive database (BioProject ID PRJNA603451) of the NCBI.

Detection of new sex-specific markers

Multiple contig alignment of the genomes of the two sexes was done using NUCmer module 3.0 (NUCleotide MUMmer, part of mummer software) to determine the maximal unique matches of a given length (350-500 bp) between the two input sequences, a step to increase the overall coverage of the alignment (Kurtz et al., 2004). A number of 100 contigs of each genome showed high matching in DNA sequences. Contig pairs with high similarity (~90%) and unique sex-specific areas of 350-500 bp (sequence similarity/difference criteria) were selected and sex-specific primers were generated (*Appendix 1*). PCR was performed using ready master mix (BioTaq Green Master Mix, Promega) and conditions were 95 °C/5 min (initial denaturation), 95 °C/30 s, 52 °C/45 s and 72 °C/1 min (40 cycles), 72 °C (final extension), then reaction was held at 4 °C. Amplicons were run on agarose gel, stained with ethidium bromide (0.3 ug/ml), then visually examined and photographed.

Detection of previously-known sex-specific markers

Resulted contigs from both sexes were blasted (ncbi-BLAST v 2.10.0) against previously-known sex-specific sequences referring to an ISSR marker namely UBC-807_{1200} (Sharma et al., 2008; Heikrujam et al., 2014), sequence-related amplified polymorphism (SRAP) (Kumar et al., 2019) determining sex in jojoba as well as *OGI/MeGI* system determining sex in persimmons (*Diospyros* spp.) (https://www.ncbi.nlm.nih.gov/nuccore/KM408640) (Akagi et al., 2014).

Results and discussion

Production of jojoba has spread in many regions of the world (Benzioni et al., 2005) including the Middle East. However, no previous comparative analysis has been made at the molecular genetic level to detect genetic distances among genotypes existing in different regions. Therefore, there is no guarantee that the genetic makeup of the genotypes in Saudi Arabia will harbor the same molecular markers published elsewhere.

In the present study, several types of molecular markers using specific primers were proven not to be useful in determining sex in jojoba plants growing in Saudi Arabia (*Appendix 2*). As models, amplicons of two RAPD (with A02 and B09 primers) and two ISSR (with 544A and HB11 primers) are shown in *Appendix 2*. We speculate one reason for the failure to detect the known sex-specific RAPD or Td-PCR markers is that these two types of markers are likely genotype-specific. Identification of molecular marker for ascertaining sex of plants at seedling stage is vital for optimal plantation of dioecious plants including jojoba. This approach has previously been followed in many plants including *Pistacia vera* (Hormaza et al., 1994), *Carica papaya* (Deputy et al., 2002) and *Mercurialis annua* (Khadka et al., 2002) using random amplified polymorphic DNA (RAPD) approach, while sex in plants like *Asparagus officinalis*

http://www.aloki.hu ● ISSN 1589 1623 (Print) ● ISSN 1785 0037 (Online)
DOI: http://dx.doi.org/10.15666/aeer/1804_50235035

(Reamson-Büttner et al., 1998), *Cannabis sativa* (Flachowsky et al., 2001; Peil et al., 2003) and *Ficus fulva* (Parrish et al., 2004) was determined using amplified fragment length polymorphism (AFLP) approach. Previous studies to detect sex-specific molecular markers in jojoba included a number of RAPD (Agrawal et al., 2007), touchdown polymerase chain reaction (Td-PCR) (Ince et al., 2010) and cleavage-amplified polymorphic sequence (CAPS) (Ince and Karaca, 2011) markers. Out of 72 RAPD primers, only one primer, e.g., OPG-5 (5`-CTGAGACGGA-3`), produced a male-specific marker of ~1.4 kb (Agrawal et al., 2007). Using Td-PCR, another male-specific marker, namely JMS900, was detected using a 10-mer primer (5`-AGACCCAGAG-3`) (Ince et al., 2010). Mohasseb et al. (2009) indicated that one reason for the failure to generate reliable information from these two types of markers is that they might be vulnerable to PCR conditions and quality of the genomic DNA.

The previous results of CAPS with the J888 marker indicated that the 888 bp digested with ClaI, HindIII and HinfI produced polymorphic fragments in male and female samples (Ince and Karaca, 2011). In the present study, this was not the case as digestion of the 888 bp amplicon with these three restriction enzymes generated no polymorphic sex-specific bands (data provided upon request). Therefore, the J888 marker was sequenced for five male and five female samples and multiple sequence alignments of the forward and reverse sequences were done using Clostal Omega (*Appendices 3* and *4,* respectively). The results indicated the presence of two sex-specific SNPs shown in both the forward [sites 138 (G > A) and 330 (C > T)] (*Table 1* and *Appendix 3*) and reverse [sites 609 (C > T) and 416 (G > A)] (*Table 1* and *Appendix 4*) directions of the clean sequences.

Table 1. *List of sex-specific SNPs either lying within restriction sites (colored boxes) or not (clear boxes) across five male (J1-J5) and five female (J6-J10) samples existing in the CAP marker J888. Sanger sequencing was done for J888 amplicon at the two (forward and reverse) directions. SNPs are mainly C/T and A/G, while restriction sites are for Bsp119I and TaqI enzymes. Note that TaqI site (T↓CGA) exists within Bsp119I site (TT↓CGAA). Red = male, blue = female. Multiple sequence alignments of the forward and reverse sequences of J888 marker using Clostal Omega are shown in Appendices 1 and 2, respectively*

Primer	J1	J2	J3	J4	J5	J6	J7	J8	J9	J10	SNP position (type)/restriction site
Forward	A	A	A	A	A	A	A	A	A	T	44 (A > T)
	G	G	G	G	G	A	A	A	A	A	138 (G > A)/TaqI
	G	G	G	G	G	G	G	G	G	A	268 (G > A)
	C	C	C	C	C	T	T	T	T	T	330 (C > T)/Bsp119I/TaqI
Reverse	G	G	G	G	G	A	A	A	A	A	416 (G > A)/Bsp119I/TaqI
	C	C	C	C	C	C	C	C	C	T	479 (C > T)
	C	C	C	C	C	T	T	T	T	T	609 (C > T)/TaqI
	T	G	G	G	G	G	G	G	G	G	678 (G > T)
	A	G	G	G	G	G	G	G	G	G	695 (G > A)

In addition, restriction analysis and maps of one randomly selected male (*Appendix 5*) and one selected female (*Appendix 6*) samples were detected using SnapGene®. The latter software predicted the occurrence of several polymorphic sex-specific bands when the amplicon is digested with either restriction enzymes TaqI or

http://www.aloki.hu ● ISSN 1589 1623 (Print) ● ISSN 1785 0037 (Online)
DOI: http://dx.doi.org/10.15666/aeer/1804_50235035

Bsp119I (*Fig. 1* and *Appendix 7*). These polymorphic bands are consequences of the two SNPs sites located within the male and female of the J888 marker sequences. For TaqI, two male-specific markers with 125 and 70 bp, while two female-specific markers with 173 and 90 bp were detected. For Bsp119I, three male-specific markers with 80, 70 and 53 bp, while two female-specific markers with 123 and 90 bp were detected. Note that the TaqI site (T↓CGA) exists within Bsp119I site (TT↓CGAA). The predicted number of restriction fragments of TaqI enzyme is much higher than that of Bsp119I as the recognition site of the first is 4-base, while 6- base for the second. We expected that DNA sequences of the 90 bp female-specific marker across the two restriction enzymes are the same. Then, we claim that we successfully detected two SNPs markers that resulted in the production of five male-specific and four female-specific markers when the J888 amplicon was digested with both TaqI and Bsp119I restriction enzymes.

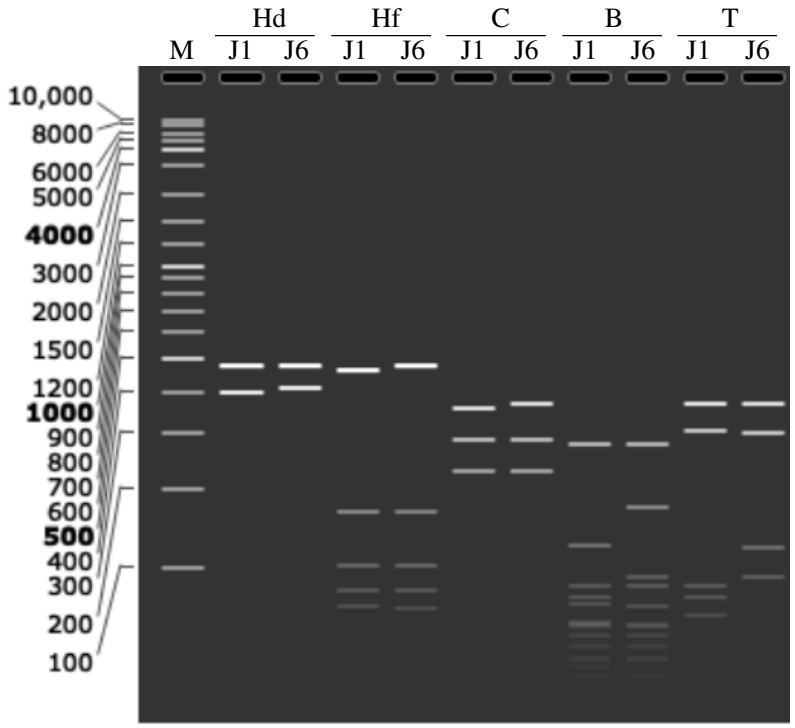

Figure 1. *Predicted restriction analysis displayed on a virtual gel for one male (sample J1) and one female (sample J6) samples existing in the CAP marker J888. Restriction enzymes involved HindIII (Hd), HinfI (Hf), ClaI (C), Bsp119I (B) and TaqI (T). Note that TaqI site (T↓CGA) exists within Bsp119I site (TT↓CGAA). M = 100 bp-ladder. Sizes of restriction fragments are shown in Appendix 3. Complete restriction maps of J888 markers for the male and female samples are shown in Appendices 4 and 5. Restriction fragment sizes and maps were detected using SnapGene®*

AFLP is a reliable approach in detecting molecular markers in dioecious plants (Mwase et al., 2007), while RAPD, a dominant marker, has several drawbacks and lacks reproducibility (Mohasseb et al., 2009). Then, AFLP has a large chance to detect sex-specific markers in jojoba (Agarwal et al., 2011) as this type of markers allows the testing of large genomic fragments at once compared with the earlier types of molecular markers that test very small regions of the genome. Previous efforts utilizing AFLP in detecting sex-specific markers resulted in the recovery of two male-specific markers of

http://www.aloki.hu ● ISSN 1589 1623 (Print) ● ISSN 1785 0037 (Online)
DOI: http://dx.doi.org/10.15666/aeer/1804_50235035

~525 and 325 bp using primer combinations EcoRI-GC/MseI-GCG and EcoRI-TAC/MseI-GCG, respectively, while only one female-specific marker of ~270 bp using the primer combination EcoRI-TAC/MseI-GCG. In the present study, the primer combination EcoRI-GC/MseI-GCG resulted in the recovery of five (428, 307, 190, 163 and 60 bp) male-specific and three (768, 401 and 25 bp) female-specific markers (*Appendix 8*), while the primer combination EcoRI-TAC/MseI-GCG resulted in the recovery of three (340, 196 and 56 bp) male-specific and three (425, 241 and 179 bp) female-specific markers (*Appendix 9*). We disconsidered sex-specific markers with > 25 bp. Dendrograms utilizing the two combinations resulted in the complete separation of the two sexes (*Figs. 2* and *3*). Then, we claim that this type of marker successfully determines sex in jojoba with high efficiency.

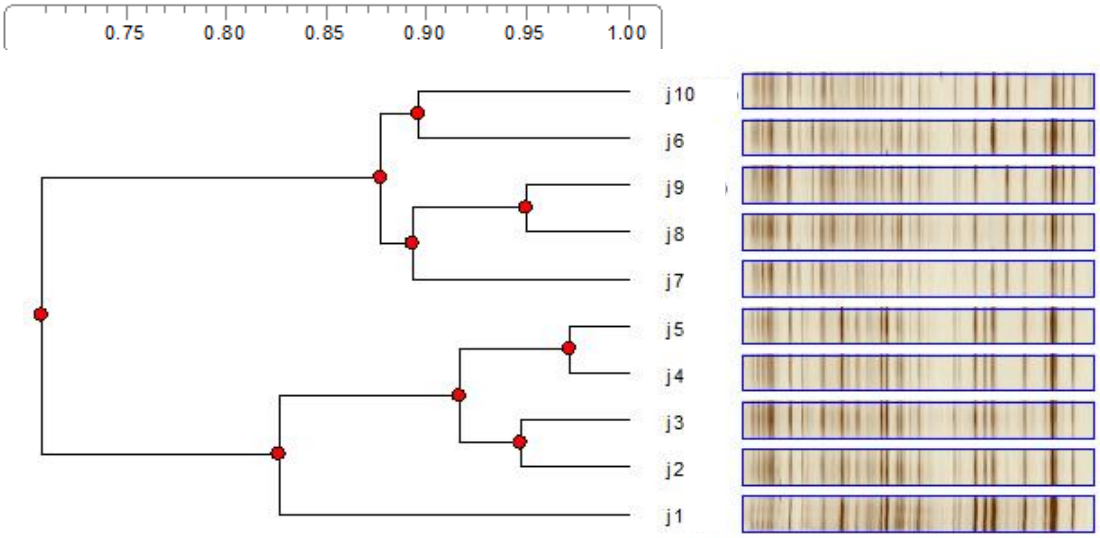

Figure 2. *Dendrogram resulted from AFLP with the primer combination EcoRI-GC/MseI-GCG to describe the relationship between male (J1-J5) and female (J6-J10) banding patterns*

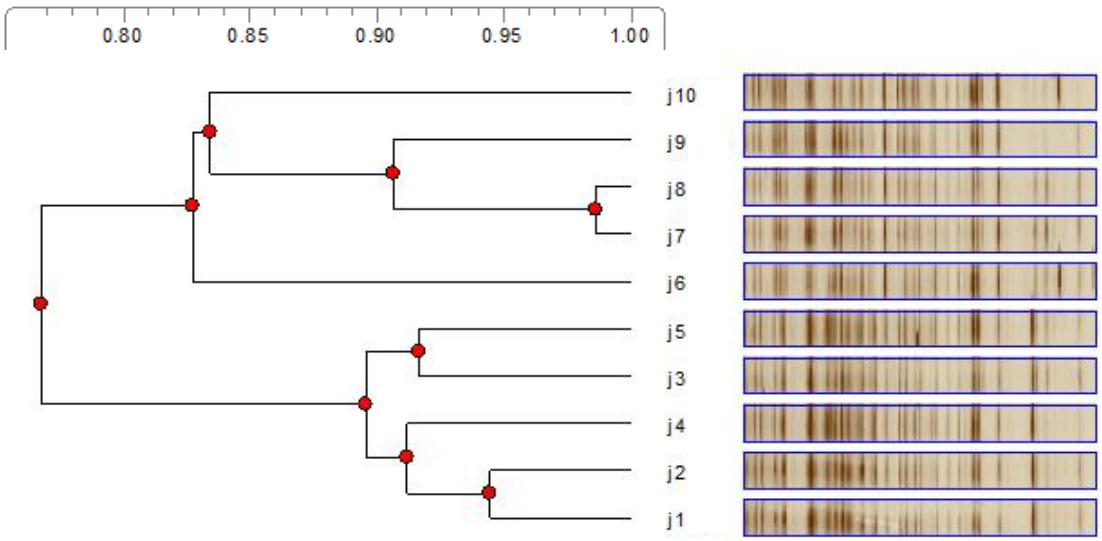

Figure 3. *Dendrogram resulted from AFLP with the primer combination EcoRI-TAC/MseI-GCG to describe the relationship between male (J1-J5) and female (J6-J10) banding patterns*

http://www.aloki.hu ● ISSN 1589 1623 (Print) ● ISSN 1785 0037 (Online)
DOI: http://dx.doi.org/10.15666/aeer/1804_50235035

Multiple contig alignment of the genomes of the two sexes done using NUCmer module 3.0 (NUCleotide MUMmer, part of mummer software) indicated a number of 18 male and 17 female unique sequences of 350-500 bp. PCR with the designed sex-specific primer combinations was done for one male and one female samples and results indicated the occurrence of four male-generated (Rx9, Rx11, Rx26 and Rx33) and two female-generated (Rx1 and Rx4) amplicons (*Appendix 2*). Interestingly, the male-generated amplicons of Rx9 and Rx11 were supposed to be possible female-specific markers. PCR for five male and female samples indicated arbitrary inconsistent presence/absence of the four male and two female-generated amplicons in the two sexes (*Appendix 2*). We speculate that the failure to detect sex-specific markers via multiple contig alignment of the genomes of the two sexes and the use of MUMmer software is due to the need for larger yield or coverage of raw reads of genomes of the two sexes or due to the lack of appropriate binding sites in the template. Low coverage results in the presence/absence of many contig sequences that are not sex-specific. Therefore, we recommend repeating the whole genome sequencing of genomes of the two sexes, but requesting larger read coverage.

Two male-specific ISSR (Sharma et al., 2008; Heikrujam et al., 2014) and sequence-related amplified polymorphism (SRAP) (Kumar et al., 2019) markers have also been validated in the present study. ISSR was previously reported to result in the recovery of a male-specific marker namely UBC-807_{1200} utilizing primer UBC-807, while SRAP was reported to result in the recovery of a male-specific marker with an amplicon size of 396 bp utilizing primer combination Em14/Me10. In the present study, we have sequenced the whole jojoba male and female genomes and blasted the *de novo* assembled contigs of the two genomes against the published sequence of the male-specific ISSR marker in the NCBI (acc. no. HQ166029). The results indicated the presence of several fragments of the marker sequence in both male (*Fig. 4* and *Appendix 10*) and female (*Fig. 4* and *Appendix 11*) genomes. Results of the blasted male and female *de novo* assembled genomes against the published sequence of the SRAP male-specific marker of Kumar et al. (2019) with primer combination Em14/Me10 are shown in *Appendices 12* and *13,* respectively. The results proved that the DNA sequence of the SRAP marker was almost completely detected in the male sample (*Fig. 5*), while completely absent in the female sample. We concluded that the SRAP marker can successfully determine males in jojoba with high efficiency, while the UBC-807_{1200} marker was not proven to be male-specific.

Dioecy is often associated with the occurrence of sex chromosomes in plant and the presence of genetic determinants of sex (Ming et al., 2011; Renner, 2014; Charlesworth, 2016). After the era of genomics and whole genome sequencing (WGS), it is now possible to decipher the architecture of sex chromosomes in several dioecious plants (Liu et al., 2004; Ming et al., 2011; Wang et al., 2012, 2013; Charlesworth, 2016; Kazama et al., 2016; Harkess et al., 2017; Muyle et al., 2017). Genetic determinants of sex were deciphered in some species, including persimmons (*Diospyros* spp.) (Akagi et al., 2014), garden asparagus (*Asparagus officinalis* L.) (Harkess et al., 2017) and kiwifruit (*Actinidia* spp.) (Akagi et al., 2018). Sex was determined in persimmons through the action of one single non-coding RNA gene located on the Y chromosome namely *OGI* gene (Yang et al., 2019). This gene produces a small-RNA sequence that targets an autosomal counterpart gene namely *MeGI* (Yang et al., 2019). The latter is thought to be a single integrator of sex expression (Akagi et al., 2014, 2016; Henry et al., 2018; Yang et al., 2019). As *OGI* gene is located on Y chromosome, we expected

http://www.aloki.hu ● ISSN 1589 1623 (Print) ● ISSN 1785 0037 (Online)
DOI: http://dx.doi.org/10.15666/aeer/1804_50235035

that if this sex determination system exists in jojoba, then existence of *OGI* gene will be a male-specific marker, while we expect that the *MeGI* gene exists in the two sexes. BLAST results of the *de novo* assembled contigs in the present study against the published sequences of the *OGI* and *MeGI* genes are shown for male (*Appendix 14* and *15,* respectively) and female (*Appendix 16* and *17,* respectively) jojoba genomes. The sequences of *OGI* and *MeGI* genes of persimmon are available in the DDBJ database, with the Illumina reads for the mRNA-Seq analysis deposited in the Short Read Archive database (BioProject ID PRJDB7688) of the NCBI. The BLAST results indicated that *OGI* gene was not detected in either jojoba sexes, while *MeGI* gene was detected in 12 and six contigs of the jojoba male and female samples, respectively. Prior information neither confirmed the existence of Y chromosome in male plants of jojoba, nor proved the existence of *OGI*/*MeGI* system in jojoba. Existence of *MeGI*, while lack of *OGI* is a question remains to be answered. In general, we confirmed that the published *OGI*/*MeGI* system does not exist to drive sex in jojoba.

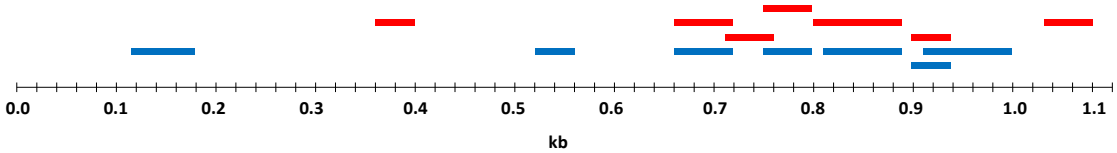

Figure 4. *BLAST results for the DNA fragments within the UBC-807$_{1200}$ sequence (acc. no. HQ166029) existed in the male (blue) and female (red) de novo assembled genomes of jojoba growing in Saudi Arabia*

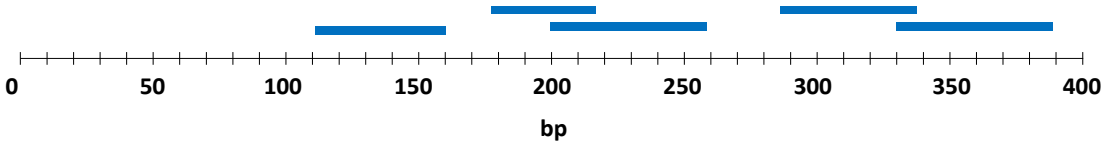

Figure 5. *BLAST results for the DNA fragments within the SRAP male-specific marker (396 bp) existed in the male de novo assembled genome of jojoba germplasm growing in Saudi Arabia*

Conclusion

Overall results of the present study indicated the possibility to utilize CAPS with either restriction enzymes TaqI or Bsp119I in detecting sex-specific markers in jojoba. Also, AFLP resulted in the recovery of several sex-specific markers, thus, seems to be very useful in separating the two sexes in jojoba very efficiently. The previously described male-specific SRAP marker was also confirmed in jojoba plants growing in Saudi Arabia. These three types of sex-specific markers might be useful in the future industry of biofuel production in Saudi Arabia and the Arab region. The study also refers to the necessity to barcode this important plant in different regions of the country and re-validate the recovered sex-specific markers way before we decide to incorporate this plant in breeding program or at commercial scale.

Acknowledgements. This project was funded by the Deanship of Scientific Research (DSR), King Abdulaziz University, Jeddah, under Grant no. (G: 368-247-1439). The authors, therefore, acknowledge with thanks DSR technical and financial support.

http://www.aloki.hu ● ISSN 1589 1623 (Print) ● ISSN 1785 0037 (Online)
DOI: http://dx.doi.org/10.15666/aeer/1804_50235035

REFERENCES

[1] Akagi, T., Henry, I. M., Tao, R., Comai, L. (2014): A Y-chromosome-encoded small RNA acts as a sex determinant in persimmons. – Science 346: 646-650.
[2] Akagi, T., Henry, I. M., Kawai, T., Comai, L., Tao, R. (2016): Epigenetic regulation of the sex determination gene MeGI in polyploid persimmon. – Plant Cell 28: 2905-2915.
[3] Akagi, T., Henry, I. M., Ohtani, H., Beppu, K., Kataoka, I., Tao, R. (2018): A Y-encoded suppressor of feminization arose via lineage-specific duplication of a cytokinin response regulator in kiwifruit. – Plant Cell 30: 780-795.
[4] Agrawal, V., Sharma, K., Gupta, S., et al. (2007): Identification of sex in *Simmondsia chinensis* (Jojoba) using RAPD markers. – Plant Biotechnol. Rep. 1: 207-210.
[5] Agarwal, M., Shrivastava, N., Padh, H. (2008): Advances in molecular marker techniques and their applications in plant sciences. – Plant Cell Rep. 27: 617-631.
[6] Agarwal, M., Shrivastava, N., Padh, H. (2011): Development of sex-linked AFLP markers in *Simmondsia chinensis*. – Plant Breed. 130: 114-116.
[7] Alstrom-Rapaport, C., Lascoux, M., Wang, Y. C., Roberts, G., Tuskan, G. A. (1998): Identification of a RAPD marker linked to sex determination in the basket willow (*Salix viminalis* L.). – J. Heredity 89: 44-49.
[8] Benzioni, A. (1995): Jojoba domestication and commercialization in Israel. – Horti. Rev. 17: 233-266.
[9] Benzioni, A., Mills, D., Van Boven, M., Cokelaere, M. (2005): Effect of genotype and environment on the concentration of simmondsin and its derivatives in jojoba seeds and foliage. – Industrial Crops and Products 21: 241-249.
[10] Charlesworth, D. (2016): Plant sex chromosomes. – Annu. Rev. Plant Biol. 67: 397-420.
[11] Chaves-Bedoya, G., Nunenz, V. (2007): A SCAR marker for the sex types determination in Colombian genotypes of *Carica papaya*. – Euphytica 153: 215-220.
[12] Coates, W., Ayerza, R., Palzkill, D. (2006): Supplemental pollination of jojoba - a means to increase yields. – Industrial Crops and Products 24: 41-45.
[13] Culley, T. M., Wolfe, A. D. (2000): Population genetic structure of the cleistogamous plant species *Viola pubescens* Aiton (Violaceae), as indicated by allozyme and ISSR molecular markers. – J. Heredity 86: 545-556.
[14] Danilova, T. V., Karlov, G. I. (2006): Application of inter simple sequence repeat (ISSR) polymorphism for detection of sex-specific molecular markers in hop (*Humulus lupulus* L.). – Euphytica 151: 15-21.
[15] Deputy, J. C., Ming, R., Ma, H., Liu, Z., Fitch, M. M., et al. (2002): Molecular markers for sex determination in papaya (*Carica papaya*, L.). – Theor. Appl. Genet. 106: 107-111.
[16] El-Mallah, M. H., El-Shami, S. M. (2009): Investigation of liquid wax components of Egyptian jojoba seeds. – J. Oleo Sci. 58(11): 543-548.
[17] Flachowsky, H., Schumann, E., Weber, W. E., Peil, A. (2001): Application of AFLP for the detection of sex specific markers in hemp. – Plant Breed. 120: 305-309.
[18] Gangopadhyay, G., Roy, S. K., Ghose, K., et al. (2007): Sex detection of *Carica papaya* and *Cycas circinalis* in pre-flowering stage by ISSR and RAPD. – Curr. Sci. 92: 524-526.
[19] Gawel, N. J., Jarret, R. L. (1991): A modified CTAB DNA extraction procedure for Musa and Ipomoea. – Plant Mol. Biol. Rep. 9: 262-266.
[20] Harkess, A., Zhou, J., Xu, C., et al. (2017): The asparagus genome sheds light on the origin and evolution of a young y chromosome. – Nat. Commun. 8: 1279.
[21] Hormaza, J. I., Dollo, L., Polito, V. S. (1994): Identification of a RAPD marker linked to sex determination in *Pistachia vera* using bulked segregant analysis. – Theor. Appl. Genet. 89: 9-13.
[22] Heikrujam, M., Sharma, K., Kumar, J., Agrawal, V. (2014): Validation of male sex-specific UBC-8071200 ISSR marker and its conversion into sequence tagged sites marker in Jojoba: a high precision oil yielding dioecious shrub. – Plant Breed. 133: 666-671.

http://www.aloki.hu ● ISSN 1589 1623 (Print) ● ISSN 1785 0037 (Online)
DOI: http://dx.doi.org/10.15666/aeer/1804_50235035

[23] Henry, I. M., Akagi, T., Tao, R., Comai, L. (2018): One hundred ways to invent the sexes: theoretical and observed paths to dioecy in plants. – Annu. Rev. Plant Biol. 69: 553-575.
[24] Ince, A. G., Karaca, M. (2011): Early determination of sex in jojoba plant by CAPS assay. – J Agric. Sci. 149: 327-336.
[25] Ince, G. A., Karaca, M., Onus, A. N. (2010): A reliable gender diagnostic PCR assay for jojoba (*Simmondsia chinensis* (Link) Schneider). – Genet. Resour. Crop Evol. 57: 773-779.
[26] Jhang, T., Kaur, M., Kalia, P., Sharma, T. R. (2010): Efficiency of different marker systems for molecular characterization of subtropical carrot germplasm. – J. Agric. Sci., Cambridge 148: 171-181.
[27] Kafkas, S., Cetiner, S., Perl-Treves, R. (2001): Development of sex-associated RAPD markers in wild *Pistacia* species. – J. Hort. Sci. Biotechnol. 76: 242-246.
[28] Karaca, M., Ince, A. G. (2008): Minisatellites as DNA markers to classify bermudagrasses (*Cynodon* spp.): confirmation of minisatellite in amplified products. – J. Genet. 87: 83-86.
[29] Karaca, M., Saha, S., Callahan, F. E., et al. (2004): Molecular and cytological characterization of a cytoplasmic-specific mutant in pima cotton (*Gossypium barbadense* L.). – Euphytica 139: 187-197.
[30] Kazama, Y., Ishii, K., Aonuma, W., et al. (2016): A new physical mapping approach refines the sex-determining gene positions on the *Silene latifolia* Y-chromosome. – Sci. Rep. 6: 18917.
[31] Khadka, D. K., Nejidat, A., Tal, M., Golangoldhirsh, A. (2002): DNA markers for sex: molecular evidence for gender dimorphism in dioecious *Mercurialis annua* L. – Mol. Breed. 9: 251-257.
[32] Kumar, J., Heikrujam, M., Sharma, K., Agrawal, V. (2019): SRAP and SSR marker-assisted genetic diversity, population structure analysis and sex identification in Jojoba (*Simmondsia chinensis*). – Industrial Crops and Products 133: 118-132.
[33] Kurtz, S., Phillippy, A., Delcher, A. L., et al. (2004): Versatile and open software for comparing large genomes. – Genome Biol. 5: R12.
[34] Li, M., Yang, H., Li, F., et al. (2010): A male-specific SCAR marker in *Calamus simplicifolius*, a dioecious rattan species endemic to China. – Mol. Breed. 25: 549-551.
[35] Liu, Z., Moore, P. H., Ma, H., et al. (2004): A primitive Y chromosome in papaya marks incipient sex chromosome evolution. – Nature 427: 348-352.
[36] Ming, R., Bendahmane, A., Renner, S. S. (2011): Sex chromosomes in land plants. – Annu. Rev. Plant Biol. 62: 485-514.
[37] Mohasseb, H. A. A., Moursy, H. A., El-Bahr, M. K., et al. (2009): Sex determination of jojoba using RAPD markers and *sry* gene primer combined with RAPD primers. – Res. J. Cell Mol. Biol. 3: 102-112.
[38] Muyle, A., Shearn, R., Marais, G. A. (2017): The evolution of sex chromosomes and dosage compensation in plants. – Genome Biol. Evol. 9: 627-645.
[39] Mwase, W. F., Erik-Lid, S., Bjørnstad, A., Stedje, B., Kwapata, M. B., Bokosi, J. M. (2007): Application of amplified fragment length polymorphism (AFLPs) for detection of sex–specific markers in dioecious *Uapaca kirkiana* Muell. – Årg. Afr. J. Biotechnol. 6: 137-142.
[40] Parrish, T. L., Koelewijn, H. P., van Dijk, P. J. (2004): Identification of a male-specific AFLP marker in a functionally dioecious fig, *Ficus fulva* Reinw. ex Bl. (Moraceae). – Sex. Plant Reprod. 17: 17-22.
[41] Passerini, E., Lombardo, P. (2000): Cosmetics. – Cosmet. News 22: 396-398.
[42] Peil, A., Flachowsky, H., Schumann, E., Weber, W. E. (2003): Sex-linked AFLP markers indicate a pseudoautosomal region in hemp (*Cannabis sativa* L.). – Theor. Appl. Genet. 107: 102-109.

http://www.aloki.hu ● ISSN 1589 1623 (Print) ● ISSN 1785 0037 (Online)
DOI: http://dx.doi.org/10.15666/aeer/1804_50235035

[43] Pinzi, S., Garcia, I. L., Lopez-Gimenez, F. J., et al. (2009): The ideal vegetable oil-based biodiesel composition: a review of social, economical and technical implications. – Energy Fuels 23: 2325-2341.
[44] Prakash, S., Van Staden, J. (2006): Sex identification in *Encephalartos natalensis* (Dyer and Verdoorn) using RAPD markers. – Euphytica 152: 197-200.
[45] Reamson-Büttner, S. M., Schondelmaier, J., Jung, C. (1998): AFLP markers tightly linked to the sex in *Asparagus officinalis*. – Mol. Breed. 4: 91-98.
[46] Renner, S. S. (2014): The relative and absolute frequencies of angiosperm sexual systems: dioecy, monoecy, gynodioecy, and an updated online database. – Am. J. Bot. 101: 1588-1596.
[47] Ruas, C. F., Fairbanks, D. J., Evans, R. P., et al. (1998): Male-specific DNA in the dioecious species *Atriplex garrettii* (Chenopodiaceae). – Am. J. Bot. 85: 162-167.
[48] Sharma, K., Agrawal, V., Gupta, S., et al. (2008): ISSR marker-assisted selection of male and female plants in a promising dioecious crop: jojoba (*Simmondsia chinensis*). – Plant Biotechnol. Rep. 2: 239-243.
[49] Shibu, M. P., Ravishankar, K. V., Anand, L., et al. (2000): Identification of sex-specific DNA markers in the dioecious tree, nutmeg (*Myristica fragrans* Houtt.). – PGR Newslet. 121: 59-61.
[50] Tan, H., Callahan, F. E., Zhang, X. D., et al. (2003): Identification of resistance gene analogs in cotton (*Gossypium hirsutum* L.). – Euphytica 134: 1-7.
[51] Tobares, L., Frati, M., Guzman, C., Maestri, D. (2004): Agronomical and chemical traits as descriptors for discrimination and selection of jojoba (*Simmondsia chinensis*) clones. – Industrial Crops and Products 19: 107-111.
[52] Torjek, O., Bucherna, N., Kiss, E., et al. (2002): Novel male-specific molecular markers (MADC5, MADC6) in hemp. – Euphytica 127: 209-218.
[53] Vaknin, Y., Mills, D., Benzioni, A. (2003): Pollen production and pollen viability in male jojoba plants. – Industrial Crops and Products 18: 117-123.
[54] Wang, J., Na, J. K., Yu, Q., et al. (2012): Sequencing papaya X and Yh chromosomes reveals molecular basis of incipient sex chromosome evolution. – Proc. Natl. Acad. Sci. USA 109: 13710-13715.
[55] Wang, Z., Jiao, Z., Xu, P., et al. (2013): Bisexual flower ontogeny after chemical induction and berry characteristics evaluation in male *Vitis amurensis*. – Rupr. Sci. Hortic. 162: 11-19.
[56] Xu, W. J., Wang, B. W., Cui, K. M. (2004): RAPD and SCAR markers linked to sex determination in *Eucommia ulmoides* Oliv. – Euphytica 136: 233-238.
[57] Yang, H. –W., Akagi, T., Kawakatsu, T., Tao, R. (2019): Gene networks orchestrated by *MeGI*: a single-factor mechanism underlying sex determination in persimmon. – Plant J. 98: 97-111.

ELECTRONIC APPENDIX

Appendix 1. *List of RAPD (Operon Technologies, USA) and ISSR primers along with their nucleotide sequences as well as sex-specific primers generated from NUCmer*

Appendix 2. *Banding patterns randomly selected for RAPD (a) and ISSR (b) analyses as well as those generated from NUCmer (c & d) in a trial to detect new sex-specific markers. As models, amplicons of two RAPD (with A02 and B09 primers) and two ISSR (with 544A and HB11 primers) are shown. (c) Patterns generated from 35 reactions (Rx) of one male and female samples, (d) patterns of five male and five female samples for selected reactions. Mw = 50bp DNA Step ladder, 1-5 = M, 6-10 = female, M = male, F = female. Primer sequences are shown in Appendix 1*

http://www.aloki.hu ● ISSN 1589 1623 (Print) ● ISSN 1785 0037 (Online)
DOI: http://dx.doi.org/10.15666/aeer/1804_50235035

Appendix 3. *Forward J888 marker sequences of five male and five female samples and multiple sequence alignments using Clostal Omega*

Appendix 4. *Reverse J888 marker sequences of five male and five female samples and multiple sequence alignments using Clostal Omega*

Appendix 5. *Restriction map of J888 marker for the male sample*

Appendix 6. *Restriction map of J888 marker for the female sample*

Appendix 7. *Virtual gel describing predicted restriction analyses of ClaI, HindIII, HinfI, TaqI and Bsp119I of the 888 bp amplicon for one male and one female samples in jojoba using SnapGene® software*

Appendix 8. *AFLP analysis for the primer combination EcoRI-GC/MseI-GCG in five male and five female samples in jojoba*

Appendix 9. *AFLP analysis for the primer combination EcoRI-TAC/MseI-GCG in five male and five female samples in jojoba*

Appendix 10. *BLAST analysis of the de novo assembled contigs of the jojoba male genome against the ISSR male-specific marker namely UBC-807$_{1200}$ generated by PCR with primer UBC-807*

Appendix 11. *BLAST analysis of the de novo assembled contigs of the jojoba female genome against the ISSR male-specific marker namely UBC-807$_{1200}$ generated by PCR with primer UBC-807*

Appendix 12. *BLAST analysis of the de novo assembled contigs of the jojoba male genome against the SRAP male-specific marker (396 bp) generated by PCR with primer combination Em14/Me10*

Appendix 13. *BLAST analysis of the de novo assembled contigs of the jojoba female genome against the SRAP male-specific marker (396 bp) generated by primer combination Em14/Me10*

Appendix 14. *BLAST results of the de novo assembled contigs of male jojoba plant against the published sequences of the OGI gene*

Appendix 15. *BLAST results of the de novo assembled contigs of male jojoba plant against the published sequences of the MeGI gene*

Appendix 16. *BLAST results of the de novo assembled contigs of female jojoba plant against the published sequences of the OGI gene*

Appendix 17. *BLAST results of the de novo assembled contigs of female jojoba plant against the published sequences of the MeGI gene*

http://www.aloki.hu ● ISSN 1589 1623 (Print) ● ISSN 1785 0037 (Online)
DOI: http://dx.doi.org/10.15666/aeer/1804_50235035

THE POSSIBILITY OF MUTUAL CONTROL OF STEM MINING WEEVILS AND POLLEN BEETLE IN OILSEED RAPE

JURAN I.* – GRUBIŠIĆ, D. – OKRUGIĆ, V. – GOTLIN ČULJAK T.

University of Zagreb Faculty of Agriculture, Svetošimunska 25, 10000 Zagreb, Croatia (phone: +385-1-239-3737)

**Corresponding author*
e-mail: ijuran@agr.hr; phone: +385-1-239-3965

(Received 21st Feb 2020; accepted 25th May 2020)

Abstract. Stem weevils and pollen beetle are significant pests that attack oilseed rape crops after winter hibernation. Correct timing of insecticide application is a key point in control of both pests. The aim of this research is whether the mutual control of both pests is possible in order to reduce insecticide input. The two-years experiment was set up according to the EPPO guidelines in random block design in four replications with nine different treatments. The optimal treatment period was determined by monitoring the occurrence and population density of stem weevils using yellow water traps. The decision threshold for pollen beetles was determined by beating terminal inflorescences into trays. The use of insecticides against rape stem weevils and pollen beetles is possible if thresholds are exceeded at the same time. All insecticides applied against stem mining weevils increased rapeseed yield, and in the absence of treatment, the average loss of oilseed rape seed yield was 37%.
Keywords: *oilseed rape, pests, integrated pest management, Curculionidae, Nitidulidae*

Introduction

Oilseed rape stem weevil (*Ceutorhynchus napi* Gyllenhal, 1837) and cabbage stem weevil (*Ceutorhynchus pallidactylus* Marsham, 1802) (Coleoptera: Curculionidae) are the first pests which attack oilseed rape plants after winter hibernation. They are often considered as a pest complex due to their biological and ecological characteristics which are similar although their life cycles are different and demand different control approach. Pollen beetle (*Brassicogethes aeneus* Fabricius, 1775) (Coleoptera: Nitidulidae) is the most important oilseed rape pest from the *Brassicogethes* genus and appears in oilseed rape fields after stem weevils when temperature exceeds 12°C (Láska and Kocourek, 1991; Alford et al., 2003; Williams, 2010). Direct damage caused by adult forms of stem weevils occurs as a result of the oviposition inside plant tissue. More significant damage occurs as a result of the larvae feeding inside leave petioles, secondary shoots and stems. In general, damages result in short and tiny plants. It is enough to find only one larva inside the plant to classify damage from the feeding of the larvae as significant. The plant deforms, stunts and decays rapidly. One day after oviposition plants begin to respond with histological changes, which are resulted by the slower development of the plant above the attacked part, the deformation of the stem and the cracking tissue at different places. Due to the destruction of the central part of the stem, a deformation of the tissue and loss of plant vigors, the number of siliques per plant is reduced. The plant produces lateral shoots and has a bushy appearance which causes a ripening maturity and makes difficulties to harvest. Feeding of adults and larvae of the pollen beetle cause bud abscission with podless stalks or siliques that can be distorted and weakened (Klukowski and Kelm, 2000; Alford et al., 2003; Krause et al., 2006; Williams, 2010). Yield losses up to 50% caused by stem weevils and up to 70% by pollen beetle have been reported (Alford et al., 2003).

http://www.aloki.hu ● ISSN 1589 1623 (Print) ● ISSN 1785 0037 (Online)
DOI: http://dx.doi.org/10.15666/aeer/1804_50375047

The number of insecticides treatments for pest control in oilseed rape as well as the cost of treatment and insecticides in Europe have been changing over the last 30 years (Walczak and Mrówczyński, 2006). Continued frequent use of insecticides may decrease effectiveness of insecticides for stem weevils and pollen beetle control and is already present in most countries in the European Union (Heimbach et al., 2006; Thieme et al., 2010; Gotlin Čuljak et al., 2013). According to Maceljski (2002) both species of stem weevils and pollen beetle are sufficiently controlled with the single insecticide application, especially with earlier applications at the beginning of the stem elongation. In other EU countries the first treatment is performed against cabbage stem weevil and the second against rape stem weevil and pollen beetle as two insecticides application in spring significantly reduces the pollen beetle populations (Wahmhoff, 2000).

The aim of this research was to determine possibility of joint control of stem weevils and pollen beetle which might reduce insecticide input and result in slower resistance development of the oilseed rape pest.

Materials and methods

The experiment was conducted in Croatia during 2017 and 2018 at two locations, Koprivnički Bregi (46°7'34.06"N 16°53'42.55"E) in Koprivnica-Križevci county and Šašinovec (45°51'2.10"N 16°11'3.01"E) in Zagreb county. Experiments were set up according to the EPPO guidelines (2014) for investigating the effectiveness of insecticides for the control of stem weevils (PP 1/219 (1)) and pollen beetles (PP 1/178 (2)). During both growing seasons, the experiment was set up according to a random block design in four replications with nine different treatments (*Table 1*). The size of each experimental plot was 30 m^2 with average plant density in harvest of 39 plants/m^2 during both investigation years. Oilseed rape had been drilled on September 5 for both experimental years with cultivar PR46W14. Row space was 14 cm and previous crop was winter wheat. The crop was fertilized with 90 kg N/ha in autumn and spring and with 40 kg S/ha in autumn. The experiment included commercial products, applied according to recommended and registered doses, with single active ingredient: lambda cyhalothrin (6.25 ml of active ingredient/ha) and deltamethrin (5 g active ingredient/ha) as well as combined products thiacloprid (55 g of active ingredient/ha) + deltamethrin (5 g active ingredient/ha) and chlorpyrifos-ethyl (450 ml active ingredient/ha) + cypermethrin (45 ml active ingredient/ha). Chlorpyrifos-ethyl belongs to organophosphates and is classified into group 1. Deltamethrin, lambda cyhalotrin and cypermethrin belong to pyrethroids and are classified into group 3. Both groups have contact action. Thiacloprid belongs to neonicotinoids and is classified into group 4 with systemic action (IRAC, 2019).

Table 1. *Treatments and active ingredients during two years experiment*

treatment	active ingredient/pests
1	lambda cyhalothrin/stem weevils
2	thiacloprid + deltamethrin/stem weevils
3	deltamethrin/pollen beetles
4	chlorpyrifos-ethyl + cypermethrin/pollen beetles
5	lambda cyhalothrin/stem weevils and deltamethrin/pollen beetles
6	lambda cyhalothrin/stem weevils and chlorpyrifos-ethyl +cypermethrin/pollen beetles
7	thiacloprid+deltamethrin/stem weevils and deltamethrin/pollen beetles
8	thiacloprid+deltamethrin/stem weevils and chlorpyrifos-ethyl + cypermethrin/pollen beetles
9	untreated control

http://www.aloki.hu ● ISSN 1589 1623 (Print) ● ISSN 1785 0037 (Online)
DOI: http://dx.doi.org/10.15666/aeer/1804_50375047

Oilseed rape crop was treated using Solo Accu Power sprayer with constant pressure of 2 bar after the decision threshold of pest population was exceeded. Optimal treatment period was determined by monitoring the occurrence and population density of stem weevils using yellow water traps. The decision threshold for pollen beetle was determined by beating 50 terminal inflorescences per each treatment into trays when flower buds were but still closed with leaves (BBCH 50). The decision threshold for *C. napi* control was 10 adult forms and for the *C. pallidactylus* control 20 adult forms caught in a yellow water traps in three consecutive days (PP 1/219 (1)). The decision threshold for pollen beetle was 0.8 - 1 adults per terminal inflorescence in growth stage when the flower buds were still covered with leaves and barely noticeable (BBCH 50) (PP 1/178 (2)). The experiment was evaluated according to EPPO guidelines (PP 1/219 (1), PP 1/178 (2)) (2014) to investigate the effectiveness of insecticides. For stem weevils, the experiment was evaluated by dissecting 10 plants taken from each treatment during the flowering (BBCH 65 - 69). The number larvae and feeding tubes were recorded. The effectiveness of insecticides for the pollen beetle control was evaluated 24 hours and three days after the insecticides application. The number of live adult forms was recorded on 50 terminal inflorescences. Harvest of each experimental plot was performed by the trial combine and seed from each experimental plot was weighed and yield was converted to hectare based on 9% seed moisture. A two-way ANOVA was performed to test the difference between treatments for the number larvae and feeding tubes caused by the larval feeding, the number of live adult forms of pollen beetle and yield. The averages are compared to Tukey's rank test. Data were statistically analysed by computer program "R" (Version 3.1.2., 2014).

Results

For the first year of experiment at Koprivnički Bregi location population dynamics of stem weevils adults, from yellow water traps, is present in *Figure 1*. Decision threshold for *C. pallidactylus* was reached on February 26 and on March 21, 24, 26 and 30. Decision threshold for *C. napi* was reached on March 30. *Table 2* presents average number of pollen beetle adults recorded by beating into trays method. Decision threshold was reached on March 29 (BBCH 50).

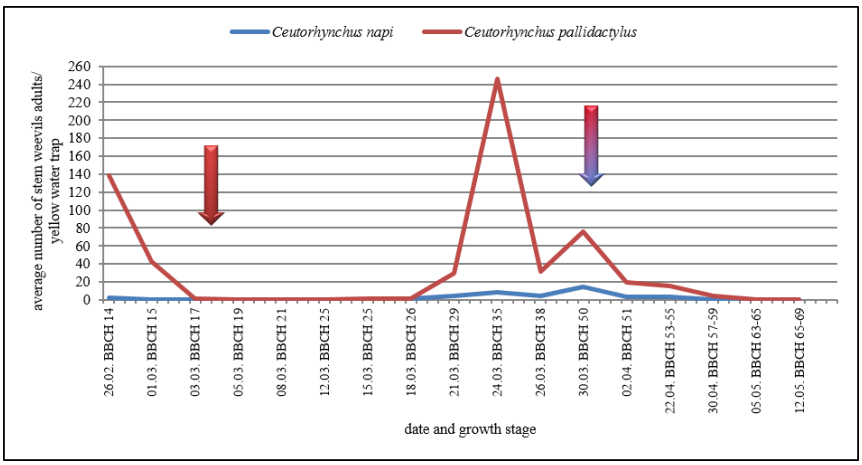

Figure 1. *Average number of adult forms of C. pallidactylus and C. napi per yellow water trap at Koprivnički Bregi site (arrows present date of insecticide application)*

http://www.aloki.hu ● ISSN 1589 1623 (Print) ● ISSN 1785 0037 (Online)
DOI: http://dx.doi.org/10.15666/aeer/1804_50375047

Table 2. *Average number of the pollen beetle adults per plant at Koprivnički Bregi site, BBCH 50*

replication treatment	I	II	III	IV
1	0.9	1.2	1.4	0.9
2	1	1.2	1.4	0.9
3	0.8	1.2	1.1	0.9
4	1.3	1.2	1.2	0.9
5	1	1.1	1.3	1.3
6	1.2	1.1	1.5	1
7	0.9	1.2	1.3	0.9
8	0.9	1.4	1.3	0.9
9	1.9	0.8	1.5	0.8

First insecticides application was conducted on treatments 1, 2, 5, 6, 7, and 8 on March 2 after threshold for *C. pallidactylus* was exceeded. Second insecticide application was conducted on March 30 after thresholds for both species of stem weevils and pollen beetle were exceeded.

For the second year of experiment at Šašinovec location population dynamics of stem weevils adults, from yellow water traps, is present in *Figure 2*. Decision threshold for *C. pallidactylus* was reached on March 1 and 5. Decision threshold for *C. napi* was reached on March 26. The average number of pollen beetle adults recorded by beating into trays method are present in *Table 3*. Decision threshold was reached on March 30 (BBCH 50) at treatments 3, 4 and 9.

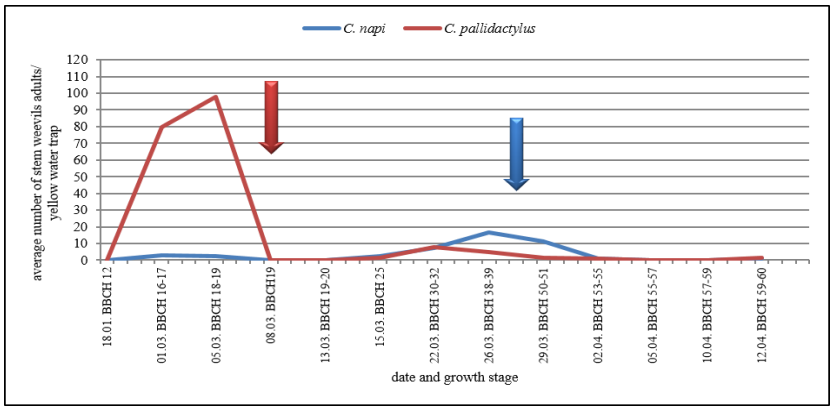

Figure 2. *Average number of adult forms of C. pallidactylus and C. napi per yellow water trap at Šašinovec site (arrows present date of insecticide application)*

Table 3. *Average number of the pollen beetle adults per plant at Šašinovec, BBCH 50*

replication treatment	I	II	III	IV
1	0.06	0.1	0.1	0.08
2	0.04	0.08	0.06	0.1
3	0.8	0.8	0.8	0.8
4	0.8	0.98	0.8	0.8
5	0.08	0.42	0.04	0.1
6	0.02	0.1	0.12	0.14
7	0.04	0.04	0.1	0.08
8	0.02	0.02	0.04	0.08
9	0.9	0.82	0.8	0.9

http://www.aloki.hu ● ISSN 1589 1623 (Print) ● ISSN 1785 0037 (Online)
DOI: http://dx.doi.org/10.15666/aeer/1804_50375047

First insecticides application was conducted on treatments 1, 2, 5, 6, 7, and 8 on March 7 after threshold for *C. pallidactylus* was exceeded. Second insecticide application was conducted on March 27 after threshold for *C. napi* was exceeded. Third insecticide application was conducted on treatments 3 and 4 on March 30 after decision threshold for pollen beetle was exceeded.

Results of a two-way ANOVA conducted to test differences between treatments for stem weevil larvae for all locations and years are present in *Figure 3*. Statistical analysis showed a significant difference between years ($F = 504.8$; $DF = 1.8$; $P < 0.001$) and between treatments ($F = 23.4$; $DF = 8.8$; $P < 0.0001$). Tukey's HSD post hoc test showed significant differences between interaction of years and treatments.

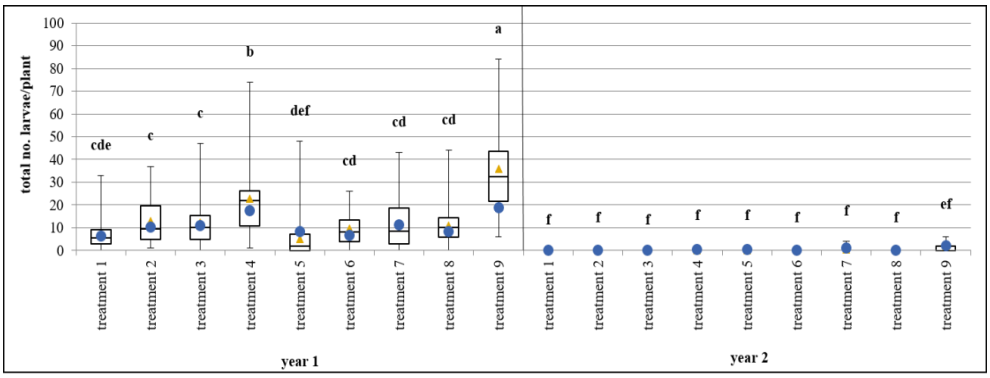

Figure 3. *Two-way ANOVA for number of stem weevils larvae per plant (each treatment is presented by upper and lower quartile, minimum and maximum values; median is presented by middle line, middle value by triangle and standard deviation by circle; ranges not connected with the same latter are significantly different)*

Results of a two-way ANOVA conducted to test differences between treatments for feeding tubes of stem weevils for all locations and years are present in *Figure 4*. Statistical analysis showed a significant difference between years ($F = 536.06$; $DF = 1.8$; $P < 0.0001$) and between treatments ($F = 8.4$; $DF = 8.8$; $P < 0.0001$) as well as interaction between treatments and years ($F = 4.7$; $DF = 8.8$; $P < 0.0001$). Tukey's HSD post hoc test showed significant differences between interaction of years and treatments.

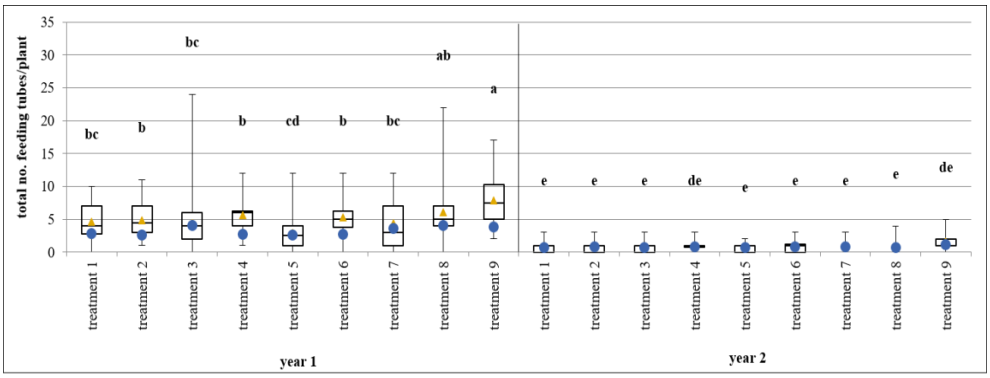

Figure 4. *Two-way ANOVA for number of stem weevils feeding tubes per plant (each treatment is presented by upper and lower quartile, minimum and maximum values; median is presented by middle line, middle value by triangle and standard deviation by circle; ranges not connected with the same latter are significantly different)*

http://www.aloki.hu ● ISSN 1589 1623 (Print) ● ISSN 1785 0037 (Online)
DOI: http://dx.doi.org/10.15666/aeer/1804_50375047

Results of a two-way ANOVA conducted to test differences between treatments for live adults of pollen beetle 24 hours after insecticides application for all locations and years are present in *Figure 5*. Statistical analysis showed a significant difference between years ($F = 86.06$; $DF = 1.8$; $P < 0.0001$) and between treatments ($F = 54.8$; $DF = 8.8$; $P < 0.0001$) as well as interaction between treatments and years ($F = 25.9$; $DF = 8.8$; $P < 0.0001$). Tukey's HSD post hoc test showed significant differences between interaction of years and treatments.

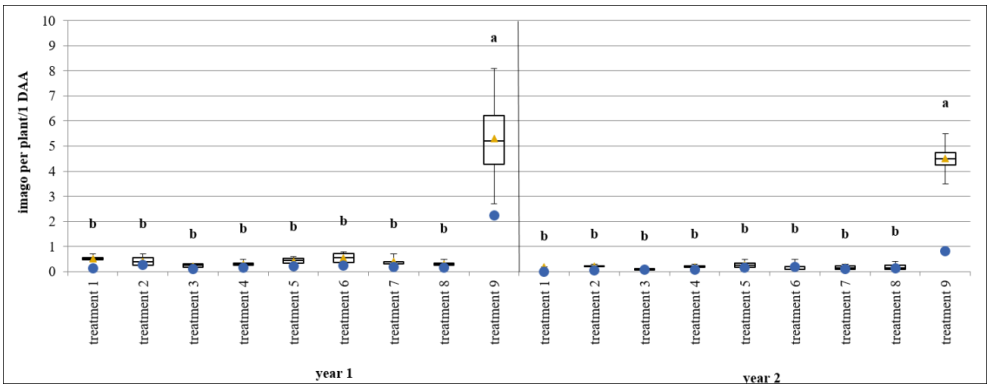

Figure 5. *Two-way ANOVA for number of live pollen beetle adults 24 hours after application (each treatment is presented by upper and lower quartile, minimum and maximum values; median is presented by middle line, middle value by triangle and standard deviation by circle; ranges not connected with the same latter are significantly different)*

Results of a two-way ANOVA conducted to test differences between treatments for live adults of pollen beetle 3 days after insecticides application for all locations and years are present in *Figure 6*. Statistical analysis showed a significant difference between years ($F = 89.5$; $DF = 1.8$; $P < 0.0001$) and between treatments ($F = 44.1$; $DF = 8.8$; $P < 0.0001$) as well as interaction between treatments and years ($F = 16.5$; $DF = 8.8$; $P < 0.0001$). Tukey's HSD post hoc test showed significant differences between interaction of years and treatments.

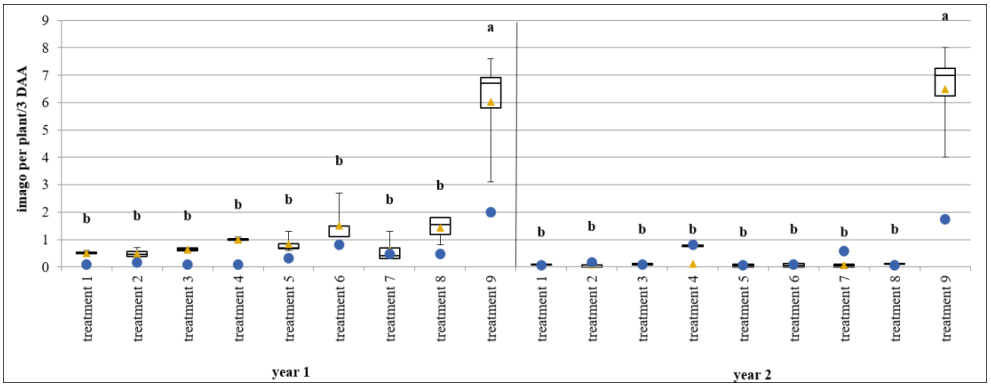

Figure 6. *Two-way ANOVA for number of live pollen beetle adults 3 days after application (each treatment is presented by upper and lower quartile, minimum and maximum values; median is presented by middle line, middle value by triangle and standard deviation by circle; ranges not connected with the same latter are significantly different)*

http://www.aloki.hu ● ISSN 1589 1623 (Print) ● ISSN 1785 0037 (Online)
DOI: http://dx.doi.org/10.15666/aeer/1804_50375047

Results of a two-way ANOVA conducted to test differences between treatments for yield of oilseed rape for all locations and years are present in *Figure 7*. Statistical analysis of data showed a significant difference between years (F = 163.3; DF = 1.8; P < 0.0001). No statistically significant differences between treatments (F = 1.5; DF = 8.8; P < 0.1922) and interaction between treatments and years (F = 1.2; DF = 8.8; P < 0.3005) were recorded.

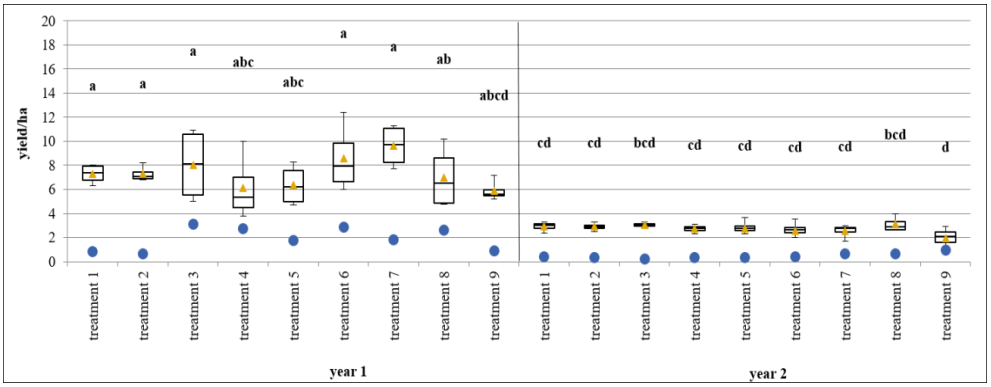

Figure 7. *Two-way ANOVA for oilseed rape seed yield per hectare (each treatment is presented by upper and lower quartile, minimum and maximum values; median is presented by middle line, middle value by triangle and standard deviation by circle; ranges not connected with the same latter are significantly different)*

Discussion

During both years of research, the first insecticide application was performed against adult forms of *C. pallidactylus*, which is coincided by the biology of this species. Another insecticide application was performed against *C. napi* and *Brassicogethes* sp. as both species reached the decision threshold at the same time.

The main indicator of the effectiveness of insecticides is the number of stem weevils larvae in plants and the yield of rapeseed (EPPO, 2014). The number of larvae and the number feeding tubes caused by the diet of stem weevil larvae in rapeseed plants, were significantly higher in the first experimental year compared with second year. The main reason is the later positioning of the yellow water traps in the crop of the first year and it is very likely that, by the time of the first application of the insecticide, the decision threshold for the control of *C. pallidactylus* had already been reached. As both sexes of *C. pallidactylus* tend to appear simultaneously (Juran et al., 2011) there is a possibility that copulation has occurred and that females have laid eggs before insecticide application, which is contrary to the results of Büchs (1998), who states that treatment of adult forms of *C. pallidactylus* may be delayed two weeks after the decision threshold is exceeded. Due to the large differences in the abundance of stem weevil larvae in plants in both years, it can be concluded that insecticides should be applied immediately after decision threshold for *C. pallidactylus* control is reached and not after two weeks when females become sexually mature as proposed by Kostal (1992), Büchs (1998) and Seidenglanz et al. (2009). The decision threshold should be considered as the number of females caught in yellow water traps, as suggested by Wahmhoff (2000). This is especially important when pests appear in high adult population and when the number of females exceeds the critical number of 10 for *C. napi* or 20 adult forms for

http://www.aloki.hu ● ISSN 1589 1623 (Print) ● ISSN 1785 0037 (Online)
DOI: http://dx.doi.org/10.15666/aeer/1804_50375047

C. pallidactylus per yellow water trap. Considering different temporal occurrence of adult stages of both stem weevil species, insecticides application at two deadlines during the spring could significantly reduce the population of adult forms (Wahmhoff, 2000). The highest efficacy in reducing larval abundance in rapeseed plants in the first year was observed with the use of a lambda cyhalothrin against adult forms (treatments 1 and 5). Systemic active ingredients should have good efficacy on larvae within plants (Tomlin, 1994) but on treatments where thiacloprid (treatments 2, 7 and 8) was used in combination with deltamethrin, the number of stem weevil larvae was not significantly reduced (Gratina et al., 2011). This may be due to lower temperatures at the first insecticide application against adult forms of *C. pallidactylus* (Seta and Wolski, 2006) at which neonicotinoids have lower efficacy (Tomlin, 1994). During second year, no significant differences were observed in the number of stem weevils larvae in rapeseed plants. Differences are not present even on treatments three and four where stem weevils were not controlled and as one reason may be the different distribution of these pests across the field (Green et al., 1991; Kuhne, 1997). Uneven distribution across the surface has also been recorded for adult forms of pollen beetle (Ferguson et al., 2003, 2005). At treatments where pollen beetle was controlled with the chlorpyrifos-ethyl and cypermethrin (treatment 4), satisfactory effects on stem weevil larvae inside the stem were not achieved during both years of the study, although the organophosphorus component penetrate deeper into plant tissue (Corteva, 2019) which is partially confirmed by Milovac et al. (2017). This is in contradiction with the results of Inđić et al. (2011), but the applied insecticide dose per hectare (1l), in their investigation was twice higher than recommended. The same authors conclude that there are no statistically significant differences in the number of larvae in the plant between the treatment of adult forms of stem weevils with chlorpyrifos-ethyl + cypermethrin and deltamethrin.

The results of the ANOVA for the number of larvae are also accompanied by the number of the feeding tubes which is to be expected since the damage depends on their presence and their number in the plant. The differences in the number of feeding tubes between treatments 1 and 6 (lambda cyhalothrin was used in both treatments to control stem weevils) could be explained by the different spatial distribution of adults across the field. Thiacloprid did not have a satisfactory effect on the number of feeding tubes in the plant due to the lower efficacy at lower temperatures (mean daily temperature ranged from 3.4 to 6.7°C) at the time of application of the insecticide (CMHS, 2019). During both years of the study, no statistically significant differences were found between treatments against adult forms of pollen beetle, although a year later, resistance to pyrethroids was confirmed in Croatia (Gotlin Čuljak et al., 2013).

Although no statistically differences were found between treatments for rapeseed yield in both years, it is important to observe the increase in yield from a biological importance, not a statistical significance level (Lovell, 2013). In all treatments where insecticides were applied, during the two years of the study, a relative increase in the yield of rapeseed ranged from 4 to 63% compared to the untreated control. Although the highest insecticide efficacy, for number of stem weevil larvae and feeding tubes was observed for the lambda-cyhalothrin (treatment 1 and 5 against stem weevils) did not ultimately affect the seed yield, as confirmed by Seta and Wolski (2006). The highest yield increasing in the first year of investigation was recorded on treatment 7 (63% increase in yield) where stem weevils were controlled with combination of thiacloprid and deltamethrin, and pollen beetle with deltamethrin, which is in contrast with the results of the statistical analysis for the number of larvae. A significant uniformity of the rapeseed yield across all treatments

http://www.aloki.hu ● ISSN 1589 1623 (Print) ● ISSN 1785 0037 (Online)
DOI: http://dx.doi.org/10.15666/aeer/1804_50375047

was observed during second year, which again demonstrates that insecticide application against adults of *C. pallidactylus* is required immediately after decision threshold is exceeded. Any application of insecticides against stem weevils results in an increase in yield regardless results cannot be statistically significant, which is confirmed by Seta and Mrówczyński (1999), Seta and Wolski (2006), Petraitiené et al. (2012). The results show that stem weevils can reduce rapeseed seed yield by up to 60% and 37% on average, as confirmed by several authors (Walczak et al., 1997; Kelm and Walczak, 1998; Kelm and Klukowski, 2000; Seta and Mrówczyński, 2000; Alford et al., 2003; Dechert and Ulber, 2004).

Conclusions

Based on the results of the control and considering the life cycle of stem weevils, the first application of insecticide against adult forms of *C. pallidactylus* is critical point in protecting rapeseed against these pest. *C. napi* can be controled with pollen beetles as the decision thresholds for these two pests coincide. Considering the confirmed resistance of pollen beetle to pyrethroids and possible resistance to organophosphorus insecticides in joint control of *C. napi* and *Brassicogethes* sp. producers should pay attention of the proper selection of insecticides and insecticides rotation to achieve effective control. For the future research, it is highly recommended to investigate the impact of stem weevils on different components of oilseed rape yield and to determine which component has the most significant impact on yield lose.

REFERENCES

[1] Alford, D. V., Nilsson, C., Ulber, B. (2003): Insect pests of oilseed rape crops. – In: Alford, D. V. (ed.) Biocontrol of oilseed rape pests. Blackwell Publishing, London.

[2] Büchs, W. (1998): Strategies to control the cabbage stem weevil (*Ceutorhynchus pallidactylus* Mrsh.) and the oilseed rape stem weevil (*Ceutorhynchus napi* Gyll.) by a reduced input of insecticides. – IOBC Bulletin 21(5): 205-220.

[3] CMHS (2019): Croatian Meteorlogical and Hydrological Service. – https://meteo.hr/index_en.php/.

[4] Corteva (2019): Corteva Agriscience. – https://www.chlorpyrifos.com/.

[5] Dechert, G., Ulber, B. (2004): Interactions between the stem-mining weevils *Ceutorhynchus napi* Gyll. and *Ceutorhychus pallidactylus* (Marsh.) (Coleoptera: Curculionidae) in oilseed rape. – Agricultural and forest entomology 6: 193-198.

[6] EPPO (2014): Guidelines for efficacy evaluation of plant protection product - insecticides & acaricides, Efficacy evaluation of insecticides - *Ceutorhynchus napi* and *Ceutorhynchus pallidactylus* on rape. – Bulletin OEPP/EPPO Bulletin 33: 65-69.

[7] Ferguson, A. W., Klukowski, Z., Walczak, B., Clark, S. J., Mugglestone, M. A., Perry, J. N., Williams, I. H. (2003): Spatial distribution of pest insects in oilseed rape: implications for integrated pest management. – Agriculture, ecosystems and environment 95: 509-521.

[8] Ferguson, A. W., Barari, H., Warner, D. J., Campbell, J. M., Smith, E. T., Watts, N. P., Williams, I. H. (2005): Distributions and interactions of the stem miners *Psylliodes chrysocephala* and *Ceutorhynchus pallidactylus* and their parasitoids in a crop of winter oilseed rape (*Brassica napus*). – Entomologia experimentalis et applicata 119: 81-92.

[9] Gotlin Čuljak, T., Jelovčan, S., Grubišić, D., Juran, I., Ilić Buljan, M. (2013): Pojava rezistentnosti repičinog sjajnika (*Meligethes* spp.) na piretroide u usjevima uljane repice (*Brassica napus* L.) u Hrvatskoj. – Glasilo biljne zaštite 5: 379-383.

http://www.aloki.hu ● ISSN 1589 1623 (Print) ● ISSN 1785 0037 (Online)
DOI: http://dx.doi.org/10.15666/aeer/1804_50375047

[10] Gratina, I., Apenite, I., Turka, I. (2011): Commonly found species of *Ceutorhynchus* (Coleoptera: Curculionidae) on the oilseed rape in Lativa. – Acta Biologica Daugavpils University 11(2): 260-264.
[11] Green, D. B., Bennison, J., Emmett, B., Walters, K. (1991): Evaluation of alphacypermethrin and phorate against cabbage stem weevil in autumn-sown oilseed rape. – Annals of Applied Biology 118: 4-5.
[12] Heimbach, U., Müller, A., Thieme, T. (2006): First steps to analyse pyrethroid resistance of different oil seed rape pests in Germany. – Nacrichten aus Deutschland Pflanzenschutzdienst 58: 1-5.
[13] Inđić, D., Vuković, S., Grahovac, M., Mrkajić, M., Gvozdenac, S., Šunjka, D., Tanaskovič, S., Stevanović, V. (2011): Validnost nekoliko parametara u oceni efekata insekticida u suzbijanju *Ceutorhynchus* spp. na uljanoj repici. – Biljni lekar 39: 481-489.
[14] IRAC (2019): Insecticide Resistance Action Committee. – https://www.irac-online.org/.
[15] Juran, I., Gotlin Čuljak, T., Grubišić, D. (2011): Rape Stem Weevil (*Ceutorhynchus napi* Gyll. 1837) and Cabbage Stem Weevil (*Ceutorhynchus pallidactylus* Marsh. 1802) (Coleoptera: Curculionidae) - Important Oilseed Rape Pests. – Agriculture Conspectus Scientificus 76(2): 93-100.
[16] Kelm, M., Walczak, B. (1998): The relationship between the stem weevil (*Ceutorhynchus pallidactylus* Marsh.) injury and losses of the flower buds. – IOBC/wprs Bulletin 21(5): 147-151.
[17] Kelm, M., Klukowski, Z. (2000): Weather as a factor determining damage caused by oilseed rape pests. – IOBC/wprs Bulletin 23(6): 119-124.
[18] Klukowski, Z., Kelm, M. (2000): *Stenomalina gracilis* (Walker), a new parasitoid reared from *Ceutorhynchus napi* Gyll. in Poland. – IOBC/wprs Bulletin 23(6): 135-138.
[19] Kostal, V. (1992): Monitoring of activity and abundance of adult pollen beetle (*Meligethes aeneus* F.) and cabbage stem weevil (*Cenutorhynchus pallidactylus* Marsh.) in winter rape stand. – Oilseed crops 38(3-4): 297-306.
[20] Krause, U., Koopmann, B., Ulber, B. (2006): Impact of rape stem weevil, *Ceutorhynchus napi*, on the early stem infection of oilseed rape by *Phoma lingam*. – IOBC/wprs Bulletin 29(7): 323-328.
[21] Kuhne, W. (1997): Studies on the distribution of infestation by the weevils *Ceutorhynchus napi* Gyll., *Ceutorhynchus quadridens* Panz. and *Ceutorhynchus assimilis* Payk. in large-scale plantings of winter rape. – Archiv für Phytopathologie und Pflanzenschutz 13(2): 109-115.
[22] Láska, P., Kocourek, F. (1991): Monitoring of flight activity in some crucifer-feeding pests by means of yellow water traps. – Acta Entomol Bohemos 88: 25-35.
[23] Lovell, D. P. (2013): Biological importance and statistical significance. – Journal of agricultural and food chemistry 61: 8340-8348.
[24] Maceljski, M. (2002): Poljoprivredna entomologija. – Zrinski, Čakovec.
[25] Milovac, Ž., Zorić, M., Franeta, F., Terzić, S., Petrović Obradović, O., Marjanović Jeromela, A. (2017): Analysis of oilseed rape stem weevil chemical control using a damage rating scale. – Pest Management Science 79(9): 1962-1971.
[26] Petraitiené, E., Brazauskiené, I., Vaitelyté, B. (2012): The effect of insecticides on pest control and productivity of winter and spring oilseed rape (*Brassica napus* L.). – In: Perveen, F. (ed.) Insecticides - Advances in Integrated Pest Management. InTech, New York.
[27] R Foundation for Statistical Computing (2014): R: A Language and Environment for Statistical Computing. – http://www.r-project.org/.
[28] Seidenglanz, M., Poslušná, J., Hrudová, E. (2009): The importance of monitoring the *Ceutorhynchus pallidactylus* female flight activity for the timing of insecticidal treatment. – Plant Protection Science 45(3): 103-112.

http://www.aloki.hu ● ISSN 1589 1623 (Print) ● ISSN 1785 0037 (Online)
DOI: http://dx.doi.org/10.15666/aeer/1804_50375047

[29] Seta, G., Mrówczyński, M. (1999): Harmfulness and possibility of cabbage stem weevil (*Ceutorhynchus pallidactylus* Marsh.) control in winter rape. – Progress in Plant Protection 39(2): 534-536.
[30] Seta, G., Wolski, A. (2006): Trial of qualification of harmfulness and effectiveness of *Meligethes aeneus* F. and *Ceutorhynchus pallidactylus* Marsh. on winter oilseed rape control in dependence of air temperature in spring time. – Progress in Plant Protection 46(2): 390-394.
[31] Thieme, T., Heimbach, U., Müller, A. (2010): Chemical control of insect pests and insecticide resistance in oilseed rape. – In: Williams, I. H. (ed.) Biocontrol-based integrated management of oilseed rape pests. Springer, Berlin.
[32] Tomlin, C. (1994): The Pesticide Manual, Incorporating The Agrochemicals Handbook. – The British Crop Protection Council and The Royal Society of Chemistry, Bath.
[33] Wahmhoff, W. (2000): Integrieter Rapsanbau: Untersuchungen zur Entwicklung integrierter Produktionsverfahren am Beispiel des Winterrapses (*Brassica napus* L.). – Erich Schmidt Verlag, Berlin.
[34] Walczak, B., Kelm, M., Karp, R., Smart, L. (1997): Use of semiochemicals in different types of traps for monitoring stem weevil (*Ceutorhynchus* sp.) flight to winter rape. – Progress in plant protection 37(2): 25-27.
[35] Walczak, F., Mrówczyński, M. (2006): The endangerment of oilseed rape by pests in Poland. – IOBC/wprs Bulletin 29(7): 163.
[36] Williams, I. H. (2010): The major insect pests of oilseed rape in Europe and their management: an overview. – In: Williams, I. H. (ed.) Biocontrol-based integrated management of oilseed rape pests. Springer, Berlin.

http://www.aloki.hu ● ISSN 1589 1623 (Print) ● ISSN 1785 0037 (Online)
DOI: http://dx.doi.org/10.15666/aeer/1804_50375047

NEW MULTIVARIATE EMPIRICAL PREDICTION EQUATION FOR RELATIVE FEED VALUE OF NATIVE GRASSES

CELIKTAS, N.[1*] – CAN, E.[1] – KAYA, S.[2] – ATIS, I.[1] – HATIPOGLU, R.[3] – ERTEKIN, I.[1]

[1]Department of Field Crops, Agricultural Faculty of Mustafa Kemal University, Antakya, 31034 Hatay, Turkey
(e-mails/ORCIDs: ecan69@hotmail.com/0000-0003-3530-6010; iatis15@hotmail.com/0000-0002-0510-9625; ibrahimertekin@mku.edu.tr/0000-0002-3030-8159)

[2]Department of Animal Science, Agricultural Faculty of Mustafa Kemal University, Antakya, 31034 Hatay, Turkey
(e-mail/ORCID: serafettinkaya@gmail.com/0000-0001-9744-8714)

[3]Department of Field Crops, Agricultural Faculty of Çukurova University, Sarıçam, 01330 Adana, Turkey
(e-mails/ORCIDs: rustu_hatipoglu@hotmail.com/0000-0002-7977-0782)

**Corresponding author*
e-mail: nafizcel@hotmail.com; phone: +90-326-245-5845/11038; fax: +90-326-245-5832;
ORCID: 0000-0002-0467-1034

(Received 6th Sep 2019; accepted 28th Nov 2019)

Abstract. Relative feed value and structural mineral differentiation of native grasses and their relationships at different plant growth stages were studied to create a more informative multivariate model to predict relative feed value. The hierarchical clustering grouped the species and their growth stages under six distinct categories with their average relative feed values of 122.6, 108.6, 99.6, 90.3, 80.9 and 71.5. The principal component analyses for the relative feed value and the mineral composition of native grasses was efficient to classify the forages with the total explained variation of 63.69% with the first two principal components. The most important predictors for relative feed value were determined as nitrogen and potassium contents of the native grasses according to beta coefficients from the partial least square regression analyses. Three partial least square regression based new empirical equations for predicting the relative feed value were constructed by using the forage nitrogen content. The coefficients of determination (R^2) and the root mean square error of prediction (RMSEP) for the equations were 0.92, 0.35, 0.81 and 2.17, 11.29, 5.88, respectively. The Fisher's F test manifested that the actual and the predicted relative feed values were not different ($P>0.05$) for all three equations.
Keywords: *forage quality index, mineral elements, pasture, plant growth stages, PLSR*

Introduction

Reaching the optimum reflection of animal genetic potential on the phenotype is only possible with an accurate diet program. In order to achieve this, delicious and highly digestible, quality roughage above the maintenance requirement of the animal is an absolute necessity. This will also lead to economic farming via reducing concentrated feed because 60 to70% of dairy or beef cattle production costs are concerned with feed inputs. Actually sustainable livestock farming requires the use of a pasture-based system. High-quality roughage feed from the pastures also encourages a healthy rumen flora by enhancing the effectiveness of the bacteria (Schroeder, 1996). This promotes nutrient intake and also conversion to energy.

In the formulation of diets for dairy cattle, the quality and the amount of forage needed to meet nutrient and fiber requirements must be considered in the first (Linn and Kuehn,

http://www.aloki.hu ● ISSN 1589 1623 (Print) ● ISSN 1785 0037 (Online)
DOI: http://dx.doi.org/10.15666/aeer/1804_50495063

1997). The fiber needed in rations for cud chewing and rumination is provided through forage. The feed requirement varies depending on both animal species and their physiological growth stages and with this aspect, there are many different criteria to express the quality of feed. Knowing this helps in forming the diet program and also foreseeing the management cost. Moreover, it is necessary to manage the natural ecosystems without any detriment for many years. Forage quality can be expressed with the subjective physical evaluations and also with the results of the chemical analysis, which entail more accurate assessments. The relative feed value (RFV) has become an important criteria for evaluating the quality of the forage. RFV is a forage quality index used widely for hay pricing. It is used for forage-quality education and also by seed producers to indicate variety improvement (Moore and Undersander, 2002) and it is an energy-based scale (Henning et al., 1999). Acid detergent fiber (ADF) estimates forage digestibility and neutral detergent fiber (NDF) provides an estimate for forage intake (Caddel and Allen, 1994). RFV is obtained on the basis of both intake and digestibility; thus, RFV reflects the forage quality in a single digit by using these two animal responses. However, the forage-quality parameters including the RFV are variable and almost everything can affect them in one way or another in native pastures. The RFV hay-grading system is based on the full-bloom alfalfa hay, which has an RFV of 100. However, grasses usually have higher concentrations of NDF than legumes at the same plant growth stages (Hodgson et al., 2014). But NDF is more digestible than alfalfa (Brown and Pittman, 1991; Ward, 2008). Therefore, comparing grasses with legumes using such a grading underestimates the nutritional value of high-quality grasses relative to legumes.

The minerals are key to many metabolic reactions most of the time. That is why the forage quality is assessed by the accumulation rate of the minerals in plant tissues one way or another. The amount of those minerals in grass tissues depend upon many factors including genetic capacity to take up minerals from the soil, availability of minerals in soil, stage of plant growth, climatic conditions, etc. (Kappel et al., 1983; Stone, 1994; Greene, 1997). Forage nutritive value is often evaluated by measuring such characteristics related to digestibility and intake. Whereas, the minerals that correlate with these factors should not be overlooked. Knowledge on plant nutrient characteristics and its relationship with RFV is vital. Also, RFV ignores the important variations in economic value caused by variation in crude protein (CP) concentrations (Weiss et al., 2012). Consequently, creating more descriptive equations for different forages is important for an accurate pricing or planning of feeding.

Chemometry is a useful tool to explain the best such relations by processing the chemical results with mathematics and statistics. Multivariate modelling that is one of the important chemometric applications is a statistical tool that uses multiple variables to predict the possible outputs. Partial least-squares regression (PLSR) has been one of the most widely applied multivariate calibration method because of the quality of calibration models produced and the ease of their implementation (Hopke, 2003). It is appreciable for constructing predictive models when the explanatory variables are many and highly collinear (Yeniay and Göktaş, 2002).

The study presented in this paper discusses the variations of relative feed values (RFVs) and the mineral compositions of the herbage obtained from some important native grasses at different plant growth stages, their relationships and the possibilities of producing new empirical equations for predicting RFV by applying multivariate analyses (MVA) and their literature based comparative accuracy.

http://www.aloki.hu ● ISSN 1589 1623 (Print) ● ISSN 1785 0037 (Online)
DOI: http://dx.doi.org/10.15666/aeer/1804_50495063

Materials and methods

Grass samples

Some of the native grass species from the natural pastures (between 36°13′04”-36°29′55”N/36°11′37”-36°14′59”E, 80 m average altitude) of Amik Plain located at the east Mediterranean coastal region of Turkey were evaluated in the study. Eight pasture sites with different directions and geog. exposure were determined for sampling (*Fig. 1*).

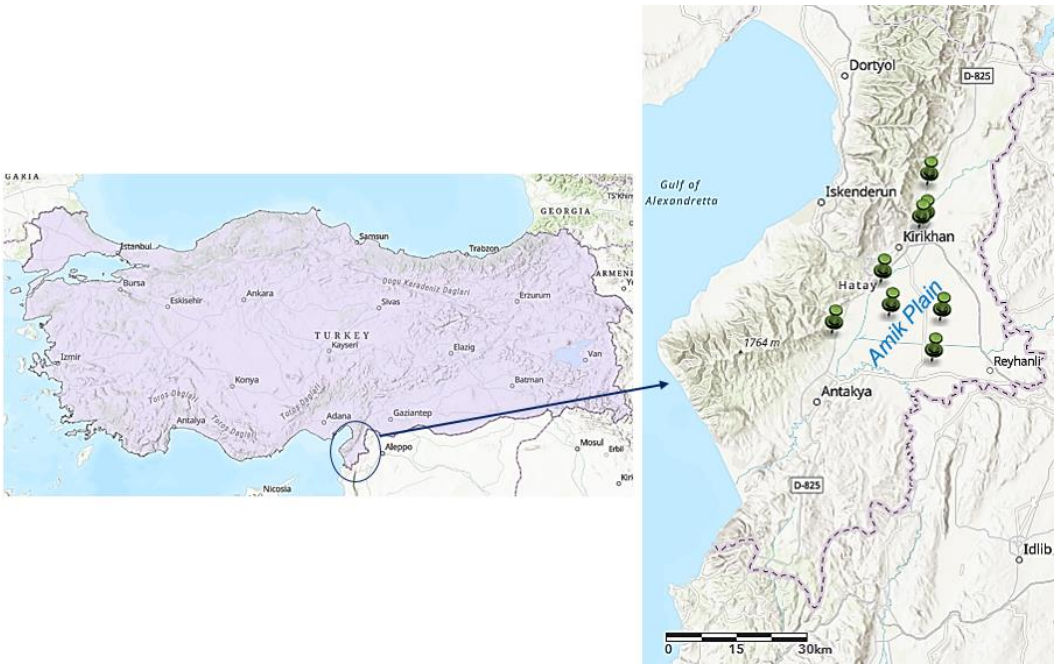

Figure 1. *The map of sampling sites from the Amik Plain of Hatay province*

The climate of the site is a Mediterranean-type with mild, wet winters and warm to hot dry summers. The seven cool-season C3 grasses and four warm season C4 grasses were studied (*Table 1*). Five phenological stages being vegetative (VEG), stem elongation (STE), head emergence and flowering (HEF), developing seed stalks (DSS) and seed ripening (SER), adapted from Cogswell and Kamstra (1976), were included in the study for relative feed values (RFV) and mineral composition.

Sample preparation, chemical analyses and calculations

Grass sampling at each plant growth stages was accomplished in the same habitat in the year of 2016. Harvested aboveground materials from 3 individual clones of each species at the stages of phenology described above were washed with continuously flowing tap water and rinsed with distilled water for possible contaminants, oven-dried at 70 °C for 48 h and homogenized by particle size reduction (< 0.5 mm). Neutral detergent fiber (NDF) and acid detergent fiber (ADF) analyses were performed as described by Goering and Van Soest (1970). Digestible dry matter (DDM), Dry matter intake (DMI) and Relative feed value (RFV) were estimated by the equations given below suggested by Undersander et al. (1993):

$$DDM\%=88.9-(0.779\times ADF\%)$$

http://www.aloki.hu ● ISSN 1589 1623 (Print) ● ISSN 1785 0037 (Online)
DOI: http://dx.doi.org/10.15666/aeer/1804_50495063

$$\text{DMI \% of body weight} = 120 \div \text{NDF\%}$$

$$\text{RFV} = (\text{DDM} \times \text{DMI}) \div 1.29$$

Powdered samples were digested with HNO_3 + $HClO_4$ mixture (Jones et al., 1991) and analyzed for calcium (Ca), magnesium (Mg), potassium (K), phosphorus (P), iron (Fe), copper (Cu), manganese (Mn), and zinc (Zn) contents by inductively coupled plasma atomic emission spectroscopy (ICP-AES Varian Liberty Series II). Nitrogen (N) content of the samples was determined by the Kjeldahl method (Kjeldahl, 1883). All chemical analyzes were performed with three repetitions.

Table 1. *The investigated grass species and the abbreviations for plant scientific names*

Species		Abbreviation
Cool-season C3 grasses	Tall fescue (*Festuca arundinaceae* L.)	*Feau*
	Tor-grass (*Brachypodium pinnatum* (L.) Beauv.)	*Brpi*
	Timothy (*Phleum pretense* L.)	*Phpr*
	Orchard grass (*Dactylis glomerata* L.)	*Dagl*
	Smooth brome (*Bromus inermis* Leyss.)	*Brin*
	Perennial ryegrass (*Lolium perenne* L.)	*Lope*
	Bulbous barley (*Hordeum bulbosum* L.)	*Hobu*
Warm-season C4 grasses	Coolatai grass (*Hyparrhenia hirta* (L.)	*Hyhi*
	Dallis grass (*Paspalum dilatatum* Poir.)	*Padi*
	Yellow bluestem (*Bothriochloa ischaemum* (L) Keng)	*Bois*
	Red oat grass (*Themeda triandra* Forssk.)	*Thtr*

Data analysis

Significance in differences of RFV means for all species at whole plant growth stages were evaluated by Duncan multiple comparison tests at the 1% significance level with SPSS software (v24 for Windows; IBM, New York, USA). Hierarchical clustering analysis was applied to group the species according to periodically changing RFV with Ward method by using the software JMP 13 (SAS Institute Inc. Cary, North Carolina, USA). Principal component analyses (PCA) which is the most commonly used ordination technique was applied to observe the behavior of RFV and the mineral compositions of native grasses at different phenological stages by reducing the dimensionality of the original data matrix. To determine the key mineral(s) affecting the RFV and the quantitative relationships between them (constructing an empirical multivariate model), partial least-squares regression (PLSR) analysis was applied. The performance of the developed empirical equations was evaluated with the coefficients of determination (R^2), root mean square error of prediction (RMSEP) and literature based comparison of the predicted RFVs. Differences between the actual RFV from the open access literature and the predicted ones obtained in the study were compared with Fisher's F test. The chemometric software XLSTAT v2016 (Addinsoft Inc., New York, USA) was used for PCA and PLSR analyses.

http://www.aloki.hu ● ISSN 1589 1623 (Print) ● ISSN 1785 0037 (Online)
DOI: http://dx.doi.org/10.15666/aeer/1804_50495063

Results and discussion

RFV differentiation depending on the plant growth stages

Mean relative feed values (RFV) of the native grass species averaged over five plant growth stages are presented in *Table 2*. As shown in *Table 2* differences between the RFV of the native species were significantly important.

Table 2. *Relative feed values (RFV) of the native grass species as an average of five plant growth stages*

Species	Range	Mean	Std. dev.	MAD[2]
Feau	79.31 - 103.49	94.67 b[1]	8.05	7.02
Brpi	70.33 - 88.54	79.13 de	6.24	5.65
Phpr	88.78 - 112.87	102.30 a	7.68	6.92
Dagl	72.68 - 103.79	84.89 c	9.36	8.17
Brin	87.02 - 100.96	93.26 b	4.33	3.68
Lope	71.20 - 123.34	103.20 a	15.45	11.70
Hobu	66.24 - 130.82	95.21 b	19.66	16.09
Hyhi	65.04 - 87.84	76.33 e	8.29	7.37
Padi	65.79 - 89.78	80.18 d	7.91	6.24
Bois	68.91 - 82.58	76.69 e	4.36	3.75
Thtr	70.12 - 88.78	78.01 de	6.18	5.76

LSD: 3.362
[1]Differences between the groups comprising different letters in the same column is statistically significant (P<0.01)
[2]MAD=Mean absolute deviation

The highest value of RFV (103.20) was determined for Perennial ryegrass but it was clustered with the same statistical group with Timothy. Coolatai-grass was evaluated as the species having the lowest RFV with 76.33 as an average of whole vegetation. However, the species of yellow bluestem, tor-grass and red oat grass were clustered together with coolatai-grass, as well. As it is expected, the RFV decreased with the advancing plant growth stages (*Fig. 2*).

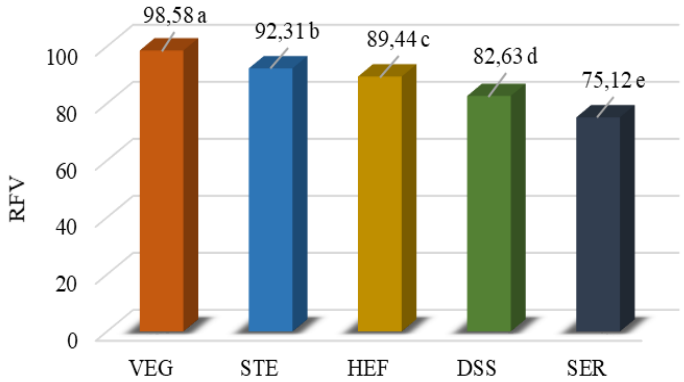

Figure 2. *Relative feed value (RFV) at different plant growth stages of native grasses (LSD=1.199, P<0.01) (VEG: Vegetative, STE: Stem elongation, HEF: Head emergence and flowering, DSS: Developing seed stalks, SER: Seed ripening)*

http://www.aloki.hu ● ISSN 1589 1623 (Print) ● ISSN 1785 0037 (Online)
DOI: http://dx.doi.org/10.15666/aeer/1804_50495063

The highest RFV was detected for the earlier phenological stages. Generally, the cool season grasses had better RFV than the warm season grasses; however, RFV of the species significantly varied depending on their growth stages (*Fig. 3*).

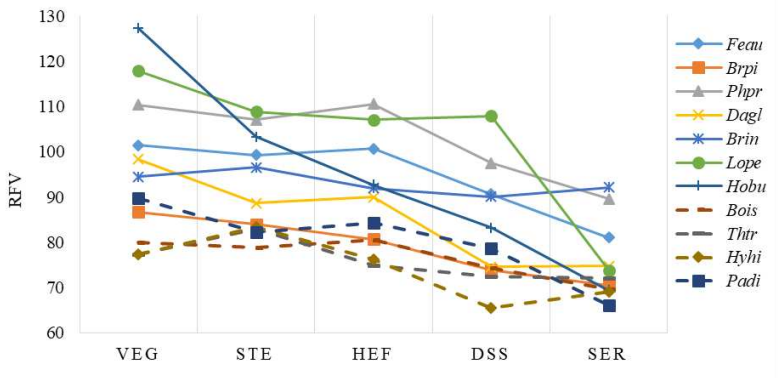

Figure 3. *Differentiation of relative feed value (RFV) of native grasses depending on the plant growth stages (Dashed lines indicate the warm season C4 grasses)*

In other words, the quality parameters were substantially under the influence of the stage of maturity. Actually, the information about mentioned fluctuations is more valuable for pasture management since the grazing period do not cover whole growth stages. In that respect, while the highest mean values were observed from perennial ryegrass (*Lope*) without any small deviation till DSS, it reached one of the lowest averages at the end stage with a severe reduction. In fact, this is a critical stage for pasture plants when the grazing process should be terminated to avoid some physiological damages to the plants. Therefore, the decline on RFV at this critical stage gives some advantages to plants in respect to storing nutrients and seed maturation. On the other hand, the decline for Timothy (*Phpr*) was not obvious as in perennial ryegrass in maturity stages. In this respect, the most remarkable reduction was recorded for bulbous barley (*Hobu*). It had the lowest RFV at SER with a distinctive reduction while it stood the highest at the beginning of the vegetation. However, it was one of the good species with a moderate RFV index as an overall average. On the other hand, it was consequently determined as the worst species in terms of dry matter digestibility together with tall fescue, which also has good RFV index (data not shown). Something similar can also be said for orchard grass (*Dagl*). Tall fescue (*Feau*) seemed to be the most stable species in terms of RFV differentiation throughout the maturity stages. The investigated four warm season C4 grasses produced the worst RFV indexes even in VEG stage. This is an expected result since the higher temperatures increase the lignocellulosic structure and reduce the soluble carbohydrates (Pearson and Ison, 1997). Therefore, the C4 species start to accumulate more lignin at earlier stages. The constellation plot in *Figure 4* summarizes the clusters formed with the RFV differentiation of the species at different plant growth stages. The hierarchical clustering grouped the species and their growth stages under six distinct clusters (Clu). The *Hobu*VEG and *Lope*VEG were constituted the first cluster (Clu1) with the highest average RFV (122.6). The warm season grasses were mostly clustered in Clu5 and Clu6 with the worst RFV (80.9 and 71.5, respectively). It is clear that the later stages of the cool season grasses such as *Feau*SER or *Phpr*SER were closely aggregated with the very early stages of the warm season grasses.

http://www.aloki.hu ● ISSN 1589 1623 (Print) ● ISSN 1785 0037 (Online)
DOI: http://dx.doi.org/10.15666/aeer/1804_50495063

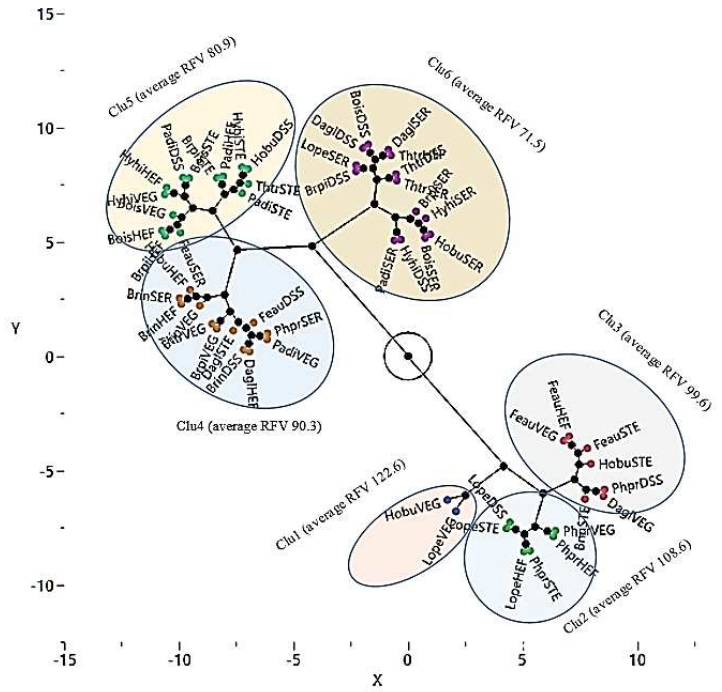

Figure 4. *The hierarchical clusters (Clu) formed with the relative feed value (RFV) differentiation of the plant species at different plant growth stages (VEG: Vegetative, STE: Stem elongation, HEF: Head emergence and flowering, DSS: Developing seed stalks, SER: Seed ripening)*

High animal gains require an adequate nutrition program. Hence, matching the forage quality to animal nutritional needs greatly increases the productivity. Producing high-quality forage requires the knowledge of the factors that affect forage quality and management accordingly. Stage of maturity when harvested or grazed is the most important factor affecting the forage quality. Relative feed value (RFV) is an index that makes it possible to compare forages based on their digestibility and intake. Forage quality is highest when pasture plants are young and vegetative. Timothy (*Phpr*) species reached the superior RFV index at HEF stage, even higher than the index calculated at its VEG while the other species tend to decrease at HEF (*Fig. 3*). This is because of the extremely poor cellulosic structure of timothy at mentioned stage. It is one of the fast-growing species that accumulates more cytoplasmic compounds (Poorter and Bergkotte, 1992; Niemann et al., 1992). Pasture or forage quality is very closely related with the amount of leaves (Lacefield et al., 2012). The leaf/stem ratio of the species at harvest; however, is one of the major determiners of lignocellulosic structure along with RFV. Ball et al. (2001) propounded that the higher the leaf content, the higher the forage quality since the NDF in legume or grass leaves is significantly more digestible than NDF in stem tissue (Hoffman et al., 2003). Timothy (*Phpr*) is a leafy species, which translates to high digestibility and intake (Peeters, 2004). It has a higher capacity to accumulate water-soluble carbohydrates (WSC) like fructose. Humphreys (1989) reported a positive correlation between WSCs and dry matter digestibility DMD. Likewise, Pearson and Ison (1997) attributed that the reason of the lower digestibility of C4 plants is related to a rapid decrease in soluble carbohydrate content as a result of the increased temperature. WSCs are also an indicator of palatability of the forages (Mayland et al., 2000). Sturla (1960)

http://www.aloki.hu ● ISSN 1589 1623 (Print) ● ISSN 1785 0037 (Online)
DOI: http://dx.doi.org/10.15666/aeer/1804_50495063

indicated that Timothy as the most palatable species followed by perennial ryegrass. Thus, the first four growth stages of Timothy species were clustered in the best quality region (Clu2 and Clu3). Therefore, it is possible to infer that the higher the RFV in forages, the more digestible and palatable they become.

In fact, forage plants differentiate so rapidly that it is possible to detect significant declines in forage quality every two or three days (Fulgueira et al., 2007). Schroeder (1996) pointed out as well that quality declines four to five times a day in RFV in the spring. That is why the rapid quality changes make the cutting or grazing time critical especially on fast-growing species. Our results targeted bloom stage (HEF) as having the maximum quality and yield for most of the investigated native species. Similarly, Lacefield et al. (2012) indicated that the RFV index of cool season grasses at vegetative-boot and boot-head stages were 101-122 and 84-101 respectively. As it is seen in *Figure 4*, the first three clusters, even the fourth cluster, are within the mentioned range with their average RFV (Clu1: 122.6, Clu2: 108.6, Clu3: 99.6 and Clu4: 90.3 respectively). The results of the chemical analyses in the current study covers the entire biomass analyses of the native species. However, the animals in pastureland selectively graze native plant parts. Hence, native grasses are able to produce higher than expected animal gains estimated by the whole plant analyses. Therefore, comparison of RFV of the native species with the other forages may result in misevaluation. Because of this, the nutritional value of the higher quality native grasses may be underestimated. Moore and Undersander (2002) indicated that a current equation to predict DMI is based on the assumption of NDF intake with a constant 1.2% of body weight. Whereas, they emphasized that "the NDF intake is not exactly a constant 1.2% of body weight". NDF intake is variable for grasses and legumes fed alone. That is why, the authors argue that different equations may be needed for alfalfa, cool-season grasses, warm season grasses, grass/legume mixtures, corn silage, etc.

The multivariate relationship between RFV and mineral contents

The mineral composition of the native grass forages at different growth stages are given in *Table 3*.

Table 3. *Values of macro and microelement composition as an average of 11 native grass species and five plant growth stages*

Macro and micro elements		Range	Mean	Std. dev.	MAD[1]
Macro minerals (g kg^{-1})	N[2]	5.82 - 26.12	14.78	5.51	4.80
	P	1.05 - 4.92	2.75	1.02	0.84
	K	5.63 - 19.33	12.88	3.73	3.19
	Ca	1.96 - 13.66	5.27	2.34	1.61
	Mg	0.87 - 2.57	1.75	0.47	0.40
Micro minerals (mg kg^{-1})	Zn	12.04 - 57.10	22.20	7.12	4.76
	Cu	3.87 - 18.89	8.65	2.85	2.15
	Fe	75.39 - 702.67	190.25	102.76	64.61
	Mn	12.41 - 191.74	64.43	48.54	37.93

[1]MAD=Mean absolute deviation
[2]N (Nitrogen), P (phosphorus), K (potassium), Ca (calcium), Mg (magnesium), Zn (zinc), Cu (copper), Fe (iron) and Mn (manganese)

http://www.aloki.hu ● ISSN 1589 1623 (Print) ● ISSN 1785 0037 (Online)
DOI: http://dx.doi.org/10.15666/aeer/1804_50495063

The range and the mean values are the averages of eleven species and five plant growth stages. The mineral content of forages varies and depends primarily on forage species and their growth stages (Rayburn, 1997). Principal component analysis (PCA) and partial least square regression (PLSR) analyses were carried out on the relationship among RFV, mineral contents, grass species and growth stages and the results were presented below.

PCA analyses

PCA analyses showed both the mentioned mineral differentiations and the relationships between the RFV of native grass species at different growth stages (*Fig. 5*).

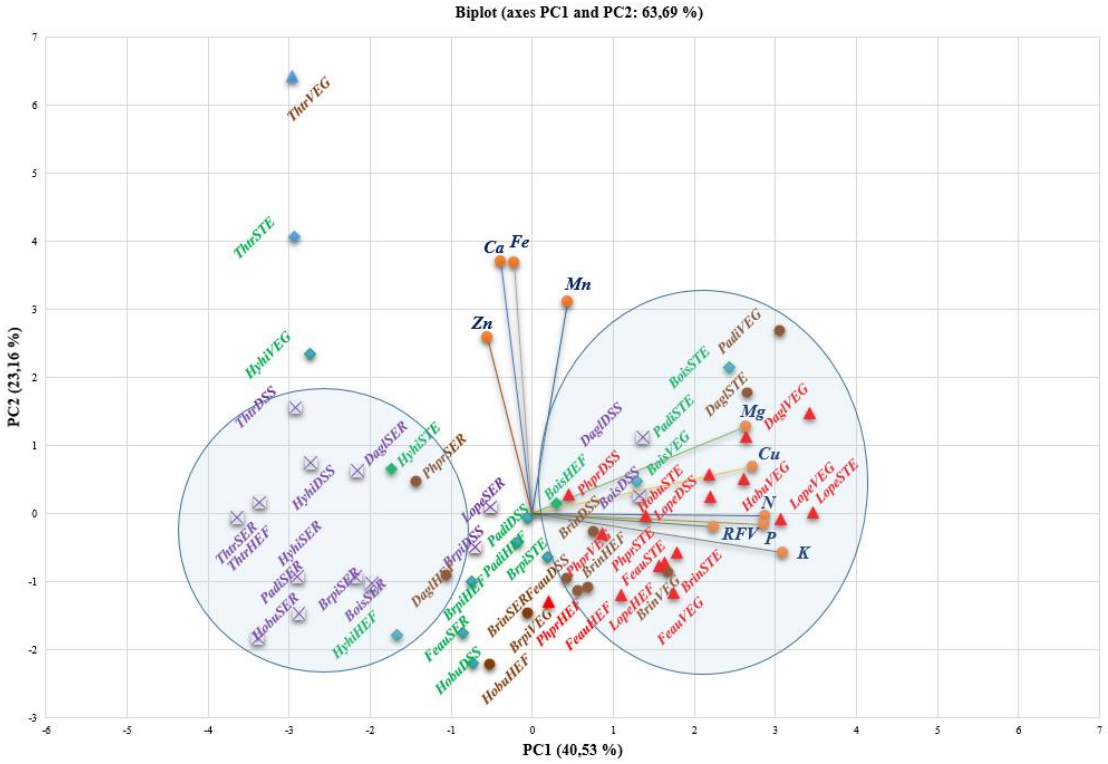

Figure 5. *Principal component analyses (PCA) for relative feed value (RFV) and the mineral composition of native grass species at different plant growth stages. (The markers "Δ" represent the clusters Clu1, Clu2 and Clu3, "O" Clu4, "◊" Clu5 and "×" Clu6)*

The PCA was effective to classify the samples explaining the total variation of 63.69% with the first two principal components (PC). The clusters of the forage samples of different species and growth stages that had higher RFV and assigned as Clu1, Clu2 and Clu3 in *Figure 4* were located up on the positive side of the PC1 axis. However, it is seen that the clusters in *Figure 3* are dispersed and the new elements are added to the area that we can define as quality zone or some of them are located beyond the boundaries of this zone. The coefficients of the eigenvectors for nitrogen (0.423), phosphorus (0.421) and potassium (0.456) were found to be about same on PC1 axes. That means the contribution of these elements on PC1 for the explanation of the variation (40.5%) is about equal. PC1 axis represents the forages that have higher minerals of N, P, K, Cu and Mg on their biochemical structure. So, the forages which had higher RFV accumulated higher

http://www.aloki.hu ● ISSN 1589 1623 (Print) ● ISSN 1785 0037 (Online)
DOI: http://dx.doi.org/10.15666/aeer/1804_50495063

amounts of these elements. As it is seen from the biplot graph, this region mostly covers the earlier plant growth stages. In this respect, the forages of perennial ryegrass (*Lope*) at VEG, STE and bulbous barley (*Hobu*) at VEG stage had good quality in view of both mineral composition and RFV. When the forages are evaluated only on the basis of RFV, the species and their growth stages contained within the clusters Clu1, Clu2 and Clu3 were prominent in view of quality (*Fig. 4*). Whereas, the multivariate relation, by adding the minerals, considered the components from Clu4 (especially *Dagl*STE, *Padi*VEG and *Brin*VEG), Clu5 (*Bois*STE, *Padi*STE and *Bois*VEG) and Clu6 (*Bois*DSS and *Dagl*DSS) moved them to the quality zone. That means that while some of the forages such as the ones from the early phenological stages of yellow bluestem (*Bois*) and dallis grass (*Padi*) were underestimated before they will be evaluated with valuable cool season grasses in the new assessment. On the other hand, some of the components of Clu2 moved towards the border of the quality zone. The plant growth stage DSS was mainly clustered around the center of the biplot graph which expresses the lower RFV and mineral accumulation. The forage samples obtained from the latest stage of SER, which were aggregated under the cluster Clu6 (*Fig. 4*), were located around the negative regions of both PC1 and PC2 axis. The eigenvectors of the iron (0.546) and calcium (0.542) were similar on PC2 axis. Therefore, the negative region of the PC2 axes covers the species and plant growth stages that have both lover RFV and Fe, Ca and Zn accumulation capacity. Even the other warm season grasses of coolatai grass (*Hyhi*) and red oat grass (*Thtr*) were evaluated as the poor RFV species and they have the important sources of the minerals Fe, Ca, Zn and Mn at earlier stages. Therefore, the versatile evaluation of any forage provided information that is more valuable to the pasture manager for managing the ration.

PLSR-based new equation construction

Partial least square regression (PLSR) was applied to relate and predict to RFV to structural mineral composition of the hay. The variable importance of the projection (VIPs) for each explanatory mineral elements showed that N, K, Mg and P contributed the most to the RFV (VIP>1) (*Fig. 6*).

On the other hand, *Figure 7* shows the standardized coefficients, which provide a comparison of the relative weight of the variables on the RFV. The higher the coefficient, the greater the impression of the corresponding variable (Perez-Arevalo et al., 2015). Thus, the most important predictors for RFV were determined as N and K at 95% confidence interval.

In most of the studies related to forage quality, data related to protein content of forage are included. The Kjeldahl method (Kjeldahl digestion) is a very common method for the quantitative determination of nitrogen contained in organic substances developed by Johan Kjeldahl in 1883. Since the 16% of the protein is nitrogen, the protein content of any forage is mostly determined by multiplying the nitrogen content with a constant of 6.25 (Mariotti et al., 2008). The Kjeldahl protocol includes the steps digestion, distillation, and titration which require sophisticated equipment (Sáez-Plaza et al., 2013). It appears to be at least as a laborious protocol as the ones for other macro or microelements. However, the advantage of the nitrogen (or protein content) is that it is a very common forage quality data. Therefore, the PLSR based equations for predicting the RFV were constructed as N% based. The equations and their prediction accuracy related statistics are given in *Table 4*.

http://www.aloki.hu ● ISSN 1589 1623 (Print) ● ISSN 1785 0037 (Online)
DOI: http://dx.doi.org/10.15666/aeer/1804_50495063

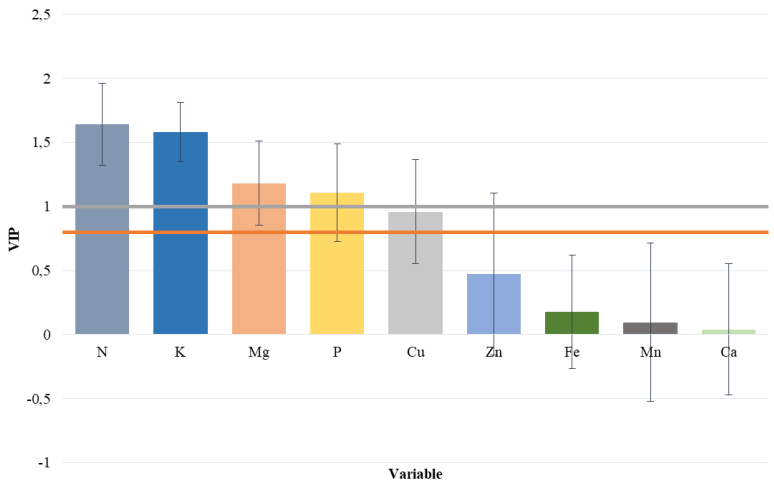

Figure 6. *The variable importance of the projection (VIPs) from partial least squares regression (PLSR) analyses for each explanatory variable of relative feed value (RFV) at 95% confidence interval*

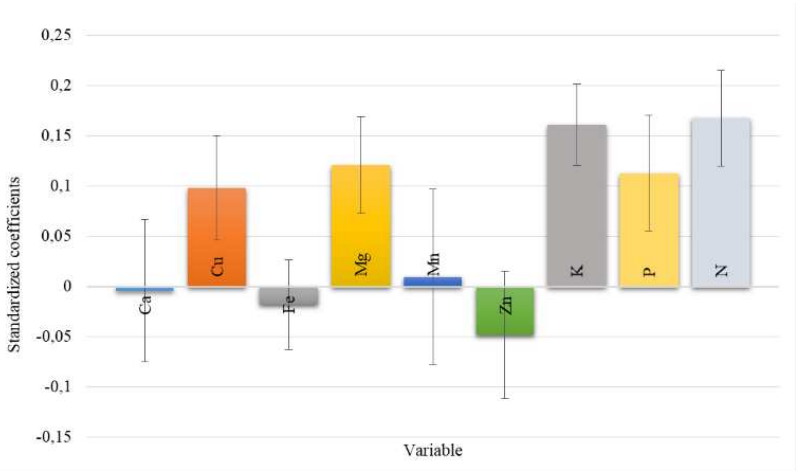

Figure 7. *Standardized/beta coefficients from partial least squares regression (PLSR) model at 95% confidence interval*

Table 4. *New PLSR based equations for predicting the RFV from forage nitrogen content along with the data range and the prediction accuracy statistics*

Equations	n	Range	Std. dev.	R^2	RMSEP
(Eq.1) RFV=57.11+20.52 N%	5	RFV: 75.12 - 98.58 N%: 0.88 - 1.84	2.80	0.92	2.17
(Eq.2) RFV=65.20+15.07 N%	55	RFV: 65.44 - 127.26 N%: 0.58 - 2.61	11.50	0.35	11.29
(Eq.3) RFV=54.25+23.95 N%	106	RFV: 65.04 - 123.84 N%: 0.52 - 2.43	5.94	0.81	5.88

http://www.aloki.hu ● ISSN 1589 1623 (Print) ● ISSN 1785 0037 (Online)
DOI: http://dx.doi.org/10.15666/aeer/1804_50495063

The empirical model *Eq. 1* was constructed with the data produced by averaging the 165 data comprising 11 grass species, 5 phenological stages and 3 repetitions. *Equation 2* is a model constructed from the average data of 11 species and 5 phenological stages whereas *Equation 3* is based on an outlier or noisy data filtering of 165 samples empirically. As it seen in *Table 4* despite data filtering, *Equation 3* has the largest and best representing data range to the entire sample. *Equation 1* has the higher coefficient of determination (R^2=0.928) with the lowest RMSEP value (2.17) that means the higher prediction accuracy. In fact, it includes the whole information about investigated species and plant growth stages. However, it reflects mainly the periodical differentiations of RFV. Multivariate modelling is highly sensitive to the existence of outliers within a dataset. Therefore, the prediction performance statistics of R^2 and RMSEP for *Equation 3* were increased with data preprocessing while they were quite low for the raw data in *Equation 2*. If the RMSEP value of *Equation 2* was within the acceptable range, the lower R^2 value may be ignored for a multivariate model. Nevertheless, it was the highest that means the predicted value can be out of range.

The estimation verification of the new equations was carried out by external validation test based on the data from literature. *Table 5* shows the predicted RFVs for each equation with the open access literature notifications.

Table 5. *The estimation verification of the new prediction equations by external validation test*

Reference	Hay type	Ref N%[+]	Ref RFV	Predicted RFV
Lacefield et al., 2012	Cool season grasses	Veg/boot 1.92-2.56	101-122	96.5-109,6[1] 94.1-103.7[2] 100.2-115.5[3]
		Boot/head 1.28-1.92	84-101	83.3-96.5[1] 84.4-94.1[2] 84.9-100.2[3]
	Warm season grasses	Pre-boot 1.6-2.24	90-104	89.9-103.1[1] 89.3-98.9[2] 92.5-107.9[3]
		Mature/head 0.96-1.6	62-90	76.8-89.9[1] 79.6-89.3[2] 77.2-92.5
Hackmann et al., 2008	Cool season grasses	1.96	90	97.3[1] 94.7[2] 101.1[3]
	Warm season grasses	2.88	109	116.2[1] 108.6[2] 123.2[3]
Lewis et al., 2006	*Tripsacum dactyloides*	2.92	100.0	117.0[1] 109.2[2] 124.1[3]
Albayrak et al., 2011	*Agropyron intermedium* Host. Beauv.	1.62 (two years average value)	89.2	90.3[1] 89.6[2] 93.0[3]
DairyOne, 2019	Grass hay (data from the years of 2000-2018)	1.74 (average of 94301 samples)	89.4 (average of 92571 samples)	92.8[1] 91.4[2] 95.9[3]

[+]It was calculated by dividing the protein content from the open access literature to 6.25
[1]Predicted RFV by *Equation 1*
[2]Predicted RFV by *Equation 2*
[3]Predicted RFV by *Equation 3*

http://www.aloki.hu ● ISSN 1589 1623 (Print) ● ISSN 1785 0037 (Online)
DOI: http://dx.doi.org/10.15666/aeer/1804_50495063

It was not expected to estimate the exact experimental results with the empirical equations. Nevertheless, it is clear that the predictions were quite close to the actual data. However, the Fisher's F test, for the 13 samples provided in *Table 5*, manifested that the actual and the predicted RFVs were not different at the significance level of 5% since having the p values for *Equations 1, 2* and *3* were 0.96, 0.13 and 0.58 respectively ($P>0.05$). Actually, RFV index classified the forages as grade 1 (>140), grade 2 (124-140), grade 3 (101-123), grade 4 (83-100), and grade 5 or supreme, good and premium (<83) (Rohweder et al., 1978) according to the limit range where the calculated RFV value is to be included. Therefore, even if the predictions from the new equations were not exactly overlapped with the actual ones, they were within the same grading class. Rohweder et al. (1978) reported another definition and physical descriptions for grass grading. According to this specification, the best pure grass hays appeared to have a grade not higher than grade 2. That is why, the grade as "prime" for grasses is with the range of the second grading step of legumes. Different grazing animals have different feed needs. Dairy cattle, cows in late-term pregnancy, heavily lactating beef cattle, pregnant heifers, and cattle in poor condition need hay of higher RFV (Nelson, 2010) and protein content. Thus, the knowledge on the variation of RFV of native pastures depending on the phenological stages and its relationships between the mineral compositions will give opportunities to the farmers to manage the harvest or grazing. Even, adjusting the stocking rate that is vital for the sustainability of native pastures might be possible with the help of new RFV equations provided here.

Conclusion

Relative feed value (RFV) is an evaluation criteria not only for marketing but also to express the forage quality. It ranks the forages based on energy. However, two forages with the same RFV do not always perform the same because the RFV index does not reveal any information on protein content. Whereas, the forage evaluation should include a complete information of nutrient composition including digestibility and crude protein (CP) because the energy requirement of livestock fed on low-quality native pastures increases and energy supplementation to diet is needed (Martin and Hibberd, 1990). Since the new PLSR models developed in the current study based on forage nitrogen content, their predictions may give more explanation about quality and protein content also. Moreover, because of the reflection of the multivariate relation between the other minerals, the PLSR based equations are more valuable and informative. However, it should not be ignored that the natural pasture composition contains many species including legumes. Therefore, the accuracy and so the effectiveness of such equations should also be supported by the future animal experiments that contain different plant families. That knowledge will improve the reliability and accuracy of the new equations in preparing rations for different animal requirements.

REFERENCES

[1] Albayrak, S., Türk, M., Yüksel, O., Yılmaz, M. (2011): Forage Yield and the quality of perennial legume grass mixtures under rainfed conditions. – Not. Bot. Horti Agrobot. Cluj-Na 39(1): 114-118.

[2] Ball, D. M., Collins, M., Lacefield, G. D., Martin, N. P., Mertens, D. A. et al. (2001): Understanding Forage Quality. – American Farm Bureau Federation, Park Ridge, IL.

http://www.aloki.hu ● ISSN 1589 1623 (Print) ● ISSN 1785 0037 (Online)
DOI: http://dx.doi.org/10.15666/aeer/1804_50495063

[3] Brown, W. F., Pittman, W. D. (1991): Concentration and degradation of nitrogen and fiber fractions in selected tropical grasses and legumes. – Trop Grassl 25: 305-312.
[4] Caddel, J., Allen, E. (1994): Forage Quality Interpretations. – Oklahoma Coop. Extension Service Facts F-2117, Oklahoma St. Univ., Stillwater, OK.
[5] Cogswell, C., Kamstra, L. D. (1976): The stage of maturity and its effect upon the chemical composition of four native range species. – J. Range Manag 29(6): 460-463.
[6] DairyOne (2019): https://dairyone.com/analytical-services/feed-and-forage/feed-composition-library/interactive-feed-composition-library. – Accessed 08.07.2019.
[7] Fulgueira, C. L., Amigot, S. L., Gaggiotti, M., Romero, L. A., Basilico, J. C. (2007): Forage quality: techniques for testing. – Fresh Produce 1(2): 121-131.
[8] Goering, H. K., Van Soest, P. J. (1970): Forage Fiber Analysis (Apparatus, Reagents, Procedures and Some Applications). – USDA Agricultural Handbook, No. 379. Agricultural Research Service, US, Dep. Agric., Washington, DC.
[9] Greene, L. W. (1997): Mineral composition of southern forages. – Proc. Mid-South Ruminant Nutr. Conf., 1-2 May, Dallas, TX.
[10] Hackmann, T. J., Sampson, J. D., Spain, J. N. (2008): Comparing relative feed value with degradation parameters of grass and legume forages. – J Anim Sci 86(9); 2344-2356.
[11] Henning, J. C., Lacefield, G. D., Donna Amaral, P. D. (1999): Interpreting Forage Quality Reports. – Online publication ID-101. Cooperative Extension Service, University of Kentucky, College of Agriculture, Lexington, KY.
[12] Hodgson, D. R., McKeever, K., McGowan, C. M. (2014): The Athletic Horse: Principles and Practice of Equine Sports Medicine. – In: Hodson, D. R. et al. (eds.) The Athletic Horse. 2nd Ed. Saunders, Elsevier Inc, Philadelphia.
[13] Hoffman, P. C., Lundberg, K. M., Bauman, L. M., Randy, D. S. (2003): The Effect of maturity on NDF digestibility. – Focus on Forage 5: 15.
[14] Hopke, P. K. (2003): The evolution of chemometrics. – Anal Chim Acta 500: 365-377.
[15] Humphreys, M. O. (1989): Water-soluble carbohydrates in perennial ryegrass breeding. III. Relationships with herbage production, digestibility and crude protein-content. – Grass and Forage Sci 44: 423-430.
[16] Jones, J. B., Wolf, B., Mills, H. A. (1991): Interpretation of results. In: Plant Analysis Handbook – a practical sampling, preparation, analysis, and interpretation guide. – Micro-Macro Publishing Inc., USA.
[17] Kappel, L. C., Morgan, E. B., Kilgore, L., Ingraham, R. H., Babcock, D. K. (1983): Seasonal changes of mineral content of Southern forages. – J Dairy Sci 68: 1822-1827.
[18] Kjeldahl, J. (1883): Neue Methode zur Bestimmung des Stickstoffs in organischen Körpern (New method for the determination of nitrogen in organic substances). – Fresenius Z Anal Chem. 22(1): 366-383.
[19] Lacefield, G. D., Henning, J. C., Smith Jr, S. R. (2012): Forages for Beef Cattle. – publications ID-108/2. University of Kentucky, Lexington, KY.
[20] Lewis, J. S., Ditchkoff, S. S., Lin, J. C., Muntifering, R. B., Chappelka, A. H. (2006): Nutritive quality of big bluestem (*Andropogon gerardii*) and eastern gamagrass (*Tripsacum dactyloides*) exposed to tropospheric ozone. – Rangeland Ecol Manag 59: 267-274.
[21] Linn, J., Kuehn, C. (1997): The effects of forage quality on performance and cost of feeding lactating dairy cows. – Proc. of Western Canadian Dairy Seminar, University of Alberta, Edmonton, Canada.
[22] Mariotti, F., Tomé, D., Mirand, P. P. (2008): Converting nitrogen into protein - beyond 6.25 and Jones' factors. – Crit Rev Food Sci Nutr 48(2): 177-184.
[23] Martin, S. L., Hibberd, C. A. (1990): Intake and digestibility of low-quality native grass hay by beef cows fed graded levels of soybean hulls. – J Anim Sci 68: 4319.
[24] Mayland, H. F., Shewmaker, G. E., Harrison, P. A., Chatterton, N. J. (2000): Nonstructural carbohydrates in tall fescue cultivars: relationship to animal preference. – Agron J 92: 1203-1206.

http://www.aloki.hu ● ISSN 1589 1623 (Print) ● ISSN 1785 0037 (Online)
DOI: http://dx.doi.org/10.15666/aeer/1804_50495063

[25] Moore, J. E., Undersander, D. J. (2002): Relative forage quality: an alternative to relative feed value and quality index. – Proc 13th Annual Florida Ruminant Nutrition Symposium. Jan. 11-12, 2002, Gainesville, FL, pp. 16-32.
[26] Nelson, M. (2010): Your Beef Cattle Operation. – In: Nelson, M. (ed.) The Complete Guide to Small-Scale Farming: Everything You Need to Know About Raising Beef and Dairy Cattle, Rabbits, Ducks, and Other Small Animals. Chapter 9. – Atlantic Publishing Company, Ocala, FL.
[27] Niemann, G. J., Pureveen, J. B. M., Gert, B. E., Poorter, H., Boon, J. J. (1992): Differences in relative growth rate in 11 grasses correlate with differences in chemical composition as determined by pyrolysis mass spectrometry. – Oecologia 89: 567-573.
[28] Pearson, C. J., Ison, R. L. (eds.) (1997): Agronomy of Grassland Systems. 2nd Ed. – Cambridge University Press, Cambridge, UK.
[29] Peeters, A. (2004): Wild and sown grasses. Profiles of a temperate species selection: ecology, biodiversity and use. – FAO & Blackwell Publishing, Rome & Hoboken, NJ.
[30] Perez-Arevalo, J. J., Callejon-Ferre, A. J., Velazquez-Marti, B., Suarez-Medina, M. D. (2015): Prediction models based on higher heating value from the elemental analysis of neem, mango, avocado, banana, and carob trees in Guayas (Ecuador). – J Renew Sustain Energy 7: 053122.
[31] Poorter, H., Bergkotte, M. (1992): Chemical composition of 24 wild species differing in relative growth rate. – Plant Cell Environ 15: 221-229.
[32] Rayburn, E. B. (1997): Forage Quality-Minerals. – Service ID-5016. West Virginia University Extension, Morgantown, WV.
[33] Rohweder, D. A., Barnes, R. F., Jorgensen, N. (1978): Proposed hay grading standards based on laboratory analyses for evaluating quality. – J Anim Sci 47: 747-759.
[34] Sáez-Plaza, P., Michałowski, T., Navas, M. J., Asuero, A. G., Wybraniec, S. (2013): An overview of the kjeldahl method of nitrogen determination. Part I. Early history, chemistry of the procedure, and titrimetric finish. – Crit Rev Anal Chem 43(4): 178-223.
[35] Schroeder, J. W. (1996): Quality Forage for Maximum Production and Return. – Educational Materials from North Dakota State University Agriculture and University Extension ID AS-1117, Fargo, ND.
[36] Stone, B. A. (1994): Prospects for improving the nutritive value of temperate, perennial pasture grasses. – New Zeal J Agr Res 37: 349-363.
[37] Sturla, F. (1960): Eggjahvítumagn og lostaetni túngrasa (Protein content and palatability of cultivated grasses in Iceland). – Atvinnudeild Háskólans, Rit landbúnaðardeildar B-Flokkur 12: 27.
[38] Undersander, D., Mertens, D. R., Thiex, N. (1993): Forage Analyses Procedures. – National Forage Testing Association (NFTA), Omaha, NB.
[39] Ward, R. (2008): Relative Feed Value (RFV) vs. Relative Forage Quality (RFQ). – Cumberland Valley Analytical Services, Inc., Hagerstown.
[40] Weiss, W. P., Eastridge, M. L., Underwood, J. F. (2012): Forages for Dairy Cattle. – Ohio State University, Columbus, OH. Extension ID-AS-0002-99.
[41] Yeniay, Ö., Göktaş, A. (2002): A comparison of partial least squares regression with other prediction methods. – Hacet J Math Stat 31: 99-111.

http://www.aloki.hu ● ISSN 1589 1623 (Print) ● ISSN 1785 0037 (Online)
DOI: http://dx.doi.org/10.15666/aeer/1804_50495063

INTERANNUAL VARIATIONS AND DISTRIBUTION OF HUMUS COMPONENTS IN SALINE-ALKALI PADDY SOILS

LIU, Q.[1,2] – TANG, J.[1*] – WANG, J.[1] – QU, Y.[1]

[1]*College of Environment and Resources, Jilin University, Changchun 130012, China*

[2]*College of Landscape Architecture, Changchun University, Changchun 130012, China*
(phone: +86-181-0431-1389)

[*]*Corresponding author*
e-mail: hamiqi.365@163.com; phone: +86-181-0431-1389

(Received 24th Oct 2019; accepted 2nd Jul 2020)

Abstract. This study analyzed saline-alkali paddy sois of different reclamation durations in the western Jilin Province of China to identify the distribution and variation of humus components so as to provide a scientific basis for rationally utilizing land resources. Test samples were collected from the former Guoerluosi irrigation area in western Jilin. Paddies with five different farming durations (1, 10, 20, 30 and 55 years) under which single-cropping rice was planted from May to October every year and where all other conditions were common, were selected as the test plots. The results showed that: (1) The ratio of Soil Humus content to organic carbon in paddy field with different cultivation years showed humin > humus carbon > humic acid > fulvic acid, and the content of Humus and its components decreased gradually with the deepening of soil layer; (2) Soil humus components were closely correlated with the content of organic carbon in soil as the regeneration and activation of soil humus had a direct bearing on the variations of the organic carbon pool in soil; (3) The HA/FA and PQ values of saline-alkali paddy soil were positively correlated with farming duration, with the biggest increase in the 20–30 cm soil layer.
Keywords: *cultivation, carbon variation, vertical distribution, saline-alkaline rice fields, humus composition*

Introduction

[Study significance] A large amount of CO_2 has accumulated in the Earth's atmosphere since the 19th century due to the conversion of natural forests and grasslands to farmland (Jonczak, 2014). Therefore, the ebb and flow of carbon in farmland soils will exert direct influences on the atmospheric CO_2 level (Shao et al., 2018). The former Guoerluosi (Qianguo) irrigation area, western Jilin Province, China, is one of the four largest irrigation areas in Northeast China and also one of the world's three largest areas of saline-alkali soil; therefore, the region is of importance for global carbon cycle studies (Tang et al., 2011). Included among recent efforts to improve land salinization in this area are the artificial enclosures of degraded grasslands and some dry land or the conversion of these areas to paddy fields. Changing carbon fixation capacity, soil fertility and CO_2 emissions of paddy soils is evident with changing land use (Ding et al., 2013; Zhang et al., 2015). Therefore, it is of great significance to study the factors driving the variations and regeneration patterns of humus components in saline-alkali soils under different farming durations so as to derive knowledge for improving the soil quality, fertility and carbon sequestration capacity of saline-alkali paddy fields. [Previous study progress] Soil humus is one of the main components of soil organic matter and is a key indicator of soil fertility and quality as its amount and composition can reflect certain soil-forming conditions and processes (Six et al., 2004; Dong et al., 2017; Wiao et al., 2020). As an organic substance formed by the decomposition of dead

http://www.aloki.hu ● ISSN 1589 1623 (Print) ● ISSN 1785 0037 (Online)
DOI: http://dx.doi.org/10.15666/aeer/1804_50655077

organisms by soil microorganisms, humus is mostly derived from plant litter and decaying roots. Humus is not a single organic compound, but rather a mixture of organic compounds with commonalities and differences in composition, structure and properties, including humus carbon (HE), humic acid (HA), fulvic acid (FA) and humin (HM) (Brady, 1974; Bunting, 1987; Brady et al., 2000; Zheng, 2019). Much research, both in China and globally, has been performed in recent years on the factors influencing the composition of soil humus (Andreetta et al., 2011; Vos et al., 2015; Dong and Dou, 2017; Daryanti et al., 2019). It has generally been shown that humus is a relatively stable soil component and is notably affected by the geographical environment and biological factors (Zhu et al., 2018). [Study approach] It is known that farming practices and duration both affect the content and distribution of soil humus to some extent (Wang et al., 2015; Li et al., 2016). Therefore, the present study has analyzed the variation in the vertical distribution of humus over time in saline-alkali paddy soil. [Proposed solutions to key problems] The present study has analyzed the variations in the composition of humus for different paddy soil layers as a result of farming duration to provide a scientific basis for the rational use of land resources so as to improve both rice yield and soil carbon sequestration capacity. Saline-alkali soil is an important reserve land resource. Through this study, the response of Humus composition to reclamation years and soil layers can be determined, which is the focus of this study, the results can provide reference for the rational development and utilization of saline-alkali land.

Materials and Methods

Study Area

The study area is located in the irrigation region of the former Guoerluosi Mongolian Autonomous County of Jilin Province (E123°35' - 125°18', N44°17' - 45°28'). This region has a temperate continental monsoon climate with four distinct seasons. Highest and lowest temperatures are approximately 36 ℃ and −36 ℃, respectively. The region is dry and windy in spring, hot and humid in summer, cool in autumn with a large diurnal temperature difference and cold in winter with little snowfall and a long freezing period. The annual averages of sunny days, hours of sunshine and temperature are 110 d, 2,879 h and 4.5 ℃, respectively. The first day of frost generally falls in the middle of or late September, whereas the final frost date generally falls between late April and early May; hence, the frost-free duration is 130 – 140 d. The average annual precipitation is 400 – 500 mm. The annual average evaporation is > 1,200 mm, with evaporation from April to May accounting for 531.2 mm or 45.2% of the annual total (Tang et al., 2012; Liu et al., 2018). Single-cropping rice seedlings are generally planted in mid-May, and the mature plants are harvested in October. The rice growth stage is mainly supported by application of urea and potassium and phosphate fertilizers. *Figure 1* shows the monthly average precipitation and temperature in the study area in 2015.

Test Design

Investigation of maps of soil types and land use types combined with the paddy field farming history and field investigation was performed to facilitate the selection of representative sampling plots and universal test results (*Fig. 2*). Sampling was conducted on plots with paddy soils farmed over five different durations (1, 10, 20, 30

http://www.aloki.hu ● ISSN 1589 1623 (Print) ● ISSN 1785 0037 (Online)
DOI: http://dx.doi.org/10.15666/aeer/1804_50655077

and 55 years) under basically the same natural conditions. Three 20 m × 20 m sampling areas were established in each sampling plot before rice planting in 2015 (early May). Each sampling area contained five S-shaped sampling points where soils were collected from five levels (0 cm -10 cm, 10 cm -20 cm, 20 cm -30 cm, 30 cm -40 cm and 40 cm -50 cm), soil samples were taken by a drill with a diameter of 10 cm. The collected soil samples were then processed to remove grit and plant residues, air-dried and then sequentially filtered with 0.2 mm and 0.125 mm sieves before being analyzed for soil organic carbon and humus components (*Fig. 3*). The basic information of the plots is shown in *Table 1*.

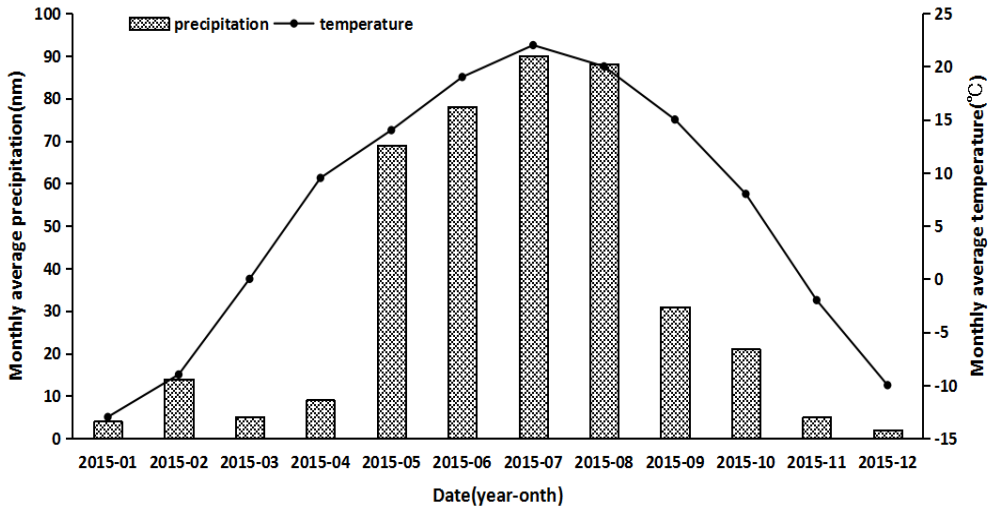

Figure 1. *Mean precipitati on and temperature in the study area in 2015*

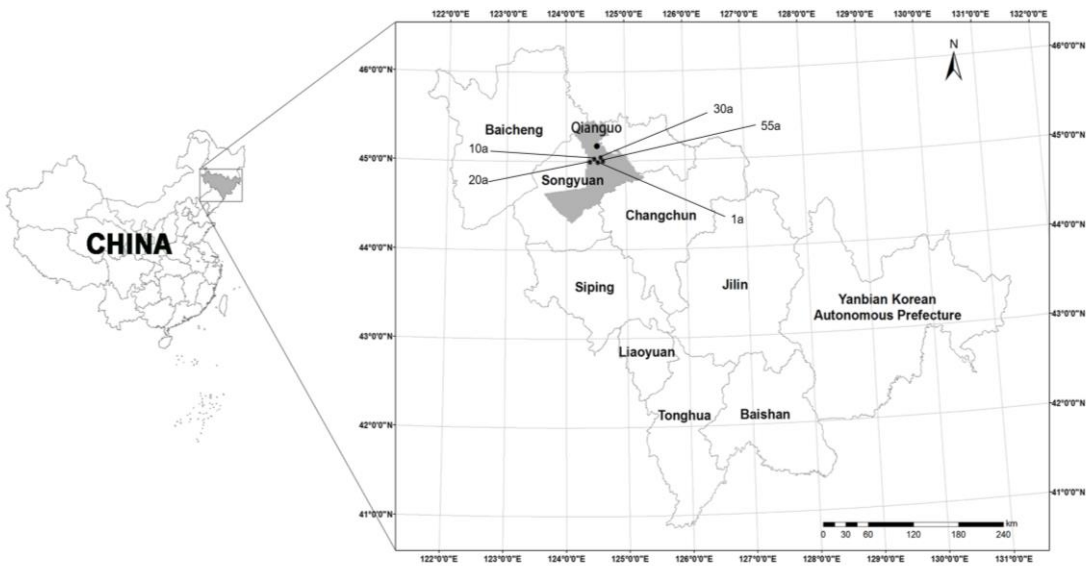

Figure 2. *The location of the study area and the distribution of the sampling points*

http://www.aloki.hu ● ISSN 1589 1623 (Print) ● ISSN 1785 0037 (Online)
DOI: http://dx.doi.org/10.15666/aeer/1804_50655077

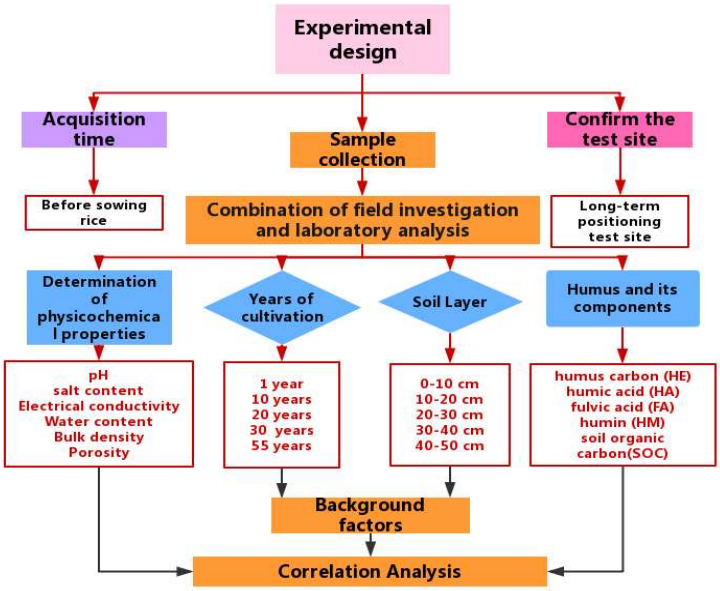

Figure 3. *Test Design and procedure*

Table 1. *Overview of study area*

Sample number	Cultivation history	Geographical location	Soil type	pH	Salt content /%	Electrical conductivity /ms·cm^{-1}	Water content /%	Bulk density /g·cm^{-3}	Porosity /%
R1	1 a	E124°42′27″, N45°00′05″	rice soil	8.7	2.088	0.306	0.54	1.01	0.63
R10	10 a	E124°41′40″, N45°00′23″	rice soil	8.53	1.923	0.218	0.48	0.87	0.67
R20	20 a	E124°40′41″, N45°00′25″	rice soil	8.56	1.961	0.211	0.50	0.83	0.70
R30	30 a	E124°42′45″, N45°01′24″	rice soil	8.12	1.784	0.132	0.47	0.90	0.66
R55	55 a	E124°43′03″, N45°00′19″	rice soil	8.07	1.736	0.104	0.48	0.92	0.64

Test Indicators and Methods

Soil organic carbon and humus components were determined using the potassium dichromate volumetry-thermodilution method (Cha, 2017). The humus components were extracted by weighing 2.5 gair-dried soil sample in 100 mL centrifuge tube, adding 0.1 mol·L^{-1} $Na_4P_2O_7 \cdot 10H_2O$, 0.1 mol·L^{-1} NaOH mixture 50 mL, shaking 145 r·min^{-1} at 70 ℃ in a constant temperature water bath oscillator, extracting for 1 h, then centrifuging and filtering, the humic acid (HE) can be extracted in a 50 mL volumetric flask. The residue in the centrifuge tube is called crude humin (HM). The Alkali extract was extracted with 30 mL in 50 mL flask, and 1 mol·L^{-1} H2SO4 was added to adjust the pH value to 1.0-1.5. Place the solution in a 60-70 ℃ water bath for 1-2 h, then leave overnight. On the next day, the solution was quantitatively filtered

http://www.aloki.hu ● ISSN 1589 1623 (Print) ● ISSN 1785 0037 (Online)
DOI: http://dx.doi.org/10.15666/aeer/1804_50655077

with medium speed filter paper, and the precipitate was HA, and the solution was FA (Zhang et al., 2004).

Data Processing

Statistical analysis was performed using SPSS 19.0 statistical software (SPSS Inc., Chicago, IL, USA). Statistical significance of soil organic carbon and humus components in different reclamation years and in different soil layers was determined by one-way analysis of variance (ANOVA) and Fisher's least significant difference (LSD) test. Multivariate analysis of variance was used to examine the differences of soil carbon and Statistical significance of soil organic carbon and humus in different reclamation years and soil layers. Pearson correlation analysis was used to estimate the relationship between organic carbon and humus components.

Results

Interannual Variation in Saline-alkali Paddy Soil Humus Components

Variations in Humus Carbon Content

The content of extractable humus carbon (HE) in reclaimed soil increased significantly, and showed an increasing trend with the extension of reclamation years. He in reclaimed soil was about 5.64 - 8.22 $g \cdot kg^{-1}$ in 55 years, which was about 10 times higher than that in unreclaimed soil. He was significantly higher in 0-10cm than in 40-50 cm *($P < 0.05$)* in different soil layers, and there was no significant difference in HE between 30-40cm and 40-50cm soil layers (*Fig. 4*).

Variations in Humic Acid Content

Humic acid (HA) is a brown to deep-brown extractable humus that is soluble in dilute alkali soil but dilute acid soil. HA has colloidal properties and is one of the relatively active parts of soil humus, playing an important role in soil structure composition (Gong et al., 2009; Chu et al., 2013). As illustrated by *Figure 5*, the HA content of each soil layer generally increased with increasing farming duration, with the lowest and highest HA contents were found in R1 and R55 soils, respectively. The HA content of the R0 0 cm–10 cm soil layer was significantly higher than those of the R1, R10, R20 and R30 soils by 48.25%, 29.01%, 17.35% and 11.19%, respectively ($P < 0.05$). For the 10 cm–20 cm soil layer, no significant difference in HA content were evident between R1, R10 and R20 soils as well as between R30 and R55 soils; however R55 HA content increased by 50% compared with R1. For the 20 cm–30 cm soil layer, no significant difference in HA content was evident between R10, R20 and R30 soils; however, R55 HA content was significantly higher than those of other farming durations, and increased by 68.87% compared with R1. For the 30 cm–40 cm soil layer, R20 soil HA content was significantly higher than those of R1, R10 and R30 soils; the R55 soil HA content was in particular higher than those of other farming years. For the 40 cm–50 cm soil layer, no significant differences in HA content were evident between R1 and R10 as well as between R20 and R30; however, that of R55 was significantly higher than those of other farming durations. A decrease in HA content with increasing depth was evident for soils of all farming durations. The soil HA contents between the 0 cm–10 cm and 40 cm–50 cm soil layers were significantly different ($P < 0.05$). The 0 cm–10 cm soil HA contents for R1, R10, R20, R30 and R55

http://www.aloki.hu ● ISSN 1589 1623 (Print) ● ISSN 1785 0037 (Online)
DOI: http://dx.doi.org/10.15666/aeer/1804_50655077

soils were higher than their respective 40 cm–50 cm layers by 1.07 g·kg^{-1}, 1.64 g·kg^{-1}, 1.4 g·kg^{-1}, 1.4 g·kg^{-1} and 1.23 g·kg^{-1}, respectively. These results indicates a buildup of soil HA with increasing farming duration. In addition, HA content decreased with increasing depth, suggesting that the surface layer gains the most HA with increasing farming duration.

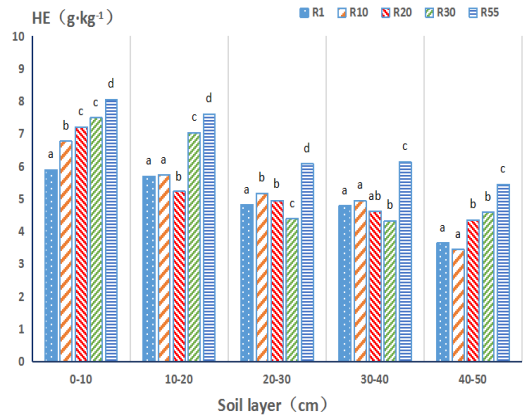

Figure 4. *Vertical distribution of humus carbon in saline-alkaline soil over different farming durations*

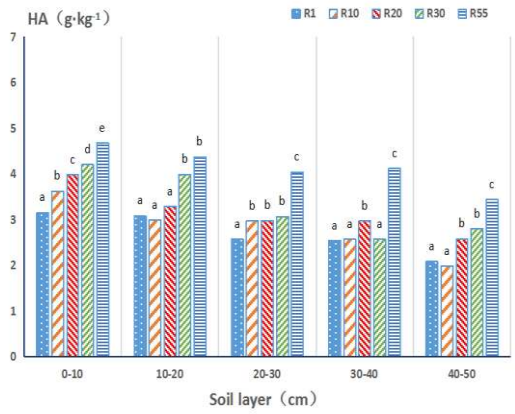

Figure 5. *Vertical distribution of humic acid in saline-alkaline soil over different farming durations*

Note: lowercase letters indicate a significant difference at P< 0.05

Variations in Fulvic Acid Content

Fulvic acid (FA) is low in molecular weight, with a brown or black surface appearance and is soluble in acid, alkali and ethanol solutions and water. FA is beneficial to soils in that it assists in the adsorption of heavy metals and in releasing nutrients (Sądej and Żołnowski, 2015; Borowska et al., 2015). *Figure 6* illustrates that the 0 cm-10 cm R1 soil layer FA content was dramatically higher than those of other farming durations *($P < 0.05$)* and those of R10, R20, R30 and R55 soils remained relatively stable across all farming durations at 3.15 g·kg^{-1}, 3.23 g·kg^{-1}, 3.29 g·kg^{-1} and 3.39 g·kg^{-1}, respectively. For the 10 cm–20 cm soil layer, no significant difference in FA was evident between Rl and R30 as well as between R30 and R55, whereas that of R30 (3.05 g kg^{-1}) was significantly lower than those of other farming durations. For the 20 cm–30 cm soil layer, no significant differences were evident between R1 and R10 as well as between R20 and R55, whereas that of R20 (1.98 g·kg^{-1}) was notably lower than those of other farming durations. For the 30 cm–50 cm soil layer, no significant difference was evident between R1 and R10 as well as between R20 and R30. No consistent pattern was evident in soil FA content for different farming durations and between soil layers. The soil FA content appeared to accumulate with increasing farming duration in the 0 cm–10 cm and 40 cm–50 cm soil layers, whereas it decreased before increasing in the 10 cm–40 cm soil layer, and was relatively low in R20 and R30 soils.

Variations of Humin Content

Humin (HM) is a humus component which combines most closely with soil minerals, and cannot be extracted by any acid, alkali or organic solvents. Therefore, as

http://www.aloki.hu ● ISSN 1589 1623 (Print) ● ISSN 1785 0037 (Online)
DOI: http://dx.doi.org/10.15666/aeer/1804_50655077

an inert humus component, it is the most resistant to decomposition and can exist in soil for over a thousand years (Newcomb, 2015). In recent years, studies have shown that HM is composed of carbonized microbial protoplasmic and plant residues, and that due to its ubiquitous presence in the natural environment, can be used as an electron mediator to promote bioremediation of organic pollutants. As a result, there is a growing interest in this substance (Kramer et al., 2004). *Figure 7* illustrates that the 0 cm–10 cm HM soil content tended to increase first and then decrease with increasing farming duration. In addition, R1 and R30 soils had the lowest and highest HM contents at 6.89 $g \cdot kg^{-1}$ and 8.06 $g \cdot kg^{-1}$, respectively, with no significant difference evident between R1 and R10 as well as between R30 and R55. HM in the 10 cm–20 cm soil layer appeared to increase with increasing farming duration. However, HM contents for this layer in the R1, R10 and R20 soils remained stable at between 6.08 $g \cdot kg^{-1}$–6.64 $g \cdot kg^{-1}$ and between 7.73 $g \cdot kg^{-1}$–7.81 $g \cdot kg^{-1}$ for R30 and R55 soils. The HM content of the 20 cm–50 cm soil layer increased, then decreased and then increased again with increasing farming duration, and was highest in the R10 and R55 soils with no significant difference between R1 and R20 soils. R55 presented the highest HM content, with values of 6.57 $g \cdot kg^{-1}$, 6.82 $g \cdot kg^{-1}$ and 5.64 $g \cdot kg^{-1}$ for the 20 cm–30 cm, 30 cm–40 cm and 40 –50 cm soil layers, respectively. All soils showed decreasing HM content with increasing soil depth, indicating that that uppermost soil layer is subject to heavier HM accumulation.

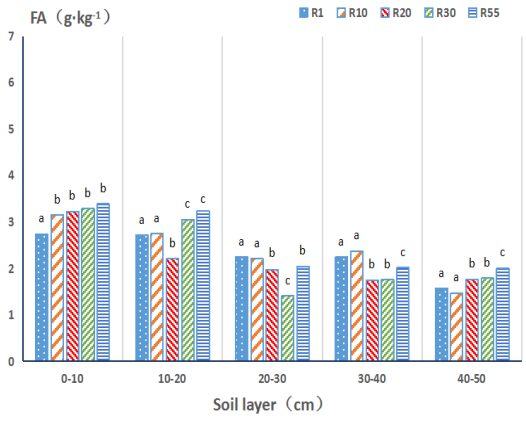

Figure 6. *Vertical distribution of fulvic acid in saline-alkaline soil over different farming durations*

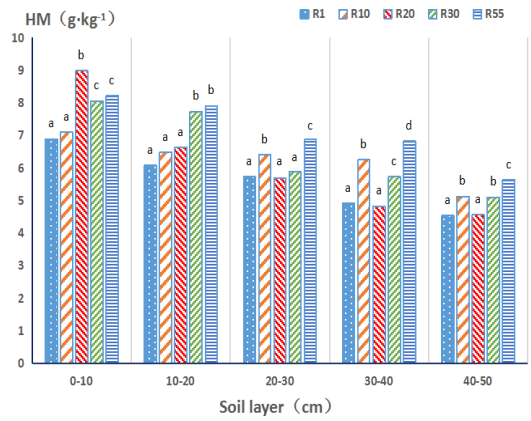

Figure 7. *Vertical distribution of humin in saline-alkaline soil over different farming durations*

Note: lowercase letters indicate a significant difference at P< 0.05

Analysis of the Variations in Humus Components in Saline-alkali Paddy Soil

Variations in the composition and content of soil humus reflect the mechanisms behind soil formation and evolution (Liu et al., 2019). *Table 2* shows the proportions of humic components (HE, HA, FA and HM) in organic carbon. It can be seen that HM accounted for the largest proportion at > 50% of soil organic carbon. Generally, the proportions of soil components in soil organic carbon was in the order of HM > HE > HA > FA, indicating that stable HM made up the majority of soil humus. In the 0 cm–10 cm, 10 cm–20 cm, 20 cm–30 cm and 30 cm–50 cm soil layers, the value of

http://www.aloki.hu ● ISSN 1589 1623 (Print) ● ISSN 1785 0037 (Online)
DOI: http://dx.doi.org/10.15666/aeer/1804_50655077

[(HM)/(SOC)]% and [(HE)/(SOC)]% decreased and increased with increasing farming duration, respectively. *Table 3* shows a consistently significant positive correlation between soil HE, HA, FA, HM and SOC across all farming durations. This indicates a close internal correlation between soil humus components. A strong correlation between soil humus components and soil organic carbon was also evident, indicating that the stability of soil organic carbon was related to humus content.

Table 2. *Soil humus composition as a proportion of organic carbon*

Sample number	Proportion of organic carbon in soil	Soil layer/(cm)				
		0–10	10–20	20–30	30–40	40–50
R1	[(HM)/(SOC)]%	53.91	51.61	54.31	50.67	55.43
	[(HE)/(SOC)]%	46.09	48.39	45.69	49.33	44.57
	[(HA)/(SOC)]%	24.65	25.30	24.36	26.16	25.40
	[(FA)/(SOC)]%	21.44	23.09	21.33	23.17	19.17
R10	[(HM)/(SOC)]%	51.19	52.21	55.31	54.02	59.74
	[(HE)/(SOC)]%	48.81	47.79	44.69	45.98	40.26
	[(HA)/(SOC)]%	26.10	25.29	25.63	24.73	23.10
	[(FA)/(SOC)]%	22.71	22.50	19.07	21.25	17.15
R20	[(HM)/(SOC)]%	55.47	55.94	53.52	50.05	51.18
	[(HE)/(SOC)]%	44.53	44.06	46.48	49.95	48.82
	[(HA)/(SOC)]%	24.58	25.44	27.89	31.43	28.96
	[(FA)/(SOC)]%	19.95	18.62	18.59	18.52	19.87
R30	[(HM)/(SOC)]%	51.83	52.34	57.25	51.99	52.63
	[(HE)/(SOC)]%	48.17	47.66	42.75	48.01	47.37
	[(HA)/(SOC)]%	27.01	27.01	29.02	30.52	28.90
	[(FA)/(SOC)]%	21.16	20.65	13.73	17.50	18.47
R55	[(HM)/(SOC)]%	50.49	50.32	50.69	52.62	50.86
	[(HE)/(SOC)]%	49.51	49.68	49.31	47.38	49.14
	[(HA)/(SOC)]%	28.69	28.80	33.49	31.79	31.02
	[(FA)/(SOC)]%	20.82	20.88	15.82	15.59	18.12

Abbreviations: humus carbon (HE), Humic acid (HA), fulvic acid (FA), Humin (HM), soil organic carbon (SOC)

Variations in Humus Composition of Saline-alkali Paddy Soil

The degree of soil humification and quality of humus are generally measured by values of HA/FA and PQ (the ratio of HA to HE), with higher values indicating better soil quality (Shu et al., 2015). The results of *Figure 8* and *Figure 9* showed that the HA/FA and PQ values of soil humus in different tillage years had the same trend, which was R55 > R30 > R20 > R10 > R1. However, the changes of HA/FA and PQ of humus in different soil layers were not completely consistent, and the changes of HA/FA and PQ of R1 and R10 showed a "W"-type trend with the depth of soil layers, the values of HA/FA and PQ of R20, R30 and R55 in the soil layers of 10-20 cm and 30-40 cm, respectively showed a trend of increasing first and then decreasing with the depth of soil layers, and the peak value was 20-30 cm. The HA/FA and PQ of Soil in different tillage years were higher than 1 and 0.5, respectively, because the humus in soil was renewed and activated every year. The values of HA/FA and PQ in 20-30 cm soil layer increased the most, and the values of HA/FA and PQ in R55 were 85.96% and 28.3% higher than those in R1 soil

http://www.aloki.hu ● ISSN 1589 1623 (Print) ● ISSN 1785 0037 (Online)
DOI: http://dx.doi.org/10.15666/aeer/1804_50655077

layer, which indicated that the tillage years could significantly increase the values of HA/FA and PQ, the proportion of humic acid increased gradually, and the soil humus quality improved gradually. In addition, we also know that soil layer and reclamation years are the two factors that control the contents of HE, HA and FA (*Table 4*).

Table 3. *Analysis of the correlation between soil humus composition and soil organic carbon*

Sample number	Index	SOC	HM	HE	HA	FA
R1	SOC	1	.979**	.977**	.988**	.959*
	HM		1	.913*	.939*	.882*
	HE			1	.995**	.996**
	HA				1	.982**
	FA					1
R10	SOC	1	.990**	.997**	.999**	.978**
	HM		1	.976**	.996**	.940*
	HE			1	.991**	.992**
	HA				1	.966**
	FA					1
R20	SOC	1	.996**	.990**	.963**	.993**
	HM		1	.974**	.938*	.984**
	HE			1	.987**	.990**
	HA				1	.955*
	FA					1
R30	SOC	1	.988**	.989**	.994**	.971**
	HM		1	.955*	.977**	.925*
	HE			1	.989**	.994**
	HA				1	.966**
	FA					1
R55	SOC	1	.994**	.995**	.910*	.936*
	HM		1	.978**	.916*	.905*
	HE			1	.894*	.954*
	HA				1	0.719
	FA					1

Note: Correlation coefficients labeled by * and ** indicate significant difference at P = 0.05 and P = 0.01, respectively. Abbreviations: humus carbon (HE), Humic acid (HA), fulvic acid (FA), Humin (HM), soil organic carbon (SOC)

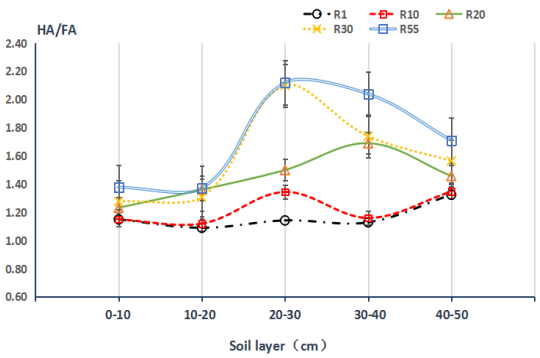

Figure 8. *Trends in the relative proportions of saline-alkaline soil (C_{HA}/C_{FA}) over different farming durations*

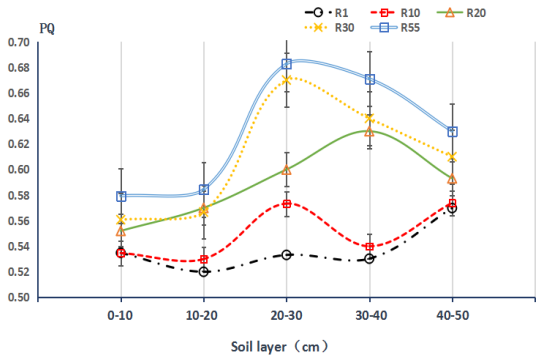

Figure 9. *Trends in PQ values of saline-alkaline soil over different farming durations*

Note: The error line in figure shows the positive and negative deviation of the value

http://www.aloki.hu ● ISSN 1589 1623 (Print) ● ISSN 1785 0037 (Online)
DOI: http://dx.doi.org/10.15666/aeer/1804_50655077

Table 4. *Multifactor Variance Analysis of Soil HE, HA and FA in Saline-alkali Rice Paddy Soil during Soil Layer, Reclamation years*

Index	Source of variation	Sum of squares	Degree of freedom	Mean square	F	P
HE	Soil layer	608.312	4	152.078	1221.48	*
	Reclamation years	1755.474	4	438.868	3524.965	*
	Soil layer * Reclamation years	62.121	16	3.883	31.184	*
HA	Soil layer	157.722	4	39.431	1163.278	*
	Reclamation years	448.556	4	112.139	3308.319	*
	Soil layer * Reclamation years	14.206	16	0.888	26.194	*
FA	Soil layer	126.172	4	31.543	1298.59	*
	Reclamation years	318.766	4	79.692	3280.811	*
	Soil layer * Reclamation years	12.144	16	0.759	31.246	*

Note: P<0.001

Discussion

Humus generally undergoes synthesis and decomposition during its formation. Soil humus composition is partly derived from the decomposition of plant residues and partly from the synthesis of microorganisms (Cu, 2015); therefore, its content is related to the process of soil mineralization and humification. In the present study, the proportions of soil humus components (HA, FA and HM) gradually increased with increasing farming duration, consistent with the results of Clark et al. (1998), Pimente et al. (2005) and Melerol et al. (2006), who showed consistent increases in soil organic carbon and humus carbon with increasing soil cultivation time. This can be explained by considering that soil microorganisms directly participate in the degradation and humification of organic residues; farming provides more suitable temperature and humidity conditions for microorganisms, thereby increasing microbial activity in soil. In this way, the decomposition of soil organic carbon is increased along with soil mineralization and humification, resulting in a rise in the soil organic carbon and humus contents (Yu et al., 2004; Watanabe et al., 2007; Wissing et al., 2013).

The variances of soil carbon content and humus components across different farming durations and soil layers has also resulted in some regular variations in the proportion of organic carbon in each component. HM was found to make up the largest proportion in soil, accounting for approximately half of organic carbon. In general, the rank proportion of each component in soil was HM > HE > HA > FA, with a significant correlation between soil humus components and organic carbon evident. This indicates that the majority of humus exists as stable HM, and that saline-alkaline paddy soils have certain potentials for carbon sequestration.

The relative variations in soil humus components can also be analyzed by comparing the values of specific indicators, namely HA/FA or PQ. The total amount of humus and the degree of soil humification increased with increasing soil maturity, with HA/FA values of 1.4, 0.5 and 0.2–0.3 for highly mature, moderately mature and relatively immature paddy soils, respectively (Liu et al., 2017). In the present study, increasing farming duration resulted in an improvement in HA content across all soil layers. Moreover, both HA, HA/FA and PQ values increased with increased duration of rice farming. This indicates that an increase in the amount of soil HA resulted in an increase

http://www.aloki.hu ● ISSN 1589 1623 (Print) ● ISSN 1785 0037 (Online)
DOI: http://dx.doi.org/10.15666/aeer/1804_50655077

in soil humification, thereby also improving soil maturity, humus quality and fertility (Liu et al., 2018). The variations in and regeneration of soil humus can not only be used to evaluate soil quality and vegetation restoration, but also bears vital significance for soil carbon sequestration. Paustian pointed out that the chemical combination of soil humus and soil minerals serves as an important mechanism for the stabilization of organic carbon and prevention of microbial degradation (Paustian et al., 1992). Therefore, further studies on the molecular structure of humus and the mechanism of regulation of molecular *in-situ* polymerization for saline-alkali paddy soils would play an important role in limiting soil microbial mineralization and improving soil organic carbon sequestration.

Conclusion

(1) Variations in soil humus were found across different farming durations and soil layers. Soil humic acid content increased significantly with increasing farming duration. In general, the soil humus components were found to decrease in value with increasing soil depth. Farming maintained soil fulvic acid content at a relatively stable level across all farming durations. Humin made up the largest proportion of humus in saline-alkaline paddy soil and increased remarkably with increased farming duration, with the largest accumulation in the top soil. (2) Soil humus components (humic acid, fulvic acid and humin) were significantly correlated with organic carbon content, and the regeneration and activation of soil humus exerted direct impacts on the variations of the soil organic carbon pool. (3) Farming duration significantly increased the values of HA/FA and PQ of saline-alkali paddy soils with the largest increase shown in the 20-30 cm soil layer.

As a stable carbon component in soil, soil humus carbon increased with the extension of cultivation years. The content of soil humus carbon after cultivation was significantly higher than that of uncultivated saline-alkali wasteland, the results showed that saline-alkali soil was improved and reclaimed as a back-up soil of farmland, and it was also beneficial to improve the function of soil carbon sink. This suggests that we should make better and reasonable use of the reserve land resources, increase production, and at the same time, improve the climate change also has a certain role in promoting.

Funding. This research was funded by National Natural Science Foundation of China (No.51179073, 41471152) and Changchun University Scientific Research and cultivation Fund (2019JBC27L40).

REFERENCES

[1] Andreetta, A., Ciampalini, R., Moretti, P., Vingiani, S., Poggio, G., Matteucci, G., Tescari, F., Carnicelli, S. (2011): Forest humus forms as potential indicators of soil carbon storage in Mediterranean environments. – Biol. Fertil. Soils 47: 31-40.

[2] Borowska, K., Koper, J., Kozik, K., Rutkowska, A. (2014): Effect of slurry fertilization on the selenium content and catalase activity in lessive soil. – Journal of elementology 19(3).

[3] Brady, N. C. (1974): The Nature and Properties of Soils(8th ed). – MacMillan Publishing Co, New York.

[4] Brady, N. C., Weil, R. R. (2000): Elements of the nature and properties of soils. – Pearson Education, USA.

http://www.aloki.hu ● ISSN 1589 1623 (Print) ● ISSN 1785 0037 (Online)
DOI: http://dx.doi.org/10.15666/aeer/1804_50655077

[5] Bunting, B. T., Lundberg, J. (1987): The humus profile - concept, class and reality. – Geoderma 40(1-2): 17-36.
[6] Cha, T. G. (2017): Physical and chemical analysis of soil. – China Forestry Press: Beijing, pp. 177-189.
[7] Chu, H., Zong, L. G., Wang, Z. Y., Xie, S. H., Yang, N., Luo, M. (2013): Dynamic changes in humus composition in vegetable soils different in cultivation Mode. – Acta Pedologica Sinica 50(5): 931-939.
[8] Clark, M. S., Ferris, H., Klonsky, K., Lanini, W. T., Bruggen, A. H. C. V., Zalom, F. G. (1998): Agronomic, economic, and environmental comparison of pest management in conventional and alternative tomato and corn systems in northern california. – Agriculture Ecosystems and Environment 68(1-2): 51-71.
[9] Cu, J. T. (2015): Studies on the role of microorganism in the formation and transformation of humus. – Jilin Agricultural University: Jilin.
[10] Daryanti, N. Y., Zulaikah, S., Mufti, N., Haryati, D. S. (2019): Characteristics of magnetic susceptibility and geochemistry of paddy soils in malang city, east java. – IOP Conference Series Earth and Environmental Science 311: 012-032.
[11] Ding, C. X., Yong, Q., Dong, Z. Y., Ruobo, W. (2013): Effects of different land use modes on physical and chemical properties of saline-alkali soil in Yellow River Delta. – Science of Soil and Water Conservation 11(2): 84-89.
[12] Dong, S.-S., Dou, S. (2017): Effect of different ways of corn stover application to soil on composition and structural characteristics of organic carbon in black soil. – Journal of Agro-Environment Science 2017-02.
[13] Dong, S.-S., Dou, S., Shao, M. J. (2017): Effect of corn stover deep incorporation with different years on composition of soil humus and structural characteristics of humic acid in black soil. – Journal of Soil Science 054(001): 150-159.
[14] Gong, W., Yan, X. Y., Wang, J. Y., Hu, T. X., Gong, Y. B. (2009): Effects of long-term fertilization on soil humus carbon and nitrogen fractions in a wheat-maize cropping system. – Plant Nutrition and Fertilizer Science 15(6): 1245-1252.
[15] Jonczak, J. (2014): Effect of land use on the carbon and nitrogen forms in humic horizons of stagnic luvisols. – Journal of elementology 19(4): 1037-1048.
[16] Kramer, R. W., Kujawinski, E. B., Hatcher, P. G. (2004): Identification of black carbon derived structures in a volcanic ash soil humic acid by fourier transform ion cyclotron resonance mass spectrometry. – Environmental Science & Technology 38(12): 3387-3395.
[17] Li, L. Q., Zhang, X. H., Wang, P. (2016): Microbial activity promoted with organic carbon accumulation in macroaggregates of paddy soils under long-term rice cultivation. – Biogeosciences 13: 6565-6586.
[18] Liu, X. J., Hu, Y. F., Shu, X. Y., Xu, H. Y., He, J. F., Wang, Q. (2017): Varying characteristics of organic carbon and humus carbon under or outside the branchy tamarisk canopy in sand land in northwest sichuan. – Agricultural Research In The Arid Areas 35(4): 15-21.
[19] Liu, P., Zhou, W. J., Tan, J., Cao, S. (2018): Research progress on structural characteristics of organic carbon and humus in paddy soil. – Southern agriculture 12(33): 183-185.
[20] Liu, Q., Tang, J., Wang, J. J., Qu, Y. K. (2018): Spatial distribution characteristics of soil organic carbon and active components in saline-alkali paddy fields in Western Jilin. – Journal of Northeast Agricultural University 49(09): 47-56.
[21] Liu, P., Zhou, W., Cui, H., Tan, J., Cao, S. (2019): Structural characteristics of humic substances in buried ancient paddy soils as revealed by ^{13}c nmr spectroscopy. – Environmental Geochemistry and Health 41: 2459-72.
[22] Melero, S., Porras, J. C. R., Herencia, J. F., Madejon, E. (2006): Chemical and biochemical properties in a silty loam soil under conventional and organic management. – Soil & Tillage Research 90(1-2): 162-170.
[23] Newcomb, C. J. (2015): Humic matter in soil and the environment, principles and controversies. – Soil Science Society of America Journal 79(5): 1520.

http://www.aloki.hu ● ISSN 1589 1623 (Print) ● ISSN 1785 0037 (Online)
DOI: http://dx.doi.org/10.15666/aeer/1804_50655077

[24] Paustian, K., Parton, W. J., Persson, J. (1992): Modeling soil organic matter in organic-amended and nitrogen-fertilized long-term plots. – Soil ence Society of America Journal 56: 476-88.
[25] Pimentel, D., Hepperly, P., Hanson, J., Douds, D., Seidel, R. (2005): Environmental, energetic, and economic comparisons of organic and conventional farming systems. – Bioscience Science 55(7): 573-582.
[26] Sądej, W., Żołnowski, A. C. (2015): Effects of different long-term fertilization systems on the content and fractional composition of humic substances in lessive soil. – 29 Congress of the Polish Society of Soil Science-soil Resources & Sustainable Development.
[27] Shao, X. W., Ran, C., Jin, F., Guo, L. Y., Geng, Y. Q. (2018): Advances and Prospects in Research of Rice Cultivation Technology in Saline-sodic Soil of Songnen Plain. – Journal of Jilin Agricultural University 40(04): 5-8.
[28] Shu, Z., Sen, D., Chen, L. Z. (2015): Effect of deep application of straw on composition of humic acid in soil aggregates. – Acta Pedologica Sinica 52(4): 747-758.
[29] Six, J., Bossuyt, H., Degryze, S. (2004): A history of research on the link between (micro)aggregates, soil biota, and soil organic matter dynamics. – Soil & Tillage Research 79(1): 7-31.
[30] Tang, J., Zhang, N., Li, Z. Y. (2011): Vertical Distribution of Soil Organic Carbon and Carbon Density Under Different Land Use Types in Western Jilin Province. – Journal of Jilin University (Earth Science Edition) 41(4): 1151-1156.
[31] Tang, J., Yun, L., Na, L., Li, Z., Hao, Z. (2012): Soil moisture content and nitrogen impacts on soil organic carbon of saline-alkali paddy field under the effect of freeze-thaw. – Ecology and Environmental Sciences 21(4): 620-623.
[32] Vos, B., Cools, N., Ilvesniemi, H., Vesterdal, L., Vanguelova, E., Carnicelli, S. (2015): Benchmark values for forest soil carbon stocks in Europe: results from a large scale forest soil survey. – Geoderma 251-152: 33-46.
[33] Wang, R., Yu, G., He, N. (2015): Latitudinal variation of leaf stomatal traits from species to community level in forests: Linkagewith ecosystem productivity. – Scientific Reports 5(5): 14454.
[34] Watanabe, T., Kimura, M., Asakawa, S. (2007): Dynamics of methanogenic archaeal communities based on rrna analysis and their relation to methanogenic activity in japanese paddy field soils. – Soil Biology & Biochemistry 39(11): 2877-2887.
[35] Wiao, X. Q., Chen, Y. W., Sun, H. (2020): Stabilization of Soil Organic Carbon in Alpine Treeline Ecotone along Altitudinal Gradient in the West of Sichuan Province. – Journal of Northwest Forestry University 35(1): 1-7, 36.
[36] Wissing, L., Kölbl, A., Hausler, W., Schad, P., Cao, Z. H., Kögel-Knabner, I. (2013): Management-induced organic carbon accumulation in paddy soils: the role of organo-mineral associations. – Soil & Tillage Research 126: 60-71.
[37] Yu, J. B., Liu, J. S., Wang, J. D., Liu, S. X., Wang, G. P. (2004): Organic carbon variation law of black soil during different tillage period. – Journal of Soil & Water Conservation 18(1): 27-30.
[38] Zhang, J. J., Dou, S. (2004): Studies on fractionation of soil humus. – Chinese journal of soil science 35(6): 706-709.
[39] Zhang, M., Chen, C., Liu, G. M., Yang, J. S., Yu, S. P. (2014): Suitable utilization of fertilizer and soil modifier to ameliorate physicochemical characteristics of saline-alkali soil and increase crop yields. – Transactions of the Chinese Society of Agricultural Engineering 10: 91-98.
[40] Zheng, Y. J., Zhang, J. B., Tan, J. (2019): Chemical Composition and Structure of Humus Relative to Sources. – Acta Pedologica Sinica 56(2): 386-397.
[41] Zhu, R. H., Zheng, Z. C., Li, T., Liu, H. (2018): Effect of tea plantation age on humus fractions in soil water-stable aggregates. – Research of Environmental Sciences 31(6): 1096-1104.

http://www.aloki.hu ● ISSN 1589 1623 (Print) ● ISSN 1785 0037 (Online)
DOI: http://dx.doi.org/10.15666/aeer/1804_50655077

EFFECT OF *ASPERGILLUS NIGER* STRAIN XF-1 ON SOIL NUTRIENTS AND GROWTH OF *AMORPHA FRUTICOSA*

WU, Q.-F.[1] – HU, H.-B.[2,3*] – HE, L.-M.[1]

[1]*School of Biological and Food Engineering, Anyang Institute of Technology, Anyang, Henan 455000, China*

[2]*Collaborative Innovation Center of Sustainable Forestry in Southern China of Jiangsu Province, Nanjing Forestry University, 159 Longpan Road, Nanjing, Jiangsu 210037, China*

[3]*Key Laboratory of Soil and Water Conservation and Ecological Restoration in Jiangsu Province, Nanjing Forestry University, 159 Longpan Road, Nanjing, Jiangsu 210037, China*

**Corresponding author*
e-mail: 531208831@qq.com

(Received 4th Nov 2019; accepted 7th Jul 2020)

Abstract. In order to reveal the interaction effect between *Aspergillus niger* (*A. niger*) and *Amorpha fruticosa* (*A. frusticosa*), to guide the large-scale production and cultivation of *A. fruticose* in ecological restoration, and to promote the greening of rock slope and improve the ecological environment, a study on the effect of fermentation broth with different dilutions of *A. niger* strain XF-1 on soil nutrient elements and the growth of *A. fruticosa* was conducted by pot experiment in a green house. The results showed that the contents of chlorophyll a, chlorophyll b and total chlorophyll in the leaves of *A. fruticosa* significantly increased with the 10^{-2} dilution. *A. niger* strain XF-1 fermentation broth, and the plant height, fresh weight and dry weight of *A. fruticosa* significantly increased. Whether the condition of planting *A. fruticosa* or not, the contents of available phosphorus, iron, copper, and zinc in soil by watering were higher in *A. niger* strain XF-1 fermentation broth than that of control (no watering *A. niger* strain XF-1 fermentation broth), and the contents of the above-mentioned nutrients by watering with the 10^{-2} dilution were the highest in soil in *A. niger* strain XF-1 fermentation broth, which could significantly promote the growth of *A. fruticosa*. Therefore, *A. niger* strain XF-1 has a good growth promotion effect on *A. fruticosa*.
Keywords: *Aspergillus niger, nutrient element, growth-promoting, Amorpha fruticosa, weathering*

Introduction

Aspergillus niger (*A. niger*) can dissolve the elements in rocks and minerals, releasing phosphorus, potassium, calcium, silicon and other elements in a form that is easy to be absorbed by plants (Wu, 2018). Meanwhile, it can also secrete oxalic acid, tartaric acid and citric acid to promote the growth of plants (Wang et al., 2018). It is a good strain used as a biological fertilizer. Zhang Lizhen et al. isolated and screened a strain of *A. niger* from caragana rhizosphere soil from a saline-alkali land, and found that this strain could convert insoluble inorganic phosphorus into available phosphorus nutrients for plants to absorb through metabolism, and improve the effective utilization rate of phosphorus (Zhang et al., 2011). Qian Linzhao found in his study that after adding *A. niger* fermentation broth, the pH value in the soil was significantly reduced, and the effective P, exchangeable Ca, Mg and effective Fe, Cu and Zn in the soil were effectively released in the acidic environment, resulting in a significant increase in the content of nutrient elements in the soil (Qian, 2014). Wang Yanqiu et al. used *A. niger* Ap-2 strain to produce biophosphorus bacterial fertilizer, and found that the content of available phosphorus in soil increased by 141.94%. The weight of single leaf, the

http://www.aloki.hu ● ISSN 1589 1623 (Print) ● ISSN 1785 0037 (Online)
DOI: http://dx.doi.org/10.15666/aeer/1804_50795092

proportion of superior tobacco and the internal quality of tobacco leaf were all better than the control (Wang et al., 1993). Li Song et al. found that secondary metabolites of *A. niger* could promote the growth of potted tomatoes and reduce the incidence of tomato root knot nematode disease (Li et al., 2011). Gong Mingbo et al. inoculated *A. niger* in the corn field experiment, and the corn yield increased by about 15% compared with the control treatment (Gong et al., 2010). Lu Jing et al. found that the chlorophyll content, photosynthetic rate and the accumulation of carbon assimilation products in wheat leaves were enhanced when 100 times of *A. niger* fermentation broth was irrigated. It also significantly promoted the nitrate reductive activity of wheat leaves and roots ($p < 0.05$), and the nitrogen metabolism rate, protein content, total phosphorus content of plant tissues in wheat seedlings (up to 61%) and biomass accumulation in wheat parts above ground all increased significantly (up to 21%). After applying *A. niger* fermentation broth diluted 100 times, the available phosphorus content of the soil increased by 122% during the experiment. The decrease of soil total phosphorus was greater than that of the corresponding control group (Lü et al., 2015). Relevant studies have shown that microorganisms can resist diseases and insect pests, absorb heavy metals, dissolve phosphorus and release potassium, therefore, they can be successfully used in bioremediation, promotion of crop growth and improvement of crop quality.

Amorpha fruticosa (*A. fruticosa*), also called *Shrubby falseindige*, is a perennial deciduous shrub, that has a strong vitality, resistance to drought (Yan et al., 2017), resistance to water dipping, resistance to cold, resistance to the sand, resistance to pests, resistance to stress, and resistance to pollution (Cui et al., 2016). It is currently an important plant in the flood control and highway defence in China, and it is also one of the common species of slope greening trees. *A. fruticose* is a good green fertilizer and animal feed, leaves of which are large and rich in nutrition. At the same time, the root wart of *A. fruticose* in the part of root plays an important role in soil improvement. When Yang Chuanxing et al. investigated the weathering soil thickness of gangue hill in semi-arid areas, they found that the weathering soil thickness of *A. fruticosa* was the thickest in the five years old young trees among *A. fruticosa*, *Robinia pseudoacacia*, *Ulmus pumila* and Seabuckthorn. Compared with other tree species, *A. fruticose* can save 50% of the cost in the greening of gangue hill. Planting *A. fruticose* can accelerate the surface weathering of gangue, forming of soil, thus afforestation cost is lower (Yang, 2008).

Plant beneficial rhizospheric microorganisms (PBRMs) are able to colonize the rhizosphere and to improve plant growth, development and nutrient use efficiency by means of a wide variety of mechanisms like organic matter mineralization, biological control against soil-borne pathogens, biological nitrogen fixation, potassium, phosphorous and zinc solubilization and root growth promotion (Meena et al., 2017; Eriola, 2018). The growth promotion effect of *A. niger* XF–1 on *A. fruticosa* was studied in a green house. We tested the effect of different concentrations of fermentation broth of *A. niger* XF-1 on the growth of *A. fruticosa*, the number of soil microorganisms, available phosphorus, iron, copper, zinc, manganese, exchangeable calcium and magnesium in soil. The physiological and biochemical characteristics of *A. fruticosa* seedling were analysed under different concentrations of *A. niger*, and the interaction effect between the *A. niger* and the *A. fruticose* was revealed, so as to provide theoretical and technical support for guiding the large-scale production and cultivation in the ecological restoration of rock side slope.

http://www.aloki.hu ● ISSN 1589 1623 (Print) ● ISSN 1785 0037 (Online)
DOI: http://dx.doi.org/10.15666/aeer/1804_50795092

Materials and methods

The tested seeds of A. fruticosa

Seeds of *A. fruticosa* were collected from Taihang mountain in Henan province. It was preserved in the Key Laboratory of Soil and Water Conservation and Ecological Restoration in Nanjing Forestry University.

Collection of soil and rock samples

Soil samples were taken from the closed mine in Jindingshan (E 120°30', N31°17') in Suzhou, Jiangsu. The content of soil organic matter (OM) was 13.67 $g \cdot kg^{-1}$, total nitrogen (N) 0.92 $g \cdot kg^{-1}$, pH 7.10, available P was 9.01 $mg \cdot kg^{-1}$, exchangeable calcium was 9.70 $cmol \cdot kg^{-1}$, exchangeable magnesium was 3.16 $cmol \cdot kg^{-1}$, effectiveness of iron, manganese, copper, zinc was 2.66, 5.24, 0.50, 1.23 $mg \cdot kg^{-1}$ respectively in tested soil. Samples were sterilized at 121 ℃ for 20 min.

The rocks used in this study are porphyritic granites. The collected samples were placed in a sterile kraft bag and stored in a refrigerator at -20 ℃. Fresh rock samples used in the experiment were washed with distilled water, dried naturally, ground, screened with 100 mesh, particle size < 90 μm, and sterilized under high pressure at 121 ℃ for 20 min.

Testing strain

A. niger strain XF-1 was activated, inoculated and fermented in PD culture solution for 72 h for later use.

Medium and preparation

PD medium (liquid): 200 g of diced potatoes were boiled for 20 min, filtered by 8 layers of gauze to remove residue. 20 g of glucose was added in it, and distilled water was added to 1000 mL. Then, the potatoes were thoroughly stirred and sterilized at 115 ℃ for 20 min (Wu, 2018).

Seed treatment and seedling cultivation of A. fruticosa

Seeds of *A. fruticosa* were soaked in sodium hypochlorite solution (2.5% of active chlorine) for 10 min to eliminate the bacteria on the surface of the seed, washed several times with sterile water, put on the sterilized tray containing quartz sand (hand knead as dough, openhanded as powder), covered with a sterile gauze, then put in the darkness of the incubator at 28 ℃. Right amount water was sprayed to maintain appropriate humidity every day, sprouting seed germinated after 4 d, the consistent germinated seeds were selected and transferred to the pot for culture.

The pots (12.5 cm in diameter and 14.5 cm in height) used in the experiment were filled with 1.0 kg of soil and 100 g of granite powder each, and were divided into two groups: one group was planted with *A. fruticosa*, and the other group was not planted with *A. fruticosa*. Three plants were planted in each pot. When the plants emerged for 10 days, *A. niger* fermentation broth was diluted by 50, 100 and 200 times respectively. and poured into the two groups of the test bowls. A total of 5 mL irrigation was applied at one time, and tap water irrigation was applied for control treatment. The experimental treatments and their codes were shown in *Table 1*. The treatments of planting *A.*

http://www.aloki.hu ● ISSN 1589 1623 (Print) ● ISSN 1785 0037 (Online)
DOI: http://dx.doi.org/10.15666/aeer/1804_50795092

fruticosa were CK (T_0-A), T_{50}-A, T_{100}-A, T_{200}-A. The treatments without *A. fruticosa* were CK (T_0), T_{50}, T_{100} and T_{200}, as shown in *Table 1*. Each treatment was repeated 10 times. The experiment began on May 20, 2017, with a growth cycle of three months, and 50 mL water was sprayed on every other day to maintain appropriate humidity.

Table 1. *The different treatments and corresponding codes*

Treatment	Without *A. fruticosa* group	Planting *A. fruticosa* group
CK	CK (T_0)	CK (T_0-A)
50 times nutrient solution of *A. niger* XF-1	T_{50}	T_{50}-A
100 times nutrient solution of *A. niger* XF-1	T_{100}	T_{100}-A
200 times nutrient solution of *A. niger* XF-1	T_{200}	T_{200}-A

Determination of microbial quantity in rhizosphere

A. fruticosa was removed from soil, 0.2 g plant roots were carefully cut and placed in 100 mL sterile water, diluted and spread on PDA solid medium, cultured at 28 ℃ for 72 h and counted. *A. niger* PDA plates were cultivated, 1 g of the soil of various treatments were taken and put in a 100 mL conical flask, 50 mL sterile water was added in it, it was diluted it into four gradient, namely 10^{-1}, 10^{-2}, 10^{-3}, and 10^{-4} in super clean workbench after 3 h, and then last two gradient coating to its corresponding medium were selected and put through the shaking table at 28 ℃. After 4 d, the number of tested fungi in the soil was observed and recorded.

Determination of soil pH value, effective P, Cu, Zn, Fe, Mn, exchangeable Ca, and Mg

PH value of soil was determined by PHS-3CT. The available phosphorus in soil was determined by sodium bicarbonate extraction–molybdenum antimony anticolorimetric method (Olsen method). The contents of exchangeable Ca and Mg in soil were determined by 1 $mol \cdot L^{-1}$ ammonium acetate exchangeable atomic absorption spectrometry (Bao, 1981). The soil availability of Cu, Zn, Fe and Mn were determined by DTPA solution extraction-atomic absorption spectrometry (Zhang, 2004).

Determination of chlorophyll content

Chlorophyll content of *A. fruticosa* was extracted by ethanol and 80% acetone mixture (V_{ethanol}: $V_{80\%\ \text{acetone}}$) = 1:1), and determined by colorimetry at wavelengths of 646 nm and 663 nm, respectively, to calculate chlorophyll content of *w*(Chla), *w*(Chlb) and *w*(Chl) (Wang et al., 2017).

Determination of plant height and biomass of A. fruticosa

Put the whole pot of *A. fruticosa* under the tap pipe, rinse the soil with slender water. Take out the whole plant, clean it with deionized water several times, and then dry the water on the root surface with absorbent paper. The *A. fruticosa* roots were cut off, the height, root length and fresh weight were measured respectively. The whole plant of *A. fruticosa* were washed with deionized water, and then water was removed at 105 ℃, and dried at 85 ℃ to a constant mass. The dry and fresh mass of each part of *A. fruticosa* were recorded, and the root-crown ratio was calculated.

http://www.aloki.hu ● ISSN 1589 1623 (Print) ● ISSN 1785 0037 (Online)
DOI: http://dx.doi.org/10.15666/aeer/1804_50795092

Scanning electron microscope observation of root complex of A. fruticosa

The root part of *A. fruticosa* was cut off with scissors, put in a 1.5 mL centrifuge tube, and placed in an oven at 40 ℃. After drying, the samples were fixed on the copper table of scanning electron microscope, and sprayed metal. The root of the plant was analyzed by Hitanchi-S3400N scanning electron microscope and energy spectrometer.

Statistical analysis method of data

Excel 2010 was used to process the data, and SPSS 20.0 was used for variance analysis.

Results

Influence of A. niger strain XF-1 on the number of microorganisms tested in soil rhizosphere

The determination results from *Figure 1* showed that all the quantity of rhizosphere microorganisms of *A. fruticosa* inoculated with *A. niger* were above 10^3 cfu·g^{-1}, which was significantly higher than that of control. With the decrease of irrigation concentration, the number of rhizosphere microorganisms decreased gradually. The number of microorganisms of *A. niger* XF-1 treated with T_{50}-A was maximum, reached 3.16×10^4, which was significantly higher than other treatments. It indicated that *A. niger* XF-1 could colonize the rhizosphere of *A. fruticosa*, and then interacted with plants to form a soil-microbe-plant system with soil.

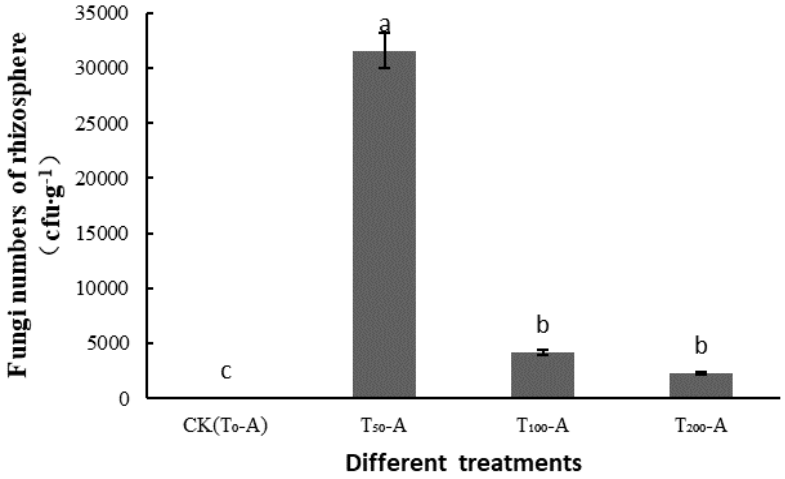

Figure 1. *Fungi numbers in A. fruticosa rhizosphere in different treatments*

Effects of A. niger XF-1 on soil pH value

As shown in *Table 2,* the pH values of the treated group after irrigation of *A. niger* XF-1 fermentation broth were significantly lower than that of the control group and were slightly acidic, indicating that irrigation of *A. niger* XF-1 nutrient solution had a significant impact on the soil pH value. The pH value of soil of planting *A. fruticosa* treated with the same *A. niger* concentration was lower than that without planting *A. fruticosa*, but the difference was not significant, indicating that the growth of *A. niger*

http://www.aloki.hu ● ISSN 1589 1623 (Print) ● ISSN 1785 0037 (Online)
DOI: http://dx.doi.org/10.15666/aeer/1804_50795092

strain XF-1 secreted organic acids to reduce the soil pH value. Compared with the control without *A. fruticosa*, the soil pH values of treatments of the control group of planting *A. fruticosa*, diluted 50 times, diluted 100 times and diluted 200 times decreased to 7.0, 6.2, 6.1 and 6.3 respectively, and the pH value of the treatment diluted 100 times decreased to the lowest, indicating that the organic acid produced by watering at this concentration was the most.

Table 2. *pH values of different dilutions of fermentation broth of A. niger strain XF-1*

Treatment	pH value
CK (T_0-A)	7.0 ± 0.09a
CK (T_0)	7.1 ± 0.12a
T_{50}-A	6.2 ± 0.11b
T_{50}	6.3 ± 0.08b
T_{100}-A	6.1 ± 0.19b
T_{100}	6.2 ± 0.07b
T_{200}-A	6.3 ± 0.13b
T_{200}	6.4 ± 0.08b

Different letters after the same column of numbers indicate significant differences at the 0.05 level

Influence of A. niger strain XF-1 on effective P, Cu, Zn, Fe and Mn in soil

As can be seen from *Table 3,* after watering *A. niger* strain XF-1 nutrient solution, the content of effective P in soil was generally higher than that of CK (T_0-A and T_0). For dilution of 50 times, 100 times and 200 times, the available P content of soil planted with *A. fruticosa* increased by 16.9%, 35.91% and 26.76%, respectively compared with CK (T_0-A), and that of soil without *A. fruticosa* increased by 17.69%, 32.24% and 23.32%, respectively compared with CK (T_0). After watering *A. niger* strain XF-1 nutrient solution, the contents of effective Fe, Cu, zinc, and Mn in the soil were higher than CK (T_0-A and T_0). The content of effective Fe of treatments of planting *A. fruticosa* diluted 50 times, 100 times and 200 times in the soil after 90 days increased by 24.04%, 27.10% and 25.95% than CK ($T_{0\text{-}A}$), respectively, the content of effective Cu in soil increased by 4.91%, 11.48% and 6.56% than CK (T_0-A), respectively, the content of effective zinc in soil increased by 6.30%, 7.87% and 7.09% than CK (T_0-A) ,respectively, the content of available Mn in soil increased by 6.65%, 11.49% and 6.85% than CK (T_0-A), respectively. For dilution of 50 times, 100 times and 200 times, the content of effective Fe of treatments without *A. fruticosa* in soil after 90 days increased by 26.89%, 26.89% and 25.76% than CK (T_0), respectively, and the content of effective Cu in soil increased by 1.61%, 11.29% and 6.45% than CK (T_0), respectively, the content of available Zn in soil increased by 5.43%, 6.30% and 4.65% than CK (T_0), respectively, and the content of available Mn in soil increased by 6.85%, 11.49% and 6.85% than CK (T_0), respectively, but the difference was not significant.

Effects of A. niger strain XF-1 on exchangeable Ca and Mg in soil

As can be seen from *Table 4,* after watering of *A. niger* XF-1 nutrient solution, the contents of exchangeable Ca and Mg in soil were higher than CK (T_0) and CK (T_0-A), but the difference were not significant. 90 days after watering, the contents of

http://www.aloki.hu ● ISSN 1589 1623 (Print) ● ISSN 1785 0037 (Online)
DOI: http://dx.doi.org/10.15666/aeer/1804_50795092

exchangeable Ca of treatments diluted 50 times, 100 times and 200 times with planting *A. fruticosa* in soil were 1.23%, 1.91% and 0.90% higher than CK (T_0-A), and the contents of exchangeable Mg of that in soil were 0.61%, 1.22% and 0.91% higher than CK (T_0-A), respectively. The contents of exchangeable Ca of treatments diluted 50 times, 100 times and 200 times without planting *A. fruticosa* in soil after 90 days increased by 1.57%, 2.68% and 1.12% than CK (T_0) respectively, and the content of exchangeable Mg of that in soil increased by 0.61%, 1.21% and 0.91% than CK (T_0), respectively, but there was no significant difference.

Table 3. *Effect of different dilution fermentation broth of A. niger XF-1 on available P, K, Cu, Zn, Fe, Mn (mg·kg^{-1}) in soil*

Treatment	P	Cu	Zn	Fe	Mn
CK (T_0-A)	7.10 ± 0.12b	0.53 ± 0.01b	1.27 ± 0.03b	2.62 ± 0.05b	4.96 ± 0.02b
CK (T_0)	7.63 ± 0.19b	0.62 ± 0.02a	1.29 ± 0.04b	2.64 ± 0.06b	4.96 ± 0.06b
T_{50}-A	8.30 ± 0.09b	0.64 ± 0.02a	1.35 ± 0.02a	3.25 ± 0.04a	5.29 ± 0.04ab
T_{50}	8.98 ± 0.13ab	0.63 ± 0.01a	1.36 ± 0.01a	3.29 ± 0.03a	5.30 ± 0.03a
T_{100}-A	9.65 ± 0.08a	0.68 ± 0.01a	1.37 ± 0.03a	3.33 ± 0.02a	5.53 ± 0.05a
T_{100}	10.09 ± 0.15a	0.69 ± 0.02a	1.37 ± 0.02a	3.35 ± 0.01a	5.53 ± 0.03a
T_{200}-A	9.00 ± 0.08a	0.65 ± 0.01a	1.36 ± 0.01a	3.30 ± 0.03a	5.30 ± 0.06a
T_{200}	9.41 ± 0.12a	0.66 ± 0.01a	1.35 ± 0.02a	3.32 ± 0.02a	5.30 ± 0.07a

Different letters after the same column of numbers indicate significant differences at the 0.05 level

Table 4. *Effect of different dilution fermentation broth of A. niger on exchangeable Ca and Mg (mg·kg^{-1}) in soil*

Treatment	Ca	Mg
CK (T_0-A)	8.92 ± 0.04a	3.29 ± 0.07a
CK (T_0)	8.94 ± 0.05a	3.30 ± 0.09a
T_{50}-A	9.03 ± 0.06a	3.31 ± 0.05a
T_{50}	9.08 ± 0.13a	3.32 ± 0.07a
T_{100}-A	9.09 ± 0.08a	3.33 ± 0.08a
T_{100}	9.18 ± 0.15a	3.34 ± 0.07a
T_{200}-A	9.00 ± 0.11a	3.32 ± 0.05a
T_{200}	9.04 ± 0.12a	3.33 ± 0.06a

Same letters after the same column of numbers indicate no significant differences at the 0.05 level

Effect of A. niger strain XF-1 on chlorophyll content of A. fruticosa

As can be seen from *Figure 2,* the photosynthetic pigment content of *A. fruticosa* seedlings could be increased to different degrees after watering dilution nutrient solution of *A. niger* at different multiples. The contents of chlorophyll a, chlorophyll b and total chlorophyll in treatments of watering diluted 100 times were the highest, higher than that in treatments of watering diluted 50 times, but the difference was not significant ($p < 0.05$). The content of chlorophyll a and total chlorophyll were significantly higher than that of watering diluted 200 times, and significantly higher than that of control ($p < 0.05$). There was no significant difference in chlorophyll b content. The contents of

http://www.aloki.hu ● ISSN 1589 1623 (Print) ● ISSN 1785 0037 (Online)
DOI: http://dx.doi.org/10.15666/aeer/1804_50795092

chlorophyll a, chlorophyll b and total chlorophyll in treatments of watering diluted 50 times were higher than that in treatments of watering diluted 200 times, but the difference were not significant ($p < 0.05$). The contents of chlorophyll a and total chlorophyll were significantly higher than that of the control group (T_0 and $T_{0\text{-}A}$), while the content of chlorophyll b was not significantly different ($p < 0.05$). The contents of chlorophyll a, chlorophyll b and total chlorophyll in the watered locust with a concentration of 200 times dilution were higher than that of the control ($T_{0\text{-}A}$), the contents of chlorophyll a and total chlorophyll were significantly higher than that of the control ($T_{0\text{-}A}$), and the content difference of chlorophyll b was not significant ($p < 0.05$). To sum up, the results showed that the contents of chlorophyll a, b and total chlorophyll of *A. fruticosa* in treatments of watering diluted 100 times were higher than that in treatments of watering diluted 50 times, and the contents of chlorophyll a, b and total chlorophyll of *A. fruticosa* in treatments of watering diluted 200 times were the lowest. The chlorophyll content was T_{100}-A > T_{50}-A > T_{200}-A in turn.

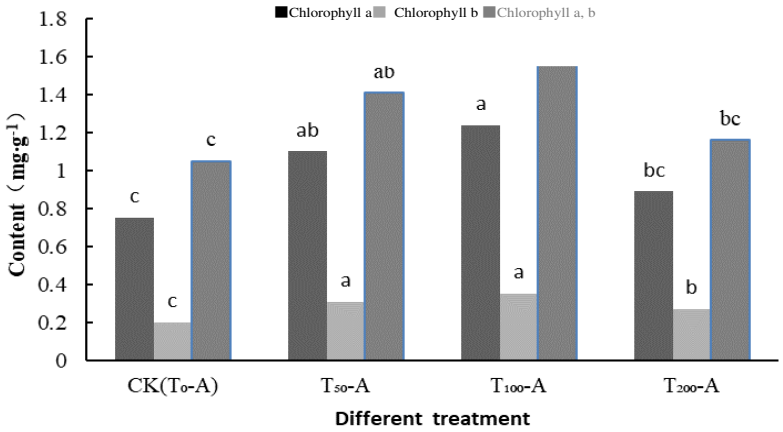

Figure 2. *Effect of different dilution fermentation broth of A. niger XF-1 on chlorophyll content of Amorpha fruticosa*

Effect of A. niger XF-1 on plant height and biomass of A. fruticosa

Effect of watering three kinds of different dilution concentrations of *A. niger* fermentation broth on plant height, root system and biomass were shown in *Figures 3* and *4* and *Tables 5* and *6*.

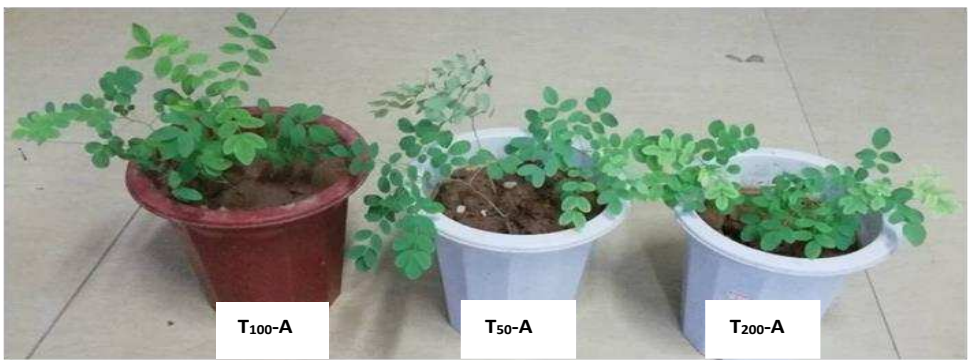

Figure 3. *Effect of different dilution fermentation broth of A. niger XF-1 on the growth of A. fruticosa*

http://www.aloki.hu ● ISSN 1589 1623 (Print) ● ISSN 1785 0037 (Online)
DOI: http://dx.doi.org/10.15666/aeer/1804_50795092

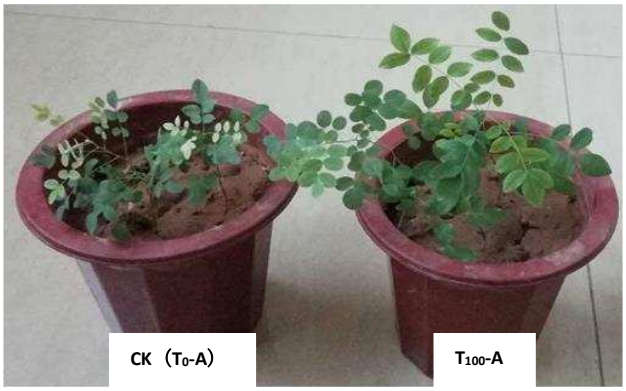

Figure 4. *Comparison of plant height of A. fruticosa between treatment T_{100}-A and CK (T_0-A)*

Tables 5 and *6* show that treatments of watering different dilution concentrations of fermentation broth of *A. niger* XF-1 can obviously promote the growth of *A. fruticosa* above ground. The analysis of plant height, fresh and dry weight above ground of *A. fruticosa* showed that the promoting effect of T_{100}-A was the best, of T_{200}-A was the second, of T_{50}-A was the worst. The plant height of *A. fruticosa* for T_{100}-A was 6.09 cm, 2.02 cm and 4.20 cm, which was significantly higher than that for T_0-A, T_{50}-A and T_{200}-A respectively. The fresh weight above ground for T_{100}-A was 0.11 g, 0.21 g and 0.24 g, which was significantly lower than that for T_{50}-A, T_{200}-A and T_0-A, respectively. The dry weight above ground for T_{100}-A was 0.04 g, 0.08 g and 0.12 g, which was significantly lower than that for T_{50}-A, T_{200}-A and T_0-A, respectively. The promoting ability of the three kinds of *A. niger* XF-1 nutrient solution to root length of *A. fruticosa* was T_{100}-A > T_{50}-A > T_{200}-A, and the root length of *A. fruticosa* for T_{100}-A was 2.34 cm, 3.92 cm, and 3.15 cm, which was significantly higher than that for T_{50}-A, T_{200}-Aand T_0-A, respectively. The root diameter circumference and dry weight of *A. fruticosa* for the three kinds of *A. niger* XF-1 nutrient solution were significantly lower than that for T_0-A. The root diameter circumference of *A. fruticosa* for T_{100}-A was 0.26 mm and 0.58 mm, which was significantly higher than that for T_{50}-A and T_{200}-A respectively, but 0.21 mm was significantly lower than that for T_0-A. Root fresh weight of *A. fruticosa* for T_{100}-A was significantly higher (0.04 g and 0.05 g) than that for T_{50}-A and T_{200}-A respectively, but 0.04 g was significantly lower than that for T_0-A. The dry weight of root system of *A. fruticosa* for T_{100}-A was significantly lower than that for T_{50}-A and T_0-A by 0.02 cm and 0.04 cm respectively, and significantly higher than that for T_{200}-A by 0.02 cm. Compared with the control T_0-A, the root cap ratio of *A. fruticosa* with different concentrations of *A. niger* XF-1 fermentation broth was significantly decreased, indicating that *A. niger* XF-1 nutrient solution improved the condition of nutrition supplies of *A. fruticosa*, was advantageous to the rapid growth of above round parts. Among them, T_{100}-A treatment promoted the growth of *A. fruticosa* the fastest, but there was no significant difference with the other two concentrations of *A. niger* XF-1 nutrient solution. On the whole, T_{100}-A treatment has the best effect in promoting the growth of *A. fruticosa*, which is suggested as a reference for ecological restoration.

Scanning electron microscope (SEM) observation of root complex of A. fruticosa

The above studies indicated that A. niger XF-1 had a significant effect on promoting A. fruticosa. In order to better study the weathering of plants and microorganisms on

http://www.aloki.hu ● ISSN 1589 1623 (Print) ● ISSN 1785 0037 (Online)
DOI: http://dx.doi.org/10.15666/aeer/1804_50795092

granite rocks, the effect of A. niger XF-1 on the granite and the roots of A. fruticosa was observed by SEM. As can be seen from *Figure 5,* the surface of the granite which is not planted with A. fruticosa and not inoculated with A. niger XF-1 was relatively smooth, angular and without a large number of fragments. However, A. niger XF-1 was distributed on the surface of the granite treated by inoculation without A. fruticosa, and there were a large number of granular substances, even the presence of fungal secretions. It can be seen that the granite underwent different degrees of weathering under the action of *A. niger* XF-1.

Table 5. *Effect of different dilution fermentation broth of A. niger XF-1 on plant height, root length and diameter circumference of A. fruticosa*

Treatment	Plant height (cm)	Root length (cm)	Diameter circumference (mm)
CK (T_0-A)	7.43 ± 0.19d	9.42 ± 0.22c	2.03 ± 0.45a
T_{50}-A	11.50 ± 0.17b	10.23 ± 0.26b	1.56 ± 0.09c
T_{100}-A	13.52 ± 0.35a	12.57 ± 0.69a	1.82 ± 0.06b
T_{200}-A	9.32 ± 0.23c	8.65 ± 0.19d	1.24 ± 0.03d

Different letters after the same column of numbers indicate significant differences at the 0.05 level

Table 6 *Effect of different dilution fermentation of A. niger XF-1 on the above ground part and root biomass of A. fruticosa*

Treatment	Fresh weight (g·plant^{-1})			Dry weight (g·plant^{-1})			Root cap ratio
	Overground	Root system	Total	Overground	Root system	Total	
CK (T_0-A)	0.40 ± 0.09d	0.45 ± 0.09a	0.85c	0.26 ± 0.09c	0.25 ± 0.09a	0.51 ± 0.09c	0.96a
T_{50}-A	0.55 ± 0.09b	0.37 ± 0.09c	0.92b	0.34 ± 0.09a	0.21 ± 0.09c	0.55 ± 0.09b	0.62b
T_{100}-A	0.66 ± 0.09a	0.41 ± 0.09b	1.07a	0.38 ± 0.09a	0.23 ± 0.09b	0.61 ± 0.09a	0.61b
T_{200}-A	0.45 ± 0.09c	0.36 ± 0.09c	0.80c	0.30 ± 0.09ab	0.19 ± 0.09d	0.49 ± 0.09d	0.63b

Different letters after the same column of numbers indicate significant differences at the 0.05 level

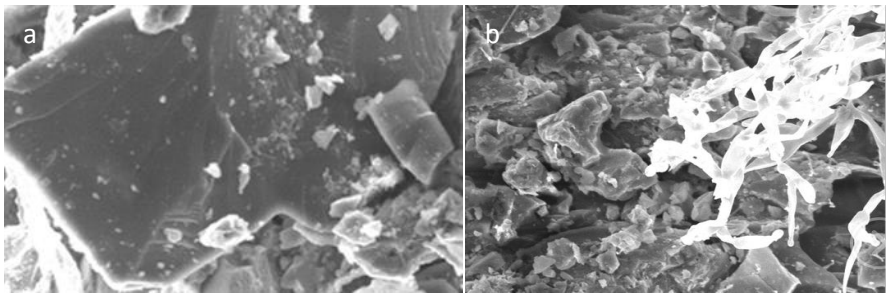

Figure 5. *SEM photos of granite surfaces without planting A. fruticosa. (a) Granite surface without A. niger strain XF-1. (b) Granite surface with A. niger XF-1*

Figure 6 showed the scanning electron microscope (SEM) images of the root system of plant and the attached granitoid particle complexes planted with *A. fruticosa* without inoculation. As can be seen from the picture, the root (or root hair) of the *A. fruticosa* can absorb fragments of granite. According to the result of energy spectrum analysis, the weathering effect of granites adsorbed on the root surface of *A. fruticosa* is not obvious.

http://www.aloki.hu ● ISSN 1589 1623 (Print) ● ISSN 1785 0037 (Online)
DOI: http://dx.doi.org/10.15666/aeer/1804_50795092

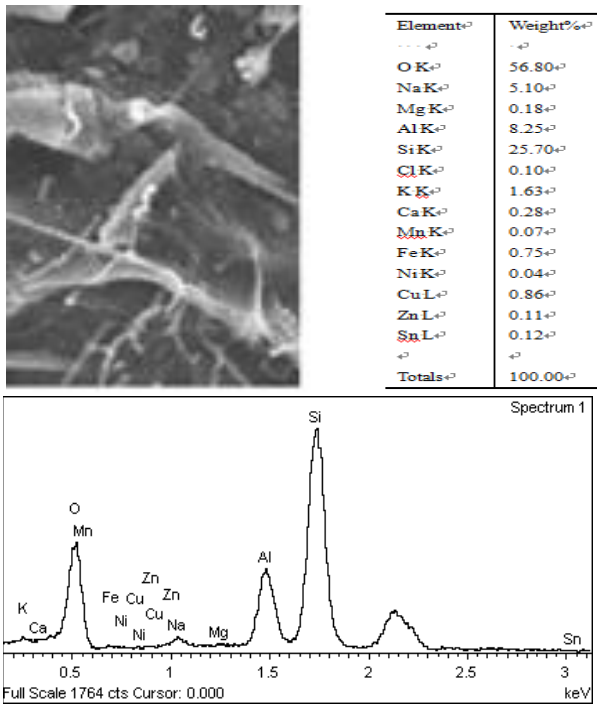

Figure 6. *SEM photos of granite planted A. fruticosa without A. niger XF-1*

Figure 7 is a scanning electron microscope image of the root system and the attached granitoid particle complex of *A. fruticosa* by inoculation. It can be seen from the figure that there were a large secretions of *A. niger* XF-1 and granites on the root system surface of *A. fruticosa* treated by inoculation. It can be seen that *A. niger* XF-1 could colonize the surface of granite rocks and root of *A. fruticosa,* and multiply to produce hyphae and secrete metabolites. According to the results of energy spectrum analysis, the surface of *A. niger* XF-1 and root system of *A. fruticosa* adsorbed a lot of elements. *A. niger* XF-1 had a significant effect on the granite weathering of the root surface of *A. fruticosa*.

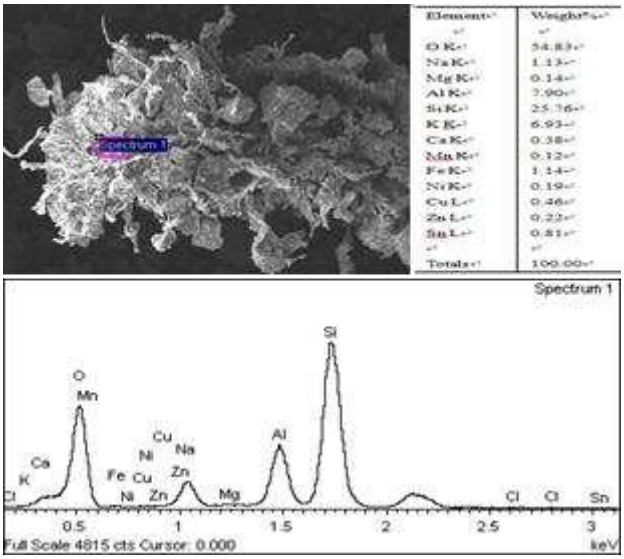

Figure 7. *SEM photos of granite, that plant A. fruticosa, treated with A. niger XF-1*

http://www.aloki.hu ● ISSN 1589 1623 (Print) ● ISSN 1785 0037 (Online)
DOI: http://dx.doi.org/10.15666/aeer/1804_50795092

Discussion

A. niger XF-1 can well colonize surfaces of plant roots and rock, appropriately reduce the soil pH value, increase the content of available phosphorus, iron, copper, zinc and manganese in the soil, and promote the growth of plants and the increase of biomass. It is a strain that can effectively dissolve soil elements and promote the growth of plants. The results of this experiment showed that the pH value of soil was decreased from 7.1 to 6.1 after watering the fermentation broth of *A. niger* star in XF-1. The decrease of pH value was due to the strain producing a large amount of oxalic acid, lactic acid and succinic acid (Wu, 2018). The secretion of organic acids is the main mechanism of releasing nutrient elements from rock minerals (Wu et al., 2017a, b). During the reproduction process in soil, microorganisms secrete organic acids, cause the increase of the number of H^+ in soil reduce the pH value in soil and can chelate with some plasmas such as iron, aluminum, calcium and so on, which makes the undissolved phosphorus render into effective phosphorus (Zhong et al., 2015), and the calcium, magnesium, iron, copper, zinc, silicon and other nutrients in soil can be activated with the increase of H^+ to improve the availability of these nutrients in the soil (Wu, 2018; Wu, 2019). Meanwhile, microorganisms can also secrete polysaccharides, amino acids and other substances to directly improve plant stress resistance (Huang et al., 2009; Li et al., 2012).

In the process of screening microbial strains of weathered rock minerals from soil, in addition to its ability to weathering rock minerals, its role in plant-microbial systems should be considered. As the rhizosphere microorganism, the function of microbial strains may be influenced by other factors (Benoit et al., 2015). As living organisms, microbial strains also secrete metabolites, which may affect plant growth and development. For example, metabolites affect the effective absorption, and deposition of nutrients, the activity of plant pathogens, the occurrence and degree of plant diseases, and the stress resistance of plants, so as to promote or inhibit the growth of plants (Jiang et al., 2000). Saxena et al. have shown that applying bioinoculated *A. niger* K7 and biochar simultaneously is a good measure to improve soil fertility and crop yield. In the soil-plant experiment, all treatments significantly increased the growth, root nodule and yield of soybean plants ($p < 0.05$) (Saxena, 2016). Rhizosphere microorganisms stimulate plant growth because they produce a variety of plant growth hormones and vitamins in solution and in plants. These compounds can promote plant growth to some extent.

Nitrogen, phosphorus and potassium are essential elements for plant growth and development. Released nutrients by weathering rock mineral and substances secreted by metabolism for single strain cannot completely meet the requirements of plant growth. Therefore, using the mutual composite of microorganisms with different functions in soil, such as compound utilization of phosphorus-soluble microorganisms and microbial strains which can resolve nitrogen or potassium, can meet the plant's nutritional requirements. At present, the compounding and use of compound bacterial preparation has become a hot research problem, and if microbial strains are used in combination with microorganisms that can decompose the remaining chemical fertilizers and pesticides in the soil, or kill pests, or sterilize bacterials, and or improve physical and chemical properties of soil, it is bound to strengthen the ability of microorganisms to adapt to the environment, optimize the structure of soil, stimulate the accumulation of the microbial metabolites, and meet the supply of plant growth nutrients, which will benefit the rapid coverage of bare rock slope vegetation and promote the sustainable development of ecological restoration.

http://www.aloki.hu ● ISSN 1589 1623 (Print) ● ISSN 1785 0037 (Online)
DOI: http://dx.doi.org/10.15666/aeer/1804_50795092

Conclusion

In this study, the number of rhizosphere microorganisms was significantly higher than that of control group after inoculation. Moreover, with the increase of irrigation concentration, the number of rhizosphere microorganisms of *A. fruticosa* increased gradually. It indicated that *A. niger* XF-1 can colonize the rhizosphere of *A. fruticosa*, which is conductive to the formation of soil-microbial-plant system.

After inoculation with *A. niger* XF-1 fermentation broth, the pH value of soil decreased significantly. The contents of exchangeable Ca and Mg in soil were generally higher than those in control. Different concentration of *A. niger* XF-1 fermentation broth could increase the photosynthetic pigment content and the growth of *A. fruticosa* seedlings significantly.

SEM results showed that the root surface of *A. fruticosa* had a large number of metabolites and granites after inoculation of *A. niger* XF-1. It indicated that XF-1 could colonize on the granite and the root surface of *A. fruticosa*, produce a large number of mycelia and secrete metabolites. The granite weathering effect on *A. fruticosa* was obvious. This study provides a new idea for ecological restoration of degraded habitats and a new model for rapid soil formation and wall greening of exposed rocks in abandoned mining areas. At present, the use of microorganisms for ecological restoration is still in the experimental stage, and the effect of mountain slope greening remains to be further studied.

Acknowledgements. This research was supported by the positioning research project of Forest Ecosystem of Changjiang River Delta in Jiangsu Province, the Engineering Project 'Three New' for Forestry in Jiangsu Province (lysx [2013] 10), a project funded by the Priority Academic Program Development of Jiangsu Higher Education Institutions, the open project of the Key Laboratory of Soil and Water Conservation and Ecological Restoration in Jiangsu Province, and the Doctoral Research Fund Project of Anyang Institute of Technology (BSJ2020003).

REFERENCES

[1] Benoit, I., van den Esker, M., Patyshakuliyeva, A. et al. (2015): Bacillus subtilis attachment to *Aspergillus niger* hyphae results in mutually altered metabolism. – Environmental Microbiology 17(6): 2099-2113.

[2] Bao, S. D. (1981): Soil Agrochemical Analysis. 3rd Ed. – China's Agricultural Publishing House Beijing.

[3] Cui, B. X., Zhang, X. X., Han, G. et al. (2016): Antioxidant defense response and growth reaction of *Amorpha fruticosa* seedlings in petroleum. – Contaminated Soil. Water, Air, & Soil Pollution 227(4): 121.

[4] Eriola, V., Glenda, S., Astrit, B. (2018): Tripartite relationships in legume crops are plant-microorganism-specific and strongly influenced by salinity. – Agriculture 8(8): 117.

[5] Gong, M. B., Fan, B. Q., Jin, Z. G. et al. (2010): Screening and application of phosphate-dissolving microorganism suitable for corn production. – Acta Microbiologica Sinica 50(12): 1619-1625.

[6] Huang, Y. H., Tang, R. S., Ye, X. Q., et al. (2009): Effect of ABA on the germination of white grain wheat seeds and growth of its seedlings. – Journal of Triticeae Crops 29(3): 503-507.

[7] Jiang, X. J., Huang, Z. X., Xie, D. T., et al. (2000): Promoting effects of the metabolites of silicate for plant growth. – Journal of Southwest Agricultural University 2(2): 116-119.

http://www.aloki.hu ● ISSN 1589 1623 (Print) ● ISSN 1785 0037 (Online)
DOI: http://dx.doi.org/10.15666/aeer/1804_50795092

[8] Li, M., Ma, Q. Q., Zhao, H. J., et al. (2012): Effect of micro-derived hardiness agent on endogenous hormones content in maize roots. – Heilongjiang Agricultural Sciences 29(8): 47-49.
[9] Li, S., Duan, Y. X., Zhu, X. F. et al. (2011): Effects of adding secondary metabolites of *Aspergillus niger* on resistance to tomato root-knot nematode. – China Vegetables 1(4): 44-49.
[10] Lü, J., Tian, X. H., Y, H. et al. (2015): Effect of *Aspergillus niger* fermentation liquid on the growth of wheat seedings in calcareous soil. – Journal of Northwest Agriculture and Forestry University (Natural Sciences Edition) 43(5): 100-106.
[11] Meena, V. S., Meena, S. K., Verma, J. P. et al. (2017): Plant beneficial rhizospheric microorganism (PBRM) strategies to improve nutrients use efficiency: a review. – Ecological Engineering 107: 8-32.
[12] Qian, L. Z., Gong, M. B., Gu, J. G. et al. (2014): Effect of two different fungi on nutrient dynamic changes in soil. – Chinese Soil and Fertilizer 41(5): 86-89.
[13] Saxena, J., Rawat, J., Sanwal, P. (2016): Enhancement of growth and yield of glycine max plants with inoculation of phosphate solubilizing fungus *Aspergillus Niger* K7 and biochar amendment in soil. – Communications in Soil Science and Plant Analysis 47(20): 2334-2347.
[14] Wang, X. H., Wang, C. D., Sui, J. K. et al. (2018): Isolation and characterization of phosphofungi, and screening of their plant growth-promoting activities. – AMB Express 8(1): 63.
[15] Wang, Y. Q., Xu, H. L., Xu, G. Y. et al. (1993): The applicable of AP-2 *Aspergillus niger* dissolve phosphorus microorganism in the planting tobacco. – Biotechnology 3(1): 4-38.
[16] Wang, Y. X., Zhang, J. C., Wu, Y. W. et a1. (2017): Effects of soil bacteria inoculation in spray seeding matrix on photosynthesis characteristics and chlorophyll fluorescence parameters of Amorpha fruticose. – Research of Environmental Sciences 30(6): 902-910.
[17] Wu, Q. F., Hu, H. B., Zhang, X. (2018): Effect of *Aspergillus niger* and its metabolites on weathering of granite. – Journal of Nanjing Forestry University (Natural Sciences Edition) 42(1): 81-88 (in Chinese).
[18] Wu, Q. F., Hu, H. B. (2019): The influence of environmental factors on Aspergillus niger granite weathering. – Applied Ecology and Environmental Research 17(1): 395-408.
[19] Wu, Y. W., Zhang, J. C., Guo, X. P., et al. (2017a): Identification of efficient strain applied to mining rehabilitation and its rock corrosion mechanism: based on boosted regression tree analysis. – Environmental Science 38(1): 283-293 (in Chinese).
[20] Wu, Y. W., Zhang, J. C., Wang, L. J. et al. (2017b): A rock-weathering bacterium isolated from rock surface and its role in ecological restoration on exposed carbonate rocks. – Ecological Engineering 101(1): 162-169.
[21] Yan, W. M., Zheng, S. X., Zhong, Y. q. W. et al. (2017): Contrasting dynamics of leaf potential and gas exchange during progressive drought cycles and recovery in Amorpha fruticosa and Robinia pseudoacacia. – Scientific Reports 7(1): 4470.
[22] Yang, C. X. (2008): Amorpha fruticosa L. is a superior aforestation tree species in semi-arid waste dump area. –Forestry Science and Technology information 4(03): 30-31.
[23] Zhang, J. (2004): Contrast determination of available Cu, Zn, Fe, Mn in soil by DTPA and M3 extraction. – Journal of Shanxi Agricultural Sciences 32(3): 30-33.
[24] Zhang, L. Z., Fan, J. J., Niu, W. et al. (2011): Isolation of phosphate solubilizing fungus (*Aspergillus niger*) from Caragana rhizosphere and its potential for phosphate solubilization. – Acta Ecologica Sinica 31(24): 7571-7578.
[25] Zhong, W. Y., Shi, F. C., Hong, M. J. et al. (2015): Phosphate solubilization and promotion of maize growth by *Penicillium oxalicum* P4 and *Aspergillus niger* P85 in a calcareous soil. – Canadian Journal of Microbiology 61(12): 1-11.

http://www.aloki.hu ● ISSN 1589 1623 (Print) ● ISSN 1785 0037 (Online)
DOI: http://dx.doi.org/10.15666/aeer/1804_50795092

EFFECT OF ROOT-SOIL PARAMETERS ON THE LODGING RESISTANCE OF SUGARCANE (*SACCHARUM OFFICINARUM* L.)

YANG, W.[1,2] – YUAN, F. W.[1] – CHEN, Y. Q.[3] – YANG, J.[1*]

[1]*College of Mechanical Engineering, Guangxi University, Nanning 530004, China*

[2]*Guangxi Key Laboratory of Manufacturing System & Advanced Manufacturing Technology, College of Mechanical Engineering, Guangxi University, Nanning 530004, China*

[3]*Xingjian College of Science and Liberal Arts, Guangxi University, Nanning 530005, China*

**Corresponding author*
e-mail: gxuyangjian@163. com

(Received 8th Nov 2019; accepted 3rd Jul 2020)

Abstract. Lodging reduce sugarcane yield, also results in the increase of harvest loss and head-splitting rate in mechanical harvesting. Although there are some researches on lodging resistance of sugarcane, there are few studies on the effects of root-soil multi-factor, which limits the discovery of the most important lodging resistance influence factors and the most effective lodging resistance technical measure of sugarcane. This study aimed at: (1) establishing the mathematical model of the relationship between $F_{30°}$ and the root and soil parameters using the artificially induced tilt experiment for sugarcane. $F_{30°}$ is the maximum pulling force in the process of the tilt angle (the angle between stem and ground) changing from 90° to 30°; (2) studying the effects of lodging resistance using the model. The results show that the established model is reasonable. The two most important influence factors of sugarcane lodging resistance are number of roots and interaction between planting depth and soil hardness. The most effective measure to improve the lodging resistance is to increase the number of roots through breeding and reasonable fertilization, and to increase the planting depth, meanwhile, to establish good drainage measures to timely drain water in typhoon season for reducing soil moisture and maintaining greater soil hardness.

Keywords: *tilt induction test, multi-factor, mathematical model, influence law, lodging resistance technical measure*

Introduction

Lodging reduces crop yields (Goodman and Ennos, 1999; Berry et al., 2000; Terashima et al., 2003; Sposaro et al., 2008; Loades et al., 2013; Manzur et al., 2014; Bian et al., 2018; Liu et al., 2018; Wu and Ma, 2018). And sugarcane (Saccharum officinarum L.) is the main sugar material in the world and China, of which, the sugarcane planting area in the world is about 26 million ha, China's sugarcane planting area is about 1.6 million ha (Li et al., 2017, 2019; Wang and Zhang, 2018). Lodging normally reduce sugarcane yield by 10-20%, and when lodging is serious, the yield can even be reduced by more than 50% (Singh et al., 2002; van Heerden et al., 2015). Meanwhile, lodging also results in the increase of harvest loss and head-splitting rate in mechanical harvesting of sugarcane (Wang et al., 2010; Ou et al., 2013). And because of its high growth height, sugarcane is more prone to lodging. Thus, it is necessary to study the lodging resistance of sugarcane. Berding and Hurney (2005) conducted the comparison tests of sugarcane planting with different planting depths and varieties. The result showed that lodging in a planting depth of 260 mm was lower than that in a depth of 120 mm. Lodging of sugarcane variety Q152 was less than that of sugarcane varieties Q187 and Q174. Babu et al. (2009) investigated the relationship between the hardness

http://www. aloki.hu ● ISSN 1589 1623 (Print) ● ISSN 1785 0037 (Online)
DOI: http: //dx.doi.org/10.15666/aeer/1804_50935107

of sugarcane skin and lodging by experiment. The result showed that the sugarcane was not prone to lodge when the hardness of sugarcane skin was high. Loganandhan et al. (2013) conducted the comparison tests of sugarcane planting with different planting depths and hilling conditions. The result showed that lodging could be diminished at a high planting depth and hilling thickness. Jongrungklang et al. (2018) studied the effects of stalk height, stalk diameter, leaf and stalk weight, root length density (RLD), root length density percentage (% RLD) on lodging of sugarcane. The results showed that high stalk dry weight is a key factor that induces lodging. The low stalk heights and stalk dry weights as well as a good partition of the root in the upper soil layer had better lodging resistance. The cultivars with large root systems in the upper soil layer should be selected in breeding for strong lodging resistance. Li et al. (2019) studied the lodging grade, fracture resistance force, basal stem diameter, middle stem diameter and brix. With the data of lodging classification, the lodging resistance index was established. The results showed that the lodging resistance index was significantly and positively correlated with the ratio of basal and middle stem diameters and brix. These authors carried out some researches on lodging resistance of sugarcane. However, there are few studies on the effects of root-soil multi-factor on the lodging resistance, which limits the discovery of the most important lodging resistance influence factors and the most effective lodging resistance technical measure of sugarcane.

The root system of sugarcane is composed of main stem and root, and its morphological structure is complex. The root system of newly planted sugarcane studied in this paper is shown in *Figure 1*. Meanwhile, the root plate (the soil–root volume that rotates in the broader soil matrix when lodging occurs) which has large influence on lodging is closely associated with the complex root and soil parameters (Sposaro et al., 2008). It is difficult to study the effect of lodging resistance by mechanical analysis alone. The objectives of the work presented here were to establish the mathematical model of the effect of root and soil parameters on lodging resistance using field experiments and regression analysis method, and to study the influence law and mechanism of root-soil parameters on the lodging resistance. The study outcomes will discover the most important lodging resistance influence factors and the most effective lodging resistance technical measure of sugarcane.

Materials and methods

Lodging resistance measurements

Test scheme and method

The lodging resistance of sugarcane is associated with the length, the diameter, the density, the tensile strength of sugarcane roots, the planting depth of sugarcane, the complex soil parameters (including density, cohesion, moisture content, internal friction angle, elastic modulus, etc.) and the comprehensive friction coefficient between sugarcane roots and soil. And the comprehensive friction coefficient between roots and soil is closely related to soil water content that significantly associate with soil hardness which is a comprehensive index to measure the properties of soil (Ren, 2011). Thus, the number of roots x_1, the length of roots x_2, the diameter of roots x_3, the planting depth of sugarcane x_4, the tensile strength of roots x_5 and the soil hardness x_6 were selected as experimental factors.

http://www. aloki.hu ● ISSN 1589 1623 (Print) ● ISSN 1785 0037 (Online)
DOI: http: //dx.doi.org/10.15666/aeer/1804_50935107

Strong lodging resistance of sugarcane required large wind load to produce the same tilting angle. Therefore, the wind load that makes sugarcane produce the same tilting angle can be regard as a measuring index of lodging resistance. However, it is difficult for different sugarcane to produce the same tilting angle by controlling wind load in field test. And the distributed wind load acting on sugarcane can be replaced by a concentrated load. Hence the test of sugarcane lodging resistance under wind load can be replaced by the artificially induced tilting experiment of sugarcane applying the pulling force (Manzur et al., 2014). Meanwhile, when the tilting angle (i.e., the angle between stem and ground) is 30°, it indicates that a severe lodging occurs (Mou et al., 2010). Thus, $F_{30°}$ was taken as the test index. $F_{30°}$ is the maximum pulling force in the process of the tilt angle changing from 90° to 30°.

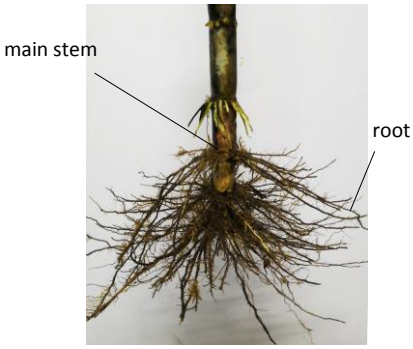

Figure 1. *Sugarcane root system*

When loading height and loading speed on the stem are different, the corresponding required pulling forces for producing the same tilting angle are different. Nevertheless, the effect of root and soil parameters on lodging resistance is not changed. Thus, to facilitate the operation of the test, the loading height of the pulling force set at 0.5 m above the ground, and the pulling force was applied slowly and uniformly. Meanwhile, the upper part of the sample sugarcane was removed for reducing the influence of gravity, and only 0.6 m of the stem was retained. Guangxi Province is main sugarcane production base in China, and its planting area accounts for more than 60% of China. Thus, in order to obtain the representative experiment results, the sugarcane with well growth, no pests and no diseases were randomly selected in different main sugarcane producing areas of Guangxi, China for the experiment. The number of test sites is 3, and the number of samples taken per sites is 15. The number of verifying test sites is 2, and the number of samples taken per sites is 4. The easy lodging period of sugarcane in Guangxi is from July to September. During this period, the root growth is different due to the different length of growth time, but it does not change the influence of root parameters on lodging resistance. Therefore, the sugarcane tilting tests were carried out from July to September in this paper.

Simultaneously, in order to obtain soil water content in the monsoon and typhoon days, artificial irrigation was carried out before the tilting experiment. During irrigation, the soil wall with a radius of about 1 m was built around the sample sugarcane, and then water was filled into the wall. Moreover, in order that water can permeate downward sufficiently, the experiments were carried out after filling the water for 24 h.

After the experiments, the root system of sugarcane was dug out and the planting depth of sugarcane was measured. And then the soil on the root system was washed

http://www. aloki.hu ● ISSN 1589 1623 (Print) ● ISSN 1785 0037 (Online)
DOI: http: //dx.doi.org/10.15666/aeer/1804_50935107

away with water, and the number, average length and diameter of roots were obtained. Finally, eight roots were randomly selected for measuring the tensile strength, and then their average value was taken as the tensile strength of individual sugarcane roots. Tensile strength test of the roots was performed using the electronic universal testing machine. To avoid root damage caused by clamping parts, the gauze was used to wind round the both ends of root. The measurement of the soil hardness and the tilt induction test were carried out simultaneously. The measured soil located near the sugarcane sample. Because the soil hardness is closely related to the soil depth (Yang et al., 2015), the soil hardness was measured in three layers according to the planting depth. Twelve test points were selected in each layer, and then the average hardness value of all test points in three layers was taken as the soil hardness.

The higher the prediction accuracy of the established mathematical model, the more induction tests are needed. However, the tilt induction test of each sugarcane needs a lot of time, thus, after comprehensive consideration, 45 sugarcane samples were selected for the test. The experimental scheme and results are shown in *Table A1* in the *Appendix*.

Test equipment and site

The main test equipment are as follows: self-made inducing sugarcane tilt test system, electronic tension meter, hardness tester, NKK-4005 microcomputer-controlled electronic universal testing machine (Shenzhen Nanfangjinke Instruments and Equipment Co., Ltd., China, the maximum load is 5 kN and the load resolution is 0.1 N), electronic balance, oven and protractor, etc. The tilt induction test system of sugarcane is shown in *Figure 2*.

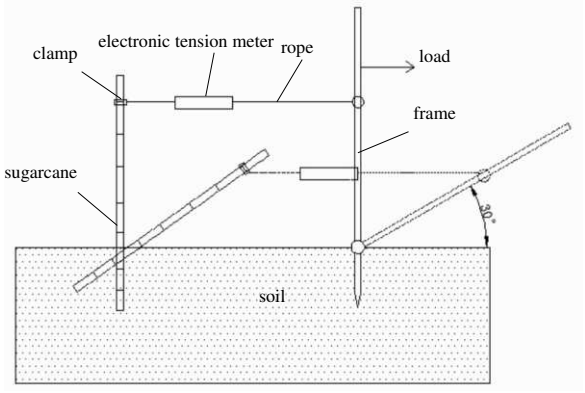

Figure 2. *The tilt induction test system of sugarcane*

The test sites and the sugarcane varieties are as follows:

(1) The sugarcane planting base is in Jinguang Farm, Nanning City, Guangxi Province, China (lat. 22°56′48.03″N, long. 107°53′43.25″E). The soil type is yellow clay. The sugarcane varieties are GT-32, GT-42, GT-46, Liucheng 07-150 and GT-22, respectively. The sugarcanes were planted in wide and narrow row alternately using machine. The wide row spacing is 1.2 m and the narrow row spacing is 0.5 m. The sugarcanes were covered by film. The planting time was from January to February 2017. 3 sugarcane was chosen in each variety, and test time is July 2017. The total number of the samples was 15.

http://www. aloki.hu ● ISSN 1589 1623 (Print) ● ISSN 1785 0037 (Online)
DOI: http: //dx.doi.org/10.15666/aeer/1804_50935107

(2) The sugarcane planting base is in Qianwei Farm, Nankang Town, Beihai City, Guangxi Province, China (lat. 21°35′47.39″N, long. 109°28′46.49″E). The soil type is sandy soil. The sugarcane varieties are GT-46, GT-22, 03-23, GY-1 and Liucheng 05-136, respectively. The sugarcanes were planted in the same row using machine. The row spacing is 1 m. The sugarcanes were covered by film. The planting time was from January to February 2017. 3 sugarcane was chosen in each variety, and test time is August 2017. The total number of the samples was 15.

(3) The sugarcane planting base is in Guizhong Farm, Liuzhou City, Guangxi Province, China (lat. 24°29′17.12″N, long. 109°40′11.93″E). The soil type is loam. The sugarcane varieties are YT 94-128, GT-22, Liucheng 05-136, ROC 22 and GT-41, respectively. The sugarcanes were planted in wide and narrow row alternately using machine. The wide row spacing is 1.3 m and the narrow row spacing is 0.5 m. Trickle irrigation was used in the middle of the narrow row. The sugarcanes were covered by film. The planting time was February 2017. 3 sugarcane was chosen in each variety, and test time is September 2017. The total number of the samples was 15.

The test sites in this paper have been marked on the map, as shown in *Figure 3*.

Figure 3. *The map with location of test sites*

Regression analysis

SPSS software is a powerful and mature mathematical statistics software. Therefore, using this software, regression analysis of the test data in *Table A1* was implemented, and the mathematical model of the relationship between $F_{30°}$ and root-soil experiment factors was established. Meanwhile, using the software's significance test function, the mathematical model and regression coefficients were tested, and the significance of the mathematical model and the order of the influence of the experimental factors on $F_{30°}$ were analyzed.

Verification of mathematical model

Firstly, $F_{30°}$ was measured by the artificial induced tilt test, meanwhile, the parameters of soil hardness and sugarcane root were obtained by the above soil and root measurement methods. Then the predicted values of $F_{30°}$ were calculated by substituting the parameters of soil hardness and root into the established mathematical model. Finally, the rationality of the mathematical model was verified by comparing the

http://www. aloki.hu ● ISSN 1589 1623 (Print) ● ISSN 1785 0037 (Online)
DOI: http: //dx.doi.org/10.15666/aeer/1804_50935107

measured and predicted values of F_{30°. The sugarcane planting bases for verification are in Jinguang Farm, Nanning City, Guangxi Province, China (lat. 22°56′48.03″N, long. 107°53′43.25″E) and Wuming County, Nanning City, Guangxi Province, China (lat. 23°13′12.89″N, long. 108°07′59.43″E). In the two bases, the soil types are yellow clay and red clay, and the sugarcane varieties are GT-32 and ROC 22, respectively. The sugarcanes were planted alternately in wide and narrow row using machine. The wide row spacing is 1.2 m and the narrow row spacing is 0.5 m. The sugarcanes were covered by film. The planting time was March 2018. The experiment time was September 2018. 4 sugarcane with no pests were randomly selected in each variety for the verified tests.

Factor influence analysis

Using the established mathematical model, the relationships between significant factors or factor interactions and F_{30° were obtained, and the influence laws of factors or factor interactions on F_{30° were analyzed. Meanwhile, combined with observation in the experiment and relevant theoretical analysis, the influence mechanisms of factors or factor interactions on F_{30° were discussed. When analyzing the relationships between a certain factor or factor interaction and F_{30°, except for the factor or factors considered, all other factors were average in the mathematical model.

Results

Regression analysis

The mathematical model of the relationship between F_{30° and root-soil experiment factors is as follows.

$$\begin{aligned} F_{30^0} &= -188.976 + 1.43x_1 + 2.355x_2 + 76.044x_3 + 9.587x_5 \\ &- 0.042x_1x_4 - 0.057x_1x_5 + 0.13x_1x_6 - 57.352x_3x_6 + 5.656x_4x_6 \end{aligned} \quad \text{(Eq.1)}$$

where x_1 is number of roots, x_2 is root length, x_3 is root diameter, x_4 is planting depth, x_5 is tensile strength of root, and x_6 is soil hardness. The significance test results of the mathematical model and regression coefficients demonstrate that the mathematical model is significant at the level of 0.0001, and the regression coefficients are also significant at the level of 0.04-0.0001. The mathematical model is highly significant and fits well. Meanwhile, the significance test of the regression coefficients indicates that the order of factors affecting F_{30° (lodging resistance of sugarcane) is number of roots and interaction between planting depth and soil hardness, root diameter and interaction between root diameter and soil hardness and interaction between number of roots and planting depth, tensile strength of root, interaction between number of roots and tensile strength of root, root length, interaction between number of roots and soil hardness.

Verification of mathematical model

The measured results of field validation tests and the predicted results according to *Equation 1* are shown in *Table 1*. *Table 1* shows that the minimum relative error between the predicted and the measured value is 5.9%, while the maximum is 15.8%, and the average relative error is 10.7%. The main existence reason of error is that the

http://www. aloki.hu ● ISSN 1589 1623 (Print) ● ISSN 1785 0037 (Online)
DOI: http: //dx.doi.org/10.15666/aeer/1804_50935107

root growth shape and soil structure are complex, and some factors could not be considered. The mathematical model is reasonable and can be used for analyzing lodging resistance of sugarcane.

Table 1. *Measured and predicted results*

Test number	Number of roots x_1/bar	Root length x_2/cm	Root diameter x_3/mm	Planting depth x_4/cm	Tensile strength of root x_5/MPa	Soil hardness $x_6/10^{-1}$MPa	Predicted maximum pulling force $F_{30°}$/N	Measured maximum pulling force $F_{30°}$/N	Relative error/%
1	62	7.78	1.8	17.5	10.95	1.49	81.27	68.4	15.8
2	56	7.44	1.68	14.2	11.3	1.29	63.95	59.6	6.8
3	94	8.51	1.98	16.5	9.05	2.61	68.27	75.3	10.3
4	108	8.81	1.82	16	6.73	1.16	75.31	63.6	15.5
5	103	11.01	2.04	17	8.26	0.84	90.26	84.9	5.9
6	114	10.17	2.28	15.8	12.15	1.88	83.29	91.7	10
7	100	9.41	2.14	19.5	10.64	2.42	99.73	87.6	12.1
8	127	8.8	1.78	17.5	8.23	1.26	91.58	83.3	9

Influence factor analysis

Single factor influence

The relationships between $F_{30°}$ and factors are shown in *Figure 4*.

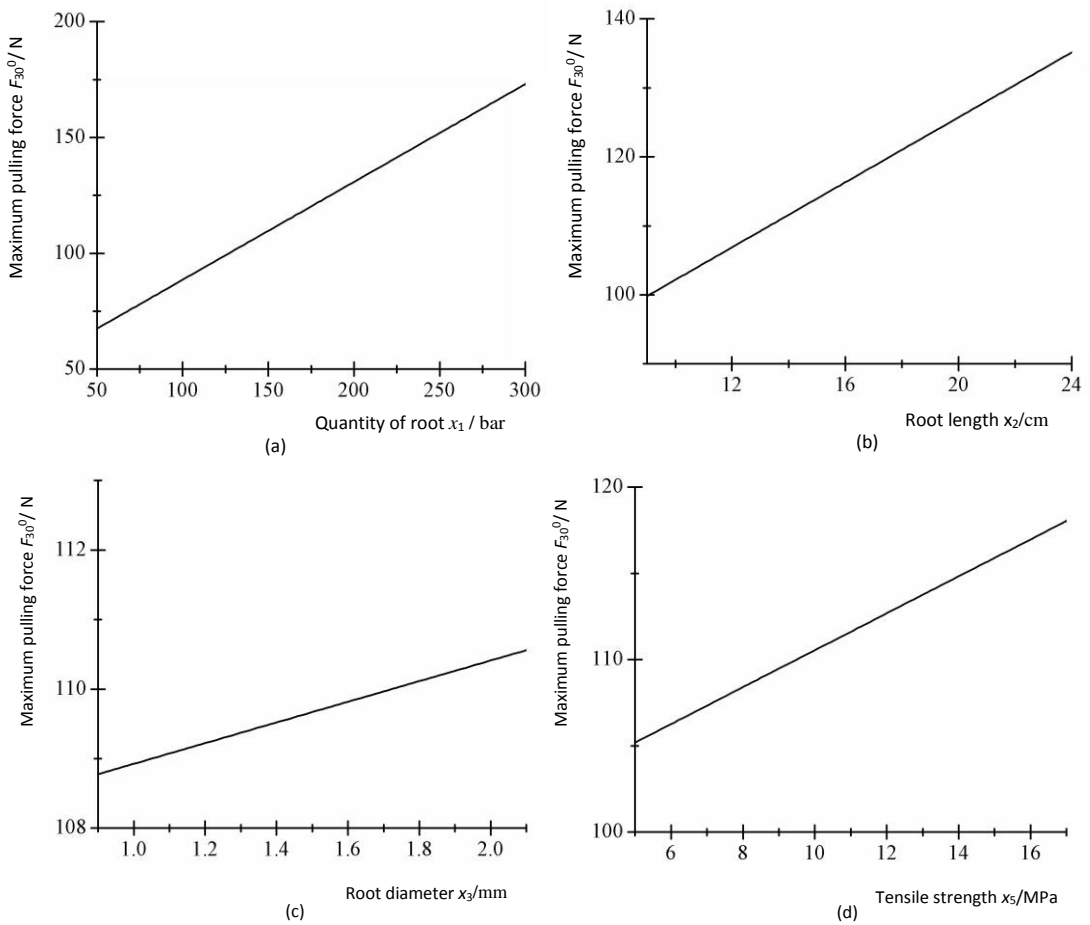

Figure 4. *Relationship between factors and maximum pulling force $F_{30°}$*

http://www. aloki.hu ● ISSN 1589 1623 (Print) ● ISSN 1785 0037 (Online)
DOI: http: //dx.doi.org/10.15666/aeer/1804_50935107

Figure 4 shows that with the increase of number of roots, root length, root diameter and tensile strength of root, F_{30° increases linearly and lodging resistance increases.

Influence of factor interaction

The relationships between F_{30° and interaction of factors are shown in *Figure 5*.

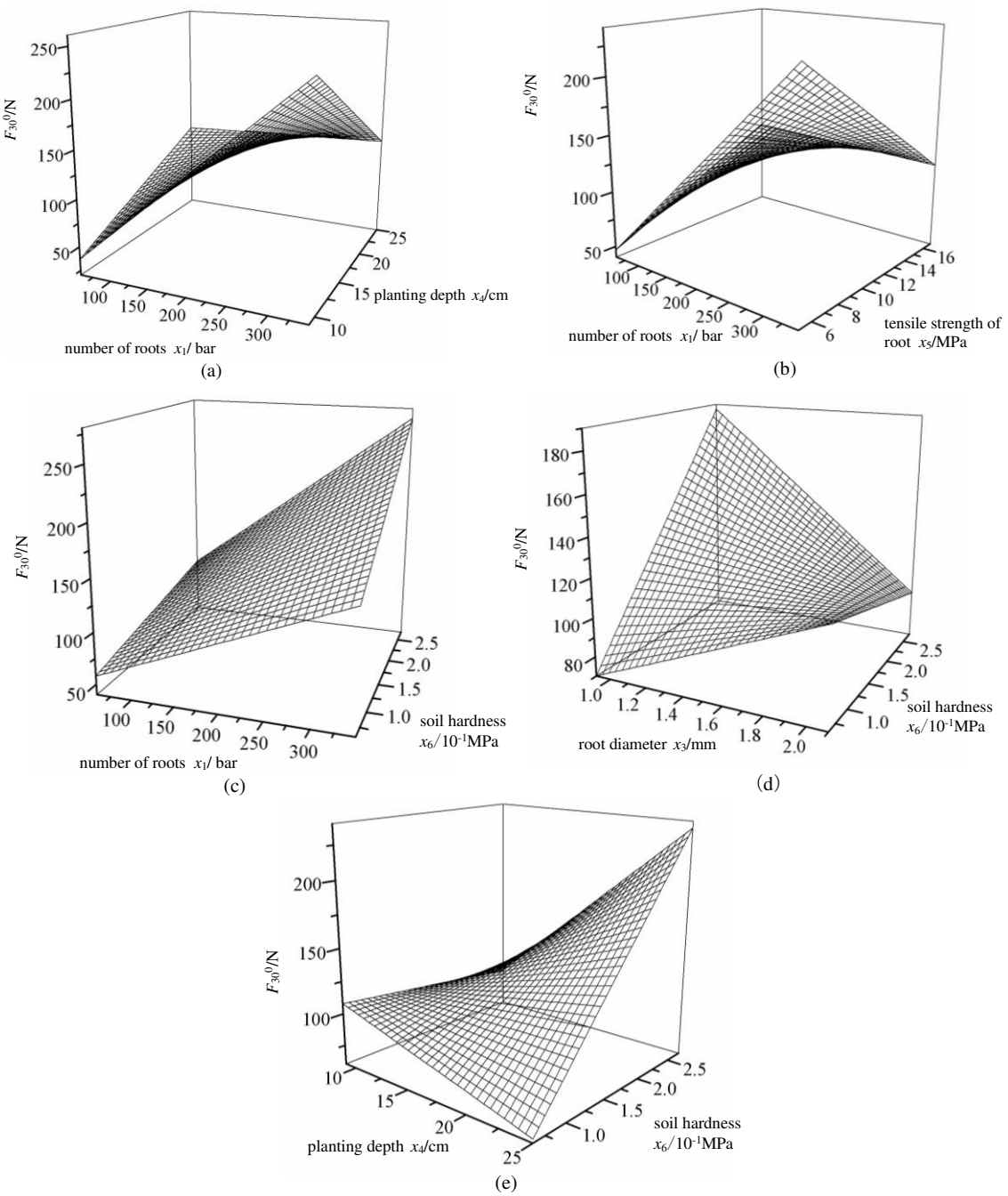

Figure 5. *Relationship between interaction of factors and* F_{30°

When number of roots is small, F_{30° increases with the increasing of planting depth, while when number of roots is large, F_{30° decreases with the increasing of planting

http://www. aloki.hu ● ISSN 1589 1623 (Print) ● ISSN 1785 0037 (Online)
DOI: http: //dx.doi.org/10.15666/aeer/1804_50935107

depth. When planting depth is small, with the increasing of number of roots, F_{30° increases, while when planting depth is large, with the increasing of number of roots, F_{30° increases slowly (*Fig. 5a*).

When tensile strength of root is small, F_{30° increases with the increasing of number of roots, while when tensile strength of root is large, F_{30° increases slowly with the increasing of number of roots. When number of roots is small, with the increasing of tensile strength of root, F_{30° increases, while when number of roots is large, with the increasing of tensile strength of root, F_{30° decreases (*Fig. 5b*).

Figure 5c shows that F_{30° increases with the increasing of number of roots and soil hardness.

When soil hardness is small, F_{30° increases with the increasing of root diameter, while when soil hardness is large, F_{30° decreases with the increasing of root diameter. When root diameter is small, F_{30° increases with the increasing of soil hardness, while when root diameter is large, F_{30° decreases with the increasing of soil hardness (*Fig. 5d*).

When soil hardness is small, F_{30° decreases with the increasing of planting depth, while when soil hardness is large, F_{30° increases with the increasing of planting depth. When planting depth is small, F_{30° decreases gently with the increasing of soil hardness, while when planting depth is large, F_{30° increases with the increasing of soil hardness (*Fig. 5e*).

In the meantime, according to the above analysis, the order of factors affecting F_{30° and *Equation 1,* we can obtain that when number of roots, root length, planting depth and soil hardness are at the maximum value, meanwhile, root diameter and tensile strength of root are at the minimum value, F_{30° is the largest, and the maximum value is 378.3 N.

Discussion

In this study, we obtained a mathematical model of the effect of multiple factors on lodging resistance of sugarcane, and the multiple factors include number of roots, root diameter, tensile strength of root, root length, planting depth and soil hardness. The order and the law of root-soil factors influencing the lodging resistance of sugarcane were clarified. And the most effective lodging resistance measure of sugarcane was proposed.

The mathematical model in this paper and the method using the model to study the influence of multiple factors on lodging resistance have not been reported in previous studies. The method can find out the order of the influence of root-soil factors on lodging resistance and analyze the influence of factor interaction on lodging resistance. The results of the effect of single factor on lodging resistance are consistent with the literature (Goodman and Ennos, 1999; Berry et al., 2000; Terashima et al., 2003; Berding and Hurney, 2005; Loades et al., 2013; Loganandhan et al., 2013; Manzur et al., 2014; Bian et al., 2016; Wu and Ma, 2018; Jongrungklang et al., 2018), while the effect of factor interaction on lodging resistance is complex.

The effect of factor interaction on lodging resistance

Number of roots and planting depth

When number of roots is small, the porosity of the root plate is relatively small. Although with the increasing of planting depth, the water penetrates downward and

http://www. aloki.hu ● ISSN 1589 1623 (Print) ● ISSN 1785 0037 (Online)
DOI: http: //dx.doi.org/10.15666/aeer/1804_50935107

moisture content of the root plate increases slightly, which cause the resistance ability of deformation and shear decrease slightly. However, the center of gravity of the root plate moves downward and the supporting force's arm of sugarcane increases. Thus, for all the above reasons, F_{30° increases. When number of roots is large, with the increasing of planting depth, the center of gravity of the root plate moves downward and the supporting force's arm of sugarcane increases. Nonetheless, moisture content of the root plate increases, and the resistance ability of deformation and shear decreases. Therefore, for all the above reasons, F_{30° decreases.

With the increasing of number of roots, the root plate increases (Berry et al., 2000; Manzur et al., 2014; Bian et al., 2018; Wu and Ma, 2018). Furthermore, when planting depth is small, the moisture content of the root plate is small. Therefore, when planting depth is small, with the increasing of number of roots, although the porosity of the root plate also increases, but the moisture content maintains lower and the resistance ability of deformation and shear maintains stronger, F_{30° increases. When planting depth is large, with the increasing of number of roots, although the root plate increases, but the moisture content increases and the resistance ability of deformation and shear decreases, thus, F_{30° increases slowly.

Number of roots and tensile strength of root

The roots with low tensile strength are the new roots, which have strong growth vigor, more branches and root hairs (*Fig. 6*). The anchoring effect of a single root on soil is strong. Thus, when tensile strength of root is small, with the increasing of number of roots, the root plate increases, which cause F_{30^o} increases. And when tensile strength of root is large, with the increasing of number of roots, the dragging effect of roots increases, however, the root plate increases slowly, which cause F_{30^o} increases slowly.

The number of roots is small, the root plate is small (Wu and Ma, 2018). Therefore, when number of roots is small, with the increasing of tensile strength of root, although the root plate decreases slightly, but the dragging effect of roots increases, which cause F_{30^o} increases. And when number of roots is large, with the increasing of tensile strength of root, although the dragging effect of roots increased, but the root plate decreases, which cause F_{30^o} decreases.

Figure 6. *Sugarcane roots*

Number of roots and soil hardness

When the number of roots is numerous and the soil hardness is large, the root plate is large, and the resistance ability of deformation and shear is strong, the lodging resistance is strong. It is consistent with the literatures (Goodman and Ennos, 1999; Loades et al., 2013).

http://www. aloki.hu ● ISSN 1589 1623 (Print) ● ISSN 1785 0037 (Online)
DOI: http: //dx.doi.org/10.15666/aeer/1804_50935107

Root diameter and soil hardness

When soil hardness is small, the moisture content is high, and the adhesion and friction between roots and soils are large (within the range of the tested soil hardness). Therefore, when soil hardness is small, with the increasing of root diameter, the new roots turn into the old roots, although the root plate decreases relatively, however, the adhesion and friction between roots and soils increase, for all the above reasons, F_{30° increases. And when soil hardness is large, the root plate decreases with the increasing of root diameter, and the adhesion and friction between roots and soils increase slowly, which cause F_{30° decreases.

When root diameter is small, with the increasing of soil hardness, although the adhesion and friction between roots and soils decrease slightly, the resistance ability of deformation and shear of the root plate increases, result in the increase of F_{30°. And when root diameter is large, with the increasing of soil hardness, although the resistance ability of deformation and shear of the root plate increases, however, the adhesion and friction between roots and soils decreases, result in the decrease of F_{30°.

Planting depth and soil hardness

The soil hardness (the average value of three soil layers) is small, the moisture content is high. And moisture content can be higher in a deeper soil depth due to the downward infiltration of water. Therefore, when soil hardness is small, with the increasing of planting depth, although the supporting force arm of sugarcane increases, but the hardness of the lower part of the root plate decreases, result in the decrease of F_{30°. And when soil hardness is large, the hardness of the lower part of the root plate decreases slightly with the increasing of planting depth, but the supporting force arm of sugarcane increases, result in the increase of F_{30°.

When planting depth is small, the supporting force arm of sugarcane is small. Therefore, when planting depth is small, with the increasing of soil hardness, although the resistance ability of deformation and shear of the root plate increases and the stabilizing effect of sugarcane also increases slightly, nevertheless, the adhesion and friction between roots and soils decrease, result in the decrease of F_{30°. And when planting depth is large, with the increasing of soil hardness, although the adhesion and friction between roots and soils decrease, nevertheless, the resistance ability of deformation and shear of the root plate increases, and the stabilizing effect of sugarcane also increases, result in the increase of F_{30°.

Lodging resistance measure

Many scholars have studied the effects of number, length, growth depth and strength of roots, planting depth, soil hardness, drainage and fertilization on crop lodging resistance, and their results showed that when the planting depth, the soil hardness, and the number, length, growth depth and tensile strength of roots were large, the crop lodging resistance was strong, however, they did not indicate which of these factors has the greatest effect on crop resistance (Goodman and Ennos, 1999; Berry et al., 2000; Terashima et al., 2003; Berding and Hurney, 2005; Loades et al., 2013; Loganandhan et al., 2013; Manzur et al., 2014; Bian et al., 2016; Jongrungklang et al., 2018; Wu and Ma, 2018; Liu et al., 2018). And according to the research in this paper, we clarified the order of the influence of root-soil factors on the lodging resistance of sugarcane. And the order is number of roots and interaction between planting depth and soil hardness,

http://www. aloki.hu ● ISSN 1589 1623 (Print) ● ISSN 1785 0037 (Online)
DOI: http: //dx.doi.org/10.15666/aeer/1804_50935107

root diameter and interaction between root diameter and soil hardness and interaction between number of roots and planting depth, tensile strength of root, interaction between number of roots and tensile strength of root, root length, interaction between number of roots and soil hardness. It shows that the number of roots and the interaction between planting depth of roots and soil hardness are the two most important influence factors of lodging resistance, meanwhile, our results show that when the number of roots, planting depth and soil hardness are large, lodging resistance is the greatest. Therefore, the most effective measure to improve the lodging resistance of sugarcane is to increase the number of roots through breeding and reasonable fertilization, and to increase the planting depth of sugarcane, meanwhile, to establish good drainage measures to timely drain water in typhoon season for reducing soil moisture and maintaining greater soil hardness.

Conclusions

In this study, a mathematical model of the effect of root-soil factors on lodging resistance of sugarcane was established by using field tilt test and regression analysis method. Using the model, the research on the influence of multiple factors on lodging resistance was carried out. The most important influence factors of lodging resistance and the influencing law of factor interaction on lodging resistance were clarified. And the most effective lodging resistance measure of sugarcane was proposed. In conclusion, we believe that the established mathematical model is reasonable. The change of sugarcane lodging resistance is the result of the comprehensive influence of number of roots, root diameter, tensile strength of root, root length planting depth and soil hardness. The two most important influence factors of sugarcane lodging resistance are number of roots and interaction between planting depth and soil hardness, while the influence of factor interaction on sugarcane lodging resistance is complex. The most effective measure to improve the lodging resistance of sugarcane is to increase the number of roots through breeding and reasonable fertilization, and to increase the planting depth of sugarcane, meanwhile, to establish good drainage measures to timely drain water in typhoon season for reducing soil moisture and maintaining greater soil hardness. Increasing the influence of root growth distribution on lodging resistance of sugarcane is the subject of future research.

Acknowledgements. This work was supported by a grant from the National Natural Science Foundation of China (Grant Nos 51565003 and 51365005), Guangxi Natural Science Foundation (Grant No. 2018GXNSFAA138196), Guangxi Key Laboratory of Manufacturing System & Advanced Manufacturing Technology (Grant No. 17-259-05S006).

REFERENCES

[1] Babu, C., Koodalingam, K., Natarajan, U. S. (2009): Assessment of rind hardness in sugarcane (Sachharum Spp. Hybrids), genotypes for development of non lodging erect canes. – Advances in Biological Research 3(1-2): 48-52.

[2] Berding, N., Hurney, A. P. (2005): Flowering and lodging, physiological-based traits affecting cane and sugar yield. What do we know of their control mechanisms and how do we manage them. – Field Crops Research 92(2-3): 261-275.

http://www. aloki.hu ● ISSN 1589 1623 (Print) ● ISSN 1785 0037 (Online)
DOI: http: //dx.doi.org/10.15666/aeer/1804_50935107

[3] Berry, P. M., Grifna, J. M., Sylvester-Bradley, R., Scott, R. K., Spink, J. H., Bakerd, C. J., Clare, R. W. (2000): Controlling plant form through husbandry to minimise lodging in wheat. – Field Crops Research 67: 59-81.
[4] Bian, D. H., Jia, G. P., Cai, L. J., Ma, Z. Y., Egrinya Eneji, A., Cui, Y. H. (2016): Effects of tillage practices on root characteristics and root lodging resistance of maize. – Field Crops Research 185: 89-96.
[5] Cao, Y. S., Chen, L. H., Liu, X. G., Yang, Y. J. (2014): The influence factors of plant roo-soil interface friction. – Tribology 34(5): 482-488.
[6] Chen, Z. D., Xiao, H. B., Zhang, C. X., Li, Z. Y., Zeng, J. J., He, B., Xie, J. Y. (2016): The impact of root distribution methods on the shear strength of root-soil composite. – Journal of Central South University of Forestry & Technology 36(8): 130-135.
[7] Goodman, A. M. and Ennos, A. R. (1999): The effects of soil bulk density on the morphology and anchorage mechanics of the root systems of sunflower and maize. – Annals of Botany 83: 293-302.
[8] Jongrungklang, N., Maneerattanarungroj, P., Jogloy, S., Songsri, P., Jaisil, P. (2018): Understanding lodging resistant traits from diverse sugarcane lines. – Philippine Journal of Crop Science 43(2): 71-80.
[9] Kazuo, T., Takeshi, T., Hitoshi, O., Takayuki, U. (2003): Effect of field drainage on root lodging tolerance in direct-sown rice in flooded paddy field. – Plant Production Science 6(4): 255-261.
[10] Li, M., Tian, H. C., Huang, Z. G. (2017): Research on the development status of sugarcane industry in China. – Sugar Crops of China 39(1): 67-70.
[11] Li, X., Li, Y. J., Liang, Q., Lin, S. H., Huang, Q. Y., Yang, R. Z., Yang, L. T., Li, Y. R. (2019): Evaluation of lodging resistance in sugarcane (Saccharum spp. hybrid) germplasm resources. – Applied Ecology and Environmental Research 17(3): 6107-6116.
[12] Liu, S. Q., Song, F. B., Li, X. N., Wang, Y., Zhu, X. C. (2018): Effect of nitrogen application on nodal root characteristics and rootlodging resistance in maize. – Pakistan Journal of Botany 50(3): 949-954.
[13] Loades, K. W., Bengough, A. G., Bransby, M. F., Hallett, P. D. (2013): Biomechanics of nodal, seminal and lateral roots of barley: effects of diameter, waterlogging and mechanical impedance. – Plant Soil 370: 407-418.
[14] Loganandhan, N., Gujja, B., Goud, V. V., Natarajan, U. S. (2013): Sustainable Sugarcane Initiative (SSI): a methodology of "more with less". – Sugar Tech 15(1): 98-102.
[15] Manzur, M. E., Hall, A. J., Chimenti, C. A. (2014): Root lodging tolerance in Helianthus annuus (L.): associations with morphological and mechanical attributes of roots. – Plant Soil 381: 71-83.
[16] Mou, X. W., Xie, F. X., Ou, Y. G., Gong, J. H. (2010): Experiments of lifting process for the lodged sugarcane. – Journal of South China Agricultural University 31(3): 98-101.
[17] Ou, Y. G., Malcolm, W., Yang, D. T., Liu, Q. T., Zheng, D. K., Wang, M. M., Liu, H. C. (2013): Mechanization technology: the key to sugarcane production in China. – International Journal of Agricultural and Biological Engineering 6(1): 1-27.
[18] Ren, L. Q. (2011): Soil Adhesion Mechanics. – Machinery Industry Press, Beijing.
[19] Singh, G., Chapman, S. C., Jackson, P. A., Lawn, R. J. (2002): Lodging reduces sucrose accumulation of sugarcane in the wet and dry tropics. – Australian Journal of Agricultural Research 53(11): 1183-1195.
[20] Sposaro, M. M., Chimenti, C. A., Hall, A. J. (2008): Root lodging in sunflflower. Variations in anchorage strength across genotypes, soil types, crop population densities and crop developmental stages. – Field Crops Research 106(2): 179-186.
[21] van Heerden, P. D. R., Singels, A., Paraskevopoulos, A., Rossler, R. (2015): Negative effects of lodging on irrigated sugarcane productivity—an experimental and crop modelling assessment. – Field Crops Research 180: 135-142.

http://www. aloki.hu ● ISSN 1589 1623 (Print) ● ISSN 1785 0037 (Online)
DOI: http: //dx.doi.org/10.15666/aeer/1804_50935107

[22] Wang, W. Z., Fang, F. X., Zhu, Q. Z., Liang, T and Luo, Y. W. (2010): Discussion on key agronomic coordinated technology of sugarcane mechanical harvest. – Chinese Agricultural Mechanization 5: 63-67.
[23] Wang, X. Q., Zhang, J. (2018): Supporting policies and related development ideas of sugarcane industry in China. – Agricultural Outlook 14(1): 43-48, 53.
[24] Wu, W., Ma, B. L. (2018): Assessment of canola crop lodging under elevated temperatures for adaptation to climate change. – Agricultural and Forest Meteorology 248: 329-338.
[25] Yang, W., Zhang, S., Yang, J., Zhou, J., Lu, H. (2015): Experimental study on soil hardness of cultivated horizon at cassava cultivated farm in harvesting period. – Journal of Agricultural Mechanization Research 37(7): 176-180.

APPENDIX

Table A1. *Test scheme and results*

Test number	Number of roots x_1/bar	Root length x_2/cm	Root diameter x_3/mm	Planting depth x_4/cm	Tensile strength of root x_5/MPa	Soil hardness $x_6/10^{-1}$MPa	Maximum pulling force $F_{30°}$/N
1	87	11.98	1.67	15.5	11.76	0.79	76.51
2	117	23.74	1.59	17	15.26	2.4	152.67
3	81	15.43	1.89	11.8	6.55	0.89	80.65
4	97	12.76	1.94	16.6	8.44	1.2	93.38
5	66	14.4	2.10	16.2	9.55	0.76	78.92
6	88	11.49	1.62	17.9	8.01	0.9	85.31
7	141	12.10	1.66	22	8.29	0.65	72.5
8	119	15.00	1.75	17	8.94	1.5	115
9	77	14.50	1.41	19.5	11.91	0.73	88.5
10	238	16.40	1.2	10.5	6.25	1.28	176.44
11	195	13.80	1.62	17.5	7.37	1.23	125.8
12	138	13.20	1.65	21	7.5	0.9	102.65
13	215	14.80	1.34	17	7.21	0.72	108.14
14	142	10.10	1.55	15.5	5.87	2	105.72
15	136	11.40	1.34	13	8.33	1.8	102.72
16	159	11.60	1.22	15.5	6.19	0.61	74.48
17	61	9.04	1.11	19.5	10.4	0.92	65.6
18	180	12.60	0.92	17.5	8.73	1.07	94.38
19	179	16.30	1.32	13.5	10.61	1.22	180.44
20	199	12.50	1.22	14	10.27	1.66	169.5
21	77	16.10	1.01	18.2	11.1	1.21	94.3
22	179	10.50	1.18	12.5	8.05	0.67	91.97
23	119	10.30	1.75	25	9.06	1.25	128.59
24	285	12.30	1.75	18.5	6.81	2.7	226.39
25	209	16	1.39	14	12.48	1.3	128.59
26	97	11.8	1.1	14.5	13.64	1.22	103.54
27	156	14.5	1.24	13	8.99	1.07	105.31
28	170	14.5	1.13	12.5	9.16	1.53	128.64
29	153	10.6	1.07	13	5.88	1.6	105.32
30	151	9.25	1.13	20	7.43	1.09	88.69
31	221	11.4	1.03	14.5	5.06	2.02	192.13
32	238	12.6	1.14	19	6.07	1.37	150.92
33	347	16.5	1.3	18.5	9.33	2.44	257.84
34	273	13.2	1.1	12.5	12.07	1.44	145.6
35	98	11.5	1.04	11.5	10.92	0.92	75.5

http://www. aloki.hu ● ISSN 1589 1623 (Print) ● ISSN 1785 0037 (Online)
DOI: http: //dx.doi.org/10.15666/aeer/1804_50935107

36	221	12.2	0.98	16	7.69	1.84	191.1
37	149	13.8	1.23	12	11.18	1.44	105.89
38	119	10.9	1.16	12.5	16.78	1.11	105.55
39	150	9.68	1.32	9	6.47	1.64	75.25
40	183	9.62	1.23	18	8.5	1.99	118.52
41	121	10.6	1.34	17.5	7.19	1.07	92.08
42	58	14.8	1.27	13	9.5	1.73	71.63
43	81	13.5	1.2	17	7.2	0.86	46.46
44	64	11.9	1.43	12.3	8.6	1.28	51.94
45	87	17.3	1.97	17.5	8.97	1.49	87.65

http://www. aloki.hu ● ISSN 1589 1623 (Print) ● ISSN 1785 0037 (Online)
DOI: http: //dx.doi.org/10.15666/aeer/1804_50935107

DISTRIBUTION AND MAINTENANCE OF VEGETATION ADJACENT TO HIGH VOLTAGE TRANSMISSION LINES, SOUTHERN BRAZIL

DUARTE, S. W.[1*] – MAÇANEIRO, J. P.[2] – FENILLI, T. A. B.[1] – SCHORN, L. A.[1] – BLUNK, L.[1] – MEDEIROS, D. S.[3]

[1]*Departamento de Engenharia Florestal, Universidade Regional de Blumenau, Box. 89030-000, Blumenau, Brazil*

[2]*Departamento de Engenharia Florestal, Universidade Federal do Paraná, Box. 80210-170, Curitiba, Brazil*

[3]*Departamento de manutenções, Companhia Estadual de Energia Elétrica do Rio Grande do Sul, Box. 91410-400, Porto Alegre, Brazil*

[*]*Corresponding author*
e-mail: swduarte0@gmail.com; phone: +55-47-3221-6043

(Received 10th Nov 2019; accepted 24th Mar 2020)

Abstract. Vegetation is the main cause of power outages; therefore, it is fundamental to carry out maintenance to prevent the interruption of electric power. In general, the maintenance of transmission lines is performed without previous studies on floristic composition. In this sense, it is necessary to establish the floristic composition and the factors that influence the establishment of the species to determine the best practices of maintenance. In this study, we evaluated which environmental and spatial factors influence species distribution in order to improve the maintenance of vegetation adjacent to high voltage transmission lines. The vegetation was sampled in 25 plots of 300 m^2, distributed randomly and prioritizing the main span of the power transmission line. The main factors that influenced species distribution were elevation, leaf area and Mg/K ratio, all associated with the spatial factor. Therefore, maintenance along transmission lines should prioritize species associated with higher elevations and leaf area, considering a risk height of 7 meters.
Keywords: *Atlantic Forest, environmental variables, electrical energy, power outages, RDA*

Introduction

The Atlantic Forest is the second largest tropical pluvial forest on the American continent, it covers approximately 1,300,000 km^2 in Brazil, being more representative in the south (Ribeiro et al., 2011; Rocha and Silva, 2013). This unit includes different forest types, climatic zones and it presents high species richness and endemism (Rocha and Silva, 2013). The Atlantic Forest is currently fragmented, with only 11.7% of its original coverage (Ribeiro et al., 2011). These forests are priority areas for the conservation of biological diversity, due to the exploitation processes and advanced stage of degradation (Ribeiro et al., 2011; Silverio Neto et al., 2015).

The process of degradation of the Atlantic Forest is usually associated with logging and conversion of Forests to agricultural and livestock areas. In addition to these activities, the installation and maintenance of power transmission lines has been causing severe environmental damage. For example, vegetation removal to build power transmission lines exposing the soil to erosive processes, as well as fragmenting ecosystems and altering natural succession (Dupras et al., 2015). Among the aspects to be evaluated in the maintenance of power transmission lines, we have metal structures

http://www.aloki.hu ● ISSN 1589 1623 (Print) ● ISSN1785 0037 (Online)
DOI: http://dx.doi.org/10.15666/aeer/1804_51095121

and the objects that can cause power cuts (e.g., arboreal vegetation) (Matikainen et al., 2016). Accidents associated with vegetation are common, both in the urban and rural areas, and it is fundamental to carry out maintenance to prevent the interruption of electric power (Ahmad et al., 2014).

Usually, previous monitoring for maintenance of transmission lines is performed by aerial and visual survey (Matikainen et al., 2016), without previous studies about the floristic composition under the transmission lines. Thus, the improvement of vegetation maintenance techniques can benefit the electrical companies and the consumer (e.g., costs and risks reduction) (Kuntz et al., 2002). In addition, the use of pruning and vegetation cutting techniques can minimize the impacts generated by transmission networks, reducing the loss of natural habitats and forest fragmentation (Young, 2010).

Regardless of the maintenance technique used, it should be considered that the vegetation maintains growth variations throughout the year (Lopes, 2013). Therefore, it is essential to analyze the floristic composition and density, annual increments and growth rates (Lopes, 2013). For example, species growth is associated with several factors, such as luminosity, elevation and soil properties (e.g., fertility, depth and soil types) (Jurinitz et al., 2013; Moraes et al., 2013; Maçaneiro et al., 2016, 2019). In this way, the relationship between environmental variations and floristic composition can positively affect the frequency and intensity of vegetation maintenance, directly influencing the practice and the cost for the company.

Therefore, it seems reasonable to evaluate the environmental and spatial factors that influence the distribution of species in order to determine the best practices of maintenance (e.g., pruning) of vegetation adjacent to the power transmission lines. Thus, the goal of this study was to evaluate the influence of environmental and spatial variables on the distribution of species of forest fragments adjacent to power transmission lines and to determine the best practices of maintenance.

Material and Methods

Study area

The object of the study is forest remnants in distinct stages of succession located in an area adjacent to the power transmission line. This transmission line was installed in 1978. Along these areas, the responsible company for the transmission line regularly performs maintenance in the vegetation. In general, pruning and removal of trees or branches that may cause a power outage are performed. The maximum height that the vegetation can be to the electrical cables is 7 meters.

The transmission line is 65 km long and it covers 14 municipalities in the state of Rio Grande do Sul, southern Brazil (*Figure 1*). The region is part of the *Guaíba* river basin and it presents an altitude variation between 90 and 600 meters.

The climate of the region, according to the classification of Köppen, is of the type humid subtropical – Cfa, without dry season and with hot summer. The annual mean temperature fluctuates between 9°C to 26°C, annual mean precipitation from 1,600 to 2,200 mm, and relative humidity between 60 and 85% (Alvares et al., 2013).

The geology of the region is formed by the *Botucatu* Formation and *Serra Geral* Formation, presenting sandstones and basalts, respectively. The predominant soils are Litholic Neosols and Regolithic Neosols (Brazilian Classification) (Santos et al., 2018), and in general have high fertility (V% > 70%).

http://www.aloki.hu ● ISSN 1589 1623 (Print) ● ISSN1785 0037 (Online)
DOI: http://dx.doi.org/10.15666/aeer/1804_51095121

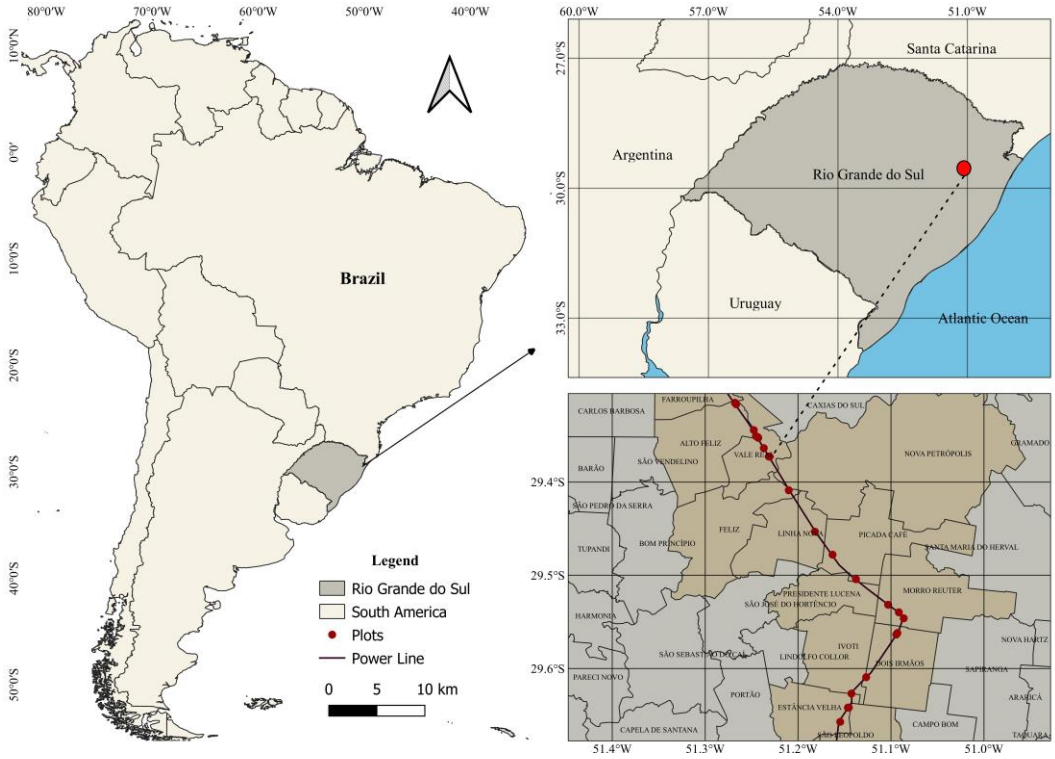

Figure 1. *Location of the study area and plots in a power transmission line, southern Brazil*

The predominant forest type is subtropical deciduous forest in distinct stages of succession. The structure of the vegetation that represents this formation is linked to the altitudinal and climatic variations, which according to Scipioni et al. (2013) guarantee heterogeneity of species in different Brazilian forest formations. Among the most representative species are *Apuleia leiocarpa* (Vogel) JF Macbr., *Trichilia claussenii* C. DC., *Sorocea bonplandii* (Baill.) WCBurger et al., *Nectandra megapotamica* (Spreng.) Mez.

Data collection

To characterize forest structure and determine environmental and spatial variables we sampled vegetation in 25 plots 300 m^2 (10 m x 30 m), parallel to the main span of the power transmission line. In each plot we sampled all arboreal individuals with diameter at breast height – DBH ≥ 5 m and height > 1.3 m. We collected the data between March/2018 and October/2018. We identified the collected botanical material by comparison with exsicates deposited in the Herbarium *Dr. Roberto Miguel Klein* and by consulting the taxonomic literature and the specialists the U*niversidade Regional de Blumenau (FURB).*

To obtain the chemical properties of the soil, in each plot we collected soil samples in the depth of 0 - 20 cm, i.e. we collected five points per plot and stirred the soil. Then, we stored the samples in plastic bags and sent them to the Laboratory of Soil Analysis of *EPAGRI (Empresa de Pesquisa Agropecuária e Extensão Rural de Santa Catarina)* to obtain the chemical variables: clay content (m/v - %), pH, phosphorus (P – mg/dm^3), potassium (K – mg/dm^3), organic matter (%), aluminum (Al – $cmolc/dm^3$), calcium (Ca – $cmolc/dm^3$), magnesium (Mg – $cmolc/dm^3$), SMP index, potential acidity (H+Al –

http://www.aloki.hu ● ISSN 1589 1623 (Print) ● ISSN1785 0037 (Online)
DOI: http://dx.doi.org/10.15666/aeer/1804_51095121

cmolc/dm^3) and calculated the cation exchange (CTC – cmolc/dm^3), aluminum saturation (m%) and base saturation (V%), base sum (S), and relation Ca:Mg, Ca:K and Mg:K (Santos et al., 2018).

To obtain the physical properties of the soil, we collected samples with volumetric rings of the Kopecky type of known volume, i.e. we collected three points per plot. After these collections, we stored and weighed the samples for later drying them in a drying kiln (105°C). With these samples, we determined the soil humidity (%) through the volumetric method and total porosity (%) and soil density (g.cm^{-3}) according to Teixeira et al. (2017).

To verify the luminosity condition of the arboreal stratum, we evaluated through the hemispherical photographies the canopy opening (Parker and Russ, 2004). In each plot we took four hemispherical photographs. We use a Nikon D3100 digital SLR camera and Nikon Fisheye Nikkor 10.5 mm lens. The camera was attached to a tripod and was facing the forest canopy at a height of 1.30 m from the ground (Silva, 2016). The photos were analyzed in the software *Hemisfer 2.2* to obtain the values of canopy opening (%) and leaf area (m^2.m^2) (Thimonier et al., 2010).

We obtained the elevation through a GPS Garmin 62CSx. We obtained the bioclimatic variables (Annual Mean Temperature, Mean Diurnal Range, Isothermality, Temperature Seasonality, Max Temperature of Warmest Month, Min Temperature of Coldest Month, Temperature Annual Range, Mean Temperature of Wettest Quarter, Mean Temperature of Driest Quarter, Mean Temperature of Warmest Quarter, Mean Temperature of Coldest Quarter, Annual Precipitation, Precipitation of Wettest Month, Precipitation of Driest Month, Precipitation Seasonality, Precipitation of Wettest Quarter, Precipitation of Driest Quarter, Precipitation of Warmest Quarter, Precipitation of Coldest Quarter), for each plot, in the data base of Fick and Hijmans (2017).

Data analysis

We calculated the values of relative density (% individuals of a species in the community) and frequency (% absolute frequency of a species in the community) through the phytosociological parameters described by Mueller-Dombois and Ellenberg (2002). During this process, we used the "spacemakeR" package in R environment (R Core Team 2013), according to the recommendations of Borcard et al. (2011) and Eisenlohr (2014).

After that, we removed collinear environmental variables through principal component analysis (PCA) in PC-ORD 6.0 (McCune and Mefford, 2011). After this procedure, the environmental variables that remained in the analysis were clay content (m/v – %), pHH_2O, SMP index, aluminum (Al – cmolc/dm^3), calcium (Ca – cmolc/dm^3), magnesium (Mg – cmolc/dm^3), potassium (K– mg/dm^3), phosphorus (P – mg/dm^3), organic matter (MO%), potential acidity (H+Al – cmolc/dm^3), cation exchange (CTC – cmolc/dm^3), aluminum saturation (m%), base saturation (V%), base sum (S), and relation Ca:Mg, Ca:K and Mg:K, soil humidity (%), soil density (g.cm^{-3}), canopy opening (%), leaf area (m^2.m^2), elevation (m), annual temperature (°C) and annual precipitation (mm).

Subsequently, we used a species composition matrix. To correct the distinct units of measure, the environmental matrix was standardized (`standardized score` transformation). The spatial matrix (MEMs) was established through the geographic coordinates (latitude and longitude). In this procedure we used the Environment R, with the package "spacemakeR" (Borcard et al., 2011). The MEMs (Moran's Eigenvector

http://www.aloki.hu ● ISSN 1589 1623 (Print) ● ISSN1785 0037 (Online)
DOI: http://dx.doi.org/10.15666/aeer/1804_51095121

Maps) were selected through the "forward" method. The environmental variables were selected through the canonical analysis of RDA. Finally, the last RDA was processed in the PC-ORD 6.0 (McCune and Mefford, 2011), using the composition matrix with the environmental (standardized) and spatial (MEMs) variables selected to verify the effect of these variables in the distribution pattern of the species in the study site. The statistical significance of the RDA ordering axes was verified by means of 999 Monte Carlo permutations (Legendre and Legendre, 2012).

Then, we performed the partitioning of the variance into the data set in order to separate the fractions relative to the environment [a], the spatially structured environment [b], only the space [c] and the undetermined variables [d]. In this analysis, we used the "vegan", "packfor", "spacemakeR" and "spdep" packages in the R Environment (R Core Team 2013).

Results

In the 25 plots along the power transmission line, a total of 1,444 individuals (total absolute density= 1,925 ind/ha) were sampled, belonging to 101 species and 38 botanic families (*Table 1*). The species with the highest density and frequency values were *Cupania vernalis, Nectandra megapotamica, Sambucus australis, Trema micrantha,* and *Allophylus edulis*.

Table 1. *Species with the highest density and frequency values in the arboreal stratum adjacent to power transmission line in southern Brazil*

Family	Specie	*DR*	*FR*
Sapindaceae	*Cupania vernalis* Cambess.	12.9	5.9
Lauraceae	*Nectandra megapotamica* (Spreng.) Mez	6.4	5.9
Adoxaceae	*Sambucus australis* Cham. & Schltdl.	6.3	2.6
Cannabaceae	*Trema micrantha* (L.) Blume	5.1	3.4
Sapindaceae	*Allophylus edulis* (A.St.-Hil. et al.) Hieron. ex Niederl.	5.1	4.6
Malvaceae	*Luehea divaricata* Mart. & Zucc.	5.0	3.7
Primulaceae	*Myrsine umbellata* Mart.	4.8	3.7
Lauraceae	*Persea americana* Mill.	3.5	1.4
Escalloniaceae	*Escallonia bifida* Link & Otto	3.4	0.6
Fabaceae	*Machaerium stipitatum* Vogel.	3.0	3.1
Euphorbiaceae	*Alchornea triplinervia* (Spreng.) Müll.Arg.	2.6	2.3
Salicaceae	*Casearia sylvestris* (Vell.) Mart.	2.4	4.0
Meliaceae	*Trichilia clausseni* C.DC.	2.1	1.7
Rubiaceae	*Psychotria suterella* Müll.Arg.	2.1	0.3
Fabaceae	*Parapiptadenia rigida* (Benth.) Brenan	1.8	3.1
-	Others species	33.5	53.7
-	**Total**	**100**	**100**

DR = relative density (%), FR = relative frequency (%)

In the redundancy analysis (RDA) (*Figure 2, Table 2*), the plots differed according to the variation in environmental and spatial variables. The eigenvalues of the first two ordering axes explained 14.6% of the data variance (axis 1 = 8.2%, axis 2 = 6.4%) and presented significance by the Monte Carlo test ($p \leq 0.05$). The environmental and spatial variables that correlated with axis 1 were MEM 1 and MEM 5, while for axis 2 were leaf area (LAI), elevation, Mg:K content and MEM 2.

http://www.aloki.hu ● ISSN 1589 1623 (Print) ● ISSN1785 0037 (Online)
DOI: http://dx.doi.org/10.15666/aeer/1804_51095121

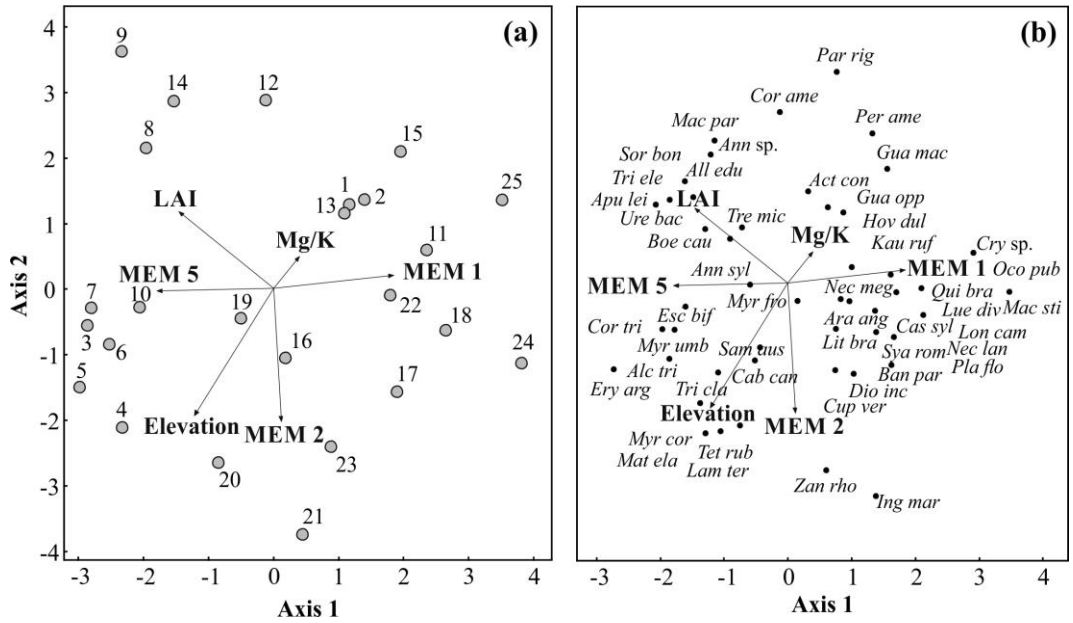

Figure 2. *Redundancy analyzes (RDA) produced by plots, species and environmental and spatial variables in forest fragments under power transmission lines in southern Brazil*

Table 2. *Environmental and spatial variables produced by the RDA for forest fragments under power transmission lines in southern Brazil. R² adjusted, F and p were obtained by ANOVA after partitioning the variance*

Predictor	R^2 adjusted (%)	F (ANOVA)	p (ANOVA)
Elevation	7.0	1.74	0.001
MEM 1	5.8	1.41	0.02
LAI	5.7	1.45	0.02
MEM 2	5.7	1.43	0.02
MEM 5	5.6	1.43	0.02
Mg/K	5.5	1.42	0.01

In the ordination diagram of the plots, we verified that the first two axes had a strong relation between area leaf and elevation and the spatial variable MEM 1, MEM 2 and MEM 5. The axes formed three groups of plots, the first one being related to the leaf area. These groups are influenced directly to the spatial variable MEM 5. The second group had strong relation with the elevation, and it was influenced by the spatial variable MEM 2. We verified the formation of a gradient between MEM 1 and the plots. In addition, we observed the formation of a short gradient related to the Mg:K relation (*Figure 2a*).

In the diagram of species ordination, we verified a strong association with the leaf area and the density of arboreal individuals of *Apuleia leiocarpa* (Vogel) J.F.Macbr., *Sorocea bonplandii* (Baill.) W.C.Burger, *Trichilia elegans* A.Juss., *Allophyllus edulis* (*Figure 2b*), therefore, distinct levels of luminosity will affect the density of these species. While in areas with open canopy we found other predominant species, like *Araucaria angustifolia* (Bertol.) Kuntze, *Nectandra megapotamica, Syagrus romanzoffiana* (Cham) Glassman, *Banara parviflora* (A.Gray) Benth., *Platymiscium floribundum* Vogel.

http://www.aloki.hu ● ISSN 1589 1623 (Print) ● ISSN1785 0037 (Online)
DOI: http://dx.doi.org/10.15666/aeer/1804_51095121

In the same sense, the formation of two gradients was observed between species with preference to soils with high Mg:K relation and areas with low elevation (e.g., *Actinostemon concolor* (Spreng.) Müll.Arg., *Persea americana*, *Guarea macrophylla* Vahl., and *Guapira opposita* (Vell.) Reitz). The species associated with higher elevation are influenced directly by the spatial variable MEM 2. Thus, some biotic variation can influence directly on the species distribution. On the other hand, the species *Sambucus australis* Cham. & Schltdl., *Trichilia clausseni, Myrsine coriacea* (Sw.) R.Br. ex Roem. & Schult., and *Matayba elaeagnoides* Radlk, are associated to areas of higher elevation and lower Mg/K relation.

Partitioning of variance revealed that fractions [a] "pure" environment (F = 1.34, p = 0.007) and [c] "pure" space (F = 1.24, p = 0.04) were significant (*Figure 3*). The fraction [b], related to space + environment, indicated that part of the analyzed environmental variables (2%) is structured in space, while the [a] "pure" environment (5%) and [c] "pure" space (3%) stood out among fractions. However, the fraction [d] relative to the undetermined variables explained most of the vegetation variation in the study area (90%).

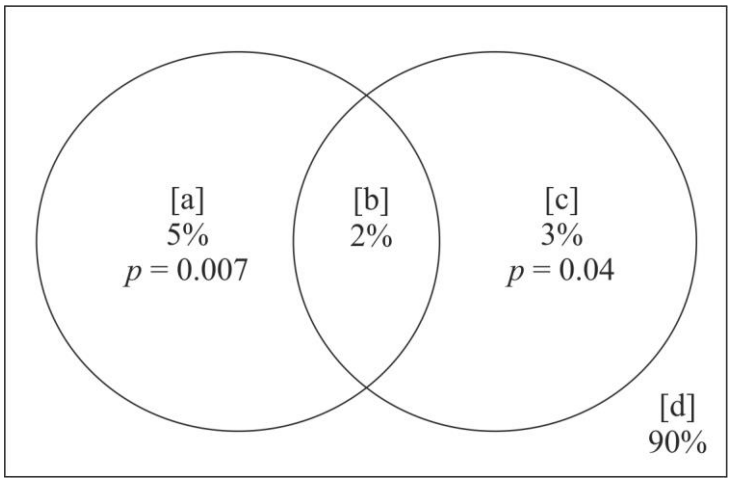

Figure 3. *Partition of the variance by the redundancy analysis to determine the fractions "pure" environment [a], space + environment [b], "pure" space [c] and undetermined variables [d] for forest fragments under power transmission line in Southern Brazil*

Discussion

In the present study we observed that some environmental variables have influence the distribution of species present in forest fragments adjacent to transmission lines. In addition, the spatial structure had a direct influence on the environmental variables, presenting a relevant role in the species distribution.

The elevation was the predictor that most influenced the distribution of the species. Studies indicate that elevation is an indirect environmental variable that influences vegetation distribution and characterization of forest types in the Atlantic Forest (Nettesheim et al., 2010; Maçaneiro et al., 2016; Duarte et al., 2019). In this study, not just the elevation has influence in the distribution of the species, but local features can directly influence the vegetation within the same altitudinal level (e.g., wind actions, watercourse) (Sanchez et al., 2013). Thus, higher elevation directly affects the floristic composition and, consequently, the maintenance of power transmission lines.

http://www.aloki.hu ● ISSN 1589 1623 (Print) ● ISSN1785 0037 (Online)
DOI: http://dx.doi.org/10.15666/aeer/1804_51095121

We observed that *Sambucus australis* has high density in plots that were inserted in the highest elevation. Generally, this specie is in slopes areas (Grings and Brack, 2009). In this study, we identified a strong relation between the species distribution and the elevation variation, probably related to the environmental heterogeneity presenting in the power transmission line. In this same sense, the species distribution is associated to the elevation, luminosity and soil properties, granting predominance of certain species (Cardoso and Schiavini, 2002).

Considering the influence of the environmental variables in the present study, we observed that the leaf area positively affects the distribution of certain species (e.g., *Apuleia leiocarpa, Sorocea bonplandii, Allophyllus edulis*). The leaf area is associated with mass and energy changes, and is directly related to evapotranspiration, hydrology and ecology of the species (Wang et al., 2005; Galvani and Lima, 2014). Studies indicate that leaf area vary according to species composition, local conditions, successional stage, forest dynamics and light conditions, among others (Leblanc and Chen, 2008). According to Moraes et al. (2013), the leaf area is associated with ecological variations in the environment, influencing the productivity, growth, and reproduction of the species. Therefore, the application of the maintenance in species adapted to higher luminosity directly affects its growth and, consequently, if carried out in the vegetative period, the growth will be positively affected, increasing the cost and number of times to be performed the maintenance.

In the same way, the Mg:K relation in the soil is associated with the presence of some species. In areas with more fertile soils, there are differences in floristic composition, density of dominant species, and lower fertility in the soil selects species with low nutritional requirements (Moreno et al., 2007). Unlike to the present study, floristic composition is generally associated with soil pH, moisture, fertility and texture (Mélo et al., 2013). According to Maçaneiro et al. (2019), floristic richness increases in relation to water availability and soil depth. In this way, shallower soils may have lower floristic richness. In addition, nutritional availability will directly affect plant growth. Overall, the area exhibits high fertility rates affecting plant growth positively.

In addition to elevation, leaf area and Mg:K content in the soil, the spatial factors were also predictors that influence the distribution of the species in fragments adjacent to power transmission lines. We observed that generally the spatial component is associated with the environmental variables that are related to the distribution of the species. We believe that it is possible that the soils variations, luminosity and elevation are conditioned to biotic and/or stochastic processes (e.g., such as dispersion and competition) (Diniz-Filho et al., 2012; Lewis et al., 2014). In this study the spatial component revealed a significant fraction on the floristic component, indicating the importance of the neutral processes on the vegetation.

In this study the distribution of *Cupania vernalis* is directly associated with biotic factors. This species presented the highest density and, therefore, is one of the species that must be taken into consideration for maintenance practices. This species is generally found in different topographic variations, but in higher density at high altitudes (~ 700 m) (Souza et al., 2015) and its growth is directly affected by the luminosity level (de Castro Lima et al., 2006). The association between the spatial predictor MEM 2 and elevation evidence that the specie can be observed in areas of higher elevation and it is being influenced of spatial component and linked to the altimetric quotes.

http://www.aloki.hu ● ISSN 1589 1623 (Print) ● ISSN1785 0037 (Online)
DOI: http://dx.doi.org/10.15666/aeer/1804_51095121

The biotic variations are usually attributed to the spatial component, like the dispersion that provides different distribution patterns of species, such as anemocory that provides a random pattern, for example the fruits and seeds are distributed randomly in space (Urbanetz et al., 2003; Maçaneiro et al., 2018). The dispersion is among the most affected ecological processes in the life cycle of the plants, besides playing a fundamental role in the colonization and evolution of the species, it varies according to the elevation (Wang and Smith, 2002; Urbanetz et al., 2003; Almeida-Neto et al., 2008; Neuschulz et al., 2016). This justifies the relation of spatial factors to elevation, whereas the processes of facilitation and competition do not depend on the physical factors of the environment and on different climatic conditions (Mélo et al., 2013). Environments with more adversity (e.g., practice of maintenance of the vegetation) directly affects the species performance providing the facilitation process and acting like an ecological filter and influencing in the floristic composition (Temperton and Hobbs, 2004). Others processes that affect the species distribution are polinization and the seeds predation, being responsible for the species maintenance and presenting adversity for the establishment of the plants (Wang and Smith, 2002). Considering this, we observed that each specie has particularities, like polinization, dispersion, and it will be directly associated to the distribution and consequently to the density/frequency that the species will be found in certain place, influencing in the intensity of the maintenance of the power transmission line. In this case, the association of the spatial factors and environmental variables in the comprehension in how the vegetation is distributed in the power transmission line to determine the best maintenance practices (e.g., pruning intensity and cutting) which may avoid the fragmentation of the forests remnants and then reducing the costs for the electrical company.

The partitioning of the variance indicated that the highest percentage of factors that interfered in distribution patterns is related to unknown fractions (90%). According to Lewis et al. (2014), variation of species composition along the plots and heterogeneity are factors that increase the unknown fractions. In addition, the environmental variables used are not necessarily the predictors that best explain the species distribution variations (Soininen, 2014). Another reason is the weakening of environmental responses when using a variance partition (Angeler et al., 2013). However, it revealed that purely environmental (5%) and purely spatial (3%) factors were statistically significant and could account for part of the distribution of species along in the power transmission line. The purely environmental fraction indicates that environmental variables are strongly related to the composition of species, while the purely spatial fraction presented a low explanation, justified by the high variation along the power transmission line. Nevertheless, the spatial component was significant in explaining species distribution patterns. In this sense, the inclusion of variables such as dispersion factors, water and light are necessary to determine the unknown fractions. In addition, the species respond interactively to environmental conditions, evidencing the complexity of the soil-plant-environment relationship (Siqueira et al., 2009).

Another hypothesis for the low environmental explanation is related to the maintenance practices that are performed in the vegetation adjacent to the transmission line, which may affect the forest structure and ensure greater homogeneity along the transmission line.

The spatially structured environment (2%) affects the spatial distribution of the species, influencing where species are distributed, i.e., the greater the distances between

http://www.aloki.hu ● ISSN 1589 1623 (Print) ● ISSN1785 0037 (Online)
DOI: http://dx.doi.org/10.15666/aeer/1804_51095121

the samples, the more floristic differences will be observed (Diniz-Filho et al., 2012). This fact is evidenced in the present study, since the power transmission lines cover an extension of 65 km, that is, the sites sampled are generally separated at great distances, with a distinction being made between ecological sequences and floristic differences. The indeterminate variables presented high percentage, this fact occurred due to the great environmental heterogeneity and not to include all the variables that can act in the distribution of the species. Therefore, the inclusion of new biotic and abiotic factors would possibly increase the explanation of the variables on species distribution (Maçaneiro et al., 2016), or the inclusion of new plots to reduce floristic and site variability.

Conclusion

In our study, given the relationship found between vegetation and spatial/environmental variations, we suggested to perform selective maintenance in the vegetation. Thus, species such as *Araucaria angustifolia, Nectandra megapotamica, Syagrus romanzoffiana, Banara parviflora, Platymiscium floribundum*, which are associated with high luminosity should be managed with pruning or, if necessary, tree suppression, before reaching the height of risk. In addition to these species, *Sambucus australis, Trichilia clausseni, Myrsine coriacea, Matayba elaeagnoides*, which are associated with elevation, must also be managed when they reach the height of risk.

Although soil (Mg:K) ratio is associated with species distribution, due to homogeneity of soil fertility along the transmission line, this factor was not used as a criterion for species selection for maintenance. Given the difficulty of selective management, it is recommended at least to manage vegetation when it reaches 7 meters in height, thereby reducing the intensity of maintenance of areas under power transmission lines, minimizing costs with this activity. and minimizing the impacts generated.

In addition, this study was developed on a local scale, in this sense, we suggest the development of other studies with complementary information such as competition, dispersion and microclimate, since the addition of these variables can increase the predictive power of floristic patterns in subtropical forests, and offers indicators to improve or plan the management of native forests under electric power lines.

Acknowledgements. The authors are grateful to *Coordenação de Aperfeiçoamento de Pessoal de Nível Superior* (CAPES) and *Conselho Nacional de Desenvolvimento Científico e Tecnológico* (CNPq) for their research fellowship grant. We also thank Luiz Henrique da Silva from FURB Idiomas for English review.

REFERENCES

[1] Ahmad, J., Malik, A. S., Abdullah, M. F., Kamel, N., Xia, L. (2014): A novel method for vegetation encroachment monitoring of transmission lines using a single 2D camera. – Pattern analysis and applications 18(2): 419-440.

[2] Almeida-Neto, M., Campassi, F., Galetti, M., Jordano, P., Oliveira-Filho, A. T. (2008): Vertebrate dispersal syndromes along the Atlantic forest: broad-scale patterns and macroecological correlates. – Global Ecology and Biogeography 17(4): 503-513.

http://www.aloki.hu ● ISSN 1589 1623 (Print) ● ISSN1785 0037 (Online)
DOI: http://dx.doi.org/10.15666/aeer/1804_51095121

[3] Alvares, C. A., Stape, J. L., Sentelhas, P. C., Gonçalves, J. L. M., Sparovek, G. (2013): Köppen's climate classification map for Brazil. – Meteorologische Zeitschrift 22(6): 711-728.
[4] Angeler, D. G., Göthe, E., Johnson, R. K. (2013): Hierarchical dynamics of ecological communities: do scales of space and time match? – PLoS One 8(7): e69174.
[5] Borcard, D., Gillet, F., Legendre, P. (2011): Numerical Ecology with R. – Dordrecht London Heidelberg, New York.
[6] Cardoso, E., Schiavini, I. (2002): Relationship between tree species distribution and topography in a forest gradient in the Panga Ecological Station (Uberlândia, MG). – Brazilian Journal of Botany 25(3): 277-289. [Portuguese].
[7] de Castro Lima Jr., É., de Alvarenga, A. A., de Castro, E. M., Vieira, C. V., Barbosa, J. P. R. A. D. (2006): Aspectos fisioanatômicos de plantas jovens de *Cupania vernalis* Camb. Submetidos a diferentes níveis de sombreamento. – Revista Árvore 30(1).
[8] Diniz-Filho, J. A. F., Siqueira, T., Padial, A. A., Rangel, T. F., Landeiro, V. L., Bini, L. M. (2012): Spatial autocorrelation analysis allows disentangling the balance between neutral and niche processes in metacommunities. – Oikos 121(2): 201-210.
[9] Duarte, S. W., Hoffmann, L. T., Maçaneiro, J. P., Fenilli, T. A. B., Schorn, L. A. (2019): Effects of the environment and spatial factors on the regeneration of *Araucaria* Forest fragments, southern Brazil. – Applied Ecology and Environmental Research 17(4): 9577-9589.
[10] Dupras, J., Patry, C., Tittler, R., Gonzalez, A., Alam, M., Messier, C. (2015): Management of vegetation under electric distribution lines will affect the supply of multiple ecosystem services. – Land Use Policy 51: 68-75.
[11] Eisenlohr, P. V. (2014): Persisting challenges in multiple models: a note on commonly unnoticed issues regarding collinearity and spatial structure of ecological data. – Brazilian Journal of Botany 37: 365-371.
[12] Fick, S. E., Hijmans, R. J. (2017): Worldclim 2: New 1-km spatial resolution climate surfaces for global land areas. – International Journal of Climatology 37: 4302-4315.
[13] Galvani, E., Lima, N. G. B. (2014): Hemispherical photographs in microclimatic studies: theoretical-conceptual and applications. – Ciência e Natura 36: 215-221. [Portuguese].
[14] Grings, M., Brack, P. (2009): Trees in the native vegetation of Nova Petrópolis, Rio Grande do Sul. – Iheringia 64(1): 5-22. [Portuguese].
[15] Jurinitz, C. F., Oliveira, A. A., Bruna, E. M. (2013): Abiotic and Biotic Influences on Early-Stage Survival in Two Shade-Tolerant Tree Species in Brazil's Atlantic Forest. – Biotropica 45(6): 728-736.
[16] Kuntz, P. A., Christie, R. D., Venkata, S. S. (2002): Optimal maintenance scheduling of overhead electric power distribution systems. – IEEE Transactions on power delivery 17(4): 1164-1169.
[17] Leblanc, S. G., Chen, J. M. (2008): A practical scheme for correcting multiple scattering effects on optical LAI measurements. – Agricultural Forest Meteorological 110(2): 125-139.
[18] Legendre, P., Legendre, L. (2012): Numerical ecology. – Elsevier, Amsterdam, Netherlands.
[19] Lewis, R. J., Pakeman, R. J., Marrs, R. H. (2014): Identifying the multi-scale spatial structure of plant community determinants of an important national resource. – Journal of Vegetation Science 25(1): 184-197.
[20] Lopes, R. F. (2013): Optimization of maintenance process in border zone of medium / high power lines. – Faculdade de Engenharia da Universidade do Porto, Porto, MSc Thesis. [Portuguese].
[21] Maçaneiro, J. P., Oliveira, L. Z., Seubert, R. C., Eisenlohr, P. V., Schorn, L. A. (2016): More than environmental control at local scales: do spatial processes play an important role on floristic variations in Subtropical Forests? – Acta Botanica Brasilica 30(2): 183-192.

http://www.aloki.hu ● ISSN 1589 1623 (Print) ● ISSN1785 0037 (Online)
DOI: http://dx.doi.org/10.15666/aeer/1804_51095121

[22] Maçaneiro, J. P., Gasper, A. L., Galvão, F., Schorn, L. A. (2018): Dispersion and aggregation patterns of tree species in *Araucaria* Forest, Southern Brazil. – Anais da Academia Brasileira de Ciências 90(2): 2397-2408.
[23] Maçaneiro, J. P., Liebsch, D., Gasper, A. L., Galvão, F., Schorn, L. A. (2019): Structural and floristic variations in an Atlantic Subtropical Rainforest in Southern Brazil. – Floresta e Ambiente 26(1): e20160101.
[24] Matikainen, L., Lehtomäki, M., Ahokas, E., Hyypä, J., Karjalainen, M., Jaakkola, A., Kukko, A., Heinonen, T. (2016): Remote sensing methods for power line corridor surveys. – ISPRS Journal of Photogrammetry and Remote Sensing 119: 10-31.
[25] McCune, B., Mefford, M. J. (2011): PC-ORD: Multivariate analysis of ecological data, Version 6. – MjM Software Design. Gleneden Beach, Oregon.
[26] Mélo, M. A., Budke, J. C., Henke-Oliveira, C. (2013): Relationships between structure of the tree component and environmental variables in a subtropical seasonal forest in the upper Uruguay River valley, Brazil. – Acta Botanica Brasilica 27(4): 751-760.
[27] Moraes, L., Santos, R. K., Wisser, T. Z., Krupek, R. A. (2013): Evaluation of leaf area from simple linear measurements of five plant species under different light conditions. – Revista Brasileira de Biosciências 11(4): 381-387. [Portuguese].
[28] Moreno, M. I. C., Schiavini, I., Haridasan, M. (2007): Influence of the edaphic factors in the Cerrado fitofisionomies. – Caminhos da Geografia 9(25): 173-194. [Portuguese].
[29] Mueller-Dombois, D., Ellenberg, H. (2002): Aims and methods of vegetation ecology. – The Blackburn Press, New Jersey, USA.
[30] Nettesheim, F. C., Menezes, L. F. T., Carvalho, D. C., Conde, M. M. S., Araújo, D. S. D. (2010): Influence of environmental variation on Atlantic Forest tree-shrub-layer phytogeography in southeast Brazil. – Acta Botanica Brasilica 24(2): 369-377.
[31] Neuschulz, E. L., Mueller, T., Schleuning, M., Böhning-Gaese, K. (2016): Pollination and seed dispersal are the most threatened processes of plant regeneration. – Scientific Reports 6(29839).
[32] Parker, G. G., Russ, M. (2004): The canopy surface and stand development: assessing forest canopy structure and complexity with near-surface altimetry. – Forest Ecology and Management 189(1-3): 1284-1307.
[33] R Core Team. (2013): R: A language and environment for statistical computing. – Vienna: R Foundation for Statistical Computing.
[34] Ribeiro, M. C., Martensen, A. C., Metzger, J. P., Tabarelli, M., Scarano, F., Fortin, M. J. (2011): The Brazilian Atlantic forest: a shrinking biodiversity hotspot. – In: Zachos, F. E., Habel, J. C. (eds.) Biodiversity hotspots. Springer, Heidelberg.
[35] Rocha, R. P., Silva, M. B. (2013): Biogeographical History of the Atlantic Forest: Opilioes (Arachnida) as a model for their inference. – In: Carvalho, C. J. B., Almeida, E. A. B. (eds.) Biogeography of South America: Standards and processes. Roca, São Paulo, Brasil. [Portuguese].
[36] Sanchez, M., Pedroni, F., Eisenlohr, P. V., Oliveira-Filho, A. T. (2013): Changes in tree community composition and structure of Atlantic rain forest on a slope of the Serra do Mar range, Southeastern Brazil, from near sea level to 1000 m of altitude. – Flora 208(3): 184-196.
[37] Santos, H. G., Jacomine, P. K. T., Anjos, L. H. C., Oliveira, V. A. V., Lumbreras, J. F., Coelho, M. R., Almeida, J. A., Cunha, T. J. F., Oliveira, J. B. (2018): Brazilian system of soil classification. – Embrapa, Distrito Federal. [Portuguese].
[38] Scipioni, M. C., Galvão, F., Longhi, S. J. (2013): Floristic composition and dispersal and regeneration strategies of woody species in Deciduous Seasonal Forests. – Floresta 43(2): 241-254. [Portuguese].
[39] Silva, D. A. (2016): Effect of harvest intensity on the remaining structure of a secondary forest managed in Guaramirim-SC. – Universidade Regional de Blumenau, Blumenau, MsC Thesis. [Portuguese].

http://www.aloki.hu ● ISSN 1589 1623 (Print) ● ISSN1785 0037 (Online)
DOI: http://dx.doi.org/10.15666/aeer/1804_51095121

[40] Silverio Neto, R., Bento, M. C., Menezes, S. J. M. C., Almeida, F. S. (2015): Characterization of Forest Cover of Protected Areas of the Atlantic Forest. – Floresta e Ambiente 22(1): 32-41. [Portuguese].
[41] Siqueira, A. S., Araújo, G. M., Schiaviani, I. (2009): Tree layer structure and soil characteristics of two deciduous dry forests in the Araguari river valley, Minas Gerais State, Brazil. – Acta Botanica Brasilica 23(1): 10-21. [Portuguese].
[42] Soininen, J. (2014): A quantitative analysis of species sorting across organisms and ecosystems. – Ecology 95(12): 3284-3292.
[43] Souza, K., Souza, C. C., Rosa, M. G., Cruz, A. P., Lima, C. L., Silva, J. O., Lazzarin, L. C., Loebens, R., Dias, R. A. R., Silva, A. C., Higuchi, P., Schimalski, M. B. (2015): Tree component structure and dispersion strategies in a subtropical forest along a topographic sequence in Alto- Uruguai. – Scientia Forestalis 43(106): 321-332. [Portuguese].
[44] Teixeira, P. C., Donagemma, G. K., Fontana, A., Teixeira, W. G. (2017): Manual of soil analysis methods. – Embrapa, Brasília. [Portuguese].
[45] Temperton, V. M., Hobbs, R. J. (2004): The search for ecological assembly rules and its relevance to restoration ecology. – In: Temperton, V. M., Hobbs, R. J., Nuttle, T., Halle, S. (eds.) Assembly rules and restoration ecology: brindging the gap between theory and practice. Island Press, New York.
[46] Thimonier, A., Sedivy, I., Schleppi, P. (2010): Estimating leaf area index in different types of mature forest stands in Switzerland: a comparison of methods. – European Journal of Forest Research 129(4): 543-562.
[47] Urbanetz, C., Oliveira, V. M., Raimundo, R. L. G. (2003): Spatial pattern and dispersion syndromes. – www2.ib.unicamp.br/profs/fsantos/relatorios/ne211r3a2003.pdf. (accessed on 20.05.2019). [Portuguese].
[48] Wang, B. C., Smith, T. B. (2002): Closing the seed dispersal loop. – Trends in Ecology and Evolution 17(8): 379-386.
[49] Wang, Q., Adiku, S., Tenhunen, J., Granie, R. A. (2005): On the relationship of NDVI with leaf area index in a deciduous forest site. – Remote Sensing of Environment 94(2): 244-255.
[50] Young, R. F. (2010): Managing municipal green space for ecosystem services. – Urban forestry and urban greening 9(4): 313-321.

http://www.aloki.hu ● ISSN 1589 1623 (Print) ● ISSN1785 0037 (Online)
DOI: http://dx.doi.org/10.15666/aeer/1804_51095121

THE EFFECT OF SOIL CONDITIONERS ON THE QUALITY OF SELECTED FORAGE GRASSES

TRUBA, M.* – JANKOWSKI, K. – WIŚNIEWSKA-KADŻAJAN, B. – SOSNOWSKI, J. – MALINOWSKA, E.

Institute of Agriculture and Horticulture, Siedlce University of Natural Sciences and Humanities, Prusa 14 Street, 08-110 Siedlce, Poland
(phone: +48-25-643-1318; fax: +48-25-643-1309)

**Corresponding author*
e-mail: milena.truba@uph.edu.pl

(Received 2nd Dec 2019; accepted 6th May 2020)

Abstract. The aim of this paper is to determine the effect of selected soil conditioners, applied separately and with mineral fertilizers, on the intake, digestibility, and feed value of cocksfoot and perennial ryegrass. The main experimental factors were three soil conditioners with the following trade names: UGmax, Eko-Użyźniacz, and Humus Active Papka, each used on its own or together with NPK fertilizers. They were applied to the soil with two forage grasses: the Bora variety of cocksfoot and perennial ryegrass of the Info variety. In the case of cocksfoot the Humus Active Papka and UGmax soil conditioners, when both used with mineral fertilizers, had the highest impact on dry matter digestibility, but for the biomass of perennial ryegrass this parameter was the highest when Humus Active Papka was used on its own, or when UGmax was applied together with mineral fertilizers. As an average effect of fertilizer combinations, perennial ryegrass had higher digestibility, dry matter content, and relative feed value than cocksfoot. Combinations of mineral fertilizers with soil conditioners, particularly with UGmax and Humus Active Papka, resulted in the highest relative feed value of perennial ryegrass. This forage met requirements of high productive dairy cows.
Keywords: *dry matter intake, dry matter digestibility, relative feed value, cocksfoot, perennial ryegrass*

Introduction

According to many publications (Fernandez-Nunez et al., 2012; Gardarin et al., 2014; Barbero et al., 2020; Deroche et al., 2020) digestibility is dependent on plant species, its variety, fertilizer application, development stage at the harvest, but also on the harvest and plant preservation methods. Jankowska-Huflejt and Wróbel (2008) found that pasture grass had the highest digestibility of 66%, with 64% for meadow hay, and 63% for meadow grass. In turn, Harasim (2006) reported that pasture grass digestibility was 80.9%, while the figure for meadow grass was 77.6%. Acid detergent fibre (ADF) and neutral detergent fibre (NDF) fractions both limit animal dry matter intake, its digestibility, and its energetic value. Additionally, many publications (Rodrigues et al., 2008; Bélanger et al., 2013; Stejskalova et al., 2013) point out that present day systems of livestock feeding for cows in particular, take into account the intake of both NDF and ADF to estimate quality of forage by working out relative feed value; thus, the NDF and ADF contents are used to determine it. Nowadays, at the time of organic farming, on the one hand, and the intensive use of mineral fertilizers and pesticides, on the other, soil conditioners are of a growing importance. They can be successfully applied to grasses, and mixtures of grasses and legumes (Sosnowski, 2012a, 2014; Sosnowski and Jankowski, 2015; Saby and Abdal-Latife, 2018; Bozhanska, 2019). Most publications on this matter deal with UGmax, and because of that, the experiment described here was set up to study the effects of other conditioners.

http://www.aloki.hu ● ISSN 1589 1623 (Print) ● ISSN 1785 0037 (Online)
DOI: http://dx.doi.org/10.15666/aeer/1804_51235133

The aim of this paper is to determine the effect of selected soil conditioners, applied separately and with mineral fertilizers, on the intake, digestibility, and feed value of cocksfoot and perennial ryegrass. These are good quality grass species of permanent grasslands, and, as many publications point out (Szkutnik et al., 2012; Tilvikiene et al., 2014; Georgieva et al., 2015; McDonagh et al., 2016), they are different from each other in regards the content of nutrients determining their digestibility, such as crude fibre, or NDF and ADF fractions.

Materials and methods

Experiment location

Set up in the autumn of 2011 the three-year research was conducted in the experimental field of the Institute of Agriculture and Horticulture at the University of Natural Sciences and Humanities in Siedlce (52.169°N, 22.280°E), Poland. The experiment was replicated three times, with a split-plot arrangement and plots of 3 m^2 as experimental units.

The experiment was conducted on the soil with the granulometric composition of light loamy sand, classified according to FAO as technosols. It was found that the soil was of neutral pH (pH = 6.8), with the concentration of carbon in organic compounds (C_{org}) of 13.50 g kg^{-1} DM, total nitrogen concentration was 1.30 g kg^{-1} DM. Assimilable phosphorus concentration of 170 mg kg^{-1} DM was high, with medium concentration of potassium (114.00 mg kg^{-1} DM), and high concentration of assimilable magnesium (84.00 mg kg^{-1} DM).

Experimental factors

The main experimental factors were three soil conditioners with the trade names of Ugmax (Bogdan, Poland), Eko-Użyźniacz (Biohumuseco, Poland), and Humus Active Papka (Ekodarpol, Poland), applied separately and together with mineral fertilizers.

The UGmax soil conditioner (described as UG in the tables and figures) is an extract from compost, containing the following concentrations of macroelements (g kg^{-1}): nitrogen - 1.2, phosphorus - 0.2, potassium - 2.9, magnesium - 0.1, sodium - 0.2, and 0.3 mg kg^{-1} of manganese as a microelement. The conditioner also contains lactic acid bacteria, photosynthetic bacteria, yeast, and actionmycetes.

The main ingredients of Humus Active Papka (described as HA) are macroelements (g kg^{-1}): nitrogen - 0.2. phosphorus - 1.3, potassium - 4.6, calcium - 3.0, magnesium - 0.5, microelements (mg kg^{-1}): manganese - 15, iron - 500, zinc - 3.0, copper - 1.0, and enriched humus with beneficial microorganisms.

Eko-Użyźniacz (described as a EU) is an extract from manure vermicompost, containing mainly macroelements (g kg^{-1}): nitrogen - 0.6. phosphorus - 0.3. potassium - 0.7, microorganisms, and enzymes regulating metabolism of earth worms.

In the present experiment soil conditioners were used every year in spring, before the growing season, at the following doses: UGmax - 0.6 dm^3 ha^{-1}, Eko-Użyźniacz – 15 dm^3 ha^{-1}, and Humus Active Papka - 50 dm^3 ha^{-1}.

Mineral fertilizers (described as NPK) were used at the following doses: N – 15, P (P_2O_5) – 80, and K (K_2O) – 120 kg ha^{-1}. Phosphorus fertilizers were used once, in spring, while nitrogen and potassium were applied at equal doses three times a year.

http://www.aloki.hu ● ISSN 1589 1623 (Print) ● ISSN 1785 0037 (Online)
DOI: http://dx.doi.org/10.15666/aeer/1804_51235133

Effects of the above soil conditioners were tested on two forage grass species (second experimental factor): cocksfoot, the Bora variety, and perennial ryegrass, the Info variety, sown in the autumn of 2011 with the sowing rates of 18 and 23 kg ha^{-1}, respectively.

Weather conditions

Meteorological data for the years of research were obtained from the Hydrological and Meteorological Station in Siedlce (*Fig. 1*).

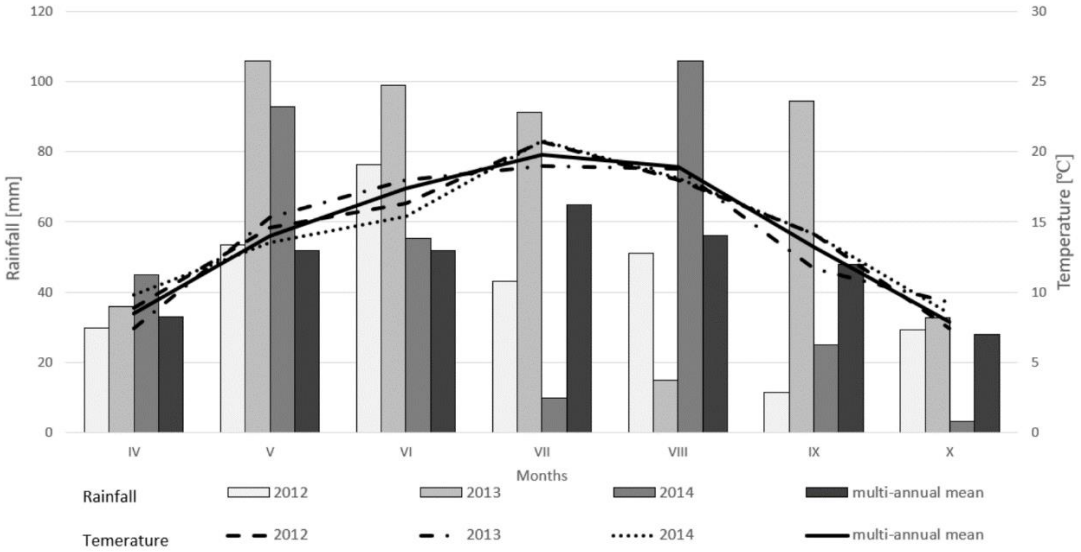

Figure 1. *Average of air temperature and sum of atmospheric precipitation in the months of the growing seasons during the research*

Based on the data from *Figure 1*, the Sielianinov's hydrothermal coefficient was calculated (Skowera and Puła, 2004) (*Table 1*):

$$K = \frac{P}{0,1} \times \sum t \qquad \text{(Eq.1)}$$

where:
K - hydrothermal coefficient value (dimensionless quantity),
P - total monthly precipitation (mm),
t - monthly sum of air temperature (ºC).

Table 1. *Sielianinov's hydrothermal coefficient values (K) during the growing seasons*

Years	Months						
	Apr.	**May**	**June**	**July**	**Aug.**	**Sept.**	**Oct.**
2012	1.12(md)	1.22(md)	1.56 (o)	0.69 (sd)	0.94 (d)	0.27 (ed)	1.32 (o)
2013	1.60 (o)	2.20 (w)	1.80 (mw)	1.50 (o)	0.25 (ed)	2.70 (sw)	1.22(md)
2014	1.53 (o)	2.29 (w)	1.20 (md)	0.16 (ed)	1.95 (mw)	0.59 (sd)	0.13 (ed)

$K \leq 0.4$ extreme drought (ed); $0.4 < K \leq 0.7$ severe drought (sd); $0.7 < K \leq 1.0$ drought (d); $1.0 < K \leq 1.3$ moderate drought (md); $1.3 < K \leq 1.6$ optimal (o); $1.6 < K \leq 2.0$ moderately wet (mw); $2.0 < K \leq 2.5$ wet (w); $2.5 < K \leq 3.0$ severely wet (sw); $K > 3.0$ extremely wet (ew)

http://www.aloki.hu ● ISSN 1589 1623 (Print) ● ISSN 1785 0037 (Online)
DOI: http://dx.doi.org/10.15666/aeer/1804_51235133

Analysis

Chemical composition of grass biomass was measured with near-infrared spectroscopy (NIRS), using the NIRFlex N-500 spectrometer (BUCHI, Poland) with the INGOT calibration package for dry feed. Acid detergent fibre (ADF) and neutral detergent fibre (NDF) concentration were used to evaluate suitability of the forage to feed livestock. It was done with Linn and Martin's test (Linn and Martin, 1989), in which a classifying parameter is relative feed value, which, in turn, was calculated using the formula:

$$RFV = \frac{DDM \times DMI}{1.29} \quad \text{(Eq.2)}$$

where:
RFV - relative feed value (dimensionless quantity),
DDM - digestible dry matter (%).

$$DDM = 88.9 - 0.779 \times ADF \quad \text{(Eq.3)}$$

DMI - dry matter intake (percentage of body weight).

$$DMI = \frac{120}{NDF} \quad \text{(Eq.4)}$$

Using range of values for RFV provided by Linn and Martin (1989), grass was classified to specific feed classes meeting requirements of corresponding cattle groups (*Table 2*).

Table 2. *Cattle forage quality as relative feed value*

Quality class	RFV range	Animal
I	> 151	Most productive dairy cows
II	125 – 151	Good quality dairy cows, young heifers selected for breeding
III	103 – 124	Good quality beef cattle, older heifers, less productive dairy cows
IV	87 – 102	Beef cattle and dry cows
V	75 – 86	Dry cows for fattening. supplemented with high-energy feeds

The results were statistically processed using analysis of variance for multi-factor experimental design. Tukey's test was used to determine $HSD_{0.05}$, and Statistica 12 software was applied for calculations.

Results and discussion

Evaluation of cocksfoot and perennial ryegrass digestible dry matter

According to Stachowicz (2010) the digestibility of grass forage, as feed for ruminants, should be at least 65%. As regards dry matter digestibility, average of experimental years and treatments, it was found that mean values of this parameter for cocksfoot and perennial ryegrass were significantly different, with 65.9% and 66.9%, respectively

http://www.aloki.hu ● ISSN 1589 1623 (Print) ● ISSN 1785 0037 (Online)
DOI: http://dx.doi.org/10.15666/aeer/1804_51235133

(*Table 3*). Other publications provide similar results (Downing and Gamroth, 2007; McDonagh et al., 2016; Cupic et al., 2019), stressing the fact that perennial ryegrass is easily digestible because it contains low amounts of such compounds as crude fibre, neutral detergent fibre, and acid detergent fibre. According to many authors (Szkutnik et al., 2012; Tilvikiene et al., 2014; Georgieva et al., 2015) cocksfoot contains too much of the above compounds, which lowers its digestibility.

Table 3. *The effects of year and fertilizer on digestible dry matter (%)*

Species / Year / Cutting	Fertilizer								Mean
	0	NPK	UG	EU	HA	UG+NPK	EU+NPK	HA+NPK	
Mean for species									
Cocksfoot	65.5^{Ba}	65.4^{Aa}	65.3^{Aa}	66.0^{Aa}	66.1^{Aa}	66.4^{Aa}	65.8^{Aa}	66.4^{Aa}	65.9^{B}
Perennial ryegrass	67.5^{Aa}	66.1^{Aa}	65.9^{Aa}	67.4^{Aa}	67.5^{Aa}	67.5^{Aa}	66.4^{Aa}	67.1^{Aa}	66.9^{A}
Mean for cuttings									
I	66.2^{Aa}	64.8^{Aa}	65.0^{Aa}	65.3^{Ba}	66.2^{Aa}	66.5^{Aa}	64.8^{Aa}	65.9^{Aa}	65.6^{B}
II	66.0^{Aab}	65.3^{Ab}	65.8^{Aab}	67.9^{Aa}	66.8^{Aab}	66.9^{Aab}	66.6^{Aab}	66.9^{Aab}	66.5^{A}
III	67.3^{Aa}	67.3^{Aa}	66.1^{Aa}	67.0^{Aa}	67.3^{Aa}	67.5^{Aa}	66.9^{Aa}	67.4^{Aa}	67.1^{A}
Mean for years									
2012	65.9^{Ab}	65.5^{Ab}	65.7^{Ab}	66.3^{ABab}	67.2^{Aab}	68.2^{Aa}	66.2^{Ab}	67.2^{Aab}	66.5^{AB}
2013	67.1^{Aab}	66.6^{Aab}	65.9^{Ab}	68.0^{Aa}	67.0^{Aab}	66.6^{ABab}	66.3^{Aab}	67.4^{Aab}	66.9^{A}
2014	66.5^{Aa}	65.3^{Aa}	65.3^{Aa}	65.9^{Ab}	66.2^{Aa}	66.1^{Ba}	65.8^{Aa}	65.7^{Aa}	65.9^{B}

Means in lines marked with the same small letters do not differ significantly. Means in columns marked with the same capital letters do not differ significantly

When both UGmax and mineral fertilizers were used not together but separately, the digestibility of forage from both plots was lower, with 65.6% and 65.8%, respectively. In the forage form those plots, with UGmax or mineral fertilizers applied, it was 1.4% lower than in the control (*Table 3*). Jankowska-Huflejt and Wróbel (2008) found similar results studying digestibility of forage from permanent grassland. They found that it ranged from 63 to 66% for green grass, while for hay it was 64%. Harasim (2006), however, presents much higher values found in research on grass from permanent grassland, with its digestibility ranging from 77.6 to 80.9%. In the experiment presented here, for both grass species and all combinations of fertilizers the digestibility of the second year forage (2013) was the highest (66.9%) and significantly different form the value of the same parameter in the third year (2014), which was 65.9%. There is a relationship between the value of hydrothermal coefficient and the above values. In the second year weather conditions were rather optimal and forage digestibility was the highest, while in the third year most of the growing season was dry to extremely dry, which resulted in lower digestibility.

Comparing forage from the two grass species from all experimental units it was found that the application of soil conditioners and mineral fertilizers did not significantly affect digestibility of cocksfoot (*Table 3*). But mineral fertilisers and UGmax, when both applied on their own, slightly lowered digestibility of perennial ryegrass, by 2.4%, compared to the control. Sosnowski (2012a) noticed a similar reaction of plants to fertilizers in an experiment with *Festulolium brauni*, where its digestibility was 60%, not

http://www.aloki.hu ● ISSN 1589 1623 (Print) ● ISSN 1785 0037 (Online)
DOI: http://dx.doi.org/10.15666/aeer/1804_51235133

being affected by a soil conditioner, while mineral fertilizers significantly lowered it to 48.5%.

Analysing dry matter digestibility in consecutive harvests in the same growing seasons it was found that it significantly increased, from 65.6% in the first one, to 67.1% in the third one.

It was found that the treatment effect on digestibility was the highest on plots where mineral fertilizers and UGmax were applied together. However, this value did not differ significantly from that in the control (*Fig. 2*), but the increase caused by this combined application (about 1.8%) was statistically significant when compared to the effect of the soil conditioner used on its own. In the case of other soil conditioners their use together with mineral fertilization or separately, did not cause significant differences.

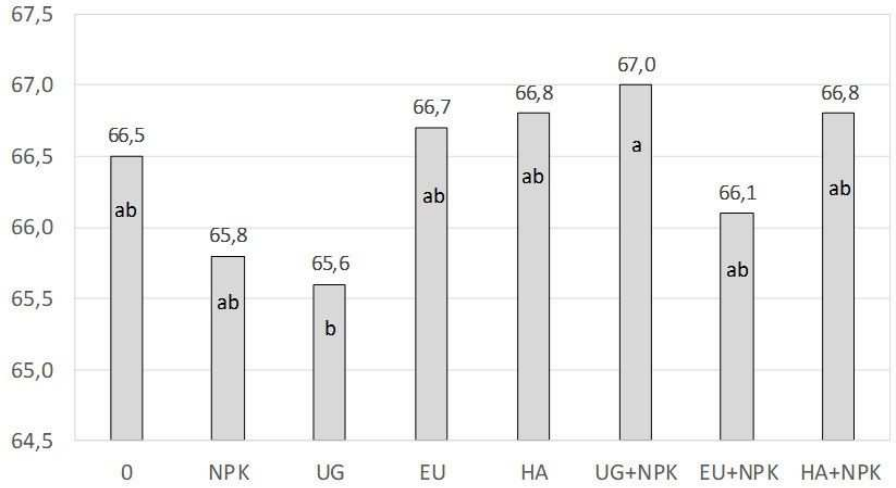

Figure 2. *The effects of fertilizer on digestible dry matter (%). Means in columns marked with the same lower case letters do not differ significantly*

Dry matter intake for cocksfoot and perennial ryegrass

According to Deroche et al. (2020) forage quality depends on the development stage at which plants are harvested. Together with plant aging its nutritional value is declining because the amount of crude fibre is going up, which in turn affects dry matter intake and dry matter digestibility.

By comparing both grass species (*Table 4*) it was found that perennial ryegrass had significantly higher dry matter intake (2.83%) than cocksfoot (2.60%). Cocksfoot from the plot where Eko-Użyźniacz was applied had a significantly higher dry matter intake (2.77%) than the same grass species from the control plot. There were no significant differences between the forage coming from other plots.

The highest dry matter intake (2.98%) was for perennial ryegrass coming from the plots where UGmax and mineral fertilizers were used together (2.98%), and from the ones where Humus Active Papka with mineral fertilizers was used (3.0%). However, the parameters did not differ significantly from the results on the control plot. Dry matter intake was significantly lower, by 9.4%, for perennial ryegrass from the plot with UGmax (2.63%). Sosnowski (2012b) proved that the UGmax soil conditioner slightly raised perennial ryegrass dry matter intake, from 2.44 to 2.52%, whereas the same conditioner slightly decreased it in cocksfoot, from 2.20 to 2.11%. The results of dry matter intake in

http://www.aloki.hu ● ISSN 1589 1623 (Print) ● ISSN 1785 0037 (Online)
DOI: http://dx.doi.org/10.15666/aeer/1804_51235133

the present experiment are higher than those provided by Jankowska-Huflejt and Wróbel (2008), who found that it ranged from 1.96% for hay, to 2.42% for pasture grass, while Moore and Undersander (2002) found that dry matter intake for forage ranged from 1.93 to 2.17%. The analysis of this parameter in different cuttings of grass for both species and all fertilizer combinations proved that it steadily increased in consecutive cuttings.

Table 4. *The effects of fertilizer and year of the experiment on dry matter intake (percentage of body weight)*

Species / Year / Cutting	Fertilizer								Mean
	0	NPK	UG	EU	HA	UG+NPK	EU+NPK	HA+NPK	
Mean for species									
Cocksfoot	2.54^{Bab}	2.45^{Ab}	2.51^{Aab}	2.77^{Aa}	2.68^{Aab}	2.61^{Bab}	2.51^{Bab}	2.69^{Bab}	2.60^{A}
Perennial ryegrass	2.91^{Aab}	2.74^{Aab}	2.63^{Ab}	2.76^{Aab}	2.75^{Aab}	2.98^{Aa}	2.87^{Aab}	3.00^{Aa}	2.83^{A}
Mean for cuttings									
I	2.72^{Aa}	2.43^{Aa}	2.41^{Aa}	2.67^{Aa}	2.59^{Aa}	2.70^{Aa}	2.56^{Aa}	2.78^{Aa}	2.61^{B}
II	2.59^{Aa}	2.56^{Aa}	2.60^{Aa}	2.84^{Aa}	2.71^{Aa}	2.80^{Aa}	2.78^{Aa}	2.83^{Aa}	2.71^{AB}
III	2.86^{Aa}	2.80^{Aa}	2.70^{Aa}	2.80^{Aa}	2.84^{Aa}	2.87^{Aa}	2.71^{Aa}	2.93^{Aa}	2.81^{A}
Mean for years									
2012	2.65^{Aab}	2.62^{Aab}	2.58^{Ab}	2.79^{Aab}	2.93^{Aab}	2.93^{Aab}	2.76^{Aab}	3.02^{Aa}	2.79^{A}
2013	2.85^{Aa}	2.66^{Aa}	2.62^{Aa}	2.93^{Aa}	2.63^{Aa}	2.69^{Aa}	2.71^{Aa}	2.84^{Aa}	2.74^{AB}
2014	2.67^{Aa}	2.50^{Aa}	2.51^{Aa}	2.58^{Aa}	2.58^{Aa}	2.75^{Aa}	2.59^{Aa}	2.68^{Aa}	2.61^{B}

Means in lines marked with the same small letters do not differ significantly. Means in columns marked with the same capital letters do not differ significantly

Analysing the effect of fertilizers on dry matter intake (*Fig. 3*), calculated by using the content of neutral detergent fibre, it was found that the lowest value of this parameter was for the forage from the plots where UGmax (2.57%) and NPK fertilizers (2.59%) where applied separately.

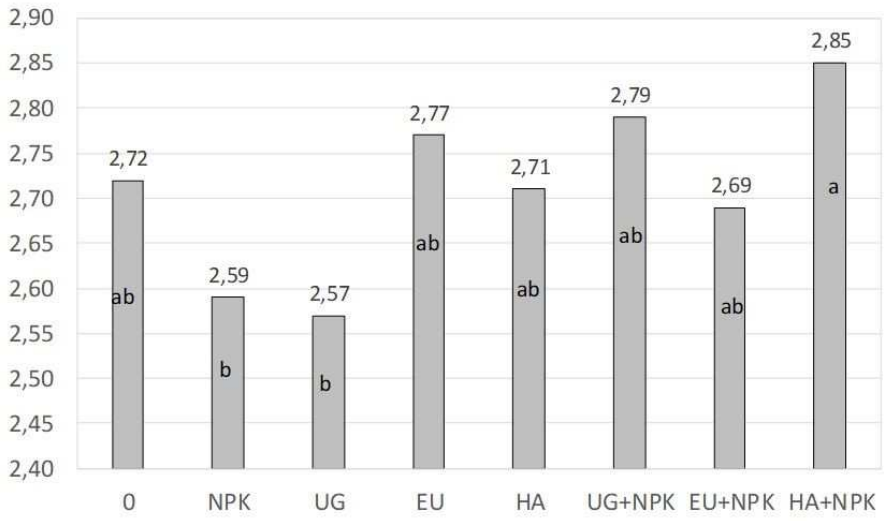

Figure 3. *The effects of fertilizer on dry matter intake (percentage of body weight). Means in columns marked with the same lower case letters do not differ significantly*

http://www.aloki.hu ● ISSN 1589 1623 (Print) ● ISSN 1785 0037 (Online)
DOI: http://dx.doi.org/10.15666/aeer/1804_51235133

However, when UGmax and NPK fertilizers were applied together, the amount of dry matter significantly increased (to 2.79%), compared to the plots where they were used separately. The highest increase of this parameter was in the grass from the plot where Humus Active Papka together with mineral fertilizers was applied (2.85%); it was about 5% higher than in the forage from the control. Comparing this parameter in each experimental year it was found that the highest dry matter intake (2.79%) was in the first year (2012), and it decreased in consecutive years. Analysing dry matter intake for all three harvests it was observed that it significantly decreased, from 2.79% in the first one, to 2.61% in the third one.

Relative feed value

Linn and Martin's test (1989) applied in the present experiment showed that, as an average for both grass species, the forage from all plots is of second quality class. Comparing experimental years only, it was discovered that the grass had the highest value in the first year (144), and it was gradually lower in the consecutive years (*Table 5*).

Table 5. *The effects of experimental year and fertilizer on dry matter relative feed value*

Species / Year / Cutting	Fertilizer								Mean
	0	NPK	UG	EU	HA	UG+NPK	EU+NPK	HA+NPK	
Mean for species									
Cocksfoot	129^{Ba}	125^{Aa}	127^{Aa}	142^{Aa}	138^{Aa}	134^{Ba}	128^{Ba}	139^{Aa}	133^{B}
Perennial ryegrass	152^{Aab}	141^{Aab}	135^{Ab}	145^{Aab}	144^{Aab}	156^{Aa}	148^{Aab}	156^{Aa}	147^{A}
Mean for cuttings									
I	140^{Aa}	122^{Aa}	122^{Aa}	135^{Aa}	134^{Aa}	140^{Aa}	129^{Aa}	143^{Aa}	133^{C}
II	132^{Aa}	130^{Aa}	133^{Aa}	150^{Aa}	141^{Aa}	146^{Aa}	144^{Aa}	147^{Aa}	140^{B}
III	150^{Aa}	146^{Aa}	139^{Aa}	146^{Aa}	148^{Aa}	150^{Aa}	141^{Aa}	153^{Aa}	147^{A}
Mean for years									
2012	136^{Aab}	133^{Aab}	132^{Ab}	144^{Aab}	152^{Aab}	155^{Aab}	142^{Aab}	158^{Aa}	144^{A}
2013	149^{Aa}	138^{Aa}	134^{Aa}	155^{Aa}	137^{Aa}	139^{Aa}	140^{Aa}	149^{Aa}	143^{AB}
2014	138^{Aa}	127^{Aa}	127^{Aa}	132^{Aa}	133^{Aa}	141^{Aa}	132^{Aa}	137^{Aa}	133^{B}

Means in lines marked with the same small letters do not differ significantly. Means in columns marked with the same capital letters do not differ significantly

Comparing both grass species (*Table 5*) it was found that perennial ryegrass had a significantly higher RFV (147) than cocksfoot (133). The results indicate that only perennial ryegrass from the plot with UGmax and mineral fertilizers applied together (156) and form the plot with Humus Active Papka and mineral fertilizers applied together (156) was of the first quality class.

The above results indicate that that forage met requirements of high productivity dairy cows. Perennial ryegrass from the control plot also had a high RVF value (152). Forage from other plots was classified to the second class, to be used to feed good dairy cows and young heifers selected for breeding. According to Sosnowski (2012b) perennial ryegrass had a lower RFV (119), but UGmax application slightly raised it (124). The same author (2012d) found that for cocksfoot relative feed value was 104 and after UGmax application this parameter decreased to 100. Comparing relative feed value of forage from

http://www.aloki.hu ● ISSN 1589 1623 (Print) ● ISSN 1785 0037 (Online)
DOI: http://dx.doi.org/10.15666/aeer/1804_51235133

different grass cuttings it was found that it increased significantly, rising from133 in the first cutting to 147 in the third.

Grass from plots where UGmax with mineral fertilizers and form plots where Humus Active Papka with mineral fertilizers were applied had the highest feed value, 145 and 148, respectively (*Fig. 4*). Compared to the plot where both of them were applied together, separate application of UGmax and mineral fertilizers lowered relative feed value by 9%.

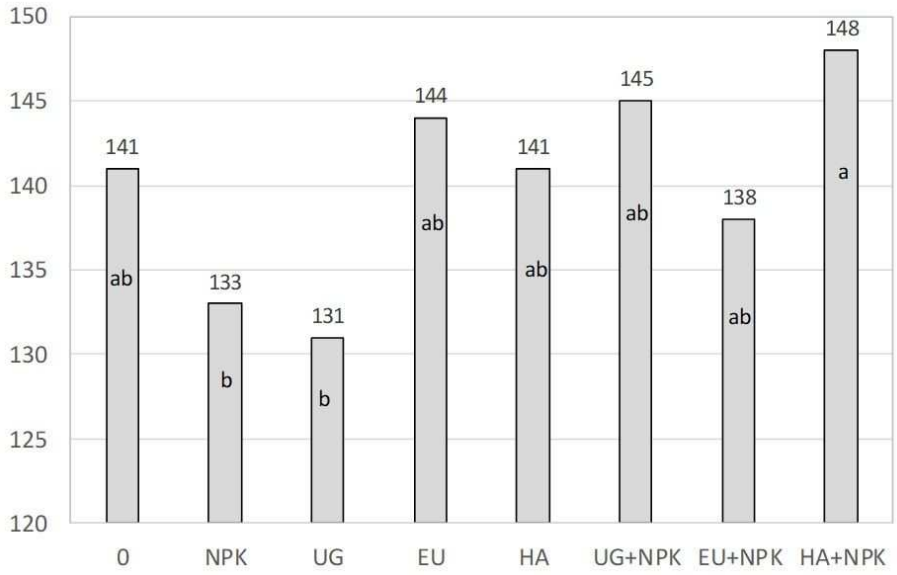

Figure 4. *The effects of fertilizer on relative feed value in dry matter (-). Means in columns marked with the same lower case letters do not differ significantly*

Conclusions

1. In the case of cocksfoot the Humus Active Papka and UGmax soil conditioners, when both used with mineral fertilizers, had the highest impact on dry matter digestibility, but in the biomass of perennial ryegrass this parameter was the highest when Humus Active Papka was used on its own, or when UGmax was applied together with mineral fertilizers.
2. As an average affect of fertilizer combinations, perennial ryegrass had higher digestibility, dry matter content, and relative feed value than cocksfoot.
3. Combinations of mineral fertilizers with soil conditioners, in particular with UGmax and Humus Active Papka, resulted in the highest relative feed value of perennial ryegrass. This forage met requirements of high productive dairy cows.
4. The diverse and inconclusive results of the experiment with the nutritional value of perennial ryegrass and cocksfoot indicate that there should be further research conducted to select the most suitable soil conditioner to be used for growing forage grass.

Acknowledgements. The research carried out under the theme No. 171/16/MN was financed from the science grant of the Ministry of Science and Higher Education – Poland.

http://www.aloki.hu ● ISSN 1589 1623 (Print) ● ISSN 1785 0037 (Online)
DOI: http://dx.doi.org/10.15666/aeer/1804_51235133

REFERENCES

[1] Barbero, R. P., Malheiros, E. B., Aguilar, N. M., Romanzini, E. P., Ferrari, A. C., Nave, R. L., Mullinks, J. T., Reis, R. A. (2020): Supplementation level increasing dry matte intake of beef cattle grazing low herbage height. – Journal of Applied Animal Research 48(1): 28-33. doi:10.1080/09712119.2020.1715985.

[2] Bélanger, G., Virkajarvi, P., Duru, M., Tremblay, G. F., Saarijarvi, K. (2013): Herbage nutritive in less – favoured areas of cool regions. – The Role of Grasslands in a Green Future, EGF, Grassland Science in Europe 18: 57-70.

[3] Bozhanska, T. (2019): Study on the influence of Lumbricl and Lumbrex bio-fertilizers over an artificial grassland of red fescue (*Festuca rubra* L.). – Bulgarian Journal of Agricultural Science 25(2): 278-282.

[4] Cupic, T., Varnica, I., Jukic, G., Krizmanic, G., Tucak, M., Popovic, S., Babic, I., Simic, A. (2019): Forage grass productivity and quality in south-western part of Pannonian basin. – Journal of Central European Agriculture 20(1): 341-352. doi:10.5513/JCEA01/20.1.2215.

[5] Deroche, B., Pradel, P., Baumont, R. (2020): Long-term evolution and prediction of feed value for permanent mountain grassland hay: Analysis of a 32-year data set in relation to climate change. – Grassland and Forage Science 75(1): 18-27. doi:10.1111/gfs.12465.

[6] Downing, T., Gamroth, M. (2007): Nonstructural Carbohydrates in Cool – season Grasses. – Oregon State University Extension Service. Special Report 1079-E.

[7] Fernandez-Nunez, E., Pires, J. M., Fernandes, A., Pires, J., Aguiar, C., Galvao, L., Moreira, N. (2012): Grazing regimes and fertilization rates: effect on dry matter yield, crude protein content and digestibility of meadows in the Northeast of Portugal. Grassland – a European Resource? – EGF. Grassland Science in Europe 17: 311-313.

[8] Gardarin, A., Garnier, E., Carrère, P., Cruz, P., Andueza, D., Bonis, A., Colace, M. P., Dumont, B., Duru, M., Farruggia, A., Gaucherand, S., Grigulis, K., Kernéïs, E., Lavorel, S., Louault, F., Loucougaray, G., Mesléard, F., Yavercovski, N., Kazakou, E. (2014): Plant trait-digestibility relationship across management and climate gradients in permanent grasslands. – Journal of Applied Ecology 51(5): 1207-1217. doi:10.1111/1365-2664.12293.

[9] Georgieva, N., Pachev, I., Katova, A., Naydenova, Y. (2015): Study of introduced varieties of Perennial grass species grown in the conditions of central northern Bulgaria. – Banat's Journal of Biotechnology 6(12). doi:10.7904/2068-4738-VI(12)-20.

[10] Harasim, J. (2006): Productivity of grassland communities used for hay and grazing as permanent grass or leys changes. – Annales UMCS sectio E Agricultura LXI: 165-173. (in Polish).

[11] Jankowska-Huflejt, H., Wróbel, B. (2008): Evaluation of usefulness of forages from grasslands in livestock production in examined organic farms. – Journal of Research and Application in Agricultural Engineering 53(3): 103-108. (in Polish).

[12] Linn, J. G., Martin, N. P. (1989): Forage quality test and interpretation. – Minnesota Extension Service, University of Minnesota, 1-5.

[13] McDonagh, J., O'Donovan, M., McEvo, M., Gilliland, T. J. (2016): Genetic gain in perennial ryegrass (*Lolium perenne*) varieties 1973 to 2013. – Euphytica 212(2): 187-199. doi:10.1007/s10681-016-1754-7.

[14] Moore, J. E., Undersander, D. J. (2002): Relative Forage Quality: An Alternative to Relative Feed Value and Quality Index. – Proceedings 13th Annual Florida Ruminant Nutrition Symposium: 16-32.

[15] Rodrigues, A. M., Andueza, D., Picard, F., Cecato, U., Farruggia, A., Baumont, R. (2008): Classification of mountain permanent grasslands based on their feed value. – Biodiversity and animal feed, EGF. Grassland Science in Europe 13: 501-503.

[16] Sabry, R. E., Abdal-Latife, S. A. (2018): Effect of bio fertilizers on growth of some turfgrass pants. – Iraqi Journal of Agricultural Sciences 48(6B): 1624-1633.

http://www.aloki.hu ● ISSN 1589 1623 (Print) ● ISSN 1785 0037 (Online)
DOI: http://dx.doi.org/10.15666/aeer/1804_51235133

[17] Skowera, B., Puła, J. (2004): Pluviometric extreme conditions in sping season in Poland in the years 1971 - 2000. – Acta Agrophysica 3(1): 171-177. (in Polish).
[18] Sosnowski, J. (2012a): Reaction of *Dactylis glomerata* L. *Festuca pratensis* Huds. and *Lolium perenne* L. to microbiological fertilizer and mineral fertilization. – Acta Scientiarum Polonorum, Agricultura 11(1): 91-98.
[19] Sosnowski, J. (2012b): Effect of soil's fertilizer used in cultivation *Lolium perenne* L., *Dactylis glomerata* L. and Festuca pratensis Huds. On relative value (RFV) of food. – Fragmenta Agronomica 29(3): 136-143. (in Polish).
[20] Sosnowski, J., Jankowski, K., Wiśniewska-Kadżajan, B. (2014): Evaluation of the impact of selected microbiological preparations on the development of the aboveground biomass of *Trifolium pretense* L. – Environmental Protection and Natural Resources 25(3): 1-4. doi:10.2478/oszn-2014-0010.
[21] Sosnowski, J., Jankowski, K. (2015): The Applicability of Soil's Fertilizers in Increasing of Production Effects in *Lolium Perenne* and *Lolium Multiflorum* Cultivation. – Journal of Life Science 9: 91-94. doi:10.17265/1934-7391/2015.03.001.
[22] Stachowicz, T. (2010): The rational use of grassland in ecological farm. – The Agricultural Advisory Centre in Brwinow, Radom. (in Polish).
[23] Stejskalova, M., Hejcmanova, P., Hejcman, M. (2013): Forage value of leaf fodder main European broad – leaved woody species. – The Role of Grassland in a Green Future, EGF. Grassland Science in Europe 18: 85-87.
[24] Szkutnik, J., Kacorzyk, P., Szewczyk, W. (2012): The content change of total protein and crude fibre depending on the dose of fertilization and phenological phase of grasses. – Grassland Science in Poland 15: 185-191. (in Polish).
[25] Tilvikiene, V., Kadziuliene, Z., Dabkevicius, Z., Sarunaite, L., Slepetys, J., Pociene, L., Slepetiene, A., Ceceviciene, J. (2014): The yield and variation of chemical composition of cocksfoot biomass after five years of digestate application. – The Future of European Grasslands, EGF. Grassland Science in Europe 19: 468-470.

http://www.aloki.hu ● ISSN 1589 1623 (Print) ● ISSN 1785 0037 (Online)
DOI: http://dx.doi.org/10.15666/aeer/1804_51235133

OCCURRENCE CHARACTERISTICS OF *STEPHANODISCUS* AND *SYNEDRA* IN RELATION TO WATER TEMPERATURE AND CONCENTRATIONS OF NUTRIENTs DURING SPRING DIATOM BLOOM IN LAKE PALDANG, KOREA

YOUN, S. J. – YU, S. J. – BYEON, M. S.*

Han River Environmental Research Center, National Institute of Environmental Research
42, Dumulmeori-gil68beon-gil, Yangser-myeon, Yangpyeong-gun, Gyeonggi-do 12585, Republic of Korea
(phone: +82-31-770-7270; fax: +82-31-773-2268)

**Corresponding author*
e-mail: zacco@korea.kr; phone: +82-31-770-7271

(Received 6th Dec 2019; accepted 6th May 2020)

Abstract. Physicochemistry was measured weekly from 2014–2017 at sites PD1, PD2, and PD3 in Lake Paldang, Korea. The effects of temperature and nutrients on the growth of the freshwater diatoms *Stephanodiscus* and *Synedra* were determined. PD2 had higher water temperature, dissolved oxygen, and conductivity than PD3. Total phosphorus and nitrogen at PD2 were the highest (0.038 mg/L and 2.181 mg/L, respectively). However, PD3 had more silicon (1.396 mg/L) than PD2 (1.027 mg/L). *Stephanodiscus* and *Synedra* bloomed mainly between March and May. At all three sites, *Stephanodiscus* was detected at 1.2–22.7°C and its density was the highest at 6.7°C. *Synedra* was detected at 1.2–32.8°C and its density was the highest at 13–15°C. *Stephanodiscus* and *Synedra* proliferated when TP was ≥ 0.020 mg/L and ≤ 0.020 mg/L, respectively, and Si was ≤ 0.4 mg/L and ≥ 0.4 mg/L, respectively. Therefore, temperature, phosphorus and silicon significantly influenced diatom growth.
Keywords: *phosphorus, silicon, Si:P ratio, springtime*

Introduction

Spring diatom bloom frequently occurs in eutrophic rivers, lakes, and seas around the world. The mass growth of *Asterionella* or *Stephanodiscus* is accompanied by malodor (Jüttner, 1983; Deng et al., 2013). When large volumes of these diatoms flow into water purification plants, they clog filter basins (Joh et al., 2011). Diatom overpopulation also causes many other problems. These problems lead to a reduction of dissolved oxygen transparency, which results in clogging and sedimentation issues in water-treatment processes and drinking water supply systems, with high diatoms biomass (Hijnen et al., 2007; Reavie et al., 2016).

Spring diatom bloom is affected by various environmental factors like light, rainfall, water temperature, and nutrient levels (Bleiker and Schanz, 1989; Marshall and Peter, 1989; Muylaert and Sabbe, 1999; Ye et al., 2007). These factors modify phytoplankton development and sustainability. They also determine species composition and seasonal succession (McCauley and Downing, 1991; Teubner and Dokulil, 2002; Lv et al., 2014). Water temperature is a major factor influencing phytoplankton growth (Masaki and Seki, 1984; Tsuchida et al., 1984). A rise in water temperature may accelerate phytoplankton growth. Nevertheless, temperature fluctuations may cause stress and reduce phytoplankton populations (Round et al., 1990; Reynolds, 2006). It was reported that a change in water temperature caused the existing predominant species to be replaced by another more competitive one at the new temperature (Tilman et al., 1981).

http://www.aloki.hu ● ISSN 1589 1623 (Print) ● ISSN 1785 0037 (Online)
DOI: http://dx.doi.org/10.15666/aeer/1804_51355147

Motile freshwater flagellate algae changed their locations according to water temperature (Clegg et al., 2003). Nutrients and water temperature affected the springtime growth of phytoplankton (Wu et al., 2013). Phosphorus and silicon have significant effects on the development and succession of phytoplankton, especially diatoms. A low Si:P ratio may partially constrain diatom growth in eutrophic lakes (Schindler et al., 1996; Schindler, 2006; Reynolds, 2006). The centric freshwater diatoms *Cyclotella* and *Stephanodiscus* are known to compete with other diatom genera for silicon (Tilman et al., 1986). They grow continuously in the springtime until the silicon is almost exhausted. Their growth is not affected by silicon concentration (cited in Shatwell et al., 2013). Contrarily, *Synedra*, *Asterionella*, and other linear Fragilariaceae prefer high silicon concentrations and are more competitive at low phosphorus levels (Tilman et al., 1982). Sommer (1985) reported that *Asterionella* was a better competitor for phosphorus than *Stephanodiscus*, and *Synedra acus* is the most successful competitor for phosphorus when the silicon levels were not limiting. Constraints on the availability of silicon restrict diatom growth to a short springtime duration. However, the interactions between physicochemical factors like water temperature and Si:P play important roles in determining diatom species distributions (Shatwell et al., 2013). Analysis of the interaction between phytoplankton and environmental factors will help us understand phytoplankton species composition under various conditions. It will improve predictions about the growth, development, and dynamics of diatoms.

The objective of this study was to identify the environmental factors affecting the growth of *Stephanodiscus* and *Synedra* by investigating the development of spring diatom blooms (*Stephanodiscus* and *Synedra*) in Lake Paldang at the confluence of the physicochemically different Bukhan and Namhan Rivers, in South Korea.

Materials and methods

Study site

Lake Paldang is located in the upper region of the Han River running through Seoul, the capital city of South Korea, in East Asia. Lake Paldang is a man-made lake constructed in 1973 at the confluences of the Bukhan and Namhan Rivers. In 1975, it was designated a protected watercourse area. It provides water to 2.4 million people, and is the largest drinking water source in South Korea. The surface area is 36.5 km^2 and the total basin area is ~23,800 km^2. The Bukhan River catchment occupies 37%, while the Namhan River catchment accounts for ~60% of the total basin area. The average depth of Lake Paldang is ~6.5 m. Therefore, the vertical distributions of both water temperature and DO are more or less uniform and no distinct stratification is observed. The Bukhan and Namhan Rivers account for 35.5% and 62.9% of the total inflow into Lake Paldang, respectively. The tributaries of Lake Paldang have different water quality characteristics. The continuous inflow of domestic sewage and livestock wastewater cause eutrophication, and, consequently, algal blooms (Park et al., 2004; Park and Jheong, 2003).

Analytical methods

A field survey was conducted at three different sites; PD1, PD2, and PD3. PD1 (N 37°31'24.5" E 127°16'56.6") was located in front of the Paldang Dam. PD2

http://www.aloki.hu ● ISSN 1589 1623 (Print) ● ISSN 1785 0037 (Online)
DOI: http://dx.doi.org/10.15666/aeer/1804_51355147

(N 37°30'00" E 127°15'00") was under the influence of the Namhan River. PD3 (N 37°35'25.2" E 127°20'24.5") was in the trajectory of the Bukhan River (*Fig. 1*). Water samples were collected weekly from March 2014 to October 2017 except when the water was frozen, and continuously measured 40 times or more each year. In our analysis, Springtime was set between March to May. Water samples were taken at a depth of 0.5 m using an 8 L water sampler (Wildco, Yulee, FL, USA).

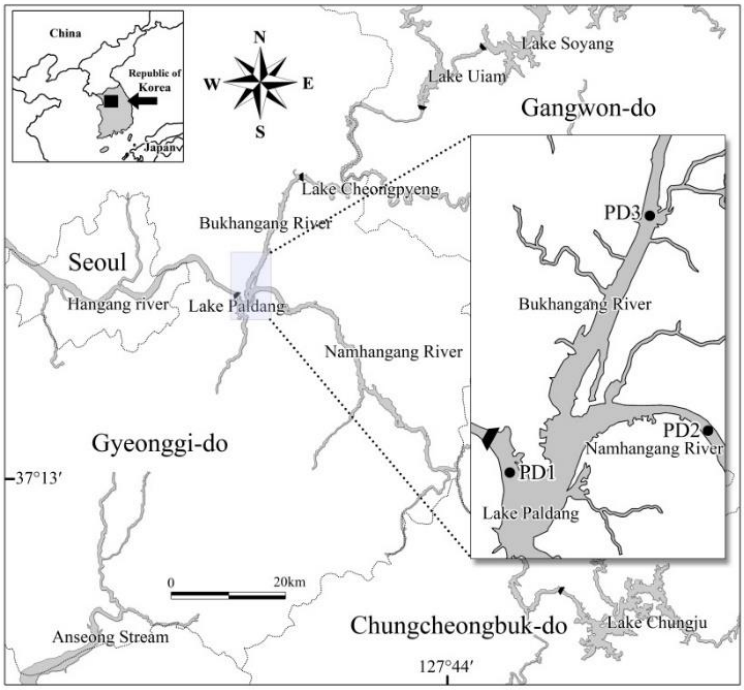

Figure 1. *Location of sampling sites in Lake Paldang*

At each sampling, water temperature (T), dissolved oxygen (DO), and conductivity (C) were measured with a multi water quality checker (YSI EXO; YSI Inc., Yellow Springs, OH, USA). An 8-L water sampler (Wildco, Yulee, FL, USA) was used and the collected samples were stored in the cold (~4°C) and dark until they were transported to the laboratory. For certain samples, total phosphorus (TP, mg/L), dissolved total phosphorus (DTP), total nitrogen (TN), dissolved total nitrogen (DTN), and silicon (Si) were measured in accordance with the Korean standard methods (ME, 2016). TP and DTP were calculated from the absorbance of molybdic acid measured by continuous flow at 880 nm. TN and DTN were determined from the absorbance of NO_2-N (nitrite nitrogen) measured by continuous flow at 550 nm. From March 2015 to October 2017, Si was analyzed using the color reactions of supersaturated oxalic acid and the absorbance was measured at 630 nm. N:P and Si:P were reported as mass ratios using the values of TN and TP. Si:P was calculated from Si and TP.

The samples for analyzing the cell counts of *Stephanodiscus* and *Synedra* were fixed by adding Lugol's iodine solution (final concentration: 2% w/v). They were then used unmodified, concentrated, or diluted depending on the phytoplankton density. One milliliter of the fixed sample was placed into a Sedgwick-Rafter counting chamber, left to settle for ≥30 min, then viewed under a microscope. Cell counts per unit area were calculated using an ECLIPSE Ni phase-contrast microscope (Nikon Instruments, Tokyo,

http://www.aloki.hu ● ISSN 1589 1623 (Print) ● ISSN 1785 0037 (Online)
DOI: http://dx.doi.org/10.15666/aeer/1804_51355147

Japan). The diatoms were identified based on the methods of John et al. (2002), Joh (2010), and Joh et al. (2010). *Stephanodiscus* and *Synedra* were differentiated from other diatoms by structural characteristics at the genus level. A Pearson correlation analysis was used to examine the relationship between environmental factors and *Stephanodiscus* and *Synedra* cell counts. Data were processed with SPSS v. 12.0 (IBM Corp., Armonk, NY, USA).

Results

Environmental characteristics of Water quality

Average annual water temperature, DO and conductivity measurements were higher at PD2 than at PD3 every year (*Table 1*). The average annual water temperature of the three sites was 16.8–20.0°C (*Table 1*). The lowest water temperatures were recorded in March (≤10°C). In July and August, the water temperature rose to ≥20°C (*Fig. 2*). The average annual DO ranged from 10.2 to 11.0 mg/L at PD1, 11.5 to 12.7 mg/L at PD2 and 9.8 to 10.4 mg/L at PD3. The average annual conductivity at PD2 was 236 to 271 μS/cm, whereas that at PD3 was 119 to 137 μS/cm. Electrical conductivity at PD2 was twice that of PD3. The conductivity at PD1 was intermediate relative to those at the other two sites (206 to 220 μS/cm). There were clear differences in some nutrients among three sites (ANOVA, $P < 0.01$): TN, TP, DTN, and DTP values were higher in PD2 compared to PD3 in all years of the survey period (*Table 1*). The average annual TP in PD3 ranged from 0.012 to 0.017 mg/L (i.e., less than 0.020 mg/L), and it had a broader range in PD2 that was typically greater than 0.030 mg/L (0.035 to 0.048 mg/L). The average annual TN was 1.857 to 2.095 mg/L at PD1, 1.959 to 2.404 mg/L at PD2 and 1.636 to 1.828 mg/L at PD3 (*Table 1*). Trends in DTN and DTP were similar to those of TN and TP, respectively. At PD1, the average annual DO ranged from 10.2 to 11.0 mg/L. Si concentrations were higher at PD3 (0.966 to 1.774 mg/L) compared to PD2 (0.922 to 1.460) (*Table 1*).

Table 1. *Differences in the values of environmental parameters at three sites in Lake Paldang from 2014 to 2017*

Site	Year	WT (°C)	DO (mg/L)	Cond. (μS/cm)	TP (mg/L)	DTP (mg/L)	TN (mg/L)	DTN (mg/L)	Si (mg/L)
PD1	2014	18.4	11.0	206	0.024	0.014	1.929	1.835	-
	2015	18.2	10.2	220	0.023	0.013	1.857	1.786	0.731
	2016	18.3	10.4	215	0.024	0.011	2.027	1.961	1.175
	2017	18.9	10.5	211	0.027	0.011	2.095	2.018	1.511
PD2	2014	18.9	12.7	236	0.038	0.020	2.173	2.046	-
	2015	19.3	12.0	271	0.035	0.019	1.959	1.862	0.922
	2016	19.1	11.6	265	0.035	0.015	2.250	2.152	1.306
	2017	20.0	11.5	263	0.048	0.023	2.404	2.299	1.460
PD3	2014	16.8	10.4	119	0.012	0.006	1.705	1.636	-
	2015	17.7	10.1	135	0.013	0.008	1.804	1.730	0.966
	2016	17.5	9.8	137	0.016	0.007	1.879	1.828	1.548
	2017	17.6	10.4	121	0.017	0.007	1.810	1.749	1.774

WT: Water temperature, DO: Dissolved oxygen, Cond.: Conductivity, TP: Total phosphorus, DTP: Dissolved total phosphorus, TN: Total nitrogen, DTN: Dissolved total nitrogen, Si: Silicon

http://www.aloki.hu ● ISSN 1589 1623 (Print) ● ISSN 1785 0037 (Online)
DOI: http://dx.doi.org/10.15666/aeer/1804_51355147

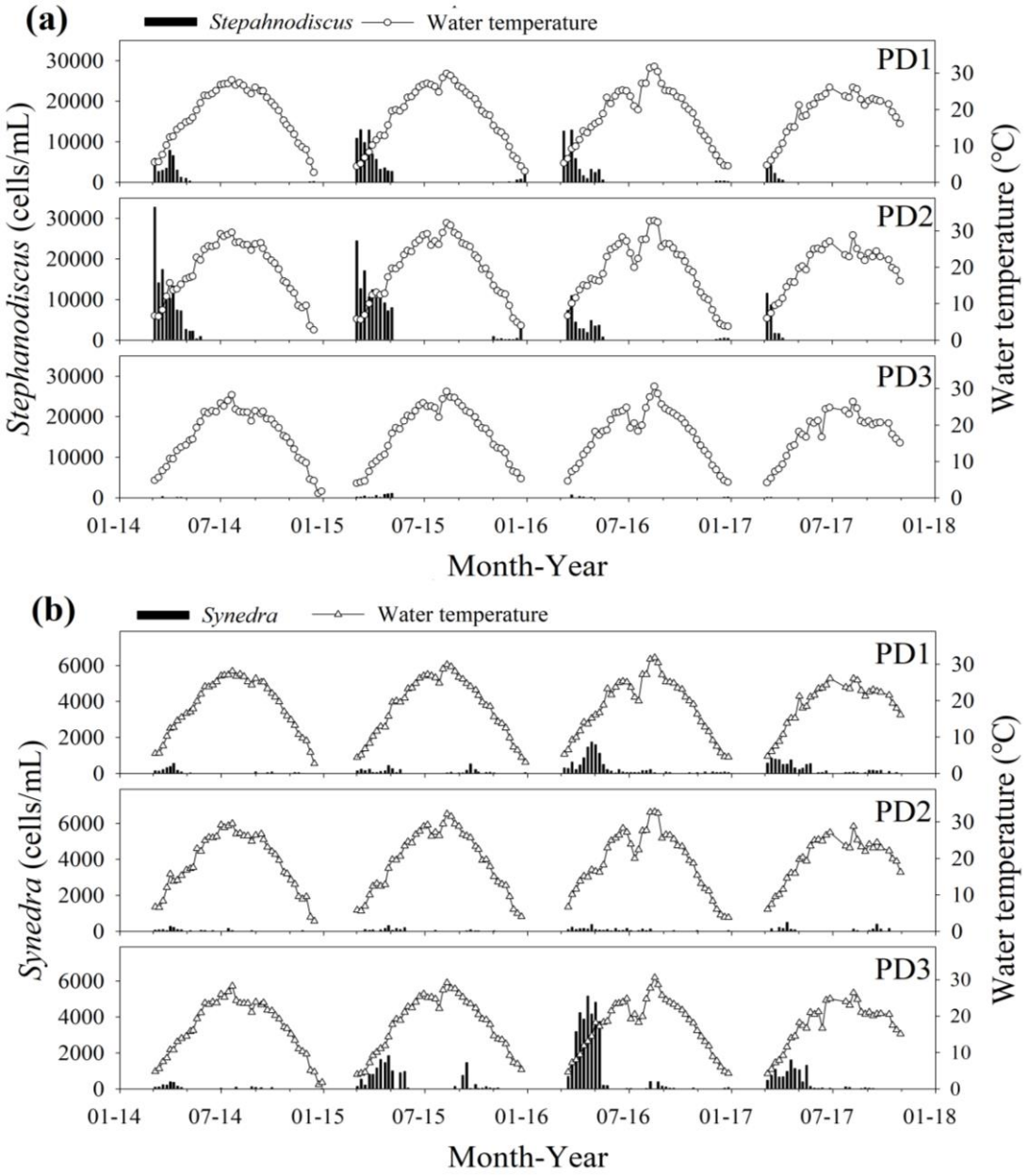

Figure 2. *Weekly variations in water temperature and abundance of Stephanodiscus (a) and Synedra (b) at Lake Paldang from March 2014 to October 2017 (except frost period)*

The concentration ranges of TP and TN in Lake Paldang were 0.006–0.279 mg/L and 1.002–3.466 mg/L, respectively. The maximum measured Si concentration in Lake Paldang was 4.107 mg/L (*Fig. 3*). TP, TN, and Si significantly increased during the summer season because of high rainfall. In fact, the values of all three parameters substantially increased in response to every rainfall event. TN concentrations were high in March at every site and steadily decreased until early June. In early March, Si was ≥1.5 mg/L at PD3, but it was ≤1.0 mg/L at PD1 and PD2. In 2016 and 2017, continuous rainfall between July and November increased Si to ≥1.5 mg/L (*Fig. 3*).

http://www.aloki.hu ● ISSN 1589 1623 (Print) ● ISSN 1785 0037 (Online)
DOI: http://dx.doi.org/10.15666/aeer/1804_51355147

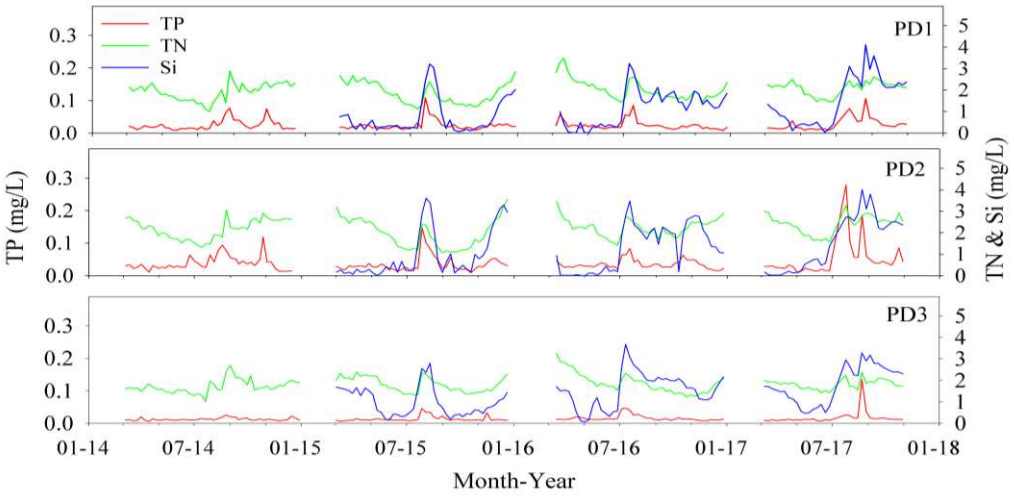

Figure 3. *Temporal variations in TP, TN, and Si from March 2014 to October 2017 (except frost period). TP: Total phosphorus, TN: Total nitrogen, Si: Silicon*

Stephanodiscus and Synedra in relation to water temperature

Stephanodiscus exhibited increased growth during spring and low growth during summer every year. Its cell counts were the highest in early March when the water temperature was <10°C, and it gradually decreased thereafter, until *Stephanodiscus* disappeared almost completely after May. As the water temperature fell once again in November, *Stephanodiscus* began to reappear. In March, PD1 had the highest cell count (12,950 cells/mL). In March 2014, PD2 had a record *Stephanodiscus* count of 32,570 cells/mL, but the cell counts decreased thereafter until May. In 2015, 2016, and 2017, the cell counts peaked in early March, followed by a steady decline (*Fig. 2a*). From PD3, *Stephanodiscus* cell counts were 1,150 cells/mL maximum, which was less than the other two points.

Stephanodiscus was detected within the temperature range of 1.2–22.7°C and had the highest biomass at 6.7°C. At PD1, the cell counts were >10,000 cells/mL within the temperature range of 4.4–9.2°C. At PD2, it was at 5.6–15.7°C that the cell counts reached >10,000 cells/mL. At PD3, the cell counts never exceeded 10,000 cells/mL (*Fig. 4a*).

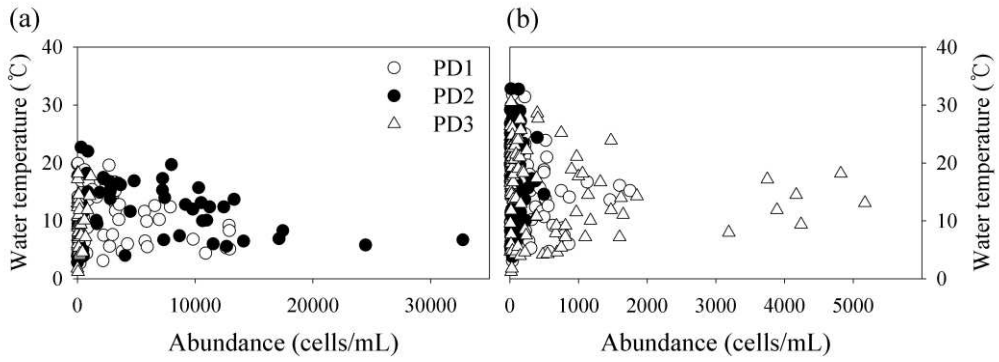

Figure 4. *Abundance of Stephanodiscus (a) and Synedra (b) relative to water temperature at the three sites at Lake Paldang. Note that cyanobacteria cell count scales are different*

http://www.aloki.hu ● ISSN 1589 1623 (Print) ● ISSN 1785 0037 (Online)
DOI: http://dx.doi.org/10.15666/aeer/1804_51355147

The temperature-dependent growth pattern of *Synedra* was essentially the same every year. *Synedra* cell counts began to increase from March and reached their maxima by mid-April when the water temperature was ~14 ± 2°C. Thereafter, the cell counts significantly decreased and remained low. PD1 had the highest *Synedra* cell counts of all three sites (1,750 cells/mL) between March and May 2016. In contrast, the *Synedra* cell counts at PD2 never surpassed 500 cells/mL and were significantly lower than those at the other two sites. The highest *Synedra* counts were obtained at PD3 (5,170 cells/mL) (*Figure 2b*). *Synedra* appeared from March to May and proliferated at 13–15°C, except in 2014, when the mean water temperature was only 11°C at that time of year.

At all three sites, *Synedra* grew under a very wide water temperature range of 1.2-32.8°C. However, cell counts ≥1,000 cells/mL were measured only at 7.2–23.9°C. At PD2, the *Synedra* cell counts never exceeded 1,000 cells/mL (*Fig. 4b*).

Effect of nutrients on the growth of Stephanodiscus and Synedra during springtime

Correlations between nutrient concentration and cell count were determined for *Stephanodiscus* and *Synedra* in springtime (March to May) when their cell counts were >85% of their annual totals. The average springtime TP concentration was the lowest at PD3 (0.011 mg/L). At the same time, PD2 had an average TP concentration of 0.027 mg/L (>2 times that of PD3). PD1 recorded a TP concentration of 0.019 mg/L, which was intermediate between those of PD2 and PD3. PD2 presented with a wider TN concentration range than PD3 (*Fig. 5*). However, the average springtime Si concentration at PD3 was 1.116 mg/L, which substantially exceeded that at PD2 (0.181 mg/L). The Si concentration at PD1 was higher than that at PD2, but lower than that at PD3 (*Fig. 5*). The cell counts of *Stephanodiscus* and *Synedra* of Lake Paldang varied with site during the springtime. The *Stephanodiscus* cell count was high at PD2 (average 6,108 ± 6,954 cells/mL) but significantly lower at PD3 (average 150 ± 264 cells/mL). In contrast, *Synedra* had a relatively lower cell count at PD2 (average 101 ± 103 cells/mL) and a comparatively high cell count at PD3 (average 1,089 ± 1,362 cells/mL).

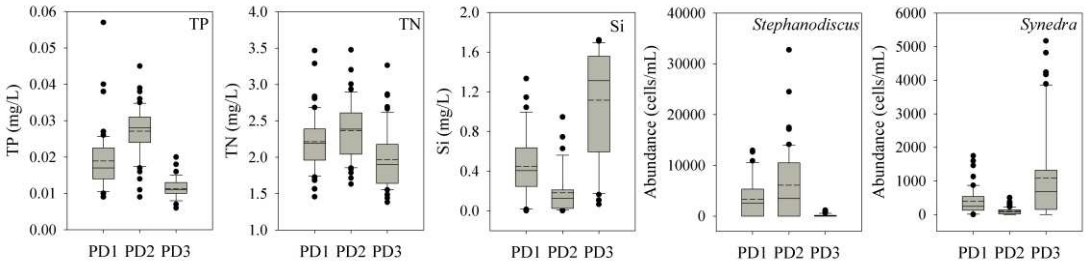

Figure 5. *Range of nutrients (TP, TN, and Si) and diatoms (Stephanodiscus and Synedra) densities during springtime (2014–2017) at Lake Paldang (Median values: horizontal dashed line; mean values: solid line; boxes: 25th and 75th percentiles; error bars: 10thth and 90th percentiles; circles; outliers). TP: Total phosphorus, TN: Total nitrogen, Si: Silicon*

The growth rates of *Stephanodiscus* and *Synedra* in the springtime varied differentially in response to nutrient concentration. *Stephanodiscus* had the highest cell counts when the concentrations of TP, TN, and Si were 0.030 mg/L, 2.688 mg/L, and

http://www.aloki.hu ● ISSN 1589 1623 (Print) ● ISSN 1785 0037 (Online)
DOI: http://dx.doi.org/10.15666/aeer/1804_51355147

0.161 mg/L, respectively. The cell counts of *Synedra* were the highest when the TP, TN, and Si concentrations were 0.020 mg/L, 2.412 mg/L, and 0.473 mg/L, respectively (*Fig. 6*). High TP and TN concentrations increased *Stephanodiscus* cell counts more than they did those of *Synedra*. When TP was ≥0.020 mg/L, *Stephanodiscus* cell counts substantially increased. On the contrary, the cell counts of *Synedra* were the highest when TP was ≤0.020 mg/L. At springtime, Si concentrations were ≤0.4 mg/L, and >70% of the total annual *Stephanodiscus* cells appeared then. In contrast, the *Synedra* cell counts were high even when Si was ≥0.4 mg/L. When TP was ≥0.020 mg/L, and Si was ≤0.4 mg/L, (Si:P ratio <20), the cell count of *Stephanodiscus* increased significantly. Contrarily, there were large numbers of *Synedra* cells when TP was ≤0.020 mg/L and Si was ≥0.4 mg/L (Si:P ratio > 20) (*Fig. 7*).

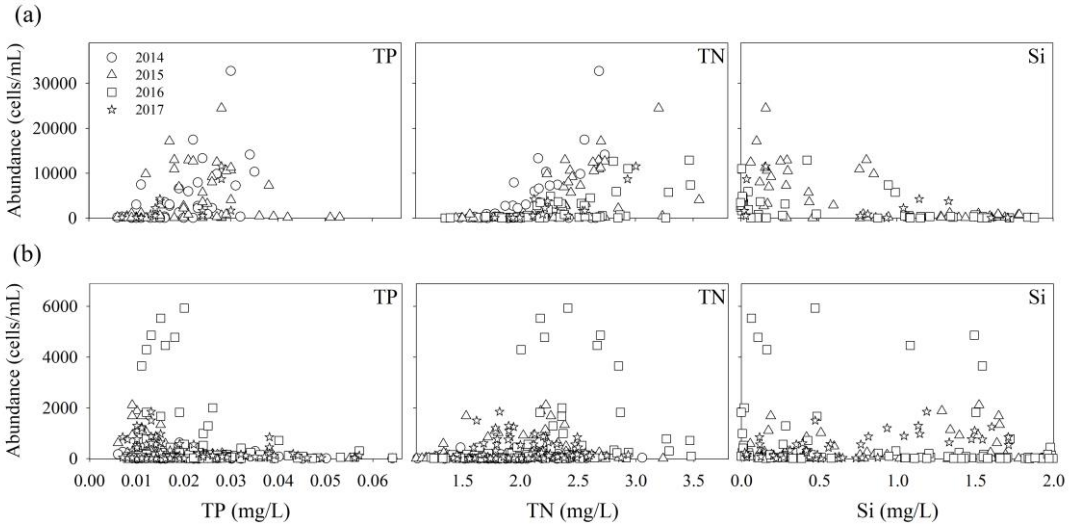

Figure 6. *Comparison of cell counts of Stephanodiscus (a) and Synedra (b) as functions of nutrient (TP, TN, and Si) concentrations in springtime from 2014 to 2017. TP: Total phosphorus, TN: Total nitrogen, Si: Silicon*

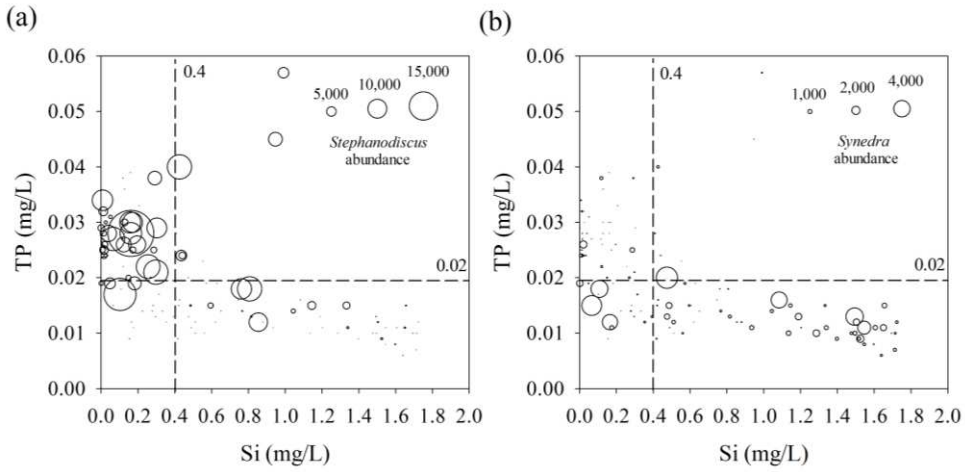

Figure 7. *Distribution of Stephanodiscus (a) and Synedra (b) abundance as functions of nutrient (TP and Si) concentrations during springtime (2015–2017). TP: Total phosphorus, Si: Silicon. Legend unit is 'cells/mL'*

http://www.aloki.hu ● ISSN 1589 1623 (Print) ● ISSN 1785 0037 (Online)
DOI: http://dx.doi.org/10.15666/aeer/1804_51355147

The cell count of *Stephanodiscus* had weak positive correlations with DO, conductivity, and TN, and weak negative correlations with water temperature, Si, and Si:P ratio. The *Synedra* cell counts had weak positive correlations with DO, TN, and N:P ratio, and weak negative correlations with water temperature, conductivity, TP, and Si (*Table 2*). In springtime, the cell count of *Stephanodiscus* had weak negative correlations with water temperature, Si, N:P ratio, and Si:P ratio. In contrast, the *Synedra* cell counts had weak positive correlations with Si, N:P ratio, and Si:P ratio during that period.

Table 2. *Pearson's correlation coefficients between the abundance of two diatoms and environmental parameters during all time periods investigated and during springtime at Lake Paldang*

Parameter	All period		Spring	
	Stephanodiscus	***Synedra***	***Stephanodiscus***	***Synedra***
W.T	-0.368**	-0.187**	-0.416**	-
DO	0.431**	0.120**	0.530**	-0.172*
Cond.	0.221**	-0.206**	0.396**	-0.372*
TP	-	-0.130**	0.442**	-0.203*
TN	0.405**	0.163**	0.584**	-
Si	-0.274**	-0.145**	-0.283**	0.233*
N:P	-	0.278**	-0.286**	0.258**
Si:P	-0.250**	-	-0.320**	0.196*

W.T: Water temperature, Cond.: Conductivity, * $P < 0.05$, ** $P < 0.01$

Discussion

In Lake Paldang, the variations in phytoplankton biomass and the spatial distributions of the dominant species comprising it were greatly affected by environmental factors. Water temperature plays an important role in modifying phytoplankton dynamics (Lee et al., 2013). The present study also showed that the growth of *Stephanodiscus* and *Synedra* were significantly affected by the water temperature of Lake Paldang. Both diatom species had the highest cell counts during spring. This pattern recurred at about the same time each year. Both species preferred low water temperatures, but their cell counts peaked at different ranges of water temperature. It was reported that *Stephanodiscus* adapted to low water temperatures and proliferated at <7°C (Ha et al., 2003). *Synedra* has a similar preference for low water temperatures. Bondarenko and Geuselnikova (2002) reported that the optimal water temperature range for the proliferation of *Synedra acus* var. *radians* was 12–14°C in vitro. The growth rates of both diatom species were negatively correlated with water temperature throughout the survey period, and they were found to prefer low water temperatures to high ones. However, *Stephanodiscus* grew at the range of 1.2–22.7°C whereas *Synedra* proliferated at 1.2–32.8°C. Accordingly, *Synedra* was detected at higher temperatures than *Stephanodiscus*. In addition, *Stephanodiscus* was dominant and had the highest cell count at ≤10°C whereas *Synedra* prevailed at the range of 10.8-15.7°C. In Lake Paldang, *Stephanodiscus* flourished at low water temperatures, and, therefore, occurred earlier than *Synedra.* Both species contributed to the spring bloom at relatively low water temperatures. However, since they have different

http://www.aloki.hu ● ISSN 1589 1623 (Print) ● ISSN 1785 0037 (Online)
DOI: http://dx.doi.org/10.15666/aeer/1804_51355147

temperature optima, they would not proliferate or compete for resources simultaneously.

The types of predominant diatoms and their population densities depend on nutrient concentrations. In the Behler See, centric diatoms increased their relative biovolumes by >60% at low Si:P ratio (<15). Contrarily, Fragilariaceae species, which are linear, had comparatively low biomasses at low Si:P ratio (Makulla and Sommer, 1993). *Stephanodiscus minutulus,* a centric diatom, required significantly more phosphorus than silicon. Its optimal Si:P (molar) ratio was ~1.0. In contrast, *Synedra* grew well despite the lack of phosphorus, but did not flourish at low silicon concentrations (Kilham et al., 1986). According to Tilman et al. (1982), *Synedra* was more competitive than *Stephanodiscus* when phosphorus was limited. In a culture with limited phosphorus (Si:P ratio> 75), *Asterionella* and *Fragilaria* predominated but *Stephanodiscus* failed to thrive (Van Donk and Kilham, 1990). In the present study, PD2 presented with *Stephanodiscus* blooms but *Synedra* was nearly absent there. Contrarily, PD3 had a low *Stephanodiscus* biomass but substantial quantities of *Synedra* (*Figure 5*). The two watershed influencing Lake Paldang (Namhan River and Bukhan River) have very different water quality properties. The Namhan River has a high nutrient concentration because it receives pollution inputs from widely dispersed point- and nonpoint sources. In contrast, the upper part of the Bukhan River is adjacent to mountains and is mesotrophic or oligotrophic (Park et al., 2004; Kim et al., 2014). In addition, the watershed of the Bukhan River is more prone to silicate weathering than that of the Namhan River. Therefore, the silicic acid concentration is higher in the Bukhan River than in the Namhan River (Ryu et al., 2008). PD2 had low silicon and high phosphorus levels; so, its average springtime Si:P ratio was as low as 8. For this reason, *Stephanodiscus* could bloom at PD2, since it prefers low Si:P ratio. As the *Stephanodiscus* population decreased at PD2, the Si:P ratio remained low there and the growth of *Synedra* was restricted, even when its optimal water temperature was attained. PD3 showed high silicon and relatively low phosphorus levels. At this site, the average springtime Si:P ratio was 109. Since *Synedra* prefers high Si:P ratio, its population density at PD3 was very high. However, *Stephanodiscus* populations were very sparse because they fail to thrive under phosphorus restriction. Consequently, *Stephanodiscus* can flourish at water temperatures <10°C, since its growth is positively correlated with phosphorus and nitrogen concentrations and the levels of this nutrient are relatively high in springtime ($r = 0.442$, $P < 0.01$, $r = 0.584$, $P < 0.01$, respectively). Therefore, its population density would be high at elevated phosphorus concentrations (>0.02 mg/L) and low Si:P ratio. Contrarily, *Synedra* prefers higher water temperatures (10.8–15.7°C) than *Stephanodiscus*. Moreover, *Synedra* tends to flourish at high silicon levels (>0.4 mg/L). *Synedra* showed weak negative correlations with silicon concentration during springtime. However, throughout the study period, there were negative correlations as silicon concentration increased during summer due to heavy rain. *Synedra* did not appear during summer because of high water temperatures. From our analysis, it can be inferred that both diatoms can grow at low water temperatures, but they have different temperature range preferences. In addition, *Stephanodiscus* and *Synedra* flourish at low Si:P ratio and high Si:P ratio, respectively.

Both *Stephanodiscus* and *Synedra* were detected at PD1. Since PD1 was located at the boundary or interface of PD2 and PD3, its nutrient levels were the combination of those for the other two sites. In springtime, the average cell count of *Stephanodiscus* was 3,291 cells/mL, which was only ~54% that of PD2. During the same period, the

http://www.aloki.hu ● ISSN 1589 1623 (Print) ● ISSN 1785 0037 (Online)
DOI: http://dx.doi.org/10.15666/aeer/1804_51355147

average cell count of *Synedra* was 391 cells/mL, which corresponded to ~36% of that of PD3. At PD1, the highest cell counts for *Stephanodiscus* were recorded in early March. The same phenomenon was observed at PD2. *Synedra* cell counts peaked in mid-April. The same trend was found at PD3 (*Figure 3*). The growth rates and patterns of both diatoms at PD1 resembled those observed at the Namhan (PD2) and Bukhan (PD3) Rivers. Relative to the inflow into Lake Paldang, the cell counts at PD1 were lower than those at the other sites. Therefore, the inflow of the Bukhan and Namhan Rivers diluted the diatoms. At PD1, then, the growth rates of *Stephanodiscus* and *Synedra* were affected mainly by the inflow from the upper regions rather than their own population densities. However, more detailed investigation is necessary in future to estimate the effects of rainfall, flow rate, and zooplankton predation on diatom growth.

Conclusions

Through this study, it was demonstrated that the timing and magnitude of spring diatom bloom are affected by physicochemical factors like water temperature, and nutrient levels and their ratios. (1) Both *Stephanodiscus* and *Synedra* prefer low water temperatures, but *Synedra* biomass reaches it maxima at higher temperatures. (2) The two diatoms have different optima for available nutrient concentrations. Low levels of phosphorus and silicon limit the growth of *Stephanodiscus* and *Synedra*, respectively. (3) Growth of these diatoms is affected both by nutrient concentrations (especially phosphorus and silicon) and water temperature. The growth rates of *Stephanodiscus* and *Synedra* are controlled by multiple factors. Optimal water temperature, and phosphorus and silicon concentrations and their ratios can promote diatom growth. These factors must be considered in the prediction of the growth trends and population densities of *Stephanodiscus* and *Synedra* in Lake Paldang. However, in order to clearly identify the effects of environmental factors on the appearances of *Stephanodiscus* and *Synedra*, future research should be conducted using various types of statistical analyses for factors such as hydraulic and hydrologic factors, competition with other species, and predation.

Acknowledgements. This research was supported by a grant from the National Institute of Environmental Research (NIER), funded by the Ministry of Environment (ME) of the Republic of Korea (NIER-2020-01-01-022).

REFERENCES

[1] Bleiker, W., Schanz, F. (1989): Influence of environmental factors on the phytoplankton spring bloom in lake Zürich. – Aquatic Sciences 51(1): 47-58.

[2] Bondarenko, N. A., Geuselnikova, N. Y. (2002): Studies on *Synedra acus* Kutz. var. *radians* (*Kutz.*) Hust. (*Bacillariophyta*) in culture. – International Journal on Algae 4(1): 85-95.

[3] Clegg, M. R., Maberly, S. C., Jones, R. J. (2003): Behavioural response of freshwater phytoplanktonic flagellates to a temperature gradient. – European Journal of Phycology 38(3): 195-203.

[4] Deng, X. W., Tao, M., Zhang, L., Xie, P., Chen, J., Zhang, J. (2013): Relationships between Odors and Algae and Water Quality in Dongting Lake. – Research of Environmental Sciences 26(1): 16-21.

http://www.aloki.hu ● ISSN 1589 1623 (Print) ● ISSN 1785 0037 (Online)
DOI: http://dx.doi.org/10.15666/aeer/1804_51355147

[5] Ha, K., Jang, M. H., Joo, G. J. (2003): Winter *Stephanodiscus* bloom development in the Nakdong River regulated by an estuary dam and tributaries. – Hydrobiologia 506(1-3): 221-227.
[6] Hijnen, W. A. M., Dullemont, Y. J., Schijven, J. F., Hanzens-Brouwer, A. J., Rosielle, M., Medema, G. (2007): Removal and fate of *Cryptosoridium parvum*, *Closteridium perfringens* and small-sized centric diatoms (*Stephanodiscus hantzschii*) in slow sand filters. – Water Research 41(10): 2151-2162.
[7] Joh, G. (2010): Algal flora of Korea 3 (1). Chrysophyta: Bacillariophyceae: Centrales. Freshwater diatoms I. – National Institute of Biological Resources, Incheon.
[8] Joh, G., Lee, J. H., Lee, K., Yoon, S. K. (2010): Algal flora of Korea 3 (2). Chrysophyta: Bacillariophyceae: Pennales: Araphidineae: Diatomaceae. Freshwater diatoms II. – National Institute of Biological Resources, Incheon.
[9] Joh, G., Choi, Y. S., Shin, J. K., Lee, J. (2011): Problematic algae in the sedimentation and filtration process of water treatment plants. – Journal of Water Supply: Research and Technology-AQUA 60(4): 219-230.
[10] John, D. M., Whittonand, B. A., Brook, A. J. (2002): The freshwater algal flora of the British Isles. – Cambridge University Press, Cambridge.
[11] Jüttner, F. (1983): Volatile odorous excretion products of algae and their occurrence in the natural aquatic environment. – Water Sciences & Technology 15(6-7): 247-257.
[12] Kilham, P., Kilham, S. S., Hecky, R. E. (1986): Hypothesized resource relationships among African planktonic diatoms. – Limnology and Oceanography 31(6): 1169-1181.
[13] Kim, D. W., Jang, M. J., Han, I. S. (2014): Determination of focused control pollutant source by analysis of pollutant delivery characteristics in unit watershed upper Paldang Lake. – Journal of Korean Society of Environmental Engineers 36(5): 367-377.
[14] Lee, K. R., Sung, E. J., Park, H. J., Park, C. H., Park, M. H., Hwang, S. J. (2013): Phytoplankton community change of Lake Paldang by increasing CO_2 and temperature during spring cold water season. – Korean Journal of Ecology and Environment 46(4): 588-595.
[15] Lv, H., Yang, J., Liu, L., Yu, X., Yu, Z., Chiang, P. (2014): Temperature and nutrients are significant drivers of seasonal shift in phytoplankton community from a drinking water reservoir, subtropical China. – Environmental Sciences and Pollution Research 21(9): 5917-5928.
[16] Makulla, A., Sommer, U. (1993): Relationships between resource ratios and phytoplankton species composition during spring in five North German lakes. – Limnology and Oceanography 38(4): 846-856.
[17] Marshall, T. C., Peters, R. H. (1989): General patterns in the seasonal development of chlorophyll *a* for temperate lakes. – Limnology and Oceanography 34(5): 856-867.
[18] Masaki, A., Seki, H. (1984): Spring bloom in hypereutrophic lake, Lake Kasumigaura, Japan-IV: Inductive factors for phytoplankton bloom. – Water Research 18(7): 869-876.
[19] McCauley, E., Downing, J. (1991): Different effects of phosphorus and nitrogen on chlorophyll concentration in oligotrophic and eutrophic lakes. – Canadian Journal of Fisheries and Aquatic Sciences 48(12): 2552-2553.
[20] Ministry of Environment (ME). (2016): Standard method for the examination of water pollution. – Ministry of Environment, Sejong.
[21] Muylaert, K., Sabbe, K. (1999): Spring phytoplankton assemblages in and around the maximum turbidity zone of the estuaries of the Elbe (Germany), the Schelde (Belgium/The Netherlands), and the Gironde (France). – Journal of Marine Systems 22(2-3): 133-149.
[22] Park, H. K., Jheong, W. H. (2003): Long-term changes of algal growth in Lake Paldang. – Journal of Korean Society on Water Environment 19(6): 673-684.
[23] Park, H. K., Byeon, M. S., Kim, E. K., Lee, H. J., Chun, M. J., Jung, D. J. (2004): Water quality and phytoplankton distribution pattern in upper inflow rivers of Lake Paldang. – Journal of Korean Society on Water Environment 20(6): 615-624.

http://www.aloki.hu ● ISSN 1589 1623 (Print) ● ISSN 1785 0037 (Online)
DOI: http://dx.doi.org/10.15666/aeer/1804_51355147

[24] Reavie, E. D., Cai, M., Twiss, M. R., Carrick, H. J., Davis, T. W., Johengen, T. H., Gossiaux, D., Smith, D. E., Palladino, D., Burtner, A., Sgro, G. V. (2016): Winter–spring diatom production in Lake Erie is an important driver of summer hypoxia. – Journal of Great Lakes Research 40(3): 608-618.
[25] Reynolds, C. S. (2006): The ecology of phytoplankton. – Cambridge University Press, Cambridge.
[26] Round, F. E., Crawford, R. M., Mann, D. G. (1990): The diatoms: biology and morphology of the genera. – Cambridge University Press, Cambridge.
[27] Ryu, J. S., Lee, K. S., Chang, H. W., Shin, H. S. (2008): Chemical weathering of carbonates and silicates in the Han River basin, South Korea. – Chemical Geology 247(1-2): 66-80.
[28] Schindler, D. W., Bayley, S. E., Parker, B. R. (1996): The effects of climatic warming on the properties of Boreal lakes and streams at the Experimental Lakes Area, Northwestern Ontario. – Limnology and Oceanography 41(5): 1004-1017.
[29] Schindler, D. W. (2006): Recent advances in the understanding and management of eutrophication. – Limnology and Oceanography 51(1): 356-363.
[30] Shatwell, T., Köhler, J., Nicklisch, A. (2013): Temperature and photoperiod interactions with silicon-limited growth and competition of two diatoms. – Journal of Plankton Research 35(5): 957-971.
[31] Sommer, U. (1985): Comparison between steady state and non-steady state competition: experiments with natural phytoplankton. – Limnology and Oceanography 30(2): 335-346.
[32] Teubner, K., Dokulil, M. T. (2002): Ecological stoichiometry of TN: TP: SRSi in freshwaters: nutrient ratios and seasonal shifts in phytoplankton assemblages. – Archiv fur Hydrobiologie 154(4): 625-646.
[33] Tilman, D., Mattson, M., Langer, S. (1981): Competition and nutrient kinetics along a temperature gradient: an experimental test of a mechanistic approach to niche theory. – Limnology and Oceanography 26(6): 1020-1033.
[34] Tilman, D., Kilham, S. S., Kilham, P. (1982): Phytoplankton community ecology: the role of limiting nutrients. – Annual Review of Ecology, Evolution, and Systematics 13(1): 349-372.
[35] Tilman, D., Kiesling, R., Sterner, R., Kilham, S. S., Johnson, F. A. (1986): Green, bluegreen and diatom algae: taxonomic differences in competitive ability for phosphorus, silicon and nitrogen. – Archiv fur Hydrobiologie 106(4): 473-485.
[36] Tsuchida, A., Hara, Y., Seki, H. (1984): Spring bloom in a ypereutrophic Lake, Lake Kasumigaura, Japan V: factors controlling natural population of phytoplankton. – Water Research 18(7): 877-883.
[37] Van Donk, E., Kilham, S. S. (1990): Temperature effects on silicon and phosphorus limited growth and competitive interactions among three diatoms. – Journal of Phycology 26(1): 46-50.
[38] Wu, Z., Cai, Y., Liu, X., Xu, C. P., Chen, Y., Zhang, L. (2013): Temporal and spatial variability of phytoplankton in Lake Poyang: the largest freshwater lake in China. – Journal of Great Lakes Research 39(3): 476-483.
[39] Ye, L., Han, X. Q., Xu, Y. Y., Cai, G. H. (2007): Spatial analysis for spring bloom and nutrient limitation in Xiangxi Bay of Three Gorges Reservoir. – Environmental Monitoring and Assessment 127(1-3): 135-145.

http://www.aloki.hu ● ISSN 1589 1623 (Print) ● ISSN 1785 0037 (Online)
DOI: http://dx.doi.org/10.15666/aeer/1804_51355147

HISTORY OF PRION PROTEIN GENE (*PRNP*) POLYMORPHISM IN SHEEP AND SCIENTIFIC FINDINGS

IQBAL, A.[1] – HE, X.[1] – YUE, D.[1] – LIU, X.[1] – MEMON, S.[2] – XI, D.[1] – DENG, W.[1*]

[1]*Yunnan Provincial Key Laboratory of Animal Nutrition and Feed, Faculty of Animal Science and Technology, Yunnan Agricultural University, Kunming, PR China*

[2]*Yunnan Animal Science and Veterinary Institute, Kunming, PR China*

**Corresponding author*
e-mail: 1692425306@qq.com

(Received 15th Dec 2019; accepted 25th May 2020)

Abstract. Scrapie is basically a kind of disease that originally was specific to European countries, but from England it spread all over the world to Canada, South Africa, Australia, New Zealand and many other countries. Scrapie is a prion disease which is fatal and results in or can be characterized by the degeneration of the nervous system. It belongs to transmissible spongiform encephalopathies (TSEs) infecting small ruminants including sheep and goat. Sheep susceptibility or resistance to classical scrapie is highly supervised by the polymorphisms at codons 136, 154 and 171 of the *PRNP*. In this review, we found that countries like Romania, Finland, Italy, Slovakia, Germany, Greece, Spain, Poland, Turkey, Iran, Brazil, England, Portugal, Hungary, Austria, and Czech Republic, are susceptible to scrapie, while in Pakistan, China, Algeria, West Africa, America, Burkina Faso, and Niger are those countries where sheep are not susceptible to this disease. From these studies, we can clearly conclude that China and Pakistan are the countries where sheep show more resistance to scrapie. We focused to summarize the *PRNP* polymorphism at 136, 154, and 171 in sheep and some important findings in major parts of the world.
Keywords: *scrapie, transmissible spongiform encephalopathies (TSEs), European countries, history, prion*

Introduction

Approximately, 70.7% of the total sheep population is present in Asia and 35.89% of the total population of sheep is present in China which has become the leading country for sheep products. But in China, no case of scrapie in sheep has been found so far, whereas in the countries like England, Greece, Turkey and other small European countries scrapie is on red alert. Where sheep (*Ovis aries*) and goat (*Capra aegagrus hircus)* have many resemblances, their scientific taxonomy eventually split, have distinct species and genus, whereas sheep and goat have 54 and 60 chromosomes simultaneously. The polymorphism of the *PRNP* gene plays a fundamental role in prion disease. Scrapie is resulting in or characterized by the degeneration of the nervous system affecting sheep and belongs to a group of a prion disease that naturally occurs in sheep. *PRNP* is responsible for negative influence on the financial loss, such as the cashmere yield, wool thickness (Lan et al., 2012) and milk yield (Vitezica et al., 2013) as well as the waistline, body length (Yang et al., 2016), rump length (Yang et al., 2018), and weight. Almost the same mutation of *PRNP* present in sheep, has also been determined in goat (White et al., 2008; Zhou et al., 2013). The only responsible factor for scrapie that has been determined until now is a prion. Scrapie is not like a viral or bacterial disease which have causal agent, rather it is a genetical disease making it difficult to cure. The possibility for the elimination of this disease is wholly associated with polymorphisms of the *PRNP*. Sheep and goat are not the only victims of prion disease as it has been reported in almost all vital living species of animals with different

http://www.aloki.hu ● ISSN 1589 1623 (Print) ● ISSN 1785 0037 (Online)
DOI: http://dx.doi.org/10.15666/aeer/1804_51495173

names (*Table 1*). The first human victimization to scrapie were the farmers or the sheep owners who were directly affected by the disease. During the 20th century, many ideas on the nature of the causative agent of TSEs were published (*Table 2*) while with the passage of time, the majority of these revealed to be unwarranted. Prion disease affects both animals and humans (Yaman and Ün, 2017) but until 1990s scientists failed to provide any evidence of transmission of disease to humans (Van Duijn et al., 1998).

Table 1. *Affected species with prion diseases (Mabbott, 2017)*

Disease	Species
Scrapie	Sheep, goats, mouflon
Iatrogenic Creutzfeldt-Jakob disease (CJD)	Human
Sporadic Creutzfeldt-Jakob disease	Human
Variant Creutzfeldt-Jakob disease	Human
Familial Creutzfeldt-Jakob disease	Human
Gerstmann-Straussler-Scheinker syndrome	Human
Kuru	Human
Fatal familial insomnia	Human
Bovine spongiform encephalopathy	Cattle
Chronic wasting disease	Elk, deer, moose
Transmissible mink encephalopathy	Mink
Feline spongiform encephalopathy	Domestic and zoological cats
Exotic ungulate encephalopathy	Nyala, kudu

Table 2. *Names of causative agents given by different scientists from 1912 to 1991*

Year	TSE agents	Reference
1914	Sarcosporidia	M'Gowan (1914)
1938	A filterable virus	Cuillé and Chelle (1938)
1954	A slow virus	Sigurdsson (1954)
1966	A replicating polysaccharide	Alper et al. (1967)
1967	A protein	Pattison and Jones (1967)
1967	A replicating membrane	Gibbons and Hunter (1967)
1968	A DNA-polysaccharide complex	Adams and Caspary (1968)
1972	A viroid	Diener (1972)
1978	A lipid	Alper et al. (1978)
1979	A Spiroplasma sp.	Bastian (1979)
1979	A virino	Dickinson (1979)
1982	A prion	Prusiner (1982)
1984	A virus	Manuelidis (1996)
1989	Mitochondria (l nucleic acid(s))	Aiken et al. (1990)
1991	A holoprion, consisting of abnormal prp (PrP in the scrapie specific conformation, the apoprion) and a (dispensible) nucleic acid (the coprion)	Weissmann (1991)

http://www.aloki.hu ● ISSN 1589 1623 (Print) ● ISSN 1785 0037 (Online)
DOI: http://dx.doi.org/10.15666/aeer/1804_51495173

Scrapie is the disease with the maximum and oldest publications as explicit journals allude to a paper going back to the year 1732 as the initial report of scrapie (Detwiler and Baylis, 2003). In 1772 scrapie was accounted for to be known for around 40 years, a point in time going back to the year 1732. This distemper disease is normally said to be remains of almost forty years in England (Comber, 1772). All scholars were devoted to the quest for the origin of the disease. A large number of proposed causes were diagnosed by all methods like the number of prescribed pathogens set forward all through the twentieth century. Since the 1930s, scrapie examination was reinforced when impressive money related misfortunes to the sheep business were brought about by expanding measurements of cases. These harms likewise advance studies on the precise idea of the infective reason, besides parasites (M'Gowan, 1914) and bacteria (Bastian, 1979) as causative agents, virus infection was the most frequently proposed principle, already formulated in 1938 (Cuillé and Chelle, 1938). In 1954, the word of a "slow virus infection" was presented the first time (Sigurdsson, 1954). Though, in 1966, a substitute to the viral origin was hypothesized as the cause, i.e., polysaccharides (Alper et al., 1966; Alper et al., 1967) or lipids (Alper et al., 1978). In 1967, for the first time, a protein was predictable as an infective cause (Pattison and Jones, 1967), and the first "protein-only- hypothesis" was articulated (Griffith, 1967), which was followed in the 1970s by the "virino" theory (Dickinson, 1979). At long last, in light of the opposition of the pathogen, in 1982, "proteinaceous irresistible molecule" (abbreviation: prion) was presented (Prusiner, 1982) and the transformation of a healthy cellular protein (PRPC) into a pathological isoform (PRPSc) as a critical event of TSE pathogenesis was proposed not long after (Oesch et al., 1985).

The investigation of scrapie was complex by the circumstance that in previous times, many new diseases like Drehkrankheit, Kreuzdrehe, and Gnubberkrankheit were confused with scrapie. Numerous scholars believed at least one of them to be indistinct with or separate from scrapie. Some particular authors attempted to recognize "Drehkrankheit," "Gnubberkrankheit," "Kreuzdrehe," and "Traberkrankheit." Whereas a lot of them segregate among "Drehkrankheit" and "Kreuzdrehe" from one viewpoint and "Traberkrankheit" on the other (Frank, 1820; Ribbe, 1821; Hering, 1849; Erdt, 1861; May, 1868), there were other writers who considered "Kreuzdrehe" and "Traberkrankheit" to be the identical but to be dissimilar from "Gnubberkrankheit" (Wagenfeld, 1829). This mistake of terms, just as the indistinct and confounding portrayal of the indications of scrapie and of different diseases, indicating scrapie recognized in the year 1750. Different terms that were utilized to make reference to scrapie are mentioned (*Table 3*).

Table 3. *Historical names of scrapie given by locals in different regions of the world*

	Name of scrapie	Country	Reference
1	Basqvilla Disease	Spain	von Richthofen (1828)
2	Cuddie Trot	Scotland	Healy et al. (2003)
3	Drab(en)	Germany	von Richthofen (1827)
4	Dreb/Deeb	Germany	Frank (1820)
5	Drehkrankheit	Germany	Schneider et al. (2008)
6	Gaubber/G(n)aup(p)er	Germany	Schneider et al. (2008)
7	Gnubberkrankheit	Germany	Cassirer (1898)
8	Knopper	Germany	Frank (1820)

http://www.aloki.hu ● ISSN 1589 1623 (Print) ● ISSN 1785 0037 (Online)
DOI: http://dx.doi.org/10.15666/aeer/1804_51495173

9	Khujali	India	Katiyar (1962)
10	Kreu(t)zdrehe(n)	Germany	von Richthofen (1827)
11	Kreutzschlagen	Germany	Albert and Brunn (1818)
12	La maladie convulsive	France	Liberski and Jaskólski (2002)
13	La maladie foll(i)e	France	Beck et al. (1964)
14	La maladie trotteurs	France	Besnoit (1899)
15	La prurigo lombaire	France	Liberski and Jaskólski (2002)
16	La Tremblante	France	Beck et al. (1964)
17	Mukoo	India	Katiyar (1962)
18	Petermännchen	Germany	Erdt (1861)
19	Prurigo lombaire	France	Besnoit (1899)
20	Prurigo lumbar	Spain	Yam (2003)
21	Reiberkrankheit	Germany	Beck et al. (1964)
22	Reiber-Uebel	Germany	von Richthofen (1827)
23	Rickets	England	Beck et al. (1964)
24	Rida	Iceland	Palsson (1979)
25	Rub/Rubbers	England	Beck et al. (1964)
26	Rubbing disease	England	Parry (1983)
27	Ruppe	Germany	Frank (1820)
28	Scabies dorsalis	Germany	Hörnlimann et al. (2001)
29	Schrucken/Schru(c)kigsein	Germany	Frank (1820)
30	Scratchie	Scotland	Liberski and Jaskólski (2002)
31	Shakings	England	Beck et al. (1964)
32	Shrewcroft	England	Liberski and Jaskólski (2002)
33	Shrugginess	England	Parry (1983)
34	Spruckigkeit	Germany	Schneider et al. (2008)
35	Tempermänner	Germany	Erdt (1861)
36	Trab(en)/Traberkrankheit	Germany	Beck et al. (1964)
37	Trotting disease	England	Schneider et al. (2008)
38	Trze ̨sawka	Poland	Liberski and Jaskólski (2002)
39	Wetzkrankheit	Germany	May (1868)
40	Yeukie pine	Scotland	Healy et al. (2003)
41	Zitterkrankheit	Germany	May (1868)

The description of literature is that scrapie was firstly born in Europe in the 18th century but until now the presence of scrapie in Europe is a dangerous sign for all over the world due to the threat of its spreading (*Fig. 1*) from England to all over the world (Detwiler and Baylis, 2003). The evidence of the scrapie in the European Union and the nearby regions from the day first till 2016 (EFSA, 2017) were as follows.

In 1987, 442 animals infected with scrapie were reported in England. In 1992, the number of animals infected with scrapie were reported as 37301. This number was reported as 1123 in 2002 and 610 animals in 2013, after that there were no reports of animals infected with scrapie. In Ireland, 15 animals were reported in 1990, in 2002, a total of 334 animals were reported, and in 2017, the disease showed peak time. Scrapie disease in France was first published in 1993, in 2002, 240 patients were reported. The first case was reported in Germany in 1991, the number of animals

http://www.aloki.hu ● ISSN 1589 1623 (Print) ● ISSN 1785 0037 (Online)
DOI: http://dx.doi.org/10.15666/aeer/1804_51495173

reported in 2002 were 7, while in 2001, 125 animals were published (EFSA, 2017). The first case of scrapie in Spain was reported in 1987, and in 2001, it was observed that the number of infected animals had been increased (Acín et al., 2004). Spain has started to work on the genotypic characterization of various races in this sense, to develop different strategies for each race and to prepare the laws governing these programs (Ugarte and Gabina, 2004). The first case of scrapie in Greece was settled in the north of the country in 1986, and the second case was diagnosed in 1997, the latter case was diagnosed after 11 years. The second case was seen near the region where the first case was observed, which was the evidence that the implemented eradication program is inadequate (Leontides et al., 2000). In 2001, there were 18 cases reported in Greece. According to the eradication program in Greece, the herds with the disease were massacred (Billinis et al., 2004). As a result of the breeding policies observed in Europe, the number of scrapie cases has decreased since 2009 (EFSA, 2014). In sheep, 933 scrapie cases were reported in the EU in 2017, which is an increase of 36.2% compared with 2016 (EFSA, 2018). In *Figure 2,* Cosseddu showed us the presence of scrapie in all over the world in 2007.

Resistance and susceptibility

Sheep can be resistant and susceptible to the disease and the majority of susceptible sheep are in European countries. Every one of these discernments lead to the European Union (EU) keeping on developing breeding projects focused at developing the frequency of safe alleles in breeds from all member-states. These European programs are established on five groups of genotypes, from extremely resistant to extremely sensitive, whose alleles ARR and VRQ are considered highly resistant and susceptible to scrapie, respectively (Hunter, 1997).

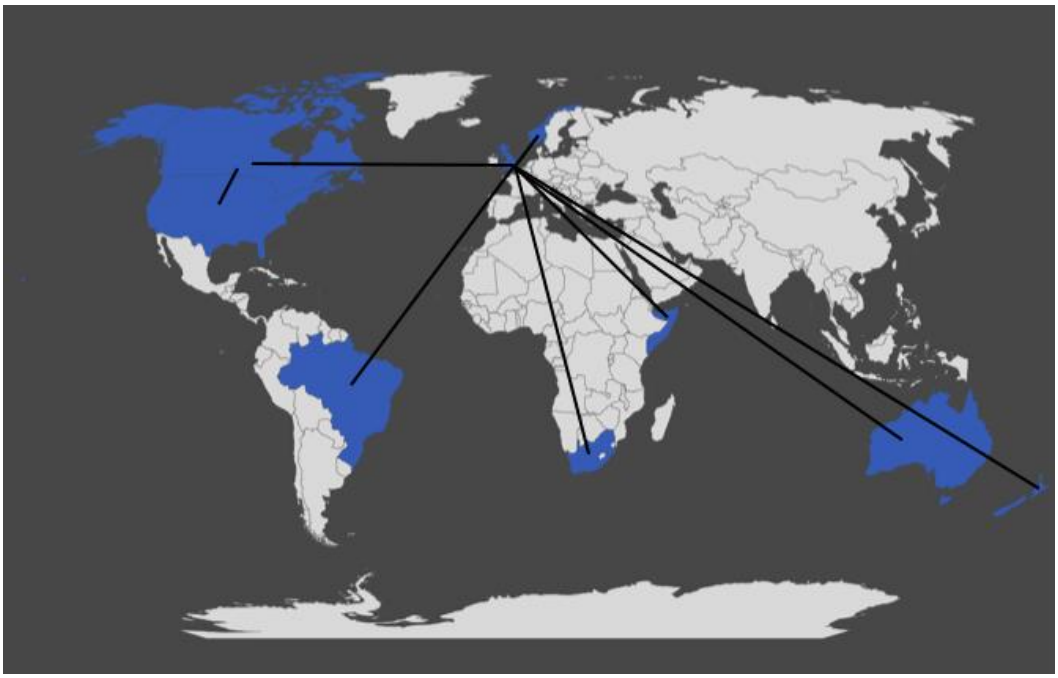

Figure 1. *Spread of scrapie from England to the major parts of the world in 2003 (Detwiler and Baylis, 2003)*

http://www.aloki.hu ● ISSN 1589 1623 (Print) ● ISSN 1785 0037 (Online)
DOI: http://dx.doi.org/10.15666/aeer/1804_51495173

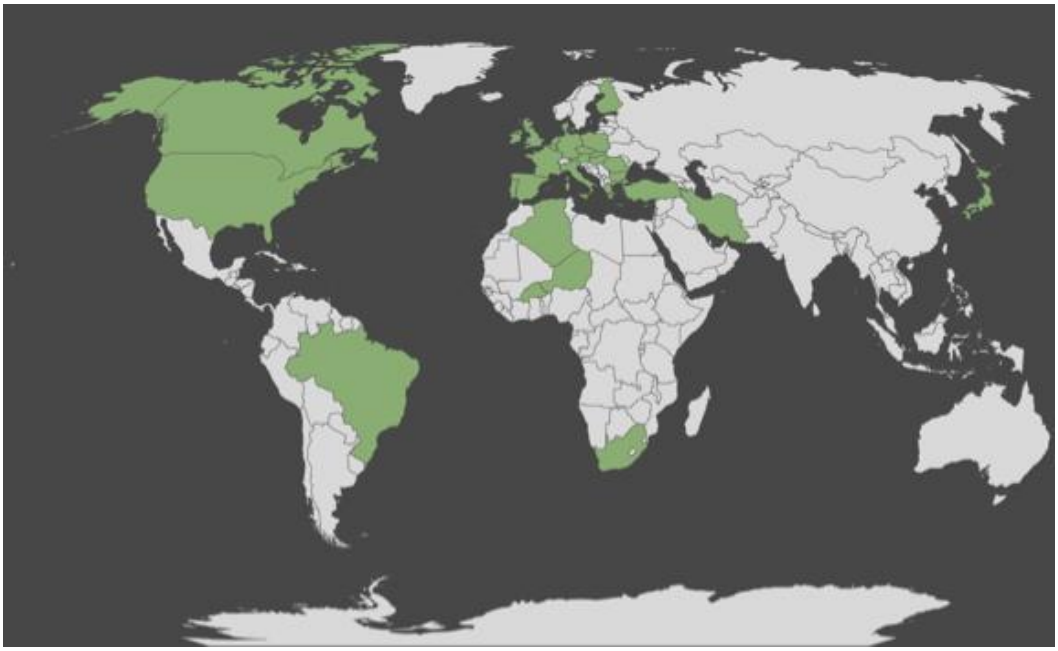

Figure 2. *Scrapie distribution in all over the world in 2007 (Cosseddu et al., 2007)*

As it is clear that polymorphisms at residues 136, 154, and 171 are associated with susceptibility to both, experimental and natural scrapie (Hunter, 1997). In sheep, breeding projects have been set up in a few European nations to expand the ARR allele as much as possible. To evade the negative outcomes of scrapie-safe alleles, it is indispensable to know their populace recurrence. Some programs are still working on the frequencies to get rid of the susceptible alleles. In *Table 4* we can see the genotype groups and the intensity of risk.

Prions and scrapie

Scrapie is a protein misfolding where the normal prp misfolds into abnormal prp that is extremely resistant to enzymatic breakdown within the cell and accumulates, ultimately leading to neurodegeneration. The disease is experimentally transmissible to cattle, goats, and laboratory animals *via* oral, parenteral, and intracerebral routes using homogenates of a brain or lymphoid tissues from infected animals (Pattison et al., 1961). Squirrel monkey was infected by feeding infected tissues and many other species like rats, mice, chimpanzees and many others were infected as well (de Mouton, 2007). The mode of transmission from ewe to lamb or between adults in field environments is not clear. However, oral exposure to fetal membranes or to pastures grazed by infected animals has been implicated as a possible route of vertical and horizontal transmission (Brotherston et al., 1968). Susceptibility to ovine scrapie is controlled by a combination of host genetics. During the course of a prion disease, a largely protease-resistant aggregated form of prp designated abnormal prp, accumulates mainly in the brain, and maybe the main or only constituent of the prion but in some species little or no signs of accumulation other than brain were found (de Mouton, 2007). The alteration of the normal prp into the abnormal prp is the vital route of transmission and pathogenesis of the prion disease in sheep. Transgenic studies say that abnormal prp acts as a template

http://www.aloki.hu ● ISSN 1589 1623 (Print) ● ISSN 1785 0037 (Online)
DOI: http://dx.doi.org/10.15666/aeer/1804_51495173

on which normal prp is refolded into a nascent abnormal prp molecule through a process facilitated by another protein. Because no differences in the primary sequence were found between normal prp and abnormal prp, the two species are believed to differ only in their conformation. After normal prp is synthesized in the endoplasmic reticulum, it transits through the Golgi to the cell surface where it is bound by a glycophosphatidyl inositol (GPI)-anchor. At or near the cell surface, normal prp is either metabolized or converted into abnormal prp (Benke et al., 2007). Normal prp seems to re-enter cells through caveolae-like domains (CLDs), a subcellular compartment defined biochemically by membranes rich in cholesterol and glycosphingolipids; this compartment also contains many GPI-anchored proteins. Polymorphisms in the prion protein gene (*PRNP*) determine the amino acid sequence of the host's prion protein and play a major role in relative susceptibility or resistance to classical scrapie. Prion protein (*PRNP*) gene is well known for affecting mammal transmissible spongiform encephalopathies (TSE) and is also reported to regulate phenotypic traits (e.g., growth traits) in healthy ruminants. As the vital control gene of fatal prion diseases or transmissible spongiform encephalopathies (TSE), the prion protein (*PRNP*) gene will always be a focus of ovine research (Houston et al., 2015; Stepanek and Horin, 2017). The *PRNP* gene encodes the prion protein (PrP), which plays a major role in the disease process (Goldmann, 2008; Houston et al., 2015). In sheep, amino acid polymorphisms at many positions (89, 94, 101, 112, 127, 128, 132, 134, 135, 136, 137, 138, 141, 143, 145, 146, 149, 151, 152, 154, 157, 159, 160, 163, 164, 167, 168, 169, 171, 172, 174, 175, 176, 180, 183, 184, 185, 189, 193, 195, 196, 199, 211, 213, 220, 224, 241) have been described (Oner et al., 2011), but the polymorphisms at codons 136, 154 and 171 have been demonstrated to be of major importance, as they modulate the susceptibility/resistance of sheep for scrapie (Clouscard et al., 1995; Hunter et al., 1996).

These polymorphisms are Alanine (A), Valine (V) or Threonine (T) at codon 136, Arginine (R) or Histidine (H) at codon 154 and Glutamine (Q), R, H or Lysine (K) at codon 171. The five most common haplotypes are ARR, ARQ, AHQ, ARH, and VRQ. New haplotypes (TRQ, ARK, VRR, AHR, VHQ, and TRR) have been reported so far. Haplotype alleles encoding three other forms of PrP (ARQ, AHQ, and ARH, where H is histidine) have intermediate associations with classical scrapie disease progression following exposure to the transmissible agent (Goldmann, 2008). Over 30 SNPs already showed that the ovine prion gene (PrP) shows an unusually high level of genetic variation (Goldmann et al., 2005). The ovine *PRNP*, mapped to chromosome 13, is a highly polymorphic gene consisting of three exons, among which only the third is translated (Lee et al., 1998). Single nucleotide polymorphisms (SNPs) leading to amino acid change in PrP were observed in over 20 codons, but most of them are rare and unrelated to disease development (Goldmann et al., 2005). It was established that polymorphisms A136V (Alanine, GCC → GTC, Valine), R154H (arginine, CGT → CAT, histidine) and Q171R (glutamine, CAG → CGG, arginine) are associated with susceptibility or resistance to scrapie (Baylis et al., 2004). Additionally, some studies reported another polymorphic variant coding for histidine at codon 171, but it is very rare (Acín et al., 2004). The combination of these polymorphisms results in the creation of 3-locus haplotypes and diploid genotypes, among which A136R154Q171 (hereafter ARQ) haplotype and AA136RR154QQ171 (hereafter ARQ/ARQ) genotype are thought to be wild-type variants. With the help of *Table 4,* we can see the severity or intensity of genotypes.

http://www.aloki.hu ● ISSN 1589 1623 (Print) ● ISSN 1785 0037 (Online)
DOI: http://dx.doi.org/10.15666/aeer/1804_51495173

Table 4. *According to the intensity of risk, scientists has classified the risk groups (Cosseddu et al., 2007)*

Risk class	Genotype	Risk intensity
1	ARR/ARR	Sheep are highly resistant to scrapie
2	ARR/AHQ ARR/ARH ARR/ARQ	Sheep are resistant to scrapie, thus require particular attention in breeding programs
3	ARQ/ARH ARQ/AHQ AHQ/AHQ ARH/ARH AHQ/ARH ARQ/ARQ	Sheep with low genetic resistance to scrapie. Their use in breeding programs must be avoided
4	AHQ/ARH	Sheep are sensitive to scrapie
5	AHQ/VRQ ARH/VRQ ARQ/VRQ VRQ/VRQ	Sheep are highly sensitive to scrapie, thus must be castrated or culled

The rapid dissemination of scrapie over the previous limited years led to the development of a specific eradication program, based on the polymorphisms within the prion protein gene (*PRNP*). The current approach encourages the selection of animals carrying the resistant ARR/ARR genotype, while other genotypes are considered not preferable. Although the strategy seems to be working quite well, farmers are concerned whether this will affect sheep productivity and subsequently decrease net profits. Current scrapie eradication program includes genotyping and subsequent selection of animals on the ARR/ARR genotype.

Genotype and haplotype

Observing the development of *PRNP* genotype and haplotype is a powerful pointer of choice weight, which is evaluated in reference class creatures alongside ages so as to dodge predisposition, while the advancement in the common populace is assessed depending on scientific models. In countries where the scrapie incidence was statistically significant (see *Tables 5* and *6*), such as from Romania (Lacaune) the genotype frequencies are (ARR/ARR: 15.1) and (ARQ/VRQ: 12.6) (Otelea et al., 2011); from Romania (Turcana) (ARR/ARR: 14.64) and (ARQ/VRQ: 12.2) (Coşier et al., 2011); from Finland (Finnish Landrace) (ARR/ARR: 1.3) and (ARQ/VRQ: 10.3) (Hautaniemi et al., 2012); from Italy (Biellese rams) (ARQ/VRQ: 1.4) and (ARQ/VRQ: 9.9) (Acutis et al., 2004); from Slovakia (Orava) (ARR/ARR; 10.9) and (ARQ/VRQ: 9.0) (Tkáčiková et al., 2003); from Slovakia (Valachian) (ARR/ARR; 10.9) and (ARQ/VRQ: 9.0) (Tkáčiková et al., 2003); rom Slovakia (Spiš) (ARR/ARR; 10.8) and (ARQ/VRQ; 8.9) (Tkáčiková et al.,

http://www.aloki.hu ● ISSN 1589 1623 (Print) ● ISSN 1785 0037 (Online)
DOI: http://dx.doi.org/10.15666/aeer/1804_51495173

2003); from Germany (Texel) (ARR/ARR; 11.7) and (ARQ/VRQ; 7.8) (Kutzer et al., 2002); from Greece (Greek Dairy Breed) (ARR/ARR; 2.2) and (ARQ/VRQ; 5.4) (Boukouvala et al., 2018a); from Spain (Rasa Aragonesa) (ARR/ARR; 2.0) and (ARQ/VRQ; 5.0) (Acín et al., 2004); from Poland (Pomorska) (ARR/ARR; 13.3) and (ARQ/VRQ; 3.3) (Lühken et al., 2008); from Poland (Pomorska) (ARR/ARR; 13.3) and (ARQ/VRQ; 3.3) (Acín et al., 2004); from Spain (Roya Bilbilitana) (ARR/ARR; 2.0) and (ARQ/VRQ; 3.0) (Acín et al., 2004); from Poland (Kaminieniecka) (ARR/ARR; 35.3) and (ARQ/VRQ; 2.9) (Szkudlarek-Kowalczyk et al., 2010); from Germany (Nolana) (ARR/ARR; 32.4) and (ARQ/VRQ; 2.8) (Kutzer et al., 2002); from Turkey (Imroz) (ARR/ARR; 29.9) and (ARQ/VRQ; 2.7) (Oner et al., 2011); from Brazil (Santa Ines sheep) (ARR/ARR; 7.4) and (ARQ/VRQ; 2.2) (Andrade et al., 2018); from Greece (Crossbred) (ARR/ARR; 7.3) and (ARQ/VRQ; 1.9) (Kioutsioukis et al., 2018); from Greece (Chios crossbred) (ARR/ARR; 2.7) and (ARQ/VRQ; 1.6) (Kioutsioukis et al., 2018); from Brazil (Dorset sheep) (ARR/ARR; 11.6) and (ARQ/VRQ; 1.5) (Andrade et al., 2018); from Iran (local sheep) (ARR/ARR; 38) and (ARQ/VRQ; 1.2) (Karami et al., 2011); from Greece (chios) (ARR/ARR; 1.2) and (ARQ/VRQ; 1.2) (Kioutsioukis et al., 2018); from Poland (Ile de France) (ARR/ARR; 72.0) and (ARQ/VRQ; 1.1) (Wisniewska and Mroczkowski, 2009); from Poland (Polish Merino) (ARR/ARR; 7.1) and (ARQ/VRQ; 1.0) (Wiśniewska et al., 2006); from Turkey (Kivircik) (ARR/ARR; 1.41) and (ARQ/VRQ; 0.7) (Oner et al., 2011); from Greece (Chios) (ARR/ARR; 0.4) and (ARQ/VRQ; 0.5) (Psifidi et al., 2011); from England (15 scrapie affected flocks) (ARR/ARR; 14.8) and (ARQ/VRQ; 0.2) (Tongue et al., 2004); from Pakistan (Kajli) (ARR/ARR; 1.9) (Babar et al., 2009); from China (Gansu Alpine Merino sheep) (ARR/ARR; 20.7) (Liu et al., 2017); from the Czech Republic (Charollais) (ARR/ARR; 61.5) (Stepanek and Horin, 2017). Breeding programs planned to increase the RR171 genotype in sheep populations and eliminate affected animals, to considerably decrease the number of classical scrapie cases in America and in the European Union (Greenlee, 2019). This is cleared that these genotypes and haplotypes are the backbone in the resistance and susceptibility of scrapie, which can be low or high. From *Table 5* we can clearly say that, in Romania, Finland, Italy, Slovakia, Germany, Greece, Spain, Germany, Brazil, Iran, Poland, Turkey, Greece, England, Portugal and Hungary sheep are highly sensitive to scrapie, therefore must be eliminated or separated and in countries like Pakistan and China resistance to scrapie was observed.

The writers propose that arginine/glutamine replacement in the 171st position of the sheep *PRNP* might have affected the scrapie incubation period. In some countries the haplotype is very significant, that can be seen in *Table 6,* like the ARR in German Blackheaded Mutton; 87.0 which is the highest ARR frequency recorded and the highest VRQ frequency is recorded in Lacunae from Romania 18.9. The countries where the VRQ frequencies are found are Romania, Poland, Greece, Germany, Italy, Slovakia, Czech Republic, Finland, Germany, Austria, Spain, Turkey, Finland, Iran, Hungary; these are highly sensitive to scrapie, thus sheep must be eliminated and breeding programs must be introduced.

From these two tables and from the graphical presentation in *Figures 3* and *4,* we can see the clear difference between the countries where the scrapie is present, or the chance of scrapie is severe. The countries like China and Pakistan must take some important steps like proper breeding programs, before doing meat or any kind of trade associated with sheep with countries like Romania, Greece and the other countries found susceptible to scrapie.

http://www.aloki.hu ● ISSN 1589 1623 (Print) ● ISSN 1785 0037 (Online)
DOI: http://dx.doi.org/10.15666/aeer/1804_51495173

Table 5. *Genotypic frequencies of PRNP gene at codon 131, 154 and 171 in various breeds of sheep in major parts of the world*

#	Country	Breed	N	ARR/ ARR	ARR/ ARQ	ARQ/ ARQ	ARR/ AHQ	ARQ/ AHQ	AHQ/ AHQ	ARR/ VRQ	VRQ/ VRQ	ARQ/ VRQ	Reference
1	Romania	Lacaune	159	15.1	33.3	20.1	5.0	5.7		6.3		12.6	Otelea et al. (2011)
2	Romania	Turcana	123	14.64	32.52	28.46	0.81	1.63		5.69		12.2	Coşier et al. (2011)
3	Finland	Finnish Landrace	232	1.3	15.9	68.8		0.4			0.4	10.3	Hautaniemi et al. (2012)
4	Italy	Biellese rams	1207	1.4	11.4	56.3	0.7	5.5	0.2	1.2	0.7	9.9	Acutis et al. (2004)
5	Slovakia	Orava	366	10.9	45.4	19.4	5.7	4.9	0.8	3.6	0.3	9.0	Tkáčiková et al. (2003)
6	Slovakia	Valachian	735	10.9	45.2	19.3	5.7	4.9	0.7	3.5	0.3	9.0	Tkáčiková et al. (2003)
7	Slovakia	Spiš	369	10.8	54.0	19.2	0.5	4.9	0.5	3.5	0.3	8.9	Tkáčiková et al. (2003)
8	Germany	Texel	231	11.7	19.5	25.1	0.4	2.2		6.5	0.4	7.8	Kutzer et al. (2002)
9	Greece	Greek Dairy Breed	4382	2.2	24.2	32.4		12.5	2.0	1.23	0.3	5.4	Boukouvala et al. (2018b)
10	Spain	Rasa Aragonesa	296	2.0	21.0	51.0	2.0	6.0	0.0	0.0		5.0	Acín et al. (2004)
11	Poland	Pomorska	30	13.3	36.7	16.7	6.7	6.7		3.3	3.3	3.3	Lühken et al. (2008)
12	Spain	Ojinegra	182	2.0	21	56	0.0	1	0.0	1.0		3.0	Acín et al. (2004)
13	Spain	Roya Bilbilitana	96	2.0	34	53	1.0	0	0.0	1.0		3.0	Acín et al. (2004)
14	Poland	Kaminieniecka	102	35.3	33.3	2.9				6.9		2.9	Szkudlarek-Kowalczyk et al. (2010)
15	Germany	Nolana	71	32.4	33.8	18.3				4.2		2.8	Kutzer et al. (2002)
16	Turkey	Imroz	147	29.9	33.3	19.0	6.1	5.4			0.7	2.7	Oner et al. (2011)
17	Brazil	Santa Ines sheep	94	7.4	21.3	47.8		17		1.1		2.2	Andrade et al. (2018)

http://www.aloki.hu ● ISSN 1589 1623 (Print) ● ISSN 1785 0037 (Online)
DOI: http://dx.doi.org/10.15666/aeer/1804_51495173

#	Country	Breed	N	ARR/ ARR	ARR/ ARQ	ARQ/ ARQ	ARR/ AHQ	ARQ/ AHQ	AHQ/ AHQ	ARR/ VRQ	VRQ/ VRQ	ARQ/ VRQ	Reference
18	Greece	Crossbred	483	7.3	28.2	31.5	5.6	12.7	1.0	0.4	0.00	1.9	Kioutsioukis al. (2018)
19	Greece	Chios crossbred	633	2.7	18.9	40.8	2.0	9.9	0.8	0.6	0.3	1.6	Kioutsioukis et al. (2018)
20	Brazil	Dorset sheep	69	11.6	43.5	39.1				4.3		1.5	Andrade et al. (2018)
21	Iran	Local sheeps	250		38	43.2						1.2	Karami et al. (2011)
22	Greece	chios	340	1.2	13.2	52.9	2.1	7.1	0.6	0.3	0.00	1.2	Kioutsioukis et al. (2018)
23	Poland	Ile de France	93	72.0	6.5					17.2	3.2	1.1	Wisniewska and Mroczkowski (2009)
24	Poland	Polish Merino	98	7.1	54.1	35.7				2.0		1.0	Wiśniewska et al. (2006)
25	Turkey	Kivircik	142	1.41	24.65	30.28	1.41	7.75				0.7	One et al. (2011)
26	Greece	Chios	1013	0.4	11.4	56.0	0.5	15.0	0.1			0.5	Psifidi et al. (2011)
27	England	15 scrapie affected flocks	3732	14.8	30.7	15.7	7.8	8.2	1.5	7.6	0.8	0.2	Tongue et al. (2004)
28	Portugal	Merino Branco	62	0.194	0.387	0.306	0.065	0.016	0.00	0.016		0.00	Mesquita et al. (2010)
29	Portugal	Saloia	52	0.096	0.231	0.442	0.038	0.135	0.00	0.019		0.019	Mesquita et al. (2010)
30	Portugal	Serra da Estrela	69	0.174	0.420	0.304	0.014	0.014	0.00	0.014		0.029	Mesquita et al. (2010)
31	Portugal	Bordaleira entre Douro e Minho	64	0.078	0.250	0.469	0.047	0.047	0.0	0.016		0.047	Mesquita et al. (2010)
32	Portugal	Churra Badana	58	0.052	0.345	0.517	0.017	0.052	0.0	0.00		0.00	Mesquita et al. (2010)
33	Portugal	Churra Galega Mirandesa	71	0.014	0.253	0.549	0.0	0.099	0.014	0.00		0.056	Mesquita et al. (2010)
34	Portugal	Churra Mondegueira	19	0.053	0.105	0.737	0.0	0.00	0.00	0.00		0.00	Mesquita et al. (2010)
35	Portugal	Merino da Beira-Baixa	65	0.092	0.231	0.523	0.0	0.31	0.00	0.031		0.077	Mesquita et al. (2010)

http://www.aloki.hu ● ISSN 1589 1623 (Print) ● ISSN 1785 0037 (Online)
DOI: http://dx.doi.org/10.15666/aeer/1804_51495173

#	Country	Breed	N	ARR/ ARR	ARR/ ARQ	ARQ/ ARQ	ARR/ AHQ	ARQ/ AHQ	AHQ/ AHQ	ARR/ VRQ	VRQ/ VRQ	ARQ/ VRQ	Reference
36	Hungary	Hungarian Tsigai	392	0.27	0.4	0.2	0.06	0.02	0.0	0.02	0.06	0.06	Mari (2016)
37	Greece	Karagouniko	100		14.5	32		6.0			7.9		Billinis et al. (2004)
38	Austria	Carynthian sheep	24	4.2	37.5	41.6		4.2			4.2		Sipos et al. (2002)
39	Turkey	Chios	124	15.32	22.58	20.16	1.61	7.26	1.61		0.8		Oner et al. (2011)
40	Poland	Olkuska	174	35.1	60.9	4.0							Kaczor et al. (2011)
41	Poland	Gorska	31	12.9	51.6	22.6	3.2	9.7					Lühken et al. (2008)
42	Poland	Wrzosowka	31	6.5	48.4	9.7	19.3	12.9	3.2				Lühken, Lipsky et al. (2008)
43	Finland	Kainuu	48		16.7	83.3							Hautaniemi et al. (2012)
44	Germany	Suffolk	87	14.9	20.7	54.0	1.1	1.1					Kutzer et al. (2002)
45	Pakistan	Awassi	21		4.8	92.2							Babar et al. (2009)
46	Pakistan	Buchi	35			100							Babar et al. (2009)
47	Pakistan	Hissardale	20	5		70							Babaret al. (2009)
48	Pakistan	Kajli	52	1.9	9.6	84.6							Babaret al. (2009)
49	Pakistan	Lohi	50		10	88							Babaret al. (2009)
50	Pakistan	Pak-Karakul	19		36.8	63.2							Babaret al. (2009)
51	Pakistan	Sipli	41			65.9							Babaret al. (2009)
52	Pakistan	Thalli	40		25	100							Babaret al. (2009)
53	Pakistan	kachi	30			100							Babaret al. (2009)
54	China	Gansu Alpine Merino sheep	111	20.7	27	46							Liu et al. (2017)

http://www.aloki.hu ● ISSN 1589 1623 (Print) ● ISSN 1785 0037 (Online)
DOI: http://dx.doi.org/10.15666/aeer/1804_51495173

#	Country	Breed	N	ARR/ ARR	ARR/ ARQ	ARQ/ ARQ	ARR/ AHQ	ARQ/ AHQ	AHQ/ AHQ	ARR/ VRQ	VRQ/ VRQ	ARQ/ VRQ	Reference
55	Algeria	Barbarine	20		20	40							Djaout et al. (2018)
56	Algeria	Berbere	20	5	20	20							Djaout et al. (2018)
57	Algeria	Hamra	27		19	11							Djaout et al. (2018)
58	Algeria	Ouled Djellal	35	8	17	11							Djaout et al. (2018)
59	Algeria	Rembi	40	8	20	18							Djaout et al. (2018)
60	Algeria	Sidaou	30		3	23							Djaout et al. (2018)
61	Algeria	Taadmit	10	20	10	10							Djaout et al. (2018)
62	Algeria	Tazegzawt	31		10	23							Djaout et al. (2018)
63	Czech Republic	Berrichone du Cher	445	54.6									Stepanek and Horin (2017)
64	Czech Republic	Charollais	3219	61.5									Stepanek and Horin (2017)
65	Czech Republic	East Friesian sheep	1864	56.5									Stepanek and Horin (2017)
66	Czech Republic	German Blackheaded Mutton	628	75.3									Stepanek and Horin (2017)
67	Czech Republic	Kent Romney)	5995	38.0									Stepanek and Horin (2017)
68	Czech Republic	Merinolandschaf	2057	33.1									Stepanek and Horin (2017)
69	Czech Republic	Oxford Down	1044	59.5									Stepanek and Horin (2017)
70	Czech Republic	Romanov sheep	3281	44.2									Stepanek and Horin (2017)
71	Czech Republic	Sumavka	3358	23.1									Stepanek and Horin (2017)
72	Czech Republic	Suffolk	12987	73.9									Stepanek and Horin (2017)

http://www.aloki.hu ● ISSN 1589 1623 (Print) ● ISSN 1785 0037 (Online)
DOI: http://dx.doi.org/10.15666/aeer/1804_51495173

#	Country	Breed	N	ARR/ ARR	ARR/ ARQ	ARQ/ ARQ	ARR/ AHQ	ARQ/ AHQ	AHQ/ AHQ	ARR/ VRQ	VRQ/ VRQ	ARQ/ VRQ	Reference
73	Czech Republic	Texel	3142	72.7									Stepanek and Horin (2017)
74	Czech Republic	Valachian sheep	1301	55.9									Stepanek and Horin (2017)
75	Czech Republic	Zwartbles	1791	39.6									Stepanek and Horin (2017)
76	West Africa	Burkina-Sahel	46		6.5	80.4	2.2	10.9					Traoré et al. (2012)
77	West Africa	Djallonké	50			86.0		12.0	2.0				Traoré et al. (2012)
78	West Africa	Mossi	46		6.5	76.1		15.2	2.2				Traoré et al. (2012)
79	West Africa	Touareg	20			40.0		55.0	5.0				Traoré et al. (2012)
80	Finland	Grey race sheep	48		16.7	83.3							Hautaniemi et al. (2012)
81	Finland	Aland sheep	56		23.2	48.2		19.6	8.9				Hautaniemi et al. (2012)
82	Finland	Taxel	71	1.4	31.0	33.8		8.5					Hautaniemi et al. (2012)
83	America	Suffolk	128	36.72	43.75	17.19							DeSilva et al. (2003)
84	America	Montadale	47	17.02	23.40	19.15							DeSilva et al. (2003)
85	America	Hampshire	91	20.88	52.75	26.37							DeSilva et al. (2003)
86	America	Dorset	62	9.68	38.71	38.71							DeSilva et al. (2003)
87	Austria	Tyrolean mountain	35	2.9	40.0	40.0	5.7	11.4					Sipos et al. (2002)
88	Austria	Forest sheep	26	111.5	15.4	57.7		11.5					Sipos et al. (2002)
89	Austria	Tyrolean stone sheep	27		29.6	40.7		22.2					Sipos et al. (2002)

http://www.aloki.hu ● ISSN 1589 1623 (Print) ● ISSN 1785 0037 (Online)
DOI: http://dx.doi.org/10.15666/aeer/1804_51495173

Table 6. *Haplotypic frequencies of PRNP gene at codons 136, 154 and 171: alanine (A), arginine (R), histidine (H), glutamine (Q) and valine (V) in various breeds of sheep in major parts of the world*

#	Country	Breed	N	ARR	ARQ	AHQ	VRQ	Reference
1	Romania	Lacaune	159	15.1	60.4	5.0	18.9	Otelea et al. (2011)
2	Poland	Ile de France	93	83.8	3.8		12.4	Wisniewska and Mroczkowski (2009)
3	Greece	Greek Dairy Breed	4382	0.1	9.4	10	11.9	Boukouvala et al. (2018b)
4	Romania	Turcana	123	34.1	53.7	1.2	8.9	Coşier et al. (2011)
5	Poland	Pomorska	30	40.0	40.0	6.7	8.3	Wiśniewska et al. (2006)
6	Germany	Texel	231	28.8	44.4	1.9	8.2	Kutzer et al. (2002)
7	Italy	Biellese rams	2414	8.3	74.4	3.8	6.8	Acutis et al. (2004)
8	Slovakia	Valachian	735	38.4	48.7	6.0	6.5	Tkáčiková et al. (2003)
9	Czech Republic	Valachian sheep	1301	74.3			5.7	Stepanek and Horin (2017)
10	Finland	Finnish Landrace	464	9.5	83.4	0.2	5.6	Hautaniemiet al. (2012)
11	Germany	Nolana	71	52.8	36.6		5.6	Kutzer et al. (2002)
12	Poland	Kaminieniecka	102	63.2	21.6		5.4	Szkudlarek-Kowalczyk et al. (2010)
13	Poland	Zelanienska	31	46.8	43.6	4.8	4.8	Lühken et al. (2008)
14	Austria	Carynthian sheep	24	23.0	64.6	4.2	4.2	Sipos et al. (2002)
15	Spain	Rasa Aragonesa	296	15.0	70.9	4.8	2.9	Acín et al. (2004)
16	Spain	Roya Bilbilitana	96	21.4	72.4	1	2.6	Acín et al. (2004)
17	Czech Republic	Romanov sheep	3281	66.3			2.5	Stepanek and Horin (2017)
18	Turkey	Imroz	147	50.0	40.1	5.8	2.4	Oner et al. (2011)
19	Greece	Chios crossbred	633	15.0	63.4	7.7	1.7	Kioutsioukis et al. (2018)
20	Czech Republic	Zwartbles	1791	63.7			1.6	Stepanek and Horin (2017)
21	Greece	Crossbred	483	25.7	55.9	11.3	1.5	Kioutsioukis et al. (2018)
22	Poland	Polish Merino	98	35.2	63.3		1.5	Wiśniewska et al. (2006)
23	Finland	Taxel	144	17.6	64.1	4.2	1.4	Hautaniemiet al. (2012)
24	Czech Republic	Charollais	3219	79.6			1.3	Stepanek and Horin (2017)
25	Turkey	Kivircik	142	30.64	39.52	6.83	0.8	Oner et al. (2011)
26	Greece	Chios	340	10	71.5	5.8	0.7	Kioutsioukis et al. (2018)

http://www.aloki.hu ● ISSN 1589 1623 (Print) ● ISSN 1785 0037 (Online)
DOI: http://dx.doi.org/10.15666/aeer/1804_51495173

#	Country	Breed	N	ARR	ARQ	AHQ	VRQ	Reference
27	Iran	Local sheeps	250		67.8		0.6	Karami et al. (2011)
28	Czech Republic	East Friesian sheep	1864	76.1			0.5	Stepanek and Horin (2017)
29	Czech Republic	Sumavka	3358	46.1			0.5	Stepanek and Horin (2017)
30	Greece	Chios	1013	6.9	76.1	8.2	0.4	Psifidi et al. (2011)
31	Turkey	Chios	124	17.25	56.69	5.63	0.4	Oner et al. (2011)
32	Czech Republic	Berrichone du Cher	445	75.5			0.4	Stepanek and Horin (2017)
33	Spain	Ojinegra	182	14.6	73.9	3	0.3	Acín et al. (2004)
34	Greece	Random breeds	5815	47.7	44.9	3.9	0.3	Boukouvala et al. (2018b)
35	Czech Republic	Texel	3142	85.9			0.2	Stepanek and Horin (2017)
36	Czech Republic	Suffolk	12987	86.28			0.1	Stepanek and Horin (2017)
37	Czech Republic	Merinolandschaf	2057	59.3			0.1	Stepanek and Horin (2017)
38	Czech Republic	Kent Romney)	5995	63.5			0.1	Stepanek and Horin (2017)
39	Hungary	Hungarian Tsigai	569	0.5	0.4	0.05	0.01	Mari (2016)
40	Czech Republic	German Blackheaded Mutton	628	87.0			0.0	Stepanek and Horin (2017)
41	Czech Republic	Oxford Down	1044	79.2			0.0	Stepanek and Horin (2017)
42	Finland	Grey race sheep	96	8.3	91.7	0	0	Hautaniemiet al. (2012)
43	Finland	Aland sheep	112	11.6	69.6	18.8	0	Hautaniemiet al. (2012)
44	Poland	Olkuska	174	65.5	34.5			Kaczor et al. (2011)
45	Poland	Polish Mountain	31	40.3	53.2	6.5		Wiśniewska et al. (2006)
46	Poland	Wrzosowka	31	41.9	38.7	19.4		Lühken et al. (2008)
47	Finland	Kainuu	48	8.3	91.7			Hautaniemi et al. (2012)
48	Greece	Karagouniko	100	28.5	66.0	3.0		Billinis et al. (2004)
49	Germany	Suffolk	87	27.0	67.2	1.1		Kutzer et al. (2002)
50	China	Xinjiang Sheeps	222	9.0	75.2	2.3		Lan et al. (2006)
51	Algeria	Barbarine	20	15	65			Djaout et al. (2018)
52	Algeria	Berbere	20	18	48	3		Djaout et al. (2018)
53	Algeria	Hamra	27	11	41	7		Djaout et al. (2018)
54	Algeria	Ouled Djellal	35	26	31	3		Djaout et al. (2018)

http://www.aloki.hu ● ISSN 1589 1623 (Print) ● ISSN 1785 0037 (Online)
DOI: http://dx.doi.org/10.15666/aeer/1804_51495173

#	Country	Breed	N	ARR	ARQ	AHQ	VRQ	Reference
55	Algeria	Rembi	40	24	43	3		Djaout et al. (2018)
56	Algeria	Sidaou	30	8	45	2		Djaout et al. (2018)
57	Algeria	Taadmit	10	30	30	10		Djaout et al. (2018)
58	Algeria	Tazegzawt	31	8	47	3		Djaout et al. (2018)
59	Burkina Faso	Burkina-Sahel	46	4.4	89.1	6.5		Traoré et al. (2012)
60	Burkina Faso	Djallonké	50		92.0	8.0		Traoré et al. (2012)
61	Burkina Faso	Mossi	46	3.2	87.0	9.8		Traoré et al. (2012)
62	Niger	Touareg	20		67.5	32.5		Traoré et al. (2012)
63	Austria	Tyrolean mountain	35	25.8	65.7	8.6		Sipos et al. (2002)
64	Austria	Forest sheep	26	19.2	71.2	5.8		Sipos et al. (2002)
65	Austria	Tyrolean stone sheep	27	14.8	70.3	11.1		Sipos et al. (2002)
66	China	Lanzhou large-tailed sheep	30	0	26	0		Lan et al. (2014)
67	China	Mongol sheep	30	0	26	0		Lan et al. (2014)
68	China	Tan sheep	30	0	25	0		Lan et al. (2014)
69	China	Gaoyuan sheep	30	0	32	0		Lan et al. (2014)
70	China	Guide fur sheep	30	0	28	0		Lan et al. (2014)
71	China	Oula sheep	30	0	30	0		Lan et al. (2014)
72	China	Lowland sheep	30	0	28	0		Lan et al. (2014)
73	China	Sishui fur sheep	30	0	21	0		Lan et al. (2014)
74	China	Small-tailed Han sheep	30	0	22	0		Lan et al. (2014)
75	China	Hu sheep	30	2	25	0		Lan et al. (2014)
76	China	Tong sheep	30	1	25	0		Lan et al. (2014)
77	China	Duolang sheep	30	1	27	0		Lan et al. (2014)
78	China	Diqing sheep	30	2	30	1		Lan et al. (2014)
79	China	Tengchong sheep	30	1	12	17		Lan et al. (2014)
80	China	Zhaotong sheep	30	1	7	22		Lan et al. (2014)
81	China	Tibetan sheep	30	3	27	0		Lan et al. (2014)

http://www.aloki.hu ● ISSN 1589 1623 (Print) ● ISSN 1785 0037 (Online)
DOI: http://dx.doi.org/10.15666/aeer/1804_51495173

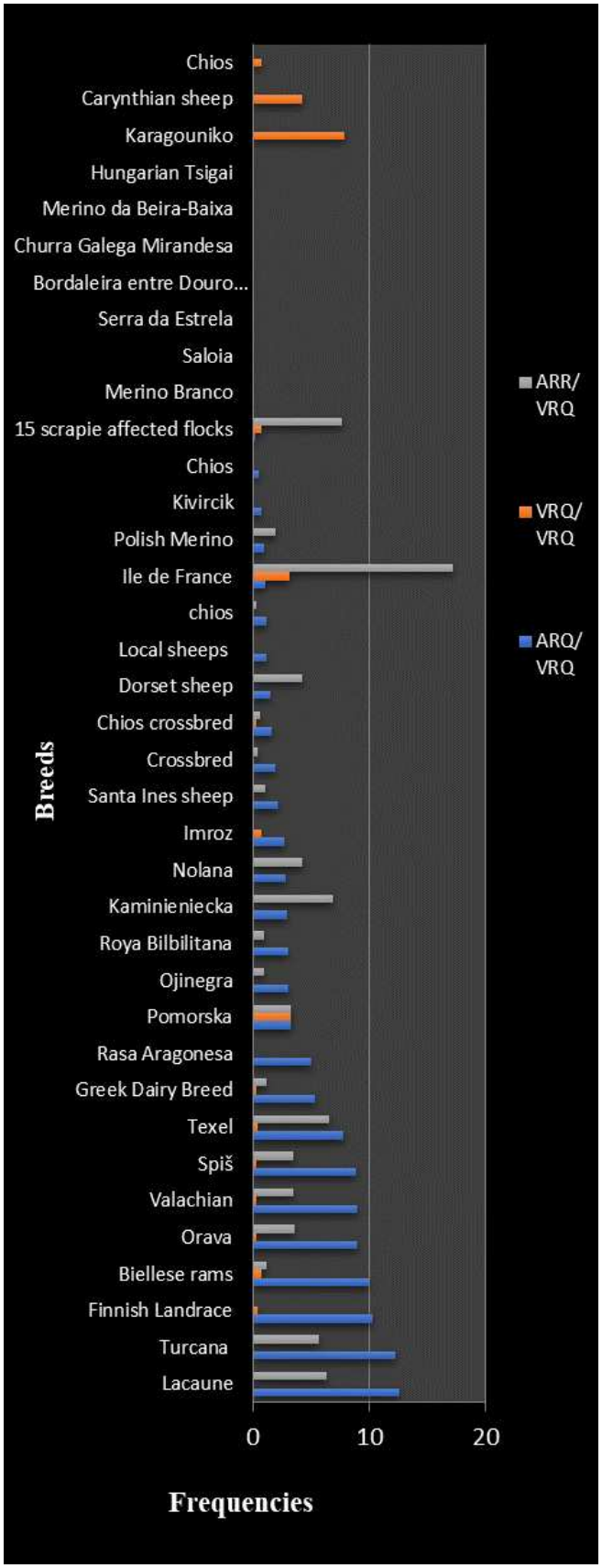

Figure 3. *Genotype frequencies of PRNP gene at codons 136, 154 and 171. (Constructed from Table 5)*

http://www.aloki.hu ● ISSN 1589 1623 (Print) ● ISSN 1785 0037 (Online)
DOI: http://dx.doi.org/10.15666/aeer/1804_51495173

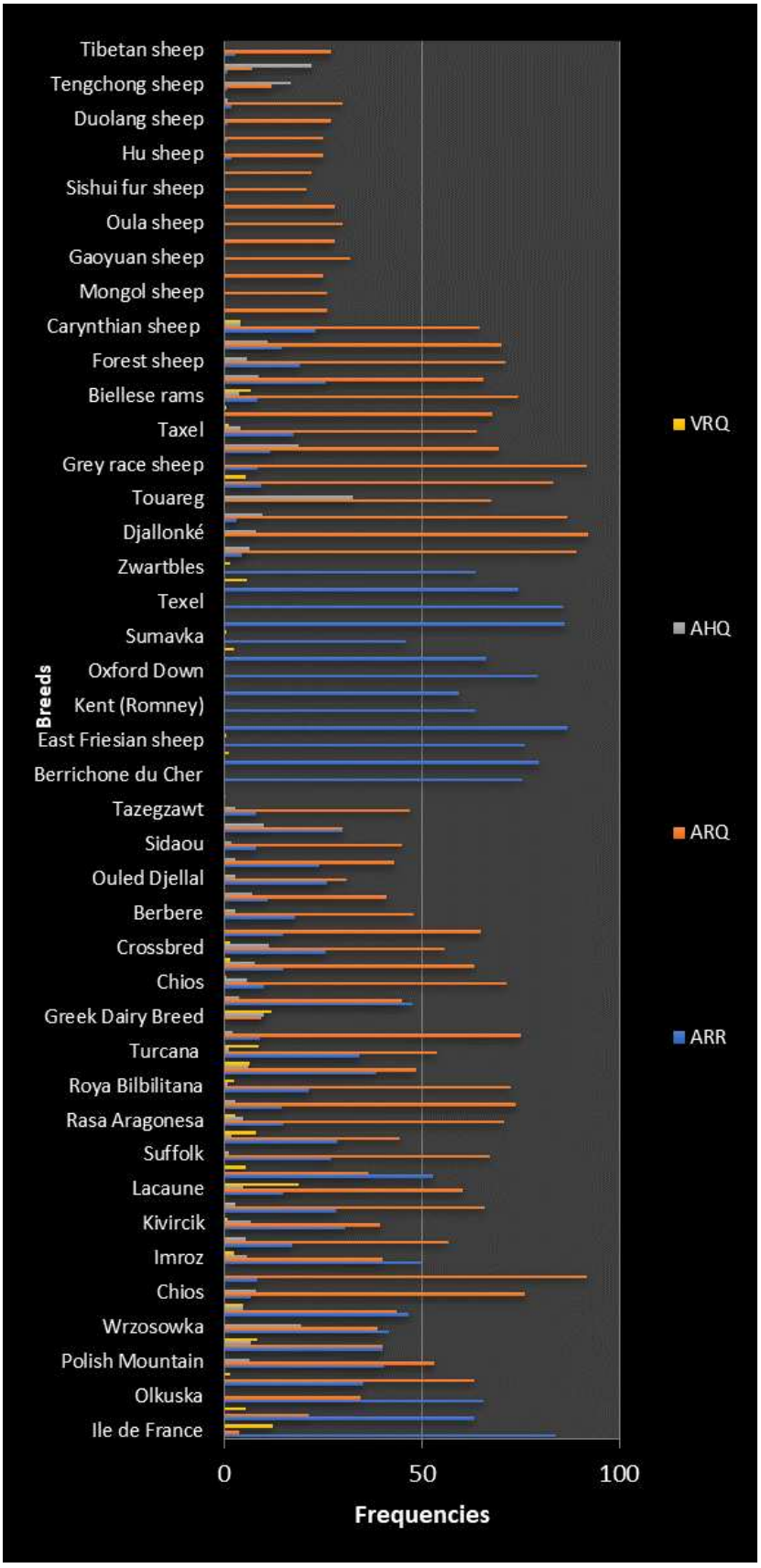

Figure 4. *Haplotype frequencies of PRNP gene at codons 136, 154 and 171. (Constructed from Table 6)*

http://www.aloki.hu ● ISSN 1589 1623 (Print) ● ISSN 1785 0037 (Online)
DOI: http://dx.doi.org/10.15666/aeer/1804_51495173

Summary

The purpose of this review is to highlight the countries where scrapie is causing problems and provide some information about the countries where scrapie is not present but there is possibility of its occurrence because scrapie is a prion disease and scientists still do not know how to cure the disease. It is very difficult to get rid of this if once entered in a country, the complete rid is only possible with the help of special breeding programs. Almost every country is working hard on breeding programs to get rid of scrapie, because these breeding programs showed positive signs in countries like Australia and New Zealand which are now scrapie free. But actual facts of scrapie in many parts of the world remain unknown due to the unsatisfactory passive surveillance system, because of which we cannot get consistent results or conclusion. As already described scrapie or any other prion disease do not have any treatment, so the only way to protect the animals is taking proper precautionary measures. The causative agent of the scrapie has still not been fully identified. All routes of transmission and their relative importance are still unknown. Animal health is directly related to humans, for the safety of humans, we must try to find some serious solutions for the well-being of animals. Like in humans, for the early diagnosis of sCJD many scientists have preferred the polysomnogram to detect earlier changes in sCJD patients may be praiseworthy. In humans, the accessory examinations of magnetic resonance imaging (MRI), electroencephalography (EEG), combined with this evidence and clinical symptom; scientists made a clinical diagnosis of sCJD. Though various drugs have been tried *in vitro* and/or *in vivo*, only four drugs have been studied in larger-scale observational or placebo-control trials: flupirtine, quinacrine, pentosan polysulfate (PPS), and doxycycline (Trevitt and Collinge, 2006). In sheep scientists must try some special drugs, any kind of hormonal changes which can prolong the survival or try to find any other way by which animal can show the clinical signs on early stage so that they can be culled or separated from healthy animals. Continuous study and research programs are needed to clear risk factor especially those affecting for human health. Yet, we do not have effective results which can lead us to the solution. The only possible solution is to carry out proper breeding programs. Continuity investigation is needed on this research for the well-being of the mankind and for the well-being of the animals. Further studies are needed to clarify the transmission of scrapie to humans.

Acknowledgements. This review is part of a project that is funded by Yunnan Provincial Key Research and Development Project (2018BB002).

REFERENCES

[1] Acín, C., Martín-Burriel, I., Goldmann, W., Lyahyai, J., Monzon, M., Bolea, R., Smith, A., Rodellar, C., Badiola, J. J., Zaragoza, P. (2004): Prion protein gene polymorphisms in healthy and scrapie-affected Spanish sheep. – Journal of General Virology 85(7): 2103-2110.

[2] Acutis, P., Sbaiz, L., Verburg, F., Riina, M., Ru, G., Moda, G., Caramelli, M., Bossers, A. V. (2004): Low frequency of the scrapie resistance-associated allele and presence of lysine-171 allele of the prion protein gene in Italian Biellese ovine breed. – Journal of General Virology 85(10): 3165-3172.

http://www.aloki.hu ● ISSN 1589 1623 (Print) ● ISSN 1785 0037 (Online)
DOI: http://dx.doi.org/10.15666/aeer/1804_51495173

[3] Adams, D., Caspary, E. (1968): Incorporation of nucleic acid and polysaccharide precursors into a post-ribosomal fraction of scrapie-affected mouse brain. – Biochemical Journal 108(5).
[4] Aiken, J. M., Williamson, J. L., Borchardt, L. M., Marsh, R. J. (1990): Presence of mitochondrial D-loop DNA in scrapie-infected brain preparations enriched for the prion protein. – Journal of Virology 64(7): 3265-3268.
[5] Alper, T., Haig, D. A., Clarke, M. C. (1966): The exceptionally small size of the scrapie agent. – Biochem Biophys Res Commun 22: 278-284.
[6] Alper, T., Cramp, W., Haig, D. A., Clarke, M. C. (1967): Does the agent of scrapie replicate without nucleic acid? – Nature 214(5090): 764.
[7] Alper, T., Haig, D., Clarke, M. (1978): The scrapie agent: evidence against its dependence for replication on intrinsic nucleic acid. – Journal of General Virology 41(3): 503-516.
[8] Andrade, C. P., Barbosa Neto, J. D., Driemeier, D. (2018): Identification of single nucleotide polymorphisms in the prion protein gene in Santa Ines and Dorset sheep. – Pesquisa Veterinária Brasileira 38(4): 624-628.
[9] Babar, M. E., Farid, A., Benkel, B. F., Ahmad, J., Nadeem, A., Imran, M. (2009): Frequencies of PrP genotypes and their implication for breeding against scrapie susceptibility in nine Pakistani sheep breeds. – Molecular Biology Reports 36(3): 561-565.
[10] Bastian, F. O. (1979): Spiroplasma-like inclusions in Creutzfeldt-Jakob disease. – Archives of Pathology and Laboratory Medicine 103(13): 665-669.
[11] Baylis, M., Chihota, C., Stevenson, E., Goldmann, W., Smith, A., Sivam, K., Tongue, S., Gravenor, M. J. (2004): Risk of scrapie in British sheep of different prion protein genotype. – Journal of General Virology 85(9): 2735-2740.
[12] Benkel, B. F., Valle, E., Bissonnette, N., Farid, A. H. (2007): Simultaneous detection of eight single nucleotide polymorphisms in the ovine prion protein gene. – Molecular and Cellular Probes 21(5-6): 363-367.
[13] Billinis, C., Psychas, V., Leontides, L., Spyrou, V., Argyroudis, S., Vlemmas, I., Leontides, S., Sklaviadis, T., Papadopoulos, O. J. (2004): Prion protein gene polymorphisms in healthy and scrapie-affected sheep in Greece. – Journal of General Virology 85(2): 547-554.
[14] Boukouvala, E., Gelasakis, A. I., Kanata, E., Fragkiadaki, E., Giadinis, N. D., Palaska, V., Christoforidou, S., Sklaviadis, T., Ekateriniadou, L. V. (2018a): The association between 171 K polymorphism and resistance against scrapie affection in Greek dairy sheep. – Small Ruminant Research 161: 51-56.
[15] Boukouvala, E., Katharopoulos, E., Christoforidou, S., Babetsa, M., Ekateriniadou, L. (2018b): Analysis of the PRNP gene polymorphisms in healthy Greek sheep during 2012–2016. – Small Ruminant Research 69(1): 839-846.
[16] Brotherston, J., Renwick, C., Stamp, J., Zlotnik, I., Pattison, I. J. (1968): Spread of scrapie by contact to goats and sheep. – Journal of Comparative Pathology 78(1): 9-17.
[17] Clouscard, C., Beaudry, P., Elsen, J., Milan, D., Dussaucy, M., Bounneau, C., Schelcher, F., Chatelain, J., Launay, J., Laplanche, J. (1995): Different allelic effects of the codons 136 and 171 of the prion protein gene in sheep with natural scrapie. – Journal of General Virology 76(8): 2097-2101.
[18] Comber, T. (1772): Real improvements in agriculture: (on the principles of A. Young, Esq.) recommended to accompany improvements of rents. – In a letter to Reade Peacock, esq; alderman of Huntingdon. To which is added, a letter to Dr. Hunter, physician in York. Concerning the rickets in sheep. Printed for W. Nicoll.
[19] Coşier, V., Vlaic, A., Vioara, M., Constantinescu, R. (2011): The genetic resistance of rams from Turcana breed to Ovine Transmissible Spongiform Encephalopathy (scrapie). – RBL 16(4): 6328-6335.

http://www.aloki.hu ● ISSN 1589 1623 (Print) ● ISSN 1785 0037 (Online)
DOI: http://dx.doi.org/10.15666/aeer/1804_51495173

[20] Cosseddu, G., Agrimi, U., Pinto, J., Schudel, A. (2007): Advances in scrapie research. – Revue scientifique et technique-Office international des épizooties 26(3): 657.
[21] Cuillé, J., Chelle, P.-L. (1938): La tremblante du mouton est-elle déterminée par un virus filtrable. – CR Acad Sci (Paris) 206: 1687-1688.
[22] de Mouton, T. (2007): Species Affected. www-cfsph.sws.iastate.edu. pp 1-14.
[23] DeSilva, U., Guo, X., Kupfer, D. M., Fernando, S. C., Pillai, A. T. V., Najar, F. Z., ... Roe, B. A. (2003): Allelic variants of ovine prion protein gene (PRNP) in Oklahoma sheep. – Cytogenetic and Genome Research 102(1-4): 89-94.
[24] Detwiler, L. A., Baylis, M. (2003): The epidemiology of scrapie. – Revue Scientifique Et Technique - Office International Des Epizooties 22(1): 121-144.
[25] Dickinson, A. G. (1979): The scrapie replication-site hypotheses and its implications for pathogenesis. – Slow Transmissible Diseases of the Nervous System 2: 13-31.
[26] Diener, T. O. (1972): Is the scrapie agent a viroid? – Nature New Biology 235(59): 218-219.
[27] Djaout, A., Chiappini, B., Afri-Bouzebda, F., Conte, M., Chekkal, F., El-Bouyahiaoui, R., ... Vaccari, G. (2018): Biodiversity and selection for scrapie resistance in sheep: genetic polymorphism in eight breeds of Algeria. – Journal of Genetics 97(2): 453-461.
[28] Erdt, W. E. A. (1861): Die Traberkrankheit der Schafe, ihre Natur, Genesis, Erkennung, Ursachen, Verhütung und Ausrottung. – Bosselmann, Berlin.
[29] Frank, E. C. (1820): Beschluß der gesammelten Erfahrungen über die Traberkrankheit der Schafe. – Verhandlungen der Königlich sächsischen ökonomischen Gesellschaft 10-24.
[30] Gibbons, R. A., Hunter, G. D. (1967): Nature of the scrapie agent. – Nature 215(5105): 1041-1043.
[31] Goldmann, W. (2008): PrP genetics in ruminant transmissible spongiform encephalopathies. – Veterinary Research 39(4): 1-14.
[32] Goldmann, W., Baylis, M., Chihota, C., Stevenson, E., Hunter, N. (2005): Frequencies of PrP gene haplotypes in British sheep flocks and the implications for breeding programmes. – Journal of Applied Microbiology 98(6): 1294-1302.
[33] Greenlee, J. J. (2019): Update on classical and atypical scrapie in sheep and goats. – Veterinary Pathology 56(1): 6-16.
[34] Griffith, J. S. (1967): Nature of the scrapie agent: self-replication and scrapie. – Nature 215(5105): 1043-1044.
[35] Hautaniemi, M., Tapiovaara, H., Korpenfelt, S. L., Sihvonen, L. (2012): Genotyping and surveillance for scrapie in Finnish sheep. – BMC Veterinary Research 8(1): 122.
[36] Hering, E. (1849): Specielle Pathologie und Therapie für Thierärzte: zum Gebrauche bei Vorlesungen und zu eigener Belehrung. – Ebner & Seubert, Stuttgart.
[37] Houston, F., Goldmann, W., Foster, J., Gonzalez, L., Jeffrey, M., Hunter, N. (2015): Comparative susceptibility of sheep of different origins, breeds and PRNP genotypes to challenge with bovine spongiform encephalopathy and scrapie. – PloS One 10(11).
[38] Hunter, N. (1997): Molecular biology and genetics of scrapie in sheep. – The Genetics of Sheep 225-240.
[39] Hunter, N., Foster, J. D., Goldmann, W., Stear, M. J., Hope, J., Bostock, C. (1996): Natural scrapie in a closed flock of Cheviot sheep occurs only in specific PrP genotypes. – Archives of Virology 141(5): 809-824.
[40] EFSA (2014): Scientific opinion on the scrapie situation in the EU after 10 years of monitoring and control in sheep and goats. – EFSA Journal 12(7): 3781.
[41] EFSA (2017): The European Union summary report on surveillance for the presence of transmissible spongiform encephalopathies (TSE) in 2016. – EFSA Journal15(11): e05069.
[42] EFSA (2018): The European Union summary report on surveillance for the presence of transmissible spongiform encephalopathies (TSE s) in 2017. – EFSA Journal 16(11): e05492.

http://www.aloki.hu ● ISSN 1589 1623 (Print) ● ISSN 1785 0037 (Online)
DOI: http://dx.doi.org/10.15666/aeer/1804_51495173

[43] Kaczor, U., Domoń, D., Martyniuk, E., Murawski, M. (2011): Polymorphism in the PRNP locus in prolific Olkuska sheep. – Bulletin of the Veterinary Institute in Puławy 55(1): 3-7.
[44] Karami, M., Amirinia, C., Kashan, N. E., Amirmozafari, N., Chamani, M., Banabazi, M. H. (2011): Polymorphisms of the prion protein gene Arabi sheep breed in Iran. – African Journal of Biotechnology 10(70): 15819-15822.
[45] Kioutsioukis, C., Papadogiannakis, E., Palaska, V., Kontos, V., Papakostaki, D., Paraskeva, S., Vassalou, E. (2018): Prion protein gene polymorphisms in classical scrapie-affected flocks of sheep in Central Macedonia. – Journal of the Hellenic Veterinary Medical Society 69(2): 931-940.
[46] Kutzer, T., Pfeiffer, I., Brenig, B. (2002): Identification of new allelic variants in the ovine prion protein (PrP) gene. – Journal of Animal Breeding and Genetics 119(4): 201-208.
[47] Lan, X. Y., Zhao, H. Y., Li, Z. J., Li, A. M., Lei, C. Z., Chen, H., Pan, C. Y. (2012): A novel 28-bp insertion–deletion polymorphism within goat PRNP gene and its association with production traits in Chinese native breeds. – Genome 55(7): 547-552.
[48] Lan, Z., Li, J., Sun, C., Liu, Y., Zhao, Y., Chi, T., ... Wang, Z. (2014): Allelic variants of PRNP in 16 Chinese local sheep breeds. – Archives of Virology 159(8): 2141-2144.
[49] Lan, Z., Wang, Z. L., Liu, Y., Zhang, X. (2006): Prion protein gene (PRNP) polymorphisms in Xinjiang local sheep breeds in China. – Archives of Virology 151(10): 2095-2101.
[50] Lee, C. A., Ironside, J. W., Bell, J. E., Giangrande, P., Ludlam, C., Esiri, M. M., McLaughlin, J. E. (1998): Retrospective neuropathological review of prion disease in UK haemophilic patients. – Thrombosis and Haemostasis 80(12): 909-911.
[51] Leontides, S., Psychas, V., Aargyroudis, S., Giannati-Stefanou, A., Paschaleri-Papadopoulou, E., Manousis, T., Sklaviadis, T. (2000): A survey of more than 11 years of neurologic diseases of ruminants with special reference to transmissible spongiform encephalopathies (TSEs) in Greece. – Journal of Veterinary Medicine, Series B 47(4): 303-309.
[52] Liu, Y. Z., Zhao, C. L., Yang, Y. Z., Wu, R., Wang, C., Wan, X. R., Wang, Y. (2017): The correlation analysis of polymorphisms of Prion-Related Doppel (PRND) with prion (PRNP) alleles in Gansu Alpine Merino sheep. – Genetics and Molecular Research 16(4).
[53] Lühken, G., Lipsky, S., Peter, C., Erhardt, G. (2008): Prion protein polymorphisms in autochthonous European sheep breeds in respect to scrapie eradication in affected flocks. – Small Ruminant Research 75(1): 43-47.
[54] M'Gowan, J. P. (1914): Investigation into the Disease of Sheep called "Scrapie" (Traberkrankheit; La Tremblante) with Especial Reference to its Association with Sarcosporidiosis. With an Appendix on a Case of Johne's Disease in the Sheep. – William Blackwood and Sons, Edinburgh.
[55] Mabbott, N. A. (2017): How do PrPSc prions spread between host species, and within hosts? – Pathogens 6(4): 60.
[56] Manuelidis, L. J. (1996): In the Community of Dinosaurs: The Viral View. – In: Court, L, Dodet, B. (eds.) Transmissible Subacute Spongiform Encephalopathies: Prion Diseases. Elsevier, Paris, pp. 375-387.
[57] Mari, K. B. (2016): Genetics of scrapie susceptibility in females of Tsigai Breed. – Doctoral Dissertation, Szent István University, Faculty of Veterinary Science, Budapest.
[58] May, G. (1868): Das Schaf: seine Wolle, Racen, Züchtung, Ernährung u. Benutzung, sowie dessen Krankheiten: in 2 Bd (Vol. 1). – Trewendt, Breslau.
[59] Mesquita, P., Batista, M., Marques, M. R., Santos, I. C., Pimenta, J., Silva Pereira, M., ... Fontes, C. M. (2010): Prion-like Doppel gene polymorphisms and scrapie susceptibility in Portuguese sheep breeds. – Animal Genetics 41(3): 311-314.

http://www.aloki.hu ● ISSN 1589 1623 (Print) ● ISSN 1785 0037 (Online)
DOI: http://dx.doi.org/10.15666/aeer/1804_51495173

[60] Oesch, B., Westaway, D., Wälchli, M., McKinley, M. P., Kent, S. B., Aebersold, R., ... Prusiner, S. B. (1985): A cellular gene encodes scrapie PrP 27-30 protein. – Cell 40(4): 735-746.
[61] Oner, Y., Yesilbag, K., Tuncel, E., Elmaci, C. (2011): Prion protein gene (PrP) polymorphisms in healthy sheep in Turkey. – Animal 5(11): 1728-1733.
[62] Otelea, M. R., Zaulet, M., Dudu, A., Otelea, F., Baratareanu, S., Danes, D. (2011): The scrapie genetic susceptibility of some sheep breeds in southeast Romanian area and genotype profiles of sheep scrapie infected. – Romanian Biotechnology Letter 16(4): 6419-6429.
[63] Pattison, I. H., Jones, K. M. (1967): The possible nature of the transmissible agent of scrapie. – Veterinary Record 80(1): 2-9.
[64] Pattison, I. H., Millson, G. C. (1961): Experimental transmission of scrapie to goats and sheep by the oral route. – Journal of Comparative Pathology and Therapeutics 71: 171-176.
[65] Prusiner, S. B. (1982): Novel proteinaceous infectious particles cause scrapie. – Science 216(4542): 136-144.
[66] Psifidi, A., Basdagianni, Z., Dovas, C. I., Arsenos, G., Sinapis, E., Papanastassopoulou, M., Banos, G. (2011): Characterization of the PRNP gene locus in Chios dairy sheep and its association with milk production and reproduction traits. – Animal Genetics 42(4): 406-414.
[67] Ribbe, J. C. (1821): Die innerlichen und äusserlichen Krankheiten des Schafviehes und deren Heilung: mit Bezug auf die Verhütung und Abwendung dieser Uebel wissenschaftlich-praktisch für gebildete Leser dargestellt: nebst einem Anhange zum Unterricht für Schäfer. – Barth, Leipzig.
[68] Sigurdsson, B. (1954): Rida, a chronic encephalitis of sheep: with general remarks on infections which develop slowly and some of their special characteristics. – British Veterinary Journal 110(9): 341-354.
[69] Sipos, W., Kraus, M., Schmoll, F., Achmann, R., Baumgartner, W. (2002): PrP genotyping of Austrian sheep breeds. – Journal of Veterinary Medicine Series A 49(8): 415-418.
[70] Stepanek, O., Horin, P. (2017): Genetic diversity of the prion protein gene (PRNP) coding sequence in Czech sheep and evaluation of the national breeding programme for resistance to scrapie in the Czech Republic. – Journal of Applied Genetics 58(1): 111-121.
[71] Szkudlarek-Kowalczyk, M., Wiśniewska, E., Milewski, S. T. A. N. I. S. Ł. A. W., Mroczkowski, S. Ł. A. W. O. M. I. R. (2010): Prion protein gene (PRNP) polymorphism in a flock of sheep of Kamieniecka breed. – Bulletin of the Veterinary Institute in Pulawy 54: 645-649.
[72] Hanušovská, E., Novák, M., Arvayová, M., Mikula, I. (2003): The PrP genotype of sheep of the improved Valachian breed. – Folia Microbiologica 48(2): 269-276.
[73] Tongue, S. C., Wilesmith, J. W., Cook, C. J. (2004): Frequencies of prion protein (PrP) genotypes and distribution of ages in 15 scrapieaffected flocks in Great Britain. – Veterinary Record 154(1): 9-16.
[74] Traoré, A., L. J., Kaboré, A., Pérez-Pardal, L., Álvarez, I., Fernández, I., ... Goyache, F. (2012): Prion protein gene polymorphism in four West African sheep populations. – Tropical Animal Health and Production 44(7): 1469-1472.
[75] Trevitt, C. R., Collinge, J. (2006): A systematic review of prion therapeutics in experimental models. – Brain 129(9): 2241-2265.
[76] Ugarte, E., Gabina, D. U. N. I. X. I. (2004): Recent developments in dairy sheep breeding. – Archiv für Tierzucht 47(6; SPI): 10-17.
[77] Van Duijn, C. M., Delasnerie-Laupretre, N., Masullo, C., Zerr, I., De Silva, R., Wientjens, D. P. W. M., ... Alperovitch, A. (1998): Case-control study of risk factors of Creutzfeldt-Jakob disease in Europe during 1993-95. – Lancet 351(9109): 1081-1085.

http://www.aloki.hu ● ISSN 1589 1623 (Print) ● ISSN 1785 0037 (Online)
DOI: http://dx.doi.org/10.15666/aeer/1804_51495173

[78] Wagenfeld, L. (1829): Ueber die Erkennung und Cur der Krankheiten der Schaafe. – Gerhard, Danzig.
[79] Weissmann, C. (1991): A 'unified theory' of prion propagation. – Nature 352(6337): 679-683.
[80] White, S., Herrmann-Hoesing, L., O'rourke, K., Waldron, D., Rowe, J., Alverson, J. (2008): Prion gene (PRNP) haplotype variation in United States goat breeds (Open Access publication). – Genetics Selection Evolution 40(5): 553-561.
[81] Wiśniewska, E., Mroczkowski, S. (2009): Different breeding strategies for scrapie resistance depending on breed-specific PrP allele and genotype frequencies in the Polish sheep. – Züchtungskunde 81(3): 180-189.
[82] Wiśniewska, E., Lühken, G., Mroczkowski, S., Erhardt, G. (2006): Prion protein (PrP) gene polymorphisms and breeding for resistance to scrapie in Polish Merino sheep. – Arch Tierz 49: 365-371.
[83] Yaman, Y., Ün, C. (2017): Genetic Resistance to Prion Diseases. – In: Tutar, Y. (ed.) Prion - An Overview. IntechOpen, London.
[84] Yang, Q., Zhang, S., Liu, L., Cao, X., Lei, C., Qi, X., ... Wang, R. (2016): Application of mathematical expectation (ME) strategy for detecting low frequency mutations: an example for evaluating 14-bp insertion/deletion (indel) within the bovine PRNP gene. – Prion 10(5): 409-419.
[85] Yang, Q., Zhang, S., Liu, L., Lei, C., Qi, X., Lin, F., ... Chen, H. (2018): The evaluation of 23-bp and 12-bp insertion/deletion within the PRNP gene and their effects on growth traits in healthy Chinese native cattle breeds. – Journal of Applied Animal Research 46(1): 505-511.
[86] Zhou, R., Li, X., Xi, J., Li, L., Zhang, Z., Zhao, Z. (2013): Genetic variability of PRNP in Chinese indigenous goats. – Biochemical Genetics 51(3-4): 211-222.

http://www.aloki.hu ● ISSN 1589 1623 (Print) ● ISSN 1785 0037 (Online)
DOI: http://dx.doi.org/10.15666/aeer/1804_51495173

EFFECTS OF PLANT-DERIVED SMOKE ON SEED GERMINATION OF SPECIES COMMON IN SUBTROPICAL CHINA

LIANG, Q.[1,2,3] – DENG, H. P.[3] – HE, P.[3]* – FANG, W.[4] – JIANG, H.[1] – LUO, T.[5]

[1]*School of Pharmacy, Guizhou University of Traditional Chinese Medicine, Guiyang, Guizhou 550025, PR China*

[2]*School of Ecological Engineering, Guizhou University of Engineering Science, Bijie, Guizhou 551700, PR China*

[3]*Chongqing Key Laboratory of Plant Resource Conservation and Germplasm Innovation, Institute of Resources Botany, School of Life Sciences, Southwest University, Chongqing, 400715, PR China.*

[4]*Chongqing Management Center for conversion of cropland to forest, Chongqing 400036, PR China*

[5]*College of Landscape Architecture and Life Science, Institute of Special Plants, Chongqing University of Arts and Sciences, Chongqing 402168, PR China*

**Corresponding author*
e-mail: lqin0857@qq.com

(Received 22nd Dec 2019; accepted 6th May 2020)

Abstract. Wildfires are predicted to increase with global climate change. Despite studies in several regions of the world indicating that burning smoke produced by wildfires may affect seed germination of some plants, little attention has been paid to this effect on wild plants in subtropical areas of China. In this study, seeds of 11 species from the Karst area of Guizhou province in China were collected for analysis. These seeds were treated with different concentrations of a plant-derived smoke solution prior to investigate seed germination parameters. We report that seven species out of the 11 tested germinated successfully, including five species which showed a positive germination response. Interestingly, we found that the seed germination percentage for *Pyracantha fortuneana* (Firethorn) and *Osbeckia opipara* seeds increased by 150% and 171% respectively following treatment with optimal smoke solution concentrations. However, smoke solution treatment had an inhibitory effect on the seed germination of one species and seed germination of one other species was unaffected by smoke solution exposure. Four species failed to germinate under our experimental conditions.
Keywords: *fire, smoke aqueous, prescribed burning, forest management, vegetation regeneration*

Introduction

Forest fire is one of the major causes of forest disturbance throughout the world. Due to climate change, the warmer, drier and more variable climate conditions predicted for the near future may further increase fire risk either in quantity or intensity. The recent wildfires all over the world have confirmed this prediction, such as Australia, Amazon region, California, and China. At the same time, prescribed burning is gradually recognized as an effective measure to reduce wildfire risk (Wang et al., 2019), and it has been promoted in many countries and regions. Prescribed burning refers to burning the accumulated fuels in the specified forest area within the specified time by

http://www.aloki.hu ● ISSN 1589 1623 (Print) ● ISSN 1785 0037 (Online)
DOI: http://dx.doi.org/10.15666/aeer/1804_51755185

controlling the fire intensity. With the increase of wildfire and prescribed burning by human, the importance of fire ecology research is further enhanced.

It is well known that the seedling regeneration for many plants is closely related to fire disturbance (Keeley and Pausas, 2018; Alahakoon et al., 2020): high temperature, burning smoke and coke are all produced by fire and can influence seed germination with variable effect sizes. Previously published studies describing the effects of plant-derived smoke on seed germination are gathering increasing attention from ecologists and physiologists all over the world, particularly in recent years (Flematti et al., 2004, 2011; Keeley et al., 2018; De Lange et al., 2018; Riveiro et al., 2019). Of particular interest is the discovery that the seed germination of many plants native to regions around the world can be induced by exposure to smoke solution, including many species the seed germination of which is difficult to induce under normal conditions or whose seeds are in a dormant phase (Flematti et al., 2011; Cédric Leperlier et al., 2018). The research carried out to date in this field has enhanced the application of plant-derived smoke in commercial or industrial settings. And the potential stimulatory effect of plant-derived smoke on seed germination has been widely recognized in some countries and regions (Kulkarni, et al., 2011). Plant smoke has become one of the most important tools in the field of fire ecology because the smoke produced by burning plant matter from wildfire can promote or inhibit the germination of seeds. Indeed, the concept of "plant-derived smoke ecology" has recently been discussed (Light, 2016), and the study of the ecological effects of plant-derived smoke is becoming a distinct and independent discipline. However, seed germination of some plant seeds is inhibited following exposure to high concentrations of smoke solution (Dixon et al., 1995; Zirondi et al., 2019).

At present, the germination response of seeds from 120 families and 1335 plants from around the world have been tested through stimulation by aqueous solutions of smoke or aerosol smoke, and many of them have been found to respond positively (Çatav et al., 2014; Light, 2016; Cembrowska-Lech and Kępczyński, 2017). These plants are denoted smoke responsive plants. According to the reports, smoke responsive plants research originate from South Africa (De lange et al., 2018), then many in the Mediterranean-climate ecosystems (Keeley and Fotheringham, 1998; Moreira et al., 2010; Çatav et al., 2014), and then expanded to many types of ecosystems around the world. However, few studies have focused on the effects of smoke on plant regeneration in subtropical ecosystems, including subtropical areas of China.

Based on the records of smoke-stimulated seed germination in many species from different areas, we hypothesized that smoke would enhance seed germination of species in subtropical areas of China. To test this hypothesis, we performed a seed germination experiment with seeds of eleven species growing in natural subtropical areas of China. The seed germination percentage and seed germination rate of each species were assessed in smoke solution treatments at different concentrations, and these results were compared to the controls to determine if smoke treatments resulted in any increment in seed germination percentage and rate. In parallel, we examined the percentage and rate of seed germination between species within the same family, to determine if the germination response of seeds to smoke solution is dependent on the genera and families of species. By conducting this experiment, we aimed to clarify the role of smoke in seed germination of species in subtropical areas of China.

http://www.aloki.hu ● ISSN 1589 1623 (Print) ● ISSN 1785 0037 (Online)
DOI: http://dx.doi.org/10.15666/aeer/1804_51755185

Materials and methods

Study area and sites

The research area is located in Bijie, a city of Guizhou province (26°21′~27°46′N; 103°36′~106°43′E). The total area of the city is 26,900 km^2, 79.31% of the total area is Karst area, and the area of rocky desertification is 24.36%. This area belongs to the humid monsoon climate zone in the middle subtropical zone. The mean annual temperature in this area is 12.5 ℃ and the annual mean precipitation is about 1000 mm with clearly defined dry and wet seasons. The precipitation is mainly concentrated in summer. Most of the vegetation in this area has degenerated into herbaceous communities and rattan thorn bush, including species of *Pyracantha fortuneana* (Firethorn)*, Cotoneaster glaucophyllus, Rosa rubus* (Mayberry)*, Deyeuxia arundinacea, Bidens pilosa*, *Galinsoga parviflora* and so on. Karst is widespread in this area and the soil is very dry. Plants here are suffering from the stresses of both drought and cold in the winter. During this period, vegetation above ground mostly dies off and fell on the ground, causing the accumulation of fuel, which may increase wildfire risk. Between the years of 2005 and 2009, a county of Bijie named Qi Xingguan was exposed to 102-237 wildfires every year. After that, a large number of human and financial resources have been invested in this area, accompanied by special wildfire control laws (Ruan et al., 2015). In recent years, the trend of aggravation of wildfires predicted by theory in this area has been changed, and the number of wildfires decreased significantly, but still occur every year.

Seed collection

Based on the dominance of species in the study area, we collected seeds of 11 species which growing in fire-prone areas in November 2013, from the typical Karst mountainous area of Bijie: *P. fortuneana, C. glaucophyllus, Osbeckia opipara, Vernonia saligna, Spiraea japonica, B. pilosa, Carpesium cernuum, Imperata koenigii* (Cogongrass)*, R. rubus, Cotoneaster adpressus, Clematis lasiandra.* The characterizations of the species seeds are as follows (*Table 1*). These plants are common and widely distributed in the subtropical areas of China. The seeds collected were taken back to the laboratory for air drying about four weeks. Healthy seeds free of pathology and pathogens were selected, packed in paper bags and stored at room temperature.

Preparation of plant-derived smoke solution

We used smoke solution throughout this study since the concentrations can be strictly controlled compared to aerosol smoke. And smoke solution and aerosol have similar effects on seed germination according to the study of Çatav et al. (2014). On the other hand, Studies have shown that the content of smoke is consistent regardless of the kind of plants that are burned (Brown and Van Staden, 1997; Çatav, et al., 2012). We therefore used the leaves of *D. arundinacea* as the raw material to produce smoke, which is widely distributed in the Guizhou area and would therefore be representative of a wildfire in the area.

Following the methods of Coons et al. (2014), we collected *D. arundinacea* leaves, then cut them and incubate in an oven at 105 ℃ for 5 min, and then at 70 ℃ to constant weight. 100 g of dried leaves were then moved to a smoker, ignited, and left to produce smoke. Smoke was guided into a chamber containing 500 ml distilled water through the pipe. This infusion was then diluted to six different concentrations (1:1000, 1:500, 1:100, 1:50, 1:2, 1:1) (v:v) before treating the seeds.

http://www.aloki.hu ● ISSN 1589 1623 (Print) ● ISSN 1785 0037 (Online)
DOI: http://dx.doi.org/10.15666/aeer/1804_51755185

Table 1. *Description of seed characterization*

Species name	Family name	Genus name	Life form	Fruit type	Seed length (mm)	Seed width (mm)	Seed mass (mg)
Pyracantha fortuneana	Rosaceae	Pyracantha	Shrub	Pome	2.48	1.31	1.39
Cotoneaster glaucophyllus	Rosaceae	Cotoneastr	Shrub	Pome	4.33	3.18	10.29
Osbeckia opipara	Melastomataceae	Osbeckia	Shrub	Capsule	0.43	0.45	0.05
Vernonia saligna	Compositae	Vernonia	Shrub	Achene	2.19	0.23	0.17
Spiraea japonica	Rosaceae	Spiraea	Shrub	Follicle	1.23	0.34	0.12
Bidens pilosa	Compositae	Bidens	Herb	Achene	8.72	0.57	1.45
Carpesium cernuum	Compositae	Carpesium	Herb	Achene	3.56	0.60	0.49
Imperata koenigii	Gramineae	Imperata	Herb	Caryopsis	1.44	0.57	0.36
Rosa rubus	Rosaceae	Rubus	Shrub	Aggregate fruit	4.56	2.62	8.46
Cotoneaster adpressus	Rosaceae	Cotoneaster	Shrub	Pome	3.86	2.84	8.39
Clematis lasiandra	Ranunculaceae	Clematis	Liana	Achene	3.73	1.73	2.68

Seed germination test

We selected approximately 900 seeds with no obvious diseases or infection with insect pests for each species. Seeds were sterilized for 10 min with 1% sodium hypochlorite solution. Floating seeds were removed at this stage. After sterilization, sedimented seeds were washed three times and dried by airing. Seeds were placed in beakers at a concentration of 100 seeds per beaker, and then soaked in sterile water (ck) or at different concentrations of smoke solution. After 24 h, seeds were leached and moved to 10 cm Petri dishes. Two layers of filter paper were positioned at the bottom of each dish, then four milliliters of sterile water or smoke solution was added, and this was incubated at (25 ±_2) ℃ 12 h / (15 ±_2) ℃ 12 h in darkness. Seeds were only exposed to light briefly during the monitoring periods. Incubation was performed under dark conditions to ensure consistent conditions between treatments. A total of seven treatments were set up including the control (ck). Each treatment was performed with four replicates of 25 seeds. The seeds were monitored for germination daily. Filter paper was moistened with distilled water or smoke solution respectively if necessary, to prevent dry conditions. Seeds were considered as germinated if they had a radicle emergence > 1 mm.

Statistical analysis

Seed germination percentage (GP) and seed germination rate (GR) were calculated for each species and treatment as follows:

$$GP(\%) = (\sum_{i=1}^{n} n_i)/\, N \times 100 \quad \text{(Eq.1)}$$

$$GR = (\sum_{i=1}^{n} n_i)/\, t_i \times 100 \quad \text{(Eq.2)}$$

http://www.aloki.hu ● ISSN 1589 1623 (Print) ● ISSN 1785 0037 (Online)
DOI: http://dx.doi.org/10.15666/aeer/1804_51755185

where n_i is the number of seeds which germinate on a given day, N is the total number of seeds sown, and t_i is the number of days from sowing to the termination of the experiment for each species. GR represents the grains of germinated seeds per 100 days.

SPSS 20 statistical software was used for statistical analysis. The seed germination percentage and germination rate of different treatments was analyzed by one-way ANOVA (One-Way ANOVA), the significance of differences were compared by Duncan's multiple comparison (a = 0.05).

Results

Seed germination percentage

Germination was successful following smoke exposure for seeds from 7 plant species (*P. fortuneana, C. glaucophyllus, O. opipara*, *C. cernuum*, *B. pilosa*, *V. saligna* and *I. koenigii*) out of 11 tested species (*Fig. 1*). In addition to *C. glaucophyllus*, seed germination of six additional germinated species was significantly affected by treatment with smoke solution, but the influence was not consistent between species.

There were five species belonged to Rosaceae out of a total of 11 tested species: *P. fortuneana*, *C. glaucophyllus*, *S. japonica*, *C. adpressus* and *R. rubus*. Only *P. fortuneana* and *C. glaucophyllus* germinated successfully from this genus. The seed germination percentage of *P. fortuneana* was 150% higher than control following smoke solution treatment at the 1:1000 dilution, but no significant differences were observed between the control treatment and higher smoke solution concentrations. For *C. glaucophyllus*, the seed germination percentage were unaffected by the presence of smoke solution at any concentration, compared with the control group.

Three species of Compositae plants were included in this study: *C. cernuum*, *B. pilosa* and *V. saligna*. Seeds of all three species germinated successfully, but the germination response was not consistent between smoke solution treatments. Smoke solution stimulated the seed germination of *C. cernuum* and *B. pilosa.* Germination of these seeds was enhanced by smoke solution at one or more of the concentrations tested. In contrast, the seed germination percentage of *V. saligna* was inhibited by smoke solution. We observed a general trend where there was an inverse correlation between smoke concentration and the seed germination percentage. At the maximum smoke solution concentration, the seed germination percentage of *V. saligna* was reduced by 70% compared to the control treatment.

Smoke solution can also promote the seed germination percentage of *O. opipara* and *I. koenigii*, both of these species' seeds showed a positive correlation with smoke solution concentration. At the maximum smoke solution concentration, the seed germination percentage was enhanced by 21.66% and 171.23% respectively. *O. opipara* was more sensitive to smoke solution treatment than *I. koenigii*, as an increased seed germination percentage was observed at lower smoke solution concentrations than *I. koenigii*. The seed germination percentage of *O. opipara* is significantly higher than that of control in all smoke solution concentrations tested.

Seed germination rate

In control treated samples, the seed germination rate of *I. koenigii* and *C. cernuum* is relatively high (up to 135 grains/100d), compared to the seed germination rate of others

http://www.aloki.hu ● ISSN 1589 1623 (Print) ● ISSN 1785 0037 (Online)
DOI: http://dx.doi.org/10.15666/aeer/1804_51755185

(*Fig. 2*). In addition to *C. glaucophyllus*, smoke solution had a significant influence on the germination rate of seeds ($P < 0.05$).

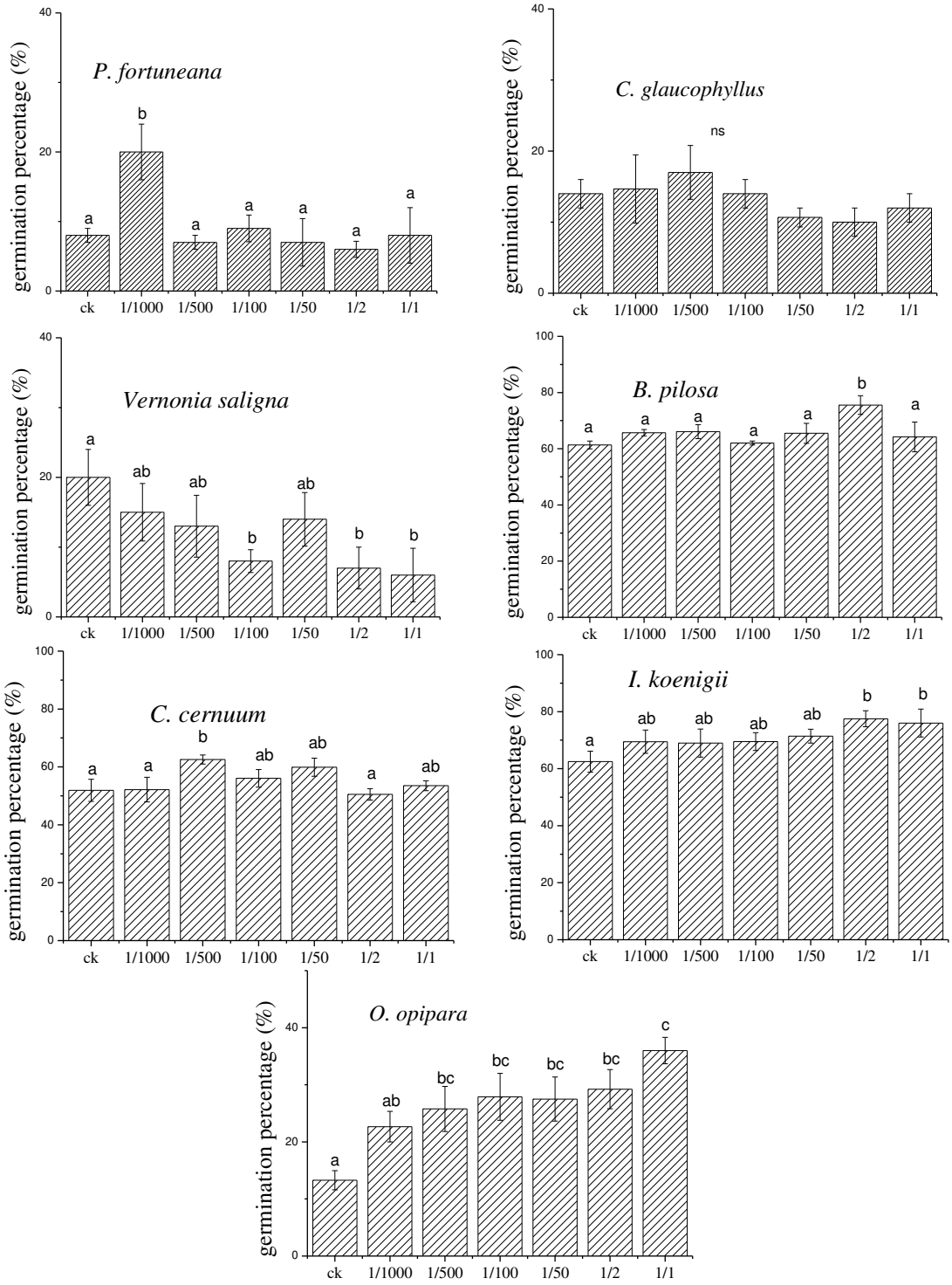

Figure 1. *Seed germination percentage under different smoke solution treatment (means + s.e., n = 4). The same letter represents no significant difference between the groups. Different letters represent a significant difference between groups (P < 0.05). ck, control; 1/1000, 1/500, 1/100, 1/50, 1/2, 1/1 represent the concentration of smoke solution (v/v). (The same applies below in Fig. 2)*

http://www.aloki.hu ● ISSN 1589 1623 (Print) ● ISSN 1785 0037 (Online)
DOI: http://dx.doi.org/10.15666/aeer/1804_51755185

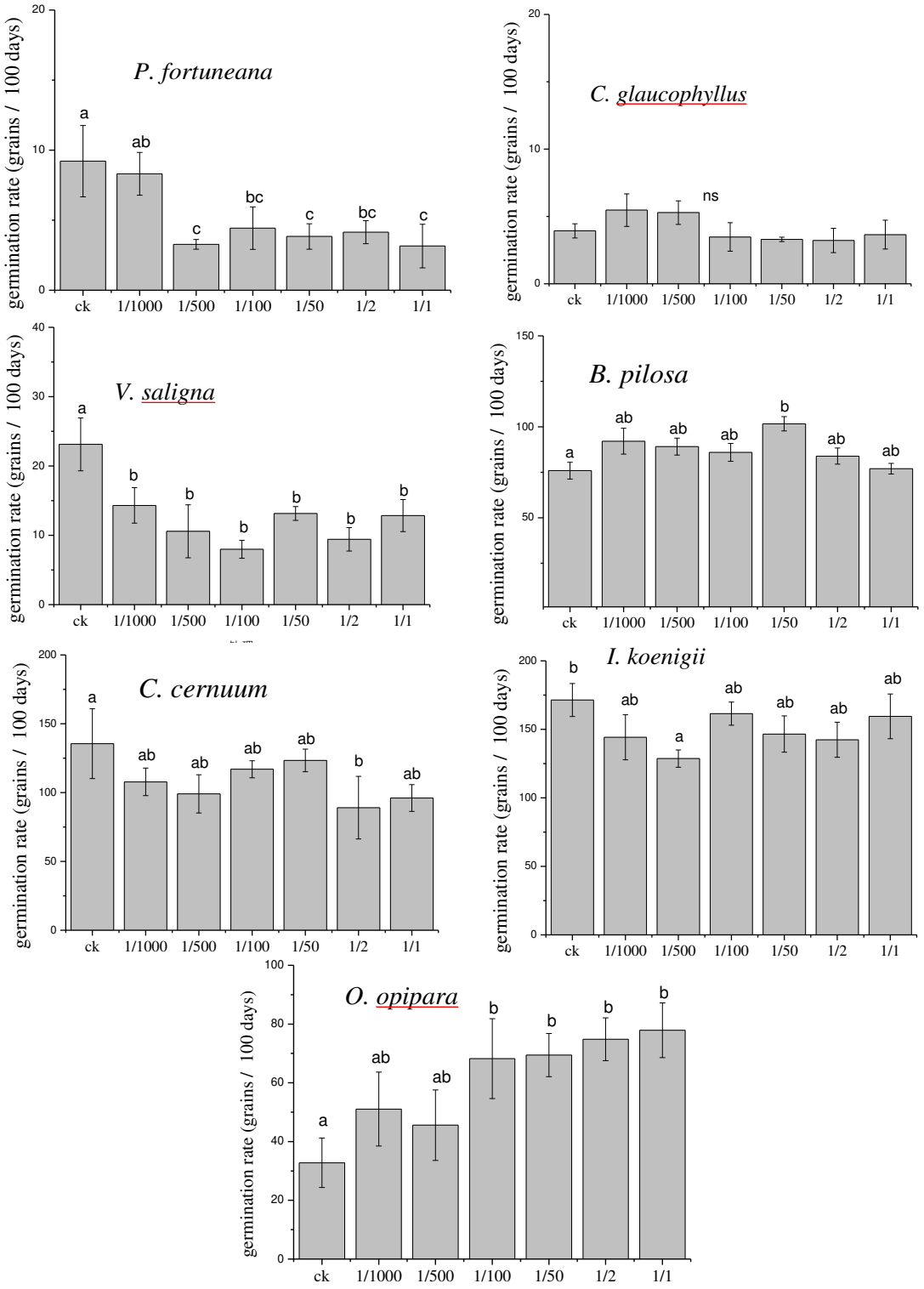

Figure 2. *Seed germination rate under different smoke solution treatment (means ± s.e., n = 4)*

The seed germination rate of *P. fortuneana* decreased significantly when the smoke solution concentration was higher than 1:500. However, smoke solution did not affect the seed germination rate of *C. glaucophyllus* significantly, even though they were belonging to the same family (Rosaceae). The seed germination rate of Compositae

http://www.aloki.hu ● ISSN 1589 1623 (Print) ● ISSN 1785 0037 (Online)
DOI: http://dx.doi.org/10.15666/aeer/1804_51755185

plant *V. saligna* and *C. cernuum* were negatively correlated with the smoke solution concentration, and the seed germination rate of *B. pilosa* improved under smoke solution treatment. The seed germination rate of *I. koenigi* was significantly slower than control at a smoke solution concentration of 1:500. The seed germination rate for *O. opipara* seeds was accelerated significantly when the smoke solution concentration was equal to or greater than 1:100. When the smoke solution concentration reached 1:1, the seed germination rate peaked at approximately 137% of the control seeds.

Discussion

There were seven species out of a total of 11 tested species germinated successfully under our experimental conditions. This study is the first to report the seed germination response of the six plant species following smoke solution treatment (Except for *B. pilosa*). This study shows that, as in Mediterranean climate zones, plant-derived smoke also promotes seed germination of plants widely distributed in the subtropical humid monsoon climate area of China. In this study, most germinated species (5/7) showed enhanced seed germination under smoke solution treatment, with a wide variety of plant characteristics for example life type and fruit type. The effects on seed germination were dependent upon the concentration of smoke solution and the species tested. This result is consistent with previous research, which showed plant-derived smoke generally stimulates seed germination, but the sensitivity of plants to smoke can vary (Çatav et al., 2014; Alahakoon et al., 2020).

This study shows that plant-derived smoke solution may promote seed germination for plants widely distributed in the subtropical areas of China, but this effect is independent of the species' family and genera. Researchers found that species even belonging to the same family (Ferraz et al., 2013; Çatav et al., 2018) or generus (Kulkarni et al., 2007) also responded differently to plant-derived smoke. This study is in keeping with this work: the smoke response of plants belonging to same family differed between the Rosaceae plants *P. fortuneana* and *C. glaucophyllus*, as well as with the Compositae plants *V. saligna* and *C. cernuum.* Based on seed germination response to smoke solution, the plants tested here can be divided into three types (*Table 2*): Type A, positive responders; Type B, neutral responders; Type C, negative responders. Type A plants are characterized by the positive response of seed germination with at least one concentration of smoke solution. These plants include *O. opipara, I. koenigii*, *P. fortuneana*, *B. pilosa* and *C. cernuum*. Type B plants, such as *C. glaucophyllus,* were not sensitive to smoke solution. Type C plants were characterized by negative response of seed germination to at least one concentration of smoke solution. Type C plants included *V. saligna*. The result is consistent with the study of Ferraz et al. (2013), in which the seed germination response of woody plants from the Amazon to smoke solution were studied. Overall, there are more A-type plants in the tested species, but there are other response types of plants, so further research is still needed to reveal the impact of smoke water on vegetation regeneration in the fire prone areas.

Although smoke solution treatment increased seed germination percentages in most species tested, the response of seed germination rate differed between species. Under smoke solution treatment, the seed germination rate of only 2/7 species accelerated significantly, but 4/7 species were slowed. smoke solution was able to increase the seed germination rate of *O. opipara* significantly, and the effect showed a positive

http://www.aloki.hu ● ISSN 1589 1623 (Print) ● ISSN 1785 0037 (Online)
DOI: http://dx.doi.org/10.15666/aeer/1804_51755185

correlation with the concentration of smoke solution. Seed germination rates of *V. saligna* were significantly inhibited by smoke solution. It is generally believed that the earlier germinating species in the open field will have advantages in community competition, because they have more resources, indicating that the smoke generated by wildfire may change the competition of communities.

Table 2. *Response types of seed germination under smoke solution*

Treatments	Type A					Type B	Type C
	O. opipara	***I. koenigii***	***P. fortuneana***	***B. pilosa***	***C. cernuum***	***C. glaucophyllus***	***V. saligna***
1/1000	0	0	+	0	0	0	0
1/500	+	0	0	0	+	0	0
1/100	+	0	0	0	0	0	-
1/50	+	0	0	0	0	0	0
1/2	+	+	0	+	0	0	-
1/1	+	+	0	0	0	0	-

"+" indicates a positive response, seed germination percentage increased significantly under smoke solution treatment. "-" indicates a negative response, seed germination percentage decreased significantly under smoke solution treatment; "0" shows seed germination rate did not differ significantly from the control seeds with smoke solution treatment

Our results show that there are three types of responses to plant smoke, and these responses are independent with the phylogenetical family of the species. Considering that the seed germination promoting effect of smoke has no obvious regularity, the seed germination of some weeds and exotic species with low economic value but high reproductive ability may be promoted. Thus, we must remain alert to the risk that plant-derived smoke generated from frequent wildfires could potentially increase weed and exotic species invasion (Mojzes and Kalapos, 2014; Alahakoon et al., 2020). Conversely, most of the tested plants are medicinal plants, garden plants or forage grasses, and it is of great value to use plant-derived smoke to improve their seed germination. In addition, the positive effect on seed germination of plant-derived smoke is of great significance. It can be used in horticulture and agriculture, and even in weeds control (by increasing the germination percentage of weeds and reducing the seed bank of weeds). Our result suggests that the plant-derived smoke can improve the species germination, thus, it can also be used as an important tool for the protection and restoration of plant communities, such as ecological restoration of mining wasteland, restoration and reconstruction of disturbed ecosystems amongst other possibilities.

Prescribed burning technologies are increasingly used in forest management in domestic and international settings. The use of prescribed fire will inevitably produce a large volume of smoke, and we cannot control the boundary and direction of the smoke just as the time and area. We do not know which species might be exposed to the smoke, nor do we know which species will be stimulated by the smoke. Thus, it is suggested that prescribed burning techniques should be used carefully before we understand the response of non - economic plants and non - target plants (such as invasive alien species) to fire and its related factors by strict control experiments.

http://www.aloki.hu ● ISSN 1589 1623 (Print) ● ISSN 1785 0037 (Online)
DOI: http://dx.doi.org/10.15666/aeer/1804_51755185

Conclusion

Plant-derived smoke can promote seed germination of several species of plants in subtropical areas of China, with few plants being insensitive to plant-derived smoke and others being inhibited by plant-derived smoke. Plant-derived smoke has different effects on seed germination of different plants and the differences are independent of family or generus. Therefore, burning smoke generated with wildfire is likely to change the subsequent recovery and species composition of burned areas. Because plant-derived smoke has different ecological effects on plants, it is necessary to evaluate the feasibility and efficacy of prescribed burning technology for the perspective of burning smoke in specific regions. Globally, wildfires are increasing, and fire products associated with wildfires increasing, therefore we must be aware of the effects of smoke produced with wildfires. And we suggest that future research could consider the following aspects:

a) Study the effect of plant-derived smoke on the growth of medicinal plants, ornamental plants and vegetation restoration plants, and to make full use of the advantages of smoking.
b) Study the germination response of dominant species or key species (such as endangered species, economic species and other target species) to plant-derived smoke and explore the impact of wildfire on the vegetation succession and community composition in fire prone area or prescribed burning area.
c) Study the response of high-risk invasive plants to plant-derived smoke in the fire prone region or prescribed burning areas, to prevent fire smoke from becoming an assistant of invasive plants.
d) The bioactive components in plant-derived smoke and its mechanisms have always been the concern of ecologists and chemists, which also needs further study.

Acknowledgments. This study was funded by the science and technology cooperation plan project of Guizhou Science and Technology Agency and Bijie Bureau of Science and Technology and Guizhou University of Engineering Science (No. Qiankehe LH zi [2017]7020). And supported by the top talents project of Guizhou Education Department (No. [2016]101), and the Science and Technology project of Guizhou Province (No. [2017] 7004) also.

REFERENCES

[1] Alahakoon, A. A. C. B., Perera, G. A. D., Merritt, D. J., Turner, S. R., Gama-Arachchige, N. S. (2020): Species-specific smoke effects on seed germination of plants from different habitats from Sri Lanka. – Flora 263: 151530.
[2] Brown, N. A. C., Van Staden, J. (1997): Smoke as a germination cue: a review. – Plant growth regulation 22: 115-124.
[3] Çatav, Ş. S., Bekar, İ., Ateş, B. S., Ergan, G., B., Oymak, F., Ülker, E. D., Tavşanoğlu, Ç. (2012): Germination response of five eastern Mediterranean woody species to smoke solutions derived from various plants. – Turkish Journal of Botany 36: 480-487.
[4] Çatav, Ş. S., Küçükakyüz, K., Akbaş, K., Tavşanoğlu, Ç. (2014): Smoke-enhanced seed germination in Mediterranean Lamiaceae. – Seed Science Research 24: 257-264.
[5] Çatav, Ş. S., Küc ¸ükakyüz, K., Tavşanoğlu, C., Pausas, J. G. (2018): Effect of fire-derived chemicals on germination and seedling growth in Mediterranean plant species. – Basic and Applied Ecology 30: 65-75.

http://www.aloki.hu ● ISSN 1589 1623 (Print) ● ISSN 1785 0037 (Online)
DOI: http://dx.doi.org/10.15666/aeer/1804_51755185

[6] Cembrowska -Lech, D., Kępczyński, J. (2017): Plant-derived smoke induced activity of amylases, DNA replication and β-tubulin accumulation before radicle protrusion of dormant Avena fatua L. caryopses. – Acta Physiologiae Plantarum 39(1): 39-39.
[7] Coons, J., Coutant, N., Lawrence, B., Finn, D., Finn, S. (2014): An effective system to produce smoke solutions from dried plant tissue for seed germination studies. – Applications in plant sciences 2(3): 1-5.
[8] De Lange, J. H., Brown, N. A. C., Van Staden, J. (2018): Perspectives on the contributions by South African researchers in igniting global research on smoke-stimulated seed germination. – South African Journal of Botany 115: 219-222.
[9] Dixon, K. W., Roche, S., Pate, J. S. (1995): The promotive effect of smoke derived from burnt native vegetation on seed germination of Western Australian plants. – Oecologia 101(2): 185-192.
[10] Ferraz, I. D. K., Arruda, Y. M. B. C., Van Staden, J. (2013): Smoke-water effect on the germination of Amazonian tree species. – South African Journal of Botany 87: 122-128.
[11] Flematti, G. R., Ghisalberti, E. L., Dixon, K. W., Trengove, R. D. A. (2004): Compound from smoke that promotes seed germination. – Science 305(5686): 977-977.
[12] Flematti, G. R., Merritt, D. J., Piggott, M. J., Trengove, R. D., Smith, S. M., Dixon, K. W., Ghisalberti, E. L. (2011): Burning vegetation produces cyanohydrins that liberate cyanide and stimulate seed germination. – Nature Communications 2(1): 1-6.
[13] Keeley, J. E., Fotheringham, C. J. (1998): Smoke-induced seed germination in California chaparral. – Ecology 79: 2320-2336.
[14] Keeley, J. E., Pausas, J. G. (2018): Evolution of 'smoke' induced seed germination in pyroendemic plants. – South African Journal of Botany 115: 251-255.
[15] Kulkarni, M. G., Sparg, S. G., Van Staden, J. (2007): Germination and post-germination response of Acacia seeds to smoke-water and butenolide, a smoke-derived compound. – Journal of Arid Environments 69: 177-187.
[16] Kulkarni, M. G., Light, M. E., Van Staden, J. (2011): Plant-derived smoke: Old technology with possibilities for economic applications in agriculture and horticulture. – South African Journal of Botany 77(4): 972-979.
[17] Leperlier, C., Riviere, J. E., Allibert, A., Dessauw, D., Lacroix, S., Fock-Bastide, I. (2018): Overcoming dormancy and light requirements in seeds of Heteropogon contortus, a target species for savanna restoration. – Ecological Engineering 122: 10-15.
[18] Light, M. E. (2016): Ecology of plant-derived smoke: its use in seed germination. – African Journal of Range & Forage Science 33: 76-76.
[19] Mojzes, A., Kalapos, T. (2014): Plant-derived smoke stimulates germination of four herbaceous species common in temperate regions of Europe. – Plant Ecology 215: 411-415.
[20] Moreira, B., Tormo, J., Estrelles, E., Pausas, J. G. (2010): Disentangling the role of heat and smoke as germination cues in Mediterranean Basin flora. – Annals of Botany 105: 627-635.
[21] Riveiro, S. F., García-Duro, J., Cruz, Ó., Casal, M., Reyes, O. (2019): Fire effects on germination response of the native species Daucus carota and the invasive alien species Helichrysum foetidum and Oenothera glazioviana. – Global Ecology and Conservation 20: 1-7.
[22] Ruan, P. L., Tang, T., Zhang, H. A. (2015): Study on the forest fire prevention in Bijjie experimental area of Guizhou Province. – Guizhou Forestry Science and Technology 43(2): 43-47.
[23] Wang, X. L., Xu, J. Y., Wu, Z. S., Shen, Y. C., Cai, Y. J. (2019): Effect of annual prescribed burning of wetlands on soil organic carbon fractions: A 5-year study in Poyang, China. – Ecological Engineering 138: 219-226.
[24] Zirondi, H. L., Silveira, F. A. O., Fidelis, A. (2019): Fire effects on seed germination: Heat shock and smoke on permeable vs impermeable seed coats. – Flora 253: 98-106.

http://www.aloki.hu ● ISSN 1589 1623 (Print) ● ISSN 1785 0037 (Online)
DOI: http://dx.doi.org/10.15666/aeer/1804_51755185

WEED SUPPRESSION IN MAIZE (*ZEA MAYS* L.) THROUGH THE ALLELOPATHIC EFFECTS OF SORGHUM [*SORGHUM BICOLOR* (L.) CONARD MOENCH.] SUNFLOWER (*HELIANTHUS ANNUUS* L.) AND PARTHENIUM (*PARTHENIUM HYSTEROPHORUS* L.) PLANTS

RASHID, H. U.[1] – KHAN, A.[1] – HASSAN, G.[2] – KHAN, S. U.[1] – SAEED, M.[3] – KHAN, S. A.[4] – KHAN, S. M.[5] – HASHIM, S.[2]

[1]*Department of Agronomy, The University of Haripur, Haripur, Pakistan*

[2]*Department of Weed Science, The University of Agriculture Peshawar, Peshawar, Pakistan*

[3]*Department of Agriculture, The University of Swabi, Swabi, Pakistan*

[4]*Department of PBG, The University of Haripur, Haripur, Pakistan*

[5]*Department of Horticulture, The University of Haripur, Haripur, Pakistan*

**Corresponding author*
e-mail: peerayub@gmail.com

(Received 19th Jan 2020; accepted 25th May 2020)

Abstract. The present study was carried out at the Weed Science Research Laboratory, The University of Agriculture, Peshawar Pakistan (June-July 2013 and Sep-Oct 2013). To evaluate the most effective and economical treatment for weed management in maize (*Zea mays* L.), the pot experiment was performed using completely randomized design (CRD) with three replications. Allelopathic effects of *Sorghum bicolor* (L.) Conard Moench., *Helianthus annuus* L., *Parthenium hysterophorus* L, and the commercial herbicide (atrazine @ 18 g L^{-1}) was used for comparison. The data were recorded on germination and seedling growth of test species (*Zea mays*, *Trianthema portulacastrum* and *Lolium rigidum*). The data showed that *S. bicolor* + *H. annuus* + *P. hysterophorus* water extract (WE) @ 33.33 + 33.33 + 33.33 (g L^{-1}) reduced dry biomass of *T. portulacastrum* and *L. rigidum* by 35 and 41% respectively, whereas the commercial herbicide by 45-47%. Maize seeds were found more tolerant than the weed species tested. Hence, it is concluded that extracts applied in mutual combination had more inhibitory effect than their sole applications, however, the efficacy of atrazine was more effective in suppressing germination and seedling growth of the tested species. The degree of toxicity for the various treatments can be placed in the following array of inhibition: Herbicide > combined extracts > isolated extracts. The current study showed that all the tested allelopathic plants contain water soluble allelochemicals which could inhibit/retard the germination percentage and seedling growth of the tested species. Hence, the findings of the current study suggest that it is possible to use these extracts as an alternative to synthetic herbicide (s) for sustainable weed management in maize. However, further studies are suggested to confirm our findings under field conditions.
Keywords: *allelochemicals, atrazine, water extracts, weed management*

Introduction

Weed infestation is and has been a major constraint in maize production systems and is reported to reduce its yield by 24-83% (Dogan et al., 2004; Usman et al., 2001). Weeds are the most ever-present class of pests that interfere with crop plants through allelopathy and competition for nutrients, moisture, solar radiation, gases and space resulting in direct loss to quantity and quality of the product (Gupta, 2004). The yield of

http://www.aloki.hu ● ISSN 1589 1623 (Print) ● ISSN 1785 0037 (Online)
DOI: http://dx.doi.org/10.15666/aeer/1804_51875197

maize could be reduced up to 32% due to horse purslane (*Trianthema portulacastrum*) infestation (Balyan and Bhan, 1989) and up to 80% due to the competition with rigid ryegrass (*Lolium rigidum*) depending on the season and infestation level (Izquierdo et al., 2003). The worst weeds competitive with *Zea mays* L. in Pakistan are purple nutsedge (*Cyprus rotundus* L.), horse purslane (*Trianthema portulacastrum* L.), bermuda grass (*Cynodon dactylon* (L.) Pers., common lambasquarters (*Chenopodium album* L.), barnyard grass (*Echinochloa crus-galli* L. Beauv.) and jungle rice (*E. colona* (L.) Link) (Muhammad et al., 2009). The predominance and competitive ability of weeds with maize or corn varies due to the geographical location, competitive ability of the variety planted, nutrients availability, availability of moisture, soil type and soil management. In the US there is a variation in weed flora from state to state, but the commonly predominant weeds include common waterhemp (*Amaranthus tuberculatus*), giant ragweed (*Ambrosia trifida*), horseweed (marestail) (*Conyza canadensis*) and velvetleaf (*Abutilon theophrasti*) (NewGenFarmer Maize + Soybean, 2020). In South Africa, common lambsquarters (*Chenopodium album*), purple nutsedge (*Cyperus rotundus*), yellow nutsedge (*Cyperus esculentus*) and bermuda grass (*Cynodon dactlon*) are ranked as the worst competitors of maize (University of Pretoria, 2020).

Weed control emerged an easy job due to the advent of 2.4-D and its analogs during the second world war era in the early 1940's. It was followed by the discovery of myriads of herbicides with varying modes of action and specificity on weeds. But this panacea started dwindling after the discovery of resistance to diclofop in Oregon state USA in the early 1980s'. Ironically the list of resistant weeds has kept growing to different herbicides and presently 512 unique cases (species x site of action) of herbicide resistant weeds, with 262 species (152 dicots and 110 monocots) have been reported globally in 93 crops in 70 countries (Heap, 2020). The non-judicious use of herbicides can create many environmental and health related problems everywhere in addition to resistance development in weeds (Jabran et al., 2008; Khan et al., 2010). Recently thirty-eight weed species have now evolved resistance to glyphosate, spread across 37 countries of the world infesting 34 different crops and six non-crop situations (Heap and Duke, 2018), which includes some of the worst weeds of the world. Hence, principal reliance on herbicides has become obscure and alternate weed control measures are indispensable. Hand weeding is labor intensive, time consuming and getting more expensive, hence mostly impracticable. Cultural methods are environment friendly, but very slow in action. Therefore, scientists realized that the alternative to herbicides should be designed for sustainable weed management by the use of allelopathic crop plants and weeds for quality production of crops and to reduce the use of synthetic herbicides to contribute to maintaining sustainable agriculture (An et al., 2005; Jabran et al., 2007, 2015; Khan et al., 2012; Hassan et al., 2018).

Several allelopathic plant species have been reported for weed management in cereal crops through the inhibitory effect on weed species. Allelopathy is a new approach to be used as an alternative to synthetic herbicides for the weed management as a source of bio herbicides. Several allelopathic plant species such as *Sorghum bicolor* (L.) Conard Moench. (Cheema and Khaliq, 2003; Weston and Duke, 2003), *Halianthus annuus* L. (Leather, 1987; Batish et al., 2002) and *Parthenium hysterophorus* L. (Adkins et al., 1996; Belz et al., 2007; Belz, 2016; Hassan et al., 2018) are inhibitory at high doses as well as stimulatory to weeds at low doses due to hormesis (Belz, 2008).

Keeping in view the importance of these allelopathic plants on weeds, the present study was designed with the objective to identify the most effective water extracts of

http://www.aloki.hu ● ISSN 1589 1623 (Print) ● ISSN 1785 0037 (Online)
DOI: http://dx.doi.org/10.15666/aeer/1804_51875197

allelopathic species applied isolated and in mixture for control of weeds in maize under Laboratory (pot conditions).

Materials and methods

Laboratory based Pot experiments were conducted at the Weed Research Laboratory, The University of Agriculture Peshawar, Pakistan during June-July 2013 and subsequently repeated in September-October 2013.

Collection of allelopathic plants

Sorghum [*Sorghum bicolor* (L.) Conard Moench.] and sunflower (*Helianthus annuus* L.) were collected from the farmers' fields in district Swabi, Pakistan while, parthenium (*Parthenium hesterophorus* L.) plants were collected from the roadsides and waste areas of Swabi. Sorghum and sunflower were collected after harvesting the crops in the field while parthenium was collected freshly at maturity stage. All the plant samples were cleaned to remove dust and other particles and then were dried in oven (Kenton; KH-120AS) for 72 h at 65 °C and were ground with the help of an electrical grinder. The grinded samples of all the three species were kept in bags and labeled properly for further use in both runs of experiments.

Preparation of water extracts

All the plants' powders were mixed with each other and with distilled water as the treatment specifications @ 1:10 (w/v). The extracts were kept at room temperature 20 ± 22 °C for 48 h and filtered through muslin cloth and finally through Whatman No.1 filter paper to collect the respective water extract. Synthetic herbicide (atrazine) and distilled water was included as check. Fungicide Topsin-M 70% @ 2 g kg $^{-1}$ was used in all treatments in order to avoid fungal infestation. Water extracts bottles were individually tagged and stored for further utilization.

Experimental details

A total of 81 plastic pots (12 cm height and 15 cm diameter) were filled with 1 kg of soil. The soil samples were analyzed for soil physicochemical properties. The soil was sandy loam in texture with almost neutral soil reaction, low in organic matter, nitrogen and phosphorus content (*Table 1*). The details of treatments are presented in *Table 2*. Each treatment was replicated three times. All the seeds of the tested species were soaked in their respective treatments for 48 h and were sown in the pots. There were 10 seeds of each species per pot. All the pots were irrigated with a mini sprayer when needed. After recording all the required data, the experiment was terminated after 45 days. The experiment was laid out in completely randomized design (CRD) and the treatment means were separated by Least Significant Difference Test (LSD) at P = 0.05.

Data recording

Germination (%) was recorded by counting the number of germinated seeds in each Pot and percentages were computed and recorded for each treatment. Seeds having 2 mm radicle were considered as germinated. On a daily basis germination% were recorded and days to 50% germination were counted for each treatment. After

http://www.aloki.hu ● ISSN 1589 1623 (Print) ● ISSN 1785 0037 (Online)
DOI: http://dx.doi.org/10.15666/aeer/1804_51875197

germination, shoot length (cm) was measured with a measuring scale for all the germinated seedlings in each treatment. Dry biomass (g) was measured on an electrical balance after drying the fresh biomass in an oven at 65 °C for 48 h. The data presented for the experiment are the pooled data of two runs since the runs were not significantly different statistically ($P > 0.05$). Experiments were discarded after 45 days data for shoot length, fresh and dry biomass were recorded.

Table 1. *Physicochemical properties of the soil used in the experiment*

Soil parameters	Tillage depths (0-30 cm)
Textural class	Silt Loam
Clay (%)	15.13
Silt (%)	60.7
Sand (%)	21.8
*p*H	7.63
EC (d Sm-1)	0.06
Organic matter (%)	0.71
Total N (%)	0.028
Available P (mg kg^{-1} soil)	4.17
Extractable K (mg kg^{-1} soil)	105

Table 2. *Treatment details of the experiment*

Factor A. Treatments (plant water extracts)		
Treatments	**Water extracts Wes species**	**Wes conc. g L^{-1}(w/v)**
1	Sorghum	100
2	Sunflower	100
3	Parthenium	100
4	Sorghum + Sunflower	50 + 50
5	Sorghum + Parthenium	50 + 50
6	Sunflower + Parthenium	50 + 50
7	Sorghum + Sunflower + Parthenium	33.3 + 33.3 + 33.3
8	Atrazine (herbicide)	18
9	Control (Distilled water)	-
Factor B. Test species		
1	Maize (*Zea mays* L.).	
2	*Trianthema partulacastrum* L. (horse purslane)	
3	*Lolium rigidum* L. (rigid ryegrass)	

Statistical analysis

The data recorded for all the individual parameters were statistically analyzed using the appropriate ANOVA suitable for Completely Randomized Design (CRD). Means were separated by using LSD test at $P \leq 0.05$ (Steel et al., 1997). The statistical Software Statistic 8.1 was used for statistical calculations.

http://www.aloki.hu ● ISSN 1589 1623 (Print) ● ISSN 1785 0037 (Online)
DOI: http://dx.doi.org/10.15666/aeer/1804_51875197

Results and discussion

Germination (%)

The statistical analysis of the data revealed that various plant extract treatments had significant effect on germination (%) of the tested species (*Table 3*). The data recorded showed the maximum germination (100%) of maize in control (distilled water) treatment, while the minimum germination (85%) was recorded at sunflower + parthenium (WEs), similarly for horse purslane seeds maximum germination (75%) was recorded in the control (distilled water) treatment while the minimum germination (36.67%) was recorded in herbicide (atrazine) treatment. Furthermore, data recorded for rigid ryegrass showing maximum germination (98.33%) was observed in control (distilled water) treatment while the minimum (40%) was equally recorded in herbicide (atrazine) and sunflower + sorghum + parthenium (WEs) treatments. Among the species means the highest germination (90.55%) was recorded in control (distilled water) treatment followed by rigid ryegrass (57.59%), whereas the lowest value (49.81%) was recorded for horse purslane. Among the treatment means, the highest value of germination (83.89%) was recorded in control (distilled water) treatment, while the lowest value (55.56%) was recorded in herbicide (atrazine) treatment followed by sunflower + sorghum + parthenium (WEs) (56.11%) (*Table 3*).

Table 3. *Allelopathic effect of different plants water extracts applied isolated and in combination on germination (%) of Z. mays, and its associated weeds under laboratory conditions (pots study*

Treatments (1:10 w/v)	Species tested			Extracts means
	Z. mays	*T. partulacastrum*	*L. rigidum*	
Sorghum	90.0 bc	56.7fg	78.3 d	75.0b
Sunflower	86.67 bc	56.7 fg	73.33 de	72.2b
Parthenium	91.67 b	58.33 f	71.67 e	73.9b
Sorghum + Sunflower (50% ea.)	86.67 bc	45.00 ij	51.67 gh	61.1bc
Sorghum + Parthenium (50% ea.)	86.67 bc	48.33 hi	51.67 gh	62.3bc
Sunflower + Parthenium (50% ea.)	85.00 c	50.00 hi	53.33 fgh	62.8c
Sunflower + Sorghum + Parthenium (33.3%ea.)	88.33 bc	40.00 jk	40.00 jk	56.1d
Atrazine (herbicide)	86.67 bc	36.67 k	40.00 jk	54.5ad
Control (distilled water)	100.00 a	75.00 de	98.33 a	91.1a
Test species means	89.07a	51.85c	62.03b	

$LSD_{0.05}$ for extracts = 3.51, for test species = 2.92 and for interaction = 6.07 and the means followed by the same letter (s) in the respective category do not differ from one another at $P \leq 0.05$ according to $LSD_{0.05}$ test

Overall encouraging results of these extracts indicate the presence of germination inhibitors in the allelochemicals released by these plant species. Leather (1983) reported that Chlorogenic acid and Iso-chlorogenic acids could reduce the seed germination of many weed species. Guenzi and McCalla (1966) isolated and identified chlorogenic acid in *Sorghum bicolor* along with other phenolic acids; similarly, Anjum et al. (2005) isolated and identified chlorogenic acid and iso-chlorogenic acid in sunflower. Therefore, the current study suggests that these extracts could be further explored for sustainable weed management in maize under ambient field condition.

http://www.aloki.hu ● ISSN 1589 1623 (Print) ● ISSN 1785 0037 (Online)
DOI: http://dx.doi.org/10.15666/aeer/1804_51875197

Days to 50% germination

The statistical analysis of the data revealed that the water extracts had significant effect on days to 50% germination of the tested species (*Table 4*). Maximum days to 50% germination (5 days) were equally recorded for sorghum + parthenium (WEs), sunflower + parthenium (WEs) and herbicide (atrazine) treatments which were statistically at par with the rest of the treatments, while minimum (3 days) was recorded for control (distilled water) treatment. Furthermore, for horse purslane the maximum (8.83 days) days to germination was recorded in sorghum + sunflowers + parthenium (WEs) treatment which was statistically at par with herbicide (atrazine), sorghum + sunflower (WEs), and sorghum + parthenium (WEs) treatments while the minimum days to 50% germination (4.50 days) was recorded in control (distilled water) treatment. Similarly, for rigid ryegrass, the maximum value (6.83 days) was recorded in herbicide (atrazine) treatment which was statistically at par with sunflower + sorghum + parthenium (WEs) treatment, while the minimum value (3 days) were recorded in control (distilled water) treatment. Among the species, means maximum days to 50% germination (7.55 days) were recorded for *Trianthema portulacstrum* (horse purslane) followed by *Lolium rigidum* (rigid ryegrass) (5.22 days), whereas the minimum (4.59 days) were recorded in maize. Among the treatment means, maximum (6.83 days) time was recorded in herbicide (atrazine) treatment whereas the minimum (3.50 days) was recorded in control (distilled water) treatment.

Table 4. *Allelopathic effect of different plants water extracts applied isolated and in combination on days to 50% germination of Z. mays, and its associated weeds under laboratory conditions (pots study)*

Treatments (1:10 w/v)	Species tested			Extracts means
	Z. mays	*T. partulacastrum*	*L. rigidum*	
Sorghum	4.50 ijk	6.33 cde	4.67ij	5.17d
Sunflower	4.83 ij	6.00 efg	4.00 k	4.94d
Parthenium	4.33jk	6.67 cd	4.50ijk	5.17d
Sorghum + Sunflower (50% ea.)	4.83 ij	8.67 a	6.17 def	6.56ab
Sorghum + Parthenium (50% ea.)	5.00 hi	8.50 a	5.67fg	6.39b
Sunflower + Parthenium (50% ea.)	5.00hi	7.33 b	5.50 gh	5.94c
Sunflower + Sorghum + Parthenium (33.3%ea.)	4.83 ij	8.83 a	6.67 cd	6.78a
Atrazine (herbicide)	5.00 hi	8.67 a	6.83bc	6.83a
Control (distilled water)	3.00 l	4.50ijk	3.00 l	3.50e
Test species means	4.59a	7.55b	5.22a	

$LSD_{0.05}$ for extracts = 0.38, for test species = 0.22 and for interaction = 0.66 and the means followed by the same letter (s) in the respective category do not differ from one another at $P \leq 0.05$ according to $LSD_{0.05}$ test

Our findings are in line with the findings of Babar et al. (2009), who concluded that chickpea seeds soaked in root extract of *Asphodelus tenuifolius* Cav. took more time for germination. Guenzi and McCalla (1966) reported that the presence of chlorogenic acid along with other responsible phenolic acids in *Sorghum bicolor* could be responsible for the delay in germination of weed species. Similarly, Anjum et al. (2005) reported that chlorogenic and isochlorogenic acids in sunflower may be attributed to the inhibition

http://www.aloki.hu ● ISSN 1589 1623 (Print) ● ISSN 1785 0037 (Online)
DOI: http://dx.doi.org/10.15666/aeer/1804_51875197

and the delay in time to germination. In crops, weed competition time to emergence is an important factor; therefore, the findings of the current study are valuable for the weed scientists to further explore the possibility of such plants water extracts for delaying the germination time in weed species and enabling the crops to capture the space prior to weed germination.

Shoot length (cm plant^{-1})

The statistical analysis of the data showed that the extracts had significant effect on shoot length (cm plant^{-1}) of test species (*Table 5*). The data recorded for maize showed that maximum shoot length (38.46 cm plant^{-1}) was recorded in control (distilled water), while minimum (29.99 cm plant^{-1}) was recorded in sunflower + sorghum + parthenium (WEs) treatment which was statistically at par with herbicide (atrazine) treatment. Furthermore, maximum shoot length of *Trianthema* (6.20 cm plant^{-1}) was recorded in control (distilled water) treatment, while the minimum (3.55 cm plant^{-1}) was recorded in herbicide (atrazine) treatment. Data recorded for the *Lolium* showed the maximum shoot length (16.96 cm plant^{-1}) in control (distilled water) treatment while the minimum (9.45 cm plant^{-1}) was recorded in herbicide (atrazine) treatment which was statistically at par with sunflower + sorghum + parthenium (WEs) treatment. Among the species means, maximum shoot length (32.36 cm plant^{-1}) was recorded for maize followed by *Lolium* with (11.76 cm plant^{-1}) whereas the lowest shoot length (4.5 cm plant^{-1}) was recorded for *Trianthema*. Among the treatment means maximum shoot length (20.54 cm plant^{-1}) was recorded in control (distilled water) treatment while minimum (14.46 cm plant^{-1}) was recorded in herbicide (atrazine) treatment which was statistically at par with sunflower + sorghum + parthenium (WEs) treatment.

Table 5. *Allelopathic effect of different plant water extracts applied sole and mixed on shoot length (cm) of Z. mays and its associated weeds under laboratory conditions (pots study)*

Treatments (1:10 w/v)	Species tested			Extracts means
	Z. mays	*T. partulacastrum*	*L. rigidum*	
Sorghum	35.51 b	5.04 n	12.12 i	17.57b
Sunflower	31.85 d	4.95 n	12.94 h	16.58c
Parthenium	32.48 c	4.95 n	12.10 i	16.51c
Sorghum + Sunflower (50% ea.)	31.39 d	4.16 o	10.28 k	15.28d
Sorghum + Parthenium (50% ea.)	30.58 e	3.99op	11.20 j	15.26d
Sunflower + Parthenium (50% ea.)	30.68 e	4.00op	11.11 j	15.26d
Sunflower + Sorghum + Parthenium (33.3%ea.)	29.99 f	3.71 op	9.70 l	14.47e
Atrazine (herbicide)	30.37ef	3.55 p	9.45 l	14.46e
Control (distilled water)	38.46 a	6.20 m	16.96g	20.54a
Test species means	32.37a	4.5c	11.76b	

$LD_{0.05}$ for extracts = 0.32, for test species = 0.18 and for interaction = 0.55. The means followed by the same letter (s) in the respective category do not differ significantly from one another at $P \leq 0.05$ according to $LSD_{0.05}$ test

Our results are also in close conformity with the findings of Javaid et al. (2009) who found that water extracts of *Withania somnifera* and *Datura alba* have bioactive compounds responsible for the inhibition of root and shoot growth of *Rumex crispus*.

http://www.aloki.hu ● ISSN 1589 1623 (Print) ● ISSN 1785 0037 (Online)
DOI: http://dx.doi.org/10.15666/aeer/1804_51875197

The presence of p-coumaric, vanillic, syringic, and ferulic acids in allelopathic plants may inhibit the shoot growth of the tested species. Our results are further similar to that of Turk and Tawah, 2002, who stated that allelopathic plants water extracts were more promising on radicle growth, as radicle emerges earlier and comes in contact with phytochemicals. Based on the current study it is suggested to exploit the utilization of these extracts for sustainable weed management in maize under field condition if infested with *Trianthema portulacastrum* (horse purslane) and *Lolium rigidum*.

Dry biomass (g plant^{-1})

The statistical analysis of the data showed that the extracts had significant effect on dry biomass (g plant^{-1}) of the tested species (*Table 6*). The data recorded for maize showed the maximum dry biomass (0.2585 g plant^{-1}) in control (distilled water) treatment, whereas the minimum (0.1895 g plant^{-1}) biomass was recorded in herbicide (atrazine) treatment. Furthermore, the data recorded for *Trianthema* showed maximum dry biomass (0.0707 g plant^{-1}) in control (distilled water), while the minimum (0.0163 g plant^{-1}) was recorded in herbicide (atrazine) treatment. Similarly, data recorded for the *Lolium* dry biomass, the maximum value (3.04 g plant^{-1}) was recorded in control (distilled water) treatment, while the minimum (1.66 g plant^{-1}) was recorded in herbicide (atrazine) treatment. Among the species means maximum dry biomass (2.14 g plant^{-1}) was recorded for *Lolium* followed by maize with (0.2126 g plant^{-1}), whereas minimum value (0.038 g plant^{-1}) was recorded for *Trianthema*. Among the treatment means maximum dry biomass (1.12 g plant^{-1}) was recorded in control (distilled water) treatment, whereas the minimum (1.62 g plant^{-1}) was recorded in herbicide (atrazine) treatment. Among the tested species maize showed tolerance to various allelopathic water extracts, whereas *Trianthema* and *Lolium* species were found more susceptible to herbicide treatment (atrazine) followed by sunflower + sorghum + parthenium (WEs) treatment.

Table 6. *Allelopathic effect of different plants water extracts applied isolated and in mixture on dry biomass (g) of Z. mays, and its associated weeds under laboratory conditions (pots study)*

	Species tested			
Treatments (1:10 w/v)	***Z. mays***	***T. partulacastrum***	***L. rigidum***	**Extracts means**
Sorghum	0.2175 b	0.0508 ij	2.32 b	0.86b
Sunflower	0.2157 b	0.0482 ij	2.33 b	0.86b
Parthenium	0.2148h	0.0440 ij	2.30 b	0.85b
Sorghum + Sunflower (50% ea.)	0.2048 bd	0.0295 j	1.99 c	0.74c
Sorghum + Parthenium (50% ea.)	0.2063 bc	0.0315 j	1.94 d	0.73c
Sunflower + Parthenium (50% ea.)	0.2092 bc	0.0283 j	1.94 d	0.73c
Sunflower + Sorghum + Parthenium (33.3%ea.)	0.1968 cd	0.0227 j	1.80 e	0.67d
Atrazine (herbicide)	0.1895h	0.0163 j	1.66 f	0.62e
Control (distilled water)	0.2585 g	0.0707 i	3.04 a	1.12a
Test species means	0.213b	0.038a	2.146c	

$LSD_{0.05}$ for extracts = 0.022, for test species = 0.013 and interaction = 0.039 and for each effect, values with the same letter (s) in a column do not differ significantly from one another at $P \leq 0.05$ according to LSD test

http://www.aloki.hu ● ISSN 1589 1623 (Print) ● ISSN 1785 0037 (Online)
DOI: http://dx.doi.org/10.15666/aeer/1804_51875197

The tolerance of maize seeds and sensitivity of weed seeds to these extracts are interesting findings which could be further explored as a tool for sustainable weed management strategies. The presence of sorgoleone, phenolics, p-coumaric, vanillic, syringic, and ferulic acids in allelopathic plants may inhibit the fresh and dry biomass (g plant^{-1}) of the tested species by inhibiting the electron transport in both photosynthesis and respiration, resulting in the reduction in chlorophyll content, and reduction in chlorophyll accumulation**.** It is concluded from the current study that allelopathic plants water extracts could decrease dry biomass (g plant^{-1}) of weeds, which is a positive indicator of such studies, although synthetic herbicides are cheaper and effective than allelochemicals, but still it seems that allelochemicals could be used in developing countries as an ecological and ecofriendly weed management tool. It is suggested to study the active ingredient of allelochemicals to understand their behaviors and plant responses to their applications.

General discussion

In the laboratory bioassays, it is observed that among the tested species maize seeds showed tolerance whereas *Trienthema* followed by *Lolium* showed more sensitivity against synthetic herbicides and other applied allelopathic water extracts. In the light of the present findings of the current study, the tolerance of maize seeds and sensitivity of weed seeds against allelopathins is a good indicator that could be explored further for the commercial use of the selective weed management strategy. Allelopathic plants/weed water extracts applied in combination had more inhibitory effect than their sole application on seed germination, time to germination, shoot length and dry biomass of the tested species. The similar trends for all the studied parameters are confirmatory to the previous findings of Einhellig (1995) and Weston and Duke (2003), who reported that application of various allelopathic plants water extracts in mutual combination had more pronounced inhibitory effect as compared to their sole applications. Likewise, Khanh et al. (2005) also illustrated that a mixture of allelochemicals may help to retard the germination and seedling growth of weed species. The more inhibitory effect in combined extracts could be due to synergistic action of various allelochemicals present in the plant species, however data recorded for shoot length (cm) and dry biomass (g) showed that inhibitory effect of synthetic herbicide had slightly more effect than combined application of extracts, but pollution, herbicide resistance development and harming the quality of product encourages to opt for the allelopathins. Our results are also in line with the work of Cheema and Khaliq (2000) and Hassan et al. (2018), who observed the inhibitory effect of allelopathic crops/weed extracts on weeds and concluded worth to be exploited for weed management in different crops.

Conclusion

It is concluded from the current study that all tested allelopathic plants species viz., sorghum, sunflower and parthenium have phytotoxic effect against the two studied weeds of maize. They have water soluble allelochemicals which could inhibit the germination% and growth parameters of weeds. Among all the treatments, Sorghum + Sunflower + Parthenium (WEs) significantly minimized the growth of the tested species almost comparable to the synthetic herbicide (atrazine). A positive indicator during the study has been that maize *(Zea mays* L.) showed more tolerance against the tested extracts thus, offering a window for selective control of weeds in maize crop

http://www.aloki.hu ● ISSN 1589 1623 (Print) ● ISSN 1785 0037 (Online)
DOI: http://dx.doi.org/10.15666/aeer/1804_51875197

consequently averting the reliance on the synthetic herbicides. Another prospect of this study is the combined use of the tested species emerged as synergistic for the effective control of weeds as compared to their sole application. It is thus, recommended that the combined extracts of the tested plants may be utilized for sustainable weed management in maize crop for environmental safety and sustainable maize production. Water extract of sorghum + sunflower + parthenium @ 33.3 + 33.3 + 33.3 g/L in mutual combination may be recommended for sustainable weed management in maize.

Acknowledgements. This study is a part of a PhD dissertation, which was submitted by the senior author to the University of Haripur Pakistan, for the award of degree. Authors are very thankful to the Higher Education Commission (HEC) Pakistan for full financial assistance under the Project HEC Indigenous 5000 PhD Fellowship Program Phase-II, Batch-I.

REFERENCES

[1] Adkins, S. W., Sowerby, M. S. (1996): Allelopathic potential of the weed, *Parthenium hysterophorus* L., in Australia. – Plant Protection Quarterly 11(1): 20-23.

[2] An, M., Pratley, E., Haig, T. (1998): Allelopathy: from Concept to Reality. – Environmental and Analytical Laboratories and Farrer Center for Conservation Farming, Charles Sturt University, Wagga NSW.

[3] Anjum, T., Stevenson, P., Hall, D., Bajwa, R. (2005): Allelopathic potential of *Helianthus annuus* L.(sunflower) as natural herbicide. – Proceedings of the 4th World Congress on Allelopathy: Establishing the Scientific Base, Wagga, Australia, 2005 August, pp. 21-26.

[4] Balyan, R. S., Bhan, V. M. (1989): Competing ability of maize, pearlmillet, mungbean and cowpea with carpetweed under different weed management practices. – Crop Research (Hisar) 2(2): 147-153.

[5] Batish, D. R., Tung, P., Singh, H. P., Kohli, R. K. (2002b): Phytotoxicity of sunflower residues against some summer season crops. – Journal of Agronomy and Crop Science 188(1): 19-24.

[6] Belz, R. G. (2008): Stimulation versus inhibition—bioactivity of parthenin, a phytochemical from *Parthenium hysterophorus* L. – Dose-Response 6(1): 80-96.

[7] Belz, R. G. (2016): Investigating a potential auxin-related mode of hormetic/inhibitory action of the phytotoxin parthenin. – Journal of Chemical Ecology 42(1): 71-83.

[8] Belz, R. G., Reinhardt, C. F., Foxcroft, L. C., Hurle, K. (2007): Residue allelopathy in Parthenium hysterophorus L.—Does parthenin play a leading role? – Crop Protection 26(3): 237-245.

[9] Cheema, Z. A., Khaliq, A. (2000): Use of sorghum allelopathic properties to control weeds in irrigated wheat in a semiarid region of Punjab. – Agriculture, Ecosystems & Environment 79(2-3): 105-112.

[10] Das, B., Das, R. (1995): Chemical investigation in *Parthenium hysterophorus* L.—an allelopathic plant. – Allelopathy J 2: 99-104.

[11] Dogan, M. N., Ünay, A., Boz, Ö., Albay, F. (2004): Determination of optimum weed control timing in maize *(Zea mays* L.*)*. – Turkish Journal of Agriculture and Forestry 28(5): 349-354.

[12] Einhellig, F. A. (1995): Mechanism of Action of Allelochemicals in Allelopathy. – In: Inderjit, K. M. M. et al. (eds.) Allelopathy. ACS, Washington, pp 96-116. DOI: 10.1021/bk-1995-0582.ch007.

[13] Guenzi, W. D., McCalla, T. M. (1966): Phenolic acids in oats, wheat, sorghum, and corn residues and their phytotoxicity. – Agronomy Journal 58(3): 303-304.

[14] Gupta, P. K. (2004): Pesticide exposure—Indian scene. – Toxicology 198(1-3): 83-90.

http://www.aloki.hu ● ISSN 1589 1623 (Print) ● ISSN 1785 0037 (Online)
DOI: http://dx.doi.org/10.15666/aeer/1804_51875197

[15] Heap, I. (2020): The International Survey of Herbicide Resistant Weeds. – www.weedscience.org (accessed on April 2, 2020).
[16] Heap, I., Duke, S. O. (2018): Overview of glyphosate-resistant weeds worldwide. – Pest Manag. Sci. 74(5): 1040-1049.
[17] Iqbal, J., Cheema, Z. A., Mushtaq, M. N. (2009): Allelopathic crop water extracts reduce the herbicide dose for weed control in cotton *(Gossypium hirsutum).* – International Journal of Agriculture and Biology 11(4): 360-366.
[18] Jabran, K. (2018): Tank mixing of allelopathic crop water extracts with pendimethalin helps in the management of weeds in canola *(Brassica napus)* field. – International Journal of Agriculture and Biology 10(3): 293-296.
[19] Jabran, K., Mahajan, G., Sardana, V., Chauhan, B. S. (2015): Allelopathy for weed control in agricultural systems. – Crop Protection 72: 57-65.
[20] Khan, M. B., Ahmad, M., Hussain, M., Jabran, K., Farooq, S., Waqas-Ul-Haq, M. (2012): Allelopathic plant water extracts tank mixed with reduced doses of atrazine efficiently control Trianthema portulacastrum in L. *Zea mays.* – Journal of Animal and Plant Sciences 22(2): 339-346.
[21] Khan, T. D., Chung, M. I., Xuan, T. D., Tawata, S. (2005): The exploitation of crop allelopathy in sustainable agricultural production. – Journal of Agronomy and Crop Science 191(3): 172-184.
[22] Leather, G. R. (1987): Weed control using allelopathic sunflowers and herbicide. – Plant and Soil 98(1): 17-23.
[23] Leather, G. R. (1983): Sunflowers (*Helianthus annuus*) are allelopathic to weeds. – Weed Science 31(1): 37-42.
[24] NewGenFartmer Maize + Soybean (2020): Top 10 worst weeds in corn and soybean. – https://www.farmprogress.com/crop-protection/top-10-worst-weeds-corn-and-soybeans.
[25] Sohaib, M., Zaheer-ud-din, K., Cheema, T. A. (2009): Distribution of weeds in wheat, maize and potato fields of Tehsil Gojra, District Toba Tek Singh, Pakistan. – Pakistan Journal of Weed Science Research 15(1): 91-103.
[26] Turk, M. A., Tawaha, A. M. (2002): Inhibitory effects of aqueous extracts of barley on germination and growth of lentil. – Pakistan Journal of Agronomy 1: 28-30.
[27] Usman, A., Elemo, K. A., Bala, A., Umar, A. (2001): Effect of weed interference and nitrogen on yields of a maize/rice intercrop. – International Journal of Pest Management 47(4): 241-246.
[28] University of Pretoria (2020): Important Weeds in Maize. – https://www.up.ac.za/sahri/article/1810372/important-weeds-in-maize. Accessed on April 7, 2020.
[29] Weston, L. A., Duke, S. O. (2003): Weed and crop allelopathy. – Critical Reviews in Plant Sciences 22(3-4): 367-389.

http://www.aloki.hu ● ISSN 1589 1623 (Print) ● ISSN 1785 0037 (Online)
DOI: http://dx.doi.org/10.15666/aeer/1804_51875197

EFFECTS OF AMELIORANT Cu^{2+}, Fe^{3+}, AND Zn^{2+} AND PALM OIL FROND COMPOST APPLICATIONS ON THE GROWTH AND PRODUCTION OF MUNG BEAN (*VIGNA RADIATA* (L.) R. WILCZEK) GROWN ON PEAT SOIL IN RIAU

SITI, Z.

Department of Agriculture, Faculty of Agriculture, Universitas Islam Riau, Jl. Kaharuddin Nasution, Marpoyan, Pekanbaru, Riau 28284, Indonesia
(e-mail: sitizahrah@agr.uir.ac.id; phone: +62-813-7104-6440)

(Received 22nd Jan 2020; accepted 25th May 2020)

Abstract. Low production of all crops cultivated due to the poor physical and chemical properties of such soil, including acid reaction; high organic acid content, which is toxic for crops; low macronutrient and micronutrient content. The use of the ameliorants Cu^{2+}, Fe^{3+}, and Zn^{2+} together with Palm Oil Frond (POF) compost can improve peat soil with a low impact on the environment. This research aimed to examine the effects of the ameliorants Cu^{2+}, Fe^{3+}, and Zn^{2+} and POF compost applications on the growth of mung bean. The first factor was the ameliorant application with four levels (without ameliorant Cu^{2+}, Fe^{3+}, and Zn^{2+}). The second factor was the POF compost doses with four levels (0, 12, 24, and 36 g per plant). Results showed that the interaction of ameliorant (Cu^{2+}, Fe^{3+}, and Zn^{2+} and POF compost applications significantly affect the percentage of fully filled pods, seed dry weight, and root volume of mung bean. The best treatment was achieved with the application of ameliorant Cu^{2+} and 24 g $plant^{-1}$ POF compost, which resulted in 26.67 g $plant^{-1}$ seed dry weight, 94.7% fully filled pods, and 27.4 cm^3 root volume, comprising increased percentages of 175.5%, 32.8%, and 109.2%, respectively, compared to no treatment.
Keywords: *marginal land, organic acid, polyvalent cation, chelating, RGR, SFR, ESFP*

Introduction

Mung bean (*Vigna radiata* (L.) R. Wilczek) is a leguminous crop that grows well in tropical regions and has high nutritional value. Currently, the demand for mung bean in Indonesia increases each year, yet its production tends to decrease every year. Mung bean production decreased from 1739 tons in 2007 to 598 tons in 2015 (Bureau, 2016). This decreased production is caused by low land productivity with non-optimal soil and crop management. Agricultural land in Riau mostly consists of marginal land with low productivity, including dry and wet land. From this land area, peat soil reaches 3.87 million hectares or 59.94% from the total peat soil in Sumatera and 25.96% from the total peat soil in Indonesia (IAARD, 2011).

Peat soil for agriculture in Indonesia is used for both plantation and food crops. The development of peat land for agriculture increases continuously owing to the decreasing dry land area, which is a result of land conversion for other purposes, while the land requirement for food production persistently increases (Darmawan et al., 2015; Nurulita et al., 2016). Although dry land extensification can be conducted, the agricultural extensification of peat land is being further explored by policy makers and researchers because peat land area is sufficiently wide in Indonesia (Jaenicke et al., 2008; Siti et al., 2013). The average production of almost all crops cultivated on peat soil, including mung bean, remains low. This condition is due to peat soil having poor physical and chemical properties, such as acid reaction; high organic acid content, which is toxic for crops; and low macronutrient and micronutrient content (Troeh and Thompson, 2005; Lampela et al., 2014). The management and sustainability associated with the chemical and physical

http://www.aloki.hu ● ISSN 1589 1623 (Print) ● ISSN 1785 0037 (Online)
DOI: http://dx.doi.org/10.15666/aeer/1804_51995209

aspects of peat soil must be performed correctly to increase peat soil productivity (Hooijer et al., 2012; Comte et al., 2013; Hoyos et al., 2015; Könönen et al., 2015).

Nutrient uptake (anion) of plant on peat soil is very low because peat soil has high negative charge. Thus, the adsorption and anion exchange capacity of peat soil is low, leading to low availability and nutrient uptake (Stevenson, 1994). Adding cations, such as Cu^{2+}, Fe^{3+}, and Zn^{2+}, into peat soil is expected to increase anion exchange capacity and the availability and nutrient uptake of crops. The outcome is especially apparent in anions where the cations Cu^{2+}, Fe^{3+}, and Zn^{2+} function as metals bridging organic acid and NO_3^- or $H_2PO_4^-$ in the chelating formation of peat soil. Complex compound formation between organic acid molecules and metal ions that form more than one bond will increase the stability of complex compounds (Abat et al., 2012).

The bond phenomenon between metal ion and organic acid enables the use of several cations in controlling the reactivity of phenolic acids so that they do not poison and endanger crops (Orlov, 1995; Shanmugam et al., 2018). The application of polyvalent cation on peat soil in Indonesia (Kalimantan and South Sumatera) can reduce the content and reactivity of phenolate acid and increase crop production (Hartatik and Nugroho, 2001; Brachia, 2006). In the current study, the application of polyvalent cations, such as Cu^{2+}, Fe^{3+}, and Zn^{2+}, as ameliorant is expected to reduce toxic organic acids, including phenolic acids and carboxylic acids, through the formation of an organo-cation complex (Gyliene and Šalkauskas, 2001; Tan, 2010). Thus, the toxic properties of these acids will be reduced to improve the crop growth and development of mung bean. Peat soil also contains very low amounts of micronutrients, such as Cu^{2+}, Fe^{3+}, and Zn^{2+}, which are strongly chelated with organic matter and are thus not available to crops (Abat et al., 2012; de A. Melo et al., 2014). The cations Cu^{2+}, Fe^{3+}, and Zn^{2+} act as ameliorant materials and are a source of nutrients for crops (Jones, 2012; Sullivan et al., 2013).

Besides applying an ameliorant material, an additional organic matter, such as compost, is required for the use of peat soil for crop cultivation. The application of Palm Oil Frond (POF) compost is expected to activate microorganisms in peat soil. The organic material is an energy source for soil microorganisms that can increase microorganism activity in the decomposition of organic materials to stabilize peat soil (Fan et al., 2007; Onwonga et al., 2010). Furthermore, the POF compost contains the macronutrients N (0.75%), P (0.47%), and K (0.80%) (Eviati, 2011). Thus, it can enrich the nutrients N, P, and K of peat soil to support the growth of mung bean. The article aimed to investigate the effects of ameliorant Cu^{2+}, Fe^{3+}, and Zn^{2+} applied with palm oil frond compost on the yield and growth of mung bean, grown on peat soil in Riau, Indonesia.

Material and Methods

This research was conducted at the experimental farm of the Faculty of Agriculture, Universitas Islam Riau, Pekanbaru, Indonesia for four months, from November 2018 to February 2019.

Experimental design

The experimental design used was a factorial 4×4 in a completely randomized design with three replications. The first factor was the ameliorant treatment application with four levels (without ameliorant, Cu^{2+}, Fe^{3+}, and Zn^{2+}). The second factor was the dose of POF compost with four levels (0, 12, 24, and 36 g per plant). This experiment consisted of 48 experimental units, with each experimental unit consisting of 8 plants (8 pots). The

http://www.aloki.hu ● ISSN 1589 1623 (Print) ● ISSN 1785 0037 (Online)
DOI: http://dx.doi.org/10.15666/aeer/1804_51995209

observational data were analyzed using analysis of variance and the honestly significant difference (HSD) test at 5% probability level (P = 0.05) (Stell and Torrie, 1980).

Variety and soil sampling

The mung bean variety used in this experiment was Vima 1. The peat soil sample originated from Pekanbaru, Riau, and was collected at a depth of 10–40 cm with the sapric decomposition level. Each pot was filled with 8 kg of peat soil (300% soil water content) or equivalent to 2 kg of absolute dry weight.

Treatment application and fertilization

The ameliorants Cu^{2+}, Fe^{3+}, and Zn^{2+} (5% maximum sorption) were applied in the form of $CuSO_4$, $FeCl_3$, and $ZnSO_4$, respectively. They were then mixed and stirred with soil three weeks before planting. POF compost was applied and stirred evenly in accordance with the treatment 1 week before planting. N fertilizer (urea 50 kg ha^{-1}), triple super phosphate (TSP) (150 kg ha^{-1}), KCl (100 kg ha^{-1}), and lime $CaMg(CO_3)_2$ were also applied a week before plantingg (1-ton ha^{-1}).

Observation parameters

The observed parameters in this study were relative growth rate (RGR), seed filling rate (SFR), effective seed filling period (ESFP), percentage of fully filled pods, seed dry weight, and root volume.

The study was conducted at the experimental farm of the Universitas Islam Riau, Riau Province, Indonesia. The experiment involved a completely randomized factorial design with three replications, *Figure 1* shows the location of experiment conducted.

Figure 1. *Location of experiment in Pekanbaru city, Riau Province, Indonesia*

Results and Discussion

RGR

From the observation of RGR (*Table 1*), the application of ameliorant materials and POF compost produce higher RGR than without both ameliorant and POF compost. This result is due to the improved plant growth response with the application of ameliorant

http://www.aloki.hu ● ISSN 1589 1623 (Print) ● ISSN 1785 0037 (Online)
DOI: http://dx.doi.org/10.15666/aeer/1804_51995209

materials and POF compost. The POF compost contains plant nutrients and a source of energy for soil microorganism for survival and activity in the soil. Hence, microorganism activities in agricultural soils profoundly influence plant nutrient availability and OM transformation (Onwonga et al., 2010). In addition, the application of organic and inorganic ameliorants into the soil can improve soil conditions and enhance plant growth (Okwuagwu et al., 2003; Rudrappa et al., 2006).

Table 1. *Relative growth rate of mung bean with ameliorant materials and POF compost treatments (g day^{-1})*

Days	Ameliorant materials	POF compost (g plant^{-1})				$\bar{X}$
		0	12	24	36	
14-21	Without ameliorant	0.106a	0.121a	0.175a	0.152a	0.139c
	Cu^{2+}	0.153a	0.189a	0.241a	0.226a	0.202a
	Fe^{3+}	0.135a	0.170a	0.219a	0.195a	0.180b
	Zn^{2+}	0.137a	0.163a	0.208a	0.184a	0.173b
	$\bar{X}$	0.133d	0.161c	0.211a	0.189b	
28-35	Without ameliorant	0.342a	0.372a	0.429a	0,394a	0.384d
	Cu^{2+}	0.423a	0.453a	0.504a	0.476a	0.464a
	Fe^{3+}	0.403a	0.435a	0.485a	0.460a	0.446b
	Zn^{2+}	0.396a	0.417a	0.472a	0.449a	0.433c
	$\bar{X}$	0.391d	0.419c	0.473a	0.445b	

The number in rows and columns followed by the same small letter show no significant difference (HSD test, at $P = 0.05$)

Table 1 also shows that the highest RGR was at the age of 14–21 and 28–35 days in the treatment of ameliorant Cu^{2+} for 0.202 and 0.464 g day^{-1}, respectively. The lowest RGR was found without ameliorant treatment at 0.139 and 0,384 g day^{-1}. Furthermore, in the main effect of POF compost application alone, the highest RGR was at the age of 14–21 and 28–35 days during the addition of as much as 24 g plant^{-1} POF compost for 0.211 and 0.473 g day^{-1}, respectively. The lowest RGR was found without compost treatment at 0133 and 0.391 g day^{-1}. The RGR of plants increased due to an increase in plant growth and photosynthesis process. The increased photosynthetic process increases plant biomass (Jumin et al., 2014).

The increased RGR is hypothesized to be caused by an increase of plant nutrient uptake by ameliorant addition. Zahrah (2010) found that the application of an ameliorant (Cu^{2+}, Fe^{3+}, and Zn^{2+}) on peat soil for several varieties of rice can increase the uptake of N, P, and K and seed dry weight. Maftu'ah et al. (2013) also reported that the application of ameliorant on peat soil increases the growth and nutrient uptake of N, P, and K on sweet corn.

Seed filling rate

The observation result of SFR of mung bean is summarized in *Table 2*. The data from *Table 2* indicate that the interaction of ameliorant materials and POF compost treatments did not significantly affect the SFR of mung bean (analysis of variance). However, the main effect of each treatment factor was significant. The SFR results (*Table 2*) show that

http://www.aloki.hu ● ISSN 1589 1623 (Print) ● ISSN 1785 0037 (Online)
DOI: http://dx.doi.org/10.15666/aeer/1804_51995209

all treatments with the addition of an ameliorant (Cu^{2+}, Fe^{3+}, and Zn^{2+}) and various doses of POF compost into the peat soil produced higher SFR than without both ameliorant addition (Cu^{2+}, Fe^{3+}, and Zn^{2+}) and POF compost. The highest SFR was obtained from additional treatment with the ameliorant Cu^{2+} (0.060 g $seed^{-1}day^{-1}$) and the addition of as much as 24 g $plant^{-1}$ (0.061 g $seed^{-1}day^{-1}$) POF compost. The increased SFR generated by the addition of ameliorant materials was due to the improved plant growth as reflected by the growth of RGR owing to the addition of ameliorant materials and POF compost into the peat soil (*Table 1*). Thus, the accumulation of dry plant materials (biomass) also increased. Jones (2012) stated that the results of plant biomass and seed development are determined by the rate of plant growth.

Table 2. *Seed filling rate of mung bean seed with ameliorant materials and POF compost treatments (g $seed^{-1}day^{-1}$)*

Ameliorant Materials	POF compost (g $plant^{-1}$)				$\bar{X}$
	0	12	24	36	
Without Ameliorant	0.038a	0.044a	0.051a	0.047a	0.045c
Cu^{2+}	0.053a	0.055a	0.070a	0.061a	0.060a
Fe^{3+}	0.050a	0.054a	0.063a	0.058a	0.056a
Zn^{2+}	0.049a	0.053a	0.059a	0.055a	0.054b
$\bar{X}$	0.047c	0.052b	0.061a	0.055b	

The number in rows and columns followed by the same small letter show no significant difference (HSD test, at $P = 0.05$)

Peat soil management with an additional appropriate ameliorant type and proper dosage improves chemical properties and soil microbiology activity to support plant growth (Bragazza et al., 2007). Therefore, a good ameliorant is one that can improve peat soil conditions, increase crop production, preserve peat soil, and reduce negative impacts on the environment (Husen and Agus, 2011; Agus et al., 2012).

Effective seed filling period

The ESFP of mung bean is presented in *Table 3*.

Table 3. *Effective seed filling period of mung bean with ameliorant materials and POF compost treatments (day)*

Ameliorant Materials	POF compost (g $plant^{-1}$)				$\bar{X}$
	0	12	24	36	
Without Ameliorant	33.33a	35.89a	34.60a	36.11a	34.98c
Cu^{2+}	30.00a	31.27a	28.32a	30.47a	30.02a
Fe^{3+}	31.19a	33.64a	32.67a	33.24a	32.68b
Zn^{2+}	29.44a	29.85a	33.85a	30.76a	30.98b
$\bar{X}$	30.99	32.66	32.65	32.65	

The number in rows and columns followed by the same small letter show no significant difference (HSD test, at $P = 0.05$)

http://www.aloki.hu ● ISSN 1589 1623 (Print) ● ISSN 1785 0037 (Online)
DOI: http://dx.doi.org/10.15666/aeer/1804_51995209

Table 3 illustrates that the effect of the interaction of ameliorant materials and POF compost treatments was not significant (analysis of variance). However, the main effect of ameliorant (Cu^{2+}, Fe^{3+}, and Zn^{2+}) application alone was significant on the ESFP of mung bean. The application of the ameliorant Cu^{2+} caused a shorter ESFP than the addition of the ameliorants Fe^{3+} and Zn^{2+} at 30.02 days. ESFP describes the time required by seeds to evolve perfectly and reach maximum dry weight (Salisbury and Ros, 1996). Therefore, the higher the SFR is, the shorter the ESFP will be. These results indicate that the highest SFR, namely, 0.070 g $seed^{-1}day^{-1}$, was obtained from the treatment combination of additional ameliorant Cu^{2+} and as much as 24 g $plant^{-1}$ (*Table 2*) POF compost with the fastest ESFP, namely, 28.32 days. The longest was 33.33 days without ameliorant and without POF compost (*Table 3*).

Percentage of fully filled pods

The percentage of fully filled pods of mung bean is shown in *Table 4*.

Table 4. *Percentage of fully filled pods of mung bean with ameliorant materials and POF compost treatments (%)*

Ameliorant materials	POF compost (g $plant^{-1}$)				$\bar{X}$
	0	12	24	36	
Without ameliorant	71.3d	82.7c	84.5c	83.4c	80.48c
Cu^{2+}	85.9bc	86.6c	94.7a	89.1b	89.08a
Fe^{3+}	83.7c	83.7c	85.6bc	85.0bc	84.70b
Zn^{2+}	83.4c	83.5c	85.6bc	84.2c	84.17b
$\bar{X}$	81.08c	84.13b	87.75a	85.43b	

The number in rows and columns followed by the same small letter show no significant difference (HSD test, at $P = 0.05$)

Table 4 shows that the addition of ameliorant (Cu^{2+}, Fe^{3+}, and Zn^{2+}) and POF compost on peat soil produced a higher percentage of fully filled pods than without both ameliorant and POF compost. The highest percentage (94.7%) of fully filled pods was derived from the highest treatment with the application of ameliorant Cu^{2+} and as much as 24 g $plant^{-1}$ POF compost, and it was significantly different from the other treatment combinations.

These results revealed that Cu^{2+} cations had a better ability to neutralize the adverse effects of organic acids on mung bean growth compared with Fe^{3+} and Zn^{2+}. Toxic organic acids in plants are neutralized through the occurrence of chelating the positive charge of metal cations with organic acids, which has a negative charge (Gyliene and Šalkauskas, 2001; Tan, 2010).

The results of the high fully filled pods were also associated with improved SFR and ESFP results with such treatment combination. The pods will be fully filled if the translocation of photosynthesis results in seeds that run smoothly and are effective. In addition, as a chelating agent of peat organic acids, Cu is a micronutrient that should be added to peat soil to achieve good growth and increase crop production. The use of tropical peat enriched with micronutrients can contribute to improving agricultural productivity because micronutrients can effectively stimulate plant growth[20]. As a micronutrient, Cu acts as an enzyme activator, regulating carbohydrate and protein metabolism and chlorophyll formation (Jones, 2012; Sullivan et al., 2013).

http://www.aloki.hu ● ISSN 1589 1623 (Print) ● ISSN 1785 0037 (Online)
DOI: http://dx.doi.org/10.15666/aeer/1804_51995209

Seed dry weight

The observation result of the seed dry weight of mung bean after analysis of variance showed that the interaction effect of ameliorant materials and POF compost treatments was significant on the seed dry weight. This result indicates that the seed dry weight of mung bean as a result of applying several doses of POF compost was not the same for different ameliorants (Cu^{2+}, Fe^{3+}, and Zn^{2+}). The result of the seed dry weight of mung bean is presented in *Table 5*.

Table 5. *Seed dry weight of mung bean with ameliorant materials and POF compost treatments (g plant^{-1})*

Ameliorant materials	POF compost (g plant^{-1})				$\bar{X}$
	0	12	24	36	
Without ameliorant	9.67j	19.00fghi	21.33de	20.33efg	17.58c
Cu^{2+}	19.67efgh	22.33cd	26.67a	24.33bc	23.25a
Fe^{3+}	18.00hij	19.67efgh	24.67ab	21.33de	20.92b
Zn^{2+}	17.33ij	18.67ghij	23.67bc	21.00ef	20.17b
$\bar{X}$	20.64d	19.92c	24.08a	21.75b	

The number in rows and columns followed by the same small letter show no significantly different (HSD test, at $P = 0.05$)

Table 5 shows that the addition of ameliorant (Cu^{2+}, Fe^{3+}, and Zn^{2+}) and POF compost into peat soil produced the higher dry weight of seed than without both ameliorant and POF compost. An increase in seed dry weight of mung bean with the application of ameliorant materials (Cu^{2+}, Fe^{3+}, and Zn^{2+}) and POF compost improved soil conditions than without ameliorant. Thus, the plant roots grew well. Good root development enhances nutrient uptake, growth, and crop production (Rudrappa et al., 2006; Štursová and Baldrian, 2011). Chelation between Cu^{2+}, Fe^{3+}, and Zn^{2+} and organic acids neutralizes the organic acids of peat so that they do not poison the plant. Phenolic acids are an intermediate compound in humus formation. At a certain concentration, this compound is toxic and will inhibit plant growth and reduce crop production (Orlov, 1995). The results of the highest dry weight of mung bean with the addition of Cu^{2+} ameliorant and as much as 24 g plant^{-1} POF compost were also related to SFR and the highest percentage of fully filled pods with such treatment (*Table 2* and *Table 4*).

Table 5 shows that the highest dry weight of the seeds was obtained from the addition of the ameliorant Cu^{2+} and as much as 24 g plant^{-1} POF compost treatments, namely, 26.67 g plant^{-1}. The lowest dry weight without ameliorant and without POF compost treatments was 9.67 g plant^{-1}. This result indicates that the Cu^{2+} cation was more effective in chelating with the organic acids of peat compared with the cations Fe^{3+} and Zn^{2+}. It can effectively suppress the adverse effects of organic acids of peat on growth and crop production. The stability of the chelating bond was Cu > Fe > Co > Ni > Zn = Mn [20]. These results also relate to the role of Cu^{2+} as a cation chelating organic acid of peat soil and a plant micronutrient involved in chlorophyll formation as well as an important coenzyme for activating several plant enzymes (Lampela et al., 2014).

Adding inorganic and organic fertilizers also improves the physical, chemical, and biological conditions of soil and, therefore, increases the production and quality of crops,

http://www.aloki.hu ● ISSN 1589 1623 (Print) ● ISSN 1785 0037 (Online)
DOI: http://dx.doi.org/10.15666/aeer/1804_51995209

including seed quality (Hooijer et al., 2012). The application of inorganic and organic ameliorants can improve soil chemical properties and stabilize peat soil, reducing greenhouse emission and increasing crop production on peat lands (Murdiyarso et al., 2010; Könönen et al., 2015).

The results of regression and correlation analyses of seed dry weight are shown in *Figure 2*.

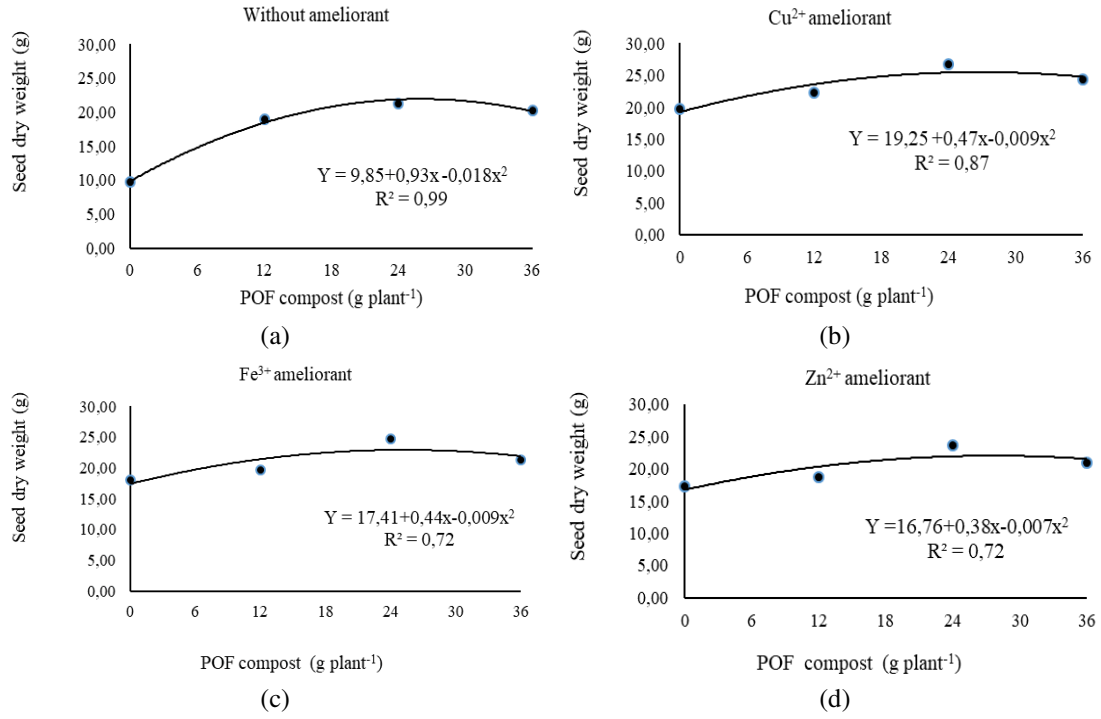

Figure 2. *Relationship between dosage of POF compost and the seed dry weight per plant on the various ameliorant materials (a) without ameliorant, (b) with Cu^{2+} ameliorant (c) with Fe^{3+} ameliorant (d) with Zn^{2+} ameliorant*

Figure 2 shows that the seed dry weight increase with increasing doses of POF compost from 0 to 24 g plant^{-1} and decreases with the addition of 36 g plant^{-1} for all ameliorant materials (Cu^{2+}, Fe^{3+}, and Zn^{2+}).

Root volume

The average of root volume for mung bean is presented in *Table 6*.

The data in *Table 6* show that the highest root volume (27.4 cm^3) was obtained from the ameliorant treatment addition of Cu^{2+} and as much as 24 g plant^{-1} POF compost; it was also significantly different from that obtained from other treatment combinations. The lowest root volume was found without both ameliorant and POF compost treatments. These results relate to the improvement of the root zone (rhizosphere) with the addition of ameliorant materials and POF compost that can increase the growth and development of plant roots, thus increasing root volume. In addition, Cu^{2+} has a role in root respiration. As root respiration increases, the uptake of plant nutrients also increases as a result of improved plant growth (Könönen et al., 2015).

http://www.aloki.hu ● ISSN 1589 1623 (Print) ● ISSN 1785 0037 (Online)
DOI: http://dx.doi.org/10.15666/aeer/1804_51995209

Table 6. *Root volume of mung bean with ameliorant materials and compost and POF compost treatments (cm^3)*

Ameliorant materials	POF compost (g plant^{-1})				$\bar{X}$
	0	12	24	36	
Without ameliorant	13.1f	16.6e	19.3cde	18.9cde	17.0c
Cu^{2+}	19.9cd	21.5bc	27.4a	22.4bc	22.8a
Fe^{3+}	18.7cde	19.8cd	23.2b	21.8bc	20.9b
Zn^{2+}	18.2de	19.3cd	21.8bc	20.1bc	19.9b
$\bar{X}$	17.5d	19.4c	22.9a	20.8b	

The number in rows and columns followed by the same small letter show no significant difference (HSD test, at $P = 0.05$)

Conclusions

The interaction of ameliorant (Cu^{2+}, Fe^{3+}, and Zn^{2+}) and POF compost applications significantly affected the percentage of fully filled pods, seed dry weight, and root volume of mung bean. The best treatment was found in the application of ameliorant Cu^{2+} and 24 g plant^{-1} POF compost. The results showed 26.67 g plant^{-1} seed dry weight, 94.7% fully filled pods, and 27.4 cm^3 root volume at increased percentages of 175.5%, 32.8%, and 109.2%, respectively, compared with no treatment. The main effect of the application of ameliorant materials alone was significant on the RGR, SFR, ESFP, percentage of fully filled pods, seed dry weight, and root volume. The best treatment was found on the ameliorant Cu^{2+}. The main effect of POF compost application alone was significant on the RGR, SFR, seed dry weight, percentage of fully filled pods, and root volume. The best treatment was achieved in the application of 24 g plant^{-1} POF compost.

Acknowledgements. Author would like to thank you to Research Institute and Community Services (LPPM), Universitas Islam Riau for funding this project and Mr. Nursamsul Kustiawan for assistance in the research experiment.

REFERENCES

[1] Abat, M., McLaughlin, M. J., Kirby, J. K., Stacey, S. P. (2012): Adsorption and desorption of copper and zinc in tropical peat soils of Sarawak, Malaysia. – Geoderma 176: 58-63.
[2] Agus, F., Wahyunto, Dariah, A., Runtunuwu, E., Susanti, E., Supriatna, W. (2012): Emission reduction options for peatlands in the Kubu Raya and Pontianak Districts, West Kalimantan, Indonesia. – Journal of Palm oil Research 24: 1378-1387.
[3] Bossio, D. A., Fleck, J. A., Scow, K. M., Fujii, R. (2006): Alteration of soil microbial communities and water quality in restored wetlands. – Soil Biol Biochem 38(6): 1223-1233.
[4] Brachia, F. (2006): Peat: Agroecosystem and Carbon Transformation. – Yogyakarta, Gajah Mada University Press.
[5] Bragazza, L., Siffi, C., Iacumin, P., Gerdol, R. (2007): Mass loss and nutrient release during litter decay in peatland: The role of microbial adaptability to litter chemistry. – Soil Biol Biochem 39(1): 257-267.
[6] Bureau, S. C. (2016): Mung bean Production in Indonesia. – Jakarta, Institute, C. S.

http://www.aloki.hu ● ISSN 1589 1623 (Print) ● ISSN 1785 0037 (Online)
DOI: http://dx.doi.org/10.15666/aeer/1804_51995209

[7] Comte, I., Colin, F., Grunberger, O., Follain, S., Whalen, J. K., Caliman, J. P. (2013): Landscape-scale assesment of soil response to long-term organic and mineral fertilizer application in an industrial palm oil plantation, Indonesia. – Agriculture, Ecosystems and Environment 169: 58-68.
[8] Darmawan, B., Siregar, Y. I., Sukendi, Zahrah, S. (2015): Physical and chemical peatsoil properties assesment in Kampar Peninsular Region, Sumatera, Indonesia. – International Journal of Science and Research (IJSR) 4: 64-68.
[9] de A. Melo, C., de Oliveira, L. K., Goveia, D., Fraceto, L. F., Rosa, A. H. (2014): Enrichment of tropical peat with micronutrients for agricultural applications: Evaluation of adsorption and desorption processes. – J. Braz. Chem. Soc. 25: 36-49.
[10] Eviati (2011): Nutrient Content of Palm Oil Frond Compost. – Laboratory of Soil Fertility, Bogor, Bogor Agriculture Institute.
[11] Fan, T., Xu, M., Zhou, G., Ding, L. (2007): Trends in grain yields and soil organic carbon in a long-term fertilization experiment in The China Loess Plateau. – Am-Euras. Journal of Agriculture and Environmental Science 2: 600-610.
[12] Gyliene, O., Šalkauskas, M. (2001): Sorption of complexed and uncomplexed Cu(II), Ni(II) and Zn(II) ions by peat. – Chemija 12: 183-188.
[13] Hartatik, W., Nugroho, K. (2001): Effect of different ameliorant sources to maize growth in peat soil from Air Sugihan Kiri, South Sumatera. – In: Rieley, J. O., Page, S. E. (eds.) Peatlands for People: Natural Resource Functions and Sustainable Management. Jakarta.
[14] Hooijer, A., Page, S., Jauhiainen, J., Lee, W., Lu, X., Idris, A., Anshari, G. (2012): Subsidence and carbon loss in drained tropical peatlands. – Biogeosciences 9: 1053-1071.
[15] Hoyos, S. J., Lomax, B., Large, D., Turner, B., Boom, A., Lopez, O. (2015): Getting to the root of the problem: Litter decomposition and peat formation in low and neotropical peatlands. – Biogeochemistry 126: 115-129.
[16] Husen, E., Agus, F. (2011): Microbial activities as affected by peat dryness and ameliorant. – American Journal of Environmental Sciences 7: 348-353.
[17] IAARD (2011): Agricultural Research and Development in Indonesia. – Jakarta.
[18] Jaenicke, J., Rieley, J. O., Mott, C., Kimman, P., Siegert, F. (2008): Determination of the amount of carbon stored in Indonesian peatlands. – Geoderma 147: 151-158.
[19] Jones, J. B. (2012): Plant Nutrition and Soil Fertility Manual (2nd ed.). – New York, CRC Press.
[20] Jumin, H. B., Rosneti, H., Agusnimar (2014): Application of crude palm oil liquid sludge sewage on maize (*Zea mays* L.) as re-cycle possibility to fertilizer. – Journal of Agriculture Technology 10: 1473-1488.
[21] Kononen, M., Jauhiainen, J., Laiho, R., Kusin, K., Vasander, H. (2015): Physical and chemical properties of tropical peat under stabilised land uses. – Mires Peat 16: 1-13.
[22] Lampela, M., Jauhiainen, J., Vasander, H. (2014): Surface peat structure and chemistry in a tropical peat swamp forest. – Plant Soil 382: 329-347.
[23] Maftu'ah, E., Maas, A., Syukur, A., Purwanto, B. H. (2013): Effectivity of ameliorant in degraded peatland to increase the growth and NPK uptake on sweet corn (*Zea mays* L. Varsaccharata). – J. Agron Indon 41(1): 16-23.
[24] Murdiyarso, D., Hergoualc'h, K., Verchot, L. V. (2010): Opportunities for reducing greenhouse gas emissions in tropical peatlands. – Proc Natl Acad Sci 107(46): 19655-19660.
[25] Nurulita, Y., Adetutu, E. M., Gunawan, H., Zul, D., Ball, A. S. (2016): Restoration of tropical peat soils: The application of soil microbiology for monitoring the success of the restoration process. – Agriculture, Ecosystems & Environment 216: 293-303.
[26] Okwuagwu, M. I., Alleh, M. E., Osemwota, I. O. (2003): The Effects of organic and inorganic manure on soil properties and yield of okra in Nigeria. – African Crop Science Conference Proceedings 6: 390-393.

http://www.aloki.hu ● ISSN 1589 1623 (Print) ● ISSN 1785 0037 (Online)
DOI: http://dx.doi.org/10.15666/aeer/1804_51995209

[27] Onwonga, R. N., Lelei, J. J., Mochoge, B. B. (2010): Mineral nitrogen and microbial biomass dynamics under different acid soil management practices for maize production. – Journal of Agricultural Science 2: 16-30.
[28] Orlov, D. S. (1995): Humic Substances of Soils and General Theory of Humification. – USA, Balkema Publ.
[29] Rudrappa, L., Purakayastha, T. J., Singh, D., Bhadraray, S. (2006): Long-term manuring and fertilization effects on soil organic carbon pools in a Typic Haplustept of Semi-arid Sub-tropical India. – Soil Till. Res. 88: 180-192.
[30] Salisbury, F. B., Ros, C. W. (1996): Plant Physiology. – California, Wadsworth Publishing Co. Inc.
[31] Shanmugam, S., Dalal, R. C., Joosten, H., Raison, R. J., Joo, G. K. (2018): SOC Stock Changes and Greenhouse Gas Emissions Following Tropical Land Use Conversions to Plantation Crops on Mineral Soils, with a Special Focus on Oil Palm and Rubber Plantations. – MDPI Agriculture 8: 133.
[32] Siti, N., Agus, F., Syahbuddin, H. (2013): Ameliorant application on variation of carbon stock and ash content on peatland South Kalimantan. – J. Trop. Soils 18: 11-16.
[33] Stell, R. G. D., Torrie, J. H. (1980): Principles and Procedures of Statistics: A Biometrical Approach. – Mcgraw-Hill Inc, New York.
[34] Stevenson, F. J. (1994): Humus Chemistry, Genesis, Composition, Reactions. – New York, John Wiley & Sons Inc.
[35] Štursova, M., Baldrian, P. (2011): Effects of soil properties and management on the activity of soil organic matter transforming enzymes and the quantification of soil-bound and free activity. – Plant Soil 338: 99-110.
[36] Sullivan, T. S., McBride, M. B., Thies, J. E. (2013): Soil bacterial and archaeal community composition reflects high spatial heterogeneity of pH, bio available Zn, and Cu in a metalliferous peat soil. – Soil Biology & Biochemistry 66: 102-109.
[37] Tan, K. H. (2010): Principles of Soil Chemistry. – Fourth Edition, New York, CRC Press, Taylor and Francis Group.
[38] Troeh, F. R., Thompson, L. M. (2005): Soils and Soil Fertility. – New York, Blackwell Publishing.
[39] Zahrah, S. (2010): The uptake of N, P, K and yield rice of various varieties with application of Cu, Zn, Fe ameliorants on peat soil. – Journal Natur Indonesia 12: 102-108.

http://www.aloki.hu ● ISSN 1589 1623 (Print) ● ISSN 1785 0037 (Online)
DOI: http://dx.doi.org/10.15666/aeer/1804_51995209

AN ANALYSIS OF GENETIC ASSOCIATION BETWEEN YIELD AND QUALITY TRAITS IN SEGREGATING POPULATION OF *ORYZA SATIVA* L.

GHOURI, F.[1] – NAEEM, M.[2*] – IQBAL, M.[2] – ALLAH, S. U.[3] – SHAHID, M. Q.[1*]

[1]*College of Agriculture, South China Agricultural University, Guangzhou, Guangdong 510642, China*

[2]*Department of Plant Breeding and Genetics, UCA & ES, The Islamia University of Bahawalpur, Bahawalpur, Pakistan*

[3]*Department of Plant Breeding and Genetics, College of Agriculture, BZU Bahaddar Sub-Campus, Layyah, Pakistan*

**Corresponding authors*
e-mail: mniub@iub.edu.pk (M. Naeem); shahidmq@gmail.com (M. Q. Shahid); phone: +92-62-925-5539; fax: +86-20-8528-0205

(Received 22nd Jan 2020; accepted 6th May 2020)

Abstract. Limited information has been reported on the genetic association of morphological and quality traits of *Oryza sativa* L. From a total of 50 genotypes, evaluated for genetic diversity using SSR markers, six diverse genotypes were selected for the generation of three crosses. Progenies of these crosses were grown to develop three F_2 populations. Morphological and quality traits were recorded and analysed for genotypic and phenotypic correlations followed by the path coefficient analysis from the genotypic correlation. Strongest association was observed for yield per plant and alkali spread value (ranging from -0.73 to -0.91 for different crosses). It was depicted from path coefficient analysis that length width ratio had a maximum direct effect on yield (ranging from 0.61 to 0.67 for different crosses), and also had a relatively high magnitude of the indirect effect to the yield via plant height, panicle length protein content and length width ratio. Although, minute differences were detected in the strength of association and direct/indirect effects for different populations, the direction of the association always remained the same. The present study showed that direct and indirect effects of traits should be considered for the selection of yield improvement instead of correlation, as a trait having high correlation may have a low direct effect and vice versa.
Keywords: *Oryza sativa L., correlation, path coefficient analysis, qualitative traits, basmati rice*

Introduction

Rice is the staple food for about half of the world population. Rice is a healthful cereal grain which owns unusual dietary requirements. In 2018-19 worlds' rice production is expected to be 510 million tonnes while world's consumption is also expected to be 503 million tonnes (FAO, 2018). Asia produced and consumed more than 90% of the world's rice (Memon et al., 2015) as three billion Asians fulfil their 35-60% of caloric requirement through rice (Guyer et al., 1998). The cooking and eating qualities of rice are important in defining its economic value in export market and for user acceptance (Pingali, 1997). The Quality of rice grain is intricate characteristic comprising several components such as appearance, cooking and eating qualities (Rabiei et al., 2004). Physicochemical properties of rice are calculated on the basis of amylose content, protein contents and alkali spread value (Rohilla et al., 2000). Quality and yield of rice grain can be enhanced by understanding the genetic mechanism

http://www.aloki.hu ● ISSN 1589 1623 (Print) ● ISSN 1785 0037 (Online)
DOI: http://dx.doi.org/10.15666/aeer/1804_52115224

controlling these traits and association between these traits which is not very well elaborated in previous studies. Correlation studies reported in past have been conducted in homozygous populations but in this study we have conducted correlation studies in segregating populations.

Complex inheritance pattern of grain yield and quality traits necessitate their thorough understanding in order to strengthen rice breeding program. Studies of genetic correlation between yield and quality traits gave understanding about the extent and direction of association between these traits. However direct and indirect effect of different yield related traits are determined by path coefficient analysis. Genetic attributes could be ranked according to their contribution by the breeder (Dewey and Lu, 1959). Dewey and Lu (1959) developed a statistical technique for path analysis which helps in understanding the cause of association and provide information about cause and effect situation. Path analysis assists plant breeders in making selection as it dissects the correlation of different traits into direct and indirect effects (Dewey and Lu, 1959; Milligan et al., 1990; Samonte et al., 2005).

The main objective of this study was to (i) assess genetic variability and correlation among yield and quality traits of various segregating populations for selecting superior genotypes, (ii) to assess the direct and indirect contribution of yield components to yield (iii) to assess the type of connection between quality and yield traits of rice.

Materials and methods

The present study was conducted in the experimental area of Department of Plant BREEDING and Genetics, University College of Agriculture and Environmental Sciences, the Islamia University of Bahawalpur, Pakistan.

Development of plant material for genetic diversity studies

Thirty rice varieties were grown in nursery during stat of May 2013 up to three leaf stage. Of each genotype 4 cm leaf sample was collected and preserved in liquid nitrogen prior to DNA extraction by CTAB method (Ul-Allah et al., 2017). Twenty µl PCR reaction mixture included DNA 2 µl, 0.2 µl Taq polymerase enzyme, 1.5 µl of each primer, 2.5 µl of 2.5 mM dNTPs, 3 µl $MgCl_2$ and2 µl PCR buffer along with 9.3 µl of ddH_2O. One hundred SSR markers (*Table 1*) were used for diversity studies. PCR product was studied on 1.5% agarose gel with Ethydium bromide as fluorescent dye. Banding pattern was scored in binary fashion for the calculation of similarity index which was deployed for the construction of dendrogram by using un-weighted pair group method with arithmetic mean (UPGMA).

Selection of diverse genotypes and development of populations

Based on dendrogram generated by UPGMA, six genetically diverse genotypes i.e., Basmati Pak, Basmati-198, Basmati-385, Super Basmati, Basmati-2000 and Shaheen Basmati were grown in field in end of May, 2013. Cross combinations were made among genotypes widely assorted in dendrogram in following fashion (Basmati Pak × HuoYou8166, Basmati-385 × HuoYou8305 and Basmati-198 × HuoJingXian) to generate F_1 seed. F_2 seed harvested from F_1 generation during September 2014 was sown in field during May 2015 adapting nursery sowing followed by field transplantation maintaining plant to plant and row to row distance of 30 cm. Soil was

http://www.aloki.hu ● ISSN 1589 1623 (Print) ● ISSN 1785 0037 (Online)
DOI: http://dx.doi.org/10.15666/aeer/1804_52115224

sandy-loam with 50:30:20 sand, silt and clay proportion. Ten rows (each having fifteen plants) of each segregating population plus five rows of each parent were grown keeping single plant per hill in non-replicated fashion. All agronomic practices and crop protection measures were observed as per standard recommendations. Weeds, insect pests and diseases were controlled following standard recommendations.

Table 1. *List of primers used in present study*

Locus name	Chr	Forward primer sequence	Reverse primer sequence	Reference
RM1	1	GCGAAAACACAATGCAAAAA	GCGTTGGTTGGACCTGAC	Panaud et al., 1996
RM2	7	ACGTGTCACCGCTTCCTC	ATGTCCGGGATCTCATCG	Panaud et al., 1996
RM3	6	ACACTGTAGCGGCCACTG	CCTCCACTGCTCCACATCTT	Panaud et al., 1996
RM7	3	TTCGCCATGAAGTCTCTCG	CCTCCCATCATTTCGTTGTT	Panaud et al., 1996
RM8	2	CACGTGGCGTAAATACACGT	GGCCAAACCCTAACCCTG	Panaud et al., 1996
RM10	7	TTGTCAAGAGGAGGCATCG	CAGAATGGGAAATGGGTCC	Panaud et al., 1996
RM11	7	TCTCCTCTTCCCCCGATC	ATAGCGGGCGAGGCTTAG	Panaud et al., 1996
RM13	5	TCCAACATGGCAAGAGAGAG	GGTGGCATTCGATTCCAG	Panaud et al., 1996
RM16	3	CGCTAGGGCAGCATCTAAA	AACACAGCAGGTACGCGC	Panaud et al., 1996
RM17	12	TGCCCTGTTATTTTCTTCTCTC	GGTGATCCTTTCCCATTTCA	Panaud et al., 1996
RM18	7	TTCCCTCTCATGAGCTCCAT	GAGTGCCTGGCGCTGTAC	Panaud et al., 1996
RM19	12	CAAAAACAGAGCAGATGAC	CTCAAGATGGACGCCAAGA	Panaud et al., 1996
RM21	11	ACAGTATTCCGTAGGCACGG	GCTCCATGAGGGTGGTAGAG	Panaud et al., 1996
RM22	3	GGTTTGGGAGCCCATAATCT	CTGGGCTTCTTTCACTCGTC	Panaud et al., 1996
RM26	5	GAGTCGACGAGCGGCAGA	CTGCGAGCGACGGTAACA	Chen et al., 1997
RM27	2	TTTTCCTTCTCACCCACTTCA	TCTTTGACAAGAGGAAAGAGGC	Chen et al., 1997
RM30	6	GGTTAGGCATCGTCACGG	TCACCTCACCACACGACACG	Chen et al., 1997
RM31	5	GATCACGATCCACTGGAGCT	AAGTCCATTACTCTCCTCCC	Chen et al., 1997
RM36	3	CAACTATGCACCATTGTCGC	GTACTCCACAAGACCGTACC	Chen et al., 1997
RM38	8	ACGAGCTCTCGATCAGCCTA	TCGGTCTCCATGTCCCAC	Chen et al., 1997
RM39	5	GCCTCTCTCGTCTCCTTCCT	AATTCAAACTGCGGTGGC	Chen et al., 1997
RM41	9	AAGTCTAGTTTGCCTCCC	AATTTCTACGTCGTCGGGC	Chen et al., 1997
RM42	8	ATCCTACCGCTGACCATGAG	TTTGGTCTACGTGGCGTACA	Chen et al., 1997
RM44	8	ACGGGCAATCCGAACAACC	TCGGGAAAACCTACCCTACC	Chen et al., 1997
RM47	7	ACTCCACTCCACTCCCCAC	GTCAGCAGGTCGGACGTC	Chen et al., 1997
RM49	3	TTCGGAAGTTGGTTACTGATCA	TTGGAGCGGATTCGGAGG	Chen et al., 1997
RM50	6	ACTGTACCGGTCGAAGACG	AAATTCCACGTCAGCCTCC	Chen et al., 1997
RM51	7	TCTCGATTCAATGTCCTCGG	CTACGTCATCATCGTCTTCCC	Chen et al., 1997
RM55	3	CCGTCGCCGTAGTAGAGAAG	TCCCGGTTATTTTAAGGCG	Chen et al., 1997
RM60	3	AGTCCCATGTTCCACTTCCG	ATGGCTACTGCCTGTACTAC	Chen et al., 1997
RM70	7	GTGGACTTCATTTCAACTCG	GATGTATAAGATAGTCCC	Chen et al., 1997
RM71	2	CTAGAGGCGAAAACGAGATG	GGGTGGGCGAGGTAATAATG	Temnykh et al.,2000
RM72	8	CCGGCGATAAAACAATGAG	GCATCGGTCCTAACTAAGGG	Temnykh et al., 2000
RM80	8	TTGAAGGCGCTGAAGGAG	CATCAACCTCGTCTTCACCG	Chen et al., 1997
RM82	7	TGCTTCTTGTCAATTCGCC	CGACTCGTGGAGGTACGG	Chen et al., 1997
RM83	12	ACTCGATGACAAGTTGAGG	CACCTAGACACGATCGAG	Chen et al., 1997
RM85	3	CCAAAGATGAAACCTGGATTG	GCACAAGGTGAGCAGTCC	Temnykh et al.,2000
RM87	5	CCTCTCCGATACACCGTATG	GCGAAGGTACGAAAGGAAAG	Temnykh et al., 2000
RM88	8	ACTCATCAGCATGGCCTTGCTC	TAATGCTCCACCTTCACCAC	Temnykh et al., 2000
RM201	9	CTCGTTTATTACCTACAGTACC	CTACCTCCTTTCTAGACCGATA	Chen et al., 1997
RM202	11	CAGATTGGAGATGAAGTCCTCC	CCAGCAAGCATGTCAATGTA	Chen et al., 1997
RM204	6	GTGACTGACTTGGTCATAGGG	GCTAGCCATGCTCTCGTACC	Chen et al., 1997
RM205	9	CTGGTTCTGTATGGGAGCAG	CTGGCCCTTCACGTTTCAGTG	Chen et al., 1997
RM206	11	CCCATGCGTTTAACTATTCT	CGTTCCATCGATCCGTATGG	Chen et al., 1997
RM207	2	CCATTCGTGAGAAGATCTGA	CACCTCATCCTCGTAACGCC	Chen et al., 1997
RM209	11	ATATGAGTTGCTGTCGTGCG	CAACTTGCATCCTCCCCTCC	Chen et al., 1997

http://www.aloki.hu ● ISSN 1589 1623 (Print) ● ISSN 1785 0037 (Online)
DOI: http://dx.doi.org/10.15666/aeer/1804_52115224

Locus name	Chr	Forward primer sequence	Reverse primer sequence	Reference
RM210	8	TCACATTCGGTGGCATTG	CGAGGATGGTTGTTCACTTG	Chen et al., 1997
RM214	7	CTGATGATAGAAACCTCTTCTC	AAGAACAGCTGACTTCACAA	Chen et al., 1997
RM215	9	CAAAATGGAGCAGCAAGAGC	TGAGCACCTCCTTCTCTGTAG	Chen et al., 1997
RM216	10	GCATGGCCGATGGTAAAG	TGTATAAAACCACACGGCCA	Chen et al., 1997
RM217	6	ATCGCAGCAATGCCTCGT	GGGTGTGAACAAAGACAC	Chen et al., 1997
RM219	9	CGTCGGATGATGTAAAGCCT	CATATCGGCATTCGCCTG	Chen et al., 1997
RM222	10	CTTAAATGGGCCACATGCG	CAAAGCTTCCGGCCAAAAG	Chen et al., 1997
RM223	8	GAGTGAGCTTGGGCTGAAAC	GAAGGCAAGTCTTGGCACTG	Chen et al., 1997
RM224	11	ATCGATCGATCTTCACGAGG	TGCTATAAAAGGCATTCGGG	Chen et al., 1997
RM225	6	TGCCCATATGGTCTGGATG	GAAAGTGGATCAGGAAGGC	Chen et al., 1997
RM228	10	CTGGCCATTAGTCCTTGG	GCTTGCGGCTCTGCTTAC	Chen et al., 1997
RM229	11	CACTCACACGAACGACTGAC	CGCAGGTTCTTGTGAAATGT	Chen et al., 1997
RM230	8	GCCAGACCGTGGATGTTC	CACCGCAGTCACTTTTCAAG	Chen et al., 1997
RM234	7	ACAGTATCCAAGGCCCTGG	CACGTGAGACAAAGACGGAG	Chen et al., 1997
RM235	12	AGAAGCTAGGGCTAACGAAC	TCACCTGGTCAGCCTCTTTC	Chen et al., 1997
RM239	10	TACAAAATGCTGGGTACCCC	ACATATGGGACCCACCTGTC	Chen et al., 1997
RM241	4	GAGCCAAATAAGATCGCTGA	TGCAAGCAGCAGATTTAGTG	Chen et al., 1997
RM242	9	GGCCAACGTGTGTATGTCTC	TATATGCCAAGACGGATGGG	Chen et al., 1997
RM244	10	CCGACTGTTCGTCCTTATCA	CTGCTCTCGGGTGAACGT	Chen et al., 1997
RM245	9	ATGCCGCCAGTGAATAGC	CTGAGAATCCAATTATCTGGGG	Chen et al., 1997
RM246	1	GAGCTCCATCAGCCATTCAG	CTGAGTGCTGCTGCGACT	Chen et al., 1997
RM247	12	TAGTGCCGATCGATGTAACG	CATATGGTTTTGACAAAGCG	Chen et al., 1997
RM248	7	TCCTTGTGAAATCTGGTCCC	GTAGCCTAGCATGGTGCATG	Chen et al., 1997
RM250	2	GGTTCAAACCAAGCTGATCA	GATGAAGGCCTTCCACGCAG	Chen et al., 1997
RM253	6	TCCTTCAAGAGTGCAAAACC	GCATTGTCATGTCGAAGCC	Chen et al., 1997
RM254	11	AGCCCCGAATAAATCCACCT	CTGGAGGAGCATTTGGTAGC	Chen et al., 1997
RM255	4	TGTTGCGTGTGGAGATGTG	CGAAACCGCTCAGTTCAAC	Chen et al., 1997
RM256	8	GACAGGGAGTGATTGAAGGC	GTTGATTTCGCCAAGGGC	Chen et al., 1997
RM257	9	CAGTTCCGAGCAAGAGTACTC	GGATCGGACGTGGCATATG	Chen et al., 1997
RM258	10	TGCTGTATGTAGCTCGCACC	TGGCCTTTAAAGCTGTCGC	Chen et al., 1997
RM259	1	TGGAGTTTGAGAGGAGGG	CTTGTTGCATGGTGCCATGT	Chen et al., 1997
RM260	11	ACTCCACTATGACCCAGAG	GAACAATCCCTTCTACGATCG	Chen et al., 1997
RM261	4	CTACTTCTCCCCTTGTGTCG	TGTACCATCGCCAAATCTCC	Chen et al., 1997
RM262	2	CATTCCGTCTCGGCTCAACT	CAGAGCAAGGTGGCTTGC	Chen et al., 1997
RM263	2	CCCAGGCTAGCTCATGAACC	GCTACGTTTGAGCTACCACG	Chen et al., 1997
RM264	8	GTTGCGTCCTACTGCTACTTC	GATCCGTGTCGATGATTAGC	Chen et al., 1997
RM266	2	TAGTTTAACCAAGACTCTC	GGTTGAACCCAAATCTGCA	Chen et al., 1997
RM267	5	TGCAGACATAGAGAAGGAAGTG	AGCAACAGCACAACTTGATG	Chen et al., 1997
RM269	10	GAAAGCGATCGAACCAGC	GCAAATGCGCCTCGTGTC	Chen et al., 1997
RM270	12	GGCCGTTGGTTCTAAAATC	TGCGCAGTATCATCGGCGAG	Chen et al., 1997
RM271	10	TCAGATCTACAATTCCATCC	TCGGTGAGACCTAGAGAGCC	Chen et al., 1997
RM272	1	AATTGGTAGAGAGGGGAGAG	ACATGCCATTAGAGTCAGGC	Chen et al., 1997
RM273	4	GAAGCCGTCGTGAAGTTACC	GTTTCCTACCTGATCGCGAC	Chen et al., 1997
RM274	5	CCTCGCTTATGAGAGCTTCG	CTTCTCCATCACTCCCATGG	Chen et al., 1997
RM275	6	GCATTGATGTGCCAATCG	CATTGCAACATCTTCAACATCC	Chen et al., 1997
RM276	6	CTCAACGTTGACACCTCGTG	TCCTCCATCGAGCAGTATCA	Chen et al., 1997
RM278	9	GTAGTGAGCCTAACAATAATC	TCAACTCAGCATCTCTGTCC	Chen et al., 1997
RM279	2	GCGGGAGAGGGATCTCCT	GGCTAGGAGTTAACCTCGCG	Chen et al., 1997
RM280	4	ACACGATCCACTTTGCGC	TGTGTCTTGAGCAGCCAGG	Chen et al., 1997
RM281	8	ACCAAGCATCCAGTGACCAG	GTTCTTCATACAGTCCACATG	Chen et al., 1997
RM282	3	CTGTGTCGAAAGGCTGCAC	CAGTCCTGTGTTGCAGCAAG	Chen et al., 1997
RM283	1	GTCTACATGTACCCTTGTTGGG	CGGCATGAGAGTCTGTGATG	Chen et al., 1997
RM284	8	ATCTCTGATACTCCATCCATCC	CCTGTACGTTGATCCGAAGC	Chen et al., 1997
RM285	9	CTGTGGGCCCAATATGTCAC	GGCGGTGACATGGAGAAAG	Chen et al., 1997

http://www.aloki.hu ● ISSN 1589 1623 (Print) ● ISSN 1785 0037 (Online)
DOI: http://dx.doi.org/10.15666/aeer/1804_52115224

Morphological and quality traits evaluation

At maturity data was recorded on one hundred fifty randomly selected guarded plants from each population for plant height, panicle length, and yield per plant. Seed samples were collected separately for the estimation of Amylose content, Alkali Spread Value, protein content and grain length/width ratio. Chemical analysis of Protein contents were accomplished according to AACC method 2000.

Correlation analysis

Correlation coefficient among the characters under study was estimated according to the statistical techniques given by Gomez and Gomez (1984).

$$r = \frac{\sum XY - \sum X.\sum Y/n}{\sqrt{[\sum X^2 - (\sum X)^2/n].[\sum Y^2 - (\sum Y)^2/n]}}$$

where n is number of observations, X is first variable, Y is second variable, while genotypic correlation was calculated according to formula

$$r = \frac{CoVF_2 - \overline{CoVp}}{\sqrt{[VF_{2(X)} - \mathrm{Vp(X)}].[VF_2 - \overline{CoVp}(\mathrm{Y})]}}$$

Path analysis

Path coefficient analysis was performed according to the method given by Dewey and Lu (1959) for the yield and quality traits of Rice, keeping yield per plant as resultant variable and rest of the traits as causal variables.

Results

Genetic diversity studies

Thirty rice genotypes having wide range of phenotypic variability (*Table 2*) for all of the traits under study were subjected to Simple sequence repeat (SSR) based genetic diversity study (*Fig. 1*). Cluster analysis revealed the genetic relatedness among 30 genotypes of rice as shown in the dendrogram (*Fig. 2*). One hundred SSR markers equally distributed on twelve chromosomes were randomly selected from the genetic map of Rice which revealed polymorphism percentage of 11.3 to 77.5%. Distribution of these genotypes in the dendrogram shows the genetic variation among the genotypes. Cluster analysis grouped the genotypes into four clusters with reference to yield and yield related traits having smallest cluster (Cluster I) with two varieties, Huo Jing Xian and HuoYou8187 and the largest cluster (Cluster IV) having nine varieties, while second and third clusters possesses eight varieties each. Huojing xian, Huoyou-8187, Huoyou-8305, Basmati-Pak, Basmati-198 and Basmati-385 on the bases of genetic divergence owing to variation in yield were selected for making three cross combinations.

http://www.aloki.hu ● ISSN 1589 1623 (Print) ● ISSN 1785 0037 (Online)
DOI: http://dx.doi.org/10.15666/aeer/1804_52115224

Correlation analysis

Genetically diverse F_2 population (*Fig. 3*) for all of the traits studied was obtained from above mentioned cross combinations. Populations from all three cross combinations are significantly different from each other for plant height, panicle length, yield per plant, alkali spread value, amylose content, L/W ratio and protein content. All the characters studied were significantly correlated with yield per plant with few exceptions (discussed below). Genotypic and phenotypic correlation coefficients of three cross combinations populations for various traits are presented in *Table 3*. Highest positive phenotypic correlation for plant height was observed with protein content values 0.61 in Basmati-198 × HuoJingXian, while it was minimum with L/W ratio 0.01 in the same cross. Phenotypic correlation of plant height was lowest with Alkali spread value -0.48 while genotypic correlation between plant height and amylase content was highest having numerical value -0.71. Highest positive phenotypic correlation for panicle length was with Yield per plant 0.73 while genotypic correlation between panicle length and ASV was -0.64. Panicle length show minimum genotypic correlation with protein content and L/W ratio having numerical values 0.04 and -0.05 respectively. Yield per plant being the most important character of plant showed strongest phenotypic and genotypic correlation with ASV -0.91 while the genotypic and phenotypic correlation between YPP vs panicle length 0.14 and YPP vs Plant height -0.54 respectively, were minimum. Genotypic correlation of ASV was strongest with YPP -0.91, but phenotypic correlation of ASV was weakest with panicle length -0.31. Alkali Spread Value showed strongest positive phenotypic correlation with amylose content 0.87. Length Width ratio show strongest positive phenotypic correlation with protein content 0.86 while strongest negative phenotypic correlation of L/W ratio was found with amylose content -0.89. Contrary to this weakest genotypic correlation of L/W ratio was observed with panicle length -0.05. Protein content shows highest positive phenotypic correlation with L/W ratio i.e. 0.72 and strongest negative genotypic correlation with ASV -0.91. Strong negative (-0.73) phenotypic correlation was observed between protein content and ASV while weakest positive (0.04) genotypic correlation was found between protein content and panicle length.

Table 2. *Mean values of various traits of parent, studied in this experiment*

S. No	VAR/TR	PH	PL	YPP	ASV	Aamyl	L/W ratio	Protein
1	BASMATIPAK	132.98^{a}	22.68^{b}	14.04a	5.59^{b}	25.67cd	4.63^{cd}	7.79^{cd}
2	M133	139.07^{a}	21.86^{a}	14.71^{a}	5.33^{ab}	25.63cd	4.65^{cd}	7.75^{def}
3	KASHMIRBAS	136.63^{a}	21.97^{ab}	14.08^{ab}	5.51^{ab}	25.79cd	4.67^{cd}	7.75^{def}
4	BASMATI198	136.53^{a}	23.18^{bc}	14.23^{ab}	5.55^{b}	25.67cd	4.93^{f}	7.83^{efg}
5	BASMATI385	137.60^{a}	23.22^{b}	14.99^{ab}	5.66^{bc}	25.06bc	4.93^{f}	7.68^{cd}
6	KS282	140.84^{a}	21.97^{ab}	14.63^{ac}	5.37^{ab}	25.10bc	4.87^{ef}	7.90^{g}
7	NIABIRRI9	128.03^{b}	22.68^{bc}	14.65^{ac}	5.42 ^{ab}	25.26bc	4.97^{efg}	7.94^{g}
8	PAK23717	127.36^{ab}	21.74^{ab}	12.12^{abc}	5.43 ^{ab}	24.88bc	4.94^{ef}	7.64^{ef}
9	IR36	116.89^{abc}	21.02^{a}	11.58^{abc}	6.25^{c}	26.44d	4.74^{c}	7.25^{ab}
10	MB385	116.48^{abc}	23.17^{abc}	10.71^{acd}	5.87^{cd}	27.05de	4.67^{cd}	7.21^{ab}
11	MB198	117.48^{abc}	22.71^{bc}	13.50^{ad}	5.27^{ab}	27.48e	4.76^{d}	7.19^{ab}
12	BAS2000	115.75^{abc}	23.47^{bc}	13.61^{ad}	5.27^{ab}	25.39bc	4.57^{c}	7.18^{ab}
13	M153	115.46^{abc}	24.27^{cd}	13.70^{abcd}	5.48^{ab}	26.38cd	4.84^{d}	7.15^{a}

http://www.aloki.hu ● ISSN 1589 1623 (Print) ● ISSN 1785 0037 (Online)
DOI: http://dx.doi.org/10.15666/aeer/1804_52115224

S. No	VAR/TR	PH	PL	YPP	ASV	Aamyl	L/W ratio	Protein
14	N185	115.36^{bc}	22.36^{b}	13.65^{abcd}	6.74^{cd}	26.49cd	4.26^{a}	7.13^{a}
15	LH18	115.36^{bc}	22.58^{bc}	13.50^{abcd}	6.32^{c}	26.47cd	4.38^{ab}	7.10^{a}
16	521	115.94^{bc}	23.46^{cd}	13.45^{abd}	6.38^{c}	24.55b	4.27^{a}	7.08^{a}
17	A1	113.14^{c}	22.73^{bc}	13.20^{abd}	5.27^{ab}	24.49b	4.39^{ab}	7.43^{cd}
18	SUPPERBAS	113.18^{c}	23.46^{c}	13.10^{abde}	5.95^{b}	25.63cd	4.71^{e}	7.24^{ab}
19	X625	113.27^{c}	24.24^{d}	12.74^{f}	5.27^{ab}	25.48bc	4.75^{e}	7.29^{c}
20	MK134	111.28^{cd}	22.36^{bc}	12.64^{f}	6.46^{cd}	23.47a	4.57^{c}	7.35^{c}
21	SWAT1	110.27^{cd}	22.68^{bc}	12.70^{f}	6.25^{bc}	23.84cb	4.26^{a}	7.36^{cd}
22	SHADAB	109.27^{cd}	23.74^{c}	11.74^{fg}	7.46^{d}	24.57b	4.27^{a}	7.25^{ab}
23	SARSHAR	108.13^{cde}	22.47^{bc}	10.72^{fgh}	5.47^{ab}	24.65b	4.37^{ab}	7.28^{ab}
24	KSK133	108.17^{cde}	22.37^{b}	10.64^{fgh}	5.61^{bc}	23.48a	4.28^{a}	7.55^{e}
25	X625	108.34^{cde}	23.58^{c}	10.54^{fgh}	5,82^{bc}	24.59b	4.76^{ed}	7.45^{cd}
26	BOYOU8166	107.48^{d}	24.57^{d}	9.78^{fhi}	5.96^{bc}	24.65bc	4.56^{c}	7.39^{cd}
27	BOYOU8305	107.47^{ef}	22.16ab	9.54^{fghi}	6.57^{c}	25.58d	4.36^{ab}	7.85^{gh}
28	HUOYOU8305	106.37^{ef}	22.38^{b}	8.49^{hij}	5.68^{bc}	23.52a	4.57^{c}	7.73^{fg}
29	HUOYOU8187	106.48^{ef}	24.27^{b}	8.43^{hij}	4.90^{a}	24.48bc	4.95^{ef}	7.63^{f}
30	HJK	105.37^{ef}	23.57^{cd}	7.21^{117}	5.27^{ab}	23.44^{a}	4.37^{ab}	7.46^{cd}

PH: plant height, PL: penical length, YPP: yield per plant, ASV: Alkali spread value, L/W ratio: length width ratio, Protein: protein content. ^{a,b,c,d} values with similar alphabets are statistically same

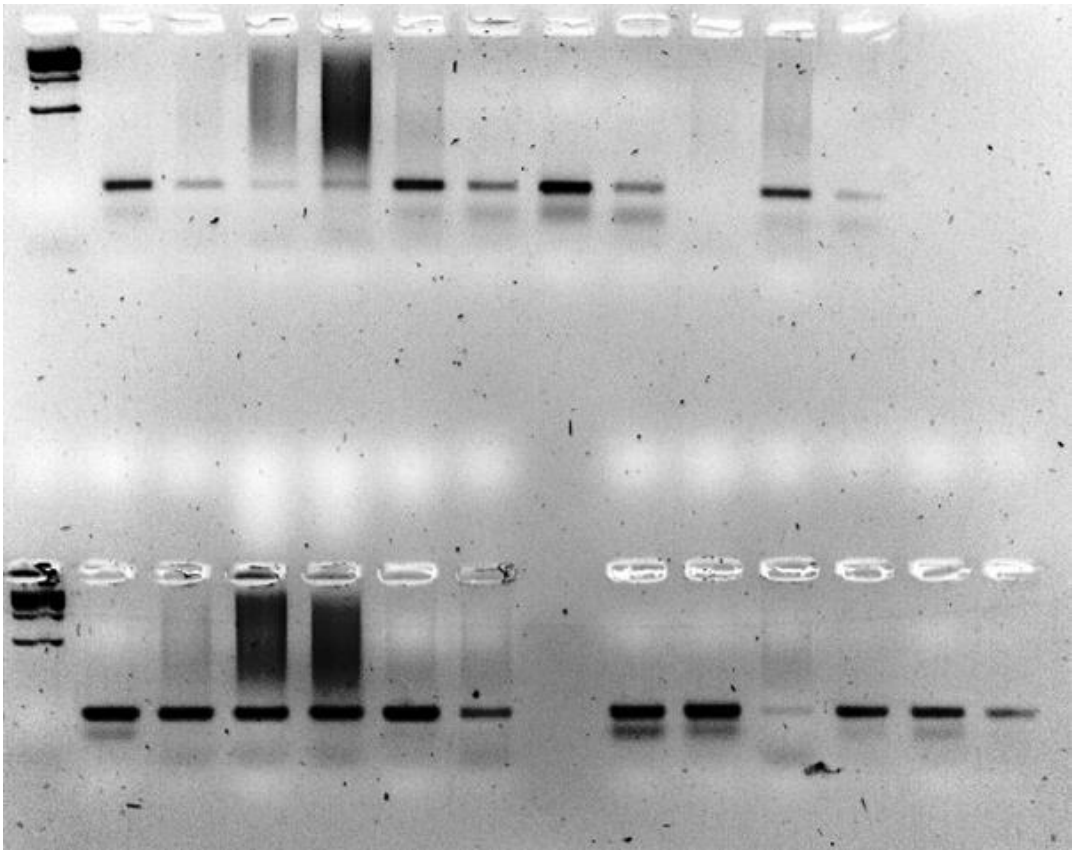

Figure 1. *Gel electrophoresis image of RM-229 with rice genotypes in present study*

http://www.aloki.hu ● ISSN 1589 1623 (Print) ● ISSN 1785 0037 (Online)
DOI: http://dx.doi.org/10.15666/aeer/1804_52115224

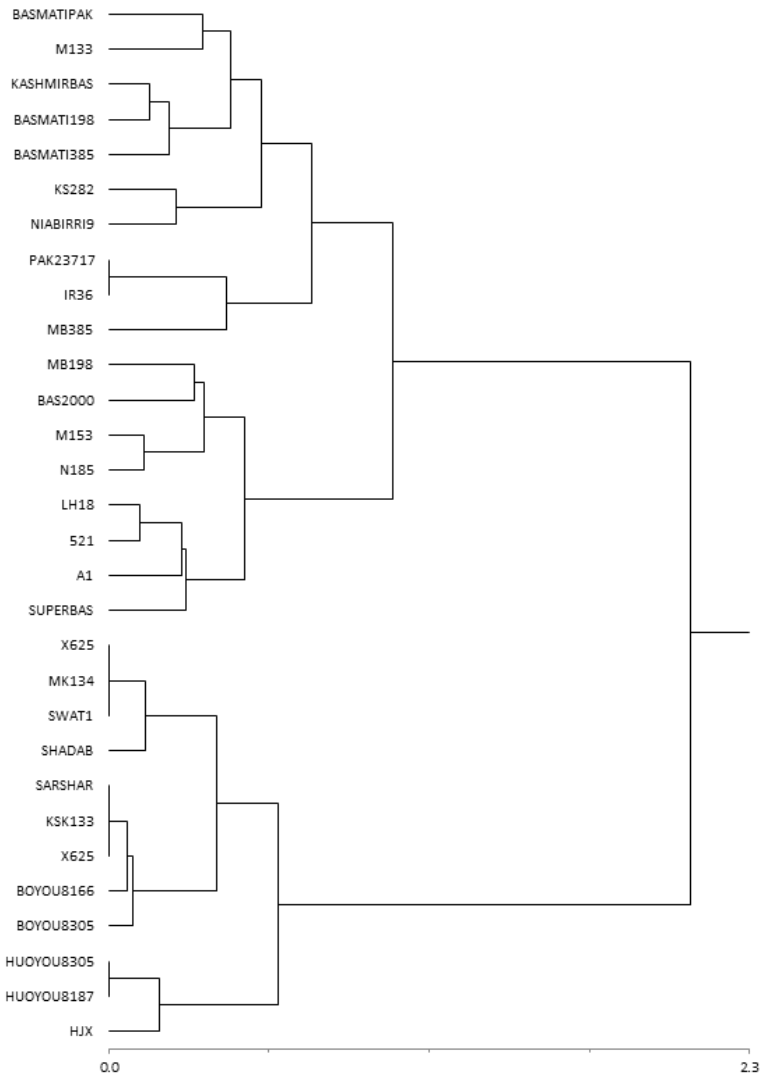

Figure 2. *UPGMA cluster analysis showing the diversity and relatedness among the 30 rice genotypes studied*

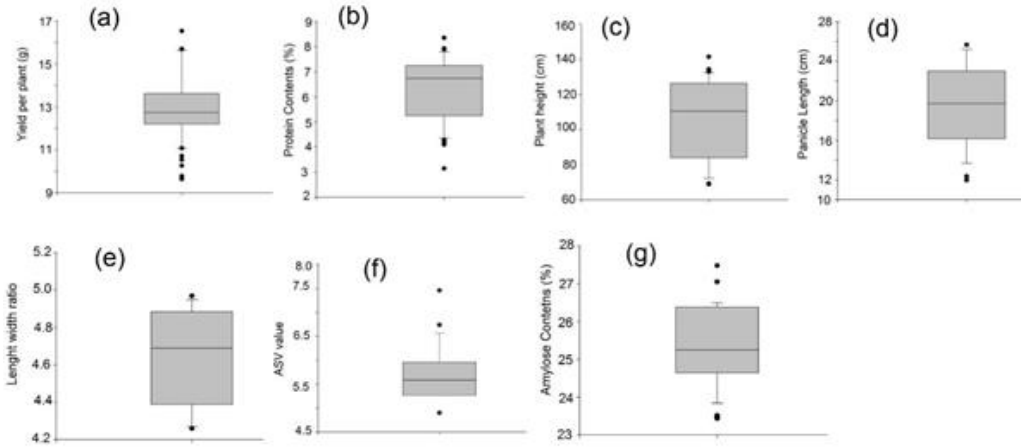

Figure 3. *Cumulative range of variability in F_2 population of all three crosses for various traits in present study*

http://www.aloki.hu ● ISSN 1589 1623 (Print) ● ISSN 1785 0037 (Online)
DOI: http://dx.doi.org/10.15666/aeer/1804_52115224

Table 3. *Phenotypic and genotypic correlation among different yield and quality traits of rice in three different F_2 populations*

Variables	PH	PL	YPP	ASV	Aamyl	L/W Ratio	Protein
Basmati Pak × HuoYou8166							
PH	**1.00**	0.12	-0.70**	-0.69**	-0.71**	0.05	0.49*
PL	0.19	**1.00**	0.16	-0.35	-0.27	-0.26	0.05
YPP	-0.68	0.67**	**1.00**	-0.91**	-0.86**	0.56**	-0.11
ASV	-0.67 **	-0.31	-0.87**	**1.00**	0.75**	-0.83**	-0.85**
Aamyl	-0.66**	-0.23	-0.82**	0.92**	**1.00**	-0.57**	-0.89**
L/W Ratio	0.09	-0.21	0.82*	-0.79**	-0.50*	**1.00**	0.62**
Protein	0.56**	0.15	-0.15	-0.83**	-0.84**	0.86**	**1.00**
Basmati-385 × HuoYou8305							
PH	**1.00**	0.17	-0.61**	-0.65**	-0.65**	0.05	0.49*
PL	0.42*	**1.00**	0.14	-0.64**	-0.58**	-0.05	0.04
YPP	-0.56**	0.53**	**1.00**	-0.83**	-0.72**	0.73**	-0.15
ASV	-0.59 **	-0.43*	-0.79**	**1.00**	0.79**	-0.69**	-0.91**
Aamyl	-0.54*	-0.25	-0.73**	0.87**	**1.00**	-0.85**	-0.87**
L/W Ratio	0.10	-0.24	0.81**	-0.67**	-0.82**	**1.00**	0.68**
Protein	0.59**	0.13	-0.17	-0.86**	-0.83**	0.81**	**1.00**
Basmati-198 × HuoJingXian							
PH	**1.00**	0.21	-0.61**	-0.50*	-0.57**	0.04	0.42*
PL	0.39	**1.00**	0.23	-0.49*	-0.38	-0.36	0.05
YPP	-0.54**	0.73**	**1.00**	-0.91**	-0.85**	0.48*	-0.12
ASV	-0.48 **	-0.42*	-0.85**	**1.00**	0.51*	-0.81**	-0.82**
Aamyl	-0.55**	-0.34	-0.81**	0.55*	**1.00**	-0.89**	-0.91**
L/W Ratio	0.01	-0.28	0.70**	-0.76**	-0.87**	**1.00**	0.72**
Protein	0.61**	0.17	-0.19	-0.73**	-0.82**	0.81**	**1.00**

Lower diagonal represents phenotypic correlation and upper diagonal represent genotypic correlation. Bold numerical values are diagonals. PH: plant height, PL: panicle length, YPP: yield per plant, ASV: Alkali spread value, L/W ratio: length width ratio, Protein: protein content. *Significant at the 5% level. **Significant at the 1% level

Path co-efficient analysis

Genetic correlation of different quality traits and yield components was further dissected to investigate the direct and indirect effects of each trait that it has on grain yield (*Table 4*). Direct effects explain the contribution of individual trait with grain yield while indirect effect explains the influence of a character on yield in association of other characters.

Direct effects

Direct effect is the contribution of the trait that directly determined the yield. The traits that have positive direct effect, with increase in them the yield will also increases. While increase in the characters having negative effect toward yield will results in decrease of yield. In the present population the results show that all the traits show positive direct effect in the yield except ASV. Highest positive direct effect was showed by L/W ratio (0.67) followed by panicle length (0.41), amylose content (0.36) while lowest positive direct effect was contributed by plant height (0.22). Alkali spread value show negative direct effect with maximum value (-0.49) and minimum value (-0.21).

http://www.aloki.hu ● ISSN 1589 1623 (Print) ● ISSN 1785 0037 (Online)
DOI: http://dx.doi.org/10.15666/aeer/1804_52115224

Table 4. *Direct and indirect effect matrix. Dependent variable is YPP. The last column shows genotypic correlations of independent variables with YPP among different yield and quality traits of rice in three different F_2 populations*

Variables	PH	PL	ASV	Aamyl	l/w ratio	Protein	YPP
Basmati Pak × HuoYou8166							
PH	0.19	0.07	-0.33	-0.31	-0.03	-0.29	-0.70
PL	0.04	0.32	-0.18	0.01	0.04	-0.07	0.16
ASV	0.12	-0.27	-0.49	0.19	0.28	-0.74	-0.91
Aamyl	0.10	0.07	-0.82	0.33	-0.73	0.19	-0.86
L/w ratio	-0.01	-0.03	-0.34	0.56	0.61	-0.23	0.56
Protein	-0.02	0.02	-0.18	0.32	-0.15	-0.1	-0.11
Basmati-385 × HuoYou8305							
PH	0.22	0.09	-0.27	-0.31	-0.02	-0.32	-0.61
PL	0.04	0.41	-0.24	0.02	0.05	-0.05	0.14
ASV	0.11	-0.15	-0.21	0.51	-0.57	-0.52	-0.83
Aamyl	0.13	0.06	-0.73	0.32	-0.68	0.22	-0.72
L/W ratio	0.03	-0.04	-0.32	0.73	0.67	-0.35	0.73
Protein	0.06	0.08	-0.15	0.21	-0.22	-0.13	-0.15
Basmati-198 × HuoJingXian							
PH	0.20	0.08	-0.35	-0.28	-0.04	-0.26	-0.61
PL	0.03	0.36	-0.20	0.02	0.06	-0.04	0.23
ASV	0.18	-0.56	-0.44	0.27	0.36	-0.63	-0.91
Aamyl	0.09	0.05	-0.78	0.36	-0.84	0.27	-0.85
L/w ratio	-0.03	-0.04	-0.43	0.57	0.65	-0.24	0.48
Protein	-0.01	0.05	-0.12	0.26	-0.14	-0.16	-0.12

PH: plant height, PL: penical length, YPP: yield per plant, ASV: Alkali spread value, L/W ratio: length width ratio, Protein: protein contents

Indirect effects

Plant height has positive indirect effect through panicle length which ranges 0.07-0.09. Negative indirect effect of plant height was present for all other traits which was minimum (-0.02) for L/W ratio while negative indirect effect was maximum (-0.35) for ASV. Panicle length has positive indirect effect with plant height, amylose content and L/W ratio which was highest for L/W ratio having value 0.06 while panicle length has minimum indirect positive effect with amylose content (0.01). Negative indirect effect of panicle length observed with ASV and protein content, being maximum for ASV (-0.24) and minimum for protein content (-0.04). Negative indirect effect of ASV was resulted with panicle length ranges (-0.15 to -0.56) and protein content ranges (-0.52 to -0.72). ASV showed positive indirect effect with plant height, amylose content and L/W ratio which is highest for L/W ratio (0.57) and lowest for (0.11). Amylose content has all the positive indirect effects except ASV and L/W ratio. Direct positive effect of amylose content was maximum through protein content (0.27) and was minimum through panicle length (0.05). Negative indirect was highest through L/W ratio (-0.84) while minimum was also through L/W ratio (-0.68). L/W ratio has all the negative indirect effect except through amylose content, the maximum negative indirect effect contributed through ASV (-0.43) while minimum through plant height (-0.01). Positive indirect effect of protein content presented through panicle length and amylose content

http://www.aloki.hu ● ISSN 1589 1623 (Print) ● ISSN 1785 0037 (Online)
DOI: http://dx.doi.org/10.15666/aeer/1804_52115224

which ranges (0.02-0.32). Negative indirect effect of Protein content ranges (-0.02 to -0.22) that are contributed through plant height, ASV and L/W ratio.

Discussion

The study was conducted to add in the existing knowledge of relationship between yield and quality traits. For the improvement of complex quantitative traits, the knowledge of inter relationship for yield contributing and quality traits are important for a breeder to evolve high yielding cultivars with improved quality traits. Negative correlation of plant height with paddy yield show higher photosynthetic accumulation in the vegetative parts due to tallness rather their accumulation in the reproductive parts (Zahid et al., 2006; Akinwale et al., 2011). Furthermore, dwarf genes have also been reported to have pleiotropic effect on yield (Zahid et al., 2006; Parsad et al., 2001; Tahir et al., 1988). However, the results were contradictory to Ranawake and Amarasinghe (2014) who reported that increase in plant height results in increased rate of photosynthesis in plant which transfer more photosynthates to grains. The contrary results may be attributed to genetic differences and environmental factors. Negative correlation between panicle length and plant height was also observed by Jayasudha and Sharma (2010) and Eradasappa et al. (2007), this may be as a result of compromise between reproductive and vegetative growth. Increase amylose content of grain will increase grain yield in rice. Positive correlation between amylose content and protein shows that increase in one character will lead to increase the in others traits and vice versa Anandan et al. (2011). For the improvement of yield direct selection through plant height will result in the reduction of grain yield per plant due its negative direct effect (Naseem et al., 2014; Hairmasis et al., 2010; Akhtar et al., 2011). Panicle length has positive direct effect on yield so increase in panicle length will enhance yield. All the genetic coefficients of correlation were less than the phenotypic coefficient of correlation in present investigation which indicates the effect of environment in the observed correlation. Panicle length was positively correlated with grain yield which showed that improvement of this character will led to improved varieties with higher yield. Plant height and quality traits like alkali spread value, amylose content and protein content decrease with the increase of yield so higher yielding varieties will produce lower amylose, ASV content and protein contents (Sarkar et al., 2007; Sabesan et al., 2009). Protein contents have negative correlation with grain yield, but this correlation was negative, therefore, selection for higher yield may not have significant impact on protein contents. Here, it is important to notice that amylose content and plant height have negative correlation with grain yield of rice but when its correlation is divided into direct and indirect effects, direct effect of these traits was in positive direction. Similar findings have also been shown in cotton case of seeds per locule and lint percentage (Ul-Allah et al., 2017). In such conditions, selection become complicated and indirectly effecting traits must be considered for an effective selection. It is concluded that plant height and panicle length are the key yield influencing traits, while protein content and amylose content are the basic quality traits which also influence yield.

This reflect that with the increase in panicle length, number of spikelets may increase that result in increase of paddy yield (Ashfaq et al., 2012; Ramkrishnan et al., 2006). Increase amylose content of grain will increase grain yield in rice. Positive correlation

http://www.aloki.hu ● ISSN 1589 1623 (Print) ● ISSN 1785 0037 (Online)
DOI: http://dx.doi.org/10.15666/aeer/1804_52115224

between amylose content and protein shows that increase in one character will leads to increase the others (Anandan et al., 2011).

Path coefficient analysis simplify the complex multiple effect of different traits on resultant traits (Ul-Allah et al., 2017) as it breaks the correlation into direct and indirect effects. Main purpose of the analysis is to identify that how different traits effect each other and modify the effect of other trait to the final yield. Plant height has positive direct effect on yield per plant as with the increase in plant height, plant produce photosynthates but due to accumulation of photosynthetic assimilate in vegetative parts, magnitude of its direct effect is low and indirect effect of plant height through various other traits lead to overall negative correlation. Plant height has indirect effect with panicle length toward the increment of yield as due to increase of plant height, panicle length also increases, which leads to higher yield. Similar correlation far panicle and plant height was identified by Jayasudha and Sharma (2010) and Eradasappa et al. (2007). Amylose content, ASV, length to width ratio and protein content have overall negative correlation with yield per plant as more photosynthates will accumulates in the vegetative parts and does not moves towards sink (Tahir et al., 1988; Zahid et al., 2006). Similar result was reported by Parsad et al. (2001). More the length of panicle more grain will produce which leads to increased grain yield (Immanue et al., 2011).

The negative direct effect of alkali spread value shows that it directly decreases the yield and also indirectly along with L/B ratio decreases the yield. Length to width ratio has positive direct effect on the yield while overall correlation with grain yield was positive, which means that with the increase in L/B ratio grain yield will increase. Nandan et al. (2010) suggested that the difference was due to different genotypes and environmental conditions. Protein content has positive direct effect on the yield and negative indirect effect via plant height, ASV and L/W ratio. While combined effect of protein with all other traits on the yield is positive.

Conclusion

It is concluded from this study that traits having positive correlation with yield may have negative direct effect and vice versa. Therefore, selection of traits for yield improvement should be made carefully by looking at direct effect of specific trait to yield as one trait with smaller direct effect may have higher correlation due to higher indirect effect of other traits. Information created from this research will help plant breeder for effective selection of traits in developing high yielding rice cultivars. High yield rice cultivars will contribute to sustainable profit of the farmers by getting higher yield without any extra inputs.

Acknowledgements. This work was supported by the National Natural Science Foundation of China (NSFC) (grant number 31850410472).

REFERENCES

[1] AACC International (2000): Approved Methods of the American Association of Cereal Chemists. 10th Ed. Methods 22-05, 38-12A, 46-12, 54-30A, 54-40A, 56-11, and 56-70. – AAAC, St. Paul, MN.

http://www.aloki.hu ● ISSN 1589 1623 (Print) ● ISSN 1785 0037 (Online)
DOI: http://dx.doi.org/10.15666/aeer/1804_52115224

[2] Akhtar, N., Nazir, M. F., Rabanawaz, A., Mahmood, T., Safdar, M. E., Asif, M., Rehman, A. (2011): Estimation of heritability, correlation and path coefficient analysis in fine grain rice (*Oryza sativa* L.). – J. Anim. Plant Sci. 21(4): 660-664.
[3] Akinwale, M. G., Gregorio, G., Nwilene, F., Akinyele, B. O., Ogunbayo, S. A., Odiyi, A. C. (2011): Heritability and correlation coefficient analysis for yield and its components in rice (*Oryza sativa* L.). – African J. Plant Sci. 5: 207-12.
[4] Anandan, A. G., Eswaran, R. R., Prakash, M. (2011): Genotypic variation and relationships between quality traits and trace elements in traditional and improved rice (*Oryza sativa* L.). – Genotypes J. Food Sci. 76: 122-130.
[5] Ashfaq, M., Khan, A. S., Khan, S. H. U., Ahmad, R. (2012): Association of various morphological traits with yield and genetic divergence in rice (*Oryza sativa* L.). – Int J. Agric. Biol. 14: 55-62.
[6] Chen, X., Temnykh, S., Xu, Y., Cho, Y. G., Mccouch, S. R. (1997): Development of a microsatellite framework map providing genome-wide coverage in rice (*Oryza sativa* L.). – Theor. Appl. Genet. 95: 553-567.
[7] Dewey, R. D., Lu, K. H. (1959): A correlation and path coefficient analysis of components of crested wheat grass seed production. – Argon. J. 51: 515-518.
[8] Eradasappa, E., Nadarajan, N., Ganapathy, K. N., Shanthala, J., Satish, R. G. (2007): Correlation and path analysis for yield and its attributing traits in rice (*Oryza sativa* L.). – Crop Research 34: 156-159.
[9] FAO (2018): Rice market monitor 21(1). – www.fao.org/3/I9243EN/i9243en.pdf.
[10] Gomez, K. A., Gomez, A. A. (1984): Statistical Procedures for Agricultural Research. 2nd Ed. – John Wiley and Sons, New York.
[11] Guyer, D., Tuttle, A., Rouse, S., Volrath, S., Johnson, M., Potter, S., Gorlach, J., Goff, S., Crossland, L., Ward, E. (1998): Activation of latent 171 transgenes in Arabidopsis using a hybrid transcription factor. – Genetics 149: 633-639.
[12] Hairmasis, A., Kustianto, B., Suwarno, S. (2010): Correlation analysis of agronomic characters and grain yield of rice for tidal swamp areas. – Indonesian J Agric Sci 11(1): 11-15.
[13] Immanue, S. C., Nagarajan, P., Thiyagarajanak, K., Bharathi, M., Rabindran, R. (2011): Genetic parameters of variability, correlation and path coefficient studies for grain yield and other yield related attributes among rice blast disease resistant genotypes of rice (*Oryza sativa* L.). – African J. Biotech. 10(17): 3322-3334.
[14] Jayasudha, S., Sharma, D. (2010): Genetic parameters of variability, correlation and path-coefficient for grain yield and physiological traits in rice (*Oryza sativa* L.) under shallow lowland situation. – Electronic J. Plant Breeding 1(5): 33-38.
[15] Memon, Q. A., Wagan, S. A., Wagan, T. A., Memon, I. H., Wagan, Z. A., Memon, H., Wagan, Z. A., Jamro, A., Wagan, S. A., Memon, I. H., Memon, A. H. (2015): Economic analysis of hybrid rice in Taluka Golarchi District Baddin Sindh, Pakistan. – International Journal of Business and Economics Research 4(6): 264-269.
[16] Milligan, S. B., Gravois, K. A., Bischoff, K. P., Martin, F. A. (1990): Crop effects on genetic relationships among sugarcane traits. – Crop Sci. 30: 927-931.
[17] Nandan, R., Sweta, Singh, S. K. (2010): Character association and path analysis in rice (*Oryza sativa* L.) genotypes. – World J. Agric Sci. 6(2): 201-206.
[18] Naseem, I., Khan, A. S., Akhter, M. (2014): Correlation and path coefficient studies of some yield related traits in rice (*Oryza sativa* L.). – International Journal of Scientific and Research Publications 4(4): 2250-3153.
[19] Panaud, O., Chen, X., Mccouch, S. R. (1996): Development of microsatellite markers and characterization of simple sequence length polymorphism (SSLP) in rice (*Oryza sativa* L.). – Mol. Gen. 252: 597-607.
[20] Parsad, B., Patwary, A. K., Biswas, P. S. (2001): Genetic variability and selection criteria for fine rice (*Oryza sativa* L.). – Asian J. Plant Sci. 1: 245-247.

http://www.aloki.hu ● ISSN 1589 1623 (Print) ● ISSN 1785 0037 (Online)
DOI: http://dx.doi.org/10.15666/aeer/1804_52115224

[21] Pingali, P. L. (1997): From subsistence to commercial production systems: the transformation of Asian agriculture. – American Journal of Agricultural Economics 79: 628-34.
[22] Rabiei, B., Valizadeh, M., Ghareyazie, B., Moghaddam, M., Ali, A. J. (2004): Identification of QTLs for rice grain size and shape of Iranian cultivars using SSR markers. – Euphytica 137: 325-332.
[23] Ramkrishnan, S. H., Anandakumar, C. R., Saravanan, S., Malini, N. (2006): Association analysis of some yield traits in rice (*Oryza sativa* L.). – Journal of Applied Science Research 2: 402-404.
[24] Ranawake, A. L., Amarasingheu, G. S. (2014): Relationship of yield and yield related traits of some traditional rice cultivars in Sri Lanka as described by correlation analysis. – Journal of Scientific Research and Reports 3(18): 2395-2403.
[25] Rohilla, R., Singh, V. P., Singh, U. S., Singh, R. K., Khush, G. S. (2000): Crop Husbandry and Environmental Factors Affecting Aroma and Other Quality Traits. –In: Sing, R. K., Sing, U. S., Khush, G. S. (eds.) Aromatic Rices. Oxford and IBH Publishing Co. Pvt. Ltd., New Delhi, India, pp 201-216.
[26] Sabesan, T., Suresh, R., Saravanan, K. (2009): Genetic variability and correlation for yield and grain quality characters of rice grown in coastal saline low land of Tamilnadu. – Electronic Journal of Plant Breeding 1: 56-59.
[27] Samonte, P. B. O. S., Sherwin, A. L., Tagle, J. S., Lales, G. M., Villegas, E. A. (2005): Path analysis of traits affecting grain yield and its components in corn. – The Philippine Agric. Scientist. 88(4): 400-407.
[28] Sarkar, K. K., Bhutia, K. S., Senapathi, B. K., Roy, S. K. (2007): Genetic variability and character association of quality traits in rice (*Oryza sativa* L.). – Oryza 44(1): 64-67.
[29] Tahir, H., Jilliani, G., Iqbal, M. Z. (1988): Integrated use of organic and inorganic N fertilizers in rice wheat cropping system. – Pakistan Journal of Soil Science 3: 19-23.
[30] Temnykh, S., Park, W. D., Ayeres, N., Cartinhour, S., Hauck, N., Lipovich, L., C. H. O., Y. G., Ishit, T., Mccouch, S. R. (2000): Mapping and genome organization of microsatellite sequences in rice (*Oryza sativa* L.). – Theor. Appl. Genet. 100: 697-712.
[31] Ul-allah, S., Iqbal, M., Naeem, M., Zahid, W. (2017): Genetic dissection of association among within boll yield components and their relationship with seed cotton yield in F3 populations of *Gossypium hirsutum* L.). Plant Genetic Resources 15: 157-164.
[32] Zahid A. M. A., Akhtar, M., Sabir, M., Manzoor, Z. T., Awan, H. (2006): Correlation and path analysis studies of yield and economic traits in Basmati rice (*Oryza sativa,* L.). – Asian J. of Plant Science 5: 643-645.

http://www.aloki.hu ● ISSN 1589 1623 (Print) ● ISSN 1785 0037 (Online)
DOI: http://dx.doi.org/10.15666/aeer/1804_52115224

DEVELOPMENT OF A REGIONAL DATA ASSIMILATION SYSTEM AND ITS APPLICATION IN TWO DISTINCT AREAS OF CHINA FOR ESTIMATING CO SURFACE FLUX

LU, L. J.[1,2*] – WANG, X. B.[3]

[1]*College of Resource and Environment, Anhui Science and Technology University Bengbu 233000, China*

[2]*School of Environment Science and Spatial Information, China University of Mining and Technology, Xuzhou 221116, China*

[3]*State Key Laboratory of Safety and Health for Metal Mines, Maanshan 243000, China*

[*]*Corresponding author*
e-mail: lijiang_lu@163.comnstitution

(Received 27th Jan 2020; accepted 22nd May 2020)

Abstract. Traditional methods are time-consuming and labor-intensive for CO flux estimations, there are generally significant uncertainties concerning the results. Data assimilation method has been adopted in recent years for flux optimization in many studies and has proven to be an effective way to improve the accuracy of the CO flux. In this study, a regional data assimilation system, i.e., TracersTracker, was developed based on the POD4DVAR (Proper Orthogonal Decomposition Four-dimensional Variational) method, the CMAQ (Community Multi-scale Air Quality) model and the WRF (Weather Research and Forecasting) model. The system was then applied in two distinct representative areas, i.e., Shangdianzi and Waliguan, for estimating the surface anthropogenic CO flux in 2016. Results show that the CO posteriors in the two study areas were generally higher than the CO priories, but the variations of the posteriors in Shangdianzi and Waliguan are quite different. The overall increase rates of the posteriors are 29.1% and 61.2% in Shangdianzi and Waliguan, respectively. Posteriors optimized by the TracersTracker system significantly improve the accuracy and the correlation of CO simulations in both study areas, which proves that the TracersTracker system is an effective tool for improving the accuracy of the CO emission flux.

Keywords: *carbon monoxide, flux inversion, CMAQ model, proper orthogonal decomposition, four-dimensional variational assimilation*

Introduction

CO is one of the six major atmospheric pollutants, these pollutants are generally generated from human productive and living activities, e.g., cement production, coal combustion. During the past 40 years of urbanization and industrialization, a large amount of CO was emitted in China, which seriously damaged the living environment and caused some social issues (Gurjar et al., 2010; Kamimura et al., 2017; Tao et al., 2019). According to the statistics of the Ministry of Environmental Protection, over 75% of cities in China cannot met the CO concentration standard established by the Ministry of Environmental Protection (MEPC, 2017). Therefore, it is very important to determine the spatial distribution and variation characteristics of anthropogenic CO emissions on the earth surface, which can help us understand the mechanism of CO migration and transformation, and provide effective way for environmental governance. In order to quantify the anthropogenic CO emission flux, many statistical methods have been carried out to obtain surface CO emissions, which is called the "bottom-up"

http://www.aloki.hu ● ISSN 1589 1623 (Print) ● ISSN 1785 0037 (Online)
DOI: http://dx.doi.org/10.15666/aeer/1804_52255246

method (Law et al., 2015). Over the last few decades, researchers have established several atmospheric pollutant emission inventory datasets at different scales in China, from province to national levels (Kilmont, 2002; Ma, 2007; Ohara, 2007; Shi et al., 2014). However, these inventories generallyhave low spatial-temporal resolutions, which increases the difficulty for forecasting and diagnosing air quality (Zheng et al., 2009). Besides, "bottom-up" CO fluxes generally are time-consuming and labor-intensive (Li et al., 2007; Lu et al., 2019), and the obtained CO fluxes generally have significant uncertainties, which needs to be verified carefully before using in realistic applications.

In recent years, the “top-down” method has been used in many researches for obtain high-accuracy fluxes. The data assimilation is one “top-down” method in which fluxes are optimized by minimizing the difference between the observations and the simulations, this method has been proved to be an effective way for improving the accuracy of flux estimations (Saide et al., 2009; Tian et al., 2014). The four-dimensional variational data assimilation (4DVAR) is one of the most widely used data assimilation methods, it can realize the effective integration of the transport model, observational sampling and emission–concentration relationships (Lu et al., 2015; Park et al., 2016). Besides, it can make full use of effective information in the surface observations in the assimilation procedure (Zhang et al., 2008; Peng et al., 2015). However, the main hamper for using the 4DVAR method is the large dimension (generally with order of 10^7–10^8) in flux estimation, which requires large amount of computing resources that it is hard to satisfy. Besides, the adjoint model must be integrated in the use of 4DVAR (Gou and Sandu, 2011; Park et al., 2016), which requires large efforts for development and maintenance because of the high nonlinearity of the chemical transport model (Tian et al., 2008; Gou and Sandu, 2011; Lu et al., 2015).

In order to solve these problems, many dimension-reduction methods have been introduced into the 4DVAR, among whom the POD4DVAR method is a good way to reduce the dimension. A data assimilation system coupled with POD method can largely reduce the dimension in the assimilation procedure that was used frequently in many realistic applications (Tian and Xie, 2009; Tian et al., 2011; Tian and Feng, 2015; Zhang et al., 2017). Some researchers also tried to integrate other mathematical algorithms, e.g., Ensemble Kalman Filter, into the assimilation system for the flux inversion, which also can reduce computing resources and improve inversion accuracy (Lu et al., 2015; Kim et al., 2018). However, current CO fluxes mainly come from statistical investigation, wich generally have a low spatial resolution.

In order to improve the spatial resolution of the CO flux, an efficient inversion algorithm, POD4DVar, was developed by coupling the POD and the 4DVAR in this paper, then massive computing problem was solved in a low dimension. Afterwards, a regional high-resolution assimilation inversion system, TracersTracker, was conducted by coupling the POD4DVAR algorithm and the CMAQ model. The TracersTracker system can effectively absorb the information from observations for eliminating "errors" in the prior fluxes, and then improve significantly the accuracy of the posterior simulations. In order to dianose the effectiveness of the system, two regions with different geographical and climatic conditions were chosen for experiments.

Details of materials and methods are given in section 2, results of the background concentrations, sensitivity experiments and flux inversions of CO are shown in section 3, conclusions are shown in section 5.

http://www.aloki.hu ● ISSN 1589 1623 (Print) ● ISSN 1785 0037 (Online)
DOI: http://dx.doi.org/10.15666/aeer/1804_52255246

Materials and Methods

The TracersTracker system is constructed by integrating the WRF model, the CMAQ model and the POD4DVAR method. The WRF model and the CMAQ model are used for providing meteorological fields and atmospheric transport simulations respectively. The POD method has proved to be an effective method for the dimension reduction, in which problems can be solved in a low-dimension space, the POD4DVAR is a combination of POD and the traditional 4DVAR.

Generally, 4DVAR can been described by minimizing the difference between the observations and the simulations as follows:

$$J(x)=(x-x_b)^T B^{-1}(x-x_b)+\sum_{t=0}^{n}\left(y_i-H_i\left[M_{t_0\to t_k}(x)\right]\right)^T R_i^{-1}\left(y_i-H_i\left[M_{t_0\to t_k}(x)\right]\right) \quad \text{(Eq.1)}$$

where the M means the transport model, the superscript T indicates a transpose, x_b is the background filed, k is the index of the observation time, H is the observation operator, R_i is the observational error covariance and B is the background error covariance.

We suppose there are S time steps in each assimilation time window: at the first time step, N first-guesses $x_{0,n}(n=1,...,N)$ should be prepared by sampling from the historical forecasts or other existing priories. Secondly, transport model, e.g., CMAQ in this paper, can been integrated with the N first-guesses until the last time step of the assimilation time window and N state variable series $x_{k,n}(k=1,...,S)$ can be obtained. With the N state variable series, the sample ensemble $X_n=(x_{0,n},...,x_{s,n})^T$ can be conducted and matrix $A=(X_1,X_2,...X_N)$ by X_N. From the ensemble perturbation, the PODs can be generated based on the matrix, and the optimization can be linearly represented by the PODs.

With the WRF model, the CMAQ model and the POD4DVAR method, TracersTracker system is developed for optimization of CO fluxes. The detail of the process for using the TracersTracker system is as follows (*Fig. 1*):

(1) Generating the first-guess perturbation ensemble. Start from a first-guess extracted from the priori and get N first-guesses from perturbations generated by Monte Carlo method.

(2) Getting N state variable series. Run the CMAQ model from the N first-guesses generated in last step over the whole assimilation time window and N state variable series can be obtained. With proper perturbations, the space of the N state variable series can capture the spatiotemporal evolution of the model state.

(3) Proper orthogonal decomposition. Obtain the base vectors Pn (PODs) from the space of the N state variable series by the proper orthogonal decomposition technique. In this way, the original N-dimensional problem can be solved in N dimensions, which greatly reduce the computing resources.

(4) Rerunning the CMAQ model. Rerun the CMAQ model from the Pn vectors and from the previous step over the assimilation time window to obtain n simulations of the state series.

(5) Generating a new emission. The optimal emission can be approximately expressed by the POD-base vectors generated from step (3). The weights of the base vectors can be determined by the performance of each POD.

http://www.aloki.hu ● ISSN 1589 1623 (Print) ● ISSN 1785 0037 (Online)
DOI: http://dx.doi.org/10.15666/aeer/1804_52255246

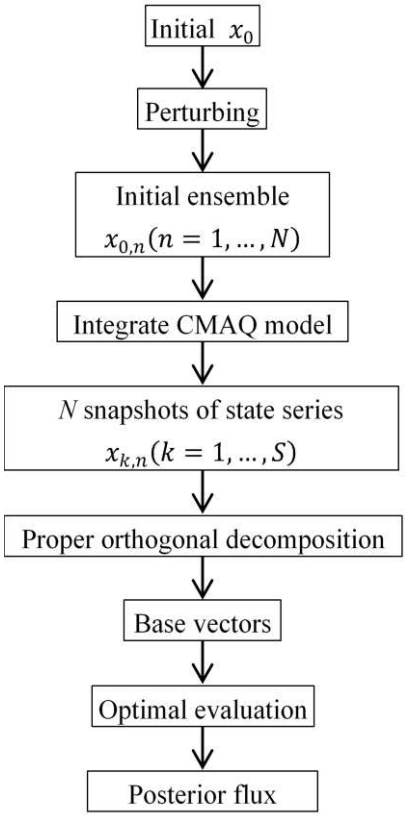

Figure 1. *Schematic diagram of the TracersTracker data assimilation system*

A carbon assimilation system involves many parameters, e.g., lag window, boundary filed, chemical mechanism, measurements, these parameters affect largely in the assimilation process and eventually the inversion results. The data assimilation system should be tested for these parameters before being applied to realistic applications. Ignoring influences of these parameters may decrease the accuracy of the inversion results or lead to incorrect results. In this section, nine sensitivity experiments were conducted for system parameters in the process of flux inversion, the detailed settings of these experiments are as follows:

Reference experiment (RE): two nesting mode (*Fig. 2*), d02 is used for providing boundary field for inner area d01, CO concentration observations are assimilated for flux optimization of the inner area. In this experiment, chemical mechanism is CB05, the number of perturbation samples is 126, lag window is not considered and the spatial resolution is 3 km. This experiment is the main experiment in this paper, results of other experiments are compared with that in this experiment.

Experiment 1 (E1): perturbing sample experiment. The number of perturbation samples is set to 60, the settings of other parameters are the same as that in RE. This experiment mainly diagnoses the influence of the perturbation samples in the TracersTracker inversion system.

Experiment 2 (E2): perturbing sample experiment. The number of perturbation samples is set to 200, the settings of other parameters are the same as that in RE, the purpose of this experiment is the same as that of E1.

http://www.aloki.hu ● ISSN 1589 1623 (Print) ● ISSN 1785 0037 (Online)
DOI: http://dx.doi.org/10.15666/aeer/1804_52255246

Experiment 3 (E3): boundary field experiment. No nesting mode is adopted in this experiment; the settings of other parameters are the same as that in RE. This experiment mainly diagnoses the influence of nested mode in the TracersTracker inversion system.

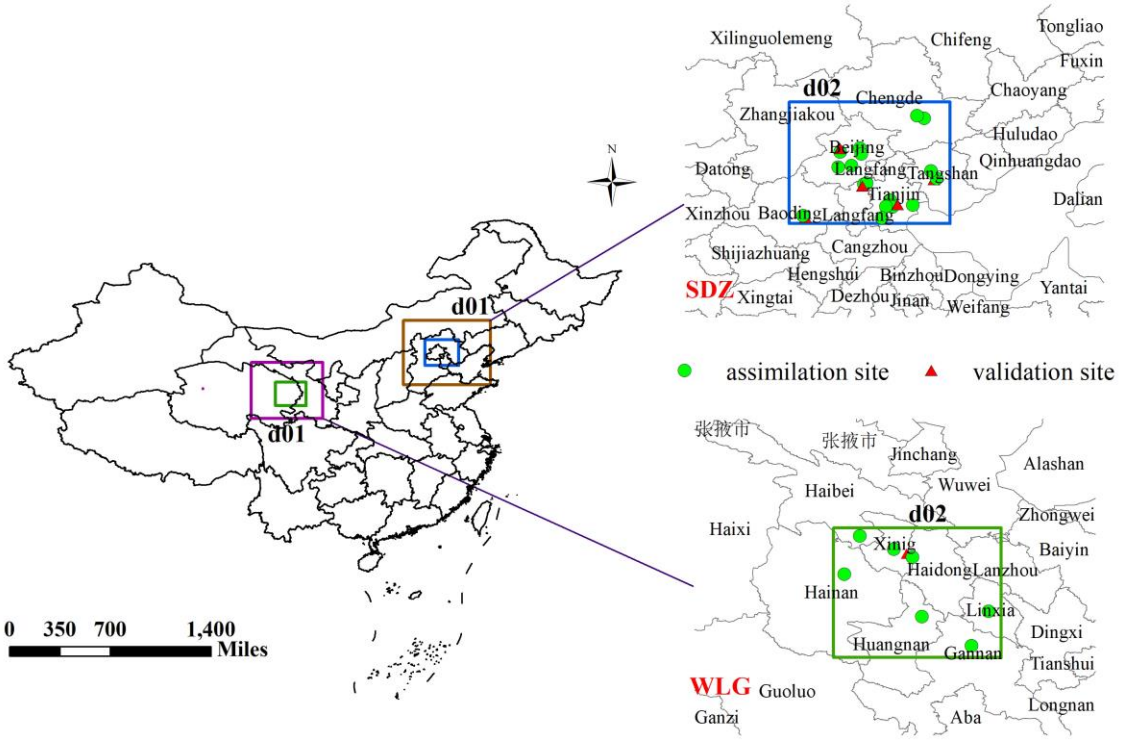

Figure 2. *The two study areas. d02 is our inner area and d01 is the boundary layer area for providing boundary fields for d02. The green dots are the CO monitoring sites used for flux inversions and the red dots are used for validation.ext of the introduction*

Experiment 4 (E4): boundary field experiment. Three nesting mode is adopted in this experiment; the settings of other parameters are the same as that in RE. The purpose of this experiment is the same as that of E3.

Experiment 5 (E5): lag window experiment. The lag window is set to 2 days in this experiment, the settings of other parameters are the same as that in RE. This experiment mainly diagnoses the influence of lag window in the TracersTracker inversion system.

Experiment 6 (E6): lag window experiment. The lag window is set to 2 weeks, the settings of other parameters are the same as that in RE. The purpose of this experiment is the same as that of E5.

Experiment 7 (E7): chemical mechanism experiment. The chemical mechanism in the model was changed into CB06 in this experiment, the settings of other parameters are the same as that in RE. The main purpose of this experiment is to test the influence of different chemical mechanisms on assimilation inversion results in the TracersTracker inversion system.

Experiment 8 (E8): spatial resolution experiment. The spatial resolution is set to 27 km in this experiment, the settings of other parameters are the same as that in RE. This experiment mainly tests the influence of spatial resolution on assimilation inversion results in the TracersTracker inversion system.

http://www.aloki.hu ● ISSN 1589 1623 (Print) ● ISSN 1785 0037 (Online)
DOI: http://dx.doi.org/10.15666/aeer/1804_52255246

After the sensitivity analysis for the TracersTracker system, the system was then applied to two distinct areas in China, i.e., Shangdianzi (hereinafter referred to as SDZ) and Waliguan (hereinafter referred to as WLG), for improving the resolution of the CO flux inversion in 2016. China has a vast land area that significant differences of CO emission exist in different regions with unbalanced development. The two distinct areas, i.e., SDZ and WLG (*Fig. 2*), to some extent, can represent two kinds of regions with different characteristics of CO emissions. SDZ, located on the North China Plain, covers the region of Jing-Jin-Tang, is one of the highest urbanized regions in china. The total population is over 60 million in this area, emitting a large amount of CO through people's daily activities. There is one Global Atmosphere Watch (GAW) station, i.e., SDZ, in this area, which lies northeast of Beijing city, with low population and industrial density. WLG, unlike SDZ, locate in a region with a underdeveloped industrial foundation, covering parts of Qinghai and Gansu provinces. In this area, variations of CO concentration are significantly different from that of SDZ regions in the whole year. The purpose of choosing these two areas is to investigate the characteristics of emission mechanisms and uncertainties for CO inversions in different areas with the support of the TracersTracker system.

In this paper, the MIX inventory of 2010 released by the MEIC team was used as the a priori in the simulation process, this inventory has information of some major anthropogenic pollutants, e.g., CO_2, CO, PM10, PM2.5, SO_2, NH_3, BC and NMVOC. The inventory files have a resolution of 0.25 degree and include emissions from five sectors, i.e., power, agriculture, residential, industry and transport.

Hourly CO concentration measurements of 2016 in the two study areas were collected for flux inversion and accuracy validation. These CO observations can be downloaded from the air quality monitoring network of The Ministry of Environment Protection of the People's Republic (http://106.37.208.233:20035/). There are 22 and 9 motoring sites in SDZ and WLG respectively, the monitoring sites used in our study are shown in *Fig. 1*, details of these monitoring site are as listed in *Table 1*. In general, even if no pollutants are released, there is still residual amounts of pollutants in the atmosphere, called the background or baseline, often referred to be the measure in pure air masses that are not perturbed by pollutant emissions. In different regions, the background concentration is obviously different, which is affected by many factors, e.g., the local topography, the climate and the CO emissions intensity, the real-time concentrations are the results of long-time migration, transformation and integration. Therefore, the background concentration of CO is not caused by the current emissions and the current CO concentration measurements generally include two part, i.e., the background part and the current emission part, the background part should be subtracted from the observations before assimilation for the current flux inversion. Before the real assimilation process in the TracersTracker system, we evaluated the CO background concentration for the 31 monitoring sites mentioned above. In order to determine the background concentration of CO, the raw data were filtered to remove the regional pollution amount. We defined a threshold for removing obviously local pollution. Pollutant concentrations above the threshold within ±6 hours were removed. Then, we calculated the mean and standard deviation (σ) for every continuous unpolluted period and removed data larger than 3σ above the mean. We repeated this step until the concentration data set was stable.

http://www.aloki.hu ● ISSN 1589 1623 (Print) ● ISSN 1785 0037 (Online)
DOI: http://dx.doi.org/10.15666/aeer/1804_52255246

Table 1. *CO observation and validation sites in SDZ and WLG*

Name	Longitude	Latitude	Location	Usage
BDCPZ	116.238	40.227	SDZ	ASSIMILATION
BJDL	116.237	40.300	SDZ	VALIDATION
BJGC	116.200	39.917	SDZ	ASSIMILATION
BJHRZ	116.647	40.308	SDZ	ASSIMILATION
BJNZG	116.471	39.947	SDZ	ASSIMILATION
BJSYXC	116.673	40.187	SDZ	ASSIMILATION
CDTL	117.978	40.924	SDZ	ASSIMILATION
CDWHZX	117.831	40.981	SDZ	ASSIMILATION
LFJLZX	116.729	39.564	SDZ	ASSIMILATION
LFKFQ	116.785	39.583	SDZ	ASSIMILATION
LFYCGS	116.698	39.525	SDZ	VALIDATION
TSSEZ	118.179	39.657	SDZ	VALIDATION
TSTCGS	118.233	39.678	SDZ	ASSIMILATION
TSWZJ	118.122	39.834	SDZ	ASSIMILATION
TJBCKJY	117.276	39.233	SDZ	ASSIMILATION
TJDLZX	117.316	39.088	SDZ	ASSIMILATION
TJWLJGY	117.432	39.135	SDZ	VALIDATION
TJTFGYY	117.186	39.097	SDZ	ASSIMILATION
TJTPW	117.103	38.861	SDZ	ASSIMILATION
TJSTC	117.744	39.130	SDZ	ASSIMILATION
BDJCZ	115.521	38.870	SDZ	VALIDATION
BDJDZX	115.471	38.914	SDZ	ASSIMILATION
GNJCZ	102.919	34.994	WLG	ASSIMILATION
HBXHZ	100.910	36.964	WLG	ASSIMILATION
HNQBQZ	100.632	36.281	WLG	ASSIMILATION
HNLWZ	102.029	35.516	WLG	ASSIMILATION
LXHBJ	103.251	35.611	WLG	VALIDATION
LXZWDX	103.223	35.609	WLG	ASSIMILATION
XNDWSC	101.522	36.726	WLG	ASSIMILATION
XNJCZ	101.756	36.649	WLG	VALIDATION
XNSLYY	101.857	36.584	WLG	ASSIMILATION

Results and Discussion

CO background concentrations

Fig. 3 is background CO concentrations at different monitoring sites in SDZ and WLG. The economic and geographical conditions of Shangdianzi region and Waliguan region are different, the CO concentration level and the varation characteristics are also different. Overall, the CO concentration in Waliguan is significantly lower than that in Shangdianzi (*Table 2*). The average annual CO concentration in Waliguan is 1.09 mg/m^3, that is 1.43 mg/m^3 in Shangdianzi area, about 1.3 times of that in Waliguan.

From January to December, the CO concentration in Shangdianzi is higher than that in Waliguan, but the difference between December and January is the largest. However, in terms of seasonal varation, the trends are similar in the two regions, the CO concentration is generally low in summer and autumn, and significantly increased in winter and spring. The background concentrations of CO are highly correlated with the observed concentration; its variation trend is basically consistent with the observed CO concentration. The average annual background concentration in Shangdianzi is 1.08 mg/m^3, and that is 0.69 mg/m^3 in Waliguan, which is significantly lower than that in Shangdianzi. In summer and autumn, the background concentration in Shangdianzi is

http://www.aloki.hu ● ISSN 1589 1623 (Print) ● ISSN 1785 0037 (Online)
DOI: http://dx.doi.org/10.15666/aeer/1804_52255246

1.53 times of that in Waliguan. In winter and spring, the background concentration in Shangdianzi is 1.55 times of that in Waliguan. Besides, it can be seen that in the same region, the spatial variation of CO background concentration is also very unbalanced. In Shangdianzi, the background concentration of CO in Tangshan, Langfang and Tianjin is much higher than that in other areas, where are the main areas of CO emissions. In Waliguan, Xining and Linxia are the main areas of CO emissions, background concentrations of where are much higher than that in other areas. These areas are mainly industrial and human settlements with active human activities and large CO emissions.

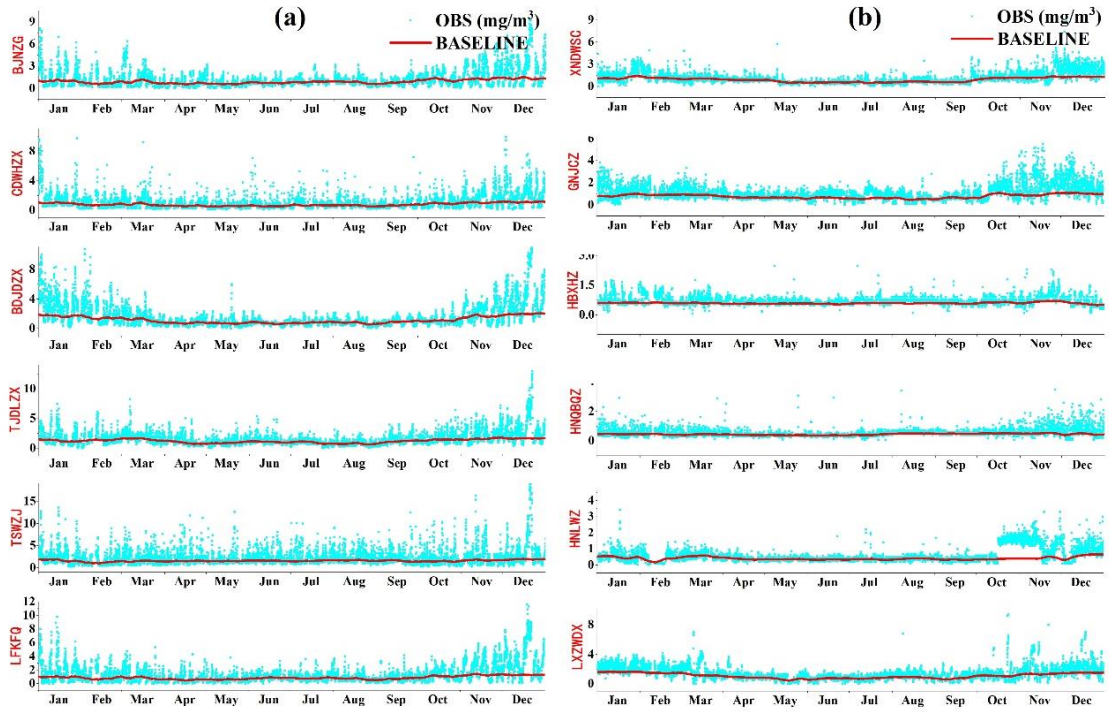

Figure 3. *CO background at monitoring sites. (a) and (b) are the CO background in SDZ and WLG respectively*

Table 2. *CO background concentrations in Shangdianzi and Waliguan. obs and bg are CO monitoring and background concentration respectively*

	SDZ (mg/m^3)		**WLG (mg/m^3)**	
	obs	bg	obs	bg
Jan	1.98	1.27	1.47	0.87
Feb	1.27	1.05	1.20	0.82
Mar	1.48	1.10	1.04	0.78
Apr	1.02	0.84	0.82	0.63
May	0.88	0.83	0.76	0.54
Jun	1.01	0.92	0.73	0.53
Jul	1.07	0.95	0.76	0.54
Aug	1.02	0.88	0.81	0.59
Sep	1.10	0.95	0.80	0.57
Oct	1.35	1.17	1.13	0.77
Nov	2.03	1.43	1.63	0.85
Dec	2.90	1.54	2.01	0.90

http://www.aloki.hu ● ISSN 1589 1623 (Print) ● ISSN 1785 0037 (Online)
DOI: http://dx.doi.org/10.15666/aeer/1804_52255246

Although there are large differences of CO concentration between the two study areas, CO concentration can both reach to a high level in some heavy pollution periods, e.g., January and December. This illustrates that even in areas with low CO emission intensity, serious pollution events can also appear because of adverse meteorological and geographical conditions. In addition, no matter in Shangdianzi or Waliguan, the CO concentration is higher in spring and winter than in the other two seasons. The main reason is that Shangdianzi and Waliguan are located in the north of China. In spring and winter, more fossil fuel is consumed by living activities, e.g., residents heating, because of low temperatur, and the CO concentration can be pushed up significantly in a short time due to these activities. However, the difference of CO concentrations between the four seasons in Waliguan is significantly smaller than that in Shangdianzi, which shows that the activity intensity of heating in spring and winter in this area is limited to a few areas and has limited impact on the whole area. Unlike the Waliguan, the CO concentration in Shangdianzi changes more violently, and there are more periods with serious pollutions.

Sensitivity experiments

Reference experiment

This experiment is the reference for other experiments in sensitivity test to diagnose the variations of assimilation results when system parameters change. Experiment results (*Table 3*) show that the priori-based CO concentration simulations are significantly lower than that in RE, the RMSE of prior-based CO simulations is 1.30 mg/m^3, it is reduced to 0.94 mg/m^3 in the posterior-based simulations in RE, the simulated accuracy improved obviously.

Table 3. *Results of sensitivity experiments for CO*

	priori	**RE**	**E1**	**E2**	**E3**	**E4**	**E5**	**E6**	**E7**	**E8**
Jan		40%	4%	44%	20%	41%	39%	23%	42%	47%
Feb		23%	2%	22%	15%	20%	22%	20%	25%	19%
Mar		31%	81%	28%	13%	32%	23%	26%	29%	25%
Apr		29%	58%	26%	20%	25%	28%	10%	29%	20%
May		26%	31%	23%	26%	24%	25%	33%	29%	18%
Jun		26%	64%	22%	25%	28%	26%	17%	27%	18%
ul		40%	43%	36%	27%	39%	36%	38%	39%	31%
Aug		29%	20%	26%	12%	26%	28%	7%	28%	24%
Sep		30%	14%	28%	17%	25%	31%	20%	29%	25%
Oct		28%	25%	26%	17%	29%	24%	41%	24%	26%
Nov		24%	78%	29%	23%	22%	23%	28%	30%	31%
Dec		23%	10%	25%	23%	21%	25%	38%	28%	28%
R	0.63	0.76	0.42	0.77	0.54	0.75	0.77	0.75	0.76	0.69
RMSE	1.30	0.94	1.47	0.86	1.35	0.97	0.87	0.99	0.92	1.05

Besides, the correlation between simulations and observations increased from 0.60 based on the a priori to 0.76 based on the posteriors. From the perspective of the whole year, the annual average flux increased from 1.14 mole/s to 1.47 mole/s with an increase rate of 29%. From the perspective of monthly variations, the CO posteriors of 12 months in 2016 increased by 40%, 23%, 31%, 29%, 26%, 26%, 40%, 29%, 30%, 28%, 24% and 23%, respectively, compared with the a prior, January and July have the

http://www.aloki.hu ● ISSN 1589 1623 (Print) ● ISSN 1785 0037 (Online)
DOI: http://dx.doi.org/10.15666/aeer/1804_52255246

largest growth rates. In terms of seasons, the growth rate of summer and autumn is significantly higher than that of spring and winter, the underestimation of summer and autumn in the a prior is much greater than that of spring and winter. With the parameters described in this experiment, the TracersTracker system can assimilate CO observations effectively, and then obtain the optimized CO flux which can reduce simulation errors and significantly improve the simulations accuracy.

Perturbing sample

The number of perturbing samples greatly affect the accuracy of the posterior fluxes. In theory, the more perturbing samples, the more spatial information the samples can represent, but the more computing resources it needs. Insufficient perturbing samples cannot fully reflect the temporal and spatial variation characteristics of the CO flux and the CO concentrations, which can lead to large errors in the assimilation inversion results. In the sensitivity experiment, 126 perturbing samples are used in the reference experiment, 60 and 200 perturbing samples are used in Experiment 2 and Experiment 3, respectively to verify the influence of perturbing samples on the assimilation inversion results. Experiment results show that there is no significant difference between 126 and 200 perturbing samples in CO simulation errors. Their correlation coefficients with 126 and 200 perturbing samples are 0.76 and 0.77, respectively, and their RMSE are also very close, i.e., 0.94 and 0.86, respectively. This shows that when the number of perturbing samples increases to a certain extent, the accuracy of assimilation inversion cannot be improved obviously. In contrast, when 60 perturbing samples are used for assimilation inversion, there is large errors in the inversion results. As can be seen in *Table 1*, the correlation coefficient of CO simulated concentration is significantly reduced to 0.42, its RMSE increased from 0.94 mg/m^3 to 1.47 mg/m^3, the simulation accuracy also decreased significantly. Flux inversion results show that the posterior with 200 perturbing samples is close to that in the reference experiment, the annual average of the posterior is 1.46 mole/s. Compared with the a prior, the 200-samples-based posterior has growth ratios of 44%, 22%, 28%, 26%, 23%, 22%, 36%, 26%, 28%, 26%, 29% and 25% in 12 months, respectively, which was basically consistent with the trend of the reference experimental inversion results (*Table 3*). In comparison, although there is no significant difference in the total amount of flux inversion results based on 60 perturbing samples, there is obvious fluctuations in monthly variations. The 12-month growth ratios are 4%, 2%, 81%, 58%, 31%, 64%, 43%, 20%, 14%, 25%, 78% and 10%, respectively, the inversion fluxes in January, February, November and December are all abnormal, which shows that there is large uncertainties in the inversion results with 60 perturbing samples (*Table 3*).

Boundary layer

Generally, boundary layers directly impact the simulated surface concentration and flux. Ignoring boundary layers in the process of assimilation can lead to additional errors in the final inversion results. In the reference experiment, two nesting domains mode is set to eliminate errors around the boundary layer, as shown in *Fig. 2*, d01 is our study area and d02 is the boundary layer area providing the boundary field for d01. In Experiment 3, no nesting mode is adopted, the dynamic evolution setting of the boundary field is removed, and the default boundary field inside the CMAQ model is adopted. According to the comparison between the posterior-based simulations and the observations (*Table 3*), the errors of CO simulations without boundary field is

http://www.aloki.hu ● ISSN 1589 1623 (Print) ● ISSN 1785 0037 (Online)
DOI: http://dx.doi.org/10.15666/aeer/1804_52255246

significant, RMSE increases from 0.94 mg/m^3 of the a prior to 1.35 mg/m^3 of the Experiment 3, and the correlation decreases from 0.76 to 0.54. After the boundary field is reset in Experiment 4, RMSE decreased to 0.97 mg/m^3, the correlation also increased to 0.75, which was slightly lower than that in the reference experiment, the simulation accuracy is significantly improved. This shows that the boundary field plays an important role in assimilation inversion system, if the boundary field is not set or the setting is not suitable, the inversion result could have large uncertainties. Suitable boundary field can provide accurate exchange data for the study area, thus significantly improving the accuracy of CO flux inversions. Without suitable boundary fields, flux inversions have great fluctuations compared to that in the reference experiment. The average flux retrieved from the Experiment 3 is 1.31 mole/s which is significantly lower than that in the reference experiment, and the monthly variations in the Experiment 3 is quite different with that in the reference experiment. In an obvious contrast, the average and monthly flux in the Experiment 4 have no significant difference with that in the reference experiment after sufficient boundary information been provided. In this paper, we use two-nested mode in all inversion processes as described in the reference experiment.

Lag window

Due to different physical and chemical characteristics of different pollutants, lag windows of them are also obviously different. In the process of assimilation inversion, the lag window should be set reasonably for a specified substance. The life time of CO is short of about two months and the study areas in this paper are small, the lag window should also be set short. In the reference experiment, the lag window is set to 0, i.e., no consideration for lag window. In contrast, the lag windows in Experiment 5 and Experiment 6 are set to 2 days and 2 weeks respectively to obtain the influence of lag window on the assimilation inversion results. The simulation results show that the errors and correlations in Experiment 5 and Experiment 6 are quite close. Compared to the reference experiment, the simulation correlation in Experiment 5 is slightly improved (R changes from 0.76 to 0.77), in experiment 6 it is slightly reduced (R changes from 0.76 to 0.75), the overall difference is not obvious. Meanwhile, the RMSEs in Experiment 5 and Experiment 6 did not change significantly, which are 0.87 mg/m^3 and 0.99 mg/m^3, respectively. The annual average flux in Experiment 5 and Experiment 6 are 1.46 mole/s and 1.43 mole/s, which only have minor differences with that in the reference experiment of 1.47 mole/s (*Table 3*).

Chemical reactions

In the CMAQ model, there are two chemical mechanisms to describe the chemical reaction mechanism of simulated substances, namely CB05 and CB06. These two chemical mechanisms have some differences in simulating the chemical reaction of trace gases, which will ultimately affect the flux inversion results. In the reference experiment, CB05 was adopted to describe the chemical reactions of CO, it is replaced to CB06 in Experiment 7 to diagnose the sensitivity of different chemical mechanisms in the inversion process. As shown in *Table 1*, simulations errors by CB05 and CB06 are quite close, and RMSE is 0.92 mg/m^3, correlation is 0.76, both are basically same as that in the reference experiment. Besides, the annual average of the CB06-based posterior is 1.48 mole/s that it almost has no difference with that in the reference experiment (*Table 3*).

http://www.aloki.hu ● ISSN 1589 1623 (Print) ● ISSN 1785 0037 (Online)
DOI: http://dx.doi.org/10.15666/aeer/1804_52255246

Spatial resolution

Inversion results of large-scale, e.g., global and continent scale, usually have coarse resolutions in degree, which cannot guarantee the requirement for high-resolution flux at regional scale. The spatial resolution of assimilation inversion system in the reference experiment 3 km, which has greatly improved the resolution in the posterior. In Experiment 8, the resolution of the assimilation inversion system is set to be 27 km to analysis detail affections of the spatial resolution on the results of flux inversions. Experiment results show that simulations errors and RMSEs (from 0.94 mg/m^3 to 1.05 mg/m^3) become larger, correlations R become worse (from 0.76 to 0.69) when the spatial resolution becomes coarser (*Table 3*). Besides, the flux inversions with 27 km have more uncertainties compared to that in the reference experiment, and the simulation accuracy of the inversion flux will be affected by the coarse spatial resolution. In summary, coarse spatial resolution will bring uncertainties to the results of flux inversion.

CO flux inversions

The posterior emissions

9 and 22 groups of CO concentration observations are collected in WLG and SDZ respectively for CO flux inversions. Based on the background concentrations of CO, the "polluted observations" are extracted for the 31 monitoring sites which are actually assimilated in the inversion process, the CO flux inversions are as shown in *Table 3* and *Fig. 4*.

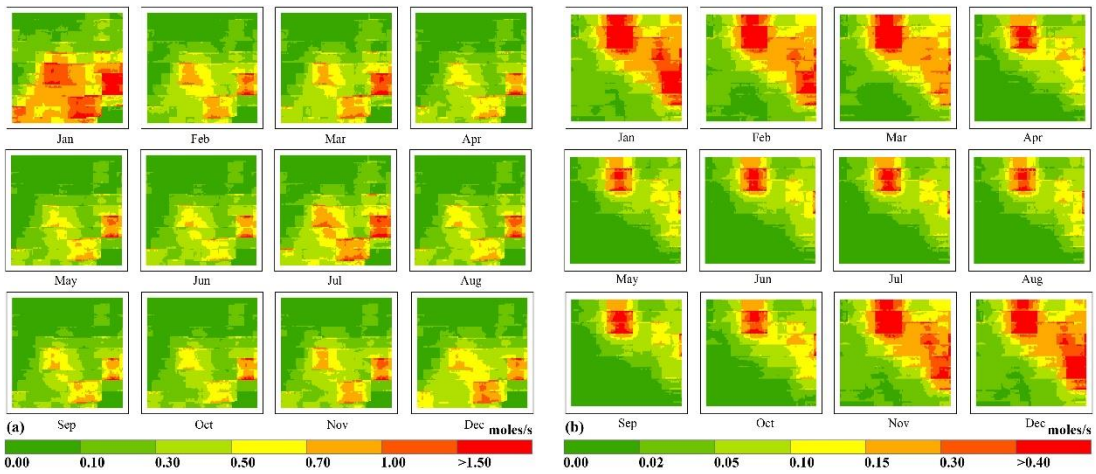

Figure 4. *Increment of CO posterior compared with the MIX priori in SDZ (a) and WLG (b)*

In SDZ, the CO posterior is higher than the a prior in most periods, flux grow rates in 12 months are 40.2%, 23.2%, 30.7%, 28.6%, 26.2%, 26%, 40.5%, 28.8%, 29.6%, 27.7%, 24.1% and 23.4%, respectively (*Table 4*), most of them are close except January and July, whose monthly increase are higher than that in other months. The average flux of the posterior is 1.47 mole/s, which is about 1.3 times of that in the a priori. The minimum growth of the posterior appears in February and December, the maximum growth is in January and July, CO posterior has significant variation after the optimization of the TracersTracker system.

http://www.aloki.hu ● ISSN 1589 1623 (Print) ● ISSN 1785 0037 (Online)
DOI: http://dx.doi.org/10.15666/aeer/1804_52255246

Table 4. *Increments and proportions of the CO posteriors in SDZ and WLG*

	SDZ *(mole/s)*			**WLG** *(mole/s)*		
	Max	**Ave**	**Percent(%)**	**Max**	**Ave**	**Percent(%)**
Jan	7.39	0.66	40.2	1.28	0.19	68.9
Feb	2.58	0.33	23.2	0.92	0.16	60.7
Mar	4.81	0.37	30.7	1.17	0.14	62.5
Apr	3.30	0.30	28.6	0.80	0.08	58.5
May	3.02	0.27	26.2	0.71	0.06	58
Jun	2.67	0.26	26.0	1.06	0.06	59
Jul	5.06	0.40	40.5	1.14	0.06	61.2
Aug	3.24	0.28	28.8	1.08	0.06	59.4
Sep	2.06	0.26	29.6	0.79	0.06	62.6
Oct	2.74	0.25	27.7	0.59	0.08	57.4
Nov	2.44	0.29	24.1	1.10	0.17	66
Dec	2.00	0.32	23.4	0.96	0.17	60.2
Annual	3.44	0.33	29.1	0.97	0.10	61.2

Compared to SDZ, the CO posterior flux in WLG is also higher than the a prior in most periods, but the growth proportion is much larger than that in SDZ. The posterior flux increased by 68.9%, 60.7%, 62.5%, 58.5%, 58%, 59%, 61.2%, 59.4%, 62.6%, 57.4%, 66% and 60.2%, respectively in 12 months of the whole year (*Table 4*). The overall increase rate is about 4 times of that in SDZ, although the overall increase rate is high, the absolute flux increment (0.10 mole/s) in WLG is much smaller than that in SDZ (0.33 mole/s), which is mainly related to the low CO priori in WLG. The annual average flux of the posterior in WLG is 0.09 mole/s, the minimum is 0.05 mole/s occurring in May and September, the maximum flux in the posterior is 0.15 mole/s appearing in December and January.

According to the spatial distribution of the posterior fluxes, the net increase and increase ration in the posteriors have significant difference. The net increase of the posterior fluxes is mainly concentrated in urban or densely populated areas. In SDZ, the area with the most flux growth is in Tangshan, followed by Tianjin and Beijing, and Chengde has the least flux growth. In WLG, the area with obvious CO flux growth is mainly located near Xining, followed by the urban area and surrounding area of Linxia, and other areas, e.g., Haibei, Hainan and Haidong, have little flux growths. Due to the productive and living activities are concentrated in the urban and nearby areas, the prior flux of CO in these areas is much larger than that in other areas, thus the net increase of CO in these areas is large with the same growth rate (*Fig. 4*). In contrast, the main areas with high growth rates are not entirely located in the urban areas, the spatial distribution of growth rate has no obvious tendency except for some periods, e.g., June, August in WLG. Whether in SDZ or WLG, the proportion of posterior incremental growth is scattered in time and space.

Comparison of observations and simulations

In order to evaluate the accuracy of the posteriors obtained by the TracersTracker system, comparisons between the observations and the posteriori-based simulations were conducted in the validation sites shown in *Fig. 1*. Some indices for the accuracy evaluation are used in this section, i.e., max absolute error (E_{max}), mean error (E_{mean}),

http://www.aloki.hu ● ISSN 1589 1623 (Print) ● ISSN 1785 0037 (Online)
DOI: http://dx.doi.org/10.15666/aeer/1804_52255246

root mean squared error (E_{rmse}), and correlation coefficient (R), indices are determined by the following equations.

$$E_{\max} = \max(e_1, e_2, ..., e_n) \quad \text{(Eq.2)}$$

$$E_{mean} = (e_1, e_2, ..., e_n)/n \quad \text{(Eq.3)}$$

$$E_{rmse} = \sqrt{(e_1^{\ 2} + e_2^{\ 2}, ..., +e_n^{\ 2})/n} \quad \text{(Eq.4)}$$

$$R = \frac{\sum_{i=1}^{n}\left(o_i - \bar{o}\right)\left(s_i - \bar{s}\right)}{\sqrt{\sum_{i=1}^{n}\left(o_i - \bar{o}\right)^2}\sqrt{\sum_{i=1}^{n}\left(s_i - \bar{s}\right)^2}} \quad \text{(Eq.5)}$$

where n is the number of comparison couples, e is the difference between the CO posterior-based simulation and the CO concentration observation, o and s mean the observations and simulations, respectively.

The CO concentration in January is significantly higher than that in July, this tendency can be grasped well in the posteriors and the a priori. However, there are large errors between the CO simulations in the a priori and ground-based observations, and these errors are largely eliminated in the posterior-based simulations (*Fig. 5* and *Fig. 6*).

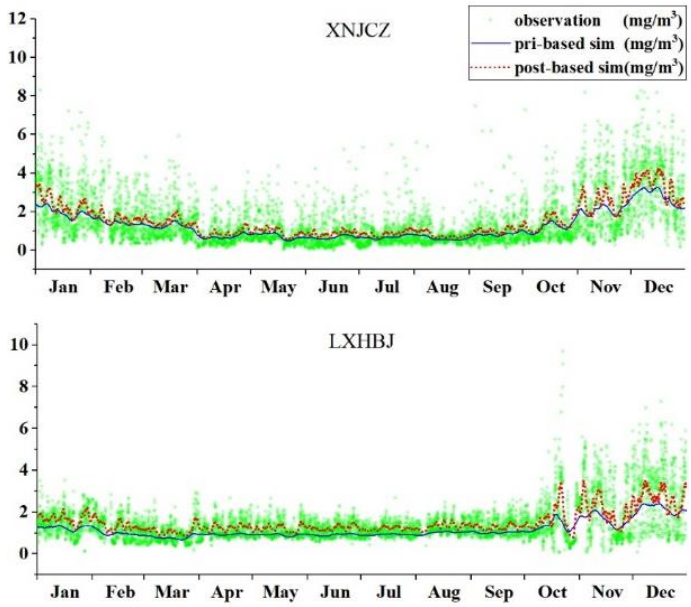

Figure 5. *Comparison of posterior-simulations and observations in WLG*

In SDZ, the correlation coefficients between the observed and simulated CO concentrations based on the a prior are 0.58, 0.66, 0.65, 0.61 and 0.52 in the five validation sites, i.e., BJDL, BDJCZ, LFYCGS, TJWLJGQ, and TSSEZ, respectively (*Table 5*). Priori-based simulations have a poor correlation with the CO observed

http://www.aloki.hu ● ISSN 1589 1623 (Print) ● ISSN 1785 0037 (Online)
DOI: http://dx.doi.org/10.15666/aeer/1804_52255246

concentrations, the main cause of this is the underestimation in the a priori. In an obvious contrast, errors between the posterior-based CO simulations and observations are significantly reduced and the simulation accuracy has been improved greatly (*Fig. 5* and *Fig. 6*). Besides, the correlation coefficients of validation sites, i.e., BJDL, BDJCZ, LFYCGS, TJWLJGQ and TSSEZ have been improved to 0.78, 0.78, 0.76, 0.76 and 0.70, respectively.

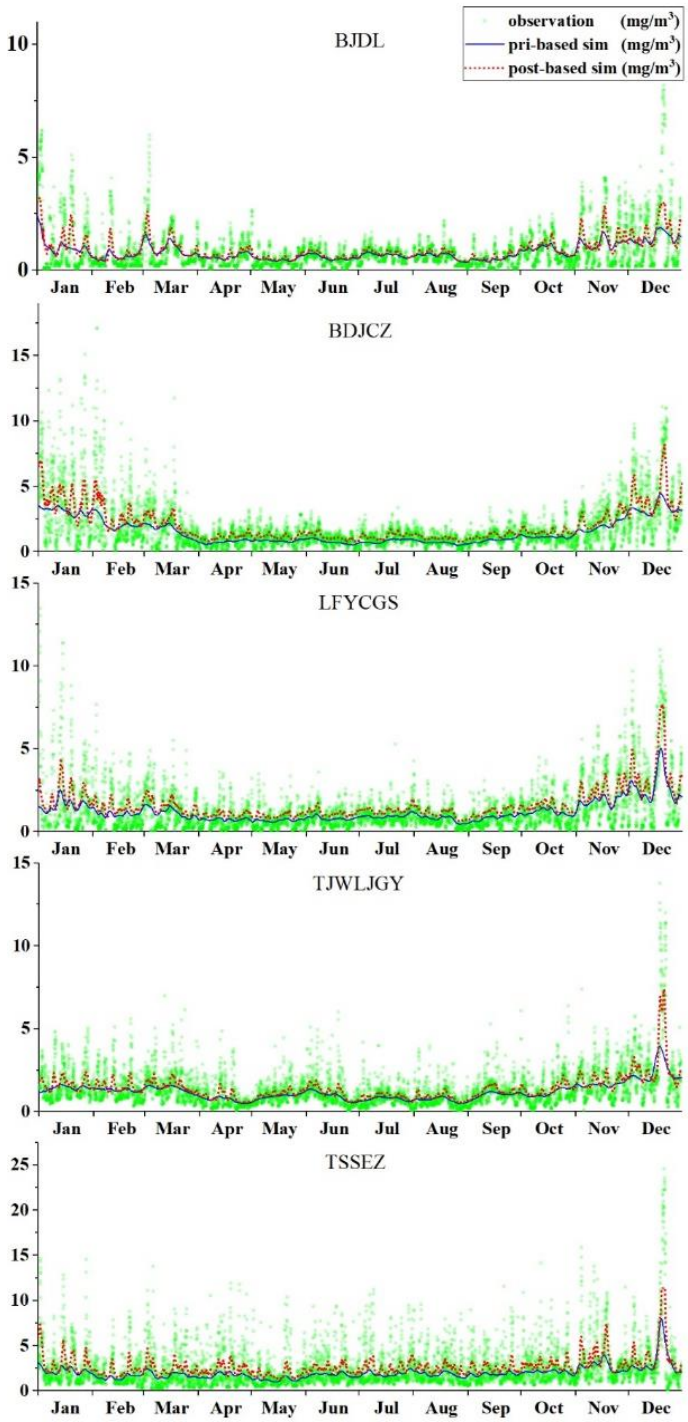

Figure 6. *Comparison of posterior-simulations and observations in SDZ*

http://www.aloki.hu ● ISSN 1589 1623 (Print) ● ISSN 1785 0037 (Online)
DOI: http://dx.doi.org/10.15666/aeer/1804_52255246

Table 5. *Errors of CO posterior-simulations and observations in SDZ and WLG*

	SDZ *(mg/m³)*					**WLG** *(mg/m³)*	
	BJDL	BDJCZ	LFYCGS	TJKG	TSSEZ	XNJCZ	LXHBJ
priori-based:							
E_{max}	7.61	13.9	12.0	9.87	18.4	7.22	8.26
E_{mean}	0.49	0.87	0.71	0.60	1.20	0.65	0.54
E_{rmse}	0.62	1.11	0.82	0.74	1.57	0.72	0.60
R	0.58	0.66	0.65	0.61	0.52	0.69	0.64
posterior-based:							
E_{max}	6.42	12.7	10.6	6.94	13.2	6.43	7.19
E_{mean}	0.43	0.76	0.75	0.54	1.21	0.62	0.48
E_{rmse}	0.49	0.90	0.68	0.58	1.19	0.63	0.52
R	0.78	0.78	0.76	0.76	0.70	0.73	0.74

In WLG, the correlation coefficients between the observed and simulated CO concentrations based on the prior flux is 0.69 and 0.64 at XNJCZ and LXHBJ, respectively (*Table 5*). The correlations are slightly higher than that based on the a priori in SDZ, but the priori-based simulations still have great errors. With the posteriori optimized by the TracersTracker system, the correlation between CO simulations and observations increased to 0.73 and 0.74 at XNJCZ and LXHBJ, respectively, and the CO simulations and observations are more consistent in the variation trend in the whole year. In addition, errors between the CO simulations and observations are also reduced obviously, the average error is reduced from 0.65 mg/m^3 to 0.62 mg/m^3 at XNJCZ and 0.54 mg/m^3 to 0.48 mg/m^3 at LXHBJ, respectively. At the same time, the maximum errors also show a stable downward trend in both SDZ and WLG. In SDZ, the maximum error of posterior-based simulations decreased by 1.19 mg/m^3, 1.2 mg/m^3, 1.4 mg/m^3, 2.93 mg/m^3 and 5.2 mg/m^3 at BJDL, BDJCZ, LFYCGS, TJWLJGQ and TSSEZ, respectively, the average decrease ration of the five monitoring sites is over 20%. In the WLG, the maximum error of posterior-based simulations decreased by 0.79 mg/m^3 and 1.07 mg/m^3 at XNJCZ and LXHBJ respectively with an average decrease of 12% (*Table 5*).

All above performance of the posterior illustrate that the TracersTracker system can greatly optimize the CO flux and significantly improve the simulation accuracy. It also shows that observation information is very important in the assimilation system, enough observations is the effective guarantee for high-precious flux inversions. Insufficient observed information could bring a lot of uncertainties, thus increases the simulations errors of the posteriors. In addition, there are both similarities and differences in simulation errors and tendencies in the a priori and posteriors no matter in SDZ and WLG. CO simulation errors in both areas tend to decrease in all validation sites, and errors range obviously shrinks in the posterior-based simulations. Although the trend of error distribution is similar in all monitoring sites, the shrink trend of error change is not in the same degree. Some of them have large contractions, e.g., TSSEZ, some have small contractions, e.g., BJDL, some have no obvious error contractions, e.g., XNJCZ, which is mainly related to the location of each validation site and the magnitude of CO observation concentration itself.

http://www.aloki.hu ● ISSN 1589 1623 (Print) ● ISSN 1785 0037 (Online)
DOI: http://dx.doi.org/10.15666/aeer/1804_52255246

Seasonal and regional variation of emissions

From the perspective of seasonal net increase of the posteriors, the net flux increase in winter is the largest among the four seasons in SDZ, reaching 0.43 mole/s, there is no significant difference in the other three seasons, which are about 0.3 mole/s, 0.31 mole/s and 0.27 mole/s in spring, summer and autumn respectively, only about two thirds of that in winter. Similar to SDZ, net flux increase in winter is the largest in WLG, reaching 0.17 mole/s, while spring and summer have the smallest net increase of 0.06 mole/s, only one third of that in winter (*Table 6*). From the perspective of annual average net increase, it is much smaller in WLG than that in SDZ.

Table 6. *Seasonal variation and increment proportions of the CO posteriors in SDZ and WLG*

Time	Max	Avg	Percent(%)
SDZ:			
Spring	3.69	0.31	28.5
Summer	3.49	0.31	31.8
Autumn	2.37	0.27	27.2
Winter	3.86	0.43	28.9
WLG:			
Spring	0.15	0.09	60.6
Summer	0.11	0.06	59.4
Autumn	0.17	0.10	59.8
Winter	0.17	0.17	65

From the perspective of seasonal net increase ration of the posteriors, there is no significant difference in the incremental ratio of the four seasons in SDZ. The growth ratio of the four seasons is basically the same, about 30%, summer has the highest increment (31.8%) which is slightly higher than that in other three seasons. In WLG, the proportions of growth in all seasons is much higher than that in SDZ, and the tendency of growth is also significantly different from that in SDZ (*Table 6*). The growth rate of WLG in winter is the largest, reaching 65%, slightly higher than that in other seasons.

Overall, the posteriors in winter have the highest growth rate in both areas. During this period, anthropogenic living activities, e.g., residential heating, push up the CO concentration in the atmosphere. With the development of economic, the demand for living activities in winter increases rapidly, thus makes the CO flux growth rate in winter higher than that in other seasons.

Fig. 7 is the scatter diagram of the seasonal error distribution in SDZ, in which the horizontal axis is the concentration of CO observations, the vertical axis is the posterior-based CO simulation, the black points are the prior-based simulations, and the red points are the posterior-based simulations. On the whole in SDZ, CO concentration in winter is the highest with a range of 0 mg/m^3 to 24 mg/m^3, which is much higher than that in other seasons and indicating that CO concentration changes frequently and greatly in winter, the main cause for this phenomenon is the activities of residents heating. For the CO simulations, the results have obvious different situations in different seasons whether in the a priori or the posteriors. Besides, the simulation accuracy of the a priori and the posteriors are better in autumn and winter than that in spring and summer, correlations of the priori-based simulations are 0.56 and 0.59 in spring and summer, 0.62 and 0.61 in autumn and winter, respectively. After the flux

http://www.aloki.hu ● ISSN 1589 1623 (Print) ● ISSN 1785 0037 (Online)
DOI: http://dx.doi.org/10.15666/aeer/1804_52255246

optimization, the trend of the posterior-based simulations is more obvious. The simulation precision is higher in autumn and winter, and the correlation coefficients are 0.75 and 0.83, respectively.

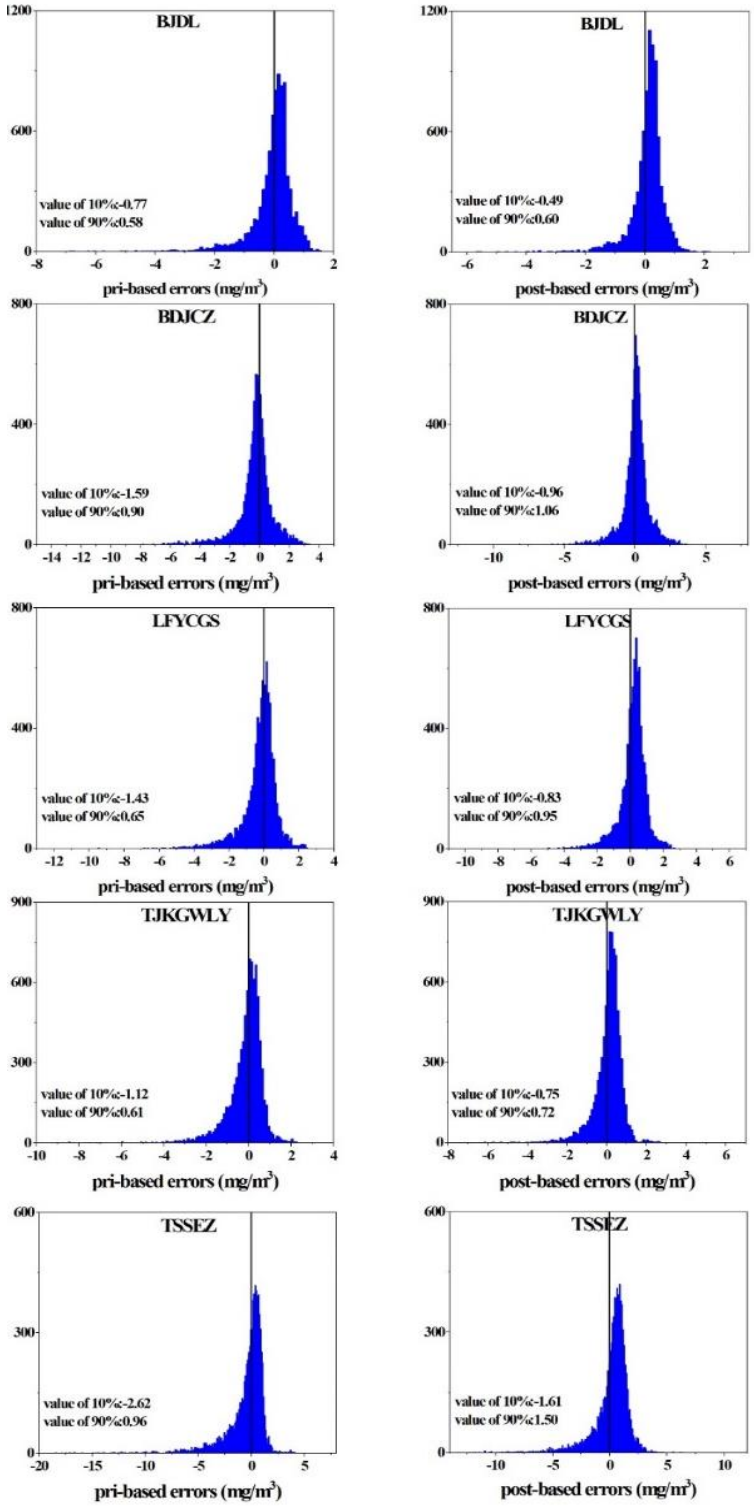

Figure 7. *Simulated errors of validation sites in SDZ. The pri-based and post-based errors are simulations errors based on the a priori and the posterior, respectively*

http://www.aloki.hu ● ISSN 1589 1623 (Print) ● ISSN 1785 0037 (Online)
DOI: http://dx.doi.org/10.15666/aeer/1804_52255246

Fig. 8 is the scatter diagram of the seasonal error distribution in WLG. Similar to that in SDZ, CO concentrations in winter is significantly higher than that in other seasons in WLG, but there are obvious differences of CO simulations between the two study areas. The correlation of priori-based simulations is very poor, especially in autumn (R is only 0.56), which is significantly lower than that in other seasons. After flux optimization, the correlation between the CO observations and the posterior-based simulations has been improved greatly especially in winter (R is 0.79) and spring (R is 0.76).

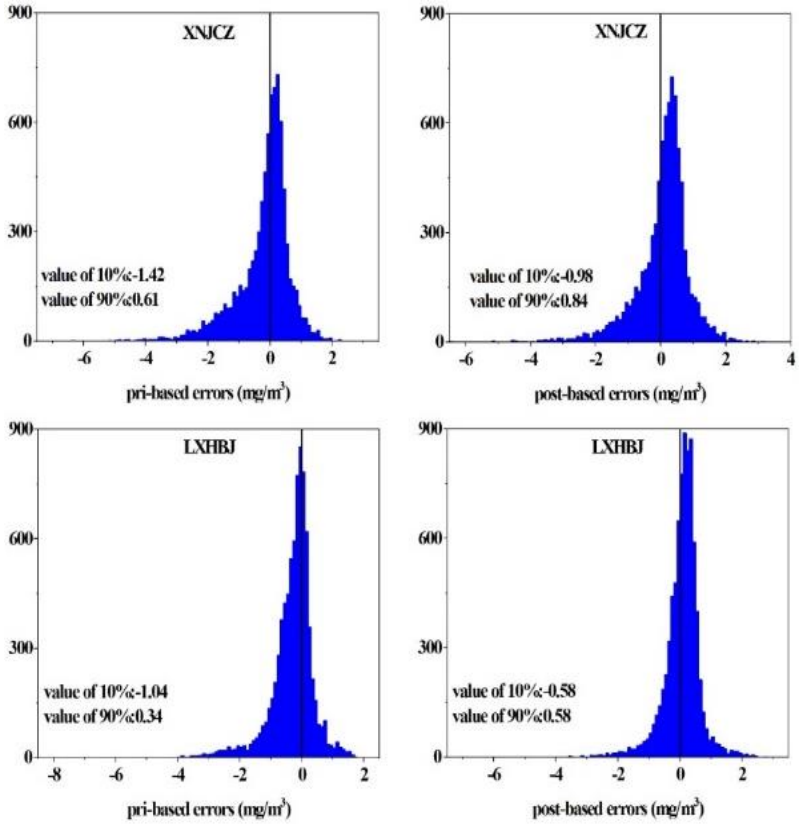

Figure 8. *Simulated errors of observation sites in WLG. The pri-based and post-based errors are simulations errors based on the a priori and the posterior, respectively*

In winter of northern China, the low temperature will increase the consumption of fossil fuels, e.g., coal and oil, thus the CO concentration in the atmosphere increase sharply in a short period. In addition, adverse weather conditions will exacerbate the increase speed, and eventually led to heavy air pollution events. In general, it will be more difficult to simulate the CO concentration with frequent variations in the atmospheric model. However, from the results shown above, CO concentration in winter with large fluctuations have better simulations than other period, which illustrate that the posterior can effectively optimize the a priori, errors are eliminated significantly in the posterior. For the period with small fluctuation of CO concentration, the accuracy of the posterior simulation is improved, but the accuracy in spring, summer and autumn are not as good as that in winter (*Fig. 9* and *Fig. 10*).

http://www.aloki.hu ● ISSN 1589 1623 (Print) ● ISSN 1785 0037 (Online)
DOI: http://dx.doi.org/10.15666/aeer/1804_52255246

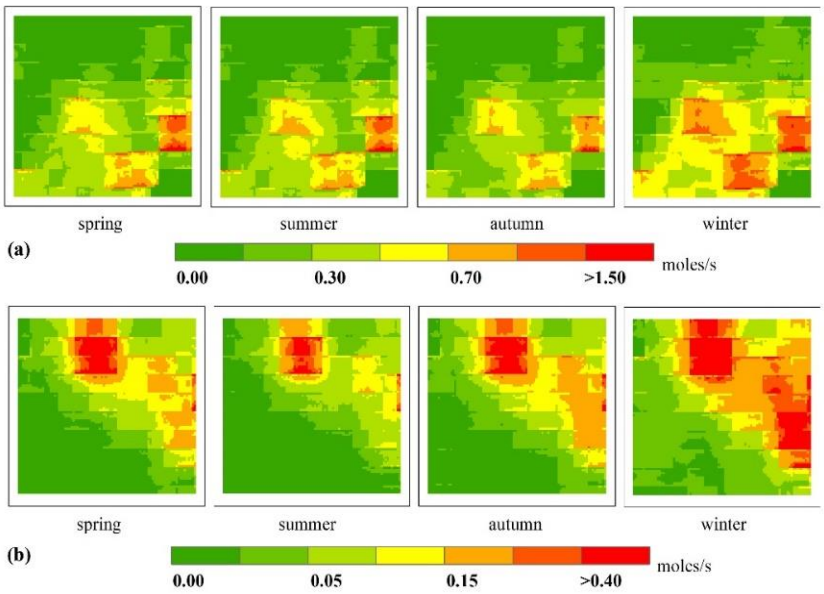

Figure 9. *Seasonal increment of the CO posteriors in SDZ (a) and WLG (b)*

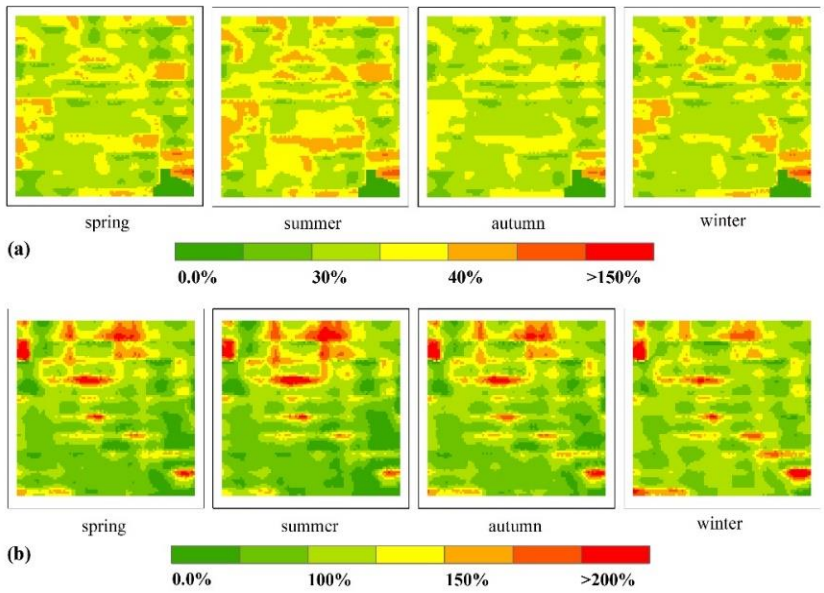

Figure 10. *Seasonal increment proportions of the CO posteriors in SDZ (a) and WLG (b)*

Conclusions

In this paper, a regional assimilation system, i.e., TracersTracker, was conducted for CO flux inversion by coupling the POD4DVAR method and the CMAQ model. The system was then applied to two distinct areas in china to diagnose the variations of CO flux inversion with different conditions. The TracersTracker system can effectively assimilate the hourly CO observations in the two study areas, the posteriors can significantly improve the accuracy of CO simulations. This study also suggested that the MIX inventory has underestimations of CO emission by 29.1% in SDZ and 61.2% in WLG. Due to the active chemical characteristics of CO, the flux inversion for CO can

http://www.aloki.hu ● ISSN 1589 1623 (Print) ● ISSN 1785 0037 (Online)
DOI: http://dx.doi.org/10.15666/aeer/1804_52255246

only be carried out in a small area, how to obtain global and continental CO fluxes should be considered in next step. In addition, in order to improve the efficiency of the assimilation inversion system, other mathematical methods with high efficiencies should be introduced into the assimilation system to obtain high-resolution CO fluxes.

Acknowledgements. This work was supported and funded by the talent introduction project of anhui university of science and tectechnology (ZRC2014460).

REFERENCES

[1] Gou, T., Sandu, A. (2011): Continuous versus discrete advection adjoints in chemical data assimilation with CMAQ. – Atmospheric Environment 45(28): 4868-4881.
[2] Gurjar, B. R., Jain, A., Sharma, A., Agarwal, A., Gupta, P., Nagpure, A. S., Lelieveld, J. (2010): Human health risks in megacities due to air pollution. – Atmospheric Environment 44(36): 4606-4613.
[3] Kamimura, A., Armenta, B., Nourian, M., Assasnik, N., Nourian, K., Chernenko, A. (2017): Perceived Environmental Pollution and Its Impact on Health in China, Japan, and South Korea. – J Prev Med Public Health 50(3): 188-194.
[4] Kilmont, Z. S. (2002): Anthropogenic emissions of non-methane volatile organic compounds in China. – Atmospheric Environment 36: 1309-1322.
[5] Kim, H., Kim, H. M., Kim, J., Cho, C. (2018): Effect of Data Assimilation Parameters on The Optimized Surface CO_2 Flux in Asia. – Asia-Pacific Journal of Atmospheric Sciences 54(1): 1-17.
[6] Law, K. J. H., Stuart, A. M., Zygalakis, K. C. (2015): Data Assimilation: A Mathematical Introduction. – Revista Brasileira De Meteorologia 26(3): 433-442.
[7] Li, P., Chai, T. F., Carmichael, G. R., Tang, Y. H., Streets, D., Woo, J.-H., Friedli, H. R., Radke, L. F. (2007): Top-down estimate of mercury emissions in China using four-dimensional variational data assimilation. – Atmospheric Environment 41(13): 2804-2819.
[8] Lu, S., Lin, H. X., Heemink, A. W., Fu, G., Segers, A. J. (2015): Estimation of Volcanic Ash Emissions Using Trajectory-Based 4D-Var Data Assimilation. – Monthly Weather Review 144: 575-589.
[9] Lu, L., Chen, B., Guo, L., Zhang, H., Li, Y. (2019): A regional data assimilation system for estimating CO surface flux from atmospheric mixing ratio observations—a case study of Xuzhou, China. – Environmental Science and Pollution Research 26(9): 8748-8757.
[10] Ma, Y. T. (2007): The Compilation of Vehicle Emission Inventory in Pearl River Delta Region and its Uncertainty Analysis. – Beijing, Peking University.
[11] MEPC (2017): Report on the State of the Environment in China 2016. – Ministry of Ecology and Environment, China.
[12] Ohara, T., Akimoto, H., Kurokawa, J., Horii, N., Yamaji, K., Yan, X., Hayasaka, T. (2007): An Asian emission inventory of anthropogenic emission sources for the period 1980-2020. – Atmos. Chem. Phys. 7: 4419-4444.
[13] Park, S., Kim, D., Lee, S., Lee, H. W. (2016): Variational data assimilation for the optimized ozone initial state and the short-time forecasting. – Atmospheric Chemistry and Physics 16(5): 3631-3649.
[14] Peng, Z., Zhang, M., Kou, X., Tian, X., Ma, X. (2015): A regional carbon data assimilation system and its preliminary evaluation in East Asia. – Atmos. Chem. Phys. 15: 1087-1104.
[15] Saide, P., Osses, A., Gallardo, L., Osses, M. (2009): Adjoint inverse modeling of a CO emission inventory at the city scale: Santiago de Chile's case. – Atmospheric Chemistry and Physics Discussions 9(2): 6325-6361.

http://www.aloki.hu ● ISSN 1589 1623 (Print) ● ISSN 1785 0037 (Online)
DOI: http://dx.doi.org/10.15666/aeer/1804_52255246

[16] Shi, Y., Xia, Y. F., Lu, B. H., Liu, N., Zhang, L., Li, S. J., Li, W. (2014): Emission inventory and trends of NO_x for China, 2000-2020. – Journal of Zhejiang University 15(6): 454-464.
[17] Tian, X., Xie, Z., Dai, A. (2008): An ensemble-based explicit four-dimensional variational assimilation method. – Journal of Geophysical Research 113(D21).
[18] Tian, X., Xie, Z. H. (2009): An explicit four-dimensional variational data assimilation method based on the proper orthogonal decomposition: Theoretics and evaluation. – Science in China Series D: Earth Sciences 52(2): 279-286.
[19] Tian, X., Xie, Z., Sun, Q. (2011): A POD-based ensemble four-dimensional variational assimilation method. – Tellus A: Dynamic Meteorology and Oceanography 63(4): 805-816.
[20] Tian, X., Xie, Z., Liu, Y., Cai, Z., Fu, Y., Zhang, H., Feng, L. (2014): A joint data assimilation system (Tan-Tracker) to simultaneously estimate surface CO_2 fluxes and 3-D atmospheric CO_2 concentrations from observations. – Atmospheric Chemistry and Physics 14(23): 13281-13293.
[21] Tian, X., Feng, X. (2015): A non-linear least squares enhanced POD-4DVar algorithm for data assimilation. – Tellus A: Dynamic Meteorology and Oceanography 67: 25340.
[22] Xue, T., Liu, J., Zhang, Q., Geng, G., Zheng, Y., Tong, D., Liu, Z., Guan, D., Bo, Y., Zhu, T., He, K., Hao, J. (2019): Rapid improvement of PM2.5 pollution and associated health benefits in China during 2013–2017. – Science China Earth Science 62: 1847-1856.
[23] Zhang, L., Constantinescu, E. M., Sandu, A., Tang, Y., Chai, T., Carmichael, G. R., Byun, D., Olaguer, E. (2008): An adjoint sensitivity analysis and 4D-Var data assimilation study of Texas air quality. – Atmospheric Environment 42(23): 5787-5804.
[24] Zhang, B., Tian, X. J., Zhang, L. F., Sun, J. H. (2017): Handling non-linearity in radar data assimilation using the non-linear least squares enhanced POD-4DVar. – Science China Earth Sciences 60: 478-490.
[25] Zheng, J., Zhang, L., Che, W., Zheng, Z., Yin, S. (2009): A highly resolved temporal and spatial air pollutant emission inventory for the Pearl River Delta region, China and its uncertainty assessment. – Atmospheric Environment 43(32): 5112-5122.

http://www.aloki.hu ● ISSN 1589 1623 (Print) ● ISSN 1785 0037 (Online)
DOI: http://dx.doi.org/10.15666/aeer/1804_52255246

ADAPTATION OF SINGAPORE DAISY (*WEDELIA TRILOBATA*) TO DIFFERENT ENVIRONMENTAL CONDITIONS; WATER STRESS, SOIL TYPE AND TEMPERATURE

AZEEM, A.[1] – JAVED, Q.[1] – SUN, J. F.[1*] – ULLAH, I.[2] – KAMA, R.[1] – DU, D. L.[1,2*]

[1]*School of the Environment and Safety Engineering, Jiangsu University, Zhenjiang 212013, China*

[2]*Key Laboratory of Modern Agricultural Equipment and Technology, Ministry of Education, Institute of Agricultural Engineering, Jiangsu University, Zhenjiang, Jiangsu, China*

**Corresponding authors*
e-mail: ddl@ujs.edu.cn (D. L. Du), zxsjf@ujs.edu.cn (J. F. Sun)

(Received 18th Dec 2019; accepted 22nd May 2020)

Abstract. Invasion success of the invasive plant species (Singapore daisy) mostly depends on environmental factors, therefore, this study was conducted to investigate the effect of temperature, 25/30 °C (outside), 30/35 °C (inside) and water fluctuation, volumetric water content at 100% field capacity (normal water), volumetric water content at 33% field capacity (water stress) in three different soil types (nutrient soil, normal soil and sandy soil) on the growth and photosynthetic traits of *Wedelia trilobata* (Wt) in Jiangsu University, Zhenjiang China. In comparison, Wt significantly performed better in outside temperature at all water levels in every soil type. Wt can tolerate high temperature at normal water level in normal and nutrient soil. At outside temperature along with water stress in sandy soil, Wt exhibited reduction in growth and photosynthetic trails, but the adverse effect was more severe at inside temperature with water stress in normal and sandy soil. After 4th week, leaf chlorophyll content of Wt decreased in water stress at outside and inside temperatures in normal and sandy soil. Furthermore, Wt maintained its water status under water stress, after the 4th week to the 8th week in every soil type, which indicated that Wt have the ability to grow in every harsh environmental condition. In conclusion Wt successfully invaded different soil types at high temperature, under water stress conditions.
Keywords: *invasive plant species, resources variation, growth, physiological traits, invasion*

Introduction

Invasive plant species are key threat to natural biodiversity and working of ecosystems (Schweiger et al., 2010). The properties that enhanced the ability of non-native plants becoming invasive are linked with their fast germination to reproductive growth stage and their high phenotypic plasticity, all of these enable them to cope with different environmental stress habitats (Baker, 1974). Not all invasive plant species show these types of characteristics (Lorenzo et al., 2010). It is the knowledge about invasive plant species, namely why they become invasive and which properties within the plant help them to become invasive, that makes us clear how to control the spread of these invasive plant species. Invasion success of invasive plant species have been explained by several hypotheses i.e. novel-weapons hypotheses (Callaway et al., 2000), propagule-pressure hypotheses (Colautti et al., 2006; Adamowski et al., 2008; Pairon et al., 2010), increased competitive ability hypotheses (Blossey et al., 1995), high reproductive with dispersal success (Moravcova et al., 2010; Van Kleunen et al., 2015; Jacquemart et al., 2015) and enemy release hypothesis (Keane et al., 2002). Many of these proposed mechanisms were taking part in the invasion success of several invasive plant species.

http://www.aloki.hu ● ISSN 1589 1623 (Print) ● ISSN 1785 0037 (Online)
DOI: http://dx.doi.org/10.15666/aeer/1804_52475261

Invasive plant species have physiological, phenotypic plasticity and may utilize the resources for its growth development and reproduction, when the enemy pressure is reduced (Ebeling et al., 2008). According to these strategies invasive plant species should maintain their growth in poor resources environment and maximize their growth under favorable environmental conditions (Gioria et al., 2014). These strategies should be investigated with the help of physiological traits of invasive plant species under poor and favorable environmental conditions, in order to directly involve resource acquisition (Van Kleunen et al., 2010). Many physiological factors involved in plant growth development like net photosynthetic rate, growth rate, leaf species area (SLA) and water use efficiency (WUE) could help invasive plant species to improve their fitness in different environmental resources containing water fluctuation and temperature variations (Zheng et al., 2009; van Kleunen et al., 2011; Javed et al., 2019). These functional traits are vital for invasive plant species for reproductive and physiological evaluation to build new populations or maintain their population in different habitats (Sun et al., 2019). Therefore, the studies linked with invasive plant species and based on physiological traits could be helpful to understand their invasion success under different environmental conditions.

Biological invasion may increase due to climate change and fluctuation of environmental resources such as precipitation, nutrient variation, temperature and substrate type (Abatzoglou et al., 2011; Azeem et al., 2020). Among these water, soil type and temperature are the main factors in the development of invasive plant species in different type of habitats. Increased temperature helps to boost the expansion of invasive plant species under higher precipitation availability and better nutrient substrate (Wang et al., 2011). Soil nutrient composition and water holding capacity has been shown to have great influence on plant productivity and stability (Callaway et al., 2004; Middleton et al., 2012; Van Der Heijden et al., 2008). Interaction effect of soil type and water fluctuation have received more attention recently (van der Putten, 2010). Similarly, interaction of temperature variations and precipitation also played an important part in growth development and reproduction of invasive plant species (Saptiningsih et al., 2019). Therefore, it is important to study the effect of each environmental factor and their interaction related to the success of the target plant.

Singapore daisy (*Wedelia trilobata,* Wt) belongs to the *Asteraceae* family and an annual invasive plant species in China, was chosen for this study (Azeem et al., 2020). It has been registered as one of the top 100 worst invasive plant species in the world (Qi et al., 2014). In 1970s, Wt was introduced to south China as a groundcover plant, but it quickly spread to the field (Weber et al., 2008). Faster clonal growth is also an important feature for their successful invasion (Song et al., 2010). Wt has ability to survival in every habitat condition. It can bear high temperature and moderate drought under different soil types. It prefers to grow in nutrient rich soil and moderate temperature range with high amount of water (Dai et al., 2016). The competitive success of Wt partially depends on its reproductive capacities. According to reproductive biology, the competitive success depends upon its physiological traits that enhances both WUE and photosynthetic rate (Quinet et al., 2015). Many researchers have done work to check response of Wt under different moisture conditions, soil nutrient combination and shading conditions (Dai et al., 2016; Saptiningsih et al., 2019). Apart from this higher temperature, water fluctuation and soil culture are also very important factors restricting plant growth (Xu et al., 2006). In addition, many researchers noted the response of invasive plant species with water stress and different

http://www.aloki.hu ● ISSN 1589 1623 (Print) ● ISSN 1785 0037 (Online)
DOI: http://dx.doi.org/10.15666/aeer/1804_52475261

temperature regime under only one type of soil (Legault II et al., 2018; Song, 2017), but none of them investigated the response of invasive plant species under combined effect of temperature variations along with water fluctuations in different soil types. Therefore, in this study our objectives were to investigate the response of Wt under water fluctuations and temperature variations within different soil types and their combined effect on physiological traits related to plant growth, water relation and their combination. Detailed physiological traits enable us to understand the invasion success of Wt under different environmental conditions. According to these we proposed hypotheses that Wt will grow better under normal water availability along with moderate temperature in every soil types but at severe temperature along with water stress, Wt sustain its growth in nutrient soil and normal soil due to their better water holding capacity and nutrient availability.

Material and methods

This study was conducted at the School of Environmental and Safety Engineering, Jiangsu University, Zhenjiang China (32.20°N, 119.45°E). This study was started in May and completed in July 2019. Ramets of Singapore daisy (*Wedelia trilobata,* Wt) were collected outside of the greenhouse where they were grown for experimental studies. Ramets of Wt were prepared in the seedling trays with sand as a culture medium. These trays were placed in the greenhouse that had 25 ± 5 °C temperature with 70% relative humidity. When these ramets had two fully expended leaves, they were transferred into plastic pots (height 10 cm, outer diameter 13 cm and lower inner diameter 6 cm), filled with three type of soil (sandy soil, normal soil, and nutrient soil). The physical and chemical characteristics of all soil types, that were used in this study are given in *Table 1*.

Table 1. *Physical and chemical characteristics of different soil types*

Parameters	Nutrient soil	Sandy soil	Normal soil	Unit
pH	7.0	6.60	6..20	-
Organic matter	38	0.34	1.75	%
Total nutrient	3.8	0.98	1.6	%
Water content	20	15	18	%
Electrical conductivity	2	1.2	1.8	ds/m

These transferred seedlings were placed under different temperature conditions 25/30 °C and 30/35 °C named as inside and outside temperature regime. All these seedlings were watered normally for one week to adopt the inside and outside (temperature) conditions. After one week of seedling transfer, treatments were started. This study was completely spilt-plot design with temperature as whole plot factor and their factorial combination of water levels, soil types serve as split-plot factors (Will et al., 2013a) with five replicates (2 × 3 × 2 × 5), 60 pots in total as shown in *Figure 1*. The water treatment was set according to pot volumetric water content. Volumetric water content at 100% field capacity was taken as normal water treatment and volumetric water content at 33% field capacity was taken as water stress treatment. Soil moisture meter (TR-6/TR-6D, China) was used to measure volumetric soil water

http://www.aloki.hu ● ISSN 1589 1623 (Print) ● ISSN 1785 0037 (Online)
DOI: http://dx.doi.org/10.15666/aeer/1804_52475261

content three time a week and watering was carried out when the volumetric soil water content fell below the set treatment level.

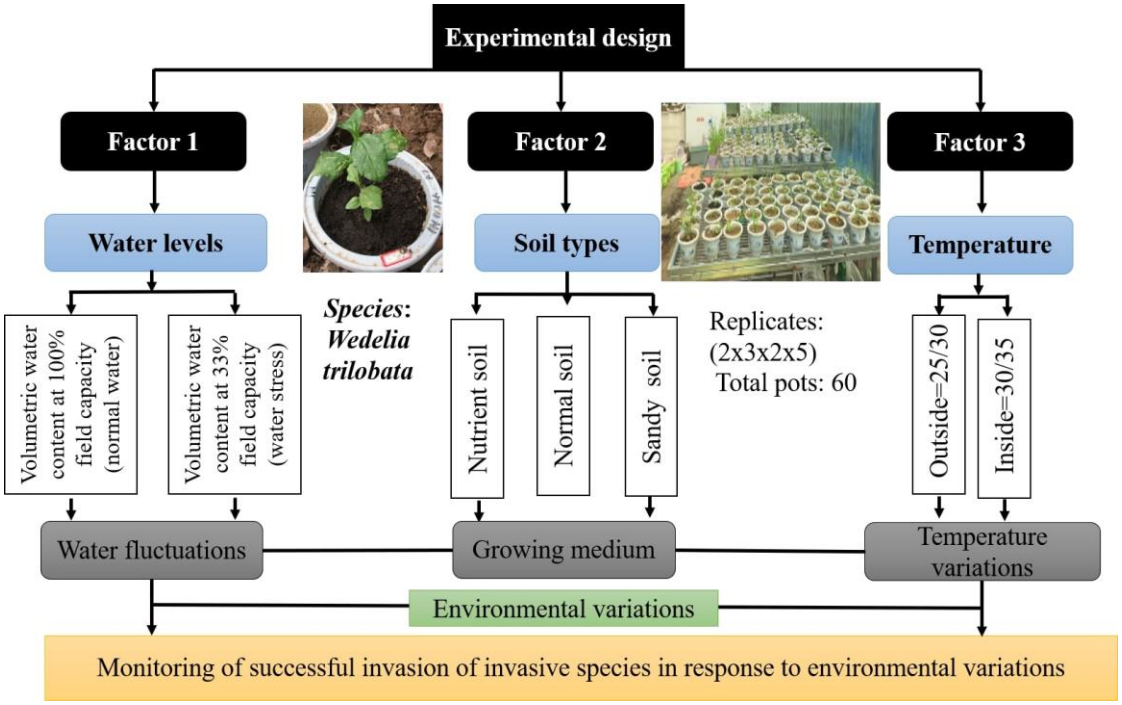

Figure 1. *Experimental design*

Set temperature values (outside and inside) were achieved in a greenhouse and the level of warming was controlled with ventilation (Valiño et al., 2014). The greenhouse at Jiangsu University, Zhenjiang, China was partitioned into two compartments in April 12, 2017. One compartment was equipped with two ventilators (380V, 2000W), and two windows and it was used for the inside temperature regime (Teitel et al., 2010; Willits, 2003). The outside temperature group was placed under a shelter made of the same material of the greenhouse. The material of the greenhouse made by solar sheet, light transmittance up to 96% (Xiaoming et al., 2008; Ureña-Sánchez et al., 2012), thus without regards to shade. Air temperature and humidity were recorded automatically every 10 min using temperature humidity recorder (TH11R, Inste, Shenzhen, China) placed 5 cm above pot edge (Fang et al., 2015; Will et al., 2013b).

Outside and inside temperature condition were received two water levels (water stress) volumetric water content at 33% field capacity and (normal water) volumetric water content at 100% field capacity in all three types of soil. The details of the treatments were explained in *Table 2*. These treatments were continued for two month and parameters related to growth were determined after every week. The photosynthetic traits and water potential were determined after the 4th and the 8th week of the study period.

Plant growth measurements

The parameters selected for plant growth measurement were plant height, number of nodes, leaves per plant and specific leaf area (SLA). The plant height was determined from the top of the soil surface to the top of first leaf with a ruler. Leaf chlorophyll

http://www.aloki.hu ● ISSN 1589 1623 (Print) ● ISSN 1785 0037 (Online)
DOI: http://dx.doi.org/10.15666/aeer/1804_52475261

content was measured with portable chlorophyll meter (SPAD; Oakoch OK-Y104, China). Moisture content was measured with moisture meter (TR-6/TR-6D, China).

Leaf area was determined with ImageJ software, then these leaves, were placed into an oven at 60 °C for two days to determine their dry weight (DW). Specific leaf area (SLA) were determined as the ratio of leaf area to leaf DW.

Table 2. *Experiment treatments detail*

Treatments	Soil type	Water level	Temperature
T_1	Nutrient	Normal water	Outside
T_2	Normal	Normal water	Outside
T_3	Sandy	Normal water	Outside
T_4	Nutrient	Water stress	Outside
T_5	Normal	Water stress	Outside
T_6	Sandy	Water stress	Outside
T_7	Nutrient	Normal water	Inside
T_8	Normal	Normal water	Inside
T_9	Sandy	Normal water	Inside
T_{10}	Nutrient	Water stress	Inside
T_{11}	Normal	Water stress	Inside
T_{12}	Sandy	Water stress	Inside

Normal water representing pot volumetric water content at 100% field capacity, water stress representing pot volumetric water content at 33% field capacity. Outside temperature = 25/30 °C, Inside temperature = 30/35 °C

Photosynthetic traits

Photosynthetic traits were determined after the 4th and the 8th week of the treatment's initiation. Gas exchange parameters like net photosynthetic rate (P_N), stomatal conductance (gs), and transpiration (Tr) were recorded by using a portable photosynthesis measurement system (LI-6400XT, LI-COR, Lincoln, NE, USA). A fully extended leaf from the top of the plant was selected for measurement. Measurement were performed under full sunshine conditions from 10 am to 11 am. The following conditions were maintained during the measurement: photosynthetically active radiation maximum up to 1000 μmol m^{-2} s^{-1}, molar flow of air 403.3 mmol m^{-2} s^{-1}, ambient CO_2 concentration 400 μmol mol^{-1}, atmospheric pressure 99.9 kPa, water vapor pressure ranged from 7.0 to 8.8 mbar.

Water use efficiency was calculated according to the following equation:

$$WUE = P_N/T_r \quad \text{(Eq.1)}$$

where P_N: net photosynthetic rate and Tr: transpiration respectively.

Plant water status

Plant water status was measured through water potential (Wp). Wp of every treatment plant was determined after the 4th and the 8th week of the treatment with the help of a dew point micro voltmeter in a C-52-SF universal sample room (Psypro, Wescor, USA).

http://www.aloki.hu ● ISSN 1589 1623 (Print) ● ISSN 1785 0037 (Online)
DOI: http://dx.doi.org/10.15666/aeer/1804_52475261

Statistical analysis

Variance analysis with four crossed fixed factors (water level, soil type, weeks, temperature) was performed to analyse soil moisture content, plant height, leaves per plant, nodes per plant and leaf chlorophyll content. Variance analysis with three crossed fixed factors (water level, soil type and temperature) was performed to analyse, gas exchange and water status parameters. Post hoc analyses were performed using the Tukey test with $p < 0.05$. All these analyses were performed on SPSS 22, software (SPSS Inc., Chicago, IL, USA). Origin pro 9.0 was used to makes graphs.

Results

Growth response

Water levels, temperature variations, soil types and duration of treatment significantly affect plant height as shown in *Table 3*. Their interactions also have significant effect on plant height ($F_{12,126} = 22.115$, $P < 0.01$). Plant height at outside temperature T_6 showed the smallest value while at inside temperature T_{11} and T_{12} both resulted in the smallest height as shown in *Figure 2A, B.*

Table 3. *Analysis of variance with four fixed factors against growth response*

Responses	Plant height	Moisture content	Leaves per plant	Nodes per plant	Leaf chlorophyll content
Temperature	1325.480**	3176.878**	46.398**	78.545**	3.177
Soil type	1770.225**	2439.745**	199.150**	72.591**	1.286
Weeks	5903.425**	235.388**	1071.506**	516.460**	10.764
Water level	1021.544**	1977.366**	869.251**	387.879**	18.034
Temperature * Soil type	617.065**	34.004**	19.537**	.045	.779
Temperature * Weeks	132.138**	4.135*	3.313*	5.753**	.336
Temperature * Water level	194.239**	50.821**	28.602**	87.515**	1.102
Soil type * Weeks	75.388**	3.004*	.372	7.982**	.675
Soil type * Water level	175.465**	344.764**	33.289**	17.924**	.217
Weeks* Water level	323.599**	.708	94.572**	34.591**	6.278**
Temperature * Soil type * Weeks	48.578**	5.319**	2.580*	.806	.893
Temperature * Soil type * Water level	395.196**	96.140**	7.961**	9.561**	2.610
Temperature * Weeks * Water level	23.958**	7.267**	1.469	4.753**	1.103
Soil type * Weeks * Water level	20.000**	1.105	10.261**	1.538	1.439
Temperature * Soil type * Weeks * Water level	22.115**	.736	2.104*	1.412	.630

Main and interactive effects (F-values) of water levels, temperature, soil type and weeks on the growth parameters of *Wedelia trilobata* over the growing period. ** and * indicate a significant level at $P < 0.01$ and $P < 0.05$

Soil moisture content was also significantly effective on temperature ($F_{1,126} = 3176.878$, $P < 0.01$), soil types ($F_{2,84} = 2439.745$, $P < 0.01$), weeks ($F_{6,36} = 235.388$, $P < 0.01$), and water levels ($F_{1,126} = 1977.366$, $P < 0.01$). Interaction effect between weeks and water levels were non-significant due to soil moisture content depends upon soil type and its water holding capacity as shown in *Table 3*. The interaction effect of temperature, soil types, weeks and water levels were non-significant ($F_{12,126} = 0.736$, $P = 0.715$). Soil moisture content at T_6 and at T_{11} and T_{12} shown lower values as compared to other treatment levels with increasing the duration of treatment period as shown in *Figure 2C, D.*

http://www.aloki.hu ● ISSN 1589 1623 (Print) ● ISSN 1785 0037 (Online)
DOI: http://dx.doi.org/10.15666/aeer/1804_52475261

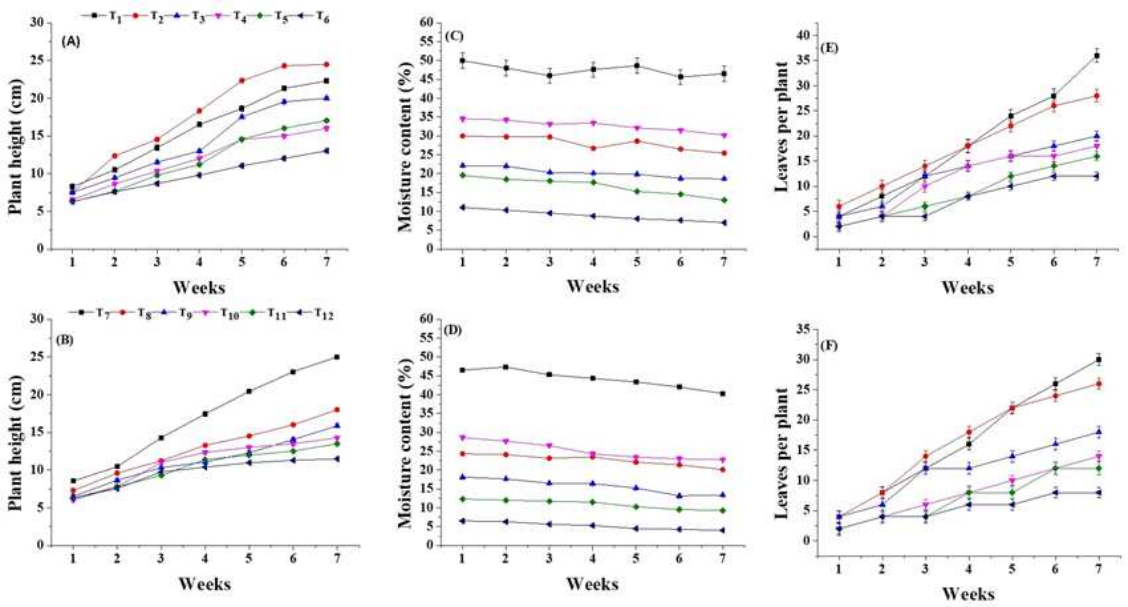

Figure 2. *Impact of outside, inside temperature, soil types and water levels against duration of treatment on Plant height (A, B) Moisture content (C, D), Leaves per plant (E, F). Data represented with mean ± SD on error bar of each treatment against weeks*

Leaves per plant also showed significant results with respect to temperature, soil types, water levels and duration of treatment as shown in *Table 3*. Interaction effect of water levels and temperature was significant ($F_{1,126} = 28.602$, $P < 0.01$) that showed with the increasing temperature plant needed more water to sustain its growth at higher temperature. Interaction effect of soil types and weeks were non-significant ($F_{12, 84} = 0.372$, $P = 0.534$) because properties of different soils with respect to water holding capacity and temperature responses does not depend upon duration of treatments. Regarding leaves per plant under outside temperature regime, T_1 showed higher values as compared to others and under inside temperature regime, T_{12} and T_{11} showed lower values as compared to other treatments as shown in *Figure 2E, F*.

Number of nodes per plant was also significantly affected by all treatments as shown in *Table 3*. Interaction effect between temperature and soil types were non-significant ($F_{2, 126} = 0.045$, $P = 0.956$) because every soil has ability to bear higher temperature and maintain their properties. Interaction effects of all factors were non-significant ($F_{12, 126} = 2.104$, $P = 0.019$), which indicated that invasive plant species have ability to maintain their growth in every habitat condition. Number of nodes per plant were decreased with decreasing amount of water and increasing temperature. At both outside and inside temperature with water stress treatments plants have lower number of nodes compared with those under normal water level treatments as shown in *Figure 3G, H.*

Leaf chlorophyll content was significantly affected by the interaction effect of water levels and weeks ($F_{6,36} = 10.764$, $P < 0.01$). Interaction effects of all other factors were non-significant as show in *Table 3*. Leaf chlorophyll content value at T_6, T_{11} and T_{12} were decreasing after the 5th week of treatments as shown in *Figure 3I, J*. This was indicated by the loss of green colour of plant leaves in plants under water stress and high temperature conditions, that is the first indication of plant under stress.

http://www.aloki.hu ● ISSN 1589 1623 (Print) ● ISSN 1785 0037 (Online)
DOI: http://dx.doi.org/10.15666/aeer/1804_52475261

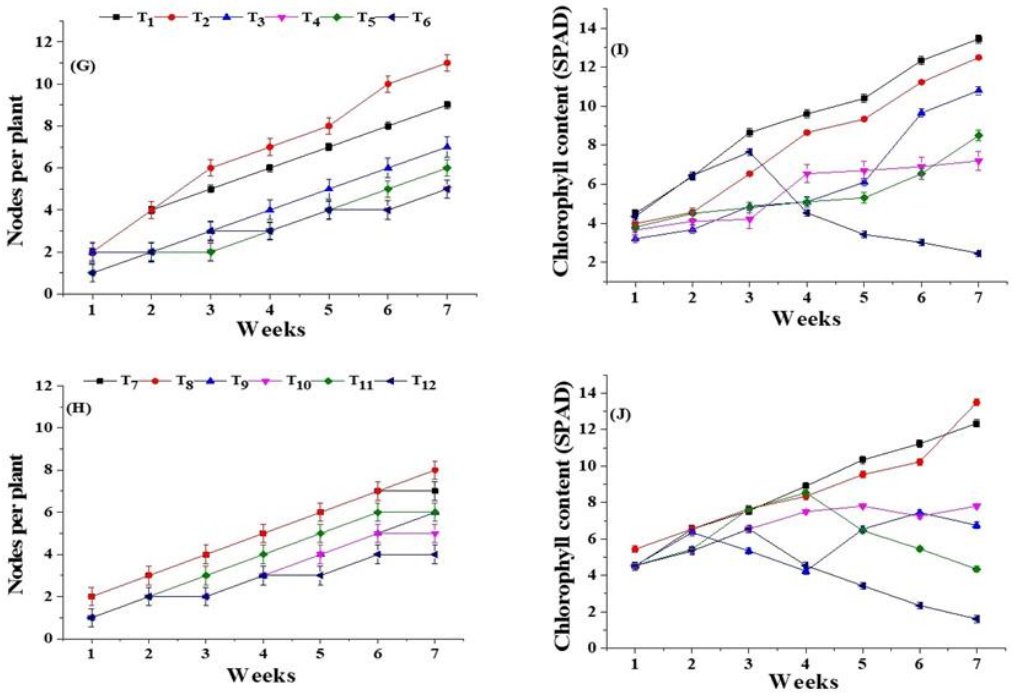

Figure3. *Impact of outside, inside temperature, soil types and water levels against duration of treatment on nodes per plant (G, H) Chlorophyll content (I, J). Data represented with mean ± SD on error bar of each treatment against weeks*

Specific leaf area (SLA) was also significantly affected by soil types, water levels and temperature after the 4th and the 8th week of treatments as shown in *Tables 4* and *5*. SLA of normal soil at T_2, T_8 under normal water at both outside and inside temperature showed a higher value as compared to other soil types as shown in *Figure 5U, V*. SLA was more affected in all soil types under water stress at inside temperature from the 4th and the 8th week, indicating that plant water requirement increased with its growth development and also with higher temperature. Interaction effect after the 4th week between soil types and temperature were non-significant ($F_{2,18} = 2.541$, $P = 0.10$), but soil types and water levels were significant ($F_{2,18} = 68.923$, $P < 0.01$), which described that every soil has different water holding capacity under same water level conditions. Similar results were found after the 8th week as shown in *Table 5*. According to the results, Wt can survive under higher temperature, if reasonable amount of water is available or growing medium has ability to hold more water content.

Photosynthetic responses

Stomatal conductance (gs) gradually decreased during the first four weeks of treatments ($F_{2,18} = 18.212$, $P < 0.01$). Soil types, water levels and temperature ($F_{2,12} = 398.988$, $P < 0.01$, $F_{1,18} = 50.536$, $P < 0.01$, $F_{1,\ 18} = 3604.34$, $P < 0.01$) had a significantly negative effect on stomatal conductance as shown in *Figure 4K, L*. After the 4th to the 8th week all these factors have significant effect on stomatal conductance as shown in *Table 5*. More negative effect of stomatal conductance was found under water stress treatment at both outside and inside temperature in every soil type as shown in *Figure 4K, L*. These results indicated that Wt water requirement increased as long as its growth increased.

http://www.aloki.hu ● ISSN 1589 1623 (Print) ● ISSN 1785 0037 (Online)
DOI: http://dx.doi.org/10.15666/aeer/1804_52475261

All treatments had significant effect on photosynthesis after the 4th and the 8th week of treatment imposition as shown in *Tables 4* and *5*. Photosynthesis of T_6, T_{11} and T_{12} were low values as compared to other treatments as shown in *Figure 4M, N*.

Table 4. *Analysis of variance after four weeks of treatment against physiological traits*

Response	gs	P_N	Tr	WUE	Wp	SLA
Soil type	398.988**	851.996**	81.822**	413.981**	117.474**	84.023**
Temperature	50.536**	1038.554**	428.889**	235.735**	63.027**	30.160**
Water level	3604.346**	3673.937**	525.208**	1461.600**	695.230**	440.059**
Soil Type * Temperature	5.856	153.133**	2.605	111.120**	8.093*	2.541
Soil Type * Water level	25.182**	229.787**	52.050**	145.823**	103.565**	68.923**
Temperature * Water level	776.286**	41.521**	36.141**	121.644**	46.066**	4.142
Soil Type * Temperature* Water level	18.212**	61.855**	30.585**	16.121**	17.914**	9.146*

Main and interactive effects (F-values) of water levels, temperature and soil type on the physiological traits of *Wedelia trilobata* after four weeks of treatments. ** and * indicate a significant level at $P < 0.01$ and $P < 0.05$. gs: stomatal conductance, P_N: photosynthetic rate, Tr: transpiration, WUE: water use efficiency, Wp: water potential and SLA: specific leaf area

Table 5. *Analysis of variance after eight weeks of treatment against physiological traits*

Response	gs	P_N	Tr	WUE	Wp	SLA
Soil type	630.385**	1332.963**	95.091**	748.037**	.050	109.562**
Temperature	472.724**	216.031**	59.751**	62.306**	.519	82.174**
Water level	6820.402**	6841.689**	745.959**	2771.657**	.030	744.589**
Soil Type * Temperature	18.735**	55.197**	22.195**	80.906**	.252	3.019
Soil Type * Water level	124.874**	33.102**	5.083	41.249**	.087	66.032**
Temperature * Water level	340.335**	178.361**	.813	176.575**	.068	1.814
Soil Type * temperature* Water level	29.152**	8.756*	30.527**	34.035**	.260	.259

Main and interactive effects (F-values) of water levels, temperature and soil types on the physiological traits of *Wedelia trilobata* after eight weeks of treatments. ** and * indicates a significant level at $P < 0.01$ and $P < 0.05$. gs: stomatal conductance, P_N: photosynthetic rate, Tr: transpiration, WUE: water use efficiency, Wp: water potential and SLA: specific leaf area

Temperature, soil types and water level had a significant effect on transpiration (Tr) of Wt ($F_{1,18} = 428.88$, $P < 0.01$, $F_{2,12} = 81.822$, $P < 0.01$, $F_{1,18} = 525.208$, $P < 0.01$), after 4 weeks of treatment imposition. Transpiration of Wt was decreased with high temperature along with water stress at both outside and inside temperature as shown in *Figure 4O, P*. After 8 weeks of treatment imposition transpiration was decreased significantly more at T_6, T_{11} and T_{12} as compared to other treatments. Interaction effect of soil types, temperature and water levels had a significant effect on transpiration as shown in *Tables 4* and *5*.

Water use efficiency (WUE) was also negatively affected by increasing temperature and decreasing water availability in every soil types as shown in *Figure 5Q, R*. After the 4th and the 8th week of treatments temperature, soil types and water levels had a significant effect on water use efficiency as show in *Tables 4* and *5*. WUE were increased from the 4th to the 8th week under normal water level in nutrient soil and normal soil at both outside and inside temperature. While under water stress level in sandy soil at outside and in normal soil and sandy soil at inside temperature, WUE were decreased because stomatal closure and increased transpiration.

http://www.aloki.hu ● ISSN 1589 1623 (Print) ● ISSN 1785 0037 (Online)
DOI: http://dx.doi.org/10.15666/aeer/1804_52475261

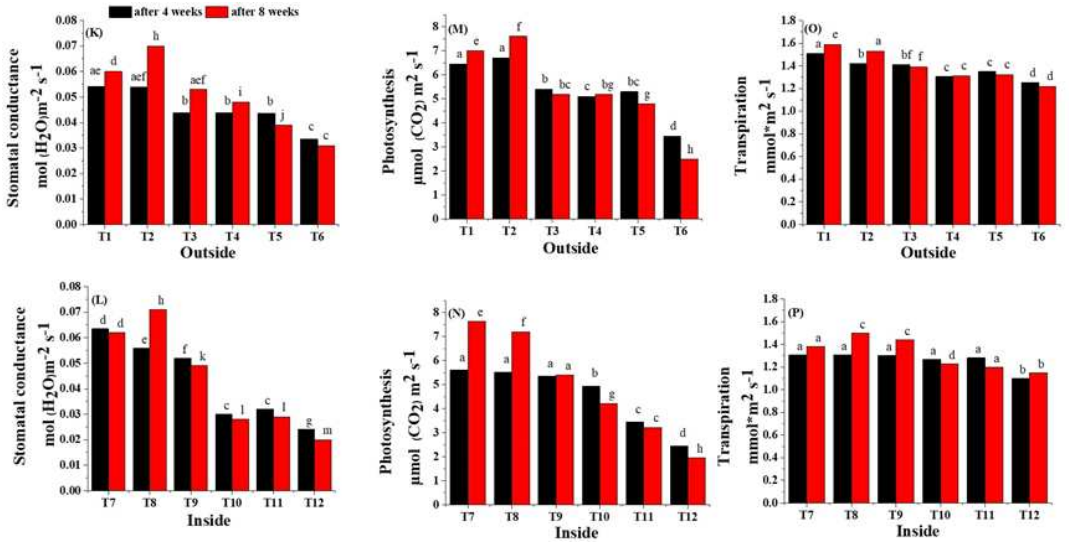

Figure 4. *Impact of water levels, temperature and soil types on stomatal conductance (K, L), photosynthesis (M, N) and transpiration (O, P) of Wedelia trilobata after the 4th and the 8th week of treatments. Different letter indicates the significant difference P < 0.05, according to Tukey test.*

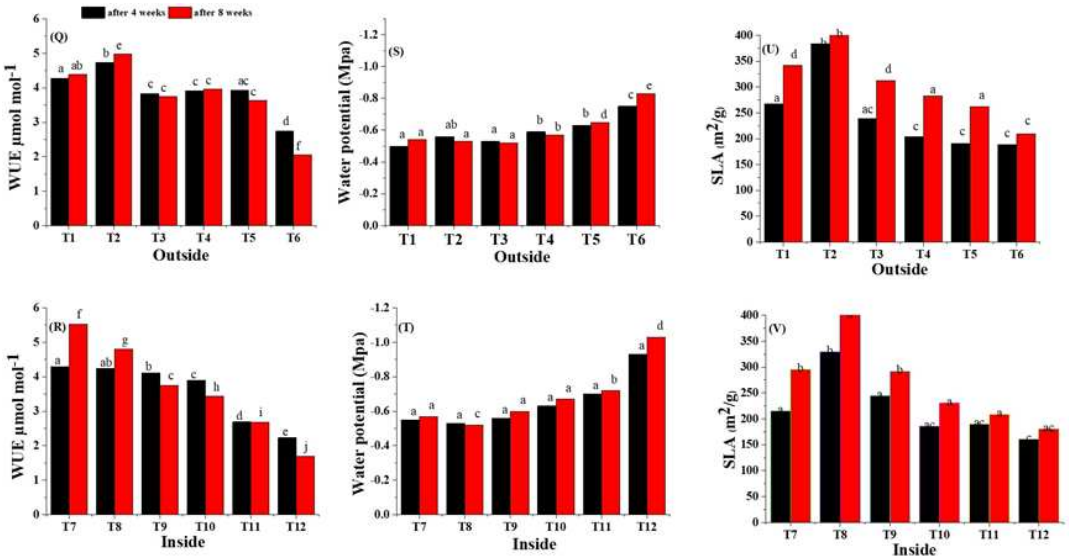

Figure 5. *Impact of water levels, temperature and soil types on WUE (Q, R) water potential (S, T) and SLA (U, V) of Wedelia trilobata after the 4th and the 8th week of treatments. Different letter indicates the significant difference P < 0.05, according to Tukey test. WUE: water use efficiency, SLA: specific leaf area*

Water status

After 4 weeks of treatment imposition water potential (Wp) was significantly affected by soil types, temperature and water level as shown in *Table 4*. Water potential of all soil types under water stress level at both outside and inside temperature were decreased significantly as shown in *Figure 5S, T*. These significant results indicated that Wt was facing difficulty to survive under these habitat conditions. After 8 weeks of treatment

http://www.aloki.hu ● ISSN 1589 1623 (Print) ● ISSN 1785 0037 (Online)
DOI: http://dx.doi.org/10.15666/aeer/1804_52475261

imposition Wp was non-significant with soil types and water levels ($F_{2,12} = 0.05$, $P = 0.22$, $F_{1,18} = 0.03$, $P = 0.475$), but significant effect of temperature ($F_{1,18} = 0.519$, $P < 0.01$) was observed. After the 8th week non-significant results indicated that for Wt it took the first four weeks to cope with habitat conditions and after the 4th week due to strong ability of Wt to tolerate all types environmental conditions it maintained steady growth.

Discussion

Effect of temperature, water stress and different soil types on physiological traits of Wt

Physiological traits that were considered in this study have often been described among characteristics that may take part in invasive plants development and consequently improve plants growth and enhance invasiveness. In this regard higher photosynthetic rate and morphological traits, that were connected with plant growth development and also with the plant invasiveness (Quinet et al., 2015; Van Kleunen et al., 2010). Especially in high temperature habitats where reasonable amount of water content is needed to maximize photon (Čuda et al., 2014). Under these experiment results SLA, plant height, number of leaves per plant and number of nodes per plant increased under normal water at inside and outside temperature in all soil types with the increasing duration of the treatments as shown in *Figure 2A-D*. This indicated that Wt has potential to tolerate higher temperature under favourable environmental conditions. Therefore, in the future due to global warming and urbanization there is some possibility that Wt will grow faster in these habitats (Song et al., 2012). Similarly, P_N, g_s, Tr and WUE decreased with increasing temperature under water stress at both outside and inside temperature after 4 and 8 weeks as shown *Tables 4* and *5* in every soil type. The treatments T_6, T_{11}, and T_{12} had lesser growth rate and photosynthetic traits, that indicated Wt was suffering with high temperature stress due to shortage of water as shown in *Figures 2* and *4*. Soil properties were also played an important role for the successful invasion under water fluctuation and temperature variations (Fang et al., 2016). In sandy soil Wt was suffering due to less water holding capacity at high temperature, similar result was observed in normal soil at inside temperature condition because with the passage of time plant water requirement was increasing (Azeem et al., 2017), but due to insufficient amount of water Wt was suffering. Soil moisture plays an important role in the survival of invasive plant species at high temperature (Song, 2017).

Nutrient soil has better effect on plant growth at both inside and outside temperature along with water stress level due to its better water holding capacity. This allowed Wt to cope with these habitat conditions and it developed better growth. Leaf chlorophyll content at the beginning of the treatments were increasing in every treatment but after the 3rd and the 4th week of the treatments, leaf chlorophyll content at T_6, T_{11} and T_{12} were decreasing as shown in *Figure 3I, J*. Leaf chlorophyll content depends upon sunlight and also the amount of water available for photosynthesis (Song, 2017), which supports our results that leaf chlorophyll content was decreasing under lower photosynthetic rate and under lower water potential (Song et al., 2010).

Invasive potential

Phenotypic plasticity allows invasive plant species to grow and expand in low resources and heterogeneous habitats (Richards et al., 2006). It has been reported that phenotypic plasticity is the characteristic that promotes invasiveness (Gioria et al.,

http://www.aloki.hu ● ISSN 1589 1623 (Print) ● ISSN 1785 0037 (Online)
DOI: http://dx.doi.org/10.15666/aeer/1804_52475261

2014). In this study growth development were tested under different environmental factors. We observed that physiological traits such as SLA, lower gs, stable P_N, Tr and adjustable Wp enable Wt to grow well in different environmental habitats. This could be the best strategy for survival under these habitat conditions (Rahlao et al., 2010). Moreover, Wt is known as fast spreading through nonsexual propagation (clonal growth). Once established in plantation Wt can also grow into a compressed groundcover and avert the revival of native plant species (Song et al., 2010). Macanawai, 2013 and Saptiningsih et al., 2019 reported that Wt can bear higher temperature, water stress and grow in every soil medium that was also confirmed in this study. According to these findings Wt is able to maintain growth development and reproduction within unfavourable conditions, which proposed that the strategy used by Wt for invasion success was very similar to the jack, trades scenario (Richards et al., 2006).

In this study we acknowledged physiological traits connected to temperature and water stress tolerance with different soil types that could indicate high phenotypic plasticity may confer competitive advantages of these invasive plant species. In meta-analysis (Van Kleunen et al., 2015) it was reported that invasive plant species had complex values for several valuable constraints of plant physiology such as P_N, WUE, leaf area, and SLA compared to native plant species. However, the competitive properties of native plant species compared with invasive plant species depend on the environmental resources (Gioria et al., 2014). Many researchers have described that invasive plant species were better contestants in water stress, with different soil textures and higher temperature regimes than native plant species, because they have expressively higher tolerance ability (Gioria et al., 2014; van Kleunen et al., 2011). In this regard studies comparing different plant species with the same family of Wt, could help us to recognize and predict future invasions. In addition, precise experiments under different environmental conditions i.e. temperature and water stress to examine the functional traits among *Asteraceae* family plants and comparing their physiological traits involved to predict the future trends of invasive species in presently invaded and potentially susceptible countries. Furthermore, future change in climate are possible to affect local, regional moisture, temperature and invasion success of Wt and may aid its spread effectively under future environmental conditions.

Conclusion

Our study confirmed that higher environmental resource accessibility (water, soil type and temperature) enhanced growth of Wt, furthermore under water stress and high temperature in normal soil and sandy soil, the growth of Wt was decreased. Wt is likely to become more aggressive in the future upcoming heat and water stress conditions. In a long-term evaluation process Wt developed an adaptive strategy to cope with high temperature and water stress in every soil medium. These facts are playing an important role in its management and control. Based on our finding we suggested that managers plan to target areas that have higher precipitation and ambient temperature to remove seedling from that places where Wt performed well. In addition, future study could be done by considering its native congener *Wedelia chinensis* along with these environmental factors under competition experiment. Therefore, investigating the growth development under competition along with these environmental factors could give us more understanding for the invasion success of Wt under these environmental conditions.

http://www.aloki.hu ● ISSN 1589 1623 (Print) ● ISSN 1785 0037 (Online)
DOI: http://dx.doi.org/10.15666/aeer/1804_52475261

Acknowledgment. This work was supported by the State Key Research Development Program of China (2017YFC1200100), the National Natural Science Foundation of China (31971427, 31570414, and 31770446), the Priority Academic Program Development of Jiangsu Higher Education Institutions (PAPD), and the Jiangsu Collaborative Innovation Center of Technology and Material of Water Treatment.

REFERENCES

[1] Abatzoglou, J. T., Kolden, C. A. (2011): Climate change in western US deserts: potential for increased wildfire and invasive annual grasses. – Rangeland Ecology & Management 64: 471-478.

[2] Adamowski, W., Tokarska-Guzik, B. (2008): Balsams on the Offensive: The Role of Planting in the Invasion of Impatiens Species. – In: Tokarska-Guzik B. et al. (eds.) Plant Invasions: Human Perception, Ecological Impacts and Management. Backhuys Publishers, Leiden, pp. 57-70.

[3] Azeem, A., Wu, Y., Javed, Q., Xing, D., Ullah, I., Kumi, F. (2017): Response of okra based on electrophysiological modeling under salt stress and re-watering. – Bioscience Journal 33.

[4] Azeem, A., Sun, J., Javed, Q., Jabran, K., Du, D. (2020): The effect of submergence and eutrophication on the trait's performance of *Wedelia trilobata* over its congener native *Wedelia chinensis.* – Water 12: 934.

[5] Baker, H. G. (1974): The evolution of weeds. – Annual Review of Ecology and Systematics 5: 1-24.

[6] Blossey, B., Notzold, R. (1995): Evolution of increased competitive ability in invasive nonindigenous plants: a hypothesis. – Journal of Ecology 83: 887-889.

[7] Callaway, R. M., Aschehoug, E. T. (2000): Invasive plants versus their new and old neighbors: a mechanism for exotic invasion. – Science 290: 521-523.

[8] Callaway, R. M., Thelen, G. C., Rodriguez, A., Holben, W. E. (2004): Soil biota and exotic plant invasion. – Nature 427: 731.

[9] Colautti, R. I., Grigorovich, I. A., Macisaac, H. J. (2006): Propagule pressure: a null model for biological invasions. – Biological Invasions 8: 1023-1037.

[10] Čuda, J., Skálová, H., Janovský, Z., Pyšek, P. (2014): Habitat requirements, short-term population dynamics and coexistence of native and invasive Impatiens species: a field study. – Biological Invasions 16: 177-190.

[11] Dai, Z.-C., Fu, W., Qi, S.-S., Zhai, D.-L., Chen, S.-C., Wan, L.-Y., Huang, P., Du, D.-L. (2016): Different responses of an invasive clonal plant Wedelia trilobata and its native congener to gibberellin: implications for biological invasion. – Journal of Chemical Ecology 42: 85-94.

[12] Ebeling, S. K., Hensen, I., Auge, H. (2008): The invasive shrub Buddleja davidii performs better in its introduced range. – Diversity and Distributions 14: 225-233.

[13] Fang, X., Zhou, G., Li, Y., Liu, S., Chu, G., Xu, Z., Liu, J. (2015): Warming effects on biomass and composition of microbial communities and enzyme activities within soil aggregates in subtropical forest. – Biology and Fertility of Soils 52: 353-365.

[14] Fang, X., Zhou, G., Li, Y., Liu, S., Chu, G., Xu, Z., Liu, J. (2016): Warming effects on biomass and composition of microbial communities and enzyme activities within soil aggregates in subtropical forest. – Biology and Fertility of Soils 52: 353-365.

[15] Gioria, M., Osborne, B. A. (2014): Resource competition in plant invasions: emerging patterns and research needs. – Frontiers in Plant Science 5: 501.

[16] Jacquemart, A.-L., Somme, L., Colin, C., Quinet, M. (2015): Floral biology and breeding system of Impatiens balfourii (Balsaminaceae): an exotic species in extension in temperate areas. – Flora-Morphology, Distribution, Functional Ecology of Plants 214: 70-75.

http://www.aloki.hu ● ISSN 1589 1623 (Print) ● ISSN 1785 0037 (Online)
DOI: http://dx.doi.org/10.15666/aeer/1804_52475261

[17] Javed, Q., Sun, J., Azeem, A., Ullah, I., Huang, P., Kama, R., Jabran, K., Du, D. (2019): The enhanced tolerance of invasive alternanthera philoxeroides over native species under salt-stress in china. – Applied Ecology and Environmental Research 17: 14767-14785.
[18] Keane, R. M., Crawley, M. J. (2002): Exotic plant invasions and the enemy release hypothesis. – Trends in Ecology & Evolution 17: 164-170.
[19] Legault Ii, R., Zogg, G. P., Travis, S. E. (2018): Competitive interactions between native Spartina alterniflora and non-native Phragmites australis depend on nutrient loading and temperature. – PloS One 13: e0192234.
[20] Lorenzo, P., González, L., Reigosa, M. J. (2010): The genus Acacia as invader: the characteristic case of Acacia dealbata Link in Europe. – Annals of Forest Science 67: 101.
[21] Middleton, E. L., Bever, J. D. (2012): Inoculation with a native soil community advances succession in a grassland restoration. – Restoration Ecology 20: 218-226.
[22] Moravcova, L., Pyšek, P., Jarošík, V., Havlíčková, V., Zákravský, P. (2010): Reproductive characteristics of neophytes in the Czech Republic: traits of invasive and non-invasive species. – Preslia 82: 365-390.
[23] Pairon, M., Petitpierre, B., Campbell, M., Guisan, A., Broennimann, O., Baret, P. V., Jacquemart, A.-L., Besnard, G. (2010): Multiple introductions boosted genetic diversity in the invasive range of black cherry (Prunus serotina; Rosaceae). – Annals of Botany 105: 881-890.
[24] Qi, S.-S., Dai, Z.-C., Miao, S.-L., Zhai, D.-L., Si, C.-C., Huang, P., Wang, R.-P., Du, D.-L. (2014): Light limitation and litter of an invasive clonal plant, Wedelia trilobata, inhibit its seedling recruitment. – Annals of Botany 114: 425-433.
[25] Quinet, M., Descamps, C., Coster, Q., Lutts, S., Jacquemart, A.-L. (2015): Tolerance to water stress and shade in the invasive Impatiens parviflora. – International Journal of Plant Sciences 176: 848-858.
[26] Rahlao, S. J., Esler, K. J., Milton, S. J., Barnard, P. (2010): Nutrient addition and moisture promote the invasiveness of crimson fountain grass (Pennisetum setaceum). – Weed Science 58: 154-159.
[27] Richards, C. L., Bossdorf, O., Muth, N. Z., Gurevitch, J., Pigliucci, M. (2006): Jack of all trades, master of some? On the role of phenotypic plasticity in plant invasions. – Ecology Letters 9: 981-993.
[28] Saptiningsih, E., Dewi, K., Santosa, S., Purwestri, Y. A. (2019): Clonal integration of the invasive plant Wedelia trilobata (L.) Hitch in stress of flooding type combination. – International Journal of Plant Biology 10.
[29] Schweiger, O., Biesmeijer, J. C., Bommarco, R., Hickler, T., Hulme, P. E., Klotz, S., Kühn, I., Moora, M., Nielsen, A., Ohlemüller, R. (2010): Multiple stressors on biotic interactions: how climate change and alien species interact to affect pollination. – Biological Reviews 85: 777-795.
[30] Song, L., Chow, W. S., Sun, L., Li, C., Peng, C. (2010): Acclimation of photosystem II to high temperature in two Wedelia species from different geographical origins: implications for biological invasions upon global warming. – Journal of Experimental Botany 61: 4087-4096.
[31] Song, U. (2017): Temperature-dependent performance of competitive native and alien invasive plant species. – Acta Oecologica 84: 8-14.
[32] Song, U., Mun, S., Ho, C.-H., Lee, E. J. (2012): Responses of two invasive plants under various microclimate conditions in the Seoul metropolitan region. – Environmental Management 49: 1238-1246.
[33] Sun, J., Javed, Q., Azeem, A., Ullah, I., Saifullah, M., Kama, R., Du, D. (2019): Fluctuated water depth with high nutrient concentrations promote the invasiveness of Wedelia trilobata in Wetland. – Ecology and Evolution. https://doi.org/10.1002/ece3.5941.

http://www.aloki.hu ● ISSN 1589 1623 (Print) ● ISSN 1785 0037 (Online)
DOI: http://dx.doi.org/10.15666/aeer/1804_52475261

[34] Teitel, M., Atias, M., Barak, M. (2010): Gradients of temperature, humidity and CO2 along a fan-ventilated greenhouse. – Biosystems Engineering 106: 166-174.
[35] Ureña-Sánchez, R., Callejón-Ferre, Á. J., Pérez-Alonso, J., Carreño-Ortega, Á. (2012): Greenhouse tomato production with electricity generation by roof-mounted flexible solar panels. – Scientia Agricola 69: 233-239.
[36] Valiño, V., Rasheed, A., Tarquis, A. M., Perdigones, A. (2014): Effect of increasing temperatures on cooling systems. A case of study: European greenhouse sector. – Climatic Change 123: 175-187.
[37] Van Der Heijden, M. G., Bardgett, R. D., Van Straalen, N. M. (2008): The unseen majority: soil microbes as drivers of plant diversity and productivity in terrestrial ecosystems. – Ecology Letters 11: 296-310.
[38] Van Der Putten, W. H. (2010): Impacts of soil microbial communities on exotic plant invasions. – Trends in Ecology & Evolution 25: 512-519.
[39] Van Kleunen, M., Weber, E., Fischer, M. (2010): A meta-analysis of trait differences between invasive and non-invasive plant species. – Ecology Letters 13: 235-245.
[40] Van Kleunen, M., Schlaepfer, D. R., Glaettli, M., Fischer, M. (2011): Preadapted for invasiveness: do species traits or their plastic response to shading differ between invasive and non-invasive plant species in their native range? – Journal of Biogeography 38: 1294-1304.
[41] Van Kleunen, M., Dawson, W., Essl, F., Pergl, J., Winter, M., Weber, E., Kreft, H., Weigelt, P., Kartesz, J., Nishino, M. (2015): Global exchange and accumulation of non-native plants. – Nature 525: 100.
[42] Wang, R. L., Zeng, R. S., Peng, S. L., Chen, B. M., Liang, X. T., Xin, X. W. (2011): Elevated temperature may accelerate invasive expansion of the liana plant Ipomoea cairica. – Weed Research 51: 574-580.
[43] Weber, E., Sun, S.-G., Li, B. (2008): Invasive alien plants in China: diversity and ecological insights. – Biological Invasions 10: 1411-1429.
[44] Will, R. E., Wilson, S. M., Zou, C. B., Hennessey, T. C. (2013a): Increased vapor pressure deficit due to higher temperature leads to greater transpiration and faster mortality during drought for tree seedlings common to the forest–grassland ecotone. – New Phytologist 200: 366-374.
[45] Will, R. E., Wilson, S. M., Zou, C. B., Hennessey, T. C. (2013b): Increased vapor pressure deficit due to higher temperature leads to greater transpiration and faster mortality during drought for tree seedlings common to the forest-grassland ecotone. – New Phytologist 200: 366-374.
[46] Willits, D. (2003): Cooling fan-ventilated greenhouses: a modelling study. – Biosystems Engineering 84: 315-329.
[47] Xiaoming, D., Changji, Z. (2008): Test and measurement of solar visible radiation transmittance of greenhouse glazing. – Transactions of the Chinese Society of Agricultural Engineering 2008(8).
[48] Xu, Z. Z., Zhou, G. S. (2006): Combined effects of water stress and high temperature on photosynthesis, nitrogen metabolism and lipid peroxidation of a perennial grass Leymus chinensis. – Planta 224: 1080-1090.
[49] Zheng, Y.-L., Feng, Y.-L., Liu, W.-X., Liao, Z.-Y. (2009): Growth, biomass allocation, morphology, and photosynthesis of invasive Eupatorium adenophorum and its native congeners grown at four irradiances. – Plant Ecology 203: 263-271.

http://www.aloki.hu ● ISSN 1589 1623 (Print) ● ISSN 1785 0037 (Online)
DOI: http://dx.doi.org/10.15666/aeer/1804_52475261

THE EFFECTS OF ARSENIC AND SILICON ON THE OXIDATIVE AND NON-OXIDATIVE ENZYMES IN THE SEEDLINGS OF THREE DIFFERENT RICE (*ORYZA SATIVA* L.) VARIETIES IN DIFFERENT GROWTH PERIODS

BOORBOORI, M. R. – LIN, W. X.* – FANG, C. X. *

Fujian Provincial Key Laboratory of Agroecological Processing and Safety Monitoring, College of Life Sciences, Fujian Agriculture and Forestry University, Fuzhou 350002, P. R. China

**Corresponding authors*
e-mail: wenxiong181@163.com, changfangxingyx@163.com

(Received 27th Jan 2020; accepted 22nd May 2020)

Abstract. Silicon plays an important role in reducing the damage done to plans by environmental stress. Arsenic is an important stress factor, and silicon can reduce arsenic-induced stress on plants. In this study, we examined the affection of silicon on different enzymatic, and non-enzymatic antioxidants in the roots and shoots of different rice that exposed to arsenic at different time periods. The rice varieties studied during this experiment included LE-WT, LE-OE, and LE-R. This study showed addition of silicon increased APX, CAT, GSH, and GST in the first and second weeks after treatment, while it also significantly decreased MDA, POD, and SOD in roots and shoots of three varieties of rice. Addition of arsenic increased MDA content the all rice, but also decreased the rest of enzymes compared to control. Treatment of seedlings with As + Si significantly decreased APX, CAT, GSH, GST, POD, and SOD in rice shoots and roots compared to control in the first and second weeks after treatment. The results indicated the effect on enzymes activity in rice roots and shoots, which are attributable to arsenic, and silicon levels in the culture medium.
Keywords: *rice (Oryza sativa L.), wild type, transgenic, silicon, arsenic (III), antioxidants*

Introduction

Arsenic (As) is a carcinogenic metalloid (Dey et al., 2014), which accumulates in soil and water is a significant problem in the environment, which negatively affects human health. In addition, contaminated soil cause a negative result on economic growth and development because of its deep effects on growth of crops (Farquhar et al., 2002; Huq et al., 2006; Celik et al., 2008). Contamination of water by As needs specific attention due to high toxicity of it, even at down concentrations, due to its rapid transfer to the environment. High concentrations of arsenic reported in France, Bangladesh, Brazil, Vietnam, China, Nicaragua, United States, and many other countries (McClintock et al., 2012), making As contamination important public health issue around the world. Therefore, special attention should be paid or the arsenic accumulation indirectly consumed crops, such as rice. Indeed, arsenic accumulates in rice, and as rice is a staple diet in many countries, this increases the risk of arsenic-related diseases in humans living in those areas (Tchounwou and Centeno, 2004; Mondal, 2008; Su et al., 2010; Fontcuberta et al., 2011; Awasthi et al., 2017). Moreover, extreme accumulation of As in soil and irrigation water negatively affects both the growth and quality of rice which presses the importance of this issue further.

Silicon (Si) is a numerous metalloid in the soil, and that is useful for rice. Si absorbed in the form of silicic acid (H_4SiO_4) in high quantities via plants. Si content in rice reach up to 10% of its dry weight. Si fertilizers commonly used to increase rice growth and

http://www.aloki.hu ● ISSN 1589 1623 (Print) ● ISSN1785 0037 (Online)
DOI: http://dx.doi.org/10.15666/aeer/1804_52635278

production capacity. Si also makes plants resistant to biological and non-biological stresses (Ma et al., 2001, 2006; Feng et al., 2011; Singh et al., 2011; Guntzer et al., 2012; Pontigo et al., 2017). Some studies showed the application of Si can reduce the biological toxicity of As, as well as As accumulation decreased in rice, which grows in pots or hydroponics (Seyfferth and Fendorf, 2012; Tripathi et al., 2013; Fleck et al., 2013).

A number of different methods have been used to reduce soil As contamination, but the application of fertilizers is one of the simplest for this purpose. Si widely uses to make a better soil condition for plant growth. Besides its suitability for basic manure, the high potential of sodium silicate to reduce As content in rice has also been reported. Effects of Si on As-induced oxidative stress is a way to increase As tolerance in the early stages of growth. In present study, we investigate effect of Si on oxidative stress behaviour on three different rice seedlings exposed to As. To recognize possible mechanisms responsible for stress responses in rice, the impact of anti-oxidative enzymes in short (one week after As and Si treatment) and long-term (two weeks after As and Si treatment) were analyzed. This experiment evaluated the time-dependent responses in rice plants after adding Si and As in both periods. We hypothesized that the addition of Si in the early stages of growth would help the rice to compensate for the toxic effects of As via anti-oxidative enzyme protective mechanisms. The present study particularly addresses the questions: (1) if does the addition of Si in the early stages of rice increases the tolerance to As toxicity, and (2) whether does the combination of As and Si in different rice varieties affects the amount of anti-oxidative enzymes.

Material and method

Planting conditions

This study was done in the greenhouse of Fujin agriculture and forestry university in Fuzhou city of China. Rice seeds selected from two different varieties of rice, Lemont wild type (Le-WT), *Lsi1*-overexpression transgenic Lemont (LE-OE), and *Lsi1*-RNAi transgenic Lemont rice (LE-R). Before planting, the seeds sterilized by 1% H_2O_2 for 15 minutes, rinsed in deionized water for 48 hours, and then kept in a Petri dish in an incubator for 4 days, at 28°C. After germination, suitable seedlings selected and transferred to the greenhouse for cultivation under hydroponic conditions. The pots (2.5 L) filled with a modified version of the nutrient solution described by Yoshida et al. (1971). The nutrient solution included: $(NH_4)2SO_4$ (48.2 mg L^{-1}), $Ca(NO_3)_2 \cdot 4H_2O$ (86.43 mg L^{-1}), K_2SO_4 (14.9 mg L^{-1}), $Na_2SiO_4 \cdot 9H_2O$ (200 mg L^{-1}), KNO_3 (18.5 mg L^{-1}), $FeSO_4 \cdot 7H_2O$ (45.7 mg L^{-1}), H_3BO_3 (1.43 mg L^{-1}), EDTA (48.44 mg L^{-1}), $CuSO_4 \cdot 5H_2O$ (0.04 mg L^{-1}), KH_2PO_4 (24.8 mg L^{-1}), $MnCl_2 \cdot 4H_2O$ (0.905 mg L^{-1}), $Na_2MoO_4 \cdot 2H_2O$ (0.045 mg L^{-1}), $ZnSO_4 \cdot 7H_2O$ (0.11 mg L^{-1}), and $MgSO_4 \cdot 7H_2O$ (135.06 mg L^{-1}). The nutrient solution pH set to 5.8 by using HCl or NaOH rice seedlings planted, when they had three leaves, and the nutrient solution changed once a week. In each pot, we planted 4 seedlings. The plants exposed to two levels of Si ($Na_2SiO_4 \cdot 9H_2O$) (0 and 0.70 mM), and two levels of As (III) ($NaAsO_2$) (0 and 30 μM), thus, four different treatments formed, control (CK, I), 0.70 mM Si + no As (II), 30 μM As + no Si (III), 30 μM As + 0.70 mM Si (IV). For each treatment we had three pots.

Random plant samples were selected one and two weeks after treatment. For both times of sampling, we harvested two seedlings from each pots. The roots and shoots of plants washed separately by distilled water, and remaining residue in the root zone washed by 0.5 mM $CaCl_2$ solution for 30 minutes before being washed with distilled

http://www.aloki.hu ● ISSN 1589 1623 (Print) ● ISSN1785 0037 (Online)
DOI: http://dx.doi.org/10.15666/aeer/1804_52635278

water again. All samples were instantly transferred to a freezer at -10°C, and stored until the enzyme activity determined.

The amount of sodium added to the solution compensated for adding $Na_2SiO_4 \cdot 9H_2O$, the equivalent of NaCl added to the solution.

Superoxide dismutase (SOD) activity measurement

SOD activity specified with some modification of the nitro blue tetrazolium method (NBT) (Dias et al., 2011; Esposito et al., 2015). Approximately, 0.5 g of samples homogenized by potassium phosphate buffer (50 mM, pH 7.8) including 1% polyvinylpolypyrrolidone, and centrifuged for 20 minutes, at 15000 × g speed, and 4°C. The supernatants used to find SOD activity (Sajedi et al., 2011). Every 3 ml of the reaction mixture included 0.2 ml of NBT (750 µM), 130 mM Met (0.2 ml), 2.2 ml of PBS (50 mM pH 7.8), 20 µM EDTA-Na_2 (0.1 ml), 100 µM riboflavin (0.2 ml), and 0.1 ml of supernatant. The enzyme activity expressed as the amount of extract requirement to control the decrease of NBT by 50%.

Catalase (CAT) activity measurement

Azevedo et al. (2007) reported, CAT activity specified by the absorbance amount of 240 nm because of H_2O_2 consumption. Reaction mixture included H_2O_2 (0.3 ml, 0.1 M), distilled water (1 ml), 50 mM PBS (1.5 ml, pH 7.8) and sample (0.2 ml).

Ascorbate peroxidase (APX) activity measurement

The supernatant was used to measure APX activity. It made by using 1 g sample homogeneous solution, 0.1 M sodium phosphate buffer (5 ml, pH 7) including 10% PVP. Then it centrifuged for 20 minutes at 12000 × g speed, and 4°C (Nakano and Asada, 1981). Reaction mixture included 0.1 mM EDTA (0.3 ml), 0.1 M phosphate buffer (0.7 ml, pH 7), 0.5 mM ascorbic acid (0.3 ml), 0.1 mM H_2O_2 (0.3 ml), and the supernatant (0.4 ml). The reaction mixture absorbance variation determined at 290 nm after 5 minutes. APX activity expressed by consuming extinction coefficient 2.8 mM^{-1} cm^{-1}, then showed decomposed ascorbic acid protein mg^{-1} min^{-1}.

Peroxidase (POD) activity measurement

POD activity characterized by some changes according to Bai et al. (2006) method. Almost 0.5 g of samples of the stored shoots and roots homogenized. We used potassium phosphate buffer (50 mM, pH 7.8) for homogenized. That included 1% polyvinylpolypyrrolidone, and centrifuged for 20 minutes, at 15000 × g speed, and 4°C. The supernatants used to find POD activity. Reaction mixture included 0.3% H_2O_2 (1.0 ml), 0.9 ml Guaiaco l0.2%, 0.05 M PBS (1 ml, pH 7.8), and supernatants (0.1 ml), and absorbance determined at 470 nm in a minute period.

Malondialdehyde (MDA) content measurement

The MDA content estimated from a reaction with Thiobarbituric Acid (Heath and Packer, 1968). We subjected sample (0.5 g) with potassium phosphate buffer (1.5 mM, PBS, pH 7.8) contains 1% polyvinylpolypyrrolidone. We centrifuged it for 20 minutes, at 15,000 × g speed, and 4°C (Sajedi et al., 2011). The supernatant (2 ml) mixed by 0.5% TBA (2 ml), and 20% TCA (2 ml). The mixture made hot with a temperature around 95°C for about 30 minutes, after that rapidly made it cold. Non-specific adsorption measured

http://www.aloki.hu ● ISSN 1589 1623 (Print) ● ISSN1785 0037 (Online)
DOI: http://dx.doi.org/10.15666/aeer/1804_52635278

at 600 nm, and reaction mixture minus absorbance from sample solution at 532 nm. To find MDA content, contraction coefficient (155 mM^{-1} cm^{-1}) used.

Glutathione reduced (GSH) content measurement

GSH content measured by Sedlak and Lindsay (1968) method. The plant sample (1 g) was prepared in a homogeneous solution; 5% (w / v) SSA (5 ml) including EDTA (10 mM), then it centrifuged for 20 minutes, at 10,000 × g speed, and 4°C. The supernatant (10 µl) added to reaction mixture (140 µl). The reaction mixture included potassium phosphate buffer (100 mM, pH 7.5), 6 ml^{-1} GR, EDTA (1 mM), 5% SSA (10 µl), and 10 mM DTNB, and then put in Incubator for 3 hours at a dark room. The reaction started via increasing 2 mM NADPH (50 µl). Absorbance occurred at 412 nm with a spacing of 1 minute and 5 minutes. We found GSH content by a standard curve, then demonstrated as $nmol.g^{-1}$ (FW).

Glutathione-S-transferase (GST) activity measurement

The roots and shoots (1 g) homogenized by 100 mM Tris-HCl (5 ml, pH 7.5) including 14 mM β-mercaptoethanol, 7.5% PVP (w/v), and EDTA (2 mM) (Ando et al., 1988). The collected supernatants centrifuged for 15 minutes, and 15,000 × g speed, and 4°C. Measurement did in 100 mM potassium phosphate buffer (2 ml, pH 6.5), which included 1 mM CDNB (250 ml), 5 mM GSH, and extracted enzyme (0.5 ml). The absorbance changes determined at 340 nm with a spacing of 1 minute and 5 minutes. The GST activity computed by consuming an extinction coefficient (9.6 mM^{-1} cm^{-1}), then showed as $U.min^{-1}.mg^{-1}$ protein.

Statistical analyses

This experiment arranged in the completely randomized factorial design, and three replications. All the findings analyzed by one-way ANOVAs pursued by LSD test ($p \leq 0.05$), and SPSS software (19.0).

Results and Discussion

Effects of Si and As on SOD activity of rice roots and shoots

In our study, we tried to understand the result of Si in reducing As stress by measuring physiological responses of rice to different treatments, at different periods. Our results show that SOD activity in roots and shoots of different rice decreased As exposure compared to CK ($p \leq 0.05$). The highest reduction observed in LE-R line root in the first week, but the highest decrease observed in the roots of LE-WT after two weeks (*Fig. 1*). In addition, Si treatment showed a significant difference in SOD activity of rice roots and shoots compared to CK ($p \leq 0.05$). The greatest decrease in the first and second weeks after exposure to Si treatment observed in the roots of LE-R. In the present study, reduction in SOD activity observed in the seedlings, which treated by As + Si in shoots and roots in both exposure periods. The highest decrease was in the roots of LE-R in the first and second weeks.

Abiotic stress same as metalloids and heavy metals increases the amount of reactive oxygen species (ROS) in plants, and stimulates oxidative stress. ROS, by containing $O2^{-}$, OH and H_2O_2 attack important metabolic functions via destroying vital biomolecules

http://www.aloki.hu ● ISSN 1589 1623 (Print) ● ISSN1785 0037 (Online)
DOI: http://dx.doi.org/10.15666/aeer/1804_52635278

same as proteins, lipids, and nucleic acids. Plants have several defense mechanisms against ROS. One of those defense pathways in plants is through different enzymes same as SOD, POD, and CAT. These enzymes detoxify ROS, and destroy free radicals, that are responsible for cellular signaling. The effects of SOD, POD, and CAT highly majored to produce one of them usually turns into another enzyme-substrate, resulting in the production of non-toxic substances. First defensive line of organisms versus the toxicity of ROS is SOD, and it catalyzes the disproportionate reaction of $O2^{-}$ to hydrogen peroxide, oxygen, and works as a significant defense mechanism versus ROS. Thus, SOD considered a suitable index for assessing toxicity in nature.

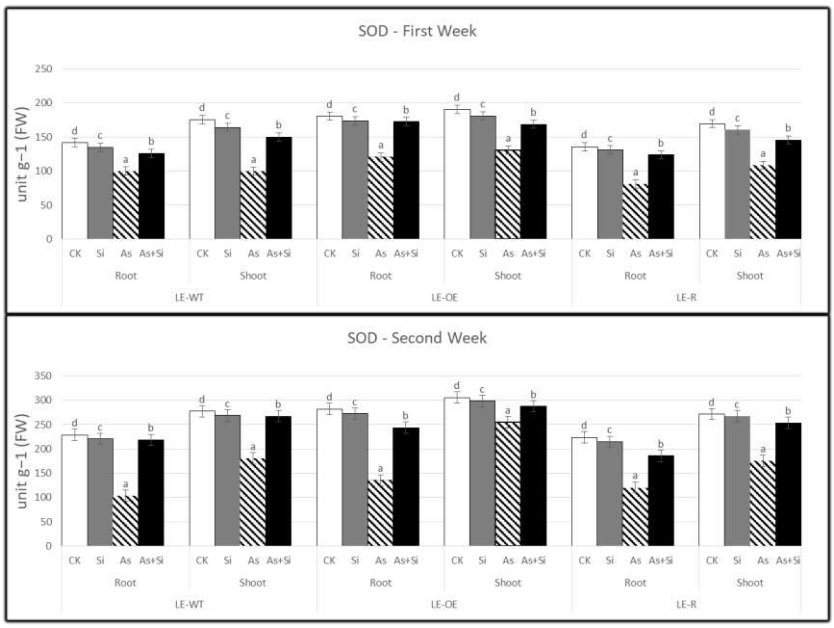

Figure 1. *SOD activity in shoots and roots of LE-WT, LE-OE line and LE-R first and second weeks after adding different treatments*

In theory, as ROS increases, plants increase SOD activities to remove ROS. In this study, SOD activity was significantly reduced with increasing ROS, which indicates rice seedlings tolerated oxidative stress caused by As toxicity. Including giving less area for As accumulation in rice, or oxidative stress that damages SOD, thereby diminishing SOD activity, or stresses that cause intense loss to rice cells, leading to restraint of more SOD amount (Shen et al., 2010; Farooq et al., 2013; Wu et al., 2017). In our study, As + Si treatment significantly grew SOD activity compared to the single As treatment, which indicates Si can activate SOD to eliminate additional free radicals, and can effectively increase defense capacity versus oxidative stress caused via As toxicity in rice. Some studies showed SOD activities will also increase under other stress in rice (Song et al., 2009; Tripathi et al., 2013; Ju et al., 2017). Moreover, we also observed the reduction in SOD activity in roots under As stress was greater than in the shoots, indicating that the reduction in SOD activity related to rice tissue characteristics, too (Zeng et al., 2011).

Effects of Si and As on CAT activity of rice roots and shoots

Treatment containing As decreased CAT activity compared to CK ($p \leq 0.05$). The highest reduction observed both in the first week and second weeks in the roots of LE-WT

http://www.aloki.hu ● ISSN 1589 1623 (Print) ● ISSN1785 0037 (Online)
DOI: http://dx.doi.org/10.15666/aeer/1804_52635278

(63.98% and 44.79% decrease compared to CK, respectively) (*Fig. 2*). The present study showed Si treatment in different rice in the first week and second weeks increased CAT activity. The highest increase in CAT activity observed in LE-R shoots compared to CK ($p \leq 0.05$). The increase in CAT activity in the first week and second weeks was respectively 13.84% and 12.3% compared to CK. By adding As + Si treatment, CAT activity significantly reduced in roots and shoots of different rice compared to CK ($p \leq 0.05$). The highest reduction saw in LE-WT roots, which was 54.62% lower in the first week than in the control, and in the second week decreased by 38.62% compared to control.

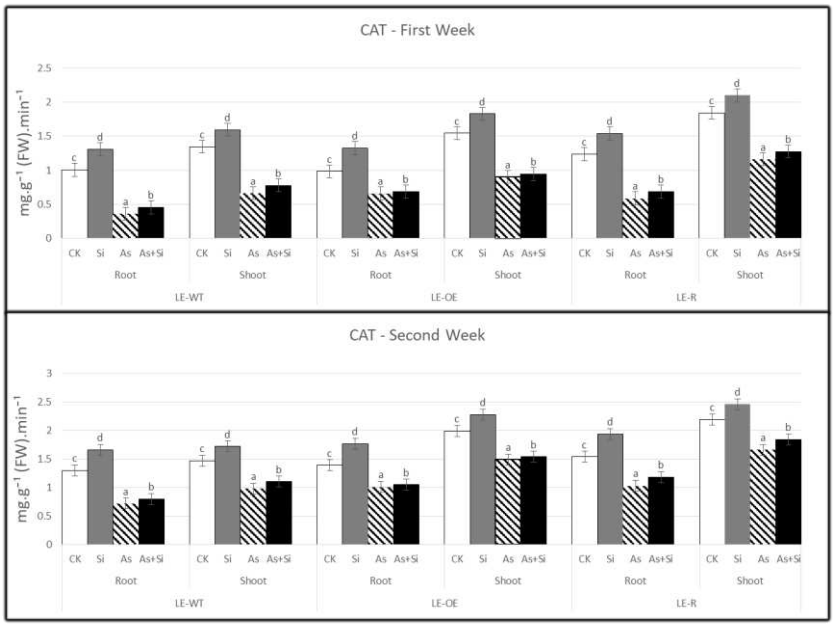

Figure 2. *CAT activity in shoots and roots of LE-WT, LE-OE line and LE-R first and second weeks after adding different treatments*

There are some non-enzymatic and enzymatic ROS elimination systems in plants. These systems act as a vital role in the membrane defense systems structure and function, and in maintaining the redox state of cells (Chen et al., 2018). SOD naturally converts $O2^{-}$ to harmful H_2O_2 and O_2, and although H_2O_2 is still harmful, CAT can instantly transform that to water (Liu et al., 2015). CAT is likely to be an important enzyme in facilitating ROS modification in rice, making that essential section of ROS detoxification system, and a key in defense mechanism versus ROS. Thus, CAT activity is ever subject to increased oxidative stress (Wang et al., 2015). As treatments significantly decreased CAT activity, which can be because of 1) ROS levels are higher than those CAT is able to control 2) CAT may have a less role in detoxifying As in rice. In the latter case this maybe because As inhibits rice growth, or stronger oxidative stress damages CAT. Similar results related in rice and other plants (Shi et al., 2005; Song et al., 2009; Zeng et al., 2011; Farooq et al., 2013; Tripathi et al., 2015; Rahman et al., 2017). Treatments with both As and Si increased CAT activity compared to As alone treatment, probably due to the CAT synthesis increasing effect of Si. Higher CAT activities increased via Si addition may further eliminate ROS as well as H_2O_2, and defense rice organs against As membrane oxidative damage. Other studies have shown similar results in different plants under

http://www.aloki.hu ● ISSN 1589 1623 (Print) ● ISSN1785 0037 (Online)
DOI: http://dx.doi.org/10.15666/aeer/1804_52635278

different stress, and this indicates different effects on different varieties, plant growth stages, and even plant tissue types (Shi et al., 2005, 2010, 2014; Song et al., 2009, 2011; Zeng et al., 2011; Farooq et al., 2013; Habibi and Hajiboland, 2013; Zhang et al., 2013; Vaculíková et al., 2014; Tripathi et al., 2015; Kang et al., 2016; Ju et al., 2017; Rahman et al., 2017; Wu et al., 2017; Shekari et al., 2017).

Effects of Si and As on APX activity of rice roots and shoots

Compared to CK, APX activity significantly ($p \leq 0.05$) decreased in both roots and shoots of all three rice verities, when they were exposed to As, with the highest decrease observed for both the first and second weeks in the roots of LE-WT (*Fig. 3*). In addition, Si treatment showed a significant ($p \leq 0.05$) grow in APX activity both in the shoots and roots of rice plants compared to control. The highest increase was observed in the LE-OE line shoots in the first week and second weeks after treatment with Si, which respectively represents 8.85% and 14.40% growth compared to CK. APX activity was decreased in plants treated with As + Si compared to CK ($p \leq 0.05$), and the largest reduction saw in the roots of LE-WT. One week after treatment this decrease was 28.02%, and was 22.80% two weeks after treatment. When we compared APX activity in shoots, the highest reduction in APX activity observed in LE-WT shoots. APX activity decreased 2.94%, one week after treatment, and 5.57%, two weeks after treatment, indicating different effects of the same treatment on different tissues. APX is important in the ascorbate-glutathione cycle, and can break down H_2O_2 (Mittler et al., 2004; Liang et al., 2005; Mhamdi et al., 2010; Zeng et al., 2011; Foyer and Noctor, 2011). Since Si has a positive effect on APX activity in rice, which are under stress, treating plants with Si, can effectively increase the defense capacity versus oxidative stress, either caused by arsenic or other stressors. The function of APX to eliminate H_2O_2 partially overlaps with that of CAT in non-photosynthetic tissues, and research has shown, that APX's role in eliminating H_2O_2 in rice can be replaced or offset by CAT (Zhao et al., 2018).

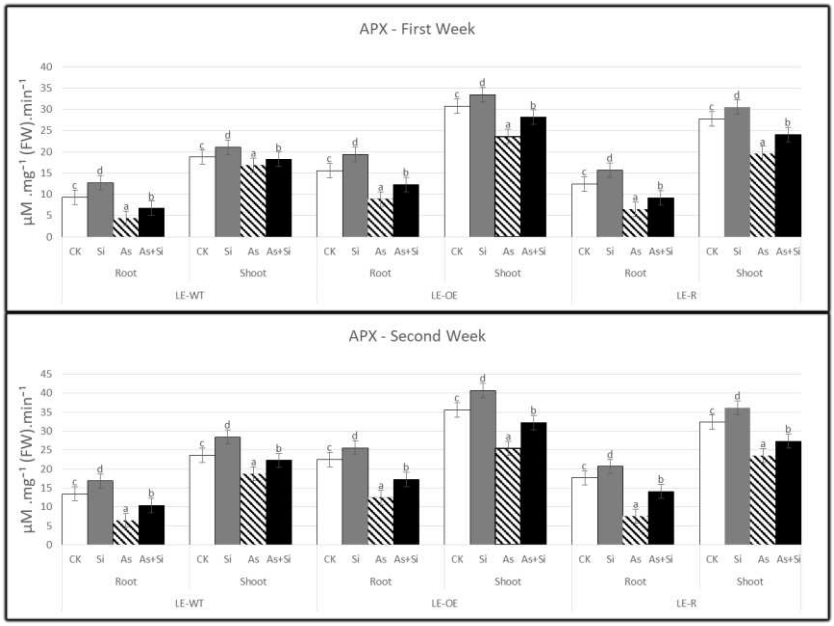

Figure 3. *APX activity in shoots and roots of LE-WT, LE-OE line and LE-R first and second weeks after adding different treatments*

http://www.aloki.hu ● ISSN 1589 1623 (Print) ● ISSN1785 0037 (Online)
DOI: http://dx.doi.org/10.15666/aeer/1804_52635278

Effects of Si and As on POD activity of rice roots and shoots

Treatment of seedlings by Si significantly ($p \leq 0.05$) decreased POD activity in both the first and second weeks after treatment with the lowest POD activity being observed in LE-WT shoots (*Fig. 4*). POD activity decreased by 9.99% in the first week after treatment but only reduced 5.95% in the second week. One and two weeks after As treatment, POD activity was significantly different in the roots and shoots of rice, when it was compared to CK ($p \leq 0.05$). The lowest POD activity observed in the shoots of LE-WT in the first week (47.51% decreased compared to control), and in the roots of LE-WT in the second week (39.16% reduceed compared to control). However, POD activity in rice treated with As + Si was higher than in rice treated only with As. This indicates that the addition of Si positively affects POD activities and effectively enhances the defense capacity versus oxidative stress-induced via As exposure in rice. Same results found in rice treated by heavy metals, acidic rain, and other stresses, and also was seen in different plants like barley ،Brassica Chinensis *L.* ،cotton, xerophyte Zygophyllum xanthoxylum ،peas ،peanut, pakchoi ،banana, dill ،pistachio (Song et al., 2009; Shi et al., 2010; Zeng et al., 2011; Li et al., 2012; Zhang et al., 2013; Bharwana et al., 2013; Farooq et al., 2013; Habibi and Hajiboland, 2013; Kang et al., 2016; Rahman et al., 2017; Shekari et al., 2017; Ju et al., 2017). Furthermore, the efficacy of Si addition can depends on plant varieties and tissues (Song et al., 2009; Shi et al., 2010; Zeng et al., 2011; Zhang et al., 2013; Kang et al., 2016). At extreme As doses CAT activity may not be sufficient in protecting the plants against the large amounts of released H_2O_2 and, the POD enzyme can be involved in the detoxification process. POD can take part in lignin biosynthesis to create physiological obstacles versus heavy metal stress, and it also can detoxify H_2O_2 using different substrates (same as phenols) as an electron donor. Thus, POD activity changes considered as the most trustworthy oxidative stress indicators, the decrease in POD may be because of severe oxidative stress damage (Farooq et al., 2013).

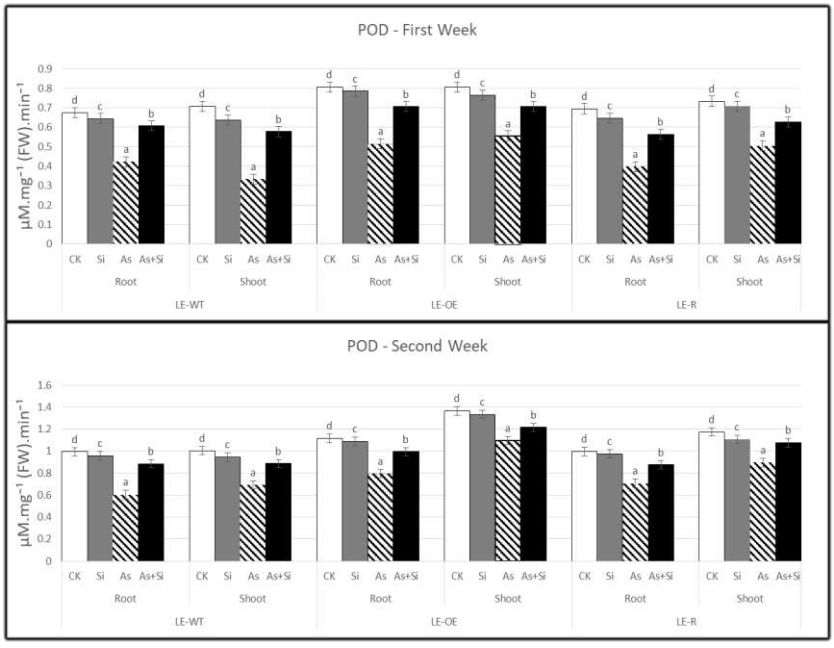

Figure 4. *POD activity in shoots and roots of LE-WT, LE-OE line and LE-R first and second weeks after adding different treatments*

http://www.aloki.hu ● ISSN 1589 1623 (Print) ● ISSN1785 0037 (Online)
DOI: http://dx.doi.org/10.15666/aeer/1804_52635278

Effects of Si and As on MDA content of rice roots and shoots

MDA levels increased after adding As to the culture solution compared to CK ($p \leq 0.05$); the highest MDA content in the first week was observed in shoots of LE-R line (*Fig. 5*). However, the highest MDA content in the second week was observed in the LE-WT shoots. This increase in MDA content compared to CK respectively was 186% and 98%. In most of the plants, free radicals inevitably made in non-infected plants and plants, which evolved elimination systems (non-enzymatic antioxidants, and antioxidant enzymes) to control ROS levels and prevent excessive accumulation of ROS. This balance can be broken by environmental stresses. The excessive presence of heavy metals in plants causes accumulation of free radicals. Accumulation of As stimulates the increase of ROS, the effect on the activity of chlorophyll synthesis and biomass, membrane permeability, enzymes, and photosynthetic reactions. ROS dou to As directly attack to the hydrogen atom on the methylene group alongside an unsaturated carbon atom, thus, peroxidation, as the chain of degenerate fatty acids, polyunsaturated fatty acids, induce membranes, and eventually produce lipid peroxides. MDA is an important product of the degradation of unsaturated fatty acids by hydroperoxides, is generally regarded as an indirect index of oxidative stress. in present experiment, MDA content grew in whole rice treated with As compared to CK, and it shows As can cause superoxide radicals. Increasing the MDA content proves that rice was under oxidative stress conditions. In addition, the increase in MDA in a rice cultivar indicates that the cultivar is weak against As stress. This can be related to rice tissue, rice genotype, stages and conditions of plant growth, and the concentration and duration of As exposure. Studies showed similar results for MDA content in different plants under different stresses (Liu et al., 2009; Song et al., 2011; Vaculíková et al., 2014; Tripathi et al., 2015; Begum et al., 2016; Wu et al., 2017).

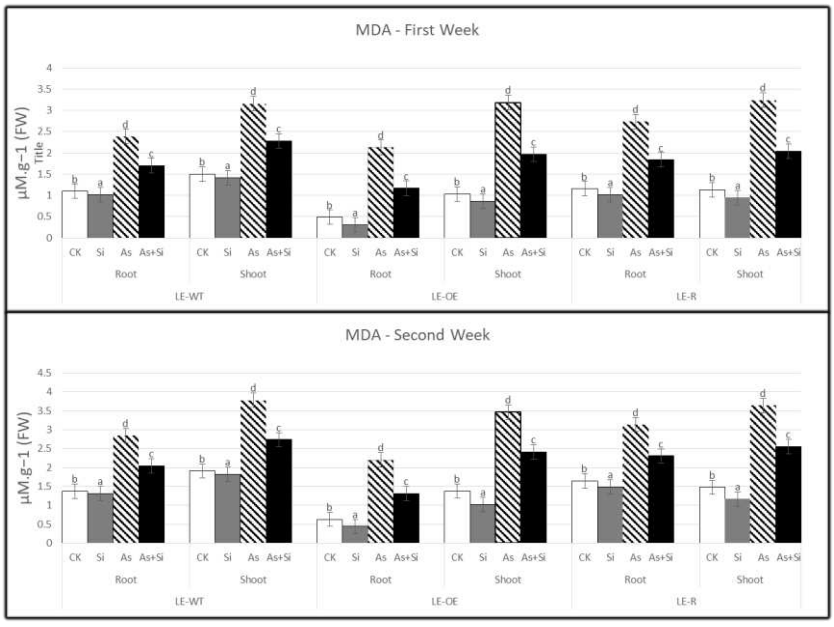

Figure 5. *MDA content in shoots and roots of LE-WT, LE-OE line and LE-R first and second weeks after adding different treatments*

Treated with Si rice seedlings significantly reduced MDA content, with the lowest MDA content, observed in the first and second weeks being in roots of Lsi1-OE line

http://www.aloki.hu ● ISSN 1589 1623 (Print) ● ISSN1785 0037 (Online)
DOI: http://dx.doi.org/10.15666/aeer/1804_52635278

(37.61% and 30.11% decrease, compared to CK ($p \leq 0.05$), respectively). MDA content in rice treated with As + Si grew compared to CK ($p \leq 0.05$), and the highest MDA content, both in the first and second weeks, was observed in LE-WT shoots (52.11% and 43.39% increase, respectively). In the present study, MDA contents in roots and shoots of different rice varieties treated by As + Si decreased compared to As exposure, indicating Si, indeed, is important in ROS metabolism of rice subjected to stress, and mitigates effect of As toxicity. The reason maybe that 1) Si reduces superoxide accumulation, and H_2O_2 radicals, as a result reducing LPO in As-stressed rice, and improving the antioxidant defense system, or 2) Si minimizes the penetrate plasma cell membranes by increasing the lipid strength and preventing harm to the structures and function of rice cell membranes during stress (Shi et al., 2005, 2014; Liu et al., 2009; Song et al., 2009, 2011; Li et al., 2012; Bharwana et al., 2013; Farooq et al., 2013; Tripathi et al., 2013, 2015; Cao et al., 2015; Vaculíková et al., 2014; Wu et al., 2017).

Effects of Si and As on GSH content of rice roots and shoots

Si treatment significantly ($p \leq 0.05$) increased GSH content in roots and shoots of different rice compared to control (*Fig. 6*). The highest GSH content observed in the LE-WT shoots both in the first and second weeks (12.81% and 8.68% increase compared to CK, respectively). GSH content significantly decreased in all rice cultivars, which treated with As. When compared to CK, the highest decrease of GSH content was in LE-WT roots, both in the first and second weeks (80.78% and 66.16% decrease, respectively). At the time of application of As + Si treatment, GSH content increased compared to the application of As alone, but it decreased in all rice cultivars in both the first and second weeks. The highest decrease observed in the roots of LE-WT in both first and second weeks, with respectively, 68.67% and 52.84% decreases compared to CK ($p \leq 0.05$).

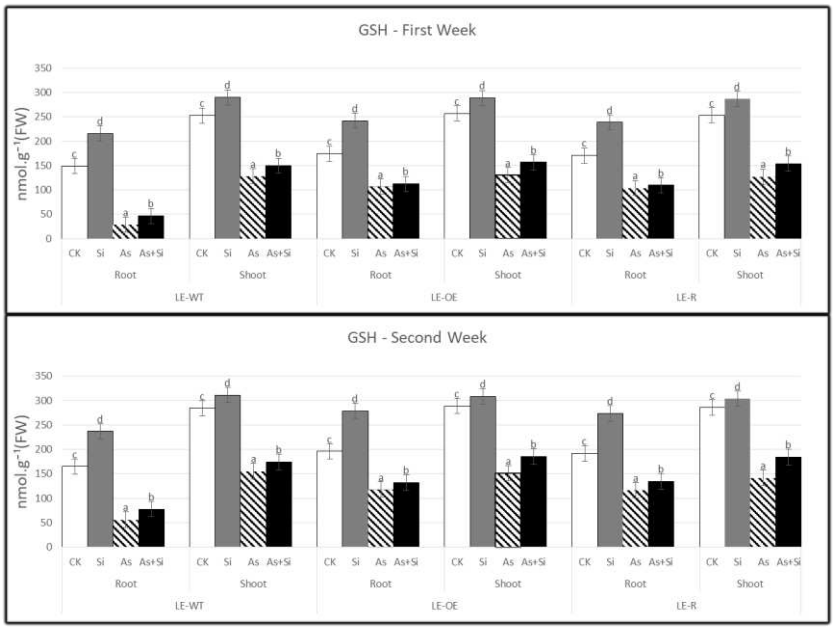

Figure 6. *GSH content in shoots and roots of LE-WT, LE-OE line and LE-R first and second weeks after adding different treatments*

http://www.aloki.hu ● ISSN 1589 1623 (Print) ● ISSN1785 0037 (Online)
DOI: http://dx.doi.org/10.15666/aeer/1804_52635278

GSH is an important non-protein triols sources in plant cells. High levels of GSH effect on reducing the toxicity of heavy metals via direct cleaning of ROS or making a complex with the toxic metals by GST activity. Meanwhile, GSH is involved in the biological transmission of As. GSH is used as an enzymatic or non-enzymatic depressant to decrease As (V) to As (III), therefore, GSH is a good indicator for assessing the toxicity of As in the environment. Binding of inorganic GSH to As is a good mechanism by which may control the toxicity of As. GSH uses GST to synthesize toxic molecules. GST is a present enzyme, which stimulates with toxic metals, in detoxification by combining GSH to toxic molecules. GSH nucleophilic attack on the electrophilic center of toxic compounds, and targets them for ATP-dependent transport into the vacuole, and it protects plant cells against their detrimental effects. In this experiment, the presence of As clearly decreased GSH content in three rice. This decrease in GSH levels may be due to 1) shortening of NAD(P)H as a substrate in possible reaction, through the reduction of GSSG to GSH by GR; 2) its reduction phytoclutins via acute or chronic exposure to stress; 3) Interference with the reproduction of AsA from its oxidized form in AsA-GSH cycle (Shi et al., 2005; Ellis et al., 2006; Hasanuzzaman et al., 2017). In our study adding Si increased GSH content in different rice roots and shoots, indicating an increase in GSH activity by Si application. According to reports, Si is important in the activity enzymes of ROS inhibitors in chloroplasts, in ASA-GSH pathway. When rice is in a stressful environment, Si will be involved in ROS metabolism. Similar results observed in rice under heavy metals stress, and other stress. According to similar studies, Si has a different effect on GSH content in different plant tissues as well as different rice (Shi et al., 2005; Song et al., 2009; Liu et al., 2009; Li et al., 2012; Wang et al., 2015; Cao et al., 2015; Rahman et al., 2017).

Effects of Si and As on GST activity of rice roots and shoots

In our study, GST activity levels significantly decreased by As treatments compared to CK ($p \leq 0.05$). The highest reduction in GST activity compared to control observed in LE-WT shoots in both first and second weeks (32.26% and 31.07% decline, compared to CK, respectively) (*Fig. 7*). When As + Si treatment added, GST activity increased compared to the As application alone. However, the GST activity under As + Si treatment showed a significant reduction compared to CK ($p \leq 0.05$). The highest reduction observed in LE-WT shoots, with 6.39% and 4.20%, respectively decreased compared to CK, in the first and second weeks. Treating rice seedlings with Si ($p \leq 0.05$) significantly increased GST activity compared to control in both the first and second weeks after treatment. The highest GST activity observed in LE-OE line roots in the first week, and the highest GST activity in the second weeks observed in LE-OE line shoots, showing a 23.22% and 20.31% increase compared to control, respectively.

GSTs are concentrated in apoplast, cytosol, chloroplast, mitochondria, and nucleus (Gechev et al., 2006). GST activity has important function in the ascorbate-glutathione cycle relate to ascorbate, and its regulatory enzymes. GSTs do detoxification in plants via combining toxic molecules with GSH (Ellis et al., 2006). Increased GST activity in rice seedlings treated by As + Si compared to treated with As alone indicates Si prevents oxidative damage induced by As, probably by reducing GSSG to GSH (Tripathi et al., 2013). Same results reported for the effects of GST activity against various stresses on the tissues of rice, pea, maize, wheat and Phragmites (Mauch and Dudler, 1993; Marrs and Walbot, 1997; Dixit et al., 2001; Iannelli et al., 2002; Adamis et al., 2004; Zhang et al., 2013).

http://www.aloki.hu ● ISSN 1589 1623 (Print) ● ISSN1785 0037 (Online)
DOI: http://dx.doi.org/10.15666/aeer/1804_52635278

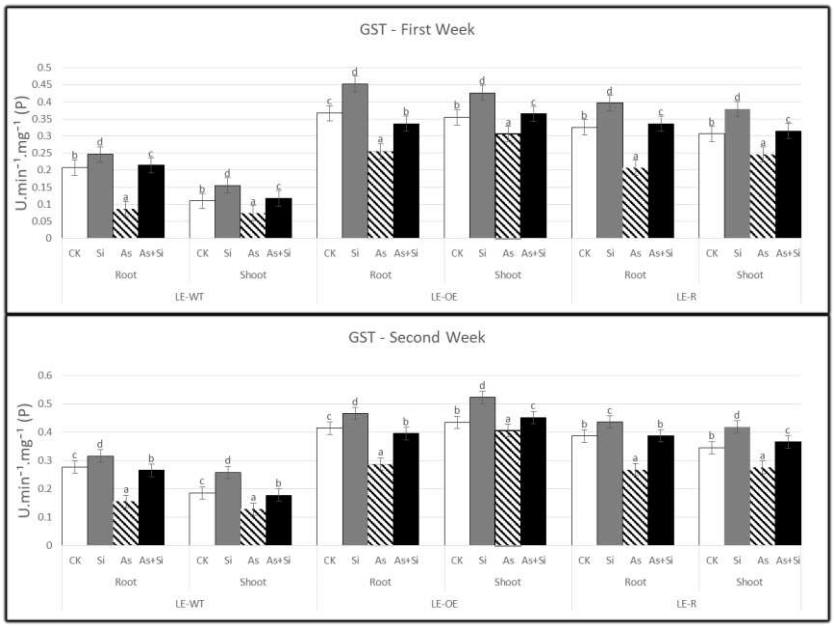

Figure 7. *GST content in shoots and roots of LE-WT, LE-OE line and LE-R first and second weeks after adding different treatments*

Conclusions

By decreasing the antioxidant capacity, exposure to As in rice plants can be harmful to the plant. The use of Si with As-toxicated plants partially reduces the harmful effects of As alone by modulating the antioxidant activities. Si application can also reduce stress induced by As by reducing MDA content in rice seedlings. Findings of the present experiment partly indicate Si is capable to enhance significantly the antioxidant defense capacity in rice seedlings, thus, it increases the resistance of different plant organs to As stress over time.

We also found that different varieties of rice have different resistance to As stress, and the addition of Si in different varieties has a different effect on the plant's resistance to As stress. Therefore, choosing As tolerant varieties, along with the use of Si in fertilizers can substantially reduce the damage caused in rice, and compensate for the economic loss. Also, suggest doing RNA-seq and Transgenic experiments, to know more details about the mechanisms and the genes relate to As and Si in these three rice varieties.

Acknowledgements. We thank Dr. Gabor Pozsgai for his thoughtful comments and useful suggestions to make better the quality of this paper. There were not declared any conflicts of interest. This work was supported by the Outstanding Youth Scientific Fund of Fujian Agriculture and Forestry University (Grant No. xjq201805).

REFERENCES

[1] Adamis, P. D. B., Gomes, D. S., Pinto, M. L. C. C., Panek, A. D., Eleutherio, E. C. A. (2004): The role of glutathione transferases in cadmium stress. – Toxicology letters 154: 81-88.

http://www.aloki.hu ● ISSN 1589 1623 (Print) ● ISSN1785 0037 (Online)
DOI: http://dx.doi.org/10.15666/aeer/1804_52635278

[2] Ando, K., Honma, M., Chiba, S., Tahara, S., Mizutani, J. (1988): Glutathione transferase from Mucor javanicus. – Agricultural biological chemistry 52: 135-139.
[3] Awasthi, S., Chauhan, R., Srivastava, S., Tripathi, R. D. (2017): The journey of arsenic from soil to grain in rice. – Frontiers in plant science 8: 1007.
[4] Azevedo, M.-M., Carvalho, A., Pascoal, C., Rodrigues, F., Cássio, F. (2007): Responses of antioxidant defenses to Cu and Zn stress in two aquatic fungi. – Science of the total environment 377: 233-243.
[5] Bai, L.-P., Sui, F.-G., Ge, T.-D., Sun, Z.-H., Lu, Y.-Y., Zhou, G.-S. (2006): Effect of soil drought stress on leaf water status, membrane permeability and enzymatic antioxidant system of maize. – Pedosphere 16(3): 326-332.
[6] Begum, M. C., Islam, M. S., Islam, M., Amin, R., Parvez, M. S., Kabir, A. H. (2016): Biochemical and molecular responses underlying differential arsenic tolerance in rice (*Oryza sativa* L.). – Plant Physiology Biochemistry 104: 266-277.
[7] Bharwana, S., Ali, S., Farooq, M., Iqbal, N., Abbas, F., Ahmad, M. (2013): Alleviation of lead toxicity by silicon is related to elevated photosynthesis, antioxidant enzymes suppressed lead uptake and oxidative stress in cotton. – J Bioremed. Biodeg. 4.
[8] Cao, B.-L., Ma, Q., Zhao, Q., Wang, L., Xu, K. (2015): Effects of silicon on absorbed light allocation, antioxidant enzymes and ultrastructure of chloroplasts in tomato leaves under simulated drought stress. – Scientia horticulturae 194: 53-62.
[9] Celik, I., Gallicchio, L., Boyd, K., Lam, T. K., Matanoski, G., Tao, X., Shiels, M., Hammond, E., Chen, L., Robinson, K. A. (2008): Arsenic in drinking water and lung cancer: a systematic review. – Environmental research 108: 48-55.
[10] Chen, R., Lai, U. H., Zhu, L., Singh, A., Ahmed, M., Forsyth, N. R. (2018): Reactive oxygen species formation in the brain at different oxygen levels: the role of hypoxia inducible factors. – Frontiers in cell developmental biology 6: 132.
[11] Dey, T. K., Banerjee, P., Bakshi, M., Kar, A. (2014): Groundwater arsenic contamination in West Bengal: current scenario, effects and probable ways of mitigation. – International Letters of Natural Sciences 13: 45-58.
[12] Dias, A. P., Dafré, M., Rinaldi, M. C., Domingos, M. (2011): How the redox state of tobacco 'Bel-W3'is modified in response to ozone and other environmental factors in a sub-tropical area? – Environmental pollution 159: 458-465.
[13] Dixit, V., Pandey, V., Shyam, R. (2001): Differential antioxidative responses to cadmium in roots and leaves of pea (Pisum sativum L. cv. Azad). – Journal of Experimental Botany 52: 1101-1109.
[14] Ellis, D. R., Gumaelius, L., Indriolo, E., Pickering, I. J., Banks, J. A., Salt, D. E. (2006): A novel arsenate reductase from the arsenic hyperaccumulating fern Pteris vittata. – Plant physiology 141: 1544-1554.
[15] Esposito, J. B. N., Esposito, B. P., Azevedo, R. A., Cruz, L. S., Da Silva, L. C., De Souza, S. R. (2015): Protective effect of Mn (III)–desferrioxamine B upon oxidative stress caused by ozone and acid rain in the Brazilian soybean cultivar Glycine max "Sambaiba". – Environmental Science and Pollution Research 22: 5315-5324.
[16] Farooq, M. A., Ali, S., Hameed, A., Ishaque, W., Mahmood, K., Iqbal, Z. (2013): Alleviation of cadmium toxicity by silicon is related to elevated photosynthesis, antioxidant enzymes; suppressed cadmium uptake and oxidative stress in cotton. – Ecotoxicology environmental safety 96: 242-249.
[17] Farquhar, G. D., Buckley, T. N., Miller, J. M. (2002): Optimal stomatal control in relation to leaf area and nitrogen content. – Silva Fennica 36: 625-637.
[18] Feng, J., Yamaji, N., Mitani-Ueno, N. (2011): Transport of silicon from roots to panicles in plants. – Proceedings of the Japan Academy, Series B 87: 377-385.
[19] Fleck, A. T., Mattusch, J., Schenk, M. K. (2013): Silicon decreases the arsenic level in rice grain by limiting arsenite transport. – Journal of Plant Nutrition 176: 785-794.

http://www.aloki.hu ● ISSN 1589 1623 (Print) ● ISSN1785 0037 (Online)
DOI: http://dx.doi.org/10.15666/aeer/1804_52635278

[20] Fontcuberta, M., Calderon, J., Villalbí, J. R., Centrich, F., Portana, S., Espelt, A., Duran, J. (2011): Total and inorganic arsenic in marketed food and associated health risks for the Catalan (Spain) population. – Journal of agricultural food chemistry 59: 10013-10022.
[21] Foyer, C. H., Noctor, G. (2011): Ascorbate and glutathione: the heart of the redox hub. – Plant physiology 155: 2-18.
[22] Gechev, T. S., Van Breusegem, F., Stone, J. M., Denev, I., Laloi, C. (2006): Reactive oxygen species as signals that modulate plant stress responses and programmed cell death. – Bioessays 28: 1091-1101.
[23] Guntzer, F., Keller, C., Meunier, J.-D. (2012): Benefits of plant silicon for crops: a review. – Agronomy for Sustainable Development 32: 201-213.
[24] Habibi, G., Hajiboland, R. (2013): Alleviation of drought stress by silicon supplementation in pistachio (*Pistacia vera* L.) plants. – Folia Horticulturae 25: 21-29.
[25] Hasanuzzaman, M., Nahar, K., Anee, T. I., Fujita, M. (2017): Glutathione in plants: biosynthesis and physiological role in environmental stress tolerance. – Physiology Molecular Biology of Plants 23: 249-268.
[26] Heath, R. L., Packer, L. (1968): Photooxidation in isolated chloroplast: I. Kinetics stoichiometry of fatty acid peroxidation. – Archives of Biochemistry and Biophysics 125(1): 189-198.
[27] Huq, S. M. I., Joardar, J. C., Parvin, S., Correll, R., Naidu, R. (2006): Arsenic contamination in food-chain: transfer of arsenic into food materials through groundwater irrigation. – J Health Popul Nutr. 24(3): 305-316.
[28] Iannelli, M. A., Pietrini, R., Fiore, L., Petrilli, L., Massacci, A. (2002): Antioxidant response to cadmium in Phragmites anstrals plants. – Plant Physiol. Biochem. 40: 977-982.
[29] Ju, S., Yin, N., Wang, L., Zhang, C., Wang, Y. (2017): Effects of silicon on *Oryza sativa* L. seedling roots under simulated acid rain stress. – PloS one 12.
[30] Kang, J., Zhao, W., Zhu, X. (2016): Silicon improves photosynthesis and strengthens enzyme activities in the C3 succulent xerophyte Zygophyllum xanthoxylum under drought stress. – Journal of Plant Physiology 199: 76-86.
[31] Li, L., Zheng, C., Fu, Y., Wu, D., Yang, X., Shen, H. (2012): Silicate-mediated alleviation of Pb toxicity in banana grown in Pb-contaminated soil. – Biological trace element research 145: 101-108.
[32] Liang, Y., Wong, J., Wei, L. (2005): Silicon-mediated enhancement of cadmium tolerance in maize (*Zea mays* L.) grown in cadmium contaminated soil. – Chemosphere 58: 475-483.
[33] Liu, J.-J., Lin, S.-H., Xu, P.-L., Wang, X.-J., Bai, J.-G. (2009): Effects of exogenous silicon on the activities of antioxidant enzymes and lipid peroxidation in chilling-stressed cucumber leaves. – Agricultural Sciences in China 8(9): 1075-1086.
[34] Liu, T., Zhong, S., Liao, X., Chen, J., He, T., Lai, S., Jia, Y. (2015): A meta-analysis of oxidative stress markers in depression. – PloS one 10.
[35] Ma, J. F., Miyake, Y., Takahashi, E. (2001): Silicon as a beneficial element for crop plants. – Studies in plant Science 8: 17-39.
[36] Ma, J. F., Tamai, K., Yamaji, N., Mitani, N., Konishi, S., Katsuhara, M., Ishiguro, M., Murata, Y., Yano, M. (2006): A silicon transporter in rice. – Nature 440: 688-691.
[37] Marrs, K. A., Walbot, V. (1997): Expression and RNA splicing of the maize glutathione S-transferase Bronze2 gene is regulated by cadmium and other stresses. – Plant physiology 113: 93-102.
[38] Mauch, F., Dudler, R. (1993): Differential induction of distinct glutathione-S-transferases of wheat by xenobiotics and by pathogen attack. – Plant Physiology 102: 1193-1201.
[39] McClintock, T. R., Chen, Y., Bundschuh, J., Oliver, J. T., Navoni, J., Olmos, V., Lepori, E. V., Ahsan, H. (2012): Arsenic exposure in Latin America: Biomarkers, risk assessments and related health effects. – Science of the Total Environment 429: 76-91.
[40] Mhamdi, A., Hager, J., Chaouch, S., Queval, G., Han, Y., Taconnat, L., Saindrenan, P., Gouia, H., Issakidis-Bourguet, E., Renou, J.-P. (2010): Arabidopsis glutathione reductase1 plays a crucial role in leaf responses to intracellular hydrogen peroxide and in ensuring

http://www.aloki.hu ● ISSN 1589 1623 (Print) ● ISSN1785 0037 (Online)
DOI: http://dx.doi.org/10.15666/aeer/1804_52635278

appropriate gene expression through both salicylic acid and jasmonic acid signaling pathways. – Plant Physiol. 153(3): 1144-1160.
[41] Mittler, R., Vanderauwera, S., Gollery, M., Van Breusegem, F. (2004): Questions and future challenges. – Trends in Plant Science 10: 490-498.
[42] Mondal, D. (2008): Rice is a major exposure route for arsenic in Chakdaha block, Nadia district, West Bengal, India: A probabilistic risk assessment. – Applied Geochemistry 23: 2987-2998.
[43] Nakano, Y., Asada, K. (1981): Hydrogen peroxide is scavenged by ascorbate-specific peroxidase in spinach chloroplasts. – Plant cell physiology 22: 867-880.
[44] Pontigo, S., Godoy, K., Jiménez, H., Gutiérrez-Moraga, A., de la Luz Mora, M., Cartes, P. (2017): Silicon-mediated alleviation of aluminum toxicity by modulation of Al/Si uptake and antioxidant performance in ryegrass plants. – Frontiers in Plant Science 25(8): 642.
[45] Rahman, M. F., Ghosal, A., Alam, M. F., Kabir, A. H. (2017): Remediation of cadmium toxicity in field peas (*Pisum sativum* L.) through exogenous silicon. – Ecotoxicology Environmental Safety 135: 165-172.
[46] Sajedi, N. A., Ardakani, M. R., Madani, H., Naderi, A., Miransari, M. (2011): The effects of selenium and other micronutrients on the antioxidant activities and yield of corn (*Zea mays* L.) under drought stress. – Physiology Molecular Biology of Plants 17: 215-222.
[47] Sedlak, J., Lindsay, R. H. (1968): Estimation of total, protein-bound, and nonprotein sulfhydryl groups in tissue with Ellman's reagent. – Analytical biochemistry 25: 192-205.
[48] Seyfferth, A. L., Fendorf, S. (2012): Silicate mineral impacts on the uptake and storage of arsenic and plant nutrients in rice (*Oryza sativa* L.). – Environmental science technology 46: 13176-13183.
[49] Shekari, F., Abbasi, A., Mustafavi, S. H. (2017): Effect of silicon and selenium on enzymatic changes and productivity of dill in saline condition. – Journal of the Saudi Society of Agricultural Sciences 16: 367-374.
[50] Shen, Q., Zhang, B., Xu, R., Wang, Y., Ding, X., Li, P. (2010): Antioxidant activity in vitro of the selenium-contained protein from the Se-enriched Bifidobacterium animalis 01. – Anaerobe 16(4): 380-386.
[51] Shi, Q., Bao, Z., Zhu, Z., He, Y., Qian, Q., Yu, J. (2005): Silicon-mediated alleviation of Mn toxicity in *Cucumis sativus* in relation to activities of superoxide dismutase and ascorbate peroxidase. – Phytochemistry 66: 1551-1559.
[52] Shi, G., Cai, Q., Liu, C., Wu, L. (2010): Silicon alleviates cadmium toxicity in peanut plants in relation to cadmium distribution and stimulation of antioxidative enzymes. – Plant Growth Regulation 61: 45-52.
[53] Shi, Y., Zhang, Y., Yao, H., Wu, J., Sun, H., Gong, H. (2014): Silicon improves seed germination and alleviates oxidative stress of bud seedlings in tomato under water deficit stress. – Plant Physiology Biochemistry 78: 27-36.
[54] Singh, V. P., Tripathi, D. K., Kumar, D., Chauhan, D. K. (2011): Influence of exogenous silicon addition on aluminium tolerance in rice seedlings. – Biological trace element research 144: 1260-1274.
[55] Song, A., Li, Z., Zhang, J., Xue, G., Fan, F., Liang, Y. (2009): Silicon-enhanced resistance to cadmium toxicity in Brassica chinensis L. is attributed to Si-suppressed cadmium uptake and transport and Si-enhanced antioxidant defense capacity. – Journal of Hazardous Materials 172: 74-83.
[56] Song, A., Li, P., Li, Z., Fan, F., Nikolic, M., Liang, Y. (2011): The alleviation of zinc toxicity by silicon is related to zinc transport and antioxidative reactions in rice. – Plant Soil 344: 319-333.
[57] Su, Y.-H., McGrath, S. P., Zhao, F.-J. (2010): Rice is more efficient in arsenite uptake and translocation than wheat and barley. – Plant Soil 328: 27-34.
[58] Tchounwou, P. B., Centeno, J. A. (2004): Arsenic toxicity, mutagenesis, and carcinogenesis–a health risk assessment and management approach. – Molecular cellular biochemistry 255: 47-55.

http://www.aloki.hu ● ISSN 1589 1623 (Print) ● ISSN1785 0037 (Online)
DOI: http://dx.doi.org/10.15666/aeer/1804_52635278

[59] Tripathi, P., Tripathi, R. D., Singh, R. P., Dwivedi, S., Goutam, D., Shri, M., Trivedi, P. K., Chakrabarty, D. (2013): Silicon mediates arsenic tolerance in rice (*Oryza sativa* L.) through lowering of arsenic uptake and improved antioxidant defence system. – Ecological engineering 52: 96-103.
[60] Tripathi, D. K., Singh, V. P., Prasad, S. M., Chauhan, D. K., Dubey, N. K. (2015): Silicon nanoparticles (SiNp) alleviate chromium (VI) phytotoxicity in *Pisum sativum* (L.) seedlings. – Plant Physiology Biochemistry 96: 189-198.
[61] Vaculíková, M., Vaculík, M., Šimková, L., Fialová, I., Kochanová, Z., Sedláková, B., Luxová, M. (2014): Influence of silicon on maize roots exposed to antimony–Growth and antioxidative response. – Plant physiology biochemistry 83: 279-284.
[62] Wang, S., Wang, F., Gao, S. (2015): Foliar application with nano-silicon alleviates Cd toxicity in rice seedlings. – Environmental Science Pollution Research 22: 2837-2845.
[63] Wu, Z., Liu, S., Zhao, J., Wang, F., Du, Y., Zou, S., Li, H., Wen, D., Huang, Y. (2017): Comparative responses to silicon and selenium in relation to antioxidant enzyme system and the glutathione-ascorbate cycle in flowering Chinese cabbage (*Brassica campestris* L. ssp. chinensis var. utilis) under cadmium stress. – Environmental Experimental Botany 133: 1-11.
[64] Yoshida, S., Forno, D. A., Cock, J. H. (1971): Laboratory manual for physiological studies of rice. – Los Banos, Philippines.
[65] Zeng, F.-R., Zhao, F.-S., Qiu, B.-Y., Ouyang, Y.-N., Wu, F.-B., Zhang, G.-P. (2011): Alleviation of chromium toxicity by silicon addition in rice plants. – Agricultural Sciences in China 10: 1188-1196.
[66] Zhang, Y., Liu, J., Zhou, Y., Gong, T., Wang, J., Ge, Y. (2013): Enhanced phytoremediation of mixed heavy metal (mercury)–organic pollutants (trichloroethylene) with transgenic alfalfa co-expressing glutathione S-transferase and human P450 2E1. – Journal of hazardous materials 260: 1100-1107.
[67] Zhao, Q., Zhou, L., Liu, J., Du, X., Huang, F., Pan, G., Cheng, F. (2018): Relationship of ROS accumulation and superoxide dismutase isozymes in developing anther with floret fertility of rice under heat stress. – Plant physiology biochemistry 122: 90-101.

http://www.aloki.hu ● ISSN 1589 1623 (Print) ● ISSN1785 0037 (Online)
DOI: http://dx.doi.org/10.15666/aeer/1804_52635278

METABOLIC ENGINEERING OF MEP PATHWAY FOR OVERPRODUCTION OF LYCOPENE IN *SACCHAROMYCES CEREVISIAE* USING PESC-LEU AND PTEF1/ZEO VECTORS

ALSHEHRI, W. A.[1] – GADALLA, N. O.[2,3] –EDRIS, S.[4,5,6] – ATEF, A.[4] – HEMEG, H.[7] – AL-QUWAIE, D. A. H.[8] – ALSUBHI, N. H.[8] – KABLI, S. A.[4] – BAHIELDIN, A.[4,6*]

[1]*Department of Biology, College of Science, University of Jeddah, Jeddah, Saudi Arabia*

[2]*Department of Arid Land Agriculture, Faculty of Meteorology, Environment and Arid Land Agriculture, King Abdulaziz University, Jeddah, Saudi Arabia*

[3]*Genetics and Cytology Department, Genetic Engineering and Biotechnology Division, National Research Center, Dokki, Egypt*

[4]*Department of Biological Sciences, Faculty of Science, King Abdulaziz University, Jeddah, Saudi Arabia*

[5]*Princess Al Jawhara Albrahim Centre of Excellence in Research of Hereditary Disorders (PACER-HD), King Abdulaziz University, Jeddah, Saudi Arabia*

[6]*Department of Genetics, Faculty of Agriculture, Ain Shams University, Cairo, Egypt*

[7]*Department of Medical Laboratory Technology, Faculty of Applied Sciences, Tiba University, Al-Madina Al-Monawara, Saudi Arabia*

[8]*Department of Biological Sciences, Rabigh College of Science and Arts, King Abdulaziz University (KAU), Rabigh, Saudi Arabia*

**Corresponding author*
e-mail: abmahmed@kau.edu.sa; phone: +966-506-329-922

(Received 29th Jan 2020; accepted 2nd Jul 2020)

Abstract. Recent studies indicated that overexpression of *dxs* and *idi* genes in bacteria transformed with *crtEBI* genes dramatically improved the production of lycopene. The aim of the present study was the assessment of *crtEBI*-transformed *S. cerevisiae* overexpressing the bacterial synthetic *dxs* and yeast *idi* genes for lycopene production. The two genes were driven by galactose-induced promoters namely *GAL1 and GAL10*, respectively, of the pESC-LEU yeast vector of which gene cassettes were inserted in pTEF1/Zeo vector. The synthetic *dxs* gene was constructed in accordance with the preferred codon usage in *S. cerevisiae* with no change in the resulting amino acid sequences. The RT-PCR analysis indicated that the two genes were efficiently transcribed in *crtEBI*-transformed *S. cerevisiae* cells. The highest production of lycopene (6755 µg lycopene/g dry cell weight) was reached for yeast cells transformed with the two genes, which is higher than the previously reported lycopene levels in yeast. The level of Acetyl-Coenzyme A (Acetyl-CoA) was negatively related to that of lycopene in transformed *S. cerevisiae* cells, suggesting that lycopene and Acetyl-CoA biosyntheses compete for the use of pyruvate.
Keywords: *GAL1 promoter, GAL10 promoter, RT-PCR, zeocin resistance, Acetyl-CoA, pESC-LEU yeast vector, pTEF1/Zeo vector*

Abbreviations: IPP, isopentenyl pyrophosphate; DMAPP, dimethylallyl diphosphate; DXP, 1-deoxy-D-xylulose 5-phosphate; DXS, 1-deoxy-D-xylulose 5-phosphate synthase; GAP, glyceraldehyde-3-phosphate; IPDP, isopentenyl diphosphate; FPP, farnesyl diphosphate; DCW, dry cell weight; TCA, tricarboxylic acid; MDH, malate dehydrogenase; ANOVA, analysis of variance; LSD, least significant differences

http://www.aloki.hu ● ISSN 1589 1623 (Print) ● ISSN 1785 0037 (Online)
DOI: http://dx.doi.org/10.15666/aeer/1804_52795292

Introduction

Lycopene is an important naturally occurring intermediate metabolite directly converted into β-carotene. Lycopene received major interest among carotenoids as it may be beneficial in diseases such as cancer, coronary heart disease and many other chronic conditions including osteoporosis. It is also used as an antioxidant to reduce cellular or tissue damage (Sevgili and Erkman, 2019). Metabolic engineering was successfully employed in improving industrial strains (Lee et al., 2005; Price et al., 2004) through the overproduction of a desired product via expression/overexpression of certain metabolic genes (Herrgård et al., 2006; Kirschner, 2005). Isoprenoids, basically formed from two precursors, isopentenyl pyrophosphate (IPP) and its isomer dimethylallyl diphosphate (DMAPP), have many applications in biotechnology and industry (Lange and Croteau, 1999; Römer et al., 2000). Biosynthesis of these two precursors utilizes the 2-C-methyl-D-erythritol 4-phosphate (MEP) pathway in eukaryotes and eubacteria (Eisenreich et al., 2004). This pathway supports the synthesis of the major pigments, including lycopene, hormones and mono- and di-terpenes (Eisenreich et al., 2004) by initiation of a reaction catalyzed by the enzyme 1-deoxy-D-xylulose 5-phosphate (DXP) synthase (DXS) using pyruvate and glyceraldehyde-3-phosphate (GAP) as substrates (*Fig. 1a*) to yield DXP (Lange et al., 1998; Lois et al., 1998). The latter is converted into a mixture of IPP and DMAPP compounds through six consecutive enzymatic reactions (Lange et al., 2000; Rodrıguez-Concepción and Boronat, 2002). The fluctuation in ratio of these two compounds is based on the expression of a gene encoding isopentenyl diphosphate (IPDP) isomerase (the *idi* gene), a key enzyme that has been shown to exert a positive effect on lycopene production (Lee and Schmidt-Dannert, 2002). Recent studies indicated that overexpression of *dxs* and *idi* genes in *E. coli* transformed with *crtEBI* genes resulted in the production of lycopene at 8.57 mg/g dry cell weight (DCW), which is ~ 6-fold higher than the control *crtEBI-E. coli* strain (1.48 mg/g DCW) (Choi et al., 2010). On the other hand, the overexpression of the *mdh* gene, which encodes malate dehydrogenase (MDH) of the tricarboxylic acid (TCA) cycle, in conjunction with *idi* and *dxs* genes, resulted in a slightly higher level of lycopene (9.98 mg/g DCW) (Choi et al., 2010). TCA cycle has no direct connection with MEP pathway for lycopene production, except that NADH generated by MDH action is required for the synthesis of isopentenyl diphosphate (IPP) or dimethylallyl diphosphate (DMAPP) via the MEP pathway. *In cilico* analysis for improving lycopene production in *E. coli* (Choi et al., 2010) indicated that the flux from pyruvate to Acetyl-CoA (*Fig. 1b*) is decreased and flux from pyruvate to DXP is increased due to overexpression of *dxs* and *idi* genes. This indicates that the MEP pathway (for lycopene biosynthesis) and Acetyl-CoA biosynthesis (precursor for the TCA cycle, glyoxylate cycle and histone acetylation) might compete for the use of pyruvate in *E. coli* (*Fig. 1*).

More recently, Sun et al. (2014) has utilized a completely different approach to accumulate higher levels of lycopene (6.5 mg/g DCW) in engineered *E. coli*. This approach relies on the deletion of genes (e.g., *crtY* and *crtX*) functioning downstream the final step of lycopene biosynthesis. The authors also used ribosome binding site libraries to modulate expression of *dxs*, *idi* and the *crt* genes and optimal strain produced as high as 50.6 mg/g DCW. More recently, the overexpression of *OLE1* gene, encoding stearoyl-CoA 9-desaturase, in combination with the *STB5* gene, encoding a transcription factor involved in NADPH production, in the yeast with increasing membrane flexibility and NAPDH production resulted in the production of up to

http://www.aloki.hu ● ISSN 1589 1623 (Print) ● ISSN 1785 0037 (Online)
DOI: http://dx.doi.org/10.15666/aeer/1804_52795292

41.8 mg/g DCW of lycopene (Hong et al., 2019). These two genes can be further used in addition to the genes under study in order to maximize the production of lycopene in yeast (*S. cerevisiae*).

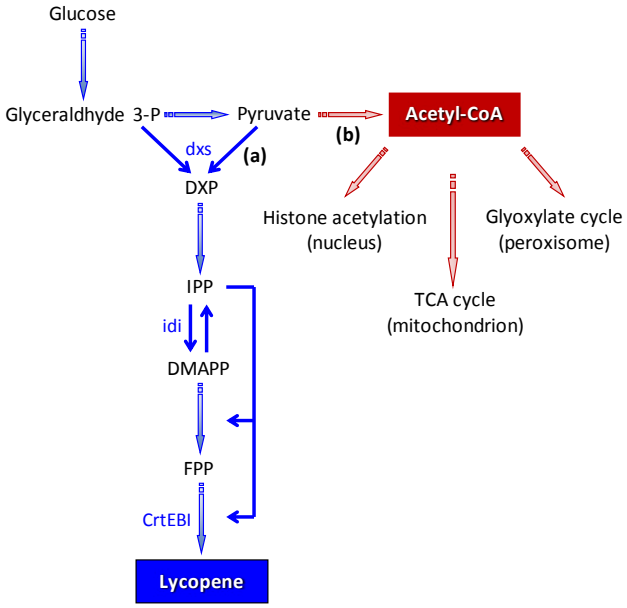

Figure 1. *Engineered MEP pathway (in blue) for lycopene biosynthesis (a) by inducing the conversion of pyruvate to DXP due to the action of the bacterial dxs and overexpressing the yeast idi gene in crtEBI-transformed S. cerevisiae cells. Acetyl-CoA biosynthesis (b) and downstream metabolic processes (in red) in the nucleus (histone acetylation), mitochondrion (TCA cycle) and peroxisome (glyoxylate cycle) are favored in nature due to the conversion of pyruvate to Acetyl-CoA. Abbreviations: DXP, 1-deoxy-D-xylulose-5-phosphate; IPP, isopentenyl pyrophosphate; DMAPP, dimethylallyl diphosphate; FPP, farnesyl diphosphate*

The aim of the present study was the assessment of *crtEBI*-transformed *S. cerevisiae* line overexpressing the bacterial *dxs* and the yeast *idi* genes for lycopene production. The sequence of the bacterial *dxs* gene was optimized according to the preferred codon usage of *S. cerevisiae*. The two genes were efficiently expressed under the control of *GAL1 and GAL10* promoters, respectively, contained within the pESC-LEU vector (cat. no. 217452, Agilent Technologies, Santa Clara, CA 95051, USA).

Materials and methods

Strain and its growth conditions

Master plates and cell cultures of *Saccharomyces cerevisiae* DSY-5 strain (Dualsystems Biotech AG, Schlieren, Switzerland) were prepared as indicated earlier (Bahieldin et al., 2014).

Construction of yeast expression vector with the synthetic bacterial dxs and the native yeast idi genes

The synthetic *dxs* gene (1863 bp) was constructed by Bioneer corporation (Daejeon, Republic of Korea; NCBI submission ID no. 1719788) and inserted in the pKS1

http://www.aloki.hu ● ISSN 1589 1623 (Print) ● ISSN 1785 0037 (Online)
DOI: http://dx.doi.org/10.15666/aeer/1804_52795292

(6.65 bp) shuttle vector (cat. no. P03305, KickStart™ Dualsystems Biotech AG, Schlieren, Switzerland). The gene was synthesized in reference to the corresponding native gene from *E. coli*, strain K-12 (acc. no. HG738867, region: 340298-342160 bp) and the codon preference of *S. cerevisiae*. The replacement of nucleotides between the native and synthetic gene resulted in the reduction of GC contents from ~56% to ~46%. Added-on restriction sites of *Bam*HI and *Kpn*I were inserted at the 5` and 3` ends of the synthesized gene, respectively, to facilitate further ligation of the gene to the *Bam*HI/*Kpn*I-digested pESC-LEU vector (7.8 kb) downstream of the *GAL1* promoter (*Fig. 2*). The yeast *idi* full-length open reading frame (acc. no. NM_001183931, 867 bp) was amplified from *S. cerevisiae* DSY-5 strain by PCR using primers (*idi*_F: 5` attagaattc-ATGACTGCCGACAACAATAGTA 3` and *idi*_R: 5` attagagctcTTATAGCATTCTATGAATTTGCCTGTC 3`) with *Eco*RI and *Sac*I restriction sites added-on at the 5` and 3` ends, respectively. Primers were designed using the Universal ProbeLibrary Assay Design Center (Roche, www.roche-applied-science.com, 2012). PCR was performed in a 20-µl reaction mixture and conditions consisted of denaturation at 94 °C for 4 min (first cycle), then denaturation for 15 s, annealing at 48 °C for 30 s, and extension at 72 °C for 1 min (40 cycles). Amplicons were run on a 1.2% agarose gel stained with ethidium bromide and visualized using the Gel Doc XR (Bio-Rad Laboratories; Hercules, CA, USA). *Eco*RI/*Sac*I-digested PCR products were ligated to *Eco*RI/*Sac*I-digested pESC-LEU vector downstream of the *GAL10* promoter (*Fig. 2*). Generated P-*GAL1*/*dxs*/T-*CYC* and P-*GAL1*/*dxs*/T-*CYC*::P-*GAL10*/*idi*/T-*ADH1* cassettes were digested with *Apa*I/*Not*I and ligated to *Apa*I/*Not*I-digested pTEF1/Zeo vector (3.56 kb, cat. no. V503-20, Life Technologies Inc., Grand Island, NY, USA) to generate pTEF1/Zeo/*dxs* and pTEF1/Zeo/*dxs*/*idi* yeast expression vectors.

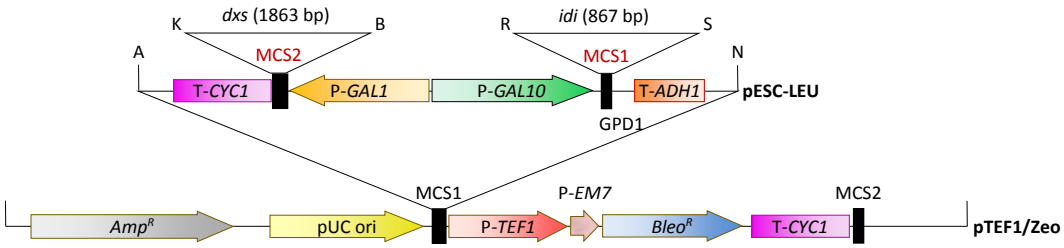

Figure 2. *Schematic representation of P-GAL1/dxs/T-CYC::P-GAL10/idi/T-ADH1 gene cassette (~ 4.23 kb) of yeast expression pESC-LEU vector construct after genes were inserted between R/S and B/K sites of MCS1 and MCS2 (red), respectively. Gene cassette was inserted between N/A sites of MCS1 (black) of yeast expression pTEF1/Zeo (~ 3.56 kb) vector construct. Abbreviations: T-CYC1 and T-ADH1: yeast CYC1 and ADH1 terminators, P-GAL1 and P-GAL10: yeast GAL1 and GAL10 divergent promoters, MCS1 and MCS2: multiple cloning sites 1 and 2, Amp^R: ampicillin prokaryotic resistance gene, pUC ori: origin of replication, P-TEF1 and P-EM7: TEF and EM7 eukaryotic and prokaryotic promoters, respectively, Bleo^R: Zeocin prokaryotic and eukaryotic resistance gene. Abbreviations of restriction enzymes: A: ApaI, K: KpnI, B: BamHI, R: EcoRI, S: SacI, N: NotI*

Transformation of S. cerevisiae with a vector harboring the idi/dxs genes

The *S. cerevisiae* cell Line 2 with pKS1 harboring synthetic *crtEBI* genes (Bahieldin et al., 2014) was transformed with pTEF1/Zeo, pTEF1/Zeo/*dxs* or pTEF1/Zeo/*dxs*/*idi* yeast expression vector following protocol in the manufacturer's manual (KickStart™

http://www.aloki.hu ● ISSN 1589 1623 (Print) ● ISSN 1785 0037 (Online)
DOI: http://dx.doi.org/10.15666/aeer/1804_52795292

Dualsystem protein expression kit protocol, Schlieren, Switzerland). The *S. cerevisiae* cell Line 2 as well as those harboring the pTEF1/Zeo derivatives were grown under optimized growth conditions (35 °C with YPD medium adjusted at pH 6.0 and supplemented with 0.5% glucose and 80 μg/ml G418) as described earlier (Bahieldin et al., 2014). Yeast cell Line 2 harboring pTEF1/Zeo derivatives were originally selected on 100 μg/ml zeocin (cat. no. R250-01, Life Technologies Inc., Grand Island, NY, USA) with no galactose added to the medium. Transformed cells with robust growth on YPD plates were recovered and stored as glycerol stocks at -80 °C. Then, the growth behavior in terms of biomass production of the original *S. cerevisiae* DSY-5 transformed cell Line 2 was tested in the presence of zeocin (0, 50, 100 and 200 μg/ml) in the medium to detect the concentration completely inhibiting cell growth. This concentration of zeocin was used in evaluating yeast cells transformed with different pTEF1/Zeo derivatives. Biomass was determined under optimized conditions (cells were grown in YPD medium with 0.5% glucose at pH 6.0/35 °C, see Bahieldin et al., 2014), in the presence of 200 μg/ml zeocin) in five randomly selected *S. cerevisiae* Line 2 transformed with pTEF1/Zeo, pTEF1/Zeo/*dxs* or pTEF1/Zeo/*dxs*/*idi* expression vector. Turbidity was monitored by spectrophotometer at 546 nm across growth time (0, 5, 25, 45 and 65 h), in three replicates. The best performing *S. cerevisiae* Line 2 transformed with pTEF1/Zeo, pTEF1/Zeo/*dxs* and pTEF1/Zeo/*dxs*/*idi* expression vectors were used in further experiments.

RT-PCR analysis

Transcript levels of the *dxs* and/or *dxs*/*idi* genes in selected single events (based on biomass production) of *S. cerevisiae* cell Line 2 with pTEF1/Zeo/*dxs* or pTEF1/Zeo/*dxs*/*idi* yeast expression vector, grown at optimized conditions in the presence of galactose (2%) for 65 h, were analyzed by RT-PCR. Transformed yeast cells with pTEF1/Zeo vector only were used as a control. RNAs were extracted with QIAzol® (Qiagen, Düsseldorf, Germany) from different transformed derivatives of the *S. cerevisiae* cell Line 2. Then, RNAs were treated with RNase-free DNase (Promega, Madison, WI, USA). First-strand cDNA was synthesized using 1 μg of total RNA, 0.5 μg oligo reverse primers of each gene (*Table 1*) and Superscript II reverse transcriptase (Invitrogen, Carlsbad, CA, USA) to a final volume of 20 μl. PCR with forward and reverse primers (*Table 1*) for amplifying either gene consisted of denaturation at 94 °C for 4 min (first cycle), then denaturation for 15 s, annealing at 48 °C for 30 s, and extension at 72 °C for 45 s (40 cycles) to amplify 294 bp for *dxs* gene and 288 bp for *idi* gene. Amplicons were run on a 1.2% agarose gel stained with ethidium bromide and visualized using the Gel Doc XR (Bio-Rad Laboratories; Hercules, CA, USA). To ensure the absence of DNA contamination, PCR for the original RNA samples was run and results were negative (data not shown). Yeast *actin* gene (acc. no. L00026.1) was used as a reference to amplify 337 bp (*Table 1*).

Quantification of lycopene and acetyl-coenzyme A in S. cerevisiae dxs- and dxs/idi-transformed cells

Quantification of lycopene in *S. cerevisiae* cell Line 2 as well as in single selected transformed yeast cell with pTEF1/Zeo, pTEF1/Zeo/*dxs* or pTEF1/Zeo/*dxs*/*idi* expression vector was performed as described (Bahieldin et al., 2014). First, cells were harvested by centrifugation and lyophilized. The extracted lycopene was subjected to

http://www.aloki.hu ● ISSN 1589 1623 (Print) ● ISSN 1785 0037 (Online)
DOI: http://dx.doi.org/10.15666/aeer/1804_52795292

high-performance liquid chromatography (HPLC) as described (Miura et al., 1998a). The *S. cerevisiae* cell Line 2 was used as a control. Galactose was added to the optimized medium at different concentrations (0, 1, 2, 3 and 4%) and measurements were made after 65 h growth. Concurrently, Acetyl-Coenzyme A Assay kit (cat. no. MAK039, Sigma-Aldrich, St. Louis, MO, USA) was used to detect concentration of Acetyl-CoA in nmole/µl after 65 h growth as described in the manufacturer's manual. Deproteinized samples were collected from the different *dxs*- or *dxs*/*idi*-transformed lines as well as from *S. cerevisiae* cell Line 2 (control). Then, time-dependent profiles of lycopene and Acetyl-CoA syntheses in different transformed cells were tested across time (0, 5, 25, 45 and 65 h) when cells were grown under optimized growth condition and optimal concentration of galactose. Experiments were statistically analyzed via two-way analysis of variance (ANOVA) with three replicates. ANOVA was performed based on the data of lycopene and Acetyl-CoA levels for the four yeast transformants with different vectors under the five different galactose concentrations. Multiple comparisons were performed within and across these two factors based on the least significant differences (LSD) at 5%. P-values were estimated for the variances among transformants with different vectors (V) and among different galactose (G) concentrations as well as for the variance due to the interaction between these two factors (e.g., V x G).

Table 1. *Primer names, sequences, expected sizes and locations of amplicons in the coding regions of the synthetic dxs of bacterial origin (E. coli, strain K-12) and yeast endogenous idi genes along with the house-keeping gene actin of S. cerevisiae*

Primer	Accession no.	Sequence (5` - 3`)	Size of amplicon (bp)
*dxs*_RT_F	HG738867	GAA GCT ATG AAC CAT GCA GG	294
*dxs*_RT_R		AAC ATC ATG ACC ATC AAC TGG	
*idi*_RT_F	NM_001183931	ACG TCA AAT GAC GAA AGC G	288
*idi*_RT_R		ACA TAG TGG ATG AGA GCA GC	
actin-F	L00026.1	CCA ATT GCT CGA GAG ATT TC	337
actin-R		CAT GAT ACC TTG GTG TCT TG	

Results

Yeast strains tend to respond to antibiotics differently. Zeocin antibiotic was tested at different concentrations (0, 50, 100 and 200 µg/ml) against the yeast Line 2 transformed with the three *crtEBI* genes (Bahieldin et al., 2014) and results indicated that zeocin at 200 µg/ml completely inhibited growth of yeast cells in terms of biomass production. This concentration was used to select one, out of five, single transformed yeast cell - in terms of biomass production - with pTEF1/Zeo vector or that harboring *dxs* or *dxs*/*idi* genes, both functions upstream the *crt* genes in the MEP pathway. There is no significant difference in terms of biomass within each of the three transformants (with pTEF1/Zeo or derivatives) after 45 and 65 h indicating that cell growth almost reached a growth plateau (*Fig. 3*) in accordance with the findings of Bahieldin et al. (2014), where they found that 45 h were sufficient to recover the highest biomass production of *crtEBI* transformants. The *crtEBI* genes were inserted in the pKS1 vector under the control of *ADH2* promoter, while the other two upstream genes were inserted in the pTEF1/Zeo vector under the control of *GAL1* promoter for *dxs* gene and the control of

http://www.aloki.hu ● ISSN 1589 1623 (Print) ● ISSN 1785 0037 (Online)
DOI: http://dx.doi.org/10.15666/aeer/1804_52795292

GAL10 promoter for *idi* gene. Expression of the *crt* genes requires the depletion of glucose, while expression of the latter two genes requires the presence of galactose. It was decided to use the transformed Line *EBI-Nil2* with pTEF1/Zeo vector only (*Fig. 3a*), the transformed Line *EBI-D4* with *dxs* gene (*Fig. 3c*) and transformed Line *EBI-DI2* with *dxs*/*idi* genes (*Fig. 3b*) in the presence of 200 µg/ml zeocin in the optimized medium (Bahieldin et al., 2014) in further experiments.

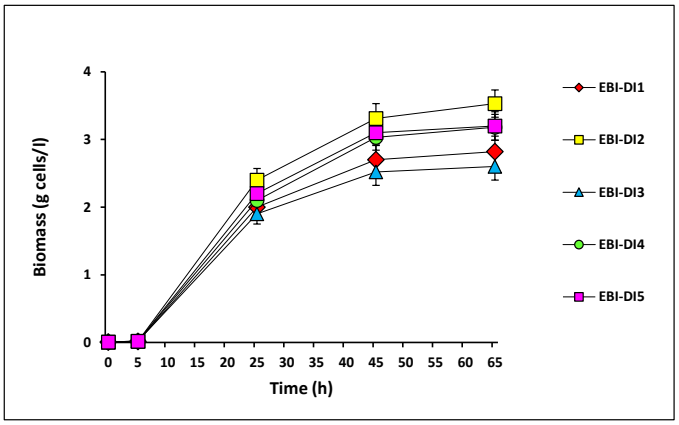

a

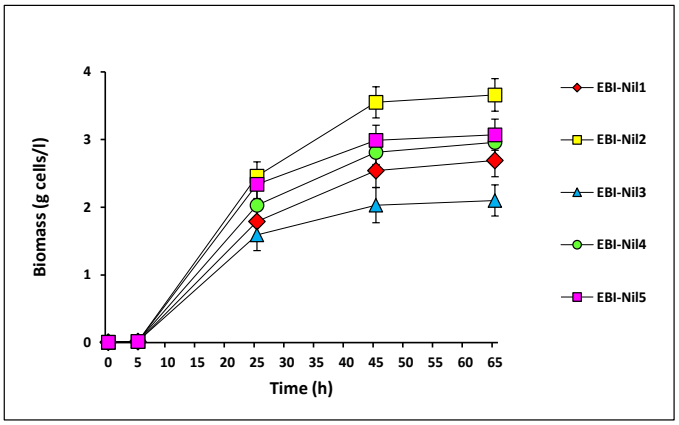

b

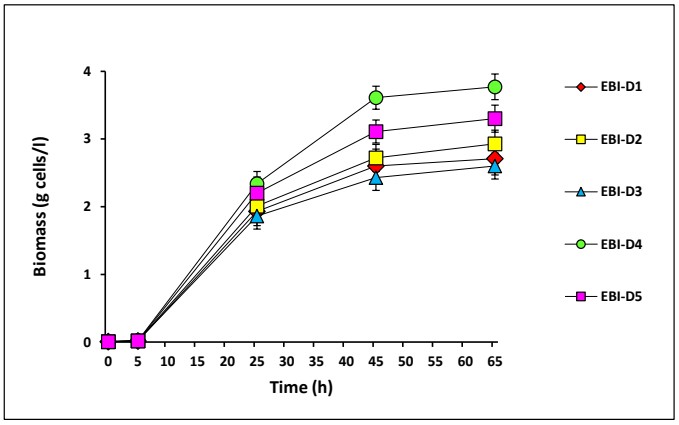

c

Figure 3. *Growth profile of different S. cerevisiae Line 2 transformed with pTEF1/Zeo (a), pTEF1/Zeo/dxs (b) or pTEF1/Zeo/dxs/idi (c) expression vector under optimized conditions (growth in YPD medium with 0.5% glucose at pH 6.0/35 °C in the presence of 200 µg/ml zeocin). Bars refer to values of standard error. Lines were marked via excel*

http://www.aloki.hu ● ISSN 1589 1623 (Print) ● ISSN 1785 0037 (Online)
DOI: http://dx.doi.org/10.15666/aeer/1804_52795292

Expression of dxs and idi genes in transformed S. cerevisiae lines

Lines *EBI-D4* and *EBI-DI2*, grown for 65 h at optimized conditions with galactose at 2%, were subjected to molecular analysis to detect the expression of the *dxs* and *idi* genes. Line 2 transformed with pTEF1/Zeo served as a control. The RT-PCR analysis (*Fig. 4*) revealed that the two genes were transcribed, where appropriate, and amplicons were recovered at the expected sizes. The RT-PCR analysis of transcripts from control cell resulted in the recovery of no amplicons for *dxs* gene (*Fig. 4,* lane 4). Amplicon intensities of *idi* gene were much higher for the two Lines *EBI-D4* and *EBI-DI2* as compared to the control yeast cell (*Fig. 4,* lanes 4-6, respectively), which indicates the low expression level of the endogenous *idi* gene in the control (*Fig. 4,* lane 6) as compared to that in the two Lines *EBI-D4* and *EBI-DI2* (*Fig. 4,* lanes 4 and 5, respectively) where the gene is driven by *GAL10* promoter.

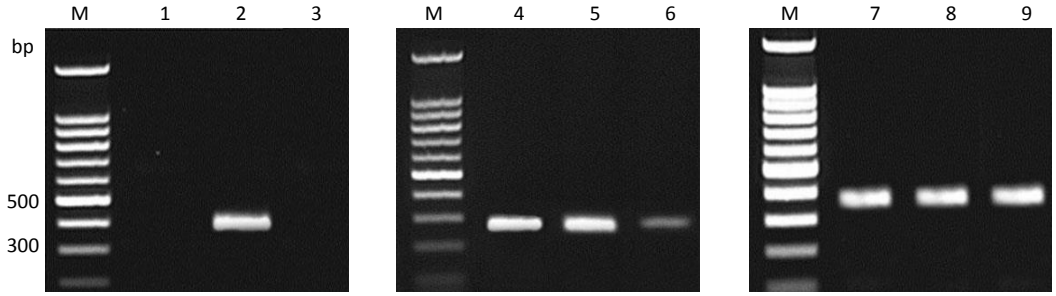

(a) *dxs* (b) *idi* (c) *actin*

Figure 4. *Analysis by RT-PCR of dxs and idi transcripts in EBI-D4 (lanes 1 and 4, respectively) and EBI-DI2 (lanes 2 and 5, respectively) transformed Lines of S. cerevisiae. Control cell of S. cerevisiae Line 2 (lanes 3 and 6, respectively) was transformed with the pTEF1/Zeo. Primers used for PCR (Table 1) were specific to dxs gene (a) to generate amplicons of 294 bp; idi gene (b) to generate amplicons of 288 bp; and actin gene (c) to generate amplicons of 337 bp. Primers specific to actin gene were used to demonstrate the transcription activity in EBI-D4 (lane 7) and EBI-DI2 (lane 8) transformed Lines of S. cerevisiae as well as S. cerevisiae Line 2 (lane 9) transformed with the pTEF1/Zeo. M refers to the 100-bp ladder (Bioron, Ludwigshafen, Germany)*

Synthesis of lycopene and Acetyl-CoA in S. cerevisiae transformed with dxs or dxs/idi genes

Lycopene and Acetyl-CoA were examined for the two transformed Lines *EBI-D4* and *EBI-DI2* as well as for the transformed cell Line 2 w/o pTEF1/Zeo (controls) under optimized conditions in the presence of galactose at different concentrations (0, 1, 2, 3 and 4%) and measurements were made after 65 h cell growth (*Table 2*). The results of lycopene and Acetyl-CoA levels indicated no significant differences among different *S. cerevisiae* Line 2 and pTEF1/Zeo derivatives in the absence of galactose. However, the two Lines *EBI-D4* and *EBI-DI2* showed much higher significant levels of lycopene in the presence of galactose. This is reasonable because the onset of *GAL1 and GAL10* promoter activities necessary for the expression of *dxs and idi* genes, respectively, depends on the presence as well as the concentration of galacose in the medium. The highest levels of lycopene were scored at 2% galactose for both lines *EBI-D4* and *EBI-DI2*. The latter line with both *dxs* and *idi* genes significantly synthesized higher level of lycopene (6755 μg/g dry cell weight) as compared to the first line with *dxs* gene

http://www.aloki.hu ● ISSN 1589 1623 (Print) ● ISSN 1785 0037 (Online)
DOI: http://dx.doi.org/10.15666/aeer/1804_52795292

(5214 µg/g dry cell weight), only (*Table 2*). These results indicate the efficacy of inducing the two genes that function upstream the *crtEBI* genes in the MEP pathway. The same procedure was used to synthesize lycopene in *E. coli* but resulted in much higher levels (e.g., 8.57 mg/g dry cell weight, see Choi et al., 2010). The results of Acetyl-CoA levels across galactose concentrations indicated no significant increase or decrease within Line 2 (e.g., Line pKS1-*crtEBI*) as well as within its pTEF1/Zeo derivative with the increase of galactose concentration in the medium (e.g., Line *EBI-Nil2*) (*Table 2*). However, the levels of Acetyl-CoA within Lines *EBI-D4* and *EBI-DI2* significantly decreased with the increase of galactose concentration in the medium up to 2%. These two lines showed significantly lower levels of Acetyl-CoA as compared to either Line 2 or *EBI-Nil2*. The levels of lycopene and Acetyl-CoA at 65 h with 2% galactose in the medium reversely related among *S. cerevisiae* Line 2 with pKS1-*crtEBI* and pTEF1/Zeo derivatives. This indicates that biosynthesis of lycopene and Acetyl-CoA compete for the use of pyruvate (see *Fig. 1*) in yeast.

Table 2. *Means (± SE) of lycopene (µg) (a) and Acetyl-CoA (µmoles) (b) levels per g dry cell weight (DCW) of S. cerevisiae Line 2 transformant (Line pKS1-crtEBI) and those with pTEF1/Zeo derivatives. Cells were grown for 65 h under optimized condition with different concentrations of galactose to induce expression of bacterial dxs gene and overexpress yeast idi genes. Measurements were performed three times and means with standard errors at 5% are presented P-values were estimated based on the variances among transformants with different vectors and among different galactose concentrations and the variances due to the interaction between the two factors*

(a) Lycopene (µg)

Vector	Galactose (%)				
	0	**1**	**2**	**3**	**4**
Line 2 (Line pKS1-*crtEBI*)	3327 ± 23	3219 ± 41	3281 ± 42	2992 ± 38	3106 ± 46
pTEF1/Zeo (Line *EBI-Nil2*)	3207 ± 31	3310 ± 37	3601 ± 38	3100 ± 27	3123 ± 28
pTEF1/Zeo/*dxs* (Line *EBI-D4*)	3311 ± 44	4302 ± 28	5214 ± 51	5030 ± 46	5100 ± 19
pTEF1/Zeo/*dxs*/*idi* (Line *EBI-DI2*)	3219 ± 39	4730 ± 32	6755 ± 23	6196 ± 76	6208 ± 42

Sources of variance	**F value**	**P-value**
Transformant (V) (df = 3)	3.37	0.0277
Galactose % (G) (df = 4)	6.23	0.0005
V x G (df = 12)	2.89	0.0058

(b) Acetyl-CoA (µmoles)

Vector	Galactose (%)				
	0	**1**	**2**	**3**	**4**
Line 2 (Line pKS1-*crtEBI*)	3.66 ± 0.2	3.45 ± 0.2	3.19 ± 0.2	3.62 ± 0.3	3.55 ± 0.2
pTEF1/Zeo (Line *EBI-Nil2*)	3.51 ± 0.2	3.31 ± 0.2	3.33 ± 0.3	3.26 ± 0.2	3.41 ± 0.3
pTEF1/Zeo/*dxs* (Line *EBI-D4*)	3.62 ± 0.3	2.80 ± 0.2	1.67 ± 0.1	1.99 ± 0.1	1.93 ± 0.1
pTEF1/Zeo/*dxs*/*idi* (Line *EBI-DI2*)	3.49 ± 0.2	2.61 ± 0.3	1.50 ± 0.1	1.91 ± 0.1	1.85 ± 0.1

Sources of variance	**F value**	**P-value**
Transformant (V) (df = 3)	4.11	0.0124
Galactose % (G) (df = 4)	2.92	0.0329
V x G (df = 12)	2.37	0.0205

http://www.aloki.hu ● ISSN 1589 1623 (Print) ● ISSN 1785 0037 (Online)
DOI: http://dx.doi.org/10.15666/aeer/1804_52795292

Biosynthesis of the two compounds were also studied across yeast growth time up to 65 h and results indicated similar conclusions to those reached in the last experiment, where we observed an increase in lycopene synthesis in Lines *EBI-D4* and *EBI-D12* (*Fig. 5a,* triangles and circles, respectively) as compared to those in Line 2 or pTEF1/Zeo derivative (e.g., Line *EBI-Nil2*) (*Fig. 5a,* diamonds and squares, respectively). However, there were no significant changes in biosynthesis of lycopene across Line 2 and all pTEF1/Zeo derivatives beyond 45 h of cell growth (*Fig. 5a*). These results also indicate that growth of yeast cells beyond 45 h time point for commercial production of lycopene is unnecessary. These results align with that of the biomass production as yeast cells have gained no significant weight beyond 45 h of cell growth. Biosynthesis of Acetyl-CoA was increased across time up to 25 h for transformants *EBI-D4* and *EBI-DI2* (*Fig. 5b,* triangles and circles, respectively), while continued to increase for Lines 2 and *EBI-Nil2* up to 65 h (*Fig. 5b,* diamonds and squares, respectively). On the other hand, levels of Acetyl-CoA were almost unchanged for Lines *EBI-D4* and *EBI-DI2* beyond 25 h time point. These results confirm our previous findings that biosyntheses of lycopene and Acetyl-CoA compete for the use of pyruvate in yeast.

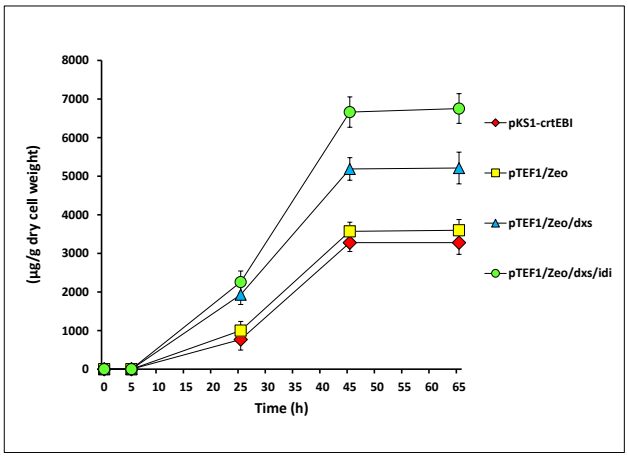

(a) Lycopene

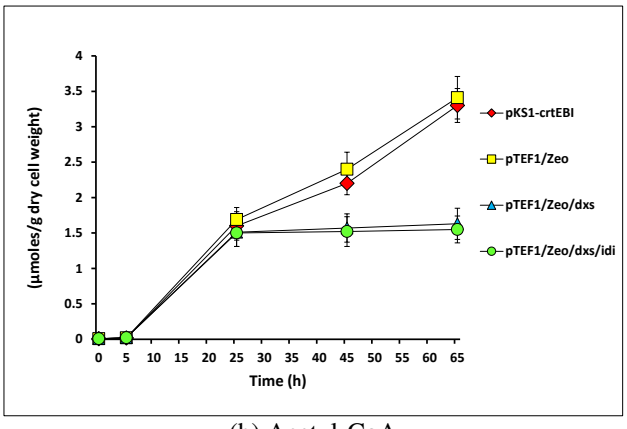

(b) Acetyl-CoA

Figure 5. *Time-dependent changes across time (0, 5, 25, 45 and 65 h) in lycopene (a) and Acetyl-CoA (b) levels in EBI-D4 and EBI-DI2 transformed Lines of S. cerevisiae as well as S. cerevisiae Line 2 w/o the pTEF1/Zeo under optimized condition. Measurements were performed three times and means with standard errors at 5% are presented. Bars refer to values of standard error. Lines were marked via excel*

http://www.aloki.hu ● ISSN 1589 1623 (Print) ● ISSN 1785 0037 (Online)
DOI: http://dx.doi.org/10.15666/aeer/1804_52795292

Discussion

Promoters used for the expression of *crt* genes in previous studies of *C. utilis* and *S. cerevisiae* were *P14* and *P57*, *PMA*, *GAP*, *PGK* (Miura et al., 1998a, b) and *ADH2* (Bahieldin et al., 2014). The highest lycopene levels (1100 and 3280 ug/g dry cell weight, respectively) were reached when *crtE* gene was driven by *GAP* promoter, *crtB* gene was driven by *P14* promoter, and *crtI* gene was driven by *PGK* promoter (Miura et al., 1998a, b) or when the three *crt* genes were driven by *ADH2* promoter (Bahieldin et al., 2014). In the present study, we can claim that the use of *GAL10* promoter resulted in higher expression of *idi* gene as well as higher levels of lycopene production. This conclusion cannot be applied for *GAL1* promoter driving the *dxs* gene as no information is available for the efficacy of utilizing this or other promoters in driving the *dxs* gene in terms of lycopene production in yeast.

However, Lee and DaSilva (2005) also reported the superior performance of the *ADH2* promoter relative to the inducible *CUP1* and *GAL1* promoters in driving the *lacZ* gene. We can also claim that the use of synthetic genes with codons preferred to *S. cerevisiae* cells in order to overexpress foreign genes like *dxs* is a successful approach. These synthetic *crt* as well as *dxs* genes had a high AT ratio as compared to the native genes. The results of the present work also indicate that lycopene can be produced at high levels not only by utilizing the *Saccharomyces cerevisiae ADH2* promoter in driving the three *crt* genes but also by utilizing *GAL1* and *GAL10* promoters in driving the bacterial *dxs* and the yeast *idi* genes, respectively. The main advantage of the *ADH2* promoter relative to other non-yeast promoters is the inducer-free characteristic allowing uninterrupted bioreactor operations during industrial fermentation processes (Michael Lee and DaSilva, 2005). A library of the *TEF1* promoter mutants was also screened by Alper et al. (2005) and results indicated the possible generation of precise genetic control that is also a useful characteristic for industry.

Yeast (*Saccharomyces cerevisiae*) is considered as an attractive organism for metabolic engineering as compared to *E. coli* and *Candida utilis* as it is classified as a GRAS (generally regarded as safe) organism. The yeast cell wall does not contain any toxic components (such as pyrogens in the case of *E. coli*). In industry, yeast is easy to cultivate and requires no sophisticated instruments or supplies. Previous studies have indicated that *S. cerevisiae* transformed with native (Miura et al., 1998a, b) or synthesized (Bahieldin et al., 2014) *crt* genes accumulate lycopene. In the present study, we employed synthetic bacterial *dxs* and overexpressed yeast *idi* genes. The first was constructed according to the preferable codon usage of *S. cerevisiae*, for the lycopene production. This is the first report to use *S. cerevisiae* transformed with these two genes for the successful recovery of lycopene at higher levels (6755 µg/g dry cell weight) than those reported earlier. The *idi* gene is endogenously expressed in yeast, however, overexpression resulted in higher expression of the gene as well as higher level of lycopene production. These results prove the utility of metabolic engineering in the commercial production of lycopene.

Lycopene can be extracted from tomatoes, however, its content in the fruit is low (~0.02 g/kg), and the extraction method is difficult and relatively expensive (Sun et al., 2014). Lycopene can also be produced by chemical analysis, but this approach is complex and includes hazardous materials (Sun et al., 2014). Therefore, microbial fermentation can be considered as the method of choice (Alper and Stephanopoulos, 2008; Choi et al., 2010; Kim et al., 2011) as lycopene overproduction can take place via several strategies involving overexpression of genes required for isoprenoid synthesis to

http://www.aloki.hu ● ISSN 1589 1623 (Print) ● ISSN 1785 0037 (Online)
DOI: http://dx.doi.org/10.15666/aeer/1804_52795292

encode compounds of the MEP pathway (e.g., *crtEBI*, *dxs* and *idi*). This strategy was successfully utilized in *E. coli* (Choi et al., 2010; Liu et al., 2020) and yeast (the present study) engineered to overproduce lycopene. Other strategies involve the knockout of (or deleting) genes functioning downstream the lycopene biosynthetic pathway (e.g., *crtY* and *crtX*) (Sun et al., 2014) or the increase of IPP (isopentenyl pyrophosphate) supply (Yoon et al., 2007). In addition, fermentation processes can be optimized to overproduce lycopene by adding auxiliary carbon source (Kim et al., 2011) or maintaining high O_2 levels and pH values (Yoon et al., 2006). Most recently, Sun et al. (2014) has successfully utilized ribosome binding site libraries to modulate expression of *crtEBIYX*, *dxs* and *idi* genes towards the production of substantial levels of lycopene production.

In general, we suggest that biosynthesis of lycopene and Acetyl-CoA compete for the use of pyruvate. The same conclusion was reached by Choi et al. (2010) in their study in *E. coli*. It is notable that the decrease in Acetyl-CoA level due to the engineering in MEP pathway is not severe as this co-enzyme is crucial for the cell in many metabolic pathways (Fatland et al., 2005). Acetyl-CoA is important for pyruvate decarboxylation, which occurs in the matrix of the mitochondria (*Fig. 1*), then, it enters the citric acid cycle (Choi et al., 2010). It is also an important component in the biogenic synthesis of the neurotransmitter acetylcholine and plays an essential role in regulating fatty acid synthesis and degradation (Wright et al., 2006).

Conclusion

The study aims at the assessment of *crtEBI*-transformed *S. cerevisiae* overexpressing two bacterial synthetic *dxs* and yeast *idi* genes driven by galactose-induced promoters for lycopene production. Gene cassettes constructed in pESC-LEU were inserted in pTEF1/Zeo vector. Expression levels of the two genes were proven in *crtEBI*-transformed *S. cerevisiae* cells resulted in highest production of lycopene (6755 μg lycopene/g dry cell weight). In contrast, the levels of Acetyl-Coenzyme A (Acetyl-CoA) was lowest in *crtEBI*-transformed *S. cerevisiae* cells indicating the competition for the use of pyruvate in biosynthesizing lycopene and Acetyl-CoA. We strongly recommend the use of yeast as a host for the production of lycopene utilizing metabolic engineering approaches in future trials to further improve its levels at commercial scale.

Acknowledgments. The authors acknowledge Prof. Dr. Khalid M. Al-Ghamdi, head of Department of Biological Sciences, Faculty of Science, King Abdulaziz University, Jeddah, KSA, for providing physical and logistic supports for this study.

Conflict of interests. The authors declare that they have no competing interests.

REFERENCES

[1] Alper, H., Stephanopoulos, G. (2008): Uncovering the gene knockout landscape for improved lycopene production in *E. coli*. – Applied Microbiology & Biotechnology 78: 801-810.

[2] Alper, H., Fischer, C., Nevoigt, E., Stephanopoulos, G. (2005): Tuning genetic control through promoter engineering. – Proceedings of the National Academy of Sciences 102: 12678-12683.

http://www.aloki.hu ● ISSN 1589 1623 (Print) ● ISSN 1785 0037 (Online)
DOI: http://dx.doi.org/10.15666/aeer/1804_52795292

[3] Bahieldin, A., Gadalla, N. O., Al-Garni, S. M., et al. (2014): Efficient production of lycopene in *Saccharomyces cerevisiae* by expression of synthetic crt genes from a plasmid harboring the ADH2 promoter. – Plasmid 72: 18-28.
[4] Choi, H. S., Lee, S. Y., Kim, T. Y., Woo, H. M. (2010): *In silico* identification of gene amplification targets for improvement of lycopene production. – Applied Environmental Microbiology 76: 3097-3105.
[5] Eisenreich, W., Bacher, A., Arigoni, D., Rohdich, F. (2004): Biosynthesis of isoprenoids via the non-mevalonate pathway. – Cellular & Molecular Life Sciences CMLS 61: 1401-1426.
[6] Fatland, B. L., Nikolau, B. J., Wurtele, E. S. (2005): Reverse genetic characterization of cytosolic acetyl-CoA generation by ATP-citrate lyase in Arabidopsis. – The Plant Cell 17: 182-203.
[7] Herrgård, M. J., Lee, B.-S., Portnoy, V., Palsson, B. Ø. (2006): Integrated analysis of regulatory and metabolic networks reveals novel regulatory mechanisms in *Saccharomyces cerevisiae*. – Genome Research 16: 627-635.
[8] Hong, J., Park, S. H., Kim, S., et al. (2019): Efficient production of lycopene in *Saccharomyces cerevisiae* by enzyme engineering and increasing membrane flexibility and NAPDH production. – Applied Microbiology & Biotechnology 103: 211-223.
[9] Kim, Y.-S., Lee, J.-H., Kim, N.-H., et al. (2011): Increase of lycopene production by supplementing auxiliary carbon sources in metabolically engineered *Escherichia coli*. – Applied Microbiology & Biotechnology 90: 489-497.
[10] Kirschner, M. W. (2005): The meaning of systems biology. – Cell 121: 503-504.
[11] Lange, B. M., Croteau, R. (1999): Genetic engineering of essential oil production in mint. – Current Opinion in Plant Biology 2: 139-144.
[12] Lange, B. M., Wildung, M. R., McCaskill, D., Croteau, R. (1998): A family of transketolases that directs isoprenoid biosynthesis via a mevalonate-independent pathway. – Proceedings of the National Academy of Sciences 95: 2100-2104.
[13] Lange, B. M., Rujan, T., Martin, W., Croteau, R. (2000): Isoprenoid biosynthesis: the evolution of two ancient and distinct pathways across genomes. – Proceedings of the National Academy of Sciences 97: 13172-13177.
[14] Lee, P., Schmidt-Dannert, C. (2002): Metabolic engineering towards biotechnological production of carotenoids in microorganisms. – Applied Microbiology & Biotechnology 60: 1-11.
[15] Lee, S. Y., Lee, D.-Y. and Kim, T. Y. (2005): Systems biotechnology for strain improvement. – Trends in Biotechnology 23: 349-358.
[16] Liu, N., Liu, B., Wang, G., et al. (2020): Lycopene production from glucose, fatty acid and waste cooking oil by metabolically engineered *Escherichia coli*. – Biochemical Engineering Journal 155: 107488.
[17] Lois, L. M., Campos, N., Putra, S. R., et al. (1998): Cloning and characterization of a gene from *Escherichia coli* encoding a transketolase-like enzyme that catalyzes the synthesis of D-1-deoxyxylulose 5-phosphate, a common precursor for isoprenoid, thiamin, and pyridoxol biosynthesis. – Proceedings of the National Academy of Sciences 95: 2105-2110.
[18] Michael Lee, K., DaSilva, N. A. (2005): Evaluation of the *Saccharomyces cerevisiae ADH2* promoter for protein synthesis. – Yeast 22: 431-440.
[19] Miura, Y., Kondo, K., Saito, T., et al. (1998a): Production of the carotenoids lycopene, β-carotene, and astaxanthin in the food yeast *Candida utilis*. – Applied Environmental Microbiology 64: 1226-1229.
[20] Miura, Y., Kondo, K., Shimada, H., et al. (1998b): Production of lycopene by the food yeast, *Candida utilis* that does not naturally synthesize carotenoid. – Biotechnology & Bioengineering 58: 306-308.
[21] Price, N. D., Reed, J. L. and Palsson, B. Ø. (2004): Genome-scale models of microbial cells: evaluating the consequences of constraints. – Nature Reviews Microbiology 2: 886.

http://www.aloki.hu ● ISSN 1589 1623 (Print) ● ISSN 1785 0037 (Online)
DOI: http://dx.doi.org/10.15666/aeer/1804_52795292

[22] Rodriguez-Concepción, M., Boronat, A. (2002): Elucidation of the methylerythritol phosphate pathway for isoprenoid biosynthesis in bacteria and plastids. A metabolic milestone achieved through genomics. – Plant Physiology 130: 1079-1089.
[23] Römer, S., Fraser, P. D., Kiano, J. W., et al. (2000): Elevation of the provitamin A content of transgenic tomato plants. – Nature Biotechnology 18: 666.
[24] Sevgili, A., Erkman, O. (2019): Improved lycopene production from different substrates by mated fermentation of Blakeslea trispora. – Foods 8: 120.
[25] Sun, T., Miao, L., Li, Q., et al. (2014): Production of lycopene by metabolically-engineered *Escherichia coli*. – Biotechnology Letters 36: 1515-1522.
[26] Wright, T. C., Cant, J. P., Brenna, J. T., McBride, B. W. (2006): Acetyl CoA carboxylase shares control of fatty acid synthesis with fatty acid synthase in bovine mammary homogenate. – Journal of Dairy Science 89: 2552-2558.
[27] Yoon, S. H., Lee, Y. M., Kim, J. E., et al. (2006): Enhanced lycopene production in *Escherichia coli* engineered to synthesize isopentenyl diphosphate and dimethylallyl diphosphate from mevalonate. – Biotechnology & Bioengineering 94: 1025-1032.
[28] Yoon, S.-H., Kim, J.-E., Lee, S.-H., et al. (2007): Engineering the lycopene synthetic pathway in *E. coli* by comparison of the carotenoid genes of Pantoea agglomerans and *Pantoea ananatis*. – Applied Microbiology & Biotechnology 74: 131-139.

http://www.aloki.hu ● ISSN 1589 1623 (Print) ● ISSN 1785 0037 (Online)
DOI: http://dx.doi.org/10.15666/aeer/1804_52795292

ANALYSIS OF SPATIOTEMPORAL CHARACTERISTICS OF DROUGHT IN AN ARID REGION OF NORTHWEST CHINA

WEI, W.[1] – PANG, S. F.[1*] – XIE, B. B.[2] – ZHOU, J. J.[1] – ZHOU, L.[3]

[1]*College of Geography and Environmental Science, Northwest Normal University, 967 Anning East Road, Lanzhou 730070, Gansu, China*
(e-mails: weiweigis2006@126.com – W. Wei; 540628961@qq.com – J. J. Zhou)

[2]*School of Urban Economics and Tourism Culture, Lanzhou City University, Lanzhou 730070, Gansu, China*
(e-mail: 116543885@qq.com)

[3]*Faculty of Geomatics, Lanzhou Jiaotong University, Lanzhou 730070, Gansu, China*
(e-mail: zhougeo@126.com)

**Corresponding author*
e-mail: psfei1993@163.com; phone: +86-181-9419-9139

(Received 4th Feb 2020; accepted 22nd May 2020)

Abstract. Drought, as a natural disaster, affects the local environment and agricultural production. Drought monitoring plays a crucial role in preventing and mitigating drought, especially Meteorological and Agricultural Drought (IMAD) monitoring. To better monitoring IMAD, a new comprehensive drought index, called Meteorological and Agricultural Drought Index (MADI), was developed in this study, which combined the Standardized Precipitation Evapotranspiration Index (SPEI) and the Temperature Vegetation Dryness Index (TVDI). And, the spatiotemporal characteristics of drought were analyzed by the methods of the frequency, comparison and regionalization in Gansu Province of China during 2000-2016. The results showed that: (1) The meteorological and agricultural drought always occurred, while there was a difference in time of appearance; the IMAD in Gansu Province was mainly light and moderate, becoming serious from southeast to northwest. (2) MADI was temporally well-matched to the drought affected area, soil moisture and NPP. (3) The IMAD based on MADI can reflect both meteorological and agricultural drought well in time and space. (4) According to the drought frequency, the study area was divided into six regions, and most of the study area was the stable drought type. For different regions, government should take timely measures to prevent drought.
Keywords: *SPEI, TVDI, MADI, integrated meteorological and agricultural drought (IMAD), arid region, China*

Introduction

Drought caused by the unbalance supply of water, is one of the most frequent, widespread, disastrous and costly natural disasters in the world (Lloyd-Hughes and Saunders, 2002). It can significantly impact on socio-economy, agricultural production, water resources and ecosystem function (Lei et al., 2016). With climate warming, drought occurred frequently in China during the past decades (Liang et al., 2014; Yu et al., 2014; Zhang et al., 2018), especially in the northwestern region (Ren et al., 2014). Gansu Province is a typical arid area and sensitive to drought in the northwestern China, where the crop production and people's lives are largely affected by drought. Therefore, studying the drought characteristics in this area is conducive to comprehensively exploring the drought conditions in arid areas, and can provide more useful suggestions for drought in similar areas in the world.

http://www.aloki.hu ● ISSN 1589 1623 (Print) ● ISSN 1785 0037 (Online)
DOI: http://dx.doi.org/10.15666/aeer/1804_52935314

Drought is generally classed into the meteorological, agricultural, hydrological, socio-economic drought (Maity et al., 2016). The meteorological drought (MeD) and agricultural drought (AD) are closely related to national food security and social stability (Liu et al., 2015). MeD refers to the water deficiency caused by the unbalance between precipitation and evapotranspiration, and AD refers to soil moisture less than the water requirement of vegetation (Sheffield and Wood, 2012). Various indices of MeD and AD have been proposed by many scholars (Zargar et al., 2011; Hao and Singh, 2015).

MeD indices are widely applied to monitor drought (Zhang et al., 2011), such as the percentage of Precipitation anomaly (Pa) (Van Rooy, 1965), Standardized Precipitation Index (SPI) (McKee et al., 1993), Standardized Precipitation Evapotranspiration Index (SPEI) (Vicente-Serrano et al., 2010), Palmer Drought Severity Index (PDSI) (Palmer, 1965), and Compound Index (CI) (Zou et al., 2010). Among them, while SPI and Pa are simple to calculate, they only consider precipitation and cannot reflect drought change as the climate warming (Guo et al., 2018). PDSI can be calculated by temperature, precipitation, runoff and soil moisture, whereas it is complicated to calculate and cannot reflect multi-scale characteristics of droughts (Yao et al., 2017). CI is a comprehensive index, but it always exaggerates the actual drought situation. However, SPEI not only is a standardized and multi-scale drought monitoring index, but also considers precipitation and evapotranspiration which can reflect the drought condition accurately as the climate warming (Begueria et al., 2014). Thus, SPEI is the most suitable index to monitor meteorological drought.

Most of AD indices are remote sensing indices, which can objectively reflect the drought condition. And those indices can be classified into three categories: some indices detect AD by Land Surface Temperature (LST), such as Apparent Thermal Inertia (ATI) (Price, 1985); some indices use the vegetation change monitoring to detect drought, such as Anomaly Vegetation Index (AVI) (Chen et al., 1994) and Vegetation Condition Index (VCI) (Kogan, 1995); some indices based on the feature space of LST and vegetation indices, such as Vegetation Supply Water Index (VSWI) (Carlson et al., 1994) and Temperature Vegetation Dryness Index (TVDI) (Sandholt et al., 2002). Different indices above has different application conditions. For example, ATI is only suitable in bare or low vegetation coverage area (Wu et al., 2012); AVI and VCI always lag behind the drought monitoring (Sun et al., 2012); VSWI and TVDI have high requirements for the study area where the vegetation coverage should vary from bare to high vegetation (Yang et al., 2009). According to the vegetation coverage of the Gansu Province, TVDI was selected to monitor AD because of its simple computation and high precision (Bai et al., 2017).

Due to the independence and interaction of MeD and AD, the integrated drought based on MeD and AD is crucial in the development of drought research. Many scholars have developed the comprehensive drought indices and minoring drought characteristics. For example, Hao and AghaKouchak (2013) developed Multivariate Standardized Drought Index (MSDI) based on SPI and Standardized Soil Moisture Index (SSM); Li et al. (2017) improved MSDI and developed Modified Multivariate Standardized Drought Index (MMSDI) based on SPEI and SSI, which makes up the deficiencies of MSDI. However, the physical significance, calculation methods and monitoring accuracy of these drought indices may need to be improved. Besides, it is lack of the comprehensive drought indices for the arid areas. Thus, there are some issues to be considered in the future research: (1) how to develop a comprehensive and

http://www.aloki.hu ● ISSN 1589 1623 (Print) ● ISSN 1785 0037 (Online)
DOI: http://dx.doi.org/10.15666/aeer/1804_52935314

accurate comprehensive based on a simple calculation? (2) how to minoring comprehensive drought characteristics by a new drought index?

Given the introduction above, this study aims to develop a new comprehensive drought index to investigate the drought characteristics in Gansu Province of the northwest China: (1) select the optimal indices of MeD and AD for the arid region, and analyze the MeD and AD characteristics; (2) develop Meteorological and Agricultural Drought Index (MADI) based on SPEI and TVDI, and analyze the spatiotemporal characteristics of Integrated Meteorological and Agricultural drought (IMAD); (3) validate the MADI from several aspects; (4) determine the drought partitions according to the drought frequency of IMAD, and provide targeted suggestions.

Data and methods

Study area

Gansu Province is located in the northwest region of China (32°11′-42°57′N, 92°13′-108°46′E), which covers various climatic types from humid to semi-humid, and from semi-arid to arid (*Fig. 1*). The annual average temperature ranges from 0 to 16 ℃ and the annual precipitation ranges from 30 mm to 860 mm. Gansu Province lies among the Loess Plateau, the Tibetan Plateau and the Mongolian Plateau. The landscape is complex and diverse, including plateaus, mountains, valleys and deserts, and it is covered from bare areas to high vegetation. And there are six geomorphic units, including the Gannan Plateau, the Longnan Mountainous Region, the Loess Plateau in the middle and east of Gansu, the Qilian Mountain Region, the Hexi Corridor and the northern zone of the Hexi Corridor. Affected by climate, topography, geographic location and human activities, natural disasters in the study area occur frequently, and drought is the most serious disaster, which has a major impact on agriculture, economy and human health.

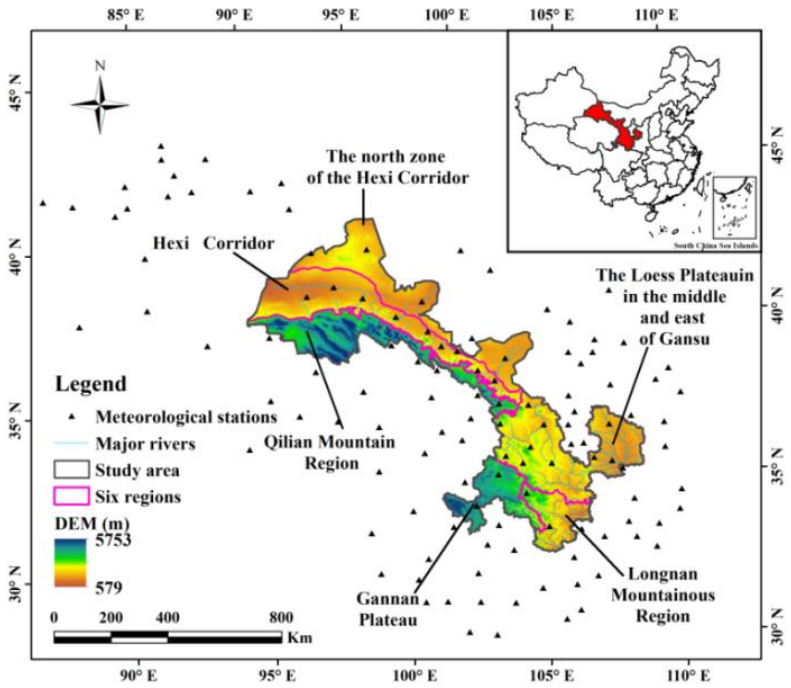

Figure 1. *The location of the study area*

http://www.aloki.hu ● ISSN 1589 1623 (Print) ● ISSN 1785 0037 (Online)
DOI: http://dx.doi.org/10.15666/aeer/1804_52935314

Data and processing

Meteorological station data

The meteorological data from 1960 to 2016 were obtained from the China Meteorological Data Sharing Service System (http://cdc.cma.gov.cn/), including monthly precipitation and temperature. In order to reduce error of spatial distribution, 35 stations were eliminated in the original datasets due to the observation data less than 30 years during 1961-2016 or missing observation data more than one year during 2000-2016. And 120 meteorological gauge stations were selected, including 26 stations in Gansu, 8 stations in the Inner Mongolia, 9 stations in Ningxia, 23 stations in Qinghai, 16 stations in Shanxi, 20 stations in Sichuan and 18 stations in Xinjiang. In this study, the meteorological drought index was calculated based on monthly precipitation and temperature data from 1960 to 2016. However, the meteorological data and remote sensing data were different in time range, and there were difference between the results of meteorological drought index and agricultural index. Therefore, the result of meteorological drought index during 2000-2016 was extracted to show and analyze drought in this study.

Remote sensing data

The Moderate Resolution Imaging Spector radiometer (MODIS) data were obtained from National Aeronautics and Space Administration (NASA), including four products of Normalized Difference Vegetation Index (NDVI) (MOD13A2), LST (MOD11A1), Net Primary Productivity (NPP) (MOD17A3) and surface reflectance (MOD09A1) (*Table 1*). Four tiles (h25v04, h25v05, h26v04, h26v05) were used to cover the study area. *Table 1* provides the detailed information on the MODIS products.

Table 1. *MODIS data information*

Production	Time	Spatial resolution	Temporal resolution	Source
MOD13A3 NDVI	2000-2016	500 m	16- Day	NASA (http://modis.gsfc.nasa.gov)
MOD11A2 LST	2000-2016	1 km	8-Day	
MOD09A1 surface reflectance (Band 6 and Band 7)	2000-2016	1 km	8-Day	Numerical Terradynamic Simulation Group (NTSG) at the University of Montana (http://www.ntsg.umt.edu/project/mod16)
MOD17A3 NPP	2000-2015	1 km	Year	

Global land data assimilation system (GLDAS) soil moisture data

Global Land Data Assimilation System (GLDAS) data from NASA (https://disc.gsfc.nasa.gov/) is the global land surface assimilation data based on satellite data, land surface models and ground observation data jointly released by NASA and the National Oceanic and Atmospheric Association (NOAA). The GLDAS soil moisture data (0.25° × 0.25°, unit of kg/m^2) are global monthly data generated by the GLDAS-Noah model, including 4 layers of 0-10 cm, 10-40 cm, 40-100 cm, and 100-200 cm. These data have been widely used worldwide and show actual soil moisture (Zawadzki and Kedzior, 2015). In addition, soil moisture data in the soil layer of 0-10 cm can

http://www.aloki.hu ● ISSN 1589 1623 (Print) ● ISSN 1785 0037 (Online)
DOI: http://dx.doi.org/10.15666/aeer/1804_52935314

better reflect drought conditions (Pang et al., 2019), so the soil moisture in the 0-10 cm soil layer from 2000 to 2016 was selected to evaluate the proposed drought index.

Other data

Disaster data were obtained from the crop and disaster database of the Ministry of Agriculture and Rural Affairs of the People's Republic of China, including types, area and degree of disaster. In this study, crop area affected by drought in Gansu Province during 2000-2016 was expressed the actual drought condition and verified the results of this study.

Drought indices

Standardized precipitation evapotranspiration index (SPEI)

The SPEI can show the water deficit for a certain temporal scale at a location to the historical average of the cumulative moisture deficit (Li et al., 2012). In this study, SPEI is calculated using the SPEI package in the R software environment (Santiago Beguería and Vicente-Serrano, 2013). There are nine categories of SPEI according to the World Meteorological Organisation, National Standard of Meteorological and Agricultural Drought in China, and the actual situation in Gansu (WMO, 2012; Ramkar and Yadav, 2018) (*Table 2*). It reflects different drought characteristics based on SPEI in different time scales, and SPEI-3, SPEI-6, and SPEI-12 represent seasonal, half a year, and annual accumulated drought condition, respectively (Shi et al., 2017). Therefore, SPEI-12 was selected to monitoring drought in this study.

Table 2. *Classification of SPEI*

Category	SPEI value	Category	SPEI value
Extreme Wet (EW)	(2.0, + ∞)	Light Drought (LD)	(-1, -0.5]
Severe Wet (SW)	(1.5, 2]	Moderate Drought (MD)	(-1.5, -1]
Moderate wet (MW)	(1, 1.5]	Severe Drought (SD)	(-2, -1.5]
Light Wet (LW)	(0.5, 1]	Extreme Drought (ED)	(-2, -∞)
Normal (N)	(-0.5, 0.5]		

Temperature vegetation dryness index (TVDI)

The obviously negative correlation between NDVI and LST is closely related to soil moisture (Yu and Chen, 2010). The scatter plot of NDVI and LST has a triangular shape when vegetation coverage and soil moisture vary widely (Price, 1990). In the NDVI-LST triangle feature space (*Fig. 2*), the point A and B indicate the dry and wet bare soil, respectively. The point C indicates the area where soil moisture is sufficient and the surface is completely covered by vegetation with strong transpiration. With the surface vegetation coverage increasing, LST decreases and evaporation increases at the same time. The edge AC, as the dry edge of the NDV-LST feature space, indicates low soil moisture and low surface evapotranspiration in the area. The edge BC, as the wet edge of the NDVI-LST feature space, indicates a sufficient soil moisture and equal evapotranspiration and potential evapotranspiration in the area.

Based on the relationship between NDVI and LST, the Temperature Vegetation Dryness Index (TVDI), can monitor the soil moisture (Sandholt et al., 2002). As TVDI

http://www.aloki.hu ● ISSN 1589 1623 (Print) ● ISSN 1785 0037 (Online)
DOI: http://dx.doi.org/10.15666/aeer/1804_52935314

increases, soil moisture decreases and the drought becomes more severe. According to the actual drought condition, the classifications of TVDI were shown in *Table 3* (Liu et al., 2017).

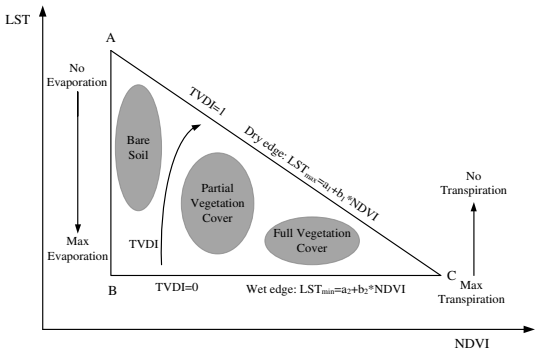

Figure 2. *The NDVI-LST triangle space and definition of the TVDI*

Table 3. *Classification of TVDI*

Category	TVDI value	Category	TVDI value	Category	TVDI value
EW	[0, 0.1]	LW	(0.3, 0.4]	MD	(0.7, 0.8]
SW	(0.1, 0.2]	N	(0.4, 0.6]	SD	(0.8, 0.9]
MW	(0.2, 0.3]	LD	(0.6, 0.7]	ED	(0.9, 1]

Meteorological and agricultural drought index (MADI)

For better monitoring both MeD and AD at the same time, a new IMAD index, called Meteorological and Agricultural Drought Index (MADI), was proposed based on the Euclidean distance method. The Euclidean distance can measure the absolute distance between points in multi-dimensional space (Mesquita et al., 2017). Due to the objectivity, scientific nature and universality of Euclidean distance, it has been widely used in various geographically related fields, such as dry monitoring, ecological quality assessment, and vegetation monitoring (Amani et al., 2017; Shi et al., 2018; Li and Tian, 2013). The Euclidean distance can be expressed as (*Eq. 1*):

$$D(X,Y) = \sqrt{\sum_{i=1}^{n}(x_i - y_i)^2} \quad \text{(Eq.1)}$$

where D(X,Y) is the Euclidean distance between the point X(x_1, x_2, x_3..., x_n) and the points Y(y_1, y_2, y_3..., y_n); n is the multidimensional space.

Based on the above introduction, the MADI is developed as follows: first, a reference point is set (for research purposes, this point is the wettest point), and then, the Euclidean distance is calculated from each point to this reference point. When the calculated distance is longer, the drought value is higher; otherwise, the drought value is lower. The MADI value ranges from 0-200 and the higher MADI is drier. Its calculation is as follows (*Eq. 2*):

$$MADI = \frac{\sqrt{2}}{2}\sqrt{(NSPEI - NSPEI_{max})^2 + (NTVDI - NTVDI_{min})^2} \quad \text{(Eq.2)}$$

http://www.aloki.hu ● ISSN 1589 1623 (Print) ● ISSN 1785 0037 (Online)
DOI: http://dx.doi.org/10.15666/aeer/1804_52935314

where $NSPEI_{max}$ and $NTVDI_{min}$ represent the driest status. NSPEI and NTVDI represent the normalized value of SPEI and TVDI in a point.

Due to the differences in ranges of drought classifications among different drought indices, a similar classification should be established to make these indices comparable (Esfahanian et al., 2017). Therefore, associated ranges were assigned and nine categories were identified, including four drought categories (light drought, moderate drought, severe drought, and extreme drought), four wet categories (light wet, moderate wet, severe wet, and extreme wet) and a normal category (normal). To obtain the drought score of each category of SPEI and TVDI, each drought index and category should be normalized using the linear scaling technique (*Table 4*).

Table 4. *The normalized formula of each category using the linear scaling technique*

Category	Formula	Category	Formula
LW	$I_N = \frac{I-a}{b-a}(0-25)$	LD	$I_N = \frac{I-a}{b-a}(40-20)+20$
MW	$I_N = \frac{I-b}{c-b}(25-50)-25$	MD	$I_N = \frac{I-b}{c-b}(60-40)+20$
SW	$I_N = \frac{I-c}{d-c}(50-75)-50$	SD	$I_N = \frac{I-c}{d-c}(80-60)+20$
EW	$I_N = \frac{I-d}{e-d}(75-100)-75$	ED	$I_N = \frac{I-d}{e-d}(100-80)+20$
N	$I_N = \frac{I-p}{q-p}(20-0)$		

I is the original drought/wet index value; IN is the normalized value of drought/wet index; p and q are the associated range of the normal category; a and b are the associated range of the light drought/wet category; b and c are the associated range of the moderate drought/wet category; c to d is the associated range of the severe drought/wet category; d to e is the associated range of the extreme drought/wet category

The classification of MADI was acquired from the classification of NSPEI and NTVDI. The calculation of MADI was shown as follows (*Eq. 3*):

$$\begin{aligned} MADI_m &= \sqrt{(NSPEI_m - NSPEI_{max})^2 + (NTVDI_m - NTVDI_{min})^2} \\ &= \sqrt{(NSPEI_m + 100)^2 + (NTVDI_m + 100)^2} \end{aligned} \quad \text{(Eq.3)}$$

where $MADI_m$ represent the boundary value of every category of MADI. $NSPEI_m$ and $NTVDI_m$ are the boundary value of every category of SPEI and TVDI.

The NSPEI, NTVDI and MADI classification were shown in *Table 5*.

Table 5. *Classification of NSPEI, NTVDI and MADI*

Category	NSPEI and NTVDI value	MADI value	Category	NSPEI and NTVDI value	MADI value
EW	[-100, -75]	[0, 25]	LD	(20, 40]	(120, 140]
SW	(-75, -50]	(25, 50]	MD	(40, 60]	(140, 160]
MW	(-50, -25]	(50, 75]	SD	(60, 80]	(160, 180]
LW	(-25, 0]	(75, 100]	ED	(80, 100]	(180, 200]
N	(0, 20]	(100, 120]			

http://www.aloki.hu ● ISSN 1589 1623 (Print) ● ISSN 1785 0037 (Online)
DOI: http://dx.doi.org/10.15666/aeer/1804_52935314

Analysis methods

The frequency analysis of drought

The drought frequency indicates the probability of drought occurrence and can be calculated as follows:

$$F = \frac{n}{N} \times 100\% \quad \text{(Eq.4)}$$

where n is the number of drought occurrence in the time series. N is the total number of time points in the time series.

Comparative analysis of the drought indices

In the temporal scale, SPEI, TVDI and MADI are quantitatively compared using Probability of Detection (POD), False Alarm Ratio (FAR), Critical Success Index (CSI), and Effect of Detection (EOD) methods (*Table 6*) (Hao and AghaKouchak, 2014).

Table 6. *The quantitative compared methods*

Method	POD	FAR	CSI	EOD
Formula	$\frac{H}{H+M}$	$\frac{F}{H+F}$	$\frac{H}{H+M+F}$	$\frac{H+HN}{A}$

H (Hit) denotes the grid number where SPEI or TVDI is drought and MADI is drought; M (Miss) denotes the grid number where SPEI or TVDI is drought and MADI is not drought; F (False Alarm) denotes the grid number where SPEI or TVDI is not drought and MADI is drought; HN (Hit Null) denotes the grid number where SPEI, TVDI, MADI are not drought; A (all) denotes the total number of grid

In the spatial scale, the consistent of meteorological drought, agricultural drought and IMAD based on SPEI, TVDI and MADI were analyzed using the coding method (*Table 7*). (a, b, c) is the code, among which a, b, c represents the drought condition of SPEI, TVDI and MADI, respectively. 1 and 2 indicate respectively drought and no drought.

Table 7. *The code and type of consistency*

Type		Code (a, b, c)
The monitoring drought result of SPEI, TVDI, MADI are all consistent	SPEI, TVDI, MADI are all dry	(1, 1, 1)
	None of SPEI, TVDI, MADI is dry	(2, 2, 2)
The monitoring drought result of SPEI, TVDI, MADI are not consistent	MADI and SPEI are dry, but TVDI is not dry	(1, 2, 1)
	SPEI is dry, but TVDI and MADI are not dry	(1, 2, 2)
	TVDI and MADI are dry, but SPEI is not dry	(2, 1, 1)
	TVDI is not dry, but MADI and SPEI are not dry	(2, 1, 2)

The method of drought type partition

In order to better prevent and mitigate drought, drought type partition was obtained taking into consideration of the frequency of IMAD (*Table 8*). There are three types,

http://www.aloki.hu ● ISSN 1589 1623 (Print) ● ISSN 1785 0037 (Online)
DOI: http://dx.doi.org/10.15666/aeer/1804_52935314

including Stable Drought (StD), Stable Non-Drought (SND), and Fluctuation type of Drought and Non-Drought (F-D-ND). The StD includes Stable Light Drought (SLD), Stable Moderate Drought (SMD), Stable Severe Drought (SSD), Stable Extreme Drought (SED), and Fluctuation type of LD, MD, SD (F-LD-MD-SD).

Table 8. *The partition type of drought*

Type		Frequency	
Stable Non-Drought (SND)		0 ≤ frequency of drought ≤ 20%	
Fluctuation type of Drought and Non-Drought (F-D-ND)		20% < frequency of drought ≤ 70%	
Stable Drought (StD)	Stable Light Drought (SLD)	Frequency of LD > 70%	Frequency of drought > 70
	Stable Moderate Drought (SMD)	Frequency of MD > 70%	
	Stable Severe Drought (SSD)	Frequency of SD > 70%	
	Stable Extreme Drought (SED)	Frequency of ED > 70%	
	Fluctuation type of Light Drought, Moderate Drought, Severe Drought (F-LD-MD-SD)	Frequency of LD ≤ 70%, frequency of MD ≤ 70%, frequency of SD ≤ 70%, and frequency of ED ≤ 70%	

Results

The characteristics of meteorological and agricultural drought

The characteristics of MeD based on SPEI-12

SPEI-12 value fluctuated around -0.5 and drought duration was long in each drought period (*Fig. 3*), indicated that the MeD always occurs in the study area. The northwest and southeast region was mainly affected by LD and N, respectively (*Fig. 4a*). LD occurred every year with occupying the largest area; the MD occurred in 12 years, and its largest occupied area occurred in 2000 and 2009; the SD occurred in 2006 and 2009; the ED only occurred in 2009 (*Fig. 4b*). Moreover, the largest drought area and the most drought categories were occurred in 2009, which indicated the most serious drought occur in 2009.

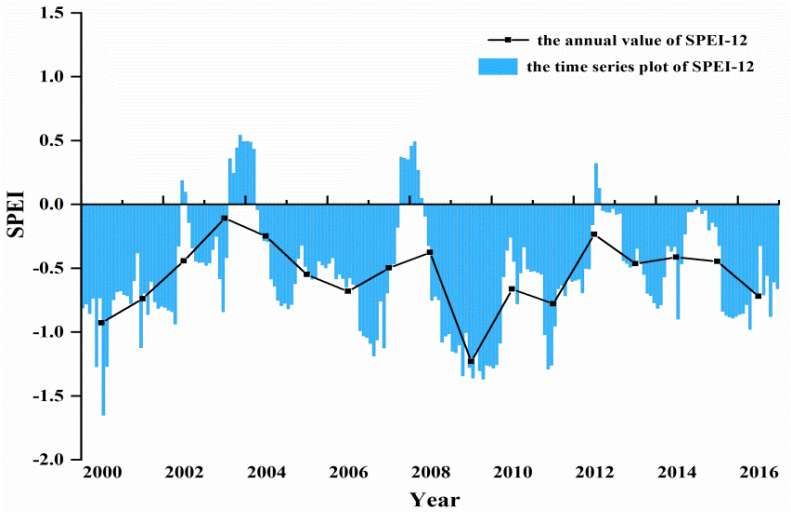

Figure 3. *Time series plot of SPEI-12*

http://www.aloki.hu ● ISSN 1589 1623 (Print) ● ISSN 1785 0037 (Online)
DOI: http://dx.doi.org/10.15666/aeer/1804_52935314

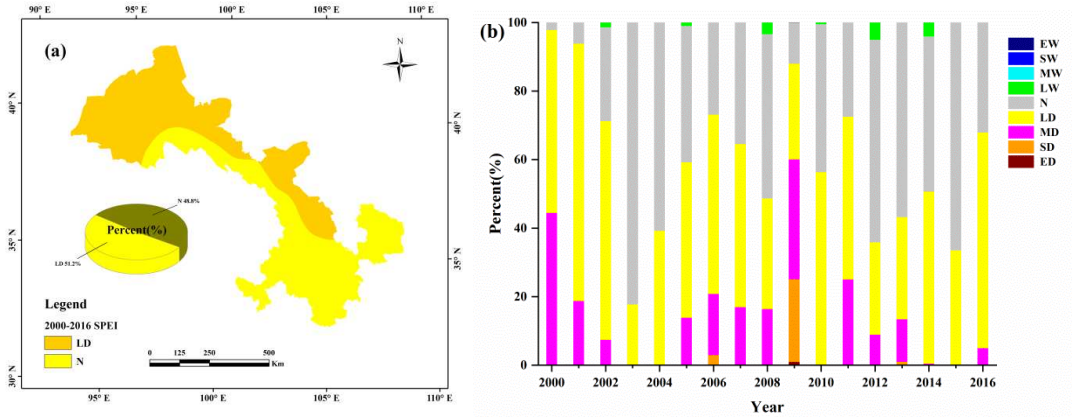

Figure 4. *The spatiotemporal distribution of MeD based on the annual SPEI-12 values during 2000-2016: (a) the spatial distribution of the annual average values of SPEI-12 (b) and the yearly change of area percent of different MeD categories in years*

The drought frequency value showed an increasing trend from southeast to northwest (*Fig. 5*). And the high drought frequency, approaching 60%, mainly occurred in the northwestern region of the study area, especially the northern zone of the Hexi Corridor. The low drought frequency, less than 48%, was mainly in the southeastern region, especially in the Longnan Mountainous Region and the Gannan Plateau. The frequency of LD and MD was higher than other drought categories; the frequency of ED was the least throughout the Province; the higher frequency value of light, moderate, severe, extreme drought all appeared in the northwestern Gansu and the northern zone of the Hexi Corridor. In a word, MeD was spatial and temporal in character.

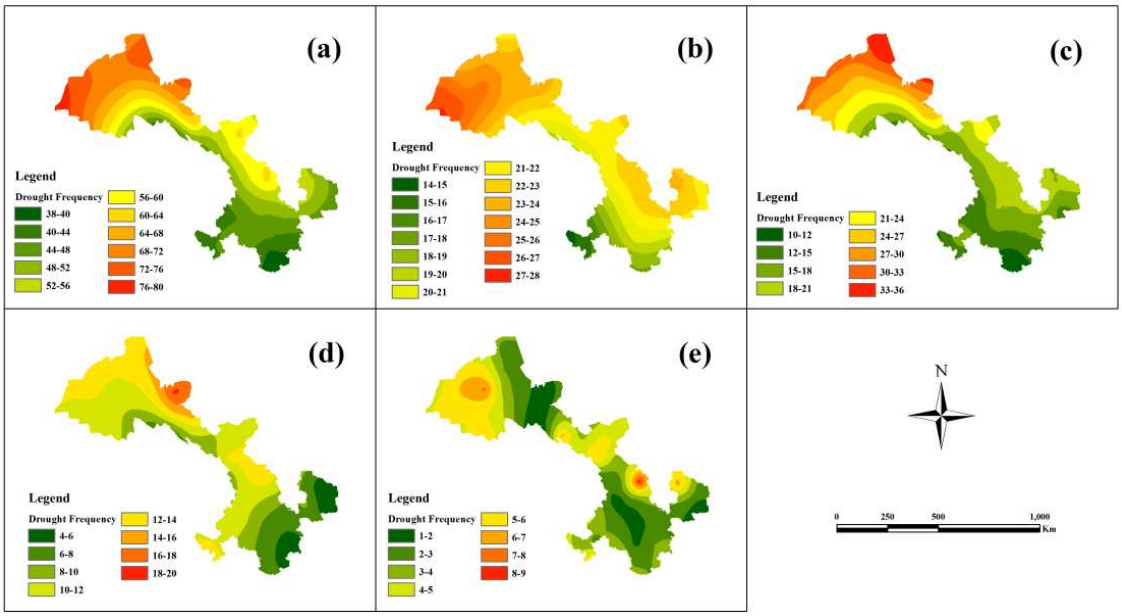

Figure 5. *The spatial distribution of MeD occurrence frequency from 2000 to 2016: the frequency distribution of (a) drought occurrence, (b) LD occurrence, (c) MD occurrence, (d) SD occurrence, (e) ED occurrence*

http://www.aloki.hu ● ISSN 1589 1623 (Print) ● ISSN 1785 0037 (Online)
DOI: http://dx.doi.org/10.15666/aeer/1804_52935314

The characteristics of agricultural drought based on TVDI

During 2000 to 2016, the mean TVDI value had a slight fluctuation around -0.69 (*Fig. 6*). And this study area was mainly affected by light and moderate drought. The lightest and most serious drought occurred in 2012 and 2002, respectively. Overall, AD always occurred in the past years and small changed in intensity.

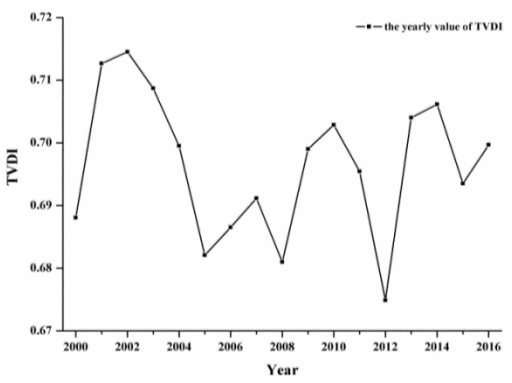

Figure 6. *Time series plot of TVDI*

Seed from annual average value of TVDI in 17 years (*Fig. 7a*), most of the study area was affected by light, moderate and severe drought, which was up to 85% in percentage; the MD percentage amounted to 40%, and distributed widely; the ED percentage was approximately 5% and concentrated in the desert; the percent of wet category approaches 7%, mainly in the mountain regions. And the percent of drought was about 80% in the most years, among which the percent of MD was the most, followed by SD and LD, and ED was the least (*Fig. 7b*).

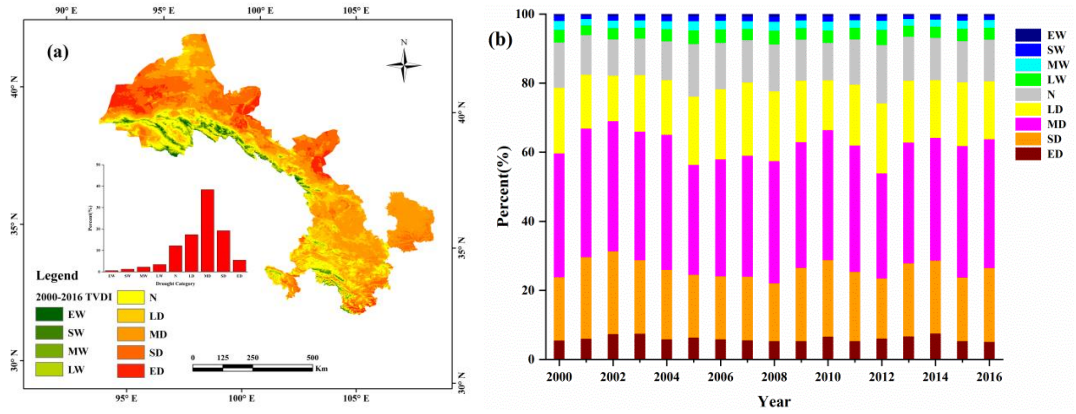

Figure 7. *The spatio-temporal distribution of AD based on the annual TVDI values during 2000-2016: (a) the spatial distribution of the annual average values of TVDI (b) and the yearly change of area percent of different AD categories in years*

The drought frequency was from 0 to 100 and it increased from southeast to northwest (*Fig. 8*): the highest drought frequency, up to 90%, was mainly in the northwestern region, especially the northern zone of the Hexi Corridor; the least drought frequency, less than 20%, mainly occurred in Qilian Mountain Region. However, the

http://www.aloki.hu ● ISSN 1589 1623 (Print) ● ISSN 1785 0037 (Online)
DOI: http://dx.doi.org/10.15666/aeer/1804_52935314

frequency of different AD categories differed significantly. The frequency of LD and MD occurrence was relatively higher than other drought categories: the high frequency of LD was mainly distributed in the Loess Plateau of the middle and east of Gansu, the Hexi Corridor, surrounding areas of Qilian Mountain Region and the northern zone of the Hexi Corridor; the high frequency of MD mainly represented in Hexi Corridor and the northern zone of the Hexi Corridor; the high frequency of SD was mainly concentrated in the desert area; the frequency of ED was less than 10% in the whole province. Overall, AD had obvious spatiotemporal characteristics and small changed.

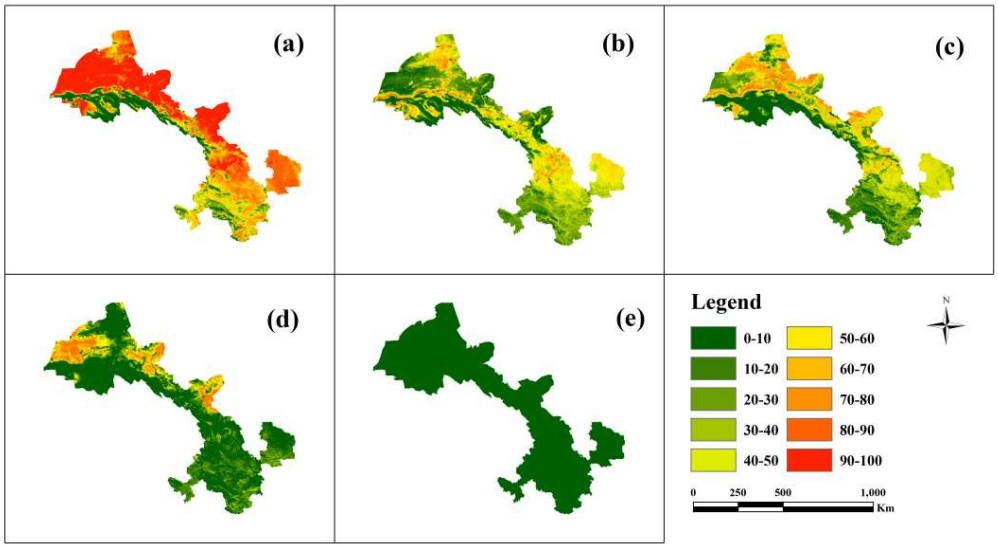

Figure 8. *The spatial distribution of AD occurrence frequency from 2000 to 2016: the frequency distribution of (a) drought occurrence, (b) LD occurrence, (c) MD occurrence, (d) SD occurrence, (e) ED occurrence*

The characteristics of IMAD based on MADI

From the time series plot of MADI during 2000-2016, slight fluctuation was from 130 to 145 in mean MADI value (*Fig. 9*). And this study area was mainly affected by LD in 17 years and only MD in 2009. Moreover, the lightest and most serious drought occurred in 2012 and 2009, respectively. From distribution of MADI (*Fig. 10*), most of the study area occurred IMAD and the sum area of LD and MD account for about 80%. And area percentages of LD and MD accounted for the majority in17 years; the largest area and range of SD occurred in 2009, and ED also mainly occurred in 2009.

From the occurrence frequency of IMAD at 1-year interval in 17 years (*Fig. 11*), the drought frequency ranged from 0 to 100, gradually increasing from southeast to northwest. The high drought frequency, over 90%, was in the large part of the study region. The least drought frequency, less than 10%, was concentrated in the Qilian Mountain Region. Moreover, the frequency differences of different drought categories were relatively high: the occurrence frequency of LD and MD were higher than other drought categories, being in the largest region of the whole province and in the northern zone of the Hexi Corridor, respectively; the high frequency of SD occurred in the desert area of the northern zone of the Hexi Corridor; the frequency of ED was nearly 2% around the Province. Overall, IMAD had obvious spatiotemporal characteristics in Gansu Province.

http://www.aloki.hu ● ISSN 1589 1623 (Print) ● ISSN 1785 0037 (Online)
DOI: http://dx.doi.org/10.15666/aeer/1804_52935314

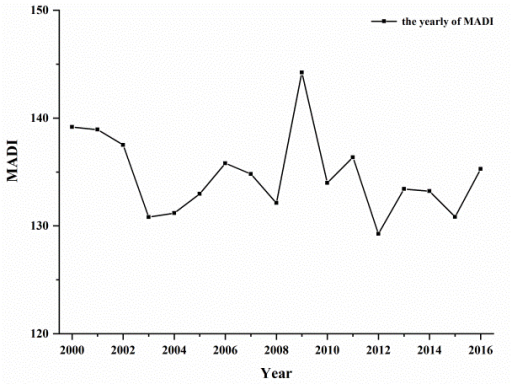

Figure 9. *Time series plot of MADI*

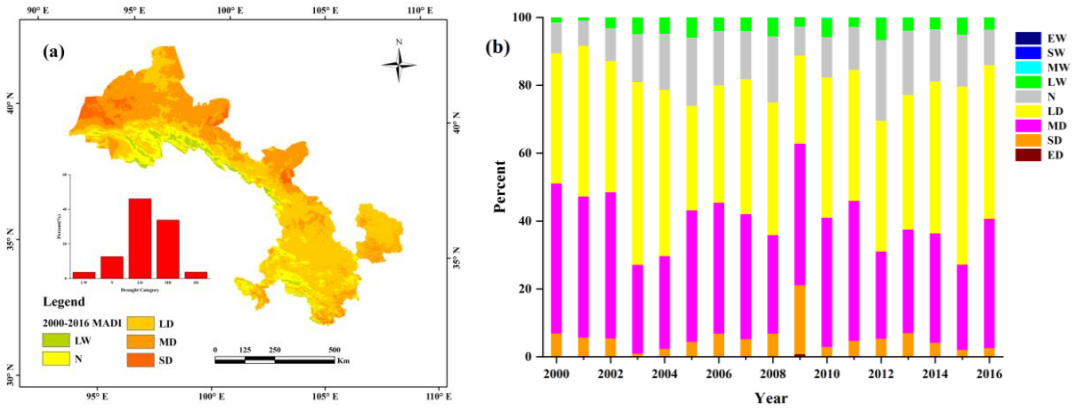

Figure 10. *The spatiotemporal distribution of IMAD based on the annual values of MADI during 2000-2016: (a) the spatial distribution of the annual average values of MADI (b) and the yearly change of area percent of different IMAD categories in years*

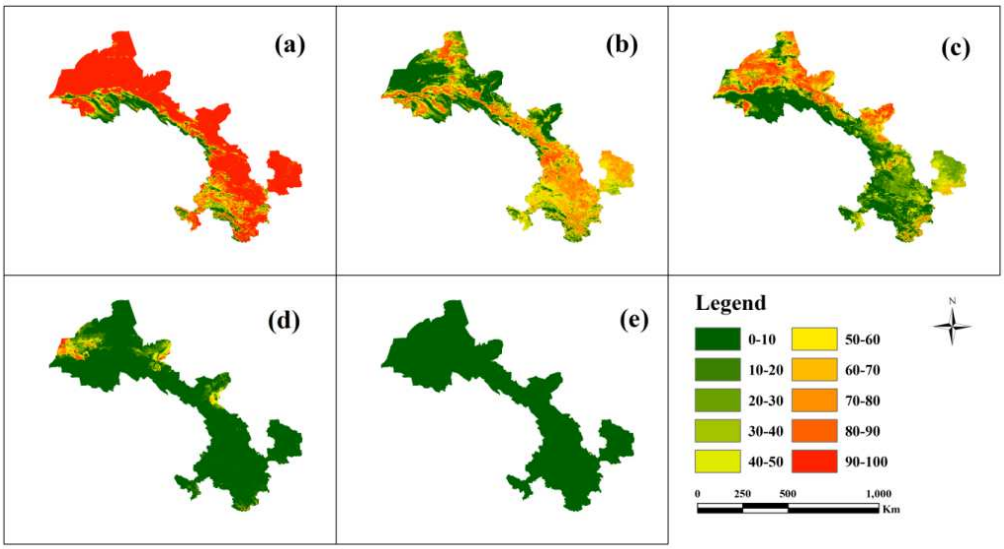

Figure 11. *The spatial distribution of IMAD occurrence frequency from 2000 to 2016: the frequency distribution of (a) drought occurrence, (b) LD occurrence, (c) MD occurrence, (d) SD occurrence, (e) and ED occurrence*

http://www.aloki.hu ● ISSN 1589 1623 (Print) ● ISSN 1785 0037 (Online)
DOI: http://dx.doi.org/10.15666/aeer/1804_52935314

Discussion

The validation of the MADI

Drought affected area

The drought affected area can directly reflect the drought impact extent and is often used for the accuracy validation of drought index (Du et al., 2013). The MADI was in good agreement with the variation of drought affected area (*Fig. 12*). The MADI showed a good positive linear correlation with the drought affected area, with the correlation coefficient R value reaching 0.7263 and passing 0.01 significance test. Meanwhile, the fluctuation changes, peaks and troughs of MADI were generally consistent with drought affected area in the 17 years. For example, MADI detected the worst drought in 2000 and 2009, and the drought affected areas in 2000 and 2009 were also relatively high; MADI detected the lightest drought in 2012, and the lowest drought affected areas also occurred in 2012. Thus, according to the above, MADI has a good accuracy in monitoring drought affected area.

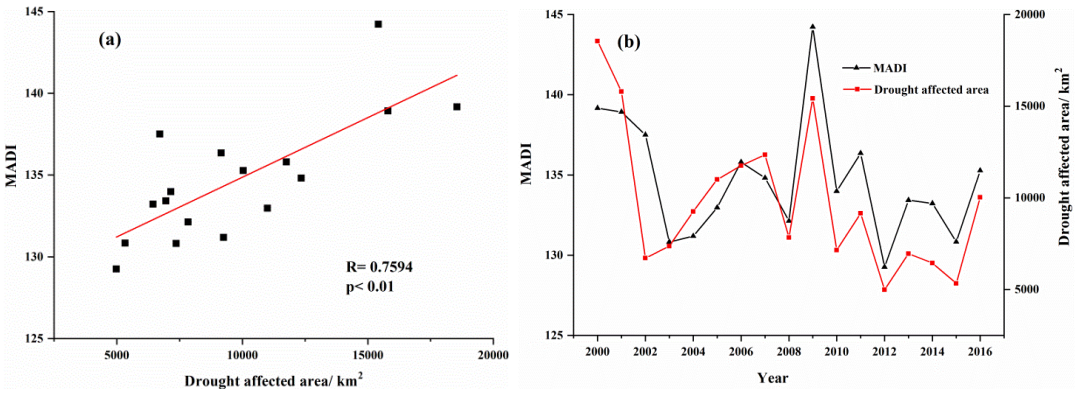

Figure 12. *The relationship between MADI and drought affected area from 2000 to 2016*

GLDAS soil moisture and NPP

Soil moisture, playing an important role in the formation and development of drought, is a direct indicator of the dry-wet condition in the land surface and is often verified the drought index (Cong et al., 2017; Hauser et al., 2016). Therefore, GLDAS soil moisture from 2000 to 2016 was selected for the accuracy of MADI. Due to the GLDAS soil moisture with 0.25°×0.25° spatial resolution, Inverse Distance Weighted (IDW) interpolation was performed to improve the spatial resolution to 1 km × 1 km. And the correlation between soil moisture and MADI was conducted based on pixels from 2000 to 2016 (*Fig. 13a*). The results showed that there was a negative correlation between soil moisture and MADI, accounted for about 85.34% of the study area. It proved that the drought change detected by MADI well matched the soil moisture change. Thus, MADI can better reflect the soil moisture change in the most areas.

Vegetation is an important feedback to the drought. When vegetation is subjected to drought stress, it will exhibit adaptive traits such as decreased photosynthesis and respiratory metabolism, thus reducing productivity (Drake et al., 2017). Therefore, the NPP can be as an effective tool to verify the MADI and directly reflect the drought distribution (*Fig. 13b*). It should be noted that the correlation between NPP and MADI was only distributed in the vegetation zone. Result showed the R value between the

http://www.aloki.hu ● ISSN 1589 1623 (Print) ● ISSN 1785 0037 (Online)
DOI: http://dx.doi.org/10.15666/aeer/1804_52935314

NPP and the MADI was negatively correlated in 88% of the regions with vegetation, indicating that the changes between the MADI and the NPP in most regions are consistent. Thus, the MADI can reflect the vegetation production status and better detect drought.

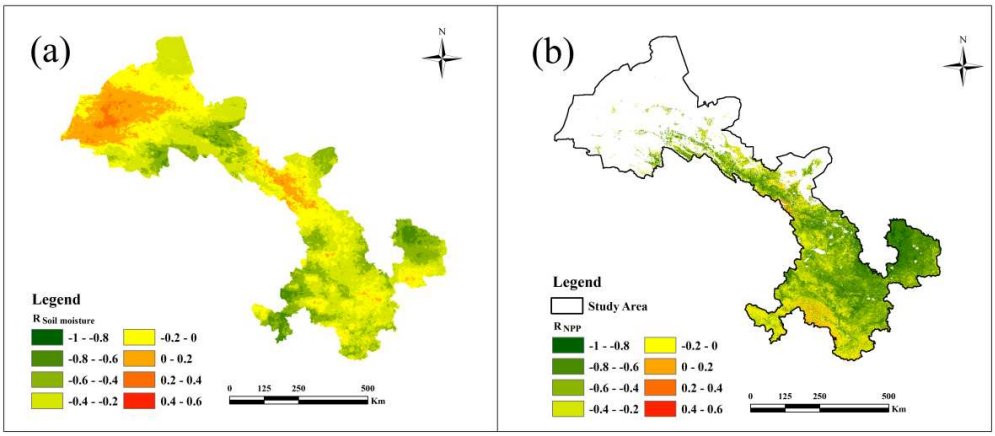

Figure 13. *The spatial distribution of correlation coefficient R: (a) soil moisture and MADI (b) and NPP and MADI*

The difference of the MADI among MeD, AD and IMAD based on SPEI, TVDI and MADI

POD, EOD, CSI and FAR can be used to evaluate the accuracy of IMAD in detecting of MADI from temporal aspect (*Fig. 14*). Result showed that POD, CSI and EOD had similar change characteristics and their values were closed to 0.9 from 2000 to 2016. The POD indicated that IMAD occurred in the same time and place when MeD/AD occurred; the EOD indicated that there was high the success rate to detect occurrence and no occurrence of IMAD and Med/AD. Moreover, the values of FAR were nearly 0 but not equal to 0, proving that IMAD was not only the simple addition of Med and AD, but also monitor the dry areas that cannot be monitored in Med and AD monitoring. Therefore, IMAD not only reflect MeD and AD, but also is more comprehensive to reflect drought than MeD and AD.

Comparing MeD, AD and IMAD spatially (*Fig. 15*), the area where MeD, AD and IMAD occurred and did not occur together, accounted for 59.3% of the study area: the type of (1,1,1) that MeD, AD and IMAD occurred together, was mainly distributed in Hexi Corridor, the northern zone of the Hexi Corridor and the northern region of the Loess Plateau in China; the type of (2,2,2) that MeD, AD and IMAD all did not occur, was mainly distributed in the most parts of Qilian Mountain Region, parts of the Gannan Plateau and the Longnan Mountainous Region. Moreover, the different area of MeD, AD and IMAD accounts for 40.7%, including four types (2,1,1), (1,2,2), (1,2,1) and (2,1,2): the type of (2,1,1), which AD and IMAD occurred but MeD did not occur, was distributed in the middle of Hexi Corridor, the most regions of the Loess Plateau, some parts of the Gannan Plateau and the Longnan Mountainous Region; the type of (1,2,2) which AD and IMAD did not occurred but MeD occurred, was mainly in the western mountain area of Qilian Mountain Region.

In a word, the MADI is a good index and IMAD monitored by MADI can well reflect both Med and AD whether from temporal or spatial perspectives.

http://www.aloki.hu ● ISSN 1589 1623 (Print) ● ISSN 1785 0037 (Online)
DOI: http://dx.doi.org/10.15666/aeer/1804_52935314

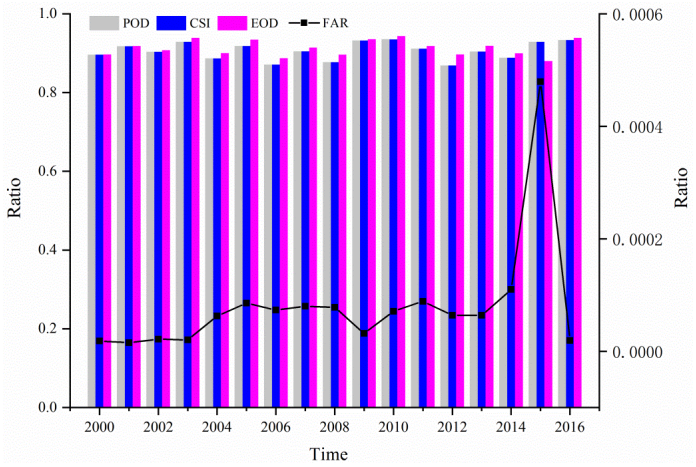

Figure 14. *The temporal comparation among MeD, AD and IMAD with the trend of POD, CSI and EOD from 2000 to 2016*

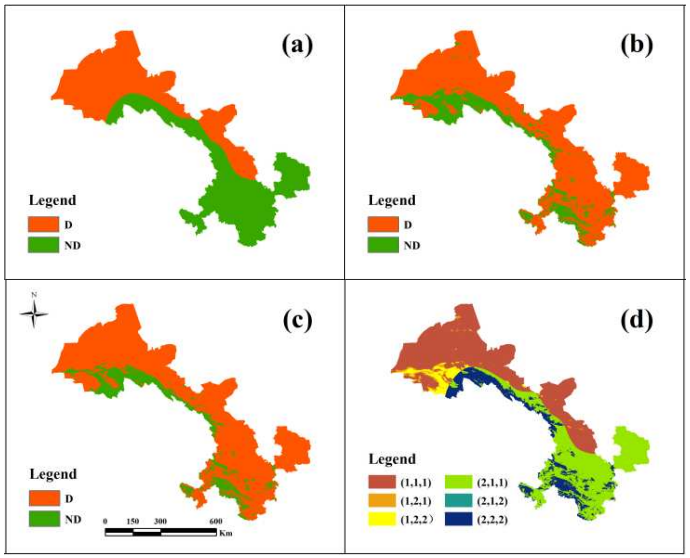

Figure 15. *The spatially comparation among MeD, AD and the IMAD: the spatial distribution of (a) MeD based on SPEI, (b) AD based on TVDI, (c) IMAD based on MADI, (d) and comparative result. D and ND referred to occurrence of drought and no drought*

Application in different drought partitions

In accordance with the drought frequency, the study area was divided in to 6 partitions (*Fig. 16*), including SND, F-D-ND, F-LD-MD-SD, SLD, SMD, and SSD (*Table 8*). The area percentage of each was in the order: F-LD-MD-SD (29.8%) > SLD (25.5%) > SMD (21.3%) > F-D-ND (12.2%) > SND (9.7%) > SSD (1.5%). In different partitions, different measures for drought prevention and mitigation should be recommended.

(1) The region of SND is mainly distributed in high-vegetation mountains and grasslands. Because of low temperature and good water conservation, this region is rich in water resources. Moreover, the main agricultural type is animal husbandry with low water requirement. Therefore, the drought does not occur in this region (Xu, 2004). To

http://www.aloki.hu ● ISSN 1589 1623 (Print) ● ISSN 1785 0037 (Online)
DOI: http://dx.doi.org/10.15666/aeer/1804_52935314

maintain the current non-drought condition, the government should reduce the size and quantity of grazing, avoid excessive deforestation, and strengthen the protection and construction of grassland-forest. Meanwhile, the drought monitoring system and mountain reservoir should be established to monitoring drought conditions.

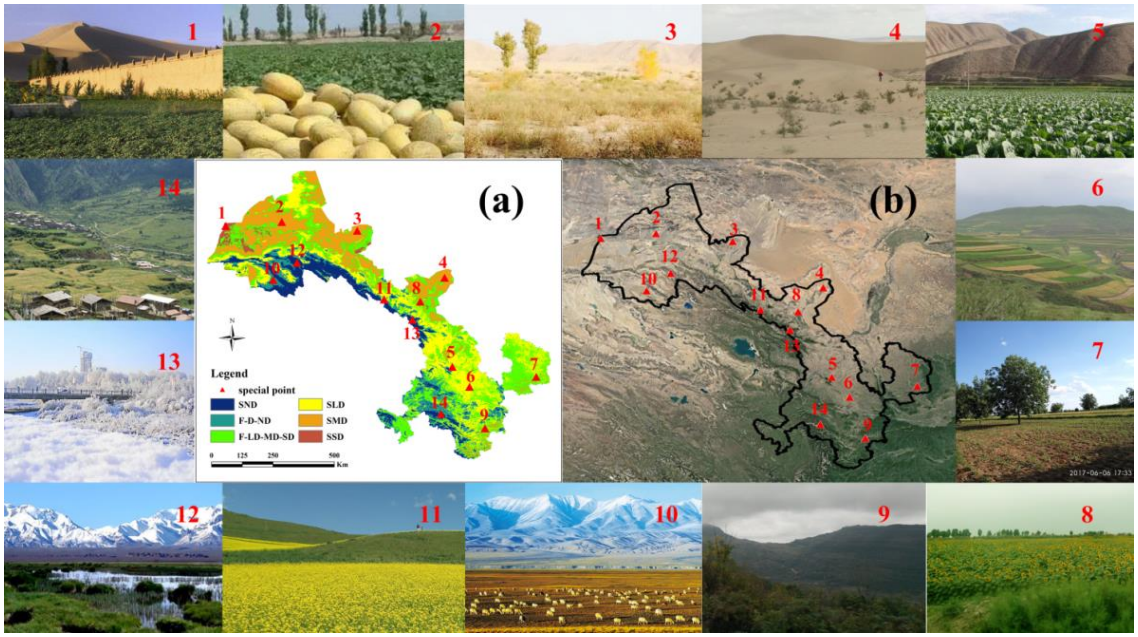

Figure 16. *The partitions of IMAD in the study area: (a) the regionalization based on the drought frequency of MADI (b) and the Google map of the study area. The sample of 1-14 is the typical point in different regions: the picture of 1 represents SSD; the picture of 2, 3, 4 represent SMD; the picture of 5, 6, 7 represent SLD; the picture of 8, 9 represent F-LD-MD-SD; the picture of 10, 11 represent F-D-ND; and the picture of 12, 13, 14 represent SND*

(2) The region of F-D-ND is mainly distributed around the high mountains. The land use and agriculture type in this region was the same as SND. Hence, government should makes the similar measures with the region of SND to prevent and mitigate drought.

(3) The region of SLD is the main rained agriculture region with the scarce resources of surface water. Its main agricultural type is crop farming, with the main crops being wheat, maize and potato (Tian and Chen, 2011). In this region, government should promote the technology of "terracing + plastic film + rain collection + structural adjustment" and select various irrigation types, such as well canal joint irrigation, drip irrigation and infiltration. In addition, the government should invest in the construction of water conservancy facilities, reservoirs and rainwater collection facilities to increase the utilization of rainwater resources. Finally, famers should avoid wasting water resources and select the most suitable crops in dry area.

(4) The region of SMD is mainly distributed in desert, because of low precipitation vegetation coverage, high land surface temperature, and water shortage (Peng, 2011). From the perspective of desertification management, drought-tolerant plants, such as Tamarisk, Calligonum and white thorn, should be widely planted to enhance the ability of drought resistance and sand fixation; from the perspective of crop farming, the local government should take measures to encourage farmers to plant more drought-tolerant crops, such as cotton, cantaloupe, sunflower, red date, grape (Shi, 2013); and in terms of

http://www.aloki.hu ● ISSN 1589 1623 (Print) ● ISSN 1785 0037 (Online)
DOI: http://dx.doi.org/10.15666/aeer/1804_52935314

irrigation, the government should advocate water-saving irrigation, vigorously develop drip irrigation under mulch to reduce evaporation and leakage, and increase the utilization efficiency of water (Hou et al., 2009).

(5) The region of SSD is distributed in the desert area of the northwestern desert. The main crops are cotton and cantaloupe in this region. In order to deal with serious drought, the planting structure should be changed to reduce the proportion of food crops. And high-efficiency water-saving agriculture, featuring red globe grasps and special vegetables planting, should be promoted. In addition, farmers should raise their awareness of water conservation and build water storage facilities (Shu, 2012).

(6) The region of F-LD-MD-SD. In this region, the measures of prevent and mitigate drought should be similar with SLD, SMD and SSD.

Research prospects

This study started from two aspects of meteorology and agriculture, and combined a common meteorological drought index SPEI and agricultural drought index TVDI to develop a new comprehensive index MADI. And it proved that the MADI has advantages in drought monitoring: (1) It has good accuracy, which can well reflect the drought affected area, soil moisture and NPP situation; (2) It can well monitor the meteorological and agricultural drought at the same time, and can be applied to IMAD monitoring. However, the index uses meteorological station data from station observations and remote sensing data from satellite observations in the calculation, which may cause some errors in the results. Therefore, in future research, the data in index calculation should be improved and remote sensing data should be used as much as possible.

Conclusions

In this study, the MADI was developed based on SPEI and TVDI, validated and applied in Gansu Province of China. Results showed that the MeD and AD always occurred, but the most serious and lightest droughts occur at different times; according to the classification of MADI value, the study area was mainly affected by light and moderate IMAD, being gradually serious from southeast to northwest; the serious drought occurred in the northern zone of the Hexi Corridor and the non-drought occurred in the Qilian Mountain Region. Seen from the validation result of the MADI, MADI was well-matched to the drought affected area, soil moisture and NPP; MADI is a better monitor index than SPEI and TVDI, and can well monitor IMAD in the study area. Seen from the different drought partitions, the study area was divided into six regions according to the drought frequency, including SND, F-D-ND, F-LD-MD-SD, SLD, SMD, and SSD. Some suggestions were proposed for different drought partitions: in the regions of SND and F-D-ND, the drought monitoring system and mountain reservoir should be established; in the regions of F-LD-MD-SD, SLD, SMD, and SSD, government should adopt positive measures in drought-tolerant crops, agricultural construction, irrigation types and water conservancy projects. In summary, MADI is a good IMAD monitoring index, which can be used for future drought monitoring; a comprehensive single index method can be used to construct a drought index; different regions should make different drought prevention measures according to different drought characteristics.

http://www.aloki.hu ● ISSN 1589 1623 (Print) ● ISSN 1785 0037 (Online)
DOI: http://dx.doi.org/10.15666/aeer/1804_52935314

REFERENCES

[1] Amani, M., Salehi, B., Mahdavi, S., Masjedi, A., Dehnavi, S. (2017): Temperature-Vegetation-Soil Moisture Dryness Index (TVMDI). – Remote Sensing of Environment 197: 1-14.

[2] Bai, J. J., Yuan, Y. U., Di, L. (2017): Comparison between TVDI and CWSI for drought monitoring in the Guanzhong Plain, China. – Journal of Integrative Agriculture 16: 389-397.

[3] Begueria, S., Vicente-Serrano, S. M., Reig, F., Latorre, B. (2014): Standardized Precipitation Evapotranspiration Index (SPEI) revisited: parameter fitting, evapotranspiration models, tools, datasets and drought monitoring. – International Journal of Climatology 34: 3001-3023.

[4] Carlson, T. N., Gillies, R. R., Perry, E. M. (1994): A method to make use of thermal infrared temperature and NDVI measurements to infer surface soil water content and fractional vegetation cover. – Remote Sensing Reviews 9: 161-173.

[5] Chen, W. Y., Xiao, Q. G., Shen, Y. W. (1994): Application of the anomaly vegetation index to monitoring heavy drought in 1992. – Remote Sensing of Environment 9: 106-112.

[6] Cong, D. M., Zhao, S. H., Chen, C., Duan, Z. (2017): Characterization of droughts during 2001-2014 based on remote sensing: a case study of Northeast China. – Ecological Informatics 39: 56-67.

[7] Drake, J. E., Power, S. A., Duursma, R. A., Medlyn, B. E., Aspinwall, M. J., Choat, B., Creek. D., Eamus, D., Maier, C., Pfautsch, S., Smith, R. A., Tjoelker, M. G., Tissue, D. T. (2017): Stomatal and non-stomatal limitations of photosynthesis for four tree species under drought: a comparison of model formulations. – Agricultural and Forest Meteorology 247: 454-466.

[8] Du, L. T., Tian, Q. J., Yu, T., Meng, Q. Y., Jancso, T., Udvardy, P., Huang, Y. (2013): A comprehensive drought monitoring method integrating MODIS and TRMM data. – International Journal of Applied Earth Observation and Geoinformation 23: 245-253.

[9] Esfahanian, E., Nejadhashemi, A. P., Abouali, M., Adhikari, U., Zhang, Z., Daneshvar, F., Herman, M. R. (2017): Development and evaluation of a comprehensive drought index. – Journal of Environmental Management 185: 31-43.

[10] Guo, H., Bao, A. M., Liu, T., Jiapaer, G. L., Ndayisaba, F., Jiang, L. L., Kurban, A., Maeyer, P. D. (2018): Spatial and temporal characteristics of droughts in Central Asia during 1966-2015. – Science of the Total Environment 624: 1523-1538.

[11] Hao, Z., AghaKouchak, A. (2013): Multivariate standardized drought index: a parametric multi-index model. – Advances in Water Resources 57: 12-18.

[12] Hao, Z., AghaKouchak, A. (2014): A nonparametric multivariate multi-index drought monitoring framework. – Journal of Hydrometeorology 15: 89-101.

[13] Hao, Z., Singh, V. P. (2015): Drought characterization from a multivariate perspective: a review. – Journal of Hydrology 527: 668-678.

[14] Hauser, M., Orth, R., Seneviratne, S. I. (2016): Role of soil moisture versus recent climate change for the 2010 heat wave in western Russia. – Geophysical Research Letters 43: 2819-2826.

[15] Hou, F. J., Chang, S. H., Nan, Z. B. (2009): Establish the pastoral agriculture system for desertification control in Minqin. – Pratacultural Science 26: 68-74.

[16] Kogan, F. N. (1995): Application of vegetation index and brightness temperature for drought detection. – Advances in Space Research 15: 91-100.

[17] Lei, T. J., Pang, Z. P., Wang, X. Y., Li, L., Fu, J., Kan, G. Y., Zhang, X. L., Ding, L. Q., Li, J. R., Huang, S. F., Shao, C. L. (2016): Drought and carbon cycling of grassland ecosystems under global change: a review. – Water 8: 460.

http://www.aloki.hu ● ISSN 1589 1623 (Print) ● ISSN 1785 0037 (Online)
DOI: http://dx.doi.org/10.15666/aeer/1804_52935314

[18] Li, Q., Zhang, Q., Huang, Q. Z., Shi, P. J. (2017): Nonparametric integrated agro-meteorological drought monitoring in China: new monitoring technique and applicability. – Acta Geographica Sinica 73: 67-80.
[19] Li, W. G., Hou, M. T., Chen, H. L. (2012): Study on drought trend in south China based on standardized precipitation evapotranspiration index. – Journal of Natural Disasters 21: 84-90.
[20] Li, Z., Tan, D. (2013): The second modified perpendicular drought index (MPDI1): a combined drought monitoring method with soil moisture and vegetation index. – Journal of the Indian Society of Remote Sensing 41: 873-881.
[21] Liang, L., Zhao, S. H., Qin, Z. H., He, K. X., Chen, C., Luo, Y. X. (2014): Drought change trend using MODIS TVDI and its relationship with climate factors in China from 2001 to 2010. – Journal of Integrative Agriculture 13: 1501-1508.
[22] Liu, L. Y., Liao, J. S., Chen, X. Z., Zhou, G. Y., Su, Y. X., Xiang, Z. Y., Wang, Z., Liu, X. D., Li, Y. Y., Wu, J. P., Xiong, X., Shao, H. Y. (2017): The Microwave Temperature Vegetation Drought Index (MTVDI) based on AMSR-E, brightness temperatures for long-term drought assessment across China (2003-2010). – Remote Sensing of Environment 199: 302-320.
[23] Liu, X. F., Zhu, X. F., Pan, Y. Z., Li, S. S., Liu, Y. X. (2015): Agricultural drought monitor: progress, challenges and prospect. – Acta Geographica Sinica 70: 1835-1848.
[24] Lloyd-Hughes, B., Saunders, M. A. (2002): A drought climatology for Europe. – International Journal of Climatology 22: 1571-1592.
[25] Maity, R., Suman, M., Verma, N. K. (2016): Drought prediction using a wavelet based approach to model the temporal consequences of different types of droughts. – Journal of Hydrology 539: 417-428.
[26] McKee, T. B., Doesken, N. J., Kleist, J. (1993): The relationship of drought frequency and duration to time scales. – Eighth Conference on Applied Climatology, Anaheim, California 17: 17-22.
[27] Mesquita, D. P. P., Gomes, J. P. P., Júnior, A. H. S., Nobre, J. S. (2017): Euclidean distance estimation in incomplete datasets. – Neurocomputing 248: 11-18.
[28] Palmer, W. C. (1965): Meteorological Drought, 30. – US Department of Commerce, Weather Bureau, Washington.
[29] Pang, S. F., Wei, W., Guo, Z. C,, Zhang, J., Xie, B. B. (2019): Agricultural drought characteristics and its influencing factors in Gansu Province based on TVDI. – Chinese Journal of Ecology 38(9): 1849-1860.
[30] Peng, J. F. (2011): Application of anti-drought measures in afforestation in arid desert area. – Gansu Forestry 1: 37-38.
[31] Price, J. C. (1985): On the analysis of thermal infrared imagery - the limited utility of apparent thermal inertia (for Heat Capacity Mapping Mission data of surface temperature). – Remote Sensing of Environment 18: 59-73.
[32] Price, J. C. (1990): Using spatial context in satellite data to infer regional scale evapotranspiration. – IEEE Transactions on Geoscience and Remote Sensing 28: 940-948.
[33] Ramkar, P., Yadav, S. M. (2018): Spatiotemporal drought assessment of a semi-arid part of middle Tapi River basin, India. – International Journal of Disaster Risk Reduction 28: 414-426.
[34] Ren, P. G., Zhang, B., Zhang, T. F., Li, X. Y., Chen, L., Lu, L. P. (2014): Trend analysis of meteorological drought change in Northwest China based on Standardized Precipitation Evapotranspiration Index. – Bulletin of Soil and Water Conservation 34: 182-187.
[35] Sandholt, I., Rasmussen, K., Andersen, J. (2002): A simple interpretation of the surface temperature/vegetation index space for assessment of surface moisture status. – Remote Sensing of Environment 79: 213-224.
[36] Santiago Beguería, Vicente-Serrano, S. M. (2013): Package 'SPEI'. – http://digital.csic.es/handle/10261/10002.

http://www.aloki.hu ● ISSN 1589 1623 (Print) ● ISSN 1785 0037 (Online)
DOI: http://dx.doi.org/10.15666/aeer/1804_52935314

[37] Sheffield, J., Wood, E. F. (2012): Drought: past problems and future scenarios. – International Journal of Digital Earth 5: 456-457.
[38] Shi, B. L., Zhu, X. Y., Hu, Y. C., Yang, Y. Y. (2017): Drought characteristics of Henan Province in 1961-2013 based on Standardized Precipitation Evapotranspiration Index. – Journal of Geographical Sciences 27: 311-325.
[39] Shi, S. E., Wei, W., Yang, D., Hu, X., Zhou, J. J., Zhang, Q. (2018): Spatial and temporal evolution of eco-environmental quality in the oasis of SRB based on RSEDI. – Chinese Journal of Ecology 37: 1152-1163.
[40] Shi, S. Y. (2013): High-yielding cultivation techniques of red globe grapes in arid desert in Gansu Province. – Fruit Tree Technology and Information 5: 11-12.
[41] Shu, C. (2012): Study on problems and countermeasures of agricultural development in Dunhuang City. – Social Sciences Review 4: 59-60.
[42] Sun, H., Chen, Y. H., Sun, H. Q. (2012): Comparisons and classification system of typical remote sensing indexes for agricultural drought. – Transactions of the Chinese Society of Agricultural Engineering 28: 147-154.
[43] Tian, W. H., Chen, R. Y. (2011): Study on water saving agriculture model in northwest arid area. – Water Resources and Hydropower Technology of Gansu 47: 47-50.
[44] Van Rooy, M. (1965): A rainfall anomaly index independent of time and space. – Notos 14: 43-48.
[45] Vicente-Serrano, S. M., Beguería, S., López-Moreno, J. I. (2010): A multi-scalar drought index sensitive to global warming: the Standardized Precipitation Evapotranspiration Index. – Journal of Climate 23: 1696-1718.
[46] WMO (2012): Standardized Precipitation Index User Guide. – WMO-No. 1090, Geneva.
[47] Wu, L., Zhang, Y. Z., Xie, W. H., Li, Y., Yang, S. C. (2012): The inversion of soil water content by the improved apparent thermal inertia. – Remote Sensing for Land and Resources 25: 44-49.
[48] Xu, F. H., Cui, Y., Ma, C. B. (2004): Status quo of development of dryland water saving agriculture in Australia and its enlightenment. – World Agriculture 26: 27-29.
[49] Yang, X., Wu, J. J., Yan, F. (2009): Assessment of regional soil moisture status based on characteristics of surface temperature/vegetation index space. – Acta Ecologica Snica 29: 1205-1216.
[50] Yao, N., Li, Y., Lei, T. J., Peng, L. L. (2017): Drought evolution, severity and trends in mainland China over 1961-2013. – Science of the Total Environment 616-617: 73-89.
[51] Yu, M., Cheng, M. H. (2010): Drought monitoring Heilongjiang Province Based on NDVI-Ts Space. – Journal of Applied Meteorological Science 21: 221-228.
[52] Yu, M. X., Li, Q. F., Hayes, M. J., Svoboda, M. D., Heim, R. R. (2014): Are droughts becoming more frequent or severe in China based on the standardized precipitation evapotranspiration index: 1951~2010? – International Journal of Climatology 34: 545-558.
[53] Zargar, A., Sadiq, R., Naser, B., Khan, F. I. (2011): A review of drought indices. – Environment Reviews 19: 333-349.
[54] Zawadzki, J., Kedzior, M. (2015): Soil moisture variability over Odra watershed: comparison between SMOS and GLDAS data. – International Journal of Applied Earth Observation and Geoinformation 51: 110.
[55] Zhang, Q., Zhang, L., Cui, X. C., Zeng, J. (2011): Progresses and challenges in drought assessment and monitoring. – Advances in Earth Science 26: 763-778.
[56] Zhang, Q., Yao, Y. B., Wang, Y., Wang, S. P., Jinsong Wang, J. S., Yang, J. H., Wang, J., Li, Y. P., Shang, J. L., Li, W. J. (2018): Characteristics of drought in Southern China under climatic warming, the risk, and countermeasures for prevention and control. – Theoretical and Applied Climatology 136: 3-4.
[57] Zou, X. K., Ren, G. Y., Zhang, Q. (2010): Droughts variations in China based on a compound index of meteorological drought. – Climatic and Environmental Research 15: 371-378.

http://www.aloki.hu ● ISSN 1589 1623 (Print) ● ISSN 1785 0037 (Online)
DOI: http://dx.doi.org/10.15666/aeer/1804_52935314

APPENDIX

Abbreviations

AD: agricultural drought
ATI: Apparent Thermal Inertia
AVI: Anomaly Vegetation Index
CI: Compound Index
CSI: Critical Success Index
ED: Extreme Drought
EOD: Effect of Detection
EW: Extreme Wet
FAR: False Alarm Ratio
F-D-ND: Fluctuation type of Drought and Non-Drought
F-LD-MD-SD: Fluctuation type of LD, MD, SD
GLDAS: Global Land Data Assimilation System
IMAD: Integrated Meteorological and Agricultural Drought
LD: Light Drought
LST: Land Surface Temperature
LW: Light Wet
MADI: Meteorological and Agricultural Drought Index
MD: Moderate Drought
MeD: meteorological drought
MW: Moderate wet
N: Normal
Pa: percentage of Precipitation anomaly
PDSI: Palmer Drought Severity Index
POD: Probability of Detection
MMSDI: Modified Multivariate Standardized Drought Index
MODIS: Moderate Resolution Imaging Spector radiometer
MSDI: Multivariate Standardized Drought Index
NASA: National Aeronautics and Space Administration
NOAA: National Oceanic and Atmospheric Association
NPP: Net Primary Productivity
NDVI: Normalized Difference Vegetation Index
SD: Severe Drought
SED: Stable Extreme Drought
SLD: Stable Light Drought
SMD: Stable Moderate Drought
SND: Stable Non-Drought
SPEI: Standardized Precipitation Evapotranspiration Index
SPI: Standardized Precipitation Index
SSD: Stable Severe Drought
SSM: Standardized Soil Moisture Index
StD: Stable Drought
SW: Severe Wet
TVDI: Temperature Vegetation Dryness Index
VCI: Vegetation Condition Index
VSWI: Vegetation Supply Water Index

http://www.aloki.hu ● ISSN 1589 1623 (Print) ● ISSN 1785 0037 (Online)
DOI: http://dx.doi.org/10.15666/aeer/1804_52935314

GENOTOXICITY OF WASTEWATER SAMPLES FROM THE TEXTILE INDUSTRY DETECTED BY BROAD BEAN (*VICIA FABA*) MICRONUCLEUS TEST ASSAY

ZGÓRSKA, A.* – BORGULAT, A.

Central Mining Institute in Katowice, Department of Water Protection
Plac Gwarków 1, 40-166 Katowice, Poland
(Zgórska, A. e-mail: azgorska@gig.eu; phone: +48-32-259-2480; fax: +48-32-259-2154)
(Borgulat, A. e-mail: aborgulat@gig.eu; phone: +48-32-259-2697; fax: +48-32-259-2154)

**Corresponding author*
e-mail: azgorska@gig.eu; phone: +48-32-259-2480; fax: +48-32-259-2154

(Received 5th Feb 2020; accepted 22nd May 2020)

Abstract. The textile wastewater induces a significant number of environmental problems, and while its toxicity has been extensively described in literature, its genotoxic and cytotoxic potential is not well known. The presence of non-biodegradable and highly toxic compounds in textile effluents make textile wastewater a possible source of ecological concern. Therefore, new data in subject matter may be very useful for their risk assessment. In the study the cytotoxicity and genotoxicity of textile wastewater derived from leather dyeing in reference to meristematic *Vicia faba* (*V. faba*) root cells has been studied. The study results show that textile wastewater decreased the mitotic index (MI) as well as significantly enhanced the micronucleus frequencies (MCN) and number of chromosomal aberrations (CA) in root cells. The MCN frequencies for wastewater samples were in the range of tested concentration 6.5 – 43.5 times higher than the negative control (NC). Also the correlation between the decreasing MI ratio and increasing wastewater concentration were detected. For the highest wastewater concentration the MI value was over 9 times lower than in the NC. The results indicate that textile wastewater has a genotoxic effect on plant cells and exposure to untreated wastewater can pose a potential cytotoxic and genotoxic risk.
Keywords: *cytotoxicity, dye, chromosome aberrations, micronuclei, mitotic index*

Introduction

Environmental impact of textile and dyeing industry is directly associated with significant amount of water consumption and significant quantities and types of chemicals used along all of the textile processing steps. Textile wastewater is a heterogeneous, poorly characterized complex mixture of several contaminants which contains a large amounts of dyes, pigments, biocides, metals, salts, surfactants, solvents, detergents and other non-biodegradable organic matters (Liang et al., 2018; Castro et al., 2019). Most of these substances poses a serious threat to exposed ecosystems. Toxicity and biodegradability of individual textile wastewater components has been the subject of many studies. Many of dyes and pigments widely used in the textile industry have been found to be toxic and genotoxic. The toxicity of dyes as individual components of textile wastewater has been widely described by authors who applies a battery of ecotoxicological tests contest organisms belonging to different trophic level and with a wide range of sensitivities (e.g. *Daphnia magna*, *Artemia salina*, *Raphidoceli subcapitata*, *Aliivibrio fischeri*, *Lemna minor*, *Cucumis sativum*, *Lycopersicon esculentum*, *Eisenia fetida*, etc.) (de Souza et al., 2007; Liang et al., 2018; Oliveira et al., 2018; Castro et al., 2019). Additionally, the publication describing the cytotoxicity, gentoxicity and mutagenicity of dyes detected using the techniques like mouse lymphoma assay, bone marrow micronucleus test and comet assay can also be found. The above-mentioned topics were the subject of work Fernandes et al. (2019) and Jha et al. (2016).

http://www.aloki.hu ● ISSN 1589 1623 (Print) ● ISSN 1785 0037 (Online)
DOI: http://dx.doi.org/10.15666/aeer/1804_53155323

However, in relation to textile wastewater, it should be noticed that wastewater are a complex mixture in which the dyes are only a part. Thus, the assessment of the toxicity of a single component is not sufficient to predict the interactions and joint toxicity of pollutant present in mixture even at low concentration and does not reflect the real environmental threat. While information about the potential toxicity of textile wastewater as a complex mixture can be found in trade literature (Castro et al., 2019), the knowledge about the genotoxicity and cytotoxicity of textile wastewater is still insufficient. Therefore, in order to enrich knowledge about the environmental threat posed by untreated or insufficiently treated textile wastewater the aim of the present study was to evaluate the genotoxic potential of raw textile wastewater by the use of *V. faba* micronucleus test assay. *V. faba* micronucleus test is a low cost, easy to handle short term assay which has been extensively used for environmental monitoring and genotoxicity assessment of various types of chemicals and wastewater (Duan et al., 1999; Iqbal, 2016). *V. faba* micronucleus test does not only provide information about cytotoxic and genotoxic potential of analyzed samples but also its mechanism of action on genetic material.

Materials &Methods

Wastewater sampling

Textile wastewater samples were obtained from textile industry located in GZM Metropolis (Silesia, Poland). Within the study an average daily wastewater sample were used. The samples were collected directly from the dyeing process line in July 2019. The daily average sample was a mixture of hourly samples taken during the 24-hour production cycle. During the daily production cycle, a sample of wastewater was taken every hour and placed in a collecting vessel. Two containers of 5 L capacity were taken for the test. Directly after collection, a part of wastewater was sent for physicochemical analysis the rest was portioned and storage in refrigerator until use. Before each genotoxicity test the wastewater samples were thawed and filtered.

Physico-chemical analysis

Within the study an average daily wastewater sample were used. The collected textile wastewater sample was analyzed for physico-chemical parameters like: pH, temperature, biochemical oxygen demand (BOD_5), chemical oxygen demand (COD), electrical conductivity (EC), total phosphorus (Ptot), total nitrogen (Ntot), total organic carbon (TOC) and suspended solids. Within the analyses the concentration of sulfate and chloride ions in wastewater sample was also determined. *Table 1* showed some special phasico-chemical parameters of the analyzed wastewater samples.

Test concentration and control

The essence of the micronucleus test is the assessment of damage of genetic material occurring during the cell division. The genetic damages are observed in plant cells in the division phase, therefore it is importent to use the samples that do not affect the total inhibition of the mitosis process. In order to determine an appriopriate range of textile wastewater concentrations for *V. faba* micronucleus test assay an initially the root growth inhibition test for meristematic part of broad been was carried out. The root growth inhibition test was performed for 8 wastewater concentration in a range 0.78%-

http://www.aloki.hu ● ISSN 1589 1623 (Print) ● ISSN 1785 0037 (Online)
DOI: http://dx.doi.org/10.15666/aeer/1804_53155323

100.00% (OECD, 1984). Based on root growth inhibition test result the EC_{50} value for meristematic part of *V. faba* was estimated (*Table 2*). According to the guidelines the target *V. faba* micronucleus test was carried out for wastewater concentrations in the range below the EC_{50}. Therefore, the *V. faba* micronucleus test was carried out for 5 test concentrations. The highest concentration corresponded to estimated EC_{50} value (15.40%) and amounted 12.50%. Subsequent wastewater concentrations were prepared by the dilution method, maintaining a dilution factor of 1: 2. Simultaneously, according to OECD (2014) recommendations in the field of genetic toxicology studies, the test was carried out using two types of test control: negative control (NC) and positive control (PC). As a NC an aerated tap water was used. The NC was used as a medium ensuring optimal culture growth conditions. A PC was used to observe damage induced by compounds with proven cancerogenic and mutagenic activity. In the micronucleus test a 1.12 g/L solution of maleic hydrazide (Sigma Aldrich, $C_4H_4N_2O_2$) was used as a PC. This compound is considered a potential carcinogen whose ability to cause micronuclei and chromosomal aberrations in plant cells has contributed to the widespread use of this compound in genotoxicity assessment (Hajjouji et al., 2007; Marcato-Romain et al., 2009; Sta et al., 2012).

Table 1. *Characteristics of untreated textile wastewater*

Parameter	Unit	Value	±SD
pH	-	6.6	*0.2*
Electrical conductivity (EC)	Ms/cm	7 500	*380*
Temperature	°C	14.5	-
COD	mg/L	17 500	*2 600*
BOD_5	mg/L	2 750	
TOC	mg/L	3 100	*460*
N_{tot}	mg/L	380	*57*
P_{tot}	mg/L	27.5	*2.8*
Suspended Solid	mg/L	2 000	*200*
Chloride	mg/L	635	*64*
Sulphates	mg/L	2 070	*210*

Table 2. *Impact of raw textile wastewater on growth inhibition of V.faba root*

Sample	Control		Textile wastewater concentration [%]							
	NC	**PC**	**100**	**50**	**25**	**12.5**	**6.25**	**3.13**	**1.56**	**0.78**
Mean root length [cm]	4.68	1.10	0.68	0.91	1.94	2.37	2.88	3.54	4.57	5.38
± SD	±1.*52*	*±0.21*	*±0.37*	*±0.31*	*±0.22*	*±0.66*	*±0.88*	*±2.47*	*±2.00*	*±3.75*
Growth inhibition [%]	-	76.5	85.3	80.5	58.5	49.3	38.3	24.3	2.32	-15.1
EC_{50} [%]	-	-	15.45							

Procedure for seeds treatment

In the test untreated broad bean (*V. faba*) seeds variety of White Windsor were used. The seeds were obtained from a local farmers' market. 72 hours before the proper micronucleus test, healthy, equal size *V. faba* seeds were pre-sterilized using a 2% H_2O_2 solution. After sterilization the seeds were soaked in tap water for 24 h and placed on moist surface to germinate for 2÷3 days at 20÷22°C. Incubations were carried out until the roots reached the required length of 1.5-2.5 cm. The required length should be

http://www.aloki.hu ● ISSN 1589 1623 (Print) ● ISSN 1785 0037 (Online)
DOI: http://dx.doi.org/10.15666/aeer/1804_53155323

understood as the length of the root obtained after seed germination, which allows to immersed the root in the tested medium without soaking the seed which protects the tested material against rotting. For each of the test concentrations and controls five seeds of *V. faba* were used. One seed means one measurement series.

Micronucleus test procedure

The *V. faba* micronucleus test was conducted based on the modified procedure described by Minissi and Lombi (1997). *V. faba* micronucleus test assay is a modification of the micronucleus test procedure recommended by OECD (2014) guidelines. After reaching by the *V. faba* roots a required length the seeds were peeled from the skin covering the endosperm. The seeds were handled carefully in a way that prevents damage the visible germ or seed shell. Prepared seeds were placed on styrofoam platforms covering the glass cuvette filled with adequate concentrations of textile wastewater and respectively controls solutions. The Styrofoam platform has been constructed in a way ensuring permanent contact of plant roots with the tested medium (form of hydroponic farming). After 44 h of incubation, *V. faba* roots were cut at 1.5-2 cm length and transferred to freshly prepared Carnoy solution (99% ethanol and glacial acetic acid in a 3: 1 ratio). Prepared samples were stored in 4÷7^{o}C in dark for 24 h. After 24 h, the roots were rinsed with distilled water. Within the test the possibility of indirect microscopic analysis was used. For this purpose, the roots were fixed in a 70% ethyl alcohol solution (PPH Stanlab sp. J.). Samples for analysis were stored in a refrigerator (4°C). In order to prepare microscopic preparations, the roots were washed in dH_2O and subjected to hydrolysis in 1N hydrochloric acid solution (POCH S. A.), at a temperature of 55÷60^{o}C for a time of 5-7 minutes. After hydrolysis the roots were washed in dH_2O and placed on microscope slides. 1.0÷1.5 mm meristem was cut, stained with a 2% orcein solution (2% orcein in 45% glacial acetic acid) and left for 2÷5min (dye penetration time). A cover slip was applied. Microscopic observation was carried out at 1000x magnification (10 × 100) using a Motic light microscope. Pictures of the cells were taken with the MOTICam 100 camera and developed in the Motic Images program. For each of the test concentrations and controls, the test was performed in 5 replicates. In each replication, microscopic observations were made for 1000 cells (1 series = 5000 cells analyzed / concentration). Based on the results of microscopic analysis, the following parameters were assessed: the value of the mitotic index (IM), the frequency of chromosome aberrations in cells during mitotic division (CA), as well as the incidence of micronucleus aberrations in the observed cells (MCN).

Scoring the mitotic indexd (MI)

Five slides for each wastewater concentration and control were prepared. Nearly 5000 cells (1000 cells per slide) were subjected to microscopic analysis to determine the mitotic index (MI). The MI value was calculated as the quotient of a total number of dividing cells to total number of cells examined.

Scoring the micronucleus (MCN) and chromosomal aberrations (CA) frequency

About 1000 meristematic cells were scored for each slide. The MCN frequency was calculated from the number of cells with scored MCN aberrations divided by the total cells scored for slide and expressed in terms of MCN/1000 cells. Adequately, the CA

http://www.aloki.hu ● ISSN 1589 1623 (Print) ● ISSN 1785 0037 (Online)
DOI: http://dx.doi.org/10.15666/aeer/1804_53155323

were analyzed by microscope observing about 400 cells at the stage of mitosis per slide. During the analyses a different types of the aberration cells were observed and recorded.

Statistical analysis

Statistical analysis was performed using MS EXcel software. The obtained results are expressed as an average value and standard errors.

Results & Discussion

MI is considered as an indicator that allows to estimate the frequency of cellular division. The results of the analysis (*Table 3*) show that textile wastewater induced mitotic delay and decrease MI frequency in meristematic root cell of *V. faba*. The MI index was significantly different for all analyzed samples, however in all test series a reliable and reproducible results were obtained. Compared to NC, MI frequencies decreased with increasing wastewater concentration. Textile wastewater affected the inhibition of the cell division from 13.67% to 54.85%. The 54.85% reduction of MI versus NC were detected in the *V. faba* root tips after treatment with the highest wastewater concentration (12.50%). Similar results were obtained by Giorgetti, which evaluates the geneotoxicity of raw effluents from textile industry. Estimated MI value was heavily reduced from 19.58% in the NC to 3.82% for raw effluent. For undiluted textile wastewater the mitosis activity inhibition was 80.49% (Giorgetti et al., 2011).

Table 3. *Value of mitotic index (MI) in root tip cells of V. faba treated with textile wastewater in various concentrations*

Wastewater concentration	**Mitotix index per 1000 *Vicia faba* cells in 5 root tips [%]**						
Series	1	2	3	4	5	Mean	±SE
12.5%	2.13	1.45	0.74	2.56	2.09	1.79	±0.71
6.25%	7.05	8.14	8.62	6.99	6.2	7.40	±0.97
3.125%	8.3	7.12	8.34	9.76	8.98	8.45	±0.99
1.56%	10.15	10.78	11.14	15.12	11.23	11.68	±1.97
0.78%	13.56	15.24	14.98	10.77	16.2	14.15	±2.11
NC	14.23	16.53	18.34	15.23	17.65	16.39	±1.69
PC	1.89	1.76	0.96	1.45	1.15	1.44	±0.39

The determined values of MI confirms the results obtained in growth inhibition test. Root growth reflects the toxicity in the elongation plant zone, as root growth inhibition is caused by the occurrence of chromosol aberration and a reduction in the root length of *V. faba* exposed to textile wastewater (Bhat et al., 2017). Both test results (growth inhibition, micronucleus test) confirm that textile wastewater in concentration above 12.50% are highly toxic and affect significant growth inhibition, which exceeds the 80% for wastewater concentration above 50%. Maximum inhibition of cell division noted in the micronucleus test directly coincides to a EC_{50} (15.45%) estimated in growth inhibition test for meristematic part of *V. faba* (*Table 2*). A comparable impact level of textile wastewater on plant cells has been shown by Samuel (2010). Estimated EC_{50} value of textile industry effluent for rhizosphere part of *Allim cepa* amounted 16% after 96 h of exposition.

http://www.aloki.hu ● ISSN 1589 1623 (Print) ● ISSN 1785 0037 (Online)
DOI: http://dx.doi.org/10.15666/aeer/1804_53155323

The genotoxic effects expressed as the number of micronuclei (MCN) induced in *V. faba* root cells are given in *Table 4*. The reference point in the text is the PC that induced a significantly high number of micronuclei in root tips of *V. faba* (24.42‰). The number of micronuclei inducted by textile wastewater was lower according to PC (twice lower) and simultaneously much higher in reference to NC (43 times higher). Conducted studies proves that textile wastewater, even at low concentrations, causes damage to the genetic material of tested plants. The number of micronuclei identified in root cells exposed to wastewater sample at the lowest concentration reach 1.58‰ (wastewater concentration 0.78%) and increased with increasing wastewater concentration up to value 10.44‰ (wastewater concentration 12.50%). Examples of micronucleus aberrations observed in *V. faba* meristematic cells are presented in *Figure 1*.

Table 4. *MCN frequencies in root tip cells of V. faba treated with textile wastewater in individual concentrations*

Wastewater concentration	**MCN per 1000 *Vicia faba* cells in 5 root tips [‰]**					**Mean**	
Series	1	2	3	4	5	Mean	±SE
12.5%	11.89	10.98	9.77	11.02	8.56	10.44	±1.29
6.25%	6.54	9.28	7.13	7.25	6.14	7.27	±1.21
3.125%	4.56	10.56	5.12	4.16	6.55	6.19	±2.61
1.56%	2.94	3.15	3.89	2.06	3.85	3.18	±0.75
0.78%	1.03	0.99	1.45	2.43	2.01	1.58	±0.63
NC	0.78	0.00	0.00	0.12	0.32	0.24	±0.33
PC	24.32	21.34	19.87	26.75	29.84	24.42	±4.03

The study result shows a clastogenic effect, evidenced by the induction of CA at used concentration. During the micronucleus test the major CA were noted as fragments, laggards, vagrants and chromosomal bridges (*Figure 2*). The lowest CA frequency was observed to be 0.39% in control sample (NC). In turn the highest frequency of CA (18.78%) was found to be in 12.50% concentration of textile wastewater. A PC, whose genotoxicity has been confirmed, induced chromosomal aberrations at the level 3.52%. An increasing with wastewater concentration percentage of CA showed positive correlation with sample concentration (*Table 5*).

Additionally, the studies proved the usefulness of *V. faba* micronucleus test for assessing the genotoxic potential of such complex mixtures as textile wastewater. Similar conclusions based on research were formulated by Bhat (2017). Author indicate in his work that the *V. faba* (broad bean) bioassay is used extensively to evaluate toxic substances in the environment and is an excellent bioassay for toxicological observations. As an advantage of the method author indicates the high sensitivity and economic profitability of the test. Moreover, author marks the that broad bean cells are quite large which makes the chromosomes more visible and finally makes the chromosomal-aberration evaluation easier (Bhat et al., 2017). The study result confirm that plant test model based on the analysis of induced changes in meristematic cells of *V. faba* is effective and appropriate assay for detection of genotoxicity and cytotoxicity of environmental samples.

http://www.aloki.hu ● ISSN 1589 1623 (Print) ● ISSN 1785 0037 (Online)
DOI: http://dx.doi.org/10.15666/aeer/1804_53155323

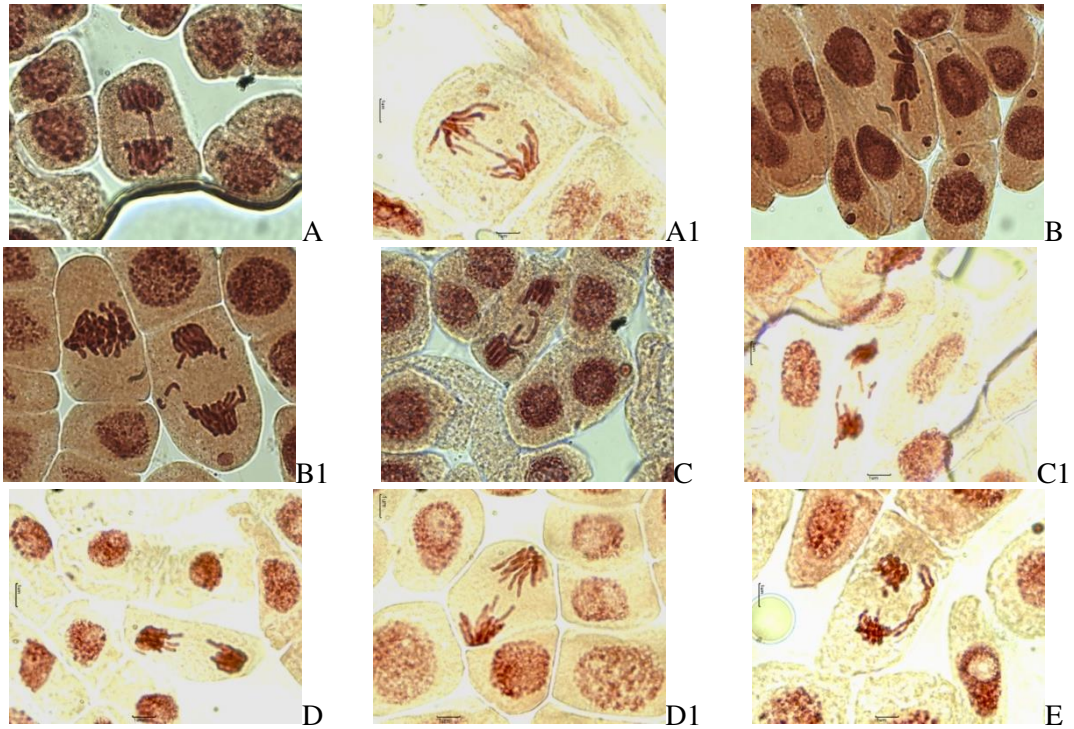

Figure 1. *Examples of micronucleus and chromosomal aberrations observed in Vicia faba root cells after exposure to textile wastewater: [A,A1]chromosome bridge; [B,B1]fragments of chromosome; [C,C1]lagger chromosome; [D,D1]vagrant chromosome; [E]multi aberration*

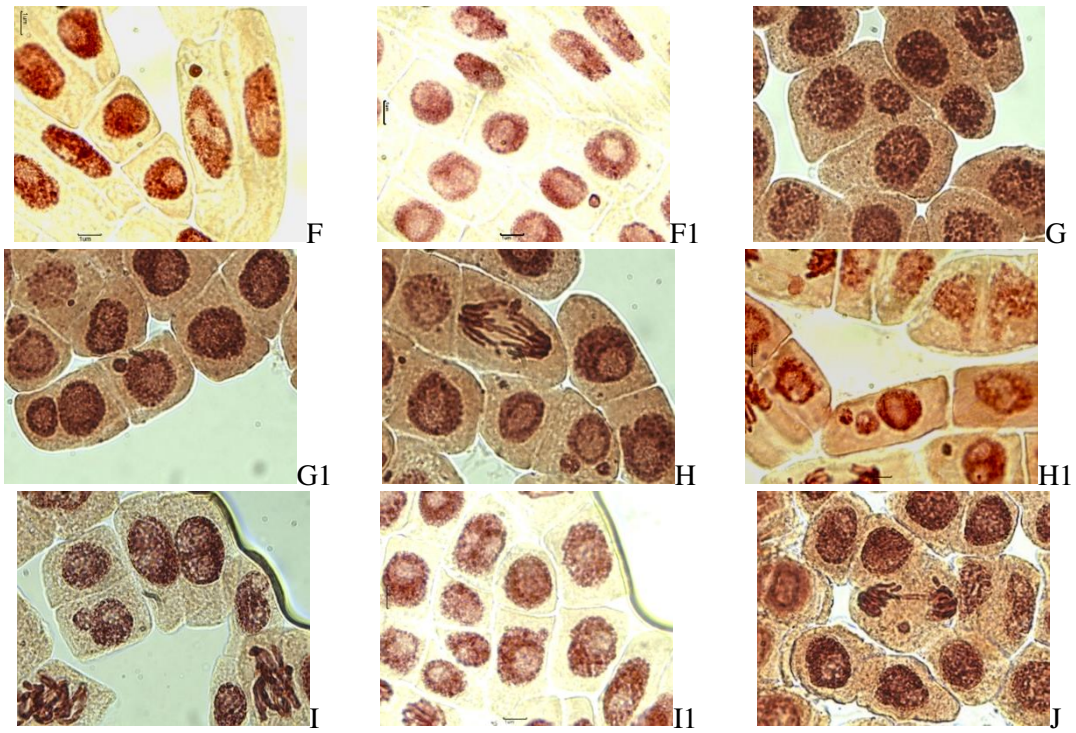

Figure 2. *Examples of micronucleus aberration observed in V.faba root cells after exposure to textile wastewater: [F,F1]micronuclei; [G,G1]meganuclei,[H,H1] multinuclei; [I,I1]bud chromosome; [J]micronuclei in anaphase*

http://www.aloki.hu ● ISSN 1589 1623 (Print) ● ISSN 1785 0037 (Online)
DOI: http://dx.doi.org/10.15666/aeer/1804_53155323

Table 5. *CA frequencies in root tip cells of V. faba treated with textile wastewater in individual concentrations*

Wastewater concentration	**CA per 400 *Vicia faba* cells in 5 root tips [%]**						
Series	1	2	3	4	5	Mean	±SE
12.5%	18.67	17.34	21.14	18.32	18.45	18.78	±1.41
6.25%	11.23	10.98	9.87	11.34	12.14	11.11	0.82
3.125%	7.85	7.64	8.14	6.14	7.33	7.42	±0.76
1.56%	3.87	4.1	2.88	3.95	4.13	3.79	±0.52
0.78%	2.65	1.89	2.54	2.32	1.99	2.28	±0.33
NC	0.65	0.45	0.00	0.87	0.00	0.39	±0.39
PC	3.45	4.21	2.98	3.21	3.75	3.52	±0.48

Conclusion

The results of the study showed toxic effect posed by untreated textile wastewater on the meristematic cell of *V. faba*. The test results demonstrated a positive correlation between the wastewater concentration and toxic effect expressed in the indicators form as MI, MCN frequencies and CA. Conducted research proves that textile wastewater have a genotoxic potential. The results imply that the wastewater could result in environmental contamination even at low concentration and exposure to wastewater might posed potential risk conducted cytogenetic damages induced in exposed organisms cells. Additionally, the study results imply that *V. faba* micronucleus assay as a sensitive and repeatable method can successfully use for testing cytotoxic and genotoxic risk for both, individual (chemical) substances, which have been already proved, as well as complex mixtures, such as textile wastewater which often forming a difficult to identify. Moreover, described method is cheaper than other techniques that may be used in genotoxicological studies (e.g. FISG, GISH or RT-PCR) and, what is particularly important, does not require sterile working conditions.

Acknowledgements. The work was carried out in Central Mining Institute as a part of the statutory work №11158019 co-funded by the Polish Ministry of Science and Higher Education.

REFERENCES

[1] Bhat, S. A., Singh, J., Singh, K., Vig, A. P. (2017): Genotoxicity Monitoring of Industrial Wastes Using Plant Bioassays and Management through Vermitechnology: A Review. – Agriculture and Natural Resources 51(5): 325-37.

[2] Castro, A. M. , Nogueira, V., Lopez, I., Rocha-Santos, T. (2019): Evaluation of the Potential Toxicity of E Ffl Uents from the Textile Industry before and after Treatment. – Applied Sciences 9: 3804. doi:10.3390/app9183804.

[3] De Souza, U., Guelli, S. M. A., Forgiarini, E., Augusto, A. (2007): Toxicity of Textile Dyes and Their Degradation by the Enzyme Horseradish Peroxidase (HRP). – Journal of Hazardous Materials 147(3): 1073-78.

[4] Duan, C. Q., Hu, B., Jiang, X. H., Wen, C. H., Wang, Z., Wang, Y. X. (1999): Genotoxicity of Water Samples from Dianchi Lake Detected by the Vicia Faba Micronucleus Test. – Mutation Research - Fundamental and Molecular Mechanisms of Mutagenesis 426(2): 121-25.

http://www.aloki.hu ● ISSN 1589 1623 (Print) ● ISSN 1785 0037 (Online)
DOI: http://dx.doi.org/10.15666/aeer/1804_53155323

[5] Fernandes, F. H., de Aragão Umbuzeiro, G., Fávero-Salvadori, D. M. (2019): Genotoxicity of Textile Dye C.I. Disperse Blue 291 in Mouse Bone Marrow. – Mutation Research - Genetic Toxicology and Environmental Mutagenesis 837: 48-51.
[6] Giorgetti, L., Talouizte, H., Merzouki, M., Caltavuturo, L., Geri, C., Frassinetti, S. (2011): Genotoxicity evaluation of effluents from textile industries of the region Fez-Boulmane, Morocco: A case study. – Ecotoxicology and Environmental Safety 74(8): 2275-2283.
[7] Hajjouji, H. El., Pinelli, E., Guiresse, M., Merlina, G., Revel, J. C., Hafidi, M. (2007): Assessment of the Genotoxicity of Olive Mill Waste Water (OMWW) with the Vicia Faba Micronucleus Test. – Mutation Research - Genetic Toxicology and Environmental Mutagenesis 634(1-2): 25-31.
[8] Iqbal, M. (2016): Vicia Faba Bioassay for Environmental Toxicity Monitoring: A Review. – Chemosphere 144: 785-802.
[9] Jha, P., Jobby, R., Desai, N. S. (2016): Remediation of Textile Azo Dye Acid Red 114 by Hairy Roots of Ipomoea Carnea Jacq. and Assessment of Degraded Dye Toxicity with Human Keratinocyte Cell Line. – Journal of Hazardous Materials 311: 158-67.
[10] Liang, J., Ning, X., Kong, M., Liu, D., Wang, G., Cai, H., Sun, J., Zhang, Y., Lu, X., Yuan, Y. (2017): Elimination and Ecotoxicity Evaluation of Phthalic Acid Esters from Textile-Dyeing Wastewater. – Environmental Pollution 231: 115-22.
[11] Liang, J., Ning, X., Sun, J., Song, J., Lu, J., Cai, H., Hong, Y. (2018): Toxicity Evaluation of Textile Dyeing Effluent and Its Possible Relationship with Chemical Oxygen Demand. – Ecotoxicology and Environmental Safety 166: 56-62.
[12] Marcato-Romain, C. E., Pinelli, E., Pourrut, B., Silvestre, J., Guiresse, M. (2009): Assessment of the Genotoxicity of Cu and Zn in Raw and Anaerobically Digested Slurry with the Vicia Faba Micronucleus Test. – Mutation Research - Genetic Toxicology and Environmental Mutagenesis 672(2): 113-18.
[13] Minissi, S., Lombi, E. (1997): Heavy Metal Content and Mutagenic Activity, Evaluated by Vicia Faba Micronucleus Test, of Tiber River Sediments. – Mutation Research 393: 17-21.
[14] Oliveira, G. A. R., Leme, D. M., de Lapuente, J., Brito, L. B., Porredón, C., de Brito Rodrigues, L., Brull, N. (2018): A Test Battery for Assessing the Ecotoxic Effects of Textile Dyes. – Chemico-Biological Interactions 291: 171-79.
[15] Organization for Economic Cooperation and Development (1984): Terrestrial Plants, Growth Test. – Test No. 208.
[16] Organization for Economic Cooperation and Development (2014): In vitro Mammalian Cell Micronucleus Test. – Test No. 487.
[17] Samuel, O. B., Osuala, F. I., Odeigah, P. G. C. (2010): Cytogenotoxicity Evaluation of Two Industrial Effluents Using Allium Cepa Assay. – African Journal of Environmental Science and Technology 4(1): 21-27.
[18] Sta, C., Ledoigt, G., Ferjani, E., Goupil, P. (2012): Exposure of Vicia Faba to Sulcotrione Pesticide Induced Genotoxicity. – Pesticide Biochemistry and Physiology 103(1): 9-14.

http://www.aloki.hu ● ISSN 1589 1623 (Print) ● ISSN 1785 0037 (Online)
DOI: http://dx.doi.org/10.15666/aeer/1804_53155323

EFFECTS OF NANO-POTASSIUM FERTILIZER ON AMINO ACID COMPONENTS AND GLN FAMILY GENE EXPRESSION IN CHINESE CABBAGE

JIN, Z. J. – LIU, Y. – XU, W. H.* – YANG, C. – CHEN, S. L. – LI, Y. H.

College of Resources and Environmental Sciences, Southwest University, Chongqing 400715, P. R. China
(phone: +86-23-68251249; fax: +86-23-68251912)

**Corresponding author*
e-mail: xuwei_hong@163.com

(Received 15th Feb 2020; accepted 7th Jul 2020)

Abstract. This study was conducted to investigate the effects of nano potassium silicate on amino acid components and family gene expression of nitrogen metabolism-related glutamine synthetase (GS) in Chinese cabbage (Brassica rapa L. ssp. pekinensis). With ordinary potassium silicate (OKSi) and nano potassium silicate (NKSi) as different potassium fertilizers, the experiment set four potassium levels (K2O) of 0 (CK), 150, 300 and 450 kg·hm-2, respectively. Field experiments were adopted to investigate the effects of different forms and levels of potassium on the amino acid content of Chinese cabbage and GLN family gene expression in roots, stems and leaves. The total amount of essential amino acids was the highest in NKSi-300 treatment, which was 41.1% higher than that in the control (CK). In the stem of Chinese cabbage, the relative expression of GLN1.2, GLN1.3, GLN1.4 and GLN2 was up by 7.85, 3.46, 45.6 and 50.7 times compared with CK under NKSi-300 treatment. In Chinese cabbage leaves, GLN1.1, GLN1.2 and GLN1.3 had the highest relative expressions under NKSi-150 treatment, which were up by 1.984, 1.235 and 1.617 times, respectively compared to CK. GLN family gene expression was significantly or extremely significantly correlated with histidine, glycine, methionine, tyrosine and cysteine contents in the stem of Chinese cabbage.
Keywords: *nano potassium silicate, Chinese cabbage, amino acid, GLN family gene, correlation analysis*

Introduction

It has become an important goal to improve vegetable quality in today's vegetable production. Amino acids, sugars, organic acids and volatile metabolites have always acted as important indicators for evaluating nutritional and flavor quality of vegetables. To study the key enzymes and key genes involved in the synthesis of these compounds carries important significance for vegetable quality control. As one of the essential nutrients for plant growth and development, potassium participates in multiple metabolic processes of plants, which is crucial for the development of quality vegetable. However, China lacks potash fertilizer resources, potassium-ion soil deficiency is prevalent in China and Asia, and urgent solution is needed. Nanotechnology involves the understanding and control of substances at the nanoscale, i.e. new applications having unique physical, chemical and biological properties (nanomaterials, NMs) with dimensions in the range of 1-100 nm (Huang et al., 2014). Nano-fertilizers provide certain effects in improving fertilizer utilization rate and agricultural product quality. Nano-selenium fertilizer can increase the content of selenomethionine, selenium methylation cysteine, etc. in wheat (Li et al., 2017). The experiment results on combined application of low potassium and nano magnesium hydroxide showed significantly increased contents of carotene, total phenols and flavonoids in Chinese cabbage (Brassica rapa L. ssp. pekinensis), with potassium utilization efficiency significantly improved (Yuan et al., 2017). Foliar spray

http://www.aloki.hu ● ISSN 1589 1623 (Print) ● ISSN1785 0037 (Online)
DOI: http://dx.doi.org/10.15666/aeer/1804_53255342

tests on nano chelate nitrogen fertilizer and urea showed that the former can better improve the quality of pomegranate fruit (Davarpanah et al., 2017).

Since the 1930s, breeders have been emphasizing yield increase, basically ignoring vegetable quality in aspects like flavors and nutritional properties of interest to consumers (Gascuel et al., 2017). For the reason: first, it is quite difficult to obtain complex polygenic traits such as flavor; second, we lack understanding of molecular genetic basis of vegetable quality (Lim et al., 2014). These result in decline in vegetable quality and loss of flavor, indirectly producing a negative impact on vegetable consumption. Despite the continuous development of biotechnology in recent decades, breeding programs often fail in the face of complex quality traits (Mattoo et al., 2014). Advances in biotechnology and omics technology for variant traits may help us decode the underlying genetic basis of complex traits, so that it is possible to implant optimal allele to vegetables by hybridization, genetic engineering, transgenic techniques or new plant breeding techniques (NPBT) to improve vegetable quality (Gascuel et al., 2017). To this end, this study adopted field experiments to investigate the effect of nano potassium silicate on amino acid composition of Chinese cabbage, and explore the effect of nano potassium silicate on the family gene expression of amino acid metabolism and nitrogen metabolism-related glutamine synthetase in Chinese cabbage. The study aims to clarify the physiological and molecular biological mechanism in amino acid metabolism regulation of vegetables by nano-potassium fertilizer, thus providing a theoretical basis for efficient utilization of potassium fertilizer resources and high-quality vegetable production.

Materials and methods

Plant material, soil and treatments

The Chinese cabbage (Brassica rapa L. ssp. pekinensis) variety for the field experiment was “Liangqing”, and the test fertilizer was the same as that in the pot experiment. The physical and chemical properties of the tested soil are shown in *Table 1*.

Table 1. *Basic soil physical and chemical properties in the field experiment*

pH Water/Soil=1/1	Organic matter /g·kg^{-1}	Total nitrogen /g·kg^{-1}	Available nitrogen /mg·kg^{-1}	Available phosphorus /mg·kg^{-1}	Available potassium /mg·kg^{-1}
5.80	25.8	1.70	140	127	77.5

The field experiment was conducted from February 18, 2017 to May 19, 2017 at Sanyuan Village, Badang Town, Bishan District, Chongqing, China. There were three potassium levels (K2O), 150, 300 and 450 kg·hm^{-2}, respectively, as well as potassium-free blank control (CK) (*Table 2*). Each treatment was repeated 3 times, and application of nitrogen (N) and phosphorus (P2O5) was consistent in all treatments. According to the customary application rate of farmers, 750 kg·hm^{-2} nitrogen-phosphorus compound fertilizer (15-15-0) was converted into urea and superphosphate and applied to the soil by means of furrow application. Only nitrogen fertilizer was applied in late topdressing, and the dosage was 300 kg·hm^{-2} urea. The test plot area was 2 m × 5 m = 10 m^2, a total of 21 plots. 60 strains of Chinese cabbage seedlings with uniform growth conditions were

http://www.aloki.hu ● ISSN 1589 1623 (Print) ● ISSN1785 0037 (Online)
DOI: http://dx.doi.org/10.15666/aeer/1804_53255342

transplanted in each plot, arranged in random blocks, with a spacing of 0.5 m between the plots for easy management. Also, guard rows were set around. Field management was carried out in accordance with conventional management. After the Chinese cabbage matured, 5 representative plants were selected and harvested from each plot. Different organ samples of Chinese cabbage were collected by portable liquid nitrogen tanks and stored in a -80 °C ultra-low temperature refrigerator for subsequent gene expression determination. Part of the harvested plants were used for determination of vegetable quality indicators, while part was killed at 105 °C, dried, crushed and stored at 65-80 °C for analysis and detection of plant nutrients.

Table 2. *Field experiment design and fertilization amount*

Treatment	N-P_2O_5-K_2O/kg·hm^{-2}
CK	112.5-112.5-0
OKSi-150	112.5-112.5-150
OKSi-300	112.5-112.5-300
OKSi-450	112.5-112.5-450
NKSi-150	112.5-112.5-150
NKSi-300	112.5-112.5-300
NKSi-450	112.5-112.5-450

Amino acid component determination

Measurement was carried out using L-8800 automatic amino acid analyzer (Hitachi, Japan).

RNA extraction

RNA was extracted from the roots, stems and leaves of Chinese cabbage using EZ-10 DNAaway RNA Mini-Preps Kit (Sangon Biotech Co., Ltd, China). Please refer to the operating instruction on the kit for the specific procedures. The sample RNA was stored in -80 °C refrigerator for later use.

RNA concentration and quality detection

Using RNase-Free Water as a reference, the concentration and quality of extracted RNA were detected using a NanoDrop 2000C spectrophotometer (500 ng/band) (Thermo Scientific, Wilmington, DE, USA), and RNA degradation degree and quality were measured by 1% agarose gel electrophoresis. The results are shown in *Table 3* and *Figure 1*.

The detection results of NanoDrop 2000C spectrophotometer show that RNA concentration is greater than 125 ng·μL^{-1}, OD260/280 is between 1.8-2.21, and OD260/OD230 is greater than 2.0, indicating that there is no protein or phenolic substances, carbohydrate, salt pollutions and quality and concentration are qualified.

The results of RNA agarose gel electrophoresis (*Figure 1*) show that 28S band is brighter than 18S band, 5S band is the darkest or invisible, the characteristic bands are clear, the degradation is unobvious. Quality and concentration are assessed as qualified by luminance method (Li et al., 2018) and usage for follow-up experiments like reverse transcription is possible.

http://www.aloki.hu ● ISSN 1589 1623 (Print) ● ISSN1785 0037 (Online)
DOI: http://dx.doi.org/10.15666/aeer/1804_53255342

Table 3. *Concentration and quality test results of RNA extracted from Chinese cabbage in the field experiment*

No.	Treatments	RNA concentrations /ng·μL^{-1}	OD_{260}/ OD_{280}	OD_{260}/OD_{230}
1	CK-BrR	672.4	2.17	2.32
2	OKSi-150-BrR	815.8	2.18	2.38
3	OKSi-300-BrR	565.0	2.17	2.29
4	OKSi-450-BrR	1172.4	2.21	2.36
5	NKSi-150-BrR	492.8	2.14	2.19
6	NKSi-300-BrR	1056.3	2.19	2.33
7	NKSi-450-BrR	560.6	2.15	2.24
8	CK-BrS	224.8	2.16	2.17
9	OKSi-150-BrS	232.4	2.17	2.25
10	OKSi-300-BrS	212.7	2.17	2.23
11	OKSi-450-BrS	213.9	2.18	2.23
12	NKSi-150-BrS	126.3	2.17	2.14
13	NKSi-300-BrS	140.5	2.18	2.14
14	NKSi-450-BrS	135.9	2.19	2.09
15	CK-BrL	1348.1	2.19	2.34
16	OKSi-150-BrL	1629.1	2.2	2.35
17	OKSi-300-BrL	1210.5	2.2	2.33
18	OKSi-450-BrL	1071.3	2.21	2.37
19	NKSi-150-BrL	1076.5	2.16	2.27
20	NKSi-300-BrL	1894	2.16	2.27
21	NKSi-450-BrL	847.2	2.16	2.22

Note: BrR/S/L indicates the root/stem/leaf of Chinese cabbage, the same below

RNA purification and reverse transcription

gDNA removal and reverse transcription were performed using TaKaRa PrimeScript® Reagent Kit. For specific procedures, refer to the kit's operating instructions. The reverse transcription product cDNA was stored in a -20 °C refrigerator.

Detection of reverse transcription product cDNA

With cDNA as a template, F26Sq+R26Sq was used as a primer (primer sequence was 5'-GTTACCACAGGGATAACTGGCTTG-3' + 5'-CTAACCTGTCTCACGACGG TCTAA-3'), and 26SrRNA gene was amplified by 25 μL system and detected by agarose gel electrophoresis. The reaction system is as follows (*Table 4*).

The PCR reaction procedure was as follows: predenaturation at 94 °C for 2 min; denaturation at 94 °C for 1 min, annealing at 60 °C for 30 s, extension at 72 °C for 30 s, repetition by 18 cycles and 35 cycles; extension at 72 °C for 10 min and at 4 °C for 2 min.

The results of cDNA electrophoresis (*Figure 2*) show that a clear band of about 173bp is obtained by agarose gel electrophoresis except for No.6 (*Figure 2A*), indicating successful reverse transcription. However, RNA reverse transcription efficiency differs due to different RNA concentrations and purities, so 173 bp bands show slightly different brightness, and No.6 only has weak brightness. As can be seen from Figure *2B*, No. 6 has been reverse transcribed successfully, though the reverse transcription efficiency is low.

http://www.aloki.hu ● ISSN 1589 1623 (Print) ● ISSN1785 0037 (Online)
DOI: http://dx.doi.org/10.15666/aeer/1804_53255342

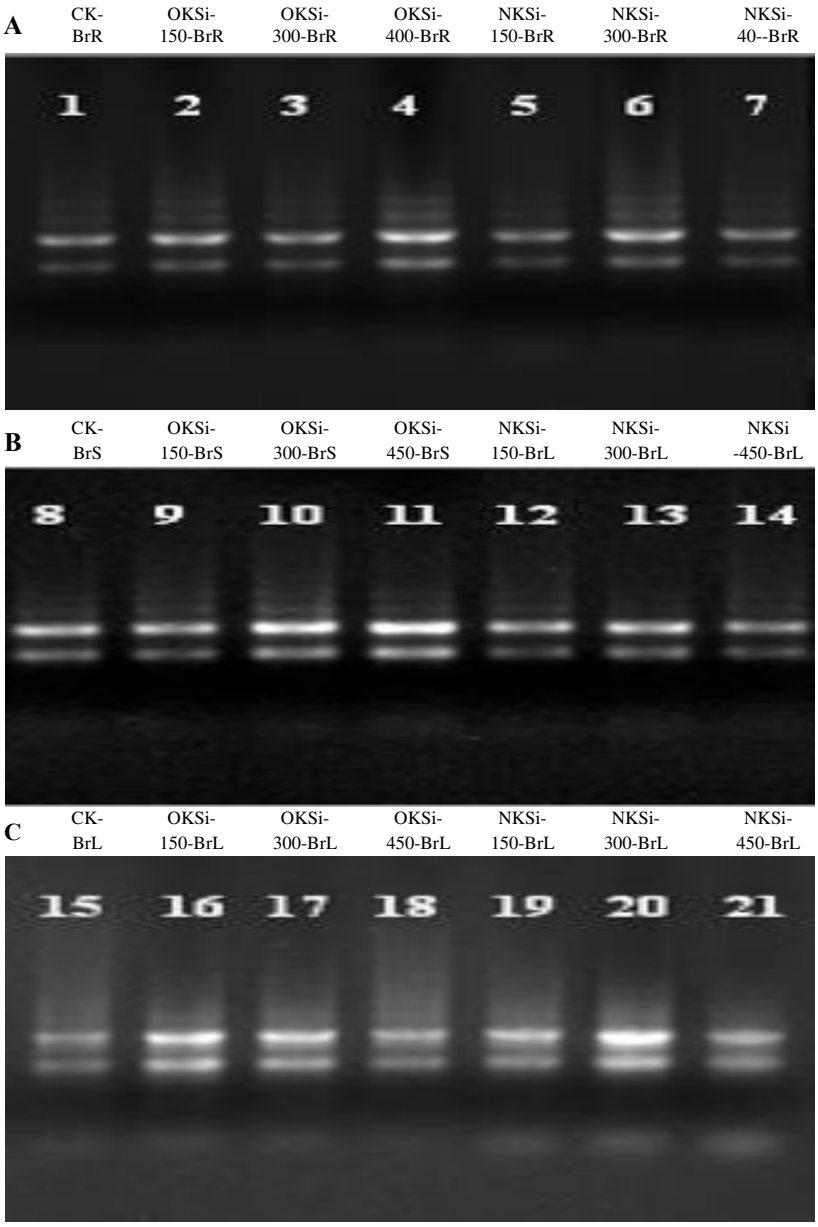

Figure 1. *Agarose gel electrophoresis detection results of RNA extracted from Chinese cabbage. Note: No.1-21 has the same meaning as Table 3, M-Trans 2K Plus Marker*

Table 4. *Amplification system of reverse transcription product PCR*

Reagents	Volume/μL
ddH_2O	20.15
cDNA	0.50
dNTPs /10 $mmoL \cdot L^{-1}$	0.50
F26Sq /10 $\mu moL \cdot L^{-1}$	0.50
R26Sq /10 $\mu moL \cdot L^{-1}$	0.50
10×Easy Taq Buffer (Mg^{2+})	2.50
Easy-Taq DNA PoLymerase /5$U \cdot \mu L^{-1}$	0.35
Total volume	25.0

Note: F-Forward primer, R-Reverse primer

http://www.aloki.hu ● ISSN 1589 1623 (Print) ● ISSN1785 0037 (Online)
DOI: http://dx.doi.org/10.15666/aeer/1804_53255342

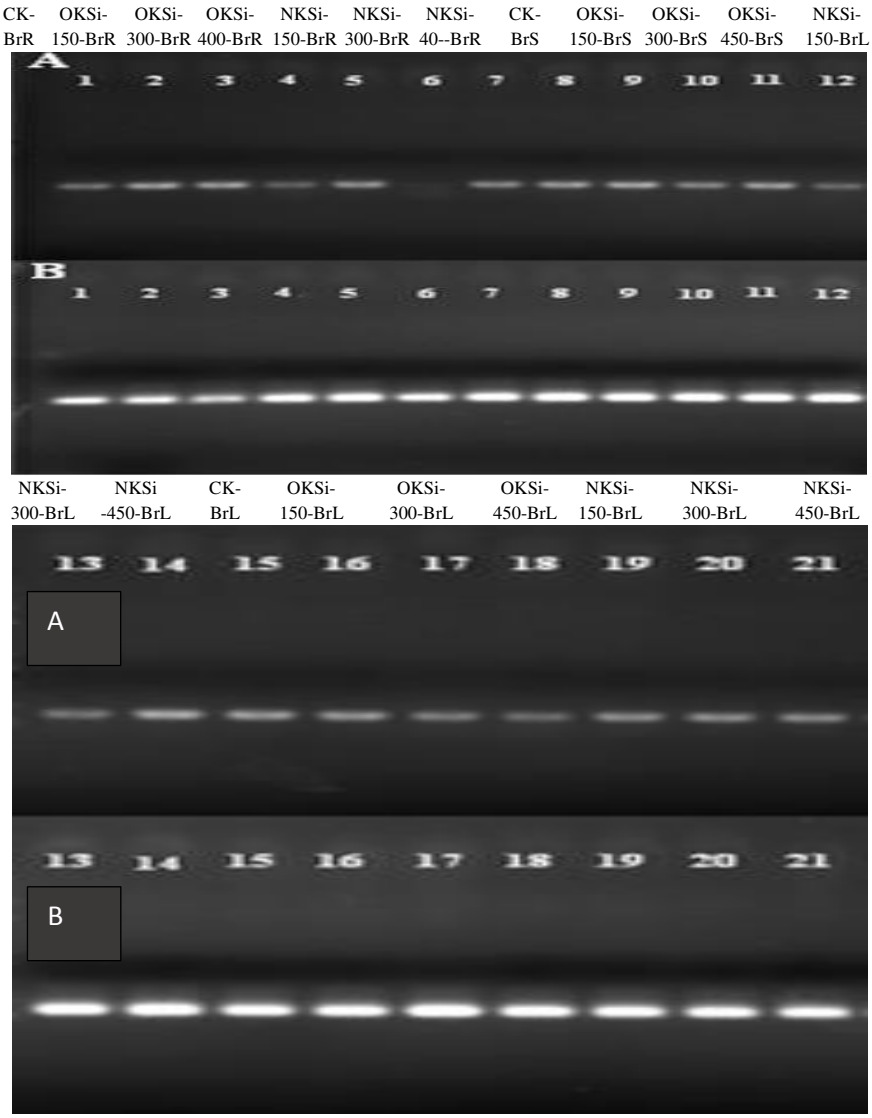

Figure 2. *Agarose gel electrophoresis results of reverse transcription product cDNA. Note: 18A-PCR amplified cyclic electrophoresis results; 35 B-PCR amplified cyclic electrophoresis results, number 1-21 has the same meaning as those in Table 3, M-Trans 2K Plus Marker*

Electronic cloning of GLN family gene

The locus number of the Arabidopsis thaliana L. GLN family gene was accessed from Arabidopsis thaliana L. database. BLAST was performed on NCBI website, Organism was defined as Arabidopsis thaliana L. and Brassica rapa L. ssp. pekinensis, respectively. The database was defined as Reference RNA sequence (refseq_rna), Reference genomic sequences (refseq_ genomic) and Transcriptome Shotgun Assembly (TSA). The reference RNA sequences, reference chromosomal sequences and TSA sequences of Arabidopsis thaliana L. and Brassica L. ssp. pekinensis GLN family genes were obtained from BLAST results; sequences were created using Vector NTI Advance 11.5. Then, using the Arabidopsis thaliana L. GLN family gene sequence as a basic sequence, the above sequence tags were added one by one for alignment until multiple alignments were completed.

http://www.aloki.hu ● ISSN 1589 1623 (Print) ● ISSN1785 0037 (Online)
DOI: http://dx.doi.org/10.15666/aeer/1804_53255342

GLN family gene primer design

Based on the electronic cloning results of GLN family genes, corresponding qRT-PCR primers were designed based on sequence difference sites between the species (*Table 5*).

Table 5. *qRT-PCR primers of GLN family gene of Chinese cabbage*

Primers	Primer Sequence (5'→3')	Predicted annealing temperature
FBrGLN1.1	CTGGCATCAACATTAGTGGCATC	60.0
RBrGLN1.1	TGTGTCTCAGTCCCAATTTATCG	60.0
FBrGLN1.2	GTATGCTGGAATTAACATCAGTGG	62.0
RBrGLN1.2	CTTGATTATCTCGTATCCTCCTTC	62.0
FBrGLN1.3	TCCGACCAACAAGAGGCACAA	62.0
RBrGLN1.3	CGAAGCTGACATTTACACCAGAGA	62.0
FBrGLN1.4	GTCTTTACGCCGGAATCAATGT	62.0
RBrGLN1.4	GTGTTCCTTGTGACGCAATCCA	62.0
FBrGLN2	CAGGTGATCATGTTTGGTGTGC	62.0
FBrGLN2	TGCTTTCCGGTCAACCTTCTC	62.0

Note: F-forward primer, R-reverse primer, Br-Chinese cabbage, GLN-glutamine synthetase

Primer annealing temperature gradient test

The mixed cDNA of Chinese cabbage in each treatment was used as a template, and six temperature gradients at 55 °C, 57 °C, 59 °C, 60 °C, 61 °C and 62 °C were set for the combination of (forward primer and reverse primer) in *Table 2* with 60 °C as the criterion. The 25 μL standard semi-quantitative RT-PCR system was used to amplify the GLN family genes in each sample at different temperatures. The amplified products were subjected to 1% agarose gel electrophoresis to detect the optimum annealing temperature for each primer. The reaction system is as follows (*Table 6*):

Table 6. *Primer annealing temperature gradient test on PCR amplification system*

Reagents	Volume /μL
ddH_2O	11.0
cDNA	0.5
Forward primers /10 μmol·L^{-1}	0.5
Reverse primers /10 μmol·L^{-1}	0.5
FastStart Essential DNA Green Master	12.5
Total volume	25.0

PCR reaction procedure was as follows: pre-denaturation at 94 °C for 2 min; denaturation at 94 °C for 1 min, annealing at T0 °C for 30 s, extension at 72 °C for 30 s, repetition for 40 cycles; extension at 72 °C for 10 min and at 4 °C for 2 min (T0 °C means predicted annealing temperature of different primers). GLN1.1-GLN1.4 electrophoresis bands of Chinese cabbage had gradually increased brightness with increasing temperature, reaching the top at 62 °C, and GLN2 bands basically had no differences in brightness. Therefore, the annealing temperature of Chinese cabbage GLN family was set at 62 °C (*Figure 3*) and the annealing temperature of qRT-PCR could be uniformly set to 62 °C.

http://www.aloki.hu ● ISSN 1589 1623 (Print) ● ISSN1785 0037 (Online)
DOI: http://dx.doi.org/10.15666/aeer/1804_53255342

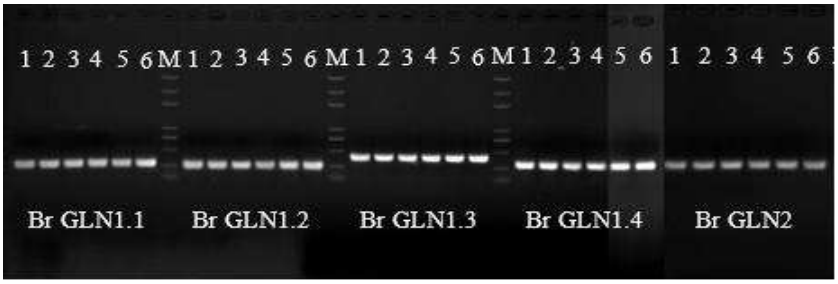

Figure 3. *Agarose gel electrophoresis detection results of Chinese cabbage GLN family gene annealing temperature gradient test. Note:1: 55 ℃,2: 57 ℃,3: 59 ℃,4: 60 ℃,5: 61 ℃,6: 62 ℃, M: Trans 2K Plus Marker*

qRT-PCR detection of GLN family gene

The cDNA of reverse transcription products of Chinese cabbage in 7 different treatments was diluted 30-fold as a template, 26SrRNA was used as an internal reference gene, and (forward primer and reverse primer) in *Table 2* was used as a combination to detect expression differences of Chinese cabbage GLN family genes in different organs under different treatments by qRT-PCR (CFX96TM Real-Time System, New England Biolabs, USA). Each treatment of each gene was repeated by 3 times. The reaction system is as follows (*Table 7*):

Table 7. *qRT-PCR reaction system*

Reagents	Volume /μL
ddH_2O	1.5
cDNA	2.5
Forward primers /10 μmol·L^{-1}	0.5
Reverse primers /10 μmol·L^{-1}	0.5
FastStart Essential DNA Green Master	5.0
Total volume	10.0

qRT-PCR reaction procedure was as follows: pre-denaturation at 95 °C for 10 min; denaturation at 95 °C for 10 s, annealing at T1 °C for 30 s, repetition by 45 cycles; addition of melting curve ranging from 65 °C to 95 °C (T1 °C was the optimum annealing temperature for different primers).

Statistical analysis

Three-way analysis of univariate ANOVA and correlation analysis were performed using SPSS version 21.0package (SPSS, 2009).

Results and analysis

Amino acid component

As can be seen from *Table 8*, essential amino acids (BI), total non-essential amino acids (BD) and total amino acids (BT) of Chinese cabbage increase with the increasing application of ordinary potassium silicate (OKSi) and nano potassium silicate (NKSi). The total amount of essential amino acids is the highest in NKSi-300 treatment, which is

http://www.aloki.hu ● ISSN 1589 1623 (Print) ● ISSN1785 0037 (Online)
DOI: http://dx.doi.org/10.15666/aeer/1804_53255342

41.1% higher than that of control (CK), followed by OKSi-450 which is by 31.0% higher than that of the control. Both OKSi and NKSi treatments improve lysine (Lys) content, but NKSi has greater improvement than OKSi under the same application rate. Under 150, 300 and 450 kg·hm^{-2} application rate, OKSi-Lys is increased by 33.4%, 45.5% and 64.3%, respectively compared with control, NKSi-Lys is increased by 104%, 170% and 132%, respectively compared with control, and NKSi-Lys is 53.2%, 85.3% and 41.5% higher than OKSi-Lys, respectively. OKSi treatment increases methionine (Met) content and there is greater increase with the increasing application rate of OKSi, while NKSi demonstrate an effect opposite to that of OKSi. Met content is decreased with the increasing application rate. At application rates of 150, 300 and 450 kg·hm^{-2}, OKSi-Met is increased by 33.1%, 35.2% and 101% respectively compared with the control, while NKSi-Met is decreased by 53.8%, 57.9% and 65.5%, respectively compared with the control. The ratio of essential amino acid to total amino acid (BI/BT) shows an upward trend, reaching the highest in NKSi-300 treatment, which is 22.3% higher than CK. Non-essential amino acid ratio (BD/BT) shows an opposite effect, with the lowest in NKSi-300 treatment, which is 11.3% lower than CK. The ratios of total essential amino acids and non-essential amino acids (BI/BD) in adult are higher than that of CK under potassium silicate treatment, with NKSi-BI/BD higher than OKSi-BI/BD at the same application rate. NKSi-300 has the highest ratio, which is 37.7% higher than CK.

The above analysis shows that application of both OKSi and NKSi can increase amino acid content of Chinese cabbage, with superior effect in NKSi than OKSi.

Expression characteristics of GLN family gene

As can be seen from *Figure 4*, GLN family gene in Chinese cabbage root (BrR) shows the following tendency under potassium silicate treatment: under ordinary potassium silicate (OKSi) treatment, expression of GLN1.1, GLN1.2, GLN1.3 and GLN2 is first down-regulated and then up-regulated, with the highest expression under OKSi-450 treatment, which is up by 1.84, 5.47, 5.20 and 5.57 times, respectively, compared with control (CK). Expression of GLN1.4 is gradually up-regulated with the increasing OKSi application rate, but the increase range is first increased and then increased, which is up by 4.37, 1.25 and 99.5 times respectively compared with CK under 150, 300 and 450 kg·hm^{-2} application rates. Under nano potassium silicate (NKSi) treatment, GLN1.1 and GLN1.2 expressions are only up-regulated under 300 kg·hm^{-2} treatment, which are up by 34.4 and 40.7 times, respectively compared with CK. GLN1.3 and GLN2 expressions are up-regulated at 300 and 450 kg·hm^{-2} treatments, up by 119, 1.91 and 67.2, 0.108 times, respectively compared with CK. GLN1.4 is up-regulated under 150, 300 and 450 kg·hm^{-2} treatments, up by 9.57, 1305 and 6.48 times compared with CK, respectively. Compared with CK, GLN1.1, GLN1.2, GLN1.3, GLN1.4 and GLN2 genes have the highest relative expression under the treatment of 300 kg·hm^{-2} NKSi, showing the order of expression of GLN1.3 (158)>GLN1. 1 (154)>GLN1.4 (139)>GLN2 (125)>GLN1.2 (82.0). GLN1.1, GLN1.2, GLN1.3 and GLN2 expressions are down-regulated under 150 kg·hm^{-2} application rate, but OKSi has greater down-regulation than NKSi. On the other hand, GLN1.4 expression is up-regulated, but NKSi brings greater up-regulation effect than OKSi. Under 450 kg·hm^{-2} application rate, all of OKSi-GLN1.1, GLN1.2, GLN1.3, GLN1.4 and GLN2 show up-regulated expressions, NKSi-GLN1.1 and GLN1.2 show down-regulated expression, while GLN1.3, GLN1.4 and GLN2 show up-regulated expressions. The expression levels of each gene are higher in OKSi treatment than in NKSi treatment at 450 kg·hm^{-2} potassium feitilizer treatment.

http://www.aloki.hu ● ISSN 1589 1623 (Print) ● ISSN1785 0037 (Online)
DOI: http://dx.doi.org/10.15666/aeer/1804_53255342

Table 8. *The amino acid component and content in the aboveground parts of Chinese cabbage treated with potassium silicate*

Treatments	Lys*	Met*	Ile*	Leu*	Phe*	Val*	Thr*	BI	His	Arg	Glu	Ser	Gly	Ala	Tyr◆	Pro	Asp	Cys◆	BD	BT	BI/BT	BD/BT	BI/BD
	g•kg^{-1} DW																				% DW		
CK	3.14	1.45	5.11	8.03	5.76	4.77	3.66	31.9	1.85	2.43	23.8	4.71	5.15	6.67	1.91	1.8	9.36	0.44	58.1	90.1	35.4	64.5	0.549
OKSi-150	4.19	1.93	5.86	9.01	6.02	6.23	4.41	37.7	2.02	2.64	25.7	5.40	5.71	7.36	2.37	6.20	10.4	0.640	68.5	106	35.6	64.6	0.550
NKSi-150	6.42	0.670	4.57	7.80	4.95	5.64	3.63	33.7	2.28	2.6	15.1	3.23	5.65	7.25	0.960	1.27	8.72	0.280	47.4	81.1	41.6	58.4	0.711
OKSi-300	4.57	1.96	5.60	9.18	5.50	5.99	4.13	36.9	1.98	2.41	23.1	4.77	5.39	6.55	2.17	5.71	10.2	0.590	62.8	100	36.9	62.8	0.588
NKSi-300	8.47	0.610	6.05	10.6	7.00	7.44	4.75	45.0	3.07	3.59	17.2	4.61	7.34	8.51	1.34	1.55	11.9	0.321	59.5	104	43.3	57.2	0.756
OKSi-450	5.16	2.92	5.99	9.98	6.65	6.48	4.59	41.8	2.44	2.75	24.5	4.84	5.95	7.76	3.01	1.81	10.6	0.660	64.3	106	39.4	60.7	0.650
NKSi-450	7.30	0.500	5.43	8.91	5.71	6.63	5.21	39.7	2.64	3.49	20.8	4.75	6.82	8.90	0.920	1.35	12.00	0.360	62.1	102	38.9	60.9	0.640

Note: "*" means essential amino acids for adults, "◆" means conditionally essential amino acids; Lys-lysine, Met-methionine, Ile-isoleucine, Leu-leucine, Phe-phenylalanine, Val-valine, Thr-threonine, BI-total essential amino acids in adults; His-histidine, Arg-arginine, Glu-glutamic acid, Ser-serine, Gly-glycine, Ala-alanine, Tyr-tyrosine, Pro-proline, Asp-asparaginic acid, Cys-cysteine, BD-total non-essential amino acids in adults, BT-total amino acid; BI/BT-A ratio of total essential amino acids in adults to total amino acids, BD/BT - ratio of total non-essential amino acids in adult to total amino acids, BI / BD - the ratio of total essential amino acids in adults to total non-essential amino acids, the same below

http://www.aloki.hu ● ISSN 1589 1623 (Print) ● ISSN1785 0037 (Online)
DOI: http://dx.doi.org/10.15666/aeer/1804_53255342

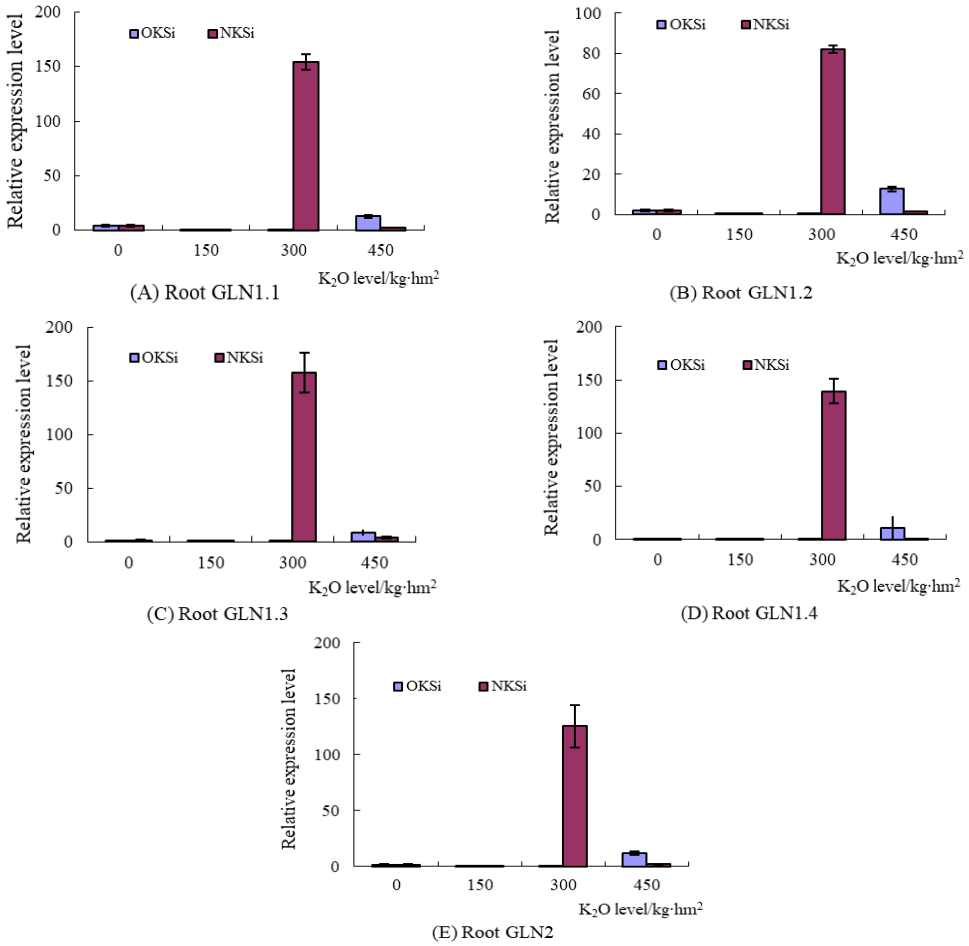

Figure 4. *Relative expression of GLN family genes in Chinese cabbage root under different potassium silicate treatments*

As can be seen from *Figure 5*, GLN family gene in Chinese cabbage stem (BrS) shows the following trend under potassium silicate treatment: under ordinary potassium silicate (OKSi) treatment, GLN1.1, GLN1.2 and GLN1.3 expressions are gradually down-regulated with the increasing application rate, while GLN1.4 expression first decreases and then increases. The relative expression is the highest under OKSi-300 treatment, while that under OKSi-300 and OKSi-450 treatments is up by 1.16 and 0.088 times compared with the control (CK), respectively. GLN2 shows up-regulated expression, which is up by 1.79, 10.1 and 4.03 times compared with CK, respectively, under application rates of 150, 300 and 450 kg·hm^{-2}. Under nano potassium silicate (NKSi) treatment, relative expressions of GLN1.1, GLN1.2, GLN1.3, GLN1.4 and GLN2 are up-regulated under each treatment, showing higher increase range than that of OKSi. The relative expression of GLN1.1 is the highest under NKSi-450 treatment, which is 0.603 times higher than CK. GLN1.2, GLN1.3, GLN1.4 and GLN2 have the highest relative expression under NKSi-300 treatment, which is up by 7.85, 3.46, 45.6 and 50.7 times, respectively compared with CK, showing the order of expression of GLN1.4 (1.30)<GLN1.2(3.38)<GLN1.3(4.46)< GLN2 (4.87). The above analysis indicates that NKSi treatment can significantly up-regulate GLN family gene expression in Chinese cabbage stem, with superior up-regulation effect than OKSi.

http://www.aloki.hu ● ISSN 1589 1623 (Print) ● ISSN1785 0037 (Online)
DOI: http://dx.doi.org/10.15666/aeer/1804_53255342

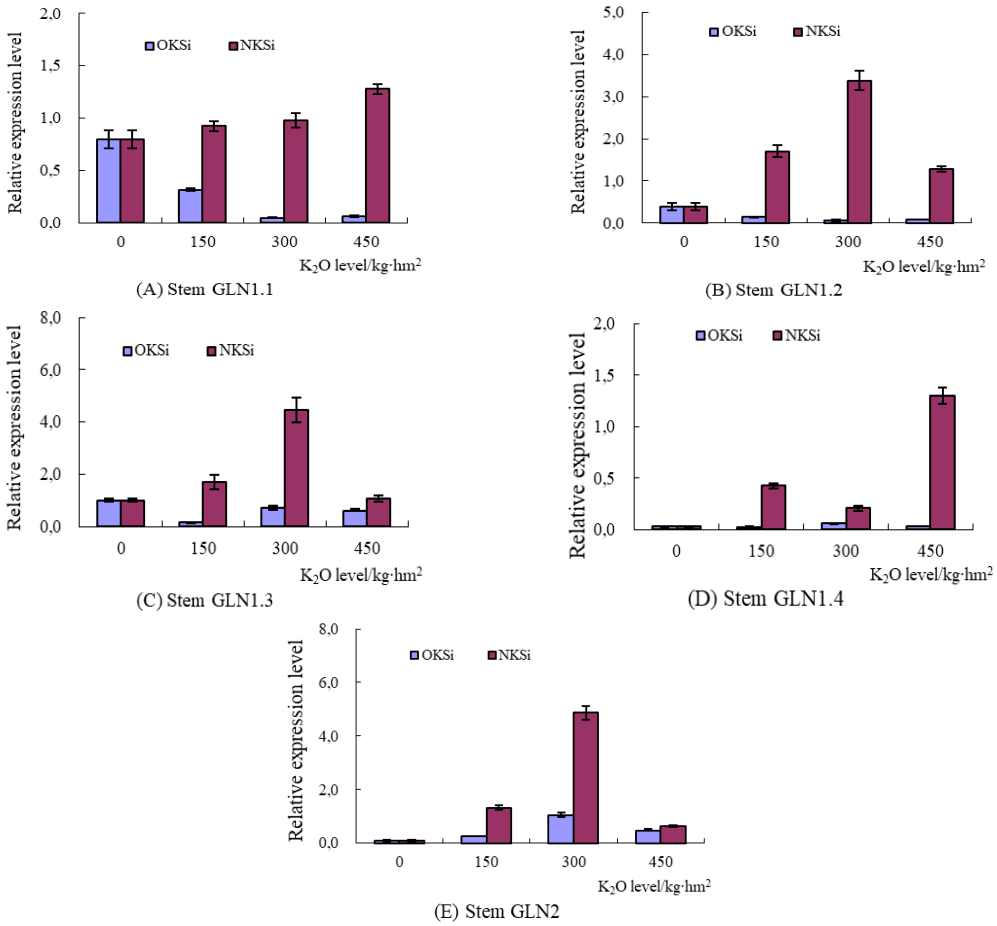

Figure 5. *Relative expression of GLN family genes in Chinese cabbage stem under different potassium silicatetreatments*

As can be seen from *Figure 6*, GLN family gene shows the following trend in Chinese cabbage leaves (BrL) under potassium silicate treatment: relative expression of GLN1.1, GLN1.2, GLN1.4 and GLN2 is gradually up-regulated with increasing application rate under ordinary potassium silicate (OKSi) treatment, reaching the highest under OKSi-450 treatment, which is 2.19, 6.29, 1.63 and 58.7 times higher than that of the control (CK), and the following order of expression of GLN1.4 (1.25)<GLN1.1 (2.07)<GLN1.2 (6.12)<GLN2 (6.48) is shown. GLN1.3 expression is first down-regulated and then up-regulated, with the highest relative expression in OKSi-300 treatment, followed by OKSi-450, which is up by 9.59 and 8.96 times, respectively, compared with CK. Under nano potassium silicate (NKSi) treatment, expression of GLN1.1, GLN1.2 and GLN1.3 is first up-regulated and then down-regulated, showing the highest relative expression under NKSi-150 treatment, which is up by 0.984, 0.235 and 0.617 times, respectively, compared with CK. Only NKSi-150 brings higher expression level than OKSi-150, while other relative gene expression levels are higher in OKSi treatment under the same application rate. The relative expression of GLN1.4 is down-regulated while that of GLN2 is up-regulated, both of which are lower than that of OKSi treatment under the same application rate. The above analysis suggests that OKSi treatment can significantly up-regulate GLN family gene expression in Chinese cabbage leaves, showing superior up-regulation effect than NKSi.

http://www.aloki.hu ● ISSN 1589 1623 (Print) ● ISSN1785 0037 (Online)
DOI: http://dx.doi.org/10.15666/aeer/1804_53255342

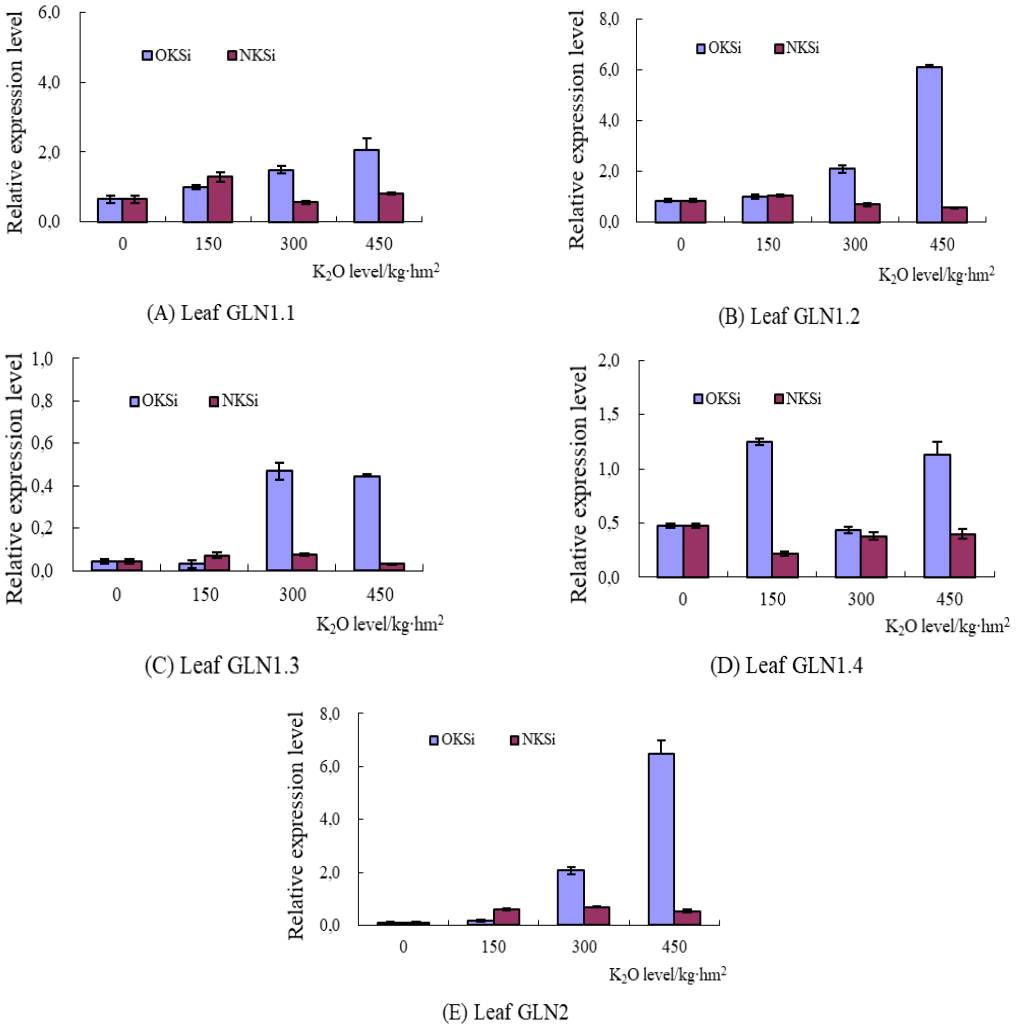

Figure 6. *Relative expression of GLN family genes in Chinese cabbage leave under different potassium silicate treatments*

Correlation analysis between GLN family gene expression and amino acid component

As can be seen from *Table 9*, BrRGLN1.1 (r=0.779*), BrRGLN1.2 (r=0.794), BrRGLN1.3 (r=0.784*), BrRGLN1.4 (r=0.783*) and BrRGLN2 (r=0.786*) are significantly positively correlated with histidine (His), BrRGLN1.3 (r=0.759*) is significantly positively correlated with glycine (Gly); BrSGLN1.1 (r= -0.922**, -0.900** and -0.898**) is significantly negatively correlated with methionine (Met), tyrosine (Tyr) and cysteine (Cys), BrSGLN1.2 (r=0.866* and 0.820*), BrSGLN1.3 (r=0.758* and 0.775*), BrSGLN1.4 (r=0.808* and 0.811) *) and BrSGLN2 (r = 0.762* and 0.781*) are significantly positively correlated with lysine (Lys) and His, and BrSGLN1.2 (r = -0.762* and -0.799*) is significantly negatively correlated with Met and Cys, BrSGLN1.2 (r=0.780*) and BrSGLN1.4 (r=0.763*) are significantly positively correlated with Gly; BrLGLN1.2 (r= 0.822* and 0.757*) and BrLGLN1.4 (r=0.834* and 0.782*) are significantly positively correlated with Met and Tyr, BrLGLN1.4 (r=0.757*) is significantly positively correlated with Cys, while other amino acids show no significant or highly significant correlation with GLN family gene.

http://www.aloki.hu ● ISSN 1589 1623 (Print) ● ISSN1785 0037 (Online)
DOI: http://dx.doi.org/10.15666/aeer/1804_53255342

Table 9. *Correlation coefficient (r) between amino acid component (AAs) and GLN family genes in Chinese cabbage under different potassium silicate treatments*

Amino acids	GLN family genes											
	BrRGLN1.1	BrRGLN1.2	BrRGLN1.3	BrRGLN1.4	BrRGLN2	BrSGLN1.1	BrSGLN1.2	BrSGLN1.3	BrSGLN1.4	BrSGLN2	BrLGLN1.2	BrLGLN1.4
Lys	0.667	0.667	0.683	0.676	0.673	0.589	0.866*	0.758*	0.808*	0.762*	-0.207	-0.347
Met	-0.359	-0.309	-0.384	-0.357	-0.348	-0.922**	-0.762*	-0.597	-0.595	-0.473	0.822*	0.834*
Ile	0.470	0.502	0.461	0.473	0.480	-0.414	0.005	0.147	0.196	0.315	0.382	0.473
Leu	0.708	0.743	0.701	0.714	0.720	-0.236	0.335	0.471	0.510	0.617	0.379	0.405
Phe	0.714	0.749	0.697	0.710	0.720	-0.136	0.304	0.454	0.463	0.518	0.351	0.257
Val	0.678	0.699	0.687	0.691	0.691	0.106	0.562	0.545	0.635	0.678	0.101	0.052
Thr	0.327	0.348	0.336	0.331	0.337	0.205	0.245	0.177	0.241	0.255	0.091	0.096
His	0.779*	0.794*	0.784*	0.783*	0.786*	0.480	0.820*	0.775*	0.811*	0.781*	-0.017	-0.199
Arg	0.673	0.673	0.685	0.673	0.675	0.635	0.748	0.659	0.695	0.642	-0.242	-0.340
Glu	-0.450	-0.430	-0.465	-0.457	-0.449	-0.639	-0.827*	-0.716	-0.721	-0.636	0.389	0.559
Ser	0.008	0.019	0.003	0.003	0.009	-0.397	-0.415	-0.309	-0.285	-0.196	0.151	0.371
Gly	0.749	0.754	0.759*	0.752	0.754	0.531	0.780*	0.714	0.763*	0.731	-0.168	-0.273
Ala	0.481	0.495	0.491	0.483	0.487	0.581	0.598	0.459	0.515	0.441	-0.085	-0.288
Tyr	-0.224	-0.177	-0.250	-0.223	-0.215	-0.900**	-0.689	-0.501	-0.498	-0.374	0.757*	0.782*
Pro	-0.290	-0.305	-0.280	-0.278	-0.287	-0.665	-0.537	-0.471	-0.397	-0.268	-0.032	0.309
Asp	0.536	0.546	0.544	0.536	0.541	0.254	0.390	0.380	0.420	0.451	-0.038	0.051
Cys	-0.388	-0.351	-0.403	-0.383	-0.378	-0.898**	-0.799*	-0.667	-0.634	-0.502	0.633	0.757*
BI	0.697	0.730	0.696	0.705	0.710	-0.013	0.468	0.513	0.575	0.636	0.289	0.225
BD	-0.044	-0.024	-0.048	-0.043	-0.038	-0.493	-0.452	-0.368	-0.318	-0.213	0.279	0.474
BT	0.282	0.312	0.279	0.287	0.293	-0.358	-0.112	-0.032	0.032	0.136	0.337	0.451

http://www.aloki.hu ● ISSN 1589 1623 (Print) ● ISSN1785 0037 (Online)
DOI: http://dx.doi.org/10.15666/aeer/1804_53255342

Discussion

Amino acids are important nutrients for vegetables. The content of amino acid components directly affects its nutritional value, which is closely related to human taste (Ou et al., 2007). Potassium is an activator of various enzymes in plant cells. Potassium deficiency affects nitrogen metabolism, which in turn affects the composition of free amino acids and total amino acids (Eppendorfer et al., 1996). In this study, the essential amino acids (BI), total non-essential amino acids (BD) and total amino acids (BT) of Chinese cabbage increased with the increasing application rate of ordinary potassium silicate (OKSi) and nano potassium silicate (NKSi). It indicates that proper application of potassium fertilizer contributes to the synthesis of amino acids in Chinese cabbage, which is similar to the research results of Tang et al. (2013). The mixture of salt compound of aspartic acid and glutamic acid and free acidic amino acids can lower the umami threshold with obvious synergistic effect and freshening effect, which is therefore known as umami amino acid, a major umami flavoring substance (Lioe et al., 2005). In this experiment, with the increasing application rate of ordinary potassium silicate (OKSi) and nano potassium silicate (NKSi), the concentration of umami amino acids showed an upward trend, suggesting that moderate application of potassium fertilizer in field experiment could improve content of umami amino acids in Chinese cabbage, which is consistent with the findings of Lin et al. (2003). On the whole, application of ordinary potassium silicate (OKSi) and nano nanosilicate (NKSi) can increase the content of sweet amino acids (glycine, alanine, threonine, and serine) in Chinese cabbage to some extent. Under NKSi-450treatment, glycine, alanine, threonine and serine were increased by 32.4%, 33.4%, 42.3% and 0.8%, respectively, compared with CK. The above results indicate that: under the experimental conditions of this study, application of potassium fertilizer can increase the total amount of amino acids in Chinese cabbage, greatly improve umami amino acids and sweet amino acids, thereby improving the nutritional value and flavor quality of Chinese cabbage. Nanotechnology has been applied to fertilizer modification and development of new fertilizers (Conesa et al., 2010; Adhikari et al., 2015). Thanks to the unique properties of nanomaterials, nanofertilizers have achieved good yield increase benefits in various crop applications. In the present study, NKSi-BI/BD was higher than OKSi-BI/BD under the same application rate, with the highest under NKSi-300 treatment. Principal component analysis method was used for dimensionality reduction and comprehensive evaluation of amino acids (AAs). The results showed that AAs comprehensive score was the highest under NKSi-300 treatment. The above analysis indicates that nano-potassium fertilizer has better benefits in improving amino acid components of Chinese cabbage and perfecting its flavor quality compared with traditional potassium fertilizer. It may be related to the fact that nano-fertilizer particles have better physical properties, which can enhance permeability of cell wall and cell membranes of plants, so that it is more easily absorbed by plant cells (Adhikari et al., 2015). This is similar to the finding by Lee et al. that mung bean and wheat have significant absorption effects on nano-copper (Lee et al., 2010).

Glutamine synthetase (GS) constitutes one of the key enzymes in the nitrogen metabolism pathway of higher plants (Feng et al., 2015). The ammonium directly absorbed by plants from the outside world and the ammonium obtained from nitrate reduction are further assimilated into amino acids via glutamine synthetase (GS)/ glutamate synthase (GOGAT) circulation (Lea and Miflin, 1974). Schuller et al. (1986)

http://www.aloki.hu ● ISSN 1589 1623 (Print) ● ISSN1785 0037 (Online)
DOI: http://dx.doi.org/10.15666/aeer/1804_53255342

found that: potassium application could increase nitrogen metabolism-related key enzyme activities in soybean and Sesbania rostrata. The synthesis of biomacromolecules such as enzymes is regulated by gene expression. The activity of glutamine synthetase (GS) is subject to influence of the expression level of GLN family genes. It is one of the focuses of this study to determine the effect of treatment with different concentrations of OKSi and NKSi on GLN family genes of Chinese cabbage under field experimental conditions. In this study, application of ordinary potassium silicate (OKSi) and nano potassium silicate (NKSi) have a certain up-regulation effect on GLN family gene expression in the roots, stems and leaves of Chinese cabbage. NKSi and OKSi treatments have different effects on expression of GLN family genes in different parts of Chinese cabbage. NKSi can better up-regulate GLN family gene expression in roots and stems of Chinese cabbage than OKSi, but the latter has better up-regulation effect on leaves than NKSi. This may be because potassium promotes the uptake of NO3- in plant roots, thus accelerating the process of plant nitrogen metabolism, and promoting the synthesis of amino acids (Edward, 1981). The completion of nitrogen metabolism is inseparable from catalytic action of related key enzymes (GS, GOGAT, etc.). That is to say, potassium may up-regulate GLN family gene expression by a certain mechanism to increase the content of nitrogen metabolism-related enzymes in roots and stems, thereby achieving efficient conversion of nitrogen. Compared with ordinary potassium fertilizer, Chinese cabbage has higher absorption rate of nano potassium fertilizer. NKSi treatment may increase absorption of potassium ions in roots and stems of Chinese cabbage, thus showing superior up-regulation effect on GLN family gene than OKSi. The main organ for plant uptake and transport of nitrogen is root system (Fan et al., 2010). NKSi can better up-regulate GLN family genes in roots and stems of Chinese cabbage than OKSi, which means that NKSi has superior effect on root and stem vegetables than on leaf vegetables.

Conclusion

The ratio of essential amino acids to total amino acids (BI/BT) in Chinese cabbage increased with the increasing application rate of OKSi and NKSi, reaching the highest under NKSi-300 treatment. NKSi-BI/BD was higher than OKSi-BI/BD at the same application rate, with the highest under NKSi-300 treatment. NKSi treatment can significantly up-regulate GLN family genes in roots and stems of Chinese cabbage, showing superior up-regulation effect than OKSi, while OKSi treatment can significantly up-regulate GLN family genes in Chinese cabbage leaves, showing superior up-regulation effect than NKSi. There exists a significant or extremely significant correlation between GLN family gene expression in Chinese cabbage and the contents of histidine, glycine, methionine, tyrosine and cysteine in the stems of Chinese cabbage. Nano potassium silicate (NKSi) could increase the content of amino acid components in Chinese cabbage, showing better effect than ordinary potassium silicate (OKSi) at the same application rate, and NKSi-300 was the most appropriate. NKSi treatment significantly up-regulated the expression of GLN family genes in roots and stems of Chinese cabbage, showing superior up-regulation effect than OKSi.

Nanotechnology is a new material and technology. With the development of material science, nano-fertilizer and other nano-products are being gradually applied to agricultural production. Compared to the traditional fertilization techniques, nano-fertilizers improve plant production and nutrient use efficiency by consuming a small amount of resources (Kashyap et al., 2015). Furthermore, nanoparticles (NPs) can

http://www.aloki.hu ● ISSN 1589 1623 (Print) ● ISSN1785 0037 (Online)
DOI: http://dx.doi.org/10.15666/aeer/1804_53255342

increase crop yield and nutritional value by promoting plant metabolism (Ghormade et al., 2011) due to their unique physicochemical properties. In recent research, the effects of nano-potassium fertilizer on amino acid composition and gene expression of GLN family in Chinese cabbage were discussed in detail. However, the research of nano-fertilizer on the physiological mechanism of crop, especially the micro-mechanism, needs to be strengthened. On the other hand, it has been reported that some nano-fertilizers show some toxicity to crops (Gui et al., 2015; Rico et al., 2017), so it is important to carry out toxicological research on nano-fertilizers. The emergence of nano-fertilizer plays an important role in promoting and innovating agricultural production mode, but there are still a lot of research on nano-fertilizer.

Acknowledgments. This work was supported by Fund of China Agriculture Research System (CARS-23), and the National Key Research and Development Program of China (2018YFD0201200), and the National College students Innovation and Entrepreneurship training Program (201910635054).

REFERENCES

[1] Adhikari, T., Kundu, S., Biswas, A. K., Tarafdar, J. C., Subba Rao, A. (2015): Characterization of zinc oxide nano particles and their effect on growth of maize (*Zea mays* L.) plant. – Journal of Plant Nutrition 38(10): 1505-1515.

[2] Conesa, H. M., Wieser, M., Gasser, M., Hockmann, K., Evangelou, M. W. H., Studer, B., Schulin, R. (2010): Effects of three amendments on extractability and fractionation of Pb, Cu, Ni and Sb in two shooting range soils. – Journal of Hazardous Materials 181(1-3): 845-850.

[3] Davarpanah, S., Tehranifar, A., Davarynejad, G., Aran, M., Abadía, J., Khorassani, R. (2017): Effects of foliar nano-nitrogen and urea fertilizers on the physical and chemical properties of pomegranate (Punica granatum cv. Ardestani) fruits. – HortScience 52(2): 288-294.

[4] Edward, E. (1981): Potash Fertilizer and Increased Tolerance to Stress. – Agriviews 1, No. I. Canada. Foth, R. D.

[5] Eppendorfer, W. H., Bille, S. W. (1996): Free and total amino acid composition of edible parts of beans, kale, spinach, cauliflower and potatoes as influenced by nitrogen fertilization and phosphorus and potassium deficiency. – Journal of the Science of Food and Agriculture 71(4): 449-458.

[6] Fan, J. B., Zhang, Y. L., Turner, D., Duan, Y. H., Wang, D. S., Shen, Q. R. (2010): Root physiological and morphological characteristics of two rice cultivars with different nitrogen-use efficiency. – Pedosphere 20(4): 446-455.

[7] Feng, W. J., Xing, G. F., Niu, X. L., Dou, C., Han, Y. H. (2015): Progress and application prospects of glutamine synthetase in plants. – Chin J Biotech 31: 1301-1312.

[8] Gascuel, Q., Diretto, G., Monforte, A. J., Fortes, A. M., Granell, A. (2017): Use of natural diversity and biotechnology to increase the quality and nutritional content of tomato and grape. – Frontiers in Plant Science 8: 1-24.

[9] Ghormade, V., Deshpande, M. V., Paknikar, K. M. (2011): Perspectives for nano-biotechnology enabled protection and nutrition of plants. – Biotechnology Advances 29(6): 792-803.

[10] Gui, X., Zhang, Z. Y., Liu, S. T., Ma, Y. H., Zhang, P., He, X., Li, Y. Y., Zhang, J., Li, H. F., Rui, Y. K., Liu, L. M., Cao, W. D. (2015): Fate and phytotoxicity of CeO2 nanoparticles on lettuce cultured in the potting soil environment. – Plos One 10(8): e0134261.

http://www.aloki.hu ● ISSN 1589 1623 (Print) ● ISSN1785 0037 (Online)
DOI: http://dx.doi.org/10.15666/aeer/1804_53255342

[11] Huang, S., Wang, L., Liu, L., Hou, Y., Li, L. (2014): Nanotechnology in agriculture, livestock, and aquaculture in China. A review. – Agronomy for Sustainable Development 35(2): 369-400.
[12] Kashyap, P. L., Xiang, X., Heiden, P. (2015): Chitosan nanoparticle based delivery systems for sustainable agriculture. – International Journal of Biological Macromolecules 77: 36-51.
[13] Lea, P. J., Miflin, B. J. (1974): Alternative route for nitrogen assimilation in higher plants. – Nature 251(5476): 614-616.
[14] Lee, C. W., Mahendra, S., Zodrow, K., Li, D., Tsai, Y. C., Braam, J., Alvarez, P. J. J. (2010): Developmental phytotoxicity of metal oxide nanoparticles to Arabidopsis thaliana. – Environmental Toxicology and Chemistry 29(3): 669-675.
[15] Li, T., Sun, F. Y., Gong, P., Wang, A., Yuan, L. X., Yin, X. B. (2017): Effects of Nano-selenium fertilization on selenium concentration of wheat grains and quality-related traits. – Journal of Plant Nutrition and Fertilizer 23(02): 427-433.
[16] Li, Y. H., Qin, Y. L., Xu, W. H., Chai, Y. R., Chi, S. L., Li, T., Zhang, C. L., Yang, M., He, Z. M., Feng, D. Y. (2019): Differences of Cd uptake and expression of MT and NRAMP2 genes in two varieties of ryegrasses. – Environmental Science and Pollution Research 26: 13738-13745.
[17] Lim, W., Miller, R., Park, J., Park, S. (2014): Consumer sensory analysis of high flavonoid transgenic tomatoes. – Journal of Food Science 79(6): S1212-S1217.
[18] Lin, D., Huang, D. F. (2003): Effects of potassium levels on photosynthesis and fruit quality of muskmelon in medium culture. – Acta Horticulturae Sinica 30: 221-223.
[19] Lioe, H. N., Apriyantono, A., Takara, K., Wada, K., Yasuda, M. (2005): Umami taste enhancement of MSG/NaCl mixtures by subthreshold L-α-Aromatic amino acids. – Journal of Food Science 70(7): s401-s405.
[20] Mattoo, A., Nath, P., Bouzayen, M. (2014): Fruit Ripening: Physiology, Signalling and Genomics. – CABI, Oxfordshire.
[21] Ou, X. Q., Ren, X. J., Zhou, Y. (2017): Analysis on the amino acid content and the composition in the vegetable sweet potato tips. – Journal of Chinese Institute of Food Science and Technology 7: 120-125.
[22] Rico, C. M., Johnson, M. G., Marcus, M. A., Andersen, C. P. (2017): Intergenerational responses of wheat (*Triticum aestivum* L.) to cerium oxide nanoparticles exposure. – Environmental Science: Nano 4(3): 700-711.
[23] Schuller, K. A., Day, D. A., Gibson, A. H., Gresshoff, P. M. (1986): Enzymes of ammonia assimilation and ureide biosynthesis in soybean nodules: effect of nitrate. – Plant Physiology 80: 646-50.
[24] Wang, X. J., Chen, Y., Wang, F., Wang, Z. Y. (2015): Effects of potash fertilizer on cabbage′s quality in cadmium polluted soils. – Journal of Agricultural Resources and Environment 32(1): 40-47.
[25] Yuan, T., Wang, Z. Y., Gu, S. K., Wang, F., Yang, D., Cheng, Y. (2017): Effect of combined application of low-level potassium fertilizer with nano-Mg(OH)2 on Chinese cabbage quality. – Journal of Plant Nutrition and Fertilizer 23: 254.

http://www.aloki.hu ● ISSN 1589 1623 (Print) ● ISSN1785 0037 (Online)
DOI: http://dx.doi.org/10.15666/aeer/1804_53255342

STUDY ON THE CONTENT OF GENIPOSIDIC ACID IN DIFFERENT PARTS OF *EUCOMMIA ULMOIDES* ON KARST PLATEAU OF GUIZHOU PROVINCE, CHINA

QIAN, C. J.[1,2] – OU, M. C.[2] – YU, L. F.[1*] – YAN, L. B.[1] – HUANG, Z. S.[1] – FU, Y. H.[2]

[1]*Guizhou University, The Key laboratory of Plant Resource Conservation and Germplasm Innovation in Mountainous Region (Ministry of Education), Collaborative Innovation Center for Mountain Ecology & Agro-Bioengineering (CICMEAB) Guiyang 550025, Guizhou, China*

[2]*Guizhou Education University, Guiyang 550018, Guizhou, China*

**Corresponding author*
e-mail: gdyulifei@163.com

(Received 15th Feb 2020; accepted 7th Jul 2020)

Abstract. This study aims to explore the content of (geniposidic acid, GPA) in the leaves, trunk bark and root bark of *Eucommia ulmoides* on Xingyi karst plateau mountains of Guizhou Province, China. There was no significant difference in the content of GPA in *Eucommia ulmoides* planted in different directions on the same slope. The content of GPA in leaves, trunk bark and root bark of *Eucommia ulmoides* planted on the sunny slope varied significantly, where the GPA content in root bark was the highest (32.7851 mg/g), There was no significant difference in GPA content in leaves and root bark of *Eucommia ulmoides* planted on the shady slope, but the GPA content in trunk bark was significantly different from that in leaves and root bark, where the GPA content in trunk bark was the highest (30.3958 mg/g), There was no significant difference in GPA content in trunk bark and root bark of *Eucommia ulmoides* planted in different slope directions, and the GPA content in leaves of *Eucommia ulmoides* planted on shady slope was significantly (36.71%) higher than that on sunny slope. The GPA content in different parts of Eucommia ulmoides on both sunny or shade slope was GAP content in root bark was the largest followed by that in leaves, and that in trunk bark was the lowest. These results expand the source sites and provide new ideas for the comprehensive utilization and further research of *Eucommia ulmoides* resources.

Keywords: *sunny slope and shady slope, different directions, root bark, trunk bark, leaves, high performance liquid chromatography*

Introduction

The karst area in southwest China is the largest karst core area in the world (Wang et al., 2013). The exposed area of carbonate rocks in Guizhou is 12.8×10^4 km^2, accounting for 73% of the total area of the province, which makes Guizhou the province with the most developed karst landform in China. Of the province's 86 counties (cities), 68 have more than 50% karst area. Environmental degradation is prominent in karst areas (Cai, 1996), and problems such as soil-forming difficulties, lack of transition layer of limestone formed by carbonate rocks (Yang, 1990), thin soil, discontinuous soil cover and low ecological capacity also need to be addressed (Li et al., 2016). There are many factors restricting plant growth and development in karst environment. The central production areas of *Eucommia ulmoides* Oliver include Guizhou, Sichuan, Hubei, Hunan, Shaanxi and Henan (Li et al., 2001). The *Eucommia ulmoides* does not have strict requirements on environment and soil, and can grow on fertile hills, plains, barren red soil and harsh rock cliffs (Jiao, 2016). The *Eucommia ulmoides* is characterized by cold tolerance, drought resistance, poverty resistance, which can be

http://www.aloki.hu ● ISSN 1589 1623 (Print) ● ISSN 1785 0037 (Online)
DOI: http://dx.doi.org/10.15666/aeer/1804_53435353

grown in a wide range of area (Liu, 2012) with soil pH ranging from 5.0 to 8.4 (Du, 2003). There are plantations of *Eucommia ulmoides* in the harsh environment of Guizhou karst plateau.

As a unique deciduous tree of single species and single genus in China, The *Eucommia ulmoides* is a rare medicinal material unique to China as well asa widely used plant tonic. *Eucommia ulmoides* tea is a popular beverage in Asia and a new dual-purpose food resource for blood pressure medicine (Bai et al., 2015; Zhu and Sun, 2018). The *Eucommia ulmoides* contain abundant chemical constituents such as cycloene ether terpenes, bphenylpropanoids, flavonoids and phenols, which have a variety of medicinal values (Hussain et al., 2016; Yan et al., 2018). The Medicinal components of *Eucommia ulmoides* have anti-diabetes, anti-inflammatory, blood pressure lowering and diuretic effects (Peng and Li, 2013; Sugawa et al., 2016; Wang et al., 2016), anti-obesity effect (Hirata et al., 2011), anti-virus effect (Sun et al., 2004), effect of liver protection and gallbladder protection (Lou et al., 2011), and effect of improving hyperuricemia (Fang et al., 2019). The total flavonoids of *Eucommia ulmoides* have inhibitory effects on cell proliferation, migration and invasion of glioblastoma, one of the malignant primary brain tumors (Wang et al., 2019). The trunk bark extract of *Eucommia ulmoides* can reduce the serum level in liver injury (Lee et al., 2014). The leaf extract of *Eucommia ulmoides* has the effect of treating non-alcoholic fatty liver disease (Lee et al., 2019), and can be used as a new drug for treating male erectile dysfunction caused by diabetes (Fu et al., 2019). The GPA, chlorogenic acid, ginipinidine, rosin diglucoside, rutin and quercetin are the main components of *Eucommia ulmoides* (He et al., 2014). The GPA as the representative ingredient of terpenoids has the functions of anticancer, lowering blood pressure (Du et al., 2011). The GPA can change bile composition and prevent the formation of cholesterol stones (Huang et al., 2002), with anti-mutation activity and antiviral effect (Ong and Tan, 2007). Therefore, the studies on *Eucommia ulmoides* mainly focus on the pharmacology and the medicinal components of the bark and leaves of *Eucommia ulmoides.* In this study, the high-performance liquid chromatography (HPLC) was used to determine the content of GPA in leaves, trunk bark and root bark of *Eucommia ulmoides* in karst plateau mountains. The influence of different slope directions on the content of GPA in three parts as well as the content of GPA in leaves of *Eucommia ulmoides* planted in different slope directions were analyzed, with the purpose of providing a new idea for expanding the source site of *Eucommia ulmoides*.

Materials and methods

The *Eucommia ulmoides* samples were collected from Pishanlin village, Jingnan town, Xingyi city, Guizhou province, China (*Fig. 1*), which is a typical karst plateau mountainous area with a subtropical humid monsoon climate, where the soil type is lime soil, the average annual temperature is 16.1 ℃ and the average annual rainfall is 1531.6 mm. The longitude of the sunny slope is 104°49’11” E, the latitude is 24°55’29” N, and the altitude is 1670 m; The longitude of the shady slope is 104°52’21” E, the latitude is 24°55’ 20” N, and the altitude is 1610 m.

The *Eucommia ulmoides* was planted in 1996 as a pure forest, and the samples collection date was May 29, 2017. Three 20 m × 20 m quadrats were set on the sunny slope and the shady slope, respectively, with a total of 6 quadrats. According to the kraft grading principle, three dominant trees were selected from each quadrat, including a

http://www.aloki.hu ● ISSN 1589 1623 (Print) ● ISSN 1785 0037 (Online)
DOI: http://dx.doi.org/10.15666/aeer/1804_53435353

total of 18 plants of *Eucommia ulmoides*, of which the leaves, trunk bark and root bark were collected. The *Eucommia ulmoides* leaves without pests and diseases were selected from the east, south, west and north of the tree canopy. The trunk bark samples of *Eucommia ulmoides* were collected by ring stripping. The ring was cut 130 cm from the ground, and the second incision was cut 30 cm upward from this point. All the openings were cut longitudinally between the two incisions to obtain the trunk bark. The root bark samples were collected from the rough root. After digging out all the *Eucommia ulmoides* roots, the root bark was peeled off after removing the soil (*Fig. 2*). There were 36 samples of *Eucommia ulmoides* leaves on the sunny slope and the shady slope, respectively; there were 9 samples of *Eucommia ulmoides* trunk bark on the sunny slope and on the shady slope, respectively; there were 9 samples of *Eucommia ulmoides* root bark on the sunny slope and on the shady slope, respectively. In total, there were 108 samples. The samples of leaf, trunk bark and root bark of *Eucommia ulmoides* were placed in the self-sealing bags, labeled with the corresponding sample name, and then dried in the lab before use.

Figure 1. *The habitat of Eucommia ulmoides*

Figure 2. *Digging the root of Eucommia ulmoides dominant wood*

http://www.aloki.hu ● ISSN 1589 1623 (Print) ● ISSN 1785 0037 (Online)
DOI: http://dx.doi.org/10.15666/aeer/1804_53435353

The apparatuses used in the experiment include a single channel pipette (I53066G, R39656F; Eppendorf China Co., Ltd.), the circulating water type multipurpose vacuum pump (SHZ - D (Ⅲ) (single; Shanghai to the China Instrument and Equipment Co., Ltd.), Agilent1260 high performance liquid chromatograph (Agilent Technology Co., Ltd.), chromatographic column (Agilent ZORBAX Eclipse Plus C18; Agilent Technology Co., Ltd.), electronic balance (Accuracy: Ten thousandth, ATY224; Shanghai Shengke Instrument Co., Ltd.), ultrasonic cleaner (SG8200HPT; Shanghai Guante Ultrasonic Instrument Co., Ltd.), electric blast drying oven (101-3A), high-speed universal pulverizer (FW80, Tianjin Taisite Instrument Co., Ltd.), low-speed multi-tube frame automatic balancing centrifuge (TDZ5-WS; Hunan Xiangyi Laboratory Instrument Development Co., Ltd.), ultra-pure water meter (Direct-Q8 UV system; Shanghai Merck Chemical Technology Co., Ltd.)

Research methods and data analysis

Chromatographic condition

The chromatographic column was ZORBAX Eclipse Plus C18 column (4.6 × 250 mm, 5 μm; Agilent); The column temperature was 30 ℃. The mobile phase was acetonitrile (A) -0.1% phosphoric acid solution (B) (97:3). Injection quantity 5 μL, Volume flow rate 1.0 mL/min; Detection wavelength 235 nm (Lv et al., 2012; Jiang et al., 2013; Qing et al., 2018). Qualitative test was conducted according to the retention time of the reference solution, and GPA content was calculated according to the peak area.

Preparation of reference solution

The GPA reference sample was weighed and dried to constant weight (0.2200 mg) in a 120 ℃ oven and placed in a 10 mL brown volumetric bottle. Then, the solution was dissolved with addition of methanol, diluted, and shaken well to obtain a GPA 0.0220 mg/mL control solution, which was stored in a refrigerator at 4 ℃ for later use (Lv et al., 2012; Jiang et al., 2013; Qing et al., 2018).

Preparation of sample solution

The samples of dried leaves, trunk bark and root bark of *Eucommia ulmoides* (the weight of each sample was 1.0000 g) were placed in 250 mL conical flasks, and then 50 mL of 70% methanol were added for each flask. Ultrasonic treatment was performed for 30 min (30 ℃, 300 W, 40 Hz) for extraction. The solution was transferred to a 100 mL centrifuge tube, centrifuged (4000 r/min) for 60 min, filtered and diluted to 50 mL, mixed well. After that, the solution was subjected to a 0.45 μm Millipore filter before collecting filter liquor and transferring it to a 2.5 mL injection bottle to obtain the sample solution (Lv et al., 2012; Jiang et al., 2013; Qing et al., 2018).

Data processing

After the experimental data were input into EXCEL2010 for preliminary sorting, SPSS24.0 statistical software was used for data analysis. The One-Way ANOVA and LSD method were used for pair-wise comparison between groups (Tamhane's T2 was used if the variances were not equal). The difference was considered statistically significant when $p < 0.05$.

http://www.aloki.hu ● ISSN 1589 1623 (Print) ● ISSN 1785 0037 (Online)
DOI: http://dx.doi.org/10.15666/aeer/1804_53435353

Results and analysis

Effect of slope direction on GPA content in different parts of Eucommia ulmoides

The average GPA content in leaves, trunk bark and root bark of *Eucommia ulmoides* planted on sunny slope was 18.8755 mg/g, 9.8154 mg/g and 32.7851 mg/g, respectively, where the average GPA content in root bark was the highest, which was 1.73 times that in leaves and 3.34 times that in trunk bark. The average GPA content in leaves, trunk bark and root bark of *Eucommia ulmoides* planted on shady slope was 29.8228 mg/g, 12.4351 mg/g, 30.3958 mg/g, respectively, where the average GPA content in root bark was the highest, which was 1.02 times that in leaves and 2.44 times that in trunk bark. The average GPA content in leaves and trunk bark of *Eucommia ulmoides* planted on shady slope was 36.71% and 21.07% higher than that of *Eucommia ulmoides* planted on sunny slope. However, the average GPA content in root bark of *Eucommia ulmoides* planted on sunny slope was 7.29% higher than that planted on shady slope (*Fig. 3*).

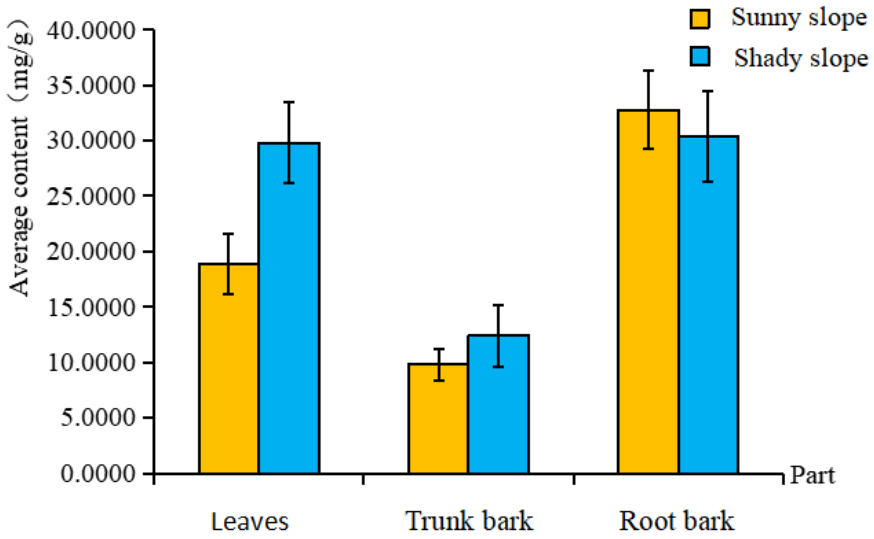

Figure 3. *The Average GPA content in different parts of Eucommia ulmoides. The GPA content in different parts is an average value of 9 Eucommia ulmoides plants, GPA content in leaves is the average value of 36 samples in 4 directions of 9 plants; The error line in the figure is made by the standard deviation value obtained by SPSS software analysis, the following is the same*

Of all *Eucommia ulmoides* plants planted on sunny slope of 3 quadrats, the east, south and west leaves of three *Eucommia ulmoides* plants planted on sunny slope of quadrat 2 had the largest average GPA contents, which was 32.8512 mg/g in the east, 24.8759 mg/g in the south and 22.7506 mg/g in the west, respectively (*Table 1*). Of all *Eucommia ulmoides* plants planted on shady slope of 3 quadrats, the east, north and west leaves of three *Eucommia ulmoides* plants planted on sunny slope of quadrat had the largest average GPA contents, which was 41.3838 mg/g in the east, 38.8765 mg/g in the north and 32.8861 mg/g in the west, respectively (*Table 1*). The GPA contents in the leaves in different directions of *Eucommia ulmoides* on the shady slope were generally higher than those on the sunny slope, 32.15% higher in the east direction, 31.98% higher in the south direction, 30.97% higher in the west direction, 51.27% higher in the north direction, and 36.71% higher on average (*Fig. 4*).

http://www.aloki.hu ● ISSN 1589 1623 (Print) ● ISSN 1785 0037 (Online)
DOI: http://dx.doi.org/10.15666/aeer/1804_53435353

Table 1. *The GPA contents of Eucommia ulmoides leaves in different directions (unit: mg/g)*

Sample name	East		South		West		North	
	Content	Average content	Content	Average content	Content	Average content	Content	Average content
Sunny slope 1-1	15.6373		22.1938		15.0186		18.2852	
Sunny slope 1-2	26.1185	20.8990	22.8177	23.4366	20.8589	22.2403	12.4141	16.4362
Sunny slope 1-3	20.9413		25.2982		30.8435		18.6092	
Sunny slope 2-1	44.9994		34.4299		28.4599		26.8174	
Sunny slope 2-2	32.0135	32.8512	24.3969	24.8759	22.5436	22.7506	12.4932	14.3284
Sunny slope 2-3	21.5406		15.8008		17.2484		3.6747	
Sunny slope 3-1	10.4001		7.2360		6.4477		8.7534	
Sunny slope 3-2	19.7992	11.4774	19.5079	11.6257	18.5480	11.9259	23.1472	13.6592
Sunny slope 3-3	4.2329		8.1332		10.7820		9.0769	
Shady slope 1-1	37.1771		27.0310		30.1355		24.9982	
Shady slope 1-2	40.4021	41.3838	26.7918	30.9979	24.5900	32.8861	44.9588	38.8765
Shady slope 1-3	46.5721		39.1708		43.9328		46.6726	
Shady slope 2-1	26.3005		37.5194		41.8741		35.7397	
Shady slope 2-2	11.6734	24.8509	7.3637	25.5007	11.2789	24.5347	13.6083	28.2587
Shady slope 2-3	36.5787		31.6190		20.4510		35.4281	
Shady slope 3-1	46.4620		41.4126		35.5867		39.1191	
Shady slope 3-2	24.0767	29.8985	34.4809	31.6244	26.3403	25.0267	19.8311	24.0347
Shady slope 3-3	19.1569		18.9797		13.1531		13.1538	

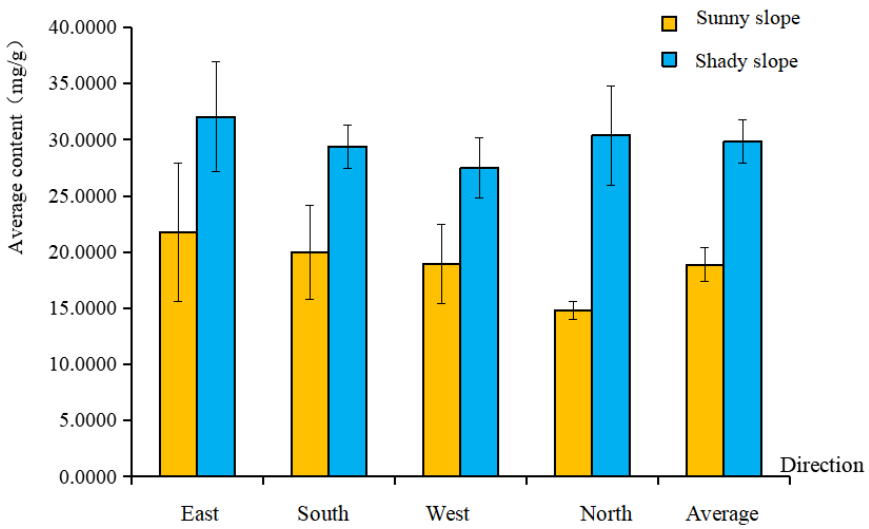

Figure 4. *The average GPA contents of leaves in different directions of Eucommia ulmoides on sunny slope and shady slope. The GPA content of leaves in different directions of Eucommia ulmoides is the mean value of the content in corresponding directions of 9 plants (9 samples)*

There was no significant difference in the GPA content of leaves of *Eucommia ulmoides* in different directions ($p > 0.05$). The GPA content of leaves in different directions on the sunny slope was 21.7425 mg/g in the east, 19.9794 mg/g in the south, 18.97234 mg/g in the west, 14.8079 mg/g in the north, respectively (*Fig. 5*). There was no significant difference in GPA content of leaves in different directions for *Eucommia ulmoides* planted on shady slope ($p > 0.05$). The GPA content of leaves in different directions on the shady slope was32.0444 mg/g in the east, 29.3743 mg/g in the south,

http://www.aloki.hu ● ISSN 1589 1623 (Print) ● ISSN 1785 0037 (Online)
DOI: http://dx.doi.org/10.15666/aeer/1804_53435353

27.4825 mg/g in the west, 30.3900 mg/g in the north, respectively, which is slightly different from the results of *Eucommia ulmoides* planted on sunny slope (*Fig. 5*).

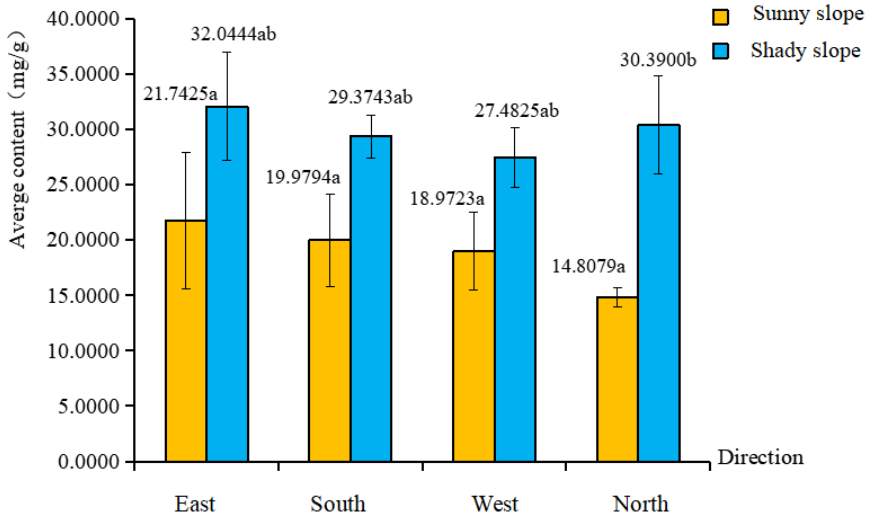

Figure 5. *The difference analysis of GPA content in Eucommia ulmoides leaves in different directions on the sunny slope and the shady slope. The GPA content of Eucommia ulmoides leaves in each direction is the average value of 9 samples in the corresponding direction of 9 plants*

There was a significant difference in GPA content in leaves, trunk bark and root bark of *Eucommia ulmoides* planted on sunny slope ($p < 0.05$), and the GPA in root bark was 42.43% higher than that in leaves and 70.06% higher than that in trunk bark ($p < 0.05$). The GPA content in leaves was significantly higher than that in trunk bark ($p < 0.05$) by 48.00% for of *Eucommia ulmoides* planted on sunny slope. The GPA content in root bark was the largest followed by that in leaves, and that in trunk bark was the lowest (*Fig. 6*).

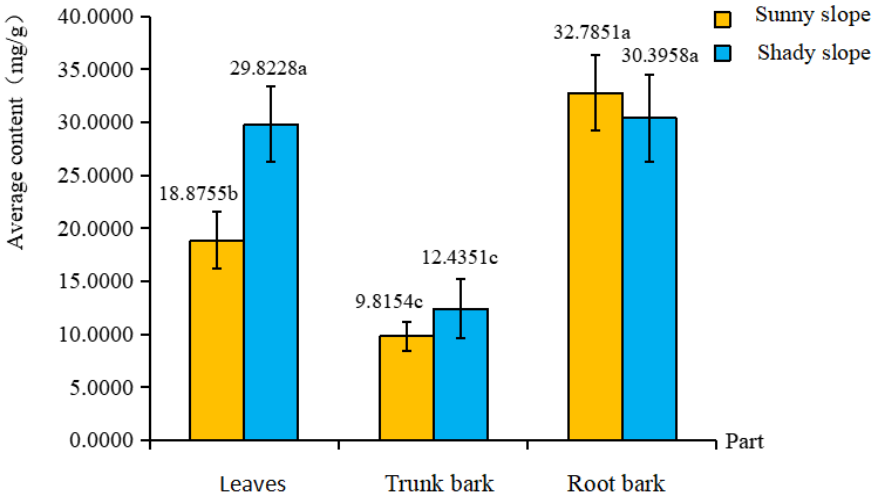

Figure 6. *The difference analysis of GPA content in different parts of Eucommia ulmoides on the sunny slope and the shady slope. The GPA content in leaves was the mean value of 36 samples in 4 directions of 9 plants, while the GPA content in trunk bark and root bark content was the mean value of 9 plants*

http://www.aloki.hu ● ISSN 1589 1623 (Print) ● ISSN 1785 0037 (Online)
DOI: http://dx.doi.org/10.15666/aeer/1804_53435353

The GPA contents in leaves and root bark of *Eucommia ulmoides* on shady slope showed no significant different ($p > 0.05$). The GPA contents in leaves and root bark of *Eucommia ulmoides* on shady slope were significantly higher than GPA content in trunk bark by 58.30% and 59.09%, respectively ($p < 0.05$). The GPA content in different parts of *Eucommia ulmoides* on the shady slope in root bark was the largest followed by that in leaves, and that in trunk bark was the lowest (*Fig. 6*).

Difference analysis of GPA contents in leaves of Eucommia ulmoides in different directions on sunny and shady slope

There was no significant difference in GPA content of Eucommia ulmoides leaves in different directions on both sunny slope and the shady slope ($p > 0.05$). In the east, south and west directions, there was no significant difference in GPA content in leaves of Eucommia ulmoides on both the sunny slope and the shady slope ($p > 0.05$). In the north, the GPA content of Eucommia ulmoides leaves on the shady slope was 51.27% higher than that on the sunny slope ($p < 0.05$). In the different directions, the GPA content in Eucommia ulmoides leaves on the shady slope was higher than that on the sunny slope, which was 32.15% higher in the east, 31.98% higher in the south, 30.97% higher in the west, and 51.27% higher in the north (*Fig. 5*).

Difference analysis of GPA content in different parts of Eucommia ulmoides on sunny slope and shady slope

There was a significant difference in GPA content in leaves, trunk bark and root bark of *Eucommia ulmoides* on the sunny slope ($p < 0.05$). For *Eucommia ulmoides* on shady slope, there was no significant difference between the GPA content in leaves and that in root bark ($p > 0.05$), while the GPA content in trunk bark was significantly different from that in leaves and that in root bark ($p < 0.05$). The GPA content in *Eucommia ulmoides* leaves on shady slope was 36.71% higher than that on sunny slope ($p < 0.05$). There was no significant difference between GPA content in trunk bark of *Eucommia ulmoides* on sunny slope and that on shady slope ($p > 0.05$). There was no significant difference between the GPA content in root bark of *Eucommia ulmoides* on sunny slope and that on shady slope ($p > 0.05$). There was a significant difference in GPA content in leaves between *Eucommia ulmoides* on shady slope and that on sunny slope, the GPA content in leaves and trunk bark of *Eucommia ulmoides* on shady slope was higher than that on sunny slope by 36.71% and 21.07%, respectively. The GAP content in root bark of *Eucommia ulmoides* on sunny slope was 7.29% higher than that on shady slope (*Fig. 6*).

Discussion

At present, the Eucommia ulmoides-related researches are mainly focused on the GPA contents in leaves and bark (Xu, 2007; Wei, 2016; Yan, 2018), the GPA content in seeds (Liu, 2013) and the GPA content in male flowers (He, 2010). However, there have been no systematic study on the GPA contents in leaves, trunk bark and root bark of Eucommia ulmoides in different directions on the sunny slope and the shady slope. In the karst plateau mountainous area studied, the GPA content in different parts of Eucommia ulmoides on both sunny or shade slope was GAP content in root bark was the largest followed by that in leaves, and that in trunk bark was the lowest. This is not consistent with the study (Jiang et al., 2013) which reports that the GPA content in the

http://www.aloki.hu ● ISSN 1589 1623 (Print) ● ISSN 1785 0037 (Online)
DOI: http://dx.doi.org/10.15666/aeer/1804_53435353

bark of Eucommia ulmoides from the same origin is higher than that in the leaves of Eucommia ulmoides, and also not consistent with the study (Lv et al., 2012) which reports that the GPA content of GPA in the bark of Eucommia ulmoides is higher than that in the leaves in Hunan province. Such different may be related to differences in sampling time and habitats of Eucommia ulmoides in different areas. In this study, the GPA content of Eucommia ulmoides root bark was studied for the first time, and it was found that the GPA content of Eucommia ulmoides root bark is higher than that of trunk bark and leaves, which may have higher medicinal value of root bark. Currently, the root bark of Eucommia ulmoides has not been included in the 2015 edition of Chinese pharmacopoeia as the medicinal part. Further study on the GPA content of root bark of Eucommia ulmoides will have important guiding significance for making full use of Eucommia ulmoides resources.

Conclusion

In the karst plateau mountains where *Eucommia ulmoides* samples are collected, the GPA content in *Eucommia ulmoides* leaves in different directions on shady slope was generally 36.71% higher than that on sunny slope. There was no significant difference in the GPA content in leaves in different directions for *Eucommia ulmoides* on the same slope direction. Except that the GPA of *Eucommia ulmoide*s leaves in the north on the shady slope was significantly higher (by 51.27%) than that in the north of the sunny slope, there was no significant difference in the GPA of *Eucommia ulmoides* leaves in the other three directions. Therefore, if GPA in the *Eucommia ulmoides* leaves is the target medicinal component, it is most suitable to collect *Eucommia ulmoides* leaves in the north on shady slope.

The GPA contents in different parts of *Eucommia ulmoides* on sunny are the GPA content in root bark (32.7851 mg/g), that in leaves (18.8755 mg/g) and that in trunk bark (9.8154 mg/g). In contrast, the results are GPA content in the root bark (30.3958 mg/g), that in the leaf (29.8228 mg/g), that in the trunk bark (12.4351 mg/g) for *Eucommia ulmoides* on shady slope.

The GPA content in different parts of *Eucommia ulmoides* on both sunny or shade slope was GAP content in root bark was the largest followed by that in leaves, and that in trunk bark was the lowest. If the GPA in *Eucommia ulmoides* is taken as the target component, the root bark is the best resource. This study expands the medicinal source part of *Eucommia ulmoides* and provides a new idea for the comprehensive utilization of *Eucommia ulmoides* resources. In the later stage, it will strengthen the research on the content of other medicinal components in the root bark, trunk bark and leaves of *Eucomia ulmoides* on the karst plateau mountain areas, further explore the influencing factors of the content of medicinal components in different parts of *Eucomia ulmoides* in the harsh karst environment, and explore the relationship between the biomass and the content of medicinal components in each part.

Acknowledgements. This work is supported by the 13th Five-year National Key Research and Development Plan (2016YFC0502604), Construction Program of Biology First-class Discipline in Guizhou (GNYL[2017]009), the Project of Promoted Innovation of Colleges and Universities of Guizhou Province (Qian Jiao He Collaborative Innovation [2014]01), National Natural Science Foundation of China (51868008), Guizhou provincial first-class major (biological science) project (Education

http://www.aloki.hu ● ISSN 1589 1623 (Print) ● ISSN 1785 0037 (Online)
DOI: http://dx.doi.org/10.15666/aeer/1804_53435353

department of guizhou province[2019]46); and Guizhou First-class Teaching Team Construction Project (Qian Jiao Gao Fa [2017] 158)].

REFERENCES

[1] Bai, M. M., Shi, W., Tian, J. M., Zhang, K. J., Kim, J. H., Sun, Y. N., Kim, Y. H., Gao, J. M. (2015): Soluble epoxide hydro-lase inhibitory and anti-inflammatory components from the leaves of *Eucommia ulmoides* Oliver (duzhong). – Journal of Agricultural and Food Chemistry 63(8): 2198-2205.

[2] Cai, Y. L. (1996): Preliminary research ecological reconstruction in karst mountains poverty areas of Southwest China. – Advances in Earth Science 11(6): 602-606.

[3] Du, H. Y. (2003): The progress in research of the active component from *Eucommia ulmoides* and its pharmacology. – Economic Forest Researches 2: 58-61, 82.

[4] Du, H. Y., Li, Q., He, J. J., Liu, C. Y., Liu, P. F. (2011): Comparison of the main active components contents in barks of different variance types of *Eucommia ulmoides*. – Forest Research 24(02): 230-233.

[5] Fang, C., Chen, L. Y., He, M. Z., Luo, Y. Y., Zhou, M. J., Zhang, N., Yuan, J. F., Wang, H. L., Xie, Y. Y. (2019): Molecular mechanistic insight into the anti-hyperuricemic effect of *Eucommia ulmoides* in mice and rats. – Pharmaceutical Biology (57)1: 112-119.

[6] Fu, H., Bai, X., Le, L., Tian, D., Gao, H., Qi, L. X., Hu, K. D. (2019): *Eucommia ulmoides* Oliv. leaf extract improves erectile dysfunction in streptozotocin-induced diabetic rats by protecting endothelial function and ameliorating hypothalamic-pituitary-gonadal axis function. – Evidence-Based Complementary and Alternative Medicine. https://doi.org/10.1155/2019/1782953.

[7] He, J. J. (2010): Studies on Variation of Secondary Metabolites in Eucommia Bark and Eucommia Male Flower. – Henan University, Henan.

[8] He, X., Wang, J. H., Li, M. X., Hao, D. J., Yang, Y., Zhang, C. L., He, R., Tao, R. (2014): *Eucommia ulmoides* Oliv.: ethnopharmacology, phytochemistry and pharmacology of an important traditional Chinese medicine. – Journal of Ethnopharmacology 151(1): 78-92.

[9] Hirata, T., Kobayashi, T., Wada, A., Ueda, T., Fujikawa, T., Miyashita, H., Ikeda, T., Tsukamoto, S., Nohara, T. (2011): Antiobesity compounds in green leaves of *Eucommia ulmoides*. – Bioorganic & Medicinal Chemistry Letters 21(6): 1786-1791.

[10] Huang, R. H., Xiang, Y., Liu, X. Z., Zhang, Y., Hu, Z., Wang, D. C. (2002): Two novel antifungal peptides distinct with a five-disulfide motif from the bark of *Eucommia ulmoides* Oliver. – Federation of European Biochemical Societies 521(01): 87-90.

[11] Hussain, T., Tan, B. E., Liu, G., Oladele, O. A., Rahu, N., Tossou, M. C., Yin, Y. L. (2016): Health-promoting properties of *Eucommia ulmoides*: a review. – Evidence-Based Complementary and Alternative Medicine. https://doi.org/10.1155/2016/5202908.

[12] Jiang, X. F., Zhang, C. L., Li, Q., Du, H. Y., Du, L. Y., Fu, J. M. (2013): Determination of three active components in leaves and bark of *Eucommia ulmoides* from different habitats by RP-HPLC. – Jiangsu Agricultural Sciences 41(08): 314-316.

[13] Jiao, H. L. (2016): Study on the Extraction and Quality of *Eucommia Ulmoides* Seed Oil. – Henan University of Technology, Henan.

[14] Lee, G. H., Lee, M. R., Lee, H. Y., Kim, S. H., Kim, H. K., Kim, H. R., Chae, H. J. (2014): *Eucommia ulmoides* cortex, geniposide and aucubin regulate lipotoxicity through the inhibition of lysosomal BAX. – PLoS ONE 9(2): 1-14.

[15] Lee, G. H., Lee, H. Y., Park, S. A., Shin, T. S., Chae, H. J. (2019): *Eucommia ulmoides* leaf extract ameliorates steatosis induced by high-fat diet in rats by increasing lysosomal function. – Nutrient 11(426): 1-15.

[16] Li, F. D., Du, H. Y. (2001): *Eucommia ulmoides* Oliver. – China Press of Traditional Chinese Medicine, Beijing, pp. 260-280.

http://www.aloki.hu ● ISSN 1589 1623 (Print) ● ISSN 1785 0037 (Online)
DOI: http://dx.doi.org/10.15666/aeer/1804_53435353

[17] Li, J. X., Xiong, G. M., Xu, W. T., Zong, Q. X. (2016): Distribution of shrublands in relation to soil and climate in mid-subtropical China. – Journal of Plant Ecology 9(4): 393-401.
[18] Liu, P. F. (2012): Isolation, Identification and Sequence Characterization of Full Length cDNA of MEP Pathway Related Genes in *Eucommia ulmoides*. – Chinese Academy of Forestry, Beijing.
[19] Liu, T. T. (2013): The New Technology for Multistage Efficient Utilization of Eucommia Ulmoide Oliver. Resources. – Northeast Forestry University, Harbin.
[20] Lou, L. J., Chen, B. Q., Du, H. Y., Fu, J. M., Du, L. Y., Li, Q. (2011): Protection effects of *Eucommia ulmoides* male flower tea on carbon tetrachloride induced liver injury in mice. – Journal of Henan University (Medical Science) 30(1): 24-26.
[21] Lv, Q., Peng, M. J., Lan, W. J., Peng, S., Zhang, L. J. (2012): Effect of processing methods on the content of several active ingredients in barks and leaves of *Eucommia ulmoides* Oliver. – Chemistry and Industry of Forest Products32(01): 75-79.
[22] Ong, V. Y. C., Tan, B. K. H. (2007): Novel phytoandrogens and lipidic augmenters from *Eucommia ulmoides*. – BMC Complementary and Alternative Medicine 7(01): 1-11.
[23] Peng, H. M., Li, X. Z. (2013): Pharmacological research and application of duzhong. – Acta Chinese Medicine 28(176): 72-73.
[24] Qing, J., Wei, Y. X., Wang, D. H., Wang, L., Liu, P. F., Du, H. Y., Du, Q. X. (2018): Study on genetic variation of main active components in leaves of Eucommia ulmoides. – Acta Botanica Boreali-Occidentalia Sinica 38(2): 316-323.
[25] Sugawa, H., Ohno, R. I., Shirakawa, J. I., Nakajima, A., Kanagawa, A., Hirata, T., Ikeda, T., Moroishi, N., Nagaia, M., Nagai, R. (2016): *Eucommia ulmoides* extracts prevent the formation of advanced glycation end products. – Food & Function 7(6): 2566-2573.
[26] Sun, Y. R., Dong, J. X., Wu, S. G. (2004): Studies on chemical constituents from *Eucommia ulmoides* Oliver. – Journal of Chinese Medicinal Materials 27(5): 341-343.
[27] Wang, J. W., Zhou, Y., Xiao, B. X., Li, J. S. (2013): Progress of study on karst soil moisture characteristics of Southwest China. – Soil and Water Conservation in China 2: 37-42.
[28] Wang, J. Y., Yuan, Y., Chen, X. J., Fu, S. G., Zhang, L., Hong, Y. L., You, S. F., Yang, Y. Q. (2016): Extract from *Eucommia ulmoides* Oliv. ameliorates arthritis via regulation of inflammation, synoviocyte proliferation and osteoclastogenesis in vitro and in vivo. – Journal of Ethnopharmacology 194: 609-616.
[29] Wang, Y. S., Tan, X. R., Li, S., Yang, S. L. (2019): The total flavonoid of *Eucommia ulmoides* sensitizes human glioblastoma cells to radiotherapy via HIF-α/MMP-2 pathway and activates intrinsic apoptosis pathway. – Onco Targets and Therapy (12): 5515-5524.
[30] Wei, Y. X. (2016): Study on variability of main active components and rubber content in *Eucommia ulmoides*. – Chinese Academy of Forestry 1-87.
[31] Xu, Y. M. (2007): The Effects of External Hormones on the Content of Secondary Metabolites in *Eucommia ulmoides* Oliver. – Northwest Agricultural and Forestry University of Science and Technology, Shaanxi.
[32] Yan, Y. (2018): Studies on quality evaluation of Eucommiae Cortex. – Nanjing University of Chinese Medicine 1-148.
[33] Yan, Y., Zhao, H., Chen, C. H., Zou, L. S., Liu, X. H., Chai, C., Wang, C. C., Shi, J. J., Chen, S. Y. (2018): Comparison of multiple bioactive constituents in different parts of *Eucommia ulmoides* based on UFLC-QTRAP-MS/MS combined with PCA. – Molecules 23(643): 1-11.
[34] Yang, M. D. (1990): On the fragility of the karst environment. – Yunnan Geographic Environment Research 2(01): 21-29.
[35] Zhu, M. and Sun, R. (2018): *Eucommia ulmoides* Oliver: a potential feedstock for bioactive products. – Journal of Agricultural and Food Chemistry 66(22): 5433-5438.

http://www.aloki.hu ● ISSN 1589 1623 (Print) ● ISSN 1785 0037 (Online)
DOI: http://dx.doi.org/10.15666/aeer/1804_53435353

THE EFFECT OF SOWING METHOD ON THE YIELD OF GRASSPEA (*LATHYRUS SATIVUS*) CULTIVATED IN AN ORGANIC SYSTEM

KSIĘŻAK, J. – BOJARSZCZUK, J.*

Institute of Soil Science and Plant Cultivation – State Research Institute, Puławy, Czartoryskich 8 Str., 24-100 Puławy, Poland
(phone: +48 81 4786796; fax: +48 81 4786900)

**Corresponding author*
e-mail: jolanta.bojarszczuk@iung.pulawy.pl

(Received 17th Feb 2020; accepted 22nd May 2020)

Abstract. The field experiment was conducted to evaluate how intercropping of the lentil with barley *Hordeum vulgare* or oats (*Avena sativa* L.) as a supporting plant impacts the yield of grasspea (*Lathyrus sativus)* in an organic system. The height of the plants, the height to the first and last pod, the number of pods and seeds on the plant, the weight of seeds on the plant, the air dry weight of the stem of one plant and the weight of the pods, the number and weight of grain per cereal plant, weight of one thousand grains, plant height and number of production shoots were also determined. The field experiment was conducted at the Agricultural Experimental Station in Grabów belonging to the Institute of Soil Science and Plant Cultivation in Puławy. The experimental factors were as follows: (A) the grasspea cultivar (cv.): Derek and Krab; (B) cropping method: sole cropping (without a supporting crop), row intercropping with a supporting crop – barley (cv. Ella) and oat (cv. Bingo). The grasspea seed yield obtained in the treatments with a supporting crops was higher by 11.4% compared with the sole cropped plots. The yield of both grasspea cultivars grown in pure stand and in mixed with cereals, was similar. Seed yield percentage of cv. 'Derek' grown with supporting crops was lower than that of cv. 'Krab'. Higher 1000 seed weight, number of pods, seeds and weight per plant were recorded for both cultivars grown in pure sowing than with supporting crops. Moreover, cv. 'Krab' characterized more favorable structure elements affecting yielding than cv. 'Derek'.
Keywords: *pure sowing, evaluation, supporting plant, cultivar, effect, organic farming*

Introduction

Grasspea (*Lathyrus sativus*) is one of the oldest species of cultivated plants. It was already known around 8000 years ago in ancient Egypt, India, and Roman Empire (Lambein and Kuo, 1997). This species probably originates from the Mediterranean Sea and the Middle and Far East (Lambein and Kuo, 1997). According to Smartt (1984), the center of grasspea origin is south-eastern and central Asia. In the Mediterranean region, the most common to be found are coarse-grained. According to Milczak et al. (1997) on the area of Poland, it appeared the earliest in the Podlasie region. Most probably, grasspea migrated with the settlers as a weed of lentil, and over the years, it became the dominant species due to a higher yield potential than the original species.

Grasspea is characterized by a strong, deep, soil-penetrating, pile root system reaching 1.5 m (Dziamba, 1997; Campbel et al., 1994), which makes it stand out from other legume species due to its high tolerance to abiotic stress (Mc Cutchan, 2003; Vaz Patto et al., 2006). According to Hanbury et al. (1999) and Milczak et al. (2001), its high tolerance to water stress, allows grasspea to be cultivated on weaker soils. The higher productivity of this species in unfavorable (deficit) water conditions compared to other legume species is also pointed out by many authors (Abd El-Moneim, 2000;

http://www.aloki.hu ● ISSN 1589 1623 (Print) ● ISSN1785 0037 (Online)
DOI: http://dx.doi.org/10.15666/aeer/1804_53555366

Hanbury et al., 2000; Mc Cuthan, 2003; Rybiński, 2003; Rybiński and Bocianowski, 2006; Rybiński et al., 2010). According to Vaz Patto et al. (2006), taking into account the role of the grasspea in crop rotation, its significant tolerance to diseases and pests, and high nutritional value of the seeds, it is a model species for sustainable agriculture. Due to its low habitat requirements, it may be a competitive species with respect to yellow lupine.

The grasspea seeds were also used for grain, fodder, biomass and green fertilization (Mikić et al., 2010; Basaran et al., 2011). Due to its high biological potential, grasspea have the ability to develop well in a cultivar of environmental conditions and capacity to improve soil fertility (Wani et al., 2012). In general, three main characteristics of this grain legume consist of its massiveness, drought tolerance, and adaptability to a wide range of soil types, including the marginal lands (Ahmadi et al., 2012; Sidorova et al., 2013; Kosev and Vasileva, 2019). There is a growing interest in cultivation of this culture, dictated by the need to restore particularly eroded soils (Polignano et al., 2009).

Grasspea seeds contain a lot of protein and constitute a valuable source of energy components, nutritional fibre and many mineral elements, such as: zinc, copper, sodium, magnesium and calcium (Grela and Günter, 1995; Lampart-Szczapa, 1997; Pisulewska et al., 1997; Hanbury, 2000; Kasprzak and Pzedzicki, 2008; Karadag and Yavuz, 2010). In addition, grasspea seeds are also a rich source of a number proactive non-nutritional components of food, such as inhibitors of prostheses, tannins and neurotoxins, mainly β-ODAP, which may limit the use of seeds, especially in the raw state (Deshpande and Campbell, 1992; Grela et al., 2000; Rybiński and Pokora, 2002; Urga and Fufa, 2005). Moreover, these seeds are considered to have hypocholesterolemic (Fruhbeck et al., 1997) and anticancer properties (Pawlęga et al., 1995). High protein content in seeds of this species makes it suitable for feed and nutrition purposes (Grela et al., 2011). Moreover, restrictions from animal protein in human nutrition, which are caused by health reasons and the popularity of vegetarian diet, cause an increase in the consumption of legume proteins in Poland as well.

The aim of the study was to evaluate the effect of cultivar and sowing method on grasspea yielding cultivated under organic farming system.

Material and methods

Field experiment and cultivation management

During the period from 2017 to 2018, a controlled field experiment was conducted at the Agricultural Experimental Station in Grabów [51°21′18″N 21°40′09″E] (Masovian Voivodeship) belonging to the Institute of Soil Science and Plant Cultivation – State Research Institute in Puławy (Lublin voivodeship) (*Fig. 1*). The experiment was established on a soil belonging to a good rye complex, class IVa. The soil was characterized by the following nutrient content: (mg·100 kg^{-1} soil): P – 11.1-13.0; K – 15.1-20.4 and Mg – 4.0-6.2. Soil pH, as determined in 1 N KCl, was 5.5-6.3. The experimental factors were as follows: (A) – the grasspea cultivar: Derek and Krab; (B) – sowing method: sole cropping (without a supporting crop), and row intercropping with barley (Ella cultivar) and oat (Bingo cultivar).

The experiment was set up as a split-plot design with four replicates. The area of a single plot was 40 m^2 and for harvest – 35 m^2. Each year the total number of plots in the experiment was 48.

http://www.aloki.hu ● ISSN 1589 1623 (Print) ● ISSN1785 0037 (Online)
DOI: http://dx.doi.org/10.15666/aeer/1804_53555366

Figure 1. *Localization of the study site (Public Domain, https://commons.wikimedia.org/w/index.php?curid=89531)*

The density (units·m^{-2}) of grasspea in pure cropping was 100, in row intercropping - 50; oat as supporting plant – 250 and barley – 150. Sowing was conducted in the first decade of April. Row spacing is 20 cm. Cereals were sown separately in the interrows of the lentil crop. Mineral fertilization was not applied. The plots were harrowed twice to control weeds in the mixtures. Plants were harvested at the full maturity stage of mixture components at the first decade of August.

The height of the plants, the height to the first and last pod, the number of pods and seeds on the plant, the weight of seeds on the plant, the air dry weight of the stem of one plant and the weight of the pods were determined before harvest. The number and weight of grain per cereal plant, weight of one thousand grains, plant height and number of production shoots were also determined. After harvest, the seed mixtures yield, grasspea seed yield, component percentage in yield and weight of one thousand seeds at 14% humidity were determined.

Weather conditions

Weather conditions during the study period varied substantially between the years (*Table 1*). In 2017 the highest amount of precipitation was recorded in April, exceeded by 77% the long-term average, which made it difficult to perform mechanical maintenance. In June and the first decade of July was recorded a small amount of precipitation (32.6 and 9.7 mm, respectively) and was lower than the long-term average by 54.1 and 65.0%, respectively. It had a negative influence on the growth and development of the plants. In the first decade of August there were occurred very small amount of precipitation (0.9 mm). The average air temperature in this vegetative season exceeded the long-term average by 1.4°C. In 2018, the amount of precipitation in May (97.4 mm) and July (118.5 mm) exceeded the average from multi-years by 70.9 and 41.1%, respectively, which favoured the yields of grasspea. During April and June the total precipitation was only 65% and 63% of the long-term average, respectively. The average air temperature in this vegetative season exceeded the long-term average by 2.4°C.

http://www.aloki.hu ● ISSN 1589 1623 (Print) ● ISSN1785 0037 (Online)
DOI: http://dx.doi.org/10.15666/aeer/1804_53555366

Table 1. *Course of weather conditions during the vegetation periods*

Specification	Month						Sum /Mean III-VIII
	III	IV	V	VI	VII	VIII	
2017							
Precipitation (mm)	35.8	69.1	34.4	32.6	86.3	55.3	313.5
Temperature °C	5.7	7.5	13.9	18.1	18.6	19.6	13.9
2018							
Precipitation (mm)	14.1	25.3	97.4	44.6	118.5	70.6	370.5
Temperature °C	-0.1	13.3	17.0	18.4	20.4	20.2	14.9
Mean precipitation from multiyear*	30.0	39.0	57.0	71.0	84.0	75.0	356.0
Mean temperature from multiyear °C	1.6	7.7	13.4	16.7	18.3	17.3	12.5

*Mean from 1871-2000

Chemical analysis of grass pea seeds

The following were determined in seed samples: N (mineralization in sulfuric acid and oxygenated water; determination by the Kjeldahl distillation method; titration detection), P (mineralization in sulfuric acid and oxygenated water; determination by the vanadium-molybdate spectrophotometric method), K (mineralization in sulfuric acid and oxygenated water; determination by flame photometry). Moreover, total protein (mineralization in sulfuric acid; determination by the Kjeldahl distillation method; titration detection), fat content (Soxhlet method) were also determined.

Statistical analysis

Assessing the significance of the impact of the considered factors on the features was based on the variance analysis, indicating Tukey's confidence half-intervals at a significance level of 0.05.

Results and discussion

The yield of grasspea was significantly influenced by the cultivar, cropping method, species of supporting crops, and the course of weather conditions during the growing season. Higher total precipitation in the growing season and a more favorable distribution of precipitation contributed to a much better grasspea yield in 2018 than in 2017 (*Table 2*). The higher yield was the result of higher number of pods and seed weight per plant (*Table 3 and Table 4*). In the both years of the study, the grasspea seed yield obtained in the treatments with a supporting crops was higher by 11.4% compared with the sole cropped plots. The highest yield was obtained by grasspea with oat used as supporting crop compared to cultivation grasspea with barley or sole cropping (statistically significant differences). However, significantly higher yields of grasspea seeds, both of 'Derek' and 'Krab' cultivars, were obtained in sole cropping than in cultivation with supporting crops. Average for 2 years, the yield of both grasspea cultivars grown in pure stand and in mixed with cereals, was similar, whereas in a drier year (2017) cv. 'Krab' yielded better, while in the year with more evenly distributed precipitation (2018), cv. 'Derek' yielded better. Until now, very few studies have been carried out on grasspea taking into account agrotechnical factors, especially cultivation

http://www.aloki.hu ● ISSN 1589 1623 (Print) ● ISSN1785 0037 (Online)
DOI: http://dx.doi.org/10.15666/aeer/1804_53555366

with supporting crops. Rachoń (1995) states that the yield of grasspea cropped with triticale or with oats was higher than that of grasspea in sole cropping, and the yields of mixtures with triticale were higher than with oats. Moreover, the yield of the grasspea and cereal mixture, irrespective of the cereal species, increased with an increase in the percentage of cereal in the weight of sown seeds (from 5% to 25%). Karadag and Yavuz (2010) reported that the average seeds yield of from the assessed grasspea lines was 1288 kg·ha^{-1} and ranged from 1079 to 1583 kg·ha^{-1}. Cichy and Rybiński (2007) recorded a very similar yield of seeds as 'Krab' and 'Derek'. It was higher than the yield obtained in own research; 'Krab' by 4.8% and 'Derek' by 6.0%.

Table 2. *Total seeds yield of grasspea and supporting plant and thousand seeds weight of grasspea depending on cropping method*

Cropping method	Seeds yield (t·ha^{-1})			Thousand seeds weight (g)		
	2017	2018	Mean	2017	2018	Mean
Derek cv. – pure sowing	2.22^{b*}	3.52^{c}	2.87	122^{ab}	120^{ab}	121
Derek cv. + barley	2.00^{a}	3.84^{d}	2.92	114^{b}	112^{b}	113
Derek cv.+ oat	3.30^{c}	4.03^{cd}	3.67	103^{a}	99^{a}	101
Krab cv. – pure soving	2.53^{b}	3.32^{a}	2.93	176^{cd}	183^{cd}	180
Krab cv. + barley	2.13^{a}	3.44^{b}	2.79	161^{d}	167^{c}	164
Krab cv. + oat	3.44^{c}	3.63^{ab}	3.54	156^{c}	158^{bc}	157
Mean	2.60	3.63	-	139	140	-

*Values followed by a different letter are significantly different ($p<0.05$), Source: own study

Table 3. *Number of pods per plant grasspea depending on cropping method*

Cropping method	2017	2018	Mean
Derek cv. – pure sowing	5.53^{bc*}	6.37^{c}	5.95
Derek cv. + barley	4.18^{c}	5.40^{ab}	4.79
Derek cv.+ oat	2.65^{b}	4.90^{a}	3.78
Krab cv. – pure soving	6.73^{d}	7.10^{bc}	6.92
Krab cv. + barley	3.75^{ab}	5.30^{ab}	4.53
Krab cv. + oat	2.15^{a}	5.03^{b}	3.59
Mean	4.17	5.68	-

*See Table 2, Source: own study

Table 4. *Seed weight and number per plant grasspea depending on cropping method*

Cropping method	Seeds number per plant (units)			Seed weight per plant (g)		
	2017	2018	Mean	2017	2018	Mean
Derek cv. – pure sowing	22.1^{bc*}	23.1^{d}	22.6	2.68^{ab}	2.75^{bc}	2.72
Derek cv. + barley	12.6^{c}	19.3^{bc}	16.0	1.43^{b}	1.92^{bc}	1.68
Derek cv.+ oat	7.10^{ab}	17.0^{c}	12.1	0.73^{a}	1.49^{ab}	1.11
Krab cv. – pure soving	21.8^{bc}	17.7^{c}	19.8	3.83^{c}	3.26^{d}	3.55
Krab cv. + barley	6.58^{b}	13.8^{ab}	10.2	1.55^{b}	2.30^{c}	1.93
Krab cv. + oat	4.83^{a}	13.0^{ab}	8.9	0.74^{a}	2.05^{b}	1.40
Mean	12.5	17.3	-	1.83	2.30	-

* See Table 2, Source: own study

http://www.aloki.hu ● ISSN 1589 1623 (Print) ● ISSN1785 0037 (Online)
DOI: http://dx.doi.org/10.15666/aeer/1804_53555366

The share in the yield of seeds of cv. 'Derek' cropped with supporting plants was lower than that of cv. 'Krab' (*Table 5*). Moreover, oat was more competitive compared to grasspea than barley, which resulted in a lower percentage of legume seeds in the yield. The share in the yield of grasspea seeds grown with supporting crops, regardless of the cultivar, was much smaller than in the case of sowing, especially in cultivation with oats.

Table 5. *The share and seeds yield of grasspea depending on cropping method*

Cropping method	Grasspea share (%)			Seeds yield of grasspea ($t \cdot ha^{-1}$)		
	2017	2018	Mean	2017	2018	Mean
Derek cv. – pure sowing	-	-	-	2.22^{c*}	3.52^{bc}	2.87
Derek cv. + barley	33.8	46.2	40.0	$0.68a^{b}$	1.77^{c}	1.23
Derek cv.+ oat	11.0	39.7	25.4	0.37^{a}	1.52^{b}	0.95
Krab cv. – pure soving	-	-	-	2.53^{d}	3.32^{bc}	2.93
Krab cv. + barley	42.5	47.0	44.8	0.91^{bc}	1.62^{ab}	1.27
Krab cv. + oat	15.0	39.6	27.3	0.51^{b}	1.44^{a}	0.98
Mean	25.6	43.1	-	0.62	1.59	-

* See Table 2, Source: own study

Higher weight of one thousand seeds, number of pods, number of seeds, weight per plant and dry weight of stems and pods of one plant were characteristic for both cultivars grown in sole cropping than with cereals (statistically significant differences) (*Tables 3, 4, 5, 6*). Irrespective of the cropping method, cv. 'Krab' was characterized by higher weight of 1000 seeds, weight of seeds, and number of pods per plant than cv. 'Derek' (*Tables 2, 4, 5*). Cichy and Rybinski (2007) recorded a similar seeds size of these cultivars. According to Milczak et al. (1997), 'Krab' is classified as a medium-seeded cultivar (MTN 193 g) and 'Derek' as a small-seeded cultivar (MTN 115 g). According to Rybiński and Grela (2007), cv. 'Derek' was characterized by higher number of pods and seeds per plant, while lower weight of seeds per plant than cv. 'Krab'. However, Rybiński and Bocianowski (2006) found several times higher number of pods and seeds per plant than in own research. Cultivation of grasspea with spring cereals had little effect on the height of the first pod on the shoot, caused slightly higher settling of the last pod and increased shoot length, especially cultivated with oats (*Table 7*). Moreover, these features showed little difference between the two cultivars. Rybiński and Grela (2007) stated that cv. 'Derek' produced longer shoots and formed the first pod on the shoot higher than cv. 'Krab'. However, in the study by Rybiński and Bocianowski (2006), the mean height of a grasspea was 106 cm (range: 154-40) and the mean height of the lowest pod set was 12.0 cm (range: 18-4 cm).

Talukdar (2009) reported considerable differences in morphological characters such as plant height, number of branches, grain yield and developmental characteristics among grass pea lines. According to Mera et al. (2003), Kumari and Prasad (2005) characteristics such as morphological traits, plant height, number of seed per pod, 100-seed weight, biological yield and harvest index are the most important in grass pea improvement for increasing grain yield. According to Ahmadi et al. (2015) reported that harvest index, 100-seed weight and plant height explained 75% of yield variation. Thus,

http://www.aloki.hu ● ISSN 1589 1623 (Print) ● ISSN1785 0037 (Online)
DOI: http://dx.doi.org/10.15666/aeer/1804_53555366

these characters can be effective in yield improvement. Mihailovic et al. (2013) reported that number of plants, plant height, number of stems and lateral branches, number of internodes, green forage yield were highly significantly correlated.

Table 6. *Stem dry matter of one plant and dry matter of siliques depending on cropping method (g)*

Cropping method	Stem dry matter of one plant			Dry matter of siliques		
	2017	2018	Mean	2017	2018	Mean
Derek cv. – pure sowing	0.64^{c*}	0.70^{c}	0.67	0.22^{b}	0.17^{c}	0.20
Derek cv. + barley	0.31^{ab}	0.55^{b}	0.43	0.13^{a}	0.13^{b}	0.13
Derek cv.+ oat	0.16^{a}	0.37^{a}	0.27	0.11^{a}	0.03^{ab}	0.07
Krab cv. – pure soving	0.89^{bc}	0.88^{bc}	0.89	0.29^{c}	0.21^{bc}	0.25
Krab cv. + barley	0.24^{b}	0.53^{b}	0.39	0.12^{a}	0.14^{b}	0,13
Krab cv. + oat	0.16^{a}	0.45^{ab}	0.31	0.10^{a}	0.14^{b}	0,12
Mean	0.40	0.58	-	0.16	0.14	-

* See Table 2, Source: own study

Table 7. *Height to the 1st pod, height of the last pod and height to top of grasspea (cm)*

Cropping method	Height to the 1st pod			Height of the last pod			Height to top		
	2017	2018	Mean	2017	2018	Mean	2017	2018	Mean
Derek cv. – pure sowing	30.4	33.6	32.0	42.3	45.8	44.0	56.3	58.5	57.4
Derek cv. + barley	31.0	30.6	30.8	42.8	41.8	42.3	59.4	52.3	55.8
Derek cv.+ oat	32.0	33.9	32.9	44.3	53.4	48.8	58.9	62.3	60.6
Krab cv. – pure soving	32.5	33.6	33.1	44.6	48.7	46.6	58.2	59.6	58.9
Krab cv. + barley	33.2	34.4	33.8	45.3	45.9	45.6	59.3	58.9	59.1
Krab cv. + oat	36.6	38.1	37.4	47.5	49.5	48.5	60.1	63.1	61.6
Mean	32.6	34.0	-	44.5	47.5	-	58.7	59.1	-

Source: own study

Kosev and Vasileva (2019) reported that the main factor for higher productivity of the varieties was not the maximum display of certain characteristics, but their optimal combination.

A significantly higher protein, crude fibre and phosphorus content was determined in cv. 'Krab' seeds regardless of the cropping method. Whereas cv. 'Derek' contained slightly less fat (*Table 8 and Table 9*). According to Rybiński and Grela (2007), Cichy and Rybiński (2007), cv. 'Derek' seeds collected more protein than cv. 'Krab'. According to Karadagi and Yavuz (2010), the average protein content in seeds was 256.9 $g \cdot kg^{-1}$ DM (from 251.2 to 274.4) and fat content was 42.1 $g \cdot kg^{-1}$ DM (from 32.2 to 50.7). Whereas Rybiński et al. (2013) evaluating many cultivars of grasspea, noted small differences in protein content (statistically insignificant differences), while fat content did not exceed 10 $g \cdot kg^{-1}$ DM. These authors proved a positive correlation between protein amount and fat and linolenic acid content. Sammour et al. (2007) found significant variation for seed weight and seed protein content in accessions of grass pea

http://www.aloki.hu ● ISSN 1589 1623 (Print) ● ISSN1785 0037 (Online)
DOI: http://dx.doi.org/10.15666/aeer/1804_53555366

from different geographical regions. Grela and Winiarska (1997) indicate a high dietary value of grasspea, which in their opinion, is similar in composition and usefulness to soybean oil. Williams et al. (1994) reported that the average fat concentration in the tested seeds of the cultivars was about 6.0 $g \cdot kg^{-1}$ DM. According to Grela and Winiarska (1997), the phosphorus content in the grasspea seeds ranged from 0.1 to 5.5, while potassium from 1.0 to 10.4 $g \cdot kg^{-1}$ DM. The limited amount of precipitation (in 2017) favourably influenced the protein concentration in the seeds, but also caused a higher accumulation of fibre and phosphorus. Cultivation of grasspea in row intercropping with cereals did not significantly affect the accumulation of nutrients in the seeds.

Table 8. *Concentrations of protein, crude fibre and crube fat in grasspea seeds depending cropping method ($g \cdot kg^{-1}$DM)*

Cropping method	Protein content			Fat content			Crude fibre		
	2017	2018	Mean	2017	2018	Mean	2017	2018	Mean
Derek cv. – pure sowing	269^{a*}	257^{a}	263	12.0^{ab}	13.0^{bc}	12.5	50.3^{a}	39.4^{a}	44.8
Derek cv. + barley	270^{a}	258^{a}	264	11.0^{b}	14.0^{c}	12.5	51.2^{a}	42.3^{c}	46.7
Derek cv.+ oat	269^{a}	258^{a}	263	11.0^{b}	13.0^{bc}	12.0	52.1^{a}	41.7^{b}	46.9
Krab cv. – pure soving	294^{b}	270^{b}	282	10.0^{a}	12.0^{a}	11.0	68.3^{b}	49.6^{ab}	58.9
Krab cv. + barley	291^{b}	270^{b}	281	11.0^{b}	13.0^{bc}	12.0	69.1^{b}	52.3^{bc}	60.7
Krab cv. + oat	293^{b}	272^{b}	283	12.0^{b}	12.0^{b}	12.0	67.8^{b}	51.9b^{c}	59.8
Mean	281	260	-	11.0	13.0	-	59.8	46.2	-

* See Table 2, Source: own study

Table 9. *Concentrations of phosphorus and potassium in grasspea seeds depending on cropping method ($g \cdot kg^{-1}$DM)*

Cropping method	Phosphorus content			Potassium content		
	2017	2018	Mean	2017	2018	Mean
Derek cv. – pure sowing	5.8^{a*}	4.5^{ab}	5.1	11.2^{b}	12.0^{a}	11.6
Derek cv. + barley	5.8^{a}	4.7^{b}	5.2	11.4^{b}	11.9^{a}	11.6
Derek cv.+ oat	6.2^{b}	4.6^{c}	5.4	12.1^{c}	12.2^{a}	12.1
Krab cv. – pure soving	6.9^{c}	4.9^{bc}	5.9	12.1^{c}	12.0^{a}	12.1
Krab cv. + barley	6.5^{ab}	5.1^{d}	5.8	10.8^{a}	12.3^{a}	11.6
Krab cv. + oat	6.6^{ab}	5.2^{d}	5.9	11.1^{b}	11.9^{a}	11.5
Mean	6.3	4.8	-	11.4	12.1	-

* See Table 2, Source: own study

The studied grasspea cultivars had a relatively weak effect on the height of barley and oat plants, the number of grains per plant, and the number of production shoots of both cereal species (*Table 10 and Table 11*). Moreover, higher 1000 grain weight characterized the mixtures of barley grown with the grasspea of cv. 'Krab' and the mixtures of oats with the grasspea of cv. 'Derek'. Higher grain weight was recorded in oat grown with grasspea of the cv. 'Krab'.

http://www.aloki.hu ● ISSN 1589 1623 (Print) ● ISSN1785 0037 (Online)
DOI: http://dx.doi.org/10.15666/aeer/1804_53555366

Table 10. *Number, weight of cereals grain per plant and thousand seeds weight of cereals depending on cropping method*

Cropping method	Number of cereals grain per plant (units)			Weight of cereals grain per plant (g)			Thousand seeds weight of cereals (g)		
	2017	2018	Mean	2017	2018	Mean	2017	2018	Mean
Derek cv. + barley	52.6^{a*}	54.7^{a}	53.6	2.32^{a}	2.39^{a}	2.36	43.0^{c}	47.5^{c}	45.3
Derek cv.+ oat	56.3^{b}	56.9^{ab}	56.6	2.40^{b}	2.48^{b}	2.44	29.3^{b}	33.5^{a}	31.4
Krab cv. + barley	54.5^{a}	55.8^{b}	55.1	2.31^{a}	2.40^{a}	2.36	45.8^{c}	48.5^{c}	47.1
Krab cv. + oat	57.4^{b}	58.3^{c}	57.8	2.46^{b}	2.56^{b}	2.51	28.8^{a}	32.2^{b}	30.5
Mean	55.2	56.4	-	2.37	2.45	-	36.7	40.4	-

* See Table 2, Source: own study

Table 11. *Height plant and number of fruiting shoots depending on cropping method*

Cropping method	Height plant (cm)			Number of fruiting shoots (units)		
	2017	2018	Mean	2017	2018	Mean
Derek cv. + barley	32.0	56.0	44.0	2.63	3.63	3.13
Krab cv. + barley	34.0	56.0	45.0	2.65	3.18	2.92
Derek cv.+ oat	44.0	83.0	64.0	1.95	1.73	1.84
Krab cv. + oat	45.0	87.0	66.0	1.50	1.70	1.60
Mean	39.0	70.0	-	2.18	2.56	-

Source: own study

Conclusions

1) The grasspea seed yield obtained in the treatments with a supporting crops was higher by 11.4% compared with the sole cropped plots. The yield of both grasspea cultivars grown in pure stand and in mixed with cereals, was similar.
2) Seed yield percentage of the 'Derek' cultivar grown with supporting crops was lower than that of cultivar 'Krab'.
3) Higher 1000 seed weight, number of pods, seeds and weight per plant were recorded for both cultivars grown in pure sowing than with supporting crops. Moreover, 'Krab' cultivar characterized more favorable structure elements affecting yielding than 'Derek' cultivar.

REFERENCES

[1] Abd El-Moneim, B., Dorrestein, M., Mulugeta, W. (2000): Improving the nutritional quality and yield potential of grasspea (*Lathyrus sativus* L.). – Food and Nutrition Bulletin 21(4): 493-496.
[2] Ahmadi, J., Vaezi, B., Shaabani, A., Khademi, K. (2012): Multi-environment Yield Trials of Grass Pea (*Lathyrus sativus* L.) in Iran Using AMMI and SREG GGE. – Journal of Agricultural Science and Technology 14: 1075-1085.
[3] Ahmadi, J., Vaezi, B., Pour-Aboughadareh, A. (2015): Assessment of heritability and relationships among agronomic characters in grass pea (*Lathyrus sativus* L.) under rainfed conditions. – Biharean Biologist 9(1): 29-34.

http://www.aloki.hu ● ISSN 1589 1623 (Print) ● ISSN1785 0037 (Online)
DOI: http://dx.doi.org/10.15666/aeer/1804_53555366

[4] Basaran, U., Mut, H., Önal-Asci, Ö., Acar, Z., Ayan, İ. (2011): Variability in forage quality of Turkish grass pea (*Lathyrus sativus* L.) landraces. – Turkish Journal of Field Crops 16(1): 9-14. http://www.fieldcrops.org/assets/pdf/product512fafd825cd8.pdf.

[5] Campbell, S. G., Mehra, R. B., Agraval, S. K., Chen, Y. Z., Abd El Moneim, A. M., Khawaja, H. I. T., Yadow, C. R., Tay, J. U., Araya, W. A. (1994): Current status and future research strategy in breeding grasspea (*Lathyrus sativus* L.). – Euphytica 73: 167-175.

[6] Cichy, H., Rybiński, W. (2007): The yielding ability of grasspea (*Lathyrus sativus* L.) mutants and cultivars in field trials (Ocena zdolności plonowania wybranych mutantów lędźwianu siewnego (*Lathyrus sativus* L.) w doświadczeniach polowych). – Zeszyty Problemowe Postępów Nauk Rolniczych 522: 177-185. (in Polish).

[7] Deshpande, S. S., Campbell, C. G. (1992): Genotype variation in BOAA, condensed tannins, phenolcs and enzyme inhibitors of grasspea (*Lathyrus sativus*). – Canadian Journal of Plant Science 72: 1037-1047.

[8] Dziamba, S. (1997): Biology and agrotechnic of grasspea (Biologia i agrotechnika lędźwianu siewnego). – Conference materials „Lędźwian siewny – agrotechnika i wykorzystanie w żywieniu zwierząt i ludzi." Radom, 9-10.06.1997, pp. 27-33. (in Polish).

[9] Fruhbeck, G., Montreal, I., Santidrian, S. (1997): Hormonal implications of the hypocholesterolemic effct of intake of field beans (*Vicia faba*) by young men with hypercholesterolemia. – American Journal of Clinical Nutrition 66: 1421-460.

[10] Grela, E. R., Günter, K. D. (1995): Fatty acid composition and tocopherol content of some legume seeds. – Animal feed science and technology 52: 325-331.

[11] Grela, R., Winiarska, A. (1997): Chemical composition and nutritional value of grasspea (*Lathyrus sativus* L.) Skład chemiczny i wartość pokarmowa nasion lędźwianu siewnego (*Lathyrus sativus* L.). – International Scientific Symposium „Lędźwian siewny - agrotechnika i wykorzystanie w żywieniu zwierząt i ludzi". Radom, 9-10.06.1997, pp. 49-55. (in Polish).

[12] Grela, E., Studziński, T., Winiarska, A. (2000): Latinism in humans and animals (Latyryzm u ludzi i zwierząt). – Medycyna Weterynaryjna 59(9): 558-562. (in Polish).

[13] Grela, E., Rybiński, W., Sobolewska, S. (2011): Nutritional and dietary value of grass pea (*Lathyrus sativus* L.) and dwarf chickling (*Lathyrus cicera* L.) seeds. (Wartość odżywcza i dietetyczna nasion lędźwianu siewnego (*Lathyrus sativus* L.) i czerwonego (*Lathyrus cicera* L.)). – Problemy Higieny i Epidemiologii 92(4): 887-889. (in Polish).

[14] Hanbury, C. D., Siddique, K. H. M., Galwey, N. W., Cocks, P. S. (1999): Genotype environment interaction for seed yield and β-ODAP concentration of *Lathyrus sativus* L. and *Lathyrus cicera* L. in Mediterranean-type environments. – Euphytica 110: 45-60.

[15] Hanbury, C. D., White, C. L., Mullan, B. P., Siddique, K. H. M. (2000): A review of the potential of *Lathyrus sativus* L. and *L. cicera* L. grain for use an animal feed. – Animal Feed Science and Technology 87: 1-27.

[16] Karadag, Y., Yavuz, M. (2010): Seed yield and biochemical compounds of grasspea (*Lathyrus sativus* L.) lines grown in semi-arid regions of Turkey. – African Journal of Biotechnology 9: 8343-8348.

[17] Kasprzak, M., Rzedzicki, Z. (2008): Application of Everlasting Pea Wholemeal in Extrusion-cooking Technology. – International Agrophysics 22: 339-347.

[18] Kosev, V. I., Vasileva, V. M. (2019): Morphological characterization of grass pea (*Lathyrus sativus* L.) varieties. – The Journal of Agricultural Sciences - Sri Lanka 14(2): 67-76. http://dx.doi.org/10.4038/jas.v14i2.8509.

[19] Kumari, V., Prasad, R. (2005): Model plant type in Khesari (*Lathyrus sativus* L.) suitable for hill farming. – Lathyrus Lathyrism Newsletter 4: 1-17.

[20] Lambein, F., Kuo, Y. H. (1997): *Lathyrus sativus*, a neolithic crop with a modern future? An overview of a present situation. – International Scientific Symposium „Lędźwian siewny - agrotechnika i wykorzystanie w żywieniu zwierząt i ludzi". Radom, 9-10.06.1997. pp. 6-12.

http://www.aloki.hu ● ISSN 1589 1623 (Print) ● ISSN1785 0037 (Online)
DOI: http://dx.doi.org/10.15666/aeer/1804_53555366

[21] Lampart-Szczapa, E. (1997): Legume seeds in human nutrition: Biology and technological value. (Nasiona roślin strączkowych w żywieniu człowieka: Wartość biologiczna i technologiczna). – Zeszyty Problemowe Postępów Nauk Rolniczych 238: 235-237. (in Polish).
[22] McCutchan, J. S. (2003): A brief history of grasspea and its use in crop improvement. – Lathyrus Lathyrism Newsletter 3: 18-20.
[23] Mera, M., Montenegro, A., Espinoza, N., Gaete, N., Barrientos, L. (2003): Heritability of seed weight in an inbred population of large seeded *Lathyrus sativus*. – Lathyrus Lathyrism Newsletter 3: 24-25.
[24] Mihailovic, V., Mikic A., Cupina, B., Krstic, D. (2013): Forage yields and forage yield components in grass pea (*Lathyrus sativus* L.). – Legume Research 36(1): 67-69.
[25] Mikić, A., Mihailović, V., Ćupina, B., Krstić, D., Vasiljević, S., Milić, D. (2010): Forage and seed yield components in four French landraces of grass pea (*Lathyrus sativus* L.). – In: Huyghe, C. (ed.) Sustainable Use of Genetic Diversity in Forage and Turf Breeding. Springer Science+Business Media, Dordrecht, pp. 127-130. https://www. springer.com/us/book/9789048187058.
[26] Milczak, M., Pędziński, M., Mnichowska, H., Szwed-Urbaś, K. (1997): Creative breeding of grasspea (*Lathyrus sativus* L.) - summary of the first stage (Hodowla twórcza lędźwianu siewnego (*Lathyrus sativus* L.) – podsumowanie pierwszego etapu. Międz. Sym. Nauk. „Lędźwian siewny – agrotechnika i wykorzystanie w żywieniu zwierząt i ludzi." Radom, 9-10.06.1997, pp. 13-22. (in Polish).
[27] Milczak, M., Pędziński, M., Mnichowska, H., Szwed-Urbaś, K., Rybiński, W. (2001): Creative breeding of grasspea (*Lathurus sativus*) in Poland. – Lathyrus lathyrism Newsletter 2: 85-88.
[28] Pawlęga, J., Rachtan, J., Dyba, T. (1995): Can legumes prevent cancer? (Czy warzywa strączkowe mogą zapobiegać rakowi jajnika). – Żywienie Człowieka 22: 351-360. (in Polish).
[29] Pisulewska, E., Hanczakowski, P., Szymczyk, B., Dziamba, Sz. (1997): Comparison of chemical composition and seeds nutrition value of three forms grasspea (Porównanie składu chemicznego oraz wartości pokarmowej nasion trzech form lędźwianu siewnego). – Zeszyty Problemowe Postępów Nauk Rolniczych 446: 349-353. (in Polish).
[30] Polignano, G. B., Bisignano, V., Tomaselli, V., Uggenti, P., Alba, V., Gatta, C. D. (2009): Genotype × Environment Interaction in Grass Pea (*Lathyrus sativus* L.) Lines. – International Journal of Agronomy: Article ID: 898396. DOI:10.1155/2009/898396.
[31] Rachoń, L. (1995): Yielding of grasspea (*Lathyrus sativus* L.) in pure and mixed sowing (Plonowanie lędźwianu siewnego (*Lathyrus sativus* L.) w siewie czystym i mieszanym). – Materiały Konferencyjne Ogólnopolskiej Konferencji Naukowej „Nauka Praktyce Ogrodniczej". Akademia Rolnicza Lublin, pp. 661-664. (in Polish).
[32] Rybiński, W., Pokora, L. (2002): Effect of helium-neon laser light and chemomutagene (MNU) on traits variability of grass pea (*Lathyrus sativus* L.) in M1 generation (Wpływ światła lasera helowo-neonowego i chemomutagenu (MNU) na zmienność cech lędźwianu siewnego (*Lathyrus sativus* L.) w pokoleniu M1). – Acta Agrophysica 62: 127-134. (in Polish).
[33] Rybiński, W. (2003): Mutagenesis as a tool for improvement of traits in grasspea (*Lathyrus sativus* L.). – Lathyrus Lathyrism Newsletter 3: 27-31.
[34] Rybiński, W., Bocianowski, J. (2006): Variability of morphological traits and yield structure in grasspea mutants (*Lathyrus sativus* L.). – Biuletyn IHAR 240/241: 291-297. (in Polish).
[35] Rybiński, W., Grela, E. R. (2007): Genetic variation of traits and chemical composition of seeds in grasspea mutants (*Lathyrus sativus* L.). – Zeszyty Problemowe Postępów Nauk Rolniczych 517: 613-627. (in Polish).
[36] Rybiński, W., Pankiewicz, K. (2010): Grasspea (*Lathyrus sativus* L.) – pulse crop with a perspective future: characteristics, variability and use on the example of collected

http://www.aloki.hu ● ISSN 1589 1623 (Print) ● ISSN1785 0037 (Online)
DOI: http://dx.doi.org/10.15666/aeer/1804_53555366

accessions. (Lędźwian siewny (*Lathyrus sativus* L.) – perspektywiczna roślina strączkowa- charakterystyka, zmienność i wykorzystanie na przykładzie materiałów kolekcjach). – Zeszyty Problemowe Postępów Nauk Rolniczych 555: 361-372. (in Polish).

[37] Rybiński, W., Bocianowski, J., Starzycki, M., Starzycka, E. (2013): Estimation of variability of selected traits of species of the genus Lathyrus maintained in the germplasm collection (Ocena zróżnicowania w rodzaju Lathyrus na podstawie wybranych cech w materiałach kolekcyjnych). – Polish Journal of Agronomy 12: 49-63. (in Polish).

[38] Sammour, R., Mustafa, A. E. Z., Badr, S., Tahr, W. (2007): Genetic variations in accessions of *Lathyrus sativus* L. – Acta Botanica Croatica 66(1): 1-13.

[39] Sidorova, K. K., Levko, G. D., Shumny, V. K. (2013): Investigation of nodulation and nitrogen fixation in annual species and varieties of vetchling, genus Lathyrus. – Russian Journal of Genetics: Applied Research 3(3): 197-202.
DOI: https://doi.org/10.1134/s2079059713030106.

[40] Smartt, J. (1984): Evaluation of grain legumes. I. Mediterranean pulses. – Experimental Agriculture 20: 275-296.

[41] Talukdar, D. (2009): Recent progress on genetic analysis of novel mutants and aneuploidy research in grass pea (*Lathyrus sativus* L.). – African Journal of Agricultural Research 4: 1549-1559.

[42] Urga, K., Fufa, H. (2005): Evaluation of *Lathyrus sativus* cultivated in Ethiopia foe proximate composition, minerals, β-ODAP and antinutritional components. – African Journal of Food, Agriculture, Nutrition and Development 5(1): 1-15.

[43] Vaz Patto, M. C., Skiba, B., Pang, E. C. K., Ochatt, S. J., Lambein, F., Rubiales, D. (2006): Lathyrus improvement for resistance against biotic and abiotic stresses: From classical breeding to marker assisted selection. – Euphytica 147: 133-147.

[44] Wani, M. R., Khan, S., Kozgar, M. I. (2012): Genetic enhancement of mungbean [*Vigna radiate* (L.) Wilczek] through induced mutagenesis. – Crop Research 43(1, 2 & 3): 189-193. https://www.scitechnol.com/abstract.php?abstract_id=3100.

[45] Williams, P. C., Bhatty, R. S., Deshpande, S. S., Hussein, L. A., Savage, G. P. (1994): Improving nutritional quality of col season food legumes. – In: Muchlbauer, F. J., Kaiser W. J. (eds.) Exfuture panding the production and use cool season food legumes. Kluwer Academic Publishers, Dordrecht, Netherlands, pp. 113-129.

http://www.aloki.hu ● ISSN 1589 1623 (Print) ● ISSN1785 0037 (Online)
DOI: http://dx.doi.org/10.15666/aeer/1804_53555366

EFFECTS OF MIXED CONTROLLED RELEASE AND NORMAL UREA ON MAIZE (*ZEA MAYS* L) GROWTH, GRAIN YIELD AND NITROGEN BALANCE AND USE EFFICIENCY IN NORTHEAST CHINA

LI, C. L.[1,2] – CAO, Y. Q.[1,2] – WANG, Y.[1,2*] – LI, X. Y.[1,2] – LI, Y. X.[1,2] – ZHU, L.[1,2] – ZHAO, X. H.[1,2] – GAO, Q.[1,2]

[1]*College of Resources and Environmental Science, Jilin Agricultural University, Changchun 130118, China*

[2]*Key Laboratory of Soil Resource Sustainable Utilization for Jilin Province Commodity Grain Bases, Changchun, China*

[*]*Corresponding author*
e-mail: wy1986410@163.com (Dr. Yin Wang)

(Received 18th Feb 2020; accepted 2nd Jul 2020)

Abstract. Mixed application of controlled release urea (CRU) and normal urea (NU) are effective N fertilization plural to improve crop yield and nitrogen use efficiency (NUE). In this study, field experiments were conducted for two consecutive years in 2018 and 2019 on two contrasting soil types. The treatments included one solely NU and four mixture ratios of CRU and NU under an identical N rate of 180 kg N ha^{-1} as single basal fertilizer before sowing. The results showed that the highest maize yields were obtained from the CRU30% treatment, increasing by 24% on sandy soil and 11% on clay soil as compared to CRU0% treatment. The yield improvements were mainly attributed to increased seed setting percentage and grain numbers per ear. Maize plants grown in CRU30% treatment accumulated more dry biomass (DM) and N uptake after silking, and thereby increasing grain yield and NUE. This work demonstrates that the appropriate mixture of CRU and NU increases maize yield and NUE while reducing N loss, by optimizing N fertilizer release and soil N availability to match the crop N demand, and 30%CRU and 70%NU was determined as the optimal mixture ratio on both sandy and clay soils in Northeast China.
Keywords: *maize, controlled release urea, grain yield, N uptake, DM accumulation, N loss*

Abbreviations. AE, agronomic efficiency; CRU, controlled release urea; CRU0%, 100% normal urea as basal fertilizer; CRU15% (30%,45% and 60%), 15% (30%,45% and 60%) of CRU was mixed application with normal urea as basal fertilizer; DM, dry biomass; K, potassium; NU, normal urea; NUE, N use efficiency; P, phosphorus; PFP, partial factor productivity; RE, recovery efficiency

Introduction

Global food demand is expected to double by 2050 due to rapid population growth (Tilman et al., 2011). Considering the limited expansion of cultivated land area, it is essential to increase crop yield per unit cultivated land area and thereby enhance the total productivity (Burney et al., 2010; Cui et al., 2013). In the past few decades, crop yields were considerably increased by applying mass inorganic fertilizers in the intensive cropping system in China and many other countries (Chen et al., 2014). However, excessive N input reduced N use efficiency (NUE) (Cassman et al., 2002), and also adversely affected surface water, groundwater and the atmosphere through runoff, N leaching and reactive gaseous N emission (Drecht et al., 2003; Galloway et al., 2008; Cui et al., 2013). Therefore, further optimal N management practices are required in intensive

http://www.aloki.hu ● ISSN 1589 1623 (Print) ● ISSN1785 0037 (Online)
DOI: http://dx.doi.org/10.15666/aeer/1804_53675382

crop production to synchronously achieve food security, higher NUE and lower environmental impacts (Guo et al., 2016).

Maize is an important crop for food and feed, has surpassed wheat and rice as the largest cereal crop in China and the whole world (FAD, 2017). Northeast China is the most important maize cropping region, accounting for 31.5% and 32.8% of the national maize planting area and production, respectively (China Agriculture Press, 2018). Traditionally, all N fertilizers are applied by local farmers for maize as single basal fertilizer before sowing, thus always causing mass N loss at the early stage and reduced final yield and NUE (Gao et al., 2012). In the local best N management method, split N fertilization (i.e. 40% as basal fertilizer and 60% as topdressing at jointing stage) is recommended to meet maize N demand for improving yield and NUE (Gao et al., 2012; Yan et al., 2016). However, the topdressing is generally unacceptable by farmers due to the operational inconvenience and high labor cost. Moreover, the split fertilization method is facing more challenges with the aging of the population and continually increasing labor cost in China (Liu and Griffiths, 2011).

Controlled release urea (CRU) is a new type of N fertilizer, which is designed and produced to control N release process for matching crop N demand during the growing period, has been widely used for various crops in many countries (Song et al., 2014). CRU is usually prepared by encapsulating water-soluble granular urea with a low-permeability hydrophobic membrane, and the key principle is using a physical barrier to reduce N dissolution rate (Shavit et al., 1997). Numerous researchers have found that the application of CRU effectively improved maize yield and NUE (Haderlein et al., 2001; Kondo et al., 2005; Sun et al., 2010; Geng et al., 2016; Zheng et al., 2016), and reduced nitrate leaching and N loss (Shoji et al., 2001; Zvomuya et al., 2003), as compared to the normal urea (NU) application. However, the use of CRU for cereal crops is generally limited because of its expensive prices (Shaviv, 2001). Therefore, some researchers proposed to apply the mixture of CRU and NU with an appropriate ratio, to provide an optimal N supply for crop demand to reduce N loss, improve NUE and also decreased N fertilizer costs (Noellsch et al., 2009; Zheng et al., 2016; Guo et al., 2017). The optimal ratio of CRU for maize differed at various countries or regions due to the differences in soil and climate conditions, crop yield level and growth duration, which was determined as 70% at 180 kg N ha^{-1} or 30% at 240 kg N ha^{-1} in North China, and 70% at 180 kg N ha^{-1} in Brazil (Guo et al., 2017; Garcia et al., 2018).

The mixed application of CRU and NUE is a promising alternative to farmers' practice of one-time fertilization and recommended split N fertilization in Northeast China, however, the optimal mixture ratio of CRU and NU is still not clear for local maize production. Therefore, in this study, consecutive two-year field experiments were conducted at two contrasting soil types in Northeast China, the N release rate of CRU in soil, the dynamics changes of maize plant dry biomass (DM) and N uptake, grain yields and yield components, N balance and loss in soil-plant system were investigated. The objectives of this study were: to investigate the possibility of mixed application of CRU and NU to synchronize the nutrient release with maize N uptake demand and to determine the optimal mixture ratio at different soil types in Northeast China. The results would provide new N management techniques to achieve higher maize yield and NUE with lower environmental impacts.

http://www.aloki.hu ● ISSN 1589 1623 (Print) ● ISSN1785 0037 (Online)
DOI: http://dx.doi.org/10.15666/aeer/1804_53675382

Materials and Methods

Experiment site description

Field experiments were conducted in 2018 and 2019 at two sites in Jilin Province, Northeast China, i.e. Fu-jia-jie (N43°22',E124°05') and San-ke-shu (N43°20', E124°00') (*Figure 1*). The two sites are only 4 km away from each other, and have the nearly identical meteorological condition (Feng et al., 2019). The experimental region is located in the warm-temperate and has a semi-humid continental monsoon climate with a hot and rainy summer and a cold and dry winter, and the annual precipitation ranges between 400 and 600 mm. The detailed daily average temperature and rainfall during the maize growing season are shown in *Figure 2*. The total precipitation showed significant difference between two experimental years, which was 354.5 mm in 2018 and 533.4 mm in 2019. Obviously, the climate was drier in 2018 as compared with 2019, especially during sowing and seed germination in spring (May and June).

Figure 1. *Distribution of experimental site in the Fu-jia-jie and San-ke-shu, Jilin province, Northeast China*

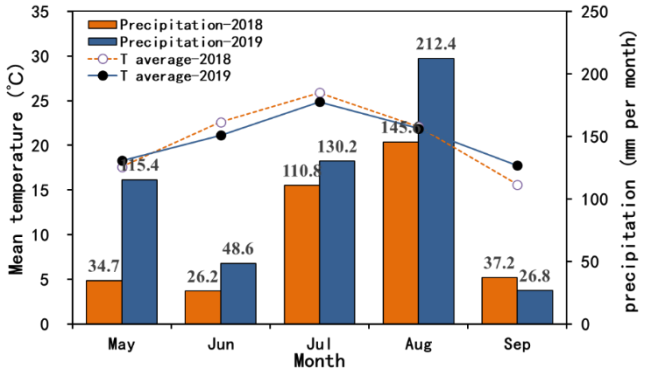

Figure 2. *Daily average temperatures (℃) and precipitation (mm) during the maize growing seasons in 2018 and 2019. The numbers above the bars indicate the total precipitation in the corresponding months*

http://www.aloki.hu ● ISSN 1589 1623 (Print) ● ISSN1785 0037 (Online)
DOI: http://dx.doi.org/10.15666/aeer/1804_53675382

The soils in Fu-jia-jie and San-ke-shu are classified as Aeolian sandy soil and Black soil, respectively, according to the Chinese Soil Taxonomy (CRGCST, 2001). The soil texture in Fu-jia-jie is sandy soil with 79.6% sand, 9.6% silt, and 10.8% clay, and the main properties of topsoil layer (0-20 cm) are: pH 6.04, organic matter 12.4 g kg^{-1}, total N 0.81 g kg^{-1}, NO_3^--N 13.92 mg kg^{-1}, NH_4^+-N 9.22 mg kg^{-1}, available P 24.9 mg kg^{-1} and available K 93.2 mg kg^{-1}. While the soil texture in San-ke-shu is clay soil with 32.5% sand, 25.2% silt, and 42.3% clay, and the main properties of topsoil layer are: pH 5.58, organic matter 30.1 g kg^{-1}, total N 2.09 g kg^{-1}, NO_3^--N 26.11 mg kg^{-1}, NH_4^+-N 14.1 mg kg^{-1}, available P 40.1 mg kg^{-1} and available K 142.5 mg kg^{-1}.

Experimental design and field management

Each field experiment consisted of six N treatments with three replications: N0 (without N fertilizer), CRU0 (100% NU), CRU15% (15%N CRU mixed with 85%NU), CRU30% (30%N CRU mixed with 70%NU), CRU45% (45%N CRU mixed with 55% NU) and CRU60% (60%N CRU mixed with 40%NU). In N fertilization treatments, all the N fertilizers were one-time applied before sowing at 185 kg ha^{-1} (N). Across all the treatments, P and K fertilizers were also one-time applied before sowing at 87 kg ha^{-1} (P_2O_5) and 90 kg ha^{-1} (K_2O), respectively. Conventional fertilizers used in this study included NU (46%N), calcium superphosphate (16%P_2O_5) and potassium chloride (60%K_2O). The CRU, manufactured by Shandong Maoshi Ecological fertilizer Inc, Dezhou, China, is a polymer-coated urea with a N content of 44%.

Field experiment was a completely randomized block design with a total of 18 plots in each site, and the plot size was 48 m^2 (6×8 m). Maize variety Liangyu 99, a widely cultivated variety in Northeast China, was sown in early May (May 9 and 5 in 2018 and 2019, respectively) and harvested in early October (October 3 both in 2018 and 2019). Plant density was 65,000 plants ha^{-1} with a 60 cm space between rows across the sites and years. In both two years, the weeds, diseases and pests were well controlled as needed according to the local best management practice, and no irrigation was done during the entire growing seasons.

Sampling and chemical analyses

Plant samples were collected at the seedling stage (V5-V6), jointing stage (V12), silking stage (R1), grain filling stage (R3) and physiological maturity stage (R6), i.e. 27, 46, 79, 109 and 140 days after sowing (DAS) in both years. Five adjacent maize plants were sampled in each plot and separated into stems (including leaf sheath, tassel and cob), leaves (including leaves and bracts) and grains, and then dried to the constant weights at 70°C for determining DM. Dried plant samples were ground to powder for further determining N concentration by H_2SO_4-H_2O_2 digestion and the micro-Kjeldahl procedure (Douglas et al., 1980). At physiological maturity, grain yield was manually harvested from an area of 18 m^2 (3.6 by 5 m) in the middle of each plot and standardized to a moisture content of 15.5%.

Recovery efficiency (RE_N), agronomic efficiency (AE_N) and partial factor productivity (PFP_N) of N fertilizer were calculated using *equations (1), (2)* and *(3)* below (Dobermann, 2007).

$$RE_N = (U - U_0) / N \times 100 \quad \text{(Eq.1)}$$

$$AE_N = (Y_N - Y_0) / N \quad \text{(Eq.2)}$$

http://www.aloki.hu ● ISSN 1589 1623 (Print) ● ISSN1785 0037 (Online)
DOI: http://dx.doi.org/10.15666/aeer/1804_53675382

$$PFP_N = Y_N / N \quad \text{(Eq.3)}$$

where N is the N fertilizer rate (kg ha^{-1}), U_0 and U are the plant N uptake (kg ha^{-1}) at maturity in N_0 and N fertilization treatments, respectively, Y_0 and Y_N are the grain yield (kg ha^{-1}) at maturity in N_0 and N fertilization treatments, respectively.

Basic soil sample was collected randomly from 0 to 20 cm soil layer in each site before tillage, to analyze physical and chemical properties followed the soil testing methods of Page et al. (1982). In addition, fresh soil samples were also collected randomly at 0-100 cm in each plot with a 20-cm increments by using an auger, before sowing and after harvest in each year. These soil sample were extracted with 100 ml 0.01M $CaCl_2$ to analyze soil NO_3^--N and NH_4^+-N contents using Continuous Flow Analysis (AA3 Auto Analyzer system, Seal Analytical GmbH, Norderstedt, Germany). During the maize growing seasons, the amounts of apparent soil N mineralization (kg ha^{-1}) and N loss (kg ha^{-1}) were calculated according to the balance methods described by Guo et al. (2017).

Test of CRU release in the field

The N release rate of CRU was tested in field condition with a buried bag method (Kaneta et al., 1994). Before fertilization, 10.0 g of CRU was accurately weighed and placed in small nylon net bags (15×10 cm) with 150 cm^2 mesh size. In each site, a total of 24 CRU fertilizers bags were buried in no-fertilized areas neighboring the experimental plots while fertilization, and three bags were collected each time at 2, 5, 7, 21, 42, 70, 105 and 140 days after burial. After sampled bags were opened with scissors, CRU granules were removed and rinsed with distilled water to remove the attached soil, and then placed in a vacuum oven at 60°C for 48 h to obtain the constant weight for determination of the N release rate from CRU (Kaneta et al., 1994; Guo et al., 2017).

Statistical analyses

All data across the N treatments, soil types and years were pooled for analysis of variance (ANOVA) with a three-factor analysis program by using the SAS statistical analysis package (version 9.4, SAS Institute, Cary, NC, USA). The least significant difference test (LSD) was performed to compare the differences among N treatments at the 5% significance level.

Results

CRU release in the field conditions

The N release curves from CRU were significantly affected by experimental years and soil types (*Figure 3*). On average, total N release amounts of CRU during the maize growing seasons were 83.9% and 90.8% in 2018 and 2019, respectively. N release from CRU was severely limited due to the rainless climate in 2018. The CRU granules had similar total N release amounts on sandy and clay soils, with the averages of 86.7% and 88.0%, respectively, but they showed contrasting release processes between soil types. In 2018, about 20% of N was released at 42 and 28 days on sand and clay soils, respectively, and the durations for 80% of N release were 116 and 98 days, respectively. In 2019, about 20% of N was released at 20 and 15 days on sand and clay soils, respectively, and the durations for 80% of N released were 79 and 71 days. Obviously, N release from CRU was slowed on sandy soil as compared with clay soil, especially under the adverse climatic condition.

http://www.aloki.hu ● ISSN 1589 1623 (Print) ● ISSN1785 0037 (Online)
DOI: http://dx.doi.org/10.15666/aeer/1804_53675382

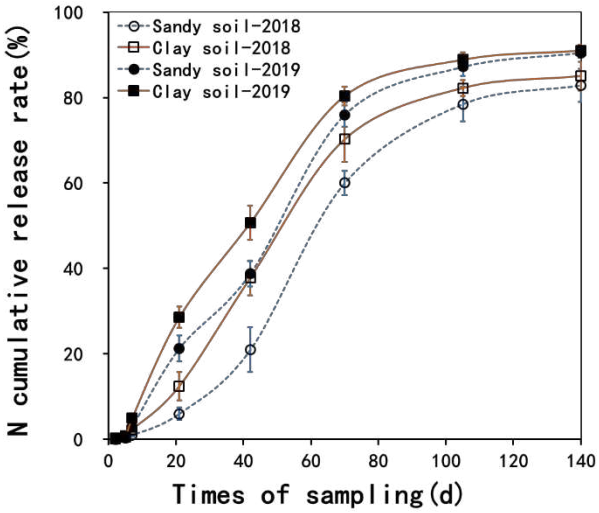

Figure 3. *Nitrogen release curves of controlled release urea in field conditions in 2018 and 2019. The vertical bars indicate standard error of the mean in the nitrogen release curves*

Maize yield and yield components

Maize yield was significantly affected by soil type, year, N treatment, and all the two-factor interactions (*Table 1*). In 2018, across the different N treatments, the average maize yield was 11.3 t ha^{-1} on clay soil, which was 36.7% higher than that of 8.3 t ha^{-1} on sandy soil. In 2019, the average yield was 13.2 t ha^{-1} on clay soil and which was 19.0% higher than that of 11.1 t ha^{-1} on sandy soil. Obviously, maize yields were limited on sandy soil as compared with clay soil, especially under the rainless climate in 2018. Across the soil types and years, maize yields were increased with N fertilizers application relative to N0 treatment, and those in mixed CRU treatments were as or higher than that in CRU0% treatment. The CRU30% treatment showed the highest yields with an average of 12.6 t ha^{-1}, but had no significant differences with other mixed CRU treatments except for CRU60% treatment on sandy soil in 2018. Compared with CRU0% treatment, the yield increase in CRU30% treatment was 27.6% in 2018 and 21.3% in 2019 on sandy soil, respectively, and those were 11.1% and 11.3% on clay soil, respectively.

In terms of yield components, all the parameters were better for plants grown on clay soil as compared with sandy soil, and which were better in 2019 than those in 2018. Among the different N fertilization treatments, no significant differences were observed in seed setting percentage and 100-grain weight on clay soil, while grain numbers per ear was higher in all mixed CRU treatments as compared with CRU0% treatment. In contrary, the responses of yield components to N treatments were greater on sandy soil, all the parameters were affected by N fertilization treatments except for the seed setting percentage in 2019. Compared with CRU30% treatment, CRU0% treatment showed the lowest parameters and followed by CRU60% treatment on sandy soil, while other mixed ratio treatments had no significant differences. The increases of yield components in CRU30% treatment was 5.5% for seed setting percentage, 10.4% for grain numbers per ear and 9.6% for 100-grain weight in 2018, respectively, relative to CRU0% treatment; and these increases were 2.0%, 6.4% and 8.3% in 2019.

http://www.aloki.hu ● ISSN 1589 1623 (Print) ● ISSN1785 0037 (Online)
DOI: http://dx.doi.org/10.15666/aeer/1804_53675382

Table 1. *Maize yield and yield components as affected by N treatments and soil types in 2018 and 2019*

Soil type	Year	Treatment	Grain yield t ha^{-1}	Seed setting percentage %	Grain number per ear No. ear^{-1}	100-grain weight g
Sandy soil	2018	N0	5.5 d	82.3 c	406 d	21.7 c
		CRU0%	7.9 bc	91.3 ab	482 bc	23.5 b
		CRU15%	10.0 a	96.3 a	535 a	25.7 a
		CRU30%	10.1 a	96.3 a	532 ab	25.8 a
		CRU45%	8.9 ab	95.3 ab	487 abc	25.3 a
		CRU60%	7.2 c	88.7 bc	476 c	23.7 b
	2019	N0	4.3 c	78.7 b	331 c	21.3 c
		CRU0%	11.0 b	98.0 a	564 b	27.1 b
		CRU15%	12.9 a	99.3 a	582 ab	29.3 a
		CRU30%	13.3 a	100.0 a	600 a	29.4 a
		CRU45%	12.8 a	99.0 a	578 ab	29.1 a
		CRU60%	12.3 ab	99.3 a	558 b	29.6 a
Clay soil	2018	N0	9.8 b	95.3 b	539 b	25.4 a
		CRU0%	10.8 ab	99.3 a	564 b	26.8 a
		CRU15%	11.7 a	98.7 a	595 a	27.1 a
		CRU30%	12.0 a	100.0 a	617 a	27.0 a
		CRU45%	11.7 a	98.7 a	613 a	27.3 a
		CRU60%	11.6 a	98.7 a	608 a	27.1 a
	2019	N0	8.0 c	97.3 b	447 c	24.7 b
		CRU0%	13.3 b	99.0 a	607 b	29.2 a
		CRU15%	14.5 ab	99.7 a	669 a	29.4 a
		CRU30%	14.8 a	99.3 a	670 a	29.6 a
		CRU45%	14.6 ab	99.3 a	656 a	29.7 a
		CRU60%	14.2 ab	99.3 a	651 a	29.4 a
ANOVA						
Soil type (S)			***	***	***	***
Year (Y)			***	**	***	***
N treatment (N)			***	***	***	***
S × Y			**	*	*	**
S × N			*	***	**	**
Y × N			***	ns	***	***
S × Y × N			ns	*	ns	ns

Means within each column, soil type and year followed by different letters are significantly different at P = 0.05. ns, no significant; * significant at $p < 0.05$; ** significant at $p < 0.01$; *** Significant at $p < 0.001$

Hence, mixed application of CRU and NU could effectively improve maize yield as compared with sole NU application, and showed better performance in yield improvements on sandy soil, even under the adverse climatic condition in 2018. The best yield improvements in CRU30% treatment could be attributed to the dramatically increased grain numbers per ear and 100-grain weight, in combination with a slightly enhanced seed setting percentage.

Plant DM accumulation

The total DM of maize plants at maturity was obviously lower in 2018 than 2019, mainly associated with the limited DM accumulation at seedling stage (*Figure 4*). On average, the total DMs were 18.9 and 13.8 t ha^{-1} on clay and sandy soils in 2018, respectively, while which were 21.6 and 16.8 t ha^{-1} in 2019, respectively. Compared with sandy soil, maize plants grown on clay soil accumulated 37.4% and 28.9% more total DM

http://www.aloki.hu ● ISSN 1589 1623 (Print) ● ISSN1785 0037 (Online)
DOI: http://dx.doi.org/10.15666/aeer/1804_53675382

in the two years, respectively. During the entire maize growing season, plant DM accumulation was lower in N0 treatment than N fertilization treatments across the soil types and years, and the DM gaps enlarged obviously in 2019 due to the continuous soil N consumption. Compared with CRU0% treatment, higher total DMs at maturity were observed in all the mixed CRU treatments except for CRU60% on sandy soil in 2018. Plant DM accumulation had no difference between the treatments with or without CRU at the vegetative growth periods, thus the differences in total DMs at maturity were attributed to the different DM accumulation after silking. Obviously, the post-silking DM percentages in the mixed CRU treatments were higher than those in CRU0% treatment under the most soil and climate conditions, especially in CRU30% treatment (*Figure 5*).

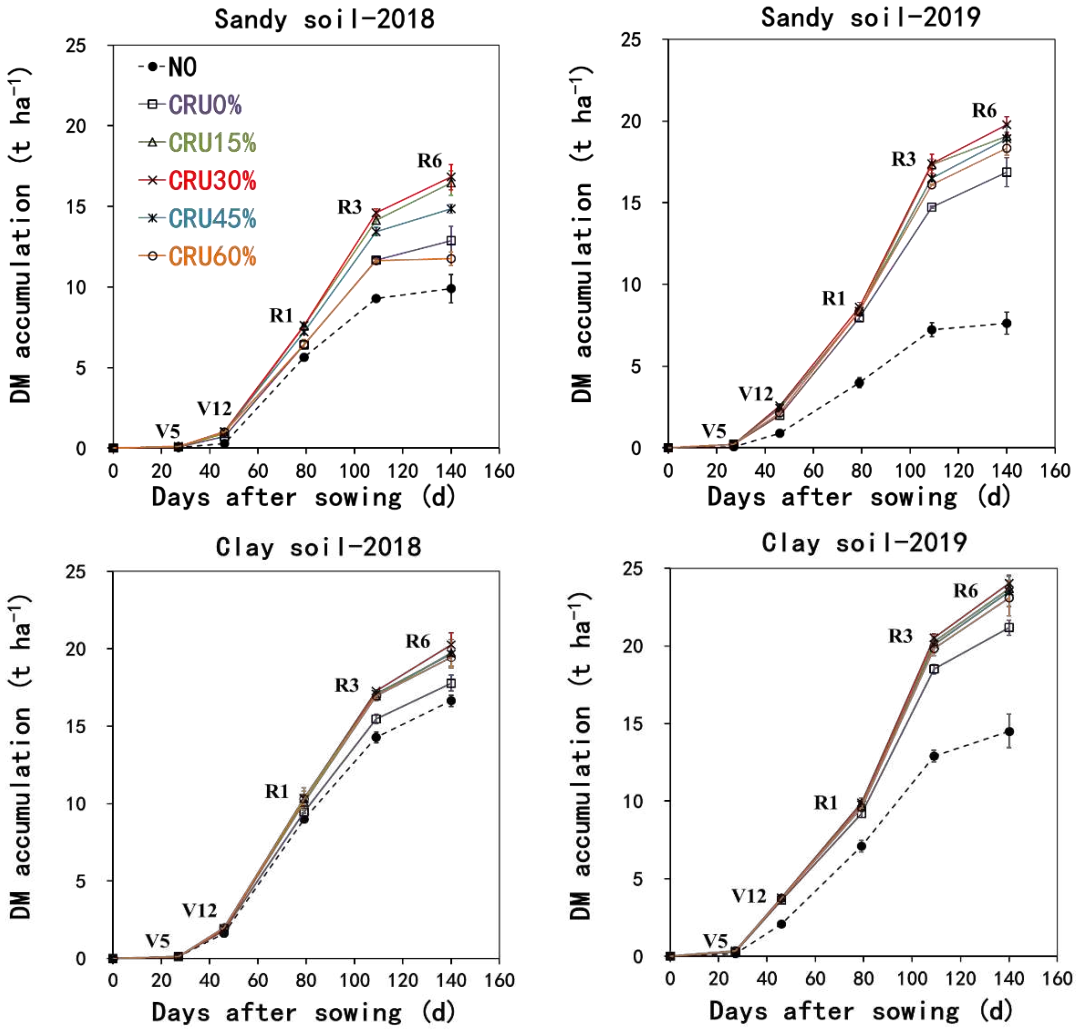

Figure 4. *DM accumulation dynamic of maize plants as affected by N treatments and soil types in 2018 and 2019. The vertical bars indicate standard error of the mean*

Across the soil types and years, no differences were observed in plant DM accumulation among the mixed CRU treatments during the maize growing seasons, except for sandy soil in 2018 (*Figure 4*). On average, CRU30% treatment showed the highest total DM at maturity of 20.2 t ha^{-1}, and followed by CRU15% (19.7 t ha^{-1}), CRU

http://www.aloki.hu ● ISSN 1589 1623 (Print) ● ISSN1785 0037 (Online)
DOI: http://dx.doi.org/10.15666/aeer/1804_53675382

45% (19.2 t ha^{-1}) and CRU60% (18.2 t ha^{-1}). In 2018, the total DMs in CRU30% treatment were 30.7% and 17.3% higher than those in CRU0% treatment on sandy and clay soils, respectively, and the increases were 14.0% and 13.5% in 2019, respectively. Mixed application of CRU and NU showed greater improvements in plant DM accumulation on sandy soil as compared with clay soil, especially under rainless climate in 2018.

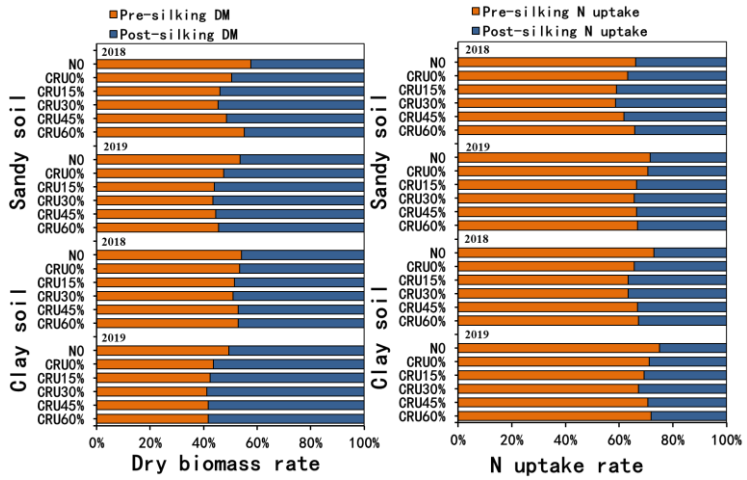

Figure 5. *The pre- and post-silking percentages of plant DM and N uptake for maize as affected by N treatments and soil types in 2018 and 2019*

Plant N uptake

The N uptake of maize plants showed similar responses to soil types, inter-annual climate and N treatments, as compared with plant DM accumulation (*Figure 6*). On average, the total N uptakes at maturity were 131.1 and 183.3 kg ha^{-1} in 2018 and 2019 on clay soil, respectively, which were 47.7% and 29.4% higher than those of 88.7 and 141.7 kg ha^{-1} on sandy soil, respectively. The N uptakes were obviously reduced by adverse soil and climatic conditions. Compared with plant DM, plant N uptake suffered greater limitation by N deficiency in the N0 treatment, which showed significant differences with N fertilization treatments at silking stage (R1) on clay soil in 2018 and at seedling stage (V5) in the other conditions. Compared with CRU0% treatment, higher total N uptakes at maturity were observed in all the mixed CRU treatments except for CRU60% on sandy soil in 2018. The differences in N uptake became significant since the late vegetative stage (V12) between the treatments with or without CRU. Moreover, the pre- and post-silking N uptake also showed obvious differences between these treatments (*Figure 5*). The post-silking N uptake percentages were higher in CRU30% and CRU15% treatments, as compared with other N fertilization treatments.

In both two years, no differences were observed in total N uptakes among the mixed CRU treatments on clay soil. However, these mixed CRU treatments showed different total N uptakes on sandy soil especially in 2018. Overall, the highest N uptake was obtained in CRU30% treatment, and followed by CRU15% treatment. The average N uptake in CRU30% treatment were 141.6 and 179.1 kg ha^{-1} on sandy and clay soils, respectively, which were 24.3% and 19.8% higher than those in CRU0% treatment. Therefore, mixed CRU and NU at an appropriate ratio could improve plant N uptake, while the sole NU application or the over-mixture of CRU resulted in counterproductive effects.

http://www.aloki.hu ● ISSN 1589 1623 (Print) ● ISSN1785 0037 (Online)
DOI: http://dx.doi.org/10.15666/aeer/1804_53675382

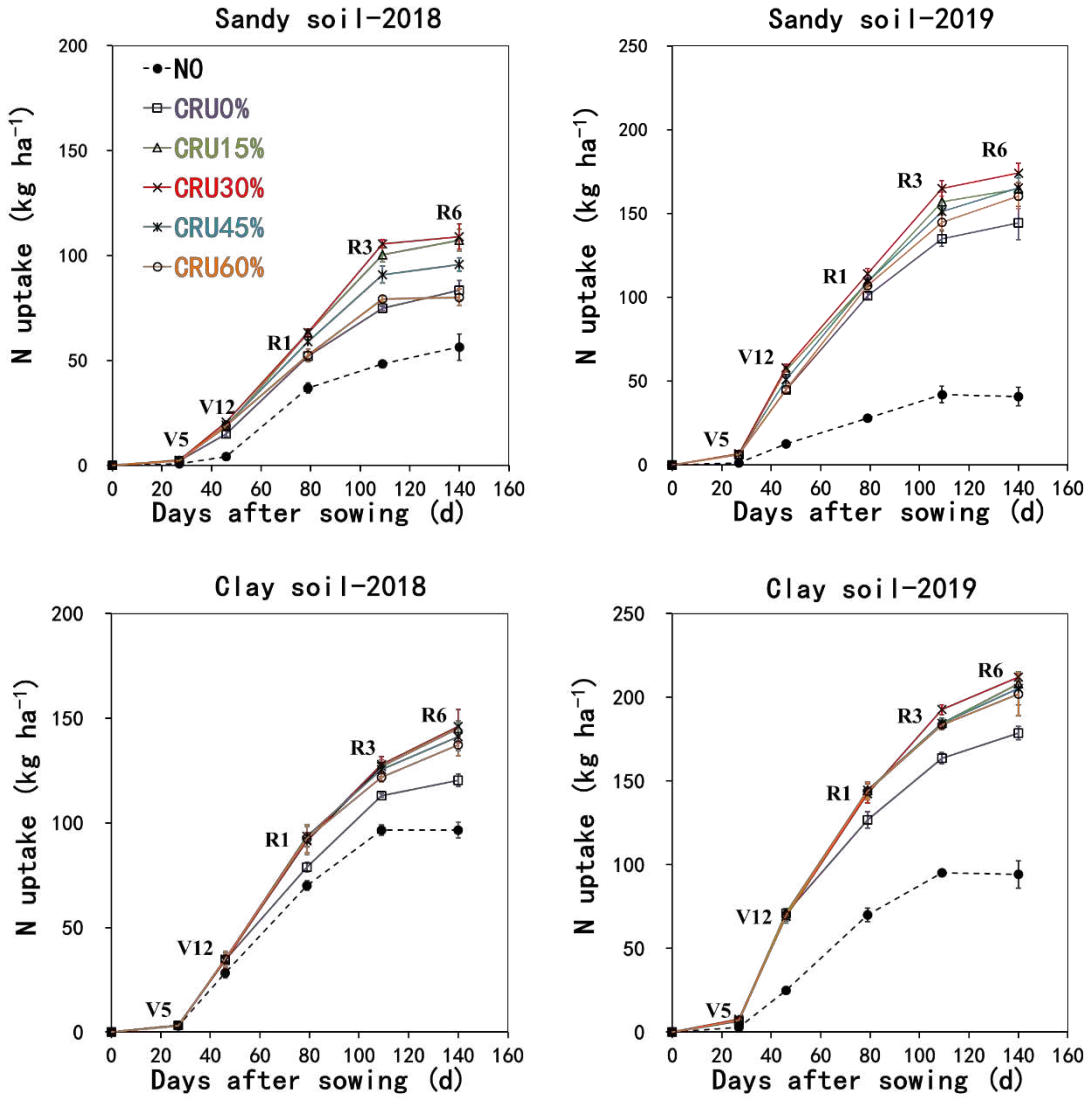

Figure 6. *N uptake dynamic of maize plants as affected by N treatments and soil types in 2018 and 2019. The vertical bars indicate standard error of the mean*

Nitrogen balance and loss

The N balance and apparent N loss were estimated based on the difference between N inputs and outputs in the soil-plant system, and all the related parameters were affected by soil type, year and N treatments (*Table 2*). The initial soil Nmin contents were much lower on sandy soil than clay soil. In both two years, soil N mineralization were also considerably less on sandy soil, and the total mineralization amounts was only 40% of that on clay soil. In contrary, N losses were higher on sandy soil as compared with clay soil. On average, the total N loss were 180.8 kg ha^{-1} across years and N treatments on sandy soil, which were 8.0% higher than that of 167.4 kg ha^{-1} on clay soil. Between experimental years, soil N mineralization of sandy soil was higher in 2018 than 2019, but which showed opposite trends on clay soil. While N losses showed consistent trends between soil types, both of which were obviously higher in 2018 than 2019.

http://www.aloki.hu ● ISSN 1589 1623 (Print) ● ISSN1785 0037 (Online)
DOI: http://dx.doi.org/10.15666/aeer/1804_53675382

Table 2. *Nitrogen balance (kg N ha^{-1}) as affected by N treatments and soil types in 2018 and 2019*

Years	N balance parameter	Sandy soil						Clay soil					
		N0	CRU0%	CRU15%	CRU30%	CRU45%	CRU60%	N0	CRU0%	CRU15%	CRU30%	CRU45%	CRU60%
2018	A. N input												
	(1) N fertilizer	0	185	185	185	185	185	0	185	185	185	185	185
	(2) Soil Nmin before sowing	73	73	73	73	73	73	155	155	155	155	155	155
	(3) Apparent soil N mineralization	36	36	36	36	36	36	59	59	59	59	59	59
	B. N output												
	(1) Plant N uptake	56	84	10	109	9	80	96	120	145	146	141	137
	(2) Soil Nmin at harvest	53	64	69	75	77	85	118	145	145	147	141	142
	C. Apparent N loss: A-B	0	146	118	110	121	129	0	134	109	106	117	120
2019	A. N input												
	(1) N fertilizer	0	185	185	185	185	185	0	185	185	185	185	185
	(2) Soil Nmin before sowing	51	62	70	75	81	84	121	147	157	154	147	150
	(3) Apparent soil N mineralization	24	24	24	24	24	24	82	82	82	82	82	82
	B. N output												
	(1) Plant N uptake	41	144	165	174	165	161	102	179	208	212	205	202
	(2) Soil Nmin at harvest	34	47	63	65	72	69	101	149	162	166	165	171
	C. Apparent N loss: A-B	0	80	51	45	53	63	0	86	54	43	44	44
2018-2019	A. N input												
	(1) N fertilizer	0	370	370	370	370	370	0	370	370	370	370	370
	(2) Soil Nmin before sowing	73	73	73	73	73	73	155	155	155	155	155	155
	(3) Apparent soil N mineralization	58	58	58	58	58	58	144	144	144	144	144	144
	B. N output												
	(1) Plant N uptake	97	228	272	283	261	241	198	299	353	358	346	339
	(2) Soil Nmin at harvest	34	47	63	65	72	69	101	149	162	166	165	171
	C. Apparent N loss: A-B	0	226	166	153	168	191	0	221	154	145	158	159

After consecutive two cropping seasons, soil Nmin contents in all N fertilization treatments showed decreasing trends on sandy soil, and the largest reduction of 35.6% was observed in CRU0% treatment, which were considerably higher than those of 1.4%-13.7% in the mixed CRU treatments. In contrary, soil Nmin contents increased by 4.5-10.3% in the mixed CRU treatments on clay soil, while only decreased by 3.9% in CRU0% treatment. Regardless of soil types and years, the N losses in CRU0% treatment were significantly higher than those in the mixed CRU treatments, and the lowest values were observed in CRU30% treatment. Compared with CRU0% treatment, total N loss in CRU30% treatment reduced by 32.3% and 34.4% on sandy and clay soils, respectively.

Nitrogen use efficiency

All the soil type, year, and N treatment factors showed significant individual effects on the NUE parameters, except for the RE_N response to soil type (*Table 3*). Between experimental years, the RE_N, AE_N and PFP_N were significantly higher in 2019 than 2018. Between soil types, sandy soil showed higher AE_N but lower PFP_N as compared with clay soil. Among the N fertilization treatments, the highest RE_N, AE_N and PFP_N were observed in CRU30% treatment, and all of which were significantly higher than those in CRU0% treatment. Across the two years, the average RE_N, AE_N and PFP_N in CRU30% treatment

http://www.aloki.hu ● ISSN 1589 1623 (Print) ● ISSN1785 0037 (Online)
DOI: http://dx.doi.org/10.15666/aeer/1804_53675382

were 50.3%, 36.7 kg kg^{-1} and 63.1 kg kg^{-1} on sandy soil, which were 42.4%, 49.9% and 24.0% higher than those in CRU0% treatment; the average RE_N, AE_N and PFP_N in CRU 30% treatment were 45.3%, 24.3 kg kg^{-1} and 72.6 kg kg^{-1} on clay soil, which were 54.6%, 42.9% and 11.2% higher than those in CRU0% treatment. The NUE parameters in other mixed CRU treatments showed no differences with CRU30% treatment, except for CRU60% treatment on sandy soil. In addition, the significant soil type × year interaction indicated that the responses of REN and PFP_N to soil types were affected by inter-annual climatic conditions, their gaps between years were larger on sandy soil as compared with clay soil.

Table 3. *Recovery efficiency (REN), agronomic efficiency (AEN) and partial factor productivity (PFPN) of N fertilizer for maize as affected by N treatments and soil types in 2018 and 2019*

Soil type	Year	Treatment	RE_N (%)	AE_N (kg kg^{-1})	PFP_N (kg kg^{-1})
Sandy soil	2018	CRU0%	14.7 bc	12.8 ab	42.6 bc
		CRU15%	27.5 ab	24.0 a	53.8 a
		CRU30%	28.5 a	24.6 a	54.3 a
		CRU45%	21.3 abc	18.3 ab	48.1 ab
		CRU60%	12.9 c	9.3 b	39.1 c
	2019	CRU0%	56.0 b	36.1 b	59.3 b
		CRU15%	67.0 ab	46.6 a	69.8 a
		CRU30%	72.1 a	48.8 a	71.9 a
		CRU45%	67.3 ab	46.2 a	69.4 a
		CRU60%	64.7 ab	43.6 ab	66.7 ab
Clay soil	2018	CRU0%	12.9 a	5.3 a	58.6 a
		CRU15%	26.3 a	10.1 a	63.3 a
		CRU30%	26.9 a	11.8 a	65.0 a
		CRU45%	24.2 a	10.0 a	63.3 a
		CRU60%	22.1 a	9.3 a	62.5 a
	2019	CRU0%	45.6 b	28.7 a	72.0 b
		CRU15%	61.6 a	34.9 a	78.2 ab
		CRU30%	63.7 a	36.8 a	80.1 a
		CRU45%	60.1 a	35.4 a	78.7 ab
		CRU60%	58.2 ab	33.4 a	76.6 ab
ANOVA					
Soil type (S)			ns	***	***
Year (Y)			***	***	***
N treatment (N)			***	**	***
S × Y			*	ns	*
S × N			ns	ns	ns
Y × N			ns	ns	ns
S × Y × N			ns	ns	ns

Means within each column, soil type and year followed by different letters are significantly different at P = 0.05. ns, no significant; * significant at $p < 0.05$; *** Significant at $p < 0.001$

Discussion

Numerous studies have indicated that the mixed application of CRU and NU can increased maize yield and NUE, and reduced N loss, such as in North China Plain, Brazil, and the United States (Noellsch et al., 2009; Zheng et al., 2016; Guo et al., 2017; Garcia et al., 2018). Similar result was also found in the present study in Northeast China. Compared with the sole NU application, the mixed application of CRU and NU increased generally maize yield and NUE and reduced N loss across the contrasting soil types.

http://www.aloki.hu ● ISSN 1589 1623 (Print) ● ISSN1785 0037 (Online)
DOI: http://dx.doi.org/10.15666/aeer/1804_53675382

Moreover, the present study determined the optimal mixture ratio of CRU as 30% for maize in Northeast China, which can synchronously achieve higher yield, NUE and environmental benefits. The optimal mixture ration of CRU for maize were 70% in both North China and Brazil at the N rate of 180 kg N ha^{-1} (Guo et al., 2017; Garcia et al., 2018), which were much higher than that determined in this study, the big difference is mainly associated with the soil types and fertility, climatic conditions, crop yield level and cultivation practices among the various regions. The soil basic fertility and crop yield levels determined the amount of nitrogen fertilizer applied, and climatic conditions and cultivation practices determined the release rate of controlled release urea in the field. The application rate of nitrogen fertilizer and the release rate of controlled release urea in the field determined the optimal mixture ration of controlled release urea and normal urea.

Modern high-yield maize varieties have a larger N demand, and the sufficient plant N uptake in the middle-late growth periods are more important for seed development and yield formation (Liu et al., 2014; Guo et al., 2017). The previous studies showed that the percentages of DM and N demand were 47%-60% and 12%-32% for modern high-yield maize, respectively, and the higher post-silking DM and N uptake are essential to obtain high yield and NUE (Meng et al., 2016). Compared with recommended split N fertilization, the high basal N fertilization adopted by farmers could not well match the maize N demand during the growing season, thus causing substantial N loss at the seedling stage and subsequently insufficient N supply for reproductive growth and grain yield at the late stage. Moreover, high N supply at the seedling stage reduce generally root growth and distribution in the deeper soil and thereby limit plant nutrient uptake (Wang et al., 2019). In this study, the total N loss reached 224 kg ha^{-1} by applying sole NU as basal fertilizer before sowing, which accounting for 60.5% of the total N rate. It is necessary to reduce soil available N level at the early stage while ensure sufficient N supply at the late stage. This aim could be achieved by applying CRU and NU with an appropriate mixture ratio, in which the mixed CRU delayed N release at the early stage and provides sufficient N supply for crop growth at the late stage (Zheng et al., 2016; Guo et al., 2017). In this study, the post-silking percentages of DM and N uptake were 49%-59% and 33%-41% in CRU30% treatment, which were comparable and even higher than those reported by Meng et al. (2016), and thereby improved grain yield and NUE. The mechanism for better performance in the CRU30% treatment might be related to the optimized root growth and reduced N loss at the seedling stage by reducing available N in soil, and the increased N uptake and plant photosynthetic production because of the sufficient N supply at the reproductive growth, and subsequent improved yield components at maturity.

Soil and climatic conditions are important factors to affect field crop growth as well as the effectiveness of fertilizer application. In this study, the drought limited seed emergence and maize seedling growth in 2018, therefore showed lower grain yields as compared with those in 2019. Moreover, maize plant growth was also limited on sandy soil due to the lower fertility and poor retention capacity for water and nutrients, and thus obtained significantly lower grain yields relative to the plants grown on clay soil (Feng et al., 2019). In addition to crops, the N release from fertilizers is also affected by the soil environmental factors. The hydrolysis rate of urea is relatively fast and could be quickly dissolved in soil and converted into available N, which is easily lost if it cannot be effectively maintained in soil or absorbed by crop root. In this study, the sole NU application provided excessive available N that exceed retention capacity of sandy soil, and thus mass N was lost might via NH_3 volatilization, especially under the rainless

http://www.aloki.hu ● ISSN 1589 1623 (Print) ● ISSN1785 0037 (Online)
DOI: http://dx.doi.org/10.15666/aeer/1804_53675382

climate condition in 2018. In this case, maize plant growth would consume the mineralized N from organic matter at the late stage, and further reduced soil N contents at harvest. For CRU products, the N release into soil was delayed or controlled by using envelope technology and thus could effectively reduce N loss (Shavit et al., 1997). However, the N release rate is considerably affected by environmental factors, especially soil moisture and temperature. Christianson (1988) has found that drought and low temperatures limited N release from CRU, may cause plant N deficiency at the early stage. In our study, the N release of CRU was obviously delayed due to reduced rainfall and soil moisture content, while the N loss was also reduced and thus could still ensure the soil N supply at the later stage of maize growth, therefore showed better crop performance in terms of grain yield, NUE and environmental impacts as compared with the sole NU application. Moreover, compared with clay soil, the relatively improving effectiveness of mixed application of CRU and NU was better on sandy soil. However, it should be noted that, in addition to sole NU treatment, the soil Nmin contents in the mixed CRU treatments also showed decreases at harvest on sandy soil due to plant consumption. Hence, the N fertilizer rate might need to be properly increased on sandy soil when adopting mixed CRU and NU application method, and the optimal N rate require further investigation in the further researches.

Conclusions

The results of this study showed that the mixed application of CRU and NU significantly increased the maize yield, aboveground DM accumulation and N uptake. Among them, the highest maize yields were obtained in CRU30% treatment, which increased by 24% on sandy soil and 11% on clay soil as compared with CRU0% treatment. Maize plants grown in CRU30% treatment accumulated more DM and N uptake after silking, which accounted for 49%-59% and 33%-41% of the total DM and N uptake at maturity, respectively, and thereby increased grain yield and NUE. Compared with CRU 0% treatment, total N loss in CRU30% treatment reduced by 32.3% and 34.4% on sandy and clay soils, respectively. In sum, the mixed application of 30%CRU and 70%NU was suitable to increase maize yield, NUE and reduce N loss, which would provide a theoretical basis for the mixed application of CRU and NU and sustainable development of agriculture with rational fertilizing in Northeast China. Researchers should pay more attention to their environmental effects while paying attention to the agronomic and economic effects of the mixed application of controlled release urea and normal urea.

Acknowledgments. This work was supported by the National Key Research and Development Program of China (2016YFD0200403).

REFERENCES

[1] Burney, J. A., Davis, S. J., Lobell, D. B. (2010): Greenhouse gas mitigation by agricultural intensification. – Proceedings of the National Academy of Sciences 107(26): 12052-12057.
[2] Cassman, K. G., Dobermann, A., Walters, D. T. (2002): Agroecosystems, nitrogen-use efficiency, and nitrogen management. – Ambio 31(2): 132-140.
[3] Chen, X. P., Cui, Z. L., Fan, M. S., Vitousek, P., Zhao, M., Ma, W. Q., Wang, Z. L., Zhang, W. J., Yan, X. Y., Yang, J. C., Deng, X. P., Gao, Q., Zhang, Q., Guo, S. W., Ren, J., Li, S. Q., Ye, Y. L., Wang, Z. H., Huang, J. L., Tang, Q. Y., Sun, Y. X., Peng, X. L., Zhang, J.

http://www.aloki.hu ● ISSN 1589 1623 (Print) ● ISSN1785 0037 (Online)
DOI: http://dx.doi.org/10.15666/aeer/1804_53675382

W., He, M. G., Zhu, Y. J., Xue, J. Q., Wang, G. L., Wu, L., An, N., Wu, L. Q., Ma, L., Zhang, W. F., Zhang, F. S. (2014): Producing more grain with lower environmental costs. – Nature 514(7523): 486-489.

[4] China Agriculture Press. (2018): China agriculture yearbook. – China Agric Press, Beijing, China.

[5] Christianson, C. B. (1988): Factors affecting n release of urea from reactive layer coated urea. – Nutrient Cycling in Agroecosystems 16(3): 273-284.

[6] CRGCST (Cooperative Research Group on Chinese Soil Taxonomy). (2001): Chinese Soil Taxonomy. – Science Press, Beijing and New York, pp. 166-167.

[7] Cui, Z. L., Yue, S. C., Wang, G. L., Meng, Q. F., Wu, L., Yang, Z. P., Zhang, Q., Li, S. Q., Zhang, F. S., Chen, X. P. (2013): Closing the yield gap could reduce projected greenhouse gas emissions: a case study of maize production in China. – Global Change Biology 19(8): 2467-2477.

[8] Dobermann, A. (2007): Nutrient use efficiency-measurement and management. – IFA International Workshop on Fertilizer Best Management Practices, Brussels, Belgium.

[9] Douglas, L. A., Riazi, A., Smith, C. J. (1980): A semi-micro method for determining total nitrogen in soils and plant material containing nitrite and nitrate. – Soil Science Society of America Journal 44(2): 431-433.

[10] Drecht, G. V., Bouwman, A. F., Knoop, J. M., Beusen, A. H. W., Meinardi, C. R. (2003): Global modeling of the fate of nitrogen from point and nonpoint sources in soils, groundwater, and surface water. – Global Biogeochemical Cycles 17(4): 1115.

[11] FAO. (2017): FAOSTAT. – Verified 20 April 2018.

[12] Feng, G. Z., Wang, Y., Yan, L., Zhou, X., Wang, S. J., Mi, G. H., Gao, Q., Cui, Z. L. (2019): Effects of nitrogen and three soil types on maize (*Zea Mays* L.) grain yield in Northeast China. – Applied Ecology And Environmental Research 17(2): 4229-4243.

[13] Galloway, J. N., Townsend, A. R., Erisman, J. W., Bekunda, M., Cai, Z., Freney, J. R., Seitzinger, S. P., Sutton, M. A. (2008): Transformation of the nitrogen cycle: recent trends, questions, and potential solutions. – Science 320(5878): 889-892.

[14] Gao, Q., Li, C. L., Feng, G. Z., Wang, J. F., Cui, Z. L., Chen, X. P., Zhang, F. S. (2012): Understanding Yield Response to Nitrogen to Achieve High Yield and High Nitrogen Use Efficiency in Rainfed Corn. – Agronomy Journal 104(1): 165-168.

[15] Garcia, P. L., González-Villalba, H. A., Sermarini, R. A., Trivelin, P. C. O. (2018): Nitrogen use efficiency and nutrient partitioning in maize as affected by blends of controlled-release and conventional urea. – Archives of Agronomy and Soil Science 64(14): 1944-1962.

[16] Geng, J. B., Chen, J. Q., Sun, Y. B., Zheng, W. K., Tian, X. F., Yang, Y. C., Li, C. L., Zhang, M. (2016): Controlled Release Urea Improved Nitrogen Use Efficiency and Yield of Wheat and Corn. – Agronomy Journal 108(4): 1666-1673.

[17] Guo, J. M., Wang, Y. H., Fan, T., Chen, X. P., Cui, Z. L. (2016): Designing Corn Management Strategies for High Yield and High Nitrogen Use Efficiency. – Agronomy Journal 108(2): 922-929.

[18] Guo, J. M., Wang, Y. H., Blaylockc, A. D., Chen, X. P. (2017): Mixture of controlled release and normal urea to optimize nitrogen management for high-yielding (>15 Mg ha^{-1}) maize. – Field Crops Research 204: 23-30.

[19] Haderlein, L., Jensen, T. L., Dowbenko, R. E., Blaylock, A. D. (2001): Controlled Release Urea as a Nitrogen Source for Spring Wheat in Western Canada: Yield, Grain N Content, and N Use Efficiency. – The Scientific World Journal 1(S2): 114-121.

[20] Kaneta, Y., Awasaki, H., Murai, T. (1994): The non-tillage rice culture by single application of fertilizer in a nursery box with controlled-release fertilizer. – Japanese Journal of Soil Science and Plant Nutrition 65(4): 385-391. (In Japanese).

[21] Kondo, M., Singh, C. V., Agbisit, R., Murty, M. V. R. (2005): Yield Response to Urea and Controlled-Release Urea as Affected by Water Supply in Tropical Upland Rice. – Journal of Plant Nutrition 28(2): 201-219.

http://www.aloki.hu ● ISSN 1589 1623 (Print) ● ISSN1785 0037 (Online)
DOI: http://dx.doi.org/10.15666/aeer/1804_53675382

[22] Liu, S., Griffiths, S. M. (2011): From economic development to public health improvement: China faces equity challenges. – Public Health 125(10): 669-674.
[23] Liu, J. L., Zhan, A., Bu, L. D., Zhu, L., Luo, S. S., Chen, X. P., Cui, Z. L., Li, S. Q., Hill, R. L., Zhao, Y. (2014): Understanding Dry Matter and Nitrogen Accumulation for High-Yielding Film-Mulched Maize. – Agronomy Journal 106(2): 390-396.
[24] Meng, Q. F., Yue, S. C., Hou, P., Cui, Z. L., Chen, X. P. (2016): Improving yield and N use efficiency simultaneously for maize and wheat in China. – Pedosphere 26(2): 137-147.
[25] Noellsch, A. J., Motavalli, P. P., Nelson, K. A., Kitchen, N. R. (2009): Corn response to conventional and slow-release nitrogen fertilizers across a Claypan Landscape. – Agronomy Journal 101(3): 607-614.
[26] Page, A., Miller, R., Keeney, D. (1982): Methods of Soil Analysis. Part 2. – American Society of Agronomy. Inc., Madison, WI.
[27] Shavit, U., Shaviv, A., Shalit, G., Zaslavsky, D. (1997): Release characteristics of a new controlled release fertilizer. – Journal of Controlled Release 43(2-3): 131-138.
[28] Shaviv, A. (2001): Advances in controlled-release fertilizers. – Advances in Agronomy 71(1): 1-49.
[29] Shoji, S., Delgado, J., Mosier, A., Miura, Y. (2001): Use of controlled release fertilizers and nitrification inhibitors to increase nitrogen use efficiency and to conserve air and water quality. – Communications in Soil Science and Plant Analysis 32(7-8): 1051-1070.
[30] Song, C., Guan, Y., Wang, D., Zewudie, D., Li, F. M. (2014): Palygorskite-coated fertilizers with a timely release of nutrients increase potato productivity in a rain-fed cropland. – Field Crops Research 166: 10-17.
[31] Sun, K. G., He, A. L., Hu, Y., Li, B. Q. (2010): Study on the effect of the control released urea in the wheat-corn rotation system. – Chinese Journal of Soil Science 41(5): 1125-1129. (in Chinese).
[32] Tilman, D., Balzer, C., Hill, J., Befort, B. L. (2011): Global food demand and the sustainable intensification of agriculture. – Proceedings of the National Academy of Sciences 108(50): 20260-20264.
[33] Wang, Y., Zhang, X. Y., Chen, J., Chen, A. J., Wang, L. Y., Guo, X. Y., Niu, Y. L., Liu, S. R., Mi, G. H., Gao, Q. (2019): Reducing basal nitrogen rate to improve maize seedling growth, water and nitrogen use efficiencies under drought stress by optimizing root morphology and distribution. – Agricultural Water Management 212(2019): 328-337.
[34] Yan, L., Zhang, Z. D., Zhang, J. J., Gao, Q., Feng, G. Z., Abelrahman, A. M., Chen, Y. (2016): Effects of improving nitrogen management on nitrogen utilization, nitrogen balance, and reactive nitrogen losses in a Mollisol with maize monoculture in Northeast China. – Environmental Science and Pollution Research 23(5): 4576-4584.
[35] Zheng, W. K., Zhang, M., Liu, Z. G., Zhou, H. Y., Lu, H., Zhang, W. T., Yang, Y. C., Li, C. L., Chen, B. C. (2016): Combining controlled-release urea and normal urea to improve the nitrogen use efficiency and yield under wheat-maize double cropping system. – Field Crops Research 197: 52-62.
[36] Zvomuya, F., Rosen, C. J., Russelle, M. P., Gupta, S. C. (2003): Nitrate leaching and nitrogen recovery following application of polyolefin-coated urea to potato. – Journal of Environment Quality 32(2): 480-489.

http://www.aloki.hu ● ISSN 1589 1623 (Print) ● ISSN1785 0037 (Online)
DOI: http://dx.doi.org/10.15666/aeer/1804_53675382

MORPHOLOGICAL, PHYSIOLOGICAL AND BIOCHEMICAL RESPONSES OF CURLY PONDWEED (*POTAMOGETON CRISPUS* L.) TO UV-B RADIATION STRESS

WANG, J. Q.[1*] – SONG, Y. Z.[1] – XUE, Y.[2]

[1]*School of Applied Meteorology, Nanjing University of Information Science & Technology, Nanjing 210044, China*

[2]*School of Environmental Science and Engineering, Nanjing University of Information Science & Technology, Nanjing 210044, China*

[*]*Corresponding author*
e-mail: w_j_q2000@hotmail.com

(Received 18th Feb 2020; accepted 2nd Jul 2020)

Abstract. Causes of *Potamogeton crispus* population decline in the late spring and early summer are not fully understood. Given that strong UV-B radiation can penetrate the water column and damage aquatic organisms, it may be a key factor in the *P. crispus* decline. In this study, adult *P. crispus* plants were exposed to different intensities of UV-B radiation for 6 hours every day, the control group was only exposed to UV-A and photosynthetically active radiation. All groups were exposed to UV-A and photosynthetically active radiation at the same intensity. We monitored the morphological changes, and physiological and biochemical indexes. The results showed that plant height, internode length, and leaf area decreased with corresponding increases in radiation intensity. Additionally, photosynthetic pigment content could be improved with low-intensity UV-B radiation (<10.8 kJ/m^2), inhibited with continuous radiation, and decreased by high-intensity of UV-B radiation (>10.8 kJ/m^2). Catalase activity improved by short-term radiation, but inhibited by long-term radiation. Superoxide dismutase activity increased gradually with longer irradiation time. The malonaldehyde content increased at the beginning but then decreased with continuing radiation. These results suggest that UV-B radiation may contribute to the mass mortality of *P. crispus* in late spring and early summer.
Keywords: *plant height, chlorophyll content, superoxide dismutase activity, malondialdehyde, mass mortality*

Introduction

The significant depletion of the ozone layer over Antarctica, the mid-latitudes and high-latitudes, has raised concerns about the impact of solar ultraviolet-B (UV-B) radiation on marine and freshwater ecosystems. UV-B radiation, which is harmful to plants and human beings (Ulm and Jenkins, 2015), is attenuated rapidly in the water column (Cory et al., 2015). The penetration depth of 10% of surface UV-B radiation is usually less than a few meters, but it can reach several meters in some clear lakes (Williamson, 1995), or even tens of meters in the clearest seaes (Williamson, 1995; Buma et al., 2001). The incident depth of 10% of incident UV-B radiation is 7.7 m in Tahoe Lake (America), 10.8 m in Bessvatn (Norway), 12.8 m in Laguna Negra (Chile), and 9 m in the Bcllingshausen Sea, even 19.8 m in the Sargasso Sea (Williamson, 1995). Many studies have indicated that increasing UV-B exposure is detrimental to organisms, which causing mutations or even death to aquatic organisms (Buma et al., 2001; Pereira et al., 2014; Al-Aidaroos et al., 2015; Häder et al., 2015; Kim et al., 2015; Liu and Wang, 2017; Aksakal and Ciltas, 2018) and leading to a decrease in biomass (Choudhary and Agrawal, 2015). Recent studies have shown that phytoplankton

http://www.aloki.hu ● ISSN 1589 1623 (Print) ● ISSN1785 0037 (Online)
DOI: http://dx.doi.org/10.15666/aeer/1804_53835397

communities are extremely sensitive to UV radiation (Liu and Wang, 2017), and phytoplankton of the freshwater is more vulnerable to damage from UV radiation than of the marine (Williamson, 1995; Kim et al., 2015). Some studies have shown that UV-B radiation can affect photosynthesis, nitrogen fixation, protein biosynthesis and survive of cyanobacteria, but some protective strategies of Cyanobacteria have been developed to counteract the damaging effects of UV-B radiation (Häder et al., 2015; Mloszewska et al., 2018). UV radiation is harmful to many freshwater zooplankton, acting as a potential driving force for zooplankton community structure in some lakes. The disadvantage effects of ultraviolet radiation on zooplankton include limitations in nutrient uptake, inhibition of photosynthesis, DNA damage, and finally cell death. Earlier studies have suggested that zooplankton move into deep water by vertical migration avoid predation, however, recent researches suggested they maybe escape from surface intense UV radiation (Al-Aidaroos et al., 2015; Dumont, 2019). UV-B radiation can produce a series of biological effects on macroalgae at the molecular, cellular, individual and community levels, UV-B radiation can inhibit the growth of several macroalgae, especially for the damage of red algae, brown algae and green algae, by restraining its photosynthesis (Xu et al., 2018). UV-B radiation may affect the physiological and ecological functions of seagrass, and ultimately affect the coastal environment by changing the spatial distribution, species and community functional structure of seagrass (Bischof et al., 2006; Sunny, 2017). Rae et al. (2001) investigated the sensitivity of freshwater macrophytes to UV radiation in New Zealand soon lake, and found that different species of plants have different sensitive degree to UVR and also the different recovery capacity for the damage. Most researches have been focused on the phytoplankton, zooplankton, macroalgae, and seagrass, however, few studies were conducted on the submerged plants, especially freshwater submerged macrophytes.

Potamogeton crispus (Potamogetonaceae) is a submerged herbaceous perennial plant that grows in freshwater lakes, ponds, paddy fields, and rivers worldwide, and produces large quantities of biomass (Wang et al., 2017). The plants usually remain underwater in the early growth stages. Thus, the impact of light on their growth is limited. In the later growth period, when the plant penetrates the water surface after rapid growth in late spring and early summer, intense light begins to inhibit its growth, resulting in the decline of *P. crispus* (Su et al., 2001). But an observation indicated that *P. crispus* grew throughout the year in an artificial lake on an open experimental site where a glass rooftop had been installed. And the plant height of the *P. crispus* was 2-3 times higher than that in the field, but the branches are significantly lower than in the wild. The illumination difference between the inside and outside of the experimental site was small after filtration by the glass, but ultraviolet radiation—especially UV-B—decreased significantly. In general, PAR penetrates a glass greenhouse at an 80% to 85% rate, and UV-A radiation at a 60% to 70% rate; by contrast, UV-B radiation only does so at a 2% to 5% rate. Could this be why *P. crispus* continuously grows in an open experimental site with glass? Jian et al. (2003) found that mass mortality of *P. crispus* is strongly associated with intense light in late spring and early summer. Thus, we have reason to believe that UV-B radiation may contribute to the mass mortality of *P. crispus* in late spring and early summer.

The aim of this study is to understand the effect of UV-B radiation on growth of *P. crispus*, it is helpful to understand the reasons for mass mortality of *P. crispus* in late spring and early summer.

http://www.aloki.hu ● ISSN 1589 1623 (Print) ● ISSN1785 0037 (Online)
DOI: http://dx.doi.org/10.15666/aeer/1804_53835397

Materials and Methods

Experimental design

The experiment was conducted in an open experimental site where a glass rooftop had been installed (32.11°N, 118.91°E). *P. crispus* plants were collected from the Hongze Lake Nature Reserve on April 15, 2012, in China (*Figure 1*). These adult plants were transferred into flower pots, of which the upper diameter, base diameter, and the height were 18.0, 12.5, and 15.0 cm, respectively. 15-20 plants were included in each pot. The average plant height was 63±1.8 cm. The roots were fixed with a small amount of clay and gravel in every disk to reduce the effect of sediment. These pots were placed in 200-L plastic buckets, of which the upper diameter, base diameter, and height were 64×52×72 cm, respectively.

Figure 1. *Experimental site (left) and some partial experimental equipment (right)*

UV-B lamps made of stainless steel were suspended 120 cm above the plants. The UV-B lamps were manufactured by Nanjing Huaqiang Special Light Source Factory (40 W, peak 313 nm). The treatment intensity was achieved by adjusting the lamp's heights. The UV-B lamps were hung in an east-west direction in order to reduce the influence of the lamps' shade and to ensure that each treatment group obtained equivalent amounts of photosynthetically active radiation (*Figure 1*). The water temperature was maintained by 23±2℃, the day length was between 13.63 h and 14.18 h, and the sunshine duration was 7.0-11.8 h of sunshine.

The overlying water was tap water with an added nutrient solution. The depth was 70 cm in all treatments.

UV-B intensity setting

UV-B Radiation intensity recorded from April to August in 2004 and 2008 in the Nanjing field were used as the reference values for the experimental intensity (*Table 1*). In this study, *P. crispus* plants were exposed to UV-B radiation at different intensity (50 μW/cm^2, 100 μW/cm^2, 150 μW/cm^2, and 200 μW/cm^2) for 6 hours (9:00 to 15:00 in local time each day), so that the cumulative daily intensity of UV-B radiation was 10.8 kJ/m^2, 21.6 kJ/m^2, 32.4 kJ/m^2, and 43.2 kJ/m^2, respectively. The treatment groups were marked as T50, T100, T150, and T200. The control group had a polyester film (125 μm thickness, Shanghai Texiang electrical material Co., Ltd) to filter small amounts of UV-B radiation in the open experimental site with a glass rooftop, so the

http://www.aloki.hu ● ISSN 1589 1623 (Print) ● ISSN1785 0037 (Online)
DOI: http://dx.doi.org/10.15666/aeer/1804_53835397

control group was only exposed to UV-A and PAR from the solar radiation; the control group was marked as T0. All treatment groups received the same intensity of UV-A and PAR from the solar radiation. The experiment began on May 10, 2012, and the duration of the experimental period was 31 days. UV-B dosimetry was set through the SpectroSense2 (British SKYE company) to connect the SKU 430UV-B sensor (280 - 315 nm). Each group included three replicates. Because the UV-B intensity released from the thick tube was more intense than that released from the thin tube at the same power, T50 and T100 were subjected to the thin UV-B lamps (diameter 14 mm), whereas T150 and T200 were subjected to the thick UV-B lamps (diameter 26 mm). PAR radiation was set in the same condition for all groups, and measured at the beginning and on the 7th day of the experiment (*Table 2*).

Table 1. *UV-B radiation intensity ($\mu W \cdot cm^{-2}$) from April to August in 2004 and 2008 in the Nanjing, China*

Year	April	May	June	July	August
2004	170.24	172.91	239.80	156.17	147.66
2008	131.20	178.82	109.51	177.50	139.50

Table 2. *Light intensity($W \bullet m^{-2}$) received at the surface of the experimental water*

Time	T0	T50	T100	T150	T200	Random error
10 May, 2012	181.6	167.7	167.4	164.3	178.6	7.7
17 May, 2012	47.0	47.6	45.1	44.4	45.7	1.3

The ability of UV-B to penetrate the water should be considered. Taking T150 as an example, the UV-B intensity at the surface water was 62.4% of the air intensity, but the intensity was reduced to 54.0%, 30.5%, 10.1%, 3.5%, 1.4%, and 0.7% at depths of 10, 20, 30, 40, 50, and 60 cm, respectively. Irradiation time was controlled by a digital timer. UV-B radiation can attenuate exponentially in the water, and the attenuation model is in accordance with the following formula: $E_d=E_0e^{-K \bullet d}$, where E_0 is the incident UV-B intensity, K is the attenuation coefficient, and d is the depth of the water (Bernhard et al., 2018; Overmans and Agustí, 2020), K is 0.0868 in this experiment. According to calculation, T150 and T200 could penetrate to the underwater depth of 90 cm, while T100 and T50 could penetrate to the underwater depth of 80cm. However, the experimental water was only 70cm deep, so UV-B radiation could penetrate to the bottom all four treatments.

Determination of monitoring indexes

Plant height: The lengths of 15-20 plants in the three parallel treatment groups were measured from the border to the top of the main plant stem using a stainless steel ruler, and the average length was calculated.

Internode length: The 10-15th internode length from the top was also measured in the three parallel treatment groups, 15-20 internode lengths were measured and the average value was calculated each time.

Leaf area: The first three to five fully expanded leaves from the top to the bottom of the plants were selected to measure the leaf area. The length of the main leaf's veins was measured using a ruler, and the leaf width was measured at the leaf's widest point.

http://www.aloki.hu ● ISSN 1589 1623 (Print) ● ISSN1785 0037 (Online)
DOI: http://dx.doi.org/10.15666/aeer/1804_53835397

20-30 leaves were measured in each treatment and the average value was calculated at every sampling time. The leaf area of *P. crispus* was calculated by the following *equation (1)* (Wang et al., 2016):

$$\text{leaf area} = 0.87 \times \text{leaf length} \times \text{leaf width-0.21} \quad \text{(Eq.1)}$$

The plant height, internode length and leaf area were measured at 9 o'clock at the beginning of the experiment, and at days 16, 24, and 31, respectively.

Chlorophyll concentrations were measured by extracting fresh leaf tissue with 80% acetone and centrifuging the sample at 3000 g for 5 mins. The absorbance of the extract was determined at 663, 645, and 440 nm. Chlorophyll concentrations were calculated using the published formulae (Strain and Svec, 1966).

Catalase activity (CAT) was determined by measuring the decrease in absorbance of the reaction mixture at 240 nm (Havir and McHale, 1987). The activity was assayed for 1 min in a reaction solution composed of 2.9 mL potassium phosphate buffer 50 mmol (2.85 mL, pH 7.0), H_2O_2 12.5 mmol (50 μL), and 100 μL of crude extract.

Superoxide dismutase (SOD) activity was determined by measuring the ability to inhibit the photochemical reduction of nitro blue tetrazolium chloride (NBT) according to the method of Beauchamp and Fridovich (1971). One enzyme unit of SOD activity was defined as the amount of enzyme that inhibits 50% NBT reduction measured at 560 nm. The blue formazan produced by NBT photoreduction was measured as an increase in absorbance at 560 nm.

Lipid peroxidation of leaves was determined using a thiobarbituric acid (TBA) test by measuring the malondialdehyde (MDA) level (Heath and Packer, 1968). The extinction coefficient was determined at 600 nm, 532 nm, and 450 nm (De Vos et al., 1989).

The physiological and biochemical parameters were determined at the beginning of the experiment, and at days 16, 23, and 31, respectively, 150-180 leaves were sampled in each treatment at every sampling time.

Statistical analysis

Data from three replicates of all treatments were subjected to analysis of variance using SPSS 16.0. All data were presented as the mean ± SE. Comparisons between treatments were performed using two-way ANOVA, and Tukey's post-test was performed to determine the significant differences between different treatment groups on the same sampling day, different sampling date for the same treatment group. The significance of treatment effects was determined at the 0.05 probability level, the level of probability was set at 95% confidence interval (p<0.05).

Results

Growth status

The leaves near the water surface in the groups from T100 to T200 were bleached from 7 d to 31 d, whereas the leaves growing underwater remained healthy. The harmful effects in all treatment groups increased with increasing radiation intensity. Some plants from the T150 and T200 groups died, but the roots of some of these plants were still linked to the stem at 16 d. At 22 d, the leaves in all treatment began to shrink, T0, T50,

http://www.aloki.hu ● ISSN 1589 1623 (Print) ● ISSN1785 0037 (Online)
DOI: http://dx.doi.org/10.15666/aeer/1804_53835397

and T100 also showed a declining trend at 22 d, two new branches appeared in T0, and T150 and T200 had no intact plants, with more broken branches and stem fractures in the roots, and they were beginning to float on the water (*Table 3*). At 31 d, there were 18 well-developed specimens in T0 in the three parallel groups, including 6 new branches, and some branches were broken from the original plants, whereas T50, T100 only had 9, 7 intact plants and more broken branches, the broken branches of T150 and T200 have been decomposed. During the whole experiment, the plant height, intermode length, and leaf area in T50-T200 decreased continuously with corresponding increases in UV-B radiation intensity.

Table 3. *Number of intact specimens in the three parallel groups*

Treatment	0d	16d	22d	31d
T0	50	50	38	18
T50	52	45	16	9
T100	50	37	17	7
T150	58	22	0	/
T200	58	13	0	/

Morphological indexes

The plant heights of T100, T150, and T200 reduced after 16 days of UV-B radiation, but the heights of T0 and T50 plants increased slightly by 2.1% and 0.9%, respectively, from the beginning of the experiment (*Table 4*), whereas the heights of T100, T150, and T200 remained relatively consistent, decreased by 1.6%, 8.3%, and 2.0% from the beginning, respectively ($p>0.5$). The heights of T50, T100, T150, and T200 decreased from the beginning by 12.5%, 11.0%, 22.6%, and 24.1%, respectively at 24 d. T0 increased continuously after from 24 d to 31 d. Although all treatment groups had a significant difference at 24 d compared with the values at the beginning of the experiment ($p<0.05$), the heights of T50-T200 decreased more significantly as the radiation intensity increased. After 24 days of UV-B radiation, the heights of T50, T100, T150, and T200 were lower than that of T0 by 21.4%, 22.9%, 28.2%, and 34.1%, respectively. The plants in T150 and T200 died at 31 d. Although T0-T100 still grew, the growth rates decreased from those at the beginning of the experiment. This decrease became more significant from 24 d to 31 d ($p<0.05$).

The internode lengths of T50, T100, T150, and T200 differed significantly ($p<0.05$) after days 16 of UV-B radiation compared with the beginning (*Table 4*), and were lower than that of T0 by 59.5%, 71.7%, 77.4%, and 71.6%, respectively. At 24 d, the internode lengths of all groups decreased, but the differences were not significant between the treatments ($p>0.05$). The average internode length of T50 was 3.8% greater than T0, T100 was lower than T0 by 8.0%, but the internode lengths of T150 and T200 were significantly lower than T0 (38.7% and 36.3%, respectively) at 24 d. The internode lengths of T0, T50, and T100 at 31 d differed significantly from those at the beginning of the experiment ($p<0.05$), but the differences among those treatments were much less.

The leaf area of T0 at 16 d had increased by 13.8% (*Table 4*), and thereafter decreased continuously. The leaf areas for T50-T200 decreased significantly ($p<0.05$) from the beginning to the day 24, and were 48.7%, 51.9%, 57.3%, and 58.1% lower than those at the beginning, respectively. The leaf areas of T0, T50, and T100 decreased

http://www.aloki.hu ● ISSN 1589 1623 (Print) ● ISSN1785 0037 (Online)
DOI: http://dx.doi.org/10.15666/aeer/1804_53835397

significantly (p<0.05) at 31 d compared with those at the beginning, accounting for 63.7%, 70.4%, and 70.5% decreases.

Table 4. *Morphological change of P. crispus affected by UV-B radiation*

Morphological indexes	Treatment	0d	16d	24d	31d
Plant height/cm	T0	64.1±2.3Aa	65.4±1.2Aa	70.6±1.7Ba	55.3±4.2Ca
	T50	63.4±3.4Aa	64.0±1.4Aa	55.5±3.4Bb	54.3±3.7Ba
	T100	61.2±3.2Aa	60.2±1.9Ab	54.4±1.6Bb	53.3±2.0Ba
	T150	65.4±3.2Aa	60.0±1.9Bb	50.7±3.1Cb	
	T200	61.3±2.2Aa	60.0±1.9Ab	46.5±1.5Bc	
Internode length/cm	T0	3.1±0.4Aa	3.5±0.6Ba	1.1±0.1Ca	0.6±0.1Da
	T50	3.1±0.6Aa	1.4±0.3Bb	1.1±0.1Ba	0.6±0.0Ca
	T100	3.4±0.1Aa	1.0±0.2Bb	1.0±0.2Ba	0.6±0.1Ca
	T150	3.5±0.6Aa	0.8±0.2Bc	0.7±0.1Bb	
	T200	3.3±0.4Aa	1.0±0.2Bb	0.7±0.1Cb	
Leaf area/cm^2	T0	1.5±0.2Aa	1.7±0.2Aa	0.8±0.1Ba	0.6±0.0Ca
	T50	1.5±0.1Aa	1.1±0.1Bb	0.8±0.1Ca	0.5±0.1Db
	T100	1.6±0.1Aa	1.0±0.2Bb	0.8±0.2Ba	0.5±0.0Cb
	T150	1.6±0.1Aa	0.8±0.1Bc	0.8±0.1Ba	
	T200	1.6±0.1Aa	0.6±0.1Bc	0.7±0.1Ba	

Lowercase letters indicate statistical differences between different treatment groups on the same sampling day, capital letters indicate statistical differences between different sampling date for the same treatment group, the equal letters indicate no differences and different letters indicate significant differences. The same situation was applied to the following monitoring indicators and parameters in the tables below.

Chlorophyll content

From 16 d to 31 d, chlorophyll a (Chla) and chlorophyll b (Chlb) concentrations in all treatments were significantly different (p<0.05) from the values at the beginning of the experiment (*Table 5*), Chla and Chlb concentrations of the T0 and T50 treatments increased, however, the concentrations of T50-T200 decreased with increasing radiation intensity. At 23 d, the values were significantly different from those at the beginning, whereas T0 increased continually, T50 decreased slightly, Chla and Chlb concentrations of T100-T200 increased from the values at 16d, but they still decreased with increasing radiation intensity. Chla and Chlb concentrations of T0-T100 decreased with increasing radiation intensity at 31 d.

Table 5. *Chlorophyll content of P. crispus affected by UV-B radiation*

Chlorophyll content	Treatment	0d	16d	23d	31d
Chlorophyll a content($mg \cdot L^{-1}$)	T0	2.18±0.17Aa	2.32±0.14Aa	4.20±0.15Ba	4.70±0.17Ca
	T50	2.24±0.13Aa	3.75±0.11Bb	3.23±0.08Cb	4.26±0.12Db
	T100	2.18±0.15Aa	1.34±0.13Bc	2.51±0.10Cc	3.05±0.12Dc
	T150	2.00±0.16Aa	1.16±0.06Bc	2.33±0.09Cc	
	T200	2.08±0.13Aa	1.14±0.09Bc	2.00±0.12Ad	
Chlorophyll b content($mg \cdot L^{-1}$)	T0	0.77±0.09Aa	0.95±0.07Aa	1.63±0.07Ba	1.71±0.04Ba
	T50	0.81±0.06Aa	1.53±0.06Bb	1.37±0.07Cb	1.75±0.08Da
	T100	0.82±0.09Aa	0.51±0.07Bc	1.05±0.07Cc	1.23±0.07Db
	T150	0.79±0.08Aa	0.54±0.07Bc	0.99±0.08Cc	
	T200	0.76±0.06Aa	0.46±0.08Bc	0.84±0.07Cd	

http://www.aloki.hu ● ISSN 1589 1623 (Print) ● ISSN1785 0037 (Online)
DOI: http://dx.doi.org/10.15666/aeer/1804_53835397

CAT activity

CAT activities of T0 and T50 were higher at the beginning of the experiment (*Table 6*). At 16 d, T50-T200 groups increased with increasing radiation intensity, and had a significant difference compared with the beginning (p<0.05); the CAT activity of T200 was 143.2% greater than that of T0, CAT activities of T50 and T100 had no significant difference than the beginning (p>0.05). While the activities of T150 and T200 were 31.3% and 383.3% higher than the beginning and higher than T0 at 23 d. At 31 d, the CAT activities of T0-T100 still had no significant difference compare with the beginning (p>0.05), and increased with the increasing intensity.

Table 6. *CAT activity, SOD activity and malonaldehyde content of P. crispus by UV-B radiation*

Physiological and biochemical parameters	Treatment	0d	16d	23d	31d
CAT activity/(U·g^{-1} FW·min^{-1})	T0	4.4±0.4Aa	3.2±0.5Ba	4.1±0.4Aa	3.8±0.4Aa
	T50	4.5±0.4Aa	4.9±0.4Ab	4.9±0.3Ab	4.6±0.4Ab
	T100	4.6±0.4Aa	4.9±0.2Ab	4.9±0.3Ab	4.9±0.5Ab
	T150	4.6±0.2Aa	6.1±0.5Bc	6.0±0.5Bc	
	T200	4.1±0.2Aa	7.8±0.5Bd	19.7±1.7Cd	
SOD activity/(U·g^{-1} FW)	T0	25.4±1.4Aa	18.8±1.8Ba	53.6±2.2Ca	109.1±8.5Da
	T50	24.3±1.6Aa	21.9±2.0Aa	56.3±2.5Ba	86.0±1.2Cb
	T100	24.6±1.3Aa	32.4±2.0Bb	59.6±1.7Cb	65.0±1.3Dc
	T150	26.3±1.2Aa	76.9±4.4Bc	82.5±3.4Bc	
	T200	23.5±1.2Aa	78.7±1.5Bc	71.4±2.3Cc	
MDA content/(n mol·g^{-1} FW)	T0	30.9±2.1Aa	26.9±2.0Aa	24.4±1.4Ba	25.1±2.1Ba
	T50	29.6±2.9Aa	29.9±1.9Aa	28.9±1.1Ab	20.2±1.5Bb
	T100	30.9±1.1Aa	35.1±1.1Bb	23.1±1.0Ca	18.3±0.5Db
	T150	30.9±2.2Aa	50.7±3.3Bc	21.8±1.2Ca	
	T200	30.9±2.1Aa	43.1±2.1Bd	20.5±0.8Cc	

SOD activity

SOD activity of each group produced a significant difference from the beginning (p<0.01) (*Table 6*) after 16 days of radiation, the activity gradually increased in T50 to T150, and all treatments were higher than that of T0. The activities of T0, T50 were slightly lower than what was measured at the experiment's onset. Each treatment's SOD activity significantly increased at 23 d (p<0.01) compared with the beginning, and T150 maintained the highest value among all treatments, and the activity of T150 and T200 had increased by 213.3%, 204.0% compared to the beginning, the activities in T0 to T150 continually increased. At 31 d, T0 to T100 had increased significantly compared with their respective values at 23 d (p<0.05), but they maintained a downward trend during the experimental period. The SOD activity of T0 reached the highest value of all groups, increasing by 329.5% compared to its initial value.

MDA content

At 16 d, the MDA concentrations of T0 and T50 remained basically unchanged, but the MDA concentrations in T150 and T200 increased significantly (63.9% and 39.3%, respectively) with the beginning (p>0.05) (*Table 6*). At 23 d, the concentrations in all

http://www.aloki.hu ● ISSN 1589 1623 (Print) ● ISSN1785 0037 (Online)
DOI: http://dx.doi.org/10.15666/aeer/1804_53835397

treatment groups decreased, but there were no significant differences compared with the beginning (p>0.05); The concentrations of T100, T150, and T200 decreased significantly from the experiment's onset (p<0.05), accounting for 25.2%, 29.5%, and 33.8% decreases, respectively, and the concentrations of T100, T150, and T200 were also lower than those of T0 and T50. At 31 d, the MDA concentrations in T0 to T100 were lower than those at the beginning, and decreased with the increasing intensity.

Discussion

Although ultraviolet radiation can be attenuated by the water column, 10% of incident UV-B radiation is still present at substantial depths: from several to dozens of meters. In the middle and lower reaches of the Yangtze river area in China, the maximum depth of UV-B penetration is approximately 2.25 m, the harmful ultraviolet radiation can reach the lake bed in some lakes, threatening aquatic organisms (Zhang et al., 2005). The UV-B radiation may not only affect the creatures in the water, but also damage the benthos (Puthumana et al., 2017).

UV-B radiation can attenuate exponentially in the water, and the attenuation model is in accordance with the following formula: $E_d=E_0e^{-K\bullet d}$, where E_0 is the incident UV-B intensity, K is the attenuation coefficient, and d is the depth of the water (Bernhard et al., 2018; Overmans and Agustí, 2020). Based on the above theory, the higher the incident UV-B radiation, the greater the UV-B radiation that can penetrate into the water in this experiment. UV-B radiation will permeate deep into the water column and increase the damage to *P. crispus*. *P. crispus* plants were collected from the Hongze Lake Nature Reserve before the start of the experiment, the plants submerged in deeper water, the ultraviolet radiation in the sunlight was not strong in winter and spring. When the experiment began, the plants grew rapidly to the surface and were exposed to UV-B radiation. The top leaves of the plants are usually injured more severely because of continuous radiation from the top and then died, so the plant height decreased. Because plant biomass is mainly concentrated on the top of the plant, the injuries at the top of the plants due to the increasing radiation intensity will rapidly affect the physiological functions of the plant, and limit plant growth. This may be the reason why all plants of T150 and T200 declined and then decayed after 24 days of continuous UV-B radiation.

Chlorophyll concentration is closely related to photosynthesis in plants and can reflect light-energy utilization by chloroplasts (Huang et al., 2013). Enhanced UV-B radiation can decrease the chlorophyll concentrations of plants (Ma et al., 2016; Zhang et al., 2017). However, the sensitivity of chlorophyll to UV-B radiation can be quite different among different species, and the decline in chlorophyll concentration may be due to inhibition of chlorophyll biosynthesis (Gao et al., 2019), enhancement of chlorophyll photodegradation (Petrović et al., 2017), or a combination of both. However, low intensity UV-B radiation can make pigment molecules of LHCII (light-harvesting pigment protein complex II) absorb more energy and transfer more energy to the PSII core to stimulate photosynthesis (Teramura et al., 1991). It has been reported that T50 treatment for a short period increases chlorophyll concentration, but high-intensity radiation results in a strong bleaching effect on leaf pigment cells (Wang et al., 2010). Some pigment proteins can absorb UV-B energy, and they produce specific photochemical reactions that decrease chlorophyll concentration (Castenholz and Garcia-Pichel, 2014). The top leaves of T100 to T200 plants were damaged when they approached the water surface, and chlorophyll concentration decreased significantly

http://www.aloki.hu ● ISSN 1589 1623 (Print) ● ISSN1785 0037 (Online)
DOI: http://dx.doi.org/10.15666/aeer/1804_53835397

under intense UV-B radiation. In particular, when the radiation intensity surpassed 21.6 kJ/m^2, acute injury occurred, and the top leaves were strongly bleached (Wang et al., 2010). Chlorophyll concentration decreased gradually with increasing radiation intensity. At 23 d, the biomass of the top of the plants declined when the radiation intensity was greater than 21.6 kJ/m^2, which resulted in decreased plant height because new-growth leaves were used in the measurements, so the chlorophyll concentration of T150 and T200 showed an increasing trend compared with 16 d. At 23 d, because T50 received low-intensity radiation, the chlorophyll concentration was only slightly lower than that of the control group; by contrast, the chlorophyll concentration in the other groups decreased substantially with increasing radiation intensity. The leaves were farther from the radiation source and received less radiation at 31 d. Therefore, injury to the plants was reduced, and the concentration of the chlorophyll increased compared with the aforementioned cases.

UV-B radiation can induce generation of reactive oxygen species (ROS) (Yokawa et al., 2016), and increased ROS causes lipid peroxidation and protein oxidation (Pospíšil and Yamamoto, 2017). These ROS are highly reactive because they can interact with a number of cellular molecules and metabolites, leading to a number of destructive processes that cause cellular damage (Choudhury et al., 2017). Plants contain antioxidant metabolites, enzymes and nonenzymes to a variable extent, which have the ability to detoxify ROS (Abid et al., 2018). CAT and SOD can play key roles in eliminating superoxide (O_2^-) and hydrogen peroxide (H_2O_2) (Chen et al., 2016). CAT are important protective enzymes that remove H_2O_2 and decompose H_2O_2 into O_2 and H_2O, protecting plants from the toxicity associated with H_2O_2. SOD is an enzyme capable of superoxide anion radical scavenging, and it can convert superoxide radicals to molecular oxygen and hydrogen peroxide (Perry et al., 2010). CAT and SOD activities in *P. crispus* increase under adverse conditions, such as heavy metal stress (Hu et al., 2007; Xu et al., 2010) and high nutrients (Zhang et al., 2009). If the stress exceeds a certain threshold, the enzyme activity decreases. UV-B radiation can produce the same effect on the antioxidant enzyme system of *P. crispus*. In this experiment, reactive oxygen concentrations increased with increasing radiation intensity in the initial radiation stage, and the antioxidant enzyme system was enhanced for scavenging reactive oxygen species. SOD activity also increased with increasing radiation intensity because it could decompose the superoxide anion into hydrogen peroxide and oxygen. However, the decomposition products could aggravate the H_2O_2 concentration in the leaves. In this study, CAT activities increased more than SOD activity, and they reached the highest levels at the early stage of radiation treatment; by contrast, SOD activity continued to grow with radiation. In general, the activities of all kinds of antioxidant enzymes rose with increasing radiation intensity, and this might have been inhibited by UV-B radiation. Furthermore, damage to enzymatic activities in the plants was irreversible under intense radiation conditions, which ultimately caused the plants to die. After 16 days of radiation, the plants apparently entered an emergency reaction period, and the activities of CAT reached their highest levels for the entire monitoring period. The plants' resistance was more obvious with increasing radiation intensity. SOD activity gradually increased with increasing radiation time and intensity. Because the T200 group received the highest radiation intensity, the damage was the most obvious in these plants. The SOD activity showed a decreasing trend, likely because the radiation intensity exceeded its tolerance threshold. Physiological function was reduced by increasing irradiation time, and reactive oxygen species increased. Therefore, SOD

http://www.aloki.hu ● ISSN 1589 1623 (Print) ● ISSN1785 0037 (Online)
DOI: http://dx.doi.org/10.15666/aeer/1804_53835397

activities at 23 d were decreased. The plants died at 31 d due to excessive radiation; the activities of CAT and SOD in the other groups were gradually reduced. Thus, the active oxygen produced in plants increased with UV-B radiation, whereas the scavenging activity of the plants decreased, resulting in a gradual increase in CAT activity. Additionally, because the top leaves of the plants were gradually dying, the plant heights decreased, so the received radiation intensity of the plants declined. The leaves used for analysis were new-growth leaves, which may also explain why the antioxidase activity was lower than in the initial stages of radiation.

Under a ray of light or under the action of free radicals, one hydrogen molecule breaks from the lipid molecules (LH) and forms a lipid free radical (L·). The L can then react with oxygen to form peroxy radicals (LOO), which can attack other lipid molecules, seize the hydrogen atom, and produce new free radicals and lipid hydroperoxide (LOOH) (Ayala et al., 2014). This reaction repeats and results in continuous consumption of lipid molecules and the generation of a number of lipid peroxides (Ayala et al., 2014). In studies of terrestrial plants, UV-B radiation increased the levels of lipid peroxidation products (MDA) significantly (Singh et al., 2014; Gęgotek et al., 2017; Chen et al., 2019), and it changed the membrane fatty acid composition, decreased the unsaturation index, and eventually injured the plants. In the present study, *P. crispus* plants produced a large amount of peroxides under intense radiation during the initial stage. As a result, leaf MDA concentration reached its maximum at 16 d. Concurrently, mass production was reduced, possibly because of continuous consumption of lipid peroxides. Membrane permeability was also increased with long-term radiation, causing gradual bleaching or death of the plants' top leaves and leading to decreased plant height. When middle leaves replaced the top leaves and became the new top leaves, the actual radiation intensity received was reduced, and the MDA concentrations in the leaves were lowered. Because the new top leaves received less radiation due to the decreased plant height, the release of peroxides in the top leaves was also tempered; this explains why the MDA concentrations of the T50-T200 groups decreased at 23 d and why the T0-T150 groups showed a decreasing trend at 31 d. This variation may suggest that oxidation products were gradually reduced because the lipid molecules were continuously oxidated.

Conclusion

UV-B radiation can accelerate plants' decline when the exposure intensity exceeds 32.4 kJ/m^2, the plants that received this level of radiation declined and died within 31 days, whereas a few plants still grew when the exposure intensity less than 21.6 kJ/m^2. UV-B radiation reduced the plant heights, and also shortened internode length and shrunk leaf area. Chla and Chlb contents all decreased under UV-B radiation when the UV-B radiation intensity surpassed 10.8 kJ/m^2, and the inhibition effects were further elevated as the radiation intensity increased. CAT activities were improved under radiation for a short time and gradually increased with increasing radiation intensity. However, CAT activities were inhibited with continuing exposure to radiation. SOD activity increased gradually with prolonged irradiation time and increased radiation intensity. MDA content was improved at the beginning of the UV-B radiation, and then gradually increased with increasing radiation intensity, but decreased with prolonged exposure. These results indicate that UV-B radiation may be an important factor leading to mass mortality of *P. crispus* in late spring and early summer.

http://www.aloki.hu ● ISSN 1589 1623 (Print) ● ISSN1785 0037 (Online)
DOI: http://dx.doi.org/10.15666/aeer/1804_53835397

Accordingly, we deduce that the sharp enhancement of ultraviolet radiation on the land surface in the late spring and early summer leads to mass mortality of the wild *P. crispus* population. However, further research is necessary to study whether UV-B radiation acts with other environmental factors to affect physiological activity and contribute to the decline of *P. crispus*.

Acknowledgements. This work was supported by MOE (Ministry of Education in China) Project of Humanities and Social Sciences [Project No. 15YJCZH167] and Jiangsu Government Scholarship for Overseas Studies [Project No. JS-2018-51 under grant]. We would like to thank the following: Dr. Guoxiang Wang for their help in the experimental site.

REFERENCES

[1] Abid, M., Ali, S., Qi, L. K., Zahoor, R., Tian, Z., Jiang, D., Snider, J. L., Dai, T. B. (2018): Physiological and biochemical changes during drought and recovery periods at tillering and jointing stages in wheat (*Triticum aestivum* L.). – Scientific reports 8: 4615.

[2] Aksakal, F. I., Ciltas, A. (2018): The impact of ultraviolet B (UV-B) radiation in combination with different temperatures in the early life stage of zebrafish (*Danio rerio*). – Photochemical & Photobiological Sciences 17: 35-41.

[3] Al-Aidaroos, A. M., El-Sherbiny, M. M. O., Satheesh, S., Mantha, G., Agustī, S., Carreja, B., Duarte, C. M. (2015): Strong Sensitivity of Red Sea Zooplankton to UV-B Radiation. – Estuaries and Coasts 38: 846-853.

[4] Ayala, A., Muñoz, M. F., Argüelles, S. (2014): Lipid peroxidation: production, metabolism, and signaling mechanisms of malondialdehyde and 4-hydroxy-2-nonenal. – Oxidative medicine and cellular Longevity 2014: 360438.

[5] Beauchamp, C., Fridovich, I. (1971): Superoxide dismutase: improved assays and an assay applicable to acrylamide gels. – Biochemistry 44: 276-287.

[6] Bischof, K., Gomez, I., Molis, M., Hanelt, D., Karsten, U., Lüder, U., Roleda, M. Y., Zacher, K., Wiencke, C. (2006): Ultraviolet radiation shapes seaweed communities. – Reviews in Environmental Science and Biotechnology 5: 141-166.

[7] Buma, A. G. J., Boer, M. K. D., Boelen, P. (2001): Depth distribution of DNA damage in Antarctic marine phyto- and bacterioplankton exposed to summertime UV radiation. – Journal of Phycology 37: 200-208.

[8] Castenholz, R. W., Garcia-Pichel, F. (2014): Cyanobacterial responses to UV radiation. – In: Whitton, B. A., Potts, M. (eds.) The Ecology of Cyanobacteria. Springer Netherlands, pp: 591-611.

[9] Chen, Y., Liu, Q., Chen, D. (2016): CO_2 laser enhances the chilling tolerance of wheat seedlings by stimulating NO synthesis. – Canadian Journal of Plant Science 96: 796-807.

[10] Chen, Z., Ma, Y., Weng, Y., Yang, R., Gu, Z., Wang, P. (2019): Effects of UV-B radiation on phenolic accumulation, antioxidant activity and physiological changes in wheat (*Triticum aestivum* L.) seedlings. – Food Bioscience 30: 100409.

[11] Choudhary, K. K., Agrawal, S. B. (2015): Effect of elevated ultraviolet-B on four tropical soybean cultivars: quantitative and qualitative aspects with special emphasis on gas exchange, chlorophyll fluorescence, biomass and yield. – Acta Physiologiae Plantarum 37: 31.

[12] Choudhury, F. K., Rivero, R. M., Blumwald, E., Mittler, R. (2017): Reactive oxygen species, abiotic stress and stress combination. – The Plant Journal 90: 856-867.

[13] Cory, R. M., Harrold, K. H., Neilson, B. T., Kling, G. W. (2015): Controls on dissolved organic matter (DOM) degradation in a headwater stream: the influence of photochemical and hydrological conditions in determining light-limitation or substrate-limitation of photo-degradation. – Biogeosciences Discuss 12: 9793-9838.

http://www.aloki.hu ● ISSN 1589 1623 (Print) ● ISSN1785 0037 (Online)
DOI: http://dx.doi.org/10.15666/aeer/1804_53835397

[14] De Vos, C. H., Vooijs, R., Schat, H., Ernst, W. H. (1989): Cooper-induced damage to the permeability barrier in roots of Silenecucubalus. – Journal of Plant Physiologyogy 135: 165-169.
[15] Dumont, H. J. (2019): Zooplankton vertical migration in two Sahara lakes with contrasting biotic environments. – Limnetica 38: 95-101.
[16] Gao, L., Liu, Y., Wang, X., Li, Y., Han, R. (2019): Lower levels of UV-B light trigger the adaptive responses by inducing plant antioxidant metabolism and flavonoid biosynthesis in Medicago sativa seedlings. – Functional Plant Biology 46: 896-906.
[17] Gęgotek, A., Rybałtowska-Kawałko, P., Skrzydlewska, E. (2017): Rutin as a Mediator of Lipid Metabolism and Cellular Signaling Pathways Interactions in Fibroblasts Altered by UVA and UVB Radiation. – Oxidative Medicine and Cellular Longevity 2017: 4721352.
[18] Häder, D.-P., Williamson, C. E., Wängberg, S.-Å., Rautio, M., Rose, K. C., Gao, K. S., Helbling, E. W., Sinha, R. P., Worrest, R. (2015): Effects of UV radiation on aquatic ecosystems and interactions with other environmental factors. – Photochemical & Photobiological Sciences 14: 108-126.
[19] Havir, E. A., McHale, N. A. (1987): Biochemical and developmental characterization of multiple forms of catalase in tobacco leaves. – Plant Physiology 84: 450-455.
[20] Heath, R. L., Packer, L. (1968): Photoperoxidation in isolated chloroplasts—I. Kinetics and stoichiometry of fatty acid peroxidation. – Archives of Biochemistry and Biophysics 125: 189-198.
[21] Hu, J. Z., Shi, G. X., Xu, Q. S., Wang, X., Yuan, Q. H., Du, K. H. (2007): Effects of Pb^{2+} on the active oxygen-scavenging enzyme activities and ultrastructure in *Potamogeton crispus* leaves. – Russian Journal of Plant Physiology 54: 414-419.
[22] Huang, J. L., Qin, F., Zang, G. C., Kang, Z. H., Zou, H. Y., Hu, F., Yue, C. L., Li, X. Y., Wang, G. X. (2013): Mutation of OsDET1 increases chlorophyll content in rice. – Plant Science 210: 241-249.
[23] Jian, Y. X., Li, B., Wang, J. B., Chen, J. K. (2003): Control of turion germination in *Potamogeton crispus*. – Aquatic Botany 75: 59-69.
[24] Kim, B. M., Rhee, J. S., Lee, K. W., Kim, M. J., Shin, K. H., Lee, S. J., Lee, Y. M., Lee, J. S. (2015): UV-B radiation-induced oxidative stress and p38 signaling pathway involvement in the benthic copepod *Tigriopus japonicus*. – Comparative Biochemistry and Physiology Part C: Toxicology & Pharmacology 167: 15-23.
[25] Liu, J., Wang, W. X. (2017): The protective roles of TiO_2 nanoparticles against UV-B toxicity in *Daphnia magna*. – Science of The Total Environment 593-594: 47-53.
[26] Ma, X., Ou, Y. B., Gao, Y. F., Lutts, S., Li, T. T., Wang, Y. (2016): Moderate salt treatment alleviates ultraviolet-B radiation caused impairment in poplar plants. – Scientific reports 6: 32890.
[27] Mloszewska, A. M., Cole, D. B., Planavsky, N. J., Kappler, A., Whitford, D. S., Owttrim, G. W., Konhauser, K. O. (2018): UV radiation limited the expansion of cyanobacteria in early marine photic environments. – Nature Communications 9: 3088.
[28] Overmans, S., Agustí, S. (2020): Unraveling the Seasonality of UV Exposure in Reef Waters of a Rapidly Warming (Sub-) tropical Sea. – Frontiers in Marine Science, https://doi.org/10.3389/fmars.2020.00111.
[29] Pereira, D. T., Schmidt, É. C., Bouzon, Z. L., Ouriques, L. C. (2014): The effects of ultraviolet radiation-B response on the morphology, ultrastructure, and photosynthetic pigments of *Laurencia catarinensis* and *Palisada flagellifera* (Ceramial , Rhodophyta): a comparative study. – Journal of Applied Phycology 26: 2443-2452.
[30] Perry, J. J., Shin, D. S., Getzoff, E. D., Tainer, J. A. (2010): The structural biochemistry of the superoxide dismutases. – Biochimica Et Biophysica Acta 1804: 245-262.
[31] Petrović, S., Zvezdanović, J., Marković, D. (2017): Chlorophyll degradation in aqueous mediums induced by light and UV-B irradiation: An UHPLC-ESI-MS study. – Radiation Physics and Chemistry 141: 8-16.

http://www.aloki.hu ● ISSN 1589 1623 (Print) ● ISSN1785 0037 (Online)
DOI: http://dx.doi.org/10.15666/aeer/1804_53835397

[32] Pospíšil, P., Yamamoto, Y. (2017): Damage to photosystem II by lipid peroxidation products. – Biochimica et Biophysica Acta (BBA) - General Subjects 1861: 457-466.
[33] Puthumana, J., Lee, M. C., Park, J. C., Kim, H. S., Hwang, D. S. (2017): Ultraviolet B radiation induces impaired lifecycle traits and modulates expression of cytochrome P450 (CYP) genes in the copepod *Tigriopus japonicus*. – Aquatic Toxicology 184: 116-122.
[34] Rae, R., Hanelt, D., Hawes, I. (2001): Sensitivity of freshwater macrophytes to UV radiation: relationship to depth zonation in an oligotrophic New Zealand lake. – Marine and Freshwater Research 52: 1023-1032.
[35] Singh, V. P., Kumar, J., Singh, S., Prasad, S. M. (2014): Dimethoate modifies enhanced UV-B effects on growth, photosynthesis and oxidative stress in mung bean (*Vigna radiata* L.) seedlings: Implication of salicylic acid. – Pesticide Biochemistry and Physiology 116: 13-23.
[36] Strain, H. H., Svec, W. A. (1966): Extraction, speration, estimation and isolation of chlorophyll. – In: Vernon, L. P., Seely, G. R. (eds.) Chlorophylls. pp: 21-66.
[37] Su, S. Q., Sheng, Y. L., Tang, H. Y., Yao, W. Z. (2001): Effects of temperature, light intensity and phonphotosynthesis in *Potamogeton Crispus* L. – Journal of Southwest Agricultural University 23: 532-534.
[38] Sunny, A. R. (2017): A review on effect of global climate change on seaweed and seagrass. – International Journal of Fisheries and Aquatic Studies 5: 19-22.
[39] Teramura, A. H., Ziska, L. H., Sztein, A. E.(1991): Changes in growth and photosynthetic capacity of rice with increased UV-B radiation. – Physiologia Plantarum 83: 373-380.
[40] Ulm, R., Jenkins, G. I. (2015): How do plants sense and respond to UV-B radiation? – BMC Biology 13: 45.
[41] Uveges, B. T., Teece, M. A., Fulton, J. M., Junium, C. K. (2018): Environmental controls on pigment distributions in the freshwater microbialites of Fayetteville Green Lake. – Organic Geochemistry 125: 165-176.
[42] Wang, G. H., Hao, Z. J., Anken, R. H., Lu, J., Liu, Y. (2010): Effects of UV-B radiation on photosynthesis activity of *Wolffia arrhiza* as probed by chlorophyll fluorescence transients. – Advances in Space Research 45: 839-845.
[43] Wang, J. Q., Song, Y. Z., Zheng, Y. F., Cao, Y. (2016): Effect of sediment deposition on turion sprouting and early growth of *Potamogeton crispus* L. – Journal of Freshwater Ecology 31: 261-269.
[44] Wang, J. Q., Song, Y. Z., Wang, G. X. (2017): Causes of large *Potamogeton crispus* L. population increase in Xuanwu Lake. – Environmental Science and Pollution Research 24: 5144-5151.
[45] Williamson, C. E. (1995): What role does UV-B radiation play in freshwater ecosystems? – Limnology and Oceanography 40: 386-392.
[46] Xie, Y. H., Yu, D., Geng, X. H., Yang, Y. Q., Huang, Y. M. (2004): Phenotypic plasticity in the submersed macrophyte *Potamogeton crispus* as a response to elevated [CO_2]. – Journal of Freshwater Ecology 19: 701-708.
[47] Xu, Q. S., Hu, J. Z., Xie, K. B., Yang, H. Y., Du, K. H., Shi, G. X. (2010): Accumulation and acute toxicity of silver in *Potamogeton crispus* L. – Journal of Hazardous Materials 173: 186-193.
[48] Xu, J., Zhang, X., Fu, Q., Gao, G., Gao, K. (2018): Water depth-dependant photosynthetic and growth rates of *Gracilaria lemaneiformis*, with special reference to effects of solar UV radiation. – Aquaculture 484: 28-31.
[49] Yokawa, K., Kagenishi, T., Baluška, F. (2016): UV-B induced generation of reactive oxygen species promotes formation of BFA-induced compartments in cells of Arabidopsis root apices. – Frontiers in plant science. https://doi.org/10.3389/fpls.2015.01162.
[50] Zhang, Y. L., Qin, B. Q., Ma, R. H., Zhu, G. W., Chen, W. M. (2005): Attenuation of solar ultraviolet radiation and analysis of attenuators in typical macrophytic, algal lake zones of Lake Taihu. – Acta Ecologica Sinica 25: 2254-2261.

http://www.aloki.hu ● ISSN 1589 1623 (Print) ● ISSN1785 0037 (Online)
DOI: http://dx.doi.org/10.15666/aeer/1804_53835397

[51] Zhang, M., Cao, T., Ni, L. Y., Xie, P., Li, Z. Q. (2009): Carbon, nitrogen and antioxidant enzyme responses of *Potamogeton crispus* to both low-light and high-nutrient stresses. – Environmental and Experimental Botany 68: 44-50.
[52] Zhang, X. R., Chen, Y. H., Guo, Q. S., Wang, W. M. (2017): Short-term UV-B radiation effects on morphology, physiological traits and accumulation of bioactive compounds in *Prunella vulgaris* L. – Journal of Plant Interactions 12: 348-354.

http://www.aloki.hu ● ISSN 1589 1623 (Print) ● ISSN1785 0037 (Online)
DOI: http://dx.doi.org/10.15666/aeer/1804_53835397

PHYSICOCHEMICAL EVALUATION OF SOME NEW SOFT SEEDLING STRAINS AND LOCAL CULTIVARS OF DATE (*Phoenix dactylifera* L.) FRUITS UNDER THE CONDITIONS OF THE NORTH DELTA, EGYPT

OMAR, A. K.[1,2*] – EL-MORSHEDY, F. A.[1] – MAZROU, Y. S.[3,4] – ABDALLAH, S. S.[1] – SALAMA, A.[1]

[1]*Horticulture Dept., Faculty of Agriculture, Kafresheikh University, Kafr El-Sheikh 33516, Egypt*

[2]*Institute of Research and Consulting, King Faisal University, Hofuf, Kingdom of Saudi Arabia*

[3] *Business Administration Dept., Community College, King Khaled University, Abha, Kingdom of Saudi Arabia*

[4]*Agriculture College, Tanta University, Tanta, Egypt*

[*]*Corresponding author*
e-mail: alaa.omr@agr.kfs.edu.eg, akomar@kfu.edu.sa; phone: +20-109-740-8240

(Received 18th Feb 2020; accepted 25th May 2020)

Abstract. This research was conducted during 2017 and 2018 seasons on some soft seedling strains and local date palm cultivars grown under the condition of Baltim, Kafr ElSheikh Governorate (North Delta), Egypt. Twelve soft seedling strains (Limony, Elhamra, Elhelowa, Nwat Elbahr, koppy, Zenat Ahmer, Zenat Asmar, Ostora, Nwat zaghloul, Nemery, Om Makatif, and Meghal) and three local cultivars: Hayany, Samany and Araby (control) were evaluated using fruit characteristics. Results revealed that, Elhamra had the highest values of yield, bunch weight, fruit diameter, fruit and flesh weight, and flesh thickness during both seasons, while, Nemery strain seedlings recorded the highest seed diameter, seed weight, SSC, total and reducing sugars. On the other hand, Araby cultivar recorded the lowest values in fruit length, flesh weight, (Soluble solids Content (SSC)) and Hayany cv., in total and reducing sugars. This study could be recommended for marketing new soft strains seedling date palms (Elhamra and Nemery) the most desirable commercial attributes of local or international standards under North Delta district, Egypt conditions.
Keywords: *parameters, firmness, bunch weight, SSC, total sugars, reducing sugars, fruit quality*

Introduction

Egypt is a subtropical country which lies between 22° and 31° North latitudes and between 25° and 35° East longitudes. Winter is a mix of mild and wet (November - April) and summer is hot and dry (May - October) are suitable for the production of many field and Horticultural crops (Directorate of Intelligence, 2011). Egypt is the world first date (*Phoenix dactylifera* L.) producer with annual production of more than 1.7million tones and contributing 18.3% in total world production (FAO, 2018). Dates can be classified into three types based on fruit moisture content; soft, semi-dry and dry cultivars (Selim et al., 1970). Cultivars Hayany, Samany and Araby are the main local soft date cultivars that grown in North Delta, Egypt. Biodiversity conservation of date palm is important in sustaining the various number of date cultivars in Egypt (Abdalla, 1986; Rizk et al., 2004). There are actually some date cultivars that are underutilized, which expected to be distinct or completely lost, and thereby affect date palm biodiversity in Egypt if it is not regularly maintains (Bazza, 2007). To

http://www.aloki.hu ● ISSN 1589 1623 (Print) ● ISSN 1785 0037 (Online)
DOI: http://dx.doi.org/10.15666/aeer/1804_53995409

simplify over view framework on the identification, description and documentation the agro-biodiversity of soft date cultivars in Egypt, systematical relationships of twenty one Egyptian soft date cultivars were described based on one hundred and three morphological attributes (Abd-El Hamed et al., 2017). Most of the cultivars identification studies are enumerative, based on local names, which vary from one place to another (Abd-Alla, 2010; Abdul-Hamid et al., 2018). These cultivars are location specific, and could be known by different names in different places. Moreover, only one name could be assigned to different cultivars in different places. This could cause ambiguity in classifying cultivars based on local names. There is no scientific characterization of cultivars to use more legitimate names that can be used to distinguish cultivars (Abd El-Baky, 2012). Most of the female cultivars are identified using fruit characteristics such as size, shape or color (Bekheet, 2013). Fruit length generally ranged from 2.80 cm in Aglany date to 5.92 cm in Zaghloul date (Mansour, 2005). Average fruit length in Bent-Aisha cultivar is about 3.69 cm, while it reaches 5.92 cm in Zaghloul cultivar (Sakr et al., 2010). Abdalla et al. (1996) stated that grading of date cultivars is mainly considered on fruit physical characteristics and general appearance, as well as moisture and sugar content. Conventionally, date fruit have been used for treating diseases, such as sore throat and fever (Chao and Krueger, 2017). Fruit also inhibit and suppress several diseases.

The aim of this work is to characterize and evaluate some new soft seedling strains and compared to local cultivars of date palm using fruit characteristics under North Delta, Egypt conditions.

Materials and methods

This study was conducted during 2017 and 2018 seasons at a private orchard in Baltim district (located at North Delta region Kafr-El-Sheikh Governorate (31° 15' 35" N, 31° 9' 36" E), Egypt. Baltim's climate is typical to the northern coastal line which is the most moderate in Egypt. It features a hot desert climate, but prevailing winds from the Mediterranean Sea greatly moderate the temperatures, making its summers moderately hot and humid while its winters mild and moderately wet (*Fig. 1*).

Figure 1. *Baltim district, Kafr El-Sheikh, Egypt*
(Source: https://www.google.com/maps/place/Baltim)

http://www.aloki.hu ● ISSN 1589 1623 (Print) ● ISSN 1785 0037 (Online)
DOI: http://dx.doi.org/10.15666/aeer/1804_53995409

Fifteen soft seedling strains (Limony, Elhamra, Elhelowa, Nwat Elbahr, koppy, Zenat Ahmer, Zenat Asmar, Ostora, Nwat zaghloul, Nemery, Om Makatif, and Meghal) were selected from a big number of excellent seedling palms beside threes trees of local cultivars (Hayany, Samany and Araby) as a standard control. The selected palms were about 15-17 years old, grown in sandy loam soil and they characterized by high yield and fruit quality (*Fig. 2*).

Figure 2. *Experimental Orchard date palm trees in Baltim, Kafr El Sheikh Governorate, Egypt*

As usual the selected palms were subjected to normal cultural practices (irrigation, fertilization, plant protections, etc.). All seedling strains and Hayany, Samany and Araby cultivars (control) were pollinated in April using pollen grains from male palm (Meghal) grown in the same location in both seasons to avoid xenia and metaxenia effects. Each of the selected tree was represented by 3 bunches as 3 replicates. Fruit samples of sixty fruit each were collected, during fruit season at Khalal (maturity) stage. Fruit weight, length, diameter, and fruit length/diameter ratio (L/D) were recorded. Same fruit were used to measure pulp and seed weight (g), and then fruit/pulp percentage were calculated. Fruit firmness (kg/cm^2) was measured at two equatorial points on the fruit using pressure tester (Penetrometer ST 308, Italy) with tips = 6.4 mm at 25°C. SSC were determined according to A.O.A.C (2000) methods.. Total and reducing sugars were determined according to the methodology of Lane and Eynon described by the A.O.A.C (2000).

Statistical analysis

Experiment was designed in a randomized complete block system, and data were analyzed using analysis of variance (ANOVA) (Snedecor and Cochran, 1980). Mean comparison was carried out using Duncan multiple range test (DMART).

http://www.aloki.hu ● ISSN 1589 1623 (Print) ● ISSN 1785 0037 (Online)
DOI: http://dx.doi.org/10.15666/aeer/1804_53995409

Results and discussion

Yield (kg/palm) parameters, bunch weight (kg/bunch) and fruit length (cm)

Results showed that Elhamra seedling strain had the maximum yield and bunch weight recorded 200.00, 192.00, 31.00 and 29.00 kg/bunch, respectively during both seasons (*Table 1* and *Fig. 3*). Elhelowa seedling strain recorded the following highest yield in both season and recorded 180.00 and 181.00 kg/pam. While Zenat Ahmer seedling strain flowed the highest bunch weight in both seasons and recorded 24.00 and 26.00 kg/bunch. On the other hand, koppy seedling strain recorded (77.00 and 76.00 kg/palm; 11.00 and 11.00 kg/bunch) the lowest values in the same characters (yield and bunch weight). The longest fruit length (6.10 and 6.03 cm) was recorded by Ostora seedling strain during 2017 and 2018 seasons.

Table 1. *Yield parameters, bunch weight and fruit length of some new seedling strains and Samany, Araby and Hyany cultivars during 2017 and 2018 seasons*

Strains/cultivars		Yield (kg/palm)		Bunch weight (kg/palm)		Fruit length (cm)	
		2017	2018	2017	2018	2017	2018
1	Zenat Asma	188.67b	167.67c	31.0a	28.33ab	4.20f	4.35d
2	Zenat Ahmer	187.70b	162.33d	24.00b	26.67b	4.40ef	4.17de
3	Om Makatif	133.67d	129.00g	17.00cde	15.67f	5.40c	5.03b
4	koppy	77.00g	76.67k	11.00g	11.00g	5.03d	4.60c
5	Meghal	161.0c	155.67e	23.33b	24.00c	4.40ef	4.68c
6	Nwat Elbar	122.0e	180.67b	19.00c	19.00d	4.33ef	4.03ef
7	Nwat zaghlou	122.0e	121.00h	16.00def	16.00ef	5.80b	4.68c
8	Elhelowa	180.33b	181.00b	29.00a	29.00a	5.35c	4.10de
9	Limony	120.00e	125.33gh	16.00def	16.00ef	4.35ef	4.15de
10	Ostora	96.00f	96.00i	14.03f	14.67f	6.10a	6.03a
11	Nemery	90.33f	91.00j	18.33cd	19.33d	4.22f	4.30de
12	Elhamra	200.00a	192.33a	31.03a	29.00a	5.03d	4.96b
13	Samany cv.	138.33d	140.67f	15.33ef	15.00f	5.03d	4.62c
14	Araby cv.	97.00f	90.00j	25.00b	24.50c	4.17f	3.83f
15	Hayany cv.	141.67d	158.33de	19.00c	18.00de	3.55g	5.03b

Means with the different letters within the same colume are significantly different at $P \leq 0.05$ according Duncan multiple range test (DMART).

Figure 3. *The fruit of selected soft seedling strains date palm & Samany, Araby and Hyany cultivars*

http://www.aloki.hu ● ISSN 1589 1623 (Print) ● ISSN 1785 0037 (Online)
DOI: http://dx.doi.org/10.15666/aeer/1804_53995409

Nwat zaghlou and Om Makatif seedling strains flowed the longest fruit length during 2017 and 2018 and recorded 5.80 and 5.03 cm, respectively. While Araby cultivar recorded the shortest fruit length (4.17 and 3.83 cm) during both seasons. Fruit quality is basically determined based on fruit shape, size and texture, while nutritional quality requires chemical analysis of sensory attributes (Al-Jasass et al., 2015). Results are in consistent with those of Rizk and Nahed (2006) found that Sewy cv., gave the highest yield followed by the strain Ghazal, while the strains Karama and Tagtaggt showed the lowest significant values in both seasons. Also agreement with El-Merghany et al. (2013) they found that Barhy cv., gave the highest yield/palm in the second season. El-Makhtoune and AbdelKader (1990), mentioned that the average bunch weight ranged from 4.22 to 34.40 kg according the date palm cultivar. Baliga et al. (2011) stated that fruit shape and organoleptic properties could indicate the differences among varieties. Habib et al. (1984), Hussein et al. (1984, 2001) and Al-Ghamdi (1996) noticed significant differences in fruit length among cultivars.

Fruit diameter (cm), fruit weight and flesh weight (g)

The weight of Fruit pulp and seed (g) are shown in *Table 2* and *Fig. 3*. Maximum values of fruit diameter and weight, as well as pulp weight were noticed in Elhamra seedling strain by 3.60 and 4.10 cm – 38.84 and 37.27 g – 33.70 and 35.31 g during 2017 and 2018 seasons.

Table 2. *Fruit diameter (cm), fruit weight (g), flesh weight (g) of some new seedling strains and Samany, Araby and Hyany cultivars during 2017 and 2018 seasons*

Strains/cultivars		Fruit diameter (cm)		Fruit weight (g)		Flesh weight (g)	
		2017	2018	2017	2018	2017	2018
1	Zenat Asma	2.99c	3.03cd	21.50d	20.70f	18.18e	27.68c
2	Zenat Ahmer	3.03bc	2.77ef	21.53d	20.87f	19.43d	18.83e
3	Om Makatif	2.17e	2.37g	18.59e	16.46h	12.75h	12.31j
4	koppy	2.99c	2.87e	24.42c	27.43b	22.65b	34.69b
5	Meghal	3.53a	2.49g	34.00b	31.84b	14.71g	14.08h
6	Nwat Elbar	2.47d	2.33g	24.52c	21.20f	17.27f	17.60f
7	Nwat zaghlou	2.60d	2.99d	20.6d	17.75g	33.97a	18.47e
8	Elhelowa	2.47d	2.37g	16.48f	14.26i	10.8i	8.97k
9	Limony	3.17bc	3.17c	21.35d	22.38e	19.58d	19.53d
10	Ostora	3.17bc	2.49g	24.87c	26.60d	22.54b	16.67g
11	Nemery	3.10bc	3.37b	23.57c	20.55f	21.47c	18.81e
12	Elhamra	3.60a	4.10a	38.84a	37.27a	33.70a	35.31a
13	Samany cv.	3.00c	3.03cd	14.89g	17.75g	18.47e	18.49e
14	Araby cv.	2.46d	2.43g	16.47f	16.21h	14.20g	12.31j
15	Hayany cv.	2.43d	2.68f	14.69g	15.76h	13.22h	13.50i

Means with the different letters within the same colume are significantly different at $P \leq 0.05$ according Duncan multiple range test (DMART).

The flowed values for fruit diameter were in Nemery seedling strain by 3.17 and 3.37 cm, for fruit weight were 34.00 and 31.84 g, for flesh weight were 22.65 and 34.69 g during both seasons. The smallest values were 2.17 g for fruit diameter in Om Makatif, 14.69 g in for fruit weight in Hayany cultivar, also 21.22 g for flesh weight in Hayany cultivar during first season.

http://www.aloki.hu ● ISSN 1589 1623 (Print) ● ISSN 1785 0037 (Online)
DOI: http://dx.doi.org/10.15666/aeer/1804_53995409

Results are in consistence with previous reports of Attala et al. (2001) in different date palm cultivars. Mansour (2005) recorded that fruit weight of Samany cultivar (23.80 g) and Bent-Aisha cultivar (11.06 g) were almost similar to our results.

Seed length (cm), seed diameter (cm), seed weight (g) and flesh thickness (cm)

The physical characters composition tests were carried out to seed length, seed diameter, seed weight and flesh thickness of various date palm seedling strains during 2017 and 2018 seasons (*Table 3* and *Fig. 3*). Samany seedling strain recorded the smallest seed length by 2.10 cm in comparison to other seedling strains, Hayany had the highest values by 3.80 cm, followed Nwat zaghlou seedling strain (2.63 cm) in second season. Fruit diameter was significantly different among date palm seedling strains and cultivars. Nemery seedling strain showed the highest diameter of 1.15 cm, followed by Zenat Ahmer (1.04 cm) Samany (1.00 cm), Limony (1.00 cm). Result indicated that Nemery seedling strain showed the highest seed weight (2.97 g) followed by Samany (2.39 g), while, Nwat Elbar seedling strain had the lowest (0.45 g) values in comparison with other seedling strains and cultivars. Fruit thickness was also significantly different from one strain to another. Elhamra seedling strain had the highest thickness (1.50 g) compared to other seedling strains and cultivars, while Om Makatif seedling strain recoreded the lowest thickness (0.57 cm) in fruits during both seasons. These results are in confirming the previous reports of Saeed and Yousof (2014). Average fruit length, width, and length/width ratio were similar to those reported by Shattir et al. (2002) and Sulieman et al. (2007, 2012), while flesh thickness, was little higher than values reported by Sulieman et al. (2012) and Saeed and Yousof (2014). Rizk et al. (2004), reported that the maximum seed weight was noticed in Siwy cultivar, while the lowest values were found in Freahy cultivar.

Table 3. *Seed length (cm), seed diameter (cm), seed weight and flesh thickness (cm) of some new seedling strains and Samany, Araby and Hyany cultivars during 2017 and 2018 seasons*

Strains/cultivars		Seed length (cm)		Seed diameter (cm)		Seed weight (g)		Flesh thickness (cm)	
		2017	2018	2017	2018	2017	2018	2017	2018
1	Zenat Asma	2.83bcd	2.63defgh	0.97abcd	1.00abc	2.37ab	2.28ab	0.90bc	0.80bcde
2	Zenat Ahmer	3.20abc	2.50fgh	1.04ab	1.03ab	2.01ab	1.79ab	1.03bc	0.70de
3	Om Makatif	3.17abc	2.57efgh	0.83bcd	1.00abc	1.59b	1.91ab	0.57d	0.63e
4	koppy	3.20abc	2.33gh	0.80bcd	0.83bcd	2.09ab	1.90ab	1.00bc	1.03bc
5	Meghal	3.10abc	2.93cdef	1.07ab	0.86bcd	2.24ab	2.57a	1.00bc	0.77cde
6	Nwat Elbar	2.80cd	3.03cde	0.70d	0.53e	0.59c	0.45c	0.77cd	0.97bcd
7	Nwat zaghlou	3.20abc	2.63ab	0.83bcd	0.87bcd	2.19ab	2.19ab	0.97bc	0.87bcde
8	Elhelowa	2.40ef	2.80cdefg	0.73cd	0.73d	1.63b	1.28b	0.83cd	0.73cde
9	Limony	3.27ab	3.60ab	0.97abcd	1.00abc	1.77b	1.96ab	1.03bc	1.07b
10	Ostora	2.57de	2.27h	0.97abcd	0.80cd	2.13ab	2.47a	1.13ab	0.73cde
11	Nemery	2.23ef	3.10cd	1.15a	1.10a	2.97a	2.49a	0.83cd	0.77cde
12	Elhamra	3.03abc	2.80cdefg	0.70d	0.93abcd	2.01ab	2.27ab	1.30a	1.50a
13	Samany cv.	2.10f	2.20h	1.00abc	1.00abc	2.11ab	2.39a	1.17ab	1.03bc
14	Araby cv.	2.33ef	3.27bc	0.90abcd	0.83bcd	2.39ab	1.51ab	0.80cd	0.73cde
15	Hayany cv.	3.33a	3.80a	0.90abcd	0.83bcd	1.77b	1.79ab	0.57d	0.73cde

Means with the different letters within the same colume are significantly different at $P \leq 0.05$ according Duncan multiple range test (DMART).

http://www.aloki.hu ● ISSN 1589 1623 (Print) ● ISSN 1785 0037 (Online)
DOI: http://dx.doi.org/10.15666/aeer/1804_53995409

Firmness (kg/cm^2), SSC (%), total and reducing sugars (%)

Fruit, firmness (kg/cm^2), SSC, total and reducing content (%) were shown in *Table 4* and *Fig. 3*. Maximum fruit firmness was noticed in Samany seedling strain by 950.00, while for SSC, total and reducing percentages were in Nemery seedling strain by 39.97, 46.33 and 35.00% for SSC percentages, respectively. Hayany cultivar recorded the followed value (893.33 kg/cm^2) in fruit firmness, Nwat Elbar seedling strain in SSC percentage 30.53% and Nwat zaghlou seedling strain in total and reducing sugars in 39.6 and 29.33%, respectively. The smallest values were 100.00 kg/cm^2 for fruit firmness in Om Makatif seedling strain, for SSC was 18.83% in Araby cultivar, 27.00 and 16.60% for total and reducing sugars in Hayany cultivar, respectively. Fruit chemical characteristics have been reported by Attala et al. (2001), Al-Eid (2006), Al-Farsi et al. (2007), Alkhateeb (2008), El-Sohaimy and Hafez (2010) and El-Merghany and Zaen El-Daen (2013). The results are in agreement with many researchers such as Gadalla et al. (2013), Idris et al. (2014), Mortazavi et al. (2015), Nasir et al. (2015), El-Salhy et al. (2016), Qadri et al. (2016), Abd-El Hamed et al. (2018) reported that Barhy at khalal stage gave the lowest total sugars percentage (51 and 50%) in both season. Youssef et al. (1998) found that total sugars concentration in fruits of eight date palm cultivars (from different areas in south Egypt) were ranged between 73.65 and 81.77% for dry cultivars. Saeed et al. (2015) stated that fruit chemical analysis of five cultivars showed that the majority of date cultivars was soft and characterized by the dominance of reducing sugars. El-Merghany, and Zaen El-Daen (2013) studied some date cultivars grown under Toshky region conditions. Seven date palm cultivars were evaluated and classified to two groups: dry date palm cultivars (Sakkoty, Bartamoda, Gondela, Malkaby and Balady [Maghal]) and soft date palm cultivars (Barhee and Sokkary). Sokkary (soft date palm cultivar) gave the highest reducing sugars (%) in the two seasons. Evaluation study revaluated that Sakkoty and Bartamoda were the best dry date palm cultivars. Wherever, Sokkary cultivar was the best soft date palm cultivars growing under Toshky conditions.

Table 4. *Firmness (kg/cm^2), SSC (%), total and reducing sugars (%) of some new seedling strains and Samany, Araby and Hyany cultivars during 2017 and 2018 seasons*

Strains/cultivars		Firmness (kg/cm^2)		SSC (%)		Total sugars (%)		Reducing sugars (%)	
		2017	2018	2017	2018	2017	2018	2017	2018
1	Zenat Asma	253.33h	843.33c	28.90bc	28.07b	38.00b	36.67bcd	28.67b	26.67bcde
2	Zenat Ahmer	620.00e	626.67f	27.93c	29.37b	37.33bc	36.67bcd	27.00bc	28.00bcd
3	Om Makatif	100.00j	486.67g	29.73bc	29.47b	36.00bcde	36.33bcd	26.33bc	26.67bcd
4	koppy	423.33g	875.00b	27.73c	28.17b	34.33cdef	34.67cde	23.67bcd	25.00bcde
5	Meghal	186.67i	710.00e	28.93bc	26.69b	29.00g	30.33fg	19.33de	21.33efg
6	Nwat Elbar	650.00d	636.67f	30.53bc	29.47b	32.67f	33.33def	21.67bc	23.67cdefg
7	Nwat zaghlou	770.00b	713.33e	30.53bc	29.30b	38.67b	39.67b	27.67b	29.33b
8	Elhelowa	493.33f	710.00e	27.33c	27.00b	36.00bcde	35.67cd	25.33bc	26.67bcd
9	Limony	813.33a	820.00c	28.50c	28.17b	33.00ef	31.33efg	23.67bcd	21.00fg
10	Ostora	653.33d	650.00f	29.93bc	29.50b	36.30bcd	38.00bc	27.00bc	28.67bc
11	Nemery	656.86d	631.67f	39.00a	39.97a	46.00a	46.33a	35.67a	35.00a
12	Elhamra	440.00g	750.00d	33.40b	29.70b	34.00def	34.33cde	27.00bc	24.00cdefg
13	Samany cv.	814.33a	950.00a	25.27c	22.43bc	32.00f	33.00def	21.83cd	23.00defg
14	Araby cv.	736.67c	750.67d	19.47d	18.83c	29.00g	30.00fg	21.50cd	20.00g
15	Hayany cv.	760.00bc	893.33b	20.00d	21.00bc	27.00g	29.00g	16.60e	19.47g

Means with the different letters within the same colume are significantly different at $P \leq 0.05$ according Duncan multiple range test (DMART).

http://www.aloki.hu ● ISSN 1589 1623 (Print) ● ISSN 1785 0037 (Online)
DOI: http://dx.doi.org/10.15666/aeer/1804_53995409

Generally, Aseeded date palm samples characterized in this study displayed a considerable diversity for most of the selected fruit characters evaluated as compared to the control (Samany, Hayani and Eraby cvs.). Furthermore, in the present study, fruit characteristics showed significant variation among the different new seeded and cultivars samples were therefore considered as useful for the identifying particular morph-types. Morphological fruit descriptors are easy to assess and widely applied by farmers, traders, processors and consumers (Kalia et al., 2011). The results showed that, Elhamra strain had the highest values in yield, bunch weight, fruit diameter, fruit and flesh weight, and flesh thickness during both seasons. While, Nemery strain seedling recorded the highest seed diameter, seed weight, SSC, total and reducing sugars. Also, results were agreement with Morell et al. (1995), who reported that qalitative characteristics of fruit quality such as fruit shape, fruit apex and fruit stalk depth, are less prone to influences from environmental factors but are considered to be subjective to a certain extent. Baliga et al. (2011) reported that fruit shape and organoleptic characteristics can be used to differentiate between varieties. Habib et al. (1984), Hussein et al. (1984, 2001) and Al-Ghamdi (1996) noticed a significant difference in fruit dimaions and other quality parameters among date cultivars.

Conclusion

The fruit characteristics showed significant variation among the different new seeded and cultivars samples were therefore considered as useful for the identifying particular morph-types. Elhamra and Nemery strains seedling were the better compared to other indigenous cultivars studied, in terms of most physical and chemical characteristics. Elhamra seedling strain had the highest values, flowed Nemery seedling strain. Morphological fruit descriptors are wanted and easy to assess and widely applied by farmers, traders, processors and consumers (Rodríguez-Burruezo et al., 2003; Kalia et al., 2011). Even nursery operators can easily identify fruits of desired landraces suitable variety. It is concluded that Elhamra and Nemery for marketing new soft strains seedling date palms as the most desirable commercial attributes of local or international standards.

Acknowledgements. The authors extend their appreciation to the Deanship of Scientific Research at King Khalid University for funding this work through Program of Research Groups under grant number (R.G.P 2/28/40).

REFERENCES

[1] Abdalla, M. Y. (1986): Morphological and chemical studies through flowering and fruiting stages on date palm. – Ph. D. Thesis. Fac. Agric., Cairo Univ. 190p.
[2] Abdalla, M., Sabour, A., EL-Makhtoun, F., Ahmed, A. (1996): Effects of some environmental conditions on vegetative, yield and fruit properties of Sewy date cultivar. – Zagazig J. Agric. Res. 23(2).
[3] Abd-Alla, M. M. (2010): Genetic stability on Phoenix dactylifera var. Karama produced in vitro. – N Y Sci J 3: 70-75.
[4] Abd El-Baky, M. A. (2012): Using morphological and anatomical features as taxonomical evidences to differentiate between some soft and semi-dry Egyptian cultivars of date palm – J Hort Sci Ornam Plants 4: 195-200.

http://www.aloki.hu ● ISSN 1589 1623 (Print) ● ISSN 1785 0037 (Online)
DOI: http://dx.doi.org/10.15666/aeer/1804_53995409

[5] Abd-El Hamed, K., Darwesh Rasmia, S. S., Zayed, E. M. M. (2017): Evaluation physical and chemical characteristics of some seedlings date palm fruits (Maghal) in the North Delta Egypt. – International Journal of Advances in Agricultural Science and Technology 4(7): 13-32.
[6] Abdul-Hamid, N. A., Mustaffer, N. M., Maulidiani, A., Mediani, A., Ismail, I. S., Tham, C. L., Shadid, K., Abas, F. (2018): Quality evaluation of the physical properties, phytochemicals, biological activities and proximate analysis of nine Saudi date palm fruit varieties. – Journal of the Saudi Society of Agricultural Sciences 19(2): 151-160.
[7] Al-Eid, S. M. (2006): Chromatographic separation of fructose from date syrup. – Int. J. Food Sci. Nutr. 57(1-2): 83-96.
[8] Al-Farsi, M., Al-Asalvar, C., Al-Abid, M., Al-Shoaily, K., Al-Amry, M., Al-Rawahy, F. (2007): Compositional and functional characteristics of dates, syrups and their by-products. – Food Chem. 104(3): 943-947.
[9] Al-Ghamdi, A. S. (1996): Field evaluation of date palm (*Phoenix dactylefera* L.) cultivas produced through tissue culture techniques. 3- Fruit physical properties. – Bulletin of Fac. of Agric. Univ. of Cairo 47(1): 153-165.
[10] Al-Jasass, F. M., Siddiq, M., Sogi, D. S. (2015): Antioxidants activity and color evaluation of date fruit of selected cultivars commercially available in the United States. – Adv. Chem. Article ID: 567203.
[11] Alkhateeb, A. (2008): Comparison effect of sucrose and date palm syrup on somatic embryogenesis of date palm (*Phoenix dactylifera* L.). – Am. J. Bioche. Biotech. 4(1): 19-23.
[12] AOAC. (2000): Official methods of analysis (17th edition). – Association of official analytical chemists, Arlington, VA, USA.
[13] Attala, A. M., Ibrahim, A. M., El-Kobbia, A. M. (2001): Comparative studies of leaf, pit and fruit physical and chemical characteristics of four Date Palm cultivars, 1- seasonal fluctuation of physical and chemical characteristics of pinnae. – The Fifth Arabian Horticulture Conference, Ismailia, Egypt, March 24-28.
[14] Baliga, M., Baliga, B. R., Kandathil, S. M., Bhat, H. P., Vayalil, P. (2011): A review of the chemistry and pharmacology of the date fruits (*Phoenix dactylifera* L.). – Food Res. Int. 44: 1812-1822.
[15] Bazza, M. (2007): Irrigated date palm production in the Near East. – Workshop on irrigation of date palm and associated crops, in collaboration with Faculty of Agriculture, Damascus University Damascus, Syria, 27-30 May.
[16] Bekheet, S. A. (2013): Date palm biotechnology in Egypt. – App Sci Rep 3: 144-152.
[17] Chao, C. T., Krueger, R. R. (2017): The Date Palm (*Phoenix dactylifera* L.): Overview of biology, uses, and cultivation. – Am. Soc. Hortic. Sci. 42: 1077-1082.
[18] Directorate of Intelligence. (2011): "CIA - World Fact-book". – Information on the history, people, government, economy, geography, communications, transportation, military, and transnational issues for 267 world entities. January 17 2013. https://www.cia. gov/library/publications/the-world-factbook/index. html.
[19] El-Makhtoun, F. M. B., Abd-El-Kader, A. M. M. (1990): Effect of different pollen types on fruit setting, yield and some physical properties of some date palm varieties. – Agricultural Research Journal 68(5): 957-971.
[20] El-Merghany, S., Zaen El-Daen, E. M. A. (2013): Evaluation of some date palm cultivars grown under toshky conditions. – J. Plant Production, Mansoura Univ. 4(8): 1207-1218.
[21] El-Salhy, A. M., Ibrahim, R. A., Gadalla, E. G., Khalil, H. K. H. (2016): Evaluation of some seeded dry date palm grown under Aswan climatic condition. – Assiut J. Agric. Sci. 47(4): 136-155.
[22] El-Sohaimy, S. A., Hafez, E. E. (2010): Biochemical and Nutritional Characterizations of Date Palm Fruits (*Phoenix dactylifera* L.). – Journal of Applied Sciences Research 6(8): 1060-1067.
[23] FAO Statistics. (2018): http://www.fao.org/statistics/en. – Accessed on 23 July 2018.

http://www.aloki.hu ● ISSN 1589 1623 (Print) ● ISSN 1785 0037 (Online)
DOI: http://dx.doi.org/10.15666/aeer/1804_53995409

[24] Gadalla, E. G., Abeer, H. I., Ahmed, E. F. S. (2013): Behavior of some Egyption dry cultivars and Barhee cv. Date palm produced from tissue culture under Shark Al-Oinat condition El –Wadi El –Gadid governorate. – J of Appl. Sci. 32(12).
[25] Habib, S. S., Nawal, M. G., Nour, G. M., Hussein, A. A. (1984): Evaluation of some date palm varieties grown in North Sinai Governorate. – Agric. Res. Review. 62(3A): 277-288.
[26] Hussein, A. A., Nawal, M. G., Nour Habib, S. S. (1984): Evaluation of some date palm varieties grown in South Sinai Governorate. – Agric. Res. Review. 62(3A): 289-303.
[27] Hussein, A. A. M., Attia, N. M. I., Osman, S. M. (2001): Survay and evaluation of fruit cultivars for some species grown under Siwa Oasis. II- Date palm. – Annals of Agric. Sc., Moshtohor 39(2): 1265-1278.
[28] Idris, T. I. M., Hussein, F. A., Said, A. E., Elsadig, E. H. (2014): Evaluation of some dry seedling date selections from the Northern State, Sudan. – Sudanese Journal of Agricultural Sciences 1: 30-35.
[29] Kalia, R. K., Mai, M. K., Kalia, S., Singh, R., Dhawan, A. K. (2011): Microsatellite markers: an overview of the recent progress in plants. – Euphytica 177: 309-334.
[30] Mansour, H. M. (2005): Morphological and Genetic Characterization of Some Common *Phoenix dactylifera* L. Cultivars in Ismailia Region. – M. Sc. Thesis Botany Department, Faculty of Science, Suez Canal University.
[31] Mortazavi, S. M. H., Azizollahi, F., Moalemi, N. (2015): Some quality attributes and biochemical properties of nine Iranian date (*Phoenix dactylifera* L.) cultivars at different stages of fruit development. – International Journal of Horticultural Science and Technology 2(2): 161-171.
[32] Nasir, M. U., Hussain, S., Jabbar, S., Rashid, F., Khalid, N., Mehmood, A. (2015): A review on the nutritional content, functional properties and medicinal potential of dates. – Science Letters 3(1): 17-22.
[33] Qadri, R. W. K., Waheed, S., Haider, M. S., Khan, I., Naqvi, S. A., Bashir, M., Khan, M. M. (2016): Physiochemical characterization of fruits of different date palm (*Phoenix dactylifera* L.) varieties grown in Pakistan. – The Journal of Animal & Plant Sciences 26(5): 1268-1277.
[34] Rizk, R. M., El-Sharabasy, Sh., El-Bana, A. (2004): Morphological Diversity of Date palm (*Phoenix dactylifera* L.) in Egypt. I. Dray date cultivars. – Egyptian Journal of Biotechnology 16: 482-500.
[35] Rizk, R. M., El-Sharabasy, Sh. (2004): Morphological Diversity of Date palm (*Phoenix dactylifera* L.) in Egypt. I.Semi dray date cultivars. – Egyptian Journal of Biotechnology 17: 218-234.
[36] Rizk, S. A., Nahed Rashed, A. K. (2006): Morphological chemical and genetical studies on some date palm cultivars and strains grown under Siwa Oasis conditions. – Egypt. J. of App. Sci. 21(8): 158-176.
[37] Rodríguez-Burruezo, A., Prohens, J., Nuez, F. (2003): Wild relatives can contribute to the improvement of fruit quality in pepino (*Solanum muricatum*). – Euphytica 129: 311-318.
[38] Saeed, I. K., Yousof, D. E. (2014): Nutritional changes in date fruits Barakawi cv infested by date palm dust mite Oligonychus afrasiaticus Meg. measured by physical and chemical parameters. – Persian Gulf Crop Protection 3(1): 46-51.
[39] Saeed, I. K., El-Rauof, F. A., Dawoud, H. D. (2015): Physioco-chemical evaluation of some introduced date palm fruits cultivars grown under Sudanese conditions. – Int J Appl Sci Biotechnol 3(4): 731-736.
[40] Sakr, M. M., Abu Zeid, I. M., Hassan, A. E., Baz, A-G. I. O., Hassan, W. M. (2010): Identification of some Date palm (*Phoenix dactylifera*) cultivars by fruit characters. – Indian Journal of Science and Technology 3(3): 338-343.
[41] Selim, H. H. A., Mahdi, M. A. M., El-Hakeem, M. S. (1970): Studies on the evaluation of fifteen local date cvs grown under desert conditions in Siwa Oasis. U.A.R. – Bull. De L'Inst. Du Desert d'Egypte 38(1): 137-155.

http://www.aloki.hu ● ISSN 1589 1623 (Print) ● ISSN 1785 0037 (Online)
DOI: http://dx.doi.org/10.15666/aeer/1804_53995409

[42] Shattir, A. E., Abu-Goukh, A. A., Karam-Alla, K. M. (2002): Physical and chemical characteristics and yield components of 'Barakawi' and 'Gondeila' dry dates. – Sudan Journal of Scientific Research 8(1): 119-131.
[43] Snedecor, G. W., Cochran, W. G. (1980): Statistical Methods. – Oxford and J. B. H. Publishing Comm., 6th edition.
[44] Sulieman, A. E., Saleh, Z. A., Alssed, A. A. (2007): Use of Some Sudanese Local Varieties of Date Palm in Manufacturing of Date's Honey for Consumption and Exportation. – Proceedings of 4th Sypmosium on Date Palm. Al-Hassa, Saudi Arabia.
[45] Sulieman, A. E., Abd Elhafise, I. A., Abdelrahim, A. M. (2012): Comparative Study on Five Sudanese Date (*Phoenix dactylifera* L.) Fruit Cultivars. – Food and Nutrition Sciences 3(9): 1245-1251. DOI: 10.4236/fns.2012.39164.
[46] Youssef, M. K., El-Rify, M. N., El-Geddawy, M. A., Ramadan, B. R. (1999): Nutrient elements and vitamins content of some new valley dates and certain date products. – The international conference on Date Palm, 9-11 November, Assuit University for Environmental Studies, Egypt.

http://www.aloki.hu ● ISSN 1589 1623 (Print) ● ISSN 1785 0037 (Online)
DOI: http://dx.doi.org/10.15666/aeer/1804_53995409

OPTIMAL LIME APPLICATION RATES FOR AMELIORATING ACIDIC SOILS AND IMPROVING THE YIELD AND QUALITY OF TOBACCO LEAVES

JIANG, C.[1*] – SHEN, J.[1] – CUI, Q.[1] – YAN, Y.[1] – LIU, Y.[2] – ZU, C.[1*]

[1]*Tobacco Research Institute, Anhui Academy of Agricultural Sciences, Hefei 230031, China*

[2]*Anhui provincial tobacco company, Hefei 230071, China*
(phone: +86-551-6514-8970; fax: +86-551-6514-8991)

[*]*Corresponding authors*
e-mail: chaoqjiang@163.com, lcz2468@sina.com

(Received 21st Feb 2020; accepted 2nd Jul 2020)

Abstract. Liming is a common practice for improving plant growth and yield on acidic soils. However, knowledge is still limited on the effect of liming on tobacco growth and leaf quality planted on acidic soil. In this study, effects of lime ($Ca(OH)_2$) (0, 0.75, 1.5 and 3 t ha^{-1}) on soil nutrient status (Ca^{2+} and Mg^{2+} in particular), growth, nutrient accumulation and quality of flue-cured tobacco was investigated in an acidic soil located in Anhui province, China. The results showed that liming significantly increased soil pH both 30 days after transplanting and after the harvest of the tobacco. In comparison with CK (no lime application), liming at a rate of 1.5 t ha^{-1} increased leaf number and leaf dry weight by 15% and 11%, and enhanced the appearance and smoking quality of cured leaves by 7% and 9%, respectively. Moreover, liming significantly increased calcium concentration, while decreased nitrogen and magnesium concentration in the cured leaves. The increase in cured leaf quality was attributed to the improvement of chemical composition, particularly the increase in reducing sugar content. Together, our results suggest that $Ca(OH)_2$ application at a rate of 1.5 t ha^{-1} may alleviate soil acidification and improve yield and quality of flue-cured tobacco in Anhui province, China.
Keywords: *flue-cured tobacco, soil acidity, calcium, cured leaves quality, soil improvement*

Introduction

Soil acidity is a serious limitation to plant growth and crop production in many regions of the world, since about 40-50% of the world's arable soils are acidic (Kochian et al., 2015). Extreme acidity in subsoil (pH <5.0) limits plant growth and development, which is particularly harmful to root growth and function, and therefore inhibits root water and nutrient acquisition (Lynch and Wojciechowski, 2015; Wang et al., 2017). In less acidic soils (pH >5.0), the inhibition of plant growth and yield is more likely due to nutrient deficiencies and toxicities (Karaivazoglou et al., 2007; Hue, 2011). However, these inhibitions for plants may act independently or commonly work together (Karaivazoglou et al., 2007; Kochian et al., 2015). There are various causes for soil acidification, and excess nitrogen (N) fertilizer application has become a major cause in agricultural soils (Guo et al., 2010; Qu et al., 2013; Shaaban et al., 2015). Most of the tobacco (*Nicotiana tabacum* L.) fields have been affected by acidification due to the intensive cropping and excessive N fertilizer inputs in Anhui province, China (Zhang et al., 2014; Jiang et al., 2015a). Therefore, it is imperative to ameliorate acid soils and improve the yield and quality of tobacco leaves in these areas. However, optimal measure for ameliorating acid soils in tobacco growing area is still lacking in Anhui province at present.

http://www.aloki.hu ● ISSN 1589 1623 (Print) ● ISSN 1785 0037 (Online)
DOI: http://dx.doi.org/10.15666/aeer/1804_54115423

Considerable measures have been made to ameliorate acid soils, improve crop yield and quality, such as lime application (Jiang et al., 2015a; Shaaban et al., 2015; Kunhikrishnan et al., 2016), straw retention (Liao et al., 2018), biochar application (Tarin et al., 2019), green manure and biological organic fertilizer application (Deng et al., 2019). Traditionally, surface application of lime materials (including lime, calcite and dolomite) is one of the most common measures to overcome the problems associated with soil acidity (Shaaban et al., 2014; Kunhikrishnan et al., 2016). Previous studies have shown that lime application increases soil pH, improves plant growth and leaf yield of tobacco (Karaivazoglou et al., 2007; Jiang et al., 2015a; Deng et al., 2019). Karaivazoglou et al. (2007) reported that hydrated lime ($Ca(OH)_2$) application at a rate of 3 t ha^{-1} may alleviate soil acidification and increase the yield of flue-cured tobacco in an acid soil (pH 5.3), while lead to a decrease in potassium (K) concentration in cured leaves. Moreover, recently, Deng et al. (2019) found that lime application at a rate of 2.25 t ha^{-1} significantly increased the soil pH from 5.05 to 5.38 but did not significantly enhanced the yield of flue-cured tobacco. Although the application of lime can increase the soil pH and alleviate soil acidification, different studies have found diverse conclusions on the effect of lime on the yield and quality of tobacco leaves. The differences in the effect of liming on tobacco are likely to be due to the different type and rate of lime materials, fertilizer application, tobacco varieties and cultivation environment (Karaivazoglou et al., 2007; Jiang et al., 2015a; Deng et al., 2019). Therefore, the suitable type and rate of lime application on tobacco acid soils is limited and needs to be further explored.

Tobacco is an important industrial crop in China, and plays an important economic role for both the national tax income (Zou et al., 2018). Especially, flue-cured tobacco is a main source of many farmers' income, due to the good quality of tobacco leaves in Anhui province (Dong et al., 2015). Soil acidity has always been the main factor limiting tobacco leaves yield and quality, particularly in Anhui province due to the inherent low soil pH and excessive application of N fertilizer (Jiang et al., 2015a). Previous studies have shown that the soil pH for producing high quality tobacco is range from 5.5 to 6.5 (Shao et al., 2012; Jiang et al., 2015a). At present, liming is a common practice for ameliorating acid soils and improve crop yield, and is widely applied to the tobacco acid soils in southern China (Jiang et al., 2015a; Zou et al., 2018). However, research on the effect of liming on plant growth and leaves quality of flue-cured tobacco in the acidic soil is still limited. Therefore, in this study, a pot experiment was carried out to determine the effect of liming on soil nutrient status (Ca^{2+} and Mg^{2+} in particular), plant growth, nutrient (including micronutrients) accumulation and quality characteristics of tobacco leaves in an acidic soil in Anhui province, China.

Materials and methods

Experiment site and growth conditions

The pot experiment was carried out under greenhouse conditions in Chizhou, a major tobacco-producing area of Anhui province, China. The soil was collected from the tobacco field (0–20 cm), with a pH of 5.35, 18.2 g kg^{-1} organic matter, 152.8 mg kg^{-1} alkali-hydrolyzed N, 17.6 mg kg^{-1} available phosphorus (P) and 168.3 mg kg^{-1} available K. During the experiment, the tobacco plants were kept in a greenhouse with a (29±3)°C/(19±3)°C day/night temperatures, and a 70±10% relative humidity.

http://www.aloki.hu ● ISSN 1589 1623 (Print) ● ISSN 1785 0037 (Online)
DOI: http://dx.doi.org/10.15666/aeer/1804_54115423

Experimental design and Management

Treatments consisted of four levels of lime ($Ca(OH)_2$), namely 0 (CK), 0.75 (Ca1), 1.5 (Ca2) and 3.0 t ha^{-1} $Ca(OH)_2$ (Ca3) in the experiment. In tobacco growing area of Chizhou, the tobacco plants were cultured in 1.2 m spaced rows with 0.5 m distance. Therefore, it should add 0, 6.67, 13.33, 26.67 g $Ca(OH)_2$ per pot cultivating one tobacco plant for the CK, Ca1, Ca2 and Ca3, respectively. The pot was 35 cm in diameter and 28 cm in height, containing 20 kg of air-dried and 2 mm-sieved soil. The $Ca(OH)_2$ (AR) powder and all the fertilizers needed for the flue-cured tobacco were applied as basal and fertilizer and mixed thoroughly with soil in the pot two days before the seedlings transplanting. Fertilizers were use as Jiang et al. (2015b).

Flue-cured tobacco (*Nicotiana tabacum* L., cv. Yunyan 87) seedlings were transplanted to individual pots when they were about 12 cm in height. The pots were placed neatly according to the plant spacing of 120 cm and the row spacing of 50 cm. Each treatment was replicated three times and each replicate included six plants (i.e. 18 plants per treatment). During the period of 60–65 days after transplanting, when approximately 50% of the plants in each plot were at full bloom, they were topped (Karaivazoglou et al., 2007). Tobacco leaves were harvested five times by hand starting 70–80 days after transplanting. Three or five leaves were removed by hand at 7- or 8-day intervals when the leaves were mature and turn yellow from bottom to top, and cured immediately in a flue-curing barn. Photos of the experimental culture were shown in *Figure 1*.

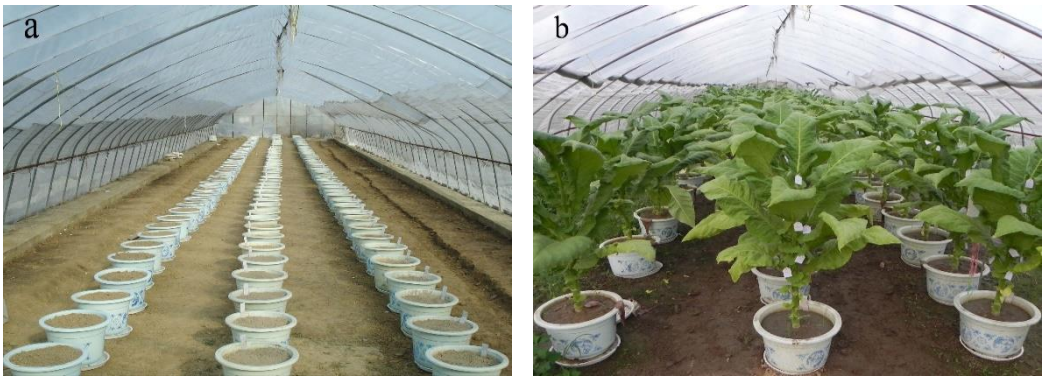

Figure 1. *Photos of the experimental culture before the seedlings transplanting (a) and 90 days after transplanting (b)*

Sample collection and determination

Plant height, leaf number and stem diameter were measured after topping of the tobacco plant. The plants were divided into leaves, stems and roots, and dry weights were measured after being dried to constant weight at 65 °C.

The cured leaves (from nodes 8 to 12) were used to determine appearance quality, smoking quality and the concentrations of elements. Both the appearance quality and the smoking quality of the leaves were graded using a scale from 1 to 10 (quality index) (Karaivazoglou et al., 2007). The appearance quality included maturity, structure, status, oil, color and chroma of the cured leaf. The smoking quality included aroma quality and quantity, fineness, roundness, hygroscopicity and uniformity of the cured leaf. For elements analysis, the leaves samples were dried to constant weight at 65 °C,

http://www.aloki.hu ● ISSN 1589 1623 (Print) ● ISSN 1785 0037 (Online)
DOI: http://dx.doi.org/10.15666/aeer/1804_54115423

and milled into powder. The N concentration was analyzed according to the method of Karaivazoglou et al. (2007). The K, calcium (Ca) and magnesium (Mg) concentration were determined according to the method of Shao et al. (2012) and Tang et al. (2013).

Before the experiment, soils were collected to determine the basic fertility. At 30 days after transplanting, soils of each treatment were sampled for determining the soil pH. After harvest, soil samples were collected from each treatment for pH, exchangeable Ca and exchangeable Mg analysis. Soil pH, organic matter, alkali-hydrolyzed N, available P, available K, exchangeable Ca and exchangeable Mg were determined according to the method of Shao et al. (2012) and Tang et al. (2013).

Statistical analysis

Statistical analyses were performed using one-way ANOVA with SPSS 19.0 (SPSS Inc., Chicago, IL, USA). The treatments were compared by the method of least significance difference at $P < 0.05$.

Results

Effect of liming on plant height, leaf number, and dry weight of tobacco plant

As showed in *Table 1*, Ca application had a significant effect on plant height, leaf number, and dry weight of the tobacco plant. The plant height and leaf number of Ca2 were significantly increased by 9% and 15% compared with the CK, respectively, but no significant difference was found between the Ca2 and Ca3 treatments. However, the stem diameter of tobacco plant was not significantly affected by Ca application at the rate of 0.75 to 3.0 t ha^{-1} $Ca(OH)_2$. The leaf and total dry weight of the tobacco plant was highest in Ca2 treatment, which was 11% and 17% higher than that of the CK, respectively. Similarly, Ca2 treatment achieved the highest root and leaf dry weight among all treatments. The root/shoot ratio of Ca2 treatment was significantly higher than that of the CK, Ca1 and Ca3 treatments.

Table 1. *Effects of $Ca(OH)_2$ application on plant height, leaf number, stem diameter and dry weight of tobacco plant*

Treatments	Plant height (cm)	Number of leaves per plant	Stem diameter (cm)	Dry weight (g plant^{-1})			Root/shoot
				Root	Leaves	Total	
CK	88.0 b	20.3 b	83.0 a	22.1 b	72.0 b	117.4 b	0.23 b
Ca1	90.3 b	21.0 b	84.7 a	22.8 b	73.9 b	121.0 b	0.23 b
Ca2	95.7 a	23.3 a	88.7 a	29.3 a	79.6 a	136.9 a	0.27 a
Ca3	92.0 ab	21.7 ab	86.7 a	25.0 b	75.6 ab	126.7 ab	0.25 b

Means within a column that have different letters are significantly different from each other at $P < 0.05$. The CK, Ca1, Ca2 and Ca3 are respectively 0, 0.75, 1.5 and 3.0 t ha^{-1} $Ca(OH)_2$

Effect of liming on concentrations of elements in tobacco leaf

As showed in *Table 2*, lime application significantly decreased the N concentration in tobacco leaves. However, liming did not significantly affect the K concentration in tobacco leaves. The Ca concentration in leaves of Ca1, Ca2 and Ca3 was significantly increased by 43%, 59% and 109% than that of the control without Ca, respectively. The

http://www.aloki.hu ● ISSN 1589 1623 (Print) ● ISSN 1785 0037 (Online)
DOI: http://dx.doi.org/10.15666/aeer/1804_54115423

Ca concentration in leaves was significantly increased with an increased Ca application rate. However, the Mg concentration in leaves declined with an increase of the Ca application rate, and the Ca2 and Ca3 treatments resulted in 23% and 30% decrease of Mg concentration in leaves compared with the CK, respectively. Similarly, Ca application also decreased the P concentration in leaves. Under the Ca3 treatment, the P concentration in leaves was reduced by 15% than that of the CK.

Table 2. *Effect of $Ca(OH)_2$ application on concentrations (g kg^{-1} DW) of N, P, K, Ca and Mg in leaves of tobacco plant*

Treatments	N	P	K	Ca	Mg
CK	30.9 a	5.29 a	19.8 a	30.2 c	4.18 a
Ca1	27.0 b	4.75 ab	21.4 a	43.3 b	4.05 a
Ca2	27.3 b	4.91 ab	21.2 a	47.9 b	3.23 b
Ca3	28.1 b	4.48 b	20.3 a	63.2 a	2.92 b

Means within a column that have different letters are significantly different from each other at $P < 0.05$. The CK, Ca1, Ca2 and Ca3 are respectively 0, 0.75, 1.5 and 3.0 t ha^{-1} $Ca(OH)_2$

The effect of Ca application on concentrations of microelements in tobacco leaf was showed in *Table 3*. The application of Ca resulted in a reduction of iron (Fe), manganese (Mn), copper (Cu) and zinc (Zn) in tobacco leaf. Compared with the CK, the Ca3 treatment significantly decreased Fe, Mn, Cu and Zn in tobacco leaf by 52%, 71%, 45% and 51%, respectively; and the Ca2 treatment significantly decreased Fe, Mn and Zn in tobacco leaf by 34%, 37% and 29%, respectively. In contrast, Ca application significantly increased the chloride (Cl) concentration in tobacco leaf compared with the CK, and the Cl concentration in leaves was increased with the increase of Ca application rate.

Table 3. *Effect of $Ca(OH)_2$ application on concentration of micronutrients in leaves of tobacco plant*

Treatments	Fe (mg kg^{-1})	Mn (mg kg^{-1})	Cu (mg kg^{-1})	Zn (mg kg^{-1})	Cl (g kg^{-1})
CK	530.7 a	749.1 a	12.10 a	109.6 a	3.32 c
Ca1	447.0 ab	659.7 a	10.84 a	98.2 ab	4.25 b
Ca2	350.5 bc	473.3 b	9.70 ab	77.9 bc	4.67 ab
Ca3	258.5 c	215.1 c	6.60 b	53.7 c	4.91 a

Means within a column that have different letters are significantly different from each other at $P < 0.05$. The CK, Ca1, Ca2 and Ca3 are respectively 0, 0.75, 1.5 and 3.0 t ha^{-1} $Ca(OH)_2$

Effect of liming on appearance and smoking quality of cured leaf

The application of Ca had a significant effect on the appearance and smoking quality of cured leaves (*Fig. 2*). Both the appearance and smoking quality of cured leaves were highest in Ca2, and increased by 7% and 9% compared with the control, respectively. However, there was no significant difference was observed between treatments Ca1 and Ca2 in the appearance and smoking quality of cured leaves. Moreover, Ca3 treatment

http://www.aloki.hu ● ISSN 1589 1623 (Print) ● ISSN 1785 0037 (Online)
DOI: http://dx.doi.org/10.15666/aeer/1804_54115423

did not significantly affect the smoking quality of cured leaves or even showed a declining trend in appearance quality compared with the control.

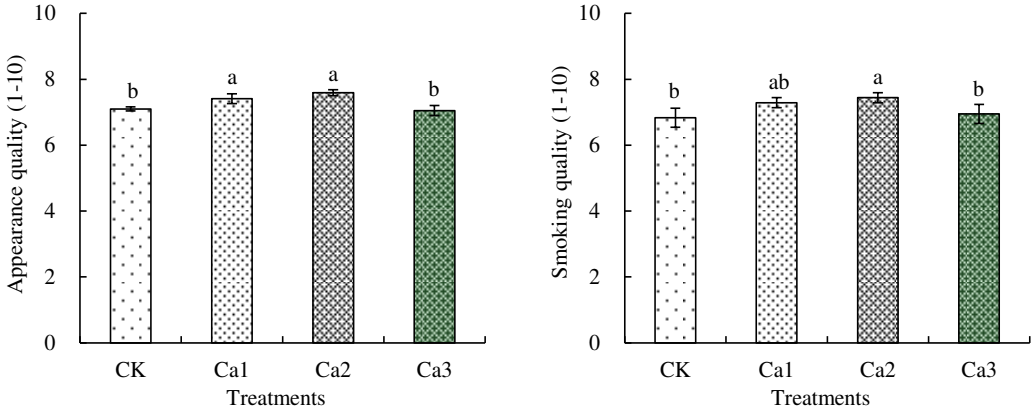

Figure 2. *Effect of $Ca(OH)_2$ application on appearance and smoking quality of tobacco leaves. The CK, Ca1, Ca2 and Ca3 are respectively 0, 0.75, 1.5 and 3.0 t ha^{-1} $Ca(OH)_2$. The error bars indicate standard error. Columns with different letters indicate significant difference among different treatments ($P < 0.05$)*

Effect of liming on soil pH and calcium and magnesium content

As showed in *Figure 3*, Ca application significantly increased the soil pH 30 days after transplanting and after harvest. Compared with the CK, the soil pH was significantly increased by 0.30, 0.61 and 0.81 units in Ca1, Ca2 and Ca3 treatments 30 days after transplanting, respectively; and by 0.24, 0.36 and 0.73 units, respectively. After harvest, the highest soil pH was found in Ca3 treatment (6.02), which was significantly higher than the other treatments; however, there was no significant difference in soil pH between the CK and Ca1 treatments.

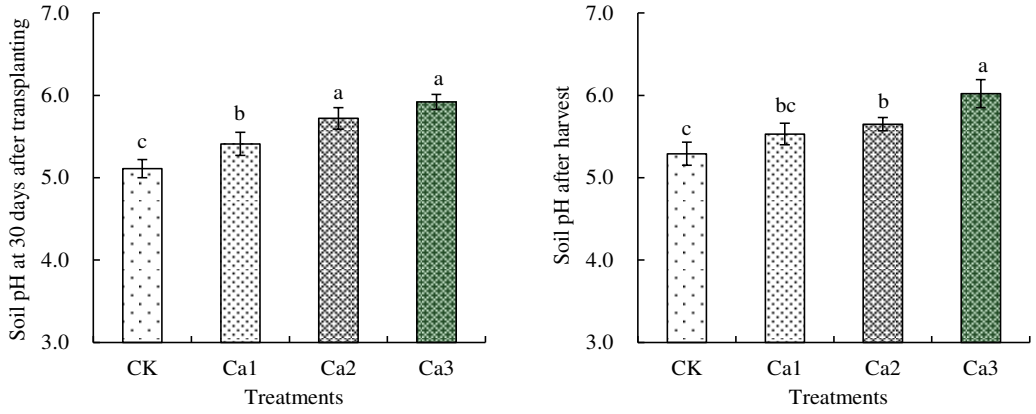

Figure 3. *Effect of $Ca(OH)_2$ application on soil pH. The CK, Ca1, Ca2 and Ca3 are respectively 0, 0.75, 1.5 and 3.0 t ha^{-1} $Ca(OH)_2$. The error bars indicate standard error. Columns with different letters indicate significant difference among different treatments ($P < 0.05$)*

http://www.aloki.hu ● ISSN 1589 1623 (Print) ● ISSN 1785 0037 (Online)
DOI: http://dx.doi.org/10.15666/aeer/1804_54115423

Furthermore, the effect of liming on soil exchangeable Ca^{2+} and Mg^{2+} was investigated. The exchangeable Ca content of soil was increased with an increased Ca application rate (*Fig. 4* and *Fig. 5*). Compared with the CK treatment, Ca2 and Ca3 significantly increased the exchangeable Ca content of soil by 16%, 100% and 147%, respectively. In contrast, the exchangeable Mg content of soil was decreased with the increase of Ca application rate. The Ca2 and Ca3 treatments resulted in 24% and 29% decrease in exchangeable Mg content of soil compared with the CK, respectively. However, there was no significant difference in both the exchangeable Ca and Mg content of soil between the CK and Ca1 treatment.

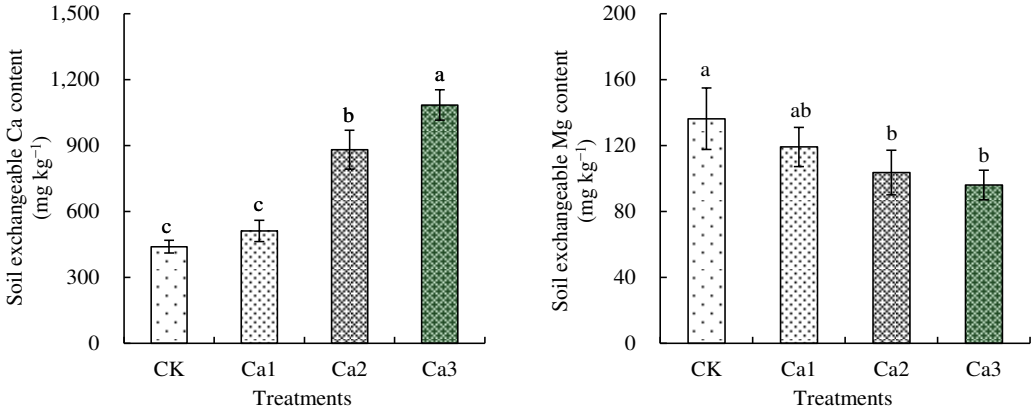

Figure 4. *Effect of $Ca(OH)_2$ application on exchangeable Ca and Mg content of soil. The CK, Ca1, Ca2 and Ca3 are respectively 0, 0.75, 1.5 and 3.0 t ha^{-1} $Ca(OH)_2$. The error bars indicate standard error. Columns with different letters indicate significant difference among different treatments ($P < 0.05$)*

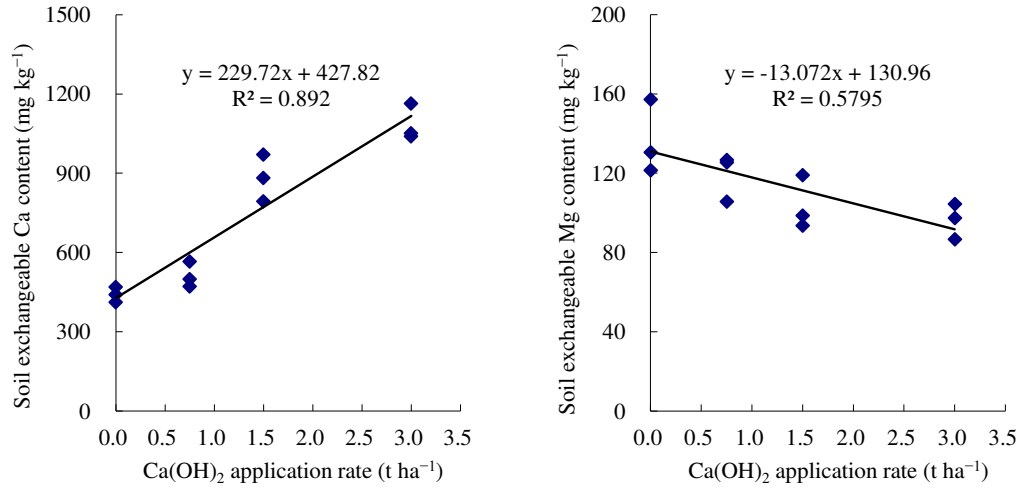

Figure 5. *Relationship between $Ca(OH)_2$ application rate and soil exchangeable cations (Ca and Mg) content. Data were the means of three replicates*

http://www.aloki.hu ● ISSN 1589 1623 (Print) ● ISSN 1785 0037 (Online)
DOI: http://dx.doi.org/10.15666/aeer/1804_54115423

Discussion

Liming is a common practice to alleviate soil acidification and improve crop yield in acidic soils (Crusciol et al., 2016; Holland et al., 2018; Liao et al., 2018). In this study, lime ($Ca(OH)_2$) application significantly enhanced leaves plant dry weight of flue-cured tobacco on an acidic soil, which is consistent with previous studies in Virginia tobacco (Karaivazoglou et al., 2007), rice (Jiang et al., 2018), and sugarcane (Pang et al., 2019). The improvement plant growth and dry weight in flue-cured tobacco were associated with the increase in plant height and higher leaf number per plant (*Table 1*), in agreement with the findings of Karaivazoglou et al. (2007) in flue-cured tobacco. Crop yield was increased by liming in acidic soils was mainly due to increase soil pH and improving the availability of soil nutrients (López-Lefebre et al., 2001; Zeng et al., 2017; Liu et al., 2018). In this study, soil pH was significantly increased by 0.36 units in the treatment received 1.5 t ha^{-1} in comparison to without liming (pH 5.29) (*Fig. 3*), and the plant total dry weight was increased by 17% (*Table 1*). Although numerous studies have shown that liming significantly increased crop yield on acidic soils, continuous or excessive application of lime also lead to a significant decrease in crop yield (Zhang and Zheng, 1987; Zeng et al., 2017). The present results showed that the application of lime at a relatively high rate (3.0 t ha^{-1}) did not significantly affect the plant total dry weight, plant height and leaf number per plant (*Table 1*), in contrast to previous studies (Karaivazoglou et al., 2007). The optimal rate of lime to improve acidic soil and enhance crop yield was quite various in different studies may be due to rainfall and soil water content as these factors affect the rate and extent of lime dissolution and subsequent plant response (Liu et al., 2004; Hu et al., 2016; Zhang et al., 2019). We recognize that more field trials are needed to provide more evidences that liming can improve the growth and yield of flue-cured tobacco. The present study provides clear evidence that the optimal rate of liming was 1.5 t ha^{-1} for flue-cured tobacco growth and development in an acidic soil with a pH below 5.5.

Furthermore, appropriate rate (1.5 t ha^{-1}) of lime application on acidic soil significantly improved the appearance and smoking quality of tobacco leaves (*Fig. 2*). The results are in agreement with Karaivazoglou et al. (2007), reported that liming significantly increased the quality index of cured leaves of Virginia tobacco. Also, many studies have shown that lime application increased the quality of tobacco cured leaves (Tang and Xiong, 2003; Zhu et al., 2016a,b; Deng et al., 2019). In relevant research, Zhu et al. (2016b) reported that tobacco plant growth and leaf quality were significantly improved at the lime application rate of 1.5 t ha^{-1} for alleviating acidity of yellow soil (pH 5.0). Moreover, the physical and chemical properties and the smoking quality of tobacco leaves were increased by lime application rate of 2.25 t ha^{-1} for the sustainable remediation of acid soil (Deng et al., 2019). One possible explanation for the improvement in smoking quality of tobacco leaves would be that liming of acid soils improved chemical composition availabilities of the cured leaves, particularly enhanced reducing sugar content in cured leaves (Zhu et al., 2016a; Deng et al., 2019). We also found that the reducing sugar content of cured leaves was increased at the lime application rate of 0.75 and 1.5 t ha^{-1} (data not shown). However, there are still unclear how the lime application affected the sugar accumulation in tobacco leaves. Therefore, more attention should be paid on the relationship of Ca concentration and sugar content in tobacco cured leaves.

As expected, leaf Ca concentration increased significantly with increasing $Ca(OH)_2$ application rates in the soil. These results are in agreement with those reported by

http://www.aloki.hu ● ISSN 1589 1623 (Print) ● ISSN 1785 0037 (Online)
DOI: http://dx.doi.org/10.15666/aeer/1804_54115423

Karaivazoglou et al. (2007), who reported that leaf Ca concentration was significantly increased by 10%, as $Ca(OH)_2$ application increased from 0 to 3 t ha^{-1}. López-Lefebre et al. (2001) also found that the Ca concentration in the leaves accumulated progressively with increasing $CaCl_2$ application in the culture medium. The increase in leaf Ca was mainly due to the increase in soil exchangeable Ca in the $Ca(OH)_2$ application treatments, because the Ca uptake in tobacco leaf was significant positive correlation with the content of soil available Ca (Zou and Xiong, 2010; Liu et al., 2017). However, excessive Ca concentration may result in a decline in the sensory quality of tobacco cured leaves (Duan et al., 2010; Dai et al., 2017). We found that the smoking quality of cured leaf of the Ca3 was significantly lower than that of the Ca1 and Ca2 (*Fig. 2*), which may probably due to the Ca3 greatly increased the Ca concentration of tobacco leaves (*Table 2*). Many studies have shown that Ca concentration of high quality tobacco leaves should be less than 35 g kg^{-1} (Hu et al., 1997; Duan et al., 2010). Therefore, a suitable concentration of Ca in tobacco leaves must be considered for determining the optimal lime dosage for improving acidic soil.

In contrast, increasing the $Ca(OH)_2$ application rates diminished the leaf Mg concentration, the lowest concentration of Mg being found in Ca3 treatment, with a 30% decrease in comparison with the CK (*Table 2*). In agreement with our findings, López-Lefebre et al. (2001) reported that increasing CaCl application in the culture medium caused a gradual decline in Mg concentration in the roots and leaves. Duan et al. (2010) indicated that Mg concentration in leaf was increased by decreasing the soil Ca^{2+}/Mg^{2+}, i.e. an increase in soil exchangeable Ca will lead to the decrease of Mg concentration in tobacco leaves. In this study, the soil Ca^{2+}/Mg^{2+} was significantly increased from on average 3.2 to 11.3 (*Fig. 4*), and the Mg concentration in leaf was decreased from 4.18 to 2.92 g kg^{-1} (*Table 2*) by applying 3.0 t ha^{-1} $Ca(OH)_2$ in acid soil. However, Karaivazoglou et al. (2007) found that Mg concentration of cured leaves was not significantly affected by $Ca(OH)_2$ application in acid soil. It was reported that the Mg concentration of superior tobacco leaves usually ranged from 4 to 15 g kg^{-1}, and low Mg concentration would reduce the quality of cured leaves (Xu et al., 2007; Duan et al., 2010). Therefore, the application of lime should increase the soil pH in acidic soil without reducing the Mg concentration to ensure the quality of tobacco leaves.

In addition, many studies have shown that K concentration is one of the most important indexes to evaluate the quality of tobacco leaves, and the K concentration of good quality tobacco leaves should be up to 25 g kg^{-1} (Wei et al., 2011; Li et al., 2015; Yan et al., 2018). Karaivazoglou et al. (2007) reported that leaf K concentration was significantly decreased by 10% and 12% under the application of 1.5 and 3.0 t ha^{-1} $Ca(OH)_2$ in flue-cured tobacco. In contrast, both Li et al. (2005) and Wei et al. (2011) found that calcium application improved the K uptake and increased the K concentration in flue-cured tobacco leaves. In this study, the leaf K concentration was numerically higher in the lime application treatments than in the control, but was not statistically significant (*Table 2*). The K concentration in tobacco leaves increased by lime application was probably due to Ca can have a direct, positive effect on K uptake, promoting the accumulation of K by the tobacco plant (Qiang et al., 2001; Wei et al., 2011). However, the positive effect of lime on K accumulation in tobacco leaves was not clearly reflected in the present study. Thus, further experiments, especially long-term field trials are needed to confirm whether and how the effect of liming on K accumulation in tobacco leaves.

http://www.aloki.hu ● ISSN 1589 1623 (Print) ● ISSN 1785 0037 (Online)
DOI: http://dx.doi.org/10.15666/aeer/1804_54115423

Conclusion

The experiment explored the effect of liming on soil nutrient status, plant growth, nutrients accumulation and quality characteristics of flue-cured tobacco in an acid soil. The results confirmed that positive response of liming on ameliorating acidic soils, improving plant growth and yield. We found that liming enhances the growth and yield of flue-cured tobacco in an acid soil, and the appearance and smoking quality of cured leaves was improved with lime application at a rate of 1.5 t $Ca(OH)_2$ ha^{-1}. Furthermore, the soil pH was significantly increased from 5.29 to 5.65 in the treatment received 1.5 t $Ca(OH)_2$ ha^{-1}. Although long-term field experiments are needed to investigate the influence of liming on K concentraion and quality in tobacco cured leaves, our results suggest that application of $Ca(OH)_2$ at a rate of 1.5 t ha^{-1} may alleviate soil acidity, improve yield and quality of flue-cured tobacco, especially in soil with a pH below 5.5.

Acknowledgements. This study was funded by the Discipline Team Project of Anhui Academy of Agricultural Sciences (No. 2019YL039 and No. 2020YL059), the Science and Technology Project of Anhui Province Tobacco Company (No. 20170551022 and No. 20180551009).

REFERENCES

[1] Crusciol, C. A., Artigiani, A. C., Arf, O., Carmeis Filho, A. C., Soratto, R. P., Nascente, A. S., Alvarez, R. C. (2016): Soil fertility, plant nutrition, and grain yield of upland rice affected by surface application of lime, silicate, and phosphogypsum in a tropical no-till system. – Catena 137: 87-99.

[2] Dai, H., Zhang, S., Wang, A., Zhou, H., Liang, T., Song, J., Zhang, Y., Yin, Q. (2017): Contents of some mineral nutrient elements in flue-cured tobacco and their relationship with sensory quality. – Tobacco Science & Technology 50(4): 1-9.

[3] Deng, X., Huang, J., Yang, L., Chen, J., Li, Y., Tian, M., Zhou, M., Tian, F., Zhang, M. (2019): The synergistic effect of lime, green manure and bio-organic fertilizer on restoration of acid field and improvement of tobacco production efficiency. – Journal of Plant Nutrition and Fertilizers 25(9): 1577-1587.

[4] Dong, J., Wang, X., Zhang, L. (2015): Development and management of Anhui tobacco with high quality and good characteristics. – Chinese Tobacco Science 36(4): 106-109.

[5] Duan, Z., Zheng, B., Lu, Y., Hu, W., Liu, D., Yin, S. (2010): Effects of Ca^{2+}/Mg^{2+} regulation on Mg, K and Ca uptake in the different parts of flue-cured tobacco leaf. – Soil and Fertilizer Sciences in China 5: 61-65.

[6] Guo, J., Liu, X., Zhang, Y., Shen, J., Han, W., Zhang, W., Christie, P., Goulding, K., Vitousek, P., Zhang, F. (2010): Significant acidification in major Chinese croplands. – Science 327: 1008-1010.

[7] Holland, J. E., Bennett, A. E., Newton, A. C., White, P. J., McKenzie, B. M., George, T. S., Pakeman, R. J., Bailey, J. S., Fornara, D. A., Hayes, R. C. (2018): Liming impacts on soils, crops and biodiversity in the UK: A review. – Science of the Total Environment 610: 316-332.

[8] Hu, G., Zhao, Y., Cao, Z., Zhao, X., Zhao, Z., Chen, J., Zhang, X., Zhou, X., Li, Z. (1997): The evaluation of the chemical elements and some organic components in flue-cured leaf tobacco from the main tobacco production provinces of China. – Acta Tabacaria Sinica 3(1): 36-44.

[9] Hu, M., Xiang, Y., Lu, J. (2016): Effects of lime application rates on soil acidity and barley seeding growth in acidic soils. – Scientia Agricultura Sinica 49(20): 3896-3903.

[10] Hue, N. V. (2011): Alleviating soil acidity with crop residues. – Soil Science 176: 543-549.

http://www.aloki.hu ● ISSN 1589 1623 (Print) ● ISSN 1785 0037 (Online)
DOI: http://dx.doi.org/10.15666/aeer/1804_54115423

[11] Jiang, C., Dong, J., Xu, J., Shen, J., Xue, B., Zu, C. (2015a): Effects of soil amendment on soil pH, plant growth and heavy metal accumulation of flue-cured tobacco in acid soil. – Soils 47(1): 171-176.
[12] Jiang, C., Zu, C., Shen, J., Shao, F., Li, T. (2015b): Effects of selenium on the growth and photosynthetic characteristics of flue-cured tobacco (*Nicotiana tabacum* L.). – Acta Societatis Botanicorum Poloniae 84(1): 71-77.
[13] Jiang, Y., Liao, P., van Gestel, N., Sun, Y., Zeng, Y., Huang, S., Zhang, W., van Groenigen, K. J. (2018): Lime application lowers the global warming potential of a double rice cropping system. – Geoderma 325: 1-8.
[14] Karaivazoglou, N. A., Tsotsolis, N. C., Tsadilas, C. D. (2007): Influence of liming and form of nitrogen fertilizer on nutrient uptake, growth, yield, and quality of Virginia (flue-cured) tobacco. – Field Crops Research 100: 52-60.
[15] Kochian, L. V., Pineros, M., Liu, J., Magalhaes, J. (2015): Plant adaptation to acid soils: the molecular basis for crop aluminum resistance. – Annual Reviews of Plant Biology 66: 571-598.
[16] Kunhikrishnan, A., Thangarajan, R., Bolan, N. S., Xu, Y., Mandal, S., Gleeson, D. B., Seshadri, B., Zaman, M., Barton, L., Tang, C., Luo, J., Dalal, R., Ding, W., Kirkham, M. B., Naidu, R. (2016): Functional relationships of soil acidification, liming, and greenhouse gas flux. – Advances in Agronomy 139: 1-71.
[17] Li, J., Zhang, M., Lin, Q., Chen, Z., Xie, G., Peng, J., Xiong, D. (2005): Effects of interaction of potassium, calcium and magnesium on flue-cured tobacco growth and nutrient absorption. – Journal of Anhui Agricultural University 32(4): 529-533.
[18] Li, J., Zhang, X., Li, T., Zheng, Z., Wang, Y. (2015): Effect of potash management on potassium absorption and utilization of flue-cured tobacco. – Journal of Plant Nutrition and Fertilizers 21(4): 969-978.
[19] Liao, P., Huang, S., van Gestel, N. C., Zeng, Y. J., Wu, Z. M., van Groenigen, K. J. (2018): Liming and straw retention interact to increase nitrogen uptake and grain yield in a double rice-cropping system. – Field Crops Research 216: 217-224.
[20] Liu, D., Helyar, K. R., Conyers, M. K., Fisher, R., Poile, G. J. (2004): Response of wheat, triticale and barley to lime application in semi-arid soils. – Field Crops Research 90: 287-301.
[21] Liu, K., Zhou, J., Li, Q., Wang, M., Li, H., Zhou, W., Wang, R. (2017): Tobacco planting soil of calcium and magnesium content exchange and influence on calcium and magnesium content in tobacco leaves. – Southwest China Journal of Agricultural Sciences 30(9): 2065-2070.
[22] Liu, X., Rezaei Rashti, M., Esfandbod, M., Powell, B., Chen, C. (2018): Liming improves soil microbial growth, but trash blanket placement increases labile carbon and nitrogen availability in a sugarcane soil of subtropical Australia. – Soil Research 56: 235-243.
[23] López-Lefebre, L. R., Rivero, R. M., García, P. C., Sánchez, E., Ruiz, J. M., Romero, L. (2001): Effect of calcium on mineral nutrient uptake and growth of tobacco. – Journal of the Science of Food and Agriculture 81: 1334-1338.
[24] Lynch, J. P., Wojciechowski, T. (2015): Opportunities and challenges in the subsoil: pathways to deeper rooted crops. – Journal of Experimental Botany 66(8): 2199-2210.
[25] Pang, Z., Tayyab, M., Kong, C. B., Hu, C., Zhu, Z., Wei, X., Yuan, Z. (2019): Liming positively modulates microbial community composition and function of sugarcane fields. – Agronomy 9(10): 808.
[26] Qiang, J., Wan, H., Li, F., Wu, S., Xu, S. (2001): Effect of various levels of calium fertilizer on Ca and K absorption by flue-cured tobacco. – Journal of Yunnan Agricultural University 2: 120-123.
[27] Qu, Z., Wang, J., Almøy, T., Bakken, L. R. (2013): Excessive use of nitrogen in Chinese agriculture results in high $N_2O/(N_2O+ N_2)$ product ratio of denitrification, primarily due to acidification of the soils. – Global Change Biology 20: 1685-1698.

http://www.aloki.hu ● ISSN 1589 1623 (Print) ● ISSN 1785 0037 (Online)
DOI: http://dx.doi.org/10.15666/aeer/1804_54115423

[28] Shaaban, M., Peng, Q., Lin, S., Wu, Y., Zhao, J., Hu, R. (2014): Nitrous oxide emission from two acidic soils as affected by dolomite application. – Soil Research 52: 841-848.
[29] Shaaban, M., Peng, Q., Hu, R., Wu, Y., Lin, S., Zhao, J. (2015): Dolomite application to acidic soils: a promising option for mitigating N_2O emissions. – Environmental Science and Pollution Research 22: 19961-19970.
[30] Shao, F., Jiang, C., Zu, C., Xue, B., Xu, J., Shen, J. (2012): Influence of sulfur and stillage fertilizer on the growth, quality of flue-cured tobacco, and pH in alkaline soil. – Acta Botanica Boreali-Occidentalia Sinica 32(12): 2479-2485.
[31] Tang, L., Xiong, D. (2003): Effects of applying lime on the properties of acid soil and the leaves quality in flue-cured tobacco. – Chinese Journal of Eco-Agriculture 11(3): 81-83.
[32] Tang, X., Su, J., He, K., Han, Y., Li, Z., Xie, B., Yang, Q. (2013): Exchangeable Ca and Mg contents in various purple soils and their effects on Ca and Mg contents in flue-cured tobacco. – Chinese Tobacco Science 34(4): 1-4.
[33] Tarin, M. W. K., Fan, L. L., Shen, L., Lai, J. L., Tayyab, M., Sarfraz, R., Chen, L. Y., Ye, J., He, T. Y., Rong, J. D., Chen, L. G., Zheng, Y. S. (2019): Effects of different biochars ammendments on physiochemical properties of soil and root morphological attributes of Fokenia hodginsii (Fujian Cypress). – Applied Ecology and Environmental Research 17(5): 11107-11120.
[34] Wang, H., Li, Y., Hou, J., Huang, J., Liang, W. (2017): Nitrate reductase-mediated nitric oxide production alleviates Al-induced inhibition of root elongation by regulating the ascorbate-glutathione cycle in soybean roots. – Plant and Soil 410: 453-465.
[35] Wei, Z., Shen, F., Wang, L., Fan, D., Yin, Y., Yi, F., Gu, M. (2011): Effects of calcium and magnesium application on uptake, circulation and content of potassium in flue-cured tobacco. – Chinese Tobacco Science 32(40): 66-70.
[36] Xu, Z., Li, Y., Xiao, H., Li, H., Liu, C. (2007): The contents of exchangeable calcium and magnesium in Hunan tobacco-growing soils and their effects on tobacco quality. – Acta Ecologica Sinica 27(11): 4425-4433.
[37] Yan, T., Wang, Y., Lu, D., Liu, X., Zhang, H., Wang, H., Yang, G. (2018): Effects of root-zone potassium fertilizer on the yield， potassium concentration and potassium uptake of flue-cured tobacco. – Soil and Fertilizer Sciences in China 5: 70-76.
[38] Zeng, T., Cai, Z., Wang, X., Liang, W., Zhou, S., Xu, M. (2017): Integrated analysis of liming for increasing crop yield in acidic soils. – Scientia Agricultura Sinica 50(13): 2519-2527.
[39] Zhang, X., Zheng, G. (1987): Effects of continuous liming on crop growth and their absorption of nutrients. – Acta Pedologica Sinica 24(4): 343-350.
[40] Zhang, G., Zhu, Q., Guo, X., Xiang, Z., Wang, S., Shen, S., Ji, X. (2014): Amelioration of dolomite on acidity of flue-cured tobacco soil in south Anhui. – Soils 46(3): 534-538.
[41] Zhang, L., Li, Y., Deng, X., Tian, M., Zheng, M., Zhou, Z., Peng, S., Chen, Z. (2019): Dynamic change of soil pH and physicochemical properties after application of lime, green manure and biological organic fertilizer. – Acta Tabacaria Sinica 25(3): 60-66.
[42] Zhu, J., Zhang, Y., Liu, Q., Jiang, W., Feng, Y., Liang, Y., Huo, Q., Xia, H., Li, Z. (2016a): Effects of application of lime and potassium humate on flue-cured tobacco yield and quality on newly recovered lands. – Southwest China Journal of Agricultural Sciences 29(2): 346-351.
[43] Zhu, J., Li, Z., Liu, Q., Liang, Y., Huang, C., Huo, Q., Peng, Y., Xia, H., Zhang, Y. (2016b): Influence of lime dosage on soil acidity of acidified yellow soil in renovated flue-cured tobacco field and application effects. – Soil and Fertilizer Sciences in China 3: 43-48.
[44] Zou, W., Xiong, D. (2010): Effects of soil available calcium on some physiological metabolism of flue-cured tobacco. – Journal of Anhui Agricultural University 37(2): 369-373.

http://www.aloki.hu ● ISSN 1589 1623 (Print) ● ISSN 1785 0037 (Online)
DOI: http://dx.doi.org/10.15666/aeer/1804_54115423

[45] Zou, C., Li, Y., Huang, W., Zhao, G., Pu, G., Su, J., Coyne, M. S., Chen, Y., Wang, L., Hu, X., Jin, Y. (2018): Rotation and manure amendment increase soil macro-aggregates and associated carbon and nitrogen stocks in flue-cured tobacco production. – Geoderma 325: 49-58.

http://www.aloki.hu ● ISSN 1589 1623 (Print) ● ISSN 1785 0037 (Online)
DOI: http://dx.doi.org/10.15666/aeer/1804_54115423

SEED SOAKING WITH SODIUM SILICATE PRIMES SALT TOLERANCE IN RICE (*ORYZA SATIVA* L.) SEEDLINGS WITHOUT ANY NEGATIVE EFFECT ON GROWTH

XU, C. C.[1,2#] – ZHANG, Q. R.[3#] – HU, L.[4] – WANG, R. M.[1] – SHI, Q.[2] – CHEN, J.[1] – SONG, Y. Y.[1] – CHEN, D. M.[1] – ZENG, R. S.[1*]– SUN, Z. X.[1*]

[1]*Key Laboratory of Ministry of Education for Genetics, Breeding and Multiple Utilization of Crops, College of Agriculture, Fujian Agriculture and Forestry University Fuzhou 350002, China*

[2]*College of Life Sciences, Fujian Agriculture and Forestry University, Fuzhou 350002, China*

[3]*Crop Research Institute, Fujian Academy of Agricultural Sciences, Fuzhou 350013, China*

[4]*Key Laboratory of Beibu Gulf Environment Change and Resources Utilization of Ministry of Education, Nanning Normal University, Nanning 530001, China*

[#]*These authors equally contributed to the study.*

[*]*Corresponding authors*
e-mail: szx@fafu.edu.cn (Sun, Z. X.), rszeng@fafu.edu.cn (Zeng, R. S.)
phone: +86-184-5263-6956; fax:+86-591-8378-9483)

(Received 27th Feb 2020; accepted 2nd Jul 2020)

Abstract. Rice is one of the most important cereal crops and is susceptible to salinity stress. To enhance biotic and abiotic stress tolerance in crops, the application of silicon (Si) during seedling culture and seed priming are two effective approaches. However, whether seed priming with silicon can enhance salinity stress tolerance in rice seedlings, and what the optimal concentration of Si treatment is largely unclear. In this study, rice seeds were pretreated with sodium silicate, and the hydroponically grown rice seedlings were exposed to sodium chloride. Our results show that seed soaking with Si can significantly improve the growth of rice seedlings under salinity-stress, as evidenced by enhanced fresh weight, dry weight, leaf relative water content, photosynthetic pigment level, soluble protein content, as well as the activities of POD and SOD enzymes. Moreover, Si-pretreated seeds showed accelerated seed germination, increased seedling height and reduced root length. Furthermore, qRT-PCR analysis showed that seed soaking with Si induced the transcription of genes encoding Na^+/H^+ exchangers and H^+-pyrophosphatase. Our results imply that seed priming with Si enhances seedling tolerance to salinity stress without negative effect on growth and it can be used as an effective strategy.
Keywords: *Na_2SiO_3, priming, salinity stress, OsNHX1, OsVPI*

Introduction

Rice (*Oryza sativa* L.) is one of the most important food crops in the world (Higham and Lu, 1998). It feeds more than one half of the global population (Mather et al., 2007). However, in many regions of rice production, the yield is markedly reduced due to salinity (Tuteja, 2007; Sakadevan and Nguyen, 2010). The cultivation of salt-tolerant varieties and efforts to reduce soil salinity are two common approaches to minimize the effects of salinity stress on crops (Ganie et al., 2019). However, salt-tolerant rice varieties are not readily available or their yield is low, and reducing soil salinity is costly.

Seed priming has been shown to be a simple, low cost and effective approach to enhance seed germination, early seedling growth and yield under stress conditions

http://www.aloki.hu ● ISSN 1589 1623 (Print) ● ISSN1785 0037 (Online)
DOI: http://dx.doi.org/10.15666/aeer/1804_54255436

(Hameed et al., 2013). Priming seeds with certain bioactive chemicals such as hormones and antioxidants has been reported to enhance crop performance under harsh conditions (Guntzer et al., 2012; Hameed et al., 2013; Etesami, 2018). For example, seed priming with salicylic acid (SA) improved seedling emergence, root, shoot and length, seedling fresh and dry weight both at optimal and low temperatures (Farooq et al., 2008).

Silicon (Si) is the second most abundant element found in the soil, next to oxygen (Sahebi et al., 2015). As a fertilizer, biostimulant or plant protectant, Si plays a pivotal role in plant growth and productivity, especially in stress regimes (Savvas and Ntatsi, 2015). Over the last two decades, numerous studies have demonstrated that the application of Si can enhance plant resistance to biotic stresses caused by microbial pathogens and insect herbivores, as well as abiotic stresses, such as drought, waterlogging, freezing, high temperature, and UV, as well as salinity, nutrient deficiencies, and metal toxicity (Guntzer et al., 2012; Ma and Takahashi, 2002; Balakhnina and Borkowska, 2013; Rizwan et al., 2015). Si application can also enhance maize seed germination, seedling growth (Guan et al., 2009) and tolerance to alkaline stress (Abdel Latef and Tran, 2016). Hameed and Sheikh (Hameed et al., 2013) reported that priming wheat seeds with sodium silicate improved seed germination and seedling growth under water-deficit stress.

Rice is known as a Si accumulator, and therefore is a good model crop to investigate the impacts of Si on plant performance and tolerance to environmental stresses (Ma et al., 2006). In the present study, we determined the impacts of seed soaking with different concentration gradients of Si on growth and salinity stress tolerance of rice plants. After discovering the optimal concentration of Si treatment, we examined the possible effects of Si pre-treatment on growth traits, including seedling biomass, root length and shoot height, as well as physiological traits such as levels of chlorophyll (Chl) a and b, carotenoids, malondialdehyde (MDA), proline and the activities of antioxidant enzymes of rice seedlings grown in nutrient solution with different concentrations of sodium chloride.

Materials and Methods

Seeds induction and germination

The experiment was performed in the Experimental Farm of Fujian Agriculture and Forestry University, Fuzhou, China (119º54′ E, 26º05′ N) in May 2018 using a salinity stress-sensitive rice (*Oryza sativa* L. cv. Shishoubaimao). Rice seeds were sterilized with 1% sodium hypochlorite solution for 10 min and rinsed with sterile distilled water. The sterilized seeds were divided into six groups: the first group (Control) was treated with distilled water, and the other five groups were treated with 2.5, 5.0, 10.0, 15, 20 mM sodium metasilicate ($Na_2SiO_3.9H_2O$) solutions for 48 h, separately. After treating with sodium silicate, the seeds were germinated on wet cotton cloth for 5 d. The germination potential of the primed and non-primed rice seeds was examined using the seed test of the Association of Official Seed Analysts (AOSA). To test seed germination and seedling vigor under salinity stress, 20 seeds of each treatment with four replicates were germinated in petri dishes (12 cm in diameter) at 25°C. A seed was considered to have germinated when a 2-3 mm long coleoptile and radicle was formed. Seed germination was counted twice a day at different time intervals (24, 48 h) starting from the first day and terminated when maximum germination was attained.

http://www.aloki.hu ● ISSN 1589 1623 (Print) ● ISSN1785 0037 (Online)
DOI: http://dx.doi.org/10.15666/aeer/1804_54255436

Rice cultivation and salt stress treatment

After 5 d of germination, the seedlings were placed in plastic pot with normal nutrient solution for another 7 d. Then the seedlings were transplanted in nutrient solution with sodium chloride, NaCl (120 mM) for 7 d. The degree of leaf damage was determined by the percentage of yellow area of leaf: If the whole leaf is green, we count it as 0; if the percentage of yellow area of the whole leaf ≤ 25%, we count it as 0.25; if the percentage of yellow area of the whole leaf between 25% and 50%, we count it as 0.5, if the percentage of yellow area of the whole leaf between 50% and 75%, we count it as 0.75, if the percentage of yellow area of the whole leaf ≥ 75%, we count it as 1. This criteria are based on Renganayaki et al. (2002).

Effect on seedling growth

For growth response, rice seedlings were allowed to continue to grow after collecting the data for germination. Fifteen days old seedlings were then harvested for comparison of growth under nutrient solution after seed priming treatments. Root and shoot lengths were then quantified. The fresh weight of rice seedlings was estimated after washing with deionized water, and blotting on paper towels. Their dry biomass was weighed after oven drying at 80°C to constant weight. The dried tissues were stored in clean sealed glasses at room temperature for later analysis.

Effect on water content under salinity stress and photosynthetic pigments

Leaf relative water content (LRWC) was determined using the method described in Garíca-Mata and Lamattina, using the equation:

$$\mathrm{LRWC}(\%) = \frac{\text{Fresh weight} - \text{Dry weight}}{\text{Turgid weight} - \text{Dry weight}} * 100 \qquad \text{(Eq.1)}$$

The contents of chlorophyll a, b and carotenoid in fresh leaves were assessed spectrophotometrically as described previously (Lichtenthaler and Wellburn, 1983). The fully expanded young leaves (0.05 g) of 15-day-old plants were treated with 120 mM NaCl for 24 and 48 h. The leaves were used for pigment extraction in 80% acetone. The extract of pigments was measured versus a blank of pure 80% acetone at 663, 644, and 452.5 nm for Chl a, Chl b, and carotenoid contents, respectively.

Determination of soluble protein, proline and MDA content

Total soluble protein content in leaves of rice after 7 days under salinity stress was measured as described previously (Gao, 2006). Total soluble protein content in leaves of rice after 7 days under salinity stress was measured according to the method described by Bates et al (1973). Malondialdehyde (MDA) is the main product of membrane lipid peroxidation when plants are under stress, and its content represents the degree of cell membrane damage. Malondialdehyde content was determined according to the thiobarbituric acid (TBA) reaction as described by Draper et al. (1993). Fresh leaf sample (0.5 g) was homogenized with 5% trichloroacetic acid and centrifuged at 4,000 g for 10 min. Two milliliters of extract were mixed with 2 mL of 0.6% TBA, and the mixture was placed in a boiling water bath for 10 min. Subsequently, the absorbances were read at 532, 600, and 450 nm, separately. The MDA content was calculated using the formula:

http://www.aloki.hu ● ISSN 1589 1623 (Print) ● ISSN1785 0037 (Online)
DOI: http://dx.doi.org/10.15666/aeer/1804_54255436

$$6.45 * (A532 - A600) - 0.56 * A450 \quad \text{(Eq.2)}$$

Assays for antioxidant enzyme activities

Samples were extracted from the fresh leaves as described previously (Mukherjee and Choudhuri, 1983). The fresh leaves (0.5 g) were frozen in liquid nitrogen and ground in 10 mL of 100 mM phosphate buffer (KH_2PO_4/K_2HPO_4) pH 7.0, containing 0.1 mM Na_2EDTA and 0.1 g of polyvinylpyrrolidone (PVP). The homogenate was centrifuged at 15,000 g at 4°C for 10 min. Subsequently, the supernatant was stored at 4°C until use for assays of superoxide dismutase (SOD) and peroxidase (POD). SOD activities were assayed as described previously (Giannopolitis and Ries, 1977). POD and SOD are important antioxidant components of plant tolerance to salinity stress (Sudhakar et al., 2001).

RNA extraction and cDNA synthesis

Fresh leaf samples (100 mg) of rice plant were collected after 0, 1, 3 and 5 days of treatment with 120 mM NaCl, and immediately transferred to liquid nitrogen and stored at -80°C. Total RNAs were isolated from flash-frozen tissues using the Eastep Super Total RNA Extraction Kit (Promega, Madison, WI, United States) and quantified by measuring the absorbance at 280 and 260 nm. Then the equal RNAs from three replicates were reverse-transcribed with a GoScript Reverse Transcription System (Promega), which were used for qRT-PCR analysis.

Quantitative real-time PCR (qRT-PCR) analysis

To validate the gene expression, quantitative real-time PCR (qRT-PCR) was performed on an Applied Biosystems StepOne Plus Real-Time PCR System in a 10 μL reaction volume consisting of 5 μL of 2× SYBR GoTaq qPCR Master Mix (Promega), 0.4 μL of each gene-specific primers (10 μM), 1 μL cDNA equivalent to 50 ng total RNA and sterilized water to reach the final volume. PCR conditions were set as: 1 cycle of 95°C for 10 min; 40 cycles of 95°C for 15 s, 55°C for 30 s and 72°C for 30 s. The reference gene actin (TIGR ID *Os*03g50885) was used as the internal control. A dissociation curve analysis program was performed to check the homogeneity of the PCR product. Relative standard curves of actin and target genes were generated by using 10- fold serial dilutions cDNA to calculate the amplification efficiencies of primers. The relative mRNA levels were normalized against actin using the $2^{-\Delta\Delta Ct}$ method (Livak and Schmittgen, 2001). Three independent biological repeats were performed, each sample had two technical replicates, and a calibrator sample was used to make comparisons between different plates. All the primers were listed on *Table 1*. All designed primers were synthesized at BioSune Biotechnology Co., Ltd. (Shanghai, China).

Statistical analysis

Data were statistically analyzed by the analysis of variance (ANOVA) with SPSS software, using Dunnett's multiple range test at the 0.05 level of significance ($p < 0.05$). Data represented in the Tables and Figures are means ± standard error of at least three independent replicates.

http://www.aloki.hu ● ISSN 1589 1623 (Print) ● ISSN1785 0037 (Online)
DOI: http://dx.doi.org/10.15666/aeer/1804_54255436

Table 1. *Primers used for qPCR analysis in this study*

Gene	Forward primer (5‘ to 3‘)	Reverse primer (5‘ to 3‘)
OsActin	TGGACAGGTTATCACCATTGGT	CCGCAGCTTCCATTCCTATG
OsASIE1	TGGTCTGATTTGGTAGCC	TCCAAGAACTGGCAGACGA
OsNHX1	CCTGGAGACAGCAAGTTGT	CTCTGCTCGGTTGGTGATC
OsVP1	AAGATGACCCAAGAAACCCA	GGTACAGCATAGGAGTGAAT

Results

Seed soaking with Si enhances tolerance of rice against salinity stress

To examine the effect of Si pretreatment on rice salinity stress, the rice seeds were soaked with distilled water (control group) or sodium silicate and then the rice seedlings were exposed to salinity stress. NaCl (120 mM) treatment led to severe damage for plant growth (*Fig. 1A*). However, compared with the control and 2.5 mM group, rice seed soaking with Si at ≥ 5 mM (5, 10, 15 and 20 mM) concentrations significantly decreased the degree of leaf damage by NaCl (*Fig. 1A* and *1B*). The Si-soaked seedlings showed more green leaves and vital stems (*Fig. 1A*).

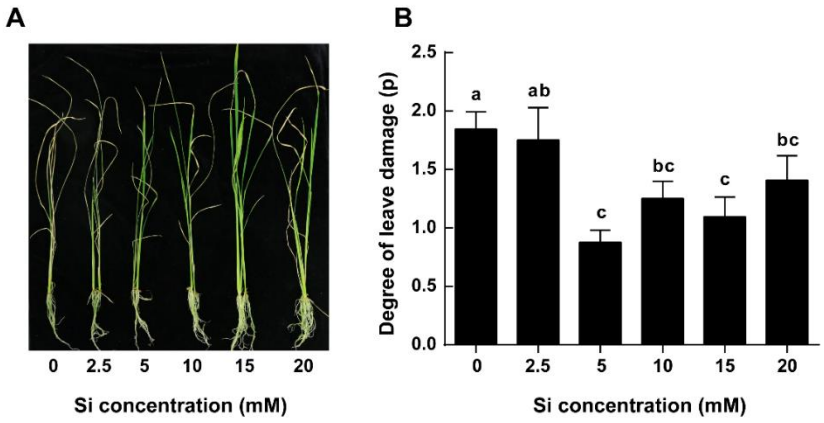

Figure 1. *Effect of seed soaking with sodium silicate on salinity tolerance of rice seedlings. Phenotypes (A) and degree of leaf damage (B) of rice seedlings treated with 120 mM NaCl for 3 d after seed soaking with different concentrations of sodium silicate for 48 h. Data are expressed as means ± SE (n = 6). Different letters above the bars indicate significant differences among treatments (P < 0.05 according to Dunnett's multiple range test)*

Seed soaking with Si improved seed germination and seedling growth

After seed soaking with Si solutions at ≥ 5 mM the seed germination rates were significantly higher 24 h after incubation relative to control (*Fig. 2A*). Seeds soaked in a solution with 20 mM Si showed the highest germination rate. However, there was no significant difference between control and five treatments at 48 h after incubation (*Fig. 2A*), implying that seed soaking with Si only accelerated the seed germination, but did not improve the final germination rate.

Seven days after transplantation seed soaking with Si solutions at ≥ 10 mM had shorter root lengths (*Fig. 2B*), but had longer shoot lengths, although only the 15 mM Si treatment showed significant effect compared to the control (*Fig. 2C*). Based on the results from

http://www.aloki.hu ● ISSN 1589 1623 (Print) ● ISSN1785 0037 (Online)
DOI: http://dx.doi.org/10.15666/aeer/1804_54255436

Fig. 1 and *Fig. 2*, 10 and 15 mM concentrations of sodium silicate were chosen as the optimal concentrations for the following experiments.

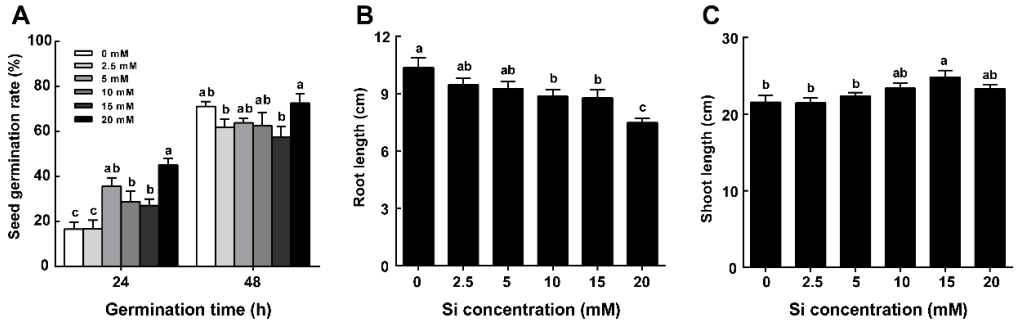

Figure 2. *Effect of seed soaking with sodium silicate on seed germination (A) and root length (B) and shoot length (C) of rice seedlings treated with NaCl. After seed soaking with different concentrations of sodium silicate for 48 h, the seeds were germinated for 2 d and rice plants were grown for 7 days in nutrient solution containing 120 mM NaCl. Data are expressed as means ± SE (n = 6). Different letters above the bars indicate significant differences among treatments (P < 0.05 according to Dunnett's multiple range test)*

Seed soaking with Si increases rice biomass, leaf relative water content and photosynthetic pigments

After seed pretreatment with Si for 48 h, fresh weight, dry weight and leaf relative water content (LRWC) of rice seedlings were measured 1, 3, 5 and 7 days after NaCl treatment. Compared with control group, seed pretreatment with Si enhanced the fresh weight on day 3 and day 7 (*Fig. 3A*) and dry weight on day 3-7 (*Fig. 3B*). On day 7, seed pretreatment with 15 mM Si increased leaf relative water content (LRWC) (*Fig. 3C*).

In order to understand physiological mechanism of enhanced salt tolerance of rice seedlings by seed soaking with sodium silicate, we measured the contents of chlorophyll a, b and carotenoid in fresh leaves of rice seedlings. We found that prior treatment of seeds with 10 or 15 mM Si significantly increased contents of Chl a and b at 24 h after salinity stress (*Fig. 3D* and *3E*). Contents of Chl a were also increased by seed treatment with 15 mM Si for 48 h (*Fig. 3D*). Prior treatment of seeds with 10 or 15 mM Si significantly increased contents of carotenoid 48 h after exposure to salinity stress (*Fig. 3F*).

Seed soaking with Si increased soluble protein and decreased proline and MDA

The soluble protein content in rice leaves was determined 7 days after exposure to salt stress. Si treatments at 10 mM and 15 mM led to 60% and 80% increase in soluble protein compared with Si-untreated control (*Fig. 4A*). The content of proline in rice plants was significantly reduced by 15 mM Si pretreatment 5 days after exposure to salt stress (*Fig. 4B*). Our results showed that in the rice leaves content of MDA significantly accumulated 3 days after exposure to salt stress. However, seed soaking with 10 mM and 15 mM Si led to 38% and 37% reduction in MDA contents 3 d after salinity stress, and 43% and 55% reduction 5 d after salinity stress, respectively (*Fig. 4C*).

http://www.aloki.hu ● ISSN 1589 1623 (Print) ● ISSN1785 0037 (Online)
DOI: http://dx.doi.org/10.15666/aeer/1804_54255436

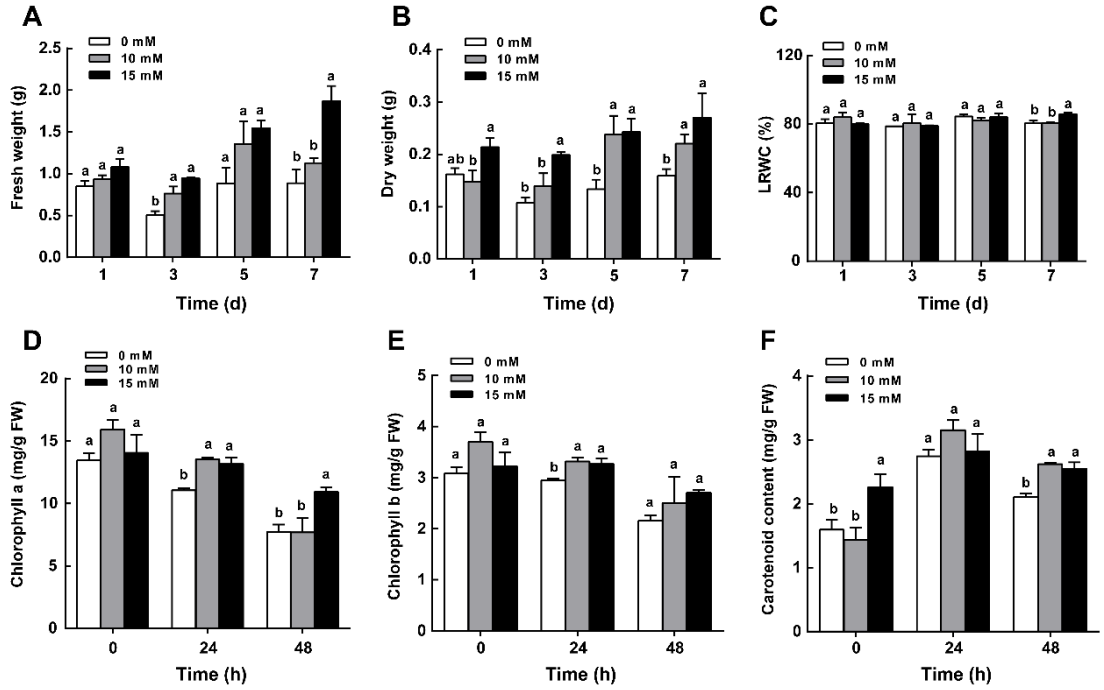

Figure 3. *Effect of seed soaking with sodium silicate on fresh weight (A), dry weight (B), LRWC (C), chlorophyll a (D), chlorophyll b (E) and carotenoid content (F) of rice seedlings treated with NaCl. Rice seedlings were cultivated in nutrient solution containing 120 mM NaCl. Data are expressed as means ± SE (n = 3-5). Different letters above the bars indicate significant differences among treatments (P < 0.05 according to Dunnett's multiple range test)*

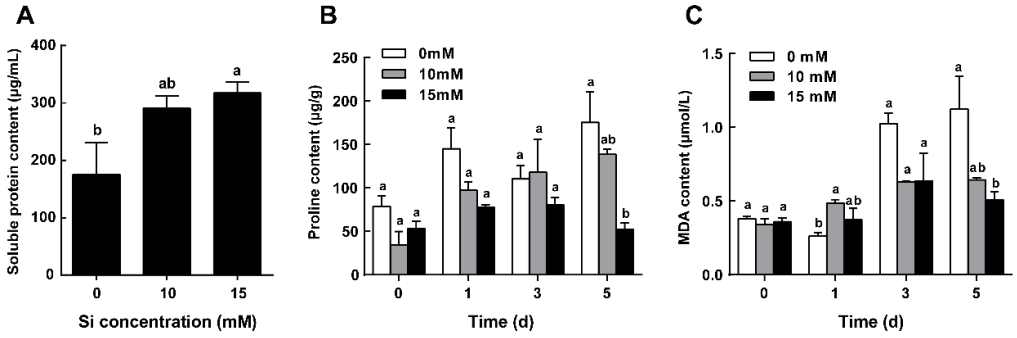

Figure 4. *Effect of seed soaking with sodium silicate on soluble protein (A), proline content (B) and MDA content (C) in the leaves of rice seedlings treated with NaCl. Rice seedlings were cultivated in nutrient solution containing 120 mM NaCl. Data are expressed as means ± SE (n = 3-5). Different letters above the bars indicate significant differences among treatments (P < 0.05 according to Dunnett's multiple range test)*

Seed soaking with Si enhanced antioxidant enzymes

Our results showed that seed soaking with 15 mM Si significantly enhanced activities of POD and SOD. Seed soaking with 15 mM Si increased POD by about 50% (*Fig. 5A*) and SOD by 20% relative to the control (*Fig. 5B*).

http://www.aloki.hu ● ISSN 1589 1623 (Print) ● ISSN1785 0037 (Online)
DOI: http://dx.doi.org/10.15666/aeer/1804_54255436

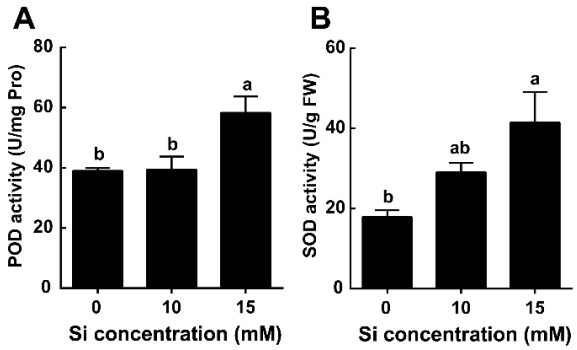

Figure 5. *Effect of seed soaking with sodium silicate on the activities of peroxidase (POD) (A) and superoxide dismutase (SOD) (B) in the rice leaves under salt stress for 7 days. Data are means ± SE (n = 5). Different letters above the bars indicate significant differences among treatments (P < 0.05 according to Dunnett's multiple range test)*

Seed soaking with Si induced transcription of salt tolerance-related genes

We want to know whether seed soaking with Si enhance salinity stress tolerance by inducing the transcription of genes encoding *OsASIE1*, *OsNHX1* and *OsVP1*. Real-time PCR analysis showed that compared with control, the *OsASIE1* gene expression was up-regulated in rice plants pretreated with 10 mM Si 1 days after exposure to salt stress and 15 mM Si 1, 3 and 5 days after salt stress (*Fig. 6A*). The expression of *OsNHX1* was significantly enhanced in rice plants pretreated with 15 mM Si 3 days after exposure to salt stress (*Fig. 6B*). The expression of *OsVP1* was up-regulated in rice plants pretreated with 15 mM Si 3 and 5 days after exposure to salt stress (*Fig. 6C*).

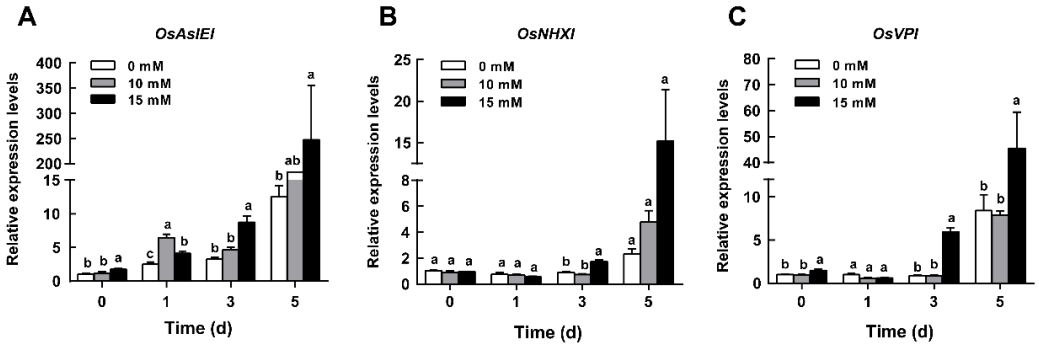

Figure 6. *Effect of seed soaking with sodium silicate on the expression of OsASIE1 (A), (B) OsNHX1 (B), OsVP1 (C) in the rice leaves under salt stress for 0, 1, 3, 5 days. Data are expressed as means ± SE (n = 5). Different letters above bars indicate significant differences among treatments (P < 0.05 according to Dunnett's multiple range test)*

Discussion

Soil salinity is a major abiotic stress that can lead to a substantial decrease in crop yields (Rengasamy, 2010). Rice plants are particularly vulnerable to salt stress and therefore there has been great interest in improving rice resistance to salinity. Si plays an important role in conferring plant resistance to a wide range of biotic and abiotic stresses (Reynolds et al., 2016), including salinity, as has been shown for crops such as wheat,

http://www.aloki.hu ● ISSN 1589 1623 (Print) ● ISSN1785 0037 (Online)
DOI: http://dx.doi.org/10.15666/aeer/1804_54255436

maize, barley, cucumber, etc (Liang et al., 1996; Zhu et al., 2004; Tuna et al., 2008). We show here that soaking seeds in Si solutions for a short term (48 h) can enhance tolerance to salinity stress and lead to several positive consequences for rice plant performance. The degree of stress-induced leaf damage was also significantly reduced in rice plants grown from Si-primed seeds as compared to plants from untreated seeds. The reduction in photosynthetic pigments of rice leaves after NaCl treatment found in this study (*Fig. 3D, E, F*) supports the findings of Kariola et al. (2005). The decrease in chlorophyll content under salinity stress may be due to increased oxidative stress that causes injury to chloroplast structure and an increase in the activity of chlorophyllase, which is responsible for the chlorophyll degradation (Tarja et al., 2005; Abdel Latef and He, 2014). Si treatment increased the chlorophyll and carotenoid contents in rice plants exposed to salinity stress, which could result in the increase in seedling fresh and dry weight, as well as the increase in green pigments per unit area. It must have also safeguarded the chlorophyll from ROS by reinforcing the carotenoid levels.

In general, increased resistance occurs with simultaneous growth inhibition. We found the opposite; Si treatment enhanced the speed of seed germination, but did not significantly affect final germination success. It also increased seedling height compared with untreated group (*Fig. 2C*) (Hameed et al., 2013; Etesami, 2018). These results imply that priming of salt tolerance by seed soaking with sodium silicate does not affect rice performance.

Salt tolerance of plants may be reflected in a number of parameters, including the contents of chlorophyll a and b, carotenoids, malondialdehyde and proline, as well as the activities of antioxidant enzymes. In maize plants, it has been shown that the content of soluble proteins increase under high alkaline pressure (Abdel Latef, 2010; Abd-Alla et al., 2014; Mohsenian and Roosta, 2015). Here, the increase in soluble protein content of rice plants under salinity stress was accompanied by a marked reduction in growth. This suggests that under salinity stress, rice plants divert much of the synthesized proteins from growth to resistance responses. The highest soluble protein level was observed in the rice seedlings that developed from seeds soaked in 15 mM Si. It is known that proline can serve as an important osmotic adjustment substance in plant cells (Silveira et al., 2003) and proline content can be used as a physiological index of a plant's resistance to stress tolerance (Toyooka et al., 2009). The accumulation of proline was reduced in the Si-pretreated seedlings, which suggests that seed priming with Si could protect cells by keeping the accumulation of proline to an optimum level (*Fig. 4B*).

Under salinity stress, the increase of reactive oxygen species leads to lipid peroxidation in cell membranes. Malondialdehyde is the main product of membrane lipid peroxidation, and the levels at which it is produced therefore represents the degree of cell membrane damage (Silveira et al., 2003). We found that malondialdehyde levels increased in rice leaves under salinity stress, but this increase was significantly mitigated by Si treatment of the seeds (*Fig. 4C*). Furthermore, seed priming with Si also resulted in a significant increase in SOD and POD activities in rice seedlings exposed to salinity stress relative to plant treated with NaCl alone. These results indicate that Si enhances antioxidant activity that protects plants against salinity induced oxidative damage (*Fig. 5*).

Certain plant membrane transporters particularly Na^+ and K^+ transporters are involved in plant resistance to salt stress. *OsSOS1* (Na^+/H^+ antiporters) (Kumar and Sinha, 2013; Amin et al., 2016), *OsCAX1* (H^+/Ca^+ antiporter) (Kumar and Sinha, 2013), *OsAKT1* (K^+ inward-rectifying channel) (Yang et al., 2014), *OsKCO1* (K^+ outward-rectifying channel) (Kumar and Sinha, 2013), *OsCLC1* (Cl^- channel) (Diédhiou and Golldack, 2006),

http://www.aloki.hu ● ISSN 1589 1623 (Print) ● ISSN1785 0037 (Online)
DOI: http://dx.doi.org/10.15666/aeer/1804_54255436

OsNRT1;2 (nitrate transporter) (Yang et al., 2014), and *OsTPC1* (Ca^{2+} permeable channel) (Kurusu et al., 2012) have all been shown to play a role in rice resistance to salt stress. In our study we found that seed soaking with Si induced transcription of genes encoding Na^+/H^+ exchangers (*OsNHX1*) and H^+ -pyrophosphatase (*OsVP1*) (*Fig. 6*). *OsASIE1* may participate in abiotic stress response by regulating the expression of downstream genes with DRE and GCC box binding. Overexpression of *OsASIE1* improves rice tolerance to salt stress (Wu et al., 2011). In this study, *OsNHX1* showed a quick response to salinity stress in 10 Mm treatment but not change in the following days due to the reason that *NHX* genes increase salt tolerance by reducing Na^+ contents in the leaves. This is in accordance with Liu et al. (2010) who found that the overexpression of *OsNHX1* and *OsVP1* in tonoplasts improved rice tolerance to salt and drought.

Conclusion

In conclusion, seed priming with Si significantly improved rice tolerance to salinity without any negative effect on growth. This treatment may therefore serve as a highly effective strategy to improve rice tolerance to salinity stress. The detailed molecular mechanism should be further investigated.

Acknowledgements. We thank Professor Ted Turlings for revising the manuscript. This work was supported by the Talent Program of Fujian Agriculture and Forestry University (KXJQ19009), National College Student Innovation Program, China (202010389013), Natural Science Fund project of Fujian Province (2020J01130966), National Natural Science Foundation of China (31870361), and Fujian Provincial Excellent Youth Science Foundation (2017J06010).

REFERENCES

[1] Abd-Alla, M. H., El-Enany, A. W. E., Nafady, N. A., Khalaf, D. M., Morsy, F. M. (2014): Synergistic interaction of Rhizobium leguminosarum bv. viciae and arbuscular mycorrhizal. ungi as a plant growth promoting biofertilizers for faba bean (*Vicia faba* L.) in alkaline soil. – Microbiol Res 169(1): 49-58.

[2] Abdel Latef, A. (2010): Changes of antioxidative enzymes in salinity tolerance among different wheat cultivars. – Cereal Res Commun 38(1): 43-55.

[3] Abdel Latef, A. A. H., He, C. X. (2014): Does inoculation with glomus mosseae improve salt tolerance in pepper plants? – J Plant Growth Regul 33(3): 644-653.

[4] Abdel Latef, A. A., Tran, L.-S. P. (2016): Impacts of priming with silicon on the growth and tolerance of maize plants to alkaline stress. – Front Plant Sci 7: 243.

[5] Amin, U., Biswas, S., Elias, S. M., Razzaque, S., Haque, T., Malo, R., Seraj, Z. I. (2016): Enhanced salt tolerance conferred by the complete 2.3 kb cDNA of the rice vacuolar Na^+/H^+ antiporter gene compared to 1.9 kb coding region with 5′ UTR in transgenic lines of rice. – Front Plant Sci 7: 14.

[6] Balakhnina, T., Borkowska, A. (2013): Effects of silicon on plant resistance to environmental stresses. – Int Agrophys 27(2): 225-232.

[7] Bates, L. S., Waldren, R. P., Teare, I. (1973): Rapid determination of free proline for water-stress studies. – Plant Soil 39(1): 205-207.

[8] Diédhiou, C., Golldack, D. (2006): Salt-dependent regulation of chloride channel transcripts in rice. – Plant Sci 170(4): 793-800.

[9] Draper, H. H., Squires, E. J., Mahmoodi, H., Wu, J., Agarwal, S., Hadley, M. (1993): A comparative evaluation of thiobarbituric acid methods for the determination of malondialdehyde in biological materials. – Free Radical Bio Med 15(4): 353-363.

http://www.aloki.hu ● ISSN 1589 1623 (Print) ● ISSN1785 0037 (Online)
DOI: http://dx.doi.org/10.15666/aeer/1804_54255436

[10] Etesami, H. (2018): Can interaction between silicon and plant growth promoting rhizobacteria benefit in alleviating abiotic and biotic stresses in crop plants? – Agr Ecosyst Environ 253: 98-112.
[11] Farooq, M., Aziz, T., Basra, S. M. A., Cheema, M. A., Rehman, H. (2008): Chilling tolerance in hybrid maize induced by seed priming with salicylic acid. – J Agron Crop Sci 194(2): 161-168.
[12] Ganie, S. A., Molla, K. A., Henry, R. J., Bhat, K., Mondal, T. K. (2019): Advances in understanding salt tolerance in rice. – Theor Appl Genet 132(4): 851-870.
[13] Gao, J. (2006): Experimental guidance for plant physiology. – China Higher Education Press, Beijing (Chinese).
[14] Giannopolitis, C. N., Ries, S. K. (1977): Superoxide dismutases: I. Occurrence in higher plants. – Plant Physiol 59(2): 309-314.
[15] Guan, Y. J., Jin, H. U., Wang, X. J., Shao, C. X. (2009): Seed priming with chitosan improves maize germination and seedling growth in relation to physiological changes under low temperature stress. – J Zhejiang Univ 10(6): 427-433.
[16] Guntzer, F., Keller, C., Meunier, J.-D. (2012): Benefits of plant silicon for crops: a review. – Agron Sustain Dev 32(1): 201-213.
[17] Hameed, A., Sheikh, M. A., Jamil, A., Basra, S. M. A. (2013): Seed priming with sodium silicate enhances seed germination and seedling growth in wheat (*Triticum aestivum* L.) under water deficit stress induced by polyethylene glycol. – Pakistan J Life & Social Sci 11(1): 19-24.
[18] Higham, C., Lu, L. D. (1998): The origins and dispersal of rice cultivation. – Antiquity 72(278): 867-877.
[19] Kariola, T., Brader, G., Li, J., Palva, E. T. (2005): Chlorophyllase 1, a damage control enzyme, affects the balance between defense pathways in plants. – Plant Cell 17(1): 282-294.
[20] Kumar, K., Sinha, A. K. (2013): Overexpression of constitutively active mitogen activated protein kinase kinase 6 enhances tolerance to salt stress in rice. – Rice 6(1): 25.
[21] Kurusu, T., Hamada, H., Koyano, T., Kuchitsu, K. (2012): Intracellular localization and physiological function of a rice Ca^{2+}-permeable channel *OsTPC1*. – Plant Signal & Behav 7(11): 1428-1430.
[22] Liang, Y., Shen, Q., Shen, Z., Ma, T. (1996): Effects of silicon on salinity tolerance of two barley cultivars. – J Plant Nutr 19(1): 173-183.
[23] Lichtenthaler, H. K., Wellburn, A. R. (1983): Determinations of total carotenoids and chlorophylls a and b of leaf extracts in different solvents. – Biochem Soc Trans 11(5): 591-592.
[24] Liu, S., Zheng, L., Xue, Y., Zhang, Q., Wang, L., Shou, H. (2010): Overexpression of *OsVP1* and *OsNHX1* increases tolerance to drought and salinity in rice. – J Plant Biol 53(6): 444-452.
[25] Livak, K. J., Schmittgen, T. D. (2001): Analysis of relative gene expression data using real-time quantitative PCR and the $2^{-\Delta\Delta CT}$ method. – Methods 25(4): 402-408.
[26] Ma, J. F., Takahashi, E. (2002): Soil, fertilizer, and plant silicon research in Japan. – Elsevier Science B. V.
[27] Ma, J. F., Tamai, K., Yamaji, N., Mitani, N., Konishi, S., Katsuhara, M., Ishiguro, M., Murata, Y., Yano, M. (2006): A silicon transporter in rice. – Nature 440(7084): 688.
[28] Mather, K. A., Caicedo, A. L., Polato, N. R., Olsen, K. M., Susan, M. C., Purugganan, M. D. (2007): The extent of linkage disequilibrium in rice (*Oryza sativa* L.). – Genetics 177(4): 2223.
[29] Mohsenian, Y., Roosta, H. R. (2015): Effects of grafting on alkali stress in tomato plants: datura rootstock improve alkalinity tolerance of tomato plants. – J Plant Nutr 38(1): 51-72.
[30] Mukherjee, S., Choudhuri, M. (1983): Implications of water stress-induced changes in the levels of endogenous ascorbic acid and hydrogen peroxide in Vigna seedlings. – Physiol Plantarum 58(2): 166-170.

http://www.aloki.hu ● ISSN 1589 1623 (Print) ● ISSN1785 0037 (Online)
DOI: http://dx.doi.org/10.15666/aeer/1804_54255436

[31] Renganayaki, K., Fritz, A. K., Sadasivam, S., Pammi, S., Harrington, S. E., Mccouch, S. R. (2002): Mapping and progress toward map-based cloning of brown planthopper biotype-4 resistance gene introgressed from into cultivated rice. – Crop Sci 42(6): 2112.
[32] Rengasamy, P. (2010): Soil processes affecting crop production in salt-affected soils. – Funct Plant Biol 37(7): 613-620.
[33] Reynolds, O. L., Padula, M. P., Zeng, R., Gurr, G. M. (2016): Silicon: potential to promote direct and indirect effects on plant defense against arthropod pests in agriculture. – Front Plant Sci 7: 744.
[34] Rizwan, M., Ali, S., Ibrahim, M., Farid, M., Adrees, M., Bharwana, S. A., Zia-Ur-Rehman, M., Qayyum, M. F., Abbas, F. (2015): Mechanisms of silicon-mediated alleviation of drought and salt stress in plants: a review. – Environ Sci Pollut R 22(20): 15416-15431.
[35] Sahebi, M., Hanafi, M. M., Siti, N. A. A., Rafii, M. Y., Azizi, P., Tengoua, F. F., Nurul, M. A. J., Shabanimofrad, M. (2015): Importance of silicon and mechanisms of biosilica formation in plants. – Biomed Res Int 2015: 396010.
[36] Sakadevan, K., Nguyen, M. L. (2010): Chapter two–extent, impact, and response to soil and water salinity in arid and semiarid regions. – Ad Agron 109(109): 55-74.
[37] Savvas, D., Ntatsi, G. (2015): Biostimulant activity of silicon in horticulture. – Sci Horticamsterdam 196: 66-81.
[38] Silveira, J. A. G., de Almeida Viégas, R., da Rocha, I. M. A., de Oliveira Monteiro Moreira, A. C., de Azevedo Moreira, R., Oliveira, J. T. A. (2003): Proline accumulation and glutamine synthetase activity are increased by salt-induced proteolysis in cashew leaves. – J Plant Physiol 160(2): 115-123.
[39] Tarja, K., Günter, B., Jing, L., Tapio, P. E. (2005): Chlorophyllase 1, a damage control enzyme, affects the balance between defense pathways in plants. – Plant Cell 17: 282-294.
[40] Toyooka, K., Goto, Y., Asatsuma, S., Koizumi, M., Mitsui, T., Matsuoka, K. (2009): A mobile secretory vesicle cluster involved in mass transport from the golgi to the plant cell exterior. – Plant Cell 21(4): 1212-1229.
[41] Tuna, A. L., Kaya, C., Higgs, D., Murillo-Amador, B., Aydemir, S., Girgin, A. R. (2008): Silicon improves salinity tolerance in wheat plants. – Environ Exp Bot 62(1): 10-16.
[42] Tuteja, N. (2007): Mechanisms of high salinity tolerance in plants. – Methods in Enzymology 428: 419-438.
[43] Wu, H.-M., Huang, L.-Y., Pan, Y.-J., Jin, P., Fu, B.-Y. (2011): Function of gene *OsASIE1* in response to abiotic stress in rice. – Acta Agro Sin 37(10): 1771-1778.
[44] Yang, T., Zhang, S., Hu, Y., Wu, F., Hu, Q., Chen, G., Cai, J., Wu, T., Moran, N., Yu, L. (2014): The role of a potassium transporter *OsHAK5* in potassium acquisition and transport from roots to shoots in rice at low potassium supply levels. – Plant Physiol 166(2): 945-959.
[45] Zhu, Z., Wei, G., Li, J., Qian, Q., Yu, J. (2004): Silicon alleviates salt stress and increases antioxidant enzymes activity in leaves of salt-stressed cucumber (*Cucumis sativus* L.). – Plant Sci 167(3): 527-533.

http://www.aloki.hu ● ISSN 1589 1623 (Print) ● ISSN1785 0037 (Online)
DOI: http://dx.doi.org/10.15666/aeer/1804_54255436

THE EFFECT OF DIFFERENT IRRIGATION LEVELS AND MULCH APPLICATION ON SOME QUALITY CRITERIA IN TABLE TOMATOES (*LYCOPERSICON ESCULENTUM* MILL.)

KARAER, M.[1*] – KUSCU, H.[2] – GULTAS, H. T.[1]

[1]*Department of Biosystems Engineering, Faculty of Agriculture and Natural Sciences, Bilecik Şeyh Edebali University, Bilecik, Turkey*

[2]*Department of Biosystems Engineering, Faculty of Agriculture, Bursa Uludag University, Bursa, Turkey*

**Corresponding author*
e-mail: murat.karaer@bilecik.edu.tr; phone: +90-228-214-1797

(Received 2nd Mar 2020; accepted 3rd Jul 2020)

Abstract. The aim of the study was to measure the response of tomato (*Lycopersicon esculentum* Mill.) grown in open field to mulch and different irrigation levels. This study was carried out in Bilecik, Turkey in the growing season of 2017 and 2018. The research was designed as a split plot design with 3 replications. The treatments consist of two mulch [black nylon mulch (M) and no mulch (NM)] and four irrigation levels of pan evaporation (Epan) replenishment [1.00×Epan (I_{100}), 0.75 × Epan (I_{75}), 0.50×Epan (I_{50}), 0.25×Epan (I_{25})]. As a result of the research, irrigation water level and mulch application was found to have significant effects on some quality criteria. The study shows that pH, fruit puncture resistance, fruit diameter, fruit length and total soluble solids/titration acidity ratio increased with increasing amount of irrigation water. As irrigation water level in mulch application increased, fruit diameter, weight, pH and fruit puncture resistance values increased. Mulch application yielded better results than application without mulch irrespective of irrigation levels.
Keywords: *colour, fruit puncture, semi-arid climate, titration acidity, total soluble solids*

Introduction

The rapid increase in population is expected to bring food shortages along with water shortages. The problem is the imbalance between the global increase in food demand and the reduction in available water resources. Therefore, existing water resources should be well protected and used rationally.

When we look at the sectoral use of the existing water resources in the world, agricultural use ranks first with 70%, industry with 19% and domestic use with 11% approximately (FAO, 2013; Anonymous, 2014). These rates show that the rational use of water resources in agricultural sector, which is the largest user of water becomes more important. However, increasing water demand for domestic use and industry, irregularity in the precipitation regime due to global climate change, pollution of usable water resources and/or the desiccation of some of these sources will make it necessary to limit the amount of water to be allocated to agriculture in the near future. While the amount of irrigated land all over the world was 170 million ha in the 1970s, this ratio reached 304 million ha in 2008 and by 2025 it is estimated to reach 330 million ha (FAO, 2011). However, it is predicted that the population of the world will be 8 billion by 2025. In order to meet the needs of the population by 2025, the amount of irrigated land should be higher than 20% of the total amount of agricultural land and the crop yield obtained from irrigated land should be 40% higher than that currently obtained

http://www.aloki.hu ● ISSN 1589 1623 (Print) ● ISSN 1785 0037 (Online)
DOI: http://dx.doi.org/10.15666/aeer/1804_54375447

(Lascano and Sojka, 2007). This makes it necessary to use the soil and water potential allocated for agricultural purposes with the highest possible efficiency and to obtain the highest yield from a unit of water used. Therefore, the approach in irrigated agriculture has been focusing on obtaining more products with less water. Deficit irrigation and partial root drying (PRD) techniques are water-saving methods that reduce the amount of water supplied to plants compared to full irrigation (Ahmadi et al., 2010).

The aim of deficit irrigation is to increase the efficiency of plant water use by reducing the amount or frequency of irrigation water. The plant which is made deficit irrigation is exposed to water stress at any period of development or during the growing season and it is expected to save water without causing a significant decrease in yield. Deficit irrigation can also be used to create new irrigation areas where water resources are sufficient. The plant type to be chosen is also important in deficit irrigation. Plant's response to deficit irrigation and the water-saving should be at the forefront. Tomato is a plant which requires much water is the most grown vegetable in the world and in Turkey. In this respect, it is a suitable plant in terms of the reactions to be achieved by shortened irrigation.

Tomato (*Solanum lycopersicum* L.) is a single-year vegetable species of the eggplant family (Solanoceae), native to South and Central America, widely used in human nutrition. Approximately 1.1 billion tons of fresh vegetables are produced in the world annually and about 177 million tons of this are tomatoes. This makes tomato to be ranked as the most grown vegetable among other vegetables and it covers the largest area with 4.8 million ha. With 176.000 ha area, Turkey has the 4 th biggest area of tomato production after China, India and Egypt. In addition to this, with 12.2 million tons of production, Turkey is the 4 th biggest producer of tomato after China, India and America (FAO, 2018).

Many irrigation studies have shown that tomato is sensitive to water stress (Locascio and Smasjstrla, 1996; Patanè and Cosentino, 2010). Water and nutrient stress leads to reduction in marketable yields and quality. In order to obtain high yields, seasonal water requirement of tomatoes range from 400 to 800 mm with a daily evapotranspiration rate of 4 to 6 mm (Salokhe et al., 2005; Hanson and May, 2006; Mukherjee et al., 2010).

Irrigation water level and scheduling of irrigation application significantly affect tomato yield and fruit quality (Wang et al., 2012). Previous studies show that deficit irrigation can increase water use efficiency (WUE) and improve tomato quality in the tomato plant (Zegbe-Dominguez et al., 2003; Favati et al., 2009; Kuşçu et al., 2014). On the other hand, deficit irrigation practices can result the fruits to be small in size, lower marketable yields and higher susceptibility to various diseases (Favati et al., 2009).

The use of mulch has many benefits in agriculture as it reduces weed output which causes yield losses and diseases. Moreover, it provides better root growth by increasing soil temperature. It reduces surface evaporation and maintains soil moisture, thus saves water. Furthermore, the use of mulch has a significant impact on earliness, productivity and fruit quality (Abak et al., 1990; Koçar, 2001; Ünlü et al., 2006; Ekinci and Dursun, 2009; Kurtar, 2010; Korkmaz and Balkaya, 2016). However, the number of studies on the effect of both different irrigation regimes and mulch applications on the quality characteristics of table tomatoes is quite limited. In addition, the response of plants to cultural practices in different varieties, climatic and soil characteristics may also change. Therefore, this study was conducted to determine the effects of different irrigation levels and mulch application on the quality of table tomatoes in Bilecik, a semi-arid climate zone.

http://www.aloki.hu ● ISSN 1589 1623 (Print) ● ISSN 1785 0037 (Online)
DOI: http://dx.doi.org/10.15666/aeer/1804_54375447

Materials and methods

The research was carried out in the open field, in the growing season of 2017 and 2018, in the Research and Application Area of Bilecik Şeyh Edebali University, Faculty of Agriculture and Natural Sciences. The experiment area is located at 40° 6' N, 30°.0' E; altitude 500 m above the sea level. Both the climate of Marmara Region and Central Anatolia Region are influential in Bilecik province. According to the long-term meteorological data, the average annual rainfall in the region is 450 mm and the average temperature is 12.5 °C. According to annual rainfall, the study area is defined as semi-arid. Climate data for the years of study are given in *Tables 1 and 2*.

Table 1. *Climate data for 2017*

	Jan	Feb	Mar	Apr	May	Jun	Jul	Aug	Sep	Oct	Nov	Dec	Yearly
Average temperature (°C)	0.4	5.7	9.3	11.7	16	21	23.8	23.1	21.4	13.2	9	6.6	13.5
Average Highest Temperature (°C)	3.7	9.8	15	18.6	22.5	27.1	31.2	29.9	29.5	19	13.7	9.9	19.2
Average Lowest Temperature (°C)	-2.2	1.5	5.2	6.4	11.4	15.3	17.8	18.4	15.4	8.9	5.7	4.3	9
Average of Total Monthly Rainfall (mm)	51.0	9.3	26	64.4	56.7	69.9	7.0	16	3.0	44.4	21.1	66.2	435

Table 2. *Climate data for 2018*

	Jan	Feb	Mar	Apr	May	Jun	Jul	Aug	Sep	Oct	Nov	Dec	Yearly
Average temperature (°C)	4	7.3	12.9	16	18.2	21.2	23.8	24.1	19.5	14.7	9.6	3.5	14.6
Average Highest Temperature (°C)	7.2	11.7	16.5	23.3	24.2	28.1	30	31.2	26.1	19.9	13.7	5.8	19.8
Average Lowest Temperature (°C)	1.4	4.5	7	9.8	14	15.7	18.4	18.7	14.7	11.3	6.8	5.8	10.7
Average of Total Monthly Rainfall (mm)	40.9	37.6	66.1	18.6	80.8	39.5	14.2	17.8	89.4	46.4	37	107.3	595.6

The study area has a clay loam soil structure (38.66% sand, 32.81% clay and 28.53% loam). The physical analysis results of the soil of the trial area are given in *Table 3*. Total rainfall during the plant growing season was 94.7 mm in 2017 and 116.3 mm in 2018.

Table 3. *The physical analysis results of soil samples*

Depth (cm)	Grain size			Texture	Volume weight (g/cm^3)	Field capacity (PW %)
	Sand	Silts	Clay			
0-30	38.66	32.81	28.53	CL	1.26	27.87
30-60	42.05	32.11	25.84	L	1.21	24.57
60-90	39.71	34.34	25.95	L	1.27	26.67

The working area was first plowed and the land surface was leveled and suitable conditions for planting were prepared. Weed control was done by hand and hoeing three times until the first harvest. Nitrogen, phosphorus and potash fertilizers were used in fertilization. Fertilization was given to plants by drip irrigation system after planting.

http://www.aloki.hu ● ISSN 1589 1623 (Print) ● ISSN 1785 0037 (Online)
DOI: http://dx.doi.org/10.15666/aeer/1804_54375447

In the study, Zahide F1 tomato variety was used. It is suitable for spring and summer planting. Its fruits are flat and round. It is an early variety and the average harvest time is 70-90 days.

Treatments were arranged in the field according to a split-plot experimental design with three replications in both seasons. The mulch treatments were randomized in the main plots and irrigation levels in the sub-plots. The treatments consist of two mulch [black nylon mulch (M) and no mulch (NM)] and four irrigation levels of pan evaporation (Epan) replenishment [1.00×Epan (I_{100}), 0.75 × Epan (I_{75}), 0.50 × Epan (I_{50}), 0.25 × Epan (I_{25})]. The irrigations were carried out at 5-day intervals according to the drip irrigation method. Each experimental plot was 6 m long and 3.2 m wide (19.2 m^2), with 4 rows. Plots are placed leaving two meters buffer zones between. The row spacing was 0.8 m and plan-plant spacing was 0.4 m.

The irrigations were carried out according to five-days evaporation amount cumulated in Class A pan. The amount of irrigation water was determined by multiplying the measured evaporation value with the kp coefficient, wetting percentage, kc coefficient, and area (*Eq. 1;* Kanber, 1984).

$$I = A \times Ep \times kp \times P \times kc \quad \text{(Eq.1)}$$

In *Equation 1, I* is irrigation water applied to the parcel (litres), *A* is parcel area (m^2), *Ep* is accumulated evaporation amount from open water surface (mm), *kp* is coefficient for experiment treatments, *P* is wetting percentage, and *kc* is coefficient at different growth periods.

The *kc* coefficient was taken 0.60 in the initial period, between 0.60-1.15 in the development period, 1.15 in the medium period, and 1.15-0.80 in the last period (Allen et al., 1998). *Table 4* shows that coefficients for experimental treatments.

Table 4. *Coefficients for irrigation treatments*

Irrigation treatment	kp coefficient
I_{100}	1.00
I_{75}	0.75
I_{50}	0.50
I_{25}	0.25

Throughout the growing season, the measurement of the crop-water requirement is made based on 0-90 cm depth increment of the soil as in *Equation 2* (Garrity et al., 1982).

$$ET = I + P \pm \Delta S - D \quad \text{(Eq.2)}$$

In *Equation 2, ET* is plant water consumption (mm), *I* is irrigation water (mm), *P* is precipitation amount (mm), *D* is deep drainage losses (mm), and ΔS is refers to the moisture change (mm) in the soil profile.

For the harvest, the edge rows of each parcel were discarded and the two rows in the middle were determined as the harvest area. Harvestes continued until mid-October.

Quality characteristics of fruit were determined by examining 20 fruit samples randomly selected from each parcel. In order to determine the quality characteristics, the

http://www.aloki.hu ● ISSN 1589 1623 (Print) ● ISSN 1785 0037 (Online)
DOI: http://dx.doi.org/10.15666/aeer/1804_54375447

diameter, length, pH ratio, perforation resistance and total soluble solids (TSS) and titration acidity (TA) of the fruit were examined.

The average fruit width was determined by measuring the widest diameter of the fruit with a digital calliper. The average fruit length was determined by measuring the distance between the stem pit and floral nose with a digital calliper. In order to determine the pH ratio, fruit juices were obtained through a blender after the tomatoes were harvested and measurements were carried out by pH meter (Cemeroğlu, 2010). Fruit perforation resistance was measured by flat-tipped hand penetrometer at 3 different locations in the equator region of the fruit and the results were expressed as kg cm^{-2}. Tomato juice was titrated with 0.1 N NaOH until the pH of the tomato juice reached up to 8.1. The amount of acid consumed was calculated in terms of citric acid (mg/100 g citric acid) and titration acidity was found. The fruit juice obtained by blending the tomatoes was filtered in order to determine total soluble solids. Then, the sample taken from the filtered fruit juice was dropped onto the hand refractometer and the results were read and determined as % (Cemeroğlu, 2010). TSS/TA value was obtained by dividing the obtained TSS and TA values. In determining the colours of tomato samples, a and b values were measured by colour measurement device. Minitab18 package program was used for statistical evaluation of the obtained results.

Results and discussion

Results of variance analysis (ANOVA) of the data are given in *Table 5*. The results show that the effect of irrigation regimes on all measured parameters was significant at $P < 0.01$ level. Mulch application was significant at $P < 0.01$ level for fruit diameter, length, and colour parameters. On addition, the effect of interactions between irrigation and mulch was significant at $P < 0.01$ level, on all parameters.

Table 5. *Result of variance of fruit diameter, length, pH ratio, perforation resistance and TSS/TA ratio for the irrigation and mulch treatments*

Variables	pH	Fruit perforation resistance	Fruit diameter	Fruit length	Colour a	Colour b	TSS/TA ratio
Year (Y)	ns	ns	**	**	ns	ns	**
Irrigation level (I)	**	**	**	**	**	**	**
Mulch application (MA)	ns	ns	**	**	**	**	ns
I × MA	**	**	**	**	**	**	**
Y × I × MA	**	**	**	**	**	**	ns

*, **, and ns: F-test significant at $p \leq 0.005$, $p \leq 0.01$, respectively, and not significant

Irrigation water applied and evapotranspiration

In this study, 15 mm water was given to the all test plots immediately after planting. Then, 30 mm of irrigation water in total was given to the plants in two times until the beginning of all subjects' irrigation application. In this study, irrigation was launched on the 18th of June for both years. In 2017, 19 irrigations, and in 2018, 18 irrigations were performed. Irrigations were performed in 5 days intervals after planting. The amount of irrigation water applied to the experiment subjects and the crop water consumption amounts of the subjects are given in *Table* 6 and the cumulative amount of irrigation water is shown in *Figures 1* and *2*.

http://www.aloki.hu ● ISSN 1589 1623 (Print) ● ISSN 1785 0037 (Online)
DOI: http://dx.doi.org/10.15666/aeer/1804_54375447

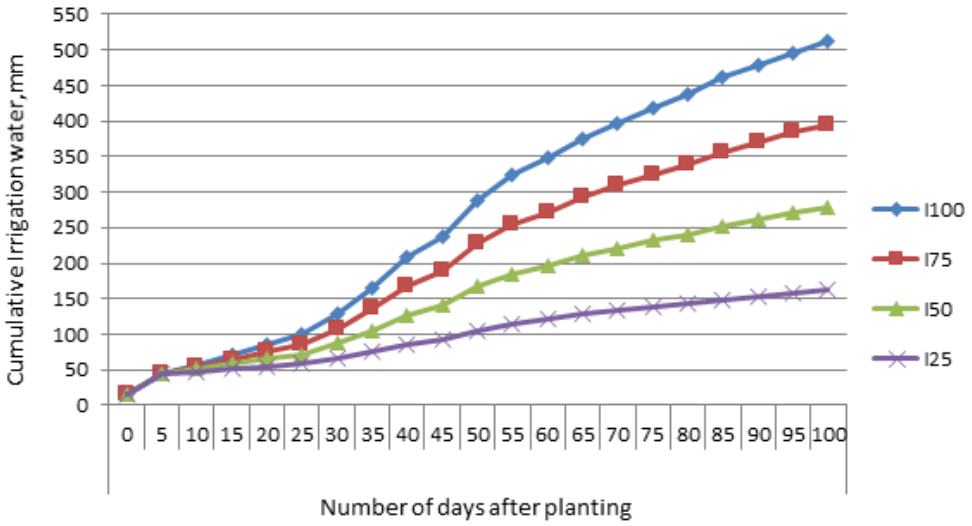

Figure 1. *The amount of cumulative irrigation water in 2017*

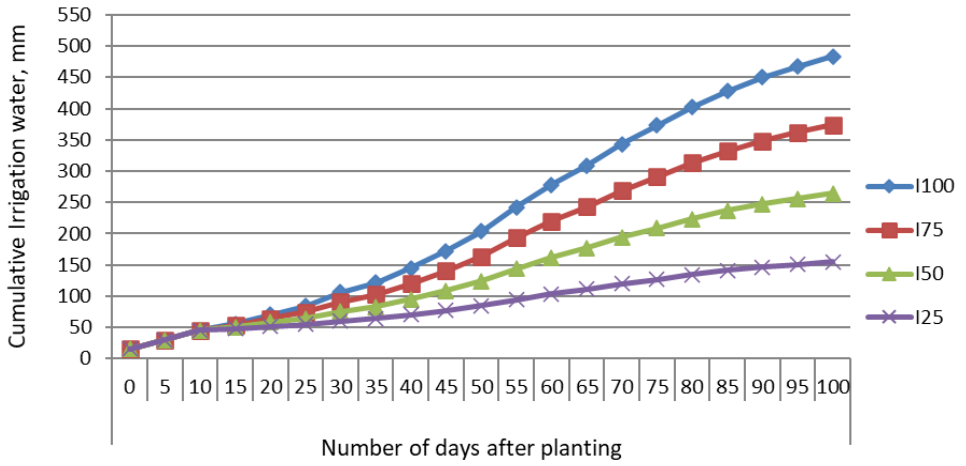

Figure 2. *The amount of cumulative irrigation water in 2018*

Table 6. *Irrigation water applied (IWA) and seasonal evapotranspiration (ET)*

Applications	IWA (mm)		ET (mm)	
	2017	2018	2017	2018
$I_{25}M$	161	154	266	276
$I_{25}NM$	161	154	247	268
$I_{50}M$	278	264	374	358
$I_{50}NM$	278	264	326	350
$I_{75}M$	395	373	450	474
$I_{75}NM$	395	373	488	510
$I_{100}M$	512	483	558	579
$I_{100}NM$	512	483	570	593

http://www.aloki.hu ● ISSN 1589 1623 (Print) ● ISSN 1785 0037 (Online)
DOI: http://dx.doi.org/10.15666/aeer/1804_54375447

Irrigation continued at intervals of 5 days in 100 days after the planting as shown in *Figures 1* and *2*. Irrigation water and evapotranspiration values changed according to the experimental treatments. In 2017, irrigation water ranged from 161 to 512 mm and evapotranspiration ranged from 266 to 570 mm. In 2018, irrigation water ranged between 154-483 mm and evapotranspiration ranged from 276-593 mm. The highest evapotranspiration was obtained from I_{100} × NM and the lowest water consumption was obtained from I_{25} × NM in both years. Mukherjee et al. (2010) obtained the highest water consumption from the subject without mulch where irrigation started, when the cumulative pan evaporation was 25 mm. Similarly, Hatami et al. (2012) obtained the highest water consumption from the subject without mulch.

Quality characteristics

pH is a criterion taken into consideration in the evaluation of tomato quality. The differences in the fruit pH among irrigation regimes were significant both for 2017 and 2018. The pH decreased as the irrigation rate was decreased. The highest pH values, 4.60 and 4.57 were obtained in the I_{100}×M and I_{100}×NM combination in 2017 respectively. On the other hand, the highest pH value, 4.62 was obtained in the I_{100}×M combination in 2018. Similar results were obtained in some studies on this subject and it was observed that the pH content decreased as irrigation water amount decreased (Ünlü et al., 2006; Lahoz et al., 2016; Tarı and Sapmaz, 2017).

The perforation resistance of fruits in table tomatoes is an important quality criterion and is significantly affected by agricultural processes applied in cultivation. The results of the presents study shows that perforation resistance of the fruits decreases as the irrigation rate decreases. The highest perforation resistance values, 1.618 and 1.613 bar were obtained in the I_{100}×M and I_{100}×NM combination in 2017, respectively. The highest perforation resistance value, 1.64 was obtained in the I_{100}×M and I_{100}×NM in 2018. Lahoz et al. (2016), Ünlü et al. (2006) and Tarı and Sapmaz (2017), have reached similar results in their studies.

The highest fruit diameter was obtained in full irrigation (I_{100}) application in both years. Mulch application was found to be statistically significant and fruit diameter was found to be higher in mulch applications. Fruit diameter values ranged between 44.62-62.02 mm in 2017 and ranged between 51.73-66.40 mm in 2018. The highest values were obtained in I_{100} × M application from 62.02 mm to 66.40 mm respectively in both years. The lowest values were obtained in I_{25}×NM application from 44.62 to 51.73 mm respectively in both years. Fruit diameter was observed to increase as irrigation water increased. The same situation was also observed in mulch application. Özbahçe and Tarı (2009), Ertek et al. (2012) have reached similar results in their studies and reported fruit diameter was increase as irrigation water increased. Biswas et al. (2015) and Samaila et al. (2011) reported that fruit diameter was increased with mulch application

The highest fruit length was obtained in full irrigation (I_{100}) application in both years. Mulch application was found to be statistically significant and fruit length was found to be higher in mulch applications. Fruit length values ranged between 34.00-46.79 mm in 2017 and it ranged between 42.50-48.06 mm in 2018. In 2017, the highest fruit length was obtained from I_{100} × M, I_{100} × NM and I_{75} × NM interactions as 46.99 mm, 46.71 mm and 46.57 mm respectively. In 2018, it was obtained from I100 × M interaction as 48.06 mm. The results show that the fruit size increased as the irrigation level increased. The same is valid for the mulch application. Ertek et al. (2012) and Biswas et al. (2015), have reached similar results in their studies.

http://www.aloki.hu ● ISSN 1589 1623 (Print) ● ISSN 1785 0037 (Online)
DOI: http://dx.doi.org/10.15666/aeer/1804_54375447

The TSS/TA ratio has a better effect on the acid on fruit taste than soluble solids or titratable acidity. This is because the acid content tends to decrease with the ripening of the fruit while the sugar content tends to increase (Zoran et al., 2014). In the present study, mulch was not found to be statistically significant, but it was observed that irrigation level affected the TSS/TA ratio statistically. In 2017, the highest TSS/TA values were obtained from I_{100} × M, I_{75}× M and I_{75} × NM interactions as 23.12, 22.62, and 22.61 respectively. In 2018, the highest value was obtained from I_{75} × NM as 26.84. Irrigation level was found to be significant in both years and I_{75} irrigation gave the best results statistically.

Colour b value of the fruit is a quality criterion that expresses the yellowness of the fruit surface. Mulch and irrigation level were found to be statistically significant for the colour value of the fruit. It was observed that the b value gets higher when the irrigation level decreases. In 2018, the highest b values were obtained from the interactions of I_{25} × NM, I_{75} × M, I_{50} × NM and I_{25} × M, respectively, as 30.36, 29.76, 29.61, and 29.58. In conclusion, mulch, irrigation and mulch × irrigation interaction were found to be statistically significant.

Colour a value of the fruit is a quality criterion that expresses the redness of the fruit surface. Mulch and irrigation level were found to be statistically significant for colour a value in the fruit. The a value of the fruit varied between 32.89 and 34.45 in mulch application and between 32.16 and 37.39 in no mulch application. The highest a value was obtained from I_{100} × NM and I_{25} × NM interactions, as 37.39 and 36.58, respectively. In conclusion, mulch, irrigation and mulch × irrigation interaction were found to be statistically significant (*Table 7*).

Table 7. *Irrigation × mulch application interactions for the fruit quality parameters*

pH			**Fruit perforation resistance**		
Irrigation	**Mulch**	**No mulch**	**Irrigation**	**Mulch**	**No mulch**
2017 yr			**2017 yr**		
I_{25}	4.343 c	4.320 c	I_{25}	1.266 c	1.240 c
I_{50}	4.433 bc	4.426 bc	I_{50}	1.386 abc	1.333 bc
I_{75}	4.500 ab	4.496 ab	I_{75}	1.486 abc	1.586 ab
I_{100}	4.603 a	4.570 a	I_{100}	1.618 a	1.613 a
2018 yr			**2018 yr**		
I_{25}	4.360 d	4.326 d	I_{25}	1.286 cd	1.206 d
I_{50}	4.423 cd	4.426 cd	I_{50}	1320 bcd	1.286 d
I_{75}	4.506 bc	4.503 bc	I_{75}	1.480 abc	1.513 ab
I_{100}	4.623 a	4.583 ab	I_{100}	1.640 a	1.640 a
Fruit diameter			**Fruit length**		
Irrigation	**Mulch**	**No mulch**	**Irrigation**	**Mulch**	**No mulch**
2017 yr			**2017 yr**		
I_{25}	47.49 cd	44.62 d	I_{25}	35.52 c	34.00 c
I_{50}	54.09 b	46.87 cd	I_{50}	42.51 b	35.55 c
I_{75}	58.83 ab	53.09 bc	I_{75}	44.14 b	46.71 a
I_{100}	62.02 a	59.16 ab	I_{100}	46.79 a	46.57 a

http://www.aloki.hu ● ISSN 1589 1623 (Print) ● ISSN 1785 0037 (Online)
DOI: http://dx.doi.org/10.15666/aeer/1804_54375447

2018 yr			**2018 yr**		
I_{25}	52.90 c	51.73 c	I_{25}	44.12 c	42.50 d
I_{50}	56.14 bc	55.10 bc	I_{50}	44.69 c	44.20 c
I_{75}	59.99 b	57.91 b	I_{75}	46.01 b	46.07 b
I_{100}	66.40 a	58.72 b	I_{100}	48.06 a	46.76 b
TSS/TA ratio			**Colour a**		
Irrigation	**Mulch**	**No mulch**	**Irrigation**	**Mulch**	**No mulch**
2017 yr			**Average of two years**		
I_{25}	19.87 b	19.67 b	I_{25}	34.45 b	36.58 a
I_{50}	21.17 ab	21.20 ab	I_{50}	33.20 c	3216 c
I_{75}	2262 a	22.61 a	I_{75}	33.15 c	35.02 b
I_{100}	23.12 a	21.36 ab	I_{100}	32.89 c	37.39 a
2018 yr			**Average colour b**		
I_{25}	23.19 bc	25.54 ab	I_{25}	29.58 a	30.36 a
I_{50}	21.98 c	24.89 abc	I_{50}	29.37 ab	29.61 a
I_{75}	26.22 ab	26.84 a	I_{75}	29.76 a	27.29 c
I_{100}	25.52 abc	23.22 bc	I_{100}	28.24 bc	27.80 c

Conclusions

According to the results of this research, irrigation water level, mulch application and irrigation water-mulch interaction had significant effects on the quality of tomato. The study shows that pH, fruit puncture resistance, fruit diameter, fruit length and TSS/TA ratio increased with increasing amount of irrigation water. Mulch application was found to increase these quality criteria regardless of irrigation water levels. The best results were obtained from fully irrigated (I_{100}) subjects in both years. In some quality parameters, there was no significant difference between I_{75} and I_{100} applications. As a result, it can clearly be stated that as the irrigation level increased, the quality criteria characteristics examined within this study gave better results.

Acknowledgements. This paper is extracted from the PhD dissertation of the first author from the Biosystems Engineering Department of Agriculture and Natural Sciences Faculty of Bilecik Şeyh Edebali University. Authors are also grateful to Bilecik Seyh Edebali University Scientific Research Projects Department for supporting the experiment through Project no: 2018-01. BSEÜ.06-01 at Bilecik location.

REFERENCES

[1] Abak K., Pakyürek A. Y., Gürsöz N., Onsinejad R. (1990): Effect of mulch applications on soil temperature in greenhouse, yield and earliness of some vegetables. – Turkey V. Greenhouse Symposium, 17-19 October, İzmir, 55-62.

[2] Ahmadi, S. H., Andersen, M. N., Plauborg, F., Poulsen, R. T., Jensen, C. R., Sepaskhah, A. R., Hansen, S. (2010): Effects of irrigation strategies and soils on field grown potatoes: yield and water productivity. – Agricultural Water Management 97(11): 1923-1930.

http://www.aloki.hu ● ISSN 1589 1623 (Print) ● ISSN 1785 0037 (Online)
DOI: http://dx.doi.org/10.15666/aeer/1804_54375447

[3] Allen, R. G., Pereira, L. S., Raes, D., Smith, M. (1998): Crop evapotranspiration. guidelines for computing crop water requirements. – FAO Irrigation Drainage Paper No. 56, FAO, Rome, Italy.
[4] Anonymous (2014): Water and water management in Turkey condition new approach: environmental perspectives. – Nature Conservation Center. www.tbcsd.org, www.dkm.org.tr.
[5] Biswas, S. K., Akanda, A. R., Rahman, M. S., Hossain, M. A. (2015): Effect of drip irrigation and mulching on yield, water-use efficiency and economics of tomato. – Plant, Soil and Environment 61(3): 97-102.
[6] Cemeroğlu, B. (2010): Food Analyzes. Expanded 2nd Ed. – Food Technology Association Publications, No: 34, Ankara.
[7] Ekinci, M., Dursun, A. (2009): Effects of different mulch materials on plant growth, some quality parameters and yield in melon (*Cucumis melo* L.) cultivars in high altitude environmental condition. – Pakistan Journal of Botany 41(4): 1891-1901.
[8] Ertek, A., Erdal I., Yilmaz H. I., Senyigit U. (2012): Water and nitrogen application levels for the optimum tomato yield and water use efficiency. – J. Agric. Sci. Technol. 14: 889-902.
[9] FAO (2011): The State of the World's Land and Water Resources for Food and Agriculture: Managing Systems at Risk. – Land and Water Division, FAO/Earthscan, Rome/London.
[10] FAO (2013): Aquastat 2013. – http://www.fao.org/nr/water/aquastat/main/index.stm.
[11] FAO (2018): FAOSTAT. – http://www.fao.org/faostat/en/#home.
[12] Favati, F., Lovelli, S., Galgano, F., Miccolis, V., Di Tommaso, T., Candido, V. (2009): Processing tomato quality as affected by irrigation scheduling. – Scientia Horticulturae 122(4): 562-571.
[13] Garrity, D. P., Watts, D. G., Sullivan, C. Y., Gilley, J. R. (1982): Moisture deficits and grain sorghum performance: evapotranspiration-yield relationships 1. – Agronomy Journal 74(5): 815-820.
[14] Hanson, B. R., May, D. M. (2006): Crop evapotranspiration of processing tomato in the San Joaquin Valley of California, USA. – Irrigation Science 24(4): 211-221.
[15] Hatami, S., Nourjou, A., Henareh, M., Pourakbar, L. (2012): Comparison effects of different methods of black plastic mulching and planting patterns on weed control, water-use efficiency and yield in tomato crops. – International Journal of Agri Science 2(10): 928-934.
[16] Kanber, R. (1984): Irrigation of first and second product peanuts by utilizing open water surface evaporation in Çukurova conditions. – Regional Groundwater Research Institute Publications 114: 64-93.
[17] Koçar, G. (2001): Effects of mulching with different colored polyethylene on lettuce production on greenhouse. – Journal of Aegean Agricultural Research Institute 11(1): 47-55.
[18] Korkmaz S. S., Balkaya, A. (2016): The effects of different coloured mulch application on earliness, yield and quality in snap bean (*Phaselous vulgaris* L.) cultivation during autumn season. – Journal of Atatürk Central Horticultural Research Institute 45(2): 278-282.
[19] Kurtar, E. S. (2010): The effects of mulch applications on summer squash (*Cucurbita pepo* L.) production in an unheated glasshouse in autumn season. – Harran Journal of Agricultural and Food Science 14(2): 69-76.
[20] Kuşçu, H., Turhan, A., Demir, A. O. (2014): The response of processing tomato to deficit irrigation at various phenological stages in a sub-humid environment. – Agricultural Water Management 133: 92-103.
[21] Lahoz, I., Pérez-de-Castro, A., Valcárcel, M., Macua, J. I., Beltrán, J., Roselló, S., Cebolla-Cornejo, J. (2016): Effect of water deficit on the agronomical performance and quality of processing tomato. – Scientia Horticulturae: 200: 55-65.

http://www.aloki.hu ● ISSN 1589 1623 (Print) ● ISSN 1785 0037 (Online)
DOI: http://dx.doi.org/10.15666/aeer/1804_54375447

[22] Lascano, R. J., Sojka, R. E. (2007): Irrigation of Agricultural Crops. 2nd Ed. – ASA Agronomy Monograph, 30. American Society of Agronomy, Madison.
[23] Locascio, S. J., Smajstrla, A. G. (1996): Water application scheduling by pan evaporation for drip-irrigated tomato. – Journal of the American Society for Horticultural Science 121(1): 63-68.
[24] Mukherjee, A., Kundu, M., Sarkar, S. (2010): Role of irrigation and mulch on yield, evapotranspiration rate and water use pattern of tomato (*Lycopersicon esculentum* L.). – Agricultural Water Management 98(1): 182-189.
[25] Patanè, C., Cosentino, S. L. (2010): Effects of soil water deficit on yield and quality of processing tomato under a Mediterranean climate. – Agricultural Water Management 97(1): 131-138.
[26] Salokhe, V. M., Babel, M. S., Tantau, H. J. (2005): Water requirement of drip irrigated tomatoes grown in greenhouse in tropical environment. – Agricultural Water Management 71(3): 225-242.
[27] Samaila, A. A., Amans, E. B., Babaji, B. A. (2011): Yield and fruit quality of tomato (Lycopersicon esculentum Mill) as influenced by mulching, nitrogen and irrigation interval. – International Research Journal of Agricultural Science and Soil Science 1(3): 90-95.
[28] Tarı, A. F., Sapmaz, M. (2017): The effect of different irrigation levels on the yield and quality. – Soil Water Journal 6(2): 11-17.
[29] Ünlü, H. Ö., Ünlü, H., Karataş, A., Padem, H., Kitiş, Y. E. (2006): The effect of different mulch color on the yield and quality properties of tomato. – Alatarım 5(1): 10-14.
[30] Wang, Q., Li, F., Zhang, E., Li, G., Vance, M. (2012): The effects of irrigation and nitrogen application rates on yield of spring wheat (longfu-920), and water use efficiency and nitrate nitrogen accumulation in soil. – Australian Journal of Crop Science 6(4): 662-672.
[31] Zegbe-Dominguez, J. A., Behboudian, M. H., Lang, A., Clothier, B. E. (2003): Deficit irrigation and partial rootzone drying maintain fruit dry mass and enhance fruit quality in 'Petopride' processing tomato (*Lycopersicon esculentum*, Mill.). – Scientia Horticulturae 98(4): 505-510.
[32] Zoran, I. S., Nikolaos, K., Ljubomir, Š. (2014): Tomato Fruit Quality from Organic and Conventional Production. – In: Pilipavicius, V. (ed.) Organic Agriculture Towards Sustainability. InTech Europe, Rijeka, Croatia, pp: 147-169.

http://www.aloki.hu ● ISSN 1589 1623 (Print) ● ISSN 1785 0037 (Online)
DOI: http://dx.doi.org/10.15666/aeer/1804_54375447

PHYLOGENETIC STUDY OF THE GENERA *MICHAUXIA* L'HÉRIT., *ASYNEUMA* GRISEB. ET SCHENK AND *LEGOUSIA* DURAND (CAMPANULACEAE) IN THE KURDISTAN REGION-IRAQ

SHILAN, A. H.* – JAWHER, F. S.

Department of Biology, College of Education, Salahaddin University-Erbil, Iraq

**Corresponding author*
e-mail: shilan.husain@su.edu.krd; phone: +96-4075-0456-8479

(Received 2nd Mar 2020; accepted 25th May 2020)

Abstract. Campanulaceae are a highly diverse clade of angiosperms. Chloroplast markers have greatly improved our understanding of this clade, but many relationships remain unclear primarily due to low levels of molecular evolution and recent and rapid divergence. Furthermore, focusing solely on maternally inherited markers such as those from the chloroplast genome may obscure processes such as hybridization. We explore the phylogenetic utility of two low-copy nuclear loci from the pentatricopeptide repeat gene family (PPR). Rapidly evolving nuclear loci may provide increased phylogenetic resolution in clades containing recently diverged or closely related taxa. We present results based on chloroplast and low-copy nuclear loci, and discuss the utility of such markers to resolve evolutionary relationships and infer hybridization events within Campanuloideae clade. The phylogeny of the genera *Michauxia*, *Asyneuma* and *Legousia* in Kurdistan Region was investigated by using eight in-group species and one out-group related genus *Campanula conferta*, based on the *matK*-KIM intergenic region of chloroplast DNA and internal transcribed spacer of nuclear ribosomal DNA. Individual and combined analysis of *matK*-KIM and ITS2 sequence data indicated monophyly of the *Asyneuma* and *Legousia* genera, the results for bayesian and maximum parsimony displayed three clades of *Michauxia, Asyneuma,* and *Legousia* with high supports (bs=76%, pp=0.100).
Keywords: *Bellflower family, matK-KIM, ITS2, evolutionary relationships, phylogeny*

Introduction

The genera *Michauxia*, *Asyneuma,* and *Legousia,* belong to the family Campanulaceae (Bellflower family), which is the second-largest family in the Asterales and third most abundant family in the campanulate, Jussieu formally described it in 1789 (Hansen, 2016). Campanulaceae family belonged to the Orders: Campanulate, Subclass: Asteridae and Class: Magnoliopsida (Cronquist, 1981; Watson and Dallwitz, 1992).

The family includes 84 genera and 2330 species, which are widespread in the world except for the major desert regions (Byng, 2014), while in the Kurdistan region of Iraq, the family includes 4 genera and 26 species distributed in different districts (Ghazanfar and Edmondson, 2013). The family (Campanulaceae s. str.) classification systems have historically followed the arrangements of Boissier (1875) and Schönland (1889), along with the refinements of Charadze (1949, 1970, 1976), Fedorov (1957), which can eventually be traced back to the arrangement of De Candolle (1839) who divided the family into two subtribes, the Campanuleae and the Wahlenbergeae, based on the mode of capsule dehiscence although Schönland split the family into three subtribes, Platycodon A. DC., Musschia Dum. and Microcodon A. DC segregated. The Platycodinae subtribe is based on the calyx lobe position concerning the locules of the ovary. Such natural classifications were necessarily based on the morphology of the calyx (e.g., the presence or absence of appendages between the lobes) or of the mode of capsule

http://www.aloki.hu ● ISSN 1589 1623 (Print) ● ISSN1785 0037 (Online)
DOI: http://dx.doi.org/10.15666/aeer/1804_54495460

dehiscence (e.g., whether it is apical and valvate or lateral and porate). Many authors (e.g., Hutchinson, 1969; Carolin, 1977; Cronquist, 1988; Takhtajan, 2009) considered *Cyananthus* A. DC. to be the most primitive genus within the family based on its superior ovary (Eddie et al., 2003).

Phylogenetic reconstruction is now an essential tool for biologists to understand the processes that govern the evolution of organisms. Restoration of divergence times and past biogeographical ranges has grown in importance. It is reflected in the multitude of new methods developed to infer organisms' spatial and temporal evolution (Sanderson, 2002; Thorne and Kishino, 2002; Ree et al., 2005; Drummond et al., 2006). Molecular and phylogenetic methods allow researchers to obtain large, multi-gene datasets for phylogenetic studies, because of highly conserved genome organization, gene order, and gene content of the chloroplast genome across much of angiosperm diversity (Cosner et al., 1991; Haberle, 2006).

In plants, chloroplast DNA (Evans et al., 2015), nuclear ribosomal DNA (Faghir et al., 2014), and mitochondrial DNA are three molecular variations tapped for phylogenetic purposes (Yu et al., 2018). The ITS region consists of three parts: the ITS1, ITS2, and the highly conserved 5.8S rDNA exon locate between them. The Campanulaceae family undertook few molecular phylogenetic studies among it's the study of Cosner and Jansen (1993) and Cosner et al. (2004) which used structural rearrangements of chloroplast DNA (cpDNA) to establish a family phylogeny based on 18 genera, while *rbc*L sequences for several genera were determined by Cosner et al. (1994) as part of the Campanulales interfamily relationship study.

Eddie et al. (2003) investigated the morphology of most genera of the family Campanulaceae by using cladistic and phonetic methodologies, in addition to the molecular variation of 23 to 29 taxa, he also used internal transcribed spacers (ITS2) and *mat*K-KIM -intron sequence data from nuclear ribosomal (nrDNA) and cpDNA in another hand Eddie et al. (2003) used 93 taxa comprising 32 genera to estimate family phylogeny based on ITS sequences of nuclear ribosomal DNA also including the sequences of chloroplast genes *mat*K and *rbc*L, as well as chloroplast genome rearrangements and morphology data.

One of the most comprehensive studies on the Campanulaceae family was presented by Crowl et al. (2016), providing a broad phylogenetic and phylogeographic perspective that included chromosomal and morphological data. Previously, Crowl et al. (2014) had produced a first phylogenetic analysis conjointly applying several molecular markers used in previous studies within the subfamily Campanuloideae, namely the chloroplast markers atpB, matK, petD, rbcL, and trnL-F and the nuclear region ITS.

DNA barcoding is a technique in which sequences of a specific DNA region are compared for species identification. Establishing the most suitable region for plants has taken a little longer. The partial *matK* gene was recently adopted as the 'plant barcode' by the Consortium for the Barcoding of Life (CBOL Plant Working et al., 2009) after much deliberation. However, there are still significant challenges that need to be overcome using these DNA regions. There have been three main sets of supposedly 'universal' *matK* primers proposed so far: namely, 390F and 1326R, XF and 5R and 1R-KIM and 3F-KIM (Dunning and Savolainen, 2010).

The internal transcribed spacer 2 (ITS2) region of nuclear ribosomal DNA is regarded as one of the candidate DNA barcodes because it possesses several valuable characteristics, such as the availability of conserved regions for designing universal primers, the ease of its amplification, and sufficient variability to distinguish even closely

http://www.aloki.hu ● ISSN 1589 1623 (Print) ● ISSN1785 0037 (Online)
DOI: http://dx.doi.org/10.15666/aeer/1804_54495460

related species. However, a general analysis of its ability to discriminate species in a comprehensive sample set is lacking (Yao et al., 2010).

The present study aims to investigate the relativeness between the genera of *Michauxia, Asyneuma* and *Legousia* based on the phylogenetic relationships and comparing with the nearest genus. For this purpose, two regions were selected, the first region is chloroplast DNA *matK*-1RKIM and the second is nuclear ribosomal DNA ITS2. This manuscript is a part of the author's Ph.D. dissertation.

Material and Methods

Taxon Sampling

The plant taxa used in the present study were collected from the different districts of Kurdistan region-Iraq during the period between 2017-2018 that preserved in the Herbarium of the College of Education/ Salahaddin University-Erbil and all plant samples were collected from Duhok, Zawita, Gali Ali Bag, Gali Zanta, Gara mountain, Piramagroon, Hawraman mountain and Shaqlawa (*Fig. 1*). Nine distinct taxa consist of eight in-group taxa and one out- group *Campanula conferta* were used in the analysis.

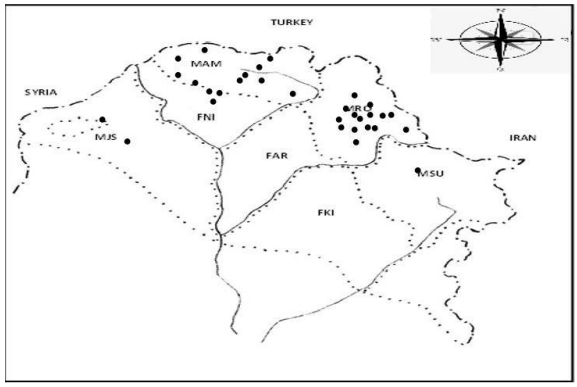

Figure 1. *A map shows the distribution of the three genera species in Kurdistan Region-Iraq*

DNA Extraction

According to the manufacturer's instructions, genomic DNA was extracted from collected plant specimens through the Presto™ Mini gDNA Bacteria Kit (Geneaid, Taiwan); extract was eluted with an elution buffer of 100 µL. Before running PCR, extracts were stored at -20°C. The NanoDrop 1000 spectrophotometer (ThermoFisher Scientific, USA) was used to evaluate DNA concentration and purity in which one µL of the genome DNA was used to define DNA concentration and purity.

PCR and DNA Sequencing

The two noncoding regions of nrDNA and cpDNA were amplified by using the primers *matK*-KIM of Dunning and Savolainen (2010), and ITS of White et al. (1990) for *matK*-KIM intergenic spacer and ITS region respectively (*Table 1*). The primers were ordered from Macrogen Company, Seoul, Korea. The total volume of amplification reactions was 25 µL and the Master Mix made up of 12.5 µL (the Master Mix consisting of 3 mM $MgCl_2$, 0.2% Tween® 20, 20 mM Tris-HCl pH 8.5, $(NH_4)2S0_4$, 0.2 units/µl

http://www.aloki.hu ● ISSN 1589 1623 (Print) ● ISSN1785 0037 (Online)
DOI: http://dx.doi.org/10.15666/aeer/1804_54495460

Ampliqon Taq DNA polymerase, 0.4 µM of each primer, and 0.4 mM of each dNTP.), 3 µL genomic DNA extract (density of 10 ng/µl), 2 µL of each primer, 5.5 µL free nuclease water. The PCR-Thermal cycler for *matK* gene started with 5 min for initial denaturation at 94°C followed by 35 cycles: denaturation at 94°C for 30 sec.; annealing at 54°C for 60 sec.; extension at 72°C for 60 sec. And the final extension at 72°C for 5 min. While the PCR program for the *ITS* gene started with 5 min for initial denaturation at 94°C followed by 35 cycles: denaturation at 94°C for 30 sec.; annealing at 56°C for 20 sec.; extension at 72°C for 20 sec. And the final extension at 72°C for 5 min. The resultant PCR products were checked on 1.5% agarose gel run in TAE buffer. The gel was stained with Safe red dye and photographed under UV transilluminator.

Table 1. *List of primers and their sequences that have used in the study*

Primer	Oligonucleotide Sequence	References
ITS2-S2	F: 5'-ATG CGA TAC TTG GTG TGA AT-3'	(White et al., 1990)
ITS4	R: 5'-TCC TCC GCT TAT TGA TAT GC-3'	
***mat*K-1KIM**	F: 5'-ACC CAG TCC ATC TGG AAA TCT TGG TTC-3'	(Dunning and Savolainen, 2010)
***mat*K-3KIM**	R: 5'-CGT ACA GTA CTT TTG TGT TTA CGA G-3'	

PCR products were purified by using Kits (Promega company-Madison-USA). The purified PCR products were sent to the National Science and Technology Development Agency (NSTDA) in Thailand for sequencing.

Sequence Alignment

All the DNA sequences were edited and aligned with the ClastalW option available in BioEdit, Version 7.0.4.1 (Hall, 2001), and manual adjustment. There are seven accessions for each *matK*-F and ITS regions, including the out-group species.

Phylogenetic Analyses

Maximum Parsimony Analysis

The reconstruction of the phylogenetic relationships was based on Maximum Parsimony (MP) methods. The analysis was carried out for separate and combined regions. MP analysis was performed by using PAUP* version 4.0a164 (Swofford, 2000). Using heuristic search with 100 replicates of random taxon additions, Tree-Bisection-Reconnection (TBR) branch swapping, MulTrees on, and steepest descent off was performed. The maximum numbers of saved trees were 100 for each replicate. The bootstrap values were calculated from 100 replicates; the consistency index (CI), retention index (RI), rescaled consistency, and homoplasy index (HI) were measured (Felsenstein, 1985).

Bayesian Analysis

Bayesian analysis was carried out by using the MrBayes version. 3.2 (Ronquist and Huelsenbeck, 2003). The parameters and evolutionary models were selected by the assistant of MrModeltest2 version 2.3 (Nylander et al., 2004), based on Akaike Information Criterion (AIC), which selected the GTR+G model for regions. Two independent analyses were run 1000000 generations with four chains (one cold and three

http://www.aloki.hu ● ISSN 1589 1623 (Print) ● ISSN1785 0037 (Online)
DOI: http://dx.doi.org/10.15666/aeer/1804_54495460

heated) for each generation and the temperature parameter set to 0.1. Trees were sampled every 100th generations. After that (25% of initial tree sampled) were removed by burn-in period samples, a tree with a maximum 50% (majority rule consensus tree) was plotted. The value of posterior probability (PP) was calculated, and the final tree was plotted by using FigTree software version 1.4.3 (Rambaut, 2016).

Results

The characteristics of each data matrix and tree statistics of *mat*K and ITS regions are summarized in (*Table 2*).

Table 2. *A summary of alignment and tree statistics of matK, ITS and combined analyses*

Parameters/Regions	*matK*	ITS	Combined
Aligned length	873	362	1343
Number of parsimony informative characters	208	70	204
Number of variable parsimony uninformative characters	517	231	544
Number of constant characters	148	61	595
Tree length (steps)	1134	380	1097
CI (Consistency Index)	0.873	0.934	0.846
RI (Retention Index)	0.489	0.833	0.501
RC (Rescaled Index)	0.427	0.779	0.424
HI (Homoplasy index)	0.304	0.066	0.154
Model	GTR+G	GTR+G	GTR+G

In this study, plant genomic DNA was extracted from entire plant tissue by using the Presto™ Mini gDNA Bacteria Kit. Isolated genomic DNA was electrophoresed on 0.8% agarose gel to confirm the integrity of the isolated DNA (*Fig. 2*).

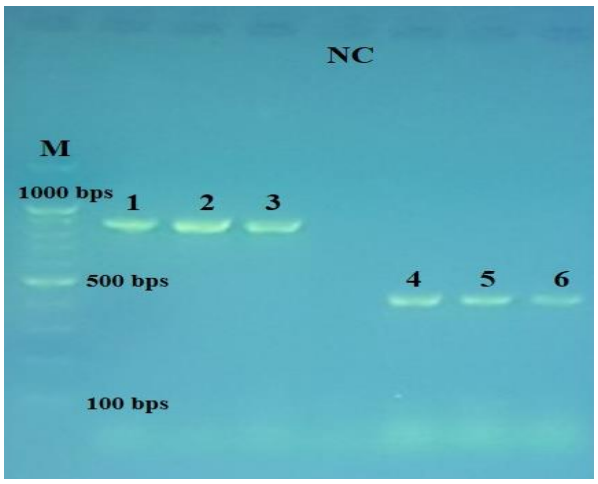

Figure 2. *Agarose gel electrophoresis of products using matK-KIM and ITS primers from studied taxa of Michauxia, Asyneuma, and Legousia. M: DNA marker with 100 bps. Lanes 1-3: positive amplification of 900 bps for matK-KIM gene (Lanes 1: M. nuda, Lanes 2: M. laevigata, Lanes 3: L. falcata). Lane NC: negative control. Lanes 4-6 positive amplification of 400 bps for ITS gene (Lanes 4: L. speculum-veneris, Lanes 5: L. pentagonia, Lanes 6: A. persicum)*

http://www.aloki.hu ● ISSN 1589 1623 (Print) ● ISSN1785 0037 (Online)
DOI: http://dx.doi.org/10.15666/aeer/1804_54495460

Phylogenetic relationships within Michauxia, Legousia and Asyneuma

Three major clades were recovered within *Michauxia, Asyneuma* and *Legousia* for *mat*K region and two major clades for nuclear ribosomal DNA ITS tree, although the positions of these clades are varied (*Figs. 3, 4 and 5*). The analyses were carried out for separate and combined regions, consisted of eight in-groups and one out-group taxa.

The clades of matK region as shown in *Figure 3* are as follow: Clade A consists of only *Michauxia nuda* with bootstrap support (bs=100%, pp=0.67); clade B consists of *Legousia falcate, Legousia speculum-veneris, Asyneuma pulchellum* and *Legousia pentagonia* and are highly supported (bs=100%, pp=0.96), while the clade C includes of *Michauxia laevigata, Asyneuma persicum* and *Asyneuma rigidum* var. *rigidum* and are highly supported (bs=100%, pp=0.59).

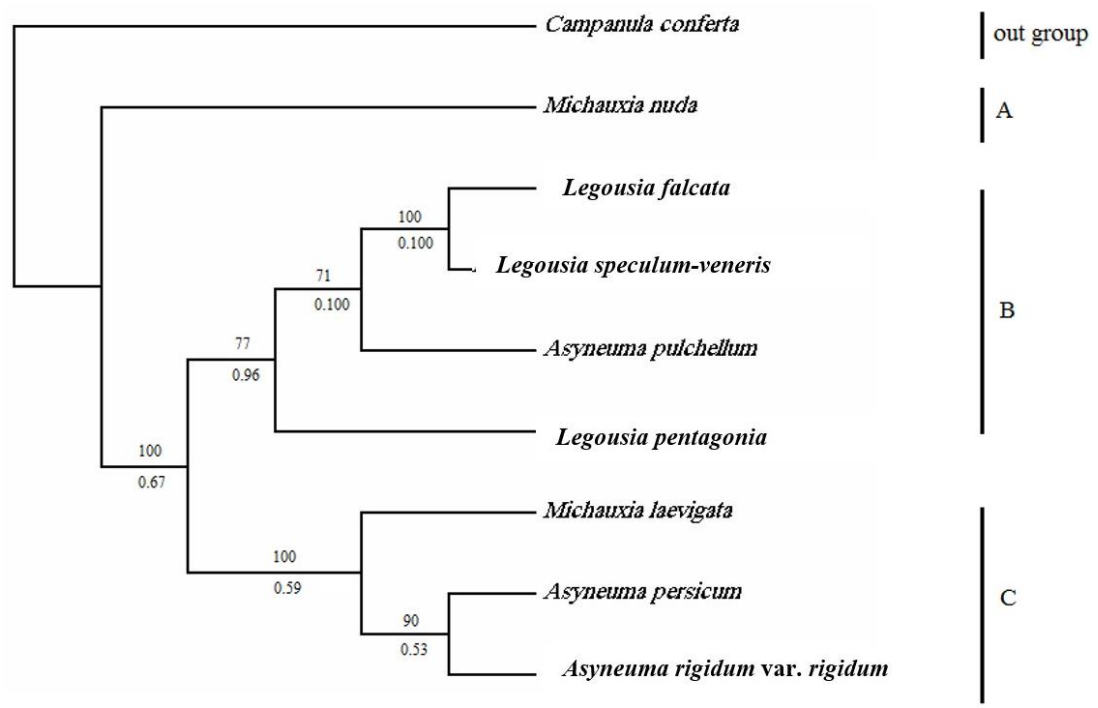

Figure 3. *Strict consensus tree of the most parsimonious tree resulting from phylogenetic analysis of the cpDNA matK sequences with a heuristic search using maximum parsimony analysis. (Tree length of 1134 steps, CI = 0.873, RI = 0.489, RC = 0.427 and HI =0.304). Numbers on the branches indicate bootstrap support, and numbers below branches are Bayesian posterior probability values and clades are identified by letters*

The clades of ITS regions as shown in *Figure 4* are as follow: Clade A consists of *L. falcate, L. speculum-veneris, A. pulchellum* and *L. pentagonia* with bootstrap support (bs=100%, pp=0.98); the clade B consists of *M. laevigata, M. nuda, A. persicum,* and *A. rigidum var. rigidum*, are highly supported (bs=98%, pp=0.90).

The clades of combined regions as shown in *Figure 5* are as follow: Clade A consists of *A. persicum, A. rigidum var. rigidum, M. laevigata* and *M. nuda* with bootstrap support (bs=76%, pp=0.52); the clade B consists of *L. pentagonia*, *A. pulchellum*, *A. pulchellum,* and *L. speculum-veneris* and are highly supported (bs=100%, pp=1.00).

http://www.aloki.hu ● ISSN 1589 1623 (Print) ● ISSN1785 0037 (Online)
DOI: http://dx.doi.org/10.15666/aeer/1804_54495460

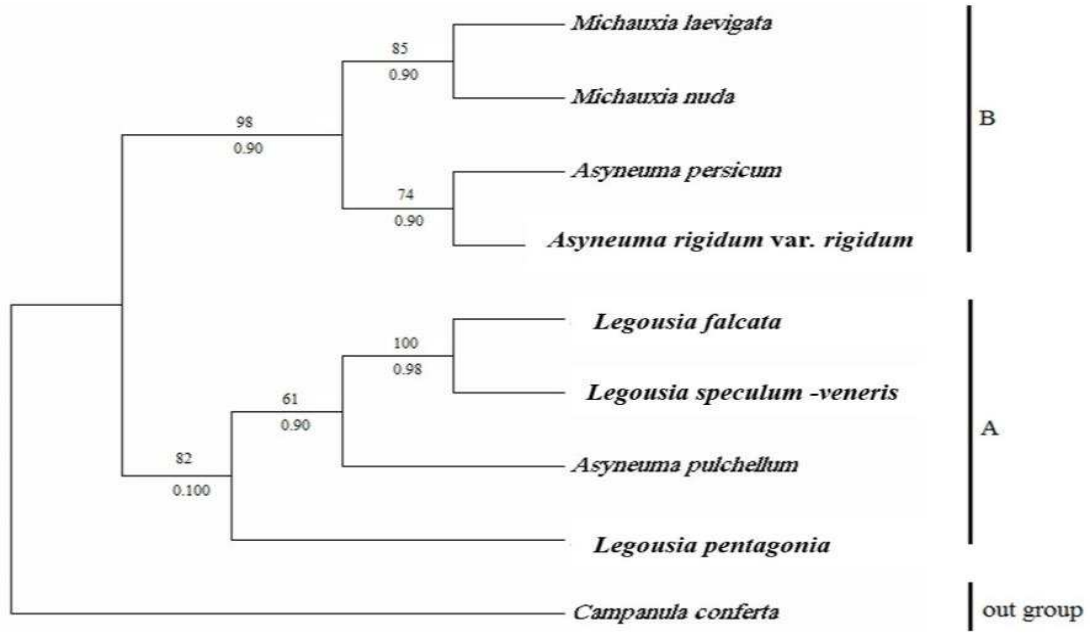

Figure 4. *Strict consensus tree of the most parsimonious tree resulting from phylogenetic analysis of the nrDNA ITS sequences with a heuristic search using maximum parsimony analysis. (Tree length of 380 steps, CI=0.934, RI=0.833, RC=0.779 and HI=0.066). Numbers on the branches indicate bootstrap support and numbers below branches are Bayesian posterior probability values and clades are identified by letters*

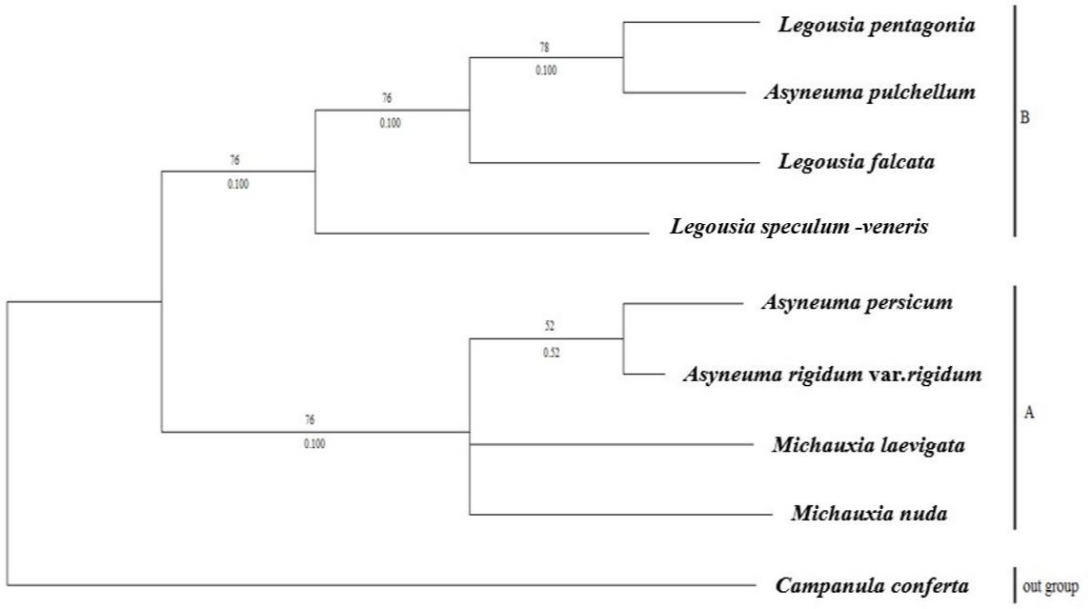

Figure 5. *Strict consensus tree of the most parsimonious tree resulting from phylogenetic analysis of the combined sequences with a heuristic search using maximum parsimony analysis. (Tree length of 1097 steps, CI = 0.846, RI = 0.501, RC = 0.424 and HI=0.154). Numbers on the branches indicate bootstrap support and numbers below branches are Bayesian posterior probability values and clades are identified by letters*

http://www.aloki.hu ● ISSN 1589 1623 (Print) ● ISSN1785 0037 (Online)
DOI: http://dx.doi.org/10.15666/aeer/1804_54495460

Discussion

Phylogenetic Analysis

As one of the essential markers in molecular systematics and evolution, *mat*K and ITS2 show significant sequence variability at the species level or lower. The availability of its structural information permits analysis at a higher taxonomic level, which provides additional information for improving accuracy and robustness in the reconstruction of phylogenetic trees (Coleman, 2003, 2009).

Furthermore, ITS2 is potentially useful as a standard DNA barcode to identify plants and it is regarded as one of the candidate DNA barcodes because of its valuable characteristics, including the availability of conserved regions for designing universal primers, the ease of its amplification, and enough variability to distinguish even closely related species (Chen et al., 2010).

The ITS2 sequence lengths of plants were mainly distributed in the 195–510 bps range. The identification of plant using DNA barcoding techniques is one of the main tasks in natural museums and research institutes. The length of the ITS2 region is sufficiently short to allow amplification of even degraded DNA (Meyer and Paulay, 2005).

Recently,the ITS2 region has been found to vary in primary sequences and secondary structures in a way that correlates highly with taxonomic classification. Several researchers have already demonstrated the potential for using ITS2 for taxonomic classification and phylogenetic reconstruction at both the genus and species levels for eukaryotes, including animals, plants, and fungi (Schultz et al., 2005; Coleman, 2007; Schultz and Wolf, 2009).

Based on the analysis of nuclear chloroplast matK data, the species *M. nuda* shared a single sister branch for all other taxa with supports (bs=100%, pp=0.6), due to the unusual occurrence and habit. It has differed with both clades B and C in some features as the species has between 7-9 number of calyx, corolla and stamens, present of small appendages of calyx, the shape of the inflorescence is narrowly conical and also the color of the flower is yellow (Fedorov, 1999). Phylogenetic relationships of clade B include four species. *L. falcata* phylogenetically nearest to *L. speculum-veneris*, they are monophyletic in this clade (bootstrap support (bs=100%, pp=0.100)) and differs morphologically from each other by calyx lobes, in *L. falcata*, the calyx lobes reflexed or curved downwards while in *L. speculum-veneris* the calyx lobes are erect and ascending (Ghazanfar and Edmondson, 2013). The species *A.pulchellum* has related with the monophyletic group in this clade (bs=71%, pp=0.100), the main difference among related monophyletic group is biennial herbs with *A. pulchellum* and annual herbs in the monophyletic group, in the other hand, *L. pentagonia* was related to above-closed group (bs=77%, pp=0.96). The *L. pentagonia* distinguishes with the related monophyletic group by the calyx lobes, which is half as long as the ovary and its capsule not constricted at the apex (Damboldt and Davis, 1978).

The clade C comprises three species, which include *M. laevigata*, with(and) the monophyletic group *A. persicum* and *A. rigidum* var. *rigidum*. The phylogenic relationship within this clade is that *A. persicum* and *A. rigidum* var. *rigidum* was classified in a monophyletic group with bootstrap support (bs=90%, pp=0.53) due to that both species are perennial herbs with black violet flowers and five stamens which are free while they differ in the shape of capsule and leaves. The capsule in *A. persicum* with nodding shape and dehiscent by 3 valves to the middle of the apex and the leaves shape are between linear to lanceolate while in the closed species, the capsule is oblong and

http://www.aloki.hu ● ISSN 1589 1623 (Print) ● ISSN1785 0037 (Online)
DOI: http://dx.doi.org/10.15666/aeer/1804_54495460

dehiscent by 3 valves to the end of the apex with the presence of oblong leaves (Rechinger, 1965). The species *M. laevigata* related monophyletic to the two first species in this clade with (bs=100%, pp=0.59). The main difference was observed within this clade is the number of stamens and colors of flowers. The stamens number of *M. laevigata* is between 8-10, and the intensity of flower color is yellow, while in both species in the monophyletic group, the number of the stamens is 5 and the color of the flower is violet (Tutin et al., 1993).

Phylogenetic analysis of the nrDNA ITS sequences showed two clades A and B with out-group *Campanula conferta*. The clade A includes four species. *L. falcata* phylogenetically nearest to *L. speculum-veneris* (bootstrap support (bs=100%, pp=0.98)) and differs morphologically from each other by the shape of corolla lobes, in *L. falcata*, the corolla lobes are acute. In contrast, in *L. speculum-veneris,* the corolla lobes are mucronate (Wahlsteen and Tyler, 2019).

The species *A.pulchellum* has related to the monophyletic group in this clade (bs=61%, pp=0.90), this species differs by having free corolla lobs, while the species in the monophyletic group have united corolla lobs (Ghazanfar and Edmondson, 2013). On the other hand, the species *L. pentagonia* was related to the above closed group (bs =82%, pp=0.100), this species discriminates from other species in this clade by having longer calyx lobes than the corolla tube and has ciliated filaments at the base. The clade B consist of four species in two monophyletic groups, the first group consists of *M. nuda* and *M. laevigata* (bs=85%, pp=0.90) due to the two species are biennial herbs and share in many features, while the second monophyletic group includes the two species *A. persicum* and *A. rigidum* var. *rigidum* (bs=74%, pp=0.90) because both are perennial herbs and have dilated filament at base (Rechinger, 1965).

Conclusions

In the present study three major clades within the species of the genera *Michauxia*, *Asyneuma* and *Legousia* were identified in the *matK*-KIM tree compared to combined tree which consists of only two clades, in the *matK*-KIM tree the clade A consists only of *M. nuda*; clade B consists of *L. falcate, L. speculum-veneris*, *A. pulchellum* and *L. pentagonia* while the clade C consists of *M. laevigata*, *A. persicum* and *A. rigidum var. rigidum* while in the combined tree the species *M. nuda* found in the clade A within the species *M. laevigata*, *A. persicum* and *A. rigidum var. rigidum*, the clade B in both trees are similar. The clades of ITS regions consist of two clades are as follow: Clade A consists of *L. falcate, L. speculum-veneris*, *A. pulchellum* and *L. pentagonia,* the clade A in ITS tree is similar to the clade B of the combined tree while the clade B in ITS tree is similar to the clade A in the combined tree. We suggest phylogenic analysis for all genera in the campanulacese family in Iraq and that helps to know the more molecular relationship among the family genera.

REFERENCES

[1] Boissier, E. (1875): Campanulaceae. – Flora orientalis 3: 884-962.
[2] Byng, J. W. (2014): The flowering plants handbook: A practical guide to families and genera of the world. – Plant Gateway Ltd.
[3] Carolin, R. C. (1977): The systematic relationships of Brunonia. – Brunonia 1: 9-29.

http://www.aloki.hu ● ISSN 1589 1623 (Print) ● ISSN1785 0037 (Online)
DOI: http://dx.doi.org/10.15666/aeer/1804_54495460

[4] CBOL Plant Working Group (Hollingsworth, P. M., Forrest, L. L., Spouge, J. L., Hajibabaei, M., Ratnasingham, S., Van Der Bank, M., Chase, M. W., Cowan, R. S., Erickson, D. L.) (2009): A DNA barcode for land plants. – Proceedings of the National Academy of Sciences 106: 12794-12797.
[5] Charadze, A. (1949): A treatment of the systematics of the Caucasian species of the genus Campanula section Medium A. DC. – Zametki Sist. Geogr. Rast 15: 13-33.
[6] Charadze, A. (1970): On the florogenesis of the Caucasian Campanulas. – Zametki Sist. Geogr. Rast 28: 89-102.
[7] Charadze, A. (1976): The genus Campanula L. sl in the Caucasus (Conspectus). – Zametki Sist. Geogr. Rast 32: 45-56.
[8] Chen, S., Yao, H., Han, J., Liu, C., Song, J., Shi, L., Zhu, Y., Ma, X., Gao, T., Pang, X. (2010): Validation of the ITS2 region as a novel DNA barcode for identifying medicinal plant species. – PloS One 5.
[9] Coleman, A. W. (2003): ITS2 is a double-edged tool for eukaryote evolutionary comparisons. – TRENDS in Genetics 19: 370-375.
[10] Coleman, A. W. (2007): Pan-eukaryote ITS2 homologies revealed by RNA secondary structure. – Nucleic Acids Research 35: 3322-3329.
[11] Coleman, A. W. (2009): Is there a molecular key to the level of "biological species" in eukaryotes? A DNA guide. – Molecular phylogenetics and evolution 50: 197-203.
[12] Cosner, M., Jansen, R., Crawford, D. (1991): Structural Variation and Evolution of Chloroplast DNA in the Campanulaceae. – American Journal of Botany 78: 92.
[13] Cosner, M., Jansen, R. (1993): Evolution of chloroplast DNA structure in the Campanulaceae. – American Journal of Botany 80: 140.
[14] Cosner, M. E., Jansen, R. K., Lammers, T. G. (1994): Phylogenetic relationships in theCampanulales based onrbcL sequences. – Plant systematics and evolution 190: 79-95.
[15] Cosner, M. E., Raubeson, L. A., Jansen, R. K. (2004): Chloroplast DNA rearrangements in Campanulaceae: phylogenetic utility of highly rearranged genomes. – BMC evolutionary biology 4: 27.
[16] Cronquist, A. (1981): An integrated system of classification of flowering plants. – Columbia University Press.
[17] Cronquist, A. (1988): The evolution and classification of flowering plants. – Thomas Nelson & Sons Ltd., London.
[18] Crowl, A. A., Mavrodiev, E., Mansion, G., Haberle, R., Pistarino, A., Kamari, G., Phitos, D., Borsch, T., Cellinese, N. (2014): Phylogeny of Campanuloideae (Campanulaceae) with emphasis on the utility of nuclear pentatricopeptide repeat (PPR) genes. – PLOS One 9(4): e94199.
[19] Crowl, A. A., Miles, N. W., Visger, C. J., Hansen, K., Ayers, T., Haberle, R., Cellinese, N. (2016): A global perspective on Campanulaceae: Biogeographic, genomic, and floral evolution. – American journal of botany 103: 233-245.
[20] Damboldt, J., Davis, P. (1978): Flora of Turkey. – Edinburgh.
[21] De Candolle, A. (1839): Campanulaceae. Prodromus systematis naturalis regni vegetabilis. – Paris: Treuttel et Würtz.
[22] Drummond, A. J., Ho, S. Y., Phillips, M. J., Rambaut, A. (2006): Relaxed phylogenetics and dating with confidence. – PLoS Biology 4.
[23] Dunning, L. T., Savolainen, V. (2010): Broad-scale amplification of matK for DNA barcoding plants, a technical note. – Botanical Journal of the Linnean Society 164: 1-9.
[24] Eddie, W., Shulkina, T., Gaskin, J., Haberle, R., Jansen, R. K. (2003): Phylogeny of Campanulaceae s. str. inferred from ITS sequences of nuclear ribosomal DNA. – Annals of the Missouri Botanical Garden 9: 554-575.
[25] Evans, T. M., Jabaily, R. S., De Faria, A. P. G., De Sousa, L. D. O. F., Wendt, T., Brown, G. K. (2015): Phylogenetic relationships in Bromeliaceae subfamily Bromelioideae based on chloroplast DNA sequence data. – Systematic Botany 40: 116-128.

http://www.aloki.hu ● ISSN 1589 1623 (Print) ● ISSN1785 0037 (Online)
DOI: http://dx.doi.org/10.15666/aeer/1804_54495460

[26] Faghir, M. B., Attar, F., Farazmand, A., Osaloo, S. K. (2014): Phylogeny of the genus Potentilla (Rosaceae) in Iran based on nrDNA ITS and cpDNA trnL-F sequences with a focus on leaf and style characters' evolution. – Turkish Journal of Botany 38: 417-429.
[27] Fedorov, A. (1957): Campanulaceae. – In: Shishkin, B. K. (ed.) Flora of the USSR, Vol. 24. Akademia Nauk. Moskva Press, Russia.
[28] Fedorov, A. A. (1999): Flora of Russia, Рипол Классик.
[29] Felsenstein, J. (1985): Confidence limits on phylogenies: an approach using the bootstrap. – Evolution 39: 783-791.
[30] Ghazanfar, S., Edmondson, J. (2013): Flora of Iraq. – Royal Botanic Gardens, Kew, London, pp.180-185.
[31] Haberle, R. C. (2006): Phylogeny and comparative chloroplast genomics of the Campanulaceae. – Dissertation, The University of Texas at Austin.
[32] Hall, R. E. (2001): The stock market and capital accumulation. – American Economic Review 91: 1185-1202.
[33] Hansen, K. M. (2016): Phylogeny, Biogeography, Floral Morphology Of Cyphocarpoideae (Campanulaceae). – Northern Arizona University.
[34] Hutchinson, J. (1969): Evolution and phylogeny of flowering plants: dicotyledons, facts and theory. – Academic Press, 717p.
[35] Meyer, C. P., Paulay, G. (2005): DNA barcoding: error rates based on comprehensive sampling. – PLoS Biology 3.
[36] Nylander, J. A., Ronquist, F., Huelsenbeck, J. P., Nieves-Aldrey, J. (2004): Bayesian phylogenetic analysis of combined data. – Systematic biology 53: 47-67.
[37] Rambaut, A. (2016): FigTree version 1.4. 0. – Available at http://tree. bio. ed. ac. uk/software/figtree. Accessed November.
[38] Rechinger, K. (1965): Flora Iranica (150 parts published out of a projected 170). – Granz-Austria: Akademische Drucku: Verlagsanstalt, 1977.
[39] Ree, R. H., Moore, B. R., Webb, C. O., Donoghue, M. J. (2005): A likelihood framework for inferring the evolution of geographic range on phylogenetic trees. – Evolution 59: 2299-2311.
[40] Ronquist, F., Huelsenbeck, J. P. (2003): MrBayes 3: Bayesian phylogenetic inference under mixed models. – Bioinformatics 19: 1572-1574.
[41] Sanderson, M. J. (2002): Estimating absolute rates of molecular evolution and divergence times: a penalized likelihood approach. – Molecular biology and evolution 19: 101-109.
[42] Schönland, S. (1889): Campanulaceae. – Die Naturichen Planzenfamilien. A. E. K. Prantl. Leipzig, W. Engelman IV. 5: 40-70.
[43] Schultz, J., Maisel, S., Gerlach, D., Müller, T., Wolf, M. (2005): A common core of secondary structure of the internal transcribed spacer 2 (ITS2) throughout the Eukaryota. – Rna 11: 361-364.
[44] Schultz, J., Wolf, M. (2009): ITS2 sequence–structure analysis in phylogenetics: a how-to manual for molecular systematics. – Molecular phylogenetics and evolution 52: 520-523.
[45] Swofford, D. (2000): PAUP (Phylogenetic Analysis Using Parsimony). Documentation for Version 4.0 b4a Sinauer Associates. – Inc. Publishers, Sunderland, Massachusetts.
[46] Takhtajan, A. (2009): Flowering plants. – Springer Science & Business Media.
[47] Thorne, J. L., Kishino, H. (2002): Divergence time and evolutionary rate estimation with multilocus data. – Systematic biology 51: 689-702.
[48] Tutin, T. G., Burges, N. A., Chaterj, A. O., Edmondson, R., Heywood, V. H., Moore, D. M., Valentine, D. H. (1993): Flora Europaea. – Cambridgeshire, UK, Cambridge University Press.
[49] Wahlsteen, E., Tyler, T. (2019): Morphometric analyses and species delimitation in Legousia (Campanulaceae). – Willdenowia 49: 21-33.
[50] Watson, L., Dallwitz, M. (1992): The families of flowering plants: descriptions, illustrations, identification and information retrieval. – University of New Orleans.

http://www.aloki.hu ● ISSN 1589 1623 (Print) ● ISSN1785 0037 (Online)
DOI: http://dx.doi.org/10.15666/aeer/1804_54495460

[51] White, T. J., Bruns, T., Lee, S., Taylor, J. (1990): Amplification and direct sequencing of fungal ribosomal RNA genes for phylogenetics. – PCR protocols: a guide to methods and applications 18: 315-322.
[52] Yao, H., Song, J., Liu, C., Luo, K., Han, J., Li, Y., Pang, X., Xu, H., Zhu, Y., Xiao, P. (2010): Use of ITS2 region as the universal DNA barcode for plants and animals. – PloS One 5: 1-9.
[53] Yu, F., Bi, C., Wang, X., Qian, X., Ye, N. (2018): The complete mitochondrial genome of Citrus sinensis. – Mitochondrial DNA Part B 3: 592-593.

http://www.aloki.hu ● ISSN 1589 1623 (Print) ● ISSN1785 0037 (Online)
DOI: http://dx.doi.org/10.15666/aeer/1804_54495460

MARINE DEBRIS ACCUMULATION ON THE BEACH IN LIBONG, A SMALL ISLAND IN ANDAMAN SEA, THAILAND

PRADIT, S.[1,2*] – NITIRATSUWAN, T.[3] – TOWATANA, P.[1,2] – JUALAONG, S.[4] – SORNPLANG, K.[1,2] – NOPPRADIT, P.[1,2] – JIRAJARUS, M.[1,2] – DARAKAI, Y.[1] – WEERAWONG, C.[5]

[1]*Marine and Coastal Resources Institute, Faculty of Environmental Management, Prince of Songkla University, Songkhla 90110, Thailand*
(phone: +66-74-282-329; fax: +66-74-212-782)

[2]*Coastal Oceanography and Climate Change Research Center, Prince of Songkla University, Hat Yai, Songkhla 90110, Thailand*

[3]*Faculty of Science and Fisheries Technology, Trang Campus, Rajamangala University of technology Srivijaya, Tuang 92150, Thailand*

[4]*Marine and Coastal Resources and Development Center, The Eastern Gulf of Thailand, Department of Marine and Coastal, Rayong Province, Thailand*

[5]*Mu Ko Libong Non-hunting Area, Department of National Parks, Wildlife and Plant Conservation, Thailand*

[*]*Corresponding author*
e-mail: *siriporn.pra@psu.ac.th; phone*: *+66-74-282-320; fax*: *+66-74-212-782*

(Received 6th Mar 2020; accepted 2nd Jul 2020)

Abstract. Marine debris is a global issue and a hot topic in Thailand. This study involved collecting and quantifying various types of debris at Libong Island. The study area is Libong Island, a small Island in Andaman Sea, with high biodiversity and an important source of sea grass providing a significant and vital habitat for endangered dugongs. Debris was collected on sandy beach and mud beach areas between May and August 2019. The results indicated that the ceramic and glass debris was found in the greatest number followed by plastic and other debris, thin plastic and hard plastic. The major contributing factor for the debris abundance in Libong beach was the shoreline and recreational activities which showed that the land-based sources provided major inputs of plastic pollution at the beaches. The calculation of the Clean Coastal Index (CCI) of Libong Island yielded a result of 5.8 at the sandy beach whereas at the mud beach was 0.65. Thus, the sandy beach was classified as moderately clean and the mud beach was classified as very clean.
Keywords: *marine litter, plastic, mud beach, dugongs, Thailand*

Introduction

Marine debris accumulates on virtually all coasts from the poles to the equator (Haynes, 1997; Convey et al., 2002). Marine debris is defined as all solid materials of anthropogenic origin that are discarded at the sea or reach the sea (Rayon-Vina et al., 2018). It can be found on the coast, at the sea surface, on the seabed, and even in remote areas (Ivar do Sul et al., 2009; Hirai et al., 2011; Eriksen et al., 2014). Marine anthropogenic debris or debris is generally defined as "any persistent, manufactured or processed solid material discarded, disposed or abandoned in the marine and coastal environment" (Galgani et al., 2010). Ingestion of marine debris (Tomás et al., 2002; Goldstein and Goodwin, 2013) and entanglement by marine organisms, including turtles and seabirds (Matsuoka et al., 2005), have been reported from various parts of the world. Humans are also affected by marine debris, which contributes heavily to landscape degradation (Somerville et al., 2003; Wyles

http://www.aloki.hu ● ISSN 1589 1623 (Print) ● ISSN1785 0037 (Online)
DOI: http://dx.doi.org/10.15666/aeer/1804_54615474

et al., 2015; Sarafraz et al., 2016). Landscape degradation by debris is not only a matter of aesthetics, but also economy (Rayon-Vina et al., 2018). As industrial development has accelerated and the manufacture and disposal of plastics have increased, concerns on plastic pollution are growing (Chae and An, 2018). There is no doubt today that plastic waste generated by the world's populations is accumulating in our seas and oceans at large amounts. Numerous marine species including fishes, seabirds, marine mammals and turtles have been reported to either ingest plastic or get entangled in marine debris (Kühn et al., 2015; Gall and Thompson, 2015). The production of plastics has grown continuously since the 1950s, with an increase of 37% over the last decade (Plastic Europe, 2016).

At present, plastic pollution is considered as a crucial environmental problem (UNEP, 2014), and it is identified alongside climate change as an emerging issue that might affect human health and biological diversity in the near to medium-term future (Sutherland et al., 2010). Plastic debris and marine wastes are currently important problems of Thailand, ASEAN and the world. Thailand is presently ranked as the world's 6th largest marine waste releasing country and therefore, the problems of plastic waste and marine wastes in the marine and coastal ecosystems are the urgent problems that need to be solved as well as other environmental problems caused by other types of pollution. Marine pollution caused by floating plastics in the sea certainly affects numerous marine species. As those sea creatures eat plastic waste into their bodies or plastic wastes entangle around their bodies, this finally causes their fatal injuries and a huge impact on the marine and coastal ecosystems. For example, it causes the deaths and injuries of rare sea animals such as sea turtles, dolphins and whales, etc. at the rate of 60-70 animals/year. In June 2019, a short-finned pilot whale died from eating 85 plastic bags at Jana District, Songkhla Province and the source of marine waste released by the main activities of communities on the shore related to landfills, piers, beach tourism, transportation, fishery, etc. Therefore, the management of municipal waste is likely to face the problem regarding the increase in amount of municipal waste due to the inadequate reduction of amount of waste caused by no efficiency in debris separation at the beginning as well as lack of complete operation of waste management including luxury plastic bag consumption.

Islands, especially the tropical and subtropical zones, are hotspots of biodiversity, hosting diverse ecosystems such as seagrass beds, mangroves and coral reefs (Nurse et al., 2001; de Scisciolo et al., 2016). At the same time, islands are one of the most vulnerable environments on Earth and a diversity of processes severely threaten them. These processes include climate change (Campbell and Barnett, 2010), sea level rise (Leatherman and Beller-Simms, 1997; Williams et al., 2018), unsustainable use of local resources (UNEP, 2009), overpopulation (Rangel-Buitrago et al., 2018), and marine debris (Bergmann and Gutow, 2015; Lavers and Bond, 2017; Lavers et al., 2019; Williams and Rangel-Buitrago, 2019). The study area of this study is Libong Island, Trang Province, which is an island with high biodiversity and an important source of sea grass providing a significant habitat of endangered dugongs. It is currently encountering waste management problems since most islanders get rid of their debris by dumping some of the waste directly into the sea. This has certainly affected marine animals such as the dugongs eating sea waste resulting in blocking movement of food in their intestines and finally causing the death, etc. It can be obviously seen that the problem of marine wastes has a serious adverse impact on the environmental integrity and living organisms including human food security as well. Therefore, the objective of this investigation was to study the types and amounts of marine waste in the sand and mud beach ecosystems of Libong Island which was the first study of recording the waste type separation data showing the amount of each type of

http://www.aloki.hu ● ISSN 1589 1623 (Print) ● ISSN1785 0037 (Online)
DOI: http://dx.doi.org/10.15666/aeer/1804_54615474

marine wastes found. This definitely provides valuable information for finding suitable ways to manage marine debris for this small island that has the high potential to support tourist activities in the future.

Materials and methods

Study area

Libong Island is located at latitude 07°14'-07°17' N and longitude 99° 22'-09° 27' E on the western coastline of Kantang District, Trang Province, and approximately 2-3 km away from the mainland (*Fig. 1*). Libong Island has a diverse ecosystem, including coral reefs, mangrove forests and extensive seagrass beds. The study site is situated on the east coast of the island where the large seagrass bed and mud flat can be found.at a depth between 0.5-2.8 m above sea level (Wirachwong and Holmer, 2010). Libong Island is also important ecological area because it is the significant and vital habitat of the endangered dugongs in Trang Province (Adulyanukosol and Thongsukdee, 2006). Libong islanders presently earn their living by fishing and gardening. The villages located on the island of Libong consist of 4 villages, which are Ban Sai Kaew (Village No. 7), Ban Batu Poo Tae (Village No. 4), Ban Lang Khao (Village No. 5) and Ban Kok Sa Ton (Village No. 1), Libong Island Subdistrict with a total population of 717 people. The research area was Village No. 7 with both mud and sandy beach ecosystems. Our investigation is the first study regarding the waste contamination on the Libong Island. This beach was the best choice for being selected since it is the largest area of sea grass in the island of Libong. This sea grass source is biodiversity importance as well as a food source for dugongs. Thus, its ecological system is very delicate and sensitive to marin waste pollution. Moreover the mud beach area is a buffer zone between the sandy beach and the sea grass area.

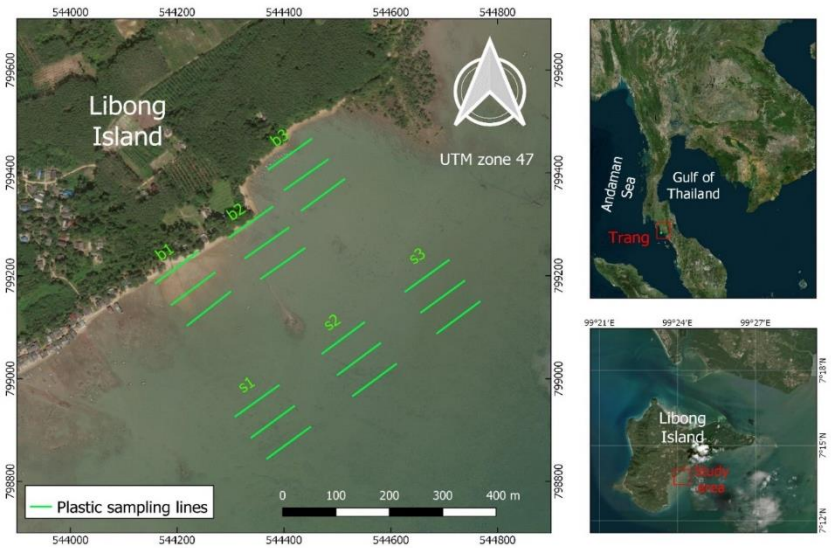

Figure 1. *Marine debris sampling areas at Village No. 7, Libong Island Subdistrict, Kantang District, Trang Province. The sandy beach sampling area included b1 (beachhead) with a residential area, b2 (the middle of the beach) possessing vacant land and b3 (the end of the beach) with a residential area mixed with a small pier and a few boats. The mud beach sampling area* was *composed of 3 sites: s1 (beachhead), s2 (the middle of the beach) and s3 (the end of the beach)*

http://www.aloki.hu ● ISSN 1589 1623 (Print) ● ISSN1785 0037 (Online)
DOI: http://dx.doi.org/10.15666/aeer/1804_54615474

Survey method

Our study on marine and plastic waste type in 2 ecosystems (sandy and mud beaches) was conducted by surveying and classifying marine waste according to the UNEP / IOC Guideline on Survey and Monitoring of Marine Litter (Cheshire and Adler, 2009). Then, the collected data from the UNEP / IOC method was converted and transferred into a record form of International Coastal Cleanup (ICC, 2009) which was classified marine waste by activity. Marine debris investigation was conducted by collecting marine debris samples 1 time per month at Village No. 7, Libong Island Subdistrict, Kantang District, Trang Province, between May - August 2019. This sample collection represented the samples ofrainy season (May - October) underthe southwest monsooninfluence . The monsoon wind blowstoward the sampling area and therefore during this time tide and wind will certainlyblow more waste into the study area thanthat of other seasons. There were 6 sampling sites consisting of 3 sites of sandy and rocky beaches which were b1 (beachhead) with a residential area, b2 (the middle of the beach) possessing vacant land and b3 (the end of the beach) with a residential area mixed with a small pier and a few boats. The rest was composed of 3 sites of the mud beach: s1 (beachhead), s2 (the middle of the beach) and s3 (the end of the beach). Each debris sampling area covered 100 x 100 m (consisting of 3 transects with 100 m long for each transect). Walking along the transect and collecting all the visible debris were conducted. The collected debris was brought back, separated and weighted according to their types.

Classification and quantification

This study divided the marine debris into 6 types which were hard plastic, thin plastic, fabric and fiber, polymer compound, glass and ceramics and others (foam, steel, metal, paper, wood, etc.). Furthermore, debris released from various activities was divided into 5 broad categories of origin as follows: 1) Shoreline and recreational activities discarded the debris from communities or tourists. 2) Fishing activities and sailing released the debris from various types of vessels and fishing equipment. 3) Medical equipment released the debris related to sanitary and medical waste. 4) Large size debris was abandoned as electrical appliance waste, construction materials, furniture and car equipment. 5) Other debris was debris that could not be specified the type of activities that generated the debris.

Calculation of the Clean Coastal Index (CCI) was done for assessing the cleanliness level of the coast (Alkalay et al., 2007). It was employed as a tool for evaluation of the "Clean Coastal" program that took place in Israel. According to Alkalay et al. (2007), this index was calculated using the formula below, with coefficient K (value = 20) inserted into the equation for statistical and convenient reasons. The index only took plastic items into account. The result corresponded to the beach CCI rank as: "very clean", 0–2; "clean", 2–5; "moderate", 5–10; "dirty", 10–20; or "extremely dirty", 20 and higher.

$$CCI = ((\text{Total number of plastic parts}) / (\text{Sampled area})) \times K \qquad \text{(Eq.1)}$$

It was important to notice that this method only regarded plastic items with a size greater than 2 cm (Marin et al., 2019). Thus, for this study, all items greater than 2 cm were recorded.

The statistical analysis was used to calculate the minimum, maximum, average and standard deviation by excel program.

http://www.aloki.hu ● ISSN 1589 1623 (Print) ● ISSN1785 0037 (Online)
DOI: http://dx.doi.org/10.15666/aeer/1804_54615474

Results and discussion

Quantity of marine debris

The survey of marine debris samples between May and August 2019 found a total of 1,400 pieces of marine debris in the study from all the stations (*Fig. 2*). In June, the largest number of debris found was 579 pieces, followed by 509, 191 and 121 pieces of debris were found in May, July and August, respectively. The total weight of the debris from all the stations from May to August 2019 was 53.4 kg. In May, the highest weight of debris was 27.1 kg, followed by 16.3, 6.2, 3.8 kg were found in June, August and July respectively since May was the first month of sampling and therefore resulting in a large amount of debris was collected. Collecting debris every month consecutively was carried out and caused the amount of debris to gradually decrease, such as in July and August, the amount and weight of debris found less than half of the amount and weight of debris in May. Moreover, the amounts of all the types of debris found in the sandy beach in each month were much higher than those of the mud beach (*Table 1*) and therefore, the sandy and rock beaches were much more dirty than the mud beach. It may be because the sandy and rock beaches are close to the highest tide line and receive the waste from the community nearby and therefore causing more accumulation of debris than that of the other areas located offshore.

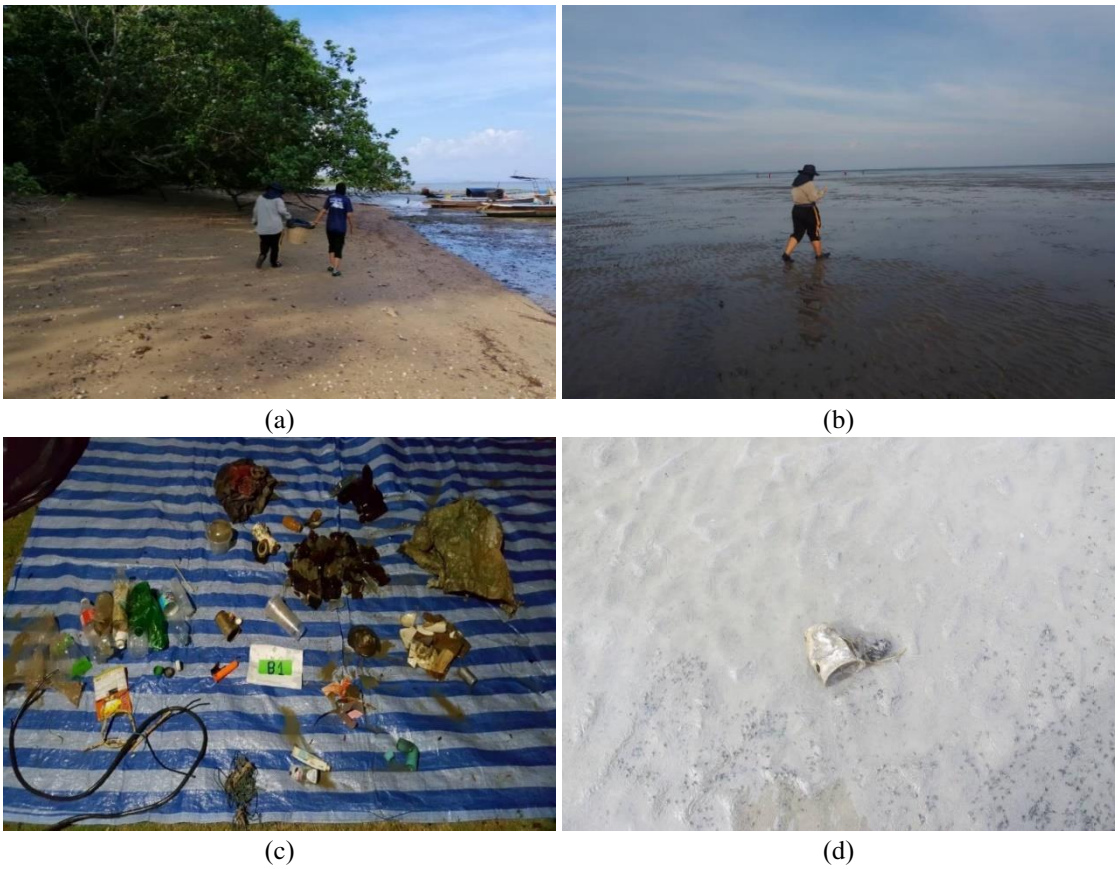

(a) (b)

(c) (d)

Figure 2. *Collecting marine debris samples on* (*a*) *sandy beach* (*b*) *mud beach; Samples of marine debris found at Libong Island* (*c*) *debris from staion b1* (*beachhead*) *with a residential area and* (*d*) *plastic glass found on mud beach*

http://www.aloki.hu ● ISSN 1589 1623 (Print) ● ISSN1785 0037 (Online)
DOI: http://dx.doi.org/10.15666/aeer/1804_54615474

Table 1. *Abundance and weight of debris collected on Libong Island from May-August 2019*

Sampling location/month	Debris type						
	Plastic (hard)	**Plastic (soft/thin)**	**Fabric or fiber**	**Polymer compounds**	**Glass or ceramic**	**Other**	**Total**
A. Sandy beach							
a. Number of debris (piece)							
May 2019	58	28	10	0	313	75	484
June 2019	77	107	24	4	254	113	579
July 2019	18	18	2	2	64	44	148
Aug 2019	21	23	6	3	38	30	121
Total	174	176	42	9	669	262	1332
Average	43.50	44	10.50	2.25	167.25	65.5	333
SD	28.80	42.20	9.57	1.71	136.79	36.83	255.90
b. Weight of debris (kg)							
May 2019	1.51	0.42	1.64	0.00	7.61	6.68	17.86
June 2019	1.33	1.17	1.70	0.38	6.58	5.11	16.27
July 2019	0.01	0.01	0.01	0.00	1.01	2.75	3.78
Aug 2019	0.33	0.27	2.03	0.29	1.46	1.79	6.18
Total	3.18	1.87	5.38	0.67	16.66	16.33	44.08
Average	0.79	0.47	1.35	0.17	4.17	4.08	11.02
SD	0.74	0.50	0.91	0.20	3.42	2.22	7.98
B. Mud beach							
a. Number of debris (piece)							
May 2019	0	6	0	0	0	19	25
June 2019	0	0	0	0	0	0	0
July 2019	8	25	1	0	3	6	43
Aug 2019	0	0	0	0	0	0	0
Total	8	31	1	0	3	25	68
Average	2	7.75	0.25	0	0.75	6.25	17
SD	4	11.84	0.50	0	1.50	8.96	26.80
b. Weight of debris (kg)							
May 2019	0.00	0.24	0.00	0.00	0.00	9.00	9.24
June 2019	0.00	0.00	0.00	0.00	0.00	0.00	0.00
July 2019	0.01	0.00	0.00	0.00	0.00	0.00	0.02
Aug 2019	0.00	0.00	0.00	0.00	0.00	0.00	0.00
Total	0.01	0.24	0.00	0.00	0.00	9.00	9.26
Average	0.00	0.06	0.00	0.00	0.00	2.25	2.32
SD	0.01	0.12	0.00	0.00	0.00	4.50	4.63

Remark: SD=Standard deviation

May was the first waste collection month. From the obtained data of villager interview, there was no waste collection in the study area before. Hence, the amount of the collected marine waste in May was the accumulate amount of waste before our study. The highest amount of glass waste on the sandy beach in May was observed and decreased in the following months whereas the reverse was true for plastic waste. It might be possible that the waste was transported by sea due to the influence of the southwest monsoon or the

http://www.aloki.hu ● ISSN 1589 1623 (Print) ● ISSN1785 0037 (Online)
DOI: http://dx.doi.org/10.15666/aeer/1804_54615474

wind blew plastic waste from the community to accumulate on the beach. Therefore the amount of waste on the beach in June was greater than that in May.

The high amount of glass and ceramic types found in the sandy beach monthly gave the high average quantities of the collected glass and ceramic debris with the high standard deviation as compared to other types of debris (*Table 1*) since the amounts of glass and ceram found varied quite a lot among each month (May to August 2019). Furthermore, the average number of soft/thin plastic debris found in the mud beach was highest as compared to the other debris types (*Table 1*). This implied that soft/thin plastics probably had some potential to accumulate in the mudflat and could be harmful to the marine organism in this area.

The calculation of the Clean Coastal Index (CCI) of Libong Island was 5.8 at sandy beach whereas at mud beach was 0.65. Hence, the sandy beach was classified as moderate clean and the mud beach was classified as very clean. However, it probably depends on the season since Libong Island is affected by both Southwest monsoon and Northeast monsoon.

From *Table 1*, collecting waste samples was carried out 1-2 days every month during the study. This might not be representative amount of the month. However, Libong island beach is relatively clean and still natural with less population and tourist activities. Therefore, it was expected that the collected waste was accumulated for many days. For this research, only one beach sample was collected at Libong Island. The area next to the beach is the mud beach and the largest sea grass area of Libong Island with conservation area for dugong habitat and no residential area.

Types of marine debris

The survey found that the collection of marine debris samples on both the sand and mud beaches between May and August 2019, the most common types of debris were glass and ceramics = 672 pieces, weight 24.7 kg, followed by other debris = 287 pieces, weight 25.3 kg, thin plastic = 207 pieces, weight 2.1 kg, hard plastic = 182 pieces, weight 3.2 kg, fabric and fiber = 42 pieces, weight 5.4 kg and polymer compound = 10 pieces, weight 0.7 kg, which was contrary to the study results of Khananurux (2012). She studied the amount of each type of marine debris per area of Bangsaen Beach, Chonburi Province and found that plastic debris had the highest amount of 34.60 ± 16.03 pieces/ 100 m^2, followed by cigarette / cigarette butt =7.84 ± 5.67 pieces/100 m^2 and rubber = 6.74 ± 3.78 pieces/100 m^2. This was due to the different characteristics of beach area utilization. Bang Saen Beach is utilized in the form of tourist attractions and beach activities. Most of the debris at Bang Saen Beach is caused by tourists but the sampling areas of Libong Island are not a tourist attraction and have communities located nearby the beach. There is a pier for small fishing boats in front of the beach and one homestay located at study area. The study at Rajamangala Beach located at the mainland of Trang Province showed that the total of marine debris found was 296 pieces, total weight 10,433 g consisting of styrofoam (51.35%), hard plastic (16.89%) and fiber and fabric (29.89%) (Thammavichan et al., 2014). The number of pieces was concordant with our study since Libong Island like Trang Province was affected by monsoon wind. Thus, the debris found on beach was probably released from the communities or influenced by the southwest monsoon during May to October.

The amounts of debris found of each sampling area in sand and rock areas at b1, b2 and b3 and mud beach areas at s1, s2 and s3 classified by the type of debris (*Figs. 3-4*) were as follows.

http://www.aloki.hu ● ISSN 1589 1623 (Print) ● ISSN1785 0037 (Online)
DOI: http://dx.doi.org/10.15666/aeer/1804_54615474

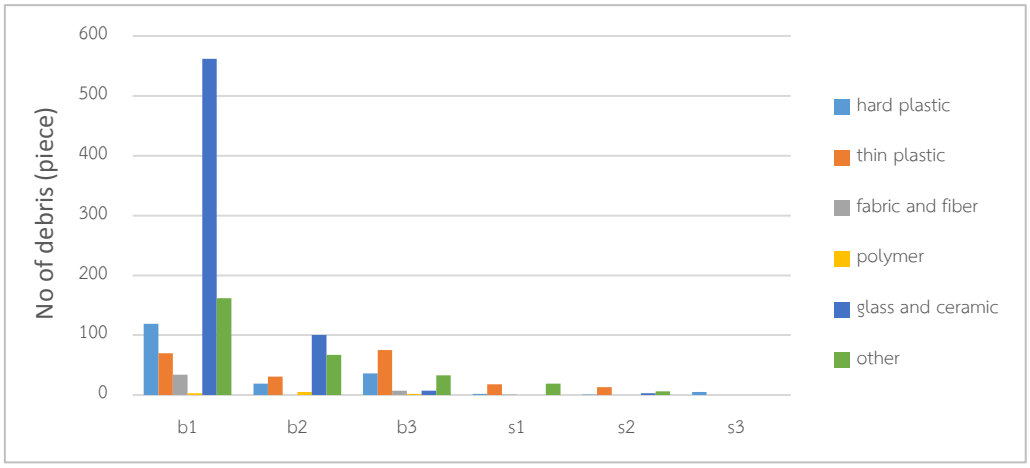

Figure 3. *The amount of marine debris (pieces) in each sampling area classified by debris types between May - August 2019. The sandy beach* sampling area *included b1 (beachhead) with a residential area, b2 (the middle of the beach) possessing vacant land and b3 (the end of the beach) with a residential area mixed with a small pier and a few boats. The* mud *beach sampling area was composed of 3 sites of the mud beach: s1 (beachhead), s2 (the middle of the beach) and s3 (the end of the beach)*

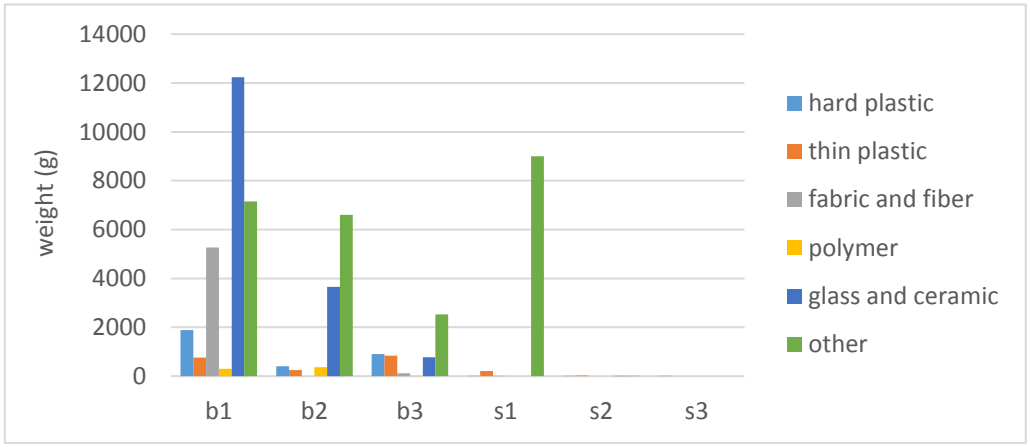

Figure 4. *The weight of marine debris (grams) in each sampling area classified by debris types between May - August 2019. The sandy beach sampling area included b1 (beachhead) with a residential area, b2 (the middle of the beach) possessing vacant land and b3 (the end of the beach) with a residential area mixed with a small pier and a few boats. The mud beach sampling area was composed of 3 sites of the mud beach: s1 (beachhead), s2 (the middle of the beach) and s3 (the end of the beach)*

1) Sand and rock beach floors at b1 area had the highest amount of glass and ceramic waste = 562 pieces, weight 12.2 kg followed by the other debris = 162 pieces, weight 7.1 kg and hard plastic =119 pieces, weight 1.8 kg. For the b2 area, the most type found was glass and ceramics = 100 pieces, weight 3.7 kg, followed by other debris = 67 pieces, weight 6.6 kg and thin plastic = 31 pieces, weight 0.3 kg. The b3 area, the most commonly found type was the thin plastic = 75 pieces, weight 0.8 kg followed by the hard plastic = 36 pieces, weight 0.9 kg and other debris = 33 pieces, weight 2.5 kg.

http://www.aloki.hu ● ISSN 1589 1623 (Print) ● ISSN1785 0037 (Online)
DOI: http://dx.doi.org/10.15666/aeer/1804_54615474

2) Mud beach area at s1 area possessed the largest amount of other debris = 19 pieces, weight 9 kg, followed by the thin plastic = 18 pieces, weight 0.2 kg and the hard plastic = 2 pieces, weight 0.01 kg whereas the s2 area, the most type found was the thin plastic =13 pieces, weight 0.03 kg followed by the other debris = 6 pieces, weight 0.01 kg. For the s3 area, 5 pieces of hard plastic with the weight of 1 kg were found.

The plastic debris abundance on Libong Island beach was shown in *Table 2*. The most occurrence was plastic bag (25.96%), followed by bottle and tumbler (15.68%) and food wrapper (12.85%). Moreover, thin plastic was found at the mud station, whereas hard plastic was absent. It probably implied that the lighter debris such as pieces of plastic bags could travel longer distance from shore than that of the hard ones with more weight. Many studies (e.g. Galgani et al., 2000; Hess et al., 1999) report plastic as the major debris collected from coastal zones. On most beaches, plastic items corresponded to over 80% of the total items collected. Particularly, plastic debris on beaches can be easily fragmented yielding a large amount of microplastics that cannot be collected and can pose significant threats to the marine environment (Andrady, 2017; Song et al., 2017).

Table 2. *Plastic debris composition on beach at Libong Island from May-August 2019*

No	Plastic debris type	Number (piece)	Occurrence %
1	Bottle and tumbler	61	15.68
2	Cups and dish	21	5.40
3	Spoon and fork	4	1.03
4	Container	13	3.34
5	Bottle cap	12	3.08
6	Straw	6	1.54
7	Plastic bag	101	25.96
8	Food wrapper	50	12.85
9	Toothpaste tube and toothbrush	4	1.03
10	Other	117	30.08
Total		389	100.00

The amount of marine debris classified by sources of activity

The survey showed the collection of marine debris samples between May and August 2019 as follows: The debris from shoreline and recreational activities was found the most amount of 1,185 pieces, weight 30.7 kg followed by fishing and sailing activities = 32 pieces, weight 11.8 kg, large size debris = 164 pieces, weight 10.5 kg, other debris = 17 pieces, weight 0.4 kg and sanitary and medical debris = 2 pieces, weight 0.06 kg (*Fig. 5* and *Fig. 6*), which was consistent with the study results of Thamwichan et al. (2014). They found that the marine debris at the Rajamangala Beach, Trang Province and Tung Khen Bay, Phuket Province was mostly generated by shoreline and recreational activities by more than 50 percent followed by fishing and sailing activities 30 percent. That most debris came from land activities which was abandoned and blown to a river and then flown along the water path into the sea. The rest came from coastal activities related to various types of boats such as fishing boats, cargo vessels, piers, fishing, etc.

From the survey of the amounts and types of marine debris in each month, it was found that the sampling area that received the most debris was b1 (beachhead) at the sand and rock beach since there were communities nearby with a pier for small fishing boats in

http://www.aloki.hu ● ISSN 1589 1623 (Print) ● ISSN1785 0037 (Online)
DOI: http://dx.doi.org/10.15666/aeer/1804_54615474

front of the beach. The activities that caused the most amount of debris were shoreline and recreational activities. This was probably caused by most debris coming from neighboring communities and the influence of the passing southwest monsoon wind. This corresponded to the sampling area of s1 (beachhead) at the mud beach where most debris from shoreline and recreational activities was found. This study found that the most activities generating debris were certainly caused by shoreline and recreational activities which was well agreed with the previous study of Kumar et al. (2016).

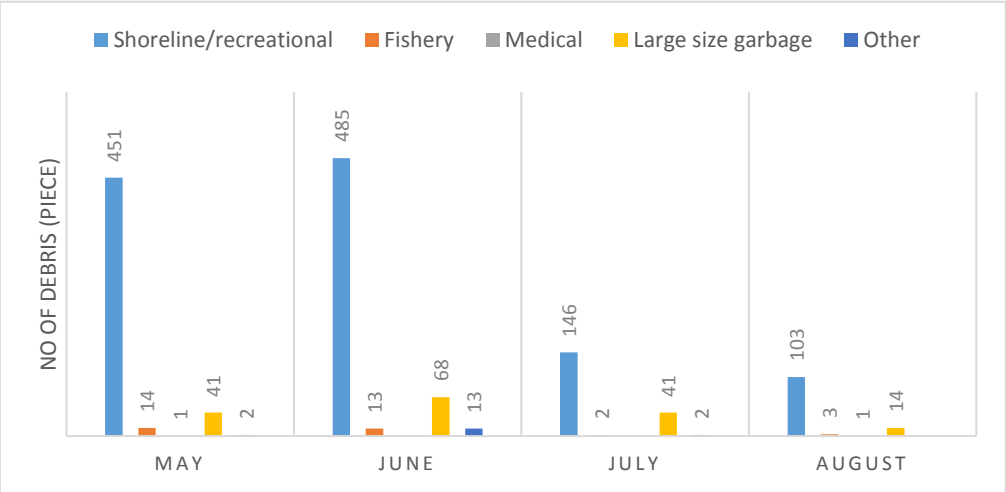

Figure 5. *The amount of marine debris (pieces) classified by debris-generating activities between May - August 2019*

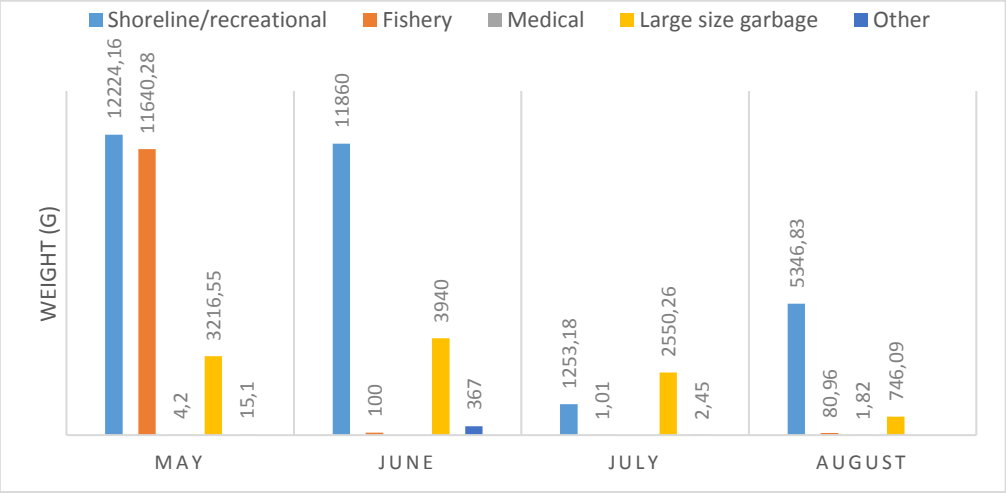

Figure 6. *The weight of marine debris (g) classified by debris-generating activities between May - August 2019*

The amount of marine debris classified by sources of habitat

The amounts of debris in each sampling area at the sand and rock beach areas namely b1, b2 and b3, and the mud beach areas namely s1, s2 and s3 based on the classification of debris-generating activities were found as follows:

http://www.aloki.hu ● ISSN 1589 1623 (Print) ● ISSN1785 0037 (Online)
DOI: http://dx.doi.org/10.15666/aeer/1804_54615474

1) Sand and rock beach

Debris was mostly found in the area of b1 approximately 950 pieces, weight 27.6 kg, which was the most debris from shoreline and recreational activities (808 pieces, weight 19.8 kg), followed by large size waste (110 pieces, weight 5.1 kg) and fishing and sailing activities (amount 20 pieces, weight 2.3 kg), followed by b2 area, 222 pieces, weight 11.3 kg. The debris of b2 consisted of the debris released from shoreline and recreational activities (172 pieces, weight 5.9 kg), followed by large size debris (43 pieces, weight 4.9 kg) and other debris (4 pieces, weight 0.04 kg). For the total debris of b3 found was 160 pieces, weight 5.2 kg, which were the most debris generated from shoreline and recreational activities (144 pieces, weight 4.6 kg), followed by large size debris (8 pieces, weight 0.5 kg) and the debris from the activities of fishing and sailing (7 pieces, weight 0.1 kg).

2) Mud beach

The s1 area had the most amount of debris found (40 pieces, weight 9.2 kg) consisting of the most amount of debris from shoreline and recreational activities (38 pieces, weight 0.3 kg), followed by fishing and sailing activities (2 pieces, weight 8.9 kg). For the s2 area possessed the total amount of 23 pieces, weight 0.45 kg that consisted of the most debris generated from shoreline and recreational activities (19 pieces, weight 0.05 kg) followed by large size debris (3 pieces, weight 0.03 kg) and other debris (1 piece, weight 0.01 kg). The total amount of debris found at the s3 area was 5 pieces, weight 0.01 kg, which were mostly generated from shoreline and recreational activities (4 pieces, weight 0.07 kg), followed by fishing and sailing activities (1 piece, weight 0.04 kg).

The above study results were consistent with the study results of Kaikaew et al. (2017). They found the distribution of plastic debris at Tha Wang Beach by collecting samples along a perpendicular line transecting along the coast starting from the highest tide line down to the sea with a length of 50 m. Therefore, the nature of the accumulation of debris with high amount at the beginning of the line transect and gradually reduced to the end which was attributed to the nature of the surveyed area with almost entirely rocky area. The current normally carries plastic debris into rock beach during the high tide and the debris will be trapped during the low tide. The characteristics of the aforementioned study area was similar to the Libong Island sampling areas having a sandy beach with about 10-20 m long (from the highest sea level) and next to it was rock and mud beaches. Thus, it caused more debris in the sampling areas of sand and rock beaches (b1, b2 and b3) than that of the mud beach (s1, s2 and s3). Apart from that the spatial distribution of marine debris depends on the density differences of the materials, as lighter ones will be transported further (Ryan et al., 2009). Thus, the removal of large-sized plastic debris from coastal areas is the most practical approach to reduce the accumulation of debris including microplastics (Lee et al., 2019).

Conclusion

From the collection of marine waste 4 times between May - August 2019 in the area of the sand and mud beaches revealed that the most common found wastes were ceramic and glass debrises, followed by plastics mostly consisting of the plastic bags. The marine wastes found in our invetigation came from coastal and recreational activities. However, further research is needed to identify the sources of the wastes whether they came from the communities on the island of Libong or were transported by currents from the coast of Trang Province or waves from the sea.

http://www.aloki.hu ● ISSN 1589 1623 (Print) ● ISSN1785 0037 (Online)
DOI: http://dx.doi.org/10.15666/aeer/1804_54615474

The data obtained from this study can help to indicate material types of marine debris in Libong Island. The result showed that the beaches of Libong Island were still fairly clean and had not much plastic debris accumulation as compared to other areas. Regular monitoring of marine debris are suggested since Libong Island is a hotspot of biodiversity as well as vital and important habitat of endanger species, dugongs.

From the research, it was concluded that Libong Island is a small island with agricultural communities on the island. It has sandy and mud beach ecological systems and seagrass that is still natural. The research team proposed the suggestion regarding the marine waste management by increasing the waste collection area to cover the remaining beaches of the island especially the beaches with no community since a lot of plastic wastes were found during May - October. They were probably transported by the influence of the southwest monsoon. The people responsible for implementing waste management activities should consist of the personnel of Libong Island Non-Hunting Area providing waste management plan and budget, the Libong Island School supporting labor and Libong Island Subdistrict Administrative Organization supporting the tools (waste handling equipment). Research groups from Prince of Songkla University and Rajamangala University of Technology Srivijaya, Trang Campus had research knowledge on Libong Island waste management and a role to coordinate among government and private organizations. They proposed the use of various technologies and participate in surveying, collecting, classifying waste and inventing new products from the wastes (innovation) of the Libong Island area.

Acknowledgments. This work was financially supported by by Grand Challenges Thailand: Thai Ocean Waste Free, National Research Council of Thailand (Sub project: Marine litter and microplastic at Libong Island, Trang Province). We would like to express our sincere appreciation to the Department of National Parks, Wildlife and Plant Conservation for allowing us to conduct the research at Libong Island. We owe many thanks to reviewers for assisting us to complete the manuscript.

REFERENCES

[1] Adulyanukosol, K., Thongsukdee, S. (2006): Dugong Survey at Muk-Talibong Islands, Trang Province. – Marine and Coastal Resources Research & Development Institute, Bangkok.
[2] Alkalay, R., Pasternak, G., Zask, A. (2007): Clean-coast index—A new approach for beach cleanliness assessment. – Ocean & Coastal Management 50: 352-362.
[3] Andrady, A. L. (2017): The plastic in microplastics: A review. – Marine Pollution Bulletin 119: 12-22.
[4] Bergmann, M., Gutow, L., Klages, M. (2015): Marine Anthropogenic Litter. – Springer International Publishing, Cham.
[5] Campbell, J., Barnett, J. (2010): Climate Change and Small Island States. – Routledge.
[6] Chae, Y., An, Y.-J. (2018): Current research trends on plastic pollution and ecological impacts on the soil ecosystem: A review. – Environmental Pollution 240: 387-395.
[7] Cheshire, A., Adler, E. (2009): UNEP/IOC Guidelines on Survey and Monitoring of Marine Litter. – United Nations Environment Programme (UNEP), Nairobi.
[8] Convey, P., Barnes, D., Morton, A. (2002): Debris accumulation on oceanic island shores of the Scotia Arc, Antarctica. – Polar Biology 25: 612-617.
[9] Eriksen, M., Lebreton, L. C. M., Carson, H. S., Thiel, M., Moore, C. J., Borerro, J. C., Galgani, F., Ryan, P. G., Reisser, J. (2014): Plastic Pollution in the World's Oceans: More

http://www.aloki.hu ● ISSN 1589 1623 (Print) ● ISSN1785 0037 (Online)
DOI: http://dx.doi.org/10.15666/aeer/1804_54615474

than 5 Trillion Plastic Pieces Weighing over 250,000 Tons Afloat at Sea Dam, H.G. – PLoS ONE 9: e111913.

[10] Galgani, F., Leaute, J., Moguedet, P., Souplet, A., Verin, Y., Carpentier, A., Goraguer, H., Latrouite, D., Andral, B., Cadiou, Y., Mahe, J., Poulard, J., Nerisson, P. (2000): Litter on the Sea Floor Along European Coasts. – Marine Pollution Bulletin 40: 516-527.

[11] Galgani, F., Fleet, D., van Franeker, J., Katsanevakis, S., Maes, T., Mouat, J., Oosterbaan, L., Poitou, I., Hanke, G., Thompson, R., Amato, E., Birkun, A., Janssen, C. (2010): Marine Strategy Framework Directive: Task Group 10 Report Marine Litter. – Office for Official Publications of the European Communities, Luxembourg.

[12] Gall, S. C., Thompson, R. C. (2015): The impact of debris on marine life. – Marine Pollution Bulletin 92: 170-179.

[13] Goldstein, M. C., Goodwin, D. S. (2013): Gooseneck barnacles (Lepas spp.) ingest microplastic debris in the North Pacific Subtropical Gyre. – PeerJ 1: e184.

[14] Haynes, D. (1997): Marine debris on continental islands and sand cays in the Far Northern Section of the Great Barrier Reef Marine Park, Australia. – Marine Pollution Bulletin 34: 276-279.

[15] Hess, N. A., Ribic, C. A., Vining, I. (1999): Benthic Marine Debris, with an Emphasis on Fishery-Related Items, Surrounding Kodiak Island, Alaska, 1994–1996. – Marine Pollution Bulletin 38: 885-890.

[16] Hirai, H., Takada, H., Ogata, Y., Yamashita, R., Mizukawa, K., Saha, M., Kwan, C., Moore, C., Gray, H., Laursen, D., Zettler, E. R., Farrington, J. W., Reddy, C. M., Peacock, E. E., Ward, M. W. (2011): Organic micropollutants in marine plastics debris from the open ocean and remote and urban beaches. – Marine Pollution Bulletin 62: 1683-1692.

[17] International Coastal Cleanup (2009): Guide to marine debris and International Coastal Cleanup. – Ocean conservancy, Washiton.

[18] Ivar do Sul, J. A., Spengler, Â., Costa, M. F. (2009): Here, there and everywhere. Small plastic fragments and pellets on beaches of Fernando de Noronha (Equatorial Western Atlantic). – Marine Pollution Bulletin 58: 1236-1238.

[19] Kaikaew, S., Jitpraphai, S. M., Kettratad, J. (2018): Distribution of Plastic Marine Debris in Intertidal Zone at Sichang Island, Chonburi Province. – the 55th Kasetsart University Annual Conference: 19-26. Bangkok.

[20] Khananurux, N. (2012): Types and Sources of Marine debris in Bangsaen beach, Chonburi Province. – PhD thesis, Chulalongkorn University, Bangkok.

[21] Kühn, S., Bravo Rebolledo, E. L., van Franeker, J. A. (2015): Deleterious Effects of Litter on Marine Life. – In: Bergmann, M., Gutow, L., Klages, M. (eds.) Marine Anthropogenic Litter. Springer International Publishing, pp. 75-116.

[22] Kumar, A. A., Sivakumar, R., Reddy, Y. S. R., Raja, M. V. B., Nishanth, T., Revanth, V. (2016): Preliminary study on marine debris pollution along Marina beach, Chennai, India. – Regional Studies in Marine Science 5: 35-40.

[23] Lavers, J. L., Bond, A. L. (2017): Exceptional and rapid accumulation of anthropogenic debris on one of the world's most remote and pristine islands. – Proceedings of the National Academy of Sciences 114: 6052-6055.

[24] Lavers, J. L., Dicks, L., Dicks, M. R., Finger, A. (2019): Significant plastic accumulation on the Cocos (Keeling) Islands, Australia. – Scientific Reports 9: 7102.

[25] Leatherman, S. P., Beller-Simms, N. (1997): Sea-Level rise and small island states; an overview. – Journal of Coastal Research 24: 1-16.

[26] Lee, J., Hong, S., Lee, J. (2019): Rapid assessment of marine debris in coastal areas using a visual scoring indicator. – Marine Pollution Bulletin 149: 110552.

[27] Marin, C. B., Niero, H., Zinnke, I., Pellizzetti, M. A., Santos, P. H., Rudolf, A. C., Beltrão, M., de Souza Waltrick, D., Polette, M. (2019): Marine debris and pollution indexes on the beaches of Santa Catarina State, Brazil. – Regional Studies in Marine Science 31: 100771.

[28] Matsuoka, T., Nakashima, T., Nagasawa, N. (2005): A review of ghost fishing: scientific approaches to evaluation and solutions. – Fisheries Science 71: 691-702.

http://www.aloki.hu ● ISSN 1589 1623 (Print) ● ISSN1785 0037 (Online)
DOI: http://dx.doi.org/10.15666/aeer/1804_54615474

[29] Nurse, L. A., Sem, G., Hay, J. E., Suarez, A. G., Wong, P. P., Briguglio, L., Ragoonaden, S. (2001): Small island states. – In: McCarthy, J. J., Canziani, O. F., Leary, N. A., Dokken, D. J., White, K. S. (eds.) Climate Change 2001: Impacts, Adaptation and Vulnerability.Contribution of Working Group II to the Third Assessment of the Intergovernmental Panel on Climate Change. Cambridge University Press, Cambridge.
[30] Plastics Europe (2016): Plastics- the Facts 2016: an Analysis of European Plastics. – Plastics Europe, Brussels.
[31] Rangel-Buitrago, N., Williams, A., Anfuso, G. (2018): Killing the goose with the golden eggs: Litter effects on scenic quality of the Caribbean coast of Colombia. – Marine Pollution Bulletin 127: 22-38.
[32] Rayon-Viña, F., Miralles, L., Gómez-Agenjo, M., Dopico, E., Garcia-Vazquez, E. (2018): Marine litter in south Bay of Biscay: Local differences in beach littering are associated with citizen perception and awareness. – Marine Pollution Bulletin 131: 727-735.
[33] Ryan, P. G., Moore, C. J., van Franeker, J. A., Moloney, C. L. (2009): Monitoring the abundance of plastic debris in the marine environment. – Philosophical Transactions of the Royal Society B: Biological Sciences 364: 1999-2012.
[34] Sarafraz, J., Rajabizadeh, M., Kamrani, E. (2016): The preliminary assessment of abundance and composition of marine beach debris in the northern Persian Gulf, Bandar Abbas City, Iran. – Journal of the Marine Biological Association of the United Kingdom 96: 131-135.
[35] Scisciolo, T. de, Mijts, E. N., Becker, T., Eppinga, M. B. (2016): Beach debris on Aruba, Southern Caribbean: Attribution to local land-based and distal marine-based sources. – Marine Pollution Bulletin 106: 49-57.
[36] Somerville, S., Miller, K., Mair, J. (2003): Assessment of the aesthetic quality of a selection of beaches in the Firth of Forth, Scotland. – Marine Pollution Bulletin 46: 1184-1190.
[37] Song, Y. K., Hong, S. H., Jang, M., Han, G. M., Jung, S. W., Shim, W. J. (2017): Combined Effects of UV Exposure Duration and Mechanical Abrasion on Microplastic Fragmentation by Polymer Type. – Environmental Science & Technology 51: 4368-4376.
[38] Sutherland, W. J., Clout, M., Côté, I. M., Daszak, P., Depledge, M. H., Fellman, L., Fleishman, E., Garthwaite, R., Gibbons, D. W., Lurio, J. De, Impey, A. J., Lickorish, F., Lindenmayer, D., Madgwick, J., Margerison, C., Maynard, T., Peck, L. S., Pretty, J., Prior, S., Redford, K. H., Scharlemann, J. P. W., Spalding, M., Watkinson, A. R. (2010): A horizon scan of global conservation issues for 2010. – Trends in Ecology & Evolution 25: 1-7.
[39] Thammavichan, J., Manyagase, K., Manakij, J., Noomnual, W. (2014): Study of amount, material type and source of marine debris along the Andaman sea in Trang and Phuket province. – The 4th Marine Science Conference: 646-652.
[40] Tomás, J., Guitart, R., Mateo, R., Raga, J. A. (2002): Marine debris ingestion in loggerhead sea turtles, Caretta caretta, from the Western Mediterranean. – Marine Pollution Bulletin 44: 211-216.
[41] UNEP (2014): United Nations Environment Programme Year Book 2014: emerging issues in our global environment.
[42] Williams, A. T., Rangel-Buitrago, N., Pranzini, E., Anfuso, G. (2018): The management of coastal erosion. – Ocean & Coastal Management 156: 4-20.
[43] Williams, A. T., Rangel-Buitrago, N. (2019): Marine Litter: Solutions for a Major Environmental Problem. – Journal of Coastal Research 35: 648-663.
[44] Wirachwong, P., Holmer, M. (2010): Nutrient dynamics in 3 morphological different tropical seagrasses and their sediments. – Aquatic Botany 93: 170-178.
[45] Wyles, K. J., Pahl, S., Thomas, K., Thompson, R. C. (2016): Factors That Can Undermine the Psychological Benefits of Coastal Environments. – Environment and Behavior 48: 1095-1126.

http://www.aloki.hu ● ISSN 1589 1623 (Print) ● ISSN1785 0037 (Online)
DOI: http://dx.doi.org/10.15666/aeer/1804_54615474

CHEMICAL CUES MEDIATING BEHAVIORAL AND ELECTROPHYSIOLOGICAL RESPONSES OF *FOPIUS ARISANUS* (HYMENOPTERA: BRACONIDAE): THE ROLE OF HERBIVORE-INDUCED PLANT VOLATILES

CAI, P.M.[1,2,3] – SONG, Y.Z.[1] – HUO, D.[1] – LIN, J.[2,3] – ZHANG, H.M.[1] – ZHANG, Z.H.[1] – HUANG, F.M.[1] – XIAO, C.M.[1] – JI, Q.E.[2,3*]

[1]*Department of Horticulture, College of Tea and Food Science, Wuyi University, Wuyishan, 354300 Fujian Province, China*
(e-mails: caipumo@163.com – P.M. Cai; 1023554932@qq.com – Y.Z. Song; hawda1090@163.com – D. Huo; z15159754369@163.com – H.M. Zhang; Zhangzihao1095@163.com – Z.H. Zhang; Ulikexx123@163.com – F.M. Huang; XGM2352033@163.com – C.M. Xiao)

[2]*Institute of Beneficial Insects, Plant Protection College, Fujian Agriculture and Forestry University, Fuzhou, 350002 Fujian Province, China*
(e-mail: Lin14787861578@163.com – J. Lin)

[3]*Key Lab of Biopesticide and Chemical Biology, Ministry of Education, Fuzhou, 350002 Fujian Province, China*

**Correspondence author*
e-mail: jiqinge@yeah.net; phone: +86-591-8378-9420; fax: +86-591-8378-9421

(Received 25th Mar 2020; accepted 2nd Jul 2020)

Abstract. The aim of the present study was to establish how a selection of herbivore-induced plant volatiles (HIPVs) regulate the behavioral response of *Fopius arisanus*. A total of ten HIPVs were selected which are major bioactive components produced by fruits immediately after being infested with eggs of *Bactrocera dorsalis*, a common pest parasitized by *F. arisanus*. The behavioral and electroantennogram (EAG) responses of both sexes of *F. arisanus* to these chemicals were investigated. Our results suggest that all tested HIPVs can elicit different levels of antennal and behavioral response for both sexes at a variety of concentrations. There were no significant differences in response levels between sexes for all compounds, except trans farnesol at a concentration of 10^{-2} ml/ml (*v/v*), indicating that it may be of value in biological control programs using *F. arisanus*. Furthermore, we observed that the behavioral and EAG dose-dependent curves of both sexes of *F. arisanus* could be largely divided into four types, namely steady decrease (ethyl octanoate, methyl octanoate, linalool, tetradecane, pentadecane), steady increase (trans farnesol), inverted V (cis-3-hexenyl acetate, β-myrcene, β-ocimene) and fluctuating (benzaldehyde). The ecological role of these HIPV components in the host location process of *F. arisanus* is discussed.
Keywords: *HIPVs, biological control, EAG response, behavioral responses, infochemicals*

Introduction

Within the context of biological control programs, the effectiveness of a parasitoid relies heavily on its capacity to search for suitable hosts (Godfray, 1994). Insects have developed multisensory systems for perceiving various cues from their habitats, including visual, chemical and vibrational cues, which are utilized in an interactive manner to make foraging choices (Schellhorn et al., 2014). Of these, chemical cues play the most important role and influence activities such as food finding, mate searching and escaping natural enemies and competition. These, in turn, affect the large-scale

http://www.aloki.hu ● ISSN 1589 1623 (Print) ● ISSN 1785 0037 (Online)
DOI: http://dx.doi.org/10.15666/aeer/1804_54755489

geographical distribution of insect populations (Schoonhoven et al., 2005; Vinatier et al., 2011). Chemical cues from either the phytophagous host or its habitat may be used by parasitoids at long- and short-range. Generally, cues derived from the host are less detectable but a more reliable indication of the presence of herbivorous hosts. Cues from the host plant, on the other hand, are less reliable but more detectable, which presents the parasitoid with a reliability-detectability dilemma (Vet and Dicke, 1992).

Parasitoids have developed diverse tactics to overcome this predicament, one of which is the utilization of herbivore-induced plant volatiles (HIPVs) as reliable cues to find their herbivorous hosts in a complex odorous environment. This also has the indirect effect of defending host habitats from infestation (Vet and Dicke, 1992; Ngi-Song et al., 2000). These volatiles usually comprise hundreds of chemical components distributed within the green leaf volatiles, and include esters, aromatic compounds, monoterpenes, sesquiterpenes and homoterpenes (Degenhardt et al., 2009); however, not all components of HIPVs trigger behavioral responses in parasitoids. In some tritrophic contexts, single critical compounds only or a blend of compounds with specific ratios have been found to affect the recruitment and recognition of insects (Bruce and Pickett, 2011). This indicates that it is necessary to investigate how parasitoids respond to volatile infochemicals for each parasitoid-host system and to characterize which infochemicals are involved.

The subject of the present research is *Fopius arisanus* Sonan (Hymenoptera: Braconidae), an egg-pupal endoparasitoid originating in the Indo-Pacific region and known to parasitize the eggs and first instars of approximately 40 frugivorous tephritid fruit fly species (Bautista and Harris, 1996; Rousse et al., 2007a). This parasitoid was introduced into Hawaii at the end of the 1940s and into French Polynesia later in 2002; in both cases it rapidly became the dominant parasitoid of tephritid pests, greatly suppressing the populations of *Bactrocera dorsalis* Hendel and *Ceratitis capitata* Wiedemann (Diptera: Tephritidae), respectively (Vargas et al., 2007, 2012, 2013). These cases of successful application demonstrated that *F. arisanus* possessed a huge potential for augmentative biological control, alone or in combination with other management measures to control fruit flies (Harris et al., 2000).

The biology of *F. arisanus* is well-known, and its host-searching behavior has been reported on coffee fruits infested by *C. capitata* eggs (Wang and Messing, 2003). Furthermore, many studies have investigated the relationships between fly-infested plants and the ovipositional behavior or parasitism performance of parasitoids (Liquido, 1991; Harris and Bautista, 1996; Bautista et al., 2004; Ayelo et al., 2017). Additionally, *F. arisanus* was fascinated with fresh guava and orange fruits (Altuzar et al., 2004), and infestation by *Anastrepha* eggs enhanced this attraction (Rousse et al., 2007b; Pérez et al., 2013). In recent years, our research team has analyzed the volatile components of four host crops, namely guava (*Psidium guajava* L. [Myrtales: Myrtaceae], banana (*Musa paradisiaca* L. [Zingiberales: Musaceae]), citrus (*Citrus sinensis* L. [Sapindales: Rubiaceae]) and tomato *Solanum lycopersicum* Mill. [Tubiflorae: Solanaceae], by gas chromatography-mass spectrometry (GC-MS). We found that after egg deposition by *B. dorsalis*, host fruits can emit ten new chemical components in comparison with non-infested fruits (Gu et al., 2017). When we compared these volatile compounds with the volatile profile of the egg surface of *B. dorsalis* (Ji et al., 2016), we found that the emitted compounds derived from the fruits, rather than from the host pest. Until now, the ecological role of HIPVs emitted from fruits after *B. dorsalis* infestation in the host-location behavior of *F. arisanus* is poorly understood.

http://www.aloki.hu ● ISSN 1589 1623 (Print) ● ISSN 1785 0037 (Online)
DOI: http://dx.doi.org/10.15666/aeer/1804_54755489

The purpose of the present research was to construct dose-response curves of key bioactive HIPVs that modulate the tritrophic system using electrophysiological and behavioral assays. Understanding how parasitoids respond to such chemicals will significantly contribute to the current knowledge on insect chemical communication and hopefully improve their effectiveness as biological control agents against destructive fruit pests like *B. dorsalis*.

Materials and methods

Parasitoid rearing

The initial colony of parasitoid *F. arisanus* was obtained from a field culture, reared on *B. dorsalis* eggs as described by Manoukis et al. (2011). Experimental parasitoids were kept at the insect mass rearing chamber of the Beneficial Insects Institute, Fujian Agriculture and Forestry University (BII, FAFU), Fujian Province, China under conditions of 25 ± 1 °C, 65 ± 5% relative humidity (RH), and a L:D photoperiod of 10:14 h. The laboratory-reared strains were periodically introduced with a parasitoid population collected from the field to prevent genetic decline and to preserve the original behavioral properties of the species. Naïve mated parasitoid females and males aged 7–12 days (without previous exposure to host or plant odors) acquired from the fifth to sixth generation were used in the assays. All experiments were conducted between 08:00 and 16:00.

Chemical components

Ten chemical standards, namely ethyl octanoate, benzaldehyde, methyl octanoate, linalool, tetradecane, pentadecane, cis-3-hexenyl acetate, β-myrcene, trans farnesol and β-ocimene, were used in electroantennogram (EAG) and behavioral assays. Information on these standards is listed in *Table 1*. Each compound was dissolved into n-hexane (purity > 99%; Beijing solabo Technology Co., Ltd, Beijing, China) and diluted to concentrations of 10^{-1}, 10^{-2}, 10^{-3}, 10^{-4} and 10^{-5} ml/ml (*v*:*v*) for the dose-response tests. Diluted standards were maintained in a refrigerator at 4 °C until required.

Table 1. *Details of the ten chemical standards*

Chemicals	Formula	CAS no.	Purity (%)	Storage condition	Source
Benzaldehyde	C_7H_6O	100-52-7	98.5	Room temperature	Shanghai Macklin Biochemical Technology Co., Ltd
Ethyl octanoate	$C_{10}H_{20}O_2$	106-32-1	99	Room temperature	Shanghai Macklin Biochemical Technology Co., Ltd
Methyl octanoate	$C_9H_{18}O_2$	111-11-5	99	Room temperature, dry, sealed	Shanghai Macklin Biochemical Technology Co., Ltd
Linalool	$C_{10}H_{18}O$	78-70-6	98	Room temperature	Shanghai Macklin Biochemical Technology Co., Ltd
Tetradecane	$C_{14}H_{30}$	629-59-4	98	Room temperature	Shanghai Macklin Biochemical Technology Co., Ltd
Pentadecane	$C_{15}H_{32}$	629-62-9	98	Room temperature	Shanghai Macklin Biochemical Technology Co., Ltd
cis-3-hexenyl acetate	$C_8H_{14}O_2$	3681-71-8	98	Room temperature	Shanghai Macklin Biochemical Technology Co., Ltd
β-myrcene	$C_{10}H_{16}$	123-35-3	90	2–8 ℃	Aladdin reagent (Shanghai) Co., Ltd
Trans farnesol	$C_{15}H_{26}O$	106-28-5	97	2–8 ℃	Shanghai Macklin Biochemical Technology Co., Ltd
β-ocimene	$C_{10}H_{16}$	13877-91-3	90	Room temperature	Shanghai Macklin Biochemical Technology Co., Ltd

http://www.aloki.hu ● ISSN 1589 1623 (Print) ● ISSN 1785 0037 (Online)
DOI: http://dx.doi.org/10.15666/aeer/1804_54755489

Choice measurements

This bioassay was designed to determine whether different concentrations of HIPVs imposed differing impacts on the behavioral responses of *F. arisanus*. This was done using a six-choice olfactometer as described by Gu et al. (2018). The test area comprised a release area, an adapting area, a selection area and six 100-ml odor bottles. Humidified and charcoal-filtered air was passed through the test area uniformly at a rate of 200 ml/min. A piece of cotton wool was placed in each odor bottle which was moistened with 200 µl of the test component; one concentration was used for each bottle and pure n-hexane served as the control group. Each trial was tested with only one chemical type. Prior to the experiment, *F. arisanus* adults were starved for 1 h to improve their sensitivity to odor. One group of 30 parasitoids of the same sex were then concomitantly introduced into the release area. Based on pre-observations, most parasitoids need about 30 min to adapt to this experimental apparatus and then make a "choice". Therefore, after 30 min the number of parasitoids that stayed at each area for at least 10 s or trapped in each odor bottle was documented. The response rate was then calculated using the following formula:

$$R_{response} = \frac{N_{response}}{N_{release}} \times 100$$

$N_{response}$ denotes the number of selected males or females and $N_{release}$ denotes the total number of released males or females. After each trial, the parasitoids were removed and not used again in the experiment. The apparatus was then cleaned using an abluent and then 75% ethanol, rinsed using distilled water, and thereafter dried for several hours with an air-blowing drier. After each individual trial, different chemicals of various concentrations were randomly deposited into odor bottles to eliminate any positional effects. Six replicates were performed for each six-choice experiment of each chemical type.

Antennal preparation and EAG measurements

In order to evaluate the dose-dependent effects of each volatile component, the EAG technique was used to determine the electrophysiological responses of the antennae of male and female *F. arisanus* to volatile components at different concentrations. The antennae of *F. arisanus* adults were completely excised with the aid of a stereomicroscope and a few top flagellar segments of the antennae were cut off.

Thereafter, the cut antennal tips were inserted into Ag-AgCl glass electrodes filled with saline solution, which was used to maintain an electrical connection between the electrodes. The EAG response signals were passed through a high impedance amplifier (IDIC-2, Syntech, Hilversum, Netherlands) and further processed with EAG software (Syntech).

Different concentrations of the tested components diluted with n-hexane (control) were exposed in ascending order to abate the effect of olfactory adaptation possibly caused by strong stimulation. Stimulus solutions were prepared by first pipetting 20 µl of each solution onto individual filter papers (6 × 15 mm), and thereafter allowed to adequately diffuse for 2 min before the assay. The stimuli were pipetted onto filter paper strips and were immediately deposited in disposable Pasteur pipettes that in turn were connected to an air flow control device (Syntech CS-05, Netherlands Syntech Co., Ltd.) which continuously flowed purified and humidified air over the prepared antennae

http://www.aloki.hu ● ISSN 1589 1623 (Print) ● ISSN 1785 0037 (Online)
DOI: http://dx.doi.org/10.15666/aeer/1804_54755489

at a rate of 100 ml/min. Each air tube was placed 10 mm from the antenna. The control stimulus containing n-hexane was tested both at the beginning and end of each trial to ensure that the preparations were functional throughout. Five antennae were used for each chemical, and each assay was replicated five times. The electrophysiological response of *F. arisanus* to each chemical was expressed by the EAG relative value (RV_{EAG}), which was calculated using the following formula:

$$RV_{EAG} = \frac{V_1 + V_2}{V_{c1} + V_{c2}}$$

V_1 and V_2 denote the two EAG values of the test compounds, and V_{c1} and V_{c2} denote the two EAG values of the control treatments at the start and the end of each replicate, respectively.

Statistical analysis

Statistical differences between concentrations for both the behavioral responses and EAG relative values were evaluated using Tukey's honestly significant differences (HSD) test for multiple mean comparisons after ANOVA. A comparison of the differences between male and female parasitoids was conducted using a independent t-test. In both cases $P < 0.05$ was considered statistically significant. All statistical analyses were performed using SPSS 17.0 for Windows (SPSS Inc., Chicago, IL, USA).

Results

The tendencies of response rates and EAG relative values of F. arisanus to ten synthetic HIPVs at different concentrations

Our results show that all dosages of the tested components can elicit different levels of antennal and behavioral response in *F. arisanus* (both male and female). The response rates and EAG relative values of both sexes of *F. arisanus* to the same component showed some significant differences between concentrations (*Figs. 1-10; F* and *P* values see *Table 2*).

The dose threshold that can trigger the statistically highest behavioral and antennal response for each compound is shown in *Table 2*. It can be seen that both parasitoid females and males have a diverse dose threshold range for different chemicals. Furthermore, for each chemical, there was no difference in trend between males and females for both the response rate and EAG relative values. Benzaldehyde is an exception to this rule, for which the EAG relative values steadily decreased as the dose increased whereas the behavioral response rates of parasitoid males fluctuated with concentration (*Fig. 2*). The tendencies of the response rates and EAG relative values of *F. arisanus* males and females could be divided into the 4 types described below.

Steady decrease

Response rates and EAG relative values of both male and female *F. arisanus* declined as the dose increased for ethyl octanoate, methyl octanoate, linalool, tetradecane and pentadecane (*Figs. 1* and *3-6*). For benzaldehyde, both male and female EAG relative values and female response rates belonged to this type (*Fig. 2B*).

http://www.aloki.hu ● ISSN 1589 1623 (Print) ● ISSN 1785 0037 (Online)
DOI: http://dx.doi.org/10.15666/aeer/1804_54755489

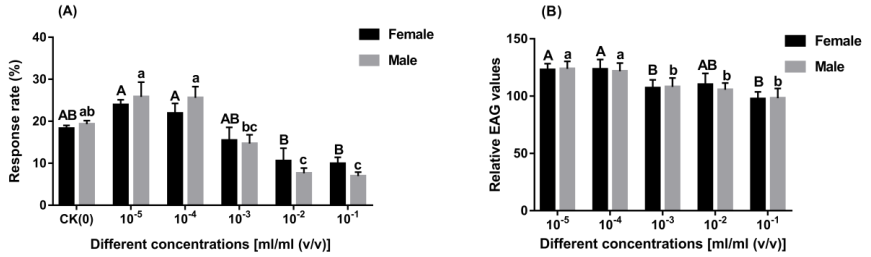

Figure 1. *Behavioral (A) and EAG (B) dose-responses of F. arisanus to ethyl octanoate. The data are expressed as mean ± SE. Different uppercase (female) or lowercase (male) letters indicate significant differences between concentrations (Tukey's HSD test after ANOVA, P < 0.05)*

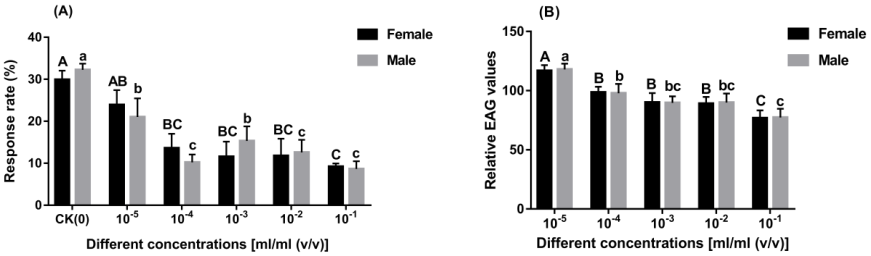

Figure 2. *Behavioral (A) and EAG (B) dose-responses of F. arisanus to benzaldehyde. The data are expressed as mean ± SE. Different uppercase (female) or lowercase (male) letters indicate significant differences between concentrations (Tukey's HSD test after ANOVA, P < 0.05)*

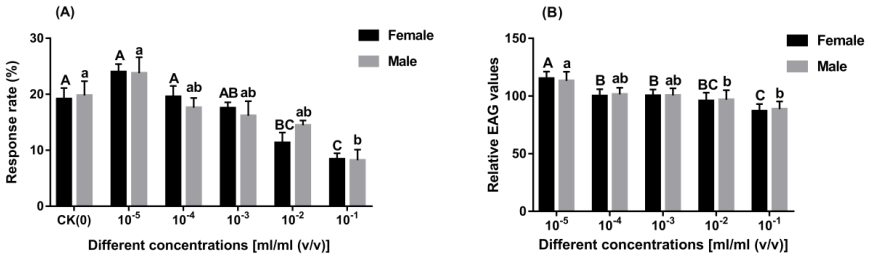

Figure 3. *Behavioral (A) and EAG (B) dose-responses of F. arisanus to methyl octanoate. The data are expressed as mean ± SE. Different uppercase (female) or lowercase (male) letters indicate significant differences between concentrations (Tukey's HSD test after ANOVA, P < 0.05)*

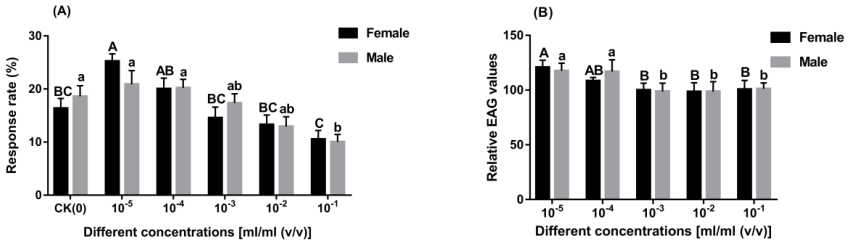

Figure 4. *Behavioral (A) and EAG (B) dose-responses of F. arisanus to linalool. The data are expressed as mean ± SE. Different uppercase (female) or lowercase (male) letters indicate significant differences between concentrations (Tukey's HSD test after ANOVA, P < 0.05)*

http://www.aloki.hu ● ISSN 1589 1623 (Print) ● ISSN 1785 0037 (Online)
DOI: http://dx.doi.org/10.15666/aeer/1804_54755489

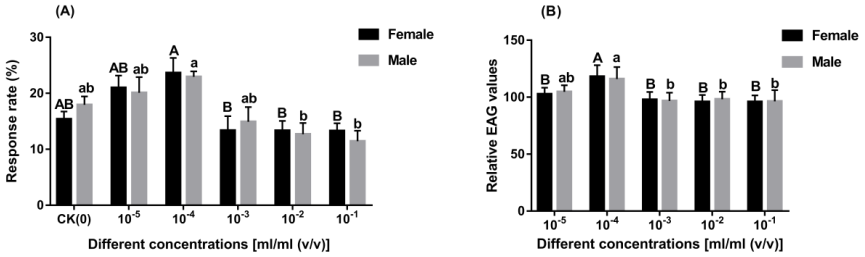

Figure 5. *Behavioral (A) and EAG (B) dose-responses of F. arisanus to tetradecane. The data are expressed as mean ± SE. Different uppercase (female) or lowercase (male) letters indicate significant differences between concentrations (Tukey's HSD test after ANOVA, P < 0.05)*

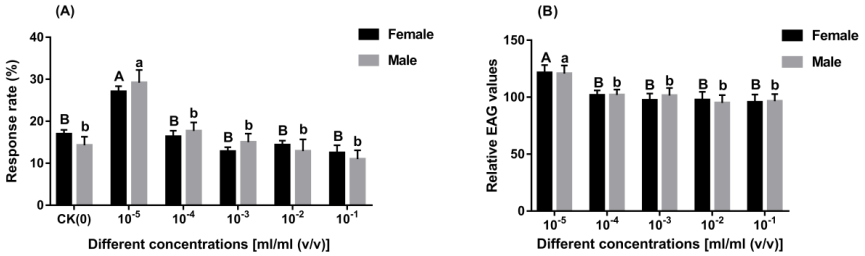

Figure 6. *Behavioral (A) and EAG (B) dose-responses of F. arisanus to pentadecane. The data are expressed as mean ± SE. Different uppercase (female) or lowercase (male) letters indicate significant differences between concentrations (Tukey's HSD test after ANOVA, P < 0.05)*

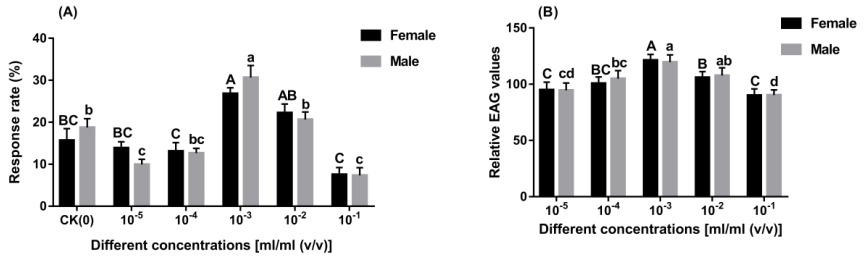

Figure 7. *Behavioral (A) and EAG (B) dose-responses of F. arisanus to cis-3-hexenyl acetate. The data are expressed as mean ± SE. Different uppercase (female) or lowercase (male) letters indicate significant differences between concentrations (Tukey's HSD test after ANOVA, P < 0.05)*

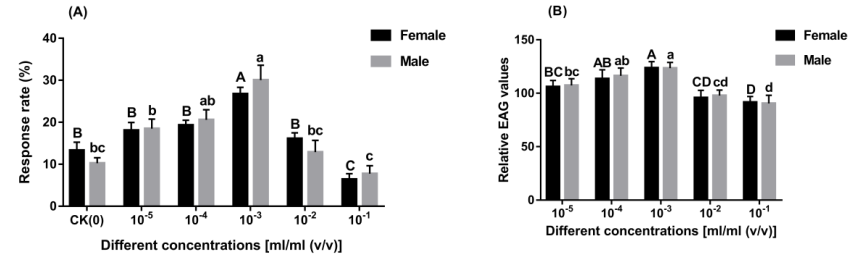

Figure 8. *Behavioral (A) and EAG (B) dose-responses of F. arisanus females to β-myrcene. The data are expressed as mean ± SE. Different letters indicate significant differences between concentrations (Tukey's HSD test after ANOVA, P < 0.05)*

http://www.aloki.hu ● ISSN 1589 1623 (Print) ● ISSN 1785 0037 (Online)
DOI: http://dx.doi.org/10.15666/aeer/1804_54755489

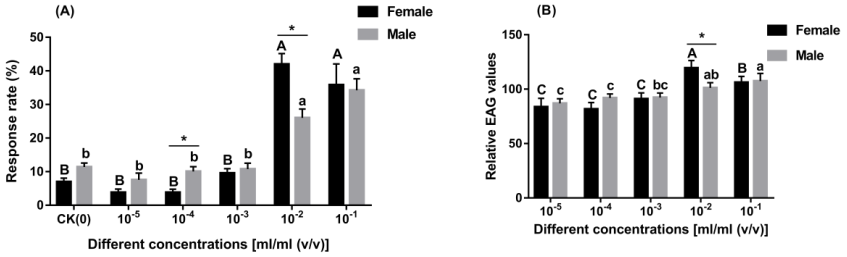

Figure 9. *Behavioral (A) and EAG (B) dose-responses of F. arisanus to trans farnesol. The data are expressed as mean ± SE. Different uppercase (female) or lowercase (male) letters indicate significant differences between concentrations (Tukey's HSD test after ANOVA, P < 0.05). Asterisks indicate significant differences between females and males using an independent t-test at P < 0.05*

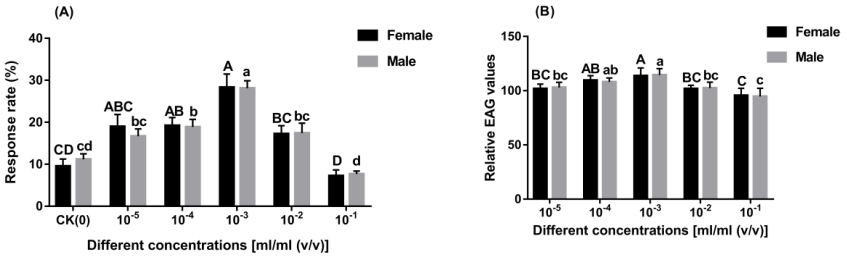

Figure 10. *Behavioral (A) and EAG (B) dose-responses of F. arisanus to β-ocimene. The data are expressed as mean ± SE. Different uppercase (female) or lowercase (male) letters indicate significant differences between concentrations (Tukey's HSD test after ANOVA, P < 0.05)*

Steady increase

Response rates and EAG relative values increased as the dose increased and peaked at the highest concentration. This applied only to trans farnesol (*Fig. 9*).

Inverted V

Response rates and EAG relative values increased as the doses increased and peaked at a specific dose, then reduced as the dose further increased. The group comprised the results for cis-3-hexenyl acetate, β-myrcene and β-ocimene (*Figs. 7, 8* and *10*).

Fluctuating

Only one trend was recorded as having this type: the response rates of *F. arisanus* males to benzaldehyde which first decreased, then increased, then decreased as the concentration increased (*Fig. 2A*).

Differences between sexes in their behavioral and antennal responses

In most cases, there were no significant differences in either the EAG relative values or the response rates of parasitoids between males and females at each concentration. However, for trans farnesol significant differences in response rates were observed at concentrations of 10^{-4} ($F = 0.007$, $t = 3.892$, $P = 0.004$) and 10^{-2} ml/ml (*v/v*) ($F = 2.230$,

http://www.aloki.hu ● ISSN 1589 1623 (Print) ● ISSN 1785 0037 (Online)
DOI: http://dx.doi.org/10.15666/aeer/1804_54755489

t = -3.683, P = 0.004) (*Fig. 9A*) and for the EAG relative values at 10^{-2} ml/ml (*v*/*v*) (F = 0.005, t = -2.749, P = 0.021) (*Fig. 9B*).

Table 2. *Concentration threshold (ml/ml) of different components that trigger the statistically highest response rate and EAG relative values of F. arisanus*

Chemicals	Behavioral response				EAG relative values			
	Female		Male		Female		Male	
	Threshold	*F* and *P*	Threshold	*F* and *P*	Threshold	*F* and *P*	Threshold	*F* and *P*
Benzaldehyde	0–10^{-5}	*F*=7.061, *P*<0.001	0	*F*=9.272, *P*<0.001	10^{-5}	*F*=30.163, *P*<0.001	10^{-5}	*F*=24.399, *P*<0.001
Ethyl octanoate	0–10^{-3}	*F*=6.992, *P*<0.001	0–10^{-4}	*F*=15.802, *P*<0.001	10^{-5}–10^{-4}, 10^{-2}	*F*=10.801, *P*<0.001	10^{-5}–10^{-4}	*F*=11.532, *P*<0.001
Methyl octanoate	0–10^{-3}	*F*=13.277, *P*<0.001	0–10^{-2}	*F*=5.746, *P*=0.001	10^{-5}	*F*=13.794, *P*<0.001	10^{-5}–10^{-3}	*F*=7.913, *P*=0.001
Linalool	10^{-5}–10^{-4}	*F*=8.506, *P*<0.001	0–10^{-2}	*F*=5.120, *P*=0.002	10^{-5}–10^{-4}	*F*=9.645, *P*<0.001	10^{-5}–10^{-4}	*F*=7.142, *P*=0.001
Tetradecane	0–10^{-4}	*F*=4.891, *P*=0.002	0–10^{-3}	*F*=4.708, *P*=0.003	10^{-4}	*F*=8.905, *P*<0.001	10^{-5}–10^{-4}	*F*=5.093, *P*<0.001
Pentadecane	10^{-5}	*F*=17.590, *P*<0.001	10^{-5}	*F*=7.483, *P*<0.001	10^{-5}	*F*=14.349, *P*<0.001	10^{-5}	*F*=13.000, *P*<0.001
cis-3-hexenyl acetate	10^{-3}–10^{-2}	*F*=12.120, *P*<0.001	10^{-3}	*F*=19.917, *P*<0.001	10^{-3}	*F*=21.630, *P*<0.001	10^{-3}–10^{-2}	*F*=16.451, *P*<0.001
β-myrcene	10^{-3}	*F*=18.641, *P*<0.001	10^{-4}–10^{-3}	*F*=10.917, *P*<0.001	10^{-4}–10^{-3}	*F*=19.490, *P*<0.001	10^{-4}–10^{-3}	*F*=21.823, *P*<0.001
Trans-farnesol	10^{-2}–10^{-1}	*F*=32.970, *P*<0.001	10^{-2}–10^{-1}	*F*=24.057, *P*<0.001	10^{-2}	*F*=31.240, *P*<0.001	10^{-2}–10^{-1}	*F*=14.070, *P*<0.001

Discussion

Plants can alter the emission of their volatile profile in response to herbivore foraging or pest oviposition (Hilker and Meiners, 2011). The selective exploration of HIPVs by parasitoids when searching their phytophagous hosts has been recorded on different parasitoids species (Dicke and van Loon, 2000), concentrated on those that parasitize folivorous larvae. Recently, various methods of parasitoid-based pest control have been developed that incorporate the use of volatile infochemicals as part of non-toxic, low-cost and effective strategies (Pickett et al., 2014). Infochemicals are disseminated through plants as a defense mechanism to directly and/or indirectly protect themselves from infestation by pests (Khan et al., 2010). For example, foraging parasitoids use HIPVs (a type of infochemicals) as reliable cues at both long- and short-range to locate their hosts in nature; this effectively protects the infested plant from their pests (Ngi-Song et al., 2000). Numerous studies have demonstrated that infestation by tephritid fruit flies, including *B. dorsalis*, enhances the attraction of *F. arisanus* adults to diverse crops species (Rousse et al., 2007b; Pérez et al., 2013; Ayelo et al., 2017; Gu et al., 2017). Thus, using infochemicals from the host habitats of pests will help design and enhance parasitoid-based biological control programs. It is essential to evaluate which volatile composition are identified at the olfactory level along with the minimum dosages required to evoke behavioral responses in a particular parasitoid (James, 2005).

Our research group has previously qualitatively and quantitatively compared the volatile profiles of four kinds of host crops before and after oviposition by *B. dorsalis*.

http://www.aloki.hu ● ISSN 1589 1623 (Print) ● ISSN 1785 0037 (Online)
DOI: http://dx.doi.org/10.15666/aeer/1804_54755489

The results suggested that ten compounds were exclusive to infested crops compared to healthy ones, and are generated by the host crop rather than the pest (Gu et al., 2017; Ji et al., 2016). Indeed, we concluded that guava fruits release benzaldehyde, cis-3-hexenyl acetate, tetradecane, pentadecane and trans farnesol, and that citrus fruit release ethyl octanoate, methyl octanoate, pentadecane, β-ocimene, linalool and β-myrcene in response to infestation by *B. dorsalis* (Gu et al., 2017). The emissions of most of these HIPVs is possibly attributed to the infested crop's active defense response because they are only detected after herbivore infestation and they are not emitted from healthy fruit, which is important in the host location process of parasitoids. Our present study revealed that these ten HIPV components, at different concentrations, can elicit different levels of electrophysiological and behavioral response in both sexes of *F. arisanus*. This provides yet more evidence that *F. arisanus* uses chemical cues derived from host crops, in concordance with speculations by other authors (Altuzar et al., 2004; Ayelo et al., 2017)

Insects are equipped with a highly sensitive olfactory system that enable them to probe and distinguish related volatile infochemicals with a high level of specificity and selectivity (Bruce and Pickett, 2011). By using electrophysiological and behavioral studies, it is possible to identify potentially bioactive volatile compounds and establish their biological function in parasitoids (Webster et al., 2010). In the present research, behavioral choice and EAG assays in *F. arisanus* confirmed 10 synthetic HIPVs to be biologically active. It is worth noting that among these volatile components, many single components have been demonstrated as eliciting positive behavioral or/and EAG responses in other braconids parasitoids [e.g. linalool for *Cotesia marginiventris* Cresson (Ngumbi and Fadamiro, 2012), ethyl octanoate for *Psyttalia concolor* Szépligeti (Benelli et al., 2013), benzaldehyde for *Lysiphlebia japonica* Ashmead (Hou et al., 2008), tetradecane and cis-3-hexenyl acetate for *Microplitis croceipes* Cresson (Morawo et al., 2016; Chen and Fadamiro, 2007), β-myrcene and β-ocimene for *Aphidius ervi* Haliday (Corrado et al., 2007; Takemoto and Takabayashi, 2015) (Hymenoptera: Braconidae)] or in other hymenopteran parasitoids [e.g. pentadecane for *Trichogramma exiguum* Pinto and Platner (Paul et al., 2002) (Hymenoptera: Trichogrammatidae) and trans farnesol for *Diaeretiella rapae* M'Intosh (Hymenoptera: Aphidiidae)] (Reed et al., 1995).

The behavioral and EAG dose–response curves of the ten compounds studied in the present research can be divided into four types: steady decrease, steady increase, inverted V and fluctuating. Regarding the group "steady decrease", the strongest response was obtained at the lowest dose, whereas for "steady increase", this was obtained at the highest dose. We therefore speculated that *F. arisanus* may have a dosage threshold for perceiving different components which can trigger corresponding levels of behavioral responses and physiological activities. For example, if the dosage is lower than the threshold value, the olfactory sensitivity of the parasitoids would elevate as the dose increased; however, if the dosage is higher than the threshold, sensitivity would descend as the dose increased. According to this, the concentration threshold of the volatile components that belonged to the group "inverted V" could be easily determined, i.e. cis-3-hexenyl acetate, β-ocimene and β-myrcene at 10^{-3} ml/ml (*v*/*v*). The step-like ability of benzaldehyde to lure *F. arisanus* was observed at our tested concentrations. Hiroyuki and Junji (2015) also reported a similar response in a braconid parasitoid to a volatile substance: using a Y-tube olfactometer, they found that *A. ervi* females, an effective natural enemy of several aphid species, were significantly attracted

http://www.aloki.hu ● ISSN 1589 1623 (Print) ● ISSN 1785 0037 (Online)
DOI: http://dx.doi.org/10.15666/aeer/1804_54755489

to α- phellandrene at doses of 30 and 0.1 ng, but not at 10- and 1- ng. Both our findings and those of Hiroyuki and Junji (2015) indicate that HIPVs can carry information at a variety of dose ranges, instead of being restricted to a single optimal dose range. The reason why *F. arisanus* has evolved to respond to two dose ranges in their host location behavior warrants further investigation.

The behavioral dose-response curves of volatile substances belonging to the "steady decrease" group are of particular interest. Of these compounds, only benzaldehyde at a concentration of 10^{-5} ml/ml (*v*/*v*) attracted significantly fewer parasitoids compared to the control group, whereas in contrary to other compounds in this group. This suggested that benzaldehyde at our tested concentrations may impose a dose-dependent repellant effect on *F. arisanus*. The ecological role of benzaldehyde on parasitoids deserves further investigation. Regarding the differences between sexes, both the behavioral and EAG responses exhibited similar trends. Only one compound showed a significant difference, i.e. trans farnesol at 10^{-4} and 10^{-2} ml/ml (*v*/*v*) for behavioral responses and 10^{-2} ml/ml (*v*/*v*) for EAG responses. We hypothesize that both female and male *F. arisanus* may utilize the same olfactory receptors to perceive the other nine infochemicals (although with varying sensitivity), whilst having distinct sensing mechanisms for trans farnesol. In parasitoid-based biological control programs, the female has a vital role in pest suppression, directly resulting in the death of pests (Mills and Getz, 1996); thus, trans farnesol may be a more valuable volatile component.

In summary, HIPVs are considered as kairomones for several parasitoid species (Carrasco et al., 2005; Dweck et al., 2010; Benelli et al., 2013) and have already been successfully applied in the field (Uefune et al., 2012). However, detailed knowledge concerning the effect of HIPVs on the host-seeking behavior of biological control agents in the field requires further investigation prior to any possible commercial utilization (Kaplan, 2012). Besides recruiting beneficial arthropods, we believe that suitable HIPV candidates for field application should also possess additional useful features: (1) improving the defensive activities of intrinsic or imported biological control agents; (2) repelling pests or impose negative effects on the colonization and development of damaging pests; (3) exerting positive effects on the crop of economic importance; (4) without any adverse effects on non-target organisms or environment. For example, methyl salicylate at a certain concentration can not only attract *Aphidius gifuensis* Ashmead females (Hymenoptera: Braconidae) (Song, 2019), but can also inhibit the colonization and development of *Myzus persicae* Sulzer (Hemiptera: Aphididae) on tobacco leaves and provide a repellant effect (Liu et al., 2013). Furthermore, this substance can improve the parasitism performance of *Anagrus nilaparvatae* Pang et Wang (Hymenoptera: Mymaridae) towards eggs of *Nilaparvata lugens* Stal (Homoptera: Delphacidae) eggs (Wang and Lou, 2013).

Outside of direct field application, HIPVs also could be applied to enhance the effectiveness of mass-rearing beneficial insects since these compounds can improve the parasitization performance on alternative hosts. In another use, the host-seeking ability of *F. arisanus* females could be augmented by associative learning using the bioactive volatile compounds: the compounds could be incorporated into the diet of parasitoids at different phases and/or through a "reward" strategy before field release. As such, HIPVs with multiple positive ecological roles could achieve many things simultaneously, thus enhancing the efficiency of a series of plant protection strategies. Accurately characterizing these chemicals, along with investigating their potential in a variety of applications, is therefore of great value in integrated pest management.

http://www.aloki.hu ● ISSN 1589 1623 (Print) ● ISSN 1785 0037 (Online)
DOI: http://dx.doi.org/10.15666/aeer/1804_54755489

Conclusion

Infochemicals are produced from either the herbivorous host or its habitat and are used by parasitoids use to search for their hosts. A greater understanding of the tritrophic context of fruit – fruit fly – parasitoid systems will help improve the effectiveness of biocontrol programs that use parasitoids against destructive pests. In the present study, our results demonstrated that individually applied HIPVs can elicit different levels of antennal and behavioral responses from both sexes of *F. arisanus* when used at a variety of concentrations. This indicates that the tested components could be utilized to modulate parasitoid behavior, at least under laboratory conditions. However, thus far, the field application of a specific infochemical has only been reported for the pest sex pheromone, where it was used to improve parasitoid foraging activity. The use of infochemicals in pest control therefore appears to be a desirable tactic and thus we strongly recommend that field investigations are performed to both evaluate their practical effects in nature and comprehensively understand their ecological roles. We hope that the findings of the present study will help to screen for appropriate HIPV components, and enhance biocontrol efforts in sustainably suppressing fruit fly populations.

Acknowledgements. We thank Dr. Yanchuan Yang for helping to conduct part of the bioassay, and Ms. Shumei Wang for helping to rear insects. This research was financially supported by Industry University Research Project of Fujian Science and Technology Department (2019N5003), Advanced Talents Introduction Project of Wuyi University (YJ201910), Education and Scientific Research Project for Young and Middle-aged Teachers in Fujian Province (JAT190801, JAT190805), National Key R&D Program of China (2017YFD0201008) and Scientific Research Team Jointly Build By Teachers and Students of Wuyi University (for Chunhua Ma). We are also grateful to Mr. Alexander Barton of englishedit.co.uk for editing the English language of our manuscript.

Conflict of interests. The authors declare that they have no conflicts of interest. The funders had no role in the design of the study; in the collection, analyses, or interpretation of data; in the writing of the manuscript, or in the decision to publish the results.

REFERENCES

[1] Altuzar, A., Montoya, P., Rojas, J. C. (2004): Response of *Fopius arisanus* (Hymenoptera: Braconidae) to fruit volatiles in a wind tunnel. – Florida Entomologist 87: 616-618.

[2] Ayelo, P. M., Sinzogan, A. A., Bokonon-Ganta, A. H., Karlsson, M. F. (2017): Host species and vegetable fruit suitability and preference by the parasitoid wasp *Fopius arisanus*. – Entomologia Experimentalis et Applicata 163: 70-81.

[3] Bautista, R. C., Harris, E. J. (1996): Effect of fruit substrates on parasitization of tephritid fruit flies (Diptera) by the parasitoid *Biosteres arisanus* (Hymenoptera: Braconidae). – Environmental Entomology 25: 470-475.

[4] Bautista, R. C., Harris, E. J., Vargas, R. I., Jang, E. B. (2004): Parasitization of melon fly (Diptera: Tephritidae) by *Fopius arisanus* and *Psyttalia fletcheri* (Hymenoptera: Braconidae) and the effect of fruit substrates on host preference by parasitoids. – Biological Control 30: 156-164.

[5] Benelli, G., Revadi, S., Carpita, A., Giunti, G., Raspi, A., Anfor, G., Canale, A. (2013): Behavioral and electrophysiological responses of the parasitic wasp *Psyttalia concolor* (Szépligeti) (Hymenoptera: Braconidae) to *Ceratitis capitata*-induced fruit volatiles. – Biological Control 64: 116-124.

http://www.aloki.hu ● ISSN 1589 1623 (Print) ● ISSN 1785 0037 (Online)
DOI: http://dx.doi.org/10.15666/aeer/1804_54755489

[6] Bruce, T. J. A., Pickett, J. A. (2011): Perception of plant volatile blends by herbivorous insects—finding the right mix. – Phytochemistry 72: 1605-1611.
[7] Carrasco, M., Montoya, P., Cruz-Lopez, L., Rojas, J. C. (2005): Response of the fruit fly parasitoid *Diachasmimorpha longicaudata* (Hymenoptera: Braconidae) to mango fruit volatiles. – Environmental Entomology 34: 576-583.
[8] Chen, L., Fadamiro, H. Y. (2007): Differential electroantennogram response of females and males of two parasitoid species to host-related green leaf volatiles and inducible compounds. – Bulletin of Entomological Research 97: 515-522.
[9] Corrado, G., Sasso, R., Pasquariello, M., Iodice, L., Carretta, A., Cascone, P., Ariati, L., Digilio, M. C., Guerrieri, E., Rao, R. (2007): Systemin regulates both systemic and volatile signaling in tomato plants. – Journal of Chemical Ecology 33: 669-681.
[10] Degenhardt, J., Köllner, T. G., Gershenzon, J. (2009): Monoterpene and sesquiterpene synthases and the origin of terpene skeletal diversity in plants. – Phytochemistry 70: 1621-1637.
[11] Dicke, M., van, Loon, J. J. A. (2000): Multitrophic effects of herbivore-induced plant volatiles in an evolutionary context. – Entomologia Experimentalis et Applicata 97: 237-249.
[12] Dweck, H. K. M., Svensson, G. P., Gündüz, E. A., Anderbrant, O. (2010): Kairomonal response of the parasitoid *Bracon hebetor* Say to the male-produced sex pheromone of its host the greater waxmoth *Galleria mellonella*. – Journal of Chemical Ecology 36: 171-178.
[13] Godfray, H. C. J. (1994): Parasitoids: Behavioral and Evolutionary Ecology. – Princeton University Press, Princeton.
[14] Gu, X. H., Cai, P. M., Yang, Q. Y., Ji, Q. E., Chen, J. H. (2017): Behavioral responses of *Fopius arisanus* (Sonan) (Hymenoptera: Braconidae) to volatiles from fruits infested by *Bactrocera dorsalis* (Hendel) (Diptera: Tephritidae) and analysis of volatile components. – Journal of Environmental Entomology 39: 820-829.
[15] Gu, X. H., Cai, P. M., Yang, Y. C., Yang, Q. Y., Yao, M. Y., Idrees, A., Ji, Q. E., Yang, J. Q., Chen, J. H. (2018): The response of four braconid parasitoid species to methyl eugenol: Optimization of a biocontrol tactic to suppress *Bactrocera dorsalis*. – Biological Control 122: 101-108.
[16] Harris, E. J., Bautista, R. C. (1996): Effects of fruit fly host, fruit species, and host egg to female parasitoid ratio on the laboratory rearing of *Biosteres arisanus*. – Entomologia Experimentalis et Applicata 79: 187-194.
[17] Harris, E. J., Bautista, R. C., Spencer, J. P. (2000): Utilization of the Egg-Larval Parasitoid, *Fopius* (*Biosteres*) *arisanus*, for Augmentative Control of Tephritid Fruit Flies. – In: Tan, K. H. (ed.) Area-Wide Control of Fruit Flies and Other Insect Pests. Penerbit Universiti Sains Malaysia, Penang, Malaysia.
[18] Hilker, M., Meiners, T. (2011): Plants and insect eggs: How do they affect each other? – Phytochemistry 72: 1612-1623.
[19] Hou, Z. Y., Yan, F. S., Chen, X. (2008): Olfactory responses of *Lysiphlebia japonica* to volatile chemicals and fresh leaves of the host plants of cotton aphids in olfactometer. – Insect Science 3: 49-57.
[20] James, D. G. (2005): Further field evaluation of synthetic herbivore-induced plant volatiles as attractants for beneficial insects. – Journal of Chemical Ecology 31: 481-495.
[21] Ji, Q. E., Bi, K., Chen, J. H. (2016): Response of egg-pupal parasitoid *Fopius arisanus* (Sonan) to infochemicals from the host eggs' surface of *Bactrocera dorsalis* (Hendel). – Journal of Asia-Pacific Entomology 19: 1151-1157.
[22] Kaplan, I. (2012): Attracting carnivorous arthropods with plant volatiles: the future of biocontrol or playing with fire? – Biological Control 60: 77-89.
[23] Khan, Z. R., Midega, C. A. O., Bruce, T. J. A., Hooper, A. M., Pickett, J. A. (2010): Exploiting phytochemicals for developing a 'push-pull' crop protection strategy for cereal farmers in Africa. – Journal of Experimental Botany 61: 4185-4196.

http://www.aloki.hu ● ISSN 1589 1623 (Print) ● ISSN 1785 0037 (Online)
DOI: http://dx.doi.org/10.15666/aeer/1804_54755489

[24] Liquido, N. J. (1991): Effect of ripeness and location of papaya fruits on the parasitization rates of Oriental fruit fly and melon fly (Diptera: Tephritidae) by braconid (Hymenoptera) parasitoids. – Environmental Entomology 20: 1732-1736.
[25] Liu, T., Li, W. Z., You, X. F., Chai, X. L., Fu, G. X., Yuan, G. H. (2013): Repellent and anti-settling activity of common plant-derived volatiles on *Myzus persicae* (Sulzer). – Acta Tabacaria Sinica 19: 77-84.
[26] Manoukis, N., Geib, S., Seo, D., McKenney, M., Vargas, R. I., Jang, E. (2011): An optimized protocol for rearing *Fopius arisanus*, a parasitoid of tephritid fruit flies. – Journal of Visualized Experiments (53): e2901.
[27] Mills, J., Getz, W. M. (1996): Modelling the biological control of insect pests: a review of host-parasitoid models. – Ecological Modelling 92: 121-143.
[28] Morawo, T., Burrows, M., Fadamiro, H. (2016): Electroantennogram response of the parasitoid *Microplitis croceipes* to host-related odors: The discrepancy between relative abundance and level of antennal responses to volatile compound. – F1000Research 5: 2725.
[29] Ngi-Song, A. J., Njagi, P. G. N., Torto, B., Overholt, W. A. (2000): Identification of behaviourally active components from maize volatiles for the stemborer parasitoid *Cotesia flavipes* Cameron (Hymenoptera: Braconidae). – International Journal of Tropical Insect Science 20: 181-189.
[30] Ngumbi, E., Fadamiro, H. (2012): Species and sexual differences in behavioural responses of a specialist and generalist parasitoid species to host-related volatiles. – Bulletin of Entomological Research 102: 710-718.
[31] Paul, A. V. N., Singh, S., Singh, A. K. (2002): Kairomonal effect of some saturated hydrocarbons on the egg parasitoids *Trichogramma brasiliensis* (Ashmead) and *Trichogramma exiguum* Pinto & Platner (Hymenoptera: Trichogrammatidae). – Journal of Applied Entomology 126: 409-416.
[32] Pérez, J., Rojas, J. C., Montoya, P., Liedo, P., Castillo, A. (2013): *Anastrepha* egg deposition induces volatiles in fruits that attract the parasitoid *Fopius arisanus*. – Bulletin of Entomological Research 103: 318-325.
[33] Pickett, J. A., Woodcock, C. M., Midega, C. A. O., Khan, Z. R. (2014): 'Push-pull' farming systems. – Current Opinion in Biotechnology 26: 125-132.
[34] Reed, H. C., Tan, S. H., Haapanen, K., Killmon, M., Elliott, N. C. (1995): Olfactory responses of the parasitoid *Diaeretiella rapae* (Hymenoptera: Aphidiidae) to odor of plants, aphids, and plant-aphid complexes. – Journal of Chemical Ecology 21: 407-418.
[35] Rousse, P., Chiroleu, F., Domerg, C., Quilici, S. (2007a): Naive *Fopius arisanus* females respond mainly to achromatic cues. – Biological Control 43: 41-48.
[36] Rousse, P., Chiroleu, F., Veslot, J., Quilici, S. (2007b): The host- and microhabitat olfactory location by *Fopius arisanus* suggests a broad potential host range. – Physiological Entomology 32: 313-321.
[37] Schellhorn, N. A., Bianchi, F., Hsu, C. L. (2014): Movement of entomophagous arthropods in agricultural landscapes: links to pest suppression. – Annual Review of Entomology 59: 559-581.
[38] Schoonhoven, L. M., Van, Loon, J. J. A., Dicke, M. (2005): Insect-Plant Biology. – Oxford University Press, Oxford.
[39] Song, Y. Z. (2019): The effects of tobacco volatiles on behavioral orientation of *Aphidus gifuensis*. – Master's Thesis, Fujian Agriculture and Forestry University.
[40] Takemoto, H., Takabayashi, J. (2015): Parasitic wasps *Aphidius erviare* more attracted to a blend of host-induced plant volatiles than to the independent compounds. – Journal of Chemical Ecology 41: 801-807.
[41] Uefune, M., Choh, Y., Abe, J., Shiojiri, K., Sano, K., Takabayashi, J. (2012): Application of synthetic herbivore-induced plant volatiles causes increased parasitism of herbivores in the field. – Journal of Applied Entomology 136: 561-567.

http://www.aloki.hu ● ISSN 1589 1623 (Print) ● ISSN 1785 0037 (Online)
DOI: http://dx.doi.org/10.15666/aeer/1804_54755489

[42] Vargas, R. I., Leblanc, L., Putoa, R., Eitam, A. (2007): Impact of introduction of *Bactrocera dorsalis* (Diptera: Tephritidae) and classical biological control releases of *Fopius arisanus* (Hymenoptera: Braconidae) on economically important fruit flies in French Polynesia. – Journal of Economic Entomology 100: 670-679.

[43] Vargas, R. I., Leblanc, L., Harris, E. J., Manoukis, N. C. (2012): Regional suppression of *Bactrocera* fruit flies (Diptera: Tephritidae) in the Pacific through biological control and prospects for future introductions into other areas of the world. – Insects 3: 727-742.

[44] Vargas, R. I., Stark, J. D., Banks, J., Leblanc, L., Manoukis, N. C., Peck, S. (2013): Spatial dynamics of two oriental fruit fly (Diptera: Tephritidae) parasitoids *Fopius arisanus* and *Diachasmimorpha longicaudata* (Hymenoptera: Braconidae) in a guava orchard in Hawaii. – Environmental Entomology 42: 888-901.

[45] Vet, L. E. M., Dicke, M. (1992): Ecology of infochemical use by natural enemies in a tritrophic context. – Annual Review of Entomology 37: 141-172.

[46] Vinatier, F., Tixier, P., Duyck, P. F., Lescourret, F. (2011): Factors and mechanisms explaining spatial heterogeneity: A review of methods for insect populations. – Methods in Ecology and Evolution 2: 11-22.

[47] Wang, P., Lou, Y. G. (2013): Screening and field evaluation of synthetic plant volatiles as attractants for *Anagrus nilaparvatae* Pang et Wang, an egg parasitoid of rice planthoppers. – Chinese Journal of Applied Entomology 50: 431-440.

[48] Webster, B., Bruce, T. J. A., Pickett, J. A., Hardie, J. (2010): Volatiles functioning as host cues in a blend become nonhost cues when presented alone to the black bean aphid. – Animal Behaviour 79: 451-457.

http://www.aloki.hu ● ISSN 1589 1623 (Print) ● ISSN 1785 0037 (Online)
DOI: http://dx.doi.org/10.15666/aeer/1804_54755489

WATER LEVEL FLUCTUATIONS DETERMINE THE SPATIAL AND TEMPORAL DISTRIBUTION OF MANCHURIAN WILD RICE (*ZIZANIA LATIFOLIA*) IN SIX YANGTZE RIVER FLOODPLAIN LAKES, CHINA

WANG, H. L.[1] – ZHANG, X. K.[1*] – JIN, B. S.[2*] – WANG, M. D.[2] – CHEN, W. X.[1] – LIU, D.[1]

[1]*College of Life Science, Anqing Normal University, Anqing 246133, China*
(e-mail: 350041761@qq.com – Wang, H. L.; 2722016526@qq.com – Chen, W. X.; 3304717426@qq.com – Liu D.)

[2]*College of Resource and Environment Science, Anqing Normal University, Anqing 246133, China*
(e-mail: 3039894838@qq.com – Wang, M. D.)

[*]*Corresponding author*
e-mail: zxksgsg@163.com; jinbsh@aqnu.edu.cn

(Received 27th Mar 2020; accepted 2nd Jul 2020)

Abstract. *Zizania latifolia* is a common emergent macrophyte in lakes along the lower reaches of the Yangtze River. To investigate the factors driving the expansion or decline of *Z. latifolia* populations, the spatial and temporal distribution patterns of *Z. latifolia* in six Yangtze floodplain lakes were analyzed from 2007 to 2016 using remote sensing and geographic information system tools. In combination with hydrological data and other environmental factors, the main influencing factors were determined. The results showed that distribution of *Z. latifolia* among the six lakes exhibited obvious differences. Plant cover was the highest in Wuchang and Huangda lakes, which had relatively stable water levels. Spearman correlation analyses showed that the lake morphological variables, climatic variables, and water quality variables had no significant effects on the distribution of *Z. latifolia*. Regarding variables related to hydrology, excluding the rate of water level change and timing of extreme water level annually, the other four groups of hydrological variables (a total of 20 indicators) all had significant effects on the distribution of *Z. latifolia*. At last, the reasons for difference in cover in different lake types were analyzed and appropriate strategies for the ecological management of *Z. latifolia* populations in different lake types were recommended.
Keywords: *hydrology, water level regulation, ecological restoration, emergent plant, remote sensing*

Introduction

The Yangtze River floodplain is one of the most important ecosystems globally. Thousands of shallow freshwater lakes are distributed in the ecosystem, with a total area of 15770 km^2 (Wang et al., 2016). Historically, all the lakes were freely connected with the Yangtze mainstream, and constituted the river-floodplain ecosystem, also known as the river-lake complex ecosystem (Wang and Wang, 2009). Aquatic plants, representing the major primary producers, are one of the most important structural and functional components in such complex ecosystems. They play important roles in nutrient cycling, energy flows, water purification, and provision of habitats for other aquatic organisms (Bornette and Puijalon, 2011; Zhang, 2013). In the course of evolution, such plants have gradually adapted to natural water level fluctuations (WLF), and formed various ecological groups with different WLF requirements (Lytle and Poff, 2004; Toogood et al., 2008; Yang et al., 2020). However, most lakes along the Yangtze River have been disconnected from the Yangtze mainstem by sluices over the recent decades to facilitate

http://www.aloki.hu ● ISSN 1589 1623 (Print) ● ISSN 1785 0037 (Online)
DOI: http://dx.doi.org/10.15666/aeer/1804_54915503

aquaculture and flood control activities (Wang et al., 2016). River-lake disconnection has not only significantly altered the community structures of lake plants, but has also altered the WLF of these lakes to various degrees (Zhang et al., 2015; Wang et al., 2016).

Zizania latifolia (Griseb.) Turcz. ex Stapf is a tall emergent plant with well developed underground parts. It can reproduce sexually through seeds or asexually via rhizomes and tiller buds (Wang et al., 2014, 2018). In the Yangtze River basin, *Z. latifolia* has been extensively cultivated as an aquatic vegetable in association with *Ustilago esculenta*, an epiphyte (Guo et al., 2007). Due to its rapid growth rate and high competitive ability, the species is the dominant emergent macrophyte in most lakes along the Yangtze River (Zhang et al., 2016; Li et al., 2018). However, spatial and temporal distributions of *Z. latifolia* in the lakes have displayed different patterns following river-lake disconnection. In some lakes, considerable terrestrialization has occurred due to the overgrowth of *Z. latifolia* populations, while the decline or elimination of emergent macrophytes has been observed in other lakes (Li et al., 2018; Wang et al., 2018). Both situations have resulted in ecological management challenges in lakes in this region. To effectively manage and exploit such *Z. latifolia* populations, it is necessary to determine the major factors influencing their distribution, which could provide a theoretical basis for the ecological management of the *Z. latifolia* populations and lakes in the Yangtze River floodplain.

WLF maintain ecological integrity and regulate ecological processes in floodplain lakes, which are usually described using amplitude, water depth, frequency, timing, and rate of change (Deegan et al., 2007; Yuan et al., 2017). Previous studies conducted in the region have reported that aquatic plant communities are structured considerably by the WLF components (Zhang et al., 2015, 2018). Therefore, alteration of WLF could be the major factor influencing temporal and spatial differences in *Z. latifolia* populations in the Yangtze floodplain lakes. In the present study, six typical floodplain lakes were selected as model ecosystems in the lower reaches of the Yangtze River. Remote sensing and geographic information system (GIS) technologies were used to determine the distribution of *Z. latifolia* populations in the six lakes from 2007–2016. The aims of the present study were: 1) to determine the temporal and spatial distribution patterns of *Z. latifolia* populations in different lakes; 2) to determine the key WLF parameters influencing the distribution of *Z. latifolia* populations; and 3) to develop water level regulation strategies for the effective management of *Z. latifolia* populations in different lakes. The results of the present study could not only have significant implications for the management of floodplain lakes, but also provide an eco-hydrological basis for the regulation of regional water resources.

Materials and methods

Study area

The six typical floodplain lakes selected in the present study, including Shengjin Lake, Caizi Lake, Pohu Lake, Huangda Lake, Wuchang Lake, and Pogang Lake, which are located in the lower reaches of the Yangtze River, China. The six lakes are also in a key region of floodplain wetlands along Anqing city, Anhui province. The region, which experiences a subtropical monsoon climate, has adequate rainfall and four distinct seasons. The annual average rainfall and air temperature among the six lakes have minimal differences, ranging from 16.1–16.6℃ and 1241.3–1554.4 mm (*Table 1*).

http://www.aloki.hu ● ISSN 1589 1623 (Print) ● ISSN 1785 0037 (Online)
DOI: http://dx.doi.org/10.15666/aeer/1804_54915503

Table 1. *Locations and environmental parameters of the six study lakes*

Lakes	Location	Lake area (km^2)	Lake bottom elevation (m)	Catchment area (km^2)	Shoreline length (km^2)	Average water depth (m)	Annual average rainfall (mm)	Annual average temperature (℃)
Shengjin Lake	N: 30°15′-30°28′, E: 116°58′-117°14′	126.6	8.4	1554	217.5	2.54	1554.4	16.1
Caizi Lake	N: 30°43′-30°58′, E: 117°01′-117°09′	181.2	8.5	3234	276.1	1.94	1241.3	16.5
Pohu Lake	N: 30°04′-30°15′, E: 116°19′-116°33′	151.9	10	4941	202.4	2.97	1291.3	16.6
Huangda Lake	N: 29°56′-30°08′, E: 116°14′-116°33′	266.5	10.5	7849	212.4	2.38	1291.3	16.6
Wuchang Lake	N: 30°14′-30°20′, E:116°36′-116°53′	100.6	10	1083.7	96.4	2.13	1299.6	16.5
Pogang Lake	N: 30°33′-30°42′, E: 117°04′-117°13′	28.4	8.7	346	46.3	2.49	1389.1	16.5

The lake with the largest surface area is Huangda Lake, at 266.5 km^2, followed by Caizi Lake, Pohu Lake, and Shengjin Lake, at 181.2, 151.9, and 126.6 km^2, respectively. Wuchang Lake and Pogang Lake have the lowest surface areas, at 100.6 and 28.4 km^2, respectively (*Table 1*). In the past, all the six lakes were freely connected with the Yangtze mainstem, and the water regime in the Yangtze mainstem greatly influenced WLF in the lakes. However, all the six lakes have become river-lake disconnected lakes due to the building of sluices, to facilitate aquaculture and flood control activities. The overgrowth of *Z. latifolia* in the Wuchang and Huangda Lakes has caused serious ecological problems, while relatively poor distribution has been observed in the other four lakes following the construction of sluices. The geographical location and basic environmental parameters of the six lakes are presented in *Fig. 1* and *Table 1*.

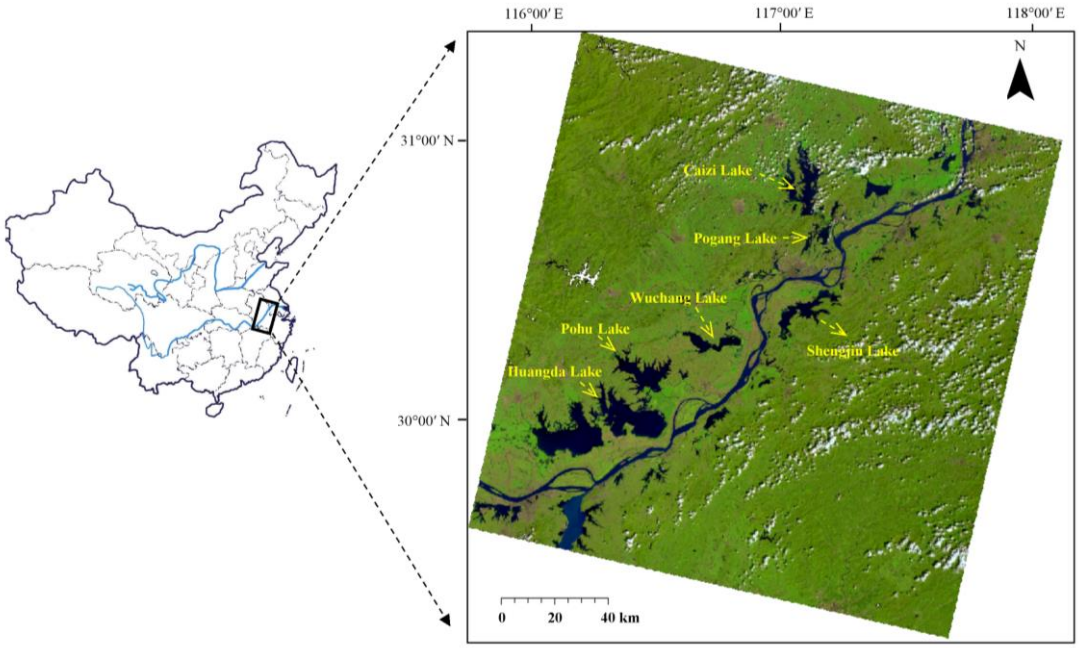

Figure 1. *Locations of the study lakes along the Yangtze River*

http://www.aloki.hu ● ISSN 1589 1623 (Print) ● ISSN 1785 0037 (Online)
DOI: http://dx.doi.org/10.15666/aeer/1804_54915503

Study methods and data analyses

To determine the spatial and temporal distribution patterns of *Z. latifolia* in the six lakes, MSS/TM/ETM+/OLI remote sensing images from 2007–2016 were obtained from the US Landsat satellite. All the Landsat images were downloaded from the US Geology Survey site (http://glovis.usgs.gov). The track numbers of the MSS and TM/ETM+/OLI sensors are 130–39 and 121–39, respectively, with resolutions of 80×80 m and 30×30 m, respectively. Considering the coverage of *Z. Latifolia* reaches the maximum in autumn, autumn images with no more than 30% cloud cover were selected in each year. To improve the accuracy of image interpretation, the ENVI v.4.7 (ITT Visual Information Solutions) was used to perform geometric correction, band combination, image fusion, and enhancement for the 10 scene remote sensing images. The images were then interpreted and classified, and the spatial distribution and areas of distribution were calculated using ArcGIS 10.2 (http://www.esri.com/software/arcgis). To verify the accuracy of plant coverage detection, field survey was conducted in May, 2017.

The environmental factors used for analyses were in four categories, including lake morphological variables, climatic variables, water quality variables, and water level fluctuation related hydrological variables. The lake morphological variables include lake surface area, lake bottom elevation, shoreline length, and catchment area. The lake bottom elevation and catchment area were derived from available literatures (Wang and Dou, 1998; Compilation Commission of Anhui Local Records, 1998; Jin, 2008), and the lake area and shoreline length were measured. The climatic variables included annual average rainfall, annual average temperature, and annual average sunshine hours, while the water quality variables included total nitrogen, total phosphorus, and transparency. All the climatic and water quality data were obtained from available literatures (Wang and Dou, 1998; Gu et al., 2014; Wu et al., 2016; Wu, 2018). The WLF variables can be divided into six groups, i.e. G1 (Fluctuating amplitude), G2 (Monthly mean water depth), G3 (Annual extreme water depth), G4 (Timing of annual extreme water level), G5 (Rate of water level changes), and G6 (Frequency of water level changes). A total of 28 indicators were included in the six groups (*Table 2*). The water level data of the studied lakes during the study period were obtained from the Hydrology Bureau of Anqing city or downloaded from the flood and drought information network of Anhui province (http://61.191.22.157/Default.aspx) (water level data for several lakes were missing in some years). The hydrological data were used to classify the six lakes into different categories using Two-Way Indicator Species Analysis (TWINSPAN), which was performed using PC-ORD for Windows (McCune and Mefford, 1997). Life history information on *Z. latifolia* was obtained from published studies (Zhang et al., 2016).

In the present study, the water level data from 2007–2016 in the six lakes were analyzed first, and then the spatial and temporal distribution patterns of *Z. latifolia* were determined based on the remote sensing images. Indicators of Hydrologic Alteration software (The Nature Conservancy, Charlottesville, Virginia) was used to calculate the related 28 indicators of the six groups. Spearman correlation was used to determine the effects of lake morphological variables, climatic variables, water quality variables, and WLF related variables on the distribution of *Z. latifolia,* and the cover data was used in the analysis. Factors influencing the variable cover in the different lake categories were also analyzed, and appropriate recommendations were provided for the ecological management of *Z. latifolia*.

http://www.aloki.hu ● ISSN 1589 1623 (Print) ● ISSN 1785 0037 (Online)
DOI: http://dx.doi.org/10.15666/aeer/1804_54915503

Table 2. *Comparison of the water level fluctuations in six floodplain lakes. The values in the table are the average values for 2007-2016.*

Items	Shengjin Lake	Caizi Lake	Pohu Lake	Huangda Lake	Wuchang Lake	Pogang Lake
G1: Fluctuating amplitude (m)						
Amplitude	7.02	6.52	4.31	3.90	3.40	1.89
G2: Monthly mean water depth (m)						
January	0.67	0.41	2.01	1.56	0.90	2.06
February	0.49	0.39	1.85	1.47	0.93	2.10
March	0.71	0.62	1.87	1.50	1.20	2.08
April	1.48	1.00	2.31	1.68	1.36	2.20
May	2.72	1.74	2.81	2.02	1.73	2.23
June	4.02	2.86	3.80	2.77	2.48	2.55
July	5.36	4.77	5.00	3.70	3.59	3.29
August	5.12	4.50	4.96	3.88	3.68	3.24
September	4.43	3.50	4.00	3.56	3.40	3.06
October	2.75	1.96	2.89	2.77	2.87	2.71
November	1.82	0.84	2.02	1.96	2.09	2.27
December	0.86	0.67	2.10	1.72	1.32	2.11
G3: Annual extreme water depth (m)						
1-day min	0	0.27	1.30	1.18	0.83	1.86
3-day min	0	0.28	1.30	1.19	0.84	1.89
7-day min	0	0.29	1.32	1.20	0.85	1.91
30-day min	0.28	0.40	1.48	1.29	0.87	1.95
90-day min	0.65	0.50	1.71	1.45	1.00	2.02
1-day max	6.31	5.74	5.26	4.13	4.23	3.63
3-day max	6.28	5.72	5.24	4.13	4.23	3.62
7-day max	6.23	5.64	5.23	4.12	4.20	3.60
30-day max	5.87	5.30	5.19	4.07	4.07	3.49
90-day max	5.16	4.47	4.84	3.81	3.68	3.27
G4: Timing (Julian date) of annual extreme water level						
Date 1-day min	32.4	50.0	169.0	146.0	153.4	153.3
Date 1-day max	214.6	213.8	218.3	231.6	218.2	219.2
G5: Rate of water level changes (cm/d)						
Rise rate	12.59	7.76	4.27	3.68	4.16	3.08
Fall rate	-11.70	-6.25	-3.87	-2.97	-2.81	-2.32
G6: Frequency of water level changes						
Reversals	81.4	43.7	67.3	48.7	48.6	83.0

Results

WLF in the study lakes

WLF in the six study lakes varied greatly (*Fig. 2*; *Table 2*). Shengjin Lake and Caizi Lake had the highest fluctuation amplitudes, which were 7.02 and 6.51 m, respectively. In addition, the mean water depths in the two lakes were lower than 1.0 m from winter to early spring, while they were more than 5.0 m in summer. Water level change rate

http://www.aloki.hu ● ISSN 1589 1623 (Print) ● ISSN 1785 0037 (Online)
DOI: http://dx.doi.org/10.15666/aeer/1804_54915503

was also highest in the two lakes, which were more than 11 cm/d and 6 cm/d, respectively. The fluctuation amplitude was also high in Pohu Lake (4.31 m), but the lake maintained a high mean water depth of 2.0 m from winter to early spring. WLF in Wuchang Lake and Huangda Lake were similar, and the fluctuation amplitudes were 3.4 m and 3.9 m, respectively. In addition, the mean water depths in the two lakes were approximately 1.1 m and 1.5 m, respectively, from winter to early spring. Water level was relatively stable in Pogang Lake, and the fluctuation amplitude was only 1.89 m. However, the lake also maintained a high mean water depth of 2.0 m from winter to early spring. Otherwise, the highest water level was observed in 2016 in all the six lakes from 2007–2016, followed by 2010. However, the lowest water levels were observed in different years in the six lakes.

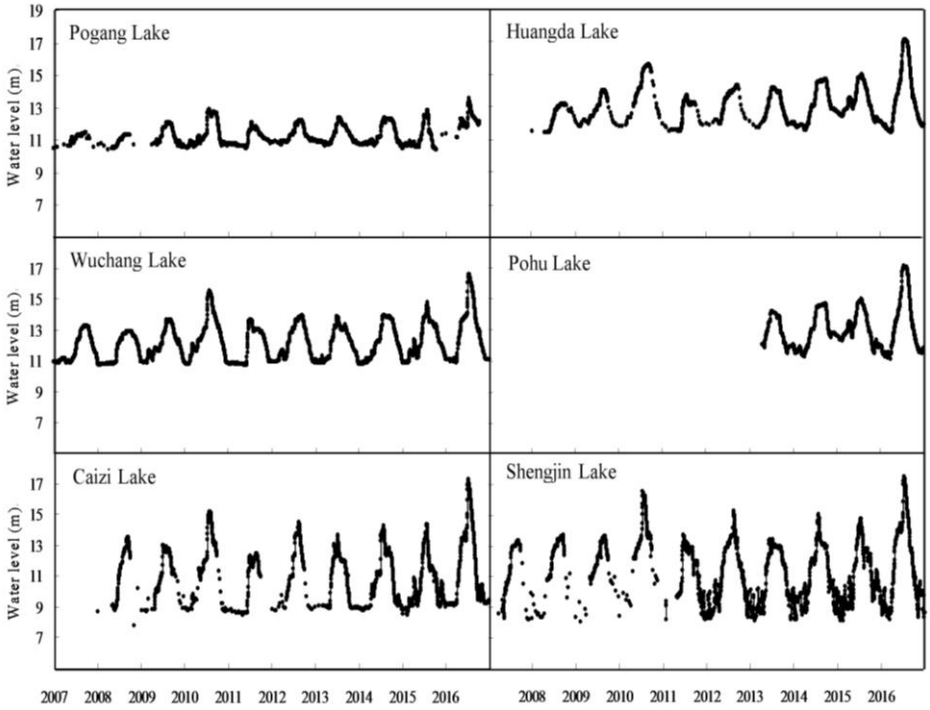

Figure 2. *Water level fluctuations in six floodplain lakes from 2007–2016*

Spatial and temporal distribution of Z. latifolia

The spatial and temporal distribution of *Z. latifolia* in the six lakes varied considerably, and the mean cover of *Z. latifolia* in Shengjin, Caizi, Pohu, Huangda, Wuchang, and Pogang Lakes were 1.54%, 1.41%, 2.93%, 17.85%, 26.01%, and 3.56%, respectively (*Fig. 3*). The distribution of *Z. latifolia* in Huangda Lake and Wuchang Lake was obviously higher than in the other four lakes, and the cover in the two lakes was more than 40% in 2007, 2008, and 2011, while it was lower than 2% in both lakes in 2016. Shengjin Lake had a patchy distribution in the southern area of the lake in 2007, 2008, and 2015, while Caizi Lake had minimal distribution in the northern area of the lake area in 2007, 2008, and 2011. However, in the other years, the two lakes had nearly no distribution of *Z. latifolia*. Pogang Lake had relatively high distributions in 2007 and 2008, which were 12.17% and 9.71%, respectively. In the other years, cover in Pogang Lake was lower than 5%.

http://www.aloki.hu ● ISSN 1589 1623 (Print) ● ISSN 1785 0037 (Online)
DOI: http://dx.doi.org/10.15666/aeer/1804_54915503

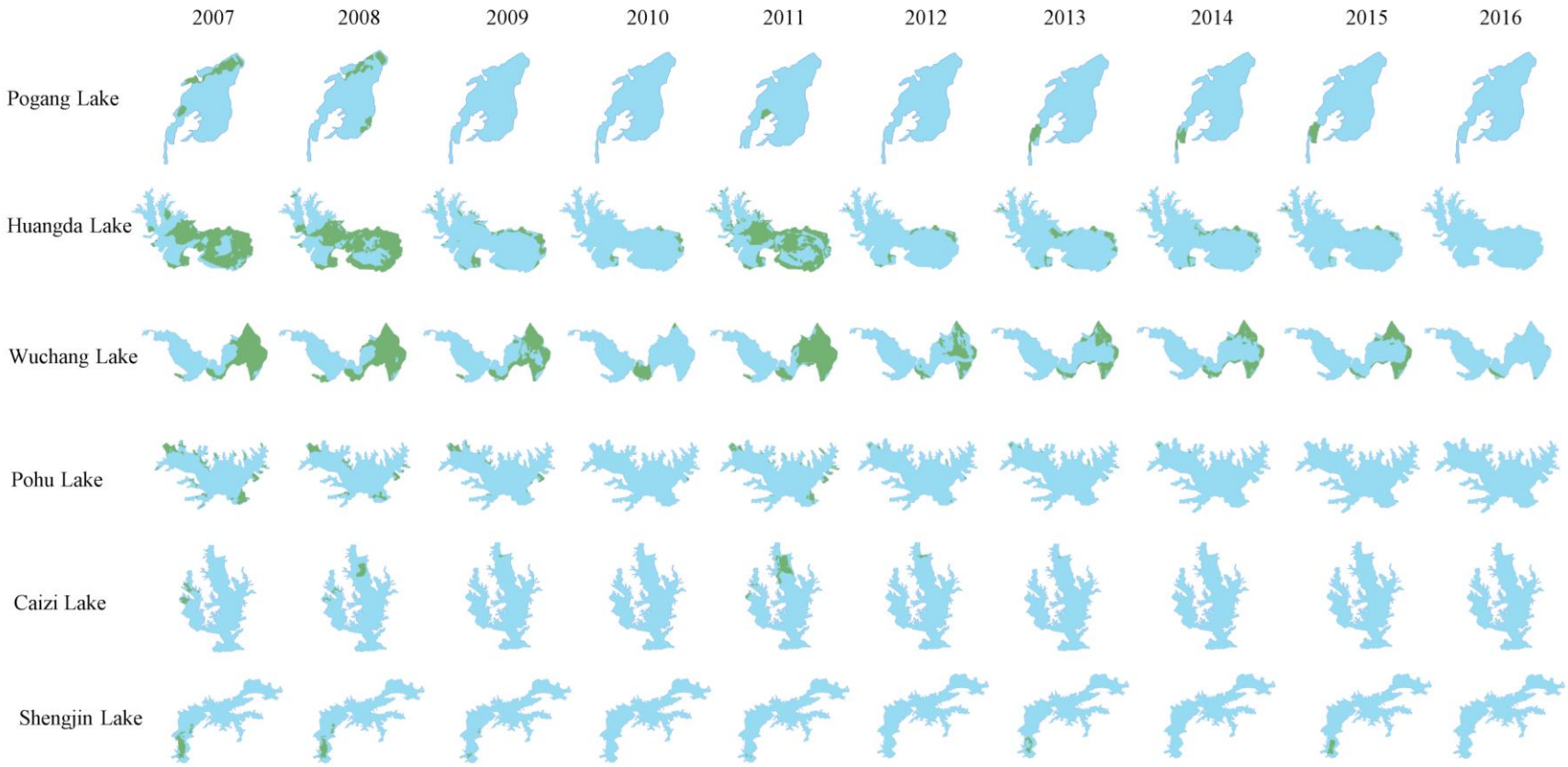

Figure 3. *Spatial and temporal distribution patterns of Z. latifolia in the study lakes from 2007-2016*

http://www.aloki.hu ● ISSN 1589 1623 (Print) ● ISSN 1785 0037 (Online)
DOI: http://dx.doi.org/10.15666/aeer/1804_54915503

Major factors influencing distribution

Spearman correlation analyses revealed that the lake morphological variables, climatic variables, and water quality variables had no significant effects on the distribution of *Z. latifolia*. With regard to the WLF related variables, all the four groups (a total of 20 indicators) except the G4 and G6 groups had significant effects on the distribution of *Z. latifolia* (*Table 3*).

Table 3. *Spearman correlation between WLF variables and Z. latifolia cover. Only the WLF and cover data in Wuchang and Huangda lakes were used in the analysis*

Items	*R*	*P*
G1: Fluctuating amplitude (m)		
Amplitude	-0.700**	**0.0078**
G2: Monthly mean water depth (m)		
January	-0.561*	**0.0297**
February	-0.810***	**0.0004**
March	-0.393	0.1069
April	-0.792 ***	**0.0001**
May	-0.933***	**0.0000**
June	-0.852***	**0.0000**
July	-0.743***	**0.0003**
August	-0.839***	**0.0000**
September	-0.665***	**0.0019**
October	-0.022	0.9302
November	0.259	0.2834
December	-0.038	0.8846
G3: Annual extreme water depth (m)		
1-day min	-0.665*	**0.0132**
3-day min	-0.657*	**0.0146**
7-day min	-0.694**	**0.0084**
30-day min	-0.720**	**0.0055**
90-day min	-0.645*	**0.0174**
1-day max	-0.777***	**0.0001**
3-day max	-0.782***	**0.0001**
7-day max	-0.782***	**0.0001**
30-day max	-0.819***	**0.0000**
90-day max	-0.837***	**0.0000**
G4: Timing (Julian date) of annual extreme water level		
Date 1-day min	0.073	0.8045
Date 1-day max	0.145	0.5540
G5: Rate of water level changes (cm/d)		
Rise rate	-0.415	0.1581
Fall rate	-0.705**	**0.0071**
G6: Frequency of water level changes		
Reversals	-0.264	0.3826

http://www.aloki.hu ● ISSN 1589 1623 (Print) ● ISSN 1785 0037 (Online)
DOI: http://dx.doi.org/10.15666/aeer/1804_54915503

Reasons for varied cover

After the first level division using TWINSPAN, the six lakes were split by 1-day max into two groups (Shengjin, Pohu, and Caizi lakes with high 1-day max water depth, and the other three lakes with low 1-day max water depth) (*Fig. 4*). Further analyses divided all the six lakes into four groups based on January mean water depths (Pohu Lake and Pogang Lake with high water depth in January, and the other four lakes with low water depth in January) (*Fig. 4*).

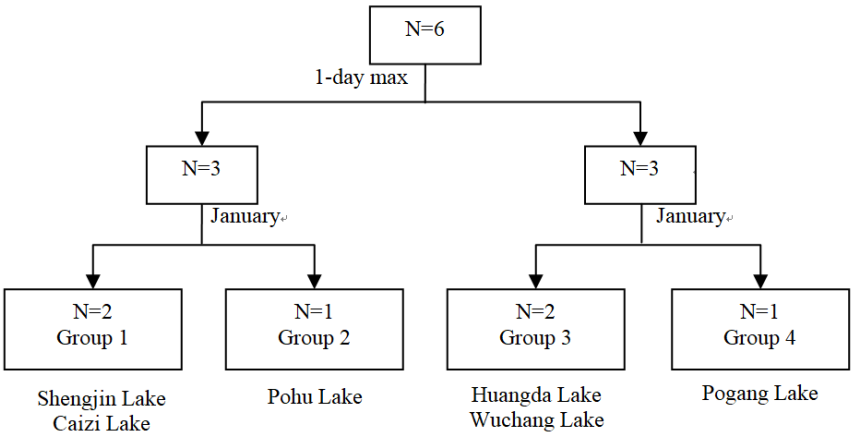

Figure 4. *TWINSPAN dendrogram of the study lakes based on water level fluctuation parameters*

The life history of *Z. latifolia* can be divided into germination period, rapid growth and expansion period, dispersal period, and dormancy period (*Fig. 5*). Combined with the major hydrological indicators (*Table 3*), the reason for low *Z. latifolia* cover in Pogang Lake could be the high water depths in winter to early spring limiting germination. In addition to the high water depth in the germination period, the high fluctuation amplitude could be a key reason for the low *Z. latifolia* cover in Pohu Lake. With regard to Caizi Lake and Shengjin Lake, although the water depth was low in the germination period, the high fluctuation amplitude and water level change rate was unfavorable for the growth and dispersal of *Z. latifolia*. WLF in Huangda Lake and Wuchang Lake were relatively adequate and met the requirements of *Z. latifolia*, which facilitated the maintenance of relatively high cover.

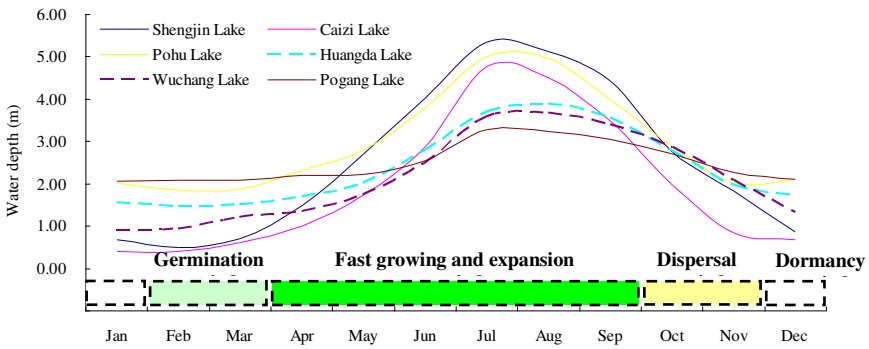

Figure 5. *Life history of Z. latifolia and monthly mean water depth in six floodplain lakes*

http://www.aloki.hu ● ISSN 1589 1623 (Print) ● ISSN 1785 0037 (Online)
DOI: http://dx.doi.org/10.15666/aeer/1804_54915503

Discussion

The Yangtze River floodplain lakes play important roles in the maintenance of regional species diversity and sustainable economic development (Fang et al., 2006; Wang and Wang, 2016). Although most floodplain lakes have become river-lake disconnected over the past few decades, WLF in the lakes are different largely due to different aquaculture and flood control activities. For instance, Pogang Lake is mainly used for aquaculture, and water level is high and stable throughout the year following the construction of a sluice, while annual mean water level has decreased in Wuchang Lake due to flood control activities (Zhang et al., 2016). In addition, the catchment area and number of tributaries could affect WLF. In Shengjin Lake and Caizi Lake, which had high fluctuation amplitudes, the catchment areas were 3234 km^2 and 1554 km^2, respectively, while in Pogang Lake, which had the lowest fluctuation amplitude, the catchment area was only 346 km^2 (Wang and Dou, 1998).

Spearman correlation analyses revealed that the lake morphological variables, climatic variables, and water quality variables had no significant effects on the distribution of *Z. latifolia.* This could be largely because the variables changed minimally from 2007–2016. Among the six groups of WLF parameters, excluding the frequency of WLF (G4) and the timing of annual extreme water level (G6), the other four groups of water level parameters had significant effects on the distribution of *Z. latifolia*. The frequency of WLFs in lakes are generally low compared with the frequency of WLF in rivers; therefore, the frequency of WLF in lakes has minimal effect on species distribution, and other studies have reported similar findings (Zhang et al., 2015, 2018). The timing of annual extreme water level had no significant impact on the distribution of *Z. latifolia* potentially because the maximum water level of all the lakes was observed in summer, while the lowest water level was observed in winter. In the present study, the fluctuation amplitude was significantly negatively correlated with the distribution of *Z. latifolia*, which indicated that water bodies with relatively stable fluctuation amplitudes could be more appropriate for the growth and development of *Z. latifolia*. Some studies have shown that habitat heterogeneity in lakes decreases with decrease in fluctuation amplitudes, while intraspecific and interspecific competition among plants increases (Zhang, 2013). *Z. latifolia* is often the dominant species under such conditions due to its high competitive ability and its capacity to tolerate flooding (Zhang et al., 2016).

In addition, mean water depths in January–February and April–September were significantly negatively correlated with the distribution of *Z. latifolia*. The low water depth in January–February could significantly improve the underwater light conditions and physico-chemical properties of the sediment (Yang et al., 2020a,b), in turn promoting the germination of *Z. latifolia* individuals. The mean water depth in April-September may have considerable influences on the growth and development of *Z. latifolia*, since numerous studies have shown that the high water depths are not conducive for growth and biomass accumulation in *Z. latifolia* (Wang et al., 2014, 2018; Li et al., 2018). The annual extreme water depths also had significant effects on the distribution of *Z. latifolia*, and the distribution of *Z. latifolia* considerably declined with increase in maximum or minimum water depth. This could be mainly due to increasing stress on growth of *Z. latifolia* with increase in water depth (Mauchamp et al., 2001; Wang et al., 2007; Yang et al., 2020a). In the present study, plant cover in all the six lakes was the lowest in 2010 and 2016, which had the highest water levels, which is consistent with the observation that growth decreases with increase in water level.

http://www.aloki.hu ● ISSN 1589 1623 (Print) ● ISSN 1785 0037 (Online)
DOI: http://dx.doi.org/10.15666/aeer/1804_54915503

The rate of change in water levels is also one of the key hydrological factors influencing the distribution of wetland plants (Yuan et al., 2017). Studies have shown that aquatic plants tolerate rapid changes in water levels to a certain degree; however, when the water levels change too rapidly, aquatic plants may not have adequate time adapt morphologically, and the plants would maintain intermediate and suboptimal states (Vretare et al., 2001). In the present study, the distribution of *Z. latifolia* was significantly negatively correlated with the rate of decline in water level, indicating that a high rate of decline was not conducive for the growth and spread of *Z. latifolia*.

Conclusion

This study showed that the lake morphological variables, climatic variables, and water quality variables had no significant effects on the distribution of *Z. latifolia* in lakes along the lower reaches of the Yangtze River. The WLF was the main factor determining the spatial and temporal distribution of *Z. Latifolia*. The results of the present study have significant implications for the ecological management of *Z. latifolia* in the Yangtze River floodplain lakes. We suggest that in lakes that require the restoration of *Z. latifolia* populations, water levels should be regulated. We recommend the maintenance of a low fluctuation amplitude and a low rate of change in water level. In addition, it is critical to consider that low water depth promotes germination. Conversely, in lakes with *Z. latifolia* overgrowth, we propose the increase of the fluctuation amplitude within a growth year, and the increase of water depth to limit germination. In addition, increasing the rate of change in water level would inhibit seedling growth and spread of *Z. latifolia* in environments in which they are overgrown. Finally, it is highly recommend that future researches carry out more studies to determine the specific WLF requirements of *Z. latifolia*, so as to provide a theoretical basis for the quantitative regulation of lake water levels.

Acknowledgements. This work was supported by the Natural Science Foundation of Anhui Province (2008085QD164), the key Project of Natural Science Foundation for Universities of Anhui Province (KJ2019A0550 and KJ2018A0373), and the National Natural Science Foundation of China (41401042).

REFERENCES

[1] Bornette, G., Puijalon, S. (2011): Response of aquatic plants to abiotic factors: a review. – Aquatic Science 73: 1-4.

[2] Compilation Commission of Anhui Local Records. (1998): Record of Anhui Province (Record of Natural Environment). – Fangzhi Press, Beijing.

[3] Deegan, B. M., White, S. D., Ganf, G. G. (2007): The influence of water level fluctuations on the growth of four emergent macrophyte species. – Aquatic Botany 86: 309-315.

[4] Fang, J., Wang, Z., Zhao, S., Li, Y., Tang, Z., Yu, D., Ni, L., Liu, H., Xie, P., Da, L., Li, Z., Zheng, C. (2006): Biodiversity changes in the lakes of the Central Yangtze. – Frontiers in Ecology and the Environment 4(7): 369-377.

[5] Gu, Y., Li, F., Li, C., Huang, W., Yao, J., Zhang, H. (2014): Comprehensive evaluation of Anqing Yangtze River wetland eutrophication of lakes. – Journal of Anqing Teachers College (Natural Science Edition) 20(4): 121-124.

[6] Guo, H., Li, S., Peng, J., Ke, W. (2007): *Zizania latifolia* Turcz. cultivated in China. – Genetic Resources and Crop Evolution 54: 1211-1217.

http://www.aloki.hu ● ISSN 1589 1623 (Print) ● ISSN 1785 0037 (Online)
DOI: http://dx.doi.org/10.15666/aeer/1804_54915503

[7] Jin, B. S. (2008): The distribution and characteristics of drainage systems in the natural protection area of Anqing Wetland along the Yangtze River. – Chinese Agricultural Science Bulletin 24(7): 445-449.
[8] Li, Z. F., Zhang, X. K., Wang, H. L., Wan, A., Xie, J. (2018): Effects of water depth and substrate type on rhizome bud sprouting and growth of *Zizania latifolia*. – Wetlands Ecology and Management 26(3): 277-284.
[9] Lytle, D. A., Poff, N. L. (2004): Adaptation to natural flow regimes. – Trends in Ecology and Evolution 19: 94-100.
[10] Mauchamp, A., Blanch, S., Grillas, P. (2001): Effects of submergence on the growth of *Phragmites australis* seedlings. – Aquatic Botany 69: 147-164.
[11] McCune, B., Mefford, M. J. (1997): Multivariate Analysis of Ecological Data (PC-ORD). – MjM Software, Gleneden Beach, Oregon.
[12] Toogood, S. E., Joyce, C. B., Waite, S. (2008): Response of floodplain grassland plant communities to altered water regimes. – Plant Ecology 197: 285-298.
[13] Vretare, V., Weisner, S. E. B., Strand, J. A., Graneli, W. (2001): Phenotypic plasticity in *Phragmites australis* as a functional response to water depth. – Aquatic Botany 69: 127-145.
[14] Wang, S. M., Dou, H. S. (1998): Lakes of China. – Science Press, Beijing.
[15] Wang, L., Hu, J. M., Song, C. C., Yang, T. (2007): Effects of water level on the rhizomatic germination and growth of typical wetland plants in Sanjiang Plain. – Chinese Journal of Applied Ecology 18(11): 2432-2437.
[16] Wang, H. Z., Wang, H. J. (2009): Ecological Effects of River-lake Disconnection and Restoration Strategies in the Midlower Yangtze River. – In: Wang, Z. Y. (ed.) Ecological Management on Water and Sediment in the Yangtze River Basin. Science Press, Beijing.
[17] Wang, Q., Chen, J., Liu, F., Li, W. (2014): Morphological changes and resource allocation of *Zizania latifolia* (Griseb.) Stapf in response to different submergence depth and duration. – Flora 209: 279-284.
[18] Wang, H. Z., Liu, X. Q., Wang, H. J. (2016): The Yangtze River floodplain: threats and rehabilitation. – American Fisheries Society Symposium 84: 263-291.
[19] Wang, H. L., Zhang, X. K., Wan, A. (2018): Morphological responses of Zizania latifolia seedlings at different ages to short-term submergence. – Journal of Lake Science 30(1): 192-198.
[20] Wu, Y., Wang, L., Xu, M., Wang, H., Zhou, Z. (2016): Community dynamics of phytoplankton and related affecting factors in Shengjin Lake. – Journal of Biology 33(5): 34-39.
[21] Wu, Q. L. (2018): Effects of Water Level Fluctuations on Phytoplankton in Huayang River Lake Group. – Master Thesis, Anhui University, Hefei.
[22] Yang, Z. D., Davy, A. J., Liu, X. Q., Yuan, S. B., Wang, H. Z. (2020a): Responses of an emergen macrophyte, *Zizania latifolia*, to water-level changes in lakes with contrasting hydrological management. – Ecological Engineering 151: 105814.
[23] Yang, W., Xu, M., Li, R., Zhang, L., Deng, Q. (2020b): Estimating the ecological water leves of shallow lakes: a case study in Tangxun Lake, China. – Scientific Reports 10: 5637.
[24] Yuan, S., Yang, Z., Liu, X., Wang, H. (2017): Key parameters of water level fluctuations determining the distribution of Carex in shallow lakes. – Wetlands 37: 1005-1014.
[25] Zhang, X. K. (2013): Water level fluctuation requirements of plants in the Yangtze floodplain lakes. – Doctoral Dissertation, University of Chinese Academy of Sciences, Beijing.
[26] Zhang, X. K., Liu, X. Q., Wang, H. Z. (2015): Effects of water level fluctuations on lakeshore vegetation of three subtropical floodplain lakes, China. – Hydrobiologia 747: 43-52.

http://www.aloki.hu ● ISSN 1589 1623 (Print) ● ISSN 1785 0037 (Online)
DOI: http://dx.doi.org/10.15666/aeer/1804_54915503

[27] Zhang, X. K., Wan, A., Wang, H. L., Zhu, L. L., Yin, J., Liu, Z. G., Yu, D. P. (2016): The overgrowth of *Zizania latifolia* in a subtropical floodplain lake: changes in its distribution and possible water level control measures. – Ecological Engineering 89: 114-120.
[28] Zhang, X. K., Qin, H. M., Wang, H. L., Wan, A., Liu, G. H. (2018): Effects of water level fluctuations on root architectural and morphological traits of plants in lakeshore areas of three subtropical floodplain lakes in China. – Environmental Science and Pollution Research 25(34): 34583-34594.

http://www.aloki.hu ● ISSN 1589 1623 (Print) ● ISSN 1785 0037 (Online)
DOI: http://dx.doi.org/10.15666/aeer/1804_54915503

PRIMARY NON-RESPONSE IN INFLAMMATORY BOWEL DISEASE, DEFINITION, POTENTIAL CAUSES, THERAPEUTIC DRUG MONITORING AND MICROBIOTA – A REVIEW

ALATAWI, H.[1,2*] – MOSLI, M.[3,5] – SAADAH, O.[4,5] – DULAI, P. S.[6] – AL-HINDI, R. R.[1] – BAHIELDIN, A.[1,7] – EDRIS, S.[1,7,8]

[1]Department of Biological Sciences, Faculty of Science, King Abdulaziz University, Jeddah 21589, Saudi Arabia (phone/fax: +966-2-460-0000)

[2]Department of Biological Sciences, University Collage of Haqel, University of Tabuk, Tabuk, Saudi Arabia

[3]Department of Medicine, King Abdulaziz University, Jeddah, Saudi Arabia (phone: +966-12-640-8272; fax: +966-12-695-2538)

[4]Department of Pediatrics, Faculty of Medicine, King Abdulaziz University, Jeddah, Saudi Arabia (phone: +966-12-640-8272; fax: +966-12-695-2538)

[5]Inflammatory Bowel Disease Research Group, King Abduklaziz University, Jeddah, Saudi Arabia (phone: +966-12-640-8272; fax: +966-12-695-2538)

[6]University of California San Diego, 9500 Gilman Drive, La Jolla, CA, USA

[7]Department of Genetics, Ain Shams University, Cairo, Egypt

[8]Princess Al Jawhara Albrahim Centre of Excellence in Research of Hereditary Disorders (PACER-HD), King Abdulaziz University, Jeddah, Saudi Arabia (phone/fax: +966-2-460-0000)

**Corresponding author*
e-mail: halatwi@ut.edu.sa; phone: +966-53-938-0024; fax: +966-2-460-0000

(Received 27th Mar 2020; accepted 7th Jul 2020)

Abstract. Tumor necrosis factors (TNF-α) are pro-inflammatory cytokines centrally involved in autoimmunity. Monoclonal antibodies against TNF-α are used to treat several autoimmune diseases including inflammatory bowel disease (IBD). The proportion of patients who experience primary non-response (PNR) to anti-TNF treatment is approximately 13–40%. Secondary loss of response (LOR) to anti-TNF agents happens in 23–46% of IBD patients leading to a drug discontinuation rate of 5–13%. A combination of factors including disease characteristics (e.g., phenotype, location, and severity), drug response (e.g., pharmacokinetics, pharmacodynamics, or immunogenicity), and treatment strategy (e.g., dosing regimen) has been associated with PNR and LOR. Therapeutic drug monitoring (TDM) relies on the measurement of serum concentrations of anti-TNF agents and anti-drug antibodies. TDM can be utilized to identify PNR and LOR and to assist clinicians in their decision-making. Additionally, TDM is used to optimize drug therapy (e.g., dose escalation) for patients who exhibit LOR. Recently, gut microbiota was believed to play a central role in immune regulation, and influence response to TNF-α antagonists. Microbial diversity for certain taxa can become a prognosis factor to monitor the response to treatment. In this article, we aim to review PNR and LOR, and discuss microbiota profiles associated with their occurrence.

http://www.aloki.hu ● ISSN 1589 1623 (Print) ● ISSN 1785 0037 (Online)
DOI: http://dx.doi.org/10.15666/aeer/1804_55055525

Keywords: *secondary loss of response, tumor necrosis factors (TNF)- α, therapeutic drug monitoring, ulcerative coliti, Crohn's disease, infliximab, adalimumab, pharmacokinetic and pharmacodynami failure*

Abbreviations: TNF: tumor necrosis factors, IBD: inflammatory bowel disease, PNR: Primary non-response, LOR: secondary loss of response, TDM: therapeutic drug monitoring, UC: ulcerative colitis, CD: Crohn's disease, IFX: Infliximab, ADL: Adalimumab, CZP: Certolizumab, GOL: Golimumab, CRP: C-reactive protein, ADAs: antidrug antibodies, AZA: Azathioprine, SCFAs: short-chain fatty acids, SpA: spondyloarthritis, NSAID: nonsteroidal anti-inflammatory drugs

Background

Tumor necrosis factors (TNF-α) are pro-inflammatory cytokines produced by certain cell types, such as T-cells and macrophages (Ebert et al., 2008). The number of these cells is increased in the intestinal mucosa of patients with inflammatory bowel disease (IBD). Accordingly, these cells are used as therapeutic targets. TNF-α functions as a component of the intestinal mucosa-mediated defensive line against mucosal pathogens and destructive inflammation (Allendoerfer and Deepe, 1998). TNF-α antagonists are monoclonal antibody drugs that are considered a revolutionary treatment for IBD. It has been demonstrated that TNF-α antagonists contribute to improving life quality of IBD patients and limit the requirement for surgeries and hospitalizations (Wang et al., 2019). Treatment guidelines encourage early utilization of TNF-α antagonists for IBD patients, particularly for patients who are refractory to other classes of medications and have been found to exhibit high-risk features at baseline (Gomollón et al., 2016). TNF-α antagonists are approved for the induction and maintenance of remission for both types of IBD, e.g., ulcerative colitis (UC) and Crohn's disease (CD) (Ha et al., 2012).

In cases of moderate-to-severe CD, intensive treatment regimens incorporating TNF-α antagonists, such as infliximab (IFX), adalimumab (ADL) and certolizumab (CZP) have been proven to be effective and can lead to clinical remission and mucosal healing (Hazlewood et al., 2015). IFX, ADL and GOL (golimumab) have been approved for the induction and maintenance of remission in UC. Despite this, the use of TNF-α antagonists is limited due to the cost and possibility of unpredictable side-effects, including infusion reactions, infections and lymphoma (Singh et al., 2011; Ben-Horin and Chowers, 2011). A small percentage (5%) of IBD patients has been recorded to experience adverse drug reactions with severity ranging from simple skin rashes to anaphylactic reactions. It has been estimated that 10-30% of patients treated with TNF-α antagonists may not respond, and these patients are referred to as primary non-responders (PNRs). Additionally, 23-46% of patients may experience loss of response (LOR) over time, and this situation is accordingly referred to as secondary LOR (Roda et al., 2016). While LOR is mainly attributed to pharmacokinetic derangements, the precise etiologies underlying PNR are unknown (Ebert et al., 2008; Ben-Horin and Chowers, 2011; Billioud et al., 2011). The gut microbiota is recently thought to play a central role in immune regulation, and the accumulating literature on this process suggests that it also influences response to TNF-α antagonists (Zhang et al., 2015; Rajca et al., 2014).

Mechanisms underlying PNR can be attributed to pharmacokinetic failure (Rocha et al.), pharmacodynamic failure (Ainsworth et al., 2008) and immunogenicity failure (Rojas et al., 2005). The causes of PNR to anti-TNF therapy are unknown, however, the possible factors contributing to PNR can be classified into four categories, patient-related factors, microbiome-related factors, disease-related factors and treatment-related factors (Ding et al., 2016). PNR can be often managed through optimization of dosing regimen (Hanauer et al., 2002) and combination therapy (Colombel et al., 2010; Coutinho et al.,

http://www.aloki.hu ● ISSN 1589 1623 (Print) ● ISSN 1785 0037 (Online)
DOI: http://dx.doi.org/10.15666/aeer/1804_55055525

1995). Therapeutic drug monitoring (TDM) play a fundamental role to determine the appropriate assessment time for PNR occurs which at weeks 12 to 14 following induction (Papamichael et al., 2014; Cornillie et al., 2014). The human gut contains more than 100 trillion different microbial organisms, including more than 1000 species of bacteria, viruses, fungi and protozoa, collectively referred to as the microbiome (Honda and Littman, 2012). Four phyla are predominant and represent more than 99% of intestinal bacteria, which are *Firmicutes*, *Bacteroidetes*, *Proteobacteria*, and *Actinobacteria* (Eckburg et al., 2005; Ley et al., 2008). The *Firmicutes* and *Bacteroidetes* phyla represent the main commensal microbiota in healthy subjects, while *Proteobacteria* and *Actinobacteria* are significantly higher in IBD patientsqw (Sheehan et al., 2015; Andoh, 2016). Fecal microbiota transplantation (FMT) aims to recover the gut microbial level in patients via transferring fecal suspension from a healthy donor (Wang et al., 2017). In this article, we aim to explore PNR and LOR with a focus on the underlying causes of PNR and the possible involvement of gut microbiota.

Primary non-response (PNR) definition

A precise definition of PNR has not been determined, however, the accepted definition of PNR in connection with the use of anti-TNF-α drugs is failure to achieve clinical remission following the induction therapy period (Sprakes et al., 2012). It has been demonstrated that anti-TNF antagonists such as CZP, ADL and IFX are efficient for eliciting prompt remission and to prevent relapse in IBD. Despite the known efficacy of these drugs, it is recommended that clinicians estimate the improvement in the clinical signs after 8, 12 and 14 weeks, respectively, following the initial infusions/injections with these drugs in PNR patients (Hanauer et al., 2002; Sands et al., 2004). Data from clinical trials and clinical practice differ in regard to the incidence of PNR, which ranges from 10 to 30% (Sprakes et al., 2012; Hanauer et al., 2002; Ford et al., 2011).

Several factors may contribute to the risk of PNR, including a disease duration of longer than 2 years, small bowel involvement, smoking, elevated C-reactive protein (CRP) and genetic mutations in apoptosis-related genes, such as FAS-L and caspase-9 (Ben-Horin et al., 2014). PNR can be minimized by optimization of the initially selected dosing regimens, by increasing the dose or reducing the intervals between doses, and by combining TNF-α antagonists with immunosuppressants, such as thiopurines or methotrexate (*Table 1*) (Ding et al., 2016; Roda et al., 2016). The latter approach is supported by data from several clinical trials. PNR is typically managed by switching to a different type of TNF-α antagonist that could be beneficial. However, several studies have demonstrated that the treatment outcome following a switch to a second anti-TNF antagonist in PNR patients is still poor with a response rate of approximately 50–65% (Allez et al., 2010). Switching to an out-of-class medication that acts through different mechanisms may provide a worthwhile resolution to this problem (Sands et al., 2014). The proportion of PNR can differ among clinical trials (36–40%) and according to clinical practice (13–33%) (Ford et al., 2011).

http://www.aloki.hu ● ISSN 1589 1623 (Print) ● ISSN 1785 0037 (Online)
DOI: http://dx.doi.org/10.15666/aeer/1804_55055525

Table 1. *A comparison between primary non-response (PNR) and secondary loss of response (LOR) (Ding et al., 2016; Roda et al., 2016)*

	Primary non-response (PNR)	**Secondary loss of response (LOR)**
Definition	Remission does not occur during the induction of therapy period and clinical signs and symptoms are continuous (no healing)	The patients who respond to the initial induction of therapy but subsequently suffer from clinical relapse and lack of remission albeit maintenance of therapy
Percentage of those who do not respond	10-30%	23-46%
Incidence	Differs between clinical trial and clinical practice from 10–20% to 13–30%	Its incidence is 13% for Infliximab (IFX) and 24% for Adalimumab (ADA)
Risk factors	- Disease longer than 2 years - Small bowel involvement - Smoking - C reactive protein - Genetic mutations such as FAS-L and caspase-9 in the apoptosis related genes	- Formation of antibodies against TNFα antagonists (immunogenicity) - Use of episodic TNFα antagonists in 5–13% of patients
Management	- Optimization of the dosing regimen - Combination therapy	Use of concomitant immunomodulators with Anti -TNFα antagonists
Therapeutic options	- Switching to another anti- TNF could be beneficial - Switch out of the therapeutic groups that are characterized by other working mechanisms	- Change to another TNFα antagonist agent was associated with a complete or partial response in 92% of patients - Switching within a therapeutic class to another anti-TNF agent may restore clinical response
Strategy	- Dose escalation based on the pharmacokinetic - Therapeutic drug monitoring (TDM)	Therapeutic drug monitoring (TDM)

Proposed mechanisms underlying PNR

Three mechanisms that could explain PNR to TNF-α antagonists are presented in *Figure 1.*

Pharmacokinetic failure

This phenomenon occurs when suboptimal levels of TNF-α antagonists circulate either because of suboptimal dosing or interaction with anti-drug antibodies (Rocha et al.) that leads to accelerated drug clearance (non-immune) via tissues or through the systemic circulation. The three fundamental mechanisms implicated in pharmacokinetic failure include:

i. Proteolytic catabolism that occurs in the reticuloendothelial system due to the ability of monoclonal antibodies to bind to Fc gamma receptors (Fc, or Fragment/crystallizable, is a surface protein, and the term is derived from the proteins' specificity to bind a part of an antibody known as the Fc region.
ii. Degradation that occurs in lysosomes as a result of interaction with membrane-bound TNF (Keizer et al., 2010; Ordás et al., 2012).

http://www.aloki.hu ● ISSN 1589 1623 (Print) ● ISSN 1785 0037 (Online)
DOI: http://dx.doi.org/10.15666/aeer/1804_55055525

iii. Ulcerated mucosa that leads to clearance and drug loss through the mucosal membrane as a result of non-immune clearance, ultimately resulting in considerable loss of protein and electrolytes in addition to loss of drug (Brandse et al., 2015).

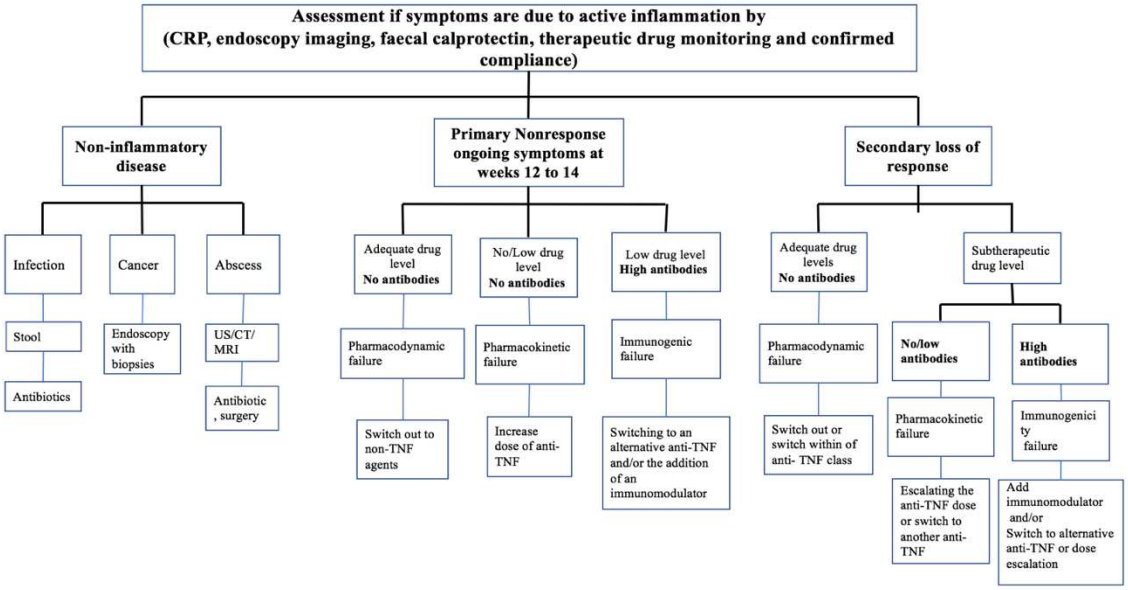

Figure 1. *Management of primary nonresponse and secondary loss of response. Taken from (Ding et al., 2016; Roda et al., 2016)*

Pharmacodynamic failure

This type of failure occurs when no improvement in clinical symptoms occurs despite the presence of adequate circulating drug and absence of Antidrug antibodies (ADAs) (Ainsworth et al., 2008). The most favorable alternative avenue would be to switch to an out-of-class medication, such as a leukocyte trafficking inhibitor or an anti-cytokine (Ding et al., 2016).

Immunogenicity failure

This scenario is characterized by a lack of improvement in symptoms in the presence of low circulating serum TNF-α antagonists and high levels of ADAs. One of the strongest factors linked to non-response is the formation of ADAs against anti-TNFα antagonists. Antibodies possess the ability to interfere with TNF receptors and to accelerate the clearance of the drug through the reticuloendothelial system. Low levels of ADAs have been implicated in effectively achieving remission (Rojas et al., 2005). Neutralizing and non-neutralizing antibodies and low drug concentrations have been reported in up to 83% of PNRs (Echarri et al., 2014). Additionally, the effective induction of remission in PNRs by using a second TNF-α antagonist occurs in only 50% of IBD patients (Gisbert et al., 2015). The perfect option is to switch to an alternative anti-TNF or to incorporate the use of an immunomodulator. Following a drug switch, therapeutic drug monitoring should be repeated to determine if antibody disappearance has occurred (Ding et al., 2016).

http://www.aloki.hu ● ISSN 1589 1623 (Print) ● ISSN 1785 0037 (Online)
DOI: http://dx.doi.org/10.15666/aeer/1804_55055525

Potential causes of PNR to anti-TNF therapy

The causes of PNR to anti-TNF therapy are unknown; however, the possible factors contributing to PNR can be classified into four categories (see *Fig. 2*).

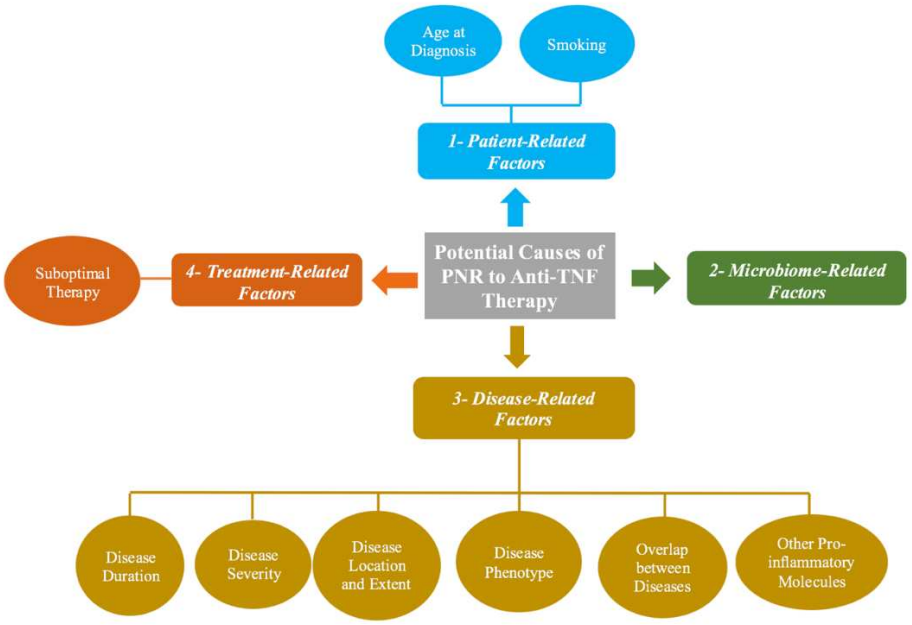

Figure 2. *Potential causes of PNR to anti-TNF therapy*

Patient-related factors

Factors like gender, lack of concomitant immunosuppression, age, prolonged duration of disease, smoking, CD phenotype, and disease not limited to the colon may contribute to the response to anti-TNF α agents (Danese et al., 2011). The two most patient-related factors include:

Age at diagnosis

The connection between age at the time of diagnosis and PNR is controversial (Juillerat et al., 2014), although diagnosis at an early age (less than 17 years) is often associated with poor outcome (Grover et al., 2014). Interestingly, younger patients tend to respond better to anti-TNF therapy in comparison with older patients (Vermeire et al., 2002).

Smoking

Smoking is an environmental factor that likely plays a role in reducing patient responsiveness to anti-TNF agents. A relationship between smoking and PNR has been previously reported. Approximately 30% of patients who are smokers are non-responsive to IFX at week 4 (Arnott et al., 2003). Smoking has been found to decrease the influence of anti-TNF drugs and to increase the likelihood of non-response (Cohen et al., 2011; Chaparro et al., 2011). According to a study performed on 221 ADL-treated patients,

http://www.aloki.hu ● ISSN 1589 1623 (Print) ● ISSN 1785 0037 (Online)
DOI: http://dx.doi.org/10.15666/aeer/1804_55055525

21.2% of the patients were smoking at the time of induction (OR 0.52, P = 0.049) (Ding et al., 2016; Kiss et al., 2011). Additionally, PRECISE-3 data indicated that smokers had more active disease compared to non-smokers (HR: 1.404; 95% CI: 1.09–1.77; P = 0.007) (Sandborn et al., 2015).

Microbiome-related factors

The exact role of the gut microbiota in PNR is not well understood. Several studies have observed no significant difference in the gut microbiota composition before and after treatment with TNF-antagonists (Zhang et al., 2015). In contrast, results published by Bazin et al. (2018) indicated that gut microbial composition could be used as a biomarker that is predictive of clinical response to anti-TNF treatments. Additionally, microbial diversity in the presence or absence of particular taxa has been used as a prognostic factor to monitor the response to treatment or the presence of several diseases, including colorectal cancer (Gagnière et al., 2016; Bazin et al., 2018). It has been found that in some diseases, such as melanoma, particular microbiota species, can be used as biomarkers to determine the correlation between the colitis and resistance to immunotherapy (Dubin et al., 2016).

Recent study compared the microbial composition among anti-TNF therapy-treated UC patients; responders showed increase of the concentrations of *Faecalibacterium prausnitzii* and decrease of the rate of dysbiosis compared with non-responders. Furthermore, both responders and non-responders had a featured mucosal antimicrobial peptides expression patterns (Magnusson et al., 2016). In addition, another recent study showed that in the case of discontinuation of using anti-TNF-α treatment, low abundance of *F. prausnitzii* can be used as a biomarker to predict the early incidence of Crohn's disease (Rajca et al., 2014). In rheumatology, dysbiosis in the oral and gut microbiota of rheumatoid arthritis patients had been monitored. This dysbiosis can be partly treated by using disease-modifying antirheumatic drugs (DMARD) (Zhang et al., 2015). However, the influence of rheumatoid arthritis was moderate on the gut microbiota compared to the oral microbiota. Moreover, decrease of risk factor and low concentration of *Holdemania filiformis* and *Bacteroides* species have been observed in the responder patients after therapy (Zhang et al., 2015).

Disease-related factors

A range of disease-related factors has been associated with PNR. They are the following:

Disease duration

According to several studies, patients with shorter disease durations (< 2 years) exhibit better responses and higher long-term remission rates compared to those of patients who have had the disease for more than 2 years. For instance, the Crohn's Trial of the Fully Human Antibody Adalimumab for Remission Maintenance (CHARM) study was performed to determine the rates of response and remission to ADL. Assessments were performed at week 26 to evaluate the impact of disease duration on response and remission rates. More patients with a short disease duration experienced response compared to patients with a disease duration of > 2 years or > 5 years (56%, 35% and 37%, respectively) (Colombel et al., 2007). Similar results were observed in the PRECISE 2 study that evaluated remission and response to certolizumab pegol (CZP) in CD at week 26. Of the CD patients treated with CZP, 62% exhibited PNR

http://www.aloki.hu ● ISSN 1589 1623 (Print) ● ISSN 1785 0037 (Online)
DOI: http://dx.doi.org/10.15666/aeer/1804_55055525

(p = 0.02) (Schreiber et al., 2010). Additionally, greater rates of response and remission were observed in CD patients with disease duration of < 2 years compared to those of patients with disease duration of ≥ 5 years (Reinisch et al., 2009; Colombel et al., 2015).

Disease severity

Several studies suggest that disease severity is one of the main factors that contribute to non-response (Castro-Laria et al., 2016; Reinisch et al., 2011). The efficacy of anti-TNF treatment has been observed to be lower in severely inflamed tissue. This is likely due to hastening of non-immune drug clearance (Fasanmade et al., 2009, 2011). PNR could also be attributed to the use of inadequate induction dosages. It has been proposed that fecal loss of anti-TNF drugs via ulcerated, denuded mucosa contributes to PNR (Brandse et al., 2015).

Disease location and extent

Although some studies suggest the presence of a correlation between localized ileal stricture disease and PNR, much of the data regarding this correlation remains conflicting (Louis et al., 2007). One study proposed ileal resection as an effective treatment for localized ileal stricture disease, but a separate study suggested that the localization of disease did not directly affect the response rate. The study compared two categories of patients who were treated with anti-TNF therapy, e.g., patients with isolated ileal stricture disease and patients with stricture disease at an unspecified location. The results indicated that both patient categories required surgery at the same rate (Moran et al., 2014).

Disease phenotype

An association between disease phenotype and response to anti-TNF therapies has been suggested in several studies. In Kiss et al. (Kiss et al., 2011; Ding et al., 2016), which included 201 CD patients treated with ADL, at week 52, PNR with continued clinical remission had been observed in patients who have active luminal disease (OR: 3.89; 95% CI: 1.43–10.6; P = 0.008). Moreover, at week 12, it had been noticed that the presence of two pathological phenotypes, luminal and fistulizing in CD patients led to decrease of remission rates. Otherwise, this rate was sort of high in CD patients with only luminal phenotype (42.5% vs. 56.3%, P = 0.06).

Overlap between diseases

An overlap between inflammatory diseases such as Spondylarthritis (SpA) and IBD is possible. For instance, 5–10% of SpA patients may have concomitant IBD, while up to 30% of IBD patients may also experience inflammatory arthritis (Bazin et al., 2018). Additionally, 60% of SpA patients have microscopic gut inflammation (Lin et al., 2014; Van Praet et al., 2012). These overlaps may often explain resistance to treatment with TNF antagonists.

Other pro-inflammatory molecules

Theoretically, IBD patients characterized as PNR may not benefit from switching between IFX and ADL since both drugs possess the same chemical structure and function (Dassopoulos, 2005). Accordingly, a lack of response to anti-TNF agents could be due to specific disease characteristics, with dose intensification would not achieve the required

http://www.aloki.hu ● ISSN 1589 1623 (Print) ● ISSN 1785 0037 (Online)
DOI: http://dx.doi.org/10.15666/aeer/1804_55055525

result. A potential explanation for this is that pro-inflammatory molecules other than TNF-α may be responsible for the pathogenesis of the disease (Gisbert et al., 2015).

Treatment-related factors

A range of treatment-related factors is associated with PNR. They are the following:

Suboptimal therapy

The common indicators of suboptimal therapy are dose escalation of anti-TNF and discontinuation of treatment. Among the anti-TNF patients, 25.8% of UC patients required dose-escalation and 19.2% of CD patients required increased doses. The underlying reason for these therapeutic alterations is the worsening of clinical signs and symptoms (94.2% UC and 94.5% CD). Among UC patients, the cause of discontinued initial anti-TNF therapy was the appearance of negative clinical symptoms (45.6%) or the occurrence of an adverse reaction (23.2%). Additionally, 49.5% of discontinued UC patients were switched to an alternate anti-TNF therapy. Among CD patients, the cause of discontinued initial anti-TNF therapy was uncontrolled symptoms (36.3%) or an adverse reaction (27.4%). Additionally, 62.7% of discontinued CD patients were switched to another anti-TNF therapy (Lindsay et al., 2017).

Rescue therapeutic strategies in cases of PNR

PNR is often managed through the following two strategies:

Optimization of dosing regimen

Data derived from CLASSIC 1 (Clinical Assessment of Adalimumab Safety and Efficacy Studied as Induction Therapy in Crohn's Disease) demonstrated that a higher dosage of ADL could achieve better remission rates at week 4 of treatment compared to that of lower dosages. Similarly, data from the PRECISE-2 (Pegylated Antibody Fragment Evaluation in Crohn's Disease: Safety and Efficacy) and ACCENT-1 (A Crohn's Disease Clinical Trial Evaluating Infliximab in a New Long-Term Treatment Regimen) trials demonstrated that higher dosages of CZP and IFX during the induction period are associated with a lower risk of PNR (Hanauer et al., 2002).

Combination therapy

Results obtained from the SONIC (Study of Biologic and Immunomodulator Naïve Patients in Crohn's disease) suggested that AZA (Azathioprine) exerts an additive influence on mucosal healing at week 26 when combined with IFX. Accordingly, combining anti-TNF drugs with immunosuppressive therapy appears to enhance drug efficacy and can theoretically help to prevent PNR (Colombel et al., 2010; Coutinho et al., 1995).

The role of therapeutic drug monitoring (TDM) in PNR

The appropriate assessment time for PNR occurs at weeks 12 to 14 following induction therapy (Papamichael et al., 2014; Cornillie et al., 2014). In week 4, 5 mg/mL serum concentration of adalimumab was used as an indicator to identify the risk of antibody formation. In a study on adalimumab-treated CD patients (n = 168), mucosal healing is

http://www.aloki.hu ● ISSN 1589 1623 (Print) ● ISSN 1785 0037 (Online)
DOI: http://dx.doi.org/10.15666/aeer/1804_55055525

associated with a trough level, and this can be utilized to predict clinical response. The median concentrations of ADL in serum were 8.6 lg/mL (interquartile range (IQR): 6.5–10.8) at week 2 and 5.3 lg/mL (IQR, 2.8–10.9) at week 4. At week 4, a comparison was performed between two types of patients, including those who received 80/40 mg and those who received 160/80 mg as a loading dose. The second patient group exhibited higher adalimumab serum concentrations (3.6 vs. 11.6 lg/mL; $P < 0.0001$) and possessed a lower incidence of PRN "as needed" (odds ratio [OR]: 0.02; 95% CI: 0.003–0.2; $P < 0.0001$) (Karmiris et al., 2009; Ding et al., 2016). A serum trough concentration of < 5 mg/mL has been associated with an increased future risk of the formation of antibodies specific to ADL (HR: 25.12; 95% CI: 5.64–111.91; $P = 0.0002$) (Baert et al., 2016).

A prospective study that examined serum drug concentrations of 32 CD patients treated with IFX (n = 15) and ADL (n = 17) at week 14 demonstrated that responders possessed a higher trough concentration than that of non-responders (FX [5.60 lg/mL]. ADL was compared to non-responders using the Harvey–Bradshaw Index, C-reactive protein (CRP) or fecal calprotectin concentration [IFX 0.032 lg/mL and ADL 2.62 lg/mL; $P = 0.01$]) (Echarri et al., 2014). At week 6, high trough concentrations of IFX (> 3 lg/mL) and ADL (> 4.5 lg/mL) were used, and > 90% remission and response rates were achieved. Additionally, sustained anti-drug antibody levels were observed in 26% of the IFX-treated patients and in 0% of the ADL-treated patients. In general, it has been suggested that the observation of adequate anti-TNF concentrations at weeks 4 to 6 is highly predictive of response to anti-TNF therapy. At week 14, a low anti-TNF drug concentration and the occurrence of antibody formation can predict primary non-response (Ding et al., 2016).

Proactive and reactive therapeutic drug monitoring

Proactive TDM is applied during remission. The aim of this approach is to modify the dose of IFX depending on individual pharmacokinetics and pharmacodynamics to avoid sub-therapeutic dosing and the risk of failure or to minimize the intensity of the therapy to reduce the financial costs associated with supra-therapeutic dosing. In contrast, reactive TDM is applied as a result of treatment failure despite the previous use of IFX therapy to achieve a successful outcome. This approach depends on pharmacokinetics and pharmacodynamic in response to IFX intensification, change to another TNF inhibitor, or the use of a new biologic drug class (Steenholdt, 2018).

Recent data suggest that proactive TDM of IFX leads to successful therapeutic outcomes in IBD. Despite this, the clinical benefits of proactive infliximab have not been confirmed after first reactive testing. A retrospective cohort study was carried out from September 2006 to January 2015 on IBD patients who underwent to maintenance IFX treatment and received an initial reactive testing (Papamichael et al., 2018). The purpose of this study was to compare outcomes at long-term between proactive infliximab monitoring after reactive testing and just reactive testing in IBD patients. Patients were divided into two groups; Group A represented a proactive infliximab monitoring after reactive testing while Group B represented a reactive testing alone. Treatment failure was defined as drug discontinuation due to either LOR or the occurrence of a serious adverse event. The total number of IBD patients was 102 (n = 70, 69% with CD; Group A, n = 33 and Group B, n = 69) were followed for a median of 2.7 years (interquartile range [IQR], 1.4–3.8 years). Multiple Cox regression analysis determined that patients who had proactive following reactive TDM were independently associated with less treatment

http://www.aloki.hu ● ISSN 1589 1623 (Print) ● ISSN 1785 0037 (Online)
DOI: http://dx.doi.org/10.15666/aeer/1804_55055525

failure (hazard ratio [HR] 0.15; 95% confidence interval [CI] 0.05–0.51; P = 0.002) and fewer IBD-related hospitalizations [HR: 0.18; 95% CI 0.05–0.99; P = 0.007]. Conclusion of this study was the proactive infliximab monitoring following reactive testing led to better drug stability and decrease of hospitalizations among IBD patients compared to reactive testing alone (Papamichael et al., 2018).

A multicenter retrospective cohort study was performed from June 2006 until December 2015 on IBD patients who underwent to maintenance adalimumab therapy (Papamichael et al., 2019). The study aimed to evaluate long-term the outcomes between IBD patients who had at least one proactive TDM of ADL with standard of care and/or reactive TDM. Treatment failure was defined as drug discontinuation due to secondary LOR, the occurrence of a serious adverse event, or the need for IBD-related surgery. The total number of IBD patients was 382 (Crohn's disease, n = 311, 81%) received at least one proactive TDM (n = 53) or the standard of care (empirical dose escalation, n = 279; reactive TDM, n = 50). Patients were followed for a median of 3.1 years (interquartile range, 1.4-4.8 years). Multiple Cox regression analyses demonstrated that obtaining at least one proactive TDM led to decrease the risk of treatment failure (hazard ratio [HR]: 0.4; 95% confidence interval [CI]: 0.2–0.9; p = 0.022). The study provided the foremost evidence that reducing of risk of treatment failure may be attributed to proactive TDM of ADL compared with standard of care (Papamichael et al., 2019).

Microbiota profiles and primary non-response to anti-TNF agents

The human gut has more than 100 trillion various microbial organisms, including more than 1000 species of bacteria, viruses, fungi and protozoa, collectively referred to as the microbiome (Honda and Littman, 2012). Four phyla are predominant and represent more than 99% of intestinal bacteria, which are *Firmicutes*, *Bacteroidetes*, *Proteobacteria*, and *Actinobacteria* (Eckburg et al., 2005; Ley et al., 2008). The *Firmicutes* and *Bacteroidetes* phyla represent the main commensal microbiota in healthy subjects, while *Proteobacteria* and *Actinobacteria* are significantly higher in IBD patients (*Figs. 3* and *4;* Sheehan et al., 2015; Andoh, 2016).

Functional composition of gut microbiota in IBD patients

Taxa of *Faecalibacterium*, *Odoribacter*, *Leuconostocaceae*, *Phascolarctobacterium* and *Roseburia* provide short-chain fatty acids (SCFAs) through a process that involves the fermentation of undigested carbohydrates. SCFAs are responsible for the regulation of trans-epithelial transport, colonocyte proliferation and differentiation, mucosal inflammation, intestinal motility, and barrier function (Smith et al., 2013; Peng et al., 2009). The concentration of SCFAs is significantly reduced in IBD patients, and this is likely a result of a decrease in the bacteria that produce them. *Bifidobacterium* synthesizes vitamins such as vitamin K and the water-soluble B vitamins (LeBlanc et al., 2011). At the functional metagenomic level, amino acid synthesis required for the production of these vitamins is decreased and amino acid transporter genes are increased due to an increase in auxotrophic and pathobiont bacteria (Ahuja, 2015). Increased glutathione and riboflavin metabolism and increased toxin secretion are associated with an increase in sulphate-reducing bacteria, such as *Desulfovibrio* (Ahuja, 2015; Erickson et al., 2012).

http://www.aloki.hu ● ISSN 1589 1623 (Print) ● ISSN 1785 0037 (Online)
DOI: http://dx.doi.org/10.15666/aeer/1804_55055525

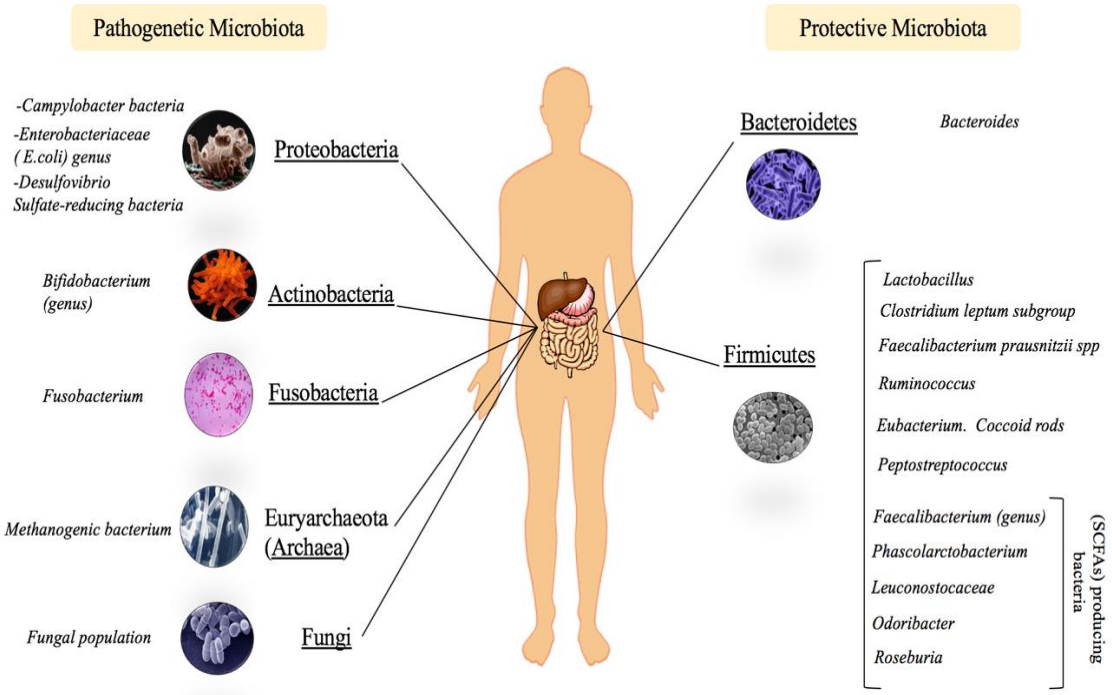

Figure 3. *Composition of gut microbiota (pathogenic and protective)*

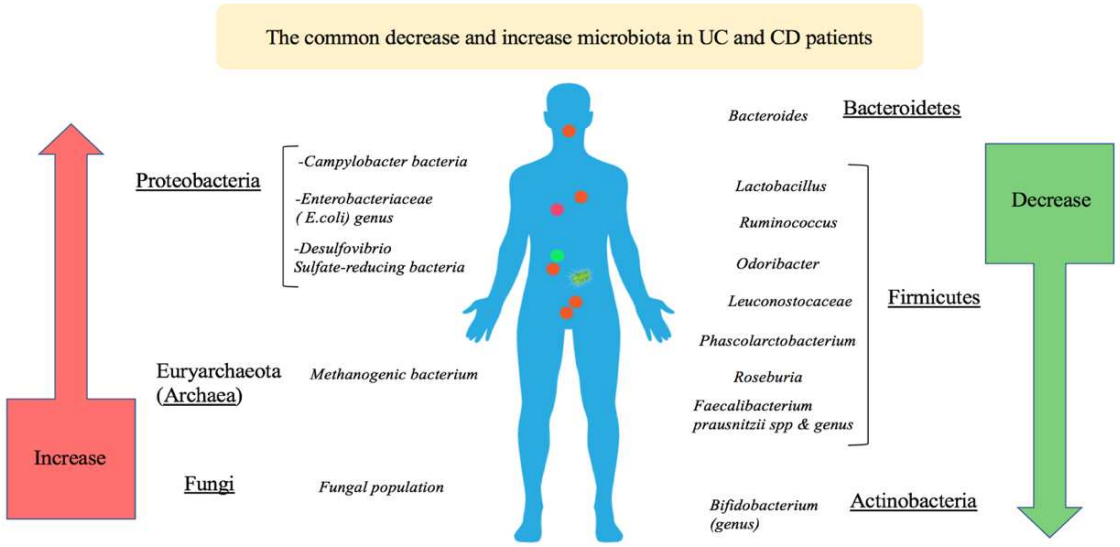

Figure 4. *The common decrease and increase of microbiota in UC and CD patients*

The clinical response to therapy is highly dependent upon the quantity and quality of bacterial taxa and upon any changes in bacterial taxa that occur in response to treatment. Accordingly, patients with few changes in their taxa in response to treatment typically exhibit improved drug responses. In contrast, patients who exhibit drastic changes in many bacterial taxa following treatment are believed to exhibit poorer drug responses. This hypothesis suggests that patients possessing an unstable gut microbial composition

http://www.aloki.hu ● ISSN 1589 1623 (Print) ● ISSN 1785 0037 (Online)
DOI: http://dx.doi.org/10.15666/aeer/1804_55055525

may possess a higher risk for anti-TNF-α treatment failure (Bazin et al., 2018). Additionally, TNF-α inhibitors may affect the composition of the gut microbiota, either directly or indirectly. TNF-α inhibitors are characterized by their ability to cure and downregulate inflammation in the infected gastrointestinal tract mucosa. These drugs also seek to repair wounded digestive epithelium and rebalance the composition of mucosal microbiota. These functions of TNF-α inhibitors may indirectly affect the microbiota composition of the gut (Baert et al., 1999).

Bazin et al. (2018) demonstrated that the gut microbial composition could be used as a predictive biomarker for clinical response to anti-TNF. Interestingly, such a predictive characteristic of anti-TNF inhibitors has been confirmed in several studies examining a number of different diseases. Additionally, microbial diversity in the presence or absence of particular taxa has been used as a prognostic factor to monitor diseases such as colorectal cancer or response to treatment (Bazin et al., 2018). For instance, an increase in the quantity of cyclomodulin-producing *E. coli*, *enterotoxigenic Bacteroides fragilis*, and *Fusobacterium nucleatum* was observed in cases of advanced colorectal cancer (Gagnière et al., 2016). Similarly, alteration in the microbiota composition has been used to explain resistance to immunotherapy in melanomas. It has also been postulated that some microbiota species possess the capacity to modify and improve the effects of therapy (Dubin et al., 2016; Routy et al., 2018).

A recent study demonstrated a decrease in dysbiosis and an increase in the quantity of *Faecalibacterium prausnitzii* exists in patients with UC who respond to anti-TNF therapy when compared to these factors in non-responders (Magnusson et al., 2016). Additionally, the results of this study demonstrated that responders and non-responders exhibit distinct expression patterns of mucosal antimicrobial peptides. Their findings also suggested that a relationship exists between decreased concentrations of *F. prausnitzii* and clinical relapse in CD patients treated with anti-TNF-α therapy (Rajca et al., 2014).

For the treatment of inflammatory diseases such as IBD and Spondyloarthritis (SpA), a therapeutic revolution occurred after the identification of tumor necrosis factor-alpha (TNF-α) antagonists, and this was particularly true for patients who had previously failed to respond to NSAID and conventional DMARDs (Sedger and McDermott, 2014; Ward et al., 2016). A number of studies have demonstrated that changes in the composition of the gut and mouth microbiome occur following the onset of several diseases. Subsequently, altered gut and mouth microbiomes are again partially modified in response to treatment, and these alterations can potentially predict response to treatment (Zhang et al., 2015; Phillips, 2015).

The effect of treatment on the gut microbiome is considered moderate when compared to these effects on the oral microbiome. It has been suggested that a higher probability of response occurs in patients who possess a significant number of virulence factors prior to therapy (Phillips, 2015).

Variations in the gut microbiota signature

In 2015, Zhang et al. (2015) performed an experiment on rheumatoid arthritis patients. They reported that differences observed in the gut microbiota composition before and after non-biologic DMARDs treatment were not significant. Additionally, Busquets et al. (2015) demonstrated that treatment with a TNF-α inhibitor such as ADL can affect the gut microbial composition of CD patients via recovery of *Firmicutes*, *Bacteroides*, and *Actinobacteria* phyla and a decrease in E. coli during treatment. This result was not observed in the study by Bazin et al., which may be owing to the different patient

http://www.aloki.hu ● ISSN 1589 1623 (Print) ● ISSN 1785 0037 (Online)
DOI: http://dx.doi.org/10.15666/aeer/1804_55055525

population that was studied and the therapies that were used (Bazin et al., 2018). Coyte et al. (2015) reported that an unstable microbiota composition was observed in non-responders over time. Considerable alteration in the microbiota composition has been linked to inflammatory diseases such as neurodevelopmental disorders and IBD, but it has not been associated with Spondyloarthritis. Magnusson et al. (2016) observed that UC patients who possess the capacity to respond to the induction of anti-TNF-α therapy exhibited a high abundance of *F. prausnitzii* compared to that of non-responder patients. A significant proportion of *Lactobacillus delbrueckii* has been previously observed in responder patients. These bacteria possess the ability to ferment kefir and are used as probiotics for IBD therapy (Rocha et al., 2014).

Several studies that were performed on humans have confirmed that the *Bacteroidetes* population is greater than that of *Firmicutes* in IBD patients compared to healthy controls (Wright et al., 2015). However, conflicting data were reported in a study by Rooks et al. (2014) compared mice that were treated with anti-TNF antibodies post colitis to mice that were treated with an antibiotic; *Firmicutes* populations were increased and the proportions of *Bacteroidetes* were decreased in the mice treated with anti-TNF antibodies. These contrasting results highlight the finding that microbial responses are different after anti-TNF treatment. Based on this, patient responses to anti-TNF treatment may also differ (Chiodini et al., 2013). *Firmicutes* is considered the most common phylum that is restored in CD patients treated with ADL. E. coli levels are also often increased in CD patients (Busquets et al., 2015). Bazin et al. also observed that the majority of non-responders exhibited changes in the order *Bacteroides* quantity, where two patients exhibited a decrease in these bacteria and five patients exhibited an increase. Responders, however, did not exhibit any changes in the *Bacteroides* order. This illustrates that the proportion of the order Bacteroides differs significantly for IBD conditions. The relationship between microbiota composition clusters and clinical response has been demonstrated without the presumption of causality. Fecal microbiota signatures could be used to predict clinical response to anti-TNF-α therapy, particularly in the absence of reliable biomarkers (Bazin et al., 2018). A balanced diversity in the composition of symbiotic microbiota, such as bacteria, fungi, and viruses may be used to predict a positive outcome to treatment (Ciccia et al., 2016).

Fecal microbiota transplantation

Fecal microbiota transplantation (FMT) aims to recover the gut microbial level in patients via transferring fecal suspension from a healthy donor. FMT is associated with recurrent *Clostridium difficile* infection (CDI). CDI is an appropriate situation for FMT, as it refers to gastrointestinal dysbiosis with *Clostridium difficile* overgrowth (Cohen et al., 2010). A study cohort from Shanghai Children's Hospital, China, was used to investigate the influence of IFX on the composition and function of the fecal microbiota of CD patients and healthy controls (CD [n = 11], healthy control [n = 16], all fecal samples [n = 48], CD patient samples [n = 32], baseline [n = 8], various times during IFX therapy [n = 24], healthy individuals [n = 16]). Prior to IFX therapy in pediatric CD patients, a lower biodiversity in fecal microbiome composition, an increase in *Enterococcus,* and a decrease in SCFA-producing bacteria including *Anaerostipes*, *Blautia*, *Coprococcus*, *Faecalibacterium*, *Lachnospira*, *Odoribacter*, *Roseburia*, *Ruminococcus*, and *Sutterella*, were observed. Additionally, alterations in metabolic functions of the gut microbes in CD patients were noted. In post-IFX samples, IFX treatment restored the gut microbiota to a normal state in pediatric CD patients, and the

http://www.aloki.hu ● ISSN 1589 1623 (Print) ● ISSN 1785 0037 (Online)
DOI: http://dx.doi.org/10.15666/aeer/1804_55055525

abundance of SCFA-producing bacteria (the genera *Blautia*, *Faecalibacterium*, *Odoribacte*r, and *Sutterella*) was associated with sustained therapeutic response. The gut microbiota were also improved in terms of richness and diversity. During IFX treatment, levels of *Enterococcaceae*, *Planococcaceae*, and *Streptococcaceae* were reduced in pediatric CD patients. In contrast, *Coprococcus*, *Lachnospira*, *Roseburia*, and *Ruminococcus* levels were elevated in the CD patients after treatment with IFX; however, their increases were unstable (Wang et al., 2017).

A study that was performed on adult CD patients (n = 33) aimed to identify alterations in the gut microbiota after IFX withdrawal. In this study, Rajca et al. (2014) noticed that CD patients exhibiting long-term remission possessed higher concentrations of *Firmicutes* compared to that of the relapsed CD patients. Additionally, relapsed CD patients possessed low levels of *F. prausnitzii* and *Bacteroides* during the year prior to IFX withdrawal.

Conclusion

PNR and LOR are important challenges faced by clinicians who treat patients with IBD. Although the precise cause of PNR is not well characterized, the most acceptable reason for LOR to TNF antagonists is immunogenicity that leads to the development of ADAs, which ultimately neutralize the drug or hasten its clearance. Therapeutic drug monitoring (TDM) is useful for aiding appropriate therapeutic decisions in cases of treatment failure. Through the use of TDM, clinicians can choose among dose intensification, the addition of an immunomodulator, or switching between classes of drugs. Future research should focus on the underlying mechanisms responsible for the development of PNR and on strategies to overcome LOR. The exact role that the gut microbiota plays in the process of treatment failure remains poorly understood. Microbial diversity in the presence or absence of particular taxa can be used as a prognosis factor to monitor the response to treatment. Strongly recommended increasing the prospective clinical trials to study the modification of the gut microbiota composition and determine which microbe(s) are responsible for primary non-response or loss of response and thereby used as a biomarker predictive. Therefore, the modification of microbiota composition can be used to improve the research of probiotic by creating new medications based on the patient's microbiota composition (if possible).

REFERENCES

[1] Ahuja, V. (2015): Inventory of a reservoir: friends & foes. – The Indian Journal of Medical Research 142: 4.

[2] Ainsworth, M. A., Bendtzen, K., Brynskov, J. (2008): Tumor necrosis factor-alpha binding capacity and anti-infliximab antibodies measured by fluid-phase radioimmunoassays as predictors of clinical efficacy of infliximab in Crohn's disease. – The American Journal of Gastroenterology 103: 944.

[3] Allendoerfer, R., Deepe, G. S. (1998): Blockade of endogenous TNF-α exacerbates primary and secondary pulmonary histoplasmosis by differential mechanisms. – The Journal of Immunology 160: 6072-6082.

[4] Allez, M., Karmiris, K., Louis, E., Van Assche, G., Ben-Horin, S., Klein, A., Van der Woude, J., Baert, F., Eliakim, R., Katsanos, K. (2010): Report of the ECCO pathogenesis workshop on anti-TNF therapy failures in inflammatory bowel diseases: definitions, frequency and pharmacological aspects. – Journal of Crohn's and Colitis 4: 355-366.

http://www.aloki.hu ● ISSN 1589 1623 (Print) ● ISSN 1785 0037 (Online)
DOI: http://dx.doi.org/10.15666/aeer/1804_55055525

[5] Andoh, A. (2016): Physiological role of gut microbiota for maintaining human health. – Digestion 93: 176-181.
[6] Arnott, I., Mcneill, G., Satsangi, J. (2003): An analysis of factors influencing short-term and sustained response to infliximab treatment for Crohn's disease. – Alimentary Pharmacology & Therapeutics 17: 1451-1457.
[7] Baert, F., Kondragunta, V., Lockton, S., Casteele, N. V., Hauenstein, S., Singh, S., Karmiris, K., Ferrante, M., Gils, A., Vermeire, S. (2016): Antibodies to adalimumab are associated with future inflammation in Crohn's patients receiving maintenance adalimumab therapy: a post hoc analysis of the Karmiris trial. – Gut 65: 1126-1131.
[8] Baert, F. J., D'haens, G. R., Peeters, M., Hiele, M. I., Schaible, T. F., Shealy, D., Geboes, K., Rutgeerts, P. J. (1999): Tumor necrosis factor α antibody (infliximab) therapy profoundly down-regulates the inflammation in Crohn's ileocolitis. – Gastroenterology 116: 22-28.
[9] Bazin, T., Hooks, K. B., Barnetche, T., Truchetet, M.-E., Enaud, R., Richez, C., Dougados, M., Hubert, C., Barré, A., Nikolski, M. (2018): Microbiota composition may predict anti-tnf alpha response in spondyloarthritis patients: an exploratory study. – Scientific reports 8: 5446.
[10] Ben-Horin, S., Chowers, Y. (2011): loss of response to anti-TNF treatments in Crohn's disease. – Alimentary Pharmacology & Therapeutics 33: 987-995.
[11] Ben-Horin, S., Kopylov, U., Chowers, Y. (2014): Optimizing anti-TNF treatments in inflammatory bowel disease. – Autoimmunity reviews 13: 24-30.
[12] Billioud, V., Sandborn, W. J., Peyrin-Biroulet, L. (2011): Loss of response and need for adalimumab dose intensification in Crohn's disease: a systematic review. – The American Journal of Gastroenterology 106: 674.
[13] Brandse, J. F., Van den Brink, G. R., Wildenberg, M. E., Van der Kleij, D., Rispens, T., Jansen, J. M., Mathôt, R. A., Ponsioen, C. Y., Löwenberg, M., D'haens, G. R. (2015): Loss of infliximab into feces is associated with lack of response to therapy in patients with severe ulcerative colitis. – Gastroenterology 149: 350-355. e2.
[14] Busquets, D., Mas-de-Xaxars, T., López-Siles, M., Martínez-Medina, M., Bahí, A., Sàbat, M., Louvriex, R., Miquel-Cusachs, J. O., Garcia-Gil, J. L., Aldeguer, X. (2015): Anti-tumour necrosis factor treatment with adalimumab induces changes in the microbiota of Crohn's disease. – Journal of Crohn's and Colitis 9: 899-906.
[15] Castro-Laria, L., Argüelles-Arias, F., García-Sánchez, V., Benítez, J. M., Fernández-Pérez, R., Trapero-Fernández, A. M., Gallardo-Sánchez, F., Pallarés-Manrique, H., Gómez-García, M., Cabello-Tapia, M. J. (2016): Initial experience with golimumab in clinical practice for ulcerative colitis. – Revista Española de Enfermedades Digestivas 108: 129-132.
[16] Chaparro, M., Panes, J., García, V., Mañosa, M., Esteve, M., Merino, O., Andreu, M., Gutierrez, A., Gomollón, F., Cabriada, J. L. (2011): Long-term durability of infliximab treatment in Crohn's disease and efficacy of dose "escalation" in patients losing response. – Journal of Clinical Gastroenterology 45: 113-118.
[17] Chiodini, R. J., Dowd, S. E., Davis, B., Galandiuk, S., Chamberlin, W. M., Kuenstner, J. T., Mccallum, R. W., Zhang, J. (2013): Crohn's disease may be differentiated into 2 distinct biotypes based on the detection of bacterial genomic sequences and virulence genes within submucosal tissues. – Journal of Clinical Gastroenterology 47: 612-620.
[18] Ciccia, F., Rizzo, A., Triolo, G. (2016): Subclinical gut inflammation in ankylosing spondylitis. – Current Opinion in Rheumatology 28: 89-96.
[19] Cohen, R. D., Lewis, J. R., Turner, H., Harrell, L. E., Hanauer, S. B., Rubin, D. T. (2011): Predictors of adalimumab dose escalation in patients with Crohn's disease at a tertiary referral center. – Inflammatory Bowel Diseases 18: 10-16.
[20] Cohen, S. H., Gerding, D. N., Johnson, S., Kelly, C. P., Loo, V. G., Mcdonald, L. C., Pepin, J., Wilcox, M. H. (2010): Clinical practice guidelines for Clostridium difficile infection in adults: 2010 update by the society for healthcare epidemiology of America (SHEA) and

http://www.aloki.hu ● ISSN 1589 1623 (Print) ● ISSN 1785 0037 (Online)
DOI: http://dx.doi.org/10.15666/aeer/1804_55055525

the infectious diseases society of America (IDSA). – Infection Control & Hospital Epidemiology 31: 431-455.

[21] Colombel, J. F., Sandborn, W. J., Rutgeerts, P., Enns, R., Hanauer, S. B., Panaccione, R., Schreiber, S., Byczkowski, D., Li, J., Kent, J. D. (2007): Adalimumab for maintenance of clinical response and remission in patients with Crohn's disease: the CHARM trial. – Gastroenterology 132: 52-65.

[22] Colombel, J. F., Sandborn, W. J., Reinisch, W., Mantzaris, G. J., Kornbluth, A., Rachmilewitz, D., Lichtiger, S., D'haens, G., Diamond, R. H., Broussard, D. L. (2010): Infliximab, azathioprine, or combination therapy for Crohn's disease. – New England Journal of Medicine 362: 1383-1395.

[23] Colombel, J. F., Reinisch, W., Mantzaris, G., Kornbluth, A., Rutgeerts, P., Tang, K., Oortwijn, A., Bevelander, G., Cornillie, F., Sandborn, W. (2015): Randomised clinical trial: deep remission in biologic and immunomodulator naïve patients with Crohn's disease–a SONIC post hoc analysis. – Alimentary Pharmacology & Therapeutics 41: 734-746.

[24] Cornillie, F., Hanauer, S. B., Diamond, R. H., Wang, J., Tang, K. L., Xu, Z., Rutgeerts, P., Vermeire, S. (2014): Postinduction serum infliximab trough level and decrease of C-reactive protein level are associated with durable sustained response to infliximab: a retrospective analysis of the ACCENT I trial. – Gut 63: 1721-1727.

[25] Coutinho, A., Kazatchkine, M. D., Avrameas, S. (1995): Natural autoantibodies. – Current Opinion in Immunology 7: 812-818.

[26] Coyte, K. Z., Schluter, J., Foster, K. R. (2015): The ecology of the microbiome: networks, competition, and stability. – Science 350: 663-666.

[27] Danese, S., Fiorino, G., Reinisch, W. (2011): causative factors and the clinical management of patients with Crohn's disease who lose response to anti-TNF-α therapy. – Alimentary Pharmacology & Therapeutics 34: 1-10.

[28] Dassopoulos, T. (2005): When the love is lost: adalimumab for patients with an attenuated response to infliximab. – Inflammatory Bowel Diseases 11: 948-949.

[29] Ding, N., Hart, A., De Cruz, P. (2016): Systematic review: predicting and optimising response to anti-TNF therapy in Crohn's disease–algorithm for practical management. – Alimentary Pharmacology & Therapeutics 43: 30-51.

[30] Dubin, K., Callahan, M. K., Ren, B., Khanin, R., Viale, A., Ling, L., No, D., Gobourne, A., Littmann, E., Huttenhower, C. (2016): Intestinal microbiome analyses identify melanoma patients at risk for checkpoint-blockade-induced colitis. – Nature Communications 7: 10391.

[31] Ebert, E., Das, K., Mehta, V., Rezac, C. (2008): Non-response to infliximab may be due to innate neutralizing anti-tumour necrosis factor-α antibodies. – Clinical & Experimental Immunology 154: 325-331.

[32] Echarri, A., Ferreiro, R., Fraga-Iriso, R., Barreiro-de Acosta, M., Cid, J., De-Castro, L., Pereira, S., Fernández-Villaverde, A., Soto, S., Carpio, D. (2014): Sa1264 drug trough levels and primary nonresponse to antiTNF therapy in moderate-severe Crohn disease. Results of the optimiza study. – Gastroenterology 146: S-247.

[33] Eckburg, P. B., Bik, E. M., Bernstein, C. N., Purdom, E., Dethlefsen, L., Sargent, M., Gill, S. R., Nelson, K. E., Relman, D. A. (2005): Diversity of the human intestinal microbial flora. – Science 308: 1635-1638.

[34] Erickson, A. R., Cantarel, B. L., Lamendella, R., Darzi, Y., Mongodin, E. F., Pan, C., Shah, M., Halfvarson, J., Tysk, C., Henrissat, B. (2012): Integrated metagenomics/metaproteomics reveals human host-microbiota signatures of Crohn's disease. – PloS One 7: e49138.

[35] Fasanmade, A. A., Adedokun, O. J., Ford, J., Hernandez, D., Johanns, J., Hu, C., Davis, H. M., Zhou, H. (2009): Population pharmacokinetic analysis of infliximab in patients with ulcerative colitis. – European Journal of Clinical Pharmacology 65: 1211.

http://www.aloki.hu ● ISSN 1589 1623 (Print) ● ISSN 1785 0037 (Online)
DOI: http://dx.doi.org/10.15666/aeer/1804_55055525

[36] Fasanmade, A. A., Adedokun, O. J., Blank, M., Zhou, H., Davis, H. M. (2011): Pharmacokinetic properties of infliximab in children and adults with Crohn's disease: a retrospective analysis of data from 2 phase III clinical trials. – Clinical therapeutics 33: 946-964.

[37] Ford, A. C., Sandborn, W. J., Khan, K. J., Hanauer, S. B., Talley, N. J., Moayyedi, P. (2011): Efficacy of biological therapies in inflammatory bowel disease: systematic review and meta-analysis. – The American Journal of Gastroenterology 106: 644.

[38] Gagnière, J., Raisch, J., Veziant, J., Barnich, N., Bonnet, R., Buc, E., Bringer, M.-A., Pezet, D., Bonnet, M. (2016): Gut microbiota imbalance and colorectal cancer. – World Journal of Gastroenterology 22: 501.

[39] Gisbert, J., Marín, A., Mcnicholl, A., Chaparro, M. (2015): Systematic review with meta-analysis: the efficacy of a second anti-TNF in patients with inflammatory bowel disease whose previous anti-TNF treatment has failed. – Alimentary Pharmacology & Therapeutics 41: 613-623.

[40] Gomollón, F., Dignass, A., Annese, V., Tilg, H., Van Assche, G., Lindsay, J. O., Peyrin-Biroulet, L., Cullen, G. J., Daperno, M., Kucharzik, T. (2016): 3rd European evidence-based consensus on the diagnosis and management of Crohn's disease 2016: part 1: diagnosis and medical management. – Journal of Crohn's and Colitis 11: 3-25.

[41] Grover, Z., Biron, R., Carman, N., Lewindon, P. (2014): Predictors of response to Infliximab in children with luminal Crohn's disease. – Journal of Crohn's and Colitis 8: 739-746.

[42] Ha, C., Ullman, T. A., Siegel, C. A., Kornbluth, A. (2012): Patients enrolled in randomized controlled trials do not represent the inflammatory bowel disease patient population. – Clinical Gastroenterology and Hepatology 10: 1002-1007.

[43] Hanauer, S. B., Feagan, B. G., Lichtenstein, G. R., Mayer, L. F., Schreiber, S., Colombel, J. F., Rachmilewitz, D., Wolf, D. C., Olson, A., Bao, W. (2002): Maintenance infliximab for Crohn's disease: the ACCENT I randomised trial. – The Lancet 359: 1541-1549.

[44] Hazlewood, G. S., Rezaie, A., Borman, M., Panaccione, R., Ghosh, S., Seow, C. H., Kuenzig, E., Tomlinson, G., Siegel, C. A., Melmed, G. Y. (2015): Comparative effectiveness of immunosuppressants and biologics for inducing and maintaining remission in Crohn's disease: a network meta-analysis. – Gastroenterology 148: 344-354. e5.

[45] Honda, K., Littman, D. R. (2012): The microbiome in infectious disease and inflammation. – Annual Review of Immunology 30: 759-795.

[46] Juillerat, P., Sokol, H., Froehlich, F., Yajnik, V., Beaugerie, L., Lucci, M., Burnand, B., Macpherson, A. J., Cosnes, J., Korzenik, J. R. (2014): Factors associated with durable response to infliximab in Crohn's disease 5 years and beyond: a multicenter international cohort. – Inflammatory Bowel Diseases 21: 60-70.

[47] Karmiris, K., Paintaud, G., Noman, M., Magdelaine–Beuzelin, C., Ferrante, M., Degenne, D., Claes, K., Coopman, T., Van Schuerbeek, N., Van Assche, G. (2009): Influence of trough serum levels and immunogenicity on long-term outcome of adalimumab therapy in Crohn's disease. – Gastroenterology 137: 1628-1640.

[48] Keizer, R. J., Huitema, A. D., Schellens, J. H., Beijnen, J. H. (2010): Clinical pharmacokinetics of therapeutic monoclonal antibodies. – Clinical Pharmacokinetics 49: 493-507.

[49] Kiss, L., Szamosi, T., Molnar, T., Miheller, P., Lakatos, L., Vincze, A., Palatka, K., Barta, Z., Gasztonyi, B., Salamon, A. (2011): Early clinical remission and normalisation of CRP are the strongest predictors of efficacy, mucosal healing and dose escalation during the first year of adalimumab therapy in Crohn's disease. – Alimentary Pharmacology & Therapeutics 34: 911-922.

[50] Leblanc, J., Laiño, J. E., Del Valle, M. J., Vannini, V. V., Van Sinderen, D., Taranto, M. P., De Valdez, G. F., De Giori, G. S., Sesma, F. (2011): B-Group vitamin production by lactic acid bacteria–current knowledge and potential applications. – Journal of Applied Microbiology 111: 1297-1309.

http://www.aloki.hu ● ISSN 1589 1623 (Print) ● ISSN 1785 0037 (Online)
DOI: http://dx.doi.org/10.15666/aeer/1804_55055525

[51] Ley, R. E., Hamady, M., Lozupone, C., Turnbaugh, P. J., Ramey, R. R., Bircher, J. S., Schlegel, M. L., Tucker, T. A., Schrenzel, M. D., Knight, R. 2008. Evolution of mammals and their gut microbes. –Science 320: 1647-1651.

[52] Lin, P., Bach, M., Asquith, M., Lee, A. Y., Akileswaran, L., Stauffer, P., Davin, S., Pan, Y., Cambronne, E. D., Dorris, M. (2014): HLA-B27 and human β2-microglobulin affect the gut microbiota of transgenic rats. – PloS One 9: e105684.

[53] Lindsay, J. O., Armuzzi, A., Gisbert, J. P., Bokemeyer, B., Peyrin-Biroulet, L., Nguyen, G. C., Smyth, M., Patel, H. (2017): Indicators of suboptimal tumor necrosis factor antagonist therapy in inflammatory bowel disease. – Digestive and Liver Disease 49: 1086-1091.

[54] Louis, E., Boverie, J., Dewit, O., Baert, F., De, M. V., D'haens, G. (2007): Treatment of small bowel subocclusive Crohn's disease with infliximab: an open pilot study. – Acta Gastro-Enterologica Belgica 70: 15-19.

[55] Magnusson, M. K., Strid, H., Sapnara, M., Lasson, A., Bajor, A., Ung, K.-A., Öhman, L. (2016): Anti-TNF therapy response in patients with ulcerative colitis is associated with colonic antimicrobial peptide expression and microbiota composition. – Journal of Crohn's and Colitis 10: 943-952.

[56] Moran, G. W., Dubeau, M. F., Kaplan, G. G., Yang, H., Seow, C. H., Fedorak, R. N., Dieleman, L. A., Barkema, H. W., Ghosh, S., Panaccione, R. (2014): Phenotypic features of Crohn's disease associated with failure of medical treatment. – Clinical Gastroenterology and Hepatology 12: 434-442. e1.

[57] Ordás, I., Feagan, B. G., Sandborn, W. J. (2012): Therapeutic drug monitoring of tumor necrosis factor antagonists in inflammatory bowel disease. – Clinical Gastroenterology and Hepatology 10: 1079-1087.

[58] Papamichael, K., Gils, A., Rutgeerts, P., Levesque, B. G., Vermeire, S., Sandborn, W. J., Vande Casteele, N. (2014): Role for therapeutic drug monitoring during induction therapy with TNF antagonists in IBD: evolution in the definition and management of primary nonresponse. – Inflammatory Bowel Diseases 21: 182-197.

[59] Papamichael, K., Vajravelu, R. K., Vaughn, B. P., Osterman, M. T., Cheifetz, A. S. (2018): Proactive infliximab monitoring following reactive testing is associated with better clinical outcomes than reactive testing alone in patients with inflammatory bowel disease. – Journal of Crohn's and Colitis 12: 804-810.

[60] Papamichael, K., Juncadella, A., Wong, D., Rakowsky, S., Sattler, L. A., Campbell, J. P., Vaughn, B. P., Cheifetz, A. S. (2019): Proactive therapeutic drug monitoring of adalimumab is associated with better long-term outcomes compared with standard of care in patients with inflammatory bowel disease. – Journal of Crohn's and Colitis 13: 976-981.

[61] Peng, L., Li, Z.-R., Green, R. S., Holzman, I. R., Lin, J. (2009): Butyrate enhances the intestinal barrier by facilitating tight junction assembly via activation of AMP-activated protein kinase in Caco-2 cell monolayers. – The Journal of Nutrition 139: 1619-1625.

[62] Phillips, R. (2015): Rheumatoid arthritis: microbiome reflects status of RA and response to therapy. – Nature Reviews Rheumatology 11: 502.

[63] Rajca, S., Grondin, V., Louis, E., Vernier-Massouille, G., Grimaud, J.-C., Bouhnik, Y., Laharie, D., Dupas, J.-L., Pillant, H., Picon, L. (2014): Alterations in the intestinal microbiome (dysbiosis) as a predictor of relapse after infliximab withdrawal in Crohn's disease. – Inflammatory Bowel Diseases 20: 978-986.

[64] Reinisch, W., Lofberg, R., Louis, E., Kron, M., Camez, A., Robinson, A., Pollack, P. F. (2009): T1215 Subanalysis of remission rates by duration of disease in adalimumab-treated patients with Crohn's disease: the care trial. – Gastroenterology 136: A-523-A-524.

[65] Reinisch, W., Sandborn, W. J., Hommes, D. W., D'haens, G., Hanauer, S., Schreiber, S., Panaccione, R., Fedorak, R. N., Tighe, M. B., Huang, B. (2011): Adalimumab for induction of clinical remission in moderately to severely active ulcerative colitis: results of a randomised controlled trial. – Gut 60: 780-787.

[66] Rocha, C. S., Gomes-Santos, A. C., Moreira, T. G., De Azevedo, M., Luerce, T. D., Mariadassou, M., Delamare, A. P. L., Langella, P., Maguin, E., Azevedo, V. (2014): Local

http://www.aloki.hu ● ISSN 1589 1623 (Print) ● ISSN 1785 0037 (Online)
DOI: http://dx.doi.org/10.15666/aeer/1804_55055525

and systemic immune mechanisms underlying the anti-colitis effects of the dairy bacterium Lactobacillus delbrueckii. – PLoS One 9: e85923.

[67] Roda, G., Jharap, B., Neeraj, N., Colombel, J.-F. (2016): Loss of response to anti-TNFs: definition, epidemiology, and management. – Clinical and Translational Gastroenterology 7: e135.

[68] Rojas, J. R., Taylor, R. P., Cunningham, M. R., Rutkoski, T. J., Vennarini, J., Jang, H., Graham, M. A., Geboes, K., Rousselle, S. D., Wagner, C. L. (2005): Formation, distribution, and elimination of infliximab and anti-infliximab immune complexes in cynomolgus monkeys. – Journal of Pharmacology and Experimental Therapeutics 313: 578-585.

[69] Rooks, M. G., Veiga, P., Wardwell-Scott, L. H., Tickle, T., Segata, N., Michaud, M., Gallini, C. A., Beal, C., Van Hylckama-Vlieg, J. E., Ballal, S. A. (2014): Gut microbiome composition and function in experimental colitis during active disease and treatment-induced remission. – The ISME Journal 8: 1403.

[70] Routy, B., Le Chatelier, E., Derosa, L., Duong, C. P., Alou, M. T., Daillère, R., Fluckiger, A., Messaoudene, M., Rauber, C., Roberti, M. P. (2018): Gut microbiome influences efficacy of PD-1–based immunotherapy against epithelial tumors. – Science 359: 91-97.

[71] Sandborn, W., Melmed, G., Mcgovern, D., Loftus Jr, E. V., Choi, J., Cho, J., Abraham, B., Gutierrez, A., Lichtenstein, G., Lee, S. (2015): Clinical and demographic characteristics predictive of treatment outcomes for certolizumab pegol in moderate to severe Crohn's disease: analyses from the 7-year PREC i SE 3 study. – Alimentary Pharmacology & Therapeutics 42: 330-342.

[72] Sands, B. E., Anderson, F. H., Bernstein, C. N., Chey, W. Y., Feagan, B. G., Fedorak, R. N., Kamm, M. A., Korzenik, J. R., Lashner, B. A., Onken, J. E. (2004): Infliximab maintenance therapy for fistulizing Crohn's disease. – New England Journal of Medicine 350: 876-885.

[73] Sands, B. E., Feagan, B. G., Rutgeerts, P., Colombel, J.-F., Sandborn, W. J., Sy, R., D'haens, G., Ben-Horin, S., Xu, J., Rosario, M. (2014): Effects of vedolizumab induction therapy for patients with Crohn's disease in whom tumor necrosis factor antagonist treatment failed. – Gastroenterology 147: 618-627. e3.

[74] Schreiber, S., Colombel, J.-F., Bloomfield, R., Nikolaus, S., Schölmerich, J., Panés, J., Sandborn, W. J. (2010): Increased response and remission rates in short-duration Crohn's disease with subcutaneous certolizumab pegol: an analysis of PRECiSE 2 randomized maintenance trial data. – The American Journal of Gastroenterology 105: 1574.

[75] Sedger, L. M., Mcdermott, M. F. (2014): TNF and TNF-receptors: from mediators of cell death and inflammation to therapeutic giants–past, present and future. – Cytokine & Growth Factor Reviews 25: 453-472.

[76] Sheehan, D., Moran, C., Shanahan, F. (2015): The microbiota in inflammatory bowel disease. – Journal of gastroenterology 50: 495-507.

[77] Singh, J. A., Wells, G. A., Christensen, R., Ghogomu, E. T., Maxwell, L. J., Macdonald, J. K., Filippini, G., Skoetz, N., Francis, D. K., Lopes, L. C. (2011): Adverse effects of biologics: a network meta-analysis and Cochrane overview. – Cochrane Database of Systematic Reviews. DOI: 10.1002/14651858.CD008794.pub2.

[78] Smith, P. M., Howitt, M. R., Panikov, N., Michaud, M., Gallini, C. A., Bohlooly, Y. M., Glickman, J. N., Garrett, W. S. (2013): The microbial metabolites, short-chain fatty acids, regulate colonic Treg cell homeostasis. – Science 341: 569-573.

[79] Sprakes, M. B., Ford, A. C., Warren, L., Greer, D., Hamlin, J. (2012): Efficacy, tolerability, and predictors of response to infliximab therapy for Crohn's disease: a large single centre experience. – Journal of Crohn's and Colitis 6: 143-153.

[80] Steenholdt, C. (2018): Proactive and reactive therapeutic drug monitoring of biologic therapies in inflammatory bowel disease are complementary, not mutually exclusive. – Clinical Gastroenterology and Hepatology 16: 597-598.

http://www.aloki.hu ● ISSN 1589 1623 (Print) ● ISSN 1785 0037 (Online)
DOI: http://dx.doi.org/10.15666/aeer/1804_55055525

[81] Van Praet, L., Jacques, P., Van den Bosch, F., Elewaut, D. (2012): The transition of acute to chronic bowel inflammation in spondyloarthritis. – Nature Reviews Rheumatology 8: 288.
[82] Vermeire, S., Louis, E., Carbonez, A., Van Assche, G., Noman, M., Belaiche, J., De Vos, M., Van Gossum, A., Pescatore, P., Fiasse, R. (2002): Demographic and clinical parameters influencing the short-term outcome of anti-tumor necrosis factor (infliximab) treatment in Crohn's disease. – The American Journal of Gastroenterology 97: 2357.
[83] Wang, S., Ye, Q., Zeng, X., Qiao, S. (2019): Functions of macrophages in the maintenance of intestinal homeostasis. – Journal of Immunology Research. https://doi.org/10.1155/2019/1512969.
[84] Wang, Y., Gao, X., Ghozlane, A., Hu, H., Li, X., Xiao, Y., Li, D., Yu, G., Zhang, T. (2017): Characteristics of faecal microbiota in paediatric Crohn's disease and their dynamic changes during infliximab therapy. – Journal of Crohn's and Colitis 12: 337-346.
[85] Ward, M. M., Deodhar, A., Akl, E. A., Lui, A., Ermann, J., Gensler, L. S., Smith, J. A., Borenstein, D., Hiratzka, J., Weiss, P. F. (2016): American College of Rheumatology/Spondylitis Association of America/Spondyloarthritis Research and Treatment Network 2015 recommendations for the treatment of ankylosing spondylitis and nonradiographic axial spondyloarthritis. – Arthritis & Rheumatology 68: 282-298.
[86] Wright, E. K., Kamm, M. A., Teo, S. M., Inouye, M., Wagner, J., Kirkwood, C. D. (2015): Recent advances in characterizing the gastrointestinal microbiome in Crohn's disease: a systematic review. – Inflammatory Bowel Diseases 21: 1219-1228.
[87] Zhang, X., Zhang, D., Jia, H., Feng, Q., Wang, D., Liang, D., Wu, X., Li, J., Tang, L., Li, Y. (2015): The oral and gut microbiomes are perturbed in rheumatoid arthritis and partly normalized after treatment. – Nature Medicine 21: 895.

http://www.aloki.hu ● ISSN 1589 1623 (Print) ● ISSN 1785 0037 (Online)
DOI: http://dx.doi.org/10.15666/aeer/1804_55055525

DIVERSITY AND SPATIAL DISTRIBUTION OF SOIL CYANOBACTERIA ALONG AN ALTITUDINAL GRADIENT IN MARRAKESH AREA (MOROCCO)

HAKKOUM, Z.[1] – MINAOUI, F.[1] – DOUMA, M.[1,2] – MOUHRI, K.[1] – LOUDIKI, M.[1*]

[1]Laboratory of Water, Biodiversity and Climate Change; Phycology, Biotechnology and Environmental Toxicology Research Unit, Faculty of Sciences Semlalia Marrakesh, Cadi Ayyad University, Av. Prince My Abdellah P.O. Box 2390, Marrakesh 40000, Morocco (e-mails: zineb.hakkoum@gmail.com, minaoui.farah@gmail.com)

[2]Polydisciplinary Faculty of Khouribga (FPK), Sultan Moulay Slimane University, Khouribga, Morocco (e-mail: douma_mountasser@yahoo.fr; phone: +212-661-967-057)

**Corresponding author e-mail: loudiki@uca.ac.ma; phone: +212-670-099-329; fax: +212-524-436-769; ORCID: https://orcid.org/0000-0002-3624-9225*

(Received 27th Mar 2020; accepted 7th Jul 2020)

Abstract. Cyanobacteria, are a photoautotrophic component of soil biological crusts in arid areas. They have attracted increasing interest worldwide due to their potential applications in agriculture bio-fertilization, rehabilitation of soil environments, biotechnology, natural products and medicine. However, biocrust cyanobacteria are not well investigated in North African countries where drylands are dominant. This study aims to explore the soil cyanobacterial diversity, to isolate interesting strains and to investigate the effect of soil properties and land use on their distribution in the Marrakesh area (Morocco). The sampling of biocrusts and measurement of soil physicochemical characteristics were done at five sampling sites during two campaigns. The morphological characterization of cyanobacterial strains was done by direct microscopy and soil culture inoculums in nutrient media. A total of 26 taxa were identified. Oscillatoriales constituted the most diversified order (84.62%), followed by Chroococcales (11.54%) and Nostocales (3.84%). Three species are reported for the first time in Morocco. Six strains were isolated in soil culture in nutrient media. The results showed that the distribution of cyanobacteria was mainly influenced by humidity, soil texture, land use and vegetation cover. This survey provides a first inventory and data ecology of the soil cyanobacterial assemblages in the Moroccan mountainous region needed for understanding their potential in biotechnological restoration and in agricultural biofertilization.
Keywords: *biocrust cyanobacteria, taxonomy, ecology, edaphic factors, High Atlas Mountains*

Introduction

Cyanobacteria are the oldest photoautrophic component of Biological Soil Crusts communities (BSCs) which include bacteria, algae, fungi, lichens and mosses (Rivera-Aguilar et al., 2006; Maestre et al., 2011). These biocrusts occur on and within the top centimeters of the soil surface all over the world, including the most hostile environments like extremely arid and dryland areas where cyanobacteria are often the most important primary producers (Hoffmann, 1989; Heckman et al., 2006; Belnap et al., 2016).

Cyanobacteria play a key role in carbon and N-cycling, nutrient dynamics, and ecosystem productivity (Hackl et al., 2004). They furnish nutrients to the soil as a good bio-fertilizer and stabilize soil structure by the production of the extracellular polysaccharides that aggregate soil particles, and sometimes increase their porosity and

http://www.aloki.hu ● ISSN 1589 1623 (Print) ● ISSN 1785 0037 (Online)
DOI: http://dx.doi.org/10.15666/aeer/1804_55275545

water-holding capacity (Liu et al., 2017). Most filamentous cyanobacteria are responsible for biocrust formation and are also the most abundant component in some soil types (Janatková et al., 2013).

Their many adaptations allow them to colonize unstable substrates and their presence may also enhance the ecological role and biocrust functions (Garcia-Pichel et al., 2009; Büdel et al., 2016). Due to their oxygenic photosynthesis and capability to fix carbon, atmospheric nitrogen and solubilize phosphate compounds, the bio-prospecting of cyanobacteria is increasing for their potential use in agriculture bio-fertilization (Singh et al., 2014; Rossi et al., 2017), restoration and rehabilitation of soil environments (Acea et al., 2001; Malam Issa et al., 2007).

Cyanobacteria has also gained immense interest due to its natural products and various secondary metabolites, including vitamins, enzymes, and pharmaceuticals substances (Hu et al., 2008). Moreover, these microorganisms have been identified as a rich source of biologically active compounds with antiviral, antibacterial, antifungal and anticancer activities (Abed et al., 2009).

Although several researches have shown that cyanobacteria are a precious bio-resource in agriculture, ecosystem, and environmental sustainability (Singh et al., 2016; Bag et al., 2019), studies on cyanobacterial diversity of biocrusts have begun only recently and more than 320 species are known to occur in biocrusts on different continents.

However, in Africa, data about the diversity of biocrust cyanobacteria remains fragmentary and strongly heterogenous between the different regions. Although Africa is one of the largest continents with considerably larger dryland areas, only 83 cyanobacteria species have been reported in biocrusts (Büdel et al., 2016). In the Northern part of Africa with larger arid and hyperarid landscapes, little is known about the biocrusts communities who are still underexplored and where there is a need for much more biodiversity assessments.

At the local scale, abiotic factors other than climate may control the type of biocrusts present. Soils properties such as moisture and texture, nutrient content, land use and vegetation cover are extremely important. Also, the species composition of biocrust community could be regulated by anthropogenic activities and environmental stressors across temporal and spatial scales (Belnap et al., 2016).

In Morocco, a Northwest African arid and semiarid country, cyanobacteria are well studied in aquatic ecosystems (Loudiki et al., 2002; Douma et al., 2009). However, soil cyanobacteria of biocrusts have not yet been explored and require further attention, especially in mountains such as the High Atlas and the hyperarid and desert southern areas. Soil environments in high-altitude ecosystems provide habitats for numerous cyanobacteria despite being related to extreme environmental pressures, such as freezing and desiccation (Kastovská et al., 2005; Nemergut et al., 2007; Blanco et al., 2012).

Biodiversity of soil cyanobacteria in high mountains biocrusts and their geographical distribution have received great attention worldwide (Řeháková et al., 2011). In Mediterranean dryland ecosystems, known by their fragility and vulnerability, many studies showed that biocrust cyanobacteria play a crucial role in their ecological functioning and improve both erosion protection and biofertilization of soils (Zancan et al., 2006; Maestre et al., 2011).

Therefore, this work explored the soil cyanobacteria biodiversity in the high mountains of a Moroccan area (High Atlas of Marrakesh) along an altitudinal gradient, aiming to identify and isolate some interested taxa and to assess the effect of different environmental variables in the distribution of soil cyanobacteria.

http://www.aloki.hu ● ISSN 1589 1623 (Print) ● ISSN 1785 0037 (Online)
DOI: http://dx.doi.org/10.15666/aeer/1804_55275545

Material and methods

Study area

The study was conducted in the Ourika watershed (31°N and 31°21'N, 7°30'W and 7°60'W) located in the High Atlas Mountain, at 40 km south of Marrakesh city, Morocco (*Fig. 1*). The watershed covers an area of 576 km^2 and has an altitude of 1070-4000 m. Its bioclimate is semi-arid to sub-humid from the lower altitudinal to the higher mountain parts. Its average rainfall varies from 450 to more than 650 mm on the piedmont and from 800 to 1000 mm on the high summits. The vegetation cover of the basin is scattered and quite degraded and forests occupy only 35.6% of which 25% are open forests dominated by green oak, thuja and juniper. More than half of the basin area has no forest cover with 49.74% for spiny xerophytes and 13.86% for bare soil and crops (*Fig. 1*). The data on land use, vegetation type and cover in the Ourika basin were documented by Ouhammou (2005), Haroni et al. (2009), Meliho et al. (2016) and Nduwayo et al. (2017).

This mountainous basin is very sparsely populated and the built-up area plus the river beds account for only 0.78%. Food crops occupy only 7% and cattle and goat breeding is the most dominant in some valleys. The pastoral activity and grazing are also developed especially in high altitude areas such as Oukaimeden.

The study area is located in a natural mountainous zone from the granitic highlands of Oukaimeden (2634 m) to sedimentary Haouz arid plain (765 m).

Sampling sites and soil sampling

Five sampling sites located in different zones along an altitudinal and vegetation gradient (from a high mountain to arid steppe) were prospected. These sampling sites were selected based on different land use type including grassland, open forest, moderately dense forest, shrub land and steppe land (*Fig. 1*). *Table 1* provides the sampling sites characteristics and their vegetation type.

Table 1. *Sampling sites characteristics*

Sampling sites	Coordinates	Altitude (m)	Climate (Ouhammou, 2005)	Nature of the substrate	Vegetation cover (Haroni et al., 2009)	Land use (Nduwayo et al., 2017)
Site1: *Oukaimeden*	N: 31°11.620' W: 007°51.207'	2634	Wet and humid	Eruptive, metamorphic and ancient rocks of phanerozoic	Spiny xerophytes, peeler, asylvatic zone	Grassland, pasture land and bare land
Site 2: *Aleppo Pine* forest	N: 31°15, 754' W: 007° 49.226'	1565	Wet and humid	Red sandstone of Permotrias	Clear forest reforestation of *Aleppo pine*	Forest land
Site 3: Green Oak Forest (*Quercus ilex*)	N: 31°18.565' W: 007°45, 340'	1111	Semiarid to subhumid	Schistose-type formation and conglomerates	Green Oak forest	Shrub land
Site 4: *Barbary thuja forest (Tetraclinis articulata)*	N: 31° 20.991' W: 007°45.876'	935	Semiarid to subhumid	Conglomerate, Permotrias sandstone, salt rocks, clay soil	Dense vegetation, *Thuja*, red *Juniperus, Oxycedrus*, green oak	Forest land
Site 5: Jujube steppe *(Ziziphus lotus)* of Haouz	N: 31°25.224' W: 007°50.237'	765	Arid	Sedimentary substrate	Steppe with *Zizyphus lotus*	Steppe land and bare soil

http://www.aloki.hu ● ISSN 1589 1623 (Print) ● ISSN 1785 0037 (Online)
DOI: http://dx.doi.org/10.15666/aeer/1804_55275545

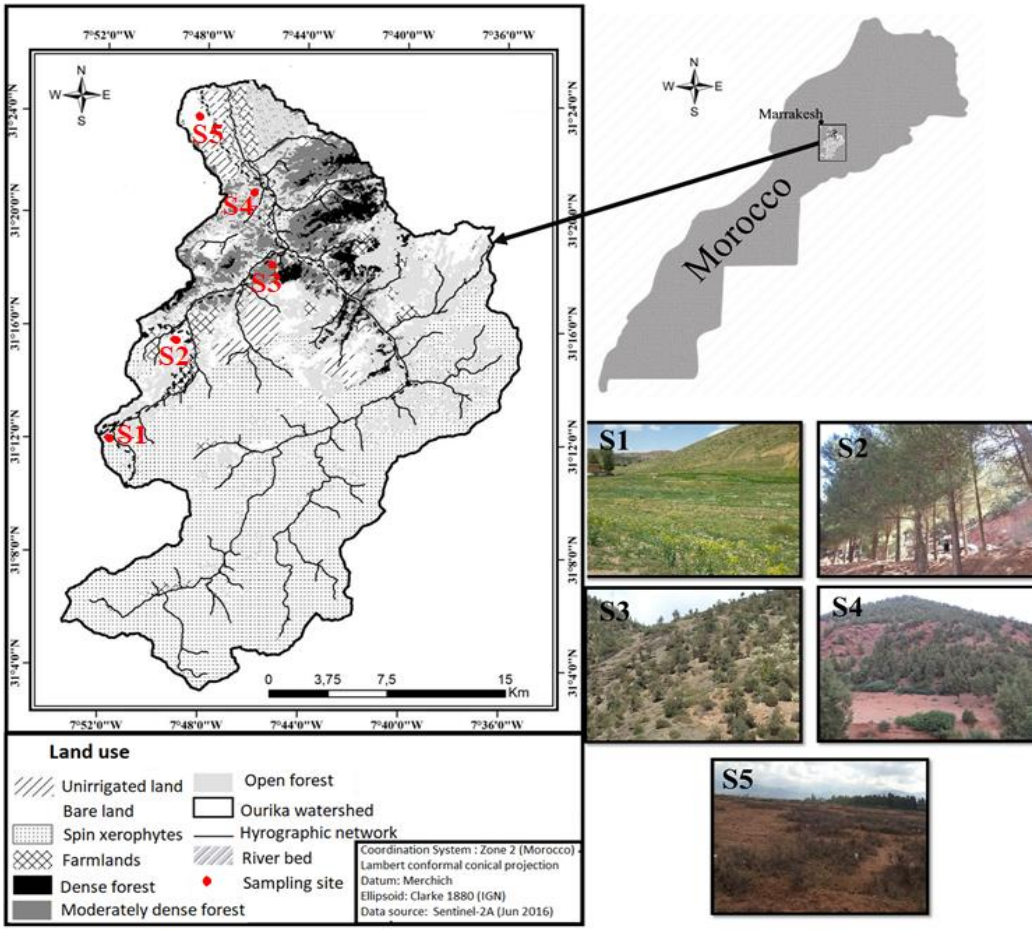

Figure 1. *Location of sampling sites in Ourika basin. S1: Oukaimeden; S2: Aleppo Pine Forest; S3: Green Oak Forest; S4: Thuja forest; S5: Haouz arid steppe. (The land use map of the Ourika basin is carried out by Nduwayo et al., 2017; modified figure)*

In each sampling site, we performed two soil samples during two campaigns (February 14th and May 4th of 2016). A composite biocrust samples (made up of number of smaller samples of 10 cm^2 and 1-3 cm deep) were taken randomly with a sterile spatula. At each site, an area of 500–1000 m^2 was explored to choose the representative points developed biocrusts, showing a range of colonization states, from early successional (lightly pigmented: light biocrusts) to late successional (darkly pigmented: dark biocrusts) (Belnap et al., 2008), avoiding those dominated by moss or lichen, as previously described by Garcia-Pichel et al. (2016). In total, 50 soil samples (5 sites × 10 replicates) were collected in sterilized Petri-dishes (90 mm diameter) for cyanobacterial microscopy examination, culturing and isolation. A second composite sample, for physicochemical analysis, was taken from the upper bare surface layer (1-3 cm) of soil according to Řeháková et al. (2011). This last sample was placed in clean polyethylene bags and kept at 4 °C until further analysis.

Soil physico-chemical characteristics

In the laboratory, the soil samples were sieved (< 2 mm) and air-dried at room temperature for physico-chemical analysis (El Khalil et al., 2013). All soil analyses

http://www.aloki.hu ● ISSN 1589 1623 (Print) ● ISSN 1785 0037 (Online)
DOI: http://dx.doi.org/10.15666/aeer/1804_55275545

were conducted on the < 2 mm size fraction according to NF ISO 10390. A conductivity meter (Cond 1970i WTW GmbH, Weilheim, Germany) was used to measure the electrical conductivity. pH was assessed using a pH meter (pH 1970i WTW GmbH, Weilheim, Germany). The method of Anne (Aubert, 1978) was used to determinate total organic carbon. This method allows to evaluate the organic matter content of soil samples. Available phosphorus was measured by the Olsen method (Olsen et al., 1954). The content of ammoniacal nitrogen ($N\text{-}NH_4^+$) was determined according to the norm instructions (AFNOR, 1975). Soil moisture was measured gravimetrically according to the standard method (AFNOR, 2000). The soil samples were oven-dried at 105 °C for 48 h based on the oven drying method. The soil texture of samples was obtained using the classic method (Soltner, 2005). The soil chlorophyll a content was performed by boiling ethanol extraction after cleaning all vascular plants (ISO, 1992).

Taxonomic identification of cyanobacteria

The morphological identification of cyanobacterial taxa was carried out using both field and cultured material (Mansour and Shaaban, 2010).

The representative subsamples of biocrusts, were selected, mixed together, and homogenized to form a composite sample (Muñoz-Martín et al., 2019). A suspension of each biocrust sample was prepared by dissolution of 1 g of mixed soil diluted 10 ml fold in sterilized distilled water. A few drops of this suspension were immediately examined using research light microscope (Motic BA210, China; 400× and 1000× magnification) to make a preliminary identification of the cyanobacteria present taxa. Then, they were identified using recent cyanobacteria monographs (Anagnostidis and Komarek, 1990; Komarek and Anagnostidis, 1998, 2005; Komarek, 2013).

Strain isolation and culture conditions of cyanobacteria

After sieving and grinding soil samples, a series of 5 dilutions ranged from 10^{-1} to 10^{-5} were prepared. Under aseptic conditions, 1 ml of the soil suspension of each dilution was inoculated in triplicate on solid (1.5% agar) and then on liquid media. Z8 medium was used for the strain isolation and growth (Kotai, 1972). The cultures were maintained under controlled conditions (temperature 26 °C ± 1, light intensity 60 $\mu mol.m^{-2}.s^{-1}$, light – dark cycle of 15/9 with continuous aeration) for 8 to 12 days. After cyanobacteria growth, a series of successive transplants of the isolated strains onto new medium were made to obtain monoalgal and purified culture. Monoalgal strains were used for profound morphological identification of species under the light microscopy (Motic BA210, China) using the imaging software analysis (Motic Images + 2.0).

Data analysis

All soil parameters analysis was done in three replicates. The results are expressed as mean ± standard Error (SE). One-way analysis of variance (ANOVA) with the Tukey test was used to determine the differences between sampling sites. The significance of the results was compared at $p < 0.05$.

A multivariate analysis was performed to identify correlations between different cyanobacteria taxa and soils properties using a Principal Component Analysis (PCA). In the data matrix, the individuals are the sampling sites; the variables are the cyanobacteria taxa and the average of physico-chemical parameters. A hierarchical

http://www.aloki.hu ● ISSN 1589 1623 (Print) ● ISSN 1785 0037 (Online)
DOI: http://dx.doi.org/10.15666/aeer/1804_55275545

classification was made from the coordinates of individuals and variables to establish a soil typology and assess the degree of similarity of the investigated sites.

The statistical analysis was performed by XLSTAT 2016 version 18.02.01.27444; Addinsoft, France.

Results

Soil physico-chemical parameters

The comparison of soils physico-chemical parameters showed spatiotemporal variations and significant differences ($p < 0.05$) were observed between soils in different land uses (*Table 2*). The pH values were slightly acidic to neutral ranging between 6.49 and 7.90 and decreasing significantly ($p < 0.05$) with altitude. The low altitude sites (S3, S4, S5) have slightly neutral to alkaline values, while the grassland high altitudinal one (S1) has slightly acidic value.

Electrical conductivity also showed a significant decreasing gradient ($p < 0.05$) with altitude. The highest values were registered in low lands, with 380 and 257.5 µS/cm in S3 and S5, respectively. While, the high land (S1) showed the minimal value (69.15 µS/cm). Indeed, the Oukaimeden grassland soil was significantly less mineralized ($p < 0.05$) compared to other soils.

In all the sites, the soil moisture ranged from 3 to 8.9% with higher values and a relative stability in February campaign (8.45-8.9%), whereas it decreased in May campaign (up to 3%), especially at S2, S3 and S4. The soil moisture of grassland (S1) was significantly higher ($p < 0.05$) than the other land uses.

During the two campaigns, the total organic carbon content varied from 2.16 to 4.66% and showed a significant difference between different soils. Soils from lower forest and steppe lands (S3, S4, S5) have the highest concentration of total organic carbon. Ammonia nitrogen and available phosphorus contents were very low and fairly similar with often no significant difference between sites. The soil texture is clay in all sites, except sites 1 and 3 where it is silty clay and clay silt, respectively.

Soil biotic indicator

On May 4th, the soil algal biomass, assessed by chlorophyll a content, increased significantly ($p < 0.05$) along the altitudinal gradient, varying from 10.48 µg/g soil at site 5 to 31 µg/g soil at sites 1 and 2 (*Fig. 2*). Unlike the February campaign, the chlorophyll a concentration increased significantly ($p < 0.05$) in May and showed a clear spatial disparity with higher level measured at the two altitudinal sampling sites.

Cyanobacterial diversity: identification and strain isolation

In all studied sites, a total of 26 cyanobacteria taxa were identified (*Table 3*), belonging to 3 orders, 8 families and 9 genera (*Fig. 3b*). Oscillatoriales constitute the most diversified order with 84.62 of all taxa, followed by Chroococcales (11.54%) and Nostocales (3.84%) (*Table 4*). The three genera *Leptolyngbya* (7 taxa), *Phormidium* (6 taxa), *Pseudanabaena* (6 taxa) are the most represented (*Fig. 3c*). In order of occurrence, the common species present in most soil crusts were *Nostoc muscorum* (5 sites), *Phormidium crassivaginatum* (4 sites), *Leptolyngbya faveolarum* (3 sites); while *Leptolyngbya* sp 1 and *Leptolyngbya* sp 2 were represented in some specific soils (2 sites). The highest number of taxa (12 taxa) were observed in the highly altitude station

http://www.aloki.hu ● ISSN 1589 1623 (Print) ● ISSN 1785 0037 (Online)
DOI: http://dx.doi.org/10.15666/aeer/1804_55275545

(S1) (*Fig. 3a*). Based on the most updated Moroccan checklist of cyanobacteria (Douma, 2010), three species are reported for the first time in Morocco (*Phormidium priestleyi, Phormidium crassivaginatum, Pseudanabaena minima*) (*Fig. 4*). It should be noted that for many taxa (10 in total), morphological taxonomic identification was stopped at the genera level. Further modern identification techniques (polyphasic approach) remain necessary to accurately confirm the identity of these taxa. Six species of soil cyanobacteria were successfully isolated from the studied soils and culturing in laboratory. These species were *Phormidium articulatum, Nostoc muscorum, Lyngbya* sp *Pseudanabaena* sp1*, Leptolyngbya* sp1 *and Synechocystis* sp1 (*Fig. 4*).

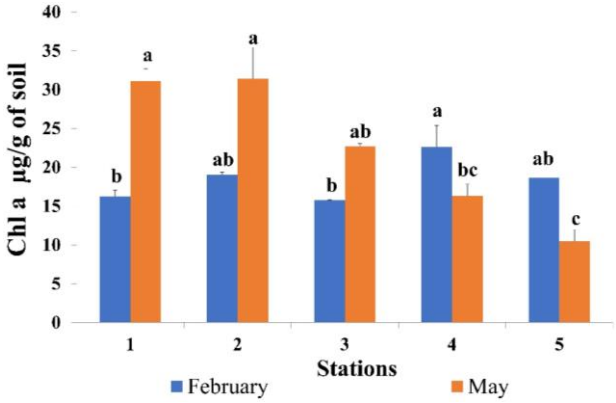

Figure 2. *Chlorophyll a concentration (µg/g soil) in the studied soils. Data are means ± standard error (n = 3). Different letters indicate significant differences (p < 0.05 by Tukey's HSD test) between sampled sites*

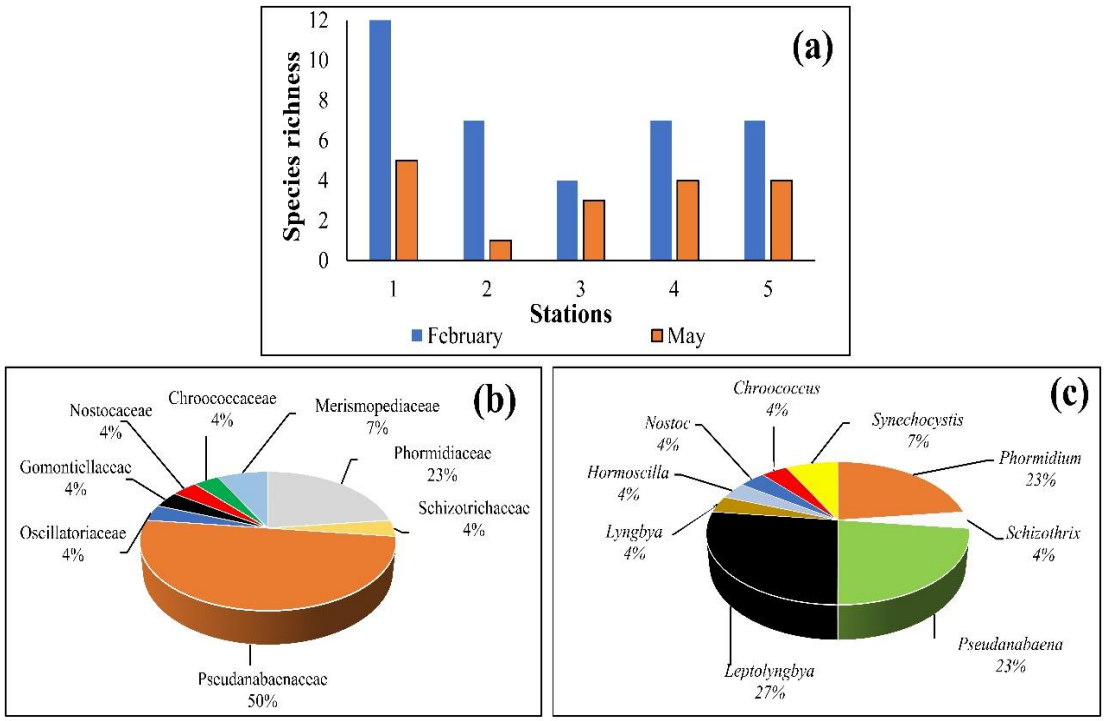

Figure 3. *Species richness (a), spectrum families (b) and spectrum genera (c) of cyanobacteria in the studied soils*

http://www.aloki.hu ● ISSN 1589 1623 (Print) ● ISSN 1785 0037 (Online)
DOI: http://dx.doi.org/10.15666/aeer/1804_55275545

Table 2. *Physico-chemical characteristics of sampled soils*

Parameter	Site 1		Site 2		Site 3		Site 4		Site 5	
	F	M	F	M	F	M	F	M	F	M
pH	6.98±0.08^{c}	6.49±0.085^{c}	7.22±0.005^{bc}	7.90±0.056^{a}	7.80±0.05^{a}	7.73±0.296^{a}	7.47±0.03^{ab}	7.29±0.014^{b}	7.42±0.39^{abc}	7.83±0.025^{a}
CE	120±10^{d}	69.2±2.35^{d}	73.15±0.15^{e}	185.7±0.45^{a}	380±6^{a}	157.6±0^{b}	139.4±0.75^{c}	161.2±0.2^{b}	257.5±7.5^{b}	101.7±1.9^{c}
H	8.9±0.01^{a}	7.7±0.06^{a}	7.4±0.01^{c}	3±0.14^{b}	8.6±0.03^{b}	4.4±0.09^{b}	8.7±0.02^{b}	3±0.06^{b}	8.5±0.02^{c}	8.7±0.05^{c}
TOC	3.02±0.15^{e}	2.16±0.16^{e}	3.28±0.43^{d}	2.91±2.31^{c}	3.33±1.33^{c}	2.66±0.66^{d}	4.66±0.66^{a}	4.33±1.2^{a}	4.16±1.01^{b}	3.83±0.72^{b}
P-PO_4	0.039±0^{ab}	0.007±0.021^{c}	0.039±0.004^{ab}	0.006±0.012^{c}	0.034±0.001^{b}	0.004±0.003^{d}	0.045±0.004^{a}	0.034±0.039^{a}	0.038±0.001^{ab}	0.016±0.031^{b}
N-NH_4^+	0.029±0.002^{a}	0.040±0.001^{a}	0.014±0.002^{b}	0.033±0.001^{b}	0.017±0.001^{b}	0.032±0.001^{b}	0.032±0.005^{a}	0.025±0.001^{c}	0.016±0^{b}	0.022±0.001^{c}
Texture	Silty clay		Clay		Clay silt		Clay		Clay	

The values are denoted as mean ± standard error (n = 3). Different letters indicate significant differences ($p < 0.05$ by Tukey's HSD test) between sampled sites. EC: Electrical conductivity in (µs/cm); H: humidity in (%); TOC: total organic carbon in (% C); N-NH_4^+: Ammoniacal nitrogen in (%); P-PO_4: available phosphorus in (mg/g soil). F: February; M: May

Table 3. *Inventory of cyanobacteria taxa in the study sites (F: February; M: May)*

Taxa	S 1		S 2		S 3		S 4		S 5	
	F	M	F	M	F	M	F	M	F	M
Order/Oscillatoriales F/Phormidiaceae										
Phormidium priestleyi Fri. (PPRI)	X									
Phormidium crassivaginatum An. et Kom. (PCRA)	X		X				X	X		X
Phormidium Kuetzingianum An. (PKUE)	X									
Phormidium molle Gom. (PMOL)	X	X								
Phormidium articulatum Clau. (PART)					X	X	X	X		
Phormidium paulsenianum (Boy.) Nov. (PPAU)									X	
F/Schizotrichaceae										
Schizothrix sp (Ssp)									X	
F/Pseudanabaenaceae										

http://www.aloki.hu ● ISSN 1589 1623 (Print) ● ISSN 1785 0037 (Online)
DOI: http://dx.doi.org/10.15666/aeer/1804_55275545

Pseudanabaena starmachii An. (PSTA)	X									
Pseudanabaena minima An. (PMIN)	X	X								
Pseudanabaena moniliformis Kom. (PMON)			X							
Pseudanabaena balatonica Sche. And Kol. (PBAL)							X	X		
Pseudanabaena galeata Böch. (PGAL)									X	X
Pseudanabaena sp 1 (Psp)	X									
Leptolyngbya lurida (Gom.) An. et Kom. (Llur)	X									
Leptolyngbya faveolarum (Rab.) An. et Kom. (LFAV)	X	X			X	X	X	X		
Leptolyngbya tenuis (Gom.) An. et Kom. (LTEN)									X	
Leptolyngbya pseudovalderiana (Vor.) An. et Kom. (LPSE)									X	X
Leptolyngbya sp 1 *(*Lsp1)	X	X			X	X				
Leptolyngbya sp 2 *(*Lsp2)	X	X	X	X						
Leptolyngbya sp 3 *(*Lsp3)			X							
F/Oscillatoriaceae										
Lyngbya sp *(*LYsp)									X	X
F/Gomontiellaceae										
Hormoscilla sp (Hsp)							X			
O/Nostocales **F/Nostocaceae**										
Nostoc muscorum Ag. (NMUS)	X		X		X		X		X	
O/Chroococcales **F/Chroococcaceae**										
Chroococcus sp (Csp)			X							
F/Merismopediaceae										
Synechocystis sp 1 *(*Ssp1)							X			
Synechocystis sp 2 (Ssp2)			X							
Total of taxa/site	12	5	7	1	4	3	7	4	7	4

http://www.aloki.hu ● ISSN 1589 1623 (Print) ● ISSN 1785 0037 (Online)
DOI: http://dx.doi.org/10.15666/aeer/1804_55275545

Table 4. *Importance of taxonomic level of cyanobacteria in studied soils*

Order (O/)	Taxonomic level			
	Family	Genera	Species	Total (%)
O/Oscillatoriales	5	6	22	84.62
O/Chroococcales	2	2	3	11.54
O/Nostocales	1	1	1	3.84
Total	8	9	26	100

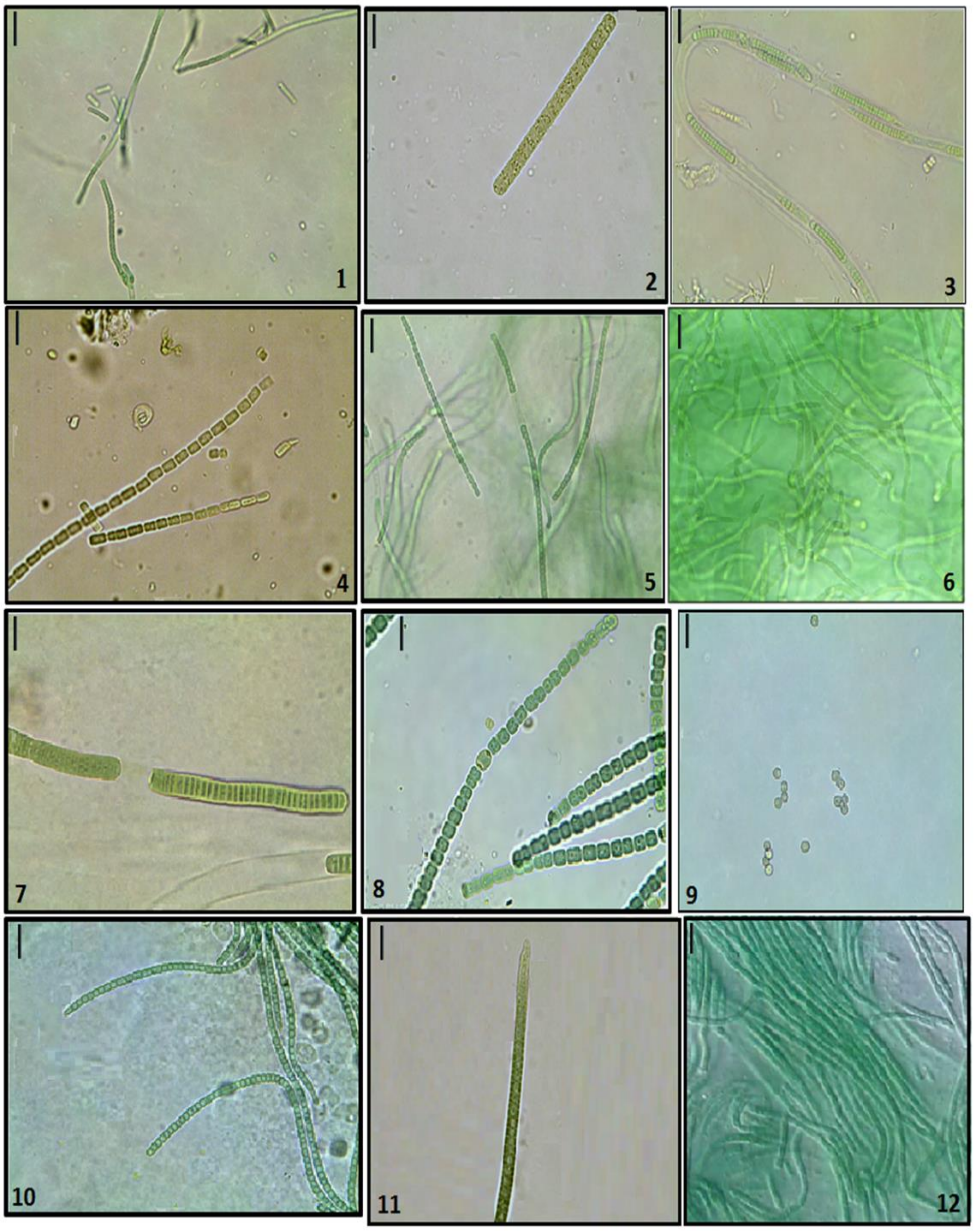

Figure 4. *Microphotographs of identified cyanobacterial strains. 1: Phormidium priestleyi; 2: Phormidium Kuetzingianum; 3: Schizothrix* sp*; 4: Pseudanbaena minima; 5: Pseudanabaena balatonica; 6: Leptolyngbya faveolarum; 7: Lyngbya* sp*; 8: Nostoc muscorum; 9: Synechocystis* sp 1*; 10: Phormidium articulatum; 11: Phormidium crassivaginatum; 12: Leptolyngbya* sp 1. *Scale Bar = 10 μ*

http://www.aloki.hu ● ISSN 1589 1623 (Print) ● ISSN 1785 0037 (Online)
DOI: http://dx.doi.org/10.15666/aeer/1804_55275545

Multivariate analyses

A principal component analysis (PCA) was performed on a data matrix consisting of 8 variables (humidity, pH, conductivity, total organic carbon, available phosphorus, ammonia nitrogen, granulometry, chlorophyll a) and 26 individuals (taxa) distributed along the five studied sites (*Fig. 5*). The variables were mainly correlated with two axes (F1 and F2) in which 53.86% of the total variance in the data was found.

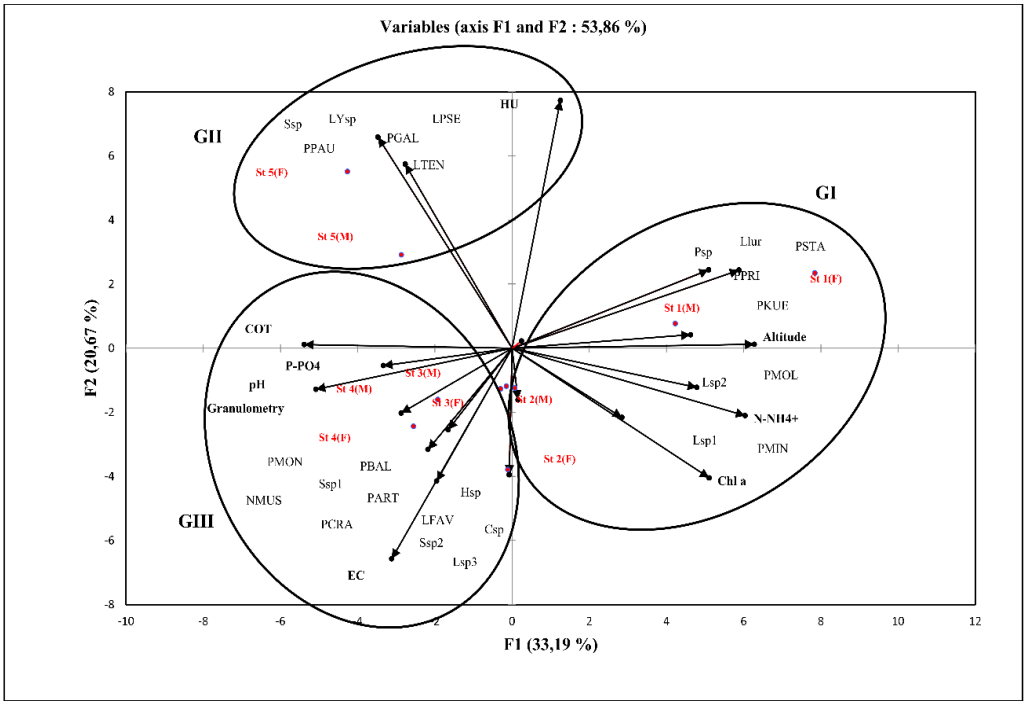

Figure 5. *Projection of variables (physicochemical parameters and cyanobacteria taxa) and sampling sites (in red) on the factorial level (1 x 2)*

The first axis F1 with 33.19% of total variance was strongly correlated on the positive side with ammonia nitrogen, chlorophyll a and altitude. The second axis F2 with 20.67% was positively formed in correlation with humidity. The PCA analysis results revealed that the group of taxa *Phormidium priestleyi* (PPRI), *Phormidium Kuetzingianum* (PKUE), *Phormidium molle* (PMOL), *Pseudanabaena starmachii* (PSTA), *Pseudanabaena minima* (PMIN), *Pseudanabaena* sp1 (Psp), *Leptolyngbya lurida* (Llur), *Leptolyngbya* sp2 (Lsp2) and *Leptolyngbya* sp1 (Lsp1) showed the highest correlation to ammonia nitrogen ($N\text{-}NH_4^+$), chlorophyll a (Chl a) and altitude. However, the group of taxa *Phormidium paulsenianum* (PPAU), *Schizothrix* sp (Ssp), *Pseudanabaena galeata* (PGAL), *Leptolyngbya tenuis* (LTEN), *Leptolyngbya pseudovalderiana* (LPSE) and *Lyngbya* sp (LYsp) has the highest correlation to humidity (HU). A third group of taxa *Phormidium articulatum* (PART), *Phormidium crassivaginatum* (PCRA), *Pseudanabaena moniliformis* (PMON), *Synechocystis* sp2 (Ssp2), *Chroococcus* sp (Csp), *Nostoc muscorum* (NMUS), *Leptolyngbya* sp3 (Lsp3), *Pseudanabaena balatonica* (PBAL), *Hormoscilla sp* (Hsp), *Synechocystis* sp1 (Ssp1) and *Leptolyngbya faveolarum* (LFAV) has the highest association to pH, conductivity (EC), available phosphorus content ($P\text{-}PO_4^-$), total organic carbon (COT) and granulometry.

http://www.aloki.hu ● ISSN 1589 1623 (Print) ● ISSN 1785 0037 (Online)
DOI: http://dx.doi.org/10.15666/aeer/1804_55275545

Furthermore, cluster analysis was performed to separate the taxa into distinct groups based on environmental factors. Three groups of taxa could be distinguished from the dendrogram based on the hierarchical cluster (*Fig. 6*):

I. Taxa with positive correlation to ammonia nitrogen, chlorophyll a and altitude; and with negative correlation to pH and total organic carbon. This first group is associated with the taxa of sites 1 and 2.

II. Taxa with highest correlation to humidity. This second group is composed of the taxa from site 5.

III. Taxa with positive correlation to pH, conductivity, available phosphorus content and granulometry. This third group brings together taxa from sites 3 and 4.

The results of the data analysis revealed that nutrient content (ammonia nitrogen, available phosphorus), altitude, humidity, pH and conductivity were the main factors influencing the spatial distribution of cyanobacteria communities along the studied altitudinal gradient.

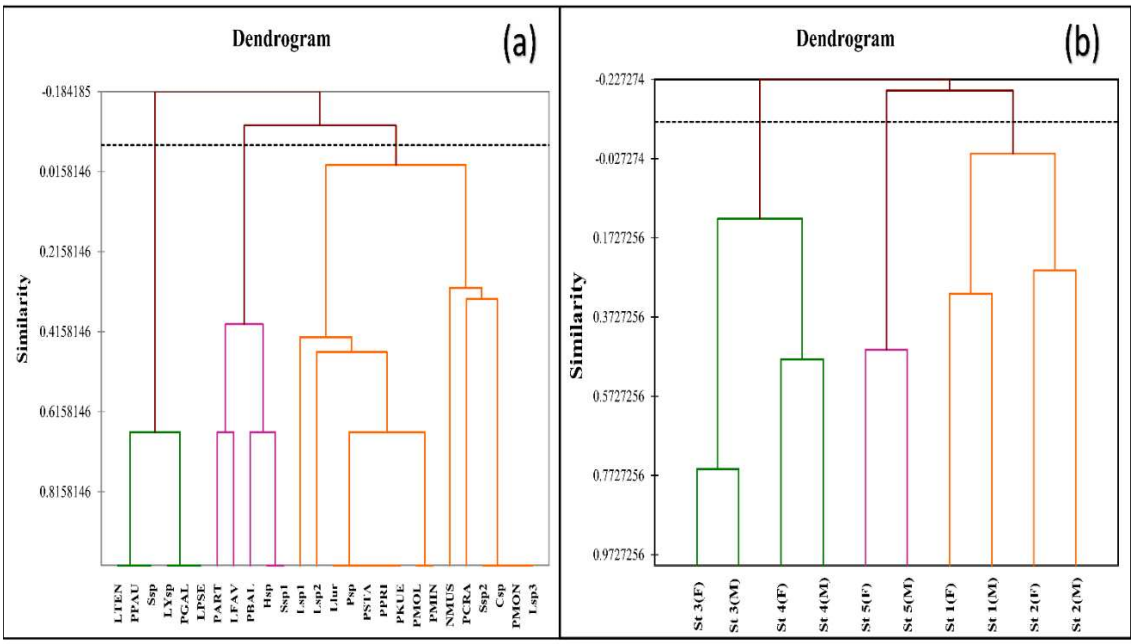

Figure 6. *Cluster dendrogram of cyanobacteria groups (a) and the sampling sites (b) based on physico-chemical parameters*

Discussion

The biomass of BSCs was mainly created by cyanobacterial and microalgal taxa, which are important primary producers within soil crusts all around the world (Janatková et al., 2013). The species composition, abundance and distribution of cyanobacteria biocrusts were influenced by various ecological and edaphic factors (Davey and Rothery, 1993). All the physico-chemical analyses and biological data (*Table 2*) showed that the characteristics of the soils along the natural altitudinal transect (S5 to S1) were mainly influenced by the substrate type, topographic and climatic conditions, land use and vegetation cover (e.g. grassland, forest land, shrub land, steppe land). These environmental factors induce a spatial variability in the soil moisture, texture and chemical composition. Compared to forest and steppe land, the

http://www.aloki.hu ● ISSN 1589 1623 (Print) ● ISSN 1785 0037 (Online)
DOI: http://dx.doi.org/10.15666/aeer/1804_55275545

soil of altitudinal grassland was slightly acidic, relatively wetter, weakly mineralized, and very poor in organic carbon and nutrients.

The obtained results show that cyanobacteria taxa exist in all studied soils, but they reveal a significant presence, especially in altitudinal grassland soil (S1). These results are in agreement with certain studies confirming that this group of microorganisms has an extraordinary resistance to extreme conditions in high altitudes (Řeháková et al., 2011). However, this observation is in contrast with other research, which suggest that cyanobacterial diversity is negatively correlated with acidity and altitude (Choudhary and Singh, 2013).

It is known that various cyanobacteria have a large ecological distribution and seem to be frequent both in high and low altitude soils. Our results showed that many cyanobacteria are ubiquitous and were inventoried at least in four different sites. Among these taxa we found *Phormidium crassivaginatum, Leptolyngbya faveolarum* and *Nostoc muscorum.* The cyanobacterial distribution and diversity in soil are the result of the complex influence of substrate, soil properties, vegetation type and climatic conditions (Quesada et al., 1998).

In this study, it was observed that the highest number of cyanobacteria was recorded in clay-silty soils (S1). This is consistent with the study of Kobbia et al. (1988) which shows that the clay soil has a high water retention and is suitable for the growth of cyanobacteria (Haider et al., 2017). The PCA analysis results revealed that humidity was among the main factors influencing the distribution of cyanobacterial communities along the studied altitudinal gradient. It was also noticed that the highest moisture value was measured in grassland soil (8.89%) which appears to be less affected by temporal variations of rainfall compared to other soil land uses. This result corroborates that of Niu et al. (2015) which showed that soil moisture condition was affected by different land uses and that the higher soil moisture content was exhibited by the grassland followed by cropland, forest land and shrub land. Our observations have confirmed that land use plays a key role in controlling spatial and temporal variations of soil moisture as well as the soil water dynamic. Therefore, water content in soil plays a very important role in the distribution and diversity of soil microalgae (Lin et al., 2013). This situation helps cyanobacteria to keep a longer period of metabolic activity and accumulate more biomass (Zhang et al., 2011).

Furthermore, soil mineralization also influences distribution of soil cyanobacteria. In the studied altitudinal transect, the average values of conductivity were rather low ranging between 73.15 and 380 µS/cm. These values are smaller than those recorded in Iraq (233.8 µS/cm-3072 µS/cm) (Haider et al., 2017). It is known that salinity leads to a decrease in the growth of cyanobacteria, but its effect on growth inhibition varies from one species to another given their morphological and molecular diversity. Consequently, the distribution of cyanobacteria in various environments is not equal, due to their adaptability and tolerance to extreme conditions such as saline environments (Rejmánková et al., 2004).

The studied soils were characterized by relatively low nitrogen, phosphorus and high organic matter content. Our results are similar to those of Zancan et al. (2006). Previous studies have shown that the concentration and quality of nutrients are probably more important in the blue-green-algal diversity. Vijayan and Ray (2015) showed that availability of phosphates and nitrates are the important factors that favor the abundance of cyanobacteria in ecosystems. In the forest land soils especially with dense vegetation (S4), the relatively high organic carbon content was related to the land use type, which

http://www.aloki.hu ● ISSN 1589 1623 (Print) ● ISSN 1785 0037 (Online)
DOI: http://dx.doi.org/10.15666/aeer/1804_55275545

plays a very important role in the soil enrichment by the organic matter and litter (Kooch et al., 2008). Despite their high organic matter content, these forests soils have the lowest number of cyanobacterial taxa. This finding was in harmony with that obtained by Vijayan and Ray (2015), who reported that the vegetation density causes a decrease in light intensity. These results highlighted that soil light condition could be influenced by different land uses. Indeed, the light is an important factor that contributes to the cyanobacterial and microalgal abundance and distribution in natural environments (Řeháková et al., 2011).

The obtained results show that cyanobacteria were found in all examined soils but they reveal a significant variation in their species richness. A comparative analysis of the total cyanobacteria richness showed a similarity with other works (Řeháková et al., 2011; Al-Sodany et al., 2018). This survey highlighted the existence of 26 taxa, distributed on 3 orders and 9 genera; with 3 species reported for the first time in Morocco (*Phormidium priestleyi, Phormidium crassivaginatum, Pseudanbaena minima).* This richness is very important and constitutes a substantial addition to soil cyanobacteria inventories around the world (35 taxa in Eastern Himalayas of India (Choudhary and Singh, 2013); 31 taxa in High altitude at Taif city of Saudi Arabia (Al-Sodany et al., 2018); 81 taxa in mountain tundras of the Polar and Subpolar Urals of Russia (Patova et al., 2018)).

The Oscillatoriales constitute the most diversified order, followed by Chroococcales and Nostocales. This result is in accordance with the findings of Řeháková et al. (2011) who reported that the Oscillatoriales are generally more abundant in finer textured soils that contain relatively high concentrations of organic matter. In contrast, the order of Chroococcales may have increased with altitude because, as unicellular organisms with rapid growth rates, they do not require a stable substrate with a high organic matter content. Whereas, the Nostocales are usually thought to be able to colonize young undeveloped soils because of their ability to fix nitrogen, which might be the limiting nutrient (Kaštovská et al., 2005).

In addition, the Nostocales, represented in this study by *Nostoc muscorum*, are found in all sites but have larger thallus in wet high mountain soil. This observation is consistent with that of Řeháková et al. (2011) who observed that Nostocales were predominated at high altitude. Indeed, they are better adapted to desiccation and cold conditions, due to their well-developed mucilaginous sheath. *Nostoc* species could also behave at high altitude because their biovolume is independent of the concentration of organic matter, unlike other species. Generally, this genus can usually colonize young undeveloped soils because of its ability to fix nitrogen (Whitton and Pott, 2012), which might be the limiting nutrient in these types of soils.

Six strains were successfully isolated in culture of soils in nutrient media. *Pseudanabaena* and *Lyngbya* strains were known by their potential toxicity (Shimizu, 2003; Olvera-Ramírez et al., 2010). However, the other isolated taxa can be considered by their high potential biotechnological value (*Nostoc muscorum, Phormidium articulatum*, *Leptolyngbya* sp and *Synechocystis* sp). In a recent work, Shariatmadari et al. (2013) showed that the application of the strains of *Anabaena vaginicola* and *Nostoc* sp increased the organic C and N content of the surface soil and enhanced plant growth and plant ion uptake; therefore, they are appropriate candidates for a good biofertilizer. Also, the work of Nonibala and Singh (2015) shows that *Nostoc muscorum* and *Synechocystis* sp have promising antifungal activity that can serve as promising biocontrol agents in current agricultural practices. Previous studies focusing on the role

http://www.aloki.hu ● ISSN 1589 1623 (Print) ● ISSN 1785 0037 (Online)
DOI: http://dx.doi.org/10.15666/aeer/1804_55275545

of microalgae in the removal of heavy metals from the soil showed that some cyanobacteria taxa such as *Stigonema* sp, *Phormidium molle*, *Leptolyngbya* sp and *Synechococcus* sp were resistant to heavy metals and thus used for the removal of soil contaminated by heavy metals (Rahman et al., 2011).

Conclusion

This exploratory survey provides a first inventory and data ecology of the cyanobacterial assemblage of soil crusts in a Moroccan mountainous region. This study reveals the existence of a significant cyanobacterial diversity (26 taxa) in the soils of five sampling sites with different land use and vegetation cover along an altitudinal gradient. The studied soils were characterized by significant cyanobacteria richness, with the presence of cosmopolitan and ubiquitous taxa (such as *Phormidium crassivaginatum, Leptolyngbya faveolarum, Nostoc muscorum* and *Schizothrix* sp).

Ultimately, the distribution of soil-cyanobacteria was mainly influenced by altitude, humidity and soils texture, land use and vegetation cover. Cyanobacteria composition and species richness were correlated to the soil physico-chemical characteristics especially nutrients content (ammonia nitrogen and available phosphorus), soils moisture, pH and conductivity.

In this first study, the soil-cyanobacterial inventory was far from being exhaustive in relation to the existing potential. Further investigations are necessary using an experimental approach based on soil culture in nutrient media and identification taxa by molecular methods. More field surveys will be necessary to complete and evaluate the effects of others environmental factors on the diversity, distribution and ecological trends of cyanobacteria in Moroccan terrestrial environments.

Acknowledgements This work was supported by the Water, Biodiversity, and Climate Change Laboratory, Faculty of Sciences Semlalia, University Cadi Ayyad, Marrakesh (Morocco). We would like to express also our gratitude to anonymous reviewers for their useful comments.

REFERENCES

[1] Abed, R. M., Dobretsov, S., Sudesh, K. (2009): Applications of cyanobacteria in biotechnology. – J. Appl. Microbiol 106(1): 1-12. https://doi:10.1111/j.1365-2672.2008.03918.x.

[2] Acea, M. J., Diz, N., Prieto-Fernandez, A. (2001): Microbial populations in heated soils inoculated with cyanobacteria. – Biol Fertil Soils 33(2): 118-125.https://doi:10.1007/s003740000298.

[3] AFNOR (1975): Standard T90-1110. – Water Test: Determination of Total Kjeldahl Nitrogen.

[4] AFNOR (2000): Soil improvers and growing media. Preparation of samples for physical and chemical testing, determination of dry matter content, moisture content and laboratory compacted density. – French Association of Normalization, NF EN 13040.

[5] Al-Sodany, Y. M., Issa, A. A., Kahil, A. A., Ali, E. F. (2018): Diversity of Soil Cyanobacteria in Relation to Dominant Wild Plants and Edaphic Factors at Western Saudi Arabia. – ARRB 26(3): 1-14. https://doi:10.9734/ARRB/2018/40492.

[6] Anagnostidis, K., Komarek, J. (1990): Modern approach to the classification system of cyanophytes, 5-Stigonematales. – Algolo Stud 86: 1-74.

[7] Aubert, G. (1978): Soil Analysis Methods. – CRDP Edition, Marseille.

http://www.aloki.hu ● ISSN 1589 1623 (Print) ● ISSN 1785 0037 (Online)
DOI: http://dx.doi.org/10.15666/aeer/1804_55275545

[8] Bag, P., Ansolia, P., Mandotra, S. K., Bajhaiya, A. K. (2019): Potential of Blue-Green Algae in Wastewater Treatment. – In: Gupta, S. K., Bux, F. (eds.) Application of Microalgae in Wastewater Treatment. Springer, Cham. https://doi.org/10.1007/978-3-030-13913-1_17.

[9] Belnap, J., Phillips, S. L., Witwicki, D. L., Miller, M. E. (2008): Visually assessing the level of development and soil surface stability of cyanobacterially dominated biological soil crusts. – Journal of Arid Environments 72(7): 1257-1264. DOI: 10.1016/j.jaridenv.2008.02.019.

[10] Belnap, J., Weber, B., Büdel, B. (2016): Biological Soil Crusts as an Organizing Principle in Drylands. – In: Weber, B. et al. (eds.) Biological Soil Crusts: An Organizing Principle in Drylands. Ecological Studies 226. Springer, Cham, pp. 3-13. https://doi.org/10.1007/978-3-319-30214-0_1.

[11] Blanco, Y., Prieto-Ballesteros, O., Gómez, M. J., Moreno-Paz, M., García-Villadangos, M., Rodríguez-Manfredi, J. A., ... Parro, V. (2012): Prokaryotic communities and operating metabolisms in the surface and the permafrost of Deception Island (Antarctica). – Environmental Microbiology 14(9): 2495-2510. https://doi.org/10.1111/j.1462-2920.2012.02767.x.

[12] Büdel, B., Dulic, T., Darienko, T., Rybalka, N., Friedl, T. (2016): Cyanobacteria and Algae of Biological Soil Crusts. – In: Weber, B. et al. (eds.) Biological Soil Crusts: An Organizing Principle in Drylands. Ecological Studies 226. Springer, Cham, pp. 55-80. DOI: 10.1007/978-3-319-30214-0_4.

[13] Choudhary, K. K., Singh, R. K. (2013): Cyanobacterial diversity along altitudinal gradient in Eastern Himalayas of India. – J. Algal Biomass Utln 4(2): 53-58.

[14] Davey, M. C., Rothery, P. (1993): Primary colonization by microalgae in relation to spatial variation in edaphic factors on Antarctic fell field soils. – J. Ecol 81: 335-343. https://doi.org/10.2307/2261503.

[15] Douma, M. (2010): Biodiversité des Cyanobactéries des zones humides continentales du Maroc: taxonomie, distribution géographique, écologie, phylogénie et potentiel toxique. – PhD Thesis, Faculty of Sciences Semlalia, University of Cadi Ayyad Marrakech, Morocco.

[16] Douma, M., Loudiki, M., Oudra, B., Mouhri, K., Ouahid, Y., Francisca, F., del Campo, F. (2009): Taxonomic diversity and toxicological assessment of Cyanobacteria in Moroccan inland waters. – Rev. Sci. Eau 22(3): 435-449. https://doi.org/10.7202/037781ar.

[17] El Khalil, H., Schwartz, C., El Hamiani, O., Kubinick, J., Morel, J. L., Boularbah, A. (2013): Distribution of major elements and trace metals as indicators of technosolisation of urban and suburban soils. – J Soils Sediments 13: 519-530.https://doi.org/10.1007/s11368-012-0594-x.

[18] Garcia-Pichel, F., Felde, V. J. M. N. L., Drahorad, S. L., and Weber, B. (2016): Microstructure and Weathering Processes within Biological Soil Crusts. – In: Weber, B. et al. (eds.) Biological Soil Crusts: An Organizing Principle in Drylands. Ecological Studies 226. Springer, Cham, pp. 237-255. DOI: 10.1007/978-3-319-30214-0_13.

[19] Hackl, E., Bachmann, G., Zechmeister-Bolternstern, S. (2004): Microbial nitrogen turnover in soils under different types of natural forest. – Forest Ecol. Manage. 188: 101-112.

[20] Haider, A. A., Haifaa, M. J. (2017): Effect of physicochemical factors on cyanobacteria biodiversity in some agricultural soil of Al-Diwaniyah City during spring period. – JGPT 2(9): 43-52.

[21] Haroni, S. A., Alifriqui, M., Ouhammou, A. O. (2009): La diversité floristique des pelouses humides d'altitude: cas de quelques sites du Haut Atlas Marocain. – Acta Botanica Malacitana 34: 91-106.

[22] Heckman, K. A., Anderson, W. B., Wait, D. A. (2006): Distribution and activity of hypolithic soil crusts in a hyperarid desert (Baja California, Mexico). – Biol Fertil Soils 43: 263-266.https://doi:10.1007/s00374-006-0104-7.

http://www.aloki.hu ● ISSN 1589 1623 (Print) ● ISSN 1785 0037 (Online)
DOI: http://dx.doi.org/10.15666/aeer/1804_55275545

[23] Hoffmann, L. (1989): Algae of terrestrial habitats. – Bot Rev 55(2): 77-105.
[24] Hu, Q., Sommerfeld, M., Jarvis, E., Ghirardi, M., Posewitz, M., Seibert, M., Darzins, A. (2008): Microalgal triacylglycerols as feedstocks for biofuel production: perspectives and advances. – Plant J 54(4): 621-639. https://doi: 10.1111/j.1365-313X.2008.03492.x.
[25] ISO 10260 (1992): Water Quality, Measurement of Biochemical Parameters; Spectrometric Determination of the Chlorophyll-a Concentration. – Beruth Verlag, Berlin.
[26] Janatková, K., Řeháková, K., Doležal, J., Šimek, M., Chlumská, Z., Dvorský, M., Kopecký, M. (2013): Community structure of soil phototrophs along environmental gradients in arid Himalaya. – Environ. Microbiol 15(9): 2505-2516. https://doi.org/10.1111/1462-2920.12132.
[27] Kaštovská, K., Elster, J., Stibal, M., Šantrůčková, H. (2005): Microbial assemblages in soil microbial succession after glacial retreat in Svalbard (High Arctic). – Microb Ecol 50: 396-407. https://doi.org/10.1007/s00248-005-0246-4.
[28] Kobbia, I. A., Shabana, E. F. (1988): Studies on the soil algal flora of Egyptian Bahariya Oasis. – Egypt. J. Bot 31: 1-3.
[29] Komarek, J. (2013): Cyanoprokaryota 3. Heterocytous genera. – In: Ettl, H., Gartner, G., Heynig, H., Mollenhauer, D. (eds.) Süsswasserflora von Mitteleuropa. Band 19/3. Spektrum Verlag, Heidelberg, pp. 1-1087.
[30] Komarek, J., Anagnostidis, K. (1998): Cyanoprokaryota 1. Chroococcales. – In: Ettl, H., Gartner, G., Heynig, H., Mollenhauer, D. (eds.) Süsswasserflora von Mitteleuropa. Vol. 19/1. Spektrum Verlag, Heidelberg, pp. 1-548.
[31] Komarek, J., Anagnostidis, K. (2005): Cyanoprokaryota 2. Oscillatoriales, Vol. 19/2. – In: Budel, B., Gartner, G., Krienitz, L., Schagerl M. (eds.) Süsswasserflora von Mitteleuropa. Spektrum Verlag, Heidelberg, pp. 1-757.
[32] Kooch, Y., Jalilvand, H., Bahmanyar, M. A., Pormajidian, M. R. (2008): The use of principal component analysis in study of physical, chemical and biological soil properties in southern Caspian forests (north of Iran). – Pakistan J Biol Sci 11(3): 366-372. https://doi:10.3923/pjbs.2008.366.372.
[33] Kotai, J. (1972): Instructions for Preparation of Modified Nutrient Solution Z8 for Algae. – Norwegian Institute for Water Research, Oslo.
[34] Lin, C. S., Chou, T. L., Wu, J. T. (2013): Biodiversity of soil algae in the farmlands of mid-Taiwan. – Bot Stud 54(1): 41. https://doi.org/10.1186/1999-3110-54-41.
[35] Liu, Y., Xing, Z., Yang, H. (2017): Effect of biological soil crusts on microbial activity in soils of the Tengger Desert (China). – J. Arid. Environ 144: 201-211. http://dx.doi.org/10.1016/j.jaridenv.2017.04.003.
[36] Loudiki, M., Oudra, B., Sabour, B., Sbiyyaa, B., Vasconcelos, V. (2002): Taxonomy and geographic distribution of potential toxic Cyanobacterial strains in Morocco. – Ann. Limnol 38(2): 101-108.https://doi.org/10.1051/limn/2002008.
[37] Maestre, F. T., Bowker, M. A., Cantón, Y., Castillo-Monroy, A. P., Cortina, J., Escolar, C., Lázaro, R.,Martínez, I. (2011): Ecology and functional roles of biological soil crusts in semi-arid ecosystems of Spain. – J. Arid. Environ 75(12): 1282-1291. https://doi.org/10.1016/j.jaridenv.2010.12.008.
[38] Malam Issa, O., Defarge, C., Bissonnais, Y. L., Martin, B., Duval, A., Bruand, A., D'Acqui, L. P., Nodernberg, S., Annerman, M. (2007): Effects of the inoculation cyanobacteria on the microstructure and the structural stability of a tropical soil. – Plant Soil 290(1): 209-219. https://doi.org/10.1007/s11104-006-9153-9.
[39] Mansour, H. A., Shaaban, A. S. (2010): Algae of soil surface layer of Wadi Al-Hitan protective area (world heritage station), El-Fayum depression, Egypt. – Am. J. Sci 6(8): 243-255.
[40] Meliho, M., Khattabi, A., Mhammdi, N., Hongming, Z. (2016): Impact of land use and vegetation cover on risks of erosion in the Ourika watershed (Morocco). – American Journal of Engineering Research (AJER) 5(9): 75-82.

http://www.aloki.hu ● ISSN 1589 1623 (Print) ● ISSN 1785 0037 (Online)
DOI: http://dx.doi.org/10.15666/aeer/1804_55275545

[41] Muñoz-Martín, M. Á., Becerra-Absalón, I., Perona, E., Fernández-Valbuena, L., Garcia-Pichel, F., Mateo, P. (2019): Cyanobacterial biocrust diversity in Mediterranean ecosystems along a latitudinal and climatic gradient. – New Phytologist 221(1): 123-141. https://doi.org/10.1111/nph.15355.
[42] Nduwayo, E., Khattabi, A., El Abidine, A., Ouhammou, A. (2017): Evaluation de l'état de formations végétales forestières dans le bassin versant de l'Ourika dans une optique de restauration des espaces dégradés. – Revue Paysages Géographiques 4: 19.
[43] Nemergut, D. R., Anderson, S. P., Cleveland, C. C., Martin, A. P., Miller, A. E., Seimon, A., Schmidt, S. K. (2007): Microbial community succession in an unvegetated, recently deglaciated soil. – Microb Ecol 53: 110-122. https://doi.org/10.1007/s00248-006-9144-7.
[44] NF ISO 10390. (1992): Soil quality - Determination of pH. – ISO, Geneva.
[45] Nonibala, K., Singh, N. I. (2015): Screening of cyanobacteria from the soil of paddy field for biotechnological applications. – J. Mycopathol. Res 53(1): 55-58.
[46] Olsen, S. R., Cole, C. V., Watanabe, F. S., Dean, L. A. (1954): Estimation of available phosphorus in soils by extraction with sodium bicarbonate. – US Dep. Agric. Circ 939: 18-19.
[47] Olvera-Ramírez, R., Centeno-Ramos, C., Martínez-Jerónimo, F. (2010): Toxic effects of *Pseudanabaena tenuis* (Cyanobacteria) on the cladocerans Daphnia magna and Ceriodaphnia dubia. – Hidrobiológica 20: 203-212.
[48] Ouhammou, A. (2005): Flore et végétation du Parc National de Toubkal (Haut-Atlas de Marrakech, Maroc): typologie, écologie et conservation. – Th. D'état, Université Cadi Ayyad, Marrakech.
[49] Patova, E. N., Novakovskaya, I. V., Deneva, S. V. (2018): The influence of edaphic and orographic factors on algal diversity in biological soil crusts on bare spots in the polar and subpolar Urals. – Eurasian J. Soil Sci 51(3): 309-320. https://doi.org/10.1134/S1064229318030109.
[50] Quesada, A., Nieva, M., Leganés, F., Ucha, A., Martín, M., Prosperi, C., Fernández-Valiente, E. (1998): Acclimation of Cyanophytal communities in rice fields and response of nitrogenase activity to light regime. – Microb Ecol 35: 147-155.https://doi.org/10.1007/s002489900069.
[51] Rahman, M. A., Soumya, K. K., Tripathi, A., Sundaram, S., Singh, S., Gupta, A. (2011): Evaluation and sensitivity of cyanobacteria, *Nostoc muscorum* and *Synechococcus* PCC 7942 for heavy metals stress-a step toward biosensor. – Environ Toxicol Chem 93(10): 1982-1990. https://doi.org/10.1080/02772248.2011.606110.
[52] Řeháková, K., Chlumská, Z., Doležal, J. (2011): Soil Cyanobacterial and microalgal diversity in dry mountains of Ladakh, NW Himalaya, as related to station, altitude, and vegetation. – Microb Ecol 62: 337-346. DOI: 10.1007/s00248-011-9878-8.
[53] Rejmánková, E., Komárek, J., Komárková, J. (2004): Cyanobacteria—a neglected component of biodiversity: patterns of species diversity in inland marshes of northern Belize (Central America). – Diversity and Distributions 10(3): 189-99. https://doi.org/10.1111/j.1366-9516.2004.00077.x.
[54] Rivera-Aguilar, V., Montejano, G., Rodriguez-Zaragoza, S., Duran-Diaz, A. (2006): Distribution and composition of cyanobacteria, mosses and lichens of the biological soil crusts of the Tehuacan Valley, Puebla, Mexico. – J. Arid. Environ 67: 208-225.https://doi:10.1016/j.jaridenv.2006.02.013.
[55] Rossi, F., Li, H., Liu, Y., De Philippis, R. (2017): Cyanobacterial inoculation (cyanobacterisation): perspectives for the development of a standardized multifunctional technology for soil fertilization and desertification reversal. – Earth-Science Reviews 171: 28-43. https://doi.org/10.1016/j.earscirev.2017.05.006.
[56] Singh, H., Khattar, J. S., Ahluwalia, A. S. (2014): Cyanobacteria and agricultural crops. – Vegetos 27(1): 37-44. DOI: 10.5958/j.2229-4473.27.1.008.

http://www.aloki.hu ● ISSN 1589 1623 (Print) ● ISSN 1785 0037 (Online)
DOI: http://dx.doi.org/10.15666/aeer/1804_55275545

[57] Singh, J. S., Kumar, A., Rai, A. N., Singh, D. P. (2016): Cyanobacteria: a precious bio-resource in agriculture, ecosystem, and environmental sustainability. – Front Microbiol 7: 529. DOI: 10.3389/fmicb.2016.00529.

[58] Shariatmadari, Z., Riahi, H., Seyed Hashtroudi, M., Ghassempour, A., Aghashariatmadary, Z. (2013): Plant growth promoting cyanobacteria and their distribution in terrestrial habitats of Iran. – J. Soil Sci. Plant Nutr 59(4): 535-547.http://dx.doi.org/10.1080/00380768.2013.782253.

[59] Shimizu, Y. (2003): Microalgal metabolites. – Curr Opin Microbiol 6(3): 236-243. https://doi:10.1021/cr00021a002.

[60] Soltner, D. (2005): The Bases of Plant Production. The Soil and Its Improvement. Vol. I, 24th Ed. – Science Collection and Agricultural Techniques, Sainte-Gemmessur-Loire.

[61] Vijayan, D., Ray, J. G. (2015): Ecology and diversity of Cyanobacteria in Kuttanadu paddy wetlands, Kerala, India. – Am. J. Plant Sci 6: 2924-2938. DOI: 10.4236/ajps.2015.618288.

[62] Whitton, B. A., Pott, M. (2012): The Ecology of Cyanobacteria II: Their Diversity in Time and Space. – Springer, Dordrecht. https://doi:10.1007/978-94-007-3855-3_10.

[63] Zancan, S., Trevisan, R., Paoletti, M. (2006): Soil algae composition under different Agro-Ecosystems in North-Eastern Italy. – Agr Ecosyst Environ 112(1): 1-12. https://doi.org/10.1016/j.agee.2005.06.018.

[64] Zhang, B., Zhang, Y., Downing, A., Niu, Y. (2011): Distribution and composition of cyanobacteria and microalgae associated with biological soil crusts in the Gurbantunggut Desert, China. – Arid Land Res Manag 25(3): 275-293.https://doi:10.1080/15324982.2011.565858.

http://www.aloki.hu ● ISSN 1589 1623 (Print) ● ISSN 1785 0037 (Online)
DOI: http://dx.doi.org/10.15666/aeer/1804_55275545

ASSESSMENT OF THE ALLELOPATHIC POTENTIAL AND IDENTIFICATION OF THE PHYTOTOXIC SUBSTANCES FROM THE STRAW OF BANGLADESHI INDIGENOUS RICE VARIETY 'GORIA'

MASUM, S. M.[1,2] – AKAMINE, H.[3] – HOSSAIN, M. A.[3*] – SAKAGAMI, J. I.[4] – ISHII, T.[3] – GIMA, S.[5]

[1]*United Graduate School of Agriculture Sciences, Kagoshima University, Kagoshima, Japan*

[2]*Department of Agronomy, Sher-e-Bangla Agricultural University, Dhaka, Bangladesh*

[3]*Faculty of Agriculture, University of the Ryukyus, Okinawa, Japan*

[4]*Faculty of Agriculture, Kagoshima University, Kagoshima, Japan*

[5]*CRAC, University of the Ryukyus, Okinawa, Japan*

**Corresponding author*
e-mail: amzad@agr.u-ryukyu.ac.jp; phone: +81-98-895-8824

The first two authors contributed equally to this work.

(Received 28th Mar 2020; accepted 2nd Jul 2020)

Abstract. Straw from Bangladeshi indigenous rice (*Oryza sativa* L. ssp. *indica*) variety 'Goria' was incorporated into a gray soil to observe the phytotoxic effects on *Echinochloa oryzicola.* The residues of 'Goria' caused inhibition on the growth and dry weight of *E. oryzicola*. The rate of 'Goria' straw incorporation was sequentially evaluated to observe autotoxicity in the cultivation of the same rice variety. An improvement was found on the growth and yield parameters of rice due to the straw incorporation into the soil. Aqueous methanol extracts of 'Goria' straw inhibited the seedling growth of *Lepidium sativum* L. and *E. oryzicola*, which suggested that this variety might contain phytotoxic substance(s). Two biologically active compounds, (-)-loliolide and 3*β*-hydroxy-5*α*,6*α*-epoxy-7-megastigmen-9-one, were isolated using several chromatographic steps. The phytotoxic potential of these two compounds was assayed in vitro on the seedling growth of test flora to validate it. The inhibitory activity of 3*β*-hydroxy-5*α*,6*α*-epoxy-7-megastigmen-9-one was greater than that of (-)-loliolide, as demonstrated by comparison of the I_{50} values. However, the two compounds synergistically suppressed the growth of *L. sativum* and *E. oryzicola* more strongly than the individual compounds. The results suggest that incorporation of allelopathic rice Goria-straw could help suppress *E. oryzicola* in rice to achieve non-herbicidal weed control.
Keywords: *allelochemicals, autotoxicity, inhibitory bioactivity, Echinochloa oryzicola, weed management*

Introduction

Rice (*Oryza sativa* L. ssp. *indica*) is the primary crop of Bangladesh, covering approximately 75% of the total crop area (BBS, 2017). The dramatic increase in the use of agricultural chemicals has contributed considerably to increasing rice productivity worldwide and in Bangladesh in the last half century (Erisman et al., 2008). However, in Bangladesh, rice cultivation is seriously threatened by several factors and circumstances including pesticide and fertilizer use. The current trend in agriculture focuses on reducing the use of herbicides because of their adverse effects on nature. Anxiety about the potential connections between public health, environmental

http://www.aloki.hu ● ISSN 1589 1623 (Print) ● ISSN 1785 0037 (Online)
DOI: http://dx.doi.org/10.15666/aeer/1804_55475560

conditions, and farming output exposes the rising demand to address the long-term sustainability of existing agricultural practices and determine which agricultural technologies will be safe and economically productive.

Rice is heavily infested with several noxious weeds, including *E. crus-galli* (Kraehmer et al., 2016). In Bangladesh, *E. oryzicola* is one of the primary weeds, which is difficult to control because it is a mimic of rice and easily adapts to both the transplanted and direct-sowing rice growing environments. Several methods are used to control weeds. Depending on the weed types and critical period of weed competition, we must intelligently select and adopt different weed management techniques based on the available resources. Allelopathy is a phytotoxic inference in which a plant or plant residue releases phytochemicals exerting an impact (generally adverse) on the adjacent or successive plants (Yang and Kong, 2017; Kong et al., 2019). Using allelopathy in crop production, reducing synthetics and ensuing environmental degradation, and developing efficient methods for sustainable crop production and agroecological schemes are the primary motivations for research on allelopathy (Han et al., 2013).

To develop herbicides, allelochemicals have been on the research interest of phytochemists recently (Chung et al., 2017). A tremendous opportunity is available to use rice residues as a source of bio-herbicides (Amb and Ahluwalia, 2016). Mulching or incorporation of allelopathic plant materials provides convenient weed management (Jabran et al., 2015) and reduces the adverse effects on an agroecosystem (Cheema et al., 2004). The adoption of mechanized agriculture has brought in leaving a significant amount of rice straw that is available for most rice farmers as organic material. Thus, we can use this rice straw for recycling in agricultural practices. Chung et al. (2001) and Xuan et al. (2005) describe suppression activities of rice residues on weeds including *Echinochloa* species. The content of phytotoxic compounds in rice straw is vast and manifold (Kong et al., 2006; Kato-Noguchi et al., 2012). Significant amounts of stubble remained in the fields after rice harvest also contain and release phytotoxins (Kong et al., 2006; Cao et al., 2008) and reduce soil erosion and effectively prohibit the growth of weeds (Ramakrishna et al., 2006). Furthermore, removal of straw from the field diminishes reserves of soil K and Si, whereas incorporation of the remaining plant parts into the soil deposits nutrients and assists in conserving soil nutrient resources for an extended period (Dobermann and Fairhurst, 2002). Thus, straw incorporation can increase soil fertility and improve soil organic matter content, which can influence the nutritional and physiological aspects of crop growth. Generally, rice straw is applied back into rice and vegetable fields as an organic substance, and particularly in greenhouse cropping. Rice straw mulching had a notable impact on controlling weed growth under zero tillage wheat (*Triticum aestivum* L.) in experimental field conditions following rice in Bangladesh (Rahman et al., 2005). Hence, weed prevention coupled with yield enhancements by rice straw mulching would benefit integrated weed management systems, while minimizing the effects of agrochemicals, which are an essential concern in current agricultural activities. Regrettably, Schreiber (1992), Lund et al. (1993) and Inderjit et al. (2004) conveyed that the incorporation of straw into the soil was the primary cause for the suppression of crop growth in the next season.

Evolution of weed resistance against herbicides demands that new classes of herbicides are created with new modes of action that have not been previously exploited and that can be used in organic agriculture. Moreover, using synthetics for weed suppression also requires public acceptance (Dayan et al., 2009; Anwar et al., 2019). Allelochemicals can be familiarized as potential natural herbicides because of their

http://www.aloki.hu ● ISSN 1589 1623 (Print) ● ISSN 1785 0037 (Online)
DOI: http://dx.doi.org/10.15666/aeer/1804_55475560

inhibitory activities on the emergence, growth, physiological response, and biochemical contents of receivers (Weir et al., 2004; Khanh et al., 2009), which ultimately manipulate the population structure and dynamics during secondary succession of flora, their vegetation pattern in communities, and farm management and output (Weidenhamer and Callaway, 2010). In agriculture, allelochemicals are considered as a supplement because they are less persistent and eco-friendly (Weston and Duke, 2003). Allelopathic substances such as momilactones A and B, form rice straw and their phytotoxic inference on weeds have been documented (Chung et al., 2001). Therefore, the present study was planned to consider the use of Bangladeshi indigenous rice straw for the control of weeds, to observe autotoxicity in rice, and to isolate and identify potential phytotoxic substances and determine their bioactivity on the growth of *E. oryzicola*.

Materials and methods

Plant materials

The Bangladesh indigenous rice (*Oryza sativa* L. spp. *indica*) variety 'Goria' as allelopathic (Masum et al., 2016) were grown in pots (Wagner pot, 0.02 m^2) from April to July 2016 in a glasshouse of the University of the Ryukyus for 120 days and then allowed to sundry in the glasshouse for an additional period (21 days). Seeds of *L. sativum* L. were purchased from the Green Field Project (Kumamoto, Japan), and seeds of *Echinochloa crus-galli* L. Beauv. var. *oryzicola* were collected from the rice field of the University of the Ryukyus, Japan.

Pot studies

Pot (Wagner pot, area 0.02 m^2; height 19.7 cm; diameter 17.3 cm) studies were undertaken in a two-step procedure, with both steps conducted in a glasshouse at the University of the Ryukyus, Japan. The first step was to verify the effect of rice straw incorporation into the soil on *E. oryzicola* growth, and the second step was to observe rice growth. In the first step, each pot was filled with 4 kg of gray soil (coarse sand 3.61%, fine sand 30.94%, silt 24.32%, and clay 32.84%; apparent density 0.90 g cm^{-3}; pH 7.43; C 1.83% and N 0.14%; and in mg g^{-1} soil, HPO_4^{2-} 0.44, K^+ 0.75, Ca^{2+} 4.99, Mg^{2+} 0.70, SO_4^{2-} 1.39, Fe^{3+} 0.64, Mn^{2+} 0.41, Zn^{2+} 0.47, Na^{2+} 1.01, Cu^{2+} 0.41, and Al^{2+} 0.81). Soils with the chaff (1–2 cm) of 'Goria' rice at the rate of 0.5, 1.0, 1.5 and 2.0 t ha^{-1} were completely incorporated in pots. The untreated pots contained soil only. The incorporated soils were moistened for 30 days to decompose appropriately. Two pre-germinated *E. oryzicola* seeds were placed in each pot. Weed-inhibition was determined from the difference of the growth parameters and dry weights of plants between treated and untreated pots.

In the second step, each pot was filled as in the first step, and four treatments were applied: control, 'Goria' straw (2.0 t ha^{-1}), commercial fertilizers, and 'Goria' straw (2.0 t ha^{-1}) with commercial fertilizers. Residues were decomposed as previously described. Commercial fertilizers were applied at the rate of 0.063, 0.05, 0.025, 0.031, and 0.005 g kg^{-1} soil in the form of urea, triple superphosphate (TSP), muriate of potash (MOP), gypsum and zinc sulphate, respectively, one day before transplanting; urea was applied in three equal splits one day before transplanting and at 20 and 40 DAT (days after transplanting). Twenty-five-day-old seedlings of Bangladesh

http://www.aloki.hu ● ISSN 1589 1623 (Print) ● ISSN 1785 0037 (Online)
DOI: http://dx.doi.org/10.15666/aeer/1804_55475560

indigenous rice variety 'Goria' were transplanted at 1 seedling per pot. Growth and yield contributing parameters of rice were observed. After the harvest of the crop, the experimental soil core was carefully removed from the pot. About 200 g of soil samples were collected from the inner area of the core up to bottom layer at 5- cm intervals, air-dried, grounded, and the roots were separated by sieving with a 2.5-mesh sieve.

Straw extract bioassay

Dried straw (leaves and stems) of 'Goria' variety was blended and kept at -40 °C until used for extraction. Extraction was performed using a slight modification of the method developed by Kato-Noguchi et al. (2011). The powder (40 g) placed in a 1000-mL flask containing 500 mL of 80% (v/v) aqueous methanol, and stirred for 48 h at room temperature. Extracts were filtered through Whatman No. 42 filter paper (Toyo, Tokyo, Japan). The residue was re-extracted with 500 mL of methanol and filtered following the above methods. Then, the two filtrates were mixed and evaporated to dryness in vacuo.

An aliquot of the aqueous concentrate (0.001, 0.003, 0.01, 0.03, 0.1 and 0.3 g dry weight [DW] equivalent extract per mL final assay concentration) was evaporated to dryness on a rotary evaporator at 40 °C. Then, the dried sample was re-dissolved in cold methanol (0.2 mL), placed on a sheet of filter paper (no. 2) in a 3 cm Petri dish, desiccated in a draft chamber and then soaked in 0.8 mL of 0.05% (v/v) aqueous solution of Tween 20 (polyoxyethylene sorbitan monolaurate; Nacalai Tesque Inc., Kyoto, Japan) as a surfactant. For the control treatments, methanol (0.2 mL) was used and desiccated as described above. Ten uniform germinated seedlings of *L. sativum* or *E. oryzicola* were placed on the filter paper and then incubated at 25 °C in a dark incubator. The root and shoot lengths of the test species were determined after 48 h of incubation. The percentage of growth inhibition was calculated with respect to the control (without extracts) seedlings.

Extraction of rice straw for purification of growth inhibitors

Extracts were prepared using the method described by Kato-Noguchi et al. (2011) for isolating allelochemicals. A total of 2.4 kg of finely ground dry straw was extracted as described above. Then, the supernatant was concentrated under vacuum to prepare the aqueous concentrate (100 mL). This aqueous concentrate was adjusted to pH 7.0 and suspended in ethyl acetate and evaporated to obtain ethyl acetate extracts (12.4 g). The active ethyl acetate fraction was chromatographed on a column of silica gel (70 g, silica gel 60N, 70-230 mesh; ASTM, Kanto Chemical Co., Inc., Tokyo, Japan), eluting with a stepwise gradient of ethyl acetate (each step 10%, v/v; 150 mL) and methanol (300 mL) in n-hexane, affording 11 fractions. The inhibition effect of the collected fractions was scrutinized using the L. sativum growth bioassay according to the above procedure, and complete inhibition was observed in fractions attained by elution with 80% ethyl acetate in n-hexane. After drying, the concentrate (1.4 g) was filtered through a column of Sephadex LH-20 (60 g, GE Healthcare Bio-Sciences AB SE-75184; Uppsala, Sweden), eluting with aqueous methanol (20, 40, 60 and 80%, v/v; 150 mL each step) and methanol (300 mL). The most effective fraction was eluted with 60% aqueous methanol and subsequently concentrated until dryness. The concentrate (254 mg) was dissolved in 20% aqueous methanol (v/v, 2 mL) and loaded onto a reverse-phase C18 Sep-Pak

http://www.aloki.hu ● ISSN 1589 1623 (Print) ● ISSN 1785 0037 (Online)
DOI: http://dx.doi.org/10.15666/aeer/1804_55475560

cartridge (Waters Corporation, Milford, Massachusetts, USA) and purified with aqueous methanol (20, 40, 60, and 80%, v/v) and methanol (15 mL each step). The most effective fraction (20% aqueous methanol) concentrated until dryness. The concentrate (71 mg) was finally purified by C18 reversed-phase HPLC (COSMOSIL 5C18-AR-II; Nacalai Tesque, Inc., Kyoto, Japan), eluting with 50% aqueous methanol at a flow rate of 3 mL/min and detecting at 220 nm. Complete inhibition was detected for two peaks that eluted at 22.0 and 24.0 min as colorless substances. Mass spectrometry with electro-spray ionization (ESI-MS) analysis was conducted on a Waters mass spectrometer. NMR spectra were computed on a Bruker NMR spectrometer (500 MHz for 1H and 125 MHz for 13C), available at the Central Instrumental Center, University of the Ryukyus. All chemical shifts were reported relative to tetramethylsilane (TMS). Optical rotation was calculated in chloroform on a JASCO P-1010 polarimeter. There are two kinds of compounds were isolated and identified in this study. Soil nutrient contents were also measured where N and C by NC-220F (SUMIGRAPH Model, Sumika Analysis Services Ltd., Osaka, Japan) and rest nutrients by ICPE-9000 (ICP-AES Multitype ICP Emission Spectrometer, SHIMADZU, Kyoto, Japan).

Evaluation of biological activities of the compounds

The isolated compounds were dissolved in methanol to make the concentrations of 0.01, 0.03, 0.1, 0.3, 1, 3, 10, 30, 100, 300 and 1000 μM for each compound, in addition to 0.01, 0.03, 0.1, 0.3, 1, 3, 10, 30, 100 and 300 μM for a mixture of the two compounds at the ratio of 8:3, with the concentration the sum of the both phytochemicals. The biological activity against *L. sativum* and *E. oryzicola* seedlings was examined using the above procedure.

Statistical analysis

Linear regression was used to determine the relationship between the rates of materials (straw, extracts, and compounds) and their effects on the test plants, and Fisher's Protected Least Significant Difference test was used for mean separations. The experimental designs were completely randomized with triplicates. The Type I error was set at 0.05 and 0.01 for all statistical comparisons. The I_{50} (concentration of approximately 50% inhibition of the growth rate) value in the assays was calculated from the regression equation of the concentration curves.

Results

Pot studies

Residues of tested rice inhibited the growth parameters and dry matter of *E. oryzicola* at the highest amounts of 1.5 and 2 t ha^{-1}, whereas less straw incorporation had no effect (*Fig. 1*). In the second step of the pot studies, the growth and yield contributing parameters of 'Goria' rice were not significantly different between commercial fertilizer application and the combination of straw incorporation with commercial fertilizer (*Table 1*). However, positive responses were observed in the parameters for the combination of straw incorporation and commercial fertilizers, except for panicle length (*Fig. 2*). Based on the results of soil analysis after harvest, numerically highest amount of plant nutrients remained under the combination of straw incorporation and commercial fertilizers (*Table 2*).

http://www.aloki.hu ● ISSN 1589 1623 (Print) ● ISSN 1785 0037 (Online)
DOI: http://dx.doi.org/10.15666/aeer/1804_55475560

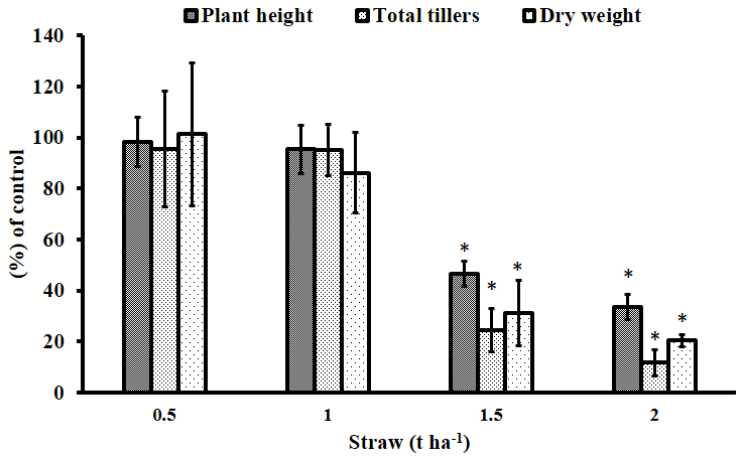

Figure 1. *Effect of straw incorporation on growth and dry weight of E. oryzicola. Bars represent ± SD of values obtained from three biological replicates. Asterisks indicate significant differences between the control and treatment: *P < 0.01*

Table 1. *Effect of allelopathic straw incorporation into the soil on growth and yield contributing parameters of Bangladesh indigenous rice variety 'Goria'*

Treatment	Plant height (cm)	Total tillers plant^{-1} (Nos.)	Effective tillers plant^{-1} (Nos.)	Panicle length (cm)	Total grain plant^{-1} (Nos.)	Filled grain percentage plant^{-1}	Thousand seed weight (g)
Control	87.67±2.52^{c}	5.33±0.58^{c}	2.67±0.58^{c}	18.33±1.53^{b}	49.26±7.76^{c}	46.91±9.74^{c}	17.98±0.21^{b}
Straw 2 t ha^{-1}	109.00±3.61^{b}	17.00±1.00^{b}	4.00±1.00^{b}	19.00±1.00^{b}	72.83±2.72^{b}	74.30±5.88^{b}	18.26±0.18^{b}
Chemical Fertilizer	117.67±2.52^{a}	25.67±1.53^{a}	8.33±1.53^{a}	20.73±0.64^{a}	89.60±2.11^{a}	96.03±2.36^{a}	20.09±0.70^{a}
Chemical fertilizer +Straw 2 t ha^{-1}	120.67±3.06^{a}	26.33±2.08^{a}	9.33±0.58^{a}	20.50±0.50^{a}	90.55±2.36^{a}	96.96±2.14^{a}	20.21±0.79^{a}

Means having similar letter(s) in a column are statistically similar and those having dissimilar letter(s) differ significantly at 0.01 level of probability

Figure 2. *Effect of Bangladesh indigenous rice variety 'Goria' straw incorporation on same rice variety*

http://www.aloki.hu ● ISSN 1589 1623 (Print) ● ISSN 1785 0037 (Online)
DOI: http://dx.doi.org/10.15666/aeer/1804_55475560

Table 2. *Effect of straw incorporation into the soil on plant nutrients in soil after rice harvest*

Treatment	Plant nutrients								
	C (%)	N	HPO_4^{2-}	K^+	Ca^{2+} (mg g^{-1} soil)	SO_4^{2-}	Mg^{2+}	Fe^{3+}	Zn^{2+}
Control	1.61±0.02	0.11±0.01	0.34±0.01	0.63±0.08	4.60±0.33	1.25±0.01	0.65±0.06	0.47±0.01	0.46±0.01
Straw 2 t ha^{-1}	1.77±0.12	0.13±0.01	0.42±0.13	0.74±0.08	5.01±0.34	1.38±0.15	0.70±0.06	0.64±0.30	0.47±0.03
Chemical fertilizer	1.87±0.06	0.14±0.01	0.36±0.02	0.67±0.09	4.72±0.19	1.40±0.04	0.63±0.07	0.47±0.01	0.45±0.01
Chemical fertilizer +straw 2 t ha^{-1}	2.23±0.01	0.16±0.01	0.36±0.02	0.73±0.05	4.53±0.30	1.47±0.33	0.70±0.06	0.48±0.01	0.45±0.01

Phytotoxic effects of aqueous methanol extracts

High concentrations of the aqueous methanol extracts inhibited the growth of the test species; whereas with very low concentrations (0.01 g DW equivalent per mL), stimulation or no effect on test species was observed (*Fig. 3A, B*). At 0.3 g DW equivalent extract per mL of rice plants, the root growth of *L. sativum* and *E. oryzicola* was 3 and 5% compared with that of the control root, respectively. At the same concentration, the shoot growth of *L. sativum* and *E. oryzicola* was 6 and 29% of control shoot growth, respectively. The obtained results reveal that the rice straw of 'Goria' may have potential growth inhibitory allelopathic substances.

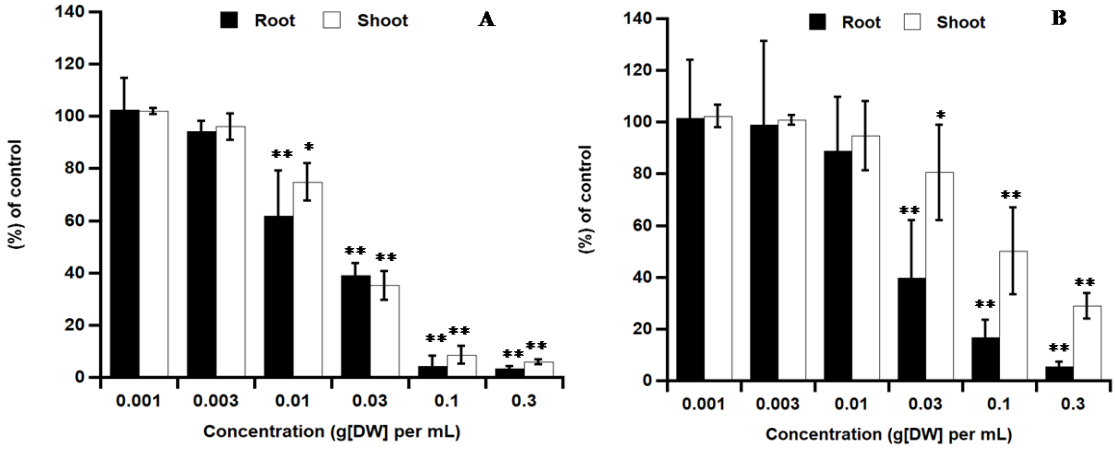

Figure 3. *Effect of aqueous methanol-extract of rice straw on root and shoot growth of L. sativum (A) and E. oryzicola (B). Bars represent ± SD of values obtained from three biological replicates. Asterisks indicate significant differences between the control and treatment: *P < 0.05; **P < 0.01*

Structural identification of isolated compounds

Two biologically active compounds were obtained from the repeated column chromatography of the aqueous methanol extracts of Bangladeshi rice straw variety 'Goria'.

Compound 1 (3.8 mg) had a molecular formula of $C_{11}H_{16}O_3$ (LR-ESI-MS *m/z* 197 $[M + H]^+$) and a specific rotation of $[\alpha]_D^{20}$ -68.8 (*c* 0.01, MeOH). The following were

http://www.aloki.hu ● ISSN 1589 1623 (Print) ● ISSN 1785 0037 (Online)
DOI: http://dx.doi.org/10.15666/aeer/1804_55475560

obtained for NMR spectra: ^{1}H-NMR (500 MHz, CD_3OD) δ: 1.27 (3H, s, H-9), 1.47 (3H, s, H-8), 1.53 (dd, J = 14.6 and 3.7 Hz, H-7), 1.78 (3H, s, H-10), 1.79 (dd, J = 13.5 and 4.1 Hz, H-5), 1.98 (dt, J = 14.5 and 2.6 Hz, H-7), 2.46 (dt, J = 14.1 and 2.6 Hz, H-5), 4.33 (m, H-6), 5.70 (s, H-3); and ^{13}C-NMR (125 MHz, CD_3OD) δ: 27.0 (C-10), 26.5 (C-9), 30.6 (C-8), 35.9 (C-4), 45.6 (C-7), 47.3 (C-5), 66.8 (C-6), 86.7 (C-7a), 112.9 (C-3), 171.9 (C-2), 182.4 (C-3a). These data were compared with the data reported by Park et al. (2004), and the compound was recognized as (-)-loliolide (*Fig. 4*).

Compound 2 (1.5 mg) had a molecular formula of $C_{13}H_{20}O_3$ (LR-ESI-MS *m/z* 225 $[M + H]^+$ and 247 $[M + Na]^+$) and a specific rotation of $[\alpha]_D^{25}$ -10.6 (*c* 0.01, $CHCl_3$). The following were obtained for NMR spectra: ^{1}H-NMR (400 MHz, $CDCl_3$) δ: 0.98 (s, H-11), 1.19 (s, H-12 and 13), 1.26 (m, H-2β), 1.64 (dd, J = 14.7 and 1.7 Hz, H-4α), 1.65 (dd, J = 14.4 and 8.6 Hz, H-2α), 2.28 (s, H-10), 2.39 (ddd, J = 14.4, 5.0 and 1.6 Hz, H-4β), 3.90 (m, H-3), 6.29 (d, J = 15.6 Hz, H-8), 7.03 (d, J = 15.6 Hz, H-7); and ^{13}C-NMR (100 MHz, $CDCl_3$) δ: 19.9 (C-13), 25.0 (C-11), 28.3 (C-10), 29.3 (C-12), 35.1 (C-1), 40.6 (C-4), 46.7 (C-2), 64.0 (C-3), 67.2 (C-5), 69.5 (C-6), 132.6 (C-8), 142.3 (C-7), 197.4 (C-9). Therefore, the structure was 3*β*-hydroxy-5*α*,6*α*-epoxy-7-megastigmen-9-one (*Fig. 4*), which corresponds with the data reported by Duan et al. (2002).

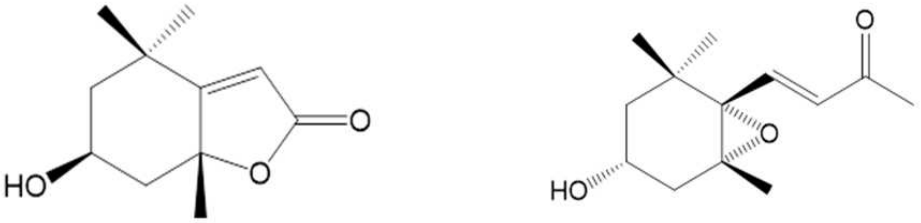

Compound **1**
(-)-Loliolide
Chemical Formula: $C_{11}H_{16}O_3$

Compound **2**
3*β*-hydroxy-5*α*,6*α*-epoxy-7-megastigmen-9-one
Chemical Formula: $C_{13}H_{20}O_3$

Figure 4. *Structures of isolated allelochemicals (-)-loliolide (Compound 1) and 3β-hydroxy-5α,6α-epoxy-7-megastigmen-9-one (Compound 2) from the Bangladeshi indigenous rice straw var. 'Goria'*

The endogenous concentrations of (-)-loliolide and 3*β*-hydroxy-5*α*,6*α*-epoxy-7-megastigmen-9-one were at least 8 and 3 μmol/kg, respectively, because 3.8 and 1.5 mg of the respective substances (MW 196 and 224, respectively) were isolated from 2.4 kg DW of rice straw. With decomposition of 1 kg of rice straw in 1 L of soil water, the concentration of (-)-loliolide and 3*β*-hydroxy-5*α*,6*α*-epoxy-7-megastigmen-9-one would be 8 and 3 μM, respectively.

Biological activity of compounds

Both identified compounds showed concentration and species-depended biological activities on seedling growth of test species (*Figs. 5A, B* and *6A, B*). The results demonstrated that significant inhibitory effects of (-)-loliolide began at concentrations as low as 10 μM on the root and shoot growth of *L. sativum* and at 10 and 30 μ*M* on the root and shoot growth of *E. oryzicola* seedlings, respectively. However, significant inhibitory effects of 3*β*-hydroxy-5*α*,6*α*-epoxy-7-megastigmen-9-one began at the

http://www.aloki.hu ● ISSN 1589 1623 (Print) ● ISSN 1785 0037 (Online)
DOI: http://dx.doi.org/10.15666/aeer/1804_55475560

concentrations 0.3 µM on the root and shoot growth of *L. sativum* and 0.3 and 1 µM on the root and shoot growth of *E. oryzicola* seedlings, respectively. The mixture effect of the two compounds at concentrations as low as 0.03 and 0.1, and 1 µM showed significant inhibition of the root and shoot growth of *L. sativum* and *E. oryzicola* seedlings (*Figs. 7* and *8*). Additionally, the inhibitory effects increased with increasing concentrations of the compounds. The concentrations causing approximately 50% growth inhibition in the assay (defined as I_{50}) for *L. sativum* roots and shoots were 28.23 and 53.4, 1.26 and 2.14, and 0.26 and 0.33 µM for (-)-loliolide, 3*β*-hydroxy-5*α*,6*α*-epoxy-7-megastigmen-9-one and their mixture, respectively. For *E. oryzicola* roots and shoots, the I_{50} values were 64.62 and 162.92, 43.28 and 137.64, and 2.31 and 17.86 µM for (-)-loliolide, 3*β*-hydroxy-5*α*,6*α*-epoxy-7-megastigmen-9-one and their mixture, respectively (*Table 3*).

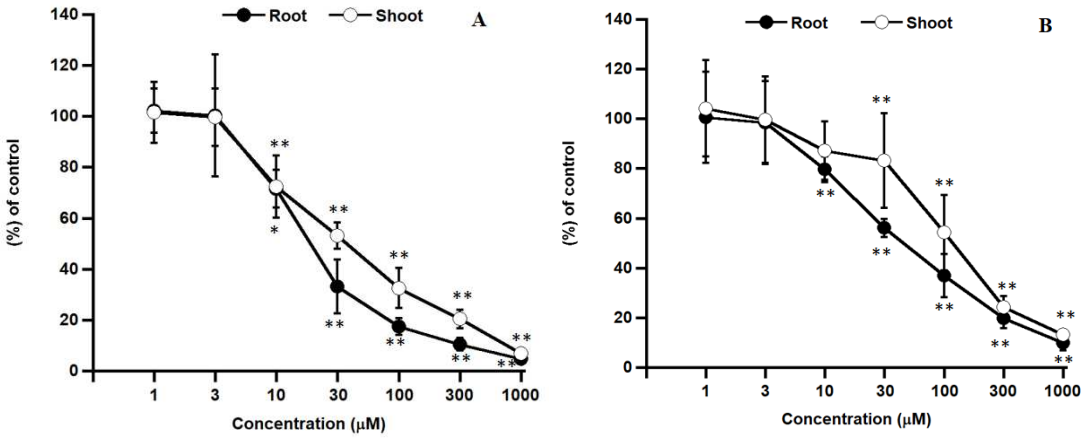

Figure 5. *Inhibition of root and shoot growth of L. sativum (A) and E. oryzicola (B) at different concentrations of (-)-loliolide. Bars represent ± SD of values obtained from three biological replicates. Asterisks indicate significant differences between the control and treatment: *P < 0.05; **P < 0.01*

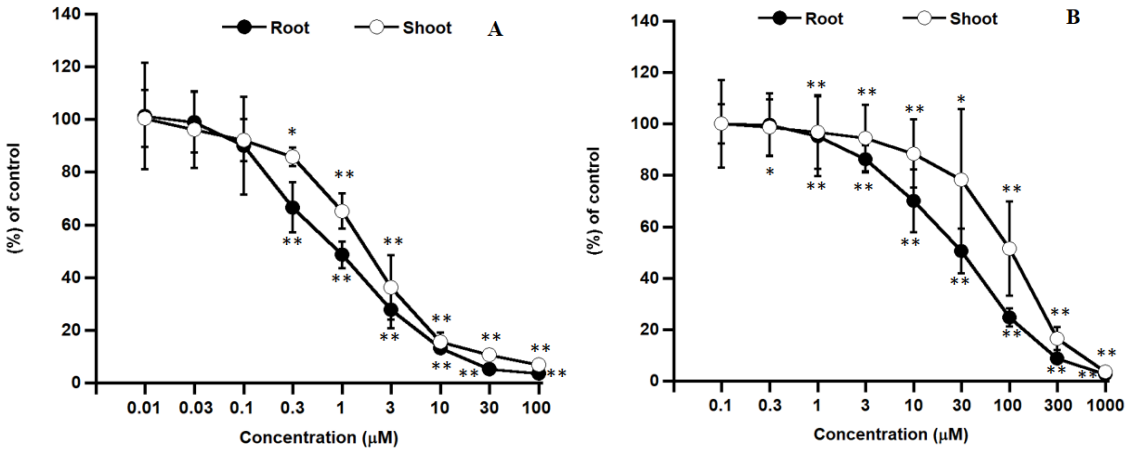

Figure 6. *Inhibition of root and shoot growth of L. sativum (A) and E. oryzicola (B) at different concentrations of 3β-hydroxy-5α,6α-epoxy-7-megastigmen-9-one. Bars represent ± SD of values obtained from three biological replicates. Asterisks indicate significant differences between the control and treatment: *P < 0.05; **P < 0.01*

http://www.aloki.hu ● ISSN 1589 1623 (Print) ● ISSN 1785 0037 (Online)
DOI: http://dx.doi.org/10.15666/aeer/1804_55475560

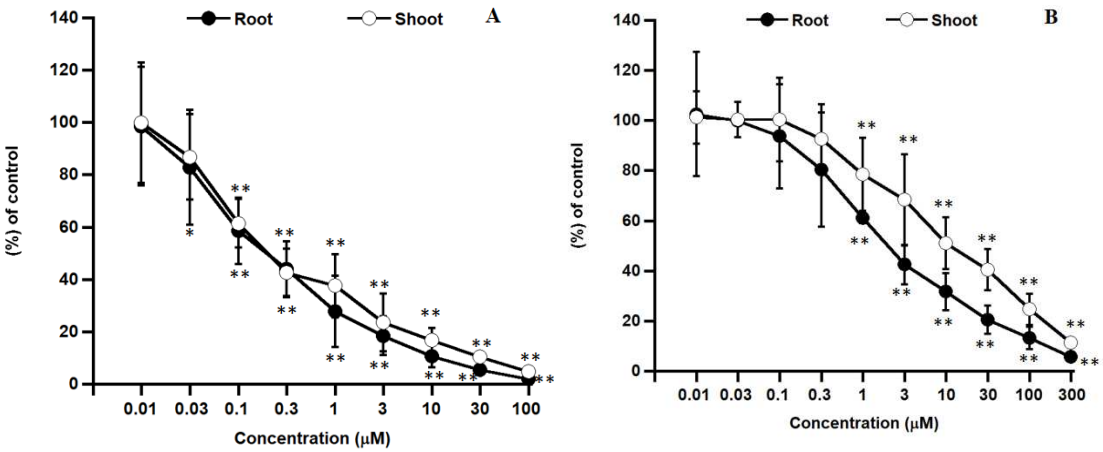

Figure 7. *Inhibition of root and shoot growth of L. sativum (A) and E. oryzicola (B) at different concentrations of (-)-loliolide and 3β-hydroxy-5α,6α-epoxy-7-megastigmen-9-one. The concentration of 100 μM represents 25 μM (-)-loliolide and 25 μM 3β-hydroxy-5α,6α-epoxy-7-megastigmen-9-one. Bars represent ± SD of values obtained from three biological replicates. Asterisks indicate significant differences between the control and treatment: *P < 0.05; **P < 0.01*

Table 3. *Regression analyses of dose response curves for effects on L. sativum and E. oryzicola growth at different concentrations of the isolated compounds and their mixture*

Test species	Compound	On root			On shoot		
		Regression equation	r^2	I_{50} (μM)	Regression equation	r^2	I_{50} (μM)
L. sativum	1	y = -0.502x + 64.17	0.729	28.23	y = -0.403x + 71.50	0.916	53.40
	2	y = -13.54x + 67.03	0.949	1.26	y = -17.49x + 87.46	0.970	2.14
	Mixture	y = -31.31x + 58.03	0.924	0.26	y = -21.41x + 57.14	0.644	0.33
E. oryzicola	1	y = -0.422x + 77.27	0.870	64.62	y = -0.202x + 82.91	0.932	162.92
	2	y = -0.467x + 70.21	0.946	43.28	y = -0.216x + 79.73	0.962	137.64
	Mixture	y = -12.96x + 79.89	0.922	2.31	y = -0.919x + 66.41	0.840	17.86

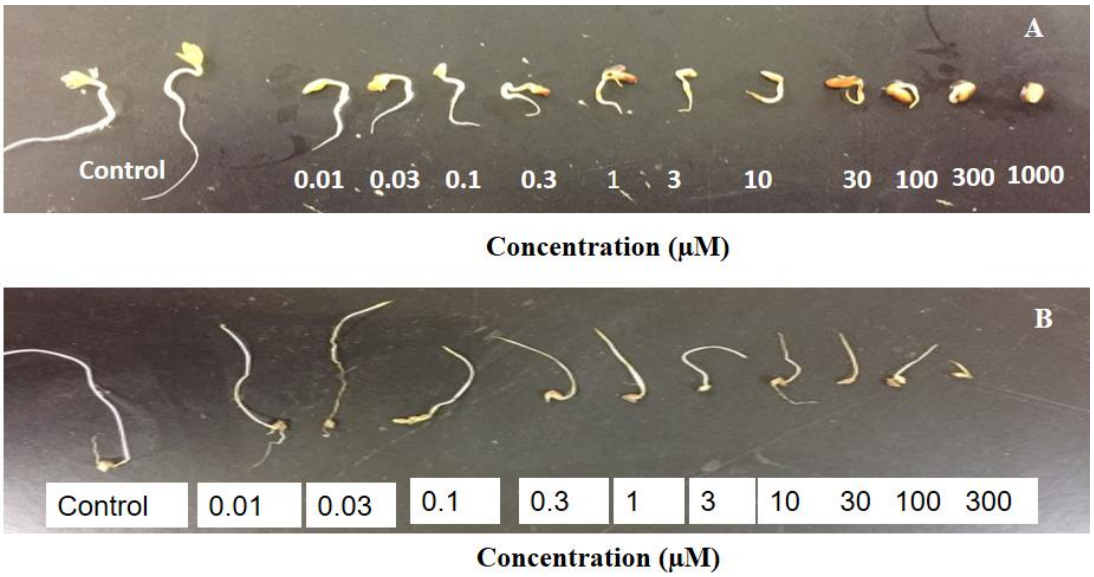

Figure 8. *Effect of (-)-loliolide and 3β-hydroxy-5α,6α-epoxy-7-megastigmen-9-one mixture at different concentrations on (A) L. sativum and (B) E. oryzicola seedlings*

http://www.aloki.hu ● ISSN 1589 1623 (Print) ● ISSN 1785 0037 (Online)
DOI: http://dx.doi.org/10.15666/aeer/1804_55475560

Discussion

The results described here clearly shown that 'Goria' rice straw was very toxic to *E. oryzicola* with significant reductions in seedling growth and dry weight. These results indicate that decomposing rice straw contained inhibitory substances that can reduce the growth of weeds. Kong et al. (2006) found that the weed growth reduction in rice straw incorporated soils through release of allelochemicals. A sharp increase of rice growth and yield parameters was observed in the rice culture in pot studies. Therefore, no autotoxicity effect on the growth and yield parameters of rice was found due to the incorporation of rice residues. The rice plant may develop adaptive mechanisms to avoid a severe autotoxic effect due to the surplus impact of disintegrating rice residues (Chou, 1980). Xuan et al. (2005) reported that incorporation of allelopathic rice straw at 1-2 t ha^{-1} decreased weed dry matter by about 70% and boosted rice yield by almost 20% compared with the respective controls. According to Dobermann and Fairhurst (2002), incorporation of rice straw by shallow tillage at the 5-10 cm depth has beneficial effects on soil fertility in intensive rice-rice systems, which include increased soil aeration during fallow periods, more complete carbon (C) turnover (approximately 50% of the C with 30-40 days), minimized negative effects (e.g., phytotoxicity) of the products of anaerobic decomposition on early rice growth, amplified N mineralization and soil P release to the next crop, and lessened weed growth. Moreover, results of rice straw incorporation are very encouraging since it helps in buildup of organic carbon (Nagargade et al., 2018). The aqueous methanol extract of Bangladeshi indigenous rice 'Goria' straw reduced the root and shoot growth of the test plant species, and with increases in the concentration of the extract, the inhibition increased. Xiao et al. (2020) demonstrated that allelopathic rice straw extract exerted inhibition effects on lettuce (*Lactuca sativa* Linn.) seed germination. Kawther et al. (2006) reported that rice straw extract potentially controlled *E. crus-galli* and *E. colona*. Anuar et al. (2015) also found that the radicle length of *E. crus-galli* was significantly reduced in the increased extract concentration of rice straw. In our studies, both stimulatory and inhibitory effects were found. Duke (2015) reported that allelopathic activity could have stimulatory results at a low concentration and an inhibitory effect at a high concentration depending on the allelopathic compounds. Inderjit and Duke (2003) also found different allelopathic responses for asymmetrical test plants due to the different selectivity of allelopathic substances. Grabarczyk et al. (2015) noted that (-)-loliolide inhibited the development of certain plants, and Islam et al. (2017) also found that loliolide reduced the seedling growth of *E. crus-galli*. Duan et al. (2002) isolated 3*β*-hydroxy-5*α*,6*α*-epoxy-7-megastigmen-9-one from *Saussurea medusa* as an immunosuppressive constituent. Masum et al. (2018) found that 3*β*-hydroxy-5*α*,6*α*-epoxy-7-megastigmen-9-one inhibited the radicle growth of *E. crus-galli*. Lu et al. (2011) isolated (-)-loliolide and 3*β*-hydroxy-5*α*,6*α*-epoxy-7-megastigmen-9-one from *Gracilaria lemaneiformis* and described their allelopathic potential on the alga *Skeletonema costatum*. Growth inhibition of test species increased significantly with the mixture of the two compounds compared with the inhibition of the individual compounds. Chotsaeng et al. (2017) reported that allelopathic effects depend on the concentrations, the combination of phytotoxins and sensitivity of flora and suggested that allelopathic compound mixtures could collectively reach sufficiently high concentrations to be bioactive on weeds. Hence, verified allelochemicals could be leads for new herbicide innovation efforts (Kong et al., 2019).

http://www.aloki.hu ● ISSN 1589 1623 (Print) ● ISSN 1785 0037 (Online)
DOI: http://dx.doi.org/10.15666/aeer/1804_55475560

Conclusion

Bangladesh indigenous allelopathic rice 'Goria' straw incorporation into the soil gave inhibitory effects on the growth and dry weight of *E. oryzicola* but had no autotoxicity on the growth of rice variety. Isolated two biologically active compounds from straw extracts, (-)-loliolide and 3*β*-hydroxy-5*α*,6*α*-epoxy-7-megastigmen-9-one had a strong synergistic inhibitory effect on the growth of tested weed. Thus, our current work suggests that Bangladesh indigenous rice straw variety 'Goria' could be useful in multidisciplinary approaches for suppressing weeds and/or decreasing the synthetical quantities and for soil nutrient improvement. Overall, based on such studies, the use of rice residues for overcoming weeds problem in crop production might be considered as a noteworthy accomplishment for the retrieving of straw in rice growing countries such as Bangladesh, which will be displayed in reductions of the effects of environmental pollution. These results also provide fundamental information for developing natural herbicides.

Acknowledgements. The authors acknowledge the Ministry of Education, Culture, Sports, Science and Technology (MEXT), Japan for providing scholarship to the first author.

Conflict of interests. The authors declare no conflict of interests.

REFERENCES

[1] Amb, M. K., Ahluwalia, A. S. (2016): Allelopathy: potential role to achieve new milestones in rice cultivation. – Rice Science 23: 165-183.

[2] Anuar, F. D. K., Ismail, B. S., Ahmad, W. J. W. (2015): Allelopathy effect of rice straw on the germination and growth of *Echinochloa crus-galli* (L.) P. Beauv. – AIP Conference Proceedings 1678: 020014.

[3] Anwar, T., Ilyas, N., Qureshi, R., Qureshi, H., Gilani, N., Khan, S., Khan, S. A., Fatimah, H., Waseem, M., Maqsood, M. (2019): Evaluation of phytotoxic potential of selected plants against weeds. – Applied Ecology and Environmental Research 17: 12683-12696.

[4] BBS (Bangladesh Bureau of Statistics) (2017): Year book of agricultural statistics-2016. – http://bbs.portal.gov.bd/sites/default/files/files/bbs.portal.gov.bd/page/1b1eb817_9325_4354_a756_3d18412203e2/Yearbook-2016-Final-19-06-2017.pdf. Accessed 6 July 2017.

[5] Cao, N. Y., Wang, P., Kong, C. H. (2008): Effects of lignin from allelopathic and non-allelopathic rice straws on *Echinocholoa crus-galli* and soil microorganisms. – Allelopathy Journal 22: 397-402.

[6] Cheema, Z. A., Khaliq, A., Saeed, S. (2004): Weed control in maize (*Zea mays* L.) through sorghum allelopathy. – Journal of Sustainable Agriculture 23: 73-86.

[7] Chotsaeng, N., Laosinwattana, C., Charoenying, P. (2017): Herbicidal activities of some allelochemicals and their synergistic behaviors toward *Amaranthus tricolor* L. – Molecules 22: 1841.

[8] Chou, C. H. (1980): Allelopathic researches in subtropical vegetation in Taiwan. – Comparative Physiology and Ecology 5: 222-234.

[9] Chung, I. M., Ahn, J. K., Yun, S. J. (2001): Identification of allelopathic compounds from rice (*Oryza sativa* L.) straw and their biological activity. – Canadian Journal of Plant Science 81: 815-819.

[10] Chung, I. M., Kim, S. H., Oh, Y. T., Ali, M., Ahmed, A. (2017): New constituents from *Oryza sativa* L. straw and their algicidal activities against blue-green algae. – Allelopathy Journal 40: 47-62.

http://www.aloki.hu ● ISSN 1589 1623 (Print) ● ISSN 1785 0037 (Online)
DOI: http://dx.doi.org/10.15666/aeer/1804_55475560

[11] Dayan, F. E., Cantrell, C. L., Duke, S. O. (2009): Natural products in crop protection. – Bioorganic & Medicinal Chemistry 17: 4022-4034.
[12] Dobermann, A., Fairhurst, T. H. (2002): Rice Straw Management. – In: Armstrong, D. L., Griffin, K. P (eds.) Better Crops International. Vol 16. International Plant Nutrition Institute, Saskatchewan, pp. 7-11.
[13] Duan, H., Takaishi, Y., Momota, H., Ohmoto, Y., Taki, T. (2002): Immunosuppressive constituents from *Saussurea medusa*. – Phytochemistry 59: 85-90.
[14] Duke, S. O. (2015): Proving allelopathy in crop–weed interactions. – Weed Science 63: 121-132.
[15] Erisman, J. W., Sutton, M. A., Galloway, J., Klimont, Z., Winiwarter, W. (2008): How a century of ammonia synthesis changed the world. – Nature Geoscience 1: 636-639.
[16] Grabarczyk, M., Winska, K., Mączka, W., Potaniec, B., Aniol, M. (2015): Loliolide - the most ubiquitous lactone. – Folia Biologica et Oecologica 11: 1-8.
[17] Han, X., Cheng, Z. H., Meng, H. W., Yang, X. L., Ahmad, I. (2013): Allelopathic effect of decomposed garlic (*Allium sativum* L.) stalk on lettuce (*L. sativa* var. *crispa* L.). – Pakistan Journal of Botany 45: 225-233.
[18] Inderjit, Duke, S. O. (2003): Ecophysiological aspects of allelopathy. – Planta 217: 529-539.
[19] Inderjit, Rawat, D. S., Foy, C. L. (2004): Multifaceted approach to determine rice straw phytotoxicity. – Canadian Journal of Botany 82: 168-176.
[20] Islam, M. S., Iwasaki, A., Suenaga, K., Kato-Noguchi, H. (2017): Isolation and identification of two potential phytotoxic substances from the aquatic fern *Marsilea crenata*. – Journal of Plant Biology 60: 75-81.
[21] Jabran, K., Mahajan, G., Sardana, V., Chauhan, B. S. (2015): Allelopathy for weed control in agricultural systems. – Crop Protection 72: 57-65.
[22] Kato-Noguchi, H., Salam, M. A., Suenaga, K. (2011): Isolation and identification of potent allelopathic substances in a traditional Bangladeshi rice cultivar Kartikshail. – Plant Production Science 14: 128-134.
[23] Kato-Noguchi, H., Tamura, K., Sasaki, H., Suenaga, K. (2012): Identification of two phytotoxins, blumenol A and grasshopper ketone, in the allelopathic Japanese rice variety Awaakamai. – Journal of Plant Physiology 169: 682-685.
[24] Kawther, G. E. R., El-Shahawy, T. A., Sharara, F. A. (2006): New approach to use rice straw waste for weed control. II. The effect of rice straw extract and Fusilade (herbicide) on some weeds infesting soybean (*Glycin max* L.). – International Journal of Agriculture & Biology 8: 269-275.
[25] Khanh, T. D., Cong, L. C., Xuan, Y., Uezato, Y., Deba, F., Toyama, T., Tawata, S. (2009): Allelopathic plants: 20 hairy beggarticks (*Bidens pilosa* L.). – Allelopathy Journal. 24: 243-254.
[26] Kong, C. H., Li, H. B., Hu, F., Xu, X. H., Wang, P. (2006): Allelochemicals released by rice roots and residues in soil. – Plant and Soil. 288: 47-56.
[27] Kong, C. H., Xuan, T. D., Khanh, T. D., Tran, H. D., Trung, N. T. (2019): Allelochemicals and signaling chemicals in plants. – Molecules 24: 2737.
[28] Kraehmer, H., Jabran, K., Mennan, H., Chauhan, B. S. (2016): Global distribution of rice weeds — a review. – Crop Protection 80: 73-86.
[29] Lu, H., Xie, H., Gong, Y., Wang, Q., Yang, Y. (2011): Secondary metabolites from the seaweed *Gracilaria lemaneiformis* and their allelopathic effects on *Skeletonema costatum*. – Biochemical Systematics and Ecology 39: 397-400.
[30] Lund, M. C., Carter, P. R., Oplinger, E. S. (1993): Tillage and crop rotation affect corn, soybean and winter wheat yields. – Journal of Production Agriculture 6: 425-431.
[31] Masum, S. M., Hossain, M. A., Akamine, H., Sakagami, J. I., Bhowmik, P. C. (2016): Allelopathic potential of indigenous Bangladeshi rice varieties. – Weed Biology and Management 16: 119-131.

http://www.aloki.hu ● ISSN 1589 1623 (Print) ● ISSN 1785 0037 (Online)
DOI: http://dx.doi.org/10.15666/aeer/1804_55475560

[32] Masum, S. M., Hossain, M. A., Akamine, H., Sakagami, J. I., Ishii, T., Gima, S., Kensaku, T., Bowmik, P. C. (2018): Isolation and characterization of allelopathic compounds from the indigenous rice variety 'Boterswar' and their biological activity against *Echinochloa crus-galli* L. – Allelopathy Journal 43: 31-42.
[33] Nagargade, M., Singh, M. K., Tyagi, V. (2018): Ecologically sustainable integrated weed management in dry and irrigated direct-seeded rice. – Advances in Plants & Agriculture Research 8: 319-331.
[34] Park, K. E., Kim, Y. A., Jung, H. A., Lee, H. J., Ahn, J. W., Lee, B. J., Seo, Y. (2004): Three norisoprenoids from the brown alga *Sargassum thunbergii*. – Journal of the Korean Chemical Society 48: 394-398.
[35] Rahman, M. A., Chikushi, J., Safizzaman, M., Lauren, J. G. (2005): Rice straw mulching and nitrogen response of no-till wheat following rice in Bangladesh. – Field Crops Research 91: 71-81.
[36] Ramakrishna, A., Hoang, M. T., Wani, S. P., Tranh, D. L. (2006): Effect of mulch on soil temperature, moisture, weed infestation and yield of groundnut in northern Vietnam. – Field Crops Research 95: 115-125.
[37] Schreiber, M. M. (1992): Influence of tillage, crop rotation, and weed management on giant foxtail population dynamics and corn yield. – Weed Science 40: 645-653.
[38] Weidenhamer, J. D., Callaway, R. M. (2010): Direct and indirect effects of invasive plants on soil chemistry and ecosystem function. – Journal of Chemical Ecology 36: 59-69.
[39] Weir, T. L., Park, S. W., Vivanco, J. M. (2004): Biochemical and physiological mechanisms mediated by allelochemicals. – Current Opinion in Plant Biology 7: 472-479.
[40] Weston, L. A., Duke, S. O. (2003): Weed and crop allelopathy. – Critical Reviews in Plant Sciences 22: 367-389.
[41] Xiao, Z., Zou, T., Lu, S., Xu, Z. (2020): Soil microorganisms interacting with residue-derived allelochemicals effects on seed germination. – Saudi Journal of Biological Sciences 27: 1057-1065.
[42] Xuan, T. D., Shinkichi, T., Khanh, T. D., Min, C. I. (2005): Biological control of weeds and plant pathogens in paddy rice by exploiting plant allelopathy: an overview. – Crop Protection 24: 197-206.
[43] Yang, X. F., Kong, C. H. (2017): Interference of allelopathic rice with paddy weeds at the root level. – Plant Biology 19: 584-591.

http://www.aloki.hu ● ISSN 1589 1623 (Print) ● ISSN 1785 0037 (Online)
DOI: http://dx.doi.org/10.15666/aeer/1804_55475560

ASSESSING GENETIC DIVERSITY AND DEMOGRAPHIC HISTORY OF THE MANCHURIAN WAPITI (*CERVUS CANADENSIS XANTHOPYGUS*) POPULATION IN THE GAOGESITAI, INNER MONGOLIA, CHINA

TIAN, X. M.[1,2] – YANG, M.[1] – ZHANG, M. H.[1] – WANG, X. L.[1*]

[1]*College of Wildlife and Protected Area, Northeast Forestry University, Harbin 150040, China*

[2]*College of Life Science and Technology, Mudanjiang Normal University, Mudanjiang 157011, China*

[*]*Corresponding author*
e-mail: yttuhh@yeah.net; phone: +86-138-3614-2920

(Received 30th Mar 2020; accepted 10th Jul 2020)

Abstract. This paper attempts to assess the genetic diversity and demographic history of the Manchurian wapiti (MW) population in the Gaogesitai region of Inner Mongolia, Northeast China. To this end, a survey was conducted on 108 stool samples collected in the Gaogesitai region. Then, the mitochondrial cytochrome b and 10 microsatellite loci were used to perform the species identification and individual identification, and 49 MW individuals were found. Besides, the cytochrome *b*, control region and microsatellites were also analyzed to obtain the genetic data of the MWs. The analysis found that the MW population in the Gaogesitai region experienced a recent bottleneck effect, but it did not have a significant impact on the subsequent rapid population growth; the population genetic diversity is at a medium level; gene exchange between individuals within the population is frequent, and there is no inbreeding; a high proportion (50%) of rare haplotypes in the population was detected. Thus, it is recommended to strengthen the protection and management of the MW population in this region to avoid a sharp decline in population genetic diversity.
Keywords: *genetic diversity, bottleneck, inbreeding, reintroduction, microsatellites, mitochondrial DNA, Cervus canadensis xanthopygus*

Introduction

The Manchurian wapiti distributed in Northeast China is a Class II wild animal under special state protection in China (Wang, 1998) and also the main prey of the world's most endangered species, the Siberian Tiger (*Panthera tigris altaica*) and Northeast Leopard (*Panthera pardus orientalis*) (Li et al., 2001; Qi et al., 2015). Due to habitat fragmentation and illegal poaching, the abundance and distribution area of the MWs have been on a decline, and some small subpopulations in the isolated area have been formed (Xu et al., 2000; Zhang and Zhang, 2011; Zhou et al., 2015). The Wandashan area was once the highest density distribution area of the MWs in Heilongjiang Province (Chen et al., 1997), but the population in this area is now on the verge of extinction (Tian et al., 2019). Since the establishment of a nature reserve at the end of the twentieth century in the south of the Greater Khingan Range in the Gaogesitai region of Inner Mongolia, the MW population has been effectively protected. A 2007-2008 survey found that the average density of the MW in this area was 1.1/km^2, with a population of nearly a thousand (Zhang et al., 2009). In the past ten years, the number has been increasing, and it is currently the region with the highest population density of wild MWs (Zhang, 2016). Therefore, this area can provide important germplasm resources for the rejuvenation of the wild MW population and the reconstruction of historical distribution areas.

http://www.aloki.hu ● ISSN 1589 1623 (Print) ● ISSN 1785 0037 (Online)
DOI: http://dx.doi.org/10.15666/aeer/1804_55615575

Population genetic diversity and demographic history are important indicators of species survival and utilization (Haig et al., 1990; Pinilla et al., 2018; Sinnett et al., 2018; Randone et al., 2019). Research on the conservation genetics of the MW mainly focused on the Wandashan region of Heilongjiang Province (Tian and Zhang, 2010; Tian et al., 2010, 2019; Zhang et al., 2010). The MWs in the Gaogesitai region have been studied only in quantitative surveys, intestinal parasite detection, nutrition adaptation strategies, and habitat evaluation (Zhang et al., 2009; Tao and Yan, 2014; Huang, 2015; Zhang, 2016). Therefore, using the mtDNA cytochrome *b*, control region and nuclear DNA microsatellite as molecular markers, this paper explores the genetic diversity and demographic history of the MW population in the Gaogesitai region of Inner Mongolia. This study shall provide basis for the scientific protection and management of the MWs.

Materials and methods

Survey area and sample collection

Inner Mongolia Gaogesitai-Hanwula National Nature Reserve is located at the southern foot of the Greater Khingan Range, north of Alukeerqin Banner, Chifeng City, Inner Mongolia. It has geographical coordinates 44°41′03″-45°08′44″ N, 119°03′30″-119°39′08″ E, with a total area of 1,062.8 km^2 (*Fig. 1*). The area belongs to the middle and low mountains and hilly valley terrain, with an altitude of 900-1500 m. It is in a middle temperate and semi-arid continental monsoon climate zone, with the annual average temperature of 3.8℃, the frost-free period of 115 d, the annual precipitation 437.3 mm, the annual evaporation 1958.1 mm, and a long and cold winter. Winter is from December to February of the following year, with the average temperature of -7.5-15.0℃. January is the coldest, with the average temperature of -16℃, the extreme low temperature of -42℃. In winter, the average snow cover of 30 d, and the longest snow cover of 100 d. The reserve is located in the northeast, north China, and Inner Mongolia-Xinjiang intersection area, as a typical forest-grassland interlaced zone. The diverse plant resources provide suitable habitat conditions for the MWs.

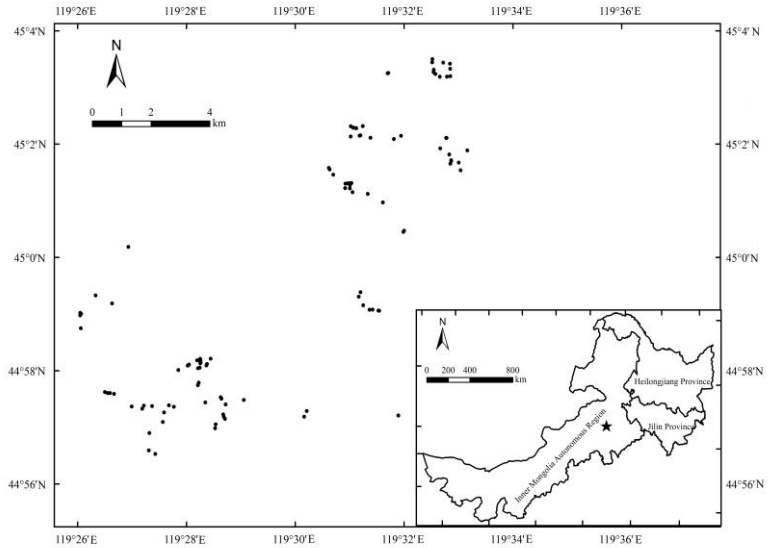

Figure 1. *Sampling location of the Manchurian wapiti in the Gaogesitai, Inner Mongolia, China*

http://www.aloki.hu ● ISSN 1589 1623 (Print) ● ISSN 1785 0037 (Online)
DOI: http://dx.doi.org/10.15666/aeer/1804_55615575

During the winter of 2017 and 2018, stools of wild MWs were collected from the entire area of the reserve as samples. The stools were found along the fresh footprint chain of the wapiti on the snow, and placed in a sealed bag for GPS (G120BD, UniStrong Inc., China) positioning. Then, another fresh footprint chain was selected for further sampling. A total of 108 stool samples were collected (*Table A1*), and stored frozen at -20℃.

DNA extraction and species identification

Stool DNA was extracted using the QIAamp DNA Stool Mini Kit (Qiagen, Germany) according to the operating manual. Select mitochondrial cytochrome b primer L14724: 5 '-CGA GAT CTG AAA AAC CAT CGT TG-3'; H15149: 5 '-AAA CTG CAG CCC CTC AGA ATG ATA TTT GTC CTC A-3' (Kocher et al., 1989; Irwin et al., 1991) for PCR amplification of stool DNA. Amplification system 50 μl: 1 U/μl KOD FX Neo DNA polymerase (Toyobo, Japan) for 1 μl, 2 × Buffer for KOD FX Neo 25 μl, 2 mmol/L dNTPs 10 μl, 10 μmol/L L14724, H15149 1.5 each μl, 10-30 ng/μl DNA 2 μl, and PCR grade water (Tiangen, China) 9 μl. Reaction conditions: pre-denaturation at 94°C for 2 min; denaturation at 98°C for 10, annealing at 59°C for 30 s, extension at 68°C for 30 s, 35 cycles; then, extension at 68°C for 10 min, and storage at 4°C. The PCR products were sent to Shanghai Shengong Biological Company for purification and two-way sequencing. The SeqMan, MegAlign, and EditSeq programs in DNAStar software (DNAStar Inc., America) were used for splicing, alignment, and correction of the forward and reverse sequences. Finally, a Blast comparison was performed in the NCBI database to determine the species source of the stools.

Individual identification and mitochondrial control region amplification

10 pairs of microsatellite primers (T507, T530, T501, C143, T156, BM848, N, OCAM, DM45, ETH225) were obtained from published research results and adapted for application to wapiti (Tian et al., 2010; Zhang, 2010; Hu et al., 2018; Yang et al., 2019). The primers were used to identify the individual DNA of the MW stool, and the 5' end of the upstream primer in each microsatellite locus was fluorescently labeled (*Table 1*). Amplification system 20 μl: 1 U/μl KOD FX Neo DNA polymerase (Toyobo, Japan) for 0.4 μl, 2 × Buffer for KOD FX Neo 10 μl, 2 mmol/L dNTPs 4 μl, 10 μmol/L upstream and downstream primers 0.6 μl each, 10-30 1 μl of ng/μl DNA 1 μl, and PCR grade water (Tiangen, China) 4 μl, while other reaction conditions were the same as the method of species identification. A multi-tube PCR amplification protocol was used, with 3 to 7 positive PCR amplifications per locus to determine the final genotype (Taberlet et al., 1996). The 10 loci were divided into two detection systems: T507, T530, T501, C143, and T156 loci; BM848, N, OCAM, DM45, and ETH225 loci. The mixed PCR products were scanned on the ABI 3730XL sequencer (Applied Biosystems Inc., America) and allele sizes were read. The software Excel microsatellite tool kit (Park, 2001) was used to find matching genotypes in the data. The principles for judging that different samples come from the same individual are: 1) The genotypes are the same at all loci; 2) Only one allele at one locus varies (Bellemain et al., 2005). When using primers L-Pro: CGT CAG TCT CAC CAT CAA CCC CCA AAG C; H-Phe: GGG AGA CTC ATC TAG GCA TTT TCA GTG (Douzery and Randi, 1997) to amplify the entire sequence of stool DNA mitochondrial control region of different individuals at the annealing temperature of 55℃, the amplification system and other amplification conditions are the same as the species identification method. All primer synthesis and sequencing were completed by Shanghai Biotech Biotechnology.

http://www.aloki.hu ● ISSN 1589 1623 (Print) ● ISSN 1785 0037 (Online)
DOI: http://dx.doi.org/10.15666/aeer/1804_55615575

Table 1. *Details of 10 microsatellite loci used for the study*

Locus	Primer sequence (5'-3')	Allele length (bp)	Repeat type	Annealing temperature (℃)
T507[1]	F: aggcagatgcttcaccatc R: tgtggagcacctcacacat	144 - 176	4	56.6
T530[1]	F: gtcctcacagcagctctatg R: gcattctttagaactccaactg	244 - 292	4	55
T501[2]	F: ctcctcattattaccctgtgaa R: acatgctttgaccaagacc	238 - 262	4	55
C143[2]	F: aaggagtctttcagttttgaga R: ggttctgtctttgcttgttg	152 - 164	4	54
T156[4]	F: tcttcctgacctgtgtcttg R: gatgaatacccagtcttgtctg	135 - 207	4	56.5
BM848[2]	F: tggttggaaggaaaacttgg R: cctctgctcctcaagacac	350 - 366	2	54.5
N[3]	F: tccagagaagcaaccaatag R: gtgtgccttaaacaacctgt	282 - 290	4	56
OCAM[4]	F: cctgactataatgtacagatccctc R: gcagaatgactaggaaggatggca	178 - 194	2	54
DM45[4]	F: caccgtttcttacaatctca R: aggggtcaggttctcagtttctac	440 - 460	2	55.5
ETH225[2]	F: gatcaccttgccactatttcct R: acatgacagccagctgctact	133 - 185	2	56

[1]Fam, [2]Hex, [3]Tamra, [4]Rox

Data analysis

Clustal X 2.1 software (Larkin et al., 2007) was used to align the sequence of mitochondrial cytochrome b and control region in different individuals. DnaSP 5.10 software (Librado and Rozas, 2009) was applied to calculate the number of mutation sites (S), number of haplotypes (H), haplotype diversity (H_d), and nucleotide diversity (P_i), calculate the Tajima's D and Fu's Fs in the detection of neutral selection, and performs a significant test. Network 4.6 (Bandelt et al., 1999) was used to construct a median-joining network, and analyze the evolutionary relationship between haplotypes.

In addition, Microchecker 2.2.3 (van Oosterhout et al., 2004) was used to detect microsatellite loci for invalid alleles or allele deletions. Gimlet 1.3.3 (Valière, 2002) was to evaluate the individual identification probability P (ID) of 10 microsatellite loci. The software GenAlEx 6.0 (Peakall and Smouse, 2006) calculated the number of alleles (N_a), the number of effective alleles (N_e), the observed heterozygosity (H_o), the expected heterozygosity (H_e), and the fixed coefficient (F_{is}). The Excel microsatellite tool kit (Park, 2001) was applied to calculate the polymorphic information content (*PIC*). The software Genepop 4.0 (Raymond and Rousset, 1995) was to measure whether the population and each locus were in line with Hardy-Weinberg equilibrium, and also tested the linkage disequilibrium between each locus. The Markov chain method was used in the probability test, setting the parameters to 10,000 de-memorization, 20 batches, and 5,000 iterations. Hardy-Weinberg equilibrium and linkage disequilibrium tests all used the Bonferroni method to correct the significance. Bottleneck 1.2 (Piry et al., 1999) tested whether the population has recently experienced bottleneck effects. The Wilcoxon test was performed under a two-phase model (TPM) and a stepwise mutation model (SMM), and repeated 1,000 times, of which TPM is considered the most suitable model for microsatellite analysis (Ellegren, 2004). This is because TPM selected 79% of the mutations to comply with SMM, and the coefficient of variation was 9% (Piry et al., 1999). Structure 2.3.4 (Pritchard et al., 2000) was to analyze the genetic structure of the population, with the

http://www.aloki.hu ● ISSN 1589 1623 (Print) ● ISSN 1785 0037 (Online)
DOI: http://dx.doi.org/10.15666/aeer/1804_55615575

parameters setting of Length of Burn-in Period 100,000, Number of MCMC Reps after Burn-in 10,000, K = 1-6, Number of Iterations 20. The calculation results were uploaded to Structure Harvester Web v0.6.94 (Earl and von Holdt, 2012) for analysis, and the grouping number K of population genetic structure was determined according to the maximum peak value of the Ln Pr (X|*K*) curve.

Results

Species identification and individual identification

The amplification products (425 bp) of Mitochondrial cytochrome b were successfully obtained in 96 of 108 stool samples. The species identification results confirmed that all 96 stool samples were from the MWs. The individual discrimination rate of 10 microsatellite loci was very high. The probability that two random individuals have the same genotype is Prod (unbias) $=1.219 \times 10^{-10}$. Even in the case of full sibs, the probability of misjudgment Prod (sibs) is only 0.033% (*Fig. 2*). The results of individual identification showed that 96 stool samples belonged to 49 individuals. Ten microsatellite loci were detected by Microchecker, to find no invalid alleles or allele deletions. The Hardy-Weinberg equilibrium test showed that the 10 microsatellite loci and the entire population met the Hardy-Weinberg equilibrium, and the fixed coefficient F_{is} values did not significantly deviate from zero (*Table 2*). The probability value of linkage disequilibrium test was corrected by Bonferroni's method, which indicated no linkage disequilibrium among 10 microsatellite loci.

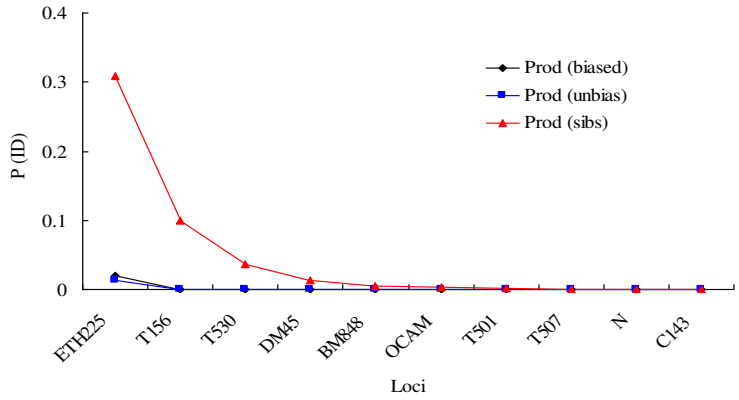

Figure 2. *Decrease in probability of identity, P (ID), for wapiti genotypes as more microsatellite loci were added*

Mitochondrial DNA sequence analysis

A total of 4 mutation sites were found in 49 mitochondrial cytochrome b sequences (425 bp), including 3 transition sites and 1 transversion site. No insertion or deletion sites were found. The nucleotide base of the sequence was composed of A, T, C, and G, with the contents of 31.9%, 29.9%, 23.7%, and 14.6%, respectively. 4 haplotypes were detected. Among 49 individuals, the distribution frequencies of haplotypes Hap1-Hap4 were 55.1%, 2.0%, 2.0%, and 40.8% (*Table 3* and *Fig. 3*).

http://www.aloki.hu ● ISSN 1589 1623 (Print) ● ISSN 1785 0037 (Online)
DOI: http://dx.doi.org/10.15666/aeer/1804_55615575

Table 2. *Variability parameters for the 10 microsatellite loci used in 49 individuals of the Manchurian wapiti*

Locus	N_a	N_e	*PIC*	H_o	H_e	F_{is}	P_{HW}
T507	6	2.349	0.520	0.551	0.574	0.041	0.242
T530	10	5.231	0.786	0.735	0.809	0.092	0.583
T501	5	2.813	0.600	0.735	0.645	-0.140	0.777
C143	4	1.415	0.261	0.347	0.293	-0.183	0.704
T156	11	7.646	0.855	0.857	0.869	0.014	0.076
BM848	7	3.515	0.679	0.714	0.716	0.002	0.745
N	3	1.476	0.287	0.265	0.323	0.178	0.189
OCAM	6	3.210	0.637	0.703	0.688	-0.022	0.575
DM45	9	4.450	0.751	0.714	0.775	0.079	0.061
ETH225	17	9.434	0.885	0.918	0.894	-0.027	0.595
All	7.8	4.154	0.626	0.654	0.659	-0.040	0.407

N_a: number of alleles found; N_e: effective number of alleles; *PIC*: polymorphism information content; H_o: observed heterozygosity; H_e: expected heterozygosity; F_{is}: fixation index; P_{HW}: probability of Hardy-Weinberg equilibrium test

Table 3. *Genetic variability at the mitochondrial cytochrome b (cyt b) and control region (CR) in the Manchurian wapiti population*

	N	*S*	*H*	H_d	P_i (%)	Tajima's D	Fu's Fs
Cyt *b*	49	4	4	0.540 ± 0.036	0.359 ± 0.106	1.601	2.169
CR	27	28	4	0.385 ± 0.108	0.805 ± 0.243	0.510	10.573**

N: number of animal individuals; *S*: number of variable sites; *H*: number of haplotypes; H_d: haplotype diversity; P_i: nucleotide diversity; significant of neutrality tests based on Tajima's D and Fu's Fs (*$P < 0.05$; **$P < 0.01$)

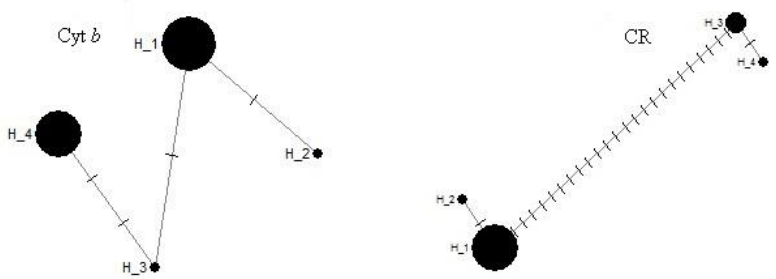

Figure 3. *The haplotype networks used the median-joining method at the mitochondrial cytochrome b (cyt b) and control region (CR) in the Manchurian wapiti population. The size of each circle represents the frequency of haplotypes. The nucleotide transitions and transversions are indicated by dashes*

Of the 49 individual samples, 27 obtained the complete sequence of mitochondrial control region (993 bp). A total of 28 mutation sites were found, including 25 transformation sites, 2 transversion sites, and 1 insertion/deletion site. The contents of A, T, C, and G were 30.2%, 31.8%, 22.2%, and 15.8%, respectively. 4 haplotypes were detected. Among 27 individuals, the distribution frequencies of haplotypes Hap1-Hap4 were 77.8%, 3.7%, 14.8%, and 3.7% (*Table 3* and *Fig. 3*).

http://www.aloki.hu ● ISSN 1589 1623 (Print) ● ISSN 1785 0037 (Online)
DOI: http://dx.doi.org/10.15666/aeer/1804_55615575

Genetic diversity

The haplotype diversity index (H_d) of the mitochondrial cytochrome b sequence was 0.540 ± 0.036, and the nucleotide diversity index (P_i) was 0.359 ± 0.106%. The H_d of the complete sequence in the mitochondrial control region was 0.385 ± 0.108, and the P_i was 0.805 ± 0.243% (*Table 3*). Microsatellite data indicates that the average number of alleles (N_a) in the population was 7.8 and the number of effective alleles (N_e) was 4.154, that is, the N_e at each locus is less than the N_a (P <0.05). The 10 microsatellite loci had a *PIC* of 0.626 (0.261-0.885). Except for loci C143 and N, the other 8 were highly polymorphic loci (*PIC*> 0.5). The expected heterozygosity (H_e) was 0.659 (0.293-0.894), and the average observed heterozygosity (H_o) was 0.654 (0.265-0.918) (*Table 2*).

Demographic history

The value of *K* at which ln Pr (X|*K*) is maximized is 1. For values $K > 1$ the ln Pr (X|*K*) dramatically decreases and the variance between independent run increases (*Fig. 4*). Based on this, there is no significant genetic differentiation in the MW population in the Gaogesitai region, and gene exchange between individuals is frequent. The microsatellite population bottleneck detection concluded that neither TPM model nor SMM model showed significant excess heterozygosity (*P*>0.05), and the allele frequency did not significantly deviate from the normal L-shaped distribution, detecting no bottleneck effect in the recent population. The neutrality test of mitochondrial cytochrome b and control region showed that both Tajima's D and Fu's Fs were non-significant positive values, and only the control region Fu 's Fs value was significantly positive, which deviated from the neutrality hypothesis (P<0.01). The mtDNA test suggests that the MW population may have experienced a weak bottleneck effect recently (*Table 3*). Microsatellite data showed that there was no significant difference between the observed heterozygosity and expected heterozygosity of the population (*P*>0.05), and the fixed coefficient (F_{is}) was -0.040, which did not significantly deviate from zero (P> 0.05), and indicated that the population did not have close inbreeding (*Table 2*).

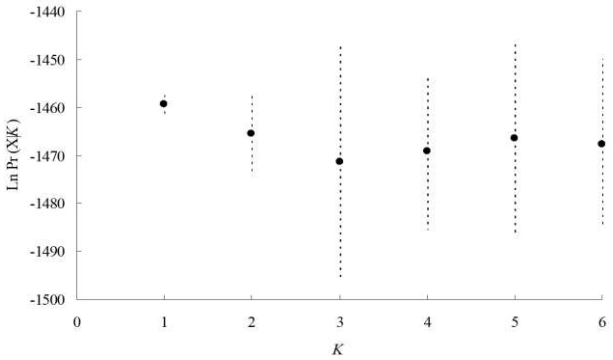

Figure 4. *Plot of the likelihood of each value of ln Pr (X|K) from twenty independent runs for K = 1-6*

Discussion

The loss of genetic diversity can lead to a decline in the ability of animals to adapt to environmental changes and even the extinction of species. The genetic diversity of populations is an important part of endangered animal protection (Frankham et al., 2010).

http://www.aloki.hu ● ISSN 1589 1623 (Print) ● ISSN 1785 0037 (Online)
DOI: http://dx.doi.org/10.15666/aeer/1804_55615575

Haplotype diversity (H_d) and nucleotide diversity (P_i) are key indicators to measure the degree of genetic variation of mtDNA in the population; taking into account the proportion of haplotypes in the population, the P_i value evaluates genetic diversity more accurately (Neigel and Avise, 1993; Ma et al., 2019). In this study, the P_i value (0.805%) of mitochondrial control region was significantly higher than that (0.359%) of cytochrome b. Many animals and plants, and humans generally have a polymorphism in the non-coding region of the gene that is higher than in the coding region (Crochet and Desmarais, 2000), mainly because the non-coding control region in the mitochondrial genome evolves faster and bears less selection pressure (Krojerová-Prokešová et al., 2013; Zorigul et al., 2019). Microsatellite data showed that the average observed heterozygosity (H_o) and expected heterozygosity (H_e) of the population were 0.654 and 0.659, respectively. Based on P_i values of mtDNA and H_e of microsatellites, the MWs were compared with other subspecies and major deer families, to find that the genetic diversity of the MW populations in the Gaogesitai region of Inner Mongolia is at a medium level (*Table 4*). Hap2 and Hap3 of mitochondrial cytochrome b, Hap2 and Hap4 of the control region each have only one individual, and the proportion of rare haplotypes was as high as 50% (4/8) (*Fig. 3*). Therefore, it's necessary to strengthen the protection and management of the WMs in this area, and especially for the rare haplotype individuals, they must be monitored to prevent a sharp decline in genetic diversity of the population.

Table 4. *Comparison of genetic variability at microsatellite loci and the mitochondrial DNA in the Cervus populations*

Species	Region	Microsatellite		Control region		Cytochrome *b*		Author
		H_o	H_e	H_d	P_i (%)	H_d	P_i (%)	
Cervus canadensis xanthopygus	Gaogesitai Reserve, Inner Mongolia, China	0.654	0.659	0.385	0.805	0.540	0.359	Tian et al. (this study)
Cervus hanglu yarkandensis	Tarim Basin, Xinjing, China	0.083	0.378	0.693	1.351	0.845	1.500	Mahmut et al., 2012; Tayerjan et al., 2018
Cervus elaphus elaphus	Šumava National Park, Czech Republic	0.401	0.405	0.511	1.270	-	-	Fickel et al., 2012
Cervus elaphus elaphus	Bavarian Forest National Park, Germany	0.416	0.459	0.385	0.974	-	-	Fickel et al., 2012
Cervus nippon mantchuricus	Lazovsky and Sikhote-Alin Reserve, Primorsky Krai, Russia	0.617	0.710	0.446	0.836	0.285	0.649	Krojerová-Prokešová et al., 2013
Cervus canadensis sibiricus	Tianshan Mountains, Xinjing, China	0.767	0.713	0.669	0.464	0.567	0.216	Zhou, 2015
Cervus canadensis wallichii	Sangri County, Tibet, China	0.519	0.719	-	-	0.897	2.781	Hu et al., 2018; Liu and Zhang, 2011
Cervus canadensis xanthopygus	Wanda Mountains, Heilongjiang, China	0.693	0.737	-	-	-	-	Tian et al., 2010
Cervus elaphus elaphus	Scotland and England, UK	0.447	0.801	0.461	0.563	-	-	Hmwe et al., 2006
Cervus canadensis canadensis	Rocky Mountain, Alberta, Canada	-	-	0.932	0.653	-	-	Speller et al., 2014
Cervus canadensis alashanicus	Helan Mountains, Ningxia and Inner Mongolia, China	-	-	-	-	0.243	0.032	Qiao et al., 2019
Cervus canadensis xanthopygus	Muling Reserve, Heilongjiang, China	0.663	0.712	-	-	0.586	0.305	Liu, 2017

The scientific name of the species referenced IUCN Red List of Threatened Species 2018

http://www.aloki.hu ● ISSN 1589 1623 (Print) ● ISSN 1785 0037 (Online)
DOI: http://dx.doi.org/10.15666/aeer/1804_55615575

Landscape pattern and species' migration ability are the most important factors affecting population genetic structure (Yuasa et al., 2007; Pérez-Espona et al., 2008). The MWs have high migration ability (Reinecke et al., 2014; Tian et al., 2019), and there are no obvious landscape barriers in the study area (Zhang, 2016), which ensures frequent gene communication between individuals, so there is no significant genetic differentiation in the population (*Fig. 4*). The historical bottleneck effect of the population was not detected based on microsatellite data, but the mtDNA detection showed that the MWs may have experienced a weaker bottleneck effect recently. The reason may be that maternal inherited mtDNA is more sensitive to population bottleneck effects than nuclear DNA (Krojerová-Prokešová et al., 2013). However, microsatellite data showed a significant lack of heterozygosity in the SMM model, which suggests that the population increased rapidly after the bottleneck event (Maruyama and Fuerst, 1985; Krojerová-Prokešová et al., 2013). The data of mitochondrial cytochrome b in this study showed that high haplotype diversity ($H_d \geq 0.5$) and low nucleotide diversity ($P_i < 0.5\%$) of the population (*Table 3*) are also considered to be results of rapid growth and mutation accumulation after bottleneck effects (Grant and Bowen, 1998; Yuasa et al., 2007). Based on the above, this study believes that the MW population in the Gaogesitai region of Inner Mongolia has experienced a recent bottleneck effect, followed by rapid population growth. Started in the 1950s, the number of wild MWs dropped sharply due to habitat destruction and over-harvesting in the Gaogesitai region; at the end of the 20th century, the population of the area reached a historical low. At the beginning of this century, especially the establishment of nature reserves taking the MW as the key protection object has helped to restore the MW population quickly (Zhang, 2009). Compared with the lowest point in history, the number of MW populations in the study area has increased by nearly 10 times. It has become the highest density distribution area in Northeast China. This study also found that Hap3 and Hap4 in the mitochondrial control region were highly variant haplotypes, which are significantly different from other haplotypes (*Fig. 3*). Meanwhile, the control region sequence of the population showed low haplotype diversity ($H_d < 0.5$) and high nucleotide diversity ($P_i \geq 0.5\%$) (*Table 3*). Some studies believe that this is often caused by isolated populations coming into contact again (Grant and Bowen, 1998). It's known that there are often incidents such as chaotic captivity, and semi-free-range MW individuals fleeing to the wild, and these escaped individuals in contact with wild populations and genetic fusion may lead to high variant haplotypes. It may also be that the number of individuals analyzed by the mitochondrial control region is small (27), resulting in a lower haplotype diversity in the population.

Conclusion

In summary, this study shows that the genetic diversity of the MW population in the Gaogesitai region of Inner Mongolia is at a medium level, and the recently weak bottleneck effect has no significant effect on the rapid population growth. Also, gene exchange is frequent among individuals, and inbreeding is not detected. The high proportion of rare haplotypes and highly mutated haplotypes in the population indicates that research areas should continue strengthening the protection and management of MW populations to avoid a sharp decline in population genetic diversity and genetic pollution. It is suggested that the individuals with rare haplotypes should be taken as the key point in monitoring and protection, and assess the field adaptability and diseases in the field. The reintroduction projects should be carrued out at the right time, so as to improve the gene exchange between individuals and accelerate the population restoration in other areas of Northeast China.

http://www.aloki.hu ● ISSN 1589 1623 (Print) ● ISSN 1785 0037 (Online)
DOI: http://dx.doi.org/10.15666/aeer/1804_55615575

Acknowledgements. Our study was funded by the Heilongjiang Provincial Basic Research Business Support Project, China (1353ZD006); National Science Foundation of China (30870309); Mudanjiang Normal College Project (GP2019005, MQP201405 and QN2019009). We thank L. Q. Zhong and J. H. Guo for help given throughout this project. We acknowledge the professional staff, guides, and drivers of Inner Mongolia Gaogesitai Hanwula National Nature Reserve.

REFERENCES

[1] Bandelt, H., Forster, P., Rohl, A. (1999): Median joining networks for inferring intraspecific phylogenics. – Molecular Biology Evolution 16(1): 37-48.
[2] Bellemain, E., Swenson, J. E., Tallmon, D., Brunberg, S., Taberlet, P. (2005): Estimating population size of elusive animals with DNA from hunter-collected feces: four methods for brown bears. – Conservation Biology 19(1): 150-161.
[3] Chen, H. P., Wu, J. P., Zhang, M. H. (1997): Heilongjiang Provincial Red Deer. – Harbin: Northeast Forestry University Press.
[4] Crochet, P. A., Desmarais, E. (2000): Slow rate of evolution in the mitochondrial control region of gulls (aves: laridae). – Molecular Biology and Evolution 17(12): 1797-1806.
[5] Douzery, E., Randi, E. (1997): The mitochondrial control region of Cervidae: Evolutionary patterns and phylogenetic content. – Molecular Biology and Evolution 14(11): 1154-1166.
[6] Earl, D. A., von Holdt, B. M. (2012): STRUCTURE HARVESTER: A website and program for visualizing STRUCTURE output and implementing the Evanno method. – Conservation Genetics Resources 4(2): 359-361.
[7] Ellegren, H. (2004): Microsatellites: simple sequences with complex evolution. – Nature Reviews Genetics 5(6): 435-445.
[8] Fickel, J., Bubliy, O. A., Stache, A., Noventa, T., Jirsa, A., Heurich, M. (2012): Crossing the border? Structure of the red deer (Cervus elaphus) population from the Bavarian-Bohemian forest ecosystem. – Mammalian Biology 77(3): 211-220.
[9] Frankham, R., Ballou, J. D., Briscoe, D. A. (2010): Introduction to Conservation Genetics (2nd edition). – New York: Cambridge University Press.
[10] Grant, W. S., Bowen, B. W. (1998): Shallow population histories in deep evolutionary lineages of marine fishes: insights from sardines and anchovies and lessons for conservation. – Journal of Heredity 89(5): 415-426.
[11] Guo, Y. W., Xie, X., Wang, B., Zhang, Y. Y., Xie, K. Z., Bu, X. N., Liu, C. J., Zhang, T., Zhang, G. X., Liu, X. Z., Dai, G. J. (2020): The establishment of a practical method for the determination of piperazine residues using accelerated solvent extraction and UHPLC-FLD. – Quality Assurance and Safety of Crops & Foods 12(1): 28-39.
[12] Haig, S. M., Ballou, J. D., Derrickson, S. R. (1990): Management options for preserving genetic diversity: reintroduction of guam rails to the wild. – Conservation Biology 4(3): 290-300.
[13] Hmwe, S. S., Zachos, F. E., Sale, J. B., Rose, H. R., Hartl, G. B. (2006): Genetic variability and differentiation in red deer (Cervus elaphus) from Scotland and England. – Journal of Zoology 270(3): 479-487.
[14] Hu, H. J., Xing, B., Yang, M., Mpemba, H., Lv, Z. H., Zhang, M. H. (2018): Population and genetic diversity of Tibetan red deer based on fecal DNA. – Journal of Forestry Research 29(1): 227-232.
[15] Huang, C. (2015): Comparative study on red deer winter nutritional strategy in Heilongjiang Muling and Inner Mongolia Gaogesitai National Nature Reserve, northeastern China. – Doctor's thesis, Northeast Forestry University, Harbin.
[16] Irwin, D. M., Kocher, T. D., Wilson, A. C. (1991): Evolution of the cytochrome b gene of mammals. – Journal of Molecular Evolution 32(2): 128-144.
[17] Kocher, T. D., Thomas, W. K., Meyer, A., Edwards, S. V., Pääbo, S., Villablanca, F. X., Wilson, A. C. (1989): Dynamics of mitochondrial DNA evolution in animals: amplification

http://www.aloki.hu ● ISSN 1589 1623 (Print) ● ISSN 1785 0037 (Online)
DOI: http://dx.doi.org/10.15666/aeer/1804_55615575

and sequencing with conserved primers. – Proceedings of the National Academy of Sciences of the United States of America 86(16): 6196-6200.
[18] Krojerová-Prokešová, J., Barančeková, M., Voloshina, I., Myslenkov, A., Lamka, J., Koubek, P. (2013): Dybowski's sika deer (Cervus nippon hortulorum): genetic divergence between natural Primorian and introduced Czech populations. – Journal of Heredity 104(3): 312-326.
[19] Larkin, M. A., Blackshields, G., Brown, N. P., Chenna, R., McGettigan, P. A., McWilliam, H., Valentin, F., Wallace, I. M., Wilm, A., Lopez, R. (2007): Clustal W and Clustal X version 2.0. – Bioinformatics 23(11): 2947-2948.
[20] Li, T., Jiang, J. S., Wu, Z. G., Han, X. D., Wu, J. C., Yang, X. J. (2001): Survey on Amur tiger in Jilin Province. – Acta Theriologica Sinica 21(1): 1-6.
[21] Li, Z. J., Chen, Y. H., Zhang, D. J., Zhang, G. F., Lu, B. X. (2019): Genetic diversity analysis and DNA fingerprinting of the main japonica rice varieties in Heilongjiang Province – Quality Assurance and Safety of Crops & Foods 11(1): 23-29.
[22] Librado, P., Rozas, J. (2009): DnaSP v5: a software for comprehensive analysis of DNA polymorphism data. – Bioinformatics 25(11): 1451-1452.
[23] Liu, Y. H., Zhang, M. H. (2011): Population genetic diversity in Tibet red deer (Cervus elaphus wallichi) revealed by mitochondrial Cyt b gene analysis. – Acta Ecologica Sinica 31(7): 1976-1981.
[24] Liu, X. X. (2017): Study on the genetic diversity between the sympatric distribution of wild sika deer (Cervus nippon) and red deer (Cervus elaphus) in Muling based on faeces molecular biology. – Master's thesis, Northeast Forestry University, Harbin.
[25] Ma, Y., Li, H. L., He, J., Zhao, Y. M., Yang, H. Q., Lu, L., Liu, Q. Y. (2019): Genetic diversity and phylogenetic relationships based on mtDNA control region sequences of Marmota himalayana. – Acta Theriologica Sinica 39(3): 285-294.
[26] Mahmut, H., Anwar, T., Noriyuki, O. (2012): Tarim Red Deer of Xinjiang in China. – Urumqi: Xinjiang University Press.
[27] Maruyama, T., Fuerst, P. A. (1985): Population bottlenecks and nonequilibrium models in population genetics. II. Number of alleles in a small population that was formed by a recent bottleneck. – Genetics 111(3): 675-689.
[28] Neigel, J. E., Avise, J. C. (1993): Application of a random walk model to geographic distributions of animal mitochondrial DNA variation. – Genetics 135(4): 1209-1220.
[29] Park, S. D. E. (2001): Trypanotolerance in west african cattle and the population genetic effects of selection. – PhD Thesis, University of Dublin.
[30] Peakall, R., Smouse, P. E. (2006): GENALEX 6: genetic analysis in Excel. Population genetic software for teaching and research. – Molecular Ecology Notes 6(1): 288-295.
[31] Pérez-Espona, S., Pérez-Barbería, F. J., Mcleod, J. E., Jiggins, C. D., Gordon, I. J., Pemberton, J. M. (2008): Landscape features affect gene flow of Scottish Highland red deer (Cervus elaphus). – Molecular ecology 17(4): 981-996.
[32] Pinilla, K., Hoinle, B., Mahecha-Groot, A., Cepeda, J. (2018): Mapping the agrodiversity in Bogotá-the platform mapeo AgroEcoBogotá. – International Journal of Design & Nature and Ecodynamics 13(4): 407-414.
[33] Piry, S., Luikart, G., Cornuet, J. M. (1999): BOTTLENECK: a computer program for detecting recent reductions in the effective size using allele frequency data. – Journal of Heredity 90(4): 502-503.
[34] Pritchard, J. K., Stephens, M., Donnelly, P. (2000): Inference of population structure using multilocus genotype data. – Genetics 155(2): 945-959.
[35] Qi, J. Z., Shi, Q. H., Wang, G. M., Li, Z. L., Sun, Q., Hua, Y., Jiang, G. S. (2015): Spatial distribution drivers of Amur leopard density in northeast China. – Biological Conservation 191: 258-265.
[36] Qiao, F. J., Li, J. L., Gao, H., Teng, L. W., Wang, J. F., Liu, Z. S. (2019): Molecular phylogenetics of the Alashan red deer (Cervus elaphus alxaicus) based on Cyt b DNA. – Chinese Journal of Wildlife 40(2): 307-311.

http://www.aloki.hu ● ISSN 1589 1623 (Print) ● ISSN 1785 0037 (Online)
DOI: http://dx.doi.org/10.15666/aeer/1804_55615575

[37] Randone, M., Bocci, M., Castellani, C., Laurent, C., Piante, C. (2019): Safeguarding marine protected areas in the growing Mediterranean blue economy— recommendations for the maritime transport sector. – International Journal of Design & Nature and Ecodynamics 14(4): 264-274.
[38] Raymond, M., Rousset, F. (1995): GENEPOP (version 1.2): population genetics software for exact tests and ecumenicism. – Journal of Heredity 86(3): 248-249.
[39] Reinecke, H., Leinen, L., Thißen, I., Meißner, M., Herzog, S., Schütz, S., Kiffner, C. (2014): Home range size estimates of red deer in germany: environmental, individual and methodological correlates. – European Journal of Wildlife Research 60(2): 237-247.
[40] Sinnett, D., Jerome, G., Smith, N., Burgess, S., Mortlock, R. (2018): Raising the standard: Developing a benchmark for green infrastructure. – International Journal of Sustainable Development and Planning 13(2): 226-236.
[41] Speller, C. F., Kooyman, B., Rodrigues, A. T., Langemann, E. G., Jobin, R. M., Yang, D. Y. (2014): Assessing prehistoric genetic structure and diversity of North American elk (Cervus elaphus) populations in Alberta, Canada. – Canadian Journal of Zoology 92(4): 285-298.
[42] Taberlet, P., Griffin, S., Goossens, B., Questiau, S., Manceau, V., Escaravage, N., Waits, L. P., Bouvet, J. (1996): Reliable genotyping of samples with very low DNA quantities using PCR. – Nucleic Acids Research 24(16): 3189-3194.
[43] Tao, Y. X., Yan, D. R. (2014): Detection of parasite eggs from manure of semi-free Cervus elaphus in Gogostai Haan Nature Reserve of Inner Mongolia. – Animal Husbandry and Feed Science 35(10): 12-13.
[44] Tayerjan, M., Tajigul, T., Buweihailiqiemu, A., Subinur, E., Mahmut, H. (2018): Influence of environmental factors on genetic diversity of Tarim red deer. – Chinese Journal of Wildlife 39(4): 754-760.
[45] Tian, X. M., Zhang, M. H. (2010): Population size and sex ratio of wapiti (Cervus elephus xanthopygus) as revealed by fecal DNA. – Acta Ecologica Sinica 30(22): 6249-6254.
[46] Tian, X. M., Zhang, M. H., Zhang, H., Yang, C. W., Jin, Z. M. (2010): Genetic diversity of wapiti population in eastern Wandashan Mountains of Heilongjiang Province, China based on microsatellite analysis. – Chinese Journal of Ecology 29(3): 543-548.
[47] Tian, X. M., Wang, X. L., Zhang, M. H. (2019): Winter home range of the Manchurian wapiti (Cervus canadensis xanthopygus) based on noninvasive sampling. – Applied Ecology and Environmental Research 17(6): 15573-15583.
[48] Valière, N. (2002): Gimlet: a computer program for analysing genetic individual identification data. – Molecular Ecology Notes 2(3): 377-379.
[49] van Oosterhout, C., Hutchinson, W. F., Wills, D. P. M., Shipley, P. (2004): MICRO - CHECKER: software for identifying and correcting genotyping errors in microsatellite data. – Molecular Ecology Notes 4(3): 535-538.
[50] Wang, S. (1998): China Red Data Book of Endangered Animals. – Beijing: Science Press.
[51] Xu, Q. X., Zhang, M. H., Lu, B. X. (2000): Study on the status of red deer population in Heilongjiang Province. – Journal of Economic Animal 4(1): 57-62.
[52] Yang, M., Sun, Y., Zhang, W. Q., Yuan, H. Y., Zhang, M. H. (2019): Variation in winter daily range area of red deer (Cervus elaphus xanthopygus) based on DNA extracted from fecal samples. – Journal of Forestry Research 30(5): 1951-1958.
[53] Yıldırım, A., Sönmezoğlu, Ö. A., Sayaslan, A., Kandemir, N., Gökmen, S. (2019): Molecular breeding of durum wheat cultivars for pasta quality. – Quality Assurance and Safety of Crops & Foods 11(1): 15-21.
[54] Yuasa, T., Nagata, J., Hamasaki, S., Tsuruga, T., Furubayashi, K. (2007): The impact of habitat fragmentation on genetic structure of Japanese sika deer (Cervus nippon) in southern Kantoh, revealed by mitochondrial D-loop sequences. – Ecological Research 22(1): 97-106.

http://www.aloki.hu ● ISSN 1589 1623 (Print) ● ISSN 1785 0037 (Online)
DOI: http://dx.doi.org/10.15666/aeer/1804_55615575

[55] Zhang, S. L., Wang, Z. L., Zhang, P., Zhang, F., Yang, Y. X., He, W. (2009): Study on the status of wild red deer populations in Chifeng city, Inner Mongolia. – Sichuan Journal of Zoology 28(5): 772-776.
[56] Zhang, H. (2010): The individual identity, parentage analysis and home range determination of wapiti based on faeces molecular biology. – Master's thesis, Northeast Forestry University, Harbin.
[57] Zhang, M. H., Tian, X. M., Li, Y. (2010): A molecular identification and rapid recognition approach for the sex determination of wild wapiti by feces pellet morphology. – Acta Theriologica Sinica 30(3): 317-321.
[58] Zhang, C. Z., Zhang, M. H. (2011): Population status and dynamic trends of Amur tiger's prey in eastern Wandashan Mountains, Heilongjiang Province. – Acta Ecologica Sinica 31(21): 6481-6487.
[59] Zhang, L. B. (2016): Winter habitat spatial structure analysis and evaluation of red deer in Gaogesitai. – Master's thesis, Northeast Forestry University, Harbin.
[60] Zhou, C. L. (2015): The study on population size, genetic structure, home range and phylogeny of Tianshan red deer (Cervus elaphus songaricus). – Doctor's thesis, Xinjiang University, Urumqi.
[61] Zhou, S. C., Sun, H. Y., Yang, J., Huang, H. J. (2015): Study on population dynamic trends of Amur tiger's prey and impact factors in eastern Wandashan Mountains. – Forestry Science & Technology 40(3): 37-40.
[62] Zorigul, I., Shamshinur, M., Buweihailiqiemu, A., Arzigul, S., Subinur, E., Mahmut, H. (2019): Influence of environmental factors on genetic diversity of Gazella subgotturosa in Xinjiang, China. – Acta Theriologica Sinica 39(3): 276-284.

APPENDIX

Table A1. *GPS positions of 108 stool samples collected in the Gaogesitai region*

Sample number	Latitude	Longitude
1	44°57'17.358"N	119°30'12.660"E
2	44°57'11.232"N	119°30'09.744"E
3	44°57'30.396"N	119°28'38.592"E
4	44°57'24.222"N	119°28'43.158"E
5	44°57'12.480"N	119°31'53.646"E
6	44°57'31.842"N	119°28'37.722"E
7	44°57'11.220"N	119°28'41.190"E
8	44°57'09.048"N	119°28'42.378"E
9	44°56'58.992"N	119°28'31.596"E
10	44°57'03.174"N	119°28'32.202"E
11	44°57'13.698"N	119°28'40.494"E
12	45°00'28.302"N	119°32'00.078"E
13	45°01'53.418"N	119°33'09.690"E
14	45°00'27.108"N	119°31'59.208"E
15	45°02'16.986"N	119°31'07.218"E
16	45°02'16.890"N	119°31'07.308"E
17	45°02'17.244"N	119°31'04.464"E
18	45°02'17.484N	119°31'03.846"E
19	45°02'18.906"N	119°31'01.206"E
20	45°02'19.068"N	119°31'14.388"E
21	45°01'42.288"N	119°32'52.020"E
22	45°01'49.128"N	119°32'49.812"E
23	45°01'39.216"N	119°32'51.006"E
24	45°01'40.458"N	119°33'00.186"E
25	45°01'32.286"N	119°33'02.364"E
26	45°03'15.420"N	119°31'42.594"E
27	45°03'15.042"N	119°31'41.748"E
28	45°02'06.792"N	119°31'22.848"E
29	45°02'09.252"N	119°31'11.892"E

http://www.aloki.hu ● ISSN 1589 1623 (Print) ● ISSN 1785 0037 (Online)
DOI: http://dx.doi.org/10.15666/aeer/1804_55615575

30	45°02'08.928"N	119°31'10.824"E
31	45°02'08.022"N	119°31'01.080"E
32	45°01'34.746"N	119°30'36.918"E
33	45°01'33.240"N	119°30'37.908"E
34	45°01'27.708"N	119°30'41.898"E
35	45°01'18.174"N	119°30'55.302"E
36	45°01'18.504"N	119°30'57.900"E
37	45°01'18.642"N	119°31'00.132"E
38	45°01'18.702"N	119°31'01.878"E
39	44°57'22.458"N	119°27'22.074"E
40	44°56'31.806"N	119°27'25.578"E
41	44°56'35.502"N	119°27'18.456"E
42	44°56'53.976"N	119°27'19.104"E
43	44°57'05.712"N	119°27'33.900"E
44	44°57'15.834"N	119°27'35.268"E
45	45°01'42.966"N	119°32'51.888"E
46	45°01'55.512"N	119°32'39.858"E
47	45°02'06.642"N	119°32'46.404"E
48	45°02'06.552"N	119°32'46.788"E
49	44°58'03.150"N	119°28'14.688"E
50	44°58'05.604"N	119°28'21.840"E
51	44°58'07.110"N	119°28'22.632"E
52	44°58'12.696"N	119°28'26.682"E
53	44°58'12.522"N	119°28'15.042"E
54	44°58'10.068"N	119°28'14.994"E
55	44°57'37.338"N	119°26'30.000"E
56	44°57'36.378"N	119°26'33.150"E
57	44°57'36.354"N	119°26'35.706"E
58	44°57'35.394"N	119°26'40.098"E
59	44°57'22.074"N	119°26'59.544"E
60	44°57'19.734"N	119°27'11.136"E
61	44°57'22.920"N	119°27'12.942"E
62	45°03'30.078"N	119°32'31.230"E
63	45°03'26.706"N	119°32'30.966"E
64	45°03'18.780"N	119°32'32.796"E
65	45°03'16.356"N	119°32'32.454"E
66	45°03'14.370"N	119°32'34.524"E
67	45°03'11.430"N	119°32'39.384"E
68	45°03'11.514"N	119°32'47.256"E
69	45°03'12.060"N	119°32'51.036"E
70	45°03'19.818"N	119°32'50.850"E
71	45°03'25.194"N	119°32'50.532"E
72	45°03'26.394"N	119°32'43.068"E
73	45°00'58.326"N	119°31'36.498"E
74	45°01'07.266"N	119°31'19.884"E
75	45°01'09.072"N	119°31'03.126"E
76	45°01'13.164"N	119°31'00.150"E
77	45°01'13.380"N	119°30'54.984"E
78	45°01'16.488"N	119°31'00.360"E
79	45°02'05.478"N	119°31'48.798"E
80	45°02'08.778"N	119°31'56.544"E
81	44°59'03.582"N	119°31'32.580"E
82	44°59'03.720"N	119°31'31.590"E
83	44°59'04.704"N	119°31'25.326"E
84	44°59'04.572"N	119°31'21.870"E
85	44°59'09.354"N	119°31'14.934"E
86	44°59'18.438"N	119°31'09.984"E
87	44°59'23.094"N	119°31'11.892"E
88	44°58'44.988"N	119°26'03.402"E
89	44°58'58.662"N	119°26'02.724"E
90	44°59'00.222"N	119°26'03.816"E
91	44°59'01.260"N	119°26'02.802"E
92	44°59'19.806"N	119°26'19.692"E
93	44°59'11.232"N	119°26'37.944"E

http://www.aloki.hu ● ISSN 1589 1623 (Print) ● ISSN 1785 0037 (Online)
DOI: http://dx.doi.org/10.15666/aeer/1804_55615575

94	45°00'11.118"N	119°26'55.830"E
95	44°57'23.394"N	119°27'40.614"E
96	44°57'21.768"N	119°27'46.140"E
97	44°57'26.436"N	119°28'20.694"E
98	44°57'29.112"N	119°29'03.222"E
99	44°57'44.682"N	119°28'12.600"E
100	44°57'47.304"N	119°28'13.470"E
101	44°58'02.616"N	119°28'12.720"E
102	44°58'07.758"N	119°28'15.198"E
103	44°58'08.376"N	119°28'15.612"E
104	44°58'11.052"N	119°28'15.414"E
105	44°58'10.896"N	119°28'11.616"E
106	44°58'06.510"N	119°28'02.718"E
107	44°58'05.424"N	119°28'01.236"E
108	44°58'00.702"N	119°27'50.928"E

http://www.aloki.hu ● ISSN 1589 1623 (Print) ● ISSN 1785 0037 (Online)
DOI: http://dx.doi.org/10.15666/aeer/1804_55615575

EFFECT OF SILICON ON CROP YIELD, AND NITROGEN USE EFFICIENCY APPLIED UNDER STRAW RETURN TREATMENTS

MABAGALA, F. S.[1] – GENG, Y. H.[1*] – CAO, G. J.[1*] – WANG, L. C.[2] – WANG, M.[2] – ZHANG, M. L.[1]

[1]*College of Resources and Environment, Jilin Agricultural University, Changchun 130118, China*

[2]*Institute of Agricultural Environment and Resources Research, Jilin Academy of Agricultural Sciences, Changchun 130033, China*

[*]*Corresponding authors*
e-mail: gengyuhui@163.com; cgj72@126.com

(Received 30th Mar 2020; accepted 3rd Jul 2020)

Abstract. Nitrogen (N) is an essential element for crop growth and for improving crop yield. A two-year field experiment was carried out in China to test the effects of silicate (Si) fertilizer with straw return on N use efficiency (NUE) and yield of spring maize. Four treatments were arranged in a randomized block design: SI+ST (straw return + 45 kg ha^{-1} Si), SI (no straw return + 45 kg ha^{-1} Si), ST (straw return + no Si) and C (no straw return + no Si). The results showed that the accumulation of dry matter and grain yield under SI were 6.5% and 8.8% higher, respectively than those under the C. The N uptake under SI increased by 15.6% compared with that under the C treatment. The N uptake of SI+ST increased by 7.6% compared to SI. The SI+ST resulted in a significant increase in the AEN, REN, and PFPN compared with SI. The above results show that the use of Si fertilizer combined with straw return significantly provides better N for maize growing stages and is recommended as an alternative method to simultaneously increase crop yield and NUE while reducing the use of chemical fertilizer to the environment.
Keywords: *crop residues, Si-based fertilizer, spring maize, N utilization, grain yield*

Introduction

Nitrogen (N) is an essential nutrient for maize growth and is considered to be the main controlling factor for plant productivity after water deficiency (Lea and Azevedo, 2006). The high yield of the crop is associated with the application of a large amount of N fertilizers (Patel et al., 2017). The N use efficiency (NUE) of plants is the primary index used to determine nutrient uptake (Yang et al., 2003). It measures the ability of crops to accumulate and utilize nutrients for maximum yields (González-Fontes et al., 2017). NUE depends on the plant's ability to take up nutrients efficiently from the soil but also depends on internal transport, storage, and remobilization (Prieto et al., 2017). Thus, it involves three major processes in plants: uptake, assimilation, and utilization of nutrients (Baligar et al., 2001; Reich et al., 2014). Cereal NUE in china was approximately 41%, and they're still the applying of excess N fertilizer, which has consequently resulted in low NUE (Omara et al., 2019). Many measures have been recommended to enhance plant NUE including proper management of rhizosphere processes (Zhu et al., 2010), the use endophytic bacteria (Prieto et al., 2017), conservation agriculture (Jat et al., 2012), through alteration of amino acid transport processes (Perchlik and Tegeder, 2017) and the use of split application of reduced nitrogen (Du et al., 2019b). Therefore, the best N fertilizer management practice has to be adopted to improve NUE in crops. Management of N is a complex task, and several approaches individually and in combination, have been engaged to manage its effectiveness (Sharma and Bali, 2018).

http://www.aloki.hu ● ISSN 1589 1623 (Print) ● ISSN1785 0037 (Online)
DOI: http://dx.doi.org/10.15666/aeer/1804_55775590

Silicon (Si) is the most abundant element on the earth's surface, which has proved to have many beneficial effects for crops (Deshmukh et al., 2017). Si has been reported to have a significant effect on yield and modify growth in crops (Luz et al., 2008). Previous research has discovered that Si can stimulate various plants to take up more macronutrients and micronutrients (Ca, P, S, Mn, Zn, Cu, Cl, Fe) from the soil (Islam and Saha, 1969; Owino-Gerroh and Gascho, 2005; Greger et al., 2018). According to previous studies (Singh et al., 2006; Jugal and Ramani, 2017; Patel et al., 2017), the application of Si has a synergistic relationship with N in rice. Recent studies have shown that Silicon (Si) also influenced the nutrient uptake and accumulation in non-stressed crops (Greger et al., 2018). Si enhances NUE, P availability, and carbon turnover in wheat crops (Neu et al., 2017). Si application influenced the availability of N uptake, which enhances the increase of biomass and prevents N starvation in plants (Haddad et al., 2018).

Crop straw is rich in plant nutrients such as nitrogen, phosphorus, and potassium, and many trace elements (Gao et al., 2009). Wang et al. (2019) reported that straw return remarkably increased N uptake and grain yield in maize-wheat rotation. The combination of organic and inorganic fertilizers enhanced the N uptake, the N use, and recovery from the soil in rice (Moe et al., 2017). Incorporation of straw into soil improved the NUE and carbon inputs (Eagle et al., 2001). Apart from the increased NUE, the use of wheat straw significantly increased the nitrogen agronomic efficiency (AEN), the nitrogen recovery efficiency (REN), the nitrogen physiological efficiency (PEN), and the nitrogen partial factor productivity (PFPN) (Hu and Zhang, 2017). Appropriate management of organic matter ensures conservation and provisions nutrients in a prolonged period in crop production (Watson et al., 2002).

The enhancement of NUE in crops has been shown mainly by the application of Si or straw individually in previous researches. There is currently no research on Si combined with straw return on NUE in crops. We hypothesized that though apply Si could stimulate plants to take up more N from the soil, however, due to the fixation of silicon fertilizer in the soil, its effect only lasts for a short time. The straw can not only increase the nutrients in the soil but can also improve Si availability at the late stages of growth. Thus, meet crop needs and enhance plant growth and development in later stages and sustainably enhance grain yield. The main objective of the study was to investigate the effect of silicate fertilizer with straw on N uptake, remobilization, NUE, and yield in spring maize. The findings of the study could add to the development strategies that improve NUE and sustainably to enhance crop yield.

Materials and Methods

Experimental design and crop management

Two field trials were established at Dong Fang Hong village (124 °31'E, 43 °55'), Nong'an County, Changchun city, Jilin Province in China, in the 2017 and 2018 growing seasons. The soil was Chernozem (soil classification is based on the Canadian system of soil classification) (Haynes, 1998) containing 27.96 and 25 g kg^{-1}, 107.31 and 109.2 mg kg^{-1} alkaline nitrogen (N), 50.73 and 33.9 mg kg^{-1} available phosphorus (P), 163.59 and 114.1 mg kg^{-1} available potassium (K), 350.19 and 357 mg kg^{-1} available silicon (Si), 8.02 and 7.7 soil pH before maize planting at a soil depth 0-20 cm in 2017 and 2018, respectively. Spring maize is the maize grown during the spring season and are sensitive to climate change.

http://www.aloki.hu ● ISSN 1589 1623 (Print) ● ISSN1785 0037 (Online)
DOI: http://dx.doi.org/10.15666/aeer/1804_55775590

The experiments had a two-way factorial design in which 12000 kg ha^{-1} (J) of straw was returned to the field in one area, and the other area had no straw returned to the field (W). The Si treatments included the S0 treatment (0 kg ha^{-1}, no Si fertilizer) and the S3 treatment (45 kg ha^{-1} of Si fertilizer). There were four treatments: C (no Si fertilizer + no straw), SI (Si fertilizer + no straw), ST (no Si fertilizer + straw) and SI+ST (Si fertilizer + straw). The treatments were arranged in a randomized block design (RBD) with three replications. Sodium silicate (Na_2SiO_3) was used as Si fertilizer. The area of each plot was 35 m^2. The maize variety Fumin 985 (produced by Jilin Fumin Seed Leaf Co., Ltd) was planted on May 7, 2017, and May 10, 2018, and then harvested on September 28, 2017, and October 2, 2018, respectively. The planting density was 65000 plants ha^{-1}. Macronutrients (nitrogen, phosphorus, and potassium) were applied in the experimental plots. The rate of N application was 240 kg ha^{-1} in each treatment, in which the base fertilizer accounted for 40% of the total N application rate, the topdressing fertilizer at the jointing stage accounted for 30% of the total N application rate, and the topdressing fertilizer at the heading stage accounted for 30% of the total N application rate. All plots were treated with phosphorus pentoxide (P_2O_5, 100 kg ha^{-1}) and potassium oxide (K_2O, 100 kg ha^{-1}), which were applied once as the base fertilizers. The remainder of the management was based on the high standard of field production.

Plant sampling and tissue nutrient analysis

Three samples of fresh plants were collected from each plot at growth stages V6 (six leaves), V12 (twelve leaves), VT (tasseling), R2 (blister aging), R3 (milking) and R6 (maturity) (June 29, July 18, July 27, August 22, September 7, and September 27 in 2017 and July 15, July 24, August 2, August 23, September 11, and September 28 in 2018, respectively). Plant samples were divided into four components: stem (including the stem, leaf sheath, and bract leaf), leaf, cob, and grain. Plant samples were heated at a constant temperature in a blast oven at 105 °C for 30 min and dried to a uniform weight at 80 °C. Each plant piece was weighed to obtain its dry weight (DW). The total N content of the different plant organs was extracted by the Kjeldahl method.

Grain yield and yield components

At maize maturity, the yield was measured in each experimental plot with a representative area of 10 m^2, and ten ears were selected according to the weight mean method to measure the grain number per ear and the 1000-grain weight. The economic yield was calculated by the air-dry weight (14% water content) of 10 grains in each plot.

Calculations

(Mi et al., 2003; Chen et al., 2014; Agegnehu et al., 2016; Du et al., 2016, 2019a; Deng et al., 2018).

Nitrogen change and N remobilization

To model the N uptake pattern, a logistic model was used to describe the progress of the plant N uptake as follows:

$$N = \frac{N_{\max}}{1 + ae^{bt}} \quad \text{(Eq.1)}$$

http://www.aloki.hu ● ISSN 1589 1623 (Print) ● ISSN1785 0037 (Online)
DOI: http://dx.doi.org/10.15666/aeer/1804_55775590

$$t_1 = -\frac{1}{b}\ln\frac{2+\sqrt{3}}{a} \quad \text{(Eq.2)}$$

$$t_2 = -\frac{1}{b}\ln\frac{2-\sqrt{3}}{a} \quad \text{(Eq.3)}$$

where is the N uptake in maize, N_{max} (kg ha^{-1}) is the asymptotic maximum N uptake by maize, and a and b are the constants to be determined. The time of the N uptake rate acceleration is t_1, the time of the N uptake rate deceleration is t_2, t_2-t_1 is the fast uptake duration of maize N.

N accumulation amount in the plant,

$$\text{NAA (kg ha}^{-1}\text{)} = \text{Plant dry weight (kg ha}^{-1}\text{)} \times \text{Plant N content (\%)} \quad \text{(Eq.4)}$$

$$\text{N remobilization amount (kg ha}^{-1}\text{)} = \text{maximum N content during the growth period - N content at maturity} \quad \text{(Eq.5)}$$

$$\text{N remobilization efficiency (\%)} = (\text{maximum Mg content during the growth period - Mg content at maturity}) / \text{maximum Mg content during the growth period} \times 100 \quad \text{(Eq.6)}$$

$$\text{Apparent contribution to grain by N remobilization (\%)} = (\text{maximum N content during the growth period} - \text{N content at maturity})/\text{grain N content at maturity} \times 100 \quad \text{(Eq.7)}$$

Nitrogen use efficiency

The AEN, REN, PEN, and PFPN were computed using the below formulas:

$$PFPN = \frac{YT}{FN} \quad \text{(Eq.8)}$$

$$AEN = \frac{AY}{NA} \quad \text{(Eq.9)}$$

$$REN = \frac{ANU}{NA} \quad \text{(Eq.10)}$$

$$PEN = \frac{AY}{ANU} \quad \text{(Eq.11)}$$

where, AEN is the increased maize grain yield (ΔY) over zero- N plots per unit area of fertilizer N applied (NA). REN is the increased total N uptake over zero-N plots (ΔNU). PFPN is the maize total grain yield (YT) per unit area of fertilizer N applied (FN) Kg of N per ha applied. PEN is the increased maize grain yield per unit area (ΔY) of increased N uptake over zero- N plots (ΔNU).

http://www.aloki.hu ● ISSN 1589 1623 (Print) ● ISSN1785 0037 (Online)
DOI: http://dx.doi.org/10.15666/aeer/1804_55775590

Statistical data analysis

Total N accumulation (kg ha^{-1}), remobilization amount (kg ha^{-1}), remobilization efficiency (%), apparent transfer to the grain (%) and total dry matter accumulation (kg ha^{-1}) at different growth stages and the grain yield and yield components were analyzed using SPSS Statistics 25.0 (SPSS, Inc., Chicago, IL, USA). Differences in mean C, SI, ST, and SI+ST treatments were tested for statistical significance by analysis of variance (ANOVA). One-way ANOVA was used to test for differences in mean C, SI, ST, and SI+ST during the maize growth. Two-way ANOVA was used to test for the effects of Si fertilizer, straw return, and their interaction of mean C, SI, ST, and SI+ST. In case of significant differences among the means, DUNCAN significant differences at $P = 0.05$ test was used. Figures were created in Origin Pro 8. Means and standard errors (S.E) from the statistical analysis were brought into Origin Pro 8, and diagrams were created using the line+ symbol and column graph tools.

Results

Maize grain yield components

As shown in *Table 1*, the yield of Si-fertilized treatments was higher than that without silicate fertilizer. Compared with the C with an average yield of 11124 kg ha^{-1}, the corn yield of SI treatment was higher, with an average yield of 11671 kg ha^{-1} in two years (*Table 1*). In both years, significant differences in grain number and 1000-grain weight observed between Si-fertilized treatments and treatments without Si fertilizer. The two-year average yield of the SI+ST treatment (11829 kg ha^{-1}) was higher than that of the SI treatment (11671 kg ha^{-1}) (*Table 1*). Averaged over two years, the crop productivity of SI increased by 4.8% on average compared with that of C (*Table 1*).

Table 1. *Showing variance analysis of grain number (per ear), 1000-grain weight (g), and yield (kg ha^{-1}), and increased productivity of maize in two consecutive years of 2017-2018*

Year	Treatment	Grain Number (per Ear)	1000-Grain Weight (g)	Yield (kg ha^{-1})	Increased Productivity (%)
2017	C	597±4c	300±11c	11196±359c	-
	SI	597±14c	330±7a	11685±221a	4.4
	ST	635±5b	314±2b	11345±11b	1.3
	SI+ST	693±33a	330±4a	11881±107a	6.1
2018	C	329±6b	527±3c	11052±155c	-
	SI	336±4ab	550±8a	11657±30a	5.3
	ST	333±21ab	542±62b	11067±24b	0.1
	SI+ST	346±4a	556±2a	11777±134a	6.4

Total dry matter accumulation in maize

Dry matter accumulation was affected by Si and straw applications over the two experimental years (*Fig. 1*). All the treatments showed a similar trend of total biomass accumulation in maize. At the V6 stage, the level of dry matter was low, and there were no differences among treatments; then, the biomass increased continuously with the age of the maize plant until maturity, and the differences between different treatments

http://www.aloki.hu ● ISSN 1589 1623 (Print) ● ISSN1785 0037 (Online)
DOI: http://dx.doi.org/10.15666/aeer/1804_55775590

gradually increased. At harvest time, the dry matter accumulation under the SI treatment increased by 6.1% on average compared to that under the C treatment. The total dry matter under the SI+ST treatment increased by 2.9% on average compared with that under the SI treatment. In both years, there was a significant difference between the straw application treatments and those with no straw.

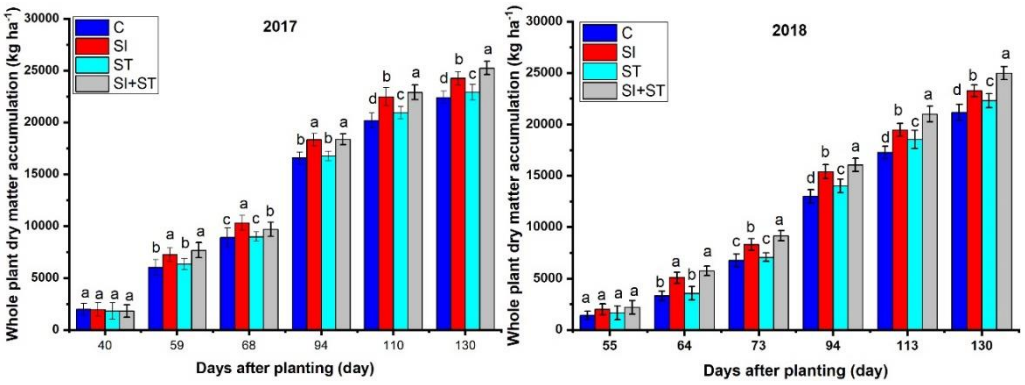

Figure 1. *The seasonal total dry matter accumulation of Si evaluated for two years, 2017 and 2018. Values are means with standard deviations shown by vertical bars (n=4). Bars with a different lowercase letter (s) in the same planting date indicate significant differences at P < 0.05 among the treatments*

Total N uptake and total N uptake rate in spring maize

N uptake in maize increased from the V6 stage to physiological maturity, and there were significant differences among the Si and straw treatments. The N uptake of the SI treatment was 15.9% higher than that of the C treatment at the maturity stage. The effect of the straw application on maize N uptake was significant (*Fig. 2*). The N uptake under the SI+ST treatment increased by 7.7% compared to that under SI treatment. During the period of the fast N uptake stage, the uptake rate under the SI treatment had a mean rate of 10.4% higher than that under the C treatment in both years. In comparison with the SI treatment, the SI+ST treatment showed a noticeable increase in N uptake by the crop. The uptake rate of SI+ST treatment had a mean rate of 3.8% higher than that of SI treatment, averaged over two years.

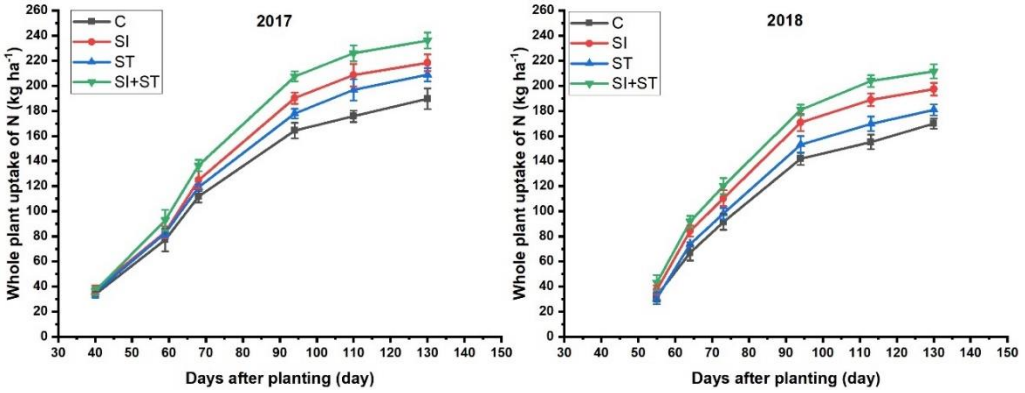

Figure 2. *The response of maize total plant N uptake for two years, 2017 and 2018. Each data point is the mean ± S.E. of three replications*

http://www.aloki.hu ● ISSN 1589 1623 (Print) ● ISSN1785 0037 (Online)
DOI: http://dx.doi.org/10.15666/aeer/1804_55775590

N remobilization in spring maize

The result showed that the remobilization of nitrogen in leaves and stems in two years under all treatments manifested the same tendency (SI+ST >SI>ST>C) (*Table 2*). Averaged over two years, the remobilization amount, the remobilization efficiency, and contribution to the grain under the SI treatment increased by 21%,4%, and 6.8%, respectively, compared to the conventional practice application (C). The remobilization amount, the remobilization efficiency, and the contribution to the grain under the plots treated with straw increased by 7.9%, 1.1%, and 3.6%, respectively, compared to that with no straw when averaged over two years.

Table 2. *Analysis of variance of the vegetative Si remobilization amount (mg kg^{-1}), remobilization efficiency (%) and contribution to the grain (%) in two successive years (2017-2018)*

		N remobilization Amount (kg ha^{-1})			**N remobilization efficiency (%)**			**Apparent contribution to grain N by N remobilization (%)**		
		leaves	stem	total	leaves	stem	total	leaves	stem	total
2017	C	31.7± 0.53b	15.5± 0.95b	47.2± 0.66c	41.2± 1.29a	50.6± 0.66b	44.4± 1.62a	29.6± 0.15c	19.3± 0.21d	48.9± 0.41d
	SI	40.3± 0.43b	17.9± 0.27ab	58.2± 0.39b	42.6± 1.28b	52.0± 1.67c	45.7± 1.48c	33.6± 0.04b	19.8± 0.25b	53.4± 0.12b
	ST	36.4± 0.24b	14.00± 0.17c	50.4± 0.24d	42.0± 1.54a	47.8± 1.49a	43.9± 1.18b	31.9± 0.11b	18.5± 0.07c	50.4± 0.10c
	SI+ST	44.1± 0.03a	17.4± 0.45a	61.5± 0.21a	43.1± 0.41b	52.4± 1.19b	46.1± 1.17c	34.6± 0.20a	20.3± 0.34a	54.9± 0.23a
2018	C	26.8± 0.76c	18.3± 1.91c	45.1± 1.35c	39.2± 1.31a	47.8± 0.97a	42.3± 2.51a	28.2± 0.19c	19.2± 0.23c	47.4± 0.49c
	SI	32.8± 0.96ab	22.8± 1.87ab	55.6± 1.87a	40.8± 0.83c	51.3± 0.22b	44.5± 1.41c	29.2± 0.05b	20.3± 0.22b	49.5± 0.22b
	ST	30.0± 0.90b	20.8± 1.39bc	50.8± 1.82b	38.7± 0.40b	51.1± 0.25b	43.0± 2.57b	28.8± 0.04b	20.0± 0.25b	48.8± 0.10b
	SI+ST	35.6± 4.33a	25.7± 1.95a	61.3± 0.68a	41.0± 1.51a	52.1± 0.23c	45.1± 3.28d	30.0± 0.21a	21.7± 0.97a	51.7± 0.29a
Anova										
F		NS	**	*	**	**	**	**	**	**
S		**	NS	**	NS	**	**	**	*	**
FS		NS	NS	NS	*	NS	NS	**	**	**
FSY		*	*	NS	NS	NS	NS	**	**	**

Note: F: fertilizer, S: straw, F × S: fertilizer with straw, FSY: fertilizer × straw × year. NS, not significant (p-value>0.05); *, significant at (p-value<0.05); **, significant at (p-value<0.01)

N use efficiency (NUE) in spring maize

The data indicated that the AEN, REN, and PFPN were significantly increased with the Si fertilizer application (*Table 3*). Compared to the C treatment, the SI treatment resulted in increases in AEN, REN, and PFPN of 13.6%, 44.9%, and 4.9%, respectively, averaged over two years. The PEN under SI treatment decreased by 26.7% compared to that of the C treatment, averaged over two years. The AEN, REN, and PFPN of the SI+ST treatment increased by 3.6%, 17.6%, and 1.3%, respectively, compared to that under SI treatment. the PEN decreased under the SI+ST treatment by 13.5% when averaged in two years.

http://www.aloki.hu ● ISSN 1589 1623 (Print) ● ISSN1785 0037 (Online)
DOI: http://dx.doi.org/10.15666/aeer/1804_55775590

Table 3. *Variance analysis of the N use efficiencies (Eq.8,9,10 and 11); - agronomic use efficiency (mg kg^{-1}), recovery use efficiency (%), and physiological use efficiency (kg ha^{-1}), and partial factor productivity of N (PFPN) in two consecutive years of 2017-2018*

	Treatments	Agronomic N Use Efficiency (AEN) kg kg^{-1}	Recovery N Use Efficiency (REN) %	Physiological N Use Efficiency (PEN) kg kg^{-1}	N partial factor productivity (PFPN) kg kg^{-1}
2017	C	16.03±0.09c	26.99±0.25d	59.39±0.15a	46.65±0.37d
	SI	18.07±0.14ab	38.89±0.68b	46.46±0.26b	48.69±0.33b
	ST	16.65±0.04b	34.94±0.29c	47.65±014b	47.27±0.17c
	SI+ST	18.88±0.37a	46.29±0.19a	40.78±0.02c	49.50±1.29a
2018	C	15.78±0.07c	24.95±0.16d	63.23±0.03a	46.05±0.08c
	SI	18.30±0.18b	36.36±0.12b	50.32±0.22c	48.57±0.22b
	ST	15.85±0.23c	29.52±0.21c	53.68±0.17b	46.11±0.03c
	SI+ST	18.80±0.37a	42.28±0.02a	44.46±0.32d	49.07±0.004a
Anova					
F		**	**	**	**
S		*	**	**	**
F S		NS	NS	**	*
FSY		NS	*	**	NS

F: fertilizer, S: straw, F × S: fertilizer with straw, FSY: fertilizer × straw × year. NS, not significant (p-value>0.05); *, significant at (p-value<0.05); **, significant at (p-value<0.01)

Discussion

Maize biomass yield, grain yield, and increased productivity

Silicon (Si) is closely related to plant growth and yield owing to strengthen the physiological attributes of the maize (Kaya et al., 2006; Amin et al., 2016). Si has proved to enhance the photosynthesis process, improves the absorption of nutrients, and increases grain yield in maize (Xu et al., 2016). The results present in *Table 1* illustrate that the maize grain and dry matter significantly influenced by Si application. The substantially higher grain yield (11685 kg ha^{-1} and 11657 kg ha^{-1}) in 2017 and 2018 were recorded due to the basal application of Si, while the lower grain (11196 kg ha^{-1} and 11052 kg ha^{-1}) were registered under the conventional practice. The treatment SI gave a 6.5% higher dry matter over C (*Fig. 1*). The result was consistent of the report by Xu et al. (2016), who found that the application of Si improved maize grain yield and dry matter accumulation.

Huang et al. (2010) mentioned the application of organic fertilizer combined with inorganic fertilizer is a good fertilization practice for modifying soil quality and attaining optimum yield. Many reports have shown that straw return provides nutrients, and it's associated with improved biomass yield and grain yield (Zhang et al., 2009; Xu et al., 2010; Wang et al., 2018). The findings from this trial demonstrate that the addition of Si fertilizer and straw increases grain yield and dry matter of maize in two years (*Table 1*). The significantly higher grain (11881 kg ha^{-1} and 11777 kg ha^{-1}) in 2017 and 2018 were recorded due to the addition of organic matter by straw application (Christensen, 1986) under the SI+ST treatment. The treatment SI+ST gave a 2.9% higher dry matter over the SI treatment (*Fig. 1*). Our findings agree with Zhang et al. (2015), who have found that straw incorporation increased grain yield and biomass yield. Therefore, the application of Si with straw return should be considered an essential practice in maize farming for improving yield and promoting sustainable soil systems.

http://www.aloki.hu ● ISSN 1589 1623 (Print) ● ISSN1785 0037 (Online)
DOI: http://dx.doi.org/10.15666/aeer/1804_55775590

Total plant N uptake and uptake rate

Cuong et al. (2017) noted that the application of Si at the level of 329 kg hm^{-2} with inorganic fertilizer would help in N uptake in rice. Si and N are said to have a synergistic effect, and Si can raise the optimum N rate in rice (Ho et al., 1980). Averaged over two years, the N uptake rate under the SI treatment increased by 10.4% than that under the C treatment (*Table 4*). We also found that the application of Si increased N uptake by 15.6% on average compared with the N uptake under the conventional practice (C) (*Fig. 2*). Our findings concerning the significant effect of Si to N uptake are broadly in line with Laîné et al. (2019).

Table 4. *Logistic equation characteristics (Eq.1,2 and 3) of the N uptake of the entire plant subjected to different Si and straw treatments in 2017 and 2018. t_1: Time of total plant N uptake acceleration t_2: Time of whole plant N uptake deceleration T: The fast uptake period of total plant N (d)*

Years	Treatments	Regression equation	R^2	t_1 (day)	t_2 (day)	T (day)	Uptake rate (kg $ha^{-1}d^{-1}$)
2017	C	$N=188.8/(1+60.1e^{-0.0714t})$	0.9970*	38.9	75.8	36.9	2.95d
	SI	$N=220.6/(1+68.8e^{-0.0669t})$	0.9981*	43.6	82.9	39.4	3.24b
	ST	$N=205.8/(1+56.8e^{-0.0693t})$	0.9940*	39.3	77.3	38.0	3.13c
	SI+ST	$N=236.6/(1+89.4e^{-0.0657t})$	0.9989*	48.3	88.4	40.1	3.41a
2018	C	$N=164.8/(1+188.7e^{-0.0746t})$	0.9901*	53.6	87.9	34.3	2.71d
	SI	$N=192.2/(1+336.6e^{-0.0714t})$	0.9856*	63.1	99.9	36.9	3.01b
	ST	$N=174.6/(1+390.4e^{-0.0744t})$	0.9872*	62.5	97.9	35.4	2.85c
	SI+ST	$N=213.4/(1+390.4e^{-0.069t})$	0.9848*	67.4	105.6	38.2	3.23a

*, significant at P<0.05; **, significant at P<0.01

Appropriate incorporation of straw has a positive effect on N mineralization and probably N uptake by rice crop (Takahashi et al., 2003). Zhang et al. (2016) demonstrated that the use of compost plus inorganic fertilizer as a practical nutrient management approach to maintain N uptake, reduce N loss and, increase soil fertility. It is evident from our study that straw return significantly improved N uptake by crop (*Table 4*). The N uptake rate under the SI+ST treatment increased by 3.8% on average than that under the SI treatment. Similarly, in treatment with the straw application (SI+ST), N uptake was 7.6% higher than that with no straw treatment (SI) (*Fig. 2*). Similar results have been reported by Hu and Zhang (2017) that straw incorporation improved N uptake and NUE in rice.

Remobilization of N in spring maize

During the vegetative phase, the leaves and stem are the sinks for N; later, during senescence or deficiency periods, this N is re-translocated for reuse in the developing grain, fruits, and even young leaves (Okumoto and Pilot, 2011; Hernandez-Apaolaza, 2014). A balanced input of N and Si fertilizers showed an effect on agronomic indexes of rapeseed crops (Laîné et al., 2019). In this study, the remobilization amount, remobilization efficiency, and contribution to the grain under SI treatment increased by 21%, 4%, and 6.8%, respectively, compared to that under C (*Table 2*). The increase of remobilization under SI treatment was probably due to the application of Si fertilizer

http://www.aloki.hu ● ISSN 1589 1623 (Print) ● ISSN1785 0037 (Online)
DOI: http://dx.doi.org/10.15666/aeer/1804_55775590

stimulated plants to take up more N (Neu et al., 2017) for remobilization. Our study corroborates with Detmann et al. (2012), who demonstrated that Si nutrition promoted N remobilization by stimulating amino acid remobilization from vegetative parts to the grains. Straw incorporation has the potential to affect agricultural management practices that improves soil nutrients (Zhou et al., 2018) as it is a readily available organic material which function to enhance soil fertility by releasing some nutrients such as N.P.K and others (Pathak et al., 2006). Organic matter applied in the form of liquid cattle manure increased N accumulation, distribution, and remobilization from leaves and stem to kernels (Dordas et al., 2008). In our study, straw application significantly affected the re-translocation of N (*Table 2*). The SI+ST treatment increased by 7.9%, 1.1%, and 3.6% of N remobilization amount, remobilization efficiency, and N contribution to the grain, respectively, compared with that of the SI treatment. This study supported previous reports Wang et al. (2017) that manure plus urea improved N accumulation and remobilization in wheat.

Si fertilization under straw return improved the NUE of maize

The Si nutrient modified nitrogen (N) use efficiency (NUE) in rice (Yogendra et al., 2013; Cuong et al., 2017) and wheat (Yogendra et al., 2013). Higher NUE observed with the application of calcium silicate (Yogendra et al., 2013). This study has clearly shown a significant effect of Si fertilizer on the NUE of maize. In the plot that received 45 kg ha^{-1} of sodium silicate, the agronomic N use efficiency (AEN), recovery N use efficiency (REN), and partial factor productivity of N (PFPN) was 13.6%, 44.9%, and 4.9%, respectively higher than that in the conventional practice plot (C). However, Si fertilizer under SI treatment decreased the physiological efficiency of N (PEN) in our results by 26.7% than that under the C treatment (*Table 3*). The result shows that there was a synergistic effect between Si and N. This study was consistent with the results of Si and N fertilization in rice (Yogendra et al., 2014) and in wheat (Neu et al., 2017) that Si fertilizer enhances the NUE's except for the PEN. Moreover, the PEN decreased with the addition of Si fertilizer, which was in harmony with the findings of (Awgchew et al., 2017), who revealed a reduced PEN with increases of fertilizer. The main reason for this phenomenon may be that the amount of nitrogen absorbed by the leaves and stems on the ground is much higher than that of the control, which reduces the yield of grain per unit of nitrogen.

Straw return and appropriate tillage approach significantly enhanced grain yield and NUE in winter wheat (Jin et al., 2017). The inorganic fertilizer, coupled with organic fertilizer, increases N uptake in rice by improving soil properties and NUE (Iqbal et al., 2019). In this study, as expected, the Si fertilizer and straw application had a significant effect on NUE. The AEN, REN, and PFPN of the SI+ST treatment were 3.6%, 17.6%, and 1.3% higher than that of SI treatment (*Table 3*). The increased NUE by straw was probably attributed to the improved organic matter status since straw served as N source (Kongchum et al., 2007). These results agree with the findings of previous studies that straw return significantly increased NUE (Eagle et al., 2000). Thus, retention of Si fertilizer plus straw return can be an option practice to improve NUE in agricultural production.

http://www.aloki.hu ● ISSN 1589 1623 (Print) ● ISSN1785 0037 (Online)
DOI: http://dx.doi.org/10.15666/aeer/1804_55775590

Conclusion

The use of silicon fertilizer can not only improve the N uptake and the N uptake rate of maize, but also promote the remobilization of nitrogen and the apparent contribution to grain N, and ultimately improve the yield. In comparison to the sole Si fertilizer application, the application of silicon fertilizer with straw return can further enhance the above effects, and at the same time, improve agronomic use efficiency, recovery use efficiency, and N partial factor productivity. There is sufficient evidence to support the claim that Si fertilizer combined with straw was of great advantage not only at improving NUE and crop yield but also reducing the effect of fertilizer on the environment, thus attaining the goals of sustainable agriculture. In further studies, long term experiments on Si fertilizer with straw return should be conducted to get more data that can provide comprehensive results on the integration of Si fertilizer and straw return on N nutrient. In addition, more studies should focus on how straw materials can be used to replace the use of Si fertilizer.

Acknowledgments. The authors would like to appreciate the National Key Research and Development Program of China (Grant No. 2017YFD0300604) and the National Key Research and Development Program of China (Grant No. 2018YFD0300203) for financial support.

REFERENCES

[1] Agegnehu, G., Nelson, P. N., Bird, M. I. (2016): The effects of biochar, compost, and their mixture and nitrogen fertilizer on yield and nitrogen use efficiency of barley grown on a Nitisol in the highlands of Ethiopia. – Science of the Total Environment 569: 869-879.

[2] Amin, M., Ahmad, R., Ali, A., Aslam, M., Lee, D. (2016): Silicon fertilization improves the maize (*Zea mays* L.) performance under limited moisture supply. – Cereal research communications 44(1): 172-185.

[3] Awgchew, H., Gebremedhin, H., Taddesse, G., Alemu, D. (2017): Influence of Nitrogen Rate on Nitrogen use Efficiency and Quality of Potato (*Solanum tuberosum* L.) varieties at Debre Berhan, Central Highlands of Ethiopia. – International Journal of Soil Science 12: 10-17.

[4] Baligar, V., Fageria, N., He, Z. (2001): Nutrient use efficiency in plants. – Communications in Soil Science and Plant Analysis 32(7-8): 921-950.

[5] Chen, Y., Xiao, C., Chen, X., Li, Q., Zhang, J., Chen, F., Yuan, L., Mi, G. (2014): Characterization of the plant traits contributed to high grain yield and high grain nitrogen concentration in maize. – Field Crops Research 159: 1-9.

[6] Christensen, B. T. (1986): Straw incorporation and soil organic matter in macro-aggregates and particle size separate. – Journal of Soil Science 37(1): 125-135.

[7] Cuong, T. X., Ullah, H., Datta, A., Hanh, T. C. (2017): Effects of silicon-based fertilizer on growth, yield, and nutrient uptake of rice in the tropical zone of Vietnam. – Rice Sci 24(5): 283-290.

[8] Deng, F., Wang, L., Li, Q. P., Ren, W. J. (2018): Relationship between nitrogen accumulation and nitrogen use efficiency of rice under different urea types and management methods. – Archives of Agronomy and Soil Science 64(9): 1278-1289.

[9] Deshmukh, R. K., Ma, J. F., Bélanger, R. R. (2017): Role of silicon in plants. – Frontiers in Plant Science 8: 1858.

[10] Detmann, K. C., Araújo, W. L., Martins, S. C., Sanglard, L. M., Reis, J. V., Detmann, E., Rodrigues, F. Á., Nunes-Nesi, A., Fernie, A. R., Da-Matta, F. M. (2012): Silicon nutrition increases grain yield, which, in turn, exerts a feed-forward stimulation of photosynthetic

http://www.aloki.hu ● ISSN 1589 1623 (Print) ● ISSN1785 0037 (Online)
DOI: http://dx.doi.org/10.15666/aeer/1804_55775590

rates via enhanced mesophyll conductance and alters primary metabolism in rice. – New Phytologist 196(3): 752-762.

[11] Dordas, C. A., Lithourgidis, A. S., Matsi, T., Barbayiannis, N. (2008): Application of liquid cattle manure and inorganic fertilizers affect dry matter, nitrogen accumulation, and partitioning in maize. – Nutrient Cycling in Agroecosystems 80(3): 283-296.

[12] Du, X., Chen, B., Zhang, Y., Zhao, W., Shen, T., Zhou, Z., Meng, Y. (2016): Nitrogen use efficiency of cotton (Gossypium hirsutum L.) as influenced by wheat–cotton cropping systems. – European Journal of Agronomy 75: 72-79.

[13] Du, X., Xi, M., Kong, L. (2019a): Split application of reduced nitrogen rate improves nitrogen uptake and use efficiency in sweet potato. – Scientific Reports 9(1): 1-11.

[14] Du, X., Xi, M., Kong, L. (2019b): Split application of reduced nitrogen rate improves nitrogen uptake and use efficiency in sweet potato. – Sci Rep 9(1): 14058.

[15] Eagle, A. J., Bird, J. A., Horwath, W. R., Linquist, B. A., Brouder, S. M., Hill, J. E., van Kessel, C. (2000): Rice yield and nitrogen utilization efficiency under alternative straw management practices. – Agronomy Journal 92(6): 1096-1103.

[16] Gao, L., Ma, L., Zhang, W., Wang, F., Ma, W., Zhang, F. (2009): Estimation of nutrient resource quantity of crop straw and its utilization situation in China. – Transactions of the Chinese Society of Agricultural Engineering 25(7): 173-179.

[17] González-Fontes, A., Navarro-Gochicoa, M. T., Ceacero, C. J., Herrera-Rodríguez, M. B., Camacho-Cristóbal, J. J., Rexach, J. (2017): Understanding calcium transport and signaling, and its use efficiency in vascular plants. – In: Hossain, M. A., Kamiya, T., Burritt, D. J., Phan Tran, L.-S., Fujiwara, T. (eds.) Plant Macronutrient Use Efficiency. Elsevier, pp. 165-180.

[18] Greger, M., Landberg, T., Vaculík, M. (2018): Silicon influences soil availability and accumulation of mineral nutrients in various plant species. – Plants 7(2): 41.

[19] Haddad, C., Arkoun, M., Jamois, F., Schwarzenberg, A., Yvin, J.-C., Etienne, P., Laîné, P. (2018): Silicon promotes the growth of Brassica napus L. and delays leaf senescence induced by nitrogen starvation. – Frontiers in plant science 9: 516.

[20] Haynes, R. H. (ed.) (1998): The Canadian system of soil classification. – 3rd edition, Soil Classification Working Group, NRC Research Press.

[21] Hernandez-Apaolaza, L. (2014): Can silicon partially alleviate micronutrient deficiency in plants? A review. – Planta 240(3): 447-458.

[22] Ho, D., Yan, H. D., Lin, Z. H., Pu, Z. X. (1980): On the silicon supplying ability of some important paddy soils in South China.−In: Proceedings of the symposium on paddy soil. Nanjing China. PP 95.

[23] Hu, Y., Zhang, H. (2017): Optimizing nitrogen management strategy under wheat straw incorporation for higher rice production and nitrogen use efficiency. – Journal of Plant Nutrition 40(4): 492-505.

[24] Huang, S., Zhang, W., Yu, X., Huang, Q. (2010): Effects of long-term fertilization on corn productivity and its sustainability in an Ultisol of southern China. – Agriculture, Ecosystems & Environment 138(1-2): 44-50.

[25] Iqbal, A., He, L., Khan, A., Wei, S., Akhtar, K., Ali, I., Ullah, S., Munsif, F., Zhao, Q., Jiang, L. (2019): Organic manure coupled with inorganic fertilizer: An approach for the sustainable production of rice by improving soil properties and nitrogen use efficiency. – Agronomy 9(10): 651.

[26] Islam, A., Saha, R. (1969): Effects of silicon on the chemical composition of rice plants. – Plant and Soil 30(3): 446-458.

[27] Jat, R. A., Wani, S. P., Sahrawat, K. L. (2012): Conservation agriculture in the semi-arid tropics: prospects and problems. –Advances in agronomy 117: 191-273.

[28] Jin, C., Zheng, M. J., Pang, D. W., Yin, Y. P., Han, M. M., Li, Y. X., Luo, Y. L., Xu, X., Yong, L., Wang, Z. L. (2017): Straw return and appropriate tillage method improve grain yield and nitrogen efficiency of winter wheat. – Journal of integrative agriculture 16(8): 1708-1719.

http://www.aloki.hu ● ISSN 1589 1623 (Print) ● ISSN1785 0037 (Online)
DOI: http://dx.doi.org/10.15666/aeer/1804_55775590

[29] Jugal, K., Ramani, P. (2017): Effect of silicon on nitrogen use efficiency, yield, and N and Si contents in rice under loamy sand soil. – Research J Chem and Environ 21(4): 110-118.
[30] Kaya, C., Tuna, L., Higgs, D. (2006): Effect of silicon on plant growth and mineral nutrition of maize grown under water-stress conditions. – Journal of Plant Nutrition 29(8): 1469-1480.
[31] Kongchum, M., DeLaune, R., Hudnall, W. H., Bollich, P. K. (2007): Effect of Straw Incorporation on 15N-Labeled Ammonium Nitrogen Uptake and Rice Growth. – Communications in Soil Science and Plant Analysis 38(15-16): 2149-2161.
[32] Laîné, P., Haddad, C., Arkoun, M., Yvin, J. C., Etienne, P. (2019): Silicon Promotes Agronomic Performance in Brassica napus Cultivated under Field Conditions with Two Nitrogen Fertilizer Inputs. – Plants 8(5): 137.
[33] Lea, P. J., Azevedo, R. A. (2006): Nitrogen use efficiency. 1. Uptake of nitrogen from the soil. – Annals of Applied Biology 149(3): 243-247.
[34] Luz, J., Rodrigues, C., Goncalves, M., Coelho, L. (2008): The effect of silicate on potatoes in Minas Gerais, Brazil. – IV Silicon in Agriculture Conference 31: 67.
[35] Mi, G., Liu, J. A., Chen, F., Zhang, F., Cui, Z., Liu, X. (2003): Nitrogen uptake and remobilization in maize hybrids differing in leaf senescence. – Journal of Plant Nutrition 26(1): 237-247.
[36] Moe, K., Mg, K. W., Win, K. K., Yamakawa, T. (2017): Effects of Combined Application of Inorganic Fertilizer and Organic Manures on Nitrogen Use and Recovery Efficiencies of Hybrid Rice (Palethwe-1). – American Journal of Plant Sciences 8(5): 1043-1064.
[37] Neu, S., Schaller, J., Dudel, E. G. (2017): Silicon availability modifies nutrient use efficiency and content, C: N: P stoichiometry, and productivity of winter wheat (*Triticum aestivum* L.). – Scientific Reports 7: 40829.
[38] Okumoto, S., Pilot, G. (2011): Amino acid export in plants: a missing link in nitrogen cycling. – Molecular plant 4(3): 453-463.
[39] Omara, P., Aula, L., Oyebiyi, F., Raun, W. R. (2019): World Cereal Nitrogen Use Efficiency Trends: Review and Current Knowledge. – Agrosystems, Geosciences & Environment 2: 180045.
[40] Owino-Gerroh, C., Gascho, G. (2005): Effect of silicon on low pH soil phosphorus sorption and uptake and growth of maize. – Communications in Soil Science and Plant Analysis 35(15-16): 2369-2378.
[41] Patel, R., Patel, K., Malav, J. (2017): Status of Silicon in Rice (Oryza sativa L.) and its Correlation with Other Nutrients under Typic ustochrepts Soil. – Int. J. Curr. Microbiol. App. Sci 6(12): 2598-2611.
[42] Pathak, H., Singh, R., Bhatia, A., Jain, N. (2006): Recycling of rice straw to improve wheat yield and soil fertility and reduce atmospheric pollution. – Paddy and Water Environment 4(2): 111.
[43] Perchlik, M., Tegeder, M. (2017): Improving plant nitrogen use efficiency through alteration of amino acid transport processes. – Plant Physiology 175(1): 235-247.
[44] Prieto, K. R., Echaide-Aquino, F., Huerta-Robles, A., Valério, H. P., Macedo-Raygoza, G., Prado, F. M., Medeiros, M. H., Brito, H. F., da Silva, I. G., Felinto, M. C. C. (2017): Endophytic bacteria and rare earth elements; promising candidates for nutrient use efficiency in plants. – In: Hossain, M. A., Kamiya, T., Burritt, D. J., Phan Tran, L.-S., Fujiwara, T. (eds.) Plant Macronutrient Use Efficiency. Elsevier, pp. 285-306.
[45] Reich, M., Aghajanzadeh, T., De Kok, L. J. (2014): Physiological basis of plant nutrient use efficiency–concepts, opportunities, and challenges for its improvement. – In: Hawkesford, M., Kopriva, De Kok, L. (eds.) Nutrient use efficiency in plants. Springer, pp. 1-27.
[46] Sharma, L. K., Bali, S. K. (2018): A review of methods to improve nitrogen use efficiency in agriculture. – Sustainability 10(1): 51.

http://www.aloki.hu ● ISSN 1589 1623 (Print) ● ISSN1785 0037 (Online)
DOI: http://dx.doi.org/10.15666/aeer/1804_55775590

[47] Singh, K. K., Singh, K., Singh, R., Singh, Y., Singh, C. S. (2006): Response of nitrogen and silicon levels on growth, yield and nutrient uptake of rice (*Oryza sativa* L.). – Oryza 43(3): 220-223.
[48] Takahashi, S., Uenosono, S., Ono, S. (2003): Short-and long-term effects of rice straw application on nitrogen uptake by crops and nitrogen mineralization under flooded and upland conditions. – Plant and Soil 251(2): 291-301.
[49] Wang, L., Wang, S., Chen, W., Li, H., Deng, X. (2017): Physiological mechanisms contributing to increased water-use efficiency in winter wheat under organic fertilization. – PloS one 12(6): e0180205.
[50] Wang, X., Jia, Z., Liang, L., Zhao, Y., Yang, B., Ding, R., Wang, J., Nie, J. (2018): Changes in soil characteristics and maize yield under straw returning system in dryland farming. – Field Crops Research 218: 11-17.
[51] Wang, L., Yuan, X., Liu, C., Li, Z., Chen, F., Li, S., Wu, L., Liu, Y. (2019): Soil C and N dynamics and hydrological processes in a maize-wheat rotation field subjected to different tillage and straw management practices. – Agriculture, ecosystems & environment 285: 106616.
[52] Watson, C., Atkinson, D., Gosling, P., Jackson, L., Rayns, F. (2002): Managing soil fertility in organic farming systems. – Soil use and management 18: 239-247.
[53] Xu, Y., Nie, L., Buresh, R. J., Huang, J., Cui, K., Xu, B., Gong, W., Peng, S. (2010): Agronomic performance of late-season rice under different tillage, straw, and nitrogen management. – Field Crops Research 115(1): 79-84.
[54] Xu, H., Lu, Y., Xie, Z. (2016): Effects of silicon on maize photosynthesis and grain yield in black soils. – Emirates Journal of Food and Agriculture 28(11): 779-785.
[55] Yang, J., Jiang, N., Chen, J. (2003): Dynamic simulation of nitrogen application level effects on rice yield and optimization analysis of fertilizer supply in paddy field. – Ying Yong Sheng Tai Xue bao, The journal of applied ecology 14(10): 1654-1660.
[56] Yogendra, N., Prakash, N., Malagi, M., Kumara, B., Mohan Kumar, R., Chandrashekar, N. (2013): Effect of calcium silicate on yield and nitrogen use efficiency (NUE) of wetland rice. – Plant Archives 13(1): 89-91.
[57] Yogendra, N., Kumara, B., Chandrashekar, N., Prakash, N., Anantha, M., Jeyadeva, H. (2014): Effect of silicon on real time nitrogen management in a rice ecosystem. – African Journal of Agricultural Research 9(9): 831-840.
[58] Zhang, W., Xu, M., Wang, B., Wang, X. (2009): Soil organic carbon, total nitrogen, and grain yields under long-term fertilizations in the upland red soil of southern China. – Nutrient Cycling in Agroecosystems 84(1): 59-69.
[59] Zhang, P., Wei, T., Li, Y., Wang, K., Jia, Z., Han, Q., Ren, X. (2015): Effects of straw incorporation on the stratification of the soil organic C, total N, and C: N ratio in a semiarid region of China. – Soil and Tillage Research 153: 28-35.
[60] Zhang, Y., Li, C., Wang, Y., Hu, Y., Christie, P., Zhang, J., Li, X. (2016): Maize yield and soil fertility with the combined use of compost and inorganic fertilizers on a calcareous soil on the North China Plain. – Soil and tillage research 155: 85-94.
[61] Zhou, D. X., Su, Y., Ning, Y. C., Rong, G. H., Wang, G. D., Liu, D., Liu, L. Y. (2018): Estimation of the Effects of Maize Straw Return on Soil Carbon and Nutrients Using Response Surface Methodology. – Pedosphere 28(3): 411-421.
[62] Zhu, H., Wu, J., Huang, D., Zhu, Q., Liu, S., Su, Y., Wei, W., Syers, J. K., Li, Y. (2010): Improving fertility and productivity of a highly-weathered upland soil in subtropical China by incorporating rice straw. – Plant and Soil 331(1-2): 427-437.

http://www.aloki.hu ● ISSN 1589 1623 (Print) ● ISSN1785 0037 (Online)
DOI: http://dx.doi.org/10.15666/aeer/1804_55775590

TEMPORAL AND SPATIAL CHANGES OF HIGH TEMPERATURE HAZARD AFFECTING SINGLE-SEASON RICE IN JIANGXI PROVINCE, SOUTHEAST CHINA

YANG, J.[1] – ZHANG, Y. Z.[1] – LI, Y. C.[1] – LIU, D.[1] – JIN, G. H.[1] – TIAN, J.[1] – LI, X. X.[2] – HUANG, S. E.[1*]

[1]*Meteorological Science Research Institute of Jiangxi Province, Nanchang 330096, China*

[2]*Agro-Meteorological Center of Jiangxi Province, Nanchang 330096, China*

**Corresponding author*
e-mail: 512675442@qq.com

(Received 12th Apr 2020; accepted 10th Jul 2020)

Abstract. High temperature (HT), considered a daily average temperature (T_{ave}) ≥ 30 °C or a daily maximum temperature (T_{max}) ≥ 35 °C, during the heading-flowering period affects single-season rice production in Jiangxi Province, southeast China, and the temporal and spatial changes of HT are not yet clear in this province. Here, the meteorological data of 85 national weather stations from 1981 to 2017 were used to explore the temporal and spatial changes of HT. In addition, the effects of HT during the heading-flowering period on yield and spikelet fertility of single-season rice were investigated. Our results showed that HT in single-season rice occurred every year from 1981 to 2017. T_{ave}, T_{max}, and HT hazard events (HT for ≥ three consecutive days) increased after 2003, with severe HT (HT for ≥ eight consecutive days) increasing significantly. In addition, a greater number of HT hazard events were mainly distributed in the middle and northeast area of Jiangxi. HT mainly occurred from July 11 to August 10, and severe HT occurred more frequently from July 21 to July 31. It is worth noting that there were strong negative correlations between spikelet fertility and T_{ave}, days of T_{ave} ≥ 30 °C, and days of T_{max} ≥ 35 °C. Thus, these results should be considered for establishing effective strategies to mitigate rice HT hazard under global climate change.
Keywords: *rice, high temperature, flowering, spikelet fertility, sowing date*

Introduction

Rice (*Oryza sativa* L.) is the staple food source for more than half of the world's population. Recently, extreme high temperature (HT) events frequently affect rice production (Kim et al., 2013; Espe et al., 2017). HT beyond the critical threshold (T_{ave} ≥ 30 °C or T_{max} ≥ 35 °C) during the growth period, especially during the heading-flowering period, leads to poor fertilization and reduced spikelet fertility, which drastically reduces rice yield (Jagadish et al., 2010; Madan et al., 2012; Chaturvedi et al., 2017; Zhao et al., 2018; Stuerz and Asch, 2019). Rice grain yield could decline by 10% for each 1 °C increase in the nighttime temperature (Peng et al., 2004). Globally, the average surface temperature has increased by 0.85 °C from 1880 to 2012 (IPCC, 2013). The frequency or intensity of HT events will likely continue to increase, which could lead to the higher vulnerability of rice (Van Oort et al., 2018). Thus, current research should be focused on reducing the loss of rice yield under HT events (Ray et al., 2015; Wang et al., 2016).

Jiangxi is one of the most important two-season rice producing provinces in southeast China, as it can deliver rice to the country year-round. In recent years, due to urbanization and the shortage of the rural labor force, the production area of two-season rice has been decreasing, whereas the production area of single-season rice in Jiangxi has exceeded 460,000 hectares and is expected to increase in the future. However, HTs

http://www.aloki.hu ● ISSN 1589 1623 (Print) ● ISSN 1785 0037 (Online)
DOI: http://dx.doi.org/10.15666/aeer/1804_55915605

caused by the Pacific sub-tropical high during the heading-flowering period from July to August every year in Jiangxi tend to occur frequently, which can easily lead to HT hazard causing a huge loss of single-season rice yield (Huang et al., 2017). Therefore, improving HT resistance of single-season rice has received increasing attention.

HT is not conducive to rice production, but taking effective defense measures can reduce HT hazard (Khan et al., 2019). Previous studies have shown that the selection of heat-resistant varieties (Prasad et al., 2006; Jagadish et al., 2010), improvement of field management (Yang et al., 2015; Tang et al., 2019), and application of exogenous substances (Mohammed et al., 2009; Fahad et al., 2016; Wu et al., 2017) can effectively mitigate the negative effects of HT on rice growth and development. In addition, avoiding HT during the heading-flowering period, by varying flowering times, is another effective method against HT hazard. Rice with an early-morning flowering (EMF) trait could avoid HT-induced sterility during anthesis by flowering at a cooler temperature in the early morning (Ishimaru et al., 2010). It has been reported that EMF rice with a quantitative trait locus (QTL) named *qEMF3* mitigated heat-induced spikelet sterility under elevated temperature by completing flower opening before the air temperature reached 35 °C during the day (Hirabayashi et al., 2015).

Previous studies have been conducted on rice HT hazard in Jiangxi. By investigating the temperature data of 74 meteorological stations in Jiangxi from June to August from 1961 to 2010, Yang et al. (2012) showed that the annual frequency of occurrence of rice heat stress decreased from 1961 to 1982, while increased significantly from 1983 to 2010. Moreover, Huang et al. (2017) indicated that the changes of intensity of HT hazard events were significant, the higher hazard events for rice heat stress were mainly detected in the middle and northeast area of Jiangxi. However, the temporal and spatial changes of HT hazard affecting single-season rice in Jiangxi were still not well analyzed.

In the present study, we used meteorological data of 85 national weather stations from July to August 1981 to 2017 to (1) comprehensively investigate temporal and spatial changes of HT hazard affecting single-season rice during the heading-flowering period in Jiangxi Province, (2) study the effects of HT on yield and spikelet fertility of single-season rice, and (3) find the highest risk period to avoid HT hazard. Thus, the overall objective of this study is to provide the scientific support for the high- and stable-yield cultivation and HT resistance of single-season rice under global warming.

Material and methods

Data collection

Jiangxi Province (latitude: 24°29′ N–30°05′ N, longitude: 113°34′ E–118°29′ E) located in southeast China is dominated by a humid subtropical monsoon climate; thus, the climate is mild with abundant sunshine and rainfall. Moreover, the four seasons are evident and there is a long frost-free period (240–307 days), making Jiangxi conducive to the cultivation of crops. The average annual temperature, average annual precipitation, and average annual illumination time are 16.5–19.8 °C, 1,436–1,956 mm, and 1,327–1,927 h, respectively (Huang et al., 2017). In Jiangxi, rice can be grown as either double cropping (early or late rice) or single cropping (single-season rice). The HTs in summer (from June to August) are likely to trigger heat stress response of early rice during the grain filling period and single-season rice during the heading-flowering period.

http://www.aloki.hu ● ISSN 1589 1623 (Print) ● ISSN 1785 0037 (Online)
DOI: http://dx.doi.org/10.15666/aeer/1804_55915605

The meteorological data of daily average temperature (T_{ave}) and daily maximum temperature (T_{max}) of 85 national weather stations (*Fig. 1*) from July 11, 1981 to August 31, 2017, in Jiangxi Province were provided by the Jiangxi Meteorological Bureau. The agricultural data of single-season rice yield in seven representative regional trial sites (Fuliang, Anyi, Nanchang, Fuzhou, Pingxiang, Ji'an, and Huichang) (*Fig. 1*) over 13 years (2004–2016) were collected from the Department of Agriculture of Jiangxi Province.

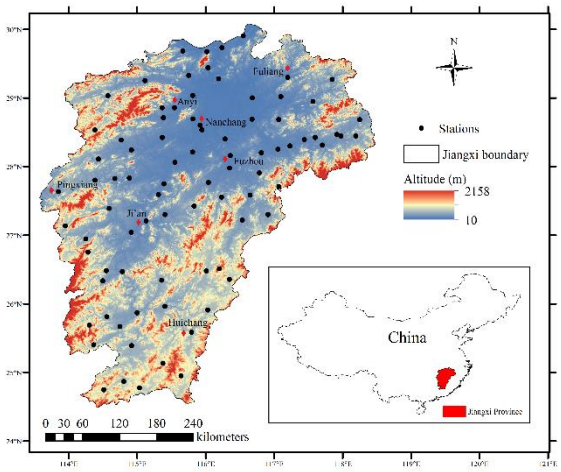

Figure 1. *Distribution of 85 national weather stations in Jiangxi Province, southeast China*

Analytical methods

Temperature anomalies

The daily T_{ave} and T_{max} data from July 11, 1981 to August 31, 2017, were compiled to analyze the temporal and spatial changes of temperature, temperature anomaly (the difference between an observed temperature and the average temperature), and accumulative anomaly (sum of the anomalies). Within the calculated temperature anomalies, the low, medium, and high anomalies were separated, where a low temperature anomaly was considered ≤ -0.50 °C, a medium temperature anomaly was -0.5–0.5 °C, and a high anomaly was ≥ 0.50 °C.

HT hazard

$T_{ave} \geq 30$ °C or $T_{max} \geq 35$ °C were considered the threshold for HT (Jagadish et al., 2010; Madan et al., 2012), and HT for three to four consecutive days was defined as slight HT hazard, five to seven consecutive days for moderate HT hazard, and ≥ eight consecutive days for severe HT hazard. Furthermore, the temporal and spatial changes of the number of stations recording the occurrence of HT hazard; the number of slight, moderate, and severe HT hazard; the number of HT days; and the greatest number of consecutive HT days at 85 national weather stations from 1981 to 2017 were analyzed.

Measures of single-season rice yield

Based on the changes in temperature, the changes in the annual yield of single-season rice (effective panicles, total grains per panicle, filled grains per panicle, spikelet

http://www.aloki.hu ● ISSN 1589 1623 (Print) ● ISSN 1785 0037 (Online)
DOI: http://dx.doi.org/10.15666/aeer/1804_55915605

fertility, 1000-grain weight, and yield) (Prasad et al., 2006) were analyzed to screen for effective traits for the identification of HT hazard during the heading-flowering period.

Statistical analysis

Excel2010, Matlab 2010a, and ArcGIS10.2 software (Huang et al., 2017) were used to analyze data and draw graphs. The correlations between meteorological parameters and rice yield were conducted by using SPSS 17.0 (Yang et al., 2015). The significance was determined using the least significant difference (LSD) test at $P < 0.05$ or $P < 0.01$, which was calculated using SPSS 17.0.

Results

Temporal changes of temperature anomalies

The temporal changes of T_{ave} and T_{max} anomalies show a consistent trend (*Fig. 2a* and *b*). The temperature anomalies and accumulative anomalies could be divided into three periods: normal temperature (1981–1992), low temperature (1993–2002), and HT (2003–2017). During the normal temperature period, the temperature anomalies and accumulative anomalies were relatively stable with 11 medium anomalies (-0.5–0.5 °C) of T_{ave} and six medium anomalies of T_{max}. During this period, the average anomaly of T_{ave} and T_{max} were 0.04 °C and 0.18 °C, respectively. During the low temperature period, the accumulative anomalies showed a downward trend with six low anomalies (≤ -0.50 °C) of T_{ave} and seven low anomalies of T_{max}; the average anomaly of T_{ave} and T_{max} during this period was -0.60 °C and -0.91 °C, respectively. During HT period, the accumulative anomalies showed an upward trend with six high anomalies (≥ 0.50 °C) of T_{ave} and seven high anomalies of T_{max}, and the average anomaly of T_{ave} and T_{max} were 0.37 °C and 0.47 °C, respectively. The increasing occurrence of temperature anomalies during the current HT period indicated that the T_{ave} and T_{max} have generally risen since 2003 ($P < 0.05$).

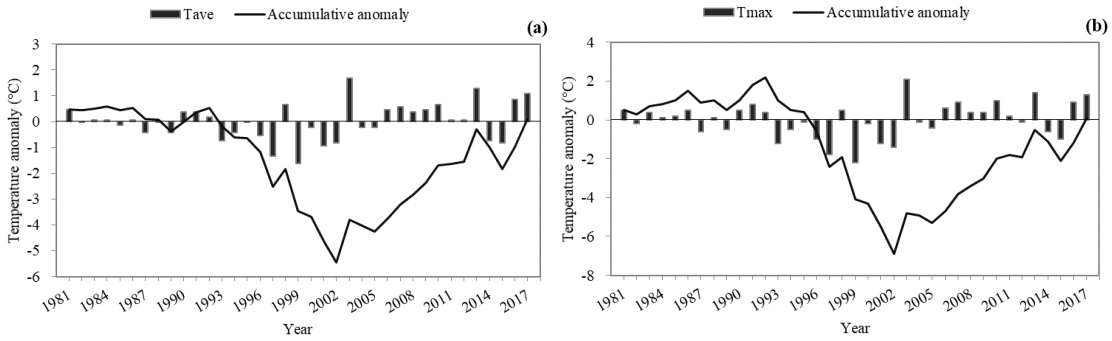

Figure 2. *Temporal changes of T_{ave} (a), and T_{max} (b) anomalies from 1981 to 2017†. †T_{ave}: daily average temperature; T_{max}: daily maximum temperature. Accumulative anomaly is the accumulation of anomalies*

Spatial distribution of temperature anomalies

The spatial distribution of T_{ave} anomalies is consistent with that of the T_{max} anomalies (*Fig. 3a* and *b*). The temperature anomalies were spatially divided into low anomaly zone, medium anomaly zone, and high anomaly zone. The medium anomaly zone (-0.5–0.5 °C)

http://www.aloki.hu ● ISSN 1589 1623 (Print) ● ISSN 1785 0037 (Online)
DOI: http://dx.doi.org/10.15666/aeer/1804_55915605

covered most of the province with 45 stations of T_{ave} and 49 stations of T_{max}. The average anomaly of T_{ave} and T_{max} in this zone were 0.47 °C and 0.11 °C, respectively. Fifteen stations of T_{ave} and 19 stations of T_{max} belonged to the low anomaly zone (≤ -0.50 °C), and the average anomaly of T_{ave} and T_{max} in this zone were -1.21 °C and -0.87 °C, respectively. The high anomaly zone (≥ 0.50 °C) was primarily located in the middle and northeast of the province with 25 stations of T_{ave} and 17 stations of T_{max}, and the average anomaly of T_{ave} and T_{max} in this zone were 0.74 °C and 0.70 °C, respectively.

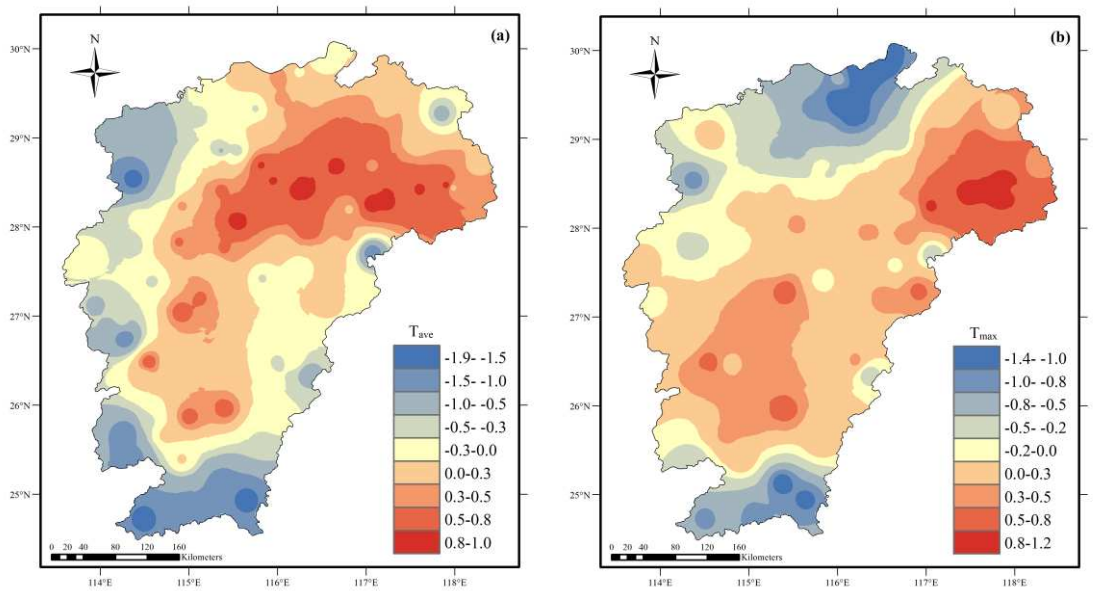

Figure 3. *Spatial distribution of T_{ave} (a), and T_{max} (b) anomalies from 1981 to 2017†. †T_{ave}: daily average temperature; T_{max}: daily maximum temperature*

Changes of daily temperature

The changes of daily T_{ave} and T_{max} are similar, showing a trend of increasing first and then decreasing (*Fig. 4*). The T_{ave} and T_{max} were 29.3 °C and 34.5 °C from July 11 to August 10, and 28.0 °C and 33.0 °C from August 11 to August 31 from 1981–2017, indicating that T_{ave} and T_{max} in mid-July to early-August were higher than that in mid- to late-August. The data presented in *Figure 4* also indicate that the temperatures of four consecutive days on July 22–25 were the highest ($T_{ave} \geq 29.6$ °C, $T_{max} \geq 34.9$ °C), especially the T_{max} of three consecutive days from July 23–25, which exceeded 35 °C. Thus, it is necessary to attend to the effects of HT on heading and flowering in single-season rice from July 22 to July 25 each year.

Temporal changes of the number of stations recording the occurrence of HT hazard

Many stations showed record of slight and moderate HT hazards each year, but no severe HT hazard events occurred in 1997 and 1999. In 1997, the number of stations recording the occurrence of HT hazard events was the lowest, with only 31 stations recording HT hazard events. In contrast, the slight, moderate, and severe HT hazard events occurred at all 85 stations in 2003 (*Fig. 5*). During the normal temperature period (1981–1992), the average number of stations recording the occurrence of slight, moderate, and severe HT hazard events was 80.92 stations, 73.75 stations, and 56.50

http://www.aloki.hu ● ISSN 1589 1623 (Print) ● ISSN 1785 0037 (Online)
DOI: http://dx.doi.org/10.15666/aeer/1804_55915605

stations, respectively. The average number of stations recording HT hazard events was 73.80 stations showing slight HT, 60.10 stations with moderate HT, 31.50 stations showing severe HT during the low temperature period (1993–2002), and 84.67 stations showing slight, 81.13 stations recording moderate, 62.80 stations recording severe during the HT period (2003–2017). The above results indicate that the number of stations recording the occurrence of slight, moderate, and severe HT hazard events have increased since 2003 ($P < 0.05$).

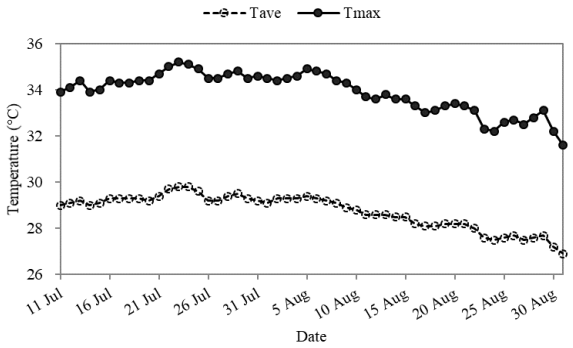

Figure 4. *Changes of daily temperature†. †T_{ave}: daily average temperature; T_{max}: daily maximum temperature*

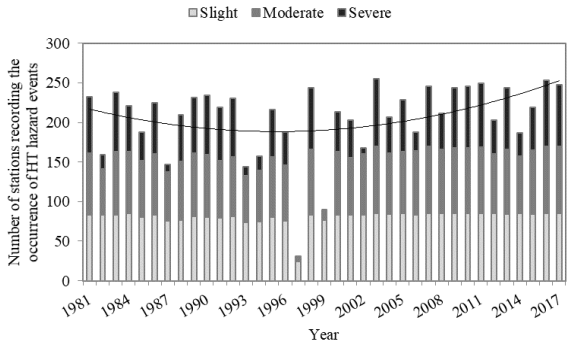

Figure 5. *Temporal changes of the number of stations recording the occurrence of slight, moderate, and severe HT hazard events from 1981 to 2017†. †HT: high temperature. T_{ave}: daily average temperature; T_{max}: daily maximum temperature. $T_{ave} \geq 30$ °C or $T_{max} \geq 35$ °C for three to four days is considered a slight HT hazard, five to seven consecutive days for moderate HT hazard, ≥ eight consecutive days for severe HT hazard*

Temporal changes of the number of HT hazard events

Over the past 37 years (1981–2017), HT hazard occurred every year in this province. The number of slight HT hazards was the highest (95.59), followed by moderate HT hazards (79.19), and severe HT hazards (72.45). In 1997, the total number of HT hazard events was the lowest, with only 33 recorded HT hazard events. In contrast, the number of HT hazard events in 2006 was the highest, reaching 405 (*Fig. 6*). During the normal temperature period (1981–1992), the average number of HT hazard events of slight, moderate, and severe HT hazards was 84.08, 82.17, and 68.23, respectively. The average number of HT hazard events for slight, moderate, and severe HT hazard events was 89.40, 65.70, and 41.90 during the low temperature period (1993–2002), and

http://www.aloki.hu ● ISSN 1589 1623 (Print) ● ISSN 1785 0037 (Online)
DOI: http://dx.doi.org/10.15666/aeer/1804_55915605

108.93, 85.80, and 93.73 during the HT period (2003–2017), respectively. This indicates that the number of slight, moderate, and severe HT hazard events has increased since 2003, with severe HT hazard events increasing significantly ($P < 0.05$).

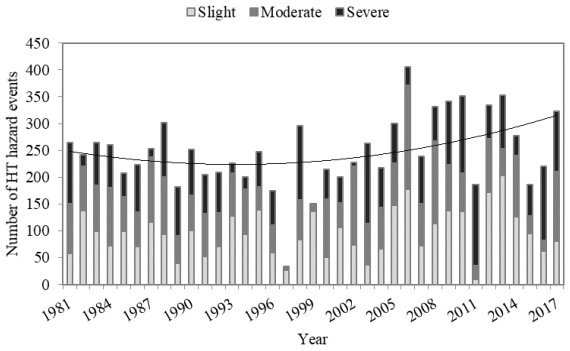

Figure 6. *Temporal changes of the number of HT hazard events from 1981 to 2017†. †HT: high temperature. T_{ave}: daily average temperature; T_{max}: daily maximum temperature. $T_{ave} \geq 30$ °C or $T_{max} \geq 35$ °C for three to four days is considered a slight HT hazard, five to seven consecutive days for moderate HT hazard, ≥ eight consecutive days for severe HT hazard*

Temporal distribution of the number of HT hazard events

Figure 7 shows that slight, moderate, and severe HT hazard events occurred in every time period (i.e., every ten days) from July 11 to August 31 in the past 37 years. The overall number of slight HT hazard events was the highest (128.97), followed by moderate HT hazards (96.35), and severe HT hazards (62.14). HT hazard events primarily occurred from July 11 to August 10, and the number of HT hazard events during the time period was 211.70, accounting for 73.65% of the total number of events. Therefore, during the heading-flowering period of rice, which falls from July 11 to August 10, the hot weather should be attended to avoid HT hazard. The fewest slight, moderate, and severe HT hazard events (33.95) occurred from August 11 to August 20, and the greatest number of HT hazard events (74.32) appeared from July 21 to July 31. The number of severe HT hazard events from July 21 to July 31 was 28.16, accounting for 45.32% of the total severe HT hazard events, indicating that this area is prone to severe HT hazard events from July 21 to July 31.

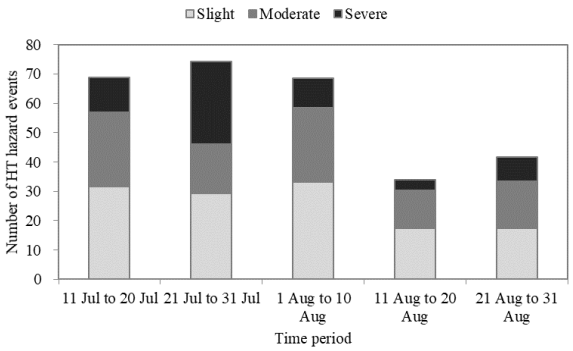

Figure 7. *Distribution of the number of HT hazard events of temporal periods (every ten days) †. †HT: high temperature. T_{ave}: daily average temperature; T_{max}: daily maximum temperature. $T_{ave} \geq 30$ °C or $T_{max} \geq 35$ °C for three to four days is considered a slight HT hazard, five to seven consecutive days for moderate HT hazard, ≥ eight consecutive days for severe HT hazard*

http://www.aloki.hu ● ISSN 1589 1623 (Print) ● ISSN 1785 0037 (Online)
DOI: http://dx.doi.org/10.15666/aeer/1804_55915605

Spatial distribution of the number of HT hazard events

The east, south, and west of Jiangxi Province are surrounded by mountains, and the north is flat, forming a large open basin that is tilted to the north. The spatial distribution of the number of HT hazard events is closely related to the topography, with more HT hazard events in plains and basins and fewer in mountains (*Fig. 8*). The spatial distribution of the total number of HT hazard events and the number of slight, moderate, and severe HT hazards (*Fig. 8a–d*) are similar, meaning that the area with a high frequency of HT hazard events is mainly distributed in the middle and northeast of this province. The total number of HT hazard events in the high frequency area was 155–174. The number of slight, moderate, and severe HT hazard events in the middle and northeast of the province were 78–86, 52–59, and 27–33, respectively. Thus, special attention should be paid to areas with a greater tendency to have HT hazard events during the heading-flowering period from July 11 to August 10 in single-season rice.

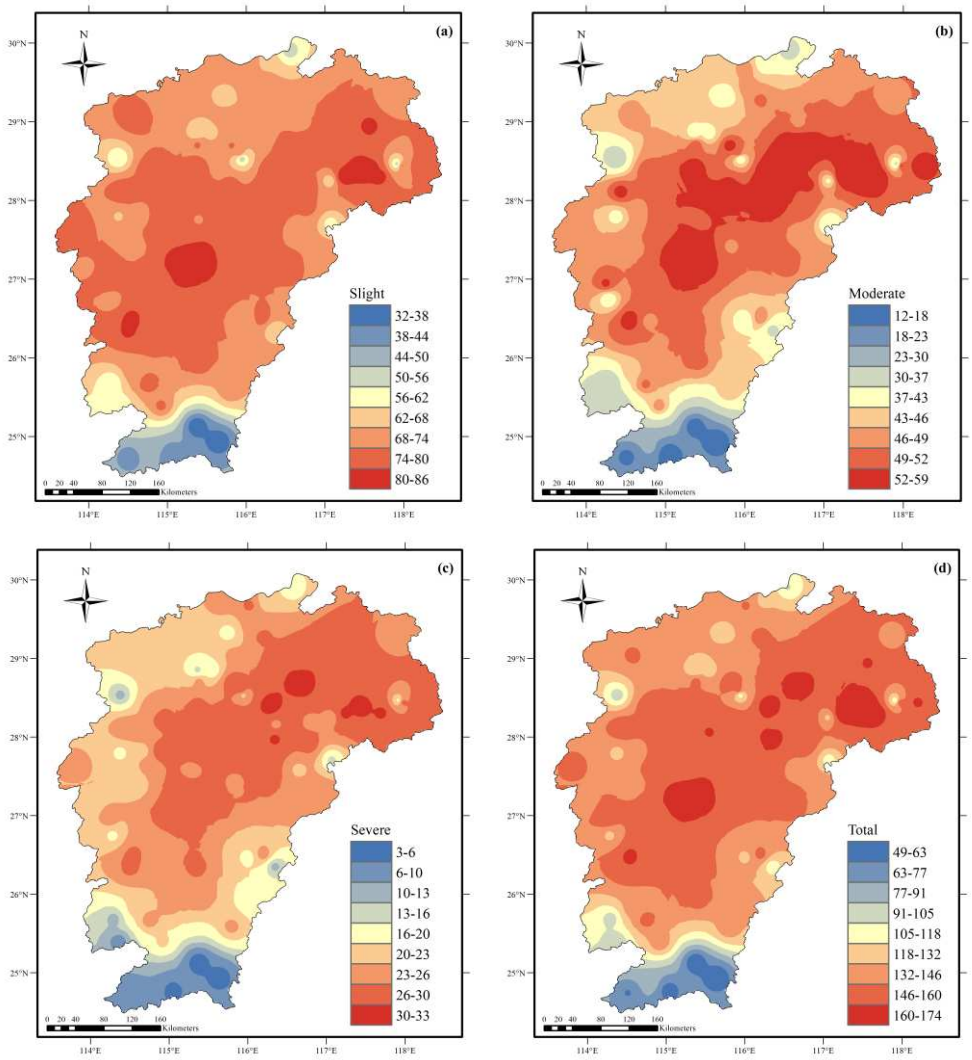

Figure 8. *Spatial distribution of the number of slight (a), moderate (b), severe (c), and total (d) HT hazard events from 1981 to 2017†. † HT: high temperature. T_{ave}: daily average temperature; T_{max}: daily maximum temperature. $T_{ave} \geq 30$ °C or $T_{max} \geq 35$ °C for three to four days is considered a slight HT hazard, five to seven consecutive days for moderate HT hazard, ≥ eight consecutive days for severe HT hazard*

http://www.aloki.hu ● ISSN 1589 1623 (Print) ● ISSN 1785 0037 (Online)
DOI: http://dx.doi.org/10.15666/aeer/1804_55915605

Temporal changes of the number of HT days and the greatest number of consecutive HT days

The temporal changes of the number of HT days of $T_{ave} \geq 30$ °C is consistent with that of $T_{max} \geq 35$ °C (*Fig. 9a* and *b*). During the normal temperature period (1981–1992), the average number of HT days of T_{ave} and T_{max} were 16.14 d and 21.36 d, respectively. The average number of HT days was 11.74 d (T_{ave}) and 15.08 d (T_{max}) during the low temperature period (1993–2002), and 20.08 d (T_{ave}) and 25.67 d (T_{max}) during the HT period (2003–2017). The number of HT days of T_{ave} and T_{max} in 1997 was the lowest, with only 1.35 d and 3.78 d, and the number of HT days in 2003 was the highest, reaching 32.31 d and 36.44 d, respectively. After 2003, the number of HT days showed an overall increase ($P < 0.05$).

The temporal changes of the greatest number of consecutive days of $T_{ave} \geq 30$ °C and $T_{max} \geq 35$ °C is similar (*Fig. 9a* and *b*). During the normal temperature period (1981–1992), the greatest number of consecutive days of T_{ave} and T_{max} were 7.88 d and 9.70 d on average, respectively. The average number of days was 5.18 d (T_{ave}) and 6.38 d (T_{max}) during the low temperature period (1993–2002), and 9.19 d (T_{ave}) and 10.98 d (T_{max}) during the HT period (2003–2017). The data presented in *Figure 9* also shows that the greatest number of consecutive days of T_{ave} and T_{max} in 1997 was the lowest, with only 0.71 d and 1.80 d, and the greatest number of consecutive days in 2003 was the highest, reaching 18.22 d and 20.94 d, respectively. Overall, the number of HT days showed an increase since 2003 ($P < 0.05$).

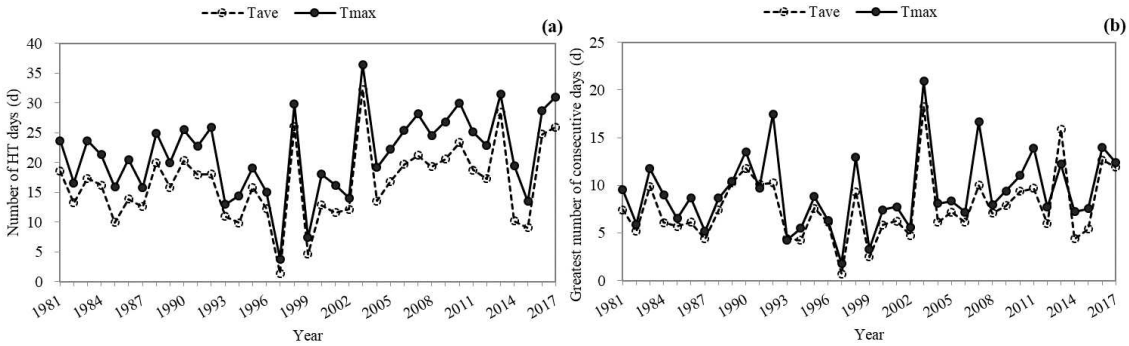

Figure 9. *Temporal changes of the number of HT days (a), and the greatest number of consecutive HT days (b) from 1981 to 2017†. †HT: high temperature. T_{ave}: daily average temperature; T_{max}: daily maximum temperature. The number of HT days is the number of days of $T_{ave} \geq 30$ °C or $T_{max} \geq 35$ °C. The greatest number of consecutive HT days is the number of consecutive days of $T_{ave} \geq 30$ °C or $T_{max} \geq 35$ °C*

Spatial distribution of the number of HT days and the greatest number of consecutive HT days

Figure 10 shows that the spatial distribution of the number of HT days of $T_{ave} \geq 30$ °C and $T_{max} \geq 35$ °C is consistent with that of the greatest number of consecutive HT days. The number of HT days and the greatest number of consecutive days of $T_{ave} \geq 30$ °C were 16.67 d and 7.72 d, respectively (*Fig. 10a* and *b*). The number of HT days and the greatest number of consecutive days of $T_{max} \geq 35$ °C were 21.49 d and 9.35 d, respectively (*Fig. 10c* and *d*). The number of HT days (≥ 21 days of $T_{ave} \geq 30$ °C or ≥ 24 days of $T_{max} \geq 35$ °C) and the greatest number of consecutive days

http://www.aloki.hu ● ISSN 1589 1623 (Print) ● ISSN 1785 0037 (Online)
DOI: http://dx.doi.org/10.15666/aeer/1804_55915605

(≥ nine days of T_{ave} ≥ 30 °C or ≥ 10.5 days of T_{max} ≥ 35 °C) were mainly distributed in the middle and northeast area of this province.

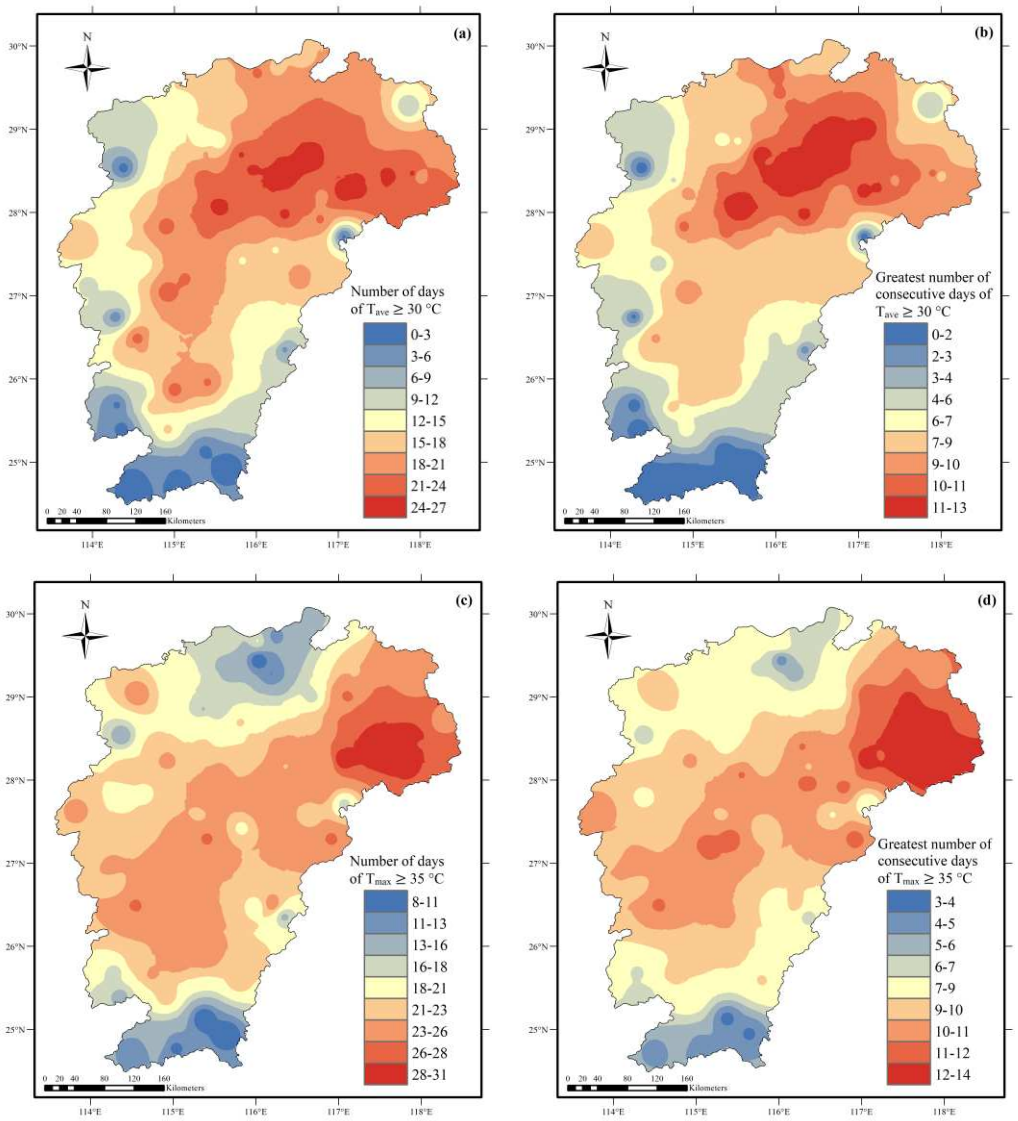

Figure 10. *Spatial distribution of the number of days of T_{ave} ≥ 30 °C (a), the greatest number of consecutive days of T_{ave} ≥ 30 °C (b), the number of days of T_{max} ≥ 35 °C (c), and the greatest number of consecutive days of T_{max} ≥ 35 °C (d) from 1981 to 2017†. †HT: high temperature. T_{ave}: daily average temperature; T_{max}: daily maximum temperature*

Relationship between spikelet fertility and temperature, number of HT days

To screen for rice agricultural traits related (data collected from 2004 to 2016) to the identification of HT hazard, the changes of temperature and measures of single-season rice yield were investigated (*Table 1*). A correlation was identified between measures of yield and temperature as well as measures of yield and the number of HT days. The relationships between spikelet fertility, temperature, and number of HT days were analyzed. As shown in *Figure 11a–d*, there were strong negative correlations between spikelet fertility and T_{ave} (P = 0.033; *Fig. 11a*), spikelet fertility and the number of days

http://www.aloki.hu ● ISSN 1589 1623 (Print) ● ISSN 1785 0037 (Online)
DOI: http://dx.doi.org/10.15666/aeer/1804_55915605

of $T_{ave} \geq 30$ °C (P = 0.020; *Fig. 11c*), and spikelet fertility and the number of days of $T_{max} \geq 35$ °C (P = 0.005; *Fig. 11d*). However, spikelet fertility was not correlated with T_{max} (P = 0.303; *Fig. 11b*), and the number of consecutive HT days (not listed in this table). Thus, in addition to meteorological factors (temperature, number of HT days), spikelet fertility can also be used as an effective trait for the identification of HT hazard in single-season rice.

Discussion

Because of its geographical location and climate, Jiangxi is prone to HT hazard events. In this study, we found that HT hazard during the heading-flowering period in single-season rice occurred every year from 1981 to 2017 in Jiangxi. Moreover, air temperature (T_{ave} and T_{max}) has generally increased since 2003, and the number of slight, moderate, and severe HT hazard events has increased since 2003, with severe HT showing a significant increase ($P < 0.05$). In addition, a greater number of HT hazard events of single-season rice was primarily distributed in the middle and northeast area of Jiangxi, which is consistent with the results of Huang et al. (2017).

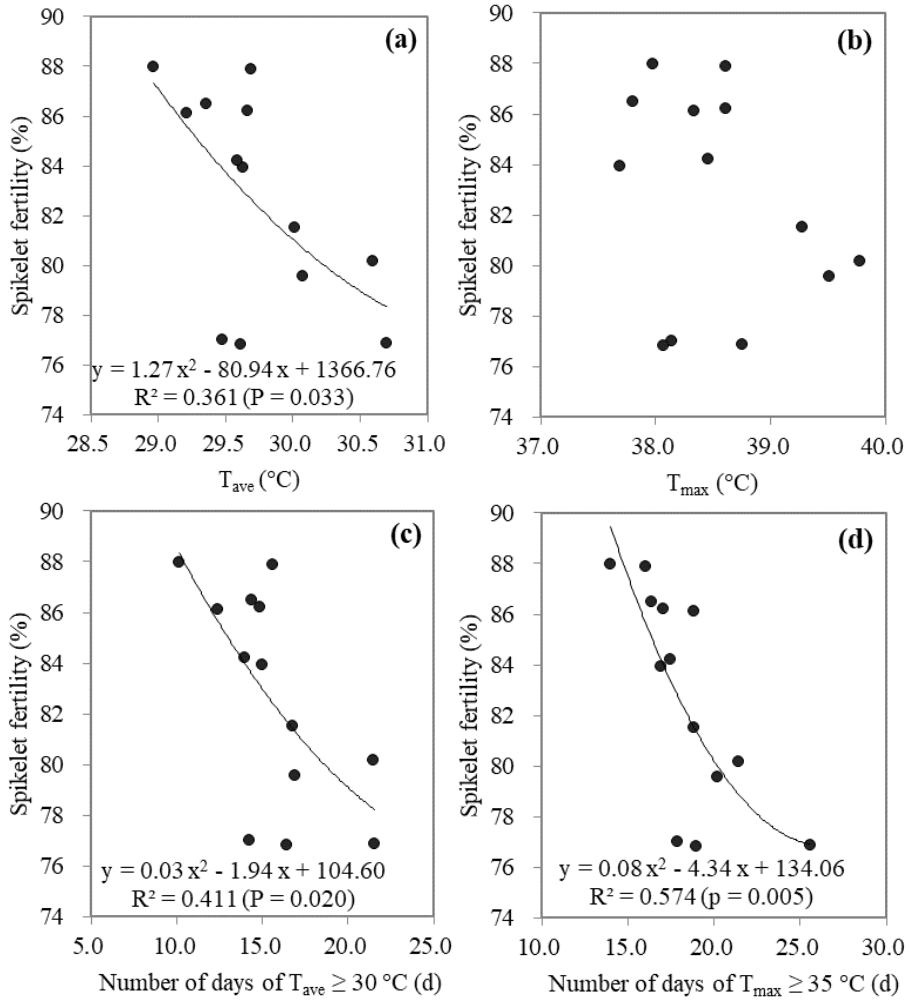

Figure 11. *Correlations between spikelet fertility and T_{ave} (a), T_{max} (b), number of days of $T_{ave} \geq 30$ °C (c), and number of days of $T_{max} \geq 35$ °C (d)†. †HT: high temperature. T_{ave}: daily average temperature; T_{max}: daily maximum temperature*

http://www.aloki.hu ● ISSN 1589 1623 (Print) ● ISSN 1785 0037 (Online)
DOI: http://dx.doi.org/10.15666/aeer/1804_55915605

Table 1. *Changes of temperature data and measures of single-season rice yield from 2004 to 2016*

Year	T_{ave} (°C)	T_{max} (°C)	Number of days of $T_{ave} \geq 30$ °C (d)	Number of days of $T_{max} \geq 35$ °C (d)	Varieties	Effective panicles (m^{-2})	Total grains per panicle	Filled grains per panicle	Spikelet fertility (%)	1000-grain weight (g)	Actual yield ($kg \cdot hm^{-2}$)
2004	29.5	38.1	14.3	17.9	Shanyou 63	16.9	129.6	99.8	77.0	28.3	7536.0
2005	29.6	38.1	16.4	19.0	Shanyou 63	15.5	140.2	107.7	76.8	29.1	7065.5
2006	29.6	37.7	15.0	16.9	II you 838	14.7	133.9	112.4	83.9	28.1	7151.1
2007	30.7	38.8	21.5	25.6	II you 838	14.7	152.3	117.1	76.9	29.6	7037.1
2008	29.7	38.6	14.9	17.1	II you 838	14.9	144.5	124.6	86.2	30.6	5233.3
2009	29.7	38.6	15.6	16.1	II you 838	15.9	123.0	108.1	87.9	30.7	7941.6
2010	30.1	39.5	16.9	20.2	II you 1308	15.0	175.7	139.8	79.6	27.5	8249.6
2011	29.6	38.5	14.0	17.5	II you 1308	15.4	170.4	143.5	84.2	28.1	8672.6
2012	29.4	37.8	14.4	16.4	Y liangyou 1	16.4	158.3	136.9	86.5	26.1	5512.9
2013	30.6	39.8	21.5	21.4	Y liangyou 1	17.5	156.4	125.4	80.2	25.6	8387.9
2014	29.2	38.3	12.4	18.8	Y liangyou 1	17.4	155.4	133.8	86.1	26.0	8718.9
2015	29.0	38.0	10.1	14.0	Y liangyou 1	17.6	157.9	138.9	88.0	26.3	8924.3
2016	30.0	39.3	16.7	18.8	Y liangyou 1	16.5	158.5	129.2	81.5	25.9	8765.4

HT: high temperature. T_{ave}: average temperature; T_{max}: maximum temperature; rice data of single-season rice yield in seven representative regional trials, and temperature data were recorded by 15 national weather stations near the trials in Jiangxi Province; the data in 2017 is not available

Rice spikelets are highly susceptible to HT exposure during the heading-flowering period. HTs greater than 35 °C leads to poor anther dehiscence, low pollen production and pollen viability, and reduced pollen germination rate on the rice stigma, which dramatically reduces spikelet fertility (Jagadish et al., 2010; Zhao et al., 2018; Shi et al., 2018). There was no significant relationship between maximum temperature and spikelets per m^2 (Peng et al., 2004). Spikelet fertility was reduced by 2.4% $(°C\ day)^{-1}$ above a threshold of 33 °C (Jagadish et al., 2007). A controlled rice experiment conducted during meiosis, with six temperatures (31, 33, 35, 37, 39, and 41 °C) and three durations (1, 3, and 5 d), showed that temperatures below 33 °C had no significant effect on spikelet fertility, but with the increase of temperature and its duration, the spikelet fertility decreased gradually; the daily relative spikelet fertility could be expressed in terms of temperature (Shi et al., 2008). In our study, spikelet fertility was negatively correlated to T_{ave} ($P < 0.05$) but not to T_{max} ($P > 0.05$) under natural conditions in Jiangxi. Spikelet fertility was negatively correlated to the number of days of $T_{ave} \geq 30$ °C ($P < 0.05$) and the number of days of $T_{max} \geq 35$ °C ($P < 0.01$). Thus, in turn, spikelet fertility can be regarded as a morphological trait to evaluate HT hazard during the heading-flowering period (Prasad et al., 2006; Jagadish et al., 2010).

HT is not conducive to rice heading and flowering; therefore, measures to protect rice from HT stress should be taken. For example, heat-resistant rice varieties can be selected and/or exogenous substances can be sprayed on foliage to effectively protect rice against HT hazard. Based on decreases in spikelet fertility under HT, previous studies have shown that the cultivars 'N22' (*O. sativa* ssp. *indica* rice from India) and 'IR64' (*O. sativa indica* rice from the Philippines) are heat-tolerant cultivars (Prasad et al., 2006; Jagadish et al., 2010). The exogenous application of plant growth regulators (ascorbic acid, alpha-tocopherol, brassinosteroids, methyl jasmonates, and triazoles), 6-benzylaminopurine, boron, and abscisic acid during the flowering period of rice affected by HT has also been shown to have a substantial effect on cell membrane stability, sugar metabolism, pollen viability, and spikelet fertility (Fahad et al., 2016; Wu et al.,

http://www.aloki.hu ● ISSN 1589 1623 (Print) ● ISSN 1785 0037 (Online)
DOI: http://dx.doi.org/10.15666/aeer/1804_55915605

2017; Shahid et al., 2018; Islam et al., 2018). In addition, avoiding HT is another effective method to reduce HT hazard. Rice with an early-morning flowering trait could allow for rice to avoid the hottest times of the day by blooming at a cooler temperature in the early morning (Ishimaru et al., 2010). Early-morning flowering rice exposed to elevated temperature could complete flowering before the air temperature reaches 35 °C during the day, which can effectively mitigate heat-induced spikelet sterility (Hirabayashi et al., 2015). In accordance with the characteristics of historical HT, optimization of sowing date can enhance rice production by avoiding HT stress during the critical period (Khan et al., 2019). In our results, HT hazard events mainly occurred from July 11 to August 10, and severe HT hazard events occurred more frequently from July 21 to July 31 in Jiangxi Province. Furthermore, our data highlight that the temperatures of four consecutive days on July 22–25 were the highest ($T_{ave} \geq 29.6$ °C, $T_{max} \geq 34.9$ °C). Thus, it is necessary to consider defense measures, such as avoiding HT, selecting heat-resistant varieties, or spraying rice foliage with exogenous substances, during the heading-flowering period of rice.

Conclusions

In this paper, we show that HT hazard events (HT for ≥ three consecutive days) in single-season rice occurred every year from 1981 to 2017, while increased after 2003. HT mainly occurred from July 11 to August 10, and occurred more frequently from July 21 to July 31. In addition, a greater number of HT hazard events was mainly distributed in the middle and northeast area of Jiangxi. It is worth noting that there were strong negative correlations between spikelet fertility and T_{ave}, days of $T_{ave} \geq 30$ °C, and days of $T_{max} \geq 35$ °C. Thus, the results of this study highlight the need for a greater understanding of how to mitigate rice HT hazard. Future studies should be considered to establish a refined regional plan for the optimal sowing dates of different maturity rice varieties under global warming.

Acknowledgements. This research was funded by the National Natural Science Foundation of China (41965008), the Jiangxi Key Research and Development Program (20192BBFL60040; 20165ABC28008; 20171BBF60032), the Jiangxi Industrial Technology System Fund for Rice Field Comprehensive Breeding (JXARS-12), the Jiangxi Key Foundation (20152ACF6009), and the Jiangxi Meteorological Technology Foundation (JMTF20170221).

REFERENCES

[1] Chaturvedi, A. K., Bahuguna, R. N., Shah, D., Pal, M., Jagadish, S. V. K. (2017): High temperature stress during flowering and grain filling offsets beneficial impact of elevated CO_2 on assimilate partitioning and sink-strength in rice. – Scientific Reports 7: 8227.

[2] Espe, M. B., Hill, J. E., Hijmans, R. J., McKenzie, K., Mutters, R., Espino, L. A., Leinfelder-Miles, M., van Kessel, C., Linquist, B. A. (2017): Point stresses during reproductive stage rather than warming seasonal temperature determine yield in temperate rice. – Global Change Biology 23: 4386-4395.

[3] Fahad, S., Hussain, S., Saud, S., Hassan, S., Ihsan, Z., Shah, A. N., Wu, C., Yousaf, M., Nasim, W., Alharby, H., Alghabari, F., Huang, J. (2016): Exogenously applied plant growth regulators enhance the morpho-physiological growth and yield of rice under high temperature. – Frontiers in Plant Science 7: 1250.

http://www.aloki.hu ● ISSN 1589 1623 (Print) ● ISSN 1785 0037 (Online)
DOI: http://dx.doi.org/10.15666/aeer/1804_55915605

[4] Hirabayashi, H., Sasaki, K., Kambe, T., Gannaban, R. B., Miras, M. A., Mendioro, M. S., Simon, E. V., Lumanglas, P. D., Fujita, D., Takemoto-Kuno, Y., Takeuchi, Y., Kaji, R., Kondo, M., Kobayashi, N., Ogawa, T., Ando, I., Jagadish, K. S., Ishimaru, T. (2015): *qEMF3*, a novel QTL for the early-morning flowering trait from wild rice, *Oryza* officinalis, to mitigate heat stress damage at flowering in rice, O. sativa. – Journal of Experimental Botany 66: 1227-1236.

[5] Huang, J., Zhang, F., Xue, Y., Lin, J. (2017): Recent changes of rice heat stress in Jiangxi province, southeast China. – International Journal of Biometeorology 61: 623-633.

[6] IPCC (2013): Climate Change 2013: The Physical Science Basis. Contribution of Working Group I to the Fifth Assessment Report of the Intergovernmental Panel on Climate Change. – Cambridge, Cambridge University Press.

[7] Ishimaru, T., Hirabayashi, H., Ida, M., Takai, T., San-Oh, Y. A., Yoshinaga, S., Ando, I., Ogawa, T., Kondo, M. (2010): A genetic resource for early-morning flowering trait of wild rice *Oryza* officinalis to mitigate high temperature-induced spikelet sterility at anthesis. – Annals of Botany 106: 515-520.

[8] Islam, M. R., Feng, B., Chen, T., Fu, W., Zhang, C., Tao, L., Fu, G. (2018): Abscisic acid prevents pollen abortion under high-temperature stress by mediating sugar metabolism in rice spikelets. – Plant Physiology 165: 644-663.

[9] Jagadish, S. V., Craufurd, P. Q., Wheeler, T. R. (2007): High temperature stress and spikelet fertility in rice (*Oryza sativa* L.). – Journal of Experimental Botany 58: 1627-1635.

[10] Jagadish, S. V., Muthurajan, R., Oane, R., Wheeler, T. R., Heuer, S., Bennett, J., Craufurd, P. Q. (2010): Physiological and proteomic approaches to address heat tolerance during anthesis in rice (*Oryza sativa* L.). – Journal of Experimental Botany 61: 143-156.

[11] Khan, S., Anwar, S., Ashraf, M. Y., Khaliq, B., Sun, M., Hussain, S., Gao, Z. Q., Noor, H., Alam, S. (2019): Mechanisms and adaptation strategies to improve heat tolerance in rice. A review. – Plants (Basel) 8: 508.

[12] Kim, H. Y., Ko, J., Kang, S., Tenhunen, J. (2013): Impacts of climate change on paddy rice yield in a temperate climate. – Global Change Biology 19: 548-562.

[13] Madan, P., Jagadish, S. V., Craufurd, P. Q., Fitzgerald, M., Lafarge, T., Wheeler, T. R. (2012): Effect of elevated CO_2 and high temperature on seed-set and grain quality of rice. – Journal of Experimental Botany 63: 3843-3852.

[14] Mohammed, A. R., Tarpley, L. (2009): High nighttime temperatures affect rice productivity through altered pollen germination and spikelet fertility. – Agricultural and Forest Meteorology 149: 999-1008.

[15] Peng, S., Huang, J., Sheehy, J. E., Laza, R. C., Visperas, R. M., Zhong, X., Centeno, G. S., Khush, G. S., Cassman, K. G. (2004): Rice yields decline with higher night temperature from global warming. – Proceedings of the National Academy of Sciences of the United States of America 101: 9971-9975.

[16] Prasad, P. V. V., Boote, K. J., Allen Jr, L. H., Sheehy, J. E., Thomas, J. M. G. (2006): Species, ecotype and cultivar differences in spikelet fertility and harvest index of rice in response to high temperature stress. – Field Crops Research 95: 398-411.

[17] Ray, D. K., Gerber, J. S., MacDonald, G. K., West, P. C. (2015): Climate variation explains a third of global crop yield variability. – Nature Communications 6: 5989.

[18] Shahid, M., Nayak, A. K., Tripathi, R., Katara, J. L., Bihari, P., Lal, B., Gautam, P. (2018): Boron application improves yield of rice cultivars under high temperature stress during vegetative and reproductive stages. – International Journal of Biometeorology 62: 1375-1387.

[19] Shi, C. L., Q., J. Z., Zheng, J. C., Tang, R. S. (2008): Quantitative analysis on the effects of high temperature at meiosis stage on seed-setting rate of rice florets. – Acta Agronomica Sinica 34: 627-631 (in Chinese).

http://www.aloki.hu ● ISSN 1589 1623 (Print) ● ISSN 1785 0037 (Online)
DOI: http://dx.doi.org/10.15666/aeer/1804_55915605

[20] Shi, W., Li, X., Schmidt, R. C., Struik, P. C., Yin, X., Jagadish, S. V. K. (2018): Pollen germination and in vivo fertilization in response to high-temperature during flowering in hybrid and inbred rice. – Plant Cell and Environment 41: 1287-1297.
[21] Stuerz, S., Asch, F. (2019): Responses of rice growth to day and night temperature and relative air humidity-dry matter, leaf area, and partitioning. – Plants (Basel) 8: 521.
[22] Tang, S., Zhang, H., Liu, W., Dou, Z., Zhou, Q., Chen, W., Wang, S., Ding, Y. (2019): Nitrogen fertilizer at heading stage effectively compensates for the deterioration of rice quality by affecting the starch-related properties under elevated temperatures. – Food Chemistry 277: 455-462.
[23] Van Oort, P. A. J., Zwart, S. J. (2018): Impacts of climate change on rice production in Africa and causes of simulated yield changes. – Global Change Biology 24: 1029-1045.
[24] Wang, P., Zhan, Z., Chen, Y., Wei, X., Feng, B., Tao, F. (2016): How much yield loss has been caused by extreme temperature stress to the irrigated rice production in China? – Climatic Change 134: 635-650.
[25] Wu, C., Cui, K., Wang, W., Li, Q., Fahad, S., Hu, Q., Huang, J., Nie, L., Mohapatra, P. K., Peng, S. (2017): Heat-induced cytokinin transportation and degradation are associated with reduced panicle cytokinin expression and fewer spikelets per panicle in rice. – Frontiers in Plant Science 8: 371.
[26] Yang, B., Shen, S., Tao, S., Li, Q., Zou, X. (2012): Spatial and temporal pattern of rice heat injury in Jiangxi. – Chinese Journal of Agrometeorology 33: 615-622 (in Chinese).
[27] Yang, J., Chen, X., Zhu, C., Peng, X., He, X., Fu, J., Ouyang, L., Bian, J., Hu, L., Sun, X., Xu, J., He, H. (2015): Using RNA-seq to profile gene expression of spikelet development in response to temperature and nitrogen during meiosis in rice (*Oryza sativa* L.). – PLoS One 10: e0145532.
[28] Zhao, Q., Zhou, L., Liu, J., Du, X., Asad, M. A., Huang, F., Pan, G., Cheng, F. (2018): Relationship of ROS accumulation and superoxide dismutase isozymes in developing anther with floret fertility of rice under heat stress. – Plant Physiology and Biochemistry 122: 90-101.

http://www.aloki.hu ● ISSN 1589 1623 (Print) ● ISSN 1785 0037 (Online)
DOI: http://dx.doi.org/10.15666/aeer/1804_55915605

UPPER EOCENE CALCAREOUS NANNOFOSSIL BIOSTRATIGRAPHY: A NEW PRELIMINARY PRIABONIAN RECORD FROM NORTHERN SAUDI ARABIA

ALJAHDALI, M. H.[1*] – ELHAG, M.[2,3] – MUFRREH, Y.[4] – MEMESH, A.[5] – ALSOUBHI, S.[4] – ZALMOUT, I. S.[4]

[1]*Marine Geology Department, Faculty of Marine Sciences, King Abdulaziz University, P. O. Box 80200, Jeddah 21589, Saudi Arabia*

[2]*Department of Hydrology and Water Resources Management, Faculty of Meteorology, Environment & Arid Land Agriculture, King Abdulaziz University, Jeddah, 21589, Saudi Arabia*

[3]*Department of Applied Geosciences, Faculty of Science, German University of Technology in Oman, Muscat 1816, Oman*

[4]*Saudi Geological Survey, Department of Paleontology, Jeddah, Saudi Arabia*

[5]*Saudi Geological Survey, Department of Sedimentary Geology, Jeddah, Saudi Arabia*

**Corresponding author*
e-mail: maljahdli@kau.edu.sa

(Received 15th Apr 2020; accepted 10th Jul 2020)

Abstract. The current research work represents the first calcareous nannofossil biostratigraphic record of the upper Eocene Rashrashiyah Formation in northern Saudi Arabia. The Rashrashiyah Formation is an Eocene carbonate sedimentary unit, exposed adjacent to the Jordanian border, and yielded rich and diverse nannofossil assemblages. The Rashrashiyah Formation overlies the Paleogene rocks of the Umm Wu'al Formation and is unconformably topped by the Neogene (Miocene) Sirhan Formation. Our nannofossil biostratigraphic data recognized 44 species belonging to 21 genera. These taxa indicate a Priabonian age based on the presence of *Chiasmolithus oamaruensis*, and the recognition of bioevents in concordance with the global Priabonian zonations. Three comparable major zones and zonal boundaries (CP14b/CP15, NP18, and CNE17) were recognized in the study section indicative of a late Eocene age. The Base common (Bc) of *Reticulofenestra erbae* was detected at the same level as the top of *Chiasmolithus grandis*, supporting the bioevent reliability in the Tethys realm. A single and more isolated occurrence of *Isthmolithus recurvus* was observed within Zones CP15 and NP18 at the maximum increase abundance of *R. erbae*. Our calcareous nannofossil biostratigraphy from the Rashrashiyah Formation has coincided with the assignment for units 2 and 3 of the Wadi Esh-Shallalah Formation in Qa' Faydat ad Dahikiya in the eastern desert Jordan.
Keywords: *paleoecology, zonation, Arabia, bioevents, Paleogene*

Introduction

Calcareous nannofossils are one of the major calcified phytoplankton that appeared and flourished in the marine photic zone since late Triassic (Gardin et al., 2012). They serve as excellent age biomarkers with wide-range correlation and sensitive indicators to trophic changes in the photic zone (Aubry, 1992; Perch-Nielsen, 1985). The Eocene epoch is one of the most significant geological times because it is characterized by a transition from a pronounced global warming to a significant large-scale glaciation (Miller et al., 1991; Pagani et al., 2005; Zachos et al., 2001). The late Eocene, therefore,

http://www.aloki.hu ● ISSN 1589 1623 (Print) ● ISSN 1785 0037 (Online)
DOI: http://dx.doi.org/10.15666/aeer/1804_56075625

represents a crucial climatic event of a major shift from a green-house world to the inception of the ice-house world in the early Oligocene when temperature and sea level played a major role in the distribution of marine microfossils (Miller et al., 2008; Pälike et al., 2006; Villa et al., 2008). This climatic shift, consequently, caused a profound decline in the diversity of calcareous nannofossils toward the early Oligocene (Aubry, 1992; Bown et al., 1991, 2004) and increased provincialism (i.e., different frequencies of taxa), between low- to high-latitude regions since the late Eocene (Aubry, 1992; Bahrawi and Elhag, 2016).

One of the major obstacles in understanding the late Eocene dynamics is that the Bartonian/Priabonian boundary is still to be determined, although several attempts have utilized calcareous nannofossil biostratigraphy (Agnini et al., 2011; Cotton et al., 2017; Farouk et al., 2015; Strougo et al., 2013). The upper Eocene carbonate sections of marine origin are widely distributed in Jordan (Bender, 1968; Farouk et al., 2015; Mustafa and Zalmout, 2002; Zalmout et al., 2000), Syria (Krasheninnikov et al., 1996), and Egypt (Strougo et al., 2013), and the very rare outcrops in Saudi Arabia have never been investigated thoroughly. During a routine geological survey in northern Saudi Arabia, a chalky exposed section, that crops out to ~10 m, was investigated. This section belongs to the Rashrashiyah Formation, located ~20 km south the Saudi-Jordanian boarders, and is overlain by the Sirhan Formation (text *Fig. 1*). Initial and tentative dating reports using echinoids and foraminifera support a late Eocene age (Meissner et al., 1990).

The aim of this study is: 1) to perform detailed calcareous nannofossil biostratigraphy which presents the first upper Eocene biostratigraphic record from Saudi Arabia, and 2) correlate local Saudi Eocene bioevents with local-regional calcareous nannofossil biostratigraphic records from Egypt and Jordan (Farouk et al., 2015; Strougo et al., 2013).

Materials and methods

Geological settings of the study area

The Sirhan Basin, also known as Azraq-Sirhan Basin (Graben/Depression/Trough), is a large scale regional synclinal structure bounds by two major faults in the northern part of the Arabian Peninsula (*Fig. 1*). It runs for several hundred kilometers from the Eastern Desert of Jordan through northern Saudi Arabia (Bahrawi and Elhag, 2019; Powers et al., 1966). The northwest-southeast oriented basin is a classical Neo-Tethyan model in origin that paleogeographically bounding the northern portion of the Arabian Carbonate Platform. As a part of the Syrian Arc System (Guiraud et al., 2001), the basin was initiated as early as Late Cretaceous by major marine transgression associated with severe compression stresses and faulting; this has resulted in the deposition and accumulation of a thick belt of carbonate and mixed sediments stretching east-west for at least 300 km in the north part of the Arabian Peninsula (Al-Rawi, 2014; Elhag and Bahrawi, 2019). During the Early Paleogene, the Sirhan Basin was affected by the Al-Jawf Rifting event which continued to accommodate carbonate sediments and to subside in response to loading along its major axis (Guiraud et al., 2001).

The development of this basin came into a halt by the end of the Alpine Orogeny tectonic event (latest Eocene-Early Oligocene) which is marked by a major drop in sea-level and the collision of Arabia with Eurasia. Subsurface data shows that the Sirhan basin has accommodated over 6 kilometers of sediments from the Paleozoic through the Neogene (Al-Rawi, 2014). Within the Sirhan Basin, Cretaceous and Tertiary sediments are exposed, while most of the Mesozoic and Paleozoic are deeply buried (Guiraud et al., 2001).

http://www.aloki.hu ● ISSN 1589 1623 (Print) ● ISSN 1785 0037 (Online)
DOI: http://dx.doi.org/10.15666/aeer/1804_56075625

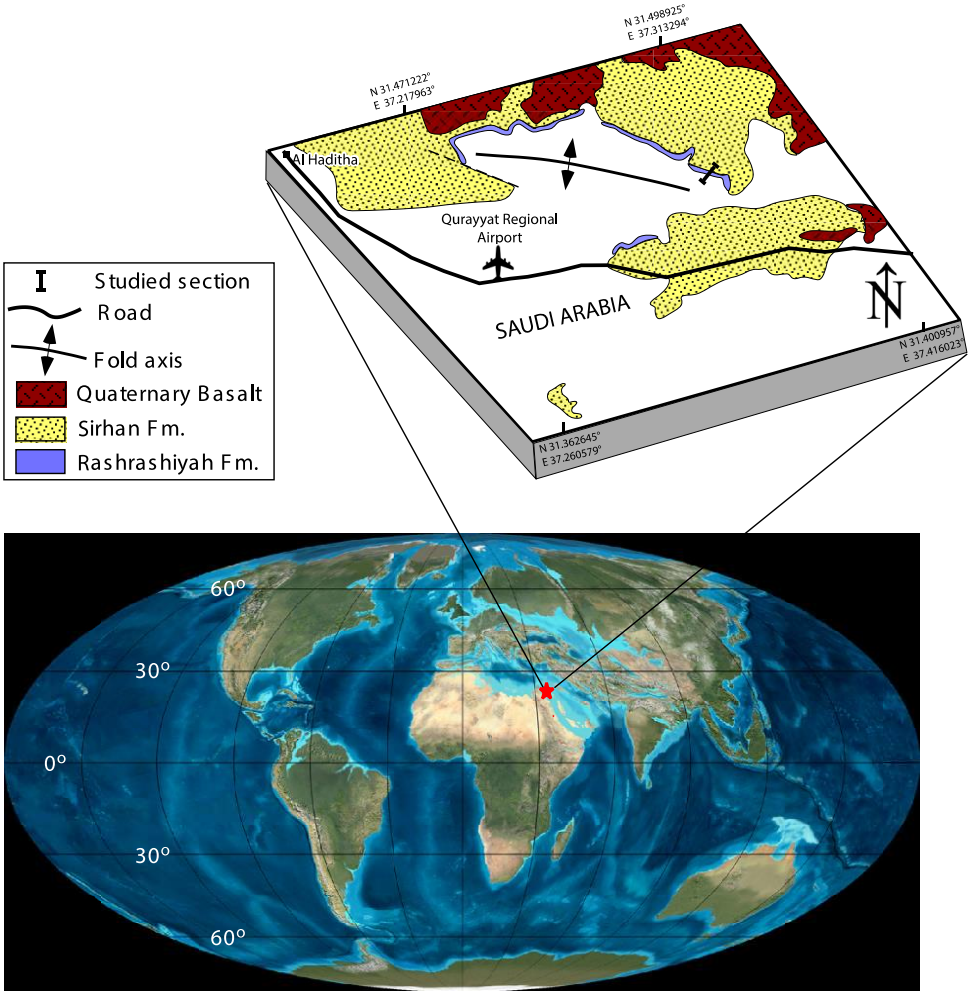

Figure 1. *Map showing the geology and paleogeography around the studied section located near the Saudi-Jordanian boarders. (A) Geological map modified after Wallace et al. (1994). (B) Paleogeographical map modified of the Eocene 38 Ma created with TSCreator (Version 7.4) (https://engineering.purdue.edu/Stratigraphy/tscreator)*

The Rashrashiyah Formation of Meissner et al. (1990) is part of the Cretaceous-Paleogene sedimentary sequence that was accommodated during the development of the Sirhan Basin (trough) in north Saudi Arabia. This formation is partially exposed within the eastern flank of the basin close and around 31°28′N and 37°17′E. The total thickness of this formation from subsurface data is estimated to be 75 m near Al Qurayyat Water well, however, the top two-thirds of it stretch out along isolated scarps and hills in the Rashrashiyah area. Lithologically, it is composed of grayish-white, massive chalk and calcareous bituminous claystone (marl), and minor crystalline limestone beds. The lower part of the formation is dominated by gypsiferous chalk, while the middle part is composed of light-brown, calcareous claystone and hard crystalline echinoidal limestone, and the upper part is grayish-white, calcareous claystone (Halawani, 2001; Meissner et al., 1990). The base of the formation overlaps the top of the Jirani Member of the Umm Wu'al Formation. The top boundaries of the formation mark a clear contact with the base of the Sirhan Formation, where a major unconformity separates its irregular eroded most

http://www.aloki.hu ● ISSN 1589 1623 (Print) ● ISSN 1785 0037 (Online)
DOI: http://dx.doi.org/10.15666/aeer/1804_56075625

younger beds (and the whole Oligocene) from the Miocene and younger strata (Meissner et al., 1990).

The topmost exposed 10 meters of the section, below the clastic Sirhan Formation, were investigated and sampled in this study (*Fig. 2*). The cliff-forming part of the section is mostly marly and argillaceous limestones (*Fig. 2*). Apparently, all the Oligocene section was subjected to erosion. As mentioned earlier, the age of the Rashrashiyah Fm. was tentatively determined to employ echnoides and foraminifera data to the late Eocene (Elhag et al., 2017; Meissner et al., 1990).

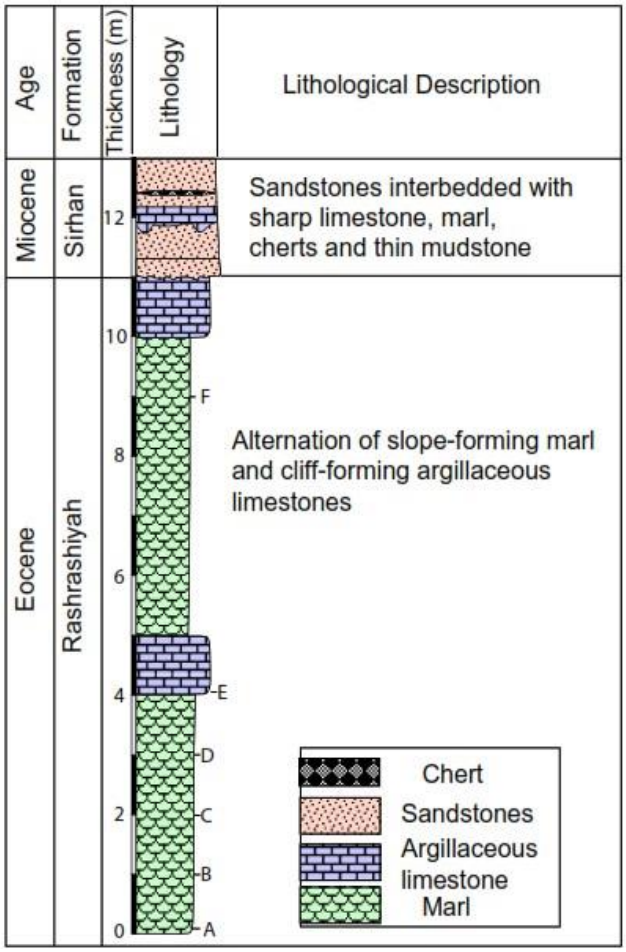

Figure 2. *Lithology of the studied section representing the upper part of the Rashrashiyah Formation and the base of the Sirhan Formation. Letters A-F represents sampling levels*

Ground survey and identification settings

Representative rock samples from the Rashrashiyah Formation were obtained every one-meter interval throughout the section as possible (*Fig. 2*). Six samples were given a prefix A-F and smear slides were prepared from freshly broken pieces of chalk based on standard techniques (Perch-Nielsen, 1985). Semi-quantitatively, at least 300 specimens were counted on random fields of view under Ziess Axiolab A1 at a magnification of 1000×. To detect rare and important biomarkers, two additional long traverses of each slide were scanned to find rare taxa. Data containing raw count were converted into percentages to detect fluctuations in abundances (see *Appendix A*). The zonations of

http://www.aloki.hu ● ISSN 1589 1623 (Print) ● ISSN 1785 0037 (Online)
DOI: http://dx.doi.org/10.15666/aeer/1804_56075625

Martini (1971), Okada and Bukry (1980), and Agnini et al. (2014) were applied for detailed calcareous nannofossil biostratigraphy. Biozone boundaries were defined and followed after Agnini et al. (2014).

Identification of Paleogene calcareous nannofossil assemblages is based on the taxonomy of Perch-Nielsen (1985), Bown and Dunkley Jones (2012) and Fornaciari et al. (2010). The state of preservation of calcareous nannofossil was qualitatively evaluated as: good, moderate, or poor, in which the former shows little dissolution and/or overgrowth and the identification to the species level was achieved, while the latter has a severe effect of dissolution and/or overgrowth and identification was hardly possible to the generic/species level. The raw count was transformed into abundance codes via Bugwin© Software in which Abundant (A) was assigned for 11-100 species, Common (C) for 6-10 species, Few (F) for 3-5 species, and Rare (R) for 1-2 species. Species list mentioned in this study is found in *Appendix B*, while raw count, and percentages are found in *Appendix A*.

Results

Calcareous nannofossils are rich and highly diverse. 21 genera and 44 species were identified in the Rashrashiyah Formation in Samples A-F (*Table 1*). The overall state of preservation showed a pattern up section ranging between good in the lower part of the section (Sample A) to poor up section (Sample F), while it is moderate in the middle of the studied section (Sample D) (*Table 1*). Species richness showed a similar pattern in being high in Sample A (39 species) and gradually declined toward the top of the section in Sample F (27 species, *Table 1*).

Zone NP18 of Martini (1971), and Zone CNE17 of Agnini et al. (2014), while two zones CP14b and CP15 of Okada and Bukry (1980) of the upper Eocene were recognized. Zone NP18, which is defined from the base of *Chiasmolithus oamaruensis* to the base of *Isthmolithus recurvus* (Martini, 1971), has a thickness of 9 m covering the entire studied interval due to the presence of *C. oamaruensis* and *R. bisecta* > 10 μm (*Table 1*). The presence of *C. oamaruensis* suggests an early Priabonian age, according to Berggren et al. (1995), for the Rashrashiyah Fm. The most common species that characterize this zone are: *Chiasmolithus grandis, Chiasmolithus oamaruensis, Coccolithus formosus, Coccolithus pelagicus, Cyclicargolithus floridanus, Discoaster barbadiensis, D. saipanensis, R. bisecta, Reticulofenestra erbae,* and *Reticulofenestra reticulata*.

Within Zone NP18, additional bioevents were recognized in samples A-F (0-9 m thickness). At the base of the section, *C. grandis* showed a rare abundance, where at Sample B (1 m) it marked the top event that defined the CP14b-CP15 boundary of Okada and Bukry (1980) (*Fig. 3*). At the same level as the top event of *C. grandis*, *Reticulofenestra erbae* substantially increased its abundance to constitute 6-8% of the total assemblage (*Fig. 3*). The increase in *R. erbae* abundance began one sample above the base of the section and continued to Sample F (9 m), where species richness declined to 27 species (*Fig. 3*). Therefore, samples A-F lies within Zone CNE17 of Agnini et al. (2014) owing to the common interval of *R. erbae*. In Sample E (4 m), a rare occurrence (2 species/slide) of *Isthmolithus recurvus* is observed with no presence in the following Sample F (9 m) (*Table 1; Fig. 3*). The rare isolated single occurrence of *Isthmolithus recurvus* cannot confidently be utilized to mark Zone NP19 (Martini, 1971), hence, Sample F still lies within Zone NP18 and therefore CNE17 (Agnini et al., 2014).

http://www.aloki.hu ● ISSN 1589 1623 (Print) ● ISSN 1785 0037 (Online)
DOI: http://dx.doi.org/10.15666/aeer/1804_56075625

Table 1. *Range chart of the Upper Eocene sampled calcareous nannofossils from the top 10 m of the Rashrashiyah Formation in NW Saudi Arabia*

Sample	F	E	D	C	B	A
Height (m)	9	4	3	2	1	0
Martini (1971)	NP18					
Okada and Bukry (1980)	CP15				CP14b	
Agnini et al. (2014)	CNE17					
Diversity	27	33	33	29	36	39
Preservation	P	M-P	M	G	M-G	G
Group Abundance	C	A	VA	VA	VA	VA
Blackites cf. *morionum*					R	C
Blackites spinosus	F	C	A	F	F	F
Braarudosphaera bigelowii	R	R				
Chiasmolithus grandis					**R**	R
Chiasmolithus oamaruensis		R	R		R	**F**
Clausicoccus subdistichtus	F	C	C	C	A	R
Coccolithus eopelagicus	C	R	R	R	R	A
Coccolithus pelagicus	A	A	A	A	A	F
Cruciplacolithus cruciformis		R	R		F	A
Cyclicargolithus floridanus < 5	A	A	A	A	A	A
Cyclicargolithus floridanus	A	A	A	A	A	F
Discoaster barbadiensis	F	F	F	F	F	A
Discoaster saipanensis	F	F	A	C	C	R
Discoaster tanii	R	R	R			R
Coccolithus formosus	C	C	R	C	C	C
Helicosphaera bramlettii	C	C	C	C	R	
Helicosphaera compacta	F	R	F	R	R	R
Helicosphaera reticulata		R	R	F		
Helicosphaera wilcoxii		R	F			
Hughesius tasmaniae						C
Isthmolithus recurvus		**R**				
Lanternithus minutus	C	F	F	C	F	F
Neococcolithes dubius			F	R	R	F
Pedinocyclus gibbsiae	F	F	C	F	C	
Pontosphaera exilis					F	F
Pontosphaera panarium				R	R	R
Pontosphaera multipora		R	R	R	F	C
Reticulofenestra bisecta	A	R	F		C	F
Reticulofenestra daviesii	R	F	R	F	F	F
Reticulofenestra cf. daviesii					F	R
Reticulofenestra umbilica	F	F	C	C	C	A
Sphenolithus cf. *furcatolithoides*		R	F	C	R	F
Sphenolithus moriformis	F	F	R	F	F	R
Sphenolithus predistentus?		R				R
Sphenolithus spiniger						R
Thoracosphaera spp.	R	R	R	F	R	C
Zygrablithus bijugatus	C	F	C	F	F	C

VA = Very Abundant, A = abundant, C = Common, F = Few, R = Rare, G = Good, M = Moderate, P = Poor

http://www.aloki.hu ● ISSN 1589 1623 (Print) ● ISSN 1785 0037 (Online)
DOI: http://dx.doi.org/10.15666/aeer/1804_56075625

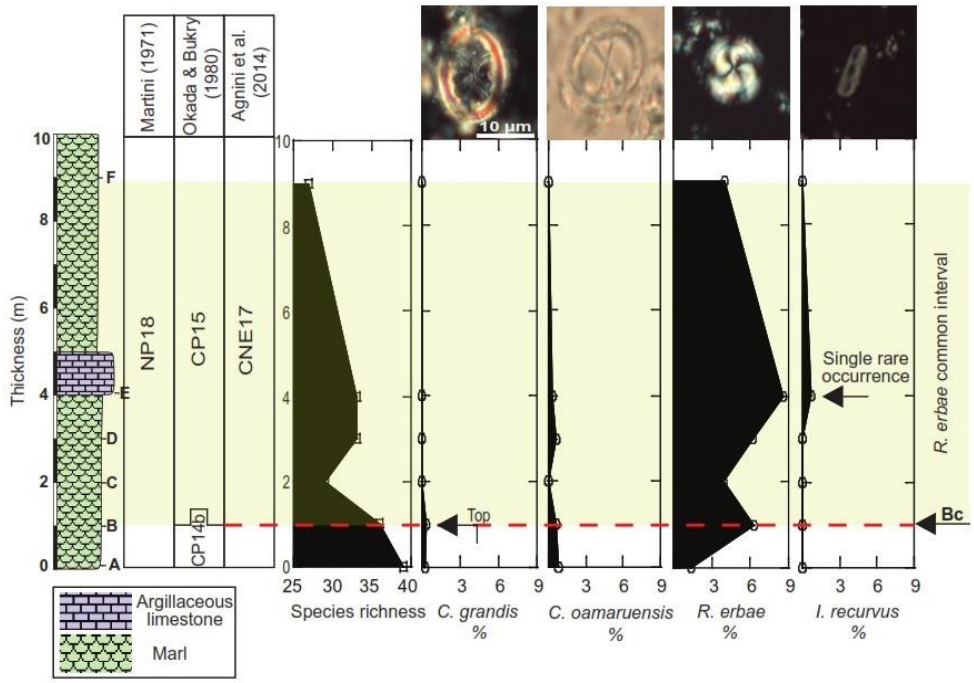

Figure 3. *Major calcareous nannofossil percentage (%) events detected in this study within the upper Eocene Rashrashiyah Formation in northern Saudi Arabia compared to the global zonation of Martini (1971), Okada and Bukry (1980) and Agnini et al. (2014). The dashed red line represents the bioevents of C. grandis, and the Base common (Bc) of R. erbae*

Discussion

Upper Eocene nannofossil bioevents in northern Saudi Arabia

Calcareous nannofossils are an excellent group of microfossils for biostratigraphic and global correlation studies (Agnini et al., 2014; Raffi et al., 2016). This is due to their high rates of speciation since their first appearance in the late Triassic (Gardin et al., 2012). In the late Eocene, calcareous nannofossils have shown profound provincialism (Aubry, 1992; Wei and Wise, 1990) as a response to the expansion of the Antarctica ice sheet (Miller et al., 1991; Zachos et al., 2001). This provincialism caused some upper Eocene nannofossil biomarkers to be unreliable for biostratigraphy and the global correlation between low- and high-latitude regions (Agnini et al., 2011; Wei and Wise, 1989, 1990; Fioroni et al., 2012). This has greatly affected the recognition of some Martini (1971) and Okada and Bukry (1980) zones throughout global localities (Perch-Nielsen, 1985), hence, no formal identification of Global Stratotype Section Point (GSSP) has been found (Agnini et al., 2011). Our section spans Zone NP18 of Martini (1971) and is correlated with the middle and upper part of the upper Eocene Wadi Esh-Shallalah Formation section (Farouk et al., 2015) in Jordan, 26 Km NW of the Rashrashiyah Formation section studied in this report. Here we discuss the occurrence of the biomarker species observed in northern Saudi Arabia and their possible correlation regionally and globally.

Top of Chiasmolithus grandis

The extinct *Chiasmolithus* genus was found to occupy high-latitude regions between the middle Eocene-Oligocene timeframe (Wei and Wise, 1989). The top of *C. grandis* was detected in Sample B slightly above the base of the section (*Fig. 4*) and primarily

http://www.aloki.hu ● ISSN 1589 1623 (Print) ● ISSN 1785 0037 (Online)
DOI: http://dx.doi.org/10.15666/aeer/1804_56075625

points out to the CP14b/CP15 boundary of Okada and Bukry (1980) zonation. This bioevent lies within Zone NP18 of Martini (1971) and Zone CNE17 of Agnini et al. (2014) due to the presence of rare-few *C. oamaruensis* and the Base common (Bc) of *R. erbae* (*Fig. 4*) just above the base of the section (*Fig. 4*). *Chiasmolithus grandis* and *C. oamaruensis* were found to overlap within the studied portion of the Rashrashiyah Formation (Figs. 3 and 4). This behavior in overlapping is documented in Egypt (Strougo et al., 2013) and in Jordan (Farouk et al., 2015), Italian Alano section (Agnini et al., 2011), and the Ocean Drilling Program (ODP) in the Indian Ocean (Fioroni et al., 2015). *Chiasmolithus grandis* exhibited a sharp top event, whereas *C. oamaruensis* was found to be within < 1% of the total assemblage with sporadic occurrence toward up section (*Fig. 3*) similar to local and regional observations (Farouk et al., 2015; Strougo et al., 2013). Additionally, the top of *C. grandis* was also observed at the same stratigraphic level of the Bc of *R. erbae* (*Fig. 4*).

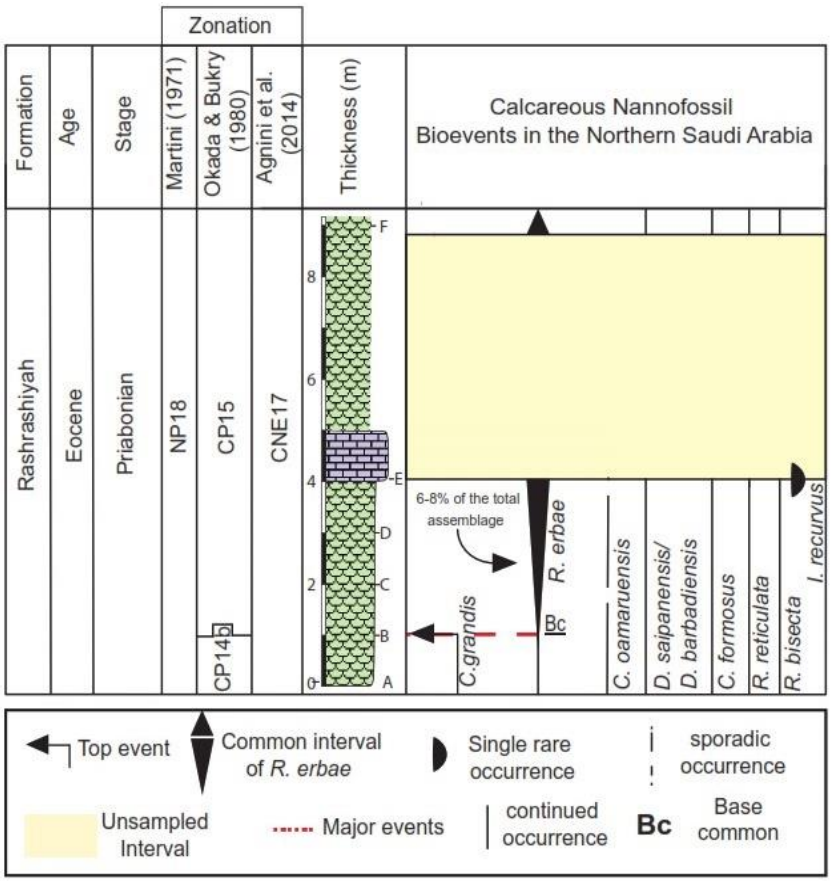

Figure 4. *Calcareous nannofossils bioevents of the studied portion of the Rashrashyiah Formation from northern Saudi Arabia aligned with Eocene nannoplanktonic zonation*

Base common (Bc) of Reticulofenestra erbae

Fornaciari et al. (2010) described two new significant middle-late Eocene biomarkers species, *R. erbae* and *R. isabellae,* that Agnini et al. (2014) utilized in their recent Paleogene zonation. *Reticulofenestra erbae* is differentiated from *R. isabellae* by size in which the latter is ≥ 12 µm (Fornaciari et al., 2010). *Reticulofenestra erbae* showed few abundances in sample A (*Table 1*), but substantially increased reached to 6-8% of the

http://www.aloki.hu ● ISSN 1589 1623 (Print) ● ISSN 1785 0037 (Online)
DOI: http://dx.doi.org/10.15666/aeer/1804_56075625

total assemblage, between samples B-F, within Zone NP18 (Martini, 1971) and base of Zone CP15 (Okada and Bukry 1980) (*Fig. 4*). The increase of *R. erbae* started at the level of sample B and continued upward throughout the rest of the studied section (*Figs. 3* and *4*), hence, we could not observe the Top common (Tc). The Bc of *R. erbae* coincides with the top of *C. grandis* (*Fig. 4*) in our section. Agnini et al. (2014) have shown that the top of *C. grandis* lies slightly above the Bc of *R. erbae* in the North Atlantic (ODP Site 1052). This earlier top event of *C. grandis* in our study (*Fig. 4*) could be related to sampling resolution or diachrony in *C. grandis* (Agnini et al., 2014; Fioroni et al., 2015). Overall, the distribution pattern of *R. erbae* with the recognizable increase abundance greatly validates the Bc *R. erbae* usefulness in northern Saudi Arabia.

Recent integrated biostratigraphic studies from local and regional sections in Jordan and Egypt have shown the presence of both *R. erbae* and *R. isabellae* together within Martini (1971) Zones NP17-18 (Farouk et al., 2015; Strougo et al., 2013). However, the two biomarker species have been observed well-spaced in time, both in deep-sea cores and land-based section (Agnini et al., 2014; Fornaciari et al., 2010). In this study, the overlapping of both species has not been detected, furthermore, even their base events did not coincide together herein. *Reticulofenestra isabellae* appeared later in Zones CNE19 (Agnini et al., 2014) and NP19/20 of Martini (1971). Morphometric measurements of random medium to large placolith (*R. erbae* and *R. reticulata*) species throughout the section were carried out to observe the size pattern and scrutinize the section for the presence of *R. isabellae* (*Fig. 5*). Within the designated study area; which is only 26 km SE of the Jordanian Qa' Faydat ad Dahikiya (Farouk et al., 2015), only *R. erbae* is found, following the description criteria of Fornaciari et al. (2010), ranging in size between 8-10 μm (*Fig. 5*), while the presence of *R. isabellae* was not recorded. Therefore, the presence of *R. isabellae* in previous local studies is possibly misidentified and/or miscalibrated in size with large specimens of *R. erbae*.

The single isolated occurrence of Isthmolithus recurvus

The base of *I. recurvus* is a bioevent utilized in the zonations of Martini (1971) and Okada and Bukry (1980) for the late Eocene. Biogeographic studies of this taxon have shown its preference and inclination toward cool-water and high-latitude regions (Wei and Wise, 1989, 1990); while it is rare with discontinuous occurrence in low-latitudes areas (Agnini et al., 2014; Farouk et al., 2015; Strougo et al., 2013; Wei and Wise, 1990; Fioroni et al., 2015) and our section in northern Saudi Arabia. *Isthmolithus recurvus* has first appeared in sample F with only 2 species (0.6%; *Fig. 3*). No *I. recurvus* was detected at sample E (*Fig. 4*). This taxon showed two distinct bioevents in the Mediterranean region (Fornaciari et al., 2010). The first appearance is short, more isolated occurrence termed 'spike' which probably here lies within Zones NP18 (Martini, 1971), CP15 (Okada and Bukry, 1980) and CNE17 (Agnini et al., 2014) (*Fig. 4*), whereas the second bioevent seems to be the lowest common occurrence (Fornaciari et al., 2010) that confidently used for base Zone NP19 of Martini (1971).

The earlier occurrence "spike" has also been observed in deep-sea cores Agnini et al., 2014; Fornaciari et al., 2010; Fioroni et al., 2015; Villa et al., 2008) which reflects a more consistent occurrence outside the Mediterranean region. The single isolated occurrence of *I. recurvus* observed in our section was found to coincide with the maximum increase in *R. erbae* (*Figs. 3* and *4*). Owing to the unsampled interval of ~5 m (*Fig. 4*), that was hindered to collect in the field due to mineralized (dolomitized rocks), concerns about the usefulness/correlation of this short occurrence remains unclear in northern Saudi Arabia

http://www.aloki.hu ● ISSN 1589 1623 (Print) ● ISSN 1785 0037 (Online)
DOI: http://dx.doi.org/10.15666/aeer/1804_56075625

despite the fact of producibility of the bioevent globally (Agnini et al., 2014; Fornaciari et al., 2010). Besides, sample E the from the top section, where species richness declined down to 27 species and preservation became moderate to poor, shows no *I. recurvus* or *R. isabellae*, indicating that the top of the studied section still lies within Zone NP18 (Martini, 1971) or Zone CNE17 (Agnini et al., 2014).

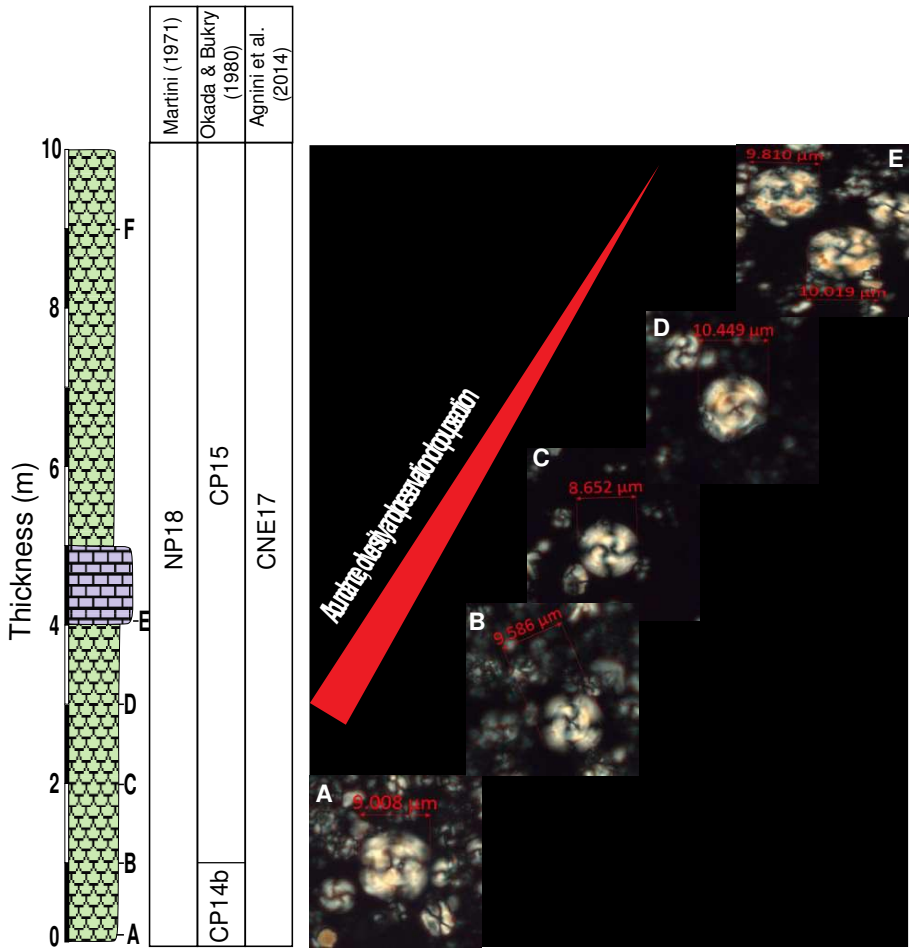

Figure 5. *Morphometric measurements of the largest Reticulofenestra erbae/R. reticulata within CNE 17 Zone, from the upper part of the Rashrashiayh Formation section in northern Saudi Arabia*

Side views of *Isthmolithus recurvus* from Egyptian and Jordanian sampled sections appeared near the base of Zone NP18 with rare occurrences (Farouk et al., 2015; Strougo et al., 2013). The calcareous nannofossil assemblage of the Rashrashiyah Formation in northern Saudi Arabia shows no side views of *I. recurvus,* only overgrown planer view of *I. recurvus* specimens were only observed in sample E (*Plate 1*).

The decline in diversity and preservation: tectonism, eustacy, and regional correlation

It is evident that a major drop in species richness accompanied by the deterioration in preservation took place toward the top of the studied section (*Fig. 5*). This drop in the species richness at the top of the Rashrashiyah Formation is a quite similar case reported

http://www.aloki.hu ● ISSN 1589 1623 (Print) ● ISSN 1785 0037 (Online)
DOI: http://dx.doi.org/10.15666/aeer/1804_56075625

from Zones NP17-18 of the Wadi Esh-Shallalah Formation section across the borders in Jordan. Below the top of the studied Saudi section, it seems that a tremendous amount of nannofossil fragmentation increased (*Plate 2*). During the late Eocene, the northern part of the Arabian Peninsula, as part of the Alpine Orogeny and the Syrian Arc Belt (Bosworth et al., 1999; Guiraud and Bosworth, 1999), witnessed severe compressional events with crustal shortening within the NW-SE direction. These compressional events produced significant topographical changes causing different depositional and erosional processes during the rest of the Eocene and later Paleogene and Neogene systems. Moreover, the presence of shallow-marine planktic foraminifera in the earliest Oligocene of the correlatable Jordanian section (Farouk et al., 2015) suggests that the basin, including our formation, was subjected to large changes in sea level.

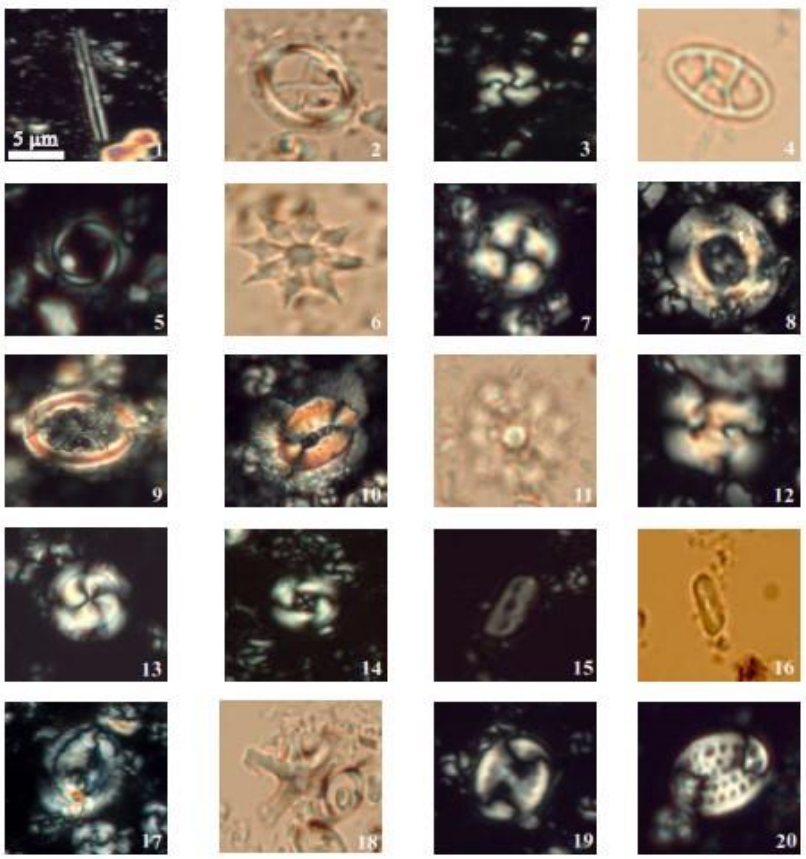

Plate 1. *Polarized and plain-light micrographs of calcareous nannofossil taxa identified in AlRashrashiyah Formation in northern Saudi Arabia. 1. Blackites spinosus, sample A. 2. Chiasmolithus oamaruensis, sample A, 3. Cyclicargolithus floridanus, sample A, 4. Neococcolithes dubius, sample A, 5. Cyclococcolithina protoannula, sample A, 6. Discoaster saipanensis, sample B, 7. Coccolithus formosus, sample A, 8. Reticulofenestra umbilicus, sample D, 9. Chiasmolithus grandis, sample A, 10. Coccolithus eopelagicus, sample C, 11. Discoaster barbadiensis, sample E, 12. Reticulofenestra bisecta, sample A, 13. Reticulofenestra erbae, sample B, 14. Reticulofenestra reticulata, sample C, 15-16. Isthmolithus recurvus, Sample E, 17. Helicosphaera compacta, sample A, 18. Discoaster tanii, sample B, 19. Pontosphaera exilis, sample A, 20. Pontosphaera multipora, sample B. (magnification of 1000×, scale bar 5 microns for all images as in A)*

http://www.aloki.hu ● ISSN 1589 1623 (Print) ● ISSN 1785 0037 (Online)
DOI: http://dx.doi.org/10.15666/aeer/1804_56075625

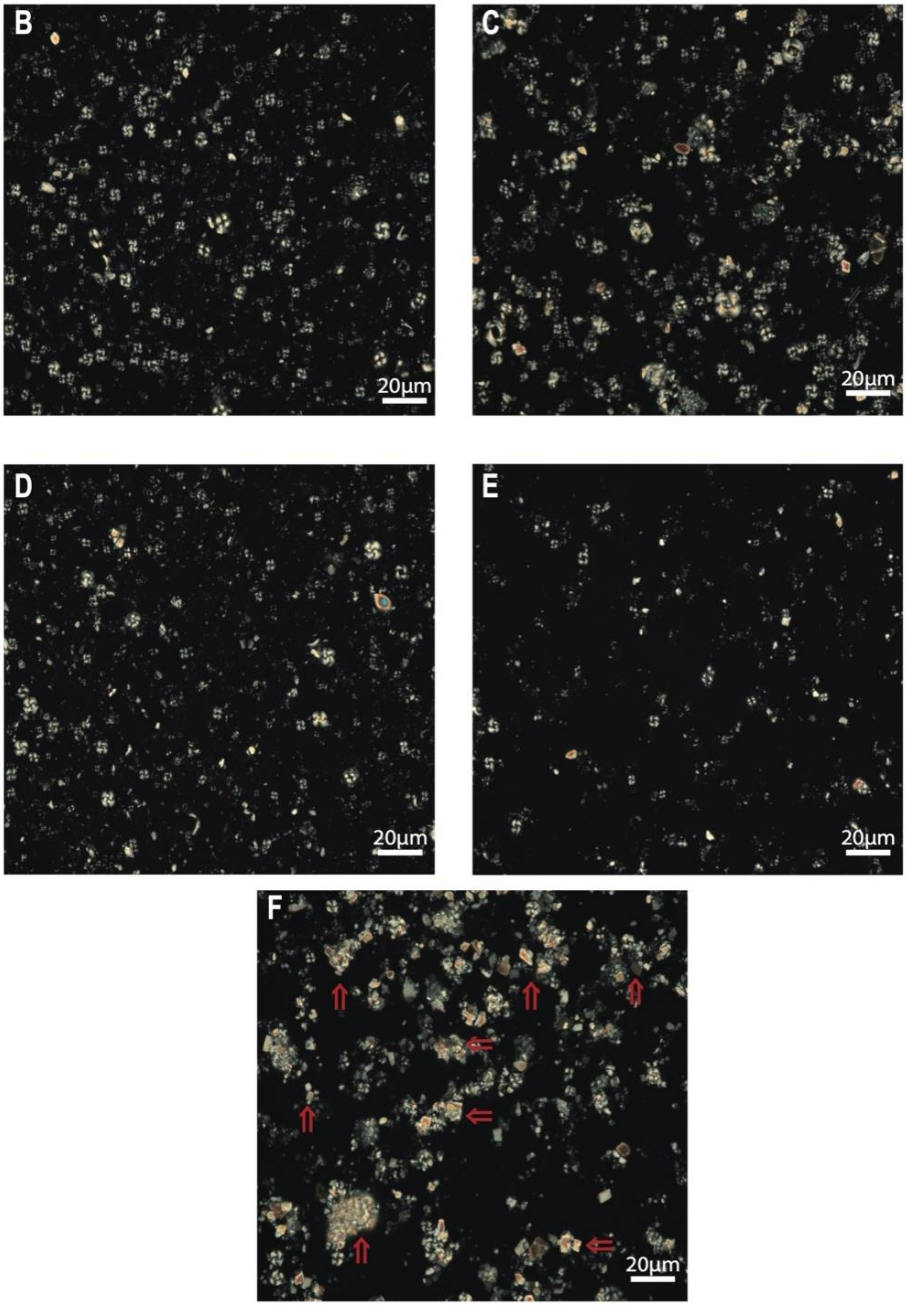

Plate 2. *Polarized views (magnification of 1000×, scale bar 20 microns) showing the degree of fragmentations (red arrows) toward up section from Samples B-F*

Conclusions

The studied part of the Rashrashiyah Formation is the only surface section to reveal a high diversity of well-preserved calcareous nannofossils at its base but deteriorate toward the top of the section. Three calcareous nannofossil zones of global zonations were recognized and all indicate an early Priabonian age based on the rare and sporadic occurrence of *C. oamaruensis* of Zone NP18. The Base common (Bc) of *R. erbae* is documented here with a common increase from 6-8% of the total assemblage and the

http://www.aloki.hu ● ISSN 1589 1623 (Print) ● ISSN 1785 0037 (Online)
DOI: http://dx.doi.org/10.15666/aeer/1804_56075625

section lies within Zone CNE17. The sharp top event of *C. grandis* was detected, at the same level of Bc of *R. erbae*, and subdivided CP14b/CP15 zones. A single and more isolated occurrence of *I. recu*rvus was observed parallel with the maximum increase of *R. erbae*. This isolated single occurrence, due to sampling resolution, cannot be compared/correlated with those sections in the Mediterranean and deep-sea cores. *Reticulofenestra isabellae*, a biomarker species found in accordance with the Lowest Common Occurrence (LCO) of *I. recurvus,* has not been observed, hence, the Rashrashiyah Formation section tentatively lies within Zone NP18/CNE17. Although the side view of *I. recurvus* specimens was recorded in Egyptian and Jordanian sections to originate at the base of NP18, only planner view specimens were observed in northern Saudi Arabia. The investigated calcareous nannofossil record at the Rashrashiyah Formation section is partially correlatable with the adjacent Jordanian Wadi Esh-Shallalah Formation section in Qa' Faydat Ad Dahikiya. The decline in species richness toward the top of our studied section is also comparable with Wadi Esh-Shallalah Formation, which reflects major tectonic activity originated during the late Eocene. The studied stratigraphic interval from the Rashrashiyah Formation, so far, is the only Eocene section to reveal calcareous nannofossils, recorded for the first time in Saudi Arabia. Hence, this report represents part of a larger ongoing investigation attempting to code the Paleogene sediments in Saudi Arabia with the global nannoplankton and foraminiferal zonation. The ongoing research plans to intergrade benthic and planktic foraminifera for more robust age determination and biostratigraphical correlation with local and regional sections. Reconstructions of Paleogene climate change and global sea-level via integrated stable isotope signature are needed from expanded outcrop sections in northern Saudi Arabia.

Acknowledgments. This project was funded by the Deanship of Scientific Research (DSR), King Abdulaziz University, Jeddah, under grant No. (D-288-150-1440). The authors, therefore, gratefully acknowledge the DSR technical and financial support. We would like to thank Prof. Giuliani Villa for her constructive comments and suggestions that improved the initial manuscript. We thank the Department of Paleontology of the Saudi Geological Survey (SGS) and the leadership of SGS represented by Saleh Al-Sefry, Nasser Aljahdali, and Wadee Kashghari for supporting fieldwork, permission to use SGS labs and equipment for this work. The authors would like to thank the editor and anonymous reviewers for their constructive comments and suggestions that substantially improved the manuscript.

REFERENCES

[1] Agnini, C., Fornaciari, E., Giusberti, L., Grandesso, P., Lanci, L., Luciani, V., Muttoni, G., Pälike, H., Rio, D., Spofforth, D. J. (2011): Integrated biomagnetostratigraphy of the Alano Section (Ne Italy): a proposal for defining the Middle-Late Eocene boundary. – GSA Bulletin 123(5-6): 841-872.

[2] Agnini, C., Fornaciari, E., Raffi, I., Catanzariti, R., Pälike, H., Backman, J., Rio, D. (2014): Biozonation and biochronology of Paleogene calcareous nannofossils from low and middle latitudes. – Newsletters on Stratigraphy 47(2): 131-181.

[3] Al-Rawi, M. M. (2014): Petroleum systems in Jordan. – GEO ExPro 11(1).

[4] Aubry, M. (1992): Late Paleogene Calcareous Nannoplankton Evolution: A Tale of Climatic Deterioration. – In: Prothero, D. R., Berggren, W. A. (eds.) Eocene-Oligocene Climatic and Biotic Evolution. Princeton University Press, Princeton, NJ.

[5] Bahrawi, J. A., Elhag, M. (2016): Simulation of sea level rise and its impacts on the western coastal area of Saudi Arabia. – Indian Journal of Geo-Marine Sciences 45(1): 54-61.

http://www.aloki.hu ● ISSN 1589 1623 (Print) ● ISSN 1785 0037 (Online)
DOI: http://dx.doi.org/10.15666/aeer/1804_56075625

[6] Bahrawi, J., Elhag, M. (2019): Consideration of seasonal variations of water radiometric indices for the estimation of soil moisture content in arid environment in Saudi Arabia. – Applied Ecology and Environmental Research 17(1): 285-303.
[7] Bender, F. (1968): Geologie Von Jordanien. – Beitraege Zur Regionalen Geologie. Region. Geol. d. Erde 7.
[8] Berggren, W. A., Kent, D. V., Swisher Iii, C. C., Aubry, M.-P. (1995): A Revised Cenozoic Geochronology and Chronostratigraphy. – In: Berggren, W. A. et al. (eds.) Geochronology, Time Scales and Global Stratigraphic Correlation. SEPM Society for Sedimentary Geology, Tulsa, OK.
[9] Bosworth, W., Guiraud, R., Kessler, L. (1999): Late Cretaceous (Ca. 84 Ma) compressive deformation of the stable platform of Northeast Africa (Egypt): far-field stress effects of the "Santonian Event" and origin of the Syrian Arc Deformation Belt. – Geology 27(7): 633-636.
[10] Bown, P. R., Dunkley Jones, T. (2012): Calcareous nannofossils from the paleogene Equatorial Pacific (IODP Expedition 320 Sites U1331-1334). – Journal of Nannoplankton Research 32(2): 3-51.
[11] Bown, P. R., Burnett, J. A., Gallagher, L. T. (1991): Critical events in the evolutionary history of calcareous nannoplankton. – Historical Biology 5(2-4): 279-290.
[12] Bown, P. R., Lees, J. A., Young, J. R. (2004): Calcareous Nannoplankton Evolution and Diversity through Time. – In: Thierstein, H. R., Young, J. R. (eds.) Coccolithophores. Springer, Berlin, pp. 481-508.
[13] Cotton, L. J., Zakrevskaya, E. Y., Van Der Boon, A., Asatryan, G., Hayrapetyan, F., Israyelyan, A., Krijgsman, W., Less, G., Monechi, S., Papazzoni, C. A. (2017): Integrated stratigraphy of the Priabonian (Upper Eocene) Urtsadzor Section, Armenia. – Newsletters on Stratigraphy 50(3): 269-295.
[14] Elhag, M., Bahrawi, J. A. (2019): Sedimentation mapping in shallow shoreline of arid environments using active remote sensing data. – Natural Hazards 99(2): 879-894.
[15] Elhag, M., Galal, H. K., Alsubaie, H. (2017): Understanding of morphometric features for adequate water resource management in arid environments. – Geoscientific Instrumentation, Methods and Data Systems 6(2): 293.
[16] Farouk, S., Faris, M., Ahmad, F., Powell, J. H. (2015): New microplanktonic biostratigraphy and depositional sequences across the Middle–Late Eocene and Oligocene boundaries in Eastern Jordan. – GeoArabia 20(3): 145-172.
[17] Fioroni, C., Villa, G., Persico, D., Wise, S. W., Pea, L. (2012): Revised Middle Eocene-Upper Oligocene calcareous nannofossil biozonation for the Southern Ocean. – Revue de micropaléontologie 55(2): 53-70.
[18] Fioroni, C., Villa, G., Persico, D., Jovane, L. (2015): Middle Eocene-Lower Oligocene calcareous nannofossil biostratigraphy and paleoceanographic implications from site 711 (Equatorial Indian Ocean). – Marine Micropaleontology 118: 50-62.
[19] Fornaciari, E., Agnini, C., Catanzariti, R., Rio, D., Bolla, E. M., Valvasoni, E. (2010): Mid-latitude calcareous nannofossil biostratigraphy and biochronology across the Middle to Late Eocene transition. – Stratigraphy 7(4): 229.
[20] Gardin, S., Galbrun, B., Thibault, N., Coccioni, R., Silva, I. P. (2012): Bio-magnetochronology for the Upper Campanian–Maastrichtian from the Gubbio Area, Italy: new results from the Contessa Highway and Bottaccione sections. – Newsletters on Stratigraphy 45(1): 75-103.
[21] Guiraud, R., Bosworth, W. (1999): Phanerozoic geodynamic evolution of northeastern Africa and the northwestern Arabian Platform. – Tectonophysics 315(1-4): 73-104.
[22] Guiraud, R., Issawi, B., Bosworth, W. (2001): Phanerozoic history of Egypt and surrounding areas. – Peri-Tethys Memoir 6: 469-509.
[23] Halawani, M. (2001): Stratigraphic column for the Phanerozoic rocks of Saudi Arabia. A compilation and synthesis with comments. – Saudi Geological Survey Technical Reports, Kingdom of Saudi Arabia SGS-TR-2001-3 2001: 4.

http://www.aloki.hu ● ISSN 1589 1623 (Print) ● ISSN 1785 0037 (Online)
DOI: http://dx.doi.org/10.15666/aeer/1804_56075625

[24] Krasheninnikov, V. A., Golovin, D. I., Mouravyov, V. I., Helou, R. (1996): The Paleogene of Syria--Stratigraphy, Lithology, Geochronology. – In: Krasheninnikov, V. A., et al. (eds.) Geologisches Jahrbuch, Reihe B, Regionale Geologie Ausland. Schweizerbart, Stuttgart.
[25] Martini, E. (1971): Standard Tertiary and Quaternary calcareous nannoplankton zonation. – Proc. II Planktonic Conference, Roma, 1970. Tecnoscienza, Roma.
[26] Meissner, C. R., Griffin, M. B. Jr., Riddler, G. P., Marcel Van Eck, Aspinall, N. C., Farasani, A. M., Dini, S. M. (1990): Preliminary Geologic Map of the Thaniyat Turayf Quadrangle, Sheet 29c, Kingdom of Saudi Arabia – Department of the Interior, US Geological Survey, Washington, DC.
[27] Miller, K. G., Wright, J. D., Fairbanks, R. G. (1991): Unlocking the ice house: Oligocene-Miocene oxygen isotopes, eustasy, and margin erosion. – Journal of Geophysical Research: Solid Earth 96(B4): 6829-6848.
[28] Miller, K. G., Browning, J. V., Aubry, M.-P., Wade, B. S., Katz, M. E., Kulpecz, A. A., Wright, J. D. (2008): Eocene–Oligocene global climate and sea-level changes: St. Stephens quarry, Alabama. – GSA Bulletin 120(1-2): 34-53.
[29] Mustafa, H., Zalmout, I. (2002): Elasmobranchs from the Late Eocene Wadi Esh-Shallala Formation Ofqa'faydat Ad Dahikiya, East Jordan. – Tertiary Research 21(1/4): 77-94.
[30] Okada, H., Bukry, D. (1980): Supplementary modification and introduction of code numbers to the low-latitude coccolith biostratigraphy (Bukry 1973; 1975). – Mar. Micropaleontol. 5: 321-325.
[31] Pagani, M., Zachos, J. C., Freeman, K. H., Tipple, B., Bohaty, S. (2005): Marked decline in atmospheric carbon dioxide concentrations during the Paleogene. – Science 309(5734): 600-603.
[32] Pälike, H., Norris, R. D., Herrle, J. O., Wilson, P. A., Coxall, H. K., Lear, C. H., Shackleton, N. J., Tripati, A. K., Wade, B. S. (2006): The heartbeat of the Oligocene climate system. – Science 314(5807): 1894-1898.
[33] Perch-Nielsen, K. (1985): Cenozoic Calcareous Nannofossils. – In: Bolli, H. M., Saunders, J. B., Perch-Nielsen, K. (eds.) Plankton Stratigraphy. Cambridge University Press, Cambridge.
[34] Powers, R., Ramirez, L., Redmond, C., Elberg, E. (1966): Geology of the Arabian Peninsula. – Geological Survey Professional Paper 560: 1-147.
[35] Raffi, I., Agnini, C., Backman, J., Catanzariti, R., Pälike, H. (2016): A cenozoic calcareous nannofossil biozonation from low and middle latitudes: a synthesis. – Journal of Nannoplankton Research 36(2): 121-132.
[36] Strougo, A., Faris, M., Abul-Nasr, R. A., Gingerich, P. D., Haggag, M. A. (2013): Planktonic foraminifera and calcareous nannofossil biostratigraphy through the Middle to Late Eocene transition at Wadi Hitan, Fayum Province, Egypt. – Journal of Paleontology 32(8).
[37] TSCreator visualization of enhanced Geologic Time Scale 2016 database (Version 7.4; 2020) James Ogg (database coordinator) https://engineering.purdue.edu/Stratigraphy/tscreator.
[38] Villa, G., Fioroni, C., Pea, L., Bohaty, S., Persico, D. (2008): Middle Eocene–Late Oligocene climate variability: calcareous nannofossil response at Kerguelen Plateau, site 748. – Marine Micropaleontology 69(2): 173-192.
[39] Wallace, C. A., Dini, S. M., Al-Farasani, A. N. (1994): Geological map of part of the Turayf Quadrangle, Sheet 31C, and An Nabk Quadrangle, Sheet 31B, Kingdom of Saudi Arabia. – Ministry of Petroleum and Mineral resources, Saudi Geological Survey: Geoscience Map Series GM-125C.
[40] Wei, W., Wise, S. W. Jr (1989): Paleogene calcareous nannofossil magnetobiochronology: results from South Atlantic DSDP site 516. – Marine Micropaleontology 14(1-3): 119-152.
[41] Wei, W., Wise, S. W. Jr (1990): Biogeographic gradients of Middle Eocene-Oligocene Calcareous nannoplankton in the South Atlantic Ocean. – Palaeogeography, Palaeoclimatology, Palaeoecology 79(1-2): 29-61.
[42] Zachos, J., Pagani, M., Sloan, L., Thomas, E., Billups, K. (2001): Trends, rhythms, and aberrations in global climate 65 Ma to Present. – Science 292(5517): 686-693.

http://www.aloki.hu ● ISSN 1589 1623 (Print) ● ISSN 1785 0037 (Online)
DOI: http://dx.doi.org/10.15666/aeer/1804_56075625

[43] Zalmout, I. S., Mustafa, H. A., Gingerich, P. D. (2000): Priabonian Basilosaurus isis (Cetacea) from the Wadi Esh-Shallala Formation: first marine mammal from the Eocene of Jordan. – Journal of Vertebrate Paleontology 20(1): 201-204.

APPENDIX

Appendix A: *Raw range chart and percentage counts.*

Sample	F	E	D	C	B	A
Height (m)	9	4	3	2	1	0
Martini (1971)	NP18					
Okada and Bukry (1980)	CP15				CP14b	
Agnini et al. (2014)	CNE17					
Diversity	27	33	33	29	36	39
Preservation	P	M-P	M	G	M-G	G
Group Abundance	C	A	VA	VA	VA	VA
Blackites cf. morionum					R	C
Blackites spinosus	F	C	A	F	F	F
Braarudosphaera bigelowii	R	R				
Chiasmolithus grandis					**R**	R
Chiasmolithus oamaruensis		R	R		R	**F**
Clausicoccus subdistichtus	F	C	C	C	A	R
Coccolithus eopelagicus	C	R	R	R	R	A
Coccolithus pelagicus	A	A	A	A	A	F
Cruciplacolithus cruciformis		R	R		F	A
Cyclicargolithus floridanus < 5	A	A	A	A	A	A
Cyclicargolithus floridanus	A	A	A	A	A	F
Discoaster barbadiensis	F	F	F	F	F	A
Discoaster saipanensis	F	F	A	C	C	R
Discoaster tanii	R	R	R			R
Coccolithus formosus	C	C	R	C	C	C
Helicosphaera bramlettii	C	C	C	C	R	
Helicosphaera compacta	F	R	F	R	R	R
Helicosphaera reticulata		R	R	F		
Helicosphaera wilcoxii		R	F			
Hughesius tasmaniae						C
Isthmolithus recurvus		**R**				
Lanternithus minutus	C	F	F	C	F	F
Neococcolithes dubius			F	R	R	F
Pedinocyclus gibbsiae	F	F	C	F	C	
Pontosphaera exilis					F	F
Pontosphaera panarium				R	R	R
Pontosphaera multipora		R	R	R	F	C
Reticulofenestra bisecta	A	R	F		C	F
Reticulofenestra daviesii	R	F	R	F	F	F

http://www.aloki.hu ● ISSN 1589 1623 (Print) ● ISSN 1785 0037 (Online)
DOI: http://dx.doi.org/10.15666/aeer/1804_56075625

Reticulofenestra cf. daviesii					F	R
Reticulofenestra dictyoda	F	C	A	C	C	F
Reticulofenestra hillae	R		R	F	F	A
Reticulofenestra lockeri	F	C	F	F	A	R
Reticulofenestra reticulata	A	A	A	A	A	A
Reticulofenestra spp. *(< 3)*	R	A	A	A	A	F
Reticulofenestra erbae	**A**	**A**	**A**	**A**	**A**	F
Reticulofenestra umbilica	F	F	C	C	C	A
Sphenolithus cf. *furcatolithoides*		R	F	C	R	F
Sphenolithus moriformis	F	F	R	F	F	R
Sphenolithus predistentus?		R				R
Sphenolithus spiniger						R
Thoracosphaera spp.	R	R	R	F	R	C
Zygrablithus bijugatus	C	F	C	F	F	C

Row count

Reticulofenestra daviesii	2	3	2	4	3	4
Reticulofenestra dictyoda	4	7	13	6	8	5
Reticulofenestra hillae	1	0	2	3	3	4
Reticulofenestra lockeri	3	10	5	5	11	4
Reticulofenestra reticulata	16	19	13	15	14	20
Reticulofenestra erbae	12	26	20	12	20	5
Reticulofenestra spp. *(< 3)*	2	21	19	27	50	76
Reticulofenestra umbilica	3	4	7	10	6	7
Sphenolithus moriformis	4	5	2	3	3	4
Sphenolithus predistentus	0	1	3	6	1	7
Sphenolithus spiniger	0	0	0	0	0	2
Thoracosphaera spp.	2	2	1	5	2	2
Zygrablithus bijugatus	7	4	8	5	5	2
Blackites spinosus	3	6	11	4	5	11
Blackites morionum	0	0	0	0	1	2
Reticulofenestra cf. *daviesii*	0	0	0	0	3	10
Discoaster 5-ray knob	0	0	0	0	3	0
Helicosphaera bramlettii	7	6	10	9	1	0
Helicosphaera wilcoxii	0	1	3	0	0	0
Braarudosphaera bigelowii	2	1	0	0	0	0
Isthmolithus recurvus	0	2	0	0	0	0
Species richness	27	33	33	29	36	39

Count percentage

Discoaster tanii	0.333333	0.662252	0.311526	0	0	0.278552
Ericsonia formosa	2.333333	2.317881	0.623053	2.95082	2.523659	1.114206
Helicosphaera compacta	1.666667	0.331126	0.934579	0.327869	0.630915	0.557103

http://www.aloki.hu ● ISSN 1589 1623 (Print) ● ISSN 1785 0037 (Online)
DOI: http://dx.doi.org/10.15666/aeer/1804_56075625

Helicosphaera reticulata	0	0.331126	0.623053	0.983607	0	0.278552
Hughesius tasmaniae	0	0	0	0	0	0.278552
Lanternithus minutus	2.333333	1.324503	1.246106	1.967213	0.946372	0.835655
Neococcolithes dubius	0	0	0.934579	0.655738	0.630915	0.835655
Cyclococcolithina protoannula	1.333333	0.993377	2.492212	1.639344	2.208202	2.506964
Pontosphaera exilis	0	0	0	0	1.26183	1.671309
Pontosphaera panarium	0	0	0	0.327869	0.315457	1.392758
Pontosphaera multipora	0	0.331126	0.623053	0.655738	1.577287	1.114206
Reticulofenestra bisecta	17.66667	0.662252	1.246106	0	2.208202	1.949861
Reticulofenestra daviesii	0.666667	0.993377	0.623053	1.311475	0.946372	1.114206
Reticulofenestra dictyoda	1.333333	2.317881	4.049844	1.967213	2.523659	1.392758
Reticulofenestra hillae	0.333333	0	0.623053	0.983607	0.946372	1.114206
Reticulofenestra lockeri	1	3.311258	1.557632	1.639344	3.470032	1.114206
Reticulofenestra reticulata	5.333333	6.291391	4.049844	4.918033	4.416404	5.571031
Reticulofenestra erbae	4	8.609272	6.23053	3.934426	6.309148	1.392758
Reticulofenestra spp. (< 3)	0.666667	6.953642	5.919003	8.852459	15.77287	21.16992
Reticulofenestra umbilica	1	1.324503	2.180685	3.278689	1.892744	1.949861
Sphenolithus moriformis	1.333333	1.655629	0.623053	0.983607	0.946372	1.114206
Sphenolithus predistentus	0	0.331126	0.934579	1.967213	0.315457	1.949861
Sphenolithus spiniger	0	0	0	0	0	0.557103
Thoracosphaera spp.	0.666667	0.662252	0.311526	1.639344	0.630915	0.557103
Zygrablithus bijugatus	2.333333	1.324503	2.492212	1.639344	1.577287	0.557103
Blackites spinosus	1	1.986755	3.426791	1.311475	1.577287	3.064067
Blackites cf. *morionum*	0	0	0	0	0.315457	0.557103
Reticulofenestra cf. *daviesii*	0	0	0	0	0.946372	2.785515
Discoaster 5-ray knob	0	0	0	0	0.946372	0
Helicosphaera bramlettii	2.333333	1.986755	3.115265	2.95082	0.315457	0
Helicosphaera wilcoxii	0	0.331126	0.934579	0	0	0
Braarudosphaera bigelowii	0.666667	0.331126	0	0	0	0
Isthmolithus recurvus	0	0.662252	0	0	0	0

Appendix B. *Species list recorded in the Rashrashiyah Formation. Taxa are alphabetically arranged with references*

Blackites morionum (Deflandre in Deflandre & Fert,1954) Varol, 1989
Blackites spinosus (Deflandre & Fert, 1954) Hay & Towe, 1962
Braarudosphaera bigelowii (Gran & Braarud 1935) Deflandre, 1947
Chiasmolithus grandis (Bramlette & Riedel, 1954) Radomski, 1968
Chiasmolithus oamaruensis (Deflandre, 1954) Hay et al., 1966
Clausicoccus subdistichus (Roth & Hay in Hay et al., 1967) Prins, 1979
Coccolithus eopelagicus (Bramlette & Riedel, 1954) Bramlette & Sullivan, 1961
Coccolithus pelagicus (Wallich 1877) Schiller, 1930
Cruciplacolithus cruciformis (Hay & Towe, 1962) Roth, 1970
Cyclicargolithus floridanus (Roth & Hay, in Hay et al., 1967) Bukry, 1971
Cyclicargolithus floridanus < 5 µm (Roth & Hay, in Hay et al., 1967) Bukry, 1971
Cyclococcolithina protoannula Gartner 1971
Coccolithus formosus (Kamptner, 1963) Wise, 1973
Discoaster barbadiensis Tan, 1927

http://www.aloki.hu ● ISSN 1589 1623 (Print) ● ISSN 1785 0037 (Online)
DOI: http://dx.doi.org/10.15666/aeer/1804_56075625

Discoaster deflandrei Bramlette & Riedel, 1954
Discoaster saipanensis Bramlette & Riedel, 1954
Discoaster tanii Bramlette & Wilcoxon 1967
Helicosphaera bramlettei (Müller, 1970) Jafar & Martini, 1975
Helicosphaera compacta Bramlette & Wilcoxon, 1967
Helicosphaera reticulata Bramlette & Wilcoxon, 1967
Helicosphaera wilcoxii (Gartner, 1971) Jafar & Martini, 1975
Hughesius tasmaniae (Edwards and Perch-Nielsen, 1975) de Kaenel and Villa, 1996
Isthmolithus recurvus Deflandre in Deflandre and Fert, 1954
Lanternithus minutus Stradner, 1962
Neococcolithes dubius (Deflandre in Deflandre and Fert, 1954) Black, 1967
Pontosphaera exilis (Bramlette & Sullivan, 1961) Romein, 1979
Pontosphaera multipora (Kamptner, 1948 ex Deflandre in Deflandre & Fert, 1954) Roth, 1970
Pontosphaera panarium (Deflandre in Deflandre & Fert, 1954) Aubry, 1986
Reticulofenestra bisecta (Hay, Mohler and Wade, 1966) Roth, 1970
Reticulofenestra daviesii (Haq, 1968) Haq, 1971
Reticulofenestra cf. *daviesii* (Haq, 1968) Haq, 1971
Reticulofenestra dictyoda (Deflandre in Deflandre & Fert, 1954) Stradner in Stradner & Edwards, 1968
Reticulofenestra erbae (Fornaciari et al., 2010) Bown & Newsam 2017
Reticulofenestra hillae Bukry & Percival, 1971
Reticulofenestra lockeri Müller, 1970
Reticulofenestra reticulata (Gartner & Smith, 1967) Roth & Thierstein, 1972
Reticulofenestra spp. (< 3 μm) Hay, Mohler & Wade, 1966
Reticulofenestra umbilica (Levin, 1965) Martini & Ritzkowski, 1968
Sphenolithus cf. *furcatolithoides* Locker, 1967
Sphenolithus moriformis (Brönnimann & Stradner, 1960) Bramlette & Wilcoxon, 1967
Sphenolithus predistentus? Bramlette & Wilcoxon, 1967
Sphenolithus spiniger Bukry, 1971
Thoracosphaera spp. Kamptner 1927
Zygrablithus bijugatus (Deflandre in Deflandre and Fert, 1954) Deflandre, 1959

http://www.aloki.hu ● ISSN 1589 1623 (Print) ● ISSN 1785 0037 (Online)
DOI: http://dx.doi.org/10.15666/aeer/1804_56075625

ANALYSIS OF LAND USE/LAND COVER CHANGE AND ITS PREDICTION IN THE MAMBASA SECTOR, DEMOCRATIC REPUBLIC OF CONGO

OPELELE, O. M.[1,2,3] – FAN, W. Y.[1,2*] – YU, Y.[1,2] – KACHAKA, S. K.[3]

[1]*School of Forestry, Northeast Forestry University, Harbin 150040, Heilongjiang, P.R. China*

[2]*Key Laboratory of Sustainable Forest Ecosystem Management - Ministry of Education, School of Forestry, Northeast Forestry University, Harbin 150040, Heilongjiang, P.R. China*

[3]*Faculty of Agronomy, University of Kinshasa, 117 Kinshasa XI, Mont-Amba/Lemba, Democratic Republic of Congo*

**Corresponding author*
e-mail: fanwy@163.com; phone/fax: +86-139-4605-5384

(Received 14th Dec 2019; accepted 22nd May 2020)

Abstract. Current information on land use/land cover change and its future evolution is required to support land management planning and policymaking in most developing countries experiencing deforestation and land degradation. Here, we explore the land use/land cover change occurring between 1987 and 2019 in the Mambasa sector, located in the Democratic Republic of Congo, and used the cellular automata model to predict the 2035 land use/land cover. The results have shown that during the last 32 years, dense forest has lost approximately 5121.54 ha, while secondary forest, fallow land and fields and, built-up area have gained 1786.23 ha, 3140.46 ha and 194.85 ha respectively. The predicted land use/land cover for the year 2035 revealed that dense and secondary forests will continue to experience a decrease of 3.85% and 13.65% respectively, while built-up area and fallow land and fields will experience an increase of 6.9% and 34.25% respectively. However, the study revealed that the unsustainable agriculture system combined with wood energy and artisanal logging have led to land use/land cover change in Mambasa. To reduce deforestation in the region, it would be necessary to improve agricultural production system, diversify the income and provide others timber product sources.
Keywords: *land cover, CA-ANN model, remote sensing, Mambasa*

Introduction

For centuries, human beings have been destroying the natural resources in order to satisfy their food needs through agricultural activities (Houghton, 1994). It is true that, for several years, the increase of human populations leads to the increase of the demand in natural resources, resulting in land degradation (Wondie et al., 2011).

Ouedraogo et al. (2010) has reported that, in tropical regions, the conversion of the natural forest areas to farmlands for the purpose of satisfying the increasing human population demand for natural resources makes agricultural activities one of the main causes of land degradation. Currently, land use/land cover change has been known for their negative effects on the survival of humankind. Indeed, in most cases, Land use/ land cover change strongly impacts crucial aspects of the functioning of the Earth (Lambin et al., 2001), especially with regard to their negative consequences on climate change (Song et al., 2018; Fan, 2015; Salazar et al., 2015; Houghton et al., 2017), degradation of soil (Alemu, 2015), global biogeochemical cycles such as carbon, nitrogen and water quality (Jain et al., 2013; Copeland et al., 1996; Schönhart et al., 2018; Le Maire et al., 2014; Spera et al., 2016; Sterling et al., 2013) as well as

http://www.aloki.hu ● ISSN 1589 1623 (Print) ● ISSN 1785 0037 (Online)
DOI: http://dx.doi.org/10.15666/aeer/1804_56275644

biodiversity loss (Haines-Young, 2009; Mantyka-Pringle et al., 2015; Wanger et al., 2010). Consequently, land use/land cover change has become one of the key environmental issues, specifically in tropical regions where deforestation is taking place at a rapid rate (Scholes and Van Breemen, 1997). Thus, performing studies on land use/ land cover change issues in these regions is important to reduce their negative consequences on humankind, and to assure the long-term persistence of natural resources.

According to Lambin et al. (2001), land cover points to the actual biophysical attributes of the Earth's surface (vegetation type, presence of water, rocks) whereas land use refers to the way in which the land cover is used. Thus, for numerous applications such as vegetation and farmland monitoring, analysis of the Earth's surface and atmosphere interactions, information on the current status of the land use/land cover is necessary (Townshend, 1992). Therefore, for the purpose of establishing sustainable land use policy with regard to natural resources, understanding the dynamics of the landscape is most important for development planners to suggest some good strategies to the current land-use for better management of natural resources and, to avoid some future unwanted negative consequences on humankind. In this context of spatiotemporal analysis, remote sensing technology can play a leading role in the frame of land use/land cover change monitoring.

Remotely sensed data, especially landsat images, have been extensively used in the frame of modeling land use/land cover change for different purposes (Ranagala et al., 2019; Song et al., 2018; Han et al., 2015; Simwanda et al., 2018; Rogan and Chen, 2004; Wu et al., 2006; Zhuravleva et al., 2013; Potapov et al., 2012; Chen et al., 2018). Indeed, for several decades, remote sensing combined with field measurements have been used with success to monitor the loss of forest cover all over the world (Defries et al., 2006). In addition, remote sensing technology possesses not only the capability to capture land use/land cover change information using different change detection techniques (Roy et al., 2002), but also, the ability to offer spatial information and repeated coverage of large areas (Lillesand et al., 2004).

Among numerous tools used for the purpose of modelling and predicting land use/land cover change, the Markov chain has not only been proved to be one of the powerful tools, but also delivered accurate results in the frame of land use/land change prediction (Halmy et al., 2015; Agarwal et al., 2002). Being a stochastic model, the Markov chain approach predicts the future evolution of one system based on the state of the initial time (Sinha and Kimar, 2013; Muller and Middleton, 1994). Numerous studies have used the Markov Cellular automata (CA) approach to predict land use/land cover change (Basse et al., 2014; Saputra et al., 2019; Li and Yeh, 2002; Nouri et al., 2014; Kumar et al., 2014; Mubea et al., 2010; Rendana et al., 2015). From these studies, it has been shown that Markov chain constitutes one of the most essential tools for land use planning and environmental change research over different regions of the world. The use of both stochastic Markov techniques and the cellular automata model seems to predict land use change better than the regression based models (Ye and Bai, 2008; Pontius and Malanson, 2005).

There are numerous tools used to model and predict land use/land cover change, but it seems that no research has been carried out to examine the land use/land cover change of the Mambasa sector, even though this region, located in amongst forested areas of the Democratic Republic of Congo, where pressures on forests are ever increasing, still experience accelerated land degradation, biodiversity loss, and climate change. And yet,

http://www.aloki.hu ● ISSN 1589 1623 (Print) ● ISSN 1785 0037 (Online)
DOI: http://dx.doi.org/10.15666/aeer/1804_56275644

accurate and current information on land use/land cover change is important to provide valuable information to decision-makers for elaborating good policies and strategies of sustainable forest management in Mambasa. Indeed, the assessment of the landscape dynamic due to human activities can provide the status of each land use/land cover type and its recent evolution so that further decision making processes can be initiated to undertake sustainable land use management Thus, the objectives of this study are (i) to analyze the spatio-temporal change of land use/land cover change of Mambasa sector from the year 1987 to 2019 and, (ii) to predict the future land use/land cover of the year 2035 using CA-ANN model.

Materials and methods

Study area

This study was conducted in Mambasa, an administrative sector of the Democratic Republic of Congo. It is located between 1°7′0″-1°29′0″N in latitude and 28°53′0″-29°7′0″E in longitude (*Fig. 1*). Its total land area is estimated at 45669.24 ha, entirely located in the Congolese central basin. The region is dominated by dense rainforest and equatorial climate. This climate is characterized by two dry seasons, notably the long dry season (between January and February) and the small dry season (between June and August). Over the two last decades, Mambasa has experienced considerable population growth that has negatively impacted its natural resources. Consequently, careful assessment of land use/land cover change is required to help decision makers for the purpose of elaborating sustainable land management planning of natural resources.

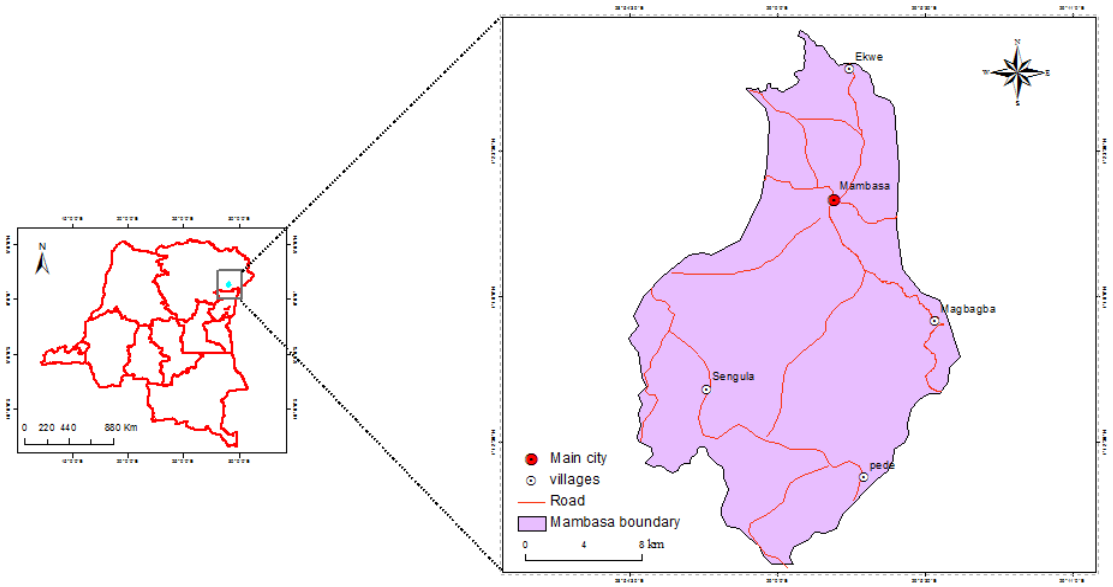

Figure 1. *Location of Mambasa sector in the Democratic Republic of Congo*

Data collection

According to the Landsat Worldwide Reference System (WRS), Mambasa is located at the Path and Row position of 174 and 59, respectively. Thus, Landsat images of the year 1987, 2003 and 2019, were freely downloaded from the website of the US

http://www.aloki.hu ● ISSN 1589 1623 (Print) ● ISSN 1785 0037 (Online)
DOI: http://dx.doi.org/10.15666/aeer/1804_56275644

Geological Survey National Center for Earth Resources Observation and Science (http://glovis.usgs.gov/), in order to extract crucial information on land use/land cover change in the Mambasa sector. In addition, as it requires to better know the region before performing supervised classification, field observations were carried out during March 2019 for the purpose of understanding the characteristics of each land use/land cover category. Thus, for each land use/land cover class, 150 training reference points were collected using the GPS receiver. The three landsat images were acquired in March and February because of cloud free images or clear sky during that period (*Table 1*). Indeed, using satellite images acquired almost in the same period remains an important advantage of land use/land cover change study. This removes the effects of change in season when investigating year-to-year change, and also minimizes the discrepancies in reflectance caused by seasonal vegetation fluxes, climatic differences and sun angle differences (Singh, 1989).

Table 1. *Characteristics of remotely sensed data used for the study*

Sensors	Acquisition date	Spatial resolution	Path/row	Band combination	Source
LT05	March 1987	30 m	174/59	5, 4, 3	http://glovis.usgs.gov/.
LE07	February 2003	30 m	174/59	5, 4, 3	http://glovis.usgs.gov/.
LC08	March 2019	30 m	174/59	6, 5, 4	http://glovis.usgs.gov/.

Land use/land cover classification and change detection

After performing the image preprocessing (radiometric calibration and atmospheric correction using the FLAASH method), we then carried out supervised classification of the 1987, 2003 and 2019 satellite images following the Yangambi vegetation classification system. Firstly, field data was collected for each land use/land cover class in order to identify the spectral signature of each one (*Fig. 2*). In addition, using the maximum likelihood algorithm, satellite images were classified into four categories, namely dense forest, fallow land and fields, secondary forest and built-up area. In fact, the maximum likelihood algorithm is a parametric decision whose rule is based on the probability that has a certain pixel belonging to a certain category. It has been reported that this algorithm provides the higher classification accuracy in land use/land cover study (Vadrevu, 2013). Ultimately, post-classification operations were applied to improve the classified images. For our research, different software were applied as each one has its strength in certain operations needed for analysis. All image processing (image preprocessing and classification, change detection and accuracy assessment) were performed in ENVI 5.3 software and QGIS, while ArcGIS 10.1 was used to produce the final map.

To describe land cover change occurring between 1987 and 2019, the transition matrix method was applied. The transition matrix corresponds to a squared matrix describing changes occurring on different elements of a system during a certain period (Bell, 1974). Cells of matrix contain values of the variable which changed the state from initial time to final time. Values of column and rows represent the proportion of an area occupied by each land cover class at the corresponding time.

Figure 3 shows the overall workflow of the study, including all the different steps from data collection to the production of the predicted land use/cover map.

http://www.aloki.hu ● ISSN 1589 1623 (Print) ● ISSN 1785 0037 (Online)
DOI: http://dx.doi.org/10.15666/aeer/1804_56275644

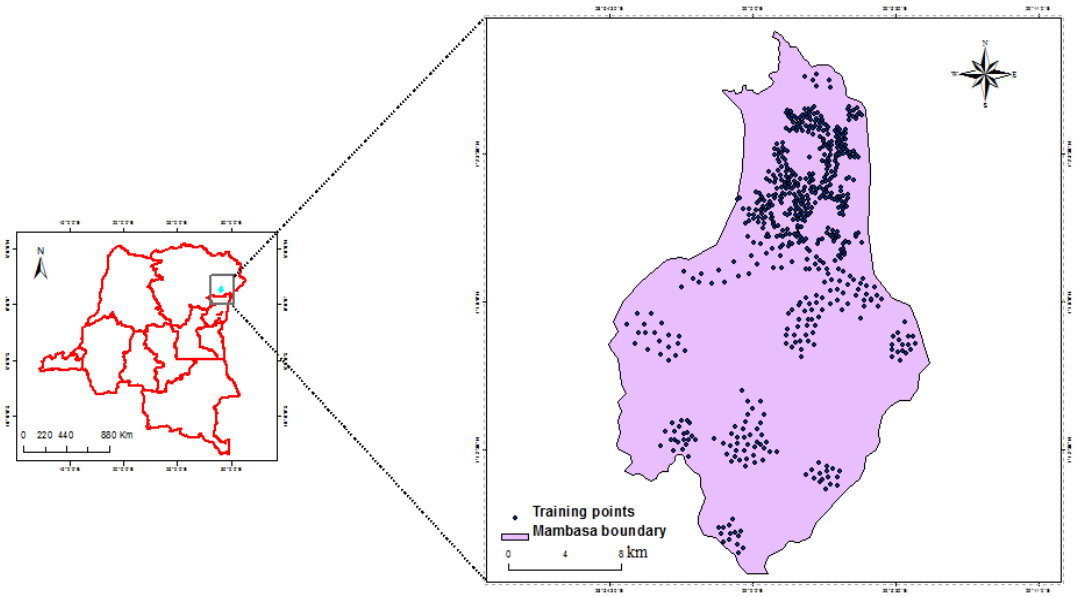

Figure 2. *Location of training reference points collected during the field survey in the Mambasa sector*

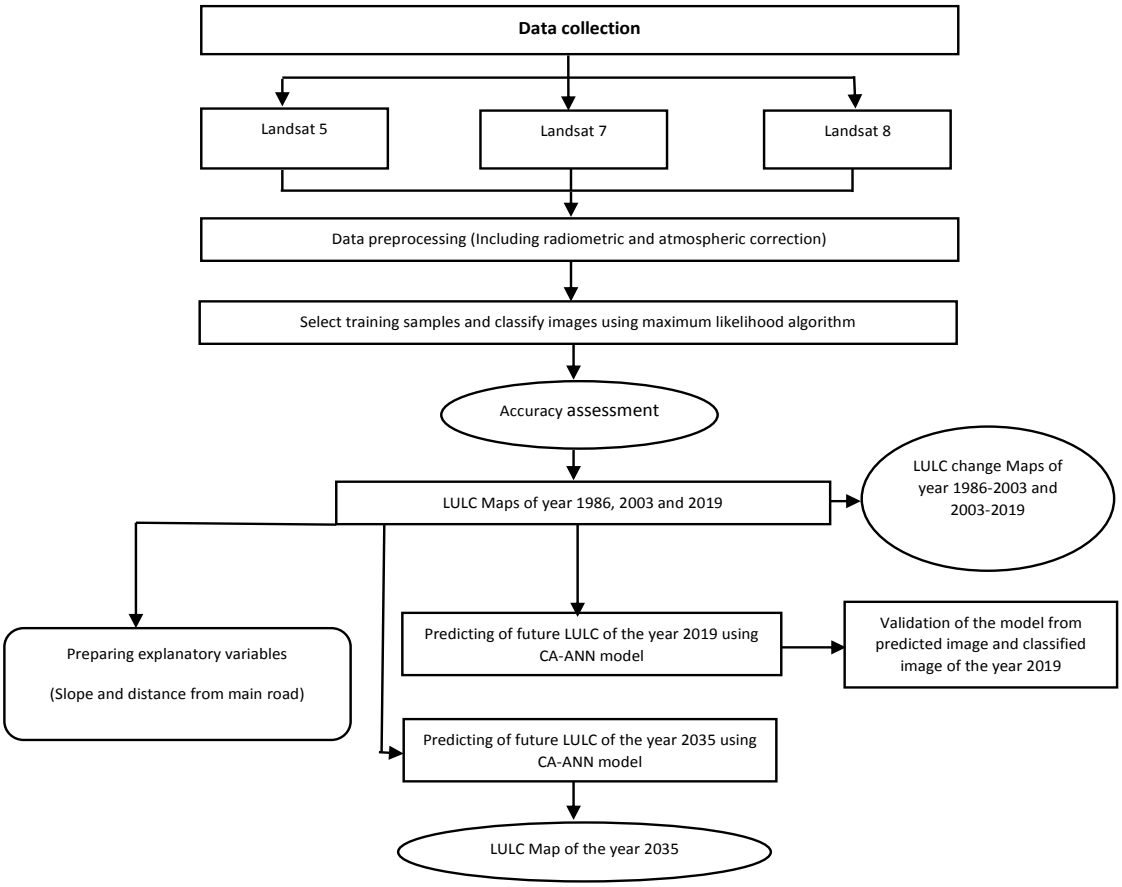

Figure 3. *Schematic diagram of the research approach*

Prediction of future land use/land cover change

http://www.aloki.hu ● ISSN 1589 1623 (Print) ● ISSN 1785 0037 (Online)
DOI: http://dx.doi.org/10.15666/aeer/1804_56275644

For the purpose of predicting land use/land cover change in the Mambasa sector, MOLUSCE plugin imbedded in QGIS software was used. The cellular automata (CA) model was then applied, and the artificial neural network (ANN) algorithm was used in the model. Indeed, Jogun (2019) has stated that the use of the machine learning algorithm such as ANN to predict land cover change, is better than other methods like linear regression. Thus, two explanatory variables namely slope and distance from main roads in the Mambasa sector, were used in order to predict the future change. Firstly, the 1987 and 2003 classified images were used to predict the 2019 land use/land cover. Then, the three map comparison method was performed for the validation of the prediction results. As the validation results have shown high accuracy, the 2035 land use/land cover was predicted by means of 2003 and 2019 classified images.

Figure 4 describes the structure of the CA-ANN model. Neurons in the input layers are considered as a set of cellular attributes, which are explanatory variables (slope and distance from main roads). It was reported that these variables explained the land use/land cover change probabilities. In the output layer, a neuron relates to a land use/land cover category. Each neuron value in the output layer represented the transition probability from the existing class to the corresponding land use class.

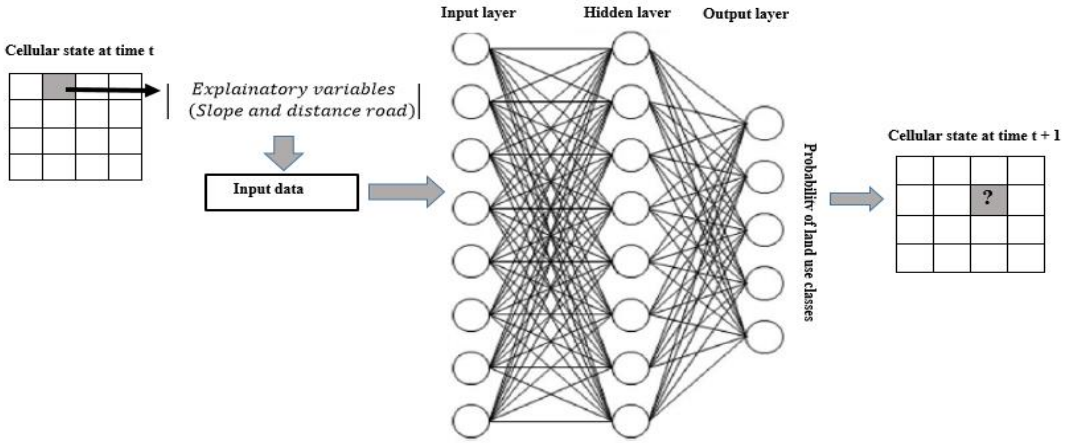

Figure 4. *Processing architecture of ANN-CA model*

Accuracy assessment

To use a land use/land cover map, it is crucial to know the accuracy of the map (Plourde and Congalton, 2003; Smits et al., 1999). Thus, accuracy assessment for the 1987, 2003 and 2019 maps was performed to appreciate the quality of information resulting from the image classification process. The confusion matrix method, which is the most common approach for appreciating image classification accuracy, was applied (Congalton, 1991). In this article, the reference data (ground truth points) were collected in March 2019 to perform the accuracy assessment of the 2019 classified image, while Google earth was used to carry out accuracy assessment for the 1986 and 2035 classified images. We then compared the observed pixels (ground truth points) of every land use/land cover class to the map pixel. The results were generated into the confusion matrix in order to assess the 1987, 2003 and 2019 final land use/land cover map accuracy. The overall user's and producer's accuracies were calculated from the confusion matrix. According to Pontius and Millones (2011), the producer's accuracy is

http://www.aloki.hu ● ISSN 1589 1623 (Print) ● ISSN 1785 0037 (Online)
DOI: http://dx.doi.org/10.15666/aeer/1804_56275644

used for determining how well an image is classified. In addition, the Kappa coefficient, one of the most statistic parameter for assessing image classification accuracy, was also computed (Rosenfield and Fitzpatrick-Lins, 1986).

Therefore, the overall accuracy of classification for the 1987, 2003 and 2019 map are 88.16% (kappa value 0.85), 89.16% (kappa value 0.86) and 93.6% (kappa value 0.91), respectively. As noted by (Weng, 2002), the minimum level for accuracy assessment in identification of land use/ land cover categories in the field of remote sensing should be at least 85%.

Results

Accuracy assessment of satellite image classification

The land use/land cover classification was successfully carried out with a high accuracy level. The overall accuracy of the 2019, 2003 and 1987 maps are 93.6% (kappa value 0.91), 89.15% (kappa value 0.86) and 88.16% (kappa value 0.85), respectively.

For the 2019 map, error matrix has been presented in *Table 2*. 159 of 170 field samples were correctly classified. The main confusion was observed between dense forest and secondary forest, with four validation points on secondary forest classified as dense forest, while two validation points on dense forest were classified as secondary forest. In addition, two validation points in secondary forest were classified as fallow land and field, while one validation point in the built-up area was classified as secondary forest.

For the 2003 map, error matrix has been presented in *Table 3*. A total of 218 reference points were checked against Google Earth image.196 of 218 validation samples were correctly classified. The main confusion was observed between dense forest and secondary forest, with seven validation points on secondary forest classified as dense forest, while six validation points in dense forest were classified as secondary forest. In addition, one validation point in secondary forest was classified as fallow land and field, while two validation points in fallow land were classified as secondary forest. Three validation points in fallow land were classified as built-up area, and three validation points in the built-up area were classified as fallow land and fields.

Table 2. *Error matrix of land cover map produced by supervised classification of 2019 image*

Number of pixels	**Reference data**					**User's accuracy (%)**
Classified image	**DF**	**SF**	**FF**	**BA**	**Row total**	
DF	61	2	0	0	63	96.3
SF	4	42	2	0	46	91.3
FF	0	0	34	2	39	92.3
BA	0	1	0	22	24	91.7
Column total	65	45	36	24		
Producer's accuracy (%)	93.9	93.3	94.7	91.7		

Overall accuracy: 93.6, Kappa statistic: 0.91

Table 3. *Error matrix of land cover map produced by supervised classification of 2003 image*

http://www.aloki.hu ● ISSN 1589 1623 (Print) ● ISSN 1785 0037 (Online)
DOI: http://dx.doi.org/10.15666/aeer/1804_56275644

Number of pixels	Reference data					
Classified image	**DF**	**SF**	**FF**	**BA**	**Row total**	**User's accuracy (%)**
DF	68	6	0	0	74	91.9
SF	7	52	1	0	60	86.7
FF	0	2	48	3	53	90.6
BA	0	0	3	28	31	90.3
Column total	75	60	52	31		
Producer's accuracy (%)	90.7	86.7	92.3	90.3		

Overall accuracy: 89.16, Kappa statistic: 0.86
DF: dense forest, SF: secondary forest, FF: fallow land and fields, BA: built-up area

Spatial and temporal changes in land use/land cover

Summary statistics of Land use/land cover change for the Mambasa sector for the years 1987, 2003 and 2019 developed from supervised classification are listed in *Table 4*.

Table 4. *Evolution of land use/cover in Mambasa sector from 1987 to 2019*

Land use/cover classes	Spatial area coverage						Annual rate of change
	1987		2003		2019		1987-2019
	Area (ha)	%	Area (ha)	%	Area (ha)	%	ha/year
Built-up area	302.76	0.66	412.02	0.9	497.61	1.09	6.09
Fallow land and fields	2763.99	6.05	4149.36	9.09	5904.45	12.93	98.14
Secondary forest	3753.54	8.22	5804.01	12.71	5539.77	12.13	55.82
Dense forest	38848.95	85.07	35303.85	77.3	33727.41	73.85	-160.05
Total	45669.24	100	45669.24	100	45669.24	100	

During our survey, Mambasa sector's landscape was classified into four land cover/land use types including dense forest, Secondary forest, Fallow land and fields, and built-up area (*Fig. 5*). On the basis of analysis carried out in 1987, it was noted that approximately 85.07%, 8.22%, 6.05% and 0.66% of the total area subject to analysis were calculated as dense forest, Secondary forest, Fallow land and fields, and built-up areas, respectively; while, in 2003, around 77.3%, 12.71%, 9.09% and 0.9% of the total area was calculated as dense forest, Secondary forest, Fallow land and fields, and built-up areas, respectively. In 2019, 73.85%, 12.13%, 12.93% and 1.09% were classified as dense forest, Secondary forest, Fallow land and fields, and built-up areas, respectively. Consequently, the land use/land cover change from 1987 to 2019 have shown an increasing in Secondary forest, Fallow land and fields, and built-up areas, by 1786.23 ha, 3140.46 ha, and 194.85 ha respectively; while in the same period dense forest underwent significant negative change. Indeed, dense forest land has strongly declined in the same period. Approximately 160.05 ha of dense forests were converted every year into other land use/land cover categories during the study period. However, the main change during the study period in the Mambasa sector was observed in the area converted from dense forest into Fallow land and fields.

http://www.aloki.hu ● ISSN 1589 1623 (Print) ● ISSN 1785 0037 (Online)
DOI: http://dx.doi.org/10.15666/aeer/1804_56275644

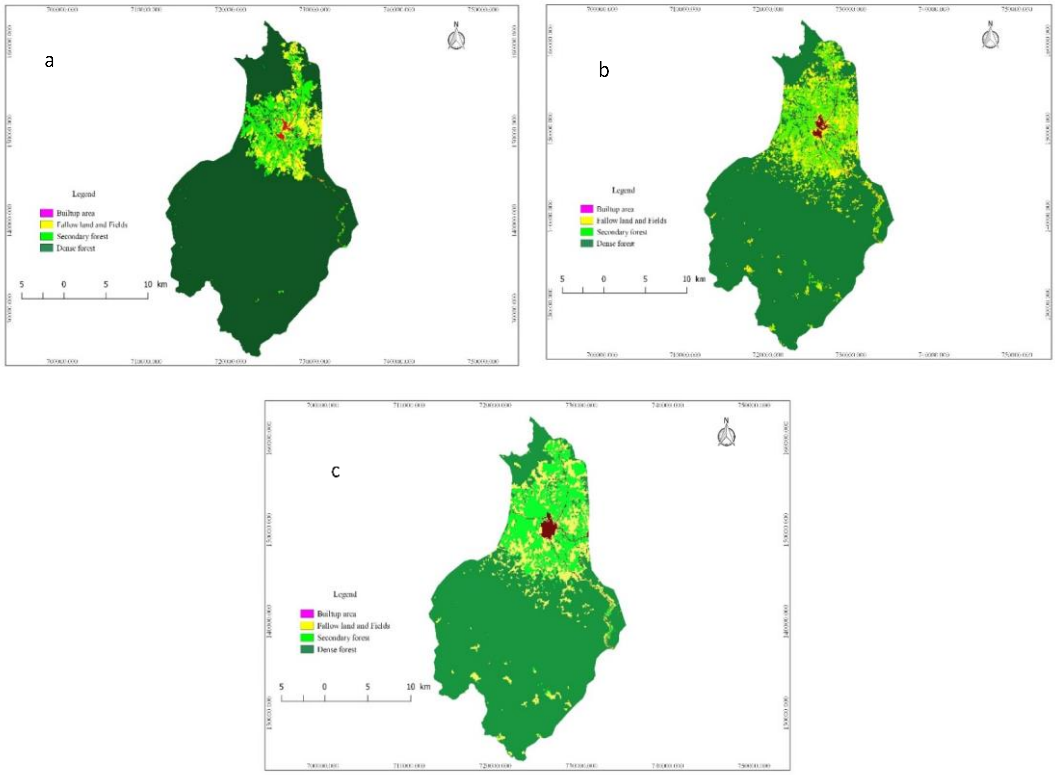

Figure 5. *Land use/land cover map for the year (a) 1987, (b) 2003 and (c) 2019*

Transition among land use/land cover types from 1987 to 2019

From the transitional probability matrix, it is easy to understand the trend in land use/land cover change occurring in the Mambasa sector during the study period. Indeed, the transitional probability matrix shows the probability of each cell of a certain land use/land cover type to be transformed into other types. Using the Markovian approach, the transitional probability matrix between the years 1987 to 2003, 2003 to 2019, and 1987 to 2019 has been performed in the MOLUSCE plugin. From *Table 5,* it can be revealed that, between 1987 and 2003, the probability of each land use/land cover category to be converted into fallow land and fields was higher than any other transition (third column). Moreover, it should be noted that, the conversion from dense forests to secondary forests is seen firstly as a conversion of dense forest into fallow land and fields; but when this land use/land cover class (fallow land and fields) is abandoned, it progresses into secondary forest by the natural process of vegetation succession. In addition, the no conversion from built-up area into dense forest was represented by zero values between 1987 and 2003, while, from 2003 to 2019, zero values represent no conversion of dense forest into built-up area. *Figure 6* represents the change maps that shows the transformation from one land use/land cover class to the others during 1987 to 2019. From the change maps, it was shown that the major part of the Mambasa landscape was converted into fallow land and fields. A total of 37426.05 ha of our study area did not change between 1987 and 2019. Among them, 33495.56 ha persisted as dense forest, 2356.01 ha as secondary forest, 1381.44 ha as fallow land and fields and 192.95 ha as built-up area. On the other hand, around 3325.47 ha, 1117.80 ha, and 81.26 ha of our study area

http://www.aloki.hu ● ISSN 1589 1623 (Print) ● ISSN 1785 0037 (Online)
DOI: http://dx.doi.org/10.15666/aeer/1804_56275644

were converted from dense forest, secondary forest, and built-up area respectively into fallow land and fields during 1987 to 2019.

Table 5. *Transition matrix of land use/cover changes in Mambasa sector from 1987 to 2019*

	Land cover category				
	To / From	Built-up area	Fallow & fields	Secondary forest	Dense forest
1987-2003	Built-up area	0.7155	0.1813	0.1031	0.0000
	Fallow and fields	0.0440	0.4007	0.5314	0.0239
	Secondary forest	0.0112	0.2032	0.6717	0.1139
	Dense forest	0.0008	0.0573	0.0459	0.8960
2003-2019	Built-up area	0.8746	0.0799	0.0443	0.0011
	Fallow and fields	0.01997	0.9290	0.0292	0.0216
	Secondary forest	0.0092	0.1809	0.7377	0.0722
	Dense forest	0.0000	0.0274	0.0317	0.9409
1987-2019	Built-up area	0.6373	0.2684	0.0859	0.0083
	Fallow and fields	0.0559	0.4998	0.4251	0.0193
	Secondary forest	0.0280	0.2978	0.6277	0.0465
	Dense forest	0.0012	0.0856	0.0510	0.8622

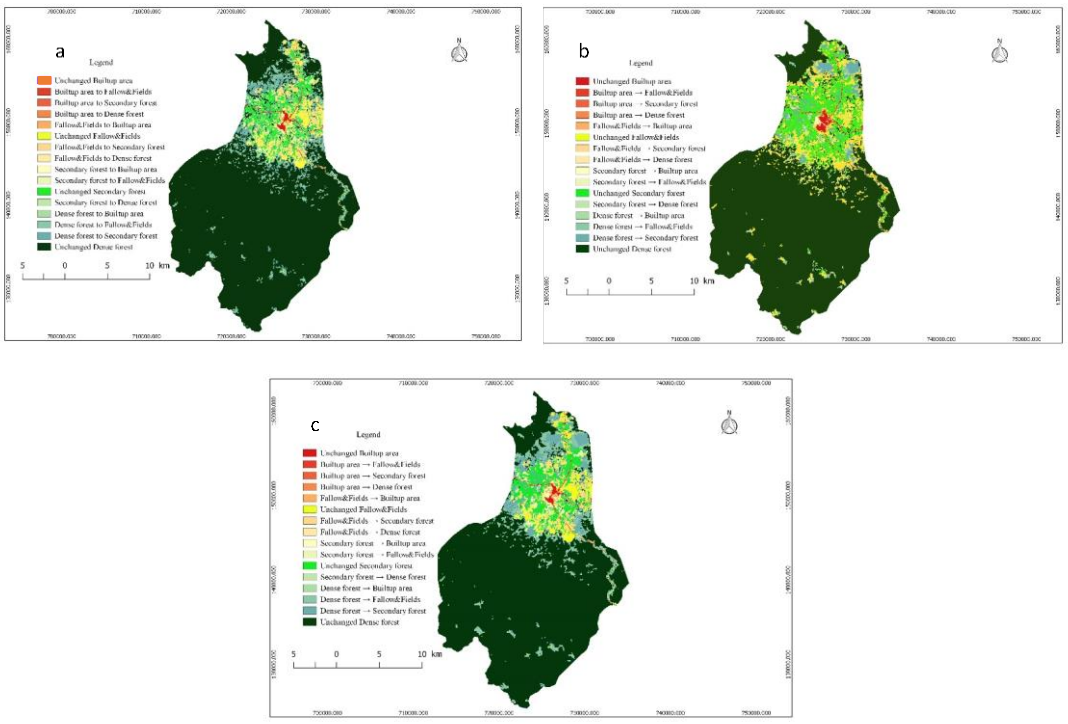

Figure 6. *LULC transformation of Mambasa sector during (a) 1987 to 2003, (b) during 2003 to 2019 and (c) during 1987 to 2019*

Prediction of the future land use change 2035

After performing the change detection analysis, the next step of this study was focused at forecasting the future land use/land cover for the year 2035. Thus, the simulated map of 2035 as shown in *Figure 7* was carried out using two spatial drivers

http://www.aloki.hu ● ISSN 1589 1623 (Print) ● ISSN 1785 0037 (Online)
DOI: http://dx.doi.org/10.15666/aeer/1804_56275644

including slope and distance from main roads. Firstly, the land use/land cover for the year 2019 was predicted by using both land use/land cover maps of the year 1987 and 2003, by means of the Cellular automata Artificial Neural Network (CA-ANN) algorithm. Then, the three map comparison method was applied to validate the prediction results. It has been demonstrated that the model, by its strong performance measured by the percentage of component agreement at 97.3%, was able to predict the future land use/land cover change almost correctly. After the validation of the model, the land use/land cover for the year 2035 was predicted from the year 2003 to 2019. In 2035, Mambasa sector will have an increase in Fallow land and fields (34.25% ha) and built-up area (6.9% h), while dense and secondary forest will lose 3.85% and 13.65% respectively (*Table 6*).

Table 6. *Summary of LULC change statistics between 2019 and 2035*

LULC classes	Area in hectare		Area change from 2019 to 2035 in (%)
	2019	2035	
Built-up area	497.61	531.90	6.9
Fallow & fields	5904.45	7926.48	34.25
Secondary forest	5539.77	4783.50	-13.65
Dense forest	33727.41	32427.36	-3.85

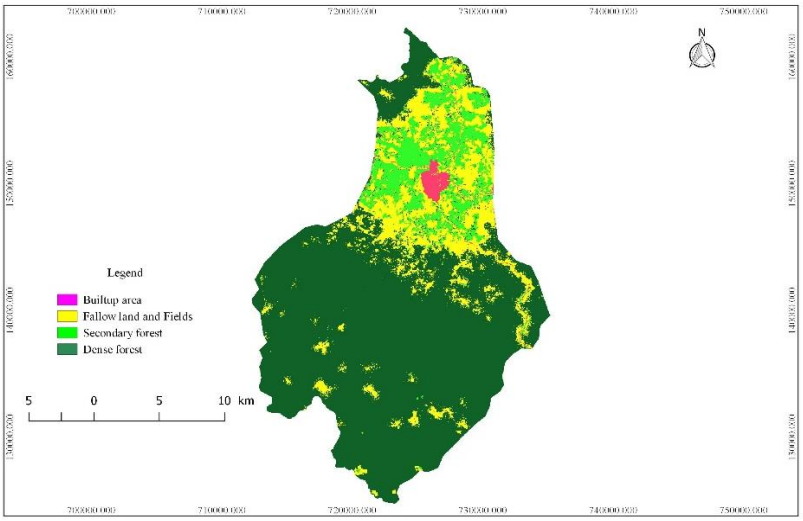

Figure 7. *Predicted LULC for the year 2035*

Discussion

Land use/land cover change from the year 1987 to 2019 and future prediction of 2035

The present study aimed to assess the land use/land cover change in the Mambasa sector from 1987 to 2019, and predict the spatio temporal change by 2035 using the Cellular automata Artificial Neural Network (CA-ANN) algorithm. The results revealed significant change in Mambasa's landscape during the study period. Indeed, Mambasa's landscape was classified into four categories namely dense forest, secondary forest, built-up areas as well as fallows and fields. During the last 32 years, dense forest has approximately lost 5121.54 ha, while secondary forest, fallow land and fields, built-up

http://www.aloki.hu ● ISSN 1589 1623 (Print) ● ISSN 1785 0037 (Online)
DOI: http://dx.doi.org/10.15666/aeer/1804_56275644

area have gained 1786.23 ha, 3140.46 ha and 194.85 ha respectively. The ratio of dense forest in the landscape declined from 85.07% in 1987, to 73.85% in 2019. Thus, the annual rate of deforestation observed in dense forest was estimated at 0.41. This rate is well above the national average, estimated between 0.2 and 0.3% over the last three decades (UN-REDD, 2012; de Wasseige et al., 2014). As for secondary forest, its area has also increased during the last three decades, from 3753.54 ha in 1987 to 5539.77 ha in 2019. Note that most of its area comes from dense forest that has been converted into fallow land and fields and, after being abandoned, it evolved to secondary forest through the natural process of succession vegetation. Fallow land and fields showed a positive evolution following the acquisition of areas mainly lost in dense and secondary forests, respectively 3325.47 ha and 1117.8 ha. Its proportion in the landscape increased from 6.05% in 1987, to 12.93% in 2019. This can be explained by the expansion of agricultural activities in this region and the increase of population in the region (*Table 7*). As reported by (Aweto, 2012), in the humid and sub-humid tropics, several hundred million people depend on agriculture system based on shifting cultivation or rotational bush fallowing for their livelihood. Indeed, agriculture system in Mambasa is based on shifting cultivation that consists in clearing primary or secondary forest to install fields. These fields can be cultivated for one or two years before soil fertility is exhausted. The field is then abandoned and the farmers move on to clear a new field elsewhere in the forest. Bamba (2010) has stated that, agriculture of DRC based on the slash-and-burn agriculture system has always been practiced for several decades. In addition, (Mpoyi et al., 2013) noted that the agriculture system in this region is based on unimproved varieties and unsustainable practices of soil fertility management. Consequently, several hectares of forest are lost every year for the benefit of crop land. Our results corroborate the findings of (Ngabinzeke et al., 2016) that reported that the expansion of slash-and-burn agriculture in the region is leading to a conversion of natural habitats. According to the study, significant changes occurred during a period of one year in the area under study. Forest and savanna areas declined by 6.5 ha (86.6 to 80.1 ha) while agricultural areas (cleared land and seasonal crops) increased from 7.3 ha to 21.8 ha. Similar results were obtained in a study conducted in the Kongo central province. In this study, it has been reported that fallow land and fields increased from 22.72% in 1960 to 54.61% in 2005; while forest land, the landscape's matrix in 1960, declined from 49.95% of the total area of landscape to 5.67% in 2005. The study has revealed that the decrease in forest area was due to the unsustainable agriculture system and demographic pressures (Bamba, 2010). In a study conducted in Isangi region, it was found that due to human activities, notably agriculture and forest logging for wood energy, the percentage of forest land decreased by 20.9% (59 004 ha to 46675 ha) during 2002–2010, while mosaic habitat-agriculture land increased by 24% (23191 ha to 28768 ha) during 2002-2010 (Ciza et al., 2015).

However, the predicted change in 2035 shows that, there will still be an increase in Fallow land and fields and Builtup area, while dense and secondary forest will experience a decrease by 1300.05 ha and 756.27 ha, respectively. The decrease in secondary forest can be attributed to the expansion of agriculture in that land cover category. In fact, after several years, secondary forest appear to be suitable for developing agriculture as well as dense forest. The decrease in dense forest can also be explained by the expansion of human activities such as agriculture, wood energy and logging.

http://www.aloki.hu ● ISSN 1589 1623 (Print) ● ISSN 1785 0037 (Online)
DOI: http://dx.doi.org/10.15666/aeer/1804_56275644

Table 7. *Evolution of population of the Mambasa sector from 1987 to 2019*

Year	Population
1987	55000
2003	128000
2019	249369

Model validation

The present study used the three map comparison method to evaluate the model performance for land use/land cover change simulation in Mambasa sector. This approach was proposed by Pontius et al. (2011), and consists of two components of agreement and three components of disagreement (Bayes and Raquib, 2012). Indeed, the components of agreement include persistence simulated correctly (correct rejection) and change simulated correctly (hits), while the components of disagreement contain change simulated as persistence (misses), persistence simulated as change (false alarm), and change simulated as change to wrong category (Wrong hits). After implementing the three-map comparison method, it has been revealed that the simulated map yields the best result in terms of the percentages of component disagreement (2.3%) and component agreement (97.7%), as presented in *Table 8*.

Table 8. *Components of agreement and disagreement of three map comparison method*

Name of component	%
Persistence simulated correctly	96.13406
Change simulated correctly	1.534867
Total agreement	97.66893
Change simulated as persistance	0.423469
Persistence simulated as change	0.737927
Change simulated as to wrong category	1.169677
Total disagreement	2.331073

Conclusions

The land use/cover change caused by direct and indirect human activities has negative consequences at spatial and temporal scales. Understanding those changes provides relevant knowledge that is most important for decision-makers and civil society. This study examines land use/cover change in the Mambasa sector between 1987 and 2019, and uses CA-ANN to predict the future land cover change by 2035. During the last 32 years, It was shown that dense forest has approximately lost 5121.54 ha, while secondary forest, fallow land and fields, built-up area have gained 1786.23 ha, 3140.46 ha and 194.85 ha, respectively. The ratio of dense forest in the landscape declined from 85.07% in 1987, to 73.85% in 2019. Thus, the annual rate of deforestation observed in dense forest was estimated at 0.41%. From the change occurred in Mambasa landscape, it was revealed that the major part for the Mambasa landscape was converted into fallow land and fields. A total of 37426.05 ha for the Mambasa landscape were considered as persistence between 1987 and 2019. Among them, 33495.56 ha persisted as dense forest, 2356.01 ha as secondary forest, 1381.44 ha

http://www.aloki.hu ● ISSN 1589 1623 (Print) ● ISSN 1785 0037 (Online)
DOI: http://dx.doi.org/10.15666/aeer/1804_56275644

as fallow land and fields and 192.95 ha as built-up area. However, around 3325.47 ha, 1117.80 ha, and 81.26 ha were converted from dense forest, secondary forest, and built-up area into fallow land and fields during 1987 to 2019. The study revealed that the unsustainable agriculture system combined with wood energy and artisanal logging led to land use/cover changes in the Mambasa landscape. The predicted change in 2035 shows that, there will still be an increase in Fallow land and fields and built-up area, while dense and secondary forest will experience a decrease by 1300.05 ha and 756.27 ha, respectively. The decrease in secondary forest can be attributed to the expansion of agriculture in that land cover category. Hence, the present results should be taken into account to support sustainable management of Mambasa forest ecosystems and efficient use of natural resources. However, further studies on the effects of land use/land cover change on biodiversity composition, and the effects of climate change on it as well, should be undertaken to provide the whole vision of the phenomenon in the Mambasa sector.

Acknowledgements. This study was supported by The Fundamental Research Funds for the Central Universities (2572019CP12).

REFERENCES

[1] Agarwal, C., Green, G. M., Grove, J. M., Evans, T. P., Schweik, C. M. (2002): A Review and Assessment of Land-Use Change Models: Dynamics of Space, Time, and Human Choice. – Gen. Tech. Rep. NE-297. Department of Agriculture, Forest Service, Northeastern Research Station, Newtown Square, PA.

[2] Alemu, B. (2015): The effect of land use land cover change on land degradation in the highlands of Ethiopia. – Journal of Environment and Earth Science 5(1): 1-12.

[3] Aweto, A. O. (2012): Shifting Cultivation and Secondary Succession in the Tropics. – CABI, Wallingford.

[4] Baillie, J., Hilton-Taylor, C., Stuart, S. N. (2004): 2004 IUCN red list of threatened species: a global species assessment. – Earth. https://doi.org/10.2305/IUCN.CH.2005.3.en.

[5] Bamba, I. (2010): Anthropisation et dynamique spatio-temporelle de paysages forestiers en République démocratique du Congo. – Fac. des Sci. - Ec. Interfacultaire des Bioingénieurs.

[6] Basse, R. M., Omrani, H., Charif, O., Gerber, P., Bódis, K. (2014): Land use changes modelling using advanced methods: Cellular automata and artificial neural networks. The spatial and explicit representation of land cover dynamics at the cross-border region scale. – Geography 53: 160-171.

[7] Bayes, A., Raquib, A. (2012): Modeling urban land cover growth dynamics using multioral satellite images: A case study of Dhaka, Bangladesh. – ISPRS International Journal of Geo-Information 1(1): 3-31.

[8] Chen, J., Du, P., Wu, C., Xia, J., Chanussot, J. (2018): Mapping urban land cover of a large area using multiple sensors multiple features. – Remote Sensing 10(6): 872.

[9] Ciza, S. K., Mikwa, J. F., Malekezi, A. C., Gond, V., Bosela, F. B. (2015): Identification des moteurs de déforestation dans la région d'Isangi, République démocratique du Congo. – Bois Forets des Tropiques 324: 29-38.

[10] Congalton, R. G. (1991): A review of assessing the accuracy of classifications of remotely sensed data. – Remote Sensing of Environment 37: 35-46.

http://www.aloki.hu ● ISSN 1589 1623 (Print) ● ISSN 1785 0037 (Online)
DOI: http://dx.doi.org/10.15666/aeer/1804_56275644

[11] Copeland, J. H., Pielke, R. A., Kittel, T. G. F. (1996): Potential climatic impacts of vegetation change: a regional modeling study. – Journal of Geophysical Research Atmospheres 101(D3): 7409-7418.
[12] Defries, R., R., Achard, F., Brown, S., Herold, M., Murdiyarso, D., Schlamadinger, B. C. J. (2006): Reducing Greenhouse Gas Emissions from Deforestation in Developing Countries: Considerations for Monitoring and Measuring. – Report of the Global Terrestrial Observing System (GTOS), Report No. 46. GTOS, Rome.
[13] de Wasseige, C., Flynn, J., Louppe, D., Hiol, F., Mayaux (2014): The Forests of the Congo Basin: State of the Forest 2013. – Weyrich, Belgium. https://doi.org/10.2788/32259.
[14] Fan, M., Shibata, H. (2015): Simulation of watershed hydrology and stream water quality under land use and climate change scenarios in Teshio River watershed, northern Japan. – Ecological Indicators 50: 79-89.
[15] Haines-Young, R. (2009): Land use and biodiversity relationships. – Land Use Policy 26: 178-186.
[16] Halmy, M. W. A., Gessler, P. E., Hicke, J. A., Salem, B. B. (2015): Land use/land cover change detection and prediction in the north-western coastal desert of Egypt using Markov-CA. – Applied Geography 63: 101-112.
[17] Han, H., Yang, C., Song, J. (2015): Scenario simulation and the prediction of land use and land cover change in Beijing, China. – Sustainability (Switzerland) 7(4): 4260-4279.
[18] Houghton, R. A. (1994): The worldwide extent of land-use change. – Bioscience 44: 305-313.
[19] Houghton, R. A., Nassikas, A. A. (2017): Global and regional fluxes of carbon from land use and land cover change 1850-2015. – Global Biogeochemical Cycles 31(3): 456-472.
[20] Jain, A. K., Meiyappan, P., Song, Y., House, J. I. (2013): CO2 emissions from land-use change affected more by nitrogen cycle, than by the choice of land-cover data. – Global Change Biology 19(9): 2893-2906.
[21] Jogun, T., Lukić, A., Gašparović, M. (2019): Simulation model of land cover changes in a post-socialist peripheral rural area: Požega-slavonia county, Croatia. – Hrvatski Geografski Glasnik 81(1): 31-59.
[22] Kumar, S., Radhakrishnan, N., Mathew, S. (2014): Land use change modelling using a Markov model and remote sensing. – Geomatics, Natural Hazards and Risk 5(2): 145-156.
[23] Lambin, E., Turner, B., Geist, H., Agbola, S., Angelsen, A., Bruce, J., Coomes, O., Dirzo, R., Fischer, G., Folke, C., George, P., Homewood, K., Imbernon, J., Leemans, R., Li, X., Moran, E., Mortimore, M., Ramakrishnan, P., Richards, J., Skånes, H., Steffen, W., Stone, G., Svedin, U., Veldkamp, T., Vogel, C., Xu, J. (2001): The causes of land-use and land-cover change: moving beyond the myths. – Global Environmental Change 11(4): 261-269.
[24] Le Maitre, D. C., Kotzee, I. M., O'Farrell, P. J. (2014): Impacts of land-cover change on the water flow regulation ecosystem service: invasive alien plants, fire and their policy implications. – Land Use Policy 36: 171-181.
[25] Li, X., Yeh, A. G. O. (2002): Neural-network-based cellular automata for simulating multiple land use changes using GIS. – International Journal of Geographical Information Science 16(4): 323-343.
[26] Lillesand, T. M., Kiefer, R. W., Chipman, J. W. (2004): Remote Sensing and Image Interpretation. – Wiley, New York.
[27] López, E., Bocco, G., Mendoza, M., Velázquez, A., Rogelio Aguirre-Rivera, J. (2006): Peasant emigration and land-use change at the watershed level: a GIS-based approach in Central Mexico. – Agricultural Systems 90(1-3): 62-78.
[28] Mantyka-Pringle, C. S., Visconti, P., Di Marco, M., Martin, T. G., Rondinini, C., Rhodes, J. R. (2015): Climate change modifies risk of global biodiversity loss due to land-cover change. – Biological Conservation 187: 103-111.

http://www.aloki.hu ● ISSN 1589 1623 (Print) ● ISSN 1785 0037 (Online)
DOI: http://dx.doi.org/10.15666/aeer/1804_56275644

[29] Mpoyi, A. M., Nyamwoga, F. B., Kabamba, F. M., Assembe-mvondo, S. (2013): Le contexte de la REDD+ en République Démocratique du Congo Causes, agents et institutions. – CIFOR, Bogor.
[30] Mubea, K. W., Ngigi, T. G., Mundia, C. N. (2010): Assessing application of markov chain analysis in predicting land cover change: a case study of Nakuru municipality. – Journal of Agriculture, Science and Technology 12(2).
[31] Muller, M. R., Middleton, J. (1994): A Markov model of land-use change dynamics in the Niagara Region, Ontario, Canada. – Landscape Ecology 9(2): 151-157.
[32] Ngabinzeke, J. S., Linchant, J., Quevauvillers, S., Muhongya, J. M. K., Lejeune, P., Vermeulen, C. (2016): Cartographie de la dynamique de terroirs villageois à l'aide d'un drone dans les aires protégées de la République démocratique du Congo. – Bois Forets des Tropiques 315(1): 21-28.
[33] Nouri, J., Gharagozlou, A., Arjmandi, R., Faryadi, S., Adl, M. (2014): Predicting Urban Land Use Changes Using a CA-Markov Model. – Arabian Journal for Science and Engineering 39: 5565-5573.
[34] Ouedraogo, I., Tigabu, M., Savadogo, P., Compaoré, H., Odén, P. C., Ouadba, J. M. (2010): Land cover change and its relation with population dynamics in Burkina Faso, West Africa. – Land Degradation and Development 21(5): 453-462.
[35] Plourde, L., Congalton, R. G. (2003): Sampling method and sample placement: how do they affect the accuracy of remotely sensed maps? – Photogrammetric Engineering and Remote Sensing 69(3): 289-297.
[36] Pontius, G. R., Malanson, J. (2005): Comparison of the structure and accuracy of two land change models. – International Journal of Geographical Information Science 19(6): 243-265.
[37] Pontius, R. G., Millones, M. (2011): Death to Kappa: birth of quantity disagreement and allocation disagreement for accuracy assessment. – International Journal of Remote Sensing 32(15): 4407-4429.
[38] Potapov, P., Turubanova, S., Hansen, M., Adusei, B., Broich, M., Altstatt, A., Mane, L., Justice, C. 2012): Quantifying forest cover loss in Democratic Republic of the Congo 2000-2010, with Landsat ETM+ data. – Remote Sensing of Environment 122: 106-116.
[39] Ranagalage, M., Wang, R., Gunarathna, M. H. J. P., Dissanayake, D. M. S. L. B., Murayama, Y., Simwanda, M. (2019): Spatial forecasting of the landscape in rapidly urbanizing hill stations of South Asia: a case study of Nuwara Eliya, Sri Lanka (1996-2037). – Remote Sensing 11(15): 1743.
[40] Reid, R. S., Kruska, R., Muthui, N., Taye, A., Wotton, S., Wilson, C., Mulatu, W. (2000): Land-use and land-cover dynamics in response to changes in climatic, biological and socio-political forces: the case of southwestern Ethiopia. – Landscape Ecology 15(4): 339-355.
[41] Rendana, M., Rahim, S. A., Idris, W. M. R., Lihan, T., Rahman, Z. A. (2015): CA-Markov for predicting land use changes in tropical catchment area: a case study in Cameron Highland, Malaysia. – Journal of Applied Sciences 15(4): 689-695.
[42] Rogan, J., Chen, D. M. (2004): Remote sensing technology for mapping and monitoring land-cover and land-use change. – Progress in Planning 61(4): 301-325.
[43] Rosenfield, G. H., Fitzpatrick-Lins, K. (1986): A coefficient of agreement as a measure of thematic classification accuracy. – Photogrammetric Engineering & Remote Sensing 52(2): 223-227.
[44] Roy, D. P., Lewis, P. E., Justice, C. O. (2002): Burned area mapping using multi-temporal moderate spatial resolution data-a bi-directional reflectance model-based expectation approach. – Remote Sensing of Environment 83: 263-286.
[45] Salazar, A., Baldi, G., Hirota, M., Syktus, J., McAlpine, C. (2015): Land use and land cover change impacts on the regional climate of non-Amazonian South America: a review. – Global and Planetary Change 128: 103-119.

http://www.aloki.hu ● ISSN 1589 1623 (Print) ● ISSN 1785 0037 (Online)
DOI: http://dx.doi.org/10.15666/aeer/1804_56275644

[46] Salovaara, K. J., Thessler, S., Malik, R. N., Tuomisto, H. (2005): Classification of Amazonian primary rain forest vegetation using Landsat ETM+ satellite imagery. – Remote Sensing of Environment 97(1): 39-51.
[47] Saputra, M. H., Lee, H. S. (2019): Prediction of land use and land cover changes for North Sumatra, Indonesia, using an artificial-neural-network-based cellular automaton. – Sustainability (Switzerland) 11(11): 3024.
[48] Scholes, R. J., Van Breemen, N. (1997): The effects of global change on tropical ecosystems. – Geoderma 79(1-4): 9-24.
[49] Schönhart, M., Trautvetter, H., Parajka, J., Blaschke, A. P., Hepp, G., Kirchner, M., Zessner, M. (2018): Modelled impacts of policies and climate change on land use and water quality in Austria. – Land Use Policy 76: 500-514.
[50] Simwanda, M., Murayama, Y. (2018): Spatiotemporal patterns of urban land use change in the rapidly growing city of Lusaka, Zambia: implications for sustainable urban development. – Sustainable Cities and Society 39: 262-274.
[51] Singh, A. (1989): Review article: Digital change detection techniques using remotely-sensed data. – International Journal of Remote Sensing 10(6): 989-1003.
[52] Sinha, P., Kimar, L. (2013): Markov land cover change modeling using pairs of time-series satellite images. – Photogrammetric Engineering & Remote Sensing 79: 1037-1051.
[53] Smits, P. C., Dellepiane, S. G., Schowengerdt, R. A. (1999): Quality assessment of image classification algorithms for land-cover mapping: a review and a proposal for a cost-based approach. – International Journal of Remote Sensing 20(10): 1461-1486.
[54] Song, X. P., Hansen, M. C., Stehman, S. V., Potapov, P. V., Tyukavina, A., Vermote, E. F., Townshend, J. R. (2018): Global land change from 1982 to 2016. – Nature 560(7720): 639-643.
[55] Spera, S. A., Galford, G. L., Coe, M. T., Macedo, M. N., Mustard, J. F. (2016): Land-use change affects water recycling in Brazil's last agricultural frontier. – Global Change Biology 22(10): 3405-3413.
[56] Sterling, S. M., Ducharne, A., Polcher, J. (2013): The impact of global land-cover change on the terrestrial water cycle. – Nature Climate Change 3(4): 385-390.
[57] Tolba, M. K., Kenya, N., El-Kholy, O. A. (1992): The World Environment 1972-1992: Two Decades of Challenge. – https://doi.org/10.1017/CBO9780511840210.008.
[58] Townshend, J. R. (1992): Land cover. – Int. J. Remote Sens. 13(6-7): 1319-1328.
[59] UN-REDD (2012): Etude qualitative sur les causes de la déforestation et de la dégradation des forêts en République Démocratique du Congo. Un-Redd Program. – UN-REDD, Geneva.
[60] Vadrevu, K. P. (2013): Introduction to Remote Sensing. Fifth Ed. – In: J. B., Campbell, Wynne, R. H. (eds.) The Photogrammetric Record. Guilford Press, New York. https://doi.org/10.1111/phor.12021.
[61] Velázquez, A. et al. (2003): Land use-cover change processes in highly biodiverse areas: the case of Oaxaca, Mexico. – Global Environmental Change 13(3): 175-184.
[62] Vieira, I. C. G., De Almeida, A. S., Davidson, E. A., Stone, T. A., Reis De Carvalho, C. J., Guerrero, J. B. (2003): Classifying successional forests using Landsat spectral properties and ecological characteristics in eastern Amazônia. – Remote Sensing of Environment 87(4): 470-481.
[63] Wanger, T. C., Iskandar, D. T., Motzke, I., Brook, B. W., Sodhi, N. S., Clough, Y., Tscharntke, T. (2010): Effects of land-use change on community composition of tropical amphibians and reptiles in Sulawesi, Indonesia. – Conservation Biology 24(3): 795-802.
[64] Weng, Q. (2002): Land use change analysis in the Zhujiang Delta of China using satellite remote sensing, GIS and stochastic modelling. – Journal of Environmental Management 64(3): 273-284.

http://www.aloki.hu ● ISSN 1589 1623 (Print) ● ISSN 1785 0037 (Online)
DOI: http://dx.doi.org/10.15666/aeer/1804_56275644

[65] Wondie, M., Schneider, W., Melesse, A. M., Teketay, D. (2011): Spatial and temporal land cover changes in the Simen Mountains National Park, a world heritage site in northwestern Ethiopia. – Remote Sens 3(4): 752-766.
[66] Wu, Q., Hong-qing, L., Ru-song, W., Juergen, P., Yang, H., Min, W., Bi-hui, W., Zhen, W. (2006): Monitoring and predicting land use change in Beijing using remote sensing and GIS. – Landscape and Urban Planning 78(4): 322-333.
[67] Ye, B., Bai, Z. (2008): Simulating land use/cover changes of Nenjiang County based on CA-Markov model. – IFIP International Federation for Information Processing 258: 321-329.
[68] Zhuravleva, I., Turubanova, S., Potapov, P., Hansen, M., Tyukavina, A., Minnemeyer, S., Lapotre, N., Goetz, S., Verbelen, F., Thies, C. (2013): Satellite-based primary forest degradation assessment in the Democratic Republic of the Congo, 2000-2010. – Environmental Research Letters 8: 024034.

http://www.aloki.hu ● ISSN 1589 1623 (Print) ● ISSN 1785 0037 (Online)
DOI: http://dx.doi.org/10.15666/aeer/1804_56275644

GENETIC DISSECTION OF PROTEIN AND GLUTEN CONTENTS IN WHEAT (*TRITICUM AESTIVUM* L.) UNDER NORMAL AND DROUGHT CONDITIONS

AHMED, H. G. M.-D.[1,2,4*] – KASHIF, M.[2] – SAJJAD, M.[3] – ZENG, Y.-W.[4*]

[1]*University of Central Punjab, Department of Botany, Punjab Group of Colleges, Bahawalpur 63100, Pakistan*

[2]*Department of Plant Breeding and Genetics, University of Agriculture, Faisalabad, Punjab 38000, Pakistan.*

[3]*Department of Biosciences, COMSATS University Islamabad (CUI), Park Road, Islamabad 45550, Pakistan*

[4]*Biotechnology and Germplasm Resources Institute, Yunnan Academy of Agricultural Sciences, Kunming 650205, China*

*****Corresponding authors*
e-mail: ahmedbreeder@gmail.com; zengyw1967@126.com

(Received 30th Dec 2019; accepted 9th Jul 2020)

Abstract. Breeding drought resistant wheat is very important for sustainable food production. In future research, each new cross from breeder will involve the modification of genome-wide gene networks that control the expression of drought and yield, especially the dynamics of change in complex gene families involved in drought adaptation. Declining water resources as a result of extreme use of water for irrigation and climate change pose a severe threat to food security. It is needed to divulge and manipulate the genetic potential of wheat (*Triticum aestivum* L.) germplasm to adapt to scarce water resources with higher/sustainable yield potential. In this regard, drought-tolerant and drought-susceptible wheat genotypes were manipulated in line (10) × tester (5) mating design in the department of PBG-UAF Pakistan to understand the genetic mechanism and effect of drought tolerance on wheat yield and quality attributes like protein and gluten contents under normal and drought conditions. It was imperative to breed wheat genotypes that withstand in drought environments having maximum yield and protein contents. The significant specific combining ability (SCA) provided the prominent non-additive genetic mechanism in the inheritance of yield and quality traits in wheat for the studied germplasm. Gene action based screening revealed that the line 9493 (L1), tester 9508 (T1) and their hybrid (L1 × T1) were ideal genetic resources to breed against drought resistance for quality and yield attributes. Therefore, hybrid breeding will be rewarding and the selection practice for superior individual plants should be delayed to advanced generations like F_4 and F_5. The superior genotype 9493 and hybrid (cross) 9493 (L1) × 9508 (T1) can be combined to develop new promising and improved hybrids/varieties for quality and yield contributing attributes under drought conditions to fulfill the wheat demand and sustainable food security.
Keywords: *breeding, gene action, additive, germplasm, food security, genotypes*

Introduction

Current wheat (*Triticum aestivum*) having three A, B and D homeologous genomes, has been evolved through a series of natural crossing and the effect of polyploidy (2n = 6x = 42, AABBDD allohexaploid) (Ahmed et al., 2017a). In the evolutionary pathway of modern wheat, allopolyploidization occurred in two phases; in first step *T. urartu* (diploid) hybridized with *Aegilops speltoides* (wild grass) that resulted into tetraploid *T. Turgidum* and in the 2nd step, tetraploid AABB, 2n = 4x = 28 crossed with diploid goat grass *A. tauschii* having the

http://www.aloki.hu ● ISSN 1589 1623 (Print) ● ISSN 1785 0037 (Online)
DOI: http://dx.doi.org/10.15666/aeer/1804_56455659

genome DD 2n = 2x = 14 which produced (hexaploid = AABBDD) modern wheat (Förster et al., 2012).

The evolution of large seeded non-shattering modern wheat cultivars from small-seeded wild cultivars with natural grain dispersal and cross pollination modified the seed shape and size. Increase in grain size might have started during the early stages of wheat evolution when cultivation of the plant was started (Peña-Bautista, 2002). Seed size is a quantitative polygenic trait which is influenced by many genes that significantly contribute to increase or decrease seed size (Peng et al., 2011).

Generally, wheat grain comprises protein (8-17%), carbohydrates (60-80%) (mainly starch), minerals (1.5-2%), fats (1.5-2%), crude fibers (2.2%), vitamins (B complex and E) and all essential amino acids except tryptophan, methionine and lysine. Gluten is a protein complex that accounts for 75 to 85% of the total protein in wheat (Fuller, 2007). Due to its nutritional worth and preference, people like to utilize wheat in daily food in the form of bread, chapati, crackers, etc. Wheat grain has distinct physical and chemical parameters of seed protein. Understanding the inheritance mechanism of wheat grain and quality traits is necessary for attaining the best genotypes on this aspect (Ali et al., 2013). Selection of best performing parental genotypes and their cross combinations are necessary for creating the desirable wheat varieties (Akram et al., 2011). The overall crop production all over the world has to be significantly increased day by day to feed a rising population, but existing production trends are not enough to meet this increasing requirement (Zeeshan et al., 2013).

Water deficit decreases the yield so it is assumed that 17 to 70% losses in the yield are due to water deficiency. Wheat yield reduced from 50 to 90% of their irrigated potential in the developing countries by water deficit conditions (Ali et al., 2013). Wheat plant suffers severe response to water deficit stress at tillering, jointing, booting, anthesis and filling stages. Tillering is a very important stage at which plant develops tillers, primodia of spike, spikelets, and flowers. Water deficit stress at this stage can cause a 46% decrease in total yield (Minhas et al., 2014). For breeding water deficit tolerance in wheat crop, it is important to know the mechanism and behavior of plant under drought environments. To stand against the water shortage conditions plant has different morphological, physiological, biochemical, anatomical and molecular developments (Noorka and Teixeira da Silva, 2014).

Genetic purity analysis for hybrid testing is compulsory to certify the hybrid seed. Hybrid testing and confirmation is essential for commercial purpose and for the production of pure hybrids. Conventionally, genetic purity examined on the basis of phenotypic data are tested in field trials and compared with improved cultivated genotypes the term used as 'Grow-Out Test' (GOT). The limitations of this test are higher cost, time consumption, requirement of large area for testing, and influence of environmental factors (Wu et al., 2010). Combining ability analysis is an effective genetic evaluation tool and therefore has been commonly implemented in plant breeding to access the performance of genotypes in hybrid/cross combinations (Kumar et al., 2011). Different types of gene actions have been estimated from combining ability variances which indicate the expression of quality, yield and yield contributing parameters. Additionally, comprehensive information about the relationship between line *per se* and hybrid potential is necessary to improve wheat breeding programs (Longin et al., 2012).

Regardless the small amount of hybrid vigor in self-pollinated crops, like in wheat the agronomic worth of their hybrids seemed to be encouraging. In China, Rice hybrid had a yield benefit of 20-30% over the commercial cultivars. In private sectors, wheat hybrids have been successfully developed in India and European countries (Cheng et al., 2007).

http://www.aloki.hu ● ISSN 1589 1623 (Print) ● ISSN 1785 0037 (Online)
DOI: http://dx.doi.org/10.15666/aeer/1804_56455659

Previously, different types of gene actions had been reported from combining ability variances which influence the expression of yield and its contributing parameters in bread wheat (Bibi et al., 2013). Yield character is a polygenic in nature which is widely affected due to environmental variations. In wheat breeding schemes the direct selection for yield and yield contributing characters may give false results especially against drought environments. Therefore, the genetic effectiveness of indirect selection is valuable than direct screening for yield and yield contributing traits in wheat breeding programs (Akram et al., 2011; Zeeshan et al., 2013).

Keeping all above in view, the experiments were planned to generate information from, combining ability studies, gene action analysis under normal and drought conditions. The information derived from these studies would be very useful for wheat breeders to exploit the new genetic potential in wheat genotypes for developing drought tolerant, better protein contents and high yielding wheat varieties for sustainable food security.

Materials and methods

The proposed research was conducted to assess the genetic mechanism of some quality and yield contributing traits in wheat under normal and drought stress conditions.

Line × tester analysis (hybridization)

The field experiment for line × tester analysis was carried out in the research area of Plant Breeding and Genetics (PBG) department, University of Agriculture, Faisalabad, Pakistan (LATITUDE = 31 - 44' N and ALTITUDE = 184.4 m). The tested ten drought tolerant genotypes namely, 9493 (L1), 9618 (L2), 9797 (L3), 9930 (L4), BWL812 (L5), DPW621 (L6), 10111 (L7), 10115 (L8), 10117 (L9) and Chakwal-86 (L10) were used as a female (line) parent and five drought susceptible wheat genotypes 9508 (T1), Millat-11 (T2), Ufaq-2002 (T3), Moomal-2002 (T4) and BARS-09 (T5) were used as male (tester) parents (Ahmed et al., 2019). These genotypes were crossed under line (L10) × tester (T5) mating design during the wheat growing seasons 2016-17.

In wheat crop anthesis starts from the center of the spike (inflorescence) and then proceeds in both directions. Hence, for emasculation purpose the suitable lateral florets were kept in the middle of the inflorescence and left over unwanted florets were detached with the help of a pair of scissors and pointed forceps. Then the small florets were supported with thumb and forefinger and 1/3 upper part of each floret was removed with a pair of scissors. The immature anthers (3) in each floret were carefully detached by using fine pointed forceps, avoiding damage to the ovary and prevent ovary from self-pollination. Glycine bags were used to cover entire spikes immediately after completion of emasculation, to minimize the chance of pollination. Male flowers with mature anthers were excluded from the female lines to avoid any chance of self-pollination. On the very next day early in the morning emasculated spike which were covered under glycine bags were pollinated by using fresh pollen from the desired male parent by hand. After completion of artificial pollination spikes of female plants were again tightly covered with their respective bags till seed setting and to avoid the contamination with other undesired pollens. These cultivars/lines were hybridized in (10) lines × (5) testers mating fashion. For each parental line 50 spikes were emasculated and pollinated with desired testers, so total 500 spikes were emasculated in this experiment. In each spike average 15 seed sets and 150 crossed seed obtained for each line with their respective testers like L1 × T1. At

http://www.aloki.hu ● ISSN 1589 1623 (Print) ● ISSN 1785 0037 (Online)
DOI: http://dx.doi.org/10.15666/aeer/1804_56455659

maturity, crossed seeds from all crosses were collected manually in separate envelops which were orderly arranged for each and every cross.

Evaluation of breeding material

Total fifty F_1 seeds along with their 15 parents genotypes were sown on November 15, 2017 in two experimental conditions (non-stressed and drought stressed experiments) in randomized complete block design (RCBD) with three replications. Each genotype was sown through maintaining plant-to-plant distance fifteen centimeters and rows-to-row distance was 30 cm. Two seeds of each genotype were dibbled/hole and one healthy seedling was reserved after germination by thinning. To abate the border effect lines of non-experimental material were sown at the border of the experiment. In normal experiment irrigations were applied at three critical stages i.e. (1) tillering (35 Days after sowing, DAS), (2) the booting stage (85 DAS) and (3) the milking stage (112 DAS) (Noorka and Teixeira da Silva, 2014). Drought stress was applied at tillering stage by upholding (missing) the irrigation treatment. One set of genotypes was irrigated at all the three-critical stages, while the other set of the same wheat genotypes was kept under drought stress. Fertilizer were applied at the rate of 46 kg nitrogen, 34 kg phosphorus and 25 kg potash per acre All regular agronomic applications like fertilizer, hoeing, weeding, etc. were implemented equivalently in both experiments to lessen the experimental faults (Ahmed et al., 2018).

Measurement of quality and yield components

At maturity, when wheat plants were fully established, data were collected of 10 plants from each replication for following some quality and yield contributing characters of fifty crosses and their fifteen parents under normal and water deficient conditions. Harvesting was done on 8-15 April, 2018. The studied traits were observed using the following methods. The flag leaf area was calculated according to (Muller, 1991) i.e., (maximum length × maximum breadth) × 0.74. Then average area of flag leaf was calculated, relative water contents (RWC) and cell membrane thermo-stability (CMT) were measured using the standard methods described by Dhanda et al. (1998) and Blum and Ebercon (1981), respectively. Number of grain per spike (GPS) was counted from the spike of mother shoot of each randomly selected plant and 1000-grain weight (TGW) was measured with electric balance from the produce each pre- selected plant. For grain yield per plant (GYP) ten randomly selected plants were harvested at maturity and threshed grains were weighed using electric balance. The yield of mother tillers was also added to the produce. Then average yield was calculated as produce was divided by number of plants. Grain quality traits like, grain protein contents (GPC) and gluten contents (GC) investigated by Kernalyser (NIR spectroscopy, ISO17025 certified and 18 mm spacer), which included grain protein percentage (%) and grain gluten percentage (%) (Liana et al., 2012; Maria et al., 2013). The data of these quality characters were measured via Near-Infrared Radiation (NIR) procedure by running the wheat genotype samples.

Biometrical analysis of line × tester

Data recorded at different stages of plants for all traits, under normal and drought stress conditions, were subjected to analysis of variance (Steel, 1997) to sort out significant differences among studied germplasm. The traits which showed, significant genotypic differences, were further analyzed for the determination of other genetic

http://www.aloki.hu ● ISSN 1589 1623 (Print) ● ISSN 1785 0037 (Online)
DOI: http://dx.doi.org/10.15666/aeer/1804_56455659

parameters. Studied characters were also subjected to line × tester analysis (Kempthorne, 1957) to calculate the combining ability, genetic components and proportional contribution under normal and drought conditions.

Results and discussion

Line × tester analysis of variances

Mean square values from line × tester analysis of variances were considered to observe the significant variation in parents and their crosses for quality and yield contributing indices under normal and water deficit conditions (*Table 1*). Highly significant differences were scored between female parents and crosses for all studied traits in the present research under normal and water deficit conditions. Under both conditions highly significant differences were scored between parents for flag leaf area, relative water contents, cell membrane thermo-stability, grains per spike, and protein contents while significant variation was observed only under normal conditions for 1000-grain weight. The GYP and GC between parents were showed non-significant variation under both conditions.

Table 1. *Mean squares values from line ×tester analysis of variances*

Sov	Df	FLA		RWC		CMT		GPS		TGW		GYP		GPC		GC	
		N	D	N	D	N	D	N	D	N	D	N	D	N	D	N	D
R	2	55.6	38.1**	140**	48.2**	53.56**	84.80**	120.00**	115.89**	10.07**	7.36	34.42**	264.78**	7.92**	4.23**	121.11**	19.98
G	64	40.4**	40.0**	191**	144**	133.33**	92.92**	117.78**	96.42**	105.21**	81.51**	129.55**	94.15**	2.40**	2.53**	41.79**	34.37**
P	14	40.6**	40.6**	155**	159.2**	86.23**	84.04**	74.41**	74.41**	10.17**	11.73	3.33	2.69	2.01**	2.01**	16.8	16.8
C	49	40.38**	40.1**	205**	143**	142.35**	81.94**	128.31**	100.14**	130.45**	100.16**	106.76**	79.16**	2.42**	2.69**	48.31**	38.83**
PvC	1	41.1**	27.4**	0.04	10.0	350.38**	754.86**	208.82**	222.36**	199.27**	144.51**	3013.3**	2109.13**	7.12**	2.44	71.95**	61.90**
L	9	56.9**	63.5**	423**	328**	124.36**	44.71**	445.44**	329.55**	420.79**	348.01**	270.32**	197.93**	5.28**	5.14**	72.43**	33.25**
T	4	29.9**	28.9**	118**	103**	394.06**	315.28**	60.71**	47.14**	40.36**	45.11**	45.01**	22.60**	1.06**	1.15	84.34**	98.76**
L×T	36	37.4**	35.5**	160**	101**	118.88**	65.33**	56.54**	48.67**	67.87**	44.31**	72.73**	55.75	1.85	2.24**	38.28**	33.57**
E	128	2.2	3.8	21.3	29.8	9.85	11.24	8.73	15.26	2.21	13.61	4.71	10.09	0.86	1.1	12.99	14.05

SOV = sources of Variations, DF, degree of Freedom, FLA = flag leaf area, RWC = relative water content, CMT = cell membrane thermostability, GPS = grain per spike, TGW = thousand grain weight, GYP = grain yield per plant, GPC = grain protein content, GC = gluten content. D = drought stressed, N = normal (non-stressed), L = line (female parent), T = tester (male parent). R = replication, G = genotype, P = parent, C = cross, L = line, T = tester, E = environment, * = significant ($P < 0.05$), ** = highly significant ($P < 0.01$)

Evaluation of the testers showed highly significant differences was for all examined characters in non-stressed and drought stressed environments except GPC which were non-significant under water deficit condition. Parent versus crosses (P vs C) exhibited non-significant results for RWC (normal and drought) and GPC (drought) while the variation in remaining traits were highly significant under normal and water deficit conditions. Considering the L × T interaction, highly significant variability existed for all tested traits under both conditions except GYP (drought) and GPC (normal) which showed non- significant behavior.

Highly significant, variability was described by wheat breeders (Kalhoro et al., 2015) for GPS and GYP. Significant results were reported (Ramani et al., 2017) for relative water contents, protein and gluten contents. Earlier scientist reported (Minhas et al., 2014) the significant results of FLA and GPS between parents and their hybrids which were in accordance with the present findings. The line × tester analysis of variances (ANOVA) showed that the genetic variability existed between parents and their crosses/hybrids for

http://www.aloki.hu ● ISSN 1589 1623 (Print) ● ISSN 1785 0037 (Online)
DOI: http://dx.doi.org/10.15666/aeer/1804_56455659

some quality and yield contributing indices in wheat under normal and water deficit conditions. So, this germplasm could be used in future for wheat hybrid breeding schemes to develop the drought tolerant and high yielding wheat varieties.

Flag leaf area (cm^2)

Flag leaf has perilous role in wheat, because its photosynthates to be stored in seed. So, it has direct relationship with grain yield. Under normal and water deficit conditions maximum flag leaf area (FLA) 39.67 cm^2 and 28.67 cm^2 respectively was scored for Line1 (L1). Among the male parents, highest mean values for FLA were 36.19 cm^2 and 31.24 cm^2 for Tester1 (T1) under both conditions, respectively (*Table 2*). Highly significant positive general combining ability (GCA) effects were revealed by the genotype L1 possessing the values 3.31 and 3.51 under normal and water deficit conditions, respectively. Among testers, the genotypes T1 had maximum positive GCA effects with the values 1.28 and 1.48 under normal and water deficit conditions, respectively (*Table 3*). Similar findings have been reported by wheat breeders (Kumar et al., 2011) for this trait in wheat crop using the same methodology as in current study.

Table 2. *The parental genotypes with highest mean values for various traits under study*

Characters	Normal	Drought
Flag leaf area	L1 (39.67), L2 (37.83), T1 (36.19)	L1 (28.67), L2 (26.83), T1 (31.24)
Relative water contents	L1 (80.32), L2 (78.32), T1 (63.32)	L1 (69.16), L2 (67.32), L3 (58.19)
Cell membrane thermo-stability	L1 (58.69), L3 (57.69), T1 (50.90)	L1 (56.6), L3 (55.6), T1 (48.60)
Grain per spike	L1 (65.63), L2 (64.34), T1 (56.34)	L1 (48.55), L2 (47.34), T1 (40.34)
Thousand grain weight	L1 (52.54), L9 (51.56), T2 (48.98)	L1 (34.31), L6 (34.31), T2 (32.98)
Grain yield per plant	L1 (33.95), L2 (33.8), T1 (27.00)	L1 (21.89), L3 (21.79), T1 (18.00)
Grain protein contents	L10 (12.92), T4 (12.83), T4 (12.83)	L1 (14.97), T1 (14.95), T5 (14.95)
Gluten contents	L10 (28), L2 (25.97), T4 (22.67)	L1 (29.93), L2 (27.9), T5 (24.9)

L = line (female parent), T = tester (male parent)

Among crosses, FLA mean values exhibited in L1 × T1 as 43.28 cm^2 and 32.17 cm^2 under normal and water deficit conditions, respectively. The estimation of SCA effects for the flag leaf area was revealed that cross combinations L1 × T1 possessed maximum positive SCA effects with the values 6.26 and 6.07 under normal and water deficit conditions, respectively (*Table 4.*). Significant GCA and SCA effects were observed earlier by many wheat scientists (Akram et al., 2011; Zeeshan et al., 2013) for this trait. Significant and positive hybrid vigor is beneficial for this character accordingly desirable for breeding program (Longin et al., 2012) but negative SCA were also found by earlier wheat breeders (Minhas et al., 2014). Flag leaf area (FLA) of wheat plant is an important character and directly influence on yield because greater area enables to produce photosynthates in higher amount, which have to translocate in seed to increase their yield.

Relative water content (%)

Soil moisture deficit is a major adverse factor in arid and semi-arid zones, causing lower leaf water potential, leading to reduced turgor and, ultimately, lower crop productivity. Under normal and water deficit conditions maximum relative water content 80.32% and 69.16% was scored in L1. Maximum mean values of relative

http://www.aloki.hu ● ISSN 1589 1623 (Print) ● ISSN 1785 0037 (Online)
DOI: http://dx.doi.org/10.15666/aeer/1804_56455659

water content 63.32% (normal) and 58.19% (drought) for T1 (*Table 2*). The magnitude of GCA effects between female parents, the highest positive GCA effects were revealed by the genotype L1 possessing the values 9.45 (normal) and 7.64 (drought). Among testers, the genotypes T3 (normal) and T1 (drought) had maximum positive GCA effects with the values 1.78 and 1.90 respectively as shown in *Table 3*. Similar research has also been confirmed by whet breeders (Ashfaq et al., 2016) using line × tester analysis.

Table 3. *The parental genotypes with highest general combining ability (GCA) effects*

Characters		Normal	Drought
Flag leaf area	L	L1(3.31), L2(2.91), L10(1.11)	L1(3.51), L2(3.11), L10(1.31)
	T	T1(1.28), T2(0.87)	T1(1.48), T2(0.42)
Relative water contents	L	L1(9.45), L7(5.04), L2(4.83)	L1(7.64), L7(5.55), L2(2.54)
	T	T3(1.78), T2(1.03)	T1(1.90), T2(0.59)
Cell membrane thermo-stability	L	L1(3.65), L2(3.54), L10(2.22)	L1(2.94), L10(0.96), L7(0.73)
	T	T1(2.72), T3(2.46)	T1(3.65), T3(1.63)
Grain per spike	L	L1(7.95), L6(6.96), L5(5.62)	L1(6.89), L6(5.75), L5(5.7)
	T	T1(1.66), T2(1.24)	T1(1.91), T2(0.42)
Thousand grain weight	L	L1(9.37), L3(4.58), L10(4.11)	L1(5.03), L3(4.77), L10(4.17)
	T	T2(1.52), T3(0.58)	T1(1.06), T3(0.34)
Grain yield per plant	L	L1(4.47), L2(4.26), L10(3.54)	L1(3.74), L2(2.86), L10(2.15)
	T	T1(1.67), T2(0.48)	T1(1.04), T4(0.43)
Grain protein contents	L	L10(1.46), L9(0.33), L6(0)	L1(1.34), L9(0.22), L4(0.20)
	T	T3(0.16), T2(0.13)	T1(0.17), T2(0.06)
Gluten contents	L	L10(3.79), L5(1.66), L6(1.60)	L1(2.27), L10(2.09), L7(1.27)
	T	T4(1.83), T3(1.52)	T3(1.78), T4(1.08)

L = line (female parent), T = tester (male parent)

Among crosses RWC mean values varied from 82.73% to 77.30% for cross L1 × T1 in non-stressed and drought stressed environments respectively and the remaining 5 superior crosses also presented in *Table 4*. The magnitudes of SCA effects for RWC revealed that cross combinations L1 × T1 possessed maximum positive SCA effects with the values 13.55 and 15.26 in non-stressed and drought stressed environments respectively (*Table 4*). Similar results were scored by many plant scientists (Ashfaq et al., 2016; Ramani et al., 2017) for SCA effects in wheat crop against relative water contents trait. This physiological characteristic has great importance when screening wheat genotypes for drought tolerance. Plant scientists showed that wheat cultivars having high RWC are more resistant to drought stress.

Cell membrane thermo-stability (%)

Cell membrane thermo-stability (CMT) is a useful parameter for the rapid evaluation of drought response in wheat breeding. This is the only adaptive and positive response beneficial to the plant under drought conditions. The line L1 had maximum cell membrane thermo-stability 58.69% (normal) and 56.60% (drought) while the tester, T1 had maximum values 50.90% (normal) and 48.60 (drought) as displayed in *Table 2*. Among female parents L1 possessed maximum positive GCA effects with the values

http://www.aloki.hu ● ISSN 1589 1623 (Print) ● ISSN 1785 0037 (Online)
DOI: http://dx.doi.org/10.15666/aeer/1804_56455659

3.65 and 2.94 in non-stressed and drought stressed environments respectively. Among testers, maximum positive GCA effects were possessed by T1 with the values 2.72 and 3.65 under non-stress and stress conditions respectively (*Table 3*). These findings are similar with the previous results reported in wheat crop under normal and drought stress conditions for this trait (Longin et al., 2012; Ramani et al., 2017). In the current study for CMT, the genotypes showing the best performance were classified as drought-tolerant, while the low performing genotypes were identified as drought-susceptible.

The CMT mean values were 64.03% (normal) and 60.70% (drought) for the crosses L6 × T3 and L1 × T1 as mentioned in *Table 4*. The magnitudes of SCA effects revealed that cross combinations L1 × T1 had positive SCA effects with the values 10.69 and 6.09 under both conditions, respectively (*Table 4*). Previously some scientists (Longin et al., 2012) inspected significant GCA and SCA effects in hexaploid wheat using line × tester mating designs and support the current study results. While some wheat breeders (Punia et al., 2011) reported the highest positive GCA effects as compared to SCA effects for CMT and their results contradicted with current study. The relative water content and cell membrane thermo-stability were also considered important selection criteria for wheat against drought stress.

Grain per spike

Under normal conditions grains per spike mean values varied from 57.34 to 65.63 for lines, in tester ranged from 49.63 to 56.34. The line L1 had maximum number of grain per spike (GPS) 65.63 and 48.55 in non-stressed and drought stressed environments, respectively. The tester, T1 had maximum values 56.34 and 40.34 under both conditions, respectively as displayed in *Table 2*. Among lines, the genotypes L1 possessed maximum positive GCA effects with the values 7.95 under non-stress and 6.89 under stress. Among testers, maximum positive GCA effects were possessed by T1 with the values 1.66 for normal and 1.91 for drought (*Table 3*). These findings match with the results of Kumar et al. (2011) and their colleagues using line × tester mating design in wheat crop for this trait.

Among crosses, grains per spike having maximum mean values 66.34 (normal) and 49.32 (drought) for L1 × T1 as mentioned in *Table 4*. The magnitudes of SCA effects revealed that cross combinations L1 × T1 and highly significant and positive SCA effects with the values 8.24 and 7.71 in non-stressed and drought stressed environments, respectively, as presented in *Table 4*. Significance SCA effects for grain per spike in wheat was estimated by wheat breeders (Kalhoro et al., 2015) which are similar with our findings. Both significant GCA and SCA effects also reported (Bibi et al., 2013; Ahmed et al., 2017b) in non-stressed and drought stressed environments and were in accordance with current findings.

1000-grain weight (g)

Under normal conditions maximum 1000 grain weight (TGW) 52.54 g was scored in L1. Maximum mean values of TGW were 48.98 g for T2 between male parents (*Table 2*). The mean values of TGW under drought conditions the line L1 had maximum TGW 34.31 g and tester T2 (32.98) as shown in *Table 2*. Among female parents L1 possessed maximum positive GCA affects with the values 9.37 and 5.03 while, between the testers maximum positive GCA effects were possessed by T2 and T1 with the values 1.52 and 1.06 in non-stressed and drought stressed environments respectively as displayed in

http://www.aloki.hu ● ISSN 1589 1623 (Print) ● ISSN 1785 0037 (Online)
DOI: http://dx.doi.org/10.15666/aeer/1804_56455659

Table 3. These findings are in line with the findings of wheat scientists (Fellahi et al., 2013; Liu et al., 2016) for this attribute in wheat crop under normal and drought stress conditions.

Table 4. *Mean and specific combining ability (SCA) values of superior crosses (hybrids) in non-stressed and drought stressed environments*

Characters	Mean		SCA	
	Normal	Drought	Normal	Drought
Flag leaf area	L1 × T1 (43.28)	L1 × T1 (32.17)	L1 × T1 (6.26)	L1 × T1 (6.07)
	L1 × T2 (42.19)	L1 × T2 (31.21)	L9 × T4 (5.58)	L10 ×T4 (6.04)
	L10 × T4 (40.5)	L10 × T4 (29.5)	L6 × T5 (5.12)	L9 × T4 (5.36)
	L2 × T2 (40.22)	L2 × T3(29.45)	L1 × T2 (4.92)	L6 × T5 (4.78)
	L2 × T3 (40.21)	L2 × T2 (29.22)	L10 × T4 (4.33)	L1 × T2 (4.72)
Relative water contents	L1 × T1 (82.73)	L1 × T1 (77.30)	L1 × T1 (13.55)	L1 ×T1 (15.26)
	L1 × T3 (82.32)	L3 × T5 (69.32)	L4 × T2 (10.03)	L9 × T1 (8.68)
	L3 × T5 (80.32)	L7 × T3 (68.67)	L10 × T4 (9.56)	L6 × T5 (8.18)
	L2 × T5 (79.66)	L1 × T3 (67.55)	L9 × T1 (7.95)	L4 × T2 (7.19)
	L1 × T2 (79.32)	L8 × T1 (67.32)	L8 × T1 (7.84)	L5 × T2 (6.99)
Cell membrane thermo-stability	L6 × T3 (64.70)	L1 × T1 (60.70)	L1 × T1 (10.69)	L1 × T1 (6.09)
	L7 × T3(64.03)	L4 × T3(60.05)	L6 × T5 (9.89)	L9 × T5 (6.07)
	L1 × T1 (62.80)	L6 × T3 (59.95)	L9 × T4 (9.27)	L8 × T2 (5.22)
	L3 × T1 (62.69)	L9 × T3 (59.75)	L9 × T5 (7.28)	L8 × T1 (5.11)
	L7 × T1 (62.69)	L8 × T1 (59.60)	L2 × T4 (7.65)	L2 × T5 (4.85)
Grain per spike	L1 × T1 (66.34)	L1 × T1 (49.32)	L1 × T1 (8.24)	L1 × T1 (7.71)
	L5 × T4 (66.04)	L5 × T4 (49.04)	L4 × T4 (6.51)	L2 × T1 (5.38)
	L6 × T2 (66.04)	L6 × T1 (48.34)	L2 × T1 (4.56)	L4 × T5 (5.15)
	L6 × T1 (65.34)	L5 × T3 (47.34)	L2 × T3 (4.56)	L10× T2 (5.06)
	L5 × T3 (64.34)	L6 × T2 (47.29)	L7 × T1 (4.08)	L4 × T4 (3.78)
Thousand grain weight	L1 × T2 (58.54)	L1 × T1 (38.54)	L1 × T2 (8.78)	L1 × T1 (7.83)
	L1 × T4 (58.54)	L10 × T3 (38.54)	L7 × T5 (8.04)	L7 × T5 (6.67)
	L1 × T1 (56.55)	L3 × T4 (38.54)	L3 × T3 (6.61)	L10× T1 (5.63)
	L1 × T3 (56.54)	L10× T1 (38.23)	L4 × T1 (5.84)	------
	L3 × T4 (55.54)	L7 × T2 (38.19)	L10 × T1 (5.59)	------
Grain yield per plant	L1 × T1 (36.91)	L1 × T1 (25.91)	L1 × T1 (6.93)	L1 × T1 (6.90)
	L1 × T 2 (33.39)	L3 × T 2 (23.35)	L6 × T4 (6.18)	L9 × T2 (6.5)
	L10 × T2 (32.39)	L1 × T3 (22.00)	L2 × T5 (6.16)	L3 × T2 (6.09)
	L3 × T2 (31.00)	L2 × T5 (22.00)	L3 × T1 (6.12)	L2 × T5 (6.09)
	L6 × T5 (30.06)	L2 × T1 (22.00)	L6 × T5 (6.08)	L5 × T3 (4.94)
Grain protein contents	L10 × T5 (14.06)	L1 × T1 (14.97)	L1 × T3 (2.22)	L1 × T1 (1.95)
	L9 × T2 (14.01)	L10 × T5 (14.95)	L7 × T3 (1.96)	L2 × T1 (1.72)
	L1 × T5 (13.98)	L6 × T2 (14.92)	L9 × T2 (1.91)	L5 × T2 (1.34)
	L7 × T2 (13.97)	L1 × T4 (14.90)	L5 × T2 (1.65)	L1 × T5 (1.26)
	L2 × T1 (13.95)	L8 × T3 (14.89)	L2 × T1 (1.03)	------
Gluten contents	L1 × T1 (28.97)	L5 × T4 (31.60)	L1 × T1 (6.75)	L1 × T1 (4.86)
	L5 × T4 (28.67)	L5× T1 (30.95)	L9 × T4 (5.11)	L9 × T4 (4.38)
	L5 × T5 (28.67)	L8 × T4 (30.90)	L2 × T2 (4.65)	L5 × T4 (4.32)
	L7 × T4 (28.67)	L8 × T3 (30.60)	L1 × T2 (4.55)	------
	L8 × T3 (28.67)	L7 × T3 (30.31)	------	------

http://www.aloki.hu ● ISSN 1589 1623 (Print) ● ISSN 1785 0037 (Online)
DOI: http://dx.doi.org/10.15666/aeer/1804_56455659

Among crosses, the highest mean values 58.54 g and 38.54 g for L1 × T1 in non-stressed and drought stressed environments as shown in *Table 4*. The magnitudes of SCA effects for 1000-grain weight revealed that cross combinations L1 × T2 and L1 × T1 in non-stressed and drought stressed environments possessed maximum positive SCA effects with the values 8.78 and 7.83 respectively (*Table 4*). Similar findings were scored (Fellahi et al., 2013; Ahmed et al., 2017b) for this character from combining ability analysis in wheat crop under normal and drought stress conditions.

Grain yield per plant (g)

In non-stressed and drought stressed environments maximum grain yield per plant (GYP) 33.95 g and 21.89 g were scored in L1 respectively. Maximum mean values for GYP 27.00 g and 18.00 g under both conditions respectively (*Table 2*). The magnitude of GCA effects between female parents revealed by the genotypes L1 and L5 possessing the highest positive values 4.47 and 3.74 while the T1 showed the highest positive GCA effects with the values 1.67 and 1.04 in non-stressed and drought stressed environments respectively (*Table 3*).

Among crosses, GYP showing highest mean values 36.91 g (normal) and 25.91 g (drought) for cross L1 × T1 as shown in *Table 4*. The magnitudes of SCA effects revealed that cross combinations L1 × T1 had positive and highly significant SCA effects with the values 6.93 and 6.90 under both conditions respectively as presented in *Table 4*. Grain yield per plant had significant GCA and SCA effects described earlier from combining ability analysis in wheat crop (Fellahi et al., 2013; Kalhoro et al., 2015) under normal and drought stress conditions while, some scientists (Kumar et al., 2011; Ahmed et al., 2018) inspected the higher positive GCA effects than SCA effects for this character which showed the contradiction with the current results. Only significant SCA effects for GYP that were exhibited the contribution of dominant genes action. Grain yield is polygenic characters which is affected environmental conditions. Significant genetic variability between wheat germplasm for yield contributing traits was found by Minhas et al. (2014), Ashfaq et al. (2016) and Ahmed et al. (2019).

Grain protein contents (%)

Under normal condition maximum grain protein contents (GPC) 12.92%was scored in L10 while, maximum mean values for GPC was 12.83% for T4. Under drought conditions, the line L1 had maximum GPC 14.97%, the GPC maximum value 14.95 for T5 as shown in *Table 2*. The highest positive GCA effects between female parents were revealed by the genotypes L10 and L1 possessing the values 1.46 and 1.34 while, the genotype T3 (3.79) and T1 (0.17) in non-stressed and drought stressed environments respectively. These results are supported by the earlier findings (Guzmán et al., 2016) in wheat genotypes from combining ability analysis using line × tester mating design.

The cross combination L10 × T5 had maximum values 14.1 under normal conditions while, 14.9 for L1 × T1 under drought environments. The magnitudes of SCA effects of GPC revealed that cross combinations L1 × T3 (normal) and L1 × T1 (drought) were possessed maximum positive SCA effects with the values 2.22 and 1.95 respectively (*Table 4*). It was perceived (Maich et al., 2017) that genetic distance was significantly and positively linked with SCA effects for grain protein contents in wheat crop under normal and drought stress conditions. From combining ability study only significant SCA effects were observed for protein contents in wheat grain. Both GCA and SCA

http://www.aloki.hu ● ISSN 1589 1623 (Print) ● ISSN 1785 0037 (Online)
DOI: http://dx.doi.org/10.15666/aeer/1804_56455659

effects were also recorded (Kraljević-Balalić et al., 1982) and exhibited significance in the inheritance of grain protein contents in wheat grain under normal and drought stress conditions.

Gluten contents (%)

Under normal condition maximum gluten contents (GC) values 28.00% was scored in L10 while 22.67% for T4 (*Table 2*). Under drought conditions line L1 had maximum GC 29.93% and maximum value 24.90% for T5 as shown in *Table 2*. Among lines, the genotypes L10 and L1 possessed maximum positive GCA effects with the values 3.79 and 2.27 while the genotypes having maximum GCA effects T4 and T3 with the values 1.83 and 1.78 in non-stressed and drought stressed environments, respectively (*Table 3*). These results are similar with the study by several wheat scientists (Peng et al., 2011; Guzmán et al., 2016) in wheat genotypes from combining ability analysis using line × tester mating design under normal drought stress conditions.

The cross combinations L1 × T1 and L5 × T4 had maximum values 28.97% and 31.60% in non-stressed and drought stressed environments, respectively. The magnitudes of SCA effects revealed that cross combinations L1 × T1 had positive SCA effects with the values 6.75 and 4.86 in non-stressed and drought stressed environments respectively as presented in *Table 4*. Gluten contents had significant GCA and SCA effects examined by wheat breeders (Arya et al., 2017) which were in line with the current study. It is the ability of an individual to transfer the best character to its cross/hybrid and designates the significant breeding value of individuals in the creation of the best hybrid (Kempthorne, 1957). It is an influential analysis to differentiate the best and poor combiners for selecting suitable parental genotypes for a specific trait in wheat breeding scheme and also delivers the evidence about the types of gene action controlling the yield and yield related characters.

Gene action

Variance due to GCA = σ2 GCA is helpful for determining the hybrid potential using the GCA effects values of their parental lines. Trial based research (Fellahi et al., 2013; Kalhoro et al., 2015) exhibited that GCA variances are more prominent than SCA variances, assortment due to GCA effects of the tester (male parent) is a favorable method, but choice of lines (female parent) with maximum GCA in crosses is essential to exploit the yield in the production of hybrid seed (Longin et al., 2012).

If general combining ability variance is greater than specific combing ability variance then selection will be done in the earlier generations due to the presence of additive types of gene action. If the values of SCA variances are higher from GCA variances, then dominant genes are supposed to be responsible for controlling the character and hybrid breeding can be proposed and selection are not useful in earlier generation. In present study the GCA:SCA ratio was less than one which indicating the preponderance of dominance types of genetic effects under both conditions in studied characters. In this case hybrid breeding may be recommended and it would be greater effective. The SCA variance was greater than GCA variance for number of tillers per plant and cell membrane thermos-stability suggesting that dominance types of genetic effects was prominent in the inheritance for these characters. Similar results have been observed by many wheat scientists (Liu et al., 2016; Longin et al., 2012) in wheat crop using line × tester mating design under normal and drought stress conditions.

http://www.aloki.hu ● ISSN 1589 1623 (Print) ● ISSN 1785 0037 (Online)
DOI: http://dx.doi.org/10.15666/aeer/1804_56455659

Due to non-additive genetic mechanism governing most of the yield relating traits, selection of the superior plants would have to be practiced with great care while handling the plant-material in segregating generations. Observing the proportional contributions of female parents, male parents and their hybrids to the total variance for studied traits (*Table 5*), lines were more prominent for the characters like flag leaf area, relative water contents, cell membrane thermo-stability, grain yield/plant, GPC and GC under normal irrigation, indicating a predominant maternal influence. Tester contribution was very low proportion, while the line × tester interaction contributed predominantly to1000-grain weight under both conditions Various scientists have suggested only dominance genetic effects (Kumar et al., 2011; Bibi et al., 2013) and some reported (Kalhoro et al., 2015) the additive genetic effects for yield and yield related traits in wheat under both conditions for improving the selection efficiency. Both types of genetic effects in yield contributing characters of wheat were suggested (Akram et al., 2011) from combining ability analysis under drought stress environments.

Table 5. *Estimates of genetic components and proportional contributions of lines and tester*

Traits	Environment	Gene action					Proportional contribution		
		σ^2 GCA	σ^2 SCA	$\sigma^2A = \sigma^2$ GCA*2	$\sigma^2D = \sigma^2$ SCA	σ^2A/σ^2D	L	T	L × T
FLA	N	0.04	11.73	0.08	11.73	0.01	26	6	68
	D	0.06	10.53	0.12	10.53	0.01	29	6	65
RWC	N	0.59	46.42	1.18	46.42	0.03	38	5	57
	D	1.00	24	2	24	0.08	42	6	52
CMT	N	36.3	0.31	72.68	0.31	234.4	16	23	61
	D	18.0	0.22	36.06	0.22	163.9	10	31	59
GPS	N	0.95	15.94	1.9	15.94	0.12	64	4	32
	D	0.68	11.14	1.36	11.14	0.12	60	4	36
TGW	N	0.83	21.89	1.66	21.89	0.08	59	3	38
	D	0.74	10.23	1.48	10.23	0.14	64	4	33
GYP	N	0.45	22.67	0.9	22.67	0.04	47	3	50
	D	0.31	15	0.62	15	0.04	46	2	52
GPC	N	0.01	0.61	0.02	0.61	0.03	35	3	62
	D	0.01	0.38	0.02	0.38	0.05	35	3	61
GC	N	0.16	7.33	0.32	7.33	0.04	32	13	55
	D	0.07	6.51	0.14	6.51	0.02	16	21	64

FLA = flag leaf area, RWC = relative water content, CMT = cell membrane thermostability, GPS = grain per spike, TGW = thousand grain weight, GYP = grain yield per plant, GPC = grain protein content, GC= gluten content. L = line (female parent), T = tester (male parent)

Breeding with drought resistance of wheat is very important for sustainable food production. In the future research, each new cross from breeder involves the modification of genome-wide gene networks (Appels et al., 2018) that control the expression of drought and yield, especially the dynamics of change in complex gene families involved in drought adaptation.

http://www.aloki.hu ● ISSN 1589 1623 (Print) ● ISSN 1785 0037 (Online)
DOI: http://dx.doi.org/10.15666/aeer/1804_56455659

Conclusion

Among parents, the line 9493 (L1) and the tester 9508 (T1) proved to be the best general combiners for most of the yield contributing indices under both conditions due to higher GCA effects. Among the hybrids L1 × T1 was the ideal specific combiner for most of the quality and yield related traits under both conditions. GCA variances were observed less than SCA variances suggesting that a dominance genetic effect was prominent in the inheritance for examined indices. Hence, the selection practice for superior individual plants should be delayed to next generations like F_4 or F_5. The superior genotypes and their cross combinations showed promising one for exploitation in wheat breeding program to develop best quality and high yielding wheat genotypes against drought stress conditions to fulfill the needs of wheat and sustainable food security.

Acknowledgement. This work was funded by the China Agriculture Research System (CARS-05-01A-04).

REFERENCES

[1] Ahmed, H. G. M.-D., Khan, A. S., Khan, S. H., Kashif, M. (2017a): Genome wide allelic pattern and genetic diversity of spring wheat genotypes through SSR markers. – International Journal of Agriculture and Biology 19: 1559-1565.

[2] Ahmed, H. G. M.-D., Khan, A. S., Kashif, M., Khan, S. H. (2017b): Genetic mechanism of leaf venation and stomatal traits for breeding drought tolerant lines in wheat. – Bangladesh Journal of Botany 46: 35-41.

[3] Ahmed, H. G. M.-D., Khan, A. S., Kashif, M., Khan, S. (2018): Genetic analysis of yield and physical traits of spring wheat grain. – Journal of the National Science Foundation of Sri Lanka 46.

[4] Ahmed, H. G. M.-D., Sajjad, M., Li, M., Azmat, M. A., Rizwan, M., Maqsood, R. H., Khan, S. H. (2019): Selection criteria for drought-tolerant bread wheat genotypes at seedling stage. – Sustainability 11: 2584.

[5] Akram, Z., Ajmal, S. U., Khan, K. S., Qureshi, R., Zubair, M. (2011): Combining ability estimates of some yield and quality related traits in spring wheat (Triticum aestivum L.). – Pak. j. bot 43: 221-231.

[6] Ali, A., Ali, N., Ullah, N., Ullah, F., Adnan, M., Ahmed, Z. (2013): Effect of drought stress on the physiology and yield of the Pakistani wheat germplasms. – International Journal of Advancements in Research & Technology 2: 419.430-2013.

[7] Appels, R., Eversole, K., Feuillet, C., Keller, B., Rogers, J., Stein, N., Pozniak, C. J., Choulet, F., Distelfeld, A., Poland, J. (2018): Shifting the limits in wheat research and breeding using a fully annotated reference genome. – Science 361: eaar7191.

[8] Arya, V. K., Singh, J., Kumar, L., Kumar, R., Kumar, P., Chand, P. (2017): Genetic variability and diversity analysis for yield and its components in wheat (Triticum aestivum L.). – Indian Journal of Agricultural Research 51.

[9] Ashfaq, W., Ul-Allah, S., Kashif, M., Sattar, A., Nabi, H. G. (2016): Genetic variability study among wheat genotypes under normal and drought conditions. – J. Glob. Innov. Agric. Soc. Sci 4: 111-116.

[10] Bibi, R., Hussain, S. B., Khan, A. S., Raza, I. (2013): Assessment of combining ability in bread wheat by using line x tester analysis under moisture stress conditions. – Pak. J. Agric. Sci 50: 111-115.

[11] Blum, A., Ebercon, A. (1981): Cell membrane stability as a measure of drought and heat tolerance in wheat. – Crop Sci 21: 43-47.

http://www.aloki.hu ● ISSN 1589 1623 (Print) ● ISSN 1785 0037 (Online)
DOI: http://dx.doi.org/10.15666/aeer/1804_56455659

[12] Cheng, S.-H., Zhuang, J.-Y., Fan, Y.-Y., Du, J.-H., Cao, L.-Y. (2007): Progress in research and development on hybrid rice: a super-domesticate in China. – Annals of botany 100: 959-966.
[13] Dhanda, S., Sethi, G. (1998): Inheritance of excised-leaf water loss and relative water content in bread wheat *(Triticum aestivum)*. – Euphytica 104: 39-47.
[14] Fellahi, Z. E. A., Hannachi, A., Bouzerzour, H., Boutekrabt, A. (2013): Line × tester mating design analysis for grain yield and yield related traits in bread wheat (Triticum aestivum L.). – International Journal of Agronomy 2013.
[15] Förster, S., Schumann, E., Weber, W. E., Pillen, K. (2012): Discrimination of alleles and copy numbers at the Q locus in hexaploid wheat using quantitative pyrosequencing. – Euphytica 186: 207-218.
[16] Fuller, D. Q. (2007): Contrasting patterns in crop domestication and domestication rates: recent archaeobotanical insights from the Old World. – Annals of botany 100: 903-924.
[17] Guzmán, C., Autrique, J. E., Mondal, S., Singh, R. P., Govindan, V., Morales-Dorantes, A., Posadas-Romano, G., Crossa, J., Ammar, K., Peña, R. J. (2016): Response to drought and heat stress on wheat quality, with special emphasis on bread-making quality, in durum wheat. – Field Crops Research 186: 157-165.
[18] Kalhoro, F. A., Rajpar, A. A., Kalhoro, S. A., Mahar, A., Ali, A., Otho, S. A., Soomro, R. N., Ali, F., Baloch, Z. A. (2015): Heterosis and combing ability in F1 population of hexaploid wheat (Triticum Aestivum L.). – American Journal of Plant Sciences 6: 1011.
[19] Kempthorne, O. 1957. An Introduction to Genetic Statistics. – John Wiley and Sons, Inc., New York.
[20] Kraljević-Balalić, M., Štajner, D., Gašić, O. (1982): Inheritance of grain proteins in wheat. – Theoretical and Applied Genetics 63: 121-124.
[21] Kumar, P., Yadava, R., Gollen, B., Kumar, S., Verma, R. K., Yadav, S. (2011): Nutritional contents and medicinal properties of wheat: a review. – Life Sciences and Medicine Research 22: 1-10.
[22] Liana, A., Alda, S., Fora, C., Diana, M., Gogoasa, I., Bordean, D., Cârciu, G., Cristea, T. (2012): Climatic conditions influence on the variation of quality indicators of some Romanian and foreign winter wheat cultivars. – Journal of Horticulture, Forestry and Biotechnology 16: 68-72.
[23] Liu, B., Asseng, S., Liu, L., Tang, L., Cao, W., Zhu, Y. (2016): Testing the responses of four wheat crop models to heat stress at anthesis and grain filling. – Global Change Biology 22: 1890-1903.
[24] Longin, C. F. H., Mühleisen, J., Maurer, H. P., Zhang, H., Gowda, M., Reif, J. C. (2012): Hybrid breeding in autogamous cereals. – Theoretical and Applied Genetics 125: 1087-1096.
[25] Maich, R. H., Steffolani, M. E., Di Rienzo, J. A., Leon, A. E. (2017): Association between grain yield, grain quality and morpho-physiological traits along ten cycles of recurrent selection in bread wheat (Triticum aestivum L.). – Cereal Research Communications 45: 146-153.
[26] Maria, A. L., Lavinia, C. L., Fora, C., Alda, S., Gogoasa, I., Despina, B. (2013): Researches regarding some winter wheat cultivars behavior under pedo-climatic conditions of Timis County. – Journal of Horticulture, Forestry and Biotechnology 17: 87-90.
[27] Minhas, N. M., Ajmal, S. U., Ahmed, Z. I., Munir, M. (2014): Genetic analysis for grain quality traits in Pakistani wheat varieties. – Pak J Bot 46: 1409-1413.
[28] Muller, J. (1991): Determining leaf surface area by means of linear measurements in wheat and triticale (brief report). – Archiv Fuchtungsforsch 21: 121-123.
[29] Noorka, I. R., Teixeira da Silva, J. A. (2014): Physical and morphological markers for adaptation of drought-tolerant wheat to arid environments. – Pakistan Journal of Agricultural Sciences 51.

http://www.aloki.hu ● ISSN 1589 1623 (Print) ● ISSN 1785 0037 (Online)
DOI: http://dx.doi.org/10.15666/aeer/1804_56455659

[30] Peña-Bautista, R. 2002. Wheat for bread and other foods. Bread wheat: improvement and production. – http://www.fao.org/3/y4011e0w.htm.
[31] Peng, J. H., Sun, D., Nevo, E. (2011): Domestication evolution, genetics and genomics in wheat. – Molecular Breeding 28: 281.
[32] Punia, S., Shah, A. M., Ranwha, B. R. (2011): Genetic analysis for high temperature tolerance in bread wheat. – African Crop Science Journal 19: 149-163.
[33] Ramani, H., Mandavia, M., Dave, R., Bambharolia, R., Silungwe, H., Garaniya, N. (2017): Biochemical and physiological constituents and their correlation in wheat (Triticum aestivum L.) genotypes under high temperature at different development stages. – International Journal of Plant Physiology and Biochemistry 9: 1-8.
[34] Steel, R. G. D., Torrie, J. H., Dickey, D. A. (1997): Principles and Procedures of Statistics: A Biometrical Approach. – McGraw Hill Book Company, New York.
[35] Wu, M., Jia, X., Tian, L., Lv, B. (2010): Rapid and reliable purity identification of F 1 hybrids of Maize (Zea may L.) using SSR markers. – Maize Genomics and Genetics 2010(1).
[36] Zeeshan, M., Arshad, W., Ali, S. (2013): Genetic diversity and trait association among some yield parameters of wheat elite lines genotypes under rainfed conditions. – J Renewable Agri 1: 23-26.

http://www.aloki.hu ● ISSN 1589 1623 (Print) ● ISSN 1785 0037 (Online)
DOI: http://dx.doi.org/10.15666/aeer/1804_56455659

DO SUBMERGED PLANTS IMPROVE THE WATER QUALITY IN MINING SUBSIDENCE RESERVOIRS?

PIERZCHAŁA, Ł.[1*] – SIERKA, E.[2]

[1]*Central Mining Institute in Katowice, Department of Water Protection*
Plac Gwarków 1, 40-166 Katowice, Poland
(phone: +48-32-259-2000; fax: +48-32-259-6533)

[2]*University of Silesia in Katowice, Faculty of Natural Sciences, Institute of Biology, Biotechnology and Environmental Protection, Jagiellońska 28, 40-032 Katowice, Poland*
(phone: +48-32-255-5873; fax: +48-32-200-9361)

[*]*Corresponding author*
e-mail: lpierzchala@gig.eu; phone: +48-32-254-2292; fax: +48-32-254-2452

(Received 31st Dec 2019; accepted 22nd May 2020)

Abstract. This paper provides an analysis of the effect of submerged vegetation on the physicochemical parameters of water with particular regard to transparency in mining subsidence reservoirs (MSR). The research encompassed 8 subsidence reservoirs with a diversified structure of submerged plants in the littoral zone. It has been proven that reservoirs where submerged vegetation coverage is greater than 25% of the water surface area are characterized by significantly greater transparency of water. High water transparency is desirable due to a greater utility value of reservoirs and their biologic diversity. The results from this research indicate that supporting the development of submerged vegetation in mining subsidence reservoirs may be an effective method for improving the water quality of such reservoirs.
Keywords: *submerged vegetation, mining subsidence reservoirs, water clarity, alternative stable states, physicochemical parameters*

Introduction

Subsidence reservoirs, as anthropogenic water ecosystems, are generally formed as a result of underground mining activity. This type of reservoirs compared to natural reservoirs (Sierka et al., 2012), frequently characterize high concentrations of dissolved substances, primarily sulfates and chlorides, and may be subject to intensive eutrophication (Raclavská et al., 2003; Strzelec et al., 2010; Kašovská et al., 2014). The water eutrophication is leading to dominance of algae, as well as reduction or even elimination of submerged plants, and cause the deterioration of water quality in reservoirs (Irfanullah and Moss, 2004). Hasler and Jones (1949), Jeppesen et al. (1990), Gross and Sütfeld (1994), Coops and Doef (1996), Bachmann et al. (2002), Nakamura et al. (2008), Kosten et al. (2009), Li et al. (2014), Phillips et al. (2016) and Verhofstad et al. (2017) have proved in their research that submerged plants have the capability to increase the clarity of water and efficiency of pollutant removal e.g. lakes. As a starting point of investigation within this paper should be the resume of general ideas behind the alternative stable states theory for shallow lakes. The theory indicates that if submerged plants are abundant, they can greatly reduce turbidity (Scheffer et al., 1993). Is the fact that the research has been conducted for almost 30 years. The problem of maintaining the clarity of water is still valid (Wang et al., 2019), because it is closely related to the searching of effective methods to maintain good status of water ecosystems. Access to the reservoirs with clear water for citizens, especially in urban and periurban areas

http://www.aloki.hu ● ISSN 1589 1623 (Print) ● ISSN 1785 0037 (Online)
DOI: http://dx.doi.org/10.15666/aeer/1804_56615672

(Woźniak et al., 2018), is important factor to enhance their well-being. Furthermore, only ecosystems with good water quality deliver suitable habitats for aquatic organisms (Tokarska-Guzik and Rostański, 1996; Pierzchała et al., 2016).

One of the water quality parameters is clarity which indicates the presence or absence of suspended matter, and hence it is a reflection of the overall quality of the water. The role of macrovegetation in reservoirs formed in subsidence basins as a factor related to improving water quality is unknown. It seems that understanding the relationship between the functioning of submerged vegetation and water parameters in mining subsidence reservoirs may be the basis for their effective restoration (Hilt et al., 2006). In natural shallow reservoirs, vegetation is not the only one parameter used for the evaluation of the ecological condition of water ecosystems. Aquatic plants, particularly species with submerged leaves, compete with algae for domination in the water ecosystems.

The main aim of this paper is to answer these questions:

1) is submerged vegetation a factor promoting water clarity in mining subsidence reservoirs as in lake?

2) does water clarity depends from submerged vegetation percentage cover surface area of the mining subsidence reservoirs?

Materials and methods

Area of research

The research was conducted within subsidence reservoirs located in Karvina county, Czechia. The area of research is part of the Ostrava-Karvina coal basin located within the Moravian-Silesian Region in the North-Eastern part of Czechia. The region is entirely industrial in nature and its landscape has been strongly affected by coal mining activities (Macoun et al., 1965; Menčik, 1983). There are also dozens of fresh water reservoirs of various size, formed due to direct activity (storage reservoirs, fish ponds) and indirect human activity (subsidence reservoirs). The accumulation of water is geologically related to Quaternary layers, primarily Quaternary sands and clayey sands that prevail in this area (Plaček, 1984). The elevated salinity of water in subsidence reservoirs is primarily the effect of washing out substances from mine waste dumps (Molenda and Rzętała, 2001). In addition, gangue (waste material from mining) is frequently used to shape the shore of the analyzed objects. The leaching of readily soluble mineral components (primarily chlorides and sulfates) from such formations leads to the higher salinity of the water.

In order to conducted research on the effect of the aqatic vegetation on water chemistry, informed by former reaserch (Raclavská et al., 2003; Stalmachová, 2003; Pertile, 2007), 8 reservoirs of diverse salinity and trophic status were selected (*Figure 1*). All of the selected reservoirs had undergone spontaneous succession for at least 10 years. The hydromorphological properties of the analyzed reservoirs are presented in *Table 1*.

Methodology

Water samples were collected from May to October in monthly intervals in 2010. The sampling points (one par lake) were determined within the littoral zone, at a distance of over 50 m from the reservoir's inlet and outlet, where water movement was

http://www.aloki.hu ● ISSN 1589 1623 (Print) ● ISSN 1785 0037 (Online)
DOI: http://dx.doi.org/10.15666/aeer/1804_56615672

undisturbed. The water transparency were measured *in situ* by Secchi Disk. The depth where the Secchi Disk settles beyond visual recognition, was determined as an index of water transparency - SD (Secchi Depth). The laboratory analyses included the following physico-chemical parameters: pH, TSS (Total Suspended Solids), TDS (Total Dissolved Substances), TN (Total Nitrogen), and TP (Total Phosphorus) were conducted in accordance with appropriate standards ISO. Seasonal mean values of the parameters were used for further computational analyses.

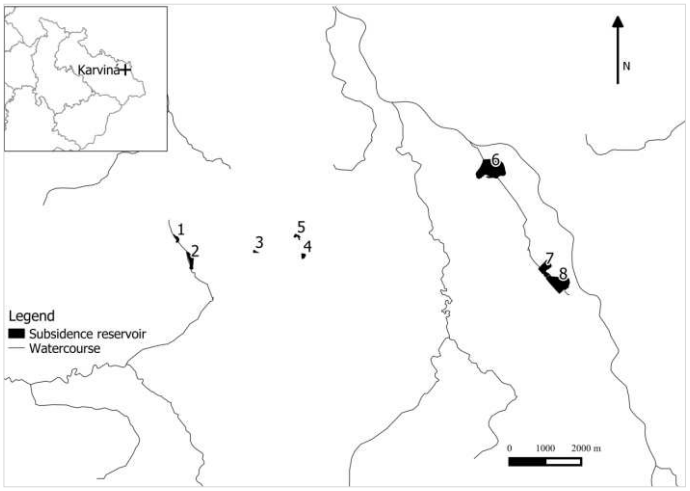

Figure 1. *Location of the research subjects. 1 - Pod lesem, 2 - Bartošůvka, 3 - František, 4 - Barbora, 5 - U cesty, 6 - Darkovské moře, 7 - Velký Myškovec, 8 - Mlýnské rybníky against the background of the hydrographic network*

Table 1. *Hydromorphological properties of the analysed reservoirs*

Subject No.	Name of the reservoir	Depth [m]	Area [ha]	Circumference of the reservoir [m]	Shore with forest covered area [%]	Flow-through reservoir
1	Pod lesem	2.5	1.34	701	85.8	Yes
2	Bartošůvka	8.5	3.95	1070	0	Yes
3	František	5	0.57	386	29.2	No
4	Barbora	4.5	1.24	740	51.3	No
5	U cesty	4.5	0.79	368	45.3	No
6	Darkovské moře	25	34.9	2311	0	Yes
7	Velký Myškovec	3.5	6.56	1106	74.1	Yes
8	Mlýnské rybník	3	17.33	2288	17.8	Yes

Vegetation research was conducted in August 2010, when there was a stable water level according to the methodology by Grulich and Vydrová (2006). Each reservoir, depending on its surface, was divided into 6-10 transects perpendicular to the shoreline. Transects were further divided into zones with regard to their depth: 0-1 m, 1-2 m, 2-3 m, >4 m (Schaumburg et al., 2004). In each zone there were 2 research plots of an area of 1 m^2. The composition of the aquatic vegetation, in terms of species and coverage of each, species was determined as a percentage: 0, 1, 10, 20, 30... 100%. To characterise the spatial structure of macrophytes of each reservoir the average percentage of vegetation coverage for individual species was calculated and this value was used for further analysis.

http://www.aloki.hu ● ISSN 1589 1623 (Print) ● ISSN 1785 0037 (Online)
DOI: http://dx.doi.org/10.15666/aeer/1804_56615672

The different aquatic vegetation were classified according to their ecological groups: *elodeids* –classified submerged macrophytes and *nymphaeids* - plants rooted in the bottom with leaves floating on the water surface.

The normality data of distribution within particular groups was confirmed using the Shapiro-Wilk test. The parametric T-test (Statistica 12.0) was employed to determine the significance of differences among particular groups with regard to the values of physico-chemical and hydromorphological indicators. The relationship between the aquatic vegetation characteristics and physico-chemical parameters of the water samples were analysed using Pearson's linear correlation coefficient.

In order to determine the habitat conditions that differentiate the type of aquatic and coastal vegetation, a linear model of ordination analysis, PCA (Principal Component Analysis) was applied. The PCA was used to: 1) identify the main differentiation patterns of aquatic vegetation and 2) determine the relationship between the differentiation of vegetation and the analyzed environmental factors. RDA (Redundancy Analysis) was employed to determine to what extent coverage of elodeids and nymphaeids affect the diversity of basic water quality parameters (SD, TN, TP, TSS). The Monte Carlo permutation test (499 permutations) was used to determine the significance of explanatory variables in the RDA model. The analysis was conducted using the CANOCO package. Prior to analysis all environmental data ver log(x+1) transformed (Šmilauer and Lepš, 2014).

In order to define the major relationships between the percent cover type of aquatic vegetation and hydromorphological and physico-chemical water parameters, a parametric test of Pearson's correlation coefficient was conducted (Statistica 12.0). Parameters that showed significant statistical correlation ($p < 0.05$) were included in the ordination analysis. Due to the length of the gradient obtained in the preliminary Canonical Correspondence Analysis (CCA) (gradient length <3), the linear model of ordination analysis (PCA and RDA) was used (Lepš and Šmilauer, 2000). Ordination analysis were conducted in CANOCO 4.1.

Results

The main species, in the reservoirs sampled forming submerged vegetation communities are *Ceratphyllum demersum, Myriophyllum spicatum,* and *Najas marina* (*Table 2*). With regard to the type of vegetation, submerged vegetation in reservoirs 6, 4, 3 and 5 plant cover a was greater than 25% of the water surface area.

The analyzed reservoirs were divided into two groups with regard to the average percentage cover of submerged vegetation. The first group encompassed reservoirs where elodeids cover was at least 25% (Group I - site 6, 4, 3, 5), while the second group included reservoirs where the submerged vegetation cover less than 25% of the water surface area (Group II - site 7, 8, 1, 2). The transparency of water in Group I reservoirs exceeded 1.8 m and this was a statistically significant difference when compared to reservoirs where submerged vegetation was scarced. Significant differences between the analyzed groups of reservoirs were also found in the values of pH, salinity (TDS) and the concentration of suspended solids. The mean concentration of total phosphorus in the group of reservoirs abundant in vegetation was within the range 0.011 - 0.06, while in the other group it was within the range 0.01 - 0.03. Moreover, no differences in nitrogen concentration were found between these groups (*Table 3*). No statistically

http://www.aloki.hu ● ISSN 1589 1623 (Print) ● ISSN 1785 0037 (Online)
DOI: http://dx.doi.org/10.15666/aeer/1804_56615672

significant differences in the morphological parameters presented in table 1 were found between the analyzed groups of reservoirs.

Table 2. *Diversity of aquatic vegetation in particular reservoirs*

Number of the reservoir	**6**	**4**	**3**	**5**	**7**	**8**	**2**	**1**
	Average cover [%]							
elodeids	57.75	38	29.17	28.5	5.76	1.56	0	0
Ceratophyllum demersum (Cer_dem)	5.25	38	28.33	4	0.20	0	0	0
Elodea canadensis (Elo_can)	0.25	0	0	0	0.10	0	0	0
Lemna minor (Lem_min)	0	4.833	1.667	0	0	0	0	0
Myriophyllum spicatum (Myr_spi)	0.75	0	0.833	24.5	0	0	0	0
Najas marina (Naj_mar)	28.5	0	0	0	2.93	1.56	0	0
Najas minor (Naj_min)	12.5	0	0	0	0	0	0	0
Potamogeton crispus (Pot_cri)	0.625	0	0	0	0.61	0	0	0
Potamogeton nodosus (Pot_nod)	2.625	0	0	0	0.30	0	0	0
Potamogeton obtusifolius (Pot_obt)	0.125	0	0	0	0	0	0	0
Potamogeton pectinatus (Pot_pec)	0.25	0	0	0	0	0	0	0
Potamogeton lucens (Pot_luc)	0	0	0	0	1.62	0	0	0
Ranunculus aquatilis (Ran_aqu)	1.125	0	0	0	0	0	0	0
Utricularia vulgaris (Utr_vul)	6.875	0	0	0	0	0	0	0
nymphaeids	1.5	6.833	1.667	1.5	0.808	1.778	0	0
Nymphea alba (Nym_alb)	0	0	0	0	0.808	0	0	0
Polygonum amphibium (Pol_amp)	0.375	2	0	1.5	0	1.778	0	0

Table 3. *Physico-chemical water parameters of the analyzed reservoirs*

Groups	**Reservoir No.**	**SD [m]*** avd ± sd	**pH^0** avd ± sd	**TP [mg·l^{-1}]** avd ± sd	**TN [mg·l^{-1}]** avd ± sd	**TDS [mg·l^{-1}]*** avd ± sd	**TSS [mg l^{-1}]*** avd ± sd
Group I	6	2.30±0.50	8.00±0.26	0.013±0.01	0.69±0.36	727.5±55.7	6.90±5.33
(coverage of	4	2.20±0.15	7.80±0.10	0.011±0.01	0.48±0.20	1701.3±312.82	3.10±1.31
submerged	3	2.00±0.12	8.00±0.13	0.044±0.04	1.18±0.18	731.2±52.53	3.60±2.96
vegetation ≥25%)	5	1.80±0.16	8.00±0.17	0.06±0,06	0.77±0.19	1067.8±19.63	5.70±2.50
Group II	7	0.70±0.24	8.00±0.36	0.03±0.01	0.88±0.26	431.6±26.69	18.4±11.04
(coverage of	8	1.00±0.30	8.00±0.18	0.02±0.01	1.10±0.25	383.3±39.36	9.30±3.84
submerged	2	0.70±0.06	7.90±0.16	0.01±0.01	1.15±0.31	684.0±65.14	7.50±4.43
vegetation <25%)	1	0.60±0.20	7.70±0.09	0.02±0.01	1.49±0.33	236.6±31.08	21.9±19.9

Statistically significant differences between the groups $p \leq 0.05$ are marked with *

The analysis of linear correlation between physico-chemical parameters of water and the type of vegetation showed the following significant: positive correlations: between water transparency (SD) and the average percentage cover of submerged vegetation (ELO) (0.95); the maximal depth of submerged vegetation (dep_lim) and water transparency (SD) (0.96); the number of species (Num_spe) and the depth (depth; 0.76) and area of the reservoir (area; 0.74); between salinity (TDS) (0.7) and water transparency (SD). The negative correlation was indicated (-0.76) between water transparency (SD) and total suspended solids (TSS) (*Table 4*).

The PCA analysis showed that the analyzed physico-chemical parameters accounted by 96.97% of the variation of vegetation. The first ordination axis (axis I) of the PCA model accounts for 52.47% of the total variation of vegetation and it has the strongest positive correlation with water of total nitrogen (TN) (0.74) and the concentration of suspended solids (-0.68) (TSS). This axis has the strongest negative correlation with

http://www.aloki.hu ● ISSN 1589 1623 (Print) ● ISSN 1785 0037 (Online)
DOI: http://dx.doi.org/10.15666/aeer/1804_56615672

transparency (0.97) (SD) and salinity (-0.69) (TDS). This axis, therefore, determines the gradient of the strongest positive correlation with the average percentage cover of submerged vegetation (ELO) The other axis (axis II) accounts for 28.48% of the total variation of vegetation and has the positive correlation with depth (0.78), area of the reservoir (0.89) (*Figure 2*). Many of submerged vegetation species has the strongest positive correlation with this axis (*Table 5*).

Table 4. *The linear correlation coefficients between seasonal mean values of physico-chemical parameters of water and the type of vegetation*

	SD [m]	**pH**	**TP**	**TN**	**TSS**	**TDS**	**Depth [m]**	**Area [ha]**
Cer_dem	0.69	-0.16	-0.04	-0.44	-0.61	**0.76**	-0.09	-0.30
Lem_min	0.54	-0.34	-0.22	-0.51	-0.49	**0.82**	-0.18	-0.32
Myr_spi	0.24	0.28	**0.81**	-0.25	-0.24	0.28	-0.11	-0.24
ELO	**0.95**	0.25	0.01	-0.70	-0.61	0.60	0.69	0.45
NYM	0.63	-0.18	-0.19	**-0.728**	-0.54	**0.86**	-0.07	-0.10
num_spec	0.52	0.53	-0.03	-0.59	-0.12	0.08	**0.76**	**0.74**
dep_lim	0.96	0.33	0.12	**-0.75**	-0.63	0.63	0.59	0.38
SD [m]	1.00	0.26	0.12	-0.68	**-0.77**	**0.71**	0.47	0.27
TP	0.12	0.42	1.00	0.03	-0.09	0.01	-0.31	-0.40
TN	-0.68	-0.29	0.03	1.00	0.55	**-0.79**	-0.23	-0.23
TSS	-0.77	-0.39	-0.09	0.55	1.00	**-0.72**	-0.03	-0.01
TDS	**0.71**	-0.09	0.01	**-0.79**	**-0.72**	1.00	-0.06	-0.25

Statistically significant values of correlation coefficient $p \leq 0.05$ are bold (N=8)

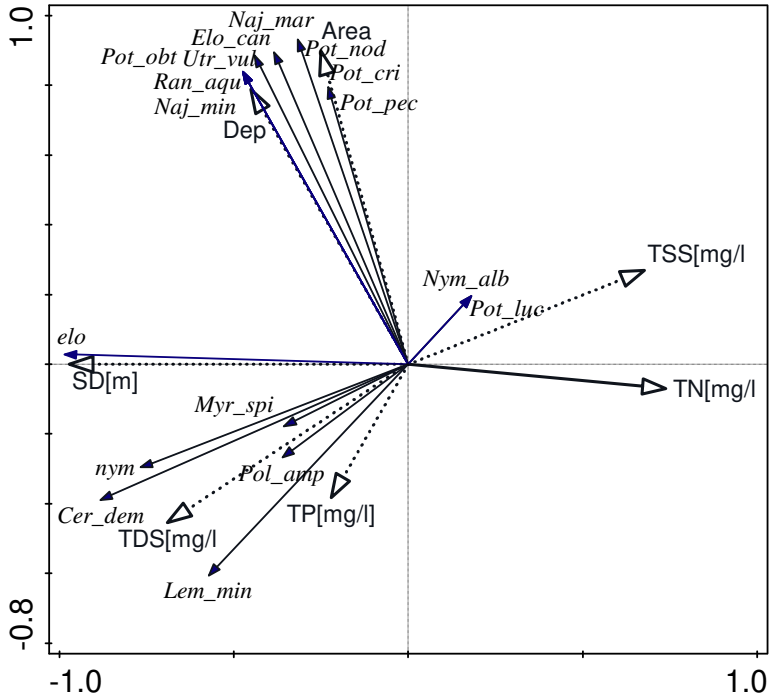

Figure 2. *Results of the Principal Component Analysis (PCA) Diversity of aquatic vegetation (Species see Table 2, elo –elodeids, nym- nymphaeids) with relation to analyzed hydromorphological (Area – surface water area of reservoirs, Dep –depth of reservoirs) and physico-chemical parameters of water (SD - water transparency, TDS – salinity, TP - total phosphorus concentration, TN - total nitrogen concentration, TSS - total suspended solid concentration)*

http://www.aloki.hu ● ISSN 1589 1623 (Print) ● ISSN 1785 0037 (Online)
DOI: http://dx.doi.org/10.15666/aeer/1804_56615672

Table 5. *Values of the correlation coefficient between hydromorphological and physico-chemical parameters of water and axes I and II of the PCA model*

Parameter	Axis I	Axis II
SD [m]	-0.97	0.00
TP [mg·l^{-1}]	-0.22	-0.38
TSS [mg·l^{-1}]	0.68	0.27
TN [mg·l^{-1}]	0.74	-0.07
TDS [mg·l^{-1}]	-0.69	-0.45
Depht [m]	-0.45	0.79
Area [ha]	-0.25	0.90

In the RDA model, canonical axes significantly account for 94.22% of the variation. The first axis is positively correlated with average percentage cover of elodeids (ELO, 0.86) and nymphaeids (Nym 0.75) and accounts for 52.15% of the variation of the main water quality parameters (SD, TN, TP, TSS). The statistical significance of the relation was confirmed by Monte Carlo test (test of first axis F value 2.7, $p<0.05$) (*Figure 3*).

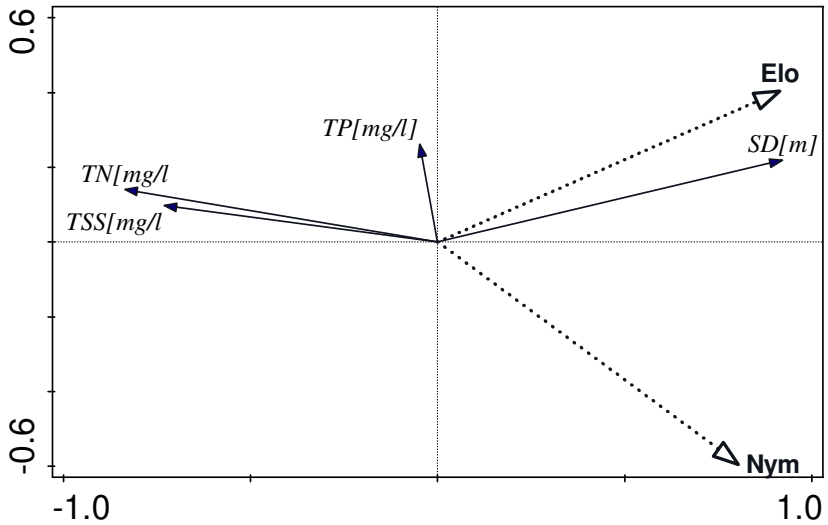

Figure 3. *Results of Redundancy Analysis (RDA). Correlations between explanatory variable (Elo - average percentage coverage of elodeids, Nym - average percentage coverage of nymphaeids) and response variable (SD - water transparency, TP - total phosphorus concentration, TN - total nitrogen concentration, TSS - total suspended solid concentration)*

Discussion

A persistent regime of transparent water is perceived as more desirable due to a greater utility value and the subsequent development of biological diversity of a fresh water reservoir (Moss, 1998; Scheffer et al., 2003; Cardinale, 2011) among water parameters. Multiple authors claim that water transparency in fresh water ecosystems greatly depends on low concentrations of phosphorus (Schindler, 1977; Kentzer, 2001; Suchowiec and Górniak, 2006; Vitense et al., 2019). Despite the fact that the concentration of phosphorus does not directly affect water transparency, low concentrations of this element may inhibit the development of phytoplankton. It has

http://www.aloki.hu ● ISSN 1589 1623 (Print) ● ISSN 1785 0037 (Online)
DOI: http://dx.doi.org/10.15666/aeer/1804_56615672

been proven within this paper that the concentration of phosphorus is not a key factor affecting the transparency of water in the analyzed reservoirs. Although there were significant differences in the transparency of water in the particular reservoirs, the concentration of phosphorus was at similar concentration in water in all of them.

Similar to phosphorus, for reservoirs with a turbid water regime (group II) there were no significant differences between the concentration of nitrogen when compared to reservoirs with a transparent water regime (group I). This indicates that the concentration of nitrogen is not important factor responsible for maintaining a regime with turbid water in the ecosystems of MSR.

The results of this study show that the depth and area of a reservoir are important factors that determine the species composition of submerged vegetation. However, these factors did not indicate significant correlation with water transparency (*Table 5*). The results of T-test also did not indicte significant differences between the two group of reservoirs (*Table 4*). As reservoir 2 are deeper than reservoirs 3, 4 and 5, it was assumed that it would have a higher level of water transpirancy. However results show, that a clarity of water is lower in Reservoir 2 (*Table 1*). This indicate that the depth is the one of many important factors which determines water quality in mining subsidence reservoirs.

Since reservoirs with a transparent water regime were characterized by elevated concentrations of dissolved compounds and a correlations between salinity and transparency were found, it appears that it is the elevated concentration of dissolved ions that may constitute a significant factor which is responsible for maintaining a transparent water regime in these ecosystems. Increased salinity (> 1000 mg TDS l^{-1}) may directly inhibit the development of phytoplankton (Raclavská et al., 2003; Redden and Rukminasari, 2008; Flöder et al., 2010; Belovsky et al., 2011). A concentration of dissolved solids exceeding 200 mg·l^{-1} may lead to an increase in water transparency by reducing the concentration of undissolved solids (Oliver et al., 1999; Nielsen and Hillman, 2000). Calcium and magnesium ions, in particular, coagulate with other particles in a column of water, and leads to their sedimentation. Nevertheless, the Bartosuvka reservoir (Reservior 2) was characterized by one of the lowest SD values (<1 m) despite high concentrations of dissolved compounds (542-790.00 mg l^{-1}). This indicates that increased salinity is not the solitary mechanism that impacts the improvement of water quality of mining subsidence reservoirs.

A regime with transparent water was maintained in all the reservoirs where the littoral zone was characterized by a significant average percentage covers usually much higher than 25% of aquatic vegetation. The percentage cover of submerged vegetation has a positive correlation with water transparency. This substantiates of results research Schefer (1998), Moss (1998, 2007) and Hejzlar (2006), that aquatic vegetation play an essential role as necessary element in maintaining a transparent water regime in freshwater ecosystems.

Tested reservoirs varied in their concentrations of both total phosphorus and nitrogen. The results appear to support the assumptions of the theory of alternative stable states, which claims that a transparent water regime may remain stable under a wide range of physico-chemical parameters since particular regimes remain constant as a result of complex bio-physico-chemical interactions that taking place in the ecosystem (Moss, 1998; Scheffer et al., 2003; Rameshkumar et al., 2019). Appropriate explanation of those interactions requires further detailed research, however, on the basis of the obtained results it may be assumed that the percentage cover of submerged vegetation is

http://www.aloki.hu ● ISSN 1589 1623 (Print) ● ISSN 1785 0037 (Online)
DOI: http://dx.doi.org/10.15666/aeer/1804_56615672

important factors responsible for maintaining a regime with transparent water in the ecosystems of mining subsidence reservoirs. The increased salinity of the water of such reservoirs does not limited the submerged vegetation from developing. TDS may cause susceptible species to retreat (Hart et al., 1991; Metzeling et al., 1995; Bailey, 1998; Bailey and James, 2000).

Presented results support the assumed hypothesis about the positive effect of submerged vegetation on the quality of water in subsidence reservoirs. Simultaneously this study show possibility the use of reclamation methods based on supporting the development of submerged vegetation in anthropogenic water reservoirs to increase the environmental and utility potential of such objects is validated by this research.

Results of presented research was obtained a few years ago, but did not lose their science value and are the complementary in the related field in investigation of the role submerged vegetation functioning in anthropogenic mining water reservoirs. Presented results are important in post-mining areas in the aspect of their revitalization of subsidence reservoirs while this issue is not wide recognized by other authors.

Conclusions

1. Submerged vegatation were proved to have the capability to increase the clarity of water in mining subsidence reservoirs.
2. If submerged vegetation cover quarter surface area of the MSR causes higher water transparency.
3. Therefore submerged plants is a good alternative in keeping a clear waterstate in mining subsidence reservoirs as in lakes.
4. Further work requires research of mining subsidence reservoirs of various sizes, controlled introduction of sumerged vegetation with different coverage, selection of species with different functional characteristics in situ and recognition of submerged and of floating plants relationships.

Acknowledgements. This work was supported by the Ministry of Science and Higher Education, Republic of Poland (Statutory Activity of the Central Mining Institute in Katowice, Poland. Work no. 11110417-342).

REFERENCES

[1] Bachmann, R. W., Horsburgh, C. A., Hoyer, M. V., Mataraza, L. K., Canfield, D. E. (2002): Relations between trophic state indicators and plant biomass in Florida lakes. – Hydrobiologia 470: 219-34.

[2] Bailey, P. (1998): Effects of Increased Salinity on Riverine and Wetland Biota. – Project UM018. Final report, LWRRDC. Canberra.

[3] Bailey, P., James, K. (2000): Riverine and Wetland Salinity Impacts. – Assessment of R.D. Land and Water Australia. Report OP25/99. Australia.

[4] Belovsky, G. E., Stephens, D., Perschon, C., Birdsey, P., Paul, D., Naftz, D., Baskin, R., Larson, C., Mellison, C., Luft, J., Mosley, R., Mahon, H., Van Leeuwen, J., Allen, D. V. (2011): The Great Salt Lake Ecosystem (Utah, USA): long term data and a structural equation approach. – Ecosphere 2: 1-40.

[5] Canoco for Windows Version 4.1. – Biometris-Plant Research International, Wageningen, The Netherlands.

http://www.aloki.hu ● ISSN 1589 1623 (Print) ● ISSN 1785 0037 (Online)
DOI: http://dx.doi.org/10.15666/aeer/1804_56615672

[6] Cardinale, B. J. (2011): Biodiversity improves water quality through niche partitioning. – Nature 472: 86-89.
[7] Coops, H., Doef, R. W. (1996): Submerged vegetation development in two shallow, eutrophic lakes. – Hydrobiologia 340: 115-120.
[8] Flöder, S., Jaschinski, S., Wells, G., Burns, C. W. (2010): Dominance and compensatory growth in phytoplankton communities under salinity stress. – Journal of Experimental Marine Biology and Ecology 395(1-2): 223-231.
[9] Gross, E. M., Sütfeld, R. (1994): Polyphenols with algicidal activity in the submerged macrophyte *Myriophyllum spicatum* L. – Acta Hortic 381: 710-16.
[10] Grulich, V., Vydrová, A. (2006): Methodology of sampling and processing of macrophytes of still waters [Metodika odberu a zpracování vzorku makrofyt stojatých vod]. – Masaryk Water Research Institute.
[11] Hart, B. T., Bailey, P., Edwards, R., Hortle, K., James, K., McMahon, A., Meredith, C., Swadling, K. (1991): A review of the salt sensitivity of the Australian freshwater biota. – Hydrobiologia 210: 105-144.
[12] Hasler, A. D., Jones, E. (1949): Demonstration of the antagonistic action of large aquatic plants on algae and rotifers. – Ecology 30: 346-59.
[13] Hejzlar, J. (2006): The EU framework directive for water policy and water quality in reservoirs. [Rámcová směrnice vodní politiky EU a kvalita vody v nádržích]. – Vodní hospodářství 56: 190-196.
[14] Hilt, S., Gross, E. M., Hupfer, M., Morscheid, H., Mählmann, J., Melzer, A., Van de Weyer, K. (2006): Restoration of submerged vegetation in shallow eutrophic lakes–a guideline and state of the art in Germany. – Limnologica-Ecology and Management of Inland Waters 36(3): 155-171.
[15] Irfanullah, H. M., Moss, B. (2004): Factors influencing the return of submerged plants to a clear-water, shallow temperate lake. – Aquatic Botany 80(3): 177-191.
[16] Jeppesen, E., Jensen, J. P., Kristensen, P., Søndergaard, M., Mortensen, E., Sortkjær, O., Olrik, K. (1990): Fish manipulation as a lake restoration tool in shallow, eutrophic, temperate lakes 2: threshold levels, long-term stability and conclusions. – Hydrobiologia 200-201: 219-28.
[17] Kašovská, K., Pierzchała, Ł., Sierka, E., Stalmachová, B. (2014): Impact of The Salinity Gradient on The Mollusc Fauna In Flooded Mine Subsidences (Karvina, Czech Republic). – Archives of Enviromental Protection 40(1): 87-101.
[18] Kentzer, A. (2001): Phosphorus and its biologically available fractions in lake sediments of various trophies. [Fosfor i jego biologicznie dostępne frakcje w osadach jezior różnej trofii]. – Wydawnictwo UMK. Hydrobiologia. Toruń.
[19] Kosten, S., Gissell Lacerot, G., Jeppesen, E., da Motta Marques, D., van Nes, E. H., Mazzeo, N., Scheffer, M. (2009): Effects of submerged vegetation on water clarity across climates. – Ecosystems 12: 1117-1129.
[20] Lepš, J., Šmilauer, P. (2000): Multivariate analysis of ecological data [Mnohorozměrná analýza ekologických dat.]. – Biologická fakulta Jihočeské univerzity v Českých Budějovicích, České Budějovice, 102p.
[21] Li, K., He, W., Hu, Q., Gao, S. (2014): Ecological restoration of reclaimed wastewater lakes using submerged plants and zooplankton. – Water and Environment Journal 28: 323-328.
[22] Macoun, J., Šibrava, V., Tyra, J., Kneblova-Vodikova, V. (1965): Outer Subcarpathia of Moravian Gate [Kvarter Ostravska a Moravske brany]. – Ústav. Geol. Praha.
[23] Menčik, E. (1983): Geology of the Moravian-Silesian Beskids and Podbeskydská Hills [Geologie Moravskoslezkých Beskyd a Podbeskydské pahorkatny]. – ÚÚG.
[24] Metzeling, L., Doeg, T., O'Connor, W. (1995): The impact of salinisation and sedimentation on aquatic biota. – Conserving Biodiversity: Threats and Solutions: 126-136.

http://www.aloki.hu ● ISSN 1589 1623 (Print) ● ISSN 1785 0037 (Online)
DOI: http://dx.doi.org/10.15666/aeer/1804_56615672

[25] Molenda, T., Rzętała, M. A. (2001): The role of natural and anthropogenic factors in the formation of coastal zones of artificial water reservoirs [Rola naturalnych i antropogenicznych czynników w kształtowaniu się stref brzegowych sztucznych zbiorników wodnych]. – Wydział Nauk o Ziemi 29(4): 52-55.
[26] Moss, B. (1998): Shallow Lakes Biomanipulation and Eutrophication. – Scope Newsletter 29: 2-45.
[27] Moss, B. (2007): Art and science of lake restoration. – Hydrobiologia 581: 15-24.
[28] Nakamura, K., Kayaba, Y., Nishihiro, J., Takamura, N. (2008): Effects of submerged plants on water quality and biota in large-scale experimental ponds. – Landscape Ecol Eng 4: 1-9.
[29] Nielsen, D. L., Hillman, T. J. (2000): The status of research into the effects of dryland salinity on aquatic ecosystems. – A discussion paper arising from a salinity workshop in Albury, NSW, on 13th December 1999. CRCFE technical report.
[30] Oliver, R. L., Hart, B. T., Olley, J., Grace, M., Rees, C., Caitcheon, G. (1999): The Darling River: Algal Growth and the Cycling and Sources of Nutrients. – Final report to the Murray-Darling Basin Commission.
[31] Pertile, E. (2007): Hydrochemistry of watered subsidence area of Karviná [Hydrochemie zvodnělých poklesových kotlin ve vymezeném území Karvinska]. – Vysoká škola báňská - Technická univerzita Ostrava. Hornicko-geologická fakulta. Ostrava, Czech Republic.
[32] Phillips, G., Willby, N., Moss, B. (2016): Submerged macrophyte decline in shallow lakes: What have we learnt in the last forty years? – Aquatic Botany 135: 37-45.
[33] Pierzchała, Ł., Sierka, E., Trząski, L., Bondaruk, J., Czuber, B. (2016): Evaluation of the suitability of anthropogenic reservoirs in urban space for ecological restoration using submerged plants (Upper Silesia, Poland). – Applied Ecology and Environmental Research 14(1): 277-296.
[34] Plaček, V. (1984): Okres Karviná. [District Karviná]. – Ostrava: Profil.
[35] Raclavská, H., Matýsek, D., Pertile, E., Šajer, J., Soldán, P., Sviták, J. (2003): Initiation of natural ecosystems in mining impected area for revitalization of Karvina district [Iniciace přírodních ekosystémů poddolované krajiny pro proces obnovy území]. – Karvinska, MŽP VaV/640/1/01. MS VŠB-TU. 2001 – 2003. Ostrava. Czech Republic.
[36] Rameshkumar, S., Radhakrishnar, K., Aanand, S., Rajaram, R. (2019): Infuence of physicochemical water quality on aquatic macrophyte diversity in seasonal wetlands. – Applied Water Science 9: 12. https://doi.org/10.1007/s13201-018-0888-2.
[37] Redden, A. M., Rukminasari, N. (2008): Effects of increases in salinity on phytoplankton in the Broadwater of the Myall Lakes, NSW, Australia. – Hydrobiologia 608: 87. https://doi.org/10.1007/s10750-008-9376-2.
[38] Schaumburg, J., Schranz, C., Hofmann, G., Stelzer, D., Schneider, S., Schmedtje, U. (2004): Macrophytes and phytobenthos as indicators of ecological status in German lakes - a contribution to the implementation of the Water Framework Directive. – Limnologica 34(4): 302-314.
[39] Scheffer, M., Hosper, S. H., Mijer, M-L., Moss, B., Jeppesen, E. (1993): Alternative equilibria in shallow lakes. – Trends in Ecology & Evolution 8(8): 275-279.
[40] Scheffer, M. Ch. H. (1998): Ecology of Shallow Lakes. – London.
[41] Scheffer, M., Szabo, S., Gragnani, A., van Nes, E. H., Rinaldi, S., Kautsky, N., Norberg, J., Roijackers, R. M. M., Franken, R. J. M. (2003): Floating plant dominance as a stable state. – Proceedings of the National Academy of Science of the United States of America 100: 4040-4045.
[42] Schindler, D. W. (1977): Evolution of Phosphorus Limitation in Lakes. – Science 21(195): 260-262.
[43] Sierka, E., Stalmachova, B., Molenda, T., Pierzchała, Ł. (2012): Environmental and social - economic importance of subsidence reservoirs. – ISBN 978-80-7300-445-3. Praha. Czech Republic.

http://www.aloki.hu ● ISSN 1589 1623 (Print) ● ISSN 1785 0037 (Online)
DOI: http://dx.doi.org/10.15666/aeer/1804_56615672

[44] Šmilauer, P., Lepš, J. (2014): Multivariate analysis of ecological data using CANOCO 5. – Cambridge University Press; Cambridge.
[45] Stalmachová, B. (2003): Recovery strategy of mining landscape [Strategie obnovy hornické krajiny]. – Technická univerzita Ostrava, Hornicko-geologická fakulta. Ostrava.
[46] Statistica ver. 12.0. – StatSoft, Inc. USA.
[47] Strzelec, M., Spyra, A., Serafiński, W. (2010): Biology of inland waters [Biologia wód środlądowych]. – Wydawnictwo Uniwersytetu Śląskiego. Katowice.
[48] Suchowiec, T. A., Górniak, A. (2006): Seasonality of water quality of small retention reservoirs in the agricultural landscape of Podlasie region [Sezonowość jakości wody małych zbiorników retencyjnych w krajobrazie rolniczym Podlasia]. – Woda Środowisko Obszary wiejskie 2(18): 347-359.
[49] Tokarska-Guzik, B., Rostański, A. (1996): The role of post-mining floods (floodplains) in the renaturalization of the industrial landscape of Upper Silesia [Rola zatopisk (zalewisk) pogórniczych w renaturalizacji przemysłowego krajobrazu Górnego Śląska.]. – Przegląd Przyrodniczy 7(3): 267-272.
[50] Verhofstad, M. J. J. M., Alirangues Núñez, M. M., Reichman, E. P., van Donk, E., Lamers, L. P. M., Bakker, E. S. (2017): Mass development of monospecific submerged macrophyte vegetation after the restoration of shallow lakes: roles of light, sediment nutrient levels, and propagule density. – Aquat. Bot. 141: 29-38.
[51] Vitense, K., Hanson, M. A., Herwig, B. R., Zimmer, K. D., Fieberg, J. (2019): Predicting total phosphorus levels as indicators for shallow lake management. – Ecological indicators 96: 278-287.
[52] Wang, L., Han, Y., Yu, H., Fan, S., Liu, Ch. (2019): Submerged Vegetation and Water Quality Degeneration From Serious Flooding in Liangzi Lake, China. – Front Plant Sci. 10: 1504.
[53] Woźniak, G., Sierka, E., Wheeler, A. (2018): Urban and industrial habitats: how important they are for ecosystem services. – Ecosystem Services and Global Ecology.

http://www.aloki.hu ● ISSN 1589 1623 (Print) ● ISSN 1785 0037 (Online)
DOI: http://dx.doi.org/10.15666/aeer/1804_56615672

UTILIZATION OF REAL-TIME PCR METHOD FOR IDENTIFICATION OF *LISTERIA SPP*. FROM HOMEMADE WHITE CHEESE ORIGINATING FROM SOUTHEAST OF TURKEY

YIGIN, A.[1*] – KILIC ALTUN, S.[2] – DEMIRCI, M.[3] – ESER, N.[4] – YOLDAS, A.[5]

[1]*Harran University Veterinary Faculty, Department of Genetics, Şanliurfa, Turkey (e-mail: akinyigin@yahoo.com)*

[2]*Harran University Veterinary Faculty, Department of Food Hygiene and Technology, Şanliurfa, Turkey (e-mail: skilicaltun@harran.edu.tr)*

[3]*Beykent University, School of Medicine, Department of Medical Microbiology, Istanbul, Turkey (e-mail: mdemirci1979@gmail.com)*

[4]*Kahramanmaras Sutcu Imam University Medical Faculty, Department of Pharmacology, Kahramanmaraş, Turkey (e-mail: esernadire01@hotmail.com)*

[5]*Kahramanmaras Sutcu Imam University Medical Faculty, Department of Anatomy, Kahramanmaraş, Turkey (e-mail: atillayoldas99@hotmail.com)*

[*]*Corresponding author*
e-mail: vetserapaltun@hotmail.com; +90-41-4318-3000

(Received 17th Jan 2020; accepted 22nd May 2020)

Abstract. This study, aimed to investigate the utilization of the real-time PCR method for the identification of *Listeria spp*., *Listeria monocytogenes* and *Listeria innocua* contamination in homemade white cheese samples produced around the southeast districts of Turkey. 103 white cheese samples were randomly selected from the local markets for investigation. ISO 11290-1/A1-2004 method was utilized for identification of *Listeria spp.* VITEK 2 GP cards were used to the identification the *Listeria spp.* using positive samples. The DNA was isolated from cheese samples directly and real-time PCR and Sanger sequencing were used to identify of *Listeria monocytogenes* and *Listeria innocua* by using specific primers designed for the *hly* and *lin02483* genes. 6.7% of samples were identified as *Listeria spp.* positive by VITEK 2, and Quantitative real-time PCR. 5.8% of samples were contaminated with *L. monocytogenes* whereas 0.97% sample was *L. innocua* positive. The results of VITEK 2 and real-time PCR were found to be similar. These findings pointed out that these products were produced under non-hygienic conditions and have potential risk for human health. Furthermore, it was revealed that real-time PCR methods were faster and as reliable as conventional methods for cheese samples directly for the determination and identification of these microorganisms.
Keywords: *Vitek 2, ISO 11290, foodborne pathogen, molecular identification, Turkey*

Introduction

White cheese is the most widely produced kind of cheese in Turkey and is commonly produced in the eastern and south-eastern parts of Anatolia. Cow cheese production in 2018 reached to 622.292 tons in Turkey in official institutions reports (Turkish Statistical

http://www.aloki.hu ● ISSN 1589 1623 (Print) ● ISSN1785 0037 (Online)
DOI: http://dx.doi.org/10.15666/aeer/1804_56735682

Institute, 2019). As a fermented dairy product, high protein content of white cheese creates a good habitat for microorganisms. White cheese varieties may contain different amounts of microorganisms due to the quality of the milk, production technique, packaging, transportation and storage. Particularly, the consumption of cheese made of non-pasteurized milk or dairy products, the containing microorganisms may cause an epidemic or cases with sporadic disease (Zamani-Zadeh et al., 2011).

Between these microorganisms, with the zoonotic character of pathogen *Listeria spp.*, contaminated food is most likely to generate infection in humans. It is also an important pathogen for agriculture and food industry that can be detected in milk and dairy products, vegetables, fish, meat products and prepared foods (Ekici et al., 2004). *Listeria spp.* can survive in humid or dry environments, soil, plants or other living organisms for months (Carter et al., 1995). *Listeria spp.* may be easily contagioned orally, nosocomially or vertically WHO/FAO 2018. Food and water contaminated with the agent, mosquitos and ticks are crucial for the contagion (Farber et al., 1991). Following the contagion, people in the risk group, which may be listed as, pregnant women, newborns, old and immune deficient people are frequently affected by listeriosis (Slutsker and Schuchat, 1999). In severe infections, septicemia, meningitis and premature stillbirths are seen in humans whereas meningoencephalitis, abortus and mastitis present in domesticated animals (Farber et al., 1991).

Among *Listeria* species, *L. monocytogenes* and *L. innocua* are important bacteria that can be found in food. Both species can live under conditions such as environments with pH values between 4.39 and 9.4 and refrigerator conditions (Vázquez-Boland et al., 2001; Zamani-Zadeh et al., 2011). *L. monocytogenes* is a potent public health issue with a 30% mortality rate when contagioned (Lou and Yousef, 1999). On the other hand, *L. innocua* is rarely associated with a disease yet commonly found during identification. Recent studies showed that in analyses conducted using the VITEK 2 system, *L innocua* may be mistaken for *L. monocytogenes* (De Lappe et al., 2014). This finding calls attention to other methods that seem to be required for confirmation of the results.

The aim of this study is to evaluate the use of the real-time PCR (Polymerase Chain Reaction) method from cheese samples directly, faster and as reliable as compared to conventional methods to identificate *L. monocytogenes* and *L. innocua* and also to find the prevalence of *Listeria spp*. *L. monocytogenes* and *L. innocua* by studying the white cheese samples collected from various local town bazaars from Şanlıurfa, Mardin, Gaziantep and Diyarbakır and demonstrate hygienic qualities of these products and the possible public health risks they constitute in this region.

Material and methods

In this study, 103 different fresh homemade white cheese samples collected from local town bazaars of the cities Şanlıurfa, Mardin, Gaziantep and Diyarbakır, were investigated. Samples were collected under aseptic conditions of the local bazaars as 200 gr each. They were brought to the Department of Food Hygiene and Technologies laboratories, Harran University in cold chain, and analyses were started the very same day. The classical microbiological analyses and VITEK 2 studies were conducted by Harran University, Food Hygiene and Technologies Department Laboratory. The DNA isolations of the positive samples in Harran University, veterinary genetics laboratory and the real-time PCR analyses of the positive sample DNAs in Medical Microbiology

http://www.aloki.hu ● ISSN 1589 1623 (Print) ● ISSN1785 0037 (Online)
DOI: http://dx.doi.org/10.15666/aeer/1804_56735682

Laboratories, Beykent University, Medical Faculty, in order to determine the molecular identifications.

Detection of Listeria spp. with conventional methods

The ISO (International Organization for Standardization) 11290-1/A1-2004 method was used for *Listeria spp.* detection following the stated protocol ISO (2004). Samples were weighed as 25 gr each with a precision balance (Cubis; Sartorius, Bohemia, NY, USA) under sterile conditions and the samples were transferred to sterile stomacher bags with an addition of 225 ml of Enrichment Broth (M863+SR142; Oxoid Ltd, Basingstoke, UK). Samples were homogenized in a stomacher (Laboratory Blender Stomacher 400; Seward, London, UK) for 2 minutes and incubated in a 30°C aerobic environment for 24 hours. Afterwards, 0.1 mL of the homogenates were added to 10 ml of a Fraiser Broth (CM895+SR156; Oxoid Ltd, Basingstoke, UK). Following incubation at 30°C for 24 hours, 0.1 mL of homogenate was taken from the Fraiser Broth and were cultivated into PALCAM Agar (CM 877+SR150; Oxoid Ltd, Basingstoke, UK) and Oxford Agar'a (CM 856+SR140; Oxoid Ltd, Basingstoke, UK). Mediums were incubated at 30°C under anaerobic conditions for 48 hours. Five colonies from any petri with a suspicion of *Listeria spp.* growth were transferred to Tryptic Soy Agar-Yeast Extract (TSA-YE, 0370; Difco, Toronto, ON) and incubated at 30°C for 24 hours for purification.

Detection of Listeria spp. By using VITEK 2

The purity of the isolated suspicious colonies was controlled with Gram staining. Also, oxidase, catalase, beta hemolysis, mannitol, rhamnose, xylose, salicin, dulcite, methyl red, Voges-Proskauer, nitrate reduction and CAMP tests were applied. All colonies added at 3 mL sterile saline solution with sterile swabs in polystyrene test tube to made homogenous 0.5 McFarland turbidity standart suspension using with Vitek 2 DensiCHEK instrument. Then the suspension tube and VITEK 2 GP card (Biomerieux, Marcy l'Etoile, France) placed in the cassette. After that the cassette loaded on Vitek 2 Systems (Biomerieux, Marcy l'Etoile, France) following the manufacturer's guidelines.

The strains, ATCC 15313 for *Listeria monocytogenes* and ATCC 33090 for *Listeria innocua* were used as positive controls.

DNA isolation

The 25 gr each cheese samples were transferred to sterile stomacher bags with 0.5 mL DNase & RNase free water. Samples were homogenized in a stomacher (Laboratory Blender Stomacher 400; Seward, London, UK) for 2 minutes and 200 µL of aqueous phase were transferred to a new 1.5 mL sterile micro centrifuge tube. After that, 400 mL of lysis buffer (0.5% N-lauryl sarcosine, 50 Mm Tris-Cl, 25 mM EDTA, pH 8.0) was added to the mixture, vortexed well and centrifuged 15.000 rpm for 5 min. The pellet was resuspended with 200 µL lysis buffer and 4 µL proteinase K, vortexed well and then incubated for 1 h at 37ºC, 300 µL of NaI solution (6 M NaI in 50 mM Tris-Cl, 25 mM EDTA, pH 8.0) and 500 µL isopropanol were added to the suspension and then centrifuged at 15.000 rpm for 5 min. The pellet was washed with 35% isopropanol, dried and then suspended in 50 µL DNase & RNase free sterile water. Isolated DNA samples were stored at -20°C until the real time PCR application (Sheela and Shrinithivihahshini, 2017; Moravkova, 2017).

http://www.aloki.hu ● ISSN 1589 1623 (Print) ● ISSN1785 0037 (Online)
DOI: http://dx.doi.org/10.15666/aeer/1804_56735682

Identification of L. monofcytogenes and L. innocua with the real-time PCR method

Following the nucleic acid isolations were performed from all cheese samples directly, the *hly* region for *L. monocytogenes* and *lin02483* region for *L. innocua* were amplified two times with real-time PCR for each sample.

The real time PCR procedure was performed using the Light Cycler 480 II (Roche Diagnostics GmbH, Mannheim, Germany) system with Light Cycler 480 Probe Master (Roche Diagnostics GmbH, Mannheim, Germany) kit. The primers and probes used for the *hly* and *lin02483* regions according to the manufacturer's guide are shown in *Table 1* (Rodríguez-Lázaro et al., 2004; Benito et al., 2017). To performed quantification, plasmid standarts with known concentrations were purchased from Bioeksen Ltd, Istanbul.

Table 1. *The primer and probe sets used in real time PCR analyses for L. monocytogenes and L. innocua identification*

***L. monocytogenes* (hly)**		**Ref.**
hlyQFa (Forward primer)	5-CAT GGC ACC ACC AGC ATC T-3	Rodríguez-Lázaro et al., 2004
hlyQRa (Reverse primer)	5-ATC CGC GTG TTT CTT TTC GA-3	
hlyQP (TaqMan probe)	5-FAM-CGC CTG CAA GTC CTA AGA CGC CA-TAMRA-3	
***L. innocua* (lin02483)**		
lipHQFa (Forward primer)	5-AAC CGG GCC GCT TAT GA-3	
lipHQRa (Reverse primer)	5-CGA ACG CAA TTG GTC ACG-3	
lipHQP (TaqMan probe)	5-FAM-TTC GAA TTG CTA GCG GCA CAC CAG T-TAMRA-3	

5 µl of isolated DNA (50 ng/µl) were added to each real time PCR reactions, making the final volume 20 µl. The real time PCR protocol used was; following the 10 min denaturation in 95°C, 45 cycles of 10 sec in 95°C, 60 sec in 62°C for a single read. The positive controls ATCC 15313 for *L. monocytogenes* and ATCC 33090 for *L. innocua* were included to all Real-time PCR experiments.

Sanger sequencing of hly and iapgene

To the confirmation of real-time PCR results, *L. monocytogenes* and *L. innocua* positive 7 samples were done Sanger sequencing using the specific primers for *hly* and *iap* genes based on Rodríguez-Lázaro et al. study in 2004, Sanger sequence were performed with the ABI 3130XL sequencing instrument (*Table 2*). The sequencer fasta files were aligned using the BLAST program against the known ones in the GenBank database of the National Centre for Biotechnology Information (NCBI, http://www.ncbi.nlm.nih.gov/).

Table 2. *Distribution of the Listeria monocytogenes identification results for VİTEK 2 GP card and "hly" Real Time PCR analysis*

Listeria monocytogenes	**VITEK 2 GP card (n)**	**Hly Real Time PCR analysis (n)**
Positive	6	6
Negative	97	97

http://www.aloki.hu ● ISSN 1589 1623 (Print) ● ISSN1785 0037 (Online)
DOI: http://dx.doi.org/10.15666/aeer/1804_56735682

Results

From 103 fresh cheese samples, 7 (6,8%) samples were found *Listeria spp.* positive using the conventional culturing method (*Table 3*). All *Listeria spp.* isolates gave Gram positive, oxidase negative and catalase positive reactions. *Figure 1* shows the *Listeria spp.* positive colonies on Oxford agar.

Table 3. *Distribution of Listeria spp. positive samples*

City	Number of samples collected (n)	*Listeria* spp. Positive (%)
Şanlıurfa	27	3 (2.91%)
Mardin	26	1 (0.97%)
Gaziantep	25	2 (1.94%)
Diyarbakır	25	1 (0.97%)
Total	103	7 (6.80%)

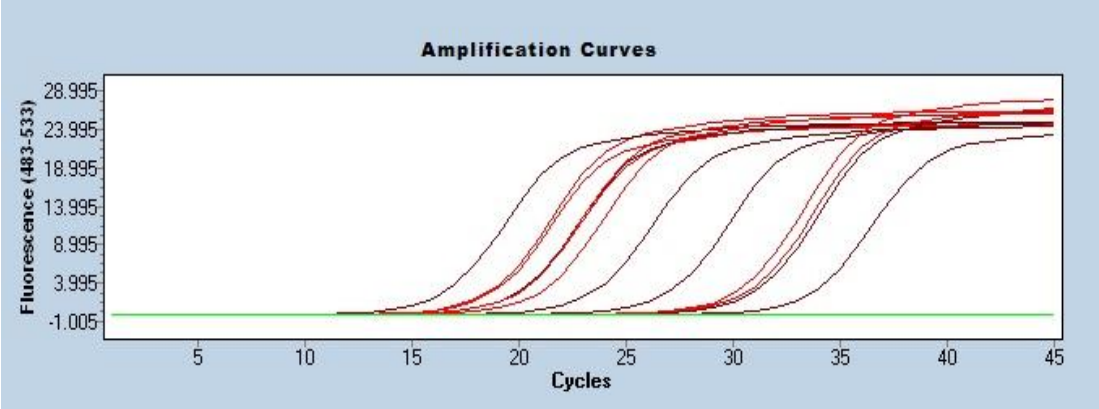

Figure 1. *Amplification curves of Real-time PCR experiments for positive samples, negative samples and standards (Red: positive samples, Brown: Standarts, Green: Negative Samples)*

Listeria spp. positive colonies were identified as *L. monocytogenes* or *L. innocua* with a 99% possibility by the VITEK 2 system GP card. The analysis on VITEK 2 system took 8.25 hours.

After DNA extraction from cheese samples directly, real-time PCR was perfomedby the amplification of the *hly* and *lin02483* regions to the detect *L. monocytogenes* or *L. innocua*, respectively. Results are shown in *Table 2* and *Table 4* for *L. monocytogenes* and *L. innocua*, respectively. The real time PCR procedure after isolation took an hour and 20 minutes on the Light Cycler 480 II system. Amplification curves of real-time PCR experiments for positive samples, negative samples and standarts are shown in *Figure 1* for *L. monocytogenes* and *L. innocua*, respectively. The results of VITEK 2 and real-time PCR were found the same at this study. All real-time PCR results were also confirmed by Sanger sequencing alignment results. *Table 5* showed that the quantification results of positive cheese samples. Although the existence of all positive samples is not suitable for human consumption, the quantitative amounts were examined considering that the situation that will make a difference may be due to quantitation with VITEK 2 System but no difference was found.

http://www.aloki.hu ● ISSN 1589 1623 (Print) ● ISSN1785 0037 (Online)
DOI: http://dx.doi.org/10.15666/aeer/1804_56735682

Table 4. *Distribution of the Listeria innocua identification results for VİTEK 2 GP card and "lin02483" Real Time PCR analysis*

Listeria innocua	VITEK 2 GP card (n)	Lin02483 Real Time PCR analysis (n)
Positive	1	1
Negative	102	102

Table 5. *Quantification results of positive cheese samples via Real-time PCR*

Name	Cp	Calculated Concentration	Known Concentration	Strain
1	17.14	5.14E+04		*L. monocytogenes*
2	18.28	2.46E+04		*L. innocua*
3	18.26	2.50E+04		*L. monocytogenes*
4	19.66	1.01E+04		*L. monocytogenes*
5	19.66	1.01E+04		*L. monocytogenes*
6	19.7	9.85E+03		*L. monocytogenes*
7	20.7	5.19E+03		*L. monocytogenes*
Standard 1	16.06	1.03E+05	100000	
Standard 2	19.6	1.05E+04	10000	
Standard 3	23	1.17E+03	1000	
Standard 4	26.61	1.14E+02	100	
Standard 5	30.69	8.23E+00	10	
Standard 6	33.25	1.41E+00	1	

Discussion

Although cow milk is commonly used for white cheese production, sheep and goat milk also has its place in production in the region. The production of white cheese sold in the local bazaars is generally done by traditional ways in family businesses, but hygienic conditions are not fully provided. Especially, the white cheese produced in Şanlıurfa, following the milking, milk is yeasted in milking temperature and strained with a thin cloth called 'parzın' to give its final shape. White cheeses are presented for consumption without any salt and no pasteurization is applied before production. Lack of pasteurization increases the risk of zoonotic foodborne pathogen contamination in dairy products. For this reason, in this study, the entity of *Listeria spp.*, an important pathogen of fresh white cheese, was investigated in fresh white cheese samples collected from local town bazaars of the region. The Turkish Food Codex regulations on Microbiological Criteria states that the existence of *L. monocytogenes* in a 25 gr cheese sample is not suitable for consumption (Turkish Food Codex, 2011). According to the regulations, 7 of 103 cheese samples studied are found to be not suitable for consumption.

As a result of this study, 7 (6.8%) of the fresh cheese samples were found to be *Listeria spp.* positive with 6 of the isolates were identified as *L. monocytogenes* and one as *L. innocua* using real-time PCR and VITEK 2 system.

When the national studies conducted on *Listeria spp.* (*L. monocytogenes* and *L. innocua)* existence in our country were investigated, no real time PCR based method is used but by the use of conventional methods statistical studies are conducted in various cities of Turkey (*Table 6*) (Kara et al., 1999; Vural et al., 2010).

http://www.aloki.hu ● ISSN 1589 1623 (Print) ● ISSN1785 0037 (Online)
DOI: http://dx.doi.org/10.15666/aeer/1804_56735682

Table 6. *Listeria spp., L. monocytogenes and L. innocua ratios in cheese determined using the classical methods*

Researcher	City	N	*Listeria* spp.	*L. monocytogenes*	*L. innocua*
Kara et al. (1999)	Erzurum	50	4 (8%)		
Sağun et al. (2001)	Van	254	13 (5.11%)	10 (3.93%)	1 (0.39%)
Gülmez and Güven (2001)	Kars	80	6 (7.5%)		
Uysal and Ang (2003)	Istanbul	275		11 (4%)	
Aygün and Pehlivanlar (2005)	Antakya	85	7 (8,23%)	2 (2,35%)	3 (3,52%)
Akkaya and Alişarlı (2006)	Afyon	100		6 (6%)	
Arslan and Özdemir (2007)	Bolu	142	47 (33.1%)	13 (9.2%)	13 (9.2%)
Azak (2012)	Erzincan	100	3 (3%)	3 (3%)	

Although national studies were not conducted using real time PCR, the ratios found are similar to other findings, with exclusion of Arslan and Özdemir (2007). Thus, it can be said that our findings are compatible with other studies conducted.

Otherwise; Dümen et al. (2011) were investigated 700 milk and dairy product samples by classical and molecular microbiological methods. 20 samples of 700 were positive as *L. monocytogenesis.* PCR results were same with classical microbiological methods. The positivity rates obtained in our study were found to be higher than Dümen's study ratio (Dümen et al., 2011).

Once international publications are taken into account, molecular and real time PCR based studies appear on identification of *Listeria spp*, *L. monocytogenes* and *L. innocua* (El-Marrakchi et al., 1993; Rossmanith et al., 2010). El-Marrakchi et al. (1993) conducted a study in Algeria and they reported *L. monocytogenes* in 1 (4.54%) of 22 fresh cheese samples. In addition, Silva et al. (2003) study, where they searched for *L. monocytogenes* in the critical checkpoints in Brazil for minas cheese production. They investigated 218 samples comprising 54 food, 107 equipment, 22 worker and 35 environmental samples and reported 13 *Listeria spp.* positive cases. Nine of the samples were identified as *L. innocua*, 2 *L. grayi* and 2 *L. monocytogenes* by Silva et al. (2003). Also, in a study where Hein et al. (2001) used the real-time PCR method for identifying *Listeria spp.* in milk, they looked for 42 *L. monocytogenes* and 33 *L. innocua* strains and showed that real-time PCR method is safe and highly reliable.

On the other hand, De Lappe et al. (2014) did a VITEK 2 system based study and reported that this method is highly reliable yet may not identify *L. monocytogenes* and *L. innocua* correctly. In our study we compared the VITEK 2 system and real-time PCR method and found no differences in their ability to identify *L. monocytogenes* and *L. innocua*. In contrary, De Lappe et al. (2014) study underlined the need of a faster and more reliable method for detection of *L. monocytogenes* that an important foodborne pathogen for human health. Regarding international publications, real time PCR method is stated as a faster and as reliable as others for *Listeria spp. L. monocytogenes* and *L. innocua* identification when compared to the conventional ISO methods (Rossmanith et al., 2010; Gianfranceschi et al., 2014).

Sallen et al. (1996) 23S rRNA and 16S rRNA regions using the primer and amplicons used for all of the *Listeria* species were analysed. However, 23S rRNA was recommended for *L. innocua* and *L. monocytogenes*, and 16S rRNA was not distinctive. Czajka et al. (1993) 16S rRNA genes (16S rDNA) of *L. innocua* and *L. monocytogenes* species were detected by using sequence analysis. Chen et al. (2017) in the cheese-borne listeriosis

http://www.aloki.hu ● ISSN 1589 1623 (Print) ● ISSN1785 0037 (Online)
DOI: http://dx.doi.org/10.15666/aeer/1804_56735682

outbreak, Schmitz-Esser et al. (2015), Lassen et al. in 2016, Salazar et al. (2018), in the outbreaks of soft cheese, *L. monocytogenes* serotypes and similar strains to determine the SNP 's made by sequence analysis. For *L. innocua*, Facinelli et al. (1993) identified strains of tetracycline in 12 strains in mozarella by DNA sequencing. Buchrieser et al. (2003) compared the genes related to the development and pathogenicity of these two *Listeria* species, which are food pathogens, with *Staphylococcus* and *Bacillus* sequence analysis. In our study, 6 *L. monocytogenes* and 1 *L. innocua* specimens which we found positive were detected by sequence analysis and confirmed.

Conclusions

Finally, our findings showed that the cheese produced in Turkey and presented for consumption is not *Listeria spp.* and *L. monocytogenes* free. The raw milk used in white cheese production without any pasteurization or heat treatment and non-hygienic production and storage conditions may be the cause of the lack of hygiene in these products. Moreover, our findings showed that the real-time PCR method is faster and as reliable as others compared to the conventional methods and can be easily applied in laboratories with experience in molecular techniques. Comprehensive studies should be conducted to identify different *Listeria spp.* by collecting much more cheese and milk samples to protect public health.

REFERENCES

[1] Akkaya, L., Alişarlı, M. (2006): An Investigation on the Presence of *Listeria monocytogenes* and *Salmonella* spp. in Retail Cheeses Consumed in Afyonkarahisar Province, Turkey. – Van Vet. J. 17: 87-91.

[2] Arslan, S., Özdemir, F. (2007): Prevalence and antimicrobial resistance of *Listeria* spp. in homemade white cheese. – Food Control 19: 360-363.

[3] Aygün, O., Pehlivanlar, S. (2005): *Listeria* spp. in the raw milk and dairy products in Antakya Turkey. – Food Control 17: 676-679.

[4] Azak, M. G., Kılıç, H., Hızlısoy, H., Abay, S. (2012): Isolation and Identification of *Listeria* spp. from Tulum Cheese of Erzincan City. – J. Fac. Vet. Med. Univ. Erciyes 9: 149-156.

[5] Benito, S., López, A., Lizana, X., Lope, S., Carbó, R., Del Valle, L. J., Piqué, N. (2017): Presence of *Listeria monocytogenes* in Prepared Foods: Analysis of Influencing Factors. – Journal of Food Processing and Preservation 41(2): e12842.

[6] Buchrieser, C., Rusniok, C., Kunst, F., Cossart, P., Glaser, P., Listeria Consortium (2003): Comparison of the genome sequences of *Listeria monocytogenes* and *Listeria innocua*: clues for evolution and pathogenicity. – FEMS Immunol. Med. Microbiol. 35(3): 207-213.

[7] Carter, G., Chengappa, M. M., Roberts, A. W. (1995): Essentials of Veterinary Microbiology. – USA, Willams and Wilkins.

[8] Chen, Y., Luo, Y., Carleton, H., Timme, R., Melka, D., Muruvanda, T., Fritzinger, A. (2017): Whole genome and core genome multilocus sequence typing and single nucleotide polymorphism analyses of *Listeria monocytogenes* isolates associated with an outbreak linked to cheese, United States 2013. – Appl. Environ. Microbiol. 83: e00633-17.

[9] Czajka, J., Bsat, N., Piani, M., Russ, W., Sultana, K., Wiedmann, M., Batt, C. A. (1993): Differentiation of *Listeria monocytogenes* and *Listeria innocua* by 16S rRNA genes and intraspecies discrimination of *Listeria monocytogenes* strains by random amplified polymorphic DNA polymorphisms. – Appl. Environ. Microbiol. 59: 304-308.

http://www.aloki.hu ● ISSN 1589 1623 (Print) ● ISSN1785 0037 (Online)
DOI: http://dx.doi.org/10.15666/aeer/1804_56735682

[10] De Lappe, N., Lee, C., O'Connor, J., Cormican, M. (2014): Misidentification of *Listeria monocytogenes* by the VITEK 2 System. – J Clin Microbiology 52: 3494-5.
[11] Dümen, E., Issa, G., İkiz, S., Bağcıgil, F., Özgür, Y., Kahraman, T., Ergin, S., Yeşil, O. (2011): Determining Existance and Antibiotic Susceptibility Status of Listeria monocytogenes Isolated from Dairy Products, Serological and Moleculer Typing of the Isolates. – Kafkas Univ. Vet. Fak. Derg. 17: 111-119.
[12] Ekici, K., İşleyici, Ö., Sağun, E. (2004): The Existence of *Listeria monocytogenes* in Milk and Milk Products. – Van Vet. J. 15: 97-101.
[13] El-Marrakchi, A., Hamama, A., Othmani, F. (1993): Occurrence of *L. monocytogenes* in milk and dairy products produced or imported into Morocco. – J. Food Prot. 56: 256-259.
[14] Facinelli, B., Roberts, M. C., Giovanetti, E., Casolari, C., Fabio, U., Varaldo, P. E. (1993): Geneticbasis of tetracyclineresistance in food-borne isolates of *Listeria innocua*. – Appl. Environ. Microbiol. 59: 614-616.
[15] Farber, J. M., Daley, E., Coates, F. (1991): Feeding trials of *Listeria monocytogenes* with a nonhuman primate model. – J. Clin. Microbiol. 29: 2606-2608.
[16] Gianfranceschi, M. V., Rodriguez-Lazaro, D., Hernandez, M., González-García, P., Comin, D., Gattuso, A., Delibato, E., Sonnessa, M., Pasquali, F., Prencipe, V., Sreter-Lancz, Z., Saiz-Abajo, M. J., Pèrez-De-Juan, J., Butrón, J., Kozačinski, L., Tomic, D. H., Zdolec, N., Johannessen, G. S., Jakočiūnė, D., Olsen, J. E., De Santis, P., Lovari, S., Bertasi, B., Pavoni, E., Paiusco, A., De Cesare, A., Manfreda, G., De Medici, D. (2014): European validation of a real-time PCR-based method for detection of *Listeria monocytogenes* in soft cheese. – Int. J. Food Microbiol. 184: 128-133.
[17] Gülmez, M., Güven, A. (2001): Investigation of *Campylobacter*, *Salmonella* and *Listeria* spp. from Turkish white and Çeçil Cheese. – Kafkas Üniv. Vet. Fak. Derg. 7: 155-161.
[18] Hein, I., Klein, D., Lehner, A., Bubert, A., Brandl, E., Wagner, M. (2001): Detection and quantification of the iap gene of *Listeria monocytogenes* and *Listeria innocua* by a new real-time quantitative PCR assay. – Res. Microbiol. 152: 37-46.
[19] ISO (International Organization for Standardization) (2004): Microbiology of Food and animal Feeding Stuffs e Horizontal Method for the Detection and Enumeration of *Listeria monocytogenes* e Part 1: Detection Method. Amendment 1: Modification of the Isolation media and the Haemolysis Test, and Inclusion of Precision Data. – ISO 11290-1: 1996/Amd 1. Geneva, Switzerland.
[20] Kara, A., Algur, Ö. F., Kaya, M. (1999): Investigation on the Isolation and Identification of the *Listeria* Species in the White and Civil Cheeses Purchased From Erzurum Region. – Tr. J. of Biol. 23: 331-337.
[21] Lassen, S. G., Ethelberg, S., Björkman, J. T., Jensen, T., Sørensen, G., Jensen, A. K., Mølbak, K. (2016): Two *Listeria* outbreaks caused by smoked fish consumption-using whole-genome sequencing for outbreak investigations. – Clin. Microbiol. Infect. 22: 620-624.
[22] Lou, Y., Yousef, A. E. (1999): Characteristics of *Listeria monocytogenes* important to food processors. – Foodborne Pathogens: 131-224.
[23] Moravkova, M., Verbikova, V., Michna, V., Babak, V., Cahlikova, H., Karpiskova, R., Kralik, P. (2017): Detection and Quantification of *Listeria monocytogenes* in Ready-to-eat Vegetables, Frozen Vegetables and Sprouts Examined by Culture Methods and Real-time PCR. – Journal of Food and Nutrition Research 5: 832-837.
[24] Rodríguez-Lázaro, D., Hernández, M., Scortti, M., Esteve, T., Vázquez-Boland, J. A., Pla, M. (2004): Quantitative Detection of *Listeria monocytogenes* and *Listeria innocua*by Real-Time PCR: Assessment of hly, iapand lin02483 Targets and AmpliFluor Technology. – Appl. Environ. Microbiol. 70: 1366-1377.
[25] Rossmanith, P., Mester, P., Wagner, M., Schoder, D. (2010): Demonstration of the effective performance of a combined enrichment/real-time PCR method targeting the prfA gene of *Listeria monocytogenes* by testing fresh naturally contaminated acid curd cheese. – Lett. Appl. Microbiol. 51: 480-484.

http://www.aloki.hu ● ISSN 1589 1623 (Print) ● ISSN1785 0037 (Online)
DOI: http://dx.doi.org/10.15666/aeer/1804_56735682

[26] Sağun, E., Sancak, Y. C., İşleyici, Ö., Ekici, K. (2001): The Presence and Prevalence of Listeria Species in Milk and Herby Cheese in and Around. – Van Turk. J. Vet. Anim. Sci. 25: 15-19.
[27] Salazar, J. K., Gonsalves, L. J., Schill, K. M., Leon, M. S., Anderson, N., Keller, S. E. (2018): Complete Genome Sequence of *Listeria monocytogenes* DFPST0073, Isolated from Imported Mexican Soft Cheese. – Genome Announc. 6: e00496-18.
[28] Sallen, B., Rajoharison, A., Desvarenne, S., Quinn, F., Mabilat, C. (1996): Comparative analysis of 16S and 23S rRNA sequences of *Listeria* species. – Int. J. Syst. Evol. Microbiol. 46: 669-674.
[29] Schmitz-Esser, S., Müller, A., Stessl, B., Wagner, M. (2015): Genomes of sequence type 121 *Listeria monocytogenes* strains harbor highly conserved plasmids and prophages. – Frontiers in Microbiol. 6: 380.
[30] Sheela, M. M., Shrinithivihahshini, N. D. (2017): Pervasiveness of *Listeria monocytogenes* in milk and dairy products. – J Food Microbiol Saf Hyg 2: 2476-2059.
[31] Silva, I. M. M., Almeida, R. C. C., Alves, M. A. O., Almeida, P. F. (2003): Occurrence of *Listeria* spp. in critical control points and the environment of minas frescal cheese processing. – Int. J. Food Microbiol. 81(3): 241-248.
[32] Slutsker, L., Schuchat, A. (1999): Listeriosis in humans. – In: Ryser, E. T., Marth, E. H. (eds.) Listeria, Listeriosis, and Food Safety. Marcel Dekker, Inc., pp.75-95.
[33] Turkish Food Codex. (2011): Regulation on Microbiological Criteria. – Authorization Law: 5996. Official Gazette: 28157.
[34] Turkish Statistical Institute. (TUİK) (2019): Production of Milk and Dairy Products. – http://www.tuik.gov.tr/PreHaberBultenleri.do?id=18717.
[35] Uysal, H. K., Ang, Ö. (2003): *Listeria* Species Isolated from Milk and Dairy Products. – Turk Mikrobiol. Cem. Derg. 33: 163-169.
[36] Vázquez-Boland, J. A., Kuhn, M., Berche, P., Chakraborty, T., Dominguez-Bernal, G., Goebel, W., González-Zorn, B., Wehland, J., Kreft, J. (2001): *Listeria* Pathogenesis and Molecular Virulence Determinants. – Clin. Microbiol. Rev. 14: 584-640.
[37] Vural, A., Erkan, M., Güran, H. Ş. (2010): The Examination of the Microbiologic Quality in Örgü Cheese (Braided Cheese) Samples. – Kafkas Univ. Vet. Fak. Derg. 4: 53-58.
[38] WHO/FAO (2018): Risk assessment of *Listeria monocytogenes* in ready-to-eat foods, Interpretative Summary. – Microbiological risk assesment series 4: 1-78. http://seafood.oregonstate.edu/.
[39] Zamani-Zadeh, M., Sheikh-Zeinoddin, M., Soleimanian-Zad, S. (2011): Prevalence and Characterization of *Listeria* Species in Domestic and Industrial Cheeses of Isfahan Region. – Iran J. Public Health 40: 98-104.

http://www.aloki.hu ● ISSN 1589 1623 (Print) ● ISSN1785 0037 (Online)
DOI: http://dx.doi.org/10.15666/aeer/1804_56735682

ACCUMULATION AND PARTITION OF DRY MASS AND NITROGEN IN THREE MAIZE (*Zea mays* L.) HYBRIDS GROWN UNDER FIVE PLANTING DENSITIES

LIU, J.[1,2] – YUAN, J.[2] – CAI, H.[2] – REN, J.[2] – LIANG, Y.[2] – HOU, W.[1*] – CHEN, G.[1*]

[1]*College of Resources and Environmental Sciences, Jilin Agricultural University Changchun 130118, China*

[2]*Institute of Agricultural Resource and Environment, Jilin Academy of Agricultural Sciences, Key Laboratory of Plant Nutrition and Agro-Environment in Northeast Region MOA, Changchun 130033, China*

[*]*Corresponding author*
e-mail: wenfenghou@163.com

(Received 19th Jan 2020; accepted 2nd Jul 2020)

Abstract. Following the development of hybrid maize (*Zea mays* L.) breeding technologies and advanced agricultural strategies, we postulated that maize grain yield and nitrogen (N) uptake and utilization could be further improved by selecting appropriate hybrids and identifying optimum planting densities. Five field experiments were conducted in 2013, 2014 and 2015 in Jilin Province, China. Our orthogonal design demonstrated significant interactive effects of maize hybrid and planting density on grain yield. The optimum planting densities, i.e., those associated with the best grain yields for hybrids ZD958, XY335 and LM33, were 74.0-81.4, 74.3-79.1, and 78.6-89.7 × 10^3 ha^{-1}, respectively, across 3 years and two sites. Increased planting density had a significant inhibitory effect on the leaf growth and development of individual plants, but this was offset by positive effects at the population level: increased planting density significantly increased the population leaf area index. Increased planting density improved dry mass and total aboveground N uptake (TNU), and promoted dry mass and N remobilization in stalks and leaves.
Keywords: *leaf area index, interaction effects, remobilization rate, nitrogen uptake, nitrogen utilization*

Introduction

Maize (*Zea mays* L.), rice (*Oryza sativa* L.) and wheat (*Triticum aestivum* L.) are the three main staple grain crops grown in China (Ma et al., 2009). Maize accounted for 43.6% of the total planted area and 42.8% of the total grain yield across these three crops in 2018 (National Bureau of Statistics, 2018). The Northeast China Plain is the major maize growing area in the country. Maize grown in Heilongjiang, Jilin and Liaoning Provinces constituted 31.5% of the total planted area and accounted for 32.8% of the grain yield (National Bureau of Statistics, 2018). Maize is an important component of the human diet, and is also used for animal feed, forage, biomass fuel, etc. (Diós et al., 2009; Chen et al., 2011; Grassini and Cassman, 2012). The grain yield of maize in the last two decades was 25% higher than over the previous 50 years; the increase has resulted from developments in breeding technology and agricultural practices (Duvick, 2005; Ciampitti and Vyn, 2012). Chen et al. (2013a) also reported that developments in breeding technology in the past 40 years have significantly increased maize yield. Half of the dry mass of a maize plant at maturity is formed after the silking stage (Tollenaar et al., 2004; Lee and Tollenaar, 2007). Chen et al. (2014) reported that almost all the grain yield at maturity is attributable to photosynthetic production after the silking stage. Leaves are the major photosynthetic organs for dry mass production in maize. Among other variables, genetic hybrids selection and plant N

http://www.aloki.hu ● ISSN 1589 1623 (Print) ● ISSN1785 0037 (Online)
DOI: http://dx.doi.org/10.15666/aeer/1804_56835699

availability are important factors influencing maize grain yield (Chen et al., 2015). With the development of modern breeding technology, new maize hybrids usually have extended periods of photosynthetic production, larger leaf area indices, delayed leaf senescence and elevated dry mass production rates (Borrell et al., 2001; Duvick, 2005; Echarte et al., 2008). The remobilization of vegetative N and N uptake after the silking stage also contributes to grain N accumulation. However, it is difficult to achieve a balance between the remobilization of vegetative N and N uptake after the silking stage, because increased leaf N remobilization decreases dry mass production after the silking stage. The choice of maize hybrids significantly affects the immobilization of leaf N, and N uptake, after the silking stage (Coque and Gallais, 2007; Ciampitti and Vyn, 2012). Modern breeding technology has produced the widely cultivated leaf-stay-green hybrids, which are generally grown under high N inputs on fertile soils (Bertin and Gallais, 2000). Compared to older hybrids, modern stay-green hybrids typically have higher N uptake after the silking stage, and a lower N remobilization rate (He et al., 2004; Pommel et al., 2006; Ciampitti and Vyn, 2012).

Yield is strongly related to hybrids, but changes in other agricultural factors, such as planting density, also affect yield responses. The production of biomass depends on photosynthesis at the whole plant level rather at the single leaf level. Therefore, increasing photosynthesis through increasing planting density may be an effective means to further increase maize biomass and grain yield. Maize planting density in China varies among agricultural zones, and according to the cultivation habits of farmers, etc. Planting density ranges from 49,850 ha^{-1} to 65,180 ha^{-1} on the Huaihai Plain, in northwestern China; both of those values are much lower than those in the USA (Meng et al., 2013; Li et al., 2016). Increases in planting density necessarily intensify competition. The effects of planting density on grain yield, the leaf area of individual plants, the population leaf area index (LAI), leaf photosynthesis, and other variables have been examined in previous works (Amanullah et al., 2007; Liu et al., 2015; Xue et al., 2015). Li et al. (2015) found that the elevated grain yield of modern maize hybrids is largely a result of enhanced stay-green characteristics and increased photosynthetic capacity after anthesis. Higher planting density leads to undesirably high leaf area indices that cause self-shading, which may reduce yield (Liu et al., 2015; Srinivasan et al., 2017). Hence, determining the effects of hybrid and planting density on leaf development will be of great significance in the management of maize cultivation.

Hybrid Xianyu335 (XY335) has elevated dry mass accumulation at silking and higher N recovery efficiency than that of Zhengdan958 (ZD958) (Chen et al., 2014). However, the differences between these two hybrids in N remobilization and N uptake after silking remain unclear. In the current study, we designed a 3-year program to develop a better understanding of the possible interaction between hybrid and planting density. We analyzed the response of grain yield, total aboveground N uptake (TNU), N partial factor productivity (NPFP), total N in the grain as a fraction of TNU (nitrogen harvest index; NHI), dry mass and N accumulation rates at silking and maturity, and stalk and leaf remobilization rates of dry mass and N in three widely used hybrids grown on the Northeast Plain of China. The aim of this study was to explore physiological mechanisms to achieve higher grain yield and N utilization efficiency by combined testing of (i) maize hybrids and (ii) planting densities.

http://www.aloki.hu ● ISSN 1589 1623 (Print) ● ISSN1785 0037 (Online)
DOI: http://dx.doi.org/10.15666/aeer/1804_56835699

Materials and methods

Experimental site

Five field experiments were conducted at Halahai (44°32′50″N, 125°09′56″E) in 2013, 2014 and 2015, and at Gongzhuling (43°29′55″N, 124°48′43″E) in 2014 and 2015. Both sites are situated in Jilin Province, which is a typical spring maize growing region in Northeast China. The respective soil physical and chemical characteristics in Halahai and Gongzhuling at the beginning of the experiments were as follows: organic matter, 25.0 and 21.0 g kg^{-1}; available N, 121.0 and 111.8 mg kg^{-1}; available phosphorus (P), 24.2 and 31.5 mg kg^{-1}; potassium (K), 166.9 and 185.9 mg kg^{-1}; and pH, 7.89 and 6.00 (under a water/soil mixture ratio of 2.5:1).

The precipitation data during the maize growth stage are presented in *Fig. 1*, which shows major precipitation in Gongzhuling in 2015, especially during the seedling stage. The growth degree units in 2013, 2014 and 2015 of Halahai were 3,055, 2,900 and 2,974 °C respectively, and that in 2013 and 2014 of Gongzhuling were 3,186 and 3,200 °C respectively.

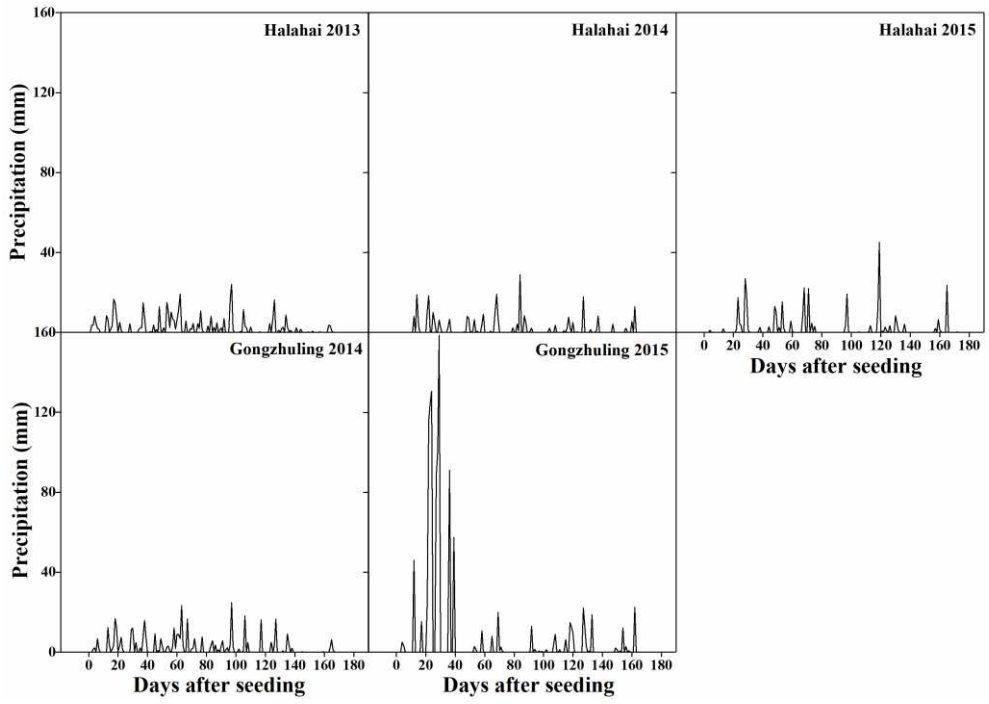

Figure 1. *Precipitation at two study sites during the maize growth stage*

Plant materials

Three maize hybrids, ZD958, XY335 and LM33, were included in the study; these are the dominant hybrids used on the Northeast China Plain (Chen et al., 2013b; Gu et al., 2017). ZD958 was developed by the Henan Academy of Agricultural Science, Henan Province, China; XY335 was developed by the Pioneer Technology Company, Tieling, Jilin Province, China; LM33 was developed by the Limin Seed Company, Songyuan, Jilin Province China. The main agronomic properties of the three maize hybrids were shown in *Table 1*.

http://www.aloki.hu ● ISSN 1589 1623 (Print) ● ISSN1785 0037 (Online)
DOI: http://dx.doi.org/10.15666/aeer/1804_56835699

Table 1. *The main agronomic properties of the three maize hybrids*

Hybrids	Authorized No.	Growing degree units (≥10℃)	Growing period (days)	Plant height (cm)	Ear length (cm)	100 grain weight (g)
ZD958	GSY20000009	2550	128	240	20.0	33.0
XY335	GSY2004017	2650	120	286	18.5	39.3
LM33	JSY2013030	2730	128	270	20.0	36.5

Experimental design

A split-plot block design with three replications was used in the five field experiments. Three hybrids were set as the main plot factors, and five planting densities (D1, D2, D3, D4 and D5: 45,000, 60,000, 75,000, 90,000 and 105,000 ha^{-1}, respectively) were set as sub-plot factors. All plots were 7 m long, and comprised eight rows spaced 0.65 m apart. Plots were fertilized with 225 kg N ha^{-1}, 90 kg P_2O_5 ha^{-1} and 90 kg K_2O ha^{-1}. All P_2O_5 and K_2O amendments were applied as base fertilizer. We applied 40% of N in the base fertilizer, and 40% and 20% at the jointing and silking stages, respectively.

Crop cultivation

Maize seeds were sown on May 3, 2013, April 29, 2014 and April 30, 2015 in Halahai, and on April 26, 2014 and April 25, 2015 in Gongzhuling with semiautomatic planters (*Fig. 2*). Maize plants were harvested on September 27, 2013, September 25, 2014 and September 27, 2015 in Halahai, and on September 26, 2014 and September 27, 2015 in Gongzhuling. All of the agricultural practices used followed the recommendations of local agricultural technology departments.

Figure 2. *Maize seeding of different planting densities with semiautomatic planters*

http://www.aloki.hu ● ISSN 1589 1623 (Print) ● ISSN1785 0037 (Online)
DOI: http://dx.doi.org/10.15666/aeer/1804_56835699

Measurements

Three representative plants from each plot were sampled at silking and maturity. All samples were separated into leaves, stalks and grain. The green leaf area of each plant at the silking stage was calculated (after separating component organs) using the following formula: length × leaf width × 0.75 (Gallais et al., 2006). Leaf area index (LAI) was the total leaf area of per unit land area. All samples were oven-dried at 105 °C for 30 minutes and then dried at 70 °C to a constant mass for dry weights measurements. After measuring the dry weights of different samples, they were ground to powder and passed through a 0.25-mm sieve. We then weighed out 0.1 g of powder from each sample and digested it in H_2SO_4 and H_2O_2 (Wolf, 1982). The N concentration in the solution was determined with a continuous flow analyzer (AA3; Seal Analytical Inc., Southampton, UK). Grain yield at maturity was determined from 20 plants and adjusted to a 14% moisture content.

Calculations

Stalk and leaf weight remobilization efficiency, the contributions to grain yield of stalk and leaf mass remobilization, stalk and leaf N remobilization efficiencies and the contributions to grain yield of stalk and leaf N remobilization were calculated as follows (Chen et al., 2014):

$$\text{Stalk mass remobilization efficiency (\%)} = (\text{stalk mass at silking} - \text{stalk mass at maturity}) / \text{stalk mass at silking} \times 100 \quad \text{(Eq.1)}$$

$$\text{Leaf mass remobilization efficiency (\%)} = (\text{leaf mass at silking} - \text{leaf mass at maturity}) / \text{leaf mass at silking} \times 100 \quad \text{(Eq.2)}$$

$$\text{Contribution to grain yield by stalk mass remobilization (\%)} = (\text{stalk mass at silking} - \text{stalk mass at maturity}) / \text{grain yield at maturity} \times 100 \quad \text{(Eq.3)}$$

$$\text{Contribution to grain yield by leaf mass remobilization (\%)} = (\text{leaf mass at silking} - \text{leaf mass at maturity}) / \text{grain yield at maturity} \times 100 \quad \text{(Eq.4)}$$

$$\text{Stalk N remobilization efficiency (\%)} = (\text{stalk N uptake at silking} - \text{stalk N uptake at maturity}) / \text{stalk N uptake at silking} \times 100 \quad \text{(Eq.5)}$$

$$\text{Leaf N remobilization efficiency (\%)} = (\text{leaf N uptake at silking} - \text{leaf N uptake at maturity}) / \text{leaf N uptake at silking} \times 100 \quad \text{(Eq.6)}$$

$$\text{Contribution to grain N by stalk N remobilization} = (\text{stalk N uptake at silking} - \text{stalk N uptake at maturity}) / \text{grain N uptake at maturity} \times 100 \quad \text{(Eq.7)}$$

$$\text{Contribution to grain N by leaf N remobilization (\%)} = (\text{leaf N uptake at silking} - \text{leaf N uptake at maturity}) / \text{grain N uptake at maturity} \times 100 \quad \text{(Eq.8)}$$

The N uptake NHI was calculated as follows (Chen et al., 2014; Hou et al., 2019):

http://www.aloki.hu ● ISSN 1589 1623 (Print) ● ISSN1785 0037 (Online)
DOI: http://dx.doi.org/10.15666/aeer/1804_56835699

$$\text{N uptake by grain (GN, kg kg}^{-1}\text{)} = \text{N content of grain} \times \text{grain mass} \quad \text{(Eq.9)}$$

$$\text{N uptake by straw (SN, kg kg}^{-1}\text{)} = \text{N content of straw} \times \text{straw mass} \quad \text{(Eq.10)}$$

$$\text{N uptake by leaf (LN, kg kg}^{-1}\text{)} = \text{N content of leaf} \times \text{leaf mass} \quad \text{(Eq.11)}$$

$$\text{Total N uptake (TNU) (kg kg}^{-1}\text{)} = \text{GN} + \text{SN} + \text{LN} \quad \text{(Eq.12)}$$

$$\text{N harvest index (NHI)} = \text{GN} / (\text{GN} + \text{SN} + \text{LN}) \quad \text{(Eq.13)}$$

The partial factor productivity of applied N (NPFP) was calculated as follows (Sun et al., 2018):

$$\text{NPFP (kg kg}^{-1}\text{)} = \text{grain yield} / \text{N rate} \quad \text{(Eq.14)}$$

Data analysis

All data were analyzed using ANOVA. Significant pairwise differences between means were identified by least significant difference (LSD) tests at the 0.05 and 0.01 levels of significance. The ANOVA that demonstrated significant effects of maize hybrid, plant density, year, site, and their interactions was executed with SPSS 17.0 software (SPSS Inc., Chicago, IL, USA). The figures were generated with Origin Pro 8.0 software (OriginLab Corp. Northampton. MA, USA).

Results

Grain yield

The effects of time, hybrid, site and planting density on grain yield are shown in *Fig. 3*. Among the experimental years, the grain yield was similar between 2013 and 2014, and both were significantly higher than that in 2015. The grain yield in 2015 was 17.3% lower on average than during the previous 2 years. The reduced grain yield in 2015 may have been a consequence of high precipitation in Gongzhuling during the seedling stage (*Fig. 1*). Among the three hybrids, XY335 had a higher grain yield that was 7.5% higher on average than Zhengdan958 (ZD958) and Limin33 (LM33). The environment also had significant effects on grain yield. The grain yield in Halahai was 12.5% higher than that in Gongzhuling. Planting density, an important agronomic measure, had a significant effect on grain yield. Grain yield increased at first, and then decreased, with increasing planting density. Density treatment D3 had the highest grain yield (*Fig. 3*).

The relationship between planting density and grain yield was described using regression equations (*Table 2*). The regression equations showed that grain yield did not always increase with planting density. In the field trials, the most appropriate planting density varied by hybrid, year and experimental site. Among the hybrids, LM33 had the highest appropriate planting density. The regression equations also showed that the lower average grain yield in 2015 was due to the lower grain yield in Gongzhuling.

http://www.aloki.hu ● ISSN 1589 1623 (Print) ● ISSN1785 0037 (Online)
DOI: http://dx.doi.org/10.15666/aeer/1804_56835699

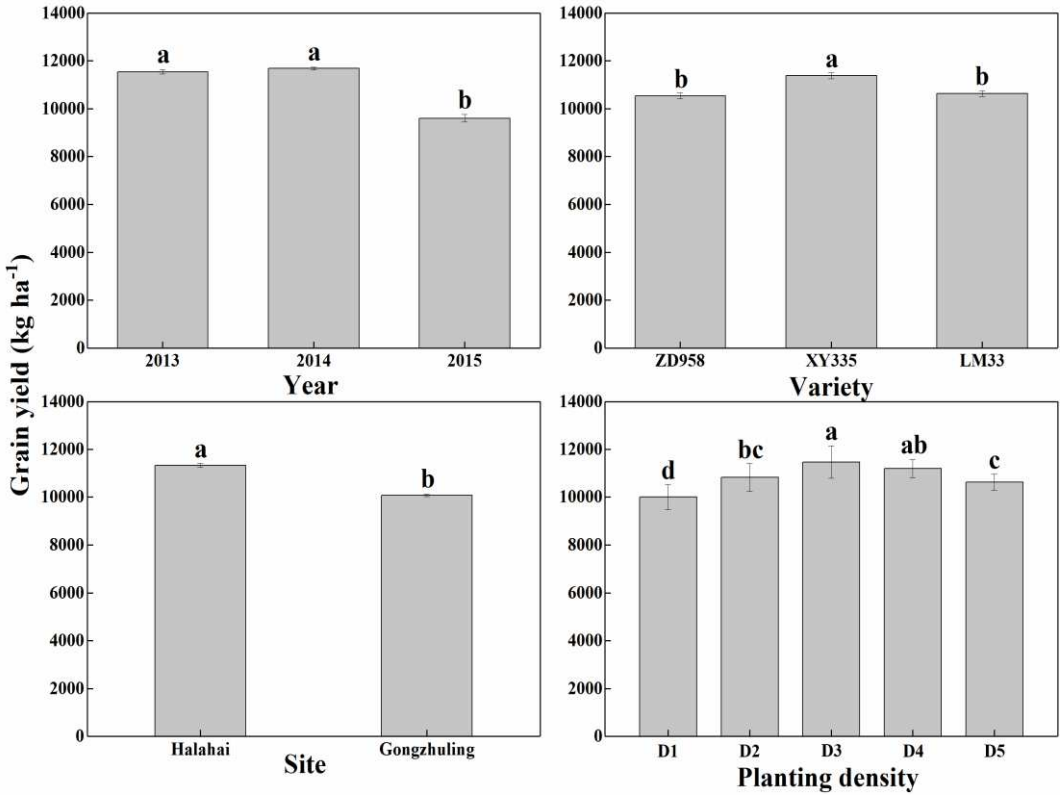

Figure 3. *Grain yields of maize by year, site, hybrids, and planting density. Values are means ± SE. Different lower case letters within panels identify significant pairwise differences between means (least significant difference [LSD] test; P < 0.05). D1, D2, D3, D4 and D5 correspond to planting densities of 45,000, 60,000, 75,000, 90,000 and 105,000 ha^{-1}, respectively*

Table 2. *Regression equations describing the relationship between planting density and yield*

Year	Site	Hybrid	Regression equation	R^2	Predicted extremum	X
2013	Halahai	ZD958	$Y = -0.8717X^2 + 138.99X + 4754$	0.9805	10265	74.0
		XY335	$Y = -0.87X^2 + 136.45X + 5477$	0.9023	10827	78.4
		LM33	$Y = -0.7019X^2 + 118.92X + 4810$	0.8568	9847	84.7
2014	Halahai	ZD958	$Y = -0.8978X^2 + 142.94X + 4286$	0.8879	9975	79.6
		XY335	$Y = -1.7201X^2 + 264.87X + 920$	0.9201	11116	77.0
		LM33	$Y = -0.7599X^2 + 136.33X + 4422$	0.9586	10536	89.7
	Gongzhuling	ZD958	$Y = -1.1598X^2 + 181.57X + 3267$	0.9397	10373	78.3
		XY335	$Y = -1.1571X^2 + 182.99X + 3726$	0.8868	10960	79.1
		LM33	$Y = -1.1241X^2 + 188.82X + 2791$	0.9802	10721	84.0
2015	Halahai	ZD958	$Y = -1.2442X^2 + 194.17X + 1888$	0.9501	9465	78.0
		XY335	$Y = -1.4991X^2 + 228.72X + 1901$	0.8477	10625	76.3
		LM33	$Y = -1.0473X^2 + 164.72X + 3133$	0.8744	9610	78.6
	Gongzhuling	ZD958	$Y = -0.7671X^2 + 124.83X + 2443$	0.8966	7521	81.4
		XY335	$Y = -0.7349X^2 + 109.27X + 4079$	0.9480	8141	74.3
		LM33	$Y = -0.5895X^2 + 98.395X + 2813$	0.9665	6918	83.5

"Predicted extremum" indicates the highest grain yield (kg ha^{-1}) obtained from the regression equation. X refers to a suitable planting density (10^3 plants ha^{-1}) at the predicted extremum obtained from the regression equations

http://www.aloki.hu ● ISSN 1589 1623 (Print) ● ISSN1785 0037 (Online)
DOI: http://dx.doi.org/10.15666/aeer/1804_56835699

Leaf development

The leaf areas of plants at the silking stage are shown in *Fig. 4*, values were highest in 2014 and lowest in 2015. Leaf area varied significantly by hybrid in the following order: ZD958 > XY335 > LM33. Leaf area did not vary significantly between the two experimental sites. Increased planting density significantly decreased leaf area. The leaf area in treatment D5 was 26.9% smaller than that in treatment D1.

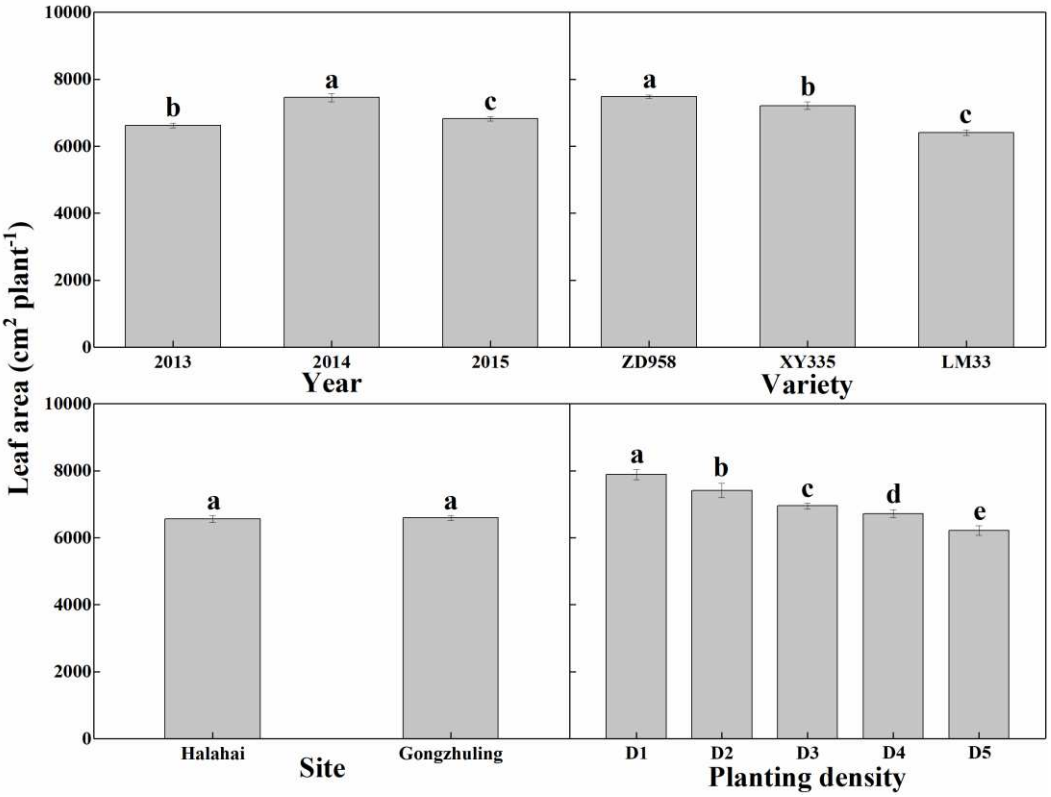

Figure 4. *Leaf areas of individual plants. Values are means ± SE. Different lower case letters within panels denote significant pairwise differences between means (LSD test; $P < 0.05$). D1, D2, D3, D4 and D5 indicate planting densities of 45,000, 60,000, 75,000, 90,000 and 105,000 ha^{-1}, respectively*

The LAI followed the same trend as leaf area/plant by year, hybrid and site (*Fig. 5*), but this was not the case for planting density: LAI significantly increased with increasing planting density. The LAI under D5 was 83.6% higher than under D1.

Dry mass accumulation, remobilization and contribution to grain yield

The dry mass accumulation, remobilization and contribution to grain yield data are listed in *Table 3*. Among three hybrids, LM33 had significantly lower stalk and leaf dry mass at silking stage than ZD958 and XY335. The stalk dry mass at maturity was not significantly different among hybrids; however, the leaf dry mass of LM33 was strikingly lower than those of ZD958 and XY335. The stalk dry mass remobilization rate and contribution to grain yield were not significantly different among hybrids. The leaves of LM33 leaf had the lowest dry mass remobilization rate and the smallest contribution to grain yield among hybrids. Compared to plants at Halahai, those at

http://www.aloki.hu ● ISSN 1589 1623 (Print) ● ISSN1785 0037 (Online)
DOI: http://dx.doi.org/10.15666/aeer/1804_56835699

Gongzhuling had significantly higher stalk and leaf dry mass accumulation rates, dry mass remobilization rates and contributions to grain yield. The dry mass accumulation rates at the silking stage, and the stalk and leaf dry mass accumulation rates at maturity, leaf dry mass remobilization rates, and stalk and leaf contributions to grain yield also increased with increasing planting density. The dry mass of stalks and leaves at silking and maturity, and dry mass remobilization rates and contributions to grain yield all increased over time.

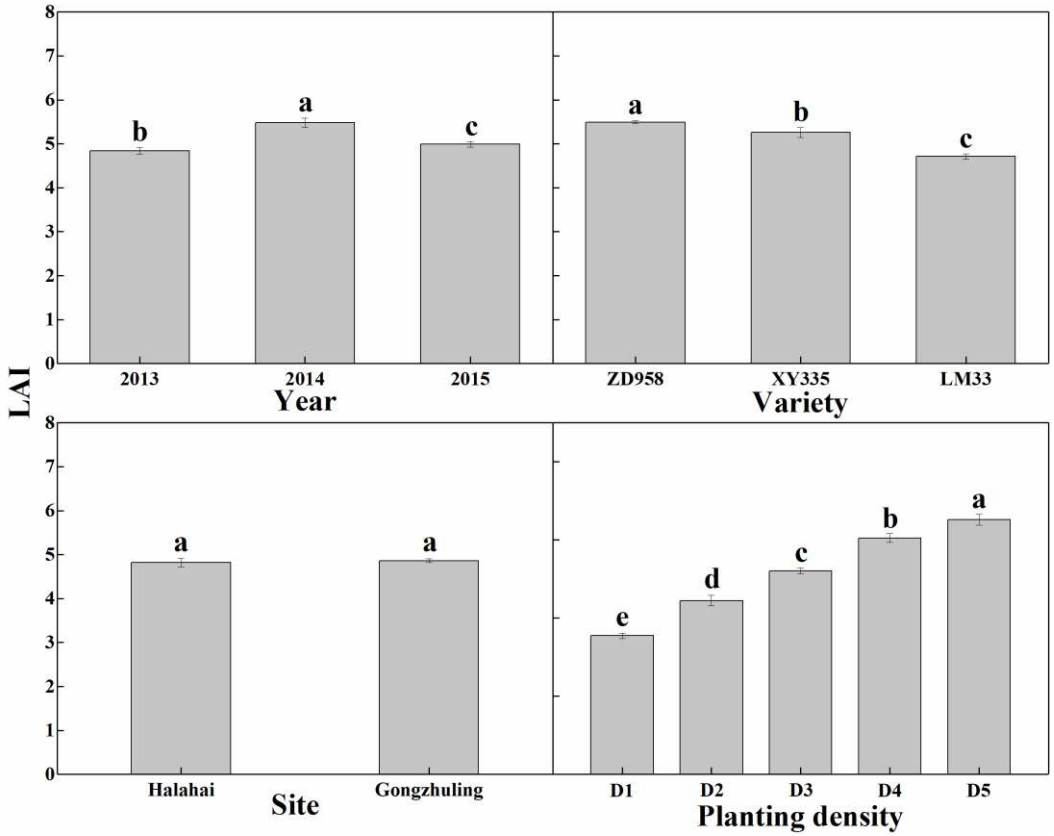

Figure 5. *Leaf area of each plant (LAI). Bars indicate standard error. Different lower case letters within panels identify significant pairwise differences between means (LSD test; P < 0.05). D1, D2, D3, D4 and D5 indicate planting densities of 45,000, 60,000, 75,000, 90,000 and 105,000 ha^{-1}, respectively*

Nitrogen uptake and utilization

The total N uptake (TNU) and utilization data are listed in *Table 4*. LM33 had the highest TNU and N uptake of 100 kg grain among the three hybrids; the respective values for LM33 were 10.6% and 10.1% higher than those of ZD958. However, the average NPFP of LM33 was the lowest among hybrids (11.8% lower than the values for ZD958 and XY335). The order of NHI values for the hybrids was as follows: XY335 > LM33 > ZD958. The TNU and NHI values for Halahai were 11.8% and 1.5% higher, respectively, than those for Gongzhuling. The NPFP and N uptake of 100 kg grain were not significantly different between sites. Increased planting density increased the TNU and N uptake of 100 kg grain, but decreased NPFP and NHI. The TNU and N uptake of 100 kg grain of D5 were 15.5% and 8.5% higher, respectively, than those of

http://www.aloki.hu ● ISSN 1589 1623 (Print) ● ISSN1785 0037 (Online)
DOI: http://dx.doi.org/10.15666/aeer/1804_56835699

D1, but NPFP and NHI under D5 were 7.9% and 5.3% lower, respectively, than under D1. Among the three experimental years, the TNU and N uptake of 100 kg grain were lowest in 2014, but NPFP and NHI highest in that year. The TNU and N uptake of 100 kg grain values were highest in 2015, but the NPFP and NHI were lowest.

TNU, NFPN, N uptake of 100 kg grain, and NHI varied significantly among the hybrids (analysis of variance [ANOVA]; $P < 0.05$). TNU, NFPN and NHI differed significantly between the two experimental sites. TNU, N uptake of 100 kg grain, and NHI varied significantly by planting density and year.

Table 3. *Dry mass (DM) accumulation, remobilization and contribution to grain yield by hybrid, site, year and planting density*

Treatments	DM at silking (kg ha^{-1})		DM at maturity (kg ha^{-1})		DM remobilization rate (%)		Contribution to grain yield (%)	
	Stalk	Leaf	Stalk	Leaf	Stalk	Leaf	Stalk	Leaf
Hybrids (H)								
ZD958	6257 a	3179 a	5562 a	2347 a	11.1 a	26.2 ab	7.7 a	9.2 a
XY335	6349 a	3189 a	5542 a	2292 b	12.7 a	28.1 a	8.2 a	9.2 a
LM33	6111 b	2989 b	5404 a	2282 b	11.6 a	23.7 b	7.7 a	7.7 b
Site (S)								
Halahai	5950 b	3044 b	5304 b	2300 a	10.9 b	24.5 b	6.6 b	7.6 b
Gongzhuling	6672 a	3231 a	5801 a	2317 a	13.1 a	28.3 a	10.1 a	10.6 a
Density (D)								
D1	5301 e	2447 e	4679 e	2055 e	11.7 ab	15.9 d	7.2 b	4.5 d
D2	5842 d	2804 d	5104 d	2187 d	12.6 a	21.9 c	7.9 b	6.6 c
D3	6378 c	3143 c	5633 c	2324 c	11.7 ab	26.1 b	7.6 b	8.3 b
D4	6699 b	3536 b	5960 b	2434 b	11.0 b	31.1 a	7.7 b	11.4 a
D5	6976 a	3665 a	6139 a	2533 a	12.0 ab	30.8 a	9.2 a	12.4 a
Year (Y)								
2013	5965 c	2688 c	5376 b	2259 a	9.8 b	16.0 b	5.9 b	4.3 c
2014	6156 b	3164 b	5478 ab	2324 a	11.0 ab	26.6 a	6.7 b	8.4 b
2015	6460 a	3289 a	5591 a	2314 a	13.5 a	29.6 a	10.5 a	11.8 a
Source of variation								
H	**	**	**	*	NS	**	NS	**
S	**	NS	**	NS	NS	NS	**	**
D	**	**	**	**	NS	**	NS	**
Y	**	**	**	NS	*	**	**	**
H × S	**	**	**	NS	NS	**	NS	**
H × D	*	NS	NS	NS	NS	NS	NS	NS
H × Y	**	**	**	**	NS	NS	NS	NS
S × D	**	NS	*	NS	NS	NS	NS	NS
S × Y	NS	**	NS	*	NS	*	**	**
D × Y	NS	**	NS	**	NS	**	NS	**
H × S × D	NS	NS	NS	NS	NS	NS	NS	NS
H × S × Y	NS	NS	**	NS	**	NS	**	NS
H × D × Y	*	NS	NS	NS	NS	NS	NS	NS
S × D × Y	NS	NS	NS	NS	NS	NS	NS	NS
H × S × D × Y	**	NS	NS	NS	NS	NS	NS	NS

Different lower case letters within columns denote significant pairwise differences between means (LSD test; P < 0.05). *, P < 0.05. **, P < 0.01. NS, no significant difference (P > 0.05). D1, D2, D3, D4 and D5 indicate planting densities of 45,000, 60,000, 75,000, 90,000 and 105,000 ha^{-1}, respectively

http://www.aloki.hu ● ISSN 1589 1623 (Print) ● ISSN1785 0037 (Online)
DOI: http://dx.doi.org/10.15666/aeer/1804_56835699

Table 4. *Total nitrogen uptake (TNU), nitrogen partial factor productivity (NPFP), nitrogen uptake of 100 kg grain and nitrogen harvest index (NHI) by hybrid, site, year and planting density*

Treatments	TNU (kg ha^{-1})	NPFP (kg kg^{-1})	N uptake of 100 kg grain (kg)	NHI
Hybrids (H)				
ZD958	168.0 c	54.2 a	1.88 b	0.644 c
XY335	179.6 b	54.9 a	1.86 b	0.684 a
LM33	185.8 a	48.8 b	2.07 a	0.672 b
Site (S)				
Halahai	185.7 a	52.9a	1.91 a	0.671 a
Gongzhuling	166.1b	52.3 a	1.95 a	0.661 b
Density (S)				
D1	159.4 c	54.2 a	1.88 c	0.678 a
D2	172.9 b	54.2 a	1.88 c	0.680 a
D3	184.7 a	53.7 a	1.90 c	0.675 a
D4	188.0 a	51.4 b	1.98 b	0.660 b
D5	184.1 a	49.9 b	2.04 a	0.642 c
Year (Y)				
2013	179.8 a	55.3 b	1.82 b	0.654 b
2014	173.5 b	58.4 a	1.73 c	0.701 a
2015	181.1 a	45.6 c	2.20 a	0.640 c
Source of variation				
H	**	*	**	**
S	**	**	NS	**
D	**	NS	**	**
Y	**	NS	**	**
H × S	NS	NS	**	**
H × D	NS	NS	NS	NS
H × Y	**	NS	**	**
S × D	NS	NS	NS	NS
S × Y	**	**	**	**
D × Y	NS	NS	*	**
H × S × D	NS	NS	NS	NS
H × S × Y	**	**	**	NS
H × D × Y	NS	NS	NS	NS
S × D × Y	NS	NS	NS	*
H × S × D × Y	NS	NS	NS	NS

Different lower case letters within columns denote significant pairwise differences between means (LSD test; $P < 0.05$). *, $P < 0.05$. **, $P < 0.01$. NS, no significant difference ($P > 0.05$). D1, D2, D3, D4 and D5 indicate planting densities of 45,000, 60,000, 75,000, 90,000 and 105,000 ha^{-1}, respectively

Nitrogen accumulation, remobilization and contribution to grain yield

Although ZD958 had the highest stalk TNU at silking and maturity, its stalk N remobilization rate was lowest among hybrids (*Table 5*). The leaf TNU values at silking and maturity, and the N remobilization rate of ZD958, were not the highest among hybrids. ZD958 had the highest stalk and leaf contributions to grain N; they were 11.9% and 14.3% higher, respectively, than the lowest values among hybrids. The stalks at Gongzhuling had higher TNU values at silking, and higher N remobilization rates and

http://www.aloki.hu ● ISSN 1589 1623 (Print) ● ISSN1785 0037 (Online)
DOI: http://dx.doi.org/10.15666/aeer/1804_56835699

contributions to grain N than stalks at Halahai. However, plants at Halahai had higher leaf TNU values at silking, N remobilization rates and contributions to grain N. Stalk and leaf TNU at maturity did not differ significantly between sites. Increases in planting density significantly increased stalk and leaf TNU values at silking and maturity, as well as leaf N remobilization rates and contributions to grain N. However, the N remobilization rate of the stalk was significantly decreased by increased planting density. The TNU, N remobilization rate, and contributions of stalk and leaf differed significantly among years.

Table 5. *Total nitrogen uptake (TNU), nitrogen remobilization rate and contribution to grain nitrogen uptake by hybrid, site, year and planting density*

Treatments	TNU at silking (kg ha^{-1})		TNU at maturity (kg ha^{-1})		N remobilization rate (%)		Contribution to grain N (%)	
	Stalk	Leaf	Stalk	Leaf	Stalk	Leaf	Stalk	Leaf
Hybrids (H)								
ZD958	62.9 a	72.4 b	28.9 a	26.9 b	54.1 b	62.8 b	31.1 a	41.6 a
XY335	58.1 c	75.9 a	23.9 b	25.8 c	58.8 a	66.0 a	27.8 b	40.8 a
LM33	59.4 b	75.0 ab	24.6 b	29.5 a	58.6 a	60.7 b	27.8 b	36.4 b
Site (S)								
Halahai	59.5 b	81.6 a	26.5 a	27.6 a	55.5 b	66.2 a	26.4 b	43.3 a
Gongzhuling	61.1 a	63.6 b	23.6 a	27.0 a	61.4 a	57.5 b	34.0 a	33.2 b
Density (D)								
D1	53.2 c	60.0 d	21.6 d	24.8 e	59.4 a	58.7 d	29.2 a	32.5 e
D2	57.9 b	68.2 c	23.1 c	26.3 d	60.0 a	61.4 c	29.5 a	35.5 d
D3	61.9 a	75.1 b	25.6 b	27.4 c	58.8 a	63.5 b	29.1 a	38.2 c
D4	63.0 a	83.4 a	28.1 a	28.5 b	55.5 b	65.9 a	28.8 a	44.2 b
D5	64.6 a	85.5 a	28.2 a	29.8 a	56.5 b	65.1 a	30.8 a	47.1 a
Year (Y)								
2013	59.6 b	81.6 a	28.2 a	27.5 b	52.8 b	66.3 a	26.8 b	46.1 a
2014	62.6 a	70.3 c	22.2 c	24.4 c	64.6 a	65.3 a	33.2 a	37.7 b
2015	58.8 b	74.9 b	27.0 b	30.2 a	54.1 b	59.7 b	27.4 b	38.4 b
Source of variation								
V	**	**	**	**	**	**	**	**
S	**	**	**	*	**	**	**	**
D	**	**	**	**	**	**	*	**
Y	**	**	**	**	**	**	**	**
H × S	*	**	*	**	NS	**	**	**
H × D	NS	NS	**	NS	NS	NS	NS	NS
H × Y	**	**	**	**	**	**	**	**
S × D	*	**	NS	**	NS	*	*	**
S × Y	**	**	NS	**	NS	**	*	*
D × Y	**	*	**	**	NS	*	NS	NS
H × S × D	NS	NS	NS	NS	NS	NS	NS	NS
H × S × Y	NS	NS	**	**	**	**	**	**
H × D × Y	NS	NS	*	NS	NS	NS	NS	NS
S × D × Y	NS	**	NS	NS	NS	**	NS	**
H × S × D × Y	NS	NS	NS	NS	NS	NS	NS	NS

Different lower case letters within columns denote significant pairwise differences between means (LSD test; $P < 0.05$). *, $P < 0.05$. **, $P < 0.01$. NS, no significant difference ($P > 0.05$). D1, D2, D3, D4 and D5 indicate planting densities of 45,000, 60,000, 75,000, 90,000 and 105,000 ha^{-1}, respectively

http://www.aloki.hu ● ISSN 1589 1623 (Print) ● ISSN1785 0037 (Online)
DOI: http://dx.doi.org/10.15666/aeer/1804_56835699

ANOVA showed that hybrid, site, planting density and year all had significant effects on the TNU, N remobilization rate, and stalk and leaf contributions to grain N.

Discussion

Grain yield

Improvements in field management practice have the potential to increase the grain yield of modern maize hybrids by 50% (Xu et al., 2017). The choice of an optimum planting density is an element of best practice that can be readily implemented by working farmers. Across China, maize planting density ranges from 49,850 ha^{-1} on the Huaihai Plain to 65,180 ha^{-1} in Northwest China (Meng et al., 2013; Li et al., 2016). However, in other regions, maize planting density ranges from 79,072 to 105,000 ha^{-1} (Kratochvil and Taylor, 2005; Robles et al., 2012; Novacek et al., 2013). Optimum planting density is an important element of efforts to maximize maize grain yield. However, optimum planting density is influenced by hybrid and environmental conditions. It is therefore difficult to identify an optimum planting density before planting (Cox and Cherney, 2012; Reeves and Cox, 2013). We found that grain yields varied significantly by year, hybrid and site (*Fig. 3*). Crop production depends on the yields of whole populations, rather than individual plants; hence, selection of an appropriate planting density is vital to realize high yields. The lowest and highest planting densities selected for the three hybrids in this study were 45,000 ha^{-1} and 105,000 ha^{-1}, respectively. Grain yield data indicated that 75,000 ha^{-1} was an appropriate planting density overall. However, the most appropriate planting density for each experiment varied among years, hybrids and sites (*Table 2*), indicating that planting density is not a fixed variable in maize cultivation. We found that the average optimum planting densities for hybrids ZD958, XY335 and LM33 were 78.3, 77.0 and 84.1 $\times$ 10^3 ha^{-1}, respectively. Xu et al. (2017) reported that the optimum planting density of ZD958 at Gongzhuling was 75.0 $\times$ 10^3 plants ha^{-1}, similar to our findings. Excessively high planting densities led to yield losses of all three hybrids in our study. Also, Amanullah et al. (2007) reported that increased maize planting density decreased the kernel number, ear size and 1,000 kernel weights, leading to an overall reduction in yield.

Leaf development

The leaf is the major photosynthetic organ of maize, and the photosynthetic capacity of this crop depends largely on leaf canopy structure and physiological characteristics. Ning et al. (2013) and Ci et al. (2012) showed that improvements in maize yield are closely related to the leaf stay-green characteristics of modern hybrids. Larger leaf area and longer leaf area duration are closely related to improve maize grain yields (Francone et al., 2014). We found significant differences in leaf area per plant (*Fig. 4*) and LAI (*Fig. 5*) among the three hybrids tested. Increasing planting density affected both the leaf area of each plant and the LAI: leaf area per plant decreased with increased planting density, but LAI increased. The negative effect of increased density on the leaf area of individual plants can be offset by concomitant increases in the population leaf area.

http://www.aloki.hu ● ISSN 1589 1623 (Print) ● ISSN1785 0037 (Online)
DOI: http://dx.doi.org/10.15666/aeer/1804_56835699

Dry mass and nitrogen remobilization

Dry mass accumulation reflects the plant growth and development status. High dry mass is fundamental to high grain yield. All dry mass gains after silking contribute to grain yield, and most of the grain yield is a product of the dry mass accumulated after the silking stage (Ning et al., 2013). In this study, increased planting density significantly increased the stalk and leaf dry mass at silking and maturity, and also increased the proportional contribution to grain yield (*Table 2*). Dordas and Sioulas (2009) reported that grain yield was mainly determined by the accumulation of dry mass. Xu et al. (2017) found that the harvest index decreased with increased planting density. However, dry mass accumulation contributes more to grain yield than the harvest index (Peng et al., 2004).

Most leaf N is mobilized and transferred to grain (Hirel et al., 2007) during the grain filling stage. Chen et al. (2014) worked with hybrid XY335 and reported that approximately 70% of the leaf N accumulated at the silking stage was transferred to the grain. We also used this hybrid in our trials and obtained a similar leaf N remobilization rate (66.0%) (*Table 5*). Improvements in breeding technology have significantly increased the uptake of N, and new maize hybrids have a higher N use efficiency than older hybrids (Lee and Tollenaar, 2007; Worku et al., 2007; Haegele et al., 2013). In this study, there were significant differences in the TNU, NPFP, N uptake of 100 kg grain and NHI values among the three hybrids (*Table 4*), thereby demonstrating the existence of inter-varietal differences in N uptake and utilization. We supplied N at a constant rate to the three hybrids included in this study. N is an essential nutrient for maize growth and development, and optimum N rate guidelines should be developed to take account of the interactions among climate, site, hybrid and planting density.

Conclusion

We demonstrated significant effects of maize hybrid and planting density on grain yield, leaf growth and development, dry mass accumulation and remobilization, as well as N uptake and utilization. The three hybrids had similar grain yield trends, but the optimum planting density varied by hybrid. The optimum planting densities for enhanced grain yield in ZD958, XY335 and LM33 were 74.0-81.4, 74.3-79.1, and 78.6-89.7 $\times$ 10^3 ha^{-1}, respectively, across years and sites, showing that LM33 had the highest density tolerance. The increase in planting density had significant inhibitory effects on the leaf growth and development of individual plants, but this was offset by positive effects at the population level. Increased planting density improved dry mass and TNU, and promoted dry mass and N transfer from stalks and leaves to grain, thereby enhancing yield. In order to get a higher grain yield, modern maize hybrids should be combined with appropriate plant densities and suitable growing environments.

Acknowledgments. This work was supported by the National Key Research and Development Program of China (No. 2017YFD0300602) and the Science and Technology Development Planning Project of Jilin Province, China (No. 20180201077NY).

http://www.aloki.hu ● ISSN 1589 1623 (Print) ● ISSN1785 0037 (Online)
DOI: http://dx.doi.org/10.15666/aeer/1804_56835699

REFERENCES

[1] Amanullah, M. J. H., Nawab, K., Ali, A. (2007): Response of specific leaf area (SLA), leaf area index (LAI) and leaf area ratio (LAR) of maize (*Zea mays* L.) to plant density rate and timing of nitrogen application. – World Applied Sciences Journal 2: 235-243.

[2] Bertin, P., Gallais, A. (2000): Genetic variation for nitrogen use efficiency in a set of recombinant maize inbred lines. I. Agrophysiological results. – Maydica 45: 53-66.

[3] Borrell, A. K., Hammer, G. L., Oosterom, E. V. (2001): Stay-green: a consequence of the balance between supply and demand for nitrogen during grain filling. – Annals of Applied Biology 138: 91-95.

[4] Chen, X., Cui, Z., Vitousek, P. M., Cassman, K. G., Matson, P. A., Bai, J., Meng, Q., Hou, P., Yue, S., Römheld, V. (2011): Integrated soil–crop system management for food security. – Proceedings of the National Academy of Sciences of the United States of America 108: 6399-6404.

[5] Chen, F., Fang, Z., Gao, Q., Ye, Y., Jia, L., Yuan, L., Mi, G., Zhang, F. (2013a): Evaluation of the yield and nitrogen use efficiency of the dominant maize hybrids grown in North and Northeast China. – Science China-Life Sciences 56: 552-560.

[6] Chen, X., Chen, F., Chen, Y., Gao, Q., Yang, X., Yuan, L., Zhang, F., Mi, G. (2013b): Modern maize hybrids in Northeast China exhibit increased yield potential and resource use efficiency despite the adverse climate change. – Global Change Biology 19: 923-936.

[7] Chen, Y., Xiao, C., Chen, X., Li, Q., Zhang, J., Chen, F., Yuan, L., Mi, G. (2014): Characterization of the plant traits contributed to high grain yield and high grain nitrogen concentration in maize. – Field Crops Research 159: 1-9.

[8] Chen, Y., Xiao, C., Wu, D., Xia, T., Chen, Q., Chen, F., Yan, L., Mi, G. (2015): Effects of nitrogen application rate on grain yield and grain nitrogen concentration in two maize hybrids with contrasting nitrogen remobilization efficiency. – European Journal of Agronomy 62: 79-89.

[9] Ci, X., Li, M., Xu, J., Lu, Z., Bai, P., Ru, G., Liang, X., Zhang, D., Li, X., Bai, L., Xie, C., Hao, Z., Zhang, S., Dong, S. (2012): Trends of grain yield and plant traits in Chinese maize cultivars from the 1950s to the 2000s. – Euphytica 185: 395-406.

[10] Ciampitti, I. A., Vyn, T. J. (2012): Physiological perspectives of changes over time in maize yield dependency on nitrogen uptake and associated nitrogen efficiencies: A review. – Field Crops Research 133: 48-67.

[11] Coque, M., Gallais, A. (2007): Genetic variation for nitrogen remobilization and post-silking nitrogen uptake in maize recombinant inbred lines: heritabilities and correlations among traits. – Crop Science 47: 1787-1796.

[12] Cox, W. J., Cherney, J. H. (2012): Lack of hybrid, seeding, and nitrogen rate interactions for corn growth and yield. – Agronomy Journal 104: 945-952.

[13] Diós, D., Szenteleki, K., Ferenczy, A. (2009): A climate profile indicator based comparative analysis of climate change scenarios with regard to maize (*Zea mays* L.) cultures. – Applied Ecology & Environmental Research 7: 199-214.

[14] Dordas, C. A., Sioulas, C. (2009): Dry matter and nitrogen accumulation, partitioning, and retranslocation in safflower (*Carthamus tinctorius* L.) as affected by nitrogen fertilization. – Field Crops Research 110: 35-43.

[15] Duvick, D. N. (2005): The contribution of breeding to yield advances in maize (*Zea mays* L.). – Advances in Agronomy 86: 83-145.

[16] Echarte, L., Rothstein, S., Tollenaar, M. (2008): The response of leaf photosynthesis and dry matter accumulation to nitrogen supply in an older and a newer maize hybrid. – Crop Science 48: 656-665.

[17] Francone, C., Pagani, V., Foi, M., Cappelli, G., Confalonieri, R. (2014): Comparison of leaf area index estimates by ceptometer and Pocket LAI smart app in canopies with different structures. – Field Crops Research 155: 38-41.

http://www.aloki.hu ● ISSN 1589 1623 (Print) ● ISSN1785 0037 (Online)
DOI: http://dx.doi.org/10.15666/aeer/1804_56835699

[18] Gallais, A., Coque, M., Quilléré, I. (2006): Modelling post-silking nitrogen fluxes in maize (*Zea mays* L.) using ^{15}N-labelling field experiments. – New Phytologist 172: 696-707.
[19] Grassini, P., Cassman, K. G. (2012): High-yield maize with large net energy yield and small global warming intensity. – Proceeding of the National Academy of Science of the United States of America 109: 1074-1079.
[20] Gu, R., Li, L., Liang, X., Wang, Y., Fan, T., Wang, Y., Wang, J. (2017): The ideal harvest time for seeds of hybrid maize (*Zea mays* L.) XY335 and ZD958 produced in multiple environments. – Scientific Reports 7: 17537.
[21] Haegele, J. W., Cook, K. A., Nichols, D. M., Below, F. E. (2013): Changes in nitrogen use traits associated with genetic improvement for grain yield of maize hybrids released in different decades. – Crop Science 53: 1-13.
[22] He, P., Zhou, W., Jin, J. (2004): Carbon and nitrogen metabolism related to grain formation in two different senescent types of maize. – Journal of Plant Nutrition 27: 295-311.
[23] Hirel, B., Gouis, J. L., Ney, B., Gallais, A. (2007): The challenge of improving nitrogen use efficiency in crop plants: Towards a more central role for genetic variability and quantitative genetics within integrated approaches. – Journal of Experimental Botany 58: 2369-2387.
[24] Hou, W., Khan, M. R., Zhang, J., Lu, J., Ren, T., Cong, R., Li, X. (2019): Nitrogen rate and plant density interaction enhances radiation interception, yield and nitrogen use efficiency of mechanically transplanted rice. – Agriculture, Ecosystems & Environment 269: 183-192.
[25] Kratochvil, R. J., Taylor, R. W. (2005): Twin-row corn production: An evaluation in the Mid-Atlantic Delmarva Region. – Crop Management 4(1): 1-7.
[26] Lee, E. A., Tollenaar, M. (2007): Physiological basis of successful breeding strategies for maize grain yield. – Crop Science 47: 202-215.
[27] Li, C., Tao, Z., Liu, P., Zhang, J., Zhuang, K., Dong, S., Zhao, M. (2015): Increased grain yield with improved photosynthetic characters in modern maize parental lines. – Journal of Integrative Agriculture 14: 1735-1744.
[28] Li, S., Wang, K., Xie, R., Hou, P., Ming, B., Yang, X., Han, D., Wang, Y. (2016): Implementing higher population and full mechanization technologies to achieve high yield and high efficiency in maize production. – Crops 4: 1-6. (in Chinese with English abstract).
[29] Liu, T., Gu, L., Dong, S., Zhang, J., Liu, P., Zhao, B. (2015): Optimum leaf removal increases canopy apparent photosynthesis: ^{13}C-photosynthate distribution and grain yield of maize crops grown at high density. – Field Crops Research 170: 32-39.
[30] Ma, W., Li, J., Ma, L., Wang, F., Sisák, I., Cushman, G., Zhang, F. (2009): Nitrogen flow and use efficiency in production and utilization of wheat, rice, and maize in China. – Agricultural Systems 99: 53-63.
[31] Meng, Q., Hou, P., Wu, L., Chen, X., Cui, Z., Zhang, F. (2013): Understanding production potentials and yield gaps in intensive maize production in China. – Field Crops Research 143: 91-97.
[32] National Bureau of Statistics. (2018): China Statistical Yearbook. – China Statistics Press, Beijing (in Chinese with English abstract).
[33] Ning, P., Li, S., Yu, P., Zhang, Y., Li, C. (2013): Post-silking accumulation and partitioning of dry matter, nitrogen, phosphorus and potassium in maize varieties differing in leaf longevity. – Field Crops Research 144: 19-27.
[34] Novacek, M. J., Mason, S. C., Galusha, T. D., Yaseen, M. (2013): Bt transgenes minimally influence maize grain yield and lodging across plant populations. – Maydica 59: 90-95.
[35] Peng, S., Huang, J., Sheehy, J. E., Laza, R. C., Visperas, R. M., Zhong, X., Centeno, G. S., Khush, G. S., Cassman, K. G. (2004): Rice yields decline with higher night

http://www.aloki.hu ● ISSN 1589 1623 (Print) ● ISSN1785 0037 (Online)
DOI: http://dx.doi.org/10.15666/aeer/1804_56835699

temperature from global warming. – Proceedings of the National Academy of Sciences of the United States of America 101: 9971-9975.
[36] Pommel, B., Gallais, A., Coque, M., Quillere, I., Hirel, B., Prioul, J. L., Andrieu, B., Floriot, M. (2006): Carbon and nitrogen allocation and grain filling in three maize hybrids differing in leaf senescence. – European Journal of Agronomy 24: 203-211.
[37] Reeves, G. W., Cox, W. J. (2013): Inconsistent responses of corn to seeding rates in field-scale studies. – Agronomy Journal 105: 693-704.
[38] Robles, M., Ciampitti, I. A., Vyn, T. J. (2012): Responses of maize hybrids to twin-row spatial arrangement at multiple plant densities. – Agronomy Journal 104: 1747-1756.
[39] Srinivasan, V., Kumar, P., Long, S. P. (2017): Decreasing, not increasing, leaf area will raise crop yields under global atmospheric change. – Global Change Biology 23: 1626-1635.
[40] Sun, M., Huo, Z., Zheng, Y., Dai, X., Feng, S., Mao, X. (2018): Quantifying long-term responses of crop yield and nitrate leaching in an intensive farmland using agro-eco-environmental model. – Science of the Total Environment 613-614: 1003-1012.
[41] Tollenaar, M., Ahmadzadeh, A., Lee, E. A. (2004): Physiological basis of heterosis for grain yield in maize. – Crop Science 44: 2086-2094.
[42] Wolf, B. (1982): A comprehensive systems of leaf analysis and its use for diagnosing crop nutrient status. – Communications in Soil Science and Plant Analysis 13: 1035-1059.
[43] Worku, M., Bänziger, M., Friesen, D., Horst, W. J. (2007): Nitrogen uptake and utilization in contrasting nitrogen efficient tropical maize hybrids. – Crop Science 47: 519-528.
[44] Xu, W., Liu, C., Wang, K., Xie, R., Ming, B., Wang, Y., Zhang, G., Liu, G., Zhao, R., Fan, P., Li, S., Hou, P. (2017): Adjusting maize plant density to different climatic conditions across a large longitudinal distance in China. – Field Crops Research 212: 126-134.
[45] Xue, H., Han, Y., Li, Y., Wang, G., Lu, F., Fan, Z., Du, W., Yang, B., Mao, S. (2015): Spatial distribution of light interception by different plant population densities and its relationship with yield. – Field Crops Research 184: 17-27.

http://www.aloki.hu ● ISSN 1589 1623 (Print) ● ISSN1785 0037 (Online)
DOI: http://dx.doi.org/10.15666/aeer/1804_56835699

EFFECT OF DIFFERENT SOWING METHODS AND NITROGEN RATES ON YIELD AND QUALITY OF WINTER WHEAT IN LOESS PLATEAU OF CHINA

NOOR, H. – KHAN, S. – SUN, M.* – YU, S. – REN, A. – YANG, Z. – HOU, F. – LI, L. – WANG, Q. – GAO, Z.

College of Agriculture, Shanxi Agricultural University, Taigu 030801, Shanxi, China

**Corresponding author*
e-mail: sm_sunmin@126.com; phone/fax: +86-354-628-7187

(Received 19th Jan 2020; accepted 2nd Jul 2020)

Abstract. In order to explore the optimum amount of nitrogen application in different sowing methods of winter wheat, a field experiment was conducted at Wenxi experimental site of Shanxi Agriculture University (2017-2018), The two sowing methods were (I) Wide Space Sowing (WSS), and (II) Drilling Sowing (DS) with seven nitrogen treatments: 0 kg.hm 90 kg·hm^{-2}, 180 kg·hm^{-2}, 210 kg hm^{-2}, 240 kg hm^{-2}, 270 kg hm^{-2} and 300 kg hm^{-2}. (WSS) significantly increased the number of spikes yield and number of kernels per spike, nitrogen rate which ultimately increased the yield. The yield was the highest at 240 kg·hm^{-2} and 210 kg·hm^{-2}, respectively. Nitrogen application significantly increased the Net Photosynthesis Rate (Pn), intercellular carbon dioxide concentration (Ci) and transpiration rate (Tr) and decreased the stomatal conductance (Gs) of post-anthesis flag leaves. Wide space sowing wheat with N_{240} was the best. Compared with other nitrogen application rates, (WSS) with the nitrogen of 240 kg· hm^{-2} increased nitrogen accumulation in all growth stage while nitrogen uptake efficiency, nitrogen use efficiency and nitrogen productive efficiency were the highest at 90 kg·hm^{-2} and lowest at 300 kg·hm^{-2}. The accumulation of soluble sugar in the middle and late stages increased and the sucrose content and starch content increased in each period after anthesis. The content of each protein component increased the albumin which was the highest at 240 kg·hm^{-2} and the globulin was the highest at 270 kg·hm^{-2}. The prolamin and glutenin (storage protein) were the highest at 300 kg·hm^{-2} and in 240 kg·hm^{-2}. The protein content at 300 kg·hm^{-2}, and protein yield at 240 kg·hm^{-2} were significantly improved compared to other nitrogen application rates. The sedimentation value, falling value, formation time, development time, wet gluten and the gluten index increased and the water absorption rate was relatively stable as nitrogen fertilizer increased.

Keywords: *nitrogen use efficiency, WSS, soil water content, photosynthesis characteristics, grain protein*

Introduction

The yield of winter wheat (*Triticum aestivum* L.) in dryland area is unstable and substantially lower than the average yield in other areas of China and other European countries. Stabilizing the yield of dryland wheat and improving the overall production and grain quality of dryland areas have always been the main task of research for cultivation work in the arid regions of North China (Li et al., 2002; Ma et al., 2005). The world's largest Loess Plateau is located in northern China, covering Shanxi, eastern Gansu, Shaanxi, and northern Henan provinces (Encyclopedia et al., 2013). The Loess Plateau in China covers about 0.65 million km^2 area and has 108 million population (Wang et al., 2010). The Loess Plateau has a semiarid climate with low and variable rainfall from 300–700 mm (Li et al., 1992). Due to the lack of irrigation resources and deep and sparse groundwater, most of the agriculture is dryland farming, which completely depends on the precipitation (Zhang et al., 2009).

Technological quality of wheat is a very complex character, which depends on the genetic potential of genotypes, applied technology and agro ecological conditions.

http://www.aloki.hu ● ISSN 1589 1623 (Print) ● ISSN 1785 0037 (Online)
DOI: http://dx.doi.org/10.15666/aeer/1804_57015726

Mineral nutrition, especially nitrogen nutrition, highly influences the technological quality. Nitrogen, in interaction with other elements of mineral nutrition, has important influence on yield and technological quality of wheat (Pepó et al., 2005; Horvat et al., 2006). Wheat is one of the most important food crops in the world and it is also an important food crop in China and its production plays an important role in China's national economic production. Improving yield and quality in production has always been an important task for wheat cultivation workers. The yield and quality of wheat are affected by varieties, environmental factors and cultivation measures (Mao et al., 2015). Different sowing methods such as drilling, wide space sowing and mulching are in practice for wheat cultivation which affect water consumption and yield (Wang et al., 2016).

In the Loess Plateau, a short summer fallow of about three months is practiced after the harvest of the previous winter wheat in late June and planting of the succeeding crop in late September to conserve soil water. Available soil moisture at sowing time depends on the tillage method used during the fallow period (Sun et al., 2018). Traditional sowing method (TS, drilled using a mechanical seeder, with rows spaced 20 cm apart without film mulching), is widely practiced on the Loess Plateau in China. Such sowing method without mulching does not conserve precipitation and soil moisture (Liu et al., 2005). Studied possibilities of direct drilling and reduced tillage in second crop silage corn. The direct seeding method gave the best result for mean of emergence dates and percentage of emerged seedling. The best result for silage yield was found in tillage combination. The lowest yield was found in the heavy-duty disc harrow tillage method. The direct seeding gives the best results for tillage efficiency parameters, such as fuel consumption, effective power requirement and field efficiency (Bayhan et al., 2006; Yalçın and Çakır et al., 2006).

The wide space and furrow sowing method, with wide space (22-25 cm wide base and 12 cm height) and furrow (depth 8 cm, sown into the top-edges of the furrow, rows spaced 12 cm) by using an all-in-one machine for ridging, fertilization and sowing, is being promoted not only for conserving precipitation and decreasing soil water evaporation, but also for avoiding contamination of soil environment with plastic. Sun et al., 2015; Li et al., 2018 reported that various sowing methods influenced wheat yield due to changes in soil water storage and water-use efficiency on the Loess Plateau in China. However, it remained unclear how different sowing methods would influence soil bacterial diversity and abundance that contribute to the changes in soil quality and micro-environment (Mann et al., 2019). Compared with flat sowing, soil moisture is not easy to be lost under the sowing condition and its water retention performance is strong (Bergeron et al., 1949). Compared with conventional seeding three-dimensional uniform sowing can increase chlorophyll content promoted photosynthesis during grain filling and can significantly reduce the number of infertile spikelet's and increase wheat yield (Li et al., 2010; Zhao et al., 2019).

The work of sowing method along with the improvement of soil water status and quality, seedling establishment, quality and crop yield can also be increased mainly through improving water infiltration and retention (Yan et al., 2008). Photosynthesis in crops is changed by the addition of water and nitrogen and nitrogen nutrition is influenced. Tridimensional uniform sowing is a modified form of conventional drilling in which seeds are distributed evenly and in the same plane (Tao et al., 2018). High nitrogen use efficiency resulting in increased grain protein content may come from improved capacity of the grain to accrue nitrogen supply to the grains (Triboı et al.,

http://www.aloki.hu ● ISSN 1589 1623 (Print) ● ISSN 1785 0037 (Online)
DOI: http://dx.doi.org/10.15666/aeer/1804_57015726

2002). Grain protein content decreased in the year with low precipitation (335.0 mm), while increased in the year with high precipitation (673.1 mm), (534.7 mm) (Sun et al., 2014). Nitrogen fertilizer expands soil fertility and crop productivity. Nitrogen is an essential mineral nutrient for plant growth (Wang et al., 2012; Ahmad et al., 2013).

Nitrogen fertilizer has a major input rate in the production of direct seeded winter wheat. In the past, recommended nitrogen application the spring using ammonium nitrate (Black et al., 1977). In China, farmers excessively apply nitrogen fertilizers because of their hope to sustain further grain yield increases but grain yield does not keep synchronous increase with excessive nitrogen application (Meng et al., 2016). Nitrogen application during the wheat growing season generally exceeds 320∼350 kg nitrogen ha^{-1} however, some farmers uses rates as high as 750 kg nitrogen ha^{-1} (Lu et al., 2015). Therefore, achieving both high yield and high nitrogen simultaneously is a major challenge (Lu et al., 2014). The efficient recovery of fertilizer nitrogen by crops is desirable both for economic reasons and to minimize environmental problems. However, various studies in China have shown that nitrogen losses following the use of fertilizer can be high (Roelcke et al., 1994; Zhang et al., 1992). Available water and nitrogen are considered the most limiting factors in wheat production in most parts of the world, especially in arid and semi-arid regions (Gonzalez et al., 2010). Therefore, supplemental irrigation and nitrogen fertilizer application are required to match soil water stress and stabilize yields (Tavakkoli et al., 2004).

The highest nitrogen uptake in the growth period occurred from reviving stage to anthesis stage. The proportion of nitrogen accumulated in leaf and stem was high before the anthesis stage and the accumulated nitrogen rate in stem reached peak at the anthesis stage (Zhao et al., 2006). The objective of this study were to find the best sowing method and optimize doses of nitrogen level to increase the yield and quality of winter wheat crop. Wide space sowing (WSS) with 240 $kg \cdot hm^{-2}$ enhances photosynthetic characteristics of flag leaves and promotes dry matter accumulation, to achieve high yield in addition, it was showed that the nitrogen metabolism of the plants improved, which was beneficial to the improvement of sugar and protein content and the quality of wheat also improved.

Materials and methods

Experimental site

The field experiment was conducted at Wenxi experimental site of Shanxi Agriculture University located in the southeastern part of the Loess Plateau (34° 35 ‘N and 110°15 ‘E) from 2017-2018. It is a typical semi-arid area with an altitude of 450-700 m. The average annual temperature is 11 to 13 °C. The average annual rainfall is 450-630 mm, 60-70% of the rainfall is concentrated in July-September. Winter wheat and maize are the main crops, irrigation conditions start for winter wheat in mid-October to the beginning of June of the following year, for corn in mid-to-late June, it is harvested in early October of the same year. The total rainfall at the test site for 2017-2018 was 240.9 mm, with rainfall for each month as shown in *Figure 1* and soil base fertility is presented in *Table 1*.

In wenxi experimental station where wheat was planted once a year without irrigation. Natural precipitation was the main source of water for crop cultivation in the same area and precipitation mainly concentrated in July-September, which was the

http://www.aloki.hu ● ISSN 1589 1623 (Print) ● ISSN 1785 0037 (Online)
DOI: http://dx.doi.org/10.15666/aeer/1804_57015726

fallow period of wheat. Precipitation from sowing to wintering and jointing to maturity were abundant, but the fallow period.

Table 1. *Soil nutrient properties from experimental location in Shanxi. (Data source: Meteorological Station of Shanxi, Wenxi)*

Soil nutrients	2017-2018	2017-2018
Soil layer (cm)	0.20	20.40
Organic matter (g kg^{-1})	12.59	10.40
Available phosphorous (mg kg^{-1})	16.26	10.71
Available potassium (mg kg^{-1})	280.65	150.65
pH	7.89	8.02

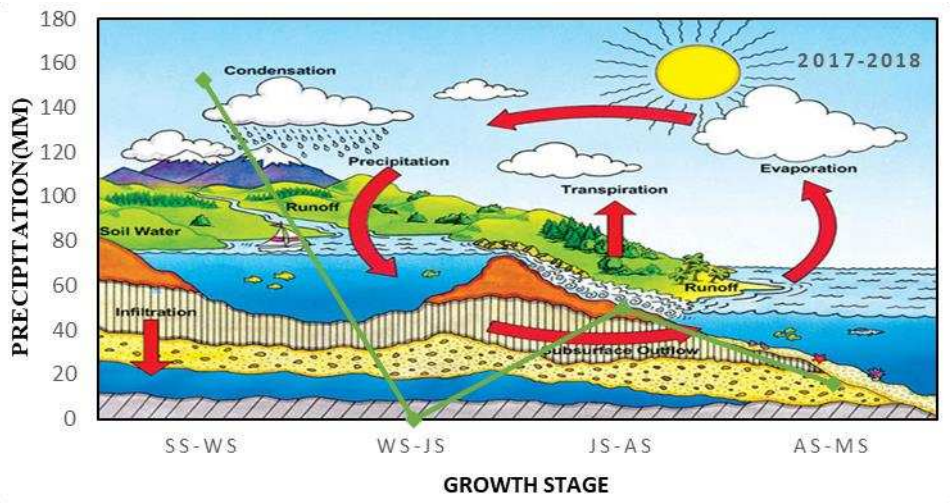

Figure 1. *Precipitation during study year (2017-2018) in different growth stages of wheat at the experimental site in Wenxi. Fallow period: SS-WS, WS-JS, JS-AS, AS-MS: 20 Jun to 30 Sep; S-W (sowing–wintering): 01 Oct to 30 Nov; W-J (wintering–jointing): 1 Dec to 25 Apr; J-A (jointing–anthesis): 26 Apr to 1 May; A-M (anthesis–maturity):2 May to 9 Jun, total growth period and total precipitation, respectively*

Experimental design and treatments

The wheat cultivar 'liangxing-99' used in this experiment was obtained from Wenxi Agriculture Jinnan. The two factors split-plot design was adopted and two sowing methods was set as (I) Wide Space Sowing (WSS) (II) Drilling Sowing (DS). The details of the machinery and sowing techniques are given in *Table 2* and *Figure 2*. Nitrogen application amount was taken as the secondary area with seven nitrogen application levels set as N_0: 0 kg hm^{-2}, N_{90}: 90 kg hm^{-2}, N_{180}: 180 kg hm^{-2}, N_{240}: 240 kg hm^{-2}, N_{270}: 270 kg hm^{-2}, N_{300}: 300 kg hm^{-2}. All treatments were replicated 3 times. The area of each plot was 30 m^2 (5 m × 6 m). Winter wheat was sown in October in 2017 and 2018 and harvested in June of the following year. Stubble (about 25 cm high) was left in field after harvesting wheat.

http://www.aloki.hu ● ISSN 1589 1623 (Print) ● ISSN 1785 0037 (Online)
DOI: http://dx.doi.org/10.15666/aeer/1804_57015726

Table 2. *Wide space sowing (WSS), drilling sowing (DS) details of sowing methods adopted during the experiment*

Sowing method	Sowing technique	Line spacing	Tillage
Wide space sowing (WS)	2BMF-12/6, tillage, auto-fertilization	Line space: 22-25 cm	Sub-soiling, rotary tillage
Drilling sowing (DS)	2BXF-12Seed driller, Nonghaha company, no-till, auto-fertilization	Line space: 20 cm	No tillage

Figure 2. *Field preparation at experimental site and tow sowing methods. (a) Wide space sowing (WSS). (b) Drilling sowing (DS) of Shanxi Agricultural University*

After the previous corn harvest, the straw was returned to the field. Before sowing, the basal application of phosphate fertilizer and potash fertilizer, P2O5 150 kg·hm^{-2}, K2O 90 kg·hm^{-2} was applied to the soil. The sowing amount was 225 kg·hm^{-2}, the nitrogen fertilizer was applied to the base ratio of 6:4 in the joint stage, with the irrigation of 60 mm, with the conventional field management. And no fertilizer was applied during growth seasons.

http://www.aloki.hu ● ISSN 1589 1623 (Print) ● ISSN 1785 0037 (Online)
DOI: http://dx.doi.org/10.15666/aeer/1804_57015726

Measurements

Determination of total tiller and plant nitrogen

Number of tillers in the population: three parallel rows of wheat sample sections with seedling emergence were selected in each growth period, with an area of 0.667 m^2 and the number of tillers in the population was investigated. After drying and comminution of plant organs in each growth period, the nitrogen content was determined by blue colorimetry of H_2SO_4-H_2O_2-indiophenol, which was calculated with reference to Li et al. (2018).

Water consumption

Water consumption in wheat fields was measured using a simplified formula as described below (Xue et al., 2019):

$$ET = P - \Delta S \quad \text{(Eq.1)}$$

where P is the effective precipitation (mm) during that stage and ΔS is reduction of soil water storage at each stage and was measured as $\Delta S = S_1 - S_2$, where S_1 and S_2 were the soil water content at the beginning and end of the stage, respectively. Whereas, runoff and drainage were considered negligible.

The water consumption intensity (CWR, mm d^{-1}) was calculated as:

$$CwR = \frac{ET_i}{d} \quad \text{(Eq.2)}$$

where ETi is the water consumption (mm) of wheat in each growth stage and d is the number of days in the growth stage.

Soil water storage

At the sowing, wintering, jointing, anthesis and maturity of wheat growth stages, 0-300 cm soil layer was drilled, carefully packed into an aluminum box to determine soil moisture content. Oven drying method was used to measure the soil water content of every 20 cm soil. Soil water storage were calculated by using the following formula (Liang et al., 2019):

$$\text{Soil water storage } (\text{mm}) = \frac{\text{wet soil weight} - \text{dry soil weight}}{\text{dry soil weight} \times 100\% \times \text{soil thickness} \times \text{soil bulk density}} \quad \text{(Eq.3)}$$

Changes in soil water storage (ΔSWS) for a specific stage of wheat will be calculated as the difference between the soil water storage at the beginning (SWS1) and at the end of the growth stage (SWS2) as follow:

$$\Delta SWS = SWS1 - SWS2 \quad \text{(Eq.4)}$$

The water consumption (CA, mm), percentage of CA to total water consumption (CP, %), and daily water consumption (CD, mm) were calculated as follow:

$$CA = P + I - \Delta SWS \quad \text{(Eq.5)}$$

$$CP = CAG / CA \quad \text{(Eq.6)}$$

http://www.aloki.hu ● ISSN 1589 1623 (Print) ● ISSN 1785 0037 (Online)
DOI: http://dx.doi.org/10.15666/aeer/1804_57015726

$$CD = \text{the CAG/d} \quad \text{(Eq.7)}$$

where P is precipitation (mm) during this period, I is the irrigation amount, CAG refers to water consumption at a certain stage, and d is the number of days in the growing stage.

$$WUE = Y/ET \quad \text{(Eq.8)}$$

where WUE is water use efficiency (kg h^{-1} mm^{-1}); Y is the yield of wheat (kg h^{-1}).

Determination of spike number

Comparison of the spike of interest with the model spike occurs in an n-dimensional vector space, which dimensions are defined by the total spikelet number of the spike of interest. The geometrical difference in GYDAS between the two spikes is based on the scalar product of these two vectors:

$$\cos\alpha\ (\vec{a},\vec{b}) = \frac{\vec{a}\cdot\vec{b}}{|\vec{a}|\cdot|\vec{b}|} \quad \text{(Eq.9)}$$

Photosynthetic characteristics i.e. leaf photosynthetic rate, transpiration rate, intercellular carbon dioxide concentration and stomatal conductance of flag leaf were measured by CI-340 hand-held photosynthesis measurement system (USA) at 9:00-11:00, 14 $_{Days}$, 21 $_{D}$, 28 $_{D}$, after flowering.

Determination of sucrose, soluble sugar and starch

After flowering period listed growth consistent and the same day flowering of wheat spike and peeling grain was placed in the oven dried at 105 °C for 20 min and then at 80 °C for 12 hours for dry weight. The quality and speed of weighing samples greatly affect the overall quality of the test. Then the grain was weighed and phenol method was used to determine the content of sucrose, and ketone color method was used to determine the total soluble total sugar content. H_2SO_4-H_2O_2-Phenol blue color method was used to determine the seed protein and its component content (Zhao et al., 2013).

Determination of grain yield, grain protein yield

At maturity, plants were randomly sampled from three 1 m^2 areas from each plot to determine grain number $spike^{-1}$ and 1,000 grain weight. All plants from the plots were harvested on 9 June 2017. Grains were air-dried whereas aboveground plant parts were oven dried until constant weight to determine the grain yield (kg ha^{-1}) and dry biomass. The harvest index (HI) was calculated dividing the grain yield by the aboveground dry biomass.

Determination of wet gluten content processing quality

The bromophenol blue water solution and isopropanol lactic acid mixture, and the settling values were determined by shock. The landing value was measured using the Landing Numerical Measurer (FN-IV). The Micro dough LAB, a micro powder instrument was produced by a Swedish company Botone (SCB) and it measured the fluidity of bread. The wet gluten content and gluten index were measured using the Gluten Index Meter (MJ-IIIB) quality analyzer. For Quality analysis dough mixed from 200 g flour was divided into small doughs weighted based on 0.25 g flour calculated as.

http://www.aloki.hu ● ISSN 1589 1623 (Print) ● ISSN 1785 0037 (Online)
DOI: http://dx.doi.org/10.15666/aeer/1804_57015726

$$Wet\ gluten(\%) = \frac{100\ \%\ flour + 2ml\ water + 10\%salt}{100} \times 0.25g\ of\ flour \quad \text{(Eq.10)}$$

Statistical analysis

The different Data were subjected to analysis of variance (ANOVA) as split-plot design using DPS and SAS 9.0. Graphics were constructed using Microsoft Excel 2010-13. Mean values were calculated and significance of the difference between treatments was tested by LSD (least significant difference) method at the significance level of P = 0.05.

Results

Nitrogen fertilizer on yield compositional factors

Wheat yield and compositional factors were more common than regular strips with a significant increase in spike, yield and an increased number of spikes (*Table 3*). The number of spikes, spike shots and the weight of thousands of grains, yield with the increased nitrogen application showed the trend of first increase and then decrease. The yield and its three elements were the highest in N_{240} and spike number and yield were significantly different from other nitrogen treatment and under DS, the yield and its constituent elements was the highest in N_{210} and the spike and yield was significantly different from other nitrogen treatment. It can be seen WSS and DS, access can optimize the output of the three elements at the same time of WSS broadcast with N_{240} and DS casting N_{210} to achieve the increase of output. Drilling sowing (DS) and wide space sowing (WWS) showed significant increase in the number of spikes and yield. With the increased nitrogen rate, the three factors of yield increased first and then decreased. For WS and DS, the yield and its three elements are the highest at 240 $kg \cdot hm^{-2}$ and 210 $kg \cdot hm^{-2}$, respectively.

Effect of different sowing methods and water consumption during the growth period for winter wheat

Effect of nitrogen fertilizers on water use of wide space sowing (WSS) of wheat influence total water consumption during the growth period. With the increase of nitrogen application, the total water consumption in the growth period of WSS wheat increased first and then decreased (*Fig. 3*). The total water consumption in the growth period of N_{240} treatment was significantly higher than in other treatments and was the lowest without nitrogen application and the differences between N_{210} and N_{270}, N_{90} and N_{180}, N0 and N_{300} were not significant. It can be seen that WSS with N_{240} increased the total water consumption during the growth period of wheat, which was conducive to the growth and development.

Effect of different sowing methods and nitrogen rates on water source of farmland and percentage for farmland water consumption

With the increase of nitrogen application, the proportion of precipitation and water content of wheat fields decreased first and then increased and water consumption of soil, storage and its proportion increased (*Table 4*). The proportion of precipitation water consumption was the lowest in N_{240} and was the highest in N_0 and N_{240} was different from other treatments and the proportion of water consumption was also the

http://www.aloki.hu ● ISSN 1589 1623 (Print) ● ISSN 1785 0037 (Online)
DOI: http://dx.doi.org/10.15666/aeer/1804_57015726

lowest in N_{240} and the highest in N_0 but the difference between treatments were not significant and the soil water storage, water consumption and its proportion were the lowest and in N_0, N_{240} and N_{240} were significantly higher than other nitrogen applications. The wide space sowing (WSS) with N_{240} reduced the dependence of wheat on precipitation and irrigation during growth and enhanced the utilization of wheat to soil water storage.

Table 3. *Effect of different sowing methods on grain protein and component contents of winter wheat*

Sowing method	N rate ($kg \cdot hm^{-2}$)	Spike number ($10^4 \cdot hm^{-2}$)	Grain number Per spike	1000-grain weight (g)	Yield ($kg \cdot hm^{-2}$)
WSS	N_0	688.25_c	29.92_b	36.42_{cd}	6433.31_e
	N_{90}	$705.75b_c$	30.69_a	37.32_c	6938.22_d
	N_{180}	716.50_c	29.73_b	40.66_b	7447.64^c
	N_{210}	728.25_c	30.56_a	41.35_{ab}	7841.61_b
	N_{240}	823.25_a	31.52_a	42.58_a	9234.26_a
	N_{270}	758.75_b	30.95^a	39.07_b	8003.31_b
	N_{300}	695.50_c	$28.08b_c$	38.90_c	6684.08_{de}
DS	N_0	511.25e	27.97_c	35.56_d	4231.12_h
	N_{90}	547.75e	28.54_{bc}	39.70_b	5139.00_g
	N_{180}	560.25e	29.88_b	40.73_b	5857.49_f
	N_{210}	628.50d	30.40_a	42.10_a	6921.53_d
	N_{240}	587.50d	29.10_b	41.28_{ab}	6092.60_f
	N_{270}	540.00e	28.02_{bc}	39.92_b	5087.64_g
	N_{300}	503.75f	27.20_c	36.84_{cd}	4356.07_h

WSS, DS indicate wide space sowing, drilling sowing and sowing technique 2BMF-12/6, tillage, auto-fertilization WSS: wide space sowing. DS: 2BXF-12 seed driller, Nonghaha Company, no-till, auto-fertilization drilling sowing

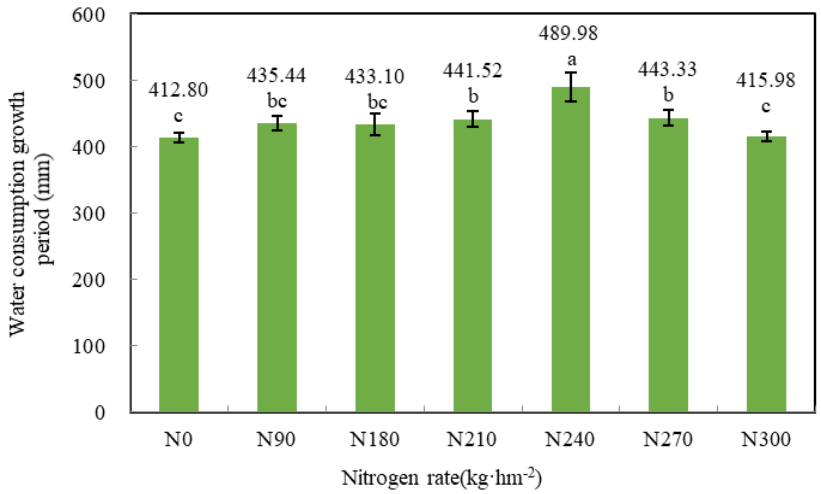

Figure 3*. Effect of different sowing methods and nitrogen rate on water consumption of soil profile, of winter wheat. Different letters indicate significant difference among treatments at the significance level of* $p \leq 0.05$

http://www.aloki.hu ● ISSN 1589 1623 (Print) ● ISSN 1785 0037 (Online)
DOI: http://dx.doi.org/10.15666/aeer/1804_57015726

Table 4. *Effect of different sowing methods and nitrogen rate on water resources of water consumption amount and ratio of winter wheat*

N rate (hm^{-2})	Precipitation		Irrigation		Soil water storage	
	Water consumption amount (mm)	Proportion ratio (%)	Water consumption amount (mm)	Proportion ratio (%)	Water consumption amount (mm)	Proportion ratio (%)
N_0	218.30	52.89_a	60.00	14.54_a	134.50_c	32.58_c
N_{90}	218.30	50.14_a	60.00	13.78_{ab}	157.14_b	36.09_b
N_{180}	218.30	50.41_a	60.00	13.85_{ab}	154.80_b	35.74_b
N_{210}	218.30	49.44_b	60.00	13.59_{ab}	163.22_b	36.97_b
N_{240}	218.30	44.55_c	60.00	12.25_b	211.68_a	43.20_a
N_{270}	218.30	49.24_b	60.00	13.53_{ab}	165.03_b	37.22_b
N_{300}	218.30	52.48_a	60.00	14.42_a	137.68_c	33.10_c

Different letters indicate significant difference among treatments at the significance level of $p \leq 0.05$

Effect of different sowing methods and nitrogen rates on grain protein and components content

The effect of nitrogen fertilizers on grain protein and its components were significantly different (*Table 5*). The contents of albumin and globulin (soluble protein) increased first and then decreased with the increase of nitrogen application. The highest value of albumin was in N_{240} and the difference between N_{270} and N_{300} were not significant. The highest value of albumin was N_{270} and the difference between N_{180}, N_{210}, N_{240} and N_{300} were not significant. The contents of glutenin (storage protein) increased with the increase of nitrogen application with the highest content of N_{300}, but the difference of glutenin content was not significant compared with N_{270} and the content of glutenin N_{300} was significantly higher than that of other nitrogen application treatments compared with N_{90}, N_{180} and N_{240} were the highest ratio of grain to alcohol but the difference was not significant. The protein contents were significantly higher than that of N_{300} and N_{240} and other nitrogen applications. The protein yield of N_{240} was significantly higher than that of other nitrogen treatments. It can be seen that nitrogen fertilizer has obvious regulation on storage protein and was more conducive to quality improvement.

Table 5. *Effect of different sowing methods nitrogen rate on grain protein and component contents at maturity stage*

N rate ($kg \cdot hm^{-2}$)	Albumin (%)	Globulin (%)	Gliadin (%)	Glutenin (%)	Glu/Gli	Protein (%)	Protein yield (kg/hm^{-2})
N_0	1.96_c	1.54_d	2.61_d	3.57_e	1.37_{ab}	10.75_d	755.79_d
N_{90}	2.09_b	1.71_c	2.88_c	4.00_d	1.39_a	11.24_c	857.56_c
N_{180}	2.12_b	1.80_{ab}	3.04_c	4.26_d	1.40_a	11.92_c	962.22_c
N_{210}	2.20_b	1.80_{ab}	3.94_b	5.24_c	1.33_b	13.40_b	1050.77_b
N_{240}	2.58_a	1.93_a	4.03_b	5.92_b	1.47_a	14.79_a	1282.54_a
N_{270}	2.46_a	1.95_a	4.30_a	5.81_b	1.35_b	14.03_b	1087.29_b
N_{300}	2.49_a	1.91_a	4.50_a	6.09_a	1.35_b	15.10_a	799.20_d

http://www.aloki.hu ● ISSN 1589 1623 (Print) ● ISSN 1785 0037 (Online)
DOI: http://dx.doi.org/10.15666/aeer/1804_57015726

Effect of different sowing methods and nitrogen rates on net photosynthesis rate (Pn) of the post-flower flag leaves

The concentration of carbon dioxide between the flag leave cells after wide space sowing (WSS) and wheat flower decreased gradually with the grouting process and the 0-7 days net photosynthesis rate increased with the amount of nitrogen applied after flowering showing a single peak increase trend (*Fig. 4*). The 14 days net photosynthesis rate after flowering was still the highest at N_{300} and not significantly different from N_{270} and N_{240}, but after flowering 21 days and 28 days net photosynthesis rate increased with nitrogen application. After flowering 28 days was still the highest with N_{240}, but the difference was not significant compared to N_{180}, N_{210}, N_{270} and N_{300}. It can be seen that the addition of nitrogen fertilizer can significantly improve the net photosynthesis rate of the flag leaves after flowering, but the treatment effect of high nitrogen (N_{270}, N_{300}) in the later grouting was weakened and the wide space sowing (WSS) with N_{240} could sustain the whole grout period.

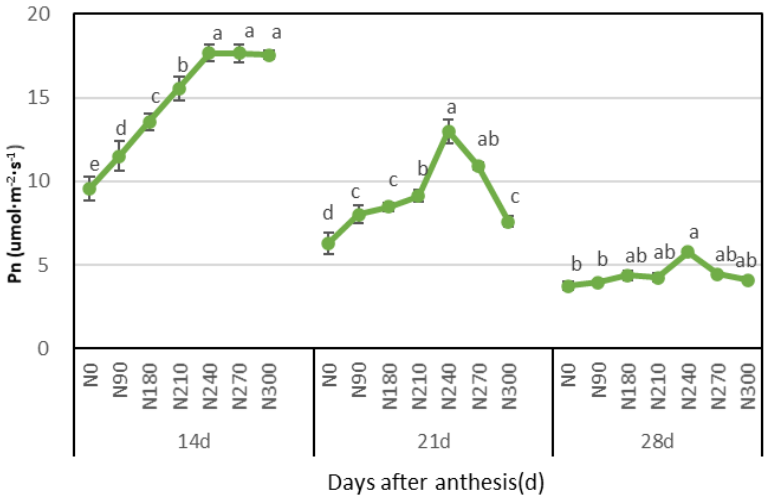

Figure 4. *Effect of different sowing methods and nitrogen rate 14 Days, 21 D, and 28 D after flowering on Net Photosynthesis Rate (Pn) of flag leaves Sowing technique2BMF-12/6, tillage, auto-fertilization WSS: wide space sowing; DS: 2BXF-12 Seed driller, Nonghaha company, no-till, auto-fertilization drilling sowing; of winter wheat*

Effect of different sowing methods and nitrogen rates on intercellular carbon dioxide concentration (Ci) in flag after flowering

The intercellular carbon dioxide concentration in the flag leaves of wide space sowing (WSS), drill sowing (DS) in wheat decreased gradually with the growing process and intercellular carbon dioxide concentration in the flag leaves decreased first and then increased with the increase of nitrogen application at different stages after flowering (*Fig. 5*). The N_{240} treatment was significantly lower than other treatments on 14 days and 21 days after flowering and N_0 was the highest N_{240} and was the lowest 28 days after flowering, but the difference was not significant compared with N_{270}. It can be seen that the increase of nitrogen fertilizer can significantly reduce the intercellular carbon dioxide concentration in the leaves of the flags after flower and the whole grouting period can be continued.

http://www.aloki.hu ● ISSN 1589 1623 (Print) ● ISSN 1785 0037 (Online)
DOI: http://dx.doi.org/10.15666/aeer/1804_57015726

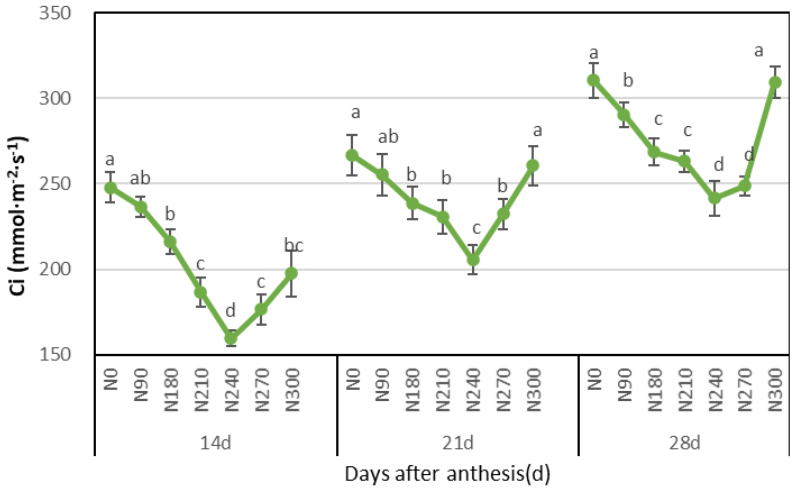

Figure 5. *Effect of different sowing methods and nitrogen rate14 Days, 21 D, and 28 D after flowering on intercellular carbon dioxide concentration (Ci) of flag leaves Sowing technique2BMF-12/6, tillage, auto-fertilization WSS: wide space sowing; DS: 2BXF-12Seed driller, Nonghaha company, no-till, auto-fertilization drilling sowing; of winter wheat*

Effect of different sowing methods and nitrogen rates on stomatal conductance (Gs) of flag leaves after flowering

The stomatal conductance of the flag leaves of wide space sowing (WSS) and drilling sowing (DS) wheat decreased gradually with the process of growing and the stomatal conductance of the flag leaves increased first and then decreased with the increase of nitrogen application at different stages after flowering (*Fig. 6*). The N_{240} treatment was significantly higher than other treatments 14 days after flowering and N_0, it was the lowest and N_{240} was the highest at 21-28 days, but the difference was not significant. It can be seen that increased nitrogen fertilizer can significantly increase stomatal conductance of flower flag leaves, but the effect lasts until the middle stage of growth and the effect weakened in the later stage.

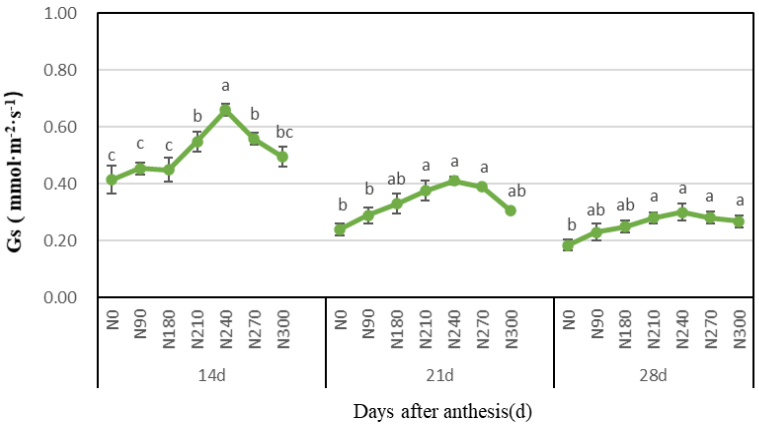

Figure 6. *Effect of different sowing methods and nitrogen rate 14 Days, 21 D, and 28 D after flowering on stomatal conductance (GS) of flag leaves Sowing technique2BMF-12/6, tillage, auto-fertilization WSS: wide space sowing; DS: 2BXF-12 Seed driller, Nonghaha company, no-till, auto-fertilization drilling sowing; of winter wheat*

http://www.aloki.hu ● ISSN 1589 1623 (Print) ● ISSN 1785 0037 (Online)
DOI: http://dx.doi.org/10.15666/aeer/1804_57015726

Effect of different sowing methods and nitrogen rates on transpiration rate (Tr) of flag leaves after flowering

The transpiration rate of flag leaves decreased gradually with the grouting process and the transpiration rate of flag leaves increased first and then decreased with the increase of nitrogen application in different stages after flowering (*Fig. 7*). The N_{240} and N_{270} treatments were significantly higher than other treatments on 14 days and 21 days, after flowering and N_0 was the lowest. After 28 days N_{240} was significantly higher than other treatments and N_0 was the lowest. It can be seen that increased nitrogen fertilizer can significantly enhance the transpiration rate of flag leaves after flowering, which could last for the whole growth period and the best effect of N_{240} was obtained in the large WSS and DS.

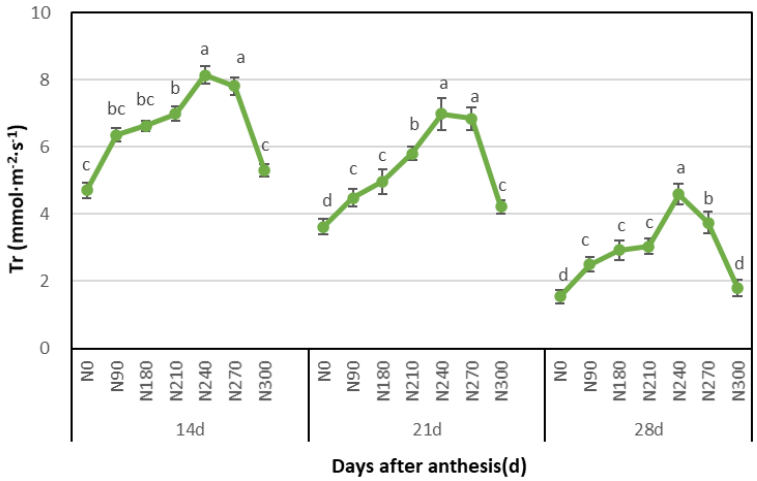

Figure 7. *Effect of different sowing methods and nitrogen rate 14 Days, 21D and 28D after flowering on transpiration rate (TR) of flag leaves Sowing technique 2BMF-12/6, tillage, auto-fertilization WSS: wide space sowing; DS: 2BXF-12 Seed driller, Nonghaha company, no-till, auto-fertilization drilling sowing; of winter wheat*

Effect of different sowing methods and nitrogen rate on soluble sugar content, sucrose content and starch content of wheat grains

The wide space sowing (WSS) method increased the soluble sugar content, sugar content and starch content in wheat grain during winter season when applied nitrogen at N300 and N270 respectively. Lowest soluble sugar content, sucrose content and starch content were count in the lower dose of nitrogen N90 and N190 as compare to control N0 and N300 (Table 6). The nitrogen application has a significant effect on soluble sugar content, sucrose content and starch content, but when nitrogen application given at certain level.

Effect of different sowing methods and nitrogen content of soil at 0-200 cm during major fertility periods

The nitrogen content of soil in different soil layers increased gradually with the increase of nitrogen application in different fertility periods and the N0 content was the lowest without the use of nitrogen treatment (*Fig. 8*). Compared between the nitrogen treatments there were no significant differences in the nitrogen content of soil in winter

http://www.aloki.hu ● ISSN 1589 1623 (Print) ● ISSN 1785 0037 (Online)
DOI: http://dx.doi.org/10.15666/aeer/1804_57015726

and no significant differences were found between the other soil layers. Among them the winter period 0-20 cm soil layer N300 was significantly higher than other nitrogen application treatment on 20-60 cm soil layer N270 and N300 were significantly higher than other treatments, 120 cm with N300 and N270 were the highest and compared with other nitrogen treatment differences significantly, maturity 0-120 cm soil nitrogen content with N300 significantly was higher than other nitrogen emissions treatment. 120-160 cm also with N300 was the highest but compared with other nitrogen treatment differences was not significant. The difference between treatments was deep as 160 cm in maturity, excessive nitrogen fertilizer was not conducive to wheat absorption of nitrogen. Wide space sowing (WWS) showed significant increase in the number of spikes, yield and an increase in the number of kernels per spike. For WS and DS, the yield and its three elements were the highest at 240 $kg \cdot hm^{-2}$ and 210 $kg \cdot hm^{-2}$, respectively. Therefore, wide space sowing (WWS) were equipped with 240 $kg \cdot hm^{-2}$ and regular strips were applied with 210 $kg \cdot hm^{-2}$ that achieved an increase in production.

Table 6. *Effect of different sowing methods and nitrogen rate on soluble sugar content, sucrose content and starch content in grains winter*

N rate ($kg \cdot hm^{-2}$)	Soluble sugar content%	Sucrose content%	Starch content%
N_0	40.35_c	17.42_b	53.31_c
N_{90}	41.31_c	20.38_b	$56.18b_c$
N_{180}	46.18_{bc}	22.82_{ab}	58.32_b
N_{210}	48.32_b	23.04_a	61.99_b
N_{240}	51.99_b	24.43_a	67.19_a
N_{270}	55.17_a	24.54_a	66.17_a
N_{300}	57.19_a	25.64_a	69.35_a

Effect of different sowing methods on plant nitrogen accumulation in main growth period

The accumulation of plant nitrogen in wide space sowing (WSS) wheat growth process increased and increase of nitrogen application the accumulation of plant nitrogen showed a trend of increasing and then decreasing in each growth periods (*Fig. 9*). The nitrogen accumulation of wheat plant in different growth stages were the highest in N_{240} treatment and showed significant difference and it was the lowest in N_0 treatment. It can be seen that N_{240} combined with wide space sowing can promote nitrogen accumulation in plants at all growth stages and provide nitrogen source for high yield. Wide space sowing (WSS) with the nitrogen of 240 $kg \cdot hm^{-2}$ could obtain nitrogen accumulation, which increased in all growth stages and the nitrogen accumulation and its proportion increased significantly during the wintering to jointing stage and proportion of nitrogen accumulation in the early growth period increased and the nitrogen accumulation of various organs increased, the nitrogen pre-anthesis nitrogen translocation amount and nitrogen accumulation amount after anthesis increased significantly, but Nitrogen uptake efficiency, nitrogen use efficiency and nitrogen productive efficiency were the highest at 90 $kg \cdot hm^{-2}$ and was the lowest at 300 $kg \cdot hm^{-2}$.

http://www.aloki.hu ● ISSN 1589 1623 (Print) ● ISSN 1785 0037 (Online)
DOI: http://dx.doi.org/10.15666/aeer/1804_57015726

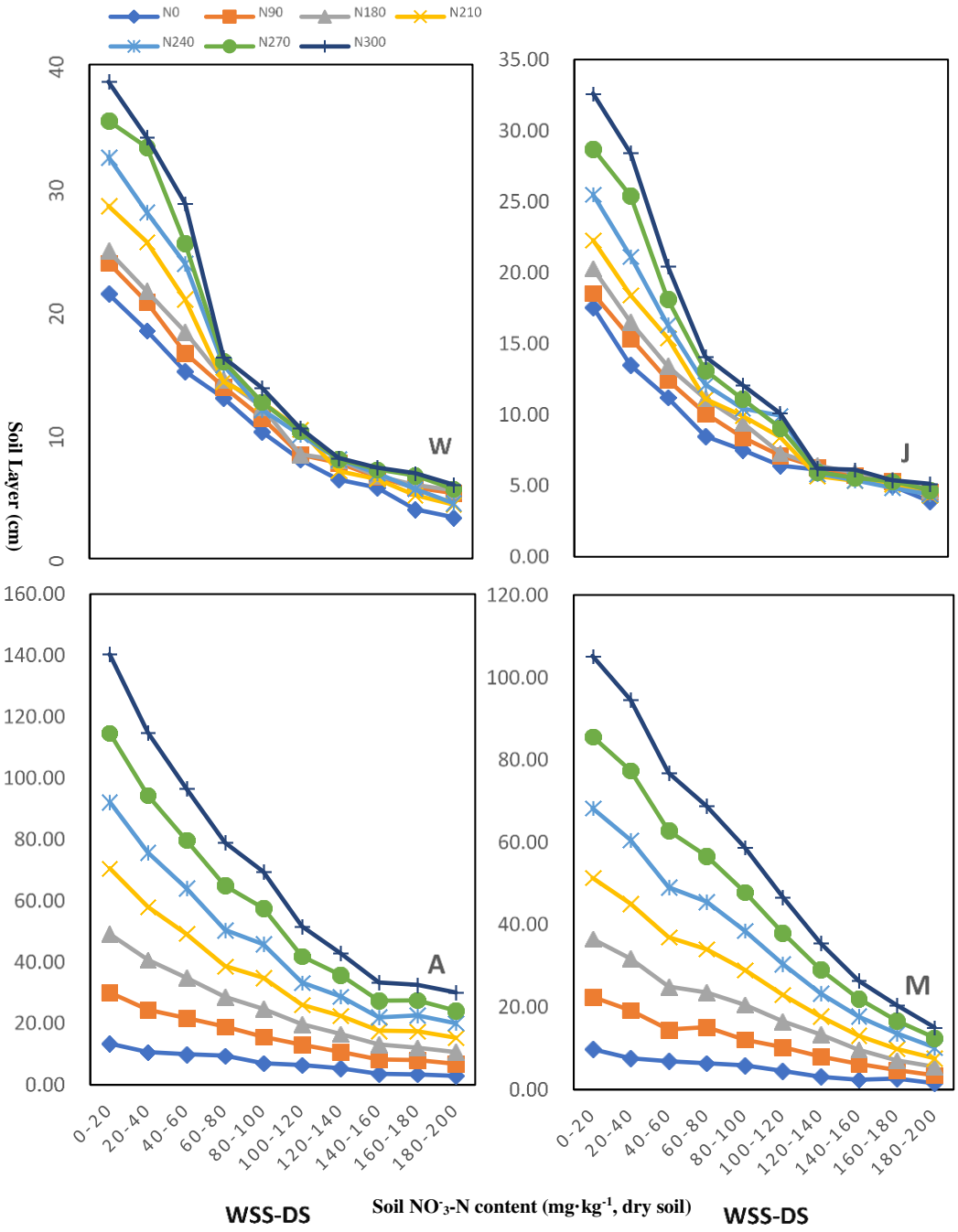

Figure 8. *Effect of different sowing methods and nitrogen rate on nitrate nitrogen content at 0-200 cm soil layers of winter wheat at different growth stages of winter wheat. W, J, A, and M indicate wintering, jointing, anthesis, and maturity stages; WSS: wide space sowing; DS drilling sowing W –J -A and M: 01 Oct to 30 Nov; W-J (wintering–jointing): 1 Dec to 25 Apr; J-A (jointing–anthesis): 26 Apr to 1 May; A-M (anthesis– maturity):2 May to 9 Jun, total growth period Sowing technique 2BMF-12/6, tillage, auto-fertilization WSS: wide space sowing; DS: 2BXF-12Seed driller, Nonghaha company, no-till, auto-fertilization drilling sowing*

http://www.aloki.hu ● ISSN 1589 1623 (Print) ● ISSN 1785 0037 (Online)
DOI: http://dx.doi.org/10.15666/aeer/1804_57015726

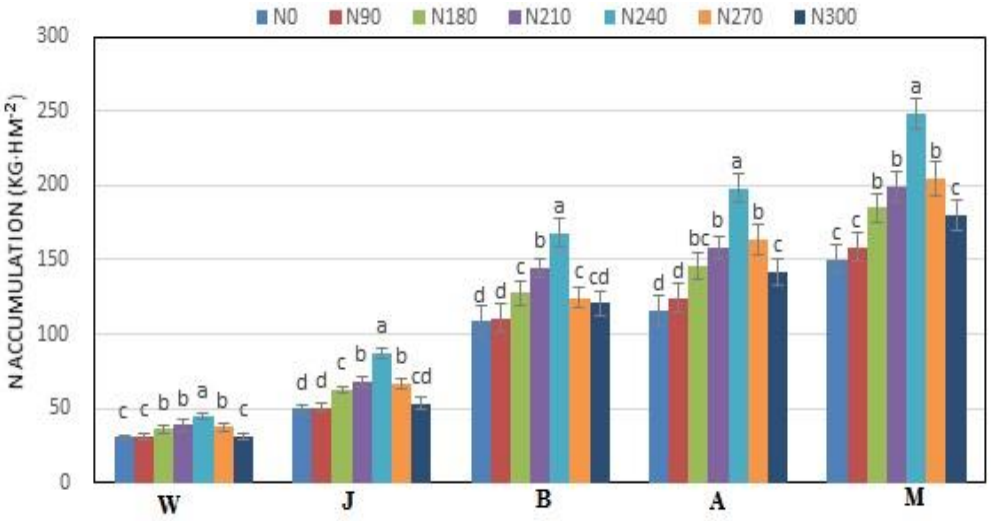

Figure 9. *Effect of different sowing methods and nitrogen rate on nitrogen accumulation of winter wheat at different growth stages of winter wheat. W, J, B, A, and M indicate wintering stage, jointing, bolting, anthesis, and maturity stages; (21 June - 30 September), sowing to wintering (1 October - 30 November), wintering to jointing (1 December T0 10 April) Jointing stage to Booting (11 April to 25 April), jointing to Anthesis (26 April - 1 May) and anthesis to maturity (2 May - 9 June) Sowing technique 2BMF-12/6, tillage, auto-fertilization WSS: wide space sowing; DS: 2BXF-12 Seed driller, Nonghaha company, no-till, auto-fertilization drilling sowing*

Correlation coefficients between water consumption and yield components at different growth stage in dryland wheat

The results of the correlation analysis of total water consumption and yield in the growth period of wide space sowing wheat showed that total water consumption in the growth period was significantly positively correlated with yield ($P < 0.01$). Further (*Fig. 10*), water consumption during growth period was closely related to yield.

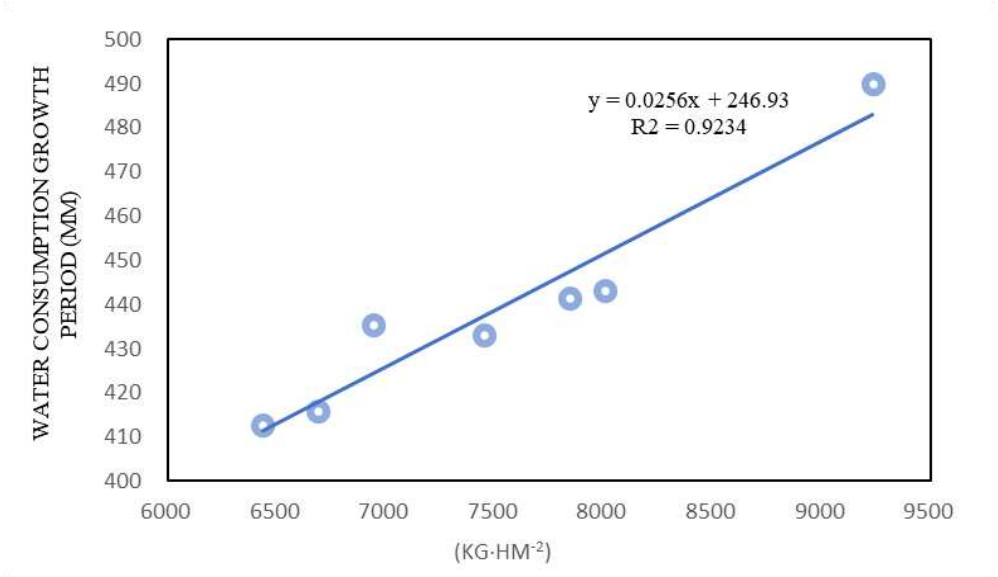

Figure 10. *Correlation coefficients between water consumption and yield in winter wheat*

http://www.aloki.hu ● ISSN 1589 1623 (Print) ● ISSN 1785 0037 (Online)
DOI: http://dx.doi.org/10.15666/aeer/1804_57015726

Discussion

Wheat production in this region are facing great challenges of a scant water supply and nutrient deficit. Due to the sparse and deep groundwater resources, rainfall is the sole water source for wheat production in the Loess Plateau, and it is limited (200-600 mm) and unevenly distributed. Only 30%-40% of annual rainfall occurs during winter wheat growing season, whereas most of the rain falls between July and September, which is concurrent with the summer fallow between two growing seasons of winter wheat (Li et al., 2015). Wheat yield in semiarid dryland areas is highly affected by the variation in the amount and distribution of seasonal precipitation (Wang et al., 2015). Precipitation is an important meteorological factor which affects soil water content. In the Loess Plateau and other dryland areas, the soil water content at the time of sowing is important for early growth of wheat and highly dependent on the precipitation during fallow season of dryland wheat (Kang et al., 2002; Rossato et al., 2017).

Effect of different sowing methods on nitrogen rates fertilizer group quality and yield formation

Soil is the basic need for plant survival the exchange of nutrients, water and gas between soil and crops affects the growth and development of crops yields then regulates the formation of yield and quality (Triboi et al., 2002). The amount of fertilization is significantly positively correlated with crop yields, so farmers pursue high yields by applying a large amount of fertilizer resulting in excessive nitrogen being dispersed in the air, water and soil causing a series of environmental and human health problems (Seong et al., 2018). The supply of nutrients in farmland is determined by the input of soil base fertility and fertilizers and the soil nutrient supply capacity and characteristics are different under different soil fertility, resulting in different characteristics of crop nutrients absorption and utilization which directly affects the utilization of nutrients (Matzen et al., 2019). The average output of WSS homogenous treatment is 8976 kg hm^{-2} compared to the DS. Relatively coordinated to promote the production composition of the three factors of growth, so as to achieve a higher production than traditional strip production (Chen et al., 2016); Dang et al., 2015). However Han et al. (2013) showed that after the use of wide, the number of spikes significantly increased but the grain weight also increased and spike but did not reach the difference level and finally achieved increased production. According to Wei et al. (2016), from the wheat growth situation under different sowing methods the difference in the number of basic seedlings winter and spring equinox between the treatments was not significant indicating that the different sowing methods had a small impact on wheat sowing and seeding and the ability of wheat sowing planted in WSS was similar to that of ordinary strips. According to Anxia et al. (2015), due to the variety difference the effect of nitrogen fertilizer on tiller number in each growth stage of wheat population is different. The growth and development characteristics of different varieties appropriate amount of nitrogen fertilizer application and top dressing time are selected to achieve reasonable control of tiller number in each growth stage of wheat population. The results of this study showed that the application of 240 kg hm^{-2} in wide and drilling significantly increased tillers in the jointing stage and the booting stage compared with other nitrogen treatments while there were no significant changes in other growth stages (Guo et al., 2016). Nitrogen application was beneficial to the ears development of

http://www.aloki.hu ● ISSN 1589 1623 (Print) ● ISSN 1785 0037 (Online)
DOI: http://dx.doi.org/10.15666/aeer/1804_57015726

wheat, increased the number of effective ears and grains per ear and achieved an increase in yield. However, excessive nitrogen application would reduce the total number of ears and 1000 grain weight of winter wheat leading to a decrease in yield. In a study of Ye et al. (2010), the three elements of wheat yield increased with the increase of nitrogen fertilizer amount, especially the 1000 grain weight and grain number per panicle reached significant levels. However, when nitrogen fertilizer amount exceeded 90 kg·hm^{-2}, grain number per panicle could not reach a significant level and when nitrogen fertilizer amount increased to 180 kg·hm^{-2} or even 210 kg·hm^{-2}, 1000 grain weight could not reach a significant level. According to Yang et al. (2018), increase of nitrogen application, the output and yield composition of the three factors will not show a single peak increase trend but show the first increase and then decrease trend in the nitrogen application of 180 kg hm^{-2}, the number of grain weight and spike reached the maximum at 240 kg hm^{-2}. The number of spike particles and yield were maximized and the differences were significant. The results of this experiment showed that with the increase of nitrogen application, the number of spikes, spike grains and thousands of grain weight, the yield increases first and then it decreases, the spike number and yield difference was significant but the difference between the number of spike and thousands of grains was not significant and the DS cast 210 kg. The number of h^{-2} spike particles and yield increased significantly and there was no significant difference between the number of spikes and the weight of thousands which showed that on the basis of the seeding method affecting the yield composition wide space sowing (WSS) was a stronger nitrogen fertilizer utilization capacity which was more consistent with the previous studies.

Effect of different sowing methods on nitrogen rates fertilizer and water utilization

Currently advocated water saving agriculture is faced with such problems as how to improve soil water utilization efficiency, reduce ineffective water consumption and strengthen wheat's utilization of water in deep soil. In addition to improving varieties adjusting crop layout and cultivation mode is a low cost efficient and fast way. The ability of wheat to adapt to changing conditions in the process of growing depends not only on the genetic characteristics of the variety itself but also on the farmland microenvironment due to changing planting patterns. The planting mode is a factor that can be controlled in agricultural production, water and nitrogen utilization efficiency is determined by multiple factors and all factors that can affect grain yield water consumption and nitrogen will directly or indirectly affect water utilization efficiency (Maaiping et al., 2009). One of a research work shows that the drilling spacing in order to reduce the basic seedlings and establish reasonable population quality can be optimized after flowering plant physiological characteristics increase capacity, improve the grain-filling ability but small planting distance contributed to the growing contradiction between individual body, poor resource utilization condition of field in the field. Therefore, by increasing the row space and width appropriately, the sowing quality can be improved the reasonable group structure can be constructed and the individual growing environment can be improved. The experimental study of Crisálida et al. (2018) shows that the wide drilling with 240 kg·hm^{-2} reduce the proportion of rainfall and irrigation water consumption, water consumption and soil water storage and its proportion increase may be due to wide drilling soil root spatial distribution promoted the root soil water use of water. The results of this study also showed that the water consumption of seeding jointing and jointing flowering increased with the

http://www.aloki.hu ● ISSN 1589 1623 (Print) ● ISSN 1785 0037 (Online)
DOI: http://dx.doi.org/10.15666/aeer/1804_57015726

adoption of WSS compared with the DS. Moreover, the total water consumption during the growth period of wide and drill was significantly positively correlated with the yield ($P < 0.01$). The drill also showed a positive correlation but not significantly. However, research conducted by Wang et al. (2013) showed that wide sowing made the inter-row plant spacing more evenly distributed. However, as the row spacing became wider the wheat population was not evenly distributed on the whole and the land cover was not complete. According to the study of Zhou et al. (2008), nitrogen application had a regulatory effect on water consumption indexes in different growth stages. Water consumption in the early stage of nitrogen application and water consumption model coefficient in the late stage of growth promoted the use of soil water and nitrogen by roots and the growth of vegetative organs. Appropriate application can improve the utilization ability of wheat to soil water storage reduce the dependence on natural precipitation and irrigation and compensate for the impact of insufficient irrigation on grain yield (Ercoli et al., 2008; Yan et al., 2012). Research showed that nitrogen fertilizer had a greater effect on water consumption in the stage and increased nitrogen fertilizer application could increase water consumption in the stage of greening-flowering and its proportion, so that the peak of water consumption moved forward. The results of this study showed that with the increase of nitrogen application, the water consumption in the early and middle stages of growth and their proportion, as well as the water consumption in the jointing flowering stage first increased and then decreased and the water consumption in the later stages first decreased and then increased. Among them the wide drilling with 240 kg hm^{-2} improved planting jointing stage and jointing stage, flowering two stage water consumption and its proportion reduced, According to Shi et al. (2008), total water consumption during the growth period of nitrogen treatment was significantly higher than that of non-nitrogen treatment. Compared with nitrogen application, the total water consumption of 210 kg hm^{-2} treatment the proportion of irrigation water and the water consumption of soil storage were the highest. Compared with other treatments the difference was significant indicating that the suitable nitrogen application of 210 kg hm^{-2} in this area promoted the utilization of soil water storage by wheat. The results of this study showed that with the increase of nitrogen application the water consumption of soil storage water and its proportion first increased and then decreased. The proportion of precipitation and irrigation water consumption of 240 kg hm^{-2} combined with wide drilling was the lowest, while the proportion of water consumption of soil storage water and its proportion were the highest. In terms of sowing characteristics wide drilling has the growth conditions to make full use of water and the coordination between water and nutrients was very important for the growth and development of crops. The utilization of soil water in wheat fields will directly affect the efficiency of nitrogen fertilizers. The studies also showed that within the scope of 0-360 kg hm^{-2} N240 kg hm^{-2} more than 180 kg hm^{-2} was the most appropriate nitrogen treatment. Nitrogen treatment increased by 9.53%, but the utilization efficiency of precipitation and water use efficiency increased by 9.54% and 21.04%, respectively (Wang et al., 2012).

Effect of different sowing methods and nitrogen fertilizer on photosynthesis characteristics of post-flower flag leaves

Photosynthetic rate, stomatal conductance, transpiration rate and chlorophyll content are important components of photosynthetic physiological characteristics of crops. Nitrogen is the main element of protein synthesis an important component of grain

http://www.aloki.hu ● ISSN 1589 1623 (Print) ● ISSN 1785 0037 (Online)
DOI: http://dx.doi.org/10.15666/aeer/1804_57015726

closely related to the life activities of crops and an indispensable nutrient limiting factor in agricultural production. As a result, nitrogen has been applied extensively in agricultural production over the past few decades to increase wheat yields. However, some studies have shown that under the condition of high nitrogen application the photosynthetic rate of leaves decreased and with the application of a large amount of nitrogen fertilizer in agricultural production the loss of fertilizer was directly caused and soil pollution was serious and the agricultural ecological environment entered a vicious circle. Wang et al. (2012) showed that the light transmittance of the large WSS and DS wheat population was significantly better than that of the traditional row spacing sowing wheat which could significantly adjust the net photosynthetic characteristics of the flower flag leaves. The results of this study showed that broad drilling with 240 kg hm^{-2} improved the photosynthetic characteristics of flag leaves, significantly increased the net photosynthetic rate, stomatal conductance and transpiration rate of flag leaves after flowering and significantly reduced the intercellular carbon dioxide concentration. This may be due to that the wide precision sowing expanded the width and row spacing, optimized the light conditions for the population in the field and at the same time, the suitable nitrogen application made reasonable use of the photo thermal resources. The nutrient conditions were good the individual plants developed well the green leaf area was large, function time was long and aging time of the whole plant in the later stage of wheat was delayed, so as to avoid the early aging of the leaves (Hu et al., 2016). Study showed that leaf photosynthesis was closely related to crop yield and leaf photosynthetic rate was an important reason for crop high yield while nitrogen fertilizer could enhance plants' ability to synthesize chlorophyll and was one of the most effective factors to regulate plant leaf photosynthetic capacity (Li et al., 2010; Fuentes et al., 2003). Their research experience define that when the soil water content was the same the Pn of wheat generally increased first and then became stable with the increase of nitrogen application and the intercellular carbon dioxide concentration transpiration rate and net photosynthetic rate generally increased first and then decreased, which also indicated that appropriate nitrogen application is beneficial for improving the photosynthetic capacity of wheat flag leaves during the filling period. Appropriate nitrogen application is also expected to improve the photosynthetic capacity of winter wheat over ground parts increase the accumulation and transfer of dry matter and promote the increase of wheat yield. The results of this study showed that the photosynthetic indexes in the flag leaves of the broad drilling with 240 kg·hm^{-2} fertilizer all reached the optimal level which may be due to the appropriate nitrogen fertilizer amount promoting the synthesis of chlorophyll. In addition, the protective enzyme activity level in the wheat plant was maintained at the same time. However, some studies have shown that increased nitrogen fertilizer is beneficial to increase the population leaf area of wheat and optimize the canopy environment. However, excessive nitrogen fertilizer will reduce leaf inclination and excessive leaf area will lead to unreasonable canopy structure resulting in wheat yield loss (Song et al., 2016).

Effect of different sowing methods and nitrogen fertilizer on nitrogen metabolism

Increasing the amount of nitrogen fertilizer can increase the effective nitrogen content of wheat field tillage layer and promote nitrogen absorption in wheat plants. Nitrogen emissions ranged from 120 kg hm^{-2} to 240 kg hm^{-2} increasing the accumulation of nitrogen in various organs during maturation but reducing the transfer rate of nitrogen accumulation to grain in the organs after flowering. According to Zhang

http://www.aloki.hu ● ISSN 1589 1623 (Print) ● ISSN 1785 0037 (Online)
DOI: http://dx.doi.org/10.15666/aeer/1804_57015726

et al. (2012), due to the increase in nitrogen application wheat organs before the operation of nitrogen and the accumulation of nitrogen in the mature period increased but the nutrient organs before the accumulation of nitrogen operation rate and the contribution rate of nitrogen to grain after flowering did not change significantly. The results of this study also show that the amount of nitrogen running before flowering increases and then decreases after the increase of nitrogen accumulation before flowering the contribution rate of nitrogen operation to grain before flowering also increases and then decreases but not significantly. The reason for the analysis may be that water fertilizer needs to be increased synchronously with increasing the amount of nitrogen applied but the lack of water in wheat fields cannot make full use of nitrogen fertilizer but is not conducive to the operation and accumulation of nitrogen in the plant (Chai et al., 2010; Guo et al., 2018). Work shows that nitrogen fertilizer recycling rate, nitrogen fertilizer agronomy efficiency nitrogen fertilizer production efficiency and nitrogen fertilizer utilization efficiency show a decreasing trend with the increase of nitrogen application when nitrogen application exceeds 240 kg hm^{-2} soil nitrogen content increases and with the extension of planting age this is more obvious. This study shows that nitrogen absorption efficiency nitrogen utilization efficiency and nitrogen production efficiency were all 90 kg hm^{-2}, soil nitrogen content with the increase of nitrogen yield and soil layer deepening, the difference between treatment can be as deep as 160 cm in maturity, Excessive application of nitrogen fertilizer was not conducive to the absorption of nitrogen in wheat, which was more consistent with previous studies.

Effect of different sowing methods and nitrogen rates fertilizer on grain quality

In recent years with the reform of agricultural structure wheat production is changing from high yield to green age. The arrival of the green era not only means the strategy of weight loss and drug reduction, the pursuit of high quality wheat, the establishment of reasonable quality evaluation standards are the most urgent tasks and in the current regulation of wheat quality of many factors nitrogen fertilizer regulation is the most effective measure (Wang et al., 2015). The total protein content and component content of wheat grains of different grains increased significantly with the increase of nitrogen application. The analysis of the proportion of each protein component of wheat grain to the total protein in this experiment showed that the protein component content increased, the protein was the highest at 240 kg, hm^{-2} the globulin was the highest at 270 kg hm^{-2} and the alcohol soluble protein and wheat gluten (storage protein) were the highest at 300 kg hm^{-2}. The globulin ratio was the highest at N240 the protein content were 300 kg hm^{-2}, 240 kg hm^{-2} and the protein yield was 240 kg hm^{-2} significantly higher than that of other nitrogen treatment. The study also found that clear protein and globulin were more regulated by nitrogen fertilizer in the grout stage, while alcohol soluble protein and wheat gluten were more sensitive to nitrogen fertilizer reaction in the later stage of grouting. However, there were also reports that with the increase of nitrogen application the increase in seed globulin and alcohol-soluble protein can be observed, while the content of clear protein and gluten has a tendency to decrease (Fuentes et al., 2003). Analysis of the reasons resulted in the consequence that varieties were the main factors affecting quality in addition according to Wang et al. (2016), that different soil fertility protein components to nitrogen application level are not the same. At the same time, it is shown that the response of strong middle and weak wheat to nitrogen fertilizer is very different. The application of the appropriate amount of nitrogen fertilizer is conducive to improving the nutritional quality of wheat and

http://www.aloki.hu ● ISSN 1589 1623 (Print) ● ISSN 1785 0037 (Online)
DOI: http://dx.doi.org/10.15666/aeer/1804_57015726

processing quality. Nitrogen application in the range of 0-300 kg hm^{-2} nitrogen and wheat actual yield and protein yield of the secondary curve relationship was conducive to improve protein, wet gluten content and sedimentation value and other indicators at the same time can extend the formation time and stability time of the dough (Cao et al., 2005). The results show that with the increase of nitrogen fertilizer, the sedimentation value, landing value and formation time, stabilization time, wet gluten and gluten index increased but the water absorption rate were relatively stable, which is consistent with the previous research results.

Conclusions

The number of spikes and production increased significantly the number of spike particles also increased. DS can optimize the output of the three elements at the same time. Further analysis shows that the wide space sowing was distributed with 240 kg hm^{-2} to reduce precipitation and irrigation increased the water consumption and proportion of soil water storage increased the water consumption in the sowing extraction and extraction flowering stages and ultimately increased the total water consumption during fertility and improved the efficiency of water utilization at the same time, reduced the high yield of each organ, increased the dry quality of each organ, increased the dry quality of the plant in the extraction-flowering and flowering maturity stage and its proportion increased the grain weight of each time after flowering, the number of spikes and yield increased significantly. The pore conductivity and steaming rate reduced the concentration of carbon dioxide between cells resulting in high yield. In addition, WSS distribution with 240 kg hm^{-2} to increase the accumulation of nitrogen in plants during the main fertility period significantly increased the accumulation of nitrogen in each stage of fertility the proportion of nitrogen accumulation increased in the pre fertility stage and the accumulation of nitrogen increased in various organs during maturity, the amount of nitrogen before flowering and nitrogen accumulation after flowering significantly increased, while ensuring the yield. It was beneficial for the improvement of sugar and protein content and the quality of wheat.

Acknowledgements. "Modern Agriculture Industry Technology System Construction" (No. CARS-3-1-24); The National Key Research and Development Program of China (No. 2018YFD020040105); The Sanjin Scholar Support Special Funds Projects; National Natural Science Foundation of China (No. 31771727); The "1331" Engineering Key Innovation Cultivation Team-Organic Dry Cultivation and Cultivation Physiology Innovation Team (No. SXYBKY201733).

REFERENCES

[1] Ahmad, W., Shah, Z., Khan, F., Ali, S., Malik, W. et al. (2013): Maize yield and soil properties as influenced by integrated use of organic, inorganic and bio-fertilizers in a low fertility soil. – Soil Environ. 32: 121–129.
[2] Anxia, Z. H., Jiang, F. et al. (2015): Effects of nitrogen fertilizer amount on population dynamics and yield of different varieties of wheat. – China Seed Industry 12: 65-67.
[3] Bayhan, Y., Kayışoğlu, B., Gönülol, E., Yalçın, H., Sungur, N. (2006); Possibilities of direct drilling and reduced tillage in second crop silage corn. – Soil and Tillage Research 88: 1-7.

http://www.aloki.hu ● ISSN 1589 1623 (Print) ● ISSN 1785 0037 (Online)
DOI: http://dx.doi.org/10.15666/aeer/1804_57015726

[4] Bergeron, T. et al. (1949): The problem of artificial control of rainfall on the globe. I. - General effects of ice-nuclei in clouds. – Tellus 1: 32^13.
[5] Black, A. L., Siddoway, F. H. et al. (1977): Winter wheat recropping on dryland as affected by stubble height and nitrogen fertilization. – Soil Sci. Soc. Am. J. 41: 1186-1190.
[6] Cao, C. F., Kong, L. C., Wang, J. L. et al. (2005): Effects of nitrogen application on yield, quality and nutrient absorption of wheat with strong and medium gluten. – Plant Nutrition and Fertilizer 1: 46-50.
[7] Chai, Y. J., Xiong, Y. S., et al. (2010): Effects of nitrogen application on nitrogen accumulation and operation of different winter wheat varieties. – Acta Botanica Sinica Northwestern 30(10): 2040-2046.
[8] Chen, C., Fan, S., Liu, G. et al. (2016): Comparison of yield and agronomic traits of spring wheat with wide-spread spread sowing and conventional strip-sowing. – Gansu Agricultural Science and Technology 1: 36-38.
[9] Crisálida, M. V., Coelho, K. P., Luz, T. R. S. A. et al. (2018): Effect of different water application rates and nitrogen fertilization on growth and essential oil of clove basil. – Industrial Crops & Products 125.
[10] Dang, W., Ma, C., Zhao, Q., Feng, Z. H. et al. (2015): Effects of wide precision sowing on wheat yield and yield components. – Hebei Agricultural Sciences 19(2): 15-17.
[11] Encyclopedia Britannica (2013): Loess Plateau. – Encyclopedia Britannica, Inc., Chicago.
[12] Ercoli, L., Lulli, L., Mariotti, M. (2008): Post-anthesis dry matter and nitrogen dynamics in durum wheat as affected by nitrogen supply and soil water availability. – European Journal of Agronomy 28(2): 138-147.
[13] Fuentes, P. J., Flury, M., Huggins, R. D. et al. (2003): Soil water and nitrogen dynamics in dryland cropping systems of Washington State, USA. – Soil and Tillage Research 71: 33-47.
[14] Gonzalez-Dugo, V., Durand, J. L., Gastal, F. (2010): Water deficit and nitrogen nutrition of crops. A review. – Agron. Sustain. Dev. 30: 529-544.
[15] Guo, L., Shi, J.-S., Wang, L.-Y. et al. (2018): Effects of nitrogen application on nitrogen uptake and utilization and soil nitrate nitrogen content in summer maize under integrated drip irrigation with water and fertilizer. – Chinese Journal of Ecological Agriculture 26(5): 668-676.
[16] Guo, M., Zhao, G., Guo, W. et al. (2016): Effects of nitrogen application and row spacing on winter wheat yield and physiological characteristics. – Journal of Nuclear Agriculture 30(4): 805-812.
[17] Han, H. F., Zhao, D. D., Shen, J. Y. et al. (2013); Effects of irrigation amount and period on yield and quality characteristics of large-area precision winter wheat. – Chinese Journal of Agricultural Engineering 29(14): 109-114.
[18] Horvat, D., Jurkovic, Z., Drezner, G., Simic, G., Novoselovic, D., Dvojkovic, K. et al. (2006); the influence of gluten proteins on technological properties of Croatian wheat cultivars. – Cereal Res. Commun. 34: 1177-1184.
[19] Hu, M. Y., Menf, Y., Zhang, Y. J., (2016); Research progress on the effects of water and nitrogen interaction on crop physiological characteristics and nitrogen utilization. – Journal of Wheat Crops 36(3): 332-340.
[20] Kang, S., Zhang, L., Liang, Y., Dawes, W. R. (2002); Simulation of Winter Wheat Yield and Water Use Efficiency on the Loess Plateau of China Using WAVES. – In: McVicar, T. R., Rui, L., Walker, J., Fitzpatrick, R. W., Changming, L. (eds.) Regional Water and Soil Assessment for Managing Sustainable Agriculture in China and Australia. ACIAR Monograph No. 84. Australian Centre for International Agricultural Research, Bruce, pp. 95-104.
[21] Li, H., Xue, J.-F., Gao, Z. -Q., Xue, N.-W., Yang, Z. -P et al. (2018); Response of yield increase for dryland winter wheat to tillage practice during summer fallow and sowing method in the Loess Plateau of China. – J. Integr. Agric. 17: 817-825.

http://www.aloki.hu ● ISSN 1589 1623 (Print) ● ISSN 1785 0037 (Online)
DOI: http://dx.doi.org/10.15666/aeer/1804_57015726

[22] Li, J., Yao, Y., Ding, Z. et al. (2010); Effects of furrow sowing on dry matter, soil water use efficiency and soil temperature of winter wheat populations. – Crop Research 24(1): 16-18.
[23] Li, N. N., Sun, M., Gao, Z. Q. et al. (2018); Study on the relationship between water consumption of deep pine and mulch seeding in upland wheat fields with extreme annual pattern and nitrogen uptake and utilization in plants. – Sci Agric Sinica 51(18): 3455-3469.
[24] Li, S. X. et al. (2002): Ways and strategies for increasing fertilizer nitrogen efficiency in dryland soil. – Acta Pedologica Sinica 39(Suppl.): 56-75.
[25] Li, S., Xiao, L. (1992); Distribution and management of drylands in the People's Republic of China. – Advances in Soil Science 18: 148-293.
[26] Li, Z., Feng, W. et al. (2015); Effects of sow spacing on water consumption characteristics of winter wheat. – Henan Agricultural Science 44(2): 22-27.
[27] Liang, Y. F., Khan, S., Ren, A. X., Lin, W., Anwar, S., Sun, M., Gao, Z. Q. (2019): Subsoiling and sowing time influence soil water content, nitrogen translocation and yield of dryland winter wheat. – Agronomy 9(1): 37.
[28] Liu, J. H., Dang, Z. P., Cao, W. X., Ai-Ping, Y. U. et al. (2005): Effect of different mulching and sowing methods on wheat yield and soil water content in Weibei. – The Journal of Applied Ecology 21(2): 351-358.
[29] Lu, D. J., Lu, F. F., Yan, P., Cui, Z. L., Chen, X. P. et al. (2014); Elucidating population establishment associated with N management and cultivars for wheat production in China. – Field Crops Research 163(1): 81 89.
[30] Lu, D. J., Lu, F. F., Pan, J. X., Cui, Z. L., Zou, C. Q., Chen, X. P., He, M. R., Wang, Z. L. et al. (2015): The effects of cultivar and nitrogen management on wheat yield and nitrogen use efficiency in North China Plain. – Field Crops Research 171: 157-164.
[31] Ma, A., Wang, J., Jing, H. et al. (2009); Effects of different sowing row spacing and density on wheat yield and water use efficiency. – Shaanxi Agricultural Sciences 55(1): 3-5.
[32] Ma, W. Q., Zhang, F. S., Zhang, W. F. et al. (2005): Fertilizer production and consumption and the resources, environment, food security and sustainable development in China. – Resource Science 27(3): 33-40.
[33] Mann, C., Lynch, D., Fillmore, S., Mills, A. et al. (2019); Relationships between field management, soil health, and microbial community composition. – Appl. Soil Ecol. 144: 12-21. DOI: 10.1016/j.apsoil.06.012.
[34] Mao, Y., Lei, B., Chen, A. et al. (2015); Effects of different no-till mulch cultivation models on the adaptation of Yunnan spring potato to seasonal drought. – Soil Bulletin 46(3): 556-561.
[35] Matzen, N., Jørgensen, J. R., Holst, N. et al. (2019); Grain quality in wheat impact of disease management. – European Journal of Agronomy 103.
[36] Meng, Q. F., Yue, S. C., Hou, P., Cui, Z. L., Chen, X. P. et al. (2016); Improving yield and nitrogen use efficiency simultaneously for maize and wheat in China: a review. – Pedosphere 26(2): 137-147.
[37] Pepó, P., Sipos, P., Gyõri, Z. et al. (2005); Effects of fertilizer application on the baking quality of winter wheat varieties in a long term experiment under continental climatic conditions in Hungary. – Cereal Res. Commun. 33: 825-832.
[38] Roelcke, M. et al. (1994); Die Ammoniak-Volatilisation nach Ausbringung von Mineraldünger-Stickstoff in carbonatreichen chinesischen Löss-Ackerböden. – PhD Dissertation, Technische Universität Braunschweig. Published in: Göttinger Beiträge zur Land- und Forstwirtschaft in den Tropen und Subtropen, Volume 92. Verlag Erich Goltze, Göttingen.
[39] Rossato, L., Alvalá, R. C., Marengo, J. A., Zeri, M., Cunha, A. P., Pires, L., Barbosa, H. A. (2017); Impact of soil moisture on crop yields over Brazilian semiarid. – Frontiers in Environmental Science 5: 73.

http://www.aloki.hu ● ISSN 1589 1623 (Print) ● ISSN 1785 0037 (Online)
DOI: http://dx.doi.org/10.15666/aeer/1804_57015726

[40] Seong-Woo, C., Chon-Sik, K., Hyeon, S. et al. (2018): Influence of protein characteristics and the proportion of gluten on end-use quality in Korean wheat cultivars. – Journal of Integrative Agriculture 17(8).
[41] Shi, X. K., Shi, Y., Zhao, J. Y. et al. (2008): Effects of nitrogen application on water consumption characteristics and grain yield of ultra-high-yield wheat variety yanong 1212. – Shandong Agricultural Sciences 50(5): 72-75.
[42] Song, M., Li, Z., Feng, H. et al. (2016); Characteristics of dry matter accumulation and yield effect of winter wheat at different water and nitrogen levels. – Chinese Journal of Agricultural Engineering 32(2): 119-126.
[43] Sun, M., Ge, X. M., Gao, Z. Q., Ren, A. X., Deng, Y., Zhao, W. F., Zhao, H. M. et al. (2014): Relationship between water storage conservation in fallow period and grains protein formation in dryland wheat in different precipitation years. – Scientia Agriculture since 47(9): 1692-1704 (in Chinese).
[44] Sun, M., Deng, Y., Gao, Z. Q., Zhao, H. M., Ren, A. X., Li, G. et al. (2015): Effects of tillage in fallow period and sowing methods on water storage and grain protein accumulation of dryland wheat. – Pakistan J. Agric. Sci. 52: 1-8.
[45] Sun, M., Ren, A. X., Gao, Z. Q., Wang, P. R., Mo, F., Xue, L. Z., Lei, M. M. et al. (2018): Long-term evaluation of tillage methods in fallow season for soil water storage, wheat yield and water use efficiency in semiarid southeast of the Loess Plateau. – Field Crops Res. 218: 24-32.
[46] Tao, Z., Wang, D., Ma, S., Yang, Y., Zhao, G., Chang, X. (2018): Light interception and radiation use efficiency response to tridimensional uniform sowing in winter wheat. – J. Integr. Agric. 17 566-578.
[47] Tavakkoli, A. R., Oweis, T. Y. et al. (2004): The role of supplemental irrigation and nitrogen in producing bread wheat in the highlands of Iran. – Agro. Water Manage. 65: 225-236.
[48] Triboı, E., Triboı Blondel, A. M. et al. (2002): Productivity and grain or seed composition: a new approach to an old problem: invited paper. – Eur J Agro 16: 163-186.
[49] Wang, C. Y., Dai, X. L., Shi, Y. H. et al. (2012): Study on the relationship between leaf area index and photosynthesis and yield of post-flowering wheat. – Chinese Journal of Plant Nutrition and Fertilizer 18(1): 27-34.
[50] Wang, H., Yu, Z., Zhang, Y., Shi, Y., Wang, D. et al. (2012): Effects of Tillage Regimes on Water Consumption and Dry Matter Accumulation in Dryland Wheat. – Acta Agron. Sin. 38: 675–682.
[51] Wang, L. F., Shangguan, Z. P. (2015): Water-use efficiency of dryland wheat in response to mulching and tillage practices on the Loess Plateau. – Scientific Reports 5: 12225.
[52] Wang, M., Zhao, G. C., Shi, S. B. et al. (2015): Effects of nitrogen application on post-flowering photosynthetic characteristics and nitrogen distribution and grain protein components of wheat with different grain colors at maturity stage. – Chinese Journal of Wheat Crops 35(6): 829-835.
[53] Wang, S., Qi, H., Wang, Y., Zhang, Q., Feng, G., Lin, Y., Liang, Q. et al. (2016): Effects of seeding rate and seeding mode on wheat growth and development and yield under wheat-cotton intercropping mode. – Journal of Shandong Agricultural University 48(7): 39-43.
[54] Wang, T., Qi, S., Guan, X. et al. (2013): Effects of population allocation on water utilization and yield of winter wheat. – North China Journal of Agronomy 28(2): 169-174.
[55] Wang, X. C., Li, J. (2010): Evaluation of crop yield and soil water estimates using the EPIC model for the Loess Plateau of China. – Mathematical and Computer Modelling 51(1112): 1390-1397.
[56] Wei, Y. Y., Jiang, H. L., Wang, B. L. et al. (2016); Effects of different sowing methods on wheat yield in Guan Zhong area. – Anhui Agricultural Science Bulletin 22(17): 49 + 68.

http://www.aloki.hu ● ISSN 1589 1623 (Print) ● ISSN 1785 0037 (Online)
DOI: http://dx.doi.org/10.15666/aeer/1804_57015726

[57] Xue, L., Khan, S., Sun, M., Anwar, S., Ren, A., Gao, Z., Lin, W., Xue, J., Yang, Z., Deng, Y. (2019): Effects of tillage practices on water consumption and grain yield of dryland winter wheat under different precipitation distribution in the loess plateau of China. – Soil and Tillage Research 191: 66-74.
[58] Yalçın, H., Çakır, E. (2006): Tillage effects and energy efficiencies of subsoiling and direct seeding in light soil on yield of second crop corn for silage in Western Turkey. – Soil and Tillage Research 90: 250-255.
[59] Yan, C. P., Zhang, Y. Q., Zhang, D. Y., Dang, J. Y. et al. (2008); Effects of sowing date and planting density on the grain's protein component and quality of strong and medium gluten winter wheat cultivars. – J. Applied. Ecol. 19(8): 1733-40.
[60] Yan, Y. R., Hao, W. P., Bai, Q. J. et al. (2012); Study on WUE effect of water stress during jointing and grouting stage of winter wheat in North China. – Chinese Journal of Irrigation and Drainage 31(1): 46-49.
[61] Yang, J., Zhao, L., Li, S. et al. (2018); Material accumulation and distribution of wheat and the formation of grain number per panicle in response to application. – Journal of Nuclear Agriculture 32(6): 1203-1210.
[62] Ye, Q. Q., Wang, G. L., Zhu, Z. et al. (2010); Effects of nitrogen application on population dynamics, yield and soil nitrogen change of high-yield wheat. – Acta Ecologica Applicata Sinica 21(2): 351-358.
[63] Zhang, M. W. et al. (2012): Effects of Nitrogen Application on Grain Yield and Quality of Wheat. – Henan Agricultural University, Henan.
[64] Zhang, S., Lovdahl, L., Grip, H., Tong, Y., Yang, X., Wang, Q. (2009): Effects of mulching and catch cropping on soil temperature, soil moisture and wheat yield on the Loess Plateau of China. – Soil & Tillage Research 102: 78-86.
[65] Zhang, S. L., Cai, G. X., Wang, X. Z., Xu, Y. H., Zhu, Z. L., Freney, J. R. et al. (1992): Losses of urea-nitrogen applied to maize grown on a calcareous fluvo-aquic soil in North China Plain. – Pedosphere 2: 171-178.
[66] Zhao, H. M. et al. (2013): Model of Drought-Resistant Wheat Cultivation Technology and Water Operating Mechanism. – Shanxi Agricultural University, Shanxi.
[67] Zhao, K., Chang, X., Wang, D. et al. (2019): Effects of three-dimensional uniform sowing and nitrogen application on winter wheat yield components and flag leaf photosynthetic performance. – Crop Magazine (1): 1-7.
[68] Zhao, M. X., Zhou, J. B., Yang, R., Zheng, X. F., Zhai, B. N., Li, S. X. et al. (2006): Characteristics of nitrogen accumulation, distribution and translocation in winter wheat on dryland. – J. Plant Nutrition and Fertilizer Science 12: 143-149.
[69] Zhou, X. B., Sun, S. J., Chen, Y. H. et al. (2008): Preliminary study on water characteristics and yield composition of winter wheat under different row spacing. – Acta Soilica Sinica 1: 188-191.

http://www.aloki.hu ● ISSN 1589 1623 (Print) ● ISSN 1785 0037 (Online)
DOI: http://dx.doi.org/10.15666/aeer/1804_57015726

EFFECT OF NITROGEN ON THE STARCH FORMATION AND YIELD OF HIGH-DENSITY SORGHUM [*SORGHUM BICOLOR* (L.) MOENCH] IN NORTHERN CHINA

YANG, G. D.[1,2] – HU, Z. Y.[2] – HUANG, R. D.[1] – HAO, Z. Y.[2] – LI, J. H.[2] – WANG, Q.[3] – MENG, X. X.[3] – ZHOU, Y. F.[1*]

[1]*College of Agronomy, Shenyang Agricultural University, No. 120 Dongling Road, Shenyang 110866 Liaoning, China*

[2]*Keshan Branch of Heilongjiang Academy of Agricultural Sciences, 161005 Heilongjiang, China*

[3]*Crop Resources Institute of Heilongjiang Academy of Agricultural Sciences, 150086 Heilongjiang, China*

**Corresponding author*
e-mail: zhouyufei2002@aliyun.com; zhouyufei@syau.edu.cn

(Received 29th Jan 2020; accepted 9th Jul 2020)

Abstract. Sorghum [*Sorghum bicolor* (L.) Moench] is an important plant in an arid and semi-arid part of China. The application of nitrogen is a basic element necessary for sorghum growth. In this study, Keza15 and Suiza7 were used as experimental materials in northern china to study the relationship among nitrogen and the accumulation of starch and the yield. The results showed that the total starch accumulation of the low-N-sensitive variety had a larger change range than the low-N-tolerant varieties. From 7 to 21 days after powder dispersal was a rapid growth period of starch accumulation and played an important role in the starch synthesis of grains. The yield of the two different genotypes of sorghum increased first and then decreased with a higher rate of nitrogen application. The best nitrogen application amount was 200 kg N ha^{-1} (N200). The application of nitrogen was beneficial for the increase of Soluble starch synthase (SSS), Starch branching enzyme (SBE), Bound starch synthetase (GBSS), Adenosine diphosphate glucose pyrophosphorylase (AGP), Uridine diphosphate glucose pyropitase activities (UGP), but the excessive nitrogen application led to a decrease. The effect of nitrogen on the activity of starch related enzymes for the low-N-sensitive sorghum was stronger than that for the low-N-tolerant sorghum.
Keywords: *sorghum, nitrogen application rates, starch synthesis, high density, key enzyme*

Introduction

Sorghum [*Sorghum bicolor* (L.) Moench] is the main food and economic crop in arid and semi-arid areas and is widely used in feed, brewing, energy, food processing and other fields (Wang et al., 2015). In the past few decades, the increase of sorghum yield were mainly attributed to the production increase in barren field (or low yield field) (Ciampitti et al., 2016). Nitrogen fertilizer is an important nutrient element in sorghum growth, reasonable application of nitrogen and sufficient nitrogen supply could alleviate the individual competition for nitrogen fertilizer, and improve the yield effectively (Mahama et al., 2014; Van weelden et al., 2016; Komla et al., 2019). However, excessive application of nitrogen fertilizer will lead to late maturity, lower harvest index, and lower nitrogen utilization efficiency (Liang et al., 2017). On the other hand, the excessive application of N results in decreased crop yields and environmental pollution (Jin et al., 2012). How to limit the negative impact of agricultural practices

http://www.aloki.hu ● ISSN 1589 1623 (Print) ● ISSN 1785 0037 (Online)
DOI: http://dx.doi.org/10.15666/aeer/1804_57275741

and increase crop production sustainability has been one of the key agricultural challenges (Ronga et al., 2019; Tilman et al., 2011).

Starch is the main component of sorghum grain, which consists of amylose and amylopectin. The proportion and quantity of amylose and amylopectin in the grain affect the quality of starch. Amylopectin content has an important impact on the palatability of sorghum and brewing quality (Ge et al., 2016). The application of nitrogen fertilizer is an effective means to improve the yield of sorghum, which can improve the accumulation of photosynthetic products, promote the formation of grain yield, which play an important role increasing production (Wang et al., 2015; Zhou et al., 2016). Nitrogen is involved in the synthesis of enzymes and their cofactors that regulate plant biochemical reactions. It is an important structural material in plants and one of the most critical elements in the process of carbon and nitrogen metabolism. Starch synthesis is a biochemical reaction process involving the coordination of many enzymes. The catalytic enzymes mainly include ADPG pyrophosphorylase, starch synthetase, starch branching enzyme, debranching enzyme and starch phosphorylase (Yan, et al., 2009).

In recent years, with the improvement of sorghum breeding level, sorghum has undergone a transformation from traditional tall-stalk and rare-planting to dwarf and high-density planting (Li et al., 2018). At present, the suitable planting density of dwarf sorghum in Heilongjiang Province is 300000 plants per hectare (Shen et al., 2013; Yang et al., 2015), which is the area with the largest sorghum planting density in China. The effect of nitrogen fertilizer on starch accumulation of sorghum grain has been reported, but the design of cultivation conditions is different. Previous studies focused on the effect of nitrogen on the yield and quality of sorghum, and high stem and sparse planting were mainly used for research background (Yu et al., 2008; Yi et al., 2014; Ge et al., 2016). There are few reports about the effect of high-density planting of sorghum starch in northern china. In this study, Keza15 and Suiza7 were used as experimental materials to study the relationship between nitrogen and starch yield, starch-related enzyme activity, and yield of different genotypes of sorghum under natural conditions. The physiological response and different mechanisms of starch accumulation and related enzyme activity of different genotypes of sorghum were clarified. It is of great significance to understand the nitrogen effect and metabolic mechanism of starch accumulation of high-density sorghum planted in an alpine area and to lay a foundation for the formulation of high-yield and high-quality cultivation technology.

Materials and methods

Trials materials

Keza15 and Suiza7 were obtained from the Keshan branch of the Heilongjiang Academy of Agricultural Sciences (Qiqihar City, Heilongjiang Province, China). Note: Keza15: the low-N-tolerant variety; Suiza7: the low-N-sensitive variety (Yang, et al., 2019) (*Fig. 1*).

Trials conditions

Agronomic trials were performed in an open field at Keshan (48°03′47″N, 125°87′57″E) (Qiqihar City, Heilongjiang Province, China) in 2017. The former crop was kidney bean, and the experimental soil was a chernozem. The 0-20 cm deep soil in

http://www.aloki.hu ● ISSN 1589 1623 (Print) ● ISSN 1785 0037 (Online)
DOI: http://dx.doi.org/10.15666/aeer/1804_57275741

the plow layer had the following characteristics: organic matter 3.2×10^4 mg·kg^{-1}, pH 6.12, alkali hydrolyzed nitrogen 173 mg·kg^{-1}, available phosphorus 28.8 mg·kg^{-1} and available potassium 307.2 mg·kg^{-1}.

Figure 1. *The field growth photos of two sorghum varieties during waxing stage under N100 treatment. (A) Keza15. (B) Suiza7*

Four nitrogen treatments were set up, and urea was used as the nitrogen source: 0 kg (N0), 100 kg (N100), 200 kg (N200) and 300 kg (N300) of pure nitrogen per hectare; 1/3 of nitrogen was applied as seed fertilizer, with 2/3 as top dressing, applied to the soil at the jointing stage. Fixed P and K (P_2O_5 150 kg and K_2O 100 kg/ha) were applied as seed fertilizer at one time. Sorghum was sown on May 15th, the trials area was 10 m long, consisting of eight ridges with a 0.65 m ridge distance and 300,000 seedlings per hectare, double row planting on ridge with row spacing of 15 cm and plant spacing of 10 cm. Three replications were conducted (*Fig. 2*).

The mean maximum and minimum air temperatures and total rainfall during the cropping cycles (May to September) were 29.3 and 7.8 °C and 357.4 mm for the year 2017 (*Fig. 3*).

1 Meter Experiment Protection Zone							
Keza15 N0	Suiza7 N0	Keza15 N100	Suiza7 N100	Keza15 N200	Suiza7 N200	Keza15 N300	Suiza7 N300
1 Meter Investigation Road							
Suiza7 N100	Keza15 N100	Suiza7 N200	Keza15 N200	Suiza7 N300	Keza15 N300	Suiza7 N0	Keza15 N0
1 Meter Investigation Road							
Keza15 N200	Suiza7 N200	Keza15 N300	Suiza7 N300	Keza15 N0	Suiza7 N0	Keza15 N100	Suiza7 N100
1 Meter Experiment Protection Zone							

Figure 2. *The experimental design*

http://www.aloki.hu ● ISSN 1589 1623 (Print) ● ISSN 1785 0037 (Online)
DOI: http://dx.doi.org/10.15666/aeer/1804_57275741

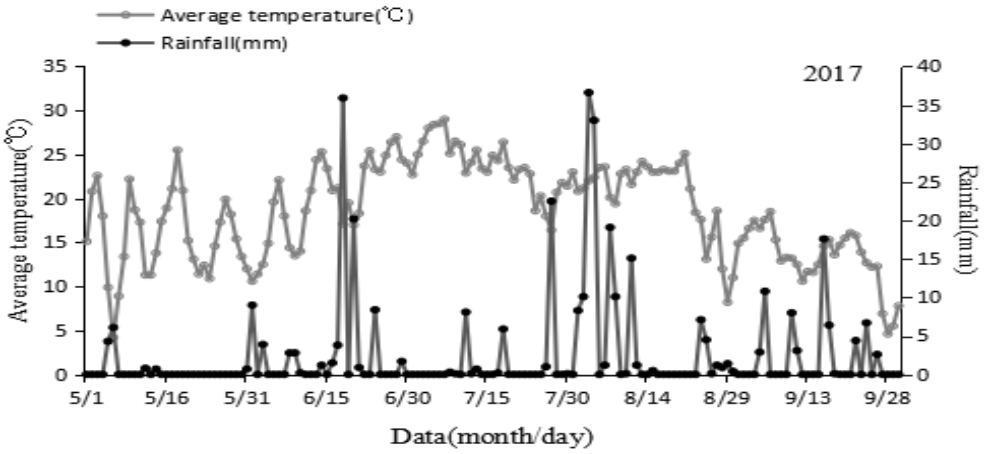

Figure 3. *Average temperature and Rainfall duration during growth period in 2017*

Sample handling

Plants of Growth uniformity were marked as samples, and the samples were taken on days 7 (August 5th), 14 (August 12th), 21 (August 19th), 28 (August 26th), 35 (September 2th) and 42 (September 9th) after the powder dispersed. Three spikes were taken each time from each treatment. Thirty grains were selected from the middle and upper parts of the spike and weighed. The seeds were frozen in liquid nitrogen and stored in an ultra-low temperature refrigerator at -70 °C. The rest of the seeds were killed at 105 °C and dried to constant weight at 80 °C for the determination of starch accumulation.

Determination of starch accumulation

Starch content determination according to the method of Fan Mingshun (Fan, et al., 2008). The main wavelength of the amylose content (%) was 620 nm, and the reference wavelength was 479 nm. The main wavelength of the amylopectin content (%) was 556 nm, and the reference wavelength was 737 nm. Both the amylose and amylopectin standard samples were obtained from the Heilongjiang Academy of Agricultural Sciences.

$$\text{Total starch content (\%)} = \text{amylose content (\%)} + \text{amylopectin content (\%)} \quad \text{(Eq.1)}$$

Determination of starch-related enzyme activity

The activity of Soluble starch synthase (SSS), Starch branching enzyme (SBE), Bound starch synthetase (GBSS), Adenosine diphosphate glucose pyrophosphorylase (AGP), Uridine diphosphate glucose pyropitase activities (UGP) was determined by enzyme-linked immunosorbent assay. The kit was provided by Shanghai Enzyme-linked Biology Co., Ltd. (Shanghai china), and the determination method was carried out according to the instructions. Three parallel measurements were made by the determination of the enzyme's activity.

Yield measurement

Grain yield and its composition: From each plot 20 plants (except from the guard area surrounding the plot) from one-meter-long ridge were harvested continuously at

http://www.aloki.hu ● ISSN 1589 1623 (Print) ● ISSN 1785 0037 (Online)
DOI: http://dx.doi.org/10.15666/aeer/1804_57275741

maturity for the determination of grain yield. The indexes included the single spike weight, grain number per spike and thousand kernel weight. The yield was converted by the weight at 14% water content.

Analysis software and analysis method

The data were processed by Excel 2013 and analyzed by SPSS 16.0 and data from each sampling data were analyzed separately. Means were separated by Duncan's multiple range test at $p < 0.05$. The data are presented as the means ± standard deviation from all replications. Different characters indicate significant differences.

Results

Effect of nitrogen application on total starch content in grains

It can be seen from *Table 1* that the total starch content of the two sorghum varieties increased with the development of the growth period. The N0 treatment was significantly lower than each nitrogen treatment. The N0 treatment of Keza15 was significantly lower than that of N application, and there was no significant difference among N application treatments.

7 d after powder dispersion, there was no significant difference in the total starch content of Suiza7 among N application treatments. From 14 d to 21 d after powder dispersion, N200 = N300 > N100 > N0 and there was no significant difference between N200 and N300. From 28 d to 42 d after powder dispersion, N200 > N100 = N300 > N0, there was no significant difference between N100 and N300.

Table 1. *Effect of nitrogen application on total starch content in grains*

Cultivars	Treatment	Total starch content (%)					
		7 d after powder dispersion	14 d after powder dispersion	21 d after powder dispersion	28 d after powder dispersion	35 d after powder dispersion	42 d after powder dispersion
Keza15	N0	6.75±0.17a	18.91±0.09b	38.07±0.38c	50.97±1.40b	58.93±0.47b	63.36±0.51b
	N100	7.53±0.53a	22.83±0.45a	42.24±0.94ab	55.07±0.26a	64.05±0.91a	68.83±0.42a
	N200	7.75±0.38a	23.43±0.21a	42.83±0.26a	55.36±0.48a	63.63±1.34a	68.53±0.32a
	N300	7.57±0.41a	22.88±0.24a	40.68±0.52b	53.89±0.06a	61.90±0.43a	67.30±0.75a
Suiza7	N0	6.38±0.31b	18.48±0.31c	35.71±0.50c	48.77±0.31c	57.46±0.30c	62.33±0.21c
	N100	7.75±0.47a	22.06±0.13b	42.17±0.47b	54.98±0.37b	63.56±0.71b	68.32±0.25b
	N200	7.96±0.38a	24.12±0.36a	44.89±0.47a	56.75±0.28a	66.61±0.61a	69.86±0.39a
	N300	7.68±0.10a	23.81±0.37a	43.94±0.12a	55.35±0.22b	62.97±0.17b	67.91±0.46b

Different letters indicate significant differences according to Duncan's test ($p \leq 0.05$)

Effect of nitrogen application on the amylopectin content in grains

The result showed that the amylopectin content of the two varieties of sorghum increased significantly from 7 d to 42 d after powder dispersion, and the amylopectin content of the nitrogen treatment was significantly higher than that of the N0 treatment (*Table 2*). There was no significant difference among nitrogen treatments with respect

http://www.aloki.hu ● ISSN 1589 1623 (Print) ● ISSN 1785 0037 (Online)
DOI: http://dx.doi.org/10.15666/aeer/1804_57275741

to the amylopectin content in Keza15 on the 7 days after powder dispersal; N100 = N200 > N300 = N0 on the 21 days after powder dispersal, there was no significant difference between N100 and N200; N200 = N100 = N300 > N0 on the 28 days after powder dispersal, there was no significant difference between N100 and N200.

There was no significant difference between N0, N100 and N200 in the amylopectin content of Suiza 7 on the 7 days after powder dispersion. From 14 to 28 days after powder dispersal, N300 = N200 = N100 > N0, and 42 days after powder dispersal, there was a significant difference between the N0 treatment and the nitrogen treatment.

Table 2. *Effect of nitrogen application on the amylopectin content in grains*

Cultivars	Treatment	Amylopectin content （%）					
		7 d after powder dispersion	14 d after powder dispersion	21 d after powder dispersion	28 d after powder dispersion	35 d after powder dispersion	42 d after powder dispersion
Keza15	N0	4.02±0.08a	14.02±0.28b	31.00±0.07b	40.98±0.95b	46.86±0.56b	49.47±0.32b
	N100	4.42±0.31a	16.63±0.30a	32.69±0.28a	43.03±0.13a	50.19±1.06a	53.36±0.16a
	N200	4.43±0.28a	17.07±0.04a	32.76±0.31a	43.18±0.24a	49.48±1.22ab	53.40±0.59a
	N300	4.39±0.31a	17.03±0.04a	31.54±0.25b	42.16±0.16ab	48.95±0.09ab	52.82±0.20a
Suiza7	N0	3.90±0.05b	13.67±0.28c	28.88±0.29c	39.72±0.31c	45.73±0.32c	49.15±0.24b
	N100	4.51±0.31ab	16.05±0.11b	32.72±0.28b	43.04±0.48b	49.78±0.35b	53.05±0.52a
	N200	4.62±0.26ab	17.88±0.07a	34.54±0.33a	44.71±0.30a	51.64±0.63a	54.19±0.43a
	N300	4.67±0.11a	18.14±0.05a	34.57±0.23a	44.24±0.20a	49.82±0.20b	53.71±0.45a

Different letters indicate significant differences according to Duncan's test ($p \leq 0.05$)

Effect of nitrogen application on the amylose content in grains

The results show that the amylose content of the two varieties increased with the development of growth (*Table 3*). The N0 treatment was significantly lower than the nitrogen treatment. 35 days after the powder dispersal of Keza15, compared with other treatments, the amylose content of N0 and N300 decreased significantly, but the difference between the N0 and N300 treatments was no significant. 42 days after powder dispersion, there was no significant difference between N200 and N300, but compared with N100 treatments, the amylose content of N200 and N300 decreased significantly.

At 7–14 days after the powder dispersal of suiza7, there was no significant difference in the content of the amylose between N100 and N200, which was significantly higher than that between N0 and N300. 21 and 35 days after powder dispersion, there was no significant difference in the amylose content between N100 and N300, but there was a significant difference between N100 and N200. There was no significant difference between N100 and N200 treatments at 28 d and 42 d after powder dispersion, which was significantly higher than the other treatments.

Effects of nitrogen application on the yield and components of sorghum

From the analysis results shown in *Table 4*, it can be seen that there was a significant positive correlation between the number of grains per spike and the 1000-grain weight of the two sorghum varieties. Within a certain range, the number of grains per spike and

http://www.aloki.hu ● ISSN 1589 1623 (Print) ● ISSN 1785 0037 (Online)
DOI: http://dx.doi.org/10.15666/aeer/1804_57275741

the 1000-grain weight of the two sorghum varieties increased with the increase of the nitrogen application amount, but when the nitrogen exceeded the N200 level, the number of grains per spike and the 1000-grain weight did not continue to increase and began to decline. From the analysis of the grain number per spike and the 1000-grain weight, the best nitrogen application amount was N200. The yield of sorghum increased first and then decreased with the increase in nitrogen application. The yield response of different sorghum genotypes to nitrogen was different. The yield of Keza15 was N100 = N200 > N300 > N0, and there was no significant difference between the N100 and N200 treatments. The yield of Suiza7 was N200 > N100 > N300 > N0 among the treatments, and there was a significant difference among the treatments.

Table 3. *Effect of nitrogen application on the amylose content in grains*

Cultivars	Treatment	Amylose content（%）					
		7 d after powder dispersion	14 d after powder dispersion	21 d after powder dispersion	28 d after powder dispersion	35 d after powder dispersion	42 d after powder dispersion
Keza15	N0	2.73±0.19a	4.89±0.21b	7.07±0.33b	9.98±0.49b	12.06±0.09c	13.89±0.22b
	N100	3.11±0.26a	6.21±0.18a	9.55±0.74a	12.03±0.13a	13.86±0.16ab	15.47±0.33a
	N200	3.32±0.14a	6.36±0.23a	10.07±0.54a	12.18±0.24a	14.15±0.37a	15.13±0.27ab
	N300	3.18±0.14a	5.85±0.21a	9.13±0.38a	11.73±0.14a	12.95±0.50bc	14.49±0.60ab
Suiza7	N0	2.48±0.27b	4.81±0.30b	6.83±0.34c	9.05±0.08c	11.73±0.28c	13.19±0.13c
	N100	3.24±0.17a	6.01±0.23a	9.45±0.21b	11.94±0.11a	13.78±0.35b	15.27±0.29a
	N200	3.34±0.23a	6.24±0.29a	10.35±0.26a	12.04±0.08a	14.97±0.09a	15.67±0.08a
	N300	3.01±0.02ab	5.68±0.33ab	9.37±0.16b	11.11±0.40b	13.15±0.17b	14.20±0.16b

Different letters indicate significant differences according to Duncan's test ($p \leq 0.05$)

Table 4. *Effect of nitrogen level on yield and components of sorghum*

Cultivars	Treatment ($kg \cdot hm^{-2}$)	Grain number per spike (Li)	Thousand grain weight (g)	Single spike weight (g)	Yield ($kg \cdot hm^{-2}$)
Keza15	N0	1018.00±10.21b	20.34±0.45b	30.18±0.52b	6210.82±75.92c
	N100	1087.70±16.41a	25.37±0.58a	37.14±1.25a	8278.23±61.97a
	N200	1069.30±6.39a	25.76±0.58a	37.85±0.86a	8262.74±89.85a
	N300	1002.00±4.51b	25.28±0.41a	35.93±0.67a	7600.17±64.28b
Suiz7	N0	948.00±17.79b	19.35±0.33b	31.75±1.55b	5504.09±62.60d
	N100	1074.00±21.66a	25.11±0.28a	37.22±0.82a	8091.52±140.98b
	N200	1086.30±6.44a	25.95±0.65a	37.35±1.10a	8457.11±61.32a
	N300	993.00±4.00b	25.27±0.45a	33.56±1.06ab	7527.93±86.88c

Different letters indicate significant differences according to Duncan's test ($p \leq 0.05$)

The correlation between nitrogen application and starch content

The results showed that the correlation among nitrogen and total starch, amylopectin content varies with varieties (*Table 5*). There was a significant positive correlation between nitrogen application and total starch, amylopectin content on the 14 days after powder dispersal, and a significant positive correlation between the nitrogen level and the content of Amylose on the 28 days after powder dispersal. There was no significant

http://www.aloki.hu ● ISSN 1589 1623 (Print) ● ISSN 1785 0037 (Online)
DOI: http://dx.doi.org/10.15666/aeer/1804_57275741

correlation between nitrogen application and starch of Keza15 in other periods. However, there was a significant positive correlation among nitrogen application and total starch, amylopectin content of Suiza7 from 7 to 42 days after powder dispersal, and the amylose content 21 days after powder dispersal. There was a significant positive correlation between nitrogen and amylose content 21 days after powder dispersal. The correlation coefficients of the two sorghum varieties were 14d > 21d > 28d > 42d > 35d > 7d after powder dispersal.

Table 5. *The coefficients of nitrogen levels and starch content*

Cultivars	Treatment ($kg \cdot hm^{-2}$)	7 d after powder dispersion	14 d after powder dispersion	21 dafter powder dispersion	28 d after powder dispersion	35 d after powder dispersion	42 d after powder dispersion
Keza 15	Total starch content	0.443	0.755**	0.466	0.497	0.402	0.559
	Amylose content	0.512	0.525	0.552	0.619*	0.351	0.200
	Amylopectin content	0.306	0.816**	0.230	0.365	0.358	0.661*
Suiza 7	Total starch content	0.584*	0.884**	0.844**	0.776**	0.649*	0.707*
	Amylose content	0.437	0.464	0.700*	0.566	0.501	0.383
	Amylopectin content	0.632*	0.946**	0.898**	0.849**	0.706*	0.797**

NS, *, **: No significance or significant at $p \leq 0.05, 0.01$

Correlation between starch content and yield

It can be seen from *Table 6* that there was a significant positive correlation between the total starch content, amylose content and 1000-grain weight, the number of grains per spike and the yield of Keza15, and a significant positive correlation between the amylopectin content and 1000-grain weight and yield. There was a significant positive correlation between the starch content and the number of grains per spike, 1000-grain weight and yield. Therefore, it can be seen that the correlation between starch and grain number per spike, 1000-grain weight and yield varies with genotypes, and the correlation coefficient of the low-N-sensitive varieties is higher than that of the low-N-tolerant varieties.

Effect of nitrogen application on the activity of SSS in grains

The change of SSS activity was shown in *Figure 4*. The activity of SSS of Keza15 and Suiza7 increased significantly on the 14th day, peaked on the 28th day, and decreased significantly on the 42nd day. The treatment of N200 and N300 of two sorghum varieties kept at a high level from 14 to 35 days after powder dispersal. During this period, the increase in SSS activity determined the synthesis ability of sorghum starch, which had a great impact on the starch content of sorghum.

There was no significant difference between the N200 and N300 treatments of Keza15 at 7–35 d after powder dispersion, but there was significant difference at 42 days after powder dispersion.

http://www.aloki.hu ● ISSN 1589 1623 (Print) ● ISSN 1785 0037 (Online)
DOI: http://dx.doi.org/10.15666/aeer/1804_57275741

Table 6. *The coefficients between starch content and production*

Cultivars	Starch content	Grain number per spike (Li)	Thousand grain weight (g)	Yield (kg·hm^{-2})
Keza 15	Total starch content	0.628*	0.927**	0.912**
	Amylose content	0.687*	0.751**	0.661*
	Amylopectin content	0.521	0.894**	0.918**
Suiza 7	Total starch content	0.818**	0.962**	0.970**
	Amylose content	0.850**	0.792**	0.901**
	Amylopectin content	0.727**	0.954**	0.913**

NS, *, **: No significance or significant at $p \leq 0.05, 0.01$

The activity of SSS of Suiza7 was N300 > N200 > N100 > N0 on the 7 days after powder dispersal, and there were significant differences among the treatments. On the 14th, 21st and 35th day after powder dispersal, the difference between N300 and N200 treatment was significant compared with N100 treatment.

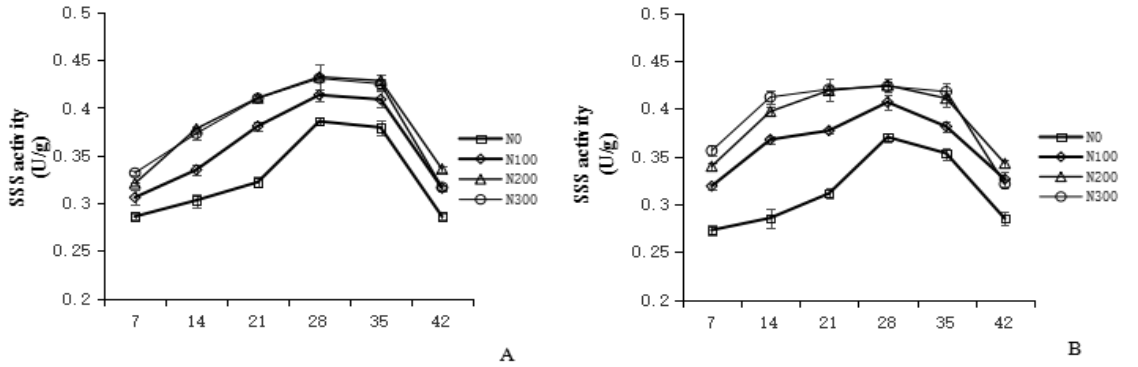

Figure 4. *(A) Effect of nitrogen application on the activity of SSS in grains of Keza15. (B) Effect of nitrogen application on the activity of SSS in grains of Suiza7. Error bars represent ± S.E. of the mean*

Effect of nitrogen application on the activity of SBE in grains

The results in *Figure 5* showed that SBE activity of two sorghum varieties with different genotypes increased first and then decreased with the advancement of grain development. It reached a peak value 28 days after powder dispersal and then began to decline. The difference between N0 and the other three treatments was very significant.

The SBE activity of Keza15 was higher at the N200 treatment from 7 to 42 days after powder dispersal. The SBE activity of the N200 and N300 treatments was significantly higher than that of the N100 treatment at 7–28 days after powder dispersal, there was no significant difference between N200 and N300. At 35–42 d, N100 and N200 were significantly higher than N300.

The SBE activity of Suiza7 was significantly increased 14 days after powder dispersion, reached the peak value 28 days after powder dispersion, and significantly decreased 35 days after powder dispersion. The SBE activity was the highest at the N300 level from 7 to 35 days after powder dispersion and was the highest at the N200 level 42 days after powder dispersion.

http://www.aloki.hu ● ISSN 1589 1623 (Print) ● ISSN 1785 0037 (Online)
DOI: http://dx.doi.org/10.15666/aeer/1804_57275741

Effect of nitrogen application on the activity of GBSS in grains

The results shown in *Figure 6* demonstrated that the GBSS activity of the two varieties of sorghum from 7 to 42 days after powder dispersal showed a single peak curve change of first increasing and then decreasing, and there was no significant difference between the GBSS activity value 42 d after powder dispersal and 7 d after powder dispersal. The N0 treatment was significantly lower than the other three treatments, indicating that low nitrogen could significantly reduce GBSS activity.

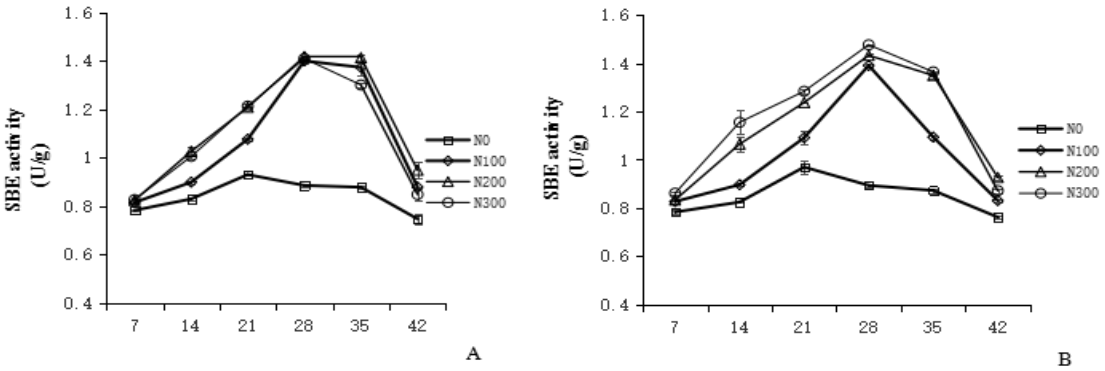

Figure 5. *(A) Effect of nitrogen application on the activity of SBE in grains of Keza15. (B) Effect of nitrogen application on the activity of SBE in grains of Suiza7. Error bars represent ± S.E. of the mean*

At the level of N0, the GBSS activity of Keza15 reached the peak value 35 days after powder dispersion, and at the level of N100 and N300, the GBSS activity reached the peak value 28 days after powder dispersion and then began to decrease significantly. At the level of N200, the activity of GBSS increased significantly 14 days after powder dispersal, peaked 35 days after powder dispersal, and decreased significantly 42 days after powder dispersal.

At the N0 level, the GBSS activity of Suiza7 reached its peak at 28 d after powder dispersal; At the N100 level, GBSS reached the peak value 28 days after powder dispersal; At the N200 and N300 levels, GBSS reached the peak value 21 days later powder dispersal, and then began to decrease significantly.

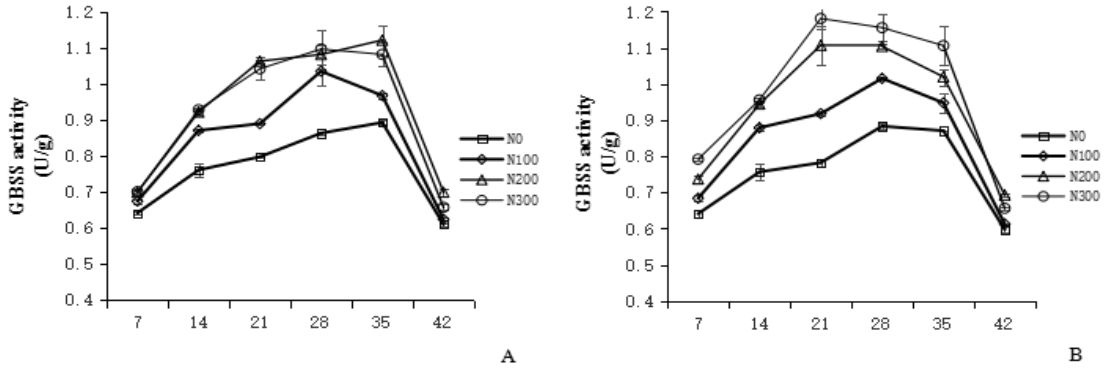

Figure 6. *(A) Effect of nitrogen application on the activity of GBSS in grains of Keza15. (B) Effect of nitrogen application on the activity of GBSS in grains of Suiza7. Error bars represent ± S.E. of the mean*

http://www.aloki.hu ● ISSN 1589 1623 (Print) ● ISSN 1785 0037 (Online)
DOI: http://dx.doi.org/10.15666/aeer/1804_57275741

The effect of nitrogen application on the activity of AGP in grains

From the analysis of *Figure 7*, it can be seen that the AGP activity of the two sorghum varieties increased first and then decreased with the development of the growth process and grain development, and the AGP activity of the N0 treatment was significantly lower than that of the other three treatments, indicating that the AGP activity of the low nitrogen treatment would be significantly reduced.

At the level of N100, N200 and N300, the AGP activity of Keza15 reached its peak at 35 d after powder dispersion, and decreased significantly at 42 d after powder dispersion.

At the N100 level of Suiza7, the AGP activity was significantly increased 21 days after powder dispersion, reached the peak value 28 days after powder dispersion, and began to decrease 35 days after powder dispersion. At the level of N200 and N300, AGP activity increased significantly at 14 days after powder dispersion, peaked at 28 days after powder dispersion, and decreased significantly at 35 days after powder dispersion. The response of different genotypes to AGP activity was different. The peak value of Keza15 was reached 35 days after powdering, and Suiza7 was advanced to 28 days. The increasing range of AGP activity between the N200 and N300 treatment and the N0 treatment of Suiza7 was significantly higher than that of Keza15.

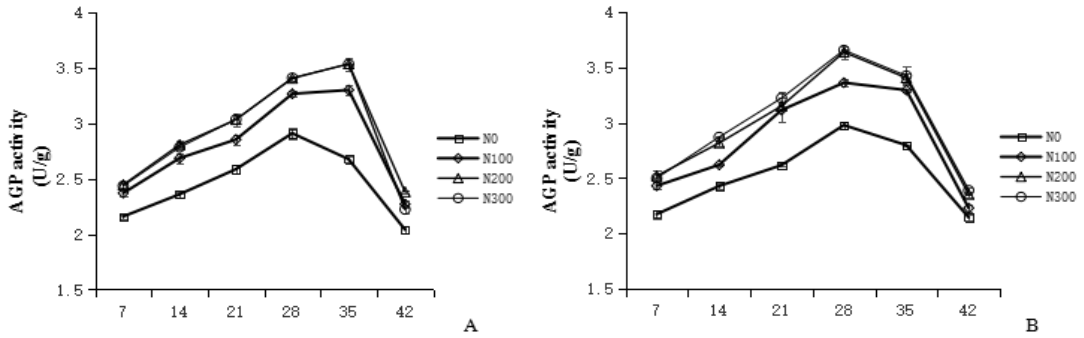

Figure 7. *(A) Effect of nitrogen application on the activity of AGP in grains of Keza15. (B) Effect of nitrogen application on the activity of AGP in grains of Suiza7. Error bars represent ± S.E. of the mean*

Effect of nitrogen application on the activity of UGP in grains

The results of *Figure 8* showed that the UGP activity of the two varieties of sorghum increased first and then decreased from 7 to 42 days after powder dispersion. The UGP activity of nitrogen application was higher than that of N0 in each period after powder dispersal. Under the level of N0, the UGP activity of Keza15 and Suiza7 increased significantly 21 days after powder dispersal, reached the peak 28 days after powder dispersal, and decreased significantly 42 days after powder dispersal.

At the N100 level, Keza15 reached the peak value 35 days after powder dispersal; at the N200 and N300 levels, at 28 days and 42 days after powder dispersal, the activity value of UGP was significantly lower than that at 7 days after powder dispersal.

At the N100 level, Suiza7 reached its peak at 28 days after powder dispersion and decreased significantly at 35 days after powder dispersion. At the level of N200 and N300, the peak value was reached at 28 days after powder dispersal and decreased significantly at 35 days after powder dispersal.

http://www.aloki.hu ● ISSN 1589 1623 (Print) ● ISSN 1785 0037 (Online)
DOI: http://dx.doi.org/10.15666/aeer/1804_57275741

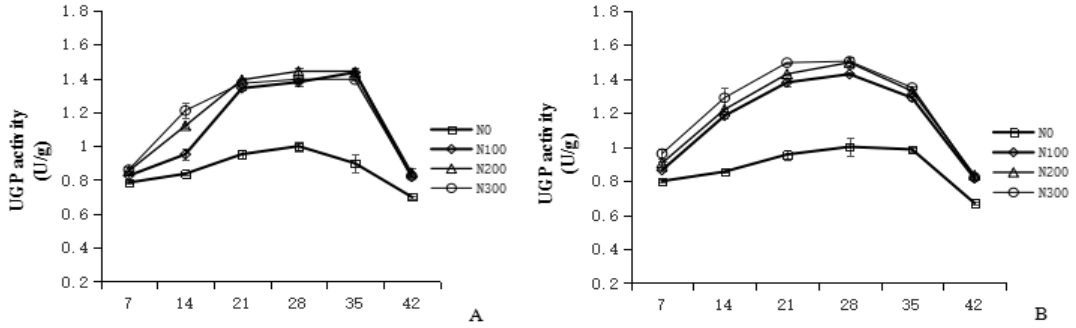

Figure 8. *(A) Effect of nitrogen application on the activity of UGP in grains of Keza15. (B) Effect of nitrogen application on the activity of UGP in grains of Suiza7. Error bars represent ± S.E. of the mean*

Discussion

Effect of nitrogen application on starch accumulation and related enzyme activities in the grain of high-density planting sorghum

Starch is an important energy storage material of plants, its content and quality will directly affect the yield and economic value of crops. There was a significant positive correlation between the amount of nitrogen application and the yield of total starch, amylopectin and amylose in a proper range, but nitrogen application played an opposite role when it exceeded a certain level (Wang et al., 2006). The starch content increased with the increase in nitrogen application in a certain range, and there were differences among varieties (Zhao et al., 2003). The results showed that there was a great change in the total starch content in the nitrogen-sensitive varieties compared with the low - nitrogen-tolerant varieties, and the difference between the treatment of Suiza7 N0 and each nitrogen application was significantly higher than that of Keza15. From 7 to 21 days after powder dispersal, the starch of the two sorghum varieties increased greatly, which was the rapid growth period of starch accumulation, and played an important role in the starch synthesis of grains. The content of amylopectin increased with the development of sorghum varieties with different genotypes. The amylose content of the two different sorghum varieties reached the peak value under the N200 treatment, and that of the N0 treatment was lower than that of the other nitrogen treatments. There was no significant difference among the nitrogen treatments of Keza15, but from 21 days after the powder dispersal of Suiza7, the N300 treatment was significantly lower than the N200 treatment, which indicated that high nitrogen was disadvantageous to amylose accumulation of nitrogen-sensitive varieties.

The AGP activity, SSS activity and GBSS activity were significantly related to the amount of nitrogen applied in the later stage. ADPG pyrophosphorylase is the key enzyme that controls the rate of starch accumulation, and starch-branching enzyme is the key enzyme that affects the synthesis of amylopectin (Li et al., 2005). It is as important in the process of grain filling as ADPG pyrophosphorylase (Kouich et al., 1992; Yang et al., 2005). The activity of SSS, SBE, GBSS, AGP and UGP increased first and then decreased with the development of grain. The results showed that the application of nitrogen was beneficial to the activity of the four enzymes, but too much of application nitrogen would lead to a decrease, which indicated that nitrogen had an important regulatory effect on the four enzymes. In this study, the N0 treatment was

http://www.aloki.hu ● ISSN 1589 1623 (Print) ● ISSN 1785 0037 (Online)
DOI: http://dx.doi.org/10.15666/aeer/1804_57275741

significantly lower than each nitrogen application, indicating that nitrogen application promoted the activity of SSS. The GBSS activity of N-sensitive sorghum was earlier than that of low-N-tolerant sorghum. The increase of GBSS activity of the N-sensitive sorghum in the low-N treatment was higher than that of the low-N-tolerant sorghum, and the AGP activity in the low-N treatment was significantly reduced. The results showed that the AGP activity of low-N-tolerant varieties was slower than that of nitrogen-sensitive varieties, which indicated that different varieties needed different nitrogen amounts, which is consistent with other research (Li et al., 2005; Tan et al., 2016).

Effect of nitrogen application on Yield of sorghum with different genotypes

The increase of corn yield by nitrogen application mainly depends on the number of grains per spike and 1000-grain weight (Yang et al., 2008). The proper application of nitrogen fertilizer could speed up grain filling rate, and too high or too low application of nitrogen fertilizer would reduce grain weight (He et al., 2005). Nitrogen fertilizer helps the decomposition of soil organic matter, promotes the absorption of nutrients by sorghum, and improves the small environment of sorghum root area (Ni et al., 2016). The application of nitrogen increased the number of spikes per unit and the grain weight, but the excessive application of nitrogen had the opposite effect on the grain weight (Sun et al., 2008). The results showed that the yield of the two sorghum varieties with different genotypes increased first and then decreased with the increase in nitrogen application. The maximum yield of Suiza7 was in the N200 treatment, and that of Keza15 was in the N100 treatment. Suiza7 was 2.16% higher than that of Keza15, which indicated that Suiza7 had a higher yield than that of the low-N-tolerant variety under the condition of sufficient nitrogen fertilizer. There were significant differences in yield between the treatments of Suiza7; the difference between N200 and N0 was 53.65%, the difference of Keza15 between N100 and N200 was not significant, and the difference between N100 and N0 was 33.3%, which indicated that the yield of the low-N-sensitive variety increased more than that of low-N-tolerant variety, and nitrogen absorption and utilization were more efficient. Nitrogen had a significant positive correlation with the number of grains per spike and the 1000-grain weight of the two sorghum varieties. When nitrogen exceeded N200, the number of grains per spike and 1000-grain weight no longer increased and began to decrease. The spike weight had the strongest direct relationship with the number of grains per spike, followed by the 1000-grain weight.

Conclusion

The response of the low-N -sensitive varieties to nitrogen was faster than that of the low-N-tolerant varieties. Under the condition of low nitrogen, the absorption and utilization of nitrogen by amylopectin of the low-N-sensitive varieties were lower than that of the low-N-tolerant varieties.

Nitrogen application is beneficial for the increase of SSS, SBE, GBSS, AGP and UGP activities, but the excessive application of nitrogen will lead to a decrease. The best nitrogen application amount was 200 kg N ha^{-1} (N200) to achieve the highest yield. Therefore, it can be concluded that N200 is optimal nitrogen application for the production potential under high plant density for sorghum production in northern China, whereas insufficient or excessive nitrogen application will lead to the decrease of starch content.

http://www.aloki.hu ● ISSN 1589 1623 (Print) ● ISSN 1785 0037 (Online)
DOI: http://dx.doi.org/10.15666/aeer/1804_57275741

Acknowledgements. This research was supported by the China Agriculture Research System (CARS-06-135-A17).

REFERENCES

[1] Ciampitti, I. A., Vara, P. P. V. (2016): Historical synthesis-analysis of changes in grain nitrogen dynamics in sorghum. – Frontiers in Plant Science 7: 275.
[2] Ge, Z. Y., Ma, S. Y., Cheng, H. J., Yan, F. Z., Wang, L. X., Zhang, S., Sui, H. J., Pan, Y. X. (2016): Effects of different nitrogen on starch content in sorghum grains. – Journal of Northeast Agricultural Sciences 41(2): 25-29.
[3] He, P., Jin, J. Y., Li, W. J. (2005): Effect of potassium application on potassium absorption characteristics and grain yield of high oil corn and common corn. – Journal of Plant Nutrition and Fertilizer 11(5): 620-626.
[4] Jin, L., Cui, H., Li, B., Zhang, J. W., Dong, S. T., Liu, P. (2012): Effects of integrated agronomic management practices on yield and nitrogen efficiency of summer maize in North China. – Field Crop. Res 134: 30-35.
[5] Komla, K. G., Bertrand, M., Malick, N., Espoir, K. G., Aliou, G., Adam, M. (2019): Defining fertilization strategies for sorghum (Sorghum bicolor (L.) Moench) production under Sudano-Sahelian conditions. – Options for Late Basal Fertilizer Application Agronomy 9: 697.
[6] Kouich, M., Koji, K., Yuji, A., Kawasaki, T., Shimada, H., Baba, T. (1992): Starch branching enzymes from immature rice seeds. – Journal of Biochemistry 112: 643-651.
[7] Li, C. Y., Feng, C. N., Zhang, Y., Guo, W. S., Zhu, X. K., Peng, Y. X. (2005): The effect of nitrogen ratio on starch synthesis and related enzyme activity of weak gluten wheat Ningmai9. – Scientia Agricultura Sinica 38(6): 1120-1125.
[8] Li, S. B., Tang, C. C., Chen, F., Xie, G. H. (2018): Temporal and spatial changes in yield and quality with grain sorghum variety improvement in China. – Scientia Agricultura Sinica 51(2): 246-256.
[9] Liang, X. H., Liu, J., Cao, X. (2017): Effects of nitrogen application rate on yield of brewing sorghum and nitrogen use efficiency. – Acta Agriculturae Boreali-Sinica 32(2): 179-184.
[10] Mahama, G. Y., Prasad, P. V. V., Mengel, D. B., Tesso, T. T. (2014): Influence of nitrogen fertilizer on growth and yield of grain sorghum hybrids and inbred lines. – Agronomy Journal 106(5): 1623-1630.
[11] Ni, Y. Q., Zhang, Q., Cao, F. Q., Yang, L. (2016): Effect of different nitrogen application on sorghum yield and plant nutrient accumulation. – Soil and Water Conservation Research 23(5): 95-99.
[12] Ronga, D., Caradonia, F., Setti, L., Hagassou, D., Giaretta, C. V., Milc, J., Pedrazzi, S., Allesina, G., Arru, L., Francia, E. (2019): Effects of innovative biofertilizers on yield of processing tomato cultivated in organic cropping systems in northern Italy. – Acta Hortic 1233: 129-136.
[13] Shen, H. J., Yang, S. R., Yang, G. Y., Shan, D. P., Tang, M., Sun, Z. H., Chen, L., Wang, F. M. (2013): Standardized cultivation techniques of dwarf sorghum Suiza7. – China Seed Industry 10: 57-58.
[14] Sun, X. S., Lin, Q., Liu, Y. G. (2008): The effect of the same amount of nitrogen application on the diurnal variation of photosynthesis in the filling stage of super high yield wheat. – Journal of Beinong 23(1): 58-162.
[15] Tan, C. X., Feng, C. N., Guo, W. S., Zhu, X. K., Li, C. Y., Peng, Y. X. (2016): Effects of gene expression of starch synthetase and starch synthesis in wheat grains. – Journal of Yangzhou University 37(2): 63-69.
[16] Tilman, D., Balzer, C., Hill, J., Befort, B. L. (2011): Global food demand and the sustainable intensification of agriculture. – Proc. Natl. Acad. Sci 108: 20260-20264.

http://www.aloki.hu ● ISSN 1589 1623 (Print) ● ISSN 1785 0037 (Online)
DOI: http://dx.doi.org/10.15666/aeer/1804_57275741

[17] Van weelden, M. T., Wilson, B. E., Beuzelin, J. M., Reagan, T. E., Way, M. O. (2016): Impact of nitrogen fertilization on Mexican rice borer (Lepidoptera: Crambidae) injury and yield in bioenergy sorghum. – Crop Protection 84: 37-43.
[18] Wang, J. S., Jiao, X. Y., Ding, Y. C., Dong, E. W., Bai, W. B., Wang, L. G., Wu, A. L. (2015): Response of grain sorghum nutrient absorption, yield and quality to nitrogen, phosphorus and potassium nutrition. – Acta Agronomica Sinica 41(8): 1269-1278.
[19] Wang, Q. (2006): Effect of Nitrogen Application on starch formation and accumulation in spring maize. Harbin, Heilongjiang. – Master Dissertation, Northeast Agricultural University, Harbin.
[20] Yan, H., Pan, X. X., Jiang, H., Wu, G. (2009): Comparison of the starch synthesis genes between maize and rice: copies, chromosome location and expression divergence. – Theoretical and Applied Genetics 119(5): 815-825.
[21] Yang, D. G., Jin, J. Y., Li, W. J. (2005): Effect of potassium application on potassium absorption characteristics and grain yield of high oil corn and common corn. – Journal of Plant Nutrition and Fertilizer 11(5): 620-626.
[22] Yang, D. G., Niu, H. Y., Zhang, H. X. (2008): Effects of nitrogen stress and non stress on yield and quality of spring maize. – Maize Science 16(4): 55-57.
[23] Yang, G. D., Hu, Z. Y., Liu, L. L., Chen, L. Q. (2015): Cultivation techniques of sorghum in the north of Heilongjiang Province. – Heilongjiang Agricultural Sciences 5: 165-166.
[24] Yang, G. D., Zhou, Y. F., Huang, R. D., Lin, F., Hu, Z. Y., Hao, Z. Y., Liang, C. B., Wang, Q., Meng, X. X., Dong, L. D. (2019): Identification of differentially expressed genes of sorghum [Sorghum bicolor (L.) Moench] seedlings under nitrogen stress by RNA-seq. – Applied Ecology and Environmental Research 17(5): 11525-11536.
[25] Yi, B., Zhou, Y. F., Gao, M. Y., Zhang, Z., Han, Y., Yang, G. D., Xu, W. J., Huang, R. D. (2014): Effect of drought stress during flowering stage on starch accumulation and starch synthesis enzymes in sorghum grains. – Journal of Integrative Agriculture 13(11): 2399-2406.
[26] Yu, Y., Huang, R. D., Zhao, S. W., Jiang, W. C. (2008): Effect of nitrogen application on starch accumulation in sorghum grains. – Crops 15: 20-24.
[27] Zhao, H. W. (2003): Study on the mechanism of carbon and nitrogen metabolism under different nitrogen nutrition levels. Harbin, Heilongjiang. – Doctoral Dissertation, Northeast Agricultural University, Harbin.
[28] Zhou, L. B., Wang, C., Lu, X. J., Zhang, G. B., Xu, Y., Wu, L. Y., Shao, M. B. (2016): Effects of fertilization amount and planting density on photosynthetic characteristics, agronomic characteristics and yield of glutinous sorghum Qiangao7. – Journal of Southern Agriculture 47(5): 644-648.

http://www.aloki.hu ● ISSN 1589 1623 (Print) ● ISSN 1785 0037 (Online)
DOI: http://dx.doi.org/10.15666/aeer/1804_57275741

STUDY ON ISOLATION, IDENTIFICATION AND LEAD BIOSORPTION CAPABILITY OF A LEAD-TOLERANT *PENICILLIUM* SP. Pb-G FROM CONTAMINATED SOIL

AN, F. Q.[1*] – LI, H. H.[1] – ZHAO, Q. Q.[1] – LI, B. H.[1] – LV, J. L.[2]

[1]*College of Environmental and Chemical Engineering, Xi'anPolytechnic University, Xi'an, Shaanxi 710048, China*

[2]*College of Natural Resources and Environment, Northwest A&F University, Ministry of Agriculture Key Laboratory of Plant Nutrition and Agri-environment in Northwest China, Yangling, Shaanxi 712100, China*

[*]*Corresponding author*
e-mail: 20130503@xpu.edu.cn; phone: +86-181-9235-9615

(Received 12th Feb 2020; accepted 9th Jul 2020)

Abstract. To acquire a potential strain that may be used for the bioremediation of lead (Pb^{2+}) contaminations, an indigenous lead-resistant fungus *Penicillium* sp. Pb-G (GenBank No.MK372218) was isolated from lead contaminated soil, and the Pb^{2+} biosorption characteristics were determined in this study. The results showed that *Penicillium* sp. Pb-G was highly tolerant to Pb^{2+}, and it could survive on PDA medium with Pb^{2+} concentration up to 4000 mg/L. Under these circumstances, the spores of the strain Pb-G becomes shrunk and malformed as observed by scanning electron microscopy (SEM). X-ray diffractometer (XRD) analysis further revealed that the *Penicillium* sp. Pb-G's mycelia had a good biosorption capability for Pb^{2+}. The best biosorption effect of strain *Penicillium* sp. Pb-G was recorded at the Pb^{2+} concentration of 1500 mg/L, with the biosorption rate and biosorption amount of 53.05% and 178.02 mg/g, respectively. Collectively, these results demonstrated that the strain of Pb-G had strong Pb^{2+} resistance and biosorption abilities, which provides an attractive application prospect in bioremediation of heavy metal contamination.
Keywords:*maximum resistance level, identification, Penicillium, scanning electron microscopy, X-ray diffractometer*

Introduction

Heavy metal pollution in soil and water has become an increasingly prominent environmental problem, among the heavy metals lead gained special attention as a pollutant due to its high persistence and toxicity. It mainly derives from minerals, metal smelting, leaded gasoline, municipal sewage, industrial waste and paint spraying (Gisbert et al., 2003; Ganesh et al., 2015). It could be taken up by various crops and then threaten human health (Szczygłowska et al., 2011; An et al., 2018). Conventional physical and chemical approaches applied for the remediation of heavy metal have several drawbacks, such as high operational cost, low removal rate and secondary pollution. Microbes are widely present in the soil, due to their large surface area, they have strong adsorption capability for heavy metals and without any undesirable effects, thus, using microorganisms as an alternative biomaterial in dealing with heavy metal contaminated wastewater and soil have been widely concerned by scientists and become the research hot spots in the field of green environmental protection (Velmurugan et al., 2010; Wu et al., 2010;Deng et al., 2011;Kayalvizhi et al., 2019).

Generally, contaminated soils are sources of heavy metal tolerant microorganisms. Recent studies indicated that there existed a certain amount of anti-heavy metal

http://www.aloki.hu ● ISSN 1589 1623 (Print) ● ISSN1785 0037 (Online)
DOI: http://dx.doi.org/10.15666/aeer/1804_57435757

microbial groups in soils that have been subjected to one or more heavy metal stresses for a long time, including bacteria, fungi, actinomycetes and algae, and these microbial groups usually have strong biosorption capacity for heavy metals (Wu et al., 2010; Jacob et al., 2013; Iram et al., 2015; Kayalvizhi et al., 2019). Fungi have been recognized as one promising class of low-cost biosorbents for the removal of heavy metal ions from aqueous waste streams. There are several mechanisms in fungi to tolerate and detoxify metals, including extra and intracellular precipitation, transformation of metals, and biosorption to cell wall. The cell walls of fungi are composed of polysaccharides, proteins, and lipids that contain reactive functional ingredients with potential metal binding capacities (Viraraghavan et al., 2011; Mohammadian et al., 2017).

Terry et al. (2018) reported that a total of 425 fungal strains were obtained from tropical forest soil, which showed heavy metal tolerance, the most common and diverse genera isolated were identified as *Penicillium*. Since the fungus *Penicillium* has strong vitality, rapid reproduction and extensive sources in environments, and it had been found as being most tolerant to many kinds of heavy metals, such as Zn, Hg, Cr and Pb (Ye et al., 2018; Kayalvizhi et al., 2019; Chang et al., 2020; Long et al., 2020), its anti-lead characteristics have been studied by some researchers particularly (Zucconi et al., 2003; Say et al., 2003; Velmurugan et al., 2010; Mohammadian et al., 2017;Ye et al., 2018). Zucconi et al. (2003) reported that a strain of *Penicillium* (*Penicillium lilacinus*) can grow in a medium containing Pb^{2+} up to 1434 mg/L. As reported by Sun et al. (2007), *Penicillium* sp. Psf-2 can grow in a solution with Pb^{2+} concentration of 4 mmol/L. Velmurugan et al. (2010) isolated a high lead-resistant strain (*Penicillium* sp. MRF-1) from South Korean mining soil, where the lead content is 357 mg/kg, the strain showed high removal efficiency of Pb^{2+}, so it would be an excellent biosorbent for the removal of lead from aqueous solution. The *Penicillium oxalicum* SL2 had tolerance to 1000 mg/L Cr^{6+} and 2500 mg/L Pb^{2+} in potato-dextrose agar, and had excellent removal efficiency of $Cr^{6+}$and Pb^{2+}via reduction with acidic metabolites and form transformation in the mycelium, the strain showed a promising new candidate for bioremediation of heavy metal pollution (Ye et al., 2018;Long et al., 2020).

Most previous reports on heavy metal resistant fungi have been focusing on the adsorption capacity of dead fungi biomass, and less on the biosorption capacity of living fungi biomass (Say et al., 2003; Fan et al., 2008; Velmurugan et al., 2010). Moreover, although these studies showed that *Penicillium* was tolerant to Pb^{2+} and had Pb^{2+} biosorption capability, their performance about tolerance and biosorption were slightly weak. Therefore, it is far-reaching significant to use living fungi to cope with the seriously lead contaminated soil for long-term bioremediation effect.

In this study, a fungus strain with high Pb-resistance was isolated and acclimated from Pb-contaminated soil, and its biological characteristics were studied. The biosorption effects of Pb^{2+} by living strains were also determined. This study would potentially provide a theoretical basis for the bioremediation of lead pollution in the environment.

Materials and methods

Collection of soil samples and Pb content analysis of soil samples

The soil samples were collected from a demonstration zone of the National Loess Fertility and Fertilizer Benefit Monitoring Base in Wuquan Town, Yangling County,

http://www.aloki.hu ● ISSN 1589 1623 (Print) ● ISSN1785 0037 (Online)
DOI: http://dx.doi.org/10.15666/aeer/1804_57435757

Shaanxi Province (34°17′51″N, 108°00′48″E), China. In the test site, 350 mg/kg Pb (in the form of $Pb(NO_3)_2$solution) was artificially added in the soil in May 2010. The surface soil (0-20 cm) was collected with the Z-shape 5-point sampling method in December 2013. After mixed, approximately 0.5 kg of soil from each site was collected. A standard soil corer device was used to collect samples without disturbing plant roots. Five collected soil cores from each plot were pooled as a replicate. A total of 3 sample replicates were transferred to laboratory. The soil samples were sieved through 2-mm mesh to remove plant residues and stones. A subsample of each soil core was sealed in a sterilized self-sealing bag in an icebox and delivered to laboratory, then stored in the refrigerator at 4℃ for isolating fungal strains. The remaining sample was air-dried at room temperature until a stable weight was reached, and air-dried soil samples were ground and passed through a 0.25-mm sieve for Pb content analysis.

Total concentration of Pb in the soils were determined by standard soil testing procedures (Bao, 2000), 5 g soil samples were digested by HNO_3:HCl:$HClO_4$(1:2:2) to extract the total Pb. Total Pb concentration was measured with ICP-MS (Thermo, model Xseries Ⅱ, USA).

Isolation of Pb-tolerant fungal strain

A total of 10 g of the collected soil sample was weighed and dissolved in 100 mL distilled water held in a 500-mL flask. The mixture was shaken at 25 ℃, 120 r/min for 2 h and kept still for 20 min, 1 mL of the suspension was removed and diluted to 10^{-1}, 10^{-2}, 10^{-3}, and 10^{-4} concentrations with a gradient-dilution method (Li et al., 2010b). With a sterilized pipettor, 100 μL of each dilution was transferred onto potato-dextrose agar (PDA) plates supplemented with 200, 300, 400 and 500 mg/L of Pb^{2+}, respectively. The plates were incubated at 28 ℃ for 5-7 d, three replications were performed for each treatment. According to fungus growing characteristics, the blooming colonies with different morphology were picked and re-inoculated onto new PDA plates until the pure strain was obtained. The obtained strains were further examined on PDA plates that contain 600, 800 and 1000 mg/L of Pb^{2+}, respectively. After isolation, the obtained pure strains were preserved with PDA slant and glycerol media. All the operations were conducted under sterilized conditions.

The above PDA culture medium formula was: peeled potato 200.0 g, glucose 15.0 g, peptone 3.0 g, $MgSO_4$ 2.0 g, KH_2PO_4 3.0 g, agar powder 15.0 g, and distilled water 1000 mL. $Pb(NO_3)_2$ solution was prepared and stored at 4 ℃ for adding to the PDA medium.

Maximum Pb resistance level of strain Pb-G

The maximum concentration of the heavy metal that a strain can tolerated is the maximum resistance level (MRL). To determine the MRL of the isolated strain, the strain was cultivated with PDA containing different concentrations of sterilized $Pb(NO_3)_2$ solution. Five Pb^{2+}concentrations (treatments) were selected, that is, 0 mg/L (CK), 1000 mg/L, 2000 mg/L, 3000 mg/L and 4000 mg/L, three replicates per treatment. After 5 days of cultivation at 28 ℃, the colonies were observed and photographed.

Molecular identification for strain Pb-G

The conservative ITS rRNA gene in fungi was used to identify the screened Pb-G strain. The ITS rRNA gene form Pb-G was amplified using the primer ITS1 (5'-

http://www.aloki.hu ● ISSN 1589 1623 (Print) ● ISSN1785 0037 (Online)
DOI: http://dx.doi.org/10.15666/aeer/1804_57435757

TCCGTAGGTGAACCTGCGG-3') and ITS4 5'-TCCTCCGCTTATTGATATGC-3') (Velmurugan et al., 2010). The PCR amplification system was 50 μL, containing 5 μL 10×LA Taq Buffer II (Mg^{2+} Plus (TaKaRa, Japan), 8 μL dNTP, 5 U LA Taq enzyme (TaKaRa), 1 μL of each primer (0.5 mmol/L), and 2 μL 10.3 ng/μL DNA template). The PCR program was as follows: pre-denaturation at 94℃ for 5 min, 31 cycles of denaturation at 94℃ for 45 s, annealing at 58℃ for 45 s, extension at 72℃ for 90 s, and finally preservation at 4℃ for less than 12 h. The PCR products were detected by agarose gel electrophoresis, and the qualified ones were sent to the Beijing Liuhe Huada Gene Technology Co., Ltd. for sequencing the ITS gene.

To analyze the homology of the strain, the sequences of the samples were aligned against NCBI databases (http://www.ncbi.nih.gov/index.html) by BLAST, and a phylogenetic tree was constructed using the software MEGA 5.05, using Neighbor-joining analysis for the ITS rRNA.

Effects of temperature and pH on the growth of Pb-G

Temperature and pH are the decisive factors affecting the growth of the strain, and the metabolic rate and growth rate of the strain will be increased at the appropriate temperature and pH. Therefore, the two factors were selected to determine the optimal growth conditions of the strain.

The *Penicillium* sp. Pb-G strain was rejuvenated on PDA medium without Pb^{2+}, and then agar dishes attached with plenty of mycelia were taken out using a sterilized hole puncher (Φ=1.2 cm). The agar dishes were put onto PDA medium and inoculated for 7 d at 20 ℃, 25 ℃, 30 ℃ and 35 ℃, respectively. The colony diameter was then measured by the Cross-crossing method at a fixed time every day. The colonial average growth rate was calculated according to *equation (1)*:

$$G_t = \frac{D_t - D_0}{t} \quad \text{(Eq.1)}$$

where, G_t (v, cm/d) is the average growth rate; D_t (φ, cm) is the average colony diameter; D_o (φ, cm) is the disk diameter, and t (d) is the culture time.

The pH of solid PDA medium was adjusted to 6.0, 7.0, 8.0 and 9.0 respectively using sterilized 1 mol/L HCl and NaOH solutions. The rejuvenated *Penicillium* sp. Pb-G were then inoculated onto these media by agar dish inoculation method using a sterilized hole puncher (Φ=1.2 cm) and cultivated at 25 °C for 7 d. Every treatment repeats three times. The colonial diameter was measured by the Cross-crossing method at a fixed time every day. The colonial average growth rate was also calculated according to equation (*Eq.1*).

Scanning electron microscopy (SEM) analysis

The scanning electron microscopy (SEM) was used to analyze the morphological characteristics of *Penicillium* sp. Pb-G cultured in different Pb^{2+} concentrations. The sterilized $Pb(NO_3)_2$ solution was added into PDA medium to get the final concentrations of 0 mg/kg (CK), 2000 mg/kg, 3000 mg/kg and 4000 mg/kg. The *Penicillium* sp. Pb-G was then inoculated in these PDA liquid media at 28℃. After 5 d, fungal biomass was harvested by centrifugation at 8000 r/min (15℃) for 10 min. To remove any loosely associated and unsequestered Pb^{2+}, the collected mycelia were soaked in 2% oxalic acid for 10 min and then soaked in distilled water for another 10 min for two times. Then the samples were dried by vacuum freeze drier (Thermo Fisher, USA), coated with gold and

http://www.aloki.hu ● ISSN 1589 1623 (Print) ● ISSN1785 0037 (Online)
DOI: http://dx.doi.org/10.15666/aeer/1804_57435757

examined under SEM (FLEXSEM1000, Hitachi, Japan), photographed with optimum magnification (Glukhova et al., 2018).

X-ray diffraction (XRD) analysis

To analyze the Pb^{2+} biosorption capability of *Penicillium* sp. Pb-G, it was cultivated in PDA liquid medium with $Pb(NO_3)_2$concentrations of 0 mg/L (CK) and 4000 mg/L respectively. Every concentration was set for three repetitions. The strain was cultured on an oscillator at 25°C, 120 r/min for 5 d, centrifuged at 6000 r/min for 15 min to precipitate the fungal biomass, the supernatant was discarded and the precipitates were rinsed with distilled water, repeat these steps twice. The precipitates were taken out and dried at 65°C. After grinding the sample was analyzed by an XRD (Nippon science Minniflex 600, Japan), and parameters were set as the light pipe current, 15 mA; the voltage, 40 kV; the width of the slit, 0.02 deg; the scanning angular velocity, 0.25 °/min; and the scanning angle ranging from 3º to 90º. The characteristics of *Penicillium* sp. Pb-G were analyzed and plotted by MDI Jade 6.5 software (Materials Data Inc. Liverpool, CA) and Origin 8.5 (Origin Lab, USA) respectively based on the average value of three repetitions.

Biosorption properties of the strain Pb-G to Pb^{2+}

The mycelium from the vigorous *Penicillium* sp. Pb-G colony was picked, inoculated into 100 mL PDA liquid medium, and cultivated on a shaker at 120 r/min and 25℃. After 5 d of inoculation, the fungus was filtered with four layers of gauze, rinsed three times with deionized water, dried together with filter paper, and then weighted.

To examine the biosorption capability of Pb-G, the collected mycelium was inoculated in $Pb(NO_3)_2$ solution (pH=7) with initial Pb^{2+} concentrations of 0 mg/L(CK), 500 mg/L, 1000 mg/L, 1500 mg/L, 2000 mg/L and 2500 mg/L respectively, three repeats per Pb^{2+} concentration. For inoculation, 1 g fungi were put into 50 mL $Pb(NO_3)_2$ solution contained in a flask, fully dispersed by a glass rod, and shaken on shaker at 25℃, 150 r/min. After 24 h, all the mycelia were filtered with the filter paper, and then the hyphae were dried to a constant weight in a drying oven at 80 °C for 12 h with the filter paper together. The weight of the filter paper was then subtracted to obtain the dry weight of the biomass. Finally, the collected mycelia weight was calculated (Pan et al., 2010). The biosorption rate (Q) and the biosorption amount (q, mg/g) of fungus *Penicillium* sp. Pb-G were calculated based on mycelium dry weight according to the equation (*Eq.2*) and (*Eq.3*), respectively.

$$Q = \frac{(C_0 - C_t)}{C_0} \times 100\% \quad \text{(Eq.2)}$$

$$q = \frac{(C_0 - C_t)}{m} \times V \quad \text{(Eq.3)}$$

where, C_0 (mg/L) is the initial Pb^{2+} concentration before biosorption; C_t (mg/L) is the final Pb^{2+} concentration after biosorption; V (L) is the volume of the reaction solution; and m (g) is the mass of dried biomass of fungi in the reaction solution.

The supernatant was digested by nitric acid (HNO_3) and hydrogen peroxide (H_2O_2) for measuring Pb^{2+}amount.

http://www.aloki.hu ● ISSN 1589 1623 (Print) ● ISSN1785 0037 (Online)
DOI: http://dx.doi.org/10.15666/aeer/1804_57435757

Data analysis

The growth rate and biosorption capability were performed with three repetitions and the data were reported as mean ± standard deviation (SD) in the figures and table. The significant differences among the treatments were evaluated using One-way analysis of variance (ANOVA) followed by LSD test at a level of $p < 0.05$ using SPSS 22.0 software for Windows (SPSS Inc., Chicago, IL, USA).

Results

The maximum resistance level of strain Pb-G

The average concentration of total Pb in collected soil samples was 331.13 mg/kg that exerted a selection pressure on microbial communities, including filamentous fungi. After isolation and culturing, a strain of fungus with high resistance capacity to Pb^{2+} was obtained, named Pb-G. The center of the colony was cyan, and the periphery of the colony showed white. The *Figure1* demonstrated that the morphology of the *Penicillium* sp. Pb-G remained same with the blue-green color and no prominent changes were detected under the different concentration of Pb^{2+} from 1000 to 2000 mg/L. Whereas, when the Pb^{2+} concentration was raised to 3000 mg/L, the growth of strain Pb-G slowed down, showing low hyphae amount, deeper color and white colony edge, which indicated that the growth of the fungi was inhibited to a certain extent and when Pb^{2+} reached up to 4000 mg/L in the medium, Pb-G strain still grew, but the number of hyphae was reduced, the colony was obviously small in diameter, and no obvious changes were found for hyphae even after 25 d of cultivation. So the MRL of the Pb-G strain was 4000 mg/L.

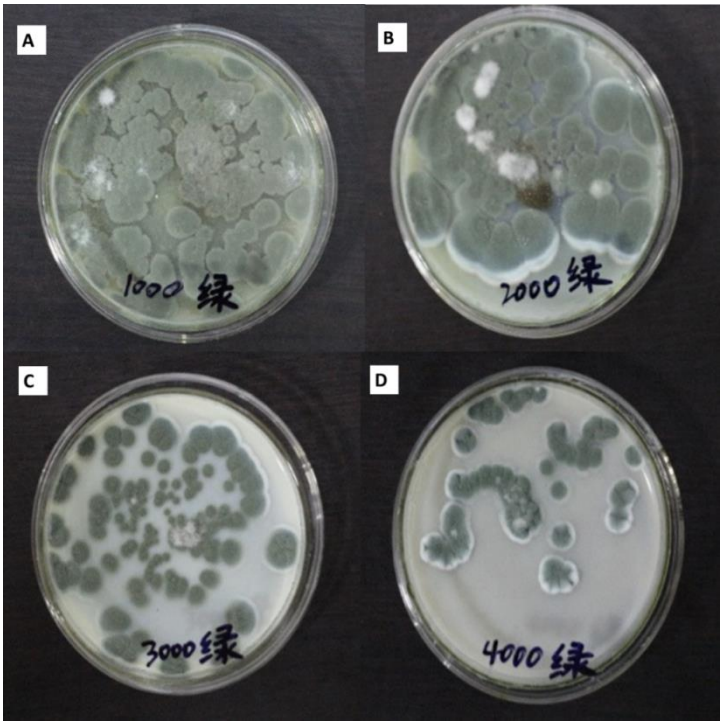

Figure 1. *The growth status of Penicillium sp. Pb-G in medium with different concentrations of Pb^{2+}. A, 1000 mg/L; B, 2000 mg/L; C, 3000 mg/L; D, 4000 mg/L*

http://www.aloki.hu ● ISSN 1589 1623 (Print) ● ISSN1785 0037 (Online)
DOI: http://dx.doi.org/10.15666/aeer/1804_57435757

Molecular identification of the Pb-tolerant microorganism (Pb-G)

The ITS rRNA gene was amplified from Pb-G stain and analyzed by software MEGA 5.05. The ITS rRNA gene in Pb-G strain was about 600 bp in length, the ITS rRNA sequence of Pb-G was deposited to GenBank and accession number was obtained, the GenBank accession was No. MK372218 (http://www.ncbi.nih.gov/index.html). A phylogenetic tree was constructed with the obtained homologous sequences from GenBank according to the sequence similarity over 97% using the ITS nuclear ribosomal RNA (Torres et al., 2018). If the similarity of ITS rRNA gene sequences was more than 99% between a studied strain and its nearest neighbor, the strain can be identified as the same species with its nearest neighbor (Mohammadian et al., 2017). In the present study the results of phylogenetic tree showed the strain Pb-G was closely related to *Penicillium* in evolution, and its nearest neighbor was the *Penicillium* JN397373.1 in the phylogenetic tree (*Figure2*). Therefore, based on the fungal morphology and sequence alignment of ITS rRNA gene, the strain Pb-G was identified as *Penicillium* genus.

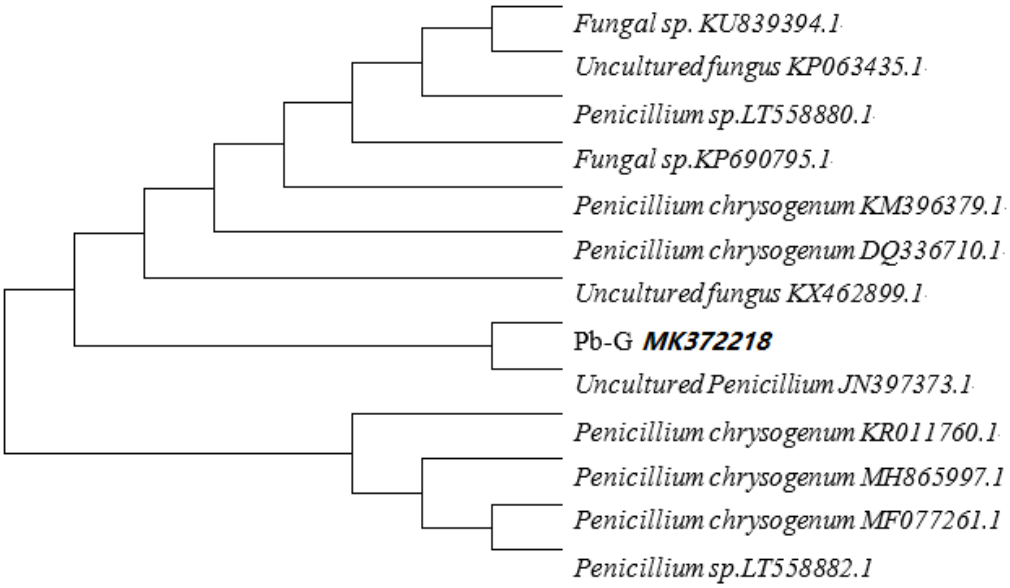

Figure 2. *The phylogenetictree of strainstolerantto* Pb^{2+}

Effects of different temperatures and pH on the growth of Pb-G

The growth rate of *Penicillium* sp. Pb-G changed under the influence of different temperatures (*Figure3*). On the first day, the *Penicillium* sp. Pb-G strain at 25 °C grew slowly, the strain at other temperatures did not change at all. On the 2-4th day, *Penicillium* sp. Pb-G had the highest growth rate at 25 °C, while they grew fast at 20 °C on the 4-7th day. For the *Penicillium* sp. Pb-G at 30 °C, they grew fast on the 2-4th day, but the growth rate decreased on the 4-7th day. The *Penicillium* sp. Pb-G was almost no obvious growth at 35°C. These results indicated that the strain Pb-G grow well within the temperature range of 20-30 °C, but inhibited at 35°C, therefore, 25 °C was the most suitable temperature for its growth.

http://www.aloki.hu ● ISSN 1589 1623 (Print) ● ISSN1785 0037 (Online)
DOI: http://dx.doi.org/10.15666/aeer/1804_57435757

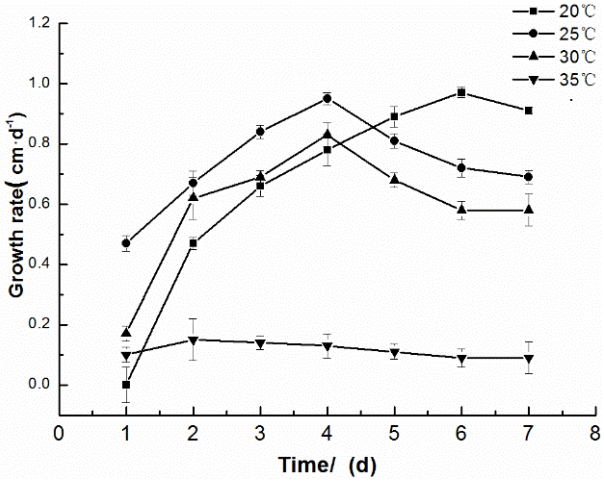

Figure 3. *Effects of different temperatures on the growth rate of Penicillium sp. Pb-G. Data are means ± SD (n=3)*

The growth rate of strain *Penicillium* sp. Pb-G also changed under the influence of different pH values (*Figure4*). The growth rate of *Penicillium* sp. Pb-G was highest at pH 7 among all pH conditions, followed by the growth rate at pH 6, while it was decreased when the pH reached up to 8 and 9. The results indicated that the pH 7 was the optimal pH value for the strain growth, and the growth rate reached the highest on the 4th day.

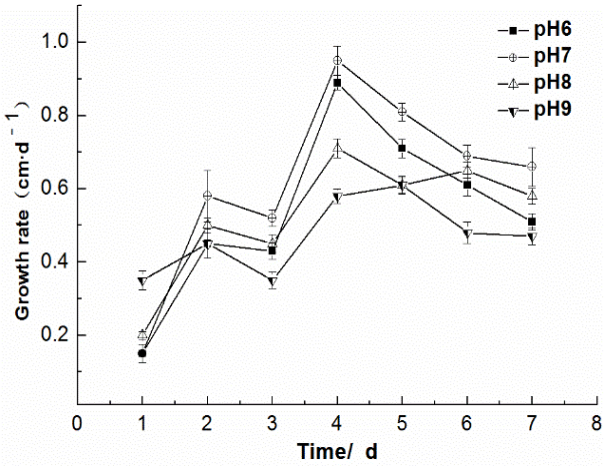

Figure 4. *Effects of different pHs on the growth rate of Penicillium sp.Pb-G. Data are means ± SD (n=3)*

Morphological characteristics of strain Pb-G's spores with different Pb^{2+} concentrations

The spore morphologies of the *Penicillium* sp. Pb-G in medium with different Pb^{2+} concentrations were observed by scanning electron microscopy. As shown in *Figure 5*, the spores of *Penicillium* sp. Pb-G in the CK group (0 mg/kg of Pb^{2+}) were more than that treated under 4000 mg/kg of Pb^{2+}, and the individuals were full and evenly

http://www.aloki.hu ● ISSN 1589 1623 (Print) ● ISSN1785 0037 (Online)
DOI: http://dx.doi.org/10.15666/aeer/1804_57435757

distributed. However, the amount of spores was reduced under different Pb^{2+} treatments, and it showed morphologies of collapse, shrinkage and deformity. Furthermore, some spores dissolved and joined into pieces in "strips" shape (as indicated by the arrows). With the increase of Pb^{2+} concentration, the phenomenon of spore shrinkage and connection into pieces also increased. After magnified, the *Penicillium* sp. Pb-G spores under the 4000 mg/kg of Pb^{2+} treatment showed obvious distortion and deformation compared with the CK group, and some of them had irregularly shaped blocky material attached, as shown by the arrows (*Figure 5*-E and F).

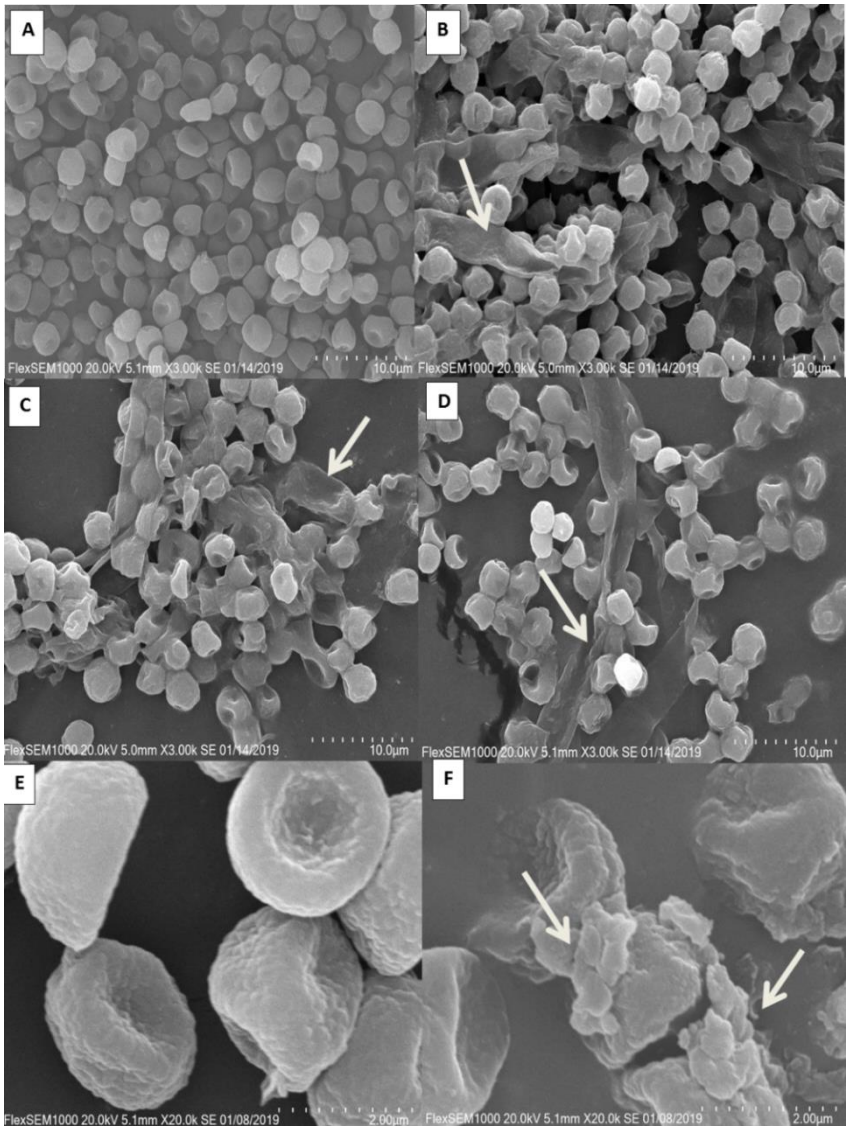

Figure 5.*Scanning electron microscopy (SEM) micrographs of strain Pb-G treated by different concentrations of* Pb^{2+}*. (A and E, 0 mg/kg (CK); B, 2000 mg/kg; C, 3000 mg/kg; D and F, 4000 mg/kg; A, B, C and D were amplified by 3000 times, and E , F were amplified by 20000 times)*

XRD analysis

The *Penicillium* sp. Pb-G grown under 0 mg/L (CK) and 4000 mg/L $Pb(NO_3)_2$ treatments were further analyzed by X-ray diffractometry. The XRD patterns of *Penicillium* sp. Pb-G cells treated with 0 and 4000 mg/L $Pb(NO_3)_2$ were different

http://www.aloki.hu ● ISSN 1589 1623 (Print) ● ISSN1785 0037 (Online)
DOI: http://dx.doi.org/10.15666/aeer/1804_57435757

(*Figure 6*). Analysis by using Jade 6.0 software and phase retrieval, it was found that the characteristic peaks of Pb-G cells under the treatment of 4000 mg/L Pb^{2+} (marked by black triangles) contained Pb elements, in which the characteristic peaks were the highest when the diffraction angle was 30.16°-30.30°. But there was no obvious characteristic peak under CK treatment and no Pb elements were found by phase retrieval. In this study, Pb-G cells treated with 4000 mg/L $Pb(NO_3)_2$ contained Pb with different compound forms, of which the characteristic peak was highest and there was no Pb element in the fungi of CK group when the diffraction angle was 30.16°-30.3°. It can be inferred that the Pb elements in Pb-G mainly come from the exogenous $Pb(NO_3)_2$ solution, indicating that the strain *Penicillium* sp. Pb-G had biosorption capability to exogenous Pb^{2+}.

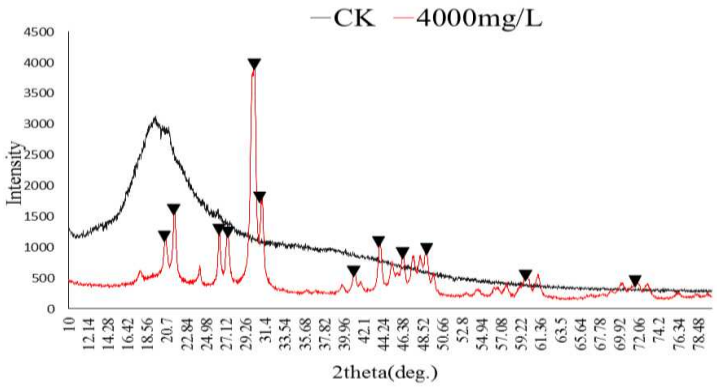

Figure 6. *X-ray diffractogram of strain Penicillium sp. Pb-G treated by different concentrations of* Pb^{2+}

Analysis of the biosorption of Pb^{2+} by the strain Pb-G

In this study, as the results shown in *Table 1*, it can be seen that the fungus *Penicillium* sp. Pb-G had good biosorption efficiency at different initial concentration of Pb^{2+}, and the trend of biosorption characteristics of Pb^{2+} by *Penicillium* sp. Pb-G was also be shown in *Figure 7*, both the biosorption capacity and biosorption rate were increasing at first and then decreasing with the increasing of Pb^{2+} concentration. When the Pb^{2+}concentration was 1500 mg/L, the biosorption influence of strain Pb-G was optimal, on which the biosorption rate and biosorption amount was 53.05% and 178.02 mg/g, respectively. When the Pb^{2+} concentration was more than 1500 mg/L, both the biosorption amount and the biosorption rate of *Penicillium* sp. Pb-G showed a rapid decline. Based on these findings, this strain has excellent biosorption capacity for Pb^{2+}.

Table 1. *The biosorption efficiency of $Pb^{2+}$by Penicillium sp.Pb-G*

The Initial concentration of Pb^{2+} (mg/L)	The residual concentration of Pb^{2+} (mg/L)	Biosorptioncapacity (mg/g)	Biosorptionrate (%)
500	426.95 ±0.66	28.25 ± 1.6 e	14.61 ± 1.9 e
1000	729.54 ±0.48	125.45 ± 3.2 b	27.05 ± 1.5 b
1500	704.25 ±0.16	178.02 ±3.9 a	53.05 ± 1.0 a
2000	1509.10 ±1.62	88.51 ± 2.8 c	24.55 ± 0.8 c
2500	2092.70 ±0.68	51.26 ± 0.9 d	16.29 ± 0.9 d

Note: Values are means ± SD, n=3. Different letters indicate significant differences among the treatment means ($p < 0.05$)

http://www.aloki.hu ● ISSN 1589 1623 (Print) ● ISSN1785 0037 (Online)
DOI: http://dx.doi.org/10.15666/aeer/1804_57435757

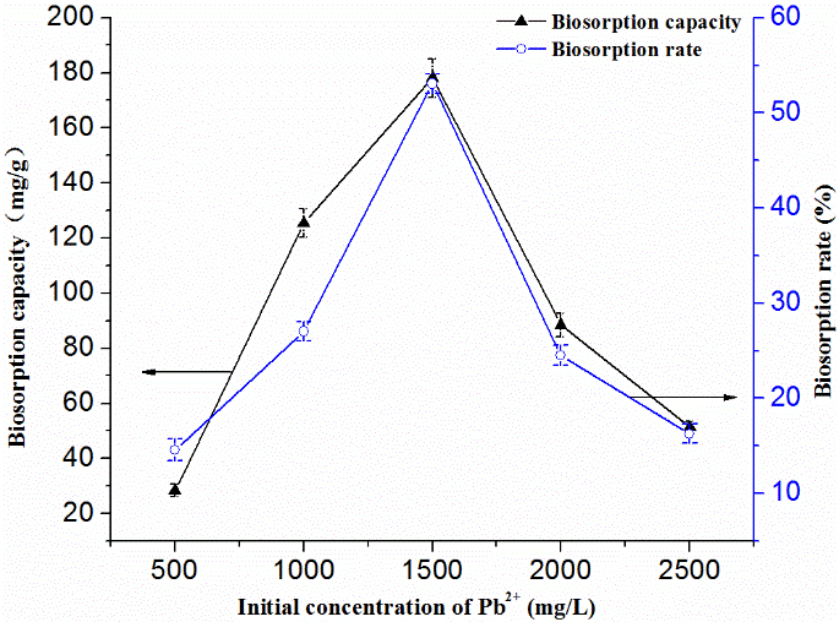

Figure 7. *Biosorption characteristics of Penicillium sp. Pb-G treated by different concentration of* Pb^{2+}

Discussion

Pb is highly toxic to living organisms. In a long-term Pb-contaminated environment, a number of microorganisms have evolved various mechanisms to counteract Pb stress and thereby improved their tolerance to Pb. Jacob et al. (2013) isolated three strains which were highly-resistant to Pb and Se from polluted seawater, namely *Aspergillus*, *Fusarium* and *Penicillium*, which can still grow on the medium contained high concentrations of Pb and Se. Iram et al. (2015) studied two strains of *Aspergillus flavus* and *Aspergillus niger* isolated from soil, which were highly resistant to Pb^{2+} and Cu^{2+}, and the biosorption capacity of *A.niger* to Pb^{2+} was 3.25-172.25 mg/g. Velmurugan et al. (2010) reported that *Penicillium* sp. MRF-1 can grow within the range of Pb^{2+} concentration from 0.31 to 1.24 g/L. Heavy metal resistant strains generally exist in areas contaminated by heavy metals, but the resistance levels of the same genus were inconsistent, and their resistance levels always depend on the level of contamination at the site of separation and the extent of heavy metal contamination in the separation test level (Jacob et al., 2013). The resistance of strain Pb-G to Pb in this study was similar to that of the previous studies. However, due to the high level of contamination at the isolation site, the strain Pb-G in this study can grow at a higher Pb^{2+} concentration and had better biosorption capacity after domestication.

It has been reported that bacteria, fungi and algae often act as biosorbent to remove a variety of heavy metal elements from the environment (Wang et al., 2006; Cain et al., 2008; Wu et al., 2010; Li et al., 2010a; Jacob et al., 2013; Iram et al., 2015), in particular, fungus in the genus of *Penicillium* had a strong biosorption capacity. Due to a large number of extracellular hyphae outside the cell wall of *Penicillium*, it had the function of adsorbing heavy metals, and some heavy metals can precipitate on the surface of the growing hyphae (Sintuprapa et al., 2000; Sun et al., 2007). The biosorption process is closely related to the concentration of heavy metal ions and the

http://www.aloki.hu ● ISSN 1589 1623 (Print) ● ISSN1785 0037 (Online)
DOI: http://dx.doi.org/10.15666/aeer/1804_57435757

biomass produced by the fungi, the biosorbent has more adsorption sites. When the adsorption site of the biosorbent reaches the saturation of the heavy metal, the biosorption amount gradually decreased (Fan et al., 2008; Pan et al., 2010; Yang et al., 2012). Therefore, as the concentration of heavy metal ions increases, the biosorption rate of the cells increases, and as the saturation of the adsorption sites increases, the biosorption capacity decreases gradually (Yang et al., 2012; Fan et al., 2013). In this study, the biosorption rate of Pb^{2+} by *Penicillium* sp. Pb-G reached the highest value, and the biosorption amount and biosorption rate began to decrease with the increasing of Pb^{2+}concentration, which indicated that the adsorption site of the added fungi may be close to saturation level in the biosorption test.

In this study, it was observed by SEM that the spores of *Penicillium* sp. Pb-G under high concentration of Pb^{2+} were deformed, collapsed and dissolved, and formed a "strip" shape in parallel. During fungal growth, the heavy metal resistant fungus can produce organic chelators and acids (Liang et al., 2016), the solubilizing effects of these compounds may be a probable reason for the spores of *Penicillium* sp. Pb-G deformed and dissolved. XRD analysis showed that *Penicillium* sp. Pb-G cells with $Pb(NO_3)_2$ treatment contained Pb, but none in CK, which indicated that Pb in *Penicillium* sp.Pb-G cells was derived from exogenously added $Pb(NO_3)_2$ solution, indicating *Penicillium* sp.Pb-G had biosorption function to Pb^{2+}. Raheem et al. (2013) reported that the *Enterobacter* sp. could produce nitrate reductase and denitrify $Pb(NO_3)_2$ to PbO when it was treated by $Pb(NO_3)_2$, and PbO peak appeared at a diffraction angle of about 30° analyzed by XRD. Liang et al. (2016) reported that *Aspergillus niger* and *Paecilomyces* grew in $Pb(NO_3)_2$-containing medium can produce phosphatase, phyticacid and glycerol-2-phosphate can be hydrolyzed by phosphatase, releasing inorganic phosphate and oxalic acid, where by $Pb(NO_3)_2$ in the solution can be precipitated into Pb-oxalate and Pb-chlorite, and the Pb-chloride can be further converted into Pb-oxalate, which is insoluble or weakly soluble. The *Penicillium* sp. Pb-G in this study showed similar characteristics to the reported strains, and the specific biosorption mechanism needs to be further studied.

The mechanism of adsorption of metal ions by fungi mainly included cell surface adsorption or complexation, intracellular enrichment and efflux, among them, enrichment was mainly achieved by transport of cell membranes inside the cells, while the stage of intracellular and extracellular excretion was when heavy metal ions reach a certain concentration, and the fungi prevented more heavy metal ions from entering the cells through efflux (Congeevaram et al., 2007; Sun et al., 2007; Deng et al., 2011). In the range of different concentrations of heavy metals, the living microbial fungus initiated two different mechanisms, one was biosorption by non-living or non-growing biomass, which was a metabolism-independent and passive uptake process, another was bioaccumulation by living and growing cells, which was mainly an intracellular accumulation (Deng et al., 2011). When the concentration of heavy metal reached a certain range that inhibiting microbial growth, the absorbing capacity of the microorganisms showed a downward trend. In this study, the biosorption rate of the strain *Penicillium* sp. Pb-G was measured in a specific concentration of Pb^{2+} solution. Within a certain concentration range, the biosorption of Pb^{2+} by the cell adsorption and enrichment achieved. When the concentration of Pb^{2+} inhibited the activity of fungi, the biosorption rate and the biosorption capacity tended to decrease.

http://www.aloki.hu ● ISSN 1589 1623 (Print) ● ISSN1785 0037 (Online)
DOI: http://dx.doi.org/10.15666/aeer/1804_57435757

Conclusions

After domestication and isolation, a strain of fungus (*Penicillium* sp. Pb-G) with high resistance to Pb was obtained, it can grow in a medium with Pb^{2+} content of 4000 mg/L. According to the morphological feature and molecular analysis, *Penicillium* sp. Pb-G had a close homology with *Penicillium*, thus the strain Pb-G was classified into the genus of *Penicillium*. The suitable temperature range for the *Penicillium* sp. Pb-G growth was 20-30°C, the most suitable pH was 7, and it had a biosorption effect on Pb^{2+}. When the Pb^{2+}concentration at 1500 mg/L, the best biosorption rate of *Penicillium* sp. Pb-G was 53.05% and the biosorption amount was up to 178.02 mg/g. This study indicated that *Penicillium* sp. Pb-G strain had high tolerance and outstanding biosorption capacity to Pb^{2+}, it could be as a potential candidate to apply in future for metal remediation from wastewater and heavy metal-contaminated soils.

Acknowledgments. This research was supported by the Social Development Project of Science and Technology Department of Shaanxi Province (2020SF-435), Scientific Research Program Funded by Shaanxi Provincial Education Department (No.18JK0354), and Doctoral scientific research foundation of Xi'an Polytechnic University (BS201922).

REFERENCES

[1] An, F. Q., Diao, Z., Lv, J. L.(2018):Microbial Diversity and Community Structure in Agricultural Soils Suffering from 4-year Pb Contamination. – Can. J. Microbiol. 64(5): 305-316.

[2] Bao, S.D. (2000): Soil and Agricultural Chemistry Analysis. – Agriculture Publication, Beijing, pp. 355-356.

[3] Cain, A., Vannela, R., Woo, L.K. (2008): Cyanobacteria as a biosorbent for mercuric ion. – Bioresour Technol 99(14): 6578-6586.

[4] Chang, J.J., Shi, Y., Si, G. Z., Yang,Q.C., Dong, J., Chen, J.Q. (2020): The bioremediation potentials and mercury(II)-resistant mechanisms of a novel fungus *Penicillium* spp. DC-F11 isolated from contaminated soil. – Journal of Hazardous Materials 396:122638.

[5] Congeevaram, S., Dhanarani, S., Park, J., Dexilin, M., Thamaraiselvi, K. (2007): Biosorption of chromium and nickel by heavy metal resistant fungal and bacterial isolates. – J Hazard Mater146(1-2): 270-277.

[6] Deng, Z. J., Cao, L. X., Huang, H. W., Jiang, X. Y., Wang, W. F., Shi, Y., Zhang, R. D. (2011): Characterization of Cd- and Pb-resistant fungal endophyte *Mucor* sp. CBRF59 isolated from rapes (*Brassica chinensis*) in a metal-contaminated soil. – J Hazard Mater 185(2-3): 717-724.

[7] Fan, T., Liu, Y.G., Feng, B.Y., Zeng, G.M., Yang, C.P., Zhou, M., Zhou, H. Z., Tan, Z. F., Wang, X. (2008): Biosorption of cadmium(II), zinc(II) and lead(II) by *Penicillium simplicissimum*: Isotherms, kinetics and thermodynamics. – J Hazard Mater160(2-3):655-661.

[8] Ganesh, K. S., Sundaramoorthy, P., Nagarajan, M. (2015): Organic Soil Amendments: Potential Source for Heavy Metal Accumulation. – World Scientific News16: 28-39.

[9] Gisbert, C., Ros, R., Haro, A. D., Walker, D. J., Bernal, M. P., Serrano, R., Navarro, A. J. (2003): A plant genetically modified that accumulates Pb is especially promising for phytoremediation. – Biochemical and biophysical research communications303(2):440-445.

[10] Glukhova, L. B., Frank, Y. A., Danilova, E. V., Avakyan, M. R., Banks, D.,Tuovinen, O. H., Karnachuk, O.V.(2018):Isolation, Characterization, and Metal Response of Novel, Acid-Tolerant*Penicillium* spp. from Extremely Metal-Rich Waters at a Mining Site in

http://www.aloki.hu ● ISSN 1589 1623 (Print) ● ISSN1785 0037 (Online)
DOI: http://dx.doi.org/10.15666/aeer/1804_57435757

Transbaikal (Siberia, Russia). – MicrobEcol76(4): 911-924.
[11] Iram, S., Shabbir, R., Zafar, H., Javaid, M. (2015): Biosorption and Bioaccumulation of Copper and Lead by Heavy Metal-Resistant Fungal Isolates. – Arabian Journal for Science &Engineering40(7):1867-1873.
[12] Jacob, J.M., Bardhan, S., Raj, M.B. (2013): Selenium and lead tolerance in fungi isolated from sea water. – International Journal of Innovative Research in Science Engineering &Technology2(7): 2975-2981.
[13] Kayalvizhi, K., Kathiresan, K. (2019): Microbes from wastewater treated mangrove soil and their heavy metal accumulation and Zn solubilization. – Biocatalysis and Agricultural Biotechnology22:101379.
[14] Li, H. F., Lin, Y. B., Guan, W. M., Chang, J. L., Xu, L., Guo, J. K., Wei, G. H.(2010a): Biosorption of Zn(II) by live and dead cells of *Streptomyces ciscaucasicus* strain CCNWHX 72-14. – J Hazard Mater179(1-3): 151-159.
[15] Li, Z. G., Luo, Y. M., Teng, Y. (2010b): Soil and environmental microbiology research method. – Science publisher, Beijing. (in Chinese).
[16] Liang, X., Kierans, M., Ceci, A., Hillier, S., Gadd, G. M. (2016): Phosphatase-mediated bioprecipitation of lead by soil fungi. – Environ Microbiol18(1): 219-231.
[17] Long, B.B., Ye, J., Ye, Z., He, J.Y., Luo, Y.T., Zhao, Y.G., Shi, J.Y. (2020): Cr(VI) removal by *Penicillium oxalicum* SL2: Reduction with acidic metabolites and form transformation in the mycelium. – Chemosphere253: 126731.
[18] Mohammadian, E., Ahari, A.B., Arzanlou, M., Oustan, S., Khazaei, S. H. (2017):Tolerance to heavy metals in filzmentous fungi isolated from contaminated mining soils in the Zanjan Province, Iran. – Chemosphere185:290-296.
[19] Pan, R., Cao, L., Zhang, R. (2010): Biosorption characteristics of heavy metals cadmium, copper, zinc, lead by *Penicillium* and *Fusarium* fungi. – Acta Scientiae Circumstantiae30(3):477-484.(in Chinese).
[20] Raheem, A.E., Shanshoury,E., Elsilk, S.E., Ateya, P.(2013):Uptake of some heavy metals by metal resistant *Enterobacter* sp. isolate from Egypt. – African Journal of Microbiology Research7(23): 2875-2884.
[21] Say, R., Yılmaz, N., Denizli, A. (2003): Biosorption of Cadmium, Lead, Mercury, and Arsenic Ions by the Fungus *Penicillium purpurogenum*. – Separation Science &Technology38(9): 2039-2053.
[22] Sintuprapa, W., Thiravetyan, P., Tanticharoen, M. (2000): A possible mechanism of Zn^{2+} uptake by living cells of *Penicillium* sp. – Biotechnology Letters22: 1709-1712.
[23] Sun, F., Shao, Z. (2007): Biosorption and bioaccumulation of lead by *Penicillium* sp. Psf-2 isolated from the deep sea sediment of the Pacific Ocean. – Extremophiles11(6): 853-858.
[24] Szczygłowska, M., Piekarska, A., Konieczka, P., Namiesnik, J. (2011): Use of Brassica plants in the phytoremediation and biofumigation processes. – Int. J. Mol. Sci. 12(11): 7760-7771.
[25] Torres-Cruz, T.J., Cedar,H.,Kuske, C. R., Alfaro, A.P. (2018): Presence and distribution of heavy metal tolerant fungi in surface soils of a temperate pine forest. – Applied Soil Ecology131:66-74.
[26] Velmurugan, N., Hwang, G., Sathishkumar, M., Choi, T. K., Lee, K. J., Taek, B.O., Lee, Y. S.(2010): Isolation, identification, Pb(II) biosorption isotherms and kinetics of a lead adsorbing *Penicillium* sp. MRF-1 from South Korean mine soil. – Journal of Environmental Sciences22(7): 1049-1056.
[27] Viraraghavan, T., Srinivasan, A. (2011):Fungal Biosorption and Biosorbents. – Springer Science Business Media B.V. Netherlands. Doi:10.1007/978-94-007-0443-5.
[28] Wang, J.L., Chen, C.(2006): Biosorption of heavy metals by *Saccharomyces cerevisiae*: a review. – Biotechnology Advances 24(5): 427-451.
[29] Wu, G., Kang, H. B., Zhang, X. Y., Shao, H. B., Chu, L. Y., Ruan, C. J.(2010): A critical review on the bio-removal of hazardous heavy metals from contaminated soils: Issues,

http://www.aloki.hu ● ISSN 1589 1623 (Print) ● ISSN1785 0037 (Online)
DOI: http://dx.doi.org/10.15666/aeer/1804_57435757

progress, eco-environmental concerns and opportunities. – J Hazard Mater174:1-8.

[30] Yang, L., Hao, R., Feng, W.U. (2012): Isolation of lead-tolerant fungus and the adsorption effect to Pb^{2+}. – Acta Scientiae Circumstantiae 32(10):2366-2374.(in Chinese).

[31] Ye, B. H., Luo, Y. T., He, J. Y., Sun, L. J., Long, B. B., Liu, Q. L., Yuan, X. F., Dai, P. B., Shi, J. Y. (2018):Investigation of lead bioimmobilization and transformation by *Penicillium oxalicum* SL2. – Bioresource Technology264:206-210.

[32] Zucconi, L., Ripa, C., Alianiello, F., Benedetti, A., Onofri, S. (2003): Lead resistance, sorption and accumulation in a *Paecilomyces lilacinus* strain. – Biology and Fertility of Soils37(1): 17-22.

http://www.aloki.hu ● ISSN 1589 1623 (Print) ● ISSN1785 0037 (Online)
DOI: http://dx.doi.org/10.15666/aeer/1804_57435757

RELATIONSHIP BETWEEN PHYTOPLANKTON FUNCTIONAL GROUPS AND ENVIRONMENTAL FACTORS IN THE HARBIN SECTION OF SONGHUA RIVER, NORTHEAST CHINA

ZHAO, F.[1,2] – SUN, X.[1] – LIU, D.[1] – SHANG, L. Y.[1] – LIU, J. M.[1] – LI, X. Y.[1] – LI, S.[1] – LI, X. C.[1] – WANG, Y. Z.[2] – SU, L. J.[2] – ZHANG, L. M.[2] – MU, Y. Y.[2] – XIAO, L.[2] – TIAN, Z.[2] – PAN, C.[2] – SUN, B.[2] – PAN, H. F.[3] – SHANG, G. Y. Q.[4] – YU, H. X.[1*] – MA, C. X.[1*]

[1]Department of Ecology, College of Wildlife and Protected Area, Northeast Forestry University, Harbin 150040, China
(e-mail: iamzhaofei@foxmail.com – F. Zhao)

[2]The Water Ecology Laboratory, Hydrology and Water Resources Survey Station in Harbin, Harbin 150028, China

[3]Greater Khingan Ling Survey, Planning and Design Institute, National Forestry and Grassland Administration, Jagdaqi 16500, China

[4]B1 West Building, WF Central, Building 1, 269 Wangfujing Street, Dongcheng District, Beijing 100006, China

[5]School of Management,Heilongjiang University of Science and Technology, Harbin 150020, China
(phone: +86-150-4586-2146)

**Corresponding author*
e-mail/phone: china.yhx@163.com/+86-131-0096-0911 (H. X. Yu); mch007@vip.163.com/+86-180-0366-8291 (C. X. Ma)

(Received 17th Feb 2020; accepted 2nd Jul 2020)

Abstract. In this study, samples were collected from 8 sites in the Harbin section of Songhua River, northeast China. We aimed to analyze how phytoplankton functional groups and environmental factors change from May to October during 2018. We identified 16 functional groups (C, D, F, G, H1, J, L0, MP, P, S1, TB, W1, W2, X1, X2 and Y) from 84 species and 7 (C, D, MP, W1, W2, X1 and X2) of them were dominant. The seasonal succession of dominant phytoplankton functional groups was the following: X2/C→X2/C/MP→X2/C/X1/MP. X2 and C always played a dominant role throughout the year. Results of the one-way ANOVA test and RDA revealed that WT, SD, NTU, Chl-a, DO, BOD5, NH4+, TP and Fe3 + were the major influencing factors. This study revealed that the dominant functional groups were positively correlated with SD and Chl-a and negatively correlated with NTU and TP.
Keywords: *phytoplankton functional groups, environmental factors, Songhua River, RDA, spatial and seasonal variation, biomass*

Introduction

Phytoplanktons are microbes that provide the foundation for aquatic food chains, and include zooplankton, fish and other aquatic animals in water environments and most important biological component in the River ecosystem. As a key part of material circulation and energy conversion in river ecosystem, phytoplankton has a very important impact on the status of aquatic ecosystem (Qiu et al., 2012). Meanwhile, phytoplankton function groups are communities of phytoplankton with similar functions in aquatic ecosystems (Reynolds et al., 2006; Crossetti et al., 2013; Huszaret al., 2015; Qu et al., 2019). It could be more directly described the growth of different species within a group in phytoplankton communities

http://www.aloki.hu ● ISSN 1589 1623 (Print) ● ISSN 1785 0037 (Online)
DOI: http://dx.doi.org/10.15666/aeer/1804_57595774

through the relatively simple classification of phytoplankton groups with observed data (Maggio et al., 2016). At present, Several studies have reflected the responsiveness of phytoplankton to environmental abiotic factors (Kruk et al., 2002; Bohnenberger et al., 2018), including water temperature (Hong et al., 2014), acidity (Klug et al., 2001), water level fluctuations (Su et al., 2019), total phosphorus and dissolved carbon (Klug et al., 2001), nutrient loading (Cupertino et al., 2019), etc. In addition, phytoplankton community development is influenced by the inter-specific interaction of organisms (Kim et al., 2020). However, most previous studies on phytoplankton functional groups had focused on the effects of a single environmental factor or a few species in a phytoplankton communities (Wang et al., 2020). The coexistence and succession of different phytoplankton functional groups under the same or similar environmental conditions have not been fully explained. The seasonal variation of environmental and biological factors are quite dynamic, they have a cumulative effect on different phytoplankton functional groups uccessions (Chuo et al., 2019). As such, more research is needed to quantify the interactions of stress effects of different factors on aquatic organisms in the future. This study can also meet the growing demand for sustainable watershed management of aquatic biota.

Songhua River, one of the 7 largest rivers in China, is the largest river in Heilongjiang Province and one of the key monitoring regions of the aquatic biodiversity conservation in China. According to the Xinhua News Agency, Songhua River of 1,900-km-long meanders through an area of 557,200 km^2, spanning Jilin Province and Heilongjiang Province, northeast China. According to the topography and channel characteristics, Songhua River is divided into three sections: the upper, middle and lower reaches. Harbin section of Songhua River is located in the middle reaches of the Songhua River. Harbin section of Songhua River starts from Sanjiazi in the upper reaches and ends at Dadingzi mountain in the lower reaches. There are two first grade tributaries, Ashi River and Hulan River. Along the Songhua River, there are Sanjiazitan wetland, Yangmingtan wetland, Jinhewan Wetland Park, Hulan estuary wetland park and other wetland parks. Songhua River would not only meet the domestic water demand of Harbin's industry and its people but also meet the ecological demand of landscape. Therefore, in order to ensure the healthy and sustainable development of the water ecological environment in the Harbin section of Songhua River, it is particularly important to investigate the changes of phytoplankton functional groups and analyze the relationship between phytoplankton functional groups and water environmental factors.

In this study, we monitored and calculated the biomass of the phytoplankton functional groups and the related water environmental factors in 2018. we analyzed the interaction between phytoplankton functional group and water environmental factors by redundancy analysis (RDA). This paper puts forward the experimental data support for the water environmental ecosystem and sustainable development of water resources of Songhua River, northeast China.

Materials and methods

Field sampling and measurements

According to the local climate and geographical characteristics, we investigated on the phytoplankton in the Harbin section of Songhua River, Heilongjaing Province, northeast China. Samples were collected seasonally (spring: May 8, 2018; summer: July 20, 2018; autumn: October 9, 2018) at eight sampling stations (*Fig. 1; Table 1*), respectively. Water samples were collected from 9:00 am to 5:00 bm.

http://www.aloki.hu ● ISSN 1589 1623 (Print) ● ISSN 1785 0037 (Online)
DOI: http://dx.doi.org/10.15666/aeer/1804_57595774

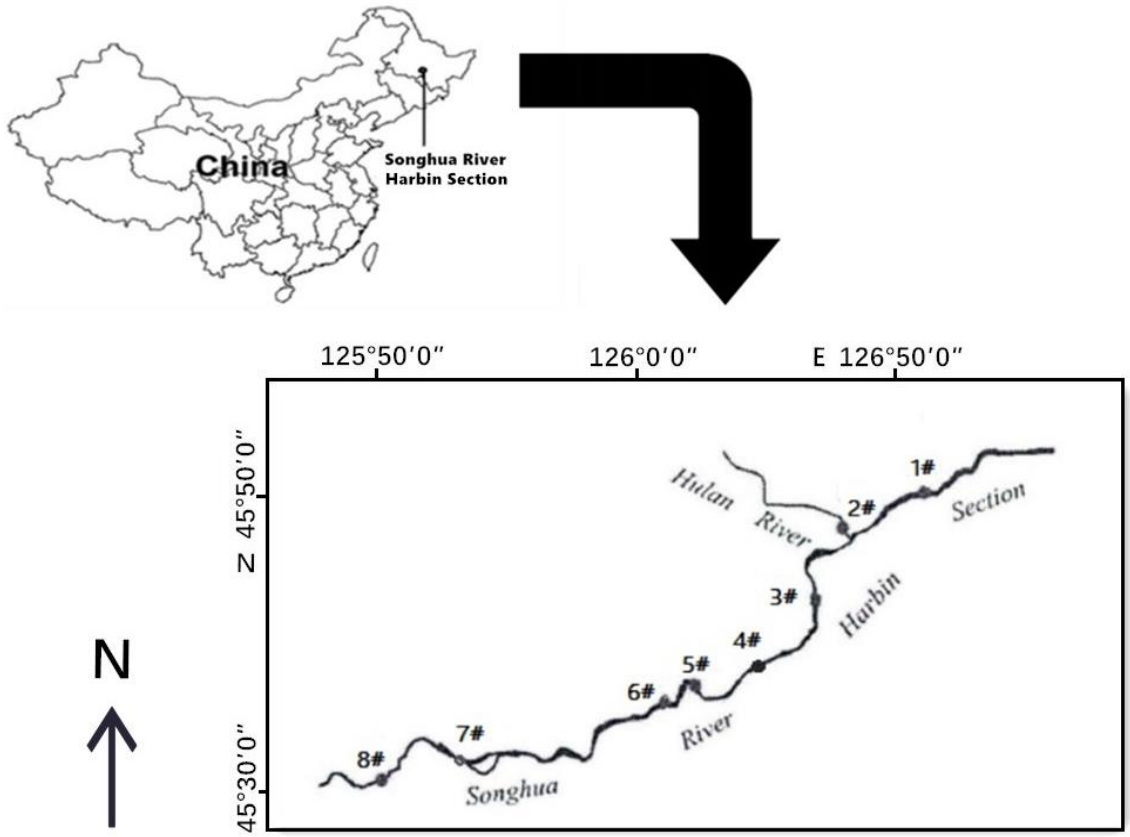

Figure 1. *The sampling stations in the Harbin section of Songhua River, Northeast China*

Table 1. *The number, GPS and water depth of each sampling station in the Harbin section of Songhua River, Northeast China*

Number	Station	GPS	Water depth (m)		
			Spring	Summer	Autumn
1#	Daliangzi village	N : 45°58′30″ E : 126°51′39″	4.50	8.30	26.80
2#	Hulan estuary wetland park	N : 45°55′28″ E : 126°47′20″	3.30	9.00	5.70
3#	Sanjiazitan wetland	N : 45°54′40″ E : 126°45′52″	7.50	3.50	4.50
4#	Cement plant	N : 45°51′44″ E : 126°42′23″	13.20	12.10	10.20
5#	The second water source	N : 45°45′23″ E : 126°32′59″	9.80	11.70	12.70
6#	Yangmingtan wetland	N : 45°46′12″ E : 126°31′13″	7.90	15.30	13.70
7#	Jinhewan wetland park	N : 45°46′10″ E : 126°28′55″	2.50	3.10	2.20
8#	Sanjiazi village	N : 45°32′23″ E : 125°53′11″	1.30	5.50	1.80

http://www.aloki.hu ● ISSN 1589 1623 (Print) ● ISSN 1785 0037 (Online)
DOI: http://dx.doi.org/10.15666/aeer/1804_57595774

Sample collection and determination

Phytoplankton samples were collected with a 5-L water sampler, and mixed samples of the upper water layer, the mid-water layer and the bottom water layer. Integrated 1000 mL water samples were preserved with acid Lugol iodine solution immediately and stored in the dark. Water sample was Siphoned to 30 mL into polythene plastic bottle after 48 h. And then qualitative and quantitative analysis was performed with 40 times magnification by optical microscope (Motic BA210, Motic Inc., China) (V = 0.1 mL) (Utermöhl, 1958). Phytoplankton species were identified using the references s from different literature (Hustedt, 1930; Prescott, 1954; Patrick et al., 1966; Komarek, 1983; Lange-Bertalot, 2001; Hu et al., 2006). The species were grouped into functional group as described by literature of science (Reynolds et al.; 2002; Reynolds, 2006; Padisak et al., 2009).

Transparency (SD) was estimated with a 20-cm diameter, black-white Secchi disc. Water depth and Flow rate (FR) were measured with the LCD digital sounder (HONDEX PS-7, HONDEX Inc., Japan) and hand-held current meter of YSI (YSI FlowTracker, YSI Inc., USA), respectively. Water temperature (WT) was measured with thermometer. PH, turbidity (NTU) and dissolved oxygen (DO) were recorded real-time by a multi-parameter water quality sonde (YSI 6600, YSI Inc., USA). Chlorophyll a (Chl-a), potassium permanganate index (COD_{Mn}), chemical oxygen demand (COD_{Cr}), 5-day biochemical oxygen demand (BOD_5), ammonium nitrogen (NH_4^+), total phosphorus (TP), total nitrogen (TN), fecal coliform (FC), and Fe^{3+} were checked and analyzed according to standard examine methods on drinking water (GB/T5750-2006) of the Chinese standard methods proposed by Ministry of Environmental Protection of People's Republic of China (MEP, 2006).

Statistical analyses

For this analysis, these phytoplankton species we selected were identified the dominant species ($y \geq 2$) of the study period, and their relative abundance > 1 at least in one sampling station (Xu et al., 1989; Lopes et al., 2005). The dominant species of phytoplankton (Y) was calculated by *Equation 1* (Lampitt et al., 1993):

$$Y = (\frac{n_i}{N}) f_i \quad \text{(Eq.1)}$$

n_i is an individual amount of the phytoplankton species, N is the sum of all individual amount (Gafan et al., 2005), f_i is the appearance frequency of the occurrence of i species in all phytoplankton samples, i is considered as the dominant species if $y \geq 0.02$.

We selected one-way analysis of covariance (ANCOVA) to establish the significant difference among physico-chemical characteristics during the study period, and the ordinations to run using computer program SPSS 16.0. All biomass data of functional groups and continuous environmental factors except for pH were $\log_{10}^{(X+1)}$ transformed to stabilize variance and reduce the influence of dominant taxa on the ordination and subjected to redundancy analysis (RDA) using down weighing of rare species (Jongman et al., 1987; ter Braak, 1988, 1990, 1994). Relationships between the phytoplankton functional groups and the environmental factors were assessed using redundancy analysis (RDA), which is a linear method of direct ordination. RDA was performed using CANOCO for Windows 4.5 (ter Braak et al., 1998), with forward selection to

http://www.aloki.hu ● ISSN 1589 1623 (Print) ● ISSN 1785 0037 (Online)
DOI: http://dx.doi.org/10.15666/aeer/1804_57595774

identify the environmental variables that explained the phytoplankton functional groups, which is a linear method of direct ordination (ter Braak, 1994). The significance of the variables and the first ordination axis was determined using Monte Carlo permutation testing (499 permutations), implemented in CANOCO.

This kind of technique can perform both regression and data ordination concurrently. The significance of the correlations between environmental factors and the species distribution was tested by one-way ANOVA test and redundancy analysis (RDA). Environmental factors measurement included WT (℃), pH, FR (m/s), SD (cm), turbidity (NTU), DO (mg/L), Chl-a/ (ug/L), COD_{Mn} (mg/L), COD_{Cr} (mg/L), BOD_5 (mg/L), NH_4^+ (mg/L), TP (mg/L), TN (mg/L), FC (mg/L), Fe^{3+} (mg/L). Only the samples which most environmental data were used in the RDA analysis to study the correlations with environmental factors on phytoplankton distribution.

Results

Characteristics of phytoplankton functional groups

A total of 84 species of phytoplankton were identified in the 24 samples collected from Harbin section of Songhua River, northeast China, belonging to 6 phyla, 8 classes, 15 orders, 26 families and 50 genera. Among these species, 37 belong to Chlorophyta, 29 belong to Bacillariophyta, and 9 belong to Cyanophyta, which represent approximately 44%, 35%, and 11% of the total species, respectively. In addition, the samples included six species in Euglenophyta (7%), two species in Cryptophyta (2%), and one species in Dinophyta (1%). And then classified into 16 functional groups namely: C, D, F, G, H1, J, L0, MP, P, S1, TB, W1, W2, X1, X2, Y (*Table 2*). There were 4 important functional groups, which with relative biomass > 20% at each sampling stations: C, MP, X2, Y. And there were 7 dominant function groups: C, D, MP, W1, W2, X1, X2 (*Table 3*). The seasonal relative biomass of functional groups in this study, X2 and C were dominant at 38.30% and 29.68% in spring, respectively; X2, C and MP were dominant at 40.97%, 15.87% and 13.20% in summer, respectively; X2, C, X1 and MP were dominant at 47.53%, 12.92%, 10.70% and 10.51% in autumn, respectively. It could be seen X2 and C were dominant in this year. In particular, X2 > 50% in 2# and 3# of spring, 2# of summer, 1#,3# and 7# of autumn, respectively. The distribution variation of phytoplankton functional groups is shown in *Figure 2*. Phytoplankton abundance was $(407.40\text{-}767.40)\times10^4$ ind./L and its mean was 524.10×10^4 ind./L in spring; it was $(51.00\text{-}156.60)\times10^4$ ind./L and its mean was 88.95×10^4 cell/L in summer; it was $(69.60\text{-}184.80)\times10^4$ cell/L and its mean was 119.03×10^4 cell/L in autumn. Biomass ranged from 3.06 to 5.10 mg/L and its mean was 3.85 mg/L in spring; it ranged from 0.45 to 1.34 mg/L and its mean was 0.79 mg/L in summer; it ranged from 0.50 to 1.79 mg/L and its mean was 1.02 mg/L in autumn.

Environmental variables

The average concentration of physico-chemical characteristics of Songhua River is shown in *Table 4*. WT ranged between 13.60-23.37 ℃ with maximum in summer and minimum in spring. WT showed distinguishing seasonal differences ($p < 0.001$) which were higher in summer and relatively lower in autumn. On the contrary, SD ranged between 10.50-58.50 cm with maximum in spring and minimum in summer. SD differed significantly seasonally ($p < 0.001$) with higher significant values in spring than

http://www.aloki.hu ● ISSN 1589 1623 (Print) ● ISSN 1785 0037 (Online)
DOI: http://dx.doi.org/10.15666/aeer/1804_57595774

in summer and autumn. NTU ranged between 7.55-170.30 with maximum in summer and minimum in spring. The river's NTU also varied seasonally ($p < 0.001$) with summer recording the highest values. The Chl-a ranged between 0.45-21.10 with maximum in spring and minimum in autumn. Chl-a differed with higher significant values ($p < 0.001$) in spring than in autumn. DO ranged between 4.70-9.75 mg/L with lower significantly values ($p < 0.001$) in summer than in spring and autumn. BOD_5 was significantly higher in spring and relatively lower in autumn ($p < 0.001$). NH_4^+ ranged between 0.07-0.83 mg/L with lower significantly values ($p < 0.001$) in autumn than in spring and summer. On the contrary, total phosphorus (TP) ranged between 0.04-0.19 mg/L with higher significantly values ($p < 0.001$) in autumn than in spring and summer. Fe^{3+} ranged between 0.10-1.64 mg/L with lower significantly values ($p < 0.001$) in spring than in summer and autumn.

Table 2. *Phytoplankton functional groups (FGs) and their relative biomass (%) in the Harbin section of Songhua River, Northeast China*

FGs	Genera	Biomass (%)
C	*Asterionella formosa, Cyclotella meneghiniana*	24.73%
D	*Nitzschia palea, Synedra acus, Synedra amphicephala, Synedra tabulata, Synedra ulna*	3.24%
F	*Oocystis parva, Oocystis elliptica, Micractinium pusillum, Kirchnerilla lunaris, Selenastrum gracile, Westella botryoides, Westellopsis linearis, Stichococcus bacillaris*	0.62%
G	*Eudorina elegans, Pandorina morum*	0.20%
H1	*Anabaena variabilis, Anabaena circinalis*	0.01%
J	*Golenkinia radiata, Chodatella quadriseta, Chodatella ciliata, Tetraëdron trigonum, Tetraëdron regulare, Actinastrum hantzschii, Crucigenia aiculata, Crucigenia quadrata, Crucigenia tetrapedia, Tetrastrum staurogeniae forme, Tetrastrum elegans, Scenedesmus ovalternus, Scenedesmus platydiscus, Scenedesmus dimorphus, Scenedesmus abundans, Scenedesmus acuminatus, Scenedesmus bijuga, Scenedesmus quadricauda*	1.97%
L0	*Gyrosigma acuminatum, Merismopedia minima, Chroococcus minutus*	0.06%
MP	*Cocconeis placentula, Achnanthes linearis, Epithemia turgida var. granulata, Surirella capronii, Surirella angustata, Cymbella ventricosa, Pinnularia major, Pinnularia gibba, Navicula exigua, Navicula radiosa, Navicula dicephala, Navicula anglica, Diatoma vulgare, Diatoma vulgare var. linearis, Coelosphaerium kützingianum, Ulothris variabilis*	5.91%
P	*Fragilaria virescens, Fragilaria brevistriata, Fragilaria ca pucina, Melosira granulata, Melosira granulata var. angustissima, Melosira granulata var. angustissima f. spiralis, Closterium sp.*	1.09%
S1	*Planktothrix agardhii, Phormidium allorgei, Phormidium beggiatoiforme, Phormidium lismorense*	0.70%
TB	*Melosira varians*	1.59%
W1	*Heteronema discomorphum, Lepocinclis steinii, Euglena oxyuris, Trachelomonas cylindrica, Strombomonas urceolata*	1.92%
W2	*Trachelomonas granulosa*	2.35%
X1	*Ankistrodesmus angustus, Ankistrodesmus acicularis, Chlorella vulgaris, Schroederia nitzschioides, Schroederia robusta*	7.73%
X2	*Chlamydomonas ovalis, Chlamydomonas globosa, Chroomonas acuta*	40.34%
Y	*Glenodinium pulvisculus, Cryptomonas ovata*	7.53%

http://www.aloki.hu ● ISSN 1589 1623 (Print) ● ISSN 1785 0037 (Online)
DOI: http://dx.doi.org/10.15666/aeer/1804_57595774

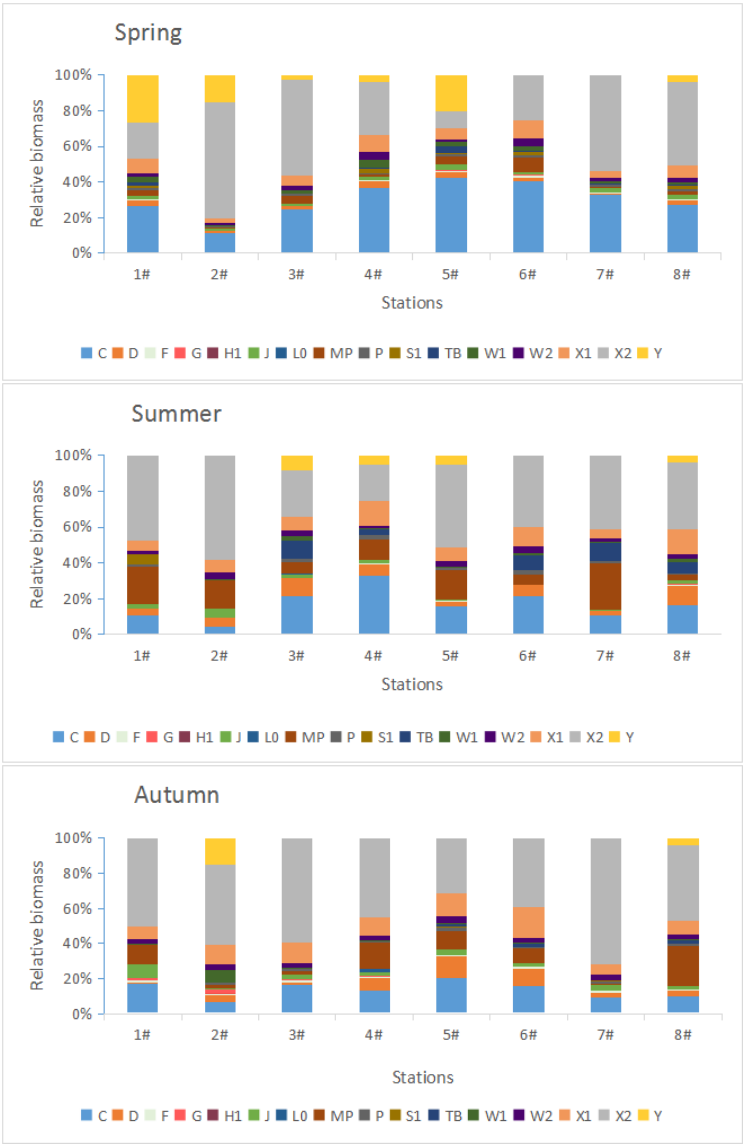

Figure 2. *Distribution of relative biomass of phytoplankton functional groups in the Harbin section of Songhua River, Northeast China*

Table 3. *Appendix list of dominant genus of phytoplankton functional groups in the Harbin section of Songhua River, Northeast China*

FGs	Phylum	Genus	Dominance		
			Spring	Summer	Autumn
D	Bacillariophyta	*Synedra acus*		0.03	0.03
C	Bacillariophyta	*Cyclotella meneghiniana*	0.47	0.32	0.25
W2	Euglenophyta	*Trachelomonas granulosa*	0.07	0.11	0.12
W1	Euglenophyta	*Trachelomonas cylindrica*	0.08	0.04	
X1	Chlorophyta	*Ankistrodesmus angustus*	0.03		
X1	Chlorophyta	*Chlorella vulgaris*	0.04	0.10	0.10
MP	Chlorophyta	*Ulothris variabilis*			0.05
X2	Chlorophyta	*Chlamydomonas ovalis*		0.02	0.03
X2	Cryptophyta	*Chroomonas acuta*	0.08	0.11	0.11

http://www.aloki.hu ● ISSN 1589 1623 (Print) ● ISSN 1785 0037 (Online)
DOI: http://dx.doi.org/10.15666/aeer/1804_57595774

Table 4. *Environmental parameters, which contained water temperature (WT), pH, flow rate (FR), Secchi depth (SD), turbidity (NTU), Chlorophyll a (Chl-a), dissolved oxygen (DO), Permanganate index (COD_{Mn}), Chemical oxygen demand (COD_{Cr}), 5-day biochemical oxygen demand (BOD_5), NH_4^+, total phosphorus (TP), total nitrogen (TN), Fecal Coliform (FC), Fe^{3+}, in each season in the Harbin section of Songhua River, Northeast China*

Parameters	Spring	Summer	Autumn	P value
WT (℃)	17.55 ± 1.63	22.9 ± 0.45	14.52 ± 0.4	0.000**
pH	7.86 ± 0.41	7.59 ± 0.18	7.72 ± 0.08	0.142
FR (m/s)	0.73 ± 0.58	0.97 ± 0.36	0.45 ± 0.24	0.070
SD (m)	37.5 ± 10.27	11.44 ± 0.82	18.5 ± 3.97	0.000**
NTU	15.91 ± 6.1	141.01 ± 26.9	43.9 ± 11.25	0.000**
Chl-a (ug/L)	14.27 ± 6.94	8.02 ± 2.45	5.98 ± 2.42	0.004**
DO (mg/L)	7.84 ± 0.93	6.6 ± 1.17	8.9 ± 0.29	0.000**
COD_{Mn} (mg/L)	5.56 ± 1	5.33 ± 0.7	4.65 ± 0.55	0.070
COD_{Cr} (mg/L)	12.25 ± 0.6	13.08 ± 1	12.53 ± 1.13	0.217
BOD_5 (mg/L)	4.74 ± 1.08	2.96 ± 0.8	2.31 ± 0.48	0.000**
NH_4^+ (mg/L)	0.43 ± 0.3	0.18 ± 0.11	0.13 ± 0.06	0.010**
TP (mg/L)	0.07 ± 0.03	0.1 ± 0.02	0.15 ± 0.03	0.000**
TN (mg/L)	2.05 ± 0.79	2.26 ± 0.46	1.83 ± 0.11	0.288
FC (mg/L)	14050.25 ± 11553.15	26284.88 ± 12806.46	22707.88 ± 12551.8	0.149
Fe^{3+} (mg/L)	0.19 ± 0.07	0.98 ± 0.22	1.23 ± 0.49	0.000**

**The environmental factors were significantly different at the level of 0.01

Correlation analysis of phytoplankton functional groups and environmental factors

The results of DCA performance by using CANOCO for Windows 4.5 showed that the Standard Deviation value was less than 3, so RDA analysis was carried out to analysis the relationship between phytoplankton functional groups and environmental factors in the Harbin section of Songhua River. The eigenvalue for RDA axis 1 (0.691) and axis 2 (0.156) together explained 84.7% of the functional groups variance out of which 69.1% of the total variability was from axis 1 (*Table 5*). The results of Monte Carlo test revealed that there were significant differences between the first axes and all canonical axes ($F = 17.921$, $p = 0.0002$, $F = 4.109$, $p = 0.004$). Axis 1 mainly positive correlated with SD ($r = 0.8729$), BOD_5 ($r = 0.7026$) and negatively correlated with Fe^{3+} ($r = –0.8241$), NTU ($r = –0.8163$). Axis 2 positively correlated with Chl-a ($r = 0.2453$) and COD_{Mn} ($r = 0.2453$) and negatively correlated with NH_4^+ ($r = –0.3812$), TP ($r = –0.3112$).

Table 5. *Summary of redundancy analysis (RDA) of phytoplankton functional groups for the first two axes*

Axes	I	II	III	IV
Eigenvalues	0.691	0.156	0.027	0.008
Species-environment correlations	0.972	0.838	0.930	0.893
Cumulative percentage variance of species data	69.1	84.7	87.4	88.2
Cumulative percentage variance of species-environment relation	78.1	95.7	98.7	99.7
Sum of all canonical eigenvalue	0.885			

http://www.aloki.hu ● ISSN 1589 1623 (Print) ● ISSN 1785 0037 (Online)
DOI: http://dx.doi.org/10.15666/aeer/1804_57595774

Discussion

Variation of phytoplankton functional groups in the Harbin section of Songhua River, Northeast China

In previous studies, the use of classification of organisms into phytoplankton functional groups have been to be the best way to explain the influence relation between factors of phytoplankton community structure and aquatic systems (Heebert et al., 2016). The Padisak J's study also showed the changes of life-history and physiological activity of phytoplankton functional groups have limited by factors of nutrient, light condition, hydrodynamic character, foraging behavior of zooplnation and hydrology dynamic change characteristics (Padisak et al., 2009). In the recent past, phytoplankton functional groups based on the morphological, as the primary producer in aquatic ecosystem, is a reliable indicator to analysis on water environmental quality and illustrate the trend of spatial and temporal variations (Li et al., 2017). Many recently studies focused on the change trend of biomass of phytoplankton functional groups in relation to their surviving environment (Mwagona et al., 2018; Ma et al., 2019; Sun et al., 2019). During the study period, the average biomass of phytoplankton was 3.85 mg/L in spring, 0.79 mg/L in summer and 1.02 mg/L in autumn. The aforesaid experimental datum were lower compared to the datum of average biomass during spring (4.03 mg/L), summer (2.78 mg/L) and autumn (5.07 mg/L) recorded by Yan (2011) in the Harbin section of Songhua River, and also lower than those during summer (2.30 mg/L) and autumn (2.57 mg/L) of Li (2013) accepted for publication in the Harbin section of Songhua River. So far, the results showed that average biomass of phytoplankton reduce continuously.

Our research showed that the main dominant phytoplankton functional groups were group C and X2 in the whole year. The two phytoplankton functional groups which we investigated were also the dominant functional groups studied by An et al. in Small Xingkai Lake and by Ma et al. Sanhuanpao wetland reservation which located in the same province (An et al., 2016; Ma et al., 2016). Group C represents the eutrophic small and medium sized lakes, and it was suitable for the water environment of no stratification or suspension (Yang et al., 2014). According to Reynolds' phytoplankton functional group theory indicated, group X2, sensitive to the filtering food zooplankton, was inhibited when the filtering food zooplankton were rich (Reynolds et al., 2002). Sampling stations (1#, 2# and 3#) were located in the middle and upper reaches in the Harbin section of Songhua River recorded high relative biomass dominated by group X2 corresponding to low filtering food zooplankton (An et al., 2016; Feng, 2014). Group MP (mainly composed of Ulothris variabilis) was important corresponding to frequently disturbed, inorganic and turbid water areas. In autumn, the wind was strong, the river was disturbed frequently, and the turbidity increased obviously, which was beneficial to the growth of MP (Yang et al., 2014). Therefore, the relative biomass of group MP is not only more than 10% in summer and autumn, but also one of the dominant functional groups in autumn.

Influence factors of water environment of Harbin section of Songhua River, Northeast China

Any environmental factors needed for phytoplankton growth, including temperature, light intensity and hydrodynamics, could be the limiting factors influenced the growth of phytoplankton, and may also be the environmental influencing factor for the

http://www.aloki.hu ● ISSN 1589 1623 (Print) ● ISSN 1785 0037 (Online)
DOI: http://dx.doi.org/10.15666/aeer/1804_57595774

distribution of phytoplankton function groups (Xiao et al., 2011). The RDA analysis was used to explain clearly the relationship between crucial factors and phytoplankton functional groups and to further explore the driving factors changing the composition and distribution of phytoplankton functional group. The results of RDA analysis displayed that phytoplankton functional groups in the Harbin section of Songhua River were affected by SD, BOD_5, Fe^{3+}, NTU, Chl-a, COD_{Mn}, NH_4^+ and TP. Among them, SD was the key of environmental factors ($r = 0.8729$), which affected the change of functional groups throughout the year.

Studies of lakes and reservoirs in different regions of country showed that, such as Tianmu Reservoir of Shahe Reservoir located in north subtropical regions, Changshou Lake located in mid-subtropical regions, Yuqiao Reservoir located in warm temperate zone and Small Xingkai Lake located in temperate zone, SD was the main environmental factors influencing and changing the phytoplankton function groups (Cui et al., 2014; Yan et al., 2018; Liu et al., 2016; An et al., 2016). According to Cui et al. (2014), it was beneficial for phytoplankton growth to be in water bodies of low NTU and high SD, and it found a positive correlation between SD and the biomass of Bacillariophyta and Chrysophyta. Similarly, most of phytoplankton functional groups for this experiment were positive correlation with SD and negative correlation with NTU in the Harbin section of Songhua River. Li et al. (2013) also recorded that the water sediment content was high, SD was low and NTU was high in perennial water of Songhua River. Compared to other water bodies, SD in our research environment was remarkably lower. For instance, in Small Xingkai Lake located in Southeast Heilongjiang Province, An et al. (2016) recorded 0.46 m, 0.21 m, and 0.21 m mean values of SD for spring, summer and autumn respectively. In Aha reservoir, one of the three drinking water sources in Guiyang, SD mean value in spring, summer and autumn was 0.90 m, 0.83 m, and 1.19 m, respectively (Li et al., 2015). According to Ostos et al. (2008), SD of El Gergal reservoir located in southwest Spain ranged from 0.2 m to 8.0 m and its mean was 1.77 m between 1979 and 2003. According to Chai et al. (2016), SD of Pearl River Estuary located in southern China ranged from 0.2 m to 3.2 m and its mean was 1.2 m in spring (March 2012) and ranged from 0.5 m to 2.0 m and its mean was 0.8 m in autumn (November 2011). There were many factors that limited SD, including not only phytoplankton, but also the concentration of sediment, the speed of FR, the amount of suspended solids and many other factors in the water (Pace et al., 1992). The faster FR will increase the suspended matter in the water, and the increase of sediment content will reduce the content of DO in the water. It was not simply to describe this with a single linear correlation (Pace et al., 1992).

Groups X2 were mainly comprised of minute-celled Chlamydomonas ovalis and Chroomonas acuta, and it was easier to be found it in waters with lower phosphorus levels (Laamanen, 1997). The study of Ma et al. (2019) also showed that group X2 with widely adaptability to nutrients was preferred to grow in slight alkaline water environment. We can see from the RDA biplot diagram in *Figure 3,* that groups X2 had a negative correlation with TP. On the one hand, the research of Siebielec et al. (2015) and da Silva and Fitzsimmons (2016) clearly proved that dissolved calcium ion will react with the phosphate in water forming insoluble calcium phosphate and other compounds that were not conducive to phytoplankton growth and propagation when the water environment was slight alkaline. On the other hand, the presence of large numbers of predators will reduce the number of filter feeders and the grazing pressure of filtering food zooplankton on group X2 (Padisak et al., 2009). Asplanchna priodonta, Polyarthra trigla and Synchaeta

http://www.aloki.hu ● ISSN 1589 1623 (Print) ● ISSN 1785 0037 (Online)
DOI: http://dx.doi.org/10.15666/aeer/1804_57595774

stylata were the dominant species (rotifer) found by Li et al. (2013) in Songhua River. Synchaeta stylata priodonta, as one kind of macrofilter-feeders, ate Dictyotaceae, filamentous algae, dinoflagellate, and other 20-50 μm zooplankton. Asplanchna and Polyarthra trigla, as group RC (predators), ate macroscopic algae, protozoa, rotifer and microcrustacea (Wen et al., 2017). It was more suitable for them to living in the alkaline water like the Songhua River with low temperature and high dissolved oxygen (Li et al., 2013). A study even showed the number of filter feeders increased and the number of phytoplankton decreased when the SD exceeded 80 cm (Li and Li, 2001).

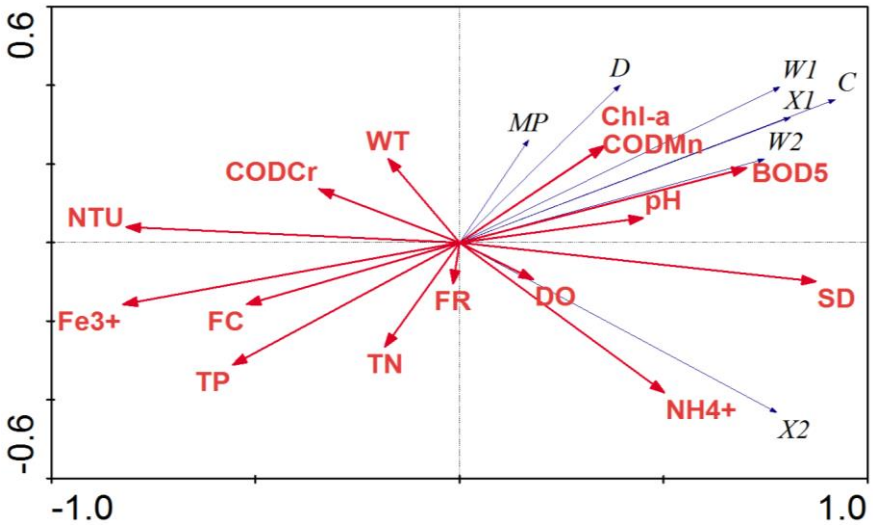

Figure 3. *Correlation plots of the redundancy analysis (RDA) on the relationship between the environment variables and phytoplankton functional groups*

Researchers had also noted that Chl-a, COD_{Mn}, BOD_5, Fe^{3+}, NH_4^+ and FC were fundamental factors in shaping phytoplankton community composition. The study of Guo et al. (2020) in Xidayang Reservoir showed that phytoplankton density and biomass were significant positive correlation with Chl-a and COD_{Mn} ($P < 0.05$) and significantly negatively correlated with NH_4^+ ($P < 0.05$). Liu et al. (2014) pointed out that Chl-a, as the main pigment of phytoplankton photosynthesis, which growth was a significant positive predicator of the rapid growth of phytoplankton. In Muling River, the researchers analyzed the COD_{Mn} was positively related with the predominant phytoplankton functional groups (Sun et al., 2019). In Dalian Songshu Reservoir, the researchers analyzed the BOD_5 was positively related with the phytoplankton density (Yang, 2019). Arnaldo concluded that the growth rate of the dominant phytoplankton community structure limited by the concentration of Fe^{3+} in the upper waters layer of the Bransfield Strait in Antarctic Peninsula (D'Amaral et al., 2015). Similarly, from the RDA results, BOD_5, Chl-a and COD_{Mn} were positive correlated with the dominant functional groups, while Fe^{3+} and NH_4^+ were negatively correlated with the dominant functional groups. Under the same experimental conditions, Mao et al. (1998) monitored the effect of phytoplankton with different densities or community composition on the amount of FC in the culture ponds. It was proved that there was a restrictive relationship between phytoplankton community composition and FC population. FC will release non-specific antibiotics substances to kill algae cells. When the amount of FC in the culture ponds was reduced, the densities of phytoplankton

http://www.aloki.hu ● ISSN 1589 1623 (Print) ● ISSN 1785 0037 (Online)
DOI: http://dx.doi.org/10.15666/aeer/1804_57595774

continued to increase within 24 h. Same as the results in this experiment, the growth of FC and the biomass of phytoplankton had a negative correlation.

Conclusions

In this current study, a total of 84 species of phytoplankton species belonging to 16 functional groups (C, D, F, G, H1, J, L0, MP, P, S1, TB, W1, W2, X1, X2 and Y) were identified in the Harbin section of Songhua River, northeast China. There were 7 dominant functional groups: C, D, MP, W1, W2, X1 and X2. The seasonal dominant functional group succession: X2/C (spring)→X2/C/MP (summer)→X2/C/X1/MP (autumn). The result of one-way ANOVA test and RDA showed that WT, SD, NTU, Chl-a, DO, BOD_5, NH_4^+, TP and Fe^{3+} were the major factors that influencing phytoplankton functional groups in the Harbin section of Songhua River, northeast China. RDA result revealed that SD and Chl-a were positive correlated with the dominant functional groups, while NTU and TP were negatively correlated with the dominant functional groups. This study revealed that the phytoplankton functional groups followed certain predictable pattern in the seasonal and spatial gradient. It could be useful for assessing and predicting the growth and development of phytoplankton in the future. At the same time, these environmental factors can also be considered as an important basis for the management and protection of rivers in northeast China for future studies.

REFERENCES

[1] An, R., Wang, F. Y., Yu, H. X., Ma, C. X. (2016): Characteristics and physical factors of phytoplankton functional groups in Small Xingkai Lake. – Research of Environmental Sciences 7: 985-994.

[2] Bohnenberger, J. E., Rodrigues, L. R., Mottamarques, D. D., Crossetti, L. O. (2018): Environmental dissimilarity over time in a large subtropical shallow lake is differently represented by phytoplankton functional approaches. – Mar. Freshw. Res 69: 95-104.

[3] Chai, C., Jiang, T., Cen, J. Y., Ge, W., Lu, S. H. (2016): Phytoplankton pigments and functional community structure in relation to environmental factors in the Pearl River Estuary. – Oceanologia 3: 201-211.

[4] Chuo, M., Ma, J., Liu, D., Yang, Z. (2019): Effects of the impounding process during the flood season on algal blooms in Xiangxi Bay in the Three Gorges Reservoir, China. – Ecol. Model 392: 236-249.

[5] Crossetti, L. O., Becker, V., Cardoso, L. D. S., Rodrigues, L. R., Da Costa, L. S., Da Motta Marques, D. (2013): Is phytoplankton functional classification a suitable tool to investigate spatial heterogeneity in a subtropical shallow lake? – Limnologica 43: 157-163.

[6] Cui, Y., Zhu, G. W., Li, H. Y., Chen, W. M., Zhou, W. P. (2014): Spatial and Temporal Distribution Characteristics of Water Quality in Shahe Reservoir within Tianmuhu Reservoir and its Relationship with Phytoplankton Community. – Journal of Hydroecology 3: 10-18.

[7] Cupertino, A., Gücker, B., Rückert, G. V., Figueredo, C. C. (2019): Phytoplankton assemblage composition as an environmental indicator in routine lentic monitoring: taxonomic versus functional groups. – Ecol. Indicat 101: 522-532.

[8] da Silva, C. B., Fitzsimmons, K. (2016): The effect of p H on phosphorus availability and speciation in an aquaponics nutrient solution. – Bioresour Technol 219: 778-781.

[9] D'Amaral, P. G. R. A., de Souza, M. S., Borges, M. C. R., Jesus, B., Tavano, V. M., Garcia, C. A. E. (2015): Photophysiological effects of Fe concentration gradients on

http://www.aloki.hu ● ISSN 1589 1623 (Print) ● ISSN 1785 0037 (Online)
DOI: http://dx.doi.org/10.15666/aeer/1804_57595774

diatom-dominated phytoplankton assemblages in the Antarctic Peninsula region. – Journal of Experimental Marine Biology and Ecology 466: 49-58.
[10] Feng, Y. M. (2014): Zooplankton Community Structure and Analysis of Correlations with Environmental Factors in Xiaoingkai Lake. – Northeast Forestry University, Heilongjiang Province, China.
[11] Gafan, G. P., Lucas, V. S., Roberts, G. J., Petrie, A., Wilson, M., Spratt, D. A. (2005): Statistical analyses of complex denaturing gradient gel electrophoresis profiles. – Journal of Clinical Microbiology 8: 3971-3978.
[12] Guo, N. N., Li, D. D., Chen, X., Qi, Y. K., Song, C., Fan, L. M., Xi, L. P., Meng, S. L., Chen, J. Z. (2020): Structural community of phytoplankton species in the Xidayang reservoir repair demonstration area during the spring and autumn. – Journal of Dalian Fisheries University. https://doi.org/10.16535/j.cnki.dlhyxb.2019-235.
[13] Heebert, M. P., Beisner, B. E., Maranger, R. (2016): A meta-analysis of zooplankton functional traits influencing ecosystem function. – Ecology 4: 1069-1080.
[14] Hong, L. V., Yang, J., Liu, L. M., Yu, X. Q., Yu, Z., Chiang, P. (2014): Temperature and nutrients are significant drivers of seasonal shift in phytoplankton community from a drinking water reservoir, subtropical China. – Environ. Sci. Pollut. Res 21: 5917-5928.
[15] Hu, H. J., Wei, Y. X. (2006): The Freshwater Algae of China: Systematics, Taxonomy and Ecology. – Science Press, Beijing.
[16] Hustedt, F. (1930): Bacillariophyta (Diatomeae). – In: Pascher, A. (ed.) Die Süsswasser Flora Mitteleuropas. GFV, Jena.
[17] Huszaret, V. L. M., Nabout, J. C., Appel, M. O., Santos, J. B. O., Abe, D. S., Silva, L. H. S. (2015): Environmental and not spatial processes (directional and non-directional) shape the phytoplankton composition and functional groups in a large subtropical river basin. – J. Plankton Res 660: 1190-1200.
[18] Jongman, R. H. G., ter Braak, C. J. F., van Tongeren, O. F. R. (1987): Data Analysis in Community and Landscape Ecology. – Pudoc, Wageningen.
[19] Kim, H. G., Hong, S., Kim, D. K., Joo, G. J. (2020): Drivers shaping episodic and gradual changes in phytoplankton community succession: taxonomic versus functional groups. – Science of the Total Environment 734: https://doi.org/10.1016/j.scitotenv.2020.138940.
[20] Klug, J. L., Cottingham, K. L. (2001): Interactions among environmental drivers: community responses to changing nutrients and dissolved organic carbon. – Ecology 82: 3390-3403.
[21] Komarek, J. (1983): Chlorophyceae (Grunalgen). Ordnung: Chlorococcales. – Die Binnengewasser 16.
[22] Kruk, C., Mazzeo, N., Lacerot, G., Reynolds, C. S. (2002): Classification schemes for phytoplankton: a local validation of a functional approach to the analysis of species temporal replacement. – J. Plankton Res 24: 901-912.
[23] Laamanen, M. J. (1997): Environmental factors affecting the occurrence of different morphological forms of cyanoprokaryotes in the northern Baltic Sea. – J Plankton Res. 10: 1385-1403.
[24] Lampitt, R. S., Wishner, K. F., Turley, C. M., Angel, M. V. (1993): Marine snow studies in the Northeast Atlantic Ocean: distribution, composition and role as a food source for migrating plankton. – Mar Biol 4: 689-702.
[25] Lange-Bertalot, H. (2001): Diatoms of Europe: Diatoms of the European Inland Waters. – Gantner Verlag, Koenigstein.
[26] Li, L., Li, Q. H., Jiao, S. L., Li, Y., Deng, L., Sun, R. G., Gao, Y. C., Luo, L. (2015): Spatial and temporal distribution characteristics of phytoplankton functional groups in aha reservoir and their influencing factors. – Acta Scientiae Circumstantiae 11: 3604-3611.
[27] Li, L., Li, Q., Chen, J., Wang, J., Jiao, S., Chen, F. (2017): Temporal and spatial distribution of phytoplankton functional groups and role of environment factors in a deep subtropical reservoir. – Chinese J Oceanol Limnol 3: 761-771.

http://www.aloki.hu ● ISSN 1589 1623 (Print) ● ISSN 1785 0037 (Online)
DOI: http://dx.doi.org/10.15666/aeer/1804_57595774

[28] Li, X. Y., Yu, H. X., Ma, C. X. (2013): Structure of phytoplankton community based on canonical correspondence analysis and biodiversity analysis in Harbin section of Songhua river. – Journal of Northeast Forestry University 10: 103-107.
[29] Li, Y. H., Li, B. C. (2001): Spending the Winter by observing water change and its biological analysis. – Fisheries Science 4: 38-41.
[30] Liu, F. F., Su, J., Moll, A., Krasemann, H., Chen, Xueen., Pohlmann, Thomas., Wirtz, Kai. (2014): Assessment of the summer-autumn bloom in the Bohai Sea using satellite images to identify the roles of wind mixing and light conditions. – Journal of Marine Systems 129: 303-317.
[31] Liu, X. B., Nie, Y., Zhao, X. G., Liu, Q. (2016): A correlation analysis of the phytoplankton community and environment factors in the Yuqiao Reservoir in spring and summer of 2014. – Environmental Monitoring in China 32: 64-67.
[32] Lopes, M. R. M., Bicudo, C. E. M., Ferragut, M. C. (2005): Short term and temporal variation of phytoplankton in a shallow tropical oligotrophic reservoir, southeast Brazil. – Hydrobiologia 542: 235-247.
[33] Ma, C. X., Yin, Z. L., Yu, H. X. (2016): Seasonal dynamics characteristics and physical factors of phytoplankton functional groups in Sanhuanpao wetland reserve. – Journal of Northeast Forestry University 11: 45-51.
[34] Ma, C. X., Mwagona, P. C., Yu, H. X., Sun, X. W., Liang, L. Q., Shahid, M. (2019): Spatial and temporal variation of phytoplankton functional groups in extremely alkaline Dali Nur Lake, North China. – Journal of Freshwater Ecology 1: 91-105.
[35] Maggio, J., Fernandez, C., Parodi, E. R., Diaz, M. (2016): Modeling phytoplankton community in reservoirs. A comparison between taxonomic and functional groups-based models. – J. Environ. Manag 165: 31-52.
[36] Mao, Z. J., Chen, C. F. (1998): A preliminary study on the relationship between phytoplankton and bacteria in culture ponds. – Reservoir Fisheries 05: 17-20.
[37] MEP (Ministry of Environmental Protection) China (2006): China's National Standard: GB/T5750-2006. Environmental Quality Standards for Surface Water. – Ministry of Environmental Protection. China Standards Press, Beijing.
[38] Mwagona, P. C., Ma, C. X., Yu, H. X. (2018): Seasonal dynamics of zooplankton functional groups in relation to environmental variables in Xiquanyan reservoir, Northeast China. – Annales de Limnologie - International Journal of Limnology 54: 33.
[39] Ostos, E. M., Pizarro, L. C., Basanta, A. B., George, D. G. (2008): The spatial distribution of different phytoplankton functional groups in a Mediterranean reservoir. – Aquat Ecol 42: 115-128.
[40] Pace, M. L., Findlay, S., Lints, D. (1992): Zooplankton in advective environments: the Hudson River community and a comparative analysis. – Fisheries and Aquatic Sciences 5: 1060-1069.
[41] Padisak, J., Crossetti, L. O., Naselli-Flores, L. (2009): Use and misuse in the application of the phytoplankton functional classification: a critical review with updates. – Hydrobiologia 1: 1-19.
[42] Patrick, R., Reimer, C. W. (1966): The Diatoms of the United States. – Monographs Philadelphia. Academy of Natural Sciences of Philadelphia.
[43] Prescott, G. W. (1954): How to Know the Fresh-Water Algae: An Illustrated Key for Identifying the More Common Fresh-Water Algae to Genus, with Hundreds of Species Named Pictured and with Numerous Aids for Their Study. Vol.1. – W. C. Brown Company, Dubuque, Iowa.
[44] Qiu, X. C., Hao, H. X., Sun, X. X. (2012): Relationships between zooplankton and water environmental factors in Shahu Lake, Ningxia of Northwest China: a multivariate analysis. – Chinese Journal of Ecology 4: 896-901.
[45] Qu, Y., Wu, N., Guse, B., Makarevi ciute, K., Sun, X., Nicola, F. (2019): Riverine phytoplankton functional groups response to multiple stressors variously depending on hydrological periods. – Ecol. Indicat 101: 41-49.

http://www.aloki.hu ● ISSN 1589 1623 (Print) ● ISSN 1785 0037 (Online)
DOI: http://dx.doi.org/10.15666/aeer/1804_57595774

[46] Reynolds, C. S. (2006): The Ecology of Phytoplankton: Ecology, Biodiversity and Conservation. – Cambridge University Press, Cambridge, UK.
[47] Reynolds, C. S., Huszar, V., Kruk, C., Naselli-Flores, L., Melo, S. (2002): Towards a functional classification of the freshwater phytoplankton. – Journal of Plankton Research 5: 417-428.
[48] Siebielec, G., Ukalska-Jaruga, A., Kidd, P. (2015): Bioavailability of Trace Elements in Soils Amended with High-Phosphate Materials. Phosphate in Soils: Interaction with Micronutrients, Radionuclides Heavy Metals. Vol. 2. – CRC Press, Boca Raton, FL.
[49] Su, M., Andersen, T., Burch, M., Jia, Z., An, W., Yu, J., Yang, M. (2019): Succession and interaction of surface and subsurface cyanobacterial blooms in oligotrophic/mesotrophic reservoirs: a case study in Miyun Reservoir. – Sci. Total Environ 649: 1553-1562.
[50] Sun, X., Mwagona, P. C., Isaac, E. S., Hou, W. J., Li, X. Y., Zhao, F., Chen, Q., Zhao, Y. X., Liu, D., Li, X. C., Ma, C. X., Yu, H. X. (2019): Phytoplankton functional groups response to environmental parameters in Muling River basin of northeast China. – Annales de Limnologie - International Journal of Limnology 55: 17.
[51] ter Braak, C. J. F. (1988): CANOCO-A FORTRAN Program for Canonical Ordination by Partial Detrended (Canonical) Correspondence Analysis, Principal Components Analysis and Redundancy Analysis (Version 2.1). – Agricultural Mathematics Group, Wageningen.
[52] ter Braak, C. J. F. (1990): Update Notes. CANOCO (Version 3.1). – Agricultural Mathematics Group, Wageningen.
[53] ter Braak, C. J. F. (1994): Canonical community ordination. Part I: Basic theory and linear methods. – Ecoscience 1: 127-140.
[54] ter Braak, C. J. F., Smilauer, P. (1998): CANOCO Reference Manual and User's Guide to CANOCO for Windows: Software for Canonical Community Ordination (version 4). – Microcomputer Power, Ithaca.
[55] Utermöhl, H. (1958): Zur Vervollkommnung der quantitativen Phytoplankton-Methodik. – Internationale Vereinigung für Theoretische und Angewandte Limnologie 9: 1-38.
[56] Wang, Y. J., Cai, Y. P., Yin, X. N., Yang, Z. F. (2020): Succession of phytoplankton functional groups in Macau's two shallow urban border reservoirs under multiple changing factors. – Journal of Cleaner Production 264: 121553.
[57] Wen, X. L., Xie, P., Zhou, J., Xi, Y. L. (2017): Reponses of the annual dynamics of functional feeding groups and dominant populations of rotifers to environmental factors in Lake Tingtang. – Acta Ecologica Sinica 23: 8029-8038.
[58] Xiao, L. J., Wang, T., Hu, R., Han, B. P., Wang, S., Qian, X., Padisák, J. (2011): Succession of phytoplankton functional groups regulated by monsoonal hydrology in a large canyon-shaped reservoir. – Water Research 45: 5099-5109.
[59] Xu, Z. L., Chen, Y. Q. (1989): Aggregated intensity of dominant species of zooplankton in autumn in the East China Sea and Yellow Sea. – Journal of Ecology 4: 13-19.
[60] Yan, Q. (2011): Study on the Community Structure of Phytoplankton and Environmental Impact Assessment in Harbin Section of Songhua River. – Northeast Forestry University, Heilongjiang Province, China.
[61] Yan, S. S., Lei, B., Liu, S. R., Yang, C. H., Xie, G. X. (2018): Seasonal variation of phytoplankton functional groups in Changshou Lake and relevant environmental factors. – Journal of Hydroecology 3: 52-60.
[62] Yang, R. F. (2019): Phytoplankton characteristics and response to environmental factors in Dalian Songshu Reservoir. – Soil and Water Conservation in China 07: 34-37.
[63] Yang, W., Zhu, J. Y., Lu, K. H., Wan, L., Mao, X. H. (2014): The establishment, development and application of classification approach of freshwater phytoplankton based on the functional group: a review. – Chinese Journal of Applied Ecology 6: 1833-1840.

http://www.aloki.hu ● ISSN 1589 1623 (Print) ● ISSN 1785 0037 (Online)
DOI: http://dx.doi.org/10.15666/aeer/1804_57595774

APPENDIX

Table A1. *Environmental parameters in each season in the Harbin section of Songhua River, Northeast China*

	WT (℃)	pH	FR (m/s)	SD (m)	NTU	Chl-a/ (ug/L)	DO (mg/L)	CODMn (mg/L)	CODCr (mg/L)	BOD5 (mg/L)	NH4+ (mg/L)	TP (mg/L)	TN (mg/L)	FC (mg/L)	Fe3+ (mg/L)
Spring1#	17.50	7.85	1.26	58.50	7.55	8.85	7.30	5.04	12.70	5.80	0.72	0.07	3.00	24196.00	0.12
Spring2#	18.00	7.88	0.83	48.00	10.00	12.25	7.00	6.00	12.40	4.30	0.83	0.10	3.32	24196.00	0.22
Spring3#	17.80	7.85	0.28	32.00	23.80	15.20	7.50	5.20	12.20	5.70	0.50	0.09	1.42	12997.00	0.10
Spring4#	18.10	7.99	0.39	31.50	15.15	19.75	7.00	5.84	12.20	5.60	0.63	0.10	2.20	24196.00	0.15
Spring5#	18.50	7.83	0.57	34.50	15.30	15.30	7.90	7.28	12.70	5.30	0.09	0.06	1.68	754.00	0.12
Spring6#	18.40	8.21	0.18	32.00	18.30	20.90	8.60	5.52	11.60	3.50	0.08	0.04	1.01	24196.00	0.23
Spring7#	18.50	8.31	1.89	29.00	24.60	21.10	7.70	5.84	13.00	4.80	0.11	0.06	1.61	393.00	0.22
Spring8#	13.60	6.95	0.41	34.50	12.55	0.80	9.75	3.76	11.20	2.90	0.48	0.04	2.18	1474.00	0.32
Summer1#	22.37	7.57	0.70	11.50	145.35	7.15	6.43	5.65	11.37	3.30	0.23	0.12	2.26	34305.00	1.00
Summer2#	22.93	7.58	0.87	11.50	170.30	10.05	5.93	5.23	13.20	3.53	0.25	0.12	2.17	36593.00	0.92
Summer3#	22.80	7.38	0.63	12.00	101.60	8.40	4.70	4.88	14.10	1.80	0.12	0.10	3.04	48392.00	0.64
Summer4#	23.30	7.64	0.64	10.50	157.65	8.45	6.63	4.85	13.27	3.73	0.38	0.11	2.01	28283.00	0.99
Summer5#	23.20	7.57	1.50	11.50	152.15	9.65	7.07	6.13	11.80	2.97	0.08	0.08	1.89	15291.00	1.28
Summer6#	23.10	7.34	1.05	11.00	146.70	8.90	6.20	4.56	14.10	1.70	0.08	0.09	2.90	17328.00	1.08
Summer7#	23.37	7.74	1.50	13.00	157.30	9.20	7.07	4.85	13.37	3.03	0.09	0.11	1.94	18975.00	1.20
Summer8#	22.10	7.88	0.84	10.50	97.00	2.35	8.80	6.51	13.47	3.63	0.22	0.06	1.88	11112.00	0.69
Autumn1#	14.55	7.73	0.23	19.00	30.30	6.05	8.60	4.56	14.00	2.20	0.19	0.08	2.05	36294.00	0.61
Autumn2#	14.35	7.72	0.29	19.00	34.60	5.65	8.75	4.48	12.95	2.05	0.23	0.16	1.84	32860.00	1.56
Autumn3#	14.50	7.78	0.29	20.00	47.50	6.80	9.30	3.76	11.80	2.60	0.07	0.14	1.70	17329.00	0.56
Autumn4#	14.75	7.68	0.66	12.50	64.65	6.75	8.75	5.36	10.60	2.95	0.16	0.19	1.86	36294.00	1.64
Autumn5#	14.90	7.63	0.45	14.00	49.45	8.65	8.75	5.20	13.55	2.90	0.09	0.15	1.89	11857.00	1.64
Autumn6#	14.00	7.84	0.94	18.00	46.80	7.30	9.40	4.08	11.50	2.30	0.07	0.17	1.72	4106.00	0.76
Autumn7#	15.10	7.77	0.29	20.00	45.40	6.20	8.75	5.04	12.95	1.55	0.18	0.17	1.82	13252.00	1.63
Autumn8#	14.00	7.59	0.47	25.50	32.50	0.45	8.90	4.72	12.85	1.95	0.09	0.16	1.79	29671.00	1.40

http://www.aloki.hu ● ISSN 1589 1623 (Print) ● ISSN 1785 0037 (Online)
DOI: http://dx.doi.org/10.15666/aeer/1804_57595774

DETERMINATION OF SILVER NANOPARTICLES IN LIQUID ENVIRONMENTAL SAMPLES

GAJEC, M.* – KUKULSKA-ZAJĄC, E. – KRÓL, A.

Oil and Gas Institute – National Research Institute, 25A Lubicz Str., 31-503 Krakow, Poland

**Corresponding author*
e-mail: gajec@inig.pl

(Received 21st Feb 2020; accepted 2nd Jul 2020)

Abstract. With the rapid increase of nanomaterial production and application, their incidental, accidental and intentional release into the environment is inevitable. Most nanoparticles (NPs) could be highly reactive, even those conventionally considered to be inert (e.g., TiO_2 and Au). Environmental transformation can remarkably alter the physicochemical properties of NPs, and consequently, their fate, transport and biological effects. Meanwhile, current facilities for wastewater treatment and waste management are not equipped to remove nanoparticles effectively and prevent their entry into the environment. The effluent from urban wastewater treatment plants (WWTPs) is considered a significant source of manufactured nanomaterial emissions into aquatic and terrestrial environments. Dissecting how the properties of nanoparticles may change once released into the environment is urgently needed to improve our understanding of their toxic effects in the environment. For this purpose, specialized methods are needed to recognize, separate and characterize nanoparticles in complex environmental media. The aim of the study was to determine silver nanoparticles in liquid environmental samples collected in Poland (surface water, treated sewage, tap water, water extraction of waste from the oil and gas mining industry) using single particle inductively coupled plasma mass spectrometry (sp ICP-MS).
Keywords: *NPs, AgNPs, sp ICP-MS, surface water, inductively coupled plasma mass spectrometry*

Introduction

Advances in nanotechnology are forecast to have a major impact on a broad range of industry sectors. The very large surface area of these nanomaterials may cause novel physical and chemical properties, such as increased catalytic activity, improved solubility or different optical behaviour. Nanotechnology offers many advantages. It allows for miniaturization, cost reduction, more sustainable use of resources among many others. Due to all its promises, nanotechnology has found an application across the fields of science and technology, ranging from scientific materials, electronics through energy, cosmetics, and agriculture to medicine, implants, and sensors. Metal nanoparticles are also widely used in the oil and gas industry sectors, e.g. during exploration, characterization of a field, drilling, cementing, production and stimulation, enhanced oil recovery (EOR), refining and processing (Krasodomski et al., 2013; Zima, 2017). The nanotechnology industry is rapidly generating new forms of waste streams because of the production and use of engineered nanomaterials (ENMs); however, only limited literature on the fate, behaviour and impacts of these waste streams on the environment and human health is available (Krasodomski et al., 2009; Aznar et al., 2013).

With the rapid increase of nanomaterials production and application, their incidental, accidental and intentional release into the environment is inevitable, and diverse types of engineered nanomaterials (ENMs), e.g., nano Ag and TiO_2, have already been detected in various environmental media (Kim, 2010; Weinberg et al., 2011; Wagner et al., 2014). Increased production and widespread use of nanomaterials can lead to NPs

http://www.aloki.hu ● ISSN 1589 1623 (Print) ● ISSN1785 0037 (Online)
DOI: http://dx.doi.org/10.15666/aeer/1804_57755788

migrating into the environment and interacting with organisms. Nanoparticles can be transported through air, water and soil and the process depends on their characteristics including size, charge, solubility, diffusion, deposition, bioavailability and biodegradability. Nanomaterials (NM) can be released into the environment in three ways: (1) during production, (2) during use, and (3) end-of-life release of products containing nanoparticles (from waste).

The release pattern and mass depend on the NP's type and its application. Metal containing nanoparticles are a significant class because their use in consumer and industrial applications makes them the fastest growing category of nanoparticles (Prasad et al., 2017). Particularly, silver nanoparticles (AgNPs) are used in many consumer products because of their proved antimicrobial properties attributable to the release of Ag^+.

The environmental impact of silver nanoparticles (AgNPs) has become a topic of interest recently, this is due to the fact that AgNPs have been included in numerous consumer products including textiles, domestic appliances, food containers, cosmetics, paints and nano-functionalised plastics. Various applications have been found in the medical field for Ag NPs; for example, they can be used for biosensors, drug delivery systems, and medical devices (Bundschuh et al., 2018).

The production, use and disposal of these AgNP containing products are potential routes for environmental exposure. Therefore, in the near future, we can expect accumulation of NPs in the environment, which can have major implications for human health and environment. Although some information on NPs emission is available, it is of high importance to quantify their amounts and concentrations in the environment. Moreover, during deposition NPs can undergo physical, chemical and biological transformations (by redox reactions, dissolution, sorption of contaminant, or bioaccumulation) forming substances of different properties and toxicity than their native form. Therefore, both NPs forms, native and after conversion, should be monitored. As a result, there is a growing need for a rapid, accurate, sensitive technique for characterizing and quantifying NPs in a wide range of sample types. Specifically, techniques are needed to determine the size and concentration of NPs in complex matrices.

The basic parameter characterizing nanomaterials is the size of their particles and the distribution of this size. At present, there are several well-known methods for such a characterization (Laborda et al., 2016). *Table 1* presents methods of nanoparticles separation from matrices of environmental samples as well as analytical techniques currently used in nanoparticles testing.

The process of nanoparticle determination consists of three basic stages: sampling and sample preparation, nanoparticle separation and identification. Sampling and preparation of the sample is a critical step in the process of nanoparticle determination as it may affect the state of dispersion. The stage of sample preparation depends to a large extent on the type of matrix being tested. Ideal sample preparation should be optimized by finding the right balance between reducing the matrix effects of the sample and maintaining its representativeness. The analysis of the data collected in *Table 1* shows that nanoparticles are separated by centrifugation, ultrafiltration, cloud point extraction (CPE) and flow fractionation in an asymmetric flow field (AF4). Due to the complexity of environmental matrices, nanoparticle separation techniques should take into account, among others, the selectivity against NPs and the influence of interference from the matrix (Majedi et al., 2016).

http://www.aloki.hu ● ISSN 1589 1623 (Print) ● ISSN1785 0037 (Online)
DOI: http://dx.doi.org/10.15666/aeer/1804_57755788

Table 1. *List of methods of nanoparticle separation and techniques for their determination in various types of matrices (Laborda et al., 2016)*

Sample type	Designated nanoparticles	Sample preparation*	Technique*
Sewage	Ag	Filtration (5µm + 0.45µm)	sp ICP-MS
	SiO_2, Al_2O_3	CPE + MW	SEM-EDS
	Ag	CPE + MW	ET-AAS
	Ag	CPE + MW	ICP-MS
	Ag	Filtration (0.45µm)	AF4-ICP-MS
	Au	SPE (magnetic matrix + acid etching)	ICP-MS
	ZnO	CPE + MW	ICP-MS
	Ag	CPE	ET-AAS
	Ag	SPE (ions exchange)	ET-AAS
	Ag	Serial filtration (0.45µm-0.1µm-10kDa)	sp ICP-MS
	Ag	Serial filtration (0.45µm-0.1µm-10kDa)	sp ICP-MS
	CuO	CPE+MW	ICP-MS
Lake water	TiO_2	Aqueous suspension	ICP-MS sp ICP-MS
	Ag	CPE + MW	ET-AAS
	Ag	CPE + MW	ICP-MS
	Ag	Filtration (0.45µm)	SEC-ICP-MS
River water	CuO	CPE	ET-AAS
	Ag	CPE + MW	ET-AAS
	Ag	SPE (ions exchange)	ET-AAS
	Ag	Sedimentation	AF4-ICP-MS
	Ag	Filtration (0.45µm)	HDC-ICP-MS
	Au	CPE	ET-AAS
	Ag	CPE	ET-AAS
Surface waters	Ag	SPE (magnetic matrix + acid etching)	ICP-MS
Sea waters	Ag	Filtration (0.45µm)	PCC
	Ag	Filtration (0.45µm)	VIP
	Ag	Filtration (0.45µm)	VIP electrochemical sensors
	Ag	Filtration (0.45µm)	VIP
	Au	SPE (magnetic matrix + acid etching)	ICP-MS
	Ag	CPE	ET-AAS
Sewage sediments	TiO_2	Centrifugation	FESEM TEM
	Ag	Filtration (0.45µm)	HDC-ICP-MS TEM
	Ag	Filtration (0.45µm)	HDC-ICP-MS
	Ag	Filtration (0.45µm)	SEC-ICP-MS
	Ag	Centrifugation	TEM-EDS
	Ag	Filtration (0.02µm)	EXAFS
	Ag	CPE + MW	ICP-MS
	ZnO	Centrifugation	EXAFS
	Ag, Au	Centrifugation	TEM-EDS EXAFS
	Ag, ZnO	Centrifugation	XANES EXAFS
Soil enriched with sewage sediment	TiO2	Centrifugation	FESEM TEM
	TiO_2	Aqueous suspension	TEM-EDS
Natural waters	Ag, TiO_2	Functionalisation + extraction in the liquid-liquid system Filtration (35µm)	ICP-MS
	Ag	Filtration (0.45µm) Ultrafiltration (3kDa)	sp ICP-MS

http://www.aloki.hu ● ISSN 1589 1623 (Print) ● ISSN1785 0037 (Online)
DOI: http://dx.doi.org/10.15666/aeer/1804_57755788

Fresh waters	Au	SPE (magnetic matrix+acid etching)	ICP-MS
	Ag	Filtration (35µm) Filtration (0.45µm) Ultrafiltration (3kDa)	NTA DLS UV-Vis
Soil extract	Ag	Filtration (0.45µm)	AF4-ICP-MS
Soil	Au	Centrifugation	ESEM FESEM
	Ag	Ultrafiltration	ESEM FESEM
	Ag	Filtration (0.02µm)	EXAFS
Artificial sea water	Ag	Filtration (0.45µm)	AF4-ICP-MS sp ICP-MS
Sewage sediment	Au	Ultracentrifugation	ESEM FESEM TEM NTA
Tap water	Ag	SPE (magnetic matrix+acid etching)	ICP-MS
	Ag	Filtration (0.45µm)	HDC-ICP-MS TEM
	ZnO	CPE + MW	ICP-MS
	Ag	CPE	ET-AAS
Soil suspension	ZnO	Particles sedimentation	AF4-ICP-MS

* Abbreviations used in the table: AF4 - asymmetric flow field-flow fractation, CPE+MW – microwave assisted cloud point extraction, DLS - dynamic light scattering, EDS - energy dispersive X-ray spectroscopy, ESEM - environmental scanning electron microscopy, ET-AAS - electrothermal atomic absorption, EXAFS - extended X-ray absorption fine structure, FESEM - field-emission scanning electron microscopy, ICP-MS - inductively coupled plasma mass spectrometry, NTA - nanoparticle tracking analysis, PCC - particle collision coulometry, SPE - solid phase extraction, sp ICP-MS - single particle ICP-MS, TEM - transmission electron microscopy, VIP - voltammetry of immobilized particles, HDC-ICP-MS - hydrodynamic chromatography coupled to ICP-MS, UV-Vis - Ultraviolet-visible spectroscopy

In complex matrices, the separation of dissolved species from NPs before their determination might be required. For instance, dissolved Ag(I) can be physically separated by ultrafiltration, ultracentrifugation, and centrifugal ultrafiltration. Solid-phase extraction (SPE) is currently one of the most widely practiced sample preparation procedures and has been shown to separate metal nanoparticles (MNPs) efficiently. Liquid phase extraction of hydrophilic NPs into water (also known as water-soluble NPs) and hydrophobic NPs into an organic solvent or a mixture of solvents has been reported for the purification and size separation of synthetic NPs. Cloud point extraction (CPE) was employed for the reversible extraction and separation of different NPs such as Au, TiO_2, multiwalled carbon nanotube (MWCNT), fullerene (C60) and Fe_3O_4 (Proulx et al., 2014; Mori, 2015; Mourdikoudis et al., 2018).

Several methods have been developed to analyse inorganic and organic nanoparticles (*Table 1*). The most common analytical methods for the determination of nanoparticles are field flow fractionation (FFF) with ICP-MS, HPLC or UHPLC coupled to high resolution mass spectrometry (HRMS), LC-UV and FFF coupled to HRMS, multi angle light scattering and dynamic light scattering. Recently, single particle inductively coupled plasma mass spectrometry (sp ICP-MS) was proposed for the simultaneous determination of NPs and dissolved ions of metals (Folens et al., 2018; Mozhayeva et al., 2019). sp ICP-MS is well suited to nanoparticle characterization as it provides determination of the particle number and size distribution, along with the concentration of both the particles and the dissolved element component.

http://www.aloki.hu ● ISSN 1589 1623 (Print) ● ISSN1785 0037 (Online)
DOI: http://dx.doi.org/10.15666/aeer/1804_57755788

The objective of this study was to determine AgNPs size distribution and particles number concentration in environmental water samples. In this study AgNPs was chosen as the representative of metallic nanoparticles due to their broad applications and potential release into the environment.

Materials and methods

Reference materials and sample preparation

Alfa Aesar reference materials, such as AgNPs with a diameter of 20 nm and a concentration of 0.02 mg/ml, AgNPs with a nominal diameter of 40 nm ± 3 nm and a concentration of 0.02 mg/ml, AgNPs with a nominal diameter of 60 nm ± 3 nm and a concentration of 0.02 mg/ml (used to determine nebulization efficiency, diluted in demineralized water to 200 ng/l) and AgNPs with a nominal diameter of 100 nm ± 3 nm and a concentration of 0.02 mg/ml were used for testing. Nanoparticles in reference solutions were stabilized by the manufacturer with 2 mM sodium citrate. Reference materials and samples were diluted to 10-200 ng/L in deionized water and sonicated for 10 minutes before dilution and before analysis, with the addition of cooling cartridges to ensure sample homogeneity. Solutions were prepared on the day of analysis. To determine the response factor (cps/ppb), the Agma standard from Sigma Aldrich TraceCERT was used at a concentration of 0.994 ± 0.003 mg/l, which was diluted to 1 µg/l in 1% nitric acid solution (HNO_3).

Samples of surface water were taken with a hand scoop with a telescopic rod near Krakow (Poland). Samples of treated sewage were collected from a domestic sewage treatment plant located near a detached house in the vicinity of Krakow. Samples of the tap water were collected in polyethylene bottles directly from the tap after 3 minutes of draining the water from the tap. Water extract of waste from the oil and gas industry was prepared in accordance with PN-EN 12457-2:2006 and PN-EN 12457-4:2006 standards. More detailed information about samples collection object is in *Table 2.*

Table 2. *Description of the places of real samples collection*

Collected sample	The description of the method and place of collection. GPS coordinates
Water from supply system collected in the area of Krakow	Three samples of tap water were taken from three different taps in one building in Krakow. 50°02'15.9"N 20°00'04.2"E
Water from supply system collected in one of the villages near Krakow	Two samples of water were collected from a tap located in a detached house in one of the towns south of Krakow. 49°58'41.3"N 20°06'48.8"E
Water from a drainage ditch	Three water samples were collected from a ditch located in one of the towns to the north of Krakow. 50°08'51.7"N 20°05'25.6"E
Water from the settling tank at a car workshop	Three water samples were taken from a settling tank at a car workshop in one of the towns north of Krakow. 50°08'44.3"N 20°05'32.0"E
Treated sewage from domestic sewage treatment system	Treated sewage taken from a domestic sewage treatment system located near a detached house in a village south of Krakow, 3 samples. 49°58'41.5"N 20°06'49.4"E
Rainwater from storage tank	Two samples taken from a rainwater storage tank situated near a house in a locality north of Krakow. 50°08'45.1"N 20°05'32.0"E
Surface water1	Water from a watercourse located in Krakow. 50°02'00.8"N 20°02'30.7"E
Surface water2	Water from a watercourse located in a village south of Krakow. 50°02'04.6"N 20°02'30.4"E
Water extract from industrial waste	Water extraction of waste from the oil and gas mining industry was prepared (excavation after the application of polymer-potassium scrubber).

http://www.aloki.hu ● ISSN 1589 1623 (Print) ● ISSN1785 0037 (Online)
DOI: http://dx.doi.org/10.15666/aeer/1804_57755788

All studies were conducted in Krakow (Poland). All samples were stored without access to light at the temperature 2-5°C. Before use, the bottles (and all flasks, pipettes and laboratory utensils used) were washed with 20% solution of HNO_3. Samples were not stabilised and were analysed up to 24 hours after collection.

Instrumentation

The mass spectrometer ICP-MS 7900 from Agilent was used for measurements. Data acquisition was done using the Agilent Mass Hunter software in the time resolved analysis (TRA) mode with a 60 s acquisition time. ICP-MS was equipped with a standard MicroMist nebulizer, nickel cones, quartz burner (1.0 mm). The samples were introduced directly into the instrument using a peristaltic pump and 1.02 mm internal diameter tubing (sample flow velocity was 0.346 ml/min). Prior to and between AgNPs analysis, the sample feed system was washed with 1% HNO_3.

The instrument was calibrated on the day of the analysis using Agilent solution (1 µg/l, Li, Co, Y, Tl, Ce, Ba w 2% HNO_3). The nebulization efficiency was in the range of 0.059-0.095. No internal standard was employed, because only ^{107}Ag was detected during the run. To ensure the absence of significant instrumental drift over time, a 200 ng/l Ag dissolved standard was run in single particles mode for every 10 AgNPs samples analyzed.

The measurement parameters used in the NPs analysis are listed in *Table 3*.

Table 3. *Parameters of analysis and mass spectrometer (sp ICP-MS) used for the determination of AgNPs*

Parameter (unit)	Value
Power RF (W)	1550
Carrier gas flow velocity (l/min)	1.05
Temperature of the mist chamber (°C)	2.0
Nebulizer pump velocity (revolutions/min.)	0.1
Sampling depth (mm)	8.0
Integration time (ms)	0.5
Data collection time (s)	60
Data collection mode	TRA
Monitored weight	^{107}Ag
Density of particles (g/ml)	10,5
Mass fraction of Ag	1

The background equivalent diameter (BED) was calculated based on the results obtained. It allows to estimate the approximate smallest detectable NPs size. Mass equivalent to instrument noise (m_{bkgnd} - background equivalent mass) is expressed by the equation (*Eq. 1*) (Laborda et al., 2016):

$$m_{bkgnd\_rm} = \frac{I_{noise}}{I_{rm}} \cdot m_{std} \quad \text{(Eq.1)}$$

$$m_{bkgnd\_unknown} = I_{noise} \cdot \frac{1}{s} \cdot t_d \cdot V \cdot \eta_{neb} \cdot 10^6 \cdot f_d \cdot \frac{1}{60} \quad \text{(Eq.2)}$$

http://www.aloki.hu ● ISSN 1589 1623 (Print) ● ISSN1785 0037 (Online)
DOI: http://dx.doi.org/10.15666/aeer/1804_57755788

BED (d_{bkgnd}, nm) can be calculated from dependency (*Eq. 3*):

$$BED = \sqrt[3]{\frac{6}{\pi} \cdot \frac{m_{bkgnd}}{10^{15} \cdot \rho_p}} \cdot 10^7 \quad \text{(Eq.3)}$$

where,
I_{noise} – signal intensity for noise (cps)),
I_{rm} – the arithmetic mean of the signal intensities for RM reference solutions (cps),
m_{std} – particulate mass of the standard (fg),
s – response rate (cps/ppb),
t_d – integration time (s),
V – sample flow velocity (ml/min),
η_{neb} – nebulisation efficiency,
f_d – molar mass of the particle/analyte,
T – total time of data collection (min),
ρ_p – density of particles (g/cm^3).

Results and discussion

This paragraph presents the test results and determination of selected validation parameters for the developed method (such as background equivalent diameter, correctness, recovery, NPs stability over time and reproducibility).

Background equivalent diameter (BED)

Equation 3 shows that BED depends on the effectiveness of nanoparticle detection. Therefore, the improvement of ionization conditions for elements with a low ionization potential, as well as the increase of ion transmission through the use of more efficient instrumental systems, may reduce the limit of particle size detection. sp ICP-MS allows to detect nanoparticles of metal above ~20 nm, while the size of oxides increases depending on their stoichiometry. In terms of mass, the detection limits are about tens of attograms per NP (Laborda et al., 2016).

The value of the smallest detectable size (BED) of silver nanoparticles obtained for the implemented method is 9-15 nm. The values obtained are similar to those provided in literature (Laborda et al., 2016). No partial results were reported due to their large number. BED was determined by the instrument for each sample.

Correctness of the method

Correctness of measurement means the conformity of a test value with a true value or an accepted reference value. Most often, correctness is expressed in terms of load, i.e. total systematic error. In order to determine the load (and verify the correctness), a standard is added, and a recovery calculation is used.

Tables 4-6 summarise the test results obtained for reference materials. *Table 4* shows the results obtained for a series of reference solutions with a nominal diameter of 20 nm; *Table 5* shows the results obtained for a series of reference solutions with a nominal diameter of 40 nm; and *Table 6* shows the results obtained for a material with a diameter of 60 nm. The correctness of the method is expressed as a percentage of recovery.

http://www.aloki.hu ● ISSN 1589 1623 (Print) ● ISSN1785 0037 (Online)
DOI: http://dx.doi.org/10.15666/aeer/1804_57755788

Table 4. *Results obtained for a series of reference solutions with a nominal diameter of 20 nm*

Parameter	Nominal diameter - mean * [nm]	Number of particles [particles/l]	Concentration of Ag [µg/l]
Value provided by manufacturer	20.0	Not provided	0.050
Measured value (n=6)*	25.58	$8.04 \cdot 10^7$	0.045
Recovery [%]	128	-	90
Value provided by manufacturer	20	Not provided	0.100
Measured value (n=4)**	20.91	$6.25 \cdot 10^7$	0.114
Recovery [%]	104.6	-	114

Table 5. *Results obtained for a series of reference solutions with a nominal diameter of 40 nm*

Parameter	Nominal diameter-mean [nm]	Number of particles [particles/l]	Concentration of Ag [µg/l]
Value provided by manufacturer	40±3nm	$4.25 \cdot 10^7$	0.050
Measured value (n=6)	40.1	$3.99 \cdot 10^7$	0.051
Recovery [%]	100	93.8	102

Table 6. *Results obtained for a series of reference solutions with a nominal diameter of 60 nm*

Parameter	Nominal diameter-mean [nm]	Number of particles/L	Concentration of Ag [µg/l]
Value provided by manufacturer	60±3nm	$1.7 \cdot 10^8$	0.200
Measured value (n=4)	54.4	$1.72 \cdot 10^8$	0.219
Recovery [%]	90.7	101	110
Value provided by manufacturer	60±3nm	$8.50 \cdot 10^7$	0.200
Measured value (n=4)	62.5	$7.15 \cdot 10^7$	0.218
Recovery [%]	104	84,1	109
Value provided by manufacturer	60±3nm	$1.7 \cdot 10^8$	0.200
Measured value (n=4)	54.4	$1.72 \cdot 10^8$	0.219
Recovery [%]	90.7	101	110
Value provided by manufacturer	60±3nm	$1.7 \cdot 10^8$	0.200
Measured value (n=6)	63.6	$1.51 \cdot 10^8$	0.218
Recovery [%]	106	89	109

The recovery obtained for the number of particles/L was within the range of 84.1-101%, while the recovery determined for the nominal diameter was within the range of 90.7-128%. The recovery value for the nominal diameter of 128% was obtained for particles of 20nm size, which are close to LOD_{size}.

On the basis of the conducted research and calculations it can be stated that the validated method of determination of AgNPs by sp ICP-MS is correct.

Figure 1 shows the particle size distribution for reference solutions of 20 nm (a), 40 nm (b), 60 nm (c) Ag NPs.

The resulting particle size distributions are wide. Reference materials are crucial for checking the quality and metrological traceability of analytical results. They are also essential for the validation of particle size analysis methods and instrument calibration. The number of reference materials for nanoparticle analysis is currently limited. In addition, matrix reference materials for nanoparticles are not commercially available.

http://www.aloki.hu ● ISSN 1589 1623 (Print) ● ISSN1785 0037 (Online)
DOI: http://dx.doi.org/10.15666/aeer/1804_57755788

Therefore, NP calibrators that are used to calibrate methods and for initial experiments should be characterized by size and size distribution (homogeneity) using scanning electron microscopy (SEM) and transmission electron microscopy (TEM).

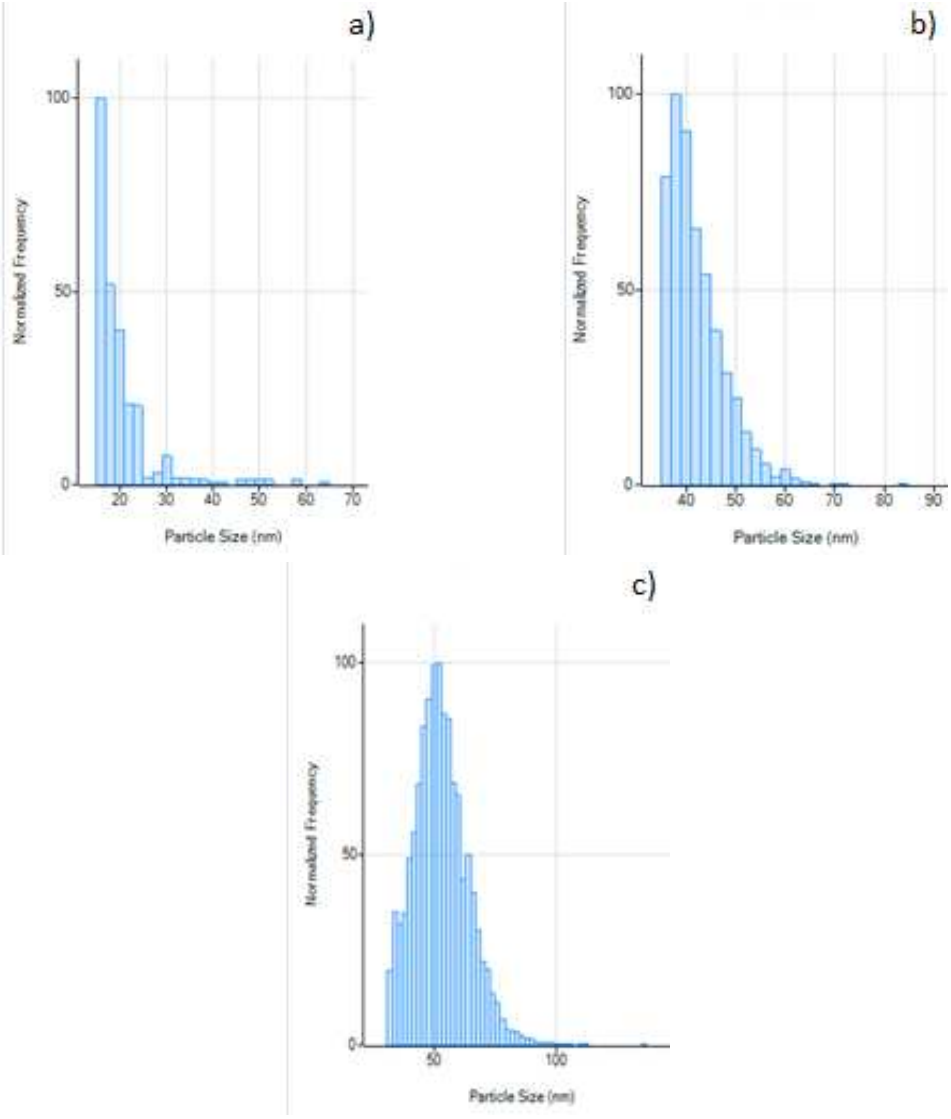

Figure 1. *Particle size distribution for 20, 40 and 60 nm AgNPs*

Reproducibility

Reproducibility is the degree of agreement between independent test results obtained under steady state conditions. Reproducibility does not refer to an actual value or other specified value. It depends only on the distribution of random errors and is a concept that describes the variability of repeated results. The reproducibility measure is usually taken as the standard deviation of the test results (the standard deviation of the sample). The higher the standard deviation, the lower the precision. RSD, i.e. relative standard deviation, is most commonly used to assess reproducibility.

http://www.aloki.hu ● ISSN 1589 1623 (Print) ● ISSN1785 0037 (Online)
DOI: http://dx.doi.org/10.15666/aeer/1804_57755788

Table 7 shows the measurement results used to determine the reproducibility of the method. The reproducibility of the method has been determined in % as the RSD (Relative Standard Deviation).

Table 7. *Measurement results used to determine the reproducibility of a method*

Value provided by manufacturer	Measured diameter [nm]	RSD [%]
60±3nm	62.0 62.8 62.0 63.1 62.6	0.366
20 nm	26.8	4.3

Calculated RSD values do not exceed 5%. The method is reproducible for the tested range

Recovery

Example results of analyses of mixtures prepared from real samples (surface waters) with the addition of a reference material with a particle size of 60 nm are presented in *Table 8*. Recovery was calculated for the mass concentration of Ag.

Table 8. *Results of analyses of mixtures prepared from real samples*

Matrix	Mean diameter of particles [nm]	Most common particle size [nm]	Number of particles per L	Mass concentration [ng NPs/L]	Recovery determined for mass concentration [%]
Surface water 1	28.6	26	$2.79 \cdot 10^8$	41.8	106
Surface water 1 + 60 nm NPs (100 µg/l)	51.4	50.7	$1.71 \cdot 10^8$	150.3	
Surface water 2	23.2	20.4	$1.83 \cdot 10^8$	14.3	86
Surface water 2 + 60 nm NPs (100 µg/l)	52.1	56	$8.23 \cdot 10^7$	98.0	

The recovery values are 86% and 106%. After adding the 60 nm standard to the analyzed samples, the number of particles/L decreased. More tests would be needed to determine the cause of this dependency (e.g. checking particle size distribution, agglomeration, optimising sonication parameters and sonication efficiency after adding the standard to the sample, tests for more diluted samples).

Stability of nanoparticles over time

Measurements were taken for the reference material 60 nm on the day of solution preparation and for the same solution 10 days after preparation. The reference solution was stored in the dark and cooled to 2-5°C. The results of the particle size distribution are shown in *Figures 2a) and 2b)* and *Table 9*.

On the basis of the conducted research it can be stated that Ag nanoparticles are not stable in aqueous solution. It is necessary to keep the samples in the dark, to cool them and possibly to add a stabilising agent to the sample, e.g. sodium citrate or 3-aminopropyltrimethoxysilane.

http://www.aloki.hu ● ISSN 1589 1623 (Print) ● ISSN1785 0037 (Online)
DOI: http://dx.doi.org/10.15666/aeer/1804_57755788

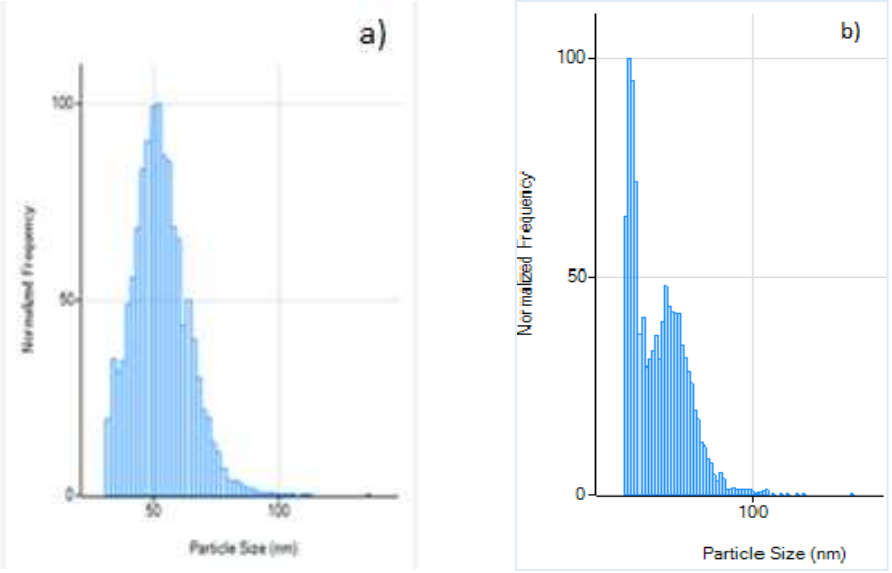

Figure 2. *Particle size distribution for a) 60 nm reference material prepared on the day of determination b) results 10 days after preparation of the solution*

Table 9. *Testing for stability of nanoparticles*

Reference solution	Most common size [nm]	Mean size of particles [nm]
60 nm	48	56.6
60 nm after 10 days	24	41.2

Nanoparticles can undergo many transformations under biological or environmental conditions. Primary nanoparticles may form larger agglomerates or aggregates, being reversible only in the first case. On the other hand, some metal-containing NPs (e.g. silver, zinc oxide) may dissolve, releasing soluble compounds.

Analysis of the data in *Table 10* shows that silver nanoparticles have been found in all environmental samples analysed. The most common nanoparticles were those of the sizes 16-28 nm.

The highest content of AgNPs was determined for one of the samples of water taken from a drainage ditch (76 ng/l). However, the total concentration obtained for this sample is not the highest. The highest concentration of silver was determined in the sample of tap water taken in Krakow. The total Ag content obtained for tap water samples does not exceed the limit given in the Minister of Health's Ordinance of 7 December 2017 on the quality of water intended for human consumption (0.010 mg/l). However, if the obtained silver concentration values were close to the limit value given in the regulation, it would be advisable to make a particle size distribution and check if the smallest size particles that may have toxic properties do not constitute a large proportion in this distribution.

The analysis of environmental samples shows that there is no direct correlation between the amount of silver nanoparticles and the concentration of silver in the sample, and therefore the interpretation of environmental data is difficult and requires the analysis of many factors.

http://www.aloki.hu ● ISSN 1589 1623 (Print) ● ISSN1785 0037 (Online)
DOI: http://dx.doi.org/10.15666/aeer/1804_57755788

Table 10. *Results obtained for real samples*

Matrix	Mean particle diameter [nm]	Most common particle size in a sample [nm]	Number of particles/L	Mass concentration of AgNPs [ng/l]	Concentration of Ag [µg/l]
Water from supply system collected in the area of Krakow	20.1	18	$1.56 \cdot 10^7$	< 0.10	0.9761
	29.6	18	$1.94 \cdot 10^7$	< 0.10	5.112
	16.2	16	$9.35 \cdot 10^6$	0.341	0.0076
Water from supply system collected in one of the villages near Krakow	19.01	16	$3.57 \cdot 10^7$	2.18	0.0095
	19.18	16	$2.07 \cdot 10^7$	1.23	0.0065
Water from a drainage ditch	33.3	24	$2.68 \cdot 10^8$	76.00	0.1059
	21.7	20	$2.33 \cdot 10^8$	14.35	0.0430
	21.5	22	$1.99 \cdot 10^8$	11.90	0.0402
Water from the settling tank at the car workshop	21.5	22	$2.06 \cdot 10^8$	12.43	0.041
	20.0	18	$2.00 \cdot 10^8$	11.84	0.036
	19.9	18	$1.53 \cdot 10^8$	7.42	0.030
Rainwater from storage tank	31.51	26	$2.95 \cdot 10^7$	8.075	0.085
	21.81	20	$9.87 \cdot 10^6$	0.648	0.021
Treated sewage from domestic sewage treatment system	18.6	18	$8.24 \cdot 10^7$	4.11	0.0183
	17.9	16	$1.28 \cdot 10^8$	4.54	0.0215
	18.0	18	$9.10 \cdot 10^7$	3.29	0.0184
Surface water1	18.1	17	$1.42 \cdot 10^7$	0.860	0.008
Surface water2	23.2	20	$1.53 \cdot 10^8$	14.25	0.029
Water extract of waste	30.00	28	$1.00 \cdot 10^7$	4.00	0.142

The graph showing the number of counts as a function of CPS time (counts per second) and the particle size distribution for a sample of tap water taken in Krakow is presented in *Figure 3*. The analyzed sample contained nanoparticles of different sizes. The mean diameter of particles was 16.2 nm, but there were also nanoparticles with a diameter above 50 nm. The particle size distribution was wide.

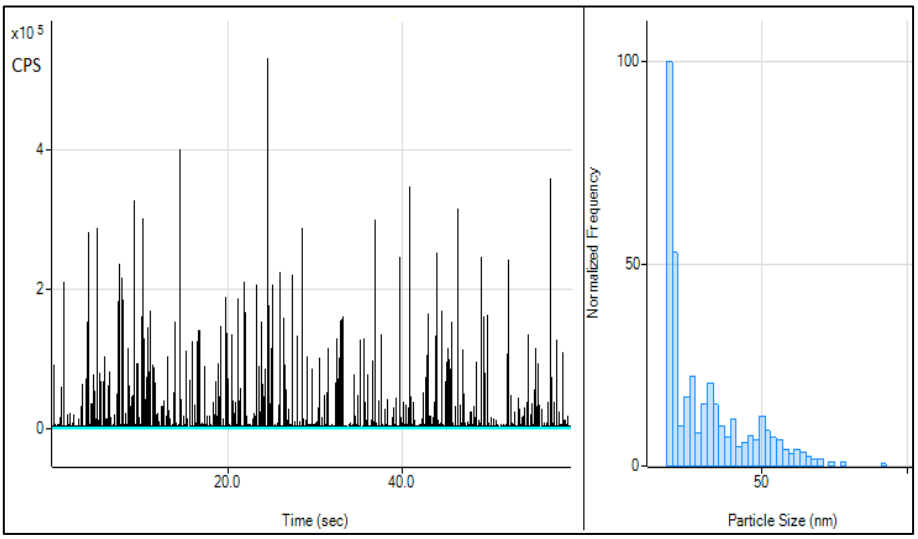

Figure 3. *CPS (counts per second) as a function of time and the particle size distribution for the sample of tap water collected in Krakow*

http://www.aloki.hu ● ISSN 1589 1623 (Print) ● ISSN1785 0037 (Online)
DOI: http://dx.doi.org/10.15666/aeer/1804_57755788

Conclusions

At present, the scale of nanoparticles' applications is enormous, which means that their presence in the environment is becoming more and more common. Nanoparticles are separated by centrifugation, ultrafiltration, cloud point extraction (CPE) and flow fractionation in an asymmetric flow force field (AF4). The most popular methods of nanoparticles determination in environmental samples are: Nanoparticle Tracking Analysis (NTA), Dynamic Light Scattering (DLS), Scanning Electron Microscopy (SEM) and Inductively Coupled Plasma Mass Spectrometry (ICP-MS, sp ICP-MS). The literature review confirmed that sp ICP-MS technique is a sensitive, effective, fast and modern technique used for the determination of metal nanoparticles in environmental samples.

The method of determination of Ag nanoparticles in liquid environmental samples using sp ICP-MS has been validated. Reproducibility, correctness, recovery, BED and stability of nanoparticles were determined. Validation of the analytical method showed its ability to determine silver nanoparticles in the matrices tested.

The results of tests of liquid real samples confirm the presence of Ag nanoparticles in the analyzed samples (e.g. environmental samples and aqueous extracts of mining waste). Nanosilver was present in most of the analysed samples at concentrations of 0.291-76 ng/l. The mean diameter of AgNPs in the examined samples was in the range of 16.2-33.3 nm. Silver nanoparticles were also found in tap water and their sizes were widely distributed over the whole range of nanometre size. The mean diameter of nanoparticles in tap water was 16.2-29.6 nm, which is quite disturbing as nanoparticles smaller than 100 nm can easily penetrate cell membranes and cause damage to all cells, including organs and brain (Zhang et al., 2019). Particle size is the main factor affecting the toxicity of AgNPs (Cho et al., 2018). The determined particle sizes are comparable to those used in nanomaterials and consumer products (Kessler, 2011).

The total Ag content obtained for tap water samples does not exceed the limit given in the Minister of Health's Ordinance of 7 December 2017 on the quality of water intended for human consumption but it would be advisable to perform a particle size distribution for samples with a concentration near the limit value given in the regulation.

Determination of NPs in environmental matrices has not been carried out in Poland so far. This study improves the knowledge on the quality of drinking and surface waters, indicates the presence of nanoparticles in environmental samples and aqueous extracts of mining waste. However, it is necessary to conduct more tests on NPs content and to extend the validation to other parameters and matrices, given the potential impact of NPs on human health. In addition, other methods of nanoparticle separation found in literature should be examined and the parameters for separating NPs from the matrix should be optimized.

REFERENCES

[1] Aznar, R., Barahona, F., Geiss, O., Ponti, J., José Luis, T., Barrero-Moreno, J. (2017): Quantification and size characterisation of silver nanoparticles in environmental aqueous samples and consumer products by single particle-ICPMS. – Talanta 175: 200-208.

[2] Bundschuh, M., Filser, J., Lüderwald, S., Mckee, M. S., Metreveli, G., Schaumann, G. E., Schulz, R., Wagner, S. (2018): Nanoparticles in the environment: where do we come from, where do we go to? – Environ. Sci. Eur. 30(1): 6.

http://www.aloki.hu ● ISSN 1589 1623 (Print) ● ISSN1785 0037 (Online)
DOI: http://dx.doi.org/10.15666/aeer/1804_57755788

[3] Cho, Y. M., Mizuta, Y., Akagi, J. I., Toyoda, T., Sone, M., Ogawa, K. (2018): Size-dependent acute toxicity of silver nanoparticles in mice. – J Toxicol Pathol. 31(1): 73-80.
[4] Folens, K., Van Acker, T., Bolea-Fernandez, E., Cornelis, G., Vanhaecke, F., Du Laing, G., Rauch, S. (2018): Identification of platinum nanoparticles in road dust leachate by single particle inductively coupled plasma-mass spectrometry. – Science of The Total Environment 615: 849-856.
[5] Kessler, R. (2011): Engineered Nanoparticles in Consumer Products: Understanding a New Ingredient. – Environ Health Perspect. 119(3): A120-A125.
[6] Kim, B., Park, C. S., Murayama, M., Hochella, M. F. Jr. (2010): Discovery and characterization of silver sulfide nanoparticles in final sewage sludge products. – Environ. Sci. Technol. 44(19): 7509-7514.
[7] Krasodomski, M., Krasodomski, W., Ziemiański, L. (2009): Nanotechnologia a przemysł naftowy. – Nafta-Gaz 65(1): 83-92.
[8] Krasodomski, W., Rembiesa-Śmiszek, A., Skibińska, A. (2013): Nanocząstki w środkach smarowych. – Nafta-Gaz 69(3): 220-225.
[9] Laborda, F., Bolea, E., Cepriá, G., Gómez, M. T., Jiménez, M. S., Pérez-Arantegui, J., Castillo, J. R. (2016): Detection, characterization and quantification of inorganic engineered nanomaterials: A review of techniques and methodological approaches for the analysis of complex samples. – Anal Chim Acta 904: 10-32.
[10] Majedi, S. M., Lee, H. K. (2016): Recent advances in the separation and quantification of metallic nanoparticles and ions in the environment. – TrAC Trends in Analytical Chemistry 75: 183-196.
[11] Mori, Y. (2015): Size-Selective Separation Techniques for Nanoparticles in Liquid. – KONA Powder and Particle Journal 32: 102-114.
[12] Mourdikoudis, S., Pallares, R. M., Thanh, N. T. K. (2018): Characterization techniques for nanoparticles: comparison and complementarity upon studying nanoparticle properties. – Nanoscale 10: 12871-12934.
[13] Mozhayeva, D., Engelhard, C. (2019): A critical review of sp ICP MS – A step towards an ideal method for nanomaterial characterization. – J. Anal. At. Spectrom., published online, DOI: 10.1039/c9ja00206e.
[14] Prasad, R., Kumar, M., Kumar, V. (2017): Nanotechnology. – Springer Nature Singapore Pte Ltd., ISBN 978-981-10-4572-1.
[15] Proulx, K., Wilkinson, K. J. (2014): Separation, detection and characterisation of engineered nanoparticles in natural waters using hydrodynamic chromatography and multi-method detection (light scattering, analytical ultracentrifugation and single particle ICP-MS). – Environ. Chem. 11: 392-401.
[16] Wagner, S., Gondikas, A., Neubauer, E., Hofmann, T., Von Der Kammer, F. (2014): Spot the difference: engineered and natural nanoparticles in the environment - release, behaviour, and fate. – Angewandte Chemie International 53: 12398-12419.
[17] Weinberg, H., Galyean, A., Leopold, M. (2011): Evaluating engineered nanoparticles in natural waters. – TrAC Trends Anal Chem. 30(1): 72-83.
[18] Zhang, M., Yang, J., Cai, Z., Feng, Y., Wang, Y., Zhang, D., Pan, X. (2019): Detection of engineered nanoparticles in aquatic environments: current status and challenges in enrichment, separation, and analysis. – Environmental Science: Nano 6: 709-735.
[19] Zima, G. (2017): Analiza wpływu nanomateriałów na właściwości osadu filtracyjnego. – Nafta-Gaz 73(5): 312-320.

http://www.aloki.hu ● ISSN 1589 1623 (Print) ● ISSN1785 0037 (Online)
DOI: http://dx.doi.org/10.15666/aeer/1804_57755788

RESPONSE OF MEXICAN PETUNIA (*RUELLIA BRITTONIANA*, L.) TO SALINITY, ORGANIC AND BIO MATERIALS

FARDOUS, M. A.[1*] – HEGAZI, M. A.[1] – EL-BABLY, S. Z.[2] – HANA, M. R.[2*]

[1]*Hort. Dept., Fac. Agric., Kafr El-Sheikh Univ., Kafr El-Sheikh, Egypt*

[2]*Research Institute, Agric. Research Center, Kafr El-Sheikh, Egypt*

**Corresponding author*
e-mail: maria_magdy_1@yahoo.com

(Received 15th Jan 2020; accepted 22nd May 2020)

Abstract. Mexican petunia (*Ruellia brittoniana*), belongs to the of family Acanthaceae. It is native to Mexico but it has escaped cultivation and established in disturbed areas in the south eastern of the United States and can be found invading habitats across the state of Florida which is regarded as the second largest producer of ornamental plants in the United States (Hodges and Haydu, 2002). Water scarcity is the greatest crisis that humanity face in the 21st century (Singh, 2008). May be water is a renewable resource, but its availability is variable and limited. Nearly every country in the world experiences water shortages during certain periods of the year (Gleick, 1993) and more than 80 countries suffer from serious water deficiency (Jin et al., 2007). To face the deficiency of fresh water for the sustainable development of agriculture, there is increasing awareness among agricultural scientists and planners in the utilization of at least diluted seawater for irrigation of crops (Liu et al., 2003). A series pot of experiments were conducted at Kaferelsheikh University Farm during 2014/2015 and 2015/2016 throughout the year. Seawater was diluted with freshwater to obtain the required percentages of 0, 5, 10, 15, 20 and 30%, in addition; the plants were foliar sprayed with organic or bio materials (humic acid, amino acids and active dry yeast). Each pot (20 cm diameter plastic pots) received 200 ml of the suitable diluted seawater every two days and foliar sprayed with organic materials fortnightly throughout the study course (Rahman et al., 2019). The obtained results showed that, plants treated with 5% seawater in combination with humic acid surpassed control one in all measured traits, namely plant height, shoot fresh and dry weights, as well as improved the root length and weight, increased the flowering number and duration, as well as total chlorophyll. All measured traits gradually declined as the seawater percentage increased in the irrigation water. Seawater at 20% in combination with amino acids treatment significantly increased plant proline content.
Keywords: *Mexican petunia, Ruellia brittoniana, L., diluted seawater, biostimulant materials*

Introduction

Ruellia brittoniana, L. (Mexican petunia) (Mexican blue bell) (Katie blue *Ruellia*) belonging to Acanthaceae family is widely used as an ornamental plant (Richard and Hamilton, 1997). It is a tender evergreen perennial, herbaceous plant spreading upright with moderate density and growth rate and is propagated by seeds or cuttings. It grows in semi shade places and has moderate tolerance to draught. It will be attractive when planted in a container or in perennial borders and can be used as ground covers (Gilman, 1999).

Salinity is one of the major environmental factors limiting plant growth and productivity. In most arid and semiarid areas the competition among agriculture, industry and landscape users for high quality water has promoted the use of alternative water sources for irrigation thus, marginal quality water, somewhat saline, became important in these areas (Chartzoulakis et al., 2002) for the irrigation of ornamental plants (Carter et al., 2005).

Seawater irrigation in agriculture should be developed in the places where there is sufficiently high saline water or seawater. Using saline water to irrigate salt-tolerant crops

http://www.aloki.hu ● ISSN 1589 1623 (Print) ● ISSN 1785 0037 (Online)
DOI: http://dx.doi.org/10.15666/aeer/1804_57895802

or halophytes is a viable strategy for developing agriculture production as well as, for saving fresh water resources.

In Egypt, the water used for irrigation is often mixed with seawater especially in the area near the coasts. It has a long sea coast, which encourages the utilization of seawater in irrigation and as a mineral fertilizer (Miyamoto et al., 1996; Glenn et al., 1998).

Salt effects involved different results due to the complex interaction among the different morphological, physiological, and biochemical processes (Singh and Chatrath, 2001) that lead to growth inhibition (Sairam and Tyagi, 2004).

Humic acid has a direct effect on plant as a hormone–like compound or indirect effect by increasing nutrients uptake through the chelating effect and retaining membrane permeability of microorganisms, serves as a buffer to neutralize both excessive soil acidity and alkalinity, it also improves both the uptake and retention of vital nutrients, stimulates root development, enhances natural resistance against diseases and stimulates over all plant growth (Atiyeh et al., 2002). Hadi et al. (2011) on *Matricaria chamomilla* L. obtained the biggest flower head diameter after spraying amino acids solution at the flowering bud stage.

Humic acid improved the vegetative growth and increased carbohydrate formation in plant as all these factors helped in prolongation of the flowering duration (Zadeh and Mirzakhani, 2012).

Amino acids can regulate both plant growth and development through their influence on the bio-synthesis of gibberellins and may also play an important role in plant metabolism and protein assimilation necessary for cell formation (Walter and Nawacke, 1978; Sadak, 2015).

Active dry yeast (*Saccharomyces cerevisia*e) is a natural source of cytokinins that stimulate cell proliferation and differentiation, control shoot and root morphogenesis, chloroplast maturation and it is a rich source of vitamin B complex, carbohydrates, sugars, enzymes, and minerals (Amer, 2004; Ezz El-Din and Hendawy, 2010).

Active dry yeast was more effective and enhanced all flowering aspects of *Dahlia pinnata* plants (Manoly and Nasr, 2008).

Ali and Hassan (2013) reported that the longest flowering duration resulted from using humic acid at 150 ppm or proline at 4 ppm, respectively with salinity of fresh water (304 ppm).

This search aimed to study the effect of diluted seawater irrigation and the effect of organic materials such as humic acid, amino acids and active dry yeast on growth and chemical composition of *Ruellia brittoniana,* L. plants.

Materials and methods

A series of pot experiments were conducted at the Experimental Farm of the Faculty of Agriculture, Kafer El-Sheikh University, Egypt, during 2014/2015 and 2015/2016 seasons to study the effect of diluted seawater irrigation combined with foliar application of biostimulant materials (humic acid, amino acids and active dry yeast) on the growth and chemical constituents of *Ruellia brittoniana, L.* Physical and chemical analysis of the experimental soil was determined and illustrated in *Table 1*.

Water salinity

Sampels of Mediterranean water (Balteem) were diluted with freshwater to obtain the required percentages (0, 10, 15, 20, 25 and 50% seawater) and pH and EC values of the obtained mixtures were measured and illustrated in *Table 2*.

http://www.aloki.hu ● ISSN 1589 1623 (Print) ● ISSN 1785 0037 (Online)
DOI: http://dx.doi.org/10.15666/aeer/1804_57895802

Table 1. *Physical and chemical properties of the experimental soil in 2014/2015 and 2015/2016 seasons*

Season	Sand %	Silt %	Clay %	pH	EC dsm^{-1}	Cations (meq/l)				Anions (meq/l)			
						Ca^{++}	Mg^{++}	Na^{+}	K^{+}	CO^{3-}	HCO^{3-}	Cl^{-}	SO_4^{-}
1st	24.12	25.67	50.21	8.59	1.42	4.08	3.63	6.50	0.32	-	3.13	7.68	3.72
2nd	24.34	25.85	49.81	8.2	1.40	3.52	2.89	6.85	0.45	-	2.19	7.60	5.41

Table 2. *pH and EC values of the different diluted seawater mixtures in 2014/2015 and 2015/2016 seasons*

Seawater %	1st season		2nd season	
	pH	Ec (dsm^{-1})	pH	Ec (dsm^{-1})
Control (0)	7.75	0.47	7.66	0.46
5%	7.67	7.20	7.55	6.95
10%	7.68	9.36	7.57	9.23
15%	7.69	11.28	7.58	11. 17
20%	7. 66	12.68	7.56	12.59
30%	7.64	14.97	7.54	14.87

Plant material and procedure

Stem cuttings of *Ruellia brittoniana, L* (average of 7 cm in length) were planted in September 1st during 2014 /2015 and 2015/2016 seasons in pots filled with a clayey soil. After two months the rooted cuttings were transplanted into plastic pots with a diameter of 20 cm (without drain holes) filled with a clayey soil.

Each pot received 200 ml of the suitable diluted seawater after two months from transplantation every two days and organic or bio stimulants (humic acid, amino acids and active dry yeast) were used as a foliar spray on plant leaves fortnightly throughout the study course. Humic acid was used at 5 ml/L, amino acids 1 g/L and active dry yeast at 5 g/L.

The experimental layout was split plot design. The experiments were conducted twice and the obtained data were subjected to one-way analysis of variance (ANOVA) and Duncan multiple range comparison test ($p < 0.05$) using them static statistical package.

Determination and measurements

At the end of the experiments on the 1st September, the following data were recorded in the two experimental seasons:

Survival %.

Plant height (cm).

Leaf area (cm^2) calculated by CI-202 Portable Laser Leaf Area Meter (CID Bio-Science Made In USA).

Shoot fresh and dry weights (g)/plant/season.

Main root length (cm).

Root fresh and dry weight (g)/plant/season.

Flowering duration (days) and number of flowers /plant/season.

http://www.aloki.hu ● ISSN 1589 1623 (Print) ● ISSN 1785 0037 (Online)
DOI: http://dx.doi.org/10.15666/aeer/1804_57895802

Leaf total green color was measured using a portable chlorophyll meter (Minolta SPAD-502, Japan).
Proline content (µ moles/100 g fresh weight) was determined and calculated on a fresh weight basis according to Baters et al. (1973).
Nitrogen (%) was determined by modified microkjeldahl method as described by A.O.A.C. (1970).
Magnesium and sodium were measured using an atomic absorption spectrophotometer (Jackson, 1973).
Chloride was assayed by titration method indicated by Jackson (1973).

Results

Effect of diluted seawater, humic acid, amino acids, active dry yeast on *Ruellia brittoniana,* L. was examined.

Vegetative growth parameters

Diluted seawater of 30% was completely lethal for plants. The highest survival percentage was recorded with control treatment (fresh water only) followed by 5% and 10% seawater then gradually declined as sea water percentage increased (*Fig. 1*).

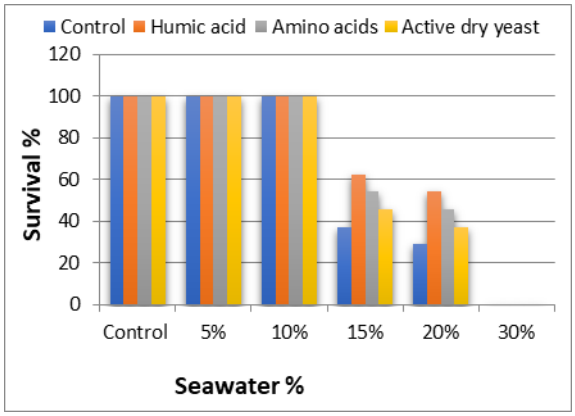

Figure 1. *Effect of diluted seawater and biostimulants and their interaction on survival % of Ruellia brittoniana, L. (mean of both seasons)*

Utilizing diluted seawater at 5% significantly improved all traits such as plant height, shoot fresh and dry weights with significant differences in between whereas control treatment recorded the widest leaves without significant differences. Raising seawater percentage in irrigation water from 10 to 20% gradually decreased all parameters of vegetative growth (*Figs. 2-7*).

As for organic or bio stimulants, humic and amino acids significantly augmented the survival%, plant height, leaf area, shoots fresh and dry weights followed by active dry yeast against the control treatments.

These results confirmed the contribution of organic or bio stimulants with seawater for improving all parameters as survival %, plant height, leaf area, shoot fresh and dry weights. Seawater at 5% combined with each of humic acid, followed by amino acids then active dry yeast improved all traits which surpassed control treatment. The

http://www.aloki.hu ● ISSN 1589 1623 (Print) ● ISSN 1785 0037 (Online)
DOI: http://dx.doi.org/10.15666/aeer/1804_57895802

combination between diluted seawater and organic or bio stimulants resulted in a gradual increment in the parameters comparing to uncombined one.

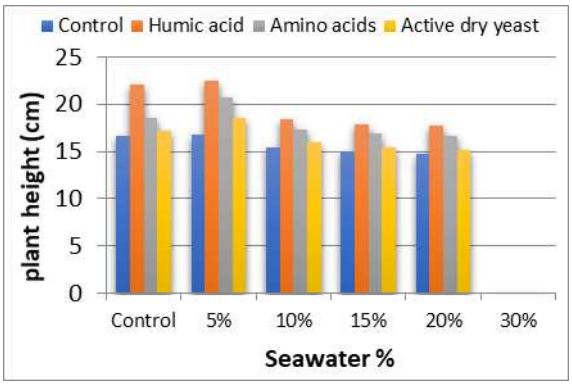

Figure 2. *Effect of diluted seawater and biostimulants and their interaction on plant height of Ruellia brittoniana, L. (mean of both seasons)*

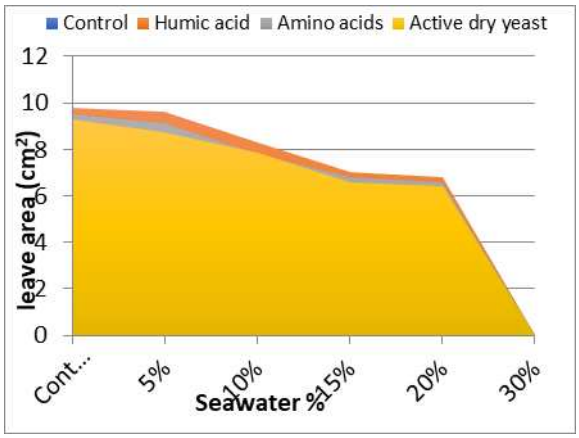

Figure 3. *Effect of diluted seawater and biostimulants and their interaction on leaf area of Ruellia brittoniana, L.*

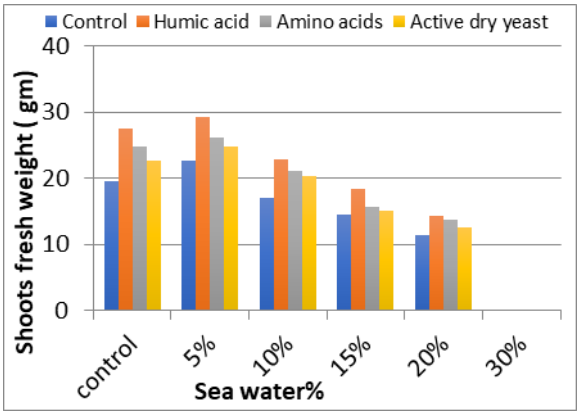

Figure 4. *Effect of diluted seawater and biostimulants and their interaction on shoots fresh weight of Ruellia brittoniana, L.*

http://www.aloki.hu ● ISSN 1589 1623 (Print) ● ISSN 1785 0037 (Online)
DOI: http://dx.doi.org/10.15666/aeer/1804_57895802

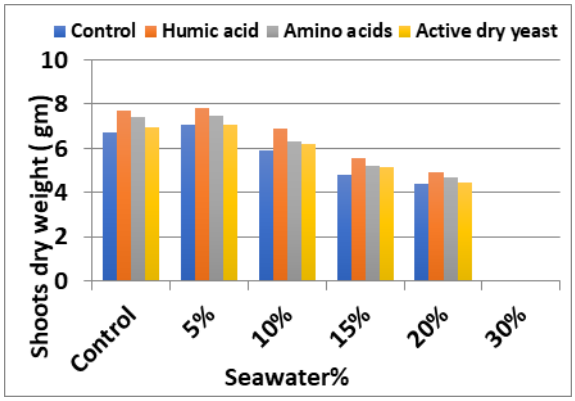

Figure 5. *Effect of diluted seawater and biostimulants and their interaction on shoots dry weight of Ruellia brittoniana, L.*

In general, increasing seawater percent from 10 to 20% combined with organic or bio stimulants significantly decreased all parameters except for 10% seawater which gave (100%) survival.

Root growth parameters

Diluted seawater (5%) treatment significantly enhanced either root length, roots fresh and dry weights which sometimes surpassed or were equivalent to control treatment. Increasing seawater percent in irrigation water from 10 to 20% gradually decreased all roots parameters (*Figs. 6* and *7*).

Adding organic or bio stimulants significantly increased root length and root fresh and dry weights.

It was noticed that, humic or amino acids increased root indices followed by active dry yeast and control.

These results are in accordance with those reported by Abourayya et al. (2013) on *Manzanillo*, who observed an increase in root length due to the reduction in the uptake of salt caused by amino acid proline and potassium humate applications which is probably due to the role of humic acid that affects root processes and increases nutrient uptake.

The interaction between seawater and biostimulant substances showed that, 5 or 0 % seawater with humic acid recorded the highest values of root length, root fresh and dry weights followed by amino acids or active dry yeast with 5% seawater. Raising seawater percentage from 10 to 20% with humic acid, amino acid or active dry yeast decreased salinity effects on root length and root fresh and dry weights.

The lowest values were obtained when seawater was used at 20% without organic or bio stimulants while diluted seawater (20%) with humic acid, amino acids or active dry yeast increased root length and root fresh and dry weights. Diluted seawater (10 or 15%) with humic acid, amino acids or active dry yeast gave higher values of root fresh and dry weights than that resulted from diluted seawater (10 or 15%) without biostimulant. These results are in agreement with those of El-Mahrouk et al. (2008) on *Conocarpus erectus L.*

Flowering characters

The longest flowering duration (days) and the highest flowers number /plant resulted from plants irrigated with diluted seawater at 5 or 10% followed by 15% diluted

http://www.aloki.hu ● ISSN 1589 1623 (Print) ● ISSN 1785 0037 (Online)
DOI: http://dx.doi.org/10.15666/aeer/1804_57895802

seawater (*Figs. 8* and *9*). The shortest flowering duration and the least flower number /plant was obtained when diluted seawater at 20% was used. These results are in accordance with those of Abdel-Maksoud et al. (2014) on *Bellis perennis.*

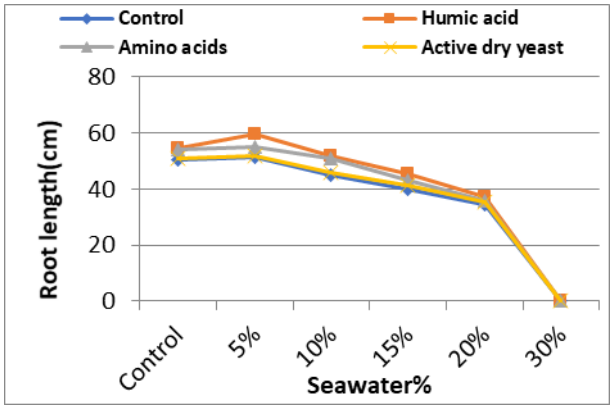

Figure 6. *Effect of diluted seawater and biostimulants and their interaction on root length of Ruellia brittoniana, L. during in the first and second seasons*

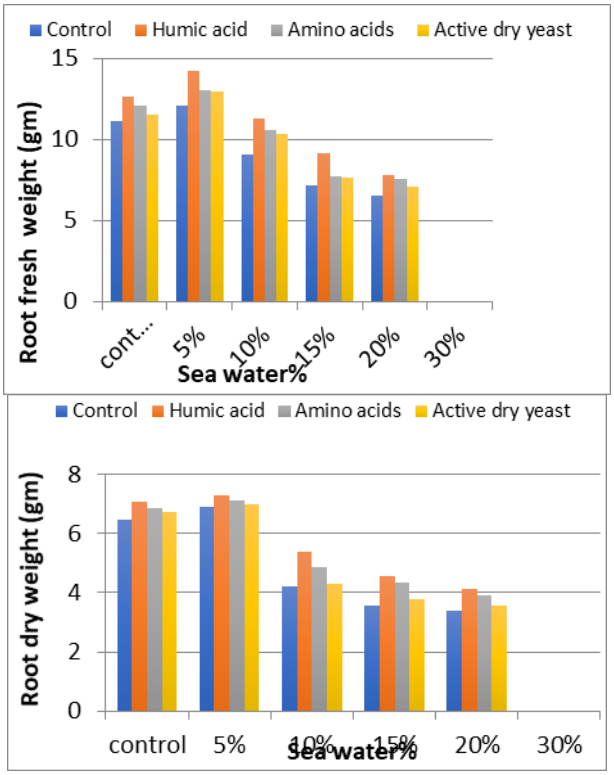

Figure 7. *Effect of diluted seawater and biostimulants and their interaction on roots fresh and dry weights of Ruellia brittoniana (mean of both seasons)*

As for organic materials, it was noticed that humic or amino acids application resulted in the significantly highest values of flowering duration and flower number/plant followed by active dry yeast compared to control (Hadi et al., 2011) on *Matricaria chamomillu,* L.

http://www.aloki.hu ● ISSN 1589 1623 (Print) ● ISSN 1785 0037 (Online)
DOI: http://dx.doi.org/10.15666/aeer/1804_57895802

The combination between diluted seawater irrigation and humic acid, amino acid or active dry yeast beside control resulted in the significantly longest flowering duration and highest flower number/plant compared to diluted seawater irrigation without organic or bio stimulants treatments (Srivastava et al., 2007) on *Gladiolus*.

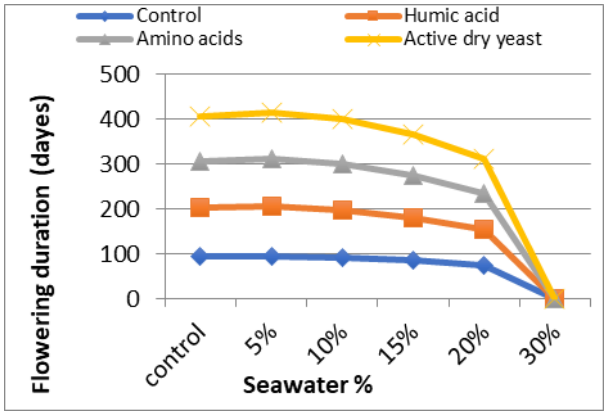

Figure 8. *Effect of diluted seawater and biostimulants and their interaction on flowering duration of Ruellia brittoniana (mean of both seasons)*

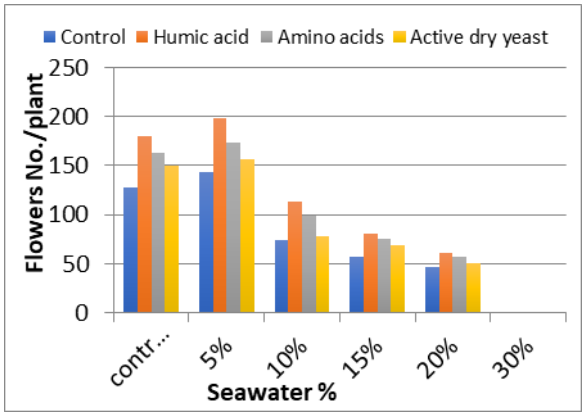

Figure 9. *Effect of diluted seawater and biostimulants and their interaction on the number of flowers/plant of Ruellia brittoniana (mean of both seasons)*

Biochemical composition

Data presented in *Table 3* cleared that using diluted seawater at 5% followed by fresh control significantly increased leaves total chlorophyll, but 20% diluted seawater significantly decreased it. Proline leaves content was significantly augmented with the increase in seawater percent in the irrigation water. Meanwhile, the deficient in leaves proline contents was observed with the lacking of seawater in the irrigation water.

Regarding organic materials, it was found that leaves total chlorophyll was significantly increased by using humic acid followed by amino acids and then active dry yeast compared to control. Amino acid and humic acid significantly increased leaves proline content followed by active dry yeast.

As for the combination between diluted seawater and organic or bio stimulants it was clear that, seawater at 5, 10% or fresh water with humic acid, amino acid or active dry

http://www.aloki.hu ● ISSN 1589 1623 (Print) ● ISSN 1785 0037 (Online)
DOI: http://dx.doi.org/10.15666/aeer/1804_57895802

yeast significantly increased leaves total chlorophyll contents. In contrast, proline content took an adverse trend as seawater at 20% only or combined with amino acid resulted the highest values of leaves proline content.

Table 3. *Effect of diluted sea water and organic or bio stimulants and their interaction on chlorophyll and proline constituents of Ruellia brittoniana (mean of both seasons)*

Seawater %	Chlorophyll (SPAD)					Proline (M.mole/100g fw.)				
	0.0	H.A	A.A	Y	Mean	0.0	H.A	A.A	Y	Mean
Control	44.55^{bcd}	49.32^{ab}	46.52^{abc}	45.22^{cde}	46.40^{b}	4.5^{f}	5.9 ^{f}	6.7^{c-f}	5.0^{f}	5.5^{d}
5%	45.29^{bcd}	50.30^{a}	49.28^{ab}	46.58^{abc}	47.86^{a}	5.2^{ef}	6.8 $^{c-f}$	7.5^{c-f}	5.8^{ef}	6.3^{cd}
10%	40.75^{d-g}	47.10^{ab}	43.13^{cde}	41.00^{d-g}	43.00^{c}	6.3^{def}	8.3^{b-f}	8.6^{b-f}	7.1^{c-f}	7.6^{bc}
15%	35.82^{hi}	42.50^{c-f}	39.58^{e-h}	36.82^{ghi}	38.68^{d}	8.7^{b-f}	10.9a^{-d}	11.5^{abc}	9.9^{a-e}	10.3^{b}
20%	32.84^{i}	37.69^{f-i}	35.87 ^{hi}	33.99^{i}	35.10^{e}	10.9^{a-d}	13.5^{a}	14.5^{a}	12.5^{abc}	12.9^{a}
30%	-	-	-	-	-	-	-	-	-	-
Mean	39.79^{c}	45.38^{a}	42.88^{b}	40.72^{bc}		7.1^{c}	9.1^{ab}	9.8^{a}	8.1^{b}	

H.A = humic acid, A.A = amino acid, Y = active dry yeast
Means of each factor designed by the same letters within a column or row are not significantly different at 5% level according to Duncan's multiple range test

Chemical composition

Nitrogen and magnesium

The percent of nitrogen and magnesium significantly declined as seawater percent in the irrigation water increased (*Table 4*).

Amino acids or humic acid followed by active dry yeast significantly increased both nitrogen and magnesium %. The least values of nitrogen and magnesium % resulted from control treatment.

As for the interaction between diluted seawater and organic or bio stimulants data presented in *Table 4* showed that, amino acids, humic acids or active dry yeast increased leaves N % and Mg %.

Table 4. *Effect of diluted sea water and organic or bi stimulants and their interaction on nitrogen and magnesium % of Ruellia brittoniana (Mean of both seasons)*

Seawater %	N%					Mg%				
	0.0	H.A	A.A	Y	Mean	0.0	H.A	A.A	Y	Mean
Control	2.59^{bcd}	2.82^{ab}	2.92^{a}	2.66^{bc}	2.75^{a}	0.62^{a}	0.66^{a}	0.68^{a}	0.63^{a}	0.65^{a}
5%	2.20^{ef}	2.36^{de}	2.45^{cde}	2.24 ^{e}	2.31^{b}	0.52^{b}	0.54^{b}	0.55^{b}	0.53b	0.54^{b}
10%	1.59^{hi}	1.80^{ghh}	1.97^{fg}	1.68^{h}	1.76^{c}	0.40 ^{cd}	0.42^{cd}	0.43^{c}	0.41^{cd}	0.42^{c}
15%	1.19^{jk}	1.31^{jk}	1. 36^{ij}	1.24 ^{jk}	1.28^{d}	0.35^{de}	0.37^{cd}	0.39^{cd}	0.36^{cde}	0.37^{d}
20%	1.07^{k}	1.28^{jk}	1.31^{jk}	1.19^{jk}	1.22^{e}	0.26^{f}	0.28f^{f}	0.30^{ef}	0.27^{f}	0.28^{e}
30%	-	-	-	-	-	-	-	-	-	-
Mean	1.73c	1.91^{b}	2.00^{a}	1.80^{bc}		0.43^{b}	0.45^{ab}	0.47^{a}	0.44^{b}	

H.A = humic acid, A.A = amino acid, Y = active dry yeast
Means of each factor designed by the same letters within a column or row are not significantly different at 5% level according to Duncan's multiple range test

http://www.aloki.hu ● ISSN 1589 1623 (Print) ● ISSN 1785 0037 (Online)
DOI: http://dx.doi.org/10.15666/aeer/1804_57895802

Diluted seawater at 20% combined with amino acids, humic acid or active dry yeast significantly increased leaves N % and Mg% while, 10 and 15% diluted seawater combined with amino acids, humic acid, active dry yeast gave intermediate values.

Sodium and chloride percentage

Diluted seawater at 20% progressively increased Na and Cl percent in the leaves whereas the percentages were gradually decreased when seawater increased in the irrigation water (*Table 5*). The lowest Na and Cl % in the leaves were obtained from control treatment.

Table 5. *Effect of diluted sea water and organic or biostimulants and their interaction on Na and Cl % of Ruellia brittoniana (mean of both seasons)*

Seawater %	Na%					Cl (mg/g D.W.)				
	0.0	H.A	A.A	Y	Mean	0.0	H.A	A.A	Y	Mean
Control	0.53^{e}	0.49^{e}	0.51^{e}	0.52^{e}	0.51^{e}	4.15^{h}	3.65^{h}	3.87^{h}	4.00^{h}	3.92^{e}
5%	1.01^{cd}	0.86^{de}	0.88^{de}	0.91^{de}	0.92^{d}	9.07^{f}	8.04^{g}	8.15^{g}	8.32^{g}	8.40^{d}
10%	1.43^{c}	1.21^{cd}	1.24^{cd}	1.32^{cd}	1.30^{c}	11.17^{e}	10.75^{e}	10.88^{e}	10.97^{e}	10.94^{c}
15%	2.53^{b}	2.11^{b}	2.20^{bc}	2.44^{b}	2.32^{b}	15.13^{d}	14.73^{d}	14.94^{d}	15.00^{d}	14.95^{b}
20%	3.82^{a}	3.41^{a}	3.71^{a}	3.75^{a}	3.67^{a}	20.42^{a}	18.74^{c}	19.07^{c}	19.80^{b}	19.51^{a}
30%	-	-	-	-	-	-	-	-	-	-
Mean	1.86^{a}	1.62^{c}	1.71^{b}	1.79^{ab}	---	11.99^{a}	11.18^{c}	11.38^{bc}	11.62^{b}	

H.A = humic acid, A.A = amino acid, Y = active dry yeast
Means of each factor noted by the same letters within a column or row are not significantly different at 5% level according to Duncan's multiple range test

Diluted seawater at 5 and 10 % combined with organic or bio stimulants decreased Na and Cl % in the leaves as compared to control treatment. These values gradually increased with increasing seawater percent. These results agree with those reported by Khaled Fawzy (2011) on *Nigella sativa* L.

Discussion

Effect of diluted seawater, humic acid, amino acids, active dry yeast on *Ruellia brittoniana*, L. was examined.

Vegetative growth

Diluted seawater of 30% was completely lethal for plants whereas 5% significantly improved all traits such as plant height, shoot fresh and dry weights. This may be due to that, salt stress inactivated proteins and enzymes as well as destroyed cell membrane structure and permeability by causing lipid oxidation (Winston, 1990). Also Parida and Das (2005) reported that, salt stress can affect plant survival, biomass and the capacity of plant to collect water and nutrient.

Organic or bio stimulants, humic and amino acids significantly augmented the survival%, plant height, leaf area, shoots fresh and dry weights followed by active dry yeast against the control treatments. This may be due to that, humic acid has a direct

http://www.aloki.hu ● ISSN 1589 1623 (Print) ● ISSN 1785 0037 (Online)
DOI: http://dx.doi.org/10.15666/aeer/1804_57895802

effect as a hormone like compound or indirect effect by increasing nutrient uptake through chelate, renewal effects and retaining membrane permeability of microorganisms, improving the physical condition of the soil and increasing shoot growth (Aliyeh et al., 2002).

Also, amino acids could directly or indirectly improve the physiological activities of the plant and regulate growth and development through their influence on the bio-synthesis of gibberllins (Walter and Nawacke, 1978) and may also play an important role in plant metabolism and protein assimilation which is necessary for cell formation (Sadak, 2015).

Active dry yeast contains cytokinines and vitamin B which increases the vegetative growth (Ezz El-Din and Hendawy, 2010).

The decrease in all parameters with increasing seawater percent from 10 to 20% combined with organic or bio stimulants may be attributed to that seawater stress has exerted the strongest effect in alleviating the harmful effect of seawater salinity (Abd el Kafie et al., 2010) on *Tuberose*.

Root growth

Salt stress may have a negative effect on roots growth. Kumar et al. (1988) observed a decrease in root length with the progressive increase in salt stress. Proline might counteract the negative effects of high salinity on carbohydrates and nitrogen metabolism which promote the whole plant growth (Lobartini et al., 1997).

Biochemical composition

The significant increase in leaves total chlorophyll by using humic acid followed by amino acids and then active dry yeast compared to control may be due to the role of humic acid in providing the plants with various nutrients necessary for synthesis of active constituents in the plant organs. This may be due to that application of NaCl significantly decreased chlorophyll contents in plant tissues (Oyetunji and Francis, 2004). These results are in accordance with those of (El sayed and Youssef, 2013) on *Jasminum sambac*. Likewise, spraying cotton plants with amino acid tended to increase proline in the leaves (Gebaly et al., 2013).

Chemical composition

Nitrogen and magnesium

High level of water salinity may reduce plant absorption of some important elements. The lowest N% and Mg% resulted from plants irrigated with 20% diluted seawater (Abdel-Fatah et al., 2008) on *Tifway* and (Caparros et al., 2017) on *Aloe vera*, *L.* Amino acids are the fundamental ingredients in the process of protein synthesis because of their nitrogen content (Kamar and Omar, 1987). Applying humic acid caused a limitation in the absorption of both Na and Cl elements (Khaled and Fawzy, 2011) on *Nigella sativa*, L.

Sodium and chloride percentage

Plants accumulate Cl ions in leaves which is more toxic in leaf tissues, plants make root production to remove excess ions and delay ion accumulation in tissues (Tozlu and Guy, 2000) on *Poncirus trifoliata* and (El-Mahrouk et al., 2008) on *Conocarpus erectus* L.

http://www.aloki.hu ● ISSN 1589 1623 (Print) ● ISSN 1785 0037 (Online)
DOI: http://dx.doi.org/10.15666/aeer/1804_57895802

Humic acid and amino acids significantly decreased Na and Cl % in the leaves followed by active dry yeast (Abdel- Fatah, 2008) on *Tifway* turf.

Conclusion

It is recommended to irrigate *Ruellia brittoniana* plants with 5% diluted seawater combined with organic or bio stimulants (humic acid 80% concentration 5 ml/L, amino acids 26.18% concentrated free amino acids 1 g/L or active dry yeast 5 g/L) as foliar spray on plant leaves fortnightly (20 spray/ season) to obtain the best growth and flowering characters.

REFERENCES

[1] A.O.A.C. (1970): Official Methods of Analysis. 10th Ed. – Association of Official Agriculture Chemists, Washington, DC.

[2] Abdel-Fatah, G. H., Boshra, A. E., Shahin, S. M. (2008): The role of humic acid in reducing the harmful effect of irrigation with saline water on Tifway turf. – J. Biol. Chem. Environ. Sci. 3(1): 75-89.

[3] Abourayya, M. S., Nabila, E. K., El-Sheikh, M. H. (2013): Effect of irrigation with saline water on fibrous root growth of Manzanillo and Picual olive cultivars. – Austral. J. of Basic and Appl. Sci. 7(1): 457-461.

[4] Ali, E. F., Hassan, F. A. S. (2013): Impact of foliar application of commercial amino acids nutrition on the growth and flowering of *Tagetes erecta*, L. plant. – J. of Appl. Sci. Res. 9(1): 652-657.

[5] Amer, S. S. A. (2004): Growth green pods yield and seeds yield of common bean (*Phaseolus vulgaris* L.) as affected by active dry yeast, salicylic acid and their interaction. – J. Agric. Sci., Mansoura Univ. 29(3): 1407-1422).

[6] Atiyeh, R. M., Lee, S., Edwards, C. A., Arancon, N. Q., Metzger, D. (2002): The influence of humic acids derived from earth worm-processed organic wastes on plant growth. – Bioresource Technol. 84: 7-14.

[7] Baters, L. S., Waldern, R. P., Teare, I. D. (1973): Rapid determination of free proline under water stress studies. – Plant and Soil 39: 205-207.

[8] Caparros, P. G., Lianderal, A., Lao, M. T. (2017): Effects of salinity on growth, water-use efficiency and nutrient leaching of three containerized ornamental. – Communication in Soil Sci. and Plant Analysis 48: 1221-1230.

[9] Carter, C. T., Grieve, C. M., Possmj, A., Suarez, D. L. (2005): Production and ion uptake of *Celosia argentea* with saline waste waters. – Sci. Hort. 106: 387-394.

[10] Chartzoulakis, K., Loupassaki, M., Ertaki, M., Androuakis, I. (2002): Effect of Nacl salinity on growth, ion content and Co_2 assimilation rate of six olive cultivars. – Sci. Hort. 96: 235-247.

[11] El-Mahrouk, M. E., El-Nady, M. F., Hegazi, M. A. (2008): Effect of diluted seawater irrigation and exogenous prolline treatments on growth, chemical composition of *Conocarpus erectus.* – J. Agric. Res. Kafrelsheikh Univ. 36(4): 420-446.

[12] El-Sayed, B. A., Youssef, H. M. A. (2013): Effect of some mutagenic and humic acid treatments on vegetative growth and chemical composition of *Jasinum sambac* Var. Double Plants. – J. Biol. Chem. Environ. Sci. 8(1): 1-14.

[13] Ezz El-Din, A. A., Hendawy, S. F. (2010): Effect of dry yeast and tea compost on growth and oil content of *Borago officinalis* plant. – Res. J. of Agric. and Biol. Sci. 6(4): 424-430.

http://www.aloki.hu ● ISSN 1589 1623 (Print) ● ISSN 1785 0037 (Online)
DOI: http://dx.doi.org/10.15666/aeer/1804_57895802

[14] Gebaly, S. F., Ahmed, M. M., Namich, A. A. M. (2013): Effect of spraying some organic, amino acids and potassium citrate on alleviation of drought stress in cotton plant. – J. Plant Production, Mansoura Univ. 4(9): 1369-1381.
[15] Gilman, E. F. (1999): *Ruellia brittoniana* (Mexican bluebell). – Environ. Hort. Dept., UF/Ifas Extention, Gainesville, FL.
[16] Glenn, E. P., Brown, J. J., O'leary, J. W. (1998): Irrigating crops with seawater. – Scientific Amer. 279: 56-61.
[17] Jackson, M. L. (1973): Soil Chemical Analysis. – Prentice-Hall of India Private Ltd. New Delhi.
[18] Kamar, M. E., Omar, A. (1987): Effect of nitrogenus levels and sprying with aminal-forte (amino acids salvation) on yield of cucumber and potatoes. – J. Agric. Sci. Mansoura Univ. 12(4): 900-907.
[19] Khaled, H., Fawzy, H. A. (2011): Effect of different levels of humic acids on the nutrient content, plant growth and soil properties under conditions of salinity. – Soil and Water Res. 6(1): 21-29.
[20] Kumar, A. B., Bahadur, B., Sharma, B. K. (1988): Effects of salinity on germination, seedling growth and some quantitative characters of *Cyamoposis tetragonoloba*, L. Taub. – New Botanist 15(1): 23-27.
[21] Lobartini, J. C., Oriole, G. A., Tan, K. H. (1997): Characterstics of soil humic acid fractions separated by ultrafilteration. – Commun. Soil Sci. Plant. 28: 787-796.
[22] Manoly, N. D., Nasr, A. A. (2008): Response of *Dahlia pinnata* plants to biofertilizer types. – Egypt. J. Exp. Biol. (Bot.) 4: 87-91.
[23] Mezanur Rahman, M. D., Mostofa, M. G., Abiar Rahman, M., Robyul Islam, M., Keya, S. S., Das, A. K., Giashuddin Miah, M. D., Robiul Kawser, A. Q. M., Ahsan, S. M., Hashem, A., Tabassum, B., Abd_Allah, E. F., Tran, L. P. (2019): Acetic cid: a cost-efective agent for mitigation of seawater-induced salt toxicity in mung bean. – Scientific Reports 9: 15186.
[24] Miyamoto, S., Glenn, E. P., Olsen, M. W. (1996): Growth, water use and salt uptake of four halophytes irrigated with highly saline water. – J Arid Environ. 32: 141-159.
[25] MSTAT Development Team (1989): Mstat User's Guide: A Microcomputer Program for the Design Management and Analysis Research Experiments. – Michigan State Univ. East Lansing, USA.
[26] Oyetunji, O. J., Francis, I. (2004): Effect of salt stress on growth, proline, glycine betaine and photosynthetic pigment concentrations on cowpea plant. – Nature and Science 2(12).
[27] Parida, A. K., Das, A. B. (2005): Salt tolerance and salinity effects on plants. A review. – Ecotoxicology and Environmental Safety 60(3): 324-349.
[28] Richard, S., Hamilton, C. W. (1997): Predicting invasions of woody plants introduced into North America. – Conservation Biology 11: 193-203.
[29] Sadak, M. S., Abdelhamid, M. T., Schmidhalter, U. (2015): Effect of foliar application of amino acids on plant yield and some physiological parameters in bean plants irrigated with seawater. – Acta Biol. Colomb. 20(1): 141-152.
[30] Sairam, R. K., Tyagi, A. (2004): Physiology and molecular biology of salinity stress tolerance in plants. – Curr. Sci. 86: 407-421.
[31] Singh, K. N., Chatrath, R. (2001): Salinity Tolerance. – In: Reynolds, M. P., Ortiz-Monasterio, J. I., Mcnab, A. (eds.) Application of Physiology in Wheat Breeding. CIMMYT, D. F. Mexico, pp. 1-110.
[32] Srivastava, R., Govil, M., Chow, K. K. (2007): Influence of biofertilizers on growth and flowering in Gladiolus cv. American Beauty. – Acta Hort. 742: 183-188.
[33] Tozlu, I. G. M., Guy, C. L. (2000): Effects of increasing NaCl concentration on stem elongation, dry mass production and macro and micro-nutrients accumulation in *Poncirus prifoliate*. – Aust. J. Plant Physiol. 27: 35-42.
[34] Walter, G. R., Nawacki, E. (1978): Alkaloid Biology and Metabolism in Plants. – Planum Press, New York.

http://www.aloki.hu ● ISSN 1589 1623 (Print) ● ISSN 1785 0037 (Online)
DOI: http://dx.doi.org/10.15666/aeer/1804_57895802

[35] Winston, G. W. (1990): Physicochemical Basis for Free Radical Formation in Cells: Production and Defenses. – In: Alscher R. G., Cumming J. R. (eds.) Stress Responses in Plants: Adaptation and Acclimation Mechanisms. Wiley-Liss Inc., New-York, pp. 57-86.
[36] Zadeh, I. Y., Mirzakhani, A. (2012): Study effect of thyme Oil., salicylic acid, *Aloe vera* gel and some chemical substances on increasing vase life of cut *Dianthus caryophyllus*. – Inter. J. Agron. Plant Production 3: 666-674.

http://www.aloki.hu ● ISSN 1589 1623 (Print) ● ISSN 1785 0037 (Online)
DOI: http://dx.doi.org/10.15666/aeer/1804_57895802

EFFECTS OF ORGANOHALOGENATED XENOBIOTICS ON GUT MICROBIOTA, OXIDATIVE REDOX, AND REPRODUCTIVE FUNCTIONS IN PIGS – A REVIEW

LARTEY, K. A.[1] – FAN, Y.[1] – NIE, F.-H.[2] – KANG, D.-J.[1] – LIN, H.-Y.[1] – NAMULA, Z.[1] – CHEN, Z.[1] – WANG, H.-C. R.[3] – GOONERATNE, R.[4] – CHEN, J.-J.[1*]

[1]*Department of Veterinary Medicine, College of Coastal Agricultural Sciences, Guangdong Ocean University, Zhanjiang, Guangdong 524088, China*

[2]*Department of Food Safety, College of Food Science and Technology, Guangdong Ocean University, Zhanjiang, Guangdong 524088, China*

[3]*Department of Biomedical and Diagnostic Sciences, The College of Veterinary Medicine, University of Tennessee, Knoxville TN 37996, USA*

[4]*Department of Wine, Food and Molecular Biosciences, Faculty of Agriculture and Life Sciences, Lincoln University, Lincoln 7647, New Zealand*

**Corresponding author*
e-mail: jjchen555@aliyun.com, chenjj@gdou.edu.cn

(Received 4th Feb 2020; accepted 22nd May 2020)

Abstract. Organohalogenated compounds contaminations in feed ingredients and feeds pose threats to the safety of food animals, and public health. Pigs are exposed through ingestions of feed contaminated with organohalogenated compounds. Microbes – organohalogens interactions in the gut cause changes in mean species diversities of bacteria, and induce gut dysbiosis. Along with metabolites from first–pass metabolisms, they affect proteins and molecular pathways that regulate ROS sensing, and induce oxidative stress. They also bind to estrogen receptors and mimic estrogen activities to impair reproductive endocrine functions. Nutritional interventions such as feed and feed ingredients substitutions, and harnessing non-conventional feed resources (NCFR) can offer sustainable alleviations. This will mitigate the risk of exposure to organohalogens whilst providing the needed nutrients to meet the animals' nutritional requirements. In addition, it will enhance the biological defense mechanisms in pigs. Phytonutrition can enhance biodegradation, and detoxification of recalcitrant organohalogenated xenobiotics. This provides a low cost, "green" strategy to alleviate adverse effects of organohalogenated xenobiotics in pigs. The low costs associated with makes this a viable remedy, especially for low income countries.
Keywords: *feed ingredients, phytonutrition, dysbiosis, metabolism, xenoestrogen*

Introduction

Pigs are the most widely consumed terrestrial food animals. Pig production is one of the fastest growing livestock enterprise. Pigs are efficient convertors of feeds to meats making pig production one of the most profitable livestock enterprise. Feeds and feed ingredients used in pig nutrition have been found to also contain xenobiotics such as organohalogens (Sapkota et al., 2007; Li et al., 2019). Organohalogenated compounds contaminations in feed ingredients and compound feeds pose threats to health, and performance of food animals, and meat safety and public health (Bernard et al., 2002; Barone et al., 2019; Das et al., 2019).

Organohalogens are ecotoxins produced as results of anthropogenic, biogenic, and geogenic activities (Xu et al., 2013). Persistence organic pollutants (POPs), pesticides,

http://www.aloki.hu ● ISSN 1589 1623 (Print) ● ISSN 1785 0037 (Online)
DOI: http://dx.doi.org/10.15666/aeer/1804_58035819

and pharmaceutical and personal care products (PPCPs) and dibutyl phthalate (DBPs) are produced from industrial, agricultural, and domestic activities (Bakhiyi et al., 2018). Polychlorinated biphenyls (PCBs) deposits in marine sediments gets transported (through microplastics) into oceans as micro pollutants (Gerdes et al., 2019). They get adsorbed by benthos, and biomagnify in adipose tissues of fish and other marine organisms at high trophic levels (Fernández-González et al., 2013; Jamieson et al., 2017; Li et al., 2019). Feed processing, and feed additives inclusions may also result in organohalogens contamination (Zijlstra and Beltranena, 2013). Environmental pollutions are the main sources organohalogenated compounds contaminations in food chains (Li et al., 2019). Oral route is the primary means of exposure in animals through the ingestion of organohalogenated compounds contaminated feeds (Sapkota et al., 2007; Li et al., 2019).

The tripartite linkage between livestock, humans, and the environment makes them prone to ecotoxins contaminations (Rabinowitz and Conti, 2013). In the setting of our time, organohalogenated xenobiotics have assume importance in food animal productions due to interdependence between livestock and the environment (Malisch, 2017). Humans and animals share health risk from environmental pollutions and zoonosis (Watanabe et al., 2010; Rabinowitz and Conti, 2013). There are increasing evidence of organohalogenated xenobiotics-induced degenerative diseases, and reproductive disorders in animals and humans (Barthold et al., 1999; Rabinowitz and Conti, 2013). Organohalogenated xenobiotic exposures in animals increase the risk of zoonosis (Barthold et al., 1999; Watanabe et al., 2010; Rabinowitz and Conti, 2013). Organohalogenated compounds have significant toxic effects even at low contaminations due to their ability to biomagnify, persist and bioaccumulate in food chains (El-Shahawi et al., 2010). Animal nutrition should therefore be critical component of comprehensive interdisciplinary preventive health strategies stipulated as in “One health” concept (Muthuvel et al., 2006). Nutritional interventions can modify the gut microbiome, and enhance the ability of (gut) bacteria to metabolize organohalogenated xenobiotics (Zhang et al., 2015b; Jin et al., 2017; Petriello et al., 2018). Utilizing plants bioactive compounds as immuno-nutritional supplement is an important nutritional intervention. The main therapeutic strategy is modulations of microbial compositions in the gut to enhance xenobiotics metabolisms (Petriello et al., 2014).

Homeostasis in the gut microbiota has been found to be critical in ensuring optimum immune, metabolic, and endocrine functions in pigs (Kim and Isaacson, 2015; Everaert et al., 2017; Patil et al., 2019). The gut serves as host to bacteria of different taxonomic diversities, referred to as microbiota (Mwaikono et al., 2018; Patil et al., 2019). The composition of bacteria taxa, and their metabolic functions defines the gut metagenome (Kim and Isaacson, 2015; Patil et al., 2019). First -pass (pre-systemic) metabolism of halogenated xenobiotics in the gut and liver produces toxic metabolites (Grimm et al., 2015). These metabolites are stored in hepatocytes, and endocrinocytes (Grimm et al., 2015).

Studies from our laboratory evaluated the adverse effects of PCBs extracted from the Zhanjiang marine offshore sediments on molecular pathways involved in gastrointestinal, metabolic, and development abnormalities in zebrafish (Liu et al., 2016; Nie et al., 2016; Yu et al., 2017). Mice have also been used as model animals to study the effect of organohalogenated xenobiotics on gut microbiota (Petriello et al., 2018; Chi et al., 2019). There is a homology in morphological, biochemical, and

http://www.aloki.hu ● ISSN 1589 1623 (Print) ● ISSN 1785 0037 (Online)
DOI: http://dx.doi.org/10.15666/aeer/1804_58035819

physiological characteristics between these model animals and some food animals (Hill et al., 2005; Chi et al., 2019). This review highlights potential effect of PCBs on underlying physiological mechanisms involved in gut health, cellular oxidative redox, and reproductive functions in pigs. Pigs are susceptible to PCB exposure, bioaccumulation, and biomagnification due to contaminations of their feeds, and bioaccumulations in their fatty tissues (Hoogenboom et al., 2004; Weber et al., 2018; Barone et al., 2019). The gut metagenome of pigs is important due to the influence on immune developments, and (reproductive) endocrine functions (Mach et al., 2015). It is also critical at post-weaning to prevent oxidative stress, a key pathophysiological disorder in pigs (Round and Mazmanian, 2009; Kim and Isaacson, 2015). Based on evidence from animal models and *in vitro* experiments, we discussed the potential effects of organohalogenated xenobiotics on gut abnormality, oxidative stress, and reproductive malfunctions in pigs. Nutritional, and husbandry interventions for "green", safe, and sustainable alleviations are also suggested in this review. This will also add to literature, as well as offer basis for future scientific research and interventions to alleviate the adverse effects of the organohalogenated compounds in pigs to enhance animal health, and public health.

Organohalogenated compounds pollutions

Organohalogenated compounds have acidic, alkaline, and thermal resistance (Xu et al., 2013). They were therefore used as coolants, and insulators in capacitors, flame-retardants, plasticizers, and a host of industrial materials (Xu et al., 2013; Bakhiyi et al., 2018). Organochlorines pesticides were used to control insect pests to improve public health, and agricultural productivities (Xu et al., 2013; Bakhiyi et al., 2018). In addition to these anthropogenic sources, geogenic events such as volcanos, and wildfires also produce polychlorinated dibenzop-dioxins and furans (PCDD/F), referred to as dioxins. Biogenic activities such as the biodegradation and biotransformation of some inorganic chemicals in biosolids also yield toxic organohalogens. Antibiotics such as fluoroquinolones, enrofloxacin, and florfenicol used for therapeutic, and subtherapeutic uses, also contain organohalogens (Fernández-González et al., 2013; Zijlstra and Beltranena, 2013).

Polychlorinated biphenyls (PCBs) largely refers to any class of organohalogenated compound prepared by a reaction of chlorine with biphenyl. Typical mixtures of PCBs contain over 100 compounds which are colorless, viscous liquids. PCBs are long-lived organic compounds, owing to their resistance to biological, photolytic, and chemical degradations (Xu et al., 2013). They are hydrophobic, and lipophilic, making them bioaccumulate, and biomagnify in fatty tissues. They have a long-range transportability making them widely present in almost every geographical location and environment, including areas they were not utilized (Bakhiyi et al., 2018). The Stockholm convention listed PCBs, and dioxins among the dirty dozen hazardous chemicals in the world (Xu et al., 2013). The chemical structure of PCB is shown in *Figure 1*.

Following the Stockholm convention in 2001, PCBs and dioxins production and utilizations have been banned, however secondary emissions from sinks, and stockpile in old gadgets continues to cause pollutions (Xu et al., 2013; Spongberg and Witter, 2007). Significant levels have been detected in marine offshore sediment in industrialized countries in the northern and middle latitude (Nie et al., 2016; Yu et al., 2017). It is worth mentioning that, over the years studies on persistent organic pollutants

http://www.aloki.hu ● ISSN 1589 1623 (Print) ● ISSN 1785 0037 (Online)
DOI: http://dx.doi.org/10.15666/aeer/1804_58035819

(POPS) have been largely focused on industrialized (and developed) regions in the northern and middle latitudes, where they were largely produced and utilized (Spongberg and Witter, 2007). However, evidence from tropical developing countries in the southern latitude have revealed significant POPs contaminations in sediments, and water bodies in these areas (Spongberg and Witter, 2007; Gioia et al., 2014). Electronic waste dumping and their improper recycling in these regions may largely account for this (Spongberg and Witter, 2007; Hogarh et al., 2012; Bakhiyi et al., 2018). PCBs concentrations have been found to be increasing in warm tropical regions in the southern latitude owing to the high water temperatures and rate of air/gas exchange (Fu and Wu, 2006; Spongberg and Witter, 2007). This may partly account for the presence of highly halogenated and toxic congeners in the tropical warms regions (Spongberg and Witter, 2007). The atmospheric total sum (∑190PCB) concentration in Agbogbloshie (in Ghana), an improper e-waste recycling hub in tropical Africa, was found to be as high as 4.64 ng/m^3 (Hogarh et al., 2012). Concentration in plumes in the area was about 11.10 ng/m^3 (Amoyaw-Osei et al., 2011). They may be carried as effluent into water bodies, and biomagnify through marine food web resulting in pollutions of marine-sourced feed resource (El-Shahawi et al., 2010).

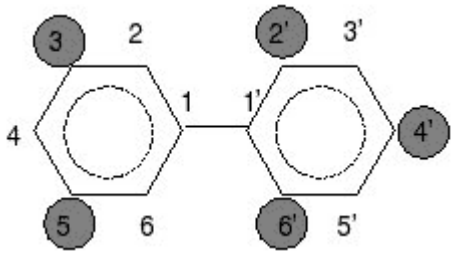

Figure 1. *Chemical structure of PCBs*

Effect of organohalogenated xenobiotics on the gut microbiota of pigs

Like most mammals, the pig's gut is the largest interface between their internal and external environments (Farhadi et al., 2003; Patil et al., 2019). It extends from the buccal cavity, passes through the intestines, and ends at the anal orifice. It contains the highest amount of bacteria of different taxonomies (Mach et al., 2015; Holmann et al., 2017). The term "gut metagenome usually includes the microbes and their metabolic interactions with the host (Patil et al., 2019). The gut bacterial ecology of pig is composed of 35% Firmicutes, 21% Bacteroidetes, 3% Proteobacteria and 2% Spirochetes (Kim and Isaacson, 2015; Patil et al., 2019). In the cecum and colon of pigs, firmicutes predominate at 75% or more, followed by proteobacteria at 13% (Kim and Isaacson, 2015; Patil et al., 2019). There is a mutually beneficial relationship between commensal bacteria and the host (Patil et al., 2019). The pigs' gut provide bacteria with nutrients, and energy for signal transductions (Kim and Isaacson, 2015). Short chain fatty acids (SCFAs) viz acetate, butyrate, and propionate are the ligands of guanine nucleotide-binding proteins (G-proteins), energy substrates for gluconeogenesis, and inhibitors of histone deacetylase (Layden et al., 2013). The probiotic (beneficial) bacteria such as *Bifidobacteria longum* and *Lactobacillus casei* biotransform primary bile acids (BA), produced in the liver, into secondary bile acids, to enable binding of the G-protein receptors to regulate intestinal barrier functions (Farhadi et al., 2003). This is important in resisting colonization of pathobionts, and preventing endotoxemia. The gut

http://www.aloki.hu ● ISSN 1589 1623 (Print) ● ISSN 1785 0037 (Online)
DOI: http://dx.doi.org/10.15666/aeer/1804_58035819

microbiota is sensitive to xenobiotics (Zhang et al., 2015b; Lefevera et al., 2016; Jin et al., 2017). The bacteria diversities exist in homeostatic state.

There are some similarities in the gut anatomy, physiologies, and biochemistry between pigs and laboratory animals such as mice, and zebrafish (Choi et al., 2010; Yu et al., 2017; Petriello et al., 2018). The observed effects of organohalogenated xenobiotics on their gut microbiota, and gut histology provide insights on the potential effects on gut abnormalities in pigs (Choi et al., 2010; Yu et al., 2017; Petriello et al., 2018). Ingested PCBs can therefore disrupt gut microbiota homeostasis, and reduce the mean species diversity as observed in mice (Choi et al., 2013; Petriello et al., 2018; Chi et al., 2019). Ingestion of 150 μmol/kg of 3 PCBs congenors (PCBs 153, 138, and 180) caused decreases in Proteobacteria species, and the overall abundance of bacteria in C57BL/6 mice (Petriello et al., 2018). They also caused a reduction in *Firmicutes* - *Bacteroidetes* ratio in the cecum (Jin et al., 2017; Petriello et al., 2018) likely due to a surge in the relative abundance of *Flavobacteria*, and *Clostridia* (Petriello et al., 2018). 2,3,7,8- tetrachlorodibenzofuran caused an increase in the level of *Flavobacteria* in the gut of mice (Zhang et al., 2015b). Similarly, oral administration of a dioxin, 2,3,7,8-tetrachlorodibenzo-p-dioxin at 24 μg/kg for 5 days caused an increase in the relative abundance of *Butyrivibrio* spp, and a decline in *Oscillibacter* spp level thereby resulting a decreased Firmicutes-Bacteroidetes ratio in cecal microbiota of mice (Zhang et al., 2015b). On the contrary, dioxin at a dose of 6 μg/kg biweekly for 26 weeks, increased Firmicutes/Bacteroidetes ratio, as results of increase in Lactobacillaceae and Desulfovibrionaceae levels and decrease in Prevotellaceae, without exacerbating streptozotocin-induced hyperglycemia in mice (Lefevera et al., 2016). It is therefore apparent that the degree of halogenation and toxicity have influence on the gut bacteria dynamics. Metabolic activities of gut bacteria are critical in biodegrading organohalogens xenobiotics, similar to soil bacteria degradations (Zhang et al., 2015a, b). Organohalide-respiring bacteria undergoes organohalide respiration to dehalogenate organohalogens (El-Shahawi et al., 2010; Zhang et al., 2015a, b; Jugder et al., 2016). The less toxic, less stable congeners further undergo aerobic and fermentative degradations to produce energy substrates such as carbon and phosphorous for the animal's biochemical and physiological processes (Zhang et al., 2015a, b). Genomes of Alistipes, Blautia, Eubacterium, Faecalibacterium, Roseburia and other core gut genera are reservoirs of (S)-2-haloacid dehalogenase genes (Shetty et al., 2017). They can chemically replace the halogen substitutes with hydrogen through a reduction reaction (Smidt and de Vos, 2004; Atashgahi et al., 2016, 2018). The reduction reaction biodegrades chemically stable (locked) organohalogens into less stable and less toxic congeners (Yim et al., 2008; Atashgahi et al., 2018). Clostridium spp (genus Desulfitobacterium) such as *C. perfringens* and *C. beijerinckii* may undergo metabolic reductive dehalogenation to dechlorinate hexachlorobiphenyl, and tetrachlorobiphenyl (toxic congeners) to pentachlorobiphenyl, and trichlorobiphenyl (Smidt and de Vos, 2004; Lefevera et al., 2006; Atashgahi et al., 2016; Jin et al., 2017). Mwaikono et al. (2018) characterized the fecal microbiota of dumpsite-scavenging pigs. Municipal dumpsites are potential sources of organohalogenated xenobiotics in the developing countries in Sub-Sahara Africa and other low-income countries (Watanabe et al., 2010). Using a high throughput Illumina MiSeq sequencing technology for 16S rRNA amplification, it was observed that the fecal microbiota of the scavenging pigs are characterized by the predominance of mobile genetic elements and pathogenic *Proteobacteria* (Watanabe et al., 2010). Increase in the relative abundance of the

http://www.aloki.hu ● ISSN 1589 1623 (Print) ● ISSN 1785 0037 (Online)
DOI: http://dx.doi.org/10.15666/aeer/1804_58035819

pathogenic phyla leads to disruption of gut microbiota homeostasis, changes in BA metabolism, and dysregulation of Farnesoid X receptor signaling pathways (Zhang et al., 2015b; Patil et al., 2019). This results in dysfunctional intestinal barriers, polydipsia and polyphagia, and liver toxicities (Lefevera et al., 2016; Petriello et al., 2018). Advances in the "omics" further support the corroboration that, a functional immune system is dependent on gut microbiome homeostasis (Round and Mazmanian, 2014; Lefevera et al., 2016; Chi et al., 2018). Suppression of antibodies production, and innate and adaptive immune responses have been linked to organohalogens-induced gut dysbiosis (Thomas and Hinsdill, 1978; Choi et al., 2010; Lefevera et al., 2016). Toll-like receptors (TLRs) are transmembrane glycoproteins involved in signal transduction to respond to active moiety of gram negative bacteria and endotoxins such as lipopolysaccharides (Round and Mazmanian, 2009; Lefevera et al., 2016). TLRs decrease in the jejunum and colon upon PCBs exposures in animals (Round and Mazmanian, 2009). Using Amarex-MT4 assay and turbidimetric immunoassay, Watanabe et al. (2010) suggested that the observed reduced plasma IgG and T4 levels in pigs scavenging on dumpsite was due to dioxin and related compounds pollutions in dumpsites. A metagenome analysis of fecal samples of pigs scavenging on dumpsites in Tanzania also showed expressions of functional pathways associated with biosynthesis of *Staphylococcus aureus* and other pathogenic infections of zoonotic potentials (Mwaikono et al., 2018). It is therefore apparent that, organohalogenated xenobiotic can cause gut dysbiosis, immunosuppression, and increase the risk of zoonotic diseases.

Effects of organohalogenated xenobiotics on oxidative stress

Gut dysbiosis from halogenated xenobiotics induce gut oxidative stress and systemic gut inflammations (Choi et al., 2010; Yu et al., 2017; Petriello et al., 2018). Gut oxidative phosphorylations, and cellular processes produce oxygen metabolites referred to as reactive oxygen species (ROS). These metabolites are by-products from partial reductions of oxygen (Ray et al., 2012; Buha et al., 2015). They include superoxide anion, hydroxyl radical, and hydrogen peroxide. At the oxidative interface, ROS may signal critical molecules for cell proliferation and survival (Ray et al., 2012). However, a disturbance in the oxidative redox causes oxidative imbalance, which induces oxidative stress (Ray et al., 2012; Buha et al., 2015).

Mechanism by which PCB ligands generates ROS is shown in *Figure 2*. Metabolism of organohalogenated xenobiotic produces four key hydroxylated metabolites viz polychlorobiphenylols (OH-PCBs), PCB-methylsulfones, PCB-catechols and PCB-epoxides (James, 2001; James et al., 2008). They are potentially toxic due to their potential effects on hepatic physiologies (Grimm et al., 2015). Incomplete degradation and slow rate of biotransformation of highly halogenated and toxic congeners leads to the storage of these toxic metabolites in the hepatocytes (Selvakumar et al., 2013; Grimm et al., 2015). This affects proteins, and molecular pathways that regulate ROS sensing and metabolic processes necessary to maintain oxidative redox (Liu et al., 2014; Grimm et al., 2015). They activate Cytochrome P450 1A1 (CYP1A1) to facilitate detoxification (Barouki and Morel, 2001). Upregulations of CYP1A1 genes however generate induce toxic metabolites (Barouki and Morel, 2001). These metabolites bind to aryl hydrocarbon receptor (AhR) to suppress AhR expressions in the hepatocytes (Barouki and Morel, 2001; Dietrich et al., 2016; Nie et al., 2016; Nielsena et al., 2017). Suppression of AhR expressions to attenuate CYP1A1-inducing cytochrome P450s,

http://www.aloki.hu ● ISSN 1589 1623 (Print) ● ISSN 1785 0037 (Online)
DOI: http://dx.doi.org/10.15666/aeer/1804_58035819

generates excess hydroxyl radicals thereby resulting in oxidative imbalance (Selvakumar et al., 2013; Liu et al., 2014; Dietrich et al., 2016; Nielsena et al., 2017). In addition, the toxic metabolites decrease the synthesis of hepatic glutathione (Muthuvel et al., 2006), and also suppress activities of antioxidant enzymes such as SOD, GPx (Liu et al., 2014). They further increases stimulation of the pro-oxidants such as Cu (Liu et al., 2014; Hong et al., 2015; Nielsena et al., 2017). Metabolites from first-pass metabolism of organohalogens can therefore reduce antioxidant capacity and induce oxidative imbalance therefore causing oxidative stress in pigs. Proliferations of proinflammatory cytokines such as tumor necrosis factor alpha (TNF-α) in the colon, ilea lesions, and intestinal inflammations have been observed in animal models upon exposure to PCBs and dioxins (Yu et al., 2017; Petriello et al., 2018). DL-PCBs caused a mild hydropic degeneration of epithelial cells in the intestine resulting in reduced intestinal folds in the gut of zebrafish larvae (Yu et al., 2017). Gut oxidative damage as result of PCBs exposure can damage, rupture or shed the intestinal villus in pigs (Choi et al., 2010; Brugman, 2016). Dioxin related compounds seem to have a potential to induce CYP1A1, and disrupt Peroxisome Proliferator-Activated Receptor (PPAR) signaling pathways in pigs (Watanabe et al., 2010; Liu et al., 2014). PPAR is critical for inflammatory response and hence disruption of the PPAR signaling pathway can cause inflammatory diseases in pigs. Oxidative stress in pigs has been identified as an underlying pathogenicity of several pathophysiological disorders such as inflammatory diseases, and heat stress in pigs (Lee et al., 2016).

Effect of PCBs on reproductive functions

The productivity, and profitability of pigs is largely as results of their high reproductive performance. Reproductive physiologies are regulated by folliculogenesis and steroidogenesis, which are driven by reproductive hormones (Pocar et al., 2011). Reproductive toxicants affect folliculogenesis and steroidogenesis, which impair reproductive functions at pre-, peri-, and post-natal stages (Pocar et al., 2011; Brevini et al., 2015).

Organohalogenated compounds share similar chemical properties with estrogens, and can bind to the estrogen receptors (Diamanti-Kandarakis et al., 2009; Nie et al., 2016; Sheng et al., 2019). They mimic estrogen activities, and this prevents estrogens from functioning properly (Brevini et al., 2015; Nie et al., 2016; Sheng et al., 2019). Findings from studies in our laboratory showed that, PCBs can induce EROD expression in zebrafish as results of Arh agonist mechanisms (Liu et al., 2016; Nie et al., 2016). Effects of the xenoestrogenic compounds on reproductive physiologies *in vivo*, and *in-vitro* provide insight into their potential adverse effects on reproductive functions in pigs (Miller et al*.,* 2004; Hill et al., 2005). Exposure to pigs can therefore induce adverse reproductive malfunctions, fetal malformation, and development toxicities (Miller et al., 2004; Pocar et al., 2011). PCB 28, PCB 105, and aroclor 1221 affected the activities of P450 arom, and inhibited modulation of Follicle Stimulating Hormone-induced aromatase activity *in vitro* (Woodhouse and Cooke, 2004). Very low concentrations (0.001-0.01 microg/ml) of Acroclor-1254 decreased oocyte maturation and development of bastocytes in an *in vitro* cumulus-oocytes complex (Campagna et al., 2008). OH-PCBs from plasma of sows treated with PCB, at 42 mg/l also induced embryotoxicities *in vitro* (Campagna et al., 2008). Blastomeres per expanded blastocyst were reduced at dose dependent manner (Campagna et al., 2008).

http://www.aloki.hu ● ISSN 1589 1623 (Print) ● ISSN 1785 0037 (Online)
DOI: http://dx.doi.org/10.15666/aeer/1804_58035819

Results from these studies therefore suggest that, organohalogenated xenobiotics can delay puberty, shorten estrous, induce abortions, and still birth, and reduce litter size in sows (Woodhouse and Cooke, 2004; Brevini et al., 2005; Campagna et al., 2008). Intergeneration toxicities lasting into F3 generations are possible (Pocar et al., 2011). Exposure to Aroclor 1221 at low-levels (0.01 – 0.1 µg/ml) during the teratogenic sensitive period induced dysregulation and complex adverse effects on the physiology, fertility, and fecundity, and sex ratio of F1 and F2 two offspring in Sprague-Dawley rats (Steinberg et al., 2008). Abnormalities in testes weight, sperm count, sperm viability, seminiferous tubule diameter (in males), and adrenocorticosteroid, estrus period, ovary weight, follicular atresia, and oocyte developmental (in female) were observed in offspring when dams were exposed to PCBs (Miller et al., 2004; Pocar et al., 2011). These could be due to impaired growth and development at the embryonic stage (Père and Etienne, 2000; Pocar et al., 2011). Cryptorchidism has been reported in F1 pigs upon maternal exposure to toxic 2,3,7,8-TCDD (most toxic dioxin congener) during the utero and lactation stages (Barthold et al., 1999). Comparing the concentrations of DRCs between dumpsite scavenging pigs and their neonates, Watanabe et al. (2010) detected higher concentrations of higher molecular weight congeners in piglets, DRCs seem to have higher bioaccumulation in breastmilk than in serum. The effect of organohalogenated compounds on reproductive and development toxicities is shown in *Figure 3*.

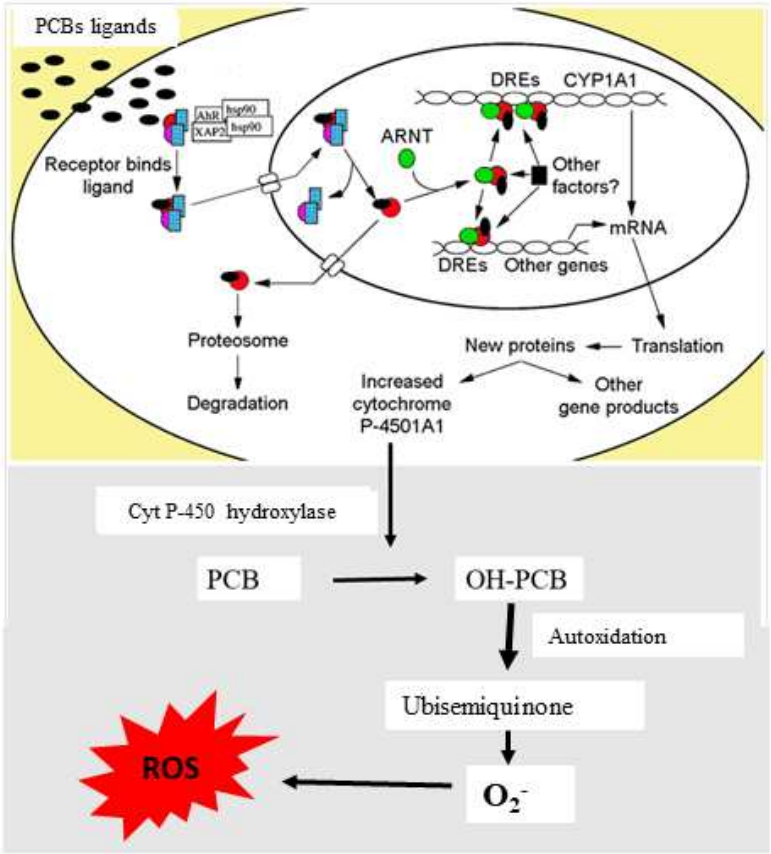

Figure 2. *ROS generation mechanism induced by organohalogenated xenobiotics. ARNT: aryl hydrocarbon receptor nuclear translocator; XAP2: aryl hydrocarbon receptor interacting protein; hsp: heat shock protein; DRE: dioxin response element*

http://www.aloki.hu ● ISSN 1589 1623 (Print) ● ISSN 1785 0037 (Online)
DOI: http://dx.doi.org/10.15666/aeer/1804_58035819

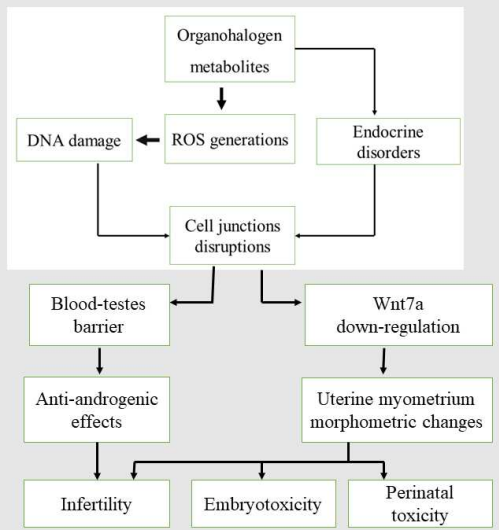

Figure 3. *Schematic diagram on reproductive malfunctions induce by organohalogenated xenobiotics*

Exposure of pigs to organohalogenated xenobiotics

Xenobiotics in animals refer to any synthetic or naturally occurring chemical substances present in the animal that are not naturally synthesized by the animal, and are hence considered foreign agents to the animal's body (Atashgahi et al., 2018). Oral intake is the commonest and primary means of exposure in farm animals (see *Fig. 4*). Inhalation from polluted air, and ocular, and dermal contacts may also occur. PCBs may be absorbed as micropollutants (ng/L - μg/L) or at higher range (μg/L -mg/L). It occurs as means of ingestion of organohalogenated contaminated feeds (Hoogenboom et al., 2004). Total equivalent quantity of DLPCBs (TEQ DL-PCBs) detected in feed samples from 16 feed ingredients was found to be 1.3 ng/kg (Fernández-González et al., 2013). This is slightly lower than the maximum level of 1.5 ng/kg TEQDL-PCBs for feeds as specified by the European Union as shown in *Table 1* (Fernández-González et al., 2013). TEQs PCDDs, PCDFs and Co-PCBs of pig feed samples in Japan was also found to be in a range of 0.13 to 0.32 pg g-1 lipid wt (Guruge et al., 2005). Animal fat (ANFA) feeds contain the highest total of PCBs (Weber et al., 2018), about 5 times higher than vegetable oil feeds (Fernández-González et al., 2013). This is largely due to the bioaccumulation of organohalogenated compounds in marine animal feed resources. Fish meals, fish oil, and shell powder have higher amounts of organohalogenated compounds compared to plant (vegetable) sources as shown in *Figure 5* (Hoogenboom, 2004). *Figure 5* shows PCB contaminations in sampled animal feeds, and feed ingredients.

Organohalogenated xenobiotics can also be transferred from lactating dams to suckling piglets at breastfeeding. The high levels of fat in piglets makes them susceptible to organohalogenated compounds bioaccumulation, and biomagnification. Biomagnification factors of 14, and 15 were observed for 2,3,7,8-TeCDF, and 1,2,3,7,8-PeCDD and 1,2,3,4,7,8- HxCDF respectively in fat of pigs (Traag et al., 2001). The biomagnification factor represents the ratio of lipid weight animal fat to mixed feed concentration. Exposure of pigs to organohalogens results in bioaccumulation in the back fat of pigs (Hoogenboom et al., 2004). Starter pigs exposed to a 10-fold contaminated feed from the recycled fat pollution (in Europe) resulted in 123 ng

http://www.aloki.hu ● ISSN 1589 1623 (Print) ● ISSN 1785 0037 (Online)
DOI: http://dx.doi.org/10.15666/aeer/1804_58035819

TEQ/kg PCBs in back fat (Hoogenboom et al., 2004). A survey on meats in France found PCBs levels in pig meats to be higher (41.8–77.7 ng g^{-1} live weight) than the EU maximum permissible levels (Barone et al., 2019). Therefore, incomplete metabolism of organohalogens xenobiotics can affect pig meat safety, in addition to the physiological and immune disorders.

Sustainable alleviation strategies

Dietary inclusion of fish meal, fish oils, and shell powder are necessary to meet pigs' demands for vitamins, digestible proteins, micronutrients, and essential fatty acids to ensure proper physiological, and immune developments in pigs (Kim and Easter, 2001; Fernández-González et al., 2013). Fish meal, and fish oil particularly contains eicosapentaenoic acid and docosahexaenoic acid, omega-3 long-chain polyunsaturated fatty acids (Kouba and Mourot, 2011; Hong et al., 2015; Saini and Keum, 2018). Animal feeds serve as a major linkage between animals and environment in the transfer of ecotoxins, through ingestion of contaminated feeds (Mizukawa et al., 2015). Safer animal nutrition and preventive health therefore needs to be important management strategies in alleviating effects of organohalogenated xenobiotics in pigs (Muthuvel et al., 2006; James et al., 2008; Zingsstag et al., 2011; Petriello et al., 2016). Improved animal husbandry and preventive animal health strategies aimed at mitigating animals' exposures to organohalogenated compounds, and enhancing their biology defenses have therefore become necessary (Muthuvel et al., 2006; James et al., 2008; Zinsstag et al., 2011; Dey et al., 2019).

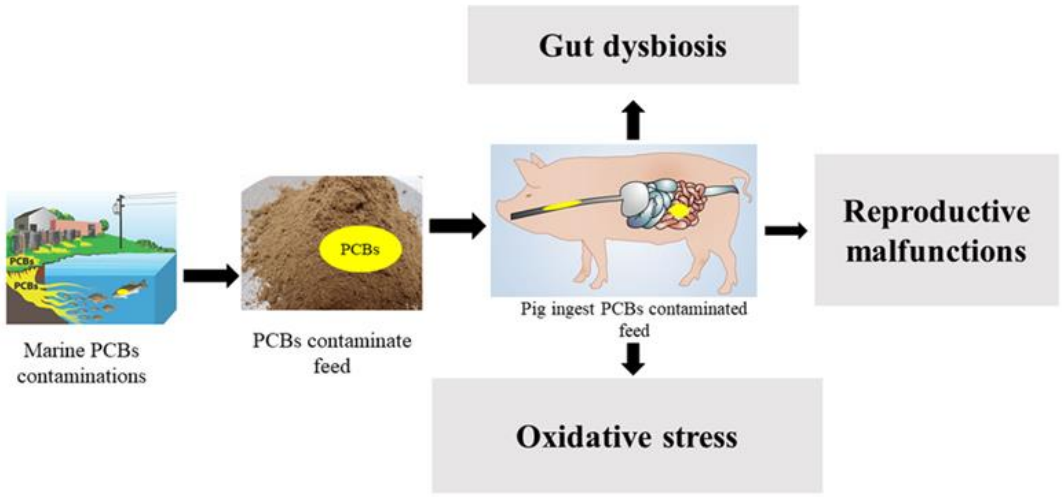

Figure 4. *Exposure of pigs to PCB contaminated fish meal*

Safety evaluation of animal feed and feed ingredients have gained important recognition in animal nutrition, and public health since feed and feed ingredient are critical components of the supply chains of (animal-derived) foods (Piskorska-Pliszczynska et al., 2019). Above the threshold levels in feeds, toxicants pose adverse effects in food animals. Ensuring that PCB levels in animal feeds are below the threshold levels is an important feed safety evaluation protocol. Maximum levels, and action levels of dioxins and DLPCBs in feed ingredients have been studied using GC-

http://www.aloki.hu ● ISSN 1589 1623 (Print) ● ISSN 1785 0037 (Online)
DOI: http://dx.doi.org/10.15666/aeer/1804_58035819

MS/MS based analytical tools. Action levels in feeds and feed ingredients are lower than the maximum values, and serve as a safer tool for early warning and detection of higher than desirable levels of PCBs in animal feed and feed ingredients (Malisch, 2017). At levels exceeding the maximum levels, feed ingredients and animal feed are prevented from entering the food chains in Europe. At levels closer or above the action level in feed (ingredients), investigations and tracing of contaminants are conducted to identify the sources of contaminations. The maximum levels and action levels of some common feed ingredient used for diets of pigs are shown in *Table 1*. This is based on the European Union maximum levels, and action thresholds of PCBs for feed ingredients laid down in Directive 2002/32/EC and amended by Commission Regulation (EU) 2019/1869 (Piskorska-Pliszczynska et al., 2019).

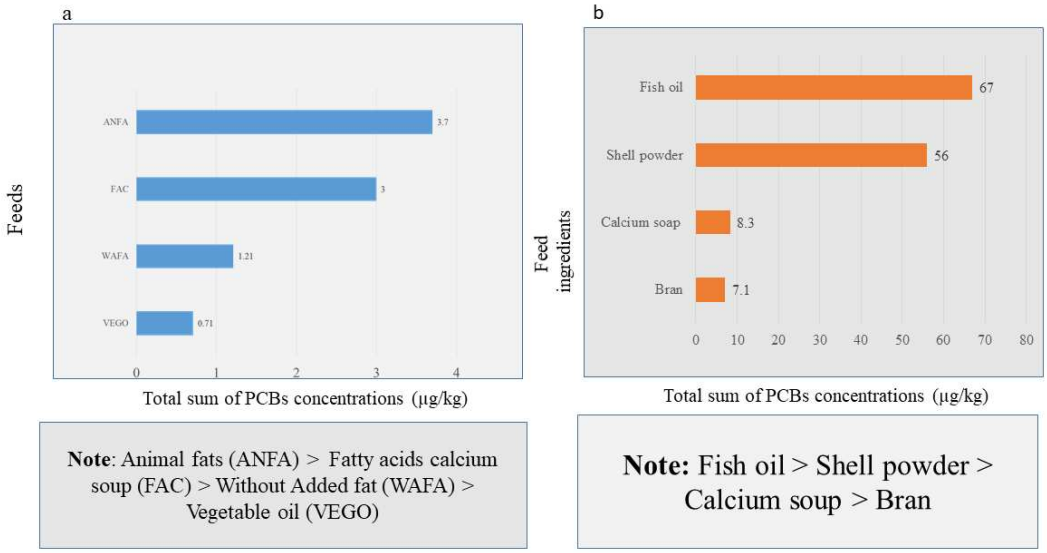

Figure 5. *Total sum of PCBs concentrations (Σ PCBs) is feeds (a) and feed ingredients (b) (Fernández-González et al., 2013)*

Table 1. *Maximum levels and action level of dioxin and DLPCBs in some feed ingredients (at moisture content of 12%)*

Feed and feed ingredients	Maximum levels		Action level	
	Dioxins (ng/kg)	$\Sigma_{Dioxin + DLPCBs}$ (ng/kg)	Dioxins (ng/kg)	Σ_{DLPCBs} (ng/kg)
Cereals	0.5	0.35	0.75	1.25
Soybean oils	0.5	0.5	0.75	1.5
Soybean meal	0.5	0.5	0.75	1.5
Calcium soaps	0.5	0.35	0.75	1
Egg shell meal	0.5	0.35	0.75	1.25
Fish oil	4	11	5	20
Fish meal	1.25	5	1.75	9
Oyster shell powder	1.25	2	1.75	4
Salts	0.5	0.5	1.75	1.5
Vitamin premix	0.5	0.35	1	1.5
Compound feed	0.5	0.5	0.75	1.5

http://www.aloki.hu ● ISSN 1589 1623 (Print) ● ISSN 1785 0037 (Online)
DOI: http://dx.doi.org/10.15666/aeer/1804_58035819

Manipulating dietary compositions to reduce the total PCB levels in feed can be an important safety protocol to mitigate exposures to pigs (Sapkota et al., 2007; Petriello et al., 2016). Substituting feed ingredients with high contaminations with less contaminated feed ingredients provides an important nutritional intervention to reduce organohalogenated compounds exposure in food animals. Replacing shell powder which are sourced from crustaceans, with egg shell powder sourced from poultry (land) can reduce organohalogenated compounds levels in animal feed since marine-origin feed bioresources have relative high contaminations (Sapkota et al., 2007; James et al., 2008; Fernández-González et al., 2013; Petriello et al., 2014; Li et al., 2019). Animal-derived feed ingredients can be replaced with plant-based ones. Replacing fishmeal, and fish oil with vegetable proteins, and vegetable oils can reduce the concentration of PCBs in animal feed. In addition, husbandry systems that expose food animals to the environment increase their exposure to ecotoxins (Piskorska-Pliszczynska et al., 2019). Unlike Europe and other developed countries where pig productions are characterized by specialized industrial production systems, productions in Sub-Sahara Africa and other low-income countries are a kind of traditional subsistence small-scale production characterized by outdoor management systems (Watanabe et al., 2010). This increases the risk of the food animal to organohalogenated compounds exposures due to the relative higher contact with the environment. Unlike confined pigs in intensive management systems, scavenging pigs in outdoor management systems burrow and wallow on dumpsites and sewerage sledges contaminated with PCBs (Mwaikono et al., 2018). Therefore, subsistence indoor pig management systems are necessary to mitigate exposure of the food animal to the environment and ecotoxins in low income countries. Simple housings systems using locally available materials have become necessary to mitigate exposures in pigs.

In addition, utilizing agro-food by-products such as groundnut cake and palm kernel cake, crop residues such as legume haulms and culled vegetables, and leaf meals from nutrient-rich herbal plants such as Alfalfa (*Medicago sativa*) and Siam weed (*Chromolaena odorata*) can also enhance feed safety. Such non-convectional feeds are safe, cheap, and environmental-friendly and hence suitable feed for pig nutrition in tropical low-income countries. Proximate analysis of such feeds have shown that they contain significant amount macro, micro-, and phyto-nutrients (Apori et al., 2000; Achilonu et al., 2018).

Phytonutrition can further enhance immunity, and biological defense systems of pigs against PCBs (Muthuvel et al., 2006; James et al., 2008; Gupta et al., 2014; Petriello et al., 2016; Dey et al., 2019). Extracts and powders from plants contain significant bioactive compounds (polyphenols), and are potential immuno-nutritional supplements against halogenated xenobiotics for sustainable pig productions (Petriello et al., 2014). They can stimulate eubiosis, xenobiotic metabolism, and steroidogenesis and folliculogenesis to enhance gut microbiota, oxidative redox, and reproductive functions in pigs (Gupta and Prakash, 2014; Dey et al., 2019). 3,3′-Di-indolylmethane, a glucosinolate from cruciferous vegetables (such as cabbage), stimulates hydroxylation, and detoxification through glucuronidation of UDP glucuronosyltransferase 1 family (UGT1A1) (James et al., 2008). An integration of such herbal feed additives, and leaf meals in pig nutrition can provide low cost, and efficient “green” technology to alleviate effects of organohalogenated xenobiotics in pigs (James et al., 2008; Gupta and Prakash, 2014; Petriello et al., 2014; Achilonu et al., 2018).

http://www.aloki.hu ● ISSN 1589 1623 (Print) ● ISSN 1785 0037 (Online)
DOI: http://dx.doi.org/10.15666/aeer/1804_58035819

Conclusion

PCBs and dioxins contaminations in feeds and feed ingredients expose pigs to organohalogenated xenobiotics. Pigs have a high magnification factor for organohalogenated xenobiotics. Enterohepatic circulations of organohalogenated xenobiotics induce gastrointestinal dysbiosis, and cellular oxidative stress. Metabolites of the endocrine disruptions compounds further induce reproductive and development abnormalities in pigs. Alleviating the adverse effects of organohalogenated xenobiotics in pigs requires nutritional interventions. Non-convectional feed resources can be harnessed to reduce pigs' exposure to organohalogenated xenobiotics whilst meeting their nutritional needs. Plants bioactive compounds also offer reliable immuno-nutritional supplements to enhance xenobiotics metabolisms, and immune-potentiation, and endocrine functions.

Acknowledgements. Supported by Marine Economy Development Project of Guangdong Province for High Quality Economic Development (GDOE2019A52).

REFERENCES

[1] Achilonu, M., Shale, K., Arthur, G., Naidoo, K., Mbatha, M. (2018): Phytochemical benefits of agroresidues as alternative nutritive dietary resource for pig and poultry farming. – Journal of Chemistry Article ID 1035071.

[2] Amoyaw-Osei, Y., Agyekum, O. O., Pwamang, J. A., Mueller, E., Fasko, R., Schluep, M. (2011): Ghana E-Waste Country Assessment. – SBC e-Waste Africa Project.

[3] Apori, S. O., Long, R. J., Castro, F. B., Ørskov, E. R. (2000): Chemical composition and nutritive value of leaves and stems of tropical weed *Chromolaena odorata*. – Grass and Forage Science 55: 77-81.

[4] Atashgahi, S., Lu, Y., Smidt, H. (2016): Overview of Known Organohalide-Respiring Bacteria - Phylogenetic Diversity and Environmental Distribution. – In: Adrian, L., Löffler, F. (eds.) Organohalide-Respiring Bacteria. Springer-Verlag, Berlin, pp. 63-105.

[5] Atashgahi, S., Liebensteiner, M. G., Janssen, D. B., Smidt, H., Stams, A. J. M., Sipkema D (2018): Microbial synthesis and transformation of inorganic and organic chlorine compounds. – Frontiers of Microbiology 9: 3079.

[6] Bakhiyi, B., Gravel, S., Ceballos, D., Flynn, M. A., Zayed, J. (2018): Has the question of e-waste opened a Pandora's box? An overview of unpredictable issues and challenges. – Environment International 110: 173-192.

[7] Barone, G., Storellia, A., Nicoletta, C., Quaglia, N. C., Dambrosio, A., Garofalo, R., Chiumarulo, R. M. M. (2019): Dioxin and PCB residues in meats from Italy: consumer dietary exposure. – Food and Chemical Toxicology 133: 110717.

[8] Barouki, R., Morel, Y. (2001): Repression of cytochrome P450 1A1 gene expression by oxidative stress: mechanisms and biological implications. – Biochemical Pharmacology 61: 511-516.

[9] Barthold, J. S., Kryger, J. V., Derusha, A. M., Duel, B. P., Jednak, R., Skafar, D. F. (1999): Effects of an environmental endocrine disruptor on fetal development, estrogen receptor (alpha) and epidermal growth factor receptor expression in the porcine male genital tract. – The Journal of Urology 162: 864-871.

[10] Bernard, A., Broeckaert, F., De Poorter, G., De Cock, A., Hermans, C., Saegerman, C., Houins, G. (2002): The Belgian PCB/dioxin incident: analysis of the food chain contamination and health risk evaluation. – Environmental Research 88: 1-18.

http://www.aloki.hu ● ISSN 1589 1623 (Print) ● ISSN 1785 0037 (Online)
DOI: http://dx.doi.org/10.15666/aeer/1804_58035819

[11] Brevini, T., Cillo, F., Antonini, S., Gandolfi, F. (2005): Effects of endocrine disrupters on the oocytes and embryos of farm animals. – Reproduction in Domestic Animals 40: 291-299.
[12] Brugman, S. (2016): The zebrafish as a model to study intestinal inflammation. – Developmental & Comparative Immunology 64: 82-92.
[13] Buha, A., Antonijević, B., Milovanović, V., Janković, S., Bulat, Z., Matović, V. (2015): Polychlorinated biphenyls as oxidative stress inducers in liver of sub acutely exposed rats: implication for dose-dependence toxicity and benchmark dose concept. – Environmental Research 136: 309-317.
[14] Campagna, C., Ayotte, P., Sirard, M., Bailey, J. (2008): An environmentally relevant mixture of organochlorines, their metabolites and effects on preimplantation development of porcine embryos. – Reproductive Toxicology 25: 361-366.
[15] Chi, Y., Lin, Y., Lu, Y., Huang, Q., Ye, G., Dong, S. (2018): Gut microbiota dysbiosis correlates with a low-dose PCB126-induced dyslipidemia and non-alcoholic fatty liver disease. – Science of the Total Environment 653: 274-282.
[16] Choi, Y. J., Seelbach, M. J., Pu, H., Eum, S. Y., Chen, L., Zhang, B., Hennig, B., Toborek, M. (2010): Polychlorinated Biphenyls disrupt intestinal integrity via NADPH Oxidase-induced alterations of tight junction protein expression. – Environmental Health Perspectives 118: 976-981.
[17] Das, A. K., Nanda, P. K., Das, A., Biswas, S. (2019): Hazards and safety issues of meat and meat products. – Food Safety and Human Health 6: 145-168.
[18] Dey, P. (2019): Gut microbiota in phytopharmacology: a comprehensive overview of concepts, reciprocal interactions, biotransformations and mode of actions. – Pharmacological Research 147: 104367.
[19] Diamanti-Kandarakis, E., Bourguignon, J. P., Giudice, L. C., Hauser, R., Prins, G. S., Soto, A. M., Zoeller, R. T., Gore, A. C. (2009): Endocrine-disrupting chemicals: an endocrine society scientific statement. – Endocrine Reviews 30: 293-342.
[20] El-Shahawi, M. S., Hamza, A., Bashammakh, A. S., Al-Saggafa, W. T. (2010): An overview on the accumulation, distribution, transformations, toxicity and analytical methods for the monitoring of persistent organic pollutants. – Talanta 80: 1587-1597.
[21] Everaert, N., Van Cruchten, S., Weström, B., Bailey, M., Van Ginneken., C., Thymann, T., Pieper, R. (2017): A review on early gut maturation and colonization in pigs, including biological and dietary factors affecting gut homeostasis. – Animal Feed Science and Technology 233: 89-103.
[22] Farhadi, A., Banan, A., Fields, J., Keshavarzian, A. (2003): Intestinal barrier: an interface between health and disease. – Journal of Gastroenterology and Hepatology 18: 479-497.
[23] Fernández-González, R., Yebra-Pimentel, I., Martínez-Carballo, E., Regueiro, J., Simal-Gándara, J (2013): Inputs of polychlorinated biphenyl residues in animal feeds. – Food Chemistry 140: 1-15.
[24] Gerdes, Z., Ogonowski, M., Nybom, I., Ek, C., Adolfsson-Erici, M., Barth, A., Gorokhova, E. (2019): Microplastic-mediated transport of PCBs? A depuration study with Daphnia magna. – PLoS ONE 14(2): e0205378.
[25] Gioia, R., Akindele, A. J., Adebusoye, S. A., Asante, K. A., Tanabe, S., Buekens, A., Sasco, A. J (2014): Polychlorinated biphenyls (PCBs) in Africa: a review of environmental levels. – Environmental Science and Pollution Research 21: 6278-6289.
[26] Grimm, F. A., Hu, D., Kania-Korwel, I., Lehmler, H. J., Ludewig, G., Hornbuckle, K. C., Duffel, M. W., Bergman, A., Robertson, L. W. (2015): Metabolism and metabolites of polychlorinated biphenyls (PCBs). – Critical Reviews in Toxicology 45: 245-272.
[27] Gupta, C., Prakash, D. (2014): Phytonutrients as therapeutic agents. – Journal of Complementary and Integrative Medicine 11: 151-169.
[28] Guruge, K. S., Seike, N., Yamanaka, N., Miyazakia, S. (2005): Polychlorinated dibenzo-p-dioxins, -dibenzofurans, and biphenyls in domestic animal food stuff and their fat. – Chemosphere 58: 883-889.

http://www.aloki.hu ● ISSN 1589 1623 (Print) ● ISSN 1785 0037 (Online)
DOI: http://dx.doi.org/10.15666/aeer/1804_58035819

[29] Hill, A. J., Teraoka, H., Heideman, W., Peterson, R. E. (2005): Zebrafish as a Model Vertebrate for Investigating Chemical Toxicity. – Toxicological Sciences 86: 6-19.
[30] Hogarh, J. N., Seike, N., Kobara, Y., Masunaga, S. (2012): Atmospheric polychlorinated naphthalenes in Ghana. – Environmental Science & Technology 46: 2600-2606.
[31] Holman, D. B., Brunelle, B. W., Trachsel, J., Allen, H. K. (2017): Meta-analysis to define a core microbiota in the swine gut. – *mSystems* 2: e00004-17.
[32] Hong, M. Y., Lumibao, J., Mistry, P., Saleh, R., Hoh, E. (2015): Fish oil contaminated with persistent organic pollutants reduces antioxidant capacity and induces oxidative stress without affecting its capacity to lower lipid concentrations and systemic inflammation in rats. – Journal of Nutrition 145: 939-944.
[33] Hoogenboom, A. P., Kan, C., Bovee, T. F. H., van der Weg, G., Onstenk, C., Traag, W. A. (2004): Residues of dioxins and PCBs in fat of growing pigs and broilers fed contaminated feed. – Chemosphere 57: 35-42.
[34] James, M. O. (2001): Polychlorinated Biphenyls: Metabolism and Metabolites. – In: Robertson, L. W., Hansen, L. G. (eds.) PCBs - Recent Advances in Environmental Toxicology and Health Effects. University of Kentucky Press, Lexington, pp. 35-46.
[35] James, M. O., Sacco, J. C., Faux, L. R. (2008): Effects of food natural products on the biotransformation of PCBs. – Environmental Toxicology and Pharmacology 25: 211-217.
[36] Jamieson, A. J., Malkocs, T., Piertney, S. B., Fujii, T., Zhang, Z. (2017): Bioaccumulation of persistent organic pollutants in the deepest ocean fauna. – Nature Ecology & Evolution 1: 0051.
[37] Jin, Y., Wu, S., Zeng, Z., Fu, Z. (2017): Effects of environmental pollutants on gut microbiota. – Environmental Pollution 222: 1-9.
[38] Jugder, B. E., Ertan, H., Susanne, Bohl, S., Lee, M., Marquis, C. P., Manefield, M. (2016): Organohalide respiring bacteria and reductive dehalogenases: key tools in organohalide bioremediation. – Frontiers in Microbiology,7: 249.
[39] Kim, H. B., Isaacson, R. E. (2015): The pig gut microbial diversity: understanding the pig gut microbial ecology through the next generation high throughput sequencing. – Veterinary Microbiology 177: 242-251.
[40] Kouba, M., Mourot, J. (2011): A review of nutritional effects on fat composition of animal products with special emphasis on n-3 polyunsaturated fatty acids. – Biochimie 93: 13-17.
[41] Layden, B. T., Angueira, A. R., Brodsky, M., Durai, V., Lowe, W. L. (2013): Short chain fatty acids and their receptors: new metabolic targets. – Translational Research 161: 131-140.
[42] Lee, I. K., Kye, C. Y., Kim, G., Kim, H. W., Gu, M. J., Umboh, J., Maaruf, K., Kim, S. W., Yun, C. H. (2016): Stress, nutrition, and intestinal immune responses in pigs — A Review. – Asian Australasian Journal of Animal Sciences 29: 1075-1082.
[43] Lefevera, D. E., Xu, J., Chen, Y., Huang, G., Tamas, N., Guo, T. L. (2016): TCDD modulation of gut microbiome correlated with liver and immune toxicity in streptozotocin (STZ)-induced hyperglycemic mice. – Toxicology and Applied Pharmacology 304: 48-58.
[44] Li, X., Dong, S., Wang, P., Xiao, O., Su, X., Fu, J. (2019): Polychlorinated biphenyls are still alarming persistent organic pollutants in marine-origin animal feed (fishmeal). – Chemosphere 233: 355-362.
[45] Liu, H., Nie, F., Lin, H., Ma, Y., Ju, X., Chen, J., Gooneratne, R. (2014): Developmental toxicity, EROD, and CYP1A mRNA expression in zebrafish embryos exposed to Dioxin-Like PCB126. – Environmental Toxicology 31: 295-303.
[46] Mach, N., Berri, M., Estellé, J., Levenez, F., Lemonnier, G., Denis, C., Leplat, J. J., Chevaleyre, C., Billon, Y., Doré, J., Rogel-Gaillard, C., Lepage, P. (2015): Early-life establishment of the swine gut microbiome and impact on host phenotype. – Environmental Microbiology Reports 7: 554-56.

http://www.aloki.hu ● ISSN 1589 1623 (Print) ● ISSN 1785 0037 (Online)
DOI: http://dx.doi.org/10.15666/aeer/1804_58035819

[47] Miller, K. P., Borgeest, C., Greenfeld, C., Tomic, D., Flaws, J. A. (2004): *In utero* effects of chemicals on reproductive tissues in females. – Toxicology and Applied Pharmacology 198: 111-131.
[48] Mizukawa, H., Nomiyama, K., Kunisue, T., Watanabe, M. X., Subramanian, A., Iwata, H., Ishizuka, M., Tanabe, S. (2015): Organohalogens and their hydroxylated metabolites in the blood of pigs from an open waste dumping site in south India: association with hepatic cytochrome P450. – Environmental Research 138: 255-263.
[49] Muthuvel, R., Venkataraman, P., Krishnamoorthy, G., Gunadharini, D. N., Kanagaraj, P., Stanley, A. J., Srinivasan, N., Balasubramanian, K., Aruldhas, M. M., Arunakaran, J. (2006): Antioxidant effect of ascorbic acid on PCB (Aroclor 1254) induced oxidative stress in hypothalamus of albino rats. – Clinica Chimica Acta 365: 297-303.
[50] Nie, F., Cai, J., Wang, X., Lin, H., Gooneratne, R., Hay, A., Ma, Y., Ju, X., Zheng, J., Chen, J. J (2016): EROD activity and CYP1A mRNA expression in zebrafish embryo exposed to marine sediment DLPCBs extract. – Asian Journal of Ecotoxicology 11: 364-368 (English abstract).
[51] Nielsena, S. D., Bauhausa, Y., Zamaratskaia, G., Junqueira, M. A., Blaabjerg, K., Petrat-Melin, B., Young, J. F., Rasmussen, M. K. (2017): Constitutive expression and activity of cytochrome P450 in conventional pigs. – Research in Veterinary Science 111: 75-80.
[52] Patil, Y., Gooneratne, R., Ju, X. H. (2019): Interactions between host and gut microbiota in domestic pigs: a review. – Gut Microbe 2019: 1-25.
[53] Père, M. C., Etienne, M. (2000): Uterine blood flow in sows: effects of pregnancy stage and litter size. – Reproduction Nutrition Development 40: 369-382.
[54] Petriello, M. C., Bradley, J., Newsome, B. J., Dziubla, T. D., Hilt, J. Z., Bhattacharyya, D., Hennig, B. (2014): Modulation of persistent organic pollutant toxicity through nutritional intervention: emerging opportunities in biomedicine and environmental remediation. – Science of the Total Environment 2014: 11-16.
[55] Petriello, M. C., Hoffman, J. B., Vsevolozhskaya, O., Morrisa, A. J., Hennigaf, B. (2018): Dioxin-like PCB 126 increases intestinal inflammation and disrupts gut microbiota and metabolic homeostasis. – Environmental Pollution 242: 1022-1032.
[56] Piskorska-Pliszczynska, J., Malagocki, P., Pajurek, M. (2019): Levels and trends of PCDD/Fs and DL-PCBs in Polish animal feeds, 2004-2017. – Food Additives & Contaminants Part A: 1-17.
[57] Pocar, P., Fiandanese, N., Secchi, C., Berrini, A., Fischer, B., Schmidt, J. S., Schaedlich, K., Rhind, S. M., Zhang, Z., Borromeo, V. (2011): Effects of Polychlorinated Biphenyls in CD-1 mice: reproductive toxicity and intergenerational transmission. – Toxicological Sciences 126: 213-226.
[58] Rabinowitz, P., Conti, L. (2013): Links among human health, animal health, and ecosystem health. – Annual Review of Public Health 34: 189-204.
[59] Ray, P. D., Huang, B. W., Tsuji, Y. (2012): Reactive oxygen species (ROS) homeostasis and redox regulation in cellular signaling. – Cell Signal 24: 981-990.
[60] Round, J. L., Mazmanian, S. K. (2009): The gut microbiota shapes intestinal immune responses during health and disease. – Nature Reviews Immunology 9: 313-323.
[61] Saini, R. K., Keum, Y. S. (2018): Omega-3 and omega-6 polyunsaturated fatty acids: dietary sources, metabolism, and significance—a review. – Life Sciences 203: 255-267.
[62] Sapkota, A. R., Lefferts, L. Y., McKenzie, S., Walker, P. (2007): What do we feed to food-production animals? A review of animal feed ingredients and their potential impacts on human health. – Environmental Health Perspectives 115: 663-670.
[63] Sheng, Z. S., Wang, C., Ren, F., Liu, Y., Zhu, B. (2019): Molecular mechanism of endocrine-disruptive effects induced by Bisphenol A: the role of transmembrane G-protein estrogen receptor 1 and integrin αvβ3. – Journal of Environmental Sciences 75: 1-13.

http://www.aloki.hu ● ISSN 1589 1623 (Print) ● ISSN 1785 0037 (Online)
DOI: http://dx.doi.org/10.15666/aeer/1804_58035819

[64] Shetty, S. A., Hugenholtz, F., Lahti, L., Smidt, H., de Vos, W. M. (2017): Intestinal microbiome landscaping: insight in community assemblage and implications for microbial modulation strategies. – FEMS Microbiology Review 41: 182-199.
[65] Smidt, H., de Vos, W. M. (2004): Anaerobic microbial dehalogenation. – Annual Review in Microbiology 58: 43-73.
[66] Spongberg, A. L., Witter, J. D. (2007): A review of PCB concentrations in tropical media, 1996-2007. – Revista de Biología Tropical 56: 1-9.
[67] Steinberg, R. M., Walker, D. M., Juenger, T. E., Woller, M. J., Gore, A. C. (2008): Effects of perinatal polychlorinated biphenyls on adult female rat reproduction: development, reproductive physiology, and second generational effects. – Biology of Reproduction 78: 1091-1101.
[68] Traag, V., Kan, K., Bovee, T., Weg, G. V. D., Onstenk, C., Portier L and Hoogenboom, R., Watanabe, M. X., Kunisue, T., Tao, L., Kannan, K., Subramanian, A., Tanabe, S., Iwata, H. (2010): Dioxin-like and perfluorinated compounds in pigs in an Indian open waste dumping site: toxicokinetics and effects on hepatic cytochrome P450 and blood plasma hormones. – Environmental Toxicology and Chemistry 29: 1551-1560.
[69] Weber, R., Herold, C., Hollert, H., Kamphues, J., Blepp, M., Ballschmiter, K. (2018): Reviewing the relevance of dioxin and PCB sources for food from animal origin and the need for their inventory, control and management. – Agricultural Sciences Europe 30: 42.
[70] Woodhouse, A. J., Cooke, G. M. (2004): Suppression of aromatase activity *in vitro* by PCBs 28 and 105 and Aroclor 1221. – Toxicology Letters 152: 91-100.
[71] Xu, W., Wang, X., Cai, Z. (2013): Analytical chemistry of the persistent organic pollutants identified in the Stockholm Convention: a review. – Analytica Chimica Acta 790: 1-13.
[72] Yim, Y. J., Seo, J., Kang, S. I., Ahn, J. H., Hur, H. G. (2008): Reductive dechlorination of methoxychlor and DDT by human intestinal bacterium *Eubacterium limosum* under anaerobic conditions. – Archives of Environmental Contamination and Toxicolology 54: 406-411.
[73] Yu, Y., Nie, F., Hay, A., Lin, H., Ma, Y., Ju, X., Gong, D., Chen, J. J., Gooneratne, R. (2017): Histopathological changes in zebrafish embryos exposed to DLPCBs extract from Zhanjiang coastal sediment. – Environmental Monitoring and Assessment 189: 289.
[74] Zhang, H. J., Jiang, X. J., Lu, L. P., Xiao, W. F. (2015a). Biodegradation of polychlorinated biphenyls (PCBs) by the novel identified *Cyanobacterium anabaena* PD-1. – PLoS One 10: e0131450.
[75] Zhang, L., Nichols, R. G., Correll, J., Murray, I. A., Tanaka, N., Smith, P. B., Hubbard, T. D., Sebastian, A., Albert, I., Hatzakis, E., Gonzalez, F. J., Perdew, G., Patterson, A. D. (2015b). Persistent Organic Pollutants modify gut microbiota–host metabolic homeostasis in mice through aryl hydrocarbon receptor activation. – Environmental Health Perspectives 123: 679-688.
[76] Zijlstra, R. T., Beltranena, E. (2013): Swine convert co-products from food and biofuel industries into animal protein for food. – Animal Frontiers 3: 48-53.
[77] Zinsstag, J., Schelling, E., Waltnertoews, D., Tanner, M. (2011): From 'one medicine' to 'one health' and systemic approaches to health and well-being. – Preventive Veterinary Medicine 101: 148-156.

http://www.aloki.hu ● ISSN 1589 1623 (Print) ● ISSN 1785 0037 (Online)
DOI: http://dx.doi.org/10.15666/aeer/1804_58035819

EFFECTS OF MANAGEMENT AND SUCCESSION PROCESS ON THE COMPOSITION OF VASCULAR HERBACEOUS PLANT SPECIES ALONG ROADSIDE AREAS IN POLAND

ŻOŁNIERCZUK, M.[1] – FORNAL-PIENIAK, B.[2*]

[1]*Garden Department, Museum of King Jan III's Palace at Wilanów, Al. Rzeczypospolitej 27A/48, 02-972 Warsaw, Poland*
ORCID: 0000-0002-6267-0929

[2]*Faculty of Horticulture and Biotechnology, Department of Environmental Protection and Dendrology, Warsaw University of Life Sciences – SGGW, Nowoursynowska 166, 02-787 Warszawa, Poland*
ORCID: 0000-0002-3834-1105

[*]*Corresponding author*
e-mail: beata_fornal_pieniak@sggw.edu.pl

(Received 21st Feb 2020; accepted 7th Jul 2020)

Abstract. Roadside areas are multifunctional elements of road surroundings (including their protective, socio-aesthetic and biocenotic functions). The purpose of the article was to determine the impact of management and succession process on the herbaceous species composition of expressways roadsides in Poland. The research was conducted on the roadsides of expressways (S7, S8) in the Mazowieckie voivodship and the S17 express road in the Lubelskie voivodship in Poland. Three roadside zones were identified during this study. 29 transects were distinguished, in each of them 4 phytosociological records were taken. It was done analysis of plant species composition in projects, floral analysis and plant cover, phytosociological analysis, synoptic table and DCA, life forms, effects of the different factors as roads age, slope of the slope^0, slope length on vegetation biodiversity. There were from four to five species of grass mixtures in roadside areas in the studied projects. Festuca rubra from 30% to 50% cover were dominating there. There were 116 species of vascular plants identified and they belong mostly to grasses communities such as Nardo-Callunetea (41%) and Molinio-Arrhenatheretea (31%). Mesohemerobes and perennial plants were dominating on roadside areas. Annual plants constitute 21% of the total while biennial plants as much as 5%. The age of road has got impact on decrease number of plants form the Poaceae family and when the slope length increases, the level of biodiversity of vegetation increases, too. On the basis of the analyzed cases, the mixtures used for sowing roadside slopes have a poor composition. This is an unfavorable situation that does not guarantee species stability. In order to preserve the spread of species composition, additional financial outlays and actions implementing the principles of sustainable development are necessary.
Keywords: *grasses, perennials, road surroundings, vegetation biodiversity*

Introduction

Roadside areas are elements of road surroundings and carry important functions, i.e. safety, socio-aesthetic, biocenotic, air quality and service quality (Coffin, 2007; Tong et al., 2015; Chen et al., 2019). In recent years, the expressway network in Poland has been under development. Back in 2001, there was only 401.5 km of this class of roads, in 2016 there were already 1533.9 km. By the beginning of 2018, 30% of the planned expressways had been built, which is a clear disproportion between 85% of motorways completed. This simple data analysis shows how much new space will appear in Poland in the coming years, which well need to be developed using plants. Most publications about vegetation of roadsides elaborate on, trees and shrubs (Hasan et al., 2016; McGrath and Henry, 2016; Perea et al., 2019). This is probably due to the fact that trees

http://www.aloki.hu ● ISSN 1589 1623 (Print) ● ISSN1785 0037 (Online)
DOI: http://dx.doi.org/10.15666/aeer/1804_58215839

and shrubs are most easily perceived and inventoried. Despite this, herbaceous vegetation is the largest contributor to roadside coverage. Its presence is appreciated by road users, who consider it proper to move trees and shrubs away from the edge of the road to create the so-called "belts forgiving drivers' mistakes" eng. forgiving roadside (Calvi, 2015). In Poland, even if trees often occur below them, only herbaceous vegetation is found. Thus, when analyzing the layout of the expressway, it should be stated that the herbaceous vegetation covers over 50% of the area of the road. Some authors, inter alia (Forman et al., 2003; Spooner and Smallbone, 2009; Kollarou and Kollaros, 2014) have observed that herbaceous roadside herbage is increasingly appreciated.

Currently, roadside slopes are mainly covered with grasses, which are one of the most resistant to road pollution plants (Koda et al., 2010). However, they do not always withstand other adverse habitat conditions (Niemandt and Greve, 2016). In Poland, this is related with, among others, the guidelines developed for establishing and maintaining roadside greenery for the needs of the General Directorate for National Roads and Motorways (GDDKiA) (Maranda et al., 2013) in which only two out the nine species listed are legumes that can be used to complete the mixture. It should be noted that there are studies indicating that the mixtures, e.g. Medicago lupulin, Lotus corniculatus (for various purposes) should be diversified (Koda et al., 2010). Unfortunately, this solution is rarely applied in Poland. The way of carrying out maintenance works on expressways in Poland has been presented, among others in the document "Guidelines for establishing and maintaining roadside greenery for the needs of the General Directorate for National Roads and Motorways" (Maranda et al., 2013). For safety reasons, 1-3 m wide strips closest to the road are cut more often (grass height should not exceed 10 cm). For further areas, mowing 2-3 times a year is used. The grass is usually cut at a height of 5 cm. Cut grass remains on the slopes. No other care treatments such as weeding or aeration are carried out. However, there are some problems related to the GDDKiA guidelines. System changes are currently being made to allow for less frequent mowing, which results, among others, from climate change - until now contractors have been obliged to carry out the number of mowing, as a result of which work was carried out even after snowfall or in hot weather, which resulted in drying out of low vegetation. Sowing is also being slowly implemented using seed mixtures for flower meadows. Polish producers have already developed a special blend composition that allows smog reduction (so-called "anti-smog seed mix"), appreciated at the international Smogathon competition.

Expressway roadsides were chosen for research because of the technical solutions and the volume of transport routes which affect the level of arduousness of road transport on the environment (Trombulak and Frissell, 2000; Pezeshki et al., 2018; Al-Taani et al., 2019) and thus on the vegetation (Trombulak and Frissell, 2000; Truscott et al., 2005; Babcock and McLaughlin, 2011).

The purpose of the article was to determine the impact of management and succession process on the species composition of herbaceous on expressway roadsides.

Research hypothesis: The species composition of herbaceous vegetation depends on management and succession process on roadsides.

Study area

The research was conducted on the roadsides of expressways (S7, S8) in the Mazowieckie voivodship and the S17 express road in the Lubelskie voivodship in

http://www.aloki.hu ● ISSN 1589 1623 (Print) ● ISSN1785 0037 (Online)
DOI: http://dx.doi.org/10.15666/aeer/1804_58215839

Poland (*Figure 1*). There are two-, five- and six-year-old expressways in this area. In order to determine the research areas, the following criteria were applied: location outside of a large city, area with potential deciduous forest habitat, neighboring agricultural area (an analysis carried out at a distance of 250 m from the road, with 50 m buffer off from buildings and noise barriers). All roadsides were sown artificially to the ground. Regardless of the location and exhibition of the escarpment, a sowing standard of 25g / m^2 was used, which is in line with the rules set by most grass mix producers available in Poland. Sowing was carried out on a 10 cm thick layer of humus. The soil is sandy with thin leyer o humus along roadside.

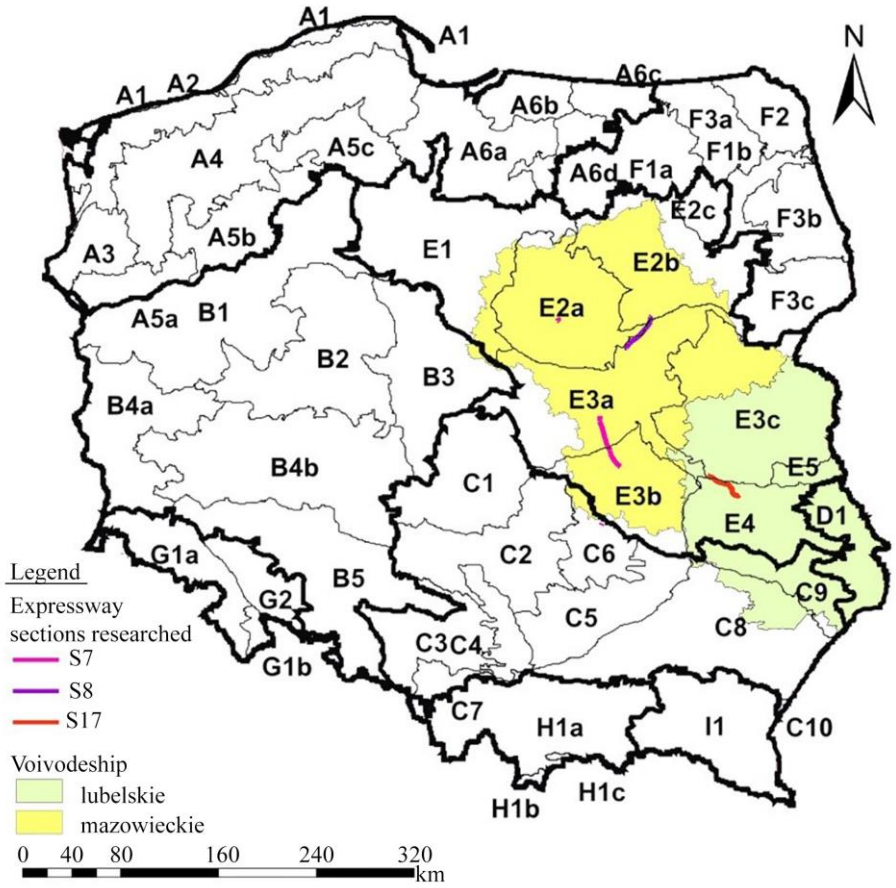

Figure 1. *Research areas against the background of voivodships, as well as divisions, lands and sub-regions in the division of Poland's geobotanical regionalization (own study based on Matuszkiewicz (1993)*

The expressways have got the roadside areas, which do not include a gravel shoulder, which could no to be overgrown by vegetation. The rest areas were diversified by plants, some parts were intensively moved, the others less moved (*Figure 2*) The slope of the slopes is wide and ranges from 1° to 50°. The lowest slope values are found on the flat surfaces behind the drainage ditch. High slope values (over 40°) occurred mainly on slopes located near road viaducts. The average slope inclination was about 32°. The greatest lengths are reached by the counter-slopes located behind the drainage ditch (length about 20 m). The average length of the slopes is about 6 m.

http://www.aloki.hu ● ISSN 1589 1623 (Print) ● ISSN1785 0037 (Online)
DOI: http://dx.doi.org/10.15666/aeer/1804_58215839

Figure 2. *View on the roadside areas (photos: M. Żołnierczuk)*

Methods and statistical approach

Research areas were designated using ArcGIS 10.5.1. At this stage, the design documentation of individual road sections was also analyzed. The composition of mixtures for sowing roadside areas available on the Polish market was carried out. Field studies were carried out and. the exact date of the survey was from 01.06. to 29.09 during the years 2016-2019.

Four roadside zones were identified during this study. 29 transects were distinguished, in each of them 4 phytosociological records were taken (one phytosociological record in each of the roadside zones). Coordnitates of research study plots (phytosociological records) were presented in *Table 1*. It was done 116 phytosociological records (one record was on 25 m^2 were taken by Dzwonko (2007)). All plants were counted on studied plot (phytosociological records).

During the research, the focus was on the roadside area, which does not include a gravel shoulder (A), which could no to be overgrown by vegetation - that's why this area (zone) was not analyzed. The research area (one transect) was divided into 3 zones, the division of which resulted from observations during pilot studies:

Zone I - a belt about 1-3 m wide, intensively mowed, for safety reasons (the vegetation must not obstruct road markings, so-called "bollards").

Zone II - the width of the third lane varies greatly and depends on the total length of the slope. It is a belt less often mowed with a uniform plant cover. Because of wider this zone, two phytosociological records were taken in this zone: the middle of the escarpment and the bottom of the escarpment at the drainage ditch.

Zone III – is located next to the drainage ditch (*Figure 3*).

http://www.aloki.hu ● ISSN 1589 1623 (Print) ● ISSN1785 0037 (Online)
DOI: http://dx.doi.org/10.15666/aeer/1804_58215839

Table 1. *Coordnitates of research study plots (Geographic Coordinate System: GCS_ETRS_1989)*

Number of plots	Location	X*	Y*
1.	top of the escarpment	21.130507	52.245953
2.	middle of the escarpment	21.130521	52.245942
3.	down of the escarpment	21.130536	52.245929
4.	counterscarp	21.130546	52.245921
5.	top of the escarpment	21.131884	52.251111
6.	middle of the escarpment	21.131930	52.251104
7.	down of the escarpment	21.131964	52.251099
8.	counterscarp	21.131998	52.251092
9.	top of the escarpment	21.133623	52.254509
10.	middle of the escarpment	21.133602	52.254512
11.	down of the escarpment	21.133577	52.254515
12.	counterscarp	21.133557	52.254517
13.	top of the escarpment	21.173512	52.273265
14.	middle of the escarpment	21.173508	52.273269
15.	down of the escarpment	21.173506	52.273271
16.	counterscarp	21.173501	52.273274
17.	top of the escarpment	21.135550	52.260838
18.	middle of the escarpment	21.135539	52.260847
19.	down of the escarpment	21.135523	52.260863
20.	counterscarp	21.135514	52.260879
21.	top of the escarpment	20.230601	52.374519
22.	middle of the escarpment	20.230581	52.374512
23.	down of the escarpment	20.230561	52.374503
24.	counterscarp	20.230515	52.374488
25.	top of the escarpment	20.232107	52.364804
26.	middle of the escarpment	20.232122	52.364807
27.	down of the escarpment	20.232139	52.364809
28.	counterscarp	20.232154	52.364812
29.	top of the escarpment	21.194791	52.282403
30.	middle of the escarpment	21.194804	52.282385
31.	down of the escarpment	21.194814	52.282368
32.	counterscarp	21.194827	52.282355
33.	top of the escarpment	21.204706	52.285571
34.	middle of the escarpment	21.204734	52.285553
35.	down of the escarpment	21.204755	52.285543
36.	counterscarp	21.204777	52.285534
37.	top of the escarpment	21.243987	52.311755
38.	middle of the escarpment	21.244004	52.311746
39.	down of the escarpment	21.244020	52.311738
40.	counterscarp	21.244036	52.311731
41.	top of the escarpment	21.254634	52.320233
42.	middle of the escarpment	21.254646	52.320228
43.	down of the escarpment	21.254658	52.320221
44.	counterscarp	21.254672	52.320211
45.	top of the escarpment	21.274219	52.332497
46.	middle of the escarpment	21.274244	52.332466
47.	down of the escarpment	21.274270	52.332442
48.	counterscarp	21.274297	52.332405

http://www.aloki.hu ● ISSN 1589 1623 (Print) ● ISSN1785 0037 (Online)
DOI: http://dx.doi.org/10.15666/aeer/1804_58215839

Number of plots	Location	X*	Y*
49.	top of the escarpment	21.274140	52.332554
50.	middle of the escarpment	21.274108	52.332573
51.	down of the escarpment	21.274063	52.332610
52.	counterscarp	21.274028	52.332647
53	top of the escarpment	22.132280	51.234303
54	middle of the escarpment	22.132280	51.234299
55	down of the escarpment	22.132280	51.234274
56	counterscarp	22.132281	51.234246
57	top of the escarpment	22.140240	51.233195
58	middle of the escarpment	22.140240	51.233181
59	down of the escarpment	22.140240	51.233175
60	counterscarp	22.140239	51.233167
61	top of the escarpment	22.152160	51.231525
62	middle of the escarpment	22.152160	51.231515
63	down of the escarpment	22.152159	51.231503
64	counterscarp	22.152160	51.231487
65	top of the escarpment	22.161559	51.230380
66	middle of the escarpment	22.161560	51.230374
67	down of the escarpment	22.161560	51.230369
68	counterscarp	22.161561	51.230360
69	top of the escarpment	22.210000	51.220622
70	middle of the escarpment	22.205997	51.220618
71	down of the escarpment	22.205994	51.220614
72	counterscarp	22.205991	51.220610
73	top of the escarpment	22.231346	51.193209
74	middle of the escarpment	22.231333	51.193210
75	down of the escarpment	22.231322	51.193210
76	counterscarp	22.231312	51.193211
77	top of the escarpment	22.232060	51.200227
78	middle of the escarpment	22.232051	51.200228
79	down of the escarpment	22.232044	51.200228
80	counterscarp	22.232038	51.200228
81	top of the escarpment	22.232027	51.201148
82	middle of the escarpment	22.232034	51.201150
83	down of the escarpment	22.232044	51.201152
84	counterscarp	22.232052	51.201154
85	top of the escarpment	22.212506	51.215109
86	middle of the escarpment	22.212520	51.215114
87	down of the escarpment	22.212534	51.215118
88	counterscarp	22.212550	51.215124
89	top of the escarpment	22.193357	51.223460
90	middle of the escarpment	22.193360	51.223482
91	down of the escarpment	22.193360	51.223491
92	counterscarp	22.193360	51.223501
93	top of the escarpment	22.140960	51.233188
94	middle of the escarpment	22.140968	51.233194
95	down of the escarpment	22.140978	51.233200
96	counterscarp	22.140986	51.233207
97	top of the escarpment	22.100455	51.252644
98	middle of the escarpment	22.100473	51.252652

http://www.aloki.hu ● ISSN 1589 1623 (Print) ● ISSN1785 0037 (Online)
DOI: http://dx.doi.org/10.15666/aeer/1804_58215839

Number of plots	Location	X*	Y*
99	down of the escarpment	22.100487	51.252661
100	counterscarp	22.100502	51.252666
101	top of the escarpment	22.075522	51.260096
102	middle of the escarpment	22.075523	51.260098
103	down of the escarpment	22.075525	51.260101
104	counterscarp	22.075526	51.260103
105	top of the escarpment	22.085278	51.254959
106	middle of the escarpment	22.085280	51.254961
107	down of the escarpment	22.085283	51.254964
108	counterscarp	22.085285	51.254966
109	top of the escarpment	22.090353	51.254770
110	middle of the escarpment	22.090360	51.254775
111	down of the escarpment	22.090368	51.254783
112	counterscarp	22.090374	51.254786
113	top of the escarpment	22.084187	51.255277
114	middle of the escarpment	22.084196	51.255284
115	down of the escarpment	22.084205	51.255291
116	counterscarp	22.084212	51.255295

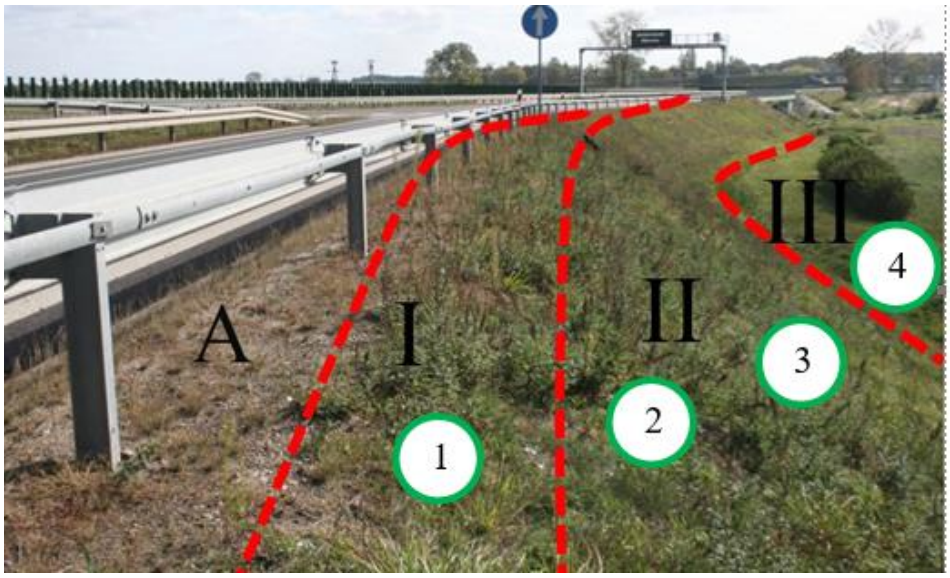

Figure 3. *Schemate of study transect: A- area (zone) not analyzed I, II, III – zones, 1, 2, 3, 4 – phytosociological records (own research)*

For the determination of plants, the key was used to identify vascular plants of lowland Poland (Rutkowski, 2004), species names were adopted after Mirek et al. (2002) and plant communities were conducted according to Matuszkiewicz (2012).

By using the 10 degree hemeroby scale (from ahemerob (natural) to metahemerobic (community completely destroyed)) there were measure a departure from naturalness. For this purpose, data from the scientific database BiolFlor were used. The Juice 5.0 program was used to determine the Shannon index (Shannon and Weaver 1963). A synoptic table was created using the TWINSPAN method - in this way, types of

http://www.aloki.hu ● ISSN 1589 1623 (Print) ● ISSN1785 0037 (Online)
DOI: http://dx.doi.org/10.15666/aeer/1804_58215839

communities have been specified, characterized by different species composition. Then DCA multifactorial analyzes were performed in the Canoco 5 program - it was used to illustrate the relationship between occurring species and the age of the road. The last stages of the study are the discussion and the conclusions.

Results

Analysis of plant species composition in projects

There were from four to five species of grass mixtures in roadside areas in the studied projects. Festuca rubra from 30% to 50% cover were dominating there. Roadside sections with a majority of Festuca ovina up to 50% and Lolium perenne up to 40% were also noticed. For sowing, it was recommended to use the species indicated by the General Directorate for National Roads and Motorways. None of the designed mixtures included an extra share of other plants, e.g. papilionaceous plants. The situation is an example illustrating the state of mixtures used for sowing roadsides in Poland. Based on the carried out analyzes, it was found that mixtures containing from 3 to 7 species are available on the Polish market, with 40% being mixtures containing 4 plant species. The key species in the mixtures are the above-mentioned Festuca rubra, Festuca ovina, Lolium perenne. The Shannon biodiversity index of the analyzed mixtures ranged from 0.64 to 1.75. It should be noted that on the market there are also several mixtures of flower meadows intended for roadside areas, whose biodiversity index ranged from 2.40 to 3.8. These types of mixtures in roadside areas are applied only sporadically.

Floral analysis and plant cover

There were 116 species of vascular plants identified. The majority (91 species) were native species, whose share in the coverage of roadside slopes was 96.78% on average. The identified species belonged to 29 families, of which the Asteraceae (28 species) and the Poaceae (20 species) clearly stood out in terms of the number of species. Additionally, a relatively high share of the Fabaceae family (9 species) was recorded. The prevalence of the families mentioned above is also visible in the analysis of the degree of coverage but in this case the Poaceae family dominates (81%), Asteraceae amounts only to approximately 7%, and the Fabaceae share exceeds just over 1% (*Table 2*).

The share of other individual families was negligible and did not exceed 1% on average. Among the species from the Poaceae family, Agrostis gigantea and Agrostis capillaris clearly stood out with an average share of 26.69% and 26.32%, respectively. A high average share was also noted in the case of Lolium perenne – 16.33%, Festuca rubra – 8.23%, and Elymus repens – 5.23%. The individual share of other species from Poaceae did not exceed 4%. The average share of individual species from Asteraceae did not exceed 1.5%. The most numerous were Artemisia vulgaris (1.41%) and Achillea millefolium (1.36%). As many as 5 species are invasive species of Conyza canadensis, Erigeron annuus, Galinsoga parviflora, Solidago canadensis, Solidago gigantea, whose overall average share is 1.18%. The plant cover was about 95% - this situation was similar in the case of all roadsides, with the lowest average value occurring on the five-year-old and six-year-old roadsides where it amounted to 92% (The whole recognized plant species in each phytosociological record are in Excel file).

http://www.aloki.hu ● ISSN 1589 1623 (Print) ● ISSN1785 0037 (Online)
DOI: http://dx.doi.org/10.15666/aeer/1804_58215839

Table 2a, b, c. *The average share of plant species from dominated families as Poaceae, Asteraceae, Fabaceaa on roadsides*

a,				
Poaceae	**Age of roadsides**			
Specie names	**2**	**5**	**6**	**16**
Agrostis capillaris	51.24%	10.00%	0.00%	0.00%
Agrostis gigantea	37.84%	27.45%	19.00%	42.14%
Agrostis stolonifera	49.00%	0.00%	0.00%	55.00%
Arrhenatherum elatius	10.00%	1.00%	0.00%	0.00%
Calamagrostis epigejos	0.00%	6.00%	0.00%	0.00%
Dactylis glomerata	0.00%	12.00%	7.50%	0.00%
Deschampsia caespitosa	0.00%	12.50%	0.00%	0.00%
Digitaria ischaemum	0.00%	0.00%	0.00%	2.00%
Elymus repens	15.80%	0.088	19.45%	19.00%
Festuca arundinacea	0.00%	10.00%	30.00%	0.00%
Festuca ovina	0.00%	5.00%	0.00%	0.00%
Festuca pratensis	0.00%	20.00%	0.00%	0.00%
Festuca rubra	0.00%	35.83%	41.67%	30.00%
Holcus lanatus	14.90%	0.00%	0.00%	0.00%
Lolium perenne	16.33%	11.88%	18.00%	5.00%
Phalaris arundinacea	0.00%	30.00%	15.00%	0.00%
Poa angustifolia	75.00%	22.79%	0.00%	15.00%
Poa trivialis	10.00%	0.00%	0.00%	0.00%
Setaria glauca	5.00%	2.40%	0.00%	0.00%
Setaria viridis	0.00%	9.50%	7.00%	5.00%
b,				
Asteraceae	**Age of roadsides**			
Specie name	**2**	**5**	**6**	**16**
Achillea millefolium	1.46%	3.59%	3.33%	8.29%
Artemisia campestris	1.00%	2.71%	0%	0.00%
Artemisia vulgaris	1.42%	5.63%	3.33%	5.00%
Bellis perennis	0.00%	1.00%	0.00%	0.00%
Carduus crispus	0.00%	1.00%	3.00%	0.00%
Centaurea jacea	0.00%	1.00%	0.00%	0.00%
Centaurea rhenana	0.00%	2.00%	0.00%	0.00%
Cichorium intybus	1.50%	3.00%	2.00%	5.00%
Cirsium arvense	1.25%	5.00%	3.00%	5.00%
Cirsium vulgare	0.00%	1.20%	0.00%	0.00%
Conyza canadensis	1.00%	2.00%	11.00%	5.00%
Erigeron annuus	1.00%	0.00%	0.00%	0.00%
Galinsoga parviflora	0.00%	4.00%	0.00%	0.00%
Helichrysum arenarium	0.00%	1.00%	0.00%	0.00%
Hieracium pilosella	0.00%	0.00%	1.50%	0.00%
Hieracium spilophaeum	0.00%	0.00%	0.00%	0.00%
Leontodon autumnalis	1.00%	0.00%	0.00%	0.00%
Matricaria chamomilla	0.00%	1.40%	2.00%	0.00%
Matriciara maritima	1.50%	1.50%	0.00%	3.00%
Senecio viscosus	0.00%	2.00%	5.00%	0.00%
Senecio vulgaris	0.00%	2.00%	0.00%	0.00%
Solidago canadensis	1.80%	3.50%	1.00%	0.00%
Solidago gigantea	1.00%	10.00%	0.00%	5.00%

http://www.aloki.hu ● ISSN 1589 1623 (Print) ● ISSN1785 0037 (Online)
DOI: http://dx.doi.org/10.15666/aeer/1804_58215839

Sonchus arvensis	2.25%	1.80%	0.00%	4.50%
Sonchus oleraceus	1.00%	1.00%	0.00%	4.00%
Tanacetum vulgare	0.00%	5.36%	2.00%	0.00%
Taraxacum officinale	2.00%	2.40%	0.00%	0.00%
Tussilago farfara	0.00%	0.00%	0.00%	10.00%
c,				
Fabaceaa	**Age of roadsides**			
Specie names	**2**	**5**	**6**	**16**
Lathyrus pratensis	0.00%	0.00%	1.00%	0.00%
Lotus corniculatus	0.00%	1.50%	0.00%	0.00%
Medicago falcata	0.00%	2.25%	2.00%	0.00%
Medicago lupulina	0.00%	4.00%	0.00%	0.00%
Vicia cracca	1.20%	5.71%	1.67%	4.00%
Vicia hirsuta	1.50%	0.00%	2.00%	0.00%
Vicia sativa	0.00%	0.00%	6.00%	0.00%
Vicia sepium	0.00%	0.00%	3.00%	0.00%
Vicia villosa	0.00%	2.40%	0.00%	0.00%

Phytosociological analysis

Plant species belong to grasses communities such as Nardo-Callunetea (41%) and Molinio-Arrhenatheretea (31%). It was determined that 9% are accompanying species, 8% belong to grasslands, 6% are forest species, 3% of species belong to lagg, and 2% are species belonging to rushes (*Table 3*). Their distribution in land cover, however, varies depending on individual years of use. On young roadside (2 years after putting the road into service) there is a dominance of species characteristic of grasslands (47% of the area) and pastures (44% of the area). It is directly related to the selection of species of seed mixtures for sowing. Five to six years after the start of use, the share of species characteristic of pastures increases significantly (from 60% to 74%). The share of ruderal species reaching 25% and accompanying species (16%) is on the increase as well. Along 16-year-old roads, the communities stabilize further - the share of species characteristic of pastures increases (67%), the share of ruderal and associated species drops down to 18% and 14%.

Table 3. *Share of characteristic plant species (%) in different vegetation types*

Vegetation types	Share of characteristic species in %
Ruderal	41
Pasture	31
Accompanying species	9
Grasslands	8
Plantings	6
Lagg	3
Rushes	2

Synoptic table and DCA

The changes taking place in the species composition are also noticeable in the synoptic table taking into account their fidelity and frequency. TWINSPAN method and 6 groups (from A to F) were distinguished. Group C (49 phytosociological records) and

http://www.aloki.hu ● ISSN 1589 1623 (Print) ● ISSN1785 0037 (Online)
DOI: http://dx.doi.org/10.15666/aeer/1804_58215839

D (47 phytosociological records) clearly stand out. In the case of phytosociological records taken along the S17 express road in the Lubelskie voivodeship, a relatively high level of homogeneity of the groups can be seen (species from group C dominate). An exemplary arrangement of groups in transects is presented in *Table 4*. Some plant species with high fidelity and frequency in the groups A –F were distinguished: group A: Artemisia campestris, Cirsium arvense, Deschampsia caespitosa, Elymus repens, Rumex thyrsiflorus, group B: Artemisia campestris, Equisetum arvense, Festuca arundinacea, Poa angustifolia, group C: Agrostis capillaris, Agrostis gigantea Achillea millefolium, Plantago lanceolata, group E: Agrostis gigantea, Daucus carota, group F: Cardamine pratensis, Carduus crispus, Festuca rubra, Hieracium pilosella, Vicia sativa (*Figure 4*).

Table 4. *Exemplary arrangement of groups in transects (own study)*

		Voivodship							
		Lubelskie Voivodeship	Masovian Voivodship						
Age of roadsides		2		5		6		16	
Location on slope	Peak of slopes	C	A	B	D	D	D	D	D
	Middle of the slopes	C	C	D	B	D	F	D	D
	Area near the drainage dich	C	C	D	B	F	D	D	D
	Counterslope	C	C	E	E	D	D	E	D

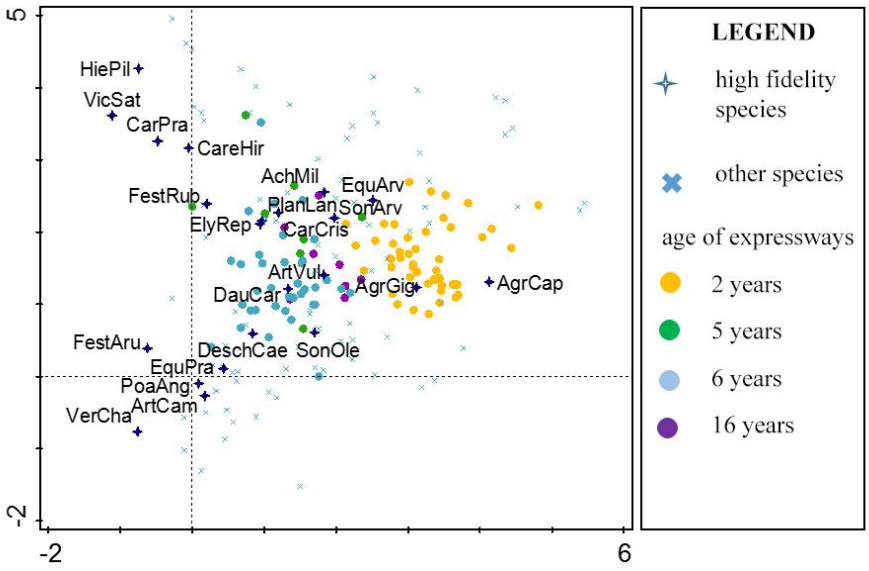

Figure 4. *Multivariate DCA analysis - relationship between species composition and road age (own research)*

Mesohemerobes plants were dominating, accounting for 25% of all plant species in general. Together with intermediate species between mesohemerobia and b-euhemerobia they constitute 47% of all species. The share of the remaining hemerobia groups was similar to each other ranging from 8% to 14%. Considering the degree of

http://www.aloki.hu ● ISSN 1589 1623 (Print) ● ISSN1785 0037 (Online)
DOI: http://dx.doi.org/10.15666/aeer/1804_58215839

coverage, grades 2 and 3 (87%) dominate in the case of young roadside. On the roadsides aged 5-6 years, a-euhemerob (up to 35%) dominates. After 16 years of use, stabilization and growth of grade 2 and 3 species of hemerobia occur (49%) (*Figure 5*).

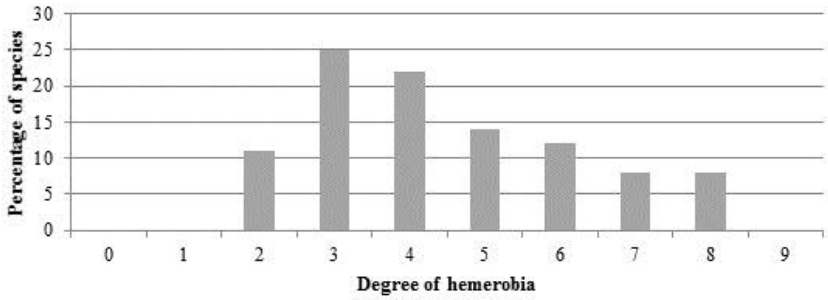

Figure 5. *Distribution of species share relative to the degree of hemerobia: 0 - ahemerob, 1 – oligohemerob (negligible human impact), 2 - intermediate form of 1 i 3, 3 - mezohemerob (moderate human impact), 4 - intermediate form of 3 i 5, 5 – b-euhemerob (strong human influence), 6*

Life forms

Perennial species are dominating (74% of the total number of species) on the studied areas. Annual plants constitute 21% of the total while biennial plants as much as 5%. When examining the degree of coverage by individual species, the dominance of perennial species is clearly visible, which on 93% of roadsides occupy 93%, five-year-old about 75%, and 16-year-old - 88%. Areas with incomplete short-circuits obtain the highest biodiversity indicators - unoccupied spots are inhabited by annual species. In places where the short circuit is greater, the value of the Shannon index decreases (r = -0,46636) (*Figure 6*).

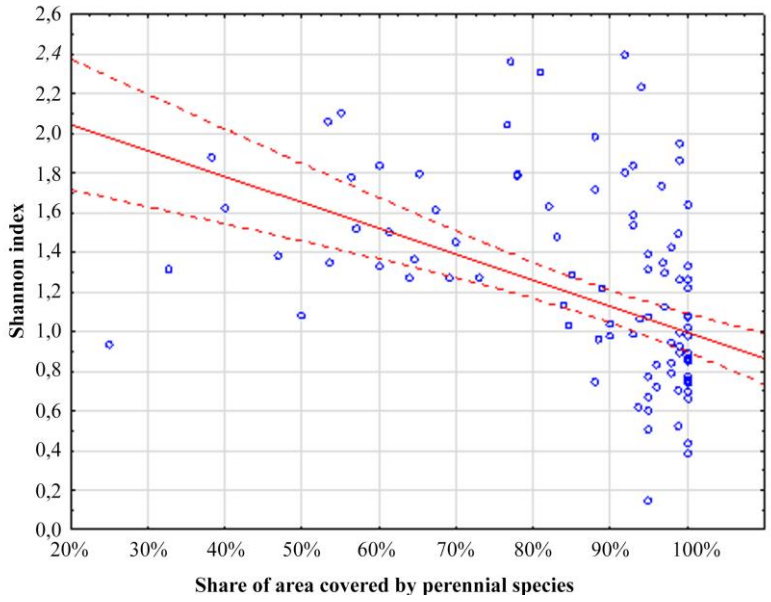

Figure 6. *A scatter chart illustrating the impact of the share of perennial species in area covered on the level of the Shannon index, r = -0,46636 (own study)*

http://www.aloki.hu ● ISSN 1589 1623 (Print) ● ISSN1785 0037 (Online)
DOI: http://dx.doi.org/10.15666/aeer/1804_58215839

Effects of the different factors as roads age, slope of the slope°, slope lengt on vegetation biodiversity

In the design documentation of the analyzed road sections it was assumed that the slopes would be sown with mixtures consisting only of grasses. During the phytosociological analysis, it was found that the share of species from the Poaceae family decreases with age of the roads (*Figure 7*). The resulting spaces are inhabited during succession mainly by species from the Asteraceae family (*Figure 8*).

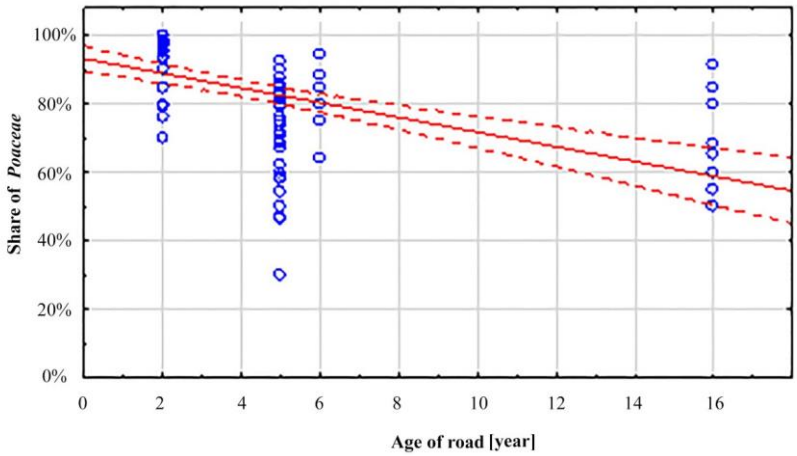

Figure 7. *Share of plant species from Poaceae depending on the age of the road. r=-,5063 (own study)*

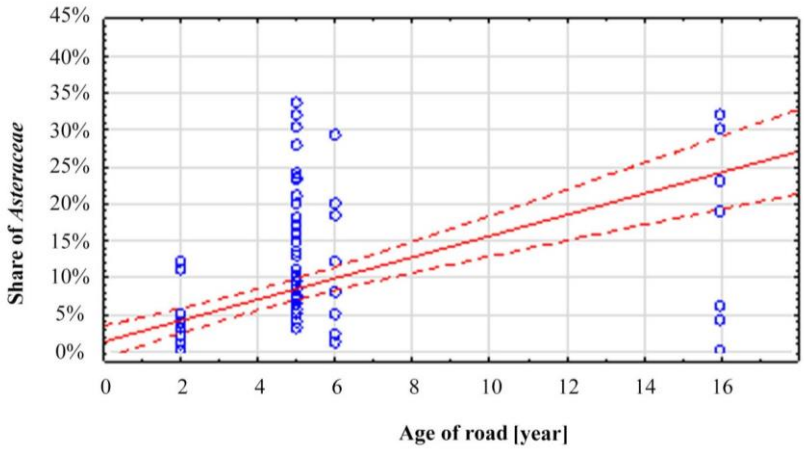

Figure 8. *Share of plant species from Asteraceae depending on the age of the road. r=-,55091 (own study)*

The analyzes show that as the angle of inclination increases, the species diversity of the vegetation decreases (*Figure 9*). This is related to, among others with higher speed of water flowing along the slopes after precipitation - an increase in water speed causes easier detachment of seeds, which together with water move towards drainage ditches.

Based on the results obtained, it can be seen that as the slope length increases, the level of biodiversity increases (*Figure 10*).

http://www.aloki.hu ● ISSN 1589 1623 (Print) ● ISSN1785 0037 (Online)
DOI: http://dx.doi.org/10.15666/aeer/1804_58215839

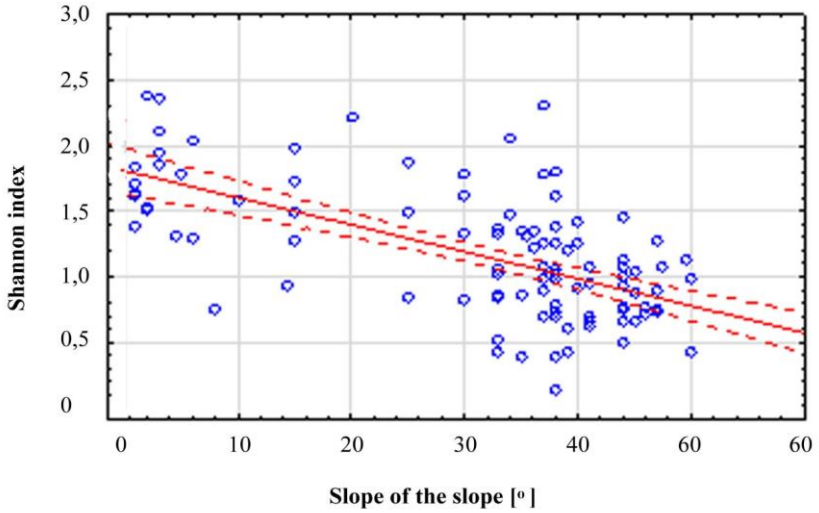

Figure 9. *Shannon index depending on slope of the slope ^{0} on the road in different ages. r=-,6085 (own study)*

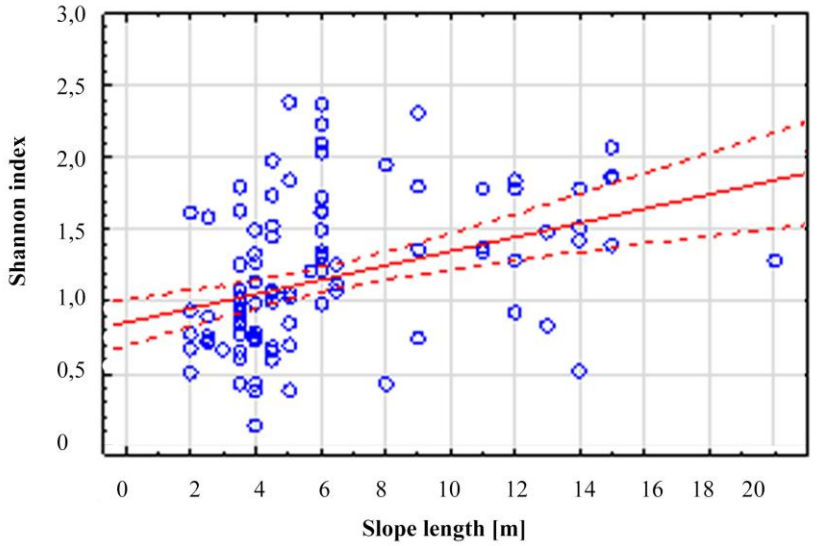

Figure 10. *Shannon index depending on slope length on the road in different ages. r=-,36855 (own study)*

Discussion

Based on the conducted research, it was found that the formulated research hypothesis was true. In the course of the study, 116 plant species were identified. This result does not differ from the results of research by other authors conducted in the studied regions (for example, Trzaskowska and Adamiec (2012) were identified 110 plant species in Lublin) but also in other climatic regions: in the research of Hayasaka et al. (2012) in Japan was noted 122 species, Zeng et al. (2011) in the Yellow River delta recognized 100 plant species, and Arenas et al. (2017) along the highway near Madrid showed the presence of 130 plant species. Slight differences that appear may be due to

http://www.aloki.hu ● ISSN 1589 1623 (Print) ● ISSN1785 0037 (Online)
DOI: http://dx.doi.org/10.15666/aeer/1804_58215839

the fact that some of the roadside areas studied by the authors were in the early stages of use. The smaller plant cover on some stands was mainly the result of technical conditions such as: lack of soil compaction, too small layer of fertile soil, large slope without additional reinforcements (geotextile, geotextile). These were the places where progressing erosion was visible (Xiao et al., 2017).

The roadside is dominated by native species (Forman et al., 2003; Szwed and Perkiewicz, 2010) which was confirmed in the research conducted by the authors where the share of alien and cultivated species slightly exceeded 3%. Alien species are mainly ruderal species of commonly considered weeds. The adjacent roadsides can potentially promote the spread of these species, which raises farmers' concerns (Chaudron et al., 2016). Understanding the factors that shape roadside vegetation makes it possible to design programs that protect biodiversity, which limits the increase in weeds that can harm crops (Chaudron et al., 2018). The predominant share of native species is associated with the formation of corridors along the roads that allow native and alien species to move (Zeng et al., 2011; Arnadottir, 2012).

Perennial species were dominating, however, their share varies over time. Based on the conducted research, the authors concluded that the process of succession takes place over time, which is consistent with the situations described by (Wysocki, 1994). Over time, the species share may decrease by as much as 17% to 33% of land cover (Wysocki and Stawicka, 2000). A similar tendency was stated by Zeng et al. (2011). The author observed that after the initial low value of biodiversity of annual plant species, their diversity increases, which is in accordance with the view presented by Forman et al. (2003), and Pickett and McDonnell (1989). This demonstrates both the succession and competition between species. The proven dominance of perennial species confirms that they are more resistant to changes in the landscape than annual species (Linborg, 2007; Chaudron et al., 2018). The obtained test results prove the need to differentiate the species composition of roadside seeding mixtures in terms of life forms.

Mesohemerobic plants were dominating, which indicates a moderate anthropogenic impact. This proves, among other things, a small amount of care work, which is limited to extensive mowing 2-3 times a year. Minimization of outlays related to care positively effects the biodiversity of plant cover as it promotes changes in species composition and an increase in the number of species (Kull and Zobel, 1991; Bernhardt-Romermann et al., 2011).

The species composition of the roadside in the first years of use clearly differs from other years, as evidenced by the obtained test results. These results are evidence that the mixtures used and their composition require modification because the sown vegetation does not withstand difficult habitat conditions and the species composition changes.

The method of management impacts the dominance of species with a competition strategy. The method of mowing particularly influences the characteristics of plants associated with the strategy C (Klimesova et al., 2008; Chaudron et al., 2016; Fried et al., 2018). There is a high probability that a change in the composition of seed mixtures used for sowing slopes and a change in the way of vegetation care (e.g. by means of mowing) will contribute to creating a certain balance between competition, stress and disturbances enabling maintaining a high level of biodiversity (Bretzel et al., 2016).

http://www.aloki.hu ● ISSN 1589 1623 (Print) ● ISSN1785 0037 (Online)
DOI: http://dx.doi.org/10.15666/aeer/1804_58215839

Conclusions

Herbaceous vegetation should be subject to rational and conscious design, constant control and care along the road lane for its proper quality and durability. These activities pose significant challenges for specialists within the realm of road problems. One of more important aspects is shaping the biodiversity of roadside spaces, which makes it possible to give them significance in the protection of native flora and fauna. Due to the direction of changes in the development of roadside space, the importance of biodiversity of herbaceous vegetation along roads will increase. One of the problems of poor vegetation associated with the appearance of areas without vegetation and progressive erosion on roadside is the manner of establishing herbaceous vegetation. As reported by Stabb et al. (2015) when selecting a seed mix, engineering constraints on roadside slopes, which are associated with specific conditions in a given area, should be taken into account as well as ensuring biodiversity. Thus, the right species selection of plants for roadside spaces makes it possible to give them importance in the protection of native flora as well as the fauna of agricultural landscapes (Spooner and Smallbone, 2009).

According to the European Landscape Convention it is necessary to take all measures to promote protection, management and landscape planning, including in roadside areas. Unfortunately, on the basis of the analyzed cases, it can be stated that the landscape's dissonance around expressways space is deepening. The mixtures used for sowing roadside slopes have a poor composition (up to 8 species). This is an unfavorable situation that does not guarantee species stability. In order to preserve the spread of species composition, additional financial outlays and actions implementing the principles of sustainable development are necessary. To promote the trend, it is advisable to diversify the composition of mixtures used in roadside areas with species from the Asteraceae and Fabaceae families. These are the species that after several years of use penetrate into empty roadside areas resulting from falling out plants that have not withstood harsh habitat conditions. In order to increase the level of biodiversity of roadside plant growing it is recommendable to apply annual and biennial species as well as ones with a high degree of hemerobia or species with a competition strategy (C). The use of these species at the time of sowing will enable integration with the surrounding space, building biodiversity as well as strengthening security, including thanks to the varied space.

Acknowledgements. The authors are grateful to Professor Czesław Wysocki for his valuable methodical remarks.

REFERENCES

[1] Al-Taani, A. A, Nazzal, Y., Howari, F. M. (2019): Assessment of heavy metals in roadside dust along the Abu Dhabi–Al Ain National Highway, UAE. – Environmental Earth Sciences 78: 411. https://doi.org/10.1007/s12665-019-8406-x.

[2] Arenas, J. N., Escudero, A., Mola, I., Casado, M. A. (2017): Roadsides: an opportunity for biodiversity conservation. – Applied Vegetation Science 20: 527-537.

[3] Arnadottir, A. L. (2012): Turf transplants for restoration of alpine vegetation: does size matter? – Journal of Applied Ecology 49: 439-446.

http://www.aloki.hu ● ISSN 1589 1623 (Print) ● ISSN1785 0037 (Online)
DOI: http://dx.doi.org/10.15666/aeer/1804_58215839

[4] Babcock, D. L., McLaughlin, R. A. (2011): Runoff water quality and vegetative establishment for groundcovers on steep slopes. – Journal of Soil and Water Conservation 66: 132-141.
[5] Bernhardt-Römermann, M., Römermann, C., Sperlich, S., Schmidt, W. (2011): Explaining grassland biomass - the contribution of climate, species andfunctional diversity depends on fertilization and mowing frequency. – Journal of Applied Ecology 48: 1088-1097.
[6] Bretzel, F., Vannucchi, F., Romano, D., Malorgio, F., Benvenut, S., Pezzarossa, B. (2016): Wildflowers: From conserving biodiversity to urban greening—A review. – Urban Forestry and Urban Greening 20: 428-436.
[7] Calvi, A. (2015): Does roadside vegetation affect driving performance? Driving simulator study on the effects of trees on drivers' speed and lateral position. – Transportation Research Record: Journal of the Transportation Research Board 2518(1): 1-8.
[8] Chaudron, C., Chauvelb, B., Isselin-Nondedeu, F. (2016): Effects of late mowing on plant species richness and seed rain in road verges and adjacent arable fields. – Agriculture, Ecosystems and Environment 232: 218-226.
[9] Chaudron, C., Perronne, R., Bonthoux, S., Di Pietro, F. A. (2018): Stronger influence of past rather than present landscape structure on present plant species richness of road-field boundaries. – Acta Oecologica 92: 85-94.
[10] Chen, M. C., Hsu, C. L., Chen, M. M. (2019): How Transportation Service Quality Drives Public Attitude and Image of a Sustainable City: Satisfaction as A Mediator and Involvement as A Moderator. – Sustainability 11(23): 6813. https://doi.org/10.3390/su11236813.
[11] Coffin, A. W. (2007): From roadkill to road ecology: A review of the ecological effects of roads. – Journal of Transport Geography 15: 396-406.
[12] Database BiolFlor. – www.ufz.de.
[13] Dzwonko, Z. (2007): Guide book to phytosociological researches. – SORU 1-308.
[14] European Landscape Convencion, Florance, 20.10.2000. – www.coe.int.
[15] Forman, R. T. T., Sperling, D., Bissonette, J. A., Clevenger, A. P., Cutshall, C. D., Dale, V. H., Fahrig, L., France, R., Goldman, C. R., Heanue, K., Jones, J. A., Swanson, F. J., Turrentine, T., Winter, T. C. (2003): Road Ecology: Science and Solutions. – Island Press, Washington, D. C. 481 p.
[16] Fried, G., Villers, A., Porcher, E. (2018): Assessing non-intended effects of farming practices on field margin vegetation with a functional approach. – Agriculture, Ecosystems and Environment 261: 33-44.
[17] Hasan, R., Othman, N., Ismail, F. (2016): Roadside Tree Management in Selected Local Authorities for Public Safety. – Procedia - Social and Behavioral Sciences 234: 218-227.
[18] Hayasaka, D., Akasaka, M., Miyauchib, D., Box, E. O., Uchida, T (2012): Qualitative variation in roadside weed vegetation along an urban–rural road gradient. – Flora 207: 126-132.
[19] Klimesova, J., Latzel, V., de Bello, F., van Groenendael, J. M. (2008): Plant functional traits in studies of vegetation changes in response to grazing and mowing: towards a use of more specific traits. – Preslia 80: 245-253.
[20] Koda, E., Osiński, P., Głażewski, M. (2010): Agrotechnical strengthening of earthworks slopes. – Scientific Review - Engineering and Environmental Sciences 4: 36-47. (in Polish).
[21] Kollarou, V., Kollaros, G. (2014): Management of roadside vegetation, road-island planting and slope cover. – In: Liakopoulos, A., Kungolos, A., Christodoulatos, C., Koutsopsyros, A. (eds.) Proceedings of the 12th International Conference on Protection and Restoration of the Environment. ISBN 978-960-88490-6-8: 647-652.
[22] Kull, K., Zobel, M. (1991): High species richness in an Estonian wooded meadow. – Journal of Vegetation Science 2: 715-718.

http://www.aloki.hu ● ISSN 1589 1623 (Print) ● ISSN1785 0037 (Online)
DOI: http://dx.doi.org/10.15666/aeer/1804_58215839

[23] Maranda, K., Karpowicz, P., Kosek, M., Kucharska, M., Materek, T., Mleczko-Król, M., Musiel, M., Ochnio, P., Siedlecki, T., Stankiewicz, E., Wójcikowska, I. (2013): Guidelines for establishing and maintaining roadside greenery for the needs of the General Directorate for National Roads and Motorways. – GDDKiA, Warszawa, 72-73. (in Polish).
[24] Matuszkiewicz, J. M. (1993): Plant landscapes and geobotanical regions of Poland. – PAN Wrocław, Warszawa, Kraków, pp. 66-83. (in Polish).
[25] Matuszkiewicz, W. (2012): Guide of plant communities in Poland. – PWN, Warszawa, 540 p. (in Polish).
[26] McGrath, D., Henry, J. (2016): Organic amendments decrease bulk density and improve tree establishment and growth in roadside plantings. – Urban Forestry and Urban Greening 20: 120-127.
[27] Mirek, Z., Piękoś-Mirkowa, H., Zając, A., Zając, M. (2002): Flowering plants and pteridophytes of Poland. A checklist. – W. Szafer Institute of Botany, Polish Academy of Sciences, Cracow.
[28] Niemandt, C., Greve, G. (2016): Fragmentation metric proxies provide insights into historical biodiversity loss in critically endangered grassland. – Agriculture, Ecosystems and Environment 235: 172-181.
[29] Pezeshki, Z., Soleimani, A., Darabi, A., Mazinani, S. M. (2018): Thermal transport in: Building materials. – Construction and Building Materials 181: 238-252.
[30] Pickett, S. T. A., McDonnell, M. J. (1989): Changing perspectives in community dynamics: A theory of successional forces. – Trends in Ecology and Evolution 4: 241-45.
[31] Piera, R., Cunha, J. S., Spadeto, C., Gomes, V. M., Moura, A. L., Rúbia, B., Fernandes, G. W. (2019): Nurse shrubs to mitigate plant invasion along roads of montane Neotropics. – Ecological Engineering 136: 193-196.
[32] Rutkowski, L. (2004): Key to determination of lowland Poland vascular plants. – PWN, Warszawa (in Polish).
[33] Shannon, C. E., Weaver, W. (1963): The mathematical theory of communication. – Urbana, The Univ. of Illionois Press.
[34] Spooner, P. G., Smallbone, L. (2009): Effects of road age on the structure of roadside vegetation in south-eastern Australia. – Agriculture, Ecosystem Environment 129: 57-64.
[35] Staab, K., Yannelli, F. A., Lang, M., Kollmann, J. (2015): Bioengineering effectiveness of seed mixtures for road verges: Functional composition as a predictor of grassland diversity and invasion resistance. – Ecological Engineering 84: 104-112.
[36] Szwed, W., Perkiewicz, F. (2010): Floristic diversity of roadsides of selected communes of Greater Poland. – Bulletin of Wielkopolska Regional Parks 16: 68-89. (in Polish).
[37] Tong, Z., Whitlow, T. H., Macra, P. F., Landers, A. J., Harada, Y. (2015): Quantifying the effect of vegetation on near-road air quality using brief campaigns. – Environmental Pollution 201: 141-149.
[38] Trombulak, S. C., Frissell, C. A. (2000): Review of ecological effects of roads on terrestrial and aquatic communities. – Conservation Biology 14: 18-30.
[39] Truscott, A. M., Palmer, S. C. F., McGowan, G. M., Cape, J. N., Smart, S. (2005): Vegetation composition of roadside verges in Scotland: the effects of nitrogen deposition, disturbance and management. – Environmental Pollution 136: 109-118.
[40] Trzaskowska, E., Adamiec, P. (2012): Aesthetic value of extensive lawns on selected objects in Lublin. – Meadows in Poland 15: 193-203. (in Polish).
[41] Wysocki, C. (1994): Studies on the functioning of lawns in urban areas. – SGGW, Warszawa, 95 p. (in Polish).
[42] Wysocki, C., Stawicka, J. (2000): Assessment of floristic changes of urban lawn. – Meadows in Poland 3: 169-176. (in Polish).
[43] Xiao, L. L., Yang, X. H., Cai, H. Y. (2017): The indirect roles of roads in soil erosion evaluation in Jiangxi Province, Chine: A large scale perspective. – Sustainbility 9: 129. doi: 10.3390/su9010129.

http://www.aloki.hu ● ISSN 1589 1623 (Print) ● ISSN1785 0037 (Online)
DOI: http://dx.doi.org/10.15666/aeer/1804_58215839

[44] Zeng, S. L., Zhang, T. T., Gao, Y., Ouyang, Z. T., Chen, J. K., Li, B., Zhao, B. (2011): Effects of road age and distance on plant biodiversity: a case study in the Yellow River Delta of China. – Plant Ecology 212: 1213-1229.

ELECTRONIC APPENDIX

This article has an electronic appendix with the basic field data.

http://www.aloki.hu ● ISSN 1589 1623 (Print) ● ISSN1785 0037 (Online)
DOI: http://dx.doi.org/10.15666/aeer/1804_58215839

ASSESSMENT OF CARBON FOOTPRINT AND LIFE CYCLE COSTS OF WINTER WHEAT (*TRITICUM AESTIVUM* L.) PRODUCTION IN DIFFERENT SOIL TILLAGE SYSTEMS

HOLKA, M.

Department of Agricultural Production Systems, Institute for Agricultural and Forest Environment, Polish Academy of Sciences, Bukowska 19, 60-809 Poznań, Poland (e-mail: malgorzata.holka@isrl.poznan.pl; phone: +48-618-475-601)

(Received 5th Mar 2020; accepted 10th Jul 2020)

Abstract. It is essential to identify the environmental impact of crop production with different soil tillage systems and to find solutions for reducing greenhouse gas emissions if we are to develop low-carbon agriculture. The aim of the study was to assess and compare the carbon footprint and costs of winter wheat production in different soil tillage systems using a life cycle approach. The winter wheat production in three soil tillage systems: conventional tillage, reduced tillage and direct sowing was analysed. The study was conducted in 2015-2017 on 15 farms in the Wielkopolska region (Poland). Inclusion of carbon sequestration into the assessment of carbon footprint allowed for a considerable reduction of the net global warming potential associated with wheat production in unploughed tillage systems. The highest average cost of wheat production per one tonne grain yield was found in reduced tillage. Conventional tillage was associated with the highest costs and greenhouse gas emissions in soil cultivation and sowing, mainly due to a higher fuel consumption and more intensive use of agricultural machinery in comparison to systems with reduced tillage and direct sowing. Pre-farm production linked with the direct input levels contributed mostly to a high overall cost of winter wheat production in the analysed tillage systems.
Keywords: *agriculture, climate change, eco-efficiency, carbon sequestration, grain crop*

Introduction

Certain amounts of raw materials and energy are consumed in agriculture for production purposes, having adverse effects on the environment such as air, water and soil pollution (Kanianska, 2016). The release of nitrous oxide (N_2O), methane (CH_4) and carbon dioxide (CO_2) contributes to the enhanced greenhouse effect (UNEP, 2010). This is a major concern due to changing climate conditions (Cihelková, 2011). It is estimated that the share of food systems in global anthropogenic greenhouse gas (GHG) emissions amounts to 19–29% and agricultural production contributes approximately 80% of the total food system emissions (Vermeulen et al., 2012). In the European Union (EU), the agricultural sector is responsible for 10% of the total GHG emissions (EEA, 2019). According to the EU Action Plan for achieving the reduction of gaseous pollutants, agriculture, as one of the economic sectors not covered by the EU Emission Trading System, must cut its GHG emissions by 30 percent by 2030 based on 2005 figures (EC, 2014). Mitigation and adaptation to climate change are important challenges facing crop production (Loboguerrero et al., 2019). Farmers, in efforts to achieve the best possible production and economic results must take into account the need to protect the environment including the issue of climate change (Liu et al., 2016). Therefore, it is essential to search for solutions and ways to prevent the depletion of natural resources and reduce the emissions of harmful substances related to crop production (Beddington et al., 2012; Campbell et al., 2016).

http://www.aloki.hu ● ISSN 1589 1623 (Print) ● ISSN 1785 0037 (Online)
DOI: http://dx.doi.org/10.15666/aeer/1804_58415855

Conventional, traditional tillage based on soil inversion by plough is a dominant soil tillage system. However, there is growing interest in unploughed tillage systems. The share of arable land on which non-inversion tillage systems were practised in Poland was 9%, while in the EU it reached 26% (CSO, 2012; Eurostat, 2018). The scientific literature relating to the soil tillage systems indicates that abandoning ploughing does not only lead to savings in labour cost, energy expenditure and time on soil preparation for sowing but also has positive influence on physical, chemical and biological soil properties (Morris et al., 2010; Vach et al., 2016). There is a wide range of agricultural machines available on the market that contributes to a growing tendency towards the unploughed tillage systems, particularly in the case of large, commercial farms. They are able to afford the purchasing cost of high-powered tractors and specialized agricultural equipment designed for the soil preparation without ploughing (Wandel and Smithers, 2000). The use of modern multi-task machines performing simultaneously the operations of soil tillage, fertilizer application and sowing enables to decrease tillage depth and reduce the number of tillage operations. Due to the fact that fuel consumption is lower, this is considered the most important way to obtain lower GHG emission and costs (Guardia et al., 2016; Townsend et al., 2016).

GHG emissions are generated at various stages of the life cycle of agricultural products. Apart from agricultural operations, off-farm processes such as extraction of raw materials, manufacture of agricultural production means, transport, use and final disposal are also potential GHG emission sources (Cooper et al., 2011; Moudrý et al., 2013a). The total amount of GHG emission resulting from all processes throughout the crop life cycle can be evaluated with the carbon footprint indicator (Pandey et al., 2011). It reflects the potential impact on global warming throughout the life cycle of a product or a process, allowing one to determine ways to reduce the negative impact (Weidema et al., 2008; BSI, 2011). Regarding the impact of the agricultural production on the carbon footprint, the soil organic carbon sequestration needs to also be taken into consideration (Hillier et al., 2009).

Wheat (*Triticum aestivum* L.) is one of the most important food crops. It occupies the third place in the world cereal production, after maize (*Zea mays* L.) and rice (*Oryza sativa* L.) and the first place in terms of cereal crop area (FAO, 2019). Research on both environmental and economic effects of wheat production, depending on tillage practices is important for achieving more environmentally friendly food production. In order to have a comprehensive comparison of soil tillage systems, the whole life cycle of the crop should be taken into account. The aim of the study was to determine the carbon footprint and life cycle costs of winter wheat grown with different soil tillage systems.

Materials and Methods

Study sites

The research was carried out on 15 agricultural farms, located at 51º-52º north latitude and 15º-19º west longitude in the Wielkopolska region, Poland (*Fig. 1*), during two consecutive growing seasons 2015/2016 and 2016/2017. The selection of farms was made with an expert advisory based on the information resources of the Wielkopolska Agricultural Advisory Centre (WAAC) in Poznan. The cooperation with the agricultural advisers of WAAC has allowed to select the farms best reflecting the criterions adopted for the research regarding to winter wheat production under three soil tillage systems:

http://www.aloki.hu ● ISSN 1589 1623 (Print) ● ISSN 1785 0037 (Online)
DOI: http://dx.doi.org/10.15666/aeer/1804_58415855

conventional tillage (CT), reduced tillage (RT) and direct sowing (DS). There were five farms chosen in each of three groups of farms representing particular soil tillage systems. The description of studied farms is presented in detail in *Table 1*. Data for analyses were gathered through face-to-face interviews with the farmers using a prepared questionnaire.

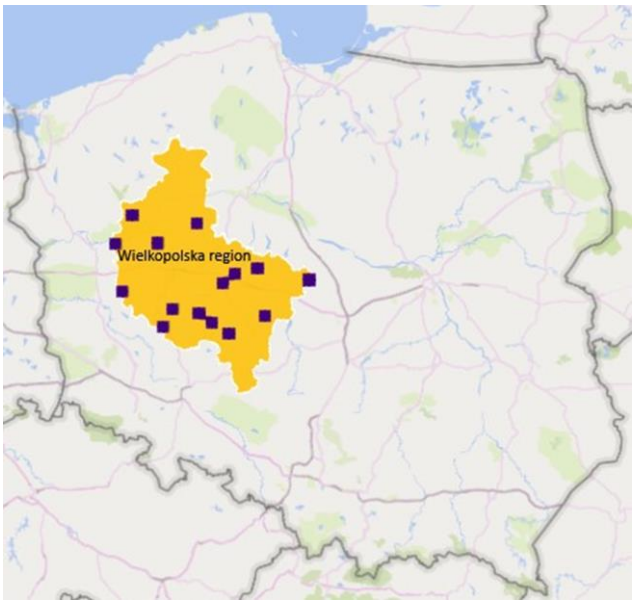

Figure 1. *Location of studied farms in the Wielkopolska region*

Table 1. *Characteristics of studied farms representing wheat production under conventional tillage (CT), reduced tillage (RT) and direct sowing (DS) systems (averages from the study years with min–max range in parentheses)*

Specification	CT	RT	DS
Number of farms	5	5	5
Utilised agricultural area (ha)	35.2 (7.8-73.1)	69.4 (18.5-156.3)	316.0 (44.5-975.0)
Share of arable lands (%)	92.4 (77.0-100.0)	99.4 (98.0-100.0)	94.0 (82.3-100.0)
Share of permanent grasslands (%)	7.6 (0.0-23.0)	0.6 (0.0-2.0)	6.0 (0.0-17.7)
Livestock density (LSU ha^{-1})	0.6 (0.0-1.0)	0.3 (0.0-1.1)	1.6 (0.0-4.9)
Cropping pattern (%)			
- cereals	85.1 (65.5-100.0)	62.0 (39.9-76.7)	66.4 (37.4-100.0)
- industrial crops	12.9 (0.0-26.7)	29.4 (21.4-40.5)	15.1 (0.0 -49.4)
- feed plants	1.1 (0.0-11.2)	1.6 (0.0-9.1)	16.3 (0.0-62.6)
- other plants	0.9 (0.0-7.2)	7.0 (0.0-20.8)	2.2 (0.0-16.7)
- catch crops	11.5 (0.0-23.0)	27.0 (0.0-45.9)	19.7 (0.0-40.2)

In the studied farms, CT included post-harvest tillage operations, ploughing to 25-30 cm depth and soil preparation before wheat sowing. For deep or shallow RT, instead of a plough, the most commonly tillage machine used was a disc cultivator or a cultivator with rigid tines. In turn, if DS system was practiced, the seeds were placed directly into the untilled soil with crop residues using a specialist direct seed drill. *Figure 2* presents winter wheat cultivation in three tillage systems. The average grain yields per hectare were 7.6, 6.9 and 6.6 tonnes in CT, RT and DS, respectively.

http://www.aloki.hu ● ISSN 1589 1623 (Print) ● ISSN 1785 0037 (Online)
DOI: http://dx.doi.org/10.15666/aeer/1804_58415855

Figure 2. *Winter wheat cultivation in conventional tillage (a), reduced tillage (b) and direct sowing (c)*

Carbon footprint

The total amount of GHG emission from the life cycle of winter wheat production under different soil tillage systems was determined with the carbon footprint indicator whose value is expressed in CO_2 equivalent. Carbon footprint was calculated according to the life cycle assessment (LCA) methodology that consists of the four phases: 1) the goal and scope definition, 2) the life cycle inventory analysis (LCI), 3) the life cycle impact assessment (LCIA), with the following steps: the selection of impact categories, category indicators and characterisation models, the assignment of LCI results (classification) and calculation of category indicator results (characterisation), 4) the interpretation of results (PKN, 2006, 2009; Caffrey and Veal, 2013).

Goal and scope

The goal of this study was to compare the carbon footprint of wheat production in different soil tillage systems. The system boundaries were from "cradle-to-farm gate", i.e. from the manufacturing of means of agricultural production to the processes of crop cultivation and harvesting (*Fig. 3*). Two phases of the life cycle, namely the pre-farm production and farm production were distinguished within the studied system. The first phase as the background included manufacture, transportation and delivery of means of agricultural production (fuel, agricultural machinery, agrochemicals, seeds etc.) to the farm gate. The farm production constituting the foreground system concerned the crop production processes as: soil cultivation, sowing, fertilization, plant protection and harvesting. The functional unit chosen was 1 tonne of wheat grain.

Life cycle inventory

In order to perform the LCA analysis, the following data were obtained from the farms: the characteristics of fields under winter wheat cultivation, the yields and detailed information on wheat production technology including type and duration of field operations, characteristics and technical specifications of agricultural machinery used, consumption of seeds, fertilizers, plant protection products, fuel and lubricants. It was assumed that the mass of spare parts constituted 30% of the mass of machinery used and the mass of repairs materials constituted 4% of mass of spare parts (Harasim, 2002). Consumption of lubricants was set to 4% of the consumption of fuel (Harasim, 2002).

http://www.aloki.hu ● ISSN 1589 1623 (Print) ● ISSN 1785 0037 (Online)
DOI: http://dx.doi.org/10.15666/aeer/1804_58415855

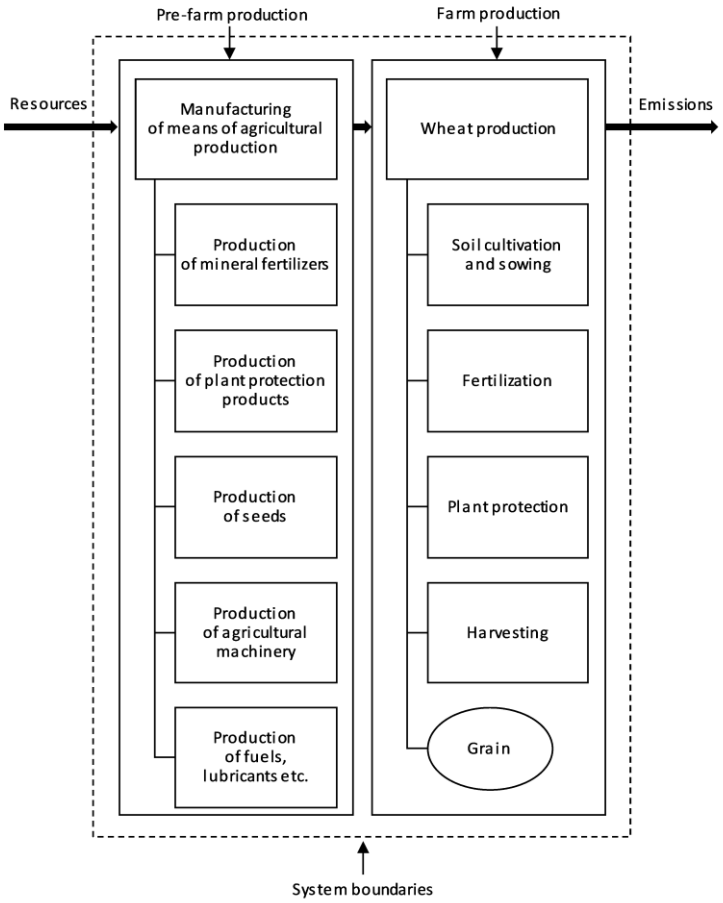

Figure 3. *System boundaries diagram of the life cycle of wheat production from "cradle-to-farm gate"*

During the second LCA phase (LCI), for each considered soil tillage system in winter wheat production, the energy and material inputs as well as the environmental emissions that contribute to the greenhouse effect were identified and calculated quantitatively per functional unit of 1 t of grain. Data on the amounts of synthetic fertilizers applied and the emission factors depending on the types of fertilizers given by the EMEP guidebook (EEA, 2013) were used to estimate the direct and indirect N_2O emissions from the mineral fertilization. Calculations of N_2O emission from crop residues were based on the methodology provided by the Intergovernmental Panel on Climate Change (IPCC, 2006). The emissions related to nitrate leaching were estimated in accordance with a method adopted by van Beek et al. (2003). Emissions from fuel combustion were estimated based on the amounts of fuel consumption in field operations according to the EMEP guidebook (EEA, 2016). For inclusion of soil organic carbon (SOC) changes in LCA, the assessment of the SOC sequestration potential in a 100-year perspective was performed (Petersen et al., 2013). The carbon inflows from crop residues of winter wheat as well as catch crops and soil tillage system were taken into account in this approach. The data source for inventory of background processes such as production of agrochemicals and agricultural machinery was the Ecoinvent version 3.0 database (Swiss Centre for Life Cycle Inventories) used with the TEAM version 5.3 software (PricewaterhouseCoopers - Ecobilan).

http://www.aloki.hu ● ISSN 1589 1623 (Print) ● ISSN 1785 0037 (Online)
DOI: http://dx.doi.org/10.15666/aeer/1804_58415855

Life cycle impact assessment and interpretation

The life cycle impact assessment was performed using the CML (Center of Environmental Science of Leiden University) methodology, based on a midpoint approach. The IPCC data were used for the estimation of the global warming potential (GWP) in a 100-year time horizon (Guinée et al., 2002; IPCC, 2007). The formula for calculating the carbon footprint indicator is given in *Equation 1* (Kowalski et al., 2007).

$$Carbon\ footprint = \sum_i m_i \cdot GWP_{a,i} \quad \text{(Eq.1)}$$

where: m_i – the quantity of the substance i emitted (in kg per functional unit), $GWP_{a,i}$ – the global warming potential for a substance i over a time horizon a (expressed relative to CO_2 per kg i).

In order to broaden the interpretation of the obtained results and to investigate the influence of the key input parameters, sensitivity analysis was performed by varying each parameter one-at-a-time by 5 percent of its original value (Guinée et al., 2002).

Life cycle costs

The life cycle costing (LCC) methodology was applied for economic evaluation all costs of the life cycle of winter wheat production in the stages from "cradle-to-farm gate" (Rebitzer and Seuring, 2003). The set of data gathered for the purposes of the LCC analysis consisted of the cost items related to the inputs for the crop production such as fertilizers, plant protection products, seeds, agricultural machinery, fuel etc. The machinery costs included the costs of owning (depreciation, insurance and housing) and operating (repairs and maintenance, fuel, labour). The results of LCC analysis were expressed in monetary values (in euros) and referenced to the functional unit of 1 tonne of grain.

Results and Discussion

An inventory table of inputs was prepared in relation to the functional unit of 1 tonne of grain yield (*Table 2*). The seed rates in RT and DS were 10-11% higher than in CT. The highest consumption of mineral fertilizers was found in wheat cultivated under DS (43.4 kg NPK t^{-1}), followed by RT (40.2 kg NPK t^{-1}). The most effective fertilization was in CT (23.6 kg NPK t^{-1}). Total consumption of active substances (a.s.) in plant protection amounted to 0.26 kg, 0.30 kg and 0.22 kg per 1 t of grain in CT, RT and DS, respectively. The highest levels of diesel oil consumed and agricultural machinery used were noted in RT despite foregoing energy-intensive ploughing. This is due to the fact that a modern, heavy equipment including high-powered tractors and multi-task machines with a large working width were mostly used in RT. Both the consumption of diesel oil and the use of agricultural machinery were the lowest in DS.

The results of LCA analysis for the life cycle of winter wheat production, based on the described system boundaries gave a total value of the carbon footprint indicator of 309.6 kg, 393.5 kg and 397.1 kg CO_2 eq. per 1 t of grain for CT, RT and DS, respectively (*Fig. 4*). It should be noted that higher GHG emissions in DS and RT occured mainly due to higher nitrogen fertilizer inputs (*Table 2*). By taking into account the differences between the levels of GHG emissions and the SOC sequestration

http://www.aloki.hu ● ISSN 1589 1623 (Print) ● ISSN 1785 0037 (Online)
DOI: http://dx.doi.org/10.15666/aeer/1804_58415855

potential, estimated due to crop residues availability and soil tillage system, it was possible to assess the net value of the carbon footprint of wheat production. Contribution of SOC sequestration to the carbon footprint was mostly present in RT and DS, allowing to decrease the carbon footprint by 32% and 19%, respectively. With regard to life cycle costs of wheat production, the highest cost was found for RT (EUR 105.4 t^{-1}), followed by DS (EUR 97.6 t^{-1}) and CT (EUR 76.0 t^{-1}).

Table 2. *Inventory data of main inputs and costs in winter wheat production under conventional tillage (CT), reduced tillage (RT) and direct sowing (DS) systems per functional unit of 1 tonne of grain*

Type of input	Consumption per 1 t of grain			Cost (EUR) per 1 t of grain		
	CT	RT	DS	CT	RT	DS
Seeds (kg)	25.0	27.8	27.5	10.8	12.0	11.6
Nitrogen fertilizers (kg N)	15.4	18.8	22.5	12.7	16.0	19.4
Phosphorus fertilizers (kg P_2O_5)	3.49	6.95	5.05	3.0	6.9	4.7
Potassium fertilizers (kg K_2O)	4.67	14.4	15.8	2.6	9.9	7.8
Herbicides (kg a.s.)	0.17	0.13	0.08	7.1	5.2	3.5
Fungicides (kg a.s.)	0.08	0.09	0.09	3.3	3.6	4.0
Growth regulators (kg a.s.)	0.01	0.08	0.05	0.4	3.2	2.2
Agricultural machinery (kg)	1.56	1.62	1.04	9.4	17.8	21.8
Spare parts (kg)	0.49	0.51	0.33	2.9	5.6	6.9
Diesel oil (kg)	12.6	14.8	9.14	14.8	17.9	10.8
Lubricants (kg)	0.50	0.59	0.36	3.4	4.0	2.4

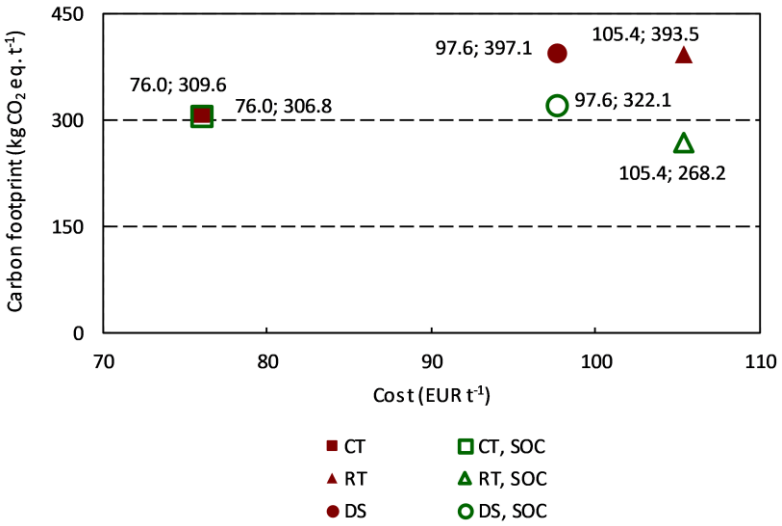

Figure 4. *Combined results of the life cycle costs and carbon footprint of the winter wheat production under conventional tillage (CT), reduced tillage (RT) and direct sowing (DS) (SOC – soil organic carbon changes included)*

A similar result of the carbon footprint of wheat production was reported by Charles et al. (2006) (381 kg CO_2 eq. t^{-1}). Studies in the Czech Republic showed that the GHG emission was higher, amounted to 558 kg CO_2 eq. per tonne of grain in wheat production under CT (Moudrý et al., 2013b). According to Sørensen et al. (2014) the total GHG emission per t of wheat grain was 655 kg CO_2 eq. for CT, 589 kg CO_2 eq. for

http://www.aloki.hu ● ISSN 1589 1623 (Print) ● ISSN 1785 0037 (Online)
DOI: http://dx.doi.org/10.15666/aeer/1804_58415855

RT and 628 kg CO_2 eq. for DS. In Finland, the differences in emissions between soil tillage systems were minor (Rajaniemi et al., 2011). Following these authors' explanation, if the carbon footprint assessment considers functional unit based on yield, the amount of GHG emissions per unit of grain is strongly dependent on the obtained yield size in the assessed system. Thus, the results of the impact assessment of crop production in different soil tillage systems may also be influenced by the differences in productivity achieved from these systems. In the presented study, the grain yield of wheat was lower in RT (by 9.2%) and DS (by 13.2%) compared to CT. Similar effects of soil tillage systems on wheat yields in the Wielkopolska region were observed by Panasiewicz et al. (2020). Townsend et al. (2016) stated that yield reductions in RT are small, suggesting that RT offers a realistic and attainable sustainable intensification of crop production. The level of the use of raw materials is an important determinant of the carbon footprint (Chiriaco et al., 2017). The production and use of nitrogen fertilizers contributes significantly to GHG emissions (Williams et al., 2010; Skowrońska and Filipek, 2014). Gan et al. (2014) showed that integrating improved practices such as fertilizing crops based on soil tests, reducing summer fallow frequencies and including grain legumes to rotation with cereals reduces the carbon footprint of spring wheat. It was also demonstrated that for each kg of grain produced, a net amount of 0.027-0.377 kg CO_2 eq. was captured from the atmosphere. In Danish studies, there were highlighted opportunities for carbon mitigation by incorporation of green manure crops (Knudsen et al., 2014). Wang and Dalal (2015) stated that implementation of no-till and stubble retention resulted in lower carbon footprint values.

Among the field operations, mineral fertilization was the major contributor to the total GHG emissions in three soil tillage systems (*Fig. 5*). Its share in the carbon footprint value was in the range from 72.5% for CT to 83.9% for DS. The soil cultivation and sowing also highly affected the carbon footprint, especially in the case of CT (20.1%) due to high fuel consumption and use of agricultural machinery. The LCC analysis indicated that the soil cultivation and sowing resulted in a considerable part of life cycle costs of wheat production under CT (representing 41.3% of all costs). The total costs of RT and DS depended mainly on the fertilization (38.1% and 42.7%, respectively).

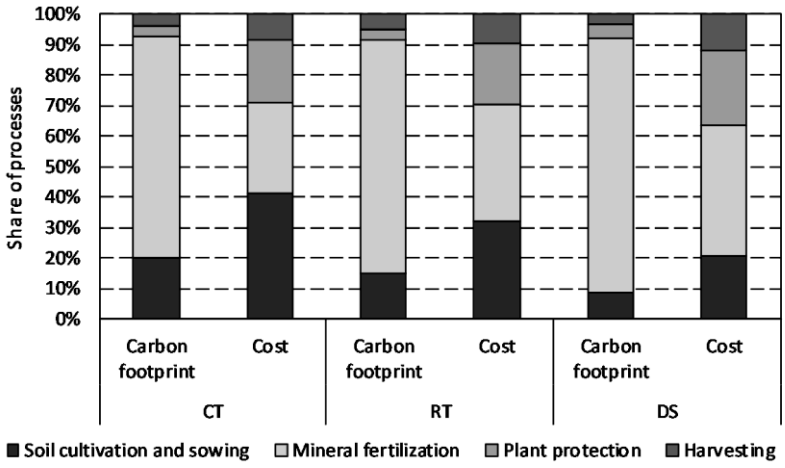

Figure 5. *Contribution of field operations with associated inputs to the carbon footprint and costs of the winter wheat production under conventional tillage (CT), reduced tillage (RT) and direct sowing (DS)*

http://www.aloki.hu ● ISSN 1589 1623 (Print) ● ISSN 1785 0037 (Online)
DOI: http://dx.doi.org/10.15666/aeer/1804_58415855

Other authors also clearly identified that the mineral fertilization is responsible for a considerable part of GHG emissions from crop production (Brock et al., 2012; Mancuso et al., 2019). This is a concern in particular nitrogen fertilizers (Yan et al., 2015). In Lithuania, the costs of soil cultivation and sowing in CT were by 5 to 50% higher than those of various variants of RT systems and by up to 3.5 times higher than the costs of DS (Sarauskis et al., 2012). According to Townsend et al. (2016), despite lower fuel and machinery costs, unploughed tillage leads to additional crop protection costs resulting from a greater risk of weed, pest and disease burdens.

As shown in *Figure 6*, the highest cost and the largest carbon footprint associated with fuel consumption for the soil cultivation and wheat sowing was noted in CT. The fuel consumption in DS involved both least cost and GHG emissions. The use of machinery caused the highest cost and the largest GHG emissions in RT, while the least cost was in CT and the lowest carbon footprint was stated in DS.

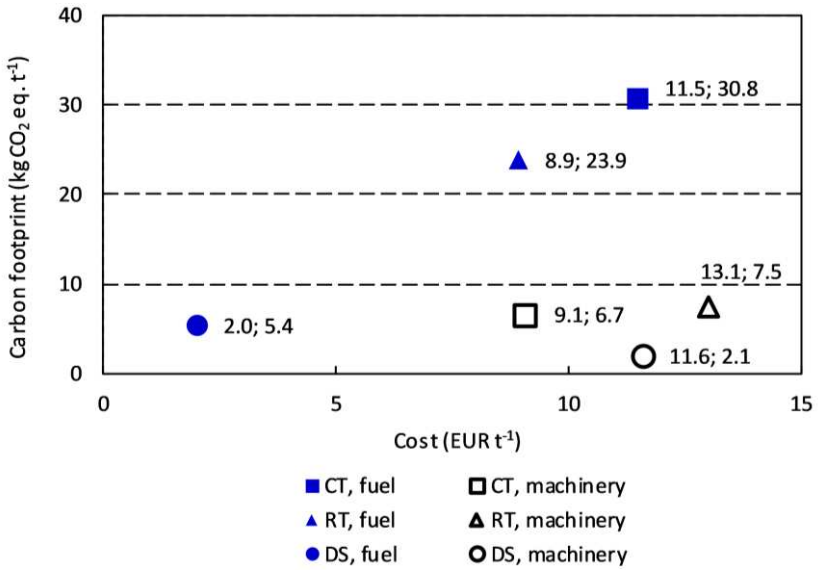

Figure 6. *Combined results of the life cycle costs and the carbon footprint related to the fuel consumption and machinery use for the soil cultivation and wheat sowing under conventional tillage (CT), reduced tillage (RT) and direct sowing (DS)*

Filipovic et al. (2006) showed that DS and RT due to lower fuel consumption for soil tillage ensured the reduction in GHG emission compared to CT. Positive effects of DS and RT on fuel savings and reduction of GHG emissions were also recorded by Stajnko et al. (2009) in studies on production of silage corn. Sørensen et al. (2014) stated that unploughed tillage generates savings in direct energy input and the amount of machinery items needed for soil tillage, thus it may lead to lower GHG emission. In studies by Sarauskis et al. (2012), the highest costs of cultivation and sowing in different tillage systems were found in small farms with areas of 2 ha. When the farm size was increased to 20 ha, the costs decreased.

In each soil tillage system, the pre-farm phase including manufacture and delivery of inputs for wheat production was more dominant in shaping the carbon footprint than the farm production phase. This also contributed more to the overall costs of the life cycle of wheat production (*Fig. 7*).

http://www.aloki.hu ● ISSN 1589 1623 (Print) ● ISSN 1785 0037 (Online)
DOI: http://dx.doi.org/10.15666/aeer/1804_58415855

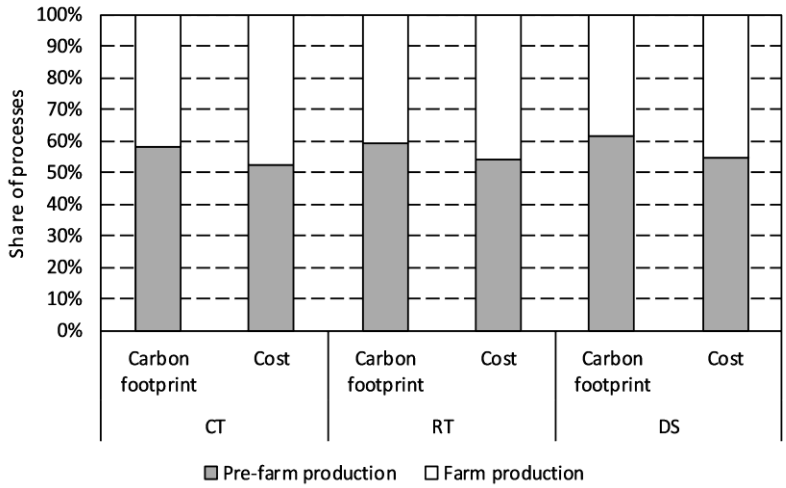

Figure 7. *Carbon footprint and life cycle costs at pre-farm production and farm production life cycle phases of winter wheat under conventional tillage (CT), reduced tillage (RT) and direct sowing (DS)*

Several studies also showed that the pre-farm production phase generated more GHG emissions than on-farm production (Biswas et al., 2008; Zhang et al., 2017). It should be stated that this results from a high share of energy- and material-consuming processes. Lares-Orozco et al. (2016) reported that the production of synthetic fertilizers accounted for 35% of the total emissions from the life cycle of wheat production. In life cycle of wheat production in Western Australia, GHG emissions from the production of fertilizers accounted for a significant portion of the impact for the pre-farm phase and the use of fertilizers was predominant for the on-farm phase (Biswas et al., 2008). Production of mineral fertilizers increases GHG emissions, mainly CO_2 from fossil fuels used in production, while application of fertilizers contributes mostly to N_2O emissions (Biswas et al., 2008; Skowrońska and Filipek, 2014).

Considering the results of sensitivity analysis of key input parameters for the carbon footprint, it can be concluded that the total amount of nitrogen (N) fertilizers applied ranked as the most influential factor (*Fig. 8*). Varying N fertilizer application rate by 5% resulted in a change of total GHG emission from the life cycle of wheat by approximately 3.7%, 3.3% and 3.2% for DS, CT and RT, respectively. Fuel consumption was the second important factor for the carbon footprint. Phosphorus (P) and potassium (K) fertilizers, as well as agricultural machinery, had much less influence. The least sensitivity for the indicator resulted from the changes in the consumption of plant protection products.

As shown in *Figure 9*, the life cycle costs of wheat production in three soil tillage systems were the most sensitive to the change in the cost of the agricultural machinery. It should be noted that the life cycle costs of wheat under DS were more sensitive to the cost of machinery (1.5%) than for wheat under RT and CT (1.1% and 0.8%, respectively). This is due to the fact that the cost of the machinery was the highest for DS. Varying the cost of fuel by 5% resulted in changes of life cycle cost of wheat by 0.9%, 0.8% and 0.5% for CT, RT and DS, respectively. The cost of N fertilizers was also an influential factor, especially in the case of life cycle costs of wheat under DS (0.9%). Other cost items including cost of P and K fertilizers, cost of agricultural

http://www.aloki.hu ● ISSN 1589 1623 (Print) ● ISSN 1785 0037 (Online)
DOI: http://dx.doi.org/10.15666/aeer/1804_58415855

machinery and cost of plant protection products led to smaller changes in the life cycle costs of wheat production.

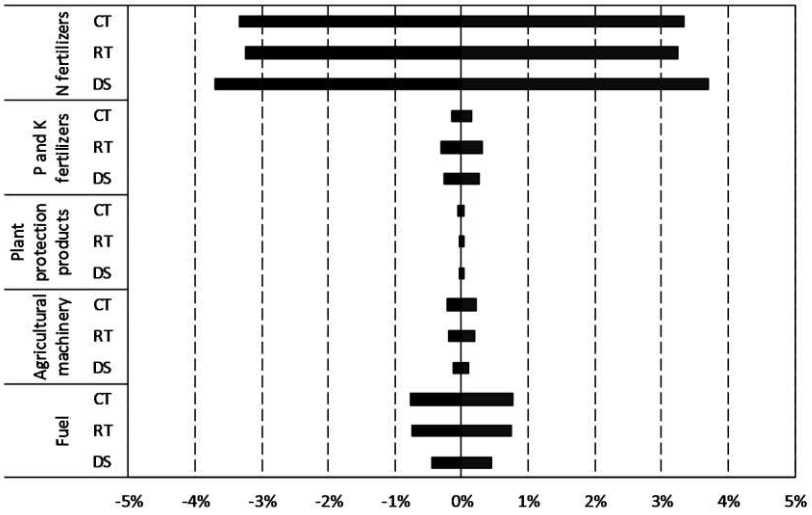

Figure 8. *The sensitivity analysis of input parameters for the carbon footprint of the winter wheat production under conventional tillage (CT), reduced tillage (RT) and direct sowing (DS)*

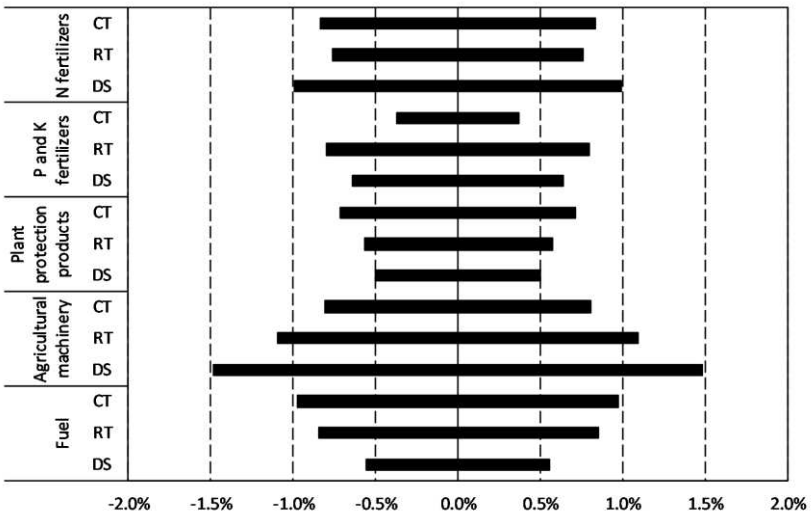

Figure 9. *The sensitivity analysis of cost parameters for the life cycle costs of the winter wheat production under conventional tillage (CT), reduced tillage (RT) and direct sowing (DS)*

Conclusions

Three soil tillage systems (conventional tillage, reduced tillage and direct sowing) for winter wheat production were compared with the use of carbon footprint and life cycle costs to present environmental and economic considerations. The research indicated that unploughed tillage combined with leaving large amounts of crop residues in the field and using catch crops leads to a lower size of the net carbon footprint in comparison with traditional tillage. Improvements in management of soil organic matter are

http://www.aloki.hu ● ISSN 1589 1623 (Print) ● ISSN 1785 0037 (Online)
DOI: http://dx.doi.org/10.15666/aeer/1804_58415855

important opportunities for the carbon footprint impact reduction. The potential for soil organic carbon retention can be increased by abandoning ploughing, growing cover crops and leaving crop residues in the field.

The fertilization process is a key factor driving the size of carbon footprint and life cycle costs of wheat production, independently from the soil tillage system. In conventional tillage, the soil cultivation and sowing provided a considerable share of the total carbon footprint and life cycle costs. Adoption of unploughed tillage systems is conducive to addressing climate change and achieving more eco-efficient performance.

The inclusion of environmental costs is recommended to be employed in future studies on the environmental burden of crop production with different tillage systems. Assessing the externalities of crop production and demonstrating the value of nature in economic terms is necessary to better inform political decision-makers and farmers to adopt practices that are more environmentally and economically sustainable.

Acknowledgements. The author would like to thank Dr Jerzy Bieńkowski, Institute for Agricultural and Forest Environment, Polish Academy of Sciences, for his valuable support in carrying out the work and Dr Tomasz Piechota, Poznań University of Life Sciences, for his contribution to preparing the photo presented in this paper. This study was carried out within the frame of the research project funded by the National Science Centre, Poland. Project no 2015/19/N/HS4/03031. Project title: "Environmental life cycle assessment and life cycle costing of grain crop production in different soil tillage systems".

REFERENCES

[1] Beddington, J. R., Asaduzzaman, M., Clark, M. E., Fernández Bremauntz, A., Guillou, M. D., Jahn, M. M., Lin, E., Mamo, T., Negra, C., Nobre, C. A., Scholes, R. J., Sharma, R., Van Bo, N., Wakhungu, J. (2012): The role for scientists in tackling food insecurity and climate change. – Agriculture and Food Security 1(1): 1-9.

[2] Biswas, W. K., Barton, L., Carter, D. (2008): Global warming potential of wheat produced in Western Australia: a life cycle assessment. – Water and Environment Journal 22(3): 206-216.

[3] Brock, P., Madden, P., Schwenke, G., Herridge, D. (2012): Greenhouse gas emissions profile for 1 tonne of wheat produced in Central Zone (East) New South Wales: A life cycle assessment approach. – Crop and Pasture Science 63(4): 319-329.

[4] BSI (2011): PAS 2050: Specification for the Assessment of the Life Cycle Greenhouse Gas Emissions of Goods and Services. – BSI, London.

[5] Caffrey, K. R., Veal, M. V. (2013): Conducting an agricultural life cycle assessment: challenges and perspectives. – The Scientific World Journal, Article ID: 472431.

[6] Campbell, B. M., Vermeulen, S. J., Aggarwal, P. K., Corner-Dolloff, C., Girvetz, E., Loboguerrero, A. M., Ramirez-Villegas, J., Rosenstock, T., Sebastian, L., Thornton, P. K., Wollenberg, E. (2016): Reducing risks to food security from climate change. – Global Food Security 11: 34-43.

[7] Charles, R., Jolliet, O., Gaillard, G., Pellet D. (2006): Environmental analysis of intensity level in wheat crop production using life cycle assessment. – Agriculture, Ecosystems and Environment 113(1-4): 216-225.

[8] Chiriaco, M. V., Grossi, G., Castaldi, S., Valentini, R. (2017): The contribution to climate change of the organic versus conventional wheat farming: a case study on the carbon footprint of wholemeal bread production in Italy. – Journal of Cleaner Production 153: 309-319.

[9] Cihelková, E. (2011): Climate change in the context of global environmental governance possibilities. – Agricultural Economics 57(9): 436-448.

http://www.aloki.hu ● ISSN 1589 1623 (Print) ● ISSN 1785 0037 (Online)
DOI: http://dx.doi.org/10.15666/aeer/1804_58415855

[10] Cooper, J., Butler, G., Leifert, C. (2011): Life cycle analysis of greenhouse gas emissions from organic and conventional food production systems, with and without bio-energy options. – NJAS - Wageningen Journal of Life Sciences 58(3-4): 185-192.
[11] CSO (2012): Characteristics of agricultural holdings - National Agricultural Census 2010. – CSO, Warsaw.
[12] EC (2014): A policy framework for climate and energy in the period from 2020 to 2030 (COM/2014/015 final). – Communication from the Commission to the European Parliament, the Council, the European Economic and Social Committee and the Committee of the Regions. EC, Brussels.
[13] EEA (2013): EMEP/EEA air pollutant emission inventory guidebook 2013. – Publications Office of the European Union, Luxembourg.
[14] EEA (2016): EMEP/EEA air pollutant emission inventory guidebook 2016. – Publications Office of the European Union, Luxembourg.
[15] EEA (2019): Climate change adaptation in the agriculture sector in Europe. EEA Report 4. – https://www.eea.europa.eu/publications/cc-adaptation-agriculture.
[16] Eurostat (2018): Agri-environmental indicator - tillage practices. Statistics Explained. – https://ec.europa.eu/eurostat/statistics-explained/index.php?title=Agri-environmental_indicators.
[17] FAO (2019): World food and agriculture - Statistical Pocketbook 2019. – FAO, Rome.
[18] Filipovic, D., Kosutic, S., Gospodaric, Z., Zimmer, R., Banaj, D. (2006): The possibilities of fuel savings and the reduction of CO_2 emissions in the soil tillage in Croatia. – Agriculture, Ecosystems and Environment 115(1-4): 290-294.
[19] Gan, Y., Liang, C., Chai, Q., Lemke, R. L., Campbell, C. A., Zentner, R. P. (2014): Improving farming practices reduces the carbon footprint of spring wheat production. – Nature Communications 5: 1-13.
[20] Guardia, G., Tellez-Rio, A., García-Marco, S., Martin-Lammerding, D., Tenorio, J. L., Ibáñez, M. A., Vallejo, A. (2016): Effect of tillage and crop (cereal versus legume) on greenhouse gas emissions and Global Warming Potential in a non-irrigated Mediterranean field. – Agriculture, Ecosystems and Environment 221(1): 187-197.
[21] Guinée, J. B., Gorrée, M., Heijungs, R., Huppes, G., Kleijn, R., de Koning, A., van Oers, L., Wegener Sleeswijk, A., Suh, S., Udo de Haes, H. A., de Bruijn, H., van Duin, R., Huijbregts, M. A. J. (2002): Handbook on life cycle assessment. Operational guide to the ISO standards. I: LCA in perspective. IIa: Guide. IIb: Operational annex. III: Scientific background. – Kluwer Academic Publishers, Dordrecht.
[22] Harasim, A. (2002): Comprehesive assessment of rotations with different percentage of cereal and root crops. – Monografie i Rozprawy Naukowe, IUNG, Puławy. (in Polish).
[23] Hillier, J., Hawes, C., Squire, G., Hilton, A., Wale, S., Smith, P. (2009): The carbon footprints of food crop production. – International Journal of Agricultural Sustainability 7(2): 107-118.
[24] IPCC (2006): IPCC Guidelines for national greenhouse gas inventories. – Institute for Global Environmental Strategies, Hayama.
[25] IPCC (2007): Climate change 2007. The physical science basis. – Contribution of Working Group I to the Fourth Assessment Report of the Intergovernmental Panel on Climate Change, Cambridge University Press, Cambridge.
[26] Kanianska, R. (2016): Agriculture and its impact on land-use, environment, and ecosystem services. – In: Almusaed, A. (ed.) Landscape ecology. The influences of land use and anthropogenic impacts of landscape creation. IntechOpen, London.
[27] Knudsen, M. T., Meyer-Aurich, A., Olesen, J. E., Chirinda, N., Hermansen, J. E. (2014): Carbon footprints of crops from organic and conventional arable crop rotations - using a life cycle assessment approach. – Journal of Cleaner Production 64: 609-618.
[28] Kowalski, Z., Kulczycka, J., Góralczyk, M. (2007): Ecological life cycle assessment of manufacturing processes. – PWN, Warsaw. (in Polish).

http://www.aloki.hu ● ISSN 1589 1623 (Print) ● ISSN 1785 0037 (Online)
DOI: http://dx.doi.org/10.15666/aeer/1804_58415855

[29] Lares-Orozco, M. F., Robles-Morúa, A., Yepez, E. A., Handler, R. M. (2016): Global warming potential of intensive wheat production in the Yaqui Valley, Mexico: a resource for the design of localized mitigation strategies. – Journal of Cleaner Production 127: 522-532.
[30] Liu, C., Cutforth, H., Chai, Q., Gan, Y. (2016): Farming tactics to reduce the carbon footprint of crop cultivation in semiarid areas. A review. – Agronomy for Sustainable Development 36: 1-16.
[31] Loboguerrero, A. M., Campbell, B. M., Cooper, P. J. M., Hansen, J. W., Rosenstock, T., Wollenberg, E. (2019): Food and earth systems: priorities for climate change adaptation and mitigation for agriculture and food systems. – Sustainability 11(5): 1-26.
[32] Mancuso, T., Verduna, T., Blanc, S., Di Vita, G., Brun, F. (2019): Environmental sustainability and economic matters of commercial types of common wheat. – Agricultural Economics 65(4): 194-202.
[33] Morris, N., Miller, P., Orson, J. H., Froud-Williams, R. (2010): The adoption of non-inversion tillage systems in the United Kingdom and the agronomic impact on soil, crops and the environment - a review. – Soil and Tillage Research 108(1): 1-15.
[34] Moudrý, J. Jr., Jelínková, Z., Jarešová, M., Plch, R., Moudrý, J., Konvalina, P. (2013a): Assessing greenhouse gas emissions from potato production and processing in the Czech Republic. – Outlook on Agriculture 42(3): 179-183.
[35] Moudrý, J. Jr., Jelínková, Z., Plch, R., Moudrý, J., Konvalina, P., Hyšpler, R. (2013b): The emissions of greenhouse gases produced during growing and processing of wheat products in the Czech Republic. – Journal of Food, Agriculture and Environment 11(1): 1133-1136.
[36] Panasiewicz, K., Faligowska, A., Szymańska, G., Szukała, J., Ratajczak, K., Sulewska, H. (2020): The effect of various tillage systems on productivity of narrow-leaved lupin-winter wheat-winter triticale-winter barley rotation. – Agronomy 10(2): 1-11.
[37] Pandey, D., Agrawal, M., Pandey, J. S. (2011): Carbon footprint: current methods of estimation. – Environmental Monitoring and Assessment 178: 135-160.
[38] Petersen, B., Knudsen, M., Hermansen, J., Halberg, N. (2013): An approach to include soil carbon changes in life cycle assessments. – Journal of Cleaner Production 52: 217-224.
[39] PKN (2006): PN-EN ISO 14040. Environmental management. Life cycle assessment. Principles and framework. – PKN, Warsaw. (in Polish).
[40] PKN (2009): PN–EN ISO 14044. Environmental management. Life cycle assessment. Requirements and guidelines. – PKN, Warsaw. (in Polish).
[41] Rajaniemi, M., Mikkola, H., Ahokas, J. (2011): Greenhouse gas emissions from oats, barley, wheat and rye production. – Agronomy Research, Biosystem Engineering 1: 189-195.
[42] Rebitzer, G., Seuring, S. (2003): Methodology and application of life cycle costing. – International Journal of Life Cycle Assessment 8: 110-111.
[43] Sarauskis, E., Buragienė, S., Romaneckas, K., Sakalauskas, A., Algirdas, J., Vaiciukevicius, E., Karayel, D. (2012): Working time, fuel consumption and economic analysis of different tillage and sowing systems in Lithuania. – Engineering for Rural Development 11: 52-59.
[44] Skowrońska, M., Filipek, T. (2014): Life cycle assessment of fertilizers: A review. – International Agrophysics 28: 101-110.
[45] Sørensen, C. G., Halberg, N., Oudshoorn, F. W., Petersen, B. M., Dalgaard, R. (2014): Energy inputs and GHG emissions of tillage systems. – Biosystems Engineering 120: 2-14.
[46] Stajnko, D., Lakota, M., Vučajnk, F., Bernik, R. (2009): Effects of different tillage systems on fuel savings and reduction of CO_2 emissions in production of silage corn in eastern Slovenia. – Polish Journal of Environmental Studies 18(4): 711-716.

http://www.aloki.hu ● ISSN 1589 1623 (Print) ● ISSN 1785 0037 (Online)
DOI: http://dx.doi.org/10.15666/aeer/1804_58415855

[47] Townsend, T. T., Ramsden, S. J., Wilson, P. (2016): Analysing reduced tillage practices within a bio-economic modelling framework. – Agricultural Systems 146: 91-102.
[48] UNEP (2010): Assessing the environmental impacts of consumption and production: priority products and materials. A report of the working group on the environmental impacts of products and materials to the international panel for sustainable resource management. – http://www.unep.fr/shared/publications/pdf/DTIx1262xPA-PriorityProductsAndMaterials_Report.pdf.
[49] Vach, M., Strašil, Z., Javurek, M. (2016): Economic efficiency of selected crops cultivated under different technology of soil tillage. – Scientia Agriculturae Bohemica 47(1): 40-46.
[50] Van Beek, C. L., Brouwer, L., Oenema, O. (2003): The use of farmgate balances and soil surface balances as estimator for nitrogen leaching to surface water. – Nutrient Cycling in Agroecosystems 67: 233-244.
[51] Vermeulen, S. J., Campbell, B. M., Ingram, J. S. I. (2012): Climate change and food systems. – Annual Review of Environment and Resources 37: 195-222.
[52] Wandel, J., Smithers, J. (2000): Factors affecting the adoption of conservation tillage on clay soils in Southwestern Ontario, Canada. – American Journal of Alternative Agriculture 15: 181-188.
[53] Wang, W., Dalal, R. C. (2015): Nitrogen management is the key for low-emission wheat production in Australia: A life cycle perspective. – European Journal of Agronomy 66: 74-82.
[54] Weidema, B. P., Thrane, M., Christensen, P., Schmidt, J., Løkke, S. (2008): Carbon Footprint - a catalyst for LCA? – Journal of Industrial Ecology 12(1): 3-6.
[55] Williams, A., Audsley, E., Sandars, D. (2010): Environmental burdens of producing bread wheat, oilseed rape and potatoes in England and Wales using simulation and system modelling. – International Journal of Life Cycle Assessment 15: 855-868.
[56] Yan, M., Cheng, K., Luo, T., Yan, Y., Pan, G., Rees, R. M. (2015): Carbon footprint of grain crop production in China - based on farm survey data. – Journal of Cleaner Production 104: 130-138.
[57] Zhang, D., Shen, J., Zhang, F., Li, Y., Zhang, W. (2017): Carbon footprint of grain production in China. – Scientific Reports 7: 1-11.

http://www.aloki.hu ● ISSN 1589 1623 (Print) ● ISSN 1785 0037 (Online)
DOI: http://dx.doi.org/10.15666/aeer/1804_58415855

MULTIVARIATE ANALYSIS OF MORPHOLOGICAL TRAITS AND THE MOST IMPORTANT PRODUCTIVE TRAITS OF WHEAT IN EXTREME WET CONDITIONS

LUKOVIĆ, K.[1*] – PRODANOVIĆ, S.[2] – PERIŠIĆ, V.[1] – MILOVANOVIĆ, M.[3] – PERIŠIĆ, V.[4] – RAJIČIĆ, V.[4] – ZEČEVIĆ, V.[5]

[1]*Centre for Small Grains, Save Kovačevića 31, 34000 Kragujevac, Serbia*

[2]*Faculty of Agriculture, University of Belgrade, Nemanjina 6, 1100 Belgrade, Serbia*

[3]*Technical Vocational College, Nemanjina 2, 12000 Požarevac, Serbia*

[4]*Faculty of Agriculture, University of Niš, Kosančićeva 4, 37000 Kruševac, Serbia*

[5]*Megatrend University, Belgrade, Faculty of Biofarming, Maršala Tita 39, 24300 Bačka Topola, Serbia*

[*]*Corresponding author*
e-mail: kika@kg.ac.rs

(Received 6th Mar 2020; accepted 9th Jul 2020)

Abstract. In these studies, 14 winter wheat (*Triticum aestivum* ssp *vulgare* L.) genotypes were analyzed in three localities across the Republic of Serbia. Some morphological and the most important productive traits were analysed in order to determine the relationship between grain yield and these traits in the year with extreme wet conditions during period of intensive wheat development (April-June period). According to our results, period of stem extension, heading and grain filling characterized by lower air temperatures and extremely high rainfall at all three localities, had detrimental effects on the grain filling process. The genotypes KG-191/5-13 and KG-1/6 achieved above average values of the most desirable traits in all three localities, and can be singled out as desirable parents in breeding programs to create new and improved varieties of wheat. Based on the principal component analysis and cluster analysis, two groups of similar genotypes were distinguished. The highest degree of positive correlation was found between diameter of the first internode and diameter of top internode; number of spikelets per spike and number of fertile spikelets per spike; grain mass/spike and grain mass/plant; plant height and length of the top internode.
Keywords: *wheat, precipitation, yield, Principal Component Analysis, clustergram*

Abbreviations: PH, plant height; LFI, length of the first internode; LTI, length of the top internode; DFI, diameter of the first internode; DTI, diameter of the top internode; LFL, length of the flag leaf; WFL, width of the flag leaf; SL, spike length; NSS, number of spikelets per spike; NFS, number of fertile spikelets; GMS, grain mass per spike; GMP, grain mass per plant; Y, grain yield; PCA, Principal Component Analysis; ANOVA, analysis of variance

Introduction

In most wheat breeding programs, the main focus is on grain yield and yield components (number of spikes per unit area, spike length, number of spikelets per spike, number of grains per spike, grain mass per spike and mass of 1000 grains). Araus et al. (2008) points out that such an approach has enabled the advancement of production in line with the growing population of the planet, while the contribution of breeding in Serbia in the second half of the 20th century is measured by increasing the genetic potential for grain yield of 32-43 kg $ha^{-1}years^{-1}$ (Mladenov et al., 2007). Today's

http://www.aloki.hu ● ISSN 1589 1623 (Print) ● ISSN1785 0037 (Online)
DOI: http://dx.doi.org/10.15666/aeer/1804_58575871

predictions about future breeding of wheat and other cereals are largely based on existing and future climate change, with drought being one of the key stress factors for production.

However, analysis of trends and intensity of precipitation, both on an annual and seasonal or monthly basis in the territory of Serbia, indicate an increase in annual precipitation sums in the northern and central parts of Serbia from the middle and the end of 1990's, as in the first decades of the 21st century, relative to the multi-year average (Stanojević, 2012; Tošić and Unkašević, 2013). Extreme wet conditions in some years were a crucial factor concerning grain yield, as well as technological quality in the period of intensive wheat development (period April-June). Xu et al. (2018) found that in this particular period of wheat development, the SPEI values of the Drought Indicator (Standardized Precipitation Evapotranspiration Index) and soil moisture status exhibit a stronger relationship with yield than other stages of growth and development. Excessive precipitation and soil water lead to losses in wheat yield (Zampieri et al., 2017), due to a stronger attack of pests and diseases, nutrient leaching from the soil, difficulty in oxygen uptakeby roots, and difficulty performing work operations (eg. harvesting). As an example, the authors cites 2016 and the yield losses recorded in France stemming from such an extreme year.

Selection of short stature wheat varieties with greater ability to utilize nutrients from fertilizers are a major feature of genetic improvement in wheat (Bhutta et al., 2006) and the basis of increased genetic potential for yield. Even so, lodging is one of the crucial factors in yield formation (Yao et al., 2011), even in short, and dwarf wheat varieties in the case of insufficient stalk strength. The existence of broad genetic variability for stem diameter, wall thickness, and stem material strength as components of stem strength has been identified, but the lack of utilization of this source of variability is due to the breeder's lack of knowledge of the importance of these traits and the difficulty in evaluating them (Berry et al., 2007; Berry and Berry, 2015). Yu et al. (2003) emphasize the necessity of combining the mechanical strength of the stem and other desirable features in order to increase the resistance to lodging.

The paper examines wheat genotypes selected at the Center for Small Grains Kragujevac (Serbia) to determine the relationship between the final grain yield and individual morphological traits as components of the mechanical strength of the stem, as well as the most important productive traits in the year with extreme wet conditions.

Material and Methods

Plant material

In these studies, 14 winter wheat genotypes were analyzed (*Triticum aestivum* ssp *vulgare* L.), of which 13 genotypes represent promising selection lines created at the Center for Small Grains in Kragujevac (KG - 47/21, KG - 52/3, KG - 1/6, KG - 60-3 / 3, KG - 52/23, KG - 40-39/3, KG - 191/5-13, KG - 162/7, KG - 28/6, KG - 307/4, KG - 199/4, KG - 244/4, KG-27/6), and one standard variety (Pobeda). The studied wheat lines and their pedigree are shown in *Table 1.*

Field trials and methods

The exploratory part of the experiment was carried out during 2013/14 in three localities: Institute of forage plants in Kruševac (21° 21' E, 43° 34' N, 166 m),

http://www.aloki.hu ● ISSN 1589 1623 (Print) ● ISSN1785 0037 (Online)
DOI: http://dx.doi.org/10.15666/aeer/1804_58575871

Agroinstitute in Sombor (19° 09' E, 45° 46' N, 87 m) and the Center for Small Grain in Kragujevac (20º 56' E, 44º 02' N, 185 m). The experiment was performed under field conditions according to a completely random block system, in three repetitions with the size of the basic plot of 5 m^2 (5 x 1 m). Within the plot, 10 rows were planted, with a row spacing of 10 cm. The sowing was done mechanically using 600-650 germinated grains per m^2 depending on the characteristics of the genotype.

Table 1. *Examined genotypes of winter bread wheat and their pedigree*

Genotypes	Pedigree
1. KG – 27/6	♀ L-100/97 x ♂ Pobeda
2. KG – 244/4	♀ (L-1165 x SSK-20/96) x ♂ Vizija
3. KG – 199/4	♀ L-35/93 x ♂ Pobeda
4. KG – 307/4	♀ Pobeda x ♂ Duga
5. KG – 28/6	♀ L-100/97 x ♂ Pobeda
6. KG – 162/7	♀ L-246/6 x ♂ Studenica
7. KG – 191/5-13	♀ [(Pi 159102 x Evropa) x Studenica] x ♂ KG-2086
8. KG – 40-39/3	♀ Vizija x ♂ KG 100
9. KG – 52/23	♀ Bujna x ♂ KG – 56-S
10. KG – 60-3/3	♀ KG 100 x ♂ SSK 50 $_{01/02}$
11. KG – 1/6	♀ KG 100 x ♂ Toplica
12. KG – 52/3	♀ Vizija x ♂ (Bujna x KG – 56-S)
13. KG – 47/21	♀ Vizija x ♂ (Lazarica x Takovčanka)
14. Pobeda	♀ Sremica x ♂ Balkan

The most important stages of the wheat development, from heading to full maturity, and 10-day periods of precipitation during May and June are presented in the *Table 2*.

Table 2. *Dates of developmental phases of wheat and precipitation during May and June 2014*

Locality	Developmental phases			
	Heading	Flowering	Milk stage	Full maturity
Kragujevac	29 April – 8 May	4 - 12 May	30 May - 5 Jun	26 Jun - 5 July
Sombor	28 April - 5 May	3 - 9 May	30 May - 2 Jun	25 Jun - 1 July
Kruševac	3 - 8 May	9-11 May	31 May -3 Jun	27 Jun - 5 July

Precipitation (mm)						
Locality	May			June		
	I	II	III	I	II	III
Kragujevac	66.6	100.7	60	6.5	23.5	36.9
Sombor	62.3	53	29.7	5.4	14.9	46.9
Kruševac	45.3	61	20.3	16.6	30.7	68

During the study, at each site, 45 plants total (three replications every with 15 plants - 3x15) were selected from each genotype tested, at the stage of full maturity, to obtain data on the following morphological and productive traits: plant height (PH), length of the first internode (LFI), length of the top internode (LTI), diameter of the first internode (DFI), diameter of the top internode (DTI), spike length (SL), number of spikelets per spike (NSS), number of fertile spikelets (NFS), grain mass per spike (GMS), grain mass per

http://www.aloki.hu ● ISSN 1589 1623 (Print) ● ISSN1785 0037 (Online)
DOI: http://dx.doi.org/10.15666/aeer/1804_58575871

plant (GMP). Length of the flag leaf (LFL), and width of the flag leaf (WFL) were measured during the stage of milk maturity. After the harvest, grain yield (Y) was measured for each plot in three replications and then converted to t ha^{-1}.

Properties of soil

The field experiment in Kragujevac was carried out on a plot of smonitza-type soil. Chemical analysis of the soil showed acidic reaction, lower humus content, provided with a moderate amountsof the total nitrogen and readily accessible phosphorus. The content of readily available potassium was high. Soil at the Kruševac locality was alluvium in degradation. Humus, total nitrogen and readily available phosphorus were moderately provided, while the amount of readily available potassium in the tiller layer was high. The basic type of soil on which the experiment was conducted in Sombor is a chernozem. It is expressed alkaline reaction, and optimum amount of humus. Total nitrogen is moderately provided while easily accessible phosphorus was provided optimally. The readily available potassium content is high (*Table 3*).

Table 3. *Agrochemical analysis of soil*

Locality	pH in KCL	Humus (%)	N (%)	P_2O_5 (mg)	K_2O (mg)
Kragujevac	4.91	2.51	0.16	17.6	29.2
Kruševac	5.45	2.97	0.146	11.3	31.08
Sombor	7.59	3.54	0.17	19.6	28.9

Climatic conditions during the trial period

The average values of monthly air temperatures and precipitation amounts by months during the trial period as well as multi-year averages are shown in *Figs. 1*, *2* and *3*. All three localities are characterized by slightly higher air temperatures during October and November. The months of December in Sombor, February in Kruševac, as well as December and February in Kragujevac, are characterized by a dry period with extremely low precipitation, which led to slower plant development (*Figs 1*, *2* and *3*).

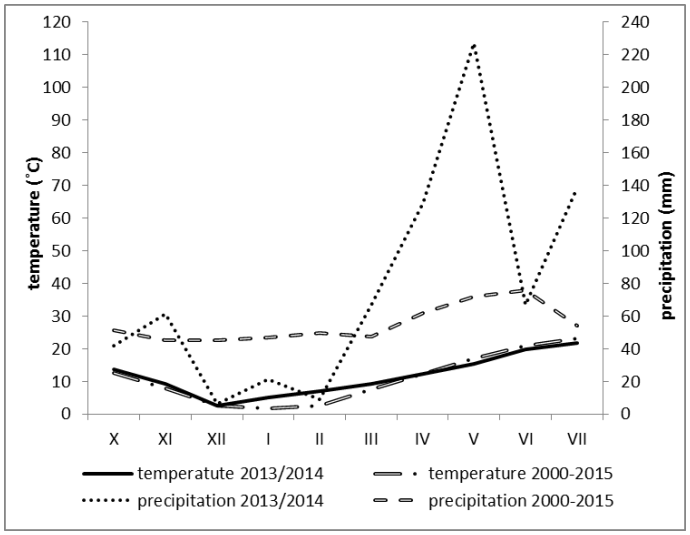

Figure 1. *Average monthly air temperatures and total amount of precipitation in Kragujevac during 2013/14 and multi-year average (2000-2015)*

http://www.aloki.hu ● ISSN 1589 1623 (Print) ● ISSN1785 0037 (Online)
DOI: http://dx.doi.org/10.15666/aeer/1804_58575871

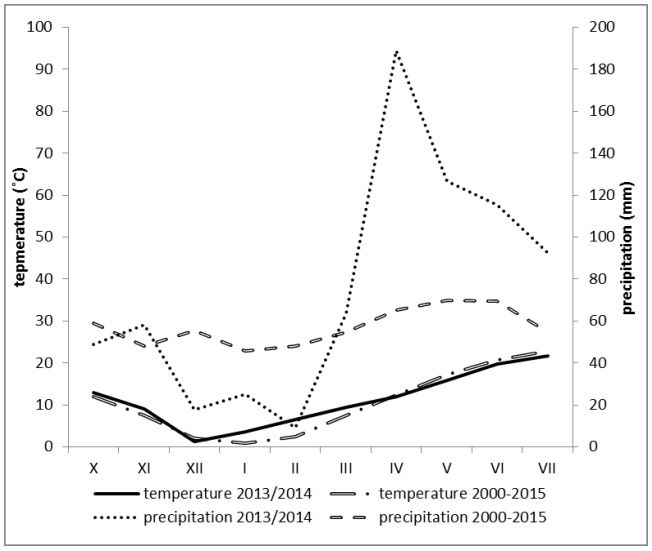

Figure 2. *Average monthly air temperatures and total amount of precipitation in Kruševac during 2013/14 and multi-year average (2000-2015)*

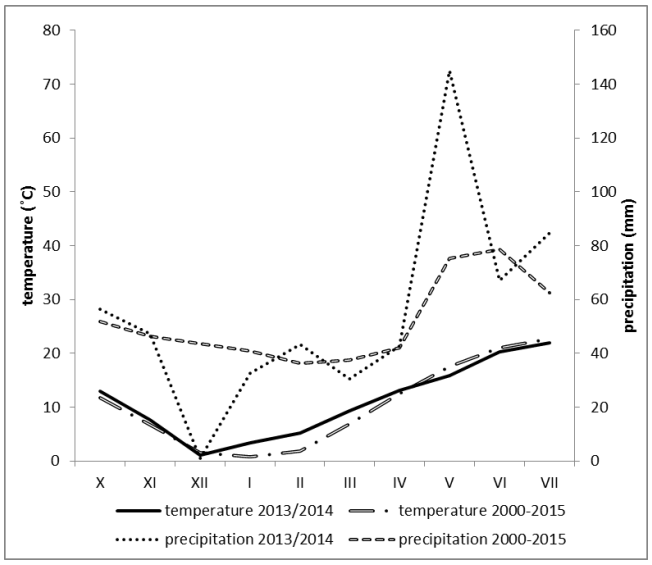

Figure 3. *Average monthly air temperatures and total amount of precipitation in Sombor during 2013/14 and multi-year average (2000-2015)*

Typically, the year of the trial is extremely high in precipitation by month. Thus, in April, 129.1 mm of precipitation occurred in Kragujevac and 188.8 mm in Kruševac, which is three times higher than the multi-year average. There were about 48.9 mm of rainfall in Sombor during the same period. The flowering period and the beginning of grain filling (during May) are characterized by lower air temperatures in all three localities, as well as extremely high rainfall, twice as high in Sombor and Kruševac (145 mm and 126.6 mm compared to the multi-year average of 75.4 mm and 66 mm, respectively), and even three times higher than the average of many years in Kragujevac (227 mm compared to 71.8 mm).

http://www.aloki.hu ● ISSN 1589 1623 (Print) ● ISSN1785 0037 (Online)
DOI: http://dx.doi.org/10.15666/aeer/1804_58575871

In April and May alone, there were 356 mm of precipitation in the Kragujevac area, which is about 50% of the total rainfall during the wheat growing season. Such large amounts of precipitation led to the excessive amounts of the surface water in the trial field in Kruševac and Kragujevac, which later reflected on the yield and quality of the wheat grain.

Statistical data processing

For all analyzed morphological and productive properties of wheat, the following parameters of descriptive statistics were calculated: mean, standard deviation as a measure of absolute variation and coefficient of variation as a measure of relative variation. Heritability in the broad sense was calculated as the ratio of genotypic to phenotypic variance.

To examine the effect of genotype and locality on the morphological and productive traits of wheat, a two-factor ANOVA model using a completely random block system was used through the SPSS-22 statistical program. Duncan's test was used for subsequent comparisons. A 5% significance level was used in all tests. To mark significant differences between genotypes, a lowercase Latin letters were used.

Principal Component Analysis (PCA) was used to examine the contribution of individual morphological and productive traits to overall variability in order to summarize data and interpret results more clearly. The number of components extracted for further analysis was determined by the Guttman-Keiser criterion. Further analysis retained components with an Eigen value greater than 1. This analysis was performed in XLSTAT software.

A clustergram was used to group genotypes by their similarity in the traits tested, as well as to group these traits by their correlation. All data are standardized (reduced to zero average and unit deviation). The Euclidean distance calculated on standardized data was used as a measure of similarity of some genotypes, and Pearson's correlation coefficient subtracted from 1. The average method was used for grouping. MATLAB R2018a was used for clustering.

Results

Analysis of morphological traits

The lowest average stem height at all three studied sites belonged to the KG-1/6 genotype (78.5 cm) while the highest was KG-162/7 genotype (102.3 cm). Compared to the standard Pobeda variety, the nine lines had lower stem height on average (*Table 4*).

The length of the first internode ranged from 3.5 cm (KG-1/6) to 5.1 cm (KG-191/5-13) on average. The highest average length of the top internode at all sites had the KG-244/4 genotype (37.7 cm) and the lowest were genotypes KG-27/6 and KG-28/6 (25.4 cm).

Different mean values of stem diameter (internode) were determined between analyzed genotypes. On average, the largest internode diameter was achieved by Pobeda (4.0 mm), and the smallest genotype KG-191/5-13 (3.5 mm), which had the smallest diameter of the top internode (3.1 mm) as well. The KG-1/6 genotype achieved, on average, the largest diameter of the top internode (4.1 mm).

http://www.aloki.hu ● ISSN 1589 1623 (Print) ● ISSN1785 0037 (Online)
DOI: http://dx.doi.org/10.15666/aeer/1804_58575871

Table 4. *Descriptive statistics and heritability for morphological traits of studied wheat genotypes*

Genotype	PH	LFI	LTI	DFI	DTI	LFL	WFL
KG-27/6	80.9^{ab*}	4^{b}	25.4^{a}	3.8^{bcd}	3.7^{cd}	20.52^{ab}	1.77^{abcd}
KG-244/4	97.7^{f}	4.1^{bcd}	37.7^{g}	3.8^{bcd}	3.9^{efg}	20.6^{ab}	1.64^{a}
KG-199/4	85.6^{cd}	4^{bc}	28.3^{cd}	3.8^{bcd}	$4f^{g}$	19.9^{a}	1.86^{bcde}
KG-307/4	92.6^{e}	4^{b}	29.6^{ef}	3.8^{bcd}	3.9^{ef}	24.29^{f}	1.66^{a}
KG-28/6	80.8^{ab}	4.1^{bcd}	25.4^{a}	3.8^{bcd}	3.7^{c}	20.2^{ab}	1.87^{de}
KG-162/7	102.3^{g}	4.5^{f}	30.7^{f}	3.9^{cd}	3.8^{cd}	21.5^{abcd}	1.69^{a}
KG-191/5-13	98.6^{f}	5.1^{f}	28.5^{de}	3.5^{a}	3.1^{a}	20.6^{ab}	1.86^{bcde}
KG-40-39/3	83^{bc}	4.2^{bcde}	28.3^{cd}	3.9^{cd}	4^{fg}	23.3^{ef}	1.87^{cde}
KG-52/23	94^{e}	4.5^{ef}	29.9^{f}	3.6^{ab}	3.5^{b}	22.3^{cde}	1.71^{ab}
KG-60-3/3	86.9^{d}	4.4^{def}	28.3^{cd}	3.8^{bcd}	3.8^{de}	21^{abc}	1.71^{ab}
KG-1/6	78.5^{a}	3.5^{a}	26.8^{b}	3.9^{cd}	4.1^{g}	21.8^{bcde}	1.92^{e}
KG-52/3	84.1^{c}	4.3^{cdef}	26.4^{ab}	3.8^{bc}	3.7^{cd}	21.7^{bcde}	1.69^{a}
KG-47/21	87.7^{d}	4.3^{cdef}	27.2^{bc}	3.7^{bc}	3.8^{de}	22.8^{def}	1.7^{a}
Pobeda	93.3^{e}	3.9^{b}	28.3^{cd}	4^{d}	3.9^{ef}	20.6^{ab}	1.72^{abc}
Average	89	4.2	28.6	3.8	3.8	21.5	1.76
CV (%)	8.6	10.9	11	5.4	7	14.65	13.7
s	7.7	0.5	3.2	0.2	0.3	3.5	0.3
h^2 (%)	98.22	93.98	96.53	62.32	95.57	86.26	73.07

Legend: PH- plant height (cm); LFI- length of the first internode (cm); LTI- length of the top internode (cm); DFI-diameter of the first internode (mm); DTI-diameter of the top internode (mm); LFL- length of the flag leaf (cm); WFL- width of the flag leaf (cm); CV (%) – coefficient of variation; s- standard deviation; h^2 (%)-heritability in the broad sense. *Distinct letters in the row indicate significant differences according to Duncan test ($P \leq 0.05$).

The highest average values of flag-leaf length were determined for the KG-47/21 genotype (22.8 cm), while the largest flag-leaf width was achieved by the KG-1/6 genotype (1.92 cm).

Productive trait analysis

The average values for the length of the primary spike indicate that 10 genotypes were better in respect to the Pobeda variety, with the highest length being KG-191/5-13 (11.6 cm) and the smallest KG-60-3/3 (7.7 cm).

The KG-27/6 genotype averaged about 23 spikelets in the primary spike, which is the highest value for all three localities, while the smallest spikelets number was distinguished by KG-60-3/3 (19.6). Grain mass per spike varied from 1.3 g (KG-27/6, KG-28/6, KG-52/3) up to 1.9 g (KG-52/23), while genotype KG-60-3/3 achieved the highest average grain mass per plant as well as the highest average yield at all localities (5.6 g; 5.6 t ha^{-1}) (*Table 5*).

Principal Components Analysis and Clustergram

Principal Component Analysis (PCA) reduced the 13 observed variables to the five principal components, which absorbed most of the variation in the observed properties. The five components account for 90.215% of the total data variation. The first major component comprises the largest part of the total variance, while each subsequent

http://www.aloki.hu ● ISSN 1589 1623 (Print) ● ISSN1785 0037 (Online)
DOI: http://dx.doi.org/10.15666/aeer/1804_58575871

component represents the largest remaining part. Thus, the first component explains 34.772% of the data variation, the second 22.525%, the third 13.966%, the fourth 10.423% and the fifth component 8.528% (*Table 6*).

Table 5. *Descriptive statistics and heritability for production traits of studied wheat genotypes*

Genotype	SL	NSS	NFS	GMS	GMP	Y
KG-27/6	10.4^{efg}	22.6^{g}	20.2^{f}	1.3^{ab}	3.6^{a}	4.5^{abcde}
KG-244/4	8.9^{b}	20.2^{ab}	19^{bc}	1.6^{bcde}	4.9^{cd}	3.9^{a}
KG-199/4	9.3^{c}	20.3^{b}	17.9^{a}	1.5^{abcd}	4.3^{abc}	4.8^{bcde}
KG-307/4	9.8^{d}	20.5^{bc}	18.5^{ab}	1.6^{cdef}	4.7^{bcd}	4.9^{cdef}
KG-28/6	10.4^{ef}	22.2^{fg}	20^{ef}	1.3^{a}	3.8^{ab}	4.4^{abcde}
KG-162/7	9.7^{d}	21.7^{ef}	20^{ef}	1.5^{abcde}	4.6^{bcd}	4.3^{abcd}
KG-191/5-13	11.6^{i}	20.7^{bcd}	19.3^{cde}	1.6^{cdef}	4.4^{abc}	4.9^{cdef}
KG-40-39/3	10.7^{h}	21.7^{ef}	19.7^{cdef}	1.5^{abcd}	4.3^{abc}	4.2^{abc}
KG-52/23	10.1^{e}	20.5^{bc}	18.5^{ab}	1.9^{f}	5.5^{d}	5.1^{ef}
KG-60-3/3	7.7^{a}	19.6^{a}	17.8^{a}	1.6^{bcde}	5.6^{d}	5.6^{f}
KG-1/6	10.6^{fgh}	21.7^{ef}	20.3^{f}	1.7^{def}	4.7^{bcd}	4.7^{bcde}
KG-52/3	10.5^{fgh}	21.2^{cde}	19^{bc}	1.3^{ab}	4.2^{abc}	4.4^{abcd}
KG-47/21	10.7^{gh}	21.7^{ef}	19.2^{bcd}	1.4^{abc}	4.3^{abc}	4.1^{ab}
Pobeda	9.5^{cd}	21.4^{de}	19.8^{def}	1.8^{ef}	5.2^{cd}	$5d^{ef}$
Average	10	21.1	19.2	1.6	4.6	4.6
CV	7.9	5.1	5.4	18.3	22.2	16.5
s	1	1.1	1	0.3	1	0.8
h^2 (%)	98.24	93.38	87.78	86.67	73.28	48.08

Legend: SL- spike length (cm); NSS- number of spikelets per spike; NFS-number of fertile spikelets; GMS-grain mass per spike (g); GMP- grain mass per plant (g); Y-yield (t ha^{-1}). CV (%)-coefficient of variation; s-standard deviation; h^2 (%)-heritability in the broad sense. * Distinct letters in the row indicate significant differences according to Duncan test ($P \leq 0.05$).

Table 6. *Eigenvalues and % of explained variability by five main components*

Factor	Eigenvalue (λ)	% of variance	Cumulative (%)
1	4.520	34.772	34.772
2	2.928	22.525	57.298
3	1.816	13.966	71.263
4	1.355	10.423	81.686
5	1.109	8.528	90.215

The value for loadings (loadings > 0.60) was used as the criterion for determining the affiliation of individual variables to the principal components. The first component was defined by six parameters (NSS, NFS, PH, LTI, GMS and GMP). The second component is in strong positive correlation with DFI and DTI, and negative correlation with LFI and SL. The third component is defined by the yield that it is positively correlated and the LTI with which it is negatively correlated. The fourth component was defined by grain mass per spike and the fifth component, which accounted for the smallest % of variability, was defined by the length of the flag leaf (*Table 7*).

http://www.aloki.hu ● ISSN 1589 1623 (Print) ● ISSN1785 0037 (Online)
DOI: http://dx.doi.org/10.15666/aeer/1804_58575871

Table 7. *Loadings of five main components*

Variable	1	2	3	4	5
PH	-0.6736	-0.2821	-0.5384	0.1307	-0.2705
LFI	-0.3802	-0.8273	-0.1208	-0.1070	0.0292
LTI	-0.6202	0.1758	-0.6184	-0.1041	-0.1959
DFI	0.3209	0.8577	-0.1152	0.0851	-0.2109
DTI	0.2042	0.9382	-0.0822	-0.0471	0.1423
SL	0.5743	-0.6174	-0.1386	0.4322	0.1302
NSS	0.8986	-0.0686	-0.1939	0.2018	-0.1510
NFS	0.7377	-0.0499	-0.2915	0.3757	-0.4106
Y	-0.5247	-0.0123	0.7661	0.1855	-0.0717
GMS	-0.6227	0.1590	0.1068	0.7017	-0.2286
GMP	-0.8546	0.2559	0.1301	0.3126	-0.1103
LFL	-0.0581	0.1394	-0.2566	0.5336	0.7766
WFL	0.5561	-0.1616	0.5308	0.1634	-0.2145

Marked loadings are >0.60, legend:PH- plant height (cm); LFI- length of the first internode (cm); LTI- length of the top internode (cm); DFI-diameter of the first internode (mm); DTI-diameter of the top internode (mm); LFL- length of the flag leaf (cm); WFL- width of the flag leaf (cm); SL- spike length (cm); NSS- number of spikelets per spike; NFS-number of fertile spikelets; GMS-grain mass per spike (g); GMP- grain mass per plant (g); Y-yield (t ha^{-1})

Biplot analysis

Biplot analysis was used to more clearly understand the relationship between genotypes and morphologically productive traits. *Fig. 4* shows the biplot PCA analysis of morphological and productive traits, whose abscission of the coordinate system is the first and the ordinate is a second major component.

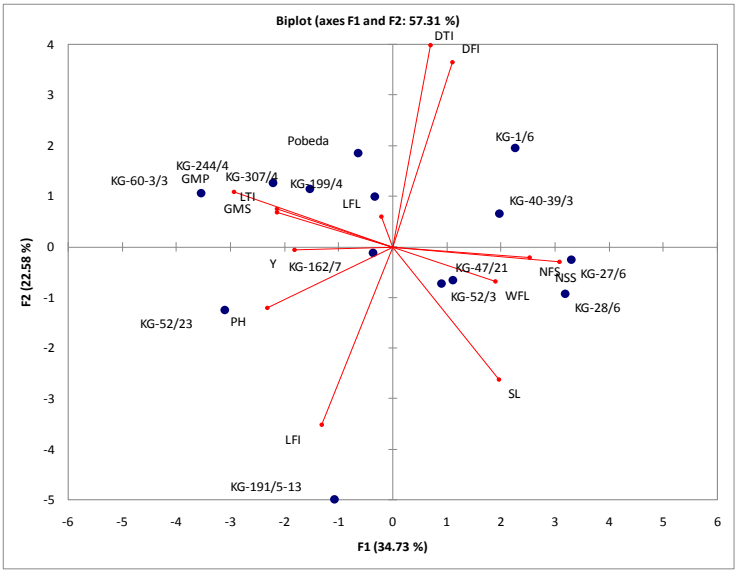

Figure 4. *Biplot for the analyzed genotypes and traits shown on the first two main components. Legend:PH- plant height (cm); LFI- length of the first internode (cm); LTI- length of the top internode (cm); DFI-diameter of the first internode (mm); DTI-diameter of the top internode (mm); LFL- length of the flag leaf (cm); WFL- width of the flag leaf (cm); SL- spike length (cm); NSS- number of spikelets per spike; NFS-number of fertile spikelets; GMS-grain mass per spike (g); GMP- grain mass per plant (g); Y-yield (t ha^{-1})*

http://www.aloki.hu ● ISSN 1589 1623 (Print) ● ISSN1785 0037 (Online)
DOI: http://dx.doi.org/10.15666/aeer/1804_58575871

The first two axes shown on the biplot explain 57.31% of the total variation of the data.

Clustergram

Figure 5 presents a clustergram of studied genotypes and morphological and productive characteristics of wheat at all three localities.

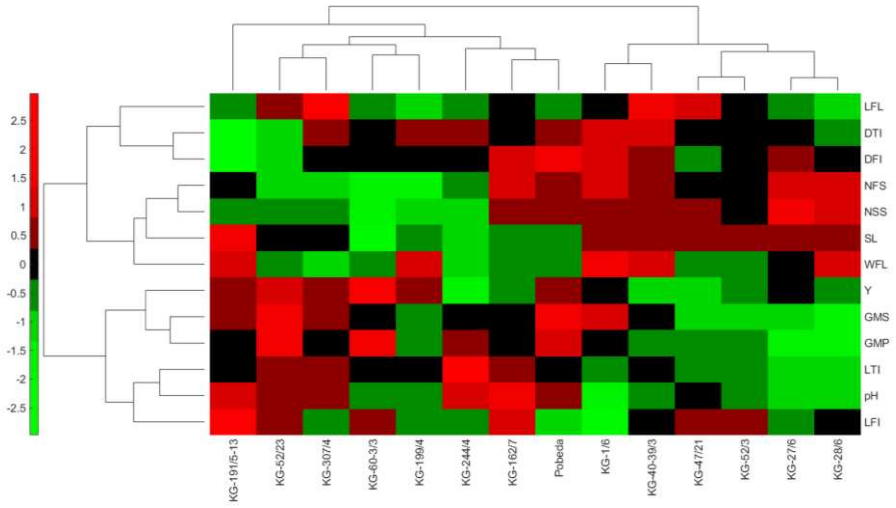

Figure 5. *Cluster diagram of analyzed genotypes and morphological and productive traits of wheat. Legend: PH- plant height (cm); LFI- length of the first internode (cm); LTI- length of the top internode (cm); DFI-diameter of the first internode (mm); DTI-diameter of the top internode (mm); LFL- length of the flag leaf (cm); WFL- width of the flag leaf (cm); SL- spike length (cm); NSS- number of spikelets per spike; NFS-number of fertile spikelets; GMS-grain mass per spike (g); GMP- grain mass per plant (g); Y-yield (t ha^{-1})*

All morphological and productive traits belong to two clusters. The first clusters consist of two subclusters: the primates DTI, DFI, and LFL and these traits are strongly correlated. They are similarly joined by another subcluster composed of NFS, NSS, SL and WF.

The second cluster consists of two subclusters: the first consisting of three productive traits, Y, GMS, GMP, and the second subcluster composed of three morphological traits (LTI, PH and LFI).

Discussion

High heritability values of the analysed morphological and productive traits are similar to research of Varsha et al. (2019), Karim and Jahan (2013) and Tripathi et al. (2011). The lowest heritability value was determined for grain yield (48.08%), which was in agreement with results obtained by Akcura (2009) and Taneva et al. (2019). Opposite to this study, Ali and Shakor (2012) found a high heritability values for bread wheat grain yield (92.60%) in arid growing conditions. Out of all the traits that are related to the mechanical strength of the stem (Berry and Berry, 2015), the stem diameter has the highest heritability value (37-56%), whereas other traits (wall thickness and stem material strength) exhibit heritability between 30 and 40%.

http://www.aloki.hu ● ISSN 1589 1623 (Print) ● ISSN1785 0037 (Online)
DOI: http://dx.doi.org/10.15666/aeer/1804_58575871

Based on biplot analysis, the first two axes, PC1 and PC2, were found to account for 57.31% of the total data variation. A similar proportion of PC1 and PC2 were determined by Sabaghnia and Janmohammadi (2014). Xhulaj et al. (2019) found that the three principal components account for 66.42% of the total data variation, where the first two components accounting for the largest part of the total variance (PC1 with 28.1% and PC2 with 24.43%). The authors emphasize that plant height, spike length, number of spikelet per spike are the most important traits in differentiating genotypes. Janmohammadi et al. (2014) found that five PCA components explained 69% of the total variation among traits. Authors emphasize that in order to develop high yielding varieties, selection may be made according to the first component defined by to grain number, floret number, tiller number, stem diameter, leaf width and spikelet number.

The NSS, NFS and SL productive traits and the WFL morphological trait are grouped on the positive side of the PCA 1 axis, with a small angle between the vectors, indicating a strong possitive correlation between them. The large angle of the vector of the mentioned properties with respect to the grain yield vector, which is located on the negative side of the PCA 1 axis, indicates a markedly negative correlation. These results were different from the results of previous studies (Zečević et al., 2004; Kumar et al., 2007; Mohammadi et al., 2012; Varsha et al., 2019) in which a positive correlation exists between the components of spike (length spike, number of spikelets per spike, grain weight and the number of grains per spike) and grain yield. However, Hristov et al. (2007, 2011), through Path analysis, identifies a negative direct effect of the number of spikelets per spike on yield per plant, indicating the need to improve their fertility. The spike fertility problem adversely affects the number of grains per spike. The authors note that although the direct effect is not significant, it must be observed since it indicates that the occurrence of sterile spikelets significantly reduces the total yield.

In these studies, the period of stem extension, heading and grain filling was characterised by lower air temperatures and extremely high precipitation at all three localities. Such adverse weather conditions had a detrimental effect on the grain filling process, causing the formation of small, poorly filled grains, which had a negative impact on the yield.

The soil on which the experiments were conducted belongs to different types, with different quality and content of macro and microelements available to the plants. However, due to heavy and unevenly distributed rainfall during the growing season, differences in the quality of the soil on which the trials were conducted did not emerge.

Depending on the temperature and amounts of rainfall at the start of grain filling stage, the coefficients of correlation between the yield and yield components, as well as the quality trait may be positive, negative or close to zero (Rharrabti et al., 2003; Terzić et al., 2018; Rajičić et al., 2019). According to Banjac et al. (2010), unfavourable water regime conditions in 2008/09 led to unexpected values of correlation coefficients, where negative mean strong correlations between plant height and spike mass were found, as well as between plant height and grain mass per spike. These authors point out that for wheat breeding it important correlations that are repeated in different conditions of growing seasons.

The study of the morphological and anatomical features of a stem is very important for a complete and thorough understanding of the processes that cause the lodging of wheat. By lodging, the yield and grain quality are reduced. Cultivars that are resistant to lodging have a wider internodes diameter and a thicker wall (Zuber et al., 1999; Pinera-Chavez et al., 2016).

http://www.aloki.hu ● ISSN 1589 1623 (Print) ● ISSN1785 0037 (Online)
DOI: http://dx.doi.org/10.15666/aeer/1804_58575871

The vectors for DTI and DFI are on the positive side of the PCA1 and PCA 2 axes and are very close, indicating a strong positive correlation between these traits as well as a strong negative correlation with the LFI and PH, located on the negative side of the PC2 axis. A strong positive correlation was found between plant height and internode length, stem diameter and leaf length (Sabaghnia and Janmohammadi, 2014), as well as between grain yields, spike length and mass of 1000 grains, whereas negative correlation was found for plant height and stem diameter. Also, a statistically significant positive correlation of grain yield was observed with the length of the spike, the number of spikelets per spike, and the mass of 1000 grains (Varsha et al., 2019). Stem diameter and stem wall thickness, as the major components, are positively correlated with the mechanical strength of the stem (Pinera-Chavez et al., 2016), while the diameter of the stem expressed the strongestrelation with grain yield.

Genotypes KG-1/6, KG-40-39/3, KG-28/6, KG-27/6, KG-47/21 and KG-52/3 are also grouped on the positive side of PCA 1 axis. This indicates that these genotypes reacted similarly in the tested environmental conditions and thus achieved the highest average values of the observed traits. According to the position they occupy on the biplot, the KG-27/6 and KG-28/6 genotypes can be concluded to be very similar to each other and characterized by higher values of NSS, NFS and lower values of GMP, GMS, LTI and PH.

The Y, GMS, GMP (productive) properties of LFL, LTI, PH, and LFI (morphological) are negatively correlated with the first basic component of PCA1 and are on its negative side. Furthermore, the small vector angles for Y, GMS, GMP, PH, and LTI indicate a positive correlation between these features. Also, genotypes KG-244/4, KG-199/4, KG-307/4, KG-162/7, KG-52/23, KG-60-3/3, Pobeda and 191/5-13 are grouped on the negative side of the PCA 1 axis, indicating that these genotypes behaved similarly under different environmental conditions.

Looking at the arrangement of wheat genotypes within the cluster, two clusters can be observed. Within each group, there are genotypes of similar productive and morphological characteristics. The first cluster contains the same genotypes as the negative side of the PCA 1 axis and consists of: Pobeda, KG-162/7, KG-244/4, KG-199/4, KG-60-3/3, KG-307/4, KG-52/23 and KG-191/5-13. Group II cluster is smaller than group I cluster and contains six wheat genotypes clustered on the positive side of PCA 1 axis (KG-1/6, KG-40-39/3, KG-47/21, KG-52/3 KG -27/6 and KG-28/6).

The cluster diagram indicates that the highest degree of positive correlation is found between the following traits: DTI and DFI; NSS and NFS; GMS and GMP; PH and LTI. In addition to the dendrogram, which shows the similarity of genotypes as well as the similarity of correlation of individual traits, an important element of the cluster is color. It shows the values of individual traits in genotypes. Light red shades indicate higher trait values than average for observed genotypes, and light green shades indicate lower trait values. Black indicates the average. While evaluating the analyzed genotypes of wheat, it is noted that in terms of productive traits, the genotypes KG-191/5-13, KG-52/23, KG-307/4 and KG-60-3/3 stood out, while genotypes KG-1/6 and KG-40-39/3 were distinguished in terms of morphological characteristics.

The analysis of wheat genotype pedigree, classified in the same cluster, reveals a similar origin. It is observed that some genotypes in their pedigree have one or both parents in common. Thus, the sister lines KG-28/6 and KG-27/6, which are in the second cluster, have a common origin (♀ L-100/97 x ♂ Pobeda) and almost identical morphological and productive features. The Vizija variety is found in the pedigree KG-

http://www.aloki.hu ● ISSN 1589 1623 (Print) ● ISSN1785 0037 (Online)
DOI: http://dx.doi.org/10.15666/aeer/1804_58575871

52/3, KG-47/21 and KG-40-39/3, which makes these lines similar to each other in most of the traits analyzed. The Pobeda variety is represented in the pedigree KG-199/4 and KG-307/4, while Studenica is found in the pedigree KG-162/7 and KG-191/5-13. These represent the basis of the similarity of these genotypes and their grouping into the first cluster. It can be observed that some related varieties are in different groups. Thus, Pobeda is in the first cluster, while the genotypes KG-27/6 and KG-28/6, whose germplasm represents the Pobeda variety as one of the parents, are in the second cluster. The difference in stem height between these genetically related genotypes and Pobeda indicates different directions in their selection.

Conclusion

Analysis of phenotypic expression of morphological and productive traits revealed the adaptability and stability of grain yield of wheat genotypes selected at the Center for Small Grains in Kragujevac (Serbia) in year with extreme wet conditions in the period of intensive wheat development. Appearance of years with prevailing extreme wet conditions is relatively rare but further researches are needed for maintaining satisfactory level of yield and quality of wheat. Genotypes KG-60-3/3 and KG-52/23 achieved the highest average grain yield in all three localities as well as the highest grain mass/plant. The KG-191/5-13 genotype achieved Y, GMS, SL, WFL, PH and LFI above average values in all three localities, while GMP, LTI and NSS were around average. Also, the KG-1/6 genotype had most of the desirable traits above average and can be singled out as a desirable parent in breeding and breeding programs to create new varieties of wheat. In order to increase and enhance biodiversity as well as to create new desirable gene recombinations, it is necessary to hybridize the genotypes of the first and second cluster groups. In progeny resulting from these hybridizations, new lines with improved morphological and productive characteristics can be expected, adapted to different environment as well as stressful environmental conditions.

Acknowledgements. This research was supported by Ministry of Education, Science and Technology Development of Republic of Serbia, Project III 46006. Autors wish to thank the Institute for forage crops in Kruševac (Dr Snežana Babić), as well as Agroinstitute in Sombor (Vladimir Sabadoš) for realization of field experiment.

REFERENCES

[1] Akcura, M. (2009): Genetic variability and interrelationship among grain yield and some quality traits in Turkish winter durum wheat landraces. – Turkish Journal of Agriculture and Forestry 33: 547-556.
[2] Ali, I. H., Shakor, E. F. (2012): Heritability, variability, genetic correlation and path analysis for quantitative traits in durum and bread wheat under dry farming conditions. – Mesopotamia Journal of Agriculture 40(4): 27-39.
[3] Araus, J. L., Slafer, G. A., Royo, C., Serret, M. D. (2008): Breeding for Yield Potential and Stress Adaptation in Cereals. – Critical Reviews in Plant Science 27: 377-412.
[4] Banjac, B., Petrović, S., Dimitrijević, M., Dozet, D. (2010): Estimation of correlation coefficient among yield parameters of wheat under stress conditions. – Annals of Agronomy 34(1): 60-68.
[5] Berry, P. M., Sylvester-Bradley, R., Berry, S. (2007): Ideotype design for lodging-resistant wheat. – Euphytica 154: 165-179.

http://www.aloki.hu ● ISSN 1589 1623 (Print) ● ISSN1785 0037 (Online)
DOI: http://dx.doi.org/10.15666/aeer/1804_58575871

[6] Berry, P. M., Berry, S. T. (2015): Understanding the genetic control of lodging-associated plant characters in winter wheat (*Triticum aestivum* L.). – Euphytica 205(3): 671-689.
[7] Bhutta, W. M., Ibrahim, M., Tahira, A. (2006): Association analysis of some morphological traits of wheat (*Triticum aestivum* L.) under field stress conditions. – Plant, Soil and Environment 52(4): 171-177.
[8] Hristov, N., Mladenov, N., Kondić-Špika, A. (2007): Environmental stability of physical traits of wheat grain. – Proceedings of the Institute of Field and Vegetable Crops, Novi Sad 43: 29-37.
[9] Hristov, N., Mladenov, N., Kondić-Špika, A., Marjanović-Jeromela, B., Jocković, B., Jaćimović, B. (2011): Effect of environmental and genetic factors on the correlation and stability of grain yield components in wheat. – Genetika 43(1): 141-152.
[10] Janmohammadi, M., Movahedi, Y., Sabaghnia, N. (2014): Multivariate statistical analysis of some traits of bread wheat for breeding under rainfed conditions. –Journal of Agricultural Sciences 59(1): 1-14.
[11] Karim Hasnat, M. D., Jahan, M. A. (2013): Study of Lodging Resistance and Its Associated Traits in Bread Wheat. – Journal of Agricultural and Biological Science 8(10): 683-687.
[12] Kumar, N., Kulwal, P. L., Balyan, H. S., Gupta, P. K. (2007): QTL mapping for yield and yield contributing traits in two mapping populations of bread wheat. – Molecular Breeding 19: 163-177.
[13] Mladenov, N., Denčić, S., Hristov, N. (2007): Breeding for grain yeld and components of yeld in wheat. – Proceedings of the Institute of Field and Vegetable Crops 43: 21-27.
[14] Mohammadi, M., Karimizadeh, R., Sabaghnia, N., Shefazadeh, M. K. (2012): Genotype environment interaction and yield stability analysis of new improved bread wheat genotypes. – Turkish Journal of Field Crops 17(1): 67-73.
[15] Pinera-Chavez, F. J., Berry, P. M., Foulkes, M. J., Molero, G., Reynolds, M. P. (2016): Avoiding lodging in irrigated spring wheat. II. Genetic variation of stem and root structural properties. – Field Crops Research 196: 64-74.
[16] Rajičić, V., Perišić, V., Madić, M., Popović, V., Perišić, V., Luković, K., Terzić, D. (2019): Grain yield and quality of winter wheat cultivars. – Proceeding of the X International Scientific Agricultural Symposium "Agrosym 2019", Jahorina.
[17] Rharrabti, Y., Garcíadel Moral, L. F., Villegasb, D., Royo, C. (2003): Durum wheat quality in Mediterranean environments III. Stability and comparative methods in analysing G × E interaction. – Field Crop Research 80: 141-146.
[18] Sabaghnia, N., Janmohammadi, M. (2014): Interrelationships among some morphological traits of wheat (*Triticum aestivum* L.) cultivars using biplot. – Botanica Lithuanica 20(1): 19-26.
[19] Stanojević, G. (2012): Analysis of annual precipitation sums in Serbia. – Journal of the Geographical Institute "Jovan Cvijić" 62(2): 1-13.
[20] Taneva, K., Bozhanova, V., Petrova, I. (2019): Variability, heritability and genetic advance of some grain quality traits and grain yield in durum wheat genotypes. – Bulgarian Journal of Agricultural Science 25(2): 288-295.
[21] Terzić, D., Đekić, V., Milivojević, M., Branković, S., Perišić, V., Perišić, V., Đokić, D. (2018): Yield components and yield of winter wheat in different years of research. – Biological Nyssana 9(2): 119-131.
[22] Tošić, I., Unkašević, M. (2013): Climate changes in Serbia. – Monography, Belgrade.
[23] Tripathi, S. N., Marker, S., Pandey, P., Jaiswal, K. K., Tiwari, D. K. (2011): Relationship between Some Morphological and Physiological Traits with Grain Yield in Bread Wheat (*Triticum aestivum* L. em.Thell.). – Trends in Applied Sciences Research 6(9): 1037-1045.
[24] Varsha, J., Verma, P., Saini, P., Singh, V., Yashvee, S. (2019): Genetic variability of wheat (*Triticum aestivum* L.) genotypes for agro-morphological traits and their

http://www.aloki.hu ● ISSN 1589 1623 (Print) ● ISSN1785 0037 (Online)
DOI: http://dx.doi.org/10.15666/aeer/1804_58575871

correlation and path analysis. – Journal of Pharmacognosy and Phytochemistry 8(4): 2290-2294.

[25] Xhulaj, D. B., Elezi, F., Hobdari, V. (2019): Interrelation ships among traits and morphological diversity of wheat (*Triticum aestivum* L.) accessions in base collection of Plant Genetic Resources Institute, Albania. – Acta Agriculturae Slovenica 113(1): 163-179.

[26] Xu, X., Gao, P., Zhu, X., Guo, W., Ding, J., Li, C. (2018): Estimating the responses of winter wheat yields to moisture variations in the past 35 years in Jiangsu Province of China. – PLoS One 13(1): 191-217.

[27] Yao, J., Ma, H., Zhang, P., Ren, L., Yang, X., Yao, G., Zhang, P., Zhou, M. (2011): Inheritance of stem strength and its correlations with culm morphological traits in wheat (*Triticum aestivum* L.). – Canadian Journal of Plant Science 91: 1065-1070.

[28] Yu, Z., Li, Z., Yan, B. (2003): Multiple correlation analysis on physical strength and properties of wheat stalk. – Hubei Agricultural Sciences 1(4): 11-14.

[29] Zampieri, M., Ceglar, A., Dentener, F., Toreti, A. (2017): Wheat yield loss attributable to heat waves, drought and water excess at the global, national and subnational scales. – Environmental Research Letters 12(6): 1-11.

[30] Zečević, V., Knežević, D., Mićanović, D. (2004): Genetic correlations and path-coefficient analysis of yield and quality components in wheat (*Triticum aestivum* L.). – Genetica 36(1): 13-21.

[31] Zuber, U., Winzeler, H., Messmer, M. M., Keller, M., Keller, B., Schmid, J. E., Stamp, P. (1999): Morphological traits associated with lodging resistance of spring wheat (*Triticum aestivum* L.). – Journal of Agronomy and Crop Science 182: 17-24.

http://www.aloki.hu ● ISSN 1589 1623 (Print) ● ISSN1785 0037 (Online)
DOI: http://dx.doi.org/10.15666/aeer/1804_58575871

JUNGLE CAT (*FELIS CHAUS* SCHREBER, 1777) POPULATION DENSITY ESTIMATES, ACTIVITY PATTERN AND SPATIOTEMPORAL INTERACTIONS WITH HUMANS AND OTHER WILDLIFE SPECIES IN TURKEY

ÜNAL, Y.[1*] – ERYILMAZ, A.[2]

[1]*Isparta University of Applied Sciences, Faculty of Forestry, 32260 Isparta, Turkey*

[2]*Isparta University of Applied Sciences, The Institute of Graduate Education, 32260 Isparta, Turkey*

[*]*Corresponding author*
e-mail: yasinunal@isparta.edu.tr

(Received 6th Mar 2020; accepted 10th Jul 2020)

Abstract. Although the jungle cat (*Felis chaus*) has been listed as a species of Least Concern – (LC status) by IUCN data, there are many threats endangering the population of the jungle cat in Turkey. Currently, relatively little is known about their population status and ecology. Our study aims to determine the jungle cat's population density, interactions among humans and other wild animals, and the diel activity patterns. This research was carried out in the northern part of Eğirdir Lake within the borders of Isparta province between March 2016 and July 2017. Presence absence studies were carried out and evaluated using 15 camera traps, placed in 193 stations based on the opportunist method in areas where trail-marks of the jungle cat were detected. Throughout the study 83 camera trap data belonging to jungle cats over 4403 camera trapping days were obtained from 193 stations. This study provides the 1st robust estimation of the jungle cat population size and spatiotemporal interactions of humans and other wildlife species in Turkey. As a result of this study, it was concluded that human activity affects wildlife behavior and that wild animals are haivng to adjust their living and feeding behaviors according to human activity. How human activity affects wildlife behavior. Our study underlines the need to consider activity patterns of wildlife for conservation and environmental management planning.
Keywords: *human-wildlife interactions, terrestrial mammals, camera trapping, capture-recapture, diurnal-nocturnal, human pressure, Turkey*

Introduction

In recent years, wildlife have been subject to increased threat by human-induced activity such as narrowed and fragmented habitats, dwindling numbers of prey in their natural areas, and inadequate nutrition due to the proximity of human settlements (Kerley et al., 2002; Treves and Karanth, 2003; Dhungana et al., 2017). Factors including industrialization, forest fires, increased tourism, as well as illegal and excessive hunting all contribute to habitat destruction (Soyumert, 2010; Ünal and Çulhacı, 2018). Despite differences in these mortality factors affecting various species in different parts of the world, researchers agree that human-induced threat is a global problem and is observed largely in carnivorous species (Durant, 1998; Bisi et al., 2007; Rawshan et al., 2012; Seoraj-Pillai and Pillay, 2016).

Despite Turkey's rich biodiversity, 8 of the 21 terrestrial predator populations have been decreasing in numbers due to the factors mentioned above (Can and Togan, 2004; Capitani et al., 2016). Among these species, the grey wolf (*Canis Lupus*), Eurasian lynx (*Lynx lynx*) (Chynoweth et al., 2015), brown bear (*Ursus arctos*) (Ambarlı et al., 2016) and caracal (*Caracal caracal*) (Giannatos et al., 2006; Ilemin and Gurkan, 2010; Oğurlu and Ünal,

http://www.aloki.hu ● ISSN 1589 1623 (Print) ● ISSN1785 0037 (Online)
DOI: http://dx.doi.org/10.15666/aeer/1804_58735890

2011; Ünal et al., 2019). The jungle cat (*Felis chaus*) is one of the five cat species still found in Turkey, along with the Eurasian lynx, Caracal, wild cat (*Felis silvestris*) and Anatolian leopard (*Panthera pardus*) (İlemin and Gurkan, 2010; Gerngross, 2014). The jungle cat is a medium-sized, long-legged cat, and the largest of the extant Felis species. The head-and-body length is typically between 59 and 76 cm (Eryılmaz, 2017). The species was first recorded in Turkey in 2007 around the Adana - Akyatan Lagoon (Avgan, 2009). Even though the jungle cat has been listed as Least Concern (LC) by 2018 IUCN data, jungles cats have struggled to survive due to increased human threat, including the conversion of swamps into agriculture areas, excessive destruction and burning of wetland reeds, eradication of rodents and extensive use of pesticides (Linnell et al., 2001; Madden, 2008; Gray et al., 2016; IUCN, 2018).

In recent years, the use of camera traps in population studies of rare terrestrial mammals has gradually increased (Silveira et al., 2003; Evcin et al., 2017). With the development of technology, reduced costs and effective results compared to other methods, camera-trapping has become the preferred method of study (Tobler et al., 2008). This method has an important role in the detection of rare terrestrial predatory mammals, including the jungle cat, and is practical for monitoring relative and absolute abundance, and obtaining data related to population condition, species behavior, habitat preferences, and diel activity patterns (Kays and Slauson, 2008; Kays et al., 2010; Linkie and Ridout, 2011). Both opportunist and systematic methods are used in wildlife studies in conjunction with camera trapping to obtain information about species populations. The Opportunist method ensures maximum data by taking into account the maximum use of space of a target species spread across a certain area (Soyumert, 2010). Data is acquired by deploying camera trap stations close to the paths, tracks and signs of the target species, their nest location, feeding places, and areas that supply water (Ünal et al., 2019).

Camera trapping studies performed on species with patterned furs, such as the jungle cat, tiger (*Panthera tigris*) (Karanth et al., 2006), lynx (Weingarth et al., 2012), and wild cat (Can et al., 2011), increases the importance of individual identification and population density research by means of fur patterns that are unique to individuals (Carbone et al., 2001; Mengüllüoğlu, 2010; Alfred, 2015).

The ability and degree to which terrestrial carnivores can coexist with humans over a sustained period of time is a considerable issue in conservation science and policy (Woodroffe et al., 2005; Dickman et al., 2011; Carter et al., 2012). Numerous research projects have been carried out to facilitate coexistence at different spatial scales. Over the past decade human and wildlife interactions have been shown as one of the most important problems limiting the number of species that can occupy an assemblage as a result of their similarity in habitats (Sillero-Zubiri and Laurenson, 2001; Di Bitetti et al., 2009). Terrestrial predators are the living group directly affected by these interactions, regardless of their size (Bisi et al., 2007). Although rural settlements consistently express negative attitudes toward large carnivores, they often constitute a minor problem compared with plant and forest pests such as microtine rodents and feral dogs (Ünal et al., 2020). If terrestrial predators do not harm agricultural areas or pets of local people, positive interactions can be mentioned rather than conflict (Durant, 1998; Rawshan et al., 2012). In such positive interactions, predatory mammals find ways to minimize spatiotemporal encounters with humans even though they have spread around human settlements (Ramesh et al., 2012). In this regard, Carter et al. (2012), report tigers in Nepal's Chitwan National park offsetting their temporal activities, especially outside the park, by being less active during the day when human activity peaked. Tiger population density is high despite the daytime human density in this protected area.

http://www.aloki.hu ● ISSN 1589 1623 (Print) ● ISSN1785 0037 (Online)
DOI: http://dx.doi.org/10.15666/aeer/1804_58735890

Capture-Recapture models are used to analyze population density. This model has become more prominent because it allows for individual diagnosis of spotted pattern structure of jungle cats in order to estimate population size. Many studies using records about target species, reveal data obtained by the statistical proportion of the captured, re-captured and freely captured individuals (Hammond, 2009; Urian et al., 2014).

Previous research conducted on observed problems including habitat loss, severe poaching of wildlife, human-jungle cat interactions, and direct threat to the jungle cat population (Oğurlu et al., 2010). Wildlife experts need comprehensive inventory data to effectively manage and conserve jungle cats in this region. Our study aims to determine the jungle cat's population density, interactions among humans and other wild animals, and the diel activity patterns.

In this study, we test three specific hypotheses: (i) despite high human density the jungle cat has a positive spatial interaction with humans if it can survive (ii) jungle cats are more active at night to avoid human disturbance and (iii) jungle cat spatiotemporal patterns overlap those of other wild animals. To test these hypotheses empirically, we used camera trapping.

Materials and methods

Study area

This research was carried out in habitats around Eğirdir lake particularly in the southern part of the north section of the lake (38015'K-30052'D), located within the borders of Eğirdir, Gelendost, Yalvaç and Senirkent districts in the province of Isparta. Eğirdir lake is the fourth-largest lake, but also the second-largest freshwater lake in Turkey. In addition to being a suitable habitat for spawning fish due to its shallowness and reed field (*Fig. 1*) (Fethi et al., 2014; Tağıl and Alevyakalı, 2014), Eğirdir Lake, shows the characteristics of being an important feeding area for jungle cats (Oğurlu et al., 2010).

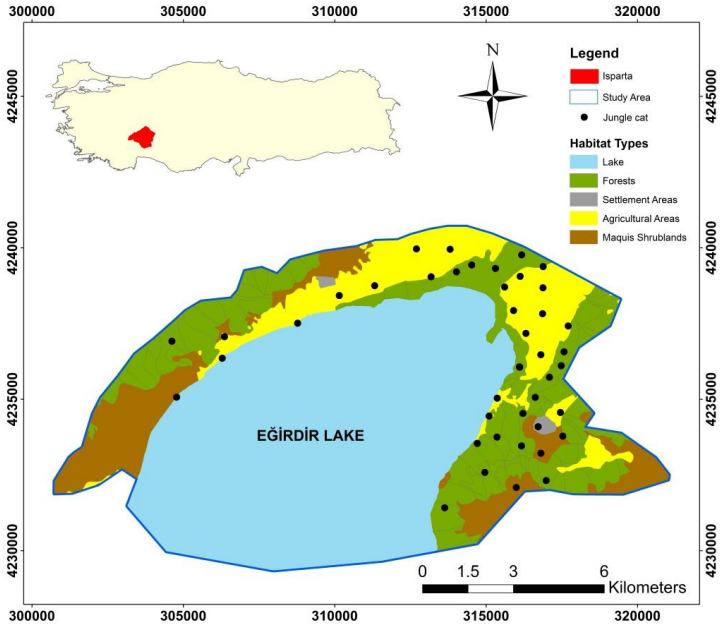

Figure 1. *Location map of the study area*

http://www.aloki.hu ● ISSN 1589 1623 (Print) ● ISSN1785 0037 (Online)
DOI: http://dx.doi.org/10.15666/aeer/1804_58735890

The area is approximately 10.7 km^2. In addition to intensive agriculture, fishing, grazing of livestock, and hunting activities are carried out in most parts of the area. There are 4 villages in the research area where the jungle cat interacts directly. 33.1% of the locals in the village are engaged in agriculture, 12.5% in livestock and 3.1% in fishing. The climate of the region is in a transition zone between Mediterranean and Central Anatolian climates. Precipitation varies 63 mm between the driest and wettest months of the year, while the average temperature throughout the year is approximately 20.2 °C.

In the research area, shrubs, such as kermes oak (*Quercus coccifera*), colutea (*Colutea melanocalyx*), terebinths (*Pistacia terebinthus*) and ephedra (*Ephedra major*), yellow jasmine (*Jasminum fruticans*), narrow-leafed ash (*Fraxinus angustifolia*) and manna ash (*Fraxinus ornus*) are found in low altitude habitats near the lake. Foetid juniper (*Juniperus foetidissima*) and European barberry (*Berberis crataegina*) were spread in relatively rugged habitats up to 1400 - 1500 meters. Above 1500 m, Junipers were scattered throughout an alpine zone (Karatepe, 2004).

Data collection

During the research period, 15 camera traps were deployed in 193 camera trap stations using the opportunist method (Harmsen et al., 2011). Google Earth, ArcMap 10.4 and Microsoft Excel programs were used to display the camera trap stations on the map. KeepGuard Color Viewer (KG860) camera traps were used, featuring non-glare infrared shooting, 12 MP maximum resolution ability, 0.25 seconds trigger time, 25-meters night vision distance, simultaneous 1-5 photo capture, and video capture (Mengüllüoğlu et al., 2019).

Camera traps were positioned in suitable and sheltered tree trunks ranging within 0.30-1.00 m from the ground (Amaya-Castaño and Palomares, 2018). Each camera trap period was designated as an average of 30 days. The total number of days that all camera traps were actively working since the date of their establishment, namely the "camera trapping day value", was calculated as 4403; (*Table 1*) (Stein et al., 2008).

Table 1. *Number of camera trappings, ratio, and days captured*

Species	Camera trap day	Num. of photos	Prop. of photos	Days captured	Num. of 100 Days Captured
Felis chaus	4.403	**83**	**3.1**	**77**	**1.89**
Human		135	5.2	88	3.07
Canis aureus		614	24.07	283	13.95
Sus scrofa		1115	43.5	358	25.32
Lepus europaea		136	5.1	95	3.09
Vulpes vulpes		224	8.7	156	5.09
Martes foina		37	1.5	37	0.84
Canis lupus		3	0.8	3	0.07
Livestock		205	8.03	123	4.66

Data analysis

The jungle cat is a long-legged and relatively short-tailed wild cat. Although individuals differ in color and patterns, they are generally gray. Individuals can be identified by unique asymmetrical patterns and lines covering both sides of the legs and body. The most distinct of these natural marks are the patterns on the hind legs. Small differences in these marks enable individuals to be distinguished from each other

http://www.aloki.hu ● ISSN 1589 1623 (Print) ● ISSN1785 0037 (Online)
DOI: http://dx.doi.org/10.15666/aeer/1804_58735890

(Fitzgerald, 2011). Individuals were recognized based on the identification of strips on their hind legs from the jungle cat camera trap records using the WildID camera trap record assessment program (Carter et al., 2013). The striped patterns on the hind legs were drawn on individuals using Microsoft Powerpoint. Images were compared and individual jungle cats were assigned a unique identifier number (Mengüllüoğlu, 2010; Avgan et al., 2014; Ünal and Culhacı, 2018) (*Fig. 2*).

Figure 2. *Two jungle cat individuals with unique fur patterns on their hind legs in the study area. Patterns were identified to based on both of camera trap and photo records using the WildID camera trap record assement program. Patterns were highlighted for visualization using Microsoft Powerpoint (Photo: Ogün Çağlayan TÜRKAY)*

Camera trap recordings were used to determine the daily activity patterns of jungle cats, other wild animals and humans. On certain occasions, individuals were captured more than once at single a camera station over a 5 minute period. Thus, to avoid pseudoreplication, we considered the 1st capture of the animal as an independent record, and subsequent captures within the 5-min time frame were censored. We tested the mean activity pattern of jungle cats, other wild animals and humans using ORIANA 4.0 Software. This software offers a wide range of analyses including rose diagrams, circular histograms, raw data plots, arrow data plots and linear histograms. The rose diagram is a histogram displayed in a circle, similar to the pie chart for linear data. However, each sector represents the frequency or number of observations that falls in the range of angles. The concentric circles show the frequency of the observations for each angular value (Hassan et al., 2009). To detect daily activity patterns of target species, the 24-hour period is divided into hourly sections, and each independent record is classified within these intervals (Pérez-Irineo and Santos-Moreno, 2016). The diel activity pattern graph was formed by evaluating camera trapping data appropriately. A rose diagram was prepared using ORIANA 4.0 (Kovach, 2011; Ünal, et al., 2019).

In order to determine the effect of human activity and presence on jungle cat and wildlife populations the risk ratio (RR) as a measure of effect size was calculated for each species. The percentage of activity that occurred at night (by camera trap) at sites or during seasons of high human disturbance (Xh) was compared with nighttime activity under low disturbance (Xl), using the *equation 1*.

$$RR = ln(Xh/Xl) \quad \text{(Eq.1)}$$

A positive RR indicated a relatively greater degree of nocturnality than diurnality in response to humans, while a negative RR indicated reduced nocturnal behavior. Sampling variance (S) of effect size was calculated using GraphPad Prism 8 random-effects models.

http://www.aloki.hu ● ISSN 1589 1623 (Print) ● ISSN1785 0037 (Online)
DOI: http://dx.doi.org/10.15666/aeer/1804_58735890

These models estimated the overall effect of human disturbance on jungle cat and other wild animals (Gaynor et al., 2010).

We used the Capture-Recapture model in order to estimate the jungle cat population (Grimm et al., 2014). This model, allows for the comparison and combination of statistical methods and identifies the minimum, maximum and average results of the population (Soria-Díaz and Monroy-Vilchis, 2015). Therefore, in the CAPTURE2 software, using Jackknife-M (h) (Silver et al., 2004), Chao M (h) (Karanth, 1995) Zippen-M (b) and Removal-M (bh) (Forbes et al., 2014) approach, we obtained the minimum and maximum population density. To evaluate the accuracy of the results, we used 3 different methods;

Lincoln-Peterson Index

$$\dot{T}: ((X + 1)(x + 1))/y + 1) - 1 \quad \text{(Eq.2)}$$

Bailey's Modification Index

$$\dot{T}: (X(x + 1))/(y + 1) \quad \text{(Eq.3)}$$

Schnabel Method

$$\dot{T}: \sum t(xy)/(\sum tX \quad \text{(Eq.4)}$$

Confidence intervals

$$(CI95\% = \dot{T} \pm 1{,}96(SE) \quad \text{(Eq.5)}$$

The Standard error (SE)

$$\sqrt{\dot{T}2(y - x)/(y + 1)(x + 2)} \quad \text{(Eq.6)}$$

The initial method of Capture-Recapture studies uses the Lincoln-Peterson Index which is considered as the standard technique (Jibasen, 2011; Bukhari et al., 2019).

In this formula, X denotes the number of individuals captured and marked in the first sampling, y is the number of individuals independently captured in the second sampling, x is the number of previously marked and recaptured individuals, and $\dot{T}$ denotes the estimated population size (Alcoy, 2013; Pochardt et al., 2019).

Results

Camera recording and density estimates

We obtained 36491 images from 193 stations that were placed using the opportunist method by means of trace and fecal surveys carried out in the field. 3104 wild animal records (8.50%) were derived. Over the course of the study, the camera trapping day value reached 4403. 83 jungle cat records (camera trap recording rate (RI) 3.1%) were obtained over 77 camera trapping days. Jungle cats were found to be spread in habitats near the lake at the rate of RI: 47.5% (Duckworth et al., 2005; Gupta et al., 2009). A total of 2550 camera trappings were obtained from other mammalian species. Apart from the jungle cat, 8 other mammal species in the region, including the golden jackal (*Canis aureus*),

http://www.aloki.hu ● ISSN 1589 1623 (Print) ● ISSN1785 0037 (Online)
DOI: http://dx.doi.org/10.15666/aeer/1804_58735890

gray wolf, red fox (*Vulpes vulpes*), European rabbit (*Lepus europaeus*), beech marten (*Martes foina*), wild boar (*Sus scrofa*) and least weasel (*Mustela nivalis*) were recorded from the camera trap surveys.

Active day values of each camera trapping were assessed and recorded (Stein et al., 2008; Wang and Macdonald, 2009). Due to the difference of monthly inspection times, lost or stolen camera traps, and unequal monthly recording times, the data were converted to fix as 100 days. For this purpose the number of records/camera trapping day number equation was used (Kinnaird and O'Brien, 2012; Keten, 2016). Due to insufficient recordings of gray wolves and least weasels, these two species were not included in the analysis.

After evaluating the results from the Lincoln-Peterson index, Bailey's Modification Index and Schnabel Index, the population size was calculated in the range of 21.82 <N> 22.50 km^2, (SI: 3.12-3.21). In the CAPTURE2 Population estimation program, Removal M (bh) was calculated as 2.34/km^2, (SI:3.16) and gave the closest population density value to index. The smallest population value of all results was calculated as Zippen-M (b): 1.96/km^2 (SI:1.89) (*Fig. 3*).

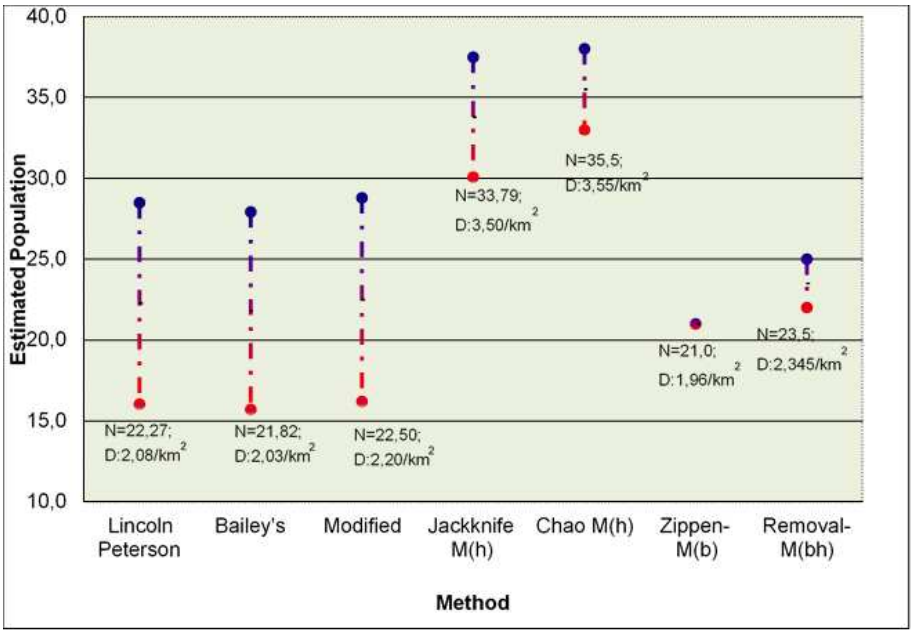

Figure 3. *Comparison of population size estimate methods*

Jungle cat, human, livestock and other wild animals species interactions

We measured the spatiotemporal activity patterns of six mammals and human activity in the research area (Shamoon et al., 2018). The daily changes of activity and graphic representation of rose diagrams were generated using Oriana 4.0 (*Fig. 4*) (Leuchtenberger et al., 2018). Our results indicated that humans were active during the day and withdrew from the field under dark conditions. Jungle cats and other wildlife on the other hand showed higher activity following human withdraw from the field. According to the GraphPad Prism 8 random-effects models no human activity was encountered between dusk and morning (RR: -1.41; S: 0.0405). Although the jungle cat is mostly nocturnal it was observed displaying diurnal behavior (RR: -0.011; S:0.0027). However, its diurnal

http://www.aloki.hu ● ISSN 1589 1623 (Print) ● ISSN1785 0037 (Online)
DOI: http://dx.doi.org/10.15666/aeer/1804_58735890

behavior occurred at a lower level compared to nocturnality. Other wild animals had positive values in the range of RR: 2.97-4.373; S: 0.0412-0.989 (*Fig. 5*). Gaynor et al. (2010) reported that nocturnality of wild animals increased positively in habitats with intense human pressure, supporting our results. Wild boar (*S. scrofa*), European rabbit (*L. europeaus*), and beech marten (*M. foina*) species, which typically show diurnal behavior in natural areas with low human pressure displayed limited daytime activity in our study and were only active at nighttime, once people had retreated from their fields (Posillico et al., 1995; Stolle et al., 2015).

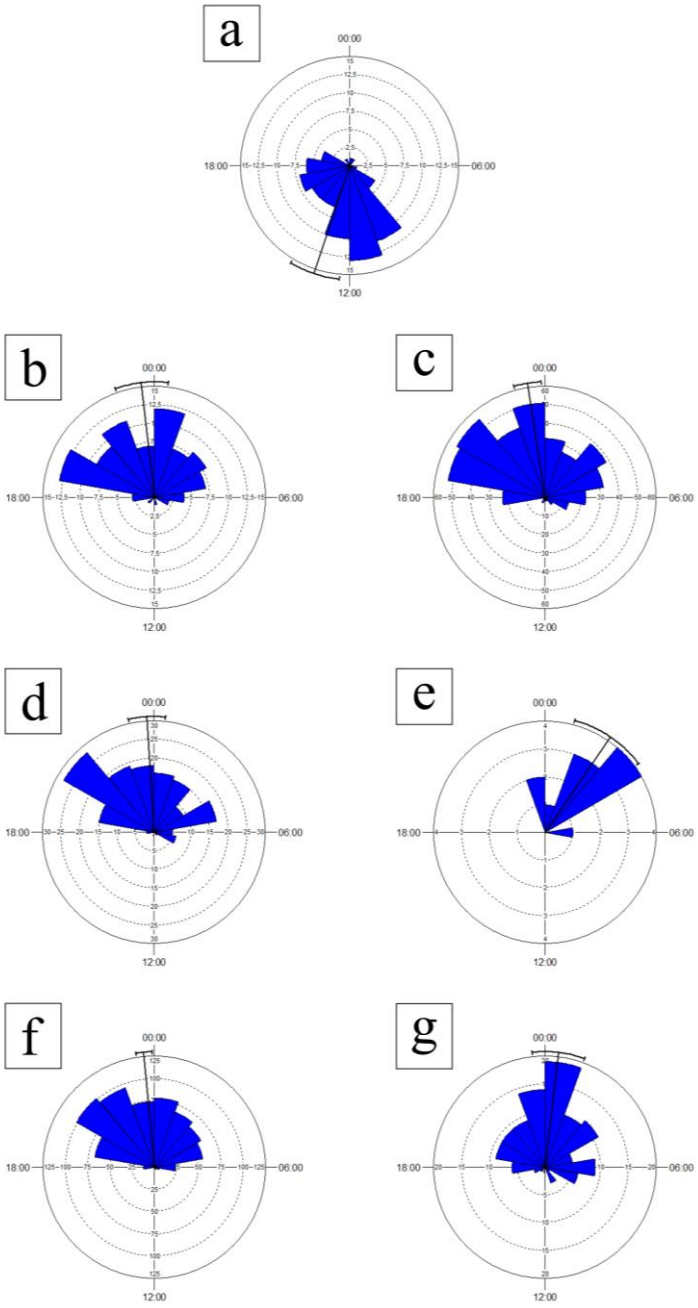

Figure 4. *Temporal activity patterns a) human, b) jungle cat, c) golden jackal, d) red fox, e) beech marten, f) wild boar, g) Eupoean hare on different habitats near the Eğirdir Lake in the Isparta, TURKEY: blue bars indicates mean dial activity with 95% confidence interval*

http://www.aloki.hu ● ISSN 1589 1623 (Print) ● ISSN1785 0037 (Online)
DOI: http://dx.doi.org/10.15666/aeer/1804_58735890

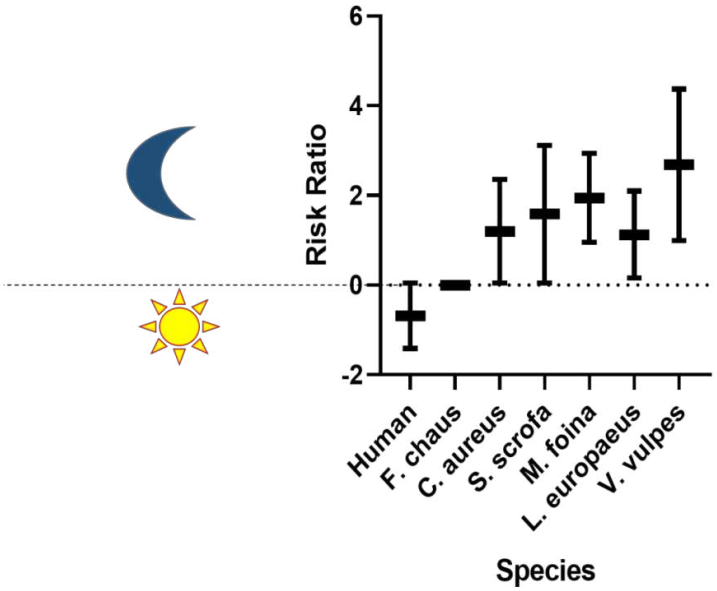

Figure 5. *GraphPad Prism 8, jungle cat, human and other wild animals random-effects models*

Discussion

This study was carried out in jungle cat habitat around Eğirdir Lake between 2016 and 2017. Few studies have been conducted so far about the population ecology of the jungle cat in Turkey (Oğurlu et al., 2010; Mert and Acarer, 2018). Our study was the first comprehensive study using emerging technologies such as camera trapping to reveal population density, diel activity pattern, habitat preference of the jungle cat, and its interactions with humans and other species. This study revealed nine terrestrial mammals species, occurring in the study area along with humans and livestock. The jungle cat was the only important and rare predator species in the study area. Our study results demonstrate how jungle cats respond to human presence at fine scales, as small as 10.7 km^2. In our research area, we found that jungle cats adjust the spatiotemporal patterns of human activity and have a positive interaction with humans despite high human density. Furthermore, as the jungle cat is often seen in areas where human presence is ubiquitous, studies that evaluate the interconnections between jungle cats and people across different land management regimes need to be developed for robust landscape-scale conservation strategies.

Research suggests that the jungle cat's global population is declining and gradually moving towards the threatened border. The European population has been reported as rapidly declining since the 1960s. Reports from Russia identify about 500 animals remaining in the wild, while a very small population exists in Georgia (Duckworth et al., 2005). Due to the jungle cats habitat proximity to rural settlements, it has been observed that jungle cats are struggling to survive from threats such as habitat fragmentation, environmental pollution, waterbird hunting, intensive pressure from vehicles, agriculture, fishing and grazing, conversion of swamps into agricultural areas, excessive destruction and burning of wetland reeds, control of rodent populations, and heavy use of pesticides (Linnell et al., 2001; Madden, 2008; Oğurlu et al., 2010). Similarly, our study confirmed some of the stated issues contributing to the declining population of jungle cats in the

http://www.aloki.hu ● ISSN 1589 1623 (Print) ● ISSN1785 0037 (Online)
DOI: http://dx.doi.org/10.15666/aeer/1804_58735890

research area. Therefore, the methodology and results of our study are vital for preserving the jungle cat populations in Turkey.

The capture-recapture model has been used for estimating densities of one of Turkey's most important predator felis species, the jungle cat. The previous conventional analyses of obtaining population density have given way to more robust methods that use the spatial information of the location of traps rather than methods that estimate the size of the effective area heuristically. It was concluded that the Capture-Recapture method gave statistically reliable results for the jungle cat population. To increase the reliability rate of results, it was ensured that the camera traps function for at least 20 days in each camera trap period, as recommended by Gupta et al. (2009) and Jansen et al. (2014). Throughout the study it was found that 15 out of 83 individuals, who were caught on camera traps over 77 trap days, were different individuals. In a camera trap period, the highest capture rate for the same camera trap was functioning as 7 records at site no_0077, near the lake. Additionally, 5 records from each of the 3 camera trap sites (fi_31, fi_106, fi_129) placed around the lake were the biggest indication that the species behaved diurnally in this habitat type (Gupta et al., 2009; Avgan et al., 2014). It is understood that the jungle cat was passive in forest habitats during the day, while it was active in habitats at point zero of the lake from the first hours of night. The jungle cat, human and livestock activity in this area appeared to be the same within the context of spatiotemporal response. Our findings suggested that jungle cats are adjusting their spatiotemporal activity patterns to people, supporting the 1st and 2nd hypotheses. The jungle cat had a positive interaction with humans despite high human density. However, there was a clear difference in temporal activity. Jungle cats were more active at night to avoid human disturbance. It is a known fact that this area is used by humans in the daytime, and by jungle cats after sunset. It is believed that the biggest reason for the jungle cat to arrive at these hours was to feed on fish scraps cleaned by fishermen or dead and live fish in the shallow part of the lake (Oğurlu et al., 2010; Oğurlu, 2015). Apart from night feeding, the jungle cat preferred to rest and isolate itself in its natural forest habitat, far from humans. The decrease in the rate of being caught on camera traps as it moved towards the forest habitats was an indicator of this case (Majumder et al., 2011).

It is clear that urban wildlife has both positive and negative interactions with humans. Historically, there has been a significant amount of research emphasis on clashes between city dwellers and wildlife. Now there is increasing recognition of the benefits that wildlife can bring (Soulsbury and White, 2015). According to our study results there was no fear of conflict between humans and jungle cats. On the contrary, cats helped farmers by eating mice on farmland and cleaned the lake environment by eating fish waste discarded by fishermen on the lakeshore. This systematic behavior of the forest cat created sympathy for the species by the locals. As a result, despite our widespread belief that terrestrial predators always clash with humans, our work has shown mutual cooperation between cats and local people (Inskip and Zimmermann, 2009; Chowdhury et al., 2015). Despite this conclusion, in order to avoid the need for human-induced harm to carnivore species in different areas, the priority of research should be focused on more human-wildlife conflict in urban areas and the human-wildlife relationship of wildlife management plans to which these species and people will be least affected. These plans need to be prepared and handled in a holistic way. There is a critical need to develop conceptual frameworks to understand human-wildlife interactions.

Jungle cats in our study site exhibited relatively high temporal overlap with other wild animals, lending some support for hypothesis 3. It was likely that jungle cats were

http://www.aloki.hu ● ISSN 1589 1623 (Print) ● ISSN1785 0037 (Online)
DOI: http://dx.doi.org/10.15666/aeer/1804_58735890

deliberately active when these species were active (*Fig. 6*). The complex landscapes consisting of agricultural area, forest and wetlands were the most preferred habitats for wild animals. The positive interaction of the jungle cat and other wild animals using these habitats existed due to a sufficient amount of nutrients for predatory species in these areas (Wegge et al., 2009). For example, prey species, such as vole and European rabbit (Prop. of photos: 5.1%), were relatively abundant for golden jackal, another large predator species (Prop. of photos: 24.07%). Therefore, there was a little conflict for food sources between predators.

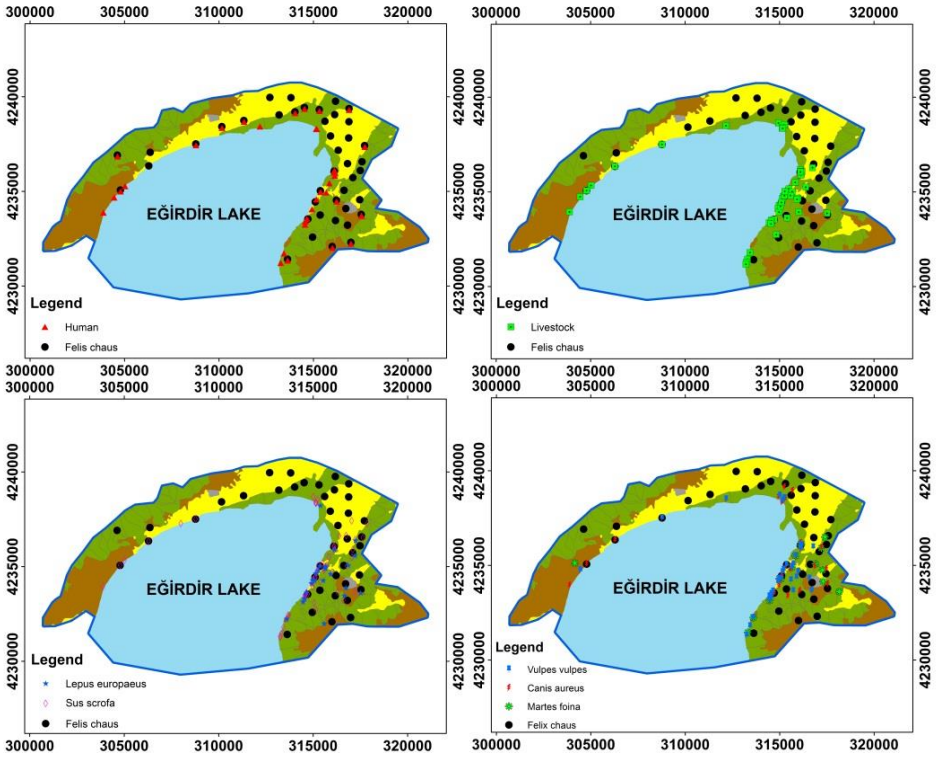

Figure 6. *Location of camera traps around Eğirdir Lake in Isparta province, capturing jungle cat, human, livestock and other important species at sampling locations within the Eğirdir Lake study area located in Turkey*

In our study, it was observed that all other wild animals, apart from the jungle cat, did not show any activity during the day (*Fig. 6*). Although humans, jungle cats and other wild animals in the area were not spatially separated, the temporal separation between them limited human contact rates (*Fig. 7*). With the exception of the jungle cat it is thought that nocturnal behavior in wild animals is preferred when humans have minimal activity, in order to comfortably feed and protect itself and its family. For this reason, jungle cats seen over the course of the study, smuggled or crushed on the highway supports this theory (Gaynor et al., 2010). Therefore changes in temporal niche should be taken into account by the Nature Conservation and National Parks Directorate. It is important that protection control is carried out after dark, throughout the night.

Based on the camera trap images, we observed no signs of jungle cat poaching by locals in the study, nor did we come across any snares while in the field (Carter et al., 2015). With the exception of human-boar conflict we did not encounter any conflicts between locals and wildlife (Carter et al., 2012). However, it is thought that poaching of

http://www.aloki.hu ● ISSN 1589 1623 (Print) ● ISSN1785 0037 (Online)
DOI: http://dx.doi.org/10.15666/aeer/1804_58735890

jungle cats is connected to fish, frog, bird and land hunters from outside the area. The fact that 5 of the camera traps installed in the study area were either broken or stolen is an indication of a problem with poachers rather than with local people (Ünal et al., 2019). The main task falls to the Ministry of Agriculture and Forestry, VI. Regional Directorate of Nature Conservation and National Parks. In order to protect an important predator species such as the jungle cat, and increase its generation, there is a need for better implementation of the laws and regulations protecting wildlife, as well as for educational and awareness-raising activities for local people (Johannesen, 2006). Eventually, it will be imperative to take conservation priority measures for the sustainable control of wildlife and biodiversity in key habitats where endangered wild animal species are spreading.

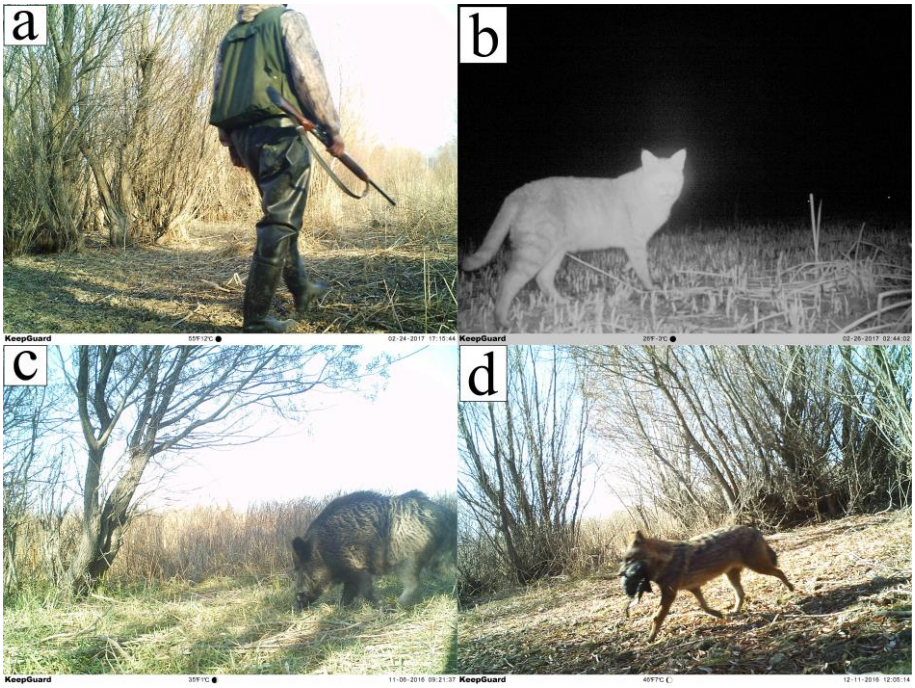

Figure 7. *Photographs of a human, b jungle cat, c wild boar, and d golden jackal captured at the same area during the study period*

A nationwide monitoring program is needed to identify wildlife population dynamics and their interactions with humans and other species. This could provide an opportunity to better understand the relationship between human restrictive factors and wildlife. We believe that this study provides important insight into the interaction of rare species such as the jungle cat with humans and other wildlife species.

In order to protect wild animals, special attention should be given to environmental and wildlife awareness training, especially for wildlife habitats and rural populations. Applicable solutions should be created to reduce the pressure of mortality factors, especially poaching of wild animals. However, as the human population grows in the developing world and shifts towards wildlife habitats, it is obvious that the damage to occur will mostly affect wild animals.

http://www.aloki.hu ● ISSN 1589 1623 (Print) ● ISSN1785 0037 (Online)
DOI: http://dx.doi.org/10.15666/aeer/1804_58735890

Conclusion

It is important to know that the response of a wild animal to different biotic and abiotic factors may vary between habitats. These responses can be positive or negative, but depend on the influence level of the factor. The greater the human pressure (population, poaching, recreation, etc.) in a living environment, the greater the variation of response in wild animal populations. Our research results show that the jungle cat and other wild animals have to adjust their daily behavior according to human activity in order to live and feed. In the research area, it was concluded that intense human activity in a small habitat such as 10.7 km^2 creates discomfort and stress for wildlife.

The jungle cat is among the endangered species in Turkey. The jungle cat is endangered due to poaching, loss of habitats, conversion of marshes into agricultural lands, the use of pesticides to control rodent populations in agriculture areas, and the consumption of poisoned rodents. In this context new scientific research should be carried out to form the basis for the conservation of the endangered jungle cat and its habitats. Additionally, Species Protection Action Plans should be prepared by expert teams. In these plans the importance for Turkey of the national and international protection status of the jungle cat (protection status within the framework of national and international legislation and contracts), determination of jungle cat population status, habitat analysis, and determination and protection status of these areas must be updated.

Funding information. This work was supported by the Ministry of Agriculture and Forestry, VI. Regional Directorate of Nature Conservation and National Parks.

Acknowledgements. We thank the fallow deer team (Ahmet Koca, Mehmet Şirin Yelsiz, Mevlüt Zenbilci, Kürşat Bal, Hasan Uysal), we thank Ogün Çağlayan Türkay for allowing us to use his photos and we gratefully thank Ibrahim Ozdemir, and Serkan Ozdemir for analysis, comments and contribution.

REFERENCES

[1] Alcoy, J. C. O. (2013): The Schnabel method: An Ecological approach to productive vocabulary size estimation. – International Proceedings of Economics Development and Research. doi: 10.7763/IPEDR. 2013. V68. 5.

[2] Alfred, J. R. B. (2015): Estimation of population trend of lesser cats by camera trap method in Buxa Tiger Reserve, West Bengal. – Nature Environment and Wildlife Socıety (News) 81p.

[3] Amaya-Castaño, G. C., Palomares, F. (2018): Effect of human influence on carnivore presence in a Mediterranean human-modified area in the Southwestern Iberian Peninsula. – Galemys 30. doi: 10.7325/Galemys.2018.A1.

[4] Ambarlı, H., Ertürk, A., Soyumert, A. (2016): Current status, distribution, and conservation of brown bear (Ursidae) and wild canids (gray wolf, golden jackal, and red fox; Canidae) in Turkey. – Turkish Journal of Zoology 40: 944-956. doi: 10.3906/zoo-1507-51.

[5] Avgan, B. (2009): Sighting of a jungle cat and the threats of its habitat in Turkey. – Cat News 50: 16.

[6] Avgan, B., Zimmermann, F., Güntert, M., Arıkan, F., Breitenmoser, U. (2014): The first density estimation of an isolated Eurasian lynx population in southwest Asia. – Wildlife Biology 20(4): 217-222.

[7] Bisi, J., Kurki, S., Svensberg, M., Liukkonen, T. (2007): Human dimensions of wolf (*Canis lupus*) conflicts in Finland. – European Journal of Wildlife Research 53: 304-314. doi: 10.1007/s10344-007-0092-4.

http://www.aloki.hu ● ISSN 1589 1623 (Print) ● ISSN1785 0037 (Online)
DOI: http://dx.doi.org/10.15666/aeer/1804_58735890

[8] Bukhari, N., Bukhari, S., Shehzad, M. A. (2019): Capture-Recapture sampling techniques: artificial and real population data analysis. – Journal of public value and administration insights 2(3): 15-16.
[9] Can, Ö. E., Togan, I. (2004): Status and management of brown bears in Turkey. – Ursus 15(1): 48-53.
[10] Can, Ö. E., Kandemir, İ., Togan, İ. (2011): The wildcat *Felis silvestris* in northern Turkey: assessment of status using camera trapping. – Oryx 45(01): 112-118.
[11] Capitani, C., Chynoweth, M., Kusak, J., Coban, E., Sekercioglu, C. H. (2016): Wolf diet in an agricultural landscape of north-eastern Turkey. – Mammalia 80: 329-334. https://doi.org/10.2192/1537-6176(2004)015<0048:SAMOBB.
[12] Carbone, C., Christie, S., Conforti, K., Coulson, T., Franklin, N., Ginsberg, J. R., Laidlaw, R. (2001): The use of photographic rates to estimate densities of tigers and other cryptic mammals. – Animal Conservation forum 4(1): 75-79.
[13] Carter, N. H., Shrestha, B. K., Karki, J. B., Pradhan, N. M. B., Liu, J. (2012): Coexistence between wildlife and humans at fine spatial scales. – Proceedings of the National Academy of Sciences 109(38): 15360-15365.
[14] Carter, K. D., Seddon, J. M., Frère, C. H., Carter, J. K., Goldizen, A. W. (2013): Fission–fusion dynamics in wild giraffes may be driven by kinship, spatial overlap and individual social preferences. – Animal Behaviour 85(2): 385-394.
[15] Carter, N., Jasny, M., Gurung, B., Liu, J. (2015): Impacts of people and tigers on leopard spatiotemporal activity patterns in a global biodiversity hotspot. – Global Ecology and Conservation 3: 149-162.
[16] Chowdhury, S. U., Chowdhury, A. R., Ahmed, S., Muzaffar, S. B. (2015): Human-fishing cat conflicts and conservation needs of fishing cats in Bangladesh. – Cat News 62: 4-7.
[17] Chynoweth, M., Coban, E., Sekercioglu, C. H. (2015): Conservation of a new breeding population of Caucasian lynx (*Lynx lynx* dinniki) in eastern Turkey. – Turkish Journal of Zoology 39: 541-543.
[18] Dhungana, R., Savini, T., Karki, J. B., Dhakal, M., Lamichhane, B. R., Bumrungsri, S. (2017): Living with tigers Panthera tigris: patterns, correlates, and contexts of human–tiger conflict in Chitwan National Park, Nepal. – Oryx 52(01): 55-65. doi:10.1017/s0030605316001587.
[19] Di Bitetti, M. S., Di Blanco, Y. E., Pereira, J. A., Paviolo, A., Pérez, I. J. (2009): Time partitioning favors the coexistence of sympatric crab-eating foxes (*Cerdocyon thous*) and pampas foxes (*Lycalopex gymnocercus*). – Journal of Mammalogy 90: 479-490.
[20] Dickman, A. J., Macdonald, E. A., Macdonald, D. W. (2011): A review of financial instruments to pay for predator conservation and encourage human–carnivore coexistence. – Proceedings of the National Academy of Sciences 108(34): 13937-13944.
[21] Duckworth, J. W., Poole, C. M., Tizard, R. J., Walston, J. L., Timmins, R. J. (2005): The jungle cat Felis chaus in Indochina: a threatened population of a widespread and adaptable species. – Biodiversity and Conservation 14(5): 1263-1280.
[22] Durant, S. M. (1998): Competition refuges and coexistence: an example from Serengeti carnivores. – Journal of Animal Ecology 67: 370-386.
[23] Eryılmaz, A. (2017): Research on the populations of jungle cat (*Felis chaus* Scheberer, 1777) around the sparking in Isparta/Eğirdir Hoyran Lake. – Master Thesis, Suleyman Demirel University Graduate School of Natural and Applied Sciences Department of Enginering of Forestry, 109p.
[24] Evcin, Ö., Küçük, Ö., Akkuzu, E., Ugış, A. (2017): Habitat preferences of roe deer (*Capreolus capreolus*) in Kastamonu: case study of elekdağı wildlife development area. – International Journal Of Engineerıng Sciences and Research Technology 6: 225-229.
[25] Fethi, F. Y., İleri, Ö., Avcı, K. M., Kocadere, B. (2014): Periodical Costal Line Changes of Eğirdir and Beyşehir Lakes Using Satellite Data and Topographic Maps. – Mineral Research & Exploration Bulletin 20: 37-45.

http://www.aloki.hu ● ISSN 1589 1623 (Print) ● ISSN1785 0037 (Online)
DOI: http://dx.doi.org/10.15666/aeer/1804_58735890

[26] Fitzgerald, A. (2011): *Felis chaus*. – Animal Diversity Web. Accessed January 09, 2020 at https://animaldiversity.org/accounts/Felis_chaus/.
[27] Forbes, K. M., Stuart, P., Mappes, T., Hoset, K. S., Henttonen, H., Huitu, O. (2014): Diet quality limits summer growth of field vole populations. – PLoS ONE 9(3): e91113. doi:10.1371/ journal.pone.0091113.
[28] Gaynor, K. M., Hojnowski, C. E., Carter, N. H., Brashares, J. S. (2018): The influence of human disturbance on wildlife nocturnality. – Science 360(6394): 1232-1235.
[29] Gerngross, P. (2014): Recent records of jungle cat in Turkey. – Cat News 61: 10-11.
[30] Giannatos, G., Albayrak, T., Erdogan, A. (2006): Status of the caracal in protected areas in southwestern Turkey. – CAT News 45: 23-24.
[31] Gray, T. N. E., Timmins, R. J., Jathana, D., Duckworth, J. W., Baral, H., Mukherjee, S. (2016): *Felis chaus*. – The IUCN red list of threatened specie. e.T8540A50651463.
[32] Grimm, A., Gruber, B., Henle, K. (2014): Reliability of different mark-recapture methods for population size estimation tested against reference population sizes constructed from field data. – PloS one 9(6): e98840.
[33] Gupta, S., Mondal, K., Sankar, K., Qureshi, Q. (2009): Estimation of striped hyena (*Hyaena hyaena*) population using camera traps in Sariska Tiger Reserve, Rajasthan, India. – Journal of the Bombay Natural History Society 106(3): 284.
[34] Hammond, P. S. (2009): Mark–recapture. – Encyclopedia of marine mammals, Academic Press. pp. 705-709.
[35] Harmsen, B. J., Foster, R. J., Silver, S. C., Ostro, L. E., Doncaster, C. P. (2011): Jaguar and puma activity patterns in relation to their main prey. – Mammalian Biology-Zeitschrift für Säugetierkunde 76(3): 320-324.
[36] Hassan, S. F., Hussin, A. G., Zubairi, Y. Z. (2009): Analysis of Malaysian wind direction data using. – Oriana 3(3): 115-119.
[37] İlemin, Y., Gürkan, B. (2010): Status and activity patterns of the caracal (*Caracal caracal*, Schreber, 1776), in Datca and Bozburun peninsulas, southwestern Turkey. – Zoology Middle East 50(1): 3-10. https://doi.org/ 10.1080/09397140.2010.10638405.
[38] Inskip, C., Zimmermann, A. (2009): Human-felid conflict: a review of patterns and priorities worldwide. – Oryx 43(1): 18-34.
[39] IUCN (2018): The IUCN Red List of threatened species v. 2017.3. IUCN. – Gland Accessed 20 Mar 2018. www.redlist.org.
[40] Jansen, P. A., Forrester, T. D., McShea, W. J. (2014): Protocol for camera-trap surveys of mammals at CTFS-ForestGEOsites. – Smithsonian Tropical Research Institute, Ancon.
[41] Jibasen, D. (2011): Capture-recapture Type Models for Estimating the Size of An Elusive Population. – An Unpublished PhD Thesis submitted to the University of Ilorin, Ilorin, Nigeria.
[42] Johannesen, A. B. (2006): Designing integrated conservation and development projects (ICDPs): illegal hunting, wildlife conservation, and the welfare of the local people. – Environment and Development Economics 11(2): 247-267.
[43] Karanth, K. U. (1995): Estimating tiger Panthera tigris populations from camera-trap data using capture—recapture models. – Biological Conservation 71(3): 333-338. doi:10.1016/0006-3207(94)00057-w.
[44] Karanth, K. U., Nichols, J. D., Kumar, N. S., Hines, J. E. (2006): Assessing tiger population dynamics using photographic capture-recapture sampling. – Ecology 87: 2925-2937. doi:10.1890/0012-9658(2006)87 [2925:ATPDUP]2.0.CO;2.
[45] Karatepe, Y. (2004): Properties and classification of sites on Eğirdir lake watershed. – İstanbul University, Institute Of Science And Technolog, Phd Thesis, 293 p. İstanbul.
[46] Kays, R. W., Slauson, K. M. (2008): Remote cameras. – In: Long, R. A., MacKay, P., Zielinski, W. J., Ray, J. C. (eds.) Noninvasive Survey Methods for Carnivores. Chapter 5, Island Press, Washington DC, USA, pp. 110-140.

http://www.aloki.hu ● ISSN 1589 1623 (Print) ● ISSN1785 0037 (Online)
DOI: http://dx.doi.org/10.15666/aeer/1804_58735890

[47] Kays, R., Tilak, S., Kranstauber, B., Jansen, P. A., Carbone, C., Rowcliffe, M. J., Fountain, T., Eggert, J., He, Z. (2010): Monitoring wild animal communities with arrays of motion sensitive camera traps. – Cornell University, arXiv preprint arXiv:1009.5718.

[48] Kerley, L. L., Goodrich, J. M., Miquelle, D. G., Smirnov, E. N., Quigley, H. B., Hornocker, M. G. (2002): Effects of roads and human disturbance on amur tigers. – Conservation Biology 16(1): 97-108. doi:10.1046/j.1523-1739.2002.99290.x.

[49] Keten, A. (2016): Spatial and temporal distribution of Carnivora (Mammalia) species in Düzce Province. – Kastamonu Univ., Journal of Forestry Faculty 16(2): 566-574.

[50] Kinnaird, M. F., O'Brien, T. G. (2012): Effects of private-land use, livestock management, and human tolerance on diversity, distribution, and abundance of large African mammals. – Conservation Biology 26(6): 1026-1039.

[51] Kovach, W. L. (2011): Oriana – circular statistics for windows, ver. 4. – Pentraeth: Kovach Computing Services, Pentraeth, Wales, UK.

[52] Leuchtenberger, C., De Oliveira, Ê. S., Cariolatto, L. P., Kasper, C. B. (2018): Activity pattern of medium and large sized mammals and density estimates of Cuniculus paca (Rodentia: Cuniculidae) in the Brazilian Pampa. – Brazilian Journal of Biology 78(4): 697-705. doi:10.1590/1519-6984.174403.

[53] Linkie, M., Ridout, M. S. (2011): Assessing tiger-prey interactions in Sumatran rainforests. – Journal of Zoology 284(3): 224-229. https:// doi.org/ 10.1111/j.1469-7998.2011.00801.x.

[54] Linnell, J. D. C., Swenson, J. E., Andersen, R. (2001): Predators and people: conservation of large carnivores is possible at high human densities if management policy is favourable. – Animal Conservation 4: 345-349. https://doi.org/10.1017/S1367943001001408.

[55] Madden, F. M. (2008): The growing conflict between humans and wildlife: law and policy as contributing and mitigating factors. – Journal of International Wildlife Law and Policy 11: 189-206. https://doi.org/10.1080/13880290802470281.

[56] Majumder, A., Sankar, K., Qureshi, Q., Basu, S. (2011): Food habits and temporal activity patterns of the Golden Jackal Canis aureus and the Jungle Cat Felis chaos in Pench Tiger Reserve, Madhya Pradesh. – Journal of Threatened Taxa 3(11): 2221-2225.

[57] Mengüllüoğlu, D. (2010): An inventory of medium and large mammal fauna in Pineforests of Beypazarı through camera trapping. – Graduate Thesis, Middle East Technical University, Ankara, Turkey.

[58] Mengüllüoğlu, D., Fickel, J., Hofer, H., Förster, D. W. (2019): Non-invasive faecal sampling reveals spatial organization and improves measures of genetic diversity for the conservation assessment of territorial species: Caucasian lynx as a case species. – PloS one14(5): e0216549.

[59] Mert, A., Acarer, A. (2018): Wildlife diversity in reed beds around Beyşehir lake. – Bilge International Journal of Science and Technology Research 2(1): 110-119. doi: 10.30516/bilgesci.399248.

[60] Oğurlu, İ., Gündoğdu, E., Yıldırım, C. (2010): Population status of jungle cat (*Felis chaus*) in Eğirdir lake, Turkey. – Journal of Environmental Biology 31: 179-183.

[61] Oğurlu, İ., Ünal, Y. (2011): A cooperation in wildlife activities by university, rural people and public authorities: wild boar census in Aksu model hunting ground. – SDU Fac For J 12: 7-12.

[62] Oğurlu, İ. (2015): Wildlife ecology, suleyma demirel university, faculty of forestry. – SDU printing house, publication number: 19, Isparta, 296 p.

[63] Pérez-Irineo, G., Santos-Moreno, A. (2016): Band size, activity pattern and occupancy of the coati Nasua narica (Carnivora, Procyonidae) in the Southeastern Mexican rainforest. – Mammalia 80(6). doi:10.1515/mammalia-2014-0136.

[64] Pochardt, M., Allen, J. M., Hart, T., Miller, S. D., Yu, D. W., Levi, T. (2019): Environmental DNA facilitates accurate, inexpensive, and multi-year population estimates of millions of anadromous fish. – Molecular Ecology Resources 20(2): 457-467. doi:10.1111/1755-0998.13123.

http://www.aloki.hu ● ISSN 1589 1623 (Print) ● ISSN1785 0037 (Online)
DOI: http://dx.doi.org/10.15666/aeer/1804_58735890

[65] Posillico, M., Serafini, P., Lovari, S. (1995): Activity patterns of the stone marten (*Martes foina* Erxleben, 1777), in relation to some environmental factors. – Hystrix, the Italian Journal of Mammalogy 7(1-2).
[66] Ramesh, T., Kalle, R., Sankar, K., Qureshi, Q. (2012): Spatio-temporal partitioning among large carnivores in relation to major prey species in Western Ghats. – Journal of Zoology 287(4): 269-275.
[67] Rawshan, K., Feeroz, M. M., Hasan, M. K. (2012): Human-carnivore conflicts in Bangladesh. – Tigerpaper 39(3): 17-21.
[68] Seoraj-Pillai, N., Pillay, N. (2016): A Meta-analysis of human–wildlife conflict: South African and Global Perspectives. – Sustainability 9(1): 34. doi:10.3390/su9010034.
[69] Shamoon, H., Maor, R., Saltz, D., Dayan, T. (2018): Increased mammal nocturnality in agricultural landscapes results in fragmentation due to cascading effects. – Biological conservation 226: 32-41.
[70] Sillero-Zubiri, C., Laurenson, K. (2001): Interactions between carnivores and local communities: Conflict or co-existence? – Conservation Biology Series, Cambridge University Press, pp. 282-312.
[71] Silveira, L., Jácomo, A. T. A., Diniz-Filho, J. A. F. (2003): Camera trap, line transect census and track surveys: a comparative evaluation. – Biological Conservation 114(3): 351-355. doi:10.1016/s0006-3207(03)00063-6.
[72] Silver, S. C., Ostro, L. E., Marsh, L. K., Maffei, L., Noss, A. J., Kelly, M. J., Ayala, G. (2004): The use of camera traps for estimating jaguar Panthera onca abundance and density using capture/recapture analysis. – Oryx 38(02): 148-154.
[73] Soria-Díaz, L., Monroy-Vilchis, O. (2015): Monitoring population density and activity pattern of white-tailed deer (*Odocoileus virginianus*) in Central Mexico, using camera trapping. – Mammalia 79(1): 43-50.
[74] Soulsbury, C. D., White, P. C. L. (2015): Human–wildlife interactions in urban ecosystems. – Wildlife Research 42(7). doi:10.1071/ wrv42n7_pr.
[75] Soyumert, A. (2010): Detection and determination of ecological characteristics of large mammal species by camera-trapping method in Northwest Anatolia forests. – Ph.D. Thesis, Hacettepe University, Ankara, Turkey.
[76] Stein, A. B., Fuller, T. K., Marker, L. L. (2008): Opportunistic use of camera traps to assess habitat-specific mammal and bird diversity in northcentral Namibia. – Biodiversity and Conservation 17(14): 3579-3587.
[77] Stolle, K., van Beest, F. M., van der Wal, E., Brook, R. K. (2015): Diurnal and nocturnal activity patterns of invasive wild boar (*Sus scrofa*) in Saskatchewan, Canada. – The Canadian Field-Naturalist 129(1): 76-79.
[78] Tağıl, Ş., Alevkayalı, Ç. (2014): Trends in Streamflow and its Relationship With Precipitation in Rivers Flowing into the Lake From the North of the Lake Eğirdir. – Balikesir University, The Journal of Social Sciences Institute 17(32): 211-229.
[79] Tobler, M. W., Carrillo-Percastegui, S. E., Leite Pitman, R., Mares, R., Powell, G. (2008): Further notes on the analysis of mammal inventory data collected with camera traps. – Animal Conservation 11(3): 187-189. doi: 10.1111/j.1469-1795.2008.00181.x.
[80] Treves, A., Karanth, K. U. (2003): Human-carnivore conflict and perspectives on carnivore management worldwide. – Conservation Biology 17(6): 1491-1499. doi: 10.1111/ j.15231739. 2003.00059.x.
[81] Ünal, Y., Çulhacı, H. (2018): Investigation of fallow deer (*Cervus dama* L.) population densities by camera trap method in Antalya Düzlerçamı Eşenadası Breeding Station. – Turkish Journal of Forestry 19(1): 57-62. https://doi.org/ 10.18182/ tjf.339042.
[82] Ünal, Y., Pekin, B. K., Oğurlu, İ., Süel, H., Koca, A. (2019): Human, domestic animal, Caracal (*Caracal caracal*), and other wildlife species interactions in a Mediterranean forest landscape. – Eur J Wildl Res 66: 5. doi:10.1007/s10344-019-1343-x.
[83] Ünal, Y., Koca, A., Kısaarslan, Y., Yelsiz, M. Ş., Süel, H., Oğurlu, İ. (2020): Population status, daily activity pattern and habitat preference of caracal (*Caracal caracal* Schreber,

http://www.aloki.hu ● ISSN 1589 1623 (Print) ● ISSN1785 0037 (Online)
DOI: http://dx.doi.org/10.15666/aeer/1804_58735890

1776) in Antalya Düzlerçamı Wildlife Development Area. – Turkish Journal of Forestry 20(4): 474-481.

[84] Urian, K., Gorgone, A., Read, A., Balmer, B., Wells, R. S., Berggren, P., Hammond, P. S. (2014): Recommendations for photo-identification methods used in capture-recapture models with cetaceans. – Marine Mammal Science 31(1): 298-321.

[85] URL (2017): https://tr.climate-data.org. – Last accessed: 02.11.2017.

[86] Wang, S. W., Macdonald, D. W. (2009): The use of camera traps for estimating tiger and leopard populations in the high altitude mountains of Bhutan. – Biological Conservation 142(3): 606-613.

[87] Wegge, P., Odden, M., Pokharel, C. P., Storaas, T. (2009): Predator–prey relationships and responses of ungulates and their predators to the establishment of protected areas: a case study of tigers, leopards and their prey in Bardia National Park, Nepal. – Biological Conservation 142(1): 189-202.

[88] Weingarth, K., Heibl, C., Knauer, F., Zimmermann, F., Bufka, L., Heurich, M. (2012): First estimation of eurasian lynx (*Lynx lynx*) abundance and density using digital cameras and capture-recapture techniques in a German National Park. – Anim. Biodivers Conserv. 35: 197-207.

[89] Woodroffe, R., Thirgood, S., Rabinowitz, A. (eds.) (2005): People and wildlife, conflict or co-existence? – (No. 9) Cambridge University Press.

http://www.aloki.hu ● ISSN 1589 1623 (Print) ● ISSN1785 0037 (Online)
DOI: http://dx.doi.org/10.15666/aeer/1804_58735890

CHARACTERISTICS OF SIZE-FRACTIONIZED PHYTOPLANKTON AND THEIR RESPONSE TO ENVIRONMENTAL FACTORS IN TYPICAL LAKES OF SOUTHEASTERN HUBEI PROVINCE, CHINA

XIE, Y.-Z.[#] – LIU, M.-Q.[#] – LIU, Z.-X. – HOU, J.-J.[*] – LIU, X.-X. – ZHOU, F. – CHEN, Q. – SUN, L.-L.

Hubei Key Laboratory of Edible Wild Plants Conservation and Utilization, Hubei Normal University, Huangshi 435002, China

Hubei Engineering Research Center of Typical Wild Vegetable Breeding and Comprehensive Utilization Technology, Hubei Normal University, Huangshi 435002, China

National Demonstration Center for Experimental Biology Education, Hubei Normal University, Huangshi 435002, China

[#]The two first authors made equal contributions to this paper

**Corresponding author*
e-mail: jjhou@hbnu.edu.cn; phone: +86-71-4651-1613

(Received 15th Mar 2020; accepted 9th Jul 2020)

Abstract. We studied the size-fractionized phytoplankton community structure characteristics and their response to environmental factors by investigating the photosynthetic pigment concentration and composition; composition and abundance of algal phyla levels; and environmental factors in typical lakes of Hubei Southeastern, China for four seasons. High-performance liquid chromatography (HLPC) results show that the total chlorophyll concentration was 36,418.62 mg/m^3, and the contribution rates of microplankton, nanoplankton, and picoplankton to the total biomass were 13.43%, 49.08%, and 37.49%, respectively. Fucoxanthin, alloxanthin, zeaxanthin, and chlorophyll b were the main photosynthetic pigments. However, the spatial and temporal distribution had significant differences in the four typical lakes. Chemical taxonomy (CHEMTAX) calculation indicates that the dominant species were *Diatoms* and *Cryptophytes* in spring, *Euglenophytes* in summer, *Euglenophytes* and *Cyanobacteria* in autumn, and *Euglenophytes* and *Cryptophytes* in winter. The *Chrysophyte* and *Dinoflagellates* have the lowest proportion for all seasons. The redundancy analysis (RDA) demonstrates that the key environmental factors for the succession were Total Nitrogen (TN) and Total Phosphorus (TP). The application of the HPLC-CHEMTAX method has provided the first analysis of the community structure of size-fractionized phytoplankton in typical lakes of Hubei Southeast, China, and environmental factors affect the succession of size-fractionized phytoplankton over time. This study provides theoretical bases that the comprehensive research on different size phytoplankton in freshwater.
Keywords: *HPLC, community structure, photosynthetic pigment, chemical taxonomy, redundancy analysis*

Introduction

East Lake (Wuchang District, Wuhan City, Hubei Province, China) is a typical semi-enclosed lake in the middle and lower reaches of the Yangtze River (Yun et al., 2015), and it is the second largest urban lake in China. The catchment area is 190 km^2, and the lake water area is 34.59 km^2. The average water depth is 2.2 m, with the highest value reaching 6 m. However, Wuhan is a typical industrial city, the domestic, industrial, and agricultural waste water discharge has significantly increased with its rapid industrialization and urbanization, which has resulted in the deterioration of the water

http://www.aloki.hu ● ISSN 1589 1623 (Print) ● ISSN 1785 0037 (Online)
DOI: http://dx.doi.org/10.15666/aeer/1804_58915905

quality of the East Lake. The trend has changed from phosphorus limitation to nitrogen restriction, and eutrophication is intensifying. Cihu Lake (Huangshi City, Hubei Province, China) is the largest lake in Huangshi with a water area of approximately 1.0×10^7 m^2, catchment area of 6.28×10^7 m^2, and average water depth of 1.75 m (Yan, et al., 2015). The effect of its geographical location (i.e., proximity to a city, low water level, and limited purification capacity) and absence of a reasonable treatment have resulted in a large amount of industrial wastewater discharge. Water pollution is serious concerning the lake's eutrophic state. Qingshan Lake (Huangshigang District, Huangshi City, Hubei Province, China), which is located in the northern part of the Cihu Lake, typical urban lake, has a catchment area of 6.2 km^2, water area of 0. 52 km^2, and depth of 16.83 m (Li et al., 2013). It consists of four sub-lakes. Qinggang Lake (Huangshigang District, Huangshi City, Hubei Province, China) is located on the west bank of the Yangtze River and east of Qingshan Lake. Compared with Qingshan Lake, Qinggang Lake, Cihu and East Lake have more domestic sewage discharge, their smaller water areas, poorer self-recovery ability, and serious water pollution are often observed to be in a nutritious state.

Phytoplankton participates in the material cycle and energy flow as the main contributors of primary productivity; they also play an important role in the freshwater ecological system (Callieri, 2008). Phytoplankton consists of microplankton (20-200 μm), nanophytoplankton (2-20 μm), picophytoplankton (0.2-2 μm), and ultraphytoplankton (< 5 μm) (Robineau et al., 1999); each type has different contributions to the primary productivity and biomass. Nishibe et al. (2015) determined that the primary production was low in winter and composed mostly of small phytoplankton (< 10 μm), whereas large phytoplankton (> 10 μm) became the major producers in spring with high production. Current studies on the phytoplankton size structure mainly focus on marine ecosystems (Wang et al., 2014; Le et al., 2014; Joan et al., 2015), which are rarely reported in freshwater waters. Therefore, the study of freshwater bodies has important theoretical and practical significance, especially with lakes as the research object. However, fresh water has a special nature because of its ecological environment, including the complexity and variability of biological factors in freshwater bodies, organisms, and the environment, which determine the study complexity in freshwater bodies.

Therefore, the current study clarifies the compositions of phytoplankton community and their relationship with environmental factors in four urban lakes (Cihu Lake, East Lake, Qingshan Lake and Qinggang Lake) with different eutrophication levels in Huangshi City or Wuhan City, Hubei Province, China by using high-performance liquid chromatography (HPLC)-chemical taxonomy (CHEMTAX) and redundancy analysis (RDA).

Materials and methods

Study area and sampling strategy

Cihu Lake (30012' N, 11503' E) is located in the center of Huangshi City, Hubei Province, China. Three sampling points (*Fig. 1A*) are set up according to the morphological characteristics, geographical location, and pollution degree of Cihu Lake. East Lake (30033' N, 114023' E) is located in Wuchang District, Wuhan City, Hubei Province, China, which composed of Guozhen Lake, Fruit Lake, Tangling Lake, Tuan Lake, Hou Lake, Xiaotan Lake, Luoyan and other small sub-lakes. Guozheng

http://www.aloki.hu ● ISSN 1589 1623 (Print) ● ISSN 1785 0037 (Online)
DOI: http://dx.doi.org/10.15666/aeer/1804_58915905

Lake is the main lake district of East Lake, where three sampling points are also set up (*Fig. 1B*). Qingshan Lake is located in the northern part of Cihu Lake, which consists of four sub-lakes: fish pond, attached lake 1, main lake district, and attached lake 2, we selected representative main lake district located in Qingshan Lake Park for sampling, three sampling points were set up (*Fig. 1C*). Three sampling points are also set up in Qinggang Lake, which is located east of Qingshan Lake and southwest of the Tiger's Head (*Fig. 1D*). The GPS latitude and longitude of each monitoring point are shown below (*Table 1*). The sampling times were March 2016, August 2015, November 2015, and January 2016 for spring, summer, autumn, and winter, respectively. Sampling once per season, a total of four lakes were sampled, each lake set up three sampling points. At each sampling point, 900 mL of surface water is collected with plexiglass sampler at a depth of 0.5 m.

Determination of photosynthetic pigment contents of the size-fractionized phytoplankton

A 900 mL water sample was collected at each sampling point and divided into three equal parts. The first water sample was directly filtered with a 0.7 μm GF/F filter membrane to obtain phytoplankton above 0.7 microns. The second water sample was first filtered with a 20 μm sieve, and then the filtrate was collected and filtered with a 0.7 μm GF/F filter membrane for store to obtain phytoplankton of 0.7 to 20 microns. The third water sample was first filtered with a pore size of 5 μm, and then the filtrate was collected and filtered with a 0.7 μm GF/F filter membrane for store to obtain phytoplankton of 0.7 to 5 microns.

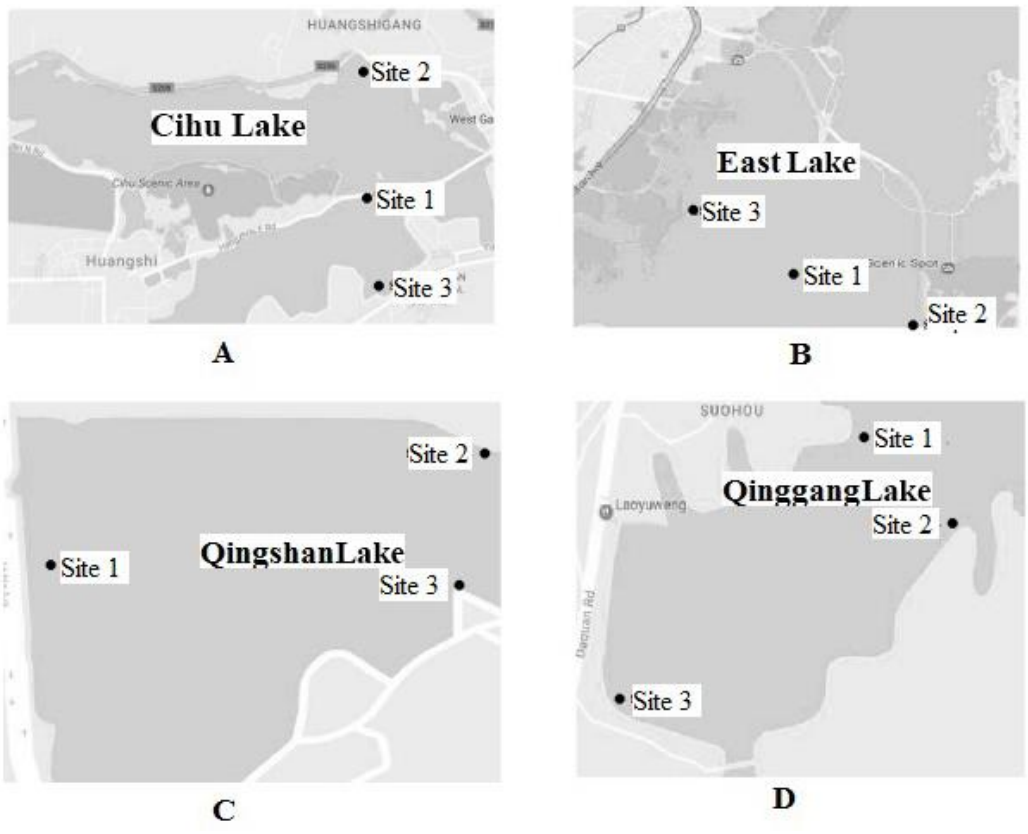

Figure 1. *Location of the sampling sites in the study area*

http://www.aloki.hu ● ISSN 1589 1623 (Print) ● ISSN 1785 0037 (Online)
DOI: http://dx.doi.org/10.15666/aeer/1804_58915905

Table 1. *The GPS latitude and longitude of each monitoring point*

Lakes	Monitoring points	longitude	latitude
Cihu Lake	Site 1	E115°3’40.8”	N30°12’39.08”
Cihu Lake	Site 2	E115°3’36.7”	N30°13’23.8”
Cihu Lake	Site 3	E115°3’35.6”	N30°11’40.3”
East Lake	Site 1	E114°23’35.7”	N30°32’44.3”
East Lake	Site 2	E114°23’53.4”	N30°32’59.8”
East Lake	Site 3	E114°22’20.3”	N30°34’19.8”
Qingshan Lake	Site 1	E115°3’251”	N30°14’12.3”
Qingshan Lake	Site 2	E115°3’18.1”	N30°13’52.9”
Qingshan Lake	Site 3	E115°3’16.6”	N30°2’0.2”
Qinggang Lake	Site 1	E115°1’59”	N30°14’4”
Qinggang Lake	Site 2	E115°1’34”	N30°14’4”
Qinggang Lake	Site 3	E115°1’33”	N30°14’2”

The membrane with the sample was cut into several 5 mm × 1 cm pieces (not excessively small or large) and placed in a 2 mL centrifuge tube. Approximately 1 mL DMF was added and shock mixed into the - 20 °C refrigerator for 40 min, centrifuged at 4,000 r/min for 5 min, filtered through a 0.22 μm filter, and mixed with an equal volume of 1 M ammonium acetate solution for the HPLC analysis according to the reference method (Liu et al., 2017). The mobile phase consisted of methanol [1 M ammonium acetate; methanol = 80:20 (pH = 7.2)] and a mobile phase B: 100% methanol. The detection wavelength was 440 nm, injection volume was 100 μL, and flow rate was 1 mL/min. The photosynthetic pigment standards include fucoxanthin (Fuco), neoxanthin (Neox), violaxanthin (Viol), zeaxanthin (Zeax), diadinoxanthin (Diad), alloxanthin (Allo), chlorophyll a (Chl a), and chlorophyll b (Chl b), which were prepared according to our patent (Chinese Number: 201410022083.4). Quantitative, gradient elution, and quantitative calculation were performed according to our published method (Liu et al., 2017). The pigment concentrations of phytoplankton in the samples were calculated by the differential method. The pigment concentrations of microphytoplankton (> 20 μm), nanophytoplankton (5-20 μm), and picophytoplankton (0.7-5 μm) were obtained by subtractive method. The characteristics of the size-fractionized phytoplankton community structure were analyzed by utilizing CHEMTAX.

Chemtax analysis of the pigment data of the size-fractionized phytoplankton

The initial pigment ratio can directly affect the Chemtax calculation (Mackey et al., 1996). In studies of different habitats, including an estuary (Lionard et al., 2008), a bay (Madhu et al., 2014), lagoons (Sarmento and Descy, 2008), and freshwater bodies (Guisande et al., 2008), many adjustments were made to the selection of the initial ratio and pigment matrix. The intent was to isolate and incubate the phytoplankton in the

http://www.aloki.hu ● ISSN 1589 1623 (Print) ● ISSN 1785 0037 (Online)
DOI: http://dx.doi.org/10.15666/aeer/1804_58915905

laboratory to discover the pigment/Chl a ratio, but the ratio for every phylum was complex. The optimal initial pigment ratios in the current study were obtained from literature (Liu et al., 2017). The pigment concentration and initial pigment ratio data were inputted utilizing the CHEMTAX software version 1.95. The new pigment ratio data were obtained from the first run. The second CHEMTAX run employed this output pigment ratio as the input pigment ratio. After five to seven repetitions, there is no change in the output of the algae composition in phylum level, which indicates that the final results have been obtained. (Latasa, 2007) reported that multiple operations of the CHEMTAX analysis lowered the dependence on the initial pigment ratio, the transformation of different pigment ratios with continuous runs was always directed towards the true value, which improves the reliability and accuracy of the results. The relative abundance of size-fractionized phytoplankton that contributes to the Chl a biomass was calculated. The spatial and temporal differences were analyzed through the ANOVA statistical analysis.

Analysis of environmental factors

Water sample environmental factors comprised temperature (T), pH, total phosphorus (TP), ammonia nitrogen (NH_4^+-N), total nitrogen (TN) and $KMnO_4$ index, measured according to Water and Wastewater Monitoring and Analysis Methods of ministry of environmental protection of the people's republic of China.

Analysis of relationship between community structure and environmental factors

First, the species variables were analyzed by detrending correspondence analysis (DCA). If the longest length of the gradient was less than or equal to 3.0, then the linear model of principal component analysis (PCA) or redundancy analysis (RDA) was more appropriate. RDA was then applied to analyze the relationship between the environmental factors and size-fractionized phytoplankton community structure. Utilizing the previous selection and Monte Carlo tests, a minimal subset of the environmental factors was adopted for the RDA analysis, which explains a significant ($P < 0.05$) variation within the species data. Only these environmental factors are shown on the biplots. The ordination plots were made by Canoco for the Windows 4.5 software.

Results

Spatial and temporal distribution of the total biomass of size-fractionized phytoplankton in typical lakes of Hubei Southeast, China

The Chl a concentration was analyzed to evaluate the size-fractionized phytoplankton biomass in the typical lakes of Hubei Southeast. The spatial and temporal distributions of the total biomass were then clarified. Results are shown in *Figure 2*. The total biomass of the size-fractionized phytoplankton in the Lake centeris higher than those of other areas. For different seasons, the total biomass of the size-fractionized phytoplankton in the same lake has a large difference, and the highest value was observed in summer. The total biomass of the size-fractionized phytoplankton in the same lake was also different, and the highest total biomass of phytoplankton was that of nanoplankton. The spatial and temporal distributions of the total biomass of size-fractionized phytoplankton in the typical lakes of Hubei Southeast are as presented follows:

http://www.aloki.hu ● ISSN 1589 1623 (Print) ● ISSN 1785 0037 (Online)
DOI: http://dx.doi.org/10.15666/aeer/1804_58915905

The contribution of the size-fractionized phytoplankton to the total biomass in Cihu Lake is shown in *Figure 2A*. The ratios of the total biomass in each site to the total biomass in all sites were 40.65%, 29.47%, and 29.89%, and the highest biomass was observed in sampling site 1. The biomass for all phytoplankton was the highest in autumn and smallest in winter. Among the microplankton, nanoplankton, and picoplankton, the highest contribution to the total biomass was that of nanoplankton. The contribution of the size-fractionized phytoplankton to the total biomass in East Lake is shown in *Figure 2B*. The ratios of the total biomass in each site to the total biomass in all sites are 45.05%, 28.77%, and 26.18%, and the highest biomass appeared in sampling site 1. The biomass for all phytoplankton was the highest in summer. The contributions of microplankton, nanoplankton, and picoplankton to the total biomass are relatively close. The contribution of the size-fractionized phytoplankton to the total biomass in QingShan Lake is shown in *Figure 2C*. The ratios of the total biomass in each site to the total biomass in all sites are 50.39%, 28.53%, and 21.08%, and the highest biomass was observed in sampling site 1. The biomass for all phytoplankton was the highest in summer. Among the microplankton, nanoplankton, and picoplankton, the highest contribution to the total biomass was that of nanoplankton. The contribution of the size-fractionized phytoplankton to the total biomass in QingQang Lake is shown in *Figure 2D*. The ratios of the total biomass in each site to the total biomass are 46.10%, 21.99%, and 31.91%, respectively, and the highest biomass was observed in sampling site 1. The biomass for all phytoplankton was the highest in summer. Among the microphytoplankton, nanophytoplankton, and picophytoplankton, the highest contribution to the total biomass was that of nanophytoplankton.

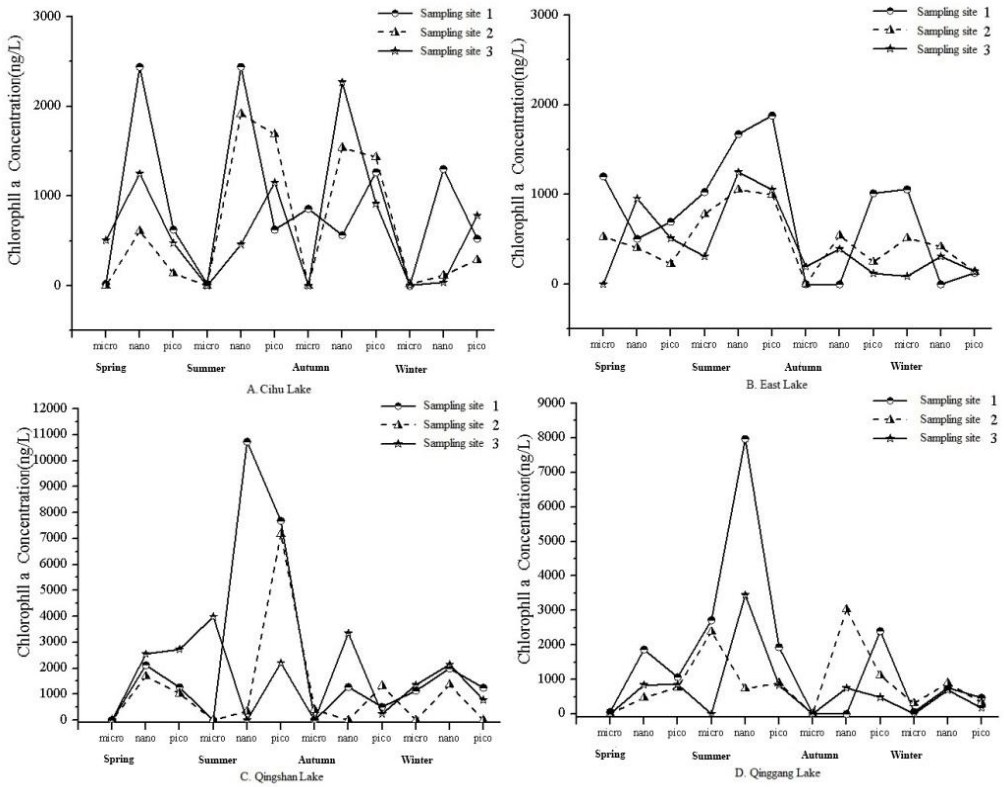

Figure 2. *Biomass of size-fractionized phytoplankton in Cihu, East, Qingshan and Qinggang lakes*

http://www.aloki.hu ● ISSN 1589 1623 (Print) ● ISSN 1785 0037 (Online)
DOI: http://dx.doi.org/10.15666/aeer/1804_58915905

Temporal and spatial distributions of the photosynthetic pigments of the size-fractionized phytoplankton

The photosynthetic pigment content of the size-fractionized phytoplankton was detected by utilizing HPLC technology in typical lakes of Hubei Southeast, China. The temporal and spatial distributions were then analyzed. The results show that the main biomark pigments in typical lakes of Hubei Southeast, China have eight types: Fuco, Neox, Viol, Allo, Lute, Zeax, Chl a, and Chl b. Among these pigments, Fuco, Allo, and Zeax were the main biomark pigments. The pigment compositions of the size-fractionized phytoplankton were similar, but the concentrations were different. Seven types of photosynthetic pigments from size-fractionized phytoplankton in the time distribution were relatively different, but their spatial distributions were relatively concentrated. The pigment concentrations in Qingshan and Qinggang Lakes were also higher. The spatial and temporal distributions of Fuco are shown in *Figure 3A*. The concentration range of Fuco was approximately 0 $\mu g/m^3$ to 2,341.91 $\mu g/m^3$, and it was highest in summer. A comparison of the Fuco concentration of the size-fractionized phytoplankton shows that nanophytoplankton was the highest in the four seasons. The spatial and temporal distributions of Neox are shown in *Figure 3B*. The concentration range of Neox was approximately 0 $\mu g/m^3$ to 262.99 $\mu g/m^3$, and it was also highest in summer. A comparison of the Neox concentration of the size-fractionized phytoplankton shows that nanophytoplankton was the highest in the four seasons. The spatial and temporal distributions of Viol are shown in *Figure 3C*. The concentration range of Viol was approximately 0 $\mu g/m^3$ to 1,024.40 $\mu g/m^3$, and it was highest in autumn. A comparison of the Viol concentration of the size-fractionized phytoplankton shows that nanophytoplankton was the highest in spring, autumn, and winter, whereas picoplankton was the highest in summer. The spatial and temporal distributions of Allo are shown in *Figure 3D*. The concentration range of Allo was approximately 0 $\mu g/m^3$ to 6,231.79 $\mu g/m^3$, and it was highest in summer. A comparison of the Allo concentration of the size-fractionized phytoplankton show that microphytoplankton was the highest in summer, whereas nanoplankton was the highest in the other seasons. The spatial and temporal distributions of Zeax are shown in *Figure 3E*. The concentration range of Zeax was approximately 0 $\mu g/m^3$ to 1,499.53 $\mu g/m^3$, and it was highest in autumn. A comparison of the Zeax concentration of the size-fractionized phytoplankton shows that nanophytoplankton was the highest in autumn, whereas picoplankton was the highest in the other seasons. The spatial and temporal distributions of Lute are shown in *Figure 3F*. The concentration range of Lute was approximately 0 $\mu g/m^3$ to 539.03 $\mu g/m^3$, and it was highest in summer. A comparison of the Lute concentration of the size-fractionized phytoplankton shows that nanophytoplankton was the highest in the four seasons. The spatial and temporal distributions of Chl b are shown in *Figure 3G*. The concentration range of Chl b was approximately 0 $\mu g/m^3$ to 4,504.55 $\mu g/m^3$, and it was highest in summer. The spatial and temporal differences among the seven photosynthetic pigments (except for Chl a) were analyzed utilizing the ANOVA statistical analysis. Results show that the photosynthetic pigment concentration had a significant difference in time ($P < 0.05$), but no significant difference in space ($P > 0.05$).

Composition of the size-fractionized phytoplankton community structure

The size-fractionized phytoplankton community structure was identified with CHEMTAX based on the pigment concentration data and initial pigment ratio. The

http://www.aloki.hu ● ISSN 1589 1623 (Print) ● ISSN 1785 0037 (Online)
DOI: http://dx.doi.org/10.15666/aeer/1804_58915905

composition of the size-fractionized phytoplankton community structure is shown in *Figure 4*. Seven phytoplankton phyla were identified in the research area: *Cryptophytes*, *Diatoms*, *Chlorophytes*, *Cyanobacteria*, *Chrysophytes*, *Euglenophytes*, and *Dinoflagellates*. The size-fractionized phytoplankton community structure in spring is shown in *Figure 4A*. The results indicate that *Diatoms* dominated the sampling area in the Cihu, East, and Qinggang Lakes, and the highest percentage of *Diatoms* (91.39%) was at sampling site 2 in East Lake. *Cryptophytes* dominated the sampling area in Qingshan Lake, and the highest percentage (94.74%) was at sampling site 1. The dominant species was different for the size-fractionized phytoplankton. *Diatoms* and *Cryptophytes* were the dominant phyla for microphytoplankton, whereas *Diatoms* were the dominant phyla for nanophytoplankton. *Cryptophytes* were the dominant phyla for picophytoplankton. The size-fractionized phytoplankton community structure in summer was shown in *Figure 4B*. The results indicate that *Euglenophytes* and *Cyanobacteria* were the dominant phyla. The community structure largely changed, and the succession occurred between the *Euglenophytes* and *Diatoms* in the Cihu, East, and QingGang Lakes. By contrast, the percentage of cyanobacteria in QingShan Lake was higher than *Euglenophytes*. The dominant phyla did not have a clear difference for the size-fractionized phytoplankton. *Euglenophytes* were the dominant species for microphytoplankton, nanophytoplankton, and picophytoplankton. The size-fractionized phytoplankton community structure in autumn was shown in *Figure 4C*. The results indicate that *Euglenophytes* and *Cyanobacteria* were the dominant phyla, and the variation range of the community structure was small in all sampling areas. The dominant phyla were different for the size-fractionized phytoplankton. *Euglenophytes* were the dominant phyla for microphytoplankton, and the percentage was the highest at sampling site 1 in Cihu Lake. Cyanobacteria were the dominant species for nanophytoplankton. The size-fractionized phytoplankton community structure in winter is shown in *Figure 4D*. The results indicate that *Euglenophytes* were the dominant phyla in the Cihu and East Lakes, and *Cryptophytes* were the dominant phyla in the Qingshan and Qinggang Lakes. The dominant species did not have an evident difference for the size-fractionized phytoplankton, and the dominant phyla were *Euglenophytes* and *Cyanobacteria*. Thus, the dominant species were *Diatoms*, *Duglenophytes*, *Cryptophytes*, and *Cyanobacteria* all year round. The percentage of dominant species in summer was more than 50%, which may cause an outbreak of water bloom. The spatial and temporal differences were analyzed by utilizing the ANOVA statistical analysis. The results indicate that the community structure had a significant difference in time ($P < 0.05$), but no significant difference in space ($P > 0.05$).

Relationship between the size-fractionized phytoplankton community structure and environmental factors

The environmental variables were first analyzed with DCA. The longest gradient length was less than three, which was suitable for the RDA analysis (*Fig. 5*). Utilizing the forward selection and Monte Carlo tests, the environmental factors showed significant ($P < 0.05$) variation within the species data in all seasons, except for autumn. The environmental factors did not significantly affect the size-fractionized phytoplankton community structure in autumn. Therefore, the relationship between the ultraphytoplankton community structure and environmental factors was clarified by RDA in spring, summer, and winter. The RDA results for spring, summer, and winter are presented as follows. The dominant phylum in spring (*Fig. 5A*) was *Diatoms*. The

http://www.aloki.hu ● ISSN 1589 1623 (Print) ● ISSN 1785 0037 (Online)
DOI: http://dx.doi.org/10.15666/aeer/1804_58915905

Diatoms were positively correlated with pH and temperature, whereas they were negatively correlated with TP, TN, and NH_4^+-N. The ordination biplot indicates that TN was the most significant environmental factor. The dominant phylum in summer (*Fig. 5B*) was *Euglenophytes*, which were positively correlated with TP, TN, and pH, whereas they were negatively correlated with temperature. The ordination biplot indicates that TP was the most significant environmental factor. The dominant phylum in winter (*Fig. 5C*) was *Euglenophytes*. *Euglenophytes* were positively correlated with NH_4^+-N, whereas they were negatively correlated with TP and TN. The ordination biplot indicates that TP was the most significant environmental factor.

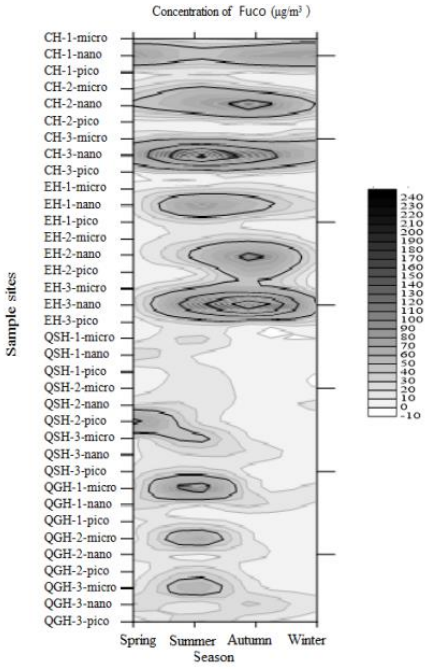

A. Fuco

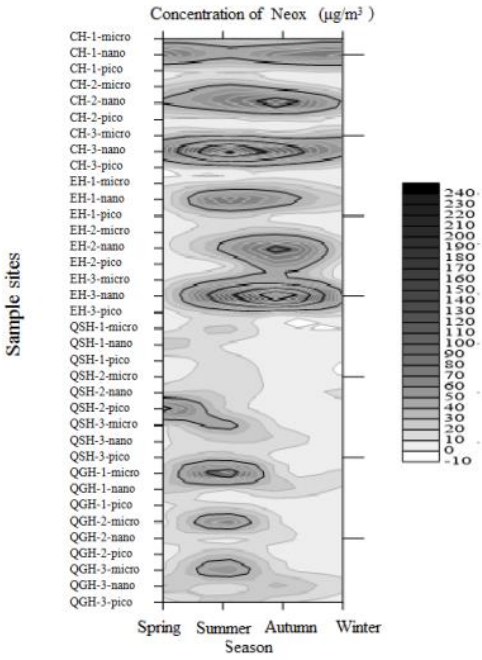

B. Neox

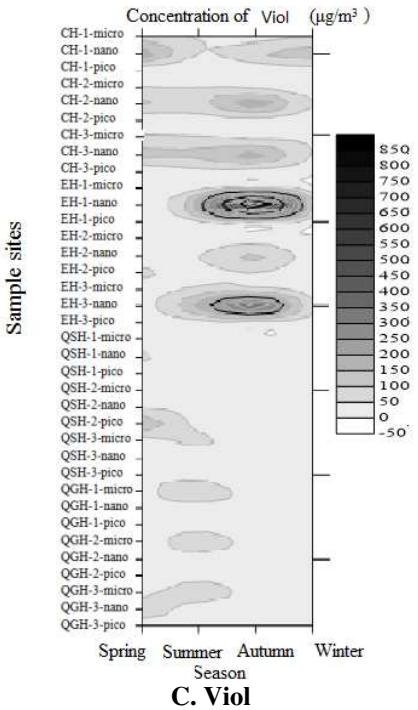

C. Viol

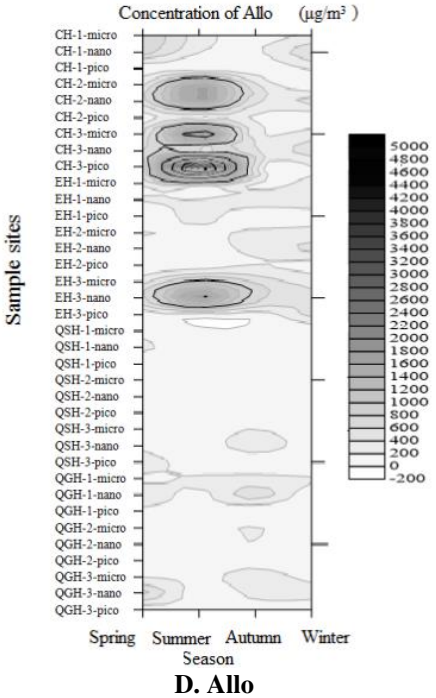

D. Allo

http://www.aloki.hu ● ISSN 1589 1623 (Print) ● ISSN 1785 0037 (Online)
DOI: http://dx.doi.org/10.15666/aeer/1804_58915905

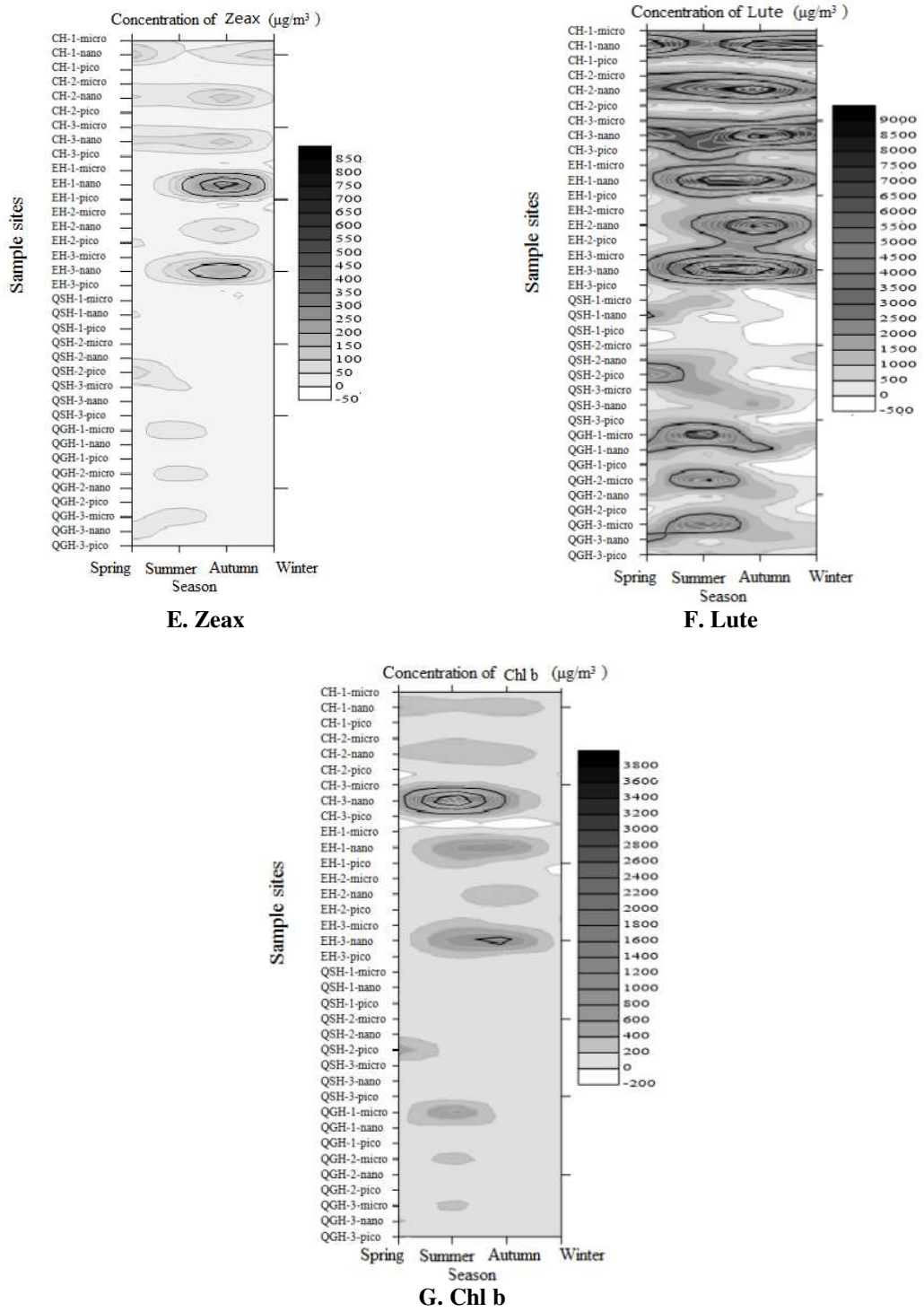

Figure 3. *Temporal and spatial distribution of photosynthetic pigments. CH: Cihu Lake; EH: East Lake; QSH: Qingshan Lake; QGH: Qinggang Lake*

Discussion

The size-fractionized phytoplankton in four seasons was analyzed. The dominant phytoplankton in the Qingshan, Qinggang, and Cihu Lakes was nanophytoplankton. However, the percentage of microphytoplankton, nanophytoplankton, and

http://www.aloki.hu ● ISSN 1589 1623 (Print) ● ISSN 1785 0037 (Online)
DOI: http://dx.doi.org/10.15666/aeer/1804_58915905

picophytoplankton in East Lake was relatively balanced. Seasonal differences were observed in the phytoplankton composition; microphytoplankton was the dominant phyla in spring and winter, whereas nanophytoplankton was the dominant phyla in summer and autumn. A significant grade structure succession occurred, which was similar to the findings (Wollschläger et al., 2015). The community structure of the size-fractionized phytoplankton in the typical lakes of Hubei Province, China has a significant difference among the seasons, but the composition of the size-fractionized phytoplankton in the same season was highly similar. Nanophytoplankton and picophytoplankton were also the dominant phyla, and these results were similar to marine ecosystem (Huang, 2018).

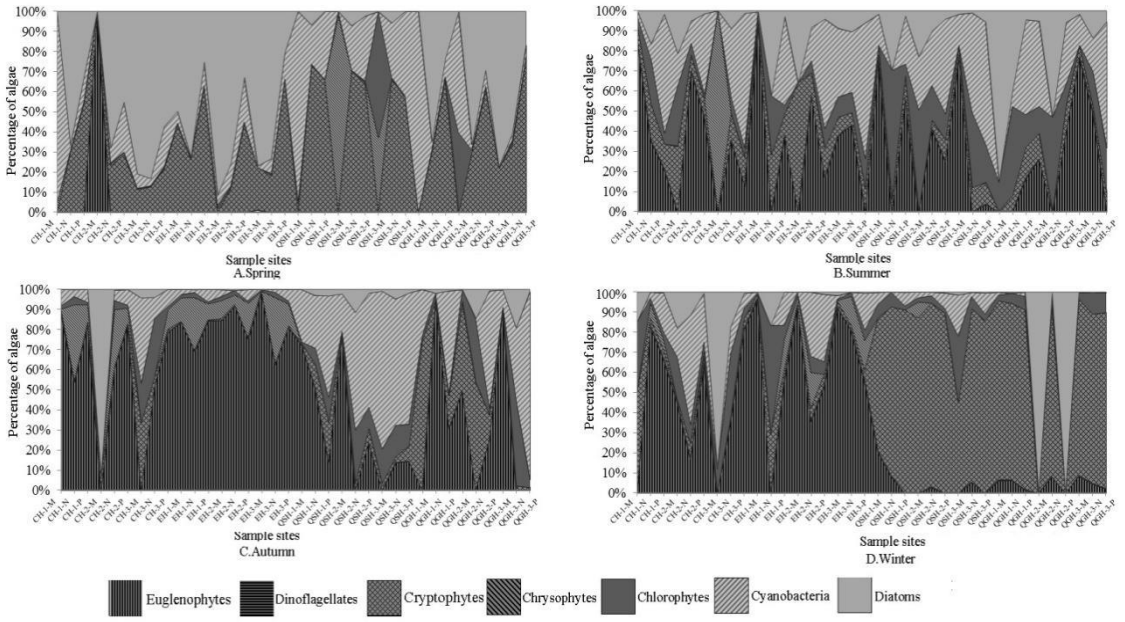

Figure 4. *The size-fractionized phytoplankton community structure. CH: Cihu Lake; EH: East Lake; QSH: Qingshan Lake; QGH: Qinggang Lake*

The community structure of size-fractionized phytoplankton was highly similar in the Cihu and East Lakes, and a small difference was observed among the seasons. The dominant phylum was *Euglenophytes.* Sun (2014) stated that *Euglenophytes* were mostly grown in water with pH 6.5 to 8.5. In our study, the pH and temperature were the optimal conditions for *Euglenophytes* growth. However, *Euglenophytes* have a strong ability of movement and migration, so they could occupy the surface and subsurface waters during the day for photosynthesis (Willén, 1992). Given this competitive relationship, other algae types could hardly reach the upper water. The surface water in this study was collected from the Cihu and East Lakes, which may be one of the reasons why the dominant phylum was *Euglenophytes*. The community structure of the size-fractionized phytoplankton in the Qingshan and Qinggang Lakes were highly similar, and a significant difference among the seasons was observed. *Cryptophytes* was the dominant phylum in spring and winter, whereas *Euglenophytes* and cyanobacteria were the dominant phyla in summer and autumn. This phenomenon is mainly related to their geographical environment. *Cryptophytes* creased to large

http://www.aloki.hu ● ISSN 1589 1623 (Print) ● ISSN 1785 0037 (Online)
DOI: http://dx.doi.org/10.15666/aeer/1804_58915905

number in the Qingshan and Qinggang Lakes in spring and winter, which may be due to the following reasons. On the one hand, *Cryptophytes* have high tolerance to low light (Marshall and Laybourn-Parry, 2002). The water in the study areas (Qingshan and Qinggang Lakes) was turbidier, which limited the light and growth of other phytoplankton, and *Cryptophytes* adapted to low light growth occupy an advantageous position. (Lewitus et al., 1991). On the other hand, the reproductive cycle was short at approximately 0.8 d to 3 d (Liu et al., 2012), this factor also provided the conditions for the *Cryptophytes* to become the dominant phylum. The dominant phylum in summer and autumn was cyanobacteria. Previous reports (Zhang et al., 2009; Li et al., 2010) states that the increasing temperature and eutrophication status are blue-green algae outbreak conditions. Results shown that the eutrophication of the Qinggang and Qingshan Lakes was more serious than the other two lakes.

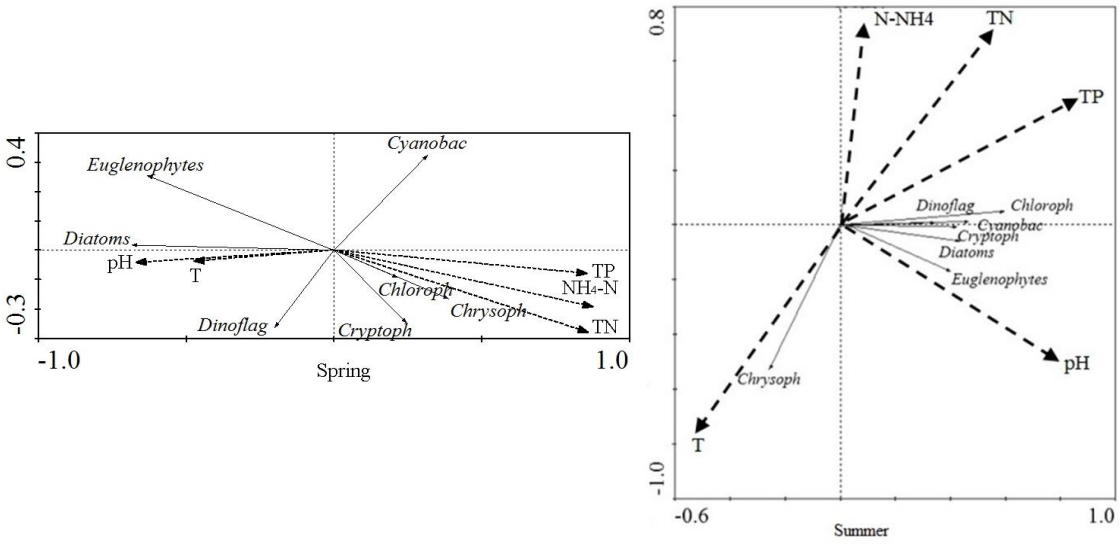

A. Spring **B. Summer**

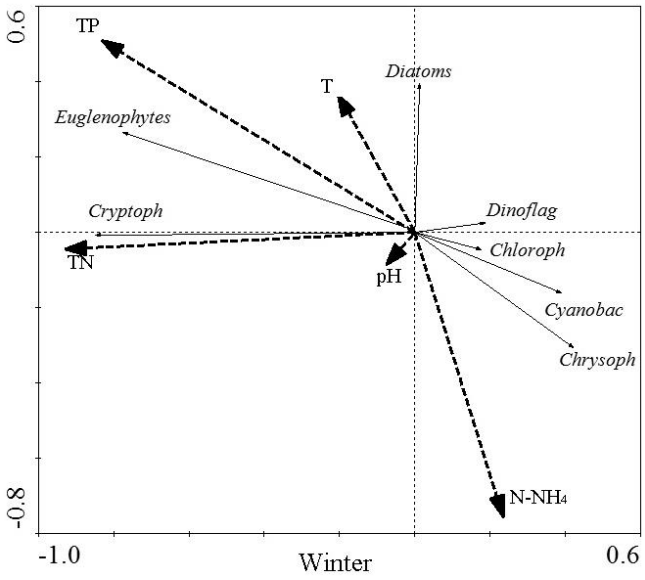

C. Winter

Figure 5. *Ordination biplot of environmental variables and the size-fractionized phytoplankton assemblages obtained by RDA for different seasons*

http://www.aloki.hu ● ISSN 1589 1623 (Print) ● ISSN 1785 0037 (Online)
DOI: http://dx.doi.org/10.15666/aeer/1804_58915905

The size-fractionized phytoplankton succession was affected by the environmental factors and nutrients. Previous reports on lakes and reservoirs states that oligotrophic systems have < 0.2 mg/L TN and < 0.01 mg/L TP, whereas eutrophic systems have TN > 0.5 mg/L and TP > 0.02 mg/L (Peng et al., 2013). The lowest values of TN and TP during the sampling period were 1.31 and 0.06 mg/L, respectively, which indicates that the typical lakes of Hubei Southeast, China fall into the category of eutrophicated water bodies. We then had to clarify the relationship between the environmental factors and ultraphytoplankton. Our findings shown that the relationship between environmental factors and size-fractionized phytoplankton had no clear significance ($P > 0.05$) in autumn, which indicates that the environmental factors did not affect the size-fractionized phytoplankton community structure in this season. By contrast, the relationship between the environmental factors and ultraphytoplankton was significant ($P < 0.05$) in the other three seasons, and the most significant environmental factors were TP and TN. The most limiting nutrient for algae growth in the freshwater ecosystem was generally phosphorus (Zhang et al., 2016). Feng et al. (2016) determined that phosphorus was the most significant factor that affects algal bloom in eutrophic conditions. Nitrogen also played an important role in the size-fractionized temporal dynamics in our study. This result was consistent with previous report (Barroso et al., 2016) that TN was the main driver of the phytoplankton structure.

Conclusions

We applied the HPLC-CHEMTAX method successfully and identified eight biomarker pigments and seven ultraphytoplankton (groups or classes) in the typical lakes of Hubei Southeast, China for the first time. The dominant phytoplankton types were *Diatoms* and *Euglenophytes*. The concentration of photosynthetic pigment had a significant difference in time ($P < 0.05$), but no significant difference in space ($P > 0.05$).

During the study period, the typical lake of Hubei Southeast, China was found to belong to the category of eutrophicated water bodies. Nanophytoplankton biomass was higher than microphytoplankton and picophytoplankton biomass, the community structure had a significant difference in time ($P < 0.05$) and was higher in summer than the other three seasons, but no significant difference in space ($P > 0.05$). Action should be taken to improve water quality to reduce the risk of harmful algal blooms.

The relationship between the environmental factors and ultraphytoplankton had a significant difference ($P < 0.05$) in the other three seasons (except autumn), and the most significant environmental factors were TP and TN, affecting size-fractionized phytoplankton succession in spring, summer and winter.

In future research, we can combine molecular biology techniques such as qPCR, high-throughput sequencing, metagenomics, single-cell sequencing with HPLC-CHEMTAX technology to study size-fractionized phytoplankton and obtain more complete information on community structure. Moreover, the biodiversity of specific groups of size-fractionized phytoplankton in freshwater lakes are requied to be further studied.

Acknowledgements. This work was supported by the National Natural Science Foundation of China (41171045), the Research Fund for Science and Technology Innovation Team of Hubei Normal University (T201504) and the Central Government Guided Local Science and Technology Development Project of Hubei Province (No.2017ZYYD008).

http://www.aloki.hu ● ISSN 1589 1623 (Print) ● ISSN 1785 0037 (Online)
DOI: http://dx.doi.org/10.15666/aeer/1804_58915905

REFERENCES

[1] Barroso, H. D., Becker, H., Melo, V. M. M. (2016): Influence of river discharge on phytoplankton structure and nutrient concentrations in four tropical semiarid estuaries. – Brazilian Journal of Oceanography 64(1): 37-48.
[2] Callieri, C. (2008): Picophytoplankton in freshwater ecosystems: the importance of small-sized phototrophs. – Freshwater Reviews 1(1): 1-28.
[3] Cui, D. Y., Wang, J. T., Tan, L. J. (2016): Response of phytoplankton community structure and size-fractionated chlorophylla in an upwelling simulation experiment in the western south China sea. – Journal of Ocean University of China 15(5): 835-840.
[4] Feng, W., Zhu, Y., Wu, F., Meng, W., Giesy, J. P., He, Z., Fan, M. (2016): Characterization of phosphorus forms in lake macrophytes and algae by solution 31P nuclear magnetic resonance spectroscopy. – Environmental Science and Pollution Research 23(8): 7288-7297.
[5] Guisande, C., Marciales, L. J., Hernández, E., Aranguren, N., Mogollón, M., Rueda-Delgado, G. (2008): Testing of the CHEMTAX program in contrasting Neotropical lakes, lagoons, and swamps. – Limnology and Oceanography: Methods 6(12): 643-652.
[6] Hong, H. S., Ruan, W. Q., Huang, B. Q., et al. (1997): The Taiwan Strait primary productivity and its regulation mechanism. – Journal of Marine Chinese, Beijing: Ocean Press 12-15 (in Chinese).
[7] Huang, D. L. (2018): Distribution and Influencing Factors of Phytoplankton Grain Size Structure in the Coastal Waters of Guangxi Beibu Gulf. – Guangxi University, Nanning (in Chinese).
[8] Joan, S., Font-Muñoz, et al. (2015): Estimation of phytoplankton size structure in coastal waters using simultaneous laser diffraction and fluorescence measurements. – Journal of Plankton Research 37(4): 740-751.
[9] Latasa, M. (2007): Improving estimations of phytoplankton class abundances using CHEMTAX. – Marine Ecology Progress Series 329(Jan): 13-21.
[10] Le, F. F., Hao, Q., Jin, H. Y., et al. (2014): 2012 in Chukchi Sea and phytoplankton in the sea area adjacent to the existing volume and primary productivity of grain structure study. – Journal of ocean 36(10): 103-115 (in Chinese).
[11] Lewitus, A., Caron, D., Miller, K. (1991): Effect of light and glycerol on the organization of the photosynthetic apparatus in the facultative heterotroph Pyrenomonas salina (Cryptophyceae). – Journal of Phycology 27: 578-587.
[12] Li, J., Ji, F. F., Hua, J. H. (2013): Community structure of phytoplankton and water quality assessment in summer in lake Qingshan. – Natural Sciences Journal of Harbin Normal University 29(5): 61-65 (in Chinese).
[13] Li, Z., Guo, J. S., Fang, F., et al. (2010): The relationship between seasonal variation of cyanobacteria in Three Gorges backwater area of Xiaojiang River and the main environmental factors. – Environmental Science 31(2): 301-309 (in Chinese).
[14] Lionard, M., Muylaert, K., Tackx, M., Vyverman, W. (2008): Evaluation of the performance of HPLC-CHEMTAX analysis for determining phytoplankton biomass and composition in a turbid estuary (Schelde Belgium). – Estuarine, Coastal and Shelf Science 76(4): 809-817.
[15] Liu, X. X., Lu, X. H., Chen, Y. W. (2012): Spatiotemporal dynamics of crypto biomass in northern taihu lake. – Lake Science (1): 144-150 (in Chinese).
[16] Liu, X. X., Li, J. Y., Bi, Y. H., Hou, J. J., Li, Y. T., He, Y. Y. (2017): Characterization of ultraphytoplankton pigments and functional community structure in Xiangxi Bay, China, using HPLC-CHEMTAX. – Journal of Freshwater Ecology 32(1): 103-118.
[17] Mackey, M. D., Mackey, D. J., Higgins, H. W., Wright, S. W. (1996): CHEMTAX-a program for estimating class abundances from chemical markers: application to HPLC measurements of phytoplankton. – Marine Ecology Progress Series 144: 265-283.

http://www.aloki.hu ● ISSN 1589 1623 (Print) ● ISSN 1785 0037 (Online)
DOI: http://dx.doi.org/10.15666/aeer/1804_58915905

[18] Madhu, N. V., Ullas, N., Ashiwini, R., Meenu, P., Rehitha, T. V., Lallu, K. R. (2014): Characterization of phytoplankton pigments and functional community structure in the Gulf of Mannar and the Palk Bay using HPLC-CHEMTAX analysis. – Continental Shelf Research 80: 79-90.
[19] Marshall, W., Laybourn-Parry, J. (2002): The balance between photosynthesis and grazing in antarctic mixotrophic crytophytes during summer. – Journal of Freshwater Ecology 47(11): 2060-2070.
[20] Nishibe, Y., Takahashi, K., Shiozaki, T., Kakehi, S., Saito, H., Furuya, K. (2015): Size-fractionated primary production in the Kuroshio Extension and adjacent regions in spring. – Journal of Oceanography 71(1): 27-40.
[21] Peng, C. R., Zhang, L., Zheng, Y. Z., Li, D. H. (2013): Seasonal succession of phytoplankton in response to the variation of environmental factors in the Gaolan River, Three Gorges Reservoir, China. – Chinese Journal of Oceanology and Limnology 31(4): 737-749 (in Chinese).
[22] Robineau, B., Legendre, L., Michel, C., Budeus, G., Kattner, G., Schneider, W., Pesant, S. (1999): Ultraphytoplankton abundances and Chlorophyll a concentrations in ice-covered waters of northern seas. – Journal of Plankton Research 21(4): 735-755.
[23] Sarmento, H., Descy, J. P. (2008): Use of marker pigments and functional groups for assessing the status of phytoplankton assemblages in lakes. – Journal of Applied Phycology 20(6): 1001-1011.
[24] Solorzano, G. G., Martinez, M. G., Vázquez, A. L., Garfías, M. B., Zuñiga, R. E., Conforti, V. (2011): Trachelomonas (Euglenophyta) from a eutrophic reservoir in Central Mexico. – Journal of Environmental Biology 32(4): 463-471.
[25] Sun, F. Z. (2014): The prevention and cure of the algae bloom in aquaculture. – Guide to the Fishing for Wealth 21: 53-53 (in Chinese).
[26] Wang, G. F, Zhou, W., Lin, G. F., et al. (2014): Validation and evaluation of the biological optical inversion model of the phytoplankton size structure in the northern South China sea. – Journal of Laser Biology 23(6): 502-515.
[27] Willén, E. (1992): Planktonic green algae in an acidification gradient of nutrient-poor lakes. – Archiv für Protistenkunde 141(1-2): 47-64.
[28] Wollschläger, J., Wiltshire, K. H., Petersen, W., Metfies, K. (2015): Analysis of phytoplankton distribution and community structure in the German Bight with respect to the different size classes. – Journal of Sea Research 99: 83-96.
[29] Yan, Z., Liu, T., Sun, J. X., Zhou, S., Zhou, Y. J., Xiao, W. S. (2015): Accumulation of heavy metals in nanoplankton in two lakes in mining area - take Daye Lake and Cihu Lake in Hubei as examples. – Safety and Environmental Engineering 22(3): 28-34 (in Chinese).
[30] Yun, X. Y., Yang, Y. Y., Liu, M. X., Wang, J. (2015): Concentrations and risk assessment of polychlorinated biphenyls and polybrominated diphenyl ethers in surface sediments from the East Lake, China. – Ecotoxicology 24(1): 172-180.
[31] Zhang, M., Cai, Q. H., Wang, L., et al. (2009): A preliminary study on the process of elimination in Xiangxi Bay of Three Gorges reservoir water algae monitoring Wahson. – Wetland Science 7(3): 230-236.
[32] Zhang, J. J., Zhang, Q., Qin, M. M., Hong, Y. (2016): Selection and characterization of eight freshwater green algae strains for synchronous water purification and lipid production. – Frontiers of Environmental Science & Engineering 10(3): 548-558.

http://www.aloki.hu ● ISSN 1589 1623 (Print) ● ISSN 1785 0037 (Online)
DOI: http://dx.doi.org/10.15666/aeer/1804_58915905

THE EFFECTS OF SUPER ABSORBENT POLYMER APPLICATION ON THE PHYSIOLOGICAL AND BIOCHEMICAL PROPERTIES OF TOMATO (*Solanum lycopersicum* L.) PLANTS GROWN BY SOILLESS AGRICULTURE TECHNIQUE

BAŞAK, H.

Department of Horticulture, Faculty of Agriculture, Kırşehir Ahi Evran University, Turkey
e-mail: hbasak@ahievran.edu.tr; phone: +90-386-280-4839; fax: +90-386-280-4832

(Received 17th Mar 2020; accepted 7th Jul 2020)

Abstract. This study, it was aimed to determine the effects of super absorbent polymers (SAP) on plant growth, yield, hormone level, leaf pigment and nutrient contents, enzyme activities, organic acid and amino acid composition, lipid peroxidation level in tomato and the amount of drained water in soilless culture. For this aim, three levels of SAPs (0, 5 and 10 g $slab^{-1}$) were applied into cocopeat slabs before planting seedlings in randomized plots. The results showed that the SAPs added to cocopeat substrate increased plant growth and yield by increasing leaf nutrient, pigment and hormone contents in tomato plants. However, SAP applications reduced lipid peroxidation, H_2O_2 content, antioxidant enzym activities and abscisic acid level. SAP treatment increased organic acid contents about 9.5-24.7%, except for butyric and maleic acid. In general, SAP treatment increased the amino acid contents in leaves, but decreased mainly proline, aspartate and hydroxyproline contents. The presence of sufficient water and nutrients in plants' root zones with low force allowed them to grow without stress. A 10 g polymer application gave better results than other doses on investigated parameters. In conclusion, SAPs can be used in soilless tomato farming, due to its beneficial effects on plant growth, yield and water saving.
Keywords: *polymers, hydroponic, leaf nutrients, fruit yield, water saving*

Introduction

Soilless culture provides significant savings in water and fertilizer use compared to conventional agriculture (Putra and Yuliando, 2015). This would provide significant benefits and protection of environment and natural resources. SAPs are hygroscopic materials consisting of acrylamide monomers (acrylic acid and sodium or potassium acrylate). The carboxyl group along the polymer chain has a high water absorption capacity, the crosslinks present in the chain prevent its complete dissolution (Bortolin et al., 2013). SAPs have hydrophilic groups with enormous capability of absorbing and retaining water or aqueous solutions of up to hundreds of times their weights (Sojka and Entry, 2000). Water and nutrients stored in SAPs are slowly released to the plant to improve growth under limited water supply (Islam et al., 2011). The application of SAPs also increases growth by increasing the soil's capacity to store water and nutrients (Tohidi-Moghadam et al., 2009). SAPs do not have any direct impact on human health and environment, therefore, the consumption of vegetable products grown with polymer application does not pose a toxicological risk (Sojka et al., 2007). SAPs increase in water retention capacity of soils, enabling to release of applied pesticides and chemical fertilizers in control (Wu et al., 2008). Nimah et al. (1983) reported that SAPs increased water retention in sandy and clay soils about 25% and 25-30%, respectively. Similarly, Başak et al. (2016) report that 25% water and nutrient savings were obtained by SAPs addition to cocopeat environment. SAPs relieve oxidative stress (Moghadam, 2017) and increasing cation exchange capacity of soils (Habibi et al., 2010). Hydrogel application to soil increases the amount of available water in the plant root zone, prolongs the time

http://www.aloki.hu ● ISSN 1589 1623 (Print) ● ISSN1785 0037 (Online)
DOI: http://dx.doi.org/10.15666/aeer/1804_59075921

between irrigations and prevents plants from water stress (Yazdani et al., 2007). Consequently, the significant saving can be achieved for water usage, labor and energy in irrigation and fertilization.

In the previous studies, the effect of SAPs application on plants was predominantly studied under salt and drought stress conditions in conventional farming (Habibi et al., 2010; Su et al., 2017; Li et al., 2019). Investigating the effects of water-retaining polymers on promoting plant growth under abiotic stress conditions will, also, increase their usage areas in non-stressed plants in soilless agriculture.

On the literature, there have not been any studies on the effect of SAPs applications on organic acid and amino acid contents of plants, except proline content. With the study, to determine the effects of SAPs aplication on organic acid and amino acid contents that play important roles on plant growth and tolerance to possible stress conditions will contribute in filling the gap on the literature on this regard. Therefore, the current study was planned to determine the effects of SAPs application on physiological and biochemical responses of tomato plants grown by soilless agriculture technique.

Material and Methods

Experimental conditions and SAPs applications

This study was conducted in the Horticulture Research Unit of Agricultural Faculty of Kırşehir Ahi Evran University (in Turkey) from May to September, in 2018. Experiments were conducted in a greenhouse with controlled climatic conditions. Since tomato is the most cultivated plant in soilless culture, hybrid cluster tomato variety (Kahraman F_1) was used as a plant material. The growing medium was cocopeat in form of slabs (100x20x16 cm). A synthetic polyacrylamide (SAP, Stockosorb 400K) with potassium salt base manufactured which is a crosslinked polymer developed to retain water in the agricultural and horticultural sector, was used in experiment. SAP was applied to the slabs before planting. Polymers weighted 5 and 10 g for each cocopeat slab were placed into 500 ml beakers and gelled by adding adequate water for two hours. The swollen polymers were, then, mixed homogeneously for each slab. Tomato seedlings were planted in cocopeat slabs as 3 plants per slab. The experiment was designed according to randomized plots with 4 replicates each including 3 plants. Before the study, Power and Sample Size analysis (PASS 15) was applied to determine the required sample size (NCSS, 2017). This sample size was sufficient for this study since the data were obtained from individual plants in controlled environment, soilless culture. Modified Hoagland nutrient solution was applied to cover the water and nutrient requirements of the plants according to their vegetative and generative stages (Hoagland and Arnon, 1950) (*Table 1*).

Table 1. *Chemical contents of nutrient solution (mg L^{-1})*

Elements	N	P	K	Mg	Ca	S	Fe	Mn	B	Cu	Zn	Mo
Concentration	210	31	234	48	200	64	2.5	0.5	0.5	0.02	0.05	0.01

The nutrient solution was placed in a root dripper of each plant and applied equally for all treatments using a timed automation system. The automation system was programmed to start the first irrigation at 8:00 am in the morning and the last irrigation at 8:00 pm in

http://www.aloki.hu ● ISSN 1589 1623 (Print) ● ISSN1785 0037 (Online)
DOI: http://dx.doi.org/10.15666/aeer/1804_59075921

the evening with an interval of 90 minutes. The first and last 2 of the total 9 irrigations were applied for 60 seconds while the other irrigations were applied for 90 seconds when the temperature was higher due to plants' higher water during these intervals. Since each dripper flows 200 ml of solution per minute, a total of 27.6 L of solution was applied daily to each application row occupied 12 plants.

Growth parameters and yield

The effects of SAP application on fruit yield per plant (g $plant^{-1}$) and morphological parameters such as plant height (cm), stem fresh weight (g) and stem diameter (mm) were determined at the end of the experiment.

Plant nutrient element analysis

Leaf macro and micro nutrients were determined on dry matter basis. Nitrogen content was determined by Kjeldahl method (Bremner, 1996). The P, K, Ca, Mg, Na, Fe and Zn contents were determined using an ICP (Inductively Coupled Plasma) spectrometer (Optima 2100 DV, ICP/OES; Perkine-Elmer, USA) (Mertens, 2005).

Leaf pigment analysis

The effect of the treatments on the leaf pigment content was determined according to the method of Arnon (1949). Fresh leaf tissues (200 mg) were homogenized in acetone (8 ml 80%). Homogenates were centrifuged at 3000 rpm and absorbances of supernatants were determined at 645, 652, 663 and 470 nm. The amounts of pigments were calculated according to the formula of Lichtenthaler and Wellburn (1983).

Antioxidant enzymes analysis

The superoxide dismutase (SOD), peroxidase (POD) and catalase (CAT) enzyme activities in the apoplastic fractions were measured by using a spectrophotometer (Sairam and Srivastava, 2002). SOD activity was determined by recording the decrease in absorbance of nitroblue tetrazolium (NBT) by the enzyme. CAT activity was measured by monitoring the decrease in absorbance at 240 nm in 50 mM phosphate buffer (pH 7.5) containing 20 mM H_2O_2. POD activity was determined (at 470 nm in 50 mM phosphate buffer (pH 5.5)) by recording the oxidation of guaiacol in the presence of H_2O_2.

Hormone analysis

Extraction and purification processes of leaf samples were executed as described by Kuraishi et al. (1991) and Battal and Tilekliоğlu (2001). Gibberellic acid, salicylic acid, indole acetic acid and abscisic acid were analyzed by HPLC using a Zorbax Eclipse-AAA C-18 column (Agilent 1200 HPLC). The hormone levels were determined by using 13% acetonitrile (pH 4.98) as the mobile phase.

Amino acid analysis

Amino acid contents were analyzed by HPLC as described by Aristoy and Toldra (1991), Antoine et al. (1999) and Henderson et al. (1999). Agilent 1200 model with single detector (UV) and Zorbax Eclipse-AAA 4.6 x 150 mm, 3.5 μm column (Agilent 1200 HPLC) was used to determine the amino acid composition of the samples.

http://www.aloki.hu ● ISSN 1589 1623 (Print) ● ISSN1785 0037 (Online)
DOI: http://dx.doi.org/10.15666/aeer/1804_59075921

Organic acid analysis

The organic acids were determined by HPLC using Zorbax Eclipse-AAA 4.6×250 mm, 5 μm columns (Agilent 1200 HPLC) and absorbance of 220 nm in UV detector. Organic acids were analyzed by using 25 mM KH_2PO_4 (pH 2.5) as the mobile phase (Siddiqui et al., 2015).

Lipid peroxidation (Malondialdehyde-MDA) and hydrogen peroxide (H_2O_2) content analysis

The level of lipid peroxidation was measured as the amount of malondialdehyde (MDA) determination by the thiobarbituric acid (TBA) reaction (Heath and Packer, 1968). The content of H_2O_2 was determined spectrophotometrically (Velikova et al., 2000). H_2O_2 content was calculated by using samples' absorbance values from the standard curve.

Determination of water drainage

The drained solution from each slab was accumulated in buckets placed at the end of the gutter to record its volume daily during the study from 24th April 2018 to 29th September 2018.

Statistical analysis

The data were analysed by GLM procedure of SPSS (Windows Version SPSS, release 20.00). Means were compared by Duncan Multiple Range Test in the same software.

Results

Growth parameters and yield

The 10 g SAP treatment increased significantly plant height and stem fresh weight compared to the control ($P \leq 0.05$). The highest plant height (387.9 cm) and stem fresh weight (3493 g) were obtained in 10 g SAP treated slabs. Without statistical significance, stem diameter decreased with increased polymer dose, and the lowest stem diameter (20.89 mm) was obtained by 10 g polymer treatment. The 10 g polymer treatment tended to increase yield compared to other treatments (*Table 2*). This difference was not statistically significant but economically valuable.

Table 2. *Effects of SAP treatments on agronomic properties of tomato plants*

Applications		**Plant height** (cm)	**Stem fresh weights** (g)	**Stem diameter** (mm)	**Yield** (g plant^{-1})
Control		337.3b*	2728b	22.35	9003.6
SAP	**5 g**	378.5ab	2893ab	21.37	9306.4
	10 g	387.9a	3493a	20.89	9679.2
SEM		0.09	136.3	0.272	352.5
P		0.047	0.050	0.080	0.747

*Means in each column with the same letters are not significantly different ($P<0.05$)

http://www.aloki.hu ● ISSN 1589 1623 (Print) ● ISSN1785 0037 (Online)
DOI: http://dx.doi.org/10.15666/aeer/1804_59075921

The nutrient contents

All determined nutrients (N, P, K, Ca, Mg, Fe and Zn), except Na and B contents were increased significantly by SAP treatments compared to the control (P<0.05) (*Table 3*). In particular, leaf K content of 10 g SAP treated plants was significantly higher than those of 5 g SAP treated plants. Without statistical significance, leaf P, Mg and Zn contents of 10 g SAP treated plants were slightly higher than those of 5 g SAP treated plants. With the effect of SAP application, the highest increase in leaf nutrient content was determined at K concentration with 21.3%, followed by P, Zn, Ca, Mg, Fe, N concentrations with the increases of 16.2%, 15.6%, 15.4%, 14.7%, 12.6% and 11.1%, respectively. Although the SAP applications tended to reduce leaf Na and B contents without any statistical significance (P>0.05).

Table 3. *Effects of SAP applications on leaf nutrient contents*

Applications		N (%)	P (mg kg^{-1})	K (mg kg^{-1})	Ca (mg kg^{-1})	Mg (mg kg^{-1})	Na (mg kg^{-1})	Fe (mg kg^{-1})	Zn (mg kg^{-1})	B (mgkg^{-1})
Control		2.17b*	1871b	4678b	4431b	355.3b	185.8	31.03b	12.34b	19.25
SAP	**5 g**	2.33a	2077ab	5002b	4895a	377.5ab	184.3	35.82a	13.69ab	18.47
	10 g	2.41a	2174a	5674a	5115a	407.5a	177.5	34.93a	14.27a	17.44
SEM		0.037	54.9	139.4	96.8	10.1	3.658	0.819	0.322	0.391
P		0.007	0.053	0.001	0.001	0.042	0.662	0.019	0.021	0.169

*Means in each column with the same letters are not significantly different (P<0.05)

Leaf pigment contents

The effect of SAP application on leaf carotenoid content was not found statistically significant (P>0.05). However, its chlorophyll a content was decreased by SAP treatments, while chlorophyll b and total chlorophyll contents were increased significantly (P<0.01). The highest chlorophyll b (1.379 mg g^{-1} FW) and total chlorophyll (5.817 mg g^{-1} FW) contents were obtained in plants treated with 10 g polymer (*Table 4*).

Table 4. *Effects of SAP treatment on leaf pigment contents (mg g^{-1} FW)*

Applications		Chlorophyll a	Chlorophyll b	T. Chlorophyll	Carotenoid
Control		2.905a*	1.043c	5.583b	1.189
SAP	**5 g**	2.871a	1.215b	5.669b	1.180
	10 g	2.828b	1.379a	5.817a	1.179
SEM		0.0098	0.0029	0.0306	0.0023
P		0.002	0.001	0.002	0.169

*Means in each column with the same letters are not significantly different (P<0.05)

Antioxidant enzymes, Lipid peroxidation (Malondialdehyde-MDA) and hydrogen peroxide (H_2O_2) content

MDA and H_2O_2 levels, which are considered as stress indicators in plants, were decreased by SAP doses. The lowest MDA (6.59 µmol g^{-1}) and H_2O_2 (17.94 mmol kg^{-1}) levels were observed in 10 g SAP treated plants. SOD, CAT and POD enzyme activities

http://www.aloki.hu ● ISSN 1589 1623 (Print) ● ISSN1785 0037 (Online)
DOI: http://dx.doi.org/10.15666/aeer/1804_59075921

were decreased significantly by SAP treatment compared to control. The lowest SOD (692 EU g leaf^{-1}), CAT (203.5 EU g leaf^{-1}) and POD (13434 EU g leaf^{-1}) enzyme activities were observed in 10 g SAP treated plants (*Table 5*).

Table 5. *Effects of SAP treatment on antioxidant enzyme activities, H_2O_2 and MDA levels*

Applications		H_2O_2 (mmol kg^{-1})	MDA (µmol g^{-1})	SOD (EU g leaf^{-1})	CAT (EU g leaf^{-1})	POD (EU g leaf^{-1})
Control		27.01a*	9.38a	1009a	233.3a	15580a
SAP	**5 g**	21.46b	8.27a	834b	215.3b	14451b
	10 g	17.94b	6.59b	692c	203.5b	13434c
SEM		1.33	0.41	845	4.51	298.9
P		0.003	0.004	0.001	0.007	0.001

*Means in each column with the same letters are not significantly different (P<0.05)

Hormone contents

Compared to control plants, SAP treatments significantly increased gibberellic acid level, while the salicylic acid and IAA contents were increased by only 5 g SAP dose. The level of ABA, which is considered as a stress hormone, was significantly decreased with SAP application (*Table 6*). The highest ABA concentration was determined in control plants as 0.18 ng µl^{-1}.

Table 6. *Effects of SAP treatment on hormone and salicylic acid contents (ng µl^{-1})*

Applications		Gibberellic acid	Salicylic acid	IAA	ABA
Control		67.77b*	17.98a	1.16b	0.18a
SAP	**5 g**	78.78a	18.48a	1.29a	0.15b
	10 g	78.08a	15.74b	1.18b	0.16b
SEM		1.972	0.436	0.038	0.007
P		0.018	0.006	0.007	0.006

*Means in each column with the same letters are not significantly different (P<0.05)

Organic acid compositions

The impacts of SAP treatments on plant organic acid concentrations were given in *Table 7*. SAP treatments increased organic acids concentrations significantly compared to control, except butyric acid and maleic acid. 10 g SAP treatment increased oxalic acid (0.778 ng µL^{-1}), propionic acid (1.768 ng µL^{-1}), malonic acid (9.935 ng µL^{-1}), citric acid (11.908 ng µL^{-1}) and succinic acid (21.258 ng µL^{-1}) concentrations when compared to other treatments. In 10 g SAP treated plants' leaves, oxalic, propionic, tartaric, malonic, malic, lactic, citric, fumaric and succinic acid contents (respectively 12.3%, 9.5%, 16.4%, 27.7%, 13.5%, 12.2%, 17.8%, 14.8% and 17.1%) were higher than those of control.

Amino acid compositions

The impacts of SAP treatments on plant amino acid compositions were given in *Table 8*. SAP treatments significantly increased asparagine, serine, arginine, cysteine,

http://www.aloki.hu ● ISSN 1589 1623 (Print) ● ISSN1785 0037 (Online)
DOI: http://dx.doi.org/10.15666/aeer/1804_59075921

valine, methionine, tryptophan, phenylalanine, isoleucine and lysine concentrations in the leaves. On the other hand, aspartate, hydroxyproline and proline contents significantly reduced by SAP applications compared to those of control plants. With the effect of SAP application, the highest increase was determined in the content of arginine with a rate of 15%, while the highest decrease was determined in the content of proline with a rate of 14.2%.

Table 7. *Effects of SAP treatment on the organic acid content (ng μl^{-1})*

Applications		Oxalic	Propionic	Tartaric	Butyric	Malonic	Malic
Control		0.693b*	1.615b	4.223b	11.520	7.970b	2.948b
SAP	5 g	0.668b	1.650ab	4.835a	12.582	8.843ab	3.332a
	10 g	0.778a	1.768a	4.915a	11.495	9.935a	3.345a
SEM		0.018	0.029	0.109	0.253	0.312	0.068
P		0.022	0.044	0.002	0.167	0.015	0.008
Applications		**Lactic Laktic**	**Citric**	**Maleic**	**Fumaric**	**Succinic**	
Control		16.070b	10.105b	3.658	4.373b	18.163b	
SAP	5 g	17.225a	11.305ab	3.693	4.873a	18.013b	
	10 g	18.023a	11.908a	3.673	5.018a	21.258a	
SEM		0.294	0.317	0.038	0.092	0.524	
P		0.006	0.042	0.944	0.000	0.002	

*Means within column not followed by the same letter differ significantly

Table 8. *Effects of SAP treatment on the amino acid content (pmol μL^{-1})*

Applications		Aspartate	Glutamate	Asparagine	Serine	Glutamine	Histidine	Glycine
Control		3657a*	2358	6127b	6904b	4599	2265	2052
SAP	5 g	3588b	2401	6158b	7276ab	4582	2326	1999
	10 g	3561b	2415	6266a	7701a	4722	2380	1961
SEM		15.192	15.23	21.89	124.08	38.39	23.38	21.72
P		0.011	0.319	0.006	0.012	0.288	0.124	0.243
Applications		**Threonine**	**Arginine**	**Alanine**	**Tyrosine**	**Cysteine**	**Valine**	**Methionine**
Control		4250	6168c	5605	954	579b	324b	1108b
SAP	5 g	4375	6668b	5623	976	628a	326b	1174ab
	10 g	4249	7093a	5449	969	651a	362a	1247a
SEM		41.08	127.29	37.93	7.79	11.36	6.44	22.99
P		0.386	0.001	0.112	0.545	0.012	0.007	0.027
Applications		**Tryptophan**	**Phenylalanine**	**Isoleucine**	**Leucine**	**Lysine**	**Hyd.pro.**	**Proline**
Control		753ab	1739b	856b	1982	1442b	2049a	254a
SAP	5 g	695b	1818ab	887b	1951	1473b	2027a	243a
	10 g	796a	1862a	939a	1873	1568a	1826b	218b
SEM		15.90	20.26	12.84	21.29	22.16	43.44	5.58
P		0.014	0.022	0.009	0.085	0.033	0.050	0.001

*Means within column not followed by the same letter differ significantly

http://www.aloki.hu ● ISSN 1589 1623 (Print) ● ISSN1785 0037 (Online)
DOI: http://dx.doi.org/10.15666/aeer/1804_59075921

The amount of water drainage

The effect of SAP application on monthly drained water are given in *Table 9*, monthly differences in drained water between SAP applications and control are presented in *Figure 1*. *Table 9* shows that there was a significant interaction between month and SAP treatment (P<0.01) according to univariate analysis. In June and July, the amount of drained water from plants in cocopeat slabs with 5 and 10 g of polymer added was higher than those of the control without polymer application. The drained water showed a linear increase during May, June and July (*Figure 1*). In addition, the amount of drained water measured in plants treated with 10 g polymer was significantly higher in June and July compared to 5 g SAP treatment (P<0.05). However, the differences in the amount of drained water between polymer-treated plants and control were not significant, especially in mid-August (*Figure 1*).

Table 9. *Effect of SAP application on drained water (ml)*

Months	Experimental groups				
	Control	**5 g SAP**	**10 g SAP**	**SEM**	**P**
May	5637.3c	6104.1abc	6947.7ab	334.8	0.273
June	3685.5dB	4878.2cB	7146.4abA	411.4	0.001
July	3929.8dC	5511.1bcB	8217.3aA	331.7	0.000
August	7123.6b	7127.7ab	6929.1ab	371.9	0.970
September	9339.1aA	7465.9aA	5359.1bB	447.9	0.001
SEM	305.9	290.4	309.1		
P	0.000	0.022	0.065		

Different letters in the same row (A,B,C) and same column (a,b,c) are statistically different (P<0.05)

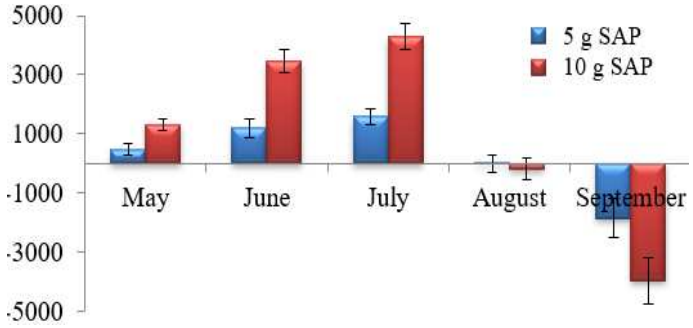

Figure 1. *Differences in drained water in SAP applications compared to that of control (ml)*

In the drainage amounts in September, the drainage amounts determined in 5 and 10 g polymer applications were determined to be 1873.2 ml and 3980 ml lower than the control application, respectively.

Discussion

Hydrophilic polymers increase water holding capacity and water usage efficiency (Dorraji et al., 2010). Furthermore, polymers stimulate the formation of new roots,

http://www.aloki.hu ● ISSN 1589 1623 (Print) ● ISSN1785 0037 (Online)
DOI: http://dx.doi.org/10.15666/aeer/1804_59075921

providing higher water and nutrient uptake. As a result, SAP treatments increase fruit yield as well as growth and development in plants. In this study, 5 and 10 g SAP applications increased stem fresh weight by 6.4% and 28%, as respective increases in yield about 3.4% and 7.5%. Consistent with our findings, the positive effects of SAPs applications on plant weight, height and yield in cucumber, pepper, and tomato and soya bean (Maboko, 2006; Yazdani et al., 2007; Sayyari and Ghanbari, 2012; Başak et al., 2016; Li et al., 2019). The increases in plant growth and yield by SAP treatment can be attributed to the presence of sufficient amount of water and nutrients which can be easily taken with low pressure in the root area.

It was determined that SAP added to the cocopite slabs increased the leaf nutrient contents about 11.1-21.3%. Similarly, Mikiciuk et al. (2015) reported that polymer application increased nitrogen and potassium contents in strawberry leaves but did not affect phosphorus, sulphur and sodium contents. Sita et al. (2005), also, indicated that the increasing doses of hydrogel treatment in chrysanthemum (*Dendrathema grandiflorum*) plant positively affected plant growth and Ca and Mg uptakes. Soilless agriculture has salinity risk in root zone, since plants are irrigated with solutions containing nutrients in every drop. The excess of Na creates problem, thus its accumulation in the root zone is not desired. Fortunately, in the present study, SAP application did not allow Na accumulation in root zone. SAPs absorb nutrients with water and, consequently, slowly release them back to plants. Thus, plants can absorb water and nutrients in the root area with less energy. The present results showed that SAP treatment had allowed plants to take the nutrients in stable and sufficient level.

Chlorophyll content is an important biochemical indicator of stress tolerance in plants (Percival et al., 2003). Therefore, the increase in chlorophyll levels of SAP treated plants can considered as an indication that plants are not experienced water and nutrient stress. In other words, these plants take water and nutrients sufficiently. SAP treatment increased, especially, N and Mg uptakes (*Table 3*), allowing to form the central ion of chlorophyll and, consequently, building a darker green leaf color (Buehner, 1956). Similar to our findings, SAP addition significantly increased the amounts of chlorophyll in cucumber (Li et al., 2019) and pepper (Sayyari and Ghanbari, 2012) plants.

The present results show that SAP application does not cause any oxidative stress in plants. On the contrary, it reduces the formation of free oxygen radicals causing cellular damage. In our findings, the decrease in free oxygen radicals was happened by decreased MDA content and SOD enzyme activity with SAP application. Also, the decreases in CAT and POD enzyme activities might be due to the decrease in H_2O_2 level. CAT and peroxidases (POD and APX) are involved in detoxification of H_2O_2 (Mittler, 2002). Similar to our findings, Habibi et al. (2010) reported that the application of SAP in corn plants reduced the level of MDA, an important indicator of oxidative damage. Su et al. (2017) found significant negative relationships between SAP water absorption capacity and proline content, peroxidase activity, H_2O_2 and MDA levels. Moghadam (2017) reported that total chlorophyll content in wheat plant were increased by SAP application doses (5 and 10 g per kg soil), while these doses decreased SOD, CAT enzyme activities and MDA content significantly. Pouresmaeil et al. (2013) determined positive and significant correlations between SOD, CAT, GPX enzyme activities with MDA content in SAP applied red bean plants.

The increase in N content of plants may increase the synthesis of hormones due to its stuructural role in protein synthesis. In this study, N content increased significantly by SAP treatment compared to control. Calcium increases IAA level while Zn and B increase

http://www.aloki.hu ● ISSN 1589 1623 (Print) ● ISSN1785 0037 (Online)
DOI: http://dx.doi.org/10.15666/aeer/1804_59075921

the auxin activity (Öktüren and Sönmez, 2005). The current results revealed that SAP treatment induced Ca and Zn uptake and, consequently, IAA content. Marulanda et al. (2009) reported linear relationships between IAA level and nutrient intake (P, Ca, Fe, Mn, Zn, B and Cu). The activity of growth regulating hormones such as indole acetic acid, cytokinin and gibberellic acid were increased by the presence of K (Marschner, 1986). The results showed that the increase in K intake with the effect of SAP treatment may be related to the increase in gibberellic acid and IAA contents (*Table 6*). Similar to our result, Özen and Onay (1999) reported that SAP treatments increased GA level but decreased ABA level. Salicylic acid, a plant growth regulator, is a signal molecule that has a regulatory role in the activation of biochemical pathways associated with stress tolerance (Sticher et al., 1997). It can be postulated that the decreases in ABA and salicylic acid levels by SAP application might be attributed to the presence of ideal moisture level in root region.

SAP treatment increased organic acid contents from 9.5 to 24.7%, except butyric and maleic acid. Although the plants were not in any stress condition in the current experiment, the increases in organic acid compositions that increase the plant tolerance against abiotic and biotic stress conditions were determined as the positive effects of SAP application.

Organic acids (oxalic, malonic, acetic, glycolic and formic acids) increase P, Ca, Fe, Zn and Mn ions uptakes in plants (Ohwaki and Hirata, 1992; Marschner, 2011). Arıkan et al. (2018) reported that the increased in organic acid content resulted in increases in plant nutrient elements, especially Fe content in peach leaves. İpek (2019) reported that the applications of rhizobacteria in raspberry plants increase the nutritional content, as well as increase the organic acid composition by 1 to 21%, excluding oxalic acid and succinic acid. This shows that SAP application may have allowed plants uptake more nutrients. In our findings, a strong linear relationship was determined between the organic acid compositions and nutrient uptake, similar to previous studies.

Amino acids, which play important roles in physiological and metabolic events of plants, have different functions. Some amino acids play significant roles in growth and development which are decreased by stress; some other are defense amino acids that increased by stress. Amino acids such as aspartate, hydroxyproline, alanine, glycine and proline accumulate in plants when exposed to stress conditions (Sanchez et al., 1998; Mansour, 2000; Maclean et al., 2009). In our findings, aspartate, hydroxyproline and proline contents were decreased by SAP application. This decrease can be explained by preventing humidity fluctuations in the root area of SAP treated plants. This might have kept plants away from stress by providing the ideal moisture level. Increasing amino acid levels that prevent cell damage and accumulation of reactive oxygen derivatives was reported important in protecting the plant under abiotic stress conditions (Keller and Torres-Martinez, 2004; Gregan et al., 2012).

Beside the direct effect of SAP application on plant growth and development, the increases in amino acid contents of plants make more tolerant to the stress conditions during vegetation period, as indirect positive effect of SAP. Amino acids and organic acids ensure osmotic balance, stabilize cellular macromolecules and neutralize free radicals produced under stress conditions (Sneha et al., 2013). In our findings, it was determined that the increases in amino acid and organic acid contents prevented the accumulation of free oxygen radicals and, consequently, significantly reduced SOD, CAT and POD enzyme activities.

http://www.aloki.hu ● ISSN 1589 1623 (Print) ● ISSN1785 0037 (Online)
DOI: http://dx.doi.org/10.15666/aeer/1804_59075921

Acting as osmoregulator, proline increases in salinity and drought stress conditions to help plants to tolerate stress conditions (Shannon, 1997; Ashraf and Foolad, 2007). The accumulation of proline in plants is also a sign that plants are under stress conditions. In our findings, it can be said that beside the effect of SAP application on reducing the proline content, the polymer provides stable moisture level in the root region, as well as increasing the uptake of nutrients effective in maintaining osmotic balance such as K, Ca, Mg. Similar studies showed that SAP application reduced the proline content in other plant species such as cucumber, *Caragana korshinskii*, sorghum, wheat, pepper and lettuce (Sayyari and Ghanbari, 2012; Being et al., 2014; Tahmasebi et al., 2015; Su et al., 2017; Rostampour, 2017; Li et al., 2019).

According to the first 3-month of the study, monthly drained water in 10 g polymer applicated cocopeat slabs were determined as 23%, 94% and 109% higher than control ones in may, july, and june, respectively (*Table 9*). In the control slabs, some amount of water in the root zone between irrigation times was consumed by the plant, some amount was both drained and evaporated. Therefore, the control plants need more water in the next irrigation. In this case, it causes the water to be absorbed more by the growing medium, causing less drainage. The amount of drainage increased by increased SAP doses supported the present hypothesis. It was determined that SAP saved the water in the environment until the next irrigation, prevented water loss especially from evaporation and drainage, and absorbed only the reduced amount of water when watering again. The excess water that cannot be absorbed, that was drained. This situation resulted in higher drainage in SAP applied slabs compared to control ones. As the amount of water supplied to all environments was equal, it can be concluded that control plants consumed more water than SAP applied plants. SAP can absorb up to 95% water and release it long time period so that potential soil moisture is available to plants (Kiatkamjornwong, 2007).

The polymers improved soil porosity, structure and water holding capacity (Karimi et al., 2009). In September, it is observed that the amount of drainage increased in control application compared to SAP applications (*Table 9*). This situation supports the current hypothesis above. In September, the decreases in water consumption of the plant and air temperatures, consequently decrease evaporation, allowing root area of the control plants remains constantly moist and a large part of the water supplied drains, causing high drainage. The maximum water holding capacity of SAPs is called as swelling equilibrium value (r), and the characteristic temperature at which the water is retained is called as phase transition temperature (LCST-Lower Critical Solution Temperature). Hydrogels absorb water when the ambient temperature is below the phase transition temperature, and release water to the environment when it is above the phase transition temperature (Altay, 2010). Lower ambient temperatures compared to phase transition temperature might have decreased the drained water in SAP treatments after mid-August. The water retention capacities of the SAPs increased as the temperatures dropped in September. The increased SAP dose caused a decrease in the amount of drainage, especially in September, confirms the present view (*Table 9*). According to this table, SAP treated slabs drained higher amount of water compared to control slab during trial. This means that the small amount of water was sufficient for plants in SAP slabs. Above all, SAP treatment affect plants growth and yield positively. This will guidance to growers when SAP contained slabs are used they can minimise water usage.

http://www.aloki.hu ● ISSN 1589 1623 (Print) ● ISSN1785 0037 (Online)
DOI: http://dx.doi.org/10.15666/aeer/1804_59075921

Conclusion

In this study, SAP application increased growth, yield, leaf chlorophyll, hormone and nutrient contents, organic acid, except butyric acid and maleic acid, and amino acid composition, except aspartate, hydroxyproline and proline, but reduced lipid peroxidasion, H_2O_2, ABA levels and antioxidant enzym activities. The present study showed that SAP applications generally increased organic acid and amino acid contents in leaves of tomato plants grown by soilless agriculture technique. This increase did not only have a positive effect on plant development, but also made plants more tolerant to the stress conditions they may encounter them during the vegetation period.

Our data showed that the applied SAP had marked effect on tomato growth in soilless culture. This positive effect is due to the considerable absorption of nutrient solution by SAP and giving gradual absorbed solution to plant root. It was understood that the better uptake of sufficient water and nutrients which are kept in the root zone with low force enabled the plant growth free from stress.

The high drainage amount determined in SAP applied plants indicated that the amount of water given can be reduced or the irrigation interval can be extended. This will allow less usage of water and chemical fertilizers in either soilless and conventional agriculture. To conclude, SAP application in soilless farming would be a good strategy for water and fertilizer economy in environmental friendly production. This allows the changes in irrigation and fertilization strategies in soilless culture. In future studies, it is recommended to investigate the effect of polymer applications under restricted irrigation conditions.

Acknowledgement. This study was supported by Kırşehir Ahi Evran University Scientific Research Projects Coordination Unit with ZRT.A4.19.026 project number.

REFERENCES

[1] Altay, A. (2010): Synthesis Of Hydrophobic Group Containing Poly (Nisopropylacrylamide) Hydrogels and Investigation of Theirs Phase Transition Temperatures (Lcst). – Master's Thesis Selçuk University, Konya, Turkey. (in Turkish).

[2] Antoine, F. R., Wei, C. I., Littell, R. C., Marshall, M. R. (1999): HPLC method for analysis of free amino acids in fish using o-phthaldialdehyde precolumn derivatization. – Journal of Agricultural and Food Chemistry 47: 5100-5107.

[3] Arıkan, Ş., Eşitken, A., İpek, M., Aras, S., Şahin, M., Pırlak, L., Turan, M. (2018): Effect of Plant Growth Promoting Rhizobacteria on Fe Acquisition in Peach (*Prunus Persica* L.) Under Calcareous Soil Conditions. – Journal of Plant Nutrition 41(17): 2141-2150.

[4] Aristoy, M. C., Toldra, F. (1991): Deproteinization techniques for HPLC amino acid analysis in fresh pork muscle and dry-cured ham. – Journal of Agricultural and Food Chemistry 39: 1792-1795.

[5] Arnon, D. I. (1949): Copper enzymes in isolated chloroplasts, polyphenoloxidase in Beta vulgaris. – Plant Physiology 24: 1-15.

[6] Ashraf, M., Foolad, M. R. (2007): Roles of glycine betaine and proline in improving plant abiotic stress resistance. – Environmental and Experimental Botany 59: 206-216.

[7] Başak, H., Şahin, E., Kıymaz, S. (2016): Effect of Water Holding Polymers and Water Restriction on Growth of Tomato Cultivated in Different Soilless Cultures. – VII International Scientific Agriculture Symposium "Agrosym 2016", Jahorina, Bosnia and Herzegovina, 6-9 October, pp. 2101-2109.

http://www.aloki.hu ● ISSN 1589 1623 (Print) ● ISSN1785 0037 (Online)
DOI: http://dx.doi.org/10.15666/aeer/1804_59075921

[8] Battal, P., Tilekliоğlu, B. (2001): The effects of different mineral nutrients on the levels of cytokinins in maize (*Zea mays* L.). – Turkish Journal of Botany 25: 123-130.
[9] Beig, A. V. G., Neamati, S. H., Tehranifar, A., Emami, H. (2014): Evaluation of chlorophyll fluorescence and biochemical traits of lettuce under drought stress and super absorbent or bentonite application. – Journal of Stress Physiology & Biochemistry 10(1): 301-315.
[10] Bortolin, A., Aouada, F. A., Mattoso, L. H., Ribeiro, C. (2013): Nanocomposite PAAm/methyl cellulose/montmorillonite hydrogel: evidence of synergistic effects for the slow release of fertilizers. – Journal of Agricultural and Food Chemistry 61: 7431-7439.
[11] Bremner, J. M. (1996): Nitrogen total. – In: Sparks, D. L. (ed.) Methods of Soil Analysis, Part III. Chemical Methods. 2nd ed. Madison, W.I., USA, Soil Science Society of America Journal pp. 1085-1122.
[12] Buehner, A. (1956): Grundsaetzlisches zur Düngung der Weinberg. – Weinberg und Keller 3: 453-462.
[13] Dorraji, S. S., Golchin, A., Ahmadi, S. (2010): The effects of hydrophilic polymer and soil salinity on corn growth in sandy and loamy soils. – Clean-Soil, Air, Water 38(7): 584-591.
[14] Gregan, S. M., Wargent, J. J., Liu, L., Shinkle, J., Hofmann, R. W., Winefield, C., Trought, M., Jordan, B. J. (2012): Effects of solar ultraviolet radiation and canopy manipulation on the biochemical composition of Sauvignon Blanc grapes. – Australian Journal of Grape and Wine Research 18: 227-238.
[15] Habibi, D., Moslemi, Z., Ardakani, M. R., Mohammadi, A. (2010): Effects of super absorbent polymer and plant growth promoting rhizobacteria (PGPR) on yield and oxidative damage of maize under drought stress. – International Conference on Chemistry and Chemical Engineering, Cape Town, South Africa.
[16] Heath, R. L., Packer, L. (1968): Photoperoxidation in isolated chloroplasts. I. Kinetics and stoichiometry of fatty acid peroxidation. – Archives of Biochemistry and Biophysics 125: 189-198.
[17] Henderson, J. W., Ricker, R. D., Bidlingmeyer, B. A., Woodward, C. (1999): Amino acid analysis using Zorbax Eclipse-AAA Columns and the Agilent 1200 HPLC. – Agilent Technologies Part No. 5980-1193E.
[18] Hoagland, D. R., Arnon, D. I. (1950): The water-culture method for growing plants without soil. – California Agricultural Experiment Station Circ. No. 347.
[19] İpek, M. (2019): Effect of rhizobacteria treatments on nutrient content and organic and amino acid composition in raspberry plants. – Turkish Journal of Agriculture and Forestry 43(1): 88-95.
[20] Islam, M. R., Xue, X., Mao, S., Zhao, X., Eneji, A. E., Hu, Y. (2011): Superabsorbent polymers (SAP) enhance efficient and eco-friendly production of corn in drought affected areas of northern China. – African Journal Biotechnology 10(24): 4887-4894.
[21] Karimi, A., Noshadi, M., Ahmadzadeh, M. (2009): Effects of super absorbent polymer (IGETA) on crop, soil water and irrigation interval. – Journal of Science and Technology of Agriculture and Natural Resources 12: 415-420.
[22] Keller, M., Torres-Martinez, N. (2004): Does UV radiation affect Winegrape composition? – Acta Horticulturae 64: 313-319.
[23] Kiatkamjornwong, S. (2007): Superabsorbent polymers and superabsorbent polymer composites. – Science Asia 33: 39-43.
[24] Kuraishi, S., Tasaki, K., Sakurai, N., Sadatoku, K. (1991): Changes in levels of cytokinins in etiolated squash seedlings after illumination. – Plant Cell Physiology 32: 585-591.
[25] Li, Y., Shi, H., Zhang, H., Chen, S. (2019): Amelioration of drought effects in wheat and cucumber by the combined application of super absorbent polymer and potential biofertilizer. – The Journal of Life and Environmental Sciences (PeerJ) 7: e6073.
[26] Lichtenthaler, H. K., Wellburn, A. R. (1983): Determinations of total carotenoids and chlorophylls a and b of leaf extracts in different solvents. – Biochemical Society Transactions 11: 591-592.

http://www.aloki.hu ● ISSN 1589 1623 (Print) ● ISSN1785 0037 (Online)
DOI: http://dx.doi.org/10.15666/aeer/1804_59075921

[27] Maboko, M. M. (2006): Growth, yield and quality of tomatoes (*Lycopersicon esculentum* Mill.) and lettuce (*Lactuca sativa* L.) as affected by gel-polymer soil amendment and irrigation management. – Master's Dissertation, Natural and Agricultural Sciences University of Pretoria, South Africa.
[28] Maclean, A. M., White, C. E., Fowler, J. E., Finan, T. M. (2009): Identification of a hydroxyproline transport system in the legume endosymbiont Sinorhizobium meliloti. – Molecular Plant-Microbe Interactions Journal 22(9): 1116-1127.
[29] Mansour, M. M. F. (2000): Nitrogen containing compounds and adaptation of plants to salinity stress. – Biologia Plantarum 43(4): 491-500.
[30] Marschner, H. (1986): Mineral Nutrition of Higher Plants. – Institute of Plant Nutrition University of Hohenheim Federal Republic of Germany, Germany, p. 850.
[31] Marschner, H. (2011): Marschner's Mineral Nutrition of Higher Plants. – 3rd ed. San Diego, C.A, Academic Press., USA.
[32] Marulanda, A., Barea, J. M., Azcón, R. (2009): Stimulation of plant growth and drought tolerance by native microor-ganisms (AM fungi and bacteria) from dry environments:mechanisms related to bacterial effectiveness. – Journal of Plant Growth Regulation 28: 115-124.
[33] Mertens, D. (2005): AOAC official method 975.03. – In: Horwitz, W., Latimer, G. W. (eds.) Metal in Plants and Pet Foods. Official Methods of Analysis, eighteenth ed. AOAC-International, Suite 500, 481, North Frederick Avenue, Gaitherburg, Maryland 20877-2417, USA, pp. 3e4 (Chapter 3).
[34] Mikiciuk, G., Mikiciuk, M., Hawrot-Paw, M. (2015): Influence of superabsorbent polymers on the chemical composition of strawberry (*Fragaria* × *ananassa* Duch.) and biological activity in the soil. – Folia Horticulturae 27(1): 63-69.
[35] Mittler, R. (2002): Oxidative stress, antioxidants and stress tolerance. – Trends in plant science 7(9): 405-410.
[36] Moghadam, H. R. T. (2017): Super absorbent polymer mitigates deleterious effects of arsenic in wheat. – Rhizosphere 3: 40-43.
[37] NCSS, L. C. (2017): Power Analysis and Sample Size. – Software (PASS 15): Kaysville, Utah, USA.
[38] Nimah, N. M., Ryan, J., Chaudhry, M. A. (1983): Effect of synthetic conditioners on soil water retention, hydraulic conductivity, porosity, and agregation. – Soil Science Society of America Journal 47: 742-745.
[39] Ohwaki, Y., Hirata, H. (1992): Differences in carboxylic acid exudation among P-starved le-guminous crops in relation to carboxylic acid contents in plant tissues and phospho-lipid level in roots. – Soil Science and Plant Nutrition 38: 235-243.
[40] Öktüren, F., Sönmez, S. (2005): The Relationship Between Plant Nutrition Elements and Some Plant Growht Regulators (Hormones). – Batı Akdeniz Agricultural Research Institute, Derim 22(2): 20-32. (in Turkish).
[41] Özen, H. Ç., Onay, A. (1999): Plant Growth and Development Physiology. – Dicle Üniversity press, Diyarbakır, p. 166. (in Turkish).
[42] Percival, G. C., Fraser, G. A., Oxenham, G. (2003): Foliar salt tolerance of Acer genotypes using chlorophyll fluorescence. – Journal of Arboriculture 29: 61-65.
[43] Pouresmaeil, P., Habibi, D., Boojar, M. M. A., Tarighaleslami, M. (2013): Effect of super absorbent polymer application on chemical and biochemical activities in red bean (*Phaseolus vulgaris* L.) cultivars under drought stress. – European Journal of Experimental Biology 3(3): 261-266.
[44] Putra, P. A., Yuliando, H. (2015): Soilless culture system to support water use efficiency and product quality: a review. – Agriculture and Agricultural Science Procedia 3: 283-288.
[45] Rostampour, M. F. (2017): Evaluation of Relative Membrane Permeability of Sorghum (*Sorghum bicolor*) Affected Super Absorbent Polymer and Water Deficit Conditions. – Journal of Crop Nutrition Science 3: 27-39.

http://www.aloki.hu ● ISSN 1589 1623 (Print) ● ISSN1785 0037 (Online)
DOI: http://dx.doi.org/10.15666/aeer/1804_59075921

[46] Sairam, R., Srivastava, G. (2002): Changes in antioxidant activity in sub-cellular fractions of tolerant and susceptible wheat genotypes in response to long term salt stress. – Plant Science 162: 897-904.
[47] Sanchez, F. J., Manzanares, M., Andres, E. F., Tenorio, J. L., Ayerbe, L. (1998): Turgor maintenance, osmotic adjustment and soluble sugar and proline accumulation in 49 pea cultivars in response to water stress. – Field Crops Research 59: 225-235.
[48] Sayyari, M., Ghanbari, F. (2012): Effects of super absorbent polymer a200 on the growth, yield and some physiological responses in sweet pepper (*Capsicum annuum* L.) under various ırrigation regimes. – International Journal of Agricultural and Food Research 1(1): 1-11.
[49] Shannon, M. C. (1997): Adaptation of Plants to Salinity. – Advances in Agronomy 60: 76-120.
[50] Siddiqui, S. N., Umar, S., Iqbal, M. (2015): Zinc-induced modulation of some biochemical parameters in a high-and a low-zinc-accumulating genotype of *Cicer arietinum* L. grown under Zn-deficient condition. – Protoplasma 252: 1335-1345.
[51] Sita, R. C. M., Reissmann, C. B., Marques, R., Oliveira, E., Taffarel, A. D. (2005): Effect of Polymers Associated with N and K Fertilizer Sources on Dendrathema grandiflorum Growth and K, Ca and Mg Relations. – Brazilian Archives of Biology and Technology 48: 335-342.
[52] Sneha, S., Rishi, A., Dadhich, A., Chandra, S. (2013): Effect of salinity on seed germination, accumulation of proline and free amino acid in *Pennisetum glaucum* (L.) R. Br. – Pakistan Journal of Biological Sciences 17: 877-881.
[53] Sojka, R. E., Entry, J. A. (2000): Influence of polyacrylamide application to soil on movement of microorganisms in runoff water. – Environmental Pollution 108(3): 405-412.
[54] Sojka, R. E., Bjorneberg, D. L., Entry, J. A., Lentz, R. D., Orts, W. J. (2007): Polyacrilamide in Agriculture and Environmental Land Management. – Advances in Agronomy 158: 233-234.
[55] Sticher, L., Mauch-Mani, B., Métraux, J. P. (1997): Systemic acquired resistance. – Annual Review of Phytopathology 35: 235-270.
[56] Su, L. Q., Li, J. G., Xue, H., Wang, X. F. (2017): Super absorbent polymer seed coatings promote seed germination and seedling growth of Caragana korshinskii in drought. – Journal of Zhejiang University Science B (Biomedicine and Biotechnology) 18(8): 696-706.
[57] Tahmasebi, N., Moghadam, H. R. T., Borzou, A. (2015): Effects of Super Absorbent Polymer on the Quantity, Quality, Physiological and Biochemical Wheat (*Triticum aestivum* L.) in soils infected with Lead. – Biological Forum 7(1): 192-197.
[58] Tohidi-Moghadam, H. R., Shirani-Rad, A. H., Nour-Mohammadi, G., Habibi, D., Mashhadi-Akbar-Boojar, M. (2009): Effect of super absorbent application on antioxidant enzyme activities in Canola (*Brassica napus* L.) cultivars under water stress conditions. – American Journal Agricultural and Biological Sciences 4: 215-223.
[59] Velikova, V., Yordanow, I., Edreva, A. (2000): Oxidative stress and some antioxidant systems in acid rain treated bean plants protective role of exogenous polyamines. – Plant Science 151: 59-66.
[60] Wu, L., Liu, M., Liang, R. (2008): Preparation and properties of a double-coated slow-release NPK compound with superabsorbent and water retention. – Bioresource Technology 99: 547-554.
[61] Yazdani, F., Allahdadi, I., Akbari, G. A. (2007): Impact of süper absorbent polymer on yield and growth analysis of soybean (*Glycine max* L.) under drought stress condition. – Pakistan Journal of Biological Sciences 10(23): 4190-4196.

http://www.aloki.hu ● ISSN 1589 1623 (Print) ● ISSN1785 0037 (Online)
DOI: http://dx.doi.org/10.15666/aeer/1804_59075921

EFFECTS OF INTERCROPPING DIFFERENT HALOPHYTES IN BARE STRIPS ON SOIL WATER CONTENT, SALT ACCUMULATION, AND COTTON (*GOSSYPIUM HIRSUTUM*) YIELDS IN MULCHED DRIP IRRIGATION

GUO, J. Z. – SHI, W. J.* – LI, J. K.

State Key Laboratory of Eco-hydraulics in Northwest Arid Region, Xi'an University of Technology, China

*Corresponding author
e-mail: shiwj@xaut.edu.cn

(Received 18th Mar 2020; accepted 9th Jul 2020)

Abstract. Mulched drip irrigation is an important water-saving irrigation method in Xinjiang, China. Three different halophytes (*Cuminum cyminum* L., *Suaeda salsa*, and *Medicago sativa* L.) were intercropped in bare soil strips between rows of plastic film in mulched drip irrigation on cotton fields to assess the distribution of soil salt. The control group (CK) was not intercropped with halophytes. The effects of the treatments on soil evaporation, accumulated soil salinity, and cotton yield were investigated. The results indicated that compared to the CK, soil evaporation was reduced by 11.4%-24.9% and 5.5%-29.2% in 2014 and 2015, respectively. Intercropping halophytes decreased the soil salinity accumulation rate by 50%-134% and 74%-125% compared to the CK in the 0-40 cm and 0-100 cm deep soil layers in both years of total area. The accumulation rate of the soil sodium ions decreased by 29%-138% and 17%-148% in the 0-40 cm and 0-100 cm deep soil layers compared to the CK and the accumulation rate was lowest for intercropping *Suaeda salsa*. Intercropping halophytes had little effect on the cotton yield but slightly decreased the water use efficiency (WUE) of the cotton plant. Intercropping halophytes represents a new method for improving saline-alkaline soils.
Keywords: *soil evaporation, soil salinity, soil sodium ions, harvest index, water use efficiency*

Introduction

The shortage of water resources and soil salinization are important factors restricting the development of agricultural production in Xinjiang, China (Li et al., 2016). Therefore, it is very important to improve the utilization efficiency of water and reduce secondary soil salinization caused by excessive evaporation (Ji and Unger, 2001). It has been shown that increasing the surface coverage and adopting drip irrigation under mulch noticeably reduced secondary salinization (Prueger et al., 1996). Mulched drip irrigation is an irrigation method that combines drip irrigation and plastic film and this method is widely used in arid and semi-arid regions of China (Li et al., 2016). Studies have shown that drip irrigation provides accurate control over the amount of water, reduces deep seepage, and decreases the damage due to salinity in the root layer of the crop (Wang et al., 2014). Drip irrigation can cause salt redistribution in the soil and results in a desalination zone under the plastic film and a salt accumulation zone in the bare strips between the two rows of plastic film. The accumulation of salt in the bare-soil strips produces a "w-shaped" distribution of salt in the fields that influences salt leaching in winter, irrigation efficiency, as well as the growth and yield of the subsequent crop (Qiao et al., 2011). Research has demonstrated that drip irrigation results in the formation of a low-salt zone in the root area after drip irrigation has been used in the cotton (*Gossypium hirsutum*) growth periods; however, salt accumulation is extensive in the bare strips where no plastic film covers the

http://www.aloki.hu ● ISSN 1589 1623 (Print) ● ISSN 1785 0037 (Online)
DOI: http://dx.doi.org/10.15666/aeer/1804_59235937

soil and where salt accumulates at the wetted edge of the drip irrigation zone (Zhang et al., 2008). The salt will accumulate in cotton fields when drip irrigation is used for long periods (Zhang et al., 2008). The development of a suitable method to control soil evaporation in the bare strips between the plastic film rows has been challenging (Tan et al., 2017). Therefore, it is of great importance to solve the problem of secondary salinization of the soil and to seek a sustainable method suitable for mulched drip irrigation systems.

Halophytes take up and accumulate high concentrations of salt in the aboveground tissues and saline soils can be improved by harvesting the plants (Manousaki and Kalogerakis, 2011; Panta et al., 2014). This process of reducing the amount of salt in the soil is called a salt pump (Sagers et al., 2017). The salt content of the soil layer in the 0-10 cm layer was reduced on average by 38.5% by planting halophytes (Zhao et al., 2003; Shaygan et al., 2017). In addition, the organic matter content of the surface soil is increased (Xiao et al., 2012). Can salinity be reduced by intercropping halophytes, and how does intercropping halophytes affect crop yields? The growth and yields of tomatoes (*Solanum lycopersicum*) were increased by planting the halophyte *Portulaca oleracea* L. (Zuccarini, 2008). The Na^+ concentration was reduced and the quality of tomatoes under salt-stress was increased by intercropping *Salsola soda* L. (Graifenberg et al., 2003; Zhang et al., 2019). The yield of watermelon (*Citrullus lanatus*) was increased by intercropping orache (Simpson et al., 2013). Saltwort intercropped with tomato was able to reduce the Na^+ concentration in both the foliage and the growing medium (Albaho and Green, 2000). Intercropping salt-tolerant plants decreased the accumulation of sodium in olive trees in an olive-grass system (Chehab et al., 2018). These previous studies have shown that intercropping halophytes could promote the absorption of soil salt and increase crop yield. The halophytes of *Cuminum cyminum* L., *Suaeda salsa,* and *Medicago sativa* L. are common plants in Xinjiang. Therefore, in this study, we chose these three halophytes for intercropping on bare soil strips between rows of plastic films in light and medium saline-alkaline soils. And the objective of this study was to investigate the effect of intercropping halophytes on soil evaporation, soil desalination, and cotton yield.

Materials and methods

Experimental site description

The field experiment was conducted at the Bazhou Irrigation Experimental Station (41°35′N, 86°09′E, 901 m a.s.l.) in the Tarim Basin of Xinjiang in northwestern China (*Figure 1*) during 2014 and 2015 (Li et al., 2016). The region is an area of irrigated agriculture and has a continental desert climate with long-term annual precipitation of 58 mm and average potential evaporation of 2788 mm (Wang et al., 2014; Li et al., 2016). The soil is a sandy loam according to the United States Department of Agriculture soil taxonomy, and the particle size distribution is 3.26% for clay, 59.96% for silt, and 36.78% for sand.

Experimental design

The planting model and drip line arrangement in the experimental field consisted of one row of film, two drip lines, and four rows of cotton (*Figure 2*). The length and width of the experimental field was 7.5 m×7.0 m, and the row spacing of the cotton was 10 cm.

http://www.aloki.hu ● ISSN 1589 1623 (Print) ● ISSN 1785 0037 (Online)
DOI: http://dx.doi.org/10.15666/aeer/1804_59235937

Four rows of cotton were covered by white plastic film and were irrigated with two drip lines with emitter intervals of 30 cm and a discharge rate of 2.2 $L \cdot h^{-1}$. The irrigation amounts during the growth period were 525 mm and 450 mm in 2014 and 2015, respectively. The drip irrigation amount in the 2014 season was higher than that in the 2015 season because the precipitation was 23.3 mm in the 2014 season and 60.8 mm in the 2015 season. The irrigation was adjusted appropriately during the season to minimize the water difference between the seasons. The cotton was sown on May 3, 2014 and April 23, 2015 and the halophytes *Cuminum cyminum* L. (IC), *Suaeda salsa* (IS), and *Medicago sativa* L. (IM) were sown in bare strips between the rows of plastic film in each treatment on May 10, 2014 and April 30, 2015 (*Figure 3*). The density of the halophyte seeds and cotton seeds were 600 seeds/m^2 and 40 seeds/m^2, respectively. The management of the cotton fields was similar to that of local farmers (Li et al., 2016). No intercropping was done in the control group (CK). All treatments were conducted in triplicate.

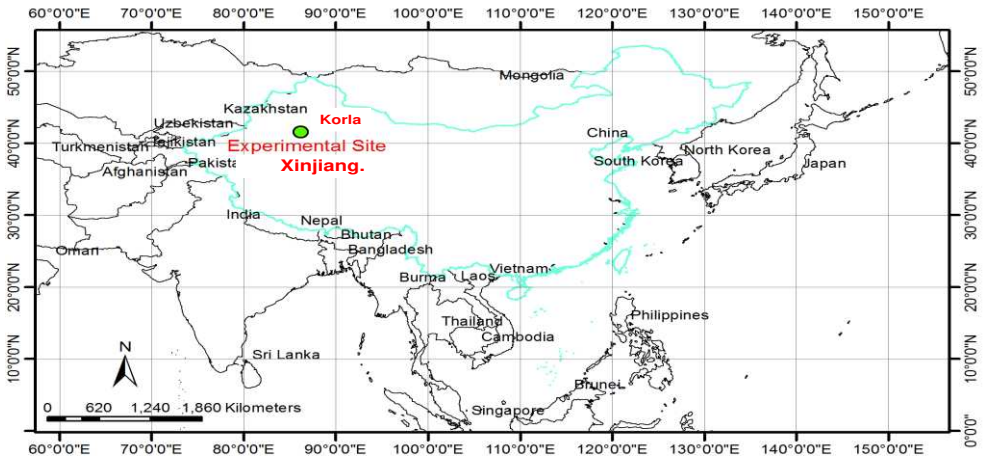

Figure 1. *Location of the experimental site in Korla City, Xinjiang, northwestern China*

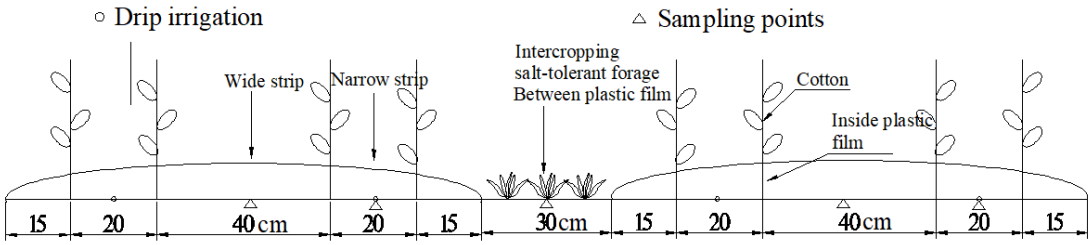

Figure 2. *Field experiment layout*

Data collection

Meteorological data

The meteorological data included precipitation, air temperature, relative humidity, and wind speed at a height of 2 m; the data were collected with a Davis wireless Vantage Pro2 weather station (Davis Instruments, California, USA), which was installed in the experimental field about 30 m away. The evapotranspiration (ET_0) during the 2014 and 2015 seasons (*Figure 4*) was calculated using the Penman-Monteith equation.

http://www.aloki.hu ● ISSN 1589 1623 (Print) ● ISSN 1785 0037 (Online)
DOI: http://dx.doi.org/10.15666/aeer/1804_59235937

Figure 3. *Field experiments of non-intercropping halophytes and intercropping halophytes in the bare strips*

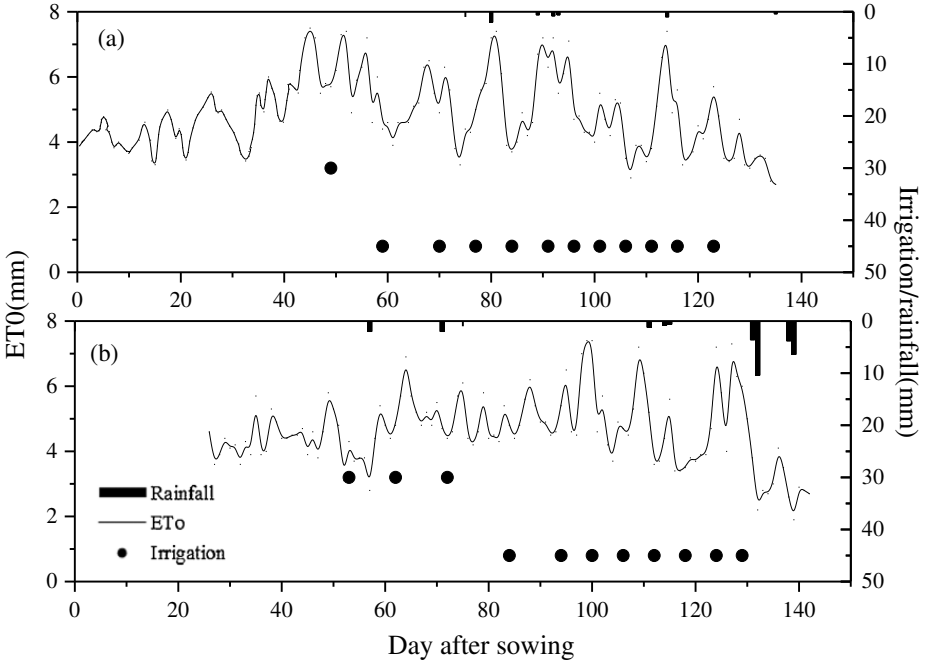

Figure 4. *Daily reference crop evapotranspiration (ET_0), rainfall, and irrigation at the experimental site during the 2014 and 2015 seasons*

Canopy cover and soil evaporation measurements

The canopy cover of the halophytes was measured using a plant canopy analyzer on July 26, 2014 and August 7, 2015. The soil evaporation of all treatments was monitored daily from July 19, 2014 to July 25, 2014 and from July 31, 2015 to August 6, 2015 at 20:00 with microlysimeters (Lage et al., 2003; Uclés et al., 2013) (13 cm diameter, 20 cm length, and 1.8 mm wall thickness), which were installed in the bare strips between the rows of plastic film.

http://www.aloki.hu ● ISSN 1589 1623 (Print) ● ISSN 1785 0037 (Online)
DOI: http://dx.doi.org/10.15666/aeer/1804_59235937

Soil water and soil salt

Soil samples were collected from the 0 to 40 cm soil layer at 10 cm intervals and from the 40 to 100 cm soil layer at 20 cm intervals using a 3.0 cm diameter auger to determine the water content, salt content and sodium ion content of the soil in the middle of the wide, narrow, and bare strips. The soil samples were collected prior to irrigation in the main growth stages of cotton (seedling, squaring, and flower-boll stage) and after harvest. The date of soil sample collection after harvest were Sep. 13, 2014 and Sep. 20, 2015. The auger holes were refilled with soil after collecting the samples to minimize the experimental error. The gravimetric soil water content (SWC) was determined by weighing the soil samples, followed by oven-drying at 105 ±2 ℃ for 24 h and reweighing. The soil volumetric water content was obtained by multiplying the mass water content with the average bulk density of each soil layer.

The electrical conductivity (EC) was determined using a DDS-307A conductivity meter (INESA, Shanghai, China) at a 1:5 soil to water extract ($EC_{1:5}$) at 25 ℃. The soil salt content was determined by converting the value of $EC_{1:5}$ for each soil sample using a linear relationship ($S=3.946\times EC_{1:5}$; $R^2=0.987$). The sodium ion contents were determined with an ion analyzer of PXSJ-216 (INESA, Shanghai, China) at a 1:5 soil to water extract ($EC_{1:5}$) at 25 ℃.

Yield and biomass measurements

The cotton (seeds and lint) was harvested from a 6.25 m^2 area in each treatment on Sep. 11, 2014 and Sep. 18, 2015. Three cotton plants from every treatment were randomly selected, collected, cut, and oven-dried at 70 ℃ until the weight remained stable to determine the aboveground biomass and harvest index (HI).

Calculations and analysis methods

Evapotranspiration calculation

The ET was calculated based on the water-balance equation:

$$ET = P_r + I + G - R - SI \pm \Delta W \quad \text{(Eq.1)}$$

$$\Delta W = SWS_f - SWS_i \quad \text{(Eq.2)}$$

where P_r is the rainfall (mm); I is the irrigation amount (mm); G is the supplementary amount of groundwater (mm); R is the surface runoff (mm); SI is the deep seepage (mm); ΔW is the change in soil water storage (SWS) in a 1.0-m profile (mm); SWS_f is the soil water storage at harvest and SWS_i is the soil water storage in the initial stage. The supplementary amount of groundwater and the surface runoff could be neglected because of the deep groundwater table (> 5 m) and the use of drip irrigation. Therefore, *Eq. (1)* was simplified in this experiment as follows:

$$ET = P_r + I \pm \Delta W \quad \text{(Eq.3)}$$

Calculation of soil water storage

SWS is defined as the amount of water stored in the soil. It is expressed as:

http://www.aloki.hu ● ISSN 1589 1623 (Print) ● ISSN 1785 0037 (Online)
DOI: http://dx.doi.org/10.15666/aeer/1804_59235937

$$SWS = \overline{\theta}_{0\sim10cm} \times r_{0\sim10cm} \times 10 + \cdots + \overline{\theta}_{80\sim100cm} \times r_{80\sim100cm} \times 20 \quad \text{(Eq.4)}$$

$$\overline{\theta}_{0\sim10cm} = \frac{2}{7}\theta_{W(0\sim10cm)} + \frac{7}{14}\theta_{N(0\sim10cm)} + \frac{3}{14}\theta_{B(0\sim10cm)} \quad \text{(Eq.5)}$$

$$\overline{\theta}_{80\sim100cm} = \frac{2}{7}\theta_{W(80\sim100cm)} + \frac{7}{14}\theta_{N(80\sim100cm)} + \frac{3}{14}\theta_{B(80\sim100cm)} \quad \text{(Eq.6)}$$

where $\overline{\theta}_{0-10cm}$ is the average water content in the 0-10 cm soil layer (cm^3 cm^{-3}); $\theta_{B(0\text{-}10cm)}$ and $\theta_{I(0\text{-}10cm)}$ are the actual water contents between the rows of plastic film and under the plastic film in the 0-10 cm soil layer (cm^3 cm^{-3}), respectively. The average soil water content of the other soil layers was determined in the same manner.

Calculation of salt and sodium ion content in the soil

The soil salt content and the accumulation rate of soil salt during both seasons were obtained as follows:

$$s_I = \frac{7}{11} \times s_N + \frac{4}{11} \times s_W \quad \text{(Eq.7)}$$

$$s_Z = \frac{11}{14} \times s_I + \frac{3}{14} \times s_B \quad \text{(Eq.8)}$$

$$D_s = \frac{s_f - s_i}{s_i} \quad \text{(Eq.9)}$$

where s_N, s_W, s_I, and s_B are the differences in the soil salt content in the narrow strips, wide strips, inside the plastic film, and the bare strips in the 40 cm or 100 cm soil profile (g/kg), respectively; s_z is the soil salt content in the entire soil layer; s_f and s_i are the soil salt contents in the entire soil layer at the harvest and late seedling stages, respectively; D_s is the accumulation rate of the soil salt from the late seedling stage to harvest.

The soil sodium ion content and the accumulation rate during both seasons were obtained as follows:

$$i_I = \frac{7}{11} \times i_N + \frac{4}{11} \times i_W \quad \text{(Eq.10)}$$

$$i_Z = \frac{11}{14} \times i_I + \frac{3}{14} \times i_B \quad \text{(Eq.11)}$$

$$D_i = \frac{i_f - i_i}{i_i} \quad \text{(Eq.12)}$$

http://www.aloki.hu ● ISSN 1589 1623 (Print) ● ISSN 1785 0037 (Online)
DOI: http://dx.doi.org/10.15666/aeer/1804_59235937

where i_N, i_W, and i_B are the soil sodium contents (Na^+ content in the soil) in the narrow, wide, and bare strips in the 40 cm or 100 cm soil profile (g/kg), respectively; i_z is the soil Na^+ content in the entire soil layer; i_f and i_i are the soil Na^+ contents in the entire soil layer at the harvest and late seedling stages, respectively; D_i is the accumulation rate of the soil sodium ions from the late seedling stage to harvest.

Harvest index

The harvest index (HI) was calculated as follows:

$$HI = \frac{Y}{B} \quad \text{(Eq.13)}$$

where *HI* is the harvest index of the cotton, %; *Y* is the yield (seeds and lint) of the cotton at harvest, kg ha^{-1}; *B* is the biomass of cotton at harvest, kg ha^{-1}.

Water use efficiency calculation

The water use efficiency (WUE) (kg/m^3) for all treatments was calculated as follows (Sun et al., 2012):

$$WUE = \frac{Y}{ET} \quad \text{(Eq.14)}$$

where *Y* is the yield (seeds and lint) of the cotton at harvest and *ET* is the total evapotranspiration (mm) during the entire growing season.

Statistical methods

Analysis of variance (ANOVA) was performed using SPSS 19.0. Multiple comparisons were performed using Duncan's test to determine the mean differences in the average evaporation, SWS, ET, soil salt, and soil sodium ion content, as well as the yield and biomass between different treatments.

Results

Soil evaporation and water balance

The soil evaporation rates of the different halophytes in the bare strips were significantly lower than that of the CK during the observation period in the 2014 and 2015 seasons, except for the IM treatment in 2015 ($P<0.05$, *Table 1*). The reductions in soil evaporation rates relative to the CK for the three halophyte treatments ranged from 11.4% to 24.9% in 2014 and from 5.5% to 29.2% in 2015. The lowest daily soil evaporation rate occurred in IS in both years. The soil evaporation rate of the IS was 2.71 mm in 2014 and 2.96 mm in 2015; these values were 24.9% and 29.2% lower, respectively than that of the CK. The canopy cover was highest for *Suaeda salsa* due to the vigorous growth and this reduced soil evaporation. The daily soil evaporation of IM was the highest of the treatments at 3.20 mm and 3.95 mm in 2014 and 2015, respectively, because of the low canopy cover of *Medicago sativa* L.

http://www.aloki.hu ● ISSN 1589 1623 (Print) ● ISSN 1785 0037 (Online)
DOI: http://dx.doi.org/10.15666/aeer/1804_59235937

Table 1. *Canopy cover and daily soil evaporation for the different treatments*

Treatment	2014			2015		
	Cover degree (%)	Average evaporation (mm day^{-1})	Reduction evaporation relative to CK (%)	Cover degree (%)	Average evaporation (mm day^{-1})	Reduction evaporation relative to CK (%)
IC	59ab	3.17b	12.2	48b	3.37b	19.4
IS	77a	2.71c	24.9	70a	2.96c	29.2
IM	33bc	3.20b	11.4	21bc	3.95a	5.5
CK	0d	3.61a	-	0d	4.18a	-

Notes: Soil evaporation in 2014 and 2015 was measured once a day from 19 July to 25 July and 31 July to 6 August, respectively. Canopy cover was measured at the start and end of the period. The canopy cover value represents the average of two measurements of canopy cover. IC stands for intercropping *Cuminum cyminum L.* in the bare strips between the rows of plastic film, IS stands for *Suaeda salsa*; IM stands for *Medicago sativa L.*, and CK stands for the control group with no intercropping. Means with different lowercase letters in the same column represent significant differences at $P<0.05$

It has been demonstrated that about 85% of cotton roots occur in the 30-50 cm soil layer under mulched drip irrigation (Kang et al., 2012); therefore, the soil layer of 0-40 cm was considered the main root zone of cotton. The SWS in the 0-40 cm soil layer is shown in *Figure 5*. For the treatment of intercropping halophytes between plastic films, the average SWS in the main root zone in the growth periods decreased 7.7%-18.77% and 5.3%-13.69% during 2014 and 2015, respectively. In contrast, the average SWS in the main root zone for the CK increased 0.26% and 2.53% during 2014 and 2015, respectively. The largest decline in the average SWS (compared to the initial SWS) was observed for *Medicago sativa* L. (18.77% decrease) and *Cuminum cyminum* L. (13.69% decrease) in 2014 and 2015. The average SWS of the main root zone decreased due to intercropping of halophytes because the halophytes consumed soil moisture.

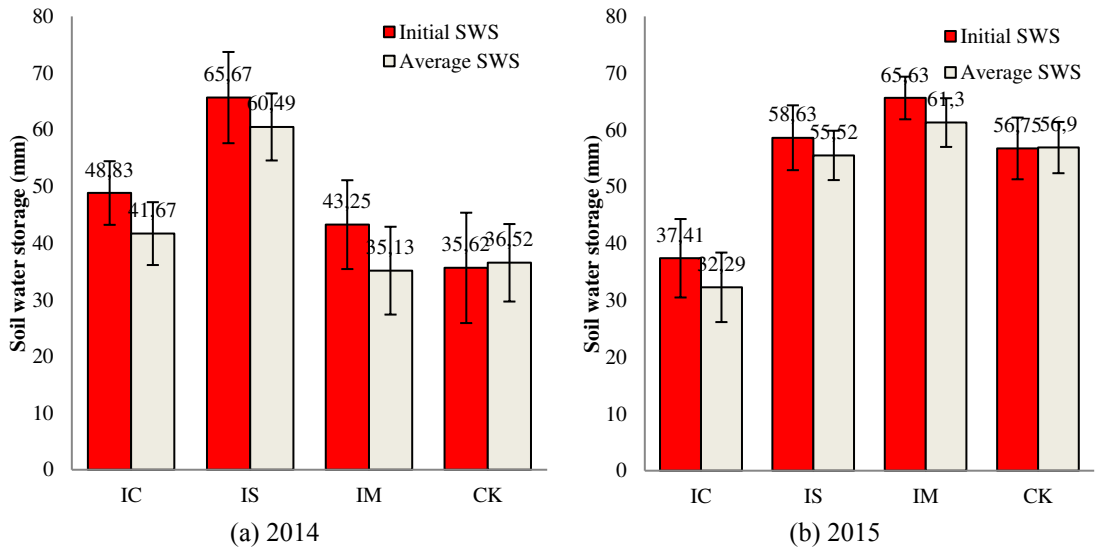

Figure 5. *The initial and average SWS at 40 cm depth for the different treatments in 2014 and 2015. Notes: IC stands for intercropping Cuminum cyminum L. in the bare strips between the rows of plastic film, IS stands for Suaeda salsa; IM stands for Medicago sativa L., and CK stands for the control group with no intercropping. Error bar represents the standard error of the mean (n=3)*

http://www.aloki.hu ● ISSN 1589 1623 (Print) ● ISSN 1785 0037 (Online)
DOI: http://dx.doi.org/10.15666/aeer/1804_59235937

ET rates differ for different crops (Allen et al., 1998). The ET was determined by calculating the changes in soil water content in the 0~100 cm soil layer at the initial stage and final stage of the experiment (*Table 2*). The initial SWS was significantly different for the treatments due to the spatial variability of the soil water content during the 2014 and 2015 seasons. There were no large precipitation events, and the planned wetting layer was between 45 mm and 50 mm during the drip irrigation; therefore, underground leakage was ignored. The ET increased by 8.54%-18.19% and 3.55%-10.40% in 2014 and 2015, respectively, due to the intercropping of halophytes between the rows of plastic film may consume a part of soil water moisture. The ET of the IS and IC treatments were not significantly different during the 2014 and 2015 seasons, and the ET was highest for the IM.

Table 2. *Water balances for the different treatments in the 100-cm soil profile*

Year	Treatment	Initial SWS (mm)	Final SWS (mm)	Rainfall (mm)	I (mm)	ET
2014	IC	146.90b	106.05a	23.3	525	589.15b
	IS	167.05a	127.96a	23.3	525	587.39b
	IM	150.84b	72.19b	23.3	525	626.95a
	CK	122.99c	127.76a	23.3	525	543.54c
2015	IC	95.49c	97.82b	60.8	450	508.47b
	IS	150.55ab	151.31a	60.8	450	510.04b
	IM	164.1a	132.83a	60.8	450	542.09a
	CK	123.81b	143.56a	60.8	450	491.05c

Notes: IC stands for intercropping *Cuminum cyminum L.* in the bare strips between the rows of plastic film, IS stands for *Suaeda salsa*; IM stands for *Medicago sativa L.*, and CK stands for the control group with no intercropping. Means with different lowercase letters in the same column represent significant differences at $P<0.05$

Changes in the soil salt

High concentrations of soil salt may reduce cotton growth, although cotton is saline tolerant (Zhang et al., 2014). The changes in the soil salinity (*Table 3*) and sodium ions content (*Table 4*) were assessed for the 0-40 cm soil layer of the main root zone and the 0-100 cm soil layer. The accumulation rate of the soil salt content was evaluated by determining the change rate of the soil salt content between the initial and final stages to avoid the influence of the initial salt content on the evaluation of the changes in the soil salt content in different treatments. The salt accumulation was higher between the rows of plastic film than under the plastic film and low salt content was maintained in the root zone of the cotton because the drip irrigation under the plastic film caused leaching, which decreased the salt concentration.

The soil salt accumulation rates of intercropping halophytes in the bare strips were lower than that of the CK in 2014 and 2015. Compared to the CK, the accumulation rates were 50%-134% and 74%-125% lower in the 0-40 cm and 0-100 cm soil layers of the total area, respectively, indicating that the salt accumulation was slowed down by intercropping halophytes in the bare strips between the rows of plastic film. The salt content of the 0-40 cm soil layer was higher than that of the 0-100 cm soil layer, showing that the soil salt accumulated in the upper layer of the soil during the cotton growth. The soil salt accumulation rate was lower in 2015 than in 2014 in the total area

http://www.aloki.hu ● ISSN 1589 1623 (Print) ● ISSN 1785 0037 (Online)
DOI: http://dx.doi.org/10.15666/aeer/1804_59235937

in the 0-40 cm soil layer and 0-100 cm soil layers. The salt accumulation rate was not different for the different locations (between the plastic film, under the plastic film, and the total area), except for the IM treatment in 2014.

Table 3. *The accumulation rate of the soil salt (s) for the different treatments between the plastic films, under the plastic film, and the total area in the 40 cm and 100 cm soil profiles in 2014 and 2015*

Year	Location	Treatment	0~40cm			0~100cm		
			Initial salinity (g/kg)	Final salinity (g/kg)	D_s/%	Initial salinity (g/kg)	Final salinity (g/kg)	D_s/%
2014	Between plastic film	IC	3.91a	7.71a	97.19	3.2a	5.08a	58.75
		IS	2.19b	4.11b	87.67	1.27b	2.09b	64.57
		IM	4.39a	2.89b	-34.17	2.02ab	2.41b	19.31
		CK	1.99b	7.76a	289.95	1.15b	4.09a	255.65
	Under plastic film	IC	5.92a	8.26a	39.53	4.14a	3.97a	-4.11
		IS	3.99a	4.74b	18.80	2.32a	2.4a	3.45
		IM	4.75a	1.97c	-58.53	2.13ab	1.37b	-35.68
		CK	1.38b	2.84c	105.8	1.33b	2.16a	62.41
	Total area	IC	5.49a	8.14a	48.33	3.94a	4.21a	6.84
		IS	3.60b	4.61b	27.76	2.10b	2.33b	11.39
		IM	4.67ab	2.17b	-53.62	2.11b	1.59b	-24.38
		CK	1.51c	3.89b	157.78	1.29b	2.57b	99.28
2015	Between plastic film	IC	3.42b	4.46b	30.41	1.76a	1.68b	-4.55
		IS	5.5a	3.91b	-28.91	2.09a	1.87b	-10.53
		IM	6.21a	9.97a	60.55	3.4a	4.14a	21.76
		CK	2.98b	8.01a	168.79	1.53a	3.73a	143.79
	Inside plastic film	IC	3.69a	4.81b	30.35	1.51a	1.86b	23.18
		IS	3.67ab	3.3b	-10.08	1.94a	1.66b	-14.43
		IM	5.17a	7.09a	37.14	2.85a	3.18a	11.58
		CK	1.98b	3.02b	52.53	0.96a	1.25b	30.21
	Total area	IC	3.63ab	4.74b	30.36	1.56a	1.82b	16.49
		IS	4.06a	3.43b	-15.54	1.97a	1.71b	-13.55
		IM	5.39a	7.71a	42.91	2.97a	3.39a	14.08
		CK	2.19b	4.09b	86.36	1.08a	1.78b	64.62

Notes: IC stands for intercropping *Cuminum cyminum L.* in the bare strips between the rows of plastic film, IS stands for *Suaeda salsa*; IM stands for *Medicago sativa L.*, and CK stands for the control group with no intercropping. Means with different lowercase letters in the same column represent significant differences at $P<0.05$

Changes in sodium ion content

Sodium ions can damage the crop and destroy the soil structure (Zhang et al., 2016; Li et al., 2019). Sodium ions may have an adverse effect on the growth and development of cotton if the sodium ion content in the soil exceeds the salt tolerance threshold of cotton (Farooq et al., 2019). The sodium ion accumulation rates of all treatments in 2015 were lower than that in 2014 in the 0-40 cm and 0-100 cm soil layers (*Table 4*) because the sodium ions were leached due to precipitation in the late growing stage of the cotton. The average soil sodium ion content was higher in the 0-40 cm soil layer than in the 0-100 cm layer at the harvest stage, showing that the sodium ions accumulated near the surface. The

http://www.aloki.hu ● ISSN 1589 1623 (Print) ● ISSN 1785 0037 (Online)
DOI: http://dx.doi.org/10.15666/aeer/1804_59235937

soil sodium ion accumulation rates of the treatment intercropping halophytes were 29% to 138% and 17% to 148% lower than that of CK in the 0-40 cm and 0-100 cm soil layers in total area, respectively. Intercropping halophytes in the bare strips between the plastic films reduced the accumulation rate of the soil sodium ions. The accumulation rate of soil sodium ions of the IS was 91% and 139% lower than that of the CK in the 0~40 cm soil layer in the total area, respectively, in 2014 and 2015. In 2014, the IS treatment had the lowest accumulation rate of sodium ions in the 0~40 cm soil layer, followed by the IC treatment and IM treatment. And in 2015, the soil sodium ion accumulation rates in the IS and IM treatments were lower than in 2014, and those of the IC treatment were higher at harvest in 2014. The accumulation rate of the soil sodium ions were lowest for the IS treatment in 2014 and 2015.

Table 4. *The accumulation rate of the soil sodium ion (Na^+) content for the different treatments between the plastic film, under the plastic film, and the total area in the 40 cm and 100 cm soil profiles in 2014 and 2015*

Year	Location	Treatment	0~40cm			0~100cm		
			Initial Na^+ content (g/kg)	Final Na^+ content (g/kg)	D_i/%	Initial Na^+ content (g/kg)	Final Na^+ content (g/kg)	D_i/%
2014	Between plastic film	IC	0.056a	0.138a	144.90	0.029b	0.079a	176.00
		IS	0.075a	0.082b	9.23	0.077a	0.055a	-28.36
		IM	0.039b	0.121a	208.82	0.021b	0.057a	173.91
		CK	0.038b	0.150a	293.94	0.018b	0.056a	206.25
	Under plastic film	IC	0.045a	0.105a	133.33	0.026b	0.066a	147.83
		IS	0.071a	0.104a	17.74	0.046a	0.071a	55.00
		IM	0.045a	0.097a	115.38	0.035ab	0.069a	100.00
		CK	0.024b	0.059a	145.83	0.012b	0.033b	175.00
	Total area	IC	0.047a	0.112a	136.59	0.027b	0.069a	154.27
		IS	0.072a	0.099a	14.29	0.053a	0.068a	28.86
		IM	0.044a	0.102a	134.21	0.032b	0.066a	110.39
		CK	0.027b	0.079a	190.72	0.013c	0.038b	185.48
2015	Between plastic film	IC	0.213a	0.362a	70.26	0.113a	0.221a	95.88
		IS	0.112bc	0.064b	-42.27	0.107a	0.038c	-64.52
		IM	0.164ab	0.309a	88.11	0.136a	0.145b	6.78
		CK	0.034c	0.108b	217.65	0.034b	0.092b	170.59
	Under plastic film	IC	0.146a	0.286a	96.13	0.168a	0.312a	85.65
		IS	0.146a	0.052b	-64.57	0.141b	0.062c	-76.42
		IM	0.201a	0.118b	-41.31	0.199a	0.121b	-67.63
		CK	0.021c	0.049b	133.33	0.023c	0.057c	147.83
	Total area	IC	0.160a	0.302a	88.77	0.156ab	0.293a	87.23
		IS	0.139a	0.055b	-60.72	0.134b	0.057c	-74.36
		IM	0.193a	0.159b	-17.86	0.185a	0.126b	-55.90
		CK	0.024b	0.062b	159.16	0.025c	0.065c	154.37

Notes: IC stands for intercropping *Cuminum cyminum L.* in the bare strips between the rows of plastic film, IS stands for *Suaeda salsa*; IM stands for *Medicago sativa L.*, and CK stands for the control group with no intercropping. Means with different lowercase letters in the same column represent significant differences at P<0.05 level

Aboveground biomass and yield of cotton

There was no significant difference in the yield and biomass between the treatments during the 2014 and 2015 seasons (*Table. 5*). The harvest index (HI) of the treatments

http://www.aloki.hu ● ISSN 1589 1623 (Print) ● ISSN 1785 0037 (Online)
DOI: http://dx.doi.org/10.15666/aeer/1804_59235937

ranged from 48.77% to 54.33% and 50.94% to 55.07% during the 2014 and 2015 seasons and the HIs of all treatments were lower in 2014 than in 2015. The reason is that the amount of irrigation in the early part of 2014 was higher and the cotton growth was better than in 2015. Compared to the CK, intercropping halophytes reduced the HI of cotton by 4.51%-10.23% and 0.78%-7.5% during the 2014 and 2015 seasons, respectively. The HI of the CK was higher than that of the intercropping halophytes because the low water consumption of the halophyte treatment between the plastic films in the early growth stage did not affect the uptake of nutrients and the halophytes competed with the cotton for soil water content and nutrients in the later growth stage. The WUE was lower in 2014 due to more irrigation. The WUE of the intercropping treatments was 6.41%-10.26% and 1.1%-4.4% lower than that of the CK during 2014 and 2015, respectively. The reason is that the halophytes compete with the cotton for soil moisture and nutrients.

Table 5. *Cotton yield, biomass, harvest index (HI), evapotranspiration (ET), and water-use efficiency (WUE) for different treatments in 2014 and 2015*

Year	Treatment	Yield (kg ha^{-1})	Biomass (kg ha^{-1})	HI (%)	WUE
2014	IC	4102.44a	8121.39a	50.51	0.70
	IS	4301.35a	8819.16a	48.77	0.73
	IM	4513.44a	8669.16a	51.88	0.72
	CK	4243.40a	7800.95a	54.33	0.78
2015	IC	4551.53a	8330.56a	54.64	0.90
	IS	4445.41a	8716.49a	50.94	0.87
	IM	4762.72a	8972.41a	53.16	0.88
	CK	4445.07a	8081.95a	55.07	0.91

Notes: IC stands for intercropping *Cuminum cyminum L.* in the bare strips between the rows of plastic film, IS stands for *Suaeda salsa*; IM stands for *Medicago sativa L.*, and CK stands for the control group with no intercropping. Means with different lowercase letters in the same column represent significant differences at $P<0.05$

Discussion

Soil surface evaporation is an important factor affecting salt accumulation in saline-alkali soils in arid areas (Schofield and Kirkby, 2003) because the evaporation in this area exceeds precipitation. Therefore, the reduction in soil surface evaporation is necessary to reduce surface salt accumulation. In our experiments, the soil evaporation was significantly reduced by growing halophytes in bare strips between the rows of plastic film in the middle and late stages in the two-year experiment (*Table 1*). Planting halophytes reduced soil surface solar radiation and decreased wind speed, thereby reducing soil evaporation (Li et al., 2013). The canopy cover was highest for *Suaeda salsa* and more solar radiation was intercepted; thus, intercropping *Suaeda salsa* in the areas between the rows of plastic film resulted in the largest reduction in soil surface evaporation. The canopy cover of halophytes was lower in 2015 than in 2014 and there was no significant difference in the evaporation rate between the IM and CK treatments in 2015. A possible reason is that the amount of irrigation in the early growth period was larger in 2014 than in 2015 (*Figure 3*) and the halophytes exhibited better growth in 2014 than in 2015. The IM treatment resulted in greater ET because the canopy cover of *Medicago sativa* L. was lower than that of the other intercropping treatments.

http://www.aloki.hu ● ISSN 1589 1623 (Print) ● ISSN 1785 0037 (Online)
DOI: http://dx.doi.org/10.15666/aeer/1804_59235937

Intercropping halophytes reduced the accumulation rate of soil salt and soil sodium ions. It decreased the soil salt accumulation rate by 50%-134% and 74%-125% in the 0-40 cm and 0-100 cm deep soil layers in both years compared to the CK. The accumulation rate of the soil sodium ions decreased by 29%-138% and 17%-148% in the 0-40 cm and 0-100 cm deep soil layers compared to the CK. There are two reasons for this: first, the canopy cover of the halophytes reduced the soil surface evaporation, which reduced the accumulation of soil salt and soil sodium ions. Second, the halophytes absorbed the soil salt and sodium ions (Zhou et al., 2019). The IS treatment resulted in a reduction in the accumulation rate of soil sodium ions, and this treatment was more effective than the other treatments. *Suaeda salsa* has a higher canopy cover than the other halophytes in arid-saline environments. Intercropping *Cuminum cyminum* L. also resulted in a reduction in the accumulation rate of the soil salt and sodium ions compared to the CK. In addition, *Cuminum cyminum* L. can be harvested because it is a good condiment with high economic value. Intercropping *Medicago sativa* L. also reduced the soil salt compared to the CK, and there was no significant difference in the desalination effect compared to the other halophytes. *Medicago sativa* L. is a forage crop with high nutritional value (Zhao et al., 2019). It is known as the king of pasture and can survive in light saline-alkali soil. Studies have shown that *Medicago sativa* L. has good salt and drought tolerance and it is a legume which could increase soil fertility and improves the soil. The halophytes (*Suaeda salsa*, *Medicago sativa* L., and *Cuminum cyminum* L.) are economic and forage crops and provide good yield; therefore, their overall benefit is higher than that of CK.

Conclusions

Intercropping halophytes (*Suaeda salsa*, *Medicago sativa* L., and *Cuminum cyminum* L.) in cotton field reduced the accumulation rate of soil salt and soil sodium ions, as well as the soil surface evaporation in the cotton field. The accumulation rate of soil sodium ions was highest for intercropping *Suaeda salsa*. Intercropping halophytes had little effect on the cotton yield and biomass. The results of this study provide guidance for the improvement of light and medium saline-alkali soils. Future studies should investigate the suitability of different halophytes in cotton fields for the removel of soil salt from different types of saline soil.

Acknowledgments. This project was supported by the National Natural Science Foundation of China (No. 51379173) and the Shaanxi Provincial Natural Science Basic Research Program (No. 2018JM5051).

REFERENCES

[1] Albaho, M. S., Green, J. L. (2000): Suaeda salsa, A Desalinating Companion Plant for Greenhouse Tomato. – Hortscience A Publication of the American Society for Horticultural Science 35: 620-623.

[2] Allen, R., Pereira, L., Raes, D., Smith, M. (1998): Irrigation and drainage paper No. 56. – FAO.

[3] Chehab, H., Tekaya, M., Gouiaa, M., Mahjoub, Z., Laamari, S., Sfina, H., Chihaoui, B., Boujnah, D., Mechri, B. (2018): The use of legume and grass cover crops induced changes in ion accumulation, growth and physiological performance of young olive trees irrigated with high-salinity water. – Scientia Horticulturae 232: 170-174.

http://www.aloki.hu ● ISSN 1589 1623 (Print) ● ISSN 1785 0037 (Online)
DOI: http://dx.doi.org/10.15666/aeer/1804_59235937

[4] Farooq, M. A., Shakeel, A., Atif, R. M., Saleem, M. F. (2019): Genotypic variations in salinity tolerance among BT cotton. – Pakistan Journal of Botany 12(51): 1945-1953.
[5] Graifenberg, A., Botrini, L., Giustiniani, L., Filippi, F., Curadi, M. (2003): Tomato growing in saline conditions with biodesalinating plants: *Salsola soda* L., and *Portulaca oleracea* L. – Acta Horticulturae 609: 301-305.
[6] Ji, S., Unger, P. W. (2001): Soil Water Accumulation under Different Precipitation, Potential Evaporation, and Straw Mulch Conditions. – Soil Science Society of America Journal 65: 442-448.
[7] Kang, Y. H., Wang, R. S., Wan, S. Q., Hu, W., Jiang, S. F., Liu, S. P. (2012): Effects of different water levels on cotton growth and water use through drip irrigation in an arid region with saline ground water of Northwest China. – Agricultural Water Management 109: 117-126.
[8] Lage, M., Bamouh, A., Karrou, M., El, M. M. (2003): Estimation of rice evapotranspiration using a microlysimeter technique and comparison with FAO Penman-Monteith and Pan evaporation methods under Moroccan conditions. – Agronomie 23: 625-631.
[9] Li, R., Hou, X., Jia, Z., Han, Q., Ren, X., Yang, B. (2013): Effects on soil temperature, moisture, and maize yield of cultivation with ridge and furrow mulching in the rainfed area of the Loess Plateau, China. – Agricultural Water Management 116: 101-109.
[10] Li, X., Jin, M., Zhou, N., Huang, J., Jiang, S., Telesphore, H. (2016): Evaluation of evapotranspiration and deep percolation under mulched drip irrigation in an oasis of Tarim basin, China. – Journal of Hydrology 538: 677-688.
[11] Li, X. Q., Xia, J. B., Zhao, X. M., Chen, Y. P. (2019): Effects of planting Tamarix chinensis on shallow soil water and salt content under different groundwater depths in the Yellow River Delta. – Geoderma 335: 104-111.
[12] Manousaki, E., Kalogerakis, N. (2011): Halophytes Present New Opportunities in Phytoremediation of Heavy Metals and Saline Soils. – Industrial & Engineering Chemistry Research 1(50): 656-660.
[13] Panta, S., Flowers, T., Lane, P., Doyle, R., Haros, G., Shabala, S. (2014): Halophyte agriculture: Success stories. – Environmental & Experimental Botany 107: 71-83.
[14] Prueger, J. H., Hipps, L. E., Cooper, D. I. (1996): Evaporation and the development of the local boundary layer over an irrigated surface in an arid region. – Agricultural & Forest Meteorology 78(3-4): 223-237.
[15] Qiao, L., Zhou, J., Li, X. (2011): Preliminary analysis of the effectiveness of desalting leaching using spring irrigation for use of brackish water for under-film drip irrigation of cotton. – Proceedings of the International Conference on Mechanic Automation & Control Engineering.
[16] Sagers, J. K., Waldron, B. L., Creech, J. E., Mott, I. W., Bugbee, B. (2017): Salinity toleranceof three competing rangeland plant species: Studies in hydroponic culture. – Ecology & Evolution 7: 1-14.
[17] Schofield, R. V., Kirkby, M. J. (2003): Application of salinization indicators and initial development of potential global soil salinization scenario under climatic change. – Global Biogeochemical Cycles 17(3): 1078.
[18] Shaygan, M., Mulligan, D., Baumgartl, T. (2017): The potential of remediation of soils affected by salt using halophytes. – Proceedings of the EGU General Assembly Conference.
[19] Simpson, C., Franco, J. G., King, S. R., Volder, A. (2013): Intercropping to Mitigate Salinity Stress on Watermelon: Halophyte Performance in a Greenhouse Pot Study. – Proceedings of the Ashs Conference.
[20] Sun, H. Y., Shao, L. W., Liu, X. W., Miao, W. F., Chen, S. Y., Zhang, X. Y. (2012): Determination of water consumption and the water-saving potential of three mulching methods in a jujube orchard. – European Journal of Agronomy 11(43): 87-95.

http://www.aloki.hu ● ISSN 1589 1623 (Print) ● ISSN 1785 0037 (Online)
DOI: http://dx.doi.org/10.15666/aeer/1804_59235937

[21] Tan, S., Wang, Q. J., Xu, D., Zhang, J. H., Shan, Y. Y. (2017): Evaluating effects of four controlling methods in bare strips on soil temperature, water, and salt accumulation under film-mulched drip irrigation. – Field Crops Research 214(12): 350-358.
[22] Uclés, O., Villagarcía, L., Cantón, Y., Domingo, F. (2013): Microlysimeter station for long term non-rainfall water input and evaporation studies. – Agricultural & Forest Meteorology 182: 13-20.
[23] Wang, Z., Jin, M., Šimůnek, J., Genuchten, M. T. V. (2014): Evaluation of mulched drip irrigation for cotton in arid Northwest China. – Irrigation Science 32: 15-27.
[24] Xiao, K. B., Wu, P. T., Lei, J. Y., Ban, N. R. (2012): Bio-reclamation of Different Halophytes on Saline-alkali Soil. – Journal of Agro-Environment Science 31(12): 2433-2440. (in Chinese).
[25] Zhang, W., Lu, X., Li, L., Liu, J., Sun, Z., Zhang, X., Yang, Z. (2008): Salt transfer law for cotton field with drip irrigation under the plastic mulch in Xinjiang Region 24: 15-19. DOI:10.3969/j.issn.1002-6819.2008.8.003.
[26] Zhang, L., Ma, H., Chen, T., Pen, J., Yu, S., Zhao, X. (2014): Morphological and Physiological Responses of Cotton (*Gossypium hirsutum* L.) Plants to Salinity. – Plos One 9: e112807.
[27] Zhang, G., Bai, J., Min, X., Zhao, Q., Lu, Q., Jia, J. (2016): Soil quality assessment of coastal wetlands in the Yellow River Delta of China based on the minimum data set. – Ecological Indicators 66: 458-466.
[28] Zhang, C. W., Tian, X. Y., Zhang, C. S. (2019): Diversity and probiotic activities of endophytic bacteria associated with the coastal halophyte Messerschmidia sibirica. – Applied Soil Ecology 143(11): 35-44.
[29] Zhao, K., Hai, F., Zhou, S., Jie, S. (2003): Study on the salt and drought tolerance of Suaeda salsa and Kalanchoe claigremontiana under iso-osmotic salt and water stress. – Plant Science 165: 837-844.
[30] Zhao. Y., Wei, X. H., Ji, X. Z., Ma, W. J. (2019): Endogenous NO-mediated transcripts involved in photosynthesis and carbohydrate metabolism in alfalfa (*Medicago sativa* L.) seedlings under drought stress. – Plant Physiol Biochem 141: 456-465.
[31] Zhou, M. X., Engelmann, T., Lutts, S. (2019): Salinity modifies heavy metals and arsenic absorption by the halophyte plant species Kosteletzkya pentacarpos and pollutant leaching from a polycontaminated substrate. – Ecotox Environ Safe 182: 10.
[32] Zuccarini, P. (2008): Ion uptake by halophytic plants to mitigate saline stress in *Solanum lycopersicon* L., and different effect of soil and water salinity. – Soil & Water Research 3(2): 62-73.

http://www.aloki.hu ● ISSN 1589 1623 (Print) ● ISSN 1785 0037 (Online)
DOI: http://dx.doi.org/10.15666/aeer/1804_59235937

WATER CHEMISTRY, PHYTOPLANKTON DIVERSITY AND SEVERE EUTROPHICATION WITH DETECTION OF MICROCYSTIN CONTENTS IN THAI TROPICAL URBAN PONDS

PRASERTPHON, R.[1] – JITCHUM, P.[2] – CHAICHANA, R.[1,3*]

[1]*Department of Environmental Technology and Management, Faculty of Environment, Kasetsart University, Bangkok, Thailand*

[2]*Department of Fishery Biology, Faculty of Fisheries, Kasetsart University, Bangkok, Thailand*

[3]*Research Group: Natural Environment in Forest and Freshwater Ecosystems, Faculty of Environment, Kasetsart University, Bangkok, Thailand*

[*]*Corresponding author*
e-mail: *fscircc@ku.ac.th; phone*: *+662-579-2945; fax*: *+662-579-2946*

(Received 20th Mar 2020; accepted 2nd Jul 2020)

Abstract. This study investigated eutrophication and the microcystin contents in urban ponds prone to the influx of excessive nutrients. We sampled urban ponds in five provinces (Khon Kaen, Chanthaburi, Chiang Mai, Bangkok and Pathum Thani) in different regions of Thailand. Water and phytoplankton samples were determined between the end of the cold and hot seasons in 2018-2019. The results revealed that all the urban ponds were in a hypereutrophic condition as indicated by the Florida trophic state index. Nutrients were exceptionally high in both the cold and hot seasons. The Cyanophyceae were common and abundant in most urban ponds and increased from the cold season into the hot season. Cluster analysis and multidimensional scaling indicated unique phytoplankton composition among the urban ponds. Dissimilarities in the phytoplankton among the urban ponds increased from the cold season to the hot season. Microcystin analysis showed that an urban pond in Pathum Thani province contained the highest mean microcystin content during cold (3.62±0.43 µg/L) and hot (3.10±0.97 µg/L) seasons. In conclusion, there is an urgent need for the restoration of urban ponds in Thailand. In particular, controlling external and internal nutrient sources should be a main focus together with regular monitoring of eutrophication.
Keywords: *chlorophyll a, cyanotoxin, microcystis, nitrogen, phosphorus, trophic state index*

Introduction

Urban ponds in urbanized landscapes are important and play several roles (Oertli and Parris, 2019). In ecosystems, ponds serve as a network of habitat patches (Hassall, 2014) and thus are inhabited by several plant and animal species. The ponds provide food sources and a breeding ground for species like invertebrates (snails and insects) and vertebrates (amphibians and fish) (Hamer et al., 2012), while maintaining ecosystem integrity and biodiversity in the city (Hassall, 2014). Ponds also provide ecosystem services to the people living in cities (Hill et al., 2017). The main services are cultural services including recreation, education and inspiration (Ghermandi and Fichtman, 2015). Urban ponds are an attraction for visitors in public parks where ponds are located. In addition, urban ponds provide regulating services such as water purification, flood control and water storage (Tixier et al., 2011; Sun et al., 2019). In particular, excess water during heavy rain can be stored in urban ponds to avoid flooding in the city areas. Although urban ponds are essential to wildlife and people, they are exposed to anthropogenic activities that have resulted in the deterioration of water quality and quantity of the urban ponds (Tixier et al., 2011).

http://www.aloki.hu ● ISSN 1589 1623 (Print) ● ISSN1785 0037 (Online)
DOI: http://dx.doi.org/10.15666/aeer/1804_59395951

Urban ponds are prone to eutrophication due to the addition of excessive nutrients (Waajen et al., 2014). Nutrient inputs of urban ponds come from several sources such as fertilizers applied on lawns, land runoff, artificial fish and bird feeding (Chaichana et al., 2011) and treated and untreated wastewater from surrounding areas (Oshima et al., 2008). Previous studies showed that urban ponds contained large quantities of nutrients and that eutrophication was present. In Belgium, for example, 42 urban ponds had high amounts of total phosphorus (0.1 mg/L) and cyanobacterial blooms were detected (such as *Anabaena*, *Aphanizomenon*, *Microcystis* and *Planktothrix*) (Peretyatko et al., 2010). In the Netherlands, eutrophication of urban ponds was induced by wastewater from communities and rainwater drainage (Total phosphorus (TP) 0.16-0.44 mg/L), with blooms of phytoplankton occurring, which were dominated by *Microcystis, Anabaena* and *Planktothrix* (Waajen et al., 2014). Eutrophication as a form of water pollution in urban ponds exerts ecological impacts. Eutrophication thus reduces potential of ponds and their usefulness since the ponds themselves remain important, but they are unable to fulfill their potential.

A particular concern is eutrophication accompanied by harmful algal blooms. Several phytoplankton species in the Division Cyanophyta produce toxic substances which can be divided into several categories such as hepatotoxin, cytotoxin, neurotoxin and dermatotoxin (Sivonen, 2009). The most common toxic substance is microcystin. Microcystin is a secondary metabolite produced by *Microcystis*, *Anabaena*, *Planktothrix* (*Oscillatoria*), *Nostoc, Hapalosiphon* and *Anabaenopsis* (Bartram and Chorus, 1999). These toxic compounds can pose a threat to wildlife and water users (Waajen et al., 2016; Tilahun et al., 2019). In Lake Zumpango, Mexico, for example, microcystin can accumulate through trophic levels and was found in the liver of *Oreochromis niloticus* (Zamora-Barrios et al., 2019).

In Thailand, eutrophication is one of the most important water pollution problems. Thailand is a tropical country where eutrophication is widespread and common due to a combination of nutrients, high temperature and abundance of sunlight throughout the year. Previous studies have revealed blooms of *Microcystis, Oscillatoria, Planktolyngbya, Planktotrix* and *Pseudanabaena* in recreational reservoirs in Khon Kaen province in north-eastern Thailand (Somdee et al., 2013). In reservoirs in northern Thailand, blooms of *Microcystis aeruginosa* resulted in microcystin being found in Nile Tilapia (*Oreochromis niloticus*) (Aroonvilairat et al., 2004; Seekhao et al., 2007; Whangchai et al., 2013). Studies of eutrophication in Thailand have so far focused on reservoirs (for drinking purposes). Relatively little attention has been given to urban ponds, which could also be at risk of eutrophication and contamination by microcystin. Therefore, this research focused on documenting eutrophication in urban ponds in Thailand. The objectives were to investigate the water quality, trophic states of urban ponds in four regions between the cold and hot seasons and to determine phytoplankton diversity and composition. The microcystin contents were assessed to provide data that could be used to help monitor and manage eutrophication in urban ponds.

Materials and Methods

Study sites

Five urban ponds located in cities of five provinces in different parts of Thailand were selected for this study as eutrophication has occurred in these urban ponds (*Fig. 1*). The names of the ponds are: 1) Bueng Nong Khot in Khon Kaen province in the northeast, 2)

http://www.aloki.hu ● ISSN 1589 1623 (Print) ● ISSN1785 0037 (Online)
DOI: http://dx.doi.org/10.15666/aeer/1804_59395951

pond in Somdej Phrachao Taksin Maharat Public Park in Chanthaburi province in the east, 3) Nong Ho in Chiang Mai province in the north, 4) the Bueng beside the Railway Hospital in Bangkok in central Thailand and 5) Bueng Yai in Pathum Thani province in central Thailand ('Bueng' and 'Nong' in Thai mean pond). Details of each urban pond are given in *Table 1*.

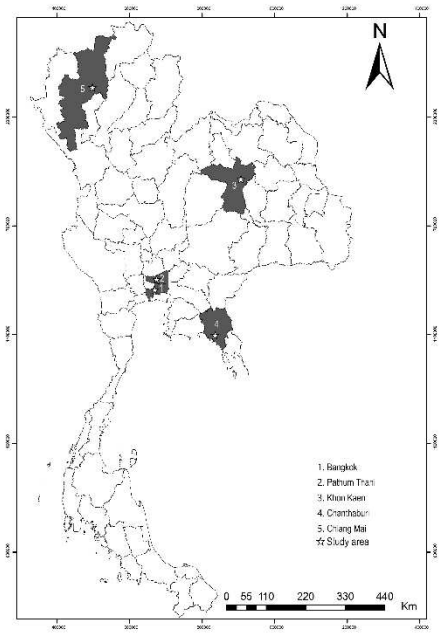

Figure 1. *Locations of five urban ponds in five provinces of Thailand*

Table 1. *Locations and details of selected urban ponds*

Detail	Khon Kaen	Chanthaburi	Chiang Mai	Bangkok	Pathum Thani
Location	Northeast	East	North	Central	Central
Coordinate (North)	16°25'55"N	12°36'18"N	18°49'15"N	13°45'05"N	13°59'42"N
Coordinate (East)	102°47'58"E	102°06'21"E	98°58'31"E	100°33'11"E	100°36'31"E
Area (m^2)	1,047,690	181,950	84,102	9,666	82,162
Depth (m)	6	6	3	3	8
Purposes	Water storage for flood control, recreation, fishing and sports	Public park, fish feeding. This pond receives discharged water from wastewater treatment plant.	Recreation, surrounded by local restaurants	Water storage, surrounded by houses and restaurants	Water storage for flood control

Sampling collection and analysist

Sampling of water and plankton

In each pond, water samples were collected from three sampling points across the ponds. Water samples were taken twice in the cold season (Dec-Jan 2019) and in the hot season (Mar-Apr 2019). We measured water quality on site based on: dissolved oxygen (DO, mg/L), pH,

http://www.aloki.hu ● ISSN 1589 1623 (Print) ● ISSN1785 0037 (Online)
DOI: http://dx.doi.org/10.15666/aeer/1804_59395951

temperature (°C), conductivity (µs/cm) and total dissolved solid (TDS, mg/L) using a multi-parameter analyser (Consort 9116). Water transparency and depth were also studied using a Secchi disk. In addition, two L of water samples were collected and kept in plastic bottles and then put in a container at four °C for further analysis in the laboratory. We analysed ammonium-N using the phenol-hypochlorite method (Strickland and Parsons, 1972), soluble reactive phosphorus (SRP) using the ascorbic acid method, total nitrogen (TN) using the Kjeldahl method, total phosphorus (TP) using the vanadomolybdate method, total suspended solid (TSS) using filtration and chlorophyll a using the acetone extraction method. All samples were analysed in triplicate at the Department of Environmental Technology and Management, Faculty of Environment, Kasetsart University and Central Laboratory, Bangkok, Thailand.

Phytoplankton was collected using a 20 µm plankton net. Sampling points for plankton were at the same locations as the water sampling points. A sample of ten L of water was passed through each plankton net. Samples were then preserved in 70% ethanol. Plankton samples were investigated by counting and classifying up to the species level using a Sedgewick-Rafter counting chamber under compound light microscope.

Toxic analysis

Microcystin was analysed using a Microcystin-Adda ELISA kit (Abraxis, USA). Samples of water were collected and then filtered using a glass microfiber filter, grade GF/C (diameter 47 mm) Whatman. Toxic analysis was done in the laboratory by measuring the absorbance at 450 nm wavelength using a microplate spectrophotometer (Powerwave 340, Biotek, USA).

Data analysis

Data presented as mean±standard deviation. We used the Florida trophic state index (TSI) to classify the urban ponds based on chlorophyll levels and the nitrogen and phosphorus concentrations (Huber et al., 1982). The trophic state index equations are:

$$CHLA_{TSI} = 16.8 + [14.4 \times LN(CHLA)] \quad \text{(Eq.1)}$$

$$TN_{TSI} = 56 + [19.8 + LN(TN)] \quad \text{(Eq.2)}$$

$$TN2_{TSI} = 10 \times [5.96 + 2.15 \times LN(TN + 0.0001)] \quad \text{(Eq.3)}$$

$$TP_{TSI} = [18.6 \times LN(TP \times 1000)] - 18.4 \quad \text{(Eq.4)}$$

$$TP2_{TSI} = 10 \times [2.36 \times LN(TP \times 1000)] - 2.38 \quad \text{(Eq.5)}$$

Limiting nutrient considerations for calculating $NUTR_{TSI}$

- If $TN/TP > 30$, then $NUTR_{TSI} = TP2_{TSI}$.
- If $TN/TP < 10$, then $NUTR_{TSI} = TN2_{TSI}$.
- If $10 < TN/TP < 30$, then $NUTR_{TSI} = (TP_{TSI} + TN_{TSI})/2$.

$$TSI = (CHLA_{TSI} + NUTRI_{TSI})/2 \quad \text{(Eq.6)}$$

In equations, CHLA is chlorophyll a (µg/L), TN is total nitrogen (mg/L), TP is total phosphorus (mg/L), LN is natural log and NUTR is nutrient. The final TSI can then be used to classify trophic state. TSI less than 60 indicates that a lake is oligotrophic to mid-eutrophic. TSI

http://www.aloki.hu ● ISSN 1589 1623 (Print) ● ISSN1785 0037 (Online)
DOI: http://dx.doi.org/10.15666/aeer/1804_59395951

between 60 and 69 indicates that a lake is mid-eutrophic to eutrophic. TSI higher than 70 indicate that a lake is hypereutrophic.

Limiting nutrient was calculated by TN/TP ratio (Lakewatch, 2000). When the TN/TP ratio is less than 10, a lake is nitrogen-limited. When the TN/TP ratio is between 10 and 17, nitrogen or phosphorus could be limiting and when the TN/TP ratio is greater than 17, a lake is phosphorus-limited.

Differences in water quality parameters and phytoplankton abundances between seasons was determined using a Student t-test by using SPSS 23. Correlation coefficient between microcystin content and cyanobacteria was also tested. The Primer seven software package was used to analyze nonmetric multi-dimensional scaling (MDS). MDS displays the spatial distribution of variables (phytoplankton) among provinces, thus indicating similarities or dissimilarities among variables. Cluster analysis was also performed to group similar variables of phytoplankton. Data were log-transformed and standardized.

Results

Water quality

The water quality analysis revealed that all urban ponds were in hypereutrophic conditions in both the cold and hot seasons as indicated by the Florida trophic state index (*Table 2*). Water quality varied among ponds and between seasons (*Table 3)*. Nutrient concentrations were exceptionally high. In the cold season, TN concentrations were in the range 2.92-13.13 mg/L. The highest TN value was in Khon Kaen province (13.13 mg/L). TP values were in the range 0.10-1.43 mg/L. The highest TP value was detected in Bangkok (1.43 mg/L). Chlorophyll a values were in the range 45.68-4,022.09 μg/L. The highest value was in Chiang Mai province (4,022.09 μg/L).

Table 2. *Florida trophic state index of sampled urban ponds*

Province	Season	Trophic State Index (Chl a)	Trophic State Index (TP)	Trophic State Index 2 (TP)	Trophic State Index (TN)	Trophic State Index 2 (TN)	Trophic State Index	State
Khon Kaen	C	83.65	-	76.85	-	-	80.25	Hypereutrophic
	H	71.71	-	-	-	-	87.95	Hypereutrophic
Chanthaburi	C	71.76	-	95.52	-	-	83.64	Hypereutrophic
	H	98.25	-	-	-	106.23	102.24	Hypereutrophic
Chiang Mai	C	110.90	-	-	-	98.80	104.85	Hypereutrophic
	H	90.34	-	-	-	101.28	95.81	Hypereutrophic
Bangkok	C	87.33	-	-	-	91.36	89.34	Hypereutrophic
	H	108.25	-	-	-	91.36	99.80	Hypereutrophic
Pathum Thani	C	114.90	-	-	-	98.80	106.85	Hypereutrophic
	H	77.41	-	-	-	106.24	91.81	Hypereutrophic

Remark**:** C = cold season, H = hot season

In the hot season, the TN concentrations were in the range 1.46-8.75 mg/L, with the highest value (8.75 mg/L) in Khon Kaen province. The TP values were in the range 0.25-34.80 mg/L, with the highest value in Chiang Mai (38.36 mg/L). The chlorophyll a values were in the range 46.00-576.61 μg/L and the highest value was in Bangkok (736.80 μg/L).

http://www.aloki.hu ● ISSN 1589 1623 (Print) ● ISSN1785 0037 (Online)
DOI: http://dx.doi.org/10.15666/aeer/1804_59395951

Table 3. *Water quality of urban ponds in Thailand in cold* (*C*) *and hot* (*H*) *seasons*

Parameter	Khon Kaen		Chanthaburi		Chiang Mai		Bangkok		Pathum Thani	
	C	**H**	**C**	**H**	**C**	**H**	**C**	**H**	**C**	**H**
DO (mg/L)	3.9±0.2	3.8±1.4	5.5±1.3	4.3±1.9	3.5±1.7	6.0±3.2	10.0±0.6*	16.0±0.5*	11.8±0.3*	7.6±1.0*
T_{water} (°C)	28±2	34±1	30±2	33±1	27±2*	35±0*	29±0*	35±0*	31±1*	34±1*
pH	8.1±0.1	8.6±0.6	7.4±0.2*	6.7±0.1*	7.2±0.1*	9.9±0.1*	8.3±0.1*	8.7±0.1*	9.4±0.3*	8.8±0.1*
TSS (mg/L)	28.9±8.4	32.0±18.8	34.4±9.3*	51.1±4.7*	59.3±33.3	81.3±4.1	98.7±124.3	70.4±8.3	181.8±123.0*	36.4±20.3*
Turbidity (NTU)	23±7	17±3	38±6*	44±3*	101±65*	111±45*	32±6*	40±7*	309±265	16±5
Trans. (cm)	43.33±7.64	28.33±7.64	26.67±5.77	20.00±0.00	12.67±21.94	15.00±4.36	30.00±5.00	24.00±22.54	11.67±16.07	29.67±13.05
TDS (mg/L)	386±3	398±10	169±3	475±27	143±12	93±1	456±3	389±1	264±3	227±2
Conductivity (µs/cm)	621±10*	714±20*	282±7	837±41	243±3	170±2	762±7	715±5	450±9	411±8
Salinity (mg/L)	0.3±0.0	0.4±0.1	0.10±0.00	0.4±0.0	0.1±0.0	0.1±0.0	0.3±0.0	0.3±0.00	0.2±0.00	0.2±0.00
Chl a (µg/L)	119.70±77.83	46.00±9.63	45.68±5.80	301.20±120.66	4022.09±6642.16	187.22±116.77	134.08±6.07*	576.51±76.95*	1288.25±1268.69	72.59±33.82
NH_4 (µg/L)	251.84±97.22	90.81±42.51	ND	2.86±19.49	152.85±243.18	0.45±5.76	12.22±14.10*	562.45±151.12*	0.67±1.25	26.16±25.59
SRP (µg/L)	13.69±4.24	7.96±5.63	9.25±1.60	19.19±5.58	10.98±7.74	14.60±3.05	773.33±4.70*	681.89±6.35*	329.33±87.77*	18.11±4.21*
TN (mg/L)	13.13±4.38*	8.75±4.38*	5.83±5.05	2.92±5.05	4.38±3.09	8.75±7.57	2.92±2.53	1.46±2.53	4.38±3.09	2.92±5.05
TP (mg/L)	0.10±0.09	0.25±0.41	0.18±0.10*	26.69± 2.36*	1.19±0.06*	34.80±4.42*	1.43±0.03*	26.69±2.36*	1.33±0.67*	17.35±5.11*

Remark**:** Values are shown as mean ±standard deviation. * indicates significant differences between cold and hot season at the 0.05 level

http://www.aloki.hu ● ISSN 1589 1623 (Print) ● ISSN1785 0037 (Online)
DOI: http://dx.doi.org/10.15666/aeer/1804_59395951

The t-test results showed that only the TN at Khon Kaen was significantly ($P < 0.05$) different between the cold and hot seasons. The TP values in most provinces (Chanthaburi, Chiang Mai, Bangkok and Pathum Thani) were significantly different between the cold and hot seasons ($P < 0.05$). Similarly, the chlorophyll a values in most provinces were significantly ($P < 0.05$) different between the cold and hot seasons (Khon Kaen, Chanthaburi, Bangkok and Pathum Thani). Furthermore, the limiting factor was calculated as shown in *Table 4*. Most ponds were nitrogen limited in both the cold and hot seasons (except Khon Kaen).

Table 4. *TN/TP ratio for sampled urban ponds*

Province	TN/TP ratio	
	Cold season	**Hot season**
Khon Kaen	131.30(P)	35(P)
Chanthaburi	32.39(P)	0.11(N)
Chiang Mai	3.68(N)	0.25(N)
Bangkok	2.04(N)	0.05(N)
Pathum Thani	3.29(N)	0.25(N)

Remark**:** (P) = P is limiting; (N) = N is limiting

The phytoplankton results revealed that the Cyanophyceae were the main group of phytoplankton in all urban ponds in both cold and hot seasons. The Cyanophyceae tended to increase from the cold season to the hot season (*Fig. 2)*. In the cold season, the dominant Division was the Cyanophyta (97% in Chiangmai, 81% in Khon Kaen and Pathum Thani and 54% in Chanthaburi). *Pseudanabaena* sp. was the dominant species in Khon Kaen with a density of 145,800 cells/L. In Chanthaburi province, *Oscillatoria* sp. was the dominant species with a density of 22,230 cells/L. *Microcystis aeruginosa* was the main species in Chiang Mai and Pathum Thani provinces with densities of 4,596,673 and 416,295 cells/L, respectively. In Bangkok the most common group was in the Division Bacillariophyceae (62%), with *Cyclotella* sp. being the most dominant species at a density of 1,668,969 cells/L.

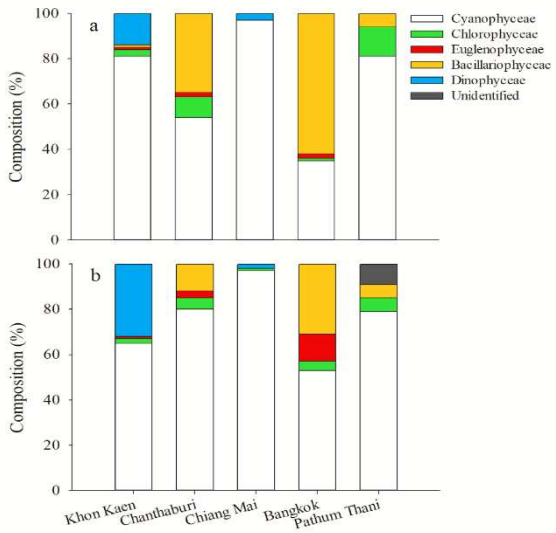

Figure 2. *Phytoplankton community succession in five urban ponds* (*a is cold season and b is hot season*)

http://www.aloki.hu ● ISSN 1589 1623 (Print) ● ISSN1785 0037 (Online)
DOI: http://dx.doi.org/10.15666/aeer/1804_59395951

In the hot season, the Division Cyanophyta comprised 97% of the community in Chiang Mai, 80% in Chanthaburi, 79% in Prathum Thani, 65% in Khon Kaen and 53% in Bangkok.*Cylindrospermopsis raciborskii* was the dominant species (density of 283,279 cells/L in Chiang Mai, 158,265 cells/L in Chanthaburi, 467,134 cells/L in Khon Kaen and 780,612 cells/L in Pathum Thani). In Bangkok, *Merismopedia minima* was the dominant species with a density of 206,107 cells/L. Details of the phytoplankton present in each province are given in *Table 5*. Statistical analysis found no significant (P> 0.05) differences in the phytoplankton between the cold and hot seasons for all provinces.

Table 5. *Phytoplankton occurrence in each urban pond and season*

Phytoplankton	Khon Kaen		Chanthaburi		Chiang Mai		Bangkok		Pathum Thani	
	C	H	C	H	C	H	C	H	C	H
Anabaena sp.	+	+	+				+	+	+	++
Anacystis sp.			+							
Chroococcus sp.										++
Cylindrospermopsis raciborskii	++	+++	++	+++	+++	+++				+++
Planktothrix sp.										+
Planktolyngbya limnetica					+					
Pseudanabaena sp.	+++	+	++	+++	+++				+	
Oscillatoria limosa							++			
Osicllatoria sp.	++	++	++	+	+++		+++	++	++	+
Spirulina platensis	+	++	++				+++	+++	+++	
Spirulina sp.				+	+++	++				
Microcystis aeruginosa	+++	++			+++	+++			+++	++
Merismopedia convoluta				+						
Merismopedia minima	+	+	+	+				+++	+	
Merismopedia punctata		+			+++					
Merismopedia sp.								+		

Remark**:** C = cold season, H = hot season, + < 5,000 cells/L, ++ = 5,001-50,000 cells/L, +++ > 50,000 cells/L

The results of the cluster analysis revealed some unique features and some similarities regarding the phytoplankton in each pond. Similarities in the phytoplankton in each pond were observed between the cold and hot seasons (*Fig. 3).* Furthermore, multidimensional scaling and cluster analysis showed more distinct differences in the phytoplankton at Chiang Mai, Pathum Thani and Bangkok in the hot season (approximately 60% similarities) than in the cold season (approximately 40% similarities). In contrast, the phytoplankton at Khon Kaen and Chanthaburi were rather similar in both the cold and hot seasons compared with the other provinces (*Fig. 4).* The stress value of the non-metric MDS indicated a fair (stress value 0.12 for cold season) and good (stress value 0.07 for hot season) goodness-of-fit.

http://www.aloki.hu ● ISSN 1589 1623 (Print) ● ISSN1785 0037 (Online)
DOI: http://dx.doi.org/10.15666/aeer/1804_59395951

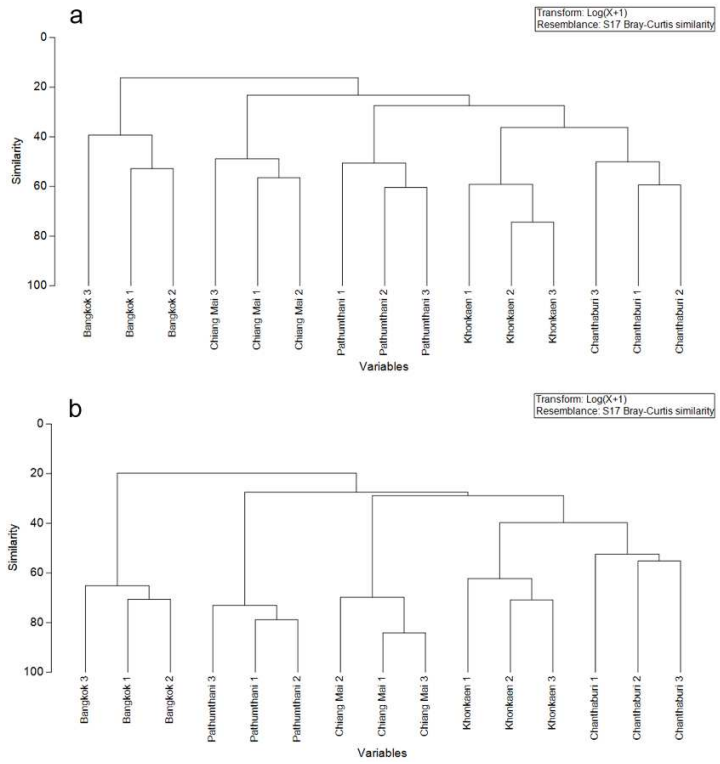

Figure 3. *Cluster analysis of phytoplankton* (*a is cold season and b is hot season*). *Variables represents sampling stations one, two, three of each pond* (*e.g. Bangkok one, two, three*)

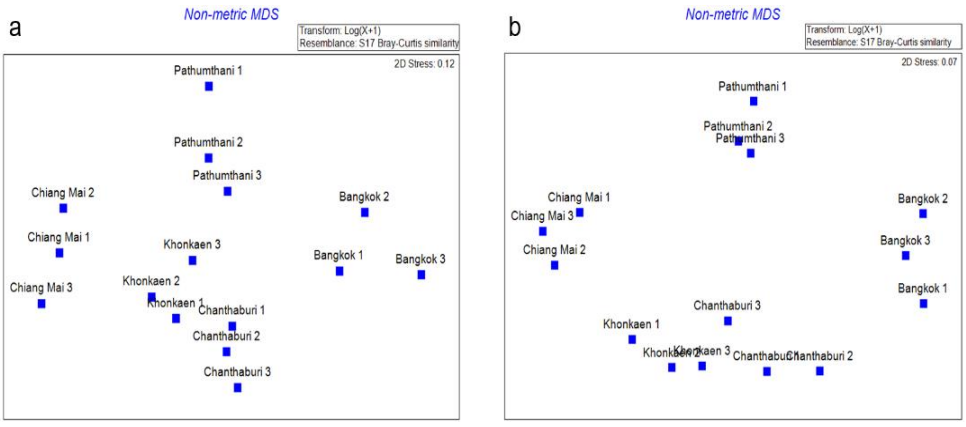

Figure 4. *Multidimensional Scaling of phytoplankton* (*a is cold season and b is hot season*)

The concentration of microcystin varied among seasons and ponds (*Table 6).* In the cold season, the highest microcystin content was detected at Pathum Thani (3.62 µg/L), followed by Chanthaburi (1.05 µg/L), Chiang Mai (0.52 µg/L) and Khon Kaen (0.063 µg/L) provinces, respectively. In the hot season, the highest microcystin content was found in Pathum Thani (3.10 µg/L), followed by Khon Kaen (0.39 µg/L), Chanthaburi (0.23 µg/L) and Chiang Mai (0.01 µg/L) provinces, respectively. In Bangkok, no microcystin content was detected.

http://www.aloki.hu ● ISSN 1589 1623 (Print) ● ISSN1785 0037 (Online)
DOI: http://dx.doi.org/10.15666/aeer/1804_59395951

Table 6. *Microcystin detected in urban ponds*

Province	Season	Microcystin (µg/L)
Khon Kaen	C	0.06±0.11
	H	0.39±0.41
Chanthaburi	C	1.05±0.99
	H	0.23±0.38
Chiang Mai	C	0.52±0.90
	H	0.01±0.02
Bangkok	C	ND
	H	ND
Pathum Thani	C	3.62±0.43
	H	3.10±0.97

Remark: MD = non detectable

Discussion

This study investigated the water quality, phytoplankton and microcystin levels in urban ponds in different regions of Thailand. The selected ponds are valuable and play crucial roles in ecosystem and human uses. However, urban ponds are in a critical condition due to exposure to nutrient pollution coming from different anthropogenic activities (e.g. wastewater from houses and restaurants) (Mayer et al., 1996). The ponds in Bangkok, Phathum Thani and Khon Kaen are functional as stormwater ponds. They are used to store runoff flow in order to mitigate flood risk during heavy rain. The ponds in Khon Kaen and Chanthaburi serve as recreational ponds, with both ponds attracting visitors coming for recreational activities such as fish feeding. Artificial feeding by the public can have adverse effects on water quality due to leftover fish feed and excretion from animals (Chaichana et al., 2011). The pond at Chanthaburi receives treated wastewater from a municipal wastewater treatment plant.

Water samples were comparatively determined between the cold season and the hot season. Water temperatures were lower in the cold season than in hot season in most ponds. The pH values were rather basic. The dissolved oxygen contents were in normal ranges and tended to be higher in ponds in Bangkok and Pathum Thani provinces, most likely due to photosynthesis. The turbidity and TSS were relatively high in the ponds in Bangkok, Chiang Mai and Pathum Thani and as a result there was lower transparency. Most ponds had high conductivity and TDS which could be due to contamination by pollutants from surrounding areas.

The Florida trophic state index suggested that all ponds were in a hypereutrophic condition (poor quality) in both the cold and hot seasons (Huber et al., 1982). The total phosphorus concentration peaked at 34.80±4.42 mg/L, which was much higher than in other urban ponds. In the Netherlands, ponds in urban areas were highly eutrophic with mean total phosphorus concentrations between 0.16 and 0.44 mg/L (Waajen et al., 2014). In Malaysia, most lake water was in a eutrophic-hypereutrophic state (Sinang et al., 2015) with total phosphorus ranging from 15 to 4,270 µg/L. It was also found that nitrogen (N) rather than phosphorus (P) appeared to be limiting factor in most ponds (except in Khon Kean). This could be explained by ponds in urban landscapes receiving P from washing wastewater and other anthropogenic P inputs (Mischler et al., 2014). This was in contrast with the rural ponds in agricultural landscapes where N appeared to be more abundant than P, and N was the major cause of nutrient enrichment (Chaichana et al., 2011).

http://www.aloki.hu ● ISSN 1589 1623 (Print) ● ISSN1785 0037 (Online)
DOI: http://dx.doi.org/10.15666/aeer/1804_59395951

The Cyanophyta was the main composition in all hypereutrophic urban ponds in Thailand. Phytoplankton in the Division Cyanophyta tended to increase toward the hot season in response to higher temperatures and sufficient sunlight that promoted the formation of phytoplankton (Chaichana and Dampin, 2016). This was in accordance with Jahan et al. (2010) stating that cyanobacterial blooms were positively correlated with temperature and pH. This study also revealed that *Osicllatoria, Pseudanabaena, Spirulina platensis, Microcystis aeruginosa* and *Merismopedia minima* were common in most urban ponds. Several studies reported Cyanobaterial species such as *Microcystis* and *Planktothrix* as being dominant in eutrophic ponds (Jahan et al., 2010; Waajen et al., 2014; Sinang et al., 2015). This study found blooming phytoplankton on the water surface. In most ponds, blooms appeared only in certain areas of the water surface, depending on the influence of waves and winds. In contrast, in Pathum Thani province, intense blooms of phytoplankton occurred across the pond indicating severe eutrophication.

The current study detected microcystin in most ponds (with a peak at 3.62±0.43 μg/L) except for the urban pond in Bangkok. Microcystin in this study was lower than in other studies (Waajen et al., 2014) and this may have been due to differences in the pond size and volume, residence time, water chemistry and climatic conditions (Olding et al., 2011; WHO, 2011). WHO (2011) has guidelines on cyanotoxins in drinking water with a value of 1 μg/L for microcystin-LR. Although the urban ponds in the current study do not provide raw water for drinking, high cyanotoxin levels could have an effect on wildlife. The highest microcystin content was in Pathum Thani and this correlated with intense blooms of Cyanobacteria, mainly *M. aeruginosa* ($r=0.407$, $P<0.05$). Other toxic-producing species such as *Oscillatoria* and *Pseudanabaena* (Marsalek et al., 2003; Teneva et al., 2009; Paerl and Otten, 2013) were also present. Toxic content was found in the urban pond in Chanthaburi even with the absence of *M. Aeruginosa*.

We observed some management actions taken by local government to solve eutrophication problems. For example, in Khon Kean, local officers are working on treatment of a nearby eutrophic pond using aluminum sulphate (phosphorus precipitation). The result (personal communication) was satisfactory and this treatment may be used to improve water quality of the Khon Kean pond. In Chiang Mai, some restaurants located inside the pond were removed to reduce external nutrient input. In Bangkok, as the ponds serve as water storage to deal with heavy rain in Bangkok, the water retention time is short. This reduces the formation of phytoplankton. In Chanthaburi, artificial feeding of fish in the pond should be stopped through a public educational campaign. The pond in Pathum Thani is still of concern since no restoration action has been taken so far. Therefore, recommendations for future research should focus on finding appropriate restoration methods (such as application of alum or phoslock, sediment removal, or biomanipulation) to improve water quality of these urban ponds.

In conclusion, this study determined eutrophication problems in some urban ponds of Thailand in a comparison between the cold and hot seasons. The results showed that the nutrient pollution levels were relatively high with intense eutrophication in all urban ponds in both the cold and hot seasons. Environmental conditions in the hot season appeared to stimulate phytoplankton growth. Most ponds were dominated by Cyanobacteria that produce toxins (*M. aeruginosa, Oscillatoria* and *Pseudanabaena*). Microcystin contents were detected with the level depending on the degree of intensity of the bloom. These findings indicated potential health risks in water use due to the presence of microcystin. Urgent management and restoration of hypereutrophic urban ponds in Thailand is needed.

http://www.aloki.hu ● ISSN 1589 1623 (Print) ● ISSN1785 0037 (Online)
DOI: http://dx.doi.org/10.15666/aeer/1804_59395951

Acknowledgements. This research was supported by the Graduate Program Scholarship from The Graduate School, Kasetsart University and partially supported by Research Group: Natural Environment in Forest and Freshwater Ecosystems, Faculty of Environment, Kasetsart University.

REFERENCES

[1] Aroonvilairat, S., Ruangyuttikarn, W., Pekkoh, J., Peerapornpisal, Y., Shen, X., Wickramasinghe, W., Shaw, G. (2004): Identification and hepatotoxicity of microcystin-LR isolated from *Microcystis aeruginosa* Kütz. in Huay Yuak reservoir, Chiang Mai province. – Chiang Mai University Journal of Natural Sciences 7: 149-162.

[2] Bartram, J., Chorus, I. (1999): Toxic cyanobacteria in water: a guide to their public health consequences, monitoring and management. – CRC Press, London.

[3] Chaichana, R., Dampin, N. (2016): Unialgal blooms of cyanobacteria in oxidation ponds of the King's Royally Initiated Laem Phak Bia environmental research and development project, Thailand. – EnvironmentAsia 9(2): 150-157.

[4] Chaichana, R., Leah, R., Moss, B. (2011): Conservation of pond systems: a case study of intractability, Brown Moss, UK. – Hydrobiologia 664: 17-33.

[5] Ghermandi, A., Fichtman, E. (2015): Cultural ecosystem services of multifunctional constructed treatment wetlands and waste stabilization ponds: Time to enter the mainstream? – Ecological Engineering 84: 615-623.

[6] Hamer, A. J., Smith, P. J., McDonnell, M. J. (2012): The importance of habitat design and aquatic connectivity in amphibian use of urban stormwater retention ponds. – Urban Ecosystems 15: 451-471.

[7] Hassall, C. (2014): The ecology and biodiversity of urban ponds. – Wiley Interdisciplinary Reviews: Water 1: 187-206.

[8] Hill, M. J., Biggs, J., Thornhill, I., Briers, R. A., Gledhill, D. G., White, J. C., Wood, P. J., Hassall, C. (2017): Urban ponds as an aquatic biodiversity resource in modified landscapes. – Global change biology 23: 986-999.

[9] Huber, W. C., Brezonik, P. L., Heany, J. P., Dickinson, R. E., Preston, S. D., Dwornik, D. S., DeMaio, M. A. (1982): A classification of Florida lakes. – Final report to the Florida Department of Environmental Regulation. PROTECTION, F. D. O. E., Florida.

[10] Jahan, R., Khan, S., Haque, M. M., Choi, J. K. (2010): Study of harmful algal blooms in a eutrophic pond, Bangladesh. – Environmental monitoring and assessment 170: 7-21.

[11] Lakewatch, F. (2000): A beginner's guide to water management–nutrients. – Department of Fisheries and Aquatic Sciences, Institute of Food and Agricultural Sciences, University of Florida, Florida.

[12] Marsalek, B., Blaha, L., Babica, P. (2003): Analyses of microcystins in the biomass of Pseudanabaena linmnetica collected in Znojmo reservoir. – Czech Phycology 3: 195-197.

[13] Mayer, T., Marsalek, J., Reyes, E. D. (1996): Nutrients and metal contaminants status of urban stormwater ponds. – Lake and Reservoir Management 12: 348-363.

[14] Mischler, J. A., Taylor, P. G., Townsend, A. R. (2014): Nitrogen limitation of pond ecosystems on the plains of eastern Colorado. – PLoS One 9: e95757.

[15] Oertli, B., Parris, K. M. (2019): Toward management of urban ponds for freshwater biodiversity. – Ecosphere 10: 1-33.

[16] Oshima, A., Shinya, M., Kitano, M., Hagiwara, T., Goto, K., Tsuchinaga, T. (2008): Eutrophication characteristics and their relationships to chlorophyll-a concentrations in urban park ponds. – Mizu Kankyo Gakkaishi Journal of Japan Society on Water Environment 31: 701-706.

[17] Paerl, H. W., Otten, T. G. (2013): Harmful cyanobacterial blooms: causes, consequences, and controls. – Microbial Ecology 65: 995-1010.

http://www.aloki.hu ● ISSN 1589 1623 (Print) ● ISSN1785 0037 (Online)
DOI: http://dx.doi.org/10.15666/aeer/1804_59395951

[18] Peretyatko, A., Teissier, S., Backer, S. D., Triest, L. (2010): Assessment of the risk of cyanobacterial bloom occurrence in urban ponds: probabilistic approach. – Annales de Limnologie - International Journal of Limnology 46: 121-133.
[19] Seekhao, I., Peerapornpisal, Y., Chantara, S. (2007): Intra-and extracellular microcystins concentrations in Mae Kuang Udomtara reservoir, Chiang Mai, Thailand in 2004–2005. – J. Sci. Fac. Chiang Mai Uni. 34: 309-318.
[20] Sinang, S. C., Poh, K. B., Shamsudin, S., Sinden, A. (2015): Preliminary assessment of cyanobacteria diversity and toxic potential in ten freshwater lakes in Selangor, Malaysia. – Bulletin of Environmental Contamination and Toxicology 95: 542-547.
[21] Sivonen, K. (2009): Cyanobacterial toxins. Encyclopedia of microbiology. – Elsevier Scientific Publ. Co, Amsterdam.
[22] Somdee, T., Kaewsan, T., Somdee, A. (2013): Monitoring toxic cyanobacteria and cyanotoxins (microcystins and cylindrospermopsins) in four recreational reservoirs (Khon Kaen, Thailand). – Environmental Monitoring and Assessment 185: 9521-9529.
[23] Strickland, J. D. H., Parsons, T. R. (1972): A practical handbook of seawater analysis. – Fisheries research board of Canada, Ottawa.
[24] Sun, Z., Sokolova, E., Brittain, J. E., Saltveit, S. J., Rauch, S., Meland, S. (2019): Impact of environmental factors on aquatic biodiversity in roadside stormwater ponds. – Scientific Reports 9: 1-13.
[25] Teneva, I., Mladenov, R., Dzhambazov, B. (2009): Toxic effects of extracts from *Pseudanabaena galeata* (Cyanoprokaryota) in mice and cell cultures in vitro. – Nat. Sci. Hum 12: 237-243.
[26] Tilahun, S., Kifle, D., Zewde, T. W., Johansen, J. A., Demissie, T. B., Hansen, J. H. (2019): Temporal dynamics of intra-and extra-cellular microcystins concentrations in Koka reservoir (Ethiopia): Implications for public health risk. – Toxicon. 168: 83-92.
[27] Tixier, G., Lafont, M., Grapentine, L., Rochfort, Q., Marsalek, J. (2011): Ecological risk assessment of urban stormwater ponds: literature review and proposal of a new conceptual approach providing ecological quality goals and the associated bioassessment tools. – Ecological Indicators 11: 1497-1506.
[28] Waajen, G. W. A. M., Faassen, E. J., Lürling, M. (2014): Eutrophic urban ponds suffer from cyanobacterial blooms: Dutch examples. – Environmental Science and Pollution Research 21: 9983-9994.
[29] Waajen, G., van Oosterhout, F., Douglas, G., Lürling, M. (2016): Geo-engineering experiments in two urban ponds to control eutrophication. – Water Research 97: 69-82.
[30] Whangchai, N., Wanno, S., Gutierrez, R., Kannika, K., Promna, R., Iwami, N., Itayama, T. (2013): Accumulation of microcystins in water and economic fish in Phayao lake, and fish ponds along the Ing river tributary in Chiang Rai, Thailand. – Agricultural Sciences 4: 52.
[31] WHO (2011): Guidelines for drinking-water quality. – IWA Publishing, London.
[32] Zamora-Barrios, C. A., Nandini, S., Sarma, S. S. S. (2019): Bioaccumulation of microcystins in seston, zooplankton and fish: A case study in Lake Zumpango, Mexico. – Environmental Pollution 249: 267-276.

http://www.aloki.hu ● ISSN 1589 1623 (Print) ● ISSN1785 0037 (Online)
DOI: http://dx.doi.org/10.15666/aeer/1804_59395951

PROMOTED AMINO SUGAR ACCUMULATION IN THE RHIZOSPHERE AND BULK SOIL OF A PADDY FIELD UNDER STRAW APPLICATION

WANG, S. N.[1,2] – TANG, J.[1,2*] – LI, Z. Y.[1,2] – LIU, Y. Q.[1,2] – ZHOU, Z. H.[1,2] – WANG, J. J.[1,2] – QU, Y. K.[1,2]

[1]*Key Laboratory of Groundwater Resources and Environment, Ministry of Education, Jilin University, Changchun 130012, China*

[2]*College of New Energy and Environment, Jilin University, Changchun 130012, China*
(phone: +86-431-8515-9440; fax: +86-431-8515-9440)

[*]*Corresponding author*
e-mail: tangjie@jlu.edu.cn

(Received 3rd Apr 2020; accepted 10th Jul 2020)

Abstract. Effects of straw application on amino sugars (a significant soil organic matter pool) in upland fields have received much attention, however, those in paddy fields remain unknown. We conducted a three-year experiment including three treatments: one without straw application (CK) and straw application at rates of 2500 (SA1) and 5000 (SA2) kg ha^{-1} yr^{-1}. SA2 stimulated a higher increase in glucosamine (GluN), muramic acid (MurA), galactosamine (GalN), fungal-derived GluN ($GluN_F$), and total amino sugars than SA1 in the rhizosphere and bulk soil in the first year. Generally, the positive effects of SA1 and SA2 on amino sugars did not differ in the last two years. Rhizosphere soil maintained a significantly higher content of MurA at 10.95%-16.35% than bulk soil. In total, rhizosphere soil accumulated insignificantly more GluN, $GluN_F$, and total amino sugars than the bulk soil, indicating a limited positive effect of the rhizosphere on microbial-derived carbon. SA1 and SA2 notably increased the ratio of $GluN_F$/MurA in bulk soil, implying that straw application increased the relative contribution of fungal-derived residues to soil organic carbon. This work may contribute to understanding the effect of straw applications on microbial residues and their contribution to soil organic carbon in paddy fields.
Keywords: *amino sugars, straw application, microbial residue, soil organic carbon, paddy soil*

Introduction

Agricultural soil contains large amounts of organic carbon (C), variations of which is critical concerning climate change and the sustainable development of agriculture (Manlay et al., 2007). Soil organic C (SOC) is very susceptible to the activity of soil microorganisms, which play a decisive role in regulating SOC (Chaparro et al., 2012). Microbial biomass and microbial residues are effective indicators for assessing the contribution of microbial processes to SOC accumulation (Liang et al., 2017). Although microbial biomass is sensitive to environmental changes (Koponen and Baath, 2016) and drives SOC turnover, microbial residues reside much longer in the soil than living microbial biomass and are believed to be a significant source of the stable C pool (Simpson et al., 2007). In the context of agriculture, soil requires SOC sequestration to maintain fertility, and better knowledge on the contribution of microbial residues to SOC is imperative.

Straw application not only proves to be highly efficient for SOC accumulation (Liu et al., 2014; Zhao et al., 2018), but could also lead to simultaneous variations in soil microbial communities and biomass (Chen et al., 2017a). However, the majority of previous studies on soil microorganisms have concentrated on the effects of straw

http://www.aloki.hu ● ISSN 1589 1623 (Print) ● ISSN 1785 0037 (Online)
DOI: http://dx.doi.org/10.15666/aeer/1804_59535964

application on microbial biomass and community composition (Hurisso et al., 2013; Fan et al., 2016; Zhao et al., 2016; Chen et al., 2017a; Wang et al., 2018). Information on the effects of straw application on microbial residues remains scarce (Simpson et al., 2004; Liu et al., 2019). The dynamics of microbial residues and their contribution to SOC can be examined and quantified by soil amino sugars (Zhang et al., 1999) due to their high abundance in microbial cells (>90%) compared to dead microbial cells (Amelung et al., 2001) and their stability against fluctuations (Glaser et al., 2004). Thus, the analysis of amino sugars could provide insight into the fate and sequestration of C and N in microbial residues and also into long-term shifts in soil organic matter quality (Joergensen et al., 2010). Among various amino sugars, galactosamine (GalN) accounts for a significant fraction of the total amino sugar pool (Glaser et al., 2004), but its origin in soil is still debated (Engelking et al., 2007). Glucosamine (GluN) originates mainly from the chitins of fungal cell walls, though a small amount originates from bacterial peptidoglycan and exoskeletons of soil invertebrates (Amelung et al., 2001; Joergensen, 2018). Muramic acid (MurA) is a unique bacterial residue biomarker because it originates exclusively from the peptidoglycans of bacterial cell walls (Engelking et al., 2007). As a result of the different origins of GluN and MurA, their ratios (GluN/MurA) have been widely used to evaluate the relative contribution of fungal- and bacterial- derived residues to SOC (van Groenigen et al., 2010).

Although some studies have investigated the effects of straw application on amino sugars in agricultural soil (Ding et al., 2013, 2015; Liu et al., 2019), they did not differentiate the effects of straw application between rhizosphere and bulk soil. By root exudates, plant roots play a vital role in regulating rhizosphere microecosystems, such as shaping rhizosphere microbiota (Wang et al., 2012; Hu et al., 2018; Zhalnina et al., 2018) and stimulating nitrogen (N) transformation (Yin et al., 2013). The effect could be appear as impacting rhizosphere bacterial communities associated with shifts in carbon metabolism (Staley et al., 2017), and facilitating or inhibiting SOC decomposition (Cheng et al., 2014). At the end, the accumulation of amino sugars in the rhizosphere and their contribution to SOC could be further influenced. An adequate description of the accumulation of amino sugars in the rhizosphere contributes to accurately evaluating the contribution of microbial residues to SOC. However, comparatively few studies have focused on amino sugar accumulation in the rhizosphere of agricultural systems as compared to bulk soil. In addition, straw application affects not only microbial biomass and community structure (Li et al., 2012; Wang et al., 2018; Jin et al., 2019; Yang et al., 2019), but also root biomass (Ma et al., 2019) and growth (Gao et al., 2018). These factors may all further alter the accumulation of amino sugars in the rhizosphere soil directly or indirectly.

Moreover, previous studies on the effects of straw application on amino sugars have focused on upland fields (i.e., maize fields, mung bean fields) (Praveen et al., 2002; Liang et al., 2007; Ding et al., 2015; Liu et al., 2019),while the effects on paddy fields remain mostly unexplored. Paddy fields in Northeast China provide the second largest grain yield in this region with large amounts of rice straw available after harvesting. In recent years, it was recommended to return rice straw to the field for maintaining fertilization and contributing to sustainable agriculture instead of conventional burning to avoid environmental pollution. The objective of this study is to reveal the effect of straw application on the amino sugar accumulation in the rhizosphere and bulk soil of paddy fields.

http://www.aloki.hu ● ISSN 1589 1623 (Print) ● ISSN 1785 0037 (Online)
DOI: http://dx.doi.org/10.15666/aeer/1804_59535964

Materials and Methods

A three-year experiment from October 2016 to August 2019 was conducted in Daan City (123°08′45″-124°21′56″E, 44°57′00″-45°45′51″N), Western Jilin province, Northeast China. The weather of study site is typical of a semi-arid and semi-humid continental monsoon climate. The average annual temperature is 4.3 °C, and the average annual precipitation is about 414 mm. The basic properties of the soil before the trial are shown in *Table 1*.

Table 1. *Soil properties at 0–15 cm depth of the experimental site (October 2016)*

SOC (g kg^{-1})	Bulk Density (g cm^{-3})	Total N (g kg^{-1})	Total P (g kg^{-1})	Total K (g kg^{-1})	Hydrolysable-N (mg kg^{-1})	pH	Particle size distribution (%)		
							sand	silt	clay
24.31	1.23	1.56	0.35	18.90	105.63	7.68	22.76	54.71	22.53

Crop management

The growth period of rice lasts from about mid-May to the end of September. For the rest of the year, the fields lie fallow. Before 2016, conventional tillage without straw application was practiced for over 25 years.

The rice seeds were sown in the greenhouse for nursery raising and seedlings were transplanted manually to the field at 30 × 18 cm plant spacing. The same fertilization rates and timing for all treatments were applied during 2017, 2018, and 2019. 150 kg N ha^{-1} (urea) was applied, 20% of which was for base fertilization, 50% of which was for the tillering period, and 30% of which was for the heading period. 100 kg P_2O_5 ha^{-1} (superphosphate) and 60 kg K_2O ha^{-1} (potassium chloride) were applied as base fertilizers. 30 kg K_2O ha^{-1} were applied during the heading period.

Experiment design

The experiment consisted of three treatments: 1) no straw application (CK); 2) straw application at a rate of 2500 kg ha^{-1} year^{-1} (SA1); 3) straw application at a rate of 5000 kg ha^{-1} year^{-1} (SA2). All the aboveground plant residues in all the plots were removed after the annual harvest. The rice straw was chopped into 5-cm-long pieces and evenly strewed onto the soil surface in SA1 and SA2 treatments by hand, then integrated into the 0–20-cm layer using a shovel and followed by raking after harvest in 2016, 2017, and 2018. The 0–20-cm soil layer in the CK treatment was mixed using a shovel and raking in the same way and at the same time as in the SA_1 and SA_2 treatments. The treatments were arranged in a randomized complete block design with three replicates. Each plot measured 2.56 m^2 (1.6 m × 1.6 m), and the space between adjacent plots was at least 1 m. Chambers (1.6 m × 1.6 m × 0.55 m) without top and bottom made of polymethyl methacrylate for the plots were pressed into the soil to a depth of 40 cm to minimize the effects from outside the plots.

Sampling and measurements

Soil samples were collected during the heading period in 2017, 2018, and 2019. Three rice plants were randomly selected in each plot, and rice plants in one row on each side of all plots were not collected to avoid border effects. Soil in between 0−15 cm depth

http://www.aloki.hu ● ISSN 1589 1623 (Print) ● ISSN 1785 0037 (Online)
DOI: http://dx.doi.org/10.15666/aeer/1804_59535964

5−10 cm distance from the rice shoot in the horizontal direction was collected as the bulk soil. Rice plants and the soil within 5 cm from their shoot in the horizontal direction were dug out to a depth of 15 cm. Rhizosphere soil was collected from soil adhering to the roots after they were thoroughly shaken. After visual plant residues and rocks were removed, soil samples were air dried, ground, and passed through a 0.25-mm sieve for SOC and amino sugar analyses.

Amino sugars were determined according to the method described by Zhang and Amelung (Zhang and Amelung, 1996). Briefly, soil samples (containing about 0.3 mg N) with 10 ml of 6 M HCl were heated for 8 h at 105 °C. After cooling, the hydrolysate with the addition of 100 μl inositol solution (1 μg ml^{-1}) was filtered. The filtrate was dried, and the residue was dissolved with distilled water and adjusted to a pH of 6.6−6.8. The solution was centrifuged and dried again. The residue was dissolved with methanol and centrifuged. The supernatant was transferred to a derivative bottle and dried using N_2 gas at 45 °C. Amino sugars were determined by gas chromatography with a flame ionization detector (Agilent 6890, Agilent Technologies, Inc., USA) after their conversion to aldononitrile acetates. The concentrations of total amino sugars were calculated as the sum of GluN, GalN and MurN.

Previous studies showed that the ratio of MurN and GluN from bacteria is 1:2, therefore, the fungal-derived GluN ($GluN_F$, mg kg^{-1}) can be calculated according to *Eq. 1* (Engelking et al., 2007).

$$GluN_F = \left(\frac{GluN}{179} - 2 \times \frac{MurN}{251}\right) \times 179 \quad \text{(Eq.1)}$$

where GluN, MurN, and $GluN_F$ are the concentrations of glucosamine, muramic acid, and fungal glucosamine, respectively. The molecular weight of GluN and MurN is 179 g mol^{-1} and 251 g mol^{-1}, respectively.

Statistical analysis

The differences between treatments and different years were tested with repeated measures analysis of variance using SPSS 22.0 (International Business Machines Corporation, New York, USA). All figures were drawn using Sigmaplot 12.5 (Systat Software Inc. San Jose, CA, USA).

Results

In CK and SA2, the contents of MurA, GalN, GluN, $GluN_F$, total amino sugars, and $GluN_F$/MurA did not differ during the trial in both rhizosphere and bulk soil (*Fig. 1*, *Fig. 2*, and *Fig. 3*). Although, the contents MurA, GalN, GluN, $GluN_F$, and total amino sugars in SA1 treatment were increased from 2017 to 2018, no significant difference was observed between 2018 and 2019 at the rhizosphere or bulk soil. The rhizosphere soil of SA1 and SA2 in 2018 and 2019 did not differ with respect to the contents of MurA, GluN, $GluN_F$, and total amino sugars, respectively, and the same was true for bulk soil.

The content of MurA in the rhizosphere soil of CK, SA1, and SA2 ranged from 42.65−44.39, 48.45−56.84, and 52.98−56.46 mg kg^{-1} during the trial, which was significantly higher by 10.95%−13.21% (4.21−5.18 mg kg^{-1}), 13.52%−16.14% (5.77−7.90 mg kg^{-1}), and 12.99%−16.35% (6.44−7.83 mg kg^{-1}) than that in bulk soil, respectively (*Fig. 1*). The content of MurA in the rhizosphere and bulk soil of CK in 2017,

http://www.aloki.hu ● ISSN 1589 1623 (Print) ● ISSN 1785 0037 (Online)
DOI: http://dx.doi.org/10.15666/aeer/1804_59535964

2018, and 2019 was significantly lower than that of SA1 and SA2, respectively. Compared to the content of MurA in the rhizosphere soil of CK (42.65 mg kg^{-1}) and SA1 (48.45 mg kg^{-1}) in 2017, that of SA2 increased significantly by 24.22% and 9.35%, respectively. The rhizosphere and bulk soil of SA1 in 2019 maintained a significantly higher content of MurA than that in 2017, respectively.

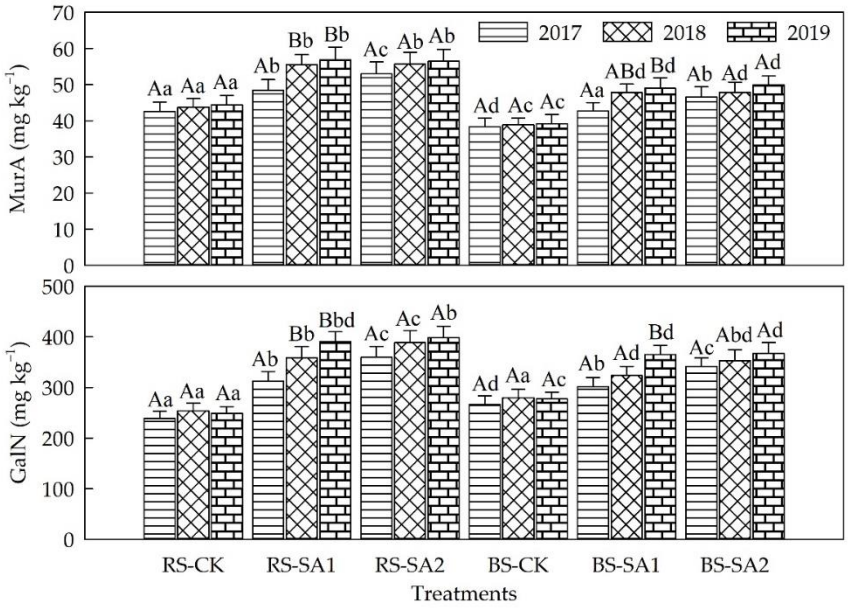

Figure 1. *Variations of muramic acid (MurA) and galactosamine (GalN) in different treatments from 2017 to 2019. Different uppercase letters indicate significant differences between the same treatments in the different year, whereas different lowercase letters indicate significant differences among different treatments in the same year (P<0.05, multiple comparison test by least significant difference).* ***RS****: rhizosphere soil;* ***BS****: bulk soil;* ***CK****: no straw application;* ***SA1****: straw application at a rate of 2500 kg* ha^{-1} $year^{-1}$*;* ***SA2****: straw application at a rate of 5000 kg* ha^{-1} $year^{-1}$*. The same below*

The content of GalN in rhizosphere soil in the CK treatment ranged from 238.74−253.65 mg kg^{-1} during the trial, which was in general lower by 9.33%−10.31% (26.1−28.42 mg kg^{-1}) than that in bulk soil (*Fig. 1*). The values of GalN in rhizosphere and bulk soil in SA1 and SA2 peaked in 2019. Compared to the content of GalN in the rhizosphere and bulk soil of CK in 2019, that of SA1 increased by 141.46 mg kg^{-1} and 87.74 mg kg^{-1}, and that of SA2 increased by 149.35 mg kg^{-1} and 89.94 mg kg^{-1}. In SA1 and SA2, rhizosphere soil contained notably higher contents of GalN than bulk soil in 2018, and 2019, respectively.

Rhizosphere and bulk soil in the same treatment and year did not differ overall in GluN and $GluN_F$. The rhizosphere soil in all treatments contained 38.69−60.15 mg kg^{-1} more GluN and 27.52−50.86 mg kg^{-1} more $GluN_F$ than the bulk soil (*Fig. 2*). At the end of the experiment, the soil content found of GluN and $GluN_F$ in the rhizosphere soil were higher by 192.36 mg kg^{-1} and 174.59 mg kg^{-1} at SA1 treatment, as well as by 208.78 mg kg^{-1} and 191.58 mg kg^{-1} at SA2 treatment than at CK treatment. Bulk soil in SA1 and SA2 in 2019 contained 201.05 mg kg^{-1} and 217.72 mg kg^{-1} more GluN, and 16 mg kg^{-1} and 202.39 mg kg^{-1} more $GluN_F$ than the bulk soil of CK.

http://www.aloki.hu ● ISSN 1589 1623 (Print) ● ISSN 1785 0037 (Online)
DOI: http://dx.doi.org/10.15666/aeer/1804_59535964

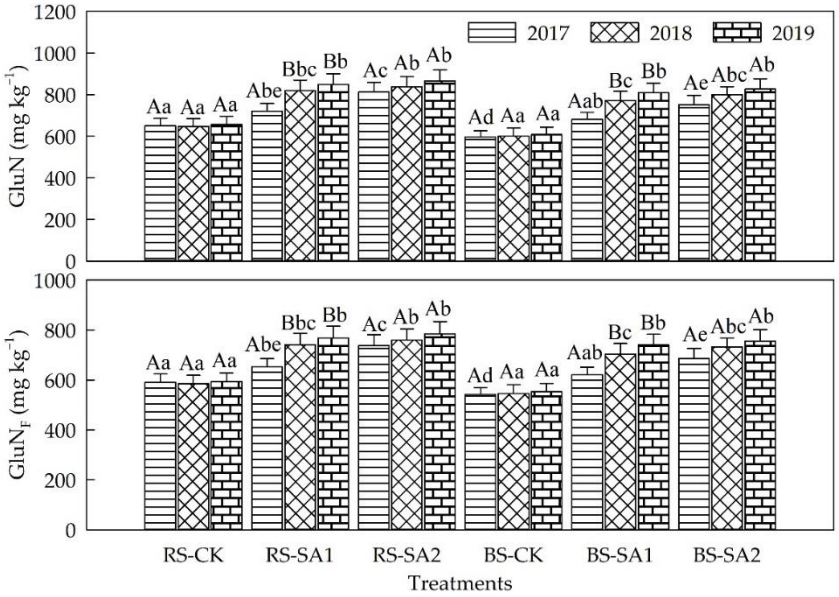

Figure 2. *Variations of glucosamine (GluN) and the fungal-derived GluN (GluN$_F$) in different treatments during the trial*

Total amino sugars among CK, SA1, and SA2 in 2017 varied significantly in both rhizosphere and bulk soil. It followed the order: SA2 (1224.95 mg kg^{-1}, RS; 1140.49 mg kg^{-1}, BS) > SA1 (1082.09 mg kg^{-1}, RS; 1025.36 mg kg^{-1},BS) > CK (932.91 mg kg^{-1}, RS; 901.36 mg kg^{-1}, BS) (*Fig. 3*). SA1 and SA2 in 2019 maintained significantly higher contents of total amino sugars by 346.28 mg kg^{-1} and 370.19 mg kg^{-1} in the rhizosphere soil and by 298.53 mg kg^{-1} and 318.41 mg kg^{-1} in the bulk soil than in the CK treatment, respectively. Just at the SA1 treatment, the content of total amino sugars in either the rhizosphere or bulk soil was notably higher in 2019 than in 2017.

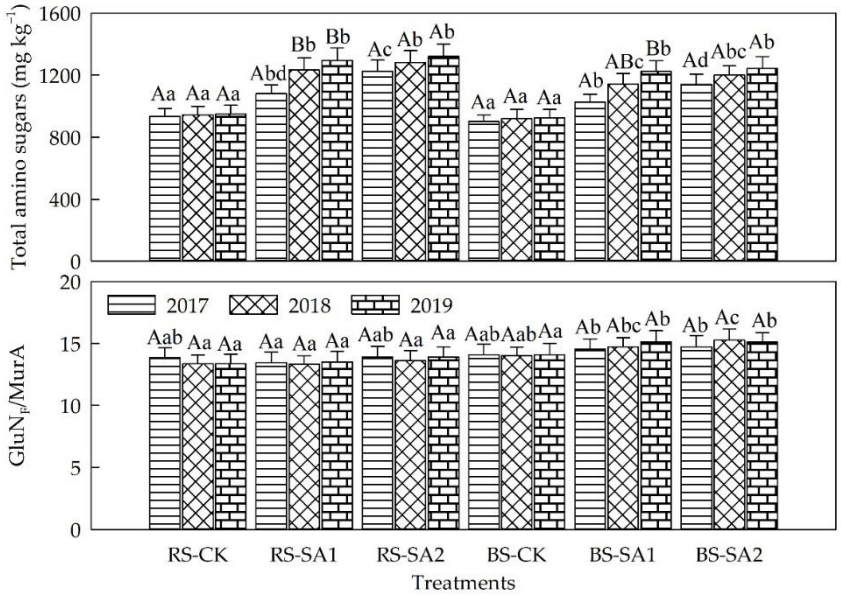

Figure 3. *Variations of total amino sugars and the ratio of GluN$_F$ and MurA (GluN$_F$/MurA) in different treatments during the trial*

http://www.aloki.hu ● ISSN 1589 1623 (Print) ● ISSN 1785 0037 (Online)
DOI: http://dx.doi.org/10.15666/aeer/1804_59535964

The values of $GluN_F$/MurA in rhizosphere soil among the three treatments in the same year did not differ (*Fig. 3*). There were no significant differences in the values of $GluN_F$/MurA among 2017, 2018, and 2019 in the rhizosphere soil in each of the three treatments. The values of $GluN_F$/MurA in the bulk soil of SA1 and SA2 in 2017 were not significantly different from and, in 2019, markedly higher than those in the CK.

Discussion

Effects of straw application on amino sugar fractions

The present results demonstrate that straw application facilitated the accumulation of amino sugars (GalN, MurA, GluN, $GluN_F$, and total amino sugars) in both the rhizosphere and bulk soil in rice fields, which was similar to the results reported for upland fields (Ding et al., 2013, 2015; Liu et al., 2019). The accumulation of amino sugars was ascribed to microbial biomass turnover as well as to the balance of microbial residue production and decomposition (Ding et al., 2013, 2015). Straw provided more available substrates and, therefore, maintained a higher microbial biomass (Chen et al., 2017b). Additionally, sugars, amino acids, and other nutrients rised from rice straw decomposition can favor a greater microbiology activity in the soil (Blagodatskaya and Kuzyakov, 2008). With continuous microbial reproduction and mortality, microbial cell wall components, such as amino sugars, are gradually released and subsequently accumulated more in the SA1 and SA2 treatments than in the CK treatment. On the other hand, association of amino sugars in aggregates can facilitate the maintenance of aggregate cohesion and stabilization (Chantigny et al., 1997), which, thus, protecting amino sugars from decomposition and reducing its decomposition, and thereby, increasing the potential of amino sugar accumulation. Xue et al. (2020) found that straw incorporation drives the formation of SOC-Fe (oxyhydr) oxides associations in aggregates, which contributes to SOC (including amino sugars) stabilization in paddy soils. The SA2 treatment could provide more available substrates, nutrients, and microbial cell wall components and better stimulate the amino sugar mediated formation of aggregates, thus, leading to an excessive accumulation of amino sugars in 2017. The lack of pronounced differences in the content of amino sugars between SA1 and SA2 in both 2018 and 2019 suggests a threshold effect of straw incorporation on microbial residue build-up in the present paddy soil. The threshold effect might result from the "saturation" of the soil aggregates with amino sugars, indicating that microbial amino sugars could be decomposed, and that the prerequisite for amino sugars contributing to a stable C pool is their combination with aggregates (Craig et al., 2018).

Although the straw application to paddy and upland fields have increased amino sugar accumulation, the degree of this accumulation is different. After a three-year straw application, compared to the treatment without straw application, our results show that total amino sugar contents increased by 32.27-38.98%. However, Liu et al. (2019) and Ding et al. (2013) reported that the content of total amino sugars in upland fields increased by 8.37% and 1.23%, respectively. These differences were perhaps due to a variation in soil aeration. The better soil aeration in upland fields greatly facilitate the decomposition of SOC (Chen et al., 2017a) (including amino sugars), thus, leading to a slower accumulation of amino sugars. Soil erosion, aggregate breakdown (Hao et al., 2019), and decreased SOC contents (Yao et al., 2019) caused by rainfall were also responsible for the increased loss of amino sugars in upland fields. Continuous flooding conditions in

http://www.aloki.hu ● ISSN 1589 1623 (Print) ● ISSN 1785 0037 (Online)
DOI: http://dx.doi.org/10.15666/aeer/1804_59535964

paddy fields provide anaerobic and relatively stable conditions (Chen et al., 2017a) to protect the amino sugars and aggregates from decomposition and physical destruction, respectively.

Amino sugars in rhizosphere and bulk soil

Our results showed that living rice roots change the accumulation of amino sugars in the rhizosphere. Root exudates (i.e., organic acids, amino acids), which are major components contributing to the rhizosphere effect, appear to shape the rhizosphere microbial community (Zhalnina et al., 2018). Rice root exudates provided not only available C for microbes (Lu et al., 2004), but also affected microbial biomass. Kong et al. (2008) found that rice root exudates resulted in a higher number of bacteria, actinobacteria, and fungi in rhizosphere than in bulk soil. Furthermore, rhizosphere aggregate stability was higher than that of non-rhizosphere soil (Caravaca et al., 2002). These aspects might favor the higher contents of MurA, GluN, and total amino sugars in the rhizosphere soil of our study. The significantly higher contents of MurA in the rhizosphere probably resulted from the fact that minor variations would lead to significant impacts on MurA because of its low content. The lack of pronounced differences in the contents of GluN and total amino sugars between rhizosphere and bulk soil were probably due to the fact that microbes had enough substrates to feed on both in rhizosphere and bulk soil. The net increase of GluN and total amino sugars caused in the rhizosphere soil was diminished when expressed on their large background in the present soil. This indicated a limited rhizosphere effect on the content of GluN and total amino sugars.

The factors that caused variations in the content of GalN appeared to be more complex. The GalN content in rhizosphere soil was lower in CK, but higher in SA1 and SA2 than that in bulk soil, respectively. Compared with MurA and GluN, little information is known about the main origin of GalN in soil (Amelung et al., 1999) and its function within microbial cells or as metabolites (Engelking et al., 2007). Engelking et al. (2007) concluded that fungi contribute larger percentages of GalN to the amino sugar pool than bacteria, which contradicted the viewpoint stated in earlier publications (Kogel and Bochter, 1985). Joergensen (2018) reported that GalN occurred mainly in bacterial extracellular polymeric substances, fungal extracellular polymeric substances, and fungal cell walls, but he did not quantify it. Ding et al. (2013) found that GalN accumulation patterns within aggregates were different from those of GluN or MurA. Therefore, further investigation is necessary to elucidate the origin and function of GalN as well as its dynamics in soil.

Variations in $GluN_F$/MurA

Previous studies showed that $GluN_F$ accumulated mainly in coarse particulate organic matter and macroaggregates, and 79% of the total MurA pool accumulated in the clay fraction (Pronk et al., 2015). Straw incorporation had a more positive impact on the macro-aggregate (> 2000 μm) and mid-aggregate (250-2000 μm) fraction than on the micro-aggregate fraction (<250 μm) in paddy fields (Huang et al., 2017). This could be responsible for the significantly increased $GluN_F$/MurA ratio in the bulk soil of SA1 and SA2 in 2018 and 2019 in the current study, indicating that straw application increased the relative contribution of fungal- over bacterial-derived residues to SOC. The insignificant variations in $GluN_F$/MurA in the rhizosphere soil of all treatments was probably due to the regulation of the bacterial and fungal communities and/or aggregates by rice root

http://www.aloki.hu ● ISSN 1589 1623 (Print) ● ISSN 1785 0037 (Online)
DOI: http://dx.doi.org/10.15666/aeer/1804_59535964

exudates instead of the litter amendments. Therefore, the rhizosphere likely mediated the relative contribution of fungal- and bacterial-derived residues to SOC and kept it stable. However, the related mechanisms remain unclear.

Conclusions

Amino sugar analysis revealed that three-year straw application enhanced the accumulation of MurA, GluN, GalN, $GluN_F$, and total amino sugars in rhizosphere and bulk soil. A high rate of straw application led to a high amino sugar accumulation in the first year only. Aggregates tended to be "saturated" with amino sugars in the last two years, indicating a limited positive effect of straw application on amino sugar accumulation. In the rhizosphere soil, the accumulation of MurA was promoted, and the contents of GluN, GalN, $GluN_F$, and total amino sugars tended to be higher than those in the bulk soil, suggesting a limited effect of the rhizosphere on GluN, GalN, $GluN_F$, and total amino sugars. Straw application increased the relative contribution of fungal-derived residues to SOC in bulk soil and did not affect the relative contribution of fungal- and bacterial- derived residues to SOC in rhizosphere soil. This work may contribute to understanding the effect of straw applications on microbial-derived C and their contribution to SOC in paddy fields. Future research should concentrate more strongly on the nature and mechanisms of microbial residue–C process during long-term agricultural practices (e.g. fertilization, water management, tillage).

Acknowledgements. This research was funded by the National Natural Science Foundation of China (51179073,41471152) and Specialized Research Fund for the Doctoral Program of Higher Education (20130061110065).

REFERENCES

[1] Amelung, W., Zhang, X., Flach, K. W., Zech, W. (1999): Amino sugars in native grassland soils along a climosequence in North America. – Soil Science Society of America Journal 63: 86-92.

[2] Amelung, W., Miltner, A., Zhang, X., Zech, W. (2001): Fate of microbial residues during litter decomposition as affected by minerals. – Soil Science 166: 598-606.

[3] Blagodatskaya, E., Kuzyakov, Y. (2008): Mechanisms of real and apparent priming effects and their dependence on soil microbial biomass and community structure: critical review. – Biology and Fertility of Soils 45: 115-131.

[4] Caravaca, F., Hernandez, T., Garcia, C., Roldan, A. (2002): Improvement of rhizosphere aggregate stability of afforested semiarid plant species subjected to mycorrhizal inoculation and compost addition. – Geoderma 108: 133-144.

[5] Chantigny, M. H., Angers, D. A., Prevost, D., Vezina, L. P., Chalifour, F. P. (1997): Soil aggregation and fungal and bacterial biomass under annual and perennial cropping systems. – Soil Science Society of America Journal 61: 262-267.

[6] Chaparro, J. M., Sheflin, A. M., Manter, D. K., Vivanco, J. M. (2012): Manipulating the soil microbiome to increase soil health and plant fertility. – Biology and Fertility of Soils 48: 489-499.

[7] Chen, Z., Wang, H., Liu, X., Zhao, X., Lu, D., Zhou, J., Li, C. (2017a): Changes in soil microbial community and organic carbon fractions under short-term straw return in a rice-wheat cropping system. – Soil & Tillage Research 165: 121-127.

http://www.aloki.hu ● ISSN 1589 1623 (Print) ● ISSN 1785 0037 (Online)
DOI: http://dx.doi.org/10.15666/aeer/1804_59535964

[8] Chen, Z. M., Wang, H. Y., Liu, X. W., Zhao, X. L., Lu, D. J., Zhou, J. M., Li, C. Z. (2017b): Changes in soil microbial community and organic carbon fractions under short-term straw return in a rice-wheat cropping system. – Soil & Tillage Research 165: 121-127.
[9] Cheng, W., Parton, W. J., Gonzalez-Meler, M. A., Phillips, R., Asao, S., McNickle, G. G., Brzostek, E., Jastrow, J. D. (2014): Synthesis and modeling perspectives of rhizosphere priming. – New Phytologist 201: 31-44.
[10] Craig, M. E., Turner, B. L., Liang, C., Clay, K., Johnson, D. J., Phillips, R. P. (2018): Tree mycorrhizal type predicts within-site variability in the storage and distribution of soil organic matter. – Global Change Biology 24: 3317-3330.
[11] Ding, X., Han, X., Zhang, X. (2013): Long-term impacts of manure, straw, and fertilizer on amino sugars in a silty clay loam soil under temperate conditions. – Biology and Fertility of Soils 49: 949-954.
[12] Ding, X., Liang, C., Zhang, B., Yuan, Y., Han, X. (2015): Higher rates of manure application lead to greater accumulation of both fungal and bacterial residues in macroaggregates of a clay soil. – Soil Biology & Biochemistry 84: 137-146.
[13] Engelking, B., Flessa, H., Joergensen, R. G. (2007): Shifts in amino sugar and ergosterol contents after addition of sucrose and cellulose to soil. – Soil Biology & Biochemistry 39: 2111-2118.
[14] Fan, X., Yu, H., Wu, Q., Ma, J., Xu, H., Yang, J., Zhuang, Y. (2016): Effects of fertilization on microbial abundance and emissions of greenhouse gases (CH_4 and N_2O) in rice paddy fields. – Ecology and Evolution 6: 1054-1063.
[15] Gao, F., Zhao, B., Dong, S., Liu, P., Zhang, J. (2018): Response of maize root growth to residue management strategies. – Agronomy Journal 110: 95-103.
[16] Glaser, B., Turrion, M. B., Alef, K. (2004): Amino sugars and muramic acid-biomarkers for soil microbial community structure analysis. – Soil Biology & Biochemistry 36: 399-407.
[17] Hao, H. X., Wang, J. G., Guo, Z. L., Hua, L. (2019): Water erosion processes and dynamic changes of sediment size distribution under the combined effects of rainfall and overland flow. – Catena 173: 494-504.
[18] Hu, L., Robert, C. A. M., Cadot, S., Zhang, X., Ye, M., Li, B., Manzo, D., Chervet, N., Steinger, T., van der Heijden, M. G. A., Schlaeppi, K., Erb, M. (2018): Root exudate metabolites drive plant-soil feedbacks on growth and defense by shaping the rhizosphere microbiota. – Nature Communications 9: 2738.
[19] Huang, R., Lan, M. L., Liu, J., Gao, M. (2017): Soil aggregate and organic carbon distribution at dry land soil and paddy soil: the role of different straws returning. – Environmental Science and Pollution Research 24: 27942-27952.
[20] Hurisso, T. T., Davis, J. G., Brummer, J. E., Stromberger, M. E., Mikha, M. M., Haddix, M. L., Booher, M. R., Paul, E. A. (2013): Rapid changes in microbial biomass and aggregate size distribution in response to changes in organic matter management in grass pasture. – Geoderma 193: 68-75.
[21] Jin, W., Hu, Z. J., Bai, Y. J., Dong, C. X., Jin, S. L. (2019): Response of rice and bacterial communities to the incorporation of rice straw in areas mined for heavy rare earth elements. – Bioresources 14: 9392-9409.
[22] Joergensen, R. G., Maeder, P., Fliessbach, A. (2010): Long-term effects of organic farming on fungal and bacterial residues in relation to microbial energy metabolism. – Biology and Fertility of Soils 46: 303-307.
[23] Joergensen, R. G. (2018): Amino sugars as specific indices for fungal and bacterial residues in soil. – Biology and Fertility of Soils 54: 559-568.
[24] Kogel, I., Bochter, R. (1985): Amino sugar determination in organic soils by capillary gas-chromatography using a nitrogen-selective detector. – Zeitschrift für Pflanzenernahrung und Bodenkunde 148: 260-267.

http://www.aloki.hu ● ISSN 1589 1623 (Print) ● ISSN 1785 0037 (Online)
DOI: http://dx.doi.org/10.15666/aeer/1804_59535964

[25] Kong, C. H., Wang, P., Zhao, H., Xu, X. H., Zhu, Y. D. (2008): Impact of allelochemical exuded from allelopathic rice on soil microbial community. – Soil Biology & Biochemistry 40: 1862-1869.
[26] Koponen, H. T., Baath, E. (2016): Soil bacterial growth after a freezing/thawing event. – Soil Biology & Biochemistry 100: 229-232.
[27] Li, P. P., Zhang, D. D., Wang, X. J., Wang, X. F., Cai, Z. J. (2012): Survival and performance of two cellulose-degrading microbial systems inoculated into wheat straw-amended soil. – Journal of Microbiology and Biotechnology 22: 126-132.
[28] Liang, C., Zhang, X., Balser, T. C. (2007): Net microbial amino sugar accumulation process in soil as influenced by different plant material inputs. – Biology and Fertility of Soils 44: 1-7.
[29] Liang, C., Schimel, J. P., Jastrow, J. D. (2017): The importance of anabolism in microbial control over soil carbon storage. – Nature Microbiology 2: 17105.
[30] Liu, S., Huang, D., Chen, A., Wei, W., Brookes, P. C., Li, Y., Wu, J. (2014): Differential responses of crop yields and soil organic carbon stock to fertilization and rice straw incorporation in three cropping systems in the subtropics. – Agriculture Ecosystems & Environment 184: 51-58.
[31] Liu, X., Zhou, F., Hu, G., Shao, S., He, H., Zhang, W., Zhang, X., Li, L. (2019): Dynamic contribution of microbial residues to soil organic matter accumulation influenced by maize straw mulching. – Geoderma 333: 35-42.
[32] Lu, Y. H., Watanabe, A., Kimura, M. (2004): Contribution of plant photosynthates to dissolved organic carbon in a flooded rice soil. – Biogeochemistry 71: 1-15.
[33] Ma, L. J., Kong, F. X., Wang, Z., Luo, Y., Lv, X. B., Zhou, Z. G., Meng, Y. L. (2019): Growth and yield of cotton as affected by different straw returning modes with an equivalent carbon input. – Field Crops Research 243: 10.
[34] Manlay, R. J., Feller, C., Swift, M. J. (2007): Historical evolution of soil organic matter concepts and their relationships with the fertility and sustainability of cropping systems. – Agriculture Ecosystems & Environment 119: 217-233.
[35] Praveen, K., Tripathi, K. P., Aggarwal, R. K. (2002): Influence of crops, crop residues and manure on amino acid and amino sugar fractions of organic nitrogen in soil. – Biology and Fertility of Soils 35: 210-213.
[36] Pronk, G. J., Heister, K., Koegel-Knabner, I. (2015): Amino sugars reflect microbial residues as affected by clay mineral composition of artificial soils. – Organic Geochemistry 83-84: 109-113.
[37] Simpson, R. T., Frey, S. D., Six, J., Thiet, R. K. (2004): Preferential accumulation of microbial carbon in aggregate structures of no-tillage soils. – Soil Science Society of America Journal 68: 1249-1255.
[38] Simpson, A. J., Simpson, M. J., Smith, E., Kelleher, B. P. (2007): Microbially derived inputs to soil organic matter: Are current estimates too low? – Environmental Science & Technology 41: 8070-8076.
[39] Staley, C., Ferrieri, A. P., Tfaily, M. M., Cui, Y., Chu, R. K., Wang, P., Shaw, J. B., Ansong, C. K., Brewer, H., Norbeck, A. D., Markillie, M., do Amaral, F., Tuleski, T., Pellizzaro, T., Agtuca, B., Ferrieri, R., Tringe, S. G., Pasa-Tolic, L., Stacey, G., Sadowsky, M. J. (2017): Diurnal cycling of rhizosphere bacterial communities is associated with shifts in carbon metabolism. – Microbiome 5: 65.
[40] van Groenigen, K.-J., Bloem, J., Baath, E., Boeckx, P., Rousk, J., Bode, S., Forristal, D., Jones, M. B. (2010): Abundance, production and stabilization of microbial biomass under conventional and reduced tillage. – Soil Biology & Biochemistry 42: 48-55.
[41] Wang, J., Li, X., Zhang, J., Yao, T., Wei, D., Wang, Y., Wang, J. (2012): Effect of root exudates on beneficial microorganisms-evidence from a continuous soybean monoculture. – Plant Ecology 213: 1883-1892.

http://www.aloki.hu ● ISSN 1589 1623 (Print) ● ISSN 1785 0037 (Online)
DOI: http://dx.doi.org/10.15666/aeer/1804_59535964

[42] Wang, N., Yu, J., Zhao, Y., Chang, Z., Shi, X., Ma, L. Q., Li, H. (2018): Straw enhanced CO_2 and CH_4 but decreased N_2O emissions from flooded paddy soils: Changes in microbial community compositions. – Atmospheric Environment 174: 171-179.
[43] Xue, B., Huang, L., Huang, Y. N., Kubar, K. A., Li, X. K., Lu, J. W. (2020): Straw management influences the stabilization of organic carbon by Fe (oxyhydr)oxides in soil aggregates. – Geoderma 358: 113987.
[44] Yang, H., Ma, J., Rong, Z., Zeng, D., Wang, Y., Hu, S., Ye, W., Zheng, X. (2019): Wheat straw return influences nitrogen-cycling and pathogen associated soil microbiota in a wheat-soybean rotation system. – Frontiers in Microbiology 10: 1811.
[45] Yao, Y., Liu, J., Wang, Z., Wei, X., Zhu, H., Fu, W., Shao, M. (2019): Responses of soil aggregate stability, erodibility and nutrient enrichment to simulated extreme heavy rainfall. – Science of the Total Environment 709: 136150.
[46] Yin, H., Li, Y., Xiao, J., Xu, Z., Cheng, X., Liu, Q. (2013): Enhanced root exudation stimulates soil nitrogen transformations in a subalpine coniferous forest under experimental warming. – Global Change Biology 19: 2158-2167.
[47] Zhalnina, K., Louie, K. B., Hao, Z., Mansoori, N., da Rocha, U. N., Shi, S., Cho, H., Karaoz, U., Loque, D., Bowen, B. P., Firestone, M. K., Northen, T. R., Brodie, E. L. (2018): Dynamic root exudate chemistry and microbial substrate preferences drive patterns in rhizosphere microbial community assembly. – Nature Microbiology 3: 470-480.
[48] Zhang, X. D., Amelung, W. (1996): Gas chromatographic determination of muramic acid, glucosamine, mannosamine, and galactosamine in soils. – Soil Biology & Biochemistry 28: 1201-1206.
[49] Zhang, X., Amelung, W., Yuan, Y., Samson-Liebig, S., Brown, L., Zech, W. (1999): Land-use effects on amino sugars in particle size fractions of an Argiudoll. – Applied Soil Ecology 11: 271-275.
[50] Zhao, S., Li, K., Zhou, W., Qiu, S., Huang, S., He, P. (2016): Changes in soil microbial community, enzyme activities and organic matter fractions under long-term straw return in north-central China. – Agriculture Ecosystems & Environment 216: 82-88.
[51] Zhao, H., Shar, A. G., Li, S., Chen, Y., Shi, J., Zhang, X., Tian, X. (2018): Effect of straw return mode on soil aggregation and aggregate carbon content in an annual maize-wheat double cropping system. – Soil & Tillage Research 175: 178-186.

http://www.aloki.hu ● ISSN 1589 1623 (Print) ● ISSN 1785 0037 (Online)
DOI: http://dx.doi.org/10.15666/aeer/1804_59535964

DIVERSITY OF CELLULOLYTIC BACTERIA ISOLATED FROM A FRESHWATER WETLAND RESERVE IN THAILAND AND THEIR CELLULOLYTIC ACTIVITY

CHANTARASIRI, A.

Faculty of Science, Energy and Environment, King Mongkut's University of Technology North Bangkok, Rayong Campus, Rayong 21120, Thailand
e-mail: aiya.c@sciee.kmutnb.ac.th; phone: +66-(0)38-627-000 #5446

(Received 10th Apr 2020; accepted 10th Jul 2020)

Abstract. Freshwater wetlands are unique aquatic ecosystems, which are a tremendous source of organic carbon. A bacterial community plays a significant role in the carbon cycle of organic matter through its cellulolytic enzymes; namely, cellulases. For this study, culturable bacteria were isolated from a freshwater wetland reserve situated in Thailand and screened for their cellulase production. Seventy-six cellulolytic bacteria were grouped by a PCR-RFLP of 16S rDNA technique and identified by a nucleotide sequencing analysis. A total of 17 different RFLP patterns were obtained, belonging to nine bacterial genera including *Acinetobacter*, *Aeromonas*, *Bacillus*, *Chromobacterium*, *Citrobacter*, *Enterobacter*, *Herbaspirillum*, *Paenibacillus* and *Vibrio*. The predominant genera of the isolated cellulolytic bacteria were *Bacillus*, *Chromobacterium* and *Herbaspirillum*. The cellulolytic bacterium isolated from the moist peat samples designated as *B. megaterium* strain S0702 could produce three types of cellulases and showed the highest CMCase activity at 4.48 ± 0.08 U/mL. The optimum pH and temperature for the CMCase activity were determined to be 45 - 50°C at a pH of 7.0 with a stability range of 25 - 60°C and pH 5.0 - 8.0. The CMCase activity was greatly enhanced by Mn^{2+} and considerably inhibited by EDTA and ethyl-acetate. This enzyme could possibly be used in various biotechnological applications.
Keywords: *aquatic ecosystem, B. megaterium, cellulase, CMCase activity, PCR-RFLP*

Introduction

Wetlands are natural or artificial, permanent or temporary areas with static or flowing water, where the depth at low tide does not exceed six meters; these include, fens, marshes, peatlands, freshwater areas and marine water areas (Bassi et al., 2014; Kalita et al., 2019). Wetlands serve as a source of biogeochemical cycles, bioremediation of contaminants, flood alleviation and production of food (Leff, 2009). Freshwater wetland is a type of saturated land, the nature of which varies based on the hydrological and plant communities. This unique nature affects the microbial communities dwelling in the wetland. Wetland soils and sediments are also a tremendous source of terrestrial carbon including decayed plants and woody organic matter (Gorham, 1991; An et al., 2019). Microbial communities also play a critical role in the detritus decomposition resulting in dissolved organic carbon and related organic compounds which maintain the nutrient cycle and wetland stableness. Cellulolytic microbes mainly provide the decomposition of cellulose-based plant litter through their cellulolytic enzymes producing the simple sugar derivatives in the sediment (Soares-Júnior et al., 2013). Microbial cellulolytic enzymes, generally called cellulase, are complex substances that comprise endoglucanases (E.C. 3.2.1.4), exoglucanases (E.C. 3.2.1.91, and E.C. 3.2.1.176) and β-glucosidases (E.C. 3.2.1.21), which synergistically work to hydrolyze the β-1,4 glycosidic linkages of cellulose polymer (Chantarasiri, 2015). Cellulases account for 20% of the world enzyme market and have biotechnological promise in various industries; such as, agriculture, animal feed, biofuel, breweries, food, laundry, paper and pulp, pharmaceuticals, textiles

http://www.aloki.hu ● ISSN 1589 1623 (Print) ● ISSN 1785 0037 (Online)
DOI: http://dx.doi.org/10.15666/aeer/1804_59655983

and waste management (Juturu and Wu, 2014; Behera et al., 2017). Furthermore, microbial cellulases have been reported in aerobic and anaerobic, mesophilic and thermophilic bacteria and fungi (Sharma and Yazdani, 2016). Cellulolytic microbes have been commonly isolated from soil, decaying organic matter, animal digestive tracts and herbivore dung (Juturu and Wu, 2014); such as, *Aspergillus* (Nwodo-Chinedu et al., 2005; Gao et al., 2008), *Bacillus* (Anand et al., 2010; Chantarasiri, 2014, 2015; Sriariyanun et al., 2016), *Cellulomonas* (Sangkharak et al., 2011), *Clostridium* (Reddy et al., 2010), *Fusarium* (Qin et al., 2010; Nwodo-Chinedu et al., 2005), *Geobacillus* (Ibrahim and El-diwany, 2007; Baharuddin et al., 2010), *Gluconacetobacter* (Wee et al., 2011) and *Penicillium* (Nwodo-Chinedu et al., 2005). Currently, most commercial cellulases in the global enzyme market have been produced by *Trichoderma reesei* and *Aspergillus* sp. (Zhang et al., 2006). Moreover, a few cellulolytic microbes have been isolated from freshwater wetlands and related environments due to their complexity and inaccessibility. The isolated cellulolytic microbes from freshwater wetlands were identified as bacteria belonging to the genera *Bacillus* (Chantarasiri et al., 2015), *Brucella* (Behera et al., 2016), *Nocardia* (Benhadj et al., 2019), *Micromonospora* (Benhadj et al., 2019) and fungi belonging to the genera *Fusarium*, *Peziza*, and *Zygomycete* (Wu et al., 2015). The search for cellulolytic microbes still has much interest, and microbial species and environmental sources of microbial isolation have been reported. However, only a few microbes can produce high cellulolytic activity, and only a few can produce all three cellulase enzymes (Sharma and Yazdani, 2016). To improve the knowledge of cellulolytic microbes and their cellulolytic performance, more research has been conducted. Isolation and screening of cellulase-producing microbes from nature is one of the important ways to obtain novel and effective cellulases.

However, sufficient data of cellulolytic microbes isolated from freshwater wetland ecosystem are required. This research consequently aimed to isolate and screen cellulolytic bacteria from Bueng Samnak Yai, a wetland reserve of Thailand. The molecular genetic methods, polymerase chain reaction-restriction fragment length polymorphism (PCR-RFLP) of 16S rDNA and nucleotide sequencing analysis, were used to describe the diversity of a cellulolytic bacterial community. All representative bacteria of each RFLP pattern were determined for their cellulolytic performance. Finally, the most effective bacterium, *B. megaterium* strain S0702, was cellulolytic characterized to evaluate its biotechnological potential.

Materials and Methods

Description of the sampling site

The study area in this research was Bueng Samnak Yai (12° 39′ N, 101° 32′ E) in Rayong province, Thailand. Bueng Samnak Yai has been designated as a wetland reserve, which uniquely combines coastal (brackish) wetland and freshwater wetland. The coastal wetland area is grown over by many characteristic plants (Chantarasiri et al., 2017) which those species are similar to those of a freshwater wetland area. Water and moist peat (partially decayed plants) samples were randomly collected from the grass islands floating in the freshwater wetland area. Twenty water samples and 30 moist peat samples were taken at a depth of 0 - 5 cm from the sampling grass islands. The sampling site covered an area of 190 ha with an average depth of water of one meter. The site comprised more than 100 floating and flowing grass islands, which their dimensions ranged from a table-sized to a soccer field-sized island. The grass islands were strongly formed by stem

http://www.aloki.hu ● ISSN 1589 1623 (Print) ● ISSN 1785 0037 (Online)
DOI: http://dx.doi.org/10.15666/aeer/1804_59655983

and rhizome networks of three dominant grass species consisting of *Lepironia articulate* (Retz.) Domin, *Imperata cylindrica* (L.) Beauv. and *Carex baccans* Nees. All samples were collected during September 2017. The samples were kept at 4°C in sterilized plastic bags and taken for bacterial isolation within 24 hours of collection. The locations of the sampling site are shown in *Figure 1*.

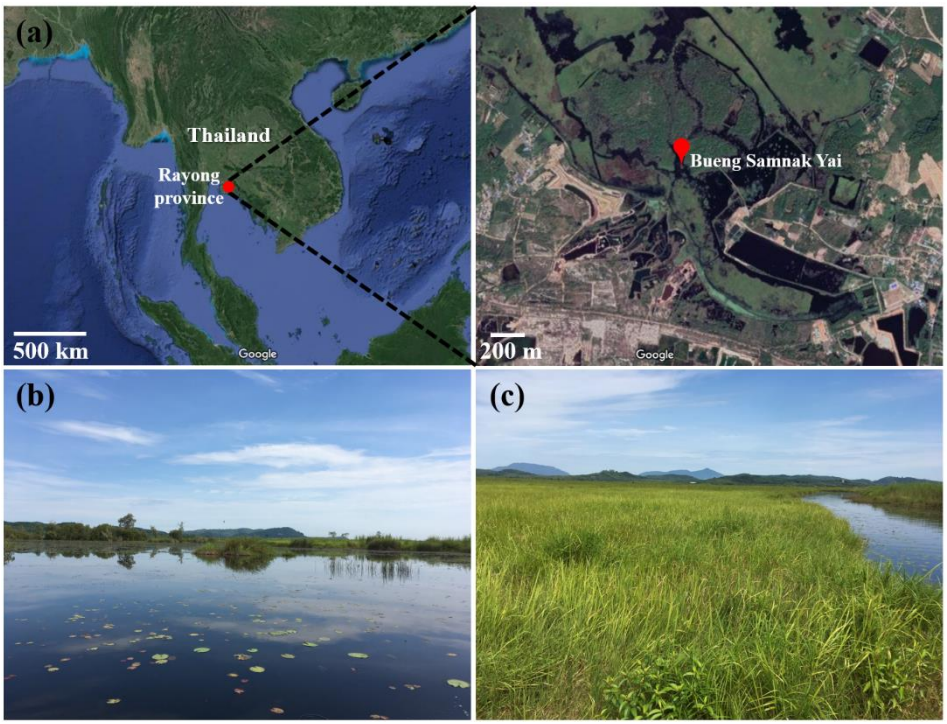

Figure 1. *Bueng Samnak Yai: (a) Map of Bueng Samnak Yai (12°39′N, 101°32′E) situated in Rayong province, Thailand (Source: Google Maps). (b) Freshwater wetland area and a few table-sized floating grass islands. (c) A scene of a soccer field-sized floating grass island*

Isolation and purification of bacteria from the freshwater wetland samples

Water and moist peat samples were serially diluted with sterilized 0.85% NaCl solution supplemented with 0.1% buffered peptone to obtain 1:10,000 dilutions (Merck, India). One hundred microliters of diluted samples were spread plated on Tryptone soya agar (HiMedia, India) and incubated at 28.5 ± 0.1°C (the average temperature of the sampling site) for 24 hours. The bacterial strains were selected based on the colony's morphology and subsequently the colony was purified by being streak plated on Tryptone soya agar.

Screening of cellulolytic bacteria

The screening of cellulolytic bacteria from an aquatic environment was conducted from that previously described (Chantarasiri, 2015). One drop (five microliters) of overnight growth culture in the Tryptone soya broth (HiMedia, India) of each isolated bacterium was spot plated on carboxymethyl cellulose (CMC) agar (0.2% $NaNO_3$, 0.1% K_2HPO_4, 0.05% $MgSO_4$, 0.05% KCl, 0.2% CMC sodium salt, 0.02% peptone and 1.7% agar). All culture plates were incubated at 28.5 ± 0.1°C for 48 hours and then flooded

http://www.aloki.hu ● ISSN 1589 1623 (Print) ● ISSN 1785 0037 (Online)
DOI: http://dx.doi.org/10.15666/aeer/1804_59655983

with iodine solution (0.33% I_2 and 0.67% KI) for 10 minutes. The bacterial isolates could produce the cellulolytic zone around the colonies after Gram's iodine staining indicated the synthesis of the extracellular cellulases by the cellulolytic candidates. The cellulolytic performance was evaluated by the hydrolysis capacity (HC) value that was calculated from the ratio between the diameter of the cellulolytic zone and the diameter of the bacterial colony. All experiments were performed in triplicate.

Polymerase chain reaction-restriction fragment length polymorphism (PCR-RFLP) of 16S rDNA

Genomic DNA of each cellulolytic bacteria was extracted by a heat treatment method (Dashti et al., 2009). Polymerase chain reaction (PCR) amplification of the 16S rRNA genes was performed using the OnePCR™ reaction mixture (Bio-Helix, Taiwan). The primer set used for the amplification of the target 16S rRNA genes included the universal forward primer 27F (5′-AGAGTTTGATCMTGGCTCAG-3′) and the universal reverse primer 1492R (5′-TACGGYTACCTTGTTACGACTT-3′) (Sigma-Aldrich, Singapore). The PCR conditions involved a preheating step at 94°C for four minutes, denaturation step at 94°C for 40 seconds, annealing step at 55°C for one minute, extension step at 72°C for 1 minute 10 seconds, and final extension step at 72°C for 10 minutes. PCR was performed for 35 amplification cycles in a Mastercycler® Nexus (Eppendorf, Germany). The 16S rDNA fragments resulting from the PCR processes were approximately 1,500 bp. The restriction fragment length polymorphism (RFLP) analysis was performed by two restriction enzymes of *Msp*I and *Alu*I (New England Biolabs, UK) in a CutSmart® buffer (New England Biolabs, UK). The 16S rDNA fragments were digested with *Msp*I and *Alu*I at 37°C for 12 hours then the digestion reaction was terminated by heating the reaction mixtures at 80°C for 15 minutes following the protocol described by New England Biolabs with minor modifications. The resulting restriction fragments were analyzed using 3% (w/v) OmniPur® agarose gel (Calbiochem, Germany) and visualized by Novel Juice (Bio-Helix, Taiwan). The PCR marker used in this study was a 100 bp DNA ladder RTU (Bio-Helix, Taiwan).

16S rDNA sequencing and phylogenetic analysis

The 16S rDNA PCR products were purified and sequenced by the nucleotide sequencing service of Macrogen Inc. (Seoul, Korea). The sequence similarity analysis of the resulting 16S rDNA was aligned using the BLASTn suite (National Center for Biotechnology Information: NCBI). The phylogenetic tree was analyzed and visualized by the SeaView software version 4.6.4 (Gouy et al., 2010) and FigTree software version 1.4.3 (Institute of Evolutionary Biology, University of Edinburgh, UK). The phylogenetic tree was generated by the neighbor-joining (NJ) method with 100,000 bootstrap replications. All the resulting nucleotide sequences of the identified cellulolytic bacteria from this study were deposited in the GenBank database of NCBI under the accession numbers MN993647, MN993849, MN993893, MN993916, MN994046, MN994069, MN994075, MN994076, MN994079 to MN994082, MN994084 and MN994270 to MN994273.

Preparation of the crude cellulases

The cellulolytic bacteria were cultured in a CMC liquid medium. All bacterial cultures were shaken under an aeration condition in a baffled flask (Schott-Duran, Germany) at

http://www.aloki.hu ● ISSN 1589 1623 (Print) ● ISSN 1785 0037 (Online)
DOI: http://dx.doi.org/10.15666/aeer/1804_59655983

150 rpm, 28.5 ± 0.1°C, for 48 hours. The bacterial cells were then removed from the liquid medium to obtain the crude cellulases by a centrifugation method at 4,500 ×*g* at 4°C for 30 minutes (Chantarasiri, 2015). The crude cellulases were concentrated by 30-kDa Amicon® ultra centrifugal filter units (Millipore, Ireland).

Cellulolytic activity assays of the crude cellulases

The cellulolytic activity assays of the crude cellulases were conducted from that previously described (Chantarasiri, 2015). The endoglucanase activity (CMCase) was measured by incubating 0.5 mL of crude cellulases with 0.5 mL of 2% CMC in an assay buffer at 50°C for 30 minutes. The exoglucanase activity (Avicelase) was measured by incubating 0.5 mL of crude cellulases with 0.5 mL of 2% Avicel® PH-101 (Sigma-Aldrich, Germany) in an assay buffer at 50°C for one hour. The reducing sugars liberated from the CMCase and Avicelase reactions were spectrophotometrically determined by a 3,5-dinitrosalicylic acid (DNS) method at 540 nm (Miller, 1959). The cellulolytic activity values of CMCase and Avicelase were calculated by a glucose standard curve. One unit (U) of CMCase and Avicelase was defined as the amount of enzyme required to release 1 μmol of the reducing sugars as glucose equivalents per minute under the assay conditions. The β-glucosidase activity was measured by incubating 0.5 mL of crude cellulases with 1 mL of 0.1% *p*-nitrophenyl-β-D-glucopyranoside (Sigma-Aldrich, Germany) in an assay buffer at 50°C for one hour. The reaction was terminated by adding 2 mL of 1 M Na_2CO_3 solution. The reaction mixture was spectrophotometrically measured at 400 nm. The cellulolytic activity values of β-glucosidase were calculated by a *p*-nitrophenol standard curve. One unit (U) of β-glucosidase was defined as the amount of enzyme required to release 1 μmol of *p*-nitrophenol per minute under the assay conditions. The assay buffer used in this study was 50 mM sodium phosphate buffer at a pH 7.0, which its pH value was conducted from Samira et al. (2011) and Shobharani et al. (2013). All experiments were performed in triplicate.

Characterization of the cellulolytic activity from the most active cellulolytic bacteria

The characterization of the cellulolytic activity was examined on the crude cellulases produced from the most active endoglucanasic bacterium, *B. megaterium* strain S0702. The study on the cellulolytic activity was determined based on its CMCase activity. The enzymatic characterization focused on three parameters, which affected the cellulolytic activity consisting of temperature, pH and some chemical additives. All experiments were performed in triplicate.

Effect of temperature on the cellulolytic activity and thermal stability

The CMCase activity was measured accordingly as mentioned in the section "Cellulolytic activity assays of the crude cellulases" at temperatures ranging from 25°C to 80°C in an assay buffer. Thermal stability was examined by pre-incubating the crude enzyme at temperatures ranging from 25°C to 80°C in an assay buffer for 24 hours, and the relative activity of CMCase was monitored using 2% CMC sodium salt as a substrate under the mentioned CMCase conditions. The assay buffer used in this study was a 50 mM sodium phosphate buffer at a pH 7.0.

http://www.aloki.hu ● ISSN 1589 1623 (Print) ● ISSN 1785 0037 (Online)
DOI: http://dx.doi.org/10.15666/aeer/1804_59655983

Effect of pH on the cellulolytic activity and pH stability

The CMCase activity was measured accordingly as mentioned above in the pH-varied buffers at 50°C. The assay buffer used in this study was a 50 mM citrate buffer (pH 4.0 - 6.0), 50 mM sodium phosphate buffer (pH 6.0 - 8.0) and 50 mM glycine-NaOH buffer (pH 8.0 - 10.0). The pH stability was examined by pre-incubating the crude enzyme in the above-mentioned buffer at 50°C for 24 hours, and the relative activity of CMCase was monitored using 2% CMC sodium salt as a substrate under the mentioned CMCase conditions.

Effect of chemical additives on the cellulolytic activity

The CMCase activity was measured accordingly as mentioned above. Crude cellulases were pre-incubated with metal ions, a chelating agent and organic solvents. Ten metal ions were used comprising Ca^{2+} (as $CaCl_2$), Co^{2+} (as $CoCl_2$), Cu^{2+} (as $CuCl_2$), Fe^{2+} (as $FeCl_2$), Hg^{2+} (as $HgCl_2$), K^+ (as KCl), Mn^{2+} (as $MnCl_2$), Ni^{2+} (as $NiCl_2$), Pb^{2+} (as $PbCl_2$) and Sr^{2+} (as $SrCl_2$). The chelating agent used in this study was ethylene diamine tetra-acetic acid (EDTA) sodium salt. The final concentration of the metal ion and chelating agent solutions was 5 mM following the study of Seo et al. (2013). The relative activity of CMCase was monitored using 2% CMC sodium salt as a substrate after being incubated with the metal ions and chelating agent at 50°C for one hour (Annamalai et al., 2013). There were six organic solvents used comprising acetone, dichloromethane, ethanol, ethyl-acetate, methanol and *n*-hexane with the final concentration of 25% of various organic solvents. The relative activity of CMCase was monitored using 2% CMC sodium salt as a substrate after being incubated with the organic solvents at 50°C for four hours (Annamalai et al., 2013).

Statistical analysis

The statistical analysis in this study was analyzed by one-way ANOVA followed by Tukey's test with a 95% confidence interval using R software version 3.6.2 (R Core Team, 2017).

Results and Discussion

Description of the freshwater wetland samples

Twenty water samples and 30 moist peat samples were randomly collected from the sampling site, Bueng Samnak Yai. The average temperature of the 50 sampling points was 28.5 ± 0.1°C. All samples were a dark brown color due to the large amount of organic matter and humic substances (Leff, 2009).

Isolation, purification and screening of bacteria from the freshwater wetland samples

Two-hundred and eight bacterial strains were isolated and purified from the freshwater wetland samples. There were 88 bacterial strains isolated from the water samples and 120 bacterial strains isolated from the moist peat samples with a dissimilar morphological colony. Most aquatic bacteria had a yellow pigmentation, circular shape, entire margin and convex elevation, whereas the moist peat bacteria usually had a white pigmentation, circular shape, entire margin and raised elevation. The percentage of the morphology of the isolated bacteria from the freshwater wetland samples is shown in *Table 1*.

http://www.aloki.hu ● ISSN 1589 1623 (Print) ● ISSN 1785 0037 (Online)
DOI: http://dx.doi.org/10.15666/aeer/1804_59655983

Table 1. *Percentage of the morphology of the isolated bacteria from the freshwater wetland samples*

Bacteria	Pigmentation (Percentage)		Shape (Percentage)		Margin (Percentage)		Elevation (Percentage)	
Aquatic Bacteria (88 strains)	Violet	11.10	Circular	90.00	Entire	80.00	Convex	34.34
	White	37.38	Irregular	7.78	Erose	4.44	Flat	32.34
	Yellow	44.85	Punctiform	2.22	Lobate	5.56	Raised	30.00
	Translucent	6.67	Filamentous	-	Undulate	10.00	Umbonate	3.32
	Total	100.00	Total	100.00	Total	100.00	Total	100.00
Moist Peat Bacteria (120 strains)	Violet	4.17	Circular	95.83	Entire	97.50	Convex	35.00
	White	68.33	Irregular	2.50	Erose	-	Flat	23.33
	Yellow	19.17	Punctiform	1.67	Lobate	1.67	Raised	40.00
	Translucent	8.33	Filamentous	-	Undulate	0.83	Umbonate	1.67
	Total	100.00	Total	100.00	Total	100.00	Total	100.00

The screening of the cellulolytic bacteria using the CMC agar method showed 22 bacterial strains isolated from the water samples (25% of the isolated aquatic bacteria) and 54 bacterial strains isolated from the moist peat samples (45% of the isolated moist peat bacteria) that were defined as active cellulolytic bacteria. The hydrolysis capacity (HC) values of the aquatic bacteria ranged from 1.54 to 3.54, while that of the moist peat bacteria ranged from 1.57 to 3.55. The aquatic bacterium strain W0105 and moist peat bacterium strain S0804 showed a maximum HC of 3.54 ± 0.13 and 3.55 ± 0.33, respectively. The cellulolytic zone around the bacterial colonies on the CMC agar plates after Gram's iodine staining is shown in *Figure 2*. Chantarasiri et al. (2015) reported that there were 87 bacterial strains (60% of the isolated bacteria) isolated from the coastal wetland soils of Bueng Samnak Yai defined as cellulolytic bacteria. The bacterium with the highest HC values of that study was the *Bacillus* sp. strain BR0302 with a HC value of 4.15 ± 0.18. From the hydrolytic performance on the CMC agar plates, it was believed that the cellulolytic bacteria dwelling in the moist peat and related terrestrial samples were more abundant than bacteria dwelling in a water sample.

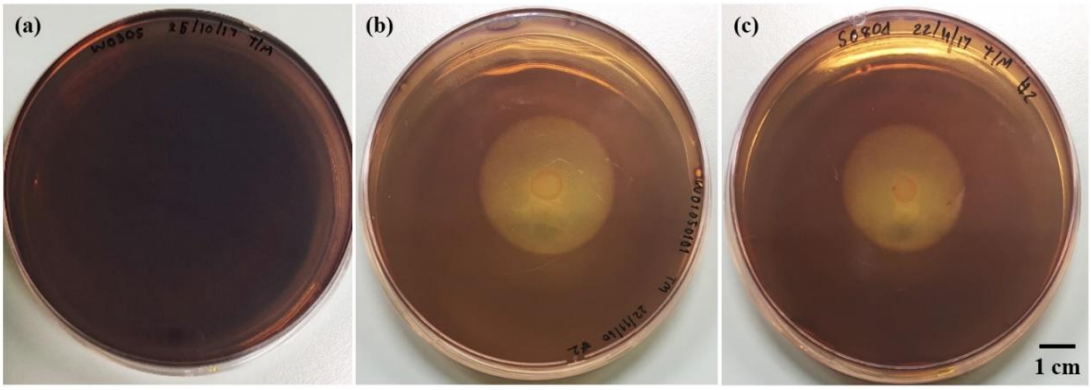

Figure 2. *The cellulolytic zone around the colonies on the CMC agar plates after Gram's iodine staining. (a) Non-cellulolytic bacterium. (b) Aquatic-cellulolytic bacterium strain W0105.(c) Moist peat-cellulolytic bacterium strain S0804*

http://www.aloki.hu ● ISSN 1589 1623 (Print) ● ISSN 1785 0037 (Online)
DOI: http://dx.doi.org/10.15666/aeer/1804_59655983

PCR-RFLP analysis of the 16S rDNA fragments amplified from the cellulolytic bacteria

The 16S rRNA genes of the isolated cellulolytic bacteria were amplified using the PCR method with a set of primers consisting of the 27F-forward primer and 1492R-reverse primer. The 16S rDNA fragments resulting from that amplification were digested by the *Msp*I and *Alu*I restriction enzymes. The resulting RFLP profiles electrophorized on agarose gel are shown in *Figure 3*. There were seven different patterns in the RFLP profile obtained from the 22 strains of cellulolytic bacteria isolated from the water samples and 10 different patterns in the profile obtained from the 54 strains of cellulolytic bacteria isolated from the moist peat samples. The different patterns of the RFLP are summarized in *Tables 2 and 3*. Patterns W1 and W7 were the ones most commonly found in the cellulolytic bacteria isolated from the water samples by 27%. Pattern W6 showed a smear arrangement; however, there was only one bacterial strain (W1401) in this pattern (*Table 2*). Therefore, it did not affect the categorization of the pattern and identification of this bacterium. Pattern S4 was the one most commonly found in the cellulolytic bacteria isolated from the moist peat samples by 37%. All patterns from the moist peat bacteria were explicit arrangements and practicable for bacterial categorization. Interestingly, several patterns of the two RFLP profiles were similar; such as, the pair of patterns W1-S4 (*Figure 3*). They were possibly believed to be the same species of cellulolytic bacteria like a pair of patterns W2-S5 and a pair of patterns W5-S1 (*Figure 3*).

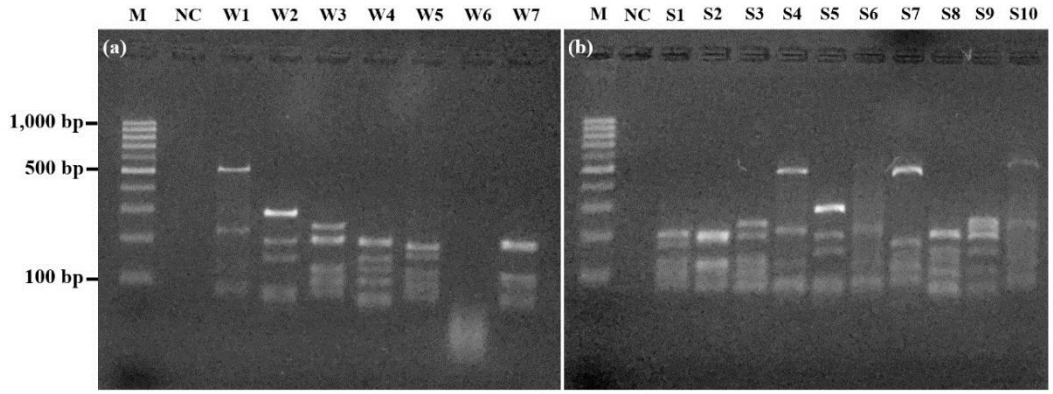

Figure 3. *RFLP profiles resulting from the PCR-RFLP analysis of the isolated cellulolytic bacteria. (a) RFLP profile of the cellulolytic bacteria isolated from the water samples (pattern W1 to W7).(b) RFLP profile of the cellulolytic bacteria isolated from the moist peat samples (pattern S1 to S10). M denoted 100 bp DNA ladder RTU. NC denoted negative control of PCR*

Table 2. *Different RFLP patterns and number of the cellulolytic bacteria isolated from the water samples*

RFLP Pattern	Bacterial Strain	Total No. of Bacterial Strains
W1	W0105, W0902, W1307, W1802, W1902, W2002	6
W2	W0203, W0301, W2003	3
W3	W0303	1
W4	W0306, W2004	2
W5	W0205, W1103, W1504	3
W6	W1401	1
W7	W0903, W1104, W1105, W1506, W1507, W1508	6
	Total	22

http://www.aloki.hu ● ISSN 1589 1623 (Print) ● ISSN 1785 0037 (Online)
DOI: http://dx.doi.org/10.15666/aeer/1804_59655983

Table 3. *Different RFLP patterns and number of the cellulolytic bacteria isolated from the moist peat samples*

RFLP Pattern	Bacterial Strain	Total No. of Bacterial Strains
S1	S0104, S0303, S2802	3
S2	S0503	1
S3	S0701, S1202, S2604, S3003	4
S4	S0103, S0201, S0204, S0703, S0804, S0902, S0903, S1103, S1302, S1304, S1306, S1702, S2004, S2303, S2601, S2605, S2803, S2804, S2904, S3004	20
S5	S0402, S0501, S0601, S0702, S0904, S0905, S0906, S0907, S0908, S1601, S1701, S2001, S2902, S2903, S2905, S2906, S2907, S3006	18
S6	S1305, S1401, S1404	3
S7	S1402	1
S8	S1602	1
S9	S2606	1
S10	S3007, S3008	2
	Total	54

Identification of the cellulolytic bacteria by 16S rDNA sequencing and phylogenetic analysis

The genomic DNA was extracted from 17 different bacterial strains based on the RFLP profiles as mentioned above. The 16S rDNA amplification was performed by the universal primers, 27F and 1492R. The 16S rDNA PCR-products were purified, sequenced and aligned. The alignment results of the cellulolytic bacteria belonged to nine genera: *Acinetobacter*, *Aeromonas*, *Bacillus*, *Chromobacterium*, *Citrobacter*, *Enterobacter*, *Herbaspirillum*, *Paenibacillus* and *Vibrio* (*Table 4*). The cellulolytic bacteria isolated from the water samples were closely similar to the bacteria in the genera of *Bacillus*, *Chromobacterium* and *Enterobacter* with a 94 - 98% identity. The cellulolytic bacteria isolated from the moist peat samples were closely similar to bacteria in the genera of *Acinetobacter*, *Aeromonas*, *Bacillus*, *Chromobacterium*, *Citrobacter*, *Herbaspirillum*, *Paenibacillus* and *Vibrio* with a 93 - 98% identity. The moist peat samples had a greater biodiversity of cellulolytic bacteria than the aquatic environment in the freshwater wetland. This could be related to their amount of organic matter and related carbon sources, which would be essential for bacterial life. The phylogenetic tree of the isolated bacteria with 100,000 bootstrap replications is shown in *Figure 4*.

The cellulolytic bacteria were designated as being closely related based on the alignment results of the 16S rDNA sequence when the identity was more than 98%; such as, *B. wiedmannii* strain W1401. The ones which were lower than a 98% identity were presented at the genus level; such as, *Bacillus* sp. strain W0105 and *Bacillus* sp. strain S0804 (the cellulolytic bacteria with the maximum HC values as previously mentioned). The alignment and phylogenetic tree results confirmed the hypothesized identification of the same RFLP patterns as mentioned above comprising patterns W1-S4, W2-S5 and W5-S1 (*Table 4*).

All the 16S rDNA sequences from this study were deposited in the GenBank database of the NCBI under the accession numbers MN993647, MN993849, MN993893, MN993916, MN994046, MN994069, MN994075, MN994076, MN994079 to MN994082, MN994084 and MN994270 to MN994273, as mentioned above in the Materials and Methods section.

http://www.aloki.hu ● ISSN 1589 1623 (Print) ● ISSN 1785 0037 (Online)
DOI: http://dx.doi.org/10.15666/aeer/1804_59655983

Table 4. *Identity percentage of the 16S rDNA sequences for the isolated cellulolytic bacteria*

RFLP Pattern	Closely Related Bacteria	GenBank Accession No. (Database)	Identity (%)*	GenBank Accession No. (Deposited)
W1	*Bacillus cereus* strain ATCC 14579	NR_074540.1	94.49	MN993849
W2	*Bacillus megaterium* strain ATCC 14581	NR_117473.1	97.98	MN993647
W3	*Chromobacterium piscinae* strain LMG 3947	NR_114953.1	97.20	MN993916
W4	*Enterobacter asburiae* strain JM-458	NR_145647.1	96.74	MN994046
W5	*Chromobacterium violaceum* strain ATCC 12472	NR_074222.1	97.55	MN993893
W6	*Bacillus wiedmannii* strain FSL W8-0169	NR_152692.1	98.83	MN994075
W7	*Chromobacterium amazonense* strain CBMAI 310	NR_136426.1	96.80	MN994069
S1	*Chromobacterium violaceum* strain NBRC 12614	NR_113595.1	98.25	MN994079
S2	*Chromobacterium vaccinia* strain MWU205	NR_109451.1	95.85	MN994081
S3	*Herbaspirillum frisingense* strain NBRC 102522	NR_114140.1	98.61	MN994082
S4	*Bacillus cereus* strain ATCC 14579	NR_074540.1	95.27	MN994076
S5	*Bacillus megaterium* strain ATCC 14581	NR_117473.1	98.54	MN994080
S6	*Aeromonas veronii* strain JCM 7375	NR_112838.1	93.09	MN994084
S7	*Paenibacillus chibensis* strain JCM 9905	NR_040885.1	97.24	MN994270
S8	*Citrobacter koseri* strain CDC-8132-86	NR_104890.1	97.43	MN994271
S9	*Acinetobacter calcoaceticus* strain NCCB 22016	NR_042387.1	97.76	MN994272
S10	*Vibrio fluvialis* strain NBRC 103150	NR_114218.1	95.51	MN994273

Remark: * The identity results were analyzed on January 28, 2020

The predominant bacterial genera of the isolated cellulolytic bacteria in this study were *Bacillus* of the Firmicutes by 63%, *Chromobacterium* of the Proteobacteria by 14%, and *Herbaspirillum* of the Proteobacteria by 5%. The previous study reported that the bacterial diversity in wetland soils showed predominant bacterial phyla belonging to Proteobacteria, Bacteroidetes, Acidobacteria, Firmicutes and Actinobacteria (Lv et al., 2014). *Bacillus* is a genus of ubiquitous bacteria frequently isolated from various environments including air, dust, soil, and water. The cellulolytic *Bacillus* in this study was isolated from both the water and moist peat samples. It was closely related to *B. cereus*, *B. megaterium* and *B. wiedmannii*. Previous reports showed that many *Bacillus* species were effective cellulolytic bacteria; such as, *B. cereus*, *B. circulans*, *B. licheniformis*, *B. megaterium*, *B. methylotrophicus* and *B. subtilis* (Chantarasiri, 2014, 2015; Azadian et al., 2016; Shahid et al., 2016). Importantly, this study has now confirmed that the *B. wiedmannii* was cellulolytic bacteria. *B. wiedmannii* was firstly isolated from a raw milk sample, named, and described in 2016 (Miller et al., 2016). It

http://www.aloki.hu ● ISSN 1589 1623 (Print) ● ISSN 1785 0037 (Online)
DOI: http://dx.doi.org/10.15666/aeer/1804_59655983

was recently defined as a rice root-associated bacterium and found its cellulase gene by molecular detection in 2020 (Khaskheli et al., 2020). *Chromobacterium* is a genus of saprophytic bacteria, which are generally isolated from soil and freshwater (Soby et al., 2013). The cellulolytic *Chromobacterium* was found in both samples similar to the *Bacillus* species. It was closely related to *C. amazonense*, *C. piscinae*, *C. vaccinia* and *C. violaceum*. *Chromobacterium* species have been previously reported as cellulolytic bacteria (Vazquez-Arista et al., 1997; Sudiana et al., 2001). *Herbaspirillum* is a genus of nitrogen-fixing bacteria associated with the roots of many grasses including rice, maize and sorghum (Kirchhof et al., 2001). *H. frisingense* was the only species of *Herbaspirillum* isolated from the moist peat samples. It has been defined as a cellulolytic species described in a previous study (Fujii et al., 2012). The other isolated genera belonging to *Acinetobacter*, *Aeromonas*, *Citrobacter*, *Enterobacter*, *Paenibacillus* and *Vibrio* had been previously reported as cellulolytic bacteria (Gao et al., 2012; Poomai et al., 2014; Pawar et al., 2015; Islam and Roy, 2018; Waghmare et al., 2018).

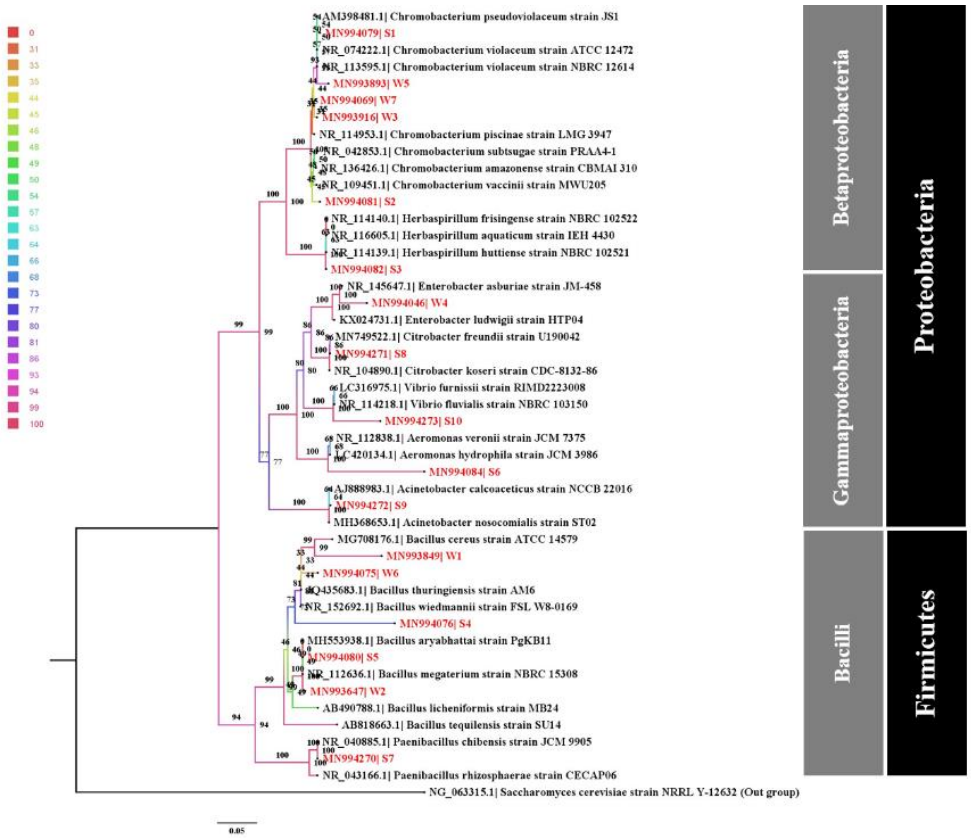

Figure 4. *Phylogenetic tree of the 16S rDNA sequences of the cellulolytic bacteria. The neighbor-joining (NJ) method with 100,000 bootstrap replications was used in the infer tree topology. The phylogenetic tree was generated and visualized by the SeaView program version 4.6.4 and FigTree program version 1.4.3. The colour-coding represents bootstrap values*

Cellulolytic activity assays of the crude cellulases

The representative bacterium from each RFLP pattern was examined for the cellulolytic activity assays consisting of endoglucanase (CMCase), exoglucanase (Avicelase) and β-glucosidase activities. The assays showed that they could yield crude

http://www.aloki.hu ● ISSN 1589 1623 (Print) ● ISSN 1785 0037 (Online)
DOI: http://dx.doi.org/10.15666/aeer/1804_59655983

cellulases from 0.57 to 4.48 U/mL of the CMCase activity, 0.06 to 0.44 U/mL of the Avicelase activity and 0.01 to 0.19 U/mL of the β-glucosidase activity (*Table 5*). All representative bacteria satisfactorily produced CMCases; however, they barely produced any Avicelases and β-glucosidases. It could be stated that endoglucanases were the mainly produced enzyme in their cellulolytic system.

Table 5. *Cellulolytic performances of the representative bacteria*

RFLP Pattern	Bacterial Representative	CMCase Activity (U/mL) with a pH 7.0	Avicelase Activity (U/mL) with a pH 7.0	β-Glucosidase Activity (U/mL) with a pH 7.0
W1	*Bacillus* sp. strain W0105	3.68 ± 0.54^{ef}	0.13 ± 0.03^{bc}	0.06 ± 0.01^{bc}
W2	*Bacillus* sp. strain W0301	3.84 ± 0.27^{fg}	0.44 ± 0.04^{d}	0.06 ± 0.01^{bc}
W3	*Chromobacterium* sp. strain W0303	0.57 ± 0.02^{a}	0.07 ± 0.01^{ab}	0.02 ± 0.00^{a}
W4	*Enterobacter* sp. strain W0306	3.91 ± 0.08^{fg}	0.08 ± 0.03^{ab}	0.06 ± 0.01^{bc}
W5	*Chromobacterium* sp. strain W1103	3.65 ± 0.17^{ef}	0.10 ± 0.03^{ac}	0.06 ± 0.00^{bc}
W6	*B. wiedmannii* strain W1401	3.87 ± 0.32^{fg}	0.08 ± 0.01^{ab}	0.03 ± 0.01^{ab}
W7	*Chromobacterium* sp. strain W0903	1.19 ± 0.24^{ab}	0.06 ± 0.00^{a}	0.02 ± 0.00^{a}
S1	*C. violaceum* strain S2802	2.15 ± 0.17^{cd}	0.15 ± 0.03^{c}	0.06 ± 0.01^{bc}
S2	*Chromobacterium* sp. strain S0503	1.01 ± 0.10^{a}	0.07 ± 0.01^{ab}	0.02 ± 0.00^{a}
S3	*H. frisingense* strain S0701	0.90 ± 0.07^{a}	0.08 ± 0.01^{ab}	0.02 ± 0.00^{a}
S4	*Bacillus* sp. strain S0804	3.17 ± 0.07^{e}	0.12 ± 0.00^{ac}	0.06 ± 0.01^{bc}
S5	*B. megaterium* strain S0702	4.48 ± 0.08^{g}	0.07 ± 0.00^{ab}	0.08 ± 0.02^{c}
S6	*Aeromonas* sp. strain S1401	2.21 ± 0.18^{cd}	0.08 ± 0.03^{ab}	0.06 ± 0.01^{bc}
S7	*Paenibacillus* sp. strain S1402	1.73 ± 0.11^{bc}	0.08 ± 0.03^{ab}	0.07 ± 0.01^{c}
S8	*Citrobacter* sp. strain S1602	2.40 ± 0.29^{d}	0.10 ± 0.03^{ac}	0.08 ± 0.02^{c}
S9	*Acinetobacter* sp. strain S2606	1.08 ± 0.17^{a}	0.07 ± 0.01^{ab}	0.01 ± 0.00^{a}
S10	*Vibrio* sp. strain S3007	3.94 ± 0.07^{fg}	0.07 ± 0.00^{a}	0.19 ± 0.02^{d}

Remark: The mean values in the same row followed by the same letter were not significantly different according to Tukey's test ($p < 0.05$) among the representative bacteria

B. megaterium strain S0702 was the significant endoglucanasic bacteria at 4.48 ± 0.08 U/mL ($p < 0.01$). It was considered as a bacterial model for the following experiments of this study because it was generally considered to be a non-pathogenic and well-known bacterium. Chantarasiri (2015) reported that *B. cereus* strain JD0404 isolated from mangrove swamp soils was an active endoglucanasic bacterium and primary degraded CMC with its endoglucanase activity. Interestingly, *B. megaterium* strain S0702

http://www.aloki.hu ● ISSN 1589 1623 (Print) ● ISSN 1785 0037 (Online)
DOI: http://dx.doi.org/10.15666/aeer/1804_59655983

was not the most active cellulolytic bacterium based on the HC value determination on the CMC agar. It exhibited only 2.27 ± 0.17, which was less than that of *Bacillus* sp. strains W0105 and S0804. This conflicting result may be due to the fluctuations in some experimental parameters which affected the cellulase producing processes described in several previous reports (Ahmad et al., 2013; Chantarasiri et al., 2015). The cellulolytic activity of *B. megaterium* strain S0702 was compared to other bacteria in the *Bacillus* genus isolated from the wetland ecosystems (*Table 6*). *Bacillus* sp. strain W0301 significantly produced the high activity of Avicelase by 0.44 ± 0.04 U/mL ($p < 0.01$); however, it could not indicate being an effective cellulolytic bacterium due to its medium CMCase and low β-glucosidase performances. This enzymatic performance was in agreement with the lack of the complete cellulolytic system of the *Bacillus* genus (Kim et al., 2012). Moreover, *Bacillus* sp. strain W0301 was closely related to *B. cereus* that was generally considered as a pathogenic bacterium. *Vibrio* sp. strain S3007 showed quite a high activity of CMCase and significant β-glucosidase activity of 0.19 ± 0.02 U/mL ($p < 0.01$). The *Vibrio* species could produce β-glucosidase for utilizing the glucans and related compounds (Wang et al., 2015). However, it was not appropriate for further experiments and industrial applications, as it was believed to be a human-pathogenic bacterium.

Table 6. *Cellulolytic performance of B. megaterium strain S0702 and the related bacteria in the Bacillus genus isolated from the wetlands and related environments*

Bacteria	Source of Isolation	CMCase Activity (U/mL)	Avicelase Activity (U/mL)	β-Glucosidase Activity (U/mL)	References
Bacillus sp. strain BR0302	Coastal wetland	0.12	ND	ND	Chantarasiri et al. (2015)
B. cereus strain JD0404	Mangrove swamp	1.78	0.08	0.05	Chantarasiri (2015)
B. licheniformis strain CDB-12	Mangrove in a river delta	98.25*	ND	ND	Behera et al. (2016)
B. subtilis strain A-53	Seawater	92*	ND	ND	Kim et al. (2009)
B. megaterium strain S0702	Freshwater wetland	4.48	0.07	0.08	This current study.

Remark: * = purified cellulases. ND = not determined

Characterization of the cellulolytic activity from B. megaterium strain S0702

Crude cellulases from *B. megaterium* strain S0702 were characterized for the CMCase performance in different experimental conditions; such as, temperature, pH and chemical additives. The optimum temperature and pH for the CMCase activity of the crude cellulases were 45 - 50°C ($p < 0.01$) with a pH 7.0 ($p < 0.01$) (*Figures 5a and 6a*). The enzyme remained stable at up to 60°C ($p < 0.01$) and a pH range of 5.0 - 8.0 ($p < 0.01$) for 24 hours (*Figures 5b and 6b*). The different buffers with the same pH were not significantly affected by the CMCase activity (*Figure 6b*). The cellulases produced from other *B. megaterium* were studied and evaluated for their CMCase activity. It was found that *B. megaterium* strain BM05 had the optimum pH and temperature of 6.5 and 50°C with a stability range of 6.0 - 8.0 and 30 - 40°C (Shahid et al., 2016). The CMCase from *B. megaterium* strain CB-sw1-I was optimally active with a pH 6.0 and temperature of

http://www.aloki.hu ● ISSN 1589 1623 (Print) ● ISSN 1785 0037 (Online)
DOI: http://dx.doi.org/10.15666/aeer/1804_59655983

60°C (Shobharani et al., 2013). The CMCases from many *Bacillus* species were active at a temperature range of 50 - 60°C and a pH range of 4.8 - 11.0 (Sadhu and Maiti, 2013; Chantarasiri, 2015). This *B. megaterium* CMCase was preferred for various industrial applications; such as, bioethanol industries and agricultural industries because the enzyme could be active and hydrolyze the cellulose-based materials under mild conditions with a neutral pH and meso-temperature.

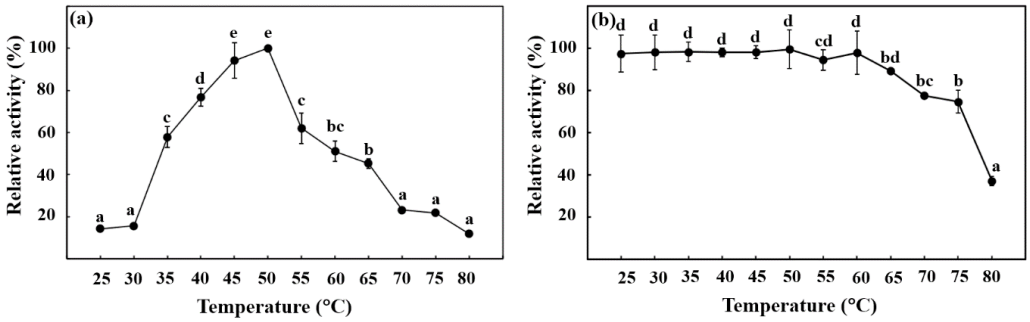

Figure 5. *Effect of temperature on the CMCase activity (a) and stability (b) from B. megaterium strain S0702. Error bars represent the standard deviation of the three replicates. The mean values followed by the same letter were not significantly different according to Tukey's test ($p < 0.05$) among the CMCase activity*

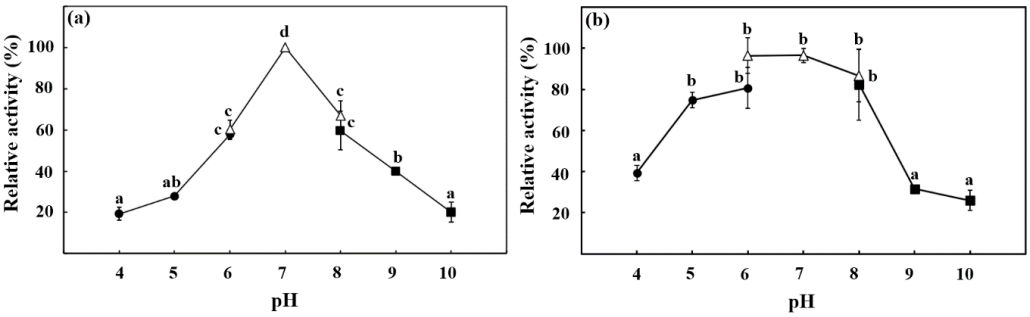

Figure 6. *Effect of pH on the CMCase activity (a) and stability (b) from B. megaterium strain S0702. The CMCase activity was measured in a citrate buffer (●), sodium phosphate buffer (△) and glycine-NaOH buffer (■). Error bars represent the standard deviation of the three replicates. The mean values followed by the same letter were not significantly different according to Tukey's test ($p < 0.05$) among the CMCase activity*

The effect of various chemical additives is shown in *Table 7*. The results of the metal ions revealed that the CMCase activity of *B. megaterium* strain S0702 was significantly enhanced by Mn^{2+}, Ca^{2+}, Co^{2+} and Sr^{2+} ($p < 0.01$). Similarly, many previous reports showed that these metal ions could activate the CMCase activity of *Bacillus* cellulases (Shobharani et al., 2013; Chantarasiri, 2015; Shahid et al., 2016). It was believed that they could possibly respond to certain amino acid residues in the active site and promote the favorable conformation of the enzyme to the substrate binding and enzyme activity (Azzeddine et al., 2013; Shahid et al., 2016). Mn^{2+} could be promised as the great activator of the CMCase in further biotechnological applications due to being less toxic than those of other metal ions. Many Mn^{2+} compounds were known; such as, manganese

http://www.aloki.hu ● ISSN 1589 1623 (Print) ● ISSN 1785 0037 (Online)
DOI: http://dx.doi.org/10.15666/aeer/1804_59655983

sulfate ($MnSO_4$) and manganese chloride ($MnCl_2$). Most metal ions and organic solvents could inhibit the CMCase activity of *B. megaterium* strain S0702. The activity was significantly inhibited by EDTA and ethyl-acetate. The reduction of the cellulolytic performance by a chelating agent EDTA revealed that the CMCase from *B. megaterium* strain S0702 could be identified as a metalloenzyme (Annamalai et al., 2013). The results indicated that this CMCase was not remarkably appropriate for any organic solvent related applications.

Table 7. *Effect of the various chemical additives on the CMCase activity from B. megaterium strain S0702*

Chemical Additives	Relative Activity (%)
Ca^{2+}	241.25 ± 7.43^{j}
Co^{2+}	221.01 ± 0.78^{i}
Cu^{2+}	77.51 ± 7.79^{ef}
Fe^{2+}	68.06 ± 5.45^{e}
Hg^{2+}	64.91 ± 6.18^{de}
K^{+}	50.52 ± 7.79^{cd}
Mn^{2+}	625.87 ± 0.78^{k}
Ni^{2+}	74.81 ± 2.06^{ef}
Pb^{2+}	63.56 ± 1.35^{de}
Sr^{2+}	199.42 ± 7.43^{h}
EDTA	23.98 ± 4.34^{ab}
Acetone	38.82 ± 4.43^{bc}
Dichloromethane	68.51 ± 7.79^{e}
Ethanol	95.05 ± 2.06^{g}
Ethyl-acetate	22.63 ± 3.12^{a}
Methanol	63.56 ± 4.05^{de}
n-Hexane	88.30 ± 0.78^{fg}

Remark: The mean values followed by the same letter were not significantly different according to Tukey's test ($p < 0.05$) among the CMCase activity

Conclusion

The freshwater wetland ecosystem is a potential source for the isolation of cellulolytic bacteria. There were nine genera of cellulolytic bacteria isolated from Bueng Samnak Yai, a freshwater wetland in Thailand based on the RFLP-PCR of a 16S rDNA and nucleotide sequencing analysis comprising *Acinetobacter*, *Aeromonas*, *Bacillus*, *Chromobacterium*, *Citrobacter*, *Enterobacter*, *Herbaspirillum*, *Paenibacillus* and *Vibrio*. The cellulolytic performance of the representative bacteria from each RFLP pattern was determined. It revealed that *B. megaterium* strain S0702 was the most active CMCase bacterium. Its CMCase was characterized and found that it could possibly be used in various biotechnological applications. This CMCase was not remarkably appropriate for some metal ions and organic solvent related applications. Finally, further study on enzyme purification, enzyme kinetic and applications of CMCase are suggested.

Acknowledgements. This research was funded by King Mongkut's University of Technology North Bangkok. Contract no. KMUTNB-61-GOV-A-72 (KMUTNB-61-GOV-03-72).

http://www.aloki.hu ● ISSN 1589 1623 (Print) ● ISSN 1785 0037 (Online)
DOI: http://dx.doi.org/10.15666/aeer/1804_59655983

REFERENCES

[1] Ahmad, B., Nigar, S., Shah, S. S. A., Bashir, S., Ali, J., Yousaf, S., Bangash, J. A. (2013): Isolation and identification of cellulose degrading bacteria from municipal waste and their screening for potential antimicrobial activity. – World Applied Sciences Journal 27: 1420-1426.

[2] An, J., Liu, C., Wang, Q., Yao, M., Rui, J., Zhang, S., Li, X. (2019): Soil bacterial community structure in Chinese wetlands. – Geoderma 337: 290-299.

[3] Anand, A. A. P., Vennison, S. J., Sankar, S. G., Prabhu, D. I. G., Vasan, P. T., Raghuraman, T., Geoffrey, C. J., Vendan, S. E. (2010): Isolation and characterization of bacteria from the gut of *Bombyx mori* that degrade cellulose, xylan, pectin and starch and their impact on digestion. – Journal of Insect Science 10: 1-20.

[4] Annamalai, N., Rajeswari, M. V., Elayaraja, S., Balasubramanian, T. (2013): Thermostable, haloalkaline cellulase from *Bacillus halodurans* CAS 1 by conversion of lignocellulosic wastes. – Carbohydrate Polymers 94: 409-415.

[5] Azadian, F., Badoei-Dalfard, A., Namaki-Shoushtari, A., Hassanshahian, M. (2016): Purification and biochemical properties of a thermostable, haloalkaline cellulase from *Bacillus licheniformis* AMF-07 and its application for hydrolysis of different cellulosic substrates to bioethanol production. – Molecular Biology Research Communications 5(3): 143-155.

[6] Azzeddine, B., Abdelaziz, M., Estelle, C., Mouloud, K., Nawel, B., Nabila, B., Francis, D., Said, B. (2013): Optimization and partial characterization of endoglucanase produced by *Streptomyces* sp. BPNG23. – Archives of Biological Sciences 65(2): 549-558.

[7] Baharuddin, A. S., Razak, M. N. A., Hock, L. S., Ahmad, M. N., Abd-Aziz, S., Rahman, N. A. A., Shah, U. K. M., Hassan, M. A., Sakai, K., Shirai, Y. (2010): Isolation and characterization of thermophilic cellulase-producing bacteria from empty fruit bunches-palm oil mill effluent compost. – American Journal of Applied Sciences 7(1): 56-62.

[8] Bassi, N., Kumar, M. D., Sharma, A., Pardha-Saradhi, P. (2014): Status of wetlands in India: A review of extent, ecosystem benefits, threats and management strategies. – Journal of Hydrology: Regional Studies 2: 1-19.

[9] Behera, B. C., Mishra, R. R., Singh, S. K., Dutta, S. K., Thatoi, H. (2016): Cellulase from *Bacillus licheniformis* and *Brucella* sp. isolated from mangrove soils of Mahanadi river delta, Odisha, India. – Biocatalysis and Biotransformation 34(1): 44-53.

[10] Behera, B. C., Sethi, B. K., Mishra, R. R., Dutta, S. K., Thatoi, H. N. (2017): Microbial cellulases-Diversity & biotechnology with reference to mangrove environment: A review. – Journal of Genetic Engineering and Biotechnology 15: 197-210.

[11] Benhadj, M., Gacemi-Kirane, D., Menasria, T., Guebla, K., Ahmane, Z. (2019): Screening of rare actinomycetes isolated from natural wetland ecosystem (Fetzara Lake, northeastern Algeria) for hydrolytic enzymes and antimicrobial activities. – Journal of King Saud University-Science 31: 706-712.

[12] Chantarasiri, A. (2014): Novel halotolerant cellulolytic *Bacillus methylotrophicus* RYC01101 isolated from ruminant feces in Thailand and its application for bioethanol production. – KMUTNB: International Journal of Applied Science and Technology 7(3): 63-68.

[13] Chantarasiri, A. (2015): Aquatic *Bacillus cereus* JD0404 isolated from the muddy sediments of mangrove swamps in Thailand and characterization of its cellulolytic activity. – Egyptian Journal of Aquatic Research 41: 257-264.

[14] Chantarasiri, A., Boontanom, P., Yensaysuk, N., Ajwichai, P. (2015): Isolation and identification of a cellulase-producing *Bacillus* sp. strain BR0302 from Thai coastal wetland soil. – KMUTNB: International Journal of Applied Science and Technology 8(3): 197-203.

http://www.aloki.hu ● ISSN 1589 1623 (Print) ● ISSN 1785 0037 (Online)
DOI: http://dx.doi.org/10.15666/aeer/1804_59655983

[15] Chantarasiri, A., Boontanom, P., Nuiplot, N. (2017): Isolation and characterization of *Lysinibacillus sphaericus* BR2308 from coastal wetland in Thailand for the biodegradation of lignin. – AACL Bioflux 10(2): 200-209.
[16] Dashti, A. A., Jadaon, M. M., Abdulsamad, A. M., Dashti, H. M. (2009): Heat treatment of bacteria: A simple method of DNA extraction for molecular techniques. – Kuwait Medical Journal 41(2): 117-122.
[17] Fujii, K., Ikeda, K., Yoshida, S. (2012): Isolation and characterization of aerobic microorganosms with cellulolytic activity in the gut of endogeic earthworms. – International Microbiology 15: 121-130.
[18] Gao, J. H., Weng-Zhu, D., Yuan, M., Guan, F., Xi, Y. (2008): Production and characterization of cellulolytic enzymes from the thermoacidophilic fungal *Aspergillus terreus* M11 under solid-state cultivation of corn stover. – Bioresource Technology 99: 7623-7629.
[19] Gao, Z. M., Xiao, J., Wang, X. N., Ruan, L. W., Chen, X. L., Zhang, Y. Z. (2012): *Vibrio xiamenensis* sp. nov., a cellulase-producing bacterium isolated from mangrove soil. – International Journal of Systematic and Evolutionary Microbiology 62: 1958-1962.
[20] Gorham, E. (1991): Northern peatlands: role in the carbon cycle and probable responses to climatic warming. – Ecological Applications 1(2): 182-195.
[21] Gouy, M., Guindon, S., Gascuel, O. (2010): SeaView version 4: A multiplatform graphical user interface for sequence alignment and phylogenetic tree building. – Molecular Biology and Evolution 27(2): 221-224.
[22] Ibrahim, A. S. S., El-diwany, A. I. (2007): Isolation and identification of new cellulases producing thermophilic bacteria from an Egyptian hot spring and some properties of the crude enzyme. – Australian Journal of Basic and Applied Sciences 1(4): 473-478.
[23] Islam, F., Roy, N. (2018): Screening, purification and characterization of cellulase from cellulase producing bacteria in molasses. – BMC Research Notes 11(445): 1-6. doi: https://doi.org/10.1186/s13104-018-3558-4.
[24] Juturu, V., Wu, J. C. (2014): Microbial cellulases: Engineering, production and applications. – Renewable and Sustainable Energy Reviews 33: 188-203.
[25] Kalita, S., Sarma, H. P., Devi, A. (2019): Sediment characterisation and spatial distribution of heavy metals in the sediment of a tropical freshwater wetland of Indo-Burmese province. – Environmental Pollution 250: 969-980.
[26] Khaskheli, M. A., Wu, L., Chen, G., Chen, L., Hussain, S., Song, D., Liu, S., Feng, G. (2020): Isolation and characterization of root-associated bacterial endophytes and their biocontrol potential against major fungal phytopathogens of rice (*Oryza sativa* L.). – Pathogens 9(3): 1-28. doi:10.3390/pathogens9030172.
[27] Kim, B. K., Lee, B. H., Lee, Y. J., Jin, I. H., Chung, C. H., Lee, J. W. (2009): Purification and characterization of carboxymethylcellulase isolated from a marine bacterium, *Bacillus subtilis* subsp. *subtilis* A-53. – Enzyme and Microbial Technology 44: 411-416.
[28] Kim, Y. K., Lee, S. C., Cho, Y. Y., Oh, H. J., Ko, Y. H. (2012): Isolation of cellulolytic *Bacillus subtilis* strains from agricultural environments. – International Scholarly Research Notices, doi: https://doi.org/10.5402/2012/650563.
[29] Kirchhof, G., Eckert, B., Stoffels, M., Baldani, J. I., Reis, V. M., Hartmann, A. (2001): *Herbaspirillum frisingense* sp. nov., a new nitrogen-fixing bacterial species that occurs in C4-fibre plants. – International Journal of Systematic and Evolutionary Microbiology 51: 157-168.
[30] Leff, L. G. (2009): Freshwater Habitats. – In: Schaechter, M. (ed.) Encyclopedia of Microbiology. Elsevier Inc., Amsterdam.
[31] Lv, X., Yu, J., Fu, Y., Ma, B., Qu, F., Ning, K., Wu, H. (2014): Meta-analysis of the bacterial and archaeal diversity observed in wetland soils. – The Scientific World Journal, doi: http://dx.doi.org/10.1155/2014/437684.
[32] Miller, G. (1959): Use of dinitrosalicylic acid reagent for determination of reducing sugar. – Analytical Chemistry 31: 426-428.

http://www.aloki.hu ● ISSN 1589 1623 (Print) ● ISSN 1785 0037 (Online)
DOI: http://dx.doi.org/10.15666/aeer/1804_59655983

[33] Miller, R. A., Beno, S. M., Kent, D. J., Carroll, L. M., Martin, N. H., Boor, K. J., Kovac, J. (2016): *Bacillus wiedmannii* sp. nov., a psychrotolerant and cytotoxic *Bacillus cereus* group species isolated from dairy foods and dairy environments. – International Journal of Systematic and Evolutionary Microbiology 66: 4744-4753.
[34] Nwodo-Chinedu, S., Okochi, V. I., Smith, H. A., Omidij, O. (2005): Isolation of cellulolytic microfungi involved in wood-waste decomposition: prospects for enzymatic hydrolysis of cellulosic wastes. – International Journal of Biomedical and Health Sciences 1: 41-52.
[35] Pawar, K. D., Dar, M. A., Rajput, B. P., Kulkarni, G. J. (2015): Enrichment and identification of cellulolytic bacteria from the gastrointestinal tract of Giant African snail, *Achatina fulica*. – Applied Biochemistry and Biotechnology 175(4): 1971-1980.
[36] Poomai, N., Siripornadulsil, W., Siripornadulsil, S. (2014): Cellulase enzyme production from agricultural waste by *Acinetobacter* sp. KKU44. – Advanced Materials Research 931-932: 1106-1110.
[37] Qin, Y., He, H., Li, N., Ling, M., Liang, Z. (2010): Isolation and characterization of a thermostable cellulase-producing *Fusarium chlamydosporum*. – World Journal of Microbiology and Biotechnology 26: 1991-1997.
[38] R Core Team (2017): R: A language and environment for statistical computing. – R Foundation for Statistical Computing, Vienna, Austria. URL https://www.R-project.org/.
[39] Reddy, H. K., Srijana, M., Reddy, M. D., Reddy, G. (2010): Coculture fermentation of banana agro-waste to ethanol by cellulolytic thermophilic *Clostridium thermocellum* CT2. – African Journal of Biotechnology 9: 1926-1934.
[40] Sadhu, S., Maiti, T. K. (2013): Cellulase production by bacteria: a review. – British Microbiology Research Journal 3(3): 235-258.
[41] Samira, M., Mohammad, R., Gholamreza, G. (2011): Carboxymethyl-cellulase and filter-paperase activity of new strains isolated from Persian Gulf. – Microbiology Journal 1(1): 8-16.
[42] Sangkharak, K., Vangsirikul, P., Janthachat, S. (2011): Isolation of novel cellulase from agricultural soil and application for ethanol production. – International Journal of Advanced Biotechnology and Research 2: 230-239.
[43] Seo, J. K., Park, T. S., Kwon, I. H., Piao, M. Y., Lee, C. H., Ha, J. K. (2013): Characterization of cellulolytic and xylanolytic enzymes of *Bacillus licheniformis* JK7 isolated from the rumen of a native Korean goat. – Asian-Australasian Journal of Animal Sciences 26(1): 50-58.
[44] Shahid, Z. H., Irfan, M., Nadeem, M., Syed, Q., Qazi, J. I. (2016): Production, purification, and characterization of carboxymethyl cellulase from novel strain *Bacillus megaterium*. – Environmental Progress & Sustainable Energy 35(6): 1741-1749.
[45] Sharma, S., Yazdani, S. S. (2016): Diversity of Microbial Cellulase System. – In: Gupta, V. (ed.) New and Future Developments in Microbial Biotechnology and Bioengineering. Elsevier Inc., Amsterdam.
[46] Shobharani, P., Yogesh, D., Halami, P. M., Sachindra, N. M. (2013): Potential of cellulase from *Bacillus megaterium* for hydrolysis of *Sargassum*. – Journal of Aquatic Food Product Technology 22: 520-535.
[47] Soares-Júnior, F. L., Dias, A. C. F., Fasanella, C. C., Taketani, R. G., Lima, A. O. S., Melo, I. S., Andreote, F. D. (2013): Endo- and exoglucanase activities in bacteria from mangrove sediment. – Brazilian Journal of Microbiology 44(3): 969-976.
[48] Soby, S. D., Gadagkar, S. R., Contreras, C., Caruso, F. L. (2013): *Chromobacterium vaccinii* sp. nov., isolated from native and cultivated cranberry (*Vaccinium macrocarpon* Ait.) bogs and irrigation ponds. – International Journal of Systematic and Evolutionary Microbiology 63: 1840-1846.
[49] Sriariyanun, M., Tantayotai, P., Yasurin, P., Pornwongthong, P., Cheenkachorn, K. (2016): Production, purification and characterization of an ionic liquid tolerant cellulase from

http://www.aloki.hu ● ISSN 1589 1623 (Print) ● ISSN 1785 0037 (Online)
DOI: http://dx.doi.org/10.15666/aeer/1804_59655983

Bacillus sp. isolated from rice paddy field soil. – Electronic Journal of Biotechnology 19: 23-28.

[50] Sudiana, I. M., Rahayu, R. D., Imanuddin, H., Rahmansyah, M. (2001): Cellulolytic bacteria of soil of Gunung Halimun National Park. – Berita Biologi 5(6): 703-709.

[51] Vazquez-Arista, M., Smith, R. H., Olalde-Portugal, V., Hinojosa, R. E., Hernandez-Delgadillo, R., Blanco-Labra, A. (1997): Cellulolytic bacteria in the digestive system of *Prostephanus truncatus* (Coleoptera: Bostrichidae). – Journal of Economic Entomology 90(5): 1371-1376.

[52] Waghmare, P. R., Patil, S. M., Jadhav, S. L., Jeon, B. H., Govindwar, S. P. (2018): Utilization of agricultural waste biomass by cellulolytic isolate *Enterobacter* sp. SUK-Bio. – Agriculture and Natural Resources 52: 399-406.

[53] Wang, Z., Robertson, K. L., Liu, C., Liu, J. L., Johnson, B. J., Leary, D. H., Compton, J. R., Vuddhakul, V., Legler, P. M., Vora, G. J. (2015): A novel *Vibrio* beta-glucosidase (LamN) that hydrolyzes the algal storage polysaccharide laminarin. – FEMS Microbiology Ecology 91: 1-10. doi: 10.1093/femsec/fiv087.

[54] Wee, Y. J., Kim, S. Y., Yoon, S. D., Ryu, H. W. (2011): Isolation and characterization of a bacterial cellulose producing bacterium derived from the persimmon vinegar. – African Journal of Biotechnology 10(72): 16267-16276.

[55] Wu, L. S., Feng, S., Nie, Y. Y., Zhou, J. H., Yang, Z. R., Zhang, J. (2015): Soil cellulase activity and fungal community responses to wetland degradation in the Zoige Plateau, China. – Journal of Mountain Science 12(2): 471-482.

[56] Zhang, Y. H. P., Himmel, M. E., Mielenz, J. R. (2006): Outlook for cellulase improvement: Screening and selection strategies. – Biotechnology Advances 24: 452-481.

http://www.aloki.hu ● ISSN 1589 1623 (Print) ● ISSN 1785 0037 (Online)
DOI: http://dx.doi.org/10.15666/aeer/1804_59655983

COMPREHENSIVE EVALUATION OF SOIL QUALITY AT DIFFERENT STAND DENSITIES OF *DENDROCALAMUS MINOR* VAR. *AMOENUS* PLANTATIONS

ZHENG, J. M.[1] – CHEN, X. Y.[2] – CHEN, L. G.[2] – HE, T. Y.[1] – RONG, J. D.[2] – LIN, Y.[3] – ZHENG, Y. S.[1,2*]

[1]*College of Arts & Landscape Architecture, Fujian Agriculture and Forestry University, Fuzhou 350002, PR China*

[2]*College of Forestry, Fujian Agriculture and Forestry University, Fuzhou 350002, PR China*

[3]*Changle Dahe State-owned Protection Forest Farm of Fujian Province, Changle, Fujian 350212, PR China*

[*]*Corresponding author*
e-mail: zys1960@163.com

(Received 19th Apr 2020; accepted 10th Jul 2020)

Abstract. Soil is considered as the fundamental media to provide nutrients to plants for their growth and development. Nevertheless, soil quality is closely related to soil microbes, enzyme activity, soil physicochemical properties, and above-ground biomass. In this study, soil quality evaluation was performed on 17 indicators, including soil physicochemical properties and enzyme activity. For this, the stand density with the highest soil quality score was selected for improving forest productivity and forest management. Stand density and soil layer factors have little effect on physical properties, mainly affecting chemical properties and enzyme activity. Different species have different adaptability to soil nutrients. The stand density of *Dendrocalamus minor* var. *amoenus* was positively correlated with total nitrogen, urease, available potassium, and available phosphorus. Nine indicators were screened by principal component analysis to explain soil quality (cumulative proportion of 92.50%). Among them, Stand H1 had the highest soil quality score, and the lower stand density is helpful in alleviating competition pressure on light resources, soil nutrition and so on. It is suggested that the future forest management of *Dendrocalamus minor* var. *amoenus* should be controlled in the range of 4300 ramet/hm^{-2}, which is more conducive to soil quality.
Keywords: *coastal sandy, ramet density, soil physicochemical, soil enzymes, clonal species, bamboo*

Introduction

Soil provides nutrients for plant growth and development. Plant litter and rhizosphere effects promote soil nutrient cycling and develop a plant-soil dynamic response relationship (Yang et al., 2016). Various biotic and abiotic factors influence soil quality, such as, soil and vegetation types (Zhang et al., 2018), which affects stand density or ramet densities. Among them, the most significant factors of soil nutrient fluctuation are site quality and stand density (Zhang et al., 2018), which can be influenced by severe and harsh climatic conditions (Japet et al., 2009). Changes in environment and resources play a significant role in regulating stand density and promoting individual climax of plant species (Maherali et al., 2001). Excessive stand density affects plant root growth, interception of light resources, and soil microbial activity in the forest; appropriate stand densities can reduce forest productivity loss caused by intra-species competition and improve the effective use of soil resources (Chen and Li, 2015; Fan et al., 2015).

http://www.aloki.hu ● ISSN 1589 1623 (Print) ● ISSN1785 0037 (Online)
DOI: http://dx.doi.org/10.15666/aeer/1804_59855996

Stand density and plant growth are restricted by site conditions (Wang et al., 2004). Studies on soil quality differences under different stand densities have been reported, such as *Larix gmelinii* forest, *Phyllostachys edulis* forest, *Pinus tabulaeformis* forest and *Acacia auriculiformis* forest stands (Zhao, 2012; Fan et al., 2015). These study sites were mainly concentrated in the mountains and hills, but a few could be found on the sandy coastal land. Recently, to overcome the rapid land degradation and low productivity of sandy coastal areas, bamboo species have been introduced for afforestation in Fujian province, China. Bamboo species have shown strong adaptability to cope with such environmental conditions with fast growth and strong reproductive capabilities. Meanwhile, bamboo species have long fiber to resist strong winds near the coastal line. The soil quality of vegetation cover is higher than that of bare land (Tu, 2014). The soil enzyme activities and nutrients under bamboo species on the sandy coastal land have greatly improved the soil quality (Tu, 2014). In order to utilize environmental resources, the relationship between different bamboo stand densities and soil quality needs to be further explored. In order to improve the soil quality of sandy land, it plays an important role in the process of artificial forest construction, forest productivity improvement and soil nutrient cycling effect.

Dendrocalamus minor var. *amoenus* is a woody bamboo species, which is native to south of Guangxi Province, China. It usually was distributed in low altitude hills. This species is clonal species with strong growth ability and drought resistance. It has been reported that soil nutrient variability in bamboo forests is strongly correlated with the response of the underground whip root system (Zhang et al., 2018). Most bamboo root distributed in 0-40 cm soil depth. The whip root system of *Pleioblastus amarus* is mainly distributed in the 0-40 cm depth (Zhao, 2009). The soil layer concentrates about 90% of the root system of *Bambusa oldhamii* in the 0-40 cm depth (Li, 2014). Although the root system of *Phyllostachys edulis* can reach more than 70 cm, the maximum of root volume range to 0-40 cm depth (Luo, 2009). For that reason, it is important to know the effects of various *Dendrocalamus minor* var. *amoenus* plantation densities on soil physicochemical properties and enzyme activities at two different vertical depth gradients. We hypothesized that plantation densities and two distinct depths will affect soil quality and enzyme activity. The best stand density plays a sustainable ecological role in regulating bamboo forest production and improving the ecological environment by comprehensive evaluation of soil quality.

Materials and Methods

Study site

The study was conducted at Dahe State-owned Protection Forest Farm, which is located (119° 40'-119° 43 'E, 25° 57'-25° 59 'N) in Changle District, Fuzhou City, Fujian Province, China (*Fig. 1*). The area falls in the subtropical climate with abundant rainfall. The annual rainy day is about 160 d, concentrated in summer. The average annual precipitation is about 1200 mm. The average annual temperature is 19.2 °C. The highest temperature occurs in July with average 35.6 °C; while the lowest temperatures occur in January with average 0 °C. The coastal climate has less frost damage, without snow cover throughout the year. The average annual wind (northeast) speed is about 4.2 $m.s^{-1}$. The annual sunshine hours are 1837.6 h. The coastal terrain is mainly sand dunes with a gentle slope, and the sandy coast is more than 10 kilometers from the coastline. These stands of *Dendrocalamus minor* var. *amoenus* were planted in 2011 at a spacing of 3 m × 3 m. Since then, no cultural or management practices were adopted until 2018. Each stand densities were surveyed in

http://www.aloki.hu ● ISSN 1589 1623 (Print) ● ISSN1785 0037 (Online)
DOI: http://dx.doi.org/10.15666/aeer/1804_59855996

August 2018, and the stand density was determined according to the number of ramets. The population structure characteristics of four kinds of stand densities are shown in *Table 1*. The sampling site had almost similar altitude within 10 m asl with 6-8° slope.

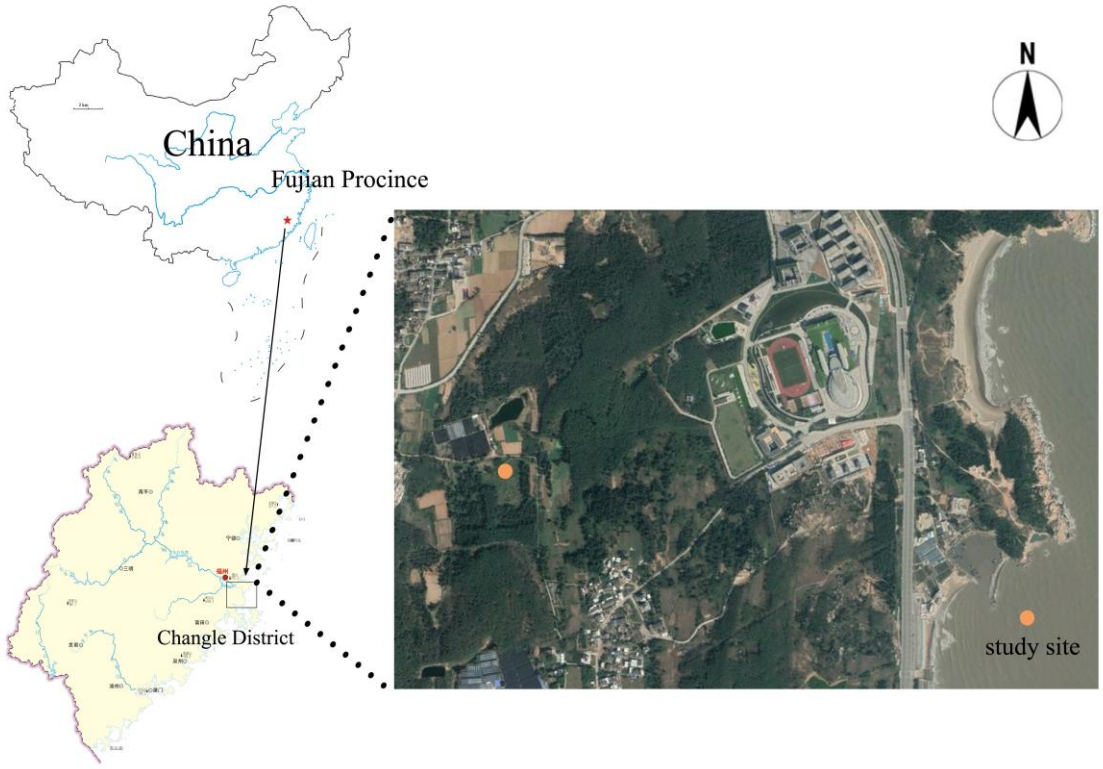

Figure 1. *The location of the sampling site*

Table 1. *Structure characteristics of Dendrocalamus minor* var. *amoenus populations*

Stand	Density (Ramet/hm^{-2})	Mean DBH (cm)	Mean height (cm)	Crown (cm)
H1	4300 ± 253	2.12	2.93	127.00
H2	5200 ± 314	2.33	3.50	105.00
H3	9400 ± 586	2.67	4.04	91.50
H4	13400 ± 599	2.66	3.95	75.80

Values are mean ± standard deviations

Methods

Soil sampling and analysis

Samples of soil were randomly collected from different directions in each stand densities (approximately 667 m^2) in summer of 2018. Each plot (10 m × 10 m) was selected for each stand density. Within each plot, soil samples collected near five randomly selected bamboos (*Fig. 2*) at three randomly selected points. We collected soil in 0-20 cm and 20-40 cm vertical depth. Roots and litters were carefully removed from the soil before sieving. Each soil sample was divided into two portions for determination of soil physicochemical properties and soil enzyme activities.

http://www.aloki.hu ● ISSN 1589 1623 (Print) ● ISSN1785 0037 (Online)
DOI: http://dx.doi.org/10.15666/aeer/1804_59855996

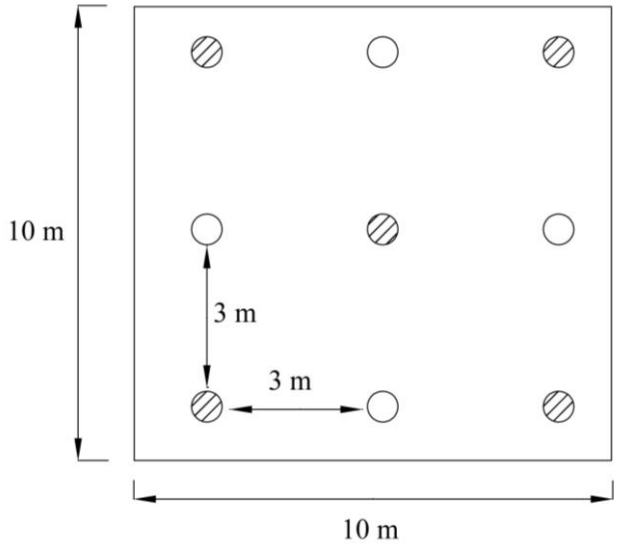

Figure 2. *Sampling at the site, which was 10 m × 10 m, and the space of the bamboo was 3 m × 3 m. The sampled bamboo is represented by the circle with oblique line*

The one portion was air dried for chemical analysis and sieved to 2 mm to get sub-samples. The 0.149-mm fraction was used for the analysis of total nitrogen (TN), total phosphorus (TP) and total potassium (TK). The 2-mm fraction was used for the analysis of pH, available nitrogen (AN), available phosphorus (AP) and available potassium (AK). The other portion (fresh soil) was stored at 4 ℃ immediately after sample collection for soil enzymatic analysis and sieved through a 1 mm sieve to remove small litter fragments.

Soil physical and chemical analysis

Volume weight, non-capillary porosity, capillary porosity, total porosity, soil aeration, soil moisture were measured by weighing fresh soil samples after and before drying at 105 ℃ to a constant weight (LY/T 1213-1999). The pH was measured at a soil: water ratio of 1:2.5 (LY/T 1239-1999). TN was measured by the sulfuric acid-mixed accelerator digestion-diffusion method, TK was measured by the sodium hydroxide melt-flame photometer method, the TP was measured by the molybdenum antimony colorimetry, and AN was measured by a sodium hydroxide (sodium hydroxide (NaOH)) hydrolytic diffusion method, AK was measured by extraction-molybdenum antimony colorimetric method, and AP was measured by ammonium acetate extraction-flame photometry. The detail of these method were under Bao (2005) construction.

Soil enzymatic activities analysis

Four enzymes were selected for analysis: acid phosphatase, sucrase, urease and catalase. The method of measuring four enzymes were previously described (Qiu et al., 2010). The results were based on three replicates. Acid phosphatase activity was measured the method of Qiu et al. (2010). Urease activity was measured by the indigo colorimetry method. The NH_3-N released by urease enzymatic hydrolysis of urea was determined colorimetrically at 578 nm, expressed as NH_3-N mg•g^{-1} •h^{-1}. The

http://www.aloki.hu ● ISSN 1589 1623 (Print) ● ISSN1785 0037 (Online)
DOI: http://dx.doi.org/10.15666/aeer/1804_59855996

p-nitrophenol (PNP) in the filtrate was determined colorimetrically at 410 nm, expressed as PNP mg•g^{-1} •h^{-1}. Sucrase activity was measured by 3,5-dinitrosalicylic acid colorimetry method. Catalase activity was measured by volumetric method.

Comprehensive evaluation of soil quality

Volume weight (X1), noncapillary porosity (X2), napillary porosity (X3), yotal porosity (X4), soil aeration (X5), soil moisture (X6), pH (X7), total nitrogen (X8), total phosphorus (X9), total potassium (X10), available nitrogen (X11), available potassium (X12), available phosphorus (X13), acid phosphatase (X14), urease (X15), sucrase (X16), catalase (X17) were normalized. Except that Volume weight is a negative effect indicators, the other indicators are positive effect indicators to soil quality. Principal component analysis was used to analyze the eigenvalues, proportion, and cumulative proportion of Principal component. The indicators were then rotated to the load matrix to calculate the σ2 of common factor. The weight of each indicator was the proportion of the σ2 of common factor to the total σ2 of common factor. Principal component correlation coefficients below 0.1 are not displayed. The comprehensive score of soil quality (F) as calculated as *equation (1)*:

$$F = \Sigma W_i \times F(X_i) \quad \text{(Eq.1)}$$

where $F(X_i)$: membership, W_i: weight of each indicators.

Data analysis

All data were collected using Microsoft Excel 2013, and SPSS 20.0 software (SPSS Inc., Chicago, USA) was used to analyze One-way ANOVA and Least-Significance Difference (LSD) for 17 soil indicators of different stand densities. Principal component analysis was used for calculation Comprehensive score of soil quality at different stand densities.

Result

Effects of stand densities on Physical properties of soil

The physical properties of soils of *Dendrocalamus minor* var. *amoenus* populations with different densities are shown in *Table 2*. The volume weight of 0-40 cm soil layer ranged from 1.15-1.28 g/m^3, noncapillary porosity ranged from 2.52-4.45%, and total porosity ranged from 56.70-66.45%, soil aeration ranged from 32.06-39.99%, and the soil moisture is between 6.78-12.24%. In the 0-20 cm soil layer, the difference between different densities is not significant. In the soil layer 20-40 cm, there are some differences in the total porosity and soil aeration of different densities. Soil aeration of stand H2 was the lowest.

Effects of stand densities on Chemical properties of soil

The soil pH and nutrient content of *Dendrocalamus minor* var. *amoenus* populations with different densities are shown in *Table 3*. pH ranged from 6.27-6.58 in 0-40 cm depth. Total nitrogen ranged from 0.08-0.26 g·kg^{-1}, total phosphorus at 0.23-0.27 g·kg^{-1}, total potassium ranged from 13.47-14.02 g·kg^{-1}, available nitrogen between

http://www.aloki.hu ● ISSN 1589 1623 (Print) ● ISSN1785 0037 (Online)
DOI: http://dx.doi.org/10.15666/aeer/1804_59855996

20.91-38.35 g·kg^{-1}, and available potassium ranged from 6.06-11.61 g·kg^{-1}. The available phosphorus was between 1.52-2.77 g·kg^{-1}. In the 0-20 cm soil depth, Stand H2 had the highest total phosphorus content. Stand H1 and H2 had the highest total nitrogen content. Stand H4 has the highest available phosphorus content. There were no significant differences in pH, total potassium, and available nitrogen at different densities. In the 20-40 cm soil layer, there were no significant differences in available potassium and available phosphorus with different densities. Stand H4 has the highest pH, stand H1 and H3 have the highest total nitrogen content.

Table 2. *Soil physical properties in Dendrocalamus minor* var. *amoenus populations*

Layer/cm	Stand	Volume weight (g/m^3)	Noncapillary porosity (%)	Capillary porosity (%)	Total porosity (%)	Soil aeration (%)	Soil moisture (%)
0-20	H1	1.28±0.09a	3.53±1.35a	62.49±2.71a	66.02±2.85a	39.99±2.03a	10.16±0.79a
	H2	1.15±0.13a	3.64±0.98a	53.06±14.74a	56.70±14.86a	35.33±8.13a	9.38±3.07a
	H3	1.25±0.14a	5.37±1.96a	55.00±6.58a	60.37±7.78a	39.16±1.75a	6.78±3.65a
	H4	1.20±0.05a	3.18±1.90a	61.51±8.07a	64.69±8.34a	38.44±3.62a	10.99±2.21a
20-40	H1	1.19±0.05a	2.52±0.80a	62.03±2.32a	64.54±3.00ab	35.46±2.10a	12.20±0.84a
	H2	1.23±0.05a	2.90±0.93a	59.15±2.32a	62.05±2.08b	32.06±2.43b	12.24±1.35a
	H3	1.25±0.05a	4.45±1.61a	59.08±3.73a	63.53±3.29ab	35.62±1.82a	12.24±1.75a
	H4	1.26±0.09a	4.14±1.68a	62.32±3.96a	66.45±4.69a	37.63±3.30a	11.50±0.92a

Different letters in the same soil layer mean that there are significant different between densities (P<0.05), the same as below. Values are mean±standard deviations. H1 means that stand densities of plantation is 4300 ± 253 ramet/hm^{-2}, details in *Table 1*

Table 3. *Chemical property of soil in Dendrocalamus minor* var. *amoenus populations*

Layer/cm	Stand	pH	TN (g·kg^{-1})	TP (g·kg^{-1})	TK (g·kg^{-1})	AN (mg·kg^{-1})	AK (mg·kg^{-1})	AP (mg·kg^{-1})
0-20	H1	6.37±0.07a	0.26±0.06a	0.26±0.01b	13.65±2.55a	33.04±3.12a	11.61±1.90ab	1.89±0.19b
	H2	6.30±0.08a	0.24±0.07a	0.27±0.02a	13.47±2.13a	38.35±10.97a	13.51±2.23a	2.09±0.23b
	H3	6.36±0.08a	0.11±0.02b	0.25±0.01b	13.65±2.28a	36.44±7.05a	9.57±2.54b	2.34±0.38b
	H4	6.42±0.15a	0.16±0.04c	0.25±0.01b	13.75±3.46a	31.54±3.48a	8.74±2.02c	2.77±0.50a
20-40	H1	6.41±0.06b	0.14±0.13a	0.25±0.03a	14.02±5.99a	32.02±3.93a	7.37±2.61a	1.52±0.16a
	H2	6.38±0.04b	0.08±0.02b	0.25±0.01a	13.66±3.08ab	32.53±5.89a	7.56±2.38a	1.64±0.49a
	H3	6.27±0.09b	0.15±0.09a	0.24±0.01ab	13.65±1.64ab	24.47±7.11b	6.51±0.30a	1.72±.016a
	H4	6.58±0.05a	0.08±0.04b	0.23±0.01b	13.58±2.48b	20.91±7.48b	6.06±1.38a	1.86±0.45a

TN: total nitrogen, TP: total phosphorus, TK: total potassium, AN: available nitrogen, AP: available phosphorus, AK: available potassium. Values are mean±standard deviations

Soil enzyme activities

The soil enzyme activities of *Dendrocalamus minor* var. *amoenus* populations with different densities are shown in *Table 4*. Soil acid phosphatase ranged from 0.02-0.09 umol·d^{-1}·g^{-1} in 0-40 cm soil layer, urease ranged from 0.19-0.41 mg·g^{-1}, sucrase was between 0.02-0.49 mg·g^{-1} and catalase was between 1.22-3.88 mg·g^{-1}. In the 0-20 cm soil layer, the content of catalase of stand H4 is the lowest. In the 20-40 cm soil layer, stand H2 had the highest urease content. Stand H3 and H4 had the lowest catalase content. There were no significant differences of sucrase between the soil densities and soil layers.

http://www.aloki.hu ● ISSN 1589 1623 (Print) ● ISSN1785 0037 (Online)
DOI: http://dx.doi.org/10.15666/aeer/1804_59855996

Table 4. *Enzyme activity of soil in Dendrocalamus minor* var. *amoenus populations*

Layer/cm	Stand	Acid phosphatase (PNP mg•g^{-1} •h^{-1})	Urease (NH_3-N mg•g^{-1} •h^{-1})	Sucrase (0.1N $Na_2S_2O_3$ mL•g^{-1})	Catalase (0.1 N $KMNO_4$ mL•g^{-1})
0-20	H1	0.08±0.01ab	0.19±0.08b	0.49±0.42a	3.88±0.92a
	H2	0.07±0.01b	0.21±0.10b	0.11±0.09a	3.88±0.92a
	H3	0.09±0.01a	0.41±0.08a	0.10±0.05a	3.47±0.63a
	H4	0.09±0.04ab	0.36±0.11a	0.10±0.10a	2.76±0.76b
20-40	H1	0.02±0.01b	0.23±0.08b	0.05±0.04a	2.65±0.92a
	H2	0.02±0.01b	0.40±0.32a	0.16±0.08a	1.63±0.63a
	H3	0.05±0.01a	0.31±0.11b	0.02±0.02a	1.22±0.00b
	H4	0.04±0.02ab	0.24±0.10b	0.05±0.08a	1.48±0.92b

Values are mean±standard deviations

Principal component analysis

Five principal component factors were extract from 17 indicators. The eigenvalue of the first principal component is 6.99, which explains 41.11% of the total proportion. The cumulative proportion of the five principal component factors is 92.50%, which can be better expressed 17 indicators (*Table 5*). There are nine indicators were screened, volume weight, noncapillary porosity, soil aeration, total phosphorus, total potassium, available nitrogen, available phosphorus, acid phosphatase and urease.

Table 5. *Principal component analysis of soil indicators*

Indicators	Principal component					σ2 of common factor	Weight
	1	2	3	4	5		
Volume weight	-0.430		-0.127	-0.127	0.879	0.9896	0.0629
Noncapillary porosity	-0.102	0.341	-0.817	-0.282	0.244	0.9330	0.0593
Capillary porosity	-0.652		0.640	0.147	0.349	0.9815	0.0624
Total porosity	-0.744		0.473		0.451	0.9878	0.0628
Soil aeration	-0.215	0.828		0.250	0.392	0.9552	0.0607
Soil moisture	-0.453	-0.623	0.589	-0.133		0.9672	0.0615
pH	-0.786	0.163	0.234		-0.118	0.7197	0.0458
Total nitrogen	0.497	0.230		0.751	0.173	0.8931	0.0568
Total phosphorus	0.913	0.151		0.289	-0.228	0.9970	0.0634
Total potassium			0.845	-0.160		0.7580	0.0482
Available nitrogen	0.914	0.285			-0.104	0.9389	0.0597
Available potassium	0.728	0.367	-0.187	0.526		0.9773	0.0622
Available phosphorus		0.903		-0.181	-0.219	0.9084	0.0578
Acid phosphatase	0.305	0.869	-0.296		0.144	0.9587	0.0610
Urease	0.118	0.128		-0.961		0.9532	0.0606
Sucrase	0.291	0.187	0.180	0.473	0.706	0.8742	0.0556
Catalase	0.631	0.575		0.445		0.9314	0.0592
Eigenvalue	6.99	3.31	2.91	1.46	1.06		
Proportion(%)	41.11	19.47	17.13	8.57	6.22		
Cumulative proportion(%)	41.11	60.58	77.71	86.28	92.50		

Comprehensive evaluation of soil quality

Nine important indicators were selected that expressed soil quality by comprehensive evaluation. The soil quality of stand H1 is highest score (*Table 6*). At the same density,

http://www.aloki.hu ● ISSN 1589 1623 (Print) ● ISSN1785 0037 (Online)
DOI: http://dx.doi.org/10.15666/aeer/1804_59855996

the 20-40 cm soil layer generally owns higher scores than the 0-20 cm soil layer, with the exception of stand H4. Stand H4 had the highest score in 0-20 cm soil layer, but lowest score in 20-40 cm soil layer.

Table 6. *Comprehensive evaluation of soil depth under different densities*

Stand	Layer/cm	Physical properties	Chemical properties	Soil enzyme activities	Score	Mean
H1	0-20	0.0326	0.1204	0.0650	0.2180	0.2279
	20-40	0.0197	0.1443	0.0738	0.2378	
H2	0-20	0.0305	0.1161	0.0608	0.2074	0.2131
	20-40	0.0439	0.1103	0.0647	0.2188	
H3	0-20	0.0231	0.1208	0.0582	0.2020	0.2116
	20-40	0.0357	0.1195	0.0659	0.2211	
H4	0-20	0.0401	0.1358	0.0647	0.2406	0.2064
	20-40	0.0090	0.0977	0.0655	0.1721	

Discussion

The relationship between soil layer and soil quality

The soil quality of different soil layers is different, mainly manifested in the differences in chemical properties and soil enzyme activities. In physical properties, the soil moisture and soil aeration in 0-20 cm soil layer are higher than those in 20-40 cm soil layer, which may be related to the soil composition. There are loose soil particles and large gaps between the gravels in 0-20 cm soil depth. Because of that, water is easily lost from topsoil to deep soil layer. Therefore, the soil moisture in 20-40 cm layer is higher.

The activity of catalase and acid phosphatase can better reflect soil nutrient condition (Qiu et al., 2010). The activity of catalase and acid phosphatase in 20-40 cm soil layer is lower than that in 0-20 cm soil layer, indicating that soil nutrition decreased with soil layer increase. Urease activity can be used to characterize soil nitrogen content (Qiu et al., 2010). The content of urease activity of stand H1 and H2 in the 0-20 cm soil layer is higher than that in 20-40 cm soil layer, while the content of urease of stand H3 and H4 has the opposite trend. The trend of total nitrogen is similar to urease. But the content of available nitrogen in 0-20 cm soil layer is better than that in 20-40 cm soil layer. The underground whiproot system of bamboo forests are sensitive to soil nutrient (Zhang et al., 2018). The content of soil nutrient in 0-20 cm is higher than that of 20-40 cm soil layer, which may be related to the distribution, secretion and residues of root can effectively accumulate nutrients, and loose soil conditions in 0-20 cm soil layer are also conducive to microbial decomposition of litter (Qi, 2009). The decomposition of litter produces a large amount of nutrients to return to the soil, so the nutrients in 0-20 cm soil layer are higher than 20-40 cm. The 20-40 cm soil layer has relatively few root systems, and soil nutrients gradually decrease with increasing soil depth. The content of nutrient elements and their supply significantly affect root competition and distribution (Markham and Halwas, 2011; Murphy et al., 2013). Plants determine the distribution of root systems by integrating resources within their habitats (Cahill et al., 2010). It can be inferred that the root systems of *Dendrocalamus minor* var. *amoenus* are mainly distributed at 0-20 cm.

http://www.aloki.hu ● ISSN 1589 1623 (Print) ● ISSN1785 0037 (Online)
DOI: http://dx.doi.org/10.15666/aeer/1804_59855996

The relationship between stand density and soil quality

Plant nutrients mainly come from soil nutrients. There was a positive correlation between total nitrogen, urease, available potassium, available phosphorus with the stand density. Soil moisture and total nitrogen are the most important factors affecting plant functional characteristics (Ding et al., 2011). The higher the soil nitrogen content, the higher the root tissue density (Yang et al., 2014). The growth of five tree species is restricted by phosphorus in sandy coast (Qiu et al., 2017). Abundant soil nutrition promoted the increase ramets density of *Dendrocalamus minor* var. *amoenus*. The higher nitrogen content in the soil, the plant allocate nutrients into the above ground, increasing the number of ramets and biomass to adapt to the environment (Yue et al., 2002, 2004, 2005). This shows that the correlation between stand density and soil quality is greater. The adaptability of different species to soil nutrients is different. The soil nutrient of *Phyllostachys edulis* rises first and descends later with the stand density (Fan et al., 2015). The stand of *Pinus tabulaeformis* and *Acacia sylvestris* showed the opposite trend, and the nutrient content decreased with the increase of the stand density (Vesterdal et al., 1995; Xu et al., 2008). There may be different strategies for resource adaptation and biomass allocation of different species (Hoffman, 2010). The ramet density of *Chimonobambusa tumidinoda* and *Pleioblastus maculata* decreased with increasing availability of water resources (Dong et al., 2002; Liu et al., 2004). In this study, there was no significant difference in soil moisture content and volume weight between different densities. It may be that the species of *Dendrocalamus minor* var. *amoenus* is more resistant to drought or has adapted to drought environment.

The activity of catalase can reflect soil nutrient condition (Qiu et al., 2010). The activity of catalase decreases with increasing stand density, indicating that stand density increases with soil nutrient decrease. In the 20-40 cm soil layer, the total phosphorus, total potassium, and available nitrogen content had a negative correlation with stand density. On a small scale, the pachymorph of clonal plants increases the contact chance of ramets and easily occupy local resource (Turkington and Harper, 1979; Dong, 2011). *Dendrocalamus minor* var. *amoenus* is a phalanx clonal plant with close arrangement of its ramets, which is likely to form a pattern of local resource monopoly. High stand density increases soil nutrient consumption and inhibits the growth of underground roots. Beside that, high canopy density also reduces light in the forest and weakens soil microbial activity (Zhao, 2009; Ren, 2012). The root system consumes soil nutrients, and the movement of nutrient elements from the soil to the plant become faster, which causes the soil nutrients gradually decrease (Shanmughavel and Francis, 1997).

Comprehensive evaluation of soil quality

In this study, nine representative indicators were screened by principal component analysis, which are different to other research results. Previous studies show that eleven and nine indicators were selected to represent the soil quality of *Phyllostachys edulis* forest in subtropical climate (Fan et al., 2015; Chen, 2015). The difference may be related to soil types, site conditions, and indicators selected. In this study, we did not measure organic matter indicator, which has certain differences with other research results. Because the sandy coast is mainly inorganic minerals and the carbon content is very small (Huang and Chen, 1994; Griffith et al., 2009).

The comprehensive scores of soil quality at different stand densities are quite different. It means that soil properties of different stand densities are different (*Table 6*).

http://www.aloki.hu ● ISSN 1589 1623 (Print) ● ISSN1785 0037 (Online)
DOI: http://dx.doi.org/10.15666/aeer/1804_59855996

In physical properties, the highest score in 0-20 cm soil layer is stand H4, but the highest score in 20-40 cm soil layer is stand H2. In the chemical properties, the highest score in 0-20 cm soil layer is stand H4, and the highest score in 20-40 cm soil layer is stand H1. In soil enzyme activities, the highest scores in 0-20 cm and 20-40 cm soil layer were stand H1. The comprehensive scores are ranked as: stand H1> stand H2> stand H3> stand H4. Thus, the higher the stand density, the lower the comprehensive score of soil quality. *Dendrocalamus minor* var. *amoenus* is a pachymorph species with many short individual spacers. These spacers are under great pressure to compete with light resources and soil nutrients. Therefore, low stand density get high comprehensive score.

Conclusion

The introduction of *Dendrocalamus minor* var. *amoenus* in sandy coast has gained good effect for stability of artificial forests and society economic. Soil properties of different densities is different. This study shows that the highest comprehensive score of soil quality with is stand H1. This stand density is good for soil quality. We recommend that diseased, old and dead ramets should be removed in future forest management. Meanwhile, topsoil should be protected, which is conducive to improving soil quality and forest productivity. Future researches should focus on the chemical elements balance in bamboo ramets, the root distribution and nutrient of different organs to reveal the fact that different stand densities could be formed with similar situation. Comparing different functional traits and their allometric growth relationships at different densities. The purpose of this study is to find a better stand density for soil quality. In coastal shelter forests, the wind resistance of bamboo clusters are also an extremely important concern, and it should be continuously paid attention in future research.

Acknowledgements. The authors are thankful to Dr Muhammad Waqqas. Khan Tarin for his help to manuscript revised. This project was jointly supported by science and technology major projects of Fujian province (2010N5002; 2013NZ0001). Foundation for Scientific and Technological Innovation of Fujian Agriculture and Forestry University (KF2015085; CXZX2017097).

REFERENCES

[1] Bao, B. D. (2005): Analysis of soil agricultural chemistry. – Beijing: Higer Education Press.
[2] Cahill, J. F. Jr., McNickle, G. G., Haag, J. J., Lamb, E. G., Nyanumba, S. M., St Clair, C. C. (2010): Plants integrate information about nutrients and neighbors. – Science 328: 1657-1657.
[3] Chen, Y. (2015): Indices and evaluation of *Phyllostachys pubescens* Forest soil fertility quality in central scenic area bamboo sea of southern Sichuan. – Sichuan Agricultural University Dissertation, 89p.
[4] Chen, Q. Q., Li, D. Z. (2015): Kin recognition in Setaria italica under the condition of root segregation. – Chinese Journal of Plant Ecology 39(12): 1188-1197.
[5] Ding, J., Wu, Q., Yan, H., Zhang, S. R. (2011): Effects of topographic variations and soil characteristics on plant functional traits in a subtropical evergreen broad-leaved forest. – Biodiversity Science 19(02): 158-167.
[6] Dong, W. Y., Huang, B. L., Xie, Z. X., Xie, Z. H., Liu, H. Y. (2002): The Ecological Strategy of Clonal Growth of Qiongzhuea tumidinoda Under Different Levels of Water

http://www.aloki.hu ● ISSN 1589 1623 (Print) ● ISSN1785 0037 (Online)
DOI: http://dx.doi.org/10.15666/aeer/1804_59855996

Resource Supply. – Journal Of Nanjing Forestry University (Natural Science Edition) 06: 21-24.
[7] Dong, M. (2011): The ecology of clonal plants. – Beijing: Science press.
[8] Fan, S. H., Zhao, J. C., Su, W. H., Yu, L., Yan, Y. (2015): Comprehensive Evaluation of Soil Quality in *Phyllostachys edulis* Stands of Different Stocking Stocking Densities. – Scientia Silvae Sinicae 10: 1-9.
[9] Griffith, A. D., Kinner, D. A., Tanner, B. R. (2009): Nutrient and Physical Soil Characteristics of River Cane Stands, Western North Carolina. – Castanea 74(3): 224-235.
[10] Hoffman, M. K. (2010): Patterns of recruitment and young culm morphology in *Arundinaria gigantea* ([Walt.] Muhl.) canebrakes in western North Carolina. – Western Carolina University Dissertations & Theses.
[11] Huang, Q. W., Chen, Y. Q. (1994): Study of the properties of coastal sandy soil in Euphoria longana Plantation. – Acta Ecologica Sinica 02: 180-187.
[12] Japet, W., Zhou, D. W., Zhang, H. X. (2009): Evidence of phenotypic plasticity in the response of *Fagopyrum esculentum* to population density and sowing date. – Journal of Plant Biology 52(4): 303-311.
[13] Li, Q., Zhou, B. Z., An, Y. F., Xu, S. H. (2014): Root system distribution and biomechanical characteristics of Bambusa oldhami. – Chinese Journal of Applied Ecology 25(05): 1319-1326.
[14] Liu, Q., Li, Y. X., Zhong, Z. C. (2004): Effects of moisture availability on clonal growth in bamboo Pleioblastus maculata. – Plant Ecology 173(1): 107-113.
[15] Luo, R. X., Zhang, C. X., Wang, F. S., Liu, G. H. (2009): A Study on the Root distribution of Three Bamboo Species and Their Soil Anti-scouribility. – Journal Of Bamboo Research 28(04): 23-26.
[16] Maherali, H., Delucia, E. H. (2001): Influence of climate-driven shifts in biomass allocation on water transport and storage in ponderosa pine. – Oecologia 129(4): 481-489.
[17] Markham, J., Halwas, S. (2011): Effect of neighbour presence and soil volume on the growth of Andropogon gerardii Vitman. – Plant Ecology & Diversity 4: 265-268.
[18] Murphy, G. P., File, A. L., Dudley, S. A. (2013): Differentiating the effects of pot size and nutrient availability on plant biomass and allocation. – Botany 91: 799-803.
[19] Qi, L. H., Zhang, X. D., Zhou, J. X., Peng, Z. H., Yue, X. H., Huang, L. L. (2009): Soil Microbe Quantities, Microbial Carbon and Nitrogen and Fractal Characteristics under Different Vegetation Restoration Patterns in Watershed, Northwest Hunan. – Scientia Silvae Sinicae 45(08): 14-20.
[20] Qiu, X. K., Dong, Y. J., Wan, Y. S., Hu, G. Q., Wang, Y. H. (2010): Effects of Different Fertilizing Treatments on Contents of Soil Nutrients and Soil Enzyme Activity. – Soils 42(02): 249-255.
[21] Qiu, L. J, Hu, H. T., Lin, Y., Ge, L. L., Wang, K. Y., He, Z. M., Dong, Q. (2017): Nutrient resorption efficiency and C:N:P stoichiometry of Eucalyptus urophylla × E. grandis of different ages in a sandy coastal plain area. – Chinese Journal of Applied & Environmental Biology 23(04): 739-744.
[22] Ren, L. N., Wang, H. Y., Ding, G. D., Gao, G. L., Yang, X. J. (2012): Effects of *Pinus tabulaeformis* Carr.plantation density on soil organic carbon and nutrients characteristics in rocky mountain area of northern China. – Arid Land Geography 35(03): 456-464.
[23] Shanmughavel, P., Francis, K. (1997): Balance and turnover of nutrients in a bamboo plantation (*Bambusa bambos*) of different ages. – Biology and Fertility of Soils 25(1): 69-74.
[24] Tu, Z., Chen, L., Yu, X., Zheng, Y. (2014): Rhizosphere soil enzymatic and microbial activities in bamboo forests in southeastern China. – Soil Science and Plant Nutrition 60: 134-144.

http://www.aloki.hu ● ISSN 1589 1623 (Print) ● ISSN1785 0037 (Online)
DOI: http://dx.doi.org/10.15666/aeer/1804_59855996

[25] Turkington, R., Harper, J. L. (1979): The growth, distribution and neighbour relationships of *Trifolium repens* in a permanent pasture: VI. Conditioning effects of neighbours. – The Journal of ecology 77(3): 734-746.
[26] Vesterdal, L., Dalsgaard, M., Felby, C. (1995): Effects of thinning and soil properties on accumulation of carbon, nitrogen and phosphorus in the forest floor of Norway spruce stands. – Forest Ecology & Management 77: 1-10.
[27] Wang, Q., Su, Z. X., Zhou, P., Xia, L. (2004): Density Regulation of Clonal Growth of Neosinocalamus affinis in Different Habitats. – Journal Of China West Normal University (Natural Sciences) 04: 380-387.
[28] Xu, S. K., Wang, X. E., Xie, T. F., Zeng, F., Huang, L. M. (2008): Soil Fertility of Young Acacia auriculiformis Stands with Different Densities. – Journal of South China Agricultural University 29(2): 79-81.
[29] Yang, S. S., Wen, Z. M., Miao, L. P., Qi, D. H., Hua, D. W. (2014): Responses of plant functional traits to micro-topographical changes in hilly and gully region of the Loess Plateau, China. – Chinese Journal of Applied Ecology 25(12): 3413-3419.
[30] Yang, Q. P., Ouyang, M., Yang, G. Y., Song, Q. N., Guo, C. L., Fang, X. M., Chen, X., Huang, L., Chen, F. S. (2016): Research on ecological stoichiometry in bamboos: From biological basis to applications in sil-viculture of bamboo forests. – Chinese Journal of Plant Ecology 40(03): 264-278.
[31] Yue, C. L., Wang, K. H., He, Q. J., Weng, F. J. (2002): Comparative research on clonal growth of *Phyllostachys praecox* in different conditions of soil nitrogen content. – Journal of Bamboo Research 21(1): 38-40, 45-45.
[32] Yue, C. L., Chang, J., Wang, K. H., Zhu, Y. M. (2004): Response of clonal growth in Phyllostachys praecox f. prevernalis to changing light intensity. – Australian Journal of Botany 52(2): 171-174.
[33] Yue, C. L., Wang, K. H., Zhu, Y. M. (2005): Morphological plasticity of clonal plant Phyllostachys praecox f. prevernalis (Poaceae) in response to nitrogen. – Annales Botanici Fennici 42(2): 123-127.
[34] Zhang, M. M., Guan, F. Y., Fan, S. H., Lu, Y. S., Zhan, M. C., Yan, Y. J. (2018): Research Progress on Influencing Factors of Soil Nutrient Variation in Bamboo Forest. – World Forestry Research 31(04): 18-22.
[35] Zhao, R. E. (2009): Root Distribution Pattern in Mixed Forest Stands of Pinus massoniana anti Pleioblastus amarus. – China Forestry Science And Technology 23(02): 77-79.
[36] Zhao, R. D., Fan, J. B., He, Y. Q., Song, C. L., Tu, R. F., Tan, B. C. (2012): Effects of Stand Density on Soil Nutrients and Enzyme Activities in Pinus massoniana Plantation. – Soils 44(02): 297-301.

http://www.aloki.hu ● ISSN 1589 1623 (Print) ● ISSN1785 0037 (Online)
DOI: http://dx.doi.org/10.15666/aeer/1804_59855996

ISOLATION OF ACC DEAMINASE PRODUCING RHIZOBACTERIA FROM WHEAT RHIZOSPHERE AND DETERMINATING OF PLANT GROWTH ACTIVITIES UNDER SALT STRESS CONDITIONS

ATEŞ, Ö.[1*] – KIVANÇ, M.[2]

[1]*Transitional Zone Agricultural Research Institute, Eskişehir, Turkey*

[2]*Eskisehir Technical University, Faculty of Science, Department of Biology, Eskisehir, Turkey*

[*]*Corresponding author*
e-mail: ozgurates@windowslive.com

(Received 27th Apr 2020; accepted 10th Jul 2020)

Abstract. Salinity in agricultural lands is a major problem worldwide and the application of 1-aminocyclopropane-1-carboxylate (ACC) producing plant growth-promoting rhizobacteria (PGPR), is a good option to reduce the effects of salt stresses on plant growth and development. This study aims to isolate ACC deaminase producing PGPR and evaluate their effect on the growth and yield of wheat (*Triticum aestivum* L.) under salt stress of conditions. 21 ACC deaminase producing bacteria were isolated from wheat rhizosphere and the effectiveness of the isolates was determined by petri, jar and pot experiments. Pot experiments were established with 5 bacterial isolates (*Bacillus cereus*, *Serratia odorifera*, *Lelliottia amnigena*, *Arthrobacter arilaitensis*, *Pseudomonas putida*) and 4 different salt levels (0.95, 3.98, 7.80, 11.05 dS m^{-1}). ACC deaminase producing bacteria increased shoot and root length under petri and jar trial. Likewise, inoculation of PGPRs under salt stress conditions had a positive effect on wheat Sodium (Na), Potassium (K), Calcium (Ca), Chlorophyll a and chlorophyll b contents compared to uninoculated control plants in pot trials. Inoculation of wheat with ACC deaminase producing PGPR alleviated the negative effects of salinity and increased plant growth. This study shows the vital role of rhizobacteria producing ACC deaminase increasing salt tolerance and eventually the development of wheat under salinity stress.
Keywords: *plant growth-promoting rhizobacteria (PGPR), abiotic stress, salinity, ethylene, pot experiments*

Introduction

Salinity is one of the most notable abiotic stress sources that affect agricultural systems and cause a decrease in the food supply in agricultural production. Salinity affects 80 million hectares of agricultural land worldwide (Munns and Tester, 2008) and saline soils increase approximately 7% per year (Tester, 2003). More than 6% of the total land that can be used for agricultural purposes is seriously affected by salt stress in arid and semi-arid regions around the world (Sarkar et al., 2018). Arid climates, low-quality irrigation water, and high temperatures with imbalances in the distribution of rain are among the main causes of soil salinity. Soluble salts accumulate in the plow layer in regions where the evaporation amount of plants is higher than the size of the leach fraction (Rajput et al., 2013). Salt deposits in the soil disrupt the physical and chemical balance of the soil and naturally adversely affect plant growth. In plants developing at high salt concentrations, reactive oxygen species, osmotic shock, ion toxicity, reduced nutrient uptake and reduction in leaf area are observed (Parihar et al., 2015). Increased soil salinity leads to a decrease in plant growth and crop yields as well as in microbial activity. Environmentally friendly, cost-effective and innovative

http://www.aloki.hu ● ISSN 1589 1623 (Print) ● ISSN1785 0037 (Online)
DOI: http://dx.doi.org/10.15666/aeer/1804_59976008

approaches are needed to minimize the effects of salinity on agricultural soils and increase crop yields. The use of bacteria known as Plant Growth Promoting Rhizobacteria (PGPR) which increases plant growth in abiotic stress conditions is one of the most appropriate and sustainable approaches for alleviating the effects of salt stress (Yang et al., 2008; Sofo et al., 2015). PGPR can increase plant growth by reducing the effects of abiotic stresses, fixing nitrogen, producing plant hormones, dissolving phosphates in the soil and also producing siderophores that increase iron intake (Shanmugam and Kanoujia, 2011; Çakmakçı, 2016). Reduced the amount of ethylene produced under stress conditions, by 1-aminocyclopropane-1-carboxylate (ACC) deaminase containing PGPR is one of the most important mechanisms of alleviating salt stress (Singh et al., 2016). Ethylene is a gaseous form and is a very important plant hormone that is produced by almost all plants and plays a role in plant growth and differentiation. Ethylene at low concentration (10 µg L^{-1}) plays a part in plant growth, seed germination, fruit maturing, flower shedding and root development. However, at high concentration (25 > µg L^{-1}) may cause root growth reduction and some plant process (Nadeem et al., 2010). A number of PGPR strains containing ACC deaminase which can break down the ethylene precursor ACC into ammonia and α-ketobuyrate thereby reduce the level of ethylene in stressful plants (Ali et al., 2014; Glick, 2014). In recent years, ACC deaminase producing bacteria have been used to reduce the amount of ethylene produced by plants under stress conditions. Research has found that PGPR containing ACC deaminase increases plant growth in abiotic stress conditions such as heavy metal (Hassan et al., 2016; Grobelak et al., 2018), flood (Ravanbakhsh et al., 2017; Ali and Kim, 2018), drought (De Zelicourt et al., 2013; Erdogan et al., 2016; Carlson et al., 2020) salinity (Afridi et al., 2019; Tahir et al., 2019). This study aims to isolate acc deaminase-containing PGPR from wheat roots grown in saline soils and to determine their effects on wheat development under salt stress conditions in pot trials.

Materials and Methods

Isolation of bacteria

For isolation, 21 soil samples were collected from saline soils of Eskişehir province TURKEY in 2014. Soil samples were taken from wheat root rhizosphere and brought into the laboratory in plastic bags. Rhizopheric bacteria were isolated by serial dilution technique. Between 10^{-4} and 10^{-6} dilution was spread on DF salt minimal medium which ACC is used as a nitrogen source (Dworkin and Foster, 1958) and bacterial isolates were purified by repeated streaking. In laboratory, we prepared salt medium as follows (per 1000 ml) 6.0 g Na_2HPO_4, 4.0 g KH_2PO_4, 2.0 g glucose, 2.0 g gluconic acid, 2.0 g citric acid, 0.2 g $MgSO_4.7H_2O$, 1 mg $FeSO_4.7H_2O$, 124.6 µg $ZnSO_4.7H_2O$, 78.22 µg $CuSO_4.5H_2O$, 10 µg H_3BO_3, 11.19 µg $MnSO_4.H2O$, 10 µg MoO_3 and 15.0 g agar (pH 7.2). We prepared 300 ml DF salt medium autoclaved and after cooling (> 35 ^oC) added 30 ml 0.5 mM ACC solution (filter sterilized). Purified ACC deaminase containing bacteria was stocked in LB medium and 20% glycerol at - 80 ^0C.

Characterization and identification of bacteria

Characterization of bacteria used in pot experiments was done by 16s rDNA method. Genomic DNA isolated from bacteria and sequence analysis was performed by

http://www.aloki.hu ● ISSN 1589 1623 (Print) ● ISSN1785 0037 (Online)
DOI: http://dx.doi.org/10.15666/aeer/1804_59976008

replicating DNA's 16s rDNA region by PCR (Barnawal et al., 2014). Nucleotide similarities were determined by NCBI-BLAST and gene bank numbers were obtained.

Inoculation of seeds with bacteria

Wheat seeds surface sterilized and coated with bacteria for further experiments. After wheat seeds were immersed to 95% ethanol for a very short time (5 seconds), kept in 2% $HgCI_2$ solution for 3 min. Seeds washed 5 times with sterilized distilled water. Seeds immersed 3 m M ACC solution for 5 min. then kept in 30 min 24-h bacterial culture (Zahir et al., 2009).

Petri experiments

In Petri experiments, 5 bacteria coated seeds placed in sterile petri dishes containing sterile filter paper under sterile conditions. After a second filter paper to cover the seeds and five ml of sterile 5 dS m^{-1} NaCl solution added to each petri dish. Petri dishes incubated seven days with 28±1 ^{o}C and shoot, root data recorded. The experiments conducted with three replication.

Jar experiments

In jar experiment, sterilized jars were used and conducted with 3 replication. 5 bacteria coated seeds were sandwiched between two sterilized filter paper which placed in 10 dS m^{-1} NaCl containing ½ strength Hoagland solution (Hoagland and Arnon, 1950). The jars were placed in the growth chamber at 25 ° C, adjusted to 16 hours light and 8 hours dark for 21 days (Zahir et al., 2009). End of the jar trials shoot length and root length recorded.

Pot experiments

Pot experiments were carried out in the greenhouse of Eskişehir Transitional Zone Agricultural Research Institute Turkey to determine the effectiveness of selected bacterial strains for plant growth of wheat under different salt conditions. Soils were taken from the land and sieved through 2 mm 4.5 kg of plastic pots were filled from the homogeneous mixture (3:1 soil, sand). Pot mixture was analyzed for some physicochemical properties i.e. saturation 56%, pH: 7.82, EC: 0.95 dS m^{-1} organic matter: 1.44%, extractable P: 4.12 mg kg^{-1} and extractable K: 120.38 mg kg^{-1}. 40 kg ha^{-1} phosphorus (together with sowing) and 180 kg ha^{-1} nitrogen (half sowing and half at the beginning of tillering) were applied to the pots.

Pot experiments were planned at 4 different salt levels with 1, 4, 8, 12 dS m^{-1} with 4 replications. The amount of NaCl calculated, dissolved in water and applied to the pots soils. Actual salinity was measured as 0.95, 3.98, 7.80 and 11.05 dS m^{-1}. 8 bacterial grafted wheat seeds were planted in the pots and after germination, the seeds were diluted 4 plants. The experiment was carried out according to the factorial experiment design in randomized plots. In the experiment, irrigation was carried out twice a week with distilled water without drainage. Na, K, Ca, chlorophyll a, and chlorophyll b were determined and analyzed. Data were analyzed by using SPSS version 25.0 (SPSS Inc., Chicago, IL, USA). differences among means were compared with Duncan multiple comparison tests.

http://www.aloki.hu ● ISSN 1589 1623 (Print) ● ISSN1785 0037 (Online)
DOI: http://dx.doi.org/10.15666/aeer/1804_59976008

Determination of leaf element contents

The first leaves, just below the flag leaf, were collected and analyzed for each plant. Leaf samples collected from plants were washed with distilled water and dried for 65 ºC 48 hours. The dried samples were ground and weighed into 0.25 g microwave tubes. 10 ml of HNO_3 mixture containing 20% $HCIO_4$ was added to the weighed sample and digested in the for 30 minutes. Na, K, and Ca were determined as mg g^{-1} dry weight (DW) by ICP-OES (Optima 8000, PerkinElmer, USA) after completing 50 ml of the digested liquid.

Determination of chlorophyll a and b content

To determine the amount of chlorophyll a and chlorophyll b in wheat leaves, 500 mg fresh weight (FW) leaf were crushed in mortar in 90% acetone and centrifuged at 9000 g for 10 minutes. After centrifugation, the supernatant was completed to 50 ml and measured at 645 and 663 nm in the spectrophotometer. Chlorophyll a (*Eq.1*) and chlorophyll b (*Eq.2*) contents were determined (Lichtenthaler, 1987).

$$\text{Chlorophyll a (mg g}^{-1}\text{ FW)} = (11.75 \times A663 - 2.35 \times A645) \times 50/500 \quad \text{(Eq.1)}$$

$$\text{Chlorophyll b (mg g}^{-1}\text{ FW)} = (18.61 \times A645 - 3.96 \times A663) \times 50/500 \quad \text{(Eq.2)}$$

Results

Petri and jar experiments

The data obtained as a result of the petri experiments showed that the root and shoot lengths of wheat which inoculated with ACC deaminase producing PGPR increased compared to the uninoculated control (*Table 1*). Inoculation with ACC deaminase containing bacteria significantly increased plant root and seedling length. The strain 20/1 caused the maximum increase in root length with 74% compared to the uninoculated control. Strain 20/1 was followed by strain 18/6 with 54%, strains 1/6 and 11/5 with 32% over the control. Among the isolates in the petri experiment, the highest shoot length was obtained from strain 17/4 with 43% over the control. Strain 10/6 and strain 1/6 increased shoot length 41% and 35% compared to uninoculated control respectively.

The jar experiments were established with 9 bacterial isolates which were determined as a promising from the petri experiments. As a result of jar trials, length of root and shoot of wheat seeds inoculated with ACC deaminase containing strains increased compared to control (*Table 2*). Strain 21/4 caused maximum increase of root length (97%) compared to uninoculated control. Strain 15/1 and strain 11/5 increased root length of 82% and 56% over the control, respectively. Similarly, strain 18/6 and 10/6 increased shoot length of 54% and 51% over the control, respectively. The maximum shoot length increase data obtained from strain 15/1 with 60% compared to control.

Pot experiments

As a result of jar trials, pot experiments were established with strain 10/6, strain 11/5, strain 15/1, strain 18/6, strain 21/4 and 4 different salt levels which 0.95, 3.98, 7.80, 11.05 dS m^{-1}. The bacterial isolates used for the pot experiments were identified as strain 10/6 *Bacillus cereus* 10/6, strain 11/5 *Serratia odorifera* 11/5, strain 15/1

http://www.aloki.hu ● ISSN 1589 1623 (Print) ● ISSN1785 0037 (Online)
DOI: http://dx.doi.org/10.15666/aeer/1804_59976008

Lelliottia amnigena, strain 18/6 *Arthrobacter arilaitensis,* and strain 21/4 *Pseudomonas putida* (*Table 3*).

Table 1. *Effect of ACC deaminase producing rhizobacteria on root and shoot length of wheat under 5 dS m^{-1} NaCl in petri trial ($p < 0.05$)*

Strain	RootLenght (cm)	ShootLenght (cm)
Control	5.85 ± 0.42**	4.98 ± 0.21
1/6*	7.70 ± 0.27	6.70 ± 0.22
2/5	6.16 ± 0.62	6.01 ± 0.50
3/4	6.02±0.48	5.24± 1.45
4/2	6.92 ± 032	6.82 ± 0.72
5/4	6.15±0.47	5.07±0.97
6/1	6.27 ± 0.37	6.50 ± 0.61
7/3	5.19±0.12	6.48± 1.11
8/4	7.13 ± 0.52	6.60 ± 0.48
9/7	6.29±1.14	6.29±1.04
10/6*	7.65 ± 0.73	7.02 ± 0.31
11/5*	7.70 ± 0.29	5.76 ± 0.19
12/1	6.00±0.79	5.15±0.71
13/4*	7.47 ± 0.56	6.14 ± 0.19
14/2	6.12±0.45	5.01±0.21
15/1*	7.02 ± 0.30	5.90 ± 0.26
16/1	7.09 ± .048	6.42 ± 0.39
17/4*	7.50 ± 0.39	7.10 ± 0.44
18/6*	9.02 ± 0.28	6.09 ± 0.13
19/3	6.12±0.77	6.08±0.51
20/1*	10.02 ± 0.87	6.30 ± 0.51
21/4*	7. 47 ± 0.21	5.90 ± 0.18

* Selected for jar trial ** Average for third replicate ± Std. Error

Table 2. *Effect of ACC deaminase producing rhizobacteria on root and shoot length of wheat under 10 dS m^{-1} NaCl in jar trial ($p < 0.05$)*

Strain	Root Lenght (cm)	Shoot Lenght (cm)
control	6.80 ± 0.75*	16.00 ± 0.53
1/6	6.60 ± 0.80	19.45 ± 1.15
10/6[a]	10.40 ± 0.89	24.20 ± 1.07
11/5[a]	10.60 ± 0.89	21.60 ± 2.60
13/4	7.60 ± 0.96	20.80 ± 0.95
15/1[a]	12.40 ± 0.96	25.60 ± 0.80
17/4	9.50 ± 0.83	20.80 ± 2,02
18/6[a]	9.20 ± 0.43	24.60 ± 1.10
20/1	8.40 ± 0.60	23.20 ± 1.28
21/4[a]	13.40 ± 0.30	23.60 ± 1.23

[a] Selected for pot trial * Average for third replicate ± Std. Error

http://www.aloki.hu ● ISSN 1589 1623 (Print) ● ISSN1785 0037 (Online)
DOI: http://dx.doi.org/10.15666/aeer/1804_59976008

Table 3. *Identification of strains*

Strain No.	Species	Accession No	Similarity (%)
10/6	*Bacillus cereus*	KP027636.1	99
11/5	*Serratia odorifera*	NR037110.1	99
15/1	*Lelliottia amnigena*	KM114915.1	99
18/6	*Arthrobacter arilaitensis*	CP012750.1	99
21/4	*Pseudomonas putida*	GQ2008822.1	99

Na^+ contents tested in salt stress wheat plants in response to ACC deaminase producing PGPR. According to the results of the analysis, the leaf Na^+ content increased due to increasing salt concentrations (*Table 4*). Bacterial applications caused reductions in Na^+ content compared to uninoculated control at 3.98, 7.80, 11.05 dS m^{-1} salinity levels. Application of *A. arilaitensis* at 7.80 and 11.05 dS m^{-1} salt levels decreased Na^+ content by 32% and 10%, respectively, compared to control. Likewise, application of *P. putida* was decreased Na^+ content of wheat by 26% and %9 at 7.80 and 11.05 dS m^{-1} salinity levels, respectively.

Table 4. *Effect of ACC deaminase producing rhizobacteria on Na, K, and Ca under differents salinity levels in pot trials*

Strain	0.95 (dS m^{-1})	3.98 (dS m^{-1})	7.80 (dS m^{-1})	11.05 (dS m^{-1})
Na^+ (mg g^{-1} DW)				
Control	0.12 h	0.15 efg	0.22 d	1.15 a
B. cereus	0.12 h	0.14 fgh	0.22 d	1.13 a
S. odorifera	0.12 h	0.13 gh	0.16 ef	1.09 b
L. amnigena	0.12 h	0.13 fh	0.21 d	1.10 b
A. arilaitensis	0.12 h	0.12 h	0.15 efg	1.04 c
P. putida	0.12 h	0.12 h	0.16 ef	1.05 c
K^+ (mg g^{-1} DW)				
Control	2.09 bc	1.98 de	1.67 hıj	1.56 k
B. cereus	2.10 bc	2.08 bcd	1.77 gh	1.57 k
S. odorifera	2.16 b	2.10 b	1.86 fg	1.57 k
L. amnigena	2.18 b	2.09 bc	1.83 fg	1.57 k
A. arilaitensis	2.50 a	2.15 b	1.90 ef	1.70 hı
P. putida	2.56 a	2,18 b	2.0 cde	1.61 ıjk
Ca^{+2} (mg g^{-1} DW)				
Control	0.80 abcd	0.74 efg	0.69 g	0.57 h
B. cereus	0.80 abcd	0.80 abcd	0.71 fg	0.59 h
S. odorifera	0.85 a	0.77 bcde	0.69 g	0.58 h
L. amnigena	0.82 ab	0.81 abc	0.75 def	0.59 h
A. arilaitensis	0.82 ab	0.82 ab	0.77 bcde	0.70 fg
P. putida	0.84 a	0.77 bcde	0.77 bcde	0.69 g

$p<0.05$ bacteria *, salinity *, bacteriaxsalinity* values with the same letter are not different according to DUNCAN

Leaf K^+ content decreased due to increased salt concentrations in trials (*Table 4*). Bacterial applications containing ACC deaminase were found to increase leaf K^+ content 0.95, 3.98, 7.80, 11.05 dS m^{-1} salinity levels compared to control. Application of *P. putida* increased leaf K^+ content at 3.98, 7.80, 11.05 dS m^{-1} salinity levels by 10%,

http://www.aloki.hu ● ISSN 1589 1623 (Print) ● ISSN1785 0037 (Online)
DOI: http://dx.doi.org/10.15666/aeer/1804_59976008

20% and 4%, respectively. Similarly, application of *A. arilaitensis* increased 9%, 14% and 9% K^+ content at 3.98, 7.80, 11.05 dS m^{-1} salinity levels, respectively.

Leaf Ca^{+2} content decreased due to increased salt concentrations similar to K^+ content. Bacterial applications increased Ca^{+2} content at, 3.98, 7.80, 11.05 dS m^{-1} salinity levels over the uninoculated control. The maximum Ca^{+2} increases data obtained from *A. arilaitensis* application at 3.98, 7.80, 11.05 dS m^{-1} salinity levels by 9%, 9% and 22%, respectively.

Chlorophyll a content of wheat significantly affected salinity (*Table 5*). Depending on the salt level, chlorophyll a content significantly decreased. ACC deaminase producing PGPR applications did not affect chlorophyll a content at 0.95 dS m^{-1} salinity levels. However, bacterial applications increased chlorophyll a content compared to control at 3.98, 7.80, 11.05 dS m^{-1} salinity levels. Application of *P. putida* increased chlorophyll a content at 3.98, 7.80, 11.05 dS m^{-1} salinity levels by 4%, 7% and 10%, respectively.

Table 5. *Effect of ACC deaminase producing rhizobacteria on chlorophyll a content of wheat under different salinity levels in pot trials (mg g^{-1} FW)*

Strain	0.95 (dS m^{-1})	3.98 (dS m^{-1})	7.80 (dS m^{-1})	11.05 (dS m^{-1})	Avarage
Control	1.95	1.80	1.73	1.60	1.77b
B. cereus	1.94	1.83	1.76	1.73	1.82ab
S. odorifera	1.94	1.85	1.77	1.72	1.82a
L. amnigena	1.94	1.87	1.77	1.74	1.83a
A. arilaitensis	1.98	1.89	1.82	1.75	1.86a
P. putida	1.97	1.89	1.84	1.75	1.86a
Average	1.95a	1.86b	1.78c	1.72d	

p<0.05 bacteria *, salinity *, bacteriaxsalinity $^{n.s.}$ values with the same letter are not different according to DUNCAN

Chlorophyll b content of wheat significantly decreased due to salinity application (*Table 6*). Bacteria applications did not affect chlorophyll b content at 0.95 dS m^{-1} salinity levels. Contrary to the 0.95 dS m^{-1} salinity levels, the amount of chlorophyll b increased with the application of ACC deaminase producing PGPR at 3.98, 7.80, 11.05 dS m^{-1} salinity levels. *A. arilaitensis* application increased the amount of chlorophyll b by 15% on average.

Table 6. *Effect of ACC deaminase producing rhizobacteria on chlorophyll b content of wheat under different salinity levels in pot trials (mg g^{-1} FW)*

Strain	0.95 (dS m^{-1})	3.98 (dS m^{-1})	7.80 (dS m^{-1})	11.05 (dS m^{-1})	Avarage
Control	1.42	1.00	0.78	0.60	0.95c
B. cereus	1.46	1.07	0.89	0.71	1.03bc
S. odorifera	1.46	1.02	0.91	0.71	1.03bc
L. amnigena	1.43	1.04	0.96	0.84	1.07ab
A. arilaitensis	1.48	1.07	0.99	0.86	1.10a
P. putida	1.46	1.07	0.98	0.79	1.08ab
Average	1.45a	1.5b	0.92c	0.75d	

p<0.05 bacteria *, salinity *, bacteriaxsalinity $^{n.s.}$ values with the same letter are not different according to DUNCAN

http://www.aloki.hu ● ISSN 1589 1623 (Print) ● ISSN1785 0037 (Online)
DOI: http://dx.doi.org/10.15666/aeer/1804_59976008

Discussion

In this study, 21 ACC deaminase containing PGPR isolated from the wheat root rhizosphere and plant growth-promoting activities of isolates tested under salt stress condition by petri trials. Based on petri trials, jar trials and according to the results of the jar trials pot trials conducted. The effect of five ACC deaminase containing PGPR (*B. cereus*, *S. odorifer, L. amnigena, A. arilaitensis, P. putida*) was evaluated for wheat growth and yield under salt stress 0.95, 3.98, 7.80, 11.05 dS m^{-1} salinity levels in pot trials. The results showed that salt stress had a strong negative effect on the development of wheat plants, while ACC deaminase containing bacterial applications increased wheat development. Previously conducted studies showed that several bacteria species, including *Serratia* and *Pseudomonas* (Zahir et al., 2009), *Arthrobacter* (Barnawal et al., 2014), *Streptomyces* (Palaniyandi et al., 2014), *Enterobacter* (Singh et al., 2016), *Staphylococcus* and *Kocuria* (Yildirim et al., 2011), *Cronobacter* (Afridi et al., 2019), increased plant growth under salt-stress conditions.

ACC deaminase containing bacterial applications increased the root and shoot length of wheat under saline conditions in petri (5 dS m^{-1}) and jar (10 dS m^{-1}) trials. Inoculation of rhizobacteria strains promoted root and shoot growth by lowering levels of ethylene caused by salt stress. It is known as the ethylene stress hormone and its synthesis is accelerated in response to different environmental stresses like salinity (Mayak et al., 2004). It has been shown that ACC-deaminase containing PGPR can help regulate endogenous ethylene levels in plants through ACC-deaminase activities and consequently promote plant growth and development (Maqshoof et al., 2011; Glick, 2014; Shimaila et al., 2014; Khan et al., 2016; Barra et al., 2016; Sarkar et al., 2018; Afridi et al., 2019). Higher concentrations of ethylene reduced plant growth. In this study, *B. cereus*, *S. odorifer, L. amnigena, A. arilaitensis, P. putida* exhibited ACC deaminase production, which cleaved ACC into α-ketobutyrate and ammonia and reduces the harsh effects of ethylene on plant growth under salinity stress.

Ionic balance is disturbed in plants under saline conditions. Salinity leads to reducing plant growth and development, as well as impairment of ionic balance, especially Na^+ and K^+ (Singh et al., 2016). One of the effects of salinity is that the high Na^+ content has an antagonistic effect on K^+ uptake. Therefore, restricting Na^+ intake by increasing K^+ intake are the main strategies commonly used by plants to maintain the desired K^+ / Na^+ ratio in the cytosol (Khan et al., 2009). In this study, Na^+ increased and K^+ decreased in plants due to increasing salt concentrations. However, in the application of bacteria that contain acc deaminase, the amount of Na^+ in the plant has decreased and the amount of K^+ has increased. Application of *A. arilaitensis*, and *P. putida* especially may help to ion homeostasis of wheat in pot trials. Also, the inoculation of bacteria increased Ca^{+2} content that improves plant growth. According to Zahir et al. (2009), low Na^+ uptake by grafted roots likely resulted from the reduction of Na^+ passive (apoplastic) flow into tissues caused by a higher proportion of the root covered with soil. Likewise, this effect has been reported in studies conducted with wheat (Singh et al., 2016, 2017; Afridi et al., 2019) and maize (El-Komy, 1998). Yue et al. (2007), Shimaila et al. (2014) and Turhan et al. (2020) shown in their studies that the plants inoculated with ACC deaminase containing bacteria have a low Na^+ and high K^+ content.

The decrease in photosynthetic efficiency takes an important place in salinity decreasing plant growth and productivity (Colmenero-Flores et al., 2007). The lack of physiological water caused by salinity stress reduces stomatal conductivity and slows down CO_2 assimilation (James et al., 2002). PGPR has an important role in increasing

http://www.aloki.hu ● ISSN 1589 1623 (Print) ● ISSN1785 0037 (Online)
DOI: http://dx.doi.org/10.15666/aeer/1804_59976008

the water intake in salt conditions and reducing the suppression of photosynthesis under salinity stress (Hashem et al., 2019). In this study, the amount of chlorophyll a and chlorophyll b decreased in salt stress conditions. On the contrary, ACC deaminase containing bacterial applications increased the amount of chlorophyll a and b compared to the uninoculated control. The findings obtained in this study are compatible with previous studies reporting an increase in photosynthetic activity in plants inoculated with ACC deaminase-producing PGPR (Singh et al., 2016, 2017; Chen et al., 2017; Afridi et al., 2019).

Conclusion

As a result, the results show that salt stress applied to wheat has strong negative effects on the growth of wheat. However, inoculation with *B. cereus*, *S. odorifer, L. amnigena, A. arilaitensis, P. putida* has a positive effect on the development of wheat plants under salt stress conditions. The results of the study show that ACC deaminase containing bacterial inoculation supports stress tolerance to wheat plants in terms of plant growth and biochemistry. For this reason, use of ACC deaminase containing bacteria great hope for the plant growth promote in saline soils. Therefore, using ACC deaminase containing bacteria to increase plant growth in saline soils is an environmentally friendly and economical option. However, this study was carried out under controlled conditions in the greenhouse. Therefore, in future studies, it will be useful to determine the yield and quality parameters of wheat in, the field conditions especially inoculation with *A. arilaitensis*, *P. putida*. In addition, suitable carrier formulations for bacteria need to be studied.

REFERENCES

[1] Afridi, M. S., Amna, S., Tariq, M., Abdul, S., Tehmeena, M., Shehzad, M. (2019): Induction of Tolerance to Salinity in Wheat Genotypes by Plant Growth Promoting Endophytes: Involvement of ACC Deaminase and Antioxidant Enzymes. – Plant Physiology and Biochemistry 139(4): 569-77.

[2] Ali, S., Kim, W.-C. (2018): Plant Growth Promotion under Water: Decrease of Waterlogging-Induced ACC and Ethylene Levels by ACC Deaminase-Producing Bacteria. – Frontiers in Microbiology 9: 1096.

[3] Barnawal, D., Nidhi, B., Deepamala, M., Chandan, S. C., Alok, K. (2014): ACC Deaminase-Containing Arthrobacter Protophormiae Induces NaCl Stress Tolerance through Reduced ACC Oxidase Activity and Ethylene Production Resulting in Improved Nodulation and Mycorrhization in Pisum Sativum. – Journal of Plant Physiology 171(11): 884-94.

[4] Barra, P. J., Inostroza, N. G., Acuña, J. J., Mora, M. L., Crowley, D. E., Jorquera, M. A. (2016): Formulation of Bacterial Consortia from Avocado (Persea Americana Mill.) and Their Effect on Growth, Biomass and Superoxide Dismutase Activity of Wheat Seedlings under Salt Stress. – Applied Soil Ecology 102: 80-91.

[5] Çakmakçı, R. (2016): Screening of Multi-Trait Rhizobacteria for Improving the Growth, Enzyme Activities, and Nutrient Uptake of Tea (Camellia Sinensis). – Communications in Soil Science and Plant Analysis 47(13-14): 1680-90.

[6] Carlson, R., Tugizimana, F., Steenkamp, P. A., Dubery, I. A., Hassen, A. I., Labuschagne, N. (2020): Rhizobacteria-Induced Systemic Tolerance against Drought Stress in Sorghum Bicolor (L.) Moench. – Microbiological Research 232: 126388.

http://www.aloki.hu ● ISSN 1589 1623 (Print) ● ISSN1785 0037 (Online)
DOI: http://dx.doi.org/10.15666/aeer/1804_59976008

[7] Chen, C. Q., Xin, K. Y., Liu, H., Cheng, J. L., Shen, X. H., Wang, Y., Zhang, L. (2017): Pantoea Alhagi, a Novel Endophytic Bacterium with Ability to Improve Growth and Drought Tolerance in Wheat. – Scientific Reports 7(1): 1-14.
[8] Colmenero-Flores, J. M., Martínez, G., Gamba, G., Vázquez, N., Iglesias, D. J., Brumós, J., Talón, M. (2007): Identification and Functional Characterization of Cation-Chloride Cotransporters in Plants. – Plant Journal 50(2): 278-92.
[9] Dworkın, M., Foster, J. W. (1958): Experiments with Some Microorganisms Which Utilize Ethane and Hydrogen. – Journal of Bacteriology 75(5): 592-603.
[10] El-Komy, M. A., Hamdia, M. A. (1997): Effect of salinity, gibberellic acid and Azospirillum inoculation on growth and nitrogen uptake of Zea mays. – Biologia plantarum 40(1): 109-120.
[11] Erdogan, Ü., Ramazan, Ç., Atafeh, V., Metin, T., Yaşar, E., Kıtır, N. (2016): Role of Inoculation with Multi-Trait Rhizobacteria on Strawberries under Water Deficit Stress. – Zemdirbyste-Agriculture 103(1): 67-76.
[12] Glick, B. R. (2014): Bacteria with ACC Deaminase Can Promote Plant Growth and Help to Feed the World. – Microbiological Research 169(1): 30-39.
[13] Grobelak, A., Kokot, P., Swiatek, J., Jaskulak, M., Rorat, A. (2018): Bacterial ACC Deaminase Activity in Promoting Plant Growth on Areas Contaminated with Heavy Metals. – Journal of Ecological Engineering 19(5): 150-57.
[14] Hashem, A., Abd_Allah, E. F., Alqarawi, A. A., Wirth, S., Egamberdieva, D. (2019): Comparing Symbiotic Performance and Physiological Responses of Two Soybean Cultivars to Arbuscular Mycorrhizal Fungi under Salt Stress. – Saudi Journal of Biological Sciences 26(1): 38-48.
[15] Hassan, W., Bashir, S., Ali, F., Ijaz, M., Hussain, M., David, J. (2016): Role of ACC-Deaminase and/or Nitrogen Fixing Rhizobacteria in Growth Promotion of Wheat (*Triticum Aestivum* L.) under Cadmium Pollution. – Environmental Earth Sciences 75(3): 1-14.
[16] Hoagland, D. R., Arnon, D. I. (1950): The water: culture method for growing plants without soil. – California Agricultural Experiment Station, Berkeley.
[17] James, R. A., Rivelli, A. R., Munns, R., Von Caemmerer, S. (2002): Factors Affecting CO2 Assimilation, Leaf Injury and Growth in Salt-Stressed Durum Wheat. – Functional Plant Biology 29(12): 1393-1403.
[18] Khan, M. A., Shirazi, M. U., Khan, M. A., Mujtaba, S. M. (2009): Role of Proline, K / Na Ratio and Chlorophyll Content in Salt Tolerance of Wheat. – Pakistan Journal of Botany 41(2): 633-38.
[19] Khan, A. S., Xue, Q. Z., Mohammed, T. J., Khalid, S. K., Asghari, B., Ren, F. S., Sajid, M. (2016): *Bacillus pumilus* Enhances Tolerance in Rice (*Oryza Sativa* L.) to Combined Stresses of NaCl and High Boron Due to Limited Uptake of Na^+. – Environmental and Experimental Botany 124: 120-29.
[20] Lichtenthaler, H. K. (1987): Chlorophylls and Carotenoids: Pigments of Photosynthetic Biomembranes. – Methods in Enzymology 148(C): 350-82.
[21] Maqshoof, A., Zahir, A., Zahir, H., Naeem, A., Asghar, M. (2011): Inducing Salt Tolerance in Mung Bean through Coinoculation with Rhizobia and Plant-Growthpromoting Rhizobacteria Containing 1-Aminocyclopropane-1-Carboxylate Deaminase. – Canadian Journal of Microbiology 57(7): 578-89.
[22] Mayak, S., Tsipora, T., Glick, B. R. (2004): Plant Growth-Promoting Bacteria Confer Resistance in Tomato Plants to Salt Stress. – Plant Physiology and Biochemistry 42(6): 565-72.
[23] Munns, R., Tester, M. (2008): Mechanisms of Salinity Tolerance. – Annual Review of Plant Biology 59(1): 651-81.
[24] Nadeem, S. M., Zahir, A. Z., Muhammad, N., Hafiz, N. A., Muhammad, A. (2010): Rhizobacteria Capable of Producing ACC-Deaminase May Mitigate Salt Stress in Wheat. – Soil Science Society of America Journal 74(2): 533-42.

http://www.aloki.hu ● ISSN 1589 1623 (Print) ● ISSN1785 0037 (Online)
DOI: http://dx.doi.org/10.15666/aeer/1804_59976008

[25] Palaniyandi, S. A., Damodharan, K., Yang, S. H., Suh, J. W. (2014): Streptomyces Sp. Strain PGPA39 Alleviates Salt Stress and Promotes Growth of 'Micro Tom' Tomato Plants. – Journal of Applied Microbiology 117(3): 766-73.
[26] Parihar, P., Samiksha, S., Rachana, S., Vijay, P. S., Sheo, M. P. (2015): Effect of Salinity Stress on Plants and Its Tolerance Strategies: A Review. – Environmental Science and Pollution Research 22(6): 4056-75.
[27] Rajput, L., Asma, I., Fathia, M., Fauzia, Y. H. (2013): Salt-Tolerant PGPR Strain Planococcus Rifietoensis Promotes the Growth and Yield of Wheat (*Triticum Aestivum* L.) Cultivated in Saline Soil. – Pakistan Journal of Botany 45(6): 1955-62.
[28] Ravanbakhsh, M., Sasidharan, R., Voesenek, L. A. C. J., Kowalchuk, G. A., Jousset, A. (2017): ACC Deaminase-Producing Rhizosphere Bacteria Modulate Plant Responses to Flooding. – Journal of Ecology 105(4): 979-86.
[29] Sarkar, A., Pallab, K. G., Krishnendu, P., Soumik, M., Tithi, S., Sanjeev, P., Monohar, H. M., Tushar, K. M. (2018): A Halotolerant Enterobacter Sp. Displaying ACC Deaminase Activity Promotes Rice Seedling Growth under Salt Stress. – Research in Microbiology 169(1): 20-32.
[30] Shanmugam, V., Kanoujia, N. (2011): Biological Management of Vascular Wilt of Tomato Caused by *Fusarium oxysporum* f. Sp. Lycospersici by Plant Growth-Promoting Rhizobacterial Mixture. – Biological Control 57(2): 85-93.
[31] Shimaila, A., Charles, T. C., Glick, B. R. (2014): Amelioration of High Salinity Stress Damage by Plant Growth-Promoting Bacterial Endophytes That Contain ACC Deaminase. – Plant Physiology and Biochemistry 80(6): 160-67.
[32] Singh, R. P., Prabhat, N. J. (2016): Mitigation of Salt Stress in Wheat Plant (*Triticum Aestivum*) by ACC Deaminase Bacterium Enterobacter Sp. SBP-6 Isolated from Sorghum Bicolor. – Acta Physiologiae Plantarum 38: 110.
[33] Singh, R. P., Prameela, J., Prabhat, N. J. (2017): Bio-Inoculation of Plant Growth-Promoting Rhizobacterium *Enterobacter cloacae* ZNP-3 Increased Resistance Against Salt and Temperature Stresses in Wheat Plant (*Triticum Aestivum* L.). – Journal of Plant Growth Regulation 36(3): 783-98.
[34] Sofo, A., Scopa, A., Nuzzaci, M., Vitti, A. (2015): Ascorbate Peroxidase and Catalase Activities and Their Genetic Regulation in Plants Subjected to Drought and Salinity Stresses. – International Journal of Molecular Sciences 16(6): 13561-78.
[35] Tahir, M., Ahmad, I., Shahid, M., Shah, G. M., Farooq, A. B. U., Akram, M., Tabassum, S. A., Naeem, M. A., Khalid, U., Ahmad, S., Zakir, A. (2019): Regulation of Antioxidant Production, Ion Uptake and Productivity in Potato (*Solanum Tuberosum* L.) Plant Inoculated with Growth Promoting Salt Tolerant Bacillus Strains. – Ecotoxicology and Environmental Safety 178(4): 33-42.
[36] Tester, M. (2003): Na^+ Tolerance and Na^+ Transport in Higher Plants. – Annals of Botany 91(5): 503-27.
[37] Turhan, E., Kıran, S., Ates, Ç., Ates, O., Sebnem, K., Sekure, S. E. (2020): Ameliorative Effects of Inoculation with *Serratia marcescen*s and Grafting on Growth of Eggplant Seedlings under Salt Stress. – Journal of Plant Nutrition 43(4): 594-603.
[38] Yang, C. W., Wang, P., Li, C. Y., Shi, D. C., Wang, D. L. (2008): Comparison of Effects of Salt and Alkali Stresses on the Growth and Photosynthesis of Wheat. – Photosynthetica 46(1): 107-14.
[39] Yildirim, E., Turan, M., Ekinci, M., Dursun, A., Cakmakci, R. (2011): Plant Growth Promoting Rhizobacteria Ameliorate Deleterious Effect of Salt Stress on Lettuce. – Scientific Research and Essays 6(20): 4389-96.
[40] Yue, H. T., Mo, W. P., Li, C., Zheng, Y. Y., Li, H. (2007): The Salt Stress Relief and Growth Promotion Effect of Rs-5 on Cotton. – Plant and Soil 297(1-2): 139-45.
[41] Zahir, Z. A., Ghani, U., Naveed, M., Nadeem, S. M., Asghar, H. N. (2009): Comparative Effectiveness of Pseudomonas and Serratia Sp. Containing ACC-Deaminase for

http://www.aloki.hu ● ISSN 1589 1623 (Print) ● ISSN1785 0037 (Online)
DOI: http://dx.doi.org/10.15666/aeer/1804_59976008

Improving Growth and Yield of Wheat (*Triticum Aestivum* L.) under Salt-Stressed Conditions. – Archives of Microbiology 191(5): 415-24.

[42] Zelicourt, de A., Al-Yousif, M., Hirt, H. (2013): Rhizosphere Microbes as Essential Partners for Plant Stress Tolerance. – Molecular Plant 6(2): 242-45.

http://www.aloki.hu ● ISSN 1589 1623 (Print) ● ISSN1785 0037 (Online)
DOI: http://dx.doi.org/10.15666/aeer/1804_59976008

EFFECT OF LOW-INTENSITY LASER IRRADIATION ON FIELD PERFORMANCE OF MAIZE (*ZEA MAYS* L.) EMERGENCE, PHENOLOGICAL AND SEED QUALITY CHARACTERISTICS

HASAN, M.[1] – HANAFIAH, M. M.[1,2*] – TAHA, Z. A.[3] – ALHILFY, I. H. H.[4]

[1]*Department of Earth Sciences and Environment, Faculty of Science and Technology, Universiti Kebangsaan Malaysia, 43600 Bangi, Selangor, Malaysia*

[2]*Centre for Tropical Climate Change System, Institute of Climate Change, Universiti Kebangsaan Malaysia, 43600 Bangi, Selangor, Malaysia*

[3]*Institute of Laser for Postgraduate Studies, University of Baghdad, Baghdad 00964, Iraq*

[4]*Department of Field Crop Science, College of Agriculture, University of Baghdad, Baghdad 00964, Iraq*

[*]*Corresponding author*
e-mail: mhmarlia@ukm.edu.my; phone: +60-389-215-865

(Received 30th Apr 2020; accepted 29th Jul 2020)

Abstract. Laser application in agriculture has attracted much interest due to the improvement of plant characteristics after laser pre-sowing seed treatment. In this study, *Zea mays* L. seeds were pre-irradiated by a single exposure to blue laser at different intensities (2 and 4 mW/cm^2) and different irradiation times of 45, 65, 85, and 105s. The field emergence characteristics (i.e., emergence %, mean emergence time, emergence index, vigor index, growth parameters, and seed quality) of laser-induced *Zea mays* L. seeds were determined and compared with those of unirradiated seeds. A randomized complete block design (RCBD) was employed with three replications. The growth characteristics of the seeds exposed to laser for 85s showed significant improvements in terms of the seedling length and leaf number. Additionally, there were observable alterations in the seed emergence percentage (91.66%), emergence index (7.25), and vigor index (520.80) in the seeds irradiated for 85s at a laser intensity of 4 mW/cm^2. In seeds irradiated for 85 s, both the oil and starch contents were increased by 6.33% and 73.11%, respectively. On the other hand, there was an increase in the protein content of maize seeds (18%) with increased laser intensity. In conclusion, the results of the present study demonstrated that 4 mW/cm^2 of blue laser and the irradiation period of 85s enhanced the emergence process of maize plants.
Keywords: *low power, blue laser, exposure time, seed stimulation, physical priming*

Introduction

Laser radiation has been found application in all spheres of engineering due to its basic characteristics, such as coherence, monochromaticity, polarization, and power density. However, these attributes of laser radiation have also made it applicable in biological and agricultural sectors. Upon exposure to laser radiation, certain changes occur in the physiological state of plants and seeds and such changes can either induce or inhibit the development of such plant or seed based on the type of laser radiation used, as well as its intensity and wavelength (Hasan et al., 2020). There are several light-absorbing molecules in nature which mediates the response of organisms to change in the natural light environment. The changes in the light parameter influence various physiological processes (i.e. intra and inter-cellular differentiation, seed germination and seedling growth, photosynthesis, flowering, etc.) depending on the species and developmental

http://www.aloki.hu ● ISSN 1589 1623 (Print) ● ISSN 1785 0037 (Online)
DOI: http://dx.doi.org/10.15666/aeer/1804_60096023

stage or studied organ (He et al., 2017). It has been reported earlier that light is an absolute factor that regulates seed germination in numerous plant species (Jala, 2011).

Several previous studies reported the effects of light on the germination and growth of seeds of plants (Hernandez et al., 2010; Aladjadjiyan, 2012; Qiu et al., 2017; Alsalhi et al., 2018). Some plant seeds require light to grow while the germination of some plant seeds can be inhibited in the presence of light (Hernandez and Michtchenko, 2011; Atif et al., 2020). According to Jala (2011), different levels of exposure time to light can have various influences on the germination parameters of different seeds. Furthermore, when low-power laser light is used on seeds, seedlings, and plants, it produces bio-stimulation (Hernandez et al., 2009, 2010, 2015; Perveen et al., 2010; Hernández and Michtchenko, 2011; Aladjadjiyan, 2012; Jia and Duan, 2013; Hasan et al., 2020).

Without a doubt, the 21st century needs to develop technologies to increase the global production of food since one of the main challenges of our time is to feed a growing world population (Foley, 2011; Muhammad-Muaz and Marlia, 2014; Hanafiah et al., 2019) which has been projected to grow by two to three billion of people by the year 2050. This implies that the world population will increase to 9000 million (FAO, 2011), with a simultaneous doubled increase in food cost, the problem of hunger will worsen. At the same time, the need to reduce damage to the environment is considered (Foley, 2011; Aziz et al., 2020a). All these, under the current context and the future climate changes, lead to threatened areas with high temperature (Harun and Hanafiah, 2018; Aziz et al., 2020b) and year forecasts are extremely unfavourable (Field et al., 2012; Fadillah and Marlia, 2016). Therefore, several methods have been introduced to increase crop yield including by laser irradiation.

Bioeffects due to low laser power in seed pre-planting and in seedlings or plants during their development have been confirmed by numerous studies using seeds of various crops (Osman et al., 2009; Aladjadjiyan, 2012; Hoseini et al., 2013; Kouchebagh et al., 2014a; Śliwka, 2014; Srećković et al., 2014). From the introduction of lasers in the '60s (Nasim and Jamil, 2014), its application began in biological systems (Bessis et al., 1962), dabbling to the agricultural sector as a bio-stimulatory element (BE) of plants and seeds with the ruby laser (Wilczek et al., 2005). He-Ne (Helium-Neon), Ar (Argon), Neodymium- YAG (Nd-YAG), carbon dioxide (CO_2) and diodes (in different wavelengths - λ) have been applied to conjecture the use of laser technology for pre-seeding treatment or during some of the phenological stages of the crops (Chen et al., 2005; Hernandez, 2009; Hernandez et al., 2010, 2015; Hernández and Michtchenko, 2011; Aladjadjiyan, 2012; Śliwka, 2014). Laser technology has evolved and has been applied in bio-stimulation processes of seeds and plants. He-Ne laser is the most applied laser as BE of seeds and/or plants since its foray into agriculture until today (Aladjadjiyan, 2012; Hernández et al., 2015; Hasan et al., 2020).

In this way, it is interesting to study the optimum laser irradiation parameters to produce favourable bioeffects and when applied in the agricultural sector, could, among other effects, increase the performance of products, stems and seeds, reduce the vegetative period, improve the quality of harvest, produce vigorous plants, improve the photosynthetic evolution of plants, break the seed dormancy, stimulate germination, recover the soil, and protect the environment against toxigenic mold and bacteria (Podleśna et al., 2015).

During the bio-stimulation of plants at various developmental phases of the plant, three kinds of photoreceptors (phytochromes, phototropins, and cryptochromes) have been found to absorb light at different wavelengths of 600-750, 320-500 and 500-630 nm,

http://www.aloki.hu ● ISSN 1589 1623 (Print) ● ISSN 1785 0037 (Online)
DOI: http://dx.doi.org/10.15666/aeer/1804_60096023

respectively (Bouly et al., 2007; Levskaya et al., 2009). This implies that the seeds, based on their respective characteristics (physical, chemical, optical, thermal, photothermal, genotypic, phenotypic, etc.) will first take in the light energy and transform it into chemical energy for use in their subsequent growth phases (Jamil et al., 2013). As such, the kinetic equilibrium of seed germination processes can be altered by exposure to laser light, thereby increasing the internal energy of the seeds (Ferdosizadeh et al., 2013) and varying the response according to the seed type and cultivar.

Based on the previous studies, the physiological quality of certain crops has been improved using He-Ne (632.8 nm) and laser diodes (650, 660 nm) bio-stimulation. Among such crops are *Zea mays* L., *Triticum* (Joshi et al., 2012; Jamil et al., 2013), *Carthamus tinctorius* L., *Helianthus annuus* L., *Brassica napus* L. (Ashrafijou et al., 2010; Perveen et al., 2010), *Medicago sativa*, *Vicia faba*, *Lathyrus sativus* L. (Qi et al., 2002; Truchliñski et al., 2002; Wilczek, 2005), *Raphanus sativus* L., *Solanum lycopersicum* L. (Álvarez et al., 2011; Jia and Duan, 2013), *Acacia farnesiana* L., *Ricinus communis* L. (Soliman and Harith, 2009), *Balanites aegyptiaca*, *Celosia argéntea*, *Beta vulgaris* L. (Metwally et al., 2013; Podleśna et al., 2015). Germination is the initial stage of development in the growth of crops. During this stage, the important seed quality parameters that can affect the plant status are the germination rate, seed vigor, and germination uniformity (Mohssen-Nasab et al., 2010). Thus, this study aims to determine the effect of different intensity of blue laser irradiation on maize seeds, in terms of their field emergence parameters, growth, and seed quality.

Materials and Methods

Study Area

This research was conducted in the experimental field located at the Faculty of Agriculture, University of Baghdad and Laser Laboratory, Institute of Laser for Postgraduate Studies, University of Baghdad (33° 16′ 26″ N, 44° 22′ 39″ E). The experimental site has a hot dry climate in summer season in 2018, the average temperature was in the range of 17.1°C to 31.6°C, with an annual average rainfall of 284.2 mm and average humidity of 45%. Soil samples were randomly collected from the field and transferred to the lab to measure the physical-chemical parameters. The soil was slightly alkaline pH (7.2), salt-free (electrical conductivity 3.8 meq/100 g soil), nitrate and ammonia nitrogen concentrations of 0.0017% and 0.009%, respectively, very high P assimilation rate (43.2 mg/kg), and high K (1.6 mg/L). The soil texture was silt (28.9 g/kg), clay (38.5 g/kg) and sand (32.6 g/kg).

Laser Irradiation Experiment

A blue laser source of 100 mW power (410 nm) was used in this study. A 100 cm distance was maintained between the laser and the seed samples. The seeds were positioned in a steady manner on the side facing the embryo and hanged in the air (supported on one side by a heat dissipater). To ensure that the laser diode operates in a normal mode for a prolonged period, it was placed in a special bed in the modules' ribbed part to provide good cooling. Optics were used in the lasers to ensure the provision of the optimum laser power. Additionally, the irradiation power intensity of the laser was set at 2 and 4 mW/cm^2, the intensity was measured using a power meter. The blue laser was used to irradiate the maize seeds for different exposure times of 45, 65, 85 and 105 s. The

http://www.aloki.hu ● ISSN 1589 1623 (Print) ● ISSN 1785 0037 (Online)
DOI: http://dx.doi.org/10.15666/aeer/1804_60096023

optimum period for each treatment was monitored using a time controller device. The parts of the device and the positioning of the treated seeds are depicted in *Table 1*.

Table 1. *Experimental conditions used for seed pre-treatment of maize*

Excremental condition	Details
Laser type	Diode laser
Wavelength	410 nm
Power intensity	2, and 4 mW/cm^2
Laser exposition time	45, 65, 85, and 105 s
Wave emission	Continuous (CW)
Beam size	2 mm
Distance from sample	100 cm
Cultivar treated	Baghdad 3

Experimental Design

In summer 2018, a 4x2 factorial experimental design was conducted for blue laser exposure times (T_1= 45, T_2= 65, T_3= 85 and T_4= 105 s) at 410 nm, two intensities (P_1= 4 and P_2= 2 mW/cm^2), and a control (without exposure to laser) in a design of complete blocks with three replications. The land was fallow, harrowed and furrowed with machinery. Planting was carried out manually in dry soil at a plant density of 6667 plants/ha, and inter-plant distance of 25 cm. In this study, 600 seeds were pretreated before sowing in the field. The size of the experimental plot was 2 meters wide by 1.5 meters long. Total irradiated seeds were 1600. This study used maize seed variety (Baghdad 3 cultivar) provided by the Office of Agriculture Research, Baghdad. The seed variety was grown during the planting season (spring-summer) in July 2018 in the experimental field. The seeds lot was first standardized with respect to size and colour, followed by seeds dipped into a sodium hypochlorite solution (1% v/v) for sterilization and then rinsed in tap water for several time periods and left to dry by room temperature prior to irradiation. From each treatment group, six seeds were selected and measured for thicknesses using a Vernier instrument. The observed average thickness of the seeds was 3.9 mm.

The fertility of the fields was improved with 520 kg/ha of compost (46:18 of N: P_2O_5) and prior to sowing, the soil was fertilized with 436 kg/ha of urea (1/2 before sowing and the rest at the flowering stage). During the growing period, weeding was done manually while insects were controlled chemically using diazinon at the rate of 6 kg/ha which was applied at 20 and 35 days after sowing. The crops were harvested manually after 110 days from the date of sowing. The drying of the ears was natural in a ventilated place and in the shade. It was manually de-grained when the moisture content of the grain was around 15% and the grain was stored at a temperature of 25°C.

Parameters Measurement

A daily count of seedling emergence was conducted while the other seedling parameters (emergence %, emergence index, vigor index) were recorded after the viable seeds have emerged (no new seed emergence observed). The mean emergence time (MET) was calculated using *Eq. 1* as follows:

http://www.aloki.hu ● ISSN 1589 1623 (Print) ● ISSN 1785 0037 (Online)
DOI: http://dx.doi.org/10.15666/aeer/1804_60096023

$$MET = \Sigma Dn / \Sigma n \quad \text{(Eq.1)}$$

where D = number of days that elapsed from the first day of sowing, and n = the number of emerged seeds on day D.

Emergence index (EI) was calculated according to The Association of Official Seed Analysis (1978) formula in *Eq. 2*:

$$EI = \text{No. of emerged seeds / Day of first count} + \ldots + \text{No. of emerged seeds/Day of final count} \quad \text{(Eq.2)}$$

Emergence speed was calculated by *Eq. 3*:

$$Es = \sum Ni / Di \quad \text{(Eq.3)}$$

where, Ni = number of seeds emerged per day. Di =Number of days (daily germination).

Seedling vigor index was calculated as below (*Eq. 4*):

$$\text{Vigor Index (VI)} = \text{emergence (\%)} \times \text{Seedling length (cm)} \quad \text{(Eq.4)}$$

Flowering dates: Dates when 100% of the plants in a plot attained anthesis and incipient silk extrusion were recorded and expressed as days after planting, as well as stem diameter, and seedling leaves number at 21th days after planting were measured.

Seedling heights at 21th day after planting: This is the measure of a distance from the surface of the soil to the flag leaf-bearing nodes. Fresh weight was determined and dry weight was calculated by drying seedling (at 21th day after planting) in an oven at 75°C until the weight remained constant. The top ear was determined from 5 randomly selected plants in a plot and the mean of the measurements was determined and presented as the plant height. The proximate composition of the grain, including protein, starch, and oil were analysed after harvesting based on the method prescribed by AACC (2000).

Statistical Analysis

The acquired data in this study were analyzed using Genstat® Statistical software version 19. The software was used to analyze the analysis of variance (ANOVA) at a significance level of $p < 0.01$; the Fisher's test was used to define the observed levels of significant differences between the means of the datasets. All the measurements were performed in triplicates.

Results

Table 2 shows the seed emergence percentage and other parameters. Evidently, each laser exposure time and intensity significantly influenced the field emergence percentage. The percentage of emergence was found to be increased over the control, reaching a maximum seed emergence percentage of 91.6% by seeds irradiated with 4 mW/cm^2 laser intensity for 85 s. A decreased percentage was observed at 65 s as the lowest seed emergence percentage of 58.6 and 62.5% was recorded from the seeds irradiated at 65 s and the un-irradiated control seeds, respectively. The increased percentage of emergence was significantly different ($p < 0.01$) when compared to the control seeds.

http://www.aloki.hu ● ISSN 1589 1623 (Print) ● ISSN 1785 0037 (Online)
DOI: http://dx.doi.org/10.15666/aeer/1804_60096023

Table 2. *Field emergence and growth components after seed pre-treatment with blue laser*

Treatments	emergence %	emergence index	emergence speed (hour)	mean emergence time (hour)	vigor index	plant height (cm/plant^{-})	leaves number/ plant	fresh weight (g)	dry weight (g)
T_1P_1	87.50^{b}	6.41^{ab}	43.33^{c}	51.00^{de}	282.80^{e}	20.20^{c}	8.20^{ab}	1.89^{a}	0.70^{a}
T_1P_2	83.33^{c}	6.33^{abc}	48.80^{d}	53.12^{e}	345.60^{c}	21.60^{bc}	7.80^{bc}	1.84^{a}	0.64^{a}
T_2P_1	58.66^{f}	4.16^{d}	63.18^{e}	64.19^{f}	148.80^{i}	18.60^{c}	8.40^{ab}	1.84^{a}	0.56^{a}
T_2P_2	83.33^{c}	6.00^{bc}	48.95^{d}	46.67^{bc}	240.00^{g}	20.00^{c}	7.00^{cd}	2.28^{a}	0.41^{a}
T_3P_1	91.66^{a}	7.25^{a}	25.71^{a}	33.00^{a}	520.80^{a}	25.13^{a}	8.20^{ab}	3.66^{a}	0.70^{a}
T_3P_2	87.50^{b}	6.58^{ab}	37.60^{b}	44.57^{b}	377.60^{b}	23.60^{ab}	8.80^{a}	4.00^{a}	0.71^{a}
T_4P_1	83.33^{c}	6.16^{abc}	43.20^{c}	49.71^{cd}	266.00^{f}	19.00^{c}	7.20^{cd}	2.70^{a}	0.50^{a}
T_4P_2	66.66^{d}	5.16^{cd}	42.50^{c}	54.25^{e}	288.40^{d}	20.60^{bc}	7.80^{bc}	2.32^{a}	0.49^{a}
Control	62.50^{e}	4.58^{d}	38.60^{b}	45.33^{b}	188.00^{h}	18.80^{c}	6.80^{d}	2.34^{a}	0.46^{a}
T	*	*	*	*	*	*	Ns	Ns	Ns
P	Ns	Ns	Ns	Ns	*	Ns	Ns	Ns	Ns
T*P	*	Ns	*	*	*	*	*	Ns	Ns
LSD	2.47	1.23	2.14	3.14	2.64	3.48	0.91	2.59	0.84

The exposure time: T_1=45 s, T_2=65 s, T_3=85 s, and T_4=105 s. Power density: P_1=4 mW/cm^2, and P_2=2 mW/cm^2. Means of treatments were compared using the least significant difference (LSD) at $p \leq 0.01$. Mean values with the same letters in the same column are statistically equal (Fisher's, a = 0.01)

A similar trend was also observed in the mean emergence time as shown in *Table 3*. The seeds irradiated with 4 mW/cm^2 laser intensity for 65 s needed 64.19 h as the average emergence time, whereas those irradiated for 85 s required only 33 h, showing a significant difference in the respective emergence times. The emergence speed was observed to be 25.7 h for seeds exposed to 4 mW/cm^2 laser intensity for 85 s, showing a considerable increase compared to seeds irradiated for 85s at a laser intensity of 2 mW/cm^2 (37.6 h) and un-irradiated treatment group (38.6 h). This reduction in emergence speed for the seeds exposed to laser treatment (T_3P_2 and T_3P_1) was significant at ($p < 0.01$) when compared to the control seeds. There was also a linear improvement in the seedling vigor index by 520 in seeds treated with a laser power intensity of 4 mW/cm^2 for 85 s compared to the other treatments. The highest emergence index of 7.25 was recorded for 85 s of 4 mW/cm^2 ($P < 0.01$), which was statistically significant in comparison to the control (4.58).

The maximum plant height, fresh and dry weights of seedling were observed in seeds treated with laser for 85 s. The plant height and the number of leaves were increased by a single exposure to laser for 85 s ($p < 0.01$) compared to the control set. Laser irradiation for 85 s at 4 mW/cm^2 significantly increased the plant height (25.13 cm) for the seedlings from the control seeds (18.8 cm). The laser treatments also significantly affected the number of leaves per maize plant as shown in *Table 2*. Increases in the number of leaves per plant for both power densities were observed. The best results (8.8 leaves/plant) were exhibited by seeds irradiated with 2 mW/cm^2 laser intensity for 85 s, followed by those irradiated with 4 mW/cm^2 laser intensity for 85 s (8.4 leaves/plant). The minimum number of leaves per plant (6.8) was obtained in the un-irradiated control. There was no statistically significant difference between the observed effects of treatments of the fresh and dry weights of the maize seeds (*Table 2*).

http://www.aloki.hu ● ISSN 1589 1623 (Print) ● ISSN 1785 0037 (Online)
DOI: http://dx.doi.org/10.15666/aeer/1804_60096023

Table 3. *Flowering and seed quality components after seed pre-treatment with blue laser*

Treatments	Protein content (%)	Oil content (%)	Starch content (%)	Stem diameter (cm)	Days to Anthesis (day)	Days to Silking (day)
T_1P_1	16.30^{ab}	3.08^{c}	68.78^{cd}	2.30^{bc}	60.40^{b}	61.50^{a}
T_1P_2	14.60^{bc}	6.22^{a}	71.25^{b}	1.90^{c}	59.33^{b}	63.90^{a}
T_2P_1	16.67^{ab}	3.95^{bc}	66.30^{cd}	2.20^{bc}	58.92^{ab}	63.30^{a}
T_2P_2	16.70^{ab}	6.18^{a}	69.40^{c}	1.90^{c}	59.13^{ab}	62.70^{a}
T_3P_1	18.00^{a}	6.33^{a}	76.83^{a}	3.50^{a}	56.20^{a}	62.25^{a}
T_3P_2	18.20^{a}	6.22^{a}	73.11^{a}	2.80^{abc}	58.72^{ab}	64.00^{a}
T_4P_1	13.70^{c}	3.81^{bc}	71.76^{b}	2.30^{bc}	61.40^{b}	64.10^{a}
T_4P_2	14.80^{bc}	4.27^{bc}	63.82^{e}	2.60^{abc}	60.83^{b}	65.40^{a}
Control	16.80^{ab}	4.37^{b}	70.12^{bc}	2.90^{ab}	61.40^{b}	63.00^{a}
T	*	*	*	Ns	*	Ns
P	Ns	*	Ns	Ns	Ns	Ns
T*P	Ns	*	*	*	*	Ns
LSD	2.47	1.23	1.76	0.91	2.97	3.60

The exposure time: T_1=45 s, T_2=65 s, T_3=85 s, and T_4=105 s. Power density: P_1=4 mW/cm^2, and P_2=2 mW/cm^2. Means of treatments were compared using the least significant difference (LSD) at $p \leq 0.01$. Mean values with the same letters in the same column are statistically equal (Fisher's, a = 0.01)

Table 3 also presents the effect of laser exposure on the oil content of the seeds. The laser-treated seeds and the control seeds presented a comparable level of oil content. As shown in *Table 3*, there were significant differences in the oil content of the seed. Generally, the oil contents of the seeds were increased by exposure to laser for different exposure times, where seeds exposed for 85 s to 4 mW/cm^2 laser intensity showed higher oil content (6.33%), followed by those exposed to 2 mW/cm^2 laser intensity (6.22%). The control seeds showed the lowest oil content (4.37%). Highest levels of total protein content and starch content were recorded in seeds exposed to laser for 85 s compared to the control ($p < 0.01$). The exposure of maize seeds to laser at different exposure times had a significant influence on the protein content of the seeds (*Table 3*). An increase in the exposure time to laser was generally found to increase the protein content of the seeds, with the highest protein content of 18.2% being observed in seeds exposed to 2 mW/cm^2 laser power for 85 s, followed by 18% for seeds exposed to 4 mw/cm^2 laser power for 85 s. The control seeds had a protein content of 16.8%. The protein content increased gradually, and the maximum activities were noted in seedlings derived from 85 s laser irradiated seeds, whereas the starch content showed maximum activity at 85 s which was found to be significant ($p < 0.01$) compared to the control group. The different energy densities of laser irradiation also increased the stem diameter during the harvest stage. Pre-sowing exposure to 4 mW/cm^2 laser power for 85 s was observed to significantly increase the stem diameter of the plants (3.5 cm) compared to the stems of the control seeds (2.9 cm).

Regarding the days to silking, *Table 3* shows a marked difference in the days to silking of the maize plants exposed to laser for different exposure times. However, there was no statistically significant difference between the observed effects. The shortest period (61.5 day) was observed in plant seeds exposed to 4 mW/cm^2 blue laser for 45 s compared to 65.4 day of the control group. There were also significant differences in the Days to Anthesis as presented in *Table 3*. In general, using different exposure times led to an

http://www.aloki.hu ● ISSN 1589 1623 (Print) ● ISSN 1785 0037 (Online)
DOI: http://dx.doi.org/10.15666/aeer/1804_60096023

increase in the Days to Anthesis. For the blue laser, 85 s of exposure at 4 mW/cm^2 has a shorter period to Anthesis (56.2 day), followed by seeds irradiated with a power density of 2 mW/cm^2 (58.72 day). The control group had the longest period to Anthesis (61.4 day).

Discussion

Seed germination is a crucial stage in plant development and can be considered as a determinant for plant productivity. Physiological and biochemical changes followed by morphological changes during germination are strongly related to seedling survival rate and vegetative growth which consequently affect yield and quality. Seed stimulates the embryo to produce phytohormones mainly gibberellic acid (GA) which can diffuse to aleurone layer and initiate a signaling cascade resulting in the synthesis of a-amylases and other hydrolytic enzymes.

Phytochromes are involved in the sensing of the light environment by seeds, and the control of germination by red and far-red light was one of earliest phytochrome-mediated responses described Phytochromes can affect the growth capacity of the embryo and/or the constraint imposed by seed tissues around it. Much evidence exists for the role of phytochromes in promoting the synthesis of gibberellins (GAs), which are important stimulants for germination (García-Martinez and Gil, 2001; Hilhorst et al., 2018; Ribalta et al., 2019). Phytochromes also play a role in regulating the sensitivity to GAs (Mishra and Khurana, 2017). Recently, phytochromes have also been shown to be involved in the degradation of abscisic acid, the major plant hormone that maintains dormancy (Miransari and Smith, 2014).

Hernandez et al. (2010, 2011) presented a detailed review of the use of laser treatment for plant stimulation. The review suggested that laser light can be used in agriculture for seeds bio-stimulation based on the additive interaction between the laser beam (polarized and monochromatic) and the photoreceptors that absorb it. This interaction activates several biological processes in the exposed seeds. However, the level of effect of laser treatment is a function of the laser wavelength, the output power, and the period of exposure.

According to several reports, various laser output powers have been investigated (Govil et al., 1991; Jia and Duan, 2013) to 5 mW (Hernandez et al., 2010). Different periods of exposure have also been studied, ranging from 30 s (Hernández and Michtchenko, 2011) to 120 min (Khalifa and El Ghandoor, 2011). In the present study, the highest emergence rate was presented by seeds exposed to 4 mW/cm^2 laser intensity for 85 s which is comparable to earlier reports by Ćwintal et al. (2010). According to several authors, laser treatment can also cause some levels of damage to plant cells and tissues (Jia and Duan, 2013). As per Salyaev et al. (2007) and Hernandez et al. (2010), there are two specific responses which can be induced upon exposure of cells to laser light: (i) a rapid stress effect which increases the level of lipid peroxidation products generation, and (ii) series of secondary reactions due to the adaptive metabolic changes which can elicit some morphogenetic processes. The present results agreed with previous findings by Taie et al. (2014) who reported the maximum germination percentage of some Merremia sp. upon exposure to laser light. In a study on Stevia seeds, Goettemoeller and Ching (1999) reported that the two weeks-delay and the low seed germination percentage observed in the control set could be attributed to the importance of light to the germination of Stevia seeds (light-requiring seeds) as the exposed seeds showed better germination

http://www.aloki.hu ● ISSN 1589 1623 (Print) ● ISSN 1785 0037 (Online)
DOI: http://dx.doi.org/10.15666/aeer/1804_60096023

percentage compared to the control. All light-requiring seeds have also been earlier reported to show dormancy (Taiz and Zeiger, 2011), while the importance of light to seed germination and plant growth has been reported (Hernandez et al., 2009).

However, upon completion of germination, Jala (2011) recorded the highest germination percentage in seeds treated with laser light. The present results on germination show deviation from Jala (2011) but in line with Colbach et al. (2002) on *Alopecurus myosuroides* and Ambika (2007) on *Chromolaena odorata* seeds. Horizontal and vertical expansion of shoot, particularly leaves, is a genetically-controlled developmental process (Tsukaya, 1998) and irradiation with blue light seems to cause imbalance in the expression of the concerned genes, leading to inhibition of leaf expansion. Furthermore, the improved rate of seed germination could be attributed to the matter and energy transfer processes involved in the germination and growth of seeds (Abu-Elsaoud et al., 2013). For instance, different intensities of laser treatment have been reported to induce the germination of wheat and maize seeds, as well as some vegetables (Asghar et al., 2016). The spectral influence of laser treatment on seed germination has also been investigated by Chen et al. (2005) in which laser light was reported to induce changes in the normal plant functions, and elicited rapid cell division, resulting in a rapid rate of initial growth and development. Therefore, the observed positive effects of laser light treatment on the seed germination parameters in the present study could be attributed to an improved rate of laser-induced cell division. Some reports have also reported that laser treatment is a physical process involves the absorption and storage of radiant energy by the cells and tissues of plants. This is also applicable to seeds as they first absorb the radiation energy before its subsequent transformation into chemical energy for subsequent use (El-Naggar et al., 2012; Hedimbi and Singh, 2012; AlSalhi et al., 2018).

According to Hernandez et al. (2010), the pre-sowing exposure of various seeds (like rice, maize, tomato, radish, peas, cucumber, lettuce, onion, etc.) to laser has a significant influence on their germination parameters. The seeds of vegetables have been reported as the most sensitive seeds to laser stimulation compared to cereals (Gładyszewska, 2006; Hernandez et al., 2015). Laser radiation of different exposure times (45, 65, 85, and 105 s) as used in the present study showed different effects on maize plants. Statistical analysis of this work reveals that plant height, number of leaves and stem diameter increased by laser treatments and this may reflect the effect of laser on cell division of shoot taps of the exposed shoots. This effect continued in the cell division of all parts of the plant at both vegetative and flowering stages. Our results reveal that the exposure to blue laser rays for 85 s and 4 mW/cm^2 laser intensity had the most pronounced effect in increasing the growth criteria for maize plant and decreased emergence time. A similar effect was also noticed by Podleśna et al. (2015). These results agree with Chen et al. (2005) who showed changes in the protein functional activities. There were also increases in the physiological and biochemical characteristics of the seedlings after exposure to laser (Chen et al., 2005; Qiu et al., 2013). The exposure time to laser radiation is very important to produce stimulation effects and these agree with the report of Rimal et al. (2014).

From the in-vitro growth data, it was observed that different exposure times to blue laser increased the germination and shoot multiplication rates of maize plants. This was supported by the reports of Hwida et al. (2012) on *Balanites aegyptiaca* and Cotoneaster horizontalis and Dănăilă et al. (2011) on Petunia hybrid and Dianthus caryophyllus plants. According to earlier reports on *Balanites aegyptiaca*, the maximum number of shootlets per explant increases with laser treatments (Lobna et al., 2014; Rania et al., 2015). The maize seeds exposed to blue laser for 85 s had the longest plants compared to the control.

http://www.aloki.hu ● ISSN 1589 1623 (Print) ● ISSN 1785 0037 (Online)
DOI: http://dx.doi.org/10.15666/aeer/1804_60096023

These results showed the same trend with the reports of Ali et al. (2014), Lobna et al. (2014), and Kouchebagh et al. (2014b). The laser-induced cell elongation has been reported to increase the level of gibberellic acid which results in increased cell vacuoles (Mahmoud and Ibrahem, 2000). Regarding the number of leaves, the seeds exposed to blue laser for 85 s has plants with the highest number of leaves per plant compared to the control. This observation agreed with the reports of earlier studies (MacLeod and Millar, 1962; Kamiya and Martinez, 1999; Aguilar et al., 2015).

Osman et al. (2009) and Aguilar et al. (2015) suggested that laser radiation could induce faster rates of enzymatic activities within the cells of the exposed seeds. This could also be due to the endogenous GA content and its role in cell growth. It is believed that GA can induce cell growth by inducing enzymes that reduce the integrity of the cell wall (MacLeod and Millar, 1962). Seeds exposed to blue laser for 85 s produced plants with the longest stem diameter and dry and fresh weights compared to the control. Plant growth is generally controlled by several factors, such as enzymes and hormones like gibberellic acid (GA_3) and cytokinin. Kamiya and Martinez (1999) observed that exposure to laser plays a significant role in GA_3 formation and endogenous level of GA_1. The resulting increase in GA_3 response manifests in better cell growth, reduced cell wall integrity, proteolytic enzymes production, increased auxin content, and increased sugar concentration; can also increase the osmotic pressure of the cell sap. The physical manifestations of the increased cell elongation due to laser radiation are increased plant height and number of branches, as well as increased number of flowers (Ali et al., 2014; Rania et al., 2015). Exposure to laser can also increase the nitrogen content and result in increased protein content. This is necessary for the development of plant organs (such as the branches and umbels) (Osman et al., 2009). The study by Mahmoud and Ibrahem (2000) showed that laser irradiation can increase cell number, nucleic acids, and phospholipids membranes. It can also increase the potassium and phosphorus contents, thereby leading to the elongation of laser-irradiated cells.

However, further details are needed on the effects of different laser irradiation as they remain inexplicable (Samuilov and Garifullina, 2007). Coherent laser light beams excite electrons and promote the biophoton and entropy emission, thereby triggering an increase in the internal energy of the exposed material. The transient action of laser irradiation has also been implicated in the stimulation of various functional activities and higher plants' resistance to biotic disease (Rassam, 2010; Podleśny et al., 2012; Srećković et al., 2014; Tang et al., 2019). The role of laser technology in the agricultural sector is being evaluated from its bio-stimulatory role. Despite the reported positive influences of laser irradiation (visible to near IR), its light-regulated mechanism and role in plants are yet to be understood (Aguilar et al., 2015). Laser irradiation is emerging as a novel agricultural practice owing to its positive role in seed germination, seeds biochemical composition, enzyme activities, plant growth, seed quality, stress resistance, fruit size, and yield characteristics. Corn seeds stained with methylene blue were treated by Hernández et al. (2011) using a laser diode, a wavelength of 655 nm with 27.4 mW of power and 5 min of exposure. In these seeds, the number of seeds infected by Fusarium spp. was reduced, suggesting the possibility of using laser irradiation as a means of disease control in maize seeds, thereby improving the quality of seeds and the final product derived from plants emerging from such seeds.

http://www.aloki.hu ● ISSN 1589 1623 (Print) ● ISSN 1785 0037 (Online)
DOI: http://dx.doi.org/10.15666/aeer/1804_60096023

Conclusion

In the present study, the pre-sowing exposure of maize seeds to blue laser light at 4 mW/cm^2 laser intensity and 85 s exposure time significantly improved the seedling emergence rate and improved the seed emergence uniformity. Significant modification was also observed in the stages of plant growth. Such use of the laser is technically feasible and could be one of the solutions to increase seed emergence, seedling growth and establishment of more efficient maize seeds. However, future study is needed to understand the mechanism underlying phytohormones by the optimum blue laser pretreatment.

Acknowledgements. This research was supported by the Ministry of Education Malaysia (FRGS/1/2018/WAB05/UKM/02/2) and UKM research grant (DIP-2019-001).

REFERENCES

[1] AACC. (2000): American Association of Cereal Chemists. International approved methods of analysis (10th ed.). – AACC International St Paul MN U.S.A.

[2] Abu-Elsaoud, A. M., Tuleukhanov, S. T. (2013): Can He-Ne laser induce changes in oxidative stress and antioxidant activities of wheat cultivars from Kazakhstan and Egypt. – Science international 1(3): 39-50.

[3] Aguilar, C. H., Pacheco, F. A. D., Orea, A. C., Tsonchev, R. I. (2015): Thermal effects of laser irradiation on maize seeds. – International Agrophysics 29(2): 147-156.

[4] Aladjadjiyan, A. (2012): Physical factors for plant growth stimulation improve food quality. – Food production-approaches, challenges and tasks, doi: 10.5772/32039.

[5] Ali, S. M., Sharbat, L. M. M., Bedour, H. A. L., Sayed, A. M. (2014): Effect of drought stress and helium neon (He-Ne) laser rays on growth, oil yield and fatty acids content in caster bean (*Ricinus communis* L.). – Agriculture Forestry and Fisheries 3(3): 203-208.

[6] AlSalhi, M. S., Tashish, W., Al-Osaif, S. S., Atif, M. (2018): Effects of He–Ne laser and argon laser irradiation on growth, germination, and physico-biochemical characteristics of wheat seeds (*Triticumaestivum* L.). – Laser Physics 29(1): 015602.

[7] Álvarez, A., Ramírez, R., Chávez, L., Camejo, Y. (2011): Effect of the treatment of seeds with radiation laser of fall promotes in a hybrid of tomato (*Solanum lycopersicum* L.). – Revista Granma Ciencia 15(2): 1-9.

[8] Ambika, S. R. (2007): Effect of light quality and intensity on emergence, growth and reproduction in Chromolaena odorata. – In: International Workshop on Biological Control and Management of Chromolaena odorata and Mikania micrantha, p.14.

[9] Asghar, T., Jamil, Y., Iqbal, M., Abbas, M. (2016): Laser light and magnetic field stimulation effect on biochemical, enzymes activities and chlorophyll contents in soybean seeds and seedlings during early growth stages. – Journal of Photochemistry and Photobiology B: Biology 165: 283-290.

[10] Ashrafijou, M., Noori, S. S., Darbandi, A. I., Saghafi, S. (2010): Effect of salinity and radiation on proline accumulation in seeds of canola (*Brassica napus* L.). – Plant, Soil and Environment 56(7): 312-317.

[11] Association of Official Seed Analysts. (1978): Rules for testing seeds. – The Association.

[12] Atif, M. J., Amin, B., Ghani, M. I., Ali, M., Cheng, Z. (2020): Variation in morphological and quality parameters in garlic (*Allium sativum* L.) bulb influenced by different photoperiod, temperature, sowing and harvesting time. – Plants 9(2): 155.

[13] Aziz, N. I. H. A., Hanafiah, M. M., Halim, N. H., Fidri, P. A. S. (2020a): Phytoremediation of TSS, NH_3-N and COD from sewage wastewater by *Lemna minor* L.*, Salvinia minima, Ipomea aquatica* and *Centella asiatica.* – Applied Sciences 10(16): 5397.

http://www.aloki.hu ● ISSN 1589 1623 (Print) ● ISSN 1785 0037 (Online)
DOI: http://dx.doi.org/10.15666/aeer/1804_60096023

[14] Aziz, N. I. H. A., Hanafiah, M. M., Gheewala, S. H., Ismail, H. (2020b). Bioenergy for a Cleaner Future: A Case Study of Sustainable Biogas Supply Chain in the Malaysian Energy Sector. - Sustainability 12: 3213.
[15] Bessis, M., Gires, F., Mayer, G., Nomarski, G. (1962): Irradiation des organites cellulaires á l'aide d'un laser á rubis. – CR Acad. Sci 255: 1010-1012.
[16] Bouly, J. P., Schleicher, E., Dionisio-Sese, M., Vandenbussche, F., Van Der Straeten, D., Bakrim, N, Ahmad, M. (2007): Cryptochrome blue light photoreceptors are activated through interconversion of flavin redox states. – Journal of Biological Chemistry 282(13): 9383-9391.
[17] Chen, Y. P., Liu, Y. J., Wang, X. L., Ren, Z. Y., Yue, M. (2005): Effect of microwave and He-Ne laser on enzyme activity and biophoton emission of isatis indigotica fort. – Journal of Integrative Plant Biology 47(7): 849-855.
[18] Colbach, N., Dürr, C., Chauvel, B., Richard, G. (2002): Effect of environmental conditions on Alopecurus myosuroides germination. II. Effect of moisture conditions and storage length. – Weed Research 42(3): 222-230.
[19] Ćwintal, M., Dziwulska-Hunek, A., Wilczek, M. (2010): Laser stimulation effect of seeds on quality of alfalfa. – Int. Agrophys 24(1): 15-19.
[20] Dănăilă-Guidea, S. I., Niculiţă, P., Esofina, R., Mona, P., Marian, R., Floarea, B., Mihaela, G. (2011): The influence of modulated red laser light on seedlings of some annual ornamental species (*Dianthus caryophyllus* and *Petunia hybrida*). – Romanian Biotechnological Letters 16(6 Supplement): 34-39.
[21] El-Naggar, A. Y., Shetaia, Y. M., Youssef, K. A., Ismail, N. A. (2012): Stimulation of the hydrocarbon compounds degrading Saccharomyces rosinii by low power laser radiation. – Der Pharma Chemica 4(4): 1424-1434.
[22] Fadillah, M. N., Marlia, M. H. (2016): Malaysian water footprint accounts: Blue and green water footprint of rice cultivation and the impact of water consumption in Malaysia. – In: AIP Publishing LLC, AIP Conference Proceedings 1784(1): 060025.
[23] FAO, IFAD, IMF, OECD, UNCTAD, WFP (2011): Price volatility in food and agricultural markets: Policy responses. – FAO: Roma, Italy.
[24] Ferdosizadeh, L., Sadat-Noori, S. A., Zare, A., Syghafi, S. (2013): Assessment of diode laser pretreatments on germination and yield of wheat (*Triticum aestivum* L.) under salinity stress. – World Journal of Agricultural Research 1(1): 5-9.
[25] Field, C. B., Barros, V., Stocker, T. F., Dahe, Q. (eds.) (2012): Managing the risks of extreme events and disasters to advance climate change adaptation: special report of the intergovernmental panel on climate change. – Cambridge University Press.
[26] Foley, J. A. (2011): Can we feed the world sustain the planet? – Scientific American 305(5): 60-65.
[27] García-Martinez, J. L., Gil, J. (2001): Light Regulation of Gibberellin Biosynthesis and Mode of Action. – Journal Plant Growth Regulation 20(4): 354-368.
[28] Gładyszewska, B. (2006): Pre-sowing laser biostimulation of cereal grains. – Technology Science 6: 33-38.
[29] Goettoeller, J., Ching, A. (1999): Seed germination in Stevia rebaudiana. – In: Jadick, J. (ed.) Perspective on new crops and new uses. ASHS Press, Alexandria, VA.
[30] Govil, S. R., Agrawal, D. C., Rai, K. P., Thakur, S. N. (1991): Physiological responses of *Vigna radiata* L. to nitrogen and argon+ laser irradiation-Short Communication. – Indian Journal of Plant Physiology 34(1): 72-76.
[31] Hanafiah, M. M., Ghazali, N. F., Harun, S. N., Abdulaali, H. S., AbdulHasan, M. J., Kamarudin, M. K. A. (2019): Assessing water scarcity in Malaysia: a case study of rice production. – Desalination and Water Treatment 149: 274-287.
[32] Harun, S. N., Hanafiah, M. M. (2018): Estimating the country-level water consumption footprint of selected crop production. – Applied Ecology and Environmental Research 16(5): 5381-5403.

http://www.aloki.hu ● ISSN 1589 1623 (Print) ● ISSN 1785 0037 (Online)
DOI: http://dx.doi.org/10.15666/aeer/1804_60096023

[33] Hasan, M., Hanafiah, M. M., Aeyad Taha, Z., AlHilfy, I. H., Said, M. N. M. (2020): Laser Irradiation Effects at Different Wavelengths on Phenology and Yield Components of Pretreated Maize Seed. – Applied Sciences 10(3): 1189.
[34] He, J., Qin, L., Chong, E. L., Choong, T. W., Lee, S. K. (2017): Plant growth and photosynthetic characteristics of *Mesembryanthemum crystallinum* grown aeroponically under different blue-and red-LEDs. – Frontiers in plant science 8: 361.
[35] Hedimbi, M., Singh, S. (2012): Laser induced fluorescence study on the growth of maize plants. – Nat. Sci. 4(06): 395.
[36] Hernandez, A. C., Dominguez-Pacheco, A., Cruz-Orea, A., Ivanov, R., Carballo-Carballo, A., Zepeda-Bautista, R., Galindo Soria, L. (2009): Laser irradiation effects on field performance of maize seed genotypes. – International Agrophysics 23: 327-332.
[37] Hernandez, A. C., Dominguez, P. A., Cruz, O. A., Ivanov, R., Carballo, C. A., Zepeda, B. R. (2010): Laser in agriculture. – International Agrophysics 24(4): 407-422.
[38] Hernández, M., Michtchenko, A. (2011): Stimulation of three Biological Systems Using Low Level Laser Radiation. – RISCE Revista Internacional de Sistemas Computacionales y Electrónicos 83(3): 30-33.
[39] Hernandez, A. C., Dominguez-Pacheco, A., Cruz-Orea, A. (2015): Thermal changes of maize seed by laser irradiation. – International Journal of Thermophysics 36(9): 2401-2409.
[40] Hilhorst, H. W. (2018): Definitions and hypotheses of seed dormancy. – Annual Plant Reviews online, pp. 50-71.
[41] Hoseini, M., Feqenabi, F., Tajbakhsh, M., Babazadeh-Igdir, H. (2013): Introduction of seed treatment techniques (seed priming). – International Journal of Biosciences (IJB) 3(5): 1-12.
[42] Hwida, M. F., Metwally, S. A., Lobna, S. T. (2012): In vitro growth behavior and leaf anatomical structure of Balanites aegyptiaca and Cotoneoster horizontalis affected by different types of laser radiation. – Journal of Applied Sciences Research 8(4): 2386-2396.
[43] Jala, A. (2011): Effects of different light treatments on the germination of Nepenthes mirabilis. – International Transaction Journal of Engineering, Management, & Applied Sciences & Technologies 2(1): 083-091.
[44] Jamil, Y., Perveen, R., Ashraf, M., Ali, Q., Iqbal, M., Ahmad, M. R. (2013): He–Ne laser-induced changes in germination, thermodynamic parameters, internal energy, enzyme activities and physiological attributes of wheat during germination and early growth. – Laser Physics Letters 10(4): 045606.
[45] Jia, Z., Duan, J. (2013): Protecting effect of He-Ne laser on winter wheat from UV-B radiation damage by analyzing proteomic changes in leaves. – Advances in Bioscience and Biotechnology 4(8): 823-829.
[46] Joshi, S., Joshi, G., Agrawal, H. (2012): Study on the effect of laser irradiation on wheat (*Triticum aestivum* L.) variety PBW-373 seeds on zinc uptake by wheat plants. – Journal of Radioanalytical and Nuclear Chemistry 294(3): 391-394.
[47] Kamiya, Y., García-Martínez, J. L. (1999): Regulation of gibberellin biosynthesis by light. – Current opinion in plant biology 2(5): 398-403.
[48] Khalifa, N. S., El Ghandoor, H. (2011): Investigate the effect of Nd-Yag laser beam on soybean (*Glycin max*) leaves at the protein level. – International Journal of Biology 3(2): 135.
[49] Kouchebagh, S. B., Farahvash, F., Mirshekari, B., Arbat, H. K., Khoei, F. R. (2014a): Seed priming techniques may improve grain and oil yields of sunflower (*Helianthus annuus* L.). – The Journal of Animal & Plant Sciences 24(6): 1863-1868.
[50] Kouchebagh, S. B., Farahvash, F., Mirshekari, B., Arbat, H. K., Khoei, F. R. (2014b): Effects of physical treatments on germination and stand establishment of sunflower (*Helianthus annuus* L. var. Hyson) under laboratory condition. – International Journal of Biosciences 5(12): 1-6.

http://www.aloki.hu ● ISSN 1589 1623 (Print) ● ISSN 1785 0037 (Online)
DOI: http://dx.doi.org/10.15666/aeer/1804_60096023

[51] Levskaya, A., Weiner, O. D., Lim, W. A., Voigt, C. A. (2009): Spatiotemporal control of cell signalling using a light-switchable protein interaction. – Nature 461(7266): 997-1001.
[52] Lobna, S. T., Hanan, A. A. T., Metwally, S. A., Hwida, M. F. (2014): Effect of laser radiation treatments on in vitro growth behavior, antioxidant activity and chemical constituents of Sequoia sempervirens. – Research Journal of Pharmaceutical Biological and Chemical Science 5(4): 1024-1034.
[53] MacLeod, A. M., Millar, A. S. (1962): Effects of gibberellic acid on barley endosperm. – Journal of the Institute of Brewing 68(4): 322-332.
[54] Mahmoud, M. M., Ibrahem, S. E. (2000): Plant physiology. – Fac. of Agric., Ain Sams Univ. pp. 164-85.
[55] Metwally, S. A., Abou-Ellail, M., Abo-Leila, B. H., Aboud, K. A. (2013): Effect of laser radiation on the growth, anatomical and biochemical genetic markers of Celosia argentea plants. – International Journal of Academic Research 5(3): 200-205.
[56] Miransari, M., Smith, D. L. (2014): Plant hormones and seed germination. – Environmental and Experimental Botany 99: 110-121.
[57] Mishra, S., Khurana, J. P. (2017): Emerging roles and new paradigms in signaling mechanisms of plant cryptochromes. – Critical reviews in plant sciences 36(2): 89-115.
[58] Mohssen, N. F., Sharafi, Z. M., Siadat, A. (2010): Study the effect of aging acceleration test on germination and seedling growth of wheat cultivars in controlled conditions (in vitro). – Crop Physiology 2(3): 59-71.
[59] Muhammad-Muaz, A., Marlia, M. H. (2014): Water footprint assessment of oil palm in Malaysia: a preliminary study. – In: American Institute of Physics, AIP Conference Proceedings 1614(1): 803-807.
[60] Nasim, H., Jamil, Y. (2014): Diode lasers: From laboratory to industry. – Optics & Laser Technology 56: 211-222.
[61] Osman, Y. A., El-Tobgy, K. M., El-Sherbini, E. S. A. (2009): Effect of laser radiation treatments on growth, yield and chemical constituents of fennel and coriander plants. – Journal Applied Science Research 5: 244-252.
[62] Perveen, R., Ali, Q., Ashraf, M., Al-Qurainy, F., Jamil, Y., Raza Ahmad, M. (2010): Effects of different doses of low power continuous wave He–Ne laser radiation on some seed thermodynamic and germination parameters, and potential enzymes involved in seed germination of sunflower (*Helianthus annuus* L.). – Photochemistry and photobiology 86(5): 1050-1055.
[63] Podlesna, A., Gladyszewska, B., Podlesny, J., Zgrajka, W. (2015): Changes in the germination process and growth of pea in effect of laser seed irradiation. – International Agrophysics 29(4): 485-492.
[64] Podleśny, J., Stochmal, A., Podleśna, A., Misiak, L. E. (2012): Effect of laser light treatment on some biochemical and physiological processes in seeds and seedlings of white lupine and faba bean. – Plant Growth Regulation 67(3): 227-233.
[65] Qi, Z., Yue, M., Han, R., Wang, X. L. (2002): The Damage Repair Role of He–Ne Laser on Plants Exposed to Different Intensities of Ultraviolet-B Radiation. – Photochemistry and photobiology 75(6): 680-686.
[66] Qiu, Z., Li, J., Zhang, M., Bi, Z., Li, Z. (2013): He–Ne laser pretreatment protects wheat seedlings against cadmium-induced oxidative stress. – Ecotoxicology and environmental safety 88: 135-141.
[67] Qiu, Z., Yuan, M., He, Y., Li, Y., Zhang, L. (2017): Physiological and transcriptome analysis of He-Ne laser pretreated wheat seedlings in response to drought stress. – Scientific reports 7(1): 1-12.
[68] Rania, A. T., Lobna, S. T., Metwally, S. A. (2015): In vitro cultures of jojoba (*Simmondsia chinensis* L.) affecting by laser irradiation. – Journal of Chemical, Biological and Physical Sciences. 5(4): 3906-3913.

http://www.aloki.hu ● ISSN 1589 1623 (Print) ● ISSN 1785 0037 (Online)
DOI: http://dx.doi.org/10.15666/aeer/1804_60096023

[69] Rassam, Y. Z. (2010): The Effect of laser light on virulence factors and antibiotic susceptibility of locally isolated Pseudomonas aeruginosa. – Journal of Applied Sciences Research 6(8): 1298-302.
[70] Ribalta, F. M., Pazos-Navarro, M., Edwards, K., Ross, J. J., Croser, J. S., Ochatt, S. J. (2019): Expression patterns of key hormones related to pea (*Pisum sativum* L.) embryo physiological maturity shift in response to accelerated growth conditions. – Frontiers in plant science 10: 1154.
[71] Rimal, B., Ranaivoson, R. M., Czarnecka, K. P., Dobrowolski, J. W. (2014): Laser biotechnology for enhanced rooting and shooting of Salix viminalis in hydroponic condition for better adaptation in industrially contaminated land. – International Journal of Environmental Bioremediation & Biodegradation 2(5): 228-230.
[72] Salyaev, R. K., Dudareva, L. V., Lankevich, S. V., Makarenko, S. P., Sumtsova, V. M., Rudikovskaya, E. G. (2007): Effect of low-intensity laser irradiation on the chemical composition and structure of lipids in wheat tissue culture in doklady. – Biological Sciences 412: 87-88.
[73] Samuilov, F. D., Garifullina, R. L. (2007): Effect of laser irradiation on microviscosity of aqueous medium in imbibing maize seeds as studied with a spin probe method. – Russian Journal of Plant Physiology 54(1): 128.
[74] Śliwka, M. (2014): Assessment of impact of coherent light on resistance of plants growing in unfavourable environmental conditions. – Journal of Ecological Engineering 15(2).
[75] Soliman, A., Harith, M. A. (2009): Effects of Laser Biostimulation on Germination of *Acacia farnesiana* (L.) Willd. – In: XIII International Conference on Medicinal and Aromatic Plants 854: 41-50.
[76] Srećković, M., Vasić, R., Dukić, M., Jevtić, S., Jovanić, P. (2014): The influence of diode and He-Ne Lasers on corn and wheat seeds. – Journal Agricultural Science and Technology 4: 165-175.
[77] Taie, H. A. A., Taha, L. S., Metwally, S. A., Fathy, H. M. (2014): Effect of laser radiation treatments on in vitro growth behavior, antioxidant activity and chemical constituents of Sequoia sempervirens. – Research Journal of Pharmaceutical, Biological and Chemical Sciences 5(4): 1024-1034.
[78] Taiz, L., Zeiger, E. (2011): A Companion to Plant Physiology in the Fifth Edition, Types of Seed Dormancy and the Roles of Environmental Factors. – Sinauer Associates Inc.
[79] Tang, Z., Yu, J., Xie, J., Lyu, J., Feng, Z., Dawuda, M. M., Hu, L. (2019): Physiological and Growth Response of Pepper (*Capsicum annum* L.) Seedlings to Supplementary Red/Blue Light Revealed through Transcriptomic Analysis. – Agronomy 9(3): 139.
[80] Truchliñski, J., Koper, R., Starczynowska, R. (2002): Influence of pre-sowing red light radiation and nitragine dressing of chickling vetch seeds on the chemical composition of their yield. – International Agrophysics 16(2): 147-150.
[81] Tsukaya, H. (1998): Genetic evidence for polarities that regulate leaf morphogenesis. – Journal of plant research 111(1): 113-119.
[82] Wilczek, M., Koper, R., Cwintal, M., Kornillowicz-Kowalska, T. (2005): Germination capacity and health status of hybrid alfalfa seeds after laser treatment. – International agrophysics 19(3): 257.

http://www.aloki.hu ● ISSN 1589 1623 (Print) ● ISSN 1785 0037 (Online)
DOI: http://dx.doi.org/10.15666/aeer/1804_60096023